

G. Sitta Sittampalam • Nathan P. Coussens • Kyle Brimacombe  
Abigail Grossman • Michelle Arkin • Douglas Auld • Chris Austin  
Jonathan Baell • Bruce Bejcek • Jose M.M. Caaveiro  
Thomas D.Y. Chung • Jayme L. Dahlin • Viswanath Devanaryan  
Timothy L. Foley • Marcie Glicksman • Matthew D. Hall  
Joseph V. Haas • James Inglese • Philip W. Iversen • Steven D. Kahl  
Stephen C. Kales • Madhu Lal-Nag • Zhuyin Li • James McGee  
Owen McManus • Terry Riss • O. Joseph Trask, Jr. • Jeffrey R. Weidner  
Mary Jo Wildey • Menghang Xia • Xin Xu

# Assay Guidance Manual

Last Updated: July 1, 2018

Eli Lilly & Company and the National Center for Advancing Translational Sciences, Bethesda (MD)

All Assay Guidance Manual content, except where otherwise noted, is licensed under a [Creative Commons Attribution-NonCommercial-ShareAlike 3.0 Unported](#) license (CC BY-NC-SA 3.0), which permits copying, distribution, transmission, and adaptation of the work, provided the original work is properly cited and not used for commercial purposes. Any altered, transformed, or adapted form of the work may only be distributed under the same or similar license to this one.

Previous Editors: Lisa Minor, PhD, Vance Lemmon, PhD, Andrew Napper, PhD, John M Peltier, PhD, Henrike Nelsen, MS, and Neely Gal-Edd, MS

Contact Information: [NCATS\\_AGM\\_Editors@mail.nih.gov](mailto:NCATS_AGM_Editors@mail.nih.gov)

Cover photo courtesy of Manju Swaroop, Research Scientist, NCATS

NLM Citation: Sittampalam GS, Coussens NP, Brimacombe K, et al., editors. Assay Guidance Manual [Internet]. Bethesda (MD): Eli Lilly & Company and the National Center for Advancing Translational Sciences; 2004-.

This eBook is a comprehensive, crucial resource for investigators optimizing assays to evaluate collections of molecules with the overall goal of developing probes that modulate the activity of biological targets, pathways or cellular phenotypes. Such probes might be candidates for further optimization and investigation in drug discovery and development.

Originally written as a guide for therapeutic project teams within a major pharmaceutical company, this manual has been adapted to provide guidelines for scientists in academic, non-profit, government and industrial research laboratories to develop assay formats compatible with **High Throughput Screening (HTS)** and Structure Activity Relationship (SAR) measurements of new and known molecular entities. Topics addressed in this manual include:

- Descriptions of assay formats that are compatible with **HTS** and determination of SAR
- Selection and development of optimal assay reagents
- Optimizations and troubleshooting for assay protocols with respect to sensitivity, dynamic range, signal intensity and stability
- Adaptations of assays for automation and scaling to microtiter plate formats
- Instrumentation
- Sources of assay artifacts and interferences
- Statistical validation of assay performance parameters
- Secondary assays for chemical probe validation and SAR refinement
- Data standards for reporting the results of screening and SAR assays
- *In vivo* assay development and validation
- Assay development and validation for siRNA-based high-throughput screens

The **National Center for Advancing Translational Sciences (NCATS)** manages the content of the Assay Guidance Manual with input from industry, academia and government experts. More than 100 authors from around the globe have contributed content to this free resource, which is updated quarterly with contributions by experienced scientists from multiple disciplines working in drug discovery and development worldwide.

For more information about the Assay Guidance Manual and related training opportunities, visit <https://ncats.nih.gov/expertise/preclinical/agm>.

## Editors

**G. Sitta Sittampalam, PhD, Editor-in-chief**, National Center for Advancing Translational Sciences, National Institutes of Health

**Nathan P. Coussens, PhD, Editor-in-chief**, National Center for Advancing Translational Sciences, National Institutes of Health

**Kyle Brimacombe, MS, Associate Scientific Editor**, National Center for Advancing Translational Sciences, National Institutes of Health

**Abigail Grossman, Associate Managing Editor**, National Center for Advancing Translational Sciences, National Institutes of Health

**Michelle Arkin, PhD**, University of California, San Francisco

**Douglas Auld, PhD**, Novartis Institutes for Biomedical Research

**Chris Austin, MD**, National Center for Advancing Translational Sciences, National Institutes of Health

**Jonathan Baell, PhD**, Monash Institute of Pharmaceutical Sciences

**Bruce Bejcek, PhD**, Western Michigan University

**Jose M.M. Caaveiro, PhD**, Laboratory of Global Healthcare Graduate School of Pharmaceutical Sciences, Kyushu University

**Thomas D.Y. Chung, PhD**, Conrad Prebys Center for Chemical Genomics, Sanford Burnham Prebys Medical Discovery Institute

**Jayme L. Dahlin, MD, PhD**, Brigham and Women's Hospital

**Viswanath Devanaryan, PhD**, Charles River Laboratories

**Timothy L. Foley, PhD**, Pfizer

**Marcie Glicksman, PhD**, Orig3n

**Matthew D. Hall, PhD**, National Center for Advancing Translational Sciences, National Institutes of Health

**Joseph V. Haas, MS**, Eli Lilly & Company

**James Inglese, PhD**, National Center for Advancing Translational Sciences, National Institutes of Health

**Philip W. Iversen, PhD**, Eli Lilly & Company

**Steven D. Kahl, BS**, Eli Lilly & Company

**Stephen C. Kales, PhD**, National Center for Advancing Translational Sciences, National Institutes of Health

**Madhu Lal-Nag, PhD**, National Center for Advancing Translational Sciences, National Institutes of Health

**Zhuyin Li, PhD**, Bristol-Myers Squibb

**James McGee, PhD**, Eli Lilly & Company

**Owen McManus, PhD**, Q-State Biosciences

**Terry Riss, PhD**, Promega Corporation

**O. Joseph Trask, Jr.**, PerkinElmer, Inc.

**Jeffrey R. Weidner, PhD**, QualSci Consulting, LLC

**Mary Jo Wildey, PhD**, Merck & Co., Inc.

**Menghang Xia, PhD**, National Center for Advancing Translational Sciences, National Institutes of Health

**Xin Xu, PhD**, National Center for Advancing Translational Sciences, National Institutes of Health

# Table of Contents

|  |      |
|--|------|
| New in Assay Guidance Manual .....   | xi   |
| Preface .....  | xiii |
| <i>G. Sitta Sittampalam and Nathan P. Coussens</i>   |      |
| Acknowledgements .....   | xix  |
| <b>Considerations for Early Phase Drug Discovery</b> .....   | 1    |
| <i>Michelle Arkin, Nathan P. Coussens, Viswanath Devanaryan, Zhuyin Li, and G. Sitta Sittampalam</i>   |      |
| Early Drug Discovery and Development Guidelines: For Academic Researchers, Collaborators, and Start-up Companies .....   | 3    |
| <i>Jeffrey Strovel, Sitta Sittampalam, Nathan P. Coussens, Michael Hughes, James Inglese, Andrew Kurtz, Ali Andalibi, Lavonne Patton, Chris Austin, Michael Baltezor, Michael Beckloff, Michael Weingarten, and Scott Weir</i> |      |
| <b>In Vitro Biochemical Assays</b> .....   | 45   |
| <i>Michelle Arkin, Douglas Auld, Kyle Brimacombe, Nathan P. Coussens, Matthew D. Hall, James Inglese, Steven D. Kahl, Stephen C. Kales, Zhuyin Li, James McGee, G. Sitta Sittampalam, and Jeffrey R. Weidner</i>               |      |
| Validating Identity, Mass Purity and Enzymatic Purity of Enzyme Preparations .....   | 47   |
| <i>John E Scott and Kevin P Williams</i>   |      |
| Basics of Enzymatic Assays for HTS .....   | 63   |
| <i>Harold B. Brooks, Sandaruwan Geeganage, Steven D. Kahl, Chahrzad Montrose, Sitta Sittampalam, Michelle C. Smith, and Jeffrey R. Weidner</i>   |      |
| Mechanism of Action Assays for Enzymes .....   | 77   |
| <i>John Strelow, Walther Dewe, Phillip W Iversen, Harold B Brooks, Jeffrey A Radding, James McGee, and Jeffrey Weidner</i>   |      |
| Assay Development for Protein Kinase Enzymes .....   | 105  |
| <i>J. Fraser Glickman</i>  |      |
| Receptor Binding Assays for HTS and Drug Discovery .....   | 129  |
| <i>Douglas S Auld, Mark W. Farmen, Steven D. Kahl, Aidas Kriauciunas, Kevin L. McKnight, Chahrzad Montrose, and Jeffrey R. Weidner</i>   |      |
| Protease Assays .....  | 177  |
| <i>Guofeng Zhang</i>   |      |
| Inhibition of Protein-Protein Interactions: Non-Cellular Assay Formats .....   | 191  |
| <i>Michelle R. Arkin, Marcie A. Glicksman, Haiyan Fu, Jonathan J. Havel, and Yuhong Du</i>   |      |
| Immunoassay Methods .....  | 221  |
| <i>Karen L. Cox, Viswanath Devanarayan, Aidas Kriauciunas, Joseph Manetta, Chahrzad Montrose, and Sitta Sittampalam</i>  |      |
| GTP $\gamma$ S Binding Assays .....  | 265  |
| <i>Neil W. DeLapp, Wendy H. Gough, Steven D. Kahl, Amy C. Porter, and Todd R. Wiernicki</i>  |      |

|  |     |
|--|-----|
| Histone Acetyltransferase Assays in Drug and Chemical Probe Discovery .....  | 279 |
| <i>Sanket Gadhia, Jonathan H. Shrimp, Jordan L. Meier, James E. McGee, and Jayme L. Dahlin</i>   |     |
| <b>In Vitro Cell Based Assays</b> .....  | 333 |
| <i>Douglas Auld, Bruce Bejcek, Kyle Brimacombe, Nathan P. Coussens, Timothy L. Foley, Marcie Glicksman, Matthew D. Hall, James Inglese, Stephen C. Kales, Madhu Lal-Nag, Zhuyin Li, Owen McManus, Terry Riss, G. Sitta Sittampalam, O. Joseph Trask, Jr., and Menghang Xia</i> |     |
| Authentication of Human Cell Lines by STR DNA Profiling Analysis .....   | 335 |
| <i>Yvonne Reid, Douglas Storts, Terry Riss, and Lisa Minor</i>   |     |
| Cell Viability Assays .....  | 357 |
| <i>Terry L Riss, Richard A Moravec, Andrew L Niles, Sarah Duellman, H el ene A Benink, Tracy J Worzella, and Lisa Minor</i>  |     |
| <i>In vitro</i> 3D Spheroids and Microtissues: ATP-based Cell Viability and Toxicity Assays .....  | 389 |
| <i>Monika Kijanska and Jens Kelm</i>   |     |
| Cell-Based RNAi Assay Development for HTS .....  | 405 |
| <i>Scott Martin, Gene Buehler, Kok Long Ang, Farhana Feroze, Gopinath Ganji, and Yue Li</i>  |     |
| FLIPR <sup>TM</sup> Assays for GPCR and Ion Channel Targets .....  | 433 |
| <i>Michelle R. Arkin, Patrick R. Connor, Renee Emkey, Kim E. Garbison, Beverly A. Heinz, Todd R. Wiernicki, Paul A. Johnston, Ramani A. Kandasamy, Nancy B. Rankl, and Sitta Sittampalam</i>   |     |
| Ion Channel Screening .....  | 465 |
| <i>Owen B McManus, Maria L Garcia, David Weaver, Melanie Bryant, Steven Titus, and James B Herrington</i>  |     |
| Automated Electrophysiology Assays .....   | 493 |
| <i>Birgit T. Priest, Rok Cerne, Michael J. Krambis, William A. Schmalhofer, Mark Wakulchik, Benjamin Wilenkin, and Kevin D. Burris</i>   |     |
| Assay Development Guidelines for Image-Based High Content Screening, High Content Analysis and High Content Imaging: Image-Based High Content Screening and Analysis .....   | 543 |
| <i>William Buchser, Mark Collins, Tina Garyantes, Rajarshi Guha, Steven Haney, Vance Lemmon, Zhuyin Li, and O. Joseph Trask</i>  |     |
| Advanced Assay Development Guidelines for Image-Based High Content Screening and Analysis .....  | 619 |
| <i>Mark-Anthony Bray and Anne Carpenter; Imaging Platform, Broad Institute of MIT and Harvard</i>  |     |
| Nuclear Factor Kappa B (NF- $\kappa$ B) Translocation Assay Development and Validation for High Content Screening: NF- $\kappa$ B Translocation Assay Development and Validation for High Content Screening .....  | 653 |
| <i>O. Joseph Trask, Jr</i>   |     |
| High Content Screening with Primary Neurons .....  | 697 |
| <i>Hassan Al-Ali, Murray Blackmore, John L Bixby, and Vance P. Lemmon</i>  |     |
| Phospho-ERK Assays .....   | 737 |

|  |      |
|--|------|
| <i>Kim E. Garbison, Beverly A. Heinz, Mary E. Lajiness, Jeffrey R. Weidner, and G. Sitta Sittampalam</i>   |      |
| IP-3/IP-1 Assays.....  | 745  |
| <i>Kim E. Garbison, Beverly A. Heinz, and Mary E. Lajiness</i>   |      |
| Cardiomyocyte Impedance Assays.....  | 753  |
| <i>Sarah D. Lamore, Clay W Scott, and Matthew F. Peters</i>  |      |
| Screening for Target Engagement using the Cellular Thermal Shift Assay - CETSA.....  | 767  |
| <i>Hanna Axelsson, Helena Almqvist, Brinton Seashore-Ludlow, and Thomas Lundbäck</i>   |      |
| Measurement of cAMP for G <sub>αs</sub> - and G <sub>αi</sub> Protein-Coupled Receptors (GPCRs).....   | 797  |
| <i>Tao Wang, Zhuyin Li, Mary Ellen Cvijic, Litao Zhang, and Chi Shing Sum</i>  |      |
| Measurement of β-Arrestin Recruitment for GPCR Targets.....  | 823  |
| <i>Tao Wang, Zhuyin Li, Mary Ellen Cvijic, Carol Krause, Litao Zhang, and Chi Shing Sum</i>  |      |
| Genome Editing Using Engineered Nucleases and Their Use in Genomic Screening.....  | 837  |
| <i>Joana R. Costa, Bruce E. Bejcek, James E. McGee, Adam I. Fogel, Kyle R. Brimacombe, and Robin Ketteler</i>  |      |
| Inhibition of Protein-Protein Interactions: Cell-Based Assays.....   | 869  |
| <i>Mark Wade, Jacqui Méndez, Nathan P. Coussens, Michelle R. Arkin, and Marcie A. Glicksman</i>  |      |
| <b>In Vivo Assay Guidelines</b> .....  | 905  |
| <i>Viswanath Devanaryan, Joseph V. Haas, and Philip W. Iversen</i>   |      |
| <i>In Vivo Assay Guidelines</i> .....  | 907  |
| <i>Joseph Haas, Jason Manro, Harlan Shannon, Wes Anderson, Joe Brozinick, Arunava Chakravarty, Mark Chambers, Jian Du, Brian Eastwood, Joe Heuer, Stephen Iturria, Philip Iversen, Dwayne Johnson, Kirk Johnson, Michael O’Neill, Hui-Rong Qian, Dana Sindelar, and Kjell Svensson</i> |      |
| <i>In Vivo Receptor Occupancy in Rodents by LC-MS/MS</i> .....   | 955  |
| <i>Cynthia D. Jesudason, Susan DuBois, Megan Johnson, Vanessa N. Barth, and Anne B. Need</i>   |      |
| <b>Assay Artifacts and Interferences</b> .....   | 967  |
| <i>Michelle Arkin, Douglas Auld, Jonathan Baell, Kyle Brimacombe, Jayme L. Dahlin, Timothy L. Foley, James Inglese, and Stephen C. Kales</i>   |      |
| Assay Interference by Chemical Reactivity.....   | 969  |
| <i>Jayme L. Dahlin, Jonathan Baell, and Michael A. Walters</i>   |      |
| Interference with Fluorescence and Absorbance.....   | 1013 |
| <i>Anton Simeonov and Mindy I. Davis</i>   |      |
| Interferences with Luciferase Reporter Enzymes.....  | 1027 |
| <i>Douglas S. Auld and James Inglese</i>   |      |
| Assay Interference by Aggregation.....   | 1043 |
| <i>Douglas S. Auld, James Inglese, and Jayme L. Dahlin</i>   |      |
| <b>Assay Validation, Operations and Quality Control</b> .....  | 1077 |



*Viswanath Devanaryan, Timothy L. Foley, Madhu Lal-Nag, Jeffrey R. Weidner, and Mary Jo Wildey*

|   |      |
|---|------|
| Development and Applications of the Bioassay Ontology (BAO) to Describe and Categorize High-Throughput Assays: Development and Applications of the BAO to Describe and Categorize High-Throughput Assays.....   | 1079 |
| <i>Uma D. Vempati and Stephan C. Schürer</i>  |      |
| Data Standardization for Results Management .....   | 1109 |
| <i>Robert M. Campbell, Julia Dymshitz, Brian J. Eastwood, Renee Emkey, David P. Greenen, Julia M. Heerding, Dwayne Johnson, Thomas H. Large, Thomas Littlejohn, Chahrzad Montrose, Suzanne E. Nutter, Barry D. Sawyer, Sandra K. Sigmund, Martin Smith, Jeffrey R. Weidner, and Richard W. Zink</i> |      |
| HTS Assay Validation .....  | 1131 |
| <i>Philip W. Iversen, Benoit Beck, Yun-Fei Chen, Walther Dere, Viswanath Devanarayan, Brian J Eastwood, Mark W. Farmen, Stephen J. Iturria, Chahrzad Montrose, Roger A. Moore, Jeffrey R. Weidner, and G. Sitta Sittampalam</i>   |      |
| Assay Operations for SAR Support .....  | 1163 |
| <i>Benoit Beck, Yun-Fei Chen, Walther Dere, Viswanath Devanarayan, Brian J. Eastwood, Mark W. Farmen, Stephen J. Iturria, Phillip W. Iversen, Steven D. Kahl, Roger A. Moore, Barry D. Sawyer, and Jeffrey Weidner</i>  |      |
| Minimum Significant Ratio – A Statistic to Assess Assay Variability .....   | 1179 |
| <i>Joseph V. Haas, Brian J. Eastwood, Philip W. Iversen, Viswanath Devanarayan, and Jeffrey R. Weidner</i>  |      |
| <b>Assay Technologies</b> .....   | 1195 |
| <i>Michelle Arkin, Douglas Auld, Kyle Brimacombe, Thomas D.Y. Chung, Nathan P. Coussens, Marcie Glicksman, Zhuyin Li, James McGee, Owen McManus, and G. Sitta Sittampalam</i>   |      |
| HPLC-MS/MS for Hit Generation .....   | 1197 |
| <i>Stefan Jon Thibodeaux, David A Yurek, and James E McGee</i>  |      |
| Impedance-Based Technologies .....  | 1219 |
| <i>Kim E. Garbison, Beverly A. Heinz, Mary E. Lajiness, Jeffrey R. Weidner, and G. Sitta Sittampalam</i>  |      |
| <b>Instrumentation</b> .....  | 1229 |
| <i>Marcie Glicksman, James McGee, and G. Sitta Sittampalam</i>  |      |
| Basics of Assay Equipment and Instrumentation for High Throughput Screening.....  | 1231 |
| <i>Eric Jones, Sam Michael, and G. Sitta Sittampalam</i>  |      |
| Calculations and Instrumentation used for Radioligand Binding Assays .....  | 1263 |
| <i>Steven D. Kahl, G. Sitta Sittampalam, and Jeffrey Weidner</i>  |      |
| <b>Pharmacokinetics and Drug Metabolism</b> .....   | 1283 |
| <i>Xin Xu</i>   |      |
| <i>In Vitro and In Vivo Assessment of ADME and PK Properties During Lead Selection and Lead Optimization – Guidelines, Benchmarks and Rules of Thumb: In Vitro / In Vivo Assessment of ADME and PK Properties During Lead Selection / Optimization</i> .....  | 1285 |
| <i>Thomas D.Y. Chung, David B. Terry, and Layton H. Smith</i>   |      |

|   |      |
|---|------|
| <b>Glossary</b> .....   | 1303 |
| Glossary of Quantitative Biology Terms .....  | 1305 |
| <i>Viswanath Devanarayan, Barry D. Sawyer, Chahrzad Montrose, Dwayne Johnson, David P. Greenen, Sitta Sittampalam, Terry Riss, and Lisa Minor</i> |      |

# New in Assay Guidance Manual

## **New Chapters**

Measurement of cAMP for Gas- and Gai Protein-Coupled Receptors (GPCRs) 20 Nov 2017

Measurement of  $\beta$ -Arrestin Recruitment for GPCR Targets 20 Nov 2017

Genome Editing Using Engineered Nucleases and Their Use in Genomic Screening 20 Nov 2017

Inhibition of Protein-Protein Interactions: Cell-Based Assays 20 Nov 2017

Histone Acetyltransferase Assays in Drug and Chemical Probe Discovery 26 Jul 2017

## **Recently Updated Chapters**

Receptor Binding Assays for HTS and Drug Discovery 01 Jul 2018

Histone Acetyltransferase Assays in Drug and Chemical Probe Discovery 01 Jul 2018

Interference with Fluorescence and Absorbance 01 Jul 2018

Interferences with Luciferase Reporter Enzymes 01 Jul 2018

Assay Operations for SAR Support 20 Nov 2017



# Preface

G. Sitta Sittampalam, PhD<sup>1</sup> and Nathan P. Coussens, PhD<sup>1</sup>

Created: May 1, 2012; Updated: March 31, 2017.

## Introduction to the Assay Guidance Manual

The Assay Guidance Manual (AGM) provides guidance on developing robust *in vitro* and *in vivo* assays for biological targets, pathways, and cellular phenotypes in the context of drug discovery and development. The proper development and implementation of such assays is critical for an appropriate evaluation of chemical compounds, probes, or siRNA collections. Chemical probes can be candidates for further optimization and development as potential therapeutics, which might require multiple variations of these assays, reagents, and analytical processes.

This manual began as the *Guidelines for Screening* in 1995 at Eli Lilly & Company and Sphinx Pharmaceuticals. With contributions from well over 100 drug discovery scientists, the manual grew substantially and was named the *Quantitative Biology Manual* in the late 1990s. Internally, the *Quantitative Biology Manual* provided valuable reference and training materials for the scientists. As the NIH Molecular Libraries and Imaging Roadmap program developed in 2003, discussions between Jim Inglese, PhD, Doug Auld, PhD, and Chris Austin, MD, at the NIH and the management at Eli Lilly and Sphinx Pharmaceuticals resulted in an agreement to publish this manual on the NIH Chemical Genomics Center (NCGC) website. The goals were to share best practices in quantitative biology and the development of robust assay methods throughout the drug discovery community in addition to enhancing academic-industrial collaborations in translational biology and medicine.

The AGM requires regular updates and the addition of new content as drug discovery technologies, assay methodologies, and best practices continue to evolve and improve. To accomplish this efficiently, the AGM was published as an eBook on the National Library of Medicine/National Center for Biotechnology Information (NLM/NCBI) website. The eBook format has several advantages: (a) it is freely available to a worldwide audience, (b) AGM chapters have PMID citations for contributing authors, and (c) high quality is maintained by a centralized submission process that accommodates updates and edits to chapters. The current eBook is an updated version of the original manual published by NCGC, which encompassed 18 chapters. The first eBook edition of the AGM, published on May 1, 2012, included three new chapters. Content is added to address emerging technologies and translational processes, and reflect best practices in assay development and validation amidst the rapidly changing drug discovery landscape. The AGM is sponsored by the National Center for Advancing Translational Sciences (NCATS) and is managed by an editorial board with members from industry, academia, and other translational research laboratories who have extensive experience (>20 years) in drug

<sup>1</sup> National Center for Advancing Translational Sciences, National Institutes of Health.

discovery and development. Our thanks and gratitude goes to the past and present editorial board members for having been diligent and committed during the past 14 years in bringing this endeavor together.

Originally written as a guide for therapeutic project teams within a major pharmaceutical company, this manual has been adapted to provide guidelines for scientists in academic, nonprofit, government, and industrial research laboratories. The scope encompasses the development of biologically, physiologically, and pharmacologically relevant assay formats compatible with high-throughput screening (HTS) and structure activity relationship (SAR) assessments of new and known molecular entities. Topics addressed in this manual include:

- a. Descriptions of assay formats that are compatible with HTS and determination of SAR
- b. Selection and development of optimal assay reagents
- c. Optimizations for assay protocols with respect to sensitivity, dynamic range, signal intensity and stability
- d. Adaptations of assays for automation and scaling to microtiter plate formats
- e. Statistical validation of assay performance parameters
- f. Secondary assays for chemical probe validation and SAR refinement
- g. Data standards for reporting the results of screening and SAR assays
- h. *In vivo* assay development and validation
- i. Assay development and validation for siRNA-based high-throughput screens

## General Definition of Biological Assays

*An assay is an analytical measurement procedure defined by a set of reagents that produces a detectable signal, allowing a biological process to be quantified.* In general, the quality of an assay is defined by the robustness and reproducibility of this signal in the absence of any test compounds or in the presence of inactive compounds. Assay quality depends on the type of signal measured (absorbance, fluorescence, luminescence, radioactivity, etc.), reagents, reaction conditions, analytical and automation instrumentation, as well as statistical models for the data analysis. Subsequently, the quality of a high-throughput screen is defined by the behavior of a given assay utilized to screen a collection of compounds. These two general concepts, assay quality and the quality of data collected for predictive analysis of biological and pharmacological activities, are discussed with specific examples in the AGM chapters.

In practice, assays developed for HTS and SAR measurements can be roughly characterized as cell-free (biochemical) or cell-based procedures. The choice of either a biochemical or cell-based assay along with the particular assay format is ultimately a balancing act. On one side of the fulcrum is the need to ensure that the measured signal is capable of providing data that is biologically relevant. On the other side is the requirement for an assay to yield robust data in microtiter plate formats where typically  $10^5$  to  $10^6$  samples are screened during an HTS operation.

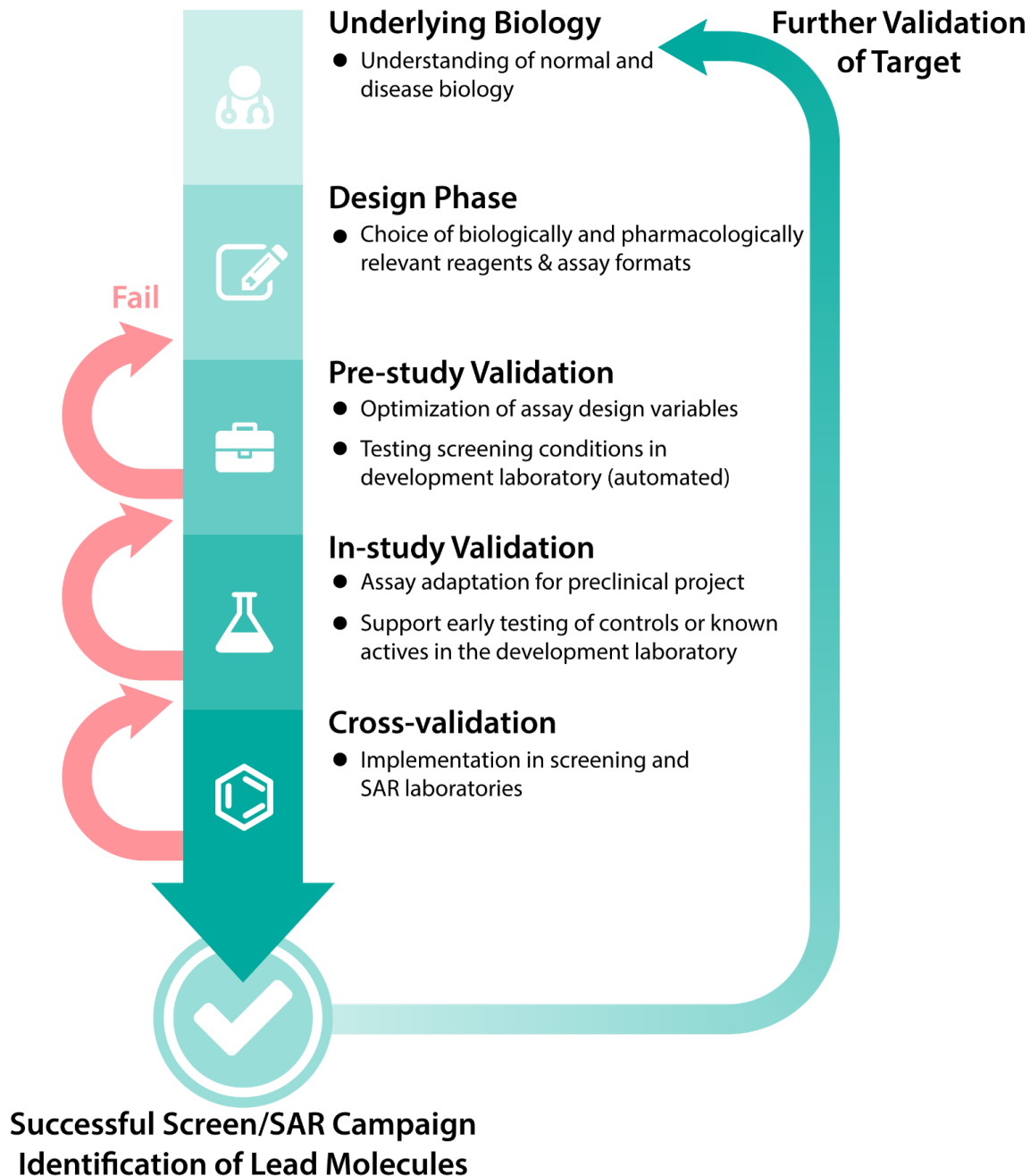


**Figure 1.** The Assay Development and Validation Cycle. The cycle begins in the design phase, which is followed by multiple validation steps that are executed at different stages throughout the assay life cycle, including: pre-study (pre-screen) validation, in-study (in-screen) validation, and cross-validation (assay transfer validation). Failure to validate the assay in any of these steps requires either addressing the deficiency or developing a new assay that meets the validation requirements (figure by Kyle Brimacombe).

## General Concepts in Assay Development and Validation

The investigator must validate a biological assay system and methodology by proceeding through a series of steps along the pathway to HTS and SAR. *The overall objective of any assay validation procedure is to demonstrate that the assay is acceptable for its intended purpose.* As mentioned above, the purpose can be to determine the biological and/or pharmacological activities of new chemical entities on pathways involved in normal and disease processes. The acceptability of an assay begins with its design, construction, and execution in automated or semi-automated procedures, which can significantly affect its performance and robustness.

The assay development and validation cycle is a process with multiple validation steps (Figure 1). Successful completion of assay validation increases the likelihood of success in a drug discovery or chemical probe development program. During the design phase, assay conditions and procedures are selected to minimize the impact of potential sources of invalidity on the measurement of an analyte or biological endpoint in targeted sample matrices or test solutions. False positive and false negative hit rates are related to the selectivity and sensitivity of an assay, respectively. Additionally, technology-related artifacts, such as interference with the reporter system, also contribute to invalid results. Many other variables including assay automation, pipetting, reagent stability, quantities of available reagent, and data analysis models impact the overall validity of an assay.

There are three fundamental areas in assay development and validation: (a) pre-study (pre-screen) validation, (b) in-study (in-screen) validation, and (c) cross-validation or assay transfer validation. These stages encompass the systematic scientific steps within the assay development and validation cycle. Rigorous validation is critical considering that assays are expected to perform robustly over several years during preclinical development.

### Pre-study Validation

The investigator is faced with a number of choices with respect to the assay format and design. For many well-characterized target classes there are a number of assays and commercially available kits. At this stage the choice of an assay format is made. Close attention must be paid to factors such as the selection of reagents with appropriate biological relevance (e.g. cell type, enzyme-substrate combination, form of enzyme/protein target, readout labels, etc.), specificity, and stability. The choice of detection is also made at this stage. If fluorescent labels are chosen, careful attention must be paid to the wavelength to ensure low interference by test compounds, compatibility with microtiter plate plastics, and the availability of appropriate filters for the plate readers. Validation of assay performance should proceed smoothly if high-quality reagents and procedures are chosen. Assessment of assay performance requires appropriate statistical analysis of confirmatory data using appropriate reagents, assay conditions and control compounds. The assessment is made from planned experiments and the analytical results must satisfy predefined acceptance criteria. If control compounds or reagents are available, the assay sensitivity and pharmacology is evaluated. The [HTS Assay Validation](#) chapter illustrates



common procedures for compound evaluation using dose-response curves. Several examples of assay design and optimization are given for well-studied target classes in other chapters of the AGM.

## In-study Validation

In-study validation is needed to verify that an assay remains acceptable during its *routine use*. For assays to be conducted in automated (larger compound screening, HTS), or even semi-automated (a series of compounds during SAR) modes, the assay must be adapted to microtiter plate volumes that are standard in preclinical screening laboratories. Therefore, plate acceptance testing is required where the assay is run in several microtiter plates (at least 96-well plates). From this data, statistical measures of assay performance, such as Z-factors, are calculated. Some assays might require additional experiments to validate the automation and scale-up that might not have been addressed in earlier stages. The plates should contain appropriate maximum and minimum control samples to serve as quality controls for each run and indicate the assay performance. If positive and negative control compounds are available, they can be used to establish maximum and minimum (or basal) signals as appropriate. This will allow the investigator to identify procedural errors and to evaluate stability of the assay over time. Examining a randomly selected subset of test compounds at multiple concentrations monitors parallelism of test and standard curve samples. The [HTS Assay Validation](#) chapter illustrates the procedures typically used to evaluate assay performance in microtiter plates and some of the common artifacts that are observed.

## Cross-validation

Cross-validation is required if an assay is transferred from the individual investigator's team to a high-throughput screening center or other laboratories collaborating on the project. More broadly, this procedure can be used at any stage to verify that an acceptable level of agreement exists in analytical results *before* and *after* procedural changes to an assay (reagents, instrumentation, personnel, lab location, etc.), as well as between results from two or more assays or laboratories. Typically, each laboratory performs the assay with a subset of compounds using the same well-documented protocols, and the agreement in results is compared to *predefined criteria* that specify the allowable performance of the assay during transfer. Considerations for adapting assays to automated robotic screening protocols are also discussed in the chapters of this manual. Note that the modification of assays to miniaturized 384- and 1536-well microtiter plate formats, which minimize costly reagent use and increase throughput, is not trivial. These formats should be rigorously validated before changing the assay operation from a 96-well format to higher density plates, because the assumption that a reduction in volume will not affect the results is not valid. Note that this might happen inadvertently if assay methods are transferred to collaborators and remote labs.

## Critical Path

The entire compound development program, whether intended for chemical probe or drug discovery efforts, encompasses a series of assays which have been subjected to the process described above. These assays are set in place to answer key questions along the path of development to identify compounds with desired properties. For example, assays acting as “counter-screens” can serve to identify direct interference with the detection technology. Orthogonal assays serve to provide additional evidence for targeted activity. Selectivity assays can provide information on the general specificity of a compound or compound series. Biophysical assays can be used to confirm direct binding of a compound to the target. Cell-based assays can be implemented to measure efficacy of a compound in disease-relevant cell types with specific biomarkers. *In vivo* assays can serve as models of the disease, while proof-of-concept clinical assays serve as a measure of efficacy in humans. Placing the right assays at the appropriate points will define the success of a program and the chosen configuration of these assays is referred to as the “critical path”.

## Additional References

1. Smith WC, Sittampalam GS. Conceptual and statistical issues in the validation of analytic dilution assays for pharmaceutical applications. *J Biopharm Stat.* 1998;8(4): 509–32. doi: [10.1080/10543409808835257](https://doi.org/10.1080/10543409808835257). PubMed PMID: 9855031.
2. Findlay JW, Smith WC, Lee JW, Nordblom GD, Das I, DeSilva BS, et al. Validation of immunoassays for bioanalysis: a pharmaceutical industry perspective. *J Pharm Biomed Anal.* 2000;21(6):1249–73. PubMed PMID: 10708409.
3. Inglese J, Johnson RL, Simeonov A, Xia M, Zheng W, Austin CP, et al. High-throughput screening assays for the identification of chemical probes. *Nat Chem Biol.* 2007;3(8):466–79. doi: [10.1038/nchembio.2007.17](https://doi.org/10.1038/nchembio.2007.17). PubMed PMID: 17637779.
4. Thorne N, Auld DS, Inglese J. Apparent activity in high-throughput screening: origins of compound-dependent assay interference. *Curr Opin Chem Biol.* 2010;14(3):315–24. doi: [10.1016/j.cbpa.2010.03.020](https://doi.org/10.1016/j.cbpa.2010.03.020). PubMed PMID: 20417149; PubMed Central PMCID: PMC2878863.
5. Dahlin JL, Inglese J, Walters MA. Mitigating risk in academic preclinical drug discovery. *Nat Rev Drug Discov.* 2015;14(4):279–94. doi: [10.1038/nrd4578](https://doi.org/10.1038/nrd4578). PubMed PMID: 25829283.

## Acknowledgements

We would like to thank our collaborators at the National Library of Medicine/National Center for Biotechnology Information (NLM/NCBI), who have been very helpful in the transition of the Assay Guidance Manual from the wiki format to the Bookshelf in 2012, and for their continued efforts in keeping the manual updated. Special thanks go to NCBI Director David Lipman and Jim Ostell, Chief, Information Engineering Branch at NCBI, and to the Bookshelf and PubMed Central development teams, especially Marilu Hoepfner and Sam Grammer.



# Considerations for Early Phase Drug Discovery

Michelle Arkin, PhD, Nathan P. Coussens, PhD, Viswanath Devanaryan, PhD,  
Zhuyin Li, PhD, and G. Sitta Sittampalam, PhD



# Early Drug Discovery and Development Guidelines: For Academic Researchers, Collaborators, and Start-up Companies

Jeffrey Strovel,<sup>1</sup> Sitta Sittampalam,<sup>2</sup> Nathan P. Coussens,<sup>2</sup> Michael Hughes,<sup>3</sup> James Inglese,<sup>2</sup> Andrew Kurtz,<sup>4</sup> Ali Andalibi,<sup>4</sup> Lavonne Patton,<sup>5</sup> Chris Austin,<sup>6</sup> Michael Baltezor,<sup>3</sup> Michael Beckloff,<sup>5</sup> Michael Weingarten,<sup>4</sup> and Scott Weir<sup>3</sup>

Created: May 1, 2012; Updated: July 1, 2016.

## Abstract

Setting up drug discovery and development programs in academic, non-profit and other life science research companies requires careful planning. This chapter contains guidelines to develop therapeutic hypotheses, target and pathway validation, proof of concept criteria and generalized cost analyses at various stages of early drug discovery. Various decision points in developing a New Chemical Entity (NCE), description of the exploratory Investigational New Drug (IND) and orphan drug designation, drug repurposing and drug delivery technologies are also described and geared toward those who intend to develop new drug discovery and development programs.

Note: The estimates and discussions below are modeled for an oncology drug New Molecular Entity (NME) and repurposed drugs. For other disease indications these estimates might be significantly higher or lower.

## Background

Medical innovation in America today calls for new collaboration models that span government, academia, industry and disease philanthropy. Barriers to translation and ultimate commercialization will be lowered by bringing best practices from industry into academic settings, and not only by training a new generation of 'translational' scientists prepared to move a therapeutic idea forward into proof of concept in humans, but also by developing a new cadre of investigators skilled in regulatory science.

As universities begin to focus on commercializing research, there is an evolving paradigm for drug discovery and early development focused innovation within the academic enterprise. The innovation process -- moving from basic research to invention and to

---

<sup>1</sup> ConverGene, LLC, Gaithersburg, MD. <sup>2</sup> National Center for Advancing Translational Sciences (NCATS), National Institutes for Health (NIH), Bethesda, MD. <sup>3</sup> Institute for Advancing Medical Innovation, University of Kansas, Lawrence, KS. <sup>4</sup> Small Business Innovation Research, National Cancer Institute, Washington, DC. <sup>5</sup> Beckloff Associates, Inc. Overland Park, KS. <sup>6</sup> NIH Chemical Genomics Center, Bethesda, MD.

commercialization and application -- will remain a complex and costly journey. New funding mechanisms, the importance of collaborations within and among institutions, the essential underpinnings of public-private partnerships that involve some or all sectors, the focus of the new field of regulatory science, and new appropriate bridges between federal health and regulatory agencies all come to bear in this endeavor.

We developed these guidelines to assist academic researchers, collaborators and start-up companies in advancing new therapies from the discovery phase into early drug development, including evaluation of therapies in human and/or clinical proof of concept. This chapter outlines necessary steps required to identify and properly validate drug targets, define the utility of employing probes in the early discovery phase, medicinal chemistry, lead optimization, and preclinical proof of concept strategies, as well as address drug delivery needs through preclinical proof of concept. Once a development candidate has been identified, the guidelines provide an overview of human and/or clinical proof of concept enabling studies required by regulatory agencies prior to initiation of clinical trials. Additionally, the guidelines help to ensure quality project plans are developed and projects are advanced consistently. We also outline the expected intellectual property required at key decision points and the process by which decisions may be taken to move a project forward.

## Purpose

The purpose of this chapter is to define:

- Three practical drug discovery and early development paths to advancing new cancer therapies to early stage clinical trials, including:
  1. Discovery and early development of a New Chemical Entity (NCE)
  2. Discovery of new, beneficial activity currently marketed drugs possess against novel drug targets, also referred to as “drug repurposing”
  3. Application of novel platform technology to the development of improved delivery of currently marketed drugs
- Within each of the three strategies, decision points have been identified along the commercial value chain and the following concepts have been addressed:
  - Key data required at each decision point, targets and expectations required to support further development
  - An estimate of the financial resources needed to generate the data at each decision point
  - Opportunities available to outsource activities to optimally leverage strengths within the institution
  - Integration of these activities with the intellectual property management process potential decision points which:
    - Offer opportunities to initiate meaningful discussions with regulatory agencies to define requirements for advancement of new cancer therapies to human evaluation



- Afford opportunities to license technologies to university start-up, biotechnology and major pharmaceutical companies
- Define potential role(s) the National Institutes of Health SBIR programs may play in advancing new cancer therapies along the drug discovery and early development path

## Scope

The scope of drug discovery and early drug development within the scope of these guidelines spans **target identification through human (Phase I) and/or clinical (Phase IIa) proof of concept**. This chapter describes an approach to drug discovery and development for the treatment, prevention, and control of cancer. The guidelines and decision points described herein may serve as the foundation for collaborative projects with other organizations in multiple therapeutic areas.

## Assumptions

1. These guidelines are being written with target identification as the initial decision point, although the process outlined here applies to a project initiated at any of the subsequent points.
2. The final decision point referenced in this chapter is human and/or clinical proof of concept. Although the process for new drug approval is reasonably well defined, it is very resource intensive and beyond the focus of most government, academic, and disease philanthropy organizations conducting drug discovery and early drug development activities.
3. The decision points in this chapter are specific to the development of a drug for the treatment of relapsed or refractory late stage cancer patients. Many of the same criteria apply to the development of drugs intended for other indications and therapeutic areas, but each disease should be approached with a logical customization of this plan. Development of compounds for the prevention and control of cancer would follow a more conservative pathway as the benefit/risk evaluation for these compounds would be different. When considering prevention of a disease one is typically treating patients at risk, but before the disease has developed in individuals that are otherwise healthy. The development criteria for these types of compounds would be more rigorous initially and would typically include a full nonclinical development program to support the human studies. Similarly, compounds being developed to control cancer suggest that the patients may have a prolonged life expectation such that long term toxicity must be fully evaluated before exposing a large patient population to the compound. **The emphasis of the current chapter is on the development of compounds for the treatment of late stage cancer patients.**
4. Human and/or clinical proof of concept strategies will differ depending upon the intent of the product (treatment, prevention, or control). The concepts and

strategies described in this chapter can be modified for the development of a drug for prevention or control of multiple diseases.

5. The cost estimates and decision points are specific to the development of a small molecule drug. Development of large molecules will require the evaluation of additional criteria and may be very specific to the nature of the molecule under development.
6. This plan is written to describe the resources required at each decision point and does not presume that licensing will occur only at the final decision point. It is incumbent upon the stakeholders involved to decide the optimal point at which the technology should move outside their institution.
7. The plan described here does not assume that the entire infrastructure necessary to generate the data underlying each decision criterion is available at any single institution. The estimates of financial resource requirements are based on an assumption that these services can be purchased from an organization (or funded through a collaborator) with the necessary equipment, instrumentation, and trained personnel to conduct the studies.
8. The costs associated with the tasks in the development plan are based on the experiences of the authors. It is reasonable to assume that variability in the costs and duration of specific data-generating activities will depend upon the nature of the target and molecule under development.

## Definitions

**At Risk Initiation** – The decision by the project team to begin activities that do not directly support the next unmet decision point, but will instead support a subsequent decision point. *At Risk Initiation* is sometimes recommended to decrease the overall development time.

**Commercialization Point** – In this context, the authors use the term to describe the point at which a commercial entity is involved to participate in the development of the drug product. This most commonly occurs through a direct licensing arrangement between the university and an organization with the resources to continue the development of the product.

**Counter-screen** – A screen performed in parallel with or after the primary screen. The assay used in the counter-screen is developed to identify compounds that have the potential to interfere with the assay used in the primary screen (the primary assay). Counter-screens can also be used to eliminate compounds that possess undesirable properties, for example, a counter-screen for cytotoxicity (1).

**Cumulative Cost** – This describes the total expenditure by the project team from project initiation to the point at which the project is either completed or terminated.

**Decision Point**<sup>1</sup> – The latest moment at which a predetermined course of action is initiated. Project advancement based on decision points balances the need to conserve scarce development resources with the requirement to develop the technology to a

commercialization point as quickly as possible. Failure to meet the criteria listed for the following decision points will lead to a *No Go* recommendation.

**False positive** – Generally related to the “specificity” of an assay. In screening, a compound may be active in an assay but inactive toward the biological target of interest. For this chapter, this does not include activity due to spurious, non-reproducible activity (such as lint in a sample that causes light-scatter or spurious fluorescence and other detection related artifacts). Compound interference that is reproducible is a common cause of false positives, or target-independent activity (1).

**Go Decision** – The project conforms to key specifications and criteria and will continue to the next decision point.

**High-Throughput Screen (HTS)** – A large-scale automated experiment in which large libraries (collections) of compounds are tested for activity against a biological target or pathway. It can also be referred to as a “screen” for short (1).

**Hits** – A term for putative activity observed during the primary high-throughput screen, usually defined by percent activity relative to control compounds (1).

**Chemical Lead Compound** – A member of a biologically and pharmacologically active compound series with desired potency, selectivity, pharmacokinetic, pharmacodynamic and toxicity properties that can advance to IND-enabling studies for clinical candidate selection.

**Incremental Cost** – A term used to describe the additional cost of activities that support decision criteria for any given decision point, independent of other activities that may have been completed or initiated to support decision criteria for any other decision point.

**Library** – A collection of compounds that meet the criteria for screening against disease targets or pathways of interest (1).

**New Chemical Entity (NCE)** – A molecule emerging from the discovery process that has not previously been evaluated in clinical trials.

**No Go Decision** – The project does not conform to key specifications and criteria and will not continue.

**Off-Target Activity** – Compound activity that is not directed toward the biological target of interest but can give a positive read-out, and thus can be classified as an active in the assay (1).

**Orthogonal Assay** – An assay performed following (or in parallel to) the primary assay to differentiate between compounds that generate false positives from those compounds that are genuinely active against the target (1).

---

<sup>1</sup> Behind each Decision Point are detailed decision-making criteria defined in detail later in this chapter

**Primary Assay** – The assay used for the high-throughput screen (1).

**Qualified Task** – A task that should be considered, but not necessarily required to be completed at a suggested point in the project plan. The decision is usually guided by factors outside the scope of this chapter. Such tasks will be denoted in this chapter by enclosing the name of the tasks in parentheses in the Gantt chart, e.g. (qualified task).

**Secondary Assay** – An assay used to test the activity of compounds found active in the primary screen (and orthogonal assay) using robust assays of relevant biology. Ideally, these are of at least medium-throughput to allow establishment of structure-activity relationships between the primary and secondary assays and establish a biologically plausible mechanism of action (1).

## Section 1 Discovery and Development of New Chemical Entities

The Gantt chart (Table 1) illustrates the scope of this chapter. The left-hand portion of the chart includes the name of each decision point as well as the incremental cost for the activities that support that task. The black bars on the right-hand portion of the chart represent the duration of the summary task (combined criteria) to support a decision point as well as the *cumulative cost* for the project at the completion of that activity. A similar layout applies to each of the subsequent figures; however, the intent of these figures is to articulate the activities that underlie each decision point.

The submission of regulatory documents, for the purpose of this example, reflects the preparation of an Investigational New Drug (IND) application in Common Technical Document (CTD) format. The CTD format is required for preparation of regulatory documents in Europe (according to the Investigational Medicinal Product Dossier [IMPD]), Canada for investigational applications (Clinical Trial Application) and is accepted by the United States Food and Drug Administration (FDA) for INDs. The CTD format is required for electronic CTD (eCTD) submissions. The advantages of the CTD are that it facilitates global harmonization and lays the foundation upon which the marketing application can be prepared. The sections of the CTD are prepared early in development (at the IND stage) and are then updated, as needed, until submission of the marketing application.



## Decision Point #1 - Target Identification

Target-based drug discovery begins with identifying the function of a possible therapeutic target and its role in the disease (2). There are two criteria that justify advancement of a project beyond target identification. These are:

- Previously published (peer-reviewed) data on a particular disease target pathway or target, OR
- Evidence of new biology that modulates a disease pathway or target of interest

Resource requirements to support this initial stage of drug discovery can vary widely as the novelty of the target increases. In general, the effort required to elucidate new biology can be significant. Most projects will begin with these data in hand, whether from a new or existing biology. We estimate that an additional investment might be needed to support the target identification data that might already exist (Table 2). However, as reflected in Table 2, if additional target validation activities proceed *at risk*, the total cost of the project at a “No Go” decision will reach approximately \$468,500 (estimated).

**Table 2:** Target Identification and Target Validation

| Task Name  | Cost             | Year 1           |    |                  |    | Year 2           |    |    |    |
|--|------------------|------------------|----|------------------|----|------------------|----|----|----|
|  |                  | Q1               | Q2 | Q3               | Q4 | Q1               | Q2 | Q3 | Q4 |
| <b>#1 Target Identification</b>                                | <b>\$200,000</b> | <b>\$200,000</b> |    |                  |    |                  |    |    |    |
| Previously published data on disease target                    | \$1,000          |                  |    |                  |    |                  |    |    |    |
| New biology that modulates a disease                           | \$199,000        |                  |    |                  |    |                  |    |    |    |
| <b>#2 Target Validation</b>                                    | <b>\$268,500</b> |                  |    | <b>\$468,500</b> |    |                  |    |    |    |
| Known molecules modulate target                                | \$100,000        |                  |    |                  |    |                  |    |    |    |
| Type of target has a history of success                        | \$1,000          |                  |    |                  |    |                  |    |    |    |
| Genetic confirmation   | \$80,000         |                  |    |                  |    |                  |    |    |    |
| Availability of known animal models                            | \$7,500          |                  |    |                  |    |                  |    |    |    |
| Low throughput target validation assay that represents biology | \$70,000         |                  |    |                  |    |                  |    |    |    |
| Intellectual property of the target                            | \$7,500          |                  |    |                  |    |                  |    |    |    |
| Marketability of the target                                    | \$2,500          |                  |    |                  |    |                  |    |    |    |
| <b>#3 Identification of Actives</b>                            | <b>\$472,500</b> |                  |    |                  |    | <b>\$941,000</b> |    |    |    |

## Decision Point #2 - Target Validation

Target validation requires a demonstration that a molecular target is directly involved in a disease process, and that modulation of the target is likely to have a therapeutic effect (2). There are seven criteria for evaluation prior to advancement beyond target validation. These are:

- Known molecules modulate the target

- Type of target has a history of success (e.g. Ion channel, GPCR, nuclear receptor, transcription factor, cell cycle, enzyme, etc.)
- Genetic confirmation (e.g. Knock-out, siRNA, shRNA, SNP, known mutations, etc.)
- Availability of known animal models
- Low-throughput target validation assay that represents biology
- Intellectual property of the target
- Market potential of the disease/target space

The advancement criteria supporting target validation can usually be completed in approximately 12 months by performing most activities in parallel. In an effort to reduce the overall development timeline, we recommend starting target validation activities *at risk* (prior to a “Go” decision on target identification). Table 2 illustrates the dependencies between the criteria supporting the first two decision points. The incremental cost of the activities supporting decision-making criteria for target validation is approximately \$268,500. However, a decision to initiate target validation prior to completion of target initiation (recommended) and subsequent initiation of identification of actives *at risk* would lead to a total project cost (estimate) of \$941,000 if a “No Go” decision were reached at the conclusion of target validation.

### Decision Point #3 - Identification of Actives

An active is defined as a molecule that shows significant biological activity in a validated screening assay that represents the disease biology and physiology. By satisfying the advancement criteria listed below for identification of actives, the project team will begin to define new composition of matter by linking a chemical structure to modulation of the target. There are five (or six if invention disclosure occurs at this stage) criteria for evaluation at the identification of actives decision point. These are:

- Acquisition of screening reagents
- Primary HTS assay development and validation
- Compound library available to screen
- Actives criteria defined
- Perform high-throughput screen
- (Composition of Matter invention disclosure)

The advancement criteria supporting identification of actives can be completed in approximately 12 months in most cases by performing activities in parallel. Table 3 illustrates the dependencies and timing associated with a decision to begin activities supporting confirmation of hits prior to a “Go” decision on decision point #3. The incremental cost associated with decision point #3 is estimated to be \$472,500 (assuming the assay is transferred and validated without difficulty). The accumulated project cost associated with a “No Go” decision at this point is estimated to be \$1.46 million. This assumes an *at risk* initiation of activities supporting decision point #4.

**Table 3:** Identification of Actives

| Task Name                                    | Cost             | Year 1 |    |                  |    | Year 2           |    |    |    | Year 3             |    |    |    |
|--|------------------|--------|----|------------------|----|------------------|----|----|----|--------------------|----|----|----|
|  |                  | Q1     | Q2 | Q3               | Q4 | Q1               | Q2 | Q3 | Q4 | Q1                 | Q2 | Q3 | Q4 |
| <b>#2 Target Validation</b>                  | <b>\$268,500</b> |        |    | <b>\$468,500</b> |    |                  |    |    |    |                    |    |    |    |
| <b>#3 Identification of Actives</b>          | <b>\$472,500</b> |        |    |                  |    | <b>\$941,000</b> |    |    |    |                    |    |    |    |
| Acquisition of screening reagents            | <b>\$100,000</b> |        |    |                  |    |                  |    |    |    |                    |    |    |    |
| Primary HTS assay development and validation | <b>\$150,000</b> |        |    |                  |    |                  |    |    |    |                    |    |    |    |
| Compound library available to screen         | <b>\$150,000</b> |        |    |                  |    |                  |    |    |    |                    |    |    |    |
| Actives criteria defined                     | <b>\$2,500</b>   |        |    |                  |    |                  |    |    |    |                    |    |    |    |
| Perform high-throughput screen               | <b>\$70,000</b>  |        |    |                  |    |                  |    |    |    |                    |    |    |    |
| (Composition of Matter invention disclosure) | <b>Variable</b>  |        |    |                  |    |                  |    |    |    |                    |    |    |    |
| <b>#4 Confirmation of Hits</b>               | <b>\$522,000</b> |        |    |                  |    |                  |    |    |    | <b>\$1,463,000</b> |    |    |    |

## Decision Point #4 - Confirmation of Hits

A hit is defined as consistent activity of a molecule (with confirmed purity and identity) in a biochemical and/or cell based secondary assay. Additionally, this is the point at which the project team will make an assessment of the molecular class of each of the hits. There are six (or seven if initial invention disclosure occurs at this stage) criteria for evaluation at the confirmation of hits decision point. These are:

- Confirmation based on repeat assay, Concentration Response Curve (CRC)
- Secondary assays for specificity, selectivity, and mechanisms
- Confirmed identity and purity
- Cell-based assay confirmation of biochemical assay when appropriate
- Druggability of the chemical class (reactivity, stability, solubility, synthetic feasibility)
- Chemical Intellectual Property (IP)
- (Composition of Matter invention disclosure)

The advancement criteria supporting decision point #4 can usually be completed in approximately 18 months, depending upon the existence of cell-based assays for confirmation. If the assays need to be developed or validated at the screening lab, we recommend starting that activity *at risk* concurrent with the CRC and mechanistic assays. Table 4 represents the dependencies and timing associated with the decision to begin activities supporting confirmation of hits prior to a “Go” decision on decision point #3. The incremental cost of confirmation of hits is \$522,000. The accumulated project cost at a “No Go” decision on decision point #4 can be as high as \$1.8 million if a proceed *at risk* decision is made on identification of a chemical lead (decision point #5).



**Table 4:** Confirmation of Hits

| Task Name   | Cost             | Year 2           |    |                    |    | Year 3 |    |                    |    | Year 4 |    |    |    |
|---|------------------|------------------|----|--------------------|----|--------|----|--------------------|----|--------|----|----|----|
|   |                  | Q1               | Q2 | Q3                 | Q4 | Q1     | Q2 | Q3                 | Q4 | Q1     | Q2 | Q3 | Q4 |
| <b>#3 Identification of Actives</b>   | <b>\$472,500</b> | <b>\$941,000</b> |    |                    |    |        |    |                    |    |        |    |    |    |
| <b>#4 Confirmation of Hits</b>  | <b>\$522,000</b> |                  |    | <b>\$1,463,000</b> |    |        |    |                    |    |        |    |    |    |
| Confirmation based on repeat assay, Concentration Response Curve (CRC)                        | \$50,000         |                  |    |                    |    |        |    |                    |    |        |    |    |    |
| Secondary assays for specificity, selectivity, and mechanisms                                 | \$400,000        |                  |    |                    |    |        |    |                    |    |        |    |    |    |
| Confirmed identity and purity   | \$10,000         |                  |    |                    |    |        |    |                    |    |        |    |    |    |
| Cell-based assay confirmation of biochemical assay when appropriate                           | \$50,000         |                  |    |                    |    |        |    |                    |    |        |    |    |    |
| Druggability of the chemical class (reactivity, stability, solubility, synthetic feasibility) | \$2,000          |                  |    |                    |    |        |    |                    |    |        |    |    |    |
| Chemical Intellectual Property (IP) (prior art search, med chemist driven)                    | \$10,000         |                  |    |                    |    |        |    |                    |    |        |    |    |    |
| (Composition of Matter invention disclosure)  | Variable         |                  |    |                    |    |        |    |                    |    |        |    |    |    |
| <b>#5 Identification of Chemical Lead</b>   | <b>\$353,300</b> |                  |    |                    |    |        |    | <b>\$1,816,300</b> |    |        |    |    |    |

## Decision Point #5 - Identification of Chemical Lead

A chemical lead is defined as a synthetically feasible, stable, and drug-like molecule active in primary and secondary assays with acceptable *specificity* and *selectivity* for the target. This requires definition of the Structure-Activity Relationship (SAR) as well as determination of synthetic feasibility and preliminary evidence of *in vivo* efficacy and target engagement (**Note: projects at this stage might be eligible for Phase I SBIR**). Characteristics of a chemical lead are:

- SAR defined
- Drugability (preliminary toxicity, hERG, Ames)
- Synthetic feasibility
- Select mechanistic assays
- *In vitro* assessment of drug resistance and efflux potential
- Evidence of *in vivo* efficacy of chemical class
- PK/Toxicity of chemical class known based on preliminary toxicity or *in silico* studies

In order to decrease the number of compounds that fail in the drug development process, a druggability assessment is often conducted. This assessment is important in transforming a compound from a lead molecule into a drug. For a compound to be considered druggable it should have the potential to bind to a specific target; however,

also important is the compound's pharmacokinetic profile regarding absorption, distribution, metabolism, and excretion. Other assays will evaluate the potential toxicity of the compound in screens such as the Ames test and cytotoxicity assay. When compounds are being developed for indications where the predicted patient survival is limited to a few years, it is important to note that a positive result in the cytotoxicity assays would not necessarily limit the development of the compound and other drugability factors (such as the pharmacokinetic profile) would be more relevant for determining the potential for development.

The advancement criteria supporting decision point #5 will most likely be completed in approximately 12-18 months due to the concurrent activities. We recommend that SAR and drugability assessments begin *at risk* prior to a "Go" on confirmation of hits. Synthetic feasibility and PK assessment will begin at the completion of decision point #4. The cost of performing the recommended activities to support identification of a chemical lead is estimated to be \$353,300 (Table 5). The accumulated project costs at the completion of decision point #5 are estimated to be \$2.1 million including costs associated with *at risk* initiation of activities to support decision point #6.

**Table 5:** Identification of a Chemical Lead

| Task Name   | Cost             | Year 2 |    |    |    | Year 3 |    |    |    | Year 4 |    |    |    |
|---|------------------|--------|----|----|----|--------|----|----|----|--------|----|----|----|
|   |                  | Q1     | Q2 | Q3 | Q4 | Q1     | Q2 | Q3 | Q4 | Q1     | Q2 | Q3 | Q4 |
| <b>#4 Confirmation of Hits</b>                        | <b>\$522,000</b> |        |    |    |    |        |    |    |    |        |    |    |    |
| <b>#5 Identification of Chemical Lead</b>             | <b>\$353,300</b> |        |    |    |    |        |    |    |    |        |    |    |    |
| SAR Defined   | \$167,900        |        |    |    |    |        |    |    |    |        |    |    |    |
| Specificity   | \$20,000         |        |    |    |    |        |    |    |    |        |    |    |    |
| Selectivity   | \$40,000         |        |    |    |    |        |    |    |    |        |    |    |    |
| Drugability   | \$107,900        |        |    |    |    |        |    |    |    |        |    |    |    |
| Solubility  | \$10,000         |        |    |    |    |        |    |    |    |        |    |    |    |
| Permeability n=50                                     | \$15,000         |        |    |    |    |        |    |    |    |        |    |    |    |
| Metabolic stability n=30 (human, murine, rat)         | \$40,000         |        |    |    |    |        |    |    |    |        |    |    |    |
| <i>In vitro</i> toxicology n=5                        | \$25,000         |        |    |    |    |        |    |    |    |        |    |    |    |
| hERG (QT prolongation) n=10                           | \$7,500          |        |    |    |    |        |    |    |    |        |    |    |    |
| Mini Ames (mutagenicity) n=3                          | \$5,400          |        |    |    |    |        |    |    |    |        |    |    |    |
| Cytotoxicity assays n=3                               | \$5,000          |        |    |    |    |        |    |    |    |        |    |    |    |
| Synthetic feasibility                                 | \$6,500          |        |    |    |    |        |    |    |    |        |    |    |    |
| Number of steps                                       | \$2,500          |        |    |    |    |        |    |    |    |        |    |    |    |
| Occupational health (starting materials and reagents) | \$2,500          |        |    |    |    |        |    |    |    |        |    |    |    |

Table 5 continues on next page...

Table 5 continued from previous page.

| Task Name  | Cost             | Year 2 |    |    |    | Year 3 |    |    |    | Year 4             |    |    |    |
|--|------------------|--------|----|----|----|--------|----|----|----|--------------------|----|----|----|
|  |                  | Q1     | Q2 | Q3 | Q4 | Q1     | Q2 | Q3 | Q4 | Q1                 | Q2 | Q3 | Q4 |
| Cost   | <b>\$1,000</b>   |        |    |    |    |        |    |    |    |                    |    |    |    |
| Availability of starting materials and reagents                  | <b>\$500</b>     |        |    |    |    |        |    |    |    |                    |    |    |    |
| Select mechanistic assays n=10                                   | <b>\$25,000</b>  |        |    |    |    |        |    |    |    |                    |    |    |    |
| No relative drug resistance issues n=10                          | <b>\$6,000</b>   |        |    |    |    |        |    |    |    |                    |    |    |    |
| Evidence of <i>in vivo</i> efficacy of chemical class (PD Study) | <b>\$10,000</b>  |        |    |    |    |        |    |    |    |                    |    |    |    |
| PK feasibility of chemical class                                 | <b>\$10,000</b>  |        |    |    |    |        |    |    |    |                    |    |    |    |
| Provisional application -composition of matter                   | <b>\$20,000</b>  |        |    |    |    |        |    |    |    |                    |    |    |    |
| <b>#6 Selection of Optimized Chemical Lead</b>                   | <b>\$302,500</b> |        |    |    |    |        |    |    |    |                    |    |    |    |
|  |                  |        |    |    |    |        |    |    |    | <b>\$2,118,800</b> |    |    |    |

### Decision Point #6 - Selection of Optimized Chemical Lead

An optimized chemical lead is a molecule that will enter IND-enabling GLP studies and GMP supplies will be produced for clinical trials. We will describe the activities that support GLP and GMP development in the next section. This section focuses on the decision process to identify those molecules (**Note: projects at this stage may be eligible for Phase II SBIR**). Criteria for selecting optimized candidates are listed below:

- Acceptable *in vivo* PK and toxicity
- Feasible formulation
- *In vivo* preclinical efficacy (properly powered)
- Dose Range Finding (DRF) pilot toxicology
- Process chemistry assessment of scale up feasibility
- Regulatory and marketing assessments

The advancement criteria supporting decision point #6 can be completed in approximately 12-15 months. As indicated above, we recommend commencing activities to support selection of an optimized chemical lead prior to a “Go” decision on decision point #5. In particular, the project team should place emphasis on 6.3 (*in vivo* preclinical efficacy). A strong lead will have clearly defined pharmacodynamic endpoints at the preclinical stage and will set the stage for strong indicators of efficacy at decision point #11 (clinical proof of concept). The cost of performing the recommended activities to support decision point #6 is estimated to be \$302,500 (Table 6). The accumulated project costs at the completion of decision point #6 are estimated to be \$2.4 million, including costs associated with *at risk initiation* of activities to support decision point #7.

**Table 6:** Selection of an Optimized Chemical Lead

| Task Name  | Cost             | Year 3 |    |                    |    | Year 4             |    |    |    | Year 5             |    |    |    |
|--|------------------|--------|----|--------------------|----|--------------------|----|----|----|--------------------|----|----|----|
|  |                  | Q1     | Q2 | Q3                 | Q4 | Q1                 | Q2 | Q3 | Q4 | Q1                 | Q2 | Q3 | Q4 |
| <b>#5 Identification of Chemical Lead</b>              | <b>\$353,300</b> |        |    | <b>\$1,816,300</b> |    |                    |    |    |    |                    |    |    |    |
| <b>#6 Selection of Optimized Chemical Lead</b>         | <b>\$302,500</b> |        |    |                    |    | <b>\$2,118,800</b> |    |    |    |                    |    |    |    |
| Acceptable <i>in vivo</i> PK                           | <b>\$32,500</b>  |        |    |                    |    |                    |    |    |    |                    |    |    |    |
| Route of administration                                | <b>\$10,000</b>  |        |    |                    |    |                    |    |    |    |                    |    |    |    |
| Bioavailability  | <b>\$7,500</b>   |        |    |                    |    |                    |    |    |    |                    |    |    |    |
| Clearance  | <b>\$7,500</b>   |        |    |                    |    |                    |    |    |    |                    |    |    |    |
| Drug distribution                                      | <b>\$7,500</b>   |        |    |                    |    |                    |    |    |    |                    |    |    |    |
| Feasible formulation                                   | <b>\$15,000</b>  |        |    |                    |    |                    |    |    |    |                    |    |    |    |
| <i>In vivo</i> preclinical efficacy (properly powered) | <b>\$165,000</b> |        |    |                    |    |                    |    |    |    |                    |    |    |    |
| Tumor size and volume                                  | <b>\$40,000</b>  |        |    |                    |    |                    |    |    |    |                    |    |    |    |
| Biomarkers   | <b>\$25,000</b>  |        |    |                    |    |                    |    |    |    |                    |    |    |    |
| Survival   | <b>\$30,000</b>  |        |    |                    |    |                    |    |    |    |                    |    |    |    |
| Target validation                                      | <b>\$30,000</b>  |        |    |                    |    |                    |    |    |    |                    |    |    |    |
| Dose frequency   | <b>\$40,000</b>  |        |    |                    |    |                    |    |    |    |                    |    |    |    |
| Dose Range Finding (DRF) pilot toxicology              | <b>\$40,000</b>  |        |    |                    |    |                    |    |    |    |                    |    |    |    |
| Process chemistry assessment of scale up feasibility   | <b>\$50,000</b>  |        |    |                    |    |                    |    |    |    |                    |    |    |    |
| Regulatory and marketing assessments                   | <b>Variable</b>  |        |    |                    |    |                    |    |    |    |                    |    |    |    |
| <b>#7 Selection of a Development Candidate</b>         | <b>\$275,000</b> |        |    |                    |    |                    |    |    |    | <b>\$2,393,800</b> |    |    |    |

## Decision Point #7 - Selection of a Development Candidate

A development candidate is a molecule for which the intent is to begin Phase I evaluation. Prior to submission of an IND, the project team must evaluate the likelihood of successfully completing the IND-enabling work that will be required as part of the regulatory application for first in human testing. Prior to decision point #7, many projects will advance as many as 7-10 molecules. Typically, most pharma and biotech companies will select a single development candidate with one designated backup. Here, we recommend that the anointed “Development Candidate” be the molecule that rates the best on the six criteria below. In many cases, a Pre-IND meeting with the regulatory agency might be considered. A failure to address all of these by any molecule should warrant a “No Go” decision by the project team. The following criteria should be minimally met for a development candidate:

- Acceptable PK (with a validated bioanalytical method)
- Demonstrated *in vivo* efficacy/activity
- Acceptable safety margin (toxicity in rodents or dogs when appropriate)
- Feasibility of GMP manufacture
- Acceptable drug interaction profile
- Well-developed clinical endpoints

The advancement criteria supporting decision point #7 are estimated to be completed in 12 months, but may be compressed to as little as 6 months. The primary rate limit among the decision criteria is the determination of the safety margin, as this can be affected by the formulation and dosing strategies selected earlier. In this case, the authors have presented a project that includes a 7-day repeat dose in rodents to demonstrate an acceptable safety margin. The incremental costs of activities to support the selection of a development candidate (as shown) are estimated to be approximately \$275,000. The accumulated project cost at this point is approximately \$2.4 million to complete decision points #6, #7, and the FDA Pre-IND meeting (Table 7). If the development plan requires a longer toxicology study at this point, costs can be higher (approximately \$190,000 for a 14-day repeat dose study in rats and \$225,000 in dogs).

**Table 7:** Selection of a Development Candidate

| Task Name   | Cost             | Year 4             |    |                    |    | Year 5             |    |    |    |
|---|------------------|--------------------|----|--------------------|----|--------------------|----|----|----|
|   |                  | Q1                 | Q2 | Q3                 | Q4 | Q1                 | Q2 | Q3 | Q4 |
| <b>#6 Selection of Optimized Chemical Lead</b>                          | <b>\$302,500</b> | <b>\$2,118,800</b> |    |                    |    |                    |    |    |    |
| <b>#7 Selection of a Development Candidate</b>                          | <b>\$275,000</b> |                    |    | <b>\$2,393,800</b> |    |                    |    |    |    |
| Acceptable PK (with a validated bioanalytical method)                   | <b>\$30,000</b>  |                    |    |                    |    |                    |    |    |    |
| Well-developed clinical endpoints                                       | <b>\$40,000</b>  |                    |    |                    |    |                    |    |    |    |
| Demonstrated <i>in vivo</i> efficacy/activity                           | <b>\$50,000</b>  |                    |    |                    |    |                    |    |    |    |
| Acceptable safety margin (toxicity in rodents or dogs when appropriate) | <b>\$125,000</b> |                    |    |                    |    |                    |    |    |    |
| GMP manufacture feasibility   | <b>\$25,000</b>  |                    |    |                    |    |                    |    |    |    |
| Acceptable drug interaction profile                                     | <b>\$5,000</b>   |                    |    |                    |    |                    |    |    |    |
| <b>#8 Pre-IND Meeting with FDA (for non-oncology projects only)</b>     | <b>\$37,000</b>  |                    |    |                    |    | <b>\$2,430,800</b> |    |    |    |

## Decision Point #8 - Pre-IND Meeting with the FDA

Pre-IND advice from the FDA may be requested for issues related to the data needed to support the rationale for testing a drug in humans; the design of nonclinical pharmacology, toxicology, and drug activity studies, including design and potential uses of any proposed treatment studies in animal models; data requirements for an IND application; initial drug development plans, and regulatory requirements for demonstrating safety and efficacy (1). We recommend that this meeting take place after the initiation, but before the completion of tasks to support decision point #7 (selection of

a development candidate). The feedback from the FDA might necessitate adjustments to the project plan. Making these changes prior to candidate selection will save time and money. Pre-IND preparation will require the following:

- Prepare pre-IND meeting request to the FDA, including specific questions
- Prepare pre-IND meeting package, which includes adequate information for the FDA to address the specific questions (clinical plan, safety assessments summary, CMC plan, etc.)
- Prepare the team for the pre-IND meeting
- Conduct pre-IND meeting with the FDA
- Adjust project plan to address the FDA comments
- Target product profile

The advancement criteria supporting decision point #8 should be completed in 12 months. We recommend preparing the pre-IND meeting request approximately 3 to 6 months prior to selection of a development candidate (provided that the data supporting that decision point are promising). The cost of performing the recommended activities to support pre-IND preparation #8 is estimated to be \$37,000.

### Decision Point #9 - Preparation and Submission of an IND Application

The decision to submit an IND application presupposes that all of the components of the application have been addressed. The largest expense associated with preparation of the IND is related to the CMC activities (manufacture and release of GMP clinical supplies). A “Go” decision is contingent upon all of the requirements for the IND having been addressed and that the regulatory agency agrees with the clinical plan. (Note: projects at this stage may be eligible for SBIR BRIDGE awards). The following criteria should be addressed in addition to addressing comments from the pre-IND meeting:

- Well-developed clinical plan
- Acceptable clinical dosage form
- Acceptable preclinical drug safety profile
- Clear IND regulatory path
- Human Proof of Concept (HPOC)/Clinical Proof of Concept (CPOC) plan is acceptable to regulatory agency (pre-IND meeting)
- Reevaluate IP positions

The advancement criteria supporting decision point #9 are estimated to be completed in 12 months, but might be compressed to as little as 6 months if necessary. We recommend initiating “*at risk*” as long as there is confidence that a qualified development candidate is emerging before completion of decision point #7 and the plan remains largely unaltered after the pre-IND meeting (decision point #8). The incremental costs of completing decision point #9 are estimated to be \$780,000. The accumulated project cost at this point will be approximately \$3.2 million (Table 8).

**Table 8:** Submit IND Application

| Task Name   | Cost             | Year 5             |    |    |    |
|---|------------------|--------------------|----|----|----|
|   |                  | Q1                 | Q2 | Q3 | Q4 |
| <b>#8 Pre-IND Meeting with FDA (for non-oncology projects only)</b> | <b>\$37,000</b>  | <b>\$2,430,800</b> |    |    |    |
| <b>#9 File IND</b>  | <b>\$780,000</b> | <b>\$3,210,800</b> |    |    |    |
| Acceptable clinical dosage form                                     | <b>\$360,000</b> |                    |    |    |    |
| Delivery, reconstitution, practicality                              | <b>\$30,000</b>  |                    |    |    |    |
| stability (at least one year)                                       | <b>\$80,000</b>  |                    |    |    |    |
| GMP quality   | <b>\$250,000</b> |                    |    |    |    |
| Acceptable preclinical drug safety profile                          | <b>\$350,000</b> |                    |    |    |    |
| Safety index (receptor profiling, safety panels)                    | <b>\$30,000</b>  |                    |    |    |    |
| Dose response (PK)  | <b>\$20,000</b>  |                    |    |    |    |
| Safety pharmacology   | <b>\$300,000</b> |                    |    |    |    |
| Clear IND regulatory path   | <b>\$30,000</b>  |                    |    |    |    |
| HPOC/CPOC plan is acceptable to regulatory agency                   | <b>\$40,000</b>  |                    |    |    |    |

## Decision Point #10 - Human Proof of Concept

Most successful Phase I trials in oncology require 12-21 months for completion, due to very restrictive enrollment criteria in these studies in some cases. There is no “*at risk*” initiation of Phase I; therefore, the timeline cannot be shortened in that manner. The most important factors in determining the length of a Phase I study are a logically written clinical protocol and an available patient population. A “Go” decision clearly rests on the safety of the drug, but many project teams will decide not to proceed if there is not at least some preliminary indication of efficacy during Phase I (decision point #10, below).

Proceeding to Phase II trials will depend on:

- IND clearance
- Acceptable Maximum Tolerated Dose (MTD)
- Acceptable Dose Response (DR)
- Evidence of human pharmacology
- Healthy volunteer relevance

We estimate the incremental cost of an oncology Phase I study will be approximately \$1 million. This can increase significantly if additional patients are required to demonstrate MTD, DR, pharmacology and/or efficacy. Our estimate is based on a 25 patient (outpatient) study completed in 18 months. The accumulated project cost at completion of decision point #10 will be approximately \$4.2 million (Table 9).

**Table 9:** Human Proof of Concept

| Task Name                               | Cost               | Year 5             |    |    |    | Year 6             |    |    |    | Year 7 |    |    |    |  |
|---|--------------------|--------------------|----|----|----|--------------------|----|----|----|--------|----|----|----|--|
|   |                    | Q1                 | Q2 | Q3 | Q4 | Q1                 | Q2 | Q3 | Q4 | Q1     | Q2 | Q3 | Q4 |  |
| <b>#9 File IND</b>                      | <b>\$780,000</b>   | <b>\$3,210,800</b> |    |    |    |                    |    |    |    |        |    |    |    |  |
| <b>#10 Human Proof of Concept</b>       | <b>\$1,000,000</b> |                    |    |    |    | <b>\$4,210,800</b> |    |    |    |        |    |    |    |  |
| IND/CTA clearance                       | <b>\$242,500</b>   |                    |    |    |    |                    |    |    |    |        |    |    |    |  |
| Acceptable Maximum Tolerated Dose (MTD) | <b>\$242,500</b>   |                    |    |    |    |                    |    |    |    |        |    |    |    |  |
| Acceptable Dose Response (DR)           | <b>\$242,500</b>   |                    |    |    |    |                    |    |    |    |        |    |    |    |  |
| Evidence of human pharmacology          | <b>\$242,500</b>   |                    |    |    |    |                    |    |    |    |        |    |    |    |  |
| Healthy volunteer relevance             | <b>\$30,000</b>    |                    |    |    |    |                    |    |    |    |        |    |    |    |  |

### Decision Point #11: Clinical Proof of Concept

With acceptable Dose Ranging and Maximum Tolerable Dose having been defined during Phase I, in Phase II the project team will attempt to statistically demonstrate efficacy. More specifically, the outcome of Phase II should reliably predict the likelihood of success in Phase III randomized trials.

- Meeting the IND objectives
- Acceptable human PK/PD profile
- Evidence of human pharmacology
- Safety and tolerance assessments

We estimate the incremental cost of an oncology Phase IIa study will be approximately \$5.0 million (Table 10). This cost is largely dependent on the number of patients required and the number of centers involved. Our estimate is based on 150 outpatients with studies completed in 24 months. The accumulated project cost at the completion of decision point #11 will be approximately \$9.2 million (Table 10).

**Table 10:** Decision Point #11 in Detail

| Task Name                                  | Cost               | Year 6             |    |    |    | Year 7             |    |    |    | Year 8 |    |    |    | Year 9 |    |    |    |  |
|--|--------------------|--------------------|----|----|----|--------------------|----|----|----|--------|----|----|----|--------|----|----|----|--|
|  |                    | Q1                 | Q2 | Q3 | Q4 | Q1                 | Q2 | Q3 | Q4 | Q1     | Q2 | Q3 | Q4 | Q1     | Q2 | Q3 | Q4 |  |
| <b>#10 Human Proof of Concept</b>          | <b>\$1,000,000</b> | <b>\$4,210,800</b> |    |    |    |                    |    |    |    |        |    |    |    |        |    |    |    |  |
| <b>#11 Clinical Proof of Concept (n=2)</b> | <b>\$5,000,000</b> |                    |    |    |    | <b>\$9,210,800</b> |    |    |    |        |    |    |    |        |    |    |    |  |
| IND/CTA clearance                          | <b>\$500,000</b>   |                    |    |    |    |                    |    |    |    |        |    |    |    |        |    |    |    |  |
| Acceptable PK/PD profile                   | <b>\$500,000</b>   |                    |    |    |    |                    |    |    |    |        |    |    |    |        |    |    |    |  |

Table 10 continues on next page...



Table 10 continued from previous page.

| Task Name                        | Cost               | Year 6 |    |    |    | Year 7 |    |    |    | Year 8 |    |    |    | Year 9 |    |    |    |
|----------------------------------|--------------------|--------|----|----|----|--------|----|----|----|--------|----|----|----|--------|----|----|----|
|                                  |                    | Q1     | Q2 | Q3 | Q4 | Q1     | Q2 | Q3 | Q4 | Q1     | Q2 | Q3 | Q4 | Q1     | Q2 | Q3 | Q4 |
| Evidence of pharmacology         | <b>\$2,500,000</b> |        |    |    |    |        |    |    |    |        |    |    |    |        |    |    |    |
| Efficacy                         | <b>\$1,250,000</b> |        |    |    |    |        |    |    |    |        |    |    |    |        |    |    |    |
| Direct and indirect biomarkers   | <b>\$1,250,000</b> |        |    |    |    |        |    |    |    |        |    |    |    |        |    |    |    |
| Safety and tolerance assessments | <b>\$1,500,000</b> |        |    |    |    |        |    |    |    |        |    |    |    |        |    |    |    |

## Section 2. Repurposing of Marketed Drugs

Drug repurposing and rediscovery development projects frequently seek to employ the 505(b)(2) drug development strategy. This strategy leverages studies conducted and data generated by the innovator firm that is available in the published literature, in product monographs, or product labeling. Improving the quality of drug development plans will reduce the time of 505(b)(2) development cycles, and reduce the time and effort required by the FDA during the NDA review process. Drug repurposing projects seek a new indication in a different patient population and perhaps a different formulated drug product than what is currently described on the product label. By leveraging existing nonclinical data and clinical safety experience, sponsors have the opportunity to design and execute novel, innovative clinical trials to characterize safety and efficacy in a different patient population. The decision points for drug repurposing are summarized in Table 11.



## Decision Point #1: Identification of Actives

For drug repurposing, actives are identified as follows (Table 12):

- Acquisition of Active Pharmaceutical Ingredients (API) for screening
- Primary HTS assay development, validation
- Actives criteria defined
- Perform HTS
- (Submit invention disclosure and consider use patent)

**Table 12:** Identification of Actives

| Decision Point   | Cost             | Year 1           |    |                  |    |    |    |    |    |    |     |     |     |  |
|--|------------------|------------------|----|------------------|----|----|----|----|----|----|-----|-----|-----|--|
|  |                  | M1               | M2 | M3               | M4 | M5 | M6 | M7 | M8 | M9 | M10 | M11 | M12 |  |
| <b>#1 Identification of Actives</b>                                  | <b>\$500,000</b> | <b>\$500,000</b> |    |                  |    |    |    |    |    |    |     |     |     |  |
| Acquisition of Active Pharmaceutical Ingredients (API) for screening | Variable         |                  |    |                  |    |    |    |    |    |    |     |     |     |  |
| Primary HTS assay development, validation                            | Variable         |                  |    |                  |    |    |    |    |    |    |     |     |     |  |
| Actives criteria defined   | Variable         |                  |    |                  |    |    |    |    |    |    |     |     |     |  |
| Perform high-throughput screen                                       | Variable         |                  |    |                  |    |    |    |    |    |    |     |     |     |  |
| (Submit invention disclosure and consider use patent)                | Variable         |                  |    |                  |    |    |    |    |    |    |     |     |     |  |
| <b>#2 Confirmation of Hits</b>                                       | <b>\$205,000</b> |                  |    | <b>\$705,000</b> |    |    |    |    |    |    |     |     |     |  |

## Decision Point #2: Confirmation of Hits

Hits are confirmed as follows for a drug repurposing project (Table 13):

- Confirmation based on repeat assay, CRC
- Secondary assays for specificity, selectivity, and mechanisms
- Cell-based assay confirmation of biochemical assay when appropriate
- (Submit invention disclosure and consider use patent)

**Table 13:** Confirmation of Hits

| Decision Point                      | Cost             | Year 1           |    |                  |    |    |    |    |    |    |     |     |     |  |
|-------------------------------------|------------------|------------------|----|------------------|----|----|----|----|----|----|-----|-----|-----|--|
|                                     |                  | M1               | M2 | M3               | M4 | M5 | M6 | M7 | M8 | M9 | M10 | M11 | M12 |  |
| <b>#1 Identification of Actives</b> | <b>\$500,000</b> | <b>\$500,000</b> |    |                  |    |    |    |    |    |    |     |     |     |  |
| <b>#2 Confirmation of Hits</b>      | <b>\$205,000</b> |                  |    | <b>\$705,000</b> |    |    |    |    |    |    |     |     |     |  |

Table 13 continues on next page...

Table 13 continued from previous page.

| Decision Point   | Cost             | Year 1 |    |    |    |    |    |    |    |    |     |     |     |
|--|------------------|--------|----|----|----|----|----|----|----|----|-----|-----|-----|
|  |                  | M1     | M2 | M3 | M4 | M5 | M6 | M7 | M8 | M9 | M10 | M11 | M12 |
| Confirmation based on repeat assay, concentration response curve (CRC) | Variable         |        |    |    |    |    |    |    |    |    |     |     |     |
| Secondary assays for specificity, selectivity, and mechanisms          | Variable         |        |    |    |    |    |    |    |    |    |     |     |     |
| Cell-based assay confirmation of biochemical assay when appropriate    | Variable         |        |    |    |    |    |    |    |    |    |     |     |     |
| (Submit invention disclosure and consider use patent)                  | Variable         |        |    |    |    |    |    |    |    |    |     |     |     |
| <b>#3 Initial Gap Analysis/ Development Plan</b>                       | <b>\$250,000</b> |        |    |    |    |    |    |    |    |    |     |     |     |

### Decision Point #3: Gap Analysis/Development Plan

When considering the 505(b)(2) NDA approach, it is important to understand what information is available to support the proposed indication and what additional information might be needed. **The development path is dependent upon the proposed indication, change in formulation, route, and dosing regimen.** The gap analysis/development plan that is prepared will take this information into account in order to determine what studies might be needed prior to submission of an IND and initiating first-in-man studies. A thorough search of the literature is important in order to capture information available to satisfy the data requirements for the IND. Any gaps identified would need to be filled with studies conducted by the sponsor. A pre-IND meeting with the FDA will allow the sponsor to present their plan to the FDA and gain acceptance prior to submission of the IND and conducting the first-in-man study (Table 14).

- CMC program strategy
- Preclinical program strategy
- Clinical proof of concept strategy
- Draft clinical protocol design
- Pre-IND meeting with the FDA
- Commercialization/marketing strategy and target product profile

Table 14: Gap Analysis/Development Plan

| Decision Point                 | Cost             | Year 1 |    |    |    |    |    |    |    |    |     |     |     |
|--------------------------------|------------------|--------|----|----|----|----|----|----|----|----|-----|-----|-----|
|                                |                  | M1     | M2 | M3 | M4 | M5 | M6 | M7 | M8 | M9 | M10 | M11 | M12 |
| <b>#2 Confirmation of Hits</b> | <b>\$205,000</b> |        |    |    |    |    |    |    |    |    |     |     |     |

Table 14 continues on next page...

Table 14 continued from previous page.

| Decision Point  | Cost             | Year 1 |    |    |    |    |    |    |             |    |     |     |     |
|---|------------------|--------|----|----|----|----|----|----|-------------|----|-----|-----|-----|
|   |                  | M1     | M2 | M3 | M4 | M5 | M6 | M7 | M8          | M9 | M10 | M11 | M12 |
| <b>#3 Initial Gap Analysis/<br/>Development Plan</b>            | <b>\$250,000</b> |        |    |    |    |    |    |    | \$955,000   |    |     |     |     |
| CMC program strategy  | Variable         |        |    |    |    |    |    |    |             |    |     |     |     |
| Preclinical program strategy                                    | Variable         |        |    |    |    |    |    |    |             |    |     |     |     |
| Clinical proof of concept strategy                              | Variable         |        |    |    |    |    |    |    |             |    |     |     |     |
| Draft clinical protocol design                                  | Variable         |        |    |    |    |    |    |    |             |    |     |     |     |
| Pre-IND meeting with FDA  | Variable         |        |    |    |    |    |    |    |             |    |     |     |     |
| Commercialization/marketing strategy and target product profile | Variable         |        |    |    |    |    |    |    |             |    |     |     |     |
| <b>#4 Clinical Formulation Development</b>                      | <b>\$100,000</b> |        |    |    |    |    |    |    | \$1,055,000 |    |     |     |     |

### Decision Point #4: Clinical Formulation Development

The clinical formulation development will include the following (Table 15):

- Prototype development
- Analytical methods development
- Prototype stability
- Prototype selection
- Clinical supplies release specification
- (Submit invention disclosure on novel formulation)

Table 15: Clinical Formulation Development

| Decision Point                             | Cost             | Year 1 |    |    |    |    |    |    |             |    |     |     |     |
|--|------------------|--------|----|----|----|----|----|----|-------------|----|-----|-----|-----|
|  |                  | M1     | M2 | M3 | M4 | M5 | M6 | M7 | M8          | M9 | M10 | M11 | M12 |
| <b>#3 Final Development Plan</b>           | <b>\$250,000</b> |        |    |    |    |    |    |    | \$955,000   |    |     |     |     |
| <b>#4 Clinical Formulation Development</b> | <b>\$100,000</b> |        |    |    |    |    |    |    | \$1,055,000 |    |     |     |     |
| Prototype development                      | Variable         |        |    |    |    |    |    |    |             |    |     |     |     |
| Analytical methods development             | Variable         |        |    |    |    |    |    |    |             |    |     |     |     |
| Prototype stability                        | Variable         |        |    |    |    |    |    |    |             |    |     |     |     |
| Prototype selection                        | Variable         |        |    |    |    |    |    |    |             |    |     |     |     |

Table 15 continues on next page...

Table 15 continued from previous page.

| Decision Point                                     | Cost             | Year 1 |    |    |    |    |    |    |    |    |     |     |     |
|--|------------------|--------|----|----|----|----|----|----|----|----|-----|-----|-----|
|  |                  | M1     | M2 | M3 | M4 | M5 | M6 | M7 | M8 | M9 | M10 | M11 | M12 |
| Clinical supplies release specification            | <b>Variable</b>  |        |    |    |    |    |    |    |    |    |     |     |     |
| (Submit invention disclosure on novel formulation) | <b>Variable</b>  |        |    |    |    |    |    |    |    |    |     |     |     |
| <b>#5 Preclinical Safety Data Package</b>          | <b>\$800,000</b> |        |    |    |    |    |    |    |    |    |     |     |     |

### Decision Point #5: Preclinical Safety Data Package

Preparation of the gap analysis/development plan will identify any additional studies that might be needed to support the development of the compound for the new indication. Based on this assessment, as well as the intended patient population, the types of studies that will be needed to support the clinical program will be determined. It is possible that a pharmacokinetic study evaluating exposure would be an appropriate bridge to the available data in the literature (Table 16).

- Preclinical oral formulation development
- Bioanalytical method development
- Qualify GLP test article
- Transfer plasma assay to GLP laboratory
- ICH S7a (Safety Pharmacology) & S7b (Cardiac Tox) core battery of tests
- Toxicology bridging study
- PK/PD/Tox studies if formulation & route of administration is different

**Table 16:** Preclinical Safety Data Package

| Decision Point  | Cost             | Year 1 |    |    |    |    |    |    |             |    |     |             |     | Year 2 |     |     |     |     |     |     |     |     |     |     |     |  |  |  |
|---|------------------|--------|----|----|----|----|----|----|-------------|----|-----|-------------|-----|--------|-----|-----|-----|-----|-----|-----|-----|-----|-----|-----|-----|--|--|--|
|   |                  | M1     | M2 | M3 | M4 | M5 | M6 | M7 | M8          | M9 | M10 | M11         | M12 | M13    | M14 | M15 | M16 | M17 | M18 | M19 | M20 | M21 | M22 | M23 | M24 |  |  |  |
| <b>#4 Clinical Formulation Development</b>                              | <b>\$100,000</b> |        |    |    |    |    |    |    | \$1,055,000 |    |     |             |     |        |     |     |     |     |     |     |     |     |     |     |     |  |  |  |
| <b>#5 Preclinical Safety Data Package</b>                               | <b>\$800,000</b> |        |    |    |    |    |    |    |             |    |     | \$1,855,000 |     |        |     |     |     |     |     |     |     |     |     |     |     |  |  |  |
| Preclinical oral formulation development                                | Variable         |        |    |    |    |    |    |    |             |    |     |             |     |        |     |     |     |     |     |     |     |     |     |     |     |  |  |  |
| Bioanalytical method development  | Variable         |        |    |    |    |    |    |    |             |    |     |             |     |        |     |     |     |     |     |     |     |     |     |     |     |  |  |  |
| Qualify GLP test article  | Variable         |        |    |    |    |    |    |    |             |    |     |             |     |        |     |     |     |     |     |     |     |     |     |     |     |  |  |  |
| Transfer plasma assay to GLP laboratory                                 | Variable         |        |    |    |    |    |    |    |             |    |     |             |     |        |     |     |     |     |     |     |     |     |     |     |     |  |  |  |
| ICH S7a (Safety Pharmacology) & S7b (Cardiac Tox) core battery of tests | Variable         |        |    |    |    |    |    |    |             |    |     |             |     |        |     |     |     |     |     |     |     |     |     |     |     |  |  |  |
| Toxicology bridging study   | Variable         |        |    |    |    |    |    |    |             |    |     |             |     |        |     |     |     |     |     |     |     |     |     |     |     |  |  |  |
| PK/PD/Tox studies if formulation & route of administration is different | Variable         |        |    |    |    |    |    |    |             |    |     |             |     |        |     |     |     |     |     |     |     |     |     |     |     |  |  |  |

*Table 16 continues on next page...*





## Decision Point #6: Clinical Supplies Manufacture

Clinical supplies will need to be manufactured. The list below provides some of the considerations that need to be made for manufacturing clinical supplies (Table 17):

- Select cGMP supplier and transfer manufacturing process
- Cleaning validation development
- Scale-up lead formulation at GMP facility
- Clinical label design
- Manufacture clinical supplies



## Decision Point #7: IND Preparation and Submission

Following the pre-IND meeting with the FDA, and conducting any additional studies, the IND is prepared in common technical document format to support the clinical protocol. The IND is prepared in 5 separate modules that include administrative information, summaries (CMC, nonclinical, clinical), quality data (CMC), nonclinical study reports and literature, and clinical study reports and literature (Table 18). Following submission of the IND to the FDA, there is a 30-day review period during which the FDA may ask for additional data or clarity on the information submitted. If after 30-days the FDA has communicated that there is no objection to the proposed clinical study, the IND is considered active and the clinical study can commence.

- Investigator's brochure preparation
- Protocol preparation and submission to IRB
- IND preparation and submission



## Decision Point #8: Human Proof of Concept

Human proof of concept may commence following successful submission of an IND (i.e. and IND that has not been placed on ‘clinical hold’). The list below provides some information concerning human proof of concept (Table 19):

- IND Clearance
- Acceptable MTD
- Acceptable DR
- Evidence of human pharmacology

**Table 19:** Human Proof of Concept

| Decision Point                          | Cost        | Year 2 |             |     |     |     |     |     |     |     |     |     |     |
|---|-------------|--------|-------------|-----|-----|-----|-----|-----|-----|-----|-----|-----|-----|
|   |             | M13    | M14         | M15 | M16 | M17 | M18 | M19 | M20 | M21 | M22 | M23 | M24 |
| #7 IND Preparation and Submission       | \$500,000   |        | \$2,855,000 |     |     |     |     |     |     |     |     |     |     |
| #8 Human Proof of Concept               | \$1,000,000 |        | \$3,855,000 |     |     |     |     |     |     |     |     |     |     |
| IND Clearance                           | Variable    |        |             |     |     |     |     |     |     |     |     |     |     |
| Acceptable Maximum Tolerated Dose (MTD) | Variable    |        |             |     |     |     |     |     |     |     |     |     |     |
| Acceptable Dose Response (DR)           | Variable    |        |             |     |     |     |     |     |     |     |     |     |     |
| Evidence of human pharmacology          | Variable    |        |             |     |     |     |     |     |     |     |     |     |     |

## Section 3. Development of Drug Delivery Platform Technology

Historically about 40% of NCEs identified as possessing promise for development, based on drug-like qualities, progress to evaluation in humans. Of those that do make it into clinical trials, about 9 out of 10 fail. In many cases, innovative drug delivery technology can provide a “second chance” for promising compounds that have consumed precious drug-discovery resources, but were abandoned in early clinical trials due to unfavorable side-effect profiles. As one analyst observed, “pharmaceutical companies are sitting on abandoned goldmines that should be reopened and excavated again using the previously underutilized or unavailable picks and shovels developed by the drug delivery industry” (SW Warburg Dillon Read). Although this statement was made more than 10 years ago, it continues to apply.

Beyond enablement of new drugs, innovative approaches to drug delivery also hold potential to enhance marketed drugs (e.g., through improvement in convenience,

tolerability, safety, and/or efficacy); expand their use (e.g., through broader labeling in the same therapeutic area and/or increased patient acceptance/compliance); or transform them by enabling their suitability for use in other therapeutic areas. These opportunities contribute enormously to the potential for value creation in the drug delivery field. Table 20 summarizes the decision points for the development of drug delivery platform technology.

**Table 20:** Summary of Decision Points for Drug Delivery Platform Technology

| Decision Point                      | Cost        | Year 1    |    |           |    | Year 2      |    |    |    | Year 3 |    |             |    | Year 4 |    |             |    | Year 5 |    |    |    | Year 6 |    |    |    |  |  |
|-------------------------------------|-------------|-----------|----|-----------|----|-------------|----|----|----|--------|----|-------------|----|--------|----|-------------|----|--------|----|----|----|--------|----|----|----|--|--|
|                                     |             | Q1        | Q2 | Q3        | Q4 | Q1          | Q2 | Q3 | Q4 | Q1     | Q2 | Q3          | Q4 | Q1     | Q2 | Q3          | Q4 | Q1     | Q2 | Q3 | Q4 | Q1     | Q2 | Q3 | Q4 |  |  |
| #1 Clinical Formulation Development | \$250,000   | \$250,000 |    |           |    |             |    |    |    |        |    |             |    |        |    |             |    |        |    |    |    |        |    |    |    |  |  |
| #2 Development Plan                 | \$300,000   |           |    | \$550,000 |    |             |    |    |    |        |    |             |    |        |    |             |    |        |    |    |    |        |    |    |    |  |  |
| #3 Clinical Supplies Manufacture    | \$500,000   |           |    |           |    | \$1,050,000 |    |    |    |        |    |             |    |        |    |             |    |        |    |    |    |        |    |    |    |  |  |
| #4 Preclinical Safety Data Package  | \$800,000   |           |    |           |    | \$1,850,000 |    |    |    |        |    |             |    |        |    |             |    |        |    |    |    |        |    |    |    |  |  |
| #5 IND Preparation and Submission   | \$500,000   |           |    |           |    |             |    |    |    |        |    | \$2,350,000 |    |        |    |             |    |        |    |    |    |        |    |    |    |  |  |
| #6 Human Proof of Concept           | \$1,000,000 |           |    |           |    |             |    |    |    |        |    | \$3,350,000 |    |        |    |             |    |        |    |    |    |        |    |    |    |  |  |
| #7 Clinical Proof of Concept        | \$2,500,000 |           |    |           |    |             |    |    |    |        |    |             |    |        |    | \$5,850,000 |    |        |    |    |    |        |    |    |    |  |  |

### Decision Point #1: Clinical Formulation Development

- Prototype development
- Analytical methods development
- Prototype stability
- Prototype selection
- Clinical supplies release specification
- (Submit invention disclosure on novel formulation)

See Table 21 for a schematic representation of the time and costs associated with development at this stage.

**Table 21:** Clinical Formulation Development

| Decision Point                                     | Cost             | Year 1           |    |                  |    |
|--|------------------|------------------|----|------------------|----|
|  |                  | Q1               | Q2 | Q3               | Q4 |
| <b>#1 Clinical Formulation Development</b>         | <b>\$250,000</b> | <b>\$250,000</b> |    |                  |    |
| Prototype development                              | Variable         |                  |    |                  |    |
| Analytical methods development                     | Variable         |                  |    |                  |    |
| Prototype stability                                | Variable         |                  |    |                  |    |
| Prototype selection                                | Variable         |                  |    |                  |    |
| Clinical supplies release specification            | Variable         |                  |    |                  |    |
| (Submit invention disclosure on novel formulation) | Variable         |                  |    |                  |    |
| <b>#2 Development Plan</b>                         | <b>\$300,000</b> |                  |    | <b>\$550,000</b> |    |

## Decision Point #2: Development Plan

Preparation of a development plan allows the sponsor to evaluate the available information regarding the compound of interest (whether at the development stage or a previously marketed compound) to understand what information might be available to support the proposed indication and what additional information may be needed. The development path is dependent upon the proposed indication, change in formulation, route, and dosing regimen. The development plan that is prepared will take this information into account in order to determine what information or additional studies might be needed prior to submission of an IND and initiating first-in-man studies. A thorough search of the literature is important in order to capture available information to satisfy the data requirements for the IND. Any gaps identified would need to be filled with studies conducted by the sponsor. A pre-IND meeting with the FDA will allow the sponsor to present their plan to the FDA and gain acceptance (de-risk the program) prior to submission of the IND and conducting the first-in-man study (Table 22).

- CMC program strategy
- Preclinical program strategy
- Clinical proof of concept strategy
- Draft clinical protocol design
- Pre-IND meeting with the FDA

**Table 22:** Development Plan

| Decision Point                             | Cost             | Year 1           |    |                  |    | Year 2 |    |    |    |
|--|------------------|------------------|----|------------------|----|--------|----|----|----|
|  |                  | Q1               | Q2 | Q3               | Q4 | Q1     | Q2 | Q3 | Q4 |
| <b>#1 Clinical Formulation Development</b> | <b>\$250,000</b> | <b>\$250,000</b> |    |                  |    |        |    |    |    |
| <b>#2 Development Plan</b>                 | <b>\$300,000</b> |                  |    | <b>\$550,000</b> |    |        |    |    |    |
| CMC program strategy                       | Variable         |                  |    |                  |    |        |    |    |    |

Table 22 continues on next page...

Table 22 continued from previous page.

| Decision Point                          | Cost             | Year 1 |    |    |    | Year 2 |    |    |    |
|---|------------------|--------|----|----|----|--------|----|----|----|
|   |                  | Q1     | Q2 | Q3 | Q4 | Q1     | Q2 | Q3 | Q4 |
| Preclinical program strategy            | <b>Variable</b>  |        |    |    |    |        |    |    |    |
| Clinical proof of concept strategy      | <b>Variable</b>  |        |    |    |    |        |    |    |    |
| Draft clinical protocol design          | <b>Variable</b>  |        |    |    |    |        |    |    |    |
| Pre-IND meeting with FDA                | <b>Variable</b>  |        |    |    |    |        |    |    |    |
| <b>#3 Clinical Supplies Manufacture</b> | <b>\$500,000</b> |        |    |    |    |        |    |    |    |

### Decision Point #3: Clinical Supplies Manufacture

- Select cGMP supplier and transfer manufacturing process
- Cleaning validation development
- Scale up lead formulation at GMP facility
- Clinical label design
- Manufacture clinical supplies

See Table 23 for a schematic representation of the time and costs associated with development at this stage.

Table 23: Clinical Supplies Manufacture

| Decision Point  | Cost             | Year 1 |    |    |    | Year 2 |    |    |    | Year 3 |    |    |    |
|---|------------------|--------|----|----|----|--------|----|----|----|--------|----|----|----|
|   |                  | Q1     | Q2 | Q3 | Q4 | Q1     | Q2 | Q3 | Q4 | Q1     | Q2 | Q3 | Q4 |
| <b>#2 Development Plan</b>                              | <b>\$300,000</b> |        |    |    |    |        |    |    |    |        |    |    |    |
| <b>#3 Clinical Supplies Manufacture</b>                 | <b>\$500,000</b> |        |    |    |    |        |    |    |    |        |    |    |    |
| Select cGMP supplier and transfer manufacturing process | <b>Variable</b>  |        |    |    |    |        |    |    |    |        |    |    |    |
| Cleaning validation development                         | <b>Variable</b>  |        |    |    |    |        |    |    |    |        |    |    |    |
| Scale up lead formulation at GMP facility               | <b>Variable</b>  |        |    |    |    |        |    |    |    |        |    |    |    |
| Clinical label design                                   | <b>Variable</b>  |        |    |    |    |        |    |    |    |        |    |    |    |
| Manufacture clinical supplies                           | <b>Variable</b>  |        |    |    |    |        |    |    |    |        |    |    |    |
| <b>#4 Preclinical Safety Data Package</b>               | <b>\$800,000</b> |        |    |    |    |        |    |    |    |        |    |    |    |

### Decision Point #4: Preclinical Safety Package

Preparation of the gap analysis/development plan will identify any additional studies that might be needed to support the development of the new delivery platform for the compound. Based on this assessment, as well as the intended patient population, the types of studies that will be needed to support the clinical program will be determined. It is



possible that a pharmacokinetic study evaluating exposure would be an appropriate bridge to the available data in the literature (Table 24).

- Preclinical oral formulation development
- Bioanalytical method development
- Qualify GLP test article
- Transfer drug exposure/bioavailability assays to GLP laboratory
- ICH S7a (Safety Pharmacology) & S7b (Cardiac Tox) core battery of tests
- Toxicology bridging study

**Table 24:** Preclinical Safety Package

| Decision Point  | Cost             | Year 1 |    |    |                    | Year 2 |                    |    |    | Year 3 |    |    |                    |
|---|------------------|--------|----|----|--------------------|--------|--------------------|----|----|--------|----|----|--------------------|
|   |                  | Q1     | Q2 | Q3 | Q4                 | Q1     | Q2                 | Q3 | Q4 | Q1     | Q2 | Q3 | Q4                 |
| <b>#3 Clinical Supplies Manufacture</b>                                       | <b>\$500,000</b> |        |    |    | <b>\$1,050,000</b> |        |                    |    |    |        |    |    |                    |
| <b>#4 Preclinical Safety Data Package</b>                                     | <b>\$800,000</b> |        |    |    |                    |        | <b>\$1,850,000</b> |    |    |        |    |    |                    |
| Preclinical oral formulation development                                      | Variable         |        |    |    |                    |        |                    |    |    |        |    |    |                    |
| Bioanalytical method development  | Variable         |        |    |    |                    |        |                    |    |    |        |    |    |                    |
| Qualify GLP test article  | Variable         |        |    |    |                    |        |                    |    |    |        |    |    |                    |
| Transfer drug exposure/<br>bioavailability assays to GLP<br>laboratory        | Variable         |        |    |    |                    |        |                    |    |    |        |    |    |                    |
| ICH S7a (Safety Pharmacology) &<br>S7b (Cardiac Tox) core battery of<br>tests | Variable         |        |    |    |                    |        |                    |    |    |        |    |    |                    |
| Toxicology bridging study   | Variable         |        |    |    |                    |        |                    |    |    |        |    |    |                    |
| <b>#5 IND Preparation and<br/>Submission</b>                                  | <b>\$500,000</b> |        |    |    |                    |        |                    |    |    |        |    |    | <b>\$2,350,000</b> |

## Decision Point #5: IND Preparation and Submission

Following the pre-IND meeting with the FDA and conducting any additional studies, the IND is prepared in common technical document format to support the clinical protocol. The IND is prepared in 5 separate modules, which include administrative information, summaries (CMC, nonclinical, clinical), quality data (CMC), nonclinical study reports and literature, and clinical study reports and literature. Following submission of the IND to the FDA, there is a 30-day review period during which the FDA might ask for additional data or clarity on the information submitted. If after 30-days the FDA has communicated that there is no objection to the proposed clinical study, the IND is considered active and the clinical study can commence (Table 25).

- Investigator's brochure preparation
- Protocol preparation and submission to IRB
- IND preparation and submission

**Table 25:** IND Preparation and Submission

| Decision Point                             | Cost             | Year 2 |                    |    |    | Year 3             |    |    |    |
|--|------------------|--------|--------------------|----|----|--------------------|----|----|----|
|  |                  | Q1     | Q2                 | Q3 | Q4 | Q1                 | Q2 | Q3 | Q4 |
| <b>#4 Preclinical Safety Data Package</b>  | <b>\$800,000</b> |        | <b>\$1,850,000</b> |    |    |                    |    |    |    |
| <b>#5 IND Preparation and Submission</b>   | <b>\$500,000</b> |        |                    |    |    | <b>\$2,350,000</b> |    |    |    |
| Investigator's brochure preparation        | <b>Variable</b>  |        |                    |    |    |                    |    |    |    |
| Protocol preparation and submission to IRB | <b>Variable</b>  |        |                    |    |    |                    |    |    |    |
| IND preparation and submission             | <b>Variable</b>  |        |                    |    |    |                    |    |    |    |

### Decision Point #6: Human Proof of Concept

Human proof of concept may commence following successful submission of an IND (i.e. and IND that has not been placed on 'clinical hold'). The list below provides some information concerning human proof of concept (Table 26):

- IND Clearance
- Acceptable MTD
- Acceptable DR
- Evidence of human pharmacology

**Table 26:** Human Proof of Concept

| Decision Point                           | Cost               | Year 3 |                    |    |    | Year 4 |    |    |    |
|--|--------------------|--------|--------------------|----|----|--------|----|----|----|
|  |                    | Q1     | Q2                 | Q3 | Q4 | Q1     | Q2 | Q3 | Q4 |
| <b>#5 IND Preparation and Submission</b> | <b>\$500,000</b>   |        | <b>\$2,350,000</b> |    |    |        |    |    |    |
| <b>#6 Human Proof of Concept</b>         | <b>\$1,000,000</b> |        | <b>\$3,350,000</b> |    |    |        |    |    |    |
| IND clearance                            | <b>Variable</b>    |        |                    |    |    |        |    |    |    |
| Acceptable Maximum Tolerated Dose (MTD)  | <b>Variable</b>    |        |                    |    |    |        |    |    |    |
| Acceptable Dose Response (DR)            | <b>Variable</b>    |        |                    |    |    |        |    |    |    |
| Evidence of human pharmacology           | <b>Variable</b>    |        |                    |    |    |        |    |    |    |

### Decision Point #7: Clinical Proof of Concept

With acceptable DR and MTD having been defined during Phase I, in Phase II the project team will attempt to statistically demonstrate efficacy. More specifically, the outcome of Phase II should reliably predict the likelihood of success in Phase III randomized trials (Table 27).

- IND Clearance
- Acceptable PK/PD profile
- Efficacy
- Direct and indirect biomarkers
- Safety and tolerance assessments

**Table 27:** Clinical Proof of Concept

| Decision Point                      | Cost               | Year 3 |    |    |    | Year 4 |    |    |    | Year 5 |    |    |    | Year 6 |    |    |    |
|-------------------------------------|--------------------|--------|----|----|----|--------|----|----|----|--------|----|----|----|--------|----|----|----|
|                                     |                    | Q1     | Q2 | Q3 | Q4 | Q1     | Q2 | Q3 | Q4 | Q1     | Q2 | Q3 | Q4 | Q1     | Q2 | Q3 | Q4 |
| <b>#6 Human Proof of Concept</b>    | <b>\$1,000,000</b> |        |    |    |    |        |    |    |    |        |    |    |    |        |    |    |    |
| <b>#7 Clinical Proof of Concept</b> | <b>\$2,500,000</b> |        |    |    |    |        |    |    |    |        |    |    |    |        |    |    |    |
| IND clearance                       | <b>Variable</b>    |        |    |    |    |        |    |    |    |        |    |    |    |        |    |    |    |
| Acceptable PK/PD profile            | <b>Variable</b>    |        |    |    |    |        |    |    |    |        |    |    |    |        |    |    |    |
| Efficacy                            | <b>Variable</b>    |        |    |    |    |        |    |    |    |        |    |    |    |        |    |    |    |
| Direct and indirect biomarkers      | <b>Variable</b>    |        |    |    |    |        |    |    |    |        |    |    |    |        |    |    |    |
| Safety and tolerance assessments    | <b>Variable</b>    |        |    |    |    |        |    |    |    |        |    |    |    |        |    |    |    |

## Section 4. Alternative NCE Strategy: Exploratory IND

The plans outlined previously in these guidelines describe advancement of novel drugs as well as repurposed or reformulated, marketed drug products to human and/or clinical proof of concept trials using the traditional or conventional early drug development, IND approach. This section of the guidelines outlines an alternative approach to accelerating novel drugs and imaging molecules to humans employing a Phase 0, exploratory IND strategy (exploratory IND). The exploratory IND strategy was first issued in the form of draft guidance in April, 2005. Following a great deal of feedback from the public and private sectors, the final guidance was published in January, 2006.

Phase 0 describes clinical trials that occur very early in the Phase I stage of drug development. Phase 0 trials limit drug exposure to humans (up to 7 days) and have no therapeutic intent. Phase 0 studies are viewed by the FDA and National Cancer Institute (NCI) as important tools for accelerating novel drugs to the clinic. There is some flexibility in data requirements for an exploratory IND. These requirements are dependent on the goals of the investigation (e.g., receptor occupancy, pharmacokinetics, human biomarker validation), the clinical testing approach, and anticipated risks.

Exploratory IND studies provide the sponsor with an opportunity to evaluate up to five chemical entities (optimized chemical lead candidates) or formulations at once. When an optimized chemical lead candidate or formulation is selected, the exploratory IND is then closed, and subsequent drug development proceeds along the traditional IND pathway.

**This approach allows one, when applicable, to characterize the human pharmacokinetics and target interaction of chemical lead candidates. Exploratory IND goals are typically to:**

- Characterize the relationship between mechanism of action and treatment of the disease; in other words, to validate proposed drug targets in humans
- Characterize the human pharmacokinetics
- Select the most promising chemical lead candidate from a group of optimized chemical lead candidates (note that the chemical lead candidates do not necessarily have the same chemical scaffold origins)
- Explore the bio-distribution of chemical lead candidates employing imaging strategies (e.g., PET studies)

Exploratory IND studies are broadly described as “microdosing” studies and clinical studies attempting to demonstrate a pharmacologic effect. Exploratory IND or Phase 0 strategies must be discussed with the relevant regulatory agency before implementation. These studies are described below.

Microdosing studies are intended to characterize the pharmacokinetics of chemical lead candidates or the imaging of specific human drug targets. Microdosing studies are not intended to produce a pharmacologic effect. Doses are limited to less than 1/100th of the dose predicted (based on preclinical data) to produce a pharmacologic effect in humans, **or a dose of less than 100 µg/subject, whichever is less.** Exploratory IND-enabling preclinical safety requirements for microdosing studies are substantially less than the conventional IND approach. In the US, a single dose, single species toxicity study employing the clinical route of administration is required. Animals are observed for 14 days following administration of the single dose. Routine toxicology endpoints are collected. The objective of this toxicology study is to identify the minimally toxic dose, or alternatively, demonstrate a large margin of safety (e.g., 100x). Genotoxicity studies are not required. The EMEA, in contrast to the FDA, requires toxicology studies employing two routes of administration, intravenous and the clinical route, prior to initiating microdosing studies. Genotoxicity studies (bacterial mutation and micronucleus) are required. Exploratory IND workshops have discussed or proposed the allowance of up to five microdoses administered to each subject participating in an exploratory IND study, provided each dose does not exceed 1/100th the NOAEL or 1/100th of the anticipated pharmacologically active dose, or the total dose administered is less than 100 mcg, whichever is less. In this case, doses would be separated by a washout period of at least six pharmacokinetic terminal half-lives. Fourteen-day repeat toxicology studies encompassing the predicted therapeutic dose range (but less than the MTD) have also been proposed to support expanded dosing in microdosing studies.

Exploratory IND clinical trials designed to produce a pharmacologic effect were proposed by PhRMA in May 2004, based on a retrospective analysis of 106 drugs that supported the accelerated preclinical safety-testing paradigm. In Phase 0 studies designed to produce a pharmacologic effect, up to five compounds can be studied. The compounds must have a common drug target, but do not necessarily have to be structurally related. Healthy volunteers or minimally ill patients may receive up to 7 repeated doses in the clinic. The goal is to achieve a pharmacologic response but not define the MTD. Preclinical safety requirements are greater compared to microdosing studies. Fourteen-day repeat

toxicology studies are required and conducted in rodents (i.e., rats), with full clinical and histopathology evaluation. In addition, a full safety pharmacology battery, as described by ICH S7a, is required. In other words, untoward pharmacologic effects on the cardiovascular, respiratory, and central nervous systems are characterized prior to Phase 0. In addition, genotoxicity studies employing bacterial mutation and micronucleus assays are required. In addition to the 14-day rodent toxicology study, a repeat dose study in a non-rodent specie (typically dog) is conducted at the rat NOAEL dose. The duration of the non-rodent repeat dose study is equivalent to the duration of dosing planned for the Phase 0 trial. If toxicity is observed in the non-rodent specie at the rat NOAEL, the chemical lead candidate will not proceed to Phase 0. The starting dose for Phase 0 studies is defined typically as 1/50th the rat NOAEL, based on a per meter squared basis. Dose escalation in these studies is terminated when: 1) a pharmacologic effect or target modulation is observed, 2) a dose equivalent (e.g., scaled to humans on a per meter squared basis) to one-fourth the rat NOAEL, or 3) human systemic exposure reflected as AUC reaches  $\frac{1}{2}$  the AUC observed in the rat or dog in the 14-day repeat toxicology studies, whichever is less.

Early phase clinical trials with terminally ill patients without therapeutic options, involving potentially promising drugs for life threatening diseases, may be studied under limited (e.g., up to 3 days dosing) conditions employing a facilitated IND strategy. As with the Phase 0 strategies described above, it is imperative that this approach be defined in partnership with the FDA prior to implementation.

The reduced preclinical safety requirements are scaled to the goals, duration and scope of Phase 0 studies. Phase 0 strategies have merit when the initial clinical experience is not driven by toxicity, when pharmacokinetics are a primary determinant in selection from a group of chemical lead candidates (and a bioanalytical method is available to quantify drug concentrations at microdoses), when pharmacodynamic endpoints in surrogate (e.g., blood) or tumor tissue is of primary interest, or to assess PK/PD relationships (e.g., receptor occupancy studies employing PET scanning).

PhRMA conducted a pharmaceutical industry survey in 2007 to characterize the industry's perspective on the current and future utility of exploratory IND studies (3). Of the 16 firms who provided survey responses, 56% indicated they had either executed or were planning to execute exploratory IND development strategies. The authors concluded that the merits of exploratory INDs continue to be debated, however, this approach provides a valuable option to advancing drugs to the clinic.

There are limitations to the exploratory IND approach. Doses employed in Phase 0 studies might not be predictive of doses over the human dose range (up to the maximum tolerated dose). Phase 0 studies in patients raises ethical issues compared to conventional Phase I, in that escalation into a pharmacologically active dose range might not be possible under the exploratory IND guidance. The Phase 0 strategy is designed to kill drugs early that are likely to fail based on PK or PK/PD. Should Phase 0 lead to a "Go" decision, however, a conventional IND is required for subsequent clinical trials, adding

cost and time. **Perhaps one of the most compelling arguments for employing an exploratory IND strategy is in the context of characterizing tissue distribution (e.g., receptor occupancy following PET studies) after microdosing.**

## Section 5. Orphan Drug Designation

Development programs for cancer drugs are often much more complex as compared to drugs used to treat many other indications. This complexity often results in extended development and approval timelines. In addition, oncology patient populations are often much smaller by comparison to other more prevalent indications. These factors (e.g., limited patent life and smaller patient populations) often complicate commercialization strategies and can, ultimately, make it more difficult to provide patient access to important new therapies.

To help manage and **expedite the commercialization of drugs used to treat rare diseases, including many cancers**, the Orphan Drug Act was signed into law in 1983. This law provides incentives to help sponsors and investigators develop new therapies for diseases and conditions of less than 200,000 cases per year allowing for more realistic commercialization.

The specific incentives for orphan-designated drugs are as follows:

- Seven years of exclusive marketing rights to the sponsor of a designated orphan drug product for the designated indication once approval to market has been received from the FDA
- A credit against tax for qualified clinical research expenses incurred in developing a designated orphan product
- Eligibility to apply for specific orphan drug grants

A sponsor may request orphan drug designation for:

- A previously unapproved drug
- A new indication for a marketed drug
- A drug that already has orphan drug status—if the sponsor is able to provide valid evidence that their drug may be clinically superior to the first drug

A sponsor, investigator, or an individual may apply for orphan drug designation prior to establishing an active clinical program or can apply at any stage of development (e.g., Phase 1 – 3). If orphan drug designation is granted, clinical studies to support the proposed indication are required. A drug is not given orphan drug status and, thus marketing exclusivity, until the FDA approves a marketing application. Orphan drug status is granted to the first sponsor to obtain FDA approval and not necessarily the sponsor originally submitting the orphan drug designation request.

There is no formal application for an orphan drug designation. However, the regulations (e.g., 21 CFR 316) identify the components to be included. **An orphan drug designation request is typically a five- to ten-page document** with appropriate literature references

appended to support the prevalence statements of less than 200,000 cases/year. The orphan drug designation request generally includes:

- The specific rare disease or condition for which orphan drug designation is being requested
- Sponsor contact, drug names, and sources
- A description of the rare disease or condition with a medically plausible rationale for any patient subset type of approach
- A description of the drug and the scientific rationale for the use of the drug for the rare disease or condition
- A summary of the regulatory status and marketing history of the drug
- Documentation (for a treatment indication for the disease or condition) that the drug will affect fewer than 200,000 people in the United States (prevalence)
- Documentation (for a prevention indication [or a vaccine or diagnostic drug] for the disease or condition) that the drug will affect fewer than 200,000 people in the United States per year (incidence)
- Alternatively, a rationale may be provided for why there is no reasonable expectation that costs of research and development of the drug for the indication can be recovered by sales of the drug in the United States

Following receipt of the request, the FDA Office of Orphan Product Development (OOPD) will provide an acknowledgment of receipt of the orphan drug designation request. The official response will typically be provided within 1 to 3 months following submission. Upon notification of granting an orphan drug designation, the name of the sponsor and the proposed rare disease or condition will be published in the federal register as part of public record. The complete orphan drug designation request is placed in the public domain once the drug has received marketing approval in accordance with the Freedom of Information Act.

Finally, the sponsor of an orphan designated drug must provide annual updates that contain a brief summary of any ongoing or completed nonclinical or clinical studies, a description of the investigational plan for the coming year, any anticipated difficulties in development, testing, and marketing, and a brief discussion of any changes that may affect the orphan drug status of the product

## Conclusion

While many authors have described the general guidelines for drug development (4,5, etc.), no one has outlined the process of developing drugs in an academic setting. It is well known that the propensity for late stage failures has led to a dramatic increase in the overall cost of drug development over the last 15 years. It is also commonly accepted that the best way to prevent late stage failures is by increasing scientific rigor in the discovery, preclinical, and early clinical stages. Where many authors present drug discovery as a single monolithic process, we intend to reflect here that there are multiple decision points contained within this process.

An alternative approach is the exploratory IND (Phase 0) under which the endpoint is proof of principle demonstration of target inhibition (6). This potentially paradigm-shifting approach might dramatically improve the probability of late stage success and may offer additional opportunities for academic medical centers to become involved in drug discovery and development.

## References

### Literature Cited

1. Pre-IND Consultation Program. US Food and Drug Administration. [Online] [Cited: August 17, 2010.] Available at: <http://www.fda.gov/Drugs/DevelopmentApprovalProcess/HowDrugsareDevelopedandApproved/ApprovalApplications/InvestigationalNewDrugINDApplication/Overview/default.htm>.
2. Apparent activity in high-throughput screening: origins of compound-dependent assay interference. Thorne N, et al. 2010, *Curr Opin Chem Biol*, p. doi: [10.1016/j.cbpa.2010.03.020](https://doi.org/10.1016/j.cbpa.2010.03.020).
3. Karara AH, Edeki T, McLeod J, et al. PhRMA survey on the conduct of first-in-human clinical trials under exploratory investigational new drug applications. *J Clin Pharmacol*. 2010;50:380–391. PubMed PMID: 20097935.
4. The price of innovation: new estimates of drug development costs. DiMasi, J.A., Hansen, R.W., and Grabowski, H.G. 2003, *Journal of Health Economics*, pp. 151-185.
5. Mehta, Shreefal S. *Commercializing Successful Biomedical Technologies*. Cambridge : Cambridge University Press, 2008.
6. Phase 0 Clinical Trails in Cancer Drug Development: From FDA Guidance to Clinical Practice. Kinders, Robert, et al. 2007, *Molecular Interventions*, pp. 325-334.

### Additional References

Eckstein, Jens. *ISOA/ARF Drug Development Tutorial*.



# *In Vitro* Biochemical Assays

Michelle Arkin, PhD, Douglas Auld, PhD, Kyle Brimacombe, MS, Nathan P. Coussens, PhD, Matthew D. Hall, PhD, James Inglese, PhD, Steven D. Kahl, BS, Stephen C. Kales, PhD, Zhuyin Li, PhD, James McGee, PhD, G. Sitta Sittampalam, PhD, and Jeffrey R. Weidner, PhD



# Validating Identity, Mass Purity and Enzymatic Purity of Enzyme Preparations\*

John E Scott, Ph.D.<sup>1</sup> and Kevin P Williams, Ph.D.<sup>1</sup>

Created: May 1, 2012; Updated: October 1, 2012.

## Abstract

When developing enzyme assays for HTS, the integrity of the target enzyme is critical to the quality of the HTS and the actives, or “hits”, identified through the screens. The incorrect identity or lack of enzymatic purity of the enzyme preparation will significantly affect the results of a screen. In this chapter, the authors discuss in detail the consequences of impure and mis-identified enzyme preparations, potential steps that can be taken to avoid measurement of the wrong activity and methods to validate the enzymatic purity of an enzyme preparation.

## Definitions

### Enzyme Identity

Enzyme identity determination is the confirmation that the protein preparation in fact contains the enzyme of interest. Enzyme identity is confirmed by demonstrating that the experimentally determined primary amino acid sequence matches the predicted primary amino acid sequence (see Identity and Mass Purity).

### Mass Purity

Mass purity refers to the percentage of the protein in a preparation that is the target enzyme or protein. For instance, 90 µg of enzyme in a solution containing a total of 100 µg of protein is considered to be 90% pure (see Identity and Mass Purity).

### Enzymatic Purity or Activity Purity

Enzymatic purity or activity purity refers to the fraction of activity observed in an assay that comes from a single enzyme. Typically, if 100% (or nearly so) of the observed activity in an enzyme assay is derived from a single enzyme then the enzyme preparation is considered enzymatically pure, even if it lacks mass purity. If two or more activities are detected in an enzyme assay then the enzyme preparation is enzymatically impure (see

---

\*Edited by Tod Holler and Andrew Napper, Ph.D.

<sup>1</sup> Biomanufacturing Research Institute and Technology Enterprise (BRITE) North Carolina Central University, Durham, NC; Email: jscott@nccu.edu; Email: kpwilliams@nccu.edu.

Validating Enzymatic Purity). Note that enzymatic purity is **not** the same as specific activity, which is enzymatic activity (in defined units) per unit mass of protein (typically mg of protein).

## Interrelationships between Identity, Mass and Enzymatic Purity

High mass purity and high specific activity are highly desirable in an enzyme used for screening because it decreases the probability of measuring contaminating enzyme activities. However, high mass purity or high specific activity alone does not guarantee enzymatic purity. On the other hand, enzymatically pure preparations may have poor mass purity. It is also possible to have an enzymatically pure preparation with all the activity coming from the wrong enzyme! For enzyme assays, enzymatic purity is absolutely essential to establish before screening (unless intentionally screening with mixed enzymes). Arguably, enzyme identity and enzymatic purity are the most critical factors. It is possible to have a valid enzyme assay with poor (or no) mass purity if it can be demonstrated that 100% of the observed activity is coming from the target enzyme.

## Consequences of using Enzymatically Impure Enzyme Preparations.

The consequences of using enzymatically impure enzyme preparations for a screen are multiple and far reaching. First, if the lot of enzyme used for assay development is enzymatically impure with the chosen substrate and format then the assay conditions could be optimized for the wrong enzyme activity. In addition, the contaminating activity may not be revealed until after the screen, when abnormally shaped  $IC_{50}$  curves are obtained (see Identity and Mass Purity). Inhibitors obtained from such a screen will likely be a mixture of inhibitors for the target and/or non-target. Depending on the fraction of signal contributed by the contaminating activity, the most potent inhibitors may be ones that are non-selective and inhibit both/all enzyme activities present. In other words, the screen may produce hits that are biased towards non-selective inhibitors, compounds that interfere with the assay format (like colored compounds), “nuisance” hits such as aggregators/reactive compounds, or a combination of these undesirable results. Thus, many or most target selective compounds may not appear as hits. Furthermore, compounds in the screening database would be annotated with false and misleading data.

## Signs of Enzymatic Contamination

- i. Inhibitor  $IC_{50}$  values  $\geq 10$ -fold different compared to literature or gold standard assay (see Inhibitor-Based Studies).
- ii. Inhibitor  $IC_{50}$  slopes are shallow (Hill slope  $< 1$ ) (see Inhibitor-Based Studies).
- iii. Unable to reach complete inhibition of activity at high concentrations of inhibitor (see Inhibitor-Based Studies).
- iv. Biphasic  $IC_{50}$  curves (see Inhibitor-Based Studies).

- v. IC<sub>50</sub> curves that plateau at significantly less than 100% enzyme activity at low inhibitor concentrations (see Inhibitor-Based Studies).
- vi. K<sub>m</sub> values do not match expected value (see Substrate-Based Studies).
- vii. Abnormally shaped K<sub>m</sub> plot (see Substrate-Based Studies).
- viii. Unexpected substrate specificities (see Substrate-Based Studies).
- ix. Lack of reproducible activity and/or IC<sub>50</sub> values between two different assay formats with the same preparation of enzyme (see Comparison Studies).
- x. Different sources of enzyme (e.g. from different vendors) or different batches of enzyme (produced in the same lab) produce different IC<sub>50</sub> values or Hill slopes (see Comparison Studies and Importance of Batch Testing) .
- xi. Post-screen: A high percentage of screen hits display Hill slopes that are very broad or do not reach complete inhibition (see Inhibitor-Based Studies) .

## Solutions for Enzymatic Contamination

- i. Purify enzyme further (add more steps to eliminate contaminating enzymes) or evaluate enzyme preparations from external or commercial suppliers.
- ii. Use a substrate that is more specific for the target enzyme.
- iii. Optimize/change buffer conditions to eliminate detection of other activities (e.g., change pH or NaCl concentration).
- iv. Change assay format to one that is more specific for the target of interest.
- v. Use multiple inhibitors for IC<sub>50</sub> experiments, instead of just one, in case the problem lies with the reference inhibitor compound.
- vi. Use inhibitors of contaminating activity in the assay buffer: The use of protease and phosphatase inhibitor cocktails may be necessary to inhibit contaminating activities. EDTA can sometimes be used to eliminate the activity of Mg<sup>2+</sup>-dependent contaminating activities, assuming the target enzyme does not require a divalent metal ion like Mg<sup>2+</sup> or Mn<sup>2+</sup>. Control experiments should be undertaken to ensure any inhibitors do not interfere with the target protein activity.

## Importance of Batch Testing

Each new batch of enzyme should be subject to some level of enzymatic purity testing since there may be contaminating enzyme present in each new preparation due to variability in expression and purification. Thus, both large and small scale purifications of enzyme need to be validated, even when the purification protocol remains the same. Batch-to-batch variability and scale-up of enzyme purifications for screening could result in subtle changes that result in, for example, differences in the percentage of target protein proteolysis or in host enzyme impurities. At minimum, new batch testing might include performing SDS-PAGE analysis for mass purity and identity along with using the most selective reference inhibitor and confirming that the IC<sub>50</sub> value and Hill slope obtained using the new batch of enzyme matches the original batch. Ideally, there should only be one or two lots of enzyme – one small one for assay development and one large bulk lot

for screening/follow-up. Multiple smaller batches can be pooled before assay development/validation. In theory, but not necessarily in practice, the screening lot should get the most rigorous validation (before screening).

## Identity and Mass Purity

Confirming enzyme identity is important because it prevents screening with the wrong enzyme. This problem arises occasionally, particularly when the target is expressed in a heterologous host. Thus, the determination of protein identity and mass purity is essential prior to any assay development and high throughput screening (HTS). In reality, no protein is purified to absolute homogeneity. After purification, the target protein may still contain contaminants derived either from the target protein itself or from host proteins. Remaining contaminants in a protein preparation may or may not interfere with the assay format under consideration.

## Methods for Confirming Identity and Mass Purity

Proteins used for HTS have typically been expressed as a recombinant form in a heterologous host. This form of expression may result in denatured, aggregated or proteolyzed forms of the target protein. Many excellent texts exist covering methods to determine protein purity including chapters in Current Protocols in Protein Sciences series (1) and Methods in Enzymology (2). A number of methods can be used to assess sample purity with the choice depending on sample availability, required accuracy and sensitivity. A simple wavelength scan also allows an assessment of non-proteinaceous contamination such as DNA/RNA.

### Protein stain of SDS-PAGE

A typical first assessment for sample purity is the use of sodium dodecyl sulfate polyacrylamide gel electrophoresis (SDS-PAGE) with either Coomassie blue staining or the more sensitive silver staining. These techniques are easy, rapid and inexpensive. Gradient SDS gels (e.g., 4-20%) allow the detection of a wide range of molecular weights and are very useful for assessing sample purity. Overloading the gel with 25-50  $\mu\text{g}$  of protein allows more sensitive detection of contaminating proteins. Densitometry of the stained gel allows some estimation of purity.

### Western blot with specific antibody

Western blotting with antibodies specific to the target protein allows a confirmation of identity and a determination of intactness of the target protein.

### Analytical gel filtration

Analytical gel filtration can be used to assess the presence of some contaminants under native conditions and also the presence and amount of target protein aggregates. A symmetrical peak eluting at the predicted molecular weight is indicative of a pure single species with no aggregation or degradation. Additional peaks eluting before the protein of

interest may be aggregates, and peaks eluting after may be degradation products. To confirm, fractions can be collected and analyzed by Western blotting and mass spectrometry to assess if the additional peaks are derived from the protein of interest.

### Reversed-phase HPLC

Reversed-phase HPLC (RP-HPLC) using a stationary phase, such as C4 or C8, is another rapid method for assessing target purity and the presence of contaminants in the protein sample. UV detection at 280 nm is typically used to monitor proteins, but when RP-HPLC is used in combination with a diode array detector, the simultaneous monitoring of a large number of wavelengths allows for detection of non-proteinaceous material as well.

### Mass Spectrometry

Mass spectrometry (MS) is the best technique (least ambiguous) for establishing protein identity because it provides an accurate direct measurement of protein mass. Mass accuracy will depend on the size of the protein but is typically around 0.01%. Furthermore, mass spectrometry provides the best approach to measuring not only the presence of impurities, but their mass as well and hence the possibility of identification. Although many labs do not possess the requisite equipment or expertise for mass spectrometry, many mass spectrometry facilities will characterize samples as a fee-based service.

### Whole mass measurement of protein

Matrix assisted laser desorption ionization (MALDI) time-of-flight (TOF) mass spectrometry is typically used for protein mass measurement because it can analyze proteins over a wide mass range, up to 200 kDa or higher. Proteins should be desalted, e.g. using a C4 ZipTip (Millipore Co.). Samples are deposited onto an  $\alpha$ -cyano-4-hydroxycinnamic acid matrix prepared in an aqueous solvent containing 50% acetonitrile and 10 mM ammonium citrate. Protein mass is determined using a MALDI TOF mass spectrometer. A comparison of the measured mass with the predicted mass allows confirmation of identity. Masses higher than predicted may indicate protein modifications, either post-translational or experimental, e.g. oxidation. Masses lower may be degradation products. Additional peaks in the spectrum may indicate the presence of contaminants although it should be remembered that ionization efficiencies may differ. For MALDI TOF, depending on the molecular size being measured and instrument used, mass accuracy is typically approximately 10 ppm to 0.01%.

### Peptide mass fingerprinting

Identity of a protein can be confirmed using peptide mass fingerprinting. In this technique, peptide fragments are generated by in-gel tryptic digestion of a Coomassie Blue stained protein band excised from a 1-D SDS-PAGE gel. The resulting peptides can be analyzed using MALDI TOF/TOF MS and observed peptide masses compared to the NCBI non-redundant database using a search algorithm such as the MASCOT MS/MS Ions search algorithm (Matrix Science: [www.matrixscience.com](http://www.matrixscience.com)). The observed masses of

all the peptides are compared to the calculated masses of the expected peptides resulting from tryptic cleavage of the target protein.

### Edman sequencing

In addition to mass spectrometry, N-terminal Edman sequencing can be used to confirm protein identity and assess the homogeneity among primary amino acid sequences in the purified target protein. To identify internal sequences from the target protein, proteins are separated by SDS-PAGE and then transferred to sequencing-grade PVDF membranes. Membranes are stained with Coomassie Blue R-250 for 3 minutes, then bands excised for tryptic peptide analysis. Peptides are separated by reversed-phase HPLC and N-terminal Edman sequencing is then performed on the peptides using a protein sequencer. A number of core facilities will perform Edman sequencing as a fee-based service.

### Crude Enzyme Preparations can be used

Enzyme assays have been developed with less than pure proteins, and even cell lysates and whole serum. For example, an activity-based probe has been developed as a highly selective substrate for measuring the activity of the protease DPAP1 in *Plasmodium falciparum* cell lysates and for Cathepsin C in rat liver extracts (3). Furthermore, whole serum has been used as a source of the enzyme PON1 to develop an enzyme assay for HTS (4). The key to this enzyme assay was the use of the highly selective, unique substrate paraoxon. PON1 is the only enzyme in serum capable of hydrolyzing the chemical paraoxon. In these cases, a highly selective substrate is used such that only the target enzyme can efficiently convert it to product in the time frame of the reaction. Enzyme assays that use these crude sources of enzyme require extra rigor in validating enzymatic purity and identity. These assays can be validated with known selective inhibitors and/or multiple methods outlined below (see Validating Enzyme Purity).

### Commercial Enzymes can be Impure or Misidentified

Commercial enzymes may be misidentified, have poor mass purity, and display poor enzymatic purity under a particular assay condition. Therefore, even for a commercially-obtained enzyme, it is recommended that the identity of the target protein be confirmed to ensure that not only is the correct protein being used, but that it is also from the correct species. Carrying out a high throughput screen on the incorrect target or on a target from the wrong species is an expensive control experiment! Identity of the target, including primary sequence confirmation, is critical.

### Co-purification of Contaminating Enzymes

Host enzymes can co-purify with the recombinant target enzyme. These contaminating host enzymes may have size and physical-chemical properties (like isoelectric point) that are indistinguishable from those of the target enzyme, making their presence in a preparation difficult to detect. This can lead to misleading purity determinations. Multiple methods of identity and mass purity determination can reveal co-purifying contaminants



that may have activity in the assay. Enzymatic purity analysis (Validating Enzyme Purity) may also reveal this contaminating activity.

## Enzyme Dead Mutant or Mock Parallel Purification

One method used to aide in establishing the identity of a recombinant enzyme preparation is to use an enzymatically inactive site-directed mutant (a mutant of the target that loses all activity) to make inactive enzyme and then apply the same purification protocol to both the wild-type enzyme and the mutant. The idea is that, unlike the wild type enzyme, the mutant-derived enzyme preparation should have no activity in the assay, demonstrating that the activity originates from the recombinant protein, not from contaminating host proteins. An assumption is that the mutation does not alter the overall structure of the enzyme. This is sometimes also done with empty vector constructs instead of mutant enzymes. While this is a useful technique, it is still recommended that all enzyme preparations to be used for screening be tested for identity, mass and enzymatic purity as outlined in this chapter.

## Reversal of Enzyme Activity by Contaminating Enzyme Activity

Contaminating enzymes can reverse the enzyme reaction by converting product back to substrate or into a different, undetected product. For instance, a contaminating phosphatase in a kinase preparation may dephosphorylate the product and alter the observed enzyme kinetics, depending on the kinase format chosen. Inhibitors of the contaminating activity, e.g. phosphatase inhibitors, can be used to prevent this. The presence of phosphatases in kinase assays may be difficult to detect. A common method is to test the kinase activity in the presence and absence of broad activity phosphatase inhibitors, such as sodium orthovanadate. Lack of an effect by these inhibitors suggests that phosphatase activity is not a problem in the assay. Increasing mass purity of the enzyme preparation can also eliminate such issues.

## Assay Design Factors that Affect the Likelihood of Detecting Enzyme Impurities

How an assay is designed and configured can influence whether or not contaminating enzyme activity is detected in the assay. In practice, if a contaminating enzyme is present, but not detected in the final assay, then there is no problem. The choice of substrate, enzyme concentration, and assay format can have a profound impact on the probability of detecting any enzyme impurities, if present.

### Substrate Selection

#### Consequences of substrate selectivity

- a. **Selective substrates:** The use of a selective substrate is an excellent method of reducing the chances of detecting any contaminating enzymes that may be present in an enzyme preparation. If only the target enzyme generates a detectable signal,

any contaminating enzymes that are present become irrelevant, since they do not contribute to the assay window. In fact, extremely selective substrates have been used to detect specific enzyme activity in whole cell lysates (e.g. luciferin for cell-based luciferase assays) or whole serum (e.g. hydrolysis of paraoxon by PON1 in serum).

- b. **Non-selective substrates:** Using less selective substrates, those that can be converted to product by many enzymes, increases the probability that contaminating enzymes will cause a problem. Therefore, the use of non-selective substrates requires the developer to obtain more data to demonstrate that the correct activity is being measured. For a kinase assay, the presence of a contaminating kinase may impact the assay depending on the selectivity of the substrate. For instance, the polymer substrate poly-[Glu,Tyr] can be phosphorylated by most tyrosine kinases, so this substrate will also detect contaminating tyrosine kinase activity, if present. In contrast, the use of a natural protein or selective peptide substrate may reduce the chances of detecting contaminating kinase activity. Another example of a non-selective substrate is para-nitrophenol phosphate (pNPP), which can be used as a substrate for a wide variety of phosphatases.

### Substrate $K_m$

Substrate selectivity has the largest impact on whether contaminating enzyme activity is detected in an assay. However, when choosing between equally selective substrates, the substrate with the lowest  $K_m$  is preferable (with all other considerations being equal). When substrates are used that have a high  $K_m$  value, higher amounts of substrate are needed in the reaction to obtain a good assay signal. However, with higher substrate concentration, especially for non-selective substrates, the chances are greater for detecting any contaminating enzyme activity that may be present. The use of substrates at concentrations at or below  $K_m$  value will select for detection of the enzyme in the preparation with the greatest activity towards the substrate. Furthermore, the substrate concentration should be kept at  $\leq K_m$  to ensure the sensitive detection of substrate competitive inhibitors, if desired.

### Enzyme Concentration

The concentration of enzyme used in an assay can determine whether contaminating enzymes, if present, are detected or not. Using high concentrations of target enzyme, based on the mass purity, increases the risk of detecting contaminating activity, especially for non-selective substrates. Conversely, using a low 1 nM enzyme concentration, for example, means that picomolar levels of contaminating activity would need to be detected to interfere with the assay. Coupled enzyme assays are particularly vulnerable to the detection of impurity activities because high concentrations of the coupling enzymes, which may also be contaminated with interfering activities, are usually added so as not to be a rate-limiting factor in the assay.

## Format Selection

Assay formats that are broadly applicable to a large class of enzymes are convenient, but increase the odds of detecting any contaminating activity present. For example, ADP detection methods for measuring kinase activity will detect all kinases in a preparation, and even any ATPases present. Thus, these types of assay formats should be used with care, and enzymatic purity should be verified by multiple methods (see Validating Enzymatic Purity). Highly specific formats will reduce the odds of detecting non-target activity. An example of this more selective format is a kinase assay that uses a natural substrate protein and an antibody to detect phosphorylation at a specific residue. Formats that allow very sensitive detection of the product may allow the use of low concentrations of enzyme, which may avoid the detection of very low activity/low concentration contaminating enzymes (see Enzyme Concentration).

## Validating Enzymatic Purity

Enzymatic purity can be assessed using inhibitor-based studies, substrate-based studies and/or comparison studies. Inhibitor-based studies are the most commonly used and the single best way to validate enzymatic purity. Combinations of these methods can also be used to enhance confidence in the assay. Enzymatic purity can be highly substrate and format dependent; that is, the same enzyme preparation can be used with one substrate/format and have 100% of the detected activity come from the intended target enzyme, but a different substrate or format may reveal multiple enzyme activities that are present in the preparation. Note that high specific activity preparations may be obtained, but there still could be multiple enzymes present that perform the same reaction and therefore the preparation would lack enzymatic purity. This can occur, if for instance, the contaminating enzyme(s) are the same size as the target or if the contaminating enzymes are present at a small percent by mass but with higher specific activity than the target enzyme.

## Inhibitor-Based Studies

Inhibitors of enzymatic activity are critical tools, and many times the only practical tool, to validate the enzymatic purity of enzyme preparations. Once an enzymatic assay has been established under kinetically valid conditions and optimized (see Basic Enzyme Assays), inhibitors described in the literature for the enzyme can be used to aide in validating that only one enzyme activity is being measured. Inhibitors are usually small organic molecules, but can also be small peptides or analogs of the natural substrate. In general, two types of inhibitors can be used for this purpose – relatively selective inhibitors and non-selective inhibitors. Selective inhibitors are preferable in verifying activity purity, but non-selective or modestly selective inhibitors are also useful when there is no practical alternative. Inhibition by selective inhibitors increases the confidence that the correct activity is being measured. However, non-selective inhibitors within a given enzyme class will frequently have a reported  $IC_{50}$  value and critical data can be ascertained concerning activity purity. For example, staurosporine is a broad spectrum

kinase inhibitor that can be used when a selective kinase inhibitor is not available. A small panel of non-selective inhibitors with a range of potencies can also be used to compare results to literature and increase confidence in the activity/purity of the assay/enzyme preparation. Any known activators of enzyme activity can also be used as evidence of enzymatic identity. **There are three important values that can be derived from concentration-response inhibition curves that aid in enzymatic purity validation: IC<sub>50</sub> value, Hill slope and maximal inhibition.**

For complete evaluation of IC<sub>50</sub> data as outlined here, maximum and minimum signal controls must be performed along with the inhibitor titration. Maximum controls should consist of enzyme reactions with no inhibitor – just DMSO. Minimum signal controls should be performed by using DMSO only (no inhibitor) and leaving enzyme out of the reaction (adding just buffer instead) to represent 100% enzyme inhibition.

### IC<sub>50</sub> value

IC<sub>50</sub> values for known inhibitors should match or be close to the literature values, with the caveat that different assay conditions (e.g. substrate concentration, total protein, pH, etc) may alter apparent potencies. Alternatively, inhibitors can be tested in a different validated assay format using the same enzyme preparation or a completely different source of enzyme, for example a commercially available enzyme. IC<sub>50</sub> values can then be compared between the different formats. IC<sub>50</sub> values are generally considered to be in close agreement if they differ by a factor of three or less.

### Hill slope

The steepness or shallowness of the IC<sub>50</sub> curve, referred to as the Hill slope, can provide valuable information as to whether a single enzyme is being inhibited. Inhibitors that bind to a single binding site on the enzyme should yield concentration response curves with a Hill slope of 1.0, based on the law of mass action (5, 6, and discussion of Hill slopes in Receptor Binding Assays). A negative sign in front of the Hill slope value may be ignored – the ± sign on a Hill slope signifies the direction of the curve, which changes if the data is plotted using percent activity or percent inhibition. Both selective and non-selective enzyme inhibitors should display a concentration response curve that has a Hill slope of close to 1.0. Thus, after plotting a concentration response curve for an inhibitor, there are three possible results when analyzing the slope (Figure 1):

- **Hill slope = 1.0.** This indicates a high probability that a single enzyme is generating the observed signal in the assay. An acceptable slope range under careful, manually-performed, experimental conditions is 0.8 to 1.2. The observation of this normal Hill slope using multiple inhibitors with a range of potencies greatly enhances confidence in the enzymatic purity of the assay. Multiple inhibitors are particularly useful when only non-selective inhibitors are available.

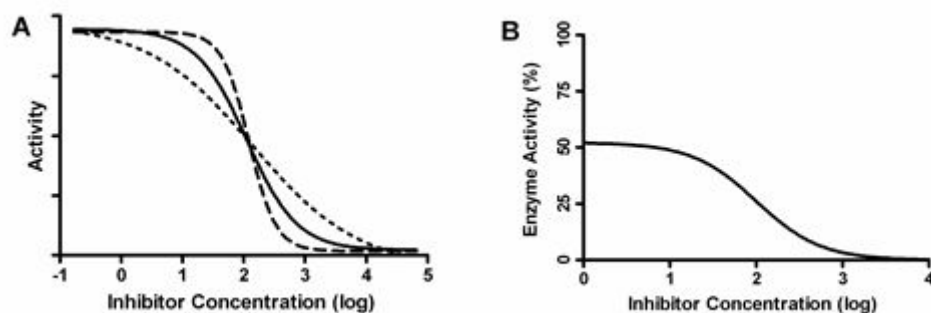


**Figure 1.** IC<sub>50</sub> curves with a Hill slope of 1.0 (solid line), 2.0 (dashed), 0.5 (dotted) (A). Partial biphasic graph (B)

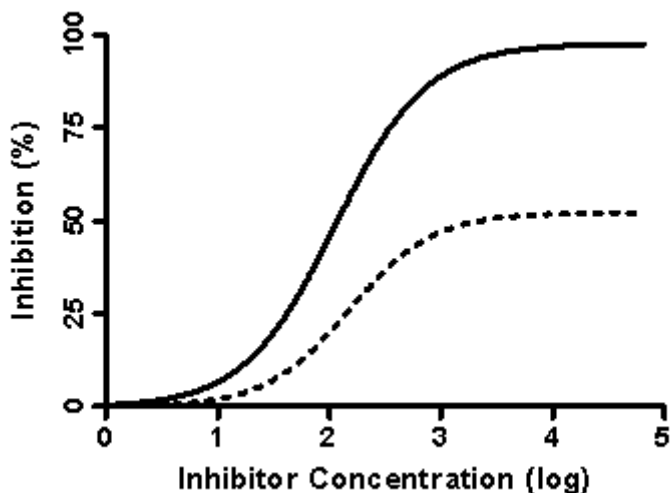


**Figure 2:** Complete IC<sub>50</sub> curve (solid line) compared to an incomplete maximal inhibition curve (dashed line). Note that both curves have a Hill slope of 1.0.

- **Hill slope < 1.0.** A shallow slope (for example <0.8) derived from the IC<sub>50</sub> curve may indicate that there is more than one enzyme that is contributing to the assay signal. This occurs when two or more enzymes are generating signal, but they have different, but non-resolvable affinities for the inhibitor. The result is a blended IC<sub>50</sub> curve that is broader than expected. If the two affinities are different enough to be resolved in the experiment, a biphasic curve will result. Thus, biphasic curves are also strongly suggestive of multiple activities present. However, in standard 10 point (1:3 dilutions) IC<sub>50</sub> curves, a partial biphasic curve may appear as a single curve where the low concentrations of inhibitor produce a plateau at significantly less than the expected 100% enzyme activity as determined by controls (Figure 1B). This type of curve can be due to multiple enzyme activities or an artifact of the

experiment caused by misleading controls due to, for example, well position or edge effects. Differentiating these two possibilities requires follow-up experiments.

- **Hill slope > 1.0.** A steep slope (Hill slope  $\gg$  1.0, for example  $>1.5$ ) may indicate that the inhibitor is either forming aggregates in aqueous solution and inhibiting non-specifically (see 7 and [Mechanism of Action assays for Enzymes](#)), chemically reacting with the enzyme or chelating a required co-factor. This type of inhibitor cannot be used in enzymatic purity validation studies. One important exception to this rule is inhibitors that have  $IC_{50}$  values lower than half the active enzyme concentration in the assay – these inhibitors are sometimes referred to as tight-binding inhibitors. These inhibitors are sometimes exquisitely specific to the enzyme target and very potent, but result in steep Hill slopes due to the fact that they are titrating enzyme. If assay sensitivity allows, it may be possible to lower the concentration of enzyme in the reaction below twice the  $IC_{50}$  value (even if only for validation studies) and thus demonstrate a Hill slope of 1.0 with tight-binding inhibitors.

#### **Tips, caveats and precautions for using Hill slope data:**

- Incomplete curves may give a less accurate Hill slope – the best data is obtained when a complete top and bottom of the curve are obtained (see  $IC_{50}$  Determination). When partial curves are obtained because high concentrations of inhibitor cannot be achieved, Hill slope information can be obtained by fitting the inhibition data using a three-parameter logistic fit with the 100% inhibition value (max or min) set equal to the average value of the “no enzyme” control. Achieving high compound concentrations in an assay may be limited by compound solubility or DMSO tolerance.
- Imprecise and/or inaccurate pipetting will shift the Hill slope.
- High assay variability or too few data points can lead to unreliable Hill slope determinations.
- Method of dilution is important –for the purpose of verifying enzymatic purity, change tips between different concentrations in a serial dilution, since this prevents carry-over of compound that could result in erroneous concentrations. For HTS hit confirmation and automated follow-up assays, tip changing is often impractical because tips are expensive or because compounds are being diluted using automated equipment with fixed tips.
- For small molecules, use 100% DMSO as diluent in the initial serial dilution series. These dilutions can then be further diluted into assay buffer for assaying. This minimizes compound precipitation at high concentration when diluted into aqueous solutions, which would alter actual compound concentrations.
- An impure compound (mixture of different inhibitors) may also generate shallow Hill slopes due to different affinities for the target.
- Compound solubility problems can result in a shallow or steep slope.
- Graphing software programs capable of fitting inhibition data with a four-parameter logistic fit will return a value for the Hill slope.

- For a Hill slope of 1.0, there should be a 81-fold inhibitor concentration difference between 10% and 90% inhibition.
- Errant data points will alter the slope – suspected outlier data points should be masked (temporarily removed from the curve) and the curve fitting repeated to see if masking the data point(s) dramatically improves the fit quality (see IC<sub>50</sub> Determination).
- Rarely, an enzyme may have more than one binding site and the Hill slope should be a higher integer (e.g., 2.0, 3.0, or higher).
- It is conceivable that multiple forms of the same enzyme might be present in the assay (for example due to heterogeneous post-translational modification) and that they may have different affinities for an inhibitor. If the two affinities cannot be resolved, the result will be a broadening of the IC<sub>50</sub> curve.
- It is theoretically possible to have two very similar enzymes (i.e. isozymes or isoforms) present in the enzyme preparation that have identical affinities for an inhibitor resulting in ideal shaped IC<sub>50</sub> curves. Isoform selective inhibitors (sometimes discovered later) may show the contamination.

A normal Hill slope is supporting evidence for enzymatic purity in the developed assay, while an unexpected Hill slope requires further investigation into the enzymatic purity of the enzyme preparation.

### Maximal inhibition.

The highest concentrations in a complete IC<sub>50</sub> curve should result in close to 100% inhibition of the assay signal based on controls with and without enzyme. **Lack of complete inhibition, even with a Hill slope = 1.0, is strongly suggestive that more than one enzyme activity is being measured.** This can occur if the inhibitor only inhibits one of the enzymes present, but does not inhibit the other enzymes that also contribute to assay signal. Such curves can have a “normal” shape, but at the highest concentrations of inhibitor, the curve plateaus (flattens out) at significantly less than 100% inhibition (Figure 2). Partial curves with normal Hill slopes are exempted from this criterion. Partial, or incomplete, curves show some inhibition at the highest concentrations of inhibitor, but lack data points displaying complete (100%) inhibition based on controls i.e. no clear plateau. Generally, the most accurate Hill slopes for partial curves will be obtained by using a three parameter fit where 100% inhibition is fixed to equal the average value from control wells that represent no enzyme activity (such as by leaving the enzyme out of the reaction). The most common cause of partial curves is simply low potency of the compound to inhibit the target enzyme. Poor compound solubility at higher concentrations could also explain lack of complete inhibition, but in that case, the curve is unlikely to have a normal appearance and a Hill slope of 1.0.

In summary, while inhibitor studies that result in expected IC<sub>50</sub> values, display expected Hill slopes and reach complete inhibition are not infallible proof of enzymatic purity, they provide strong evidence that only one enzyme species is being measured. Conversely,

inhibitor studies that result in un-expected  $IC_{50}$  values, have unexpected Hill slopes, and/or fail to achieve complete signal inhibition are not proof of contaminating enzyme activity, but are strong warning signs that should not be ignored. These results require further investigation to either rule out enzyme contamination, lay the blame elsewhere, or to prove enzyme contamination and require a change of enzyme source before proceeding. It is especially troubling when these warning signs are observed for multiple inhibitors.

## Substrate-Based Studies

If no suitable inhibitors are available, or to further confirm enzymatic purity, substrate-based studies can be employed. Two approaches can be used: substrate  $K_m$  determinations and substrate selectivity studies.

### Substrate $K_m$ determination

Substrate  $K_m$  determinations are usually done during assay development (see [Basics of Enzymatic Assays for HTS](#)). The  $K_m$  value should be close to the literature value (less than 10-fold difference), though different assay conditions can alter observed  $K_m$  values. The  $K_m$  plot (initial velocity vs. substrate concentration) should follow a single-site rectangular hyperbolic curve giving a defined  $V_{max}$ .  $K_m$  values  $\geq 10$ -fold different from literature values and/or abnormal shaped curves are suggestive of possible enzyme contamination or an error in enzyme identity. Hyperbolic curves may not be achievable if the  $K_m$  value is very high and assay format limitations preclude testing sufficiently high concentrations of substrate.

### Substrate selectivity studies

Different substrates for the same enzyme target can be tested to demonstrate selectivity. These studies can be done by performing  $K_m$  determinations and comparing  $k_{cat}/K_m$  values to the literature or expected selectivity. However, it is more easily performed by testing the different substrates at the same concentration; a concentration well below the expected  $K_m$  value. In this case, the initial velocity will be proportional to  $k_{cat}/K_m$  and therefore the measured velocities will allow a relative determination of how good a substrate is for the target. If substrate selectivity does not match expectations, then this may be a sign of contamination or mis-identification of the enzyme preparation. Similar substrates that should not result in measurable activity using the target enzyme can also be used to exclude certain enzymes that might be contaminants in the primary assay.

## Comparison Studies

For some little-studied enzymes, no or few inhibitors have been identified and substrate selectivity is unknown. For these targets, inhibitor studies and substrate studies are limited or not possible due to availability of inhibitors and substrates. In these cases, comparison studies can be done to aid in verifying purity, though the evidence for



enzymatic purity that is generated is not as strong as with the inhibitor and substrate based studies.

### Enzyme source comparison studies

The enzyme preparation under scrutiny may be compared to other enzyme preparations from different sources, such as commercially-generated enzyme. The basis for this comparison study is that different purification methods (and ideally different source organisms, e.g., mammalian vs. insect cells) are unlikely to generate the same contaminating enzymes at the same concentrations. An exception would be enzymes that co-purify due to physical association. Different enzyme sources can be compared by performing  $K_m$  determination studies with each enzyme using the same substrate. The  $K_m$  values should be within 3-fold of each other if the same enzyme activity is being measured. In addition, the curve should follow a single-site rectangular hyperbolic curve giving a defined  $V_{max}$  (assuming high enough concentrations of substrate can be used). For recombinant enzymes, one can also generate enzyme inactive mutants (at least empty vector control cells) to help establish that a host enzyme is not being measured (see Enzyme Dead Mutant or Mock Parallel Purification). For a highly selective substrate, it may also be possible to demonstrate that there is no measurable target enzyme activity in host cell lysates so there is little possibility of detecting host enzyme contaminants in the assay.

### Format comparison studies

In format comparison studies, the specific activities of the same enzyme preparation are determined using two different formats. If the same enzyme is measured in both formats (in the same assay buffer and substrate concentration), then such a comparison should yield similar activity in both assays (within 10-fold). Since different formats are used, standards would likely be required to convert assay signal to amount of product produced. Lack of activity in one format would be a potential warning sign that different enzymes are being measured in the two assays. This is most useful if one format is highly selective for the enzyme in question (e.g. a gold-standard assay) and this assay used to validate a less selective format. For example, for kinases, an assay where a specific antibody is used to detect phosphorylated protein product could be compared to an ADP detection format which detects all ATPase activity. Similar results would support the purity of the enzyme preparation. Furthermore, format comparison studies can be useful if even just one non-selective weak inhibitor is known for the target. In this case, an  $IC_{50}$  value comparison can be done using different formats to gain confidence in the enzymatic purity within the assay.

## References

1. Begg GE, Harper SL and Speicher DW (1999) Characterizing Recombinant Proteins using HPLC Gel Filtration and Mass Spectrometry. *Curr. Protoc. Protein Sci.* 16:7.10.1-7.10.15.

2. Rhodes DG, Laue TM. Determination of Protein Purity. *Meths Enzymol.* 2009;463:680–689. PubMed PMID: 19892198.
3. Deu E, Yang Z, Wang F, Klemba M, Bogyo M. Use of Activity-Based Probes to Develop High Throughput Screening Assays That Can Be Performed in Complex Cell Extracts. *PLoS One*; e. 2010;11:985. PubMed PMID: 20700487.
4. Graves TL, Scott JE. A High Throughput Serum Paraoxonase Assay for Discovery of Small Molecule Modulators of PON1 Activity. *Current Chemical Genomics.* 2008; 2008;2:51–61. PubMed PMID: 20161844.
5. H.J. Motulsky and A. Christopoulos. (2003), *Fitting Models to Biological Data using Linear and Nonlinear Regression. A practical guide to curve fitting.* GraphPad Software Inc., San Diego CA
6. GraphPad Software Inc. web site: [www.graphpad.com](http://www.graphpad.com)
7. Feng BY, Simeonov A, Jadhav A, Babaoglu K, Inglese J, Shoichert BK, Austin CP. A High-Throughput Screen for Aggregation-Based Inhibition in a Large Compound Library. *J. Med. Chem.* 2007;50:2385–2390. PubMed PMID: 17447748.

# Basics of Enzymatic Assays for HTS

Harold B. Brooks,<sup>1</sup> Sandaruwan Geeganage, Steven D. Kahl, Chahrzad Montrose,<sup>2</sup> Sitta Sittampalam,<sup>3,\*</sup> Michelle C. Smith, and Jeffrey R. Weidner<sup>4,†</sup>

Created: May 1, 2012; Updated: October 1, 2012.

## Abstract

Enzymes are important drug targets. Many marketed drugs today function through inhibition of enzymes mediating disease phenotypes. To design, develop and validate robust enzymatic assays for HTS applications, it is critical to have a thorough understanding of the enzyme biochemistry and the kinetics of enzyme action. This chapter contains basic concepts in enzyme kinetics, selection of appropriate substrates for assay design and the estimation and significance of  $K_m$  and  $V_{max}$ , the intrinsic kinetic parameters of enzyme targets. These concepts are addressed in the context of drug discovery and HTS assay development.

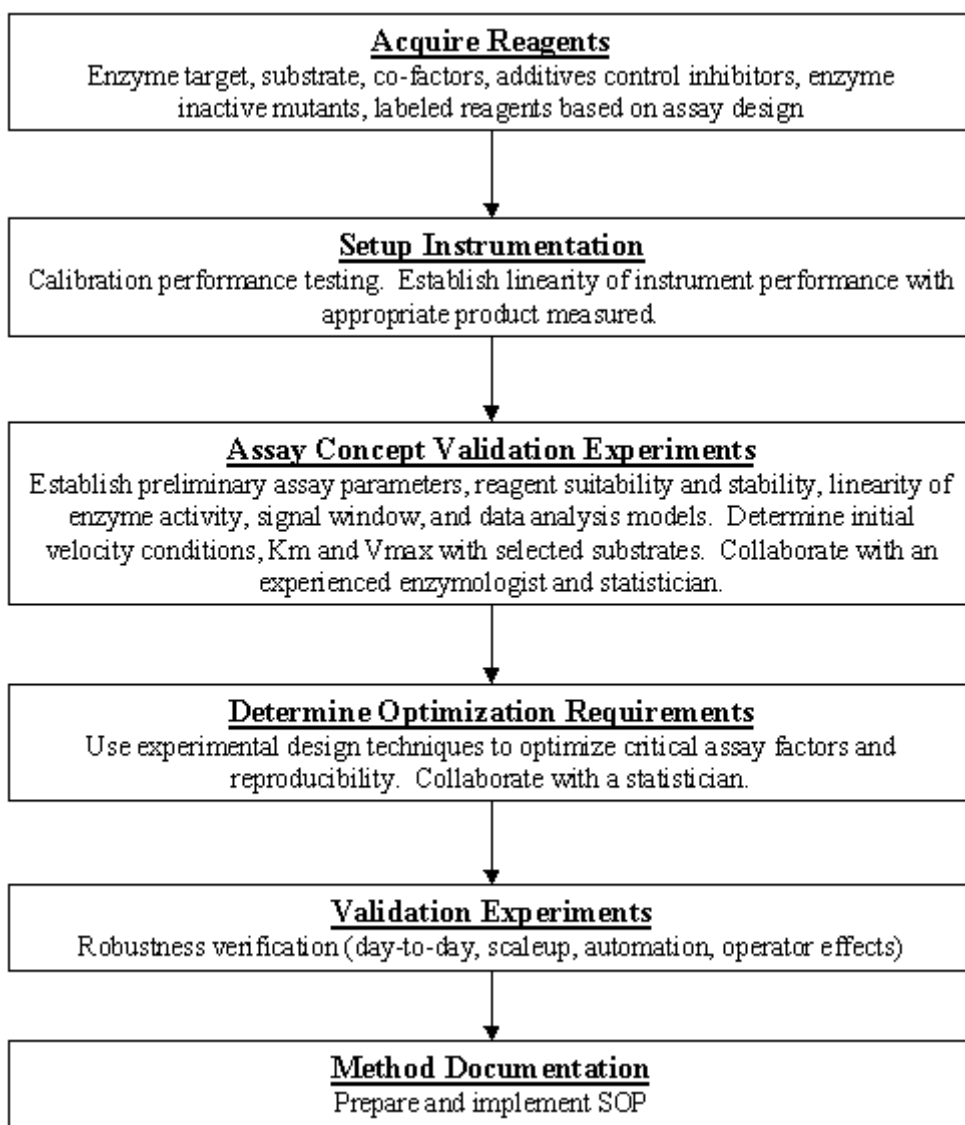
---

<sup>1</sup> Eli Lilly & Company, Indianapolis, IN. <sup>2</sup> Eli Lilly & Company, Indianapolis, IN. <sup>3</sup> National Institutes of Health, Rockville, MD. <sup>4</sup> AbbVie, Chicago, IL.

\* Editor

† Editor

## Enzyme Assay Development Flow Chart



## Introduction

Enzyme inhibitors are an important class of pharmacological agents. Often these molecules are competitive, reversible inhibitors of substrate binding. This section describes the development and validation of assays for identification of competitive, reversible inhibitors. In some cases other mechanisms of action may be desirable which would require a different assay design. A separate approach should be used if seeking a non-competitive mechanism that is beyond the scope of this document and should be discussed with an enzymologist and chemist (1).

## Concept

Enzymes are biological catalysts involved in important pathways that allow chemical reactions to occur at higher rates (velocities) than would be possible without the enzyme. Enzymes are generally globular proteins that have one or more substrate binding sites. The kinetic behavior for many enzymes can be explained with a simple model proposed during the 1900's:



where E is an enzyme, S is a substrate and P is a product (or products). ES is an enzyme-substrate complex that is formed prior to the catalytic reaction. Term  $k_1$  is the rate constant for enzyme-substrate complex (ES) formation and  $k_{-1}$  is the dissociation rate of the ES complex. In this model, the overall rate-limiting step in the reaction is the breakdown of the ES complex to yield product, which can proceed with rate constant  $k_2$ . The reverse reaction ( $E + P \rightarrow ES$ ) is generally assumed to be negligible.

Assuming rapid equilibrium between reactants (enzyme and substrate) and the enzyme-substrate complex resulted in mathematical descriptions for the kinetic behavior of enzymes based on the substrate concentration (2). The most widely accepted equation, derived independently by Henri and subsequently by Michaelis and Menten, relates the velocity of the reaction to the substrate concentration as shown in the equation below, which is typically referred to as the Michaelis-Menten equation:

$$v = \frac{[S] V_{\max}}{[S] + K_m}$$

where

$v$  = rate of reaction

$V_{\max}$  = maximal reaction rate

$S$  = substrate concentration

$K_m$  = Michaelis-Menten constant

For an enzymatic assay to identify competitive inhibitors, it is essential to run the reaction under **initial velocity conditions** with substrate concentrations at or below the  $K_m$  value for the given substrate. The substrate should either be the natural substrate or a surrogate substrate, like a peptide, that mimics the natural substrate. The optimal pH and buffer component concentrations should be determined before measuring the  $K_m$  (see Optimization Experiments).

## What is initial velocity?

- Initial velocity is the initial linear portion of the enzyme reaction when less than 10% of the substrate has been depleted or less than 10% of the product has formed. Under these conditions, it is assumed that the substrate concentration does not significantly change and the reverse reaction does not contribute to the rate.
- Initial velocity depends on enzyme and substrate concentration and is the region of the curve in which the velocity does not change with time. This is not a predetermined time and can vary depending on the reaction conditions.

## What are the consequences of not measuring the initial velocity of an enzyme reaction?

- The reaction is non-linear with respect to enzyme concentration.
- There is an unknown concentration of substrate.
- There is a greater possibility of saturation of the detection system
- The steady state or rapid equilibrium kinetic treatment is invalid

Measuring the rate of an enzyme reaction when 10% or less of the substrate has been depleted is the first requirement for steady state conditions. At low substrate depletion, i.e. initial velocity conditions, the factors listed below contribute to non-linear progression curves for enzyme reactions do not have a chance to influence the reaction.

- Product inhibition
- Saturation of the enzyme with substrate decreases as reaction proceeds due to a decrease in concentration of substrate (substrate limitation)
- Reverse reaction contributes as concentration of product increases over time
- Enzyme may be inactivated due to instability at given pH or temperature

## Reagents and Method Development

For any enzyme target, it is critical to ensure that the appropriate enzyme, substrate, necessary co-factors and control inhibitors are available before beginning assay development. The following requirements should be addressed during the method design phase:

1. Identity of the enzyme target including amino acid sequence, purity, and the amount and source of enzyme available for development, validation and support of screening/SAR activities. One should also ensure that contaminating enzyme activities have been eliminated. Specific activities should be determined for all enzyme lots.
2. Identify source and acquire native or surrogate substrates with appropriate sequence, chemical purity, and adequate available supply.
3. Identify and acquire buffer components, co-factors and other necessary additives for enzyme activity measurements according to published procedures and/or exploratory research.

4. Determine stability of enzyme activity under long-term storage conditions and during on bench experiments. Establish lot-to-lot consistency for long-term assays.
5. Identify and acquire enzyme inactive mutants purified under identical conditions (if available) for comparison with wild type enzyme.

## Detection System Linearity

Instrument capacity needs to be determined by detecting signal from product and plotting it versus product concentration. Figure 1 below demonstrates what can happen if a detection system has a limited linear range. In the Capacity 20 trace, the system becomes non-linear at concentrations of product that are greater than 10% of the total product generated. This limited linear range would severely compromise measurements, since it is essential that the enzyme reaction condition be within the linear portion of the instrument capacity. Subsequent assay analysis would be affected if the enzyme reaction were performed outside of this linear portion. The Capacity 100 trace represents a more ideal capability of an instrument that allows a broad range of product to be detected.

The linear range of detection for an instrument can be determined using various concentrations of product and measuring the signal. Plotting the signal obtained (Y-axis) versus the amount of product (X-axis) yields a curve that can be used to identify the linear portion of detection for the instrument.

## Enzyme Reaction Progress Curve

A *reaction progress curve* can be obtained by mixing an enzyme and its substrate together and measuring the subsequent product that is generated over a period of time. The initial velocity region of the enzymatic reaction needs to be determined and subsequent experiments should be conducted in this linear range, where less than 10% of the substrate has been converted to product. If the reaction is not in the linear portion, the enzyme concentration can be modified to retain linearity during the course of the experiments. Both of these steps (modifying the enzyme and analyzing the reaction linearity) can be conducted in the same experiment. An example is shown below in Figure 2.

In this set of data, product is measured at various times for three different concentrations of enzyme and one substrate concentration. The curves for the 1x and 2x relative levels of enzyme reach a plateau early, due to substrate depletion. To extend the time that the enzyme-catalyzed reaction exhibits linear kinetics, the level of enzyme can be reduced, as shown for the 0.5x curve. These curves are used to define the amount of enzyme, which can be used to maintain initial velocity conditions over a given period of time. These time points should be used for subsequent experiments.

Note that all three of the reaction progress curves shown in the example above approach a similar maximum plateau value of product formation. This is an indication that the enzyme remains stable under the conditions tested. A similar experiment performed when enzyme activity decreases during the reaction is shown in Figure 3. In this case, the

## Detection System Linearity

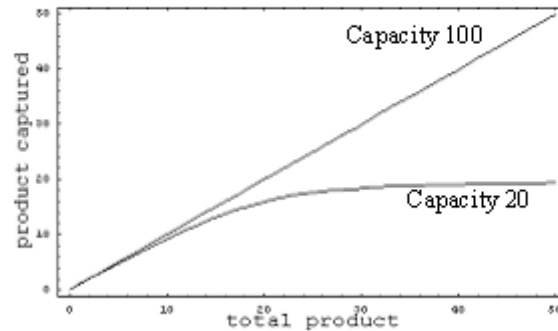


**Figure 1:** Signal saturation can lead to false measurements of assay parameters, such as  $K_m$

## Reaction Progress Curves

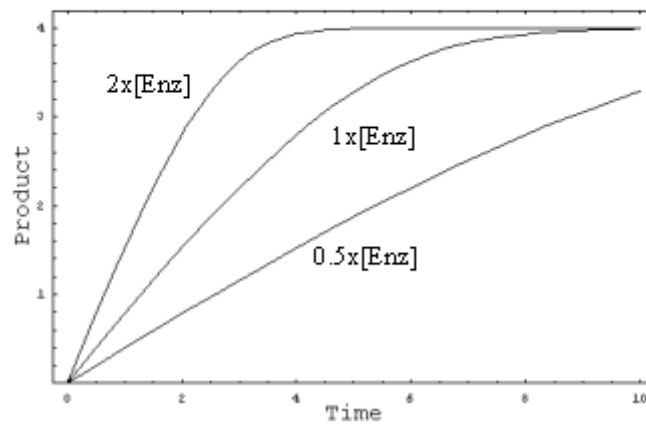


**Figure 2:** Plateau is due to substrate depletion

maximum plateau value of product formed does not reach the same for all levels of tested enzyme, likely due to enzyme instability over time.

### Measuring initial velocity of an enzyme reaction

- Keep temperature constant in the reaction by having all reagents equilibrated at the same temperature.
- Design an experiment so pH, ionic strength and composition of final buffer are constant. Initially use a buffer known for the enzyme of interest either by consulting



## Enzyme activity over time

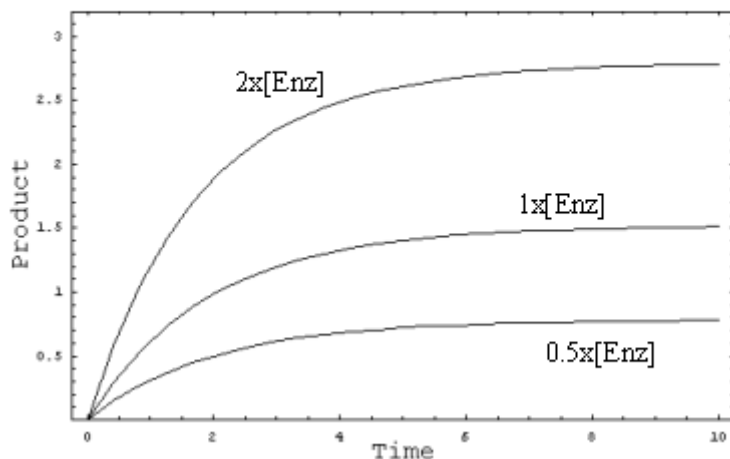


**Figure 3:** Plateau is due to loss of enzyme activity (note: plateaus do not converge)

the literature or by using the buffer recommended for the enzyme. This buffer could be further optimized in later stages of development.

- Perform the time course of reaction at three or four enzyme concentrations.
- Need to be able to measure the signal generated when 10% product is formed or to detect 10% loss of substrate.
- Need to measure signal at  $t=0$  to correct for background (leave out enzyme or substrate).

For kinase assays, the background can be determined by leaving out the enzyme or the substrate. The condition resulting in the highest background level should be used. EDTA is **not** recommended for use as the background control during validation of a kinase assay. Once the assay has been validated, if the background measured with EDTA is the same than both the no enzyme and no substrate control, then EDTA could be used.

## Measurement of $K_m$ and $V_{max}$

Once the initial velocity conditions have been established, the substrate concentration should be varied to generate a saturation curve for the determination of  $K_m$  and  $V_{max}$  values. **Initial velocity conditions must be used.** The Michaelis-Menten kinetic model shows that the  $K_m = [S]$  at  $V_{max}/2$ . In order for competitive inhibitors to be identified in a competition experiment that measures  $IC_{50}$  values, a substrate concentration around or below the  $K_m$  must be used. Using substrate concentrations higher than the  $K_m$  will make the identification of competitive inhibitors (a common goal of SAR) more difficult.

For kinase assays, the  $K_m$  for ATP should be determined using saturating concentrations of the substrate undergoing phosphorylation. Subsequent reactions need to be conducted

with optimum ATP concentration, around or below the  $K_m$  value using initial velocity conditions. However, it would be best to determine  $K_m$  for ATP and specific substrate simultaneously. This would allow maximum information to be gathered during the experiment as well as address any potential cooperativity between substrate and ATP.

A requirement for steady state conditions to be met means that a large excess of substrate over enzyme is used in the experiment. Typical ratios of substrate to enzyme are greater than 100 but can approach one million.

### What does the $K_m$ mean

- If  $K_m \gg [S]$ , then the velocity is very sensitive to changes in substrate concentrations. If  $[S] \gg K_m$ , then the velocity is insensitive to changes in substrate concentration. A substrate concentration around or below the  $K_m$  is ideal for determination of competitive inhibitor activity.
- $K_m$  is constant for a given enzyme and substrate, and can be used to compare enzymes from different sources.
- If  $K_m$  seems “unphysiologically” high then there may be activators missing from the reaction that would normally lower the  $K_m$  *in vivo*, or that the enzyme conditions are not optimum.

### How to measure $K_m$

- Measure the initial velocity of the reaction at substrate concentrations between 0.2-5.0  $K_m$ . If available, use the  $K_m$  reported in the literature as a determinant of the range of concentration to be used in this experiment. Use 8 or more substrate concentrations.
- Measuring  $K_m$  is an iterative process. For the first iteration, use six substrate concentrations that cover a wide range of substrate concentrations, to get an initial estimate. For subsequent iterations, use eight or more substrate concentrations between 0.2-5.0  $K_m$ . Make sure there are multiple points above and below the  $K_m$ .
- For enzymes with more than one substrate, measure the  $K_m$  of the substrate of interest with the other substrate at saturating concentrations. This is also an iterative process. Once the second  $K_m$  is measured, it is necessary to check that the first  $K_m$  was measured under saturating second substrate concentrations.
- Fit the data to a rectangular hyperbola function using non-linear regression analysis. Traditional linearized methods to measure  $K_m$ 's should not be used.

Figures 4 and 5 demonstrate a typical procedure to determine the  $K_m$  for a substrate. In Figure 4, reaction product is measured at various times for 8 different levels of substrate. The product generated (Y-axis) is plotted against the reaction time (X-axis). Each curve represents a different concentration of substrate. Note that all the curves are linear, indicating that initial velocity conditions (<10% of substrate conversion) have been met.

The initial velocity ( $v_0$ ) for each reaction progress curve is equivalent to the slope of the line, which is defined as the change in the product formed divided by the change in time.

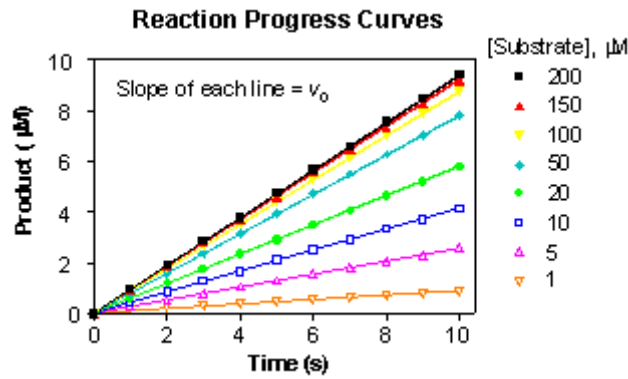


**Figure 4.** Reaction progress curves at 8 substrate concentrations

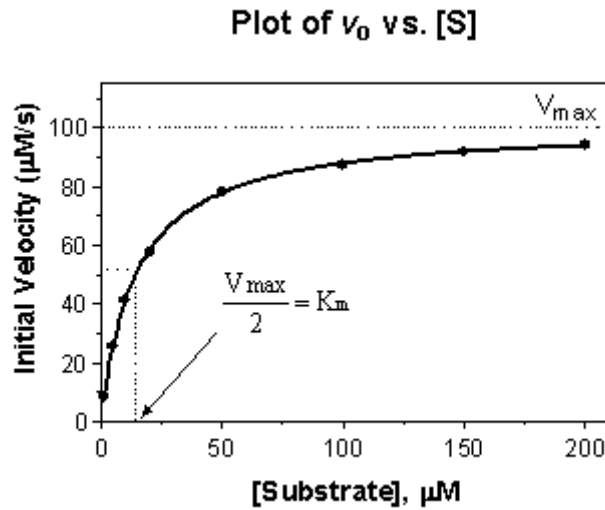


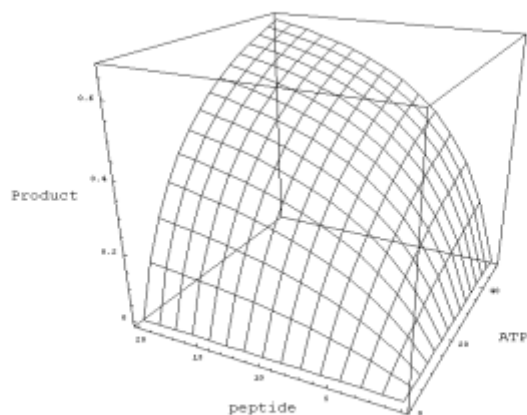
**Figure 5.** Initial velocity versus substrate concentration

This is expressed by the equation below and can be calculated using linear regression or other standard linear method:

$$\frac{\Delta Y}{\Delta X} = \text{Slope} = v_0$$

The resulting slopes (initial velocity,  $v_0$ ) for each of the reaction progress curves are plotted on the Y-axis versus the concentration of substrate (X-axis) and a nonlinear regression analysis using a rectangular hyperbola model is performed as shown in Figure 5.

## Determine $K_m$ 's for ATP and peptide/protein



- Check time dependence of four corners
- Watch for cooperativity
- Global fit at least a 4x4 matrix

**Figure 6.** Simultaneous determination of  $K_m$  for ATP and specific substrate

The  $V_{max}$  and  $K_m$  for the system is calculated from the nonlinear regression analysis. The meaning of each term is shown in Figure 5. The  $K_m$  is the substrate concentration which results in an initial reaction velocity that is one-half the maximum velocity determined under saturating substrate concentrations.

Linear transformations, such as a double reciprocal Lineweaver-Burke plot of the initial velocity/substrate concentration data (i.e.  $1/v_0$  vs.  $1/[S]$ ), should not be used for calculating the  $K_m$  and  $V_{max}$  from saturation type experiments such as those described above. These linear transformations tend to distort the error involved with the measurement and were used before programs that can perform nonlinear regression analysis were widely available.

An additional parameter, often seen in the literature, which can sometimes be useful to describe the efficiency of an enzyme, is the catalytic constant (or turnover number) that is termed  $k_{cat}$ . The  $k_{cat}$  value can be determined from saturation data (Figure 5) from the following equation:

$$k_{cat} = \frac{V_{max}}{[E]_i}$$

Where  $[E]_i$  is the initial enzyme concentration and  $V_{max}$  is the maximum velocity determined from the saturation hyperbola.

For kinase reactions where the  $K_m$  for ATP and substrate need to be determined, it is best if a multi-dimensional analysis is used to measure both  $K_m$ 's simultaneously. An example is shown in Figure 6.

If this method is used, it is important to demonstrate that in the extreme conditions (particularly low substrate, high ATP concentrations) the linearity of the instrument is maintained. In addition, it is important that linearity of the reaction is maintained at all conditions. Proper background controls must be used. The best condition would be a combination of the best signal to noise ratio while maintaining the substrate and ATP concentration as low as possible. Consult with a biochemist and statistician experienced in these techniques to ensure appropriate data analysis methods are utilized.

## Determination of $IC_{50}$ for Inhibitors

Concentration-response plots are used to determine the effects of an inhibitor on an enzymatic reaction. These experiments are performed at constant enzyme and substrate concentrations and are the primary type of analysis performed for structure-activity relationship (SAR) measurements for compounds of interest.

A typical concentration-response plot is shown in Figure 7. Fractional activity (Y-axis) is plotted as a function of inhibitor concentration (X-axis). The data are fit using a standard four-parameter logistic nonlinear regression analysis.

The concentration of compound that results in 50% inhibition of maximal activity is termed the  $IC_{50}$  (inhibitor concentration yielding 50% inhibition). It is important to use enough inhibitor concentrations to provide well-defined top and bottom plateau values. These parameters are critical for the mathematical models used to fit the data. Other criteria for successful concentration-response curves are listed in the discussion below.

## $IC_{50}$ Determination for SAR

- Use a minimum of 10 inhibitor concentrations for an accurate  $IC_{50}$  determination. Equally spaced concentration ranges (i.e. 3-fold or half-log dilutions) provide the best data sets for analysis.
- Ideally, half the data points on the  $IC_{50}$  curve are above the  $IC_{50}$  value and half are below the  $IC_{50}$  value, including a minimum and maximum signal.
- The lower limit for determining an  $IC_{50}$  is  $\frac{1}{2}$  the enzyme concentration (tight binding inhibitors, 3).
- Screening strategies for defining an initial SAR include: determination of the % inhibition at a single concentration; determination of the % inhibition at a high and a low concentration of inhibitor; and finally, determination of an apparent  $IC_{50}$  using fewer concentrations.

## Criteria for reporting $IC_{50}$ 's

- The maximum % inhibition should be greater than 50%.

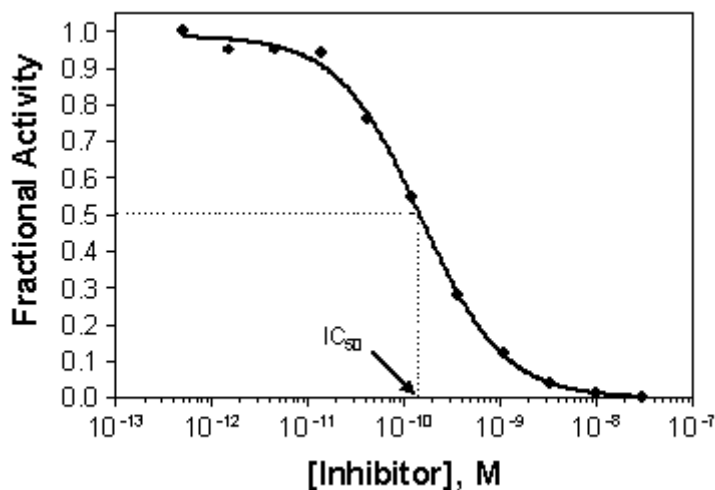


**Figure 7.** Concentration-Response plot for an enzyme inhibitor

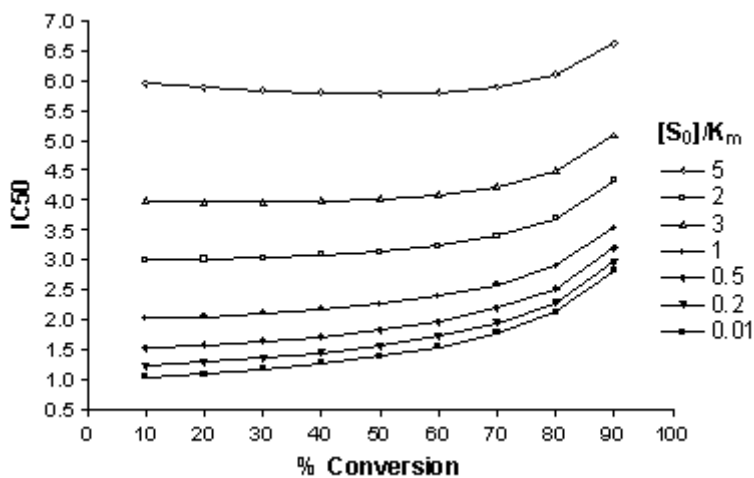


**Figure 8.** Effect of substrate concentration and % conversion on the  $IC_{50}$  for an inhibitor

- Top and bottom values should be within 15% of theory.
- The 95% confidence limits for the  $IC_{50}$  should be within a 2-5 fold range.

Since the  $IC_{50}$  value is the most common result reported for enzymatic assays, it is important to understand how experimental conditions affect  $IC_{50}$  determinations. Generally the concentrations of substrate relative to the  $K_m$  and the amount of product produced have the greatest effect on the measured  $IC_{50}$ . Figure 8 demonstrates the effect of both substrate concentration and percent conversion on measured  $IC_{50}$  values for a competitive inhibitor.

Figure 8 shows the effect of both substrate concentration and % conversion on measured  $IC_{50}$  values. Increased substrate conversion as well as increased substrate concentrations will increase the resulting  $IC_{50}$  value for a given inhibitor. The data were modeled assuming  $K_i = 1.0$  for a competitive inhibitor with no product inhibition.

## Optimization Experiments

Published literature information should be used in selecting these factors. For example a factorial design experiment could be conducted while varying:

- Divalent cations, for example  $Ca^{2+}$ ,  $Mg^{2+}$ ,  $Mn^{2+}$
- Salts, for example NaCl, KCl
- EDTA
- Reducing agents such as  $\beta$ ME, DTT, glutathione
- Bovine serum albumin
- Detergents such as Triton, CHAPS
- DMSO
- Buffer source, for example HEPES *vs.* acetate
- pH

In addition to assay conditions, enzyme stability may be affected if appropriate measures are not taken during long-term storage. Many enzymes need to be stored at  $-70^{\circ}C$  to maintain activity, but freeze-thaw cycles are not recommended. Other enzymes can be stored for long periods of time at  $-20^{\circ}C$  using an additive in the storage buffer such as 50% glycerol.

The presence of carrier proteins in the buffer (bovine serum albumin, ovalbumin, others...) as well as use of polypropylene plates (or non-binding polystyrene plates) may be essential to retain proper enzyme activity.

Enzyme instability can also occur during an assay, as demonstrated previously in Figure 3. This type of instability can occur if the active conformation of the enzyme is not stable in the chosen assay conditions of pH, temperature, ionic strength, etc. In addition, for enzymes that are dimerized, a large dilution into assay buffer may result in inactivation.

## Assay Validation

Parameters such as substrate  $K_m$  and control inhibitor  $IC_{50}$ 's need to be determined in three separate experiments to assess variability. Refer to [HTS Assay Validation](#) to assess variability of the assay.

## References

General Enzyme Kinetics references on the Internet:

<http://themedicalbiochemistrypage.org/enzyme-kinetics.php>

<http://www.ultranet.com/~jkimball/BiologyPages/E/EnzymeKinetics.html>

### Enzyme kinetics simulations:

<http://www.rpi.edu/dept/chem-eng/Biotech-Environ/Canada/enzkin.html>

<http://interactive-mathvision.com/PaisPortfolio/Ckm/EnzymeKinetics/EKJava.html>

### Software examples for fitting enzyme kinetics data:

Graphpad Prism (<http://www.graphpad.com/prism/Prism.htm>)

Sigma Plot (<http://www.sigmaplot.com/products/sigmaplot/sigmaplot-details.php>)

GraFit (<http://www.erithacus.com/grafit/>)

### Literature References:

1. Fersht, Alan. Enzyme Structure and Mechanism. WH Freeman and Co., NY, 1985, pp327-330.
2. Segel, Irwin H. Enzyme Kinetics: Behavior and analysis of rapid equilibrium and steady state enzyme systems. John Wiley and Sons, NY 1975.
3. Copeland, Robert A. Enzymes: A practical introduction to structure, mechanism and data analysis. Wiley-VCH, NY, 2nd Edition, 2000.
4. Dixon, M. and Webb, E.C. Enzymes, 3rd Edition. Academic Press, NY 1979.
5. Lai C-J. -, Wu JC A Simple Kinetic Method for Rapid Mechanistic Analysis of Reversible Enzyme Inhibitors. Assays and Drug Dev. Technologies. 2003;1(4):527–535. PubMed PMID: 15090249.



# Mechanism of Action Assays for Enzymes\*

John Strelow, Walther Dewe, Phillip W Iversen,<sup>1</sup> Harold B Brooks, Jeffrey A Radding, James McGee,<sup>2</sup> and Jeffrey Weidner<sup>3</sup>

Created: May 1, 2012; Updated: October 1, 2012.

## Abstract

Many drugs are inhibitors of enzymes involved in mediating the disease processes. Understanding the mechanism of action (MOA) of the target enzyme is critical in early discovery and development of drug candidates through extensive Structure-Activity Relationship (SAR) studies. This chapter contains a primer on the MOA of enzymes and its significance in drug discovery, types of inhibition, development and validation of MOA assays, data analysis and guidelines for performing these assays. New and experienced investigators will find this chapter useful when starting new projects involving enzyme targets.

## Overview of MOA in Drug Discovery

The purpose of a mechanism of action (MOA) study is to characterize the interaction of a compound with its target to understand how the compound interacts with the target and how natural substrates at physiologic concentrations will modulate this activity. These compounds are often inhibitors of enzymes but only rarely become drugs due to the requirements for a drug to not only inhibit the target but to have acceptable solubility, permeability, protein binding, and selectivity, metabolism and toxicity profiles. This potential for the compound to become a drug is slowly revealed through the analysis and tracking of these characteristics, as chemistry elaborates the structure-activity relationship (SAR). As described in the body of this document, certain types of biochemical behavior are associated with good drug-like properties both *in vitro* and *in vivo*.

Most biochemical screens are designed to provide a chemical starting point based upon the most robust, simple and inexpensive modality for screening. This is due to the required reproducibility in the screening process and the potentially large number of molecules to be run through the screen. Most enzymatic screens are designed to identify inhibitors regardless of their mode of action. Thus, screens are usually run at or below the  $K_m$  for the substrate(s). In the case of an enzyme with two substrates, the screen is often designed to run under pseudo-first order kinetics by running the assay under conditions where one substrate is at saturation, well above its  $K_m$ , and the second is at or below its  $K_m$  for the enzyme. One can therefore identify inhibitors that have competitive,

---

\* Edited by James McGee and Jeffrey Weidner

<sup>1</sup> Eli Lilly and Company. <sup>2</sup> Eli Lilly and Company. <sup>3</sup> AbbVie, Chicago, IL.

noncompetitive and uncompetitive behavior with regard to the substrate at or below  $K_m$  and noncompetitive or uncompetitive behavior with regard to the other substrate at well above its  $K_m$  for the enzyme.

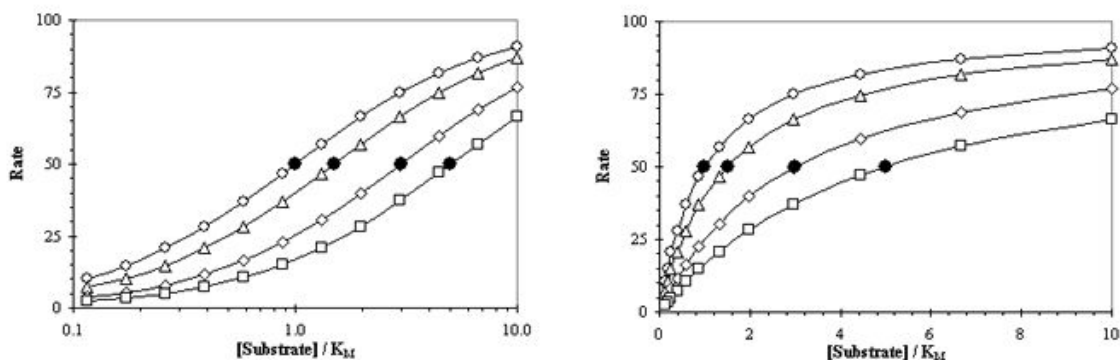
In the drug discovery process, the screening phase casts a wide net and the ability to further analyze compounds in more detail is limited, therefore the number of actives isolated from a screen for follow-up are determined by the overall hit rate, the repeat rate upon retesting and determination of the  $IC_{50}$  in a concentration response curve (CRC) test. In general, activities range from mid-micromolar to sub-micromolar for enzyme inhibitors right out of the screen. It is this piece of information (the  $IC_{50}$ ), along with an analysis of the structural classes of active molecules by a medicinal chemist, which defines the initial SAR, if there is one in the data. It is after this initial analysis that MOA studies can prove valuable by further defining the nature of the inhibitor from a biochemical point of view. MOA studies at this point in the drug discovery process define the nature of the SAR by elucidating the type of inhibition by which the discovered molecules operate. Thus, one can define if the discovered inhibitor is competitive with substrate, for example, and as described below, potentially suffers from certain liabilities associated with this mechanism.

Cell based assays of biochemical actives are usually utilized to identify promising molecules in a second round of low to medium throughput screening. If a molecule shows significant activity in a cell based assay, then it continues through the flow scheme. The lack of cell based activity of biochemically potent actives is usually attributed to lack of cellular permeability, with a wave of the hand; however, an understanding the MOA of a compound at this stage can add depth to the interpretation of cellular activity or its absence. Knowing a compound is competitive with a substrate helps establish the binding pocket and, in combination with structural and SAR information, provides an immediate direction for further chemical synthesis. However, these competitive compounds with promising structure and potent biochemical activity might compete with a cellular substrate present at high intracellular concentration thus show no significant cell based activity. Alternatively, more potent cell based activity than is biochemically predicted from  $IC_{50}$  curves might correlate with unusual kinetic behaviors such as slow binding behavior and/or slow off rates (tight binding). As there is no single, unique answer, biochemical MOA studies help in interpretation of cell based activities and provides further support for molecules with desirable characteristics to move forward in the flow scheme. Traditionally, as MOA studies were slow, laborious efforts, only a few selected molecules could be readily analyzed. With the advent of laboratory automation and enhanced data processing, it is now possible to assess a larger number of compounds rapidly. Therefore, it is feasible (and desirable) to examine the results of a screening campaign, in addition to standard cell based assays in the second tier, by an analysis of MOA.

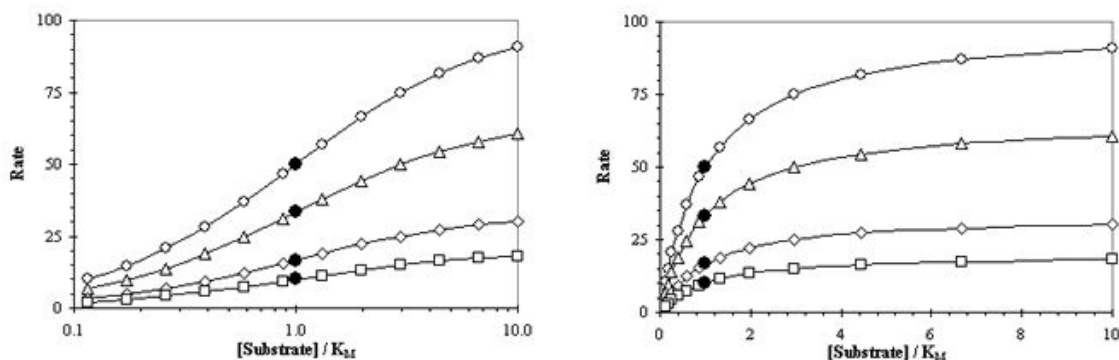
## Types of Inhibition

There are three main types of inhibition (competitive, noncompetitive, and uncompetitive) that are most commonly used to describe the binding of an inhibitor to a

### Competitive Inhibition



### Noncompetitive Inhibition



### Uncompetitive Inhibition

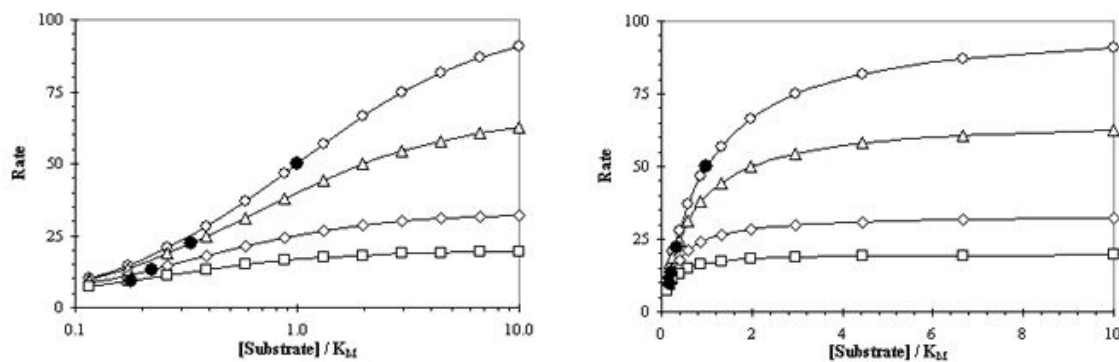


**Figure 1** – Illustrations of data demonstrating Competitive, Noncompetitive, and Uncompetitive Inhibition. The circles represent those rates obtained without the addition of inhibitor. The triangles contained  $0.5 \times K_i$  of inhibitor, the diamonds contained  $2.0 \times K_i$  of inhibitor, and the squares contained  $4.0 \times K_i$  of inhibitor. The black circles depict the shifts in the apparent  $K_M$  for each binding modality.

target enzyme (Figure 1). However, a complete analysis of the mechanism of action requires the scientist to also evaluate other potential inhibition events, including allosteric,

partial, tight-binding, and time-dependent inhibition. A review of these types of inhibition is provided in the sections that follow.

## Competitive Inhibition

A competitive inhibitor binds only to free enzyme. Often this binding event occurs on the active site of the target, precisely where substrate also binds. Although this is the case for a majority of competitive inhibitors, it is a misleading oversimplification. It is more appropriate to state that the binding of a competitive inhibitor and the binding of substrate are mutually exclusive events. Figure 2 provides illustrations of some possible mutually exclusive binding events.

Despite the differences in binding to the free enzyme illustrated in Figure 2, all competitive inhibitors have the same effects on substrate binding and catalysis. A competitive inhibitor will raise the apparent  $K_m$  value for its substrate with no change in the apparent  $V_{max}$  value. As a result, it is often stated that competitive inhibition can be overcome, observed by an increase in the apparent  $K_i$  value, at higher concentrations of substrate. This characteristic will have physiological consequences on the observed efficacy of drugs. As an enzyme's reaction is inhibited by a competitive inhibitor, there is an increase in the local concentration of substrate. Without a mechanism to clear the substrate, a competitive inhibitor will lose potency. This is not the case for a noncompetitive inhibitor.

## Noncompetitive Inhibition

A noncompetitive inhibitor binds equally well to both free enzyme and the enzyme-substrate complex. These binding events occur exclusively at a site distinct from the precise active site occupied by substrate. Figure 3 provides some illustrations of the more common noncompetitive binding events.

In contrast to a competitive inhibitor, a noncompetitive inhibitor will lower the apparent  $V_{max}$  value, yet there is no effect on the apparent  $K_m$  value for its substrate. Essentially, the  $K_i$  of the inhibitor does not change as a function of the substrate concentration.

In some circumstances, a compound may have unequal affinity for both free enzyme and the enzyme-substrate complex. This mixture of competitive and noncompetitive phenotypes is called mixed inhibition.

## Uncompetitive Inhibition

An uncompetitive inhibitor binds exclusively to the enzyme-substrate complex yielding an inactive enzyme-substrate-inhibitor complex (Figure 4). When encountered, the apparent  $V_{max}$  value and the apparent  $K_m$  value should both decrease. Despite their rarity in drug discovery programs, uncompetitive inhibitors could have dramatic physiological consequences. As the inhibitor decreases the enzyme activity, there is an increase in the local concentration of substrate. Without a mechanism to clear the buildup of substrate, the potency of the uncompetitive inhibitor will increase.

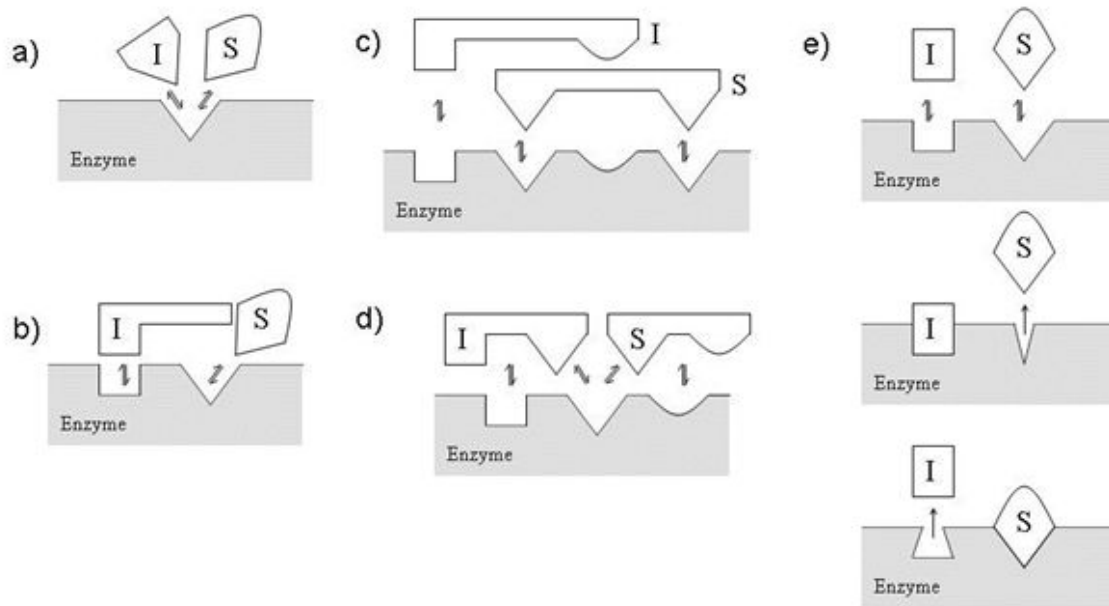


**Figure 2** – Examples of Competitive Inhibition where Substrate (S) and Inhibitor (I) binding events are mutually exclusive. (a) Classical model for competitive inhibition where S and I compete for the same precise region of the active site. (b) I does not bind to the active site, but sterically hinders S binding. (c) S and I binding sites are overlapping. (d) S and I share a common binding pocket on the enzyme. (e) I binding can result in a conformational change that prevents S binding (and vice versa). This was adapted from Segal, Enzyme Kinetics.

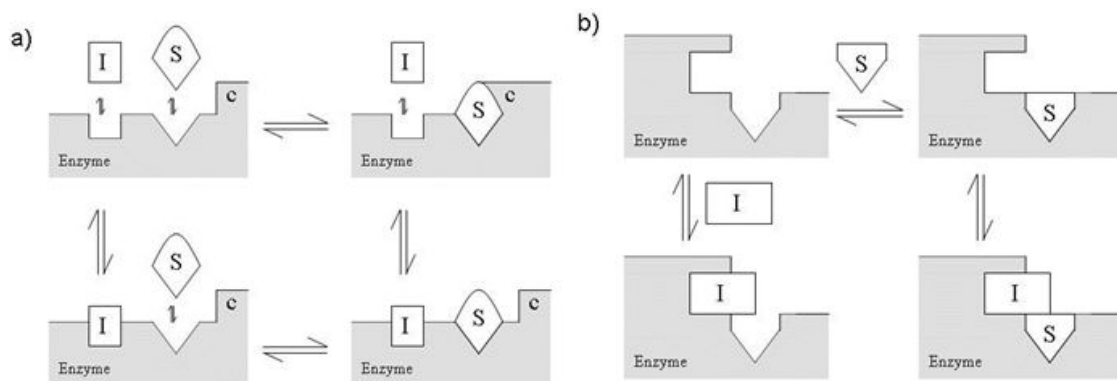


**Figure 3** – Examples of Noncompetitive Inhibition where Inhibitor (I) binding occurs at a site distinct from the Substrate (S) binding site and the Catalytic center (c) of the active site. (a) In this model, the binding of S induces a conformational change to align the catalytic center near S for catalysis. However, when I binds at a separate site, the conformational change does not occur and enzyme activity is inhibited. (b) In this model, I can sterically hinder S binding and release. However, unlike Figure 1-B, I and S can occupy the enzyme at the same time. This was adapted from Segal, Enzyme Kinetics.

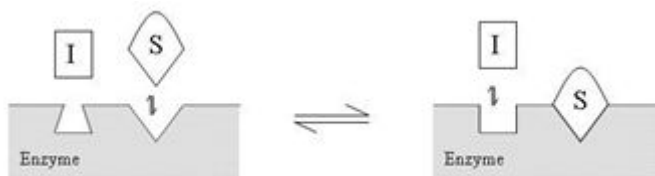


**Figure 4** – An example of Uncompetitive Inhibition where Inhibitor (I) only binds in the presence of Substrate (S).

## Allosteric Inhibition

An allosteric inhibitor decreases activity by binding to an allosteric site other than or in addition to the active site on the target. This interaction is characterized by a conformational change in the target enzyme that is required for inhibition. These conformational changes can affect the formation of the usual enzyme-substrate active site complex, stabilization of the transition state, or reduce the ability to lower the activation energy of catalysis. Figure 2e and Figure 3a are classical examples of allosteric inhibition. As such, an allosteric inhibitor may display a competitive, noncompetitive, or uncompetitive phenotype with respect to substrate binding.

## Partial Inhibition

Partial inhibition results from the formation of an enzyme-substrate-inhibitor complex that can generate product with less facility than the enzyme-substrate complex. This can be illustrated in Figure 3a. When “I” is a partial inhibitor bound in the enzyme-substrate-inhibitor complex, the catalytic center may retain some ability to align near the substrate and facilitate catalysis. As a consequence of these structural changes, partial inhibitors can also be allosteric inhibitors of enzyme activity. In direct contrast, full inhibition results in an enzyme-substrate-inhibitor complex where the catalytic center is not capable of aligning near the substrate for catalysis.

## Tight-Binding Inhibition

In this type of inhibition, the population of free, soluble inhibitor is significantly depleted by the formation of the enzyme-inhibitor or enzyme-substrate-inhibitor complex. While tight-binding inhibitors can bind to the target enzyme in a competitive, noncompetitive, or uncompetitive manner with respect to substrate binding, they can display noncompetitive phenotypes. However, a tight-binding inhibitor typically binds with an apparent affinity ( $K_i$ ) near the concentration of enzyme (active sites) present in the biochemical assay.

## Time-Dependent Inhibition

Time-dependent inhibitors bind slowly to the enzyme on the time scale of enzymatic turnover, thus displaying a change in initial velocity with time. This has the effect of

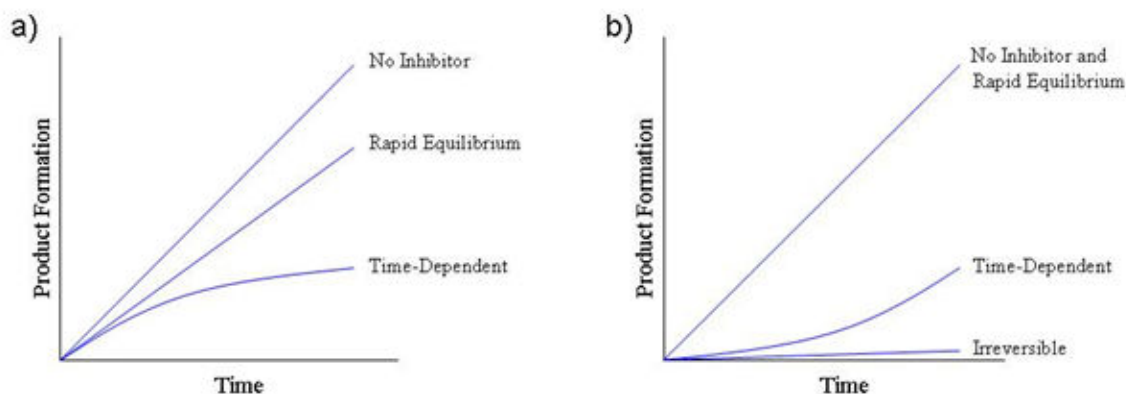


**Figure 5** – Illustrations of time-dependent inhibition. (a) This graph depicts the decrease in the initial velocity (product formed vs time) observed for classical, rapid equilibrium inhibitor and a time-dependent inhibitor. The latter yields a nonlinear progress curve consistent with a slow  $k_{on}$  value. (b) This graph depicts the recovery of enzyme activity (product formed vs time) following dilution of the enzyme-inhibitor complex with substrate. Dilutions of classical, rapid equilibrium inhibitor complexes recover full activity immediately after dilution. Dilutions of time-dependent inhibitor complexes recover enzyme activity more slowly, indicative of a compound with a slow  $k_{off}$  value. Dilutions of irreversible inhibitor complexes maintain the enzyme-inhibitor complex after dilution.

slowing the observed onset of inhibition. Time-dependent inhibitors also impede the observed recovery of enzyme activity following inhibition, resulting in slow  $k_{off}$  values. As illustrated in Figure 5, these inhibitors typically yield nonlinear initial velocities and nonlinear recoveries of enzyme activity.

Interestingly, many successful therapeutic drugs are time-dependent inhibitors. For these inhibitors with slow  $k_{off}$  values, the rate of release of inhibitor from the enzyme-inhibitor complex (recovery of enzyme activity) proceeds independent of the substrate concentration and the physiological mechanism to remove inhibitor. This makes time-dependent inhibition a very attractive and proven strategy for the discovery and development of drugs.

Some time-dependent inhibitors covalently attach to the target enzyme. For those inhibitors, the  $k_{off}$  value is zero and the inhibition is said to be irreversible. These are typically less attractive molecules, unless the formation of the covalent species is specific to the reaction mechanism of the enzyme. Some inhibitors are for all practical purposes irreversible, with very low  $k_{off}$  values, despite their inability to covalently attach to the enzyme. This stands in direct contrast to rapid equilibrium, reversible inhibitors that bind to and release from the enzyme at rates that are rapid in comparison to the rate of enzyme turnover.

## Performing MOA Studies

When performing classical steady-state mechanism of action studies, the scientist should carefully consider and incorporate the proper biochemical and statistical guidelines

provided in this section. These guidelines should assist in the initial characterization of the enzyme-inhibitor complex. However, in some cases the classical steady-state experiment is not sufficient and additional characterizations are required. Examples include compounds that display tight-binding inhibition, time-dependent inhibition, covalent modification, or nonspecific inhibition of the enzyme. Therefore, we also provide guidelines to identify these additional types of inhibitors and plan the appropriate follow-up analysis.

## Classical Steady-State Experiments

These types of studies involve measurements of the  $V_{\max}$  and  $K_M$  of a substrate at a range of inhibitor concentrations. The scientist should refer to [Basic Enzyme Assays](#) chapter of this manual, for a description of how to perform measurements of the  $V_{\max}$  and  $K_M$  for a substrate. As mentioned previously, changes in the apparent  $V_{\max}$  and  $K_M$  give the scientist a view of the binding modality (competitive, noncompetitive, or uncompetitive) and the potency ( $K_i$  and  $K_i'$ ). Figure 6 illustrates the classical steady-state experiment used to determine the binding modality and potency.

The methodology proposed here to determine the binding potency and modality of an inhibitor is derived from a steady-state model of enzyme kinetics. The term steady-state refers to a constant concentration of the enzyme-substrate complex present during the reaction. As summarized by Copeland (1) and Segal (2), there are several assumptions that simplify the mathematical treatment of the kinetics. When these assumptions fail, the steady-state MOA model proposed here is not valid.

1. The enzyme is acting catalytically and the concentration of substrate is much greater than the concentration of enzyme.
2. During the initial phase of the reaction (initial velocity), there is no buildup of any intermediate other than the enzyme-substrate complex.
3. There is very little product formed over the course of the reaction so that the depletion of substrate is minimal and the reverse reaction is insignificant.
4. The concentration of inhibitor is much greater than the concentration of enzyme so that the depletion of free inhibitor resulting from the formation of the enzyme-inhibitor complex is minimal.

The scientist should utilize the following guidelines in the design, execution, and analysis of a classical MOA experiment.

## Guidelines for Assay Design

- It is essential to ensure that the enzyme, substrate, co-factors, and buffer conditions have been fully evaluated and characterized. Wherever possible, the scientist should strive to achieve *in vitro* conditions that will best represent the physiological conditions in a robust, reproducible manner. The selection of these factors can have a large impact on the binding modality and potency observed.



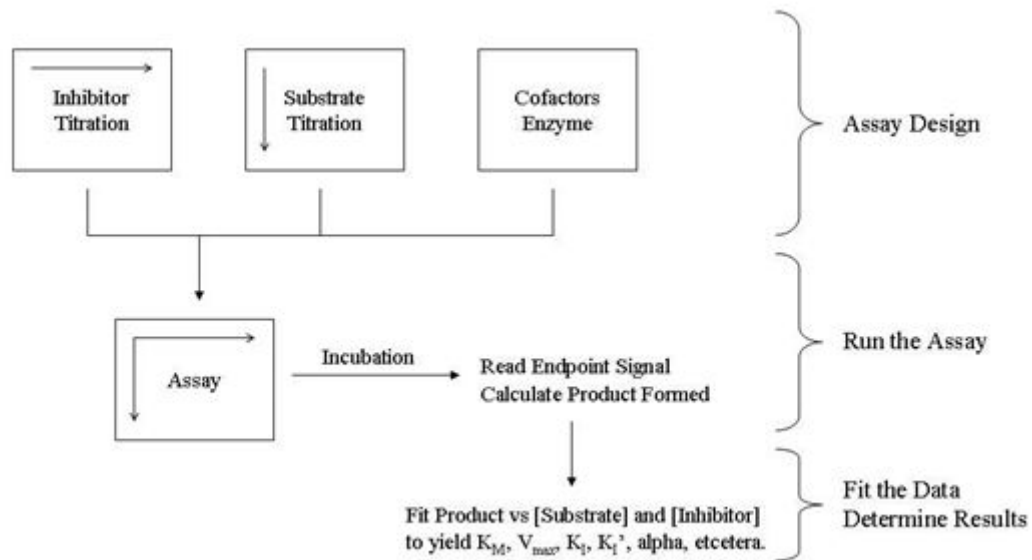


**Figure 6** – Classical Steady-State analysis of the mechanism of action. The inhibitor and substrates are serially diluted to achieve concentrations in the assay that span their respective binding constants ( $K_i$  and  $K_M$ ). The addition of enzyme and cofactors will initiate the enzymatic reaction. The order of addition typically depends on the assay in question and may be altered for time-dependent inhibitors (discussed later). The assay incubates for some period of time, the signal is read, the data is fit, and the results are analyzed.

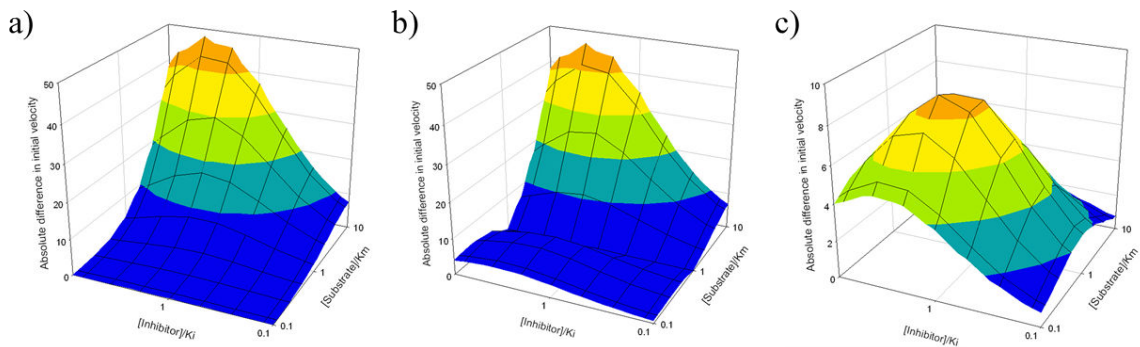


**Figure 7** – Residual plots demonstrating the difference in observed rate of enzyme activity (z-axis) at each concentration of substrate (y-axis) and inhibitor (x-axis) for 2 binding modalities. (a) Competitive Inhibition vs Noncompetitive inhibition. (b) Competitive inhibition vs Uncompetitive inhibition. (c) Noncompetitive vs Uncompetitive inhibition. Taken together, competitive inhibitors are best distinguished from noncompetitive and uncompetitive inhibitors at both high [substrate] and high [inhibitor]. Noncompetitive and uncompetitive inhibitors are best distinguished from each other at [substrate] and [inhibitor] near their binding constants ( $K_M$  and  $K_i$ ). Therefore, the range and density of concentrations tested are both important.

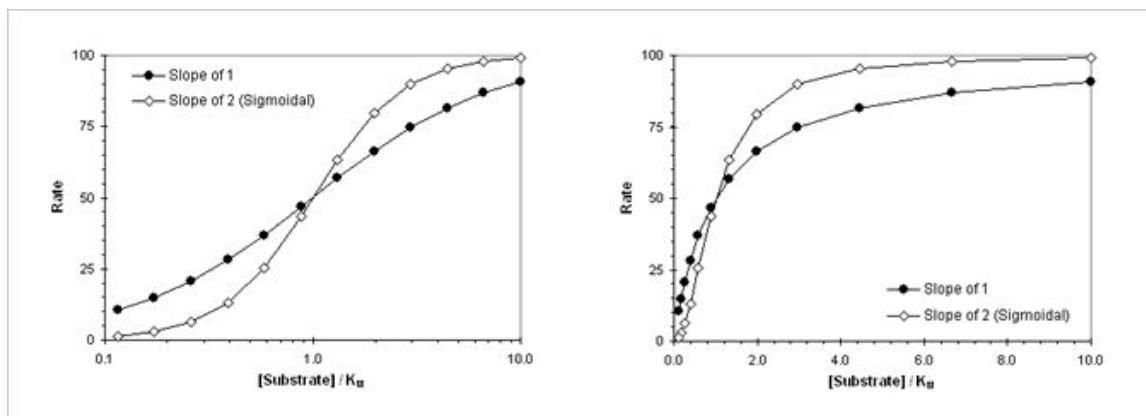


**Figure 8** – Comparison on enzyme data for a system with a proper slope of 1 and another displaying a sigmoidal relationship (ex. slope of 2) between the substrate concentration tested and the rate observed.

- An enzyme titration should be performed to determine the concentration of active sites in the assay. Consult Copeland, Enzyme 2ed, pg313 or an experienced enzymologist for more information (1).
- There should be at least 5 concentrations of substrate tested, spanning a range of at least  $\frac{1}{2} \times K_m$  to  $5 \times K_m$ , for each concentration of inhibitor tested. As illustrated in Figure 7, the ability to distinguish a competitive inhibitor from a noncompetitive or uncompetitive inhibitor is increasingly enhanced at concentrations of substrate above its  $K_m$  value. The ability to distinguish noncompetitive inhibition from uncompetitive inhibition is more challenging and can be improved with very accurate determinations of the apparent  $K_m$ . Therefore, the scientist should strive to judiciously increase the range and number of concentrations of substrate tested.
- The plot of the [substrate] vs initial velocity should not display sigmoidal kinetics, unless it is a mechanistic feature of substrate binding and catalysis for that enzyme. The impact of sigmoidal kinetics on the  $K_m$  curve is illustrated in Figure 8. Sigmoidal kinetics may be a sign of an impure enzyme or the presence of multiple isoforms of the enzyme (ex. multiple phosphorylation states of the same kinase). Refer to Copeland, Enzyme 2ed, pg382 or an enzymologist experienced with sigmoidal kinetics (1).
- The initial velocity should be measured. In order for the steady-state assumptions to hold, it is recommended that less than 10% of the substrate be converted to product. The chapter on [Basic Enzyme Assays](#) describes this in more detail. However, initial velocity conditions do not infer linearity and the user should refer to the guideline directly below.
- The formation of product should be linear with respect to time. This is best achieved by measuring the rate of product formation at the chosen concentrations of substrate using the assay conditions, detection system, and instruments that will be used for the final assay. Linearity should be assessed visually from plots of the raw data.

- There should be at least 8 concentrations of inhibitor tested at each concentration of substrate. The range of inhibitor concentrations tested should span the  $K_i$  or  $K_i'$ , depending on the binding modality. Reporting of binding constants outside of the range of concentrations tested should be avoided. It is also recommended to include inhibitor concentrations at or above  $\sim 10 \times K_i$  to ensure maximum inhibition and the identification of any potential partial inhibitors. It should be noted that any observation of partial inhibition could instead be a consequence of a compound's poor solubility.
- Where available, a control inhibitor should be evaluated under the exact conditions that will be used for the final assay.
- In addition to the experimental wells containing a matrix of substrate and inhibitor dilutions, the final assay should include both high and low controls. The high control should contain the substrate titration without inhibitor to reflect the maximum enzyme activity at each substrate concentration. The low control should contain the substrate titration without enzyme or substrate and without inhibitor. The low controls should reflect the signal expected for no enzyme activity at each substrate concentration. Depending on the composition of the inhibitor stocks, DMSO might be needed in the control wells to assure consistency across all the experiments.
- The concentration of DMSO should be kept constant in MOA experiments for a particular target. DMSO can have a significant impact on enzyme activity and the concentration of DMSO in the wells containing compound should be identical to the concentration of DMSO in the control wells (described directly above). DMSO can also impact the solubility of a compound and its observed potency. Therefore, the concentration of DMSO should be consistent in replicate MOA experiments (or in comparison to  $IC_{50}$  experiments).
- It is recommended to evaluate, in the standard assay conditions, dependence of [enzyme] on the  $IC_{50}$  of the compounds to be tested. Shifts in the  $IC_{50}$  as a function of the [enzyme] is an indication of tight-binding inhibition and/or solubility issues. When this is encountered, the scientist should consult with an enzymologist experienced with tight-binding inhibition.
- If detergents are required for enzyme activity or automation, the scientist should strive to maintain their concentrations well below the critical micelle concentration (CMC). The formation of micelles, at high concentrations of detergents, can interfere with the determinations of the binding modality and potency. An exception to this rule would include assays requiring detergents as part of the mechanistic evaluation. If the assay can only be run above the CMC, the scientist should consult with an enzymologist experienced with lipids, micelles, and surface dilution kinetics.
- The reaction should be measured under steady-state conditions that includes the following: 1) there should not be any appreciable buildup of any enzyme intermediates other than the ES complex, 2) the [substrate] should be  $\gg$  [enzyme], and 3) the initial phase of the reaction is measured so that the [product]  $\sim 0$ , the depletion of substrate is minimal, and the reverse reaction is insignificant (1).

- The concentration of a required cofactor should be  $\gg$  [enzyme].

## Statistical Validation of the Designed Assay

The requirements for statistical validation of a MOA assay can be divided into two situations: 1) high-throughput assays using automation that can test many compounds, and 2) low-throughput assays in which only one or a few compounds are tested. In the first case, a replicate-experiment study should be performed as described in the [Assay Validation](#) chapter of this manual. Briefly, 20 to 30 compounds should be tested in two independent runs. Then the MSD or MSR and limits of agreement are determined for each of the key results, including  $V_{\max}$ ,  $K_m$ ,  $K_i$ ,  $K_i'$ , and  $\alpha$  or  $\alpha_{\text{inv}}$ . Specific acceptance criteria have not been determined. The reproducibility should be judged as suitable or not for each situation. For low-throughput assays, a replicate-experiment study is not required. At a minimum, key results from the MOA experiment, such as  $V_{\max}$ ,  $K_m$ , and  $K_i$ , should be compared to previous/preliminary experiments to ensure consistency. The data from the MOA experiment should be examined graphically for outliers, goodness of fit of the model to the data, and consistency with the assumptions and guidelines for designing and running the assay (see Guidelines for Assay Design above and Guidelines for Running the Assay below).

## Guidelines for Running the Assay

- The assay should be run under the exact same conditions as developed using the guidelines above. In addition, the assay should be run within the timeframe where the reagents are known to be stable.
- When a control inhibitor is included, then the  $K_i$  (and/or  $K_i'$ ) value should be compared with legacy data to ensure robust, quality results. It is also recommended to include additional inhibitors with alternative binding modalities, if available.
- The  $K_m$  and  $V_{\max}$  values from the high controls and the signal from the low controls should be compared with the legacy values determined in identical conditions, as described above.
- A standard curve should be included for detection systems yielding signals that are nonlinear with respect to the amount of product formed. This nonlinearity is a common feature in fluorescent-based assays. The standard curve should be used to convert the signal produced to the amount of product formed. The resulting amount of product formed over the course of the assay time should be used in the data fitting methodologies. Please refer to the [Immunoassay Methods](#) chapter.

## Guidelines for Data Fitting and Interpretation

- The multivariate dataset ( $v$ ,  $[I]$ ,  $[S]$ ) should be fit using a non-linear regression analysis with the appropriate models described below. Linear transformations of the data should be avoided as they will distort the error of the experiment and were historically used only before the introduction of computer algorithms.
- The scientist should perform any necessary background corrections, before the multivariate fitting, so that a signal or rate of 0 represents that expected for

conditions lacking enzyme activity. Depending on the assay design, this may include a single background correction applied to the entire experiment or several different corrections. The latter should be used when the background signal varies with the [substrate] tested. Here there should be a background correction for each [substrate] tested.

The traditional model of general mixed inhibition is:

$$v = \frac{V_{\max} [S]}{K_m \left(1 + \frac{[I]}{K_i}\right) + [S] \left(1 + \frac{[I]}{K_i'}\right)} \quad (\text{P1})$$

Where  $v$  is the speed of the reaction (slope of product formed vs. time),  $V_{\max}$  is the upper asymptote,  $[S]$  is the substrate concentration, and  $[I]$  is the inhibitor concentration. See the glossary for definitions of  $K_m$ ,  $K_i$ , and  $K_i'$ . This model can also be written as:

$$v = \frac{V_{\max} [S]}{K_m \left(1 + \frac{[I]}{K_i}\right) + [S] \left(1 + \frac{[I]}{\alpha K_i}\right)} \quad (\text{P2})$$

$$v = \frac{V_{\max} [S]}{K_m \left(1 + \frac{[I]}{K_i}\right) + [S] \left(1 + \frac{\alpha_{\text{inv}} [I]}{K_i}\right)} \quad (\text{P3})$$

where  $\alpha = 1/\alpha_{\text{inv}} = K_i'/K_i$ . This model reduces to specific models for competitive, non-competitive, and un-competitive inhibition as described in Table 1.

Another form of this model that has better statistical properties, in terms of parameter estimation and error determination, is:

$$v = \frac{[S]}{\theta_1 + \theta_2 [I] + \theta_3 [S] + \theta_4 [I][S]} \quad (\text{P4})$$

where,

$$V_{\max} = \frac{1}{\theta_3}$$

$$K_M = \frac{\theta_1}{\theta_3}$$

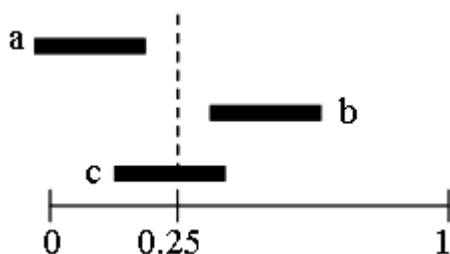
$$K_I = \frac{\theta_1}{\theta_2}$$

$$K'_I = \frac{\theta_3}{\theta_4}$$

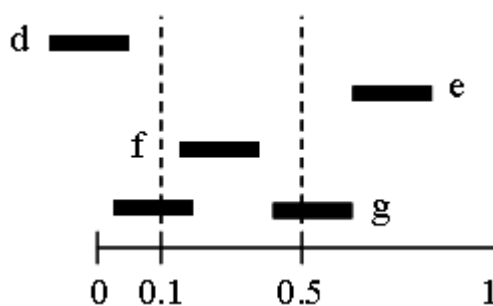
$$\alpha = \frac{\theta_2 \theta_3}{\theta_1 \theta_4} = \frac{1}{\alpha_{\text{inv}}} = \frac{K'_I}{K_I}$$

More details on these models can be found in a manuscript in preparation by the primary authors of this chapter.

1. Fit a robust multiple linear regression of  $1/v$  vs.  $1/[S]$ ,  $[I]/[S]$ , and  $[I]$ . This provides starting values of the  $\theta$  parameters for the non-linear regression in the next step.
2. Fit model P4 to the data ( $v$ ,  $[I]$ ,  $[S]$ ).
3. Calculate the parameters of interest from the  $\theta$  values.
4. Calculate confidence limits for each key parameter value using Monte Carlo simulation.
5. Make decisions of mechanism based on the value of  $\alpha$  or  $\alpha_{\text{inv}}$  and the associated confidence limits.
  - $\alpha$  or  $\alpha_{\text{inv}}$  should be used to assign the binding modality. If  $\alpha$  is less than 1, the mechanism is:
    - a. Uncompetitive if the upper confidence limit of  $\alpha < 0.25$
    - b. Noncompetitive if the lower confidence limit of  $\alpha > 0.25$
    - c. Not competitive, otherwise



- If  $\alpha_{\text{inv}} < 1$ , then the mechanism is:
  - a. Competitive if the upper confidence limit of  $\alpha < 0.1$
  - b. Noncompetitive if the lower confidence limit of  $\alpha > 0.1$
  - c. Mixed, if both confident limits are within  $[0.1, 0.5]$
  - d. Not declarable, otherwise



The details of how these cutoffs were chosen are in a manuscript in preparation.

- When the signal measured at  $10 \times K_i$  (representing full enzyme inhibition by the compound) is  $\gg 0$  (baseline corrected), the compound is displaying partial (and/or allosteric) inhibition. This difference might also be observed when the incorrect conditions were chosen for the low control to represent no enzyme activity, if there was not enough inhibitor (relative to the  $K_i$  or  $K_i'$ ) to achieve maximum inhibition, and/or if the compound tested is poorly soluble.
- When the  $K_i$  or  $K_i'$  resulting from the fit is within 10-fold of the concentration of active sites in the assay, the compound will start to display tight-binding inhibition. Inaccuracies in the binding modality and potency will result. In some cases where the inhibitor is not soluble, tight binding inhibition may exist at much higher  $K_i$  or  $K_i'$  values. As recommended previously, the dependency of the enzyme concentration on the inhibitor's potency is the best method to identify tight-binding inhibition. The scientist should consult with an expert in tight-binding inhibition to further characterize the inhibitor.
- Data suggesting that a compound is noncompetitive (and in some cases mixed) should be handled with caution. Compounds that are time-dependent, irreversible, poorly soluble, nonspecific, and/or tight-binding will display a noncompetitive/mixed phenotype in this type of classical steady-state experiment. As such, it is critical to evaluate these additional potential mechanisms of action, described herein.
- Additional recommendations for data analysis can be found in the next section.

**Table 1: Summary of competitive, non-competitive and uncompetitive inhibition models.**

| Inhibition  | Description   | $K_i$  | $K_i'$   | $K_i'/K_i$ |
|-------------|---|--------|----------|------------|
| Competitive | The inhibitor binds only to free enzyme. This binding most often occurs in the active site at the precise location where substrate or cofactor (being evaluated in the MOA study) also binds. | finite | Infinite | infinite   |
| Mixed       | These inhibitors display properties of both competitive and noncompetitive inhibition.  | finite | Finite   | $> 1$      |

*Table 1 continues on next page...*

Table 1 continued from previous page.

| Inhibition     | Description  | $K_i$    | $K_i'$ | $K_i'/K_i$ |
|----------------|--|----------|--------|------------|
| Noncompetitive | The inhibitor binds equally well to both free enzyme and the enzyme-substrate complex. Consequently, these binding events occur outside the active site. | finite   | Finite | = 1        |
| Uncompetitive  | The inhibitor binds only to the enzyme-substrate complex at a location outside the active site.  | infinite | Finite | = 0        |

## When the Steady-State Assumptions Fail

The steady-state MOA model proposed for here for data fitting requires several important assumptions hold true. While a majority of these assumptions are covered in the previous sections, the invalidation of a few key assumptions should prompt the scientist to perform additional mechanistic characterizations. These key assumptions, a mechanism to flag their breakdown in the steady-state MOA model, and a recommended plan of action are presented.

### Tight Binding Inhibition

The [inhibitor] in solution should be much greater than the [enzyme] in the assay. This assumption fails most frequently in 2 circumstances. First, some compounds bind to their target with such high affinity ( $_{app}K_i$  values within 10 fold of the [enzyme]) that the population of free inhibitor molecules is significantly depleted by formation of the EI complex. Second, some compounds are both very potent and poorly soluble. The poor solubility of the inhibitor will increase the observed  $_{app}K_i$  value (relative to the [enzyme]). In both cases, the compounds are called tight binding inhibitors.

- How can tight binding inhibitors be flagged in the steady-state MOA model?
  - Regardless of their true binding modality, they display a noncompetitive phenotype.
  - They have observed  $_{app}K_i$  values between  $\frac{1}{2}$  and 10-fold of the [enzyme] in the assay.
  - Poorly soluble compounds may also display tight binding inhibition. This is often masked by an inflated observed  $_{app}K_i$  value.
- What is the recommended plan for an appropriate characterization?
  - Calculate the dependence of the  $IC_{50}$  values on the [enzyme]. Using a fixed concentration of substrate at  $K_m$ , the  $IC_{50}$  of the inhibitor should be measured at  $\geq 5$  concentrations of enzyme. If the  $IC_{50}$  changes significantly as a function of the [enzyme], the inhibitor is displaying tight binding properties and requires further characterization. If the  $IC_{50}$  does not change significantly, the compound is not tight binding, this key assumption ([Inhibitor]  $\gg$  [Enzyme]) is true, and the steady-state MOA model is valid. These two phenotypes are illustrated in Figure 9.
  - Calculate the dependence of the  $IC_{50}$  values on the [substrate]. Using a fixed concentration of enzyme, the  $IC_{50}$  of the inhibitor should be measured at  $> 5$



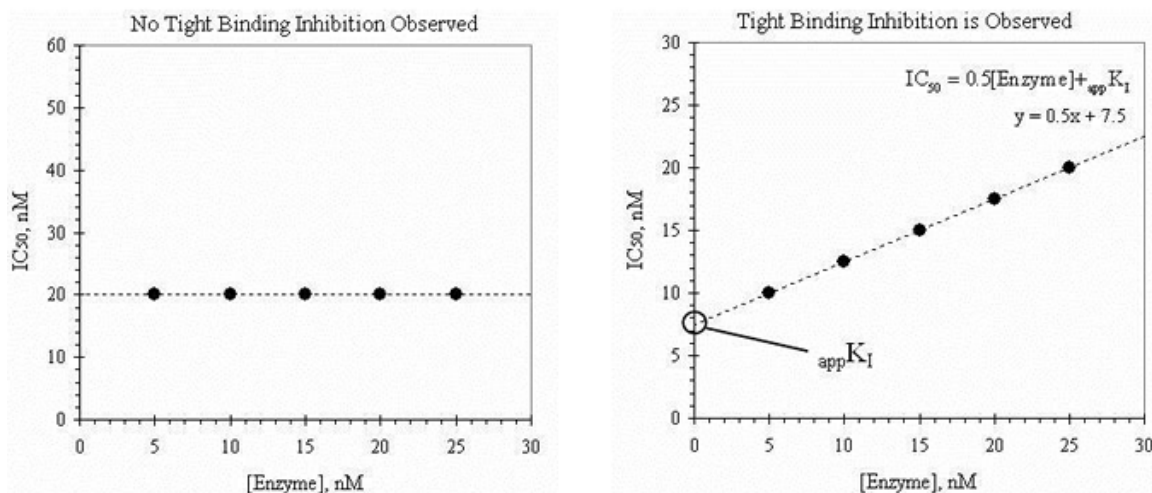


**Figure 9** – Plotting the  $IC_{50}$  vs [Enzyme] will reveal whether a compound is tight binding. As depicted on the left, no change in the  $IC_{50}$  suggests that the compound is not tight binding and the assumption ( $[I] \gg [E]$ ) holds true. As depicted on the right, a change in the  $IC_{50}$  (with a slope of 0.5) suggests that the compound is tight binding and requires additional characterization.

concentrations of substrate. The range of concentrations of substrate should span the  $K_m$  (as recommended previously). As illustrated in Figure 10, the change in the  $IC_{50}$  vs [substrate] is described by the equation listed below and yields the true binding potency ( $K_i$  and  $K_i'$ ). The ratio of  $K_i'/K_i$  (termed alpha,  $\alpha$ ) reflects the binding modality. Inhibitors with alpha values statistically equal to 1.0 are noncompetitive, values statistically less than 1.0 are uncompetitive, and values statistically greater than 1.0 are competitive.

#### **Model to Determine Tight Binding MOA:**

$$IC_{50} = \frac{[S] + K_M}{\frac{K_I}{K_I'} + \frac{[S]}{K_I'}} + \frac{[E]}{2}$$

- These methodologies are described in more detail in Chapter 9 of *Enzymes 2<sup>nd</sup>ed* by Copeland (1). We also recommend consulting with a statistician and an enzymologist experienced with tight binding inhibition.

### **Time-Dependent Inhibition**

When the reaction is started with enzyme, there should be a linear relationship between the enzyme reaction time and the amount of the product formed from that reaction. This linearity should be preserved for all enzyme reactions lacking inhibitor or having rapid equilibrium binding events outside of the time window measured. However, the addition of inhibitor may result in a nonlinear progress curve (Figure 11) with an initial burst of enzyme activity ( $v_i$ ) followed by a final, slower steady-state rate ( $v_s$ ). Although the steady-

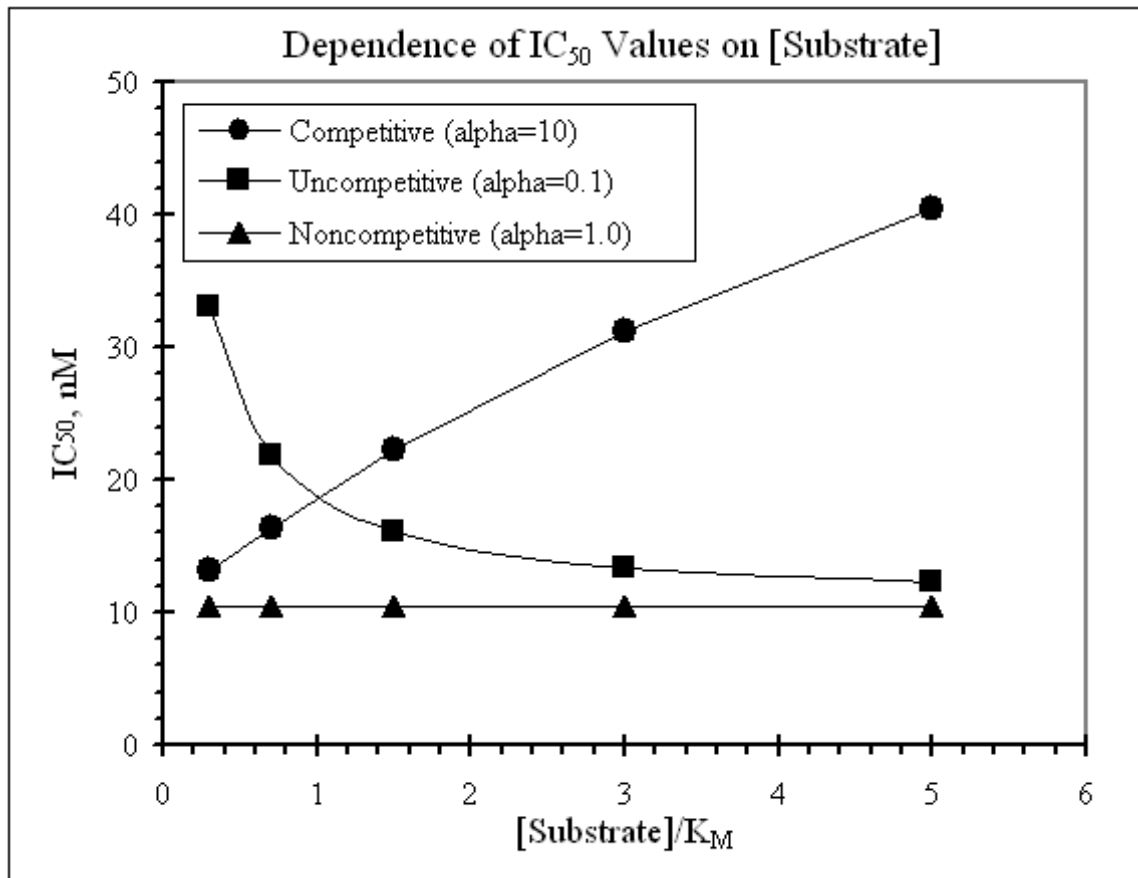


**Figure 10** – A plot of the  $IC_{50}$  vs [substrate] will reveal the binding modality for a tight binding inhibitor. The quality of this assessment is predicated on the choice of a range of substrate concentrations that span the  $K_M$ . The graph illustrates that competitive inhibition is best identified at substrate concentrations above  $K_M$ . In contrast, uncompetitive inhibition is best identified at substrate concentrations below  $K_M$ . The true  $K_i$  and/or  $K_i'$  values can be obtained from a fit using the model below.

state MOA model may still apply under some circumstances, additional characterizations are required.

- How can time dependent inhibitors be flagged in the steady-state MOA model?
  - For kinetic enzyme assays, the progress curve showing product formation over time is nonlinear (Figure 11).
  - For endpoint enzyme assays, time dependent inhibitors can display a noncompetitive phenotype regardless of their true binding modality. Otherwise, they can be identified by observing a shift in inhibitor potency with either a change in the enzyme reaction time and/or a change in the enzyme/inhibitor pre-incubation time.
- What is the recommended plan for an appropriate characterization?
  - More appropriately characterize and model the nonlinear progress curves (product formed vs time) observed. Illustrations of these progress curves and

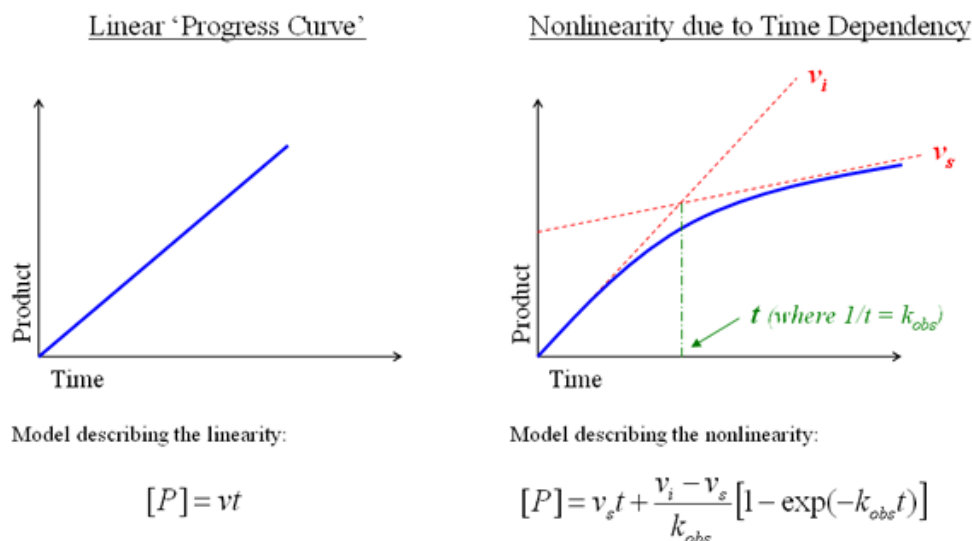


**Figure 11** – Progress curves for linear, rapid equilibrium inhibition (left) and nonlinear, time dependent inhibition (right). Nonlinear progress curves resulting from time dependent inhibition can be fit to the model shown above. The resulting fit will yield the initial velocity ( $v_i$ ), steady-state velocity ( $v_s$ ), and the rate constant for the interconversion between  $v_i$  and  $v_s$  ( $k_{obs}$ ), under the conditions tested. These values can be used to assess the true binding potency and modality.

the appropriate models to use are found below in Figure 11. The resulting fit of the data to the nonlinear model should produce the  $v_i$ ,  $v_s$ , and  $k_{obs}$  for all the [substrate] and [inhibitor] tested.

- During this evaluation,  $k_{obs}$  values reflecting timepoints ( $t$ ) outside of the window tested should be avoided. For example, valid  $k_{obs}$  values from a kinetic run starting at 2 min and ending at 60 min should range between  $0.5 \text{ min}^{-1}$  to  $0.08 \text{ min}^{-1}$ . As a general rule, the total time of the reaction should be 5 times greater than  $1/k_{obs}$ . As a result, the scientist may need to choose a smaller range of [substrate] spanning  $K_m$  and [inhibitor] spanning  $appK_i$ .
- In most cases, the initial ( $v_i$ ) and steady-state ( $v_s$ ) velocities can be fit separately to the steady-state MOA model (presented in the previous section) to yield the binding potency ( $K_i$  and/or  $K_i'$  value) and modality for each phase of inhibition.
- A more traditional approach to determine the apparent potency of the inhibitor requires the scientist to plot the  $k_{obs}$  values as a function of the [inhibitor] at a fixed

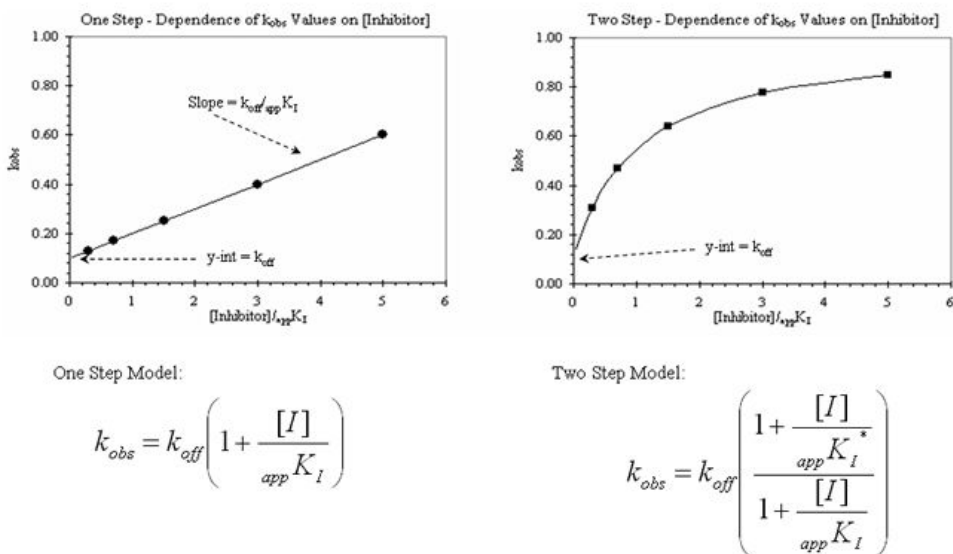


**Figure 12** – A plot of the  $k_{obs}$  vs [inhibitor] will allow for the determination of the  $appK_i$  value for a time dependent inhibitor. If the relationship between  $k_{obs}$  and the [inhibitor] is linear, the one-step model shown above should be used. If the relationship is nonlinear, the two-step model should be used.

[substrate]. This can yield 2 main types of plots illustrated in Figure 12 below: 1) If there is a linear relationship between the  $k_{obs}$  and the [inhibitor] tested, the one-step model shown should be used to determine the  $appK_i$  (potency at the steady-state velocity,  $v_s$ ). 2) If there is a hyperbolic relationship between the  $k_{obs}$  and the [inhibitor] tested, the two-step model shown should be used to determine the  $appK_i$  (potency at the initial velocity,  $v_i$ ) and the  $appK_i^*$  (potency at the steady-state velocity,  $v_s$ ).

- A more traditional approach to determine the binding modality of a time dependent inhibitor requires a determination of the  $appK_i$ , from the previous  $k_{obs}$  vs [inhibitor] plot, at each [substrate] spanning the  $K_m$ . The  $appK_i$  (and  $appK_i^*$ ) can then be graphed as a function of [substrate] and fit to the model shown below (Figure 13). The ratio of  $K_i^*/K_i$  (termed alpha,  $\alpha$ ) determined from the model below will reflect the binding modality. Inhibitors with alpha values statistically equal to 1.0 are noncompetitive, values statistically less than 1.0 are uncompetitive, and values statistically greater than 1.0 are competitive.

### **Model to Determine Time Dependent MOA**

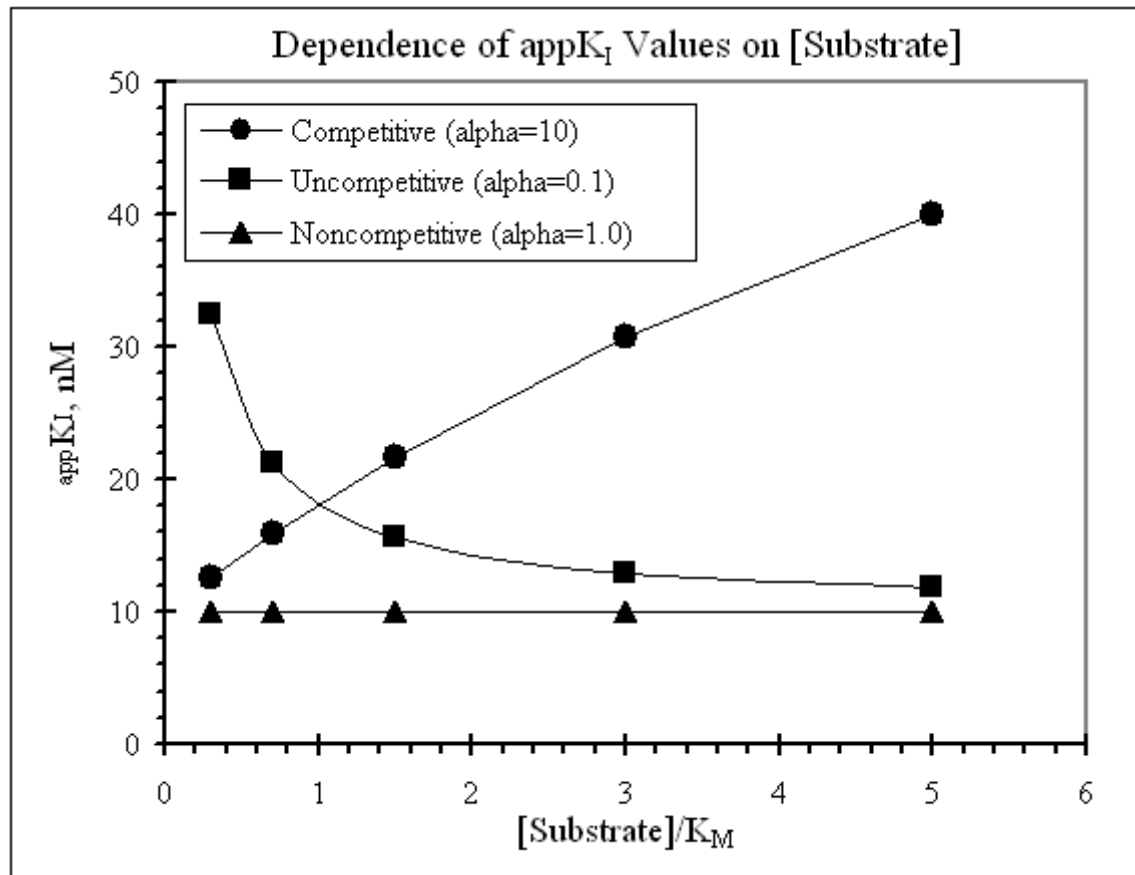


**Figure 13** – A plot of the  $\text{app}K_i$  (and  $\text{app}K_i^*$ ) vs [substrate] will allow for the determination of the true binding potency and modality. The modeled lines above are generated using the equation shown directly below where  $\alpha = K_i'/K_i$ .

$$\text{app} K_I = \frac{[S] + K_M}{\frac{K_M}{K_I} + \frac{[S]}{K_I'}}$$

Where possible, we recommend avoiding the iterative fitting into the one-step or two-step models and the model directly above. The scientist should consult with a statistician and enzymologist to perform a global fit of the data to an equation where the one-step or two-step models are solved for the  $\text{app}K_i$  shown directly above.

- A parallel approach to determine the binding modality requires the scientist evaluate the  $k_{\text{obs}}$  values as a function of the [substrate] at a fixed [inhibitor]. The  $k_{\text{obs}}$  of a competitive inhibitor will decrease with increasing [substrate] relative to  $K_M$ . The  $k_{\text{obs}}$  of an uncompetitive inhibitor will increase with increasing [substrate] relative to  $K_M$ . The  $k_{\text{obs}}$  of a noncompetitive inhibitor will not change with increasing [substrate] relative to  $K_M$ ). These trends are illustrated in Figure 14.

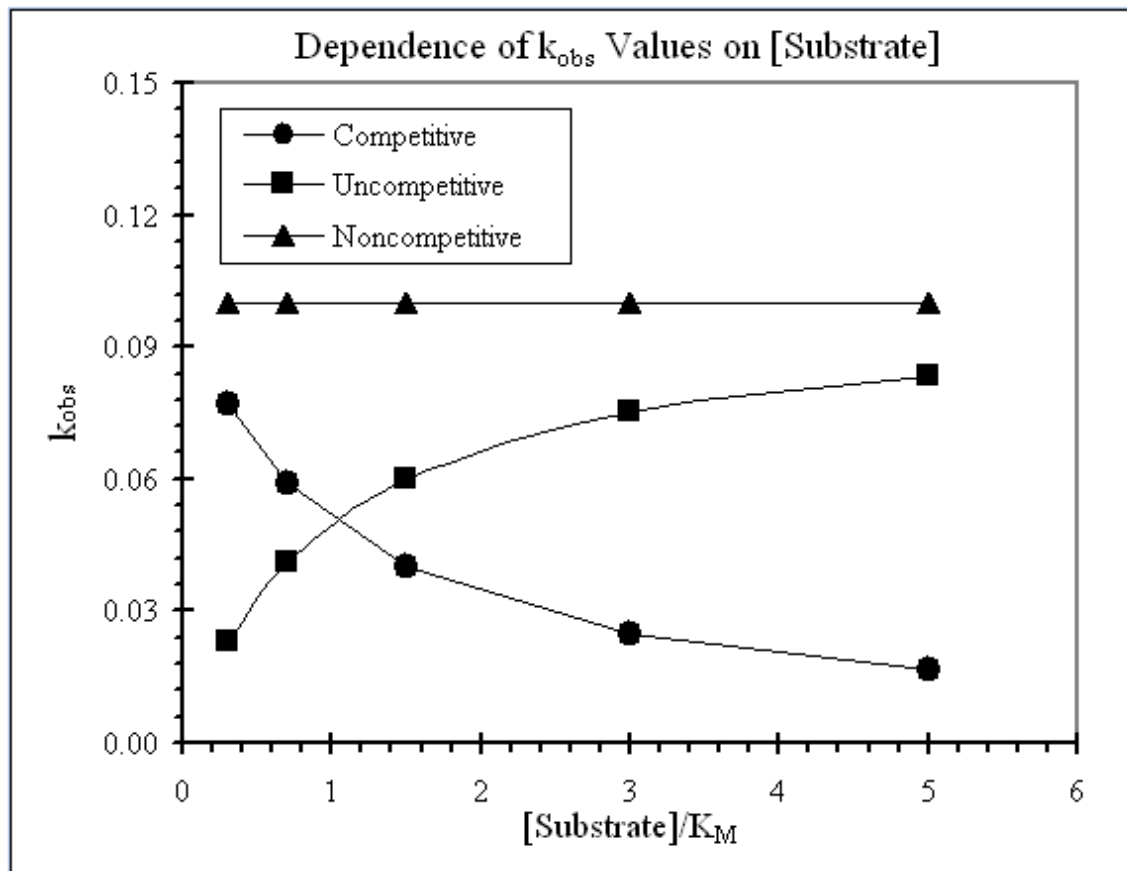


**Figure 14** – A plot of the  $k_{obs}$  vs [substrate] will reveal the binding modality for a time dependent inhibitor. It is important to choose [substrate] well above and below the  $K_m$  to improve the ability to best distinguish the true binding modality.

- These methodologies are described in more detail in Chapter 10 of *Enzymes 2<sup>nd</sup>ed* by Copeland (1). Also be aware that a compound can display both time dependent and tight binding properties. This would require a combination of experiments described above that may require the assistance of a statistician or an experienced enzymologist.

### Covalent Modification

During the initial phase of the reaction (initial velocity), there is no buildup of any intermediate other than the enzyme-substrate complex. This assumption most often fails when a compound is an irreversible inhibitor of the enzyme. This type of inhibition can be the result of an immeasurably slow  $k_{off}$  value and/or covalent modification of the enzyme.

- How can irreversible inhibitors be flagged in the steady-state MOA model?
  - Regardless of their true binding modality, they display a noncompetitive phenotype.

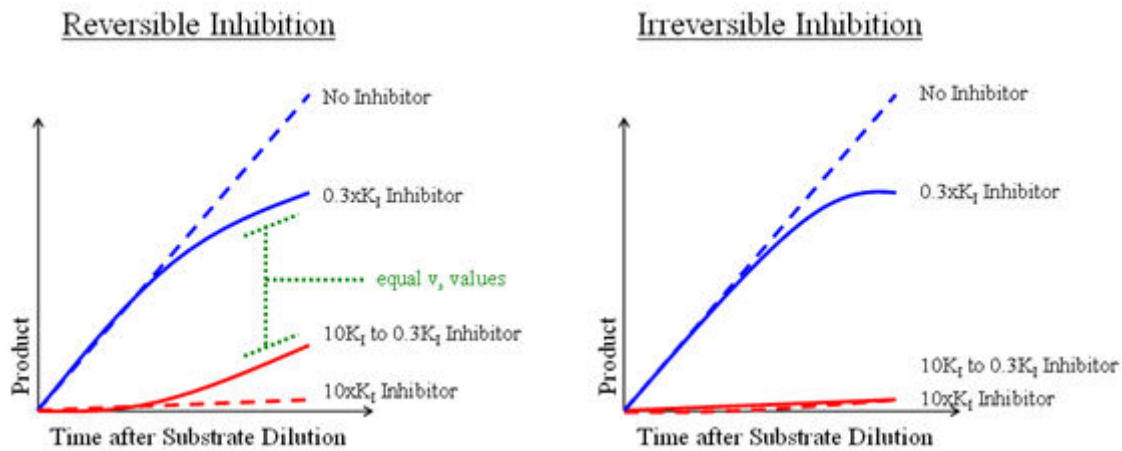


**Figure 15** – The recovery of enzyme activity following dilution of the EI complex can be an indication of the reversibility of the inhibitor. Irreversible inhibitors (right) will not recover any enzyme activity following dilution of the EI complex with substrate. In contrast, a reversible inhibitor (left) will recover enzyme activity equivalent to the  $0.3 \times K_i$  control.

- Irreversible inhibitors are time dependent with  $v_s$  values that approach zero. In contrast, reversible time dependent inhibitors have finite, non-zero  $v_s$  values. The quality of this observation can be limited by the timepoints measured and the [inhibitor] evaluated.
- The observed  $k_{off}$  value is zero. This can be observed in a plot of the  $k_{obs}$  as a function of the [inhibitor], shown in Figure 12. Irreversible inhibitors will yield a y-int ( $k_{off}$ ) of zero.
- What is the recommended plan for an appropriate characterization?
  - In addition to the characterizations described in the sections above, the scientist can measure the release of inhibitor from the enzyme-inhibitor complex. This is often performed by pre-incubating the enzyme with inhibitor at  $10 \times K_i$  to achieve 100% inhibition (all enzyme is in the EI complex reflecting  $v_s$ ), then diluting the assay 30 fold with substrate, and continuously (kinetically) measuring product formation. As illustrated in Figure 15, reversible inhibitors will regain enzyme activity while irreversible inhibitors remain inactive. This experiment can be properly interpreted when 3 controls are included containing 1) no inhibitor throughout to reflect full enzyme activity at the amount of DMSO tested, 2)  $10 \times K_i$  throughout to achieve 100% inhibition, and 3)  $0.3 \times K_i$  throughout to reflect the expected amount of inhibition remaining after substrate dilution. Assuming the  $10 \times K_i$  control is inactive, the final rate ( $v_s$ ) for the experiment can be divided by the final rate of the  $0.3 \times K_i$  control to yield the fraction of recovered activity.

It is important to remember there is no clear distinction between reversible and irreversible time dependent inhibition. The quality of the determination can often reflect the range and density of timepoints measured, [inhibitor] chosen, and other limitations

specific to the assay. Therefore, it would be wise for the scientist to consult an analytical chemist to perform a MS-based strategy to confirm irreversible inhibition resulting from covalent modification of the enzyme.

## Nonspecific Inhibition

Some compounds may form large colloid-like aggregates that inhibit activity by sequestering the enzyme. These types of compounds can display enzyme dependency, time-dependent inhibition, poor selectivity against unrelated enzymes, and binding modalities that are not competitive. This can be especially problematic when an enzyme is screened against a large diversity of compounds in a screening campaign. Although these compounds do not formally violate the steady-state assumptions, they can generate misleading results which produce inaccurate characterizations of the inhibitor-enzyme complex. The scientist is encouraged to read the Shoichet review published in *Drug Discovery Today* (3). The chart below was taken from that reference and provides an introduction to the considerations that should be made for evaluating these types of inhibitors.

**BOX 1**

**Evaluating candidate hits for aggregation-based inhibition:**

1. Is inhibition significantly attenuated by small amounts of nonionic detergent?
  - (i) If so, the compound is very likely acting through aggregation.
  - (ii) In cases where you cannot use detergent, e.g. cell-based assays, it may be possible to use high (1 mg/ml) concentrations of serum albumin instead.
2. Is inhibition significantly attenuated by increasing enzyme concentration?
  - (i) If so, the compound is very likely an aggregator. Except when the enzyme concentration to  $K_i$  ratio is high, increasing enzyme concentration should not affect percent inhibition.
3. Is inhibition competitive? If so, the compound is unlikely to be an aggregator.
4. Does the inhibitor retain activity after spinning for several minutes in a microfuge? If not, particle formation is likely (see point 5).
5. Can you directly observe particles in the 50 to 1000 nm size range? We have typically used dynamic light scattering for this. Formation of particles does not guarantee promiscuous inhibition, but it is a worrying sign.
6. Is the dose-response curve unusually steep? There are classical reasons for curves, but they too are a worrying sign.

## References



## Literature Cited

1. Copeland RA. *Enzymes: A Practical Introduction to Structure, Mechanism, and Data Analysis*, second edition. 2000, Wiley, New York.
2. Segal IH. *Enzyme Kinetics: Behavior and Analysis of Rapid Equilibrium and Steady-State Enzyme Systems*. 1975, Wiley, New York.
3. Shoichet BK. Screening in a Spirit Haunted World. *Drug Discovery Today* 2006, v11, pgs 607-615.

## Additional References

Copeland RA. Mechanistic Considerations in High-Throughput Screening. *Analytical Biochemistry* 2003, v320, pgs 1-12.

Copeland RA. *Evaluation of Enzyme Inhibitors in Drug Discovery: A Guide for Medicinal Chemists and Pharmacologists*. 2005, Wiley, New York,

Copeland RA, Pompliano DL, Meek TD. Drug-Target Residence Time and Its Implications for Lead Optimization. *Nature Reviews Drug Discovery* 2006, v5, pgs 730-739.

Fehrst A. *Structure and Mechanism in Protein Science: A Guide to Enzyme Catalysis and Protein Folding*. 1999, W.H. Freeman, New York.

Kenakin TP. *A Pharmacology Primer: Theory, Application, and Methods*. 2004, Elsevier, San Diego.

Robertson JG. Mechanistic Basis of Enzyme-Targeted Drugs. *Biochemistry* 2006, v44, pgs 5561-5571.

Swinney DC. Biochemical Mechanisms of Drug Action: What Does It Take For Success? *Nature Reviews Drug Discovery* 2004, v3, pgs 801-808.

Swinney DC. Biochemical Mechanisms of New Molecular Entities (NMEs) Approved by United States FDA During 2001-2004: Mechanisms Leading to Optimal Efficacy and Safety. *Current Topics in Medicinal Chemistry* 2006, v6, pgs 461-478.

## Glossary of MOA Terms

The definitions for these terms were gathered from references

**Active site** — the specific and precise location on the target responsible for substrate binding and catalysis.

**Allosteric activators** — an allosteric effector that operates to enhance active site substrate affinity and/or catalysis. (Copeland, *Enzymes*, pg368)

**Allosteric effector** — small molecule that can bind to sites other than the enzyme active site and, as a result of binding, induce a conformational change in the enzyme that

regulates the affinity and/or catalysis of the active site for its substrate (or other ligands). (Copeland, Enzymes, pg368)

**Allosteric repressors** — an allosteric effector that operates to diminish active site substrate affinity and/or catalysis. (Copeland, Enzymes, pg368)

**Allosteric site** — a site on the target, distinct from the active site, where binding events produce an effect on activity through a protein conformational change. (Kenakin, A Pharmacology Primer, p195).

**Alpha** — typically noted as the ratio,  $K_I'/K_I$ . It reflects the effect of an inhibitor on the affinity of the enzyme for its substrate, and likewise the effect of the substrate on the affinity of the enzyme for the inhibitor. (Copeland, Enzyme, pg268)

**Biochemical assay** — the in vitro based mechanism used to measure the activity of a biological macromolecule (enzyme).

**Cofactor** — nonprotein chemical groups required for an enzyme reaction.

**Enzyme** — protein that acts as a catalyst for specific biochemical reaction, converting specific substrates into chemically distinct products.

**Multivariate fitting** — Fitting a more than 2 variable model (Example: Response, [Inhibitor], [Substrate]) to all of the data from a MoA experiment using nonlinear regression.

**Inhibitor** — any compound that reduces the velocity of an enzyme-catalyzed reaction measured in a biochemical assay, as represented by percent inhibition or  $IC_{50}$ .

**Initial velocity** — the initial linear portion of the enzyme reaction when less than 10% of the substrate has been depleted or 10% of the product has formed. (QB Manual, Section IV, pg5)

**In vitro** — (to be defined later)

**Ligand** — a molecule that binds to the target. (Kenakin, A Pharmacology Primer, pg 198)

**Linearity** — A relationship between two variables that is best described by a straight line. In MoA experiments, the amount of product formed should be linear with respect to time.

**Substrate** — a molecule that binds to the active site of an enzyme target and is chemically modified by the enzyme target to produce a new chemical molecule (product).

**Target** — a macromolecule or macromolecular complex in a biochemical pathway that is responsible for the disease pathology. (QB manual, Section XII, pg3)

**$k_{cat}$**  — turnover number representing the maximum number of substrate molecules converted to products per active site per unit time. (Fehrst, Str Mech Prot Sci, pg109)

**$K_I$**  — the affinity of the inhibitor for free enzyme.

$K_I'$  — the affinity of the inhibitor for the enzyme-substrate complex.

$K_M$  — the concentration of substrate at  $\frac{1}{2} V_{max}$ , according to the Henri-Michaelis-Menten kinetic model (QB manual, Section IV, pg9)

$k_{off}$  — the off-rate associated with the release of inhibitor from an enzyme-inhibitor complex.

$k_{on}$  — the on-rate associated with the formation of an enzyme-inhibitor complex.



# Assay Development for Protein Kinase Enzymes

J. Fraser Glickman, M.S.P.H., Ph.D.<sup>1</sup>

Created: May 1, 2012; Updated: October 1, 2012.

## Abstract

Kinases are important drug targets that control cell growth, proliferation, differentiation and metabolism. This process involves phosphorylation of multiple substrates in cellular signal transduction pathways. Here, the authors provide a synopsis on assay technologies, mechanistic considerations for assay design and development pertaining to kinase enzymes. This chapter, along with some of the earlier chapters in this manual on basics of enzyme assays, mechanism of action and purity and identity considerations, serves as an excellent resource for beginners in HTS applications.

## Introduction

Enzymatic phosphate transfers are one of the predominant mechanisms for regulating the growth, differentiation and metabolism of cells. The post-translational modification of proteins with phosphate leads to dramatic changes in conformation resulting in the modulation of binding, catalysis and recruitment of effector molecules that regulate cellular signaling pathways. Examples include the recruitment of SH2 domain containing proteins, the activation of gene transcription pathways and the activation or deactivation of specific cell surface receptors. The practical design and implementation of these assays for drug discovery and development applications will be the focus of this section.

The keys to protein kinase assay development lie in the ability to 1) choose an appropriate “readout” technology, 2) have ample quantities of enzymes, cell lines, antibodies and reference compounds, and 3) optimize the assay for buffer conditions, reagent concentrations, timing, stopping, order of addition, plate type and assay volume. The readout technologies present many options for assay development and often depend on the laboratory infrastructure, the cost of reagents, the desired substrate and the secondary assays needed to validate the compounds and determine the structure activity relationships (Table 1). In the end, they all require the measurement of photons emitted from the assay well in a microtiter plate. They differ in how the photons are generated, and what property (ie. wavelength or polarity) of the photons are measured.

Protein kinase enzyme assays require the co-factors ATP, magnesium (and sometimes manganese) and a peptide or protein substrate (Table 2). One must have a method to detect the conversion of substrate by detecting either the formation of phosphopeptide, phosphoprotein, the disappearance of ATP, or the formation of ADP. There are many

---

<sup>1</sup> The Rockefeller University, New York, NY, 10065; Email: fglickman@rockefeller.edu.

Table 2. Kinases F. Glickman  
Assay Optimization Cycle and Typical Test Parameters

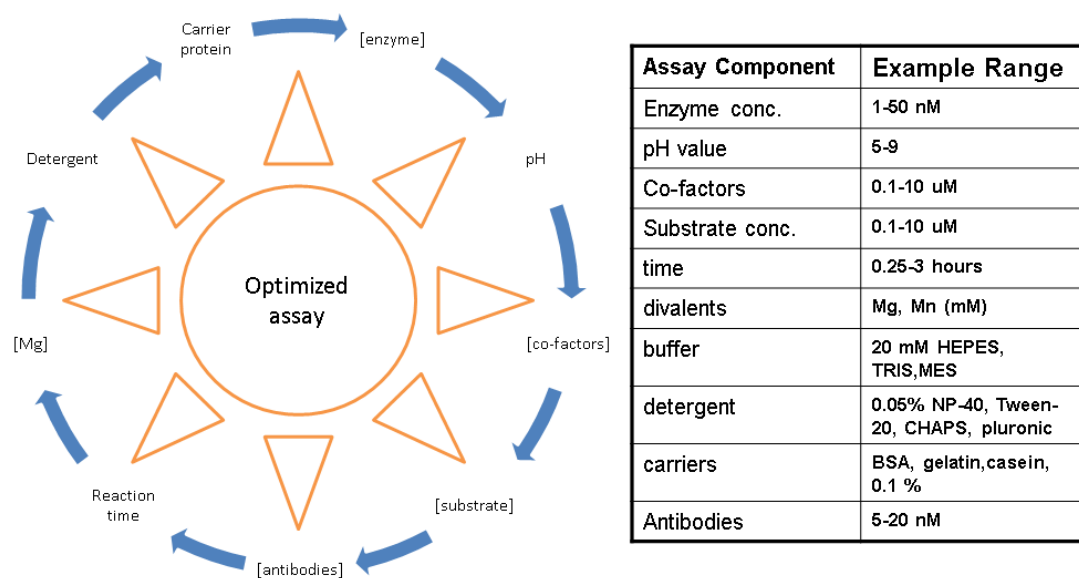


**Table 2. Assay Optimization Cycle and Typical Test Parameters**

commercially available kits and many published references describing these methodologies (Table 1). The subject of the choice of assay technologies is vast, changing and interestingly controversial (1-3) since many technologies are marketed as kits which come with strong pressure to establish “market share.” Also, in the past 15 years there has been a steady development and refinement of new kinase technologies. Examples of highlighted features in assay kits can include higher dynamic range with respect to ATP, greater sensitivity to known inhibitors, flexibility of substrate choice, statistical robustness, lowered susceptibility to artifacts and simpler assay protocol. Cost is often a consideration when choosing a technology or kit as well as the availability of instrumentation. This chapter will attempt to concisely review some of the key technologies below, highlighting the theory behind the assay, some of the underlying principles with strengths and weaknesses, in hope that the reader can make more informed decisions when reviewing the options.

**Table 1.**

| Assay Technology<br>(Commercial names<br>and aliases)                               | Technology Principles  | Advantages  | Disadvantages   | References  |
|---|--|---|---|---|
| Fluorescence Polarization (anisotropy) version 1 (InVitroGen Polar Screen)          | A fluorescently-labeled substrate peptide binds to an anti-phospho antibody after phosphorylation. A change in the Brownian motion of the peptide-antibody complex results in a change in anisotropy measured by polarization of incoming light. | high throughput, only one labeled substrate required  | susceptible to compound interference, peptide must be relatively small, precludes use of protein substrates | Parker (2000), Sills (2002), Newman (2004), Turek-Etienne (2003b) |
| Fluorescence Polarization (anisotropy) version 2 (IMAP)                             | fluorophore-labeled peptides bind to special detection beads coated with trivalent metal. Binding results in change in Brownian motion measured as with FPI.   | Versatile without need for antibody   | susceptible to compound interference, peptide must be relatively small, precludes use of protein substrates | Turek-Etienne (2003a)   |
| Scintillation Proximity (FlashPlate, SPA)   | product of reaction is a <sup>33</sup> P labeled peptide-biotin which can be captured on a detection bead which scintillates from proximity to <sup>33</sup> P. Dephosphorylation by phosphatases can be detected in a signal decrease assay     | high throughput, relatively artifact free in imaging based systems, universal readout for kinases, versatile    | radioactive waste disposal, can be less sensitive than TR-FRET  | Park (1999), Sills (2002), von Ahsen (2006)                       |
| Fluorescence Resonance energy Transfer (Quenched Fluorescence, InVitroGen Z'-LYTE)) | Peptide labeled with fluorescein and coumarin is quenched until cleaved by a protease, modification by phosphorylation or dephosphorylation by a kinase or phosphatase results in a resistance to proteolytic cleavage                           | miniaturizable, ratiometric readout normalizes for pipetting errors, can be applied to kinases and phosphatases | Coupled assay can be susceptible to protease inhibitor compounds.   | Rodems (2002)   |
| Immunsorbant Assays (enzyme-linked or fluorescent                                   | antibodies coated onto MTP wells capture kinase or phosphatase substrate and the   | Can be used as a sensitive probe for cell lysates in cell-based assays  | lower throughput and wash steps are required. Must have suitable cell                                       | Waddleton (2002), Minor   |

*Table 1 continues on next page...*

Table 1 continued from previous page.

| Assay Technology<br>(Commercial names<br>and aliases)   | Technology Principles   | Advantages   | Disadvantages   | References   |
|---|---|--|---|--|
| linked, cell signaling<br>(PathScan))   | phosphorylation state is detected by anti-phosphopeptide antibody coupled to detector dye. Can be read by time-resolved fluorescence (DELFI) technique  |  | line and antibody pair  | (2003),<br>Zhang (2007)  |
| luciferase-based ATP<br>detection (Promega<br>kinase Glo, Perkin-<br>Elmer Easylite Kinase)   | ATP-dependent luminescent signal from luciferase conversion of luminol. The kinase dependent depletion of ATP is measured.  | Versatile and non-radioactive  | Signal Decrease assay, susceptible to luciferase inhibitors   | Koresawa (2004)  |
| Luminescent Oxygen<br>Channeling (Perkin-<br>Elmer AlphaScreen,<br>Surefire)  | Antiphosphotyrosine or phosphopeptide antibodies bind only to the phosphorylated substrate. The complex is detected by streptavidin and protein A functionalized beads which when bound together results in a channeling of singlet oxygen when stimulated by light. The singlet oxygen reacts with the acceptor beads to give off photons of lowered wavelength than their excitation frequency. | Sensitive, high throughput, can be applied to cell lysates as a substitute for an ELISA type assay. Proximity distances can be very large relative to Energy transfer. Emission frequency is lower than excitation frequency, thus eliminating potential artifacts by fluorescent compounds. Can be applied to whole cell assays | Can be susceptible to interference by compounds which trap singlet oxygen. Must work under subdued or specialized lighting arrangements                     | Von<br>Leoprechting (2004),<br>Warner (2004)                       |
| Time Resolved Forster<br>Resonance Energy<br>Transfer (version 1:<br>InVitroGen<br>LanthaScreen, Perkin-<br>Elmer LANCE,<br>CysBio KinEase) | phosphopeptide formation is detected by a "Europium chelate and Ulight acceptor dye PKA substrates<br>Dephosphorylation by phosphatases can be detected in a signal decrease assay  | Very Sensitive and miniaturizable, ratiometric readout normalizes for pipetting errors   | Required two specialized antibodies, susceptible to interference, low dynamic range for substrate turnover. Binding interaction should be within restricted | Moshinsky (2003), Vogel (2006), Von Ahsen (2006), Schroeter (2008) |

Table 1 continues on next page...



Table 1 continued from previous page.

| Assay Technology<br>(Commercial names<br>and aliases)  | Technology Principles   | Advantages  | Disadvantages   | References                      |
|--|---|---|---|---------------------------------|
|  |   |   | proximity for optimal efficiency  |                                 |
| Time Resolved Forster Resonance Energy Transfer (version 2: BellBrook Labs Transcreeper, Adapta) | ADP formation by the kinase is detected by displacement of a red shifted TR-FRET system between Alexafluor647-ADP analog and a Europium-chelated- anti ADP antibody.  | High Throughput, miniaturizeable, versatile, ratiometric readout  | signal decrease assay. Binding interaction should be in close proximity (7-9 nM)                                    | Huss (2007)                     |
| Enzyme Fragment complementation (DiscoverX ED-NSIP HitHunter)                                    | Two fragments of a reporter protein fusion are brought together through a biomolecular interaction, thus reconstituting the activity of the reporter protein. Kinases can be assayed in a displacement mode using a staurosporine conjugate to one fragment and a kinase fused to the second fragment of b-galactosidase (ED-NSIP). Test compound displaces kinase-staurosporine interaction, and decreases B-gal activity. | High Throughput, sensitive, amplified enzymatic, chemiluminescent signal less susceptible to interference | coupled assay can have interference with b-galactosidase binding compounds. Compound must be competitive with probe | Eglen (2002), Vainshtein (2002) |

## Radioactive Assay Technologies

Traditional kinase assays measure the transfer of the  $^{32}\text{P}$  from the  $\gamma$  position of ATP to a peptide or protein substrate results in a  $^{32}\text{P}$  labeled peptide or protein that may be separated away from the ATP by capture on a filter and subsequent washing. The quantity of phosphoprotein is quantified by scintillation counting (4).

The availability of [ $^{33}\text{P}$ ]ATP as an alternative to  $^{32}\text{P}$  provides benefits of safety and longer half-life. The lowered energy is also better suited for scintillation proximity assays (SPAs, [www.perkinelmer.com](http://www.perkinelmer.com); 5). SPA was a major step forward because it eliminated the need for wash steps by capturing the [ $^{33}\text{P}$ ]-labeled peptide on a functionalized scintillating crystal, usually via a biotin-streptavidin interaction.

Figure 1. Scintillation Proximity Assay

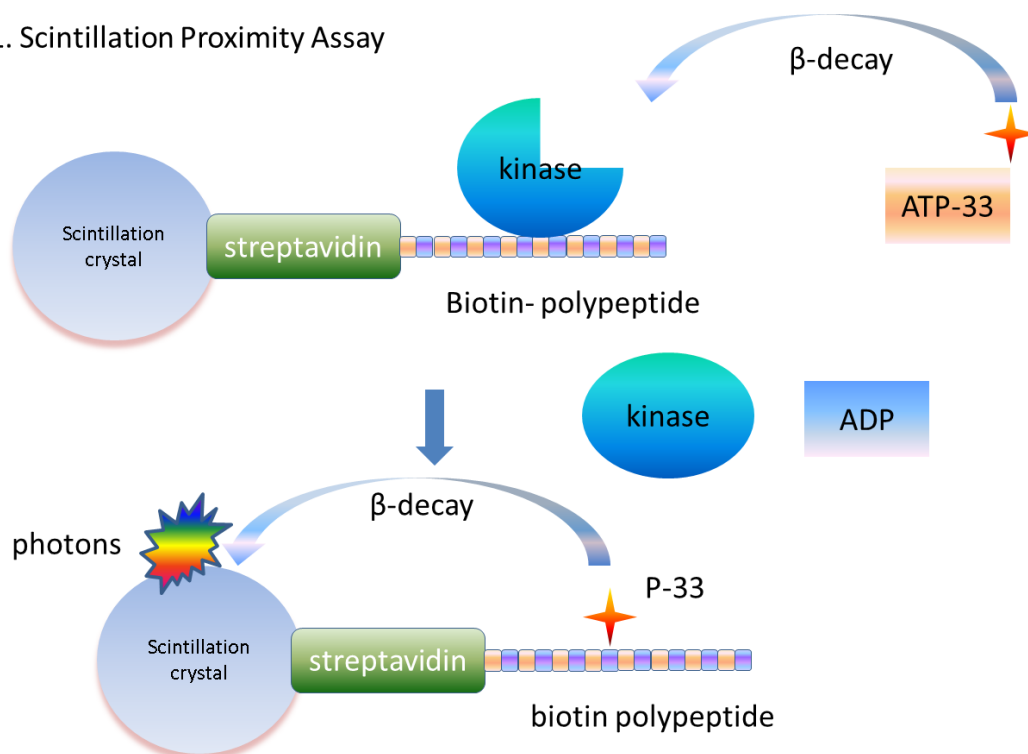


Figure 1. Scintillation Proximity Assay

The specific signal in the SPA is a consequence of a radiolabeled peptide or protein substrate becoming closely bound to the scintillation material. As a result, photons are given off due to a transfer of energy from the decaying  $^{33}\text{P}$  particle to the scintillation material. Non-specific signals (non-proximity effects) can result from decay particles emitted from free [ $^{33}\text{P}$ ]ATP molecules interacting with the scintillation material at greater distances (Figure 1).

All SPAs are based upon the phenomenon of scintillation. Scintillation is an energy-transfer that results from the interaction between particles of ionizing radiation and the delocalized electrons found in conjugated aromatic hydrocarbons or in inorganic crystals. When the decay particle collides with the scintillation material, electrons are transiently elevated to higher energy levels. Because of the return to the ground state, photons are emitted. Frequently, scintillation materials are doped with fluorophores, which capture these photons (usually in the ultraviolet spectrum) and fluoresce at a “red-shifted” wavelength more “tuned” to the peak sensitivity of the detector.

Conventionally, the scintillation materials used in bioassays were liquids composed of aromatic hydrocarbons. These bioassays required a wash step before the addition of the scintillation liquid and counting in a liquid scintillation counter. With SPA technology crystals of polyvinyltoluene (PVT), Yttrium silicate (YS), polystyrene (PS) and Yttrium oxide (YOx) are used as the scintillant. These materials are functionalized with affinity

tags to detect the decay particles directly in the bioassay without wash steps. The newer generation of “red-shifted” FlashPlates and SPA beads yields emission frequencies of around 615 nm, and thus, can be detected by CCD (charge-coupled device) imagers rather than photomultiplier tube (PMT) readers. The advantages of these “imaging” beads and plates lie in both the ability to simultaneously read all wells in a microtiter plate (MTP) and in the reduction of interference from colored compounds ([www.perkinelmer.com](http://www.perkinelmer.com)).

Because of the cost of disposing of radioactive reagents and the requirement for special safety infrastructure, the use of this approach is becoming less frequent, although it presents some distinct advantages (5). First, one needs no phosphopeptide or phosphotyrosine-specific antibodies (an advantage shared with “coupled assays”, mentioned below), as the ATP $\gamma$ <sup>33</sup>P is the only co-factor required. Second, because analyte detection is performed at only one emission wavelength, there are less potential sources of interference by light-absorbing compounds versus fluorescent assays. SPA techniques are well suited toward utilizing a variety of biologically relevant substrate proteins. Universal substrates that are biotinylated, such as poly-GlutamineTyrosine (polyEY), can be used for the tyrosine kinases. Generalized substrates such as myosin basic protein or casein, or specialized peptide substrates must be used for the serine-threonine kinases. A discussion of the choice of substrates in kinase assays is presented in the assay development section below.

## Fluorescence Assays

Although fluorescent assays are very useful in HTS, the classic issue with these assays is that they are susceptible to interference from compounds that either absorb light in the excitation or emission range of the assay, known as an inner filter effects (6), or that are themselves fluorescent resulting in false negatives. At typical compound screening concentrations of greater than 1  $\mu$ M, these types of artifacts can become significant.

There are several approaches to minimizing this interference. One approach is to use longer wavelength fluorophores (red-shifted). This reduces compound interference since most organic medicinal compounds tend to absorb at shorter wavelengths (7). The percentage of compounds that fluoresce in the blue emission (4-methyl umbelliferone) has been estimated to be as high as 5% in typical LMW compound libraries. However, this drops to <0.1% at emission wavelengths >500 nm (8). Another approach is to use as “bright” a fluorescent label as possible. Bright fluorophores have a high efficiency of energy capture and release. This means that an absorbant or fluorescent compound will have a lowered impact on the total signal of the assay. Assays with higher photon counts will tend to be less sensitive to fluorescent artifacts from compounds as compared with assays having lower photon counts. Minimizing the test compound concentration can also minimize these artifacts and one must balance the potential of compound artifacts versus the need to find weaker inhibitors by screening at higher concentrations.

The availability of anti-phosphotyrosine antibodies, anti-phosphopeptide antibodies and antibodies to fluorescent ADP analogs enabled the performance of several homogeneous

methods using fluorophores, among these time-resolved Förster resonance energy transfer (TR-FRET) and fluorescence polarization (FP).

## Fluorescence Anisotropy (Polarization)

Anisotropy can be measured when a fluorescent molecule is excited with polarized light. The ratio of emission intensity in each polarization plane, parallel and perpendicular relative to the excitation polarization plane, gives a measure of anisotropy, more commonly referred to in HTS as “fluorescence polarization” or FP. This anisotropy is proportional to the Brownian rotational motion of the fluorophore. Changes in anisotropy occur when the fluorescent small molecule binds to a much larger molecule affecting its rotational velocity. Kinase assays are set up using anti-phosphopeptide antibodies and labeled phosphopeptides (Figure 2, 9) or by using a metal ion affinity material to capture labeled phosphopeptides (10). The formation of the phosphopeptide in an enzymatic reaction causes an increase in binding to an antibody or affinity resin and consequently a change in anisotropy. The advantage of FP is that it requires only one small polypeptide labeled (instead of two labeled moieties as with TR-FRET or AlphaScreen).

FP assays are known to be susceptible to artifacts (11). In principle, the assays are ratiometric and should normalize for variations in total excitation energy applied as would occur with inner filter effects (see Assay Guidance Manual chapter on [Spectrophotometry](#)), and newer generations of red-shifted fluorophores should help to eliminate interference (7). However, introducing a test compound with fluorescent or absorbent properties at greater than 5  $\mu\text{M}$  with the typically nanomolar concentrations of fluorescently-labeled peptide in an FP assay can significantly skew the measurements. One way to reduce this potential issue is to simultaneously collect total fluorescence data and exclude those compounds which significantly affect the total fluorescence of the assay well.

## Time-Resolved (Gated) Förster Resonance Energy Transfer (TR-FRET)

These assays are based upon the use of a Europium or Terbium chelate (a transition metal-ligand complexes displaying long-lived fluorescent properties), and labeled anti-phosphopeptide or anti-phosphotyrosine antibodies that bind to phosphorylated peptides. The antibodies are usually labeled with aromatic fluorescent tags such as Cy5, Rhodamine, or fluorescent proteins such as allophycocyanin. Allophycocyanin is a light-harvesting protein which absorbs at 650 nm and emits at 660 nm (9, 12, 13). When the anti-phosphotyrosine or anti-phosphopeptide antibodies bind to a labeled phosphorylated peptide the proximity of the antibody to the labeled peptide results in a transfer of energy (Figure 3). The energy transfer is a consequence of the emission spectrum of the metal-ligand-complex overlapping with the absorption of the labeled peptide. If the donor fluor is within 7-9 nm of the acceptor fluor then Förster resonance energy transfer can occur although the optimal distance between fluorophores is also influenced by effects of proximal fluorophores on the emission lifetime in the time-gated

Figure 2. Fluorescence Anisotropy

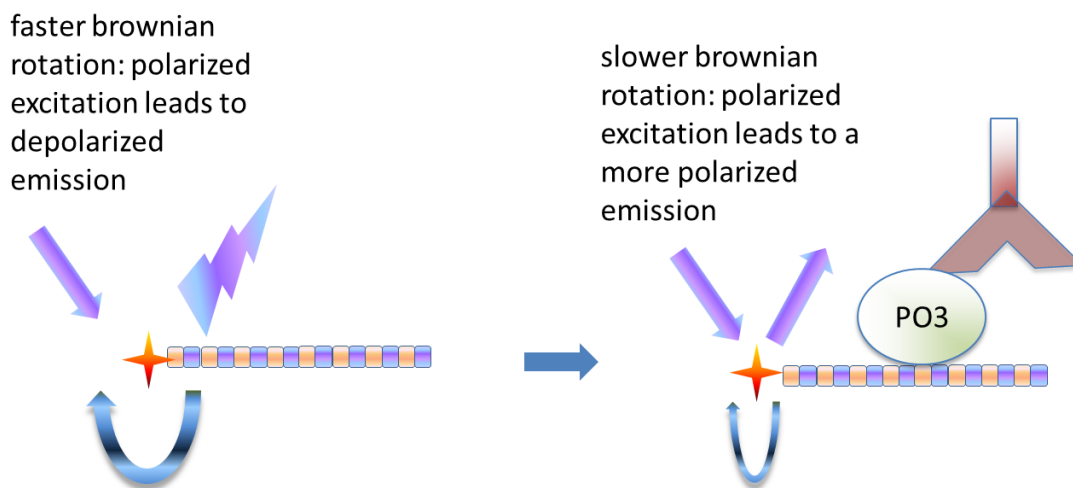


Figure 2. Fluorescence Anisotropy

system (14). The action of a kinase enzyme increases the concentration of phosphopeptide over time and results in an increased signal in such an assay.

TR-FRET assays have two main advantages. The first advantage is in the “time-gated” (the term “resolved” is commonly misused from a biophysical perspective) signal detection, which means that the emission is measured 100-900  $\mu$ s after the initial excitation frequency is applied, resulting in a reduction in fluorescence background from the microtiter plate, buffers, and compounds. Data is acquired by multiple flashes per read, to improve the sensitivity and reproducibility of the signal. The second advantage is that the one can measure the ratio of the emission from the acceptor molecule to the emission from the donor molecule. Because of this ratiometric calculation, variations in signal due to variations in pipetting volume can be reduced. Therefore, one generally observes less inter-well variation in TR-FRET assays versus other enzyme or biomolecular assay systems (15).

### Luminescent Oxygen Channeling (AlphaScreen™, AlphaLISA™)

AlphaScreen technology, first described in 1994 by Ullman and based on the principle of luminescent oxygen channeling, has become a useful technology for kinase assays (16). AlphaScreen is a bead-based, non-radioactive, Amplified Luminescent Proximity Homogenous Assay. In this assay, a donor and an acceptor pair of 250 nm diameter reagent-coated polystyrene microbeads are brought into proximity by a biomolecular interaction of anti-phosphotyrosine and anti-peptide antibodies immobilized to these beads ([www.perkinelmer.com](http://www.perkinelmer.com)). Irradiation of the assay mixture with a high intensity laser at 680 nm induces the conversion of ambient oxygen to a more excited singlet state by a photosensitizer present in the donor bead. The singlet oxygen molecules can diffuse up to

Figure 3. Time-gated forster resonance energy transfer

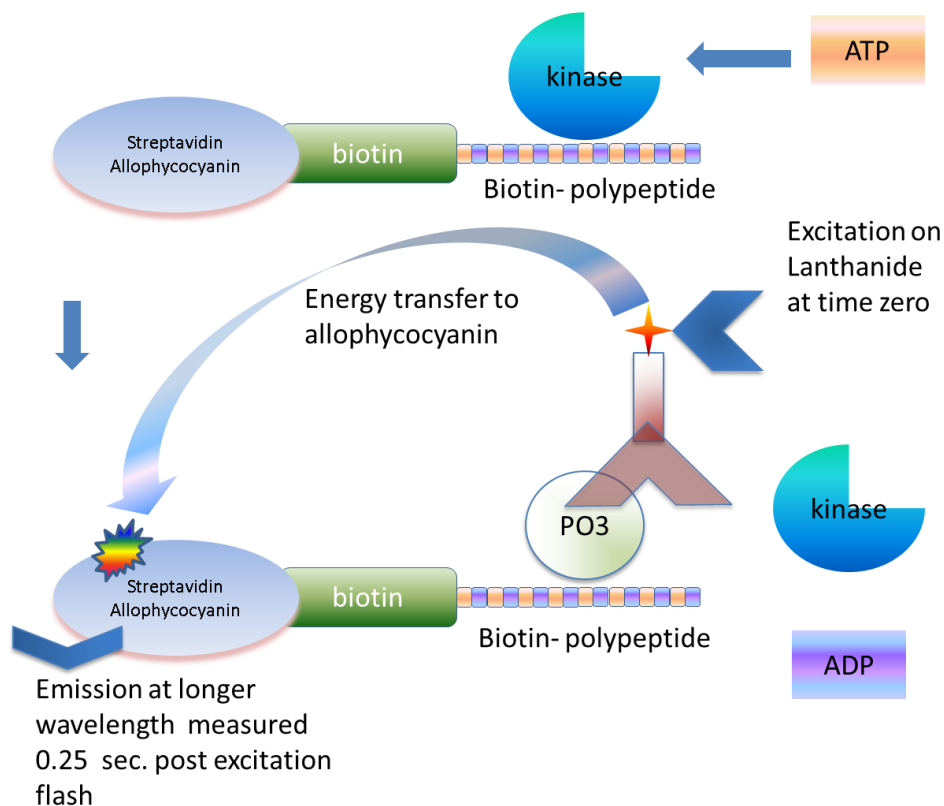


Figure 3. Time-gated Förster resonance energy transfer

200 nm and, if an acceptor bead is in proximity, can react with a thioxene derivative present in this bead generating chemiluminescence at 370 nm that further activates the fluorophores contained in the same bead. The fluorophores subsequently emit light at 520-620 nm. The donor bead generates about 60,000 singlet oxygen molecules resulting in an amplified signal. Since the signal is very long-lived, with a half-life in the one second range, the detection system can be time-gated, thus eliminating short-lived background (the AlphaScreen signal is measured with a delay between illumination and detection of 20 msec). Furthermore, the detection wavelength is of a shorter wavelength than the excitation wavelength, thus further reducing the potential for fluorescence interference. The sensitivity of the assay derives from the very low background fluorescence. The larger diffusion distance of the singlet oxygen enables the detection of binding distance up to 200 nm, whereas TR-FRET is limited to 9 nm (15), allowing the use of much larger protein substrates. A newer version of the same principle is called AlphaLISA™ (Perkin-Elmer). While AlphaScreen uses acceptor beads with an emission from rubrene, AlphaLISA acceptor beads use Europium. Thus the emission wavelength is different between AlphaScreen beads (520-620 nm) and AlphaLISA beads (615 nm). The narrow emission spectrum of AlphaLISA should, in principle, lessen interference.

Kinase assays based on the AlphaScreen principle are similar to TR-FRET assays in that they usually require a biotinylated substrate peptide and an anti-phosphoserine or tyrosine antibody. These two reagents are “sandwiched” between biotin and protein-A functionalized acceptor and donor beads. A kinase assay shows an enzyme dependent increase in antibody binding (and thus signal) over time. In some cases, the phosphorylation of an epitope will block the antibody binding which can be used as the basis of for product detection (17, 18). Like other optical assays, AlphaScreen assays are susceptible to inner filter effects (6). Additionally, compounds which react with singlet oxygen can cause false positives. One can easily re-test AlphaScreen hits in an independent AlphaScreen assay, for example measuring the effect of the compound on biotin-streptavidin bead interactions optimized to the same level of photon counts as the primary assay. Artifact compounds would be expected to inhibit this signal and can thus be eliminated as false positives.

### “Coupled” Assays

“Coupled” assays are those that require the addition to the assay of more enzymes to convert a product or substrate into a detectable signal. All coupled enzyme assays share potential artifacts from “off-target” inhibition of the enzymes used to couple the reaction to a detectable product. Thus, with all coupled assays, one must be careful that inhibitors or activator compounds are not inhibiting the coupling systems. It is usually easy to design a secondary assay system to establish that this is not the case, simply by “feeding” the coupling system with suitable substrates (in the absence of kinase enzyme) and measuring the effect of putative inhibitors on the coupling system. For protein kinases, the most common manifestation of a coupled assay uses luciferase to detect ATP formation, and yet others use proteases, ATPases and other non-disclosed commercial enzymes to produce a kinase assay kit. These are briefly described below.

### Protease Sensitivity Assays

Kinase substrates can become resistant to the actions of proteases due to phosphorylation. Thus, fluorescence quench assays for proteases can be used to measure kinase activity. With kinase assays, the formation of phosphopeptide inhibits the protease action on the peptide and the signal remains quenched and, therefore, lower when the kinase is active (19). Inhibiting the kinase results in an increase in protease sensitivity and an increase in signal.

### Luciferase-based Kinase Assays

Because kinases convert ATP into ADP, the activity of purified kinase enzymes can be measured in a “coupled” assay, which detects the ATP depletion over time by using the phosphorescence of luciferase and luciferin (commercially sold as “Kinase-Glo™”, [www.promega.com](http://www.promega.com); 13, 20). Luciferases are enzymes that produce light by utilizing the high energy bonds of ATP to convert luciferin to oxyluciferin. Oxygen is consumed in the process, as follows:

- luciferin + ATP → luciferyl adenylate + PPi
- luciferyl adenylate + O<sub>2</sub> → oxyluciferin + AMP + light

The reaction is very energy efficient: nearly all of the energy input into the reaction is transformed into light. A reduction in ATP results in a reduction in the production of photons. This type of assay has the advantage of not needing any specialized antibodies and is applicable to all kinases. It is also easy to run the assays with high ATP concentrations as a way of selecting against ATP-competitive inhibitors (21).

A potential limitation of this assay is that it is a “signal decrease assay.” In signal decrease assays, the enzyme-mediated reaction proceeds with a decrease in signal over time. As the kinase depletes the ATP over time, less light is produced by the luciferase reaction. An inhibitor compound prevents this decrease. A 50% consumption of ATP is required to obtain a two-fold signal-to-background using the 100% inhibited reaction as a control. Therefore, these assays must be run under conditions of relatively high turnover, which has the effect of slightly weakening the apparent potency of compounds (22). Another consequence of a signal decrease assay is that it can have low sensitivity for particularly low turnover enzymes (i.e., having a small  $k_{cat}$ ). For slower enzymes, one may require a long incubation time (several hours) to reach a suitable signal. With other assay formats that measure phosphopeptide formation, (especially TR-FRET, AlphaScreen), only a 2-10% conversion is required before the assay can be read, since the detecting reagents are product-specific.

Kinase assays that are coupled to luciferase have the disadvantage of being sensitive to luciferase inhibitors, which bind to the ATP-binding site of luciferase, resulting in false negatives. A kinase inhibitor which also inhibits the luciferase would result in an artificially low light signal. However, one can overcome this by additionally using a luciferase-based assay that measures ADP formation (commercially available from Promega as “ADP-Glo<sup>®</sup>”). By running Kinase-Glo<sup>™</sup> and ADP-Glo<sup>®</sup> as orthogonal assay one can identify luciferase inhibitors as these will make the signal go down in both assays while with a true kinase inhibitor the signal would go up in an Kinase-Glo assay and down in an ADP-Glo<sup>®</sup> assay (23).

The ADP-Glo system detects the ADP formed in a kinase reaction by first adding an undisclosed commercial reagent (presumably an enzyme) to deplete the ATP in the kinase reaction and then adding another undisclosed reagent to convert the ADP back into the ATP (presumably another enzyme). Coupled systems that detect ADP gain the advantage of being able to detect product formation, rather than substrate depletion, which means that small catalytic turnover percentages can be detected.

## Fluorescent Coupling

Another manifestation of coupled ADP detection is the ADP-Quest<sup>™</sup> kit (DiscoverRx, 24). In this kit, ADP is measured by a coupled enzyme reaction with pyruvate kinase and pyruvate oxidase to convert ADP to hydrogen peroxide, which is detected using a



fluorogenic substrate and horseradish peroxidase. The detection wavelength is around 590 nM, which tends to be less susceptible to inner filter effects (6).

## Assay Development

Much of the cited literature in this chapter offers good protocols as a basis for kinase assay development. A general strategy for assay development should include the following steps:

1. Choose an appropriate readout technology.
2. Synthesize, purify and characterize enzymes, substrates. Generally, highly pure preparations of kinase (greater than 98% by silver-stained SDS-PAGE or by Mass-Spectrometry) are required. It is a possibility that small amounts of contaminating kinases can result in a false detection of activity from the kinase of interest. Well-characterized preparations of enzyme are critical.
3. Design a starting protocol based on prior literature or experimental information on substrate specificity. Test the protocol for enzymatic activity and use reference inhibitors when possible.
4. Gain knowledge of kinetic and thermodynamic parameters as guidelines for assay optimization (25).
5. Set-up “matrix” experiments varying pH, ionic strength, buffers and various other parameters mentioned below to optimize signal to background ratios (Table 2.)
6. Choose volumes appropriate for HTS workstations or automated systems.
7. Test a screening protocol in a [pilot study](#) and determine assay quality based on the coefficient of variations across the assay wells, the  $Z'$  measurements (26) and dynamic range towards various control or reference compounds.

## Considerations of Mechanism

### Mechanism of Action of Kinase Inhibitors

When designing protein kinase assays it is important first to consider the desired [mechanism of action](#) (MOA) of the inhibitor MOA is quite a complex topic which is nevertheless well described in terms of drug discovery strategies by David Swinney (27); examples are given of drugs that work by a variety of mechanisms and fall into three basic categories: 1) competition with the substrate or ligand in an equilibrium or steady-state, 2) inhibiting at a site distinct from substrate binding or 3) inhibiting in a non-mass action equilibrium. (See Assay Guidance Manual section on [mechanism of action](#)).

A good overview of the [mechanism of action](#) of protein kinase inhibitors has been presented by Vogel and Zhong (28). Protein tyrosine kinase inhibitors can act by binding directly in the ATP binding site competitively, (type I inhibitors), but these tend to be less specific because of the shared characteristics of the ATP binding pocket among various kinases. More specificity can be attained with the type II inhibitors, which can extend into an allosteric site next to the ATP pocket and which is only available in the inactive (non-phosphorylated form) of the enzymes. Imatinib is an example of this, with a 200-fold

increased potency to the inactive form of the enzyme, observed in cell based assays versus enzyme assays. Often, these inhibitors bind with a slower off-rate and on-rate due to a requirement for conformational changes.

Type III inhibitors bind to sites distal to the ATP binding site and are often inactive in simple kinase enzyme assays. This apparent inactivity is because these compounds can bind to the kinase and render it a poor substrate for an activating upstream kinase, thus disabling its activation. As a consequence, a “cascade assay” or a cell-based assay might be required.

## Applying Mechanistic Principles to Assay Design

Important questions related to the desired inhibitor or agonist mechanism such as whether, in the HTS, one desires to find allosteric, competitive, slow-binding inhibitors, or inhibitors of an active or inactive form of the enzyme should be considered when designing HTS assays. These mechanisms might suggest the appropriate incubation times, substrate design and concentrations, order of addition and the appropriate recombinant construct to use. Unfortunately, the decisions of assay set up are not always straightforward. There are advantages to each type of inhibitor and it also depends largely upon the biology of the disease that is going to be treated. For example, purely ATP site competitive inhibitors might have advantages with respect to drug resistance, but disadvantages with respect to selectivity, potency and cellular activity. Small molecule inhibitors that compete with the peptide binding site are generally difficult to find since the peptide-enzyme interaction presents a large surface area. Allosteric site inhibitors might have an advantage in potency and selectivity, but also may be resistance-prone. Layered on top of this complexity is the difficulty in expressing a well-defined form of the enzyme target that is physiologically relevant.

One important consideration for assay design is that a pre-incubation step of compound with the target enzyme can be included before starting the reaction. This pre-incubation can help to favor the identification of slow, tight binding inhibitors (29), depending on the stage of the enzyme progress reaction at which the assay is stopped. The longer the reaction progress time the lower the effect of the pre-incubation step on the detection of slow-binding inhibitors. This step may add significant time to a screening protocol (pre-incubation of 15-30 minutes) and also may be difficult if the enzyme preparation is unstable. It is sometimes necessary to pre-incubate the kinase enzyme with ATP to activate it through autophosphorylation. This can be accomplished in the “stock” solution of enzyme, at stoichiometric amounts of ATP, before diluting the enzyme (and thus the ATP) into the assay. With protein kinase hit lists, it is possible to distinguish the ATP-competitive from the non-competitive inhibitors by re-screening under high and low ATP concentrations, and looking for shifts in the IC<sub>50</sub> or percent inhibition. An ATP-dependent shift in compound potency suggests competition with ATP site according to the equation, (30)

$$IC_{50} = \left(1 + \frac{S}{K_m}\right)(K_i)$$

When working with purified enzymes, it can be useful to perform a close examination of their phosphorylation state and molecular masses. Mass spectrometry is often useful for this purpose. Post-translational modifications or sequence truncations can potentially alter the compound binding sites available and can also change the structure of potential inhibitory sites. For example, with protein kinases, phosphorylations distal from the ATP binding site can inactivate the kinase whereas phosphorylations near the ATP binding site can activate the catalytic activity. Often, practice does not permit control of such situations because the purified systems are often mixtures and cannot be controlled in the commonly used recombinant expression technologies.

To favor the identification of uncompetitive or non-competitive inhibitors, one should run the assays with concentrations of substrates at least 10-fold higher than  $K_m$ . To favor competitive inhibitors, one should run the assay at or below the  $K_m$  values for the substrates. A balanced condition which provides for detection of all mechanisms is to keep the  $[S] = K_m$  (31). Thus, for making suitable conclusions for assay design, knowledge of the kinetic and binding constants of receptors and enzymes, such as  $K_d$ ,  $k_{cat}$ ,  $K_m$ ,  $B_{max}$ , is useful. Stoichiometric information, such as the number of enzyme molecules per assay, is also very useful since these can be used as guidelines to ensure that the assays are maximally sensitive to compounds with the desired **mechanism of action**. Problems in assay development often occur when the conditions required for sensitivity to the desired **mechanism of action** do not yield the best conditions for statistical **reproducibility**; therefore, compromises and balances between these two opposing factors must be often made.

The percent substrate consumption at which time the data is collected is also of importance in enzyme assay design. Typically, enzymologists like to ensure the steady-state conditions are maintained in the study of inhibitor constants such as  $K_i$  or  $IC_{50}$ . However, many assay technologies, combined with the requirements for a robust signal to background giving a good  $Z'$  factor (26), necessitate assay set-up where more turnover is required. This typically causes a trend toward the reduction of compound potency depending on the **mechanism of action**. Therefore, one must balance the need to have the most sensitive assay toward inhibition by low MW compounds with the need for sufficient signal-to-noise and signal-to-background to have statistically relevant results, for example with a coefficient of variation less than 10% around the positive and negative controls, a 5-fold difference between the positive control signal and negative control signal and/or  $Z'$  greater than 0.5. These types of effects have been modeled by Wu and Yuan (22) and additionally confirmed by empirical determination. These investigators have found that 50% inhibition at low conversion (near zero) can translate into 31% inhibition if the assay is run at 80% conversion.  $IC_{50}$  values can shift as much as three fold.

## Assay Optimization

It is very difficult to give specific guidelines for assay optimization in HTS due to the complexity of variables involved and because one often must balance cost, speed, sensitivity, statistical robustness, automation requirements and desired mechanism. The

assay development and optimization process can be thought of as a cycle in which several variables can be tested and the parameters that give a better “reading window” can be fixed, after which further parameters can be tested under the prior fixed conditions (see Table 2). Often, one observes interactions between the various parameters. For example, the optimal detergent concentration to use may not be the same for every pH and that is why the same fixed parameters must sometimes be retested under any newly-identified optimal parameters. Furthermore, the type of optimization experiments depends upon the particular technology being used. A very important aspect of optimization is to improve the [reproducibility](#) and [statistical performance](#) of the assay, by finding conditions that increase the signal-to-noise ratio with respect to positive and negative controls, and to decrease the inter-well variations that occur due to such factors as pipetting errors and temperature gradients across the microtiter plate. In general, coefficient of variations of less than 10% and Z values greater than 0.5 are desirable.

In its simplest form, building an assay is a matter of adding several reagent solutions to a microtiter plate (MTP) with a multi-channel pipette, with various incubation times, stopping the reaction if required, and reading the MTP in a plate reader. A typical procedure might involve the following steps: 1) adding the enzyme solution to a compound-containing microtiter plate and incubating for 15 minutes; 2) adding substrates and incubating for 15 minutes to 1 hour; 3) adding a stopping reagent such as EDTA; 4) adding sensor or detector reagents, such as labeled antibodies or coupling enzymes; 5) measuring in a plate reader. The particular detector reagents to use, the assay reagent volumes, the concentrations of reagents, the incubation times, the buffer conditions (Table 2), the MTP types and the assay stopping reagents are all important parameters which need to be tested in order to obtain the very high level of [reproducibility](#) yet maintain the physiological and thermodynamic conditions to find a lead compound with the desired [mechanism of action](#).

A very important aspect of assay development is making an appropriate choice of substrates. When possible, one should consider using a relatively physiological substrate. This means for example, using the substrate protein involved in the pathway of interest for serine-threonine kinases, rather than commonly used general substrates like maltose binding protein or, for example using a true-substrate-derived peptide sequence representing the phosphotyrosine site within the amino acid context that is found in the native substrate primary sequence, rather than an artificial substrate such as poly-Glu-Tyr. Once again this is not always practical because the natural substrates are either not well-characterized, and the artificial substrates often give a much higher turnover ( $k_{cat}$ ) and thus can yield a much more robust assay signal. If natural substrates are not readily available or robust, secondary assays can be designed using the natural substrates, to ensure the screening hits work equivalently under physiologic conditions. Additionally, it is often possible to perform a substrate screen where many random peptide sequences are tested to identify good substrates.

The danger of using solely statistical parameters (such as Z') in assay optimization is that these do not take into account the desired physiological or biochemical [mechanism of](#)

**action** in determining the optimal reagent concentration. For example, the optimal substrate concentration to use in an enzyme assay may not necessarily be the one that gives the best statistics with respect to **reproducibility**. The optimal salt concentration required for **reproducibility** may be far different from physiological conditions. Therefore, one must be careful to use **statistical performance** in a way that is consistent with the desired **mechanism of action** of the lead compound.

## Enzyme Preparations

One cannot over-emphasize the importance of the enzyme preparation in the ability to develop a kinase assay. First, purity is important because even the slightest contamination with another enzyme can lead one to screen with a measurement of the wrong activity. Specific reference inhibitors can be used to establish that the observed catalytic activity is the correct one. Of course, when working with novel targets, such reference inhibitors may not exist. With recombinant expression systems one can generate catalytically inactive mutations to establish that the host cell is not the source of a contaminating phosphatase or kinase. In the end, however, the key requirement is to have an extremely pure and highly active enzyme preparation. If most of the enzyme molecules are inactive or if the enzyme molecules have a very low catalytic efficiency ( $k_{\text{cat}}/K_m$ ), then one will need to have a high concentration of enzyme in the assay to obtain a good signal; this can limit the ability to distinguish between weaker and stronger inhibitors. If one needs to have a 100 nM enzyme concentration in the reaction, then inhibitors with a  $K_i$  of 10 nM cannot be distinguished from those with a  $K_i$  of 50 nM in a steady-state  $IC_{50}$  experiment.

## Assay Volumes

Assay volumes usually range from 3  $\mu\text{L}$  (for 1536-well MTPs) to 50  $\mu\text{L}$  (384-well MTPs). Within a given total assay volume, smaller volumes of reagents are added. Frequently it is convenient to add reagents into the assay in equivalent volumes of assay buffer. As an example, for a 15  $\mu\text{L}$  assay, one might add 5  $\mu\text{L}$  of compound solution, 5  $\mu\text{L}$  of enzyme solution, and 5  $\mu\text{L}$  of substrate mix, followed by 10  $\mu\text{L}$  of quench solution in a “stop” buffer. For kinase assays, this can be EDTA, which works by chelating magnesium, an essential cofactor for protein kinase catalysis. The advantages of using equal volumes are that it keeps the volumes at a level that is best for the particular pipette during automation; it minimizes the requirement for various specialized instruments and helps in the mixing of the reagents. The disadvantage of this method is that it introduces transient changes in the final concentration of reagents during the times between the various additions. In addition, enzymes are not always stable in large batches of dilute buffer required for HTS. Therefore, it can be preferred to add a low volume of a more concentrated stock solution (10X - 50X) into a higher volume of assay buffer in the well. This step often requires a liquid dispenser able to handle very low volumes of sub-microliter liquid.

Assay miniaturization helps to reduce the consumption of assay reagents, which can be very expensive. The problems encountered as one attempts to miniaturize an assay are in

the change in surface to volume ratio, the lowered sensitivity and in the low volume dispensing of materials. For instance, as one moves to smaller volumes, the surfaces available for nonspecific binding increase relative to the volume. Furthermore, the smaller the volume, the less the amount of product-sensing material can be added; thus the sensitivity of the assay is reduced.

## Plate Types

Generally, white plates are preferred for phosphorescent assays, such as those employing luciferase because they reflect emitted photons. Black plates are preferred for fluorescent assays because they reduce reflection. Transparent plates are generally used for imaging assays. Polystyrene is the material of choice because it can be molded reproducibly such that the plates are consistently-sized to fit into automated systems. Polystyrene tends to have some level of non-specific affinity for biomolecular reagents and, therefore, some manufacturers produce proprietary low binding plates. Polypropylene plates have low non-specific binding levels, but are more difficult to shape consistently. However, these plates are often useful as “source plates” for reagents due to their tolerance to freezing and their low level of “stickiness.” The use of 96-, low volume 96-, 384-, low volume 384-, or 1536-well depends on the assay volume and throughput that one needs. For 96-well plates, volumes range from 80-100  $\mu\text{l}$ ; for 384-well plates, volumes range from 15 to 100  $\mu\text{l}$ ; for 384-well, small-volume plates, volumes range from 4 to 10  $\mu\text{l}$ ; and for 1536-well MTPs, volumes range from 3 to 8  $\mu\text{l}$ .

## Incubation Times

Incubation times at different steps depend upon the binding kinetics or enzyme kinetics and can range anywhere from 10 minutes to 15 hours. It is generally preferred to read the reaction at a point before the reactants are depleted and the enzyme [progress curve](#) is slowing. Adding a short pre-incubation step of compound with enzyme before the initiation of the reaction allows for detection of slow-binding inhibitors, which require a conformational change of the enzyme to form a tight complex. Longer incubation steps can add significant amounts of plate processing time in HTS automation because incubation time often represents the rate-limiting step in the HTS process. Reaction rates can be increased by increasing the enzyme concentration or temperature and, in this fashion, incubation times can be reduced.

## Buffers and Solvents

The concentrations of detergents, buffers, carrier proteins, reducing agents, and divalent cations can affect the specific signal and the apparent potency of compounds in concentration response curves (32). In principle, it is good to stay as close to physiological conditions as possible, but for practical reasons, there are many exceptions. For example, full-length fully regulated kinases are often impossible to express, and thus, for practical purposes non-regulated kinase domains are used in screening. Furthermore, the true physiological conditions in the microcellular environment are not always known.

Sometimes carrier proteins are required for enzyme stability and to reduce nonspecific binding to reaction vessels. It is often necessary to provide additives such as protease inhibitors to prevent digestion of the assay components or phosphatase inhibitors such as vanadate to keep the product of a kinase assay intact and protected from contaminating phosphatases. Also, it is often necessary to quench assays or to add a stop reagent such as EDTA at the end of the reaction and before reading in a plate reader. A quench step or stop step is especially important when the automated HTS system does not allow for precise timing or scheduling of the assay protocol. A very good summary of solvent and buffer conditions used in kinase assay optimization is described by von Ahsen and Bomer (33).

The presence of “promiscuous” inhibitors or “aggregating” compounds in a chemical library has become a recent area of research. These compounds can cause false positives that can be reduced with certain detergents and can frequently be recognized by steep concentration response curves or by enzyme concentration-dependent shifts in the  $IC_{50}$  (34, 35). The exact mechanism of these false positives is not known but it is possible that these compounds induce the formation of compound-enzyme clusters, which reduce enzyme activity. Thus, it is important to have some non-denaturing detergent present in enzyme assays and to re-test hits in orthogonal assays to reduce the possibility of identifying promiscuous inhibitors in the HTS.

### DMSO Concentration

In most cases, the test compounds are dissolved in DMSO and are added from a source plate into the assay. Thus, the tolerance of the assay for DMSO should be tested, by looking at the activity at various increasing concentrations of DMSO. Generally, enzymatic or biomolecular binding assays are more tolerant of high DMSO concentrations (often up to 5 - 10% DMSO). Cell based assays usually can tolerate up to 0.5% DMSO.

### Detector Reagent Concentrations

Given the very large variety of assay detection methods, it is difficult to cover all the parameters needed to optimize for each detection system; however, it is important to mention that these various systems discussed in the assays readout technology section above all need to be optimized. For example, when using an antibody pair in a TR-FRET assay, it is important to find a concentration of antibodies that can trap the product efficiently at the desired time point in the reaction. In SPA, for example, an optimal SPA bead concentration should be determined empirically. In principle, the detector reagents should be present in high enough concentration to capture the analyte stoichiometrically. Having too high a concentration of detectors can be wasteful and expensive and can create higher background signals and having too low concentrations of detector reagents can compromise the dynamic range and sensitivity of the assay. A control product can sometimes be useful as a calibration standard for these types of optimization experiments.

Often times, the commercial assay kit providers provide excellent protocols in optimizing the use of the detector reagents.

## Pilot Screens

The final step in the assay development process is to run a “pilot” screen, where a small subset of libraries are screened to observe the hit rate, the distribution of the high signal and the low signal, typically employing the Z and Z-prime principle of Zhang and Chung (26) to assess quality. The Z factors combine the principle of signal to background ratio, coefficient of variation of the background and the coefficient of variation of the high signal into a single parameter, which gives one a general idea of the screening quality. One should be careful to closely examine the raw data and data trends from screening rather than to rely only on the **Z-factor** for quality control.

For pilot studies, the microtiter plates should be arrayed with reference compounds at various concentrations, to control that the screening procedure gives adequate dynamic range and sensitivity to inhibitors or activators. In general, coefficient of variations of less than 10% and Z values greater than 0.5 are desirable. The pilot studies may be used to adjust the compound concentration to obtain a reasonable hit rate; for example, one hit for every two thousand compounds tested. The hit rate will depend on the particular library screened; biased libraries may have higher hit rates than random libraries.

## Acknowledgements

The author would like to acknowledge Dr. Douglas Auld for his valuable insights and comments on the draft, and Dr's Andrew Napper, Jeff Weidner and Sittampalam Gurusingham for critical review and editing.

## References

1. Lowery RG, Vogel K, Till J. ADP detection technologies. *Assay Drug Dev Technol.* 2010 Aug;8(4):1–2author reply 1. PubMed PMID: 20804418.
2. Goueli S., Zegzouti H., Vidugiriene J. Response to the Letter of Lowery et al. *ADP Detection Technologies. Assay Drug Dev. Technol.* 2010;8(4):1.
3. Inglese J, Napper A, Auld D. Improving success by balanced critical evaluations of assay methods. *Assay Drug Dev Technol.* 2010 Aug;8(4):1. PubMed PMID: 20804419.
4. Gopalakrishna R, Chen ZH, Gundimeda U, Wilson JC, Anderson WB. Rapid filtration assays for protein kinase C activity and phorbol ester binding using multiwell plates with fitted filtration discs. *Anal Biochem.* 1992;206(1):24–35. PubMed PMID: 1456438.
5. Glickman J. F., Ferrand S. Scintillation Proximity Assays In High Throughput Screening. *Assay Drug Dev. Technol.* 2008.;6. PubMed PMID: 18593378.
6. Palmier MO, Van Doren SR. Rapid determination of enzyme kinetics from fluorescence: overcoming the inner filter effect. (2007). *Anal Biochem.* 2007 Dec 1;371(1):43–51. Epub 2007 Jul 18. PubMed PMID: 17706587.



7. Vedvik K. L., Eliason H. C., Hoffman R. L., Gibson J. R., Kupcho K. R., Somberg R. L., Vogel K. W. Overcoming compound interference in fluorescence polarization-based kinase assays using far-red tracers. *Assay Drug Dev Technol.* 2004;2(no. 2):193–203. PubMed PMID: 15165515.
8. Simeonov A, Jadhav A, Thomas CJ, et al. Fluorescence spectroscopic profiling of compound libraries. *J Med Chem.* 2008;51:2363–2371. PubMed PMID: 18363325.
9. Newman M., Josiah S. Utilization of fluorescence polarization and time resolved fluorescence resonance energy transfer assay formats for SAR studies: Src kinase as a model system. *J.Biomol.Screen.* 2004;9(no. 6):525–532. PubMed PMID: 15452339.
10. Turek-Etienne T. C., Kober T. P., Stafford J. M., Bryant R. W. Development of a fluorescence polarization AKT serine/threonine kinase assay using an immobilized metal ion affinity-based technology. *Assay Drug Dev Technol.* 2003;1(no. 4):545–553. PubMed PMID: 15090251.
11. Turek-Etienne Tammy C., Small Eliza C., Soh Sharon C., Xin Tianpei A., Gaitonde Priti V., Barrabee Ellen B., Hart Richard F., Bryant Robert W. Evaluation of fluorescent compound interference in 4 fluorescence polarization assays: 2 kinases, 1 protease, and 1 phosphatase. *J.Biomol.Screening.* 2003;8(no. 2):176–184. PubMed PMID: 12844438.
12. Moshinsky D. J., Ruslim L., Blake R. A., Tang F. A widely applicable, high-throughput TR-FRET assay for the measurement of kinase autophosphorylation: VEGFR-2 as a prototype. *J.Biomol.Screen.* 2003;8(no. 4):447–452. PubMed PMID: 14567797.
13. Schroter T., Minond D., Weiser A., Dao C., Habel J., Spicer T., Chase P., Baillargeon P., Scampavia L., Schurer S., Chung C., Mader C., Southern M., Tsinoremas N., LoGrasso P., Hodder P. Comparison of miniaturized time-resolved fluorescence resonance energy transfer and enzyme-coupled luciferase high-throughput screening assays to discover inhibitors of Rho-kinase II (ROCK-II). *J.Biomol.Screen.* 2008;13(no. 1):17–28. PubMed PMID: 18227223.
14. Vogel K. W., Vedvik K. L. Improving lanthanide-based resonance energy transfer detection by increasing donor-acceptor distances. *J.Biomol.Screen.* 2006;11(no. 4): 439–443. PubMed PMID: 16751339.
15. Glickman J. F., Wu X., Mercuri R., Illy C., Bowen B. R., He Y., Sills M. A comparison of ALPHAScreen, TR-FRET, and TRF as assay methods for FXR nuclear receptors. *J.Biomol.Screen.* 2002;7(no. 1):3–10. PubMed PMID: 11897050.
16. Ullman E. F., Kirakossian H., Singh S., Wu Z. P., Irvin B. R., Pease J. S., Switchenko A. C., Irvine J. D., Dafforn A., Skold C. N. Luminescent oxygen channeling immunoassay: measurement of particle binding kinetics by chemiluminescence. *Proc.Natl.Acad.Sci.U.S.A.* 1994;91(no. 12):5426–5430. and. PubMed PMID: 8202502.
17. Von Leoprechting A., Kumpf R., Menzel S., Reulle D., Griebel R., Valler M. J., Buttner F. H. Miniaturization and validation of a high-throughput serine kinase assay using the AlphaScreen platform. *J.Biomol.Screen.* 2004;9(no. 8):719–725. PubMed PMID: 15634799.
18. Warner G., Illy C., Pedro L., Roby P., Bosse R. AlphaScreen kinase HTS platforms. *Curr.Med.Chem.* 2004;11(no. 6):721–730. PubMed PMID: 15032726.
19. Rodems, S. M., B. D. Hamman, C. Lin, J. Zhao, S. Shah, D. Heidary, L. Makings, J. H. Stack, and B. A. Pollok. 2002. A FRET-based assay platform for ultra-high density

- drug screening of protein kinases and phosphatases. *Assay Drug Dev Technol.* 1, no. 1 Pt 1:9-19.
20. Koresawa M., Okabe T. High-throughput screening with quantitation of ATP consumption: a universal non-radioisotope, homogeneous assay for protein kinase. *Assay Drug Dev Technol.* 2004;2(no. 2):153–160. PubMed PMID: 15165511.
  21. Kashem M. A., Nelson R. M., Yingling J. D., Pullen S. S., Prokopowicz A. S. III, Jones J. W., Wolak J. P., Rogers G. R., Morelock M. M., Snow R. J., Homon C. A., Jakes S. Three mechanistically distinct kinase assays compared: Measurement of intrinsic ATPase activity identified the most comprehensive set of ITK inhibitors. *J. Biomol. Screen.* 2007;12(no. 1):70–83. PubMed PMID: 17166826.
  22. Wu Ge, Yuan Yue, Nicholas Hodge C. Determining appropriate substrate conversion for enzymatic assays in high-throughput screening. *J. Biomol. Screening.* 2003;8(no. 6):694–700. PubMed PMID: 14711395.
  23. Tanega C, Shen M, Mott BT, et al. Comparison of bioluminescent kinase assays using substrate depletion and product formation. *Assay Drug Dev Technol.* 2009;7:606–614. PubMed PMID: 20059377.
  24. Charter NW, Kauffman L, Singh R, Eglen RM. A Generic, Homogenous Method for Measuring Kinase and Inhibitor Activity via Adenosine 5'-Diphosphate Accumulation. *J. Biomol Screen.* 2006;11(4):390–399. PubMed PMID: 16751335.
  25. Pedro L, Padrós J, Beudet L, Schubert HD, Gillardon F, Dahan S. Development of a high-throughput AlphaScreen assay measuring full-length LRRK2(G2019S) kinase activity using moesin protein substrate. *Anal Biochem.* 2010 Sep 1;404(1):45–51. Epub 2010 Apr 29. PubMed PMID: 20434426.
  26. Zhang J. H., Chung T. D., Oldenburg K. R. A Simple Statistical Parameter for Use in Evaluation and Validation of High Throughput Screening Assays. *J. Biomol. Screen.* 1999;4(no. 2):67–73. PubMed PMID: 10838414.
  27. Swinney D. C. Biochemical mechanisms of drug action: what does it take for success? *Nat. Rev. Drug Discov.* 2004;3(no. 9):801–808. PubMed PMID: 15340390.
  28. Vogel Kurt W., Zhong Zhong, Bi Kun, Pollok Brian A. Developing assays for kinase drug discovery - where have the advances come from? *Expert Opin. Drug Discovery.* 2008;3(no. 1):115–129. PubMed PMID: 23480143.
  29. Glickman J. F., Schmid A. Farnesyl pyrophosphate synthase: real-time kinetics and inhibition by nitrogen-containing bisphosphonates in a scintillation assay. *Assay Drug Dev Technol.* 2007;5(no. 2):205–214. PubMed PMID: 17477829.
  30. Segal, I, 1975. *Enzyme Kinetics: Behavior and analysis of rapid equilibrium and steady-state Enzyme systems.* New York, Wiley and Sons, p106.
  31. Yang J, Copeland RA, Lai Z. Defining balanced conditions for inhibitor screening assays that target bisubstrate enzymes. *J Biomol Screen.* 2009;14:111–120. PubMed PMID: 19196704.
  32. Schröter A, Tränkle C, Mohr K. Modes of allosteric interactions with free and [<sup>3</sup>H]N-methylscopolamine-occupied muscarinic M2 receptors as deduced from buffer-dependent potency shifts. *Naunyn Schmiedebergs Arch Pharmacol.* 2000 Dec;362(6): 512–9. PubMed PMID: 11138843.
  33. Von Ahsen Oliver, Boemer Ulf. High-throughput screening for kinase inhibitors. *ChemBioChem.* 2005;6(no. 3):481–490. PubMed PMID: 15742384.

34. Feng B. Y., Shoichet B. K. A detergent-based assay for the detection of promiscuous inhibitors. *Nat.Protoc.* 2006;1(no. 2):550–553. PubMed PMID: 17191086.
35. Shoichet B. K. Interpreting steep dose-response curves in early inhibitor discovery. *J.Med.Chem.* 2006;49(no. 25):7274–7277. PubMed PMID: 17149857.

## Additional References:

- Daub H., Specht K., Ullrich A. Strategies to overcome resistance to targeted protein kinase inhibitors. *Nat.Rev.Drug Discov.* 2004;3(no. 12):1001–1010. PubMed PMID: 15573099.
- Johnston P. A., Foster C. A., Shun T. Y., Skoko J. J., Shinde S., Wipf P., Lazo J. S. Development and implementation of a 384-well homogeneous fluorescence intensity high-throughput screening assay to identify mitogen-activated protein kinase phosphatase-1 dual-specificity protein phosphatase inhibitors. *Assay.Drug Dev.Technol.* 2007;5(no. 3):319–332. PubMed PMID: 17638532.
- Lakowicz, J. R. 2006. *Principles of Fluorescence Spectroscopy*. 3rd ed. Berlin: Springer.
- Lawrence David S., Wang Qunzhao. Seeing is believing: peptide-based fluorescent sensors of protein tyrosine kinase activity. *ChemBioChem.* 2007;8(no. 4):373–378. PubMed PMID: 17243187.
- Olive D. M. Quantitative methods for the analysis of protein phosphorylation in drug development. *Expert.Rev.Proteomics.* 2004;1(no. 3):327–341. PubMed PMID: 15966829.
- Parker Gregory J., Law Tong Lin, Lench Francis J., Bolger Randall E. Development of high throughput screening assays using fluorescence polarization: nuclear receptor-ligand-binding and kinase/phosphatase assays. *J.Biomol.Screening.* 2000;5(no. 2):77–88. PubMed PMID: 10803607.
- Zegzouti H, Zdanovskaia M, Hsiao K, Goueli SA. 2009. ADP-Glo: A Bioluminescent and homogeneous ADP monitoring assay for kinases. *Assay Drug Dev Technol.* Dec;7(6): 560-72. PubMed PMID: 20105026.



# Receptor Binding Assays for HTS and Drug Discovery

Douglas S Auld,<sup>1</sup> Mark W. Farnen,<sup>2</sup> Steven D. Kahl,<sup>3,\*</sup> Aidas Kriauciunas,<sup>2</sup> Kevin L. McKnight,<sup>4</sup> Chahrzad Montrose,<sup>3</sup> and Jeffrey R. Weidner<sup>†</sup>

Created: May 1, 2012; Updated: July 1, 2018.

## Abstract

Receptor binding assay formats for HTS and lead optimization applications are discussed in detail in this chapter. Critical considerations that are discussed include appropriate selection of detection technologies, instrumentation, assay reagents, reaction conditions, and basic concepts in receptor binding analysis as applied to assay development. Sections on special circumstances that address high affinity binders and Hill slope variations are also included and may be useful for data analysis and trouble shooting. A discussion on Scintillation Proximity (SPA), filtration binding and Fluorescence Polarization (FP) assays for receptor binding analysis are also included with detailed accounts on assay development using these technologies.

## Introduction

There are two typical assay formats used for analysis of receptor-ligand interactions in screening applications, filtration and scintillation proximity assay (SPA). Both formats utilize a radiolabeled ligand and a source of receptor (membranes, soluble/purified). Receptor binding assays using non-radioactive formats (fluorescence polarization, time-resolved fluorescence, etc.) which are continually being investigated for feasibility, would have similar assay development schemes to those presented in this document.

Selection of the detection method to be used (SPA, filtration, non-radioactive) is the first step to receptor binding assay development. In some cases, investigation into more than one format may be required to meet the following desired receptor binding criteria:

- Low nonspecific binding (NSB)
- > 80% specific binding at the  $K_D$  concentration of radioligand
- Less than 10% of the added radioligand should be bound (Zone A)
- Steady-state obtained and stability of signal maintained
- For competition assays, the radioligand concentration should be at or below the  $K_D$

---

<sup>1</sup> Novartis Institutes for Biomedical Research, Boston, MA. <sup>2</sup> Eli Lilly & Company, Indianapolis, IN (Deceased). <sup>3</sup> Eli Lilly & Company, Indianapolis, IN. <sup>4</sup> University of North Carolina, Chapel Hill, NC.

\* Editor

† Editor

- No dose response in the absence of added receptor
- Reproducible
- Appropriate signal window (i.e. Z-factor > 0.4, SD window > 2 SD units)

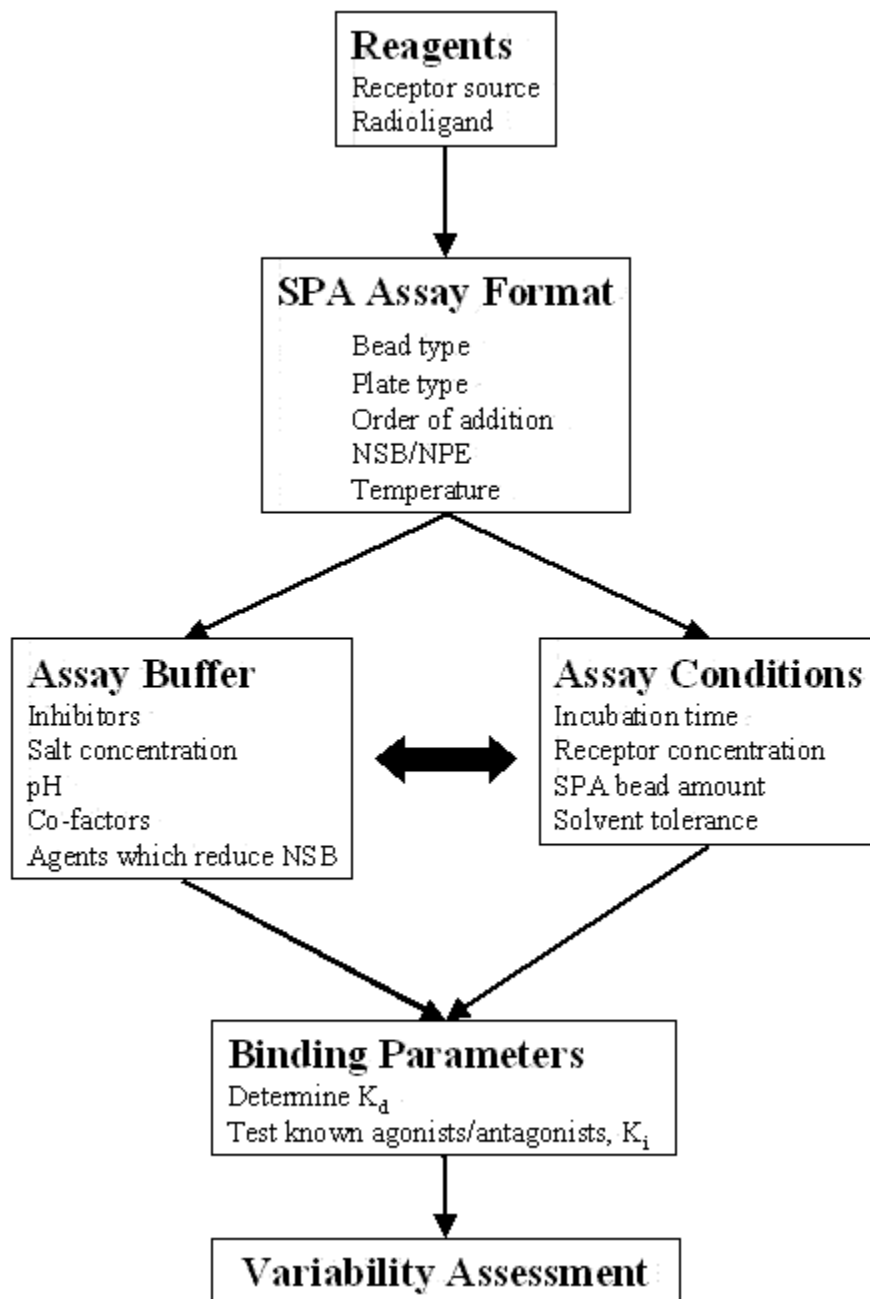
While developing receptor binding assays, some of the experiments may need to be performed in an iterative manner to achieve full optimization. In addition preliminary experiments may be required to assess the system.

In many instances, a multi-variable experimental design can be set up to investigate the impact of several parameters simultaneously, or to determine the optimum level of a factor. It is strongly recommended that full assay optimization be performed in collaboration with an individual trained in experimental design.

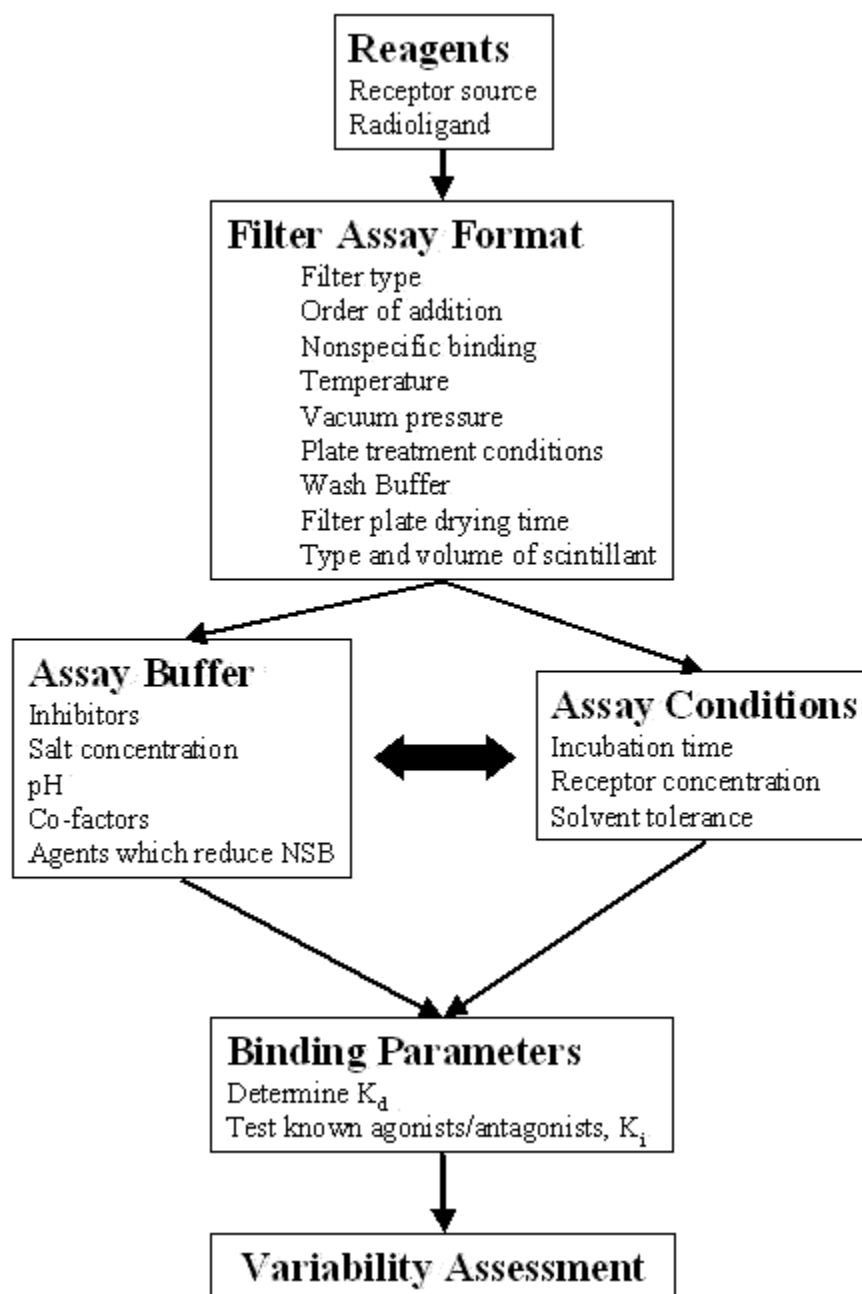
Experimental design and assay variability is addressed in detail in other sections of this handbook.

The following pages should be used as a general developmental guide to receptor binding assays using SPA or filtration formats.

## Flow Chart of Steps to Assay Development for SPA Format



## Flow Chart of Steps to Assay Development for Filter Format



### Reagents

Quality reagents are one of the most important factors involved in assay development. Validated reagents of sufficient quantity are critical for successful screen efforts over a long period of time. The primary reagents required for a radioactive receptor binding assay



which are discussed on the following pages are receptors (membranes or purified) and radioligands.

## Scintillation Proximity Assays (SPA)

### Concept

SPA assays do not require a separation of free and bound radioligand and therefore are amenable to screening applications. A diagram for a standard receptor binding SPA is shown below for a  $^{125}\text{I}$  radioligand (Figure 1).

General Steps for an SPA Assay:

1. Add and incubate test compound, radioligand, receptor and SPA beads in a plate (in some cases, the SPA beads are added at a later time point).
2. Count plates in microplate scintillation counter. The appropriate settling time needs to be determined experimentally.

| Advantages   | Disadvantages   |
|--|---|
| Non-separation method<br>No scintillation cocktail required<br>Reduced liquid radioactive waste<br>Reduced handling steps (add, incubate, read)<br>Multiple bead types (WGA, PEI-coated, etc.) | More expensive - requires license<br>Lower counting efficiency<br>Primarily for $^3\text{H}$ and $^{125}\text{I}$ ( $^{33}\text{P}$ , $^{35}\text{S}$ possible)<br>Non-proximity effects<br>Quenching by colored compounds<br>Difficult to perform kinetic experiments<br>Bead settling effects |

Many of the advantages and disadvantages are addressed in the following sections.

### SPA Assay Format

The main components of an SPA receptor binding assay format include bead type, plate type, order of addition, non-specific binding (NSB)/non-proximity effects, and temperature. Each of these items are described in detail in the sections below.

### Bead Type

The SPA bead surface-coupling molecule selected for use in a receptor binding assay must be able to capture the receptor of interest with minimal interaction to the radioligand itself. Table 1 lists the available SPA bead capture mechanisms that can be used with various receptor sources.

In addition to the capture mechanism, two types of SPA beads are available:

- Plastic SPA beads, made of polyvinyltoluene (PVT), act as a solid solvent for diphenylanthracene (DPA) scintillant incorporated into the bead

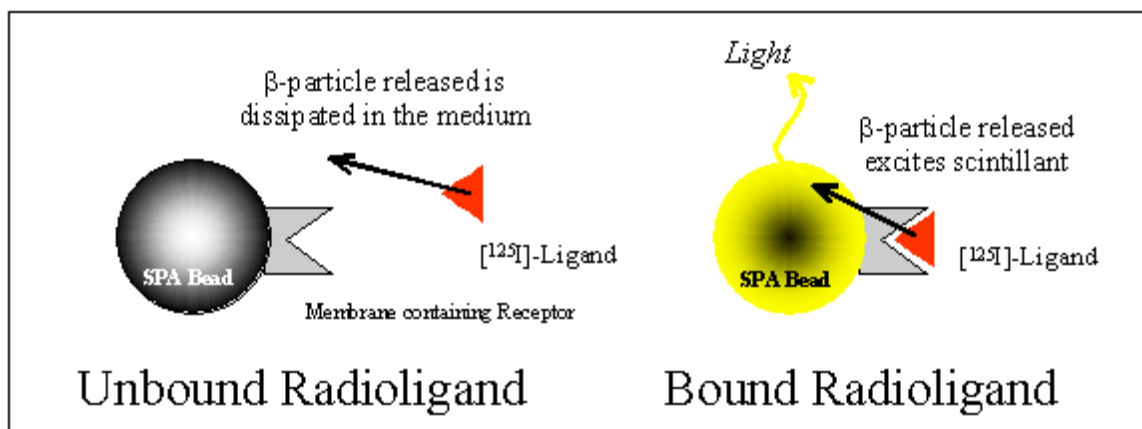


**Figure 1:** Diagram for standard receptor-binding SPA for  $^{125}\text{I}$  radioligand.

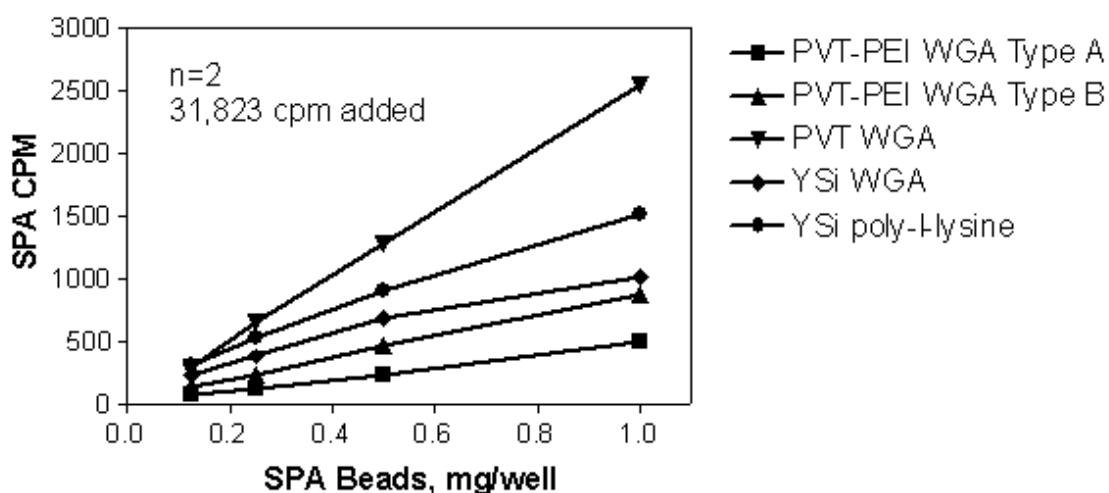


**Figure 2:** Example experiment using kit from Perkin Elmer containing several different SPA bead types (performed in absence of added membrane receptor).

- A Glass SPA bead, or Yttrium silicate (YSi), uses cerium ions within a crystal lattice for the scintillation process. In general, YSi is a more efficient scintillator than PVT is, but YSi SPA beads require continuous mixing even during dispensing.

Typical experiments to investigate nonspecific binding of radioligand to SPA beads include varying the amount of radioligand (above and below the predicated  $K_D$  value) and the amount of SPA beads (0.1 mg to 1 mg) in the absence of added membrane protein. Results from this experiment can identify the proper type of SPA beads to use in future experiments, as well as the baseline background due to non-proximity effects. An example experiment using a kit from Perkin Elmer that contains several different SPA bead types (Select-a-Bead kit, #RPNQ0250) is provided in Figure 2. For this example, which was

performed in the absence of added membrane receptor, the PVT-PEI WGA Type A SPA beads yields the lowest interaction with the radioligand and was used for further assay development. An increase in signal with an increasing amount of added SPA beads is normal. Additives may be useful in decreasing high levels of nonspecific binding of radioligand to the SPA beads (see Table 2).

**Table 1: Available SPA bead capture mechanisms**

| Receptor                | SPA Bead      | Capture Mechanism   |
|-------------------------|---------------|---------------------|
| <b>Membranes</b>        | WGA [1]       | Glycosylation sites |
|                         | Poly-L-lysine | Negative charges    |
| <b>Soluble/Purified</b> | WGA           | Glycosylation sites |
|                         | Streptavidin  | Biotinylated site   |
|                         | Antibody [2]  | Specific antibody   |
|                         | Copper        | His-Tag             |
|                         | Glutathione   | GST-fusion          |

[1] Wheat germ agglutinin (WGA) SPA beads are available in standard untreated format and two different versions that have been treated with polyethyleneimine (PEI).

[2] Secondary antibody SPA beads are available to capture specific antibodies from the following species: Rabbit, Sheep, mouse. Protein A SPA beads are also available for antibody capture.

**Table 2: Agents which reduce NSB**

|                          |              |
|--------------------------|--------------|
| BSA                      | 0.05% - 0.3% |
| Ovalbumin                | 0.05% - 0.3% |
| NP-40                    | 0.05% - 0.3% |
| Triton X-100             | 0.05% - 0.1% |
| Gelatin                  | 0.05% - 0.3% |
| Polyethylenimine         | 0.01% - 0.1% |
| CHAPS                    | 0.5%         |
| Tween-20                 | 0.05% - 0.1% |
| Fetal bovine serum (FBS) | up to 10%    |

## Plate Type

The type of plate that is used for SPA receptor binding assays may be influenced by the following factors:

- Counting instrument used (Trilux, TopCount, , LeadSeeker)
- Miniaturization (96-well, 384-well)
- Binding of radioligand to plastics
- Liquid dispensing/automation equipment

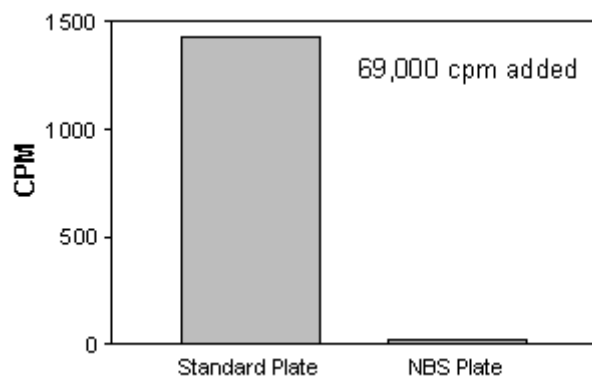


**Figure 3:** Advantage of NBS plate over standard plate when using radioligands that may bind nonspecifically to plastic plates.

Table 3 lists typical plate choices for SPA assays:

The data shown in Figure 3 demonstrates an advantage of the NBS plates when using a radioligand, which binds nonspecifically to plate plastic.

69,000 CPM of <sup>125</sup>I-labeled ligand added to the well, incubated for 60 min. Radioactivity removed and wells washed. SPA beads then added. Data demonstrates that a radioligand sticking to the plate surface can elicit an SPA signal. NBS plate yields significantly less nonspecific binding of radioligand.

**Table 3:** Typical plate choices for SPA assays

| Plate Type             | Instrument | of Wells | Comments  |
|------------------------|------------|----------|---|
| Costar #3632           | Trilux     | 96       | White/Clear-bottom, 96-well   |
| Costar #3604           | Trilux     | 96       | White/Clear-bottom, 96-well, non-binding surface (NBS), may be useful when ligands are sticky |
| Perkin Elmer 401       | Trilux     | 96       | Clear/flexible, not easily amenable to automation or liquid dispensing instrumentation        |
| Costar #3706           | Trilux     | 384      | White/Clear-bottom, 384-well  |
| Perkin Elmer Optiplate | TopCount   | 96       | White/solid bottom, 96-well   |
| Perkin Elmer IsoPlate  | Trilux     | 96       | White/Clear-bottom, 96-well   |

## Order of Addition

The order of addition for reagents may affect assay performance as well as ease of automation. Three basic formats are listed in Table 4.

Time zero or delayed additions are the most commonly used formats in HTS, with time zero addition requiring fewer manipulation steps. Experiments may be required to

determine the optimum method to be used for a particular receptor to maximize signal to background levels.

In addition, the effect of DMSO on intermediate reactants should be investigated. If compounds in DMSO are added into the wells first (most common method for screening efforts), other reagents added (i.e. radioligand, membranes, beads, etc.) may be affected by the concentration of DMSO, or if the time before reaching the final reaction mixture becomes significant.

**Table 4: Basic formats for order of addition for reagents.**

| Method                                | Advantage                                    |
|---------------------------------------|--|
| Membrane precoupled to SPA bead       | May aid in lowering NSB                      |
| Time zero (T=0) addition of SPA beads | Easily automated                             |
| Delayed addition of SPA beads         | Optimum ligand/receptor interaction possible |

## Non-Specific Binding (NSB)/Non-proximity Effects (NPE)

In order to obtain the maximum signal to noise ratio possible for SPA receptor binding assays, it is important to understand the two different types of signals associated with the radioligand and SPA beads, which may contribute to the total assay background levels.

### Non-Specific Binding (NSB) to SPA Beads

The NSB signal is attributed to the radiolabel which may adhere to the SPA beads themselves and not through a specific interaction with the receptor attached to the SPA bead (Figure 4, left). This component of background signal can be determined in the presence of an excess concentration of competitor in the absence of the membrane receptor. Reduction of this factor can be accomplished through the careful use of buffering systems and the appropriate bead type. Determination of NSB to the SPA beads is separate from the NSB associated with membrane receptor preparations.

A competition experiment using an unlabeled compound in the absence or presence of added receptor may assist in identifying nonspecific binding problems.

### Non-Proximity Effects (NPE)

NPE occurs when either the concentration of the radioligand or the concentration of SPA beads is sufficiently high enough to elicit a signal from the emitted  $\beta$ -particles. This can occur even though the labeled ligand is not attached directly to the SPA bead through the interaction with the receptor or the nonspecific interaction with the bead (Figure 4, right). In general, this signal is a linear function, directly proportional to the concentrations of each of these reagents. Therefore, a careful balance between radiolabel and SPA beads is crucial to maximize signal and sensitivity while minimizing NPE and ultimately cost. The only technique available to minimize NPE is adjustment of the SPA bead or radiolabel concentrations.

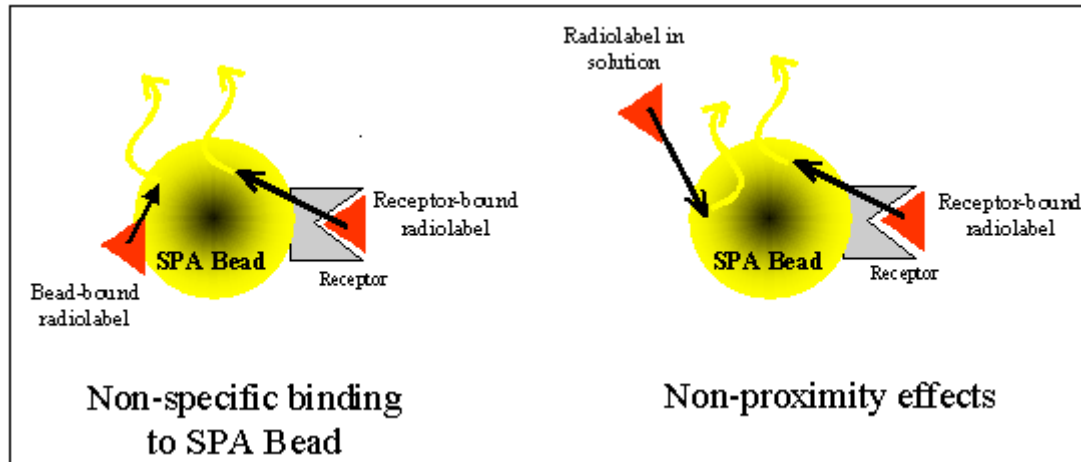


**Figure 4:** Non-specific binding (left), and non-proximity effects (right) associated with SPA beads.

For routine SPA binding assays, nonspecific binding may be a combination of nonspecific binding to SPA beads as well as nonspecific binding to the receptor, and are expressed as one. Total nonspecific binding is measured in the presence of an excess concentration of unlabeled competitor.

## Temperature

Typically, receptor binding assays used in screening efforts are performed at room temperature. Comparison experiments may be required if other temperatures are considered. A kinetic analysis may be necessary as well (Figure 5).

*Note: Since in nearly all cases, the microplate scintillation counter is at room temperature, and a 96-well plate requires approximately 12 minutes to read on a 12-detector instrument, it is difficult to perform SPA assays at temperatures other than room temperature. The information is useful in areas where there are significant variations in day-to-day laboratory temperatures.*

## Assay Buffer

Identify appropriate starting buffer from literature sources or based on experience with similar receptors. Binding assays may require  $\text{CaCl}_2$ ,  $\text{MgCl}_2$ ,  $\text{NaCl}$  or other agents added to fully activate the receptor. pH is generally between 7.0 to 7.5. Commonly used buffers include TRIS or HEPES at 25 mM to 100 mM. Protease inhibitors may be required to prevent membrane degradation

The tables below provides possible factors that can be investigated in a statistically designed experiment to improve radioligand binding to membrane receptors, or reduce radioligand binding to SPA beads (Agents which Reduce NSB – Table 2; Antioxidants/ Reducing Agents – Table 5; SPA Bead Settling Effects - Table 6; Divalent Cations – Table 7; Other Buffer Additives – Table 8). The optimization of the assay buffer may be an iterative

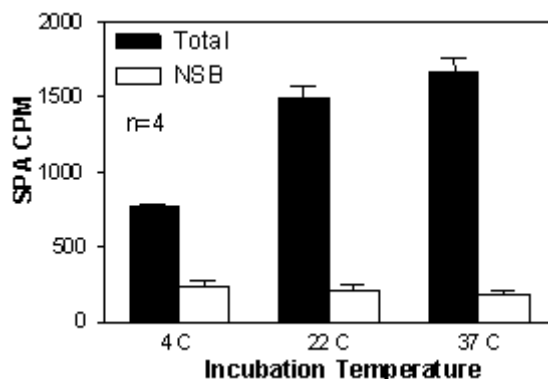


**Figure 5:** SPA receptor binding assay performed at three temperatures. Data shown at the left was generated by incubation of a limited number of wells ( $n=4$ , different plates) at the indicated temperatures and counting them rapidly in the instrument.

process in conjunction with the optimization of the assay conditions to achieve acceptable assay performance. Typical concentrations or concentration ranges for some reagents are listed in the tables below. Other reagents may be required depending on the individual receptor/ligand system.

Note that for most instances, the highest purity reagents should be tested. In some cases, such as with BSA, several forms (fatty acid free, fatty acid containing) may need to be investigated.

In addition to Aprotinin and EDTA, other protease inhibitors may be required for receptor stability. As a starting point, Complete™ tablets from Roche Molecular Biochemicals are commonly used.

**Table 5: Antioxidants/Reducing agents**

| Agent         | Concentration Range |
|---------------|---------------------|
| Ascorbic Acid | 0.1%                |
| Pargyline     | 10 $\mu$ M          |
| DTT           | 1 mM                |

**Table 6: Reduce SPA bead settling effects**

| Agent                     | Concentration Range |
|---------------------------|---------------------|
| Glycerol                  | 10 - 20%            |
| Glucose                   | 10 mM               |
| Polyethylene glycol (PEG) | 5 - 10%             |

**Table 7: Divalent cations**

| Cation                        | Concentration Range     |
|-------------------------------|-------------------------|
| Magnesium (Mg <sup>2+</sup> ) | 1 mM - 10 mM            |
| Sodium Acetate                | 10 mM - 50 mM           |
| Calcium (Ca <sup>2+</sup> )   | 1 mM - 10 mM            |
| Zinc (Zn <sup>2+</sup> )      | 10 $\mu$ M - 50 $\mu$ M |

**Table 8: Other buffer additives**

| Additive         | Concentration Range |
|------------------|---------------------|
| NaCl             | 100 mM - 150 mM     |
| KCl              | 5 mM - 80 mM        |
| TRIS             | 10 mM - 50 mM       |
| HEPES            | 5 mM - 100 mM       |
| Phosphate Buffer | 20 mM               |
| pH               | 7.0 - 8.0           |
| Aprotinin        | 500 units/ml        |
| EDTA             | 0.51 mM - 5 mM      |

**Table 9: Pharmacological profile with representative IC<sub>50</sub>, K<sub>i</sub> and rank affinity data.**

| Drug | IC <sub>50</sub> , nM | K <sub>i</sub> , nM | Relative Affinity |
|------|-----------------------|---------------------|-------------------|
| 4    | 103                   | 53                  | 1.00              |
| 5    | 190                   | 95                  | 0.56              |
| 1    | 0.25                  | 0.13                | 424               |
| 2    | 8.9                   | 4.5                 | 11.9              |
| 3    | 30.9                  | 15.5                | 3.4               |

## Solvent Interference Conditions

### Incubation Time - Signal Stability

**Setup:** Measure total binding (receptor + radioligand + SPA beads) and nonspecific binding (receptor + radioligand + excess unlabeled competitor + SPA beads) at various times using repetitive counting on the microplate scintillation counter.

**Results Analysis:** Plot total, NSB and specific binding (total binding - NSB) versus time

Since steady state will require a longer time to reach at lower concentrations of radioligand, these experiments are usually performed at radioligand concentrations below the K<sub>d</sub> (i.e. 1/10 K<sub>d</sub>) if signal strength permits. In addition, the total concentration of



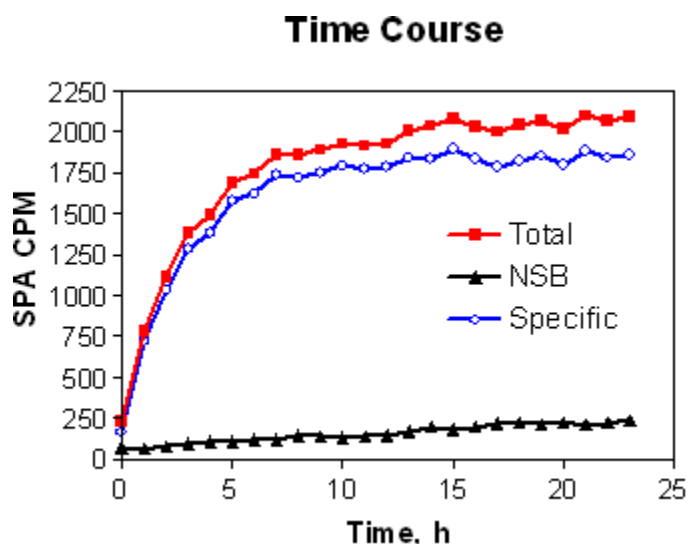


**Figure 6:** Example of incubation time course

radioligand bound should be equal to less than 10% of the concentration added to avoid ligand depletion. The receptor concentration added must be lowered, or the volume of radioligand increased, if this condition is not met.

This experiment is used to determine when a stable signal is achieved and how long a stable signal can be maintained. The signal is a combination of receptor/ligand reaching steady state and bead settling conditions. As SPA beads become packed at the bottom of the well, the efficiency of counting (particularly with  $^{125}\text{I}$ ) increases. Therefore, it is important to determine when a uniform signal is obtained and adopt this time window as standard practice. In many assays, 8-16 hours are required for stable signal counting. Use approximately 0.1-0.5 mg SPA beads depending on results from preliminary experiments.

An example of an incubation time course is provided in Figure 6. A minimum incubation time of 10 hours was chosen in this example and the interaction was stable for at least 24 hours. Failure to operate a receptor/ligand binding assay at steady state conditions may result in erroneous calculations for binding constants ( $K_D$  or  $K_i$ ).

## Receptor Concentration - Zone A

**Setup:** Measure total binding (receptor + radioligand + SPA beads) and nonspecific binding (receptor + radioligand + excess unlabeled competitor + SPA beads) at various levels of added receptor (typical  $\mu\text{g}$  amounts vary depending on the source and purity of receptor).

**Results Analysis:** Plot total and NSB versus receptor amount. Plot total bound/total added expressed as a percent versus receptor concentration. Determine the level of receptor that yields <10% total binding/total added (Zone A).

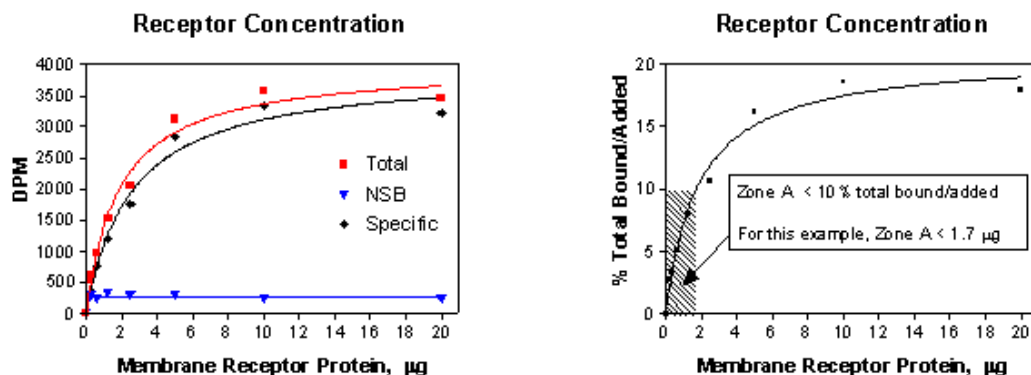


**Figure 7:** Example of radioligand at  $< 0.1 K_D$  and an increasing amount of membrane protein. Left: raw SPA data for total and NSB; right: total bound / total added expressed as a percent.

It is ideal to keep the total amount of radioligand bound at less than 10% of the total amount added to avoid ligand depletion. This is considered the acceptable limit and is commonly referred to as “Zone A”. Saturation experiments should be performed at  $< 10\%$  total ligand binding at all concentrations tested ( $0.1 \times K_D$  to  $10 \times K_D$ ), so an initial protein variation experiment at a radioligand concentration that is  $0.1 \times K_D$  is typically performed.

The example shown in Figure 7 uses radioligand at  $< 0.1 K_D$  and an increasing amount of membrane receptor protein. Two plots are shown: Figure 7, left, raw SPA data for total, NSB and specific; Figure 7, right total bound/total added expressed as a percent. In this example, receptor levels less than  $\sim 2 \mu\text{g}/\text{well}$  would meet Zone A requirements.

Total counts added (using liquid scintillation counting) are determined differently than the bound counts (SPA), therefore, in order to plot the % Total Bound/Added, the efficiency for each method must be taken into account, and any CPM data converted to DPM (described in Calculations and Instrumentation Used for Radioligand Binding Assays). You cannot compare the CPM data from one instrument/scintillation method to that of another. The Section entitled “DPM Mode for SPA” demonstrates a representative method for determining efficiency for SPA bead counting. DPM for liquid scintillation counting can be obtained from the instrument directly. The stable signal count time must be determined prior to these experiments. If the signal dips after a high concentration of receptor, then the SPA beads may be in limited amounts.

## SPA Bead Amount

**Setup:** Measure total binding (receptor + radioligand + SPA beads) nonspecific binding (receptor + radioligand + excess unlabeled competitor + SPA beads) and non-proximity effects (radioligand + SPA beads) at various SPA bead levels (typically  $0.125 \text{ mg}$  to  $1.5 \text{ mg}$ ) using the determined optimum incubation time and optimum receptor concentration.

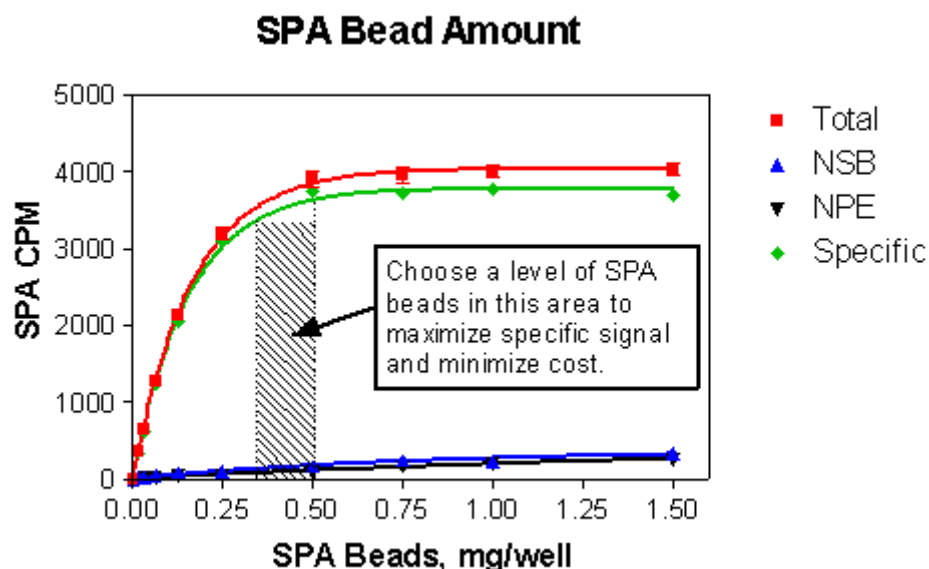


**Figure 8:** Plot demonstrating how to choose an appropriate bead concentration.

**Results Analysis:** Plot total, NSB, NPE, and specific binding (total - NSB) versus SPA bead amount. Choose a bead concentration beyond the linear range, at or near the initial saturation level on the specific binding curve (Figure 8).

Non-proximity effects (NPE) can be determined in the absence of added receptor. Ideally, the NPE signal would be identical to the nonspecific signal in the presence of unlabeled competitor. A level of SPA beads below 0.4 mg would provide the best economical signal for this example.

## Solvent Interference

**Setup:** Measure total binding (receptor + radioligand + SPA beads) and nonspecific binding (receptor + radioligand + excess unlabeled competitor + SPA beads) at various concentrations of DMSO (or other solvent) using the determined optimum incubation time, optimum receptor concentration and optimum SPA bead amount.

**Results Analysis:** Plot total and NSB versus final assay concentration of DMSO.

If the developed SPA receptor binding assay will be used to test organic compounds, interference with DMSO will need to be determined. As shown in Figure 9, there can be significant signal reduction if the DMSO concentration becomes too high.

The level of DMSO in a SPA binding assay is determined by data in experiments such as the one in the example above and by the requirement set to maintain compound solubility.

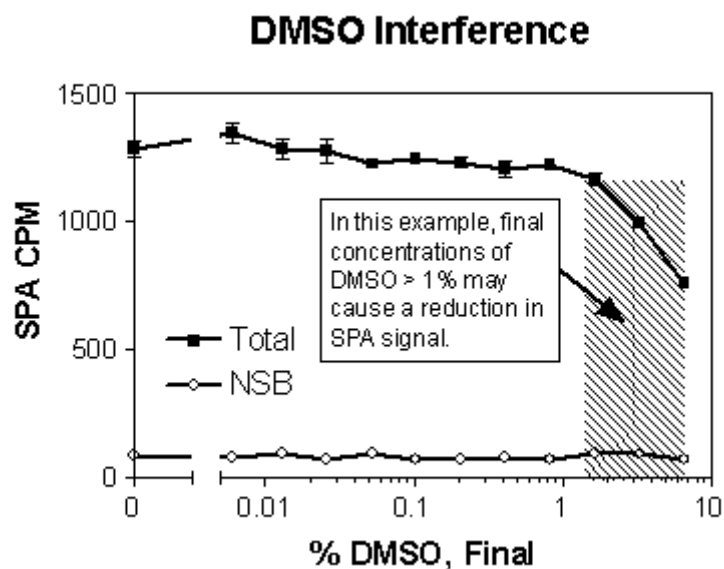


**Figure 9:** Example of DMSO interference determination and potential for signal reduction.

Additional solvents (methanol, ethanol, etc.) or other agents (i.e.  $\beta$ -cyclohexadextrin) may need to be tested if compounds will be received in these other diluents.

Once determined, the solvent should be included in any further assay development or compound testing, including controls.

As an additional verification of minimal solvent interference, test competitive binding with a known competitor in the absence or presence of solvent at the determined level to be used in assays. Ideally, the test compound will have high affinity for the receptor and be freely soluble in aqueous buffer. The  $IC_{50}$  should not change in the absence or presence of the solvent.

## Binding Parameter

The determination of the equilibrium dissociation constant for the radioligand ( $K_D$ ) or equilibrium dissociation constants for unlabeled compounds ( $K_i$ ) should be performed after the SPA receptor binding assay has been fully optimized for the conditions outlined in the prior sections.

Three methods are described for the determination of the receptor affinity for the radioligand,  $K_D$ :

- Saturation analysis
- Homologous competition
- Association rate at various radioligand concentrations

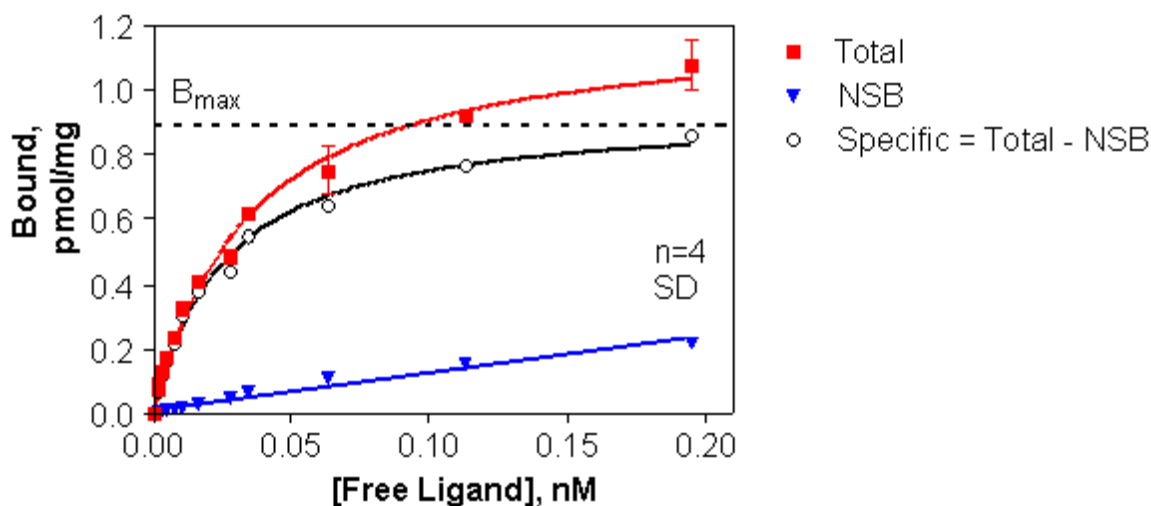


**Figure 10:** A representative saturation binding experiment. Y-axis data has been expressed in pmol/mg.

A heterologous competition binding assay is used to determine the affinity of the receptor for an unlabeled compound,  $K_i$ .

## Saturation Binding

An equilibrium saturation binding experiment measures total and nonspecific binding at various radioligand concentrations. The equilibrium dissociation constant or affinity for the radioligand,  $K_D$ , and the maximal number of receptor binding sites,  $B_{max}$ , can be calculated from specific binding (total - NSB) using non-linear regression analysis.

Requirements:

- Steady state for low concentrations of radioligand (i.e.  $1/10$  estimated  $K_D$ ) has been determined
- Ensure that  $<10\%$  of the added radioligand is bound (at all radioligand concentrations tested) to prevent ligand depletion - if this is not met, lower the receptor concentration.

The range of radioligand concentrations tested in a saturation binding experiment is typically from  $1/10 K_D$  to  $>10 \times K_D$  to yield an appropriate curve for nonlinear regression analysis methods. Radioligand specific activity, concentration or expense may prevent a wide range of concentrations from being used.

A high concentration of unlabeled compound ( $1000 \times K_i$  or  $K_D$  value) is used to determine nonspecific binding. Ideally, the unlabeled compound should be structurally different than the radioligand. Nonspecific binding should be less than 50% of the total binding at the highest concentration of  $[L]$  tested.

Calculate  $K_d$  for specific binding using a one-site binding hyperbola nonlinear regression analysis (i.e. GraphPad Prism) as shown in the equation below:

$$Bound = \frac{B_{max} \times [L]}{[L] + K_d}$$

$B_{max}$  is the maximal number of binding sites (pmol/mg), and  $K_d$  (nM, pM, etc.) is the concentration of radioligand required to reach half-maximal binding.

**Setup:** Measure total binding (receptor + radioligand + SPA beads) and nonspecific binding (receptor + radioligand + excess unlabeled competitor + SPA beads) at various concentrations of radioligand using the determined optimum incubation time, optimum receptor concentration and optimum SPA bead amount. Include the expected concentration of DMSO or other solvent for compound testing. To assess non-proximity effects (NPE), a condition without receptor can be included (radioligand + SPA beads).

**Results Analysis:** Plot total, NSB and specific binding (total - NSB) versus free concentration of radioligand. Plot NPE if no receptor condition was performed (Figure 10).

A listing of the calculations required for analysis of saturation binding data is shown below. Details for each of these calculations are shown in Calculations and Instrumentation Used for Radioligand Binding Assays

1. Determine total radioactivity added per well by counting an aliquot of each radioligand mix in a gamma counter or a liquid scintillation counter. Convert to DPM if necessary using the equation:  $DPM = CPM/Efficiency$
2. Convert binding data (total bound, NSB) from CPM to DPM data using above equation.
3. Calculate specific binding in DPM:  $Specific\ bound = Total\ Bound - NSB$
4. Calculate unbound (free) DPM:  $Free = Total\ Added - Total\ Bound$
5. Convert free DPM to concentration units (i.e. nM) using the radioligand specific activity (expressed as DPM/fmol) and the volume of sample used.
6. Convert Total bound, NSB and Specific bound DPM to pmol/mg units using specific activity expressed as DPM/fmol and the amount of receptor added per assay well in mg units.
7. Plot Bound (in pmol/mg) on Y-axis versus Free concentration of radioligand (in nM) on X-axis.
8. Determine  $K_d$  and  $B_{max}$  using a non-linear regression analysis for a single site binding (hyperbola).

## Considerations/Assumptions for Saturation Binding Experiments

The binding reaction must be at equilibrium for all concentrations of radioligand. Lower concentrations of radioligand require longer times to reach equilibrium.

Less than 10% of the total added radioligand should be bound at all concentrations of radioligand tested. At lower concentrations of radioligand, it is more likely that greater than 10% of the added radioligand will be bound (if this is the case, receptor concentration should be lowered).

If reagents and the assay system allow, radioactive concentrations of at least 10 times the  $K_D$  should be tested to provide suitable data for a nonlinear regression analysis and accurate determination of the binding parameters. The  $K_D$  and  $B_{max}$  values can be calculated from less than complete data sets, but the statistical reliability of the returned values may be lower.

Ideally, nonspecific binding should be less than 50% of the total binding. No positive or negative binding cooperativity. Binding is reversible and obeys the Law of Mass Action.

### Scatchard Plots

In the past, nonlinear saturation binding data was transformed into linear data followed by analysis using linear regression, resulting in a Scatchard (or Rosenthal) plot. Although useful for the display of data, the Scatchard plot is not used anymore for the determination of  $K_D$  or  $B_{max}$  values. These values are determined using nonlinear regression analysis as described in Saturation Binding above. Scatchard plots distort the experimental error (X-value is used to calculate Y), hence the assumptions of linear regression are violated and the resulting values are not accurate.

It is inappropriate to analyze transformed data for the determination of  $K_D$  and  $B_{max}$ .

### Homologous Competition

A homologous competition is a concentration response curve with an unlabeled compound that is identical to the radioligand being used. Radioligand concentration is constant in the experiment. Homologous competition experiments can be used as an alternative to saturation experiments to determine receptor affinity ( $K_D$ ) and density ( $B_{max}$ ), provided the criteria shown below are met. When using [ $^{125}\text{I}$ ]-ligands, a non-radioactive iodo-ligand should be used if possible.

Assumptions:

1. The receptor has identical affinity for the radioligand and unlabeled ligand.
2. There is no cooperativity.
3. No ligand depletion (<10% of the total added radioligand is bound)
4. Nonspecific binding is proportional to the concentration of labeled ligand.

The concentration-response curve should ideally descend from 90% specific binding to 10% specific binding over an 81-fold (or approximately 2 log scales) increase in concentration of the unlabeled ligand.

A homologous competition experiment has been designed correctly if the  $\text{IC}_{50}$  is between 2 and 10 times the concentration of radioligand.

Two methods can be used to analyze data from a homologous competition experiment and determine the  $K_d$  and  $B_{max}$ . They are described below as Results Analysis 1 and Results Analysis 2. The experimental setup is identical for both types of analysis.

**Setup:** Measure binding (receptor + radioligand + SPA beads) at various concentrations of unlabeled competitor using a single concentration of radioligand ( $\leq K_d$ ) and the determined optimum incubation time, optimum receptor concentration and optimum SPA bead amount. In some cases ( $^3\text{H}$ -label with low specific activity), concentrations above the  $K_d$  may be required. Total binding is determined in the absence of any added competitor. Nonspecific binding (receptor + radioligand + excess unlabeled competitor + SPA beads) is included for calculation of specific binding.

## Results Analysis 1

Plot specific bound (Bound - NSB) at each concentration of unlabeled competitor. Conversion to percent specific bound is performed using the following equation:

$$\% \text{ Specific Bound} = \frac{\text{Bound} - \text{NSB}}{\text{Total Bound} - \text{NSB}}$$

**Step 1.** Determine the  $\text{IC}_{50}$  using a sigmoidal dose-response (variable slope), which is also known as a four-parameter logistic nonlinear regression analysis (i.e. using GraphPad Prism) as shown in the equation below (use log concentration values for proper analysis) and in Figure 11.

$$Y = \text{Bottom} + \frac{(\text{Top} - \text{Bottom})}{\left(1 + 10^{(\text{LogEC}_{50} - X) + \text{HillSlope}}\right)}$$

**Step 2.** Determine the  $K_d$  and  $B_{max}$  using nonlinear regression analysis (i.e. GraphPad Prism) for the following equation:

$$Y = \frac{B_{max} \times [\text{Hot}]}{([\text{Hot}] + [\text{Cold}] + K_d)} + \text{NSB}$$

[Hot] is the concentration of radioligand used in the assay (in nM) [Cold] is the concentration of competitor, which varies, (in nM)

In GraphPad Prism, enter Y in CPM or DPM and X in log concentration of competitor.

Calculate  $K_d$  and  $B_{max}$  with above curve fit analysis. Use instrument counting efficiency and specific activity of radioligand to convert the calculated maximum signal units (CPM or DPM) to pmol/mg units.

The calculated  $\text{IC}_{50}$  for this homologous competition experiment is  $1.5 \times 10^{-10}$  M. The concentration of [L] used in this homologous competition is  $3.8 \times 10^{-11}$  M.

The calculated  $\text{IC}_{50}$  is between 2 and 10 times the concentration of added [L].



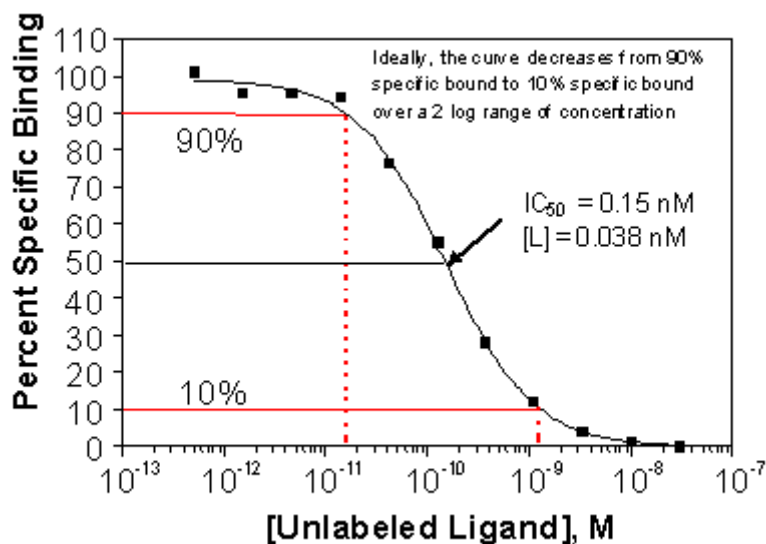


**Figure 11:** Representative data for a homologous competition.

The concentration-response curve descends from 90% specific binding to 10% specific binding over an 86-fold increase in concentration of the unlabeled ligand.

Inputting X (log concentration) and Y (Total DPM) into the homologous binding analysis equation above yields (in parentheses are the values obtained from saturation binding analysis):  $\text{Log } K_d = -9.962 \rightarrow \text{Antilog of } -9.962 = 1.09 \times 10^{-10} \text{ M} = 109 \text{ pM}$  (79 pM)  $B_{\text{max}} = 27773 \text{ DPM} \rightarrow \text{Convert using specific activity, } B_{\text{max}} = 12.5 \text{ pmol/mg}$  (5 pmol/mg)

## Results Analysis 2:

Alternatively, convert specific DPM bound to molar units (i.e. nM) bound.

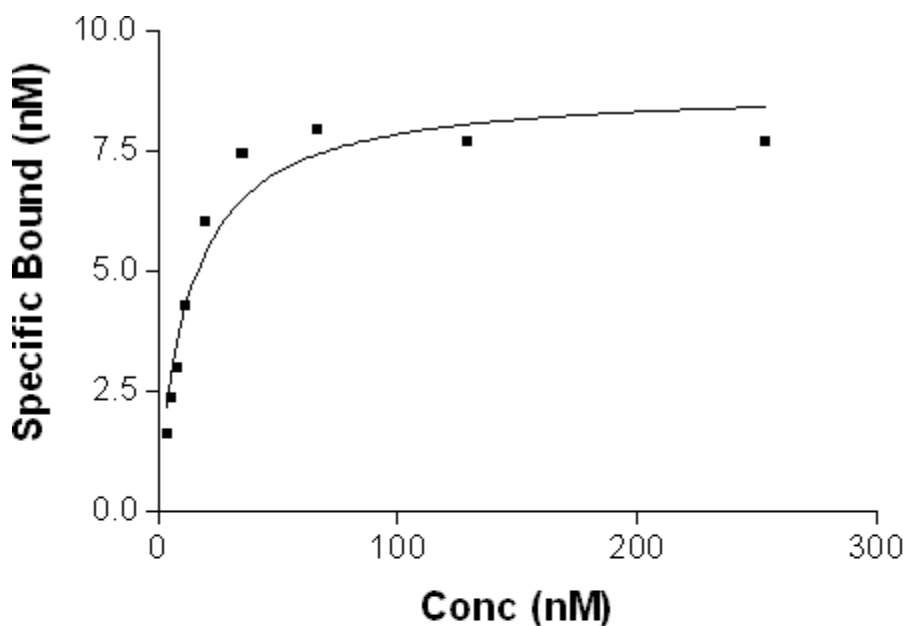
1. The molar concentration of labeled ligand ( $[L]$ ) is calculated using the DPM added per well, the specific activity and the conversion factor,  $1 \mu\text{Ci} = 2.2 \times 10^6 \text{ DPM}$ .

The formula is  $[L] \text{ nM} = (\text{specific counts}) \times (1/2200000) \times (1 / \text{Specific Activity}) \times 10000$

2. This concentration is added to all concentrations of unlabeled ligand to determine the final added ligand concentration.
3. As the added ligand concentration increases (due to increase added unlabeled ligand), the specific activity of the labeled ligand is decreased.
4. For each specific DPM bound determine the specific molar units bound by using the corresponding specific activity in that condition.

The formula is  $[RL] = (\text{added ligand}) \times (\text{specific DPM}) / (\text{DPM added per well})$ .

5. Use a one-site binding (hyperbola) similar to the saturation binding data to calculate  $K_d$  and  $B_{\text{max}}$ .



|                          |                     |
|--------------------------|---------------------|
|                          | Specific Bound (nM) |
| BMAX                     | 8.830               |
| KD                       | 12.59               |
| Std. Error               |                     |
| BMAX                     | 0.5050              |
| KD                       | 2.509               |
| 95% Confidence Intervals |                     |
| BMAX                     | 7.636 to 10.02      |
| KD                       | 6.654 to 18.52      |
| Goodness of Fit          |                     |
| Degrees of Freedom       | 7                   |
| R <sup>2</sup>           | 0.9426              |

**Figure 12:** Homologous Competition for Determination of  $K_D$ . In this example data, the  $K_D$  determined from a homologous competition experiment is 12.6 nM.

**Example:** Labeled ligand specific activity is 90 Ci/mmol and 66398 dpm are added per well (100  $\mu$ l final volume). The concentration of labeled ligand in all wells is 3.3 nM. At unlabeled ligand concentration of 125 nM, the final added ligand (unlabeled + labeled) is 128.3 nM.

If the specific binding at 125 nM unlabeled ligand condition is 3283 DPM, then the specific molar unit bound would be:

$$(3283 \times 128.3)/66398 = 6.34 \text{ nM.}$$

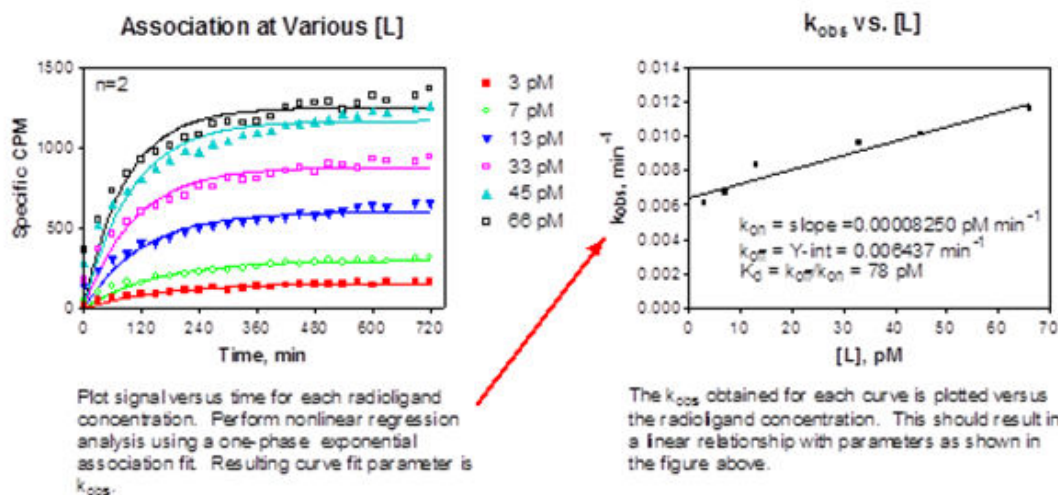


**Figure 13:** SPA Method: Reaction mix was read at different time points. The  $K_D$  calculated from saturation binding for this receptor was 35 pM.

Representative results for homologous competition analyzed using the Results Analysis 2 method is shown in Figure 12. The  $K_D$  determined from this example was 12.6 nM.

### Association Rate at Various Radioligand Concentrations (Optional)

An optional method, which can be used early in development for both determination of optimum incubation time and provide an estimate for the  $K_D$ , is to perform an association rate experiment at various radioligand concentrations.

**Setup:** Measure total binding (receptor + radioligand + SPA beads) and nonspecific binding (receptor + radioligand + excess unlabeled competitor + SPA beads) at various times and at various concentrations of added radioligand.

**Results Analysis:** Plot specific binding (total binding - NSB) versus time at each radioligand concentration tested.

Calculate the observed association rate constant ( $k_{obs}$ ) by fitting the signal versus time data to a one-phase exponential association nonlinear regression analysis for each concentration of radioligand tested. The  $k_{obs}$  value is returned as one of the resulting curve fit parameters. There will be different  $k_{obs}$  for each radioligand concentration.

Plot the observed association rate constant ( $k_{obs}$ ) versus concentration of [L].

This should result in a linear function with a slope equal to the association rate constant ( $k_{on}$ ) and the Y-intercept equal to the dissociation rate constant ( $k_{off}$ ). An estimate for the equilibrium dissociation constant ( $K_D$ ) can be calculated using the equation below with the kinetically determined rate constants (see Figure 13):

$$K_D = k_{off}/k_{on}$$

## Heterologous Competition

Experimentally, a heterologous competition is identical to a homologous competition. Heterologous competition assays measure concentration-response binding with unlabeled ligands that are **structurally different** than the radioligand. The  $IC_{50}$  for the unlabeled compound is determined from the experimental data and the equilibrium dissociation constant,  $K_D$ , can be calculated using a mathematical formula (Cheng-Prusoff equation).

**Setup:** Measure binding (receptor + radioligand + SPA beads) at various concentrations of unlabeled competitor using a single concentration of radioligand ( $\leq K_D$ ) and the determined optimum incubation time, optimum receptor concentration and optimum SPA bead amount. Total binding is determined in the absence of any added competitor. Nonspecific binding (receptor + radioligand + excess unlabeled competitor + SPA beads) is included for calculation of specific binding.

**Results Analysis:** Plot specific bound (Bound - NSB) at each concentration of unlabeled competitor. Conversion to percent specific bound is performed using the following equation:

$$\% \text{ Specific Bound} = \frac{\text{Bound} - \text{NSB}}{\text{Total Bound} - \text{NSB}} \times 100$$

Determine  $IC_{50}$  using a sigmoidal dose-response (variable slope), which is also known as a four-parameter logistic nonlinear regression analysis (i.e. using GraphPad Prism) as shown in the equation below:

$$Y = \text{Bottom} + \frac{(\text{Top} - \text{Bottom})}{\left(1 + 10^{(\text{LogEC}_{50} - X) + \text{HillSlope}}\right)}$$

where Y is the specific binding and X is the log concentration of competitor.

Calculate the equilibrium dissociation constant for the unlabeled compound ( $K_i$ ) using the Cheng-Prusoff equation (valid when Hill Slope is near unity):

$$K_i = IC_{50} / [1 + ([L]/K_D)]$$

where

- $K_i$  is the equilibrium dissociation constant for the unlabeled compound
- $IC_{50}$  is the concentration causing 50% inhibition of binding
- [L] is the concentration of radioligand
- $K_D$  is the equilibrium dissociation constant for the radioligand
- Further calculation details on the Cheng-Prusoff equation can be found in Data Standardization for Results Management.

A representative heterologous competition curve is similar to the one shown in the homologous competition section.

Several assumptions, based on specific criteria, are made to allow calculations using the Cheng-Prusoff equation to be reliable:

1. Law of Mass Action applied (10-90% of displacement occurs over 81-fold concentration range)
2. A single class of receptor binding sites
3. No ligand depletion
4. Receptor concentration  $< K_d$
5. Assay is at equilibrium or steady state
6. The concentration of the added inhibitor is equal to the free concentration of the inhibitor

For special cases associated with high affinity compounds, where ligand depletion must be accounted for; see the section on High Affinity Competitors.

## Pharmacological Profile

A pharmacological profile is a heterologous competition testing several unlabeled compounds simultaneously. The  $K_i$  for each compound can be computed and compared to each other. A rank affinity can also be calculated. The data below demonstrates a typical pharmacological profile with representative  $IC_{50}$ ,  $K_i$  and rank affinity data shown in Table 9.

Notice that different concentration ranges may be required for each drug to fully define top and bottom portions of the curves (Figure 14).

The  $IC_{50}$  is determined from experimental data, the  $K_i$  is calculated using the Cheng-Prusoff equation and the Relative Affinity is relative to a particular compound of interest (Drug 1 in this example).

$$L = 0.025$$

$$K_d = 0.025$$

$$\text{Relative Affinity} = IC_{50} \text{ for Drug 1} / IC_{50} \text{ for Drug}$$

A control compound is tested on each plate and can be used for determination of the relative affinity. This process aids in analyzing the statistical significance of differences between the individual compounds.

## Filtration Assays

### Concept

Filter assays differ from SPA because a separation of free radioligand and radioligand bound to the receptor is required for measurement. However, many of the assay development and optimization steps are the same. Specific information to the filter assay

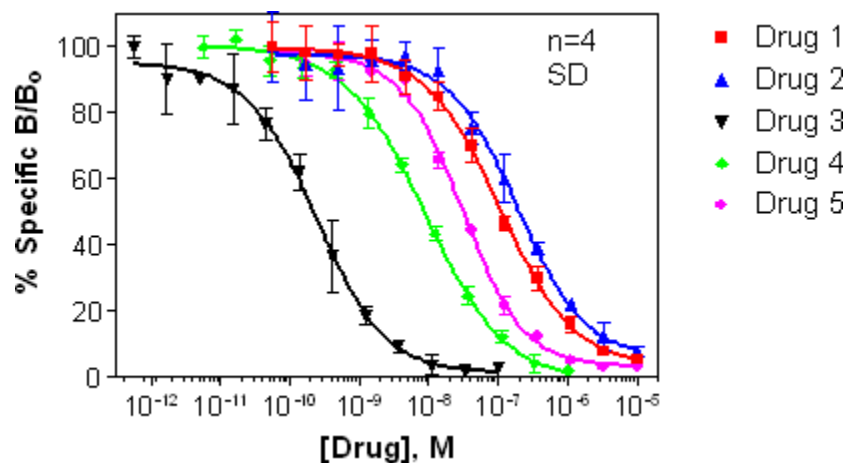


**Figure 14:** Example concentration curves for 5 drugs, calculated using the data in Table 9.

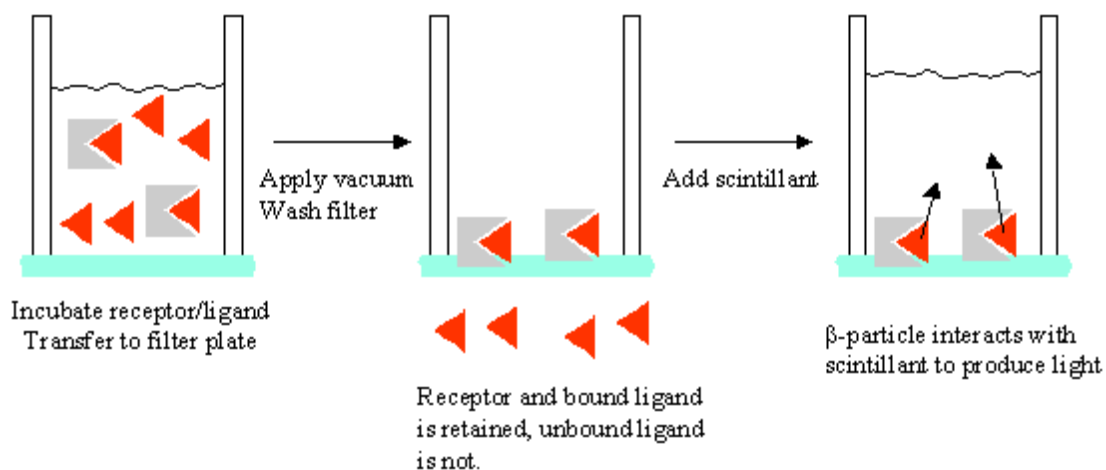


**Figure 15:** Diagram for a standard filtration assay

format is included in this section, and reference back to the text under the SPA section is made when there is no significant difference between the two formats (Figure 15).

General Steps for a filtration assay:

1. Add and incubate test compound, radioligand and receptor in a plate (this can be a separate plate or if validated, the filtration plate directly)
2. Apply vacuum to "trap" receptor and bound radioligand onto filter and remove unbound radioligand. Wash several times with an appropriate buffer to minimize nonspecific binding.
3. Allow filters to dry. Add liquid scintillation cocktail or other scintillant (i.e. solid Meltilex).
4. Count filters in microplate scintillation counter. Some time between adding the scintillant and counting may be required.

| Advantages  | Disadvantages  |
|---|--|
| Less color quenching<br>Traditional, trusted method<br>Higher efficiency than SPA<br>Kinetic experiments easier<br>Association/Dissociation | Separation method (dissociation of ligand)<br>Generated large volumes of liquid waste<br>Variable vacuum across plate<br>Nonspecific binding to filters<br>Accumulation of radioactivity on unit<br>Requires more handling steps |

## Filter Assay Format

### Exposure Time to Scintillant

#### Filter Type

The most commonly used filters for receptor binding are listed below:

- GF/B - glass fiber filters with 1.0  $\mu\text{M}$  pore size
- GF/C - glass fiber filters with 1.2  $\mu\text{M}$  pore size
- Durapore - PVDF filters with various pore sizes such as 0.22, 0.65, 1.0  $\mu\text{M}$ .

Depending on the radioligand, receptor and other assay factors, it may be necessary to perform experiments with more than one type of filter to determine the best one for the system under investigation (Table 10).

The speed of separation is important, particularly for lower affinity interactions ( $<1$  nM), and can be influenced by the filter plate type. Dissociation of bound radioligand from a receptor interaction with an affinity of 1 nM can occur in under 2 min. Lower affinity interactions can dissociate even quicker, when the separation process disrupts equilibrium.

**Table 10: Summary of plate types that can be used for filter assays.**

| Plate Type                       | Harvester Instrument       | Counting Instrument | Comments  |
|----------------------------------|----------------------------|---------------------|---|
| Unifilter GF/C or GF/B           | Packard or Brandel         | Trilux or TopCount  | Filter from an assay plate to the filter plate with washing of the assay plate possible   |
| Multiscreen-FC or Multiscreen-FB | MAP or individual manifold | Trilux or TopCount  | Removable bottom plastic piece. Requires solid white adapter for TopCount or clear plastic liner and cassette for Trilux                            |
| Multiscreen-GV                   | MAP or individual manifold | Trilux or TopCount  | 0.22 µm Durapore membrane. Removable bottom plastic piece. Requires solid white adapter for TopCount or clear plastic liner and cassette for Trilux |

## Order of Addition

The order of addition for reagents may affect assay performance as well as ease of automation. A standard format for order of reagent addition in a filtration method is as follows:

1. Test compound
2. Radioligand
3. Receptor

Experiments may be required to determine the optimum order of addition and if there is any effect by locally high concentrations of DMSO present during the initial additions into the wells.

## Non-Specific Binding

Radioligands may bind nonspecifically to components of the assay system such as tubes, pipette tips, assay plates or filters. This may lead to ligand depletion and certain binding assumptions may not be met. To test for nonspecific binding, perform an experiment in the absence of membranes. The amount of activity added can be tracked at each step of the assay to determine where any losses or nonspecific binding is occurring.

Some potential solutions to minimize nonspecific binding include the following:

- Pretreatment of tubes (siliconization)
- Additions to assay buffers (see Table 2)
- Different filter plate manufacturers (Perkin Elmer, Millipore, Brandel, Polyfiltronics, etc.)



- Different filter plate types (GF/C, GF/B, Durapore, etc.)

Since there may be non-receptor binding (to system components as described above), the use of an unlabeled ligand at a 100-fold excess may not be adequate to fully define all of the nonspecific binding.

## Temperature

See SPA section on Temperature.

The filtration format can accommodate temperatures other than room temperature easier than the SPA format. The receptor, ligand and/or compound can be incubated at the desired temperature and then filtered to capture bound radioactivity. Since the filtration process is rapid, there is not a significant temperature drop during the separation time. Once the scintillant is added, the filter plates can be counted in the microplate scintillation counter at room temperature.

## Plate Treatment Conditions

Filter plates are usually pre-wetted to ensure even distribution of the receptor/ligand reagents. If there is no ligand sticking problems, the pre-wet can be accomplished with wash buffer.

Pretreatment of filters with polyethylimine (PEI) is a common practice to minimize ligand binding to filters:

1. Presoak 30 to 60 min in 0.1% to 0.5% PEI (in water)
2. Treat at 4°C to minimize filter degradation
3. Filter away PEI, then wash with ice-cold buffer prior to filtration of receptor sample

Pretreatment with carrier proteins, serum, or detergents has also been used to minimize binding of ligands to filter plates.

**Note of Caution:** Millipore Multiscreen glass fiber filter plates have a 0.65 mm Durapore support membrane under the GF filter. Some treatments (including PEI) may change or compromise the stability of this support membrane. Appropriate experiments should be designed to test for stability when using these types of plates.

## Vacuum Pressure

The vacuum pressure used for filtration binding assays is a balance between having enough pressure to filter the samples rapidly and prevent ligand dissociation and having too much pressure which can affect filter integrity or the level of membranes retained on the filter. The pressure to be used should be determined experimentally, with a starting guideline of 5 to 10 mm Hg. If necessary, install an appropriate regulator to control consistent vacuum pressure.

## Wash Buffer

Several washes of the filters are required to remove as much unbound radioligand as possible and to maximize specific binding. Generally, an ice-cold buffer is used to prevent or reduce dissociation of bound radioligand from the receptor.

## Filter Plate Drying Time

If filters are not completely dry prior to the addition of liquid scintillant, the residual water present in the filters can interact with the scintillant to reduce counting efficiency. Dry filters require less liquid scintillant to achieve maximum signal than wetted filters. Drying filters completely may not be practical for medium or high throughput screening applications.

## Type and Volume of Scintillant

The type of microplate scintillation counter being used may dictate the type of scintillant required for proper counting conditions.

TopCount - must use a "slow" scintillator such as Microscint-20 or Microscint-40

Trilux - can use virtually any scintillant designed for microplate scintillation counting (Microscint-20/Microscint-40, Optiphase Supermix, Meltilex)

Regular liquid scintillation cocktail such as Ready Pro should not be used, as a rule, for microplate scintillation counting as their load capacities may not be adequate and they may not be compatible with microplate plastics.

General volumes of liquid scintillant used are in the range of 40 to 150  $\mu\text{l}$ . As mentioned above, the volume of scintillant used may depend on the dryness of the filters.

## Exposure Time to Scintillant

With filter plates, some of the radioligand may be embedded within the filter and require some time to become accessible to the liquid scintillant for photon generation and signal detection. Therefore, an incubation time may be required following the addition of liquid scintillant and prior to counting. In addition to increasing the maximum signal, the variability of the signal may be reduced following an incubation time as demonstrated in the figure on the following page.

When processing large numbers of plates, it is important that a stable counting signal has been reached, so that all plates from the first counted to the last counted, are comparable.

Over time, more radioactive particles will be removed from the filter and make contact with the liquid scintillant in the well. As the data in Figure 16 shows, this can improve signal strength and decrease variability.

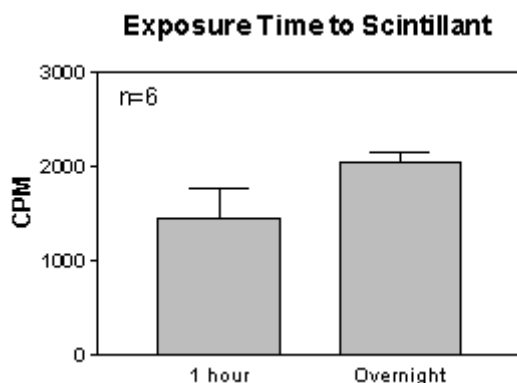


**Figure 16:** Exposure time to scintillant.

## Assay Buffer (Filter)

See the Assay Buffer section in the SPA part of this chapter. Many of the buffer additives and reagents described for the SPA format are relevant for receptor binding assays in a filtration format.

## Assay Conditions (Filter)

### Incubation Time - Signal Stability

**Setup:** Measure total binding (receptor + radioligand) and nonspecific binding (receptor + radioligand + excess unlabeled competitor) at various times.

At least two methods could be used to obtain the association/dissociation data. Both methods should yield the same result. If not, there may be a problem with receptor stability.

**Method 1:** Add and mix together enough receptor and radioligand for all time points in the experiment. At various times, filter an aliquot of the receptor/radioligand mixture and wash the filters with Wash Buffer. The last aliquots to be filtered will be the longest incubation time points.

**Method 2:** Prepare receptor and radioligand separately. At various time points, combine the two in the microplate. After all points have been added, filter the reactions at the same time. The last wells to be mixed will be the shortest incubation times.

Dissociation, which can be measured more conveniently using the filtration format than SPA, is performed by adding an excess amount of unlabeled competitor after a receptor/radioligand mixture has reached steady state (plateau on the association curve, Figure 17)

**Results Analysis:** Plot specific binding (total binding - nonspecific binding) versus time. Fit the association data to a one-phase exponential association curve and the dissociation

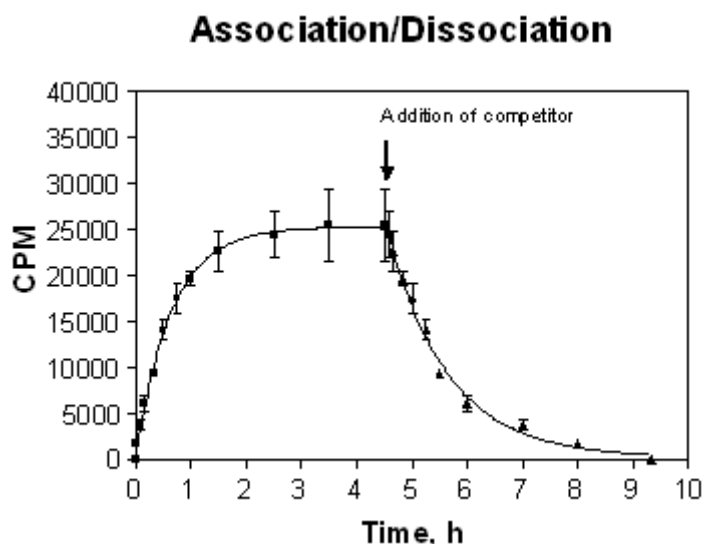


**Figure 17:** Association/dissociation experiment (total binding only shown).

data to a one-phase exponential decay curve. In the example above, a minimum reaction time of 2.5 hours would be adequate.

In addition to determination of the appropriate primary incubation time for steady state, a kinetic estimate for the equilibrium dissociation constant,  $K_d$ , can be made from the results of an association/dissociation experiment.

Association Experiment:

- Obtain  $k_{obs}$ , expressed in  $\text{min}^{-1}$ , from the nonlinear regression analysis of data

Dissociation Experiment:

- Obtain  $k_{off}$ , expressed in  $\text{min}^{-1}$ , from the nonlinear regression analysis of data

Calculate association rate constant,  $k_{on}$  (in  $\text{Molar}^{-1} \text{min}^{-1}$ )

$$k_{on} = \frac{k_{obs} - k_{off}}{[\text{radioligand}]}$$

Calculate equilibrium dissociation constant,  $K_d$  (in Molar):

$$K_d = k_{off}/k_{on}$$

## Receptor Concentration - Zone A

**Setup:** Measure total binding (receptor + radioligand) and nonspecific binding (receptor + radioligand + excess unlabeled competitor) at various levels of added receptor.

**Results Analysis:** Plot total, NSB and specific binding (total - NSB) versus receptor amount. Plot total bound/total added expressed as a percent versus receptor

concentration. Determine the level of receptor that yields <10% total binding/total added (Zone A).

See the Receptor Concentration - Zone A section in the SPA part of this document for further details and an example.

## Solvent Tolerance

**Setup:** Measure total binding (receptor + radioligand) and nonspecific binding (receptor + radioligand + excess unlabeled competitor) at various concentrations of DMSO (or other solvent) using the determined optimum incubation time and optimum receptor concentration.

**Results Analysis:** Plot total and NSB versus final concentration of solvent

See the **Solvent Tolerance** section in the SPA part of this document for further details and an example.

## Binding Parameters (Filter)

*Saturation Binding:* See the Saturation Binding section in the SPA part of this document for further details and an example.

*Homologous Competition:* See the Homologous Competition section in the SPA part of this document for further details and an example.

*Association Rate at Various Radioligand Concentrations (Optional):* See the Association Rate at Various Radioligand Concentrations (Optional) section in the SPA part of this chapter for further details and an example.

*Heterologous Competition:* See the Heterologous Competition section in the SPA part of this chapter for further details and an example.

*Pharmacological Profile:* See the Pharmacological Profile section in the SPA part of this chapter for further details and an example.

## High Affinity Competitors

For high affinity competitors, the assumption related to inhibitor depletion may not be met and an alternative analysis method can be used.

When the assay is designed properly, ligand depletion should not be a problem. However, once competitors reach an activity 2 to 3 fold lower than the ligand, inhibitor depletion can be an issue. Assuming that the hill slope for these compounds is near 1, the  $K_i$  computed using the Cheng-Prusoff equation could be compared to the  $K_i$  found by fitting the tightly bound inhibitor model below.

$$a = K_d \left( 1 + \frac{K_d}{[L]} \right)$$

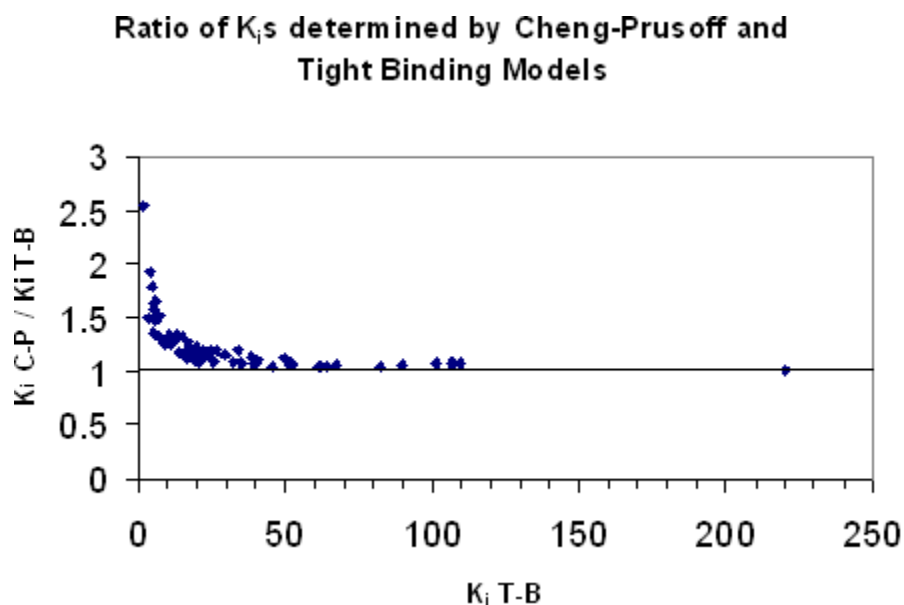


**Figure 18:** Radioligand binding results from an assay with  $K_d \approx 100$  and ligand concentration of 4 nM.

$$b = \left( [I]_t K_d + K_i [L] \left( 1 + \frac{K_d}{[L]} \right) - K_d [R]_t \right)$$

$$c = - [R]_t [L] K_i$$

$$[RL] = \frac{-b + \sqrt{b^2 - 4ac}}{2a}$$

The ligand concentration  $[L]$  and the  $K_d$  are exactly those that would be used in the Cheng-Prusoff equation. The inhibitor concentration,  $[I]_t$ , is the concentration tested. The  $K_i$  and receptor concentration  $[R]_t$  are obtained by fitting the model. In order to use this model, the response determined by the plate reader, which measures the amount of receptor ligand complex  $[RL]$ , must be converted to the same concentration units that are used for the ligand  $[L]$  and inhibitor  $[I]_t$ . This requires the specific activity of the label and a plate reader that is calibrated well.

Even though the Tight Binding (T-B) model looks much more complex than the sigmoid curve model or the one site competition model in GraphPad Prism, both the fitted curve and the  $K_i$  are virtually identical unless a substantial portion of the inhibitor is bound (Figure 18). The ratio of the  $K_i$  determined by Cheng-Prusoff to the  $K_i$  determined using the T-B model is plotted against the  $K_i$  determined by the T-B model. Inhibitor depletion will always result in understating the true potency of the molecule. Hence, the ratios are always greater than one. Also, the  $K_i$  values are virtually identical unless the  $K_i$  is much lower than the  $K_d$ .

## Hill Slope Deviations

A standard competitive binding curve that follows the law of mass action will descend from 90% specific binding to 10% specific binding over an 81-fold range of unlabeled

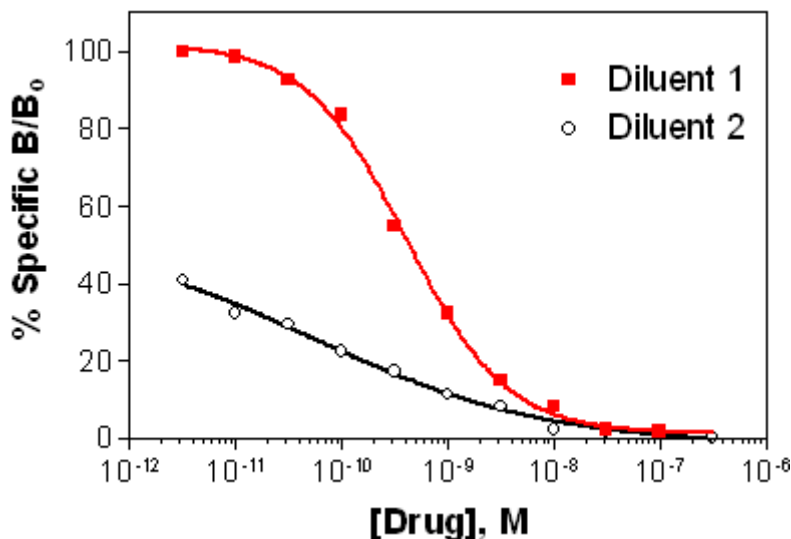


**Figure 19:** Example of a Hill slope plot for the same compound tested in two diluents.

drug concentrations. The steepness of the competition curve is given by a slope factor, called the Hill slope. This parameter is determined from a nonlinear regression analysis of the competition data when using a four-parameter logistic equation. A standard competition curve (plotted with percent bound) that meets all assumptions would have a Hill slope of -1.0. If the slope factor deviates from -1.0 significantly, then the binding may not follow the law of mass action and you may be dealing with a receptor that has more than a single class of binding sites, solubility issues or an assay artifact.

There is no adequate way to interpret the absolute value of the Hill Slope. However, there are several possible explanations when a competition curve has a calculated Hill Slope that is significantly less than 1 (shallow curve):

1. Experimental problems such as improper serial dilution of the compound
2. Curve fitting problems due to undefined top and bottom plateaus or too few data points
3. Negative cooperativity - binding on one ligand molecule reduces affinity of other binding sites
4. Heterogeneous receptors - different populations of receptors with different affinities
5. Assay variability

Although the Hill slope for a compound may not be -1.0, repetitive determinations for the same compound should yield similar Hill slopes each time. If this is not the case, further optimization of the receptor binding assay may be required.

Some compounds being tested may not be soluble in the standard solvent, DMSO. In addition, compounds at high concentrations may not be soluble. Both of these cases can affect the shape of competition curves (i.e. Hill slope, top or bottom plateau, etc.) and the

calculated parameters. Therefore, it is important to review each competition curve for the following features:

- Specific binding descends from 90% to 10% over an 81-fold concentration range
- The Hill slope is at or near -1.00
- Top and bottom plateaus have been appropriately defined
- Data points are evenly spaced along the entire range of concentrations tested

Figure 19 demonstrates a compound tested in Diluent 1 and Diluent 2. In Diluent 2, the compound appears to have limited solubility and exhibits a very shallow Hill slope and poorly defined top and bottom plateaus. In Diluent 1, the compound competes with the radioligand in the expected manner.

## Practical Use of Fluorescence Polarization in Competitive Receptor Binding Assays

### Principles of Fluorescence Polarization

Fluorescence polarization (FP) measurements have become a popular assay format for receptor binding assays. The principle of this assay is illustrated in Figure 20 and its design and implementation are also covered in Inhibition of Protein-Protein Interactions: Non-Cellular Assay Formats.

A fluorophore whose absorption vector is aligned with polarized excitation light is selectively excited. If the fluorophore tumbles rapidly relative to its fluorescent lifetime then it will be randomly orientated prior to light emission and therefore will show a low polarization value (situation A above). However, if this fluorophore's rotation is slowed down so that it tumbles slowly with respect to the fluorescent lifetime (e.g. by binding to a large receptor as shown in B above) it will not rotate much before light emission and will show a high polarization value (Figure 21).

Typical fluorophores include fluorescein- or BODIPY-labels that have fluorescence lifetimes allowing FP measurements to be made between a small labeled-ligand (<1500 Da) and a large receptor (e.g. > 10,000 Da).

The increase in polarization can be measured with several microplate readers where the fluorescence is measured using polarized excitation and emission filters. Two measurements are performed on every well. Data is obtained for the fluorescence perpendicular to the excitation plane (the "P-channel") and fluorescence that is parallel to the excitation plane (the "S-channel"). For screening applications, the millipolarization units (mP) are often calculated using:

$$mP = \left[ \frac{(S - P \times G)}{S + P \times G} \right] \times 1000$$

The proper use of S and P channel data requires two corrections. First, accurate calculation of polarization using fluorescent readers requires calculation of the instrument



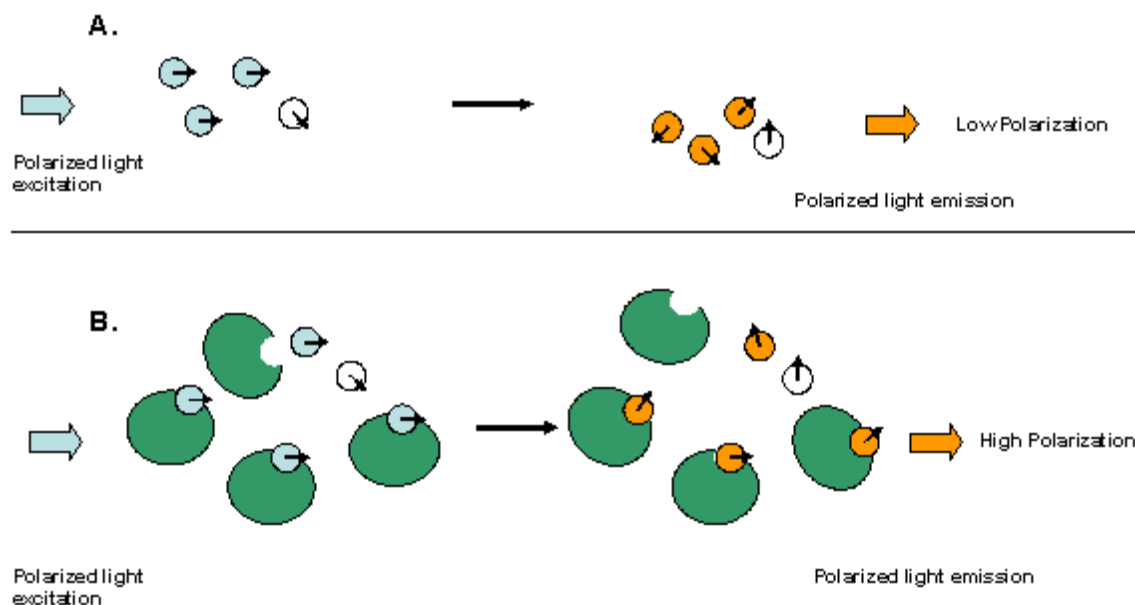


**Figure 20:** Principle of fluorescence polarization assay.

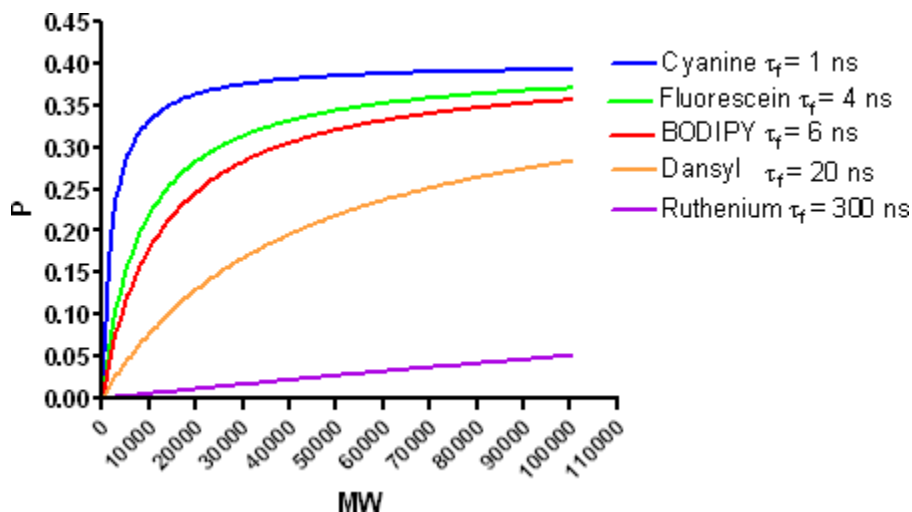


**Figure 21:** The dependence of polarization on fluorescent life-time is shown below. The graph contains simulated data using the Perrin equation (1) and taking the limiting polarization as 0.5 using  $T = 293\text{ K}$  and assuming a spherical protein in water with the fluorescence probe rigidly attached.

“G-factor”. This factor corrects for any bias toward the P channel. For microplate readers, a 1 nM fluorescein solution is typically used and the G-factor that yields a value of 27 mP is entered (27 mP is the known value for a 1 nM fluorescein solution at RT). Secondly, the S and P values should have the background fluorescence subtracted (determined using assay buffer without labeled-ligand in the well).

## Fluorescence Polarization and Receptor Binding

Receptor-binding FP assays use a small molecule labeled ligand (so called tracer) and a large unlabeled receptor. An example is a fluorescently labeled-steroidal ligand binding to a nuclear receptor-ligand binding domain (kits of this type are sold by Invitrogen/PanVera). This type of assay typically yields a minimum signal of approximately 50 mP for the unbound tracer and a maximum signal of approximately 300 mP when the tracer is fully bound to the receptor.

### Validate Activity of Fluorescent Tracer

The receptor binding activity of a fluorescent-labeled tracer can be determined in a competition assay using a radiolabeled ligand and traditional methods of receptor binding (filtration, SPA, charcoal precipitation, etc.). As shown in Figure 22, some loss of receptor binding activity may occur following fluorescent tagging. It is important to identify lower binding activity prior to further experiments with the fluorescent tracer. Functional receptor assays, such as cAMP measurement, calcium mobilization or GTP $\gamma$ S binding, can also be performed to determine if there has been a loss in biological activity as a result of the labeling process.

### Choosing Tracer and Receptor Concentrations

The  $K_D$  of the tracer and the amount of tracer bound under the chosen assay conditions will be required for analysis of competitive binding parameters. Typically, the  $K_D$  can be estimated using radioligand-binding techniques (SPA, filtration) discussed in previous sections, provided there is not significant deviation in the potency of the tracer and the unlabeled molecule (see figure above). It may be useful to perform a tracer calibration curve by varying the amount of tracer and ensuring that the polarization signal is constant over a reasonable concentration range, inclusive of the estimated  $K_D$ . By definition, the polarization signal is independent of the intensity of the tracer. This also identifies the variability at the tracer concentration to be used (Figure 23).

The amount of bound tracer can be measured in an experiment where the tracer is held at a constant concentration near its  $K_D$  and the receptor concentration is then varied. An example of this type of experiment using the glucocorticoid receptor (GR) included in the FP kit available from Invitrogen/PanVera is shown in Figure 24.

In these types of FP experiments no correction for nonspecific binding (NSB) is performed as was shown in earlier sections for radioligand-binding experiments. This is because the tracer (what is the radioactive ligand concentration in traditional assays) is held constant at a concentration usually near the  $K_D$  and the protein receptor concentration is then varied over several orders of magnitude. However, this assumption should be checked by observing the polarization of the ligand in the absence of receptor. (Caution: it is possible to observe increasing FP signals when membrane receptors are used due to light scattering. In those cases, a correction may need to be made by measuring the signal in the presence and absence of the fluorescent tracer). If binding to

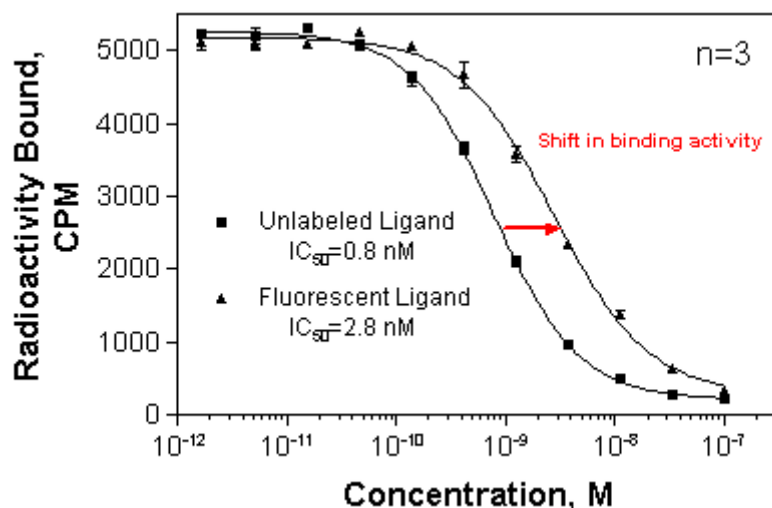


Figure 22: Example of the loss of receptor binding activity following fluorescent tagging.

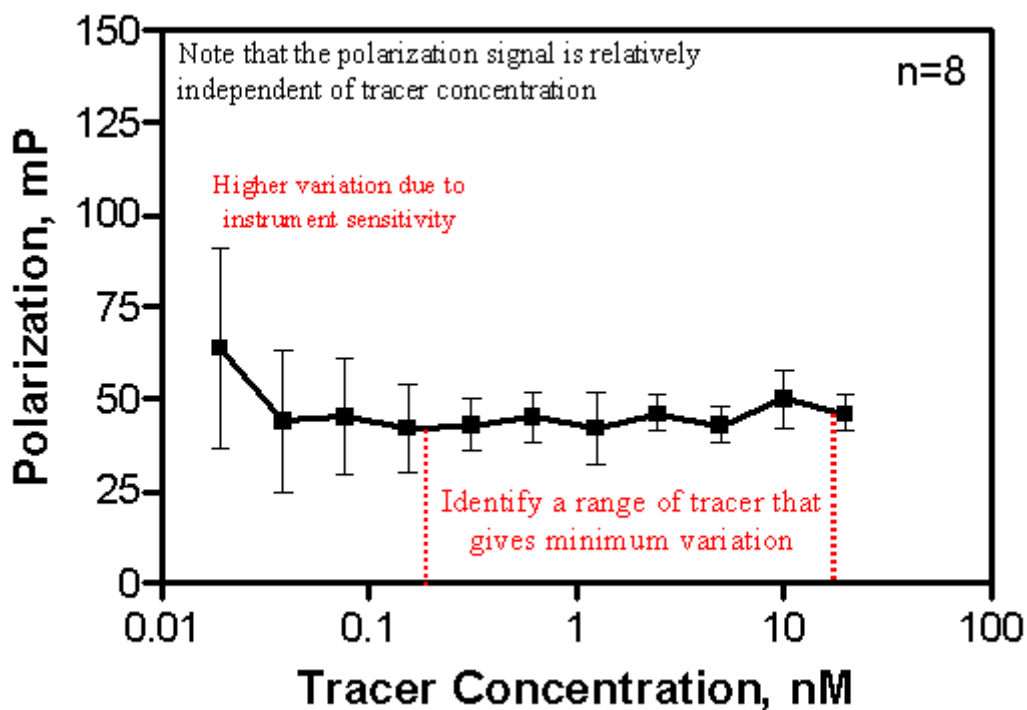
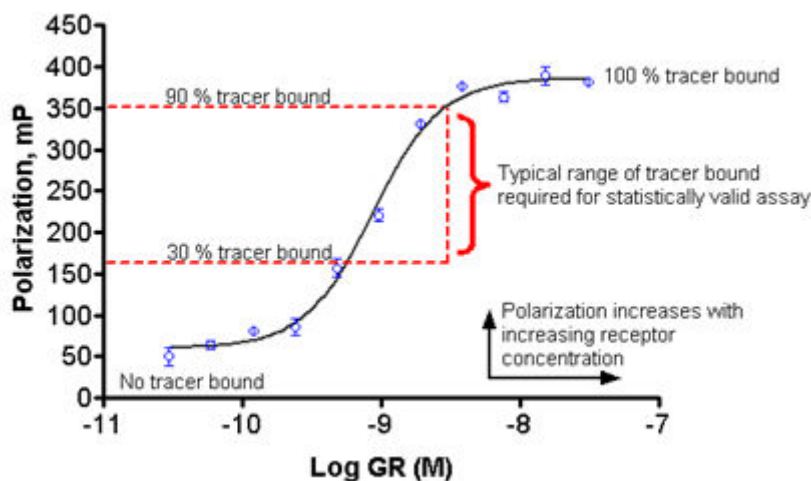


Figure 23: The polarization signal as a function of tracer concentration is shown for a representative tracer. Note that as the signal nears the limits of sensitivity for the detector, the variation increases.

non-specific buffer components or microtiter plates surfaces is observed then this tracer should be avoided. An analytical treatment of FP competitive-binding data has recently



**Figure 24:** Measuring amount of bound tracer by varying receptor concentration and keeping tracer concentration constant. Here the ligand-binding domain of GR is varied using a constant  $K_d$  concentration of a labeled-steroidal ligand (Fluormone™, Invitrogen/Panvera kits; Data provided by Pharmacopeia).

been presented by Roehrl et al. (2) that allows one to quantify the effect of non-specific binding on FP titration curves.

Examination of the curve above allows one to choose a receptor concentration that yields an acceptable assay window (typically a  $\Delta$ mP of between 150 mP and 300 mP).

## Pharmacological Profile

Sensitivity to known competitors should be checked at this stage to ensure that the developed FP assay is adequate for the intended purpose (Figure 25).

## Ligand Depletion

The FP assay format is homogenous in nature and therefore lends itself to simple “mix and read” protocols. However, to obtain an acceptable signal, the assay must be set-up with a large fraction of the tracer bound to the receptor (typically >80%). The high amount of bound tracer requires a specific set of equations to be used when interpreting FP derived competition binding results.

In these cases, where a large amount of bound tracer exists, the Cheng-Prusoff equation as mentioned in the discussion of heterologous competition-receptor binding will always lead to an overestimation of the  $K_i$  from the  $IC_{50}$ . This is because the Cheng-Prusoff equation is strictly given as:

$$K_i = \frac{IC_{50}}{1 + L_f/K_d}$$

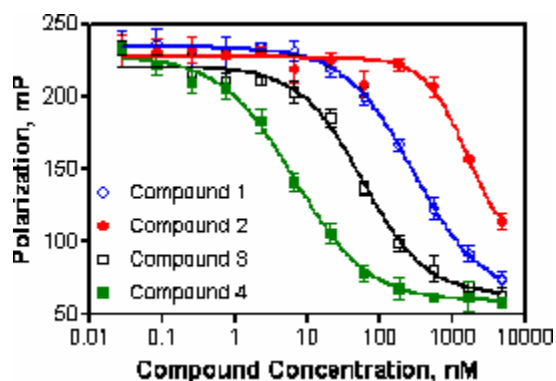


Figure 25: Example pharmacological profile using fluorescence polarization.

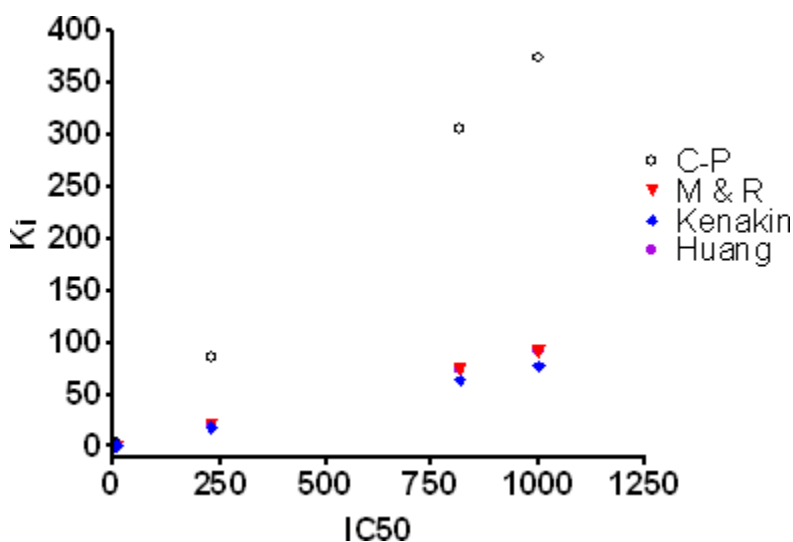


Figure 26: Graphical representation of data in Table 12.

In the case of FP displacement-binding, the free ligand term  $[L_f]$  cannot be substituted for the total ligand concentration  $[L]$  because there is little free ligand available. This differs from the typical saturation-binding experiments mentioned in previous sections.

Three equations have been presented in the literature to provide a solution to this situation for simple competitive-binding. Munson and Rodbard (3) provide a correction that takes into account the amount of bound tracer. This takes the form of:

$$K_i = \frac{IC_{50}}{1 + \frac{L_0(y_0 + 2)}{[2K_d(y_0 + 1)] + y_0}} - K_d[y_0/(y_0 + 2)]$$

Where  $y_0$  is the bound/free ratio of tracer and  $L_0$  is the total tracer concentration.

Huang provides an alternative form of this correction in terms of the fraction of bound tracer (4). Rearrangement of Equation 15 given in Huang to solve for  $K_i$  yields:

$$K_i = \frac{IC_{50}}{\frac{1}{(1-F_0)} + L_0(2-F_0)/2K_d} - K_d[F_0/(2-F_0)]$$

Where  $F_0$  is the fraction of tracer bound and  $L_0$  is the total tracer concentration. Huang's result is redundant with the earlier Munson and Rodbard equation except for expressing the equation in terms of the fraction of tracer bound (3,4). Therefore, Eq. 2 and Eq 3 yield the same correction (see below).

These equations should be used instead of Cheng-Prusoff when > 10% of the tracer is bound to the receptor in the assay. A web-based tool to convert  $IC_{50}$  values to  $K_i$  values in fluorescence-based competitive assays is also available [here](#).

Application of ligand depletion equations once a suitable choice of receptor and tracer concentrations have been made and the resulting assay has been shown to be useful for competitive binding analysis, one can calculate the amount of bound tracer under the assay conditions taking the lower and upper asymptotes as values for free and bound tracer respectively.

Some example competition-binding data (Fluormone™ kit, Invitrogen/Panvera) are shown in Table 11 to illustrate the differences between using the Cheng-Prusoff equation without correction for the amount of bound tracer or each of the above equations which correct for tracer depletion. For these competition-binding experimental results the conditions were:

- Equilibrium dissociation constant,  $K_D = 0.6$  nM (Fluormone™ ligand), determined using
- Bound Tracer Concentration,  $L_b = 0.9$  nM, determined from receptor concentration experiment at constant tracer ( $L_0$ ), by reading the mP signal and determining the % of maximum
- Total Tracer Concentration,  $L_0 = 1$  nM, concentration set near the  $K_d$  value
- Total Receptor Concentration,  $R_0 = 4$  nM (GR ligand-binding domain), determined from receptor concentration experiment at constant tracer – yields statistically valid assay with robust signal

These concentrations yield the following terms required for Equations 2-4:

- Bound/Free ratio of Tracer,  $y_0 = L_b/(L_0 - L_b) = 0.9/(1-0.9) = 9$
- Fraction of Tracer Bound,  $F_0 = L_b/L_0 = 0.9/1 = 0.9$

A graphical representation of the data is shown in Figure 26.

Application of Cheng-Prusoff under these conditions can lead to more than 10-fold overestimations of  $K_i$ . In many cases all three equations yield similar corrections and as mentioned above Munson & Rodbard and Huang yield identical values (3,4). However,

one issue with the Munson & Rodbard and Huang type corrections is that certain combinations of  $IC_{50}$ ,  $K_D$  and bound tracer yield impractical negative values of  $K_i$ . This has been discussed in the literature as a breakdown in additional assumptions buried within these equations such as competitive inhibition with a single binding site. For this reason, the Kenakin equation is commonly chosen for performing this correction. Additionally, curve fitting to the equations given in Roehrl et al. (5) can be used to examine if complete inhibition is achieved as well as the  $K_D$  of the competitor compound.

**Table 11:** Comparison of  $K_i$  values determined from ligand depletion correction formulas. Values are in nM.  $IC_{50}$  shown is the measured  $IC_{50}$  under the assay conditions described in the text. All other values are calculated values. Data provided by Pharmacopeia.

| Ligand        | $IC_{50}$ | (1) $K_i$ , nM |                |       |         |
|---------------|-----------|----------------|----------------|-------|---------|
|               |           | Cheng-Prusoff  | Munson-Rodbard | Huang | Kenakin |
| Cortisone     | 8.0       | 3.0            | 0.24           | 0.24  | 0.6     |
| Dexamethasone | 3.6       | 1.3            | -0.16          | -0.16 | 0.3     |
| Estradiol     | 815       | 306            | 74             | 74    | 63      |
| Testosterone  | 229       | 86             | 20             | 20    | 18      |
| Compound 1    | 6.4       | 2.4            | 0.09           | 0.09  | 0.5     |
| Compound 2    | 1000      | 375            | 91             | 91    | 77      |

## Detection of Fluorescence Interference from Compounds in FP Screens

All FP experiments start with measuring polarized prompt fluorescence from the assay well. This makes these experiments susceptible to fluorescence interference by compounds present in the well. However, a helpful method to address this issue has been presented by Turconi et al. (6). This paper calculates the total fluorescence intensity from a well (given by  $S + 2P$ ; see references in above paper) and the observed anisotropy [1] from the each well to flag false positive wells due to fluorescence interference. Figure 27 illustrates the use of this method.

Three cases are illustrated in Figure 27. In case A, the compounds in the wells are not active or fluorescent. Therefore the measured Fluormone tracer is bound to GR ligand-binding domain (GR-LBD) and the anisotropy values are clustered around the 0% inhibition value. Furthermore, there is no change in fluorescence intensity in the compound-containing wells relative to the control wells. In case B, the compounds in the well are active in the assay but not fluorescent. Therefore, the tracer is being displaced from the GR-LBD and the anisotropy values distribute from high to low inhibition values. Again, there is no change in the total fluorescence intensity. In case C, the compounds appear active as they show a decrease in anisotropy values suggesting that the tracer has been displaced from the GR-LBD. However there is a correlation between decreasing anisotropy and increasing fluorescence intensity in the wells with the lowest anisotropy values showing more than a 35-fold increase in the fluorescent intensity relative to control

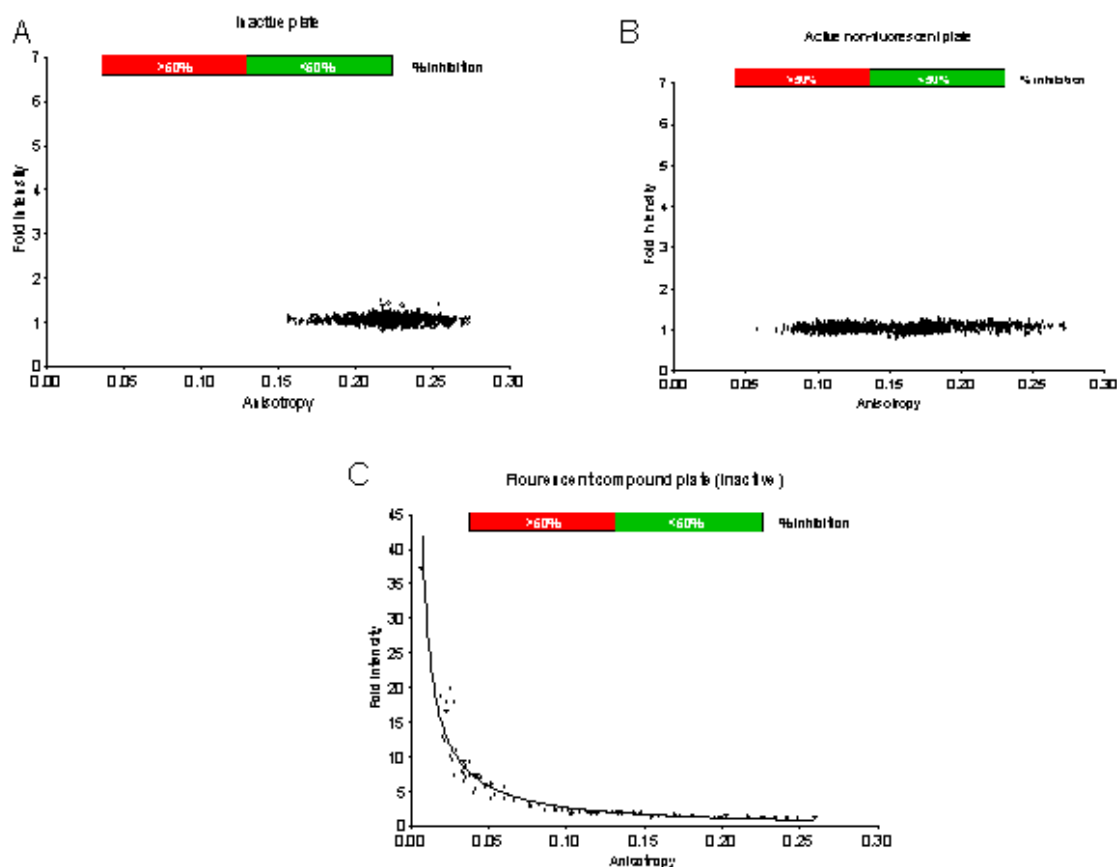


**Figure 27:** Plots of the total fluorescence intensity (normalized to the control well values, e.g. the total fluorescence intensity of the assay in the absence of compounds) versus the anisotropy. A) the compounds in the wells are not active or fluorescent. B) the compounds in the well are active in the assay but not fluorescent. C) the compounds appear active as they show a decrease in anisotropy values.

values. This suggests that the measured FP is due to the compounds themselves rather than the tracer.

In typical FP-receptor binding experiments the tracer is kept at a low nM concentration while the compounds that are being screened are typically in the  $\mu\text{M}$  range. If these compounds are fluorescent at the detection wavelengths then their fluorescence can easily overcome that of the tracer. As compounds in screening campaigns are typically of low molecular weight (<500 Da) they will exhibit low anisotropy values. Compounds in case C was of this type and subsequent secondary assays showed them to be inactive. A final case not shown above is where the compounds are both fluorescent and active. Turconi et al. present an equation that can be used to fit the fluorescent intensity data to the case where anisotropy changes without displacement of the ligand (6). The solid line in case C above shows an example of this fit. One can then evaluate outliers from this curve fit in terms of potential active but fluorescent compounds.



It is also possible to observe changes in polarization that are due to fluorescent compounds present as aggregates. In this case, the fluorescence intensity will increase along with the polarization as long as the aggregation does not quench the fluorescence. Additionally, light scattering from particulates or compound particulates can lead to apparently high polarization values. For receptor binding experiments as described above this superfluous increase in polarization may mask any decrease in polarization due to an active compound and thus result in a false negative. Careful examination of the fluorescence intensity versus polarization plots should identify these artifacts.

- 1 Anisotropy is derived by measuring the S and P channels as described above, however the fluorescence is expressed with the denominator representing the total fluorescence intensity from the sample. The equation for calculating anisotropy is given by:

$$a = \frac{(P - S)}{(S + 2P)}$$

Anisotropy and polarization are related by the equations given below where P is the polarization and a is the anisotropy:

$$P = \frac{(3a)}{(2 + a)} \text{ AND } a = \frac{2P}{(3 - P)}$$

In general, anisotropy is more useful analyzing complex systems or mixtures as the equations are simpler to express in terms of anisotropy (1). Arguably, screening data should be presented in terms of anisotropy rather than polarization but this convention has not been adopted as yet.

- [L] - Radioligand Concentration
- [R] - Receptor Concentration
- [RL] - Concentration of Receptor-Ligand complex
- $K_d$  - equilibrium dissociation constant for radioligand ([RL] yielding  $B_{max}/2$ )
- $K_i$  - equilibrium dissociation constant for an unlabeled compound
- $IC_{50}$  - concentration of unlabeled drug which results in 50% inhibition of binding activity
- $k_{on}$  - association rate constant
- $k_{off}$  - dissociation rate constant
- $k_{obs}$  - observed association rate constant
- $B_{max}$  - maximum number of binding sites
- NPE - Non-proximity Effects
- NSB - Nonspecific binding
- $K_i$  C-P =  $K_i$  Cheng-Prusoff
- $K_i$  T-B =  $K_i$  Tight-Binding

## References

## Primary References

1. Cantor and Schimmel in *Biophysical Chemistry Part II: Techniques for the study of biological structure and function*. pp. 454-465. (1980).
2. Roehrl MHA, Wang JY, Wagner G. A General Framework for Development and Data Analysis of Competitive High-Throughput Screens for Small-Molecule Inhibitors of Protein-Protein Interactions by Fluorescence. 2004. *Biochemistry*. 2004;43(51):16056–16066. PubMed PMID: 15610000.
3. Munson PJ, Rodbard D. An exact correction to the “Cheng-Prusoff” correction. *J. Receptor. Res.* 1988.;533–546. PubMed PMID: 3385692.
4. Huang X. Fluorescence polarization competition assay: The range of resolvable inhibitor potency is limited by the affinity of the fluorescent ligand. *J. Biomol. Screening*. 2003;8:34–38. PubMed PMID: 12854996.
5. Roehrl MHA, Wang JY, Wagner G. Discovery of Small-Molecule Inhibitors of the NFAT-Calcineurin Interaction by Competitive High-Throughput Fluorescence Polarization Screening. 2004. *Biochemistry*. 2004;43(51):16067–16075. PubMed PMID: 15610001.
6. Turconi S, Shea K, Ashman S, Fantom K, Earnshaw DL, Bingham RP, Haupts UM, Brown MJB, Pope A. Real experiences of uHTS: A prototypic 1536-well fluorescence anisotropy-based uHTS screen and application of well-level quality control procedures. *J. Biomol. Screening*. 2001;6:275–290. PubMed PMID: 11689128.

## Websites

1. GraphPad Prism (<https://www.graphpad.com/scientific-software/prism/>)
2. Receptor Binding Key Concepts on GraphPad Prism site ([https://www.graphpad.com/guides/prism/7/curve-fitting/index.htm?reg\\_principles\\_of\\_radioligand\\_bind.htm](https://www.graphpad.com/guides/prism/7/curve-fitting/index.htm?reg_principles_of_radioligand_bind.htm))
3. Perkin Elmer SPA Information (<http://www.perkinelmer.com/category/scintillation-proximity-assay-spa>)

## General Receptor Binding: Suggested Reading

Textbook of Receptor Pharmacology. (2003). Second Edition. Foreman, J.C. and Johansen, T., Editors. CRC Press, New York.

Kenakin, T. (1997): *Pharmacologic Analysis of Drug-Receptor Interaction*. Lippincott-Raven Publishers, Philadelphia.

*Receptor Binding Techniques*. (1999). *Methods in Molecular Biology Series*, Volume 106, Keen, M., Editor. Humana Press, New Jersey.

*The Pharmacology of Functional, Biochemical, and Recombinant Receptor Systems*. (2000). *Handbook of Experimental Biology*, Volume 148, Kenakin, T and Angus, J.A., Editors. Springer-Verlag, New York.

*Receptor-Ligand Interactions: A Practical Approach*. (1992). *The Practical Approach Series*. E.C. Hulme, Editor. Oxford University Press, New York.

- Receptor Biochemistry: A Practical Approach. (1990). The Practical Approach Series. E.C. Hulme, Editor. Oxford University Press, New York.
- Motulsky, H.J. Analyzing Data with GraphPad Prism. (1999). GraphPad Software, San Diego, CA. Available at: <http://www.graphpad.com/manuals/analyzingdata.pdf>
- Limbird, L.E. Cell Surface Receptors: A Short Course on Theory and Methods. (1996). Kluwer Academic Publishers, Boston.
- Winzor, D.J. and Sawyer, W.H. Quantitative Characterization of Ligand Binding. (1995). Wiley-Liss, Inc., New York.
- Lutz M. W., Menius J. A., Choi T. D., Gooding-Laskody R., Domanico P. L., Goetz A. S., Saussy D. L. Experimental design for high-throughput screening. *Drug Discovery Today*. 1996;1(7):277–286.
- Kahl S. D., Hubbard F. R., Sittampalam G. S., Zock J. M. Validation of a High Throughput Scintillation Proximity Assay for 5-Hydroxytryptamine1E Receptor Binding Activity. *J. Biomol. Screen*. 1997;2(1):33–39.
- Sun S., Almaden J., Carlson T.J., Barker J., Gehring M.R. Assay development and data analysis of receptor-ligand binding based on scintillation proximity assay. *Metab Eng*. 2005;7:38–44. PubMed PMID: 15721809.

### Fluorescence Polarization: Suggested Reading

- Lin S, Bock CL, Gardner DB, Webster JC, Favata MF, Trzaskos JM, Oldenburg KR. *Anal Biochem*. 2002;300:15–21. A high-throughput fluorescent polarization assay for nuclear receptor binding utilizing crude receptor extract. PubMed PMID: 11743686.
- Lee PH, Bevis DJ. Development of a homogeneous high throughput fluorescence polarization assay for G protein-coupled receptor binding. *J. Biomol. Screening*. 2000;5:415–419. PubMed PMID: 11598459.
- Banks P, Harvey M. Considerations for using fluorescence polarization in the screening of G protein-coupled receptors. *J Biomol Screen*. 2002;7:111–7. PubMed PMID: 12006109.
- Do EU, Choi G, Shin J, Jung W-S. *Anal. Biochem*. 2004;330:156–163. and Kim, S-I Fluorescence polarization assays for high-throughput screening of neuropeptide FF receptors. PubMed PMID: 15183774.
- Allen M, Reeves J, Mellor G. High throughput fluorescence polarization: A homogeneous alternative to radioligand binding for cell surface receptors. *J. Biomol. Screen*. 2000;5:63–69. PubMed PMID: 10803605.
- Burke TJ, Loniello KR, Beebe JA, Ervin KM. Development and application of fluorescence polarization assays in drug discovery. *Combinatorial Chemistry & High Throughput Screening*. 2003;6:183–194. PubMed PMID: 12678697.
- Beasely J.R., Dunn DA, Walker TL, Parlato SM, Lehrach JM, Auld DS. Evaluation of compound interference in immobilized metal ion affinity-based fluorescence polarization detection with a four million member compound collection. *Assays and Drug Development Technologies*. 2003;1:455–459. PubMed PMID: 15090182.



# Protease Assays

Guofeng Zhang, Ph.D.✉<sup>1</sup>

Created: May 1, 2012; Updated: October 1, 2012.

## Abstract

Proteases are important drug targets; the first drugs to reach the market were antihypertensives and antivirals. Designing HTS assays for these targets requires thorough understanding of the biochemistry and biology of these enzymes as well as various assay formats. In this chapter, the authors present basic properties of protease enzymes, sensitive fluorescent assay formats compatible with HTS, both in homogeneous and separation-based approaches. Sections on hit selection and data analysis concepts for identifying inhibitors are also included with an extensive set of literature references.

## Introduction

The study of proteases has a long history, and the scientific community has accumulated a wealth of knowledge, which makes the proteases one of the few well studied enzyme families. A simple search using the NIH PubMed server will find hundreds of thousands of protease related articles. In fact, the accumulated knowledge of some protease family members is comprehensive enough to make them classical teaching materials in college Biochemistry textbooks.

Proteases play critical roles in multiple biological pathways - the human genome sequencing project revealed that ~2% of our genes encode proteases - and are implicated in many diseases, including infectious diseases, inflammation, cancer, degenerative diseases, and many others (1). The search for small molecule drugs that target proteases has been an area of intensive research in both academia and industry for decades. These efforts have been noticeably productive, leading to more than two dozen FDA-approved drugs for diverse indications (<http://www.ddw-online.com/s/2003/p142685/winter-2003-edition.html>) and many more currently in clinical trials and development. A simple search for protease inhibitors in the Drugbank database (<http://www.drugbank.ca/>) returns several hundred hits, (although the majority of hits are different names for the same drug). The first protease inhibitors that became approved drugs were antihypertensives and antivirals. Since the approval of the angiotensin-converting enzyme (ACE) inhibitor Captopril from Bristol-Myers Squibb for the treatment of hypertension in

---

<sup>1</sup> Platform Technology and Science, GlaxoSmithKline, 1250 S. Collegeville Road, Collegeville, PA 19426; Email: Guofeng.2.zhang@gsk.com.

✉ Corresponding author.

\*Edited by Tod Holler and Andrew Napper, Ph.D.

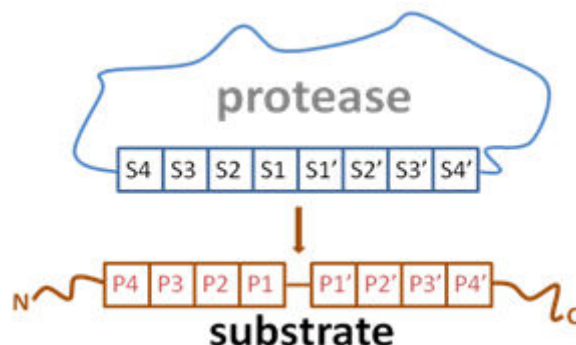


**Figure 1.** Conventional nomenclature for protease reactions. The amino acids on amino side of the scissile bond are labeled with the letter P and the ones on the carboxyl side are labeled with P'. Their corresponding binding sites on the protease are labeled with S and S', respectively.

1981, there have been eight ACE inhibitors developed by various companies and approved for the same indication. Similarly, there are now more than ten approved drugs targeting HIV proteases or HCV proteases. HIV protease inhibitors were instrumental in proving the viral etiology of AIDS; they have turned this once deadly infection into a manageable condition. The HCV protease inhibitors are revolutionizing the treatment of this disease, enabling faster, more reliable treatment (<http://www.fda.gov/ForConsumers/ByAudience/ForPatientAdvocates/HIVandAIDSActivities/ucm118915.htm>). Since these early protease inhibitors became available, protease inhibitors have proved useful in other therapeutic areas. Key examples include Argatroban from GlaxoSmithKline, the thrombin inhibitor that the FDA approved for the treatment of coagulation disorders in 2000; the DPP4 inhibitor JANUVIA<sup>®</sup> (Sitagliptin) from Merck, approved for the treatment of diabetes in 2006; and VELCADE<sup>®</sup> (Bortezomib), a proteasome inhibitor from Millennium, approved for the treatment of [multiple myeloma](#) in 2003 (2). These examples are a fraction of the total, but they represent both the large number of companies that have conducted research targeting proteases, and the diversity of disease states in which proteases are important. In this section, we will define the term “protease” broadly. The definition will include endopeptidases, which cleave peptide bonds between non-terminal [amino acids](#), and exopeptidases, which remove an amino acid from the end of a polypeptide chain. The exopeptidases include both aminopeptidases, which cleave from the amino end of a peptide and carboxypeptidases, which cleave from the carboxylic end of a peptide. We will also include protease-like enzymes that cleave isopeptide bonds, such as the deubiquitinases and de-Neddylase, in our definition. Finally, we will extend our definition to include an enzyme complex that contains multiple components, such as the 26S proteasome and the COP9 signalosome (CSN).

To clarify the terms used in this section, Figure 1 shows a general protease reaction in which the protease cleaves a scissile amide bond from the substrate, which can be either a protein or a synthetic peptide. Substrate amino acids that are on the amino (N) side of the scissile bond are numbered P1, P2, and P3 ... (called P sites) with the one closest to the scissile bond numbered P1. The same scheme applies to the residues that are on the

carboxyl (C) side of the scissile bond. In this case, the residues are numbered P1', P2', P3' ... (called P' sites). Depending on the nature of the protease, the number of amino acids on either side of the scissile bond of the substrate (shown in Figure 1) can vary. There will be only one or two amino acids on the N-terminal side of the scissile bond of aminopeptidase substrates and one or two amino acids on the C-terminal side of the scissile bond of carboxypeptidase substrates, but there will be more amino acids on both sides of the scissile bond of endopeptidase substrates.

The search for small molecules that modulate protease activity continues to be a hot area of research, with multiple targets in play. As a result, the demand for robust biochemical assays that can efficiently assess structure-and-activity relationships still exists. In addition, the discovery of new protease-like drug targets, such as the cysteine protease-like deubiquitinases and zinc-dependent COP9 signalosome (CSN), demands innovation in protease assay methodology. Like many enzyme target classes, both binding assays, which assess the interaction between a small molecule and the target protein, and functional assays, which measure a small molecule's effect on enzyme activity, are useful in the search for protease inhibitors. This section will mainly focus on biochemical assays that are amendable for high throughput screening. Binding assays in general have been recently reviewed (3, 4) and will be mentioned only briefly, when needed. Many biochemical assays exist for proteases, and they can be grouped according to the basic principles they share. To simplify the discussion, we will categorize the assays into two groups: homogenous assays and separation-based assays. In a homogenous assay, substrate turnover can be detected as a signal change directly from the reaction mixture without further sample processing. In a separation based assay, the product and/or remaining substrate are separated from the reaction mixture for detection after the enzymatic reaction is stopped.

## Homogenous Assays

A homogenous assay does not require separation of product and/or substrate from the reaction mixture. Instead, it relies on a physical change accompanying substrate turnover. This change is usually a readily-detected colorimetric or fluorescent signal from a synthetic peptide substrate. A native peptide substrate does not usually offer such convenience. Fortunately, most proteases can tolerate some degree of substrate modification. This makes it feasible to add reporter groups, for example fluorogenic or chromogenic moieties, to the substrate to assist the detection of turnover. Fluorescence-based approaches have been widely used in assays for proteases and other drug targets mainly because of their high sensitivity. This characteristic makes fluorescence-based assays particularly suitable for the dense, low volume formats employed in high throughput screening.

A number of fluorescence-based approaches have been used to measure protease activity. Those most widely used, shown in Figure 2, include (a) measuring the change in fluorescence intensity of a fluorophore chemically quenched by amide linkage to the peptide, (b) measuring the change in fluorescent signal from a pair of fluorescent dyes

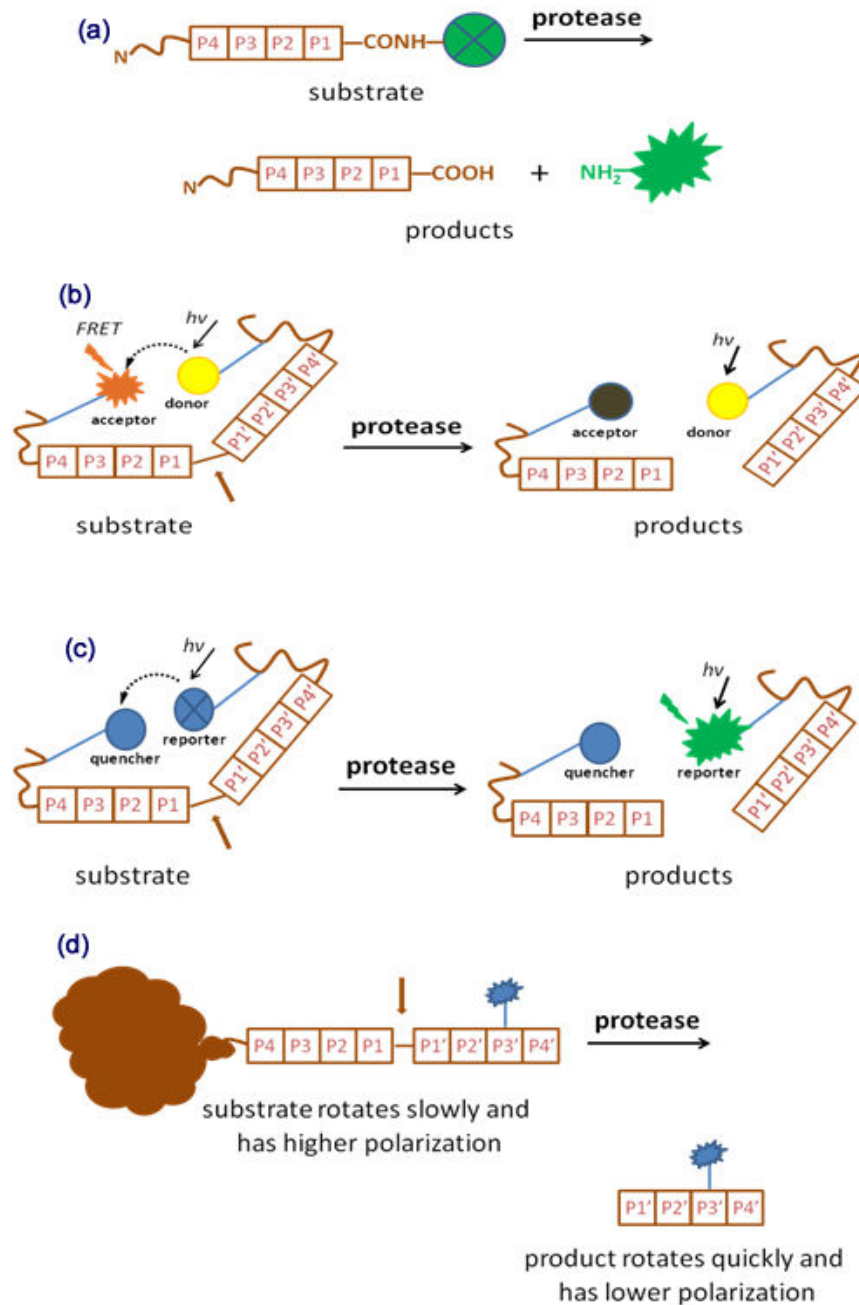


**Figure 2.** Basic principles of fluorescence-based homogenous assays for measuring protease activity. (a) Fluorescence intensity assay in which a fluorogenic group is linked to the carboxyl end of a peptide *via* an amide bond, and its fluorescence increases upon release by the action of a protease; (b) Resonance-energy-transfer-based assay in which a FRET signal can be detected when the donor and acceptor are in close proximity. The pair separates upon peptide cleavage and the FRET signal decreases; (c) Dual-label quenched-pair fluorescent assay in which the fluorescence intensity of the reporter is suppressed by the quencher because of its close proximity. The pair separates upon peptide cleavage and the fluorescence intensity from the reporter group is significantly increased; (d) Fluorescence polarization assay in which the substrate and the product give different emission polarization signals because of their different sizes (“digestive” fluorescence polarization assay).



that interact via a resonance energy transfer (FRET) system, (c) measuring the change in fluorescent intensity from a fluorescent dye that is quenched by a near-by nonfluorescent dye, and (d) measuring a change in fluorescence polarization. These four formats will be discussed in detail in the next sections.

## Fluorescence intensity assays monitoring change from chemically quenched dyes

In this approach, a fluorescent dye that contains a reactive amine group can be covalently attached to the carboxyl end of a peptide substrate *via* an amide bond. The sequence of the peptide moiety provides protease specificity, and the dye moiety functions as a reporter for enzymatic activity. The target protease will cleave the amide bond when the peptide binds and forms a productive complex. The fluorescence of the attached dye, which is quenched when covalently attached to the peptide, increases dramatically when released by a protease cleavage, as shown in Figure 2a. When the assay is configured properly, the fluorescence intensity of the released dye is linearly proportional to the enzyme activity. The most commonly used fluorophores are coumarin derivatives (5, 6), such as 7-amino-4-methylcoumarin (AMC) and 7-amino-4-(trifluoromethyl) coumarin (AFC). The fluorescent dye rhodamine has also been used in this approach. A bisamide of rhodamine is non-fluorescent, while a monoamide derivative is highly fluorescent. Rhodamine-based substrates for serine proteases (7) and a ubiquitin-linked rhodamine 110-glycine deubiquitinase substrate (8, 9) have been reported. This chemically quenched approach has been widely used in protease assays, particularly in high throughput assays designed to find inhibitors of proteases implicated in human diseases, such as cathepsins, caspases and deubiquitinases.

The chemically quenched approach applies only to proteases that can tolerate major modifications on the P1' site of the substrate (see Figure 1); it does not work for proteases that have strict specificity requirement for P1' site, such as carboxypeptidases. However, a similar approach based on colorimetric difference between substrate and product was developed for carboxypeptidases. As an example, furylacryloyl-Ala-Lys and furylacryloyl-Ala-Arg were developed as substrates for carboxypeptidase N; enzyme activity could be followed by measuring absorption decrease at 340 nm (10). Unfortunately, its application in drug discovery screening is limited by the low sensitivity of measurement and its vulnerability to interference from compounds that absorb at 340 nm.

## Fluorescence resonance energy transfer (FRET) assays

In order to use the fluorescence intensity format described above, the amino acids on the C-terminal side of the cleavage site (P' sites, Figure 1) must be replaced with a fluorogenic group, and therefore the integrity of the peptide sequence surrounding the scissile bond is sacrificed. In some cases, particularly for endopeptidases, deubiquitinase and deubiquitinase-like enzymes, maintaining the sequence integrity surrounding the cleavage site is critical, so modification of the P' sites close to the scissile bond should be avoided. For these targets, a FRET-based approach can be employed. In this approach (Figure 2b),

two fluorescent groups are placed on each side of the scissile bond, one called “donor” and the other “receptor”. The donor and the receptor are chosen such that the emission wavelength of the donor overlaps with the excitation wavelength of the receptor. The locations of the donor and receptor groups are chosen such that they will not compromise the sequence integrity near the scissile bond, but are close enough to each other that FRET can efficiently take place. Upon cleavage of the scissile bond, the fluorescent pair disassembles and the FRET signal decreases.

This particular format is limited in that it is a signal decrease assay and a relatively large percentage of substrate-turnover is required for a statistically meaningful readout in endpoint format. In addition, it can be subject to a low signal-to-noise, from time to time, due to overlap between donor and receptor fluorescence spectra. Fortunately, a practical solution had been achieved thanks to the efforts from various laboratories (11-14), which are discussed separately below.

## Fluorescence intensity assays monitoring change from dual-label quenched pairs

To convert a signal-decrease FRET assay into a signal-increase assay, one can choose a donor and receptor pair to allow a maximal overlap between the donor’s fluorescence and the receptor’s absorption, and then monitor the donor emission as readout. With the receptor in close proximity, the donor’s emission is re-absorbed upon excitation and cannot reach the detector, which results in a low level of fluorescent signal. Upon cleavage by a protease, the pair separates and the donor no longer transfers its emission to the receptor, which leads to an increase in the fluorescence intensity observed from the donor. In these cases, the donor alone takes the role as the “reporter” for enzymatic activity and the receptor functions solely as a “quencher” for the reporter’s fluorescence when they are in close proximity, as shown in Figure 2c.

Two types of quenchers exist. The early quenchers were generally a second fluorescent dye; examples include fluorescein and rhodamine (reporter and quencher) and their derivatives. The readout can be either the reporter fluorescence alone or the ratio between fluorescence of the reporter and the fluorescence of the quencher. Assays using fluorescent quenchers are usually limited by high background signal caused by incomplete separation of the reporter and quencher spectra. In the last decade a new generation of “dark quenchers” have been developed to address this issue. These quenchers do not have native fluorescence and therefore do not contribute significantly to background noise. This type of quencher offers excellent signal increase upon the separations of the energy transfer pair. Examples include Dabcyl (4,4'-dimethylaminophenylazo)benzyl (12, 15), and the “black hole quenchers” built on a polyaramatic-azo backbone (13). Recently, this approach has been extended to construct internally quenched fluorescent diubiquitin substrates for deubiquitinases (commercialized as IQF-DiUb™ by Lifesensors Inc.). This substrate maintains the isopeptide nature of the scissile bond and provides full occupancy of both the S and S' pockets from the deubiquitinases. It is hypothesized that using this substrate might increase the chance of finding inhibitors with various modes of action. A

similar approach can be designed for deneddylases and desumoylases, which catalyze the deneddylation and desumoylation in some protein modification processes by cleaving the isopeptide bonds between NEDD8 or SUMO and the protein being modified (16, 17).

## Fluorescence polarization (FP) assays

Proteases can also be assayed using an FP-based format. In this assay format, a protein or a long peptide substrate is labeled with one or more fluorescent dyes. These substrates give a high polarization signal due to their large size. Upon cleavage by a protease, the large substrate is converted into smaller fragments that give a lower polarization signal due to an increased rotation rate. This approach, which relies on the protease enzymatic activity and is sometimes referred to as a digestive fluorescence polarization assay is illustrated in Figure 2d.

In some cases, a competition binding assay can be configured using FP as the readout. In this format, the FP signal from a fluorescently labeled non-cleavable peptide substrate analog is monitored, as shown in Figure 3. Its FP signal is higher when the peptide is bound to a larger protein due to the slower rotation rate of a large complex; if the binding of a fluorescently silent small molecule prevents the binding of the peptide to the larger protein, the peptide will remain unbound in solution and tumble faster, which gives a lower FP signal. Therefore a FP signal decrease indicates the presence of a small molecule that competes with the labeled peptide analog for the protease's substrate binding site. The length of the peptide used in this approach is limited to 15 – 20 amino acids, since the difference between the FP signals of the bound and the unbound peptide decreases when its length increases, reducing the assay signal window. The affinity of the labeled peptide must be strong enough, such that the fraction of protein-bound peptide to total peptide can be set between ~0.3 - 0.7, typically at enzyme concentration well under 1  $\mu\text{M}$  (preferably at nM level). This usually gives a reasonable polarization signal window and a decent sensitivity to small molecule competition.

It is worth noting that FP measures a ratio of polarized to non-polarized fluorescence and, in general, is concentration-dependent only in a moderate range. Outside that range the signal change will not be sensitive to changes in product concentration, which limits the general application of this approach.

## Separation-Based Assays

Assays based on labeled peptides offer great advantages. Not only are they suitable for large library screening (cost and throughput), in many cases they also enable a kinetic reading of the enzymatic reaction. Kinetic reads are valuable when characterizing a compound's interaction with the target in detail, such as investigating the time-dependence of inhibition, or the on- and off-rate constants for binding to target. However, there are cases where a substrate cannot be labeled, or where a labeled substrate cannot meet the requirements for specific studies. A separation-based assay will be needed in these cases. In separation-based assays the product and/or the substrate can be isolated

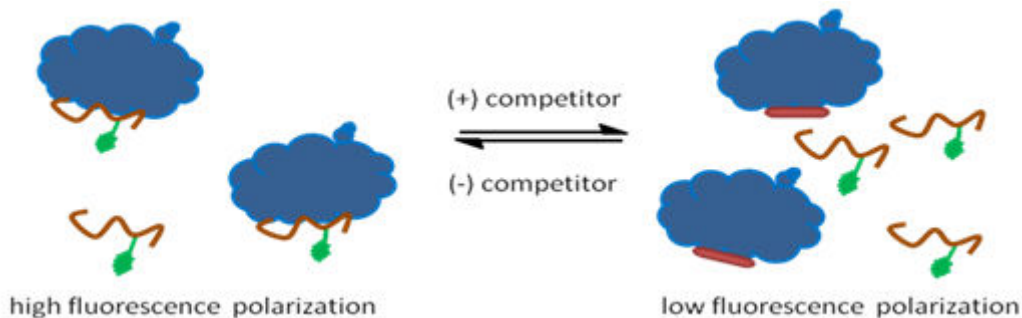


**Figure 3.** Fluorescence polarization based competition assay. Binding of a small molecule (represented by the brown bars) to the same site on target displaces the fluorescence labeled peptide analog and results in signal decrease.

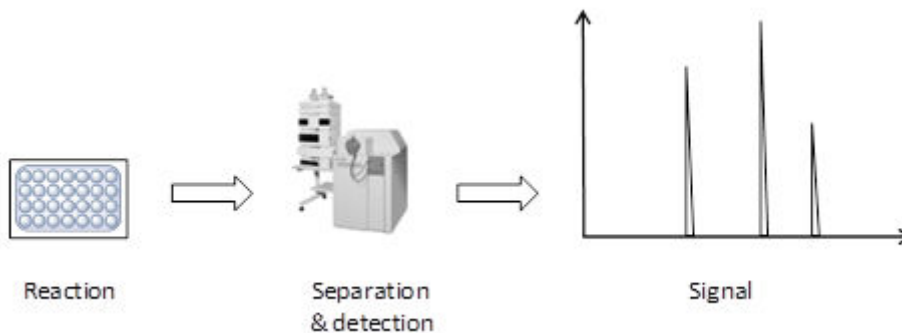


**Figure 4.** Schematic illustration of a separation-based protease assay in which the product and substrate are separated before being analyzed.

from the reaction mixture and measured independently. Typically, the reaction is stopped when its progress is within a pre-determined linear range, but enough substrate has to be turned over to give a robust signal. This approach is illustrated in Figure 4.

The substrate and the product can often be separated by liquid chromatography and then monitored either by their retention times on a column, or by their molecular weights in a mass spectrometer. The principles of liquid chromatography and mass spectrometry are well documented, and high throughput assay platforms have been developed for both. For example, a multichannel microscale HPLC systems has been developed that can run several micro-columns simultaneously (18), making it suitable for screening fairly large compound sets. Additionally, the RapidFire™ high-throughput mass spectrometry system developed by BIOCIUS Life Sciences (now part of Agilent) can run at a speed of seconds per sample (in most case, this is not total separation of product and substrate, rather it is separation from the reaction buffer) (19, 20). These technologies can be used for primary screening when labeled assays are not suitable and can also be used to confirm hits from label-based assays.

## Triaging Assay Hits

The major application of the methods described above is to find and characterize small molecule protease inhibitors, usually through screening large compound collections. It is prudent to note that all of these assays are subject to false hits. False hits can be categorized into two groups based on the origin of the interference: those that interfere with the detection of the assay signal (assay format dependent), and those that interact nonspecifically with the target enzyme (assay format independent). False hits can be misleading and should be eliminated from consideration as early as possible using a triage process. False hits that interfere with signal detection in fluorescence-based assays are either auto-fluorescent at the detection wavelength, or quench the fluorescence signal used as the enzyme activity readout. These types of interference can be detected by measuring the fluorescence signal of a stopped enzyme reaction in the presence of compounds that are added post-reaction (this way only the compound interference with detection is measured), preferably at varying compound concentrations. A signal increase will be observed if a compound is auto-fluorescent and a signal decrease will be observed if a compound is a fluorescence quencher.

Interference with signal detection can also be observed in chromatography-based assays if a compound co-elutes with substrate or product. For example, a compound will be a false inhibitor if it co-elutes with a substrate and only the substrate decrease is monitored, because there will be less “apparent” substrate decrease in the presence of this compound. Similarly, a compound will appear to be an activator if it co-elutes with product and only the product peak is monitored. This kind of interference can be addressed by changing the chromatography protocols, for example by changing the mobile phase or gradient, which may resolve the overlapping peaks, or by monitoring both substrate and product, which will allow aberrant results to be detected more easily.

The occurrence of nuisance hits that interact non-specifically with the target enzyme is usually assay format independent. A number of mechanisms of nuisance inhibition have been proposed and investigated (21), including inhibition *via* compound aggregation, *via* enzyme degradation and precipitation, *via* chemical reactivity and/or oxidation (22), and *via* trace amount of impurity, for example a metal catalyst leftover from synthesis. Cysteine proteases are generally more susceptible to nuisance inhibition *via* chemical reactivity, oxidation and trace metal contamination (23) because of the high reactivity of the thiol (or thiolate) group at the enzyme active site. Several diagnostic assays for nuisance inhibitors can be found in the literature. The kinetics of inhibition exhibited by nuisance inhibitors, for example, are usually time-dependent and non-stoichiometric, which is often manifested by a high Hill slope for the dose-response curve. Nuisance inhibitors commonly inhibit a number of unrelated enzymes, and their  $IC_{50}$  values usually show a significant shift when assay conditions are changed. Increasing the concentration of the target enzyme and including a detergent in the buffer are changes typically employed. It is not trivial, and frequently impractical, to test HTS hits in all these

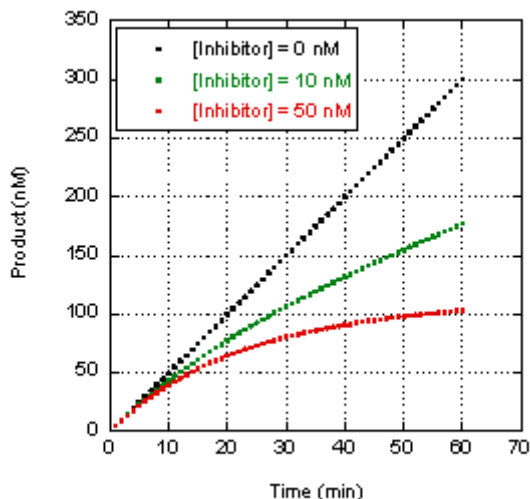


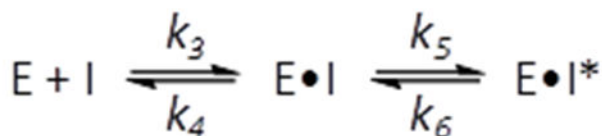
**Figure 5.** Illustration of time courses of product formation in the presence of a time-dependent inhibitor. The overall decrease in product formation rate depends on the concentration of the inhibitor added into the assay.

assays. The most reliable and efficient first filter to eliminate nuisance hits is to change the concentration of the enzyme target (24).

## Data Analysis for Time Dependent Inhibitors and Covalent Inhibitors

Data analysis for protease inhibition is not very different from other enzyme targets, in that a compound's potency is calculated based on percentage inhibition of enzymatic activity at different compound concentrations. However, this simple approach only works well when a rapid equilibrium between the free inhibitor and the enzyme-inhibitor complex is established during the assay. Time-dependent inhibitors have been developed for most proteases. Important examples include the boronic acids that inhibit serine proteases (25, 26), the ketones and aldehydes that inhibit thiol proteases (27-29), and the metal chelators that inhibit metalloproteases (30, 31). For those inhibitors, an accurate assessment of compound potency requires careful data analysis that takes into account the shift in equilibrium over time. Scheme 1, in which the rapid initial formation of an enzyme inhibitor complex (E•I) is followed by a slow isomerization step that leads to a tighter complex (E•I)\* (32).

**Scheme 1**



The presence of a time-dependent inhibitor makes the transition from free enzyme to the final stable  $E \cdot I^*$  complex more pronounced over time, and the rate of product formation (P) follows time (t) in an inverse exponential manner, as illustrated in Figure 5.

$$\text{Equation 1} \quad P = v_s t + (v_0 - v_s)(1 - e^{-kt})/k$$

where  $v_0$  is the initial reaction velocity,  $v_s$  is the steady state velocity and  $k$  is the first order rate constant for conversion of  $E \cdot I$  to  $E \cdot I^*$ .

Because many approved drugs are covalent modifiers (33, 34), it is worth mentioning that this relationship is also valid for covalent inhibitors that inactivate the enzyme irreversibly. For covalent inhibitors the final steady state velocity is zero, which reduces Equation 1 to Equation 2, as shown below.

$$\text{Equation 2} \quad P = v_0(1 - e^{-kt})/k$$

where,  $k$  is the enzyme inactivation rate constant.

Good review articles addressing data analysis of time-dependent inhibition and covalent modification of enzymes have appeared in the literature. For a discussion of this topic and examples, please refer to those articles (32, 35, 36). It is worth noting that the equations describing this phenomenon, especially equation 1 mentioned above, must be modified to account for the diminished populations of free enzyme and free inhibitor upon the formation of enzyme-inhibitor complex when dealing with time-dependent inhibitors that are also tight-binding ( $K_i \sim [E]$ ). Morrison and Walsh address the mathematical solutions explicitly (32).

## Conclusion

Proteases are important drug targets and they are among the best studied enzymes. Most assays discussed here are amenable to HTS and cost-efficient, which enables protease drug discovery in a variety of research organizations. Challenges do exist. Among them, the challenge of designing assays that are less susceptible to nuisance hits, especially for cysteine proteases, persists.

## References

1. Turk B. Targeting proteases: successes, failures and future prospects. *Nat Rev Drug Discov.* 2006;5(9):785–99. PubMed PMID: 16955069.
2. Chen D., et al. Bortezomib as the first proteasome inhibitor anticancer drug: current status and future perspectives. *Curr Cancer Drug Targets.* 2011;11(3):239–53. PubMed PMID: 21247388.

3. Zhu Z., Cuozzo J. Review article: high-throughput affinity-based technologies for small-molecule drug discovery. *J Biomol Screen*. 2009;14(10):1157–64. PubMed PMID: 19822881.
4. Mayr L.M., Bojanic D. Novel trends in high-throughput screening. *Curr Opin Pharmacol*. 2009;9(5):580–8. PubMed PMID: 19775937.
5. Zimmerman M., Yurewicz E., Patel G. A new fluorogenic substrate for chymotrypsin. *Anal Biochem*. 1976;70(1):258–62. PubMed PMID: 1259147.
6. Zimmerman M., et al. Sensitive assays for trypsin, elastase, and chymotrypsin using new fluorogenic substrates. *Anal Biochem*. 1977;78(1):47–51. PubMed PMID: 848756.
7. Leytus S.P., Melhado L.L., Mangel W.F. Rhodamine-based compounds as fluorogenic substrates for serine proteinases. *Biochem J*. 1983;209(2):299–307. PubMed PMID: 6342611.
8. Tirat A., et al. Synthesis and characterization of fluorescent ubiquitin derivatives as highly sensitive substrates for the deubiquitinating enzymes UCH-L3 and USP-2. *Anal Biochem*. 2005;343(2):244–55. PubMed PMID: 15963938.
9. Hassiepen U., et al. A sensitive fluorescence intensity assay for deubiquitinating proteases using ubiquitin-rhodamine110-glycine as substrate. *Anal Biochem*. 2007;371(2):201–7. PubMed PMID: 17869210.
10. Plummer T.H. Jr, Kimmel M.T. An improved spectrophotometric assay for human plasma carboxypeptidase N1. *Anal Biochem*. 1980;108(2):348–53. PubMed PMID: 7457880.
11. Packard B.Z., et al. Intramolecular Excitonic Dimers in Protease Substrates: Modification of the Backbone Moiety To Probe the H-Dimer Structure. *J. Phys. Chem. B*. 1998;102(10):1820–1827.
12. Grahn S., Ullmann D., Jakubke H. Design and synthesis of fluorogenic trypsin peptide substrates based on resonance energy transfer. *Anal Biochem*. 1998;265(2):225–31. PubMed PMID: 9882396.
13. Johansson M.K., Cook R.M. Intramolecular dimers: a new design strategy for fluorescence-quenched probes. *Chemistry*. 2003;9(15):3466–71. PubMed PMID: 12898673.
14. Feng B.Y., et al. High-throughput assays for promiscuous inhibitors. *Nat Chem Biol*. 2005;1(3):146–8. PubMed PMID: 16408018.
15. Tyagi S., Bratu D.P., Kramer F.R. Multicolor molecular beacons for allele discrimination. *Nat Biotechnol*. 1998;16(1):49–53. PubMed PMID: 9447593.
16. Nalepa G., Rolfe M., Harper J.W. Drug discovery in the ubiquitin-proteasome system. *Nat Rev Drug Discov*. 2006;5(7):596–613. PubMed PMID: 16816840.
17. Bedford L., et al. Ubiquitin-like protein conjugation and the ubiquitin-proteasome system as drug targets. *Nat Rev Drug Discov*. 2011;10(1):29–46. PubMed PMID: 21151032.
18. Sajonz P., et al. Multiparallel microfluidic high-performance liquid chromatography for high-throughput normal-phase chiral analysis. *J Chromatogr A*. 2007;1145(1-2):149–54. PubMed PMID: 17300788.



19. Holt T.G., et al. Label-free high-throughput screening via mass spectrometry: a single cystathionine quantitative method for multiple applications. *Assay Drug Dev Technol.* 2009;7(5):495–506. PubMed PMID: 19715455.
20. Jonas M., LaMarr W.A., Ozbal C. Mass spectrometry in high-throughput screening: a case study on acetyl-coenzyme a carboxylase using RapidFire--mass spectrometry (RF-MS). *Comb Chem High Throughput Screen.* 2009;12(8):752–9. PubMed PMID: 19531010.
21. Shoichet B.K. Screening in a spirit haunted world. *Drug Discov Today.* 2006;11(13-14):607–15. PubMed PMID: 16793529.
22. Lor L.A., et al. A simple assay for detection of small-molecule redox activity. *J Biomol Screen.* 2007;12(6):881–90. PubMed PMID: 17579124.
23. Jadhav A., et al. Quantitative analyses of aggregation, autofluorescence, and reactivity artifacts in a screen for inhibitors of a thiol protease. *J Med Chem.* 2010;53(1):37–51. PubMed PMID: 19908840.
24. Habig M., et al. Efficient elimination of nonstoichiometric enzyme inhibitors from HTS hit lists. *J Biomol Screen.* 2009;14(6):679–89. PubMed PMID: 19470716.
25. Kettner C.A., et al. Kinetic properties of the binding of alpha-lytic protease to peptide boronic acids. *Biochemistry.* 1988;27(20):7682–8. PubMed PMID: 3207699.
26. Bachovchin W.W., et al. Nitrogen-15 NMR spectroscopy of the catalytic-triad histidine of a serine protease in peptide boronic acid inhibitor complexes. *Biochemistry.* 1988;27(20):7689–97. PubMed PMID: 3207700.
27. Tavares F.X., et al. Design of potent, selective, and orally bioavailable inhibitors of cysteine protease cathepsin k. *J Med Chem.* 2004;47(3):588–99. PubMed PMID: 14736240.
28. Tavares F.X., et al. Ketoamide-based inhibitors of cysteine protease, cathepsin K: P3 modifications. *J Med Chem.* 2004;47(21):5057–68. PubMed PMID: 15456249.
29. Deaton D.N., et al. Novel and potent cyclic cyanamide-based cathepsin K inhibitors. *Bioorg Med Chem Lett.* 2005;15(7):1815–9. PubMed PMID: 15780613.
30. Agrawal A., et al. Zinc-binding groups modulate selective inhibition of MMPs. *ChemMedChem.* 2008;3(5):812–20. PubMed PMID: 18181119.
31. Jacobsen J.A., et al. To bind zinc or not to bind zinc: an examination of innovative approaches to improved metalloproteinase inhibition. *Biochim Biophys Acta.* 2010;1803(1):72–94. PubMed PMID: 19712708.
32. Morrison J.F., Walsh C.T. The behavior and significance of slow-binding enzyme inhibitors. *Adv Enzymol Relat Areas Mol Biol.* 1988;61:201–301. PubMed PMID: 3281418.
33. Robertson J.G. Mechanistic basis of enzyme-targeted drugs. *Biochemistry.* 2005;44(15):5561–71. PubMed PMID: 15823014.
34. Singh J., et al. The resurgence of covalent drugs. *Nat Rev Drug Discov.* 2011;10(4):307–17. PubMed PMID: 21455239.
35. Szedlacsek S.E., Duggleby R.G. Kinetics of slow and tight-binding inhibitors. *Methods Enzymol.* 1995;249:144–80. PubMed PMID: 7791610.
36. Duggleby R.G. Analysis of enzyme progress curves by nonlinear regression. *Methods Enzymol.* 1995;249:61–90. PubMed PMID: 7791628.



# Inhibition of Protein-Protein Interactions: Non-Cellular Assay Formats

Michelle R. Arkin, PhD,<sup>1,\*</sup> Marcie A. Glicksman, PhD,<sup>2,\*</sup> Haian Fu, PhD,<sup>3</sup>  
Jonathan J. Havel,<sup>3</sup> and Yuhong Du<sup>3</sup>

Created: March 18, 2012; Updated: October 1, 2012.

## Abstract

Protein-protein interactions (PPI) are critical in cellular signal transductions that play a key role in both normal and abnormal functions in cells. Therefore, modulating the activity of these interactions is a major focus in drug discovery research. In this chapter, the authors address the development, optimization and validation of HTS assays to identify small molecule modulators of PPI. They also discuss the sources of artifacts, detailed accounts of assay technologies compatible with HTS for PPI and validating the inhibition of PPI. An extensive set of references is provided, and is a must read for beginners and a review for experienced investigators.

## Overview and Introduction

### Introduction

Protein-protein interactions (PPI) are central to most cellular processes and, as such, are the focus of many probe- and drug-discovery programs. However, it has been difficult to identify small molecule or peptide inhibitors of PPI that bind stoichiometrically to a single site on the protein surface. Often cited reasons for this challenge include a) the flat nature of PPI interfaces, which sometimes lack deep grooves where small molecules can stick, b) the large contact area at the interface, which often exceeds the surface area of a drug-sized molecule, and c) bias in the screening libraries, which are selected by adherence to criteria – like the Rule of 5 (1, 2) – that might not suit PPI inhibitors. Furthermore, early screening approaches to PPI were prone to artifacts and tended to select hydrophobic compounds with non-drug-like mechanisms of action, such as aggregation-based inhibition or protein denaturation (3, 4, 5). Despite these challenges, there are now a number of drug-like inhibitors of PPI in the literature (5, 6, 7, 8). From these examples, we are beginning to develop “best practices” for selecting tractable targets, applying appropriate screening assays, and evaluating mechanisms of action. This chapter focuses on the selection and development of screening assays for identifying small molecules that can modulate PPI, and will touch on secondary assays used to remove

---

<sup>1</sup> University of California San Francisco, San Francisco, CA. <sup>2</sup> Harvard NeuroDiscovery Center, Boston, MA. <sup>3</sup> Emory University School of Medicine, Atlanta, GA.

\*Editor

artifacts and demonstrate binding. General introductions to assay development for HTS and to common assay equipment and instrumentation can be found in [Basics of Assay Equipment and Instrumentation for High Throughput Screening](#).

The screening assays described here monitor the binding of the two proteins, and can be used to measure inhibition or augmentation of the PPI by small molecules or other modulators (e.g. antibodies, peptides). Table 1 provides a brief summary of the assays. All assays can be used for primary high-throughput screening (HTS) at single concentrations of test compounds and for dose-response assays to obtain IC<sub>50</sub> values. These formats are regularly used in 96- and 384-well plates and can often be adapted to 1536-well plates. Traditional high-throughput assays involve binding one of the protein partners to the plate; here, we provide an overview of these ELISA-like assays, including DELFIA. Increasingly, screening scientists utilize mix-and-read assay formats such as fluorescence polarization/anisotropy (FP), fluorescent/Foerster resonance energy transfer (FRET, TR-FRET, HTRF), and bead-based assays like AlphaScreen ([Perkin Elmer](#)). These solution-phase assays are often easier to develop than ELISAs because they have fewer components, and are simpler and faster to run because they avoid multiple incubation/wash cycles. On the other hand, ELISA and DELFIA can be very sensitive and are still used for diagnostics and some high throughput screens.

**Table 1:** Overview of Assay Formats

| Method                                | FP  | ELISA/DELFLIA  | FRET   | AlphaScreen   |
|---------------------------------------|---|--|--|---|
| <b>Size of protein and/or complex</b> | Labeled ligand needs to be <1500 Da and protein needs to be >10,000 Da.           | No real limit  | Distance between donor and acceptor needs to be <9 nm  | Distance between donor and acceptor needs to be <200 nm   |
| <b>Pure protein?</b>                  | Label needs to be pure protein or small molecule                                  | Can use purified protein or complex sample                                     | Can use purified protein or complex sample             | Can use purified protein or complex sample  |
| <b>Sensitivity</b>                    | [FP probe] ~ nM; [protein] determined by K <sub>d</sub> of PPI                    | Can be as low as femtograms/well   | Depends on K <sub>d</sub> of PPI; typically 1 – 100 nM | Can be as low as femtograms/well  |
| <b>Dye(s)</b>                         | Most organic, fluorescent dyes; red-shifted preferred (e.g. Bodipy, Alexa Fluors) | Lanthanide (DELFLIA) or enzyme (Horse Radish Peroxidase, Alkaline Phosphatase) | FRET: see Table 2, below                               | Donor bead generates singlet oxygen that excites acceptor bead with organic or lanthanide fluorophore |
| <b>Need washing steps?</b>            | no  | yes  | no   | no  |
| <b>Signal range (high/low)</b>        | ~3 – 5 fold   | 4-5 log  | < 10 fold  | 2-3 log   |

*Table 1 continues on next page...*

Table 1 continued from previous page.

| Method                         | FP  | ELISA/DELFI A  | FRET  | AlphaScreen                                  |
|--------------------------------|---|--|---|--|
| <b>Cost</b>                    | Low - moderate  | Low - moderate   | Moderate - high   | High   |
| <b>Other advantages</b>        | Standard deviations tend to be low; is a direct PPI measurement                       | Low spectroscopic interference from compound                   | Ratiometric, readily controlled for spectral artifacts  | Can monitor the widest range of complex size |
| <b>Principal disadvantages</b> | Dye “propeller” rotations must be considered; fluorescence of compounds can interfere | Sensitive to off-rates, laborious, often without clear benefit | Signal window dependent on distance and dye orientation | Sensitive to ambient light                   |

## General Considerations

Screening in general, and for PPI inhibitors in particular, identifies compounds with many mechanisms of inhibition. Some of these mechanisms are undesired, such as direct assay interference, nonspecific binding, and covalent modification. To reduce the likelihood of finding such compounds, we recommend the following practices for in vitro assays:

1. **Use of detergents in biochemical assays.** Low concentrations of detergents tend to stabilize proteins, reduce nonspecific binding of proteins to assay plates, and break up compound aggregates. We favor using one detergent in a screen, then following up with alternate detergents, since no one detergent removes all aggregates. Commonly used detergents include Triton X-100 (0.01%), Tween 20 (0.005%), and Chaps (0.1%); in general, detergents should be used at concentrations below their critical micelle concentration (CMC).
2. **Use of carrier proteins.** As with detergents, non-interfering proteins such as gamma globulin, casein, or Prionex (Centerchem) can be used to reduce nonspecific binding of compounds and assay proteins. Bovine serum albumin (BSA), used in most cell-based assays, binds many compounds that are viable drug leads and may not be the best choice for primary biochemical screens. Using carrier proteins is less common than detergents, but should be considered for primary or secondary testing.
3. **Diluting compounds in DMSO.** Most HTS libraries are dissolved in DMSO, and small concentrations of DMSO (typically <0.1%) are thus carried into assays. The sensitivity of an assay to DMSO must be determined during assay development. In addition, since compounds vary in their solubility, it is best practice to limit intermediate dilutions into buffer. In particular, when running dose-response titrations, the compounds should be serially diluted in DMSO, then transferred into the assay buffer as close to the final concentration as possible. The use of nanoliter volume dispensers has made this approach practical for 384-well and higher format plates.

4. **Use of orthogonal assays.** Compounds will interfere with assays in multiple ways, some of which are difficult to predict. It is therefore important to follow up any primary assay with an orthogonal secondary assay that uses a different modality (e.g. colorimetric vs luminometric) or format (plate-bound, vs mix-and-read, vs label-free). Finally, unless the goal is to discover covalent modifiers of a PPI, reversibility of inhibition should be demonstrated. This can be accomplished by mixing the reagents at high concentration, then diluting to a condition well below the affinity of the inhibitor. Additionally, the PPI partners can be incubated with inhibitor, then analyzed by mass spectroscopy.

## ELISA-type assays

### Concept

Enzyme-Linked Immunosorbant Assays (ELISAs) follow the basic design shown in Figure 1. These formats can be used to measure PPI and thus to measure competition between a PPI and a small-molecule inhibitor. To measure a PPI, one of the proteins is attached to a plate surface and the second protein is then allowed to bind to the first protein. The second protein is detected by binding of an antibody that is linked to an enzyme. When substrate is added, the enzyme produces a measurable readout that is quantitatively linked to the amount of the second protein. ELISAs can be very sensitive, because the readout is amplified by using an enzyme. Further amplification can be achieved by using multiple layers, such as [secondary antibodies](#).

ELISA technically means that the detection event uses an antibody and enzyme-based detection; however, this term is commonly used to describe plate-bound detection of a reagent, even if the affinity reagent is not an antibody or if the detection reagent is not an enzyme. One commonly used, non-enzymatic format is called Dissociation-Enhanced Lanthanide Fluorescent Immunoassay ([DELFI](#), Perkin Elmer). In DELFIA, the detection signal is time-resolved fluorescence of a lanthanide ion (such as europium). The lanthanide ion is bound to the affinity reagent through a chemical linkage; upon adding a proprietary detergent mixture, the europium fluoresces, providing a highly sensitive measurement of the concentration of bound protein. Three features of lanthanide fluorescence lead to highly sensitive and selective assays: a) a long emission lifetime (milliseconds) allows the measurement to start after the fluorescence of organic material (proteins, test compounds) has decayed, b) the emission occurs at around 600 nm, where few biological materials absorb or emit light, and c) the narrow emission spectrum of lanthanides allow them to be multiplexed.

ELISA-style assays can be designed in many ways. Attachment of the surface-bound protein can occur by passive adsorption to a plastic plate, by capture with an adsorbed antibody, or by biotinylation and avidin capture. Detection of the second protein can occur by direct labeling the protein with a signal-generating enzyme, by binding of an enzyme-labeled antibody, by binding of an unlabeled primary antibody followed by a labeled secondary antibody, or by biotinylation followed by enzyme-linked avidin.

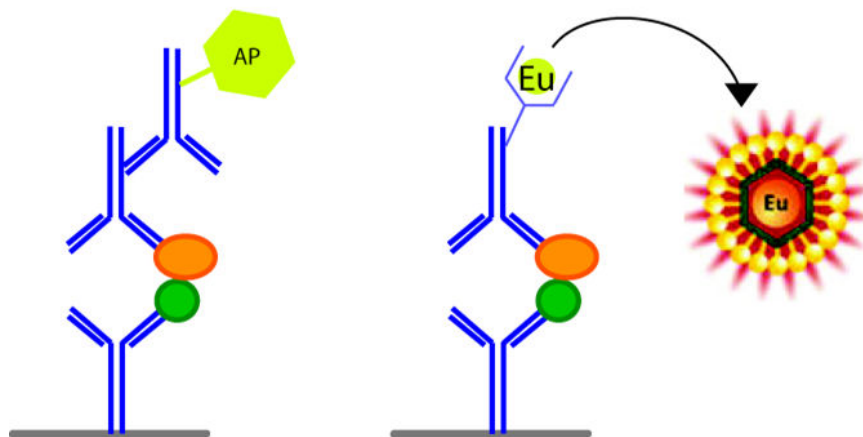


**Figure 1:** Format for ELISA and DELFIA assays. **Left:** An ELISA is built up in several steps, starting with antibody to protein 1, protein 1 (green), protein 2 (orange), anti-protein 2, and an anti-species antibody conjugated with an enzyme (AP = alkaline phosphatase). The signal produced by enzyme activity is proportional to the amount of PPI. **Right:** If protein 2 (orange) has an epitope tag, the anti-epitope antibody is often labeled with the detection reagent. In DELFIA, the detection reagent is a rare earth element such as europium.

Detection enzymes can include colorimetric, fluorogenic, or luminogenic reactions. Selection criteria for each of these steps are described below.

## General Considerations

Consider the affinity of the PPI when designing a plate-based assay. Such assays involve multiple wash steps, which will remove unbound protein. If binding kinetics are rapid, as with most weak interactions (ca.  $> 1 \mu\text{M}$ ), signals will be lower. The fewer amplification steps (e.g. direct conjugation of the enzyme to the solution-phase protein), the less signal is lost to washing. Assay format is therefore a compromise between assay complexity and signal amplification.

In principle, either member of the PPI could be immobilized, but several issues should be considered:

1. Is there a potential for avidity in the interaction? Avidity occurs when multiple contacts are made simultaneously, as with a trimeric protein binding to a trimeric ligand, or when a trimeric protein binds to a plate with a high density of ligand. This Velcro-like effect results in slowed unbinding kinetics (off-rates) and thus an apparent affinity that is tighter than the 1:1 binding affinity. For weak interactions, such avidity allows the PPI to survive washing, but it also complicates quantitative analysis. If one member of the PPI is monomeric, it is generally recommended to use this protein as the solution-phase protein, while a multimeric partner is immobilized on the plate.

2. Is one protein more likely to bind to the small molecule? Compounds are more likely to bind to the side of the PPI that is concave, such as when a bit of secondary structure from the other protein binds into a groove (examples include MDM2/p53, PDZ domains). If the grooved protein is kept in solution, then the ELISA will monitor a solution-phase binding event.
3. Is one protein more apt to precipitate or aggregate? If one protein is known to precipitate, it might be more stable as the captured, plate-bound partner.
4. Is one PPI partner limiting? Generally, more of the immobilized protein is used, so if one protein is easier to obtain and purify, it should be considered for immobilization.
5. Another option is if one of the proteins is expressed with a tag such as his or GST or FLAG, a plate coated with antibodies to the tag would serve to immobilize the protein to the plate. A protein can be biotinylated and streptavidin-coated plate can be used.

If there is no compelling reason to use one protein for surface-immobilization, then both orientations of the assay should be evaluated. In the ideal case, the same  $IC_{50}$  values should be obtained from both formats.

## Assay design and development

1. **Instrumentation:** The assays described here can be performed with most multimodal plate readers, and the readout can be selected based on available instrumentation. Typical readouts are absorbance, fluorescence, luminescence, or time-resolved fluorescence (TRF). Time-resolved fluorescence, used by DELFIA, is the least-standard modality, but most HTS facilities will have TRF-compatible instruments.
2. **Plates:** ELISA-type assays are generally performed in polystyrene microwell plates with high-binding surfaces to adsorb proteins. The color of the plate is selected based on the readout: clear (absorbance), black (fluorescence), and white (luminescence). DELFIA can be performed in clear, white or yellow plates.
3. **Binding of first protein (protein 1):** The first immobilized protein can be bound to the plate by passive adsorption or by capture. Passive adsorption is simple – the protein is added to a bare plate; however, some proteins will denature upon adsorption and the orientation of proteins on the surface will be random. After the protein is adsorbed, the rest of the well surface is blocked with a nonspecific protein, such as casein (1%), nonfat milk (5%), or bovine serum albumin (1%). Critical steps for passive adsorption include a) selecting a concentration of protein to maximize ELISA signal and b) selecting a blocking protein that reduces nonspecific binding of the second protein partner and detection reagents. At any step in the ELISA process, a blocking protein or detergent can be used to reduce nonspecific binding.

If assay sensitivity is low when the protein is adsorbed, a capture step can be added. In this format, an antibody or avidin is adsorbed to the plate first. Generally, the



capture protein is plated at a saturating condition. The plate is then blocked with nonspecific proteins and protein 1 is added. If an antibody is used for capture, it should not block the PPI and should be available in sufficient supply for the scale of the assay. If avidin is used, there are different versions (e.g. streptavidin and neutravidin) that could alter the degree of nonspecific binding. The protein to be captured must be biotinylated, which can be accomplished during expression (via [AviTag](#); Avidity) or chemically (via reaction with amines, acids, or cysteine residues). Biotinylation using AviTag sequences will provide homogeneous labeling near the N- or C-terminus of the protein.

4. **Binding of the second protein (protein 2):** Protein 2 in the PPI can also be added to the ELISA plate in several formats. The protein can be unmodified, it can be biotinylated (if the first protein was not immobilized by biotin/avidin binding), or it can be labeled directly with the detector (e.g. enzyme or DELFIA probe). As mentioned above, the decision to label or use secondary detection is a balance between the number of washing steps and signal amplification. Directly labeled proteins, such as horseradish peroxidase (HRP)-protein conjugates, can be less soluble and more prone to artifacts; compounds can also interfere with detection, such as by inhibiting the detection enzyme itself. Therefore, ELISAs usually use a secondary detection step. In either case, protein 2 should be titrated to achieve a robust but non-saturating signal. Incubation times should allow equilibrium to be reached. After incubation, the unbound protein 2 should be thoroughly washed from the plate, usually using 3 cycles of phosphate-buffered saline with 0.01% Tween 20 (or other detergent).
5. **Affinity reagents (e.g. antibodies or streptavidin):** When protein 2 is not directly labeled with a detection reagent, one or two binding steps are required to add the detector. When protein 2 is biotinylated, avidin is conjugated with the detection reagent. When the protein is unmodified, an antibody to protein 2 is usually used. This primary antibody can be labeled with detection reagent or a secondary antibody (e.g. rabbit anti-murine IgG) can be labeled and bound. The affinity reagents should be titrated to reach a maximal signal-to-background; the binding can be saturated, but care should be taken to ensure that the reagent is not binding non-specifically to wells without protein 2. Incubation time is another optimize-able parameter, and can vary from 1 hour to overnight. After incubation, the plate should be thoroughly washed to remove unbound reagents.
6. **Detection methodology:** The final step of the ELISA involves adding a substrate; when the linked enzyme turns over the substrate, a measurable change (e.g. color) occurs. Two commonly used enzymes are horseradish peroxidase (HRP) and alkaline phosphatase (AP); avidin and antibody conjugates of these enzymes are widely available, as are chromogenic and luminogenic substrates. Generally speaking, luminescent substrates are more sensitive, requiring smaller amounts of material and/or less incubation time than chromogenic substrates and have a wider dynamic range than chromogenic substrates. On the other hand, chromogenic products tend to be more stable over time. ELISAs can be read kinetically (monitoring the color change over time) or at a fixed endpoint.

Endpoint readings can include a quenching step, such as the addition of acid (e.g. equal volume of 1 M HCl or H<sub>3</sub>PO<sub>4</sub>) or base (e.g. 1 M ammonium chloride) to stop enzyme turnover and stabilize the ELISA signal.

DELFIAs are processed similarly to ELISAs. Some europium-labeled reagents are commercially available, including anti-IgGs, anti-tag antibodies (such as anti-His tag antibodies), and streptavidin, and others can be prepared in the lab or by custom synthesis (for example, see [Perkin Elmer](#) and [Cisbio](#)). Detection requires the addition of a commercial “dissociation-enhancement solution.”

## Benefits and limitations

ELISA and DELFIA have some important benefits. They are very flexible and sensitive, and can be inexpensive to run. They are also less likely to have compound interference since the compound is not present in the processing step. They also have significant limitations that have led to their reduced use in HTS. Most ELISAs have multiple incubation and washing steps, which are time-consuming for automated and bench-top assays. Washing can also disrupt weak interactions (e.g.  $K_D > 1 \mu\text{M}$ ). Finally, it is important to demonstrate that potential PPI inhibitors are not interfering with the detection system or acting nonspecifically with the proteins and detection reagents. Changing formats and using complementary detection methods (such as those described below) will help to validate potential inhibitors.

## Related technologies

PPI assays have also been performed with bead-based separation, e.g. using flow cytometry (9).

## Mix-and-read assays

Three main formats are available with both similarities and differences with regard to label, secondary detection, and maximum distance allowable between the protein partners. FRET and AlphaScreen are proximity measurements, meaning that they rely on the protein partners being within 10 – 100 angstroms. Fluorescent Polarization measures the tumbling time, related to the molecular mass, experienced by a fluorophore. A principal advantage of these mix-and-read assay formats is that they require no washing steps, leading to a wider dynamic range and higher plate throughput.

## Fluorescence polarization/anisotropy

### Concept

Fluorescence polarization (FP) is a sensitive nonradioactive method for the study of molecular interactions in solution (10). This method can be used to measure association and dissociation between two molecules if one of the molecules is relatively small and fluorescent. When a fluorescently labeled molecule is excited by polarized light, it emits light with a degree of polarization that is inversely proportional to the rate of molecular

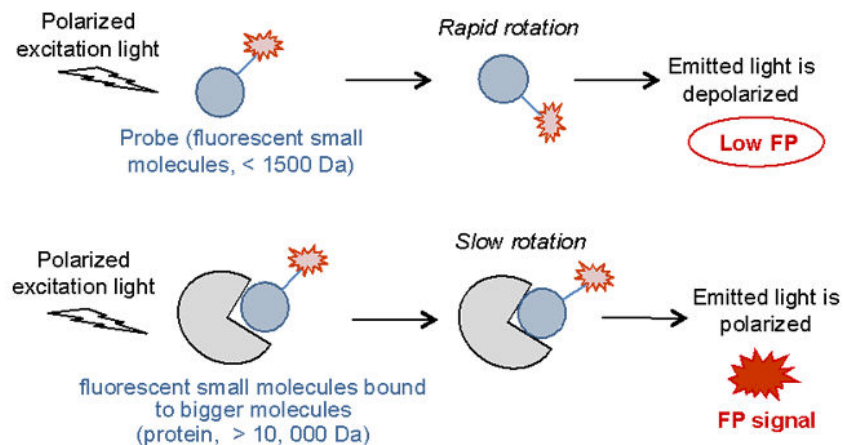


**Figure 2:** Diagram of a fluorescence polarization assay. Rapidly rotating small molecule fluorophore gives low FP signal (low mP). The association of a relatively large molecule, such as a protein, with the small molecule fluorophore slows down the motion of the fluorophore, leading to increased FP signal.

rotation. Molecular rotation is largely dependent on molecular mass, with larger masses showing slower rotation. Thus, when small, fluorescent biomolecule, such as a small peptide or ligand (typically <math>< 1500 \text{ Da}</math>), is free in solution, it will emit depolarized light. When this fluorescent ligand is bound to a bigger (e.g. > 10,000 Da) molecule, such as a protein, the rotational movement of the fluorophore becomes slower and thus the emitted light will remain polarized. Thus, the binding of a fluorescently labeled small molecule or peptide to a protein can be monitored by the change in polarization (Figure 2).

### Assay design

1. **Selection of FP probe:** Protein-protein interactions can be monitored by FP if one of the components of the PPI is small. Typically, the molecular weight of the ligand/probe is less than 1500 Da, although up to 5000 Da can be acceptable if the binding partner is very large. For most PPI, FP will be practical only a) if one side of the PPI can be minimized to a peptide, b) if there is a synthetic peptide known to bind at the interface (e.g. via phage display), or c) if an organic compound binds at the interface (or to a mutually exclusive binding site). Fortunately, there are several examples of peptides that mimic the epitope of a protein in a PPI, including PDZ domains, IAPs, Bcl2-family proteins, and others.
2. **Selection of fluorescent dye:** Once a probe molecule has been selected, it must be labeled with a fluorescent dye. Dyes are typically available in amine-reactive, cysteine-reactive, and acid-reactive forms and are chemically attached to the probe peptide/molecule using simple chemistry. Typical fluorophores used in FP are fluorescein, rhodamine, and BODIPY dyes. The BODIPY dyes have longer excited-state lifetimes than fluorescein and rhodamine, making their fluorescence polarization sensitive to binding interactions over a larger molecular weight range

- (11). Red-shifted dyes are preferable to reduce the number of compounds that will cause interference with the 405nm (e.g. fluorescein) range.
3. **Selection of buffer:** the buffer must have low fluorescence background. Frequently used buffers have neutral pH such as PBS, HEPES.
  4. **Instrumentation for FP measurement with microtiter plate:** Many commercially available instruments are capable of measuring the FP signal from solution in 96/384/1536-well microtiter plate format for high throughput screening (HTS). The fluorescence is measured using polarized excitation and emission filters. Two measurements are performed on every well and fluorescence polarization is defined and calculated as:

$$\text{Polarization} = P = (I_{\text{vertical}} - I_{\text{horizontal}}) / (I_{\text{vertical}} + I_{\text{horizontal}})$$

Where  $I_{\text{vertical}}$  is the intensity of the emission light parallel to the excitation light plane and  $I_{\text{horizontal}}$  is the intensity of the emission light perpendicular to the excitation light plane (10). All polarization values are expressed as the milli-polarization units (mP).

All commercial microplate readers have built-in software for mP calculation. Depending on the instrument used, three sets of data are generally reported, including calculated mP values, raw fluorescence intensity counts of vertical (or Parallel/S-channel) and horizontal (or perpendicular/P-channel) measurements for each well.

mP calculation for different instruments requires the proper use of measured fluorescence intensity of parallel/S-channel and perpendicular/P-channel. As optical parts of fluorometers possess unequal transmission or varying sensitivities for vertically or horizontally polarization light, such instrument artifacts should be corrected for accurate calculation of the absolute polarization state of the molecule using fluorescent readers. This correction factor is known as the "G Factor" which is instrument-dependent. G-factor corrects for any bias toward the horizontal (or perpendicular/P-channel) measurement. Most commercially available instruments have an option for correcting the single-point polarization measurement with G factor. For example, the mP values for FP measurement with Envision Multilabel plate reader are calculated as:

$$\text{mP} = 1000 * (S - G * P) / (S + G * P)$$

In practice for HTS applications, however, it is unnecessary to measure absolute polarization states; the assay window is what is important. The assay window is insignificantly changed by G Factor variation.

5. **Determining the concentrations of fluorescent probes for the FP binding assay:** In order to select the proper concentrations of fluorescent probe for the binding assay, increasing concentrations of fluorescent probe is prepared in assay buffer

without the binding protein. The fluorescence intensity (FI) in the parallel channel is then measured with defined settings in a plate reader with FP mode. A concentration of the fluorescent probe with at least 10-fold or higher FI signal compared to that of buffer only should be selected for the subsequent binding assay. Notice that the FP signal is expressed as a ratio of fluorescence intensities. Thus, the signal is not influenced by changes in intensity brought about by changes in the tracer concentration.

6. **FP Binding assay development:** To determine the binding of the fluorescent probe with the protein of interest, increasing concentrations of protein are mixed with a fixed concentration of the probe. The FP signal as expressed in mP is then measured with a plate reader. mP vs [protein] is then plotted to generate a binding isotherm for the calculation of association parameters such as K<sub>d</sub> and maximal binding. For the FP inhibition assay, select a concentration of protein that provides ca. 80% of the maximum change in polarization for the probe (e.g. 80% bound).
7. **Data analysis:** The dynamic range of the FP assay, i.e. assay window, is defined as mP<sub>b</sub> – mP<sub>f</sub>, where mP<sub>b</sub> is recorded mP value for the specific binding in the presence of a particular protein concentration and mP<sub>f</sub> is the recorded mP value for free tracer from specific binding proteins (12). Typically, the assay window is 3-5 fold (e.g. 50 mP – 150 mP).
8. **Selectivity:** once the concentrations of probe and protein are determined, the specificity of the interaction should be assessed. First, an unlabeled version of the probe is titrated into a mixture of the FP-probe and protein. As the concentration of unlabeled probe competes with bound fluor-probe, the FP should decrease. The IC<sub>50</sub> for this interaction should be similar to the K<sub>d</sub> measured above. Similarly, other known inhibitors should yield the expected IC<sub>50</sub> values.
9. **Fluorescence of the bound probe:** often the fluorescence of the probe changes when it binds to the protein. In this case, anisotropy measurements should be used in place of polarization, since unlike FP, anisotropy is directly proportional to fluorescence intensity. Anisotropy is calculated with the following expression:

$$\text{Anisotropy: } r = (I_{\text{vertical}} - I_{\text{horizontal}}) / (I_{\text{vertical}} + 2 I_{\text{horizontal}})$$

where  $I_{\text{vertical}}$  is the intensity of the emission light parallel to the excitation light plane and  $I_{\text{horizontal}}$  is the intensity of the emission light perpendicular to the excitation light plane.

### Case study: Monitoring 14-3-3 protein interactions with a homogeneous FP assay

The 14-3-3 proteins mediate phosphorylation-dependent protein-protein interactions. Through binding to numerous client proteins, 14-3-3 controls a wide range of physiological processes and has been implicated in a variety of diseases, including cancer and neurodegenerative disorders (13). We have designed a highly sensitive fluorescence polarization (FP)-based 14-3-3 assay (Figure 3), using the interaction of 14-3-3 with a

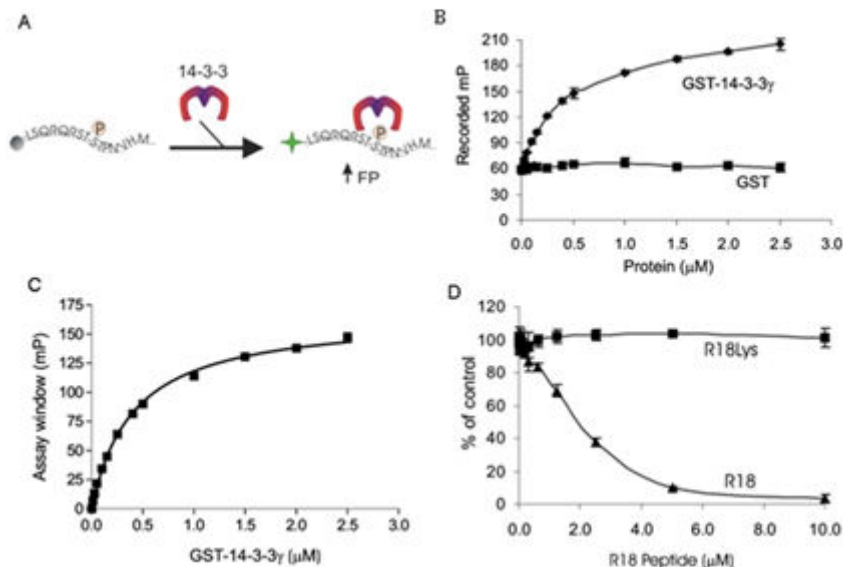


**Figure 3:** Development of FP assay for TMF-pS259-Raf/14-3-3. **A:** The interaction of 14-3-3 with TMR-pS259-Raf gave rise to a significant FP signal with a minimal background polarization with the peptide probe alone or with increasing concentrations of a nonbinding protein (GST). With increasing amounts of GST-14-3-3 $\gamma$  protein, polarization values progressively increased to reach saturation, suggesting that a greater fraction of fluorescent peptide was bound to the 14-3-3 protein. **B:** The maximum assay window ( $\Delta$ mP = mP of bound peptide – mP of free peptide) reached approximately 150 mP with an estimated dissociation constant,  $K_d$ , of  $0.412 \pm 0.01 \mu\text{M}$  for the Raf peptide. **C:** A well-known 14-3-3 antagonist peptide, R18, can compete the 14-3-3 binding as measured by a dose-dependent decrease of FP signal; however, a mutant R18 peptide cannot compete the binding (Adapted from Du, 2006).

fluorescently labeled phosphopeptide from Raf-1. The specificity of the assay has been validated with known 14-3-3 protein antagonists, e.g., R18 peptide, in a competitive FP assay format. The signal-to-background ratio is greater than 10 and a  $Z'$  factor is greater than 0.7 (12). Because of its simplicity and high sensitivity, this assay is generally applicable to studying 14-3-3/client protein interactions and for HTS.

## Materials:

1. Protein (14-3-3 $\gamma$ ): the recombinant GST-14-3-3 protein was expressed in *Escherichia coli* strain BL21 (DE3) as a GST-tagged product and purified
2. Probe (TMR-pS259-Raf): a phosphopeptide derived from Raf-1 was synthesized and labeled with 5/6 carboxytetramethylrhodamine (TMR)
3. Buffer: HEPES buffer containing 10 mM HEPES, 150 mM NaCl, 0.05% Tween 20 DTT 0.5 mM DTT, pH 7.4
4. 384-well black plate (Corning Costar Cat#: 3573)
5. Instrument for FP measurements: FP measurements were performed on Analyst HT plate reader (Molecular Devices, Sunnyvale, CA) using FP protocol. For Tetramethylrhodamine (TMR)-labeled probe (Excitation: 545 nm; Emission: 610 nm), a dichroic mirror of 565 nm was used.

## Protocol:

1. **Selection of probe concentration:** 1 nM of the TMR-pS259-Raf peptide was chosen for the binding assay based on the observation that 1 nM of the TMR-labeled peptide exhibited about 10 times more fluorescence intensity in the parallel channel than the “buffer-only” control samples.
2. **Prepare probe and protein solutions:** 2 basic solutions were prepared. Solution A contained TMR-pS259-Raf peptide in the HEPES buffer (2× solution with 2 nM of the peptide probe or as specified). Solution B contained 14-3-3 proteins in HEPES buffer (2× solution with increasing concentrations of 14-3-3 protein; a serial dilution approach is generally used for the protein titration).
3. **Binding FP assay:** The 14-3-3 FP binding assay was carried out in black 384-well microplates in a total volume of 50 µl in each well. For each assay, a 25 µl of Solution A (probe) is mixed with 25 µl of solution B (protein) in 384-well plate. Probe only without protein is always included as blank control.
4. **FP measurement:** the polarization value in mP was measured at room temperature (RT) with an AnalystHT reader immediately, or after incubating at RT as desired time period for the equilibration of the interaction.
5. **Competitive FP assays:** the specificity of the FP binding assay is generally evaluated with known antagonists, e.g, unlabeled probe, peptide or small molecule antagonists, in competitive FP assay. To achieve the desired sensitivity, the concentrations of fluorescent Raf peptide probe and 14-3-3 protein are carefully chosen to maximize the difference between the highest and lowest polarization values. Serial dilutions of competitive peptide (R18) are added to a reaction buffer containing TMR-pS259-Raf (1 nM) and GST-14-3-3γ (0.5 µM) and incubated at RT for 1 hr. The mP values were measured and the competitive effect was expressed as percentage of control mP (TMR-pS259-Raf and GST-14-3-3γ) after subtracting the background mP (TMR-pS259-Raf alone).

## Benefits and limitations:

FP-based technology has a number of key advantages for monitoring bimolecular interactions, especially for HTS applications. It is nonradioactive and is in homogenous “mix-and-read” format without wash steps, multiple incubations, or separations. FP measurement is directly carried out in solution; no perturbation of the sample is required, making the measurement faster and perhaps more native-like than immobilization-based methods like ELISA. It is readily adaptable to low volume (30 µl for a 384-well plate or 5 µl for a 1536-well plate). In addition to measuring PPI, FP assays have been used to study a wide variety of targets including protein-nucleic acid interactions, kinases, phosphatases, proteases, G-protein-coupled receptors (GPCRs), and nuclear receptors (14, 15).

As a fluorescence-based technology, FP is subject to optical interference from compounds that absorb at the excitation or emission wavelengths of the fluorescent probe. Being a ratiometric technique makes FP somewhat resistant, though enough light must be

available to obtain an emission signal. FP is also sensitive to the presence of fluorescence from test compounds. The use of red-shifted probes will minimize background fluorescence interference.

## Fluorescent/Förster resonance energy transfer and time-resolved (TR) FRET

### Concept

Fluorescence/Förster Resonance Energy Transfer (FRET) is the phenomenon of non-radiative energy transfer between two fluorophores with specific spectral properties. In order for FRET to occur, the emission spectrum of one fluorophore, i.e. the “donor,” must overlap the excitation spectrum of the second fluorophore, i.e. the “acceptor.” When the donor is excited by incident light, energy can be transferred to the acceptor via long-range dipole-dipole interactions, resulting in acceptor emission; however, this FRET event will only occur if the donor and acceptor are in sufficient proximity to one another. FRET efficiency  $E$  is defined by the equation

$$E = \frac{1}{1 + (r/R_0)^6}$$

where  $r$  is the distance between the fluorophores and  $R_0$  is the Förster distance and which FRET efficiency is 50% for the specific donor/acceptor pair. Two key factors arise from this equation. First, the amount of energy transfer decays with the sixth power of the distance between the fluorophores. Second, the term  $R_0$  depends on the spectral overlap of the donor emission spectrum and the acceptor absorbance spectrum; FRET can be observed over longer distances when the spectral overlap is large. Fortunately, the proximity limit for several donor/acceptor pairs is approximately 10 nm, which happens to be the distance over which many biomolecular interactions occur. Therefore, FRET can be used to monitor biomolecular interactions in a homogeneous mix-and-read assay format by tagging or labeling interacting biomolecules “A” and “B” with acceptor and donor fluorophores, respectively. In such a scenario, the ratio of acceptor to donor emission following donor excitation is used to quantify and monitor “AB” binding. Table 2 lists some common donor/acceptor pairs.

Due to the spectral properties of biological media and traditional FRET donor/acceptor pairs, the FRET signal can be significantly contaminated by 1) autofluorescence of biological media and test compounds; 2) a wide acceptor excitation spectrum that allows the acceptor to be directly excited by incident light; and 3) a wide donor emission spectrum that bleeds through into the acceptor emission detection window. These signal contaminants must be corrected for and can significantly diminish the sensitivity of traditional FRET assays.

One elegant solution to the problem of FRET signal contamination is the use of donor fluorophores with exceptionally long emission half-lives (up to 1500  $\mu$ s), such as the rare earth metals Europium or Terbium, in a modification of FRET known as Time Resolved



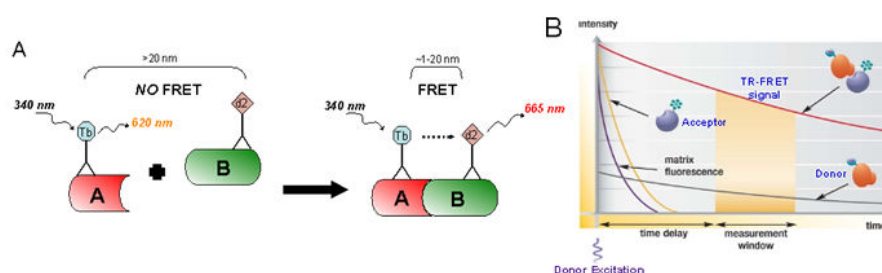


**Figure 4:** Principles of TR-FRET. **A:** Schematic of a typical FRET bioassay. Protein 1 is bound to an antibody fused to a donor fluorophore, e.g. Terbium (Tb), and Protein 2 is bound to an antibody fused to an acceptor fluorophore, e.g. d2 or XL665. If A and B interact, the donor and acceptor are brought into sufficient proximity for FRET to occur. In the case of a positive FRET event, acceptor emission is detected upon donor excitation. **B:** The primary sources of FRET signal contamination (matrix fluorescence, direct excitation of the acceptor) are avoided in TR-FRET by inserting a time delay between donor excitation and detection of acceptor emission (“measurement window”) (adapted from Degorc, 2009).

(TR) FRET (also called HTRF). In TR-FRET, Europium or Terbium cryptates (ligands that coordinate the metal ion and provide an “antenna” dye) serve as donors that have a very long luminescence half-life. This long emission decay allows for a time delay (50-150  $\mu$ s) between donor excitation and the recording of acceptor emission. During this time delay, both media autofluorescence and acceptor excitation due to incident light will rapidly decay (ns scale) and be extinguished by the time acceptor emission is measured. This essentially eliminates signal contaminants 1 and 2 above. Signal contaminant 3 – donor emission bleedthrough into acceptor detection – is attenuated by the use of acceptors with red-shifted emission (Table 2) such as allophycocyanin, Alexa 680 (Invitrogen), Cy5, or d2 (Cisbio Bioassays). Another advantage of TR-FRET is that the rare earth metals have a modestly larger proximity limit for FRET (up to 20 nm), allowing for the detection of larger biomolecular complexes. TR-FRET assays are well suited for certain HTS applications due to their homogenous mix-and-read design, high signal-to-background ratios, and enhanced proximity detection range (Figure 4).

**Table 2:** Common donor/acceptor pairs for FRET and TR-FRET/HTRF<sup>1</sup>

| Donor           | Acceptor             | $R_0$ (Å) <sup>2</sup> |
|-----------------|----------------------|------------------------|
| Fluorescein     | Tetramethylrhodamine | 55                     |
| IAEDANS         | Fluorescein          | 46                     |
| EDANS           | Dabcyl               | 33                     |
| BODIPY FL       | BODIPY FL            | 57                     |
| Fluorescein     | QSY 7 and QSY 9 dyes | 61                     |
| Alexa Fluor 488 | Alexa Fluor 555      | 70                     |

<sup>1</sup> Adapted from Invitrogen.com (FRET; Alexa dyes) and Cisbio (TR-FRET); <sup>2</sup> $R_0$  is the distance at which FRET efficiency is 50%.

Table 2 continued from previous page.

| Donor                   | Acceptor                       | $R_0$ (Å) <sup>2</sup> |
|-------------------------|--------------------------------|------------------------|
| Alexa Fluor 594         | Alexa Fluor 647                | 85                     |
| Europium (III) cryptate | XL665 (allophycocyanine) or d2 | 90                     |
| Terbium (III)           | Fluorescein                    | 70                     |

<sup>1</sup> Adapted from Invitrogen.com ([FRET](#); [Alexa](#) dyes) and Cysbio ([TR-FRET](#)); <sup>2</sup> $R_0$  is the distance at which FRET efficiency is 50%.

## Assay Design

**Instrumentation:** A plate reader capable of allowing a time delay between excitation and fluorescence detection is required. The multimodal readers Envision (PerkinElmer) and Analyst HT (Molecular Devices) and PheraStar (BMG) are well suited for this application.

2. **Plates:** TR-FRET assays are performed in black opaque plates. Assays may be performed in 96-, 384-, 1536-well formats.

3. **Buffers:** The following buffer is used routinely at the Emory Chemical Biology Discovery Center for all TR-FRET assays: 20 mM Tris, pH 7.5, 0.01% Nonidet P40, and 50 mM NaCl. However, multiple buffers can be used. As noted in the general considerations above, the use of detergents (e.g. Nonidet P40, Triton X-100, Tween 20) and carrier proteins (e.g. - Prionex) should be optimized during assay development to reduce nonspecific effects. Similarly, salt conditions can affect PPI.

4. **Labeling Reagents:** Proteins can be directly labeled with FRET donor and acceptor, using amine-, acid-, or cysteine-reactive dyes. Because random chemical coupling can disrupt the PPI, it is more common to use anti-epitope tag antibodies or streptavidin labeled with FRET and TR-FRET dyes. These general protein-dye conjugates are commercially available for proteins containing GST, HA, Flag, 6xHis, myc, or biotin tags. If it is necessary to measure binding of untagged or endogenous biomolecules, kits for labeling primary (anti-protein) antibodies with FRET and TR-FRET fluorophores are also available for purchase. FRET and TR-FRET reagents are available from [Cisbio Bioassays](#), [PerkinElmer](#), and [Invitrogen](#), among others.

5. **Assay Conditions:** FRET and TR-FRET assays are performed at room temperature. Assay performance has been shown to be stable for up to 24 hours at room temperature. In some formats, the quality of the signal improves with time and can be much better after overnight incubation. The timing for signal development and decay should be confirmed for each assay.

## Steps for developing a TR-FRET Assay

1. **Select binding partners to be used.** Typically, the greatest TR-FRET sensitivity is obtained when the purified, recombinant protein-binding domains of interacting proteins are used. However, if the binding domains are not known, full-length recombinant proteins can also be used. Additionally, if purified proteins cannot be

generated, or if it is critical to evaluate the PPI in a complex milieu, TR-FRET can also be performed using cell lysates containing over expressed, epitope-tagged versions of the interacting proteins. If using cell lysates, it may be best to develop stable cell lines expressing one of each binding pair to ensure consistent protein expression.

2. **Select protein concentrations.** When proteins are directly labeled with fluorophores, simply titrate each binding partner in a matrix to determine concentrations that yield optimal assay window, signal-to-background ratio, and  $Z'$  values. When proteins are not directly labeled, the concentrations of the PPI and the dye-conjugated antibodies/avidin must also be optimized. It is typical to start with constant concentrations of the dye-conjugated antibody/avidin, and titrate the PPI partners. Most commercial reagents suggest starting conditions; in general, the concentrations of FRET-conjugate antibodies should be higher than the concentrations of the proteins they detect (e.g. 20 nM anti-HA antibody and 10 nM HA-tagged protein).
3. **Select concentrations of (TR-)FRET reagents.** Once the PPI concentrations have been selected, the FRET-tagged antibodies/avidin should be titrated to optimize the assay window, signal-to-background, and  $Z'$  values. When concentrations of antibodies are too high, the efficiency of FRET can decrease. This effect, called “hooking,” is described in the General Consideration: Hooking Effect section below.
4. **Test effect of DMSO.** Assay performance should be measured over a range of DMSO concentrations to ensure that screening results are not skewed by vehicle effects. For HTS, DMSO generally ranges from 0.1 – 1%, but higher levels are sometimes acceptable.
5. **Assess assay performance.** Positive controls are then titrated in a competition format to ensure that  $IC_{50}$  values match expectation. Either known interaction inhibitors or non-labeled binding partners can be used as positive controls for binding competition/disruption.

### Example: Performing a TR-FRET Assay

1. All assay components are combined with assay buffer (e.g. 20 mM Tris, pH 7.5, 0.01% Nonidet P40, and 50 mM NaCl) to their optimized concentrations and 19  $\mu$ L are transferred to each well of a 384-well plate.
2. Test compounds are added. In this case, test compound stocks are at 1 mM, and 0.5  $\mu$ L is added to each well to give a final compound concentration of 25  $\mu$ M.
3. All assay plates must contain at least one column of minimal FRET/background control (e.g., all assay components minus one binding partner, usually the one that binds the acceptor fluorophore) and at least one column of maximal FRET vehicle control (i.e., all assay components plus DMSO).
4. The plate is incubated at room temperature for one hour or overnight and then the FRET signal is recorded.

5. Background is subtracted from all FRET values and test compounds are compared to the maximal FRET control to determine percent inhibition of binding for each compound.

## Benefits and Limitations

Several factors make FRET and TR-FRET attractive techniques to measure PPIs. As with the other mix-and-read formats, FRET methods are relatively easy to automate and to miniaturize. The approach is also flexible, since many dyes and dye-antibody conjugates are available. In contrast to FP, FRET can be used with a wide range of protein sizes, with the proviso that the FRET pairs must come within a few nanometers of each other. Thus, TR-FRET assays can be performed with peptides, full-length recombinant proteins, transfected cell lysates, and, in some cases, with endogenous proteins in cell lysates. This potentially allows for the development of robust HTS screening assays using binding pairs in a less artificial environment. FRET and TR-FRET are usually performed as ratiometric assays, which reduce the effects of autofluorescence and spectral interference of media and test compounds. TR-FRET further reduces the effect of autofluorescence by allowing organic fluorescence to decay before TR-FRET is measured. Finally, TR-FRET formats allow multiplexing. For instance, FRET acceptors can be multiplexed with a single lanthanide donor, allowing two or three pairs of PPI to be monitored in a single well (16, 17). TR-FRET has been multiplexed with FP, providing increased information in the primary HTS screen (18).

There are limitations to the FRET and TR-FRET formats, however. The signal window for FRET experiments depends on several factors implicit in the Forster equation, including the orientation of the dyes and the size of the complex – including the size of the FRET-labeled antibodies. For very large complexes, AlphaScreen (see AlphaScreen Format) could yield a stronger signal. Furthermore, while TR-FRET's ratiometric format does reduce interference from test compounds, those compounds that absorb a lot of UV light can inhibit excitation of the FRET donor, which absorbs in the far-UV (ca. 350 nm). Finally, if a test compound interferes with the binding of the fluorophore-tagged antibodies to their epitopes it will be detected as a hit in a TR-FRET screen, even though it has no effect on the binding of the target molecules themselves. Following up with controls and secondary assays will remove such compounds from consideration.

## AlphaScreen Format

### Concept

AlphaScreen™ is bead-based format commercialized by PerkinElmer (<http://www.perkinelmer.com>) and used to study biomolecular interactions in a microplate format. A newer, more sensitive version of the technology is called AlphaLISA. The acronym ALPHA stands for Amplified Luminescent Proximity Homogeneous Assay. The technology of AlphaScreen was originally developed under the name LOCI® (Luminescent Oxygen Channeling Immunoassay) by Dade Behring, Inc. of Germany (19). Like FRET, AlphaScreen is a non-radioactive, homogeneous proximity assay. Binding of

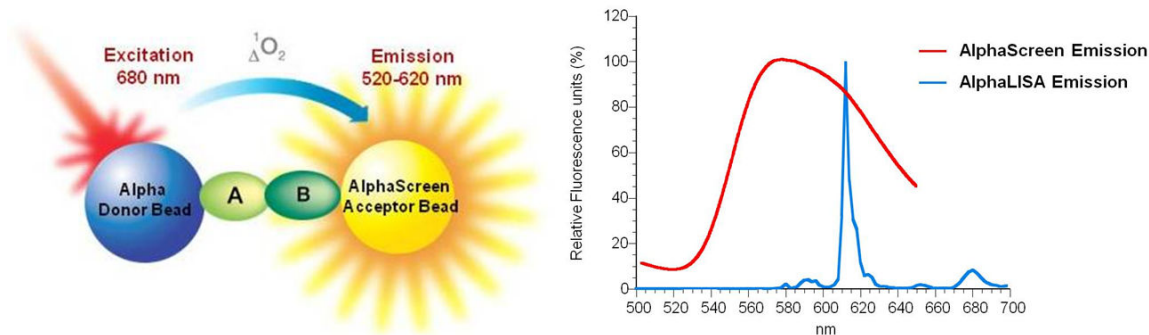


**Figure 5:** AlphaScreen and AlphaLisa. **Left:** Binding of biological partners (represented by small ovals A and B) brings Donor and Acceptor beads (represented by the large blue and yellow circles) into close proximity ( $\leq 200$  nm) and thus a fluorescent signal between 520–620 nm is produced in the case of AlphaScreen and 615 nm in the case of the AlphaLisa. When there is no binding between biological partners, Donor and Acceptor beads are not in close proximity. Singlet oxygen decays and no signal are produced. **Right:** comparison of emission spectra for AlphaScreen (red) and AlphaLisa (blue).

two molecules captured on the beads leads to an energy transfer from one bead to the other, ultimately producing a fluorescent signal. Excitation of the donor bead leads to the formation of singlet oxygen, which diffuses to the acceptor and stimulates emission. Unlike FRET, acceptor emission occurs at a higher energy (lower wavelength) than donor excitation.

The AlphaScreen assay beads are latex-based and approximately 250 nm in diameter. Both bead types (Donor and Acceptor) are coated with a hydrogel that minimizes non-specific binding and self-aggregation and provides reactive aldehyde groups for conjugating biomolecules to the bead surface. The beads are small enough that they do not sediment in biological buffers and bead suspensions do not clog the tips used commonly in liquid handling devices. The beads are typically used at  $\mu\text{g/mL}$  concentration and are very stable, even if heated to  $95^\circ\text{C}$  for example, for PCR, or lyophilized.

Donor beads contain a photosensitizer, phthalocyanine, which converts ambient oxygen to an excited form of  $O_2$ , singlet oxygen, upon illumination at 680 nm. Like other excited molecules, singlet oxygen has a limited lifetime prior to returning to ground state. Within its 4  $\mu\text{s}$  half-life, singlet oxygen can diffuse approximately 200 nm in solution. If an Acceptor bead is within that distance, energy is transferred from the singlet oxygen to thioxene derivatives within the acceptor bead, resulting in light production. Without the interaction between donor and acceptor bead, singlet oxygen falls to ground state and no signal is produced. AlphaScreen Acceptor beads use rubrene as the final fluorophore, emitting light between 520 and 620 nm. AlphaLisa acceptor beads use a Europium chelate as the final fluorophore, emitting light in a narrower peak at 615 nm (Figure 5). The AlphaLisa light is less likely to be affected by particles and other substances commonly found in biological samples (for example, plasma and serum), thereby reducing background noise and optimizing precision.

AlphaScreen assays have been developed to quantify enzymes, molecular (protein, peptide, small molecule) interactions, as well as DNA and RNA hybridizations. Due to the large diffusion distance of singlet oxygen, the binding interactions of even very large proteins and phage particles can be quantified by AlphaScreen and AlphaLISA. The high sensitivity and large distance range have led to increasing use of these technologies in HTS settings.

### General Consideration: Hooking Effect

The hook effect is a common phenomenon found when using any sandwich-type assay, including AlphaScreen, ELISA, and some of the FRET-based formats described above. When the PPI components are titrated (e.g. during assay development), both donor and acceptor beads become progressively saturated by their target molecules, and the signal increases with increasing protein concentration. At the “hook” point, either the Donor or the Acceptor component is saturated with the target molecule and a maximum signal is detected. Above the hook point, there is an excess of target molecules for the donor or the acceptor beads, which inhibits their association and causes a progressive signal decrease (Figure 6). When the affinity of the PPI is higher (weaker) than the concentrations used in the assay, the hooking effect can be masked, resulting in what looks like a traditional saturation curve that reaches a plateau, rather than hooking. In this case, two competing equilibria are occurring: the signal is decreasing because of the hooking effect on the bead, but the protein-protein interaction is still being increasing because higher concentrations of protein drive the equilibrium toward more protein-protein complex. In either event, choose a protein concentration below the hook point (or saturation point) for your assay.

### Assay Design and Development

1. **Instrumentation:** Specialized instrumentation is required to read AlphaScreens since a high-energy laser is needed to excite the donor. However, most major companies who manufacture plate readers now provide models with AlphaScreen capability. Multimode readers suitable for AlphaScreen/AlphaLisa include PerkinElmer’s Envision and Enspire, Biotek’s Synergy, BMG’s PheraStar, FluoStar, and PolarStar, and Berthold Technologies Mithras LB 940. Specialized Alpha readers include PerkinElmer’s AlphaQuest and FusionAlpha.
2. **Plates:** AlphaScreen assays are performed in white opaque plates. Assays may be performed in 96-, 384- or 1536-well formats. Some plates, such as the ProxiPlate (PerkinElmer), have been optimized for AlphaScreen to place the sample closer to the detector and therefore give an increased signal. Excitation and signal measurement are both accomplished from the top of the plate. The measured signal is in part dependent upon reflected light, therefore the reflective properties of the plate influence signal. Higher density plates (e.g. 384- vs 96-well, 1536- vs 384-well) generally provide more sensitive AlphaScreen assays. First, the higher density wells are narrower and more efficiently reflect the emitted light back to the detector. Second, higher density plates allow a higher proportion of the sample to

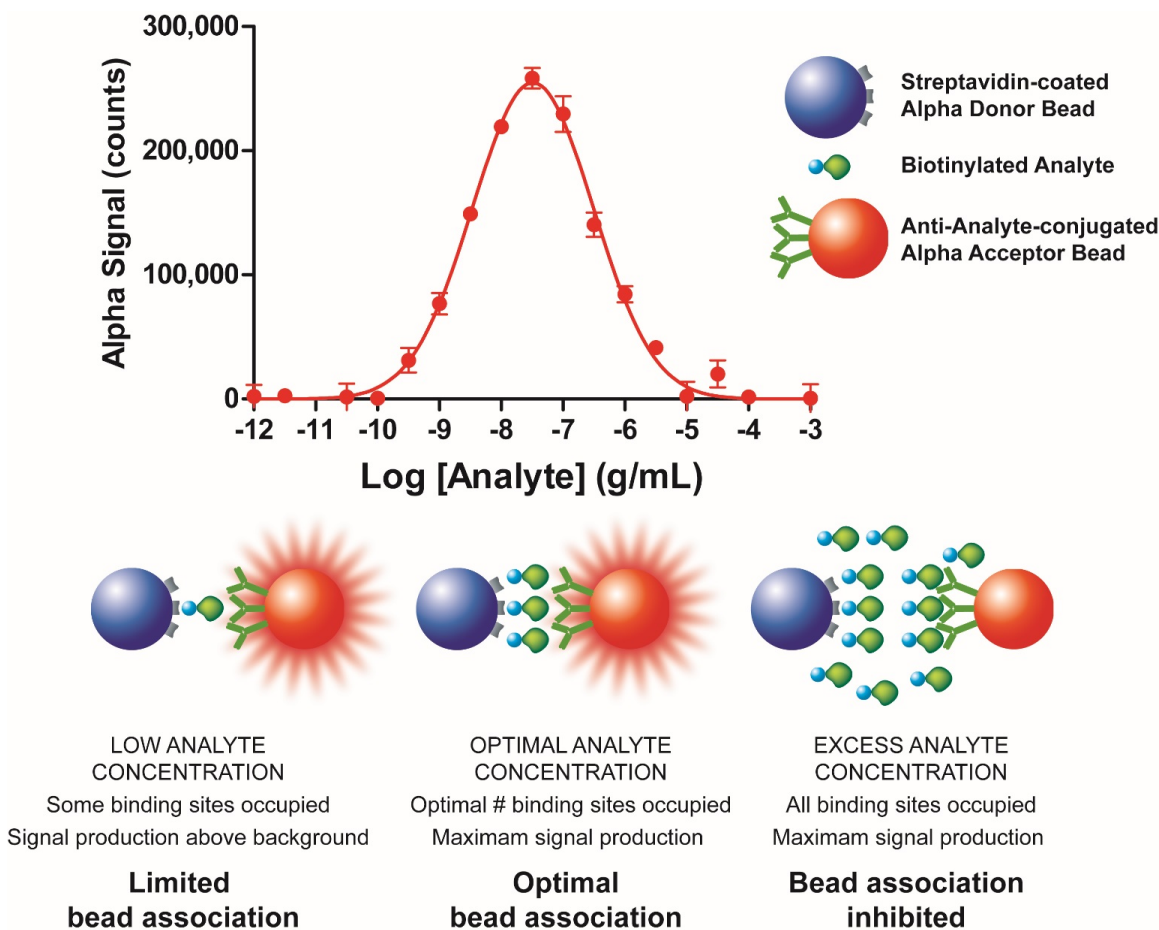


**Figure 6:** Hooking Effect in AlphaScreen. These principles hold for all sandwich-based assay formats (adapted from [PerkinElmer](#)).

be excited by the 1 mm laser beam, leading to proportionately greater signal generation. Higher density plates also allow less reagent use, lowering the overall cost of the screen.

3. **Buffers:** Choose pH buffering capacity and salt concentration that will facilitate the desired interactions between the components of the assay. The following buffers have been used without problems: Acetate, HEPES, Bis-Tris, MES, Bis-TRIS propane, MOPS, CAPS, Phosphate, Carbonate, PIPES, Citrate, Formate, and Tris. pH values between pH 2.5 to 9 are well tolerated. Higher pH is also tolerated but there may be some loss of signal. If metal co-factors are needed for the PPI, it is best to titrate these components appropriately, but note that high concentrations will quench the signal; in particular,  $\text{Al}^{2+}$ ,  $\text{Fe}^{2+}$ ,  $\text{Fe}^{3+}$ ,  $\text{Cu}^{2+}$ ,  $\text{Ni}^{2+}$  and  $\text{Zn}^{2+}$  have been shown to quench singlet oxygen in the mM and sub-mM ranges (100  $\mu\text{M}$  for  $\text{Fe}^{2+}$ ).

Detergents and/or blocking proteins should be used to reduce non-specific binding

(see General Considerations). For most AlphaScreen applications, a BSA concentration of 0.1% (w/v) is sufficient to minimize non-specific interactions; alternate blocking reagents such as casein, gelatin, heparin, poly-lysine, salmon sperm DNA, or Dextran T500 can be used (see Assay Design). The preservative azide can act as a potent scavenger of singlet oxygen and will inhibit the AlphaScreen signal, so Proclin 300 (Sigma-Aldrich) is recommended as a preservative and anti-microbial agent.

4. **Kits:** Generic detection kits from PerkinElmer include pre-coated beads that capture biotinylated, FITC-labeled, DIG-labeled, GST-tagged, 6X His-tagged, Protein A, Protein G, Protein L and anti-species beads. Unconjugated Donor and Acceptor beads are also available for direct conjugation of an antibody or other reagent of choice. Note that if you have purified your GST-tagged proteins or His-tagged proteins using an affinity column and will be using a GSH or Ni<sup>2+</sup> bead in your Alpha assay, you will need to dialyze away any glutathione or imidazole in your purified protein preparation. These components will interfere with the interaction between the tagged protein and the bead. PerkinElmer also sells specific kits for various applications.
5. **Titration of reagents:** It is important to optimize the concentrations of each protein conjugated to the Donor and Acceptor beads. On the one hand, the amount of PPI formed is dependent on the concentrations of each protein and the affinity of the interaction. Until saturation is achieved, increasing the concentration of either protein will push the equilibrium towards higher complex formation. On the other hand, each type of Alpha bead has a specific binding capacity; once the beads are saturated with associated protein, additional protein may lead to a hooking effect (see above).

Binding capacities are influenced by a number of factors, including the size of the protein and the affinity of the bead for the protein. First, there is usually a higher binding capacity for smaller proteins. For instance, streptavidin-coated beads at 20 µg/mL usually saturate at around 30 nM of biotinylated peptide (ca 1.5 KDa), but saturate at around 2-3 nM of biotinylated antibody (ca 150 KDa). Second, the saturation point of a bead varies depending on its affinity reagent. For instance, anti-GST antibody beads bind more tightly to GST-labeled proteins than do glutathione beads. Hence, the saturation point is usually 20 nM of GST tagged protein binding to anti-GST beads, but 200 nM of GST-protein binding to glutathione-conjugated beads. More information on capacity can be found at the Perkin Elmer website ([www.perkinelmer.com](http://www.perkinelmer.com)).

6. **Assay Conditions:** The beads are sensitive to light and temperature. It is important to store the beads in the dark and conduct the parts of the assay that include the beads in low light conditions (less than 100 Lux) or to use green filters. Affected areas of the lab include the bench, plate reader and liquid handler. Finally, the chemistry is designed to give best results at room temperature (e.g.: 20–25°C); do not chill plates or incubate on ice before reading. Typically the AlphaScreen signal variation is 8% per °C so consistent temperature is important.



### Steps for developing the assay:

1. Choose a suitable buffer system, noting the boundaries described above.
2. Titrate each binding partner to ascertain the optimal concentrations. For initial experiments, a final bead concentration of 20  $\mu\text{g/ml}$  is recommended for both Donor and Acceptor beads. Subsequent dilution of the beads may be assessed once it is known that a sufficiently high signal/background can be achieved. Typically, most AlphaScreen assays will utilize a final concentration of biotinylated binding partner in the nanomolar range (e.g.: 0.5 nM–30 nM with 20  $\mu\text{g/mL}$  of beads). Concentration ranges for each binding partner that interact directly with a capture molecule on the AlphaScreen beads vary considerably (ex.: 0.1 nM–300 nM) depending on the affinity of the binding partners, the efficiency of labeling, and/or stoichiometry of the capture tag/epitope.
3. It may also be necessary to vary the order of addition of the components to permit the most efficient interactions.
4. Incubation times need also to be optimized.

### Benefits and limitations

Alpha technologies have become popular in recent years, likely because they are adaptable to many assay types, are very sensitive, and are active over long distances (200 nm vs 10-20 nm for TR-FRET). The central limitations to AlphaScreen and AlphaLisa are the increased expense vs other mix-and-read formats and the sensitivity of the materials to ambient light.

Glickman, et al (20), compared FRET, TR-FRET and AlphaScreen formats (20), and concluded that the ALPHAScreen format had the best sensitivity and dynamic range. Of the three formats, TR-FRET assay had the least inter-well variation, most likely because it is a ratiometric type of measurement. Both FRET-type and AlphaScreen formats can measure a wide range of affinities ( $K_d$ 's ranging from low pM to low mM) because there are no wash steps. It is noteworthy that AlphaScreen beads have 300-3000 proteins/bead, and the protein density can be varied. This multi-valency can significantly increase sensitivity, because one PPI per bead pair leads to the maximal signal. Furthermore, high concentrations can cause avidity. On the one hand, avidity augments the apparent binding affinity of the PPI, so less material is required. On the other hand, avidity might not be desired (e.g. for high affinity PPI or high affinity inhibitors), and the apparent  $IC_{50}$  values for inhibitors could be significantly weaker than the actual affinity of the inhibitor/protein interaction. With FRET methods, each binding partner carries a single label so that if some beads are unbound, a lower signal will be generated. However, monovalency also implies that the signal will be proportional to the number of binding interactions.

### Validating drug-like binding of PPI inhibitors

The goal of primary screening is to select a set of compounds that *might be active*. Among “actives,” however, are many compounds that act by mechanisms that will not be optimizable into a qualified drug lead or biological probe. Some of the artifactual

mechanisms that lead to activity in a primary assay are specific to the assay format; as described above, compounds could autofluoresce or quench the fluorescence signal used to detect the PPI. Thus, it is very valuable to develop at least one orthogonal assay formats, or an *in vitro* assay and a cell-based assay, plus an independent way to measure binding directly.

Other artifacts are less selective to the assay methodology, though they may be somewhat selective for the proteins or assay conditions. A well-described and very common example is compound aggregation (3). Aggregates can be quite large (30-200 nM) and can interfere with protein structure in a number of pathological ways. Aggregation can also be very dependent on the assay condition; rather than thinking of compounds as “aggregators,” it is more accurate to think of aggregation as a form of molecular interaction, dependent on salt, pH, detergents, carrier proteins, and concentration of the compound. Thus, it is not sufficient to demonstrate that a compound is selective for a particular screen over other screens; to be a bona fide PPI inhibitor, the compound must bind at a distinct site(s) on one of the proteins in the complex. Binding stoichiometry is therefore a key metric for selecting useful and optimizable probes/leads.

There are a number of biophysical assays that measure binding of the small molecule to the protein. It is very beneficial to use at least two assays, since no assay is infallible, and different types of information can be gleaned from each format. Depending on the size of the protein(s), the binding affinity of the molecule, and other details, the following methods can be used:

**Optical Biosensors:** There are several related technologies for measuring the binding of a surface-immobilized “ligand” to a soluble “analyte.” In general, optical biosensors detect changes in the angle, color, or phase of light reflected off of a solid/liquid interface. Many instruments are sensitive enough to monitor the binding of a small-molecule analyte to a surface-bound protein. These systems can also be used in competition experiments, in which a PPI is monitored in the presence of increasing concentrations of inhibitor. Because the signals are proportional to the change in mass of the analyte, PPI are usually easier to monitor than protein/small-molecule interactions.

The first popular optical biosensor was the surface plasmon resonance (SPR) instrument developed by Biacore (GE Healthcare). The technology is now widely used, and numerous companies market SPR instruments (e.g. Bio-Rad, ICX, and others). Most SPR instruments use microfluidics to introduce the analyte, and monitor the binding in real time. The concentration of analyte can be varied to develop a dose-response. Through kinetic and/or steady-state experiments, SPR provides a measure of binding stoichiometry, reversibility, and affinity to a protein bound to a surface. For recent descriptions of how to analyze and evaluate small-molecule SPR data, see Rich et al, 2011 and Gianetti et al, 2008 (21, 22).

Other technologies include optical gradients (SRU BIND, Corning Epic) and interferometry (Forte Bio Octet Red). The optical gradient systems are plate-based, allowing high throughput, but more limited kinetic resolution. In interferometry, the

ligand is coated onto fiber optic sensors that are then dipped into solutions of analyte. This technology is developing rapidly, and could soon have the throughput, cost/assay, and sensitivity to rival SPR for measuring small-molecule/protein interactions.

***Nuclear Magnetic Resonance (NMR):*** NMR measures the response of nuclei in a magnetic field, and is very sensitive to the chemical environment of the nucleus. Due to the flexibility of the method, NMR has many uses in small-molecule characterization and protein structure determination. Small-molecule/protein NMR experiments come in two general formats – ligand-detected and protein-detected. Ligand-detected experiments measure the change in the compound's NMR signals (“resonances”) as a function of binding to protein. Energy can be transferred from the solvent and/or protein to the compounds (Saturation Transfer Difference, WaterLOGSY) or the apparent mass of the compound can be increased due to binding a large protein (translation, diffusion). Ligand-detected measurements are often used qualitatively, to assess the presence of binding to the target. Saturation Transfer Difference is particularly popular for moderate-throughput applications, because the protein concentration is low (micromolar) and it is particularly effective for compounds in fast exchange (weaker than micromolar). There is no limit on the protein size for ligand-detected experiments.

Protein-detected NMR provides a measurement of the effect of the compound on the protein. The most popular moderate-throughput methods are  $^{15}\text{N}$ - $^1\text{H}$  HSQC and  $^{13}\text{C}$ - $^1\text{H}$  HSQC and the related  $^{15}\text{N}$ - and  $^{13}\text{C}$ -TROSY. N-H HSQC measures the environment of the amide N-H bond, and thus provides a single peak for each amino acid in a protein sequence (except for proline; asparagine and glutamine also have primary NH signals).  $^{13}\text{C}$ - $^1\text{H}$  HSQC uses labeled methyl groups to detect changes to valine, methionine, isoleucine, and leucine. If the NMR spectrum has been assigned, changes to the resonances in the presence of compound will suggest the binding site. Even without assigning the protein resonances, however, compounds can be binned by binding site, and non-binders or multi-site binders can be identified. Protein-detected NMR used to be reserved for relatively small proteins; however, technical improvements in NMR hardware and pulse sequences, deuteration of the protein, and selective labeling have made many more proteins amenable to these experiments.

***Isothermal calorimetry (ITC):*** ITC measures the heat generated or absorbed by a binding interaction. For weakly binding PPI inhibitors (in the mid micromolar range), ITC can be challenging because protein usage is high, compound solubility can be limited, and the heats of binding are small. It is important to match the protein and compound buffers and to control for the heat-of-dilution as the compound sample is added to the protein (or vice versa). Despite these challenges, ITC can be very valuable due to the fact that unlike some other methods, ITC is truly label-free, and all components are in solution. By directly measuring the energy of binding, ITC provides information on the entropy and enthalpy of the interaction, the binding affinity (by titrating one of the partners) and the binding stoichiometry. More detail on how to conduct these studies can be found at the MicroCal website.

**Thermal stabilization - differential scanning calorimetry (DSC) and differential scanning fluorimetry (DSF, ThermoFluor, Protein Thermal Shift):** One way to define protein stability is by the temperature at which the protein unfolds. Unfolding is usually a highly cooperative process, and gives a defined melting temperature ( $T_m$ ) under a given condition of concentration, buffer, etc. When a compound binds to the protein, the complex is more stable than the protein alone, and the protein's  $T_m$  increases. To measure the binding affinity of a compound for a protein, one monitors the increase in  $T_m$  ( $\Delta T_m$ ) as the concentration of compound is increased.  $T_m$  measurements are generally done with micromolar concentrations of protein, and are therefore most sensitive to determining binding affinities in this range. This method also has the advantage that all components are in solution.

There are several methods for measuring the change in  $T_m$ . Differential scanning calorimetry (DSC) monitors the heat absorbed by the protein as the temperature is increased; the energy/degree increases at the  $T_m$ . Differential scanning fluorimetry (DSF) monitors the binding of a hydrophobic dye to the protein as the temperature is increased. The dye binds preferentially to hydrophobic portions of a protein that are exposed when a protein melts; this binding is accompanied by a change in fluorescence as a function of temperature. Typical DSF dyes include SYPRO orange and 1,8-ANS; DSF measurements are read in specialized instruments or in real-time PCR machines. The magnitude of DSC and DSF signals, and the  $\Delta T_m$ s obtained from small-molecule binding studies, is dependent on both the protein and the assay conditions. Thermodynamic statements are only valid in the cases that thermal denaturation is reversible. Nevertheless,  $\Delta T_m$  measurements can provide a rapid assessment of binding affinity, and are increasingly being used in primary screening assays as single-concentration measurements. Sample assay development guidelines can be found in Niesen, et al (23).

**Sedimentation Analysis (SA; Analytical ultracentrifugation):** Sedimentation analysis measures the sedimentation of proteins in response to a centrifugal force. The protein concentration is measured along the length a centrifugation cell using the proteins absorbance, refractive index, or fluorescence. Two general types of SA experiments are Velocity Sedimentation and Equilibrium Sedimentation. Equilibrium sedimentation gives a first-principle measurement of molecular mass, and is often used to measure self-association (e.g. dimerization) constants. It can also be used, however, to assess the binding of a small molecule to the protein, particularly if the molecule has absorbance at wavelengths distinct from the protein (e.g. > 300 nm). The compound's aggregation state and the compound's affect on the apparent molecular mass of the protein provide a quick readout of aggregation-based artifacts. Direct binding of the compound to protein can also be assessed (24). Analytical centrifuges are sold by Beckman Coulter, and add-on fluorescence detection is available from Aviv Biomedical.

**X-ray crystallography:** X-ray crystallography continues to be the gold standard for characterizing protein/small molecule interactions. The high-resolution (ca. 1.5 – 3 angstrom) structure fit from x-ray diffraction data provides information on the binding site and the specific contacts between compound and protein. The presence of a single

molecule bound to a single binding site suggests – but does not prove – that the compound's inhibition of a PPI arises from binding at that site. Co-structures of compounds and proteins are generally prepared by soaking the compound into a crystal of the protein or by co-crystallization of the protein and compound together. In many cases, it is difficult to obtain co-crystal structures, either because the protein does not crystallize well, the compound induces changes to the protein structure that inhibit crystallization (e.g. binding at a crystal contact, changing the protein conformation), or the compound is not soluble enough.

## Useful websites

### General

Microplates: <http://www.perkinelmer.com/Catalog/Category/ID/Microplates>

Avitag, for in vitro biotinylation: <http://www.avidity.com/t-technology.aspx>

### *In vitro* assays:

ELISA: <http://www.piercenet.com/browse.cfm?fldID=F88ADEC9-1B43-4585-922E-836FE09D8403#detectionmethods>

<http://www.biotek.com/resources/articles/kinetic-elisa-advantage.html>

<http://www.biocompare.com/Articles/ApplicationNote/1727/Optimisation-Of-Assays-Interference-In-Immunoassays-Recognize-And-Avoid.html>

FP: <http://www.invitrogen.com/.../Fluorescence-Polarization-FP.html>

FRET, TR-FRET: <http://www.htrf.com/technology/assaytips>

<http://www.invitrogen.com/.../Fluorescence-Resonance-Energy-Transfer-FRET.html>

<http://www.perkinelmer.com/Catalog/Category/ID/lance%20Protein%20Binding>

AlphaScreen, AlphaLISA: [http://www.perkinelmer.co.jp/tech/tech\\_ls/protocol\\_collection/AlphaScreen\\_guidebook.pdf](http://www.perkinelmer.co.jp/tech/tech_ls/protocol_collection/AlphaScreen_guidebook.pdf)

<http://www.TGR-Biosciences.com>

### Biophysical Assays

SPR: <http://www.sprpages.nl/Index.php>

Isothermal Calorimetry: <http://www.microcal.com/technology/itc.asp>

Differential Scanning Calorimetry: <http://www.microcal.com/technology/dsc.asp>

Differential Scanning Fluorimetry: <http://thermofluor.org/>

[http://www3.appliedbiosystems.com/cms/groups/mcb\\_marketing/documents/generaldocuments/cms\\_095306.pdf](http://www3.appliedbiosystems.com/cms/groups/mcb_marketing/documents/generaldocuments/cms_095306.pdf)

## References

1. Lipinski CA, Lombardo F, Dominy BW, Feeney PJ. Experimental and computational approaches to estimate solubility and permeability in drug discovery and development settings. *Adv. Drug Deliv. Rev.* 2001;46:3–26. PubMed PMID: 11259830.
2. Lipinski CA. Lead- and drug-like compounds: the rule-of-five revolution. *Drug Discovery Today: Technologies.* 2004;1:337–341. PubMed PMID: 24981612.
3. McGovern SL, Helfand BT, Feng B, Shoichet BK. A specific mechanism of nonspecific inhibition. *J. Med. Chem.* 2003;46:4365–4272. PubMed PMID: 13678405.
4. Boehm H-J, Boehringer M, Bur D, et al. Novel inhibitors of DNA gyrase: 3D structure based biased needle screening, hit validation by biophysical methods, and 3D guided optimization. A promising alternative to random screening. *J. Med. Chem.* 2000;43:2664–2674. PubMed PMID: 10893304.
5. Arkin MR, Wells JA. Small-molecule inhibitors of protein-protein interactions: progressing towards the dream. *Nature Reviews Drug Discovery.* 2004a;3:301–317. PubMed PMID: 15060526.
6. Fry D. Protein-Protein interactions as targets for small molecule drug discovery. *Biopolymers.* 2006;84:535–553. PubMed PMID: 17009316.
7. Khoury K, Dömling A. P53 Mdm2 Inhibitors. *Curr Pharm Des.* 2012;(May):29. [Epub ahead of print]. PubMed PMID: 22650254.
8. Saupé J, Roske Y, Schillinger C, et al. Discovery, structure-activity relationship studies, and crystal structure of the nonpeptide inhibitors bound to the Shank3 PDZ domain. *Chem Med Chem.* 2011;6:1411–22. PubMed PMID: 21626699.
9. Simons PC, Young SM, Carter MB, Waller A, Zhai D, Reed JC, Edwards BS, Sklar LA. Simultaneous in vitro molecular screening of protein-peptide interactions by flow cytometry, using six Bcl-2 family proteins as examples. *Nature Protocols.* 2011;6:943–952. PubMed PMID: 21720309.
10. Jameson DM, Crony JC. Fluorescence polarization: past, present and future. *Comb Chem High Throughput Screen.* 2003;6:167–73. PubMed PMID: 12678695.
11. Schade SZ, Jolley ME, Sarauer BJ, Simonson LG. BODIPY-alpha-casein, a pH-independent protein substrate for protease assays using fluorescence polarization. *Anal Biochem.* 1996;243:1–7. PubMed PMID: 8954519.
12. Du Y, Masters SC, Khuri FR, Fu H. Monitoring 14-3-3 protein interactions with a homogeneous fluorescence polarization assay. *J Biomol Screen.* 2006;11:269–76. PubMed PMID: 16699128.
13. Fu H, Subramanian RR, Masters SC. 14-3-3 proteins: structure, function, and regulation. *Ann Rev Pharmacol Toxicol.* 2000;40:617–47. PubMed PMID: 10836149.
14. Burke TJ, Loniello KR, Beebe JA, Ervin KM. Development and application of fluorescence polarization assays in drug discovery. *Comb Chem High Throughput Screen.* 2003;6:183–94. PubMed PMID: 12678697.

15. Owicki JC. Fluorescence polarization and anisotropy in high throughput screening: perspectives and primer. *J Biomol Screen*. 2000;5:297–306. PubMed PMID: 11080688.
16. Hilal T, Puetter V, Otto C, Parczyk K, Bader B. A dual estrogen receptor TR-FRET assay for simultaneous measurement of steroid site binding and coactivator recruitment. *J Biomol Screen*. 2010;3:28–78. PubMed PMID: 20150592.
17. Jeyakumar M, Katzenellenbogen JA. A dual-acceptor time-resolved Förster resonance energy transfer assay for simultaneous determination of thyroid hormone regulation of corepressor and coactivator binding to the thyroid hormone receptor: Mimicking the cellular context of thyroid hormone action. *Anal Biochem*. 2009;1:73–8. PubMed PMID: 19111515.
18. Du Y, Nikolovska-Coleska Z, Qui M, Li L, Lewis I, Dingleline R, Stuckey JA, Krajewski K, Roller PP, Wang S, Fu H. A dual-readout F2 assay that combines fluorescence resonance energy transfer and fluorescence polarization for monitoring bimolecular interactions. *ASSAY and Drug Dev Technol*. 2011;9:382–393. PubMed PMID: 21395401.
19. Ullman EF, et al. Luminescent oxygen channeling immunoassay: Measurement of particle binding kinetics by chemiluminescence. *Proc. Natl. Acad. Sci. USA*. 1994;91:5426–5430. PubMed PMID: 8202502.
20. Glickman JF, Wu X, Mercuri R, Illy C, Bowen BR, He Y, Sills M. Comparison of ALPHAScreen, TR-FRET, and TRF as Assay Methods for FXR Nuclear Receptors. *J Biomol Screen*. 2002;7:3. PubMed PMID: 11897050.
21. Rich RL, Myszka DG. Survey of the 2009 commercial optical biosensor literature. *J. Molecular Recognition*. 2011;24:892–914. PubMed PMID: 22038797.
22. Giannetti AM, Koch BD, Browner MF. Surface plasmon resonance based assay for the detection and characterization of promiscuous inhibitors. *J. Med. Chem*. 2008;51:574–580. PubMed PMID: 18181566.
23. Niesen FH, Berglund H, Vedadi M. The use of differential scanning fluorimetry to detect ligand interactions that promote protein stability. *Nature Protocols*. 2007;2:2212–2221. PubMed PMID: 17853878.
24. Arkin, MR (2004b). Sedimentation for success. *Modern Drug Discovery Nov*: 45-47. (pdf)

## Additional References

- Degorce F, Card A, Soh S, Trinquet E, Knapik GP, Xie B. HTRF: A technology tailored for drug discovery – a review of theoretical aspects and recent applications. *Curr Chem Genomics*. 2009;3:22–32. PubMed PMID: 20161833.
- Karimova G, Pidoux J, Ullmann A, Ladant D. A bacterial two-hybrid system based on a reconstituted signal transduction pathway. *Proc Natl Acad Sci U S A*. 1998;95:5752–5756. PubMed PMID: 9576956.





# Immunoassay Methods

Karen L. Cox, BS,<sup>1</sup> Viswanath Devanarayan, PhD,<sup>2</sup> Aidas Kriauciunas,<sup>1</sup> Joseph Manetta, BS,<sup>1</sup> Chahrzad Montrose, PhD,<sup>1</sup> and Sitta Sittampalam, PhD<sup>3</sup>

Created: May 1, 2012; Updated: December 24, 2014.

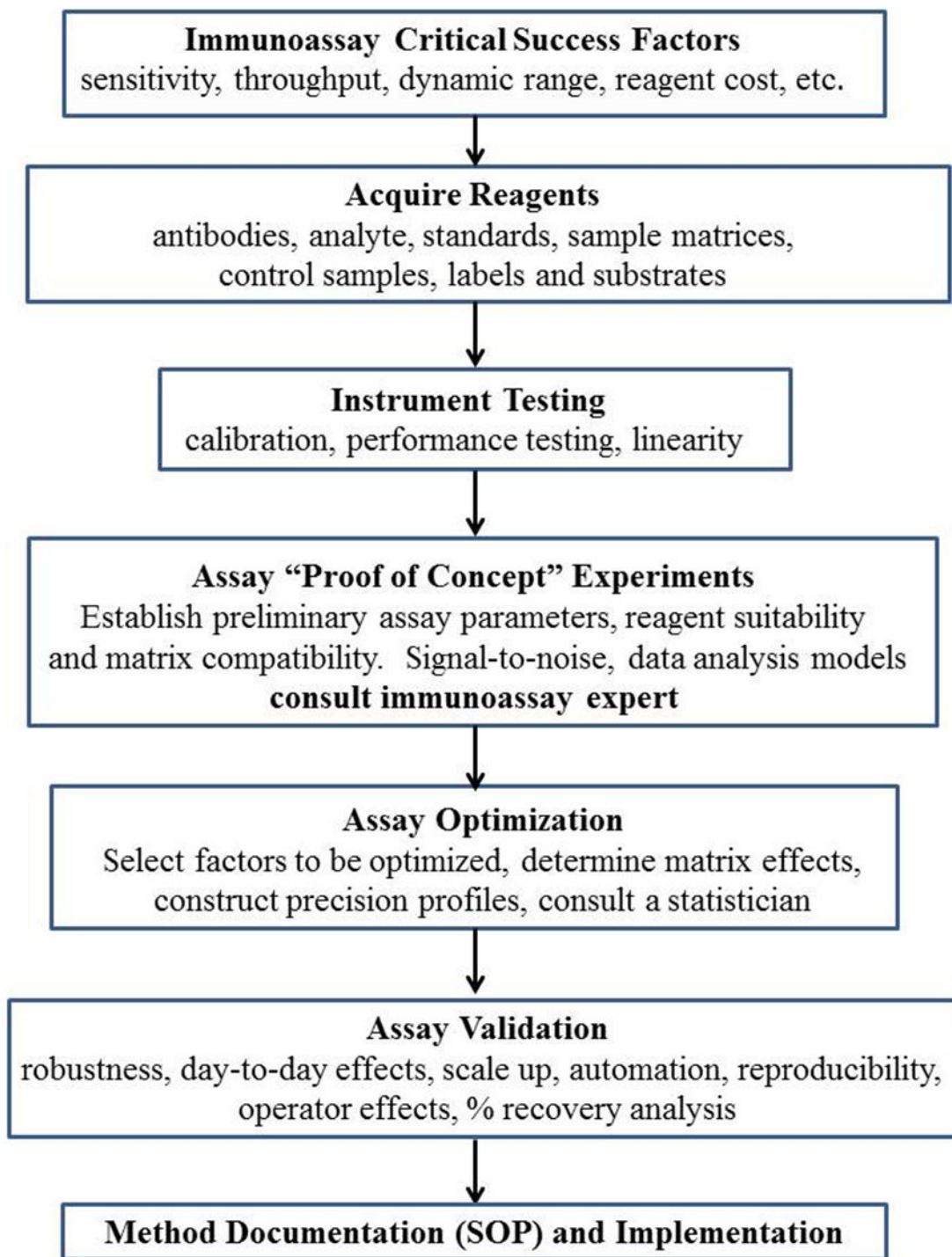
## Abstract

Immunoassays are used to quantify molecules of biological interest based on the specificity and selectivity of antibody reagents generated. In HTS and lead optimization projects, assays are designed to detect molecules that are produced intracellularly or secreted in response to compounds screened. This chapter describes the basics of designing and implementing robust, automation friendly immunoassays for HTS, modes of immunoassay formats (competitive and sandwich), instrumentation, reagent selection, experimental design and detailed data analysis concepts. The importance of an appropriate curve-fitting model for calibration curves used for quantification is also addressed in detail. This is an excellent primer for beginners as well as for experienced investigators.

---

<sup>1</sup> Eli Lilly & Company, Indianapolis, IN; Email: cox\_karen\_l@lilly.com; Email: manetta\_joseph@lilly.com; Email: montrose-rafizadeh\_chahrzad@lilly.com. <sup>2</sup> AbbVie, Chicago, IL; Email: viswanath.devanarayan@abbvie.com. <sup>3</sup> National Institutes of Health, Rockville, MD; Email: gurusingham.sittampalam@nih.gov.

## Immunoassay Development, Optimization and Validation Flow Chart



## Introduction

The intent of this document is to provide general guidelines to aid in the development, optimization and validation of an immunoassay. Following these guidelines will increase the likelihood of success in developing a robust immunoassay that will measure consistent values for unknown samples.

Immunoassays are used when an unknown concentration of an analyte within a sample needs to be quantified. To obtain the most accurate determination of the unknown concentration, an immunoassay must be developed based not only on the usual assay development criteria (standard deviation or optimal signal window) but also on how well the immunoassay can predict the value of an unknown sample. First, one needs to establish the assay critical success factors. Then the immunoassay needs to be developed, which establishes proof of concept. During the optimization phase, the quantifiable range of the immunoassay method is determined by calculating a precision profile in the matrix in which the experimental samples will be measured. A spiked recovery is then performed by spiking the analyte into the matrix and determining the percent recovery of the analyte in the matrix. If the precision profile is within the desired working range, then assaying spiked recovery samples over several days completes the validation of the immunoassay. If the precision profile limits are not within the desired working range, further optimization of the immunoassay is required prior to validation.

## Basic Steps for Developing and Running an Immunoassay

1. Establish assay critical success factors (i.e. sensitivity required).
2. Ensure appropriate antibody and antigen reagents are available.
3. Adsorb antigen or capture antibody to a solid surface.
4. Wash off unbound reagents.
5. Block nonspecific binding sites to reduce background.
6. Incubate the secondary antibody with the sample.
7. Wash off unbound reagents.
8. Incubate secondary antibody-conjugate with sample.
9. Wash off unbound reagents.
10. Incubate substrate to generate signal.
11. Calibration curve fitting, data analysis and quantitation by non-linear regression.

## Basic Steps in Using Immunoassays for High Throughput Screening (HTS)

Immunoassays are used in screening to quantify the production or inhibition of antigens/haptens related to a disease target. These antigens or haptens are characteristic of the disease process and mediated by the target, such as cytokines or growth factors. Hence the screening procedure will involve incubating compounds with the specified target, usually expressed in cells, and collecting the cell medium or lysates to quantify the activity of the compounds. Several examples of this approach for using immunoassay procedures have

been described in the literature (1-5). The critical steps in setting up a screen are as follows:

1. Develop a validated immunoassay as described above.
2. Acquire antibody, antigen/calibrator, label and buffer reagents in quantities needed for HTS.
3. Establish liquid handling and automation procedures for screening and immunoassay methods.
4. Establish stability of the capture antibody or antigen bound to a plate. Determine compound collections to be tested.
5. Develop and validate a method for incubation of compounds with a relevant target in the screening mode.
6. Develop a sample collection procedure from screening experiments.
7. Develop data analysis procedures to use immunoassay data to derive compound potency such as IC<sub>50</sub> or EC<sub>50</sub>.

## Immunoassay Parameters

It is important to define the relevant immunoassay parameters before one begins the development, optimization and validation of an immunoassay:

1. Analyte (hapten or antigen) to be measured.
2. Sample matrices in which measurements will be made (serum, plasma, cell lysates, culture media, etc.).
3. Source of antibody, analyte standards and detection reagents (labeled antibody, enzyme substrates, etc.). Availability of these reagents is a critical requirement.
4. Detection mode (colorimetric, fluorescence or chemiluminescence) and appropriate plate readers.
5. Type of immunoassay to develop: Sandwich, competitive or antigen-down formats.
6. Expected analyte concentration ranges to be measured: pg/ml, ng/ml or µg/ml in the sample matrix of choice. This would determine the detection limits and the measurable range that should be achieved in a validated assay.
7. Data analysis models and format for reporting results.
8. Validation and optimization criteria using statistical experimental design tools.
9. Recovery, accuracy and precision expected at the limits of quantification and the measurable range.
10. Sample throughput, frequency of use, automation and the number of laboratories that would run the assay.
11. Control samples that would be used for optimization, validation and quality control runs.

## Reagents

Reagents are a critical piece of any assay development process. This refers to all of the reagents that will be used in the assay. There are certain items that need to be considered when obtaining reagents:

1. Quality of standards and antibodies.
2. Quantity of standards and antibodies.
3. Purity of standards and antibodies (when possible antibodies are affinity purified).
4. Selectivity and specificity of antibodies.

## Example Plate Types

Greiner high binding plates, Costar EIA/RIA high-low binding plates, Immunotech, Falcon, Nunc

**Note:** Other plate types can also be used based on the experience of the investigator and appropriate quality control to demonstrate acceptability.

## Coating Buffers

50 mM sodium bicarbonate, pH 9.6

0.2 M sodium bicarbonate, pH 9.4

PBS - 50 mM Phosphate, pH 8.0, 0.15 M NaCl

Carbonate-bicarbonate

Phosphate Buffer: 1.7 mM  $\text{NaH}_2\text{PO}_4$ , 98 mM  $\text{Na}_2\text{HPO}_4 \cdot 7\text{H}_2\text{O}$ , 0.1%  $\text{NaN}_3$ , pH 8.5

TBS - 50 mM TRIS, pH 8.0, 0.15 M NaCl

## Blocking Buffers

1% BSA or 10% host serum in TBS, or TBS with 0.05% Tween-20

Phosphate Buffer: 73 mM Sucrose, 1.7 mM  $\text{NaH}_2\text{PO}_4$ , 98 mM  $\text{Na}_2\text{HPO}_4 \cdot 7\text{H}_2\text{O}$ , 0.1%  $\text{NaN}_3$ , pH 8.5

1% HSA in PBS

Casein Buffer: Pierce Blocker cat# 37528

Protein Free Block: Pierce cat# 37573

Pierce has many blocking buffers that are available in their catalog.

Heterophilic Blocking Reagent (HBR): Scantibodies Laboratory, Inc., cat# 3KC533

Scantibodies has many other blocking reagents that are available in their catalog.

## Wash Buffers

PBST, 0.05% Tween-20

TBST, 0.05% Tween-20

## Antibody Diluents Buffers

1% BSA or 10% host serum in TBS, or TBS with 0.05% Tween-20

1% BSA or 10% host serum in PBS, or PBS with 0.05% Tween-20

50 mM HEPES, 0.1 M NaCl, 1% BSA, pH 7.4

Blocking buffer

## Matrix Diluent

1. Serum or plasma from the sample species (this might contain the analyte to be measured which will interfere with the assay)
2. Serum or plasma from a species different from the sample (the analyte, if present, might not cross react with the antibody)
3. 0.1 M HEPES, 0.1 M NaCl, 1% BSA, 0.1% Tween-20
4. Tissue culture medium for samples
5. Cell lysates (these might contain SDS or other denaturing reagents that might interfere with the assay)

## Enzymes and Substrates

1. Horseradish peroxidase (HRP) substrates:
  - a. TMB: 3, 3', 5,5'-tetramethyl benzidine (colorimetric)
  - b. OPD: o-phenylene diamine (colorimetric)
  - c. ABTS: 2, 2'-azino-bis (3-ethylbenzthiazoline-6-sulfonic acid) (colorimetric)
  - d. Pierce Supersignal (chemiluminescent)
  - e. Pierce QuantaBlu (chemifluorescent)
  - f. Pierce QuantaRed (chemifluorescent)
  - g. Pierce has other substrates that provide strong signal and sensitivity with HRP enzyme conjugates that are available in their catalog.
2. Alkaline phosphatase substrate:
  - a. pNpp (p-Nitrophenyl Phosphate)

## Stop Solutions

1. HRP/TMB: 2M H<sub>2</sub>SO<sub>4</sub> solution (at a 1:1 volume with the HRP/TMB substrate/enzyme solution)
2. OPD: 3M H<sub>2</sub>SO<sub>4</sub> solution, (at a 1:1 volume with the OPD substrate/enzyme solution)
3. ABTS: 1% SDS

## Absorbance Readout

1. HRP TMB: 450 nm
2. OPD: 490 nm
3. ABTS: 405 nm

## Fluorescent Readout (Emax/Amax)

1. QuantaBlu 420/325
2. QuantaRed 585/570
3. FITC 518/494

## Luminescent Readout

- 1 An immunoassay technique where the antibody or the antigen is labeled with a molecule capable of emitting light during a chemical reaction. For detection, a luminescent plate reader is required (available from PerkinElmer).

## Specific Antibodies

1. Sandwich Immunoassay: matched pair of antibodies, one for analyte capture on a solid surface and one for detection that binds to the antigen/hapten/analyte. Antibodies need to be affinity purified for optimal results.
2. Competitive Immunoassay: a single antibody specific for the hapten/analyte. For optimal results affinity purified reagents are preferred.

## Standards or Antigen (Analyte)

1. The analyte to be measured is typically a recombinant form of the natural analyte or peptide.
2. Enough standard should be obtained for use in the development phase, validation phase and the continued support of the method to avoid changing lots and/or running out of standard.
3. Standard quality: Can vary from vendor to vendor and from lot to lot from a vendor.
4. Standard stability: Information on the stability of a standard can be obtained from the vendor and their recommendations should be followed in storing the standards.

## Control Samples

1. Control samples are real samples where the antigen analyte level has been determined by another validated method. Samples are aliquoted, frozen and used as control samples in each experiment to track assay performance.
2. Spiked controls are created by adding a known concentration of the standard analyte into the matrix (for example: tissue culture, serum, plasma, or cell lysates).

Spiked controls can be used to determine assay performance based on calculating the percent recovery.

## Instrumentation

### Instrument Linearity and Performance

The instrument used to read the output of the immunoassay should be tested initially for both linearity and performance. Instrument performance should be regularly calibrated according to manufacturer's specifications. The majority of plate readers employ UV-Vis Absorbance, fluorescence or chemiluminescence signals as the measured response, because the products of enzyme labels are chromophores, fluorophores or emit luminescent signals. Linearity in response to the specific enzyme product of an enzyme-linked immunoassay (ELISA) should be checked at the appropriate wavelengths and instrument settings.

### Spectrophotometric/Colorimetric Plate Readers

Lamp sources and Photomultiplier Tubes (PMT) vary in quality and performance in many plate readers. The linear range of many plate readers is generally between 0-3 Absorbance Units (AU), but other instruments have a linear range up to 4.0 AU. A malfunctioning lamp source or photomultiplier tube can significantly affect the linear response range.

### Fluorescence Plate Readers

These readers employ excitation and emission filter sets in addition to excitation lamp sources and PMTs. In addition to the lamps and PMTs, the filter sets also vary in quality, light throughput and bandwidth. Fluorescence signals are generally in Relative Fluorescence Units (RFU) and linearity should be verified with appropriate filter sets for the fluorophore employed according to instrument specifications.

### Chemiluminescence Readers

These instruments have sensitive photomultipliers to detect light emitted from a chemical reaction. No Lamp sources are necessary. These readers usually have a much larger dynamic range, thus allowing for the increase in sensitivity. Signals or responses are measured in Relative Light Units (RLU) and can be significantly different depending on the instrument design.

### Immunoassay Formats

An ELISA is one of several methods used in the laboratory to detect and quantify specific molecules. ELISAs rely on the inherent ability of an antibody to bind to the specific structure of a molecule. In order to optimize an ELISA and obtain the sensitivity and dynamic range required for the particular assay being developed, all the various



components of the assay must be evaluated. The components will vary depending on the immunoassay format selected. The following is a description of the various types of ELISA formats as well as reagents that need to be optimized in order to obtain a robust assay.

## Types of ELISA Formats

Three frequently used types of ELISA are: sandwich assays, competitive assays and antigen down assays. The format selected depends on the reagents that are available and the dynamic range required for the particular assay. Sandwich assays tend to be more sensitive and robust and therefore tend to be the most commonly used.

### Sandwich Immunoassay (ELISA)

A sandwich immunoassay is a method using two antibodies, which bind to different sites on the antigen or ligand (Figure 1). The capture antibody, which is highly specific for the antigen, is attached to a solid surface. The antigen is then added, followed by addition of a second antibody referred to as the detection antibody. The detection antibody binds the antigen at a different epitope than the capture antibody. As a result, the antigen is 'sandwiched' between the two antibodies. The antibody binding affinity for the antigen is usually the main determinant of immunoassay sensitivity. As the antigen concentration increases, the amount of detection antibody increases, leading to a higher measured response. The standard curve of a sandwich-binding assay has a positive slope. To quantify the extent of binding, different reporters can be used. These reporters (i.e. enzyme, fluorophore, or biotin) can be directly attached to the detection antibody or to a secondary antibody which binds the detection antibody (i.e. goat, anti-mouse IgG – HRP). In this latter case, the capture antibody and the detection antibody must be from different species (i.e. if the capture antibody is a rabbit antibody, the detection antibody would be from goat, chicken, etc., but not rabbit). If the detection antibody is directly labeled, then the capture and detection antibodies can be from the same species. Polyclonal antibodies often contain multiple epitopes and the same affinity purified polyclonal can be used as the capture and labeled detection antibody. The substrate for the enzyme is added to the reaction that forms a colorimetric readout as the detection signal. The signal generated is proportional to the amount of target antigen present in the sample.

The antibody linked reporter used to measure the binding event determines the detection mode. For an ELISA, where the detection is colorimetric, a spectrophotometric plate reader is used. Several types of reporters have been developed in order to increase sensitivity in an immunoassay. For example, chemiluminescent substrates have been developed which further amplify the signal and can be read on a luminescent plate reader. Also, a fluorescent readout where the enzyme step of the assay is replaced with a fluorophore tagged antibody is becoming quite popular. This readout is then measured using a fluorescent plate reader. When the detection antibody is labeled with biotin, you have the flexibility to use a number of different types of streptavidin conjugated reporters.

## Sandwich ELISA

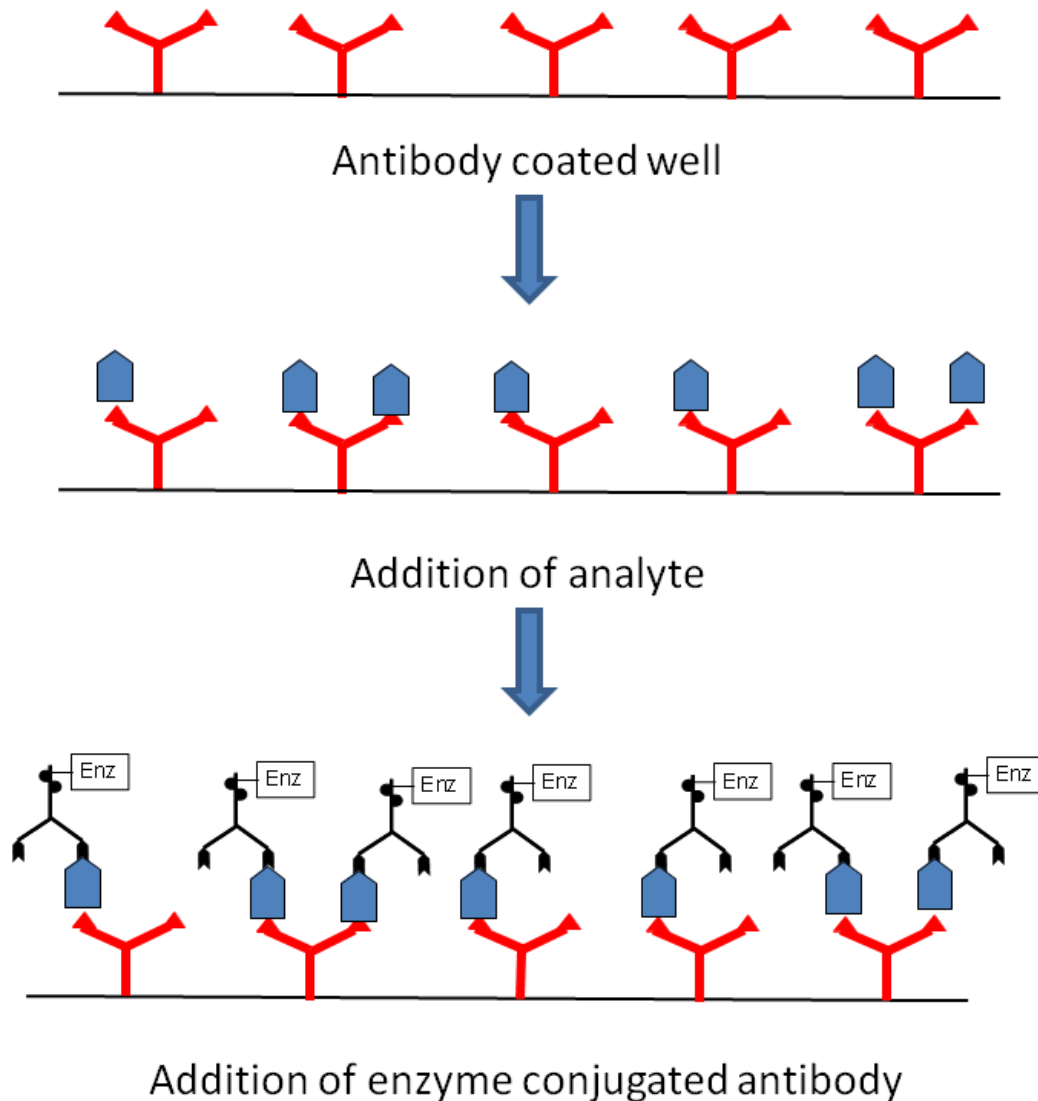


**Figure 1:** Diagram of a sandwich ELISA. The addition of the enzyme's substrate leads to color development. The amount of color (absorbance) is directly proportional to the analyte concentration.

### Competitive Binding Assay

A competitive binding assay is based upon the competition of labeled and unlabeled ligand for a limited number of antibody binding sites (Figure 2). Only one antibody is used in a competitive binding ELISA. Competitive binding assays are often used to measure small analytes. These assays are also used when a matched pair of antibodies to

## Competitive ELISA

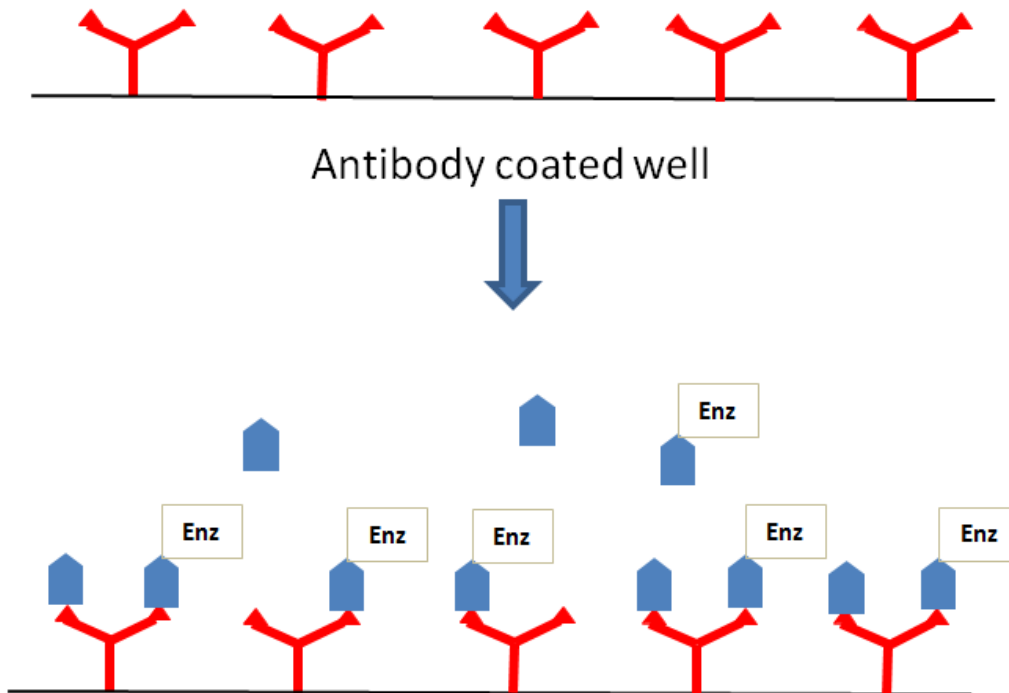


**Figure 2:** Diagram of a competitive binding assay. After addition of both the analyte and the enzyme-conjugated analyte, competition occurs between the two for binding to the antibody. The addition of the enzyme's substrate leads to color development. The amount of color (absorbance) is indirectly proportional to the analyte concentration

the analyte does not exist. A fixed amount of labeled ligand (tracer) and a variable amount of unlabeled ligand are incubated with the antibody. According to the law of mass action, the amount of bound labeled ligand is a function of the total concentration of labeled and unlabeled ligand. As the concentration of unlabeled ligand is increased, less labeled ligand can bind to the antibody and the measured response decreases. Thus the lower the signal, the more unlabeled analyte there is in the sample. The standard curve of a competitive binding assay has a negative slope. Alternatively, the antigen can be coated on the plate with the antibody and the sample in solution. Fewer antibodies will be available to bind the coated antigen as the amount of antigen in the sample increases. The antibody and labeled antigen concentrations are the important parameters that need to be optimized.

## Antigen-Down ELISA

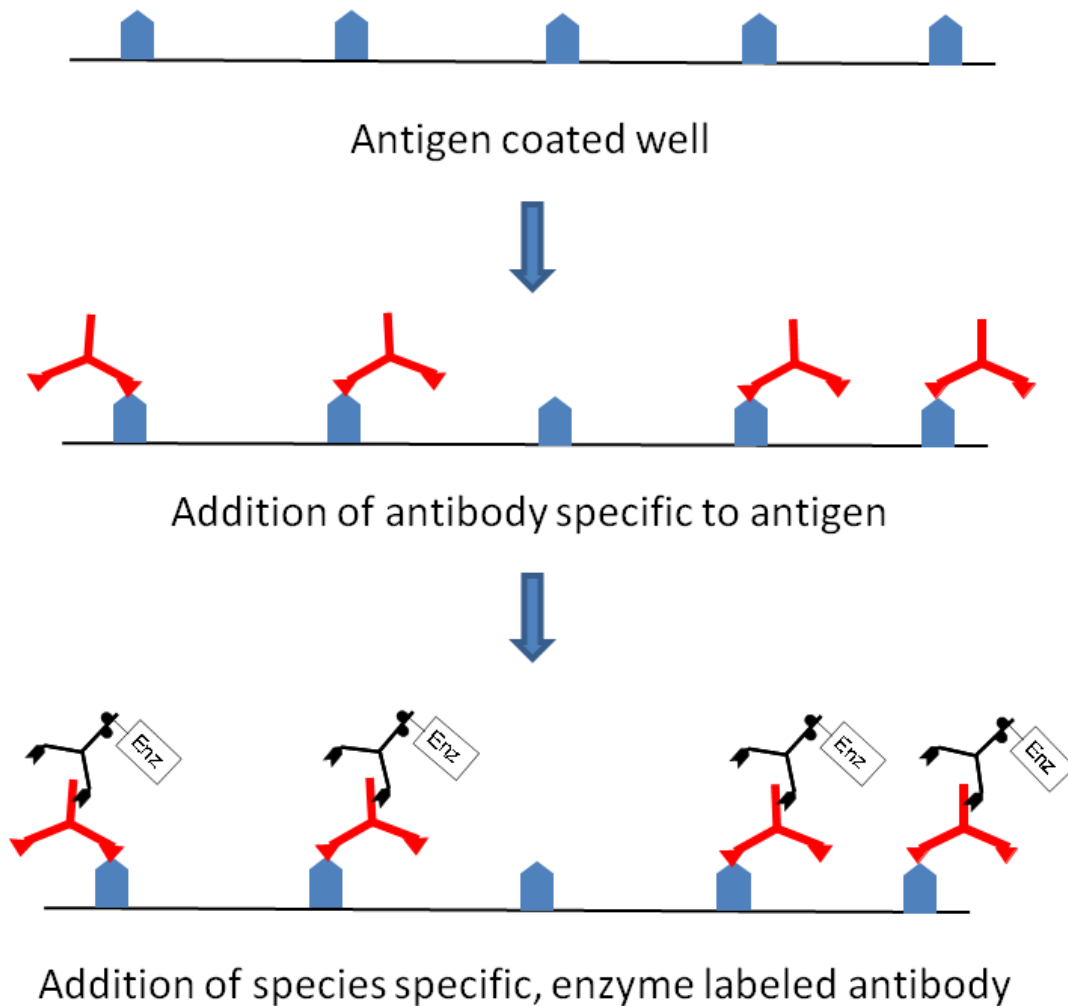


**Figure 3:** Diagram of an antigen-down ELISA. The addition of the enzyme's substrate leads to color development. The amount of color (absorbance) is directly proportional to the antigen specific antibody concentration.

### Antigen-Down Immunoassay or Immunometric Assay

An antigen-down immunoassay or immunometric assay involves binding the antigen to a solid surface instead of an antibody (Figure 3). This is done by coating the solid surface with the antigen, allowing for passive absorbance to the solid surface. Antigen-down immunoassays are used to bind antibodies found in a sample or in a competitive ELISA format (discussed above). When the sample is added (such as human serum), the

antibodies (IgE for example) from the sample bind to the antigen coated on the plate. A species-specific antibody (anti-human IgE for example) labeled with HRP is added next. The signal is directly proportional to the amount of antibody present in the sample; the more antibodies there are in the sample, the higher the signal.

## Single Antibody Two Plate ELISA Format

A single antibody ELISA format is considered when there is only one antibody available that recognizes the analyte (Figure 4). The assay is configured using the same antibody as both capture and detection. The antibody is biotinylated for use as the detection antibody. The method also utilizes two plates. The basic concept is to capture the antibody to an ELISA plate and allow the analyte of interest to bind to the capture antibody. Unbound material is removed by washing the plate and then adding an acid solution to elute the analyte from the capture antibody. The eluted analyte is then transferred to another ELISA plate containing the neutralization solution. The eluted analyte is then allowed to bind to the second ELISA plate. The unbound material is removed and the plate is blocked followed by a wash step. The detection antibody, which is biotinylated, is then added to the plate, followed by an incubation period. Another wash step is performed to remove excess detection antibody, followed by addition of a streptavidin reporter. The last wash step is performed to remove the excess reporter, followed by addition of the substrate. Below is a generic protocol that can be used to set up a Single Antibody Two Plate ELISA Method.

## Reagents and basic concepts

Included in the list below are the plate type and buffers that are a good starting point for single antibody ELISA assays.

1. One antibody that recognizes the analyte.
2. The optimal capture and detection antibody concentrations need to be determined experimentally.
3. Nunc immunoassay plate
4. Coating buffer: TBS
5. Blocking buffer: 1% BSA, TBS, 0.1% Tween-20
6. Antibody diluent buffer: 1% BSA, PBS or TBS, or 0.1% Tween-20
7. Acid elution buffer: 200 mM Acetic Acid
8. Neutralizing buffer: 1M Tris pH 9.5
9. Wash buffer: TBS 0.1% Tween-20
10. TMB and HRP are used for enzyme/substrate readout.
11. Acid stop buffer
12. The conditions for the following need to be tested and optimized for optimal assay performance: pH, buffers, incubation times, concentrations of antibodies, volumes used, etc.

## Single Antibody Two Plate ELISA

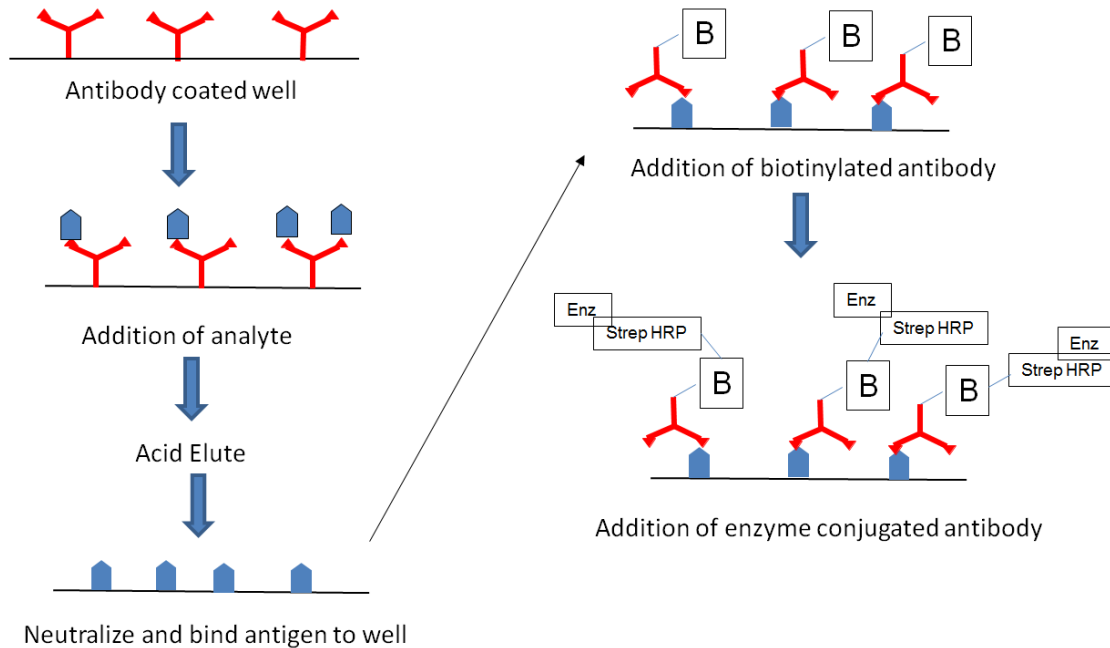


**Figure 4:** Diagram of a Single Antibody Two Plate ELISA. The addition of the enzyme's substrate leads to color development. The amount of color (absorbance) is directly proportional to the analyte concentration.

### Basic Protocol for Single Antibody Two Plate ELISA Method Day 1

1. Prepare the capture antibody in coating buffer
2. Add 100  $\mu\text{l}$  of the capture antibody in coating buffer to Plate 1- Nunc 96-well microtiter plate
3. Incubate plate with gentle shaking for 1 hour at room temperature
4. Remove the unbound capture antibody from the microtiter plate by dumping the plate
5. Wash the plate 3 times with wash buffer
6. Prepare serial dilutions of the analyte in dilution buffer
7. Add 100  $\mu\text{l}$  of the analyte to the plate
8. Incubate plate with gentle shaking for 1 hour at room temperature
9. Wash the plate 3 times with wash buffer
10. Add 65  $\mu\text{l}$  of 200 mM Acetic Acid for 5 minutes at room temperature with gentle shaking
11. Prepare Plate 2 by adding 100  $\mu\text{l}$  of 1 M Tris pH 9.5 to the microtiter plate
12. After 5 minutes of incubation transfer the 65  $\mu\text{l}$  of acidified analyte from Plate 1 to Plate 2
13. Incubate overnight at 4°C with gentle shaking

## Day2: Plate 2

1. Wash Plate 2, 3 times with wash buffer
2. Add 200  $\mu$ l of blocking buffer to the plate
3. Incubate for one hour at room temperature with gentle shaking
4. Wash the plate 3 times with wash buffer
5. Add 100  $\mu$ l of the biotinylated detection antibody (this is the same antibody that was used as the capture antibody)
6. Incubate for one hour at room temperature with gentle shaking
7. Wash the plate 3 times with wash buffer
8. Add Streptavidin HRP
9. Incubate for 20-30 minutes at room temperature with gentle shaking
10. Wash the plate 3 times with wash buffer
11. Add TMB substrate to the plate
12. Incubate according to manufacturer's suggestions with gentle shaking
13. Add Stop Solution, mix thoroughly
14. Read optical density at 450 nm

## Multiplex Immunoassay Technologies

Biomarker research has expanded over the years, producing a need to quantitatively measure multiple analytes simultaneously from one sample. In the pre-clinical research area there is a need to measure endpoints from rodents and non-human primates to determine safety and efficacy of drug candidates. Typically the samples from these animal models are limited in volume and expensive to obtain, which produces a challenge in obtaining data if more than one analyte needs to be quantified. The same issues apply to clinical samples being assayed for Biomarker, Pharmacokinetic, and Pharmacodynamic studies. A single endpoint ELISA tends to use a larger volume of sample than a multiplexed assay.

Two of the widely used multiplex technologies that have been developed are the Luminex xMAP technology (LMX) and the Meso Scale Discovery (MSD). Both technologies have well validated immunoassays that cover a wide range of secreted and intracellular proteins. In most cases, numerous analytes can be measured with sample volumes of less than 50  $\mu$ l.

Meso Scale Discovery is a multiplexed technology based on MULTI-ARRAY<sup>®</sup> technology. The technology utilizes a proprietary electrochemiluminescence detection system and an array of spots in a standard 96-well format. The electrochemiluminescence technology allows for an increase in dynamic range of the standard curve as well as an increase in sensitivity over normal ELISA readouts, such as HRP/TMB. The MSD technology utilizes a 96- or 384-well microtiter plate, allowing an immunoassay to be developed and optimized using the same variables of antibody concentrations, buffers, and incubation times that are used in a standard ELISA. The plates are read using a Sector 6000 instrument yielding Relative Light Units that can be back calibrated off the standard curve

to the analyte concentration that is being analyzed. Additional information on the MSD platform can be found at: <http://www.mesoscale.com/>.

Luminex xMAP is a bead based technology that allows capture antibodies to be coupled to color coded beads or microspheres that contain different emission spectra. A sandwich assay format is performed with the analyte added to the capture antibody bound beads, followed by the addition of a biotinylated antibody. The detection occurs by adding a streptavidin-conjugated fluorochrome to the complex containing the sandwiched immunoassay. The fluorescent readout is detected using a Luminex xMAP which is a flow cytometry based instrument. The microspheres are classified based on their emission spectra and the amount of analyte detected is directly proportional to the fluorescent signal. Additional details on the LMP technology can be found at: <http://www.luminexcorp.com/TechnologiesScience/xMAPTechnology/>.

Studies have been performed by numerous laboratories directly comparing the MSD technology to the Luminex xMAP as well as to commercially available enzyme-linked immunosorbent assays (6-12). Validation data has been generated for spiked recovery in various matrixes, including other validation parameters for both the MSD and Luminex technologies. Overall the results from numerous studies show that while there usually is a quantitative difference between the technologies (most likely due to the use of different antibodies), the relative differences are comparable. Data from these numerous studies demonstrate that multiplexed technologies are suitable for screening for trends in cytokine profiles and other secreted proteins to support pre-clinical and clinical studies.

## Important Parameters for Development of an Immunoassay

1. Capture antibody
2. Detection antibody
3. Plate type
4. Coating buffer
5. Blocking buffer/diluent buffer
6. Wash buffer
7. Coating antibody concentration
8. Coated antibody stability
9. Timing of each step in the immunoassay
10. Detection and/or secondary antibody concentration
11. Reporter concentration
12. Readout
13. Instrument linearity



## Initial Concept and Method Development for a Sandwich Immunoassay

### Initial Development Experiment

The goal is to develop a basic working method by determining the antibody which should be the capture antibody and which antibody should be the detection antibody. Determine the optimum antibody concentrations for both the capture and detection antibody. The optimal antibody for capture vs. detection can only be determined empirically. If multiple antibodies to the analyte exist, it is best to examine all possible pairs of the antibodies.

### Experiment

Coat the ELISA plate with several dilutions of each antibody that will be used as part of the sandwich assay. Add the analyte to be measured at a high, low and zero concentration. Use each of the antibodies, at several concentrations, as a detection antibody. The results of this experiment will determine which antibody is best for the capture antibody and which is best for the detection antibody. Furthermore, the dilution needed for both antibodies will also be determined.

### Reagents

Included in the list below are the plate type and buffers that will work for the majority of immunoassays. Use these conditions as a starting point.

1. Two antibodies that recognize different epitopes on the analyte.
2. The optimal antibody pair for the sandwich assay was determined empirically in the experiment above.
3. Greiner immunoassay plate
4. Coating buffer: PBS
5. Blocking buffer: 1% BSA, TBS, 0.1% Tween-20
6. Antibody diluent buffer: 1% BSA, PBS or TBS, or 0.1% Tween-20
7. Wash buffer: PBS or TBS 0.1% Tween-20
8. TMB and HRP are used for enzyme/substrate readout
9. Acid stop buffer

### Protocol (see plate layouts in Table 1 and Table 2):

1. Dilute both antibodies in coating buffer at 0.5, 1, 2 and 5  $\mu\text{g/ml}$  and add 100  $\mu\text{l}$  of each concentration to 24 wells of the 96-well microtiter plate.
2. Incubate the plate containing the capture antibody overnight at 4°C and continue the experiment the next day. (Stability of the capture antibody bound to the plate can be determined in later experiments.)
3. Remove the unbound capture antibody solution from the microtiter plates by aspirating or dumping the plate.

4. Add 200  $\mu\text{l}$  of blocking buffer to each well of the 96-well microtiter plate. Incubate the plate for one hour at room temperature.
5. Remove the blocking buffer from the plate by aspirating or dumping the plate.
6. Determine the desired working range of the analyte. This will give you the high and low concentrations to incubate with each capture antibody dilution. The zero analyte wells will give you the non-specific binding (NSB).
7. Add 100  $\mu\text{l}$  of the analyte to each well in the microtiter plate and incubate for 2.5 hours at room temperature.
8. Wash the plates 3 times with wash buffer.
9. Dilute the detection antibody serially at 1:200, 1:1000, 1:5000 and 1:25000 in diluent.
10. Add 100  $\mu\text{l}$  of detection antibody to each well of the microtiter plate and incubate for 1.5 hours at room temperature.
11. Wash the plates 3 times with wash buffer.
12. Dilute streptavidin-HRP (if detection antibodies are biotinylated) or appropriate secondary antibody (if capture and detection antibodies are from different species) according to manufacture instructions in antibody diluent and add 100  $\mu\text{l}$  to each well in the microtiter plate and incubate for 1 hour at room temperature.
13. For HRP readout add TMB as a substrate to allow color development and incubate for 10-20 minutes at room temperature.
14. Add acid stop reagent to stop the enzyme reaction.
15. Read at 450 nm for TMB/HRP.

**Table 1:** Plate 1 layout for initial experiment. H=High, L=Low and 0=Zero. High analyte or ligand concentration in combination with the low ligand concentration will give an indication of the dynamic range. Low analyte or ligand concentration will give an indication of sensitivity. Zero ligand will give the non-specific binding and indicate if there are background issues.

| Detection Antibody | Capture Antibody A |   |   |                    |   |   |                    |   |   |                      |   |   |
|--------------------|--------------------|---|---|--------------------|---|---|--------------------|---|---|----------------------|---|---|
|                    | 5 $\mu\text{g/ml}$ |   |   | 2 $\mu\text{g/ml}$ |   |   | 1 $\mu\text{g/ml}$ |   |   | 0.5 $\mu\text{g/ml}$ |   |   |
| 1:200              | H                  | L | 0 | H                  | L | 0 | H                  | L | 0 | H                    | L | 0 |
|                    | H                  | L | 0 | H                  | L | 0 | H                  | L | 0 | H                    | L | 0 |
| 1:1000             | H                  | L | 0 | H                  | L | 0 | H                  | L | 0 | H                    | L | 0 |
|                    | H                  | L | 0 | H                  | L | 0 | H                  | L | 0 | H                    | L | 0 |
| 1:5000             | H                  | L | 0 | H                  | L | 0 | H                  | L | 0 | H                    | L | 0 |
|                    | H                  | L | 0 | H                  | L | 0 | H                  | L | 0 | H                    | L | 0 |
| 1:25000            | H                  | L | 0 | H                  | L | 0 | H                  | L | 0 | H                    | L | 0 |
|                    | H                  | L | 0 | H                  | L | 0 | H                  | L | 0 | H                    | L | 0 |

**Table 2:** Plate 2 layout for the initial experiment. H=High, L=Low and 0=Zero. High analyte or ligand concentration in combination with the low ligand concentration will give an indication of the dynamic

range. Low analyte or ligand concentration will give an indication of sensitivity. Zero ligand will give the non-specific binding and indicate if there are background issues.

| Detection Antibody | Capture Antibody B |   |   |         |   |   |         |   |   |           |   |   |
|--------------------|--------------------|---|---|---------|---|---|---------|---|---|-----------|---|---|
|                    | 5 µg/ml            |   |   | 2 µg/ml |   |   | 1 µg/ml |   |   | 0.5 µg/ml |   |   |
| 1:200              | H                  | L | 0 | H       | L | 0 | H       | L | 0 | H         | L | 0 |
|                    | H                  | L | 0 | H       | L | 0 | H       | L | 0 | H         | L | 0 |
| 1:1000             | H                  | L | 0 | H       | L | 0 | H       | L | 0 | H         | L | 0 |
|                    | H                  | L | 0 | H       | L | 0 | H       | L | 0 | H         | L | 0 |
| 1:5000             | H                  | L | 0 | H       | L | 0 | H       | L | 0 | H         | L | 0 |
|                    | H                  | L | 0 | H       | L | 0 | H       | L | 0 | H         | L | 0 |
| 1:25000            | H                  | L | 0 | H       | L | 0 | H       | L | 0 | H         | L | 0 |
|                    | H                  | L | 0 | H       | L | 0 | H       | L | 0 | H         | L | 0 |

## Results

Determine the absorbance units that yield the maximum signal to noise ratio or the greatest difference between the high and low analyte concentrations with the lowest variability. These are the conditions that will be selected for the antibody to be used as the capture antibody and the dilution of the antibodies to be used in the next experiment.

- If the background signal is unacceptably high (greater than 0.2 A.U.) then run additional experiments varying the plate type, blocking buffers, blocking buffers with a diluent agent like species specific IgG, antibody diluent buffers, wash buffers, and the reporter type.
- If the above general conditions have an acceptable NSB then it can be determined if the dynamic range and sensitivity are in the appropriate range. To improve the sensitivity of the assay, the buffers, timing of incubations and matrix conditions can be varied in the next experiment.
- Antibodies are the reagents that play a major role in the sensitivity and dynamic range of an immunoassay. This is due to the actual antibody affinity for the analyte. If after attempting to develop the assay the sensitivity is still not in the desired range, different antibody pairs will need to be evaluated.

## Example 2

An ELISA was set up to measure the amounts of a protein where there is only one polyclonal antibody available. The polyclonal antibody was used as both the capture antibody and the detection antibody. In this example the detection antibody is biotinylated.

### Reagents:

1. Affinity pure polyclonal antibody
2. Analyte protein

### 3. Biotinylated affinity pure polyclonal antibody

#### Protocol:

Follow the same basic protocol above using these parameters (see plate layout in Table 3).

1. Coat the affinity purified antibody at 3 levels: 2, 1 and 0.5  $\mu\text{g/ml}$ .
2. Dilute the biotinylated antibody at 3 levels: 1:1000, 1:5000, and 1:25000.
3. Dilute the analyte protein in buffer to 50 ng/ml, 1 ng/ml, and zero.

#### Conclusions:

As seen in Table 4, the lowest NSB and best signal to noise ratio from low to high analyte concentration are the 0.5  $\mu\text{g/ml}$  concentration for the capture antibody and the 1:25000 dilution of the biotinylated detection antibody.

| Detection Antibody | Capture Antibody |   |   |         |   |   |           |   |   |  |  |  |
|--------------------|------------------|---|---|---------|---|---|-----------|---|---|--|--|--|
|                    | 2 µg/ml          |   |   | 1 µg/ml |   |   | 0.5 µg/ml |   |   |  |  |  |
| 1:1000             | H                | L | 0 | H       | L | 0 | H         | L | 0 |  |  |  |
|                    | H                | L | 0 | H       | L | 0 | H         | L | 0 |  |  |  |
| 1:5000             | H                | L | 0 | H       | L | 0 | H         | L | 0 |  |  |  |
|                    | H                | L | 0 | H       | L | 0 | H         | L | 0 |  |  |  |
| 1:25000            | H                | L | 0 | H       | L | 0 | H         | L | 0 |  |  |  |
|                    | H                | L | 0 | H       | L | 0 | H         | L | 0 |  |  |  |
|                    |                  |   |   |         |   |   |           |   |   |  |  |  |

**Table 3: Plate layout to determine the capture and detection antibody concentrations.**

**Table 4:** Results from Example 2: to determine the capture and detection antibody concentrations. Values are averages of absorbance measurements at A450.

| Capture Antibody          |         | 2 µg/ml |      |      | 1 µg/ml |      |      | 0.5 µg/ml |      |      |
|---------------------------|---------|---------|------|------|---------|------|------|-----------|------|------|
| Analyte protein ng/ml     |         | 50      | 1    | 0    | 50      | 1    | 0    | 50        | 1    | 0    |
| <b>Detection Antibody</b> | 1:1000  | 3.69    | 1.81 | 1.37 | 3.63    | 1.89 | 1.33 | 3.3       | 1.79 | 0.99 |
|                           | 1:5000  | 3.22    | 0.7  | 0.49 | 3.24    | 0.81 | 0.47 | 3.1       | 0.83 | 0.36 |
|                           | 1:25000 | 1.61    | 0.21 | 0.15 | 1.75    | 0.25 | 0.16 | 1.72      | 0.26 | 0.12 |

## Second Development Experiment-Matrix Compatibility

The goal is to determine the matrix effect or sample type on the immunoassay method. The matrix is based on what the sample is found in, for instance tissue culture media, serum, plasma, cell lysate, buffers, etc. Serum matrix, due to its complexity, can have a significant effect on the method. In this example the samples are in rat serum so the matrix effect of rat serum needs to be determined.

### Experiment

The samples that need to be measured in this assay will be in either mouse or rat serum. Use the conditions established in the first experiment for the concentration of the capture antibody and the detection antibody. Serially dilute the standard (analyte) to obtain a full standard curve in 3 different matrices (10% rat serum, 30% rat serum and the original buffer diluent used in the first experiment). This will determine the effect of the matrix used for the experimental samples.

### Reagents:

1. Use all of the reagents and buffers listed in the first experiment (Example 2).
2. Matrix diluent: 10% rat serum in antibody diluent or 30% rat serum in antibody diluent.

### Protocol:

Follow the standard protocol, changing only the matrix diluent to include rat serum.

1. Dilute the coating antibody in coating buffer at 0.5 µg/ml and add 100 µl to each well of the 96-well microtiter plate.
2. Incubate the plate containing the capture antibody overnight at 4°C and use the next day.
3. Stability of the capture antibody bound to the plate can be determined in later experiments.
4. Remove the capture antibody solution from the microtiter plates by aspirating or dumping the plate.
5. Add 200 µl of blocking buffer to each well of the 96-well microtiter plate.
6. Incubate the plate for one hour at room temperature.
7. Remove the blocking buffer from the plate by aspirating or dumping the plate.
8. Serially dilute the standard in antibody dilution buffer containing either 10% or 30% rat serum, or diluent alone.
9. Add 100 µl of the standard to each well in the microtiter plate and incubate for 2.5 hours at room temperature.
10. Wash the plates 3 times with wash buffer.
11. Dilute the detection antibody to 1:25000 in antibody diluent.
12. Add 100 µl of detection antibody diluent to each well of the microtiter plate and incubate for 1.5 hours at room temperature.
13. Wash the plates 3 times with wash buffer.
14. Dilute streptavidin-HRP according to manufacturer's instructions in antibody diluent and add 100 µl to each well in the microtiter plate and incubate for 1 hour at room temperature.
15. For HRP readout add TMB as substrate to allow color development and incubate for 10-20 minutes at room temperature.
16. Add acid stop reagent to stop the enzyme reaction.
17. Read at 450 nm for TMB/HRP.

### Results:

Use the standard curve data and construct a precision profile. Check the background levels. See the next section for standard or calibration curve model fitting. Note that the standard curves under all three matrix diluent conditions give the dynamic range and sensitivity necessary for the intended use (Figure 5). For this particular assay, no further development is needed (based on the standard curve, low background and precision profile).

### Precision Profile:

Generate the precision profile for the standard curve of the appropriate matrix for the experiment. The precision profile is a plot of coefficient of variation (CV) for the calibrated concentration levels of the replicates of each calibrator versus the nominal analyte concentration in the calibrator samples. The dynamic range of the calibration curve (quantification limits) are then defined by the concentrations where the precision profile intersects the 20% CV. The calculation of this CV has to take into consideration

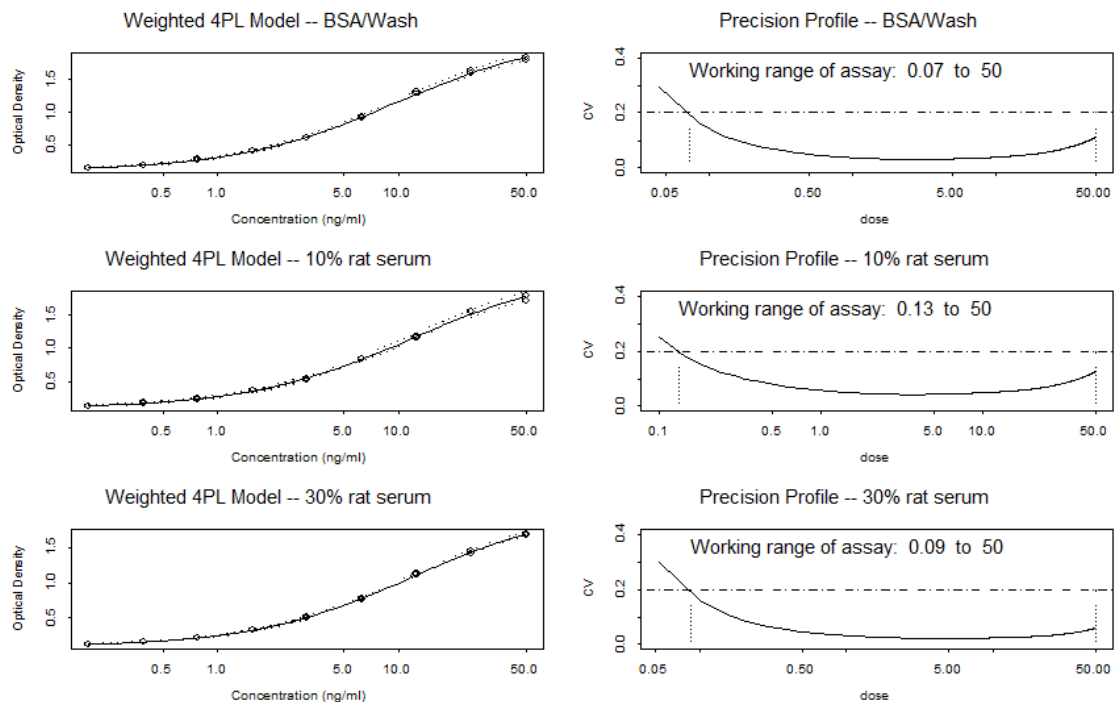


**Figure 5:** Calibration curve and precision profile for the three different matrix conditions using a Four Parameter Logistic (4PL) Model.

both the sampling variability and the lack of fit to the calibration curve, and is therefore not straightforward. A statistician should be consulted for this evaluation. An SAS program for this evaluation has been published (13).

## Calibration Curve and Precision Profile for the Three Different Matrix Conditions

### Calibration Curve Model Selection:

A significant source of variability in the calibration curves can come from the choice of the statistical model used for the calibration curve. It is therefore extremely important to choose an appropriate calibration curve model. For most immunoassays, the following models are commonly available from most instrument software.

#### Linear Model:

$$\text{Response} = a + b(\text{Concentration}) + \text{error}$$

where parameters,  $a$  and  $b$  are the intercept and slope respectively, and “response” refers to signal readout, such as optical density or fluorescence from an immunoassay. Often this linear model is fitted after log transformation of the response and concentration. This is sometimes referred as the “log-log linear model”.

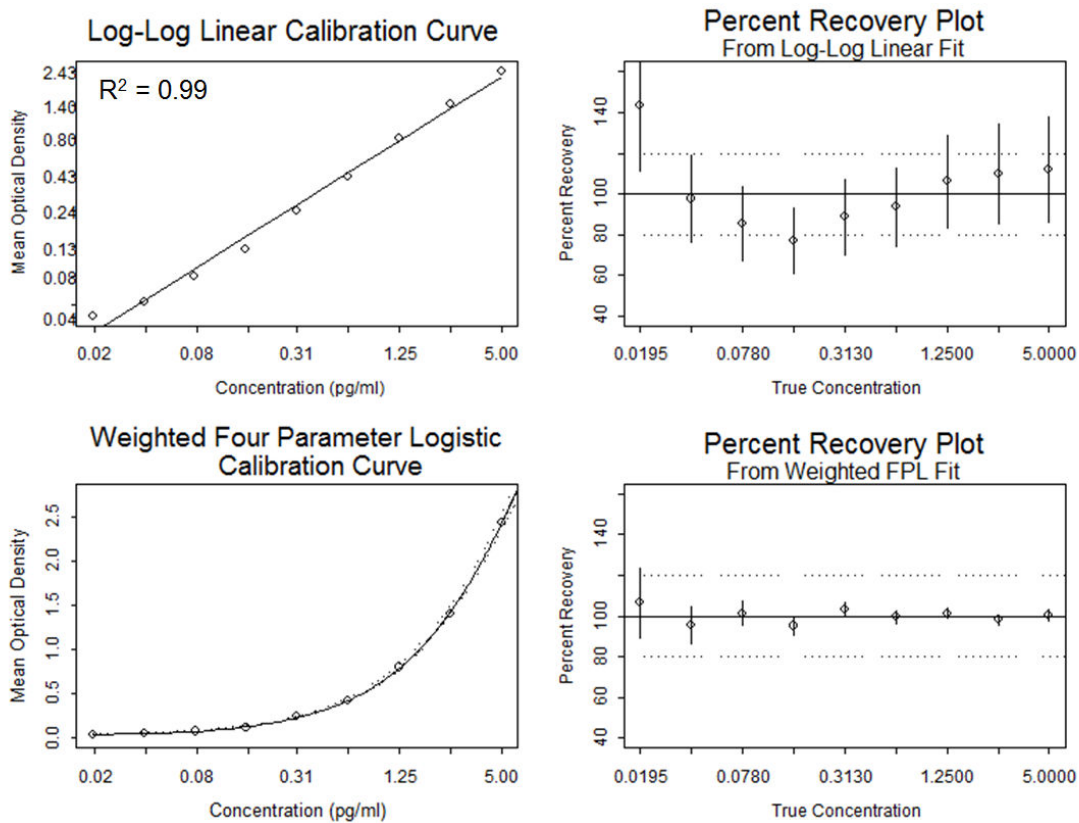


**Figure 6:** Example of log-log linear and weighted four parameter logistic calibration curves.

### Quadratic Model:

$$\text{Response} = a + b(\text{Concentration}) + c(\text{Concentration})^2 + \text{error}$$

where a, b and c are the intercept, linear and quadratic term coefficients, respectively, of this quadratic model.

### Four Parameter Logistic Model:

$$\text{Response} = \text{Top} + \frac{(\text{Bottom} - \text{Top})}{1 + \left(\frac{\text{concentration}}{\text{EC}_{50}}\right)^{\text{slope}}}$$

The four parameters to be estimated are Top, Bottom,  $\text{EC}_{50}$  and Slope. Top refers to the top asymptote, Bottom refers to the bottom asymptote, and  $\text{EC}_{50}$  refers to the concentration at which the response is halfway between Top and Bottom.

### Five Parameter Logistic Model:

$$\text{Response} = \text{Top} + \frac{(\text{Bottom} - \text{Top})}{\left[1 + \left(\frac{\text{concentration}}{\text{EC}_{50}}\right)^{\text{slope}}\right]^{\text{Asymmetry}}}$$



Asymmetry is the fifth parameter in this model. It denotes the degree of asymmetry in the shape of the sigmoidal curve with respect to “EC<sub>50</sub>”. A value of 1 indicates perfect symmetry, which would then correspond to the four-parameter logistic model. However, note that the term referred to as “EC<sub>50</sub>” in this model is not truly the EC<sub>50</sub>. It is the EC<sub>50</sub> when the asymmetry parameter equals 1. It will correspond to something very different such as EC<sub>20</sub>, EC<sub>30</sub>, EC<sub>80</sub>, etc., depending on the value of the asymmetry parameter for a particular data set.

For most immunoassays, the four or five parameter logistic model is far better than the linear, quadratic or log-log linear models. These models are available in several software packages, and are easy to implement even in an Excel-based program. As illustrated in the plots shown in Figure 6, the quality of the model should be judged based on the dose-recovery scale instead of the lack-of-fit of the calibration curve ( $R^2$ ). In this illustration, even though the  $R^2$  of the log-log linear model is 0.99, when assessed in terms of the dose-recovery plot, this model turns out to be significantly inferior to the four parameter logistic model. Before the assay is ready for production, the best model for the calibration curve should be chosen based on the validation samples using dose-recovery plots.

### Importance of Weighting in Calibration Curves

The default curve-fitting method available in most software packages assigns equal weight to all of the response values, which is appropriate only if the variability among the replicates is equal across the entire range of the response. However, for most immunoassays, the variability of assay signal among replicates of each calibrator increases proportionately with the response (signal) mean. Giving equal weight can lead to highly incorrect conclusions about the assay performance and will significantly affect the accuracy of results from the unknown samples. More specifically, lack of weighting leads to higher variability of results in the lower end of the assay range, thus greatly compromising the sensitivity of the assay. It is therefore extremely important to use a curve-fitting method/software that has appropriate weighting methods/options. This is illustrated in Figure 7 where we compare the total error results from the validation controls after fitting the calibration curves using log-log linear, four-parameter logistic and five-parameter logistic models. For this example, the performance of the validation samples is better overall when the five-parameter logistic model is used.

### Third Development Experiment

The two-step experiment detailed above is a very simple example of how to develop a sandwich ELISA method. If the dynamic range and sensitivity of the assay does not meet the experimental needs then further experimental parameters should be tested using experimental design. With experimental design all of the factors involved in the ELISA including buffers, incubation time and plate type can be analyzed.

In a sandwich ELISA method the antibodies chosen are the major drivers of the assay parameters. If at this point in the method development, the precision profile of the standard curve does not encompass the desired dynamic range and sensitivity, instead of

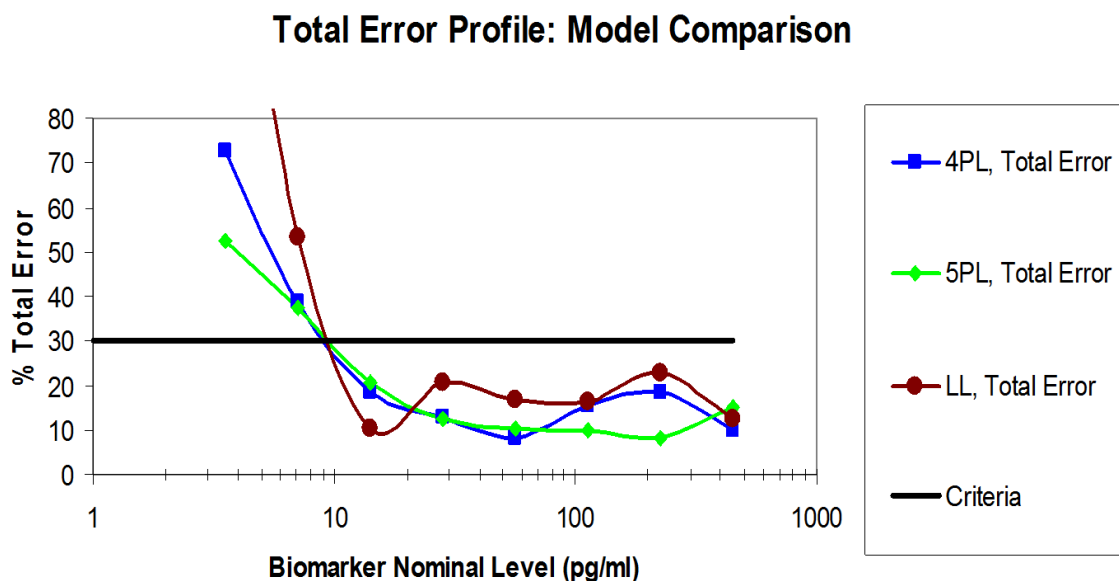


**Figure 7:** Validation samples are plotted with different calibration curve models. It is clear from the plot that the five-parameter logistic (5PL) model is better than the four-parameter logistic (4PL) and log-log linear (LL) models. For this particular assay, 5PL is the optimal choice for the in-study (production) phase.

continuing with the development experiment, antibodies should be further characterized. Changing some of the variables such as the antibody concentrations can significantly improve the calibration curve and hence its precision profile.

The goal is to determine the optimal conditions for the variables in the immunoassay, including incubation steps, buffers, substrate, etc. Also, determine the optimal antibody concentrations and the stability of the capture antibody bound to the plate.

### Experiment:

Dilute the standard in the matrix compatible to the sample (as determined in the second experiment). Vary the incubation times, dilution buffers and other variables in order to optimize the immunoassay. Analyze by using experimental design software and precision profiles.

### Reagents:

1. Antibodies
2. Coating buffers
3. Blocking buffers
4. Wash buffers
5. Antibody diluents
6. Substrate

### Protocol:

1. Coat the microtiter plate with the capture antibody at the concentration determined in the initial experiment. Incubate overnight at 4°C.
2. Discard the capture antibody solution from the microtiter plate.
3. Block the plate for 1 hour at room temperature using various blocking reagents.
4. Store plates at 4°C, desiccated, for several periods of time 0-5 days.
5. Repeat steps 1-3 the day of the actual experiment.
6. Serially dilute, using an 8-point standard curve, the known standard in the appropriate matrix for the experiment. For the control also dilute the standard in the same buffer as was used in the initial experiment. Add 100 µl of standard to each well in the 96-well microtiter plate.
7. Incubate the diluted standard with the capture antibody for 1 hour and 3 hours at room temperature and overnight at 4°C. Each time point will have to be run in a separate plate.
8. Wash plates 3 times (if background or NSB is high, try different wash buffers).
9. Add 100 µl of diluted detection antibody. If background is high again different diluents can be tested.
10. Incubate the detection antibody for different time periods and again different plates will have to be used for each time condition.
11. Wash plates 3 times.
12. Add 100 µl of substrate to the wells containing the detection antibody conjugated to the enzyme and allow incubation according to the manufacturer's conditions.
13. Add 100 µl of stop buffer.
14. Read at 450 nm.

### Data Analysis:

Compute the standard curves and their precision profiles for all the experimental design conditions. Derive the optimization endpoints using the precision profiles. Then analyze the optimization endpoints using software such as JMP (<http://www.jmp.com>) to determine the optimum levels of the assay factors. See next section for the details and illustration.

## Experimental Designs for Increasing Calibration Precision

### Step 1:

Identify all the factors/variables that potentially contribute to assay sensitivity and variability. Choose appropriate levels for all the factors (high and low values for quantitative factors, different categories for qualitative factors). Then use fractional-factorial experimental design in software such as JMP to derive appropriate experimental "trials" (combinations of levels of all the assay factors). Run 8-point calibration curves in duplicate for each trial. With each trial taking up two columns in a 96-well plate, 6 trials per plate can be tested. All trials should be randomly assigned to different pairs of columns in the 96-well plates. However, certain factors such as incubation time and

temperature are inter-plate factors. Therefore, levels of such factors will have to be tested in separate plates (see Table 5).

After the above experiment is run, the calibration curves should be fit for each trial using an appropriately weighted-nonlinear regression model. Then the precision profile for the calibration curve of each trial should be obtained along with the important optimization end-points such as working-range, lower quantitation limit and precision area (area of the region intersected by the precision profile with 20% CV). Now analyze these data to determine the optimal level of all qualitative factors and determine which subset of quantitative factors should be further investigated.

**Table 5:** Example plate layout to increase calibration precision.

|   | Trial 1                          |   | Trial 2                          |   | Trial 3                          |   | Trial 4                          |   | Trial 5                          |    | Trial 6                          |    |
|---|----------------------------------|---|----------------------------------|---|----------------------------------|---|----------------------------------|---|----------------------------------|----|----------------------------------|----|
|   | 1                                | 2 | 3                                | 4 | 5                                | 6 | 7                                | 8 | 9                                | 10 | 11                               | 12 |
| A | 8pt calibration curve; duplicate |   | 8pt calibration curve; duplicate |   | 8pt calibration curve; duplicate |   | 8pt calibration curve; duplicate |   | 8pt calibration curve; duplicate |    | 8pt calibration curve; duplicate |    |
| B | 8pt calibration curve; duplicate |   | 8pt calibration curve; duplicate |   | 8pt calibration curve; duplicate |   | 8pt calibration curve; duplicate |   | 8pt calibration curve; duplicate |    | 8pt calibration curve; duplicate |    |
| C | 8pt calibration curve; duplicate |   | 8pt calibration curve; duplicate |   | 8pt calibration curve; duplicate |   | 8pt calibration curve; duplicate |   | 8pt calibration curve; duplicate |    | 8pt calibration curve; duplicate |    |
| D | 8pt calibration curve; duplicate |   | 8pt calibration curve; duplicate |   | 8pt calibration curve; duplicate |   | 8pt calibration curve; duplicate |   | 8pt calibration curve; duplicate |    | 8pt calibration curve; duplicate |    |
| E | 8pt calibration curve; duplicate |   | 8pt calibration curve; duplicate |   | 8pt calibration curve; duplicate |   | 8pt calibration curve; duplicate |   | 8pt calibration curve; duplicate |    | 8pt calibration curve; duplicate |    |
| F | 8pt calibration curve; duplicate |   | 8pt calibration curve; duplicate |   | 8pt calibration curve; duplicate |   | 8pt calibration curve; duplicate |   | 8pt calibration curve; duplicate |    | 8pt calibration curve; duplicate |    |
| G | 8pt calibration curve; duplicate |   | 8pt calibration curve; duplicate |   | 8pt calibration curve; duplicate |   | 8pt calibration curve; duplicate |   | 8pt calibration curve; duplicate |    | 8pt calibration curve; duplicate |    |
| H | 8pt calibration curve; duplicate |   | 8pt calibration curve; duplicate |   | 8pt calibration curve; duplicate |   | 8pt calibration curve; duplicate |   | 8pt calibration curve; duplicate |    | 8pt calibration curve; duplicate |    |

## Step 2:

We now need to determine the optimum levels for the key factors determined in the previous step. Choose appropriate low, middle and high levels for each of these factors based on the data analysis results from step 1. Now use software such as JMP to generate appropriate trials (combinations of low, middle and high levels of all the factors) from a central-composite design. Then run duplicate 8-point calibration curves for each trial using a similar plate format as in step 1.

Now obtain the precision profile and the relevant optimization end-points of the calibration curve of each trial. Perform the response-surface analysis of these data to determine the optimal setting of each of the quantitative factors run in this experiment.

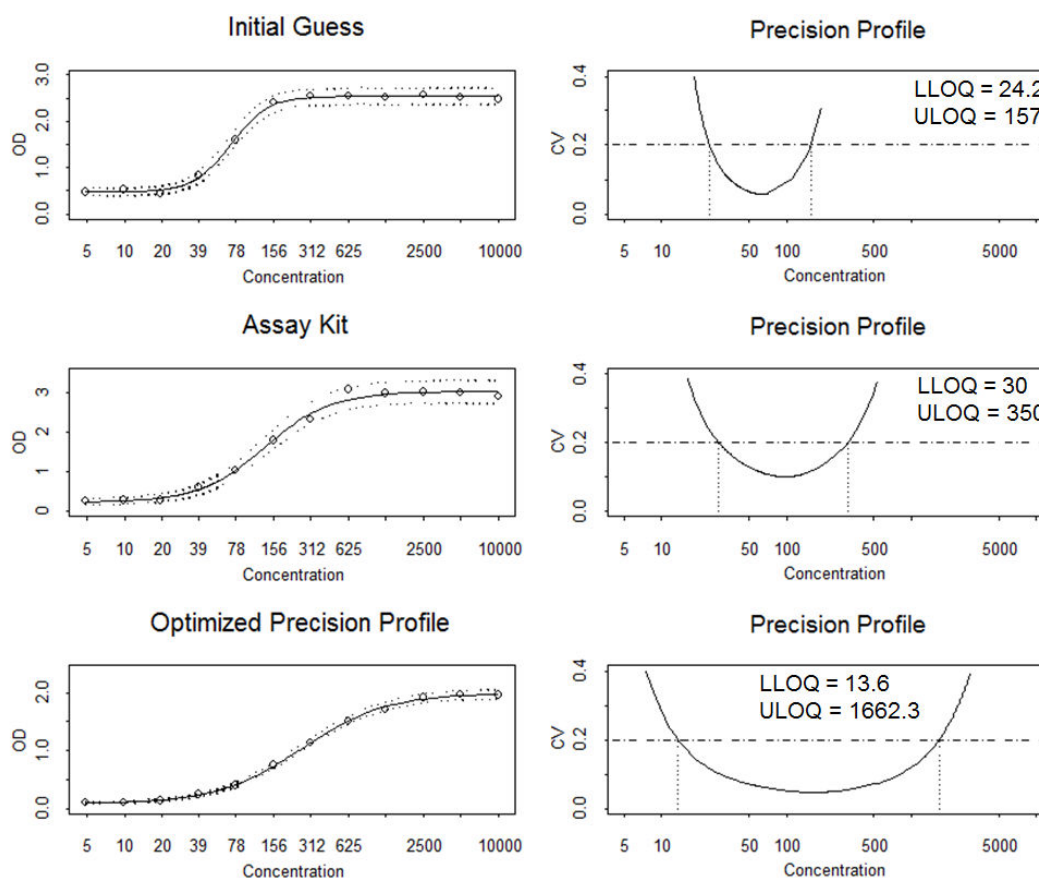


**Figure 8:** Comparison of optimized levels to pre-optimum levels and those recommended by the manufacturer.

## Illustration of Experimental Design and Analysis for Sandwich ELISA Optimization

In Table 6, we have the experiment plan from the second step of the optimization process using experimental design for a sandwich ELISA. These four factors (capture antibody, detection antibody, enzyme and volume) were picked out of the six factors considered in the first step of this optimization process (screening phase) for further optimization. We use a statistical experimental design method called central composite design to generate the appropriate combinations of the high, mid and low levels of the four factors in this second step. For example, trial #6 in this table refers to the middle level of the first, third and the fourth factors, and the low level of the second factor.

Eight-point standard curves in duplicate were generated for each of these trials, in adjacent columns of a 96-well plate. This resulted in six trials per plate, and with 36 trials in 6 plates. We computed the precision profiles of the calibration curves for each of these 36 trials. From these precision profiles, we computed the working range (lower and upper quantification limits), CV and related variability and sensitivity measures. We then used a

statistical data analysis method called "response surface analysis" on these optimization endpoints. This resulted in polynomial type models for all the factors. Using the shape of the curve and other features from this model, the optimum levels for these factors were determined. This gave us the most sensitive dynamic working range possible for this assay.

An experiment was then performed for this ELISA to compare these optimized levels to the pre-optimum levels and the assay kit manufacturer's recommendation. The results from this comparison are summarized in Figure 8.

The optimized levels derived from statistical experimental design for this ELISA resulted in the following improvements over the pre-optimum and assay kit manufacturer's recommendation.

- Lower quantification limit decreased more than two-fold to 13.6 nM.
- Upper quantification limit by up to 10-fold to 1662.3 nM.
- Precision area increased by 2-fold and the working range increased by 2-fold to two log cycles.

This improvement is evident from the precision profiles shown in Figure 8.

**Table 6:** Experimental plan from the second step of the optimization process using the experimental design for a sandwich ELISA.

| Trial # | Pattern | Capture A | Biotin A | EnzCult | Volume |
|---------|---------|-----------|----------|---------|--------|
| 1       | - - - + | 250       | 250      | 300     | 100    |
| 2       | 0 0 0 0 | 500       | 425      | 525     | 75     |
| 3       | - + + + | 250       | 600      | 750     | 100    |
| 4       | - + + - | 250       | 600      | 750     | 50     |
| 5       | - - - - | 250       | 250      | 300     | 50     |
| 6       | 0 - 0 0 | 500       | 250      | 525     | 75     |

*Table 6 continues on next page...*

*Table 6 continued from previous page.*

| Trial # | Pattern | Capture A | Biotin A | EnzCult | Volume |
|---------|---------|-----------|----------|---------|--------|
| 7       | 0 0 0 0 | 500       | 425      | 525     | 75     |
| 8       | 0 0 0 0 | 500       | 425      | 525     | 75     |
| 9       | 0 0 + 0 | 500       | 425      | 750     | 75     |
| 10      | - - + + | 250       | 250      | 750     | 100    |
| 11      | + - - + | 750       | 250      | 300     | 100    |
| 12      | 0 0 0 0 | 500       | 425      | 525     | 75     |
| 13      | 0 0 0 0 | 500       | 425      | 525     | 75     |
| 14      | + + + - | 750       | 600      | 750     | 50     |
| 15      | 0 0 0 0 | 500       | 425      | 525     | 75     |
| 16      | 0 0 0 0 | 500       | 425      | 525     | 75     |
| 17      | 0 0 0 0 | 500       | 425      | 525     | 75     |
| 18      | - + - - | 250       | 600      | 300     | 50     |

*Table 6 continues on next page...*

*Table 6 continued from previous page.*

| Trial # | Pattern | Capture A | Biotin A | EnzCult | Volume |
|---------|---------|-----------|----------|---------|--------|
| 19      | + 0 0 0 | 750       | 425      | 525     | 75     |
| 20      | 0 0 0 0 | 500       | 425      | 525     | 75     |
| 21      | 0 + 0 0 | 500       | 600      | 525     | 75     |
| 22      | - + - + | 250       | 600      | 300     | 100    |
| 23      | + + - - | 750       | 600      | 300     | 50     |
| 24      | 0 0 0 - | 500       | 425      | 525     | 50     |
| 25      | 0 0 - 0 | 500       | 425      | 300     | 75     |
| 26      | 0 0 0 + | 500       | 425      | 525     | 100    |
| 27      | 0 0 0 0 | 500       | 425      | 525     | 75     |
| 28      | 0 0 0 0 | 500       | 425      | 525     | 75     |
| 29      | 0 0 0 0 | 500       | 425      | 525     | 75     |
| 30      | + - + + | 750       | 250      | 750     | 100    |

*Table 6 continues on next page...*



Table 6 continued from previous page.

| Trial # | Pattern | Capture A | Biotin A | EnzCult | Volume |
|---------|---------|-----------|----------|---------|--------|
| 31      | + + - + | 750       | 600      | 300     | 100    |
| 32      | - - + - | 250       | 250      | 750     | 50     |
| 33      | - 0 0 0 | 250       | 425      | 525     | 75     |
| 34      | + - + - | 750       | 250      | 750     | 50     |
| 35      | + - - - | 750       | 250      | 300     | 50     |
| 36      | + + + + | 750       | 600      | 750     | 100    |

## Initial Concept and Method Development of a Competitive Assay

### Competitive Binding Immunoassay

Development and validation of a competition immunoassay requires considerable expertise in reagent characterization and method development. Sandwich and antigen-down immunoassays formats should be explored before attempting the competitive immunoassay format.

### Drawbacks Using a Competitive Immunoassay

1. A competitive immunoassay is not as sensitive as a sandwich ELISA.
2. A competitive immunoassay is more sensitive to matrix issues, especially serum matrix, which can affect assay performance.
3. Timing of the various incubation steps is less robust in a competitive assay. That is the  $IC_{50}$  of the standard curve will shift with minor changes in incubation of the various steps of the immunoassay.
4. The labeling of the hapten or analyte can change the analyte binding affinity for the antibody. Experiments need to determine the effect of the label on the binding affinity of the antibody to the analyte.

## Development of a Competitive Immunoassay

### Initial Development Experiment

The goal of the initial development experiment is to determine the optimal coating concentration of the antibody used for capture and the labeled ligand.

### Reagents

1. Antibody- mono or polyclonal, specific to the analyte.
2. Buffers- same as for a competitive assay.
3. Labeled ligand- the enzyme or biotin is labeled directly to the analyte or ligand.

### Experiment

Coat the ELISA plate with various antibody concentrations to determine the optimal concentration of antibody and labeled ligand.

### Protocol

1. Determine the desired analyte working range.
2. The capture antibody is titrated using high, low and zero analyte concentration levels.
3. Dilute the capture antibody in coating buffer at 0.1, 0.5, 1 and 2  $\mu\text{g/ml}$  and add 100  $\mu\text{l}$  to each well of the 96-well microtiter plate. The capture antibody might need to be titrated down further. The amount of antibody coated on the plate will be proportional to the sensitivity of the assay.
4. Incubate the plate containing the capture antibody overnight at 4°C and use the next day.
5. Stability of the capture antibody bound to the plate can be determined in later experiments.
6. Remove the coating antibody solution from the microtiter plates by aspirating or dumping the plate.
7. Add 200  $\mu\text{l}$  of blocking buffer to each well of the 96-well microtiter plate.
8. Incubate the plate for one hour at room temperature.
9. Remove the blocking buffer from the plate by aspirating or dumping the plate.
10. Dilute the labeled standard in antibody dilution buffer over a wide range. The desired result is the condition that gives a readable signal with the least amount of antibody coated, in combination with the least amount of labeled standard.
11. Zero concentration will give you the NSB.
12. Add 100  $\mu\text{l}$  of the labeled standard to each well in the microtiter plate and incubate for 2.5 hours at room temperature. (The standard can either be directly labeled with the enzyme or biotinylated).
13. Wash the plates 3 times with wash buffer.

14. If a biotinylated standard is used, dilute streptavidin-HRP according to the manufacturer's instructions in antibody diluent and add 100  $\mu\text{l}$  to each well in the microtiter plate and incubate for 1 hour at room temperature.
15. For HRP readout, add either OPD or TMB as a substrate to allow color development and incubate for 10-20 minutes at room temperature.
16. Add acid stop reagent to stop the enzyme reaction.
17. Read at 405 nm for TMB/HRP.
18. Determine the linearity of the instrument being used for the readout.

## Second Development Experiment

The goal of the second development experiment is to determine the potential dynamic range and sensitivity. Take the conditions established in the initial experiment for the concentration of the antibody and labeled ligand and incubate with a wide range of unlabeled analyte. The resulting standard curve and precision profile calculation will give an estimate of the sensitivity and dynamic range of the assay.

### Reagents

Reagents are the same as in the initial experiment.

### Protocol

1. Dilute the capture antibody in coating buffer at the concentration determined in the initial experiment. Add 100  $\mu\text{l}$  to each well of the 96-well microtiter plate.
2. Incubate the plate containing the capture antibody overnight at 4°C and use the next day.
3. Remove the capture antibody solution from the microtiter plates by aspirating or dumping the plate.
4. Add 200  $\mu\text{l}$  of blocking buffer to each well of the 96-well microtiter plate.
5. Incubate the plate for one hour at room temperature.
6. Remove the blocking buffer from the plate by aspirating or dumping the plate.
7. Dilute the labeled standard in antibody dilution buffer at the concentration determined in the initial experiment.
8. Dilute the unlabeled ligand in antibody dilution buffer over a wide range of concentrations.
9. Add 100  $\mu\text{l}$  of the labeled standard to each well in the microtiter plate and 100  $\mu\text{l}$  of the various dilution of the unlabeled ligand. Incubate for 2.5 hours at room temperature. This is the competitive part of the assay and will allow for the competition between the labeled and unlabeled ligand for the sites on the antibody.
10. Wash the plates 3 times with wash buffer.
11. If a biotinylated standard is used, dilute streptavidin-HRP according to the manufacturer's instructions in antibody diluent and add 100  $\mu\text{l}$  to each well in the microtiter plate and incubate for 1 hour at room temperature.

12. For HRP readout, add either OPD or TMB as a substrate to allow color development and incubate for 10-20 minutes at room temperature.
13. Add acid stop reagent to stop the enzyme reaction.
14. Read at 405 nm for TMB/HRP.

## Third Development Experiment

The goal of the third development experiment is to determine the optimal buffers, incubation periods, temperatures, matrix effects, and other variables that might affect the assay.

### Reagents

Reagents are the same as in the initial experiment.

### Protocol

Same as in the second development experiment except for the following changes at steps 8 and 9:

8. Dilute the unlabeled ligand in antibody dilution buffer, and the matrix appropriate for the experiment, over a wide range of concentrations. Again the dilution buffer can be varied according to the experimental design.
9. Add 100  $\mu\text{l}$  of the labeled standard to each well in the microtiter plate and 100  $\mu\text{l}$  of the various dilutions of the unlabeled ligand. Incubate for 2.5 hours at room temperature. This incubation time can be varied for longer and shorter periods of time to potentially increase the sensitivity and dynamic range of the assay.

## RESULTS

Analysis of the results is by the statistical software JMP or any other appropriate statistical software can be used to determine the optimal conditions for incubation timing, buffers for dilution, and matrix effects.

## Method Validation (Pre-Study)

It is important to note that the precision profile evaluation described earlier in this chapter is based on just the calibration curve. Consequently, only the calibration curve factors (quality and stability of reference standards, quality and stability of reagents, statistical validity of the calibration curve model) are taken into account for deriving these quantitation limits. Sample factors such as analyte (similar physicochemical substances), matrix (other substances that can affect analytical results) and operational factors can affect the performance of the assay/method as well. Thus the quantitation limits derived from the precision profile of a calibration curve is an optimistic assessment of the method performance. If these limits are not satisfactory the assay needs further optimization.

If the quantitation limits from the precision profile are close to the limits desired for the method's intended use, proceed to a full validation experiment as outlined below. This validation experiment is used to establish the method quantitation limits using the analysis of recovery data from validation samples (spiked standards). This experiment will take into account the three major sources of variation described above (calibration curve factors, sample factors and operational factors).

For the full validation experiment, generate the following data in at least three independent runs.

- Calibration curve in each run, preferably in triplicate.
- Validation/Quality Control (QC) samples (independent set of samples spiked with a known amount of standards) in each run at seven or more concentrations with at least two replicates; two concentrations near the precision profile estimates of the lower quantification limit and similarly two more near the upper quantification limit, and three or four that are equally spaced between lower and upper quantification limits.
- Estimate the concentrations of the validation samples of each run using the respective calibration curves. Then compute the % recovery of these validation samples using the following formula:

$$\% \text{ Recovery} = 100 \times (\text{Calibrated Concentration} / \text{Nominal Concentration})$$

- Now compute the average and standard deviation of the % recovery data of the validation samples from all runs for each concentration. The evaluation of standard deviation should be based on a separate variance component analysis of the multiple runs of validation data, and it should include the sources of variability relevant during the use of the assay in production. At the minimum, it will include inter-run and intra-run variability. Some of the other sources to consider might be analyst, plate, equipment, etc. As evident from the above formula for evaluating the percent recovery, note that the standard deviation of percent recovery can be considered as the coefficient of variation (%CV) of the calibrated results. This is essentially the intermediate precision (inter-run %CV) of the assay. We will hereafter refer to this as Intermediate Precision (IP).
- Plot the average % recovery values along with the IP (as calculated above) versus the nominal concentrations. Note that the % recovery along with the intermediate precision as determined above reflects the total error of the assay.
- The % recovery and the IP limits must be within +/- X% of the nominal value. If X is 30%, the percent recovery +/- IP must be within 70 to 130% of the nominal value. This means that the Total Error of the assay must be within 30%. The value of X should be set based on the intended use of the assay. Recommendations on the acceptance criteria are discussed later in this chapter.
- If X is set at 30%, the lower quantification limit is the lowest concentration at which the % recovery +/- IP is within 70% to 130%. The upper quantification limit is the highest concentration at which the % recovery +/- IP is within 70% to 130%.

## Method Validation (In-Study)

The in-study validation phase is about making sure that the assay continues to perform according to pre-defined specifications in each study run. During production phase, when the assays are being used for screening the unknowns, it is important to run validation/QC samples in every run, with at least 2 replicates at high, middle and low concentrations (just one or two columns of a 96-well plate). Compute the average % recovery of these samples to make sure that the average recovery is within a reasonable range of accuracy (say, 80% to 120%). This might be adequate for quality control and is a reasonable compromise for any loss in assay throughput. Various methods might be considered for setting criteria for accepting or rejecting an actual assay where samples are being tested during a study (in-study validation). This is addressed in a subsequent section in this chapter.

### Example of an Immunoassay Validation Experiment

Set up numerous aliquots of the standard and store frozen at  $-70^{\circ}\text{C}$ . If the standard concentration is much higher than the first point on your curve, pre-dilute it so that a single, simple dilution can be made in order to set up the standard curve.

Dilute the standards serially to obtain an 8-point standard curve in the matrix appropriate for the samples that need to be measured. For example, if measuring tissue culture samples then the standards should be diluted in the same tissue culture medium that the samples are in. For serum samples, the standards should be diluted in serum diluted with an optimized buffer to the same dilution that the samples will be diluted.

Set up a series of spiked samples, again in the matrix appropriate for the samples that will be measured. The spiked control samples should not be the same concentration as in the standard curve and should cover the detectable range that the samples are thought to cover.

Follow the immunoassay protocol established during the optimization experiments. Set up the plate with 3-4 replicates of the standard curve and 4 or more replicates of the spiked control samples (See Table 7).

Assay at least 3 plates over 3 different days for a complete validation.

### Validation Results from an IL-10 Immunoassay

The percent recovery and the standard error that takes into account the relevant sources of variation are plotted in Figure 9. If X is 30%, then the quantification limits are the lowest and highest concentrations where the % recovery  $\pm$  IP is within 70% to 130%. So for this assay, the lower quantification limit is the lowest concentration tested in this validation study (6.2 pg/ml), and the upper quantification limit is 3265 pg/ml (see Table 8)

|     |     |     |     |     |     |     |     |  |  |  |  |
|-----|-----|-----|-----|-----|-----|-----|-----|--|--|--|--|
| St1 | St1 | St1 | St1 | SP1 | SP1 | SP1 | SP1 |  |  |  |  |
| St2 | St2 | St2 | St2 | SP2 | SP2 | SP2 | SP2 |  |  |  |  |
| St3 | St3 | St3 | St3 | SP3 | SP3 | SP3 | SP3 |  |  |  |  |
| St4 | St4 | St4 | St4 | SP4 | SP4 | SP4 | SP4 |  |  |  |  |
| St5 | St5 | St5 | St5 | SP5 | SP5 | SP5 | SP5 |  |  |  |  |
| St6 | St6 | St6 | St6 | SP6 | SP6 | SP6 | SP6 |  |  |  |  |
| St7 | St7 | St7 | St7 | SP7 | SP7 | SP7 | SP7 |  |  |  |  |
| St8 | St8 | St8 | St8 | SP8 | SP8 | SP8 | SP8 |  |  |  |  |

**Table 7: Validation Plate Layout.**

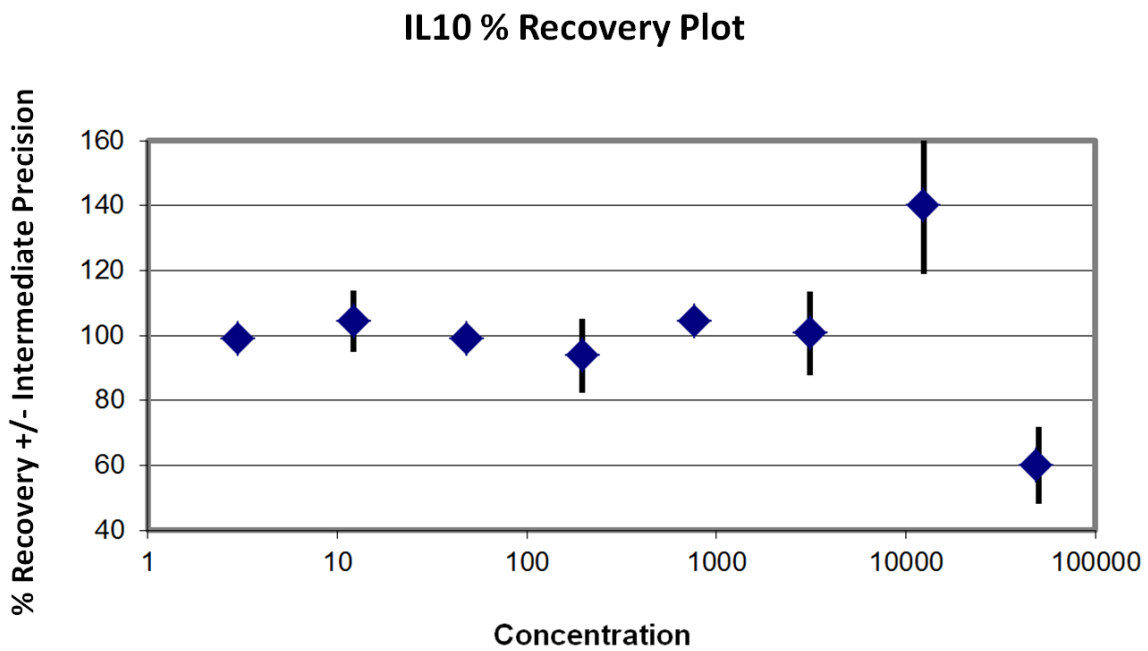


**Figure 9:** Validation results from IL-10 immunoassay.

**Table 8:** Validation results from IL-10 immunoassay

| IL-10          |               |            |
|----------------|---------------|------------|
| Expected Value | Average 4,5,6 | % Recovery |
| 40000          | 36924.96      | 92.31      |
| 11428.57       | 13846.57      | 121.16     |
| 3265.306       | 2966.42       | 90.85      |
| 932.9446       | 892.76        | 95.69      |
| 266.5556       | 242.70        | 91.05      |
| 76.15874       | 71.65         | 94.08      |

*Table 8 continues on next page...*

Table 8 continued from previous page.

| IL-10          |               |            |
|----------------|---------------|------------|
| Expected Value | Average 4,5,6 | % Recovery |
| 21.75964       | 22.32         | 102.60     |
| 6.21704        | 6.06          | 97.50      |

## Plate Uniformity and Variability Experiment

It is important to check whether there is any systematic data trend across rows or columns of the 96-well plate and whether there is any significant variability between plates. An experiment with three plates and four concentrations of the standard can be done using the plate-layout in Figure 10. In this layout, C1, C2, C3 and C4 denote the standard concentrations from lowest to highest. For the purpose of illustration, data from one of the plates and a plot of the data from this experiment are given below for a sandwich ELISA. A systematic trend across columns is evident from this plot. For determining the statistical significance of this trend and the plate to plate variability, further statistical analysis of the data can be done with the help of a statistician.

## Pre-Study & In-Study Acceptance Criteria

Different methods of quality control are available and routinely used in analytical methods. It is important that the methods used for assessment of method performance are suitable for the intended purpose. Shah et al. (14) proposed the 4-6-X rule for in-study validation phase that has become popular and widely used. This rule states that 4 out of the total 6 samples should be within X% of the nominal/reference value, and at least one out of the two samples at each level must be within X% of the reference value. The choice of X is specified a priori based on the intended use and purpose of the assay, and it was set at 20% by Shah and colleagues. DeSilva et al. (15) proposed a criteria (see Table 9) for pre-study and in-study validation phase of ligand-binding assays for assessing pharmacokinetics of macromolecules.

It should be noted that the acceptance criteria for biomarker assays will depend heavily on the intended use of the assay and should ideally be based on physiological variability as well. According to the criteria listed in Table 9, X is set at 30% for in-study validation, and the total error is set to be within 30% for the pre-study validation, along with the 20% limits for each component of total error (bias and precision). The pre-study criteria (Total Error < X %) and the in-study criteria (4-6-X rule) are not entirely consistent because the variability of the total error estimate and the consequent decision error rates are not taken into account. Thus the uncertainty in these estimates will depend on the magnitude of the errors and the number of measurements, and will in turn impact the level of decision error rates (16). The appropriate value of X in 4-6-X can be determined based on the variability of the total error estimates in pre-study validation. When it is feasible to use more QC samples in each run, 8-12-X or 10-15-X will have much better statistical outcomes than the 4-6-X criteria. In addition, the use of control charts as described by



If the plate-format is not the same as indicated below, type in the necessary changes below:

|   | 1  | 2  | 3  | 4  | 5  | 6  | 7  | 8  | 9  | 10 | 11 | 12 |
|---|----|----|----|----|----|----|----|----|----|----|----|----|
| A | C1 | C2 | C3 | C4 | C1 | C2 | C3 | C4 | C1 | C2 | C3 | C4 |
| B | C2 | C3 | C4 | C1 | C2 | C3 | C4 | C1 | C2 | C3 | C4 | C1 |
| C | C3 | C4 | C1 | C2 | C3 | C4 | C1 | C2 | C3 | C4 | C1 | C2 |
| D | C4 | C1 | C2 | C3 | C4 | C1 | C2 | C3 | C4 | C1 | C2 | C3 |
| E | C1 | C2 | C3 | C4 | C1 | C2 | C3 | C4 | C1 | C2 | C3 | C4 |
| F | C2 | C3 | C4 | C1 | C2 | C3 | C4 | C1 | C2 | C3 | C4 | C1 |
| G | C3 | C4 | C1 | C2 | C3 | C4 | C1 | C2 | C3 | C4 | C1 | C2 |
| H | C4 | C1 | C2 | C3 | C4 | C1 | C2 | C3 | C4 | C1 | C2 | C3 |

Paste the plate-data below:

|   | 1    | 2    | 3    | 4    | 5    | 6    | 7    | 8    | 9    | 10   | 11   | 12   |
|---|------|------|------|------|------|------|------|------|------|------|------|------|
| A | 1.24 | 2.53 | 1.23 | 0.81 | 2.16 | 2.61 | 1.41 | 1.02 | 1.99 | 3.27 | 1.60 | 1.10 |
| B | 2.31 | 1.29 | 0.73 | 2.12 | 3.24 | 1.75 | 1.00 | 2.12 | 3.32 | 1.81 | 1.14 | 2.27 |
| C | 1.11 | 0.91 | 1.89 | 3.08 | 1.74 | 1.03 | 1.99 | 3.61 | 1.88 | 1.30 | 2.43 | 3.36 |
| D | 0.63 | 1.95 | 2.92 | 1.64 | 1.09 | 2.30 | 3.46 | 1.92 | 1.21 | 2.51 | 3.63 | 1.90 |
| E | 1.84 | 2.63 | 1.53 | 1.06 | 2.35 | 3.41 | 1.70 | 1.15 | 2.47 | 3.45 | 1.83 | 1.27 |
| F | 2.41 | 1.90 | 1.05 | 2.09 | 3.29 | 1.79 | 1.11 | 2.35 | 3.58 | 1.90 | 1.24 | 2.38 |
| G | 1.28 | 0.86 | 2.02 | 3.50 | 1.79 | 1.13 | 2.33 | 3.56 | 1.91 | 1.24 | 2.46 | 3.50 |
| H | 0.65 | 1.82 | 2.88 | 1.72 | 1.04 | 2.22 | 3.05 | 1.85 | 1.23 | 2.33 | 3.41 | 1.99 |

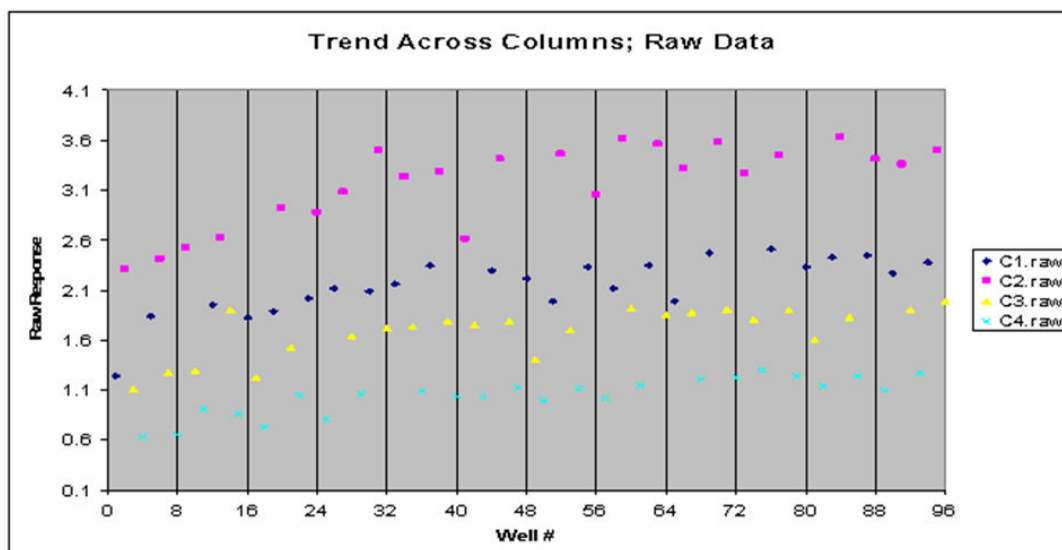


**Figure 10:** Data from one plate and a data plot from a plate uniformity and variability experiment where C1, C2, C3 and C4 denote the standard concentrations from lowest to highest.

Westgard or tolerance limits based on pre-study validation data might be considered when possible.

The concept of total error as the primary parameter, and with bias and precision as additional constraints, is very useful. This is because total error has a more practical and intuitive appeal as it relates specifically to our primary question of interest about the assay; How far are my observed test results from the reference/nominal value? Because this is the primary practical question in the minds of most laboratory scientists, the criteria on the assay performance for the in-study phase is defined with respect to this question.

**Table 9:** Criteria for pre-study and in-study validation phase of ligand-binding assays for assessing pharmacokinetics of macromolecules.

| Characteristic               | Pre-Study Validation             | In-Study Validation |
|------------------------------|----------------------------------|---------------------|
| Trueness (%Relative Bias)    | $\leq \pm 20$ ( $\pm 25$ at LQL) | -                   |
| Intermediate Precision (%CV) | $\leq 20$ (25 at LQL)            | -                   |
| Total Error                  | $\leq 30\%$                      | “4-6-30” rule       |

## Consideration of Physiological Variation for Acceptance Criteria

One of the most important considerations for defining the performance criteria of most biomarker methods is the physiological variability in the study population of interest. That is, in order to determine whether a biomarker method is ‘fit-for-purpose’, we should determine whether it is capable of distinguishing changes that are statistically significant based on the intra-subject and inter-subject variability. The term “subject” here might refer to animal or human. For example, an assay with 50% total error during pre-study validation might still be adequate for detecting a 2-fold treatment in a clinical trial for a certain acceptable sample size. Thus whenever possible, the acceptance criteria for pre-study validation should be based on physiological variation in the study. An example of the use of intra-subject and inter-subject variation for defining the pre-study acceptance criteria can be found in <http://www.westgard.com/guest17.htm> (17).

When the relevant physiological data (say, treated patients of interest) are not available during the assay validation phase, then healthy donor samples should be used to estimate the intra-subject and inter-subject variation, and hence the desired specifications on the pre-study assay validation. This can be updated at a later time when there is access to the relevant patient data. If access to healthy donor samples is also not feasible, then other flexible biological rationale should be considered and updated periodically as more information becomes available over time. In the absence of physiological data or other biological rationale, the acceptance criteria for pre-study validation should not be strictly defined. Instead, only the performance characteristics from pre-study validation such as the bias, precision and total error should be reported. Any decision regarding the acceptance of the assay (pre-study acceptance criteria) and consequently the determination of the dynamic range such as the Lower Quantification Limit (LQL) and Upper Quantification Limit (UQL) should be put on hold until adequate information related to the physiological data become available.

As the high, mid and low QC samples are used in the acceptance criteria, it is important to choose their concentrations such that they span the expected range of the study samples. For example, it is of no value to reject batches when large numbers of high concentration quality controls fail, but where the low and medium quality controls are good and when all the study sample results are in the low to medium range. Here the positioning of the high quality control based on expectation before the analysis of incurred samples is flawed – but it does not necessarily make the study sample results invalid.

## References

1. Swartzman, et al. A Homogeneous Multiplexed Immunoassay for High-Throughput Screening Using Fluorometric Microvolume Assay Technology. *Anal. Biochem.* 1999;271(2):143–151. PubMed PMID: 10419629.
2. Stockwell, et al. High-throughput screening of small molecules in miniaturized mammalian cell-based assays involving post-translational modifications. *Chem. Biol.* 1999;6(2):71–83. PubMed PMID: 10021420.
3. Martens, et al. A generic particle-based nonradioactive homogeneous multiplex method for high-throughput screening using microvolume fluorimetry. *Anal. Biochem.* 1999;273(1):20–31. PubMed PMID: 10452795.
4. Zuck, et al. Ligand-receptor binding measured by laser-scanning imaging. *Proc. Natl. Acad. Sci.* 1999;96(20):11122–11127. PubMed PMID: 10500140.
5. Kitamura, et al. A fluorescence sandwich ELISA for detecting soluble and cell-associated human interleukin-2. *J. Immunol. Methods.* 1989;121(2):281–288. PubMed PMID: 2788194.
6. Findlay, et al. Validation of immunoassays for bioanalysis: a pharmaceutical industry perspective. *J. Pharm. Biomed. Anal.* 2000;21(6):1249–1273. PubMed PMID: 10708409.
7. Pavkovic, et al. Comparison of the MesoScale Discovery and Luminex multiplex platforms for measurement of urinary biomarkers in a cisplatin rat kidney injury model. *J. Pharmacol. Toxicol. Methods.* 2014;69(2):196–204. PubMed PMID: 24333954.
8. Ray, et al. Development, validation, and implementation of a multiplex immunoassay for the simultaneous determination of five cytokines in human serum. *J. Pharm. Biomed. Anal.* 2005;36(5):1037–1044. PubMed PMID: 15620530.
9. Smolec, et al. Bioanalytical method validation for macromolecules in support of pharmacokinetic studies. *Pharm. Res.* 2005;22(9):1425–1431. PubMed PMID: 16132353.
10. Kellar, et al. Multiplexed fluorescent bead-based immunoassays for quantitation of human cytokines in serum and culture supernatants. *Cytometry.* 2001;45(1):27–36. PubMed PMID: 11598944.
11. Chowdhury, et al. Validation and comparison of two multiplex technologies, Luminex and MesoScale Discovery, for human cytokine profiling. *J. Immunol. Methods.* 2009;340(1):55–64. PubMed PMID: 18983846.
12. Elshal, et al. Multiplex bead array assays: performance evaluation and comparison of sensitivity to ELISA. *Methods.* 2006;38(4):317–323. PubMed PMID: 16481199.
13. Boulanger et al. (2007). *Statistical Considerations in Analytical Method Validation. Pharmaceutical Statistics Using SAS: A Practical Guide*, 69.
14. Shah, et al. *Pharm. Res.* 1992;9(4):588–592.
15. DeSilva, et al. Recommendations for the Bioanalytical Method Validation of Ligand-binding Assays to Support Pharmacokinetic Assessments of Macromolecules. *Pharm. Res.* 2003;20(11):1885–1900. PubMed PMID: 14661937.
16. Kringle, et al. *Pharm. Res.* 2007;24(6):1157–1164. PubMed PMID: 17373576.

17. Glasziou et al. (2007). Evidence-based medical monitoring: From principles to practice, Blackwell Publishing.

## Additional References

### Weblinks

Available at: <http://www.brendan.com/>

Available at: <http://www.waichung.demon.co.uk/webanim/Menu1.htm>

Available at: <http://www.piercenet.com/method/elisa-development-optimization>

Available at: <http://www.piercenet.com/method/overview-elisa#elisaprobes>

Available at: <http://www.piercenet.com/method/overview-detection-probes>

# GTP $\gamma$ S Binding Assays

Neil W. DeLapp,<sup>✉1,\*</sup> Wendy H. Gough, Steven D. Kahl,<sup>†</sup> Amy C. Porter, and Todd R. Wiernicki<sup>2</sup>

Created: May 1, 2012; Updated: October 1, 2012.

## Abstract

Signal transduction via G-protein coupled receptors (GPCRs) is mediated through binding of GTP to GTP-binding proteins. Evaluation of GPCR agonists in drug discovery requires GTP binding assays to confirm agonist activity. This chapter addresses the development and optimization of robust GTP $\gamma$ S binding assays with discussions on basic protocols, assay buffers, effect of required additives (Mg<sup>2+</sup>, NaCl, Saponin) and data analysis. An extensive set of recent references is included for beginners and experienced investigators.

---

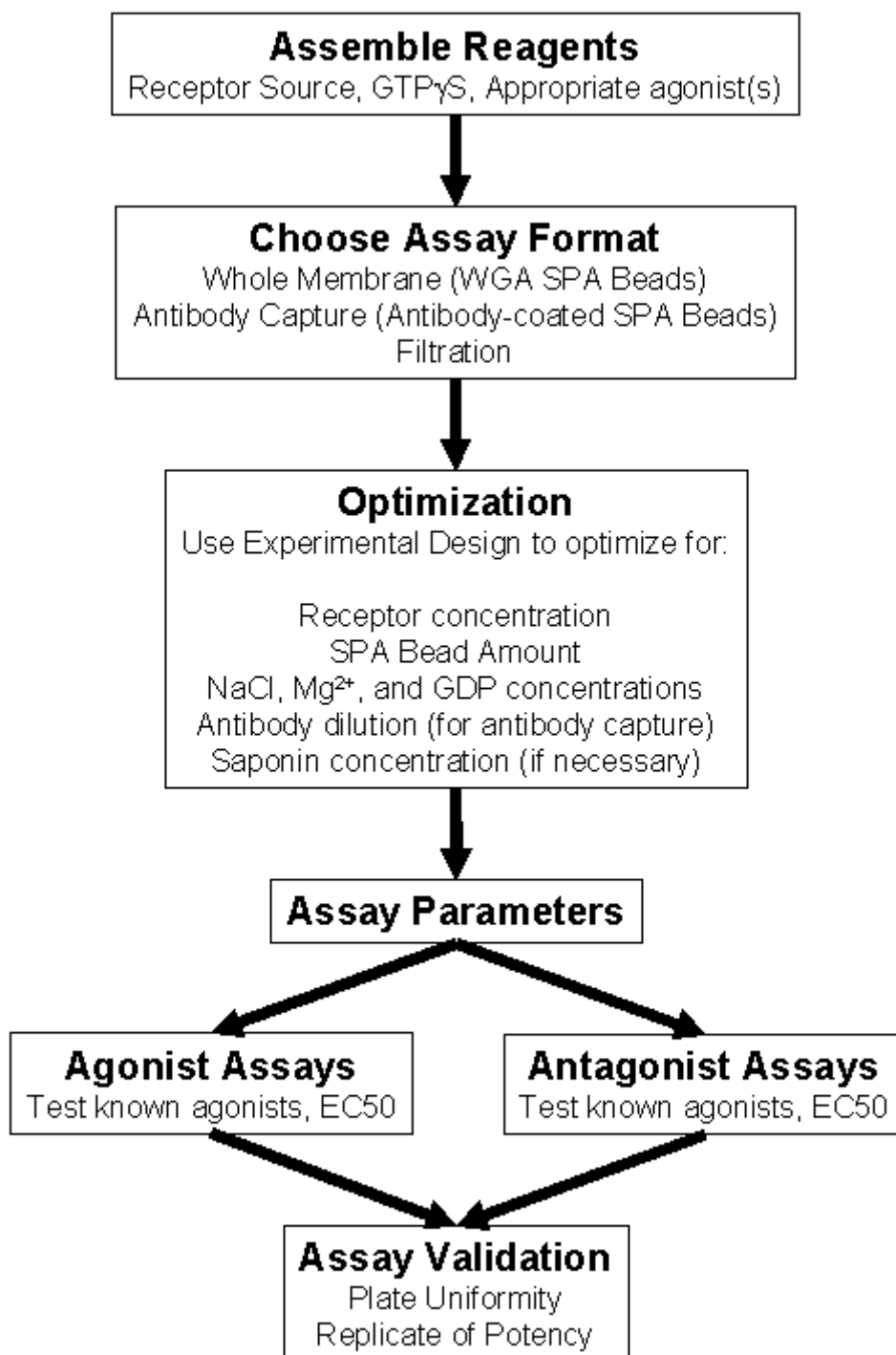
<sup>1</sup> Eli Lilly & Company, IN, USA. <sup>2</sup> Eli Lilly & Company, IN, USA.

<sup>✉</sup> Corresponding author.

\* Retired

† Editor

## Flow Chart for Assay Development



## Introduction

Binding of GTP to the alpha ( $\alpha$ ) subunit of heterotrimeric GTP binding proteins is an early event in agonist-induced activation of G-protein coupled receptors (GPCRs).

Although GTP $\gamma$ S binding assays are carried out using membrane preparations in much the same way as radioligand binding assays, these are functional assays and can thus be used to differentiate agonist, antagonist, and inverse agonist activities. Such assays are carried out using [<sup>35</sup>S]guanosine-5'-O-(3-thio) triphosphate which provides a radioactive ligand with high affinity for G-protein  $\alpha$  subunits that is highly resistant to the inherent GTPase activity of  $\alpha$  subunits such that it remains bound for sufficient periods of time to allow counting of radioactivity.

Although the classical method used for GTP $\gamma$ S binding has been filtration of radiolabeled membranes, scintillation proximity assays (SPA) are much more convenient and allow the use of an antibody capture technique which permits determination of receptor-mediated activation of specific G-protein families. There are two basic methods for running homogeneous SPA GTP $\gamma$ S binding assays in 96-well plate format: 1) whole membrane binding in which labeled membranes are bound to wheat germ agglutinin (WGA)-coated SPA beads in the same way as these beads are used for radioligand binding assays, and 2) antibody capture binding assays in which membranes are solubilized with detergent followed by isolation of the desired G-protein using a specific antibody along with capture of antibody-G-protein complexes onto anti-IgG coated SPA beads.

Advantages of GTP $\gamma$ S functional assays in comparison to determinations of second messengers produced as a result of receptor activation are:

1. The assays are very simple to run and utilize membrane preparations which can be frozen at -80°C for periods of months.
2. Because GTP exchange is an event proximal to receptor activation these assays typically have lower degrees of receptor reserve than other functional assays and are thus useful for differentiating full from partial agonists.
3. The assays are useful for determination of antagonist inhibition constants since agonists and antagonists can be equilibrated prior to starting the incubation by addition of GTP $\gamma$ <sup>35</sup>S.
4. One can often measure specific coupling of receptor subtypes to different G-protein families, even in native tissues, under very similar assay conditions.

The major disadvantage is the relatively low signal to background which limits GTP $\gamma$ S binding to medium throughput evaluations. The power of the antibody capture technique is its ability to easily generate multiple concentration response curves thus allowing true pharmacological evaluation of receptor-mediated coupling to individual G-proteins, an accomplishment that is prohibitive by older immunoprecipitation techniques.

## Materials and Reagents

The list below includes materials and reagents, which have been used successfully to enable GTP $\gamma$ S binding assays for a variety of GPCRs (1-3):

96-well plates: Costar 3632, white clear bottom

WGA SPA beads: Amersham SPQ0031

Anti-rabbit SPA beads: Amersham RPNQ 0016

Anti-mouse SPA beads: Amersham RPNQ 0017

GTP $\gamma$ <sup>35</sup>S: Perkin Elmer Life Sciences NEG030H

NP40 detergent 10%: Roche 1 332 473

Anti-G<sub>s</sub>/olf: Santa Cruz SC-383, rabbit polyclonal

Anti-G<sub>i-3</sub>: Santa Cruz SC-262, rabbit polyclonal (recognizes G<sub>i-1</sub>, G<sub>i-2</sub>, and G<sub>i-3</sub>)

Anti-G<sub>q</sub>/11: Santa Cruz SC-392, rabbit polyclonal

Anti-G<sub>o</sub>: Chemicon MAB3073, mouse monoclonal

Although the commercially available antibodies listed above have been used successfully in the antibody capture assay, certain lots of these antibodies have been found to be unsatisfactory. For this reason and because of cost considerations it may be preferable to obtain antibodies to G-proteins through in-house resources or by contracting out peptide synthesis and antibody production for specific G-proteins of interest (4–6).

## Membrane Preparations and Assay Buffers

### Types of membrane preparations used

1. Crude homogenates (7)
2. Plasma membrane preparations (P2 fraction, 1)
3. Sucrose density gradient enriched receptors (8)
4. Commercially available membranes, which include
  - i. Receptors cloned into mammalian cells (Perkin Elmer, Euroscreen, Cerep)
  - ii. Receptors cloned into *Sf9* insect cells co-expressing mammalian G-proteins (9)

### Types of Assay buffers

1. Lazareno and Birdsall buffer (7) 20 mM HEPES, 100 mM NaCl, 5 mM MgCl<sub>2</sub>, pH 7.4
2. Buffers with HEPES replaced by 50 mM Tris HCl (8,10)

## Basic Assay Protocol

### Whole membrane assay using WGA SPA beads

1. Incubate membranes, GTP $\gamma$ <sup>35</sup>S, and compounds tested in 200  $\mu$ l/well at room temperature for 30 – 60 minutes.
2. Add 50  $\mu$ l per well of suspended WGA beads (1 mg/well).
3. Seal plates and incubate for one hour or more at room temperature.
4. Centrifuge at 200 x g and count plates in a Wallac microbeta.



## Antibody Capture assay

1. Incubate membranes as for whole membrane assay.
2. Add 20  $\mu$ l per well of 3% NP40 and incubate for 15 minutes.
3. Add 20  $\mu$ l per well of primary antibody and incubate for 15 minutes.
4. Add 50  $\mu$ l per well of anti-rabbit or anti-mouse SPA beads (1 mg).
5. Seal and incubate for three hours, centrifuge as above and count.

## Assay Optimization

### Membrane protein/well and [GDP]

Using a starting buffer such as listed under assay buffer above, determine the optimal amount of membrane protein per well from 5 to 50  $\mu$ g in the presence of varying concentrations of GDP (guanosine diphosphate) from 0 – 10  $\mu$ M for transfected cell membranes and from 0 up to 300  $\mu$ M for native tissue membranes using a concentration of 200 – 500 pM GTP $\gamma$ <sup>35</sup>S. Note that G<sub>i/o</sub> coupled receptors will require higher concentrations of GDP than G<sub>s</sub> or G<sub>q</sub>-coupled receptors which may give optimal signals in the absence of added GDP. Figure 1 illustrates the marked difference in GDP requirement for determination of muscarinic agonist-stimulated GTP $\gamma$ S binding in rat brain striatal membranes measured by anti-G<sub>q/11</sub> (M1 receptor) versus anti-G<sub>o</sub> (M4 receptor).

### Effect of Mg<sup>2+</sup>

Determine the optimal Mg<sup>2+</sup> concentration for the best signal to noise over the range of 1 mM to 10 mM. Figure 2 shows the variation of Mg<sup>2+</sup> on dopamine-stimulated GTP $\gamma$ S binding mediated by D2 receptors in rat striatal membranes

### Effect of NaCl

Determine the optimal amount of NaCl for best signal to noise over the range of 0 – 200 mM. Although 100 mM NaCl is commonly used in these assays note that at times better agonist stimulation may be achieved at lower Na<sup>2+</sup> and if higher constitutive activity is desired (for evaluating inverse agonists) lowering Na<sup>2+</sup> will likely provide the best opportunity. Figure 3 demonstrates the effect of NaCl on the constitutive activity of orphan receptor 19BG.

### Effect of saponin

The effect of adding saponin at 3 – 100  $\mu$ g/ml can be explored, but recognize that while saponin may increase signal to background, it may also compromise the quality of concentration response curves. Figure 4 demonstrates the optimization of saponin to achieve the highest signal to background for an orphan receptor where constitutive activity was measured to allow evaluation of inverse agonists. Figure 5 shows how saponin may compromise the quality of some concentration response curves.

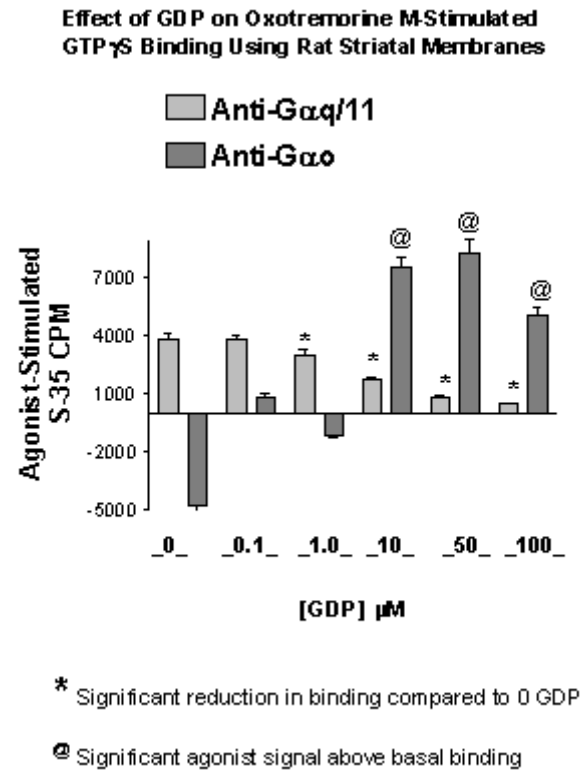


**Figure 1.** Difference in [GDP] required for G<sub>q</sub> versus G<sub>o</sub>-coupled GPCRs

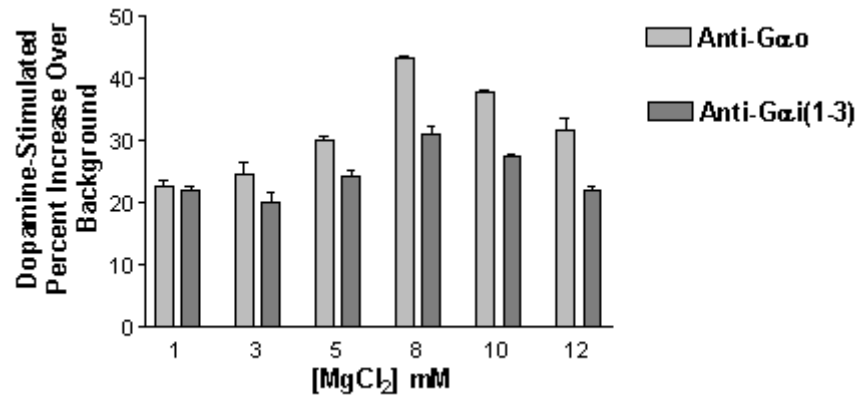


**Figure 2.** Dopamine stimulated GTP $\gamma$ S binding in brain membranes

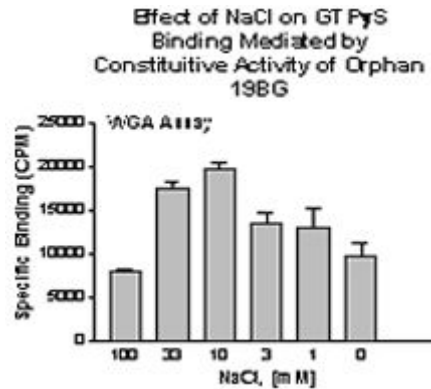


**Figure 3.** Optimization of NaCl to measure constitutive activity of an orphan GPCR

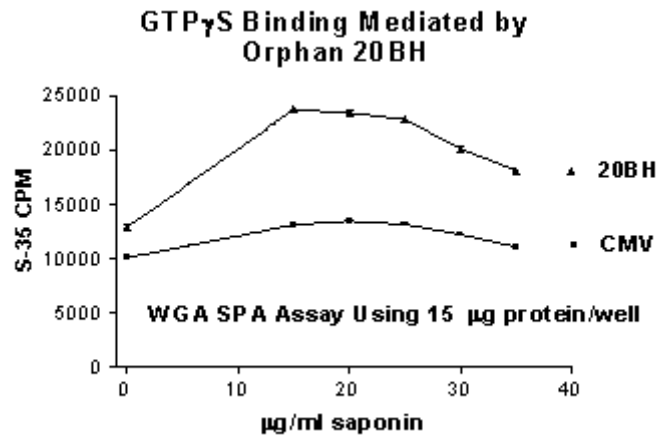


**Figure 4.** Optimization of saponin to measure constitutive activity of an orphan GPCR

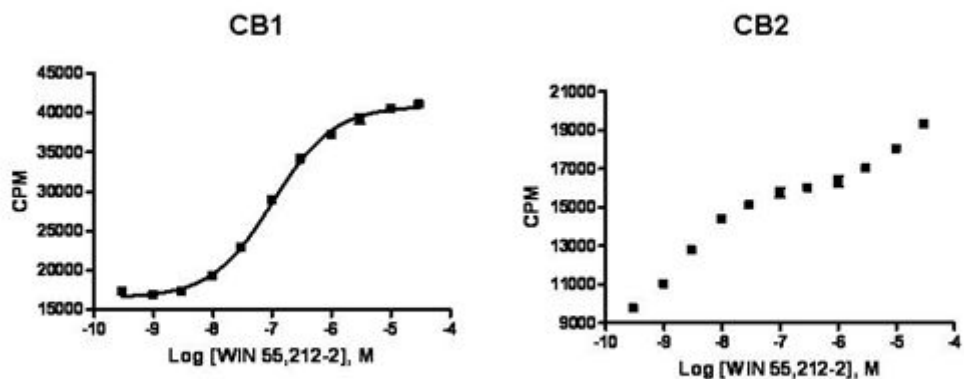
## Incubation Time

The optimal incubation time for the best signal to background may be determined, but thirty minutes is usually satisfactory for cell membranes and one hour for native tissue membranes.

## Antibody dilution for antibody capture assays

If using the antibody capture method the optimal dilution will have to be determined for each lot of antibody. Figure 6 below illustrates the effect of various dilutions of anti-G<sub>s</sub>/o1f on GTP $\gamma$ S binding mediated by the rat 5-HT<sub>6</sub> receptor.

### WIN 55,212-2 Stimulation of CB1 and CB2 CHO (Whole Membrane Capture)



100mM NaCl, 10mM MgCl<sub>2</sub>, 2uM GDP GDP, 0.2% BSA, 10ug/mL Saponin

**Figure 5:** Effect of saponin on agonist concentration response curves for some receptor subtypes

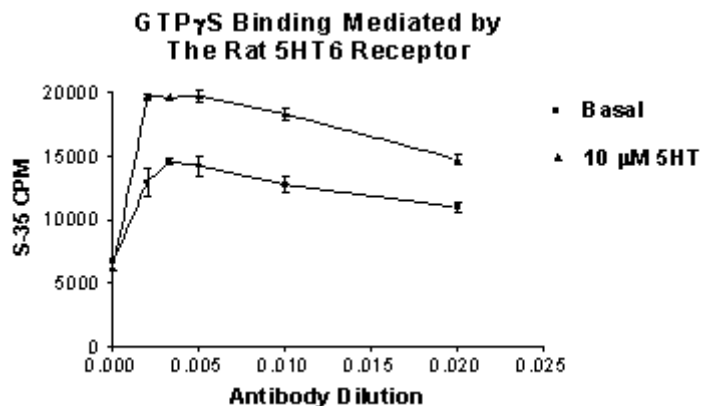


**Figure 6.** Effect of antibody dilution on basal and agonist-stimulated binding

## The use of experimental design and JMP analysis for assay optimization

Experimental design and JMP analysis are convenient tools for optimizing a variety of conditions in a small number of experiments and determining if there are any interactions among the factors. Figure 7A shows an example in which four factors were optimized in a single experiment. Figure 7B shows the two factor interaction profiles from JMP analysis. Parallel lines indicate no interaction and intersecting lines indicate interactions. For instance in this experiment there is virtually no interaction between NaCl and saponin, but there is a significant interaction between the amount of protein and GDP concentration.

### 1 $\mu$ M Methanandamide Stimulation of GTP- $\gamma$ S Binding in CB1-CHO Receptor Membranes

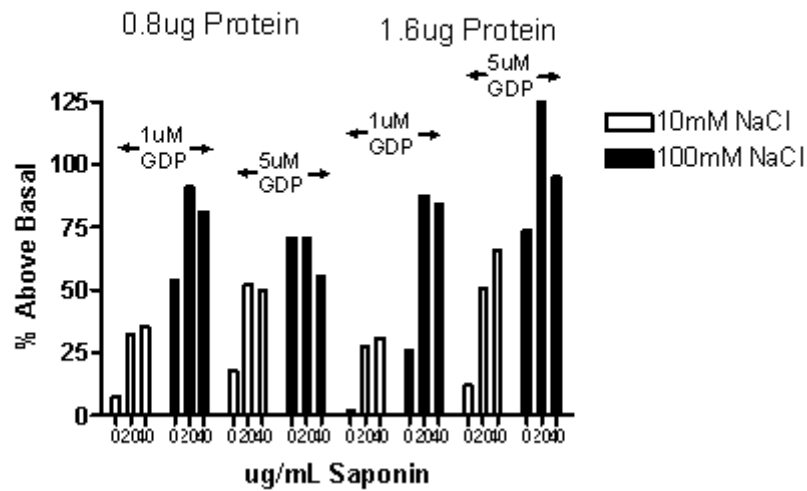


Figure 7A: Experimental design with 4 factors (GDP, Saponin, NaCl and Membrane protein)

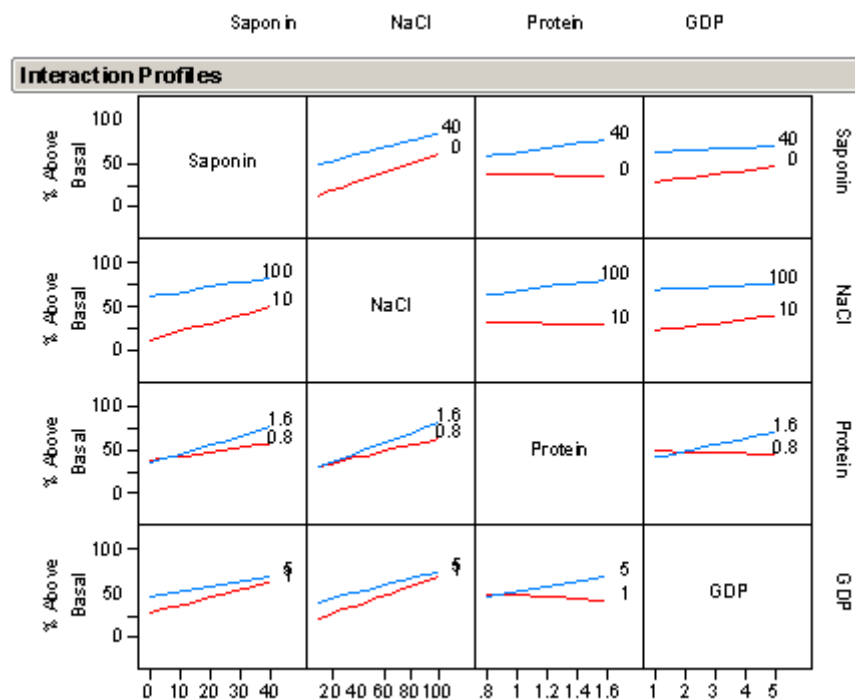


Figure 7B: Interaction Plots for Experimental Design (using JMP)

## Signal window and Z' factor

Determine the signal window for the assay under the optimal conditions by running background and maximal stimulation multiple times across assay plates on separate days. Calculate the Z' factor for the assay using the formula:

$$Z' = 1 - (3(SD_{\max}) + 3(SD_{\min}) / \text{Max} - \text{Min})$$

A Z' factor of > 0.5 indicates a useful assay. GTP $\gamma$ S binding assays can be quite reproducible and will give reliable results when signals are greater than 40-50% over background. Even with smaller signals, one can generate reliable concentration response curves by using 4 to 8 replicates per data point.

## Evaluation of standard compound concentration response curves

After determining optimal conditions for the assay concentration response curves should be run for standard agonists and antagonists to determine variability and comparability to literature values if available. Most assays will require duplicate determinations per concentration but with exceptional signals one may be able to use single data points for each.

## Choice of whole membrane versus antibody capture

Good assays for G<sub>i/o</sub> may be developed using whole membranes and WGA beads. Use of antibody capture for G<sub>i/o</sub>-coupled receptors, however, may reduce assay variability. For G<sub>q</sub>- and G<sub>s</sub>-coupled GPCRs, the antibody capture assay will most likely be superior since most cells and tissues are dominated by inhibitory G-proteins and it is often not possible to develop reliable signals without the antibody technique unless receptors are fused to G<sub>s</sub> or G<sub>q</sub> (1, 9, 11). Challiss and coworkers have found, using *post mortem* human brain tissue, that the M1 receptor signal generated using antibody capture via an anti-G<sub>q/11</sub> antibody was markedly improved by treatment of the membranes with N-ethylmaleimide (6). High throughput assays for G<sub>i</sub>-linked receptors have been reported using the WGA whole membrane technique (12,13).

## Data Analysis

As with other functional assays, concentration response data may be fitted using a four-parameter logistic equation with variable slope to determine half maximal responses. Keep in mind that GTP $\gamma$ S assays will often show some degree of receptor reserve even though typically less than a cAMP or Ca<sup>2+</sup> mobilization assay and for this reason agonist EC<sub>50</sub>'s may not agree with K<sub>i</sub> values for agonists determined in radioligand binding assays. For antagonists, K<sub>b</sub> values may be determined from rightward curve shifts in the presence of a fixed antagonist concentration or from antagonist concentration response curves run at a fixed agonist concentration (at or somewhat below the concentration that produces a maximal response). For curve shift at a single antagonist concentration the following equation may be used to determine the K<sub>b</sub>:

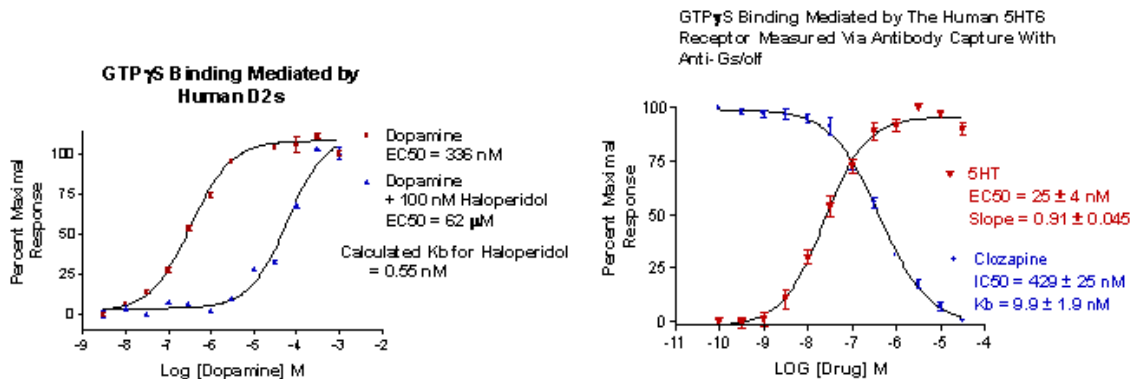


**Figure 8.** Examples of determining antagonist K<sub>b</sub> values in GTP $\gamma$ S assays with a single antagonist concentration

$$EC_{50b} = EC_{50a} (1 + [\text{antagonist}]/\text{antagonist } K_b)$$

where EC<sub>50a</sub> is the agonist EC<sub>50</sub> in the absence of antagonist and EC<sub>50b</sub> is the agonist EC<sub>50</sub> in the presence of antagonist.

For antagonist concentration responses the following equation is used (14):

$$K_b = IC_{50} / (2 + ([\text{agonist}]/\text{agonist } EC_{50})^n)^{1/n} - 1$$

where n is the slope of the agonist curve.

In antagonist concentration response experiments it is desirable to determine the agonist EC<sub>50</sub> in each experiment along with the IC<sub>50</sub> for the antagonist. Figure 8 below illustrates the use of both methods for measuring antagonist K<sub>b</sub> values. By measuring multiple shifts in agonist concentration response curves at increasing concentrations of antagonist it is possible to calculate via Schild analysis the PA<sub>2</sub> of the antagonist and to ascertain whether the antagonist is competitive (15,16).

## Filtration Assays

Filtration whole membrane assays may be used for GTP $\gamma$ S binding using the same methods employed for radioligand binding. The potential advantages of filtration assays are the lack of non-proximity effects which are present in SPA assays and the ability to use higher concentrations of GTP $\gamma$ <sup>35</sup>S. Such advantages are not usually worth sacrificing the convenience of homogeneous SPA assays. There are many examples of the use of filtration for GTP $\gamma$ S binding in the literature (7,8,10,17). As for WGA whole membrane binding, filtration assays are mostly limited to Gi/o coupled receptors since they cannot employ antibody capture.

## Muscarinic agonists-mediated GTP binding to hM4 receptors from CHO cell membrane

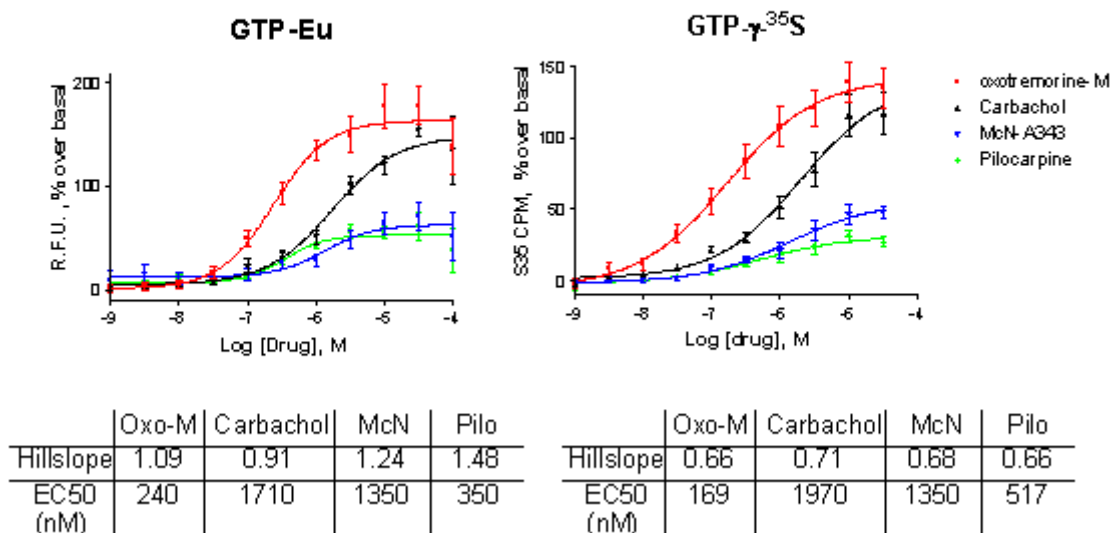


**Figure 9:** Side by side comparison of GTP-Eu vs. GTP<sup>35S</sup> assay methods.

## Non-Radiometric GTP<sub>γ</sub>S Assays

Perkin Elmer Life Sciences has developed an assay based on the use of a europium-GTP complex (11). This is a fluorescent whole membrane assay which does not require radioactivity, exhibits no non-proximity effect, and produces reliable data (Figure 9). Although the Eu-GTP<sub>γ</sub>S assay has traditionally employed a filtration step using 96 well filter plates (11), a single tube assay has been reported employing quenching resonance energy transfer (18). Eu-GTP<sub>γ</sub>S assays have not been configured to provide measurement of binding to specific G-proteins. The Eu-GTP<sub>γ</sub>S assay has been formatted to provide high throughput (19).

## References

1. DeLapp N, McKinzie J, Sawyer BD, Vandergriff A, Falcone J, McClure D, Felder CC. Determination of [<sup>35</sup>S] guanosine-5'-O-(3-thio)triphosphate binding mediated by cholinergic muscarinic receptors in membranes from Chinese hamster ovary cells and rat striatum using an anti-G-protein scintillation proximity assay. *J. Pharmacol. Exp. Ther.* 1999;289:946–955. PubMed PMID: 10215674.
2. Bymaster FP, Falcone J, Bauzon D, Kennedy JS, Schenk K, DeLapp NW, Cohen ML. Potent antagonism of 5HT<sub>3</sub> and 5HT<sub>6</sub> receptors by olanzapine. *Eur. J. Pharmacol.* 2001;430:341–349. PubMed PMID: 11711053.



3. Cussac D, Pasteau V, Millan MJ. Characterization of Gs activation by dopamine D<sub>1</sub> receptors using an antibody capture assay: antagonist properties of clozapine. *Eur. J. Pharmacol.* 2004;485:111–117. PubMed PMID: 14757130.
4. DeLapp NW. The antibody capture [<sup>35</sup>S] GTP $\gamma$ S scintillation proximity assay: a powerful emerging technique for analysis of GPCR pharmacology. *Trends Pharmacol. Sci.* 2004;25:400–401. PubMed PMID: 15276707.
5. Porter AC, Bymaster FP, DeLapp NW, Yamada M, Wess J, Hamilton SE, Nathanson N, Felder CC. M1 muscarinic receptor signaling in mouse hippocampus and cortex. *Brain Res.* 2002;944:82–89. PubMed PMID: 12106668.
6. Salah-Uddin H, Thomas DR, Davies CH, Hagan JJ, Wood MD, Watson JM, Challiss RAJ. Pharmacological Assessment of M1 Muscarinic Acetylcholine Receptor-Gq/11 Protein Coupling in Membranes Prepared from *Post Mortem* Human Brain Tissue. *J. Pharmacol. Exp. Ther.* 2008;325:869–874. PubMed PMID: 18322150.
7. Lazareno S, Birdsall NJM. Pharmacological characterization of acetylcholine-stimulated [<sup>35</sup>S]-GTP $\gamma$ S binding mediated by human muscarinic m1-m4 receptors: antagonist studies. *Br. J. Pharmacol.* 1993;109:1120–1127. PubMed PMID: 8401923.
8. Hilf G, Gierschik P, Jakobs KH. Muscarinic acetylcholine receptor-stimulated binding of guanosine 5'-O-(3-thiotriphosphate) to guanine-nucleotide-binding proteins in cardiac membranes. *Eur. J. Biochem.* 1989;186:725–731. PubMed PMID: 2514098.
9. Milligan G. Principles: Extending the utility of [<sup>35</sup>S]GTP $\gamma$ S binding assays. *Trends Pharmacol. Sci.* 2003;24:87–90. PubMed PMID: 12559773.
10. Gupta SK, Pillarisetti K, Thomas RA, Aiyar N. Pharmacological evidence for complex and multiple site interaction of CXCR4 with SDF-1 $\alpha$ : Implications for development of selective CXCR4 antagonists. *Immunology Letters.* 2001;78:29–34. PubMed PMID: 11470148.
11. Strange PG. Use of the GTP $\gamma$ S ([<sup>35</sup>S] GTP $\gamma$ S and Eu-GTP $\gamma$ S) binding assay for analysis of ligand potency and efficacy at G protein-coupled receptors. *Br. J. Pharmacol.* 2010;161:1238–1249. PubMed PMID: 20662841.
12. Ferrer M, Kolodin G, Zuck P, Peltier R, Berry K, Mandala SM, Rosen H, Ota H, Ozaki S, Inglese J, Strulovici B. A Fully Automated [<sup>35</sup>S]GTP $\gamma$ S Scintillation Proximity Assay for the High-Throughput Screening of Gi-Linked G Protein-Coupled Receptors. *Assay Drug Dev. Technol.* 2003;1:261–273. PubMed PMID: 15090191.
13. Johnson EN, Shi X, Cassaday J, Ferrer M, Strulovici B, Kunapuli P. A. 1536-well [<sup>35</sup>S]GTP $\gamma$ S scintillation proximity binding assay for ultra-high-throughput screening of an orphan G $\alpha$ i-coupled GPCR. *Assay Drug Dev. Technol.* 2008;6:327–337. PubMed PMID: 18537464.
14. Leff P, Dougall IG. Further concerns over Cheng-Prusoff analysis. *Trends Pharmacol. Sci.* 1993;14:110–112. PubMed PMID: 8516953.
15. Christopoulos A, Kenakin T. G. Protein-Coupled Receptor Allosterism and Complexing. *Pharmacol. Rev.* 2002;54:323–374. PubMed PMID: 12037145.
16. Olianias MC, Onali P. Stimulation of Guanosine 5'-O-(3-[<sup>35</sup>S] Thiotriphosphate) Binding by Cholinergic Muscarinic Receptors in Membranes of Rat Olfactory Bulb. *J. Neurochem.* 1996;67:2549–2556. PubMed PMID: 8931489.

17. Alper RH, Nelson DL. Characterization of 5-HT<sub>1A</sub> receptor-mediated [<sup>35</sup>S]GTPγS binding in rat hippocampal membranes. *Eur. J. Pharmacol.* 1998;343:303–312. PubMed PMID: 9570480.
18. Rozwandowicz-Jansen A, Laurila J, Martikkala E, Frang H, Hemmila I, Scheinin M, Pekka H, Harma H. Homogeneous GTP Binding Assay Employing QRET Technology. *J. Biomol. Screen.* 2010;15:261–267. PubMed PMID: 20103692.
19. Labrecque J, Wong RS, Fricker SP. A time-resolved fluorescent lanthanide (Eu)-GTP binding assay for chemokine receptors as targets in drug discovery. *Methods Mol. Biol.* 2009;552:153–169. PubMed PMID: 19513648.

## Additional References

1. Cussac D, Newman-Tancredi A, Duqueyroix D, Pasteau V, Millan MJ. Differential activation of Gq/11 and Gi3 proteins at 5-HT<sub>2C</sub> receptors revealed by antibody capture assays: influence of receptor reserve and relationship to agonist-directed trafficking. *Mol. Pharmacol.* 2002;62:578–58. PubMed PMID: 12181434.
2. Newman-Tancredi A, Cussac D, Marini L, Tousard M, Millan MJ. h5-HT<sub>1B</sub> receptor-mediated constitutive Gai3-protein activation in stably transfected Chinese hamster ovary cells: an antibody capture assay reveals protean efficacy of 5HT. *Br. J. Pharmacol.* 2003;138:1077–1084. PubMed PMID: 12684263.
3. Mannoury la Cour C, Vidal S, Pasteau V, Cussac D, Millan MJ. Dopamine D1 receptor coupling to Gs/olf and Gq in rat striatum and cortex: A scintillation Proximity assay (SPA)/antibody-capture characterization of benzazepine agonists. *Neuropharmacology.* 2007;52:1003–1014. PubMed PMID: 17178132.
4. Dupuis DS, Mannoury la Cour C, Chaput C, Verrielle L, Lavielle G, Millan MJ. Actions of novel agonists, antagonists and antipsychotic agents at recombinant rat 5-HT<sub>6</sub> receptors: A comparative study of coupling to GαS. *Eur. J. Pharmacol.* 2008;588:170–177. PubMed PMID: 18511034.
5. Eglen RM, Reisine T. New Insights into GPCR Function: Implications for HTS. In: *G-Protein Coupled Receptors in Drug Discovery*, series. *Methods in Molecular Biology.* 2009;551:1–13. PubMed PMID: 19521862.

# Histone Acetyltransferase Assays in Drug and Chemical Probe Discovery

Sanket Gadhia, Ph.D.,<sup>1</sup> Jonathan H. Shrimp, Ph.D.,<sup>2</sup> Jordan L. Meier, Ph.D.,<sup>2</sup> James E. McGee, Ph.D.,<sup>3</sup> and Jayme L. Dahlin, M.D., Ph.D.<sup>✉4</sup>

Created: July 26, 2017; Updated: July 1, 2018.

## Abstract

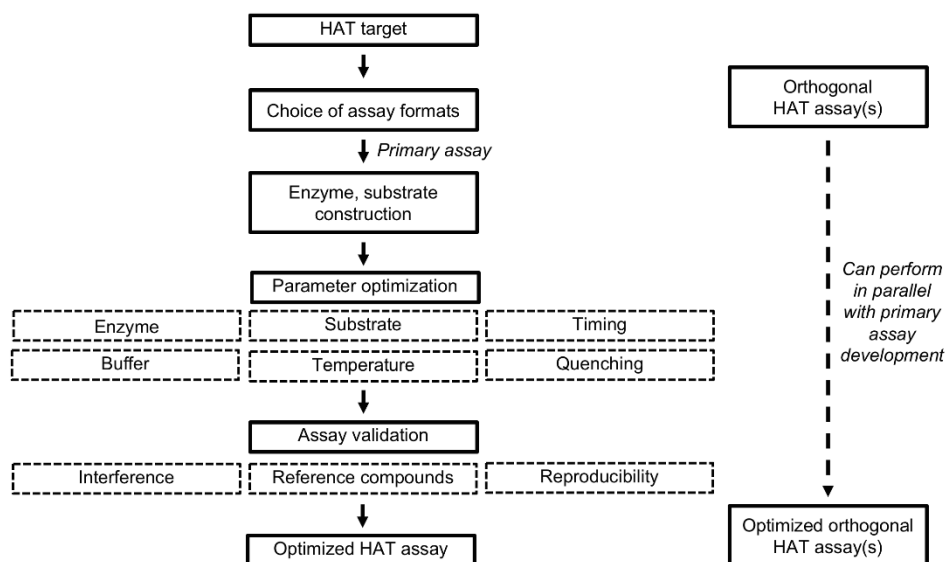
Histone acetyltransferases (HATs) are a class of epigenetic enzymes involved in critical cellular processes like nucleosome assembly, DNA damage repair, and transcriptional regulation. HATs are implicated in many human pathologies including cancers. This chapter describes essential experimental considerations for performing high-throughput screening and follow-up assays, and offers practical strategies for assay optimization and validation. Illustrative walkthroughs for several HAT assay formats are provided. This content should be useful for those performing HTS assays, orthogonal assays, and counter-screens involving HATs in the context of drug discovery, chemical biology, and molecular pharmacology.

---

<sup>1</sup> Division of Pre-Clinical Innovation, National Center for Advancing Translational Sciences, National Institutes of Health, Rockville, MD, USA. <sup>2</sup> Chemical Biology Laboratory, Center for Cancer Research, National Cancer Institute, National Institutes of Health, Frederick, MD, USA. <sup>3</sup> Quantitative Biology, Eli Lilly and Company, Indianapolis, IN, USA. <sup>4</sup> Department of Pathology, Brigham and Women's Hospital, Boston, MA, USA; Email: jdahlin@bwh.harvard.edu.

✉ Corresponding author.

## Flowchart



## Abbreviations

|            |   |
|------------|---|
| Acetyl-CoA | acetyl coenzyme A   |
| BSA        | bovine serum albumin  |
| CoA        | coenzyme A  |
| CPM        | <i>N</i> -[4-(7-diethylamino-4-methylcoumarin-3-yl)phenyl]maleimide |
| DMSO       | dimethyl sulfoxide  |
| DTT        | dithiothreitol  |
| EDTA       | ethylenediaminetetraacetic acid                                     |
| ELISA      | enzyme-linked immunosorbent assay                                   |
| FRET       | fluorescent/Förster resonance energy transfer                       |
| HAT        | histone acetyltransferase   |
| HDAC       | histone deacetylase   |
| HEPES      | hydroxyethyl piperazineethanesulfonic acid                          |
| HTS        | high-throughput screening   |
| IS         | internal standard   |
| KAT        | lysine acetyltransferase  |
| LoD        | limits of detection   |
| LoQ        | limits of quantitation  |
| MS         | mass spectrometry   |

Table continues on next page...

Table continued from previous page.

|       |                                       |
|-------|---------------------------------------|
| MSR   | minimum significant ratio             |
| NEM   | N-ethylmaleimide                      |
| PAINS | pan assay interference compounds      |
| PTM   | post-translational modification       |
| SIRT  | sirtuin                               |
| SPE   | solid-phase extraction                |
| TCEP  | <i>tris</i> (2-carboxyethyl)phosphine |

## Introduction and Background

### Introduction

HATs are a class of epigenetic enzymes involved in many critical cellular processes. Aberrancies in HAT function have been implicated in human disease. Modulators of HAT activity may therefore be highly useful for chemical probes of epigenetic systems, or potential therapeutics in HAT-related pathologies.

This chapter describes essential experimental factors needed to develop, optimize, and validate assays for the purpose of assessing compound modulation of HAT activity. Several example protocols of representative HAT assays are provided. This information should be useful for novices as well as more seasoned researchers. While this chapter specifically focuses on HAT assays, the general methodologies should also be informative to a variety of epigenetic systems (e.g., methyltransferases, deacetylases) as well as non-epigenetic bi-substrate enzymatic systems.

*Note: This chapter emphasizes biochemical HAT assays. Cell-based HAT assays are briefly discussed. However, many of the same principles discussed with respect to biochemical HAT assays should apply to cell-based HAT assays.*

### Background

Epigenetics is defined as heritable changes in gene expression that occur without altering the underlying genetic sequence. This process is regulated in part by a series of epigenetic enzymes acting *via* post-translational modifications (PTM) such as histone acetylation, methylation, phosphorylation, and ubiquitylation. Histone PTMs are regulated by histone reader, writer, and eraser enzymes.

Histone acetylation is critical for regulation of gene transcription, nucleosome assembly, and DNA repair (1,2). HATs have been implicated in a variety of human pathologies, including cancers (3). Consequently, there is great interest in developing potent and specific small-molecule modulators of HAT activity, either as chemical probes or potential therapeutics (4,5).

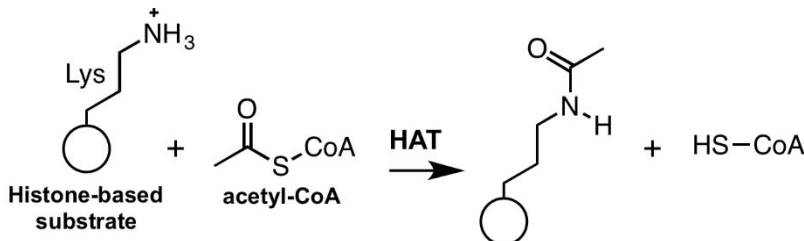


**Figure 1. Schematic of HAT reaction.** HATs catalyze the transfer of an acetyl moiety from acetyl-CoA to a histone substrate. The resulting products are free coenzyme A (“CoA-SH” or “CoA”) and an acetylated histone lysine residue.

Human HATs can be divided into several large families: MYST (TIP60, MOZ/MYST3, MORF/MYST4, HBO1/MYST2, MOF/MYST1), p300/CBP (P300, CBP), and GNAT (GCN5, PCAF, ELP3). In addition, there are also transcription factors with HAT activity and nuclear receptor co-activators. HATs are also present in other eukaryotic species, including *Drosophila* and fungi, the latter of which includes opportunistic human pathogens such as *Aspergillus*, *Candida*, and *Pneumocystis*.

HATs catalyze the transfer of an acetyl moiety from acetyl-CoA to lysine side chains present on histone proteins (**Figure 1**). Catalysis can occur through a random-order ternary complex mechanism, a compulsory-order ternary complex, or a ping-pong mechanism. The final product neutralizes the positively-charged lysine  $\epsilon$ -amino group and reduces steric bulk, which effectively “loosens” the interaction between histone proteins and negatively-charged DNA, leading to less compacted chromatin and increased transcription. Acetylated histone residues can be specifically recognized by histone reader domains called bromodomains. The biological counter-part to HATs are histone deacetylases (HDACs) and sirtuins (SIRTs), epigenetic enzymes which catalyze the removal of the acetyl moiety from acetylated histone lysines. HATs are complex bi-substrate systems, utilizing both an acetyl donor (acetyl-CoA) and an acetyl acceptor (histone protein).

HATs acetylate many histone lysine residues. (6) These occur on H2A (K5), H2B (K12, K15), H3 (K9, K14, K18, K36, K56), and H4 (K5, K8, K12, K16). Often a specific HAT can acetylate multiple histone lysine residues. HAT activity and substrate specificity can be regulated by multiple factors, including autoacetylation and chaperone proteins (7-9). Note that certain HATs can also acetylate non-histone substrates, and can also be referred more broadly as lysine acetyltransferases (KATs).

### Introduction to Common HAT Assays

Multiple biochemical HAT assays have been described (**Table 1**). These assays measure HAT activity by detecting either the acetylated histone-based product (“direct”) or the free CoA product (“indirect”).

So-called indirect methods utilize fluorescent thiol-scavenging probes or enzyme-coupling reactions. In general, these assays are inexpensive and straightforward to establish, but are highly susceptible to compound-mediated assay interference. This can necessitate multiple counter-screens and orthogonal assays to rule-out interference and confirm true compound activity. While they are usually highly amenable to HTS, the time and resources required to perform interference counter-screens and orthogonal studies to triage assay artifacts and poorly tractable chemical matter has the potential to offset the initial up-front benefits of indirect assays.

Direct HAT assays can measure the acetylated histone-based product by one of multiple technologies. These include radiolabels (e.g., filter-binding, scintillation proximity), mass spectrometry (MS), microfluidic mobility, and antibody-based techniques such as traditional enzyme-linked immunosorbent assay (ELISA), Alpha-based technologies (e.g., AlphaScreen, AlphaLISA), and FRET (including time-resolved FRET). The advantage of direct assays is that they measure the actual protein product from the HAT reaction. Direct assays can require more technical expertise, specific instrumentation, and more customized and expensive reagents compared to the most common indirect methods. Furthermore, even direct HAT assays are susceptible to compound-mediated assay interference, and should be accompanied with appropriate readout interference counter-screens and orthogonal assays.

Each HAT assay technology has characteristic advantages and disadvantages (**Table 1**). When selecting an assay type for either a primary or orthogonal assay, one should consider multiple (and often competing) factors, including but not limited to: available instrumentation, resources, expertise, project timelines, the nature of the HAT system being assayed, possible technology-related interferences, and the number and type of test compounds.

The indirect assays and most of the direct assays can be suitable for HTS (**Table 1**), while the direct and indirect assays can all be adapted for orthogonal assays. Suggestions for specific primary assay-orthogonal assay pairings are discussed in the subsequent section “Use of Orthogonal Assays/Common Interferences”.

**Table 1.** Common HAT assay formats. Each HAT assay format has advantages and disadvantages, including susceptibilities to technology-related compound-mediated assay interferences.

| Assay technology                      | Assay principle   | Advantages   | Disadvantages   | Compound-mediated readout interferences                               | General suitability for HTS | Example references |
|---------------------------------------|---|--|---|---|-----------------------------|--------------------|
| Fluorometric (thiol-scavenging probe) | Free CoA forms fluorescent adduct with probe (indirect) | -Inexpensive<br>-Easy to set-up<br>-High-throughput<br>-Label-free | -Significant potential for compound-mediated interference<br>-Enrichment of | -Light-based interferences (absorbance, auto-fluorescence, quenching, | +                           | (10-14)            |

*Table 1. continues on next page...*

Table 1. continued from previous page.

| Assay technology                          | Assay principle  | Advantages   | Disadvantages  | Compound-mediated readout interferences  | General suitability for HTS | Example references |
|---|--|--|--|--|-----------------------------|--------------------|
|   |  |  | thiol-reactive compounds<br>-Can require large concentrations of product formation for detection   | light scattering)<br>-Thiol-scavenging   |                             |                    |
| Enzyme-coupling                           | Second enzyme requires CoA, secondary product measured (indirect)                        | -Inexpensive<br>-Easy to set-up<br>-High-throughput<br>-Adaptable to continuous readout<br>-Label-free | -Significant potential for compound-mediated interference<br>-Enrichment of thiol-reactive compounds<br>-Can require large concentrations of product formation for adequate signal | -Secondary enzyme system modulation<br>-Light-based interferences (absorbance, auto-fluorescence, quenching, light scattering)<br>-Thiol-scavenging        | +                           | (15)               |
| Radiolabeled substrate (filter-binding)   | Radiolabeled acetate ( <i>via</i> acetyl-CoA) incorporated onto histone product (direct) | -High S:N<br>-Few compound-mediated interferences<br>-Label-free                                       | -Cost<br>-Radiation<br>-Lower-throughput in most settings  | -Scintillation quenching   | -                           | (10,16-18)         |
| Alpha technology (AlphaScreen, AlphaLISA) | Amplified luminescent proximity (direct)   | -High S:N<br>-Customizable<br>-No radiation<br>-Amenable to miniaturization<br>-Homogenous format      | -Cost<br>-Specialized instrumentation<br>-Dependent on antibody quality<br>-Light sensitivity  | -Singlet oxygen quenching<br>-Light-based interferences (absorbance, quenching, auto-fluorescence, light-scattering)<br>-Capture reagent disruption (e.g., | +                           | (19)               |

Table 1. continues on next page...



Table 1. continued from previous page.

| Assay technology     | Assay principle   | Advantages   | Disadvantages  | Compound-mediated readout interferences  | General suitability for HTS | Example references |
|----------------------|---|--|--|--|-----------------------------|--------------------|
|                      |   |  |  | disruption of antibody/tag interaction)  |                             |                    |
| FRET                 | Fluorescent/<br>Förster<br>resonance<br>energy transfer<br>(direct)         | -Customizable<br>-No radiation<br>-Usually<br>cheaper than<br>Alpha<br>-Can enhance<br>with time-<br>resolved FRET<br>(TR-FRET)<br>-Homogenous<br>format | Dependent on<br>antibody quality   | -Light-based<br>interferences<br>(absorbance,<br>quenching,<br>auto-<br>fluorescence,<br>light-<br>scattering)<br>-Capture<br>reagent<br>disruption<br>(e.g.,<br>disruption of<br>antibody/tag<br>interaction) | +                           | (20)               |
| Fluidic<br>mobility  | Electrophoretic<br>separation of<br>histone-based<br>products<br>(direct)   | -Monitor<br>multiply-<br>acetylated<br>substrates<br>-No radiation<br>-Adaptable to<br>continuous<br>readouts  | -Highly<br>specialized<br>instrumentation<br>-Highly-charged<br>substrates<br>challenging<br>-Large<br>substrates<br>challenging |  | +                           | (21,22)            |
| Mass<br>spectrometry | Histone-based<br>products<br>ionized and<br><i>m/z</i> measured<br>(direct) | -Highly<br>sensitive (less<br>product<br>formation<br>required)<br>-Label-free<br>-Monitor<br>multiply-<br>acetylated<br>products<br>-No radiation       | -Highly<br>specialized<br>instrumentation<br>-Throughput   | -Ion<br>suppression<br>-<br>Compound-<br>analyte<br>adducts  | +                           | (23)               |

Table 1. continues on next page...

Table 1. continued from previous page.

| Assay technology                      | Assay principle   | Advantages   | Disadvantages  | Compound-mediated readout interferences   | General suitability for HTS | Example references |
|---------------------------------------|---|--|--|---|-----------------------------|--------------------|
| Traditional antibody (ELISA, Western) | Antibody binds to acetylated histone product (direct)                     | - Straightforward to establish<br>- Highly sensitive<br>- No radiation | - Dependent on antibody quality<br>- Lower-throughput (heterogeneous format) | - Antibody interference<br>- Quenching of antibody reporter<br>- Lower dynamic ranges | -                           | (10,11,17)         |
| Scintillation                         | Radiolabeled product scintillates in proximity to capture matrix (direct) | - High S:N<br>- Homogenous format                                      | - Radiation<br>- Specialized instrumentation                                 | Scintillation quenching (24,25)   | +                           | (20,26-28)         |

## Section Summary

HATs are epigenetic enzymes involved in critical cellular processes, and have been linked to human disease. There are multiple robust, orthogonal assay platforms assessing modulation of HAT activity by test compounds.

## General Considerations for HAT Assays

### Introduction

Regardless of technology choice, HAT assays require optimization of many experimental parameters. This section describes essential experimental considerations for performing HAT assays, including optimization of enzyme and substrates, other reaction components, reaction timing, and reaction quenching.

### Enzyme/Substrate Source

HATs and histone-based substrates can be purchased commercially or produced in-house. Commercially-sourced HATs and histones have the advantage of being readily available, but often they are prohibitively expensive in amounts needed for an HTS. Proteins produced in-house can allow for greater customization and control over the purification process, but production can be time-consuming, and can be difficult to achieve at large scales and acceptable purities.

Commercially-sourced enzymes and substrates are often “one size fits all” entities, and may not have the specific features optimal for a particular HAT assay. Users may need to customize: (a) a specific affinity or purification tag, (b) the construct of the HAT enzyme

or histone (e.g., truncations), (c) the introduction of PTMs such as fluorophores, and (d) expression and purification conditions to optimize protein folding and stability. For some applications, full-length HAT or histone substrate may be necessary to capture the essential features of the native system being probed by the HTS. In other cases, users may only need the catalytic HAT domain or specific histone peptides. In some cases, supposed non-catalytic domains may have profound effects on catalysis, system stability, and substrate specificity.

Depending on the research question and HTS method, users may need to produce their own HAT or histone substrate (29). While the details of producing recombinant enzymes are beyond the scope of this chapter, we recommend first consulting any original literature on the specific HAT or histone substrate to be assayed for details about potential production and purification strategies.

The identity and purity of HAT enzymes and protein substrates should be rigorously validated, especially when performing experiments on the HTS scale. For details, refer to Validating Identity, Mass Purity and Enzymatic Purity of Enzyme Preparations.

## Acetyl-CoA

There are several important considerations with respect to the acetyl-CoA substrate:

- Acetyl-CoA is often sold in salt/hydrate preparations with variable stoichiometry. Most commercial forms are sold as a sodium or lithium salt.
- To ensure accurate  $K_M$  determination and to enhance assay precision, the concentration of acetyl-CoA should be determined spectrophotometrically. For example, acetyl-CoA (tri-lithium salt) can be measured by monitoring light absorbance at 260 nm ( $\epsilon = 16000 \text{ M}^{-1} \text{ cm}^{-1}$  in  $\text{H}_2\text{O}$ ) or at 232 nm ( $\epsilon = 8700 \text{ M}^{-1} \text{ cm}^{-1}$  in  $\text{H}_2\text{O}$ ) (30).
- In solid form, acetyl-CoA should be stored in desiccated conditions and in  $-20^\circ\text{C}$ .
- In solution, acetyl-CoA stocks should be stored at  $-20^\circ\text{C}$ . Acetyl-CoA is unstable in alkaline conditions and in highly acidic conditions. A recommended storage buffer is 50 mM sodium acetate, pH 5.0. Minimize freeze-thaw cycles.
- Commercial acetyl-CoA can contain minor amounts of free CoA. This may interfere with some types of HAT assay readouts or inhibit certain HATs by product inhibition (22). Free CoA can be treated with acetic anhydride to mitigate this effect (13).

## Histone-Based Substrates

Many choices of substrates are available for HAT assays (**Table 2**). These include (in order of complexity): histone peptides, full-length histones, histone dimers, core histones, histone-chaperone complexes, and nucleosomes.

For any given HAT assay, the optimal histone-based substrate is multifactorial. One factor is the nature of the specific HAT system being assayed, as HAT specificity and catalytic efficiency can depend on whether the histone is presented in monomeric or multimeric

form(s), or whether histone chaperones are present. Users should also consider the physiologic context of the HAT target. As with the choice of enzyme constructs, using full-length substrates and/or include chaperone proteins can potentially better approximate physiological catalysis, HAT stability, and substrate specificity. Generally speaking, it is best to approximate physiologic conditions in any given assay, but such considerations must be weighed against practical and competing factors such as compatibility with assay technology, overall system complexity, and reagent costs.

In general, histone peptides are practical and relatively easy to customize (with respect to length, sequence, labels, affinity tags), and can reduce system complexity. Depending on the particular epigenetic system, histone peptides can have a higher  $K_M$  than their full-length counterparts (31). Furthermore, a potential downside to peptide substrates is that they may not sufficiently model the physiologic context of a given HAT system.

Full-length histone products may therefore be required in this regard. Potential downsides to full-length protein use are their more challenging production procedures and the increased assay complexity due to many HATs that can acetylate multiple lysine residues. Fortunately, full-length histone monomers and multimers can be produced using recombinant technology in large scales with sufficient technique. For additional details regarding histone product production, we refer the reader to several published protocols (32-35). For full-length histone products, users should pay particular attention to protein precipitation at higher concentrations. This potential problem can often be mitigated by carefully optimizing pH and salt conditions.

Users should also consider the species of the histone-based substrate. While histones are highly conserved species in eukaryotes, subtle inter-species sequence variations may have dramatic consequences. For some applications, it may be acceptable to use histones derived from *Drosophila*, yeast, chicken, or calf thymus. In other cases, human-based histones may be required.

**Table 2.** Common histone-based substrates in HAT assays. Each substrate type has advantages and disadvantages. The optimal substrate will depend on the nature of a given HAT system, the choice of assay, and other factors.

| Substrate type              | Potential advantages  | Potential disadvantages  |
|-----------------------------|---|--|
| Histone peptide             | -Soluble<br>-Customizable<br>-Can simplify complex multi-substrate histones | -Non-native substrate<br>-Potentially higher $K_M$                       |
| Full-length histone protein | Potential physiologic substrate   | -Precipitation risk<br>-PTM heterogeneity (e.g., non-recombinant source) |

Table 2. continues on next page...

Table 2. continued from previous page.

| Substrate type              | Potential advantages            | Potential disadvantages  |
|-----------------------------|---------------------------------|--|
| Histone dimer/multimer/core | Potential physiologic substrate | -Precipitation risk<br>-Increased assay complexity<br>-PTM heterogeneity (e.g., non-recombinant source)  |
| Histone-chaperone complex   | Potential physiologic substrate | -More laborious to prepare in bulk quantities<br>-Precipitation risk<br>-Increased assay complexity<br>-PTM heterogeneity (e.g., non-recombinant source) |
| Nucleosome                  | Potential physiologic substrate | -More laborious to prepare in bulk quantities<br>-Precipitation risk<br>-Increased assay complexity<br>-PTM heterogeneity                                |

## Reaction Buffer and Additives

The essential components of a biochemical HAT reaction include buffer, salts, chelating agents, reducing agents, detergents, and carrier proteins.

- Buffer
  - Buffers are used to maintain the reaction solution within a fixed pH range optimal for HAT activity.
  - Common buffering agents include Tris HCl and HEPES, typically at 50-100 mM final concentrations.
  - Most HAT reactions are performed in slightly alkaline conditions (usually pH 7.5-8.0).
  - A common buffering agent is 50 mM Tris, pH 8.0.
- Salts
  - Most biochemical HAT assays utilize NaCl, though KCl can often be used in its place.
  - The most common ionic strength is 50-100 mM NaCl.
  - Full-length histone substrates ( $\pm$  chaperones) can be highly sensitive to salt concentrations, especially at higher concentrations.
- Chelating agents
  - Chelating agents can be added to prevent metal-catalyzed proteolysis and oxidation.
  - The most common chelating agent used in HAT reactions is ethylenediaminetetraacetic acid (EDTA), often at 0.1 mM final concentrations.
  - Be aware that certain HAT systems may show metal-dependent activity. Therefore, it is reasonable to assess the performance of a HAT assay in the

presence and absence of chelating agents like EDTA, as well as using similar methods to investigate compounds for chelation-related bioactivity. (36)

- Reducing agents
  - Reducing agents are added to prevent oxidation of protein side chains, most notably cysteine thiols. Reducing agents can also mitigate the effect of thiol-reactive screening compounds by acting as scavenging reagents (17).
  - Strong reducing agents have the potential to fuel redox-cycling, a phenomenon in which compounds produce  $H_2O_2$  *in situ* (37,38).
  - Examples of commonly used reducing agents include dithiothreitol (DTT),  $\beta$ -mercaptoethanol (BME), and *tris*(2-carboxyethyl)phosphine (TCEP).
  - The most common reducing agent is DTT, often at 1-5 mM final concentrations.
  - Note that DTT is unstable in aqueous conditions. Freshly prepare solutions containing DTT, and keep on ice.
- Detergents
  - Detergents are added for two reasons: (a) to prevent nonspecific protein adsorption to container walls, and (b) to mitigate aggregation formation by test compounds, which can nonspecifically modulate HAT activity.
  - Examples detergents include Triton X-100, Tween 20, Pluronic F-68, and Brij 35.
  - The authors have had good experience with 0.01% Triton X-100 (v/v). Triton X-100 can produce  $H_2O_2$  *in situ*, which should be considered in systems highly sensitive to oxidation. This effect can be mitigated by preparing fresh detergent-containing buffers.
  - Many detergents are highly viscous. Handling can be enhanced by preparing as 10% (v/v) solutions and pipetting slowly. Allow time (often several hours with gentle mixing) for detergents to fully dissolve in water.
- Carrier proteins
  - Carrier proteins are included in many biochemical reactions to enhance enzymatic stability, as many enzymes are unstable in dilute concentrations. Carrier proteins can prevent nonspecific adsorption of assay proteins to container walls.
  - Carrier proteins (also known as "decoy proteins" in the context of preventing aggregation) can also mitigate compound aggregation (39), and can also serve as low-level thiol-scavenging reagents to mitigate the effect of thiol-reactive screening compounds.
  - The most common carrier protein used in biochemical HAT assays is bovine serum albumin (BSA). Common concentrations of BSA range from 5 to 100  $\mu$ g/mL.
- Protease, HDAC inhibitors
  - Protease inhibitors are typically added to certain biochemical solutions to prevent proteolysis. Examples include phenylmethylsulfonyl fluoride ("PMSF") and 4-(2-aminoethyl)benzenesulfonyl fluoride ("Pefabloc"). Commercial cocktails are also widely available.

- While useful in protein purification, protease inhibitors are generally not required for most biochemical HAT assay applications.
- Inhibitors are often used at relatively high concentrations (high micromolar/low millimolar) and have the potential to cause assay interference.
- Consider adding protease inhibitors if there is evidence of significant protein degradation. Extended incubation or reaction times may also warrant trials of protease inhibitors.
- Nonspecific HDAC inhibitors such as sodium butyrate are occasionally added to prevent deacetylation. They are typically used at low millimolar concentrations. In purified systems, such inhibitors are probably unnecessary. When analyzing reactions containing cellular extracts, appropriate control experiments should be performed to determine whether HDAC inhibitors are necessary and whether they interfere with HAT activity or assay readout.
- Example reaction buffer
  - The following is a useful initial reaction buffer: 50 mM Tris, pH 8.0, 50 mM NaCl, 0.1 mM EDTA, 1 mM DTT, 0.01% Triton X-100 (v/v), 50 µg/mL BSA.
  - It is often useful to prepare reaction buffers in concentrated form. Consider making a 5X solution (250 mM Tris, pH 8.0, 250 mM NaCl, 0.5 mM EDTA, 5 mM DTT, 0.05% Triton X-100 (v/v), 250 µg/mL BSA).
  - Consider performing simple titration experiments with each reagent to determine optimal reaction conditions and components.

## Timing/Enzyme Concentration

Assay timing and enzyme concentration can usually be optimized in one experiment. Monitor HAT reactions over time at multiple enzyme concentrations at multiple time points (**Figure 2**). Optimal timing in HAT assays is during the linear reaction phase, at times feasible for the desired throughput, instrumentation, and system stability, among other factors. Sampling too soon after reaction initiation (e.g., seconds to minutes) may be impractical in many HTS settings, and may lead to imprecise results if the reaction proceeds quickly. Later sampling times are more susceptible to system stability effects (e.g., enzyme instability). For most compounds, enzyme modulation is best apparent at earlier reaction times. For inhibitors, the continued product accumulation by uninhibited enzyme can eventually confound the final readout (40). Reaction times can range from approximately five minutes to several hours, depending on the nature of the HAT system and assay specifics. Linearity can change with subtle perturbations in reaction conditions, so it is advised to periodically reassess linearity when changing assay conditions.

Optimal enzyme concentration should produce a readout intensity sufficient for robust sampling above background. Too much enzyme, and the reaction can be completed too quickly to practically measure in the linear range. Too little enzyme, and the readout is not strong enough to reliably measure relative to background signal. For reference, high picomolar to lower nanomolar concentrations of HAT enzyme are most often reported in the literature.

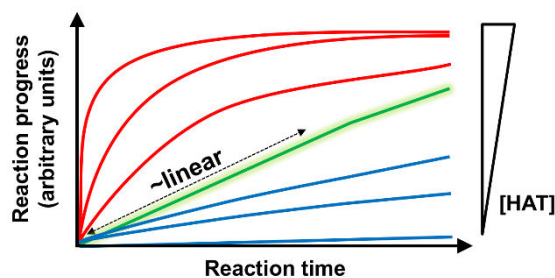


**Figure 2. Optimization of enzyme concentration and timing in HAT assays.** Optimal enzyme concentration and assay timing can be determined by a straightforward time-course experiment combined with enzyme titrations. In an ideal assay, HAT activity should be measured during the linear phase of the reaction. In this cartoon, the reaction progress curves in blue, performed with lower enzyme concentrations, are sufficiently linear but signal strength would be insufficient. The red progress curves, performed with higher enzyme concentrations, produce sufficient amounts of product but linearity is relatively transient. In this example, the green curve denotes an optimal enzyme concentration, as it is linear for sufficient duration to be assayed, and has a sufficient amount of product to measure. Assay timing should also consider other factors, including system stability, instrumentation, and workflow.

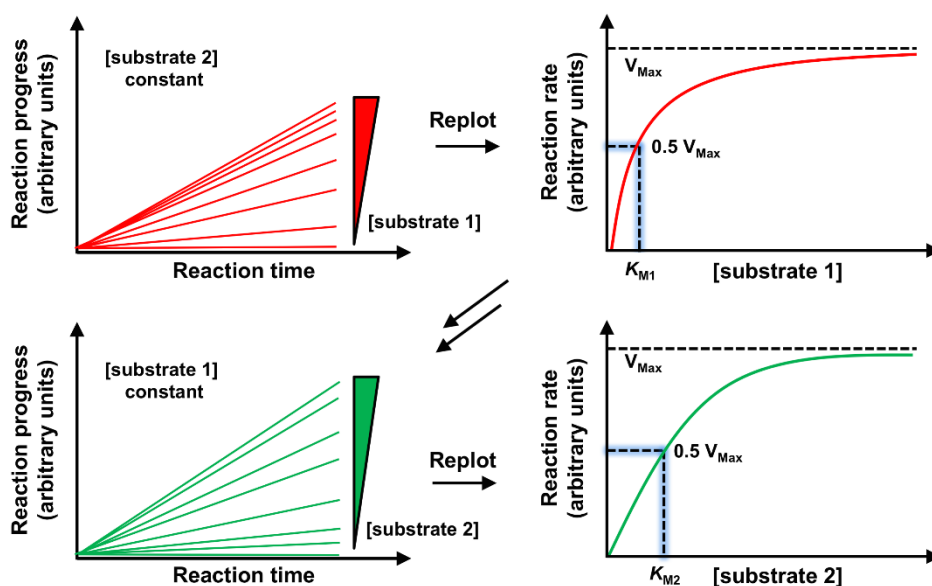


**Figure 3. Optimization of substrate concentrations in HAT assays.** Optimal substrate concentrations should be guided by the  $K_M$  for both HAT substrates. These can be determined experimentally. (Top) While keeping the concentration of substrate 2 constant (in excess), measure the enzymatic rates while titrating substrate 1, and calculate  $K_{M1}$ . (Bottom) Next, while keeping concentration of substrate 1 constant (in excess), measure the enzymatic rates while titrating substrate 2, and calculate  $K_{M2}$ .

For additional details, refer to Basics of Enzymatic Assays for HTS.



## Substrate Concentrations

The choice of substrate concentrations is an important consideration when screening for compound modulators of enzymatic activity. The choice of substrate concentrations can favor the selection of various modes of compound modulation. For instance, screening at high substrate concentrations relative to  $K_M$  will disfavor substrate-competitive inhibition, as competitive inhibitors will have more competition by the natural substrate for target binding to the substrate site. Sometimes, screening conditions are chosen to enrich certain mechanisms of target modulation. Most often, screens are performed around the  $K_M$  (so-called “balanced screening conditions”) so as not to favor any particular mechanism. In either case, the  $K_M$  for each HAT substrate must be experimentally determined under the final assay conditions.

The bi-substrate nature of HATs requires determining the  $K_M$  of each substrate: acetyl-CoA and the histone-based substrate (**Figure 3**). While holding the concentration of acetyl-CoA constant and in excess, the reaction rates can be determined with titrations of histone-based substrate, and plotted to determine the  $K_M$  of the histone-based substrate. Next, while holding the concentration of histone-based substrate constant and in excess, the reaction rates can be determined with titrations of acetyl-CoA, and plotted to determine the  $K_M$  of acetyl-CoA.

A few technical reminders on  $K_M$  determination:

- Reaction rates should be based on initial reaction velocity (linear range).
- A general guideline for excess substrate is > 100:1 substrate:enzyme.
- A guideline for substrate titrations is between 0.2-5.0  $K_M$ . Use at least eight substrate concentrations to determine  $K_M$ .
- Examine literature for reports on  $K_M$  to help guide initial conditions.

For additional details on optimizing substrate concentrations, refer to Basics of Enzymatic Assays for HTS.

Determining balanced screening conditions for bi-substrate reactions can be complex, especially in cases with significant substrate cooperativity (i.e., the concentration of one substrate significantly alters the binding behavior of another substrate). Cooperativity can be assessed by determining the  $K_M$  for each substrate at several different fixed concentrations of its partner substrate. In cases where significant cooperativity is suspected, additional mechanistic details about the HAT system should be characterized. For this undertaking, and for subsequently selecting optimal screening conditions, we recommend collaborating with an experienced enzymologist (40).

## Quenching

For end-point assays, the HAT reaction should be quenched. This prevents additional substrate consumption and guards against time-dependent enzyme modulation. This is especially important in HTS applications, as there can be a significant time lag between

reading the initial and subsequent microplates. Quenching can also have the effect of increasing assay precision by ensuring reproducible reaction and sampling times.

There are several strategies for efficiently quenching biochemical HAT assays:

- Chaotropic agents: ethanol, isopropanol, urea, guanidine HCl (often comparable in volume to reaction sample).
- Detergents such as SDS.
- Strongly basic or acidic solutions.
- Rapid freezing or heating.
- Directly spotting of the reaction solution onto filter paper.
- High concentrations of a HAT inhibitor at compound concentrations sufficient to ensure complete quenching ( $\gg IC_{50}$ ) (20,41).
- Hydroxylamine (21).

Consider several factors when picking quenching conditions.

- Depending on the specifics of the assay, quenching can be accomplished by adding the quencher to the reaction, or transferring the reaction mixture to a known quantity of quencher.
- With any of these approaches, verify that the HAT reaction is in fact quenched. This can be done by attempting to quench the reaction, and taking serial measurements to ensure a stable signal. Changing readouts usually indicate a non-quenched reaction.
- The type of quenching should be compatible with the assay readout. For example, certain quenching reagents may interfere with a given fluorescence readout, while general protein denaturants may prevent protein capture.

## Compound Solvent

Determine the optimal percentage of DMSO (or other compound solvent) in the assay. This can be done by straightforward titration of the particular compound solvent (which is usually neat DMSO in most compound libraries). This percentage is often less than 2.5% total volume, though some assays may tolerate less organic solvent. The amount of compound solvent should be kept constant regardless of compound concentration.

## Temperature

During the assay optimization process, determine the effect of temperature on the reaction system. Most biochemical HAT assays perform reactions at 30°C. This is a reasonable starting temperature point for most HAT assays. Users should experimentally determine the optimal reaction temperature that balances between convenience, reaction rate, and system stability for their particular assay application.

For HTS and even smaller scale follow-up experiments, it may be possible to conduct assays at room temperature. This convenience can circumvent the need to perform reactions in a heating oven and can reduce temperature gradient effects.

Higher temperatures can accelerate the reaction rate, which may be desirable depending on the assay timetable (this is true to a point, as too high of a temperature will eventually result in reagent or protein denaturation). Lower assay temperatures can slow the reaction rate and better stabilize the assay system, which again may be desirable for some applications.

Regardless of temperature, one should ensure assay temperature equilibration, especially if certain assay components are being kept on ice. Strategies include short pre-incubation steps and concentrated stock solutions.

## Controls/Reference Compounds

It is often useful to test the effect of positive controls or reference compounds when validating an assay. Their use can help in proof-of-concept, can monitor assay performance over time, and can help compare results from different experiments.

There are many small-molecule HAT inhibitors reported in the scientific literature, many of which are sold commercially (**Table 3**) (5). Unfortunately, to-date most are insufficiently validated with respect to target selectivity in biochemical assays, and most have not been demonstrated to show specific target engagement in cells (42,43). Many of these reported compounds contain thiol-reactive moieties, while others form aggregates in common assay conditions. Both of these properties are associated with assay interference and poor target selectivity (39,44,45). Many of these compounds have the potential to interfere with certain light-based readouts, and several appear to be chemically unstable in biological buffer (36).

Using most of these small-molecules in HAT assay development should be done with full knowledge of their considerable off-target liabilities. For example, many of their reported activities may become significantly attenuated if detergents and/or reducing agents are included in the reaction buffer. Furthermore, their reactive or aggregating tendencies may interfere with some assay readouts. Until more promising HAT inhibitors are developed (especially for HATs other than p300/CBP) that demonstrate better potency and target selectivity in biochemical and cell-based assays (among other criteria), we recommend that most currently reported small-molecule HAT inhibitors be restricted to monitoring assay performance (such as intra- and inter-run precision). Their use in more complex cell-based HAT assays should be used with extreme caution or in many cases avoided, as evidence of direct, selective target engagement in cells have not been demonstrated. While many of the reported HAT inhibitors produce decreases in histone acetylation in cells at low-to-mid micromolar compound concentrations, such readouts could also be produced by well-characterized promiscuous compounds, suggesting some observed decreases in histone acetylation may be due to a variety of nonspecific target engagements at these relatively high compound concentrations (36).

Recently, the discovery of A-485, a potent, selective indane spirooxazolidinedione inhibitor of p300 was reported by Lasko and colleagues (43). While external validation of this compound is pending, it appears promising as a useful chemical probe given strong

supporting evidence for potent and selective target engagement, including: (a) low nanomolar IC<sub>50</sub> values versus human p300/CBP, (b) approximately 1000-fold biochemical selectivity versus other HATs and greater than 100 unrelated biological targets, (c) biophysical evidence of target engagement (SPR, x-ray crystallography), (d) robust chemical characterization and SAR including the description of an inactive analog A-486, (e) nanomolar potencies in multiple cellular assays for histone acetylation, and (f) multiple lines of evidence consistent with target engagement in cells and *in vivo*. If using A-485 in HAT assays, we strongly encourage inclusion of its inactive analog A-486 as a negative control.

It is also worth mentioning Lys-CoA, a bi-substrate inhibitor (46). This compound, not a small-molecule *per se*, may be useful as a control compound in biochemical HAT assays involving p300. As it is cell-impermeable, this specific compound is not recommended in cell-based HAT assays, though cell-permeable analogs such as Tat-CoA have been reported (47).

**Table 3.** Reported HAT inhibitors. Most of the reported HAT inhibitors have structural alerts or poor physicochemical properties, and most inhibit HATs by nonspecific reactivity or aggregation. Most should be used in validating HAT assays with caution and with knowledge of their potential liabilities (36).

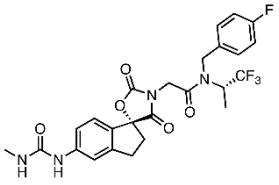
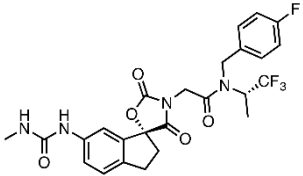
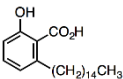
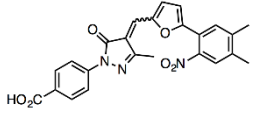
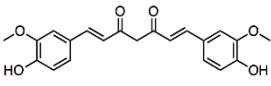
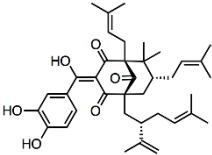
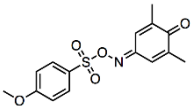
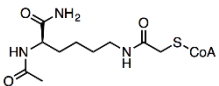
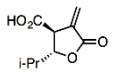
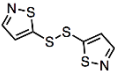
| Compound       | Chemical structure  | Reported target, <i>in vitro</i> IC <sub>50</sub> (μM) | Comments   | Reference |
|----------------|---|--|--|-----------|
| A-485          |  | p300-BHC, 0.010<br>CBP-BHC, 0.003                      | -External validation on-going, though promising potential chemical probe<br>-Nanomolar cellular activities<br>-Paired with A-486 inactive analog control | (43)      |
| A-486          |  | p300, > 50   | External characterization on-going; use with active analog A-485   | (43)      |
| Anacardic acid |  | p300, 8.5  | Aggregator   | (41)      |
| C646           |  | p300, 1.6  | Thiol-reactive   | (48)      |
| Curcumin       |  | p300, 25   | Thiol-reactive, aggregator, unstable   | (49)      |

Table 3. continues on next page...

Table 3. continued from previous page.

| Compound | Chemical structure  | Reported target, <i>in vitro</i> IC <sub>50</sub> (μM) | Comments         | Reference |
|----------|---|--|------------------|-----------|
| Garcinol |  | p300, 5  | Aggregator       | (50)      |
| L002     |  | p300, 1.98   | Thiol-reactive   | (51)      |
| Lys-CoA  |  | p300, 0.5  | Cell-impermeable | (46)      |
| MB-3     |  | Gcn5, 100  | Thiol-reactive   | (52)      |
| NU-9056  |  | Tip60, 2   | Thiol-reactive   | (53)      |

## Use of Orthogonal Assays/Common Interferences

Assay technologies are subject to various modes of compound-mediated interference (**Table 1**). Specific modes of interference for several assay technologies are also described in further detail in the subsequent section “BIOCHEMICAL HAT ASSAYS”. It is best practice to perform at least one orthogonal assay method to help confirm actual modulation of HAT activity (11,17,54). Depending on project and test compound specifics, a second orthogonal assay may also be useful to provide additional mechanistic confidence and further de-risk interference.

In the authors’ opinion, the gold standard of confirmatory biochemical HAT assays is some variation of the radiolabeled acetyl-CoA filter-binding method because: (a) it offers excellent signal:noise ratio, (b) it is a direct measurement of substrate acetylation, (c) it does not require much specialized instrumentation aside from a scintillation counter, (d) and is not prone to many of the common interference modalities seen in other assay types because test compounds are removed by filtration. While it requires specialized instrumentation, chromatographic separation coupled to mass spectrometry (i.e., LC-MS) is another high-quality HAT assay format.

There are numerous combinations of primary assays and orthogonal assays. The choice of primary and orthogonal assays will depend on a variety of factors (discussed in prior sections). In general, indirect primary assays should be paired with direct orthogonal assays, while direct primary assays can be paired with direct and/or indirect orthogonal assays (**Table 4**). Note that compound activity in both a primary and an orthogonal assay does not completely rule out compound-mediated interference. For example, many of the

assays discussed in this chapter are (in principal) susceptible to light-based interferences across multiple assay formats, which can be analyzed with appropriate interference counter-screens.

HAT systems will almost inevitably show some degree of susceptibility to generalized compound-mediated assay interferences (so-called because they will often modulate biological targets regardless of technology), such as nonspecific reactivity or aggregators. Additional studies should also confirm tractable mechanisms of target modulation by test compounds, as HATs sensitive to nonspecific modes of target modulation by thiol reactivity, redox activity, chelation, or aggregation may still show activity, albeit poorly tractable, in orthogonal assays.

**Table 4.** Potential primary assay-orthogonal assay pairings.

| Primary assay                             | Potential orthogonal assays   | Comments   |
|---|---|--|
| Fluorometric, enzyme-coupling (indirect)  | -Filter-binding radiolabel<br>-Antibody-based (Western, ELISA, Alpha)<br>-Scintillation proximity<br>-MS*<br>-Fluidic mobility* | -Pair indirect primary assay with direct orthogonal assay<br>-Caution when pairing with light-based orthogonal assay readouts without separation steps   |
| Alpha technology (AlphaScreen, AlphaLISA) | -Filter-binding radiolabel<br>-MS*<br>-Fluidic mobility*<br>-Scintillation proximity<br>-Fluorometric,<br>-Enzyme-coupling      | -Pair direct primary assay with direct and/or indirect orthogonal assays<br>-Prioritize a non-antibody-based orthogonal assay<br>-Caution when pairing with light-based orthogonal assay readouts without separation steps |
| TR-FRET                                   | -Filter-binding radiolabel<br>-MS*<br>-Scintillation proximity<br>-Fluidic mobility*<br>-Enzyme-coupling                        | -Pair direct primary assay with direct and/or indirect orthogonal assays<br>-Prioritize a non-antibody-based orthogonal assay<br>-Caution when pairing with light-based orthogonal assay readouts without separation steps |
| Fluidic mobility                          | -Filter-binding radiolabel<br>-Scintillation proximity<br>-MS*<br>-Fluorometric<br>-Enzyme-coupling                             | Pair direct primary assay with direct and/or indirect orthogonal assays  |
| MS  | -Filter-binding radiolabel<br>-Scintillation proximity<br>-Fluidic mobility*  | -Pair direct primary assay with direct and/or indirect orthogonal assays   |

\* MS and fluidic mobility orthogonal assays useful to minimize light-based compound interferences, but their implementation may be limited by available instrumentation and resources.

*Table 4. continues on next page...*

Table 4. continued from previous page.

| Primary assay           | Potential orthogonal assays  | Comments  |
|-------------------------|--|---|
|                         |  | -Can also monitor Ac-CoA depletion, CoA production by MS; non-MS-based orthogonal assay still recommended   |
| Scintillation proximity | -Antibody-based (Western, ELISA, Alpha)<br>-MS*<br>-Fluidic mobility*<br>-Fluorometric<br>-Enzyme-coupling<br>-Filter-binding radiolabel | -Pair direct primary assay with direct and/or indirect orthogonal assays<br>-Caution when pairing with light-based orthogonal assay readouts without separation steps |

\* MS and fluidic mobility orthogonal assays useful to minimize light-based compound interferences, but their implementation may be limited by available instrumentation and resources.

## Assay Validation

Assay validation represents a critical last step in assay development and optimization, but often overlooked or rushed. Best practices for HTS assay validation should include:

- Characterization of reagent stability.
- Characterization and correction of plate effects.
- Characterization and optimization of signal variability (e.g., intra-plate, inter-plate, day-to-day).
- Characterization of assay performance using reference compounds (e.g., intra-plate, inter-plate, day-to-day).
- Characterization of HTS performance using mini-compound libraries such as LOPAC (e.g., inter-plate, day-to-day).

Assay performance can be assessed with several statistical methods during both the validation and production phases:

- *Z'* factor (55). This calculation can monitor assay signal dynamic range and data variation on each microplate, as well as assay performance over time when examining multiple microplates.
- Minimum significant ratio (MSR) (56). In a robust assay, a given compound should have similar bioactivity across independent experiments. This calculation utilizes reference compound activity to monitor assay performance and variability. For an excellent discussion, the reader is referred to Minimum Significant Ratio – A Statistic to Assess Assay Variability.

For more detailed discussion on assay validation, the reader is referred to HTS Assay Validation and *In Vivo* Assay Guidelines.

## Section Summary

Constructing and validating a robust assay capable of identifying modulators of HAT activity requires careful thought and experimental optimization of multiple, often competing parameters.

## Biochemical HAT Assays

### Introduction

This section describes special considerations for multiple types of biochemical HAT assays. For several assay platforms, generic HAT assay protocols are provided.

### Filter-Binding Radiolabeled HAT Assays

Radiolabeled substrate HAT assays were some of the first HAT assays to be reported. Benefits include directly measuring acetylated histones, intrinsic high signal:noise ratios which can facilitate lower amounts of enzyme and substrate, absence of required protein labels, and resistance to certain forms of compound-mediated assay interference such as compound fluorescence. The main drawback is the use of radioisotopes, which necessitates additional safety disposal protocols and regulatory compliance.

The assay principle is relatively simple: acetyl-CoA substrate is labeled with radioactive tritium ( $[^3\text{H}]$ ) or carbon ( $[^{14}\text{C}]$ ) on the acetyl moiety. HATs catalyze the transfer of the labeled acetate to histone-based substrates, and the amount of radiation can be quantified by capturing the radiolabeled histone-based product and quantifying radioactivity, usually through a scintillation counter. HAT activity is therefore proportional to radioactivity (**Figure 4**).

Even though filter-based radiolabeled HAT assays are generally less susceptible to light-based forms of compound-mediated interference relative to homogenous light-based assay formats (because in filter-based assays most test compounds are removed by filtration prior to scintillation counting), orthogonal assay(s) should still be performed to rule out compound-mediated interference. For example, scintillation quenchers can still interfere with the assay readout if they are not separated from the radiolabeled analyte by filtration. Another source of potential interference are compounds that prevent the binding of acetylated product onto capture matrix.

In parallel with liquid scintillation counting, reaction aliquots can be separated by SDS-PAGE and analyzed by autoradiography to verify radiolabeled acetate incorporation onto the desired substrate.

The following is a sample protocol for a generic radioisotope-based HAT assay. Specific parameters may vary for a particular assay. Specific reagents, concentrations, volumes, dispensing procedures, and time intervals would need to be optimized for a particular application.



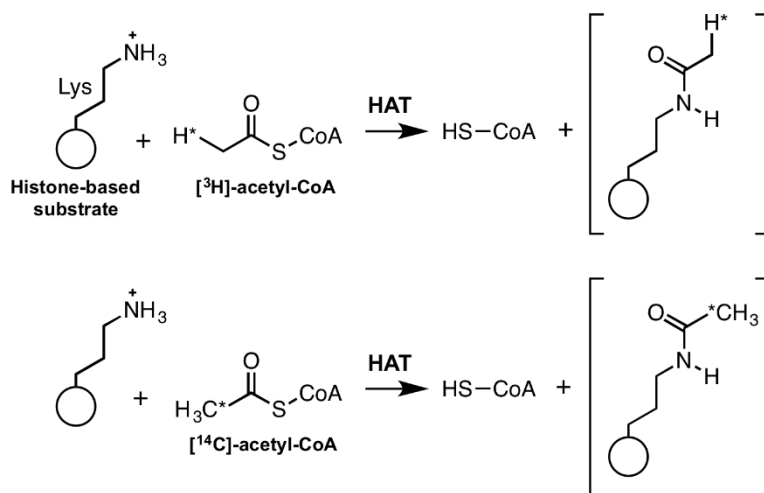


**Figure 4. General schematic of cell-free radioisotope HAT assays.** Radiolabeled acetyl-CoA is used to directly quantify HAT activity, either in the form of (top) [<sup>3</sup>H]-acetyl-CoA or (bottom) [<sup>14</sup>C]-acetyl-CoA. After the HAT reaction, histones are bound to a capture matrix (e.g., filter), and unreacted radiolabeled acetyl-CoA is removed by washing steps. The amount of radiolabeled (\*) acetate incorporated onto histone-based substrates (brackets) is proportional to HAT activity.

### Consumable specifications

- Microplates: standard-volume polystyrene 384-well microplates (final reaction volume = 15  $\mu$ L).
- For lower-throughput applications, reactions can be performed in Eppendorf-style tubes instead of microplates.

### Instrumentation specifications

- Compound dispenser: capable of dispensing in nL increments; usually acoustic droplet or pintool transfer.
  - Alternatively, serial dilutions can be made and subsequently transferred by manual pipetting. In such cases, accurate and precise compound dispensation may require higher reaction volumes.
- Fluid dispenser: capable of dispensing in 0.5  $\mu$ L increments.
  - Alternatively, solution can be dispensed by serial pipetter or multichannel pipette.
- Liquid scintillation counter.

### Solutions (for total reaction volume, 15 $\mu$ L)

- 5X reaction buffer: 250 mM Tris, pH 8.0, 250 mM NaCl, 0.5 mM EDTA, 0.05% Triton X-100 (v/v), 250  $\mu$ g/mL BSA, 5 mM DTT.
- 1X reaction buffer: 50 mM Tris, pH 8.0, 50 mM NaCl, 0.1 mM EDTA, 0.01% Triton X-100 (v/v), 50  $\mu$ g/mL BSA, 1 mM DTT.

- Reaction solution: 375 nM histones (H3H4 tetramers), 15 nM HAT enzyme in 1X reaction buffer (dilute concentrated histones and HAT enzyme with appropriate volumes of H<sub>2</sub>O and 5X reaction buffer).
- Control solution: 375 nM histones (H3H4 tetramers), 0 nM HAT enzyme in 1X reaction buffer (dilute concentrated histones with appropriate volumes of H<sub>2</sub>O and 5X reaction buffer).
- Acetyl-CoA solution: 7.5 μM [<sup>3</sup>H]-acetyl-CoA in 1X concentration (dilute concentrated enzyme stock solution with appropriate volumes of H<sub>2</sub>O and 5X reaction buffer).
- Compounds: 10 mM DMSO stocks.

### Safety and disposal considerations

- Radioactive waste should be disposed of in concordance with institutional radioactive safety protocols.
- Always wear personal protective equipment when handling radioactive material, including lab coat, gloves, and eye protection.

### Sample protocol

1. Dispense compounds and vehicle controls in microplates.
  - Ensure equal organic solvent in each reaction.
  - Add 15 nL DMSO in control wells with fluid dispenser; 15 nL test compound in test wells (to assay at 10 μM final compound concentration) with compound dispenser.
2. Dispense reaction buffer into appropriate wells.
  - Add 10 μL reaction solution into test wells and positive control wells with fluid dispenser.
  - Add 10 μL control buffer into negative control wells with fluid dispenser.
3. Allow compounds to pre-incubate for 10 min at 30°C.
  - Perform incubation in temperature-controlled microplate oven.
4. Initiate HAT reaction by adding acetyl-CoA solution.
  - Add 5 μL acetyl-CoA solution into all wells with fluid dispenser.
  - Seal microplates.
5. Allow system to equilibrate.
  - Mix reaction contents with microplate shaker for 1 min.
  - Centrifuge microplates for 1 min.
6. Allow HAT reaction to proceed for 10 min at 30°C.
  - Perform incubation in temperature-controlled microplate oven.
7. Quench reaction.
  - Transfer 12.5 μL aliquot of reaction mixture into 12.5 μL neat isopropanol with pipette. Gently mix.
8. Transfer reaction aliquots onto filter paper.

- Transfer 20  $\mu$ L aliquot of quenched reaction solution from Step 7 to Whatman P-81 phosphocellulose paper. Allow to air dry completely (approximately 30 min).
- 9. Wash filter paper.
  - Wash filter paper disks with 50 mM  $\text{NaHCO}_3$ , pH 9.0 for 5 min with gentle agitation. Repeat 3 times.
  - Wash filter paper disks with acetone for 5 min with gentle agitation. Allow to air dry completely.
- 10. Read samples.
  - Transfer washed filter paper disks from Step 9 to 20 mL liquid scintillation vials containing 5 mL liquid scintillation cocktail and briefly vortex.
  - Read radioactivity of samples using liquid scintillation counter.
- 11. Analyze data.
  - Calculate the average readout for the negative controls. This value constitutes the background signal.
  - Subtract the background signal from the remaining reactions.
  - Calculate the average readout for the positive (vehicle) controls. This value constitutes the uninhibited reaction.
  - Calculate the percent HAT modulation for each reaction. Percent HAT inhibition (%) =  $(1 - (\text{test solution}/\text{positive control})) \times 100$ .

### Miscellaneous notes

- Phosphocellulose filter disks are often used as a capture matrix (57).
- DTT and other reducing agents can be used in this assay.
- Labelled acetyl-CoA can often be mixed with unlabeled acetyl-CoA. This reduces the amount of total assay radioactivity, and expensive radiolabeled substrate. The exact ratio labelled:unlabelled acetyl-CoA will depend on the specific radioactivity of labelled acetyl-CoA, instrument settings, assay parameters, and amount of radioisotope transferred to capture matrix.
- Ensure scintillation counter is properly calibrated.
- Filter-binding assays are end point assays, but they can be adapted for continuous reaction monitoring by sampling reaction aliquots.
- Always keep solutions containing proteins and peptides on ice when not in use.

Additional examples/protocols: For additional examples of radioisotope-based HAT assays, we refer the reader to several studies (11,16,17,30,57).

### Other Radiolabeled HAT Assay Methods

Several other radiolabeled methods have been reported for assaying HAT activity:

Scintillation proximity assays (SPA) have been applied to HATs (26,43,58). SPA is a solid-phase homogenous technique that couples a scintillation matrix (beads; coated plate, “FlashPlate”) to a capture system (e.g., anti-histone antibody, or biotin-tagged histones and streptavidin-coated beads/plates). Histone-based products can be captured in close

proximity to the matrix surface. In certain cases, histone-based products can also be immobilized to the matrix (i.e., microplate) without special tags through nonspecific adsorption. When a radiolabeled product is in close proximity to the scintillator, the signal from radioactive decay of the radioisotope is amplified. Unbound radiolabeled acetyl-CoA in solution is not in close enough proximity to the scintillation matrix, and therefore does not generate signal. An advantage of SPA is that it does not require a separation event such as filter-binding. Consequently, SPA is an attractive assay technique when the detection sensitivity of radiolabels is needed in a high-throughput setting. Development and optimization of SPA-based HAT assays utilizes the same general assay development principles described in this chapter. For additional information on SPA assay development, several reviews may be useful (24,59).

Some SPA-specific comments include:

- Reducing agents such as DTT should not interfere with SPA-based technologies.
- A potential source of compound-mediated interference in SPA are compounds that disrupt scintillation (24). For example, such inner-filter effects can be quite significant in certain scintillation proximity assays where photon emission occurs in the blue region (which can be quenched by yellow-colored compounds) (25). Orthogonal assays, including filter-binding assays that remove interfering compounds, can help identify this type of assay interference.
- Excessive radiolabels can lead to high background signals, causing nonproximity effects. This can be countered by reducing the concentration of radiolabels, or aspirating reaction solution before measuring.
- Nonspecific protein binding to either beads or surfaces can also cause high background. This effect can often be mitigated with blocking agents, change of matrix, or detergent.
- Interactions between anionic acetyl-CoA and cationic histone interactions can also lead to nonspecific background signal, though these can be disrupted with appropriate selection of quenching agent to disrupt this interaction (e.g., guanidine HCl) (58). This effect can be identified by high background signal in the presence of acetyl-CoA and histone-based substrates and the absence of HAT enzyme.
- High-throughput plate-based SPA requires specialized instrumentation, such as PMT-based microplate-compatible scintillation counters or CCD-based readers (25).

Autoradiography of HAT reactions is well-described in the literature (60).

Autoradiography methods are typically employed for lower-throughput confirmatory applications. If reaction aliquots are separated by gel chromatography, they can be useful for confirming acetylation of specific substrates in multi-protein reaction mixtures (61). Reactions can also simply be applied to a capture matrix (e.g., filter paper, nitrocellulose membrane) and assayed for total radioactivity (60,62). Radiation can be quantified by radiodensitometry. The main drawback is lower-throughput. For example, gel separation requires a separate gel lane for each reaction. Furthermore, signal acquisition depends on

the specific radioisotope and the amount of radioisotope per reaction. Development can require hours to days of product exposure to film.

## Antibody-Based HAT Assays

Another common class of HAT assays probes for histone acetylation using antibodies targeting either specific acetylated histone residues (e.g., H3K27ac) or nonspecific histone acetylation (e.g., H3ac). These assays directly probe for the acetylated histone-based product. Antibody-based assays are versatile and come in several varieties, including Western blot, slot blot (a modified Western blot), and ELISA. For examples of immunoassays, we refer the reader to several studies (10,11,17).

For details on developing immunoassays, we refer readers to *Immunoassay Methods*. Some considerations for antibody-based HAT assays include:

- Certain chemotypes, such as acetimides, have been reported to interfere with acetylated histone antibodies (19). Useful counter-screens include a second, independent antibody, as well as orthogonal assays.
- Immunoassays are limited by the quality and specificity characteristics of the antibody. Verify antibody performance. Antibodies designed for specific acetylated histones have potential for significant cross-reactivity (63,64).

## Fluorometric HAT Assays

Cell-free fluorometric HAT assays are relatively inexpensive, are straightforward to establish, and require only standard HTS instrumentation. The assay principle is relatively simple: free CoA produced by the HAT reaction reacts with a sulfhydryl-scavenging probe such as *N*-[4-(7-diethylamino-4-methylcoumarin-3-yl)phenyl]maleimide (CPM), to form a highly fluorescent CoA-CPM adduct quantified by fluorescence intensity (**Figure 5**).

The actual acetylated histone product is not directly measured in this assay platform. Therefore, a significant drawback to this method is the significant burden of compound-mediated assay interference (17). The method also has a lower signal:noise ratio compared to radioisotopic methods. In principle, the detection of the CoA reaction product can serve as a convenient orthogonal assay to direct HAT assays. The decision to utilize this assay format, and whether to implement as a primary screen or orthogonal assay, will depend on multiple factors including: available resources, the availabilities of other orthogonal assays, the desired throughput and timelines at each project stage, and the expected test compound chemotypes. For instance, if many of the test compounds are colored or contain potential reactive groups, this assay format may not be an ideal choice due to the high likelihood of readout interference.

If choosing this method for assaying HAT activity, assay-specific counter-screens should be included to characterize any compound-mediated fluorescence interference (both quenching and auto-fluorescence) and CoA-scavenging reactions by test compounds. For details on performing these counter-screens, we refer the reader to several worked-out examples (14,16,17).

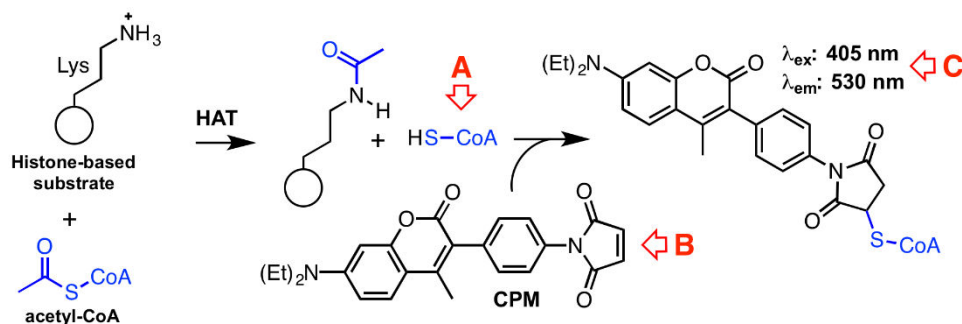


**Figure 5. General schematic of cell-free fluorometric HAT assays.** HATs produce acetylated histone-based products and free CoA (CoA-SH). After quenching the reaction, HAT activity is assayed by adding a sulfhydryl-scavenging probe, CPM, which reacts with CoA to produce highly fluorescent adducts. In absence of interference, the amount of fluorescence is proportional to HAT activity. There are three main sources of compound-mediated readout interference: (A), thiol-scavenging of CoA-SH by electrophilic test compounds; (B), formation of compound-CPM adduct by nucleophilic test compounds; and (C), fluorescence interference by test compounds (auto-fluorescence, quenching, inner-filter effects, light scattering).

Furthermore, at least one orthogonal assay that directly quantifies the protein product (acetylated histone) is all but required when utilizing this assay method.

The following is a sample protocol for a generic CPM-based HAT assay. Specific parameters may vary for a particular assay. Specific reagents, concentrations, volumes, dispensing procedures, and time intervals would need to be optimized for a particular application.

### Consumable specifications

- Microplates: low-volume black polystyrene 384-well microplates (final reaction volume = 20  $\mu$ L)
- Note: this assay can be miniaturized to 1536-well format with reaction volumes less than 5  $\mu$ L (11).

### Instrumentation specifications

- Compound dispenser: capable of dispensing in nL increments; usually acoustic droplet or pintool transfer.
  - Alternatively, serial dilutions can be made and subsequently transferred by manual pipetting. In such cases, accurate and precise compound dispensation may require higher reaction volumes.
- Fluid dispenser: capable of dispensing in 0.5  $\mu$ L increments.
  - Alternatively, solution can be dispensed by serial pipetter or multichannel pipette.
- Microplate reader: capable of reading fluorescence intensity.

### Solutions (for total reaction volume, 15 $\mu$ L)

- 5X reaction buffer: 250 mM Tris, pH 8.0, 250 mM NaCl, 0.5 mM EDTA, 0.05% Triton X-100 (v/v), 250  $\mu$ g/mL thiol-deactivated BSA.
- 1X reaction buffer: 50 mM Tris, pH 8.0, 50 mM NaCl, 0.1 mM EDTA, 0.01% Triton X-100 (v/v), 50  $\mu$ g/mL thiol-deactivated BSA.
- Substrate solution: 150  $\mu$ M histone peptide, 30  $\mu$ M acetyl-CoA in 1X reaction buffer (dilute concentrated peptide and acetyl-CoA stock solutions with appropriate volumes of H<sub>2</sub>O and 5X reaction buffer).
- Enzyme solution: 60 nM HAT enzyme; add appropriate amounts of 5X reaction buffer in 1X concentration (dilute concentrated enzyme stock solution with appropriate volumes of H<sub>2</sub>O and 5X reaction buffer)
- Quenching/probe solution (concentrated): 80  $\mu$ M CPM in 1:1 H<sub>2</sub>O:EtOH, 1% DMSO solution.
- Test compounds: 10 mM DMSO stocks.

### Sample protocol

1. Dispense compounds and vehicle controls in microplates.
  - Ensure equal organic solvent in each reaction.
  - Add 15 nL DMSO in control wells with fluid dispenser; 15 nL test compound in test wells (to assay at 10  $\mu$ M final compound concentration) with compound dispenser.
2. Dispense reaction buffer into appropriate wells.
  - Add 5  $\mu$ L reaction buffer (1X) into control wells, 2.5  $\mu$ L reaction buffer into test wells with fluid dispenser.
3. Dispense concentrated enzyme solution into appropriate wells.
  - Add 2.5  $\mu$ L enzyme in reaction buffer into test wells with fluid dispenser.
4. Allow compounds to pre-incubate for 5-10 min at 30°C.
  - Perform incubation in temperature-controlled microplate oven.
5. Initiate HAT reaction by adding concentrated acetyl-CoA solution.
  - 10  $\mu$ L substrate solution in reaction buffer into all wells with fluid dispenser.
  - Seal microplates.
6. Allow system to equilibrate.
  - Mix reaction contents with microplate shaker for 1 min.
  - Centrifuge microplates for 1 min.
7. Allow HAT reaction to proceed for 1 h at 30°C.
  - Perform incubation in temperature-controlled microplate oven.
8. Quench reaction and initiate CoA-CPM adduct formation by adding quenching/probe solution.
  - Add 5  $\mu$ L quenching/probe solution into all wells with fluid dispenser.
9. Allow thiol-probe reaction to proceed for 15 min at room temperature
  - Mix reaction contents with microplate shaker for 1 min.
  - Centrifuge microplates for 1 min.
10. Read fluorescence intensity of microplate wells.

- Settings: excitation 405 nm; emission 535 nm.
11. Analyze data.
- Calculate the average readout for the negative controls. This value constitutes the background signal.
  - Subtract the background signal from the remaining reactions.
  - Calculate the average readout for the positive (vehicle) controls. This value constitutes the uninhibited reaction.
  - Calculate the percent HAT modulation for each reaction. Percent HAT inhibition (%) =  $(1 - (\text{test solution}/\text{positive control})) \times 100$ .

### Miscellaneous notes

- DTT and other reducing agents are omitted from this assay, as they will react with the thiol-scavenging probe. This includes TCEP, whose phosphine lone pair of electrons can also react with maleimides (65).
- Besides CPM, there are several other maleimide-based fluorogenic probes available. We refer the reader to an excellent comparative study of such probes (12).
- Note some HAT enzymes may also contain free cysteine residues that may contribute to background.
- BSA can be highly useful for stabilizing HAT reactions, especially in the prolonged reaction times often necessitated in large-scale HTS settings. As BSA contains multiple cysteine residues (greater than 30 in mature BSA), free thiols on BSA must be deactivated (“capped”) to prevent interference with sulfhydryl-scavenging probes. A facile workaround involves treating BSA with excess N-ethylmaleimide (NEM) (taking into account BSA contains multiple cysteine residues), and multiple rounds of dialysis to remove excess, unreacted NEM (11,13). Ensure thiol inactivation by performing a test reaction with CPM and measuring the fluorescence intensity under assay-like conditions.
- Substrates may contain free cysteine residues. To reduce background from probe-peptide/protein adducts, it may be necessary to replace cysteine residues with alternative residues (e.g., peptide synthesis or site-directed mutagenesis for recombinant proteins), or alternatively treated with NEM or similar reagent.
- CPM and other probes can usually be prepared as 10 or 50 mM stock solutions in DMSO. Store in -20°C, protect from light.
- Protect probe solutions from light. Prepare working probe solutions fresh to prevent degradation/non-specific hydrolysis in alkaline, aqueous conditions (66).
- The reaction between free CoA and maleimide probes is relatively fast, usually on the order of minutes (12). However, during assay optimization verify the reaction is complete by monitoring fluorescence intensity over time. Look for a signal plateau to signify reaction completion. Continued increases in fluorescence intensity may indicate inadequate mixing, insufficient reaction quenching, or CPM-protein adduct formation.
- Ensure microplate reader is properly calibrated.



- Fluorometric assays are end point assays given the ability of thiol-scavenging probes to modulate HAT activity. Like filter-binding assays, they can be adapted for continuous reaction monitoring by sampling reaction aliquots.
- Always prepare solutions containing proteins and peptides on ice. Keep on ice when not in use.
- An advantage of this assay is that the protein product may also be assayed by an orthogonal method such as Western blot which may be useful for examining compound-mediated assay interference (10,17).

Additional examples/protocols: For additional examples of fluorometric HAT assays, we refer the reader to several studies (10-14).

### Microfluidic-Based HAT Assays

The development of a microfluidic mobility shift platform for cell-free, fluorescence-based HAT assays provides a useful approach for both HTS and mechanistic analysis of HAT modulators (21,22,67). The assay principle is straightforward: fluorescent HAT substrates (peptides of histones H3 and H4 tails) are acetylated by a given HAT system, altering the charge-to-mass ratio on the peptide. Subsequently, acetylated peptides are separated from non-acetylated peptides *via* electrophoretic separation, enabling distinguishable fluorescent detection of each peptide. The ratiometric measurement of substrate/product fluorescence peak heights gives the percent conversion that can be directly related to HAT enzyme activity once correcting for non-enzymatic acetylation (**Figure 6**).

An advantage of this assay platform is its versatility in facilitating compound discovery by HTS and also compound mechanism of action studies. A hydroxylamine-based reaction quench allows for uniform HAT assay conditions amenable to HTS of large compound libraries in 384-well plates. Small sample aliquots and relatively fast electrophoretic separations allow for multiple end-point measurements of a single reaction. Therefore, when the hydroxylamine-based quench is not used, consecutive measurements of HAT activity can be obtained to determine time-dependent HAT modulation. An additional advantage of this assay platform is the direct measurement of the acetylated product. Therefore, this method can be an effective counter screen to triage hits from high-throughput primary screens, such as the CPM assay, that may yield several compound-mediated assay interference molecules. Lastly, the microfluidic aspect of this assay allows for following enzymatic reactions in small reaction volumes with a minimum amount of sample, increasing its feasible applications from an economic perspective.

As this assay technique directly measures fluorescently-labeled, electrophoretic-separated acetylated histone products, the assay readout is not subject to certain types of compound-mediated interference. For instance, light-based interference compounds are usually separated by the electrophoresis. However, like the other methods described in this chapter, the enzymatic system itself will be susceptible to nonspecific sources of bioassay interference, such as redox cycling compounds, aggregators, and nonspecific reactivity. The magnitude is dependent on the experimental conditions (target, concentrations, detergent, scavenging reagents, etc.).

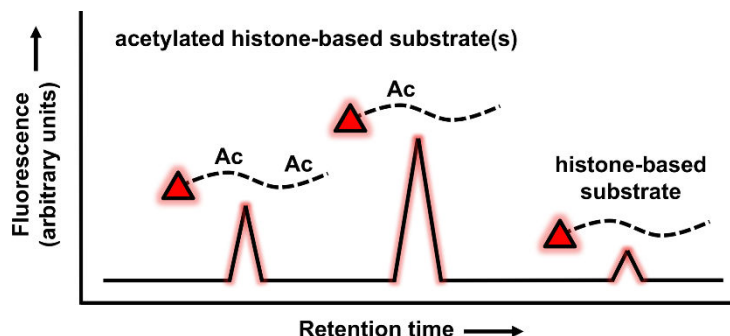


**Figure 6.** General schematic of the microfluidic mobility shift HAT assay. Acetyl-CoA and fluorescent-labeled histone peptides are the HAT substrates. Reaction aliquots are analyzed by microfluidic electrophoresis. Lysine acetylation alters the retention time of the histone peptide *via* decreasing product net charge and increasing product mass. HAT activity is proportional to the amount of acetylated product produced.

A critical factor in experimental design is substrate choice. Users should verify that the acetylated and non-acetylated histone products can be adequately resolved. This is often achievable for peptide-based histone substrates, but may be considerably more difficult for larger (> 30-mer), multiply-charged histone-based substrates, as electrophoretic separation is based upon mass/charge ratios. The net charge ideal for commercial microfluidic capillary electrophoresis instruments is from +3 to -3, and the substrate histone peptides used for HAT assays typically have net charges ranging from +3 (for the H4 peptide) and +4 (for the H3 peptide). Therefore, this system presents challenges for HAT assays requiring larger histone-based substrates (e.g., full-length histones, chaperones). The choice of fluorophore for microfluidic assays will depend on the light source and detector, as well as the spectral properties and other behaviors of the labeled analyte in the assay. Common fluorophores for the EZ-Reader include FITC, 5-FAM, and Alexa 488.

The following is a sample protocol for a generic microfluidic mobility shift HAT assay. Specific reagents, concentrations, volumes, dispensing procedures, and time intervals should be optimized for a particular application.

### Consumable specifications

- 384-well microplates from E&K Scientific (EK2253): 58  $\mu$ L well capacity volume with a U-bottom, clear, natural polypropylene (final reaction volume = 30  $\mu$ L).
- PerkinElmer ProfilerPro<sup>TM</sup> Separation Buffer (Cat# 760367): Prior to the first use of the separation buffer, add 2 mL of coating reagent 8 (CR8) that comes with the purchase of the separation buffer. CR8 is a positively-charged additive for coating the Lab-Chip sipper channels. Store separation buffer at 4°C but warm to room temperature before use.

## Instrumentation specifications

- PerkinElmer Lab-Chip EZ-Reader instrument (obtains fluorescence measurements following microfluidic electrophoresis).
  - Suggested initial electrophoresis separation conditions: downstream voltage of -500 V, upstream voltage of -2500 V, and a pressure of -1.5 psi for both FITC H3/H4 peptides
- Lab-Chip EZ Reader 12-sipper chip: capable of sipping as little as 10 nL reaction mixture while simultaneously monitoring 12 reactions (proper treatment and troubleshooting points are listed under *Miscellaneous notes*).

## Substrate peptide sequences

- FITC-H4 (3-14, FITC-Ahx-RGKGGKGLGKGG [Ahx = 6-amino-hexanoic acid])
- FITC-H3 (5-20, FITC-Ahx-TARKSTGGKAPRKQL)
- These peptides were synthesized by automated peptide synthesis on Rink amide resin, using Fmoc-based chemistry. Peptides can be synthesized in-house with appropriate instrumentation. Alternatively, custom peptides can be synthesized by commercial vendors.

## Solutions (for total reaction volume, 30 $\mu$ L)

- 10X reaction buffer: 500 mM HEPES, pH 7.5, 500 mM NaCl, 20 mM EDTA.
- Miscellaneous assay components (prepare new each experiment): 0.5% Triton X-100 (v/v) in PBS (10X), 20 mM DTT in PBS (10X), 0.5 M hydroxylamine in PBS (for reaction quench).
- Master mix solution: 1X reaction buffer, 0.05% Triton X-100 (v/v), 2 mM DTT, 2  $\mu$ M FITC-H3/H4 peptide, 150 nM p300.
- Quenching solution: 0.5 M hydroxylamine in PBS, pH 7.5.
- Test compounds: 10 mM DMSO stocks.

## Sample protocol

1. Dispense 0.5  $\mu$ L of compounds (dissolved in DMSO) and vehicle controls in screening microplates.
  - a. When screening large compound libraries for inhibitor discovery, include samples having no enzyme as this will represent the percentage of non-enzymatic acetylation.
  - b. DMSO percentage for the assay is 1.7%. Higher DMSO amounts will decrease enzyme activity.
2. Dispense 26.5  $\mu$ L master mix into appropriate wells.
3. Allow compounds to pre-incubate with master mix solution for 10 min at room temperature.
4. Initiate HAT reaction by adding 3.0  $\mu$ L of 10  $\mu$ M acetyl-CoA (total reaction volume – 30  $\mu$ L).
5. Allow HAT reaction to proceed for 10-15 min at room temperature.

- a. When performing an end-point analysis, keep product accumulation between 10-15%.
- b. For kinetic measurements, transfer the microplate to the PerkinElmer Lab-Chip EZ-Reader immediately following the addition of acetyl-CoA to begin obtaining fluorescence measurements.
6. If quenching the reaction, add 5  $\mu\text{L}$  of 0.5 M hydroxylamine to each well.
7. Read fluorescence intensity of microplate wells.
  - a. Light source: LED.
8. Analyze data.
  - a. Calculate averages and standard deviations of percent conversion for negative (no inhibitor) controls and positive (vehicle) controls.
  - b. Calculate averages and standard deviations of percent conversion for inhibitor samples.
  - c. Calculate the HAT percent activity: normalize the percent conversions by setting the negative controls to 0% and the positive control to 100% conversion.

### Miscellaneous notes

- The separation resolution (SR) is calculated using the formula  $SR = \Delta L / 2(\sigma_1 + \sigma_2)$ , where  $\Delta L$ ,  $\sigma_1$ , and  $\sigma_2$  are the distance between peaks, standard deviation of the first peak, and standard deviation of the second peak, respectively.
- Protect fluorescent peptide solutions from light to prevent photo-catalyzed degradation.
- Always prepare solutions containing proteins and peptides on ice. Keep on ice when not in use.
- Prior to use in an experiment, proper treatment for the Lab-Chip EZ Reader 12-sipper chip includes:
  - Washing entire chip with distilled water thoroughly, followed by a complete drying *via* aspiration.
  - Washing the chip wells using separation buffer (2 x 250  $\mu\text{L}$ ), followed by filling the smaller wells with 250  $\mu\text{L}$  and the two larger wells with 500  $\mu\text{L}$  of separation buffer.
- Following completion of an experiment, proper treatment for the Lab-Chip EZ Reader 12-sipper chip and EZ Reader instrument includes:
  - Filling 12 wells within a screening microplate with 5% DMSO in water and running the Lab-Chip EZ reader instrument at 15 cycles with a final delay time of 300 s. while running at a pressure of -4.0 psi. This will rinse the chip sipper channels with the 5% DMSO followed by a 300 s rinse with separation buffer.
  - For the EZ Reader instrument, switch out separation buffer for distilled water and wash the lines for 10 min prior to either starting a new experiment or shutting the instrument down. Carryover may occur from one experiment to another if lines are not washed.

- Due to evaporation of reaction solution, the maximum kinetic runtime of a single experiment is 40 h when screening microplates utilizing 500  $\mu\text{L}$  reactions. When less than 500  $\mu\text{L}$  is used, wells will dry out quicker and runtimes should be reduced. Additionally, chip wells should be refreshed by removing old separation buffer and adding fresh separation buffer every 12 h.
- It is important to be vigilant for declining chip performance, which can occur due to blockage of a sipper, presence of air bubbles, or standard wear and tear. Signs a chip may need to be refreshed or retired include a lack of reproducibility among replicate samples, broadening of peak shape, or delayed elution of peptide when compared to a properly functioning chip.
- In cases when a chip shows signs of failing (potentially due to sipper blockage or heavy usage), we have found the following protocol can be useful to refresh and restore chip performance:
  - Run the Lab-Chip EZ-Reader instrument at a positive pressure of 4.0 psi for 1 h with no microplate loaded. This can aid the clearance of any blockages from the channel. Follow this with an additional wash step, by filling 12 wells within a microplate with 5% DMSO in water and running the EZ-Reader instrument at 50 cycles with a final delay time of 300 s and pressure of -4.0 psi. This wash should be performed for approximately 1 h.
  - Purchase a fresh bottle of separation buffer. Since reaction solutions are circulated through a bottle of separation buffer, poorly performing chip sipper channels can often be resolved by simply using a fresh bottle of separation buffer.

## MS-Based HAT Assays

Mass spectrometry (MS) is an analytical technique that ionizes analytes and separates them based on their mass-to-charge ratios ( $m/z$ ). Components of HAT reactions can be ionized through one of several technologies (e.g., electrospray, MALDI), then passed through an electric field where the ionized analytes are measured based on their  $m/z$  ratios. Prior to ionization, HAT reaction components can be separated by liquid chromatography and/or subjected to various extraction/enrichment strategies such as solid-phase extraction (SPE).

MS-based detection allows for the monitoring of multiple analytes in a single injection, which facilitates the detection of substrate, product, an internal standard (IS), and/or an orthogonal reaction. For instance, the net loss of histone lysine methylation catalyzed by an  $\alpha$ -ketoglutarate-dependent recombinant demethylase can be simultaneously quantified by monitoring the production of modified histone and also succinate, with the conversion of  $\alpha$ -ketoglutarate to succinate being an orthogonal reaction (**Figure 7**). Similarly, in addition to monitoring histone-based substrates and products themselves, the production of histone acetylation states can also be validated by monitoring the deacetylation of acetyl-CoA and the production of free CoA (23). Measuring orthogonal reaction products can enable real-time identification of signal enhancement or suppression.

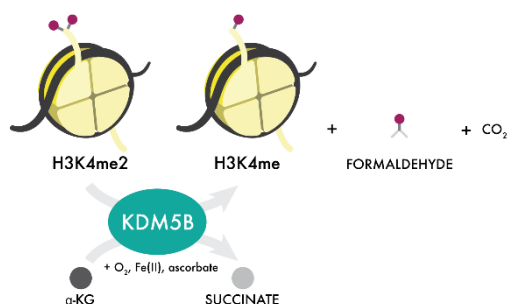


**Figure 7. Measuring histone modifications by MS.** Shown is a biochemical reaction demonstrating the KDM5B-catalyzed demethylation of H3K4 and the concurrent production of succinate. Similarly, HAT reactions can be monitored by measuring the production of acetylated histone products as well as the concurrent production of CoA/loss of acetyl-CoA (see **Figure 1**).

As a representative example of available HTS-compatible MS technology, the Agilent RapidFire (RF) MS system is a micro-SPE system enabling rapid sample analysis (7-10 s/sample) from 96- and 384-well assay plates. Aspirated sample is loaded onto a micro-SPE cartridge, washed (to remove MS-incompatible components such as salts), and immediately reverse-eluted to the mass spectrometer. The RF-MS system is amenable to wide range of SPE packing materials (e.g., C4, C18, HILIC). The SPE packing method is chosen based on the desired levels of chromatographic separation and sample clean-up, and analyte properties (e.g., polarity, solubility). Combined with the ability of pairing various mass spectrometers such as QQQ (triple quadrupole), ToF (Time of Flight), and QToF (quadrupole ToF), RapidFire analysis can offer a versatile system capable of measuring HAT-relevant analytes. Note specific instrumentation and monitoring conditions (e.g., multiple reaction monitoring with triple quadrupoles, full-scan monitoring with ToF) will depend on multiple factors, including analyte, throughput, and mass accuracy specifications.

When performing a HTS run for small molecules or biological samples, minimizing cross contamination and run times is critical. Including blank injection(s) after each sample injection reduces cross contamination due to sample carryover, although this increases run times by at least two-fold. Hence, it is vital to ensure complete elution of the sample from the SPE cartridge by altering the RF method (flow and/or duration during each step) or by using appropriate mobile phases. The optimal solvent system will depend on the specific analytes being tested. Factors to consider include the solubility, chemical stability, and chromatographic properties of the specific analyte(s) in a given solvent system.

Compound-mediated assay interference in MS-based assays can manifest as ion suppression, but this phenomena is usually mitigated through sample purification, sample chromatography, the use of internal standards, and the aforementioned monitoring of orthogonal reactions (68). Chemical modification or adduct formation of the analyte by test compounds can also interfere with accurate analyte measurement by perturbing (a)

analyte chromatographic and extraction behavior, or (b) measurement of parent ions due to mass shifts, especially when utilizing single or multiple reaction monitoring (69,70).

For additional details on MS-based assay development and optimization, refer to HPLC-MS/MS for hit generation.

The following is a sample protocol for a generic MS HAT assay. Specific reagents, concentrations, volumes, dispensing procedures, and time intervals should be optimized for a particular application.

### Sample protocol

1. Dispense 1-2  $\mu\text{L}$  enzyme mix (2X) into microplate using a liquid handling system such as Bioraptr. Centrifuge microplate briefly at 1000 rpm.
2. Dispense test compounds using a 384-head pin-tool or an acoustic dispenser
3. Dispense 1-2  $\mu\text{L}$  substrate mix (2X) using a liquid handling system to initiate the reaction and centrifuge the plate at 1000 rpm for 1 min.
4. Incubate for desired time duration.
5. Add stop solution to quench the reaction using a large volume liquid dispenser; final volume should be at least 50  $\mu\text{L}$ /well.
6. Briefly centrifuge and heat seal the plate(s) prior to RF-MS analysis. (Note: avoid using an adhesive sealer since the adhesive will clog the sipper tube in RF as well as leach on to the mass spectrometer, causing loss of signal).

*In a representative RF method for a ~20-residue histone peptide, sample can be loaded on a C4 cartridge in 0.6 s, washed for 3 s with 100% dH<sub>2</sub>O containing 0.1% (v/v) formic acid, eluted for 3 s with 80% acetonitrile containing 0.1% formic acid, and re-equilibrated for 5 s. The system can be programmed to perform a blank injection to minimize cross-contamination of subsequent samples.*

### Data processing

The Agilent RF mass spectrometry system is closely integrated with a proprietary data analysis software package (MassHunter Qualitative and Quantative Analysis) for measuring area under the curve (AUC) for each peak as well as converting the large data files into data for individual wells. Alternatively, RapidFire Integrator (Agilent) can be used for processing data from various mass spectrometer platforms (such as Sciex, Waters, and Agilent). These data can be processed further to calculate the amount of product (**Equation 1**).

$$\text{Equation 1. \% Product conversion} = \frac{\text{Product}_{\text{AUC}}}{\text{Product}_{\text{AUC}} + \text{Substrate}_{\text{AUC}}}$$

### Miscellaneous notes

- Due to the technical requirements of MS (e.g., instrumentation, chromatography/separation, troubleshooting), one may wish to consult with experienced mass spectrometrists when designing and optimizing an MS-based assay.

- The high sensitivity of many MS methods requires less product formation for detection relative to other technologies, potentially decreasing the amounts of required enzyme and substrate to complete a screening campaign.
- Polymeric detergents (e.g., Tween-20, Tween-80, Triton X-100, NP-40) are generally incompatible with MS assays, as they can broadly elude and saturate the assay signal. Monomeric detergents (e.g., CHAPS, octyl  $\beta$ -D-glucopyranoside, dodecyl  $\beta$ -D-glucopyranoside) are preferred, but can still interfere with MS assays.
- Multiple histone-based substrates have been reported for MS-based assays, including peptides and whole histone proteins (23).
- Like other detection methods, it is imperative to determine the limits of detection (LoD) and limits of quantitation (LoQ) for all analytes of interest, in presence and absence of IS. Determining the LoD and LoQ prevents detector saturation as well as determine the concentration of sample to be injected.
- Unlike LC-MS, RF-MS does not involve an elution gradient or prolonged retention times, which allows for cross contamination and carryover of samples. It is critical to establish optimal chromatography conditions for the analyte(s) of interest – appropriate SPE cartridge, alterations of load, wash and/or elute steps of RF method, along with the mass spectrometer detection method (positive or negative mode). If these manipulations fail to reduce carryover, it is advisable to incorporate blank injection(s) after each sample.
- Inclusion of an isotopically-labeled analyte (in stop solution) as an internal standard should also be considered to identify cases of incomplete sample injection, ion suppression, and matrix effects.
- Higher-throughput RF-MS can be achieved by minimizing the sample retention time on the system. This requires tubing with extremely small internal diameter combined with robust injection valves and LC-pumps. Thus, monitoring pump pressures facilitates the identification of clogs (if any), which might occur during longer runs using biological samples.
- Use of reverse-phase chromatography involving C4 or C18 cartridges requires sample preparation in 100% aqueous phase to prevent sample precipitation. In contrast, samples should be prepared in high organic (90 – 95% acetonitrile) when using HILIC cartridges (*see HPLC-MS/MS for hit generation for more details*).
- Arguably, RF-MS has lower throughput in comparison to a 1536-well biochemical assay read on a ViewLux. Multiplexing samples involving analytes that do not interfere in detection increases RF-MS throughput (71).

## Non-Radiolabeled Proximity HAT Assays

There are several non-radioisotope, proximity-based technologies available to assay HAT activity, such as AlphaScreen (Amplified Luminescent Proximity Homogeneous Assay; **Figure 8**) and FRET (Fluorescent/Förster Resonance Electronic Transfer; **Figure 9**). Each of these technologies involves the excitation of a donor system by a light source, followed by signal transmission to an acceptor system that requires proximity for efficient transmission. The acceptor system, upon excitation by the donor system, then emits a



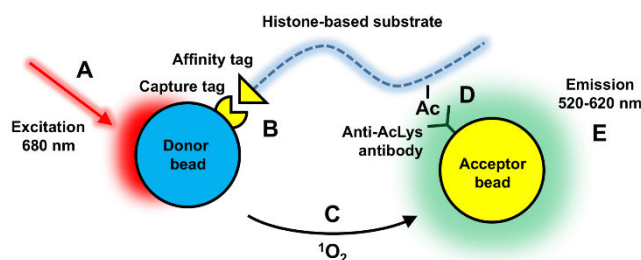


**Figure 8. Example of an AlphaScreen-based HAT assay.** A donor bead with a capture tag binds to a histone-based substrate with an affinity tag. An acceptor bead with an anti-acetyl lysine antibody binds to acetylated lysine on the histone-based substrate. Phthalocyanine from the donor bead is excited by a high-wavelength laser, which produces singlet oxygen ( $^1\text{O}_2$ ). If in close proximity to the donor bead, thioxene, anthracene, and rubrene within the acceptor bead are excited by singlet oxygen to produce an emission at a lower wavelength. In the absence of interference, HAT activity is proportional to the emission intensity at this lower wavelength. There are five main potential areas of compound-mediated readout interference: (A) interference of excitation light source by test compound (quenching/absorbance/light-scattering); (B) disruption of donor bead-substrate interaction by test compound; (C) disruption of singlet oxygen transmission by test compound (quenching, chemical reaction); (D) disruption of acceptor fluorophore construct-product interaction by test compound; and (E) acceptor bead emission interference by test compounds (auto-fluorescence, quenching/absorbance/light-scattering).

signal which can be quantified. Alpha-based technologies (AlphaScreen, AlphaLISA) utilize singlet oxygen transfer, while FRET utilizes fluorescence resonance electronic transfer. Note that AlphaScreen acceptor beads contain a thioxene/anthracene/rubrene mixture, while AlphaLISA acceptor beads contain a thioxene/europium chelate mixture. The latter configuration creates a narrower emission band that is optimized for certain biological matrices. Time-resolved FRET (TR-FRET) adaptations using lanthanide fluorophore donors are common, and can enhance signal-to-noise by coupling an excitation pulse with delayed acquisition to allow for background fluorescence decay. For a well-designed example of a TR-FRET and AlphaLISA assay versus p300, we refer readers to a recent report by Lasko and colleagues (43).

Alpha- and FRET-based HAT assays share many advantages. Compared to conventional ELISA and Western blots, Alpha and FRET technologies are homogenous assays. This eliminates many assay steps such as washing, reducing assay time and simplifying the assay workflow. Both Alpha and FRET technologies require separate capture systems for the donor and acceptor components. Typically, this involves a combination of capture and affinity tags, and an acetylated histone recognition system (i.e., antibody or bromodomain). Both technologies are versatile, and allow for extensive customization of tags, substrates, and labeling strategies. For either technology, many reagent combinations are readily commercially available (so-called “off-the-shelf” assays), or are amenable to customization by relatively straightforward techniques or commercial services.

Alpha-based HAT assays have several potential advantages, including high sensitivity, low background, good dynamic range, and miniaturization (to 1536-well plates) (72).

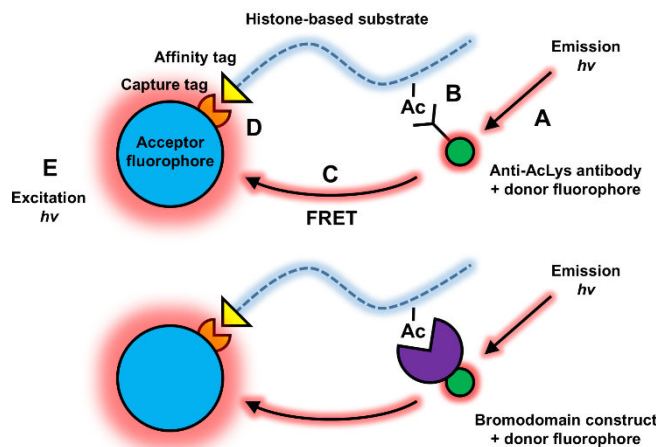


**Figure 9. General schematic of (TR)-FRET HAT assays.** A donor fluorophore conjugated to a recognition motif (top panel, antibody; bottom panel, bromodomain) binds to an acetylated lysine on the histone-based substrate. An acceptor fluorophore with a capture tag binds to the histone-based substrate with an affinity tag. The donor fluorophore is excited by a laser, which induces fluorescence. If in close proximity to the donor fluorophore, the acceptor fluorophore is excited by FRET. In the absence of interference, HAT activity is proportional to the emission intensity at this higher wavelength. There are five main potential areas of compound-mediated readout interference: (A) interference of excitation light source by test compound (quenching/absorbance/light-scattering); (B) disruption of donor fluorophore construct-substrate interaction by test compound; (C) disruption of FRET by test compound (quenching/absorbance/light-scattering); (D) disruption of acceptor fluorophore construct-product interaction by test compound; and (E) acceptor fluorophore emission interference by test compounds (auto-fluorescence, quenching/absorbance/light-scattering).

Additionally, singlet oxygen transfer can generally occur over longer distances compared to FRET. However, a disadvantage of Alpha technology can be reagent and instrumentation costs as well as light sensitivity. By contrast, TR-FRET assays may be less sensitive to DMSO (73). Both assay technologies are susceptible to specific modes of compound-mediated interference, including disruption of capture reagent systems and signal quenching (74,75).

### Miscellaneous notes

- Optimization of the capture and affinity tags is advised for either technology. This includes experimenting with different tag combinations (e.g., 6xHis-Nickel, streptavidin-biotin, GST-glutathione) as well as the location of each tag on histone-based substrate.
- These technologies are dependent on the quality of the histone recognition motif. Characterize antibody specificity and optimize antibody titers. Specificity can also be assessed by titrating purified histone-based products.
- There have been reports of compounds interfering with antibody recognition of acetylated histone substrate (19). Consider a follow-up counter-screen with a second, independent antibody.

- As with fluorescence-based assays, avoid background light contamination when acquiring FRET and Alpha readouts.
- Perform titration experiments with the various assay components. Depending on the assay format and relative concentrations of each assay component, “hook effects” may be present (76). This can occur when a capture system is saturated by excess tagged substrate/product leading to an apparent signal plateau, followed by signal attenuation with further substrate/product titrations (e.g., excess biotinylated histone-based substrate/products for available streptavidin beads).
- The absolute concentration and ratio of donor:acceptor beads is critical for optimal assay performance. Start with manufacturer recommendations and slowly titrate.
- Because many of the Alpha- and FRET-based HAT assay formats rely on several binding events, it is recommended to determine the optimal order of reagent addition (e.g., binding of capture tag to affinity tag may interfere with the binding of another the antibody-histone pair, but not vice-versa).
- For Alpha-based technologies, the manufacturer typically recommends Tween 20 (0.01-0.1% v/v), Triton X-100 (0.01-0.1% v/v), CHAPS (0.1% v/v), and/or BSA (0.1% w/v) to mitigate nonspecific interactions.
- Certain assay components may interfere with Alpha-based technologies:
  - Residual azide (a common antimicrobial used for reagent storage) may interfere with singlet oxygen transmission.
  - Certain transition metals ( $Al^{2+}$ ,  $Fe^{2+}$ ,  $Fe^{3+}$ ,  $Cu^{2+}$ ,  $Ni^{2+}$ ,  $Zn^{2+}$ ) may quench singlet oxygen at low millimolar concentrations.
- To assess for assay interference:
  - Allow the reaction to go to completion, spike reaction with test compound, and then measure assay readout. If available, an alternative is to spike purified product and compound, then measure the assay readout.
  - For Alpha-based technologies, TruHit<sup>TM</sup> beads can also be used to identify compound-mediated readout interference.
  - To assess interference with affinity tag systems, one can also test the effect of compounds on generic bead readouts that contain the affinity tag system of interest.

## Enzyme-Coupled HAT Assays

Enzyme-coupled methods “indirectly” quantify HAT activity by measuring the product of a second, coupled enzymatic reaction (**Figure 10**). This second enzyme system requires CoA substrate, which is produced from the primary HAT reaction. Additional substrates for this secondary enzyme are present in excess, so that the rate-limiting component of the final readout is the HAT reaction. Both  $\alpha$ -ketoglutarate dehydrogenase or pyruvate dehydrogenase have been successfully used as the secondary enzyme (15,30). In both cases,  $\alpha$ -ketoglutarate or pyruvate is oxidized, while  $NAD^+$  is reduced to produce NADH. This latter product can be continuously monitored by spectrophotometry at 340 nm.

Enzyme-coupled assays have characteristic advantages and disadvantages. They are relatively inexpensive and amenable to higher-throughput set-ups. In the case of NADH

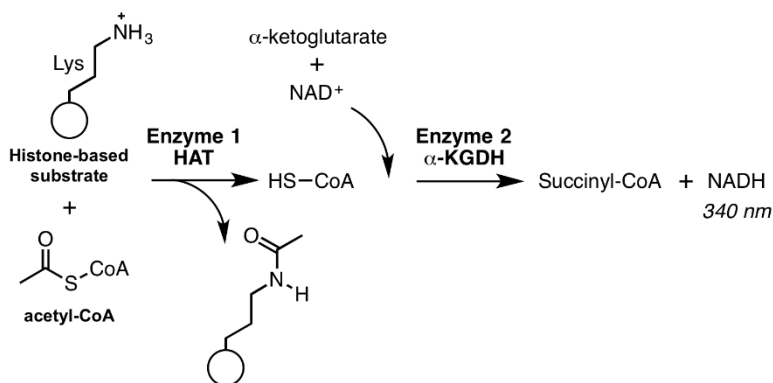


**Figure 10. General schematic of enzyme-coupled HAT assays.** Free coenzyme A produced by the HAT reaction serves as one of the substrates for a second enzymatic reaction. In the presence of excess co-substrate, the second enzymatic reaction produces a product that can be quantified. In absence of interference, HAT activity is proportional to the secondary enzyme product readout. In this example, the secondary enzyme α-ketoglutarate dehydrogenase (α-KGDH) catalyzes the conversion of free CoA and α-ketoglutarate to succinyl-CoA. The NAD<sup>+</sup> cofactor is reduced to NADH, which is monitored by absorbance at 340 nm. There are several potential areas of compound-mediated readout interference: (A) thiol-scavenging of CoA-SH by electrophilic test compounds; (B), modulation of secondary enzyme activity by test compounds; and (C), light-based interference by test compounds.

readouts, these assays typically require larger amounts of product (low micromolar) for robust detection due to their absorbance-based readout. Like thiol-scavenging HAT assays, enzyme-coupled HAT assays are susceptible to multiple modes of compound-mediated assay interference. Compounds can react with free CoA, depleting substrate for the coupled reaction and producing either a false-negative or false-positive readout depending on the absorbance properties of the compound-CoA adduct. Compounds can also modulate the secondary enzyme. Finally, test compounds can interfere with the absorbance readout.

The following are some considerations for enzyme-coupled HAT assays:

- The secondary enzyme reaction should not be rate-limiting, which can be verified by titrating each component of the secondary enzyme system. In many systems, the coupled enzyme is present in much higher concentrations than the primary (target) enzyme.
- Unlike thiol-scavenging HAT assays, DTT and other reducing agents do not typically interfere with the assay readout.
- Ensure each enzyme system components are compatible with one another, as certain HAT substrates (e.g., calf thymus histones) can interfere with previously described secondary reactions (15).
- Both α-ketoglutarate dehydrogenase or pyruvate dehydrogenase are available commercially.

- Reaction buffer should contain all of the necessary substrates and co-factors for the secondary enzyme (e.g., metals, NAD<sup>+</sup>). Reaction buffer should be optimized for both the HAT activity and secondary enzyme activity.
- Cloudy solutions or precipitation may interfere with absorbance-based readouts.
- Background controls should be included. For instance, excluding HAT enzyme allows subtraction of non-enzymatic production of CoA. Additional controls can exclude secondary enzyme or various substrates to better characterize background.

## Section Summary

There are a variety of technology platforms, each with signature advantages and disadvantages that must be carefully considered when choosing and subsequently optimizing a new HAT assay. Consideration should be given to the nature of the given HAT system being assayed, operator experience, available instrumentation, budget, project timeframe, as well as other factors. Regardless of the primary assay method, at least one orthogonal assay should be performed to confirm true compound-mediated HAT modulation.

## Cell-Based HAT Assays

### Introduction

Several cell-based HAT assays have been reported, most of which quantify histone acetylation through antibodies targeted acetylated histone lysine products. This section briefly describes common approaches to assaying HAT activity in cellular systems, as well as recommendations for their interpretation.

### Cell-Based HAT Assays

Cell-based HAT assays assess the effect of test compounds on HAT activity in the cellular context. Most cellular HAT assays involve treating cells with test compound, followed by either (a) fixing treated cells and measuring histone acetylation by immunohistochemistry, or (b) lysing treated cells and measuring histone acetylation by an antibody-based method (e.g., ELISA, Western blot, and now Alpha-based technology) (**Figure 11**). Histone acetylation is usually normalized to total histone content or cell number. More recent approaches involve live-cell imaging that links an acetylated histone recognition system (e.g., bromodomain) with a reporter-linked histone substrate (**Figure 11**). These latter approaches require transfection of engineered reporter constructs. In principle, analysis of cellular histone isolates can also be performed by MS, though such methods are generally not readily adaptable to quantitative or high-throughput analyses.

Unlike most biochemical HAT assays, histone acetylation in cellular systems is confounded by multiple variables, including HAT expression, histone deacetylase activity, histone chaperones, cell cycle effects, and rates of histone synthesis and degradation. Due to the complexities of these higher-order systems and the inherent properties of current

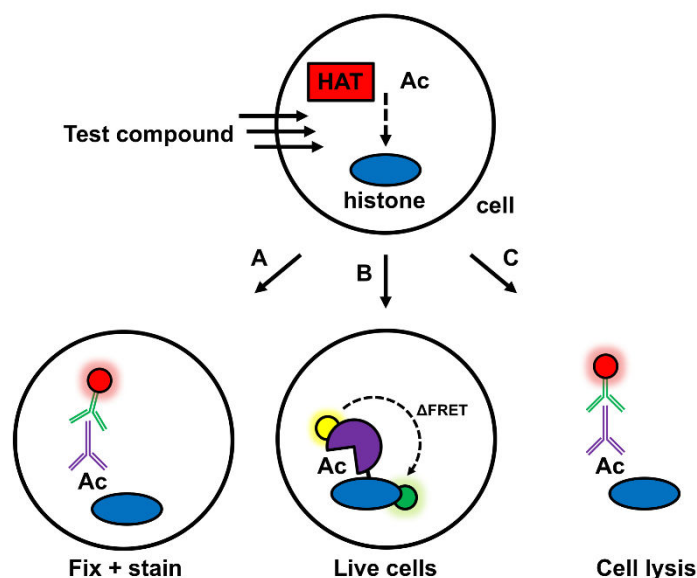


**Figure 11. Schematic of representative cell-based HAT assays.** Cells are incubated with test compound. (A) Cells can be fixed in preservative and analyzed by immunohistochemistry and related techniques. (B) HAT activity can be monitored in real-time with the introduction of special constructs, such as FRET-based systems. (C) Cells can be lysed, and histones can be probed for acetylation by antibody-based approaches, as well as mass spectrometry. Cell-based readouts should be interpreted with certain cautions (see main text).

detection technologies, many cell-based assays have smaller dynamic ranges and decreased precision than simpler biochemical assays. For these reasons, those performing cell-based HAT assays should carefully evaluate intra- and inter-assay precision and accuracy.

## Interpretation of Cell-Based HAT Assays

Many well-characterized promiscuous compounds (including known thiol-reactive, redox-active, and/or aggregators) can disrupt cell proliferation and histone acetylation in cells at low-to-mid micromolar compound concentrations, raising the strong possibility that certain histone acetylation readouts are also susceptible to off-targets (36). Therefore, caution is advised when interpreting such cell-based readouts, especially with chemical matter not sufficiently optimized or characterized for potency and selectivity. With nonspecific compounds, it is unclear whether changes in histone acetylation and other phenotypes are due to specific HAT engagement or off-target effects. It is likely that cellular HAT readouts are more interpretable with compounds possessing sufficient potency and selectivity (43).

The following are some cautions when interpreting cell-based HAT assay readouts:

- *HAT/substrate overlap.* HATs often have multiple substrates, and conversely, many histone modifications are catalyzed by more than one HAT. Changes in a particular histone acetylation after compound treatment may be due to simple engagement of

the intended HAT. However, histone acetylation may be due to engagement of other HATs with overlapping substrate specificities.

- *Deacetylase activity.* Cellular histone acetylation exists in dynamic equilibrium between acetyltransferases and deacetylases. Histone acetylation can be reversed by HDACs and sirtuins with deacetylase activity. One should carefully consider the effects of test compounds on HDAC/sirtuin activity in cellular systems.
- *Controlling for HDAC activity.* To control for HDAC activity, some researchers treat cells with HDAC inhibitors such as suberanilohydroxamic acid (SAHA) or trichostatin A (TSA). If employing this approach, one must consider the effects of HDAC inhibition in the context of the assay readout.
- *Sensitivity/acetylated histone content.* Depending on the experimental system including the specific histone acetylation, the concentration of analyte can be very low. One approach to increase measurable acetylated histones is to treat cells with HDAC inhibitors. As above, if employing this approach, again one must consider the effects of HDAC inhibition when interpreting the assay readout.
- *Cell cycle dependence.* Certain HATs and histone PTMs are cell-cycle dependent in their expression and activity. Furthermore, overall nucleosome content is cell-cycle dependent. Depending on the context, cell synchronization or cell cycle analyses may be necessary.
- *Cell proliferation.* Modulation of certain HATs can decrease cell proliferation and induce apoptosis. Decreases in cell proliferation or induction of apoptosis are not necessarily direct evidence of actual HAT engagement, and may be due to general compound toxicity.
- *Indirect readouts.* Due to complex cellular dynamics, histone acetylation is still an indirect marker of HAT engagement by a compound. Demonstrating direct target engagement in the cellular context generally requires sophisticated methodologies such as CETSA, radiolabeled compound, or chemical proteomics.

## Section Summary

Compound modulation of HAT activity should be verified in a cell-based system. Due to the complex regulation of histone acetylation, changes in bulk as well as specific cellular histone acetylation may not always be attributable to a direct compound-HAT interaction. Subsequent efforts should be made to characterize direct target engagement and specificity in the cellular context using orthogonal methods (e.g. CETSA, compound-labeling).

## Miscellaneous Considerations

The following are several miscellaneous considerations that may be especially useful in establishing and validating HAT assays:

- The relative order of compound and reagent addition may have significant effects on assay performance. It can affect enzymatic activity by altering HAT or substrate

stability, for instance (40). Experiment with several configurations during assay development and even later mechanistic studies with promising lead compounds.

- For assays utilizing affinity tags, we recommend experimenting with several different tags, tag locations (i.e., *N*-terminal or *C*-terminal), and linkages. Often the optimal tag set-up is difficult to predict, and is best determined experimentally.
- Whenever possible use the highest quality reagents possible.

## Conclusions

HATs are an emerging class of epigenetic targets in drug discovery and chemical probe development. Modulation of HAT activity by small molecules can be assayed by multiple orthogonal platforms, many of which are amenable to high-throughput formats. Designing robust and cost-effective HAT assays requires careful optimization of multiple experimental parameters. Identifying chemical matter capable of modulating HATs by tractable, useful mechanisms also requires well-designed orthogonal assays and counter-screens. Scientists investigating the effect of small molecules on HAT activity should incorporate the aforementioned strategies and principles into their assay design.

## Acknowledgements

JLD acknowledges Dr. Thomas D. Chung for helpful discussions regarding enzyme kinetics.

## Conflict of Interest Statement

The authors declare no financial conflicts of interest.

## Suggesting Readings (alphabetical order)

1. Berndsen, C. E.; Denu, J. M. *Methods*, **2005**, *36*, 321.

A well-written walkthrough of filter-binding and enzyme-coupled HAT assays.

2. Dahlin, J.L., Nelson, K.M., Strasser, J.M., Barsyte-Lovejoy, D., Szewczyk, M.M., Organ, S., Cuellar, M., Singh, G., Shrimp, J.H., Nguyen, N., Meier, J.L., Arrowsmith, C.H., Brown, P.J., Baell, J.B., Walters, M.A. Assay interference and off-target liabilities of reported histone acetyltransferase inhibitors. *Nat. Commun.* **2017**;8:1527.

Characterizes assay interference and off-target liabilities in many reported HAT inhibitors. Many widely used HAT inhibitors demonstrated nonspecific thiol reactivity, formed aggregates, and poor biochemical selectivity. Many also disrupted cell proliferation and histone acetylation similarly to several known promiscuous/interference compounds.



3. Dahlin, J. L.; Nissink, J. W. M.; Strasser, J. M.; Francis, S.; Zhou, H.; Zhang, Z.; Walters, M. J. *Med. Chem.* **2015**, *58*, 2091.  
  
Illustrative example regarding the limitations of fluorometric HAT assays. Describes the use of relevant counter-screens and other important concepts in HTS triage.
4. Falk, H.; Connor, T.; Yang, H.; Loft, K. J.; Alcindor, J. L.; Nikolakopoulos, G.; Surjadi, R. N.; Bentley, J. D.; Hattarki, M. K.; Dolezal, O.; Murphy, J. M.; Monahan, B. J.; Peat, T. S.; Thomas, T.; Baell, J. B.; Parisot, J. P.; Street, I.F. *J. Biomol. Screen.* **2011**, *16*, 1196.  
  
An excellent description on the adaptation of AlphaScreen technology to assay HATs in an HTS format, as well as describing assay-specific artifacts.
5. Lasko, L.M., Jakob, C.G., Edalji, R.P., Qiu, W., Montgomery, D., Digiammarino, E.L., Hansen, T.M., Risi, R.M., Frey, R., Manaves, V., Shaw, B., Algire, M., Hessler, P., Lam, L.T., Uziel, T., Faivre, E., Ferguson, D., Buchanan, F.G., Martin, R.L., Torrent, M., Chiang, G.G., Karukurichi, K., Langston, J.W., Weinert, B.T., Choudhary, C., de Vries, P., Van Drie, J.H., McElligott, D., Kesicki, E., Marmorstein, R., Sun, C., Cole, P.A., Rosenberg, S.H., Michaelides, M.R., Lai, A., Bromberg, K.D. Discovery of a selective catalytic p300/CBP inhibitor that targets lineage-specific tumours. *Nature.* **2017**;550:128–132.  
  
An elegant report of the discovery and optimization of A-485, a first-in-class potent, specific small-molecule inhibitor of p300/CBP with nanomolar cellular activity and *in vivo* activity.
6. Lopes da Rosa, J.; Bajaj, V.; Spoonamore, J.; Kaufman, P. D. *Bioorg. Med. Chem. Lett.* **2013**, *23*, 2853.  
  
Another example highlighting the challenges of fluorometric HAT assays. Describes several relevant orthogonal assays, counter-screens, and post-HTS mechanistic experiments.
7. Ngo, L.; Wu, J.; Yang, C.; Zheng, Y.G. *ASSAY Drug Dev. Technol.* **2015**, *13*, 210.  
  
An excellent example of SPA method development and troubleshooting.
8. Sorum, A. W.; Shrimp, J. H.; Roberts, A. M.; Montgomery, D. C.; Tiwari, N. K.; Lal-Nag, M.; Simeonov, A.; Jadhav, A.; Meier, J. L. *ACS Chem. Biol.* **2016**, *11*, 734.  
  
Describes the application of microfluidics to assay HAT activity.

## References

1. Grunstein M. Histone acetylation in chromatin structure and transcription. *Nature.* 1997;389:349–352. PubMed PMID: 9311776.

2. Strahl B., Allis C. The language of covalent histone modifications. *Nature*. 2000;403:41–45. PubMed PMID: 10638745.
3. Roelfsema J., Peters D. Rubinstein-Taybi syndrome: clinical and molecular overview. *Exp. Rev. Mol. Med.* 2007;9:1–16. PubMed PMID: 17942008.
4. Furdas S., Kannan S., Sippl W., Jung M. Small molecule inhibitors of histone acetyltransferases as epigenetic tools and drug candidates. *Arch. Pharm. (Weinheim)*. 2012;346:7–21. PubMed PMID: 22234972.
5. Simon R. P., Robaa D., Alhalabi Z., Sippl W., Jung M. KATching-up on small molecule modulators of lysine acetyltransferases. *J. Med. Chem.* 2016;59:1249–1270. PubMed PMID: 26701186.
6. Fiorentino F., Mai A., Rotili D. Lysine acetyltransferase inhibitors: structure-activity relationships and potential therapeutic implications. *Future Med. Chem.* 2018;10:1067–1091. PubMed PMID: 29676588.
7. Wapenaar H., Dekker F. Histone acetyltransferases: challenges in targeting bi-substrate enzymes. *Clin. Epigenetics*. 2016.;8. PubMed PMID: 27231488.
8. Karanam B., Jiang L., Wang L., Kelleher N., Cole P. Kinetic and mass spectrometric analysis of p300 histone acetyltransferase domain autoacetylation. *J. Biol. Chem.* 2006;281:40292–40301. PubMed PMID: 17065153.
9. Burgess R. J., Zhang Z. Histone chaperones in nucleosome assembly and human disease. *Nat. Struct. Mol. Biol.* 2013;20:14–22. PubMed PMID: 23288364.
10. Dahlin J. L., Sinville R., Solberg J., Zhou H., Francis S., Strasser J., John K., Hook D. J., Walters M. A., Zhang Z. A cell-free fluorometric high-throughput screen for inhibitors of Rtt109-catalyzed histone acetylation. *PLOS ONE*. 2013;8:e78877. PubMed PMID: 24260132.
11. Lopes da Rosa J., Bajaj V., Spoonamore J., Kaufman P. D. A small molecule inhibitor of fungal histone acetyltransferase Rtt109. *Bioorg. Med. Chem. Lett.* 2013;23:2853–2859. PubMed PMID: 23587423.
12. Gao T., Yang C., Zheng Y. G. Comparative studies of thiol-sensitive fluorogenic probes for HAT assays. *Anal. Bioanal. Chem.* 2012;405:1361–1371. PubMed PMID: 23138472.
13. Trievel R. C., Li F. Y., Marmorstein R. Application of a fluorescent histone acetyltransferase assay to probe the substrate specificity of the human p300/CBP-associated factor. *Anal. Biochem.* 2000;287:319–328. PubMed PMID: 11112280.
14. Chung C. C., Ohwaki K., Schneeweis J. E., Stec E., Varnerin J. P., Goudreau P. N., Chang A., Cassaday J., Yang L., Yamakawa T., Kornienko O., Hodder P., Inglese J., Ferrer M., Strulovici B., Kusunoki J., Tota M. R., Takagi T. A fluorescence-based thiol quantification assay for ultra-high-throughput screening for inhibitors of coenzyme A production. *ASSAY Drug Dev. Technol.* 2008;6:361–374. PubMed PMID: 18452391.
15. Kim Y., Tanner K. G., Denu J. M. A continuous, nonradioactive assay for histone acetyltransferases. *Anal. Biochem.* 2000;280:308–314. PubMed PMID: 10790315.
16. Dahlin J. L., Nissink J. W. M., Francis S., Strasser J., John K., Zhang Z., Walters M. A. Post-HTS case report and structural alert: promiscuous 4-aryloxy-1,5-disubstituted-3-hydroxy-2H-pyrrol-2-one actives verified by ALARM NMR. *Bioorg. Med. Chem. Lett.* 2015;25:4740–4752. PubMed PMID: 26318992.

17. Dahlin J. L., Nissink J. W. M., Strasser J. M., Francis S., Zhou H., Zhang Z., Walters M. A. PAINS in the assay: chemical mechanisms of assay interference and promiscuous enzymatic inhibition observed during a sulfhydryl-scavenging HTS. *J. Med. Chem.* 2015;58:2091–2113. PubMed PMID: 25634295.
18. Ait-Si-Ali S., Ramirez S., Robin P., Trouche D., Harel-Bellan A. A rapid and sensitive assay for histone acetyl-transferase activity. *Nucleic Acids Res.* 1998;26:3869–3870. PubMed PMID: 9685509.
19. Falk H., Connor T., Yang H., Loft K. J., Alcindor J. L., Nikolakopoulos G., Surjadi R., Bentley J., Hattarki M., Dolezal O., Murphy J., Monahan B., Peat T., Thomas T., Baell J., Parisot J., Street I. An efficient high-throughput screening method for MYST family acetyltransferases, a new class of epigenetic drug targets. *J. Biomol. Screen.* 2011;16:1196–1205. PubMed PMID: 22086725.
20. Michaelides, M.; Hansen, T.; Dai, Y.; Zhu, G.; Frey, R.; Gong, J.; Penning, T.; Curtin, M.; McClellan, W.; Clark, R.; Torrent, M.; Mastracchio, A.; Kesicki, E. A.; Kluge, A. F.; Patane, M. A.; Van Drie, J. H., Jr.; Ji, Z.; Lai, C. C.; Wang, C. Spirocyclic compound as HAT inhibitors and their preparation. 2016.
21. Sorum A. W., Shrimp J. H., Roberts A. M., Montgomery D. C., Tiwari N. K., Lal-Nag M., Simeonov A., Jadhav A., Meier J. L. Microfluidic mobility shift profiling of lysine acetyltransferases enables screening and mechanistic analysis of cellular acetylation inhibitors. *ACS Chem. Biol.* 2015;11:734–741. PubMed PMID: 26428393.
22. Fanslau C., Pedicord D., Nagulapalli S., Gray H., Pang S., Jayaraman L., Lippy J., Blat Y. An electrophoretic mobility shift assay for the identification and kinetic analysis of acetyl transferase inhibitors. *Anal. Biochem.* 2010;402:65–68. PubMed PMID: 20338149.
23. Rye P. T., Frick L. E., Ozbal C. C., Lamarr W. A. Advances in label-free screening approaches for studying histone acetyltransferases. *J. Biomol. Screen.* 2011;16:1186–1195. PubMed PMID: 21908798.
24. Wu S., Liu B. Application of scintillation proximity assay in drug discovery. *BioDrugs.* 2005;19:383–392. PubMed PMID: 16392890.
25. Zheng W., Carroll S. S., Inglese J., Graves R., Howells L., Strulovici B. Miniaturization of a hepatitis C virus RNA polymerase assay using a  $-102^{\circ}\text{C}$  cooled CCD camera-based imaging system. *Anal. Biochem.* 2001;290:214–220. PubMed PMID: 11237322.
26. Turlais F., Hardcastle A., Rowlands M., Newbatt Y., Bannister A., Kouzarides T., Workman P., Aherne G. W. High-throughput screening for identification of small molecule inhibitors of histone acetyltransferases using scintillating microplates (FlashPlate). *Anal. Biochem.* 2001;298:62–68. PubMed PMID: 11673896.
27. Kesicki, E. A.; Wang, C.; Patane, M. A.; Kluge, A. F.; Van Drie, J. H., Jr. HAT inhibitors and methods for their use. 2016.
28. Kesicki, E. A.; Kluge, A. F.; Patane, M. A.; Van Drie, J. H., Jr.; Wang, C. HAT inhibitors and methods for their use. 2016.
29. Marmorstein R. Biochemical and structural characterization of recombinant histone acetyltransferase proteins. *Methods Enzymol.* 2004;376:106–119. PubMed PMID: 14975301.
30. Berndsen C. E., Denu J. M. Assays for mechanistic investigations of protein/histone acetyltransferases. *Methods.* 2005;36:321–331. PubMed PMID: 16085424.

31. Dahlin J. L., Chen X., Walters M. A., Zhang Z. Histone-modifying enzymes, histone modifications and histone chaperones in nucleosome assembly: lessons learned from Rtt109 histone acetyltransferases. *Crit. Rev. Biochem. Mol. Biol.* 2015;50:31–53. PubMed PMID: 25365782.
32. Shechter D., Dormann H., Allis C., Hake S. Extraction, purification and analysis of histones. *Nat. Protoc.* 2007;2:1445–1457. PubMed PMID: 17545981.
33. Rodriguez-Collazo P., Leuba S. H., Zlatanova J. Robust methods for purification of histones from cultured mammalian cells with the preservation of their native modifications. *Nucleic Acids Res.* 2009;37:e81. PubMed PMID: 19443446.
34. Klinker H., Haas C., Harrer N., Becker P., Mueller-Planitz F. Rapid purification of recombinant histones. *PLOS ONE.* 2014;9:e104029. PubMed PMID: 25090252.
35. Tanaka Y., Tawaramoto-Sasanuma M., Kawaguchi S., Ohta T., Yoda K., Kurumizaka H., Yokoyama S. Expression and purification of recombinant human histones. *Methods.* 2004;33:3–11. PubMed PMID: 15039081.
36. Dahlin J. L., Nelson K. M., Strasser J. M., Barsyte-Lovejoy D., Szewczyk M. M., Organ S., Cuellar M., Singh G., Shrimp J. H., Nguyen N., Meier J. L., Arrowsmith C. H., Brown P. J., Baell J. B., Walters M. A. Assay interference and off-target liabilities of reported histone acetyltransferase inhibitors. *Nat. Commun.* 2017;8:1527. PubMed PMID: 29142305.
37. Johnston P. A., Soares K. M., Shinde S. N., Foster C. A., Shun T. Y., Takyi H. K., Wipf P., Lazo J. Development of a 384-well colorimetric assay to quantify hydrogen peroxide generated by the redox cycling of compounds in the presence of reducing agents. *ASSAY Drug Dev. Technol.* 2008;6:505–518. PubMed PMID: 18699726.
38. Soares K. M., Blackmon N., Shun T. Y., Shinde S. N., Takyi H. K., Wipf P., Lazo J., Johnston P. Profiling the NIH Small Molecule Repository for compounds that generate H<sub>2</sub>O<sub>2</sub> by redox cycling in reducing environments. *ASSAY Drug Dev. Technol.* 2010;8:152–174. PubMed PMID: 20070233.
39. McGovern S. L., Caselli E., Grigorieff N., Shoichet B. K. A common mechanism underlying promiscuous inhibitors from virtual and high-throughput screening. *J. Med. Chem.* 2002;45:1712–1722. PubMed PMID: 11931626.
40. Copeland, R. *Evaluation of enzyme inhibitors in drug discovery.* John Wiley & Sons: Hoboken, NJ, 2005.
41. Balasubramanyam K., Swaminathan V., Ranganathan A., Kundu T. K. Small molecule modulators of histone acetyltransferase p300. *J. Biol. Chem.* 2003;278:19134–19140. PubMed PMID: 12624111.
42. Baell J., Miao W. Histone acetyltransferase inhibitors: where art thou? *Future Med. Chem.* 2016;8:1525–1528. PubMed PMID: 27557114.
43. Lasko L. M., Jakob C. G., Edalji R. P., Qiu W., Montgomery D., Digiammarino E. L., Hansen T. M., Risi R. M., Frey R., Manaves V., Shaw B., Algire M., Hessler P., Lam L. T., Uziel T., Faivre E., Ferguson D., Buchanan F. G., Martin R. L., Torrent M., Chiang G. G., Karukurichi K., Langston J. W., Weinert B. T., Choudhary C., de Vries P., Van Drie J. H., McElligott D., Kesicki E., Marmorstein R., Sun C., Cole P. A., Rosenberg S. H., Michaelides M. R., Lai A., Bromberg K. D. Discovery of a selective catalytic p300/CBP inhibitor that targets lineage-specific tumours. *Nature.* 2017;550:128–132. PubMed PMID: 28953875.

44. Jadhav A., Ferreira R. S., Klumpp C., Mott B. T., Austin C. P., Inglese J., Thomas C. J., Maloney D. J., Shoichet B. K., Simeonov A. Quantitative analyses of aggregation, autofluorescence, and reactivity artifacts in a screen for inhibitors of a thiol protease. *J. Med. Chem.* 2010;53:37–51. PubMed PMID: 19908840.
45. Thorne N., Auld D. S., Inglese J. Apparent activity in high-throughput screening: origins of compound-dependent assay interference. *Curr. Opin. Chem. Biol.* 2010;14:315–324. PubMed PMID: 20417149.
46. Lau O. D., Kundu T. K., Soccio R. E., Ait-Si-Ali S., Khalil E. M., Vassilev A., Wolffe A. P., Nakatani Y., Roeder R. G., Cole P. A. HATs off: selective synthetic inhibitors of the histone acetyltransferases p300 and PCAF. *Mol. Cell.* 2000;5:589–595. PubMed PMID: 10882143.
47. Zheng Y., Balasubramanyam K., Cebrat M., Buck D., Guidez F., Zelent A., Alani R. M., Cole P. A. Synthesis and evaluation of a potent and selective cell-permeable p300 histone acetyltransferase inhibitor. *J. Am. Chem. Soc.* 2005;127:17182–17183. PubMed PMID: 16332055.
48. Bowers E. M., Yan G., Mukherjee C., Orry A., Wang L., Holbert M. A., Crump N. T., Hazzalin C. A., Liszczak G., Yuan H., Larocca C., Saldanha S. A., Abagyan R., Sun Y., Meyers D. J., Marmorstein R., Mahadevan L. C., Alani R. M., Cole P. A. Virtual ligand screening of the p300/CBP histone acetyltransferase: identification of a selective small molecule inhibitor. *Chem. Biol.* 2010;17:471–482. PubMed PMID: 20534345.
49. Balasubramanyam K., Varier R. A., Altaf M., Swaminathan V., Siddappa N. B., Ranga U., Kundu T. K. Curcumin, a novel p300/CREB-binding protein-specific inhibitor of acetyltransferase, represses the acetylation of histone/nonhistone proteins and histone acetyltransferase-dependent chromatin transcription. *J. Biol. Chem.* 2004;279:51163–51171. PubMed PMID: 15383533.
50. Balasubramanyam K., Altaf M., Varier R., Swaminathan V., Ravindran A., Sadhale P., Kundu T. Polyisoprenylated benzophenone, garcinol, a natural histone acetyltransferase inhibitor, represses chromatin transcription and alters global gene expression. *J. Biol. Chem.* 2004;279:33716–33726. PubMed PMID: 15155757.
51. Yang H., Pinello C., Luo J., Li D., Wang Y., Zhao L., Jahn S., Saldanha S., Chase P., Planck J., Geary K., Ma H., Law B., Roush W., Hodder P., Liao D. Small-molecule inhibitors of acetyltransferase p300 identified by high-throughput screening are potent anticancer agents. *Mol. Cancer. Ther.* 2013;12:610–620. PubMed PMID: 23625935.
52. Biel M., Kretsovali A., Karatzali E., Papamatheakis J., Giannis A. Design, synthesis and biological evaluation of a small molecule inhibitor of the histone acetyltransferase Gcn5. *Angew. Chem. Int. Ed.* 2004;43:3974–3976. PubMed PMID: 15274229.
53. Coffey K., Blackburn T. J., Cook S., Golding B. T., Griffin R. J., Hardcastle I. R., Hewitt L., Huberman K., McNeill H. V., Newell D. R., Roche C., Ryan-Munden C. A., Watson A., Robson C. N. Characterisation of a Tip60 specific inhibitor, NU9056, in prostate cancer. *PLOS ONE.* 2012;7:e45539. PubMed PMID: 23056207.
54. Aldrich C., Bertozzi C., Georg G., Kiessling L., Lindsley C., Liotta D., Merz K. J., Schepartz A., Wang S. The ecstasy and agony of assay interference compounds. *J. Med. Chem.* 2017;60:2165–2168. PubMed PMID: 28244745.

55. Zhang J., Chung T., Oldenburg K. A simple statistical parameter for use in evaluation and validation of high throughput screening assays. *J. Biomol. Screen.* 1999;4:67–73. PubMed PMID: 10838414.
56. Eastwood, B.; Farnen, M.; Iversen, P.; Craft, T.; Smallwood, J.; Garbison, K.; Delapp, N.; Smith, G. The minimum significant ratio: a statistical parameter to characterize the reproducibility of potency estimates from concentration-response assays and estimation by replicate-experiment studies. *J. Biomol. Screen.* 2--6, 11, 253-261.
57. Horiuchi K., Fujimoto D. Use of phospho-cellulose paper disks for the assay of histone acetyltransferase. *Anal. Biochem.* 1975;69:491–496. PubMed PMID: 1217715.
58. Ngo L., Wu J., Yang C., Zheng Y. G. Effective quenchers are required to eliminate the interference of substrate: cofactor binding in the HAT scintillation proximity assay. *ASSAY Drug Dev. Technol.* 2015;13:210–220. PubMed PMID: 26065557.
59. Glickman J., Schmid A., Ferrand S. Scintillation proximity assays in high-throughput screening. *ASSAY Drug Dev. Technol.* 2008;6:433–455. PubMed PMID: 18593378.
60. Poveda A., Sendra R. An easy assay for histone acetyltransferase activity using a PhosphorImager. *Anal. Biochem.* 2008;383:296–300. PubMed PMID: 18805389.
61. Han J., Zhou H., Horazdovsky B., Zhang K., Xu R.-M., Zhang Z. Rtt109 acetylates histone H3 lysine 56 and functions in DNA replication. *Science.* 2007;315:653–655. PubMed PMID: 17272723.
62. Allis C., Chicoine L., Glover C., White E., Gorovsky M. Enzyme activity dot blots: a rapid and convenient assay for acetyltransferase or protein kinase activity immobilized on nitrocellulose. *Anal. Biochem.* 1986;159:58–66. PubMed PMID: 3468811.
63. Pal S., Graves H., Ohsawa R., Huang T., Wang P., Harmacek L., Tyler J. The commercial antibodies widely used to measure H3 K56 acetylation are non-specific in human and drosophila cells. *PLOS ONE.* 2016;11:e0155409. PubMed PMID: 27187594.
64. Drogaris P., Villeneuve V., Pomies C., Lee E.-H., Bourdeau V., Bonneil E., Ferbeyre G., Verreault A., Thibaulta P. Histone deacetylase inhibitors globally enhance H3/H4 tail acetylation without affecting H3 lysine 56 acetylation. *Sci. Rep.* 2012;2:220. PubMed PMID: 22355734.
65. Shafer D. E., Inman J. K., Lees A. Reaction of Tris(2-carboxyethyl)phosphine (TCEP) with maleimide and alpha-haloacyl groups: anomalous elution of TCEP by gel filtration. *Anal. Biochem.* 2000;282:161–164. PubMed PMID: 10860517.
66. Khan M. Kinetics and mechanism of the alkaline hydrolysis of maleimide. *J. Pharm. Sci.* 1984;73:1767–1771. PubMed PMID: 6527252.
67. Shrimp J. H., Sorum A. W., Garlick J. M., Guasch L., Nicklaus M. C., Meier J. L. Characterizing the covalent targets of a small molecule inhibitor of the lysine acetyltransferase p300. *ACS Med. Chem. Lett.* 2015;7:151–155. PubMed PMID: 26985290.
68. Annesley T. Ion suppression in mass spectrometry. *Clin Chem.* 2003;49:1041–1044. PubMed PMID: 12816898.
69. Bernd O. K., Sui J., Youn A. B., Whittal R. M. Interferences and contaminants encountered in modern mass spectrometry. *Anal. Chim. Acta.* 2008;627:71–81. PubMed PMID: 18790129.

70. Kind T., Fiehn O. Advances in structure elucidation of small molecules using mass spectrometry. *Bioanal. Rev.* 2010;2:23–60. PubMed PMID: 21289855.
71. Leveridge M., Buxton R., Argyrou A., Francis P., Leavens B., West A., Rees M., Hardwicke P., Bridges A., Ratcliffe S., Chung C. W. Demonstrating enhanced throughput of RapidFire mass spectrometry through multiplexing using the JmjD2d demethylase as a model system. *J Biomol Screen.* 2014;19:278–286. PubMed PMID: 23896685.
72. Eglén R., Reisine T., Roby P., Rouleau N., Illy C., Bosse R., Bielefeld M. The use of AlphaScreen technology in HTS: current status. *Curr. Chem. Genomics.* 2008;1:2–10. PubMed PMID: 20161822.
73. Glickman J., Wu X., Mercuri R., Illy C., Bowen B., He Y., Sills M. A comparison of ALPHAScreen, TR-FRET, and TRF as assay methods for FXR nuclear receptors. *J. Biomol. Screen.* 2002;7:3–10. PubMed PMID: 11897050.
74. Schorpp K., Rothenaigner I., Salmina E., Reinshagen J., Low T., Brenke J. K., Gopalakrishnan J., Tetko I. V., Gul S., Hadian K. Identification of small-molecule frequent hitters from AlphaScreen high-throughput screens. *J. Biomol. Screen.* 2014;19:715–726. PubMed PMID: 24371213.
75. Brenke J., Salmina E., Ringelstetter L., Dornauer S., Kuzikov M., Rothenaigner I., Schorpp K., Gehler F., Gopalakrishnan J., Kieser A., Gul S., Tetko I., Hadian K. Identification of small-molecule frequent hitters of glutathione S-transferase-glutathione Interaction. *J. Biomol. Screen.* 2016;21:596–607. PubMed PMID: 27044684.
76. Acker M. G., Auld D. S. Considerations for the design and reporting of enzyme assays in high-throughput screening applications. *Perspect Sci.* 2014;1:56–73.





# *In Vitro* Cell Based Assays

Douglas Auld, PhD, Bruce Bejcek, PhD, Kyle Brimacombe, MS, Nathan P. Coussens, PhD, Timothy L. Foley, PhD, Marcie Glicksman, PhD, Matthew D. Hall, PhD, James Inglese, PhD, Stephen C. Kales, PhD, Madhu Lal-Nag, PhD, Zhuyin Li, PhD, Owen McManus, PhD, Terry Riss, PhD, G. Sitta Sittampalam, PhD, O. Joseph Trask, Jr., and Menghang Xia, PhD



# Authentication of Human Cell Lines by STR DNA Profiling Analysis

Yvonne Reid, PhD,<sup>1</sup> Douglas Storts, PhD,<sup>2</sup> Terry Riss,<sup>3,\*</sup> and Lisa Minor<sup>4,†</sup>

Created: May 1, 2013.

## Abstract

Since 1951 when the first human cell line, HeLa, was established there has been an increase in the use of human cell lines as models for human diseases such as cancer, substrates for the production of viruses for vaccine production and as tools for the production of recombinant proteins for therapeutics. Unfortunately this accelerated use of human cell lines and the lack of best practices in tissue culture have led to increase in cellular cross-contamination which has resulted in spurious results. Now a simple molecular technique, Short Tandem Repeat (STR) DNA profiling of human cell lines, is available and if applied routinely in cell culture management can greatly improve the detection of cellular cross-contamination resulting in more accurate assays.

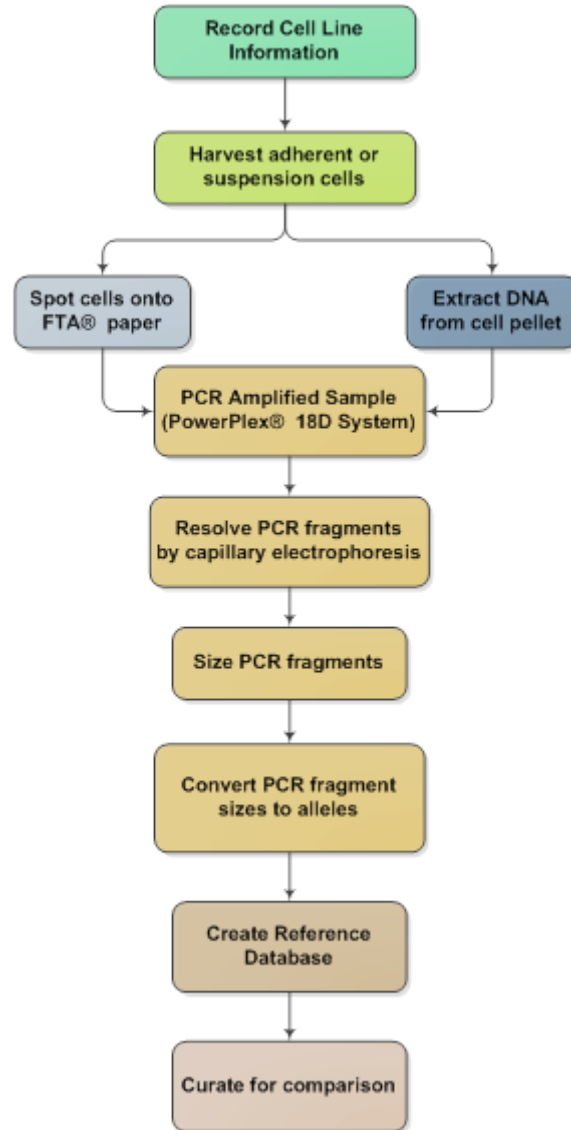
---

<sup>1</sup> ATCC; Email: yreid@atcc.org. <sup>2</sup> Promega; Email: Doug.storts@promega.com. <sup>3</sup> Promega; Email: Terry.riss@promega.com. <sup>4</sup> Promega; Email: lisakminor@yahoo.com.

\* Editor

† Editor

## Flowchart: STR DNA Analysis for Human Cell Line Authentication



### Introduction

Over the past 50 years there has been a progressive increase in the use of cells as models, substrates and tools for both basic research and industrial applications. The rapid growth in areas such as cell biology, genomics and proteomics has triggered a remarkable increase in cell culture activities, consequently resulting in an increase in the potential risk of cross-contamination of cell cultures. Cross-contamination among cultured cell lines is a persistent problem and has occurred at frequencies ranging from 16 to 35% (1, 2). Detection is particularly difficult if co-cultivated cells express similar phenotypes. Indeed,

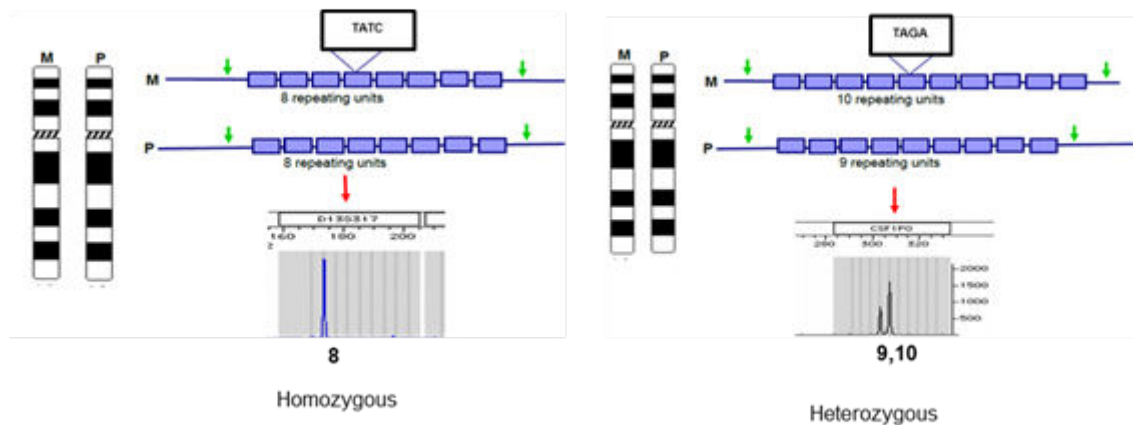


**Figure 1:** Schematic Diagram of STR Profiling Polymorphism

HeLa, a cell line derived from an invasive cervical carcinoma in 1951, was shown to contaminate more than 90 cell lines (3, 4). At one point, the number of cell lines contaminated with HeLa represented one-third of all human tumor cell lines developed for research in cancer and cell biology. In 1999 Drexler et al. found that 15% of 117 hematopoietic cell lines received from original investigators or a secondary source were cross-contaminated with other cell lines (5). More recent reports have shown cross-contaminated cell lines from breast and prostate cancers (6), thyroid cancer (7), adenoid cystic carcinoma (8), and esophagus (9). Cross-contamination of cell lines has persisted as a result of mishandling and a lack of attention to best practices in tissue culture. Advances in molecular biology have now made it possible, using Short Tandem Repeat (STR) DNA profiling, to uniquely identify human cell lines derived from the tissue of a single individual allowing researchers to ascertain if their cultures were misidentified or cross-contaminated.

The discovery of DNA hypervariable regions within genomes has made it possible to identify each human cell line derived from a single donor. In 1985 Alec Jeffreys and others (10, 11) demonstrated that hypervariable regions, which consist of variable number tandem repeat (VNTR) units from minisatellite DNA, are capable of hybridizing to many loci distributed throughout the genome to produce a DNA ‘fingerprint’. The DNA fingerprints are very complex and not easily interpretable. However, subsequent advances in the technology have given rise to the use of STR of microsatellite regions which consist of core sequences of 1-6 bp. The core sequences of these human microsatellite DNAs can serve as hotspots for homologous recombination events which are believed to maintain the variability of these loci (12). The polymorphism or informativeness of these STR markers display many variations in the number of the repeating units between alleles and among loci in unrelated cell lines and shown in detail in Figure 1. There are two copies of an allele at a given locus on the chromosome obtained from a diploid cell line; one allele derived from the mother (maternal chromosome - M) and the other allele is derived from the father (paternal chromosome - P). If the two copies of the alleles (maternal and

paternal) have the same number of repeating units, the fragments, which have the same size, will co-migrate during electrophoresis. For example, in Figure 1 the alleles 9, 10 (designated allele 8) is considered homozygous and a single peak is observed on the electropherogram. If the number of repeating units on the paternal chromosome is different from that of the maternal chromosome, at the same locus, this is considered heterozygous (for example alleles 8 and 9) and two peaks are observed in the electropherogram.

## Assay Concept: STR DNA Profiling for human cell line authentication (intraspecific identification and detection of cross-contaminating cells)

STR analysis can be performed in most laboratories that have the capabilities to execute molecular techniques. It is an easy, low cost and reliable method for the authentication of human cell lines.

When a cell line is first received into the laboratory it is essential to capture as much information as possible on its history, growth and functional characteristics. This information is important for tracking the behavior of the cells during culturing, characterization and in the event there is misidentification, see Flow chart.

Such information may include:

- Name of cell line
- Name of donor of cell line
- Name of the originator of cell line
- Date cell line was established
- Reference describing the establishment of cell line
- Tissue of origin
- Species
- Population doubling levels
- Unique characteristics and function
- Complete growth medium
- Doubling time

A plan should be developed for managing the cells during expansion and the use of cells for experiments such as the creation of a Seed Stock (Master Cell Bank) and a Distribution stock (Working Cell Bank). Upon thaw, spot about 20  $\mu\text{L}$  of cell suspension (200,000 cells) from the donor vial directly onto a FTA<sup>®</sup> paper for subsequent STR analysis to establish the baseline STR profile. The baseline STR profile from the original donor material is then used to compare against all subsequent STR DNA profiles performed on the various cell banks. The remaining cells are expanded to create a Seed stock from which a Distribution stock is prepared. Representative vials from both the Seed and Distribution stocks are subjected to another round of STR DNA profile analysis in addition to other quality control procedures. The STR DNA profiles for both Seed and

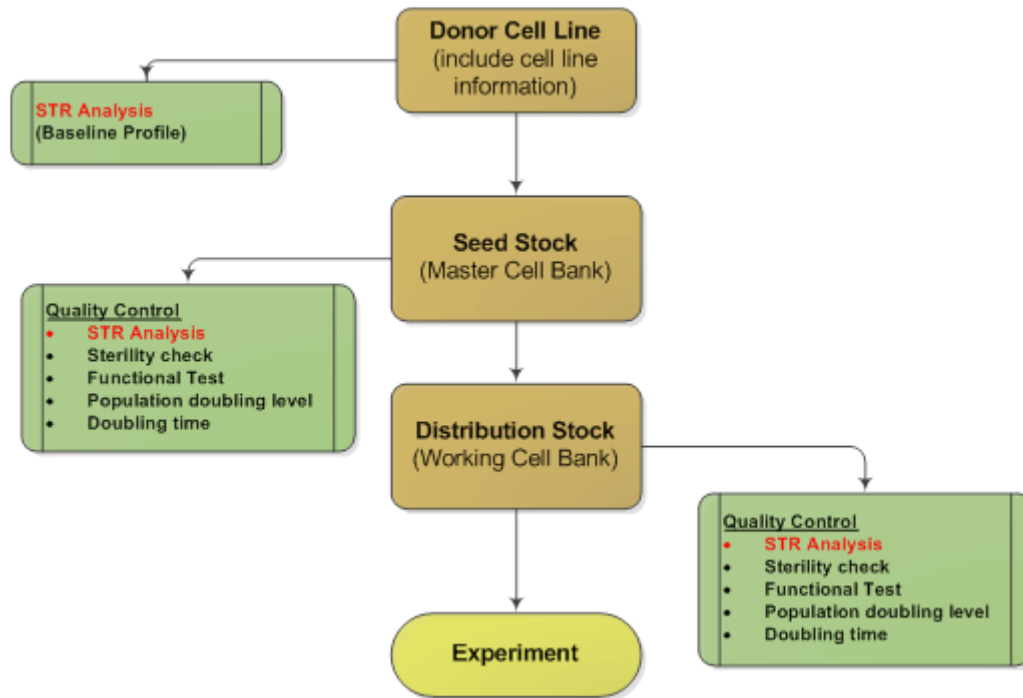


**Figure 2:** Accessioning Scheme for New Cell Line

Distribution stocks are compared to the baseline profile of the original donor material to determine if the results from these quality control tests meet the acceptance criteria ( $\geq 80\%$  match between the cell line and its original tissue or its derivatives), consistent STR profile, for a given line.

STR DNA profile analysis involves the simultaneous amplification of 17 STR markers plus amelogenin for gender determination and is capable of discriminating among human cell lines at about  $1 \times 10^{-18}$ . The amplicons from the PCR are resolved by capillary electrophoresis and sized using internal size standards (ISS). The sized fragments are then converted into alleles with comparison to the allelic ladders and the assigned alleles are converted to numeric values which are used to create a baseline profile. The baseline DNA profiles are used to create a reference database. All subsequent STR DNA profile analyses performed on the various cell banks are compared to the baseline profile of that cell line in the reference database. The STR DNA profile should also be compared to profiles of other cell lines in the reference database (Figure 2).

## Assay Development

The preparation of cell suspension obtained from adherent or suspension cultures can be used as a source of DNA. The cell suspension is either spotted directly onto FTA<sup>®</sup> paper or may be used for liquid DNA extraction. Both forms of DNA are suitable for STR DNA Profile analysis.

## Harvest of Adherent Culture

1. Remove and discard culture medium
2. Rinse cell surface by adding PBS (without calcium and magnesium) to the side of the flask (away from the cells) and rinse cells with a gentle rocking motion.
3. Remove and discard PBS.
4. Add dissociation solution, enough to cover the cells. Incubate at 37°C and rock gently until all cells detach.
5. Add medium and gently resuspend cells.
6. Centrifuge at 200 × g and for 10 minutes to pellet cells.
7. Discard supernatant and wash cell pellet twice in PBS.
8. Resuspend cell pellet in a small volume of PBS and determine cell count and viability.
9. Use cell suspension for spotting onto FTA<sup>®</sup> paper or for the isolation of DNA.

## Harvest of Suspension Culture

1. Transfer cell suspension to a centrifuge tube.
2. Centrifuge at 200 × g for 10 minutes to pellet cells.
3. Discard supernatant and wash cell pellet twice in PBS.
4. Resuspend cell pellet in a small volume of PBS and determine cell count and viability.
5. Use cell suspension for spotting onto FTA<sup>®</sup> paper or for the isolation of DNA.

Note: Isolate or prepare FTA<sup>®</sup> paper from cells harvested in log-phase of growth cycle; cells are in the exponential phase of growth and are the most viable. Use best practices in tissue culture to prevent cross-contamination of cells.

## Product Components and Storage Conditions for STR Analysis

### PowerPlex<sup>®</sup> 18D System (Cat. No DC1802, Promega Corporation)

The PowerPlex<sup>®</sup> 18D System allows co-amplification and four-color fluorescent detection of eighteen loci, D3S1358, TH01, D21S11, D18S51, Penta E, D5S818, D13S317, D7S820, D16S539, CSF1PO, Penta D, Amelogenin (gender determination), vWA, D8S1179, TPOX, FGA, D19S433 and D2S1338. The system is optimized for analysis of common database samples, such as unwashed FTA<sup>®</sup> card punches (i.e., direct amplification).

The PowerPlex<sup>®</sup> 18D System is compatible with the ABI PRISM<sup>®</sup> 3100 and 3100-Avant and Applied Biosystems 3130, 3130xl, 3500 and 3500xL Genetic Analyzers. Refer to manufacturer manual for detailed protocol.

Tables 1A and 1B provide a listing of the pre- and post-amplification components and long-term storage instruction for the PowerPlex<sup>®</sup> 18D system.



**Table 1A:** PowerPlex® 18D System pre-amplification components and storage

| Pre-amplification components*     |              | Long-term storage temperature                             |
|-----------------------------------|--------------|---|
| PowerPlex® D 5X master mix        | 1 mL         | Store at -30 °C to -10 °C                                 |
| PowerPlex® 18D 5X primer pair mix | 1 mL         | Store at -30 °C to -10 °C; light sensitive, store in dark |
| 2800M control DNA, 10 ng/μL       | 25 μL        | 2 °C to 10 °C   |
| Water, amplification grade        | 5 x 1,250 μL | Room temperature (18 °C to 22 °C)                         |

\* Recommend that the pre-amplification and post-amplification reagents are stored at different locations; use different pipette, tips and racks.

**Table 1B:** PowerPlex® 18D System post-amplification components and storage

| Post-amplification components*  |            | Long-term storage temperature  |
|---|------------|--|
| PowerPlex® 18D allelic ladder mix   | 100 μL     | Store at -30 °C to -10 °C; light sensitive, store in dark  |
| CC5 internal lane standard 500  | 2 x 300 μL | Store at -30 °C to -10 °C; light sensitive, store in dark  |
| <b>Note: Matrix standard required for initial setup of the color separation matrix (not a component of kit above)</b> |            |  |
| PowerPlex® 5-Dye Matrix standard 3100/3130  |            | Suitable for genetic analyzers: ABI PRISM® 3100, 3100-Avant Genetic Analyzers, Applied Biosystems 3130, 3130xl, 3500, 3500xL |

\* Recommend that the pre-amplification and post-amplification reagents are stored at different locations; use different pipette, tips and racks.

Available separately the proper panel and bins text files for the use with GeneMapper ID software is available for download at: [www.promega.com/geneticidtools/panels\\_bins/](http://www.promega.com/geneticidtools/panels_bins/)

## Materials

- GeneAmp® PCR System 9700 thermal cycler (Applied Biosystems) or equivalent
- MicroAmp® optical 96-well reaction plate (Applied Biosystems) or equivalent
- Microcentrifuge
- Aerosol-resistant pipet tips
- 1.2 mm Harris Micro-Punch or equivalent
- Cutting mat

## Spotting of Cells onto FTA® Card

The procedure is a modification of the protocol available at <http://www.promega.com/resources/articles/profiles-in-dna/direct-amplification-of-saliva-and-blood-samples-using-powerplex-esx-16/> (13).

1. Spot about 200,000 cells, suspended in about 20 μL of PBS onto FTA® card, or equivalent and allow to dry. **Note:** for long-term storage, cards may be stored in a cool, dry environment for further use.

2. Manually punch a 1.2 mm disk in the center of the sample spot.
3. Use plunger to eject the disk into the appropriate well of a reaction plate.

## Amplification Setup

1. Completely thaw the PowerPlex® D 5X master Mix and PowerPlex® 18D 5X Primer Pair mix.
2. Determine the number of reactions needed. Note: Include negative and positive controls and add an additional 2 reactions to compensate for pipetting errors.
3. For reaction assembly, label a clean 0.2 mL MicroAmp® plate.
4. Add reagents in the order listed in Table 2 to each sterile tube.
5. Vortex the PCR amplification mix for about 10 seconds.
6. Add 25 µL PCR amplification mix to each of the reaction tubes containing FTA® disks.
7. For the positive amplification control:
  - a. Vortex the tube of 2800M Control DNA
  - b. Dilute 2800 M Control DNA to a concentration of 5 ng/µL.
  - c. Pipet 1 µL of diluted Control DNA into reaction well containing 25 µL of PCR amplification mix.
  - d. For the negative amplification control use either a reaction well containing 25 µL amplification mix without DNA or a reaction well containing 25 µL amplification mix with FTA® disk without DNA.
8. Seal the plate and briefly centrifuge the plate to bring the disks to the bottom of the wells.

Note: Amount of cells spotted onto the FTA® card and the amount of Control DNA used to obtain positive results must be predetermined.

**Table 2:** Amplification Setup PCR Reaction Volumes

| PCR Amplification Mix Components  | Volume per reaction | × | Number of reactions | × | Final volume |
|-----------------------------------|---------------------|---|---------------------|---|--------------|
| Water, amplification grade        | 15 µL               | × |                     | × |              |
| PowerPlex® D 5X Master Mix        | 5 µL                | × |                     | × |              |
| PowerPlex® 18D 5X Primer Pair mix | 5 µL                | × |                     | × |              |
| <b>Total Reaction Volume</b>      | <b>25 µL</b>        | × |                     | × |              |

## Thermal Cycling

1. Place the MicroAmp® plate in the thermal cycler.
2. Select and run the recommended protocol provided in Table 3.
3. Store amplified Samples at 4°C after completion of the thermal cycling protocol.

Note: Optimize protocol pertaining to cycle number and injection conditions based on instrumentation used.

**Table 3:** Thermal Cycling Protocol

| Steps | Temperature | Duration   | Cycles    |
|-------|-------------|------------|-----------|
| 1     | 96 °C       | 2 minutes  |           |
| 2     | 94 °C       | 10 seconds | 27 cycles |
| 3     | 60 °C       | 1 minute   |           |
| 4     | 60 °C       | 20 minutes |           |
| 4     | 60 °C       | soak       |           |

## Detection of Amplified Fragments Using the Applied Biosystems 3500 or 3500xL Genetic Analyzer

The PowerPlex® 18D primers are covalently linked to fluorescent molecules. Multiple sets of primers with different "color" fluorescent labels are used to analyze numerous different loci in a single PCR reaction. Following the PCR reaction, internal size standards are added to the reaction mixture and the DNAs are separated by size via capillary gel electrophoresis. Once the data are collected, the GeneMapper ID-X software is used to size the amplicons based on the internal size standard. STR genotyping of each cell line is performed by converting amplicons size to alleles by comparing to allelic ladders (14). See Table 4 for a listing of the reagents that can be used in this assay.

**Table 4:** Detection of Amplified Fragment

| Material  | Manufacturer        | Catalog Number |
|---|---------------------|----------------|
| Dry heating block   | N/A                 | N/A            |
| Water bath  | N/A                 | N/A            |
| Ice-water bath or crushed iced  | N/A                 | N/A            |
| Centrifuge compatible with 96-well plates   | N/A                 | N/A            |
| Aerosol-resistant pipet tips  | N/A                 | N/A            |
| 36 cm 3500/3500xL capillary array   | Life Technologies   | 4404687        |
| 96-well retainer and base set (standard)  | Applied Biosystems  | 4410228        |
| POP-4™ polymer in a pouch for the Applied Biosystems 3500 or 3500xL genetic Analyzer  | Life Technologies   | 4393710        |
| Anode buffer container  | Life Technologies   | 4393927        |
| Cathode buffer container  | Life Technologies   | 4408256        |
| Conditioning reagent pouch for the Applied Biosystems 3500 or 3500xL genetic Analyzer | Life Technologies   | 4393718        |
| Hi-Di formamide   | Applied Biosystems  | 4311320        |
| PowerPlex® 5-Dye Matrix Standards, 3100/3130  | Promega Corporation | DG4700         |

## Sample Preparation

1. Preparation of loading cocktail:

Combine and mix CC5 Internal Lane Standard 500 and Hi-Di™ formamide as follows:

$$(1 \mu\text{L CC5 ILS 500}) \times (\text{number of injections}) + (10 \mu\text{L Hi-Di}^{\text{TM}} \text{ formamide}) \times (\text{number of injections}) = \text{amount of loading cocktail}$$

Note: the amount of internal lane standard may be adjusted based on the intensity of the size standard peak.

2. Vortex loading cocktail (formamide/lane standard mix)
3. Pipet 11  $\mu\text{L}$  of loading cocktail into each well.
4. Add 1  $\mu\text{L}$  of amplified sample or 1  $\mu\text{L}$  PowerPlex® 18D Allelic Ladder Mix.
5. Cover wells with appropriate septa.
6. Centrifuge plate briefly to remove bubbles from the wells.
7. Denature samples at 95°C for 3 minutes just prior to loading instrument.
8. Immediately chill plate on crushed ice or an ice-water bath for 3 minutes.

## Instrument Preparation and Use

Detect amplified fragments using the Applied Biosystems 3500 or 3500 xL Genetic Analyzer. Refer to the User Guide for use and care of the instrument and Promega for a detailed protocol for data analysis.

## Data Analysis

The software for data analysis is PowerPlex® 18D Panel, Bins, Stutter Text Files and GeneMapper ID-X Software, version 1.2. To facilitate the analysis of data generated with the PowerPlex 18D System, go to [www.promega.com/geneticidtools/panels\\_bins/](http://www.promega.com/geneticidtools/panels_bins/) for panel and bins text files for automatic assignment of genotypes using the GeneMapper ID-X software.

## Data Interpretation

A cell line is considered authentic when the STR profile shows a  $\geq 80\%$  match between the cell line and its original tissue or its derivatives. A STR profile match of  $\leq 56\%$  is considered unrelated. However, there are some cell lines that have a match profile between 56 and 80% match. In these cases, additional studies should be performed to confirm identity (15).

A minimum of eight core STR loci is needed to uniquely identify a human cell line. The eight loci are D5S818, D13S317, D7S820, D16S539, vWA, Th01, TPOX, CSF1PO. A unique cell line has a STR profile that is different from another unique cell line (Figure 3).

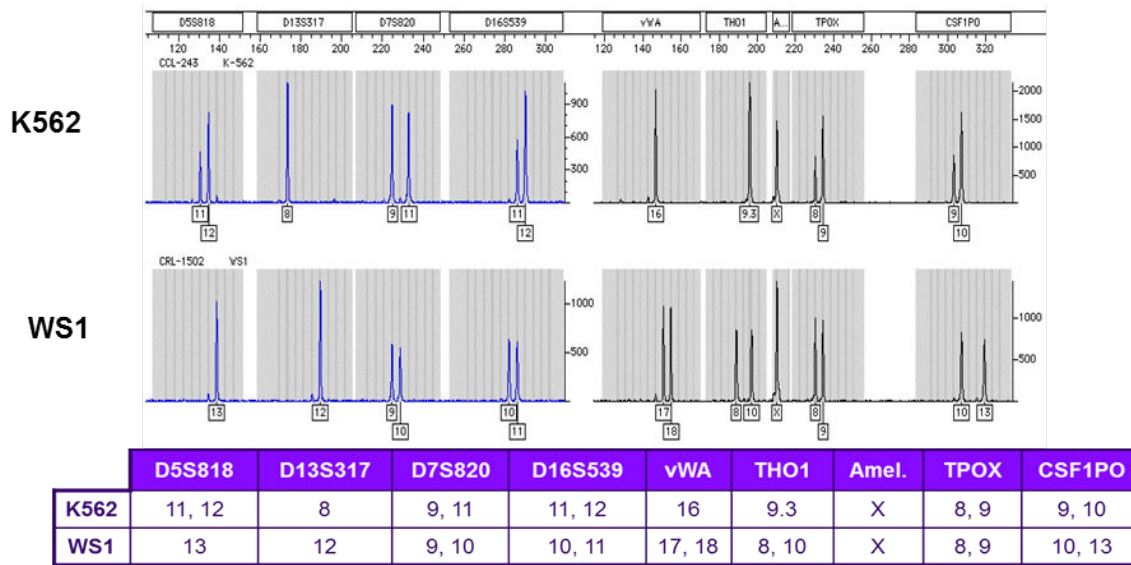


**Figure 3:** Electropherogram of two unrelated human cell lines, K562 (chronic myelogenous leukemia) and WS1 (skin fibroblast) obtained from two individuals. STR profile is different between the two cell lines. STR analysis performed with PowerPlex® 1.2. Allele numerical values are used to create database.

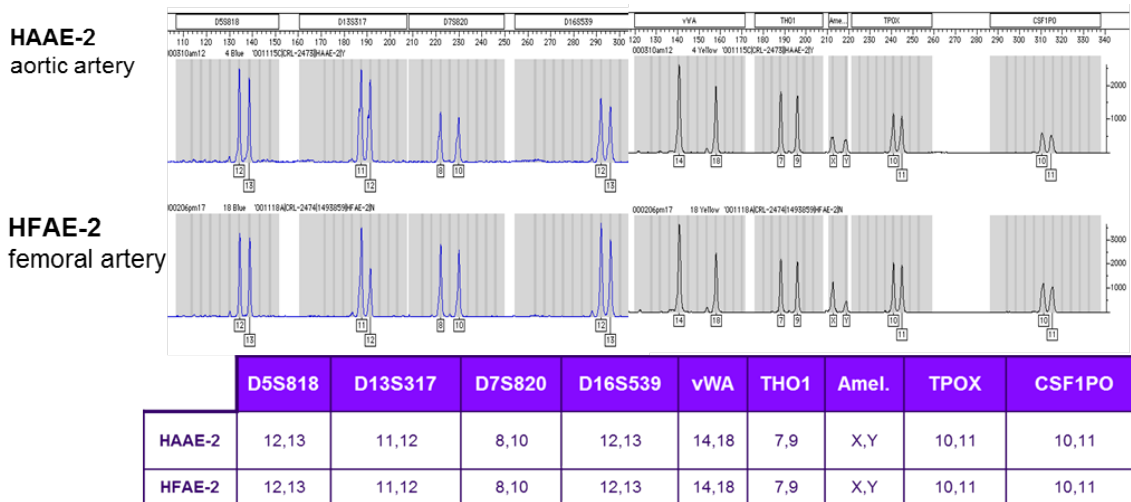


**Figure 4:** Electropherogram of two related human cell lines, HAAE-2 (human aortic artery) and HFAE-2 (femoral artery) obtained from the same individuals. STR profiles are identical between the two cell lines. STR analysis performed with PowerPlex® 1.2. Allele numerical values are used to create database.

Cell lines derived from various tissues from the same individual have the same STR profile (Figure 4).

Data interpretations of STR profiles on human cell lines, especially those derived from tumor tissue, present certain nuances such as:

- Loss of heterozygosity (LOH), also known as allele drop-out (ADO)

- Peak imbalance
- Multiple peaks at several loci

## Loss of Heterozygosity

The incidence of genetic instability in STR markers used to evaluate human cancers is not uncommon (16, 17). Most human cell lines are derived from a cancer, which differ genetically from normal tissue. Moreover, cell lines are capable of acquiring additional genetic changes while in culture. In a study of 24 lung samples, there were complete deletions of alleles at multiple loci when compared to normal tissue (18). Great care should be taken when evaluating biopsy tissue (which may contain normal tissue) for baseline STR profile to be compared to STR profile of cell line derived from tumor of that same tissue.

## Peak Imbalance

Peak imbalance is also a feature of cancer cells. The favored amplification of one allele over the over another may be due to gene duplication, aneuploidy or chimeric cell population (18). This characteristic brings a unique feature to cell line identification, see Figure 5.

## Multiple Peaks at Many Loci

Another relatively common occurrence of STR typing of human cancer cell lines is multiple peaks at several loci. Three or more peaks at one or two loci may be due to somatic mutation, trisomy or gene duplications. Events with more than three peaks at more than three loci may be due to cellular contamination. In either event, an independent method should be used to eliminate cellular cross-contamination, see Figure 6 as an example for cellular cross contamination.

## Criteria for Determining Quality STR Profile Analysis For Reliable and Interpretable Results

### Validation of Procedure

Method validation is an important element of quality control and provides the assurance that data will be reliable. Method validation is the process of demonstrating that a laboratory procedure is robust and reliable and reproducible in the hands of the laboratory personnel performing the test. The factors for method validation include: precision, accuracy, limit detection, specificity, linearity, range, robustness and system suitability. For more information on method validation of STR Systems, refer to <http://www.cstl.nist.gov/strbase/validation.htm> and Promega's Validation of STR Systems Reference Manual at <http://www.promega.com/resources/articles/pubhub/applications-notes/ge053-validation-of-str-systems-reference-manual/>.

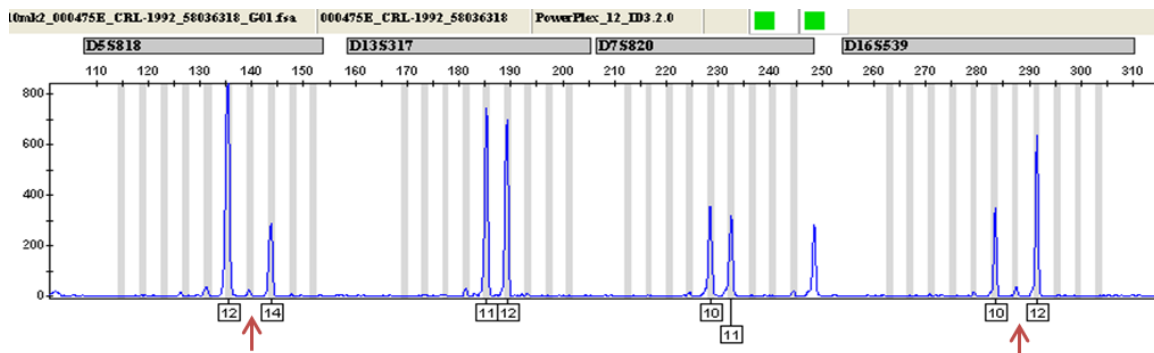


**Figure 5:** Peak imbalance (arrow) in STR profile of a tumor cell line. Most cell lines are aneuploidy with multiple copies of a chromosome and the total chromosome numbers exceeding 46.

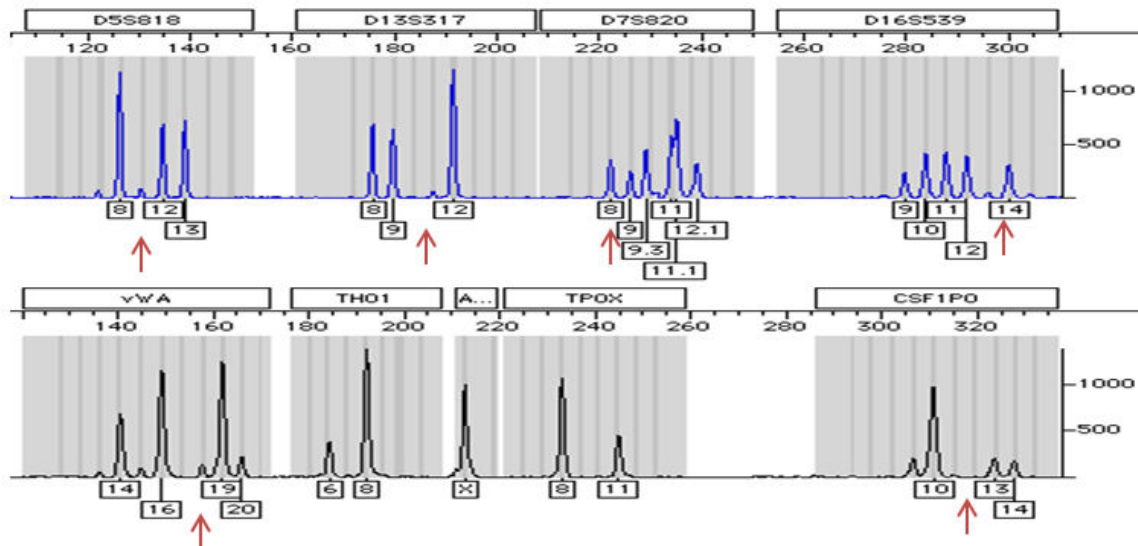


**Figure 6:** Electropherogram of cellular cross-contamination; multiple peaks at D5S818, D13S317, D7S820, D16S539, vWA, CSF1PO loci. STR typing of human cell lines with PowerPlex® 1.2.

## Setting of Analytical Thresholds and Peak Height Ratios

Each laboratory should determine the analytical threshold or the level at which detected signals are above baseline noise. Data falling below this threshold may not be suitable for allele calls; however, data at or above the threshold is of sufficient quality to determine an allele call.

## Setting the appropriate peak height or peak threshold

The genetic material for some tumor cell lines is very complex and this could lead to difficulty in distinguishing true low-level peaks from technical artifacts, including noise. There are no set rules for establishing threshold values; consequently, each laboratory

must establish peak-height thresholds for “calling” alleles as part of its validation process. Only peak-height, expressed in relative fluorescent units (RU) that exceed the accepted value will be accepted.

The threshold may be determined experimentally on the basis of observed signal-to-noise ratios or be an arbitrarily set value established by manufacturers (150 RFU) or published data. The lower threshold is a measure of the procedure sensitivity. The upper threshold is essential when reviewing data from samples with high quantity DNA. These samples have high RFU values that can oversaturate the instrument's ability to detect the sample. This can lead to difficulty in interpretation, especially when working with early stages of cellular contaminated samples.

### Use of appropriate controls (positive and negative):

Including controls during the STR profile analysis is very important as it allows the technician to identify and troubleshoot possible problems and ensure that the data is accurate and reliable.

During the amplification process, positive and negative controls are used. A positive control is a DNA sample with a known STR profile that is added to the sample set. The positive control confirms that the analysis processes are working accurately. (Positive controls are provided in the manufacturer's STR kits). A negative control which could be a reagent blank that is substituted for DNA is included and treated exactly the same manner as other samples. This allows the technician to determine if the reagents and/or techniques used may have introduced contamination.

### Ability to evaluate internal lane size standards (ISS) and allelic ladders.

All commercial STR kits include allelic ladders and internal size standards (ISS). Each sample during a run is assessed at completion for the correct calling of the ISS peaks. In general, the peaks from an ISS are uniform in size or intensity. Lack of uniformity or miscalled peaks can indicate problems with the sample, injection, and/or run.

The ISS is valuable in determining the accuracy of a capillary electrophoresis run. Temperature variations during electrophoresis can cause the in-run precision to exceed 1 base pair and evaluation of the ISS can assist analysts in identifying this issue.

Allelic ladders should be assessed to ensure that all peaks have been called correctly. Ladder peaks that have not been called or have been miscalled can indicate a problem with the ladder sample, injection, and/or run.

### Ability to evaluate and detect artifacts such as:

There are several artifacts during STR profile analysis that can lead to misinterpretation of the data. Identification and resolution of these artifacts are explained in great detail in the ANSI/ATCC ASN-0002-2011 (19).

- Stutter peaks



- Dye blobs
- Dye pull-ups
- Off-ladder alleles; microvariants

### Stutter peaks (products)

Stutter products are a common amplification artifact associated with STR analysis. Stutter products are often observed as one repeat unit below the true allele peak and, occasionally, two repeat units smaller or one repeat unit larger than the true allele peak. Frequently, alleles with a greater number of repeat units will exhibit a higher percent stutter. The pattern and intensity of stutter may differ slightly between primer sets for the same loci (see Figure 7 and Promega's manual on troubleshooting PowerPlex® 18D System).

### Dye Blobs

Dye blobs, are fairly common in STR analysis. Evidence suggests that the fluorescent dye tags attached to the primers begin to break down over time. Disassociated primer dyes can show up in the sample analysis range and can mask true data. Dye blobs are usually wider than real peaks and are typically only seen in one color. Follow the manufacturer's specifications for storage of amplification kits to avoid problems associated with free dyes. If problems persist, clean-up or re-amplify sample. See example in Figure 8 below of dye blob.

### Dye Pull-up or Bleed-through

Dye pull-up, sometimes referred to as bleed-through, represents a failure of the analysis software to discriminate between the different dye colors used during the generation of the data. Oversaturated data can also cause the dyes to "bleed" over or pull-up into another color. If pull-up occurs, inject less of the sample or re-amplify the sample with less DNA. Reoccurring pull-up (due to too much DNA) may indicate that the quantitation method or the amount of DNA used for amplification should be reevaluated. If this problem is not due to too much DNA, it may be necessary to run a new matrix and apply it to the sample.

### Off-ladder alleles or microvariants

Allelic ladders represent the most common alleles at each locus and were established through the evaluation of data from several hundred individuals. Alleles within the STR loci are known to differ significantly between individuals and the manufacturers' kit ladders do not represent all possible types of known alleles. Alleles that size outside allele categories represented in the ladder are known as off ladder (OL) alleles.

The sizing software is designed to assign allele size within one of the allele categories defined by the ladder. The software designates an allele that falls outside of these allele categories as off ladder alleles.

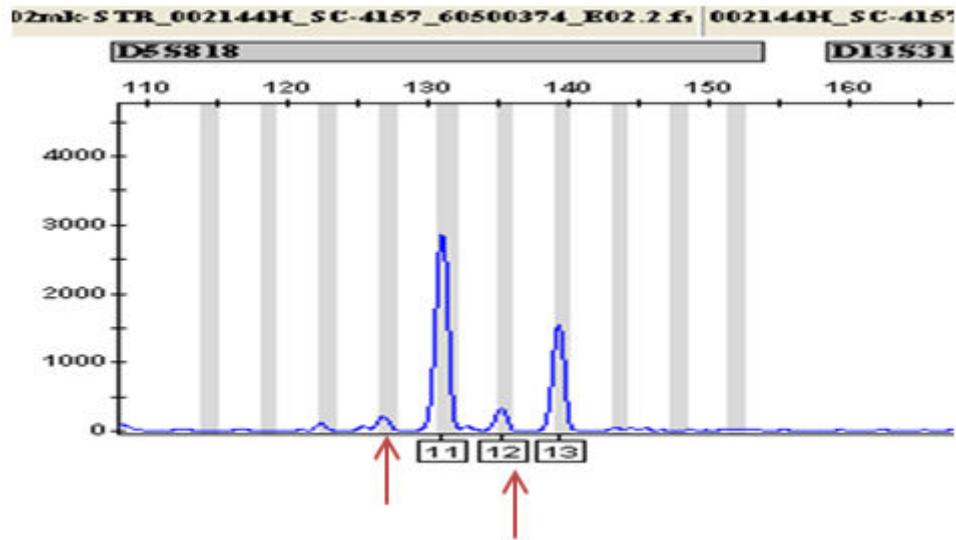


Figure 7: Stutter peaks.

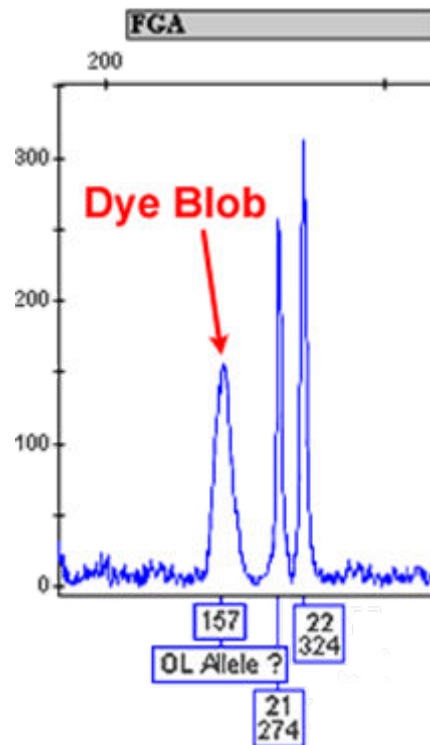
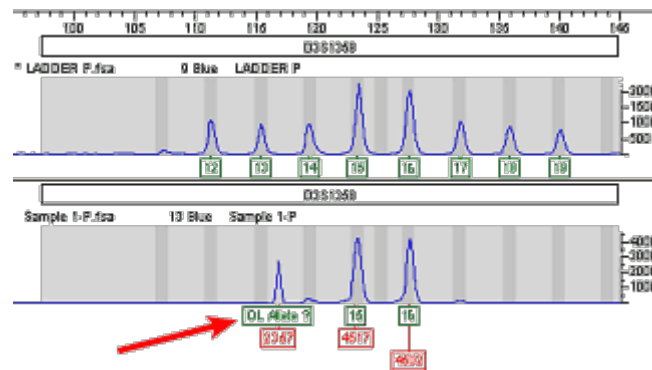


Figure 8: Dye blob

It is not unusual for STR profiling of cells from tumor tissue to see microvariants. A microvariant represents an incomplete repeat for a given allele. For instance, at D18S51 a



**Figure 9:** Off-ladder allele or microvariant.

15 allele designation means that there are 15 AGAA's along the fragment. However, a 14.2 allele designation means that there are 14 AGAA repeats along the fragment plus an additional 2 bases: AG. Microvariants are reported as the number of complete repeat units and are designated as an integer (e.g. 14). Any partial repeat is designated as a decimal, followed by the number of bases in the partial repeat, see example in Figure 9.

Many microvariants are represented in allelic ladders or have virtual allele categories within the software program; those that do not have established categories are designated as off ladder alleles.

While off ladder alleles have been well documented with forensic STR testing, some may not have been previously characterized. The National Institute of Standards and Technology (NIST) website (<http://www.cstl.nist.gov/div831/strbase/>) has a listing of off ladder alleles and can be used as a reference in these instances. If it is determined that an allele has not been characterized, it may be advisable to rerun the sample to confirm the type.

## Characteristics of STR

STRs selected for cell line authentication are chosen because they display the highest possible variation for discriminating among human cell lines and can detect cross-contaminating cells. The criteria for selecting STR loci for human cell line authentication include the following characteristics.

- High discriminating power
- High observed heterozygosity >70%
- Robust and reproducible results
- Low stutter characteristics
- Low mutation rate
- Alleles fall in the range of 90-500 bp – smaller fragments better to allow for degraded DNA

## Advantages of STR analysis

STR analysis is a universally accepted method for human cell line authentication. This method is robust in its ability to identify unique human cell lines; easy to perform; accessible to scientists and affordable. Some of the advantages of STR analysis are listed below.

- Target sequence consists of microsatellite DNA
- Typically use 1-2 ng DNA
- 1 to 2 fragments; discrete alleles allow digital record of data
- Highly variable within populations; highly informative
- Banding pattern is reproducible
- PCR amplifiable, high throughput
- Small size range allows multiplexing
- Allelic ladders simplify interpretation
- Small product size compatible with degraded DNA
- Rapid processing is attainable

## Services for STR Typing of Cell Lines

Over the past few years, several institutions are offering service for STR typing of human cell lines. When choosing a testing laboratory, considerations should be made based on experience of testing laboratory personnel to propagate human cell lines and to perform and interpret the data from STR analysis. The following are some institutions who are currently offering STR typing services.

- Cell Banks
- Paternity testing labs
- Universities
- Core labs

## Troubleshooting

### Reducing Cellular Misidentification of Cell Lines

The following list provides some suggestions to assist in reducing cellular misidentification of cell lines.

- Good documentation
- Highly trained technicians
- Good aseptic techniques
- Use one reservoir of medium per cell line
- Aliquot stock solutions/reagents
- Label flasks (name of cell line, passage number, date of transfer (use barcoded flasks when available))
- Work with one cell line at a time in biological safety cabinet

- Clean biological safety cabinet between each cell line
- Allow a minimum of 5 minutes between each cell line
- Quarantine “dirty” cell line from “clean” cell line
- Manageable work load (reduce accidents)
- Clean laboratory (reduce bioburden)
- Legible handwriting (printed labels)
- Monitor for cell line identity and characteristics contamination, routinely
- Use seed stock (create master stocks)
- Create “good” working environment
- Review and approve laboratory notebook

## Preventing contamination during PCR

Preventing contamination during PCR is of critical importance to ensure that you are getting useful results. The following list provides some suggestions of how to reduce and/or prevent contamination during PCR.

- Separate pre-amplification space (low copy) from post-amplification space (high copy)
- Use separate lab coat, gloves, tubes, pipette tip in pre-amplification room from post-amplification room
- Use aerosol-resistant pipette tips
- Keep pre-amplification and post-amplification reagents in separate rooms
- Prepare amplification reactions in a room dedicated for reaction setup
- Use a separate aliquot of DEPC water stock for each round of PCR
- Prepare your PCR mix in a hood with laminar flow. Decontaminate it with bleach, alcohol, RNase, DNase, etc...
- Use a different pipette tip when pipetting all your reagents, even the same master mix to each tube
- Keep your tubes closed during the procedure, even your master mix tube.
- Be sure that your tubes are closed when discarding the pipette tip!!! Aerosols are dangerous!!!
- Open the tubes only when necessary

## References

- Nelson-Rees WA. The identification and monitoring of cell line specificity. *Prog Clin Biol Res.* 1978;26:25–79. PubMed PMID: 218226.
- Hukku B, Halton D, Mally M. (1984). Cell characterization by use of multiple genetic markers. P 13-31. In RT Acton and DJ Lyn (eds), *Eukaryotic Cell Cultures*. Plenum Press, New York.
- Nelson-Rees WA, Flandermeyer RR. HeLa Defined. *Science.* 1976;191(4222):96–8. PubMed PMID: 1246601.

- Nelson-Rees WA, Daniels DW, Flandermeyer RR. Cross-contamination of cells in culture. *Science*. 1981;212(4493):446–52. PubMed PMID: 6451928.
- Drexler HG, Dirks WG, MacLeod RAF. False human hematopoietic cell lines: cross-contamination and misinterpretation. *Leukemia*. 1999;13:1601–1607. PubMed PMID: 10516762.
- Thompson EW, Waltham M, Ramus SJ, Hutchins AM, Armes JE, Campbell IG, Williams ED, Thompson PR, Rae JM, Johnson MD, Clarke R. LCC15-MB cells are MDA-MB-435: a review of misidentified breast and prostate cell lines. *Clin Exp Metastasis*. 2004;21(6):535–41. PubMed PMID: 15679051.
- Schweppe RE, Klopper JP, Korch C, Pugazhenthii U, Benezra M, Knauf JA, Fagin JA, Marlow LA, Copland JA, Smallridge RC, Haugen BR. Deoxyribonucleic acid profiling analysis of 40 human thyroid cancer cell lines reveals cross-contamination resulting in cell line redundancy and misidentification. *J Clin Endocrinol Metab*. 2008;93(11):4331–4341. PubMed PMID: 18713817.
- Phuchareon J, Ohta Y, Woo JM, Eisele DW, Tetsu O. Genetic Profiling Reveals Cross-Contamination and Misidentification of 6 Adenoid Cystic Carcinoma Cell Lines: ACC2, ACC3, ACCM, ACCNS, ACCS and CAC2. *PLoS ONE*. 2009;4(6):e6040. doi: [10.1371/journal.pone.0006040](https://doi.org/10.1371/journal.pone.0006040). PubMed PMID: 19557180.
- Boonstra JJ, van der Velden AW, Beerens WCW, van Marion R, Morita-Fujimura Y, Matsui Y, Nishihira T, Tselepis C, Hainaut P, Lowe AW, Beverloo BH, van Dekken H, Tilanus HW, Dinjens WNM. Mistaken Identity of Widely Used Esophageal Adenocarcinoma Cell Line TE-7. *Cancer Research*. 2007;67:7996–8001. PubMed PMID: 17804709.
- Jeffreys AJ, Wilson V, Thein SL. Hypervariable 'minisatellite' regions in human DNA. *Biotechnology*. 1985;24:467–72. PubMed PMID: 1422054.
- Nakamura Y, Leppert M, O'Connell P, Wolff R, Holm T, Culver M, Martin C, Fujimoto E, Hoff M. Variable number of tandem repeat (VNTR) markers for human gene mapping. *Science*. 1987;235(4796):1616–1622. Kumlin et al. PubMed PMID: 3029872.
- Wahls WP, Wallace LJ, Moore PD. Hypervariable minisatellite DNA is a hotspot for homologous recombination in human cells. *Cell*. 1990;60:95–103. PubMed PMID: 2295091.
- Wieczorek D, Krenke BE. (2009) [Direct amplification from buccal and blood samples preserved on cards using the PowerPlex® 16 HS System](#). *Profiles in DNA* 12(2).
- American Type Culture Collection Standards Development Organization Workgroup ASN-0002: Alston-Roberts C, Barallon R, Bauer SR, Butler J, Capes-Davis A, Dirks WG, Elmore E, Furtado M, Kerrigan L, Kline MC, Kohara A, Los GV, MacLeod RAF, Masters JR, Nardone M, Nims RW, Price PJ, Reid YA, Shewale J, Steuer AF, Storts DR, Sykes G, Taraporewala Z, Thomson J (2011). Authentication of Human Cell Lines: Standardization of STR Profiling. ANSI/ATCC ASN-0002-2011. Copyrighted by ATCC and the American National Standards Institute (ANSI). Available at: <http://webstore.ansi.org/RecordDetail.aspx?sku=ANSI%2fATCC+ASN-0002-2011> Edelman

J, Lessig R, Hering S, Horn L-C. (2004) Loss of heterozygosity and microsatellite instability of forensically used STR markers in human cervical carcinoma. *International Congress Series* 1261: 499-501.

Ronald J, Duffy KJ, Kaye MT, Shepard MT, McCue BJ, Shirley J, Shephert MS, Wisecarver ML. Loss of Heterozygosity Detected in a Short Tandem Repeat (STR) Locus Commonly Used for Human DNA Identification. *Journal of Forensic Sciences*. 2000;45(5):1087–1089. PubMed PMID: 11005185.

Peloso G, Grignani P, Rosso R, Previdere C. Forensic evaluation of tetranucleotide STR instability in lung cancer. *International Congress Series*. 2003;1239:719–721.

Master JR, Thomson JA, Daly-Burns B, Reid YA, Dirks WG, Pack P, Toji LH, Ohno T, Tanabe H, Arlett CF, Kelland LR, Harrison M, Virmani A, Ward TH, Ayer KL, Debenham PG. Short tandem repeat profiling provides an international reference standard for human cell lines. *PNAS*. 2001;98(140):8012–8017. PubMed PMID: 11416159.

Authentication of Human Cell Lines: Standardization of STR Profiling. ANSI/ATCC ASN-0002-2011.

## Additional References

ICLAC List of misidentified cell lines: [http://standards.atcc.org/kwspub/home/the\\_international\\_cell\\_line\\_authentication\\_committee-iclac/Database\\_of\\_Cross\\_Contaminated\\_or\\_Misidentified\\_Cell\\_Lines.pdf](http://standards.atcc.org/kwspub/home/the_international_cell_line_authentication_committee-iclac/Database_of_Cross_Contaminated_or_Misidentified_Cell_Lines.pdf)

Commercially available STR Multiplex Kits: <http://www.cstl.nist.gov/strbase/multiplx.htm>

## Glossary of Terms

Please refer to the “Genetics Terms” section of the “Glossary of Quantitative Biology Terms” for a list of terms and definitions used in this chapter.





# Cell Viability Assays

Terry L Riss, PhD,<sup>✉1,\*</sup> Richard A Moravec, BS,<sup>1</sup> Andrew L Niles, MS,<sup>1</sup> Sarah Duellman, PhD,<sup>1</sup> Hélène A Benink, PhD,<sup>1</sup> Tracy J Worzella, MS,<sup>1</sup> and Lisa Minor<sup>2,†</sup>

Created: May 1, 2013; Updated: July 1, 2016.

## Abstract

This chapter is an introductory overview of the most commonly used assay methods to estimate the number of viable cells in multi-well plates. This chapter describes assays where data are recorded using a plate-reader; it does not cover assay methods designed for flow cytometry or high content imaging. The assay methods covered include the use of different classes of colorimetric tetrazolium reagents, resazurin reduction and protease substrates generating a fluorescent signal, the luminogenic ATP assay, and a novel real-time assay to monitor live cells for days in culture. The assays described are based on measurement of a marker activity associated with viable cell number. These assays are used for measuring the results of cell proliferation, testing for cytotoxic effects of compounds, and for multiplexing as an internal control to determine viable cell number during other cell-based assays.

## Introduction

Cell-based assays are often used for screening collections of compounds to determine if the test molecules have effects on cell proliferation or show direct cytotoxic effects that eventually lead to cell death. Cell-based assays also are widely used for measuring receptor binding and a variety of signal transduction events that may involve the expression of genetic reporters, trafficking of cellular components, or monitoring organelle function. Regardless of the type of cell-based assay being used, it is important to know how many viable cells are remaining at the end of the experiment. There are a variety of assay methods that can be used to estimate the number of viable eukaryotic cells. This chapter will provide an overview of some of the major methods used in multi-well formats where data are recorded using a plate reader. The methods described include: tetrazolium reduction, resazurin reduction, protease markers, and ATP detection. Methods for flow cytometry and high content imaging may be covered in different chapters in the future.

---

<sup>1</sup> Promega Corporation; Email: Terry.riss@promega.com; Email: Rich.moravec@promega.com; Email: Andrew.niles@promega.com; Email: Helene.benink@promega.com; Email: Tracy.worzella@promega.com. <sup>2</sup> In Vitro Strategies, LLC; Email: lisakminor@yahoo.com.

<sup>✉</sup> Corresponding author.

\* Editor

† Editor

The tetrazolium reduction, resazurin reduction, and protease activity assays measure some aspect of general metabolism or an enzymatic activity as a marker of viable cells. All of these assays require incubation of a reagent with a population of viable cells to convert a substrate to a colored or fluorescent product that can be detected with a plate reader. Under most standard culture conditions, incubation of the substrate with viable cells will result in generating a signal that is proportional to the number of viable cells present. When cells die, they rapidly lose the ability to convert the substrate to product. That difference provides the basis for many of the commonly used cell viability assays. The ATP assay is somewhat different in that the addition of assay reagent immediately ruptures the cells, thus there is no incubation period of reagent with a viable cell population.

## Tetrazolium Reduction Assays

A variety of tetrazolium compounds have been used to detect viable cells. The most commonly used compounds include: MTT, MTS, XTT, and WST-1. These compounds fall into two basic categories: 1) MTT which is positively charged and readily penetrates viable eukaryotic cells and 2) those such as MTS, XTT, and WST-1 which are negatively charged and do not readily penetrate cells. The latter class (MTS, XTT, WST-1) are typically used with an intermediate electron acceptor that can transfer electrons from the cytoplasm or plasma membrane to facilitate the reduction of the tetrazolium into the colored formazan product.

### MTT Tetrazolium Assay Concept

The MTT (3-(4,5-dimethylthiazol-2-yl)-2,5-diphenyltetrazolium bromide) tetrazolium reduction assay was the first homogeneous cell viability assay developed for a 96-well format that was suitable for high throughput screening (HTS) (1). The MTT tetrazolium assay technology has been widely adopted and remains popular in academic labs as evidenced by thousands of published articles. The MTT substrate is prepared in a physiologically balanced solution, added to cells in culture, usually at a final concentration of 0.2 - 0.5mg/ml, and incubated for 1 to 4 hours. The quantity of formazan (presumably directly proportional to the number of viable cells) is measured by recording changes in absorbance at 570 nm using a plate reading spectrophotometer. A reference wavelength of 630 nm is sometimes used, but not necessary for most assay conditions.

Viable cells with active metabolism convert MTT into a purple colored formazan product with an absorbance maximum near 570 nm (Figure 1). When cells die, they lose the ability to convert MTT into formazan, thus color formation serves as a useful and convenient marker of only the viable cells. The exact cellular mechanism of MTT reduction into formazan is not well understood, but likely involves reaction with NADH or similar reducing molecules that transfer electrons to MTT (2). Speculation in the early literature involving specific mitochondrial enzymes has led to the assumption mentioned in numerous publications that MTT is measuring mitochondrial activity (3, 4).

The formazan product of the MTT tetrazolium accumulates as an insoluble precipitate inside cells as well as being deposited near the cell surface and in the culture medium. The

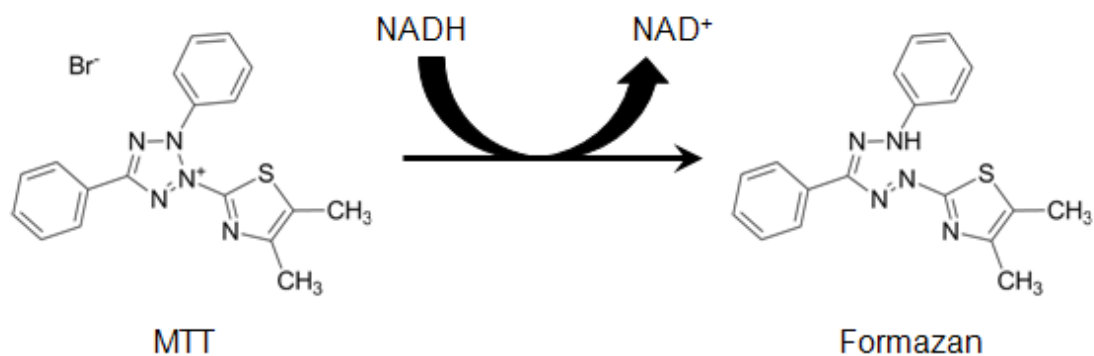


**Figure 1:** Structures of MTT and colored formazan product.

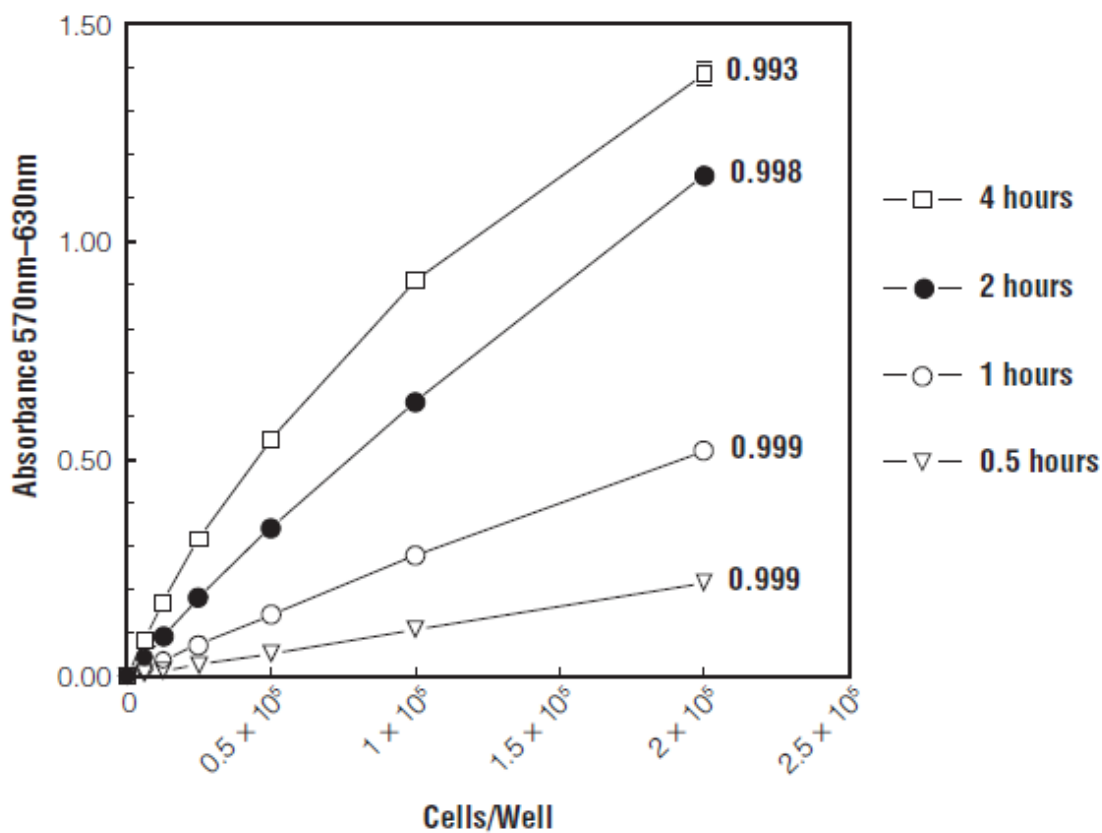


**Figure 2:** Direct correlation of formazan absorbance with B9 hybridoma cell number and time-dependent increase in absorbance. Note: there is little absorbance change between 2 and 4 hours. Adapted from CellTiter 96<sup>®</sup> Non-Radioactive Cell Proliferation Assay Technical Bulletin #112 (9).

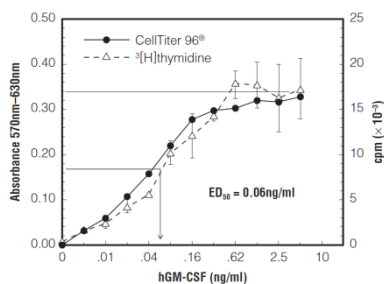


**Figure 3:** A comparison of using the MTT and  $^3\text{[H]}$ thymidine incorporation assays of hGM-CSF-treated TF-1 cells. A blank absorbance value of 0.065 (from wells without cells but treated with MTT) was subtracted from all absorbance values. Adapted from CellTiter 96<sup>®</sup> Non-Radioactive Cell Proliferation Assay Technical Bulletin #112 (9).

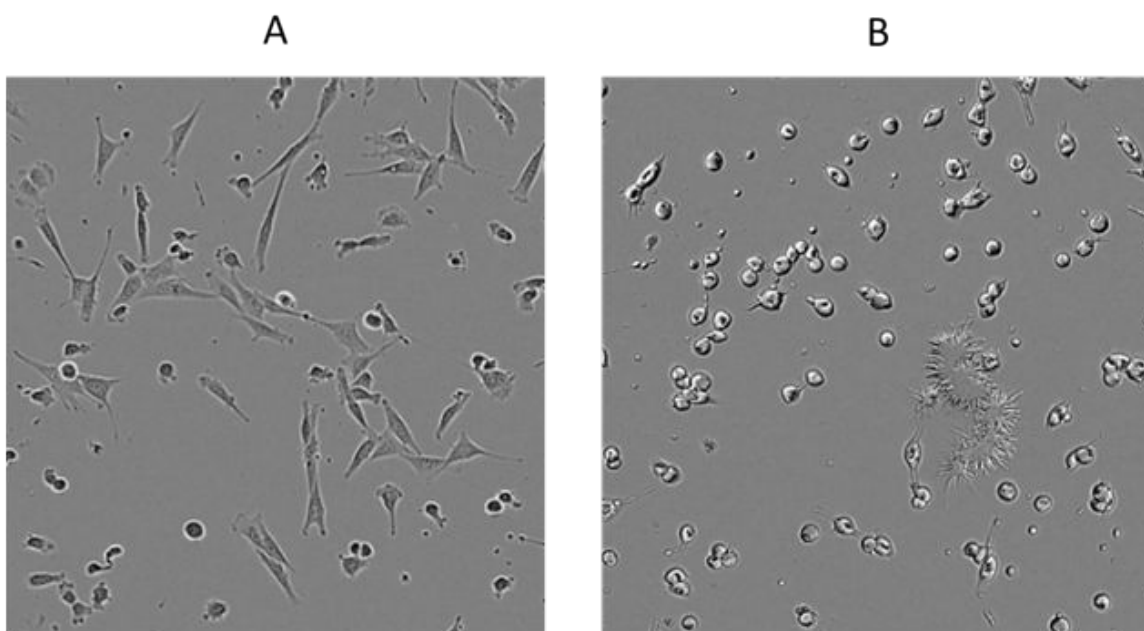


**Figure 4:** Change in NIH3T3 cell morphology after exposure to MTT (0.5 mg/ml). Panel A shows a field of cells photographed immediately after addition of the MTT solution. Panel B shows the same field of cells photographed after 4 hours of exposure to MTT. Panel B shows a change in cell morphology and the appearance of formazan crystals. Images were captured using the IncuCyte<sup>™</sup> FLR from Essen Biosciences.

formazan must be solubilized prior to recording absorbance readings. A variety of methods have been used to solubilize the formazan product, stabilize the color, avoid evaporation, and reduce interference by phenol red and other culture medium components (5-7). Various solubilization methods include using: acidified isopropanol, DMSO, dimethylformamide, SDS, and combinations of detergent and organic solvent (1, 5-7). Acidification of the solubilizing solution has the benefit of changing the color of phenol red to yellow color that may have less interference with absorbance readings. The

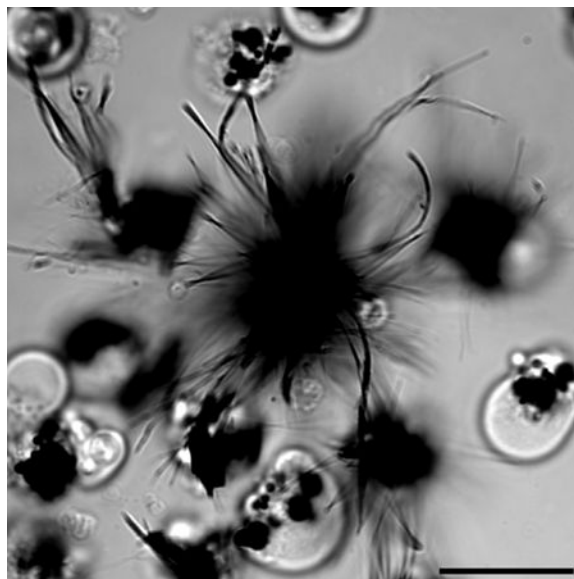


**Figure 5:** U937 cells incubated with MMT tetrazolium for 3 hours showing formazan crystals larger than the cells. Image was captured using an Olympus FV500 confocal microscope. Scale bar = 20  $\mu\text{m}$

pH of the solubilization solution can be adjusted to provide maximum absorbance if sensitivity is an issue (8); however, other assay technologies offer much greater sensitivity than MTT.

The amount of signal generated is dependent on several parameters including: the concentration of MTT, the length of the incubation period, the number of viable cells and their metabolic activity. All of these parameters should be considered when optimizing the assay conditions to generate a sufficient amount of product that can be detected above background.

The conversion of MTT to formazan by cells in culture is time dependent (Figure 2).

Longer incubation time will result in accumulation of color and increased sensitivity up to a point; however, the incubation time is limited because of the cytotoxic nature of the detection reagents which utilize energy (reducing equivalents such as NADH) from the cell to generate a signal. For cell populations in log phase growth, the amount of formazan product is generally proportional to the number of metabolically active viable cells as demonstrated by the linearity of response in Figure 2. Culture conditions that alter the metabolism of the cells will likely affect the rate of MTT reduction into formazan. For example, when adherent cells in culture approach confluence and growth becomes contact inhibited, metabolism may slow down and the amount MTT reduction per cell will be lower. That situation will lead to a loss of linearity between absorbance and cell number. Other adverse culture conditions such as altered pH or depletion of essential nutrients such as glucose may lead to a change in the ability of cells to reduce MTT.

The MTT assay was developed as a non-radioactive alternative to tritiated thymidine incorporation into DNA for measuring cell proliferation (1). In many experimental situations, the MTT assay can directly substitute for the tritiated thymidine incorporation assay (Figure 3).

However, it is worth noting that MTT reduction is a marker reflecting viable cell metabolism and not specifically cell proliferation. Tetrazolium reduction assays are often erroneously described as measuring cell proliferation without the use of proper controls to confirm effects on metabolism (10).

Shortly after addition of MTT, the morphology of some cell types can be observed to change dramatically suggesting altered physiology (11 and Figure 4).

Toxicity of the MTT compound is likely related to the concentration added to cells. Optimizing the concentration may result in lower toxicity. Given the cytotoxic nature of MTT, the assay method must be considered as an endpoint assay. A recent report speculated that formazan crystals contribute to harming cells by puncturing membranes during exocytosis (12). The observation of extracellular formazan crystals many times the diameter of cells that grow longer over time make it seem unlikely that exocytosis of those large structures was involved (Figure 4 and 5).

Growing crystals may suggest that marginally soluble formazan accumulates where seed crystals have begun to deposit.

Reducing compounds are known to interfere with tetrazolium reduction assays. Chemicals such as ascorbic acid, or sulfhydryl-containing compounds including reduced glutathione, coenzyme A, and dithiothreitol, can reduce tetrazolium salts non-enzymatically and lead to increased absorbance values in assay wells (13-17). Culture medium at elevated pH or extended exposure of reagents to direct light also may cause an accelerated spontaneous reduction of tetrazolium salts and result in increased background absorbance values. Suspected chemical interference of test compounds can be confirmed by measuring absorbance values from control wells without cells incubated with culture medium containing MTT and various concentrations of the test compound.

### **Commercial Availability**

Commercial kits containing solutions of MTT and a solubilization reagent as well as MTT reagent powder are available from several vendors. For example:

- CellTiter 96<sup>®</sup> Non-Radioactive Cell Proliferation Assay. Promega Corporation Cat.# G4000,
- Cell Growth Determination Kit, MTT based. Sigma-Aldrich Cat.# CGD1-1KT, and
- MTT Cell Growth Assay Kit. Millipore Cat.# CT02.
- Thiazolyl Blue Tetrazolium Bromide (MTT Powder). Sigma-Aldrich Cat.# M2128.

The concentration of the MTT solution and the nature of the solubilization reagent differ among various vendors. The amount of formazan signal generated will depend on variety of parameters including the cell type, number of cells per well, culture medium, etc.

Although the commercially available kits are broadly applicable to a large number of cell types and assay conditions, the concentration of the MTT and the type of solubilization solution may need to be adjusted for optimal performance.

## Reagent Preparation

### MTT Solution

1. Dissolve MTT in Dulbecco's Phosphate Buffered Saline, pH=7.4 (DPBS) to 5 mg/ml.
2. Filter-sterilize the MTT solution through a 0.2  $\mu$ M filter into a sterile, light protected container.
3. Store the MTT solution, protected from light, at 4°C for frequent use or at -20°C for long term storage.

### Solubilization Solution

1. Choose appropriate solvent resistant container and work in a ventilated fume hood.
2. Prepare 40% (vol/vol) dimethylformamide (DMF) in 2% (vol/vol) glacial acetic acid.
3. Add 16% (wt/vol) sodium dodecyl sulfate (SDS) and dissolve.
4. Adjust to pH = 4.7
5. Store at room temperature to avoid precipitation of SDS. If a precipitate forms, warm to 37°C and mix to solubilize SDS.

### MTT Assay Protocol

1. Prepare cells and test compounds in 96-well plates containing a final volume of 100  $\mu$ l/well.
2. Incubate for desired period of exposure.
3. Add 10  $\mu$ l MTT Solution per well to achieve a final concentration of 0.45 mg/ml.
4. Incubate 1 to 4 hours at 37°C.
5. Add 100  $\mu$ l Solubilization solution to each well to dissolve formazan crystals.
6. Mix to ensure complete solubilization.
7. Record absorbance at 570 nm.

### MTS Tetrazolium Assay Concept

More recently developed tetrazolium reagents can be reduced by viable cells to generate formazan products that are directly soluble in cell culture medium. Tetrazolium compounds fitting this category include MTS, XTT, and the WST series (18-23). These improved tetrazolium reagents eliminate a liquid handling step during the assay procedure because a second addition of reagent to the assay plate is not needed to solubilize formazan precipitates, thus making the protocols more convenient. The negative charge of the formazan products that contribute to solubility in cell culture medium are thought to limit cell permeability of the tetrazolium (24). This set of tetrazolium reagents is used in combination with intermediate electron acceptor reagents such as phenazine

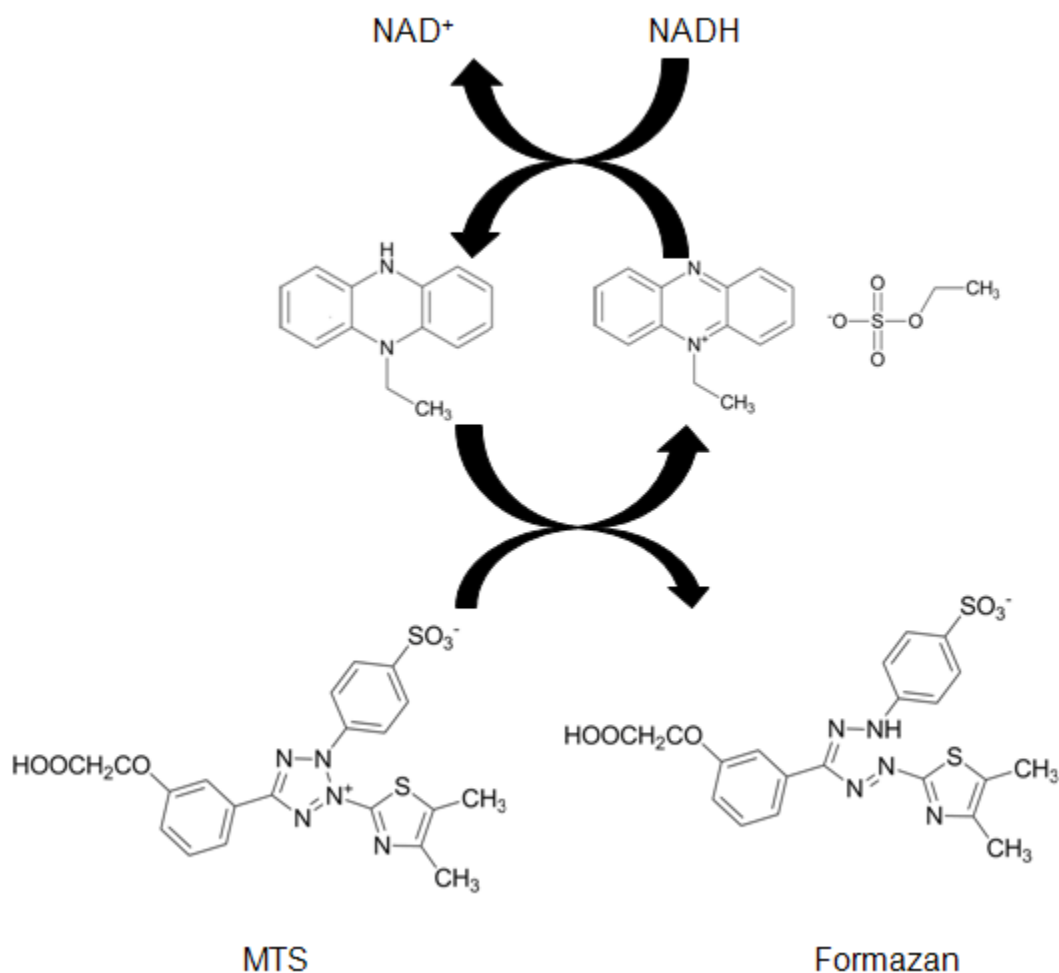


**Figure 6:** Intermediate electron acceptor phenazine ethyl sulfate (PES) transfers electron from NADH in the cytoplasm to reduce MTS in the culture medium into an aqueous soluble formazan.

methyl sulfate (PMS) or phenazine ethyl sulfate (PES) which can penetrate viable cells, become reduced in the cytoplasm or at the cell surface and exit the cells where they can convert the tetrazolium to the soluble formazan product (25). The general reaction scheme for this class of tetrazolium reagents is shown in Figure 6.

In general, this class of tetrazolium compounds is prepared at 1 to 2mg/ml concentration because they are not as soluble as MTT. The type and concentration of the intermediate electron acceptor used varies among commercially available reagents and in many products the identity of the intermediate electron acceptor is not disclosed. Because of the potential toxic nature of the intermediate electron acceptors, optimization may be advisable for different cell types and individual assay conditions. There may be a narrow



range of concentrations of intermediate electron acceptor that result in optimal performance.

### Commercial Availability

Commercial kits containing solutions of MTS, XTT, and WST-1 and an intermediate electron acceptor reagent are available from several vendors. For example:

- CellTiter 96<sup>®</sup> AQueous One Solution Cell Proliferation Assay. Promega Corporation Cat.# G3580,
- In Vitro Toxicology Assay Kit, XTT based. Sigma-Aldrich Cat.# TOX2-1KT,
- Cell Counting Kit-8 (WST-8 based). Dojindo Molecular Technologies, Inc. Cat.# CK04-01,
- MTS Reagent Powder. Promega Corporation Cat.# G1111,
- XTT sodium salt. Sigma-Aldrich Cat.# X4626.

### Reagent Preparation

#### MTS Solution (containing PES)

1. Dissolve MTS powder in DPBS to 2 mg/ml to produce a clear golden-yellow solution.
2. Dissolve PES powder in MTS solution to 0.21 mg/ml.
3. Adjust to pH 6.0 to 6.5 using 1N HCl.
4. Filter-sterilize through a 0.2  $\mu$ m filter into a sterile, light protected container.
5. Store the MTS solution containing PES protected from light at 4°C for frequent use or at -20°C for long term storage.

### MTS Assay Protocol

1. Prepare cells and test compounds in 96-well plates containing a final volume of 100  $\mu$ l/well. An optional set of wells can be prepared with medium only for background subtraction.
2. Incubate for desired period of exposure.
3. Add 20  $\mu$ l MTS solution containing PES to each well (final concentration of MTS will be 0.33 mg/ml).
4. Incubate 1 to 4 hours at 37°C.
5. Record absorbance at 490 nm.

One of the advantages of the tetrazolium assays that produce an aqueous soluble formazan is that absorbance can be recorded from the assay plates periodically during early stages of incubation. Multiple readings may assist during assay development; but caution should be taken to return the plates to the incubator between readings to maintain a nearly constant environment. Extended incubations with the tetrazolium reagent beyond four hours should be avoided.

Whereas the background (culture medium and tetrazolium without cells) absorbance at 570 nm for an MTT assay may be 0.05, in general the background absorbance for the class

of tetrazolium reagents is usually somewhat higher, in the range of 0.3 absorbance units and can depend on the type of culture medium and pH.

## Resazurin Reduction Assay Concept

Resazurin is a cell permeable redox indicator that can be used to monitor viable cell number with protocols similar to those utilizing the tetrazolium compounds (26). Resazurin can be dissolved in physiological buffers (resulting in a deep blue colored solution) and added directly to cells in culture in a homogeneous format. Viable cells with active metabolism can reduce resazurin into the resorufin product which is pink and fluorescent (Figure 7).

Addition of an intermediate electron acceptor is not required for cellular resazurin reduction to occur, but it may accelerate signal generation. The quantity of resorufin produced is proportional to the number of viable cells which can be quantified using a microplate fluorometer equipped with a 560 nm excitation / 590 nm emission filter set. Resorufin also can be quantified by measuring a change in absorbance; however, absorbance detection is not often used because it is far less sensitive than measuring fluorescence. The resazurin reduction assay is slightly more sensitive than tetrazolium reduction assays and there are numerous reports using the resazurin reduction assay in a miniaturized format for HTS applications (27).

The incubation period required to generate an adequate fluorescent signal above background is usually 1 to 4 hours and is dependent on the metabolic activity of the particular cell type, the cell density per well, and other assay conditions including the type of culture medium. The incubation period should be optimized and kept short enough to avoid reagent toxicity but long enough to provide adequate sensitivity.

The major advantages of the resazurin reduction assay are that it is relatively inexpensive, it uses a homogeneous format, and it is more sensitive than tetrazolium assays. In addition, resazurin assays can be multiplexed with other methods such as measuring caspase activity to gather more information about the mechanism leading to cytotoxicity (28 and Figure 8).

Multiplexing may require a sequential protocol to avoid color quenching by resazurin or direct chemical interference. For the multiplex example shown in Figure 8, resorufin fluorescence must be recorded first, followed by addition of the caspase reagent which contains detergent to lyse cells and reducing compounds to convert remaining resazurin and reduce interference with collecting the second fluorescent signal.

The disadvantages of the resazurin include the possibility of fluorescent interference from compounds being tested and the often overlooked direct toxic effects on the cells (Figure 9).

Some protocols describe exposing cells to resazurin for several hours or even days; however, in some systems, changes in cell morphology can be observed after only a few hours of exposure suggesting interference with normal cell function (29). It is possible

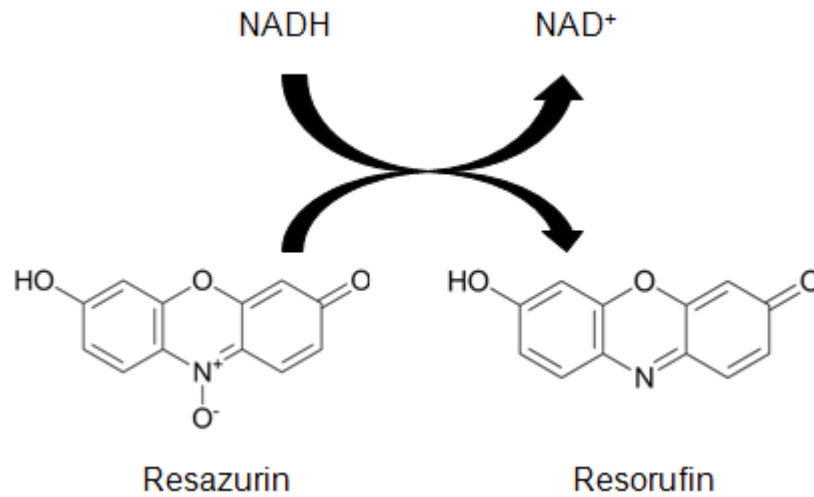


**Figure 7:** Structure of resazurin substrate and the pink fluorescent resorufin product resulting from reduction in viable cells.

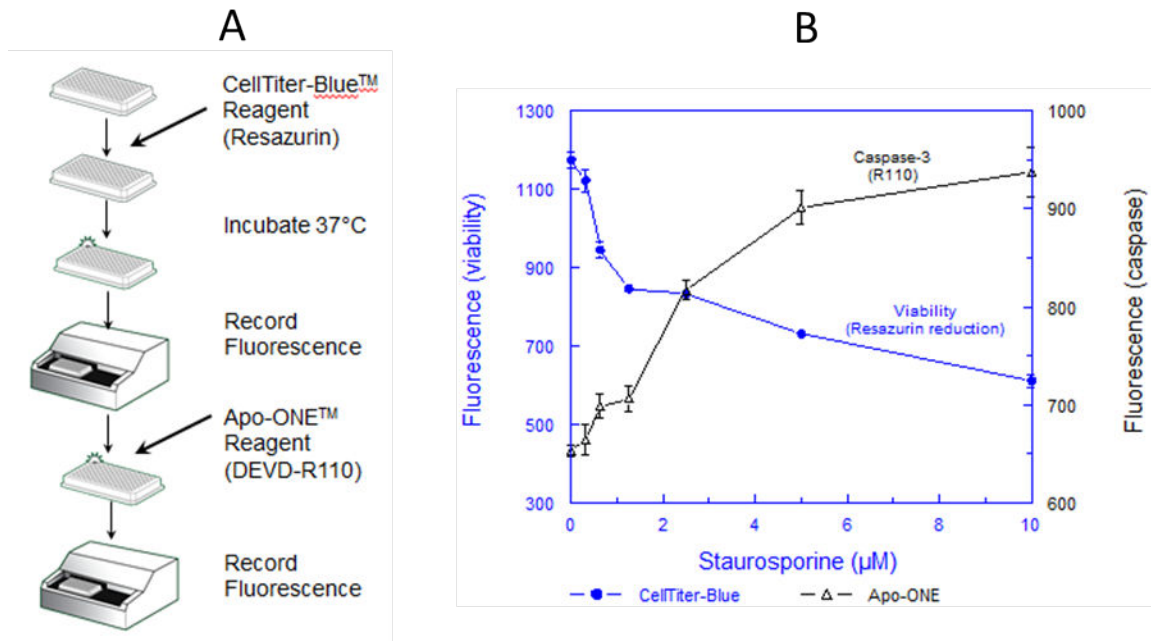


**Figure 8:** Panel A shows the steps of the sequential multiplex of a resazurin assay to measure viable cell number and a fluorometric caspase 3-assay to detect a marker of apoptosis. Panel B shows the results of treating PC3 (human prostate) cells with a range of concentrations of staurosporine for 20 hours. The resorufin (560/590 nm) and R110 fluorescence were captured at different wavelengths from the same sample as well.

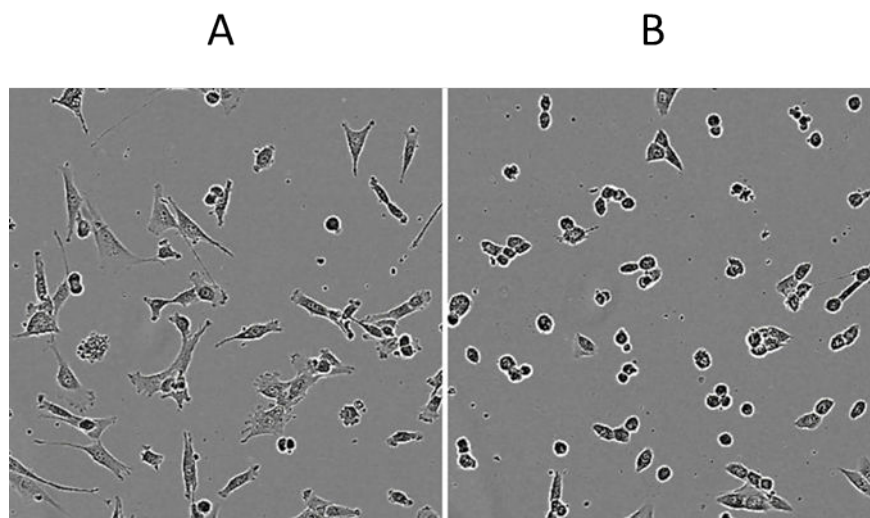


**Figure 9:** Change in NIH3T3 cell morphology after exposure to resazurin. Panel A shows a field of cells photographed immediately after addition of the resazurin solution. Panel B shows the same field of cells photographed after 4 hours of exposure to resazurin. Panel B shows a change in cell morphology. Images were captured using Incucyte from Essen Biosciences.

that exposure of cells to resazurin depletes reduced forms of nucleotides resulting in cytotoxic effects. Exposure of cells to resazurin is known to reduce the amount of ATP measured as a marker of cell viability. Figure 10 shows a decrease in ATP content of HepG2 cells exposed to resazurin for 4 and 24 hours.

### Commercial Availability

Commercial kits containing solutions of resazurin as well as resazurin powder are available from several vendors. For example:

- CellTiter-Blue<sup>®</sup> Cell Viability Assay. Promega Corporation Cat.# G8081,
- In Vitro Toxicology Assay Kit, Resazurin based. Sigma-Aldrich Cat.# TOX8-1KT,
- alamarBlue<sup>®</sup>—Rapid & Accurate Cell Health Indicator. Life Technologies, Inc. Cat.# DAL1100
- alamarBlue<sup>®</sup> AbD Serotech Cat.# BUF012B
- Resazurin sodium salt. Sigma-Aldrich Cat.# R7017-1G

Resazurin powder is readily available from chemical vendors; however, the resazurin dye content (% purity) and contamination with resorufin can lead to variability in assay results and the need to perform validation of each lot of reagent powder. Viability assay kits containing performance verified resazurin as the primary ingredient are available from different vendors; but the resazurin concentration and additional ingredients vary. The alamarBlue patent US 5,501,959 describes the use of poisoning agents to maintain the redox potential of the growth medium and prevent reduction of resazurin resulting in background signal (30). Preferred poisoning agents described include ferricyanide and

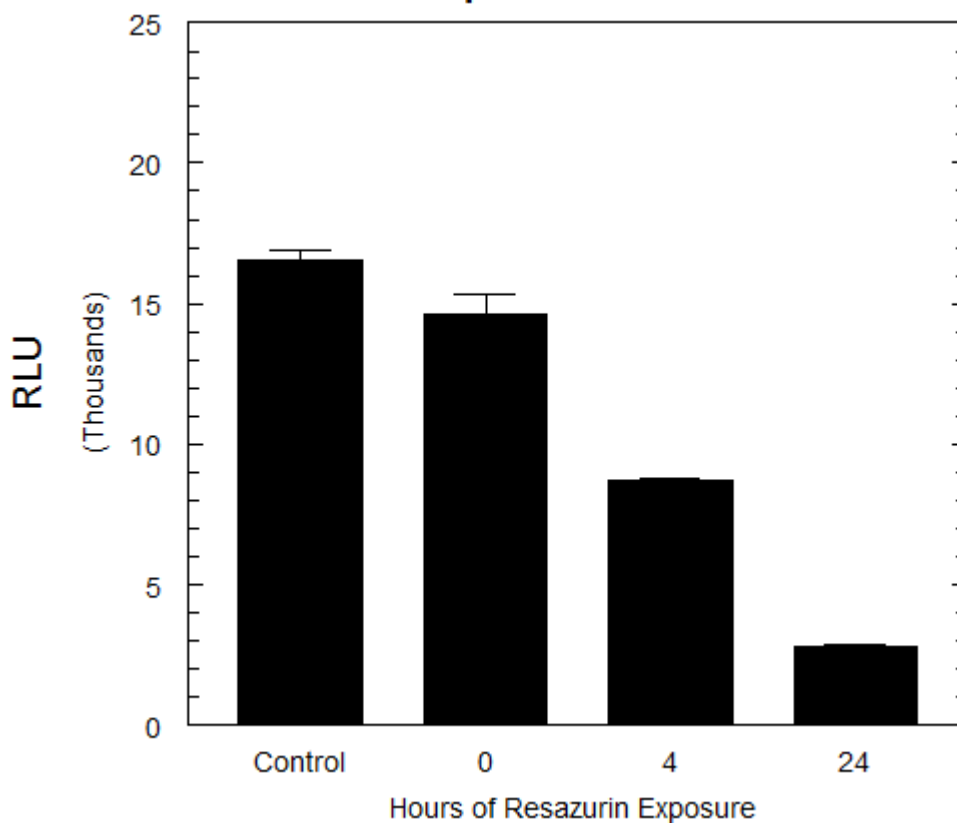


**Figure 10:** Viability (ATP content) of HepG2 cells exposed to resazurin for 0, 4, and 24 hours. Control wells did not contain resazurin. Zero hour wells contained resazurin and show quenching of luminescent signal following addition of the deeply blue colored resazurin reagent. ATP content was measured using the CellTiter-Glo<sup>®</sup> Assay.

ferrocyanide as well as methylene blue which can also serve as a redox indicator. The potential for undesired effects of additional ingredients in the proprietary alamarBlue formulation and the demonstrated performance equivalence of less complex formulations of highly purified resazurin in balanced saline solution should be considered when choosing an assay reagent.

### Reagent Preparation

1. Dissolve high purity resazurin in DPBS (pH 7.4) to 0.15 mg/ml.
2. Filter-sterilize the resazurin solution through a 0.2  $\mu\text{m}$  filter into a sterile, light protected container.
3. Store the resazurin solution protected from light at 4°C for frequent use or at -20°C for long term storage.

## Resazurin Assay Protocol

1. Prepare cells and test compounds in opaque-walled 96-well plates containing a final volume of 100  $\mu\text{l}$ /well. An optional set of wells can be prepared with medium only for background subtraction and instrument gain adjustment.
2. Incubate for desired period of exposure.
3. Add 20  $\mu\text{l}$  resazurin solution to each well.
4. Incubate 1 to 4 hours at 37°C.
5. Record fluorescence using a 560 nm excitation / 590 nm emission filter set.

A general disadvantage of both the tetrazolium and resazurin reduction assay protocols is the requirement to incubate the substrate with viable cells at 37°C for an adequate period of time to generate a signal. Incubation of the tetrazolium or resazurin reagents with viable cells increases the possibility of artifacts resulting from chemical interactions among the assay chemistry, the compounds being tested, and the biochemistry of the cell. Incubation also introduces an extra plate handling step that is not required for the ATP assay protocol described later. Extra plate manipulation steps increase the possibility of errors and are not desirable for automated assays for HTS.

## Protease Viability Marker Assay Concept

Measurement of a conserved and constitutive protease activity within live cells has been shown to serve as a marker of cell viability. A cell permeable fluorogenic protease substrate (glycylphenylalanyl-aminofluorocoumarin; GF-AFC) has recently been developed to selectively detect protease activity that is restricted to viable cells (31). The GF-AFC substrate can penetrate live cells where cytoplasmic aminopeptidase activity removes the gly and phe amino acids to release aminofluorocoumarin (AFC) and generate a fluorescent signal proportional to the number of viable cells (Figure 11).

As soon as the cells die, this protease activity rapidly disappears, thus making this protease activity a selective marker of the viable cell population. This assay approach is available as a commercial product from Promega Corporation (32). The components of the product include: GF-AFC 100mM in DMSO and an Assay Buffer for dilution of the substrate. The signal generated from the protease assay approach has been shown to correlate well with other established methods of determining cell viability such as an ATP assay (Figure 12).

One of the advantages of the GF-AFC substrate is that it is relatively non-toxic to cells in culture (Figure 13).

In addition, long term exposure of the GF-AFC substrate to cells results in little change in viability measured using ATP as a marker. This is in direct contrast to the effects of exposing cells to tetrazolium or resazurin redox indicators which have been demonstrated to be toxic to cells as described above. The non-toxic nature of the GF-AFC substrate makes it an ideal candidate for multiplexing with other assay technologies using a sequential assay protocol. After recording fluorescence data from the live cell protease

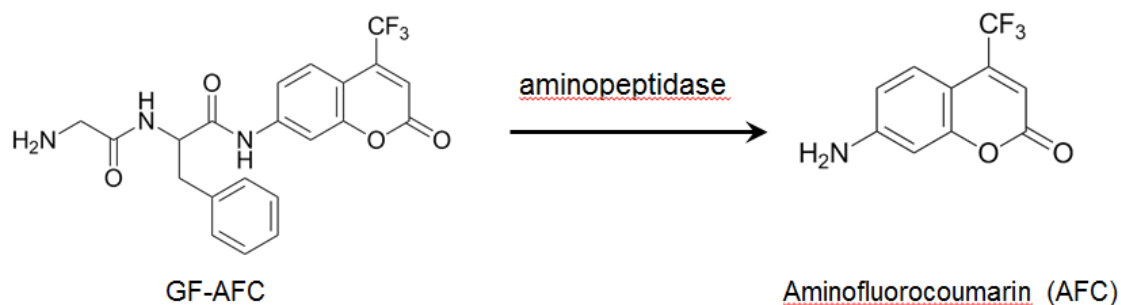


**Figure 11:** Cell permeable glycyphenylalanyl-aminofluorocoumarin (GF-AFC) substrate is converted by cytoplasmic aminopeptidase activity to generate fluorescent aminofluorocoumarin (AFC).

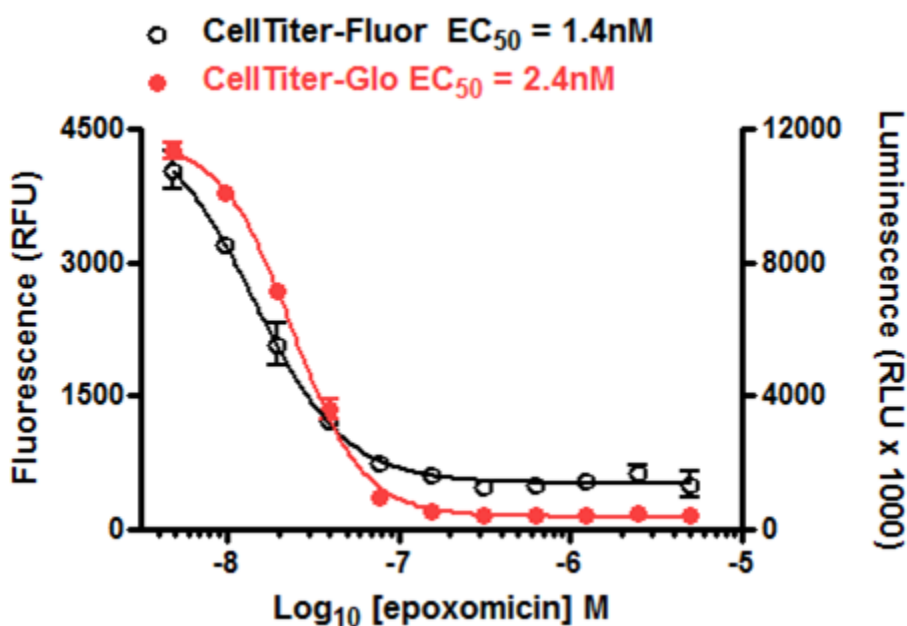


**Figure 12:** DU-145 cells treated with various concentrations of epoxomicin for 48 hours and assayed using GF-AFC reagent (CellTiter-Fluor™, open circles) and ATP detection (CellTiter-Glo® Assay, solid red circles). The similar  $EC_{50}$  values demonstrate good correlation between different methods to estimate viable cells.

assay, the population of cells remains viable and can be used for subsequent assays as long as the fluorescent signal from AFC does not interfere. This property enables “on-the-fly” detection and follow-up of cytotoxic hits during screening campaigns. Wells containing hits can be subjected to an orthogonal method to detect viable cell number or an alternate assay method to detect the mechanism leading to cell death. Figure 14 shows an example of multiplexing the live cell protease marker and a luminescent caspase assay to detect

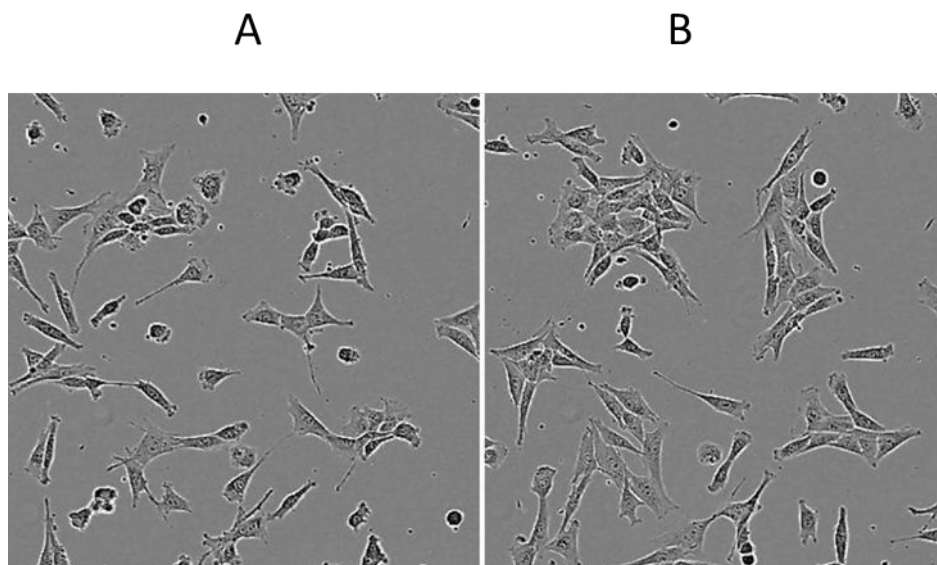


**Figure 13:** Morphology of NIH3T3 cells during exposure to GF-AFC reagent. Panel A shows a field of cells photographed immediately after additional of the GF-AFC reagent. Panel B shows the same cells photographed after 4 hours of exposure to GF-AFC. Panel B shows a little change in the cell morphology compared to the substantial changes and obvious toxicity shown for MTT and resazurin in the figures above. Images were captured using the IncuCyte™ FLR from Essen Biosciences.

apoptosis. In this example, the decrease in viability corresponds to an increase in caspase activity suggesting the mode of cell death is via apoptosis. An advantage of measuring this protease as a viability marker is that in general, the incubation time required to get an adequate signal is much shorter (30 min to 1 hour), compared to 1 to 4 hours required for the tetrazolium assays.

### GF-AFC Reagent Preparation

1. Thaw the GF-AFC substrate and Assay Buffer components from the CellTiter-Fluor™ Cell Viability Assay kit following the detailed procedure in the Technical Bulletin #371 (32).
2. Transfer 10  $\mu$ l of the GF-AFC Substrate into 10 ml of the Assay Buffer to prepare a 2X Reagent. Note: For multiplexing applications where total sample volume is a concern, a 10X Reagent can be prepared by adding 10  $\mu$ l GF-AFC Substrate to 2 ml of Assay Buffer.
3. Mix by vortexing the contents until the GF-AFC substrate is thoroughly dissolved.

**Storage:** Store the CellTiter-Fluor™ Cell Viability Assay components at  $-20^{\circ}\text{C}$ . The diluted CellTiter-Fluor™ Viability Reagent should be used within 24 hours if stored at room temperature. Unused GF-AFC Substrate and Assay Buffer can be stored at  $4^{\circ}\text{C}$  for up to 7 days with no appreciable loss of activity.



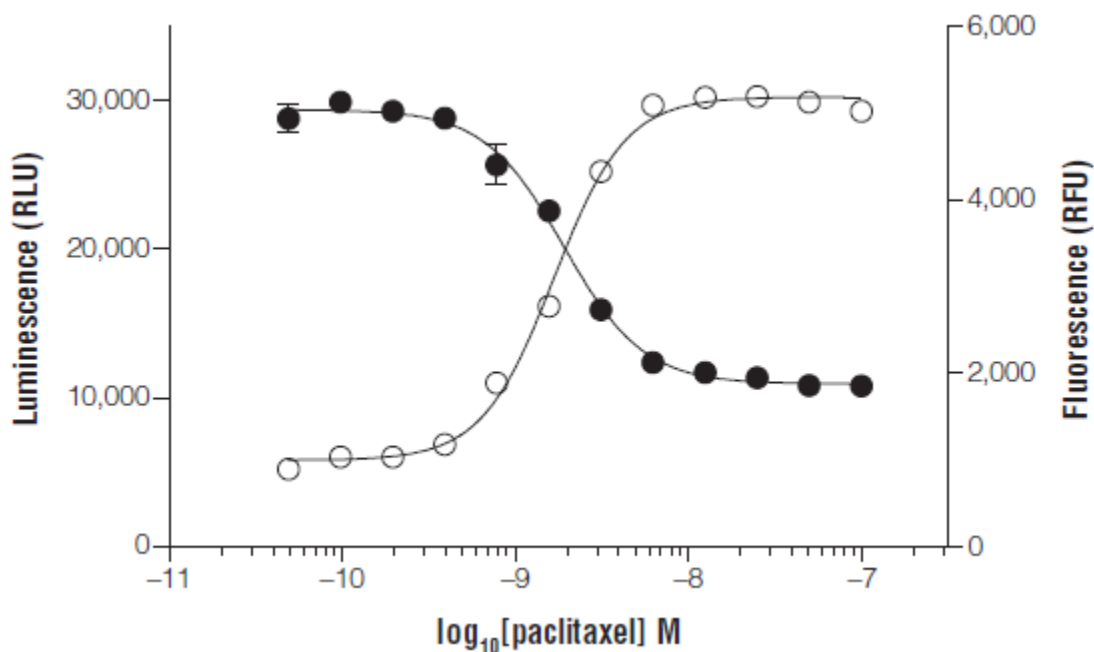


**Figure 14:** (Modified Figure 5 from TB371 32). Multiplex measurement of the live cell protease marker using GF-AFC (CellTiter-Fluor™ Assay) followed by measurement of caspase activity (Caspase-Glo® 3/7 Assay). The GF-AFC substrate was added to wells containing 10,000 cells/well, incubated for 30 minutes at 37°C and fluorescence (380–400nmEx/505nmEm) measured to estimate viable cell number. Following collection of the fluorescence data, caspase activity was measured using the luminogenic Caspase-Glo® 3/7 Reagent. Luminescence measured after 30-minutes incubation (Caspase-Glo TB323 33).

### Live Cell Protease Assay Protocol

1. Set up opaque-walled 96-well assay plates containing cells in culture medium at desired density. An optional set of wells can be prepared with medium only for background subtraction and instrument gain adjustment.
2. Add test compounds and vehicle controls to appropriate wells so that the final volume is 100  $\mu\text{l}$  in each well (25  $\mu\text{l}$  for a 384-well plate).
3. Culture cells for the desired test exposure period.
4. Add CellTiter-Fluor™ Reagent in an equal volume (100  $\mu\text{l}$  per well) to all wells, mix briefly by orbital shaking, then incubate for at least 30 minutes at 37°C. Note: Longer incubations may improve assay sensitivity and dynamic range. However, do not incubate more than 3 hours, and be sure to shield plates from ambient light.
5. Measure resulting fluorescence using a fluorometer (380–400 nm Ex/505 nm Em).

### ATP Assay Concept

The measurement of ATP using firefly luciferase is the most commonly applied method for estimating the number of viable cells in HTS applications. Data from several example HTS assays using ATP assays are publically available on [Pubchem](#) (34). ATP has been widely accepted as a valid marker of viable cells. When cells lose membrane integrity, they

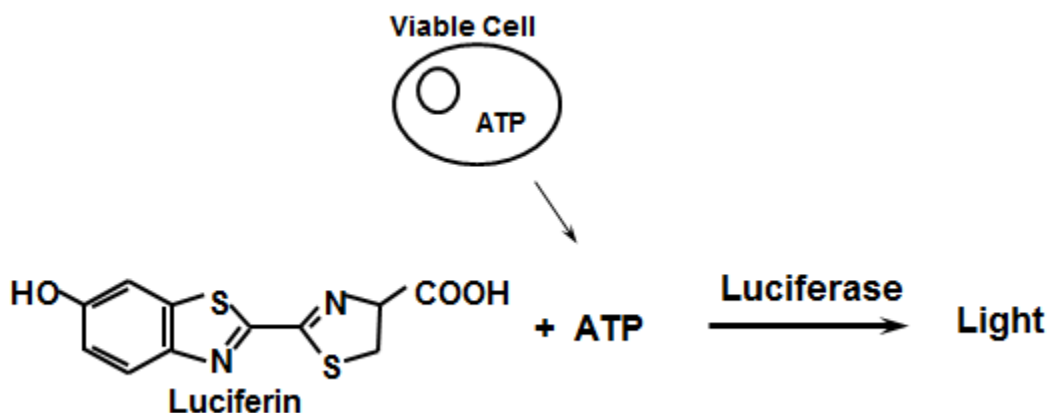


**Figure 15:** Simplified reaction scheme showing ATP and luciferin as substrates for luciferase to generate light.

lose the ability to synthesize ATP and endogenous ATPases rapidly deplete any remaining ATP from the cytoplasm. Although luciferase has been used to measure ATP for decades, recent advances in assay design have resulted in a single reagent addition homogeneous protocol that results in a luminescent signal that glows for hours. The most significant technological advancement was made under the direction of Keith Wood at Promega Corporation where directed evolution was used to select for stable molecules and generate improved versions of luciferase (35). The stable version of luciferase was the enabling technology that led to development of robust assays for HTS that can withstand harsh cell lysis conditions and are more resistant to luciferase inhibitors found in libraries of small molecules (36).

The ATP detection reagent contains detergent to lyse the cells, ATPase inhibitors to stabilize the ATP that is released from the lysed cells, luciferin as a substrate, and the stable form of luciferase to catalyze the reaction that generates photons of light. A simplified reaction scheme is shown in Figure 15.

The ATP assay is the fastest cell viability assay to use, the most sensitive, and is less prone to artifacts than other viability assay methods. The luminescent signal reaches a steady state and stabilizes within 10 minutes after addition of reagent and typically glows with a half-life greater than 5 hours. The ATP assay has the advantage that you do not have to rely on an incubation step with a population of viable cells to convert a substrate (such a tetrazolium or resazurin) into a colored compound. This also eliminates a plate handling step because you do not have to return cells to the incubator to generate signal.

The ATP assay chemistry can typically detect fewer than 10 cells per well and has been used widely in 1536-well format. The ATP assay sensitivity is usually limited by reproducibility of pipetting replicate samples rather than a result of the assay chemistry.

## Commercial Availability

Commercial kits containing reagents to measure ATP are available from several vendors. For example:

- CellTiter-Glo<sup>®</sup> Luminescent Cell Viability Assay. Promega Corporation Cat.# G7570
- ATPLite™ 1 step, Perkin Elmer Cat.# 6016731,
- Adenosine 5'-triphosphate (ATP) bioluminescent somatic cell assay kit. Sigma-Aldrich Cat.# FLASC-1KT.

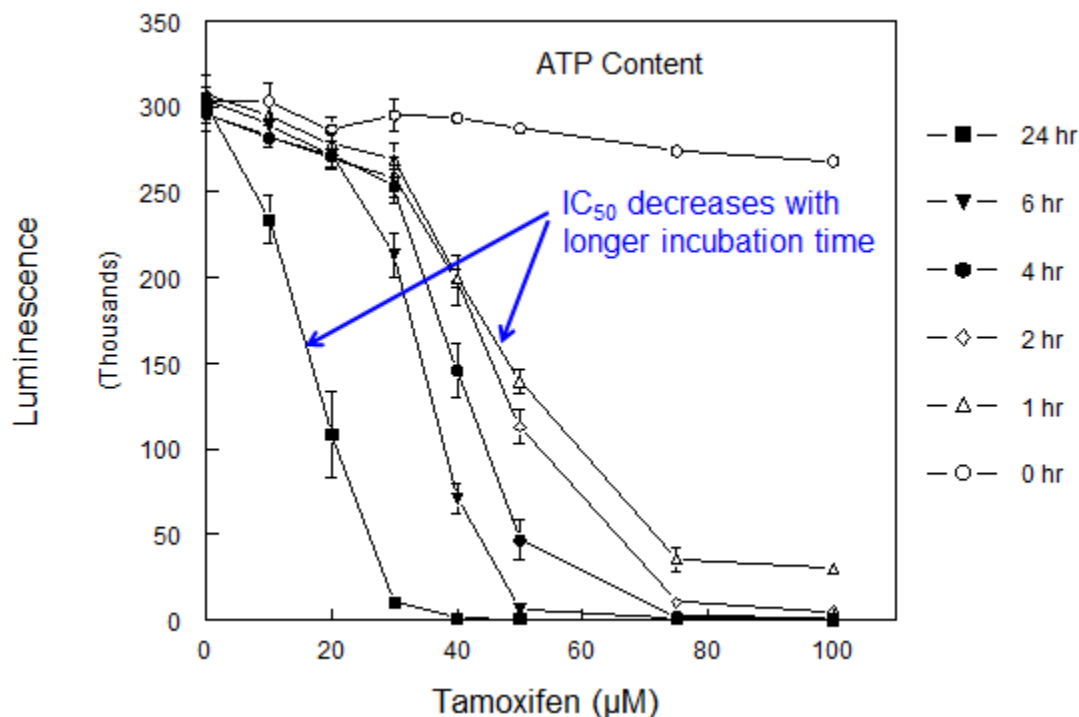
The most common version of the CellTiter-Glo<sup>®</sup> Assay kit contains a lyophilized CellTiter-Glo<sup>®</sup> Substrate and the CellTiter-Glo<sup>®</sup> Buffer which are both stored at  $-20^{\circ}\text{C}$ ; however, a bulk frozen liquid version of CellTiter-Glo<sup>®</sup> Assay also is available which eliminates the step of reconstituting the lyophilized Substrate. For more detailed information, refer to [Promega Technical Bulletin #288 \(37\)](#).

## ATP Assay Reagent Preparation

1. Thaw the CellTiter-Glo<sup>®</sup> Buffer and CellTiter-Glo<sup>®</sup> Substrate and equilibrate to room temperature prior to use. For convenience the CellTiter-Glo<sup>®</sup> Buffer may be thawed and stored at room temperature for up to 48 hours prior to use.
2. Transfer the appropriate volume (10ml for Cat.# G7570) of CellTiter-Glo<sup>®</sup> Buffer into the amber bottle containing CellTiter-Glo<sup>®</sup> Substrate to reconstitute the lyophilized enzyme/substrate mixture. This forms the CellTiter-Glo<sup>®</sup> Reagent.
3. Mix by gently vortexing, swirling or inverting the contents to obtain a homogeneous solution. The CellTiter-Glo<sup>®</sup> Substrate should go into solution easily in less than 1 minute.

## ATP Assay Protocol

1. Set up white opaque walled microwell assay plates containing cells in culture medium at desired density.
2. Add test compounds and vehicle controls to appropriate wells so that the final volume is 100  $\mu\text{l}$  in each well for 96-well plate (25  $\mu\text{l}$  for a 384-well plate).
3. Culture cells for the desired test exposure period.
4. Equilibrate plates to ambient temperature for 30 min to ensure uniform temperature across plate during luminescent assay.
5. Add CellTiter-Glo<sup>®</sup> Reagent in an equal volume (100  $\mu\text{l}$  per well for 96-well plates or 25  $\mu\text{l}$  per well for 384-well plates) to all wells.
6. Mix contents for 2 minutes on an orbital shaker to induce cell lysis.
7. Allow the plate to incubate at room temperature for 10 minutes to stabilize luminescent signal. Note: Uneven luminescent signal within standard plates can be caused by temperature gradients, uneven seeding of cells or edge effects in multiwell plates.
8. Record luminescence.



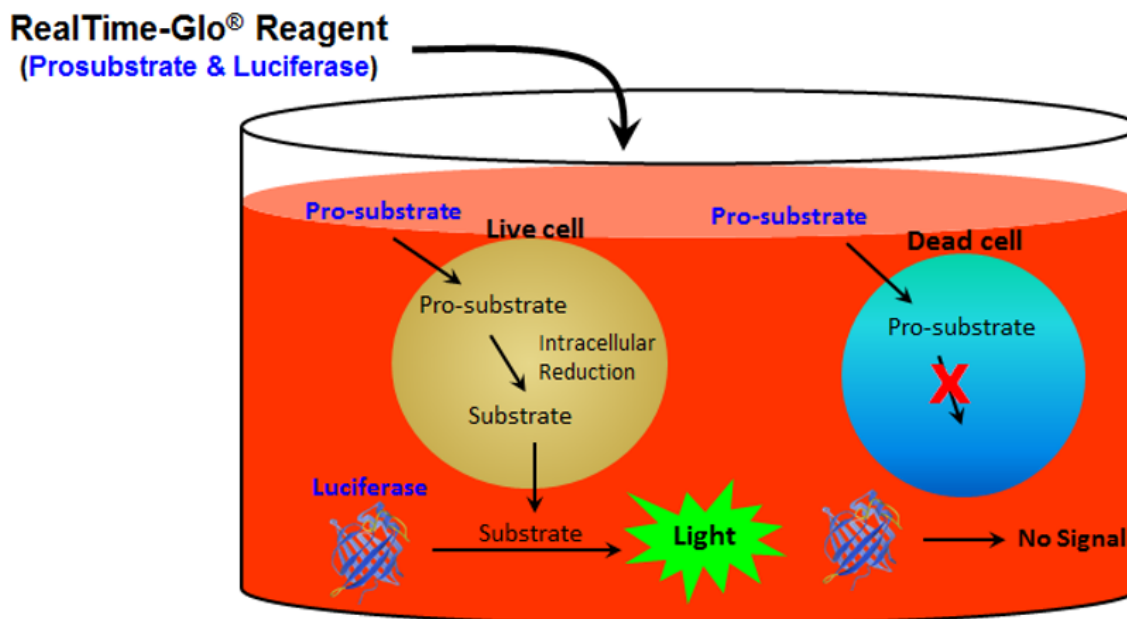
**Figure 16:** HepG2 cells (25,000 cells in 100ul medium/well) were cultured overnight in an opaque-walled 96 well plate then treated with 0-100uM tamoxifen in DMSO (final concentration of 0.2% DMSO) for various times. ATP content was measured by adding 100ul CellTiter-Glo® Reagent and recording luminescence after a 10min equilibration period. Data shown represent the mean +/- SD (n = 3). Modified from Figure 1 from Assay & Drug Devel Tech 2(1): 51, 2004 (38).

Figure 16 shows the results of an example assay characterization experiment to determine the appropriate time to record viability data for a cell-based assay.

## Real-Time Assay for Viable Cells

A recently developed approach for measuring viable cell number in “real time” utilizes an engineered luciferase derived from a marine shrimp and a small molecule pro-substrate (39). The pro-substrate and luciferase are added directly to the culture medium as a reagent. The pro-substrate is not a substrate for luciferase. Viable cells with an active metabolism reduce the pro-substrate into a substrate which diffuses into the culture medium where it is used by luciferase to generate a luminescent signal. Figure 17 shows an illustration of the assay concept.

The reagent is well tolerated by cells and is stable in complete cell culture medium at 37°C for at least 72 hours which enables measurements from the same sample for days without replenishing the pro-substrate. The assay can be performed in two formats: continuous-read or endpoint measurement. In the continuous-read format, the luminescent signal can



**Figure 17:** The real-time reagent components include a cell permeable pro-substrate and an engineered stable form of a shrimp-derived luciferase. The reagent components are added directly to cells in culture. Viable cells with an active metabolism reduce the pro-substrate to create a substrate for luciferase that generates light. Dead cells lacking metabolic activity do not generate luciferase substrate and thus do not contribute a luminescent signal.

be repeatedly recorded from the same sample wells over an extended period to measure the number of viable cells in “real time”.

Figure 18 shows example results from a toxin dose-response assay using the real time format for 3 days. The cells in the vehicle control and the lowest concentrations of thapsigargin continue to grow and show an increase in luminescence over the three day period. Samples of cells treated with the highest concentrations of thapsigargin show a decrease in luminescence over time as the cells die.

For convenience, in the continuous read format, the reagents can be added to the cell suspension prior to dispensing into assay plates. This approach eliminates a pipetting step and a potential source of variability during delivery of assay reagent into samples. In the endpoint format, the reagent can be added to cells at any time during the experimental period. A steady state develops between viable cells reducing pro-substrate to convert it into the luciferase substrate, the appearance of the substrate in the culture medium and the luciferase enzymatic reaction using the substrate to generate light. For the endpoint format, luminescence can typically be recorded within 10 minutes to an hour after adding reagent to the cells, depending on assay conditions.

The substrate produced by viable cells is used rapidly by the luciferase, thus the luminescent signal diminishes soon after cell death. Figure 19 illustrates the decrease in luminescent signal following addition of digitonin to kill the cells.

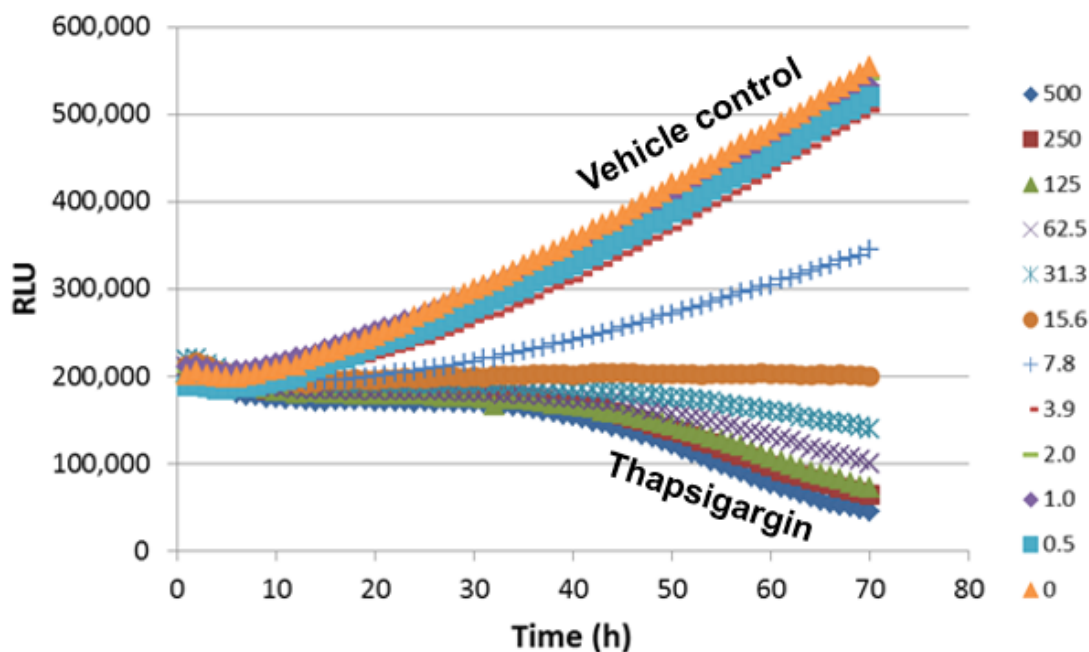


**Figure 18:** A549 cells (500/well) were plated in 40 $\mu$ L medium containing 2x RealTime-Glo™ reagents. A thapsigargin titration was prepared in medium at 2X concentrations and added to the plate at an equal volume. The final concentrations of thapsigargin ranged from 500nM - 0.5nM. The vehicle control was 0.1% DMSO. Luminescence was monitored every hour for 72 hours using a Tecan Infinite® 200 Multimode Reader with Gas Control Module (37°C and 5% CO<sub>2</sub>).

The rapid decrease in luminescent signal following cell death enables multiplexing of the real time viability assay with other luminescent assays that contain a lysis step that will kill cells. The decrease in luminescence from the real time viability assay following cell death is important to eliminate interference with subsequent luminescent assays that use firefly luciferase.

### Multiplexing with the Real Time Viability Assay

Because the real time reagent does not contain detergent (i.e. is non-lytic) and is well tolerated by most cell types, after recording viability data, the remaining sample of cells can be used for many downstream applications. Multiplexing can be achieved with a variety of other assay chemistries including: most assays with a fluorescent detection method, the luminescent ATP assay as an orthogonal approach to confirm viability data with more than one method, a luminescent caspase-3/7 assay to measure apoptosis, firefly reporter assays to monitor gene expression, and extraction of RNA that can be used to monitor gene expression.

Figure 20 illustrates an example showing the effect of a dose-response of a proteasome inhibitor on the viability of cells measured at different times from the same samples using the real time viability assay followed by multiplex measurement of ATP as an orthogonal

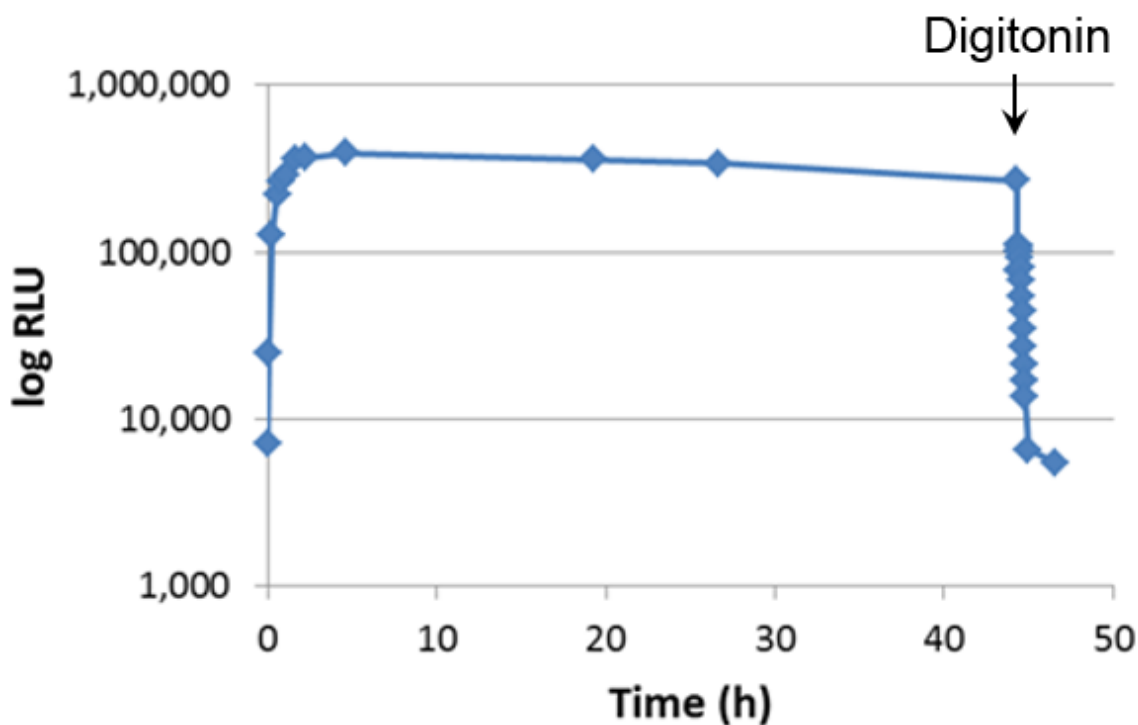


**Figure 19:** iCell cardiomyocytes (Cellular Dynamics, Inc.) were plated and grown in medium containing RealTime-Glo™ reagents (pro-substrate and NanoLuc luciferase) in a 37°C/5% CO<sub>2</sub> humidified incubator. At various time points, the luminescence signal was monitored on a Tecan M1000Pro plate reader. After 2 days, digitonin was added to a final concentration of 200 µg/ml. The luminescence was read continually, starting immediately after digitonin addition.

method to demonstrate concordance between the two viability assays. The sequential multiplexing example shows results from recording luminescence from a shrimp-derived luciferase followed by recording luminescence from a firefly-derived luciferase. The ATP assay contains detergent to lyse cells to release ATP as well as luciferin and a stable form of luciferase necessary to measure ATP (see general description above in this chapter). The detergent lysis step stops the ability of cells to generate a substrate for the shrimp luciferase and thus diminishes the luminescent signal from the real time viability assay. This sequential combination of reagents makes it possible to record two luminescent signals from two different luciferases from the same sample. The 48 hour data from the real time assay approach agrees well with the 48 hour data from the ATP assay, demonstrating concordance between these two methods. Similar agreement between assays has been observed from the combination of the real time viability assay and a constitutive firefly reporter gene assay (not shown).

Figure 21 shows another example of multiplexing the real time viability assay using the shrimp luciferase and a caspase-3/7 assay using firefly luciferase. A gradual decrease in viability and increase in caspase-3/7 activity was observed over the first ~30 hours. The decrease in caspase-3/7 activity at the longer incubation times is likely due to secondary

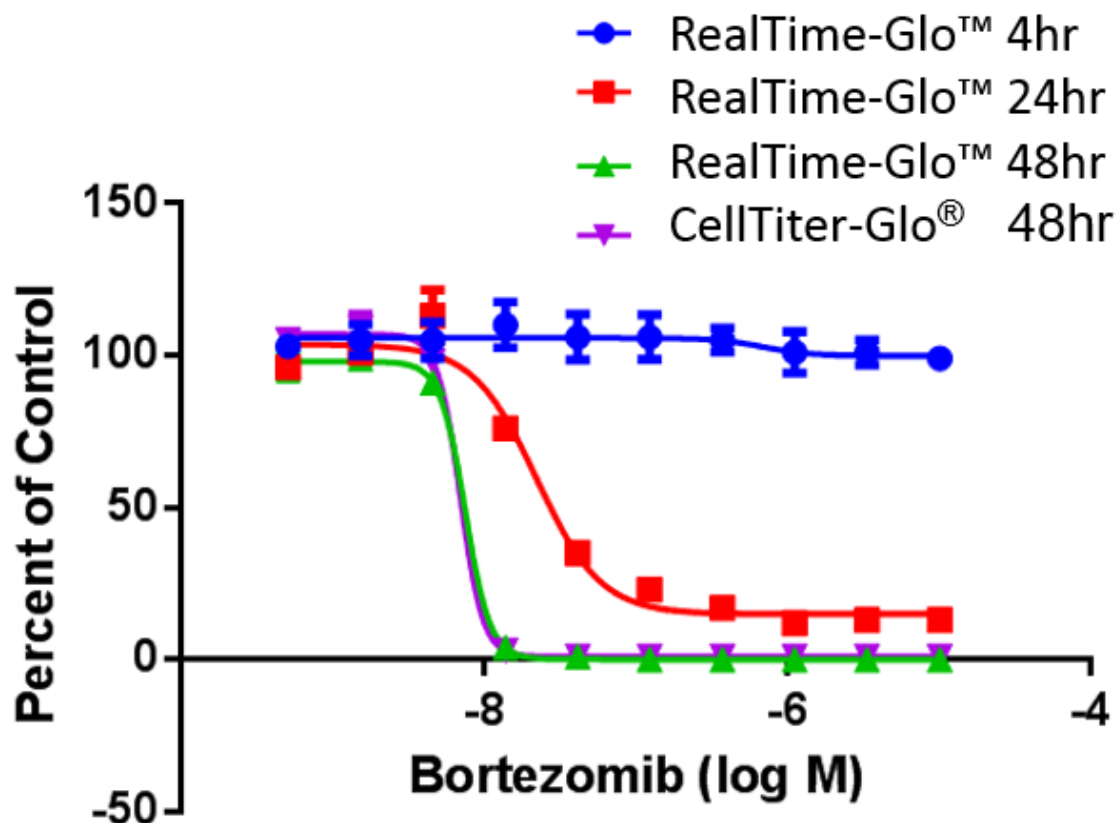


**Figure 20:** K562 cells in complete medium (RPMI medium supplemented with 10% FBS and Pen/Strep) containing the RealTime-Glo™ Reagent were seeded at 2500 cells in 50 $\mu$ l/well into 96 well opaque white plates. Bortezomib dilutions were prepared from DMSO stock as 2X final concentration in complete culture medium and 50 $\mu$ l were added to appropriate wells. The vehicle control was 0.6% DMSO in complete culture medium. Luminescence from the real time viability assay was recorded after 4, 24 and 48 hours incubation, then 100 $\mu$ l/well of the CellTiter-Glo® 2.0 Reagent was added to each well, the plate was stored at room temperature for 30 min to ensure cell lysis, then luminescence recorded. The values represent the mean  $\pm$  SD of 4 replicates and were normalized to 100% assigned to the vehicle control for each assay.

necrosis of the cells resulting in loss of activity of the caspase enzyme. This assay combination exemplifies a special case where reagent chemical compatibility during multiplexing can be a problem. Caspase assay reagent formulations typically contain reducing agents (such as dithiothreitol) which can result in some chemical reduction of the pro-substrate into substrate. The substrate generated from chemical reduction of the pro-substrate can be used by the active shrimp luciferase and contribute to background luminescence. For those situations, the addition of a specific chemical inhibitor of the shrimp luciferase eliminates signal from that enzyme so the luminescence does not interfere with the signal from firefly luciferase used in a multiplexed secondary assay.



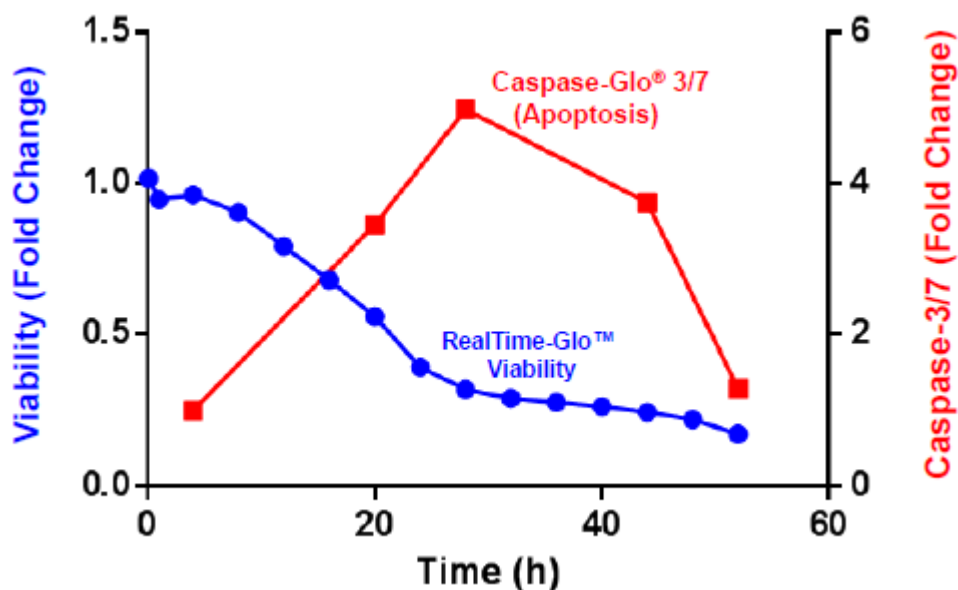


**Figure 21:** THP1 cells were grown in medium containing the RealTime-Glo™ Assay Reagent and treated with 1µM doxorubicin. Luminescence was recorded every 4 hours to monitor changes in cell viability. At selected times, Caspase-Glo® 3/7 Assay Reagent supplemented with a specific inhibitor for the shrimp luciferase was added to parallel wells. The plates were incubated at room temperature for 1 hour, then luminescence recorded from the firefly-derived luciferase in the caspase detection reagent.

The real time viability assay enables monitoring for early cytotoxic events in populations of cells exposed to drugs. Analysis of RNA extracted from a population of cells that show the first signs of cell death (i.e. when most of the cells are still viable) can provide information about which stress response genes are expressed during experimental treatments. The real time viability assay reagent has been shown to have little effect on yield or integrity of RNA. That is in contrast to the ATP assay reagent which contains a high concentration of detergent to lyse cells resulting in poor recovery and loss of integrity of RNA. Figure 22 shows the results of extracting RNA from different sizes of individual 3D spheroids of HEK293 cells after measurement of cell viability using the real time assay reagent. RNA was extracted using either a manual or an automated method. For each method, the presence or absence of the real time reagent did not affect the recovery of RNA from spheroids. In addition, the RIN values (used as an indicator of the integrity of the RNA) were in the excellent range (~8 to 9.5) and were not affected by the presence of the real time cell viability assay reagent.

A limitation of the real time assay format results from the eventual depletion of pro-substrate by metabolically active cells. In general, the luminescent signal generated correlates with the number of metabolically active viable cells; however, the length of time the luminescent signal will be linear with cell number will depend on the number of cells per well and their overall metabolic activity. Figure 23 shows luminescent signals recorded every hour for 72 hours from wells initially seeded with 750, 1500, 3000, or 6000 K562 cells/well in a 384-well plate. The signal from 750 and 1500 cells/well remain linear over

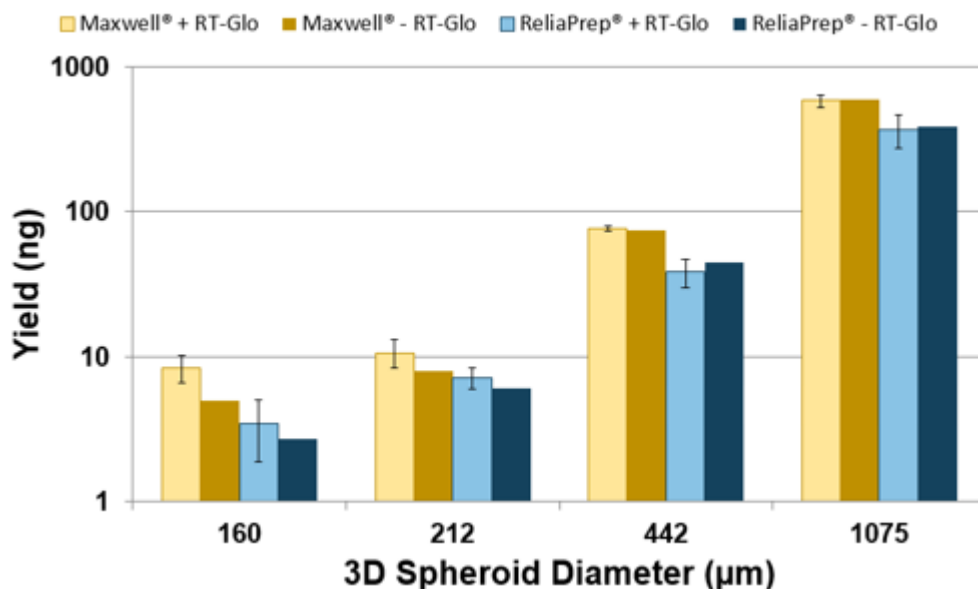


**Figure 22:** HEK293 spheroids of different sizes were prepared using the GravityPLUS™ Hanging Drop System from InSphero. RealTime-Glo™ MT Cell Viability Assay was used to measure viability of different sizes of HEK293 cell spheroids followed by RNA extraction of the same samples using a manual method (ReliaPrep™ RNA Tissue Miniprep System) and an automated method (Maxwell® 16 LEV simply RNA Tissue Kit). Each RNA extraction method was done in the presence and absence of RealTime-Glo™ Reagent for each of the different sizes of spheroid. Each bar represents the mean +/- SD of 3 spheroids.

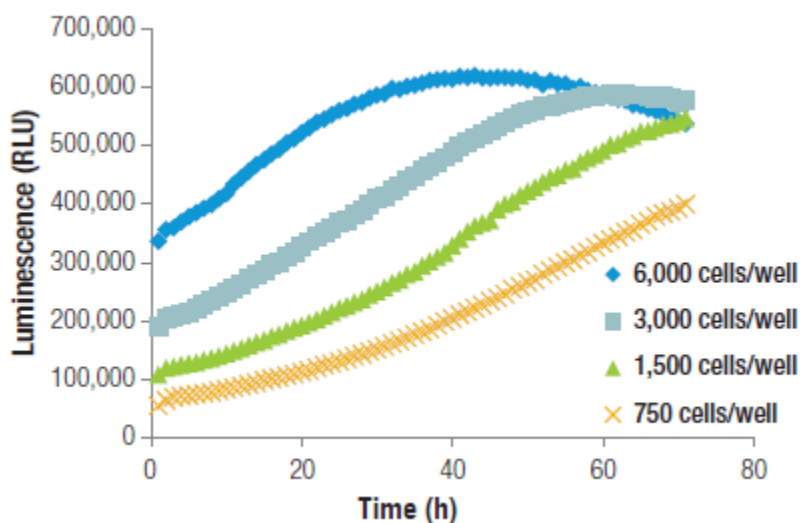


**Figure 23:** K562 cells were seeded at 750, 1500, 3000 or 6000 cells/well in a 384-well opaque white plate in 80µL of RPMI medium supplemented with 10% FBS and Pen/Strep that contained the RealTime-Glo™ Reagent. Luminescence was monitored every hour for 72 hours using a Tecan Infinite® 200 Multimode Reader with Gas Control Module (37°C and 5% CO<sub>2</sub>).

the 3 day period, whereas the signal from higher cell numbers per well lose linearity after different times of incubation. It is recommended that the maximum incubation time to maintain linearity should be empirically determined for each cell type and seeding density.

## Commercial Availability

Commercial kits containing the pro-substrate and the engineered shrimp-derived luciferase are available from Promega Corporation. RealTime-Glo™ MT Cell Viability Assay, Cat.# G9711 (100 reactions); G9712 (10x100 reactions); G9713 (1000 reactions)

## Reagent Preparation and Real Time Viability Assay Protocol

The MT Cell Viability Substrate and the NanoLuc® Enzyme are both supplied at 1000X the final recommended concentration.

For continuous read mode:

1. Equilibrate the MT Cell Viability Substrate and the NanoLuc® Enzyme to 37°C.
2. Harvest cells and adjust to desired cell density to be used in the assay.
3. Add MT Cell Viability Substrate and the NanoLuc® Enzyme to the cell suspension.
4. Dispense cell suspension containing MT Cell Viability Substrate and the NanoLuc® Enzyme into white opaque walled multiwell plates suitable for luminescence measurements.
5. Add test compound and incubate for desired length of time.
6. Record luminescence.

For endpoint mode:

1. Harvest cells and adjust to desired cell density to be used in the assay.
2. Add test compound to cells and incubate for desired length of time.
3. Equilibrate the MT Cell Viability Substrate and the NanoLuc® Enzyme to 37°C.
4. Dilute MT Cell Viability Substrate and the NanoLuc® Enzyme in cell culture medium to form 2X RealTime-Glo™ Reagent.
5. Add an equal volume of 2X RealTime-Glo™ Reagent to cells.
6. Incubate at 37°C for 10-60 min.
7. Record luminescence.

## Conclusion

There are a variety of assay technologies available that use standard plate readers to measure metabolic markers to estimate the number of viable cells in culture. Each cell viability assay has its own set of advantages and disadvantages. The ATP detection assay is by far the most sensitive, has fewer steps, is the fastest to perform, and has the least amount of interference, whereas the tetrazolium or resazurin reduction assays offer less expensive alternatives that may achieve adequate performance depending on experimental design. The fluorogenic cell permeable protease substrate is far less cytotoxic

than the tetrazolium and resazurin compounds while enabling many possibilities for multiplexing other assays to serve as orthogonal or confirmatory methods. The recently developed cell viability assay, based on generating a substrate for the shrimp luciferase, provides the opportunity for capturing data repeatedly in real time and offers many possibilities for multiplexing with other assays. Regardless of the assay method chosen, the major factors critical for reproducibility and success include: 1) using a tightly controlled and consistent source of cells to set up experiments and 2) performing appropriate characterization of reagent concentration and incubation time for each experimental model system.

## References

1. Mosmann T. Rapid colorimetric assay for cellular growth and survival: Application to proliferation and cytotoxicity assays. *J. Immunol. Meth.* 1983;65:55–63. PubMed PMID: 6606682.
2. Marshall NJ, Goodwin CJ, Holt SJ. A critical assessment of the use of microculture tetrazolium assays to measure cell growth and function. *Growth Regul.* 1995;5(2):69–84. PubMed PMID: 7627094.
3. Berridge MV, Tan AS. Characterization of the cellular reduction of 3-(4,5-dimethylthiazol-2-yl)-2,5-diphenyltetrazolium bromide (MTT): subcellular localization, substrate dependence, and involvement of mitochondrial electron transport in MTT reduction. *Arch Biochem Biophys.* 1993;303(2):474–82. PubMed PMID: 8390225.
4. Berridge M., Tan A., McCoy K., Wang R. The Biochemical and Cellular Basis of Cell Proliferation Assays that Use Tetrazolium Salts. *Biochemica.* 1996;4:14–19.
5. Tada H, Shiho O, Kuroshima K, et al. An improved colorimetric assay for interleukin 2. *J. Immunol. Methods.* 1986;93:157–65. PubMed PMID: 3490518.
6. Hansen MB, Nielsen SE, Berg K. Re-examination and further development of a precise and rapid dye method for measuring cell growth/cell kill. *J. Immunol. Methods.* 1989;119:203–210. PubMed PMID: 2470825.
7. Denizot F, Lang R. Rapid colorimetric assay for cell growth and survival. Modifications to the tetrazolium dye procedure giving improved sensitivity and reliability. *J. Immunol. Meth.* 1986;89:271–277. PubMed PMID: 3486233.
8. Plumb JA, Milroy R, Kaye SB. 1989. Effects of the pH dependence of 3-(4,5-dimethylthiazol-2-yl)-2,5-diphenyl-tetrazolium bromide-formazan absorption on chemosensitivity determined by a novel tetrazolium-based assay. *Cancer Res* 15;49(16):4435-40.
9. CellTiter 96® Non-Radioactive Cell Proliferation Assay Technical Bulletin #112. Online at [ Available at: <http://www.promega.com/~media/Files/Resources/Protocols/Technical%20Bulletins/0/CellTiter%2096%20Non-Radioactive%20Cell%20Proliferation%20Assay%20Protocol.pdf>]
10. Huyck L, Ampe C, Van Troys M. The XTT cell proliferation assay applied to cell layers embedded in three-dimensional matrix. *Assay Drug Dev Tech.* 2012;10(4): 382–392. PubMed PMID: 22574651.

11. Squatrito R, Connor J, Buller R. Comparison of a novel redox dye cell growth assay to the ATP bioluminescence assay. *Gynecologic Oncology*. 1995;58:101–105. PubMed PMID: 7789873.
12. Lü L, Zhang L, Wai MS, Yew DT, Xu J. Exocytosis of MTT formazan could exacerbate cell injury. *Toxicol In Vitro*. 2012;26(4):636–44. Epub 2012 Feb 28. PubMed PMID: 22401948.
13. Ulukaya E, Colakogullari M, Wood E J. Interference by anti-cancer chemotherapeutic agents in the MTT-tumor chemosensitivity assay. *Chemotherapy*. 2004;50(1):43–50. PubMed PMID: 15084806.
14. Chakrabarti R, Kundu S, Kumar S, Chakrabarti R. Vitamin A as an enzyme that catalyzes the reduction of MTT to formazan by vitamin C. *J Cellular Biochem*. 2000;80(1):133–138. PubMed PMID: 11029760.
15. Bernas T, Dobrucki J. Mitochondrial and nonmitochondrial reduction of MTT: interaction of MTT with TMRE, JC-1, and NAO mitochondrial fluorescent probes. *Cytometry*. 2002;47(4):236–42. PubMed PMID: 11933013.
16. Pagliacci M, Spinozzi F, Migliorati G, et al. Genistein inhibits tumour cell growth in vitro but enhances mitochondrial reduction of tetrazolium salts: a further pitfall in the use of the MTT assay for evaluating cell growth and survival. *Eur J Cancer*. 1993;29:1573–1577. PubMed PMID: 8217365.
17. Collier A, Pritsos C. The mitochondrial uncoupler dicumerol disrupts the MTT assay. *Biochem Pharm*. 2003;66:281–287. PubMed PMID: 12826270.
18. Cory A, Owen T, Barltrop J, Cory JG. Use of an aqueous soluble tetrazolium/formazan assay for cell growth assays in culture. *Cancer Commun*. 1991;3(7):207–212. PubMed PMID: 1867954.
19. Barltrop J, Owen T. 5-(3-carboxymethoxyphenyl)-2-(4,5-dimethylthiazoly)-3-(4-sulfophenyl)tetrazolium, inner salt (MTS) and related analogs of 3-(4,5-dimethylthiazolyl)-2,5-diphenyltetrazolium bromide (MTT) reducing to purple water-soluble formazans as cell-viability indicators. *Bioorg Med Chem Lett*. 1991;1:611–614.
20. Paull KD, Shoemaker RH, Boyd MR, et al. The synthesis of XTT: A new tetrazolium reagent that is bioreducible to a water-soluble formazan. *J Heterocyclic Chem*. 1988;25:911–914.
21. Ishiyama M, Shiga M, Sasamoto K, Mizoguchi M, He P. A new sulfonated tetrazolium salt that produces a highly water-soluble formazan dye. *Chem Pharm Bull (Tokyo)*. 1993;41:1118–1122.
22. Tominaga H, Ishiyama M, Ohseto F, et al. A water-soluble tetrazolium salt useful for colorimetric cell viability assay. *Anal Commun*. 1999;36:47–50.
23. Goodwin CJ, Holt SJ, Downes S, Marshall NJ. 1995. Microculture tetrazolium assays: a comparison between two new tetrazolium salts, XTT and MTS. *J Immunol Methods* 13;179(1):95-103.
24. Scudiero DA, Shoemaker RH, Paull KD, Monks A, Tierney S, Nofziger TH, Currens MJ, Seniff D, Boyd MR. Evaluation of a soluble tetrazolium/formazan assay for cell growth and drug sensitivity in culture using human and other tumor cell lines. *Cancer Res*. 1988;48(17):4827–33. PubMed PMID: 3409223.

25. Berridge MV, Herst PM, Tan AS. Tetrazolium dyes as tools in cell biology: New insights into their cellular reduction. *Biotechnology Annual Review*. 2005;11:127–152. PubMed PMID: 16216776.
26. Ahmed SA, Gogal RM, Walsh JE. A new rapid and simple nonradioactive assay to monitor and determine the proliferation of lymphocytes: An alternative to [3H]thymidine incorporation assays. *J Immunol Meth*. 1994;170:211–224. PubMed PMID: 8157999.
27. Shum D, Radu C, Kim E, Cajuste M, Shao Y, Seshan VE, Djaballah H. A high density assay format for the detection of novel cytotoxic agents in large chemical libraries. *J Enz Inhib Med Chem*. 2008;23(6):931–945. PubMed PMID: 18608772.
28. Wesierska-Gadek J, Gueorguieva M, Ranftler C, Zerza-Schnitzhofer G. A new multiplex assay allowing simultaneous detection of the inhibition of cell proliferation and induction of cell death. *J Cell Biochem*. 2005;96(1):1–7. PubMed PMID: 16052484.
29. Invitrogen alamarBlue Assay manual. Online at [ Available at: [http://tools.invitrogen.com/content/sfs/manuals/PI-DAL1025-1100\\_TI%20alamarBlue%20Rev%201.1.pdf](http://tools.invitrogen.com/content/sfs/manuals/PI-DAL1025-1100_TI%20alamarBlue%20Rev%201.1.pdf)].
30. Lancaster MV and Fields RD. Antibiotic and cytotoxic drug susceptibility assays using resazurin and poisoning agents. US Patent 5,501,959. Issued March 26, 1996.
31. Niles AL, Moravec RA, Hesselberth PE, Scurria MA, Daily WJ, Riss TL. A homogeneous assay to measure live and dead cells in the same sample by detecting different protease markers. *Anal Biochem*. 2007;366:197–206. PubMed PMID: 17512890.
32. CellTiter-Fluor® Technical Bulletin. Online at Available at: <http://www.promega.com/~media/Files/Resources/Protocols/Technical%20Bulletins/101/CellTiter-Fluor%20Cell%20Viability%20Assay%20Protocol.pdf>
33. Caspase-Glo® Technical Bulletin. Online at Available at: <http://www.promega.com/~media/Files/Resources/Protocols/Technical%20Bulletins/101/Caspase-Glo%203%207%20Assay%20Protocol.pdf>
34. PubChem BioAssay: <http://pubchem.ncbi.nlm.nih.gov/assay/>
35. Hall MP, Gruber MG, Hannah RR, Jennens-Clough ML, Wood KV. 1998. Stabilization of firefly luciferase using directed evolution. In: *Bioluminescence and Chemiluminescence—Perspectives for the 21st Century*. Roda A, Pazzagli M, Kricka LJ, Stanley PE (eds.), pp. 392–395. John Wiley & Sons, Chichester, UK.
36. Auld DS, Zhang Y-A, Southall NT, et al. A basis for reduced chemical library inhibition of firefly luciferase obtained from directed evolution. *J Med Chem*. 2009;52:1450–1458. PubMed PMID: 19215089.
37. CellTiter-Glo® Technical Bulletin #288. Online at Available at: <http://www.promega.com/~media/Files/Resources/Protocols/Technical%20Bulletins/101/Caspase-Glo%203%207%20Assay%20Protocol.pdf>.
38. Riss TL, Moravec RA. Use of multiple assay endpoints to investigate the effects of incubation time, dose of toxin, and plating density in cell-based cytotoxicity assays. *Assay Drug Dev Technol*. 2004;2(1):51–62. PubMed PMID: 15090210.
39. Duellman SJ, Zhou W, Meisenheimer P, Vidugiris G, Cali JJ, Gautam P, Wennerberg K, Vidugiriene J. Bioluminescent, Nonlytic, Real-Time Cell Viability Assay and Use

in Inhibitor Screening. *Assay Drug Dev Tech.* 2015;13(8):456–65. PubMed PMID: 26383544.

40. RealTime-Glo MT Cell Viability Assay Technical Manual. Online at Available at: <http://www.promega.com/~media/files/resources/protocols/technical%20manuals/101/realtimelo%20mt%20cell%20viability%20assay%20protocol.pdf>





# *In vitro* 3D Spheroids and Microtissues: ATP-based Cell Viability and Toxicity Assays

Monika Kijanska, Dr<sup>✉1</sup> and Jens Kelm, Dr<sup>✉2</sup>

Created: January 21, 2016.

## Abstract

*In vitro* models continuously evolve to more closely mimic and predict biological responses of living organisms. Just in the past years many novel three dimensional (3D) organotypic models, which resemble tissue structure, function and even disease progression, have been developed. However, application of more complex models and technologies may increase the risk of compromising assay robustness and reproducibility. Consequently, the first developmental stage of cell-based assays is to combine complex tissue models with standard assays - a combination that already provides more physiologically insightful information when compared to two-dimensional (2D) systems. The final goal should be to exploit the full potential of tissue-like *in vitro* models by investigating them with modern assays such as -Omics and imaging technologies. Furthermore, organotypic models will allow for a design of novel assay concepts that utilize the whole tool box of models and endpoints.

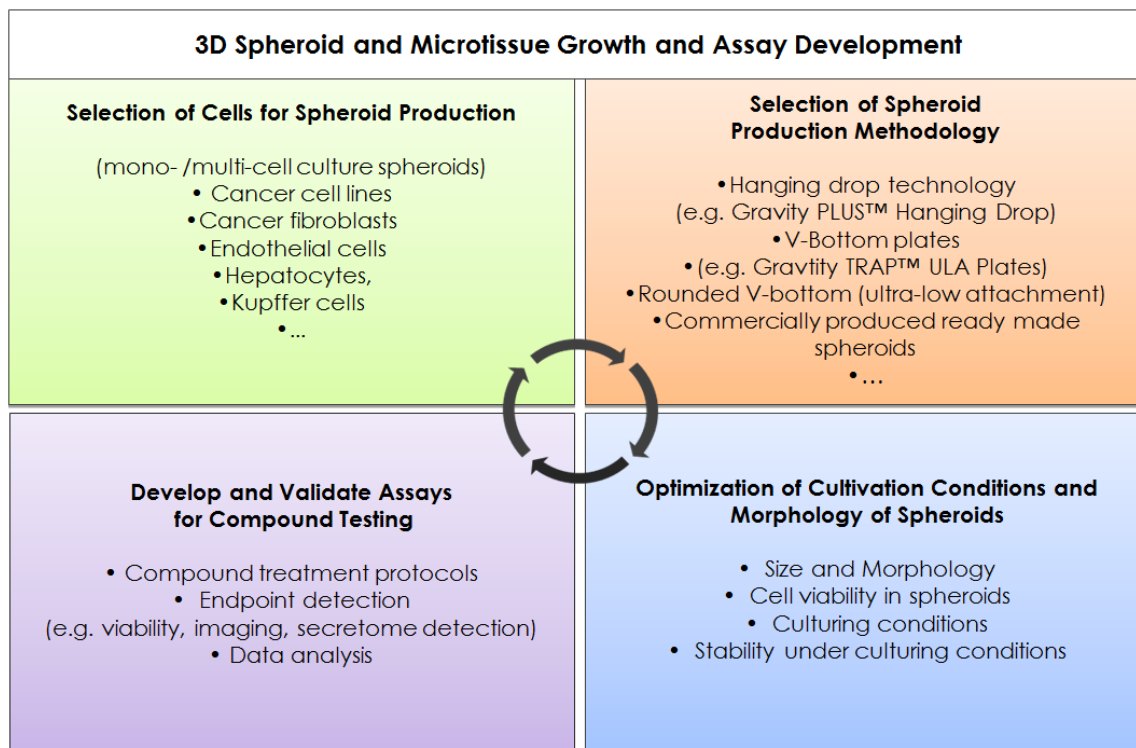
In this chapter we focus on assessment of spheroid viability by measuring intracellular ATP content. This primary assay performed on 3D cell culture system is a powerful tool to predict with high confidence health, growth and energy status of tissue of interest. The 3D spheroid model is particularly useful to mimic solid-tumors from a physiologically relevant architectural perspective, when they are grown with multiple cell types prevalent in these tumors. However, this assay is equally applicable for other non-spheroid 3D tissue models to quantify viability and toxicity.

---

<sup>1</sup> InSphero AG; Email: monika.kijanska@insphero.com. <sup>2</sup> InSphero AG; Email: jens.kelm@insphero.com.

✉ Corresponding author.

## Flow Chart: 3D Spheroid and Microtissue Growth and Assay Development



### Introduction

In recent decades cell-based assays to investigate cell biology, drug efficacy, metabolism and toxicology were dominated by technologies employing cells grown on flat plastic surfaces (2D) or in single cell suspension (1). However, biology of cells is extensively influenced by the environmental context such as cell-cell contacts, cell-matrix interactions, cell polarity or oxygen profiles.

For many years biology of avascular tumor has been recognized by cancer researchers to be particularly well mimicked by three dimensional (3D) cell cultures (2)(3). For instance, one of the earliest 3D-acknowledged effects correlating with *in vivo* clinical observations was development of multicellular resistance (MCR) to anticancer drugs in 3D culture formats. As highlighted by Desoize and Jardillier, cancer cells embedded within a 3D environment had lower sensitivity to anticancer drugs, e.g. upon Vinblastine exposure human lung carcinoma (A549) monolayer culture exhibited the  $IC_{50}$  value of  $0.008 \mu\text{mol/l}$ , whereas the  $IC_{50}$  value of spheroid culture was  $53 \mu\text{mol/l}$  (4). Importantly, drug sensitivity is a net effect of multiple factors and is highly regulated by hypoxia, which occurs in the oxygen-deficient areas of the tumor with limited access to the capillary network. Low oxygen partial pressure can lead to either higher drug sensitivity or elevated drug resistance of the tumor, depending on the drug mechanism and structure.

Additionally, extracellular acidification is yet another factor influencing response to either basic (e.g. Doxorubicin) or acidic (e.g. Chlorambucil) drugs. In this case, the uptake of basic drugs is decreased, whereas the uptake of acidic drugs is increased, resulting in higher drug resistance or higher drug sensitivity, respectively (5)(6). Therefore, tumor cells cultured in 3D formats, which are exposed to complex and heterogenic environmental context, are more relevant tool to study tumor biology and responsiveness than standard 2D cell culture.

Another example of cells with well documented influence of culturing conditions on physiology are hepatocytes. Hepatocytes are characterized by their polygonal shape and multi-polarization with at least two basolateral and two apical surfaces. Changes in cell form limit cell–cell and cell–matrix interactions, consequently leading to reduced polarization, reduced bile canaliculi formation and a loss of important signaling pathways. Dedifferentiation of hepatocytes observed in 2D monolayer cell culture results in reduction of liver-specific functions, such as metabolic competence for detoxification, due to down-regulation of phase I and II enzymes. Therefore, maintenance of hepatocyte shape and function is of the utmost importance in hepatotoxicity studies. To tackle this problem, 3D liver models employing scaffolds, hydrogels and the cellular self-assembly approach have been created. Additionally, variety of different cell types, such as HepG2, HepaRG and primary hepatocytes, is currently used to investigate liver functions. For an in depth overview of current *in vitro* liver models and application please see Godoy et al. 2013 (7).

However, a decision about application of a cell-based methodology depends not only on its physiological properties, but also on its automation-compatibility, high throughput processing and feasibility to couple it with established endpoint. A number of technologies have been developed to create 3D tissue-mimicking environment on microscale *in vitro*, with embedding cells within a hydrogel or preventing of cellular adhesion to an artificial matrix and concomitant enforced cell re-aggregation being the main ones (Table 1) (8)(9)(10)(11)(12). Both scaffold-free technologies have been used successfully to create a 3D context of cancer cells, as they allow for reconstitution of cell type-specific extracellular environment. The concept of the hanging drop technology is one of the oldest ones and it provides the benefit of aggregation of defined types and number of cells. Already used by Ross Granville Harrison, the hanging drop has proven to be a universal technology to produce a wide variety of either disease models or primary tissues (7)(13)(14)(15)(16).

A paradigm of 3D spheroid/microtissue growth and assay development summarized in Flow Chart 1, shows interplay between selection of the most suitable cell type(s) and the 3D culturing technique, followed by optimization of spheroid culturing conditions and morphology, and between the assay development and the choice of the endpoint. Tailored combinations of the above elements offer experimental freedom that makes the 3D *in vitro* testing systems fit to the purpose, and increase the amount of extracted biologically-relevant information.

**Table 1:** Overview of the three basic cell culture concepts that are employed to coax cells into a 3D environment.

|   |  |
|---|--|
| <p><b>Scaffold-free</b></p>               | <ul style="list-style-type: none"> <li>• cells produce their own ECM</li> <li>• no scaffold-associated growth factors/undefined components</li> <li>• no scaffold-associated batch-to-batch variations</li> <li>• possibility to co-culture different cell types</li> <li>• cellular aggregation in hanging drops or in ultra-low attachment plates</li> <li>• HTS-applicable</li> </ul> <p><b>Examples:</b><br/>           Multicellular tumor spheroids (14)(39)<br/>           Colorectal cancer spheroids (40)<br/>           Human liver heterotypic microtissues (26)<br/>           Cerebral organoids (41)<br/>           Myocardial microtissues (42)(23)<br/>           Neurospheres (43)<br/>           Kidney organoids (44)</p> |
| <p><b>Hydrogels/sponges/membranes</b></p> | <ul style="list-style-type: none"> <li>• mimic soft tissue stiffness and ECM composition</li> <li>• natural tissue-derived (batch-to batch variations, biological contaminants, e.g. growth factors) or synthetic</li> <li>• gel maintenance conditions may limit application</li> </ul> <p><b>Examples:</b><br/>           Mini-guts (45)</p>   |
| <p><b>Scaffolds/matrices</b></p>          | <ul style="list-style-type: none"> <li>• added (biodegradable) cellular, acellular or composite materials</li> <li>• mimick ECM</li> <li>• diversified pore geometry, mechanistic properties, size and transparency</li> <li>• regenerative medicine/implants</li> </ul> <p><b>Examples:</b><br/>           Pre-vascularized scaffolds for bone regeneration (46)</p>  |

## 1. *In Vitro* Toxicity and Drug Efficacy Testing in a 3D Spheroid Model

### 1.1. *In Vitro* Toxicity and Drug Efficacy Assay Concept

An increasing need for robust and reliable *in vitro* models for toxicity and drug efficacy testing is potentiated not only by the urge to make the process of bring therapeutics from the bench to the bedside faster and more cost-effective, but also by increasing regulatory and safety challenges. However, one of the major concerns of *in vitro* toxicity/efficacy testing remains its predictive power and translation into *in vivo* situations. As discussed in the introductory section, 3D cell culture formats such as spheroids, present a powerful alternative to standard 2D cell culture for *in vitro* studies (17)(18). The 3D spheroid model is particularly useful to mimic solid-tumors from a physiologically relevant architectural perspective, when they are grown with multiple cell types prevalent in these tumors.

The choice of the 3D model and the end point for toxicity/efficacy testing should depend on both the physiological question to be answered and the scale of the screen. In general, treatment with a toxicant can affect cellular and/or 3D cell culture morphology, viability,

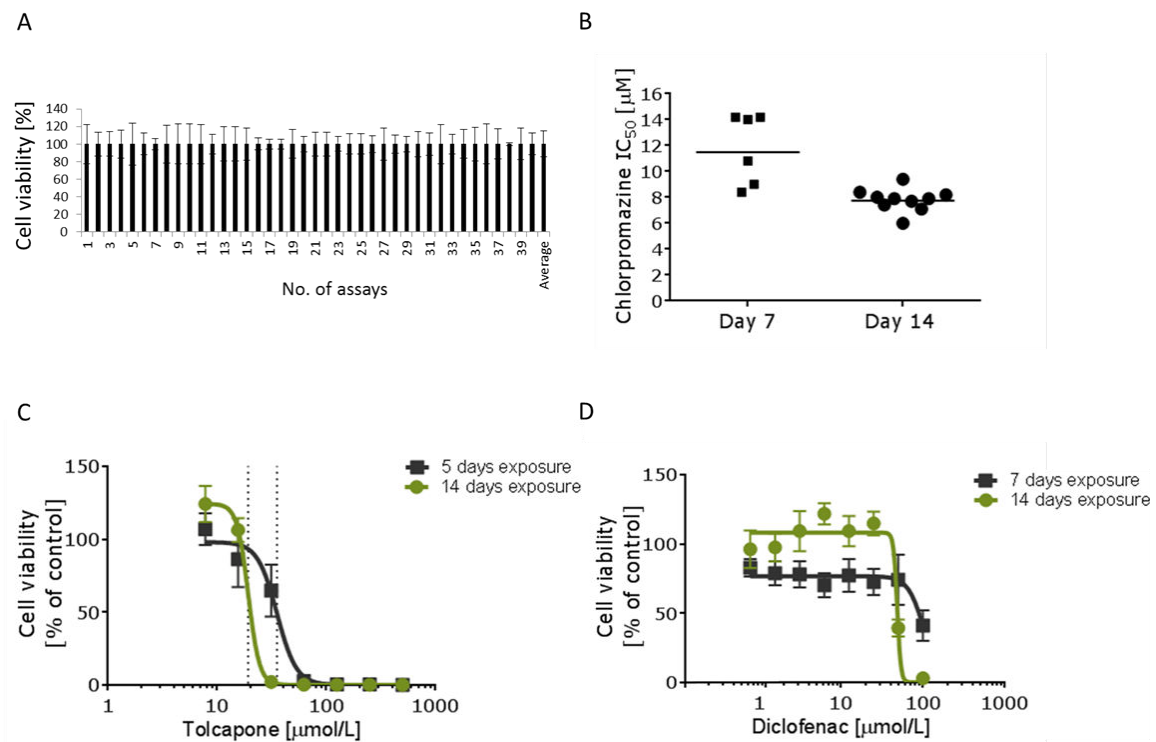


**Figure 1:** Toxicity testing in 3D heterotypic human liver microtissues - reproducibility and sensitivity of the ATP assay. (A) The human liver microtissues (hLiMTs) of co-cultured primary hepatocytes and primary NPCs were cultured for 14 days and their intra-tissue ATP content was assessed with Promega CellTiter-Glo® assay. In each assay ( $n = 40$ ) average relative light units (RLU) from triplicates (3 microtissues) was set to 100%, the relative standard deviation (SD) of the mean is depicted. Average relative SD from 40 assays is 14.6%. (B) Reproducibility of  $IC_{50}$  values of Chlorpromazine after 7 days- and 14 days-long treatment of hLiMTs. Presented are results of independent experiments and their geometric mean. Note the reproducible shift to lower  $IC_{50}$  values after increased exposure time. (C) hLiMTs were exposed to increasing concentrations of Tolcapone and of Diclofenac (D) during shorter (5 days and 7 days, respectively; 1 re-dosing) or longer (14 days; 2 re-dosing) incubation. Note the shift to lower  $IC_{50}$  values after increased exposure time. Source: InSphero AG.

metabolic activity (such as oxygen consumption or metabolic enzyme activation), or tissue-specific function. Here, the spectrum of possible tissue-specific end points is constantly widening, together with the development of specialized 3D tissue models (19) (20)(21)(22)(23)(24)(25). In case of liver microtissues of co-cultured hepatocytes and non-parenchymal cells (NPCs), established approaches include monitoring albumin and urea secretion, bile acid secretion, Kupffer cell-dependent IL-6 and TNF $\alpha$  secretion, to list a few (26). Contractile responsiveness of the myocardial microtissue model or glucose-stimulated insulin secretion by pancreatic microislets add yet further options to the growing list of functionality tests. Additionally, cultivated 3D cell culture models can be further analyzed using transcriptomic and proteomic methods, allowing for RNA and protein expression profiling upon toxicant exposure.

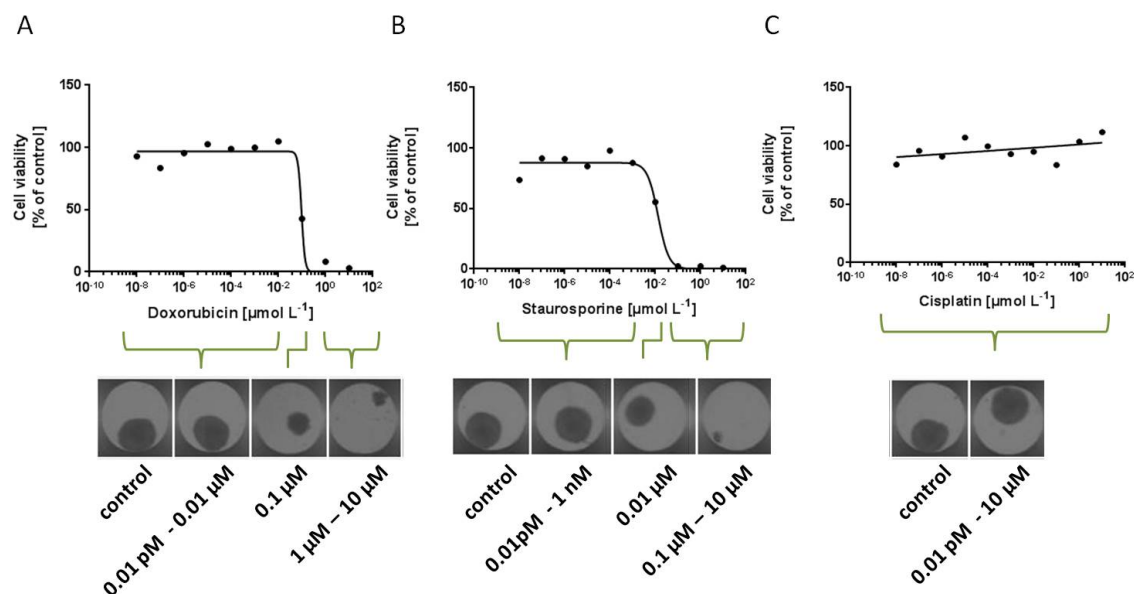


**Figure 2:** Anticancer drug efficacy testing in tumor microtissues - correlation between cell viability and tumor microtissue size suppression. Tumor microtissues grown from human ovarian cell line (HEY) were exposed to increasing concentrations of Doxorubicin (A), Staurosporine (B) and Cisplatin (C) for 10 days and their intra-tissue ATP content was assessed with Promega CellTiter-Glo<sup>®</sup> assay. Representative images of control and compound-treated microtissues show dose-dependent decrease of microtissue size upon treatment with Doxorubicin (A) and Staurosporine (B) which corresponds to decrease of microtissue viability as measured with the ATP assay. Cisplatin treatment (C) neither suppressed microtissue viability nor had an impact on size of spheroids. Source: InSphero AG.

Although very powerful and promising, the use and predictivity of the 3D models has to be carefully validated for each given application, and conditions of cultivation and sample collection need to be standardized and controlled (27)(28). For screening purposes 3D cell culture models can be treated with many classes of substances (e.g. small molecules, biologicals, siRNA/RNAi). It is good practice to include an appropriate model- or cellular process-specific control compound of known toxic effect, such as Chlorpromazine for drug-induced hepatotoxicity, Aflatoxin B for apoptotic cell death induction or Trovafloxacin for inflammation-mediated toxicity (26).

In this section we will describe an exemplary experimental design to test the toxic effects over a range of concentrations of compounds dissolved in tissue culture-grade dimethyl sulfoxide (DMSO, 0.5% v/v) on liver microtissues of primary hepatocytes co-cultured with primary NPCs, produced in a hanging drop technology (Figure 1) (26). Analogously, such an experimental set up can be applied to evaluate anticancer efficacy of drugs in spheroids derived from cancer cell lines, such as HEY - human ovarian cancer cell line, as presented in Figure 2. The effect of the toxic agents on microtissue morphology, cell viability and tissue functionality can be further investigated, depending on the study goal, endpoint of interest and compatibility with the screening approach.

### 1.1.1. Sample Protocol for a Commercially Available 3D Spheroid System

The GravityPLUS™ Hanging Drop System is designed to generate organotypic microtissues in the process of scaffold-free aggregation of cells and to enable for their prolonged cultivation and multiple compound re-dosing. Microtissues are formed within 2-4 days from cell suspensions in hanging drops on the GravityPLUS™ Plates and are subsequently harvested into the ultra-low adhesive GravityTRAP™ ULA Plates. The unique design of GravityTRAP™ ULA wells allows for numerous media exchange without microtissue disturbance as well as for microtissue imaging. This 96-well platform is compatible with liquid handling stations and suitable for HT-screening applications. Commercially available hanging drop system and microtissues for hepatotoxicity testing include:

- GravityPLUS™ 10x Kit (96-well), includes 10 GravityPLUS™ and 10 GravityTRAP™ ULA plates (InSphero, Cat.# CS-06-001)
- GravityTRAP™ ULA Plate (InSphero, Cat.# CS-09-001)
- 3D InSight™ Human Liver Microtissues from primary hepatocytes, co-culture with non-parenchymal cells (96x) (InSphero, Cat.# MT-02-002-04)
- 3D InSight™ Human Liver Microtissues from primary hepatocytes (96x) (InSphero, Cat.# MT-02-002-01)
- 3D InSight™ Rat liver microtissues formed by primary hepatocytes (96x) (InSphero, Cat.# MT-02-001-01)
- 3D InSight™ Rat liver microtissues from primary hepatocytes, co-culture with nonparenchymal cells (96x) (InSphero, Cat.# MT-02-001-04)
- 3D InSight™ Human Pancreatic Microislets (96x) (InSphero, Cat.# MT-04-001-01)

### 1.1.2. Compound Preparation

1. To adjust 0.5% DMSO (v/v) final concentration in culture medium, prepare a 200 X top compound concentration stock in DMSO.
2. Prepare 6 dilutions of the compound stock in DMSO using sterile V-bottom microplate (e.g. Greiner Bio-one, Cat.#651161). Choose the dilution factor depending on the range of concentrations to be tested in the assay.
3. Transfer 2.5 µl of each compound dilution to the corresponding well on a deep well plate (e.g. Axygen®, Cat.# 391-01-111) as presented in Figure 3 (upper panel). For each re-dosing prepare a separate deep well plate.
4. For vehicle control, pipette 2.5 µl of DMSO to columns 3 and 4 on a deep well plate.
5. Seal deep well plates with aluminum plate sealer (e.g. Greiner Bio-One, Cat.# 67609) and store in – 20°C for future re-dosing.

### 1.1.3. Compound Exposure Protocol

1. Thaw deep well plates with compound(s) to be tested and add to each experimental well 497.5 µl of pre-warmed culture medium, thereby generating 1 X

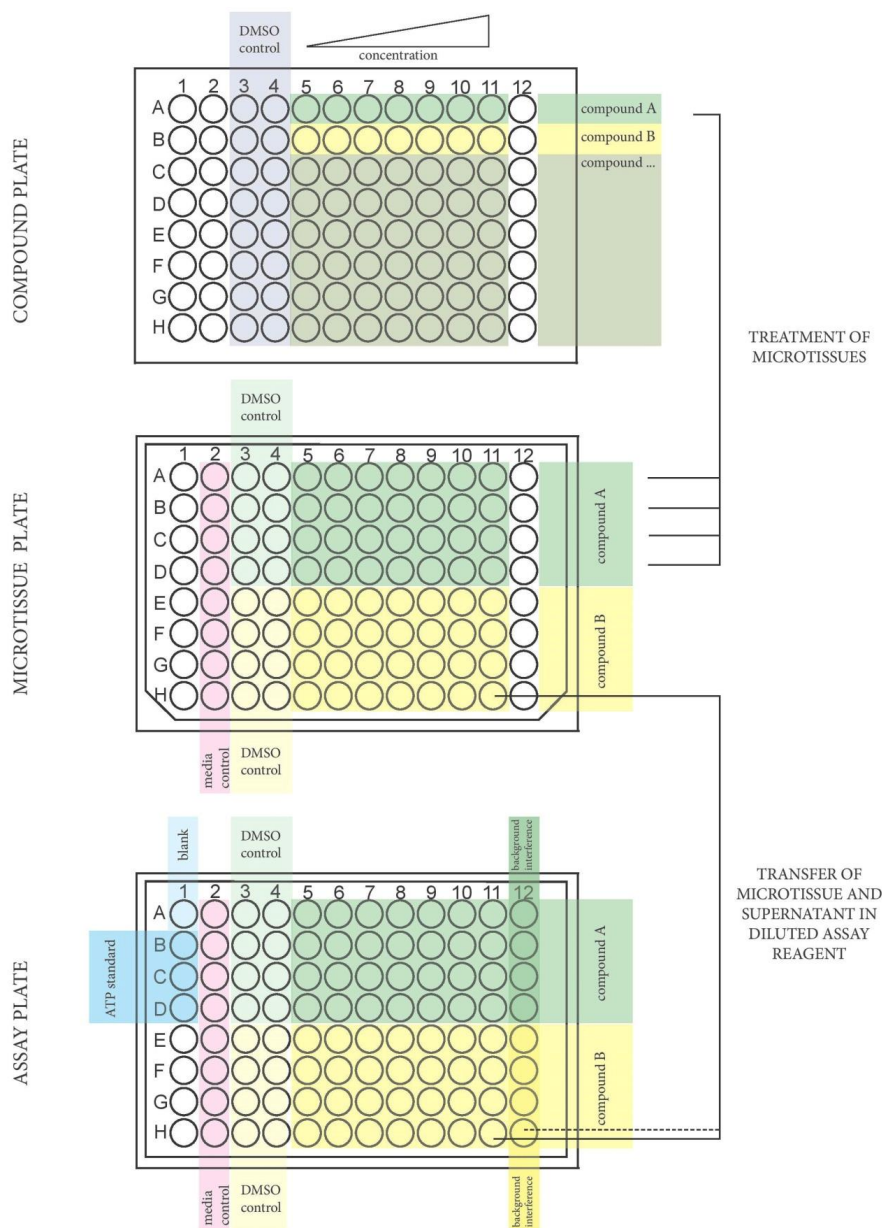


**Figure 3:** Schematic plate layout of compound-treated spheroids and of ATP measurement. Upper panel: compound deep-well plate layout. Each row contains vehicle control (column 3 and 4) and 7 compound concentrations (column 5 – 11; top concentration: column 11). Application of deep well plates reduces pipetting steps to generate 200 X dilutions of the compound and allows for dosing of experimental replicates from the same reservoir. Middle panel: dosing of microtissues in 96-well format. **Microtissues cultured in GravityTRAP™ ULA Plate are exposed to treatment with 2 compounds. Each compound concentration is tested in quadruplicate, whereas the vehicle control in octuplicate. Culture medium control is included in column 2.** Lower panel: assay plate layout for ATP measurement. Microtissues suspended in 40  $\mu$ l of diluted CellTiter-Glo® Cell Viability Assay are transferred from the **GravityTRAP™ Plate into the assay plate (column 2 to 11)**. Assay blank (A1), standard curve (A1 – D1) and the control for background interference (column 12) are included in the assay plate.



- top concentration of the compound and its corresponding dilutions in culture medium with 0.5% DMSO (v/v).
2. Gently aspirate culture medium from the GravityTRAP™ ULA Plate, leaving microtissues in the remnant volume of the medium in the V-shaped bottom of the well
  3. Thoroughly mix medium with compound in the deep well plate and dose 70 µl per microtissue in required number of replicates (Figure 3, middle panel).
  4. To control the DMSO effect on microtissues, add 70 µl of culture medium per well to column 2 on the Gravity GravityTRAP™ ULA Plate (Figure 1, middle panel).
  5. Repeat dosing at required time intervals.
  6. Determine toxicity and cell viability using CellTiter-Glo® 3D Cell Viability Assay or other suitable methods available.

## 1.2. Conclusion/Summary

Testing toxicity/drug efficacy in 3D cell culture formats presents multiple advantages over conventional 2D cell culture system. Firstly, cells aggregated into a 3D structure exhibit native tissue-mimicking organization, metabolic characteristics and specialized functions, and retain them for significantly longer periods of time, therefore enabling prolonged and repeated exposure. This in turn allows for detection of effects caused by longer exposure of lower compound concentrations, which appears frequently *in vivo*. For example, longer exposure tends to shift IC<sub>50</sub> values towards lower compound concentrations, hence increasing sensitivity of the assay and better prediction of false negative compounds (Figure 1). Additionally, a comparison between shorter and longer toxic exposures may give an idea about sensitization of the system to a given treatment. Secondly, several commercially available solutions allow for 3D cell culture cultivation in HT-friendly 96- or 384-well format with multiple re-dosing of tested compounds. On the assay development side, an appealing concept of multiplexing endpoints to generate simultaneous data-reach readouts is currently under development and shall provide more experimental flexibility.

## 2. 3D Microtissue Viability Assay

### 2.1. ATP Assay Concept

The frequently chosen primary assay for determination of 3D cell culture viability is quantification of a luminescent signal generated by conversion of luciferin by luciferase as a function of cytoplasmic ATP concentration (29)(30). Initially, architecture of the 3D cellular aggregates – their size, composition and penetration barrier, presented a challenge to assays originally tailored for the 2D cell culture models. However, by optimization of detergent composition and lysis conditions, ATP assays suitable for variable 3D cell culture formats (such as spheroids and hydrogel-based systems), have been developed (31)(30)(32)(33)(34). Available bioluminescent ATP detection assay are robust, sensitive, and scalable to high-throughput screens, and offer relatively simple work-flow and data analysis. In contrast, standard colorimetric methods based on resazurin reduction

(Alamar blue assay) or tetrazolium reduction (MTT assay), frequently used to assess number of viable cells in 2D cell culture, have been found not applicable to 3D spheroids/microtissues and collagen matrices (30)(29)(35)(36). 3D matrices and tight cell-cell junctions can affect uptake and diffusion kinetics of a dye, therefore changing readout of the assay and making results more difficult to interpret (35)(36). In parallel, development of live imagining assays linking changes of spheroid's size and morphology or localization/expression of fluorescent markers to viability of cells in 3D formats are under constant development (37)(38).

The protocol below describes how to measure viability of cells aggregated into spheroids (e.g. heterotypic liver microtissues and tumor microtissues) using CellTiter-Glo® 3D Cell Viability Assay quantifying intra-tissue ATP content (Figure 1 and Figure 2). This protocol can be easily adjusted to an automated pipetting station.

### 2.1.1. Commercial Availability

Recommended single-reagent assay for multi-well plate format:

- CellTiter-Glo® 3D Cell Viability Assay, Promega Corporation, Cat.# G9681, G9682, G9683

CellTiter-Glo® 3D Cell Viability Assay combines the enhanced penetration and lytic activity required for efficient lysis of 3D cell culture with generation of the stable ATP-dependent luminescent signal. This thereby reduces the complexity of processing multiple assay plates and HTS applications (30).

### 2.1.2. ATP Assay preparation

CellTiter-Glo® 3D Cell Viability Assay is provided as a ready-to-use solution and no additional preparation is required. The reagent should be equilibrated to room temperature before use. For stability and storage conditions please refer to the manufacturer's guidelines ([www.promega.com](http://www.promega.com)).

To perform the assay on microtissues cultured in 96-well GravityTRAP™ ULA Plates, mix 1:1 the required volume of CellTiter-Glo® 3D Cell Viability Assay (20 µl per well) and PBS without calcium and magnesium (e.g. PAN-Biotech, Cat.# P04-36500)

### 2.1.3. ATP Assay Protocol

1. Equilibrate GravityTRAP™ ULA Plates with cultured micro-tissues to room temperature.
2. Prepare 96-opaque well microplate, hereinafter refer to as assay plate (e.g. Greiner Bio-One, Cat.# 675075), by pipetting into dedicated wells (Figure 3, lower panel):
  - a. Blank – 40 µl of diluted CellTiter-Glo® 3D Cell Viability Assay
  - b. *Optional*: Standard curve – depending on the type of microtissue and the detection range of luminometer available, mix 20 µl of CellTiter-Glo® 3D Cell Viability Assay with 20 µl of 1 µM ATP (e.g. for human liver microtissues of ~ 300 µm diameter) or with 5 µM ATP (e.g. for more

metabolically active or bigger microtissues), and with corresponding ATP dilutions.

- c. *Optional:* To check background interference of the compound tested in the cytotoxicity assay, pipet 5  $\mu$ l of a culture medium from wells containing microtissues treated with the highest concentration of the compound into wells on the assay plate containing 20  $\mu$ l CellTiter-Glo<sup>®</sup> 3D Cell Viability Assay and 20  $\mu$ l of 1  $\mu$ M ATP .
3. Gently remove the culture medium from the GravityTRAP<sup>™</sup> ULA Plate by placing the pipette tip at an inner ledge of the well, leaving intact the microtissues in the remnant volume of the medium in the V-shaped bottom of the well.
4. Dispense 40  $\mu$ l of diluted CellTiter-Glo<sup>®</sup> 3D Cell Viability Assay into each well of the GravityTRAP<sup>™</sup> ULA Plate.
5. Mix and transfer content of each well from the GravityTRAP<sup>™</sup> ULA Plate into the corresponding well on the assay plate.
6. Protect the lysate from light by covering the assay plate with aluminum foil or with aluminum plate sealer (e.g. Greiner Bio-One, Cat.# 67609).
7. For effective MT lysis keep the plates on an orbital shaker for 20 min at room temperature.
8. Record luminescence with a microplate luminometer using a program recommended by the manufacturer.

#### 2.1.4. Data analysis

The absolute ATP concentration of microtissue can be calculated from the standard curve included on the same assay plate. However, for *in vitro* testing of cell toxicity of chemicals, it is often more applicable to calculate relative ATP levels of microtissues exposed to treatment as a percentage of vehicle-treated control microtissues (Figure 1, Figure 2). During prolonged cultivation of microtissues, certain cytotoxicity and a decrease in ATP levels of DMSO controls can be observed with respect to maintenance medium controls.

## 2.2. Conclusions/Summary

The type and number of cells integrated into the 3D structure as well as cultivation conditions (cell culture media compositions, time of cultivation, media exchange/re-dosing scheme) may affect physiological characteristics of the model and its responsiveness to the treatment. Therefore, standardization of intrinsic characteristics of 3D cell culture formats and extrinsic culturing parameters and protocols is crucial for further development of 3D *in vitro* assay portfolio.

Measurement of cytoplasmic ATP content is a common method for cellular viability determination in both 2D and 3D cell culture, and is a routine endpoint in toxicology/drug efficacy studies. However, 3D culture formats are characterized by development of compact structures with tight cell-cell junctions and extracellular matrix, presenting additional obstacle for effective lysis and reagent accessibility. Therefore, to allow for effective ATP release from cells, the time of lysis combined with physical disruption of the 3D structure should be determined empirically for each 3D cell culture format.

Ready-to-use assay kits, such as CellTiter-Glo® Cell Viability Assay, facilitate time-effective and standardized processing of multiple assay plates by combining lysis and luminescent signal generation into one step. However, for the best assay performance special care should be taken to ensure both the highest system reproducibility and operational reproducibility (e.g. mixing and transfer of the reagent with 3D culture from culturing plates to the assay plates, avoiding a temperature gradient within the plate and ATP contamination). Additionally, special care should be taken to ensure that the ATP levels of either large or metabolically active 3D cultures correlate with the dynamic range of luminescence output of the assay.

## References

1. Abbott A. Biology's new dimension. 2003;424(August).
2. Hirschhaeuser F, Menne H, Dittfeld C, West J, Mueller-Klieser W, Kunz-Schughart L a. Multicellular tumor spheroids: an underestimated tool is catching up again. *J Biotechnol* [Internet]. 2010 Jul 1 [cited 2014 Jul 16];148(1):3–15. Available from: <http://www.ncbi.nlm.nih.gov/pubmed/20097238>
3. Sutherland RM, Durand RE. Growth and cellular characteristics of multicell spheroids. *Recent Results Cancer Res.*[Internet] 1984;95:24–49. Available from <http://www.ncbi.nlm.nih.gov/pubmed/6396760> PubMed PMID: 6396760.
4. Desoize B, Jardillier J. Multicellular resistance: a paradigm for clinical resistance? *Crit Rev Oncol Hematol.*[Internet] 2000;36(2-3):193–207. Available from <http://www.ncbi.nlm.nih.gov/pubmed/11033306> PubMed PMID: 11033306.
5. William R., Wilson MPH. Targeting hypoxia in cancer therapy. *Nat Rev Cancer.* 2011;11:393–410. PubMed PMID: 21606941.
6. Matthew D. Halla, Catherine Martinb, David J.P. Fergusonb, Roger M. Phillipsc, Trevor W. Hambleya. Comparative efficacy of novel platinum(IV) compounds with established chemotherapeutic drugs in solid tumour models. *Biochem Pharmacol.* 2004;67(1):17–30. PubMed PMID: 14667925.
7. Godoy P, Hewitt NJ, Albrecht U, Andersen ME, Ansari N, Bhattacharya S, et al. Recent advances in 2D and 3D in vitro systems using primary hepatocytes, alternative hepatocyte sources and non-parenchymal liver cells and their use in investigating mechanisms of hepatotoxicity, cell signaling and ADME. [Internet]. *Archives of toxicology.* 2013 [cited 2014 Jul 10]. 1315-530 p. Available from: <http://www.pubmedcentral.nih.gov/articlerender.fcgi?artid=3753504&tool=pmcentrez&rendertype=abstract>
8. Lin R-Z, Lin R-Z, Chang H-Y. Recent advances in three-dimensional multicellular spheroid culture for biomedical research. *Biotechnol J* [Internet]. 2008 Oct [cited 2011 Jul 24];3(9-10):1172–84. Available from: <http://www.ncbi.nlm.nih.gov/pubmed/18566957>
9. Tibbitt Mark W., Anseth KS. Hydrogels as Extracellular Matrix Mimics for 3D Cell Culture. *Biotechnol Bioeng.*[Internet] 2009;103(4):655–63. Available from <http://www.ncbi.nlm.nih.gov/pmc/articles/PMC2997742/> PubMed PMID: 19472329.
10. Jeanie L., Drury DJM. Hydrogels for tissue engineering: scaffold design variables and applications. *Biomaterials.* 2003;24(24):4337–51. PubMed PMID: 12922147.

11. Khademhosseini A, Langer R, Borenstein JT, Vacanti JP. Microscale technologies for tissue engineering and biology. *Proc Natl Acad Sci U S A*. 2006;103(8):2480–7. PubMed PMID: 16477028.
12. Singh M, Close DA, Mukundan S, Johnston PA, Sant S. Production of Uniform 3D Microtumors in Hydrogel Microwell Arrays for Measurement of Viability, Morphology, and Signaling Pathway Activation. *Assay Drug Dev Technol*. [Internet] 2015;(November)150814092825009 Available from <http://online.liebertpub.com/doi/10.1089/adt.2015.662> PubMed PMID: 26274587.
13. Rose G, Harrison M, J. Greenman FPM and C. MJ. Observations of the living developing nerve fiber. *Anat Rec*. 1907;1(5):116–28.
14. Kelm JM, Timmins NE, Brown CJ, Fussenegger M, Nielsen LK. Method for generation of homogeneous multicellular tumor spheroids applicable to a wide variety of cell types. *Biotechnol Bioeng* [Internet]. 2003 Jul 20 [cited 2011 Jul 5];83(2):173–80. Available from: <http://www.ncbi.nlm.nih.gov/pubmed/12768623>
15. Kelm JM, Fussenegger M. Microscale tissue engineering using gravity-enforced cell assembly. *Trends Biotechnol* [Internet]. 2004 Apr [cited 2011 Jun 20];22(4):195–202. Available from: <http://www.ncbi.nlm.nih.gov/pubmed/15038925>
16. Kelm JM, Fussenegger M. Scaffold-free cell delivery for use in regenerative medicine. *Adv Drug Deliv Rev* [Internet]. Elsevier B.V.; 2010 Jun 15 [cited 2011 Aug 30];62(7-8):753–64. Available from: <http://www.ncbi.nlm.nih.gov/pubmed/20153387>
17. Grainger DW. Cell-based drug testing; this world is not flat. *Adv Drug Deliv Rev* [Internet]. 2014 Apr [cited 2014 Jun 5];69-70:vii – xi. Available from: <http://www.ncbi.nlm.nih.gov/pubmed/24709443>
18. Hartung T. 3D - A new dimension of in vitro research. *Adv Drug Deliv Rev* [Internet]. Elsevier B.V.; 2014 Apr [cited 2014 Jun 12];69-70:vi. Available from: <http://www.ncbi.nlm.nih.gov/pubmed/24721291>
19. Riss T. How to Choose a Cell Health Assay Choosing the Right Cell Health Assay Depends on What You Want to Measure. *Illum A Cell Notes Publ*. 2014;(January).
20. Thoma CR, Zimmermann M, Agarkova I, Kelm JM, Krek W. 3D cell culture systems modeling tumor growth determinants in cancer target discovery. *Adv Drug Deliv Rev* [Internet]. Elsevier B.V.; 2014 Apr 20 [cited 2014 May 28];69-70C:29–41. Available from: <http://www.ncbi.nlm.nih.gov/pubmed/24636868>
21. Ranga A, Gjorevski N, Lutolf MP. Drug discovery through stem cell-based organoid models. *Adv Drug Deliv Rev* [Internet]. Elsevier B.V.; 2014 Apr 20 [cited 2014 May 27];69-70C:19–28. Available from: <http://www.ncbi.nlm.nih.gov/pubmed/24582599>
22. Mathes SH, Ruffner H, Graf-Hausner U. The use of skin models in drug development. *Adv Drug Deliv Rev* [Internet]. Elsevier B.V.; 2014 Apr 20 [cited 2014 Jun 12];69-70C:81–102. Available from: <http://www.ncbi.nlm.nih.gov/pubmed/24378581>
23. Emmert MY, Hitchcock RW, Hoerstrup SP. Cell therapy, 3D culture systems and tissue engineering for cardiac regeneration. *Adv Drug Deliv Rev* [Internet]. Elsevier B.V.; 2014 Apr 20 [cited 2014 Jun 1];69-70C:254–69. Available from: <http://www.ncbi.nlm.nih.gov/pubmed/24378579>

24. Giese C, Marx U. Human immunity in vitro - Solving immunogenicity and more. *Adv Drug Deliv Rev* [Internet]. Elsevier B.V.; 2014 Apr 20 [cited 2014 May 27]; 69-70C:103–22. Available from: <http://www.ncbi.nlm.nih.gov/pubmed/24447895>
25. Kim D-H, Kim P, Suh K, Kyu Choi S, Ho Lee S, Kim B. Modulation of adhesion and growth of cardiac myocytes by surface nanotopography. *Conf Proc IEEE Eng Med Biol Soc.* 2005;4:4091–4. PubMed PMID: 17281132.
26. Messner S, Agarkova I, Moritz W, Kelm JM. Multi-cell type human liver microtissues for hepatotoxicity testing. *Arch Toxicol* [Internet]. 2013 Jan [cited 2013 Feb 13];87(1): 209–13. Available from: <http://www.pubmedcentral.nih.gov/articlerender.fcgi?artid=3535351&tool=pmcentrez&rendertype=abstract>
27. Roth A, Singer T. The application of 3D cell models to support drug safety assessment: Opportunities & challenges. *Adv Drug Deliv Rev* [Internet]. Elsevier B.V.; 2014 Apr 20 [cited 2014 Jun 12];69-70C:179–89. Available from: <http://www.ncbi.nlm.nih.gov/pubmed/24378580>
28. Astashkina A, Grainger DW. Critical analysis of 3-D organoid in vitro cell culture models for high-throughput drug candidate toxicity assessments. *Adv Drug Deliv Rev* [Internet]. Elsevier B.V.; 2014 Mar [cited 2014 Mar 9]; Available from: <http://linkinghub.elsevier.com/retrieve/pii/S0169409X14000301>
29. Riss TL, Niles AL, Minor L. Cell Viability Assays Assay Guidance Manual. Assay Guid Man. 2013;
30. Riss TL, Valley MP, Kupcho KR, Zimprich CA, Leippe D, Niles AL, et al. Validation of In Vitro Assays to Measure Cytotoxicity in 3D Cell Cultures. 2014;2014.
31. Messner S, Agarkova I, Moritz W, Kelm JM. Multi-cell type human liver microtissues for hepatotoxicity testing. *Arch Toxicol* [Internet]. 2012 Nov 11 [cited 2012 Nov 13]; 87(1):209–13. Available from: <http://www.pubmedcentral.nih.gov/articlerender.fcgi?artid=3535351&tool=pmcentrez&rendertype=abstract>
32. Rimann M, Laternser S, Gvozdenovic A, Muff R, Fuchs B, Kelm JM, et al. An in vitro osteosarcoma 3D microtissue model for drug development. *J Biotechnol* [Internet]. Elsevier B.V.; 2014 Nov 10 [cited 2015 May 19];189:129–35. Available from: <http://www.ncbi.nlm.nih.gov/pubmed/25234575>
33. Fey SJ, Wrzesinski K. Determination of Drug Toxicity Using 3D Spheroids Constructed From an Immortal Human Hepatocyte Cell Line. *Toxicol Sci* [Internet]. 2012 Jun [cited 2013 Feb 6];127(2):403–11. Available from: <http://www.pubmedcentral.nih.gov/articlerender.fcgi?artid=3355318&tool=pmcentrez&rendertype=abstract>
34. Rimann M, Angres B, Patocchi-Tenzer I, Braum S, Graf-Hausner U. Automation of 3D Cell Culture Using Chemically Defined Hydrogels. *J Lab Autom.*[Internet] 2013.:1–7. Available from <http://www.ncbi.nlm.nih.gov/pubmed/24132162> PubMed PMID: 24132162.
35. Bonniera F, Keatinga M.E., Wróbelb T.P., Majznerb K., Baranskac M., Garcia-Munoza A. A. Blancod HJB. No Title. *Toxicol Vitro.* 2015;29(1):124–31.
36. Walzl A, Unger C, Kramer N, Unterleuthner D, Scherzer M, Hengstschläger M, et al. The Resazurin Reduction Assay Can Distinguish Cytotoxic from Cytostatic Compounds in Spheroid Screening Assays. *J Biomol Screen.*[Internet] 2014;19(7):

- 1047–59. Available from <http://www.ncbi.nlm.nih.gov/pubmed/24758920> PubMed PMID: 24758920.
37. Sirenko O, Mitlo T, Hesley J, Luke S, Owens W, Cromwell EF. High-Content Assays for Characterizing the Viability and Morphology of 3D Cancer Spheroid Cultures. *Assay Drug Dev Technol* [Internet]. 2015 Sep [cited 2015 Sep 14];13(7):402–14. Available from: <http://www.ncbi.nlm.nih.gov/pubmed/26317884>
  38. Anastasov N, Höfig I, Radulović V, Ströbel S, Salomon M, Lichtenberg J, et al. A 3D-microtissue-based phenotypic screening of radiation resistant tumor cells with synchronized chemotherapeutic treatment. *BMC Cancer* [Internet]. 2015 Jan [cited 2015 Jun 15];15:466. Available from: <http://www.pubmedcentral.nih.gov/articlerender.fcgi?artid=4460881&tool=pmcentrez&rendertype=abstract>
  39. Alessandri K, Sarangi BR, Gurchenkov VV, Sinha B, Kießling TR, Fetler L, et al. Cellular capsules as a tool for multicellular spheroid production and for investigating the mechanics of tumor progression in vitro. *Proc Natl Acad Sci U S A* [Internet]. 2013 Sep 10 [cited 2014 Jan 24];110(37):14843–8. Available from: <http://www.ncbi.nlm.nih.gov/pubmed/23980147>
  40. Rajcevic U, Knol JC, Piersma S, Bougnaud S, Fack F, Sundlisaeter E, et al. Colorectal cancer derived organotypic spheroids maintain essential tissue characteristics but adapt their metabolism in culture. *Proteome Sci* [Internet]. 2014 Jan [cited 2014 Aug 4];12:39. Available from: <http://www.pubmedcentral.nih.gov/articlerender.fcgi?artid=4114130&tool=pmcentrez&rendertype=abstract>
  41. Lancaster M a, Renner M, Martin C-A, Wenzel D, Bicknell LS, Hurles ME, et al. Cerebral organoids model human brain development and microcephaly. *Nature* [Internet]. Nature Publishing Group; 2013 Sep 19 [cited 2014 Mar 19];501(7467):373–9. Available from: <http://www.pubmedcentral.nih.gov/articlerender.fcgi?artid=3817409&tool=pmcentrez&rendertype=abstract>
  42. Kelm JM, Ehler E, Nielsen LK, Schlatter S, Perriard J-C, Fussenegger M. Design of artificial myocardial microtissues. *Tissue Eng*. [Internet] 2004;10(1-2):201–14. Available from <http://www.ncbi.nlm.nih.gov/pubmed/15009946> PubMed PMID: 15009946.
  43. Moors M, Rockel TD, Abel J, Cline JE, Gassmann K, Schreiber T, et al. Human neurospheres as three-dimensional cellular systems for developmental neurotoxicity testing. *Environ Health Perspect* [Internet]. 2009 Jul [cited 2013 Apr 15];117(7):1131–8. Available from: <http://www.pubmedcentral.nih.gov/articlerender.fcgi?artid=2717141&tool=pmcentrez&rendertype=abstract>
  44. Alexander N. Combes\*, Jamie A. Davies† MHL. Cell-cell interactions driving kidney morphogenesis. *Curr Top Dev Biol*. 2015;112:467–508. PubMed PMID: 25733149.
  45. Sato T, Clevers H. Growing self-organizing mini-guts from a single intestinal stem cell: mechanism and applications. *Science* [Internet]. 2013 Jun 7 [cited 2014 Mar 20];340(6137):1190–4. Available from: <http://www.ncbi.nlm.nih.gov/pubmed/23744940>
  46. Giada D. G. Barabaschi, Vijayan Manoharan, Qing Li LEB. Engineering Pre-vascularized Scaffolds for Bone Regeneration No Title. *Eng Miner Load Bear Tissues*. 2015;881:79–94.





# Cell-Based RNAi Assay Development for HTS

Scott Martin,<sup>✉1</sup> Gene Buehler,<sup>1</sup> Kok Long Ang,<sup>2</sup> Farhana Feroze, Gopinath Ganji, and Yue Li

Created: May 1, 2012; Updated: May 1, 2013.

## Abstract

Gene silencing through RNA interference (RNAi) has become a powerful tool for understanding gene function. RNAi screens are primarily conducted using synthetic small interfering RNA (siRNA) or plasmid-encoded short hairpin RNA (shRNA). In this chapter, some considerations for design, optimization, validation, analysis and hit selection criteria in RNAi screens are discussed. A special emphasis is placed on pitfalls associated with off-target effects, which represent a primary limitation to the successful application of this technology.

## Introduction

RNA interference (RNAi) is a gene silencing mechanism initiated by short double-stranded RNA (dsRNA) of ~21nt in length (for a recent review see 1). Two major classes of dsRNAs harness this pathway for post-transcriptional gene regulation, including siRNAs and microRNAs (miRNAs). siRNAs direct the cleavage of mRNA transcripts that contain full sequence complementarity. Cleavage is mediated by a single strand of the siRNA duplex termed the guide strand, after loading into the RNA-induced silencing complex (RISC). Notably, the documented occurrence of naturally occurring cleavage complexes is not common in mammalian cells. Rather, it is miRNAs that use the innate RNAi machinery. miRNAs interact with transcripts possessing partial complementarity, primarily within target 3' untranslated regions (UTRs), resulting in transcript degradation and/or translation inhibition (Figure 1).

Experimentally, the ability to harness the RNAi pathway through the use of siRNAs/shRNAs (Figure 2) has paved the way for genome-wide high throughput screens. Many large-scale RNAi screens have been reported. Common variations include drug modifier screens, which combine the use of RNAi and a drug to identify genes that affect drug response, viability screens to look for vulnerabilities within specific cellular backgrounds, pathway reporter assays, pathogen-host screens to look for genes that affect pathogen spread and host response, and image-based phenotypic screens to report on genes associated with a wide variety of processes, including protein localization and disease-specific phenotypes. Many reviews cover the RNAi biology, experimental parameters and

---

<sup>1</sup> National Center for Advancing Translational Sciences. <sup>2</sup> Eli Lilly & Company, Indianapolis, IN.

<sup>✉</sup> Corresponding author.

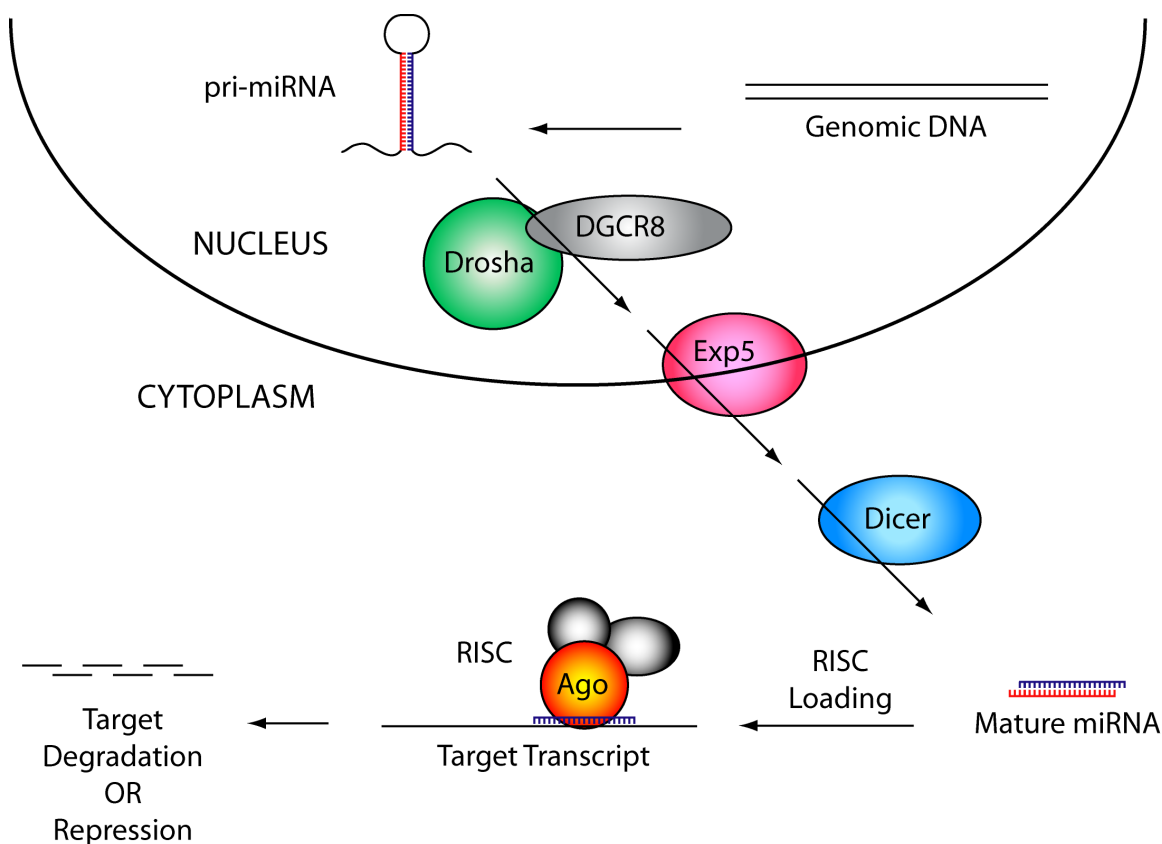


**Figure 1.** Simplified schematic of RNAi in mammalian cells. RNAi in mammalian cells is primarily mediated by endogenous miRNAs. miRNAs are expressed as primary hairpin-containing transcripts that are processed in the nucleus and cytoplasm to yield mature miRNA duplexes of ~22 nt in length. A single strand of the duplex is then loaded into an argonaute-containing silencing complex (RISC), which then guides the complex to target mRNA transcripts with partial sequence complementarity within their 3'UTRs. This interaction leads to degradation and/or translational repression.

considerations for performing screens (for example, 2-11). See table 1 for a brief summary of the differences between siRNA and shRNA reagents.

In the following sections, we have compiled our experience around RNAi-based LOF screens in mammalian cells to offer a few guidelines on best practices. As with any technology, this chapter will benefit from growing expertise and improvements in technology and methods.

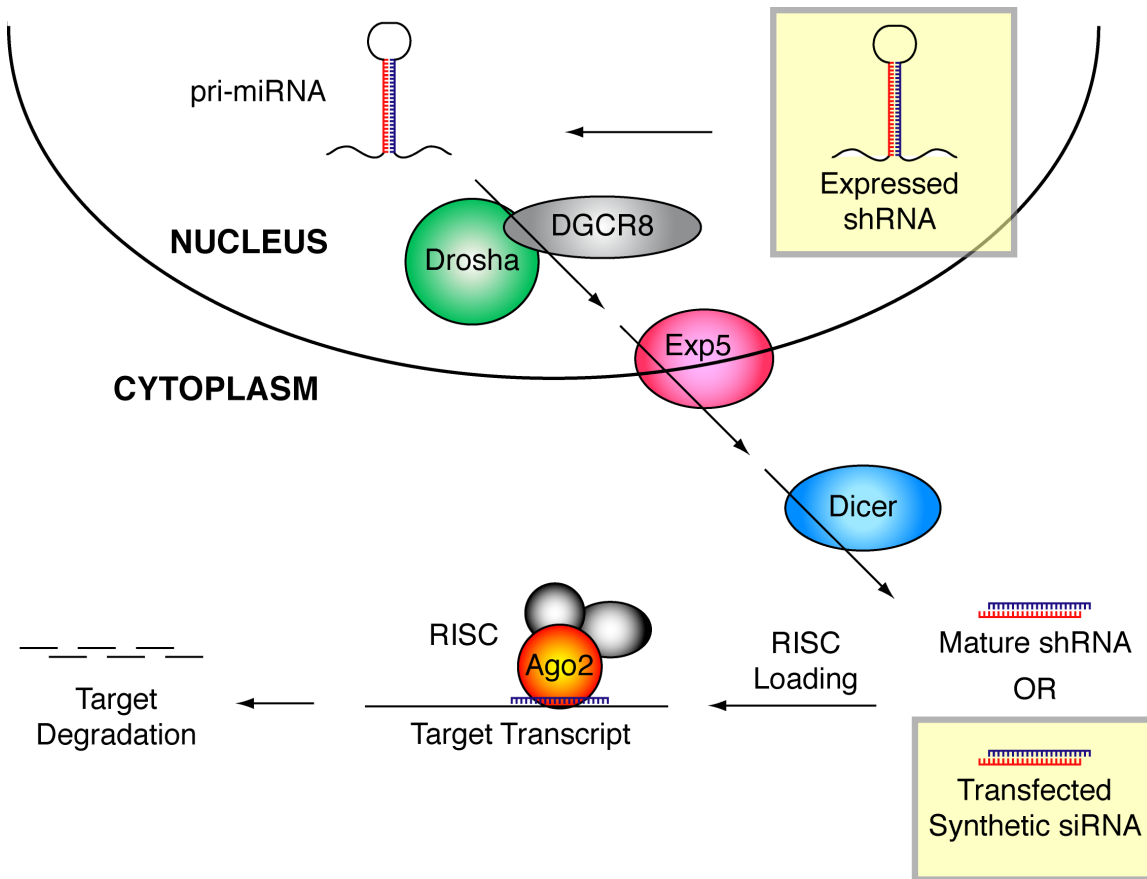


**Figure 2.** siRNAs and shRNAs harness the RNAi pathway for loss-of-function studies. shRNAs are encoded by plasmids and processed much like miRNAs to yield mature duplexes of ~22 nt in length. Alternatively, synthetic siRNAs can be introduced directly into the cell using transfection reagents. siRNAs and mature shRNAs are incorporated into a similar, if not identical, RISC complex as mature miRNAs. The loaded siRNA/shRNA strand then guides RISC to target mRNAs with full sequence complementarity, resulting in the site-specific cleavage target mRNA. Importantly, siRNA and shRNA guide strands can interact with the 3'UTRs of unintended targets through only limited stretches of sequence complementarity, much like miRNAs. These types of unintentional off-target effects can dominate the results of RNAi screens.

**Table 1:** Comparison of siRNA and shRNA-lentivirus

| siRNA   | shRNA-lentivirus   |
|---|--|
| Short-term target KD (< 1 week)                 | Long-term target KD  |
| Minimal library maintenance                     | Significant library maintenance  |
| Some cell types are not transfected efficiently | Infection is generally more effective than transfection, thus larger repertoire of cells can be used |
| Dosing to control cellular concentration        | Difficult to control cellular concentration, though inducible system possible                        |
| Chemical modifications possible                 | Stable target KD cell line can be generated.   |
| More consistent quality of reagent              | Titer of shRNA-lentiviral particles can be more variable   |

## Off-Target Effects

The ability of siRNAs/shRNAs to knockdown intended targets while minimizing or controlling for off-target effects (OTEs) is critical for the meaningful interpretation of RNAi screens. Off-target effects arise from mechanisms that can be either independent or dependent upon the siRNA/shRNA sequence. Sequence-independent effects can relate to experimental conditions (e.g., transfection reagents), inhibition of endogenous miRNA activity, or stimulation of pathways associated with the immune response. Sequence-dependent effects primarily concern the unintentional silencing of targets sharing partial complementarity with RNAi effector molecules through miRNA-like interactions. There are a number of approaches toward controlling and accounting for both types of off-target effects (discussed below).

### Sequence-Dependent Off-Target Effects: Interactions between siRNAs/shRNAs and non-targeted mRNAs

Although RNAi reagents can cause sequence-independent effects, the primary source of trouble for RNAi screeners are sequence-dependent off-target effects. Off-target effects originate from partial complementarity between RNAi effectors and off-target transcripts, in much the same way as those exhibited by endogenous miRNAs. In fact, like miRNA targets, off-targeted transcripts are enriched in those containing perfect pairing between their 3' UTRs and hexamer (nts 2–7) and heptamer (nts 2–8) sequences within 5' ends of RNAi effectors (12,13). These stretches of sequence are known as “seed sequences”. Some studies have found these effects to be non-titratable, with dose responses mirroring that of on-target transcripts (14). Others have found these effects to be concentration-dependent, whereby the use of low siRNA concentrations can significantly mitigate off-target interactions (15). Sequence-dependent off-target effects can have profound consequences. For example, Lin and colleagues determined that the top three “hits” from a siRNA-based screen for targets affecting the hypoxia-related HIF-1 pathway resulted from off-target effects (16). For two of these three “hits,” activity could be traced to interactions within the 3' UTR of *HIF-1A* itself. Additionally, Schultz and coworkers found that all active siRNAs in a TGF- $\beta$  assay reduced TGFBR1 and TGFBR2 (17).

How bad is the problem with seed-driven OTEs? It has been estimated that in a genome-wide screen using 4 siRNAs per gene, and an estimated 20 true positives in the assay, that 3,362 off-target genes would score with 1 active siRNA, 259 would score with 2 of 4 active siRNAs, and 9 would score with 3 of 4 (18). This is a sobering estimate given that the vast majority of published RNAi screens are conducted with only a single reagent per gene (pool of 4 siRNAs), and the typical bar for follow-up validation is to require that 2 members of the pool, or sometimes even 1, exhibit activity. Those approaches seem insufficient, and lead to published hit lists that are loaded with false positives, especially in cases where a simple laundry list of actives from the primary screen are presented. An additional illustration of this problem can be found in recently published host-virus screens. For example, a meta-analysis of 3 genome-wide siRNA screens conducted in

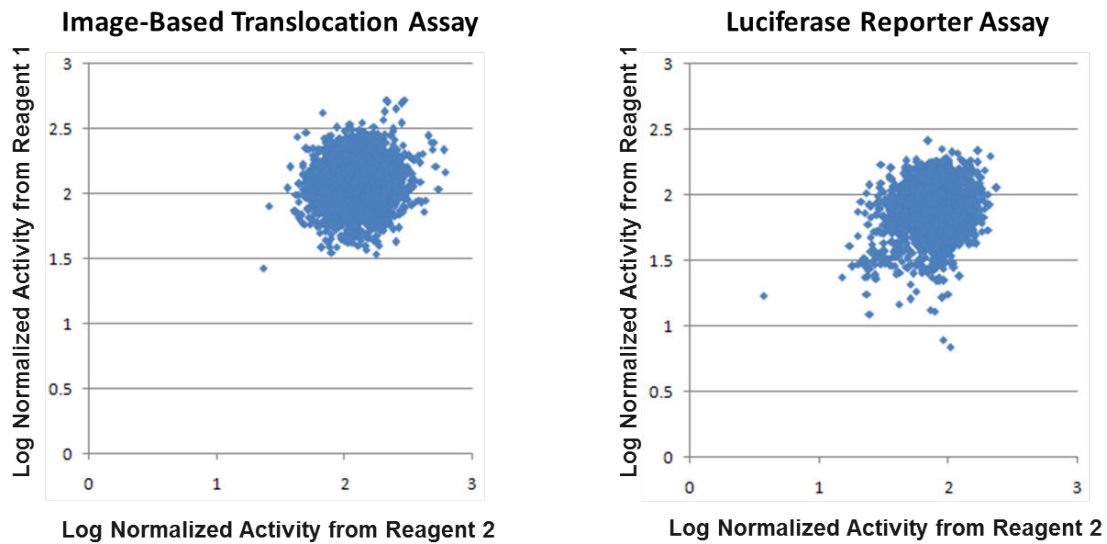


**Figure 3.** Comparing different siRNA reagents under the same exact experimental conditions. Two different screens show very little correlation between different siRNAs designed to target the same gene.

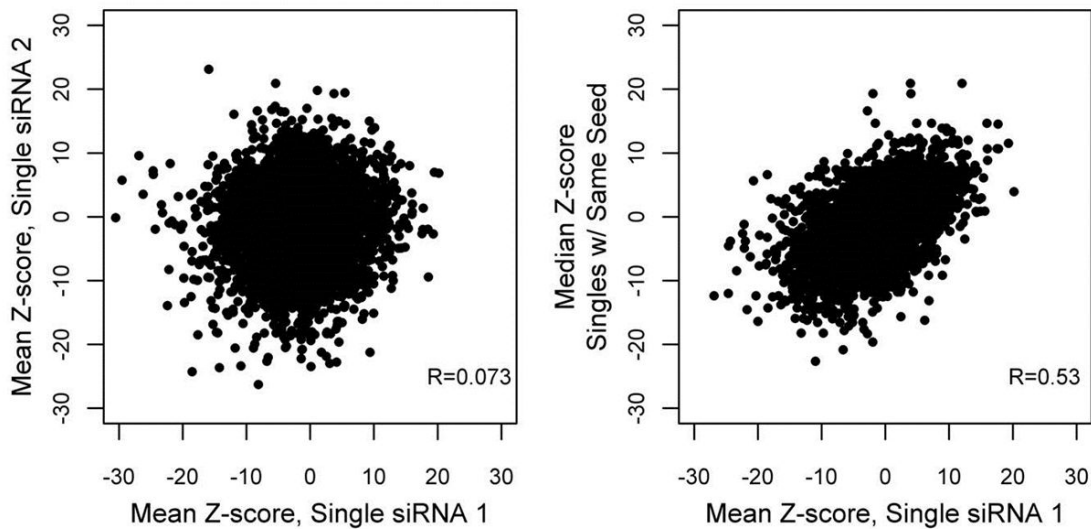


**Figure 4.** The correlation between siRNAs having the same seed is much greater than siRNAs designed to target the same gene (20). This is clear evidence that seed-dependent OTEs are the primary reason for a lack of agreement between siRNAs designed to target the same gene.

human cells to look for host genes associated with HIV revealed strikingly little overlap (19). Notably, only 3 genes were called in all 3 screens, and the pair-wise comparison of any two screens revealed only 3%-6% overlap. However, pathway analysis revealed greater similarities between the screens, and certainly false negatives (e.g, arising from reagent

deficiencies) and differences in experimental set up (e.g., cell lines and assay endpoints) are significant contributors to the lack of agreement. However, even when comparing different siRNA libraries under the same exact experimental conditions there is virtually no correlation (Figure 3). In fact, the correlation between siRNAs having the same seed is much greater than siRNAs designed to target the same gene (20, Figure 4), emphasizing the prevalence and impact of seed-driven OTEs in RNAi screen data.

There are a number of ways to help minimize the impact of sequence-dependent off-target effects. For starters, an attempt should be made to use siRNAs at relatively low concentrations. Early studies used siRNAs at  $\geq 100\text{nM}$ , but it should be possible to routinely use them at  $10\text{ nM} - 50\text{ nM}$  without loss of on-target potency. Other ways to reduce OTEs, relate to siRNA design features and chemical modifications. For example, siRNAs are now commercially available with chemical modifications to the passenger strand, which eliminate their loading into RISC, and the subsequent off-target effects that may result. Redundancy (the use of multiple reagents per gene) is another way to minimize the impact of off-target effects by requiring multiple active reagents per gene for that gene to be considered a candidate active. There are also informatic approaches to identify and even interpret off-target effects within RNAi screens. These will be discussed in more detail below. Despite all of these considerations, the occurrence of sequence-dependent off-target effects is unavoidable.

## Loss-of-Function Screens Using siRNA

### siRNA Reagents

The following choices of reagents need to be made prior to running any screens.

- **Scale:** Focused libraries (pathway collection, gene family, disease-specific library, etc.), druggable genome, or genome-wide. A variety of vendors offer these reagents (e.g., Qiagen, Dharmacon, Ambion, Sigma).
- **Format:** Some vendors provide pools of siRNAs against a given gene in an effort to guarantee knockdown. Others provide libraries in a single siRNA per well format. Recently, a variety of chemically modified siRNAs have become available. These modifications reduce off-target effects, especially arising from the passenger strand, and should be used.
- In light of the issue with OTEs, the use of multiple reagents per gene in a screen will increase the chances of identifying true positives. This is illustrated in the meta-analysis of HIV screen for example, in which genes called in 2 or 3 of the screens were more enriched in relevant pathways (19). Screening multiple reagents per gene can be a more expensive option and increase the scale of the screen. However, it is common practice to screen one reagent per gene in duplicate or triplicate. Given that the majority of variance arises from false negatives and positives (see figures 3 and 4) and that the correlation between replicates in a well-optimized assay can be quite high (see the pilot screens section below), it would seem wise to invest more in redundancy than replicates, if a choice must be made (i.e., 3 different reagents

per gene can be screened for the same cost as 1 reagent per gene in triplicate), provided that an assay has been demonstrated to be highly reproducible.

- **Negative and positive controls:** Negative and positive controls should be embedded in every assay plate. Negative controls are available from a number of vendors and are designed to lack homology with known transcripts. Positive controls should affect the assay under investigation (e.g., block the spread of virus in a virus assay). In cases where a good positive control does not exist, siRNAs should be chosen to at least report on the quality of transfection (e.g., lethal siRNAs that target essential genes or siRNAs that target the reporter used in a given assay, like GFP or luciferase). It is also important to note that negative controls are most likely not truly negative in any given assay.

## Assay Optimization

Optimization needs to be done for all screens. Table 2 lists some important parameters for consideration in RNAi optimization.

A few essential parameters (and their purpose) are worth highlighting:

- General guidelines for cell-based assays such as growth media, seeding density, growth rate, incubation time, etc. can be found in the Cell-Based Assay section in this manual.
- **Timing:** Typical siRNA screen range from 48 h to 120 h. siRNA can reach maximal silencing of mRNA transcripts within 12h – 24h, but concomitant loss or protein will depend on protein half-life. If stimuli is to be added (e.g., drug or virus), it is typical to add it 48 h – 72 h post-transfection to ensure protein knockdown for a majority of genes prior to treatment. It is also important to remember that loss of silencing will begin to occur around ~96 h, so careful considerations must be made when designing an assay.
- Transfection efficiency (below are some of the most important parameters for RNAi optimization, with reverse transfection being the preferred method for screening). See the “siRNA Transfection Optimization Experiments” section below.
  - Cell seeding density (e.g., for a viability-based experiment, you would not want to reach confluence prior to the assay endpoint).
  - Choice of transfection reagent and the amount
  - siRNA concentration (typically 10nM – 50nM)
- Determination of KD efficiency along with transfection efficiency should constitute an essential part of assay development and optimization. The extent of KD can be determined by qRT-PCR quantification of target transcript level after si/shRNA treatment. Transfection efficiency can be gauged with positive controls where a phenotypic effect (such as cell killing or reporter gene knockdown) is observed. It is ideal to use a positive control that is sensitive to knockdown efficiency, meaning that the effects are not observed under suboptimal transfection conditions. The use of such controls would also allow evaluation of both transfection and KD efficiency after a large scale screening to check performance.

- Choice of controls
  - Positive controls: cells with gene specific si/shRNAs transfected that will result in a significant change to the assay readout. For example si/shRNAs targeting UBB or PLK1 can be used as positive controls in cell proliferation or apoptosis assays. These controls can be informative in evaluating transfection efficiency and KD efficiency.
  - Negative controls: cells with non-silencing si/shRNAs (NS), also known as non-targeting control (NTC), transfected but without significant effect on the assay readout. It is also recommended to include the following as negative controls, although there may not be enough real estate in screen plates for these to be included throughout the screen:
    - Non-transfected (NT) cells: cultured cells only, without transfection/infection
    - Mock-transfected (MT) cells: cells with transfection reagent only, without si/shRNA
  - It is important to verify that transfection conditions do not significant alter the assay. For example, drug efficacy should be the same in cells transfected with negative control siRNA versus NT cells in a drug modifier screen. Similarly, cell transfected with negative control siRNA should not respond differently to virus than NT cells.
- Assay  $z'$ -factors: After identifying optimal transfection conditions, it is important to evaluate the assay  $z'$ -factor to understand if the assay signal window and variation are at an acceptable level. Although, a factor of 0.5 is widely accepted for small molecule screens, lower assay  $z'$ -factors are generally accepted and expected for RNAi screens.

**Table 2:** Important parameters in RNAi-assay optimization

| Parameter                    | Key Factors  |
|------------------------------|--|
| Cell line for screening      | transfection efficiency, growth rate, assay sensitivity  |
| Cell growth media            | should not interfere with readout or transfection efficiency                                     |
| [si/shRNA]                   | concentration must produce effective silencing and limit off-target effects                      |
| Plate format                 | medium evaporation, machine readout, barcode   |
| Negative control si/shRNA    | should have no effect on assay readout   |
| Positive control si/shRNA    | Should have large measurable effect on assay readout   |
| Transfection reagent         | should be effective in introducing RNAi reagent into cells with low toxicity and affect on assay |
| Transfection reagent diluent | should not interfere with assay readout, or transfection efficiency                              |

*Table 2 continues on next page...*



Table 2 continued from previous page.

| Parameter                                      | Key Factors  |
|--|--|
| Transfection reagent ratio                     | Toxicity vs. efficiency                                      |
| Transfection reagent incubation time           | enough time to complex RNAi reagent and transfection reagent |
| Mechanism for addition of transfection reagent | minimize well-to-well, plate-to-plate variability            |
| Complexing time                                | enough time to complex RNAi reagent and transfection reagent |
| Cell volume added                              | well-to-well, plate-to-plate variability                     |
| Cell number added                              | optimize to give greater dynamic range at readout            |
| Mechanism for addition of cells                | minimize well-to-well, plate-to-plate variability            |
| Mechanism for addition of readout reagent      | minimize well-to-well, plate-to-plate variability            |
| Incubation time for readout reagent            | optimized to give greater dynamic range at readout           |
| Readout method                                 | sensitivity, accuracy  |

## siRNA Transfection Optimization Experiments

A convenient first step in optimizing siRNA transfection conditions is to use viability assays with lethal control siRNAs. Two examples of a 96-well plate layout for transfection optimization are shown below (Figure 5). The bottom line is that a number of variables, including cell seeding density and transfection reagent identity/concentration, should be assessed.

The optimal condition is determined mainly by:

1. Negative controls should closed mimic NT; while the positive controls should achieve maximal effect as determined by the optimization experiments. Knockdown efficiency using the best condition should be verified by real-time PCR with previously validated siRNAs.
2. Controls should not exhibit high variance, which would indicate significant variation in transfection efficiency.
3. Performing experiments in clear bottom plates is also an excellent way to visualize transfection efficiency, as virtually all cells in a given well should be visibly affected by transfection with lethal controls (e.g., cell rounding).
4. After identifying potential conditions via lethal control experiments, those conditions should still be tested with assay-specific positive controls.

## Pilot Screens

Pilot screens should be performed when conducting large-scale siRNA screens. Pilot screens will help inform on assay reproducibility and data distribution. Pilot screens can be conducted with defined subsets of the genome-wide library such as the kinome. Replicate screens conducted at the same time should exhibit large correlation ( $r^2 \sim 0.8$ ) and

**A**

|   |  |   |      |      |      |       |   |      |    |      |    |  |
|---|--|---|------|------|------|-------|---|------|----|------|----|--|
| siRNA   |  |   |      |      |      |       |   |      |    |      |    |  |
| NT (no siRNA)   |  |   |      |      |      |       |   |      |    |      |    |  |
| NC  |  |   |      |      |      |       |   |      |    |      |    |  |
| NC  |  |   |      |      |      |       |   |      |    |      |    |  |
| PC  |  |   |      |      |      |       |   |      |    |      |    |  |
| PC  |  |   |      |      |      |       |   |      |    |      |    |  |
| NC/PC   |  |   |      |      |      |       |   |      |    |      |    |  |
| grey = blank  |  | 0 | 0.2x | 0.3x | 0.5x | 0.75x | x | 1.5x | 2x | 2.5x | 3x |  |
| x = transfection reagent amount recommended by manufacturer |  |   |      |      |      |       |   |      |    |      |    |  |

**B**

|    |       |  |  |    |  |  |  |    |  |       |    |
|----|-------|--|--|----|--|--|--|----|--|-------|----|
| NT | Trx.R |  |  |    |  |  |  |    |  | Trx.R | NT |
| NT | only  |  |  | NC |  |  |  | NC |  | only  | NT |
| NT |       |  |  |    |  |  |  |    |  |       | NT |
| NT |       |  |  |    |  |  |  |    |  |       | NT |
| NT | Trx.R |  |  |    |  |  |  |    |  | Trx.R | NT |
| NT | only  |  |  | PC |  |  |  | PC |  | only  | NT |
| NT |       |  |  |    |  |  |  |    |  |       | NT |
| NT |       |  |  |    |  |  |  |    |  |       | NT |

**Figure 5.** siRNA optimization plate layout examples. (A) has a wider range of transfection reagent concentrations to judge, given a fixed siRNA concentration (the edge wells are intentionally left blank); while in (B) the concentrations of siRNA and transfection reagent are optimized together. Different cell seeding density can also be tested along with the two factors in different plates. NC-negative control; PC-positive control; TRx.R – transfection reagent. In (B) each of the four blocks (4x4) in the center is a factorial design of siRNA and transfection reagent concentrations

even replicate screens conducted at different times (e.g., weeks or day apart) should be highly reproducible (see Figure 6). Pilot screen will also indicate how the data will be distributed in the larger screening campaign (e.g., normal, log-normal, or non-normal) and help indicate problems. For example, a very active screen, even if reproducible, may make it impossible to find anything of true significance in the assay, if one determines significance based on the screen population, and not a comparison to a single negative control (see hit selection below). Pilot screens can also indicate edge effects and other assay artifacts (Figure 7).

## RNAi Screen Design and Quality Control

**Plate Design:** When designing the plates one should consider including a sufficient number of control replicates to help evaluate data quality. The number of wells for each

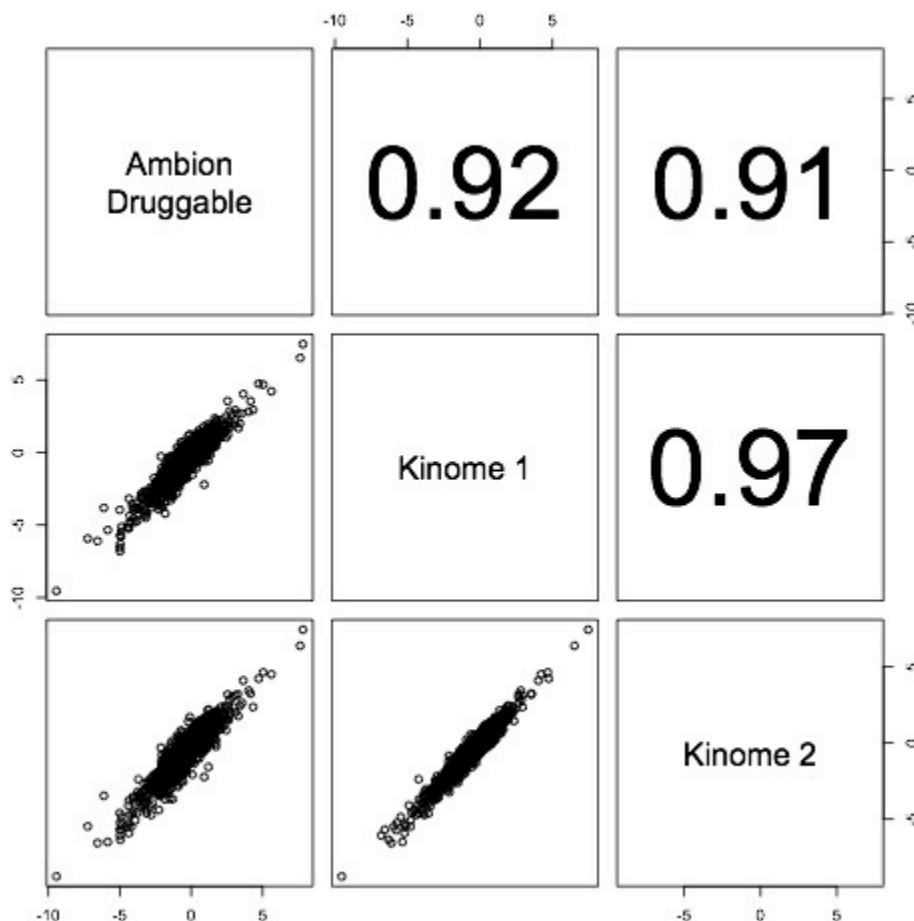


**Figure 6.** An example of a highly reproducible assay. Pilot kinome screens conducted on separate occasions indicate highly reproducible assay conditions - a prerequisite for conducting an RNAi screen. Using siRNA sequences in pilot screens that are also represented in the large-scale campaign ensures that assay performance remained unchanged (compare “Ambion Druggable” to Kinome 1 and 2).

type of control within the plate should be  $\geq 4$  for 96-well plates (preferably 8 wells); or  $\geq 8$  for 384-well plates (preferably 16 wells). See Figure 8 for a sample screen plate layout.

**Note:** Plate layouts and available wells may limit the incorporation of MT or NT controls. However, control plates should always be included in screen batches to show that negative control transfected cells respond similar to MT and NT.

**Replicates and Redundancy:** Ideally, one would incorporate numerous, different reagents per gene (redundancy) and biological replicates. Given the issues with siRNA screening, it has been suggested that 4-6 reagents per gene be screened in the primary campaign (21). Unfortunately, many off-the-shelf libraries, whether whole genome or focused, come with one reagent per gene (pool) or 3 singles per gene, requiring multiple expensive purchases

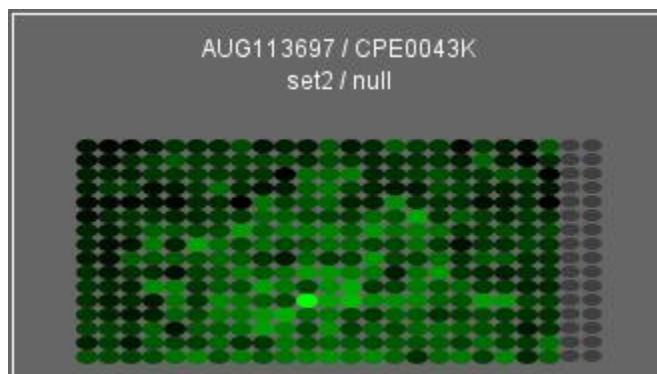


**Figure 7.** Pilot screens can indicate technical problems such as positional biases. Here, the assay signal is clearly biased toward the middle of the plate. This also emphasizes the value of data visualization.

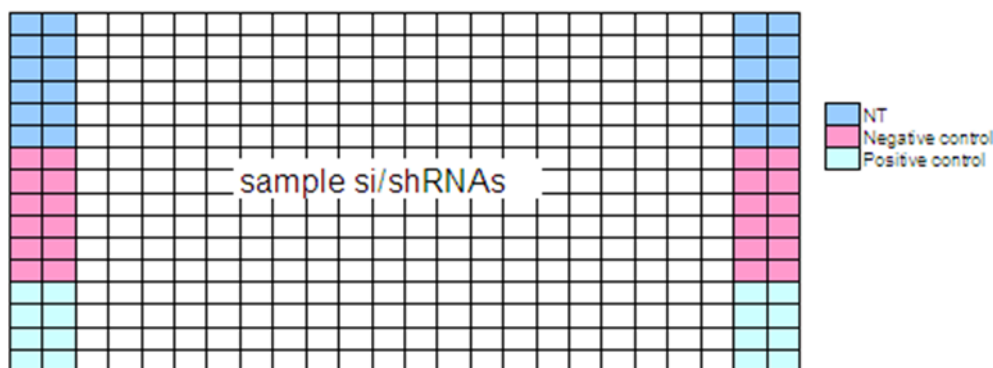


**Figure 8.** Experimental plate layout example shown in 384-well format.

to achieve that threshold. Notably, it is much easier to acquire  $\geq 4$  reagents per gene when constructing a custom library in conjunction with a vendor. Performing replicate screens can be another approach to honing in on the most reproducible actives. For example, in the meta-analysis of HIV screens by Bushman and colleagues (19), simulations using the estimated variance for one of the siRNA screens predicted that of the top 300 hits only half would be shared between two replicate screens. Increasing the number of replicates to ten would increase the overlap to 240 genes. However, the cost of running multiple reagents per gene ten times is prohibitive, requiring enough reagents (e.g., plates, tips, cell culture, transfection reagent, assay reagent, etc.) to run  $\sim 2400$  384-well plates. Given cost and throughput realities, choices must be made. For a highly reproducible assay, as determined in the pilot phase of a screening campaign, it is a given that most of the variance will come from a lack of agreement between reagents designed to target the same gene (false positives and negatives) and one may wish to devote more resources to redundancy as compared to replicates. If pilot screens indicate a high variance and very little overlap between replicates, then many replicates or a complete overhaul of the assay will be required. For smaller, focused screens, it should be practical to run multiple

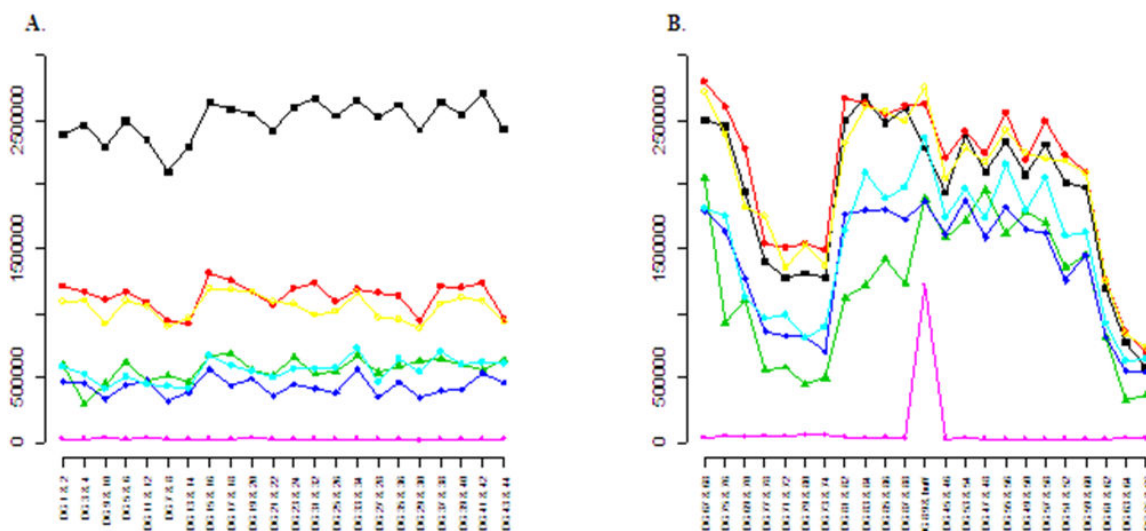


**Figure 9.** Scatter plots from two exemplar screens. Plots A and B show plate to plate variability as assessed by controls (different colors for different controls). It can be seen that the signals (Y-axis) for each kind of control are similar from plate to plate when analyzing all plates (X-axis) indicating low plate-plate variation while in plot B there is dramatic change from plate to plate, which could be corrected by some appropriate normalization method if the variation is consistent for all kinds of controls, or one needs to consider dropping some plate/wells with inconsistent variation.

reagents per gene in duplicate and beyond if necessary (the correlation between replicates can dictate the ideal number of replicates).

## Quality Control

**Uniformity:** Uniformity within-plate or from plate to plate is also a key factor to check for quality control. Heat maps are recommended to visualize each screen plate as they help to identify geometric effects due to experimental errors or systematic problems. Section II of this manual has guidelines on within-plate variation evaluation. Given the steps involved and the cell-based nature of RNAi experiments, CVs (coefficient of variation) ranging from ~15% to > 30% of the sample population are common. A scatter plot of plate-wise CVs versus the plate index may reveal plate-to-plate differences. In general most plates would be expected to yield similar CVs, but undoubtedly there will be biased plates in a given library given that libraries are not always randomly distributed (e.g., a plate may be rich in ribosomal proteins). If there are outlier plates in terms of CV, it will be important to inspect the source of those differences on a case by case basis. A replicate of that plate will ultimately determine if the aberrant CV is in fact a reflection of the biology occurring on the plate, or an assay artifact. Additionally, B-score normalization may help to minimize systematic row and column variations.

**Control Variation:** Scatter plots of common control wells across plates also help to evaluate plate-plate variation (Figure 9).

**Assay Z'-factors:** In HTS, a scatter plot of Z prime factors for every plate versus the plate index will reveal the plate-plate differences and may help to troubleshoot any existing problems, or flag plates for redo.

**Transfection / Infection Efficiency:** In many cases, the ratios between the negative control and positive control will inform on transfection/infection efficiency. For example, in a cell viability assay, the ratio of the potent positive control versus the negative controls can ideally be <5%, which can be interpreted as high (> 95%) transfection/infection efficiency. While there is no theoretically defined threshold value, often these ratios will depend on the type of assays and potency of controls. In some assays, comparing positive and negative controls will not obviously inform on transfection efficiency or homogeneity. In those cases, it may be advisable to run a control plate with siRNAs that will inform upon efficiency and heterogeneity of transfection.

**Replicates:** To evaluate the reproducibility between replicate plates (or within plate replicates), one can use Lin's Concordance Correlation Coefficient (Lin's CCC 22, 23), Bland-Altman test (24) and Pearson correlation coefficients. Please consult your statistician for the most applicable method.

## siRNA Hit Selection

**Normalization and Hit Selection:** Data is typically normalized to controls (e.g., the median of the negative control wells on each plate) or median plate activity (although the presence of biased plates may make this less appropriate). Although normalizing to the plate median may initially seem more attractive than normalizing to a negative control (which could have assay activity due to off-target effects), this will cause problems during follow-up experiments. After selections are made for follow-up, any validation experiments will be biased as will the plate median, making it impossible to compare result between primary and secondary experiments. Therefore, we consider it preferable to control for plate to plate variation by normalizing to a negative control. Please consult your statistician for most suitable method. Hit selection in large-scale siRNA screens is usually performed by converting normalized values into z-scores, or MAD-based z-scores, and then selecting actives that cross a selected threshold (e.g., 2 z-scores or MAD scores from the screen median). To apply these types of methods it is important that the data be normally distributed. Comparison to negative control using a specified cutoff with statistical and/or biological significance (e.g. > 50% loss of cell viability) may be more appropriate for smaller screens. However, using cutoffs based on departure from negative control for larger screens may lead to too many "hits". For example, it may be historically accepted that a 30% reduction in the spread of a particular virus is biological relevant and significant. However, a 30% reduction may only score one standard deviation from the screen median, meaning that ~15% of a normally distributed population would be considered active. Alternatively, the biologically significant reduction of 30% may represent a very significant departure from the screen median, and be a very appropriate threshold. For smaller screens with large number of replicates, statistical tests (such as two

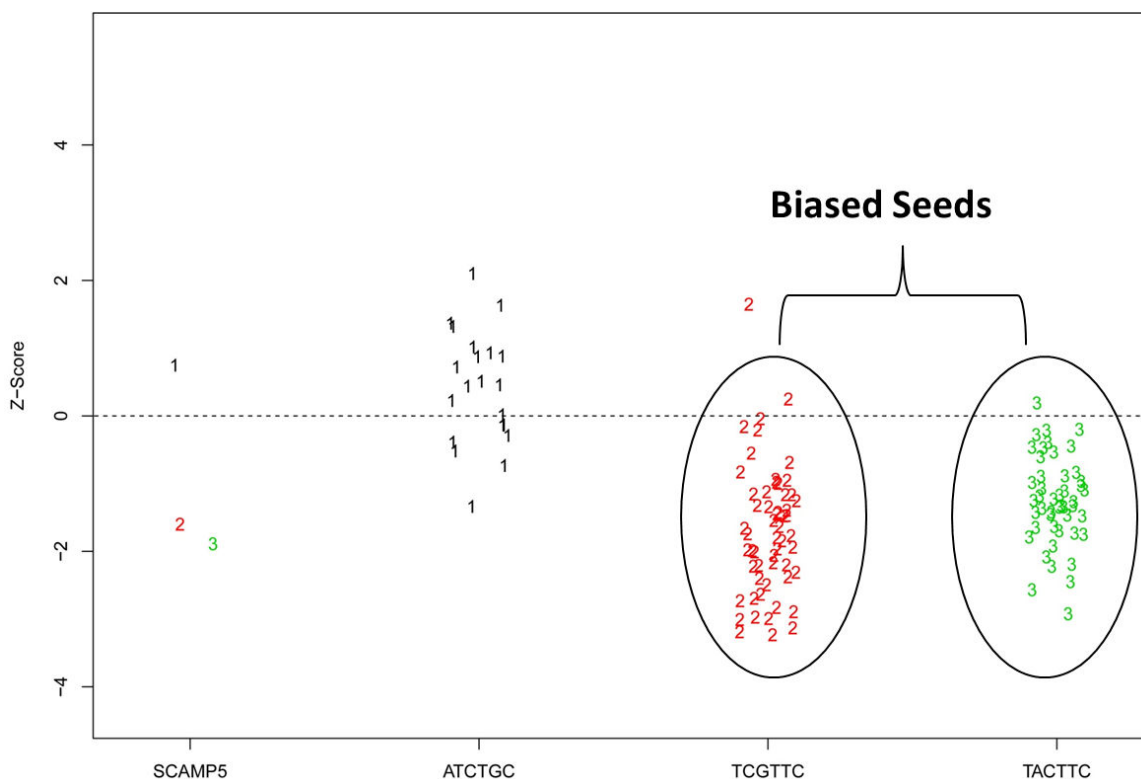


**Figure 10.** Screening a large library of non-pooled siRNAs enables determination of biased seed sequences (20). Two siRNAs targeting SCAMP5 appear to significantly down-regulate the assay response. However, siRNAs containing the same hexamer sequences exhibit a clear bias towards down-regulating the assay. Therefore, the SCAMP5 siRNAs would be flagged as highly suspicious and are most likely OTEs.

sample t-test) can be used with appropriate multiple testing correction (e.g. Tukey's, or Dunnett) if necessary.

Hits selected from screens using reagent redundancy are typically restricted to those genes with multiple active reagents. For example, one could require that 2 or more of 4 siRNAs total cross a specified threshold. A corresponding p-value and FDR can also be associated with those criteria. Similarly, redundant siRNA analysis (RSA) considers the activity of each siRNA for a given gene in an assay and generates a corresponding rank and p-value (21). Other non-parametric methods like sum of ranks can also be employed. Consult your statistician, and be sure that hits selected for follow-up are actually grounded in the screen data.

Primary screen data can and should be filtered for off-target effects. For example, by screening a large library of non-pooled siRNAs, one can analyze the data for biased seed sequences (20, Figure 10). siRNAs containing these seeds can be demoted in hit selection. Similarly, the top active siRNAs can be filtered for those containing known miRNA seed sequences with the assumption that these seeds will be highly promiscuous in terms of

off-target profiles. In addition to flagging potentially biased siRNAs, there are also tools to even interpret the underlying OTEs (25, 26).

Pathway analysis can also reveal enrichments in the data and prioritize hits for follow-up. A variety of commercial and open software are available. A potential caveat is that this type of analysis is biased towards well-annotated genes.

## Follow-up Assays

The detailed follow up plan for hits identified in a screen would depend on the nature of the investigation and the goal(s) of the study. That said, a few general suggestions are described below.

- Test additional siRNAs for targets of interest. These siRNAs should constitute different sequences than those in the primary screen. It has been traditionally accepted that 2 active siRNAs constitutes a validated active, but given the estimates described above, and the continued reports describing lack of correlation between published screens using similar systems, 2 active siRNAs seems to be an inadequate standard. However, any candidate can be examined in additional follow-up experiments for more rigorous validation.
- Target gene KD can be validated. Knockdown can be measured by QPCR over 24h or 48h. Best practices for carrying out QPCR experiments can be found elsewhere in the current or future versions of the QB manual. siRNA efficacy can also be assessed by Western blotting or immunofluorescence when possible. Clearly, a siRNA that yields a phenotype, but does not yield KD is a false positive. However, demonstrating KD does not prove that the observed phenotype is due to the on-target knockdown of that gene (i.e., an siRNA that is effective against its target has no bearing on its ability to down-regulate other transcripts and cannot be interpreted as validation). Furthermore, the number of siRNAs that have no effect on their intended target is relatively small, making it unlikely that QPCR will be a cost effective method for eliminating false-positives.
- Rescue: The current gold standard in RNAi hit validation is rescue of phenotypes by introducing siRNA-resistant cDNA. Another approach is to knockout the gene of interest by using TALEN or similar technologies. This knockout should recapitulate the siRNA-induced phenotype and can also be rescued by subsequent re-expression of the gene via cDNA. Although these experiments can be excellent validation, they can also be technically challenging and suffer from their own pitfalls.
- Test control siRNAs that retain the seed region of the original siRNA, but not its ability to cleave the transcript of interest. Recent reports have described control siRNAs where the seed region is maintained, but bases 9-11 are altered (27). The intent is to maintain the seed-driven off-target effects of a given siRNA, while eliminating its on-target effect. This initial study showed promise in separating false from true positives.

Secondary assays: This is recommended to eliminate assay artifacts and characterize target biology in more detail. Therefore, the exact nature of the assay may differ as a



function of target pathway, biological process and disease biology. Validated high-content assays may be particularly useful in this regard. These are described elsewhere in the QB manual.

## RNAi Synthetic Lethality Screens

### Synthetic Lethality Screens

A variation of a LOF screen is a synthetic lethality (or, synthetic lethal) screen which combines the use of RNAi and a drug (at single concentration or multiple concentrations) to identify knockdown events that would modulate drug response such as sensitizers that enhance drug effect. This offers a powerful approach to identify genetic determinants of drug response, especially in cancer. Most of the assay optimization and follow-up assays for si/shRNA described in part B apply here. The extra optimization and differences in data analysis will be discussed below.

### Assay Optimization


In synthetic lethality screens, the incubation time of the drug, its potency and stability also need to be evaluated. Drug dose and time response (DDTR) experiments can be carried out to optimize these conditions in either 96-well or 384-well plates. For instance, in a 96-well plate, 10-point drug dilutions with NT and negative controls (at fixed si/shRNA concentration) can be applied along each row excluding the two edge columns (Figure 11). Assay readouts need to be monitored over a period of time, say from Day 1 to Day 6. The result of such an experiment is mentioned below.

**Example:** A DDTR experiment for one drug was done from Day 1 to Day 6 to determine the appropriate drug incubation time for subsequent siRNA synthetic lethality screens. Data from Day 3 to Day 6 in Figure 8 (data from Day 1 and Day 2 data was not informative for curve fitting). Sigmoidal dose response curves of NT and NS were obtained from the experimental plates designed as above and  $IC_{50}$  values were estimated for each day. From Figure 12, we can see that:

- NS and NT produce almost exactly the same dose response curves over the various concentrations sampled
- $IC_{50}$  values of the drug (either from NT or NS curves, see vertical drop lines in Figure 12) tend to stabilize from Day 4 (for NT, Day 3: 44.59nM, Day 4: 35.78nM, Day 5: 36.54nM, Day 6: 31.77nM)
- Signal window between the zero concentration and the highest concentration of the drug tends to stabilize from Day 5 (Z prime factor calculated using NT at concentration zero and 200 nM: Day 3-0.42; Day 4-0.89; Day 5-0.73; Day 6-0.73).

Therefore 5 days of drug treatment would be recommended.

|   | 1  | 2  | 3  | 4  | 5  | 6  | 7  | 8  | 9  | 10 | 11 | 12 |
|---|----|----|----|----|----|----|----|----|----|----|----|----|
| A | NT | NT | NT | NT | NT | NT | NT | NT | NT | NT | NT | NT |
| B | NT | NT | NT | NT | NT | NT | NT | NT | NT | NT | NT | NT |
| C | NT | NT | NT | NT | NT | NT | NT | NT | NT | NT | NT | NT |
| D | NT | NT | NT | NT | NT | NT | NT | NT | NT | NT | NT | NT |
| E | NS | NS | NS | NS | NS | NS | NS | NS | NS | NS | NS | NS |
| F | NS | NS | NS | NS | NS | NS | NS | NS | NS | NS | NS | NS |
| G | NS | NS | NS | NS | NS | NS | NS | NS | NS | NS | NS | NS |
| H | NS | NS | NS | NS | NS | NS | NS | NS | NS | NS | NS | NS |


  
Drug dilution

**Figure 11.** 96-well plate layout for DDTR. NT: non-transfected; NS: non-silencing siRNA (negative control)

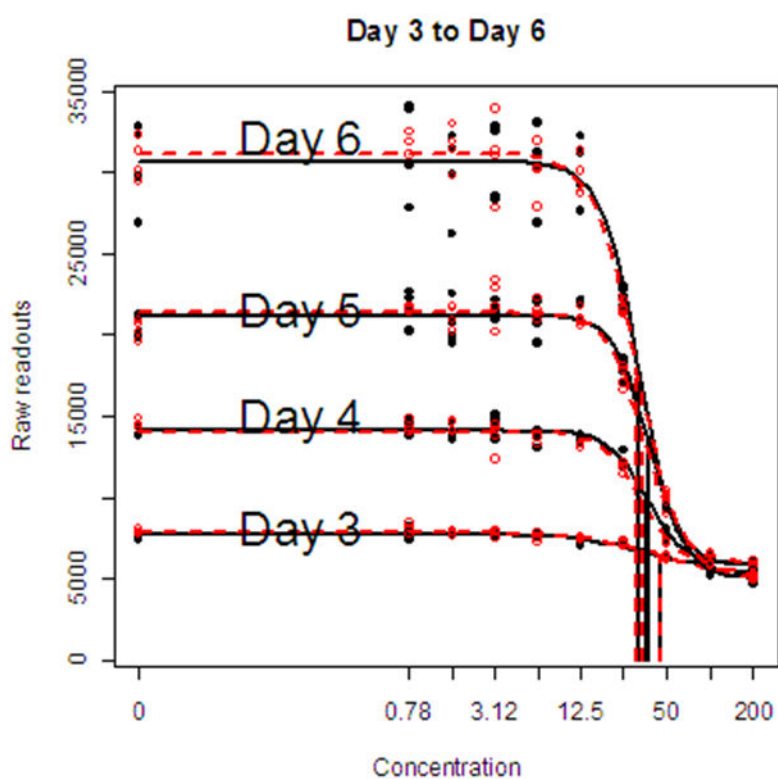


**Figure 12.** DDTR example of one experiment with four replicates from Day 1 to Day 6 (Data from Day 1 and 2 was not for curve fitting and is not shown); black solid lines and solid points are for NT, red dash lines and bullet points for NS.

## Design of Synthetic Lethality Screens

There are two main designs for synthetic lethality screens: single and multiple concentrations of drug. The hit selection strategy will vary accordingly.

- **Single-concentration experiment** - Typically drug concentrations less than the  $IC_{50}$  are chosen (e.g.  $IC_{10}$  and/or  $IC_{30}$ ). At each point including zero, we

recommend at least three replicates (may reduce to duplicates in a high-throughput screen).

- **Multiple-concentration experiment** - A full dose response curve of the drug is used. We recommend 7 doses with duplicates as a minimum. For larger scale screens where number of points and replicates are an issue, we would suggest increased dose points, provided they are chosen carefully to cover the full range of dose response.

**Note:** Several advantages exist with a RNAi synthetic lethality screen run with multiple concentrations. Non-linear curve fitting to identify biologically more relevant hits that demonstrate a 'shift' in DDR is made possible. Replicates are not as major an issue and achieving exact dose effect is not a concern due to curve fitting. In our experience, it is likely to produce more robust screen actives (less false-positives) and reduce follow-up steps.

In synthetic lethality screens, other necessary considerations are:

- Monitoring drug dose response in a large scale screen, such as control charting on drug potency ([Quantitative Biology](#)).
- Choice of sensitizer control (positive control) which may be targets related to drug MOA.
- Inclusion of extra control plates (see Appendix) along with other library plates in the screen to assess the quality of the screen especially HTS.

## Hit Selection in Synthetic Lethality Screens

Normalization methods basically are the same as described earlier for LOF screens. The basic idea of synthetic lethality experiments is to identify hits that result in maximum chemosensitization. Therefore, we suggest the following hit selection process:

1. When using a cell growth or death assay, we suggest excluding si/shRNA hits that are result in high cytotoxicity without drug. This is to prevent confounding interpretation around drug potentiation (These hits can be tested separately for any sensitization effect). As an example, in our experience, we have excluded hits that cause >60% loss of viability from the following analysis. Other threshold values can also be obtained by using population-based methods suggested by statisticians (such as 2 or 3 standard deviations from the mean).
2. After the first step,
  - In a single-concentration experiment with sufficient replicates, one can use statistical models (such as linear models) to pick statistically significant hits that demonstrate significant interaction of drug and siRNA. Furthermore, to rank hits, we suggest a non-parametric metric based on the interaction between RNAi, drug and the combination, called "potentiation score", based

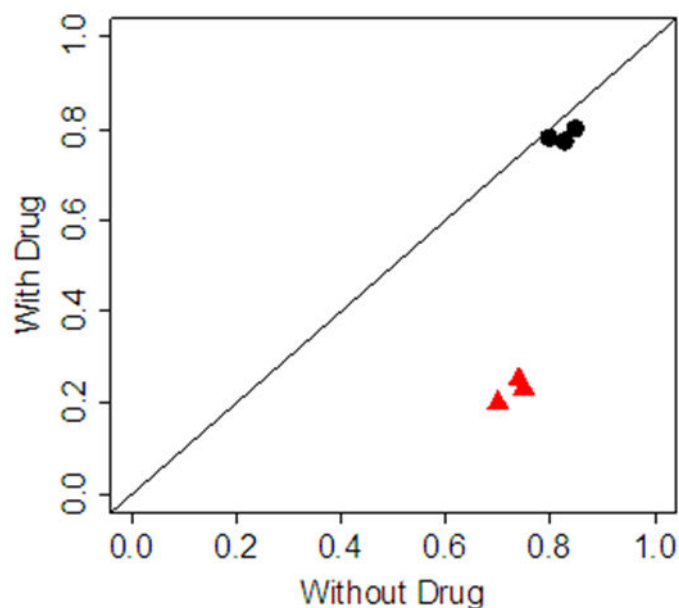


**Figure 13.** A hit from single-dose synthetic lethality screen in a cell proliferation assay. The black round points are for negative controls (NS), showing not much different effect w/ or w/o drug; the off-diagonal red triangle points are for the hit, which does not have much of an effect on its own but has significantly more effect with drug.

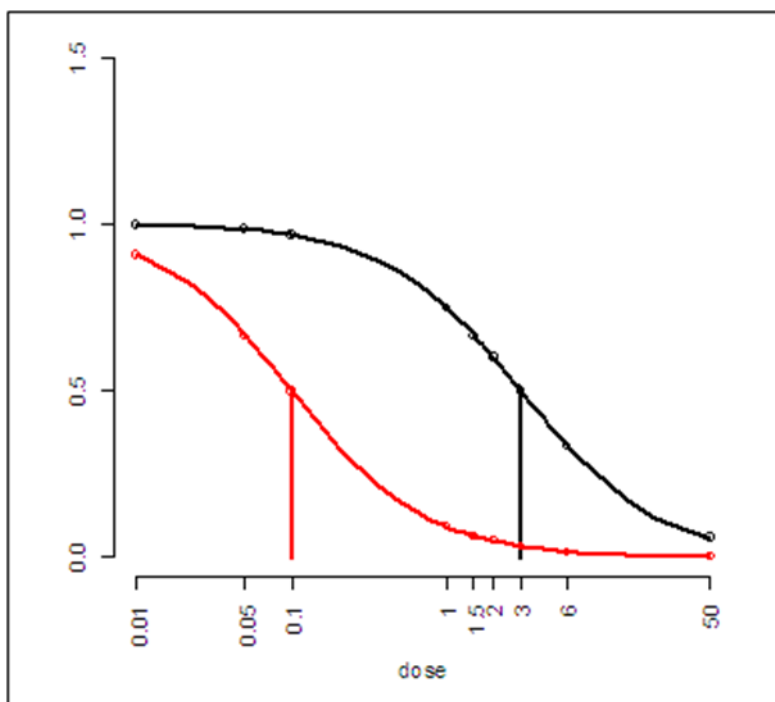


**Figure 14.** A hit in multiple-dose synthetic lethality siRNA screen in a cell viability assay. The decrease of IC50 value of the red dose response curve (the siRNA with the drug) compared to the black curve (negative control, NS with the drug) is observed (the dropping lines indicate the positions of IC50 values).

on the idea of independent events, calculated as shown below for inhibition assays, such as cell viability:

$$P = \frac{NS(T)}{NS(UT)} \times \frac{siRNAOnly(UT)}{NS(UT)} \bigg/ \frac{Combination}{NS(UT)}$$

Or, for activation assays, such as cell apoptosis:

$$P = \frac{Combination}{NS(UT)} \bigg/ \frac{NS(T)}{NS(UT)} \times \frac{siRNAOnly(UT)}{NS(UT)}$$

"UT" here refers to the untreated condition; the "drug only" and "combination" are at the same drug dose point.  $P > 1$  indicates that the combination effect is more than the product of two individual effects. The threshold values can be determined using population-based methods. An example of hits in single-concentration experiment is illustrated in Figure 13.

- In a multiple-concentration experiment, sigmoidal curve comparison is done between RNAi with and without small molecule. Using cell viability assay as an example, hits that demonstrate a significant left shift of dose response curves (Figure 14) would be of interest. One should first exclude those response curves above the negative controls (to avoid transfection artifacts) and then look for a decrease of  $IC_{50}/EC_{50}$  values. Statistical tests like t-test between  $IC_{50}/EC_{50}$  estimates, F test for two curve fittings, or information criteria can be used for testing significance (GraphPad Prism Manual). In general, we recommend hits that show at least a 2-fold  $EC_{50}$  shift with respect to the negative control.
- Apart from the follow-up mentioned above we recommend confirmation of sensitization in a multiple dose format (10-point with replicates). If available, testing related compounds for specificity is suggested.

## Loss-of-Function Screens Using **shRNA**

### General Considerations for shRNA-Lentivirus Infection

Many of the same consideration for siRNA screening can be applied to arrayed shRNA screening. However, optimization of shRNA-lentivirus infection for each cell line is a more involved process than siRNA. There are various parameters that should be considered when optimizing infection.

1. Determination of cell seeding density from performing a simple growth curve experiment
2. Determination of puromycin concentration by performing a 10-point dose response curve, ranging from 0.1 mg/ml to 10 mg/ml (a typical concentration ranges between 2-5 mg/ml)
3. Time course for puromycin treatment

4. Effect of protamine sulfate to cells
5. The amount of virus to be used for maximal infection. A detailed protocol on viral infection can be found at [http://www.broad.mit.edu/genome\\_bio/trc/publicProtocols.html](http://www.broad.mit.edu/genome_bio/trc/publicProtocols.html). Furthermore, infectability can be measured for each cell line using a cell count assay:

$$\text{Infectibility} = \left[ \frac{(\# \text{ of infected cells with puromycin}) - (\# \text{ of non-infected cells with puromycin}^*)}{(\text{Total } \# \text{ of cells without puromycin})} \right] \times 100$$

\*Refers to background (killing) i.e. just cells with puromycin added

## shRNA-Lentivirus Infection Protocol

Viral infection in 96-well microplate format. This step is similar for determination of viral titer.

1. Seed cells of interest overnight in a total volume of 50  $\mu\text{l}$  of growth media
2. Add 40  $\mu\text{l}$  of growth media with 2X of protamine sulfate (16 mg/ml) to cells. This volume is dependent of the viral supernatant added in below in Step 3.
3. Add 2-10  $\mu\text{l}$  of viral supernatant to mix above. This volume is dependent on the viral titer. The final volume of steps 2 and 3 is 50  $\mu\text{l}$ . Incubate at 37°C overnight.
4. Add 2X puromycin (4 mg/ml) in 100  $\mu\text{l}$  of growth media and incubate for 37°C overnight.
5. Wash off puromycin and replace with normal growth media.
6. Incubate for 2-4 days depending on the assays.

## Pooled shRNA Screening

Pooled shRNAs enable large-scale screens without the need for HTS infrastructure. Pooled screens are conducted by transducing cells with a soup of shRNA-containing lentiviral particles, which can comprise 1000s of unique shRNAs. Pooled screens are performed under positive or negative selection. In positive selection, a selective pressure is applied, and the identity of shRNAs in selected cells is identified. In negative selection screens, a control population of transduced cells is compared to a treated population, and shRNAs that are lost or enriched in the treated arm are identified. Pooled shRNA libraries are commercially available and corresponding protocols are provided in detail. Some general considerations include infecting cells at a low MOI (0.1 – 0.3) to ensure no more than one integrant per cell, transducing at a reasonable fold representation (e.g., 100 – 1000 fold representation for each shRNA in the pool), and maintaining adequate representation throughout all steps of the screening process. For example, harvesting genomic DNA from a number of cells that at least corresponds to the intended number of viral integrants. This will ensure that all shRNAs in the experiment population are represented.

## Appendix

### shRNA-lentivirus system

shRNA can be delivered into cells either by transfection of plasmids expressing shRNA of the gene of interest or by infection of viral-packaged shRNA of the gene of interest in the form of lentiviral vectors. The following optimization of delivery of shRNA into cells is focused on the lentiviral shRNA vectors. The lentiviral library used here is created from a pLKO1 vector that carries a puromycin resistance gene and shRNA expression is driven from a human U6 promoter (5). The puromycin resistance gene has been used as a selection marker for infected cells harboring the shRNA vectors.

Cell based phenotypic RNAi assays using shRNA lentiviral vectors involves (1) viral production where shRNA vectors are packaged into lentivirus and (2) viral infection where the lentivirus harboring the shRNA vectors are transduced into the cells of interest.

### Optimization of shRNA-lentivirus production

The production of shRNA-lentivirus involves the packaging of the shRNA vector into lentivirus and requires transfection of two plasmids which forms the packaging system, pCMVD8.9 (28, 29) and pHCMV-G (30). In the transfection process, the key factors to be optimized are the seeding density, transfection reagents used, concentration of plasmids and the ratio of transfection reagent to plasmids. For concentration of plasmids, the usual practice includes concentration ranging from 100 ng to 200 ng. The plasmid concentration to transfection reagent ratio to be tested usual includes 2:1, 3:1 and 3:2. Viral production can be performed using the protocol published by the Broad institute at [http://www.broad.mit.edu/genome\\_bio/trc/publicProtocols.html](http://www.broad.mit.edu/genome_bio/trc/publicProtocols.html).

GFP control vector is used for optimization purpose and can be viewed briefly under the microscope to assess fluorescence. The number of infectious units in the viral supernatant calculated as IU/ml is assessed by infecting cells with generally 2 ml of virus and counting survival of cells after puromycin treatment. The viral titer determination is important to assess the amount of virus to be used in infection for cell based assay. An acceptable range for viral titer is  $2 \times 10^6$  to  $2 \times 10^7$ . A variety of commercial kits (p24 ELISA) are now available to determine titer.

### shRNA-lentivirus production protocol (96-well microplate format)

1. Dilute D8.9 to 9 ng/ml, vsv-g to 1 ng/ml and shRNA to 25 ng/ml.
2. Add 6  $\mu$ l per well (150 ng) of shRNA and 5  $\mu$ l each of D8.9 (45 ng) and vsv-g (5 ng) to the shRNA.
3. Dilute transfection reagent (e.g. Fugene 6 from Roche) in Opti-Mem to a volume of 14  $\mu$ l per well, that is, 0.6  $\mu$ l of reagent to 13.4  $\mu$ l of Opti-Mem. The final ratio of transfection reagent:vDNA should be 3 ml:1mg.

4. Add diluted transfection reagent (e.g. Fugene 6 from Roche) to the plasmid mix to a final volume of 30 ml per well and incubate for 30-45 minutes at room temperature.
5. Transfer Fugene/DNA complex to HEK293T cells grown overnight seeded at 25000 cells per well in low antibiotic growth media. Incubate for 18 hours at 37°C.
6. Replace media with 170 ml of high serum growth media and incubate for further 24 hours at 37°C.
7. Harvest 150 ml of viral supernatant and add 170 ml of high serum growth media and incubate for another 24 hours at 37°C.
8. Harvest another 150 ml of viral supernatant and discard cells.
9. Pool viral supernatant and use for infection.

Examples of plate layout for control plates to quality control RNAi synthetic lethality screens.

## Acknowledgements

The authors would like to acknowledge collaborations with Translational Genomics Research Institute (Phoenix, AZ) and Genome Institute of Singapore (Singapore) that have led to joint learnings in adopting best practices for executing RNAi screens. We would like to acknowledge Seppo Karrila (Lilly Singapore Center for Drug Discovery) for introducing the potentiation score method. We also thank Pat Solenberg and Wayne Blosser (Eli Lilly and Company) for critical review and recommendations of content.

## Abbreviations

- RNAi - RNA Interference
- siRNA - Small Interfering RNA
- shRNA - Short Hairpin RNA
- miRNA - Micro-RNA
- dsRNA - Double-Stranded RNA
- KD - Knock-Down
- HTS - High Throughput Screen/Screening
- LOF - Loss-Of-Function
- QC - Quality Control
- NS - Non-Silencing
- NT - Non-Transfected
- NTC - Non-Targeting Control
- MT - Mock-Transfected
- NC - Negative Control
- PC - Positive Control
- CV - Coefficient of Variation
- SW - Signal Window
- Lin's CCC - Lin's Concordance Correlation Coefficient
- DDTR - Drug Dose Time Response



- UT/T - (Drug) Untreated/Treated

## References

### Publications:

1. Kettling RF. The many faces of RNAi. *Developmental Cell*. 2011;20(2):148–161. PubMed PMID: 21316584.
2. Mohr SE, Perrimon N. RNAi screening: new approaches, understandings, and organisms. *WIREs RNA*. 2012;3:145–158. PubMed PMID: 21953743.
3. Panda D, Cherry S. Cell-based genomic screening: elucidating virus-host interactions. *Current Opinion in Virology*. 2012;2:784–792. PubMed PMID: 23122855.
4. Chatterjee-Kishore M. From genome to phenome--RNAi library screening and hit characterization using signaling pathway analysis. *Current Opinion in Drug Discovery & Development*. 2006;9(2):231–239. PubMed PMID: 16566293.
5. Echeverri CJ, Beachy PA, Baum B, Boutros M, Buchholz F, Chanda SK, Downward J, Ellenberg J, Fraser AG, Hacohen N, Hahn WC, Jackson AL, Kiger A, Linsley PS, Lum L, Ma Y, Mathey-Prevot B, Root DE, Sabatini DM, Taipale J, Perrimon N, Bernards R. Minimizing the risk of reporting false positives in large-scale RNAi screens. *Nature Methods*. 2006;3(10):777–779. PubMed PMID: 16990807.
6. Echeverri CJ, Perrimon N. High-throughput RNAi screening in cultured cells: a user's guide. *Nature Review Genetics*. 2006;7(5):373–384. PubMed PMID: 16607398.
7. Fuchs F, Boutros M. Cellular phenotyping by RNAi. *Briefings in Functional Genomics and Proteomics*. 2006;5(1):52–56. PubMed PMID: 16769679.
8. Moffat J, Sabatini DM. Building mammalian signaling pathways with RNAi screens. *Nature Reviews Molecular Cell Biology*. 2006;7(3):177–187. PubMed PMID: 16496020.
9. Root DE, Hacohen N, Hahn WC, Lander ES, Sabatini DM. Genome-scale loss-of-function screening with a lentiviral RNAi library. *Nature Methods*. 2006;3(9):715–719. PubMed PMID: 16929317.
10. Sachse C, Krausz E, Kronke A, Hannus M, Walsh A, Grabner A, Ovcharenko D, Dorris D, Trudel C, Sonnichsen B, Echeverri CJ. High-throughput RNA interference strategies for target discovery and validation by using synthetic short interfering RNAs: functional genomics investigations of biological pathways. *Methods in Enzymology*. 2005;392:242–277. PubMed PMID: 15644186.
11. Willingham AT, Deveraux QL, Hampton GM, Aza-Blanc P. RNAi and HTS: exploring cancer by systematic loss-of-function. *Oncogene*. 2004;23(51):8392–8400. PubMed PMID: 15517021.
12. Birmingham A, Anderson EM, Reynolds A, Ilsley-Tyree D, Leake D, et al. 3'UTR seed matches, but not overall identity, are associated with RNAi off-targets. *Nature Methods*. 2006;3:199–204. PubMed PMID: 16489337.
13. Jackson AL, Burchard J, Leake D, Reynolds A, Schelter J, et al. Position-specific chemical modification of siRNAs reduces “off-target” transcript silencing. *RNA*. 2006;12:1197–11205. PubMed PMID: 16682562.

14. Jackson AL, Bartz SR, Schelter J, Kobayashi SV, Burchard J, et al. (2003). Expression profiling reveals off-target gene regulation by RNAi. *Nature Biotechnology* 21:635–3.7
15. Semizarov D, Frost L, Sarthy A, Kroeger P, Halbert DN, Fesik SW. Specificity of short interfering RNA determined through gene expression signatures. *PNAS*. 2003;100:6347–52. PubMed PMID: 12746500.
16. Lin X, Ruan X, Anderson MG, McDowell JA, Kroeger PE, et al. siRNA-mediated off-target gene silencing triggered by a 7 nt complementation. *Nucleic Acids Research*. 2005;33:4527–4535. PubMed PMID: 16091630.
17. Schultz N, Marenstein DR, DeAngelis DS, Wang WQ, Nelander S, Jacobsen A, Marks DS, Massague J, and Sander C. (2011). Off-target effects dominate a large-scale RNAi screen for modulators of the TGF- $\beta$  pathway and reveal microRNA regulation of TGFBR2. *Silence* 2: 1758-907X-2-3.
18. Sigoillot FD, King RW. Vigilance and validation: Keys to success in RNAi screening. *ACS Chemical Biology*. 2011;6:47–60. PubMed PMID: 21142076.
19. Busman FD, Malani N, Fernandes J, D’Orso I, Cagney G, Diamond TL, et al. Host cell factors in HIV replication: Meta-Analysis of genome-wide studies. *PLoS Pathogens*. 2009;5:e1000437. PubMed PMID: 19478882.
20. Marine S, Bahl A, Ferrer M, Buehler E. Common seed analysis to identify off-target effects in siRNA screens. *Journal of Biomolecular Screening*. 2012;17:370–378. PubMed PMID: 22086724.
21. Konig R, Chiang C, Tu BP, Yan SF, DeJesus PD, Romero A, Berguer T, et al. A probability-based approach for the analysis of large-scale RNAi screens. *Nature Methods*. 2007;4:847–849. PubMed PMID: 17828270.
22. Lin LI. A concordance correlation coefficient to evaluate reproducibility. *Biometrics*. 1989;45:255–268. PubMed PMID: 2720055.
23. Lin LI. A note on the concordance correlation coefficient. *Biometrics*. 2000;56:324–325.
24. Bland JM, Altman DG. Statistical methods for assessing agreement between two methods of clinical measurement. *Lancet*. 1986;I:307–310. PubMed PMID: 2868172.
25. Buehler E, Khan AA, Marine S, Rajaram M, Bahl A, Burchard J, Ferrer M. siRNA off-target effects in genome-wide screens identify signaling pathway members. *Scientific Reports*. 2012;2:428. article. PubMed PMID: 22645644.
26. Sigoillot FD, Lyman S, Huckins JF, Adamson B, Chung E, Quattrochi B, King RW. A bioinformatics method identifies prominent off-targeted transcripts in RNAi screens. *Nature Methods*. 2012;19:363–366. PubMed PMID: 22343343.
27. Buehler E, Chen YC, Martin SE. C911: A bench-level control for sequence specific siRNA off-target effects. *PLoS One*. 2012;7:e51942. PubMed PMID: 23251657.
28. Naldini L, Blömer U, Gage FH, Trono D, Verma IM. Efficient transfer, integration, and sustained long-term expression of the transgene in adult rat brains injected with a lentiviral vector. *PNAS*. 1996;93:11382–11388. PubMed PMID: 8876144.
29. Zufferey R, Nagy D, Mandel RJ, Naldini L, Trono D. Multiply attenuated lentiviral vector achieves efficient gene delivery in vivo. *Nature Biotechnology*. 1997;15:871–875. PubMed PMID: 9306402.

30. Yee J, Miyanohara A, LaPorte P, Bouic K, Burns JC, Friedmann T. A General Method for the Generation of High-Titer, Pantropic Retroviral Vectors: Highly Efficient Infection of Primary Hepatocytes. *PNAS*. 1994;91:9564–9568. PubMed PMID: 7937806.

### Additional References:

- Berns K, Horlings HM, Hennessy BT, Madiredjo M, Hijmans EM, Beelen K, Linn SC, Gonzalez-Angulo AM, Stemke-Hale K, Hauptmann M, Beijersbergen RL, Mills GB, van de Vijver MJ, Bernards R. A functional genetic approach identifies the PI3K pathway as a major determinant of trastuzumab resistance in breast cancer. *Cancer Cell*. 2007 Oct; 12(4):395–402. PubMed PMID: 17936563.
- Brideau C., Gunter B., Pikounis B., Liaw A. Improved statistical methods for hit selection in high-throughput screening. *Journal of Biomolecular Screening*. 2003;8:634–647. PubMed PMID: 14711389.
- Brummelkamp TR, Fabius AW, Mullenders J, Madiredjo M, Velds A, Kerkhoven RM, Bernards R, Beijersbergen RL. An shRNA barcode screen provides insight into cancer cell vulnerability to MDM2 inhibitors. *Nat Chem Biol*. 2006 Apr;2(4):202–6. Epub 2006 Feb 13. PubMed PMID: 16474381.
- Eggert US, Kiger AA, Richter C, Perlman ZE, Perrimon N, Mitchison TJ, Field CM. Parallel chemical genetic and genome-wide RNAi screens identify cytokinesis inhibitors and targets. *PLoS Biol*. 2004 Dec;2(12):e379. Epub 2004 Oct 5. PubMed PMID: 15547975.
- Epping MT, Wang L, Plumb JA, Lieb M, Gronemeyer H, Brown R, Bernards R. A functional genetic screen identifies retinoic acid signaling as a target of histone deacetylase inhibitors. *Proc Natl Acad Sci U S A*. 2007 Nov 6;104(45):17777–82. Epub 2007 Oct 29. PubMed PMID: 17968018.
- Gunter B., Brideau C., Pikounis B., Liaw A. Statistical and graphical methods for quality control determination of high-throughput screening data. *Journal of Biomolecular Screening*. 2003;8:624–633. PubMed PMID: 14711388.
- Iversen PW., Eastwood BJ., Sittampalam S., Cox KL. A comparison of assay performance measures in screening assays: signal window, Z' factor and assay variability ratio. *Journal of Biomolecular Screening*. 2006;11:1–6. PubMed PMID: 16490779.
- Malo N., Hanley JA., Cerquozzi S., Pelletier J., Naddon R. Statistical practice in high-throughput screening data analysis. *Nature Biotechnology*. 2006;24:167–175. PubMed PMID: 16465162.
- Root DE, Hacohen N, Hahn WC, Lander ES, Sabatini DM. Genome-scale loss-of-function screening with a lentiviral RNAi library. *Nature Methods*. 2006;3(9):715–719. PubMed PMID: 16929317.
- Sachse C, Krausz E, Kronke A, Hannus M, Walsh A, Grabner A, Ovcharenko D, Dorris D, Trudel C, Sonnichsen B, Echeverri CJ. High-throughput RNA interference strategies for target discovery and validation by using synthetic short interfering RNAs: functional

genomics investigations of biological pathways. *Methods in Enzymology*. 2005;392:242–277. PubMed PMID: 15644186.

Whitehurst AW, Bodemann BO, Cardenas J, Ferguson D, Girard L, Peyton M, Minna JD, Michnoff C, Hao W, Roth MG, Xie XJ, White MA. Synthetic lethal screen identification of chemosensitizer loci in cancer cells. *Nature*. 2007 Apr 12;446(7137):815–9. PubMed PMID: 17429401.

Willingham AT, Deveraux QL, Hampton GM, Aza-Blanc P. RNAi and HTS: exploring cancer by systematic loss-of-function. *Oncogene*. 2004;23(51):8392–8400. PubMed PMID: 15517021.

### Web sites:

1. Minimum Information About an RNAi Experiment (MIARE) - <http://miare.sourceforge.net/HomePage>
2. GraphPad Prism Manual - [http://www.broad.mit.edu/genome\\_bio/trc/publicProtocols.html](http://www.broad.mit.edu/genome_bio/trc/publicProtocols.html)

# FLIPR™ Assays for GPCR and Ion Channel Targets

Michelle R. Arkin,<sup>1</sup> Patrick R. Connor,<sup>2</sup> Renee Emkey,<sup>2</sup> Kim E. Garbison,<sup>2</sup> Beverly A. Heinz,<sup>2</sup> Todd R. Wiernicki,<sup>2</sup> Paul A. Johnston,<sup>3</sup> Ramani A. Kandasamy, Nancy B. Rankl, and Sitta Sittampalam<sup>4</sup>

Created: May 1, 2012; Updated: October 1, 2012.

## Abstract

Calcium ions (Ca<sup>2+</sup>) play a key role in cellular homeostasis involving calcium channel and GPCR function, which plays a critical role in many disease pathologies. Fluorescent Imaging Plate Reader (FLIPR™) technology to measure Ca<sup>2+</sup> flux in cells was an important development in the early 1990's and has played a significant role in HTS and lead optimization applications. In this chapter, the basic concepts in using the FLIPR instrument and assay development and optimization to measure Ca<sup>2+</sup> flux in cells are described. Although this chapter is devoted to Ca<sup>2+</sup> channel based assay development, the FLIPR™ is also useful for measuring potassium and other ion flux in cells with appropriate fluorescent dyes.

## Overview: FLIPR™ Assay Development

### **Reagents Needed:**

Cell line(s) expressing GPCRs, ion Channels, and coupling proteins.

Control cell line without target.

Suitable fluorescent dye (e.g. Fluo-3/AM, Calcein 4, etc).

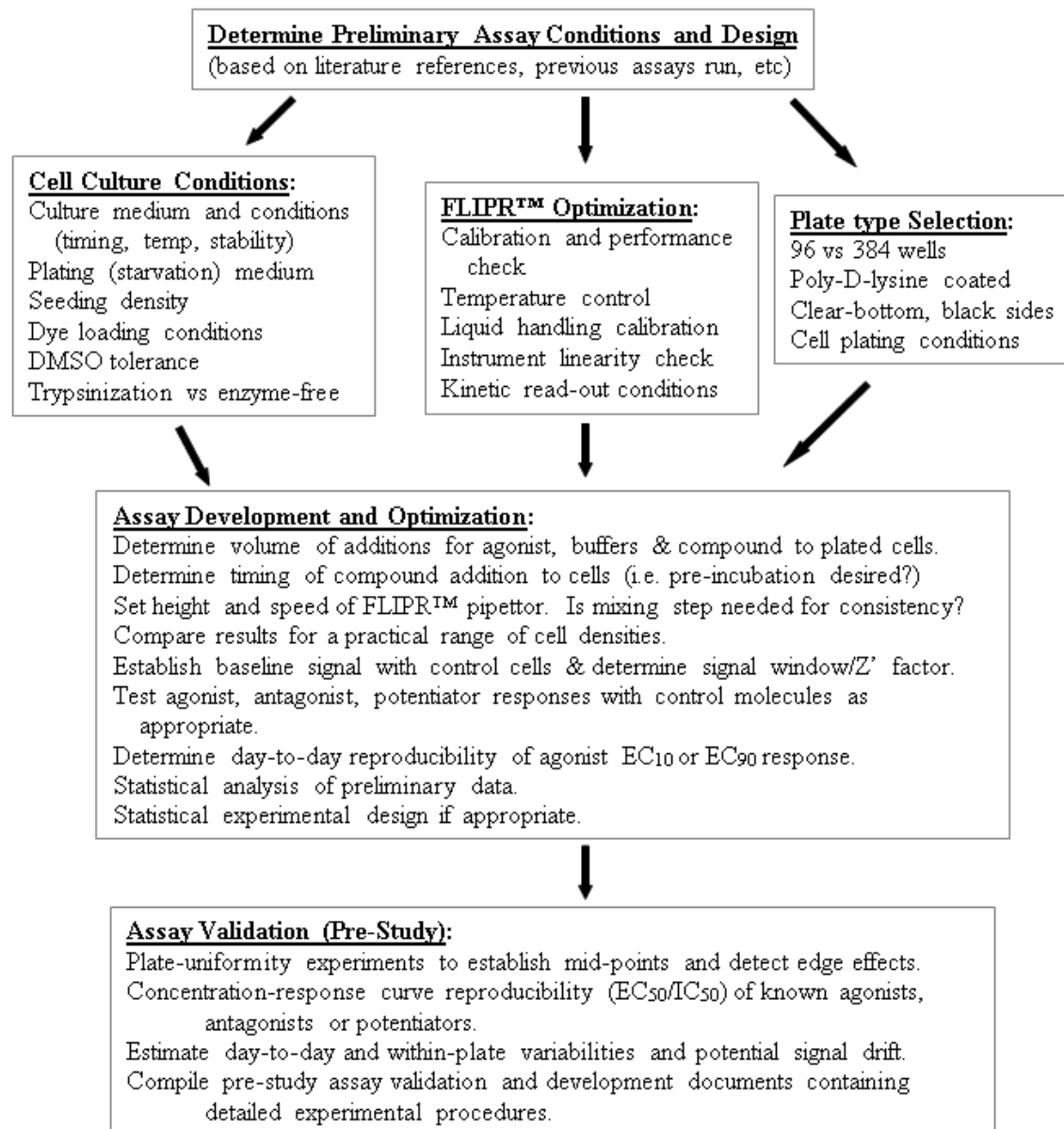
Suitable agonist or ion channel modulators.

Standard antagonists, potentiators, and control compounds.

Appropriate buffer solutions, additives, etc.

---

<sup>1</sup> University of California San Francisco, CA. <sup>2</sup> Eli Lilly & Company, IN. <sup>3</sup> University of Pittsburgh, PA. <sup>4</sup> National Center for Advancing Translational Sciences (NIH), MD.



## Introduction

The introduction of FLIPR™ (Fluorescence Imaging Plate Reader) in the 1990's provided biologists with a fast and easy method of detecting G-protein coupled receptor (GPCR) activation through changes in intracellular calcium (Ca<sup>2+</sup>) concentration. By coupling receptors to G<sub>q</sub> proteins which stimulate intracellular calcium flux upon binding, a functional response can be measured using calcium-sensitive dyes and a fluorescence plate reader. The FLIPR™ instrument has a cooled CCD camera imaging system which collects the signal from each well of a microplate simultaneously. The FLIPR™ can read at sub-second intervals, which enables the kinetics of the response to be captured, and has

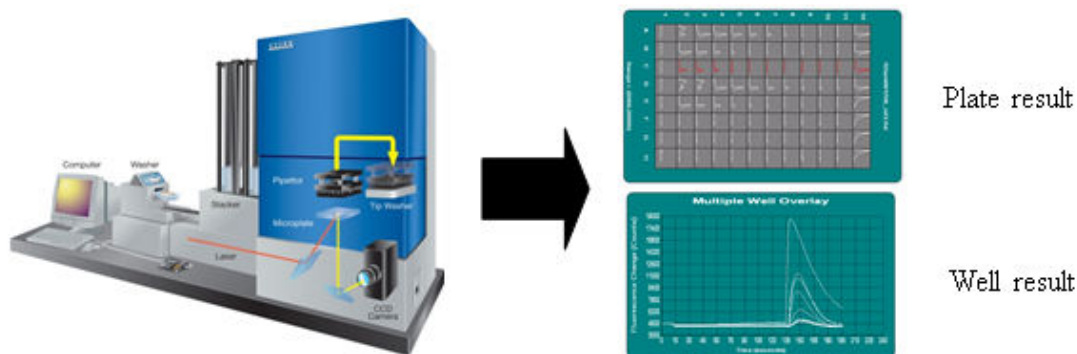


**Figure 1.** Diagram of a FLIPR™ instrument and typical kinetic tracings. The FLIPR™ collects a signal from each well of a multi-well plate at sub-second intervals, which captures and records a kinetic tracing of the calcium flux response. By successive additions to the same well, the FLIPR™ instrument allows one to distinguish between agonist, antagonist and allosteric modulators.

an integrated pipettor that may be programmed for successive liquid additions. Figure 1 provides a diagram of a FLIPR™ instrument and typical kinetic tracings.

The integrated pipettor capabilities of the FLIPR™ provide an opportunity to detect agonists, antagonists, and allosteric modulators of GPCRs all in one assay. In the first addition, compounds of screening interest are added. The timing can be adjusted to allow for a pre-incubation period with the compounds, and agonist activity is detected by monitoring the calcium flux response in this step. In the second addition, a small amount of a known agonist that results in ~10% of maximal response is added to detect potentiator activity. The third addition consists of a maximal concentration of known agonist (~90% of the maximal response) to test for antagonism. This experimental design can encompass either two or three additions depending on the specific responses to be detected.

The FLIPR™ has also been utilized to screen ion channel targets using membrane permeable fluorescent dyes, such as the bis-oxanol dye DiBAC4 (3), to measure changes in membrane potential (Table 1). Compared to the rapid sub-second kinetics of channel opening observed by electrophysiology approaches, redistribution of the dye often takes minutes to produce a measurable response, and has prompted the development of more rapid dyes compatible with the FLIPR™.

**Table 1: Comparison of the Ca<sup>2+</sup> Sensitive Dyes Fluo-3 and Fluo-4 used with the FLIPR® Fluorometric Imaging Plate Reader System.**

| Fluorescent Dye | Concentration | Loading time |
|-----------------|---------------|--------------|
| Fluo-3          | 2 μM*         | 30- 60* mins |

Suggested loading conditions (\*=Standard condition). Adapted from Molecular Devices Applications.

*Table 1 continues on next page...*

Table 1 continued from previous page.

| Fluorescent Dye | Concentration | Loading time |
|-----------------|---------------|--------------|
| Fluo-4          | 1 $\mu$ M     | 30-60 mins   |
| Fluo-4          | 2 $\mu$ M     | 30-60 mins   |

Suggested loading conditions (\*=Standard condition). Adapted from Molecular Devices Applications.

## Types of FLIPR™ Formats

### GPCR Targets Coupled to Ca<sup>2+</sup> Mobilization

GPCR targets that naturally couple via Gq produce a ligand-dependent increase in intracellular Ca<sup>2+</sup> that can be measured using a calcium-sensitive dye. GI/o-coupled receptor activation can be “switched” to induce an increase in intracellular calcium in two ways: 1) by the use of chimeric G-proteins (G $\alpha$ qi5 or G $\alpha$ qo5), or 2) by engineering the cells to over-express a promiscuous G-protein (G  $\alpha$ 16 or G $\alpha$ 15) (Figure 2).

The integrated pipettor capabilities of the FLIPR™, as well as internal software modifications, provide an opportunity to detect agonists, antagonists, and allosteric modulators all in one assay. One-, two-, or three-addition assays may be performed depending on the desired assay format. A one-addition assay can be performed to detect agonists, where the compound of interest is added to look for a response. This mode could also be used to look for allosteric modulators or antagonists if the test compounds are added “off-line”, although this is not the preferred method of operation. Until 2006, the two-addition assay was the standard assay format. In this method, the test compounds are added in the presence of an EC<sub>10</sub> dose of the agonist in the first addition to detect agonists or allosteric modulators. The second addition is an EC<sub>90</sub> dose of the max control to identify antagonists. While this scheme works, it requires a secondary assay to distinguish the agonists from the allosteric modulators; this need was abolished by the advent of a three-addition assay. In the three-addition mode, you can detect all three modes of activity in a single assay, saving considerable time and reagents. Another advantage found during testing of the three-addition assay was better mixing and a pre-incubation of the cells with compound resulting in better identification of potentiators.

Typical assay formats and the resulting curves are summarized below (Table 2).

### Ion Channels with Significant Ca<sup>2+</sup> Permeability

Ion channel targets with significant Ca<sup>2+</sup> permeability, such as the ionotropic glutamate receptor (iGluRs), produce an increase in intracellular calcium that can be measured using calcium-sensitive dyes and the FLIPR™ instrument. The methodology used is analogous to that for the GPCRs (Figure 3).



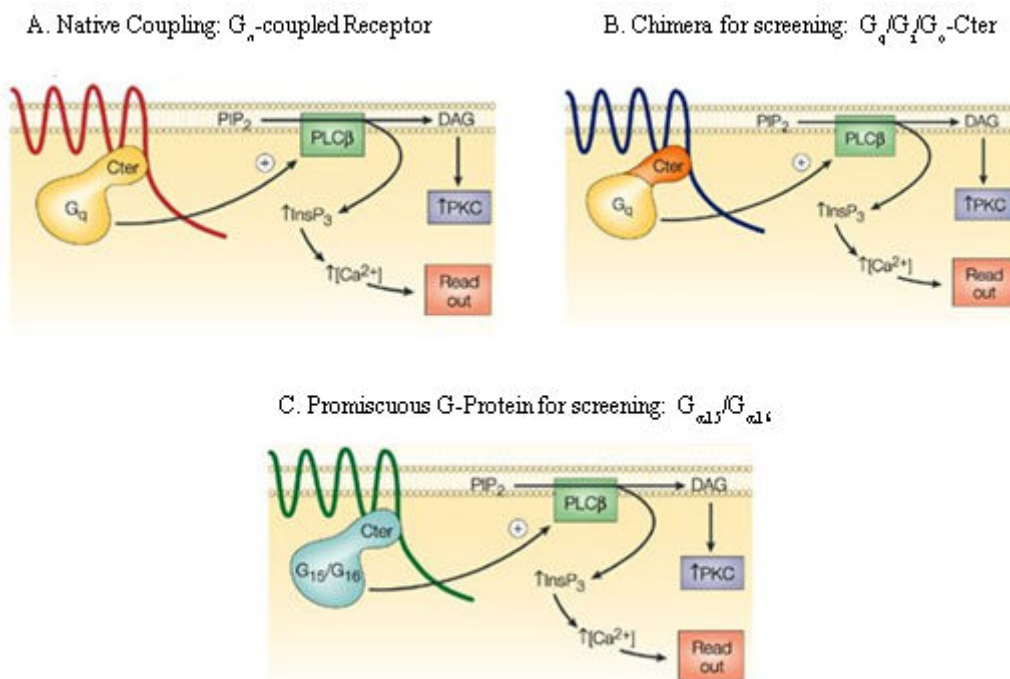


**Figure 2.** GPCR targets that couple via  $G_q$  naturally produce an increase in intracellular  $Ca^{2+}$  that can be measured using calcium-sensitive dyes and a FLIPR™ instrument. GPCR targets that naturally couple via  $G_i/o$  can be adapted to respond to agonist with a ligand-dependent increase in intracellular calcium by the use of chimeric G-protein or by the introduction of an over-expressing promiscuous G-protein ( $G_{\alpha 15}$  or  $G_{\alpha 16}$ ). (Adapted from Nature Reviews Drug Discovery)

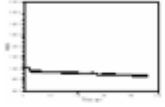
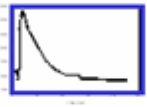
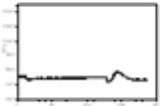
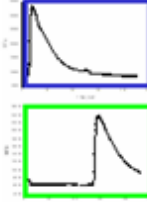
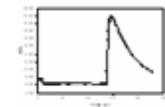
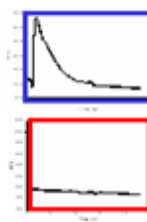
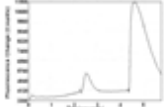
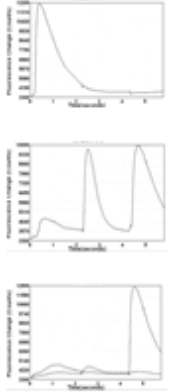
## Ion Channels which Produce Significant Changes in Membrane Potential

Ion channel targets such as the iGluRs with ion permeability that significantly affects the membrane potential can be measured using a membrane potential dye and the FLIPR™ (Figure 4) (1).

## Reagents and Buffers for Method Development

It is critical to ensure the appropriate cell lines expressing the target, control agonist and antagonist standards are available before beginning method development and validation. The minimal requirements are:

1. Transfected cell line with the  $G_q$ -coupled hGPCR target. (e.g. HEK293, CHO, THP-1 etc.). Receptors coupling through  $G_i$ ,  $G_o$ ,  $G_s$  or  $G_z$  can be coupled to  $G_q$  via promiscuous G-proteins as previously described.
2. Parental cell line control without the target and grown under identical conditions.
3. Agonist, antagonist, and allosteric modulator reference standards (with a wide range of potencies, if available).
4. Poly-D-lysine coated 96- or 384-well plates.

| Agonist | Potentiator | Antagonist | First Addition | Second Addition | Third Addition | Inactive Cmpd Profile  | "Hit" Profile  |
|---------|-------------|------------|----------------|-----------------|----------------|--|--|
| X       |             |            | Compound       | None            | None           |   |   |
| X       | X           |            | Compound       | 10% Agonist     | None           |   |   |
| X       |             | X          | Compound       | 90% Agonist     | None           |   |   |
| X       | X           | X          | Compound       | 10% Agonist     | 90% Agonist    |  |  |

**Table 2. Typical FLIPR™ Assay Formats**

- Appropriate cell growth media, buffer solutions, trypsinizing reagents.
- The reagents for ion channels are the same as for GPCRs, with the exception of the FLIPR™ buffer. It is recommended that 5mM calcium be used in the buffer for ion channel experiments. Since HBSS contains 1.3 mM calcium, 3.7 mM calcium chloride (Sigma) must be added prior to use.
- Additional reagents needed for a FLIPR assay are listed in Table 3.

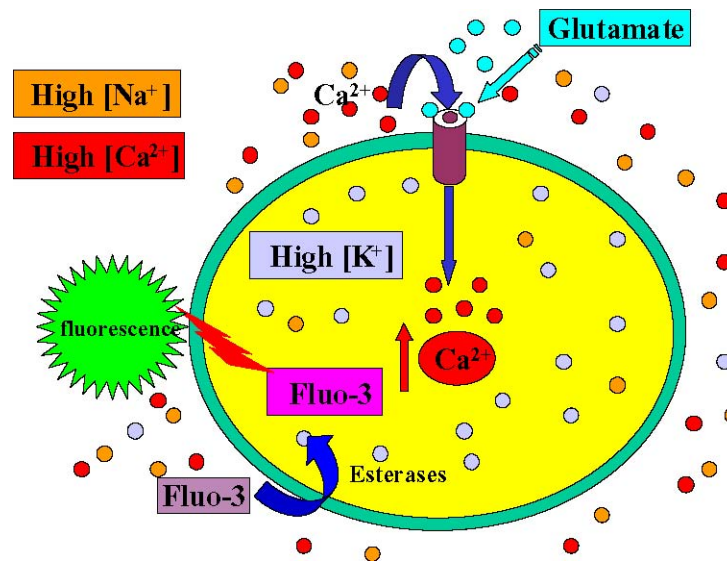


**Figure 3.** Schematic of the calcium flux response in ion channel targets. Fluo-3 dye ester is loaded into the cell and is cleaved by cell esterases to active dye.  $\text{Ca}^{2+}$  entering the cells bind to intra-cellular Fluo-3 and results in increased fluorescent emission at 520 nm.

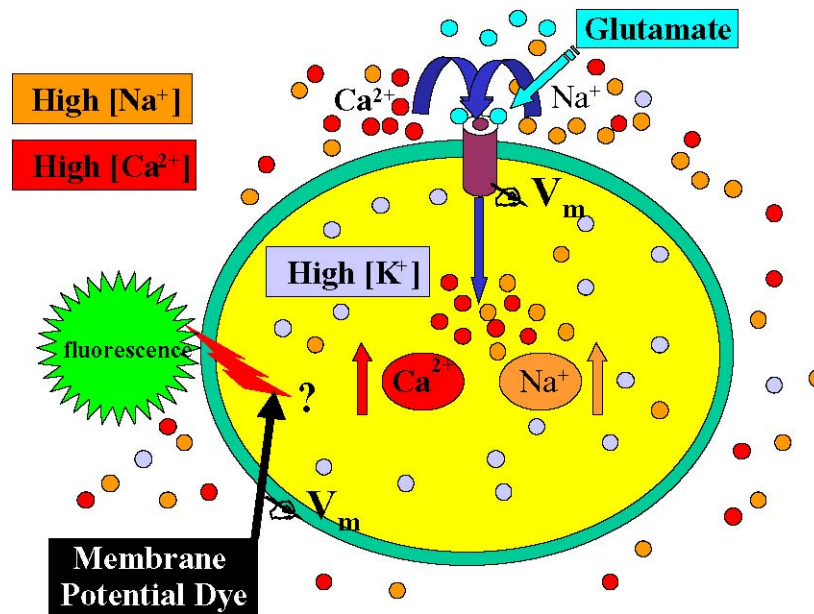


**Figure 4.** Measuring changes in membrane potential of ion channel targets.

**Table 3: Additional reagents needed for FLIPR assay**

| Reagent  | Manufacturer                        |
|--|-------------------------------------|
| Calcium dyes (Fluo-3, Fluo-4, Calcium 3, Calcium 4, etc) | Molecular Probes, Molecular Devices |

Table 3 continues on next page...

Table 3 continued from previous page.

| Reagent                | Manufacturer             |
|------------------------|--------------------------|
| HBSS                   | BioWhittaker, Invitrogen |
| HEPES                  | BioWhittaker, Invitrogen |
| Probenecid (if needed) | Sigma                    |
| Pluronic Acid          | Sigma, Molecular Devices |

## Method Development and Optimization

### Optimization Experiments for GPCR Targets Coupled to Ca<sup>2+</sup> Mobilization

Early method development should include the following experiments to demonstrate the validity of the assay concept:

1. G<sub>q</sub> coupling (or promiscuous G-protein coupling) of the cells expressing the GPCR should be demonstrated. Load selected cell clones with Fluo-3AM or other suitable dye, trigger Ca<sup>2+</sup> flux with a known agonist, and measure fluorescence signal. Select the clones with the most robust response.
2. Determine whether cells need to be constantly maintained in culture or whether they can be prepared as frozen aliquots to be thawed and plated the day prior to the assay. The use of frozen cell stocks is a convenient and efficient alternative if it can be shown that the FLIPR™ signal is sufficiently robust and stable.
3. Conduct dye-loading experiments. Select the combination of cell line, agonist and dye concentrations that produces the most significant signal window. Use a control cell line without receptor expression to establish signal base line. Choose between use of cells in culture and frozen cell stocks.
4. Conduct preliminary experiments to establish a reasonable cell density that could be further optimized in subsequent experiments as described below.
5. Using a known antagonist or potentiator, demonstrate that the Ca<sup>2+</sup> mobilization induced by the agonist can be blocked or enhanced, respectively.
6. Test poly-D-lysine coated plates with selected cell lines and conditions demonstrated in preliminary experiments. Select the plate with a stable and acceptable signal window.
7. Establish preliminary growth conditions and DMSO tolerance for the selected cell line.

Statistical experimental design can be employed to optimize these conditions and the following factors should be included:

1. Cell clones
2. Cell seeding density/well
3. Type of dye (wash vs. no-wash)
4. Dye loading concentration

5. Dye loading temperature
6. Dye loading duration
7. Coated plate type
8. Buffer additives: eg: probenecid, concanavalin A, etc.
9. Height, speed and mixing of FLIPR pipettor
10. Volume of addition

### **Notes on optimization experiments for GPCR targets coupled to Ca<sup>2+</sup> mobilization**

Some general points regarding a FLIPR™ assay for GPCRs need to be noted:

- Some receptors contain trypsin-sensitive sites in their extracellular domain that results in a loss of response if the cells are harvested by trypsinization. In these instances, cells should be harvested by either scraping or using enzyme-free dissociation buffer.
- Care should be taken when removing media and dye from the cell plate. It is common for mechanical aspiration to disrupt the cell monolayer, resulting in a deterioration of the assay performance. It is recommended to manually invert the plate and shake or “flick” the liquid out of the plate and blot onto paper towels if you are using a dye that requires washing.

Several no-wash dyes are commercially available. Testing of multiple dyes is strongly recommended, as signals differ widely. Depending on the receptor studied, media may interfere with the no-wash dyes, so testing both with and without media may be required. An example of the difference between the signal obtained from the traditional Fluo-3 dye and the new Calcium 4 no-wash dye is shown in Figure 5.

- Probenecid should be included in the dye and the buffer following dye loading whenever using CHO cells (5 mM probenecid is sufficient). This prevents the release of dye from the cells back into the medium. AV12 and HEK293 cells do not require probenecid.
- CHO cells are dye-loaded at 37°C, whereas AV12 and HEK293 cells can be dye-loaded at 25°C.
- Poly-D lysine coated plates can improve results obtained from some cell lines due to improved adhesion.
- Variability in the signal obtained on the FLIPR™ can sometimes be improved by adjusting the tip height or dispense speed on the FLIPR™.
- The standard assay buffer used in FLIPR™ experiments is HBSS with 20 mM HEPES supplemented with 0.5 mM Ca<sup>2+</sup>.
- The most common fluid addition volumes for a FLIPR assay are listed in Table 4.

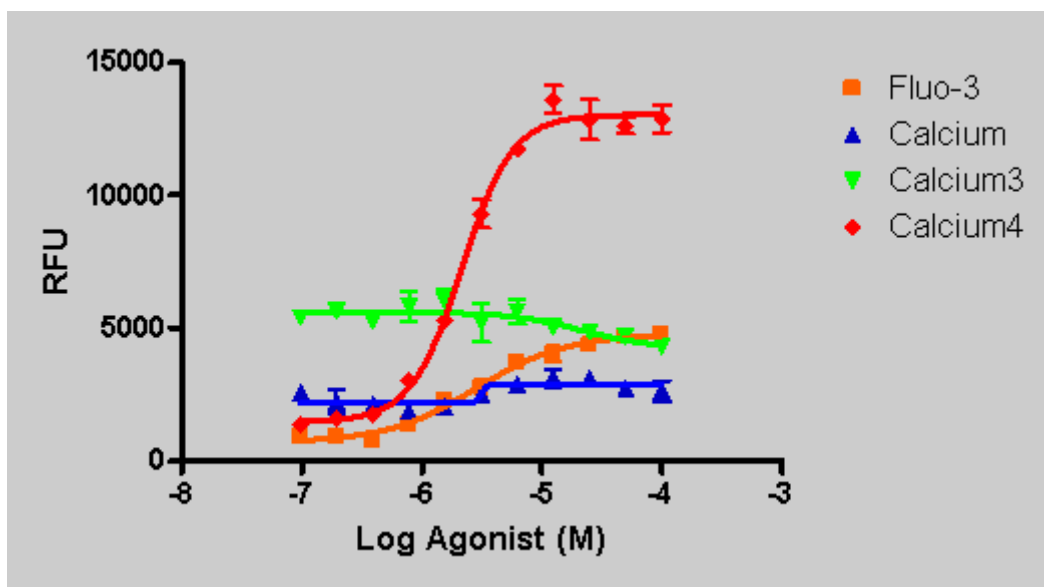


**Figure 5:** Comparison of different  $\text{Ca}^{2+}$  dyes on maximum response of a GPCR. In this example, a no-wash dye produced a significantly larger signal window than the traditional Fluo-3 dye. Signal windows are specific to receptors and cell lines, so it is recommended that testing be done during the initial optimization to ensure the appropriate choice of dye.

**Table 4:** Common fluid addition volumes for FLIPR assay

|                          | Volume per Well   |                  |
|--------------------------|-------------------|------------------|
|                          | 96 well Format    | 384 well Format  |
| Dye                      | 50 $\mu\text{l}$  | 20 $\mu\text{l}$ |
| Buffer                   | 50 $\mu\text{l}$  | 20 $\mu\text{l}$ |
| 1 <sup>st</sup> Addition | 50 $\mu\text{l}$  | 20 $\mu\text{l}$ |
| 2 <sup>nd</sup> Addition | 100 $\mu\text{l}$ | 20 $\mu\text{l}$ |

## Development of a FLIPR Assay

The development of a FLIPR assay generally requires the five experiments, described in the sections below.

### Experiment #1 - Cell density determination and incubation time

This is typically the first parameter that is examined. The best way to assess cell density requirements is to seed an entire assay plate at a single density; therefore, several plates are required to examine multiple cell seeding densities. The cells should be examined on the FLIPR™ using buffer in the first addition and a maximal concentration of agonist in the second addition. This will allow one to assess the extent of variability within the plate and detect any patterns in variability. The most common variability pattern we have observed is an edge effect which can usually be resolved by increasing the cell density or the

humidity during incubation. We recommend examining the following cell densities for the indicated cell types listed in Table 5. Some assays will perform best with a 24-hour incubation time prior to running the assay, while others may need a 48-hour pre-incubation.

**Table 5: Suggested densities for AV12, CHO, and HEK293 cell lines**

| Cell Line | Seeding Densities (cells/well) |                         |
|-----------|--------------------------------|-------------------------|
|           | 96-well Format                 | 384-well Format         |
| AV12      | 30K, 40K, 50K, 60K             | 20K, 30K, 40K, 50K, 60K |
| CHO       | 10K, 20K, 30K, 40K             | 5K, 10K, 15K, 20K, 30K  |
| HEK293    | 30K, 40K, 50K, 60K             | 20K, 30K, 40K, 50K, 60K |

## Experiment #2 - Dye loading time, dye concentration and temperature

The optimal dye loading can range from 30 minutes to 2 hours depending on the cell line and the dye used. The concentration of Fluo-3 used in the majority of FLIPR assays is 8  $\mu\text{M}$ . Lower concentrations can be examined in order to reduce the cost of the assay. The no-wash dyes have been shown to be effective at lower concentrations as well. CHO cells are dye loaded at 37°C, whereas AV12 and HEK293 cells can be dye loaded at 25°C.

## Experiment #3 - DMSO tolerance

DMSO can alter the response of the cells as well as shift the dose response curve for agonist. It is recommended to perform an agonist dose response curve in the presence of different concentrations of DMSO in order to assess the DMSO tolerance of the assay. Extreme care should be taken if a DMSO concentration >0.1% is required.

## Experiment #4 - Agonist/antagonist dose response curves

The reproducibility of the assay can be examined by performing two independent days of agonist/antagonist/or potentiator dose-response curves. The  $\text{EC}_{50}/\text{IC}_{50}$  values should remain relatively constant over the course of the two experiments.

## Experiment #5 - Full plate variability and Z' factor determination

The variability of the assay is determined by running triplicate max/mid/min plates on three days and then calculating the Z'factor (see HTS Assay Validation).

## Considerations when performing 384-well FLIPR™ assays

384-well FLIPR™ assays have a number of challenges that are not apparent in the 96-well format. The first is mixing in the well. Most 96-well experiments are designed to allow a larger volume to be added to a larger space where mixing is not a concern. In a typical 96-well assay, 50  $\mu\text{l}$  of test compound are added to 50  $\mu\text{l}$  of buffer in the cell plate at a height of approximately 80 to 95  $\mu\text{l}$ . The height is the liquid height in the well at which the tips dispense. The 384-well plate is limited to a maximum volume of a 30  $\mu\text{l}$  addition

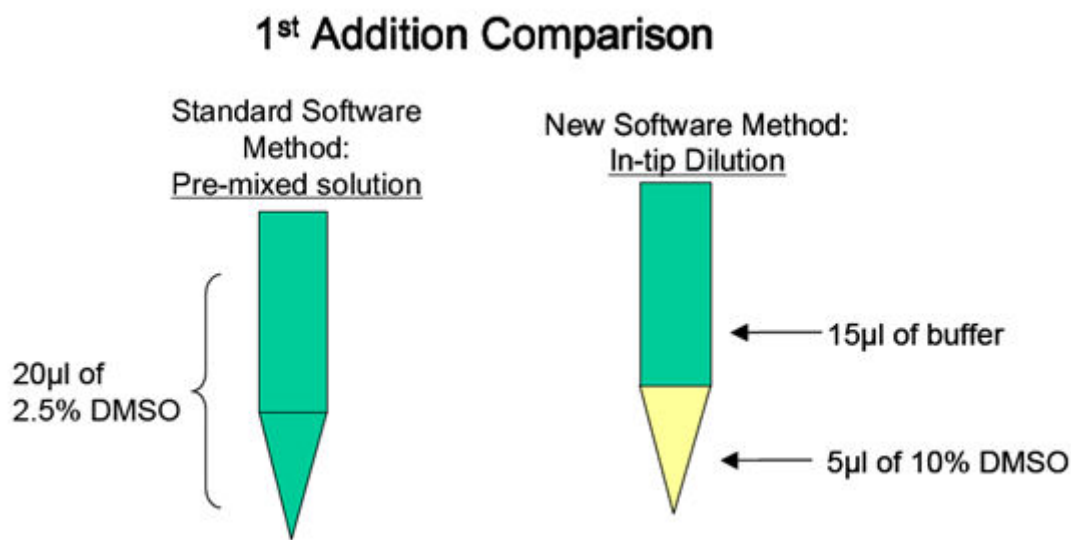


Figure 6. Schematic of in-tip dilution method.

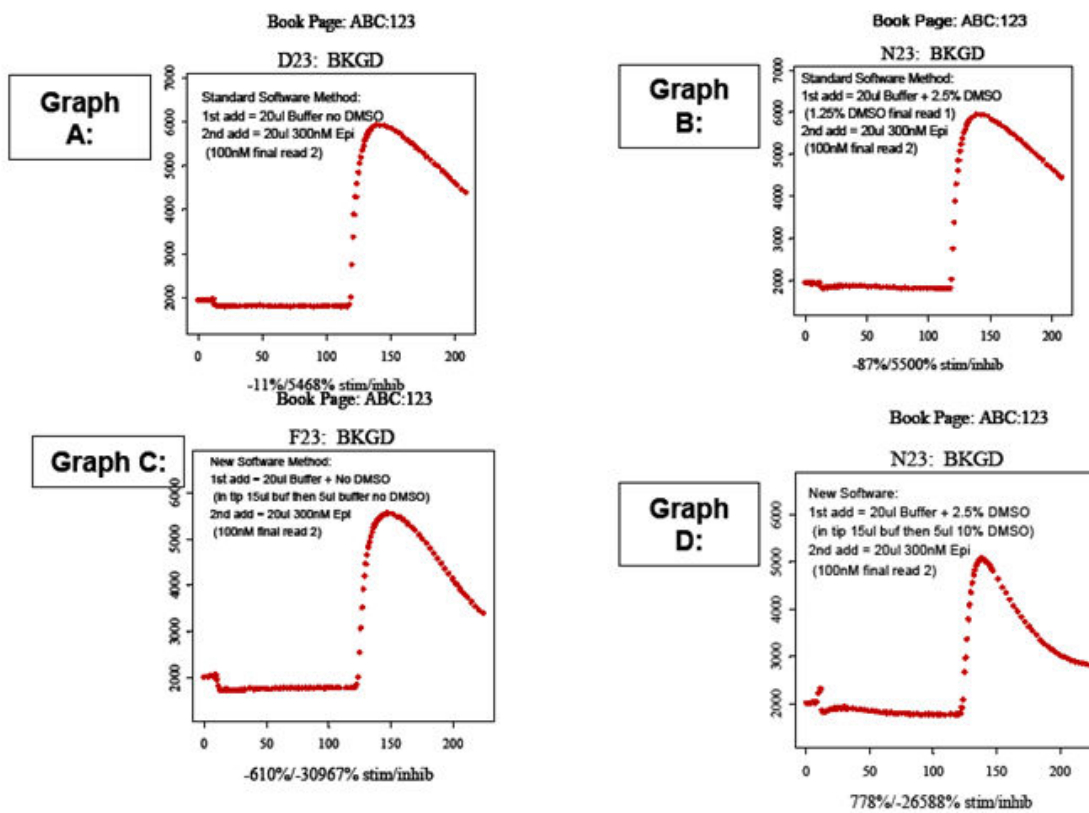
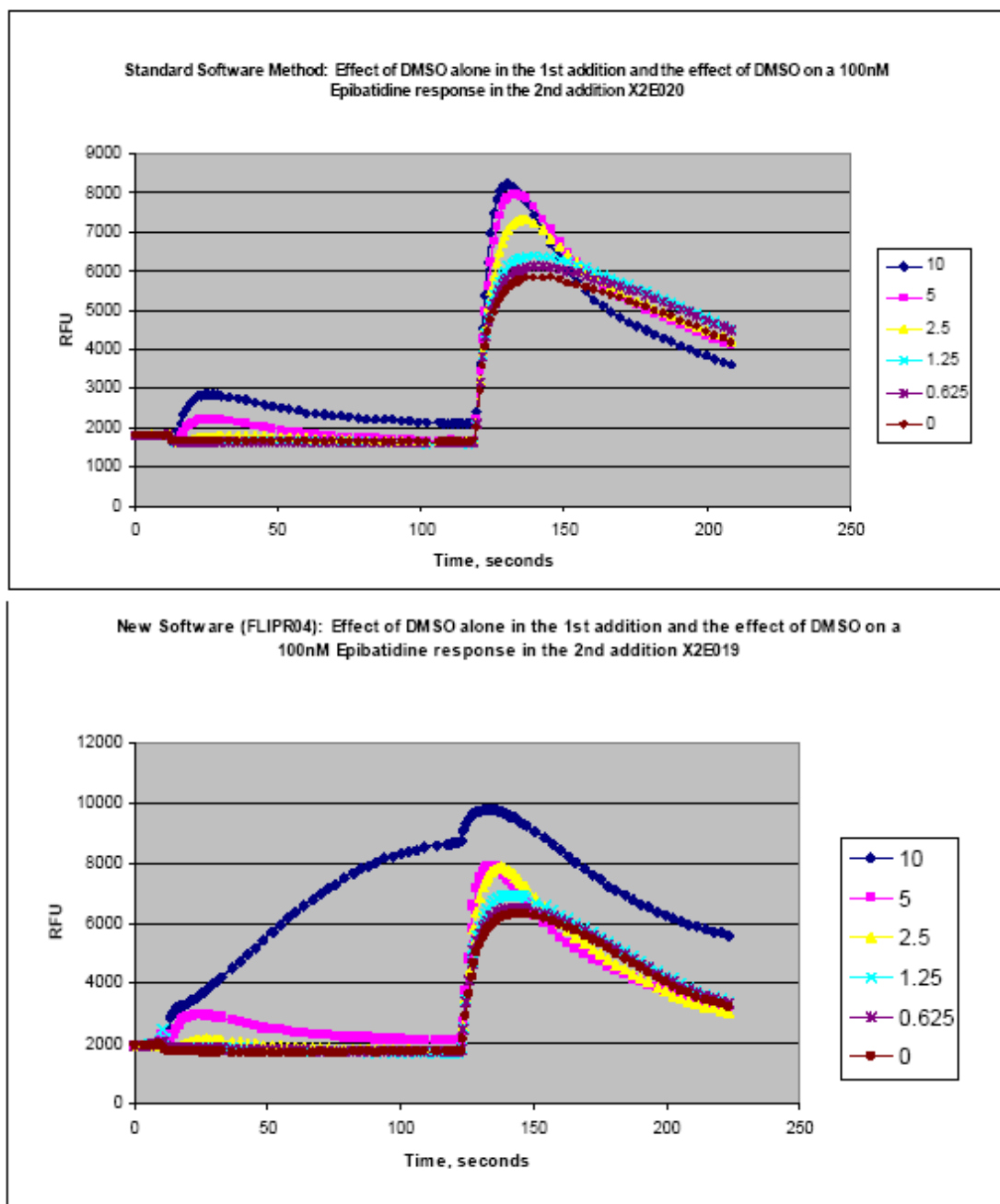


Figure 7A. Effects of bolus of DMSO on shapes of kinetic tracings.





**Figure 7B.** Effects of bolus of DMSO on shapes of kinetic tracings. Note that between 5 and 10% DMSO the response changes, possibly due to loss in membrane integrity

in a much smaller diameter well, and using the 96-well technique will result in variable response. When adding to a 384-well plate, the tips are typically in the buffer solution of the cell plate when the dispense takes place. In a number of cases, the speed of dispense has to be increased as well. These heights and speeds should be tested with buffer to check

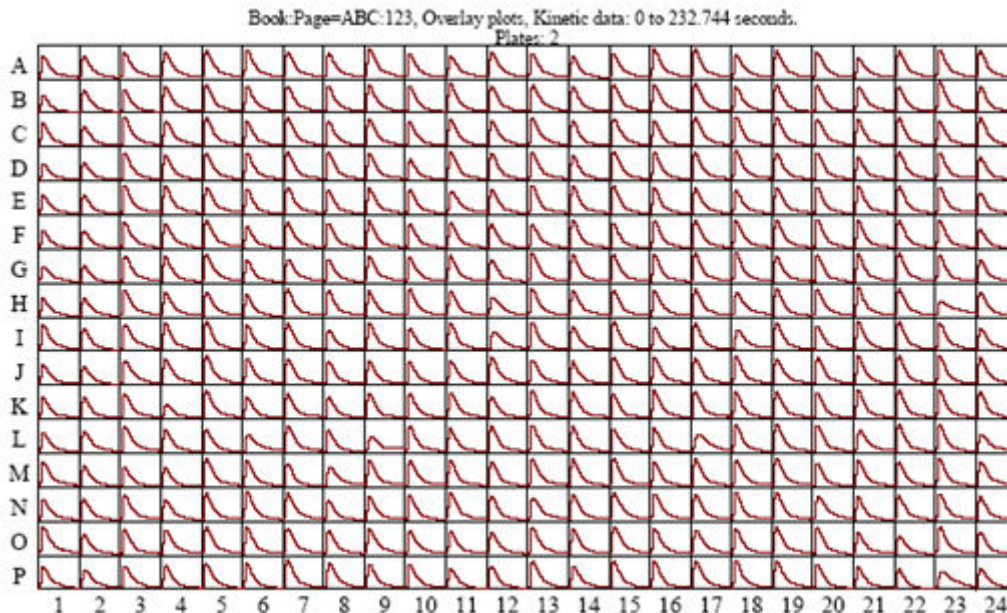


**Figure 8A.** Example of max addition with tip wash in agonist/potentiator assay.

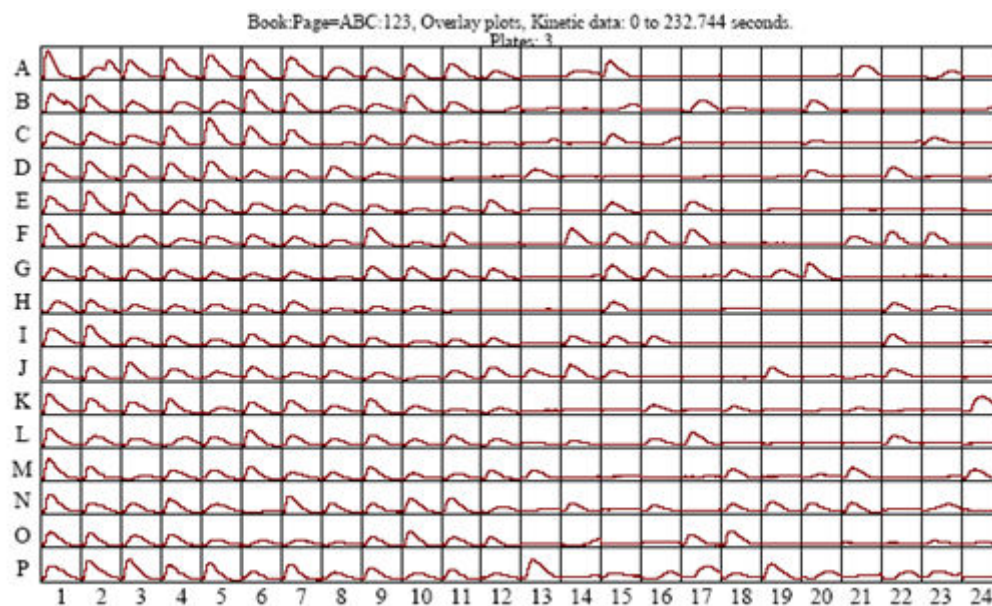


**Figure 8B.** Carry-over from tips in (a) in subsequent plate (buffer addition only).

for unwanted “pre-firing” of the cells. Another issue that arises with the 384-well format is the limited amount of diluent that can be added to the compound plate. This limitation can result in having to create intermediate dilution plates off-line, thereby slowing throughput and adding costly consumables. This has been eliminated by using an in-tip dilution on the FLIPR™ (Figure 6). Although the final DMSO concentration is the same,

the bolus of DMSO in the bottom of the tip can have an effect on the cells (Figures 7A and 7B). In our hands, a ratio of 15  $\mu$ l buffer/5  $\mu$ l compound was found to have the least DMSO effect. However since this result can be variable, different combinations should be tested during development. This in-tip dilution method can be used in both the two- and three-addition FLIPR™ methods.

**Notes on tip washing:** The FLIPR™-2 and FLIPR™-3 have tip wash stations that can be incorporated into the assay to eliminate the need to change tips. This allows one to use reservoirs without fear of cross contamination among the test compounds. In addition, a DMSO pre-wash can be performed at the tip load station with the proper adapter. When running a single-point screen of more than 100K compounds, tip washing should be tested first to minimize cost and maximize throughput. Occasionally, the compound used for the EC<sub>90</sub> addition cannot be washed off the tips, resulting in significant carry-over of active compounds in to the subsequent plate (example in Figure 8A and 8B); in these cases, the tips will have to be changed. This typically happens when peptides are added as the EC<sub>90</sub> dose.

## Optimization Experiments for Ion Channel Targets with Ca<sup>2+</sup> Permeability

Some ion channels (e.g. ionotropic glutamate receptors) differ from GPCRs in that they desensitize very quickly to agonist exposure, and in most cases, it is not possible to see a response in FLIPR™ with agonist alone. Such targets require the use of agents that decrease the rate of desensitization, which are called channel modulators or “clamps”. The choice of which channel modulator to use is dependent upon the receptor. Table 6 provides a brief summary of modulators that we have used.

Since ion channel modulators are needed to decrease the rate of desensitization of the channel to agonist, the assay design is somewhat different than for GPCRs. Like for GPCRs, the ability of the FLIPR™ to make two fluid additions to the cells enables the detection of agonists, antagonists, and allosteric modulators in one assay. Representative kinetic profiles for iGluR1 flip and flop are shown in Figure 9A. Test compounds are added in the first addition along with a 90% dose of the known agonist, in this case glutamate, which normally does not generate a measurable Ca<sup>2+</sup> response because the rate at which the receptor desensitizes is too fast to be detected on the FLIPR™. A response in the first read will indicate that the test compound is either a non-desensitizing agonist or a positive allosteric modulator (Figure 9B). The second addition consists of an optimal concentration (~90%) of a known allosteric modulator which results in maximal response by clamping the channel open and decreasing receptor desensitization. A reduced response in the second read will indicate that the compound is an antagonist (Figure 9C). The question of whether the compound is a non-desensitizing agonist or an allosteric modulator will be answered in the secondary assay in which the compound is added in the absence of any glutamate in the first read. If the compound alone elicits a response, it is a non-desensitizing agonist. Alternatively, if the compound only gives a response in the presence of glutamate (read 2), then it is a potentiator.

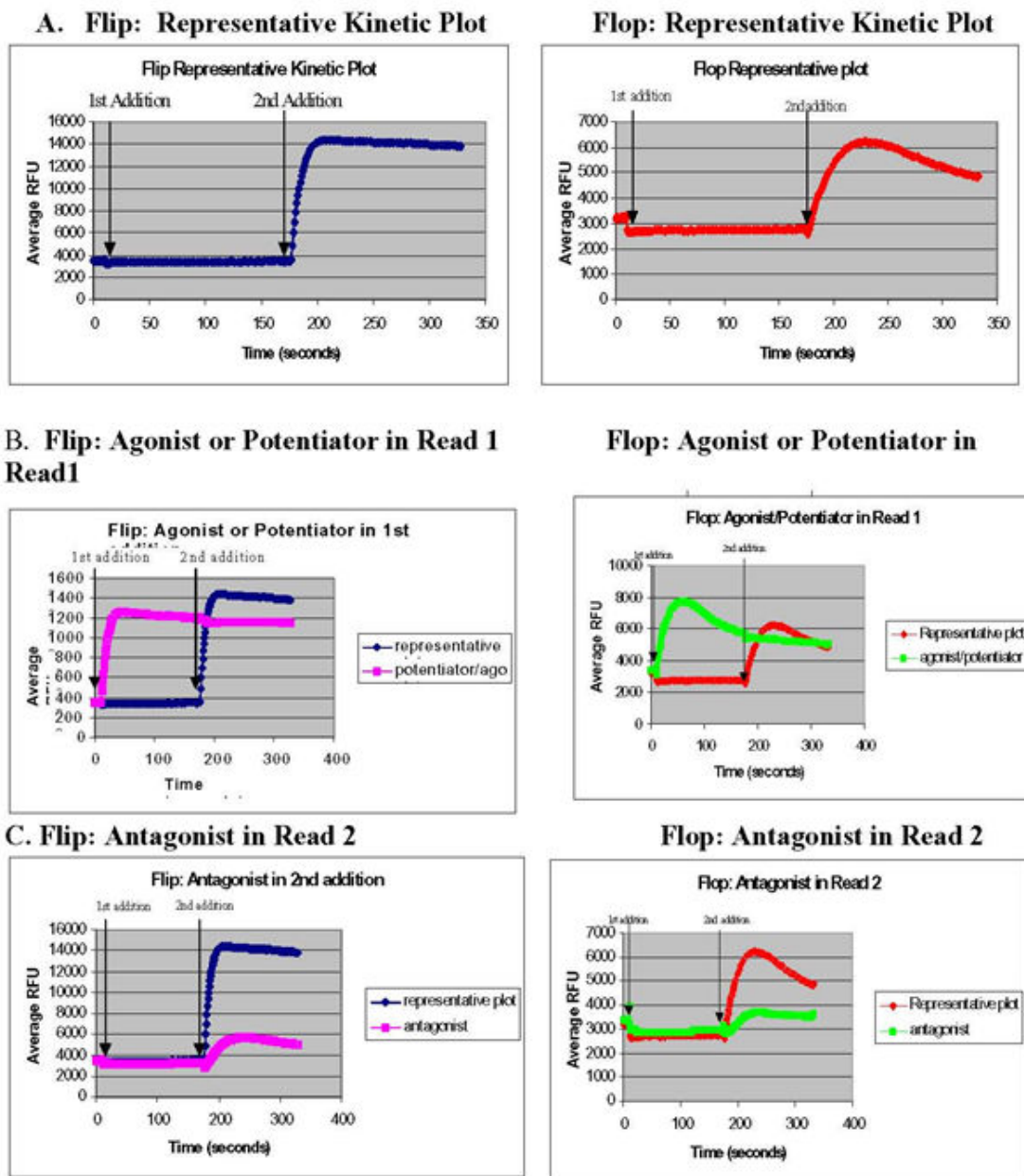


**Figure 9.** Expected kinetic profiles of iGluR1 Flip and Flop receptors.

(A) Expected kinetic profile of 0.5 mM glutamate (agonist) in the 1st addition followed by 20  $\mu$ M LY (allosteric modulator) in the 2nd addition. (B) Expected kinetic profile of an agonist or an allosteric modulator where 20  $\mu$ M LY (control potentiator) and 0.5 mM glutamate are added in 1st addition. (C) Expected kinetic profile of an antagonist where 10  $\mu$ M NBQX (control inhibitor) and 0.5 mM are added in the 1st addition, followed by 20  $\mu$ M LY in the second addition. In B and C, the test compounds will be added at the 1st addition with 0.5 mM glutamate, followed by 20  $\mu$ M LY in the 2nd addition.

In the case of the kainate receptor iGluR6, the allosteric modulator ConA needs to be incubated on the cells for a minimum of 5 minutes prior to adding agonist. ConA takes longer to bind and has an effect on receptor desensitization.

**Table 6: Summary of modulators**

| Receptor    | Channel modulator      |
|-------------|------------------------|
| iGluR1 flip | Cyclothiazide (CTZ)    |
| iGluR1 flop | LY compound            |
| iGluR4 flip | Cyclothiazide (CTZ)    |
| iGluR4 flop | LY compound            |
| iGluR5 & 6  | Concanavalin A (Con A) |

## Optimization Experiments for Ion Channel Targets with Ion Permeability that Significantly Impacts Cell Membrane Potential

Changes in membrane potential associated with ion channel activity may be measured on the FLIPR™ instrument using a voltage-sensitive dye available from Molecular Devices. The following are some of the parameters that need to be considered in developing a FLIPR™-based membrane potential assay:

### ***Cell Density:***

Optimal cell conditions for the FLIPR membrane potential assay require the creation of a confluent cell monolayer. The cell seeding density depends on the cell type and the time in culture following the plating of the cells. Receptor expression levels can change with the cell passage number or as a result of the drug-selection conditions used for cell maintenance. Thus, it is critical to monitor changes in functional activity over time. Refer to the previous in this chapter for optimizing the cell seeding density.

### ***Assay Buffer:***

HBSS + 20 mM HEPES + added CaCl<sub>2</sub> (5 mM final concentration).

### ***Preparation of Membrane potential dye:***

We recommend dissolving the dye in assay buffer. After formulation, the loading buffer can be stored frozen in aliquots for several months without loss of activity.

### ***Method of Dye Loading Cells:***

Dilute the loading buffer 1:1 with assay buffer. Aspirate the media from the cells and add 100 µl of diluted buffer per well for 96-well plates. (Note: We have not had success following the Molecular Devices recommendation of adding the dye directly to the media with the iGluR targets.) The dye:buffer ratio can be optimized to reduce cost of the assay. Dye-loading the cells should be tested at 37°C and at ambient temperature. The optimal dye loading time, on average, for HEK293 cells is 60 minutes, but the range can be wide (5-60 minutes).

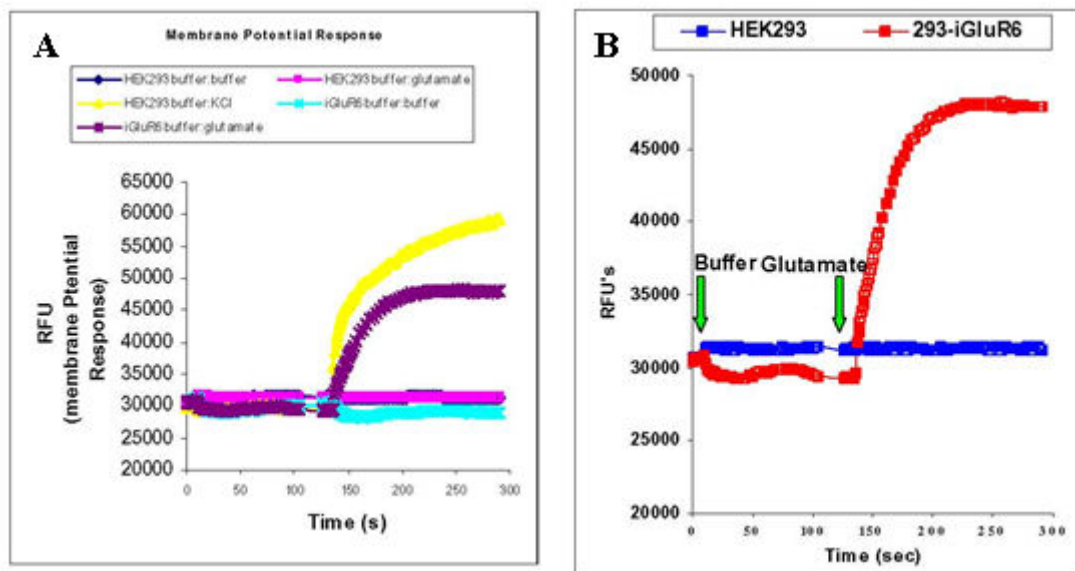


**Figure 10.** A) The HEK293 response to KCl vs the 293-iGluR6 response to glutamate. (B) HEK293 and 293-iGluR responses to glutamate.

#### **Antagonist Assays – Results Export Range:**

The kinetic profile of the calcium response to ion channel activation is prolonged when compared to the typical profiles generated by GPCR activation. As a result, agonists introduced in the first addition, read frame I, will lead to a baseline shift which will not return to baseline prior to the second addition, read frame II (see Figure 9B). This baseline shift within read frame II is due to the prolonged activation of receptor when agonists are introduced. Because the EC<sub>90</sub> challenge dose for antagonist assays is added within the initial portion of read frame II, the read frame I baseline shift due to agonists will lead to antagonist assay interference if exporting data from read frame II only (Max-Min). For this reason, one should consider exporting both read frames I and II for ion channel antagonist assays, which includes the pre-compound addition portion of read frame I, to capture the pre-compound addition or actual assay baseline (Figure 9B, time 0-350 seconds). By utilizing the pre-compound addition baseline of read frame I, false positive agonist interference in antagonist ion channel targets can be avoided.

#### **Clamp:**

Clamping agents such as Concanavalin A may be required to prevent rapid desensitization of ion channels. Depending on the incubation time required for the clamp, it could either be added with the loading buffer or it could be added with the compound.

#### **FLIPR setting:**

Choose filter #2 in the experiment setup of the FLIPR™ software to measure membrane potential. Set the background reading ~ 20000 RFU. Table 7 lists some of the recommended setup parameters for the compound (1<sup>st</sup> addition) and agonist (2<sup>nd</sup> addition) additions to a 96-well plate.

**Control:**

We recommend running a KCl dose curve as a positive control to measure changes in membrane potential independent of the ion channel activity. The following is an example of time course tracings observed with the iGluR6 assay (Figure 10).

**Table 7: Recommended setup parameters for compound and agonist additions to a 96-well plate.**

|              | Volume | Addition Speed | Pipettor Height |
|--------------|--------|----------------|-----------------|
| 1st Addition | 50 µl  | 50 µl/sec      | 100 µl          |
| 2nd Addition | 50 µl  | 50 µl/sec      | 150 µl          |

**Performing FLIPR™ using a non-adherent cell line:**

So far, we have been describing methods appropriate for adherent cells cultures. In these cases, dye can be loaded directly onto cells grown to confluency in microtiter plates. In contrast, when the transfected cell line is weakly adherent or grows in suspension culture the following procedures should be followed:

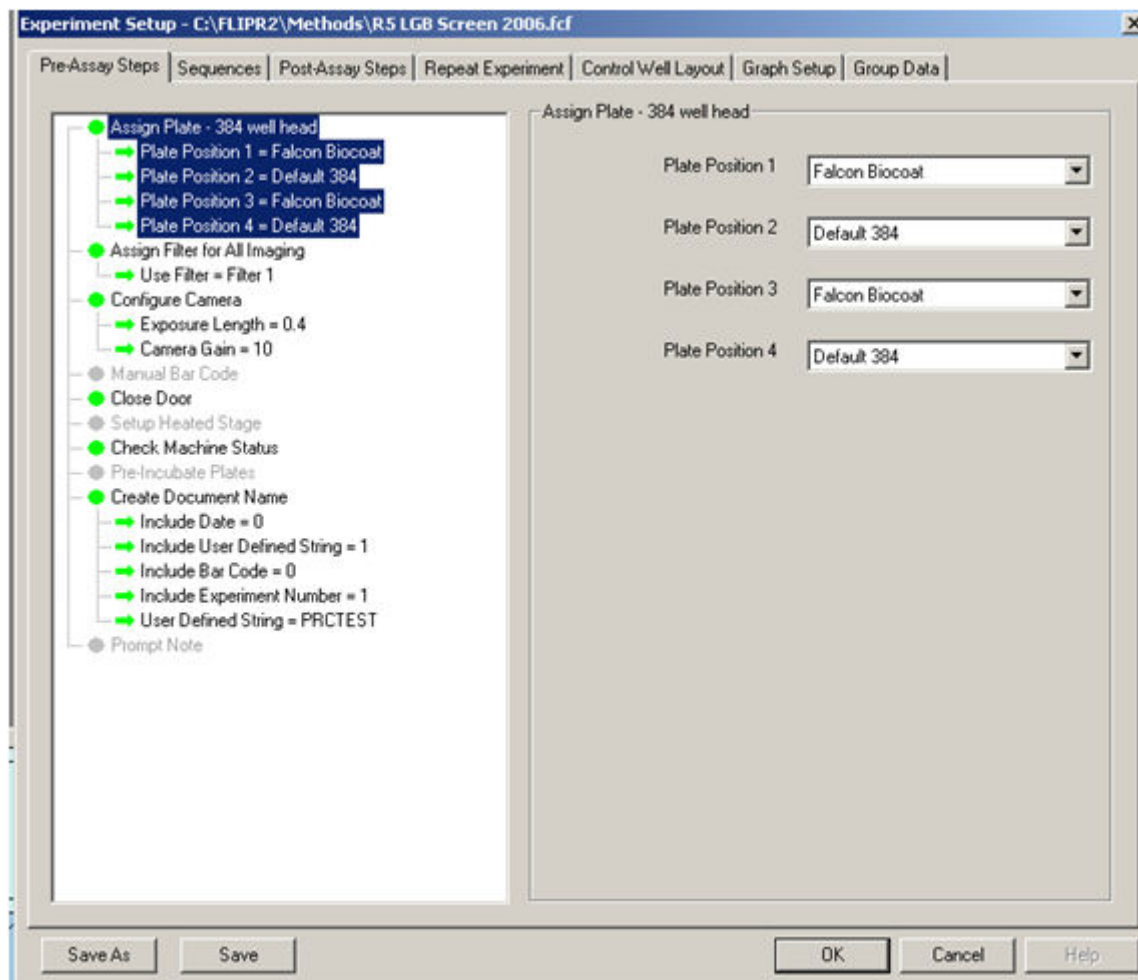
1. Remove growth media from cell culture flask.
2. Add 10 ml PBS to each flask to rinse.
3. Remove PBS and repeat rinse step.
4. Add 10 ml cell dissociation buffer to each flask.
5. Rock flask gently.
6. Add 10 ml Alpha-MEM and discard the rinse.
7. Transfer cells to 50 ml centrifuge tube.
8. Add 30 ml buffer.
9. Pellet cells for 5 min at 2000 rpm.
10. Remove supernatant.
11. Add 30 ml buffer with 30 µl Fluo-3 AM (1:1000 dilution) and 30 µl pluronic acid.
12. Cover tube with foil and shake gently.
13. Place on shaker for 60 min at 180 rpm at room temperature
14. Fill up tube with buffer and spin for 5 min at 2000 rpm and remove supernatant.
15. Repeat step #14.
16. Resuspend cells at 1 x10<sup>6</sup> cells/ml.
17. Plate 50 µl/well of Poly-D-Lysine pre-coated plates.
18. Wait 20 min and centrifuge plates for 3 min at 1500 rpm.
19. Place plates in FLIPR until ready for use.

**Notes:**

- If cells are weakly adherent, start at step #1.
- If cells are in suspension, start at step #7.
- If using a no-wash dye, skip steps #14-15.

## FLIPR Instrument Setup

### Pre-Assay Setup for FLIPR™ -2 and -3:



In this screen, which is the same for 96- or 384-well assay set-up, the user defines the labware used in the experiment from a drop-down list. The other options on this screen are the filter selection, camera configuration, and the output file setup.

1. Assign plate: This is where the user configures the deck layout. If the plate you are using is not included, there is a default 96-well and default 384-well that can be used until the correct plate is defined.
2. Camera configuration: The exposure length is typically set to 0.4 seconds. The gain is only applicable to the FLIPR™-3 with the Andor camera.

**Note:** To adjust the baseline signal of the plate, first adjust the laser intensity from the keypad before adjusting the exposure time. This should be done for each plate to set the same baseline over a run.

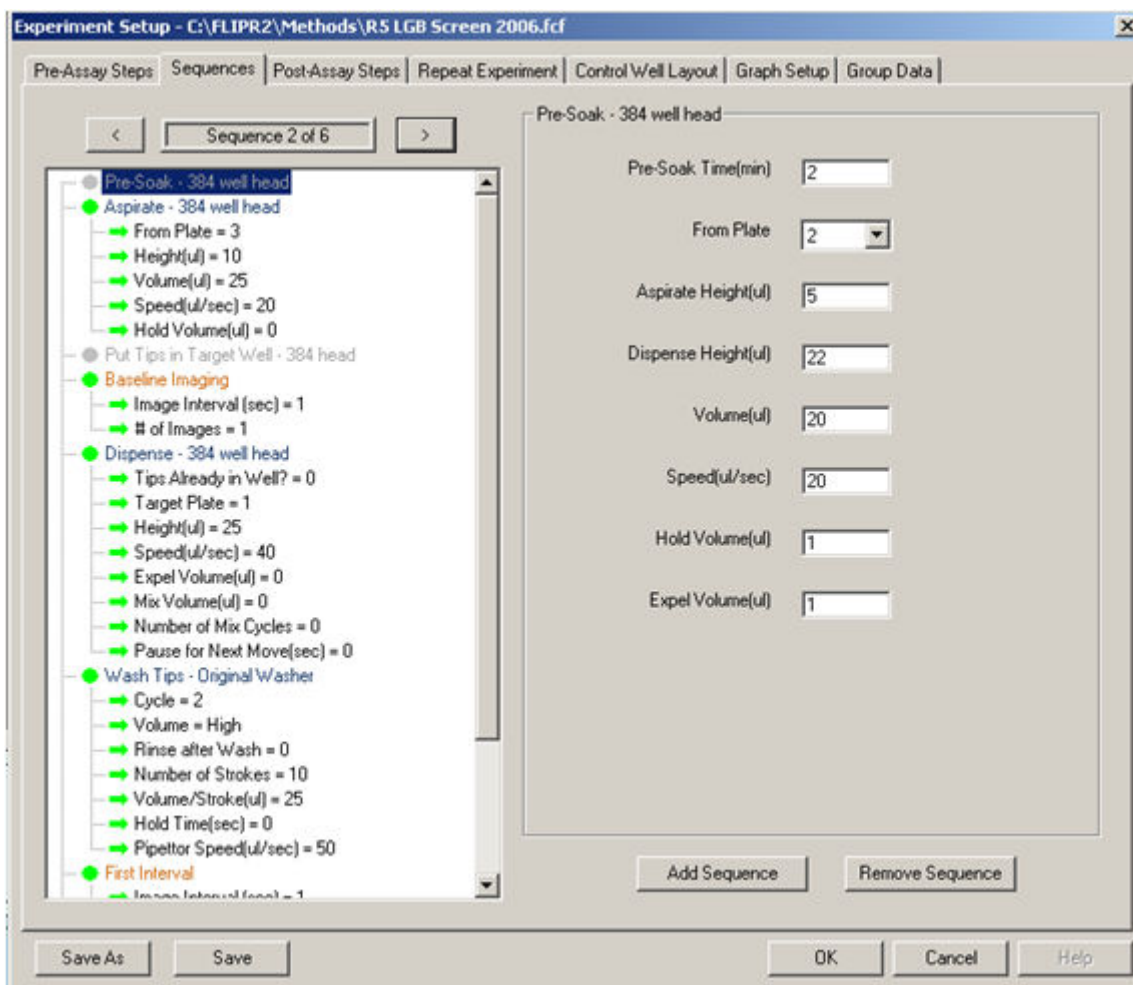


3. Filter selection: The FLIPR™ has a two-position filter slide. Typically, filter #1 is a 488-nm filter used for calcium assays, and filter #2 is either blank or a 535-nm filter for membrane potential assays.

4. Create document name: This is where the filename is created. A “1” in the field means this will be included in the file name and a “0” means it will not. A few issues deserve a warning here: If you use the date only, it is very possible that the data generated will be overwritten if another run is made on the same date. Therefore, it is a good practice to include a user-defined string in your file name. ALWAYS include the experiment number in the output. This is the flag that assigns the \_n1, \_n2, etc to the plates in the run. Failure to include this will result in every plate being labeled \_n1, thereby overwriting all previously generated data. The best practice here is to use a lab notebook number and page as the filename. An example would be: D00567\_143, where D00567 is the notebook number and 143 is the page.

#### Sequences Setup:

The sequence setup is where the entire experiment is defined. This includes defining the number of reads to be taken as well as all liquid handling steps, wash sequences, automated tip unload, etc. These settings should be done with the assistance of an automation engineer or an experienced FLIPR™ user.

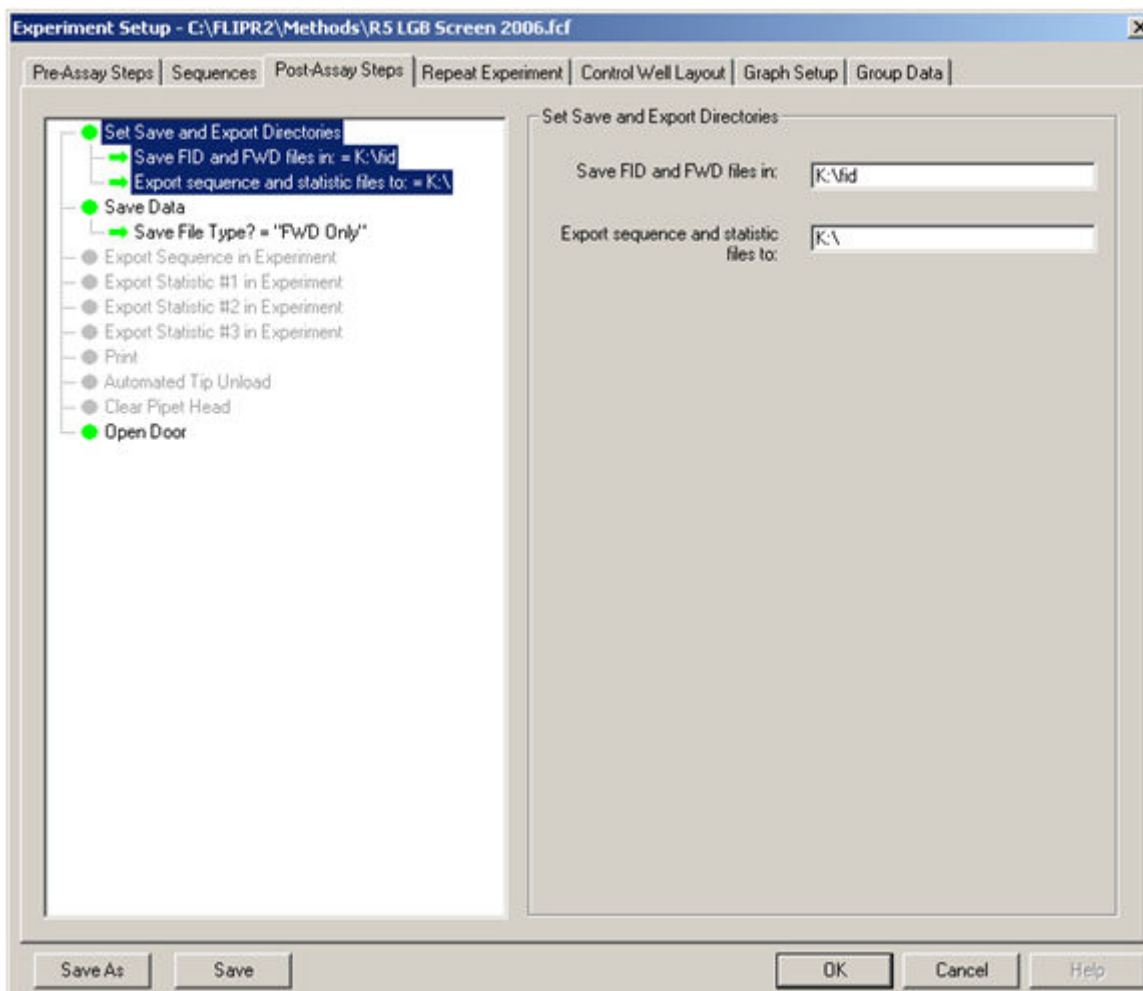


By double clicking on the circle beside each step, the user can activate/deactivate that part of the sequence. A green circle indicates the step is active while grey indicates inactive. By single clicking on the sequence step, the step's setup box appears on the right side of the window with all parameters that can be accessed by the user.

1. Pre-Soak: This is typically not used.
2. Aspirate: The FLIPR™ can aspirate from any of the four deck positions as long as a plate has been defined there in the initial setup page.
3. Put tips in target well: This will move the tips into the target plate before dispensing. Typically not used. NEVER use this if dispensing at a low height where the tips are in contact with the buffer. We have observed that this can cause a response from the compound on the outside of the tips.
4. Baseline imaging: The pipettor head will not move to the cell plate until the baseline imaging is complete. A typical setting is 1 to 5 secs.
5. Dispense: The FLIPR can dispense to any of the four deck positions as long as a plate has been defined there in the initial setup page.
6. Wash tips: This will wash tips in the wash station at position 6 if the unit has a wash station installed. A pre-wash can be performed at position 5 by clicking the

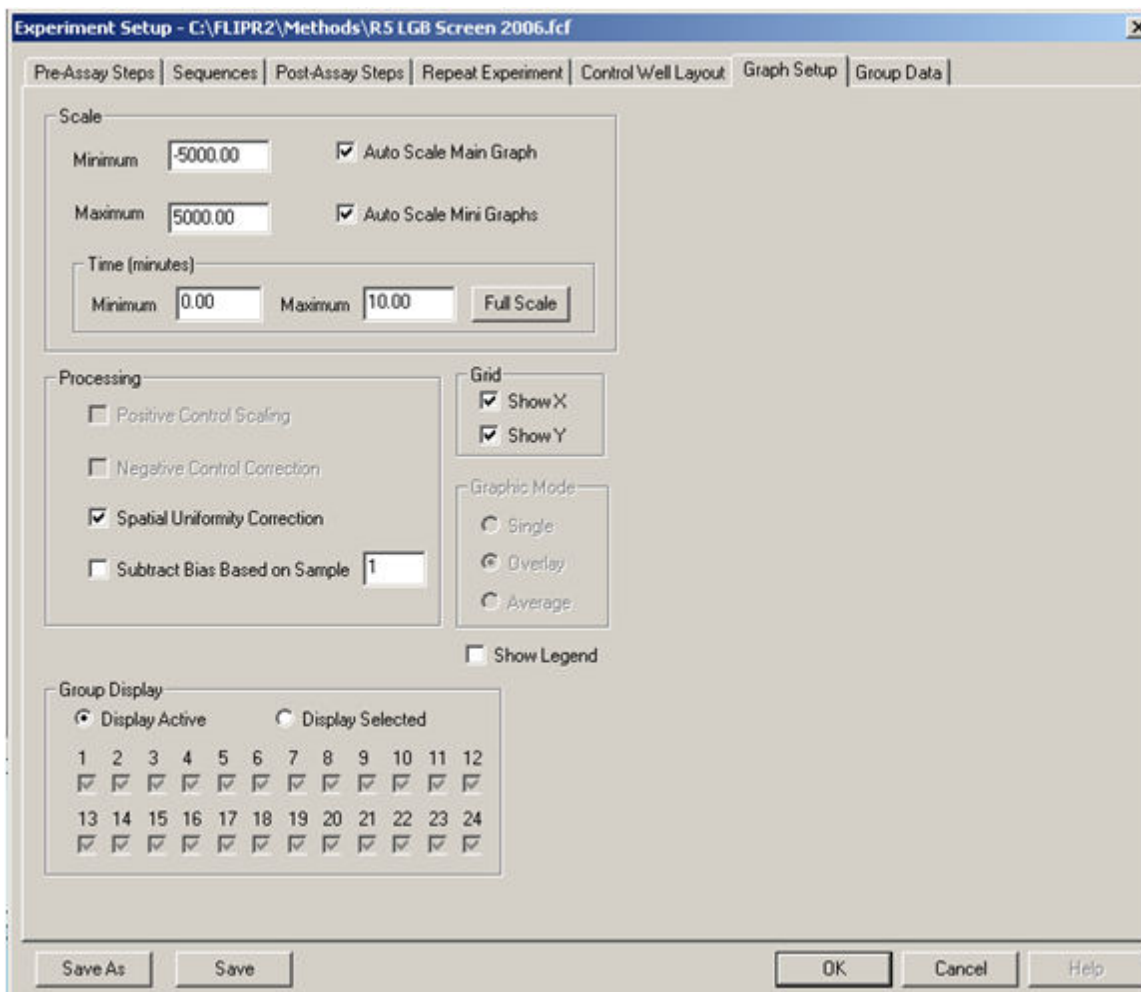
- “rinse after wash” button. This will use the same wash parameters defined, only perform them at position 5.
7. First Interval: This sets the number of images to be acquired and the interval between each image. Typically, the interval is short (1 sec) and the number of images are 30 to 60 to capture the compound addition. This should be set long enough to capture past the peak response.
  8. Second Interval: This set the number of images to be acquired and the interval between each image. Typically, the interval time is longer (3-5 secs) and the number of images is sufficient to capture when the response decreases to background. In some cases, the signal will never return to background and it is the judgment of the scientist to set this range.
  9. Automated Tip Unload: This will automatically unload the tips to the rack when all pipetting steps are completed. This should only be done in the last sequence.
  10. Clear Pipette Head: This return the pipettor head to the home position.

#### Post Assay Setup:



In the post-assay setup section, the user selects where data will be saved, what type of data to save, and considers the option to automatically export and print data at the end of each plate. When setting the save location, you must type in the exact path to the save directory. The software will generate an error if the location is invalid or if it is a network location that is not available. In most instances, only FWD files should be saved. This saves storage space, as the FID files are larger image files. In some instances, such as when a heated stage is used, the open door may need to be turned off to maintain better temperature control in the FLIPR™.

### Graph Setup:



Typically, Spatial Uniformity Correction is used without subtracting the background. Spatial Uniformity Correction is basically a software normalization that sets all wells to the average RFU of the plate when starting the experiment.

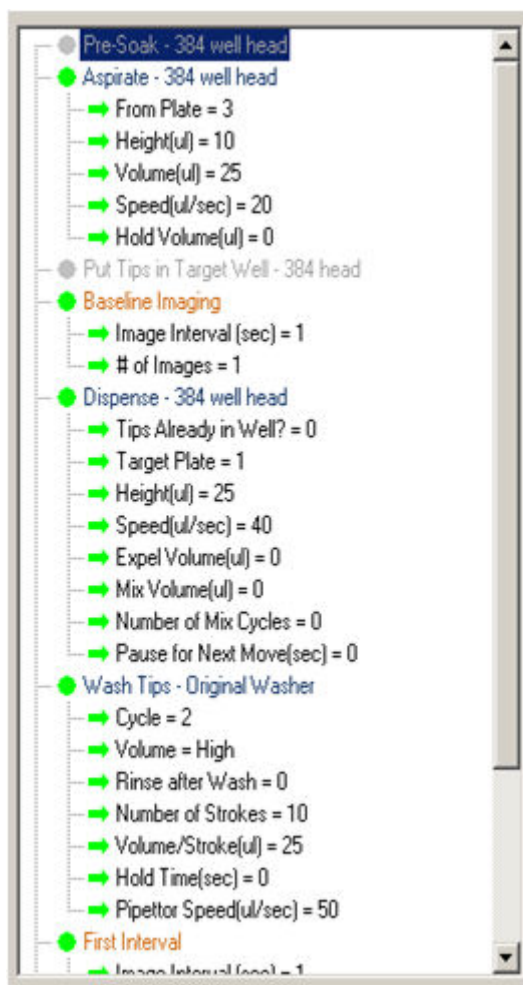
In most cases, subtract bias is not used. This will background subtract the data set which can mask the assay window. An example would be to start with a baseline of 5000 RFU and the max signal response being 6000 RFU. In most situations, this is not a screenable

window, but if the 5000 RFU background is subtracted, the window “looks” good (0 to 1000).

### One-, Two- and Three-Addition Assay Examples:

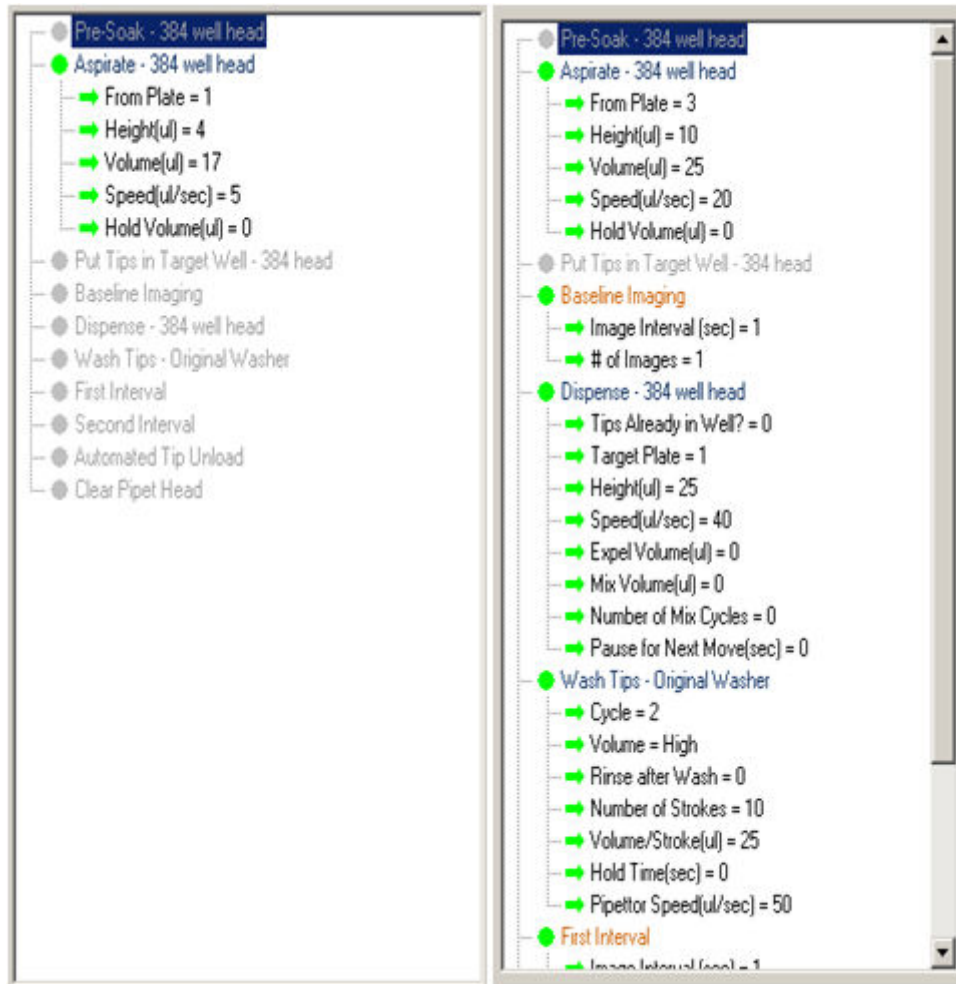
All three of these formats will require the same initial setup described above.

One-addition assays will need one or two sequences dependent upon the use of an in-tip dilution. The example below shows a 384-well aspiration from position 3 with a dispense into the cell plate at position 1 (Read Position), followed by a wash.

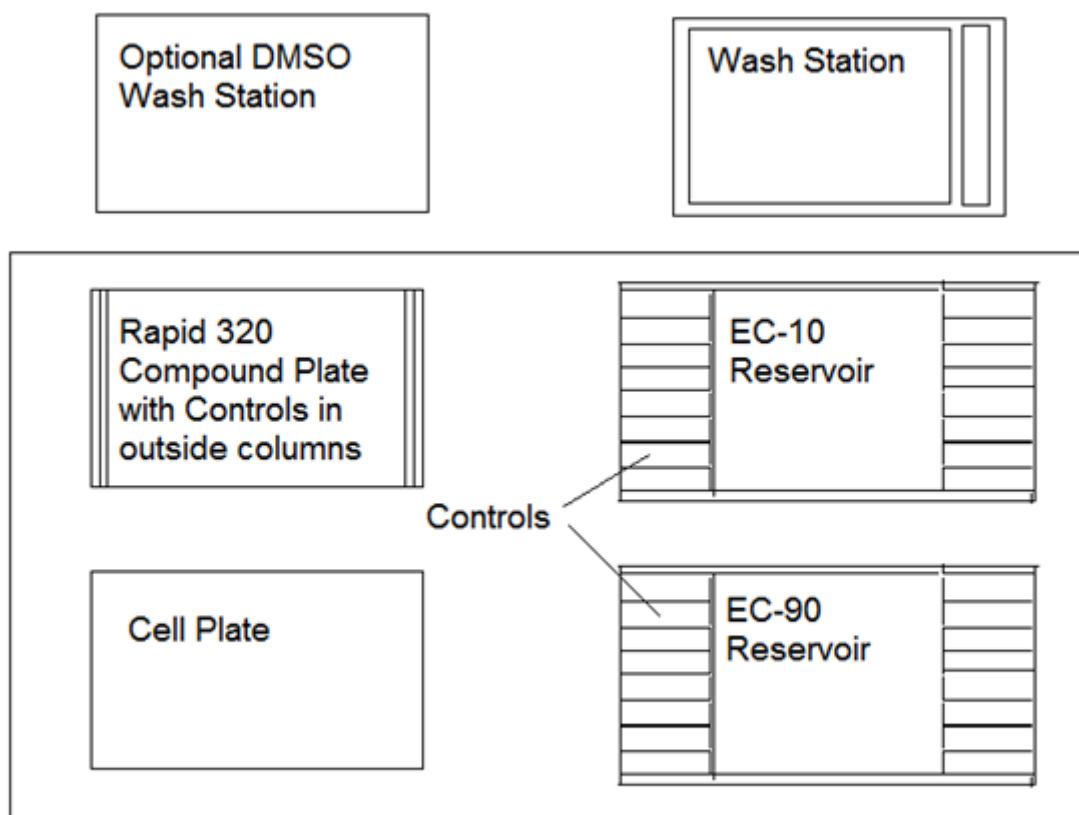


A one-addition assay with an in-tip dilution is shown below. The first step aspirates 17  $\mu\text{l}$  from plate 1 and then 8  $\mu\text{l}$  from plate 3.

Note: When performing an in-tip dilution, the volume in the second step is the final total volume aspirated (17  $\mu\text{l}$  + 8  $\mu\text{l}$ ). This is a result of the way the FLIPR™ software keeps track of the pipettor head.



A two-addition or three-addition assay can be run by simply adding sequences. It is recommended that if the assay is targeting potentiators, the in-tip dilution and pre-incubation time be used to maximize the sensitivity of the assay. Below is the complete liquid handling setup for a three-addition assay. Volumes and read times will vary.



Deck Layout for a three-addition assay

## Sequence 1

- Pre-Soak - 384 well head
- Aspirate - 384 well head
  - ➔ From Plate = 1
  - ➔ Height(ul) = 4
  - ➔ Volume(ul) = 17
  - ➔ Speed(ul/sec) = 5
  - ➔ Hold Volume(ul) = 0
- Put Tips in Target Well - 384 head
- Baseline Imaging
- Dispense - 384 well head
- Wash Tips - Original Washer
- First Interval
- Second Interval
- Automated Tip Unload
- Clear Pipet Head

## Sequence 2

- Pre-Soak - 384 well head
- Aspirate - 384 well head
  - ➔ From Plate = 3
  - ➔ Height(ul) = 10
  - ➔ Volume(ul) = 25
  - ➔ Speed(ul/sec) = 20
  - ➔ Hold Volume(ul) = 0
- Put Tips in Target Well - 384 head
- Baseline Imaging
  - ➔ Image Interval (sec) = 1
  - ➔ # of Images = 1
- Dispense - 384 well head
  - ➔ Tips Already in Well? = 0
  - ➔ Target Plate = 1
  - ➔ Height(ul) = 25
  - ➔ Speed(ul/sec) = 40
  - ➔ Expel Volume(ul) = 0
  - ➔ Mix Volume(ul) = 0
  - ➔ Number of Mix Cycles = 0
  - ➔ Pause for Next Move(sec) = 0
- Wash Tips - Original Washer
  - ➔ Cycle = 2
  - ➔ Volume = High
  - ➔ Rinse after Wash = 0
  - ➔ Number of Strokes = 10
  - ➔ Volume/Stroke(ul) = 25
  - ➔ Hold Time(sec) = 0
  - ➔ Pipettor Speed(ul/sec) = 50





Note that in sequence 3 and 5, the order of aspiration is reversed. This is due to the fact that unknown test compounds have been added to the cell plate and to aspirate from there first would be a source of contamination to the EC<sub>10</sub> reservoir. This is not the case for the 4<sup>th</sup> and 6<sup>th</sup> sequence as the tips have been washed.

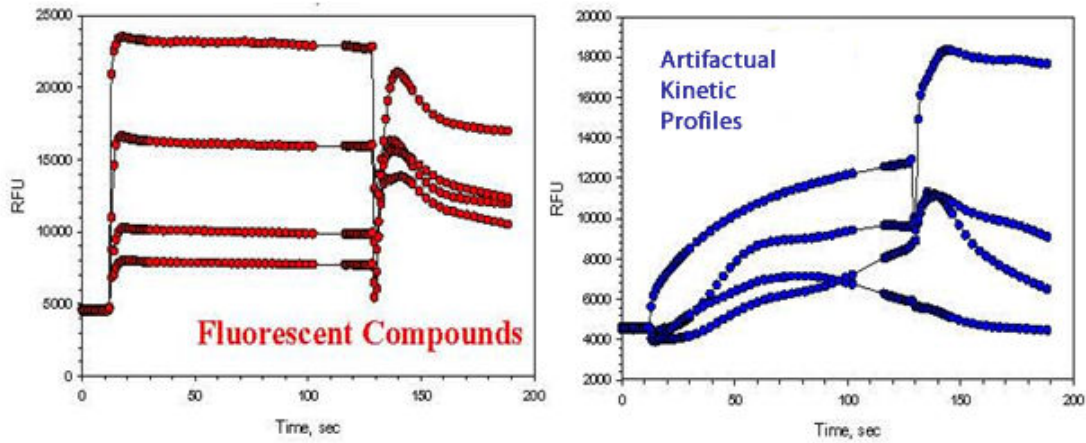


Figure 11. Typical kinetic traces that can result from FLIPR™ artifacts.

- ### Sequence 5

  - Pre-Soak - 384 well head
  - Aspirate - 384 well head
    - ➔ From Plate = 2
    - ➔ Height(ul) = 5
    - ➔ Volume(ul) = 10
    - ➔ Speed(ul/sec) = 20
    - ➔ Hold Volume(ul) = 0
  - Put Tips in Target Well - 384 head
  - Baseline Imaging
  - Dispense - 384 well head
  - Wash Tips - Original Washer
  - First Interval
  - Second Interval
  - Automated Tip Unload
  - Clear Pipet Head

### Sequence 6

  - Pre-Soak - 384 well head
  - Aspirate - 384 well head
    - ➔ From Plate = 1
    - ➔ Height(ul) = 20
    - ➔ Volume(ul) = 25
    - ➔ Speed(ul/sec) = 20
    - ➔ Hold Volume(ul) = 0
  - Put Tips in Target Well - 384 head
  - Baseline Imaging
    - ➔ Image Interval (sec) = 1
    - ➔ # of Images = 1
  - Dispense - 384 well head
    - ➔ Tips Already in Well? = 0
    - ➔ Target Plate = 1
    - ➔ Height(ul) = 25
    - ➔ Speed(ul/sec) = 40
    - ➔ Expel Volume(ul) = 0
    - ➔ Mix Volume(ul) = 0
    - ➔ Number of Mix Cycles = 0
    - ➔ Pause for Next Move(sec) = 0
  - Wash Tips - Original Washer
    - ➔ Cycle = 2
    - ➔ Volume = High
    - ➔ Rinse after Wash = 1
    - ➔ Number of Strokes = 10
    - ➔ Volume/Stroke(ul) = 25
    - ➔ Hold Time(sec) = 0
    - ➔ Pipettor Speed(ul/sec) = 50

## Potential Artifacts

Although the FLIPR™ has facilitated advances in cellular calcium mobilization screens, these assays remain difficult to configure, relatively slow, and fraught with potential artifacts. Blocked FLIPR™ tips will lead to false positives in an inhibitor screen, or false negatives in an agonist screen. Fluorescent compounds, Ca<sup>2+</sup> ionophores, and compounds that permeabilize the cell membrane can all contribute to false positives in the agonist read (Figure 11). These types of nuisance or interference compounds can often be identified from the kinetic traces of the response, but this kind of in depth data review is time consuming and requires experience to correctly recognize strange response profiles. In addition, compounds with agonist activity may interfere with antagonist reads due to desensitization or internalization of the receptor, resulting in false positives.

The utility of the FLIPR™ and calcium dye approach for screening GPCR targets has been greatly enabled by the use of over-expression of promiscuous and chimeric G-proteins that provide a method to “switch” GI/o-coupled receptor activation to an increase in intracellular calcium. However, screens designed to detect receptor activity against a backdrop of stable, high-level promiscuous G-protein expression are also susceptible to artifacts - - false positives derived presumably from other cell surface receptors hi-jacking the promiscuous G-proteins. Indeed, even in the absence of a promiscuous G-protein, any endogenous GPCR that couples through G<sub>q</sub> and induces a Ca<sup>2+</sup> response may show up as an agonist or interfere with antagonist reads. It is well documented that GPCRs, particularly those in heterologous expression systems, can activate multiple signal transduction pathways, and indeed there is also evidence for cross-talk between recombinant and native receptors that may also complicate the responses to compounds. Thus, we recommend routinely performing a secondary screen against the parent cell line that lacks the receptor of interest in order to definitively identify false positives.

## References

### Primary Reference

1. Baxter D. F., et al. A novel membrane potential-sensitive fluorescent dye improves cell-based assays for ion channels. *J. Biomolecular Screening*. 2002;7:79–85. PubMed PMID: 11897058.

### Additional Reading

- Benjamin E. R., et al. Pharmacological characterization of recombinant N-type calcium channel (Ca<sub>v</sub>2.2) mediated calcium mobilization using FLIPR. *Biochemical Pharmacology*. 2006;72:770–782. PubMed PMID: 16844100.
- Coward P., et al. Chimeric proteins allow a high-throughput signaling assay of GI-coupled receptors. *Analytical Biochemistry*. 1999;270:242–248. PubMed PMID: 10334841.

- Hodder P., et al. Miniaturization of intracellular calcium functional assays to 1536-well plate format using a fluorometric imaging plate reader. *J. Biomolecular Screening*. 2004;9:417–426. PubMed PMID: 15296641.
- Jensen A. Functional characterization of human glycine receptors in a fluorescence-based high throughput screening assay. *European J. Pharmacology*. 2005;521:39–42. PubMed PMID: 16182281.
- Liu A.M.F., et al. G- $\alpha_{16/z}$  chimeras efficiently link a wide range of G protein-coupled receptors to calcium mobilization. *J. Biomolecular Screening*. 2003;8:39–49. PubMed PMID: 12854997.
- Liu E.C-K., And Abell L. M. Development and validation of a platelet calcium flux assay using a fluorescent imaging plate reader. *Analytical Biochemistry*. 2006;357:216–224. PubMed PMID: 16889745.
- Lubin M., et al. A nonadherent cell-based HTS assay for N-type calcium channel using Calcium 3 dye. *Assay and Drug Development Technologies*. 2006;4:689–694. PubMed PMID: 17199507.
- Miret J., et al. Multiplexed G-protein-coupled receptor Ca<sup>2+</sup> flux assays for high-throughput screening. *J. Biomolecular Screening*. 2005;10:780–787. PubMed PMID: 16234348.
- New D.C., Wong Y. H. Characterization of CHO cells stably expressing a G $\alpha_{16/z}$  chimera for high throughput screening of GPCRs. *Assay and Drug Development Technologies*. 2004;2:269–280. PubMed PMID: 15285908.
- Reynen P. H., et al. Characterization of human recombinant  $\alpha_{2A}$ -adrenoreceptors expressed in Chinese hamster lung cells using Ca<sup>2+</sup> changes: evidence for cross-talk between recombinant  $\alpha_{2A}$ - and native  $\alpha_{1A}$ -adrenoreceptors. *British J. Pharmacology*. 2000;129:1339–1346.
- Robas N.M., Fidock M.D. Identification of orphan G protein-coupled receptor ligands using FLIPR assays. *Methods in Molecular Biology*. 2005;306:17–26. PubMed PMID: 15867462.
- Schroeder K. S., Neagle B. D. FLIPR: a new instrument for accurate, high throughput optical screening. *J. Biomolecular Screening*. 1996;1:75–80.
- Wolff C. Comparative study of membrane potential-sensitive fluorescent probes and their use in ion channel screening assays. *J. Biomolecular Screening*. 2003;8:533–543. PubMed PMID: 14567780.
- Zhang Y., et al. Evaluation of FLIPR Calcium 3 Assay Kit—a new no-wash fluorescence calcium indicator reagent. *J. Biomolecular Screening*. 2003;8:571–577. PubMed PMID: 14567785.

# Ion Channel Screening

Owen B McManus, Ph.D.,<sup>1,\*</sup> Maria L Garcia, Ph.D.,<sup>2</sup> David Weaver, Ph.D.,<sup>3</sup> Melanie Bryant, Ph.D.,<sup>4</sup> Steven Titus, Ph.D.,<sup>5</sup> and James B Herrington, Ph.D.<sup>6</sup>

Created: October 1, 2012.

## Abstract

Ion channels regulate a wide range of physiological processes including rapid electrical signaling, fluid, hormone and transmitter secretion, and proliferation. As such, ion channels are common targets for toxins and therapeutics. Ion channel screening assays have traditionally utilized indirect or low throughput approaches. Recent improvements in sensor technologies and instrumentation have provided fresh opportunities for ion channel screening that afford higher throughput, improved information content, and access to novel ion channel targets. Ion channels subtypes can display a variety of functional differences in gating and permeability mechanisms, which necessitates use of assay technologies that selected and adapted for a specific channel type. In order to successfully implement improved ion channel screening assays that provide pharmacologically relevant data, it is critical to carefully evaluate and control a variety of assay parameters. In this chapter, we provide an overview and assessment of some of the assay technologies commonly used in ion channel pharmacology and drug discovery efforts.

## 1. Introduction

Ion channels act as molecular transistors. Powered by ion concentration gradients, ion channels transduce a variety of signals into transmembrane ion fluxes. Ion channels have traditionally been classified according to the mechanisms that control opening-closing transitions (gating) and the types of ions that can pass through a channel (selectivity). These functional characteristics, along with control of expression and localization, determine the effector activities of each channel type. Classification of ion channels based on functional characteristics has been, in large part, supported by sequence analysis of cloned channels and by available structural studies.

---

<sup>1</sup> Johns Hopkins University; Email: Owne\_mcmanus@jhmi.edu. <sup>2</sup> Kanalis Consulting; Email: marialgarcia@gmail.com. <sup>3</sup> Vanderbilt University; Email: David.weaver@vanderbilt.edu. <sup>4</sup> University of Maryland; Email: Melbryant1@gmail.com. <sup>5</sup> GE Healthcare; Email: satitus@yahoo.com. <sup>6</sup> Genentech; Email: Herrington.james@gene.com.

✉ Corresponding author.

\* Editor

## 1.1. Gating and selectivity affect assay design

A variety of gating mechanisms are utilized in different channels to enable responses to a range of physiological stimuli including membrane potential, neurotransmitters, hormones, ions, metabolites, other proteins, temperature, lipids, pH, mechanical forces and other factors not yet identified. Multiple response capabilities may be combined such that, for instance, a single channel can gate in response to intracellular calcium and membrane potential. Some ion channels can respond rapidly to gating stimuli providing a basis for fast electrical signaling. When open, ion channels catalyze movement of (usually) charged ions across the hydrophobic barriers formed by membranes. Ion channels contain pore regions, which span the membrane, and provide a pathway for ions to traverse cell membranes following electrochemical gradients. The pore region structure provides a mechanism for distinguishing ions and thereby generating a selectivity profile for each channel type. A distinguishing characteristic of ion transport in a channel is a high flux rate, which can provide a net flux of millions of ions per second. This high transport rate can be achieved, for some channels, while also stringently selecting for a single ion type among others physiologically present.

An understanding of ion channel function is needed to effectively design and implement ion channel-specific assays. The two key issues that need to be addressed when setting up an ion channel assay are, how to control channel gating and how to measure channel activity. The mechanisms controlling channel gating and ion permeation can be best determined using electrophysiological methods, which allow rapid control of membrane potential and bath solution composition and also permit direct measurement of ion flux. For this reason, conventional voltage clamp methods are often used in early stages of ion channel drug discovery and assay development to characterize factors that control channel gating and to determine ion selectivity. This information can then be used to design assays in higher density formats that afford higher throughput at the expense of reduced flexibility, control and resolution.

Controlling channel gating can be a key challenge in designing plate-based, high density ion channel assays which often use a mix-and-read format and do not permit washout steps. Gating of ligand-gated channels with slow kinetics can be reliably triggered in this format by agonist addition, but other channel classes can require more complex approaches to trigger channel activation. For instance, voltage-gated channels respond to changes in membrane potential, which cannot be directly controlled in non-electrophysiological assays. A variety of approaches have been used to trigger voltage-gated channel opening in plate-based biochemical assays including electrical field stimulation, addition of potassium or channel modulators to the bath solution (see below) or optical triggering of membrane potential changes via co-expression of light-activated channels. A further complicating feature of assays for voltage-gated channels is that membrane potential controls channel gating, which, in turn, affects membrane potential. This feedback relationship leads to difficulties in achieving reliable channel activation in high density formats, which can be overcome by applying careful control of channel expression levels and assay parameters.

Three common measures of ion channel activity are widely used in ion channel assays. Measurements of ionic currents using voltage clamp electrophysiological methods provide a direct and linear reflection of ion channel fluxes and are still the most reliable indicators of ion channel activities. Development of automated electrophysiology instruments using planar arrays now provides a means to produce medium throughput data on thousands of compounds per day. A variety of instruments and approaches have been developed with specific advantages in either throughput or flexibility or resolution. Ion fluxes through channels affect membrane potential, which provides a second approach for following ion channel activity. Membrane potential can be measured reliably using electrophysiological methods, but few automated electrophysiology instruments provide this capability. Biochemical assays for membrane potential (see below) combining bright dye systems with fluorescent plate readers with kinetic capabilities have provided high-throughput approaches to ion channel targets that were previously inaccessible. Some limitations of this approach result from the nonlinear relation between ion channel activity and membrane potential and from sensitivity of membrane potential to alteration by a wide range of processes that are not related to the channel of interest. A more widely applied approach relies on measuring changes in ion concentration on one side of a membrane (usually the intracellular compartment) resulting from ion channel activity (see below). The ion concentrations can be measured directly using atomic absorption spectroscopy or labeled isotopes, or more commonly by using sensor molecules to detect ion concentration changes. Recent developments in chemical and genetic sensors have enabled high-throughput, robust assays for a new array of ion channels that were not previously accessible. Non-physiological ions that permeate a specific channel may be substituted for the physiological ion in some assays to provide enhanced signal-to-background ratios. For example, thallium readily permeates many potassium channels and can be detected with fluorescent probes that can be loaded into cells. This approach provides an effective surrogate for potassium flux, which would be more difficult to do by measuring potassium influx due to high background levels.

Ion channels present special challenges and opportunities for assay design. Many ion channels undergo conformational changes during gating that can provide a basis for pharmacological modulation of specific states. In some cases, a specific state may be associated with a disease condition or can present an opportunity for specific therapeutic modulation. In this way, a channel that is widely expressed may be preferentially modulated in a pathological tissue or condition. Assay formats that can control channel gating are required in order to identify compounds with functional selectivity targeting specific conditions. Recent developments in automated electrophysiology, biochemical sensors, and plate readers provide a range of options for implementing ion channel assays that can detect state-specific, or state-independent, channel modulation. Typically no single assay format can offer the ideal combination of high throughput, low cost and high information content. Ion channel drug discovery projects then typically employ a combination of assays including high throughput biochemical assays and lower throughput electrophysiological assays. A key consideration when establishing these assays is pharmacological validation of the assay such that the assay results provide a

direct and reliable measure of compound effects on the channel. Ideally, the assay results can then be used to predict compound effects in cells and tissues. For novel ion channel targets, pharmacological standards will likely not exist. An iterative approach can then be used to identify adequate pharmacological standards. An initial HTS assay format can be used in a pilot screen to identify a set of potential modulators. Mechanistic evaluation of this hit set using a different assay technology (usually electrophysiology) can be used to select appropriate pharmacological standards for further optimization of an HTS assay.

## 2. Fluorescence Assays Using Membrane Potential Sensing Dyes

### 2.1. Assay Overview

Ion channels represent a class of proteins with potential for therapeutic intervention. Human genetic studies have identified ion channel targets that are relevant for treating specific diseases with clearly unmet clinical needs. In addition, pharmacological validation exists for other ion channel targets related to medical conditions that are not well treated with current medications. The challenge for the ion channel field is to identify potent and selective ion channel modulators with appropriate features that will allow their evaluation in clinical trials. The significant improvement in technology over the last few years with automated electrophysiology instruments has provided additional platforms that can support ion channel drug development. However, none of these instruments can yet support screening of large chemical libraries (i.e. > 1 M compounds) that are typically required to identify new lead candidates for ion channel targets which lack viable probes or leads. In addition, the high cost of automated electrophysiology consumables necessitates a quest for, alternative technologies for measuring ion channel activities in high density formats. Although these technologies cannot substitute for electrophysiological evaluation of more advanced drug candidates, they can play an important role in lead identification and optimization.

Because ion channels permeate ions at a high rate when they open, the activity of these proteins can therefore cause changes in the membrane voltage. When properly tuned, the activity of ion channels expressed in mammalian cell systems can be indirectly monitored with the use of membrane potential sensing dyes that provide a fluorescence signal. These assays can operate in 96-, 384-, or 1536-well plate formats at a lower cost and higher throughput than the automated electrophysiological platforms currently available. However, for membrane potential-based assays to be useful, rigorous validation criteria must be implemented to ensure that the fluorescence signal provides a reliable measurement of channel activity. Fluorescence resonance energy transfer (FRET) with the use of a pair of dyes, a phospholipid-anchored coumarin and a hydrophobic oxanol that rapidly redistributes in the membrane according to the transmembrane field, can provide robust and reproducible signals when studying the activity of voltage-gated sodium, potassium and other channels. Indeed, the assay can be tuned to identify either activators or inhibitors of a given ion channel. The general concept when designing assays for inhibitors of potassium channels is illustrated below in Figure 1.



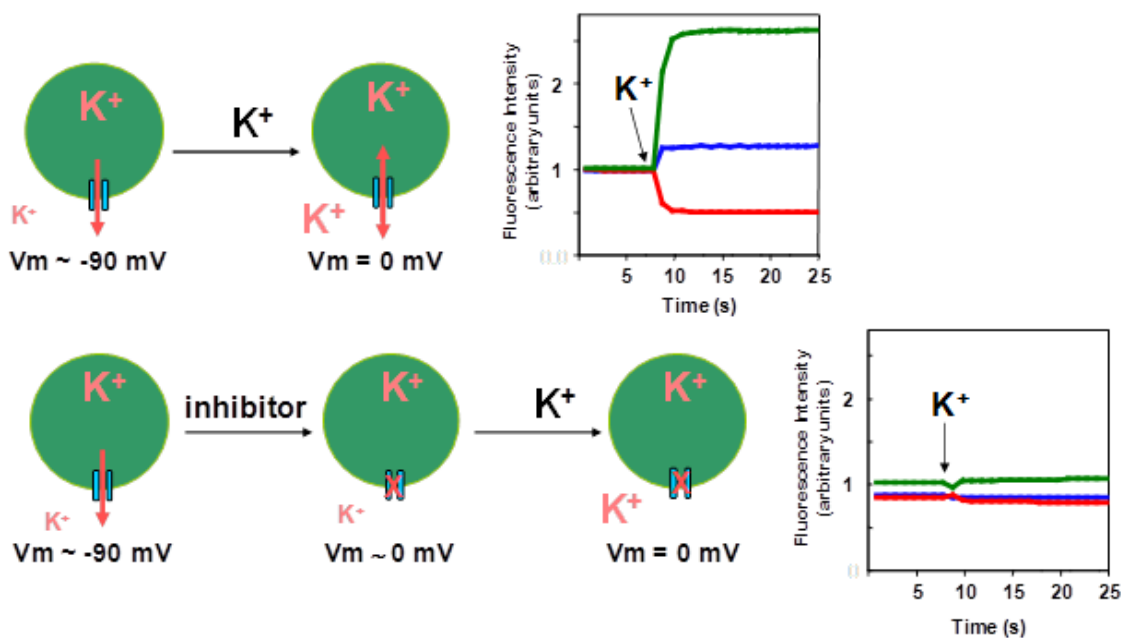


**Figure 1: Fluorescence-based Membrane Potential Assay Format for Detecting Potassium Channel Inhibitors.** Fluorescent dyes are used to measure cell depolarization following addition of high potassium concentration to the extracellular solution. A large depolarization and fluorescent signal occur in the absence of an inhibitor (top panels), while a reduced depolarization is seen after preincubation with an inhibitor.

Cell lines expressing the potassium channel of interest are constructed. In these cells, the stably expressed channel sets the resting potential at  $\sim -90$  mV. Under control conditions, addition of a high potassium solution will cause cell depolarization, and this change in voltage can be measured with the FRET dyes. In the illustrated example, the blue and red fluorescence signals represent the emission of N-(6-Chloro-7-hydroxycoumarin-3-carbonyl)-dimyristoylphosphatidylethanolamine (CC2-DMPE) and bis-(1,3-dithylthiobarbituric acid)trimethine oxonol (DiSBAC<sub>2</sub>(3)), respectively, whereas the green signal represents the ratio of CC2-DMPE to DiSBAC<sub>2</sub>(3). It can be seen that upon addition of high potassium solution (top panels of Figure 1), the emission intensity of DiSBAC<sub>2</sub>(3) decreases due to the movement of the dye to the inner leaf of the membrane. As a consequence, the emission of CC2-DMPE increases and a new fluorescence ratio is established. When cells are pre-incubated with a potassium channel inhibitor (bottom panels of Figure 1), cell depolarization will occur and further addition of the high potassium solution will not affect the FRET signal. Thus, a large assay signal can be established for identifying channel inhibitors. This assay design works well with both voltage- and non-voltage-gated potassium channels.

For identifying potassium channel activators the following assay concept can be used as shown in Figure 2.

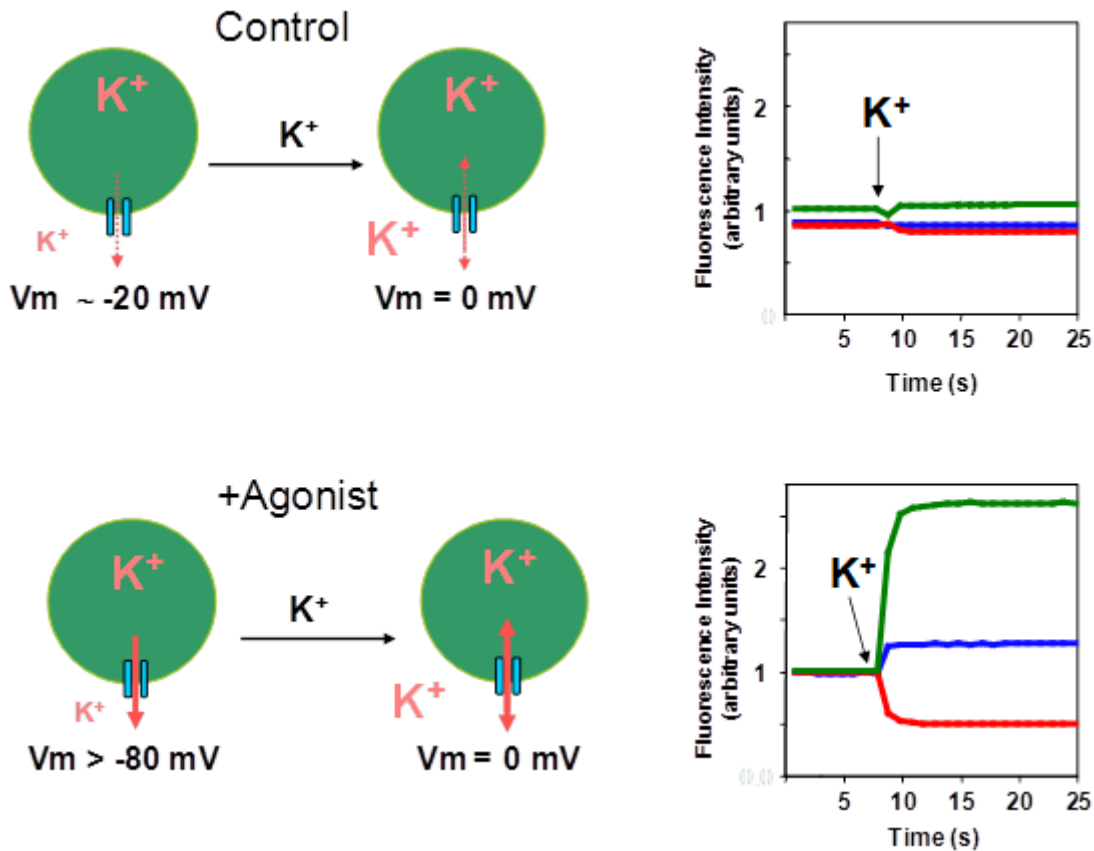


**Figure 2: Fluorescence-based Membrane Potential Assay Format for Detecting Potassium Channel Activators.** Fluorescent dyes are used to measure cell depolarization following addition of high potassium concentration to the extracellular solution. Potassium induces only a minimal change in membrane potential in control (top panels), while a large depolarization and fluorescent signal are seen after preincubation with an agonist.

Cell lines expressing the channel of interest are constructed. In these cells, the expressed potassium channel is not capable of setting the resting potential due to a combination of low expression levels and/or low open probability, and cell membrane potential is established near zero mV. However, in the presence of a channel activator (agonist) which increases channel open probability, the cell membrane potential will become hyperpolarized by shifting towards the potassium equilibrium potential. Upon addition of a high potassium solution, control cells will not display a change in the FRET signal, whereas a large change in FRET will be observed in those wells in which a channel activator is present. In the illustrated example, the blue and red fluorescence signals represent the emission of CC2-DMPE and DiSBAC<sub>2</sub>(3), respectively, whereas the green signal represents the ratio of CC2-DMPE to DiSBAC<sub>2</sub>(3).

An assay used for identification of inhibitors of voltage-gated sodium (Nav) channels can be implemented using the following scheme shown in Figure 3.

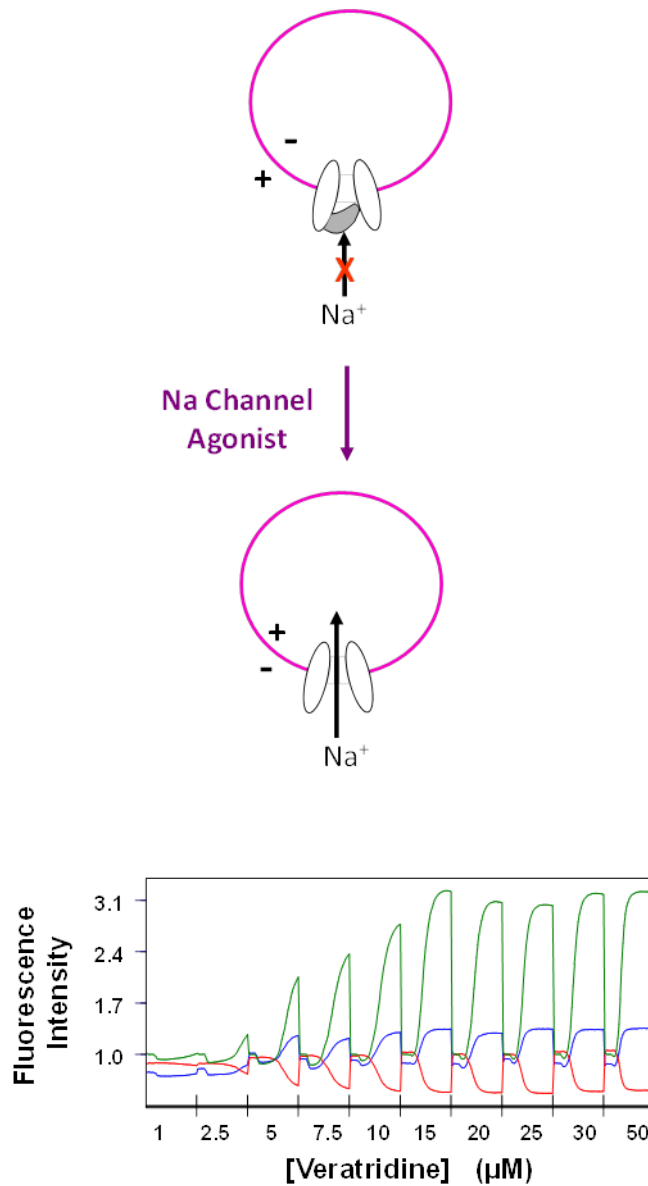


**Figure 3: Fluorescence-based Membrane Potential Assay Format for Detecting Voltage-gated Sodium Channel Inhibitors.** A sodium channel agonist (veratridine) is used to remove channel inactivation leading to sodium influx and cell depolarization measured with a fluorescent dye pair. Concentration-dependent depolarization by veratridine is shown at bottom right for 10 wells in a plate-based assay. A sodium channel inhibitor may reduce the depolarization caused by veratridine.

In mammalian cell lines, stably expressed Nav channels reside mostly in the non-conductive inactivated state due to the depolarized cell resting membrane potential (-20 to -50 mV), as sodium channels rapidly open then inactivate and remain closed in response to membrane depolarization. However, this conformation of the channel is thought to represent the high affinity state for interaction with some classes of inhibitors, and is also thought to be more prominent in some disease states. Exposure of the cells to a

Nav agonist, such as veratridine, removes inactivation and allows entry of sodium ions into the cells through open, unblocked channels, causing depolarization of cells towards the sodium equilibrium potential, with a consequent change in the FRET signal. In the illustrated example, the blue and red fluorescence signals represent the emission of CC2-DMPE and DiSBAC<sub>2</sub>(3), respectively, whereas the green signal represents the ratio of CC2-DMPE to DiSBAC<sub>2</sub>(3), and individual well responses to increasing concentrations of veratridine are shown. In the presence of a Nav inhibitor, the FRET signal will be unaltered after addition of the Nav agonist because the channel equilibrium would have been shifted toward the inactivated-drug bound state, which may not open until inhibitor dissociates. It is important to determine an optimal concentration of veratridine that affords a robust signal while not significantly affecting sensitivity to inhibitors. This assay format works well for several Nav1.X channels, although the actual agonist used to initiate sodium influx varies depending on the channel under study.

## 2.2. General Considerations

The assays described above can provide robust, reproducible signals and operate with high Z' factors in 96-, 384-, and 1536-well plates. Particular attention to cell culture conditions is critical for the success of the assay. Cells should be confluent, but not overgrown, for the assay to work properly. The operator needs to identify cell growth conditions and cell plating density that are appropriate for providing a good assay signal. The handling of the dyes is also important since these molecules are lipophilic in nature and sometimes are difficult to put into solution. Binding of these reagents to plastic surfaces has been observed and therefore it is better to use glass surfaces for preparation of the dyes' solutions.

## 2.3. Cell Lines

The assays described above can provide robust, reproducible signals and operate with high Z' factors in 96-, 384-, and 1536-well plates. Particular attention to cell culture conditions is critical for the success of the assay. Cells should be confluent, but not overgrown, for the assay to work properly. The operator needs to identify cell growth conditions and cell plating density that are appropriate for providing a good assay signal. The handling of the dyes is also important since these molecules are lipophilic in nature and sometimes are difficult to put into solution. Binding of these reagents to plastic surfaces has been observed and therefore it is better to use glass surfaces for preparation of the dyes' solutions.

## 2.4. Assay Parameters

During assay optimization, a key initial experiment is to evaluate a matrix of dye concentrations to identify those that are optimal for the particular cell line and assay under consideration. In addition to reproducibility and high Z' factors any assay needs to be further validated with the use of pharmacological channel modulators. Different structural classes and mechanisms of action agents should display effects that match the

properties observed in electrophysiological or other well-defined biochemical experiments. If not, changes in the assay parameters should be explored to achieve the most optimal conditions. For instance, for Nav channels, agonist concentration is critical to ensure a pharmacological readout that correlates well with electrophysiological values. When the agonist concentration is too high, a shift in the concentration-response curves of inhibitors to higher  $IC_{50}$  values will occur, and it may even significantly affect the response of certain structural classes of inhibitors in such a way that the assay becomes insensitive to the presence of these agents. A concentration-response curve to agonist, such as in the above illustrated example with veratridine, should be performed in a daily basis to identify the condition that provides a robust but not saturated signal. Because the concentration-response curves to agonist are quite steep it is not possible to guess the optimal agonist concentration for a given assay since other factors such as the particular state of the cells may influence the response. In general, a pre-incubation time of 30 minutes with test compound appears to be optimal. Longer incubation times than 45 minutes may start to compromise the fidelity of the assay most likely because of toxicity-related issues from the use of the dyes.

All assay plates should always contain appropriate controls. Plates that do not comply with a minimum  $Z'$  factor should be discarded. During lead optimization, concentration-response curves to standard channel modulators must be included to ensure that the pharmacological responses of novel compounds are meaningful. Particular attention must be paid to the wells positioned at the edges of the plate. If there are any issues with the assay signals from these edge wells, then the problem needs to be fixed or otherwise these wells should not be considered when calculating data. The use of several replicates per data point provides a higher accuracy when using a four parameter Hill equation to calculate  $IC_{50}$  or  $EC_{50}$  values.

## 2.5. Data Analysis

In the potassium channel assays, the FRET signal responses to the addition of a high potassium solution are a reflection of the membrane potential of the cells before this addition. Thus, in these assays, the plateau fluorescence ratio signal is used to calculate the  $IC_{50}$  or  $EC_{50}$  values for channel inhibitors or activators. In general, the plateau fluorescence ratio signal remains stable for a significant amount of time so there are no issues when using this approach. When assaying Nav channels, the situation is different. In this case, the change in membrane potential is triggered by the addition of the particular Nav activator. Ideally, one would want to measure the initial rate of signal change which should be related to the number of functional Nav channels. However, the slope of the FRET signal may not be strictly related to the number of modified functional channels and could be limited by the time response of the dyes and/or the instrument. For this reason, a 3 second time interval is identified in control wells where the signal starts approaching (~95%) plateau level. This same time interval is then used to determine the effect of test compounds.

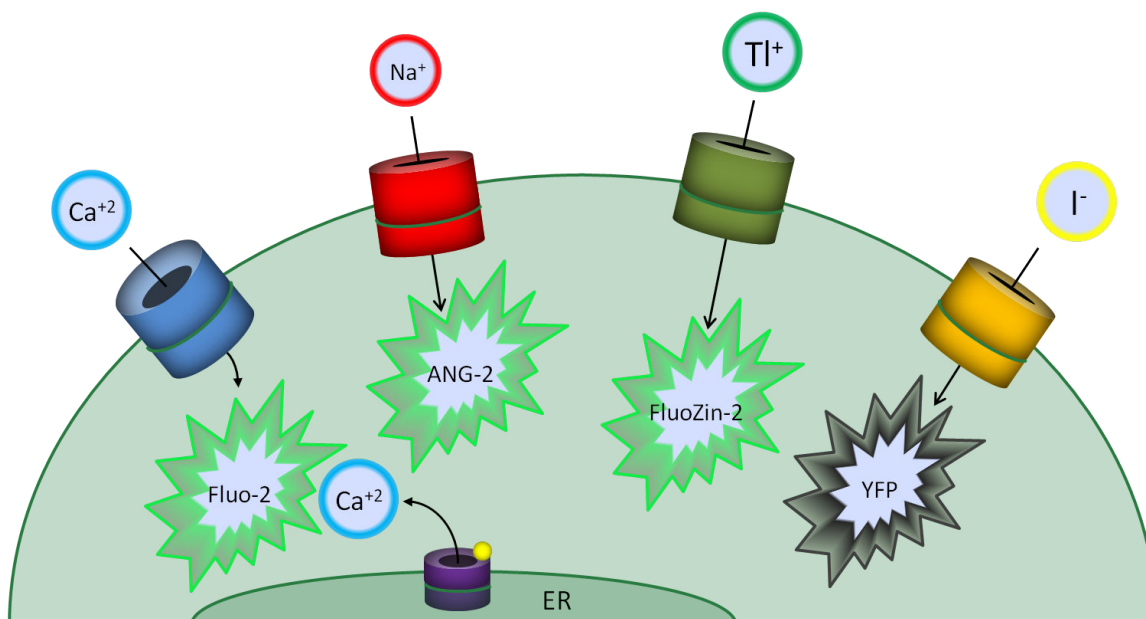


**Figure 4: Fluorescence-based Ion Flux Assay Formats.** Shown from left to right are examples of fluorescence-based ion flux assays. Plasma membrane calcium permeable channels (**BLUE**) and endoplasmic reticular (ER) calcium permeable channels (**PURPLE**) can be measured with a variety of fluorescent calcium indicator dyes like Fluo-2 and Fura-2 (not shown). Sodium permeable channels (**RED**) can be measured by sodium sensitive fluorescent dyes. Potassium channels (**GREEN**) can be assayed using a surrogate ion approach and the thallium sensitive dye, FluoZin-2. Unlike the other fluorescent dyes mentioned above, the mutant yellow fluorescent protein (YFP)-based sensor has its fluorescence effectively quenched by the surrogate ion, iodide, fluxing through a chloride channel (**YELLOW**).

All commonly used criteria to calculate statistically significant parameters from concentration-response curves of compounds should be applied to data calculation.

### 3. Ion Flux Assays

Ion channels are integral membrane proteins that conduct ions across cell membranes. Ion channels have preferences for different species of ions with some channels exhibiting a preference for cations while others prefer to pass anions. Within a given subfamily of ion channels (e.g. cation channels), some channels show preference for divalent cations versus monovalent cations, and some channels still show further specificity resulting in channels (e.g. voltage-gated sodium channels) with a high-degree of specificity for sodium over potassium, for instance.

When a concentration differential exists for an ion across a cell membrane and an open channel of appropriate specificity exists in that membrane, ions may pass through the channel down their electrochemical gradient resulting in ion flux. These ion fluxes have been used for decades as a means to measure the activity of ion channels. Early work in this area was primarily focused on radionuclide-based flux assays using ions like  $^{45}\text{Ca}^{2+}$  and  $^{22}\text{Na}^{+}$ . However, in the 1980's the development of ion-selective fluorescent dye-based

indicators revolutionized the measurement of ion flux. These indicators improved the ease of use, as well as spatial and temporal resolution of ion flux measurements. The 1980's and 1990's also witnessed the advent of genetically encoded ion flux indicators including the chemiluminescent calcium sensor, aequorin and a variety of engineered fluorescent proteins including the calcium-sensitive chameleons and anion-sensitive yellow fluorescent proteins (YFPs). More recently, the use of automated flame photometry-based ion flux assays has been proven effective as an alternative to fluorescent and radionuclide-based techniques for some ion channel assays (Figure 4).

Ion flux assays can be divided into two main categories: those that measure the flux of physiological ions (e.g. calcium, sodium, magnesium, zinc, and protons) and those that measure the flux of surrogate ions (e.g. thallium, cobalt, and iodide). For years fluorescent indicators were useful primarily for  $\text{Ca}^{2+}$  and other divalent cations while radionuclide-based approaches remained the best options for monovalent cation channels and anion channels. Recently, the new fluorescent sodium indicator, Asante Natrium Green (ANG) is showing promise as an intracellular sodium indicator. Other ions have proven more challenging; namely potassium and chloride. The discovery that the potassium congener, thallium, is capable of affecting the fluorescence of a variety of fluorescent dyes, most importantly FluoZin-2, has enabled the development of HTS-compatible assays for numerous potassium channels. Similarly, the use of surrogate anions (e.g. iodide) has allowed the development of HTS-compatible assays for chloride channels, particularly via engineered yellow fluorescent protein-based anion sensors.

In this article the main focus will be on fluorescent dye-based techniques because these are the most commonly used and most easily applied to HTS. However, many of the general principles of ion flux assay design may apply to other ion flux assay techniques. In addition, since ion channels are often effectors of signal transduction pathways, ion flux assays can be used as indirect measures of the activity of these pathways. The most common use of ion flux assays in this regard is the measurement of intracellular calcium flux mediated through the IP3 receptor downstream of  $G_q$ -couple seven transmembrane receptors (aka GPCRs).

### 3.1. General Considerations

Ion flux assays can have very broad utility for HTS. They are adaptable to a wide range of formats including 96, 384, and 1536 well plates. However, great care is required to establish appropriate cell culture and assay conditions in order to achieve highly reproducible assays capable of identifying and correctly categorizing different structural classes and modes of ion channel modulators. Special attention should be paid when non-physiological conditions are used to develop assays including but not limited to the use of surrogate ions, altered ionic gradients, compounds to promote dye retention (e.g. probenecid), and extracellular quench dyes used to establish homogenous "no-wash" assay conditions. While no-wash conditions are attractive from the point of view of speed and simplicity, some targets may be sensitive to quench dyes, while others may be affected

by the presence of signaling molecules in the assay medium which may necessitate the use of assay protocols that include wash steps.

In all cases, it is important to realize that changes in assay signals resulting from the addition of test compounds or other changes in assay conditions may not be due to a direct interaction with the ion channel but may instead be an indirect effect on some other component of the assay system. Thus, as part of an HTS screening tier, proper control experiments are necessary to establish which test compounds directly affect the ion channel target of interest, which are acting by indirectly modulating the target of interest, and which are affecting the assay signal through mechanisms unrelated to the target of interest.

### 3.2. Cell Lines

The best overall cell line for ion flux assay development will depend on the specific ion channel that is being assayed and the goals of the assay design (e.g. discovery of ion channel activators). In some cases, cell lines derived from a particular tissue of interest may be useful, particularly when the ion channel of interest is expressed in high abundance. However, it is still most common to use “reagent” cell lines as a background to over-express the ion channel target of interest. These cell lines are most commonly, but not limited to, HEK-293 and CHO cells.

In order to generate large, robust signals in flux assays, it is often advantageous to have a high level of channel expression. However, high levels of expression of some channels can be detrimental to cell health and thus may make the establishment of highly expressing stable cell lines difficult. In the event that high levels of expression pose problems for establishment for highly expressing stable cell lines, a number of strategies may be pursued. One approach is the use of inducible systems (e.g. tetracycline inducible systems). These systems use an inducible promoter to drive the expression of the ion channel of interest. Under these conditions, expression of the channel is tonically suppressed during normal propagation of the cells. On the day before/day of the assay, expression is induced to allow transient high levels of ion channel expression. Inducible systems are not perfectly controlled, however, and promoter “leakiness” can limit their utility in certain instances. In addition, care should be taken to make sure that the cell culture medium is free of the inducing agent (e.g. tetracycline). The use of certified tetracycline-free serum is recommended. In cases where inducible systems are ineffective or insufficient, ion channel inhibitors are sometimes a useful way to limit over-expression-related toxicity. In these cases, the cells are grown in the presence of the inhibitor up until just before the time of assay when the inhibitor is removed by washing. While effective in some cases, the additional manipulation required to remove inhibitors can be inconvenient in an HTS context. For some ion channels whose activity is regulated by cellular membrane potential, co-expression of a “helper” potassium channel, such as a tonically active inward rectifying potassium channel, may be useful to set the cellular membrane potential strongly negative values, as low as -90 mV, to promote a low activity state of the target. Finally, in cases where the target is completely refractory to generation



of a stable cell line, transient transfection may be pursued. While generally not as convenient as stably expressing cell lines, transiently transfected lines have proven a viable alternative to stable cell lines in some HTS assay settings.

### 3.3. Assay Parameters

There are a multitude of reagents and assay conditions to consider when developing an ion flux assay. These include plate format/density, cell number and confluence, level of channel expression, choice of indicator/assay technology, indicator concentration and loading parameters, method of activation of the ion channel, ionic composition of assay buffers, and wash versus no-wash formats. With so many variables to consider, a thorough knowledge of the ion channel target of interest, appropriate control compounds when available, an alternative reference method for measuring the ion channel's activity (e.g. electrophysiology), and a systematic approach using matrices of assay conditions are all important to the goal of establishing an assay that possesses a large signal, low background, good dynamic range, and the ability to properly detect, measure and classify ion channel modulators.

Particularly important to appropriate assay development is the selection of the best indicator, the best ionic composition, and the best mechanism of channel activation. It is important to choose indicators of the appropriate affinity and permeant ionic concentrations that are capable of producing robust signals without saturating the detector or the indicator. Conditions that result in saturation may result in left-shifted concentration response curves for channel activators and right-shifted concentration response curves for inhibitors. As a general guideline, indicator and ion concentration pairs should produce ~80% of the fully achievable signal magnitude for a given indicator/detector combination under conditions of maximal channel activation. Conditions that produce "square" wave signal profiles indicative of a saturated indicator or detector (Figure 5A) should be avoided. Also of great importance is the mechanism and degree to which a channel is activated. As shown in (Figure 5B), the concentration of extracellular potassium during test compound incubation can have a dramatic effects on the apparent potency of ion channel modulators and the amount of extracellular potassium added at the time of initiating a flux experiment with a surrogate ion can have a dramatic effect on the level of ion flux observed (Figure 5C). In these examples, potassium can affect compound potency indirectly via altering cell membrane potential or by direct interactions with the ion channel.

As described below in HTS Assay Considerations, many ion flux assays are amenable to no-wash formats. However, care must be taken to carefully validate the assays to ensure that the chosen format is most capable of detecting and correctly categorizing modulators of the target of interest. Excessive dye loading time, the use of organic ion transport inhibitors, and extracellular quench dyes should be avoided when convenient since all of these can adversely affect cell health and ion channel activity/pharmacology.

In some systems, particularly when the system shows ion flux that is rectified during the time course of the assay (e.g. calcium flux assays), multiple addition protocols can be a

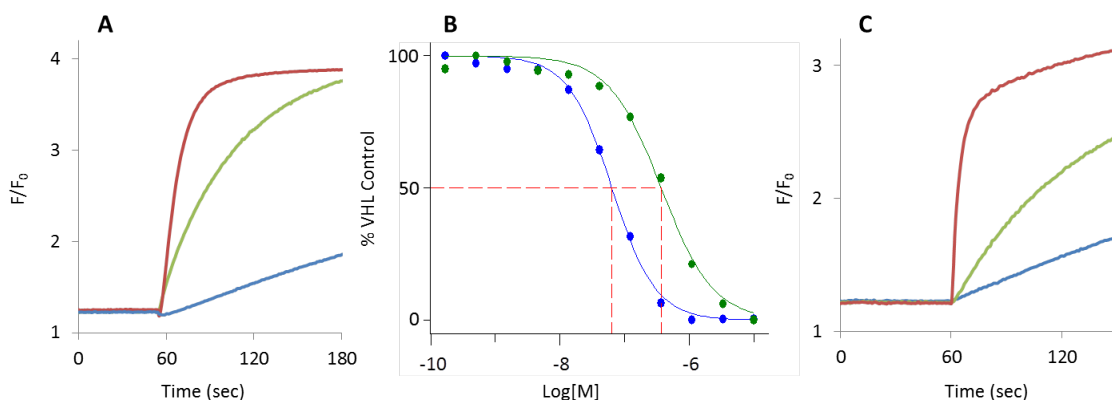


**Figure 5. Optimization of Ion Flux Assay Parameters** Shown in panel **A** are representative data demonstrating the effect of varying the concentration of permeant ion (Tl<sup>+</sup>) in a potassium channel assay. The **RED** trace is at a nearly saturating concentration of Tl<sup>+</sup> while the **GREEN** trace is a concentration producing a large, but not saturating response. The **BLUE** trace is from untransfected cells treated with the higher of the two Tl<sup>+</sup> concentrations. Panel **B** shows the effects of varying extracellular K<sup>+</sup> in the assay buffer on the potency of a voltage-gated potassium channel inhibitor. The **GREEN** curve corresponds to the compound pre-incubated in assay buffer containing 30 mM K<sup>+</sup> while the **BLUE** curve was obtained when the compound was pre-incubated in 60 mM K<sup>+</sup>-containing assay buffer. The difference in measured potency is >10-fold. Panel **C** shows the effects of varying the K<sup>+</sup> concentration in a Tl<sup>+</sup>-containing stimulus buffer when assaying a voltage-gated potassium channel. The **GREEN** trace was obtained by stimulating the cells with a Tl<sup>+</sup> containing stimulus buffer containing 5 mM K<sup>+</sup>. The **RED** trace was obtained with a stimulus buffer containing the same concentration of Tl<sup>+</sup> and 30 mM K<sup>+</sup>. The **BLUE** trace was obtained from untransfected cells with the 30 mM K<sup>+</sup> stimulus buffer.

useful way to measure more than one activity level of the system during the same experiment. The use of multiple addition protocols can be particularly beneficial for assays where there is a desire to detect positive and negative ion channel modulators. Figure 6 shows an example of a multiple addition protocol for a potassium channel using a fluorescent thallium indicator. The **GREEN** trace is representative of a vehicle control condition or the flux obtained in the presence of an inactive test compound. The **RED** and **BLUE** traces represent data that would be expected in the presence of an agonist and an inhibitor “hit”, respectively. By using a multiple addition protocol, conditions after the first addition favor the detection of activators while conditions after the second addition favor the detection of inhibitors.

Both the ability to resolve relevant levels of channel activity as judged by Z' and other HTS assay metrics, as well as the ability to measure potency and efficacy values for known classes of modulators for a target of interest are important for proper assay validation. Ideally, optimized assay conditions for ion flux assays will be calibrated against electrophysiological measures using a set of compounds that are known to be active on the ion channel target of interest and possess varying structures, potencies, and modes of efficacy. When applicable, comparison of ion flux assay performance to activity measured with control compounds in native preparations can lend further confidence that the assay conditions are able to detect and correctly classify modulators for the ion channel target of

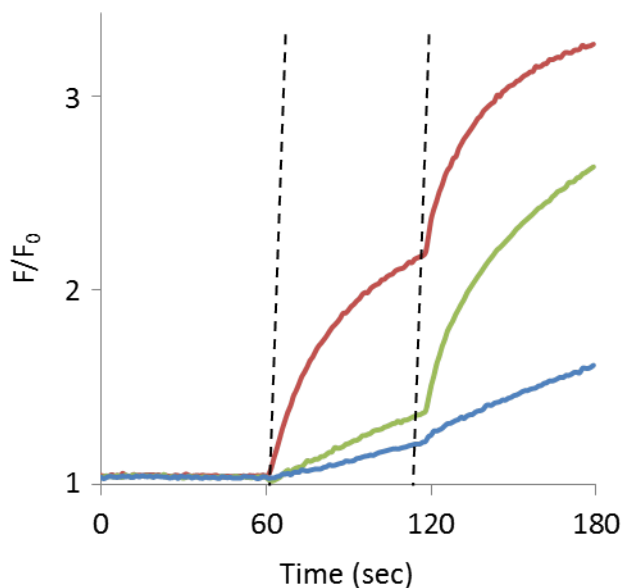


**Figure 6. Multiple Addition Assays.** Shown are data obtained using a multiple addition assay protocol for a ligand-gated potassium channel. The **BLUE** trace shows the flux in the presence of a channel inhibitor. The **GREEN** trace shows the flux resulting from first the addition of  $\sim EC_{50}$  concentration of agonist in thallium stimulus buffer followed by the addition of an  $\sim EC_{70}$  concentration of agonist. The **RED** trace shows the flux resulting from the addition of an agonist “hit” followed by an  $\sim EC_{70}$  concentration of agonist. The dotted lines, from left to right, mark the points of the first and second additions.

interest. As with other assay technologies, the inclusion of relevant control compounds and conditions throughout a screen are critical to monitoring assay performance and helping ensure the best data quality and the best ability to detect active compounds.

### 3.4. Data Analysis

A variety of analytical methods can be used for ion flux assays. The most appropriate analytical methods should be selected based on specific knowledge of assay system including limitations of the indicators, detectors, and properties of the ion channel target. Ideally, data obtained using a particular data analysis method should be compared to data obtained on an identical set of test compounds using another assay method (e.g. electrophysiology). Typical methods, depending on the in channel target, cellular background, and type of indicator used, are: amplitude, rate of change, area under the curve, and in regularly oscillating systems, frequency.

The most commonly used method is to measure signal amplitude relative to a relevant baseline at a specific time during an experimental protocol. In some cases, when data acquisition rates and indicator response time are appropriately fast, the rate of change in the initial assay signal can be an excellent way to obtain ion channel activity measurements. Finally, in assays systems where regularly spaced oscillations occur in ion fluxes, the frequency of peaks may also be a useful measure of the activity of the system.

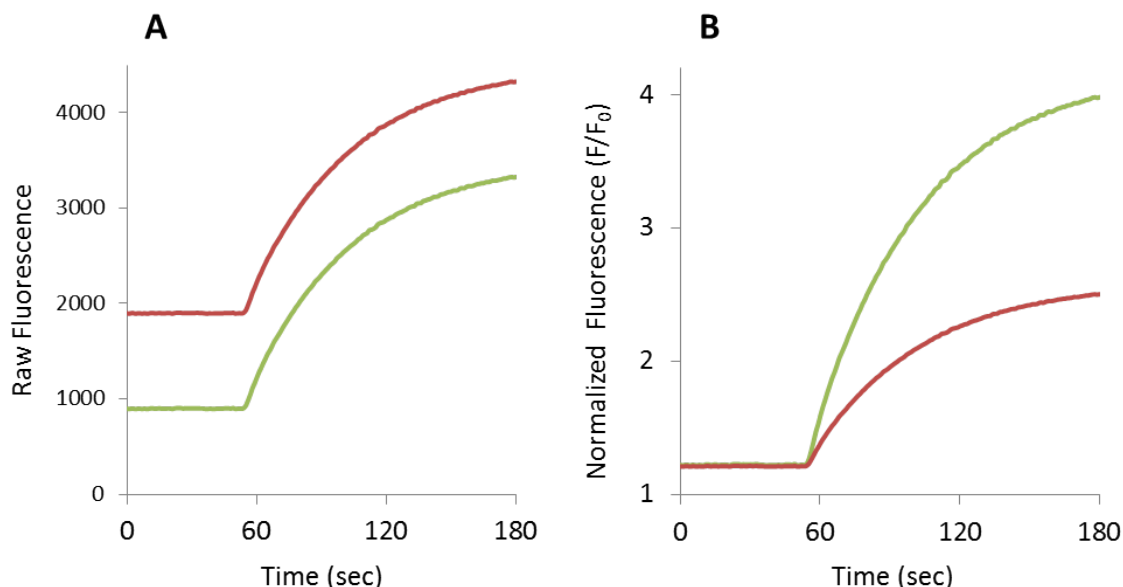


**Figure 7. Ratio Artifacts in Ion Flux Data** Shown in **A** are two waves obtained by testing a potassium channel with two compounds that are inactive at the channel. One compound is fluorescent (**RED** trace) and the other compound is non-fluorescent (**GREEN** trace). Both compounds were added before the assay was initiated and baseline values prior to compound addition were not obtained. When a commonly used data normalizing function  $F/F_0$  (aka static ratio) is performed as shown in **B**, the **RED** trace is mis-normalized and superficially appears to be an inhibitor.

In these cases, the coordinated activity of a variety of processes results in the measured properties in the assays, thus the assay may be susceptible to a great many modes of modulation many of which are not directly affecting a single specific ion channel target of interest.

In some instances, as part of the analytical process, it is valuable to subtract a relevant control waveform from a waveform that results from assaying a test compound. Subtraction of this control waveform may reveal subtle differences that may not be readily observed in raw the waveforms. Control wave subtraction may also provide a useful way to determine the time point where peak differences occur between two different assay conditions and thereby may help define the optimal time window from which to extract amplitude information (Figure 7).

When practical, it is useful to obtain measurements before and after the addition of unknown compounds in order to detect and take into account any optical properties of the test compound (e.g. fluorescence) that might affect the analysis or interpretation of the data. For instance, in the common practice of ratio normalization (e.g. division of all data points in a wave by the initial data point in the same wave,  $F/F_0$ ) is used when a fluorescent compound has been added before the first data point has been obtained, the resultant normalized values may be badly skewed resulting a false assessment of the compound's activity (Figure 7).

In all cases, standard protocols for determining well-to-well, and plate-to-plate variability can be used. Standard methods can also be used for obtaining fits and parameter estimates for concentration-response relationships.

## 4. HTS Assay Considerations

High-throughput screening is a leading method for identifying compounds for drug development, and ion channels are excellent targets for a wide range of health conditions. When optimizing cell based ion flux assays for use in HTS, there are many parameters to consider. Here we provide a list of several important assay parameters that can be examined to optimize signal to background ratio and Z-factors. We also include data and anecdotal evidence showing the effectiveness of manipulating these parameters in optimizing an HTS with a variety of cell lines.

### 4.1. Cell Growth and Harvesting

Most cell growth and harvesting parameters are specific to the cell line used for a particular assay, and are not changed when adapting an assay to high-throughput screening format. Nevertheless, changing the cell growth media, the growth temperature, the confluency at which you harvest cells, the passage number, and the method of harvesting (use of a non-proteolytic cell removal method such as versene versus trypsin) can have a significant effect on your signal. Many cell lines have been observed to stop expressing a reporter gene after reaching confluency. Additionally, some ion channels and GPCRs with large extracellular domains may be partially cleaved during incubation with trypsin, both of which can significantly affect signaling performance. Engineered cell lines can lose expression of the target of interest over time, so the use of low passage cells may be critical. In certain cases, a change in growth media or temperature the day before plating cells can favorably affect cells such that a higher signal is achieved (Figure 8).

### 4.2. Cell Plating

Altering conditions of cell plating can dramatically affect the signal in an HTS assay, and these parameters are typically the first to alter when optimizing an HTS assay. Parameters we have often changed include: plating media, cell density, incubation time, incubation temperature, plating volume, and the use of coated plates. The plating media and cell plating density will both be very dependent on the cell type used, although for 1536-well plates, 500-4000 cells per well is a good starting point. Certain cells types will yield a higher signal in low-serum media or after incubating at 32°C (Figure 9, left panel). The effect of temperature on efficient trafficking of ion channels to the plasma membrane has been described in multiple publication [1, 2]. Some cell types and receptors are less affected by low confluency, so more cells can yield higher signal amplitudes. In other cases, cells need to be very healthy and dividing to give a high signal, in which case a lower cell number, regular media, and regular growth temperature would be suggested. When using less adherent cells, consider the use of poly-D-lysine coated plates (Figure 9, right panel).

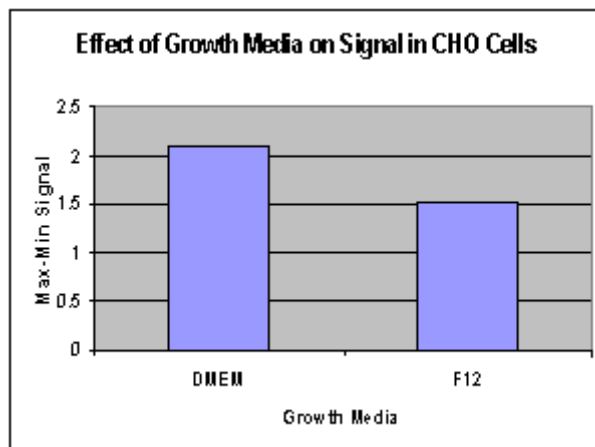


**Figure 8** CHO cells were grown in DMEM and F12 media for several days prior to plating and running. Both solutions were supplemented with 10% FBS, pen/strep, and NEAA.

### 4.3. Dyes

For cell based ion flux assays, the dyes employed play a large role in assay performance. Fluorescent dyes are compounds that emit a particular wavelength of light after excitation by another (usually shorter) wavelength of light. There are two main types of dyes used in ion flux assays: membrane potential dyes and ion binding dyes (see above). Membrane potential dyes, such as DiBAC<sub>4</sub>, respond to changes in membrane potential via redistribution within the cell membrane. This redistribution of the dye results in detectable changes in fluorescence. Ion binding dyes, in contrast, are dyes that fluoresce upon binding particular ions, such as calcium. Fluo8, from AAT Bioquest, is an example of one such calcium binding dye. Many ion binding dyes contain aminomethyl (AM) ester groups; these compounds are uncharged and membrane permeable. Once in the cytosol, the AM ester groups are cleaved by intracellular esterases, resulting in charged species that are not membrane permeable, and stay trapped inside the cell. AM ester dyes are particularly useful in ion flux assays since they help prevent background fluorescence and allow detection of changes primarily within the cell. In optimizing ion flux assays, multiple dyes can be tested and their concentration changed. A typical final concentration range of dye is 10  $\mu\text{M}$  to 100  $\mu\text{M}$ . Increasing concentration of dye can increase the signal window up to a point; however, upon reaching the upper detection limit of the instrument, any increase in dye after that point will increase the background signal and result in a lower signal window.

### 4.4. Quenchers

Fluorescent quenching agents are cell impermeable compounds that absorb fluorescence in a particular range of wavelengths [3]. Quenchers are often used in cell based ion flux assays to eliminate background fluorescence originating outside the cell membrane, thus providing a higher signal window. This is generally only necessary in no-wash assay

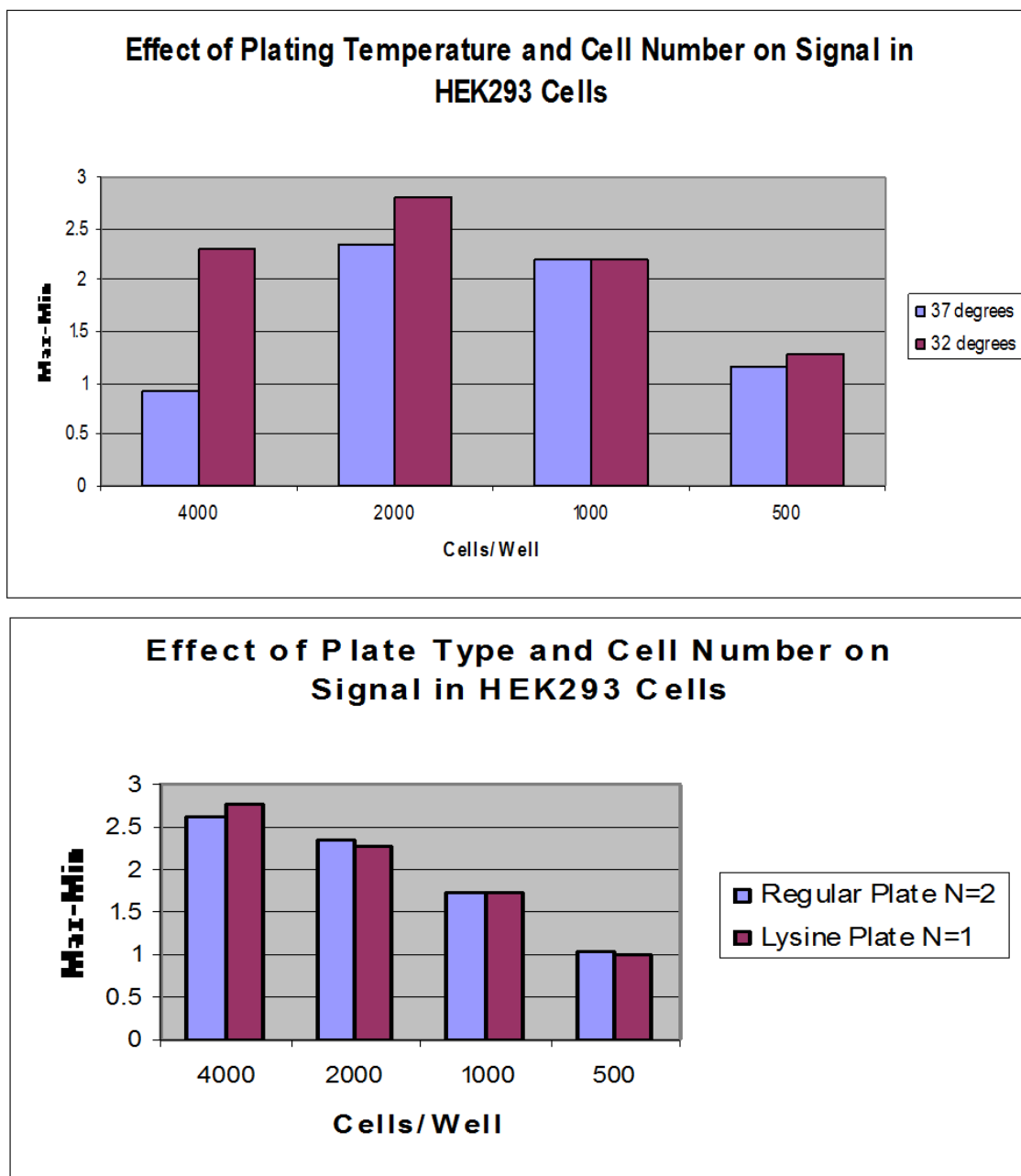


**Figure 9** Left- Effects of seeding density and outgrowth temperature on signaling in a HEK293 cell line. Cells were plated at various densities at either 32°C or 37°C overnight. Right- Effects of seeding density and plate coating. HEK293 cells were plated in either regular or poly-d-lysine coated plates at various cell densities. HEK293 cells were stimulated with a ligand causing internal calcium release.

protocols, as the wash steps are typically designed to rinse any extracellular dye out of the media. In high density format plates such as 384- and 1536-well plate assays, however, wash steps can be challenging to implement in an automated fashion and can also introduce well-to-well variations and sometimes remove less adherent cells. Therefore no-

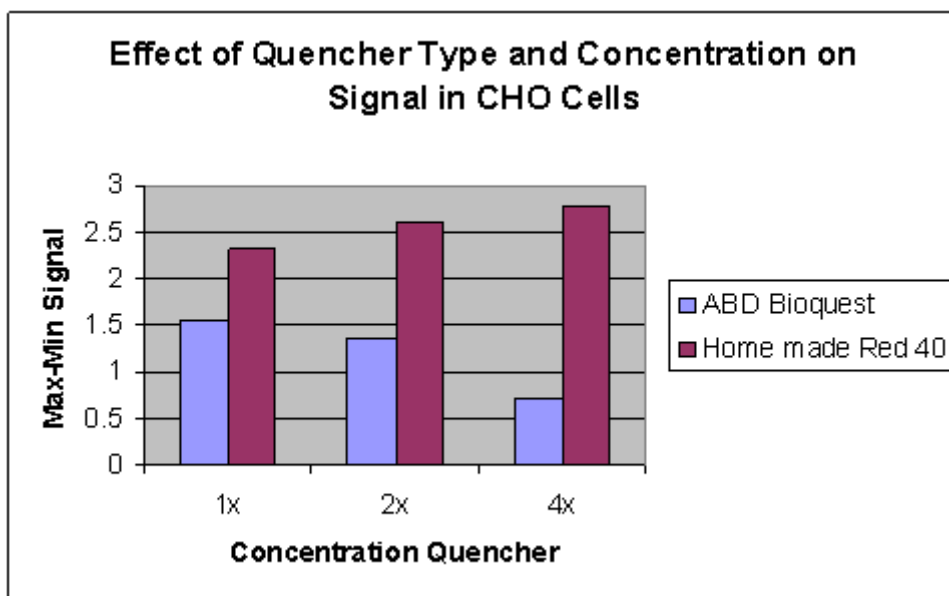


**Figure 10** CHO cells were tested with three different concentrations of two different quenchers. The signal window after stimulation of calcium release is shown.

wash assays are often preferable in high density automated HTS formats. In this case, the use of quenchers can significantly improve the signal by reducing background fluorescence, although effects of quenchers on assay pharmacology should be monitored.

There are several different types of quenchers available, both from vendors and home-made. In certain intracellular calcium assays, home-made quenchers, such as Red 40 in HBSS buffer, can equal or surpass performance of commercially available quenchers. This is an important assay parameter to test when optimizing an ion flux assay. Additionally, the optimal concentration of quencher should be evaluated, since it can dramatically affect the signal window. A typical final concentration range of quencher is 10  $\mu\text{M}$  to 100  $\mu\text{M}$  (Figure 10).

#### 4.5. Other Factors

There are several other parameters relating to dyes and quenchers that require optimization in HTS ion flux assays. These parameters include incubation time, incubation temperature, and the use of probenecid in the media. Since many dyes are toxic to cells, incubation time should be kept to a minimum while allowing adequate absorption time. The temperature at which cells are incubated with dye is specific to the dye and will be indicated in the manufacturer's instructions, however this may be altered to increase signal amplitude. In some cases, incubating at 30°C or 37°C can increase (or decrease) the signal amplitude compared with room temperature incubation, depending on the assay. Probenecid is a pan multidrug resistance-associated protein (MDR) blocker and an inhibitor of organic anion transport. Although toxic to cells at high



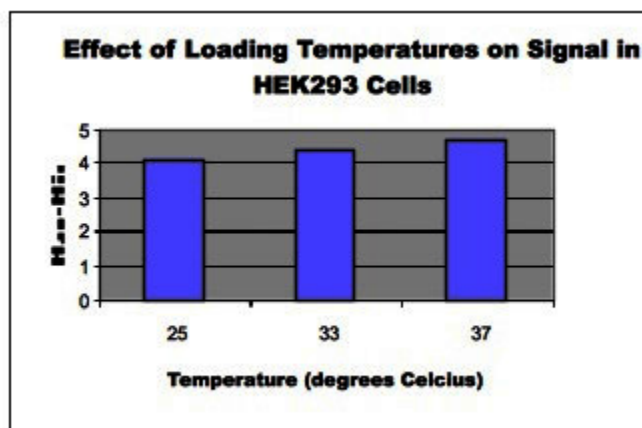


**Figure 11** HEK cells were tested after loading dye at room temperature, 33°C, and 37°C.

concentrations, it can be added to dyes in low concentrations to increase signal by preventing the active removal of dye from the cytosol. We have found a final concentration of 1mM to 10mM effective in various assays in increasing the signal window (Figure 11).

The parameters suggested in this section are all good starting places for optimizing an ion channel assay for use in an HTS format, however there are other ways to increase signal amplitude and robustness. Changes in instrument settings, such as increasing or decreasing sensitivity, adjusting pinning or pipetting settings, altering times of incubation, temperature of reading, and other factors can have substantial impact on signal robustness and assay performance. Identifying the best parameters from the list above will likely improve signal to basal ratio and Z-scores to prepare an assay for HTS.

## 5. Preparation of Cells for Automated Electrophysiology

### 5.1. Overview

The introduction of automated electrophysiological instruments has made possible the screening of large compound sets on ion channels [4]. Numerous platforms are now commercially available with varied features and potential throughputs. These systems generally employ a planar recording site where a cell suspension is added, then suction is applied to form a seal between the cell(s) and the substrate. Patch clamp whole-cell recording in either the dialyzed or perforated patch recording configuration is achieved and automated fluidics is employed to apply compound(s) to the cells.

Despite the significant advancement in throughput these systems offer relative to manual electrophysiology, a key factor in assay performance is cell preparation. A prerequisite for the creation of a robust automated electrophysiology assay is a method to reproducibly obtain suspensions of healthy, single cells. Given that there is no user-based selection of which cells to record from, as in manual electrophysiology, the need for high viability cell

preparations with minimal cell debris is even more important for automated electrophysiology.

This section will describe approaches for obtaining healthy, high density cell suspensions for automated electrophysiology. Since most researchers express ion channels in either Chinese Hamster Ovary (CHO) or Human Embryonic Kidney (HEK) cells, protocols for each will be given.

## 5.2. Cell line development

Prior to the creation of a cell line for automated electrophysiology, it is advisable to consider if the host cell line performs well on the instrument regarding electrophysiological parameters (seal quality, duration of recordings, etc.). A cell line that performs on one instrument platform may not be optimum on another platform. Ideally, the instrument to be used for the electrophysiology assay is also used to evaluate clones for functional expression [5]. Most devices now have the capability of recording from multiple cell stocks in a single assay, thus allowing the direct comparison of several clones in a single experiment. In this way, clones can be ranked not only for expression but also for performance on the instrument.

## 5.3. General Detachment Considerations

Detachment of most adherent cell lines from a culture flask to yield suspensions of predominantly single cells usually requires protease treatment. In general, enzyme treatment should be minimized to achieve this aim as cells that have been excessively treated with enzymes tend to be fragile and yield unstable recordings. If over-digestion is suspected, the enzyme solution can be diluted and/or the incubation time shortened. Cell viability following detachment should be very high (>95% as measured by trypan blue exclusion).

One of the major obstacles in obtaining cell suspensions that perform well on automated electrophysiology platforms is cell clumping. Since most recording systems require a high cell density in the final suspension (at least 1 million cells/ml), cell clumping can be significant. If clumping is due to the death of cells, DNase can be added to the enzyme solution to minimize cells sticking to the free DNA in solution. Another approach is to remove the cell clumps by passing the cell suspension through a small (40-100  $\mu$ M) nylon mesh filter (BD Biosciences). Keeping the cell suspension in serum-free media prior to use minimizes the formation of cell clumps.

All dissociation protocols require some degree of manual trituration of the cell suspension. As a general rule, trituration should always be gentle with a large bore Pasteur pipette (5 or 10 ml). Introduction of bubbles and frothing should be avoided. Only a few trituration steps should be needed to resuspend a cell pellet. If more are needed, this is an indication that enzyme treatment should be increased.

## 5.4. CHO cells

### 5.4.1. Example CHO Protocol

CHO cells are often the host cell line of choice for automated electrophysiology since they divide rapidly and have modest endogenous channel expression. Obtaining suspensions of single CHO cells is usually straightforward. As a general rule, CHO cells perform best when they are detached with a non-trypsin based enzyme treatment such as Detachin™ (Genlantis) or Accutase (Innovative Cell Technologies). Success has also been achieved with non-enzyme dissociation buffers containing EDTA (e.g. Versene).

Protocol:

1. Culture cells to 50-90% confluence in flasks. Typically, a confluent T150 flask can yield up to 40 million cells.
2. Rinse cells 1-2 times with Phosphate-Buffered Saline (PBS) without added calcium and magnesium.
3. Add Detachin™ (4 ml for T150 flask) and incubate for 5-15 minutes at 37°C until detached.
4. Once detached, add serum-free media (such as CHO SFM II; Invitrogen) supplemented with 25 mM HEPES, gently triturate the cells, and count the cell suspension and estimate viability. Viability should be very high (>98%) and the suspension should be mostly single cells. Centrifuge the cell suspension at 800 x g for 3 minutes.
5. Resuspend the cells at the appropriate cell density and place on a room temperature rotator (or the on-board cell handling station, if present on the instrument).
6. Allow the cells to recover for approximately 30 minutes prior to use. Cell suspensions can be kept for up to 4 hours in serum free media and aliquots taken for use.

### 5.4.2. Example data from CHO cell line

CHO cells were grown in F-12 media in a T-150 flask (Figure 12). Confluence was monitored with an imaging system located inside a standard tissue-culture incubator (IncuCyte™, Essen Bioscience). At near confluency (98%, Figure 12), cells were detached with Detachin™ using the standard protocol. The cell suspension was analyzed for viability (98.9%), average cell diameter (13.4 microns, Figure 13), and average circularity (0.91) with an automated cell viability analyzer (Vi-CELL™, Beckman Coulter). Example images of the cell suspension are shown in Figure 14.

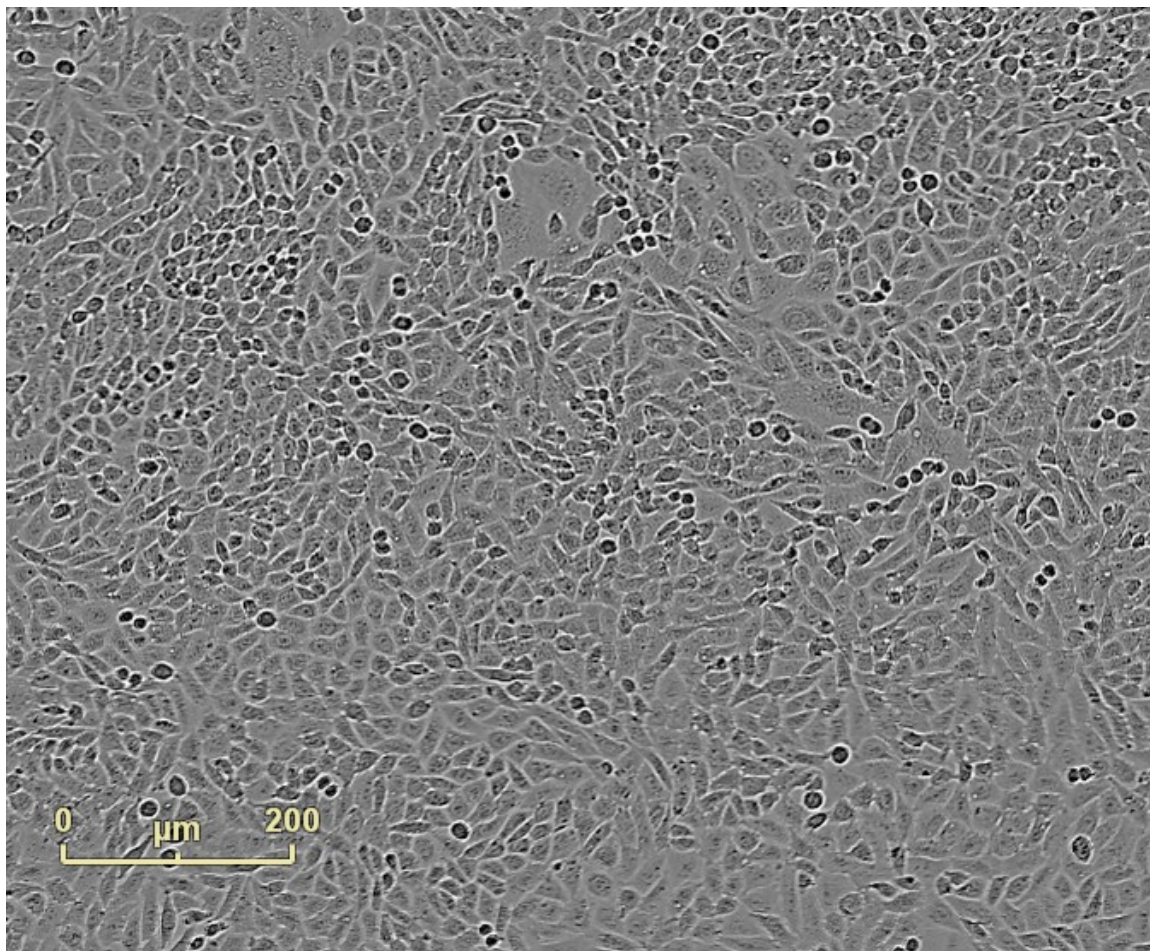


**Figure 12:** CHO cells grown to near confluency in a T-150 flask.

## 5.5. HEK Cells

### 5.5.1. Example HEK Protocol

HEK cells typically perform better on automated electrophysiology platforms when a trypsin-based enzyme solution is used. Some HEK cell lines have the tendency to form clumps which will require special precautions.

Protocol:

1. Culture cells to 50-90% confluency in flasks. If clumping is a problem, harvest the cells at lower density (may require pooling cells from more than one flask).
2. Rinse cells 1x with Phosphate-Buffered Saline (PBS) without added calcium and magnesium. Some HEK lines detach quite easily especially at higher confluency, so this step needs to be done quickly.
3. Add 1x (0.05%) trypsin-EDTA solution (4 mL for a T150 flask) and incubate at 37°C for the minimum time required for cell detachment (usually <3 minutes).

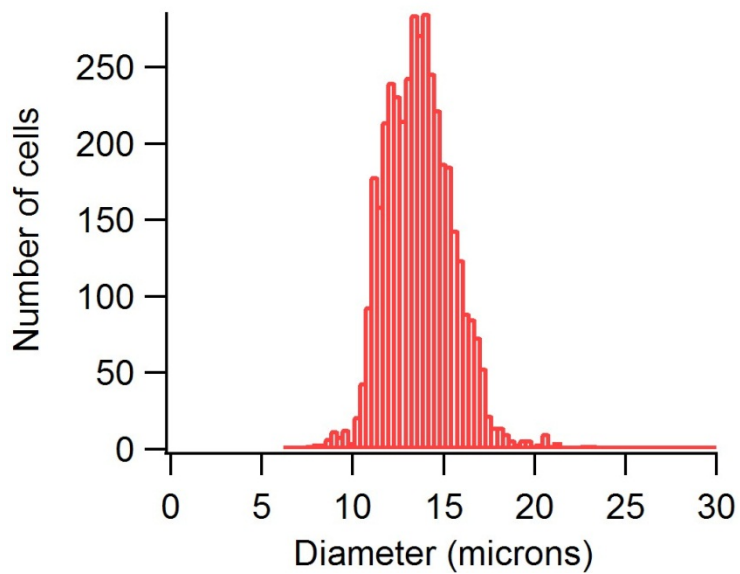


**Figure 13:** Diameter of CHO cells in suspension

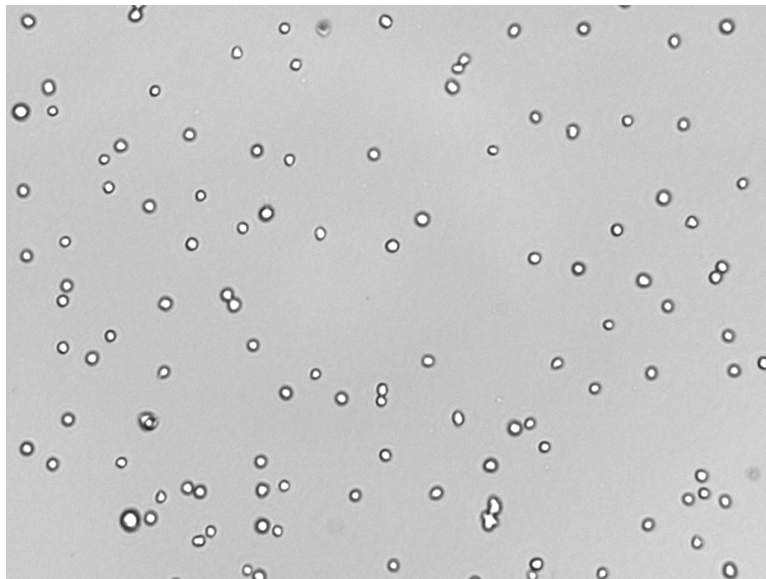


**Figure 14:** Image of CHO cells in suspension following detachment

4. Add growth media, gently triturate the cells, count the cell suspension, estimate viability, and spin the suspension at 800 x g for 3 minutes. Viability should be very high (>95%) and the suspension should be mostly single cells. If clumping is an issue, quench the enzyme with serum-free media containing soybean trypsin inhibitor.

5. Resuspend the cells at the appropriate cell density in serum-free media (with 25 mM HEPES added) and place on a room temperature rotator (or the on-board cell handling station, if present).
6. Allow the cells to recover for approximately 30 minutes prior to use. Cell suspensions can be kept for up to 4 hours in serum free media.

### 5.5.2. Example Data from HEK cell line

HEK cells were grown in high glucose DMEM media in a T-150 flask. At approximately 90% confluency, cells were treated with 1x trypsin using the standard protocol. The cell suspension was analyzed for viability (98.8%), average cell diameter (17.0 microns), and average circularity (0.62) with an automated cell viability analyzer (Vi-CELL™, Beckman Coulter). Example images of the cell suspension are shown in Figure 15.

## 5.6. Growing cells in suspension

Use of non-adherent (or weakly adherent) cell lines alleviates much of the difficulty associated with obtaining high quality cell suspensions. For example, RBL-1 is a basophilic leukemia cell line that grows in suspension that can easily be prepared for automated electrophysiology with a simple centrifugation and wash with recording saline. This line expresses an endogenous inwardly rectifying potassium channel and is quite useful for checking the performance of the recording instrument (including speed of fluid exchange) [6].

In cases where preparing a quality suspension of adherent cells is very difficult, an option to consider is converting an adherent cell line to a suspension culture. This is a time-consuming process that involves gradually reducing the amount of serum in the culture media. However, a prerequisite for this approach is that the existing adherent cell line demonstrates stable channel expression over many passages.

## 5.7. Use of acutely thawed cells

Another approach to obtaining consistent cell suspensions is to freeze ready-to-use vials of cells in liquid nitrogen. In one variation, a single vial containing up to 12 million cells per ml is rapidly thawed and resuspended in serum free media. After a period of at least 30 minutes of recovery, the cell suspension is washed with recording solution and used for recording. In general, such an approach yields lower quality recordings than the standard protocol. This approach has the advantage of allowing quick counterscreening on various channels without the need of keeping the cell line in culture regularly. In another variation, a vial of cell is thawed and cultured for 1-2 days prior to use. This approach gives the cells more time for recovery from the thaw while maintaining the advantage of using cells regularly at a particular passage. Since cells grown on culture for only 1-2 days are less likely to clump upon harvesting, this approach can also be useful for cell lines where single cell suspensions are difficult to obtain.

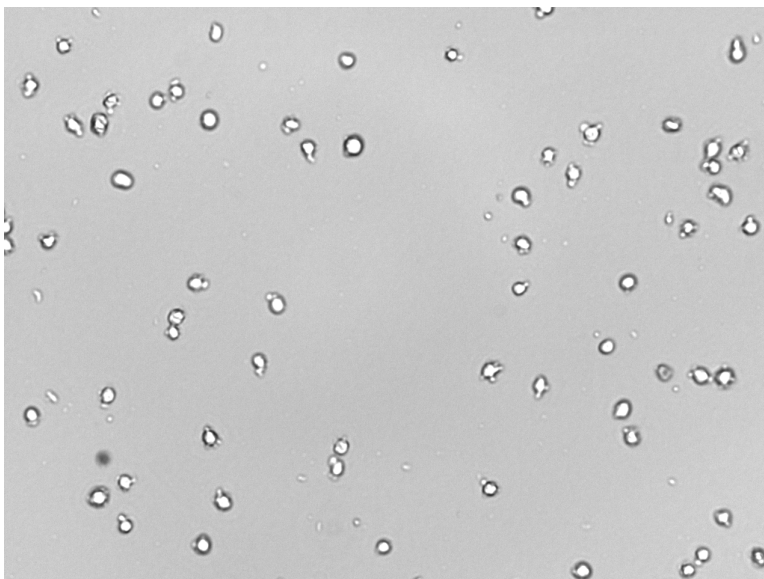


**Figure 15:** Image of HEK cells in suspension following detachment

## 5.8. Reduced temperature culture

In cases where limited channel expression is an issue, one approach that has been used successfully is to culture the cells at reduced temperature (27-30°C) for up to 3 days prior to use [2]. The lower temperature culture presumably results in a greater number of channels at the plasma membrane due to reduced channel turnover. Typically, such an approach does not impact how the cells are prepared for automated electrophysiology. Growth at the reduced temperature is severely slowed such that the cell plating density will need to be increased to achieve suitable cell numbers for the assay. As a general rule, one can expect to harvest the same number of cells that are plated following a 2 day culture at 30°C. Cultures can also be transferred to the lower temperature once they reach the desired confluency.

## 5.9. Transient expression of channels

In general, transient expression of channels using lipid-based methods is not compatible with automated electrophysiology. Membrane integrity is likely compromised by the lipid-DNA micelle to such an extent that high resistance, stable recordings are unlikely across the entire cell population. Furthermore, non-transfected cells give rise to recordings without functional channels (or reduced total current amplitude in the case of population recordings). Since such approaches are also fraught with high variability of transfection efficiency across experiments, this approach is generally not recommended.

There are now other technologies available that may be better suited for transient expression of channels for automated electrophysiology. For example, flow electroporation of cells has been used to transiently express ion channels for automated

electrophysiology (MaxCyte, Inc.). Baculovirus-mediated expression of ion channels has been successfully used to express ion channels [7] and several channel expression kits are commercially available based on this technology [8] (Invitrogen). Both electroporation and baculovirus approaches are suitable for expression of large number cell numbers coupled with freezing in liquid nitrogen and single-use thawing.

## References

1. Anderson C.L., et al. Most LQT2 mutations reduce Kv11.1 (hERG) current by a class 2 (trafficking-deficient) mechanism. *Circulation*. 2006;113(3):365–73. PubMed PMID: 16432067.
2. Chen M.X., et al. Improved functional expression of recombinant human ether-a-go-go (hERG) K<sup>+</sup> channels by cultivation at reduced temperature. *BMC Biotechnol*. 2007;7:93. PubMed PMID: 18096051.
3. Titus S.A., et al. A new homogeneous high-throughput screening assay for profiling compound activity on the human ether-a-go-go-related gene channel. *Anal Biochem*. 2009;394(1):30–8. PubMed PMID: 19583963.
4. Dunlop J., et al. High-throughput electrophysiology: an emerging paradigm for ion-channel screening and physiology. *Nat Rev Drug Discov*. 2008;7(4):358–68. PubMed PMID: 18356919.
5. Clare J.J., et al. Use of planar array electrophysiology for the development of robust ion channel cell lines. *Comb Chem High Throughput Screen*. 2009;12(1):96–106. PubMed PMID: 19149495.
6. Bruggemann A., et al. High quality ion channel analysis on a chip with the NPC technology. *Assay Drug Dev Technol*. 2003;1(5):665–73. PubMed PMID: 15090239.
7. Pfohl J.L., et al. Titration of KATP channel expression in mammalian cells utilizing recombinant baculovirus transduction. *Receptors Channels*. 2002;8(2):99–111. PubMed PMID: 12448791.
8. Beacham D.W., et al. Cell-based potassium ion channel screening using the FluxOR assay. *J Biomol Screen*. 2010;15(4):441–6. PubMed PMID: 20208034.



# Automated Electrophysiology Assays

Birgit T. Priest,<sup>✉1</sup> Rok Cerne,<sup>1</sup> Michael J. Krambis,<sup>1</sup> William A. Schmalhofer,<sup>1</sup> Mark Wakulchik,<sup>1</sup> Benjamin Wilenkin,<sup>1</sup> and Kevin D. Burris<sup>1</sup>

Created: March 9, 2017.

## Introduction

Technological breakthroughs in electrophysiological techniques, such as development of voltage-clamp and patch clamp, have enabled direct measurements of membrane currents in single cells. The low throughput of traditional electrophysiology, however has limited its use in the drug discovery process. High-throughput, non-electrophysiology based primary assays were used successfully but lack key information content, such as voltage dependence and kinetics, and may not be suitable for all ion channels. Most importantly, non-electrophysiological assays lack the ability to accurately control membrane potential, preventing the selective targeting of disease relevant conformational states of voltage-gated channels. For these reasons, substantial efforts were devoted to the development of instruments capable of automated electrophysiological recording at moderate- to high-throughput.

Early on, a number of different approaches were investigated (1). The field quickly settled on planar substrates, and in 2002 two automated electrophysiology instruments came on the market: [PatchXpress<sup>®</sup>](#) and [IonWorks<sup>™</sup> HT](#) developed at Axon Instruments and Essen BioSciences, respectively, and later sold to Molecular Devices. Several other manufacturers launched their automated instruments in subsequent years; most notably [Sophion \(QPatch\)](#), [Nanion \(Patchliner<sup>®</sup>\)](#) and [Fluxion \(IonFlux\)](#). Based on learnings obtained with first generation devices, a new set of second generation instruments was developed in more recent years.

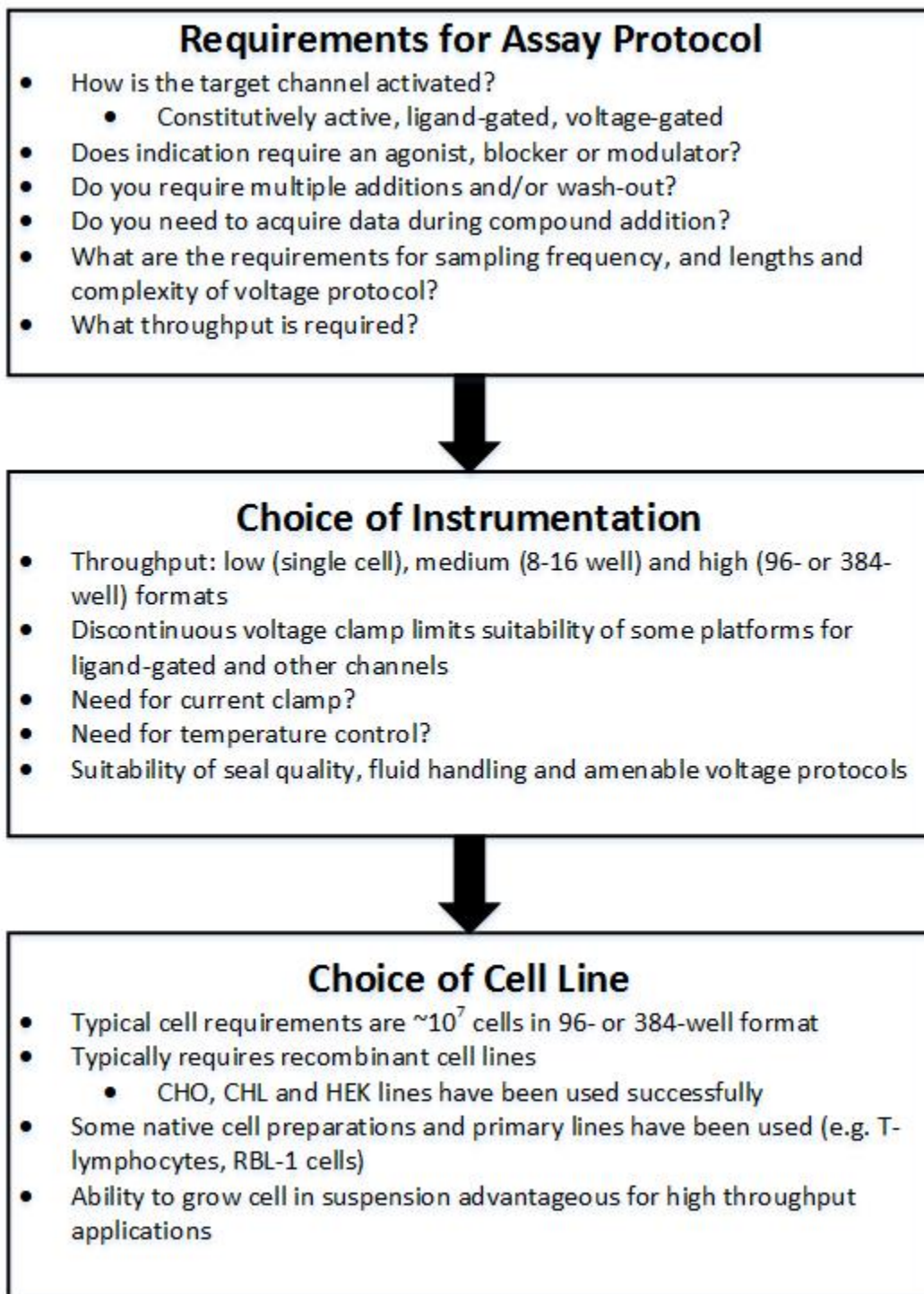
Instruments differ substantially in the composition of the patch plate, the configuration of the electrodes, liquid handling methods, and the software used to control the experiment and analyze data, and these features are discussed in greater detail below. Each platform has its strengths and weaknesses, and consideration should be given to the intended purpose before a device is purchased.

---

<sup>1</sup> Eli Lilly & Co, 355 East Merrill Street, Indianapolis, IN 46225; Email: priest\_birgit\_t@lilly.com.

<sup>✉</sup> Corresponding author.

## Flowchart



## Choice of Instrumentation

Several excellent reviews of automated electrophysiology have been published (2-5) and may be consulted for a more detailed description of the available technologies. A general overview follows below.

Manual electrophysiology is enabled by the formation of a high resistance electrical seal between cell membranes and the glass used to manufacture patch pipettes. Most of the early attempts at automating electrophysiological recordings tried to replace the glass pipette with small holes in planar glass surfaces. Some medium-throughput instruments (e.g. PatchXpress) still use this approach. Recordings on these instruments typically achieve high resistance gigaohm ( $G\Omega$ ) seals, similar to manual electrophysiology. However, from a manufacturing standpoint, producing uniform holes of 1-2  $\mu\text{m}$  diameter in planar glass represents a significant challenge. Attempts at increasing the throughput by increasing the number of parallel recordings or decreasing variability through ensemble recordings therefore employ alternative substrates. The consequence of using plastic substrates, however, is a lower seal resistance. For many applications, seal resistances in the 100-200 megaohm ( $M\Omega$ ) range are sufficient to produce reliable data. Limitations may still exist for currents with low amplitude, rapid activation kinetics or very steep voltage dependence, or for currents lacking voltage-dependent gating where the channel current may be difficult to distinguish from background leak currents. Small currents may result in a poor signal-to-noise (S/N) ratio; and insufficient response speed and accuracy of voltage control may compromise accurate measurement of rapidly activating, steeply voltage-dependent currents.

Most platforms now offer the option of recording an “ensemble” current, referred to as population patch clamp (PPC) (6). In this configuration, each well in a seal chip/patch plate contains multiple (up to 64) holes for recording of an integrated total ensemble of currents across a number of individual cells. The advantage is greater uniformity, which typically equates to higher success rates (often as high as 100%). The uniformity afforded by PPC enables endpoint assays in which currents from wells receiving the test article are compared directly to control wells, without the need for normalization to pre-compound currents.

A consequence of ensemble recordings is the requirement for much larger currents to be passed across the electrodes, particularly if seal resistances are relatively low. Large current amplitudes can contribute to electrode instability, especially on high-throughput platforms with shared ground electrodes such as IonWorks Barracuda<sup>®</sup>.

Problems with electrode instability are minimized by limiting the length of the voltage protocol, avoiding extreme voltage steps, especially in the hyperpolarizing direction, and reconditioning ground electrodes daily. For these reasons, early presentations on IonWorks Barracuda were often limited to recordings of ligand-gated channels, such as GABA-A channels. Including a silver chelator in the recording solutions may also help to avoid issues related to block of currents by silver ions emanating from the electrodes (7).

Most high-throughput electrophysiology assays for testing pharmacological agents are based on assessing whole cell currents, i.e. currents that flow across the entire cell membrane. The whole cell recording configuration can be established by two methods. Although both are technically whole cell recordings, the two methods are conventionally referred to as whole cell and perforated patch recordings, respectively. During whole cell recordings, the patch of membrane exposed to the intracellular solution, either in the patch pipette or across the hole in the planar seal chip/patch plate, is ruptured by applying negative pressure or a voltage transient. Typically the strength, duration and frequency of the negative pressure pulses can be varied and has to be optimized for each cell line such that good electrical access is achieved without damage to the cell or compromising the membrane-substrate seal. Good starting points for typically used cell lines (see below) can be obtained from the instrument manufacturers. Alternatively, perforated patch recordings establish electrical access by exposing the same membrane patch to agents that form non-selective cation pores within the lipid bilayer. More details on the choice of perforating agents follow below.

## Choice of Cell Line

All automated electrophysiology instruments use a cell suspension that is pipetted into the recording chamber, where negative pressure facilitates the placement of single cells over the holes in the planar recording substrate. Requirements for cell numbers are typically on the order of  $10^7$  cells per 96- or 384-well recording. Given the requirement for preparing a cell suspension and for large numbers of cells per experiment, non-adherent cells offer advantages. However, historically, most ion channels have been stably expressed in either adherent Chinese Hamster Ovary (CHO) cells or in adherent Human Embryonic Kidney (HEK) cells, because of the limited expression of endogenous channels, the propensity to form high resistance electrical seals on a glass surface, and the widespread use of these host cells for optical assays. Therefore, automated electrophysiology instrumentation has been optimized to work with these parental cell types. Good success rates have also been reported with Chinese Hamster Lung (CHL) and RBL-1 cells. If expression in another cell background is desired, it would be advantageous to first test the sealing properties of the parental cells on the automated electrophysiology instrument that will be used with the cell line. For other considerations regarding cell preparation and for a detailed protocol for preparing CHO and HEK cell suspensions for use on automated electrophysiology instruments, see the chapter on [Ion Channel Screening](#).

It is possible to use acutely dissociated native cells on automated electrophysiology devices; however, there are a number of important considerations and limitations (8). Cells have to be available in large numbers and the dissociation procedure has to produce a fairly homogeneous preparation of cells without a lot of cell debris. Because of these limitations, the native cell type used most successfully has been T-lymphocytes. Patchliner may offer an advantage for recording from native cells, because Nanion offers patch plates with different hole sizes and a low cell usage protocol, requiring as few as 300 cells per 16-well recording (9). Patchliner recordings from several native cell preparations have been

reported. For some applications, induced pluripotent stem cells may offer a viable alternative to native cell preparations (10).

## Choice of Solutions

The desire for higher resistance seals has led many researchers to employ intracellular solutions with high fluoride content. Intracellular solutions with  $F^-$  as the major anion lead to dramatically increased measured seal resistances; however, this may not be associated with an increase in the quality of the recording and may have unintended consequences such as changes in intracellular signaling and phosphorylation. For example, time dependent changes in sodium channel biophysics in the presence of high intracellular  $F^-$  were described in detail by Wang *et al* (11). These experiments were conducted using manual electrophysiology, but a similar lack of stability has been seen on the automated platforms. The reader is cautioned to explore alternatives and not to be persuaded by high resistance numbers alone.

High extracellular concentrations of divalent ion can also increase seal resistances, especially in the presence of high intracellular  $F^-$ . It may be helpful to temporarily expose cells to high extracellular  $Ca^{2+}$  concentrations during the sealing process, and change to a more physiological solution once seals are established. This is an approach recommended for Patchliner, which was designed with a space and protocol for use of a “seal enhancer” solution. Much of the increased seal resistance achieved by temporary exposure to a high divalent extracellular solution is maintained once the divalent concentration is lowered. While it is possible on Patchliner to exchange the intracellular solution, lowering the intracellular  $F^-$  concentration after seal formation leads to a dramatic loss of seal resistance (BTP, personal experience).

## High-Throughput Automated Electrophysiology Assays

For the purpose of this discussion, high-throughput will be defined as the parallel recording from either 96 or 384 wells.

### First Generation Instruments: IonWorks Quattro and IonWorks HT

IonWorks Quattro and IonWorks HT are distinguished by the use of single hole and PPC recording mode, respectively. Both instruments feature 48 movable electrodes and discontinuous voltage clamp and use the perforated patch configuration. The same voltage protocol is performed prior to and after a fixed incubation time with the test article.

### Single Hole versus Population Patch Clamp (PPC)

On IonWorks instruments, cells can be supplied in a trough or in individual wells; this allows the user to test multiple different cell lines in the same experiment and makes the instruments well suited to selecting stable cell lines out of multiple clones. For this application, the Single Hole mode is ideal because it provides information on the distribution of current amplitudes across cells.

For other applications, the PPC mode is typically preferred (12). Because currents are effectively averaged across 64 cells, the PPC mode mitigates against cell-to-cell variability in parameters such as current amplitudes or fractional inactivation, and recordings are much more uniform. Often it is possible to achieve 100% success rate. However, if seal rates are poor, it may be possible to acquire data from a number of higher resistance wells in Single Hole mode, whereas recordings in PPC mode will fail altogether. For this reason, the Single Hole mode should be used to troubleshoot experiments when PPC recordings report “no seal” across the entire plate. If the reason for the failure is poor cell health, the Single Hole experiment should produce some wells with seal resistances that pass the intrinsic acceptance criteria (resistance >20 M $\Omega$  during seal test). If the Single Hole experiment shows no wells with acceptable seal resistances, the reason for the failure is most likely due to instrument failure or an error in setting up the experimental protocol.

### Perforation Agent

The most commonly used perforation agent for IonWorks experiments is amphotericin B (from *Streptomyces*), although nystatin should be a viable alternative and is used more often for manual electrophysiology. There are important considerations when using amphotericin B. It is light sensitive and should be stored in the dark. Amphotericin B has limited solubility. It should always be prepared fresh on the day of the experiment, dissolved in 100% dry DMSO at approximately 30 mg/mL, sonicated for several minutes, and then diluted into the aqueous solution to a final concentration of 0.1 mg/mL. Amphotericin B of comparable quality is available from multiple vendors; however, lot differences exist and can affect various cell lines differently. Therefore it may be worthwhile to compare different lots of amphotericin B during assay development.

Although amphotericin B and nystatin form cation-selective pores, their permeability for chloride anions is not insignificant (13). This deserves some consideration when developing assays on the IonWorks platforms that employ the perforated patch method. In cases where the chloride concentration in the intracellular solution is high compared to typical cytoplasmic free chloride concentration, the cytoplasmic chloride concentration will most likely have reached steady-state at the time the actual data recording starts. However, this may not be the case; if the chloride concentration in the intracellular solution is low compared to the cytoplasmic free chloride concentration, this may lead to instability over time. Gramicidin may represent a viable alternative as a perforating agent and is much more selective for cationic currents (13).

### Voltage Protocols

The complexity of voltage protocols that can be used on IonWorks HT or IonWorks Quattro is limited. The software is best suited for single voltage steps or ramps or trains of voltage pulses at a constant frequency. Generally, the length of the voltage protocol is limited to 5 s. However, another limitation exists in the number of data points that can be acquired, and therefore the maximal length of recordings depends on the sampling frequency employed. Recordings can be performed at sample intervals ranging from 0.1 ms to 6.4 ms. A sampling interval of 0.1 ms allows for voltage protocols lasting up to 2.25

s. It is possible to include conditioning intervals or trains, during which cells are voltage clamped but no data are acquired. Adding conditioning segments can quickly extend the total time of the experiment, because recordings are performed in 8 banks of 48 recordings, and it will be important to determine the stability of currents over the time course of the experiment.

## Data Analysis

Leak subtraction is performed based on a small voltage step at the beginning of the voltage protocol. Because of the error in extrapolating from a small voltage step to the entire voltage range of the experiment and the possibility of offset potentials, the use of leak subtraction should be combined whenever possible with an offset correction based on leak currents recorded during a voltage step to 0 mV. However, this may not be possible if a membrane potential of 0 mV produces active currents. A good alternative for fast inactivating channels is the measurement of currents based on subtracting current at the end of a voltage step from the peak current.

For non-inactivating currents that operate across the voltage range, leak subtraction is not an option, and a combination of a voltage step to 0 mV to minimize the contribution of leak currents combined with a voltage ramp has been used successfully (14).

After data has been acquired, it can be filtered based on acceptance criteria such as seal resistance or current amplitude. The user then chooses one or several metrics that will be used to analyze the current traces such as the peak or average current during a particular interval. These data are stored in the form of ASCII files that can be imported into a variety of software programs for further data analysis. Overall, the analysis of IonWorks recordings is rapid and user friendly.

## Example Protocol

See Appendix 1 for a detailed protocol that can be used to evaluate block of voltage-gated sodium currents on the IonWorks platform. Other voltage-gated currents can be recorded using the same workflow with appropriate adjustments in the voltage protocols and potentially in the composition of recording solutions.

## Second Generation Instruments: IonWorks Barracuda, Qube and SyncroPatch

A key limitation of the first generation instruments is the inability to voltage clamp during test article addition. In this regard, second generation high-throughput instruments represent a significant advantage by enabling continuous voltage clamp. Another advantage of the 384 amplifiers is the shorter time required to conduct an experiment, i.e. the run time of a typical experiment is reduced from approximately one hour on IonWorks Quattro to 15-20 minutes on the second generation instruments. All platforms offer a choice between Single Hole and PPC modes, and the same considerations apply that are discussed above for IonWorks Quattro and IonWorks HT. IonWorks **Barracuda** and **Qube** (Sophion) are free-standing instruments, whereas **SyncroPatch 384PE** (Nanion

Technologies) is designed to be integrated into a liquid handling platform, such as Biomek® FX (Beckman Coulter).

## Whole Cell Access

Like the original IonWorks instruments, IonWorks Barracuda uses the perforated patch configuration, typically resulting in low access resistance that is very stable over time. In contrast, Qube and SyncroPatch obtain whole cell access by applying negative pressure to rupture the cell membrane. Different cell lines can differ substantially with regard to the negative pressure required to rupture the membrane, and the associated parameters need to be optimized carefully during assay development. In general, the user can vary the number, length and amplitude of the pressure pulses. Options may also include pressure ramps. If no or very little negative pressure is required for whole cell access, the cell membrane may have been damaged by excessive enzyme treatment and a gentler dissociation procedure should be tried.

## Voltage Protocols

Second generation instruments can handle fairly complex voltage protocols, including protocols that combine different holding potentials and sampling rates. All instruments feature graphic user interfaces for setting up voltage protocols and experimental parameters. It is reasonable to assume that protocols commonly used to characterize voltage-gated channels can be implemented on these second generation instruments, and the reader is referred to the instrument manufacturer for questions concerning specific protocols.

## Data Analysis

All second generation platforms include customized data analysis software that allow the user to subtract leak currents, set well-level criteria for data acceptance and define metrics that specify the data (such as peak current, average current during a specified time interval, etc.) that will be used for further analysis. Some software programs support further analysis of data across wells, such as IC<sub>50</sub> or EC<sub>50</sub> determination, whereas other platforms require well-level data to be exported and analyzed separately. Generally, the latter is not an impediment, because most users will already have access to analysis software that is integrated with compound management information and database publication tools. Nonetheless, real-time analysis can be a nice feature when deciding whether to repeat experiments.

## Example Protocols

See Appendix 2 for a protocol that can be used to evaluate block of KCNQ1/KCNE1 voltage-gated potassium currents on the IonWorks Barracuda platform.

Appendix 3 contains an example of a protocol that can be used to record currents from ligand-gated ion channels on IonWorks Barracuda. The example given is for GABA<sub>A</sub> currents; similar protocols can be used with other ligand-gated chloride and cationic



currents, although fluidic handling on the instrument precludes accurate recording of the most rapidly activating and inactivating channels (NMDA and nAChR  $\alpha 7$ ).

## Medium-Throughput Automated Electrophysiology Assays

Medium-throughput instruments use 8- or 16-well chambers. Currently available commercial instruments include PatchXpress, Patchliner and Qpatch. PatchXpress and Qpatch are free-standing instruments, whereas Patchliner is a bench-top instrument. A difference between these platforms is the configuration of the electrodes that can be either movable (PatchXpress and Patchliner) or embedded into the patch plate (Qpatch). Movable electrodes involve the risk of carryover of test articles between experiments, but are less prone to electrical cross-talk between electrodes, potentially leading to recording artifacts.

The PPC mode is available for Patchliner and Qube instruments.

### Scripting

The PatchXpress and Patchliner instruments offer the option of scripting, referring to protocols that are adjusted *ad hoc* based on criteria applied to the data. A commonly used example is the addition of test article once currents evoked by baseline pulses have stabilized and vary by less than 5%. Another commonly used application of scripting is to set the test pulse voltage based on the maximum current determined during a family of voltage pulses. Especially for cell lines with low expression, this type of script can help maximize the number of successful recordings. Most modulators of voltage-gated sodium and calcium channels are sensitive to the conformational state of the channel and typically interact preferentially with channels in open and inactivated states. To avoid potency differences based on cell-to-cell variability in the voltage-dependence of inactivation, scripting can be used to set the membrane potential on the fly to a voltage corresponding to a set fractional inactivation based on steady state inactivation data.

### Data Analysis

PatchXpress and Qpatch come with analysis software that is flexible but time consuming. Analysis performed by Patchliner software is limited to all-points  $IC_{50}$  values and more detailed analysis requires importing the data into another program.

Plate-based analysis software used by most pharmaceutical companies and contract research operations is incompatible with the data formats used by medium-throughput automated electrophysiology devices.

### Example Protocol with Scripting

See Appendix 4 for a protocol designed to evaluate block of voltage-gated sodium currents on the PatchXpress.

## Low-Throughput Automated Electrophysiology Assays

The [Port-a-Patch](#) offered by Nanion is comparable to manual electrophysiology in terms of throughput. Its advantages are the small footprint and ease of operation relative to manual electrophysiology. It may be a viable option for laboratories new to electrophysiology. The main disadvantage is that the experimenter does not choose the individual cells that will be voltage clamped. This limits the use with transiently transfected or acutely dissociated cells.

## Cost of Operation

The cost of consumables for any automated electrophysiology platform can be substantial and should be considered prior to purchasing an instrument. Outside of the price per patch plate/seal chip, factors that affect the cost per data point relate to the options of multiple test article additions, wash-out of test article, cell reuse, and scripting.

## References

1. Mathes C. Ion channels in drug discovery and development. *Drug Discov Today*. 2003;8:1022–1024. PubMed PMID: 14690632.
2. Wang X, Li M. Automated electrophysiology: high throughput of art. *Assay Drug Dev Technol*. 2003;1:695–708. PubMed PMID: 15090242.
3. Dunlop J, Bowlby M, Peri R, et al. Ion channel screening. *Comb Chem High Throughput Screen*. 2008;11:514–522. PubMed PMID: 18694388.
4. Dunlop J, Bowlby M, Peri R, Vasilyev D, Arias R. High-throughput electrophysiology: an emerging paradigm for ion-channel screening and physiology. *Nat Rev Drug Discov*. 2008;7:358–368. PubMed PMID: 18356919.
5. Priest BT, Swensen AM, McManus OB. Automated electrophysiology in drug discovery. *Curr Pharm Des*. 2007;13:2325–2337. PubMed PMID: 17692004.
6. Finkel A, Wittel A, Yang N, Handran S, Hughes J, Costantin J. Population patch clamp improves data consistency and success rates in the measurement of ionic currents. *J Biomol Screen*. 2006;11:488–496. PubMed PMID: 16760372.
7. Cerne R, Wakulchik M, Li B, Burris KD, Priest BT. Optimization of a High-Throughput Assay for Calcium Channel Modulators on IonWorks Barracuda. *Assay Drug Dev Technol*. 2016;14:75–83. PubMed PMID: 26716356.
8. Milligan CJ, Li J, Sukumar P, et al. Robotic multiwell planar patch-clamp for native and primary mammalian cells. *Nat Protoc*. 2009;4:244–255. PubMed PMID: 19197268.
9. Becker N, Stoelzle S, Gopel S, et al. Minimized cell usage for stem cell-derived and primary cells on an automated patch clamp system. *J Pharmacol Toxicol Methods*. 2013;68:82–87. PubMed PMID: 23567076.
10. Haythornthwaite A, Stoelzle S, Hasler A, et al. Characterizing human ion channels in induced pluripotent stem cell-derived neurons. *J Biomol Screen*. 2012;17:1264–1272. PubMed PMID: 22923790.

11. Wang DW, George AL Jr, Bennett PB. Comparison of heterologously expressed human cardiac and skeletal muscle sodium channels. *Biophys J*. 1996;70:238–245. PubMed PMID: 8770201.
12. Dale TJ, Townsend C, Hollands EC, Trezise DJ. Population patch clamp electrophysiology: a breakthrough technology for ion channel screening. *Mol Biosyst*. 2007;3:714–722. PubMed PMID: 17882333.
13. Kyrozis A, Reichling DB. Perforated-patch recording with gramicidin avoids artifactual changes in intracellular chloride concentration. *J Neurosci Methods*. 1995;57:27–35. PubMed PMID: 7540702.
14. Felix JP, Priest BT, Solly K, et al. The inwardly rectifying potassium channel Kir1.1: development of functional assays to identify and characterize channel inhibitors. *Assay Drug Dev Technol*. 2012;10:417–431. PubMed PMID: 22881347.

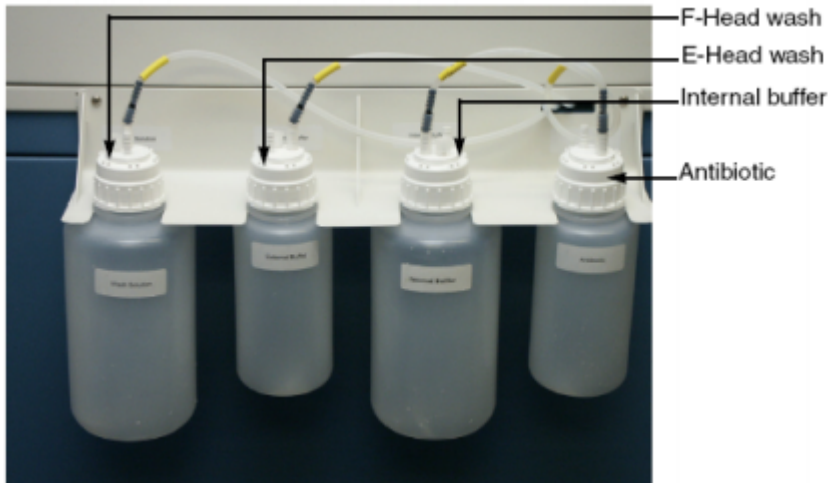
## Appendix 1: Protocol for Assessment of Use-Dependent Sodium Channel Inhibitors on IonWorks Quattro

### Overview

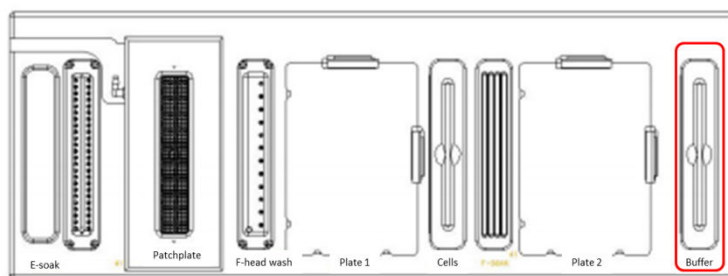
This protocol is designed to evaluate the type of use-dependent block of voltage-gated sodium channels that is seen with classic local anesthetics. After a brief period at a hyperpolarized voltage to allow recovery from inactivation, channels are subjected to a set of 26 depolarizing pulses. More pronounced inhibition of current during the later depolarizing pulses indicates use-dependent block, which typically arises from an increased affinity of test compounds for channels in open and inactivated states.

### Start of Day

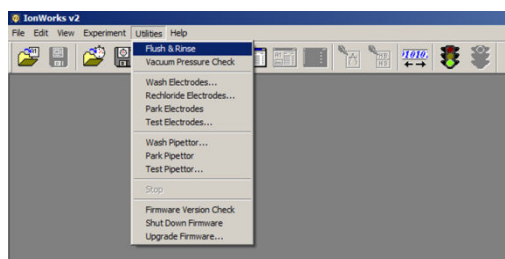
1. Turn on IonWorks Quattro using the green button located on the front of the instrument on the lower right.
2. Make sure waste bottles are empty.
3. Make sure main vacuum is on and apply vacuum to patch plate in **Patchplate** holder slot (use an old patch plate for these steps).
4. Place D-PBS without  $\text{Ca}^{2+}/\text{Mg}^{2+}$  in all buffer solution bottles on the left side of the instrument (leave waste bottles empty).



- Place a buffer trough in the **Buffer** position and fill with 5-7 mL of D-PBS without  $\text{Ca}^{2+}/\text{Mg}^{2+}$ .



- After instrument initialization, start IonWorks software.
- From the **Utilities** menu, run the **Flush & Rinse** protocol twice.



- Replace D-PBS with internal buffer solution (see below) in the bottles designated for the internal buffer solution and the antibiotic solutions. Make sure the correct lines are connected to each bottle.
- Replace the buffer in the buffer trough with 5-7 mL external buffer solution (see below).
- Run the **Flush & Rinse** protocol one time.

## Buffer Solutions

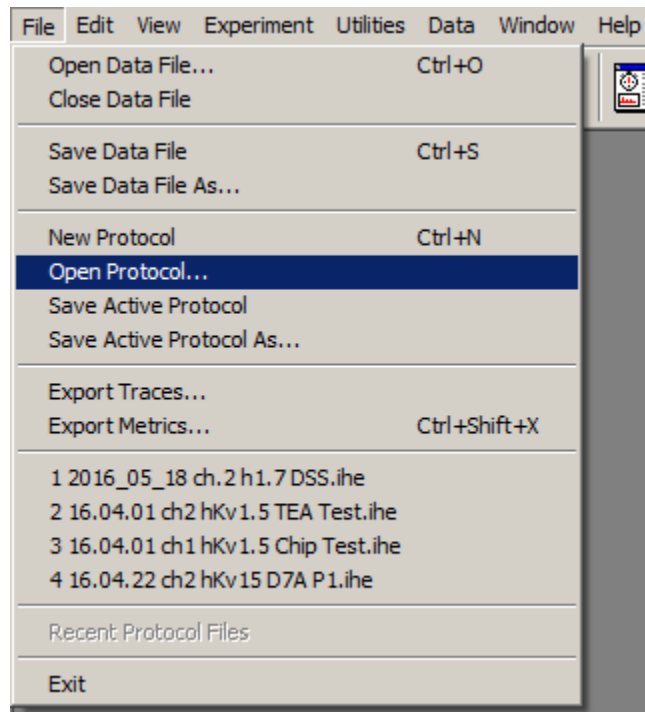
External Buffer Solution: 140 mM NaCl, 4 mM KCl, 2 mM CaCl<sub>2</sub>, 1 mM MgCl<sub>2</sub>, 10 mM HEPES, 10 mM Glucose, pH 7.4 with NaOH

Internal Buffer Solution: 70 mM KF, 70 mM KCl, 0.5 mM MgCl<sub>2</sub>, 5 mM HEDTA, 10 mM HEPES, pH 7.25 with KOH

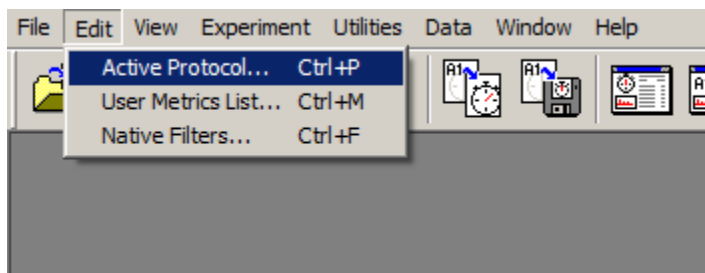
- Amphotericin B is added to internal buffer solution to a final concentration of 0.1 mg/mL to make the antibiotic solution on the day of an experiment.
  - i. Amphotericin B is weighed out and dissolved to a concentration of ~30 mg/mL in 100% anhydrous DMSO and then sonicated for 10 min.
  - ii. Amphotericin B is then added to the internal buffer solution with vigorous mixing.

## Protocol Setup

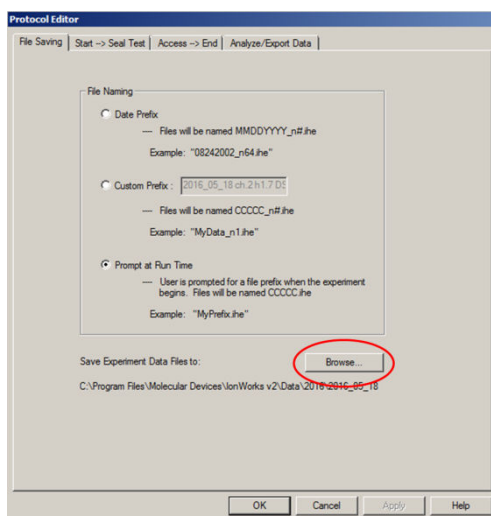
To load an existing protocol, select **Open Protocol** on the **File** menu.



Once the protocol has loaded, it may be edited from the Edit menu by selecting Active Protocol.



To set the location to save the data file, go to the **Protocol Editor** screen, select the **File Saving** tab and click the **Browse** button.



The user can also select a file format. Options are a standard **Date Prefix**, a **Custom Prefix**, or customizing the file name after the protocol has started.

**File Naming**

Date Prefix  
 --- Files will be named MMDDYYYY\_n#.ihe  
 Example: "08242002\_n64.ihe"

Custom Prefix :   
 --- Files will be named CCCCC\_n#.ihe  
 Example: "MyData\_n1.ihe"

Prompt at Run Time  
 --- User is prompted for a file prefix when the experiment begins. Files will be named CCCCC.ihe  
 Example: "MyPrefix.ihe"

On the **Start >> Seal Test** tab of the **Protocol Editor**, the user has to enter the type of patch plate (Standard or PPC) that will be used, as well as the time used for the seal test.

**Protocol Editor**

File Saving | **Start -> Seal Test** | Access -> End | Analyze/Export Data |

Start | Prime Plate | Add Cells | Seal Test

Patch-Plate Selection  
 Standard Patch-Plate  Patch-Plate PPC

Prime Plate  
 Select Plate Coverage:  
 Whole Plate  
 1/2 plate using [Full half]  
 1/4 plate using [Top quadrant]  
 1/8 plate using [Top eighth]

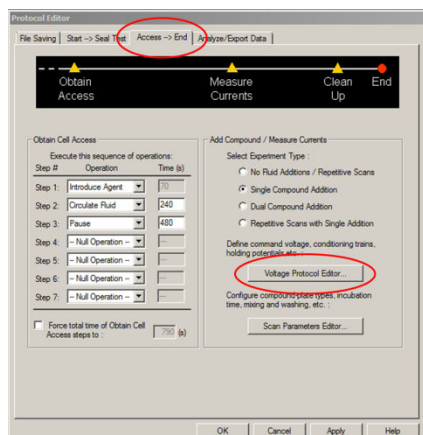
Adding Cells and Seal Test  
 Resuspend Cells before Dispense Max cycles: 2  
 Time to wait before Seal Test (s): 500

Hole Test  
 Max (mV): 0  
 Min (mV): -10

Enter Remarks  
 Prompt on Run  Enter Now

OK Cancel Apply Help

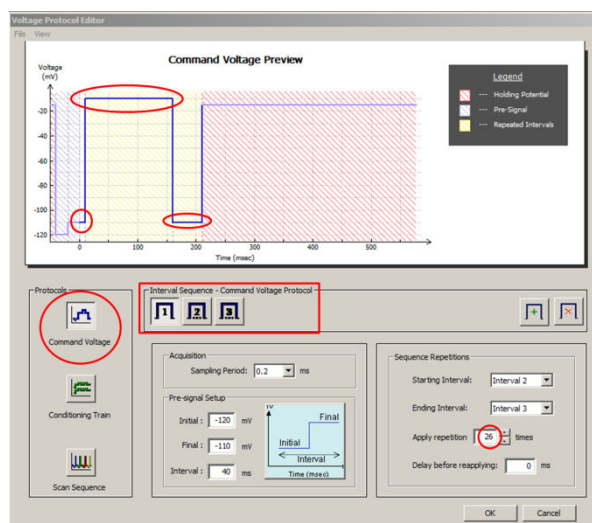
To set up/edit the voltage protocol, select the **Access >> End** tab of the **Protocol Editor** and click the **Voltage Protocol Editor**.



In the **Voltage Protocol Editor**, voltage protocols are generated by clicking **Command Voltage** and adding **Interval Sequences**. Each test pulse must be defined by an interval sequence. In the below example of a 200 ms step to -10 mV from -110 mV, the interval sequences consist of:

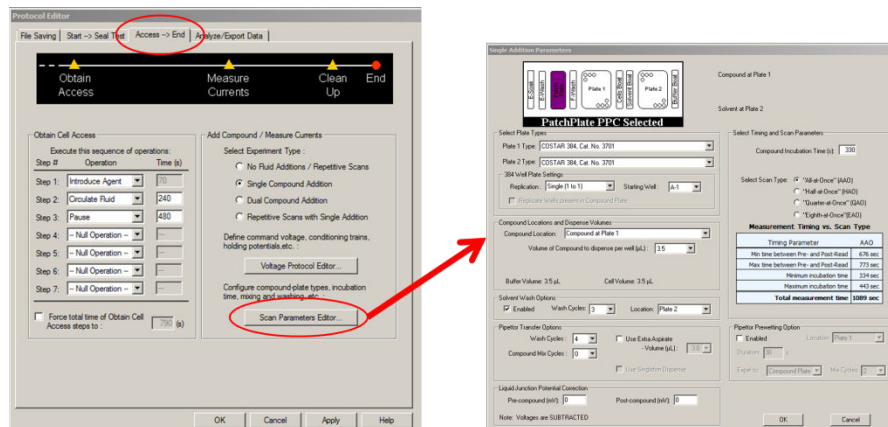
1. Holding at -110 mV for 20 ms
2. Holding at -10 mV for 200 ms
3. Holding at -110 mV for 50 ms

By selecting the **Apply repetition** function, the user can repeat any of the interval sequences up to the memory capacity of the IonWorks program. In the below example, interval sequence 2 and 3 are repeated a total of 26 times.



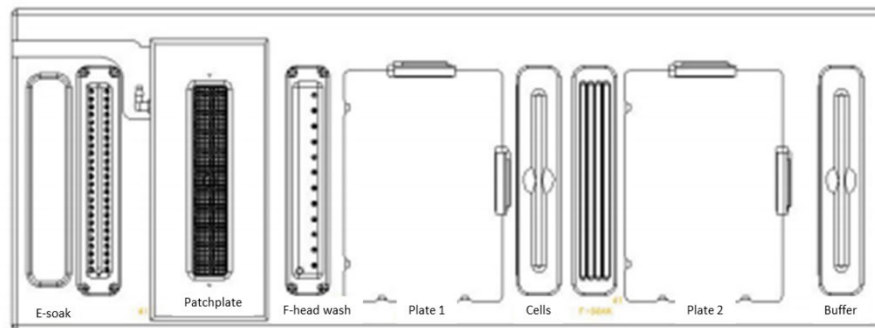
Also on the **Access >> End** tab, compound additions are controlled by using the **Scan Parameters Editor**.



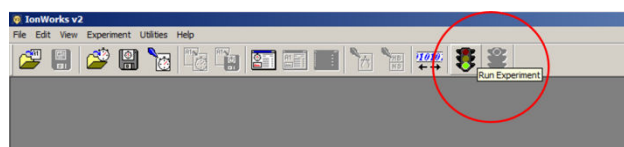


## Start of Experiment

1. Place compound plate in **Plate 1** position (for guidelines on preparing compounds, see Compound Preparation below).



2. In **Plate 2** position, place a polypropylene 384-well plate with 50  $\mu\text{l}$  per well of a 50% DMSO/water mixture to wash F-head in between compound additions.
3. In the **Buffer** position, place a buffer trough filled with fresh 5-7 mL of external buffer solution.
4. Remove patch plate used during the **Flush & Rinse** protocols. With a piece of lint-free tissue, carefully dry out the **Patchplate** area, making sure not to touch the ground electrode.
5. Place a new patch plate into the **Patchplate** area, replace the aluminum lid, and apply the vacuum. You should not be able to lift the lid after the vacuum is applied.
6. Follow Cell Preparation directions below and place cells into the instrument.
7. From main menu, click the green traffic light button to start program.



## Cell Preparation

1. Obtain one 70-80% confluent T-75 flask of HEK cells stable expressing the Nav1 channel of interest.
2. Aspirate media from flask.
3. Add 10 mL D-PBS without  $\text{Ca}^{2+}/\text{Mg}^{2+}$ , tilt gently to wash the cell monolayer.
4. Remove the D-PBS wash and add 2 mL trypsin (0.25%), tilt gently to wet the cell monolayer.
5. Place flask in 37°C, 5%  $\text{CO}_2$  incubator undisturbed until cells start to round up and dislodge.
6. Tilt flask to dislodge cells and/or tap sides of flask.
7. Add 10 mL of cell media containing 10% FBS, washing the cells down the wall of the flask.
8. Gently triturate the cells against the bottom of the flask four times.
9. Place cell suspension into a 15 mL conical centrifuge tube and centrifuge @ 1300 rpm for 3 min.
10. Aspirate supernatant and resuspend cells in 4 mL external buffer solution.
11. Gently triturate the cells using a 200  $\mu\text{l}$  pipette to break up the cell pellet. It is important that cell dispersion is carefully performed.
12. Perform cell count.
13. Cell concentration should be 2-2.5M cells/mL.
14. Dilute with external buffer solution if needed.
15. Carefully add entire contents of tube to trough located in **Cells** slot.

## Compound Preparation

For concentration response curves (CRC), create a DMSO dilution plate in a 384-well plate following the plate map below to minimize effects from potential carryover of compounds on the E-head pins.

|   | 1 | 2 | 3 | 4 | 5 | 6 | 7  | 8  | 9  | 10 | 11 | 12 | 13 | 14 | 15 | 16 | 17 | 18 | 19 | 20 | 21 | 22 | 23 | 24 |
|---|---|---|---|---|---|---|----|----|----|----|----|----|----|----|----|----|----|----|----|----|----|----|----|----|
| A |   |   | 1 | 3 | 5 | 7 | 9  | 11 | 13 | 15 | 17 | 19 | 21 | 23 | 25 | 27 | 29 | 31 | 33 | 35 | 37 | 39 |    |    |
| B |   |   | 1 | 3 | 5 | 7 | 9  | 11 | 13 | 15 | 17 | 19 | 21 | 23 | 25 | 27 | 29 | 31 | 33 | 35 | 37 | 39 |    |    |
| C |   |   | 2 | 4 | 6 | 8 | 10 | 12 | 14 | 16 | 18 | 20 | 22 | 24 | 26 | 28 | 30 | 32 | 34 | 36 | 38 | 40 |    |    |
| D |   |   | 2 | 4 | 6 | 8 | 10 | 12 | 14 | 16 | 18 | 20 | 22 | 24 | 26 | 28 | 30 | 32 | 34 | 36 | 38 | 40 |    |    |
| E |   |   | 1 | 3 | 5 | 7 | 9  | 11 | 13 | 15 | 17 | 19 | 21 | 23 | 25 | 27 | 29 | 31 | 33 | 35 | 37 | 39 |    |    |
| F |   |   | 1 | 3 | 5 | 7 | 9  | 11 | 13 | 15 | 17 | 19 | 21 | 23 | 25 | 27 | 29 | 31 | 33 | 35 | 37 | 39 |    |    |
| G |   |   | 2 | 4 | 6 | 8 | 10 | 12 | 14 | 16 | 18 | 20 | 22 | 24 | 26 | 28 | 30 | 32 | 34 | 36 | 38 | 40 |    |    |
| H |   |   | 2 | 4 | 6 | 8 | 10 | 12 | 14 | 16 | 18 | 20 | 22 | 24 | 26 | 28 | 30 | 32 | 34 | 36 | 38 | 40 |    |    |
| I |   |   | 1 | 3 | 5 | 7 | 9  | 11 | 13 | 15 | 17 | 19 | 21 | 23 | 25 | 27 | 29 | 31 | 33 | 35 | 37 | 39 |    |    |
| J |   |   | 1 | 3 | 5 | 7 | 9  | 11 | 13 | 15 | 17 | 19 | 21 | 23 | 25 | 27 | 29 | 31 | 33 | 35 | 37 | 39 |    |    |
| K |   |   | 2 | 4 | 6 | 8 | 10 | 12 | 14 | 16 | 18 | 20 | 22 | 24 | 26 | 28 | 30 | 32 | 34 | 36 | 38 | 40 |    |    |
| L |   |   | 2 | 4 | 6 | 8 | 10 | 12 | 14 | 16 | 18 | 20 | 22 | 24 | 26 | 28 | 30 | 32 | 34 | 36 | 38 | 40 |    |    |
| M |   |   | 1 | 3 | 5 | 7 | 9  | 11 | 13 | 15 | 17 | 19 | 21 | 23 | 25 | 27 | 29 | 31 | 33 | 35 | 37 | 39 |    |    |
| N |   |   | 1 | 3 | 5 | 7 | 9  | 11 | 13 | 15 | 17 | 19 | 21 | 23 | 25 | 27 | 29 | 31 | 33 | 35 | 37 | 39 |    |    |
| O |   |   | 2 | 4 | 6 | 8 | 10 | 12 | 14 | 16 | 18 | 20 | 22 | 24 | 26 | 28 | 30 | 32 | 34 | 36 | 38 | 40 |    |    |
| P |   |   | 2 | 4 | 6 | 8 | 10 | 12 | 14 | 16 | 18 | 20 | 22 | 24 | 26 | 28 | 30 | 32 | 34 | 36 | 38 | 40 |    |    |

Numbers listed in the plate map correspond to individual test compounds.

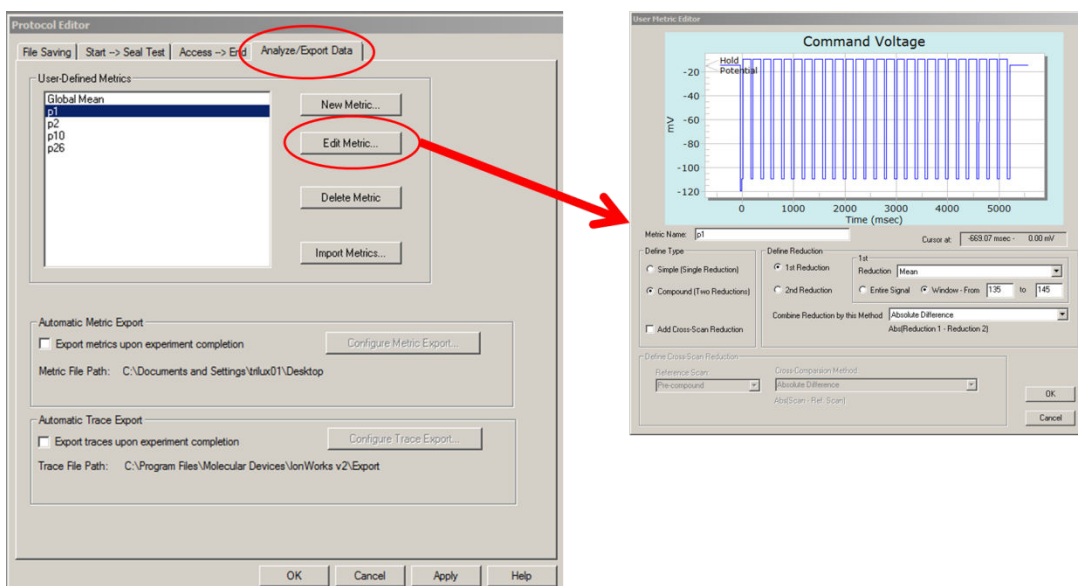
Concentrations for each test compound should start with the lowest concentration in row

A or C and go up in concentration as one moves down the plate (i.e. the highest concentration should be in row N or P).

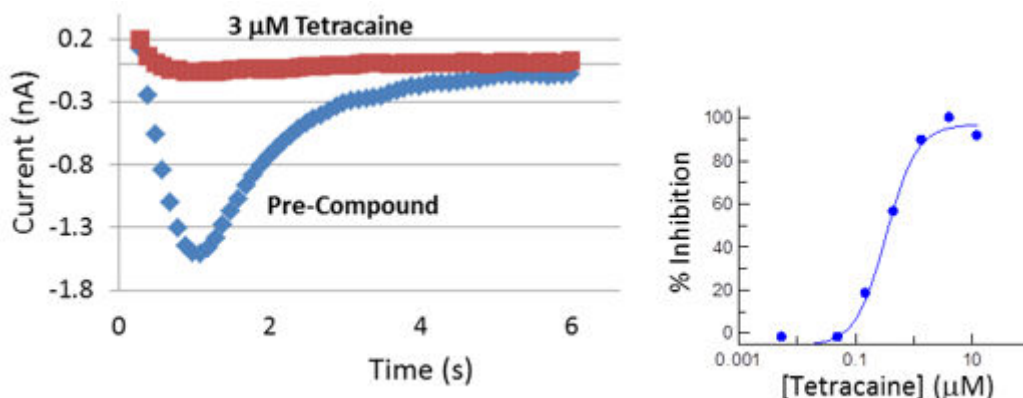
For single point testing, compounds can be placed in any order.

## Data Analysis

During an experiment, the IonWorks software generates an ASCII file based on one or more user defined analysis metrics. The metrics are defined under the **Analyze/Export Data** tab in the **Protocol Editor**. Examples of simple metrics, called **Simple (Single Reduction)** include peak current within a voltage interval and average current during a user defined time interval. Simple calculations, such as the difference or ratio between two currents, can also be applied to the data by selecting **Compound (Two Reductions)**.



Nav1 current traces recorded on IonWorks Quattro are shown below before (blue) and after (red) addition of 3  $\mu\text{M}$  tetracaine. For the protocol described, a typical concentration-response curve (CRC) is shown for tetracaine. To generate this CRC, block during the last depolarization was determined at the well level by comparing Nav1 current amplitude before and after compound application, and data were exported out of the IonWorks software as % block, defined as  $(\text{current in compound} - \text{current in control}) / \text{current in control} \times 100$ . Data were further analyzed by fitting a standard Hill equation to the data using Excel Fit.



## End of Day

1. Replace external and internal buffer solutions with 70% ethanol.
2. Place a buffer trough in the **Buffer** position and fill with 5-7 mL of 70% ethanol.
3. On the **Utilities** menu, run **Flush & Rinse** protocol once.
4. Close IonWorks Software and turn off IonWorks Quattro.

## Appendix 2: Protocol for Assessment of KCNQ1/KCNE1 Currents on IonWorks Barracuda

### Overview

This protocol is designed to evaluate inhibition of the voltage-gated potassium channel KCNQ1/KCNE1 during 3 s depolarizing test pulses repeated under control conditions and after addition of test compound.

### Buffer Solutions (prepared in advance and stored at 4°C)

External Buffer Solution: 140 mM NaCl, 5 mM KCl, 2 mM CaCl<sub>2</sub>, 1 mM MgCl<sub>2</sub>, 10 mM HEPES, 10 mM Glucose, pH 7.4 with NaOH. Osmolarity 310-320 mOsm

Internal Buffer Solution: 90 mM KGluconate, 40 mM KCl, 3.2 mM MgCl<sub>2</sub>, 3.2 mM EDTA, 5 mM HEPES, pH 7.2 with KOH. Osmolarity 290-300 mOsm

- Amphotericin B is added to internal buffer solution to a final concentration of 0.1 mg/mL to make the antibiotic solution on the day of an experiment.
  - i. Amphotericin B is weighed out and dissolved to a concentration of ~30 mg/mL in 100% anhydrous DMSO and then sonicated for 10 min.
  - ii. Amphotericin B is then added to the internal buffer solution with vigorous mixing.

## Building Protocols

### Setup Protocol

On the **Edit Setup Protocol** screen, input the following criteria into each of the different folder tabs:

The screenshot displays the 'Edit Setup Protocol' interface. The main workspace shows a grid of red waveform icons. The right-hand side contains several panels:

- Experiment:** Fields for 'Experiment Name', 'Date', and 'Protocol'.
- Protocol:** Fields for 'Protocol Name', 'Protocol Description', and 'Estimated Run Time'.
- Experiment Mode:** Radio buttons for 'Ready Development Mode', 'Multiple Protocol Mode', and 'Single Protocol Mode'.
- Event View:** A list of events and a graph showing 'Current (pA)' vs 'Time (sec)'. The graph displays a red curve that rises and then plateaus.

Buffer Wash Before Cell Addition

Edit settings for buffer wash before cell addition

**Buffer Wash Settings:**

Number of wash cycles: 1

Volume (µL): 20

Dispense tip height: MEDIUM

Dispense speed (µL/s): 5

Exchange plenum fluid with internal buffer

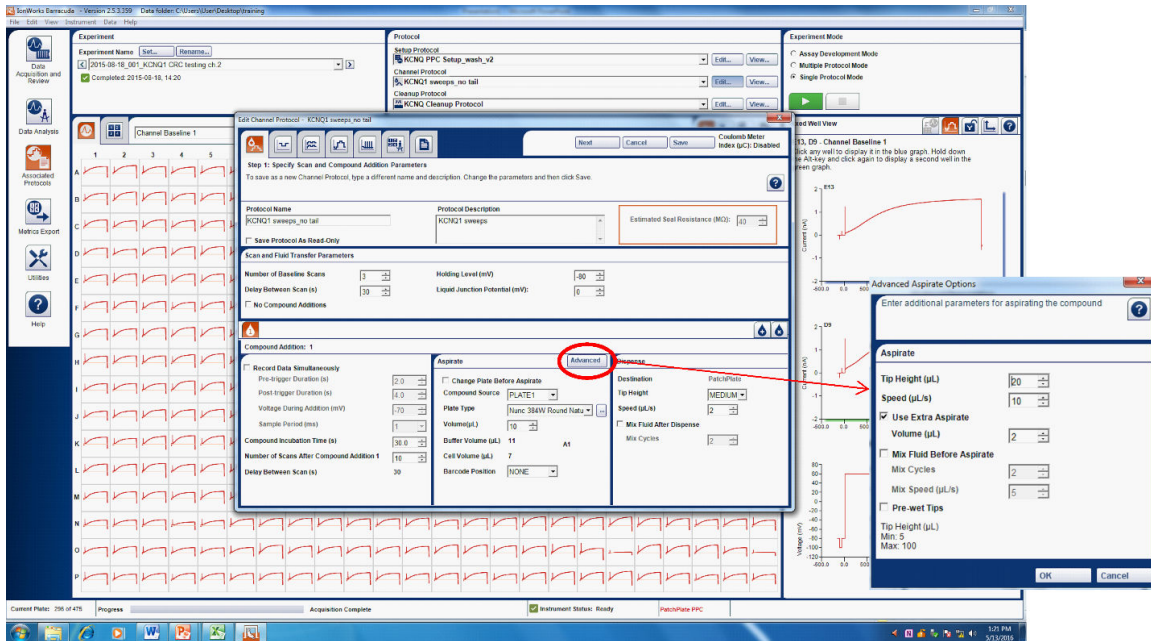
Number of cycles: 1

OK Cancel

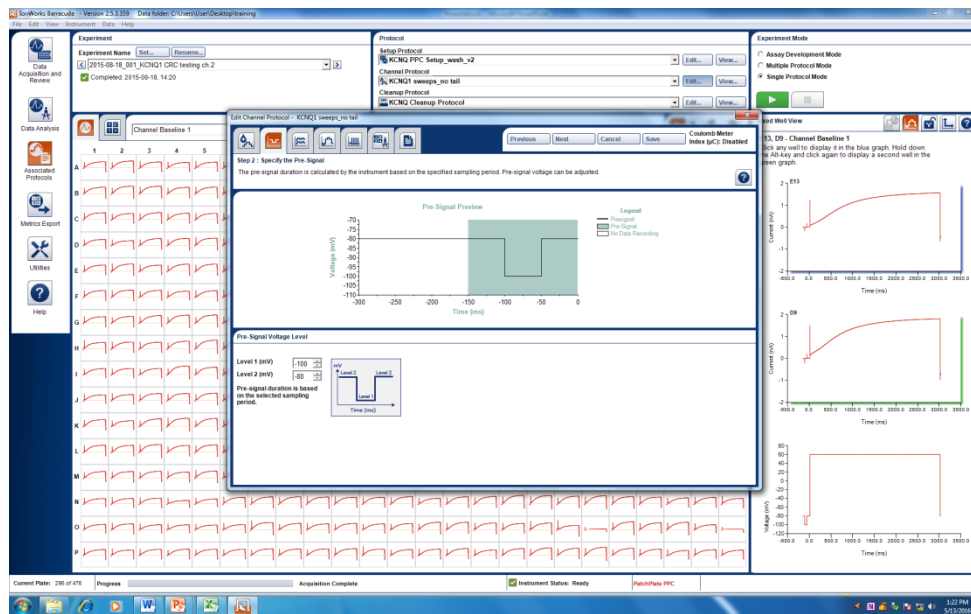
## Channel Protocol

On the **Edit Channel Protocol** screen, input the following criteria into each of the different folder tabs:

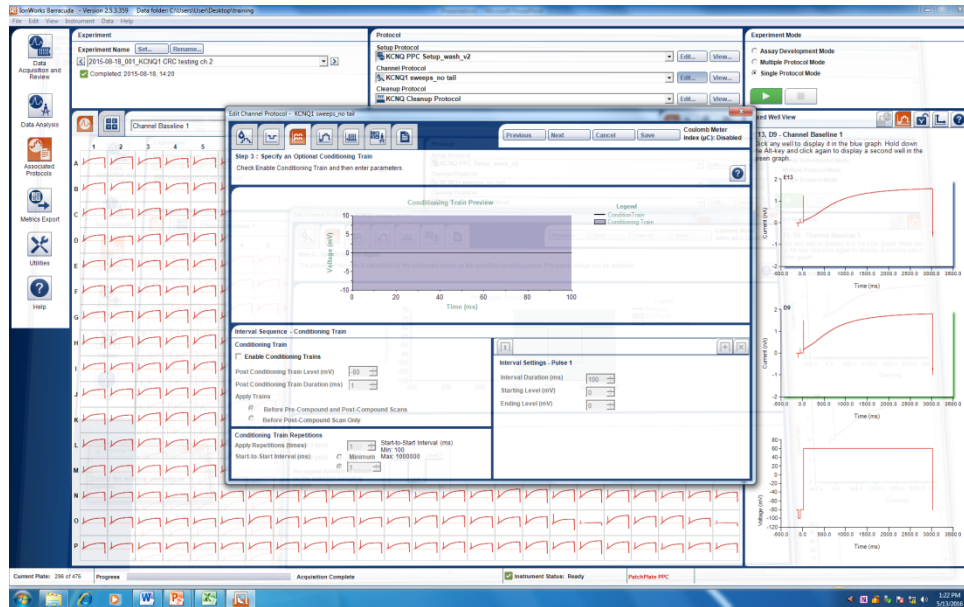
**Step 1** specifies the scan and compound addition parameters. Please note the **Advanced** aspirate options as indicated.



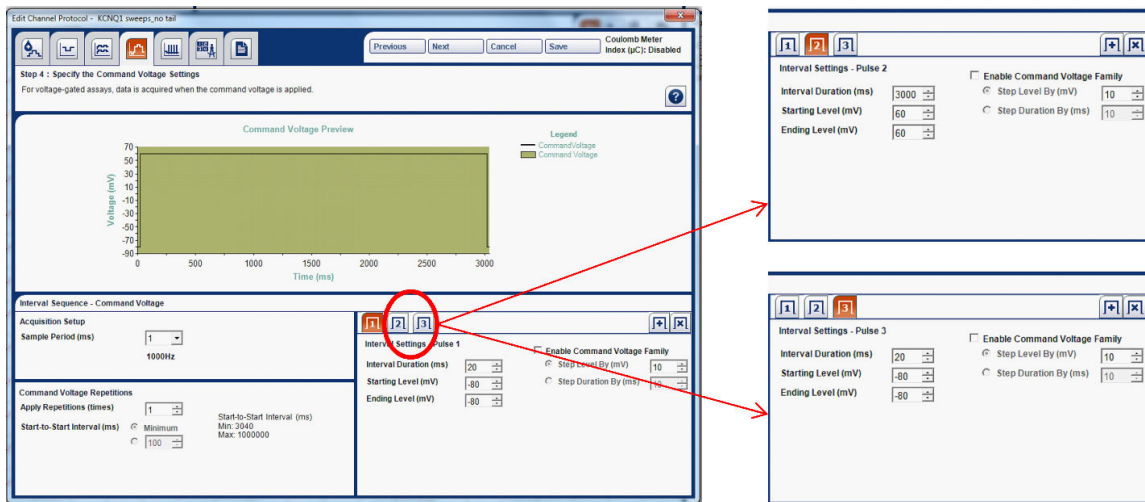
Step 2 specifies the pre-signal criteria.



Step 3 specifies the conditioning train criteria. Please note that a conditioning graph train is not utilized for this particular protocol example.

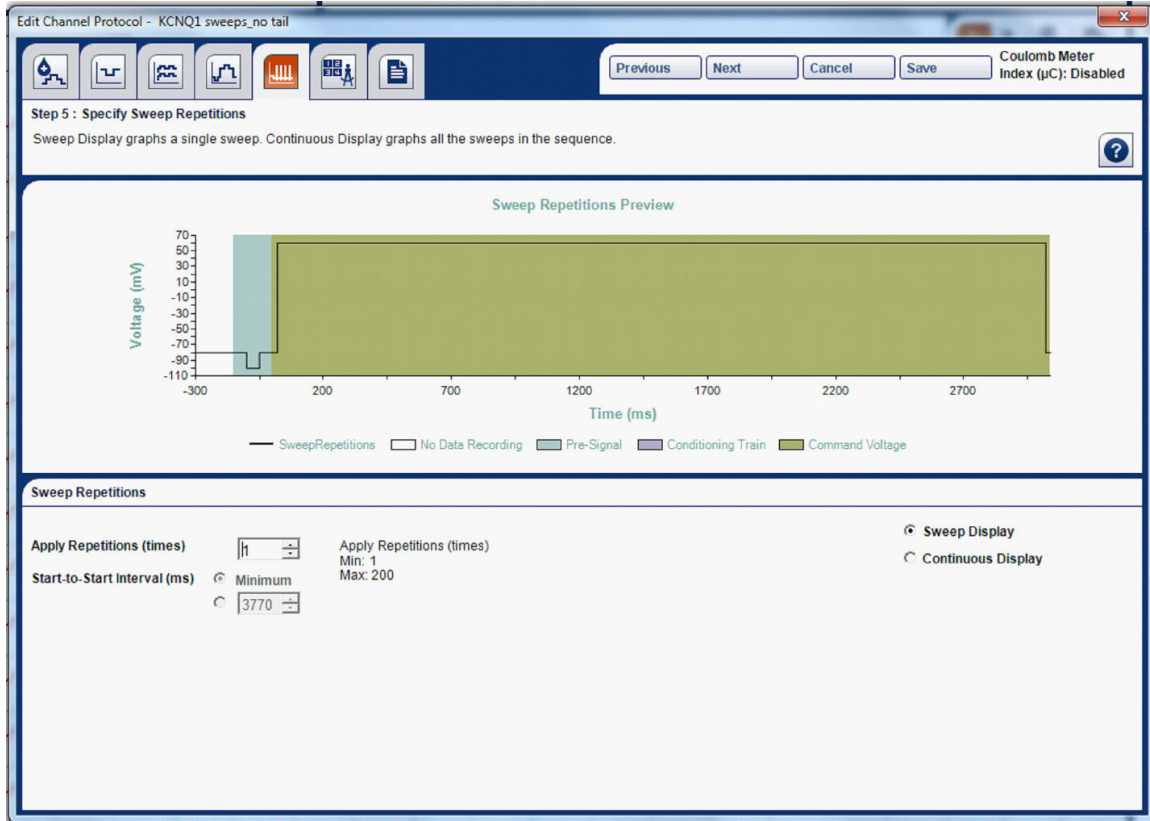


**Step 4** specifies the different command voltage settings available.

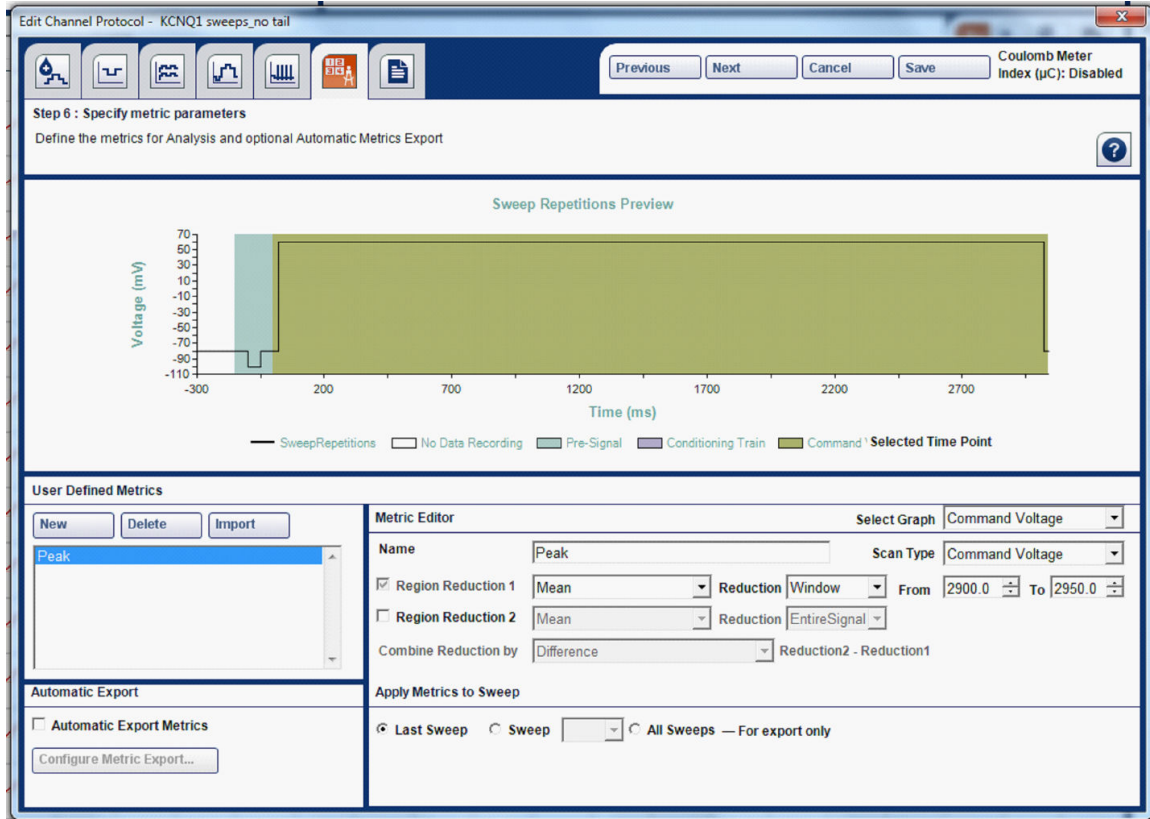


**Step 5** specifies the sweep repetitions and timeline display of the command voltage protocol (by sweep or continuous display).



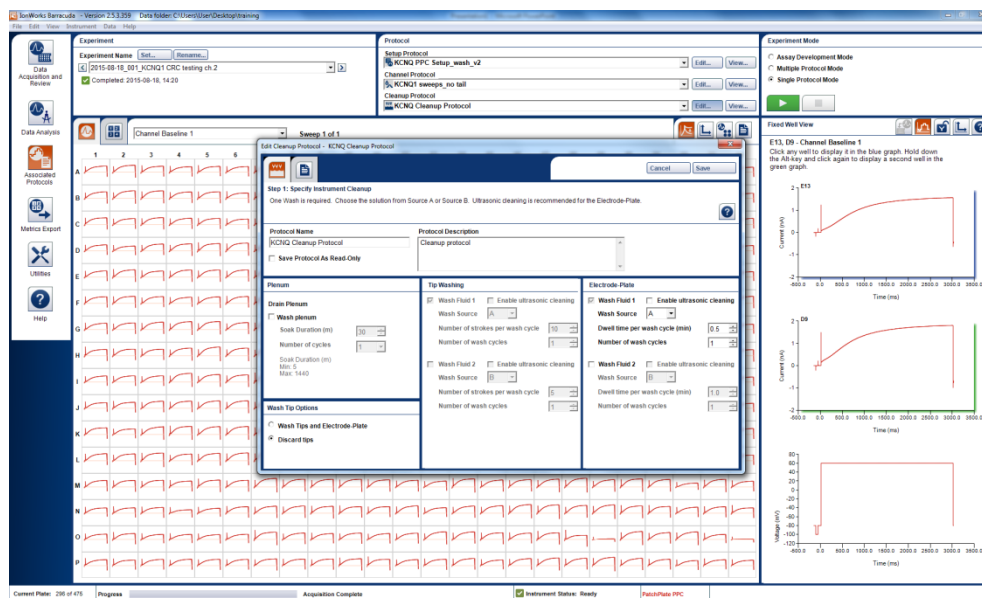


**Step 6** specifies the metric definitions. Please note that automatic export of metrics is turned off so as to allow manual inspection and rejection/acceptance of well traces before committing to metrics export.



## Cleanup Protocol

On the **Edit Cleanup Protocol** screen, input the following criteria into each of the different folder tabs:



## Running Experiments

### Start of Day

1. Turn on IonWorks Barracuda Instrument/computer using the switch located on right side of instrument.
2. Open the IonWorks Barracuda Control Software.
3. The instrument will go through an initialization.
4. Make sure all waste containers are empty.
5. Make sure there is 0.9% NaCl in both A & B wash containers.
6. External solution bottle should be filled with DPBS (not external solution) that does not contain Mg and Ca.
7. On the **Utilities** menu, select **Load Cell Pipettor** and follow the prompts.
8. Fill both amphotericin B and Internal Solution bottles with internal solution containing 0.1 mg/mL amphotericin B.
9. Place Model Cell on support pins above wash station.
10. Insert ground electrodes into plenum (they must have soaked for at least 20 min in internal solution).
11. Make sure a blank patch plate is inserted over the plenum and click **Start of Day Flush** from the **Utilities** menu.

### Cell Preparation

1. Start with >70% confluent T-150 flask of CHO cells stably expressing KCNQ1/KCNE1.
2. Aspirate media, rinse with DPBS, and add 3 mL TrypLE™.
3. Incubate 8 min at 37°C.
4. Resuspend in 9 mL of growth media lacking selection factors.
5. Spin cells at 1000 rpm for 3 min and resuspend in external solution at a density of 2-3 million cells/mL. A minimum of 5 mL of cell suspension are required.
6. Place cells on IonWorks Barracuda.

### Start of Experiment

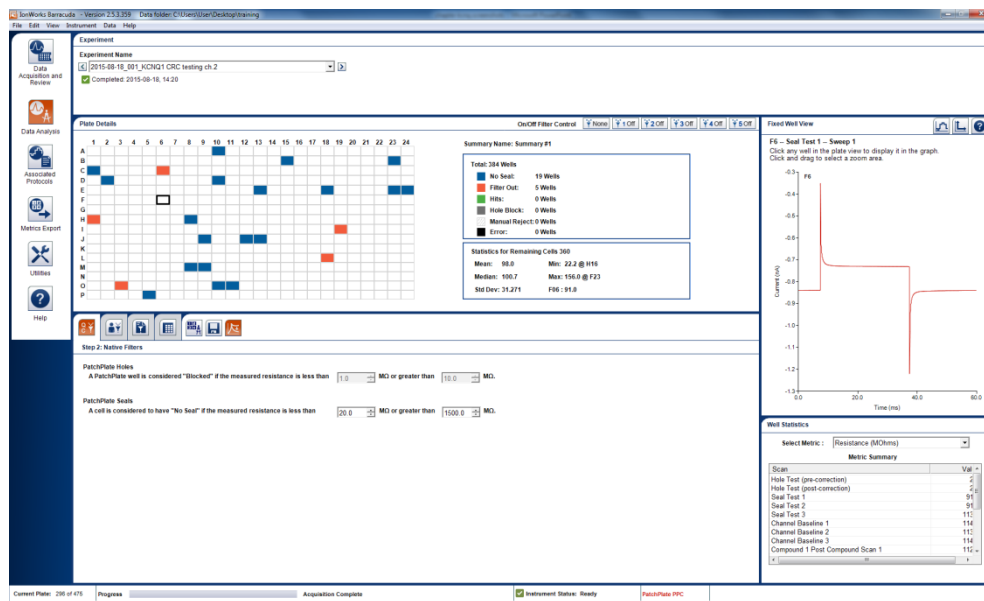
1. In **Set Default Folders** window, select the folders where the data and protocol files will reside.



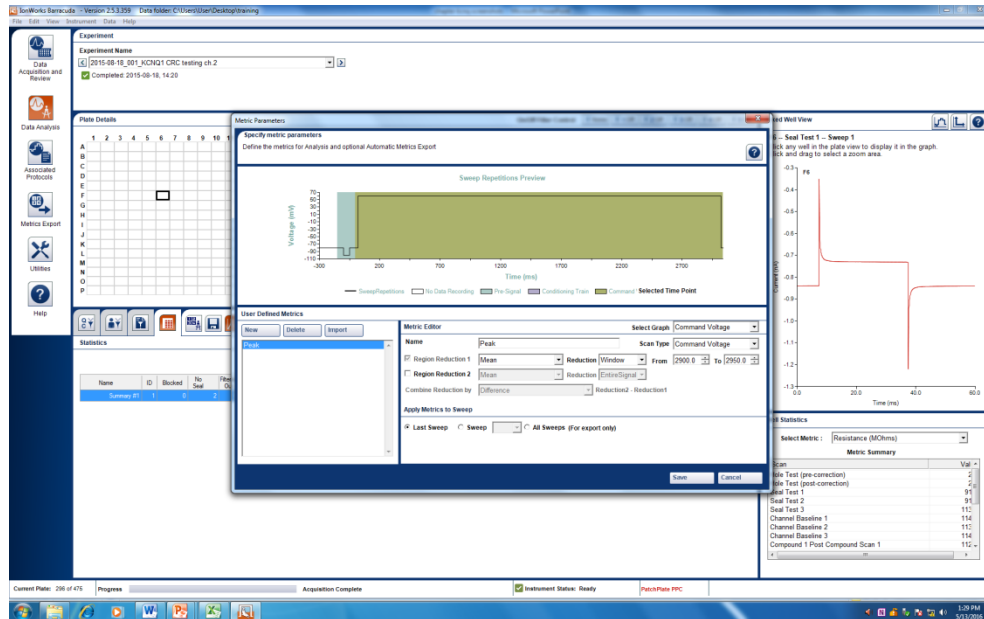
2. Select the desired **Setup**, **Channel**, and **Cleanup Protocols** (as previously described).
3. Replace patch plate used for **Start of Day** protocol with a fresh patch plate.
4. Replace Model Cell with proper recording E-Head.
5. Make sure tips, buffer boats, and compound plates are seated correctly on the instrument deck.
6. Make sure cells and empty cell dispense plate are seated correctly.
7. Set the experiment name.
8. Click the green **Play** button to start the experiment.

## Data Analysis

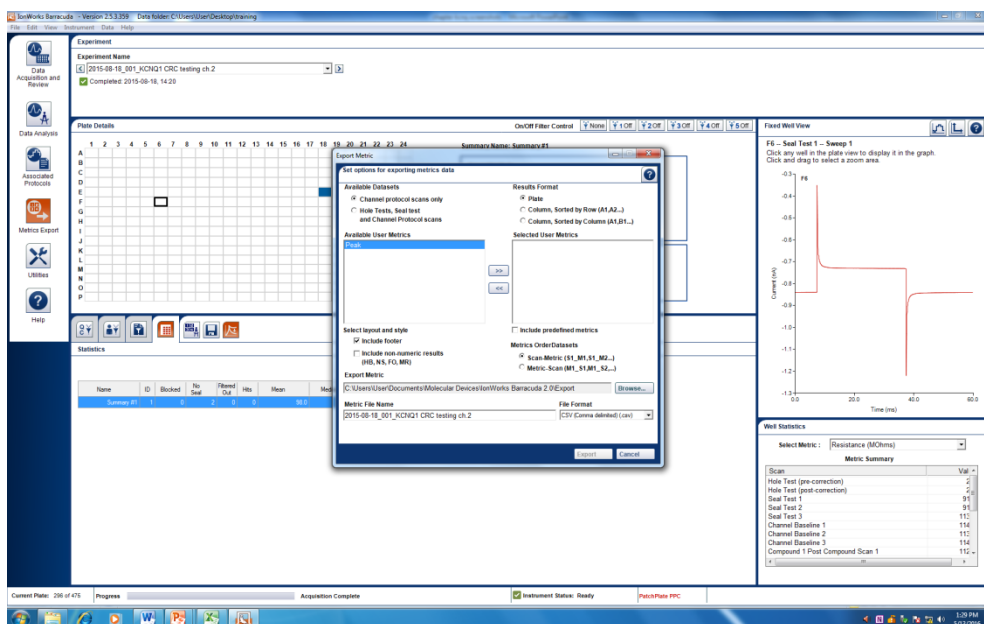
1. From the **Data Analysis** button on the left, see below for an example of all the tabs that can be opened to configure data analysis and export.



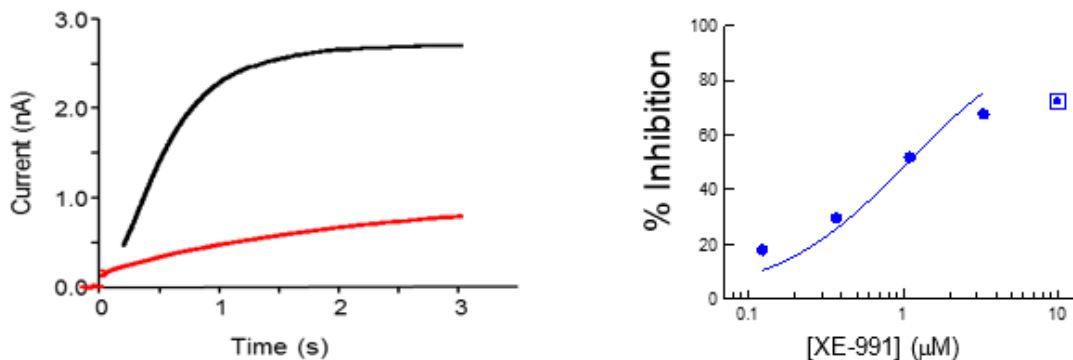
2. On the **Define Filters** tab, set your desired hole/seal resistance, peak current amplitude, and/or other criteria for removing well data from the analysis.
3. Open up the **Metrics Editor** and set the desired time and value measurements (an example is below):



4. Click the **Metric Exports** button on the left and define how and which metrics should be exported.



KCNQ1/KCNE1 current traces recorded on IonWorks Barracuda are shown below before (black) and after (red) addition of XE-991. For the protocol described, a typical concentration-response curve (CRC) is shown for XE-991. Percent inhibition was calculated by averaging the last 10 ms of the current traces during the baseline depolarizations and during the last depolarizing step following the compound addition. Data were further analyzed by fitting a standard Hill equation to the data using Excel Fit.



## End of Day Flush

1. Make certain 50% EtOH is in the alcohol wash bottle.
2. Disconnect external solution bottle, amphotericin B bottle, and internal solution bottle and replace with empty 50 mL conical vials.
3. Run **End of Day** protocol from the **Utilities** menu.
4. Remove ground electrodes and place them back into internal solution soak.
5. Shut everything off.

## Appendix 3: Protocol for Assessment of GABA<sub>A</sub> Current Block on IonWorks Barracuda

### Overview

This protocol is designed to evaluate inhibition of GABA-induced currents in a two-addition protocol. Small modifications allow this protocol to be used for agonists or allosteric modulators.

### Buffer Solutions (prepared in advance and stored at 4°C)

External Buffer Solution: 140 mM NaCl, 5 mM KCl, 2 mM CaCl<sub>2</sub>, 1 mM MgCl<sub>2</sub>, 10 mM HEPES, 10 mM Glucose, pH 7.4 with NaOH. Osmolarity 310-320 mOsm

Internal Buffer Solution: 90 mM KGluconate, 40 mM KCl, 3.2 mM MgCl<sub>2</sub>, 3.2 mM EDTA, 5 mM HEPES, pH 7.2 with KOH. Osmolarity 265-275 mOsm

- Amphotericin B is added to internal buffer solution to a final concentration of 0.1 mg/mL to make the antibiotic solution on the day of an experiment.
  - i. Amphotericin B is weighed out and dissolved to a concentration of ~30 mg/mL in 100% anhydrous DMSO and then sonicated for 10 min.
  - ii. Amphotericin B is then added to the internal buffer solution with vigorous mixing.

### Cell Suspension (prepared immediately prior to experimental run)

1. Start with 80-90% confluent T-150 flask of HEK cells stably expressing GABA<sub>A</sub> (same protocol is used for all GABA<sub>A</sub> isotypes).
2. Aspirate media, rinse with DPBS, and add 3 mL TrypLE.
3. Incubate 8 min at 37°C.
4. Transfer to 15 mL conical tube, add 9 mL of growth media lacking selection factors and triturate (7-10 times).
5. Spin cells at 1000 rpm for 3 min, aspirate supernatant and resuspend in external solution at a density of 3 million cells/mL.
6. There should be at least 5 mL of cell suspension ready to be placed on IonWorks Barracuda.

### Test Compounds

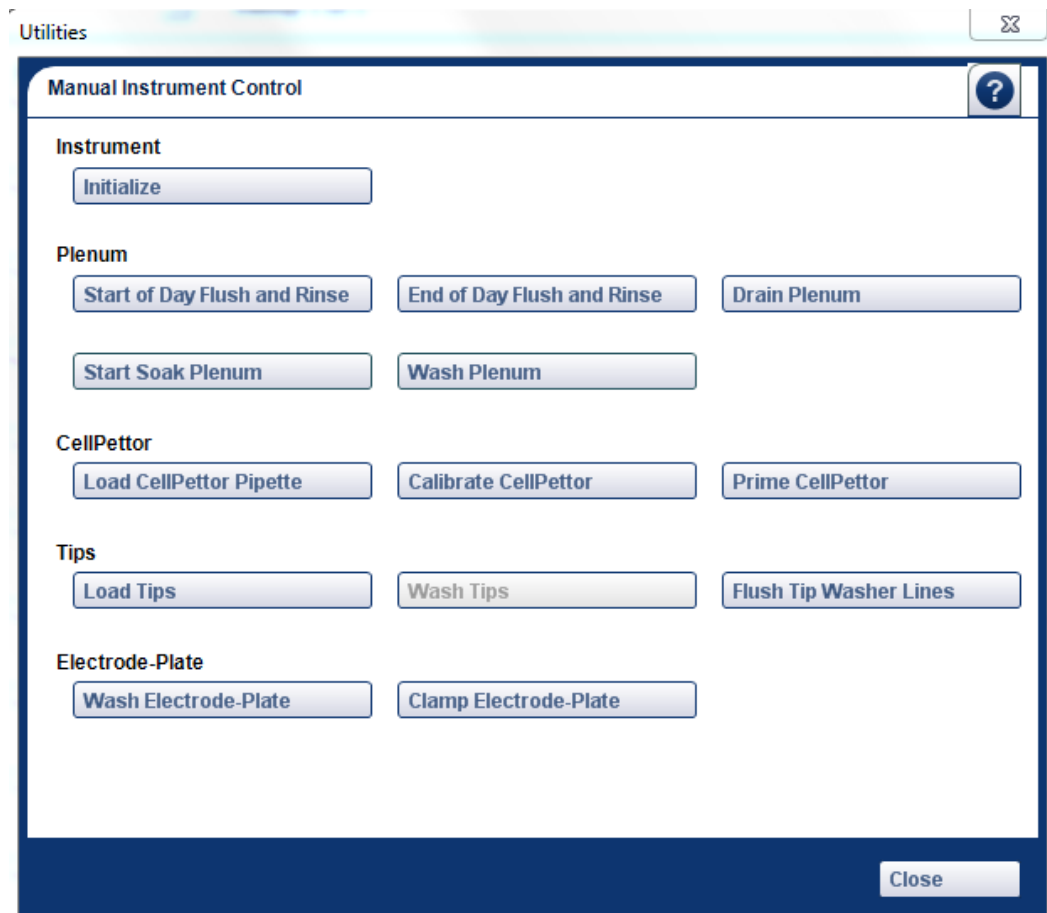
1. Prepare a Mother Plate:
  - a. Plate 50 µL of sample dissolved in 100% DMSO in columns 3 and 13 of 384-well plate.
  - b. Serially dilute (10 point CRC with 1:3 steps) using liquid handler robot.
  - c. Spin plate at 600 rpm for 1 min to collect all solution in the bottom of the well.

- d. Seal under argon and store at room temperature for up to one month (may not be suitable for all samples).
2. Prepare Daughter Plates. On the day of experiment prepare compound and agonist plates:
  - a. Dispense 100  $\mu$ L of external solution into each well of a 384-well plate (Compound Plate).
  - b. Dispense 100  $\mu$ L of 1mM GABA containing external solution into each well of a 384-well plate (Agonist Plate).
  - c. Add positive and negative controls to columns 1, 2, 23 and 24 of the compound plate.
  - d. Immediately prior to the experiment, transfer 1  $\mu$ L of DMSO stock solution from Mother Plate to Compound Plate and to Agonist Plate.
  - e. Mix three times and spin plate at 600 rpm for 1 min.

### Start IonWorks Barracuda (Start of Day)

1. Turn on IonWorks Barracuda instrument/computer using the switch located on the right side of instrument.
2. Open IonWorks Barracuda control software (the instrument will initialize automatically).
3. Make sure all waste containers are empty.
4. Make sure there is 0.9% NaCl in both A & B wash containers (approximately 4 L).
5. External solution bottle should be filled with DPBS without  $Mg^{2+}$  and  $Ca^{2+}$  (prevents deposits).
6. On the Utilities menu, select **Load Cell Pipettor** and follow the prompts:

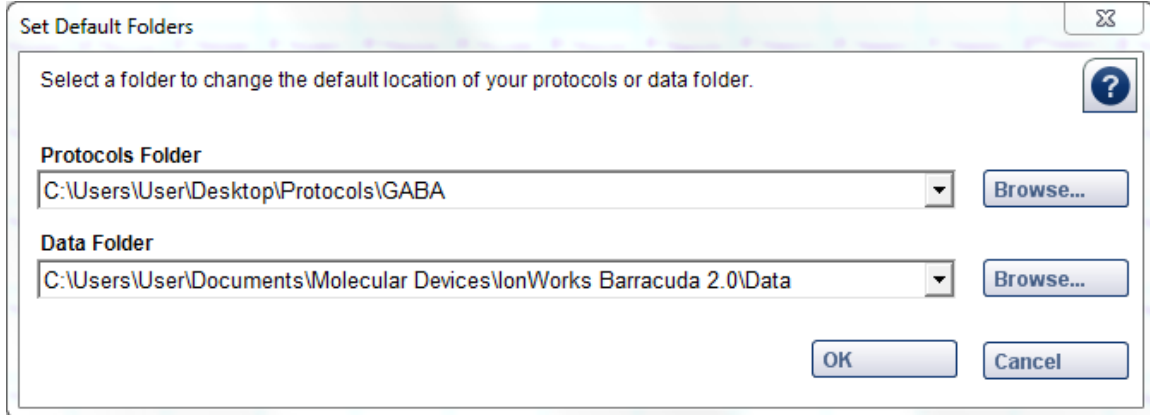




7. Fill both amphotericin B and Internal Solution bottles with internal solution containing 0.1 mg/mL amphotericin B.
8. Place Model Cell on support pins above wash station.
9. Insert ground electrodes into plenum (they must have soaked for at least 20 min in internal solution).
10. Make sure that a blank (uncontaminated with compounds) patch plate is correctly positioned in the **Patch Plate** position on the plenum.
11. On the **Utilities** menu, select **Start of Day Flush**.

## Select Data and Protocol Folders

On the **File** menu, select **Set Data Folders**:

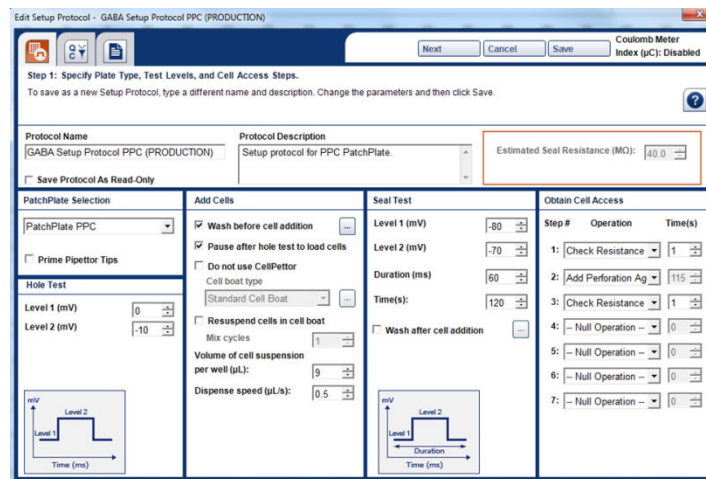


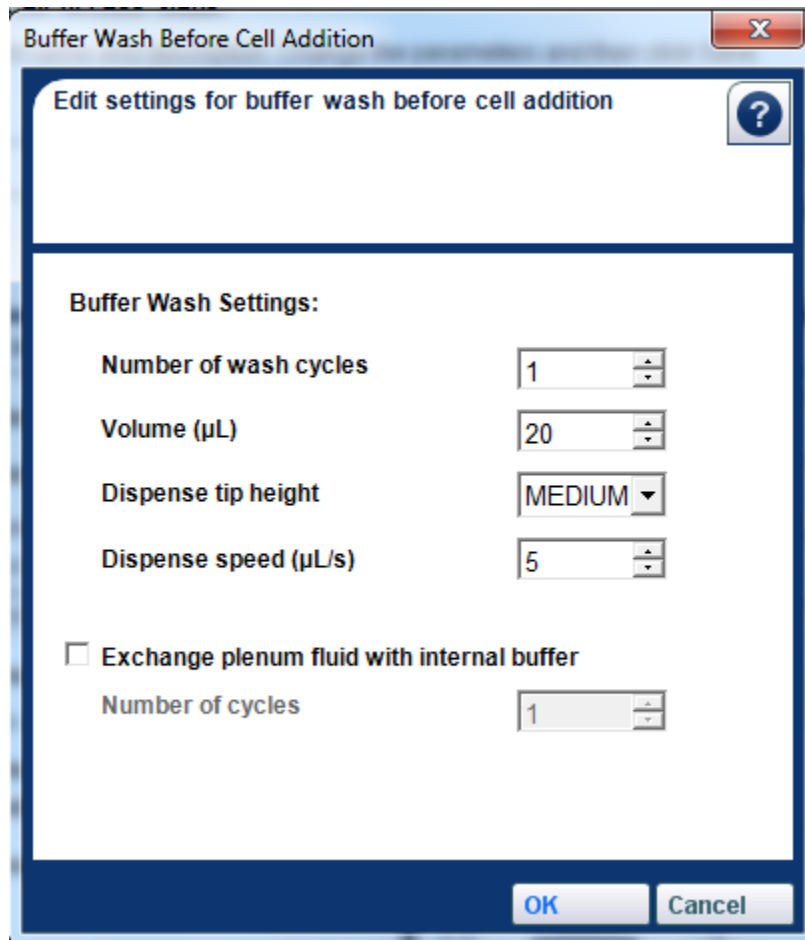
## Select IW-Barracuda Protocols for GABA<sub>A</sub>

On the **Protocol** window select **Setup**, **Command Voltage** and **Cleanup** protocols:

### Setup Protocol

From the **Setup Protocol** menu, input the following criteria into each of the different folder tabs:





1. In the **Add Cells** panel select **Wash before cell addition** and specify the wash criteria
2. In case that amphotericin B is not added to Internal Solution bottle, then **Create Cell Access** needs to be modified by the addition of **Wait 240 s** following the **Add Perforation Agent**

## Channel Protocol

From the drop down “Channel Protocol” menu, select appropriate protocol.

1. First compound addition:
  - a. Set holding potential to -80 mV.
  - b. Aspirate 10 µL of solution from **Compound Plate** (position **Plate 2**). Dispense at medium height at 5 µL/s.
  - c. Record current 2 s prior and 30 s after compound addition with sampling frequency at 1 kHz.

- d. Follow with 3 min compound incubation.
- e. No scans are recorded prior or after compound addition.

Step 1: Specify Scan and Compound Addition Parameters  
To save as a new Channel Protocol, type a different name and description. Change the parameters and then click Save.

Protocol Name: GABA Ag-Antag Protocol (3min Incubation)  
Protocol Description: GABA channel protocol with compound first and agonist second addition.  
Estimated Seal Resistance (MO): 40

Scan and Fluid Transfer Parameters

Number of Baseline Scans: 0  
Delay Between Scan (s): 10  
Holding Level (mV): -80  
Liquid Junction Potential (mV): 0

Compound Addition: 1

Record Data Simultaneously:   
Pre-trigger Duration (s): 2.0  
Post-trigger Duration (s): 30.0  
Voltage During Addition (mV): -80  
Sample Period (ms): 1  
Compound Incubation Time (s): 180.0  
Number of Scans After Compound Addition 1: 0  
Delay Between Scan (s): 10

Aspirate

Change Plate Before Aspirate:   
Compound Source: PLATE2  
Plate Type: Nunc 384W Round Natio  
Volume (µL): 10  
Buffer Volume (µL): 11  
Cell Volume (µL): 9  
Barcode Position: NONE

Dispense

Destination: PatchPlate  
Tip Height: MEDIUM  
Speed (µL/s): 5  
Mix Fluid After Dispense:   
Mix Cycles: 2

2. Second compound addition:
  - a. Maintain holding potential at -80 mV
  - b. Aspirate 10 µL of solution from “Agonist Plate” (position **Plate 1**). Dispense at medium height at 5 µL/s
  - c. Record current 2 s prior and 30 s after compound addition with sampling frequency at 1 kHz
  - d. No scans are recorded prior or after compound addition

Edit Channel Protocol - GABA Ag-Antag Protocol (3min Incubation)

Next Cancel Save Coulomb Meter Index (µC): Disabled

Step 1: Specify Scan and Compound Addition Parameters  
To save as a new Channel Protocol, type a different name and description. Change the parameters and then click Save.

Protocol Name: GABA Ag-Antag Protocol (3min Incubation)  
Protocol Description: GABA channel protocol with compound first and agonist second addition.  
Estimated Seal Resistance (MΩ): 40

Save Protocol As Read-Only

Scan and Fluid Transfer Parameters

Number of Baseline Scans: 0  
Delay Between Scan (s): 10  
Holding Level (mV): -80  
Liquid Junction Potential (mV): 0  
No Compound Additions

Compound Addition: 2

Record Data Simultaneously

Pre-trigger Duration (s): 2.0  
Post-trigger Duration (s): 30.0  
Voltage During Addition (mV): -80  
Sample Period (ms): 1  
Compound Incubation Time (s): 35.0  
Number of Scans After Compound Addition 2: 0  
Delay Between Scan (s): 10

Aspirate

Change Plate Before Aspirate  
Compound Source: PLATE1  
Plate Type: Nunc 384W Round Natu  
Volume (µL): 10  
Buffer Volume (µL): 11 A1  
Cell Volume (µL): 9  
Barcode Position: NONE

Dispense

Destination: PatchPlate  
Tip Height: MEDIUM  
Speed (µL/s): 5  
Mix Fluid After Dispense  
Mix Cycles: 2

For both, first and second dispense, adjust the **Advanced Aspirate Option** to the tip height of 20 µL, speed of 10 µL/s and extra volume to 2 µL. This setting minimizes the introduction of bubbles on dispense.

Advanced Aspirate Options

Enter additional parameters for aspirating the compound

**Aspirate**

Tip Height (µL) 20

Speed (µL/s) 10

Use Extra Aspirate

Volume (µL) 2

Mix Fluid Before Aspirate

Mix Cycles 2

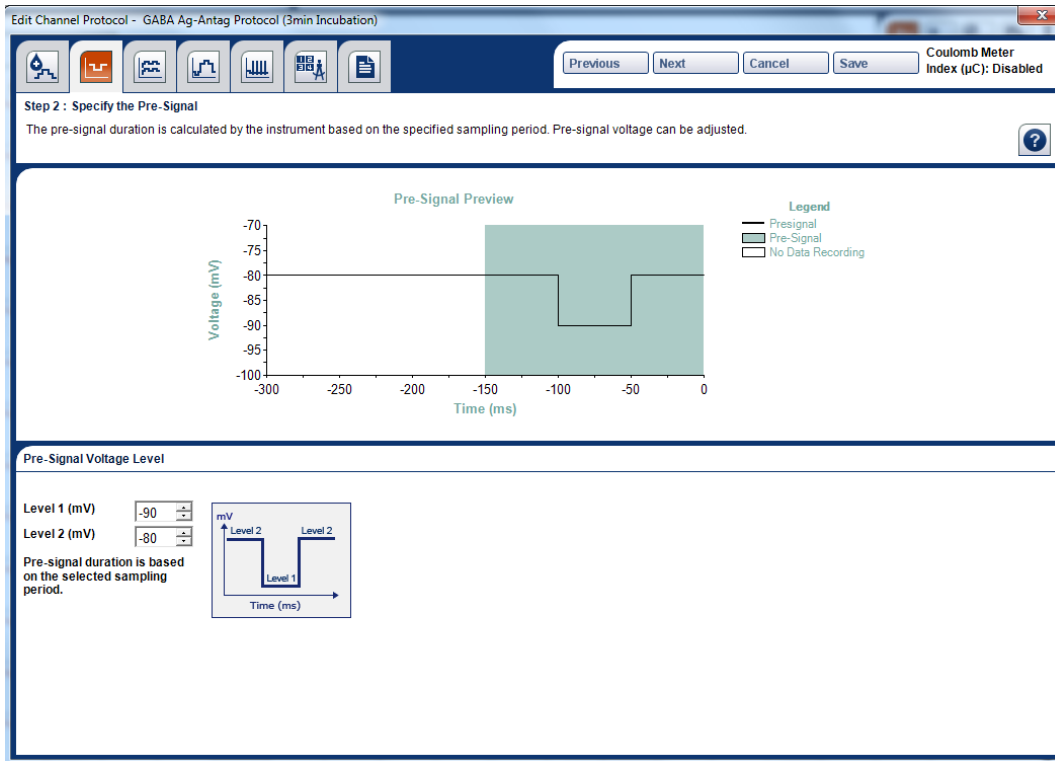
Mix Speed (µL/s) 5

Pre-wet Tips

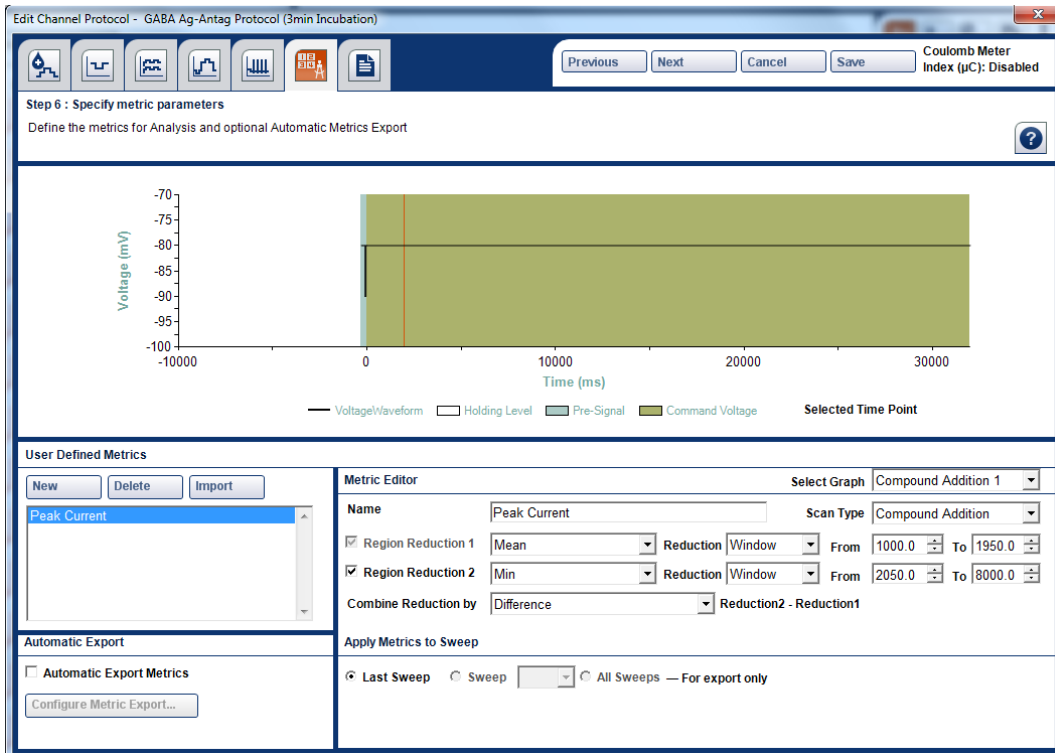
Tip Height (µL)  
Min: 5  
Max: 100

OK Cancel

3. Set the resistance pulse (pre-signal):



4. Set the metric parameters:



NOTE: In this metric, 'automated export metrics' is not used. This permits manual inspection and rejection of traces. The only measured parameter is peak current. Alternative measurements such as AUC or absolute current amplitude are not measured.

## Cleanup Protocol

From the **Cleanup Protocol** menu, input the following criteria into each of the different folder tabs:

**Edit Cleanup Protocol - GABA Cleanup Protocol (PRODUCTION)**

**Step 1: Specify Instrument Cleanup**  
One Wash is required. Choose the solution from Source A or Source B. Ultrasonic cleaning is recommended for the Electrode-Plate.

**Protocol Name:** GABA Cleanup Protocol (PRODUCTION)  
 Save Protocol As Read-Only

**Protocol Description:** GABA cleanup protocol. Ultrasonic cleaning applied for E-Plate washing (2x0.5min). F-head tips are discarded.

| Plenum   | Tip Washing  | Electrode-Plate  |
|--|--|--|
| <b>Drain Plenum</b><br><input type="checkbox"/> Wash plenum<br>Soak Duration (m): 30<br>Number of cycles: 1<br>Soak Duration (m) Min: 5, Max: 1440 | <input checked="" type="checkbox"/> Wash Fluid 1 <input type="checkbox"/> Enable ultrasonic cleaning<br>Wash Source: A<br>Number of strokes per wash cycle: 10<br>Number of wash cycles: 1<br><input type="checkbox"/> Wash Fluid 2 <input type="checkbox"/> Enable ultrasonic cleaning<br>Wash Source: B<br>Number of strokes per wash cycle: 5<br>Number of wash cycles: 1 | <input checked="" type="checkbox"/> Wash Fluid 1 <input checked="" type="checkbox"/> Enable ultrasonic cleaning<br>Wash Source: A<br>Dwell time per wash cycle (min): 0.5<br>Number of wash cycles: 2<br><input type="checkbox"/> Wash Fluid 2 <input type="checkbox"/> Enable ultrasonic cleaning<br>Wash Source: B<br>Dwell time per wash cycle (min): 1.0<br>Number of wash cycles: 1 |
| <b>Wash Tip Options</b><br><input type="radio"/> Wash Tips and Electrode-Plate<br><input checked="" type="radio"/> Discard tips                    |  |  |

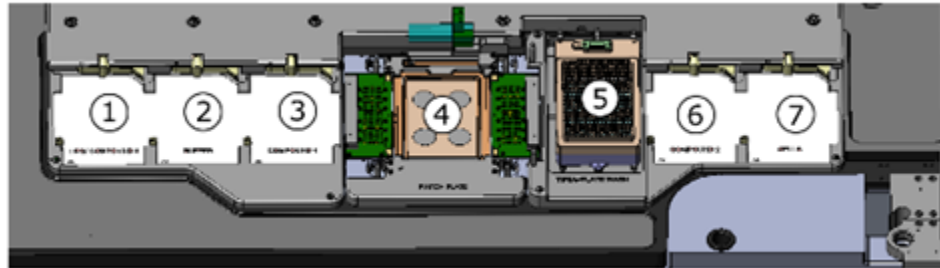
NOTE: This protocol discards tips and sonicates the electrode plate in aqueous solution. To further minimize compound carryover, an additional manual wash of the e-plate in 70% ethanol was performed off the instrument.

## Run Experiment

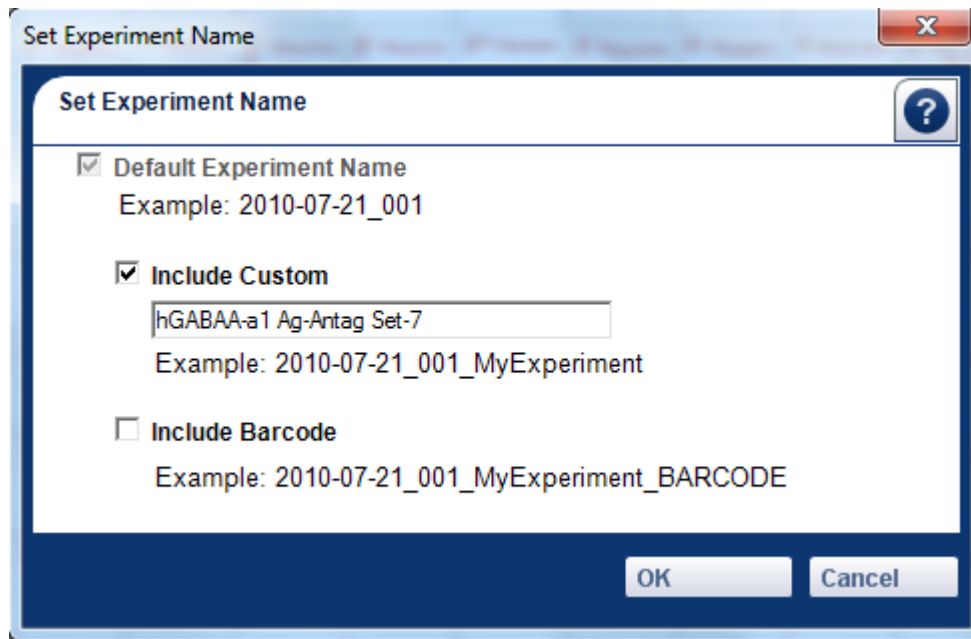
1. On **Set Default Folders** window, select the proper default folders for where the data and protocol files will reside.
2. Select the desired **Setup, Channel, and Cleanup Protocols** (as previously described) from the drop down menus.
3. Load the instrument deck. Make sure tips, boats, and plates are seated correctly:



- a. Pipette tips are in position **Tips** (position labeled 1 in the diagram below)
- b. External buffer boat is in position **External Buffer** (position 2)
- c. Agonist plate is in position **Compound 1** (position 3)
- d. Appropriate new patch plate (SH or PPC) is in position **Patch Plate** (position 4)
- e. Correct electrode plate is positioned on **Wash Station** (make sure that the plate is lying flat and in correct orientation) (position 5)
- f. Compound plate is in position **Compound 2** (position 6)
- g. Clean cell boat is in position **Cell Boat** (position 7)



4. Make sure that the cells position is empty (conical vial has been removed).
5. Set the experiment name.

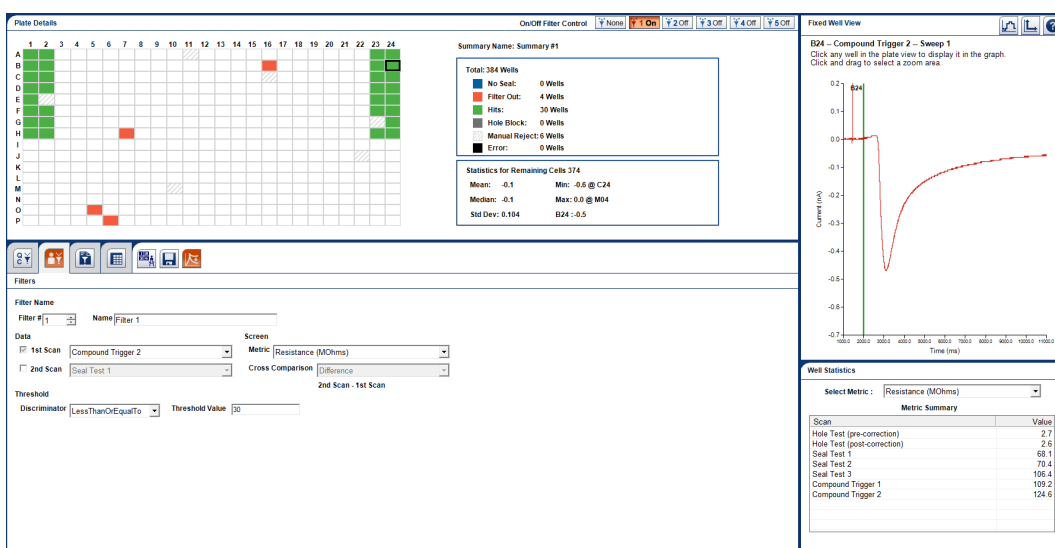


6. Click the green **Play** button to start the experiment.

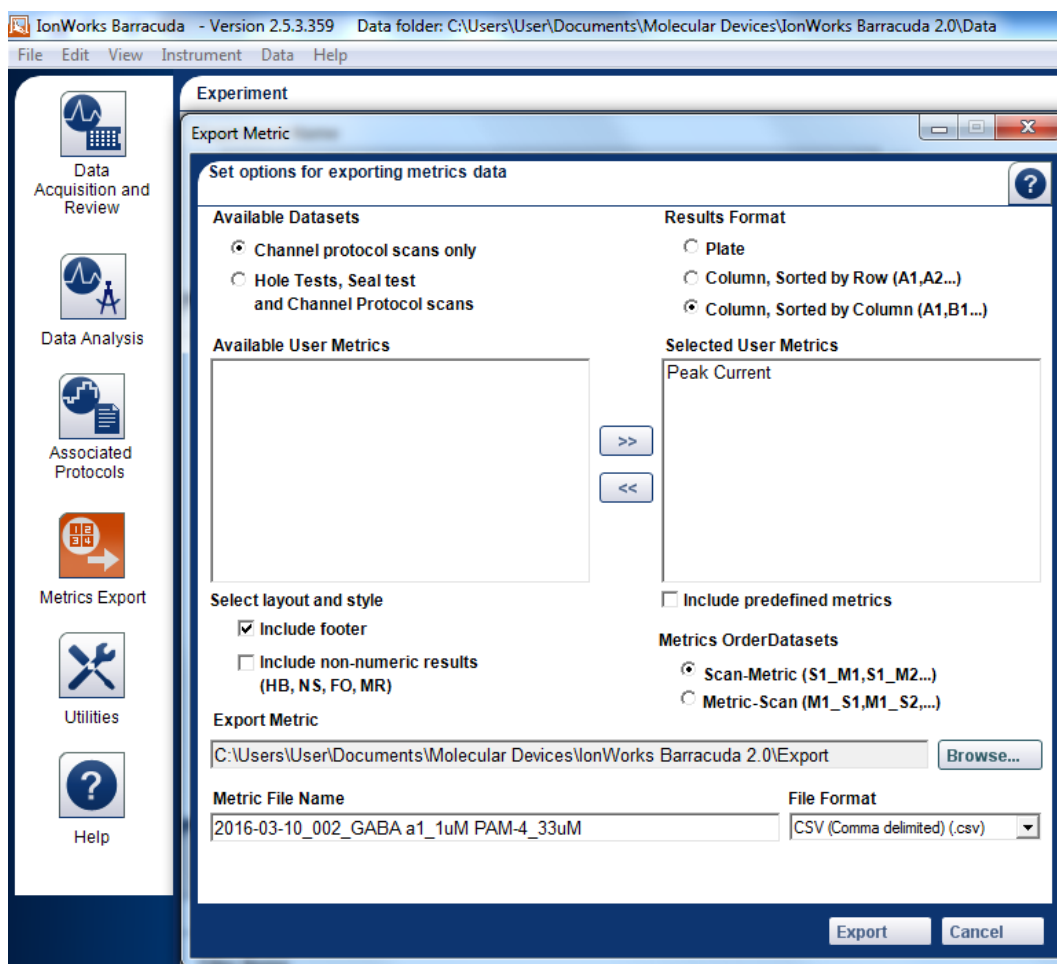
7. When the instrument pauses to load cells (after Hole Test) add the conical vial with cell suspension.
8. At the end of the run, remove and discard conical vial, tip box, agonist plate and compound plate. Remove the cell boat, wash it with H<sub>2</sub>O and wipe dry. Remove the electrode plate and wash by dipping in 70% ethanol followed by 0.9% NaCl solution. Buffer reservoir can be left on the deck if additional runs are planned.

## Analyze Data

1. From the **Data Analysis** button on the left, see below for an example of all the tabs that can be opened to configure data analysis and export.



2. In the **Define Filters** tab, set your desired hole/seal resistance, peak current amplitude, and/or other criteria for removing well data from the analysis. Additional filtering can be performed by visual inspection of traces and manual removal of wells.
3. Click the **Metric Exports** button on the left and define how your metrics should be exported.



## End of Day Flush and Rinse

1. Make certain 50% EtOH is in the alcohol wash bottle.
2. Disconnect external solution bottle, amphotericin B bottle, and internal solution bottle and replace with empty 50 mL conical vials.
3. Replace the electrode plate with model cell.
4. Replace the contaminated patch plate with an un-contaminated (has not been exposed to compounds) used patch plate.
5. Run **End of Day Flush & Rinse** protocol from the **Utilities** menu.
6. Remove ground electrodes and place them back into internal solution soak.
7. Power off the IonWorks Barracuda.

## Modifications of IW-Barracuda Protocols for Assessment of Agonists and Allosteric Modulators of GABA<sub>A</sub> Channels

### Agonist

Use the same protocol as described for assessment of current block. Compound plate should contain 1 mM GABA in position designated as maximum control (Col 1, 2, 23 and 24). In the analysis, select scan 1 instead of scan 2.

### Positive Allosteric Modulator (PAM)

Use the same protocol as described for assessment of current block. Adjust the agonist concentration in “agonist Plate” to GABA EC<sub>20</sub>. Add appropriate positive and negative controls to “Agonist Plate” (Col. 1, 2, 23 and 24). Analyze scan 2.

### Negative Allosteric Modulator (NAM)

Use the same protocol as described for assessment of current block. Adjust the agonist concentration in “agonist Plate” to GABA EC<sub>60</sub>. Add appropriate positive and negative controls to “Agonist Plate” (Col. 1, 2, 23 and 24). Analyze scan 2.

## Appendix 4: Protocol for Assessment of State-Dependent Sodium Channel Inhibitors on PatchXpress

### Overview

This protocol is designed to evaluate block of voltage-gated sodium channels at depolarizing voltages that favor interactions of test compounds with inactivated states of the channel.

### Voltage Protocol using scripting

Cells are sealed and whole cell configuration attained according to defined patch protocols that can be obtained from Molecular Devices. Sampling rate is adjusted to the maximal available rate of 31.25 kHz (32 μs sampling interval). Once a stable whole cell configuration is achieved, cells are held at -120 mV and currents are monitored with short (5-20 ms) test pulses to a voltage near the peak of the current-voltage curve until currents reach stable amplitude. At this point, a standard protocol is executed to determine the voltage dependence of steady-state inactivation, for example this protocol may consist of a set of 1 s conditioning pulses to voltages ranging from -120 mV to -20 mV followed by a short test pulse to the same voltage used during the previous test pulses. A software script is used to select a new holding potential that corresponds to approximately 40% channel inactivation. Current amplitudes are again allowed to stabilize at the new inactivated potential for approximately 2-3 minutes while applying test pulses at 0.1 Hz. Following current stabilization at the inactivated potential, a 10 pulse train at 5 Hz is applied. Following the pulse train, currents are again allowed to stabilize at 0.1 Hz prior to the first

compound addition. Two compound additions occur approximately 15 s apart, and effects on current amplitude are monitored by test pulses at 0.1 Hz. Once the software script determines that stable current amplitudes have been reached, a second 5 Hz pulse train determines use-dependent effects. Wash-out occurs at the inactivated potential for approximately one minute before the holding potential is returned to -120 mV with continued wash-out until current recovers to 80% of its initial control amplitude. Assuming satisfactory wash-out has occurred, the cell may be used for further compound additions until cell health and/or current amplitude do not remain stable.

## Typical Solutions

External Buffer Solution: 137 mM NaCl, 4 mM KCl, 1.8 mM CaCl<sub>2</sub>, 0.2 mM MgCl<sub>2</sub>, 10 mM HEPES, 10 mM D-mannitol, adjust pH to 7.4 using NaOH. Final osmolality: 300-310 mOsm

Internal Buffer Solution: 60 mM CsF, 70 mM CsCl, 5 mM NaCl, 10 mM EGTA, 10 mM HEPES, adjust pH to 7.4 using CsOH. Final osmolality: 290-300 mOsm

Notes:

-Slightly lower osmolality in the internal solution compared to the external solution often helps with sealing.

-Some F<sup>-</sup> in the internal solution helps to maintain seal resistances; however, higher F<sup>-</sup> concentrations can lead to time-dependent shifts in the voltage dependence of inactivation.

-At room temperature the Na<sup>+</sup> reversal potential for this solution is approximately +84 mV.

## Start of Day

1. Allow external and internal solutions to come to room temperature, if stored refrigerated.
2. Turn on PatchXpress 7000A Instrument using switch located on left side of instrument.
3. The associated CPU will need to be restarted to initialize settings between CPU and Hardware.
4. Open the PatchXpress Control Software.
5. When prompted by PatchXpress Commander, log on to the server housing the database.
6. After initialization, the instrument will prompt you to begin **Start of Day** procedure.
7. Make sure there is H<sub>2</sub>O in the wash (thin) container and that the waste (large) container inside the PatchXpress cabinet is empty.
8. Load external and internal solutions onto the PatchXpress Instrument.

9. Begin **Start of Day** procedure - this replaces the H<sub>2</sub>O in the lines with the internal and external assay buffers- using the blank seal chip stored in the instrument.
10. Prime wash station (hardware fluidics).
11. Add pipette tips.

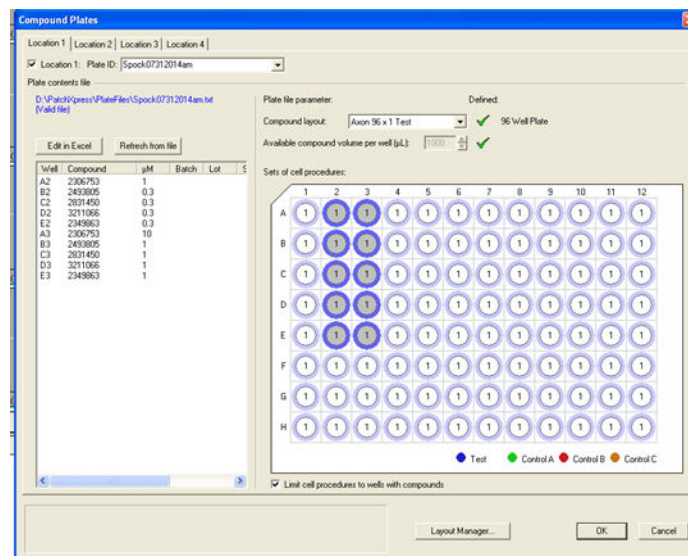
## Cell preparation

1. Start with >70% confluent T-75 flask (or equivalent) of HEK cells expressing the Nav1 channel of interest.
2. Pour off media, and add 2 mL TrypLE .
3. Incubate with TrypLE for 30-120s, tap flask to dislodge cells and add 3 mL of media.
4. Triturate with 5 mL pipette.
5. Transfer to 15 mL conical tube and spin at 1300-1500 rpm for 3 min.
6. Aspirate supernatant and resuspend cell pellet in 4-8 mL of media.
7. Triturate with 1 mL pipette and add 1 mL each of the cell suspension to 4-6 small Eppendorf tubes.
8. Store uncapped in incubator for at least 30 min and up to 3 h (optimal timing may differ between cell lines).
9. At the start of an experiment, spin cells at 2000 rpm for 2 min, remove supernatant, resuspend in 200 µL external buffer solution, triturate lightly and place the tube into the PatchXpress instrument

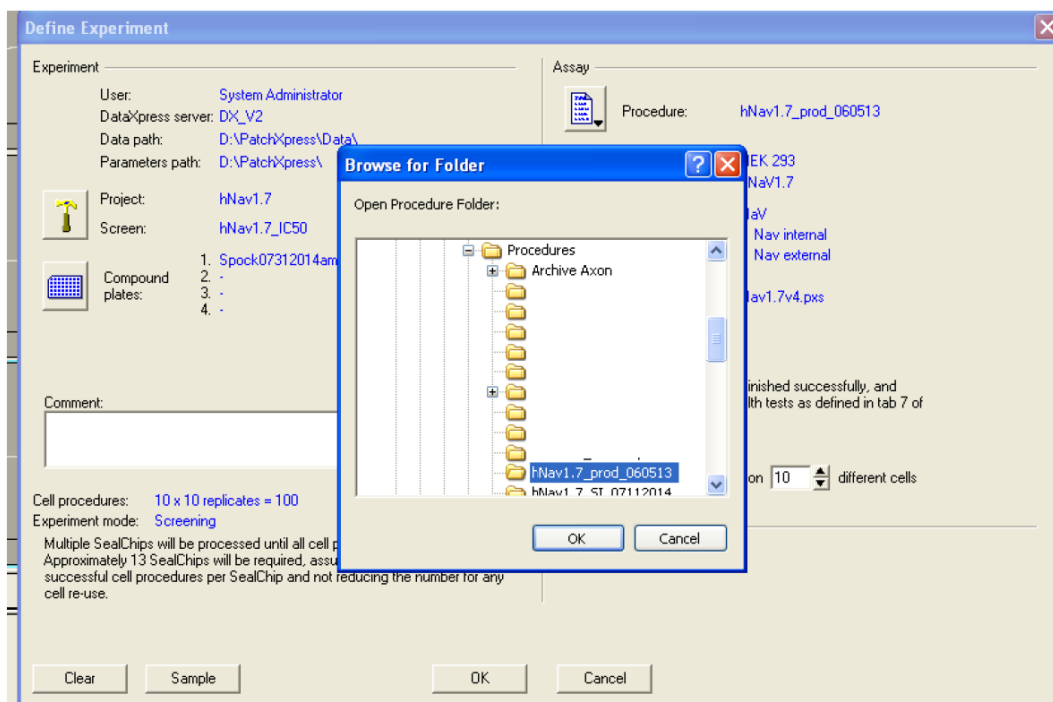
## Start of Experiment

The following settings must be established to define the experiment on the PatchXpress prior to loading the Seal chip:

1. In **Define Experiment** window, select the proper project from the menu.
2. Create a table using Excel that specifies the location and concentration of each compound to be tested in the compound plate and select this table in the PatchXpress software.



3. Select the proper procedure from the dropdown box in **Procedure** window:



4. Check **Re-use cells** with 10 replicates.
5. Under **Select Cell**, select cell, i.e. the parental cell background – typically HEK293 or CHO, and channel, e.g. Nav1.x, from the drop down boxes.
6. Select the appropriate internal and external solutions.
7. Select the appropriate patch settings. Molecular Devices provides standard settings for HEK293 and CHO cells that can be modified for optimal results with a particular cell line of interest.

8. Select **Screening mode** which means that the software will keep track of which compounds and concentrations have been tested successfully.

Once the experiment has been defined:

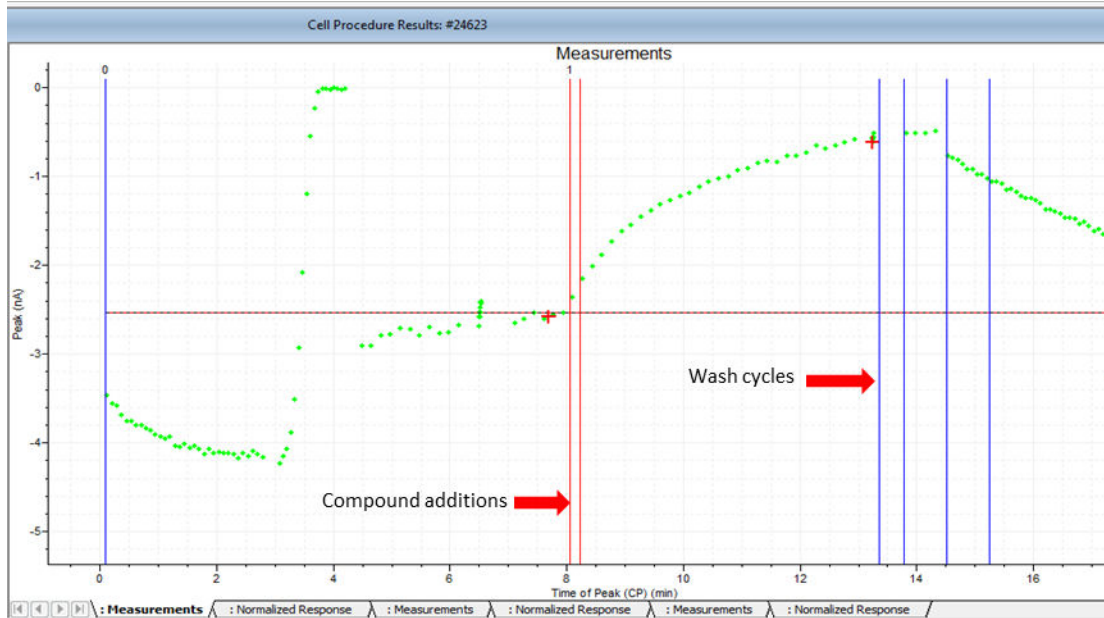
- Place test compounds onto the deck of the PatchXpress instrument. Test compounds need to be dissolved in external buffer solution and can be presented in a 96-well plate or in glass vials inserted into a plastic rack provided by Molecular Devices.
- Wash station may need to be primed again, if too much time has passed since this step was performed last.
- Resuspend an aliquot of cells in External Buffer Solution (see last step of Cell Preparation protocol) and place into the PatchXpress instrument.
- Remove a seal chip from the glass vial and flick out the remaining water. Blow the seal chip dry using the tool inside the PatchXpress cabinet and place the seal chip into the receiver on the deck of the PatchXpress with the straight edge to the back.
- Click the green **Play** button to start the experiment. Once the instrument initializes, it will request a barcode. Enter the barcode from the seal chip vial using the barcode reader (this step is optional).
- After the seal chip is loaded, the instrument will “call for cells”, requiring the user to enter information regarding the cell line for future reference (examples include cell line, passage number and time after dissociation).

## Analysis

Aggregate data from multiple single concentration additions are plotted and fit using the Hill equation. Use-dependence based on the last pulse of the 5 Hz pulse trains may also be reported. Run down correction may be employed on a limited basis.

This procedure overview is summarized below for a compound which demonstrates inhibition:





## End of Day

1. Replace external and internal buffer solutions with water.
2. Run **End of Day** protocol.
3. Turn off the computer and PatchXpress instrument.



# Assay Development Guidelines for Image-Based High Content Screening, High Content Analysis and High Content Imaging

William Buchser, Ph.D.,<sup>1</sup> Mark Collins, Ph.D.,<sup>2</sup> Tina Garyantes, Ph.D.,<sup>3</sup> Rajarshi Guha, Ph.D.,<sup>4</sup> Steven Haney, Ph.D.,<sup>5</sup> Vance Lemmon, Ph.D.,<sup>6,\*</sup> Zhuyin Li, Ph.D.,<sup>7,†</sup> and O. Joseph Trask, B.S.<sup>8,‡</sup>

Created: October 1, 2012; Updated: September 22, 2014.

## Abstract

Automated microscope based High Content Screening (HCS, or HCA, HCI) has gained significant momentum recently due to its ability to study many features simultaneously in complex biology systems. HCS can be used all along the preclinical drug discovery pipeline, it has the power to identify and validate new drug targets or new lead compounds, to predict *in vivo* toxicity, and to suggest pathways or molecular targets of orphan compounds. HCS also has the potential to be used to support clinical trials, such as companion diagnostics. In this chapter, state of the art HCS approaches are detailed, and challenges specific to HCS are discussed. It should serve as an introduction for new HCS practitioners. More chapters will follow on specific assay examples and on high level informatics analysis.

## 1. Introduction

### 1.1. What is High Content Screening (HCS)?

High Content Screening (HCS) or automated microscope-based screening measures biological activity in single cells or whole organisms following treatment with thousands of agents, such as compounds or siRNAs, in multi-well plates. Typically, multiple features of the cell or organism are measured with one or more fluorescent dyes leading to the

---

<sup>1</sup> Washington University in St. Louis School of Medicine, Department of Genetics; Email: wbuchser@genetics.wustl.edu. <sup>2</sup> PurpleBio Consulting; Email: Collinsusa2010@gmail.com. <sup>3</sup> MaxSAR Biopharma; Email: garyante@optonline.net. <sup>4</sup> National Center for Advancing Translational Sciences, National Institutes of Health (NCATS/NIH); Email: Rajarshi.guha@nih.gov. <sup>5</sup> Eli Lilly and Company; Email: Shaney314@gmail.com. <sup>6</sup> Miami Project to Cure Paralysis, University of Miami; Email: vlemmon@med.miami.edu. <sup>7</sup> Bristol-Myers Squibb; Email: Zhuyin.Li@bms.com. <sup>8</sup> The Hamner Institutes for Health Sciences; Email: jtrask@thehamner.org.

✉ Corresponding author.

\* Editor

† Editor

‡ Editor

term High Content. At times, HCS has been called high content analysis (HCA) high content imaging (HCI) or image cytometry (IC). Generally, HCA, HCI and IC refer to lower throughput automated microscope based assays (<100,000 samples or data points), although HCA sometimes refers to the analysis portion of HCS. The term HCS was first used in a 1997 paper by Giuliano et al (1). It appears to be the natural successor to the automation of clinical histology (2) and an extension of HTS plate reader systems, with early references to the automation of the analysis of microscope images dating back to the advent of the desk top computing (3). Examples of early systems were the Onco Videometric150, the BDS chromosome painting and the Meridian ACIS Ca<sup>2+</sup> image tracker, among others. Our modern automated analysis solutions owe their origins to Metamorph and ImagePro as well as a 1969 publication by Rosenfeld (4).

In contrast to traditional HTS, which has a single read out of activity, HCS allows a scientist to measure many properties or features of individual cells or organisms at once. The ability to study many features and multiplex simultaneously is both what gives HCS tremendous power and challenging complexity. Like its predecessor technologies such as standalone low throughput automated image analysis systems and screening instruments including the FMAT (5), HCS can be quite effectively used simply to provide improved signal to background or signal to noise. But it can also enable both targeted and phenotypic assays that measure movement within a cell or between cells or allow analysis of specific sub-populations of cells in a heterogeneous mix that would be difficult or impossible to run with other techniques. Most powerfully, HCS can be used to help predict the efficacy of potential drugs in unique cellular niches when applied to physiologically relevant cellular systems. The predictive power of such systems can often be enhanced by working with primary cells or differentiated stem cells and in 3-D culture rather than with cell lines in a traditional 2-D culture where many unique aspects of cellular physiology have been lost (6,7). Bickmore focused on this critical problem when she noted “the exquisite cell-type specificity of regulatory elements revealed by the ENCODE studies emphasizes the importance of having appropriate biological material on which to test hypotheses” in the 2012 publication of the data from the ENCODE project (8).

## 1.2. Uses of HCS

The most obvious applications of HCS are primary screens of potential leads, molecules that can be further optimized into drug candidates, for cellular activities that cannot be easily measured by a single endpoint, such as spatially localized proteins or measurements of cellular morphology. In almost all instances, there are alternative assay formats that can be used for primary screening, but HCS increases the power of the experiment by measuring. For example, HCS can be used to measure the formation of gap junctions by mixing cells that have been preloaded with fluorescent dye with non-loaded cells, and measuring the spread of the fluorescent dye between cells over time in culture (9). This is a very robust way to measure the establishment of functional gap junctions; however, alternatively, a binding assay could be established that looked for an increase in the expression of the gap junction proteins on the cell surface as a primary screen. That kind

of HTS approach could not, however, assess functional gap junctions, the way HCS can. Likewise, cellular differentiation can be monitored by measuring an increase in the expression of a marker of the differentiated cell type and/or a decrease in the expression of a marker of the undifferentiated cell type. However, coupling these measurements with a visual measure of differentiation can increase confidence in the outcome.

Cellular morphology changes, such as neurite outgrowth can only be measured in a microscopic image, with or without a molecular marker to confirm the relevance of observed morphology changes. Cell morphology can also be an important measure of cellular differentiation (10) such as the differentiation of epithelial cells to mesenchymal cells (11) or of precursor cells into oligodendrocytes, astrocytes and neurons (12). Here too, the concomitant use of a differentiation marker can help confirm initial analyses and clarify the lineage. Intracellular morphological changes such as protein expression, trafficking or translocation can also be studied. An example of protein translocation, NF- $\kappa$ B translocation will be discussed in a separate chapter. Movement between the cytoplasm and the nucleus or other organelles can be measured or trafficking between organelles and the cell surface can be studied. Likewise, one can measure internalization of proteins or vesicles. Similarly, movement of cells across a well, such as models of wound healing, migration, or chemotaxis, can all be evaluated with HCS (13, 14).

In addition, there are many useful lead identification applications that could be done with more traditional HTS techniques but where HCS provides an advantage. Because HCS provides more than just the endpoint, off-target effects such as cytotoxicity or fluorescence from the test compounds are easily identified. Additionally, signal to background can often be improved; for example, cell surface binding can be seen in the presence of background noise by using confocal imaging and co-localizing the signal with a cellular surface marker. Alternatively, there are assays where the statistical power of a single read out is not sufficient to enable screening in singlicate but is enabled by combining multiple features to improve the predictive power of the assay.

### 1.3. Applications of HCS beyond lead identification

The utility of HCS goes well beyond the identification of lead compounds for the development of pharmaceuticals. HCS can be used all along the drug discovery pipeline for the identification or validation of appropriate drug targets, for predicting the pathway or molecular target of compounds identified in phenotypic screens, for lead optimization and toxicity prediction or for the analysis of clinical data. Outside of biological assays, HCS systems have also found utility in chemistry and material science, for instance for screening of crystallization conditions, corrosion resistance or ceramic formation/structure.

Target identification and validation is a very common application of HCS. Potential drug targets can be identified by assaying the effect of increasing or knocking-down RNA expression in an assay that could later be used for compound screening. The cell used in the assay must be amenable to transfection and the cell culture conditions will often need to be modified to allow for translation, transcription and expression of the desired protein

to be over expressed or alternatively for the degradation of the existing mRNA of a protein to be knock-down. Alternatively, new targets and pathways can be identified by screening compounds with known mechanisms of action against a phenotype. Not surprisingly, the potential targets identified by these two approaches are often complementary rather than confirmatory since there is a bias in the timing of the effects (15, 16). Overexpression of proteins can occur very quickly, within minutes of transfections. In contrast, RNAi mediated knockdown can take 48 hours or longer to reduce protein levels. These same techniques can also be used for validating suspected targets although clinical or human genetic data is needed for full validation.

HCS can be used for target prediction or pathway profiling. Pathway profiling is an approach used to identify the pathway or target of an orphan compound coming from a phenotypic screen where assays known to be sensitive to the regulation of a pathway or target are used to suggest the mechanism of action, MOA, of an orphan compound. For example, Lonza-Odyssey Thera (17) and the Broad Institute's Metabolite profiling platform (<http://www.broadinstitute.org/scientific-community/science/platforms/metabolite-profiling-platform/metabolite-profiling-platform>) both have existing platforms for assigning MOA to compounds with unknown MOA.

HCS can also be used to improve our understanding of the on and off target effects of compounds identified by traditional HTS as they progress through lead optimization. For instance, a cellular enzyme activity assay can be used to confirm that a compound known to affect enzyme activity in a biochemical assay retains activity in the cellular environment. Alternatively, compounds identified by traditional screens can be clustered by cellular phenotype in an imaged based screen to suggest both selectivity and toxicity issues. More directly, *in vitro* micronuclei formation assays (18) use HCS to predict which compounds are likely to lead to DNA damage *in vivo* and developmental toxicity assays run on whole embryos can warn of potential reproductive toxicity liabilities that will need to be further evaluated (19).

Even further down the pharmaceutical pipeline, HCS is used to evaluate both *ex vivo* and clinical samples for relevant activity. For instance, both preclinical and clinical blood samples can be assays for biomarker activity of particular cell types by HCS (20).

## 1.4. HCS Challenges

Even with the tremendous processing capacity of modern computers, high speed interconnections, and relatively cheap data storage available with today's computers, the application of HCS has significant technical challenges that need to be considered. Although many instruments come with powerful, easy to use image analysis software, HCS practitioners often find that third party analysis software is needed to improve the performance of an occasional assay. In these cases, fluid partnership between the assay developer and an image analysis expert can greatly reduce assay development time by balancing the effort put into optimizing each. At the same time, due to lack of image and data format standards, many solutions for data storage, data transfer, and data annotation, do not translate well between platforms. In addition, the total size of data collecting and

manipulated in HCS can be daunting. Storage needs for a single academic lab are typically a few terabytes per year. The costs for on-line storage with RAID and off-line backup are not trivial (between \$20K - \$100K in 2012) and decisions will eventually have to be made about what data to keep and what to discard. Anticipating data and image transfer and sharing needs during the installation of your HCS solution will ultimately make your solution much more satisfying.

The other area that needs careful contemplation before embarking on an HCS campaign is the consistency and reproducibility of your cellular model. It is common for variables that would not be noticeable in a traditional HTS to become a major source of variance. Consider the effects of mechanical forces or thermal fluctuation on cellular stress responses (21, 22). Differentiation assays are acutely sensitive to changes in proliferation rates that vary with donor age (23, 24). Likewise, proliferation assays are sensitive to differentiation. Gene translation rates may be affected by what phase of the cell cycle cells begin in. The power of HCS to measure basic biological phenomenon, means that the practitioner also needs to be acutely aware of controlling the assay conditions and of interpreting results, with the latter being one of the most important aspect of HCS.

## 1.5. Summary

HCS has the power to identify new drug targets or new lead compounds, help predict cellular *in vivo* toxicity, suggest molecular targets of orphan compounds, and assess *in vivo* activity among other yet to be explored uses. HCS can be used to measure the effects of compounds and biological molecules such as plasmids carrying cDNAs, or RNAis on subpopulations of cells and specific cell types in mixed cultures. It can be used to measure movement, be it intracellular, cellular or intercellular. Any phenomenon that can be seen reproducibly in a microscope can ultimately be assayed with HCS. Important considerations and state of the art approaches will be detailed in rest of the chapter.

## 2. Image Technologies and Instruments

### 2.1. Introduction to Image Technologies

In theory, any instruments that produce multiparametric analysis of cellular or organismal phenotypes can produce high content data. Fluorescent Activated Cell Sorters (FACS) with multiple lasers can do this, as can MALDI-TOF mass spectrophotometers. But the term is most conventionally applied to automated microscopes using fluorescent and transmitted light to image cells, tissues, or small organisms such as Zebrafish embryos, *C. Elegans* or *Drosophila* larva followed by sophisticated image and data analysis. There are many commercial vendors of instruments in the High Content Analysis (HCA) arena and it is impossible to describe them all as the market and models are constant changing. Nonetheless, it is possible to divide the most widely used instruments into just three categories: wide-field imagers, confocal imagers and laser scanning cytometers. Basic descriptions of features that define each category will be provided along with representative examples.

### 2.1.1. High Content Screening requires speed

Effective screening campaigns required that the instrumentation have as high a throughput as possible. In the high content arena many choices have to be made to enable fast data acquisition. Lower magnification allows larger image fields that can capture larger numbers of cells which is needed to obtain statistically meaningful results. Similarly, cameras with larger chips (2048×2048 pixel vs 1040×1400 pixel) can image larger fields. Use of high intensity light sources such as lasers or optimizing fluorescence staining or fluorescent reporter expression so the fluorescent signals are bright will reduce integration exposure time and therefore the image acquisition time, as does using an objective with relatively high numerical aperture. If essential phenotypic features can be recognized with two channels as opposed to three, four or more channels, large savings in screening times can be achieved. During the assay development phase selecting the appropriate features that discriminate positive and negative controls can dramatically speed the final screen design to achieve the highest throughput possible. It is important to keep in mind that the goal is not necessarily to produce attractive images of individual cells, of the sort acquired with high magnification on a confocal microscope. Rather the goal is to detect and quantify critical features from the captured image that define a large phenotypic space from hundreds of cells in a particular treatment condition in as short a time as possible.

### 2.1.2. High Content Imagers versus Microscopes

High content imagers (HCI) at the present time typically consist of an automated microscope or components of a microscope in a box supplied with image analysis software and commonly have image management packages to store images on a server/data storage system. They generate very large image sets and associated meta-data that can be greater than a 0.5 TB per day at full capacity in screening campaigns. Compared to research microscopes, the configuration choices are much more limited. For example, a particular instrument may have only one fluorescent light source option, one or two camera options and no choices regarding objectives. But they have rapid autofocus and very precise stages optimized for multi-well plates and most systems offer environmental control for live cell imaging.

### 2.1.3. High Content Analysis versus High Content Screening

HCI can be used in two contexts. In a research environment, HCA is often a medium throughput activity where a few hundred or a few thousand perturbagens (compounds, drugs, siRNAs, cDNAs) are tested and scores of parameters are recorded from each individual cell using multiple imaging channels. The readouts can be kinetic or single endpoint using live or fixed cells respectively. The images are retained and perhaps reanalyzed with the goal of getting a very complex assessment of different subpopulations of cells in each well. The purpose could be basic research or to serve as a tertiary screen to study the toxicological properties of hits from a target based screen. In contrast, HCS is like other HTS methods aimed at screening 100,000s of perturbagens. The goal is to identify hits for additional testing. The readout is typically a fixed endpoint to reduce



noise and facilitate automation. A smaller number of parameters are often selected during the assay development phase to speed screening and reduce the data storage requirements.

#### 2.1.4. Background Information on Microscopy

Fluorescence imaging is widely used in biomedical research so a detailed introduction is not appropriate here. Several commercial and non-commercial websites provide extremely detailed information about microscopy and readers are encouraged to explore them to learn details about different fluorescent techniques listed in the links provided in below:

- Florida State University
  - Home: <http://micro.magnet.fsu.edu/primer/index.html>
  - Microscopy: <http://micro.magnet.fsu.edu/primer/index.html>
  - Fluorescence microscopy: <http://micro.magnet.fsu.edu/primer/index.html>
  - Objectives: <http://micro.magnet.fsu.edu/primer/anatomy/objectives.html>
  - Filters: <http://micro.magnet.fsu.edu/primer/lightandcolor/filtershome.html>
  - Confocal: <http://micro.magnet.fsu.edu/primer/techniques/confocal/index.html>
  - Numerical Aperture: <http://micro.magnet.fsu.edu/primer/anatomy/numaperture.html>
  - Airy Disc: <http://micro.magnet.fsu.edu/primer/java/imageformation/airydiskbasics/index.html>
  - Nipkow: <http://micro.magnet.fsu.edu/primer/techniques/fluorescence/spinningdisk/index.html>
  - Laser light sources: <http://micro.magnet.fsu.edu/primer/lightandcolor/lasersintro.html>
  - Fluorescent Proteins: <http://micro.magnet.fsu.edu/primer/techniques/fluorescence/fluorescentproteins/fluorescentproteinshome.html>
  - FRET: <http://micro.magnet.fsu.edu/primer/techniques/fluorescence/fret/fretintro.html>
- Olympus
  - Microscopy: <http://www.olympusmicro.com/primer/anatomy/anatomy.html>
  - Fluorescence microscopy: <http://www.olympusmicro.com/primer/techniques/fluorescence/fluorhome.html>
  - Objectives: <http://www.olympusmicro.com/primer/anatomy/objectives.html>
  - Filters: <http://www.olympusmicro.com/primer/lightandcolor/filter.html>
  - Confocal: <http://www.olympusmicro.com/primer/techniques/confocal/index.html>
  - Numerical Aperture: <http://www.olympusmicro.com/primer/anatomy/numaperture.html>
  - Airy Disc: <http://www.olympusmicro.com/primer/techniques/confocal/resolutionintro.html>

- Nipkow: <http://www.olympusmicro.com/primer/techniques/confocal/confocalscanningsystems.html>
- Bleed-through: <http://www.olympusmicro.com/primer/techniques/confocal/bleedthrough.html>
- Non-laser light sources: <http://www.olympusmicro.com/primer/techniques/confocal/noncoherentsources.html>
- Laser light sources: <http://www.olympusmicro.com/primer/techniques/confocal/confocallaserintro.html>
- Fluorescent Proteins: <http://www.olympusmicro.com/primer/techniques/confocal/applications/opticalhighlighters.html>
- FRET: <http://www.olympusmicro.com/primer/techniques/fluorescence/fret/fretintro.html>
- Nikon:
  - Home: <http://www.microscopyu.com>
  - Microscopy: <http://www.microscopyu.com/articles/optics/components.html>
  - Fluorescence microscopy: <http://www.microscopyu.com/articles/fluorescence/fluorescenceintro.html>
  - Objectives: <http://www.microscopyu.com/articles/optics/objectiveintro.html>
  - Filters: <http://www.microscopyu.com/articles/fluorescence/filtercubes/filterindex.html>
  - Confocal: <http://www.microscopyu.com/articles/confocal/index.html>
  - Numerical Aperture: <http://www.microscopyu.com/articles/formulas/formulasna.html>
  - Airy Disc: <http://www.microscopyu.com/articles/optics/mtfintro.html>
  - Nipkow: <http://www.microscopyu.com/articles/confocal/confocalintrobasics.html>
  - Bleed-through: <http://www.microscopyu.com/tutorials/java/cubeprofiles/triple/index.html>
  - Fluorescent Proteins: <http://www.microscopyu.com/articles/livecellimaging/fpintro.html>
  - FRET: <http://www.microscopyu.com/articles/fluorescence/fret/fretintro.html>
- Zeiss:
  - Home: <http://zeiss-campus.magnet.fsu.edu/index.html>
  - Microscopy: <http://zeiss-campus.magnet.fsu.edu/articles/basics/index.html>
  - Fluorescence microscopy: <http://zeiss-campus.magnet.fsu.edu/articles/basics/fluorescence.html>
  - Objectives: <http://zeiss-campus.magnet.fsu.edu/articles/basics/objectives.html>
  - Filters: <http://zeiss-campus.magnet.fsu.edu/tutorials/matchingfiltersets/index.html>
  - Confocal: <http://zeiss-campus.magnet.fsu.edu/tutorials/opticalsectioning/confocalwidefield/index.html>
  - Numerical Aperture: <http://zeiss-campus.magnet.fsu.edu/print/basics/resolution-print.html>

- Airy Disc: <http://zeiss-campus.magnet.fsu.edu/tutorials/basics/airydiskbasics/index.html>
- Nipkow: <http://zeiss-campus.magnet.fsu.edu/articles/spinningdisk/index.html>
- Dual-spinning disc confocal: <http://zeiss-campus.magnet.fsu.edu/articles/spinningdisk/introduction.html>
- Bleed-through: <http://zeiss-campus.magnet.fsu.edu/articles/spectralimaging/introduction.html>
- Non-laser light sources: <http://zeiss-campus.magnet.fsu.edu/articles/lightsources/index.html>
- Laser light sources: <http://micro.magnet.fsu.edu/primer/lightandcolor/lasersintro.html>
- Fluorescent Proteins: <http://zeiss-campus.magnet.fsu.edu/articles/probes/index.html>
- FRET: <http://zeiss-campus.magnet.fsu.edu/articles/spectralimaging/spectralfret.html>

### 2.1.5. Excitation Sources for High Content Imaging

There are three basic types of light sources for microscopy: lamps, lasers and light emitting diodes. Lamps provide a relatively broad excitation source from UV to IR. Lamps are likely to be able to excite many fluorescent dyes and proteins but the power in a given region may be low. Lamps may need to be replaced frequently and be realigned to give optimal excitation. Xenon lamps have a broad spectrum but relatively little UV and substantial IR that is beyond the region used to excite most dyes and fluorescent proteins. Halogen lamps also have a broad spectrum but, like Xenon lamps, give off large amounts of useless IR and heat. Mercury lamps have sharp and narrow emission bands that require a careful selection of filters. They offer strong UV excitation but have relatively short useful lifetimes, compared to other light sources. Conventional lasers provide a fixed monochromatic wavelength per laser. Power is substantial but may not offer optimal excitation for certain targets. White light and tunable lasers are entering the market but have not yet been used in commercially available HC imagers. Lasers have long lifetimes but are relatively expensive to replace, although this is changing. LEDs are now bright enough to be used in microscopy and have made a rapid entry into the HC arena. LEDs offer long-life and are much more stable light output. They have much less fluctuations on the second time scale compared to lamps and also do not slowly dim in intensity on the week/month timescale the way lamps do. This can substantially reduce noise in HC assays as images are acquired across a plate.

### 2.1.6. Objectives

Anyone using microscopy as a primary tool needs to be familiar with microscope objectives. The imaging sites listed above provide outstanding introductions to this important knowledge area (Figure 1). Some key facts to know include the following:



**Figure 1:** Important properties of objectives are indicated on the barrel of the objective, these include magnification, numerical aperture, working distance, immersion medium and coverslip thickness. Taken from <http://www.olympusmicro.com/primer/anatomy/specifications.html>

1. Objectives are designed with a certain working distance and plate or coverglass thickness in mind. To get the best image there should not be a mismatch.
2. Objectives are designed to be used dry (an air gap between the objective and the specimen) or use water or oil between the objective and the plate/coverglass to enhance numerical aperture multiplier. A dry objective cannot be used with fluid and vice versa.
3. As a rule of thumb, for a given magnification, for example 20x, the objective with the higher numerical aperture (N.A.) will collect more light, reducing exposure times and increasing throughput. Similarly, water and oil objectives collect more light than dry lenses. In fluorescence applications, more light is better and in HCS, since speed is important, anything that can be done to reduce imaging time will speed screening. But using emersion objectives (water or oil) makes microscopy much more difficult, especially in a screening environment. Therefore, most HCI uses dry objectives but with as high a N.A. as possible (Figures 2 and 3).

### 2.1.7. Airy Discs

When light comes from a point in a specimen and goes through an object to form a part of an image, the light from the point does not form a point in the image. Rather it forms a diffraction pattern with a central maximum surrounded by a few rings (Figure 4). The

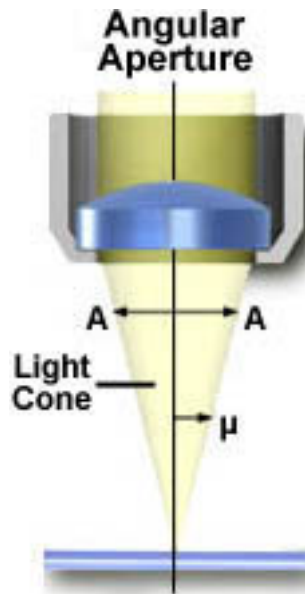


**Figure 2:** Numerical aperture is dependent on the half angle of the aperture ( $\mu$ ) and the refractive index of the medium ( $n$ ) between the objective and the specimen. Taken from <http://www.olympusmicro.com/primer/anatomy/numaperture.html>

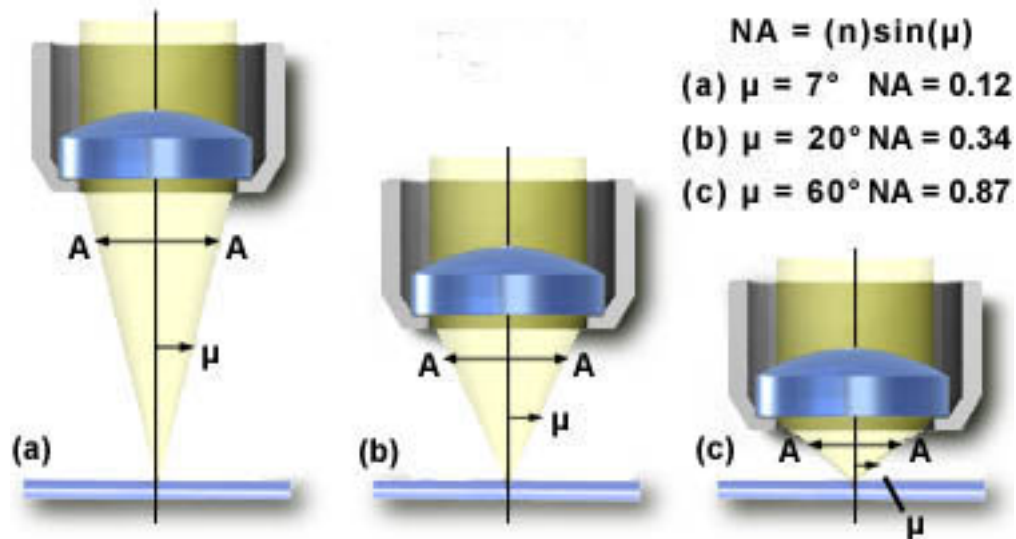


**Figure 3:** As the angle increases from 7° to 60° there is a 7 fold increase in N.A. Taken from <http://www.olympusmicro.com/primer/anatomy/numaperture.html>

central maximum, usually called an Airy Disc, contains most (>80%) of the energy. The minimum distance between airy discs then can be resolved defines the resolution of the objective and varies with the wavelength of the light ( $r_{\text{Airy}} = 0.61 \times (\lambda_{\text{Ex}} / \text{NA}_{\text{Obj}})$ ). The

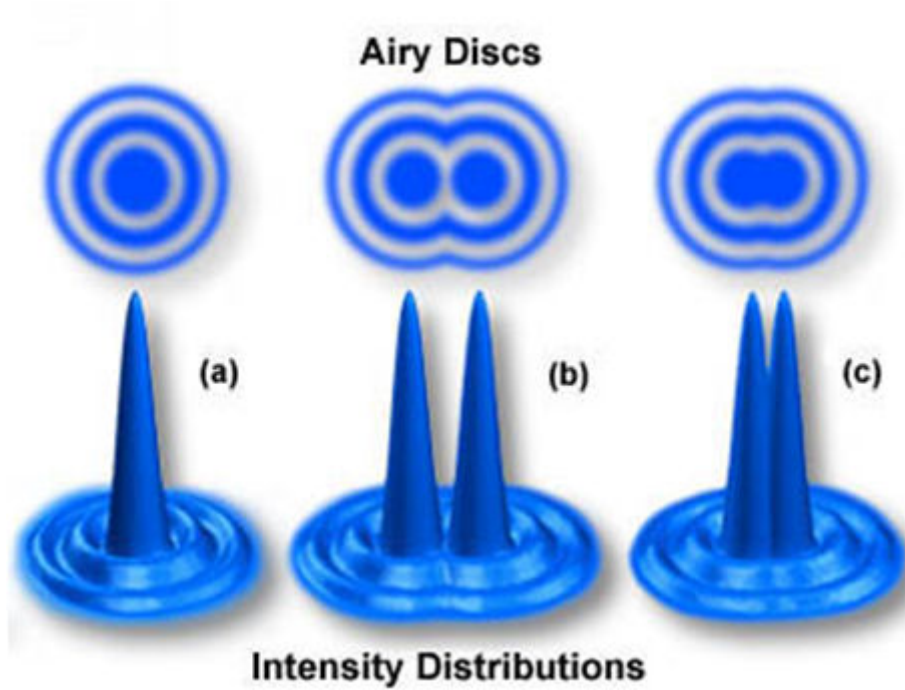


**Figure 4:** Schematic representation of Airy Disc intensity distributions. Adapted from <http://www.olympusmicro.com/primer/anatomy/numaperture.html>

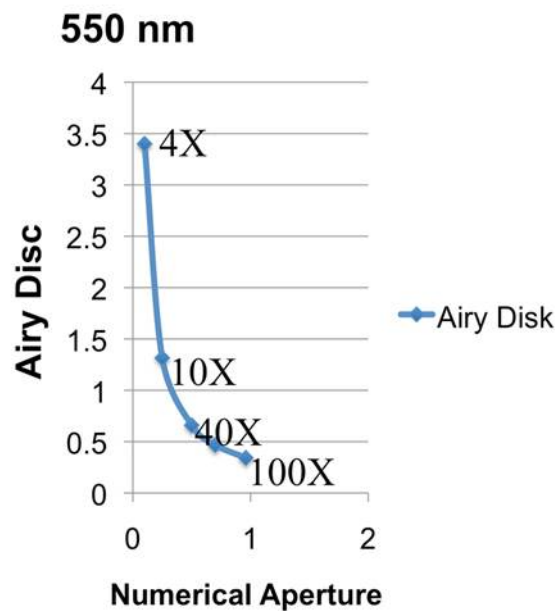


**Figure 5:** Airy disc versus numerical aperture (N.A.). As N.A. increases, the airy disc decreases.

higher the N.A. of the objective, the smaller the airy disc and the better the resolution (Figure 5).

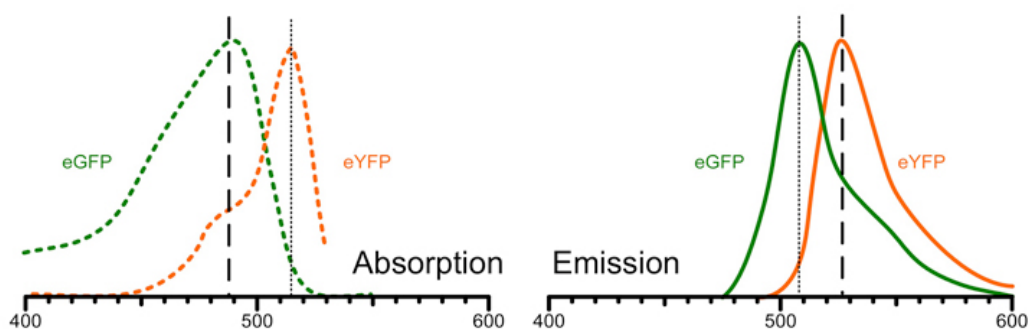


**Figure 6:** Fluorescent proteins often have overlapping excitation and emission spectra. eGFP and eYFP have substantial overlap, making clear separation of the signals difficult, even with the best filter choices.

### 2.1.8. Bleed Through

An important consideration for HCA is that the fluorescent dyes and proteins used in assays typically have broad excitation and emission spectra. As a result there can be significant bleed through from one fluorescent probe to another. At least four things can be done to minimize this:

1. The excitation wavelengths chosen should take into account the peak properties of the fluorescent targets to minimize cross excitation. With laser or LED light sources this is less of a burden. With other light sources, such as halogen, xenon or mercury lamps, careful selection of filters in the excitation path is required. In any case, absorption bands have tails towards shorter wavelengths. So a narrow band chosen to excite green fluorescent protein (GFP) will likely also excite a yellow fluorescent protein (YFP) (Figure 6).
2. The filters in the emission path must be optimized to minimize cross talk between the different fluorescence emitters and that is directly dependent on the dichroic filter in the optical path. Emission bands have tails towards the longer wavelengths. Fluorescence from GFP will bleed into the YFP channel. Keep in mind that imperfections in glass, optical materials and coatings used on filters in fluorescence detection commonly display multiple excitation or emission peaks; therefore it is recommended to review the specifications of the filters to understand how they perform.
3. Adopt a strategy to reduce problems with cross talk by having the brighter signal in the longer wavelength channels (Table 1).
4. Routinely assess cross talk between different channels. At a minimum, there should be control wells where the bleed through from the shorter wavelength channel into the longer wavelength channel is measured. In High Content Assays using primary and secondary antibodies, new lots of antibodies or just variations in handling on different days can lead to significant changes in fluorescent signals, with consequences for relative signal strengths in different channels. So controls need to be done on a routine basis.

**Table 1: Making sure the signal from the emitter in the longer wavelength is brighter than the signal from the emitter in the short wavelength can minimize cross-talk between fluorescence emitters. If the brighter signal is from the shorter wavelength emitter, much of the signal detected in the long wavelength channel will be from the “wrong” emitter.**

| Fluorescence |              | Detection          |                   |                   |                     |
|--------------|--------------|--------------------|-------------------|-------------------|---------------------|
| Green Label  | Yellow Label | Green Channel      |                   | Yellow Channel    |                     |
|              |              | From Green (~100%) | From Yellow (~0%) | From Green (~50%) | From Yellow (~100%) |
| ++           | ++           | ++                 | ~                 | +                 | ++                  |
| ++           | ++++         | ++                 | ~                 | +                 | ++++                |
| ++++         | ++           | ++++               | ~                 | ++                | ++                  |
| ++++         | ++++         | ++++               | ~                 | ++                | ++++                |

### 2.1.9. Detectors

HCI use two major types of detectors; digital cameras and photomultiplier tubes (PMTs). Digital cameras for HCS benefit from the large market for personal cameras that lead to decreased costs and increased chip size and defense needs for high sensitivity. HCI often use CCDs, EMCCDs and sCMOS cameras with high frame rates (100 FPS), large dynamic ranges (>20,000:1), broad spectral sensitivity (400-900 nm and higher), and high resolution (>2000 × 2000 pixels). While these cameras can provide high quality images, the files are large with consequences for image storage systems. The cameras are usually monochrome cameras. Color images are produced by acquiring images of the same field serially, using different optical filters. PMTs are based on a very mature technology, have extreme sensitivity to measure very low light intensity and fast responses with wide spectral sensitivity and are almost always used in conjugation with a laser source. To produce images, they are used in conjunction with a scanning technology that moves a light beam, typically a laser beam, across a sample. In HCS, the scanning is relatively slow but several PMTs can be used simultaneously to acquire data in different fluorescent channels.

### 2.1.10. Autofocus

HCI use two different approaches to focusing on the specimens. These are 1) laser-based systems that detect the bottom of the plate and 2) image analysis-based systems that step through the specimen and use algorithms to determine the optimal focus plane. Since focusing takes time it is usually not done every time an image is acquired in HCS. Testing is needed to determine the minimum number of times focusing needs to be done to provide reliable data, which is related to the plate material used. The laser-based systems are fast but can perform poorly if the plates are not extremely flat or if the specimens are thick. The image analysis-based approaches are comparatively slow and have the caveat if fluorescent debris, artifacts, material or even clumps of cells which are not within the Z focus plane of uniformed cells in the well, the focusing typically fails. For these reasons it



may be prudent to focus on fluorescence outside of typical lint debris that fluorescence in blue to violet wavelength.

### 2.1.11. Environmental Controls

HCA can be done on live cells to study cell movement, cell proliferation, cell death, and also to use various reporters to monitor protein interactions, membrane potentials or intracellular  $\text{Ca}^{2+}$  levels. This will require that the instruments control temperature, humidity and  $\text{CO}_2$  levels. The larger instruments from most vendors have environmental controls as standard features or optional packages. If long-term time lapse imaging is planned then testing different instruments prior to purchase is recommended. While temperature and  $\text{CO}_2$  are relatively easy to control, humidity is not and evaporation from multiwell plates can affect cell behavior. In addition, intense illumination of cells with lasers or lamps can damage or kill the cells. Therefore it is important to verify that the imager can detect critical features over time without causing cell damage.

### 2.1.12. Liquid Handling

Some instruments offer liquid handling to permit the addition of compounds, drugs, etc. to cells in individual wells. This is almost always done in live cell imaging situations to measure cell responses using fluorescence reporters to monitor membrane potentials or intracellular  $\text{Ca}^{2+}$ . Typically the liquid handling is done with a pipette like device, some with disposable tips.

### 2.1.13. High Content Imagers

There are many HCI on the market, with vendors releasing new models regularly. Therefore, it is impossible to have a resource that is truly comprehensive and current. Individuals interested in acquiring a new instrument are encouraged to survey the current market after first developing a detailed user requirements specification. International meetings, such as the Society for Laboratory Automation and Screening, PittCon, or CHI High Content Analysis are excellent venues to view demonstrations from many HCS vendors. There are a number of social media websites such as LinkedIn and Facebook focused on HCS/HCA that have members providing feedback about these instruments as well as dedicated user group websites. The Cold Spring Harbor Meeting on High Throughput Phenotyping is an exciting place to learn about cutting edge approaches.

### 2.1.14. Image and Data Analysis

Often the major factors that differentiate the High Content platforms from different vendors are in the software that acquire, analyze, and manage HC images. Most software packages from major vendors now offer advanced data analysis systems that allow tracking of entire screening campaigns. Perhaps more important, the software needs to have a comprehensive and user friendly system for developing a High Content Assay. While scientists often have a basic idea of the type of assay that will run, the optimal image analysis algorithms and features or parameters that need to be measured in a screen have to be determined using positive and negative referenced controls. The ease and speed

at which this can be done is highly dependent on image analysis tools provided by the vendor. Newer software packages have improved GUIs based on real world workflows. Anyone acquiring a new HCA system should include image analysis tools in the user requirement specification.

## 2.2. Wide Field Imagers

These instruments are similar to and, indeed are often built around inverted research microscopes from major vendors such as Olympus, Nikon, Zeiss, etc. The hardware solutions offered by different vendors have evolved rapidly over the past 10-15 years and are now robust and provide excellent images quickly.

BD Biosciences distributes the BD Pathway 435<sup>tm</sup>, a unit with metal halide and transmitted light sources. This is also equipped with a Nipkow spinning disk for confocality (Note: BD is discontinuing their HCS instruments but there are many in academic labs and core facilities)

GE Healthcare markets the IN Cell Analyzer 1000 and 2000. The InCell 2000 is the new generation instrument; it uses a metal halide lamp. Camera options are 1392 × 1040 or 2048 × 2048 pixels. Transmitted light modes include bright field, phase and differential interference contrast.

IDEA Bio-Medical has a large instrument, the WiSCAN that uses a mercury light source for fluorescence and LEDs for transmitted light. The instrument uses a 512 × 512 water-cooled EMCCD camera for fast, sensitive imaging in a HCS environment. The Hermes 100 is a small bench-top instrument for individual labs. It uses LED light sources to allow two-color and transmitted light image acquisition.

MAIA Scientific markets the MIAS-2<sup>tm</sup>. This instrument can acquire 5 different transmitted light channels with a halogen light source and up to 8 fluorescent channels using a xenon light source. Imaging is done with a color camera and an intensified B&W camera.

Molecular Devices has one wide field imager, the ImageXpress Micro HCS system, which has an integrated fluidics system for delivering reagents in live cell imaging applications. It uses a xenon lamp and can use air or oil objectives.

Perkin Elmer sells the Operetta, a bench top widefield unit with a xenon lamp and an LED for transmitted light. It has a spinning disk confocal option

ThermoFisher (Cellomics) developed the first commercial HCS imager and now sells three wide field instruments. The ArrayScan VTI HCS Reader is an instrument suitable for a core facility or large laboratory. It uses a metal halide or LED light source and can be enhanced with a spinning disc confocal option. The Cellinsight is designed as a “personal” imager. It also uses an LED light source and is designed for use with four common dyes; Hoechst, FITX, TRITC and Cy5. The ToxInsight IVT Platform is designed to focus on

identifying potential toxic liabilities in newly identified compounds. It is also a small footprint instrument using LEDs and a four-color approach to HCA.

Vala Sciences manufactures a Kinetic Image Cytometer (KIC) designed for kinetic analysis of calcium dynamics in an HCS system. It uses LEDs and large format cameras to acquire data.

### 2.3. Confocal HCA Imagers

Confocal microscopes use a light barrier with a fixed or adjustable pinhole to eliminate light that is in front or behind the focus plane of an objective. This gives much better depth resolution and improved contrast by rejecting light from out of focus sources. But it causes reductions in the light signal. It also only works for a single point in the specimen at any given moment. To overcome this problem the sample must be moved across the sampling point or the light beam and pinhole need to be scanned across the sample. One approach is the Laser Scanning Confocal Microscope (LSCM). The other is the Nipkow spinning disk that has multiple small pinholes or curved slits to increase illumination and the number of points in the specimen that can be imaged simultaneously. To obtain an optimal image with regards to light transmission and Z-axis resolution, the pinhole size must be matched precisely to the objectives Airy Disc. LSCMs have adjustable pinholes that can be varied depending on the objective and other factors, such as the wavelength of the illuminating light source. But the intense laser beam can bleach the specimen and it often takes a few seconds to scan a region of interest (ROI). Spinning discs sacrifice most of the illuminating light used to excite fluorescence in the specimen but can scan a ROI in a few hundred milliseconds and result in less bleaching and increases throughput. They are preferred for live cell imaging. Yokogawa has devised a dual spinning disc technology with lenses in the first disk that focus light on the pinholes in the second disc. This increases the illumination of the specimen and, importantly for HCS, decreases image acquisition time.

Confocal imaging is usually more expensive in terms of capital investment and screening time. It is best used for imaging small intra-cellular structures, small cells, complex 3-D structures and samples with strong background fluorescence. HCS campaigns have been run using confocal imagers to eliminate the need to wash stains from cells, a big advantage if the cells are loosely adherent. Furthermore, the sharper images obtained via confocal methods could make image analysis process easier.

BD Biosciences distributes the BD Pathway 855<sup>tm</sup>, a Nipkow spinning disk system with mercury halide and transmitted light sources. It has an integrated liquid handler and integrated environmental control. It can also be used in wide field mode. This imager is often used for kinetic studies of signals relevant to physiologists, such as membrane potential or calcium (**Note:** BD is discontinuing their HCS instruments but there are many in academic labs and core facilities).

GE Healthcare markets the IN Cell Analyzer 6000. This is a line scanning LSCM with a variable aperture. It has 4 laser lines (405, 488, 561, 642) and an LED for transmitted light

and a large format sCMOS camera. It has an integrated liquid handler and environmental control.

Perkin Elmer sells the Opera, a HTS system designed with water immersion lenses to give higher N.A. It uses laser based excitation combined with a Yokogawa dual spinning disc system to give confocality.

Molecular Devices has a point scanning LSCM, the ImageXpress ULTRA. This machine has four lasers and 4 PMTS that can be operated simultaneously or sequentially. It has options for air or oil objectives.

Yokogawa has two confocal imagers that exploit their dual spinning disc technologies. They have discs with different size pinholes, depending on objectives in use. The CellVoyager CV1000 is designed for long term live cell imaging with the option for oil immersion lenses. The CellVoyager CV7000 is an instrument designed for HTS, taking advantage of three large chip (2560 x 2160) cameras and a choice of lasers as well as halogen lamp and a LED for UV imaging. Live cell imaging is provided as well as liquid handling and water immersion lenses.

## 2.4. Laser Scanning Cytometers

These imagers are conceptually similar to a flatbed scanner with laser beams scanned across the entire surface of the plate and fluorescence detected with PMTs. They produce images equivalent to at maximum a low NA 20X objective and are good at detecting cells, including DNA content and colonies and even model organisms such as zebrafish, but not subcellular features or processes. LSCs have a very large depth of focus. They are often used to identify fluorescent intensities above a threshold. An example is nuclear translocation assays, where a diffusely localized protein in the cytoplasm gives a low signal but when concentrated in the nucleus gives a high signal. Other applications include cell proliferation, cell toxicity, protein kinase activation, and cell cycle analysis. This approach might be considered a medium content, high throughput technology.

The Acumen <sup>e</sup>X3 has 3 lasers (405, 488, 633nm) and 4 PMTS and has been used in many HTS projects.

Molecular Devices ImageXpress Velos Laser Scanning Cytometer (formerly IsoCyte) uses 2 lasers (selected from 405, 440, 488, 532, 633nm), 4 PMTs. It also uses light scattering as a method to detect non-fluorescent objects such as colonies.

The Compucyte iCyte is a hybrid instrument that uses laser scanning on an inverted microscope with objectives (10, 20, 40, 60, 100x) and up to four lasers (selected from 405, 488, 532, 561, 594, 633nm). It also uses 4 PMTs.

Slide based scanners: Some instruments offer measurement of transmitted light in different wavelengths using line scanners. When used with conventional histological stains, this can provide very useful images and information from tissues that could be of

interest in disease models. A major advantage of line-based scanners is the elimination or minimization of tiling to produce very large, high magnification images.

Aperio sells three slide scanners aimed at the pathology market. The ScanScope FL uses a mercury lamp, a 20x objective and a TDI line-scan camera to acquire images in up to 4 color channels. The ScanScope CS has 2 objectives (20x, 40x). The ScanScope AT has a 20x objective but is designed for automation with a slide loader that can hold up to 400 slides.

Hamamatsu markets the NanoZoomer, which uses TDI line-scans to acquire both transmitted light images of tissues stained, for example with H&E, PAS, or NBT stains and also fluorescence. It uses a 20x objective, a mercury lamp for fluorescence.

The Leica SCN400 and SCN400F uses a linear CCD device to acquire brightfield images, The SCN400F also can acquire fluorescence channels.

## 2.5. FACS like instruments

As mentioned previously FACS provides multidimensional data that can be considered in a high content approach. There are some instruments that cross the border from FACS to HCA by acquiring images and not just intensity data.

The Amnis ImageStream X uses lasers and LEDs to give darkfield, side scatter (785 nm) and fluorescence images of cells using 5 lasers (405, 488, 561, 592, 658) of cells passing through a flow cuvette.

## 3. Assay Concept and Design

Living cells, the basic building blocks of life, are an integrated and collaborative network of genes, proteins and innumerable metabolic reactions that give rise to functions that are essential for life. Conversely, dysfunctions in these same vital networks give rise to a host of diverse diseases and disorders. Although much less complex than *in vivo* models or complete organisms, cells possess the systemic complexity needed to study the interactions between different elements of the network and the responses of the network to external stimulations. Therefore more and more physiologically relevant cellular models are being used to validate targets or to evaluate drug efficacy and to predict potential adverse side-effects. Furthermore, advancements in cell isolation, cell line generation and cell differentiation technologies have led to more scalable and affordable cellular models, which in turn facilitate screening using more physiologically relevant cellular models. Due to its information-rich nature, high-content screening (HCS) has become the choice for many scientists to examine the complex effects of compounds or other reagents in physiologically relevant cellular models, not only against their intended targets, but also against other cellular targets and pathways (25-29).

Like standalone high-resolution microscopes, automated HCS systems can be utilized to study many cellular processes. Some of these processes, such as protein phosphorylation, cell surface ligand binding, molecular uptake, protein expression, cell cycle regulation,

enzyme activation, and cell proliferation, can be analyzed by conventional methods, though image-based methods can often deliver comparably high quality results with multiple parameters. The strength of HCS is based on its ability to enable both target-based and phenotype-based assays for otherwise intractable cellular processes. These processes often play pivotal roles in cell survival and division, and can be visualized as intracellular protein translocation, organelle structure changes, overall morphology changes, cell subpopulation redistribution, and three dimensional (3-D) structure modifications. These assays not only have been used to study fundamental biological processes and disease mechanisms, but also have been applied to new drug discoveries and toxicity investigations.

### 3.1. Intracellular protein translocation:

Examples of HCS assays monitoring intracellular protein redistribution include translocation of a transcription factor from the cytoplasm to the nucleus to initiate or modulate gene transcription, internalization of G-protein coupled receptors (GPCR) to initiate a signaling cascade (30, 31), translocation of glucose transporter from the cytoplasm to the cell surface to facilitate glucose uptake (32), and recruitment of LC3B, an autophagy-related protein, to the autophagosome under conditions of stress (33, 34). In order to follow the translocation event, the protein must be labeled with a fluorescent probe, often by tagging/expressing the protein directly with a conjugated fluorescent protein marker (such as green or red fluorescent proteins (GFP or RFP)). This system then can be used to study the spatial and temporal effects of external stimulants in both kinetic and end-point fashions.

Different protein tagging technologies have been developed as potential substitutions of fluorescent proteins. For example, the SNAP-tag, which is a 20 kDa mutant of the DNA repair protein O6-alkylguanine-DNA alkyltransferase that reacts specifically and rapidly with benzylguanine (BG) derivatives ([www.neb.com](http://www.neb.com)) The BG moiety can then be used to irreversibly label the SNAP-tag with a fluorophore. This technology allows one to label the protein in question using chemical fluorophores with different wavelengths and cell permeability, thus facilitating multiplex readout from the same cells. Halo-tag ([www.promega.com](http://www.promega.com)) and fluorogen activating protein (FAP) ([www.spectragenetics.com](http://www.spectragenetics.com)) are based on similar concepts, but using different proteins and probes. These proteins and their associated probes have no endogenous eukaryotic equivalent and are not toxic to cells when expressed at low levels. The covalent nature of these technologies makes them versatile for both live and fixed cell images.

The protein tagging technologies described above require overexpression of the proteins of interest. Sometimes stable cell lines are not feasible, and inducible expression systems could be used to circumvent the situation. Not surprisingly, this approach will require more intensive assay validations due to potential variations associated with the inducible expression systems. Overexpression of some proteins may disturb the delicate balance of the cellular network or the tags may disrupt the function or trafficking of the proteins in unknowable ways, and lead to results that are not physiologically relevant. Because of this,

most scientists prefer antibody staining methods to track the intracellular locations of such proteins. However, antibody staining methods generally require chemical fixation of the cells, and so are limited to end-point reads (with the exception of cell surface proteins). There are many commercially available kits for specific protein translocations. These kits are validated by vendors but their uses are narrowly defined, and one has very limited options to change the compositions of the reagents as needed. Alternatively, there are many well-characterized antibodies available via different sources. Assay developers usually need to screen multiple antibodies to find one that works in the bioimaging-based assay, and to validate the assay using known stimulators and inhibitors. If assay developers decide to use proprietary antibodies raised in house, the selectivity of the antibodies must be critically examined, and the assay must be fully validated using known stimulators and inhibitors in related and unrelated pathways to ensure the observed translocation of proteins is specific to the biological event(s) of interest.

Lastly but not least important, it is imperative to develop image analysis algorithms and phenotype clustering statistical methods (if applicable) concurrently with the development of biological assays to make sure that the assay has optimal sensitivity towards the desirable phenotypes. These algorithms and methods must be validated using known stimulators, inhibitors and/or tool compounds. For compound screening, the same compound at different concentrations could lead to different phenotypes, due to the compound's different potencies on different pathways or due to toxic effects. Therefore, it is essential to test tool compounds in a broad dose response concentration range to find all potential phenotypes associated with the assay. This information can be used to define POSITIVE calling criteria for primary screening to minimize false positives and false negatives. These principles are applicable to all HCS assay formats.

### 3.2. Organelle structure changes

Examples of organelle structure change assays include the evaluation of mitochondrial membrane potential as a marker of cell health, cytoskeletal remodeling, quantification of lipid droplet formation in metabolic disease, formation of micronuclei during genotoxicity, and quantification of endocytosis or internalization for intracellular drug delivery (35, 36). Over the years, Molecular Probes® (Life Technologies) has developed many organelle-specific chemical dyes and fluorescently labeled antibodies against specific organelle markers. Recently, they also adapted the BacMam technology to express GFP-fusion constructs of different organelle markers. These dyes, antibodies and organelle markers cover a broad spectrum of wavelengths and can be used to examine the location and structure of multiple organelles simultaneously.

Development of HCS-amenable assays for structural changes can be a challenge, due to the heterogeneous morphologies of cells in dissociated cell cultures. Cell behavior is strongly influenced by local environment. There is evidence that some cell types at the edge of a colony will behave very differently than cells in the center of the colony (37-39). Recent developments in micro-patterned plate technology could be used to address this issue. These micro-patterned plates could provide niches that mimic the extra cellular

matrix (ECM) of cells in tissues, and the organized patterns facilitate more uniform cell placement and adhesion to plates, thus making assay development and image analysis straightforward (40-43).

### 3.3. Morphology changes

Morphology change is a hallmark assay for high-content based screening. Many assays monitor cell process extension or tube formation as markers of disease. These include the measurement of angiogenesis for anti-cancer indications, oligodendrocyte differentiation for multiple sclerosis and other neurodegenerative diseases, and neurite outgrowth for different CNS indications (44). Another important area is related to cell differentiation associated morphology changes. Epithelial-mesenchymal transition (EMT) for oncology or fibrosis indications and stem cell differentiation are two notable examples (45-47).

Morphology changes can be directly monitored using bright-field image technology, or using fluorescent images with dyes or other markers that define the boundary of cells. However, assays reliant solely on morphological changes must be tightly controlled to avoid misinterpretation of results. For example, neurons, oligodendrocytes and astrocytes have very similar branched morphology, and differentiate from neural progenitor cells, though their functions are very different. Therefore, it is important to include cell-type specific markers in assays for phenotyping, preferably including both up regulated and down regulated markers, before making final conclusions.

### 3.4. Cell subpopulation redistribution

Most automated cellular imaging systems allow one to view a large population of cells at a time, often at the individual cell and organelle level. This allows one to run subpopulation analysis, including co-culture of multiple cell types to mimic tissue environment, cell-cell communication for signal transduction between cells (9 Li 2003), and determination of stem cell differentiation efficiency. Together with the multi-variant analysis ability, HCS technology empowers one to learn more about the interactions between the elements of the cellular network, such as the influence of cell cycle regulation and microenvironment on different signaling pathways, and gain in depth knowledge of the basic building blocks of our body.

The assay categories described above cover many bioassays under different biology events in different pathways and/or different cellular systems (Table 2, and Figure 7).

Furthermore, a complex biological event could include multiple steps in different pathways. Frequently, there are specific imaging based assays for different steps involved in the complex biological event. Figure 8 illustrates key steps involved in apoptosis and available imaging methods ([www.lifetechnologies.com](http://www.lifetechnologies.com)). Apoptosis is a very highly regulated process leading to cell death. The biochemical and morphological changes that characterize apoptosis include the activation of caspases, the loss of mitochondrial membrane potential, the loss of plasma membrane asymmetry, the condensing and fragmentation of the cellular DNA, cytoplasmic membrane blebbing, and apoptotic body formation. Finally, apoptotic cells will be destroyed by phagocytes. Inappropriate



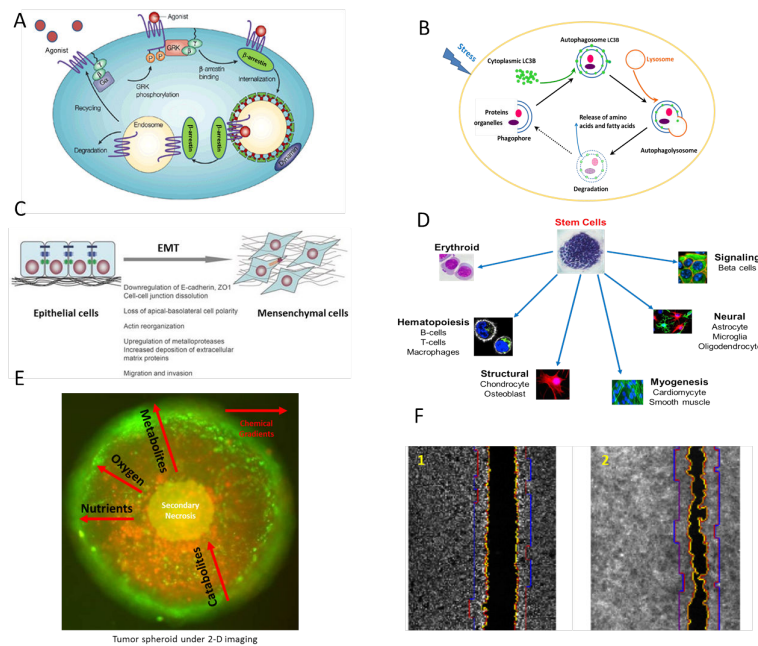


**Figure 7:** **A) Beta-arrestin mediated GPCR internalization** (Figure adapted from Nature.com with modifications). First, agonist-activated GPCRs are phosphorylated by GRKs (G-protein coupled receptor kinases) on their carboxyl-terminal tails. Second, arrestins translocate to and bind to the agonist-occupied, GRK-phosphorylated receptors at the plasma membrane. Third, arrestins target the desensitized receptors to clathrin-coated pits for endocytosis. Finally, receptors and arrestins are recycled or degraded. HCS can detect the internalization of GPCR by following GFP-tagged beta-arrestin (30, 31, 48). **B) Autophagy:** it is hypothesized that autophagy is up-regulated in cancer cells to promote survival in response to chemotherapy or other stresses. Autophagy includes multiple steps. The first step involves the formation and elongation of isolated membranes, or phagophores; in the second step, which involves the LC3B protein, the cytoplasmic cargo is sequestered, and the double-membrane autophagosome is formed. Fusion of a lysosome with the autophagosome to generate the autolysosome is the penultimate step. In the fourth and final phase, the cargo is degraded, and amino acids and fatty acids are released as nutrient for the cell. HCS can be used to monitor the aggregation of LC3B protein, thus following autophagy events (33,34). **C) Epithelial-mesenchymal transition (EMT,** Figure adapted from Nature.com with modifications): it is hypothesized that EMT is a key step toward cancer metastasis or toward tissue fibrosis. During EMT, cell morphology is changed from cobblestone shaped epithelial cells to elongated mesenchymal cells. Meanwhile, epithelial cell markers, such as ZO-1 and E-cadherin, are down regulated, and expression of extracellular matrix proteins, such as collagens, is increased. Using cell-mask dyes for morphology changes and specific antibodies for different cell markers, HCS can be used to detect EMT (45). **D) Stem cell differentiation:** under certain physiologic or experimental conditions, stem cells can be induced to become tissue- or organ-specific cells with special functions. These specialized cell types have distinguished shapes and biomarkers and can be picked up by HCS using cell-mask dyes and specific antibodies for different cell lineage markers (46,47). **E) 3-D multiple cell type tumor spheroids** show many differences in biological functions compared to 2-D cultures (e.g. the chemical gradients within the 3-D tumor spheroids are much similar to *in vivo* while 2-D models lack such gradients), and resemble *in vivo* tumor tissue structure (Figure adapted from Dr. Michael A. Henson Group website with modifications. Green: live cells; red: dead cells). Therefore, the spheroids have gained momentum for applications in drug discovery. HCS technology with confocality provides ways to study the 3-D structure of the spheroids (49,50). **F) HCS technology** can be used to quantify cell migration, invasion and chemotaxis in 2-D or 3-D cellular models for wound healing, cancer metastasis and inflammation studies. Mechanic scratch or micro-patterned plate technologies could be used to create a cell-free area prior to assay start. Migration of cells into the cell-free area could be measured. The key for this assay is to distinguish migrated cells from proliferated cells in the scratched area. Micro-pattern technology also is used to create micro-conduit array plates with steady chemical gradients for chemotaxis assays (51, 52).

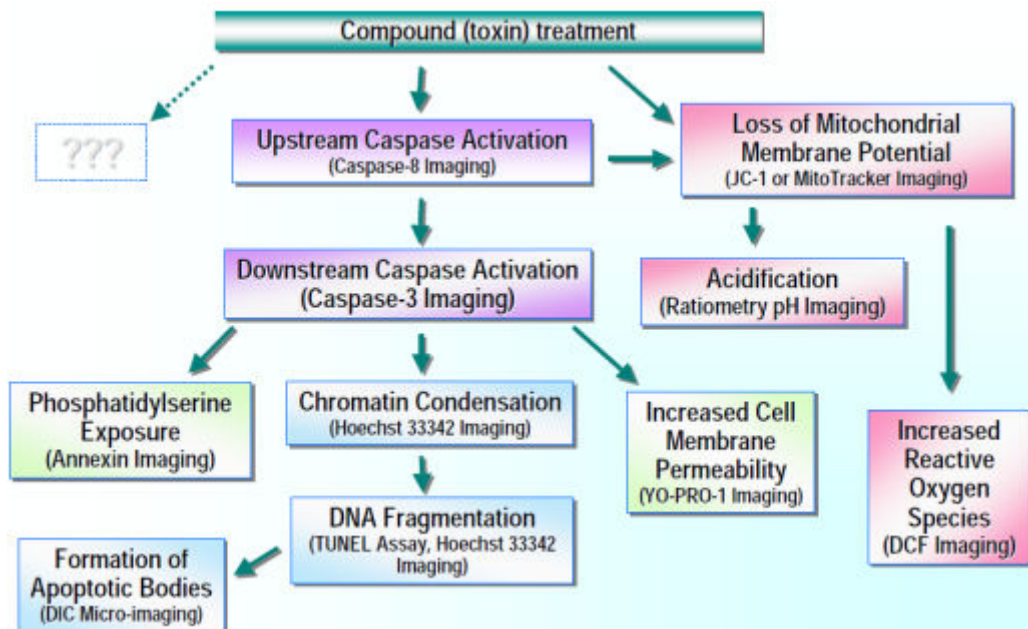


**Figure 8:** Key apoptotic steps and available imaging methods.

regulation of apoptosis could lead to diseases like neurodegeneration, autoimmune, AIDS, ischemia-associated injury, and cancers. Since there is no single parameter that defines apoptosis, a combination of imaging methods is recommended for reliable detection of apoptosis when conducting HCA. However, for high throughput compound screening, one may pick one or two imaging methods due to cost and screening logistic concerns. Choosing which imaging method(s) to be used is very dependent on the goal of the screening. To detect early stage apoptosis, caspase 8 activation and/or mitochondrial membrane potential assays could be used. To detect middle stage apoptosis, phosphatidylserine exposure or membrane permeability could be considered. Finally, to detect late phase apoptosis, DNA fragmentation assays could be used. However, in follow up assays, the hits from primary screening should be examined by a combination of multiple imaging methods in order to better understand the mechanism of actions.

**Table 2:** Examples of bioassays

| Assay Categories                      | Examples of Biology Events                  | Examples of Assays   |
|---------------------------------------|---|--|
| Intracellular Protein Redistributions | Apoptosis                                   | Caspases, cathepsins, calpains, Cyclins and PARP protein levels                        |
|                                       | Autophagy                                   | Autophagy protein LC3B aggregations  |
|                                       | Cytoplasm-nucleus translocation for nuclear | AR, ER, GR, 5-LOX, ATF-2, ATM, beta-catenin, c-Jun, CREB ERK2, NF-κB, p53, SMAD, STATs |

*Table 2 continues on next page...*

Table 2 continued from previous page.

| Assay Categories                            | Examples of Biology Events  | Examples of Assays   |
|---|---|--|
|   | receptors or transcriptional factors                                  |  |
|   | Trafficking for cell surface receptors, ion channels and transporters | Beta-arrestin for GPCR internalization; ligand or receptor internalization for CB1, CB2, CRTH2, CXCR4, EGFR; Cytoplasm-cell surface membrane translocation for ion channels or transporters such as Glut1, Glut4 |
| Organelle Structure and/or Function Changes | Apoptosis   | Annexin V assay to detect externalization of phosphatidylserine, DNA fragmentation, mitochondria membrane potential, membrane permeability, nuclear condensation   |
|   | Autophagy   | Autolysosome formation, mitochondria degradation   |
|   | Cell Division   | Mitotic spindle structure by alpha-tubulin stain   |
|   | Cell polarization   | Cytoskeletal re-arrangement by actin stain   |
|   | Drug delivery   | Internalization of drugs via endocytosis   |
|   | Genotoxicity  | Micronucleus assay to quantitate micronuclei in multinucleate cells; DNA damage indicated by phosphorylation of H2AX   |
|   | Lipid uptake and storage  | Lipid droplet size and number  |
| Morphology changes                          | Cell differentiation  | Stem cell differentiation, epithelial-mesenchymal transition (EMT), oligodendrocyte differentiation  |
|   | Process extension   | Angiogenesis, neurite outgrowth  |
| Cell Subpopulation Redistributions          | Anti-infectious   | Percentage of cells infected   |
|   | Cell differentiation  | Stem cell differentiation, epithelial-mesenchymal transition (EMT), oligodendrocyte differentiation  |
|   | Cell migration  | Chemotaxi, wound healing, and cancer cell metastasis.  |

## 4. Cellular Models for High Content Experiments

High Content experiments depend on cell systems that serve as models for *in vivo*, typically human, biology. All models are measured by the extent to which they perform well in an assay and to the extent that they respond to stimuli in an authentic manner. Controversy exists concerning how well of *in vitro* cell systems accurately portray *in vivo* biology. Plating a single cell line on a two-dimensional surface in media with high levels of both oxygen and serum/growth factors may not model the *in vivo* situation sufficiently well for all investigations. Such systems give very robust signals in proliferation and apoptosis assays, but such responses are frequently muted *in vivo*, due to the target cells growing in an environment with multiple additional cell types. This section will explore how to insure that HCS assays best provide biologically or clinically meaningful results.

A discussion of cellular models must follow one on what needs to be modeled. In general, cell growth and the regulation of canonical signaling pathways have been modeled most frequently, particularly in the contexts of common cancers, glucose dysregulation in diabetes, neurodegeneration, pathological inflammation and toxicology. In these contexts, standard cell lines and culture conditions may be inadequate, but in other cases, such conditions may be fine. We will begin with experiments where the models are easier to establish and can be considered standard, and work towards models for more complex biological questions.

### 4.1. Cellular models for signal transduction pathways and other cell-autonomous responses

Much of pharmaceutical and biotechnology research is focused on finding modulators (typically inhibitors, but increasingly also to find agonists, potentiators and inverse agonists) of specific cellular target proteins. Studies on signaling pathways are also important to academic research. Such target-based research can make the search for a suitable model fairly straightforward. The easiest cellular models are immortalized and cancer cell lines. Although transformed, there are many examples of cell lines that retain the characteristics of the cell types they originated from. This includes important signaling pathways, such as estrogen receptor signaling in breast and ovarian lines, insulin signaling in hepatic lines, and TNF- $\alpha$  responsiveness in immune cell-derived lines. Not all derivatives of a given cell type retain such properties, for example some breast cell lines have lost estrogen signaling. In these cases, the cell lines are better models of specific forms of cancer than of the original cell type, but then again, it is necessary to study signaling dysregulation in such diseases. Therefore, if you have a signaling pathway in mind, options for cell models can be found with a quick search of the literature. It is important to verify these cell lines are functional using known reference compounds, proteins, or other stimuli during assay development to ensure the desirable pathways are performing well in these cell lines.

The advantage of working with cell lines that are well-represented in the literature is that many additional properties of the lines that are important to consider will already be

characterized and be manageable. Properties such as growth and metabolic rates can affect many assay types because some lines need to be attended more frequently than others. Other properties impact imaging assays more than other types. Colony morphology is one example. If the cells grow as clumps or clusters, then many cells will grow away from the well surface, making the imaging process more difficult than for lines that grow uniformly spread. Cell adherence can be a problem for imaging assays that require fixation and staining, as these steps add additional treatments and washing cycles to the process. Loosely adherent cells will be lost at each step unless care is taken to avoid disturbing them. This can be accomplished through automating sample preparation, where some instruments can control the rate and the placement of the reagent additions and wash steps. Common properties that can vary significantly between cell lines are summarized in Table 3.

Cancer cell lines and immortalized lines (lines that are not derived from tumors, but have inactivated senescence barriers) are easier and cheaper than primary cells, as they can be passaged in theory indefinitely; however mutations and functional response typically diminish over time. This allows both a single line to be used in experiments for many months or even years, and to expand cells prior to a screen, so that all of treatments (compounds, peptides, siRNAs, etc.) are used on cells of the same passage. Although cell lines are capable of near infinite growth, their properties do change over time and these changes can be exacerbated by inconsistent management of their growth. Understanding proper handling of cell lines by managing growth rate characteristics and cell passage number limitation is essential for consistent and biologically relevant studies. Sometimes it is necessary to sort cells to enrich the desirable cell type population. There are a few additional steps that ought to be taken when working with cell lines. Misidentification of cell lines is not rare (more than 20% error rates have been reported!). Cell lines can be mislabeled, contaminated or mishandled, making them inappropriate for the intended study. Examination of the cellular properties is essential; genotyping is inexpensive, so it is worth considering a deliberate evaluation phase for any line that is acquired through a commercial source or a collaborator.

Some cell lines are engineered for screening specific pathways. The cell lines used are chosen on the basis of their properties in cell-based assays, and the monitoring activity of the pathway through fluorescent proteins such as GFP fusion can make sample preparation much easier. In fact, they can be imaged live to better understand biological function and kinetics. Transcription factors expressed as GFP fusion proteins are common. Examples include FOXO and STAT family members, beta-catenin and TCF4/TCF7L2, NF- $\kappa$ B, CREB and many others. GFP fusions to other proteins are used in other robust assays, including GPCR signaling components such as PTH receptor internalization and beta-Arrestin (30, 31, 48), even protein kinases such as p38-MAPKAP2 (53), AKT kinases are activated through a transient localization to the plasma membrane and MAP/ERK family kinases can be localized to the nucleus.

In cases where the screen or assay is not specifically tied to a single pathway, but is in fact targeting a cellular response, multiple pathways may contribute to the response. The effect

may be different across cell lines, even lines that are genetically and phenotypically very similar. This heterogeneity has made it difficult for many experimental results to be extended, particularly to clinically significant therapeutics. This is becoming a well-recognized issue, and some groups, both academic and industrial, have transitioned to using panels of cell lines that are defined by both signaling characteristics and genetic background, including amplification of oncogenes and chromosomal imbalances (54). The goal is to generate data that reflects properties of cell lines grouped by common properties as reflected in the disease state in question (such as cancer subtype). The process of selecting lines is the same as outlined above, but many cell lines would need to be selected and screened. The logistical challenges are out of the scope for this chapter, but scientists looking for novel therapeutic strategies should be aware of this approach. Phenotypic questions addressed by such panels include demonstrating that blocking autophagy, ER stress response or other survival mechanisms will lead to cell death (55). Image-based approaches to phenotypic assays present unique and very valuable additions to biology and drug discovery, but the value in a discovery made in a single cell line is potentially limited unless it can be generalized or placed in a tractable signaling context.

**Table 3: Summary of common properties that can vary between cell lines**

| Property                | Impact   |
|-------------------------|--|
| Growth rate             | Increase in cell number; affects confluence (some properties are affected by confluence and may need to be split more frequently)  |
| Metabolic rate          | Consumption of energy and nutrients; can change health of the cell, as well as assay conditions (pH in particular)   |
| Colony morphology       | Pattern of growth as cells divide; some lines will spread evenly, others will clump  |
| Adherence               | How strongly the cells bind to the plate; influenced by the materials used to coat the plate, some lines adhere better to a collagen or fibronectin coating on the plate surface |
| Heterogeneity           | Cell lines that appear as mixed populations morphologically  |
| Proportion of cytoplasm | Some lines have very little cytoplasm, making many imaging assays very difficult   |

## 4.2. Primary cell models.

### 4.2.1. Models using differentiated primary cells

Primary cells are intrinsically more difficult to acquire and handle than most cell lines. Primary cells have limited capacities for expansion (the Hayflick Limit), or may even be post-mitotic and cannot be expanded through normal cell passaging. It can be difficult to obtain many primary cell types. Most human cell types, including pancreatic  $\beta$ -cells, adipose, primary tumor and tumor-associated fibroblasts, kidney and liver hepatocytes or macrophages frequently require research collaboration or material transfer agreements with hospitals or specialized procurement facilities. Commercial sources are available, but are expensive. Primary cells from animal models, particularly rodent, are much more common. On-site animal facilities can make procurement simpler to plan for, but may

require a researcher to isolate the cells themselves. The two biggest logistical challenges to using differentiated primary cells as experimental models are (a) donor consistency and (b) delivery schedule. These can be more manageable for animal sources but both can be major problems for human samples, particularly irregular delivery schedules.

Differentiated human cells are collected during surgical or post-mortem procedures. Although disease tissue is frequently sought as a bona-fide model of the disease itself, sample heterogeneity is typically much greater and some samples cannot be used. This is true for non-cancerous samples as well, including hepatocytes or  $\beta$ -cells from diabetics and synovium samples from patients with Rheumatoid Arthritis. Even when samples can be used, there is frequent variability. Some primary cell models require media changes during the first few hours in culture, and the timing can vary from sample to sample. Samples are typically collected, isolated (purified) and shipped fresh within hours of collection, so advance warning is limited and a lab that depends on these will need to be prepared. In some cases, cells can be cryopreserved, greatly simplifying the experimental process.

#### 4.2.2. Models using primary cells produced from differentiated stem cells

An alternative to using differentiated primary cells is to differentiate stem cells in the lab for the assays. Various adult stem cell types are available, and each can be used to generate different types of cells. Mesenchymal stem cells can be used to generate hepatocytes, skeletal muscle, adipose cells, and others. The extent to which they differentiate can be variable, creating a *de facto* co-culture system with cells that did not fully differentiate. In some cases, splitting and purifying the cells is not practical. Hepatocytes form very tight junctions, making separating them difficult and adipocytes have the unexpected property of being buoyant when they have accumulated significant lipid stores. In addition to the use of partially differentiated stem cells, protocols exist for differentiating pluripotent stem cells and iPS cells. These approaches are still under development and rather specialized.

#### 4.2.3. Establishing primary cell models

Primary cells are valuable because they retain properties beyond what cell lines can provide. All cell lines have significant genetic and regulatory alterations. The price for a steady supply of cells is that many cell type-specific properties are greatly diminished or lost entirely. Loss of CDK inhibitors and telomerase, frequent activation of p53 and at least some chromosomal changes result in the degradation of cell type-specific functions; indeed many cell types are terminally differentiated, and this post-mitotic state is essential for physiology and morphology of the cell. Primary cells have a greater capacity to retain these properties, but they are affected by culture conditions, and therefore establishing proper culture conditions is essential to leveraging the benefits of using primary cells. For most cell models there is a strong primary literature history that describes the critical properties of the cell type in question and the culture conditions necessary to maintain them, although exceptions exist and some scholarship researching the models under consideration is important. Typically, conditions that need to be specified include media

and supplements or the need for supporting feeder cells to produce native growth factors. Supplements in media for primary cells are typically titrated carefully to support growth but to avoid being higher than necessary. As such, the media may expire more rapidly than standard media preparations. In general, it is better to avoid proprietary media or supplement formulations because it is not possible to specify the experimental conditions and inter-lot variability can lead to failed assays. Therefore, some reverse engineering may be required to adapt the cell culture system to one that is appropriate for the assay being developed. As a quick example, primary human hepatocyte culture has been optimized for toxicological studies using commercial ITS (insulin-transferrin-selenium) formulations, but the level of insulin is far higher than normal, and precludes any insulin sensitivity of the hepatocytes. To adapt the hepatocyte culture system to one that can be used for the study of glucose regulation, the commercial ITS solution needs to be replaced with individual component stock solutions that can be independently varied. For proprietary formulations, manufacturers are typically reluctant to fully describe their composition, although they will often confirm whether specific materials or growth factors are present when asked as a specific question. Nevertheless, a lack of complete understanding of the culture conditions may lead to surprises later on.

Beyond the media requirements, there are frequently additional specifications regarding seeding conditions. Cell density requirements are typically fairly rigid, particularly if they are high. Many post-mitotic cell types are plated at confluence, and deviating from this will cause the cells to dedifferentiate. This can be a very difficult step to optimize, as the fraction of surviving cells capable of adhering to the culture matrix will vary from sample to sample; for new samples, it may be necessary to plate cells across a range of seeding densities. The ability to work with a single batch of cryopreserved cells helps tremendously with this step more than any other. Addition of support extra-cellular matrices, such as collagen, laminin or fibronectin coated plates or basement membrane gels (e.g. Matrigel™) may be required. This is especially important for studies on certain cancer cells, such as breast cancer lines, primary neurons and hepatocytes. Often, it is not possible to omit these and maintain the cells for any length of time. Neurons, in particular are very sensitive to changes in substrate conditions. Different concentrations or types of poly-lysine, laminin or proteglycans produce dramatic changes in neuronal phenotypes. Even under optimal conditions in *ex-vivo situations*, these post mitotic cells will have a defined life span.

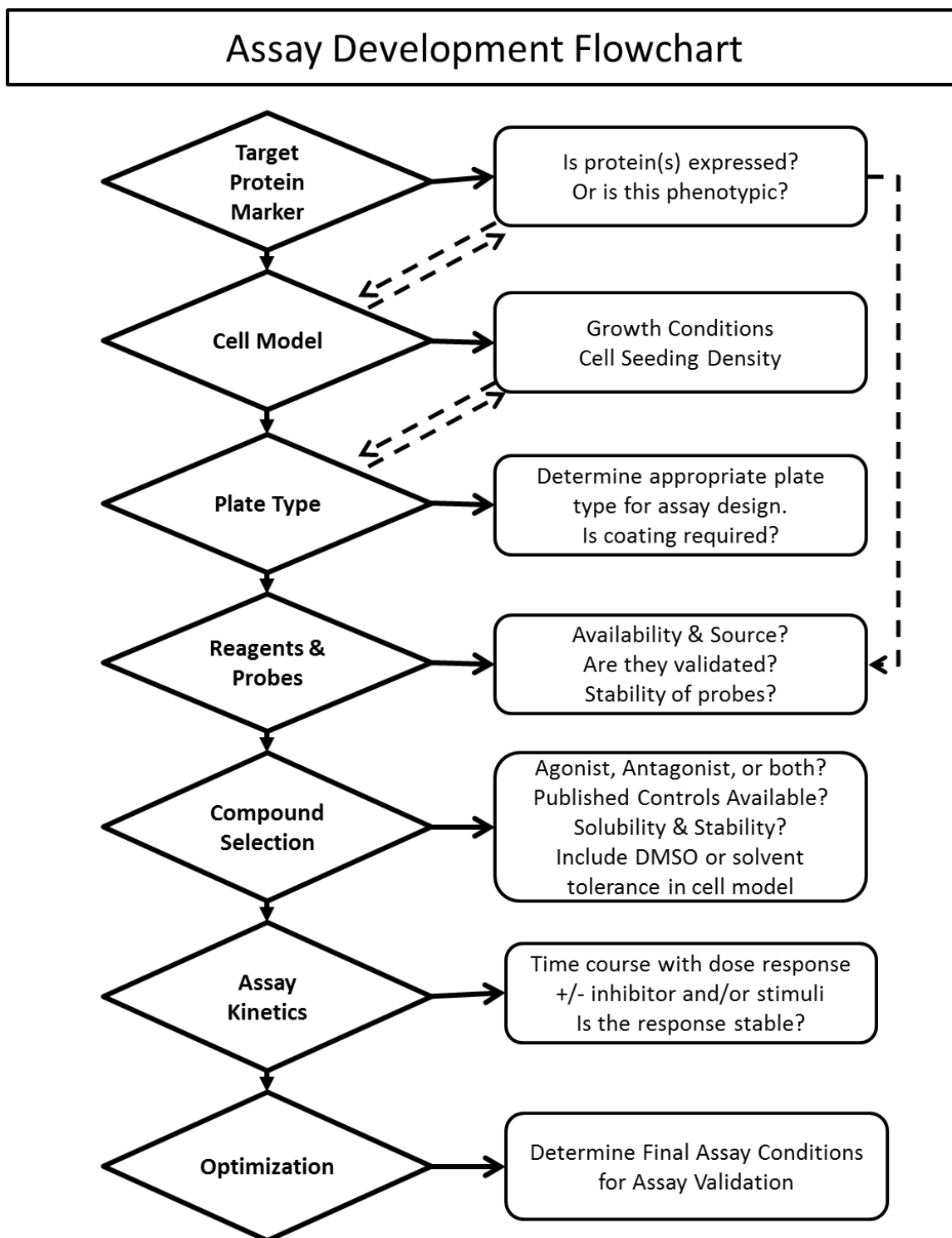
Standardizing primary cell culture conditions is essential for robust assay performance. For experiments where cells are used from a new source (patient or animal) for each experiment, responsiveness will vary, and separate normalizations will be required for each experiment. Endothelial cells, a proliferating primary cell used in angiogenesis experiments, form tube-like channels when plated on a basement membrane matrix. The dynamics of this process is affected by modest changes in source or lot, seeding density, passage number, basement membrane matrix composition and media. The first three factors mean that the assay responsiveness will change during repeated runs of an experiment, so historical performance comparisons are difficult. There is a significant



literature from the HTS field on the number of controls that are needed per plate to give reliable normalization across plates and experiments (56). This is relevant to HCS as well.

## 5. Assay Development Considerations and Troubleshooting

### 5.1. Assay Development Flowchart



## 5.2. Target, Protein, Marker

It is important to consider the goals of the assay and whether the desired target protein/s is/are expressed in the cell model of interest, if the protein expression is constitutively active or requires activation or stimulation. It is suggested to examine relevant reference literature or the Gene Expression Omnibus for microarray data, then measure activity with a validated assay (e.g. Western Blot, ELISA, flow cytometry, etc). Another consideration is location, location, location; verify the location of the protein or marker probe expression within the cell model to determine if it is amenable for HCS.

## 5.3. Cell Model

### Which Cell Line Should I Use?

It is highly recommended to review the literature and references to determine if the appropriate cell model or cell line is documented for the specific assay of interest. If the cell model or cell line of interest is not referenced in the literature then it is recommended to cross validate a known cell model or cell line with a known biological endpoint before proceeding with any unknown or orphan cell models. The source of the cell line must have documentation; if using a cell line from a collaborator or colleague then obtain as much background information as possible about the history and growth characteristics. Phenotype and genotype the cell line as required. If starting with a known documented cell line, it is best to purchase from established cell bank, e.g., ATCC with history of lot details and cell growth profile specifications. If using primary cells, stem cells, *ex-vivo* tissue then establish and document as much about the growth behavior in culture before transitioning to multiwell plates for further reference, reproducibility and evaluation of likelihood of success. For transient, stable, or inducible transfection or infection of reporter proteins, such as fluorescent proteins (i.e. GFP), then steps must be taken to further validate the cell line to determine the percentage of cells expressing the reporter after cell seeding, stimulation, and other treatment.

### 5.3.2. Growth Conditions

Define the media, serum, and other growth factors for optimal biological response. Please note, while the optimization of health of the cells and biological conditions are needed, high levels of serum can lead to compound absorption in the assay affecting the results. When and if possible reduce the amount of serum used to a minimal level without sacrificing the overall health conditions of the cells. When miniaturizing the assay to multi-well plates, it is required to verify and/or validate if it is able to reproduce the correct biological response. It is important to know how long cells can survive and respond “normally” in culture when designing these types of assays. Determine the sensitivity of the cells outside of normal optimal environmental conditions, i.e., outside of the incubator at room temperature to mimic plate handling timing, and if the cells can tolerate changes in temperature, pH or osmolarity fluctuations. Also consider whether the addition of HEPES buffer will minimize pH changes without altering the biological model response.

### 5.3.3. Cell Seeding Density

Determine the cell seeding density by initially plating cells to achieve at or near confluence of the monolayer or at desired density for biological outcome. For cell types that tend to form clumps, a cell strainer could be used to de-clumping. As a general rule, cells approximately 10 microns in diameter and proliferation doubling time less than 24 hours, seed ~5,000 cells per well for 96-well plates or ~1,500 cells per well for 384-well plate. From this point forward, dilute cells by increments of 500 to 1000 cells per 96-well in replicates and incubate overnight. Label cells with an indicator to identify cells, i.e., nucleic acid dye such as Hoechst 33342, DAPI, DRAQ5, or others; this can be counterstained with a cytoplasmic indicator such as Cell Mask<sup>TM</sup> or other live cell indicator such as CM-FDA (5-Chloromethylfluorescein Diacetate) or Calcein-AM. These fluorescent indicators will be used to determine if the image analysis algorithm can properly identify, segment (separate) individual cellular objects. Perform statistical analysis of number of cellular objects per field or well to determine minimal number that can be used to provide a robust assay (see Section 6).

## 5.4. Plate Type

Often overlooked, the plate type chosen is critical to a successful screening campaign; keep in the mind the following when choosing a plate type.

### 5.4.1. Plate Material

Plates are generally made of glass, quartz, polystyrene or other composite materials. Each plate material has its advantages and disadvantages, so it is important to carefully consider what type is chosen to provide the best result in the assay.

1. **Glass and quartz** are one of the flattest and best optical materials made but are also expensive to purchase and therefore they are typically only used in specialized cases where the need for enhanced optics and flatness of the plate is required to resolve detection of subcellular structures or if capturing an entire well with a high numerical aperture, high magnification objective, i.e. 40X, 60X, 63X, 100X. Keep in mind glass and quartz material will likely require substrate coating for proper cell attachment.
2. **Polystyrene** based materials are the most common in HTS and have been adopted for HCS. The advantage of these plates is the cost is relatively low and most cell types can attach without basement substrate materials or coating.

### 5.4.2. Substrate requirements

The use of poly-D-lysine (PDL) coating can enhance attachment and spreading in many cells. This is commonly used in to improve attachment during compound treatment and subsequent processing and labeling steps, such as cytotoxicity assays. Extracellular matrix (ECM) proteins are used to coat plates to establish or mimic appropriate biological conditions of the assay. The most common ECM base substrates include Collagen-I, Collagen-IV, Fibronectin, Laminin, and Matrigel. If using glass bottom plates, then it is

absolutely necessary to coat plates with ECM or PDL coating to promote cell adhesion and attachment. For cell spreading and migration assays it is important to test individual ECMs or a combination of these substrates as the outcome is highly dependent on the cell adhesion molecules expressed by the cells and the matrix molecules they interact with. In primary cells it is almost always necessary to use a biological substrate material to achieve appropriate conditions for an assay if feeder cells are not used. For example, appropriate substrates are required for optimal axon and dendrite outgrowth from neurons. Commercially available plates with pre-coated substrate materials are offered by many manufactures. It is recommended testing more than one lot of these plates to verify assay performance and robustness as variability in manufacturer lots are not uncommon.

### 5.4.3. Physical dimensions of the plate

Most plate manufactures follows SLAS standard format. Table 4 shows the approximate surface area and maximum volume for a single well, based on plate manufacturer. The flatness and bottom thickness of a plate are also important parameters. When matching a plate with numerical aperture (NA) microscope objective lenses, it is important to carefully determine the plate thickness. For example, higher NA objectives such as a 40X/0.95NA objective lens likely has a coverslip thickness of 0.17 mm. Be sure the plate bottom thickness is at or near the coverslip thickness of the objective lens and is appropriate for the working distance of the objective. In this case, do not use plate thickness near 1 mm as the microscope objective lens with high NA will fail to focus on the cells with clarity.

It is also important to determine if there is a need for evaporation wells or barriers to prevent loss of liquid in wells over time for longer term incubations, depending on your assay. Test plate types to ensure cell morphology and biological outcome are not altered. Additionally it is important that the plate does not leak over time before scanning; if the wells dry out from leaks or from wicking, the autofocus (image based and laser based) will likely fail. Be cautious of this as potential damage from salt based storage buffer solution including sodium azide ( $\text{NaN}_3$ ) on optics and electrical components inside the imager is possible.

**Table 4: Approximate surface area and maximum volume for a single well**

| Plate Type | Surface Area / well    | Volume   |
|------------|------------------------|----------|
| 96-well    | 0.32 cm <sup>2</sup>   | < 300 uL |
| 384-well   | 0.06 cm <sup>2</sup>   | < 110uL  |
| 1536 well  | 0.0023 cm <sup>2</sup> | < 10uL   |

### 5.5. Reagents, Buffers, and Probes.

When beginning a new assay, if and when possible use a validated assay kit, commercial if available, to become familiar with the steps involved in performing the assay. Then decide if the assay will continue with the “kit” or if a “home-brew” assay will be developed. A home-brew kit requires further optimization, validation, and time, but often offers cost

savings in larger screening campaigns. Buffers used for imaging assays include the following:

1. **Salt based solutions:** most common solutions are Hank's Balanced Salt Solution (HBSS), Phosphate Buffered Saline (PBS), and Tris Buffered Saline (TBS).
2. **Permeabilization buffers:** salt solutions or water containing detergents such as Triton X-100, Tween-20, SDS, NP-40, or other detergents.
3. **Blocking buffers:** for antibody labeling, these are salt solution buffers containing protein such as BSA, fractionated antibody chains, or whole or fractionated serum from animal species that correspond to any secondary antibodies that will be used in the assay.
4. **Fixation buffers:** for cell preservation include formaldehyde, paraformaldehyde, glutaraldehyde, ethanol, methanol, acetone, and commercial customized propriety formulas. Typically the alcohol based fixatives serve as both a fixative and a permeabilization agent and useful for phospho-protein labeling. Combinations of multiple fixatives or even double fixation methods can improve preservation and fluorescent signal. Glutaraldehyde can provide stabilization of protein labeling but it auto-fluoresces so it is best avoided or used a low concentration, i.e. 0.01%. The presence of auto-fluorescence can be reduced with specialized treatments or quenchers but these may bring about other problems.
5. **Post staining buffer solutions:** prevent microbial growth includes salt solution (HBSS, PBS, TBS) with 0.01%  $\text{NaN}_3$ . Be cautious as  $\text{NaN}_3$  is toxic and can be dangerous when combined with metals or acids, so precautions are needed.

### 5.5.1. Optimization and development of an un-validated assay

Antibody and organelle probe selection requires researching the literature and other resources to determine a starting point of antibody or probe choice. Choosing an antibody typically involves choosing one or more antibody sources for differences in epitope recognition site or phosphorylation recognition. When choosing a probe, it is important to understand the different chemistry for binding to organelles or proteins, spectral properties of the probe, how the kinetics are altered over time, and stability of probes in live or fix end point assays.

#### 5.5.1.1. Antibody optimization

As with other antibody based staining methods, blocking with serum from the same animal species as the primary antibody is best; an alternative is to use at least 3% w/w bovine serum albumin (BSA). As a general rule, use the recommended dilution by the supplier of the antibody or if not stated start at 1:50 dilution and dilute by 2-fold. If no signal is observed, increase the antibody concentration. Use 50  $\mu\text{L}$  per well for cells seeded in 96-well plate and dilute as necessary for other plate types; confirm the cell monolayers are completely covered with antibody solution. For example, if the supplier of the antibody suggests 1:100, use a titration scheme outlined in Table 5.

Incubate primary antibody for a minimum of 60 minutes at RT. Longer incubation times may be required to improve antibody binding or to optimize work flow process such as overnight incubation at 4°C. Use a secondary antibody reporter that is well established and be sure to measure secondary antibody staining alone without primary antibody to determine non-specific binding. Include no antibody staining to measure and establish background fluorescence of the cell type used, as some cell types are notorious for autofluorescence such as liver derived cells. By lowering the concentration of the fluorescent secondary reporter, the signal to noise ratio may improve. If two or more primary antibodies are used it is important to prove the secondary antibodies do not cross-react with an inappropriate primary antibody. If the signal in the antibody labeling is weak or undetectable, the use of other enhancement techniques may be required to boost the signal such as streptavidin binding complex or tyramide signal amplification.

**Table 5: Example titration scheme for primary antibody**

| Content                 | Concentration of primary antibody                          |
|-------------------------|--|
| Negative Control        | Unstained – No primary Ab and No secondary Ab              |
| Negative Control        | Non-specific Binding - Secondary Antibody Only, no primary |
| Experimental Conditions | 1:50   |
|                         | 1:100  |
|                         | 1:200  |
|                         | 1:400  |
|                         | 1:800  |
|                         | 1:1600   |

## Probe optimization

Probes include functional dyes such as calcium indicators, liposomes, lysosomes, mitochondria indicators, cytoplasmic, and nucleic acid probes. Dilute desired probe starting at the recommended manufacturer's concentration by 2-fold; additional increase concentration by 2-fold for at least one or more concentrations for a total of not less than 5 data points. Repeat concentration curve if signal is either too weak or if saturation is reached and reduce the concentration curve less than 2-fold to “dial-in” on the optimal concentration.

Not all probes are fixable and must be analyzed using live cell imaging techniques; proper design of live cell experiments with time dependent kinetics is absolutely critical to successful outcome. When planning a live cell experiment with untested bioprobes it is important to account for the time required for an HCS imaging device to acquire cells, fields or wells on a plate. For example, if a mitochondria probe requires 30 minutes to properly load in cells and fluorescence begins to decay or results in toxicity in 2 hours, then it is absolutely necessary the image acquisition is completed within this time period.

For fixable probes, determine the stability of the fluorescent signal following fixation and analyze plates appropriately. For example, measure probe fluorescent signal at time 0 post-fixation, then measure signal at day 1, 2, 3... and so on to determine the overall stability of the signal. It is also critical to establish the stability of the light source (lamp-based, laser, LED) in the high content imager to ensure it is functioning properly during the testing period. Use a known standard fluorescent dye, cells with label or other inert material to reference daily fluorescence during the study. As a general rule, most nucleic acid probes bind tightly and are very stable but organelle probes tend to be leaky and less stable over time.

## 5.6. Reference Compounds and Stimuli

If there are no known published reference compounds for the assay, then use untreated control or untreated control plus vehicle (i.e., DMSO) as a baseline to normalize the data. This is an acceptable approach and may be used for orphan targets or in phenotypic screenings assays when “references” are not established.

For known reference compounds, consider the commercial availability, the stability of the reference compound, and its solubility in solvent, media, or buffer. Also determine if a specific or specialized solvent is required, and its specificity for activation or inhibition.

Refer to literature to determine potential reagents to use as stimuli for signaling pathways. A few things to consider when selecting stimuli for assay are:

- What is the signal to noise ratio and window for the assay?
- Is the stimulus biologically relevant (e.g. cell types, pathways...)?
- Is it constitutively active
- Is the stimulus specific, or does it activate multiple pathways?
- Would different stimuli for the same receptor lead to activation of different signaling pathways?
  - If so, did you select the correct stimulus for the assay of interest?
- Is more than one stimulus required for the assay or to obtain an improved S.N? And is it biologically relevant?
- Does media, sera, or growth factor used to maintain the cells activate the signaling pathway in question or alter morphology or migration?
  - If so, one may need to search for suppliers for “conditional media” or find ways to remove the stimuli.
  - If the pathway is activated by serum, it may be necessary to incubate the cells in serum-free media for a few hours prior to starting the assay.

Determine the tolerance of the cells in the assay to chemical compound solvents, such as acetone, acetonitrile, chloroform, dimethyl sulfoxide (DMSO), ethanol, ethyl acetate, hexane, methanol, tetrahydrofuran, toluene, or water used to solubilize chemical compounds. Determine the maximum concentration of solvent a cell model or cells can withstand before assay performance is altered and/or results in detachment of cells or cytotoxicity.



DMSO is the most common solvent used in biological drug discovery and many compound libraries are delivered in DMSO. In most cases, a working concentration of DMSO for *in vitro* assays between 0.1 and 1% is acceptable; however, this needs to be confirmed for every assay model. Perform DMSO tolerance by beginning at either 8 or 4%, dilute 2-fold in media used in the assay to include 8, 4, 2, 1, 0.5% DMSO, then include 0.2, 0.1, 0.05, 0.01% DMSO. Also include an untreated (no DMSO) control. DMSO tolerance is used in the assay model design by mimicking compound addition for the assay. If a stimulus is applied, include DMSO concentration curve for both un-stimulated and stimulated to determine if the stimuli has an effect on DMSO tolerance. Based on these results chemical compounds stocks for screening can be made at the appropriate concentration for maximum solubility and delivery to cell plates for assay validation process. If dose response curves will be done in the assay, all wells need to have the same final concentration of vehicle (such as DMSO) to reduce variability and eliminate artifacts caused by synergies between the vehicle and compounds at some concentrations but not others, and to prevent compounds from crashing out in the solution. Other solvents mentioned above require a similar concentration curve as DMSO and may require a larger concentration range to determine both tolerance of cells to solvent and solubility of the chemical compound.

## 5.7. Kinetics of the Assay

### 5.7.1. Assay response stability

Determine if the response for the assay is stable or prone to degradation by performing a time course experiment. This is critical in fast response assays such as using an agonist to trigger calcium mobilization or in using a stimulus to activate signal transduction pathways. The time course will be dependent on the assay type chosen. For example, calcium flux assays must be performed in live cells and measured within seconds. Alternatively, for signal transduction pathways, you must determine the half-life activation time following addition of stimuli in increments not less than 5 minutes for the first 30 minutes and increments not less than 10 minutes between 30 and 60 minutes.

Determine if inhibitor compounds can be added simultaneously or if a pre-incubation of inhibitor compound is required before adding stimulus. Be sure to determine this timing with the adaptation of automation and liquid handling devices in the laboratory. If simultaneously delivery of inhibitor compound and stimuli is not possible, determine the time course required to pre-incubate with the inhibitor compound starting at 5 minutes and increasing to 30 minutes or more as necessary to optimize work flow logistics for screening and determine if it improves signal to noise ratio. It is important in fast signaling pathways that the pH and temperature are stable during compound and stimuli additions as these can affect the biological outcome. Be sure to pre-warm stimuli plates, media and compounds to room temperature if necessary. Once a method is adopted, it is critical to maintain it throughout the validation process.

For assays with long incubation time, samples in the wells at the outskirts of the plate are frequently problematic due to evaporation or inconsistent temperature controls. To

minimize impacts of evaporation, for small sample numbers, one could fill the outskirt wells with buffer or media only, and use other wells for your samples; for large scale screening, one could put a tray of water with antibiotics or  $\text{NaN}_3$  in an incubator to provide sufficient humidity; for assays that are very sensitive to evaporation, one could put plates in small boxes padded with wet paper towels. To minimize effects of temperature fluctuations across the plate, one should make sure all plates and reagents used for the assay are warmed up to room temperature prior to the addition of cells, pre-plate the cells in the tissue culture hood, allow the cells to attach before moving the plates to the incubator; for assays that are extremely sensitive to temperature changes, one should not stack plates in the incubator.

### 5.7.2. Cell growth characteristics

Determine if serum withdraw or serum free conditions, or addition of supplementary cell growth components or chemicals affect cell morphology, migration, or assay endpoint in cells over time. These considerations are important in several assay endpoints including

- **Cell cycle analysis:** if cells reach confluence or if they are starved of serum or growth components, cell cycle arrest can occur, which can affect the endpoint measurement.
- **Dendrite, axon or neurite extension:** typically require growth factors from supplements or from feeder cells.
- **Cell motility and migration:** typically affected by serum withdrawal and addition of serum or growth factor supplements.
- **Signal Transduction Pathway:** serum withdrawal or low serum can increase the signal in assays such as NF- $\kappa$ B (see NF- $\kappa$ B Translocation Assay Development and Validation for HCS ), MAPK kinase pathways such as ERK phosphorylation or p38 (53).

### 5.7.3. Live cell imaging

Not all live cell imaging assays need to be performed with an environmental controlled chamber; however, in screening operations it is important to know the challenges and difficulty to control the work flow if disrupted by automation mishaps or other failures. If the sequence of processing plates is interrupted, this typically will result in variable in the assay data. To determine if your assay is amenable to live cell imaging conditions with or without environmental control in screening operations, you should perform a time-course study on the HCS instrument following assay treatment or in environmental-controlled conditions such as in an incubator. For example, once a bioprobe indicator completes recommended incubation time for detection, acquire images on the HCS device at time zero ( $t=0$ ), then in subsequent time points over a 60 minute period, capturing images at 5 or 10 minutes intervals. There are several conditions that need to be considered when performing this operation including the image acquisition time per well or per plate and the exposure time per fluorescent probe. Photobleaching and phototoxicity are possible and may affect the results. When appropriate, use more than one plate and analyze multiple wells to measure the overall variability. If the time required to capture every well

or selected wells on a plate does not exceed the degradation of the fluorescent probe measured then the assay, it can be used in screening operations as long as each plate has appropriate control wells for normalization.

## 5.8. Optimization

Verify methodology through documentation of all previous established assay conditions along with the DMSO or other solvent used for optimal assay performance for preparation of assay validation. Standardize and create an SOP protocol that will be referenced for assay validation. To reiterate, image analysis method should be developed alongside with the biological assay development to ensure optimal sensitivity is obtained for the desirable phenotypes.

# 6. Image Acquisition, Analysis and Data Interpretation

## 6.1. Introduction

Computer assisted image analysis is the key component to most high-content screening endeavors, since a microscope generated image can contain an immense amount of information. The goals of image analysis are simple – identify objects (usually cells), accurately measure features within, about or between these objects and extract knowledge from the features. But before an image can be analyzed a few things should be quickly reviewed.

### 6.1.1. Capturing a Good Image

Use your imaging platform to capture *good* representative images in an unbiased manner (see Section 2 – Image Technologies and Instruments). Verify that your workflow allows for automated capture of information about the identity of the plate being scanned (user information, time, plate ID, barcode, etc). Double check the location of well A1 to ensure the plate is not loaded in reverse. Having a designated well lacking cells or containing fluorescent beads can allow unambiguous identification of plate position. Ensure that your workflow will annotate the data with assay conditions and compound treatments that will be needed for data analysis.

Every image captured regardless of the quality generates data, good or bad, so it is imperative a *good* image is captured for subsequent analysis. Some aspects of acquiring a good set of images are predetermined by the experimental design. Images should include all the fluorescent and/or brightfield channels needed for the analysis. If the analysis will require 3-D analysis or different sample or time points in a series that are required for analysis, these images must be appropriately captured. Image fields should be taken in appropriately located, predefined positions within the sample wells (cells near the edge of the well can behave differently or the images may be distorted). Pixel resolution and magnification must also be selected to balance the level of detail vs. the number of objects (eg. cells) available for analysis and will depend on the type of objects you are setting out

to analyze. Sometimes multiple fields of images from the same well must be taken to obtain enough objects with appropriate resolutions.

Two aspects that may require fine adjustment on a day-by-day basis for a given screening campaign are the focus and exposure. An out-of-focus image, even slightly, will impact the apparent size and intensity of the objects and sub-objects within the image, and can quickly increase the noise within the analysis. Most platforms provide multiple ways to auto-focus fields before taking the image, and they should be tested for their accuracy, speed and robustness. A good exposure is also very important, and should aim to optimize the *dynamic range* of the detector such as a monochrome CCD camera or PMT (photo multiplier tube). The result is a gradient scale with dark intensity in an image as black pixels and bright intensity as white pixels representing low and high numbers respectively.

Finally, do the settings used to capture an image of a neutral control field also allow other images in the experiment to be acquired accurately and with high quality? Depending on the dynamic range of the image acquisition system and the intensities in different fluorescent or brightfield channels, it may be necessary to adjust the image acquisition settings using positive or negative controls. Compromises may need to be made because it is usually preferable to have all the images within one experiment taken with exactly the same parameters rather than have to spend time normalizing after the acquisition.

In the process of taking a good image you may want try to limit the time it takes to actually acquire the images; for example, ensure that exposure times are not needlessly long or that resolution is unnecessarily high. Long exposures generally mean more time needs to be spent in image acquisition, High Throughput and High Content Screening often need to balance the amount of time taken to achieve the desired assay quality with the throughput needed for the screening.

### 6.1.2. Overview of Image Analysis

You have the images, so now what?

Analyzing an image with the goal of measuring features within the image or objects requires several steps (Figure 9). Once the image is acquired, it often needs to be adjusted to get the best quality by use of flat-field or post acquisition background correction. Next a threshold is applied to identify objects from background followed by segmentation to separate individual objects. These objects are often further selected based on a variety of criteria and finally the features are extracted. While the primary object identification is usually done using a nuclear or cytoplasm specific stain in one channel to identify the cell, additional objects are often identified with other stains and acquisition channels to generate additional feature data from the image. All these steps will be discussed in detail in the following sections.

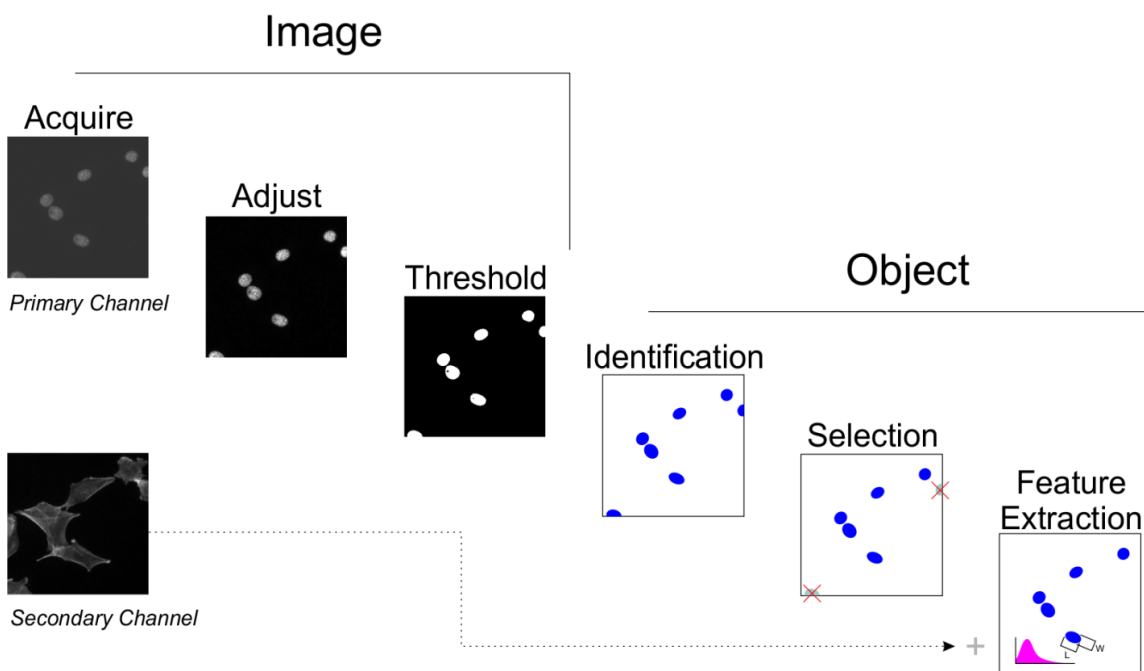


**Figure 9: Typical Steps of Image Analysis.** After acquisition, an image is adjusted to reduce noise and optimize the signal, then a threshold is applied and the information is converted into an object-based format. The objects are selected based on criteria and features of each object are extracted.

## 6.2. Segmentation (Image Processing)

Computer based image processing has been an important part of most industries since the late sixties when the first graphics programs were developed (57). Now, image analysis and processing is a normal end point for many biological assays. Most images processing in biology has a simple goal—to separate the *signal* from the *background*. This is accomplished in a few steps that involve optimizing the image, reducing background artifacts, and then applying a threshold.

### 6.2.1. Notes about Images

Images come in many forms, including different file types, resolutions, color depth, pages, stacks, montages, and usually have associated metadata. Image formats vary, and different platforms provide options for how to acquire and store images. These same considerations will also be important when processing the image.

#### 6.2.1.1. File Type

There currently is no universal image standard for HCS, although OME offers one such solution. Use a lossless format to work with images, such as TIF or BMP raster formats. Copies can be made in JPEG or PNG, but these formats will lose information so they should not be used as primary storage.

### 6.2.1.2. Resolution

Generally the image should be analyzed at the same resolution it was captured. In some situations, where the signal to noise is low, an image can be “binned” so that a group of pixels (2×2 for example) will be averaged into one pixel. This process decreases the resolution, noise and the image size for storage. It is generally more beneficial to do this during image acquisition, because it can reduce scan time, but could also be beneficial during analysis in some cases.

### 6.2.1.3. Color depth

Color or bit depth is a very important parameter of the image. It is the number of bits (1 and 0s) used to represent the staining intensity. The more bits associated with an image, the more shades of gray or color that can be represented. Larger bit depths expand the intensity range, allowing for the inclusion of pixels with fewer photons (previously black) or many more photons (previously white). Most professional cameras (including those used in HCS) operate in the 12 bit range, giving 4096 shades of intensity to work with, and this is generally preferred for image analysis due to practicality considerations. Larger dynamic range cameras may be used including 14-bit ( $2^{14}=16,384$  shades) or 16-bit ( $2^{16}=65,536$  shades). Unfortunately, the majority of computer displays (PC, Mac, Linux) are only capable of displaying 8 bits (256 shades) of information per color channel, causing some information in the acquired image to be lost upon viewing. 12-bit images will generally show up as black if you use standard software to display them. Programs like ImageJ are useful as they provide a solution to automatically stretch the color depth to fit into the 8-bit range so it can be properly displayed, but remember that the actual image is actually more nuanced.

Users will commonly see images that are labeled 16 bit and 24 bit as well. 16 bit TIF images are a common “container” that can hold 12, 14, and 16 bit images, so if your camera is 12 bit, then these are actually 12 bit images in a 16 bit container. Similarly, 24 bit images are often combinations of the three color channels (R, G, B) each of which are 8 bit. Most image based software can read and translate these image variations.

Proprietary formats often group images together within one file. For example, TIF images support groupings of images, but this can make the TIF images complicated to work with. Often, multiple color channels will be saved in one TIF image. It is also possible to bundle multiple pages, frames of a time lapse, Z-stacks of images, or even montages of images within one image format. These types of groupings may not be natively read by image processing software and will therefore need conversion to separate and store individual images. The diversity of storage solutions adapted by instrument manufacturers makes reanalysis of images across software platforms challenging.

## 6.2.2. Image Optimization and Background Correction

Before an image can be processed for object identification, it often needs to be “adjusted” or optimized to achieve optimal contrast and reduce errors that would otherwise be confused as objects or alter the object tracing. There are two common “types of error” that

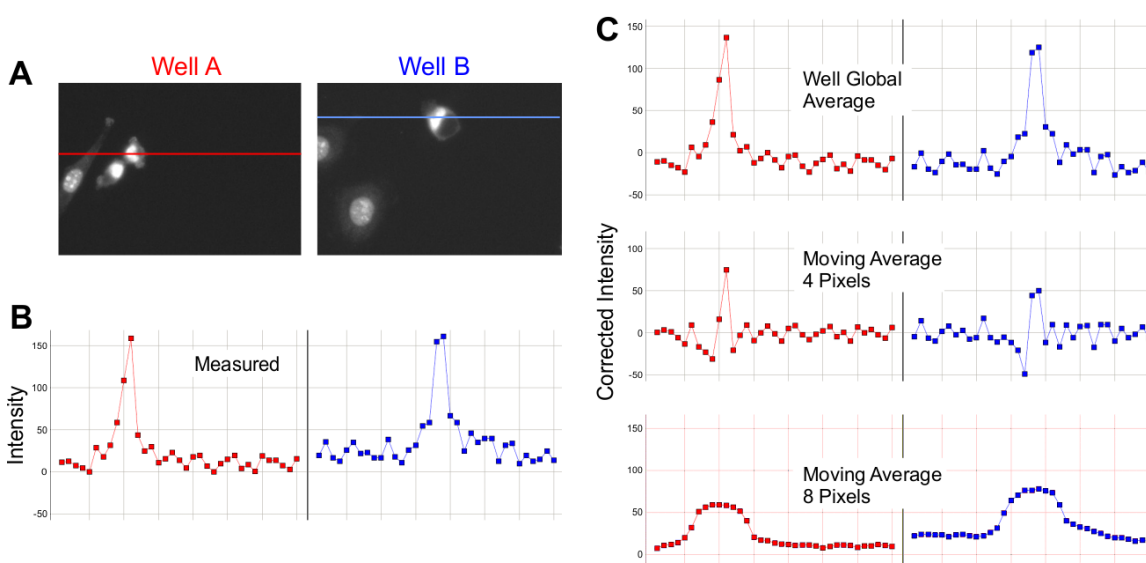


**Figure 10: Background correction can have significant effects on image analysis.** A) Two images from different “wells” are shown in raw grayscale, pre-corrected. A “line scan” is done across the image producing two scatter plots. B) Measuring the raw intensity for each well. C) Application of basic background correction on the two line scans. First, each point is simply subtracted from the global average of the scan. This preserves the full detail but shifts the baselines so they fall at zero. If a moving average (rolling ball) is applied with a radius of 4 pixels, the result is drastic, actually decreasing the signal-to-noise ratio and burying the peaks. An increase of the moving average radius to 8 pixels reduces the background noise and smoothes the scan.

are seen with microscopic images. These can be thought of as bias and imprecision or systematic and random. Bias or systematic errors are reproducible or predictable. Bias is an overall or local deviation in image intensity, which can be caused by variation in the output from the light source, uneven field illumination, optical aberrations, an artifact floating in the well, focus failures, or other reasons. On the other hand, all images contain some *imprecision* or random error, which we call noise. Random error arises from variations in the number of observed events (photons) stimulating a dye molecule, number of dye molecules, electrons emitted per stimulation, etc. These two classes of errors are present in any kind of measurement and imaging is no exception.

Bias correction is usually called “background correction” imaging platforms. Since background imperfections are generally low frequency (not in sharp focus), they are easily dealt with by two methods. The first group of methods takes the form of a moving average (a smoothing function) and can both reduce noise and reduce background. These functions are also called “rolling ball” methods. Background correction of this type is usually defined by a pixel radius to sample from and depends on both the size of the objects you are trying to identify and the size of the objects that tend to be causing artifacts. Slight changes in the sample size of the background function can have major effects on the image (Figure 10). For instance, if the background correction averages

across 4 pixels and you are looking for features that are on average 4 pixels across, you will lose most of your sensitivity to that feature.

Filtering the image based on spatial frequency is also an effective way to eliminate out of focus background artifacts (a high pass filter will remove variations that change slowly, across many pixels, such as something that is out of focus, while retaining abrupt changes seen in objects in focus). In addition, microscope systems often provide a way of eliminating common artifacts produced in the optic pathway of the instrument. These are often termed “peripheral illumination” or “illumination” errors, and are produced as the light is channeled through the various lenses and apertures. The peripheral illumination artifacts can be easily corrected by sampling an empty plate, and using that image to compute a “flat field”. This operation may not eliminate the need for additional computational adjustments.

### 6.2.3. Object Identification

The primary goal of image processing is to distinguish the *signal* from the *background*. Once the background has been corrected, a threshold is typically set which cuts off the pixels which are too dim (in a fluorescent image) or too bright (in a brightfield image) and are thus ignored as background. Setting the threshold can be simple if images are taken with consistent exposures and with a very stable dye (Hoechst or DAPI for example). In these cases it is often possible to have a manual or fixed threshold which works across an entire plate. In other cases, more sophisticated approaches must be taken that account for changes in signal intensity with time or position.

Automated thresholding algorithms analyze the pixel intensities to determine which pixels are associated with background and which belong to the objects. If certain assumptions can be made, then these automated methods work well. The most common methods assume that the majority of the image pixels will be background, and uses an offset from the mode of the image histogram (Figure 11) to set the threshold.

The result of thresholding is a “binary” image or mask, which has only negative and positive pixels. After thresholding, image “segmentation” can divide positive pixels into separate entities or “objects”. This process can be a simple algorithm which scans through the image until a positive pixel is found, then scans all connected positive pixels which are added into the first object. This process is repeated until all the positive pixels are accounted for by objects.

Another type of segmentation is often preformed either before or after object identification with the goal of splitting apart two objects that are associated with one another. This is achieved, for example, by applying a watershed algorithm on the binary image (“fills” the image with water until boundaries are established) or searching for intensity peaks or computing shape features. Other segmentation algorithms may divide the entire image into a grid for subsequent object or pixel based segmentation. Improving and developing segmentation algorithms is an active area of research.



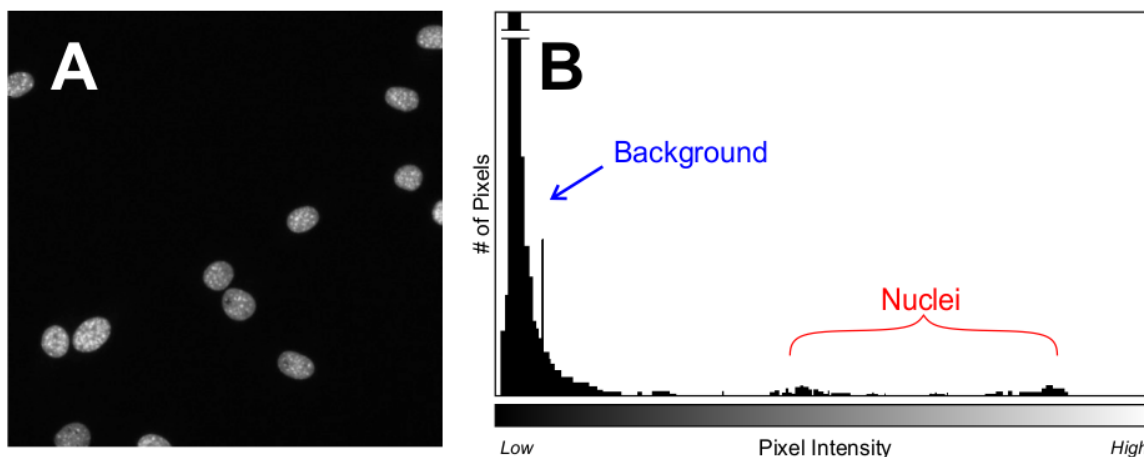


**Figure 11: Image and Corresponding Histogram.** A histogram plotting the number of pixels (Y-axis) which have a particular intensity (X-axis). Here, almost all the pixels are close to black, and only a small number occupy the lighter bins of the histogram.

### 6.2.3.1. Border or Edge Objects

Most image analysis software has options for inclusion or exclusion of objects which intersect the border of the image. These objects should only be included if complete sampling is most important (total counts for instance) and it is known that a small gap exists between image fields. If there is no gap between fields then these objects would be counted twice, which would overestimate the total count. Border objects should be excluded if information about particular object shape or structure is most important (i.e. size of cell or length of neurites).

The processing of objects provides a new set of feature data from the analytical software. Each object has many properties, i.e., shape, size, texture, and intensity that can be used in analysis. But usually objects are first “selected” to determine whether they are of interest in the analysis or just part of the noise. Object selection requires a training set or specific parameters to refine objects by their properties. For example, if objects are identified to represent cell nuclei in a homogenous culture of cells, then it is likely that the object area and object intensity criteria will be in a relatively small range, and all other objects are considered noise, debris or something else in the well. Processing can be done to identify objects similar to a known object or to identify objects that are different from a known object (i.e. training).

### 6.2.3.2. Secondary and Tertiary objects

To extract other features or to gain information about entities near the primary object, secondary and tertiary “sub-objects” are often identified. The simplest algorithm uses a mask or halo around the primary object at a predefined pixel width. Other algorithms use additional channels (from actin or cytoplasmic staining for example) to define the border of the secondary objects.

### 6.3. Feature Extraction (Object Processing)

The actual measurements generated from an image are called “features”. Usually these are cell or object-based measurements like number, size, shape, intensity, texture, or kinetic measurements. Most software analysis packages provide many more features per cell than is useful to ultimately report from a high content screen and therefore in it is important to understand what the features represent and how they are derived. This understanding will allow you to choose appropriate set to analyze.

There are no standards for output data features; therefore, there remains a wide range of interpretation of the generated output features for each manufacturer’s image analysis algorithms. The specifics for each feature vary from platform to platform, but a few stand out for their broad use such as object counts, object size / shape and object intensity. It is important to read the manufacturer’s description of each feature and to remember that features can be used in combinations.

For each of these measurements, there are two basic ways to determine their inclusion in downstream analysis. First, hypothesis driven: is a particular cellular feature which is being directly measured by a feature relevant to the dataset and worthy of inclusion. The advantage is that it will always be easy to interpret this data. The disadvantage is that these hypothesized features are often *not* the most robust features for measuring differences between samples and controls. The second method looks to best compare the sample phenotype to that of the controls. Both positive and negative controls could be used for comparison.

Before starting on analysis, it is very important to think about the organization of the various forms of data. This is primarily the images, the results of image analysis, and the metadata (experimental setup, etc). Other sections of the book will discuss this in detail (see Section 8 – Data Management for High Content Screening).

#### 6.3.1. Intensity measures

Measuring intensity should be simple, it is after all the most basic measurement that comes from the image sensor and is related to the number of photons captured on the sensor during the exposure time. The numbers attained are usually just called intensity *units*, since the camera isn’t scaled or calibrated. Raw intensities are processed over some unit of area to give a meaningful value. The unit of area is a single pixel, set of pixels, or an object area (a cell or nucleus). Usually, at least two measurements are given for a particular object. The “Sum” or “Total” measurement, and an “Average” or “Mean” measurement. The Sum or Total intensity represents an aggregation of all the pixel intensities combined to make up the unit area, so these are directly affected by object size. This is also sometimes called integrated intensity. The Average intensity feature is an average accumulation of pixel intensities across an area so that the number of pixels doesn’t affect the measurement as compared to Sum intensity, and therefore is a feature that is orthogonal to area measurements. There can also be intensity features related to the variation of the intensity compared to surrounding pixel intensities.

### 6.3.2. Nuclear features

With the appropriate fluorescent probes, nuclear stain is one of the best markers for cell identification because of its distinct edge detection and relatively uniform staining. Common features include the “Nuclear Area” and the “Nuclear Intensity”, which are simple and useful calculations. Most screening paradigms should include these measures at least in quality control assessment to identify abnormal nuclei. Cell death and proliferation can dramatically impact other features, and should be considered assessed for removal from primary analysis or used in gating strategies for measuring subpopulations. In cell death, apoptotic nuclei are often smaller and more intense, while necrotic nuclei can be larger. In addition, dividing cells may have smaller or brighter nuclei. For cell cycle assays, the Total or Sum nuclear intensity is the most useful measurement for distinguishing G0/G1 and G2/M phases but not S-phase due to variability of intensity measurements, since it most closely reflects DNA content.

### 6.3.3. Position measurement

Each object can be tracked for its relative XYZ position within the coordinate system of the platform or relative to other features of the cell or neighboring cells. As before, careful reading of the manufacturer’s description of these measures is necessary to avoid confusion. Position measurements are very important for any analysis that involves populations of cells (clusters, colonies, stem cells, population analysis). Proximity to neighboring cells has also been shown to be an important factor in predicting viral infection, neurite outgrowth, autophagy and a host of other phenomenon (40). The user should be concerned with two things – from which point is the *reference* for the position measurement (the field or image, well, entire plate), and what position within the cell *itself* (upper left point, centroid, bounding box).

### 6.3.4. Regional analysis

Measuring specific regions or compartments within or around a cell is important for many assays. As with NF- $\kappa$ B translocation, for example, the cytoplasm must be distinguished from the nucleus to assess which compartment the protein is occupying. The fastest algorithms to process this information use a mask or halo, which is dilated out or contracted in from the primary object. If a nuclear stain was used a Nuclear Mask is constructed either by directly copying the primary object, or often constricting by 1 or 2 pixels. The Cytosolic Mask is then constructed by dilating a few pixels away from the nucleus and then is active over an additional width of pixels (creating a ring overlaying the cytoplasm, Figure 12). There are two important considerations when defining the width and distances of these masks. First, should the perinuclear area be part of the nuclear mask, the cytoplasmic ring, or excluded? Many biological processes (autophagy, nuclear import/export, protein synthesis, etc) take place in this perinuclear area, so its placement is often relevant. Second, how far out should the cytoplasmic ring or halo extend? Most cells have projections which extend some distances, but if this mask is being used to identify cytosol then extending the mask too far will include too much background, decreasing the value of the measurement. On the other hand, if a spot or

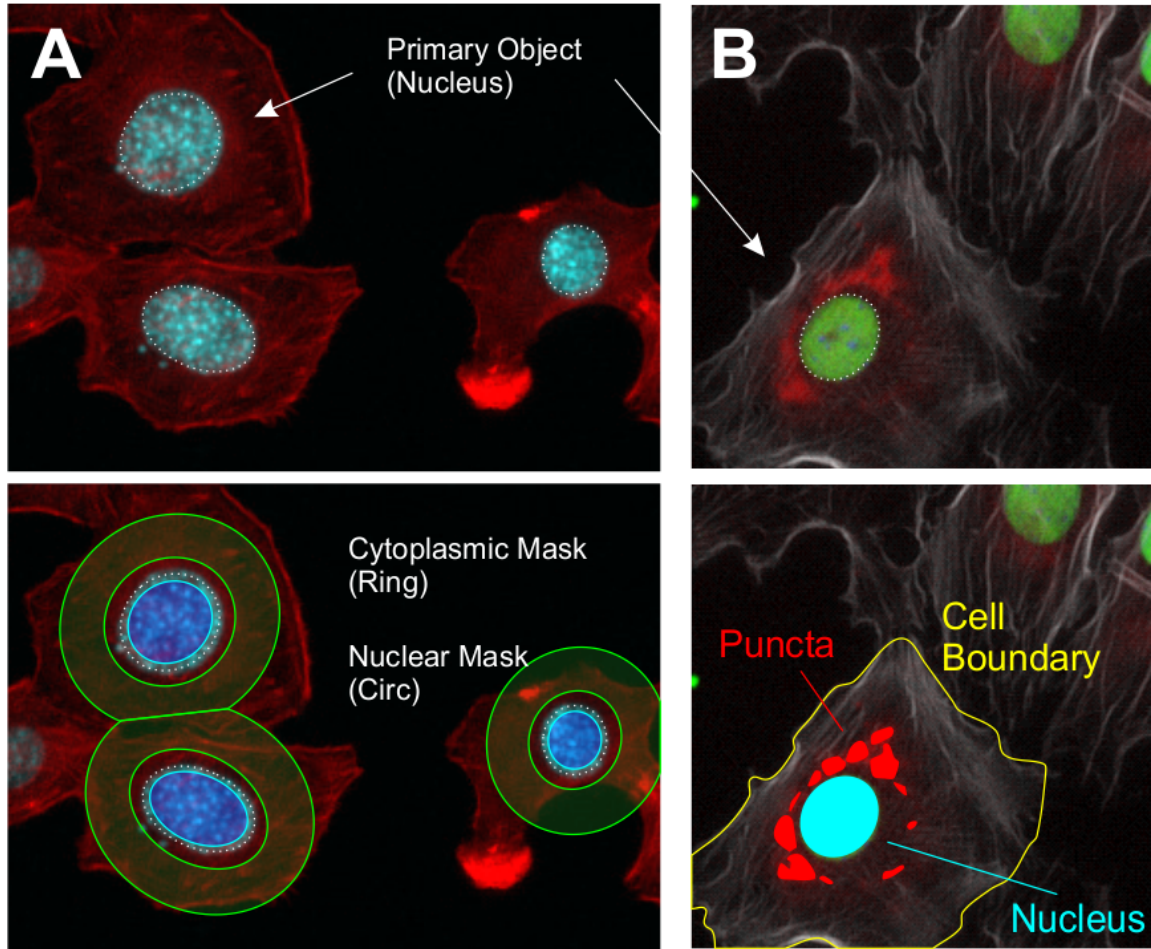


**Figure 12: Regional Analysis, Masks, and Common Features.** Images of cells in culture demonstrate primary object identification (dotted outline) and secondary analyses in the lower panels. A) Renal carcinoma cells stained with phalloidin (red) and Hoechst (blue) above. Below a 1 unit contracted nuclear mask (light blue outline) and a 2 unit dilated cytoplasmic ring (green). The relevance of the width of the ring is evident, since if the actin adhesion in the cell on right was an important feature, it would have been excluded from the mask. On the other hand, the masks on the two cells at the left do a good job of including cytoplasm and excluding background. B) mouse fibroblasts stained with phalloidin (gray), a nuclear protein (HMGB1, green), and an autophagic protein (LC3, red). Analysis of the cell boundary as well as cytoplasmic puncta in the red channel are displayed.

strand (see below) is expected out in these processes, then the mask should be extended. Sometimes this outer ring is used to detect nearby objects that aren't even part of the cell, so it could be dilated quite far depending on the assay.

### Cell area

Although the cytoplasmic ring discussed above produces a boundary whose area can be measured, the shape of this simple object doesn't reflect the true cellular boundary (also known as the cellular *extent*). Secondary object algorithms that use an additional channel which demark the cytoplasm, cytoskeleton, or membrane can return an accurate

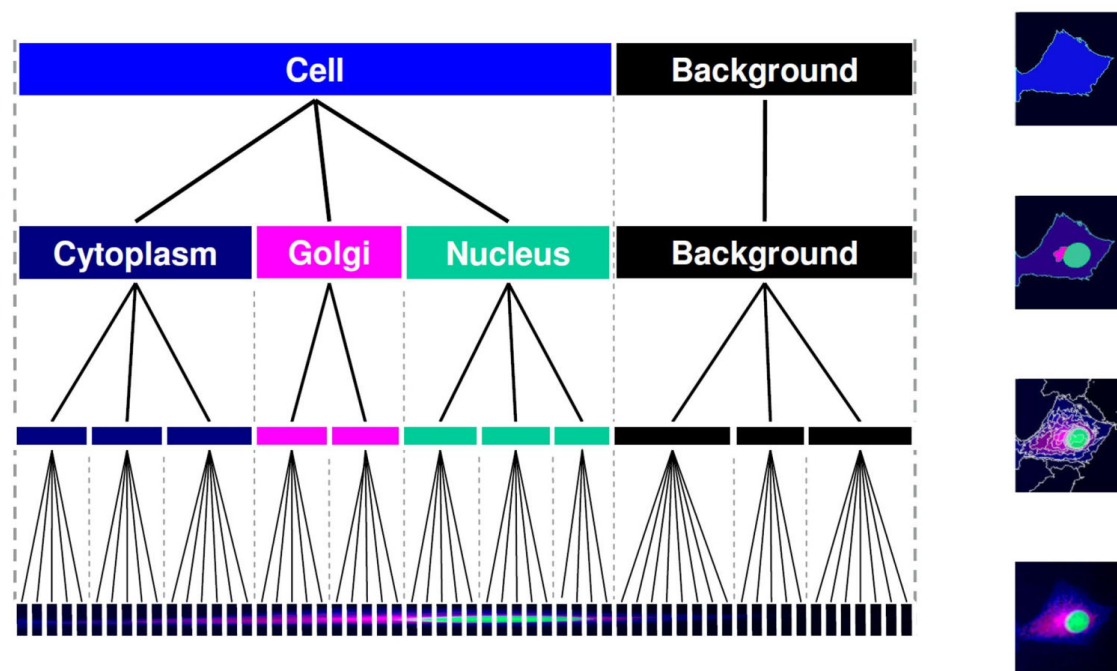


**Figure 13:** Pixels to objects. Using microscope channels that are derived from different cell strains, groups of pixels can be combined into a variety of objects, as in this example from Definiens: the cytosol, the golgi, and the nucleus.

measurement of the cellular area. These other channels can build up objects from the pixels, where groups of similar pixels are combined into groups that are eventually defined as a particular kind of object (Figure 13).

### 6.3.6. Puncta identification

Spots, strands and sub-regions are important measures in many cell biological assays. Most image analysis software includes feature extraction to look for “sub-objects” or “spots” within a primary object. These are powerful measurements, but rely on consistent primary object identification and cell extents (at least approximated) to be useful. Sub-object identification usually works by setting another threshold and operates within a boundary defined by a mask (Cytoplasmic Mask or Cell Area for example). Puncta (spots or small regions) can be identified in these regions (Figure 12). Typical examples of small punctate regions that can be identified and measured are lipid rafts, ribosomes, micronuclei, mitochondria and autophagosome to name a few. Strands like actin or tubulin filaments can also be identified in a similar manner.

### 6.3.7. Edges

Tracing and analyzing neurites often uses different types of algorithms due to the semi one dimensional nature of these extensions. Algorithms rely on a basic method sometimes called “skeletonize”. This involves converting pixels into line segments, which branch out

and behave just like axons or dendrites. These lines can then be pruned to remove small extensions (noise) and are analyzed for length and branching. Gap junction or tight junction formation between neighboring cells could be analyzed by the similar way.

## 6.4. Informatics Analysis

High content screening seems simple: take good images, get good data. But once it is time to look at the data, it gets complicated. Once the images are analyzed, the results are a number of different features that quantitatively describe each and every cell present in the imaged samples. This means not only a lot of data, but a lot of multi-dimensional (multiple parameters) and hierarchical (embedded groups, cells are all related inside a well, wells are related by experimental treatments) data. This section will act as a quick description of points to think about when starting informatics analysis, and will be followed by advanced chapter(s) in areas such as machine-learning, image analysis for whole-organism, phenotypic clustering etc..

### 6.4.1. A Brief Informatics Pipeline

An analytical pipeline (Figure 14) starts out with the raw cell-based image data. Immediately after, the metadata that describes the experimental conditions should be connected to raw data. A good next step is for a few standardized reports to be automatically generated. These reports should show well layout and plate overviews. The purpose of these reports is to get an overview of the current experiment and briefly check for large errors that can be easily spotted (such as edge effects).

A quality control / quality assurance step should be placed early in the pipeline. Many kinds of errors can occur during image acquisition or downstream analysis and common ones for the platform should be checked for in an automated or semi-automated way. Focus imperfections, incorrect exposures, background problems, artifacts, and tracing errors need to be identified so records which are affected by them can be excluded. At some point in a HCS campaign (at least in the beginning and the end, if not more frequently) images with mask overlays visible should be directly reviewed by a human observer to vet the images and ensure that tracing is correct. This process of manual image vetting can be assisted by software which let the user directly annotate the image or an attached data table with their findings ([www.fastpictureviewer.com](http://www.fastpictureviewer.com) for example). Vetting the image analysis early in the screen can help to hone the algorithms and produce better data.

The data may be normalized at this point if normalization controls are built in. Some form of normalization is likely to be necessary to compare screening runs from separate days, etc.

The final steps of the analysis involve aggregating cell information together until the data can be analyzed at the treatment level (i.e. each record or row of the data table represents a particular compound or gene or condition tested in the assay). The simplest form of aggregation is to take the average (mean) or median, but one additional measure should

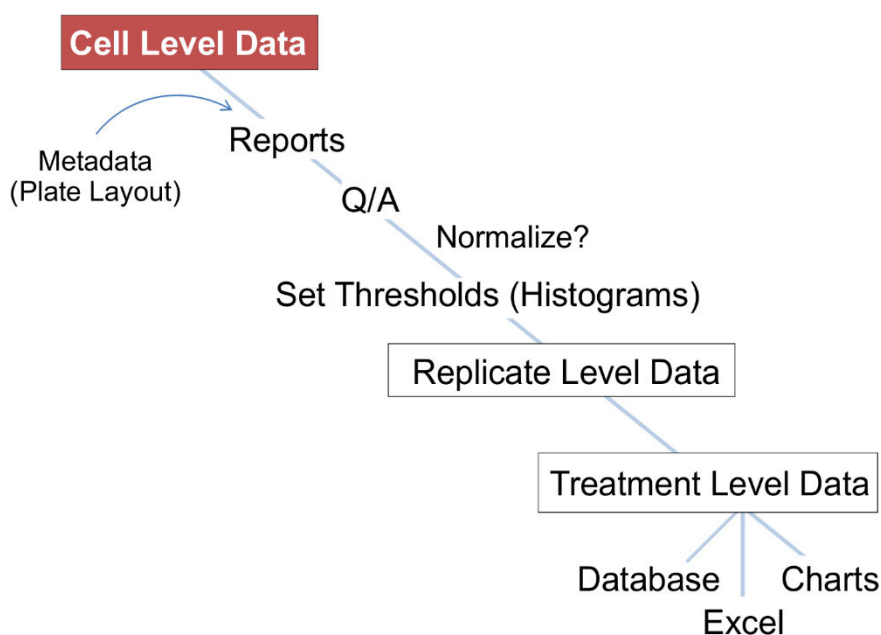


**Figure 14:** Informatics analysis pipeline

often be included. While analyzing the cell-based data, thresholds should be set for measurements of interest. Due to the fact that most measurements are not normally distributed, averages may produce inaccurate results. Therefore setting a threshold and aggregating the % of records above or below the threshold is sometimes preferred. Flow cytometry assays commonly call for this type of analysis called “gating”. Some form of a histogram (bar, cumulative, or 2 dimensional) is often utilized to aid in setting the threshold or gate.

Cell-level data may be aggregated up to treatment level directly, or taken to an intermediate “replicate-level” first. If replicate wells were used in the experiment, then the average nuclear intensity (for example) may be average for all cells within a well to produce replicate-level data. These replicates can then be further aggregated to treatment level, allowing for a different set of statistics to be used. The reasons to aggregate to different levels are usually statistical or based on weighting.

Finally, at the treatment level, the data should be in the simplest form, but still retain deviation information so statistics can be performed. All the data, but especially the treatment level data should be stored in a database and/or exported as charts. In addition, it should be possible to easily export the primary treatment data to software (such as Excel or Spotfire DecisionSite) so that personnel have easy access to it (also see Section 8, Data Management for High Content Screening)

#### 6.4.2. Software for Data Analysis

To choose the best software to analyze the high content data, remember that ultimately, the purpose of the analysis is to make a decision or a figure. Decisions will need to be

made about whether to proceed with a particular gene or compound, or whether an assay is working. Usually a figure with statistics will be needed to convince someone else of that decision. The ideal software would allow all the different forms of data to be present (completeness), and be able to operate on them quickly (speed). Being able to change the representation or the form of the data non-destructively (dynamically) is also an ideal characteristic. Below: a list of a few solutions.

Tibco Spotfire <http://spotfire.tibco.com/>

Databases (Microsoft Access for example) <http://office.microsoft.com/>

MATLAB <http://www.mathworks.com/products/matlab/>

R <http://cran.r-project.org/>

CellProfiler Analyst <http://www.cellprofiler.org/>

## 6.5. Image Analysis Solutions

HCS platforms are discussed elsewhere in this book (see Section 2 – Image Technologies and Instruments). Most of these vendors also produced Image analysis software that runs in real-time or just after the acquisition. But several good image analysis solutions exist that are free and open source. Two of these are listed below with examples demonstrating their basic use.

### 6.5.1. Free Open Source Image Analysis Software

#### 6.5.1.1. ImageJ

ImageJ is a freely available open source, multi-platform project from the NIH. A closely related package “FIJI” (FIJI Is Just ImageJ) is usually preferred since it includes many useful modules and keeps itself up-to-date. Fiji and ImageJ are toolbox based and work much more like classic graphics software where an image is loaded, and then commands are run on it in real time and are destructive (i.e. they will change the image that has been loaded, such that if you save by accident, it would destroy the original image).

ImageJ can take advantage of multicore processors on most modern desktop and laptop machines. This means that programs can be written directly with multithread capabilities or that multiple scripts can be run simultaneously to greatly decrease the processing time (<https://www.ncbi.nlm.nih.gov/pubmed/17936939>).

*Example:*

Example image used are human renal cancer cells stained with Hoechst to mark the nucleus. The following case shows how to identify objects based on the nuclei.

1. File > Open Next Image (Figure 15A)
2. Background Subtraction (rolling ball)
  - a Or FFT and get rid of all the really low frequency stuff (but slower)
3. Image > Adjust > Window/Level > “Auto”



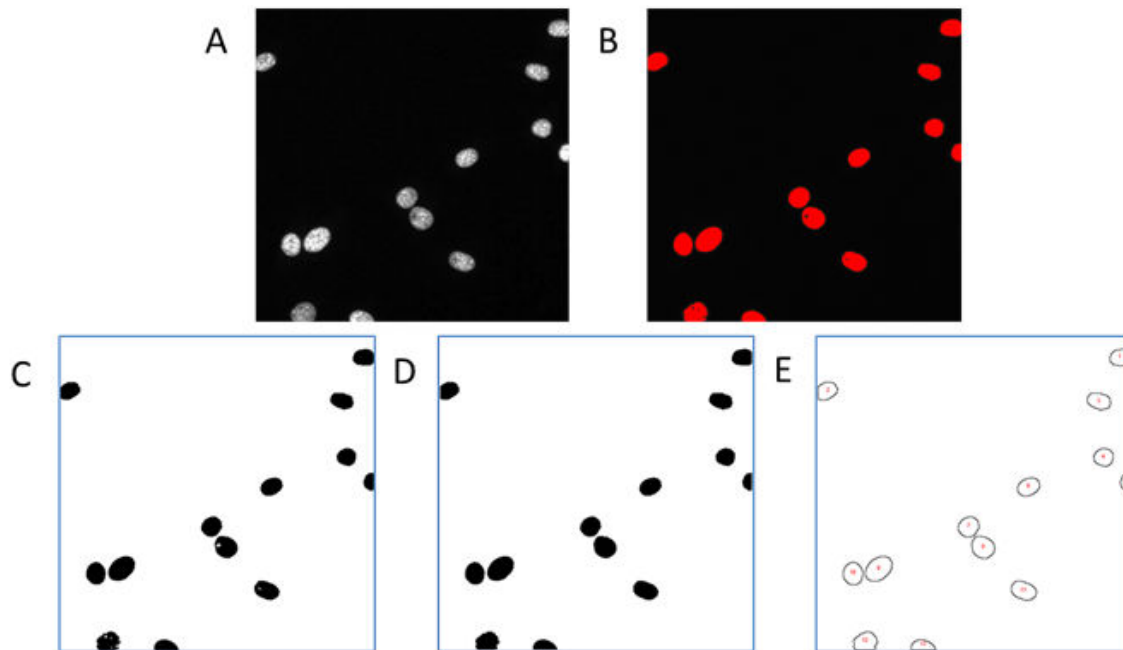




**Figure 15: Example images from ImageJ analysis software.** A) Representative image from Step 1. B) Representative image from Step 4 C and D) Representative images from step5 and 5a. E) Representative image from step 7.

4. Image > Adjust > Threshold (Figure 15B)
5. Process > Binary > Make Binary (Figure 15C)
  - a Fill holes / Close (Figure 15D)
6. Process > Binary > Watershed (of touching)
7. Analyze > Analyze Particles (Figure 15E)
8. Apply Mask to original image, and other channels
9. Measure
10. Export results

### 6.5.1.2. CellProfiler

CellProfiler (<http://www.cellprofiler.org/>) is a free, open-source image analysis package that comes out of MIT's Broad Institute from David Sabatini and Polina Golland's lab by Anne Carpenter and Thouis Jones. It is a "pipeline" based tool which lets you add simple modules that work on a sequence of images <http://genomebiology.com/2006/7/10/R100>. Unlike more classic software, the modules don't run until scheduled (by clicking analyze), and they are completely non-destructive. These tools allow for quick assay design since they are already tuned for the processing of cell biological images (for the most part). Below we load an example image (Figure 16).

Step 1:   LoadImages – use “elsewhere” and specify a directory, enter in a part of the filename or TIF or BMP etc

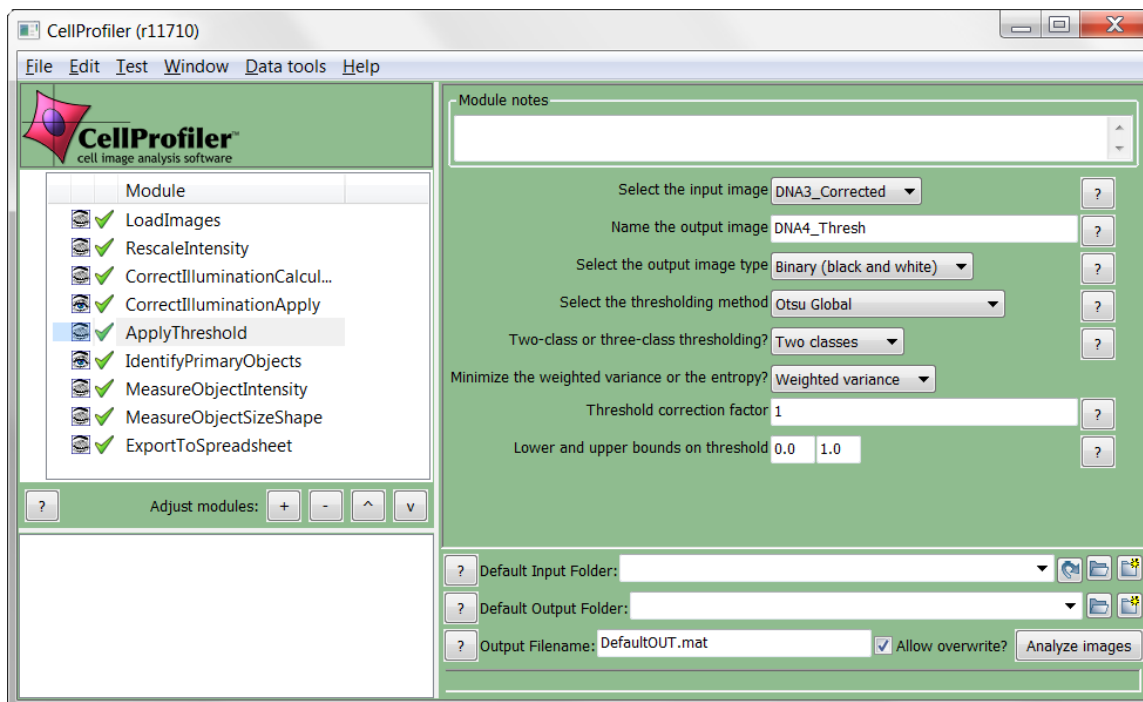


**Figure 16:** Example CellProfile image.

Step 2: RescaleIntensity and background correction (Figure 17).

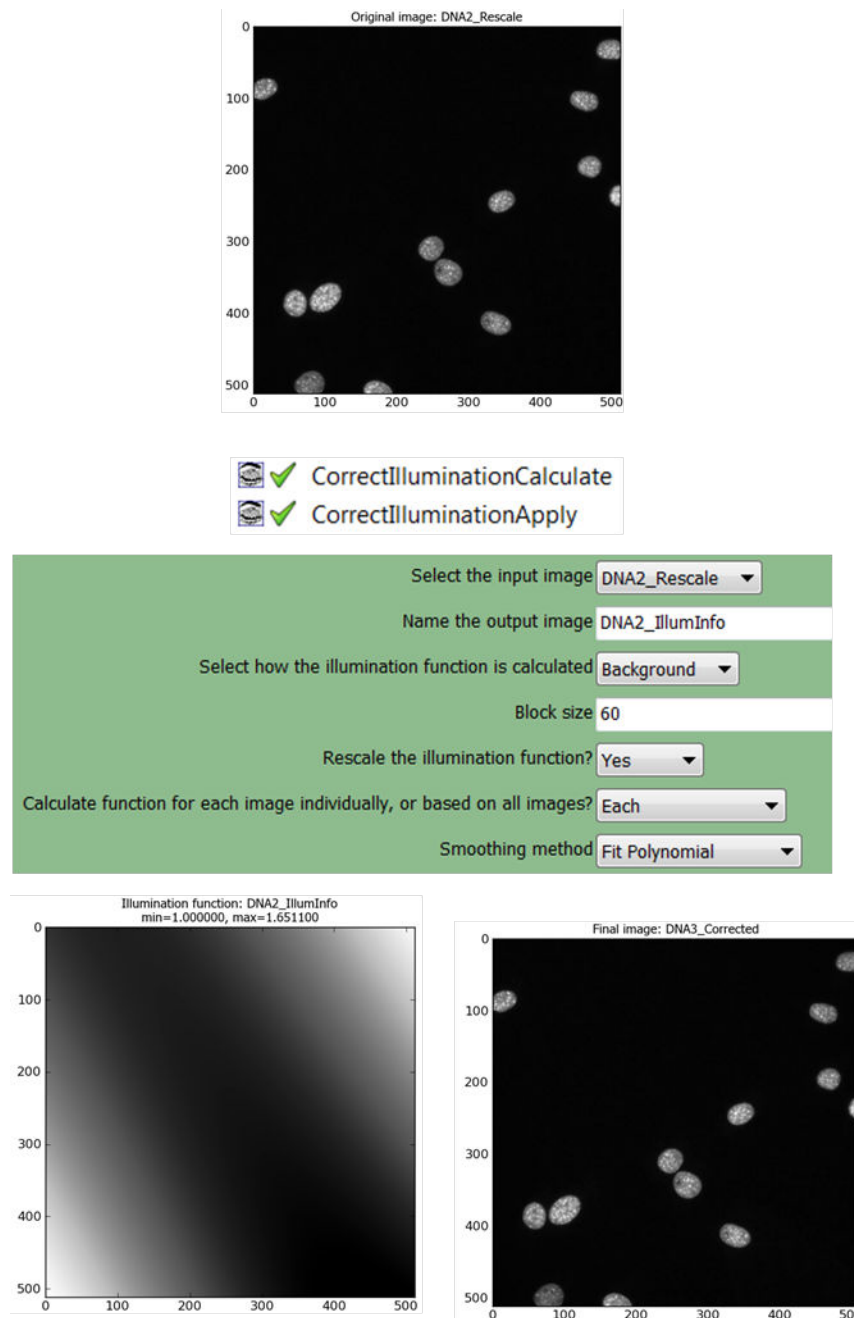
Step 3: Check “Allow Overwrite”.

See Figure 17 for representative images using CellProfiler for analysis.



Step 4: ApplyThreshold

Threshold (as above) can be done in an automated way or manually. Although CellProfiler has thresholding built into its PrimaryObjectIdentification module, it is nice to do it separately so that the results of the threshold are clear. Aside from manual, Otsu, MoG (Mixture of Gaussian) and Background methods are provided (global is usually the best sub-option). Otsu is the most automated, while MoG and Background assume that the amount of background vs. foreground is known. If it is constant among the images (for example because cultures had a very constant confluence) then these will give slightly better results. The background method is similar to many classic methods which assume the background predominates in the image and uses the mode of the histogram to set the threshold. In this example (Figure 18a), Otsu global is used (with all the other defaults – Figure 18b).

Then just have to take the measurements that you are interested in and export to spreadsheet!



**Figure 17:** Representative screen captures using CellProfiler for image analysis.

  MeasureObjectIntensity  
  MeasureObjectSizeShape


For Object Intensities – there is more than just the object mask information to consider, there is also which image should the masks be overlaid to make the intensity calculations. Here we selected the raw nuclear image, but one could easily select a background-

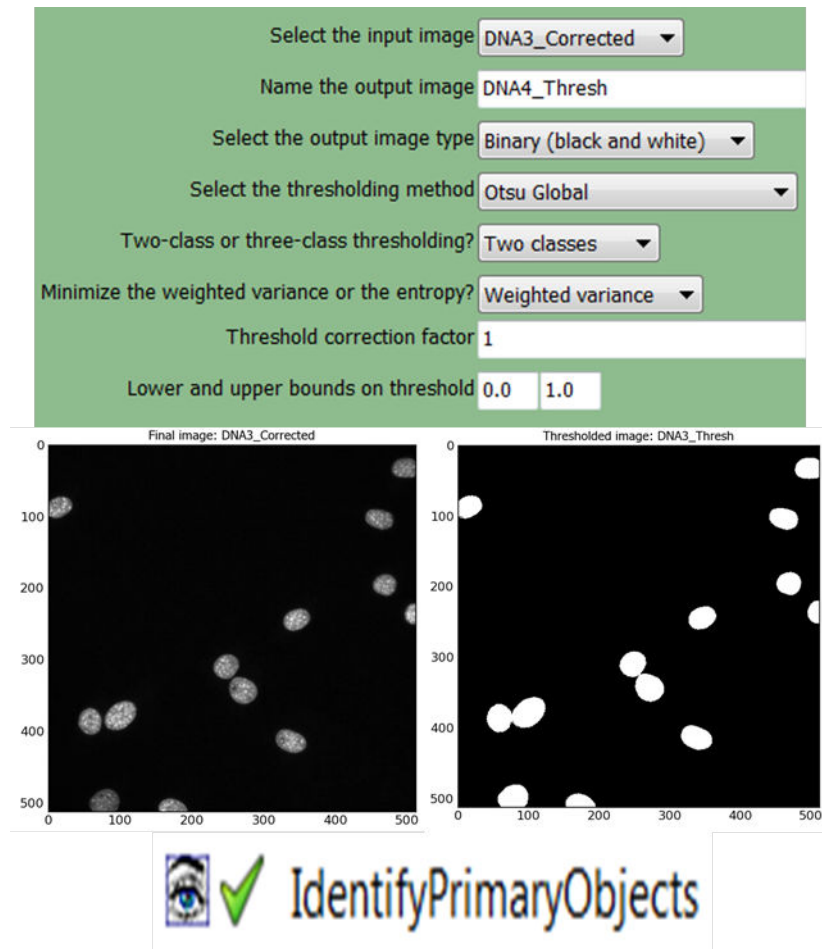


**Figure 18a:** Example using Otsu global

corrected image or even another channel. In CellProfiler, the MEAN Intensity measure is called “Intensity\_MeanIntensity\_” and the TOTAL Intensity measure is called “Intensity\_IntegratedIntensity\_”.

To measure the object size, area and shape, only the object mask is needed, so no image input is necessary. You will probably also want to uncheck the Zernicke features box, since these polynomials take a longer time.

  ExportToSpreadsheet

After export, two files will appear in the default output director: “DefaultOUT\_Image.csv” and “DefaultOUT\_Nuclei.csv”. The first, “DefaultOUT\_Images.csv” is important because it gives the list of images that were analyzed and the corresponding ID (an index) which can be used to match up additional information from the other spreadsheets.

CellProfiler has many powerful functions that are completely focused on Life Sciences research, including time lapse, worms, neuronal tracing, texture/granularity and

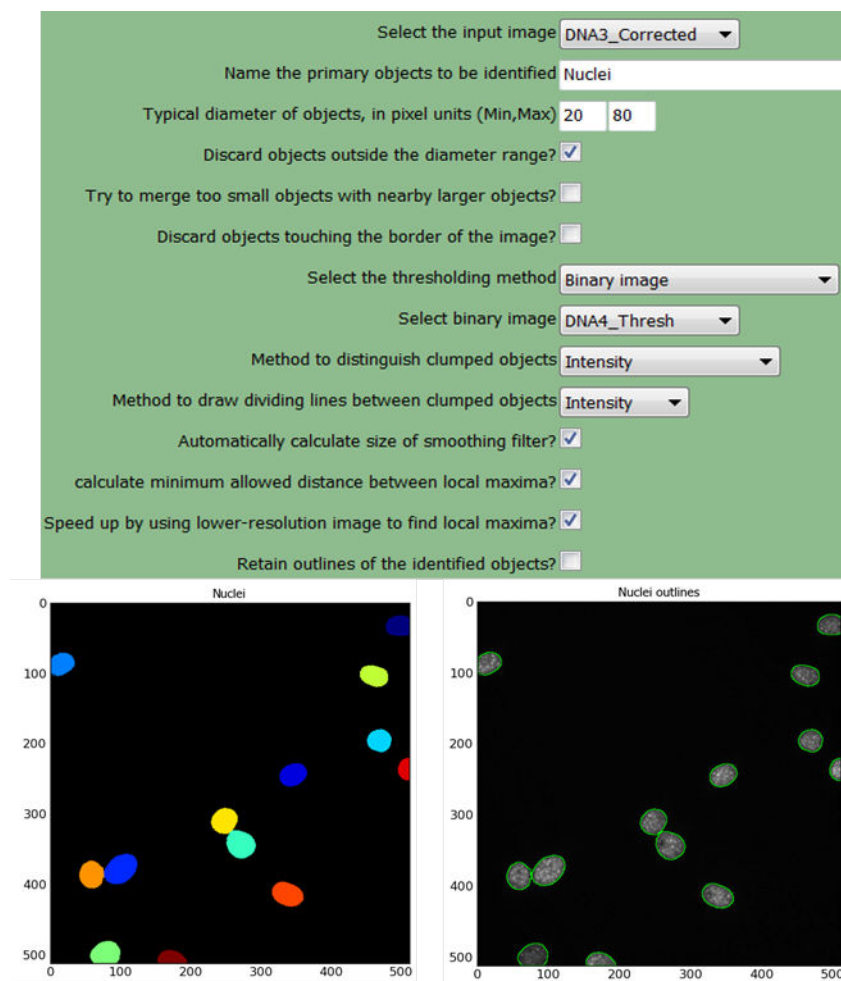


**Figure 18b:** Default Settings except for using the already-thresholded binary image and setting the typical diameter to match with the nuclear size of these cells.

neighbors. It is also helpful to free up some space by letting CellProfiler dispose its internal images using “Other > Conserve Memory”. CellProfiler can run very effectively on an enterprise multi-processor architecture (cluster computing), but is not currently configured to be able to run with parallel processes on a standard consumer machine.

### 6.5.2. Proprietary Image Analysis Software

In addition to the open source software described above, there are many proprietary image analysis software programs available. Table 6 provides a listing of some of these software programs.

Unlike the top four products, neither the Adobe nor Corel products are designed for image analysis. Since they are pervasive, many add-ons and custom scripts have been written for these to allow fairly sophisticated image analysis processes. But they are likely to require substantial more development.

**Table 6: Examples of proprietary image analysis software**

| Company           | Product               | Website   |
|-------------------|-----------------------|---|
| Definiens         | TissueStudio          | <a href="http://www.definiens.com/">http://www.definiens.com/</a>   |
| Media Cybernetics | ImagePro+             | <a href="http://www.mediacy.com/">http://www.mediacy.com/</a>   |
| Mathworks         | MATLAB                | <a href="http://www.mathworks.com/products/matlab/">http://www.mathworks.com/products/matlab/</a>                           |
| Molecular Devices | Metamorph/MetaExpress | <a href="http://www.moleculardevices.com/">http://www.moleculardevices.com/</a>   |
| Adobe             | Photoshop / Lightroom | <a href="http://www.adobe.com/products/photoshop-lightroom.html">http://www.adobe.com/products/photoshop-lightroom.html</a> |
| Corel             | Photopaint            | <a href="http://www.corel.com/">http://www.corel.com/</a>   |

## 7. Assay Validation for HCA Screens

This section on High Content Screen Assay Validation serves as an introduction to the topic but the reader is referred to the AGM [HTS Assay Validation](#) chapter.

HCA screens can be target defined but more often are phenotypic in nature and include measurements of dozens of features. Measured features include size, shape, intensity, texture, and dynamics. Simple examples include nuclear area and intensity, or derived measurements, such as nuclear or cytoplasmic translocation. The data is usually based on analysis of the phenotype of single cells or objects within cells. The data can be reported for individual cells or the data from cells may be aggregated to produce data at the well or treatment level. HCA screens, unlike HTS cell based screens, often have large variability because of heterogeneous cellular populations in a given well. The data can also have large variability because the distributions of particular features are non-Gaussian when measured at the single cell level. There are many reasons for this, but the local cellular environment can have a very major effect on a given cell's response to a perturbation (38-40, 58). There can be especially large inter-plate variability in HCA screens and this can be approached by each plate having appropriate positive and negative control wells that can be used to normalize data across plates and days (56, 59).

In HTS research plate variability studies commonly use a minimal of two signals: "Positive" and "Negative" signals. This makes the assumption that the study involves perturbagens, typically compounds that are known to be active in the assay. Many HCA phenotypic screens involve siRNAs or shRNAs to knockdown mRNA levels and subsequently protein levels or cDNA overexpression to express various proteins. In these cases it is not possible to construct dose response curves or even predict perturbagens that give "Negative" signals. Therefore standards used in HTS variability studies may not be useful in HCS assays using RNAi or over-expression approaches. During the assay development phase, it may be necessary to determine the mean response to a large number of treatments (100-1000) and then identify two or three treatments that reproducibly give a response at the level of the mean of the total set of treatments. This prescreen phase may also uncover treatments that can serve as robust positive controls. These can then be used in each plate to allow normalization across plates. The number of

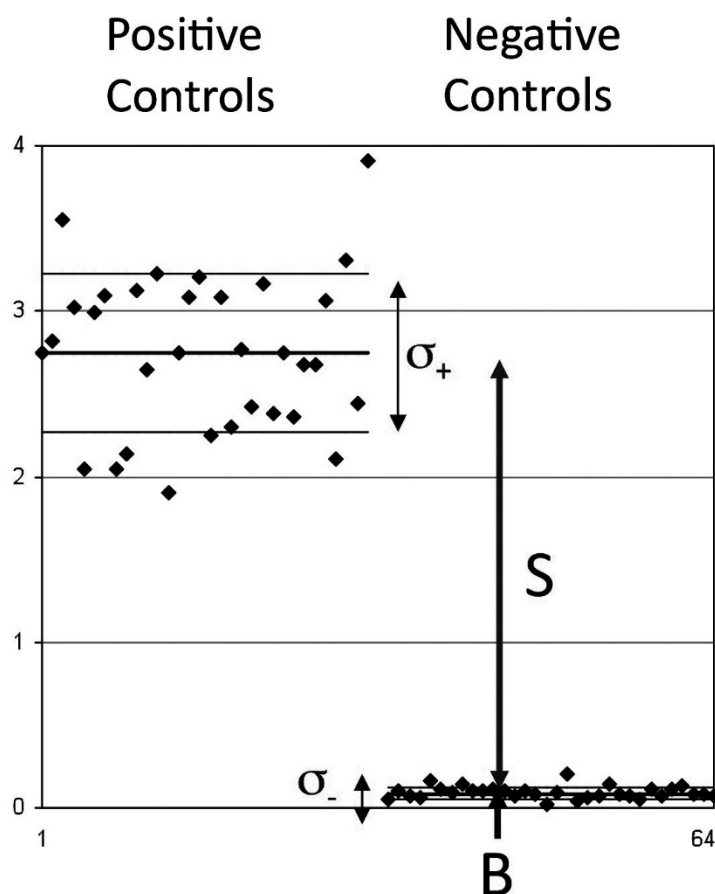


**Figure 19:** Standard measures of HTS assay performance:  
 Signal = mean of (C+) - mean (C-). Background = median (C-).  
 Signal to Background = S/B.  $\sigma_+$  = Std Dev (C+),  $\sigma_-$  = Std Dev (C-).  
 $N = \text{SqRt}(\sigma_+^2 + \sigma_-^2)$  Signal to Noise = S/N

wells per plate in the negative reference group has a large impact on reliability of genome wide screens (56) and varies with the number of wells per plate. In 384 well plates, 16 negative control wells are acceptable and 20 or more is preferable to have acceptable false non-discovery rates (Figure 19).

There are different measurements of assay performance. Classic ones include signal to noise (S/N) and signal to background (S/B). The most widely used measurement to assess an assay is the so-called Z'-factor (60). This measurement gives insight into how much negative and positive controls are separated. The formula of Z' factor depends on the means of the positive and negative controls ( $\mu_+$ ,  $\mu_-$ ) and their standard deviations ( $\sigma_+$ ,  $\sigma_-$ ).

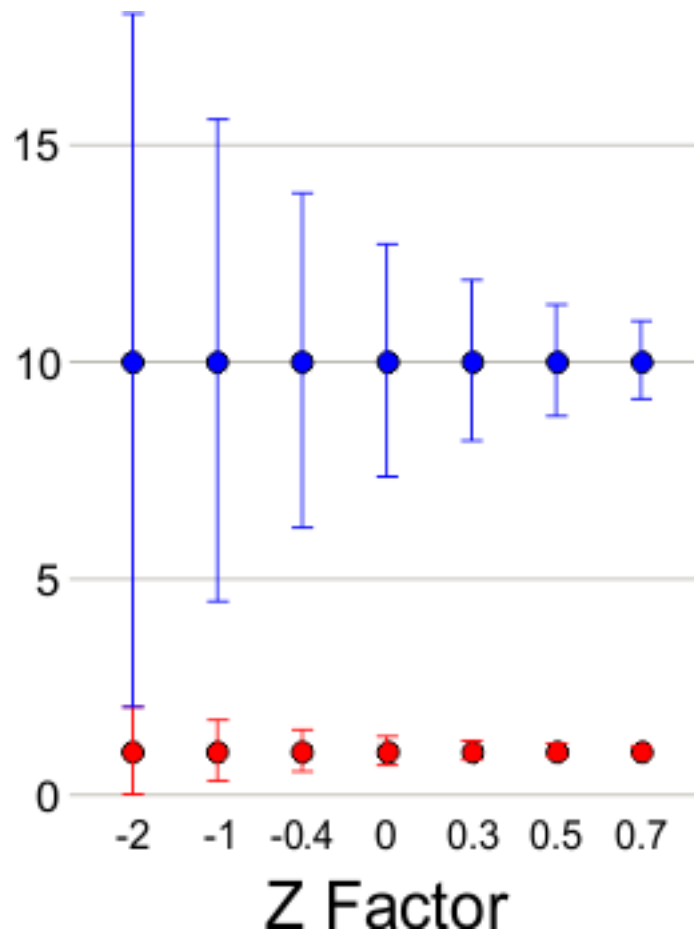


**Figure 20:** Z Factors comparing negative (red) and positive (blue) controls. The averages are fixed at 1 and 10, but the standard deviation is varied from 1 to 0.1 for the negative and 8 to 1 for the positive. A Z factor of -1 might still give significant results in a HCS assay.

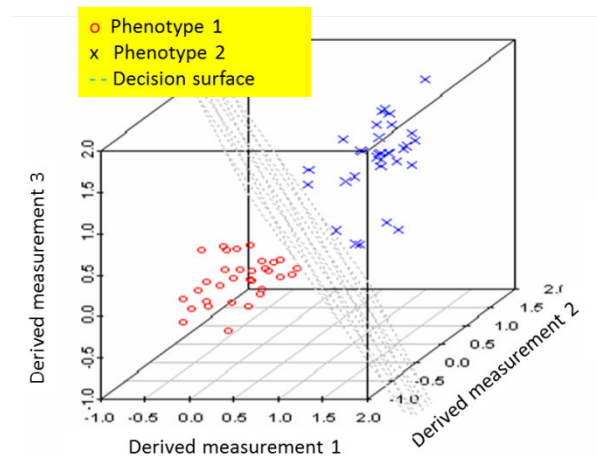


**Figure 21:** Validation of bioimaging based assay for primary screening using multiple parameter analysis.



$$Z' \text{ factor} = 1 - \frac{(3\sigma_+ + 3\sigma_-)}{|\mu_+ - \mu_-|}$$

The constant factor “3\*” assumes the data has a Gaussian distribution and that 3 standard deviations would encompass 99% of the values. Assays with a Z’-factor between 0.5 and 1 are considered excellent. However, often HCA data is not Gaussian and can have long tails in one or both directions. Neurite length distributions are well known for having distributions with a very long tail in one direction. An experimental approach to dealing with non-Gaussian data is to use the one-tailed Z’ factor which only uses samples between the positive and negative population means (CellProfiler Statistics Module). A recently introduced measure, which is an alternative to Z- factor, is the strictly standardized mean difference (SSMD) (61).

Once an assessment measurement, such as the Z-factor, is selected, then a series of validation experiments should be performed. These include:

1. A full plate with minimum and maximum signal conditions to determine Z’-factor
2. Full plates (5-10 plates at a minimum) with minimum and maximum signal conditions to assess edge effects and other patterns of variability (pipetting, etc.) between plates
3. Full plates with a range of DMSO concentrations to assess solvent tolerance
4. Full plates with minimum and maximum signal conditions in a compound dilution scheme to ensure expected EC<sub>50</sub>/IC<sub>50</sub> determinations are accurate
5. Three days of EC<sub>50</sub>/IC<sub>50</sub> runs with reference compounds to demonstrate reproducible Z’-factor and EC<sub>50</sub>/IC<sub>50</sub> values. Without reproducible EC<sub>50</sub>/IC<sub>50</sub> values, it is not possible to do reliable SAR studies.

Edge effects are readily observed in HCA screens, so much so that one should assume they exist and explicitly test for them at the beginning of assay development. There are several strategies to deal with edge effects, the most common being media-only wells around the outside of the plate and specialized plates which have water “motes” built in (from Thermo Fisher, Nunc, and Aurora Bio, for example), or simply use a water tray in the incubator or surround assay plates with wet paper towels. Another common practice is to pre-plate the cells in the tissue culture hood, allowing the cells to attach before moving the plates to the incubator, which normalizes seeding densities on the plate (62). Position effects are important, so having controls scattered through the plate and avoiding having hits always in the same part of the plate is advantageous (also see Section 5.7.1 Assay Response Stability).

Involving statisticians during the planning process of HTS and HCA campaigns is wise. Power analyses are generally better suited for non-discovery studies; therefore, HTS approaches which seek to control the false discovery rate (FDR) (63) and balance it with the false non-discovery rate (64) are generally used (65). Finding appropriate and realistic negative and positive controls is important in this effort, and negative controls often end up being especially difficult with HCA since the treatment procedures (transfection, for example) often manipulates some of the many parameters being measured. Because

screening campaigns now can involve very large numbers of perturbagens, especially compounds, special statistical methods may be called for to eliminate systemic biases introduced into an entire screen or into some plates of a screen (66)

It is also very important to understand the signal derived from a particular analytical algorithm. A common issue with HCA is to misinterpret a particular parameter due to very strong results comparing the positive and negative control. For example, many small molecule inhibitors that produce a strong effect on the parameter of interest can also diminish or enhance cell viability. Changes in overall cell health tend to have a direct impact on other measured parameters. Cell morphology changes can be due to reduced viability or increased proliferation, with many cells “rounding” up, appearing as a decreased in size. With everything else being the same, the average intensity measurements of a cytosolic marker will increase since the cell occupies less horizontal space and more vertical space. The problem can be made worse by inappropriate use of background correction or other normalization schemes. The net result is that a small effect in the parameter of interest is made to look large and significant when compounded with other variables that the investigators may not actually be interested in studying. It is a multi-parameter analysis after all, so make sure to take into account all the parameters measured.

A review of recent HCA assay development papers shows that most published HCA assays, such as nuclear translocation assays and beta-arrestin internalization, involving compound screens have  $Z'$  factors greater than 0.7. However, most HCA screens of complex biological processes, such as neurite growth, angiogenesis and tube formation, do not report  $Z'$  factors. Those studies that do provide  $Z'$  factors report values of around 0.5 or less. This is considered within the range of screenable HTS biochemical assays. However, even lower  $Z'$  factor screens can contain considerable information and a  $Z'$  factor for a single parameter around 0 may still allow hits to be identified reliably (Figure 20). Importantly, the  $Z'$  factor and most other calculations only inform the user of the strength of the positive and negative controls, and may not necessarily inform about the assay if these controls are not realistic or appropriate.

For many large scale, truly multiple-parameter HCS based compound screens, it may be difficult to validate an assay using  $Z'$  factor calculated based on only one parameter, even on a derived parameter. An advantage of HCA screens is that by combining data from multiple output parameters including ratiometric scoring it is possible to improve  $Z'$  factors from 0.3 to 0.7 (67). Figure 21 illustrates one such alternative. In this assay, each derived measurement (or classifier) alone is unable to distinguish phenotype 1 and 2 (if one projects both red and blue does onto a single axis, there will be significant overlap between the two populations). But when all 3 derived measurements are used in a three-dimensional plot, one can make a clear decision surface to separate these two populations. These advanced statistical analysis and computation need support from experienced statisticians or informatists, and must have comparable high-speed computational infrastructure in the research facility. Future HCS chapters will discuss alternatives to the  $Z'$  factor in greater detail.

## 8. Data Management for High Content Screening

High throughput screening technologies by definition generate large amounts of data. Within this field, however, high content screening methods stand out as they are capable of generating massive amounts of data – even when run in a non-high throughput mode. This is largely driven by the fact that a given well is characterized not by a single experimental readout (say, fluorescence) but first by a set of images with associated metadata and second, multiple numerical readouts derived from the well images. Given (uncompressed) image sizes on the order of 3 MB, a single 384 well plate imaged using a single field of view leads to 1.1 GB of image data alone. Assuming a small pilot screen of 10 plates run in single dose format, this generates 10 GB of data for that single run. While this is not particularly large, given today's storage systems, a medium sized lab can easily generate tens of such screens a month, and if dose response is considered, the image storage requirements increase by an order of magnitude. This implies corresponding increases in storage requirements including investment in software (for data management and analysis). Software costs are likely one-time investments (or will only increase slowly). It is useful to note that Open Source solutions can be employed on the software side, reducing initial costs, though of course, such solutions invariably require customization and maintenance and dedicated manpower.

### 8.1. Not Just Images

However, image capture and storage is just the first step in a high content screening experiment. Following imaging, the images must be registered in a repository, suitable for long-term storage and supporting efficient access by screening campaign, plate barcode and well location. Images will be processed to generate descriptors, numerical features that characterize aspects such as the number of cells, their shape, size, intensity, and texture and more complex features such as translocation of proteins, number of neurites and so on. Such analysis protocols can easily generate tens to hundreds of such features for *each* cell in a well – leading to millions of data points for a single plate. This numerical dataset must be stored and linked to the images (via plate barcode, well location and cell identifier). Finally, imaging and analysis metadata must also be recorded. This includes information such as focus settings, wavelength details, object masks, operator information and so on. These pieces of information are associated with different “levels” of the screening analysis– some are associated with the screen itself, others are relevant to individual plates or images and so on. Importantly, users may generate some metadata after the screen. Examples of this type of metadata are annotations, where a user might highlight a set of wells or even a selection of cells within a well for follow-up and include some free-text comment indicating their interest in the selection. Thus, this metadata must also be stored and linked back to images and numerical results. Any useful data management solution must be capable of supporting all these data types as well provide the flexibility to query this information in a variety of ways (68).

## 8.2. Image repositories

The key component of a HCS data management solution is a centralized location to collect images. In absence of a formalized management solution, the simplest approach is to simply acquire images in a file folder and inform users of folder location. This is clearly a crude and brittle approach that does not scale beyond one or two users. Invariably, folder locations may be forgotten, there is no explicit link between images and downstream data and images may not be accessible over a network easily. In addition, one must always work with the raw images, even though for many purposes (e.g., thumb nailing) they may not be required.

Most modern image repositories will employ a file system-based approach – where images are organized using a hierarchy of folders, usually located on a network-accessible storage device. But more importantly, the repository will also usually include a relational database system that records the file system path to the individual images along with metadata such as plate barcodes, well location, imaging details (focus setting, wavelength, etc.). Import of images into a repository will usually convert them to some standardized image format specified by the system, generate thumbnail views, record meta-data and so on.

A user versed in SQL, MySQL, or Oracle can query the database to locate individual images via the database. But obviously such an approach does not lend itself to daily usage by bench scientists! To address this most vendors of image repositories will provide a graphical user interface allowing users to easily browse the image collection, searching for individual plates or wells, retrieve or archive, record notes and so on. In addition, some vendors will also include an application programming interface (API) that allows users to develop their own applications that interact with the image repository, without having to directly work with the internals (which may be subject to arbitrary changes).

Most image repositories are designed to work in an integrated fashion with a vendors imaging platform. All such repositories allow one to export and import images, though this task may not be easy. Usually, when loading images into a repository, they are converted into a common image format, such as TIFF. Some repositories may use specialized versions (OME employs the OME-TIFF format, which is a superset of the standard TIFF format).

The fact that the image repository is usually tightly integrated with a HC instrument's platform usually means that one is constrained to using the repository that is provided by the vendor. In other words, mixing and matching components of a HCS platform is not easy and in many cases impossible. Thus one cannot (usually) employ an image repository from vendor X and expect that the analysis or viewing applications from vendor Y will work seamlessly. More often than not, such a mix will not work without significant investments in time and effort from the vendor (or custom development on the part of the user, requiring manual export of images from one repository and possibly manual import into another repository). For smaller laboratories, such restrictions on interoperability may not be a problem, given that they may only work with a single platform. For larger facilities, however, the lack of interoperability can become a major hindrance to the

effective use of multiple imaging platforms. Recent software upgrades from several of the vendors are addressing this issue but it is an on-going concern of the HCA community.

There are certain software platforms that have been designed to work with multiple imaging vendor platforms. An example would be GeneData (<http://www.genedata.com/>), a commercial software package, which can access images and data stored by PerkinElmer, Thermo Fisher, Molecular Devices and OpenBIS.

### 8.3. Data retention policies

It is important to realize that while image repositories can be very large (greater than 50-100 TB), they are finite in size. As a result, it is infeasible to continuously add images to a repository, without some policy in place to delete or archive images. Such data retention policies are obviously local to an organization. In some cases, with low enough throughput, one can retain raw images for many years. But invariably this is not practical. A more realistic goal would be to provide sufficient space to store raw images for say two years on high-speed disk (exactly how much space would be required would depend on estimates of screening throughput) after which images would be converted to a lossy compressed form (such as JPEG). These images could be retained on the high-speed disk or else moved to a slower device such as tape. This set of data would be retained for longer periods – say 5 to 10 years. This of course will depend on the study design and format. In cases of GLP, longer-term data retention policies are mandated.

A primary role of retaining the raw images is to go back to them, say for reanalysis or visual examination. In many scenarios one can get away by conversion to a format that supports different levels of compression – allowing one to quickly access a high-resolution version or a low-resolution version from the same image. A primary example is the JPEG2000 format. One could argue that a reasonable level of image compression might not affect image analysis (though we are not aware of any benchmarks that have quantitatively measured this), and thus one could directly store images in a compressed format such as JPEG instead of the raw data (even compressed TIFFs).

### 8.4. Linking images and data

Handling images is obviously the core responsibility of a HCS data management system. However, images are just the first step and a standard task is to process the images to evaluate numerical features (cell counts, shape, size, intensity, etc.). As noted above, a 384-well plate can easily lead to millions of data points being generated. All this data must be stored and efficiently retrieved. In addition to numerical features, other forms of image related data such as overlays and masks must also be stored for rapid access. Most HCS management systems will make use of a backend relational database, and these are usually suitable to support the large storage requirements of high content image analyses. The use of such databases allows users to easily write back new numerical results or updated pre-existing data, say based on a new or updated calculation procedure. Obviously, it is vital that this numerical data be linked to the actual images (and even cells within an image) that they are associated with. For management systems provided by vendors, this link is

always present. However, when one analyzes an image using software different from the vendor provided software, the link between numerical data, overlays, etc. and images is not present – unless somehow explicitly made. This is a bottleneck for many larger organizations that operate multiple imaging platforms, and solutions to this involve using an external data management system such as GeneData, Pipeline Pilot, or OpenBIS, or developing custom software to capture links between images and numerical analyses, overlays, compound IDs and other related information.

## 8.5. Commercial and Open Source solutions

All imaging hardware vendors provide a HCS data management system. In some cases, the default system may contain a small amount of functionality, sufficient for handling and viewing images of a single instrument used by a few operators. But in most cases, a more comprehensive management system will also be available. As noted above, such commercial management systems are invariably proprietary.

Depending on the scale of the HCS operation, one solution may be favored over another. Thus, a small lab, using a single instrument, is probably well served by employing the vendor provided data management system. For many such groups, the tools provided by the vendor to browse, analyze and annotate are sufficient. While we do not comment on a preferred system, most of the commercial vendors provide a capable image management solution. All of these platforms are able to export images in a variety of formats and also export numerical data obtained from image processing in standard formats (tab delimited, comma separated, etc.). In addition, many of these can be integrated with advanced visualization and reporting tools such as GeneData, SAS JMP, and Spotfire (<http://spotfire.tibco.com/>). However, given the high costs associated with these tools, they may be out of reach for smaller groups and in such cases it is paramount that image and feature data be exportable to tools such as Matlab, Excel, R and so on.

For larger operations that have multiple imaging platforms, the lack of interoperability between vendors is a significant bottleneck in the development of a unified interface to all the imaging data generated across platforms. While some progress has been made by commercial tools external to the imaging platform (such as Spotfire and GeneData), an integrated solution invariably requires custom development by the organization (69).

Such custom development can be impossible, when vendors employ completely closed systems and are unwilling to provide access to the internals via a public API. While such cases are becoming fewer, lack of a public API to all aspects of a vendors data management system should be considered a significant shortcoming and hindrance to integration with an organizations pre-existing informatics infrastructure.

On the Open Source side, there are relatively few comprehensive HCS data management systems. The two primary systems that are currently undergoing active development are the Open Microscopy Environment (OME <http://www.openmicroscopy.org/site>) and OpenBIS (<http://www.cisd.ethz.ch/software/openBIS>). The former system provides a comprehensive file system-based image repository, coupled with the use of PostgreSQL as

the relational database that stores image locations, metadata and so on. The infrastructure provides a browser-based interface to the system and allows users to access images and perform some simple operations on them. Importantly, the OME infrastructure supports varying levels of security, allowing one to restrict images and their data to certain individuals or groups, with varying degrees of accessibility (read only, read write, etc.). A key feature of this system is that it provides a completely open, well defined API, allowing users to develop applications that interact with all aspects of the repository. This makes it much easier to integrate an OME repository with an organizations pre-existing infrastructure. It is important to note that the OME platform focuses only on image data management and not other aspects of a HCS workflow such as image analysis. However, a number of open source software packages such as ImageJ and CellAnalyst (associated with CellProfiler) can interact with an OME installation, thus enabling a fully Open Source HCS data workflow.

The OpenBIS platform is a more general biological data management platform that supports a variety of technologies including high content screening, sequencing and proteomics. In terms of functionality the system supports image export and import, metadata and annotations and also links to the KNIME workflow tool to allow integrated analyses. In addition, the system comes with a number of analysis modules built in. As with the OME platform, it exposes an API allowing users to develop novel applications on top of the OpenBIS platform.

## 8.6. Visualization and reporting

Efficient and robust management of imaging data is a key to ensuring reproducible and rigorous scientific studies. But equally important is the ability to interact with the data to enable mining and visualization of phenotypic data. There is an abundance of tools and techniques for the visualization of data, though visualizing datasets characteristic of high content screens requires certain capabilities. Primary among them is the ability to handle millions of data points on a plot, yet retain interactivity. Importantly, plots with millions of data points are not usually informative, so visualization platforms should have the ability to generate on the fly summaries of the entire datasets (e.g., density and contour plots, binned plots, etc.). A common visualization platform is Spotfire, which has extensive capabilities and is able to connect to a number of HCS data management systems. This allows it to integrate images with various plots – click on a data point in a scatter plot displays the image(s) associated with that data point. Such integration is vital to the analysis and exploration of high content data; in the absence of image viewing capabilities, one is faced with a mass of (usually uninterpretable) numbers. Another commercial platform for such visualization tasks is GeneData. However, Spotfire and GeneData are commercial tools and can be very expensive for smaller groups. Alternatives include Miner3D (<http://www.miner3d.com/>) and Tableau (<http://www.tableausoftware.com/>). While there are a number of cheaper or free visualization tools, they are not always intuitive to use and some (such as R) while providing very sophisticated visualization capabilities, lack easy interactivity.

It is important to note that most visualization platforms will also be tightly coupled to data mining capabilities, as one usually wishes to perform some analytical operation (clustering, predictive modeling, etc.) on the phenotypic data. While data mining of phenotypic data is out of the scope of this section we note that the platforms such as SAS JMP, Spotfire and GeneData provide extensive modeling capabilities.

Another class of application that is commonly used to interact with HCS data are workflow tools such as Pipeline Pilot and KNIME. Both tools allow non-experts to easily construct analysis pipelines, in which individual components perform specific tasks such as retrieve images from repository, perform thresholding and then calculate summary statistics over a plate. Note that such tools do not play a direct role in terms of managing HCS data, but serve to hide the data management system from the users, enabling them to interact with the data in a sophisticated manner. Some significant progressions have been made in this area (69).

## 8.7. Towards a Unified HCS Management System

Given the variety of vendors in the HCS field, it is not surprising that there are a many choices of HCS data management system solutions. However, given that the fundamental goal of such a system is to keep track of images, their meta-data and downstream analytical results, it is not unreasonable to desire a unified management system that allows interoperability between different vendor solutions. Unfortunately, this is currently not the case.

Given the current state of HCS management systems, any unified approach must recognize that some imaging systems will be black boxes and cannot be replaced with a common repository and associated components. One unification strategy is to implement a software interface that hides the details of individual HCS data management systems, shown schematically in Figure 22. The interface would provide access to raw images, thumbnails (if present) and associated meta-data. Depending on the scope of the repository, it may also provide read/write access to numerical data calculated from images. However, the latter is very specific to individual installations and in general the interface proposed here focuses on image repositories.

Then, new applications that are developed communicate with each system via the intermediate software interface. While this certainly allows one to have a uniform interface to multiple vendor platforms this is not an ideal situation. It is completely dependent on individual vendor platforms to provide a public, documented API, which is not always the case. Furthermore while such an interface allows an organization to develop custom applications across all their imaging platforms, it does not necessarily allow specific vendor platforms to interact with other platforms (say, vendor platform X imports image from platform Y, performs an analysis and stores results in platform Z). In the end, this approach does not solve the fundamental interoperability problem.

What are the requirements for a unified HCS data management infrastructure? In fact very little! It is perfectly fine for each individual vendor to have a proprietary database



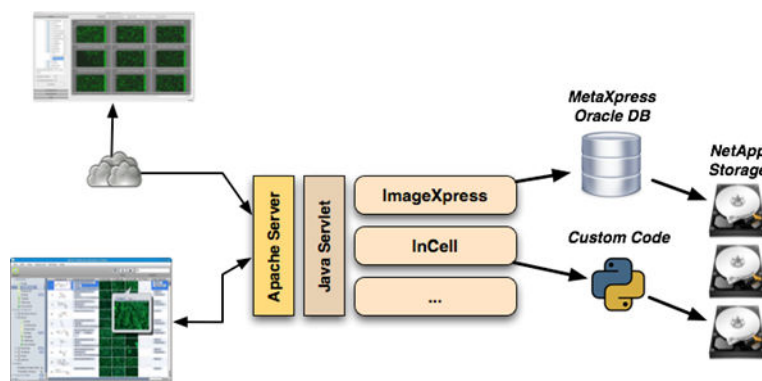


**Figure 22:** An overview of a software interface approach to providing a uniform interface to multiple imaging vendor platforms

with their own schema and formats. However, the key to supporting interoperability is the provision of a uniform API to all the data. If such an API were available, one vendor would be able to develop their applications independent of where the images and associated data are stored. One could argue that certain platforms provide certain advantages that are not available on other platforms. While this is certainly true on the hardware side, it is not clear how much vendors can (and do) differentiate themselves in terms of the actual data types that are managed by their systems. From this point of view, a set of industry standards for data management is not unthinkable.

## 9. References

1. Giuliano KA, DeBiasio RL, Dunlay RT, et al. High-Content Screening: A new approach to easing key bottlenecks in the drug discovery process. *J Biomol Screen.* 1997;2:249–259.
2. Pernick B, Kopp RE, Lisa J, et al. Screening of cervical cytological samples using coherent optical processing: Part 1. *Appl Opt.* 1978;17:21–34. PubMed PMID: 20174348.
3. Goldrosen MH, Miller GA, Warshaw WB. Comput A program for the control of an image analysis system used in in vitro assays of cell-mediated immunity. *Programs Biomed.* 1982;14:121–5. PubMed PMID: 7044672.
4. Rosenfeld A. Pictorial pattern recognition. *Curr Mod Biol.* 1969;3:211–20. PubMed PMID: 5359039.
5. Swartzman EE, Miraglia SJ, Mellentin-Michelotti J, et al. A homogeneous and multiplexed immunoassay for high-throughput screening using fluorometric microvolume assay technology. *Anal Biochem.* 1999;271:143–51. PubMed PMID: 10419629.
6. Liu H, Lin J, Roy K, et al. Effect of 3D scaffold and dynamic culture condition on the global gene expression profile of mouse embryonic stem cells. *Biomaterials.* 2006;27:5978–89. Epub 2006 Jul 7. PubMed PMID: 16824594.

7. Levin VA, Panchabhai S, Shen L, Baggerly KA. Protein and phosphoprotein levels in glioma and adenocarcinoma cell lines grown in normoxia and hypoxia in monolayer and three-dimensional cultures. *Proteome Sci.* 2012;10:5. PubMed PMID: 22276931.
8. Ecker JR, Bickmore WA. Genomics: ENCODE explained. *Nature.* 2012;489:52–66. Barroso Ines, et al. PubMed PMID: 22955614.
9. Li Z, Yan Y, Powers EA, Ying X, et al. Identification of gap junction blockers using automated fluorescence microscopy imaging. *J Biomol Screen.* 2003;8:489–499. PubMed PMID: 14567776.
10. Chang KH, Zandstra PW. Quantitative screening of embryonic stem cell differentiation: endoderm formation as a model. *Biotechnol Bioeng.* 2004;88:287–298. PubMed PMID: 15486933.
11. Lim J, Thiery JP. Epithelial-mesenchymal transitions: insights from development. *Development.* 2012;139:3471–86. PubMed PMID: 22949611.
12. Lagarde WH, Benjamin R, Heerens AT, et al. A non-transformed oligodendrocyte precursor cell line, OL-1, facilitates studies of insulin-like growth factor-I signaling during oligodendrocyte development. *Int J Dev Neurosci.* 2007;25:95–105. PubMed PMID: 17306496.
13. Mastuyugin V, McWhinnie E, Labow M, Buxton F. A quantitative high-throughput endothelial cell migration assay. *J Biomol Screen.* 2004;9:712–718. PubMed PMID: 15634798.
14. Vidali L, Chen F, Cicchetti G, et al. Rac1-null mouse embryonic fibroblasts are motile and respond to platelet-derived growth factor. *Mol Biol Cell.* 2006;17:2377–2390. PubMed PMID: 16525021.
15. Moreau D, Scott C, Gruenberg J. A novel strategy to identify drugs that interfere with endosomal lipids. *Chimia (Aarau).* 2011;65:846–8. PubMed PMID: 22289369.
16. Schulte J, Sepp KJ, Wu C, et al. 2011, High-content chemical and RNAi screens for suppressors of neurotoxicity in a Huntington's disease model. *PLoS One.* 2011;6(8):e23841. PubMed PMID: 21909362.
17. Westwick JK, Lamerdin JE. Improving drug discovery with contextual assays and cellular systems analysis. *Methods Mol Biol.* 2011;756:61–73. PubMed PMID: 21870220.
18. Shi J, Bezabhe R, Szkudlinska A. Further evaluation of a flow cytometric in vitro micronucleus assay in CHO-K1 cells: a reliable platform that detects micronuclei and discriminates apoptotic bodies. *Mutagenesis.* 2010;25:33–40. PubMed PMID: 19843589.
19. Hill A, Mesens N, Steemans M, et al. Comparisons between in vitro whole cell imaging and in vivo zebrafish-based approaches for identifying potential human hepatotoxicants earlier in pharmaceutical development. *Drug Metab Rev.* 2012;44:127–40. PubMed PMID: 22242931.
20. Wickström M, Danielsson K, Rickardson L, et al. 2007, Pharmacological profiling of disulfiram using human tumor cell lines and human tumor cells from patients. *Biochem Pharmacol.* 2007;73:25–33. PubMed PMID: 17026967.
21. Xu Q, Schett G, Li C, et al. Mechanical stress-induced heat shock protein 70 expression in vascular smooth muscle cells is regulated by Rac and Ras small G-

- proteins but not mitogen-activated protein kinases. *Circ Res.* 2000;86:1122–8. PubMed PMID: 10850962.
22. Mackanos MA, Helms M, Kalish F, Contag CH. Image-guided genomic analysis of tissue response to laser-induced thermal stress. *J Biomed Opt.* 2011;16:058001. PubMed PMID: 21639585.
  23. Lohmann M, Walenda G, Hameda H, et al. Donor age of human platelet lysate affects proliferation and differentiation of mesenchymal stem cells. *PLoS One.* 2012;7(5):e37839. PubMed PMID: 22662236.
  24. Mantovani C, Raimondo S, Haneef MS, et al. Morphological, molecular and functional differences of adult bone marrow- and adipose-derived stem cells isolated from rats of different ages. *Exp Cell Res.* 2012;318:2034–48. PubMed PMID: 22659169.
  25. Giuliano KA, Johnston PA, Gough A, Taylor DL. Systems cell biology based on high-content screening. *Methods in Enzymology.* 2006;414:601–619. PubMed PMID: 17110213.
  26. Dragunow M. High-content analysis in neuroscience. *Nature Reviews Neuroscience.* 2008;9:779–788. PubMed PMID: 18784656.
  27. Haney SA. Increasing the robustness and validity of RNAi screens. *Pharmacogenomics.* 2007;8:1037–1049. PubMed PMID: 17716236.
  28. Heynen-Genel S, Pache L, Chanda SK, Rosen J. Functional genomic and high-content screening for target discovery and deconvolution. *Expert Opin Drug Discov.* 2012; (Aug):4. PubMed PMID: 22860749.
  29. Taylor DL. A personal perspective on high-content screening (HCS): from the beginning. *J. Biomol Screen.* 2010;15:720–725. PubMed PMID: 20639498.
  30. Pierce KL, Premont RT, Lefkowitz RJ. Seven-transmembrane receptors. *Nature Reviews Molecular Cell Biology.* 2002;3:639–650. PubMed PMID: 12209124.
  31. Garippa RJ, Hoffman AF, Gradl G, Kirsch A. High-throughput confocal microscopy for beta-arrestin-green fluorescent protein translocation G-protein-coupled receptor assays using the Evotec Opera. *Methods in Enzymology.* 2006;414:99–120. PubMed PMID: 17110189.
  32. Baus D, Yan Y, Li Z, Garyantes T., et al. A robust assay measuring Glut4 translocation in rat myoblasts overexpressing Glut4-myc and AS160\_v2. *Anal. Bio.* 2010;397:233–240. PubMed PMID: 19854150.
  33. Zhang L, Yu J, Pan H, et al. Small molecule regulators of autophagy identified by an image-based high-throughput screen. *PNAS.* 2007;104:19023–19028. PubMed PMID: 18024584.
  34. Yang Z, Klionsky DJ. Eaten alive: a history of macroautophagy. *Nature Cell Biology.* 2010;12:814–822. PubMed PMID: 20811353.
  35. Delehanty JB, Boeneman K, Bradburne CE, et al. Peptides for specific intracellular delivery and targeting of nanoparticles: implications for developing nanoparticle-mediated drug delivery. *Therapeutic Delivery.* 2010;1:411–433. PubMed PMID: 22816144.
  36. Rajendran L, Knolker HJ, Simons K. Subcellular targeting strategies for drug design and delivery. *Nature Reviews Drug Discovery.* 2010;9:29–42. PubMed PMID: 20043027.

37. Altschuler SJ, Wu LF. Cellular heterogeneity: do differences make a difference? *Cell*. 2010;141:559–563. PubMed PMID: 20478246.
38. Snijder B, Pelkmans L. Origins of regulated cell-to-cell variability. *Nature Reviews Molecular Cell Biology*. 2011;12:119–125. PubMed PMID: 21224886.
39. Snijder B, Sacher R, Ramo P, et al. Population context determines cell-to-cell variability in endocytosis and virus infection. *Nature*. 2009;461:521–523. PubMed PMID: 19710653.
40. Schauer K, Duong T, Bleakley K., et al. Probabilistic density maps to study global endomembrane organization. *Nature Methods*. 2010;(7):560–566. PubMed PMID: 20512144.
41. Chevrollier A, Cassereau J., Ferre M, et al. Standardized mitochondrial analysis gives new insights into mitochondrial dynamics and OPA1 function. *Int J Biochem Cell Biol*. 2012;44:980–988. PubMed PMID: 22433900.
42. Gautrot J, Wang C, Liu X, et al. Mimicking normal tissue architecture and perturbation in cancer with engineered micro-epidermis. *Biomaterials*. 2012;33:5221–5229. PubMed PMID: 22541538.
43. Samora CP, Mogessie B., Conway L, et al. MAP4 and CLASP1 operate as a safety mechanism to maintain a stable spindle position in mitosis. *Nature Cell Biology*. 2011;13:1040–1050. PubMed PMID: 21822276.
44. Blackmore MG, Moore DL, Smith RP, et al. High content screening of cortical neurons identifies novel regulators of axon growth. *Mol Cell Neurosci*. 2011;44:43–54. PubMed PMID: 20159039.
45. Xu J, Lamouille S., Derynck R. TGF-beta-induced epithelial to mesenchymal transition. *Cell Research*. 2009;19:156–172. PubMed PMID: 19153598.
46. Erdmann G, Volz HC, Boutros M. Systematic approaches to dissect biological process in stem cells by image-based screening. *Biotechnology Journal*. 2012;7:768–778. PubMed PMID: 22653826.
47. Desbordes SC, Placantonakis DG, Ciro A., et al. High-throughput screening assay for the identification of compounds regulating self-renewal and differentiation in human embryonic stem cells. *Cell Stem Cell*. 2008;2:602–612. PubMed PMID: 18522853.
48. Zhang J, Ferguson SS, Barak LS, et al. Molecular mechanisms of G-protein-coupled receptor signaling: role of G-protein-receptor kinases and arrestins in receptor desensitization and resensitization. *Receptors Channels*. 1997;5:193–199. PubMed PMID: 9606723.
49. Iwanicki MP, Davidowitz RA, Ng MR., et al. Ovarian cancer spheroids using myosin-generated force to clear the mesothelium. *Cancer Discovery*. 2011;1:1–14. PubMed PMID: 22303516.
50. Labarbera DV, Reid BG, Yoo BH. The multicellular tumor spheroid model for high-throughput cancer drug discovery. *Expert Opinion*. 2012;7:819–30. PubMed PMID: 22788761.
51. Quintavalle M, Elia L, Price J, et al. 2011. A cell-based, high content screening assay reveals activators and inhibitors of cancer cell invasion. *Science Signaling*. 4:183 ra49
52. Gough W, Hulkower KI, Lynch R, et al. A quantitative, facile and high-throughput image-based cell migration method is a robust alternative to the scratch assay. *J. of Biomol Screen*. 2011;15:155–163. PubMed PMID: 21297103.

53. Trask OJ, Baker A, Williams RG, Nickischer D, et al. Assay development and case history of a 32K-biased library high-content MK2-EGFP translocation screening to identify p38 mitogen-activated protein kinase inhibitors on the ArrayScan 3.1 imaging platform. *Methods Enzymol.* 2006;414:419–439. PubMed PMID: 17110205.
54. Barretina J., et al. The Cancer cell line Encyclopedia enables predictive modeling of anticancer drug sensitivity. *Nature.* 2012;483:603–607. PubMed PMID: 22460905.
55. Edinger AL, Thompson CB. Death by design: apoptosis, necrosis and autophagy. *Curr Opin Cell Biol.* 2004;16:663–669. PubMed PMID: 15530778.
56. Zhang XD, Heyse JF. Determination of sample size in genome-scale RNAi screens. *Bioinformatics.* 2009;25:841–844. PubMed PMID: 19223447.
57. Hiltzik, MA. *Dealers of lightning: Xerox PARC and the dawn of the computer age.* 1999. (1st ed.). New York: HarperBusiness. ISBN 0-88730-891-0.
58. Singh DK, Ku CJ, Wichaidit C, Steininger RJ 3rd, Wu LF, Altschuler SJ. Patterns of basal signaling heterogeneity can distinguish cellular populations with different drug sensitivities. *Mol Syst Biol.* 2010;6:369. PubMed PMID: 20461076.
59. Buchser W.J., Slepak T.I., Gutierrez-Arenas O., Bixby J.L., Lemmon V.P. Kinase/ phosphatase overexpression reveals pathways regulating hippocampal neuron morphology. *Mol Syst Biol.* 2010;6:391. PubMed PMID: 20664637.
60. Zhang JH, Chung TD, Oldenburg KR. A Simple Statistical Parameter for Use in Evaluation and Validation of High Throughput Screening Assays. *J Biomol Screen.* 1999;4:67–73. PubMed PMID: 10838414.
61. Zhang X.D. Illustration of SSMD, z score, SSMD\*, z\* score, and t statistic for hit selection in RNAi high-throughput screens. *J Biomol Screen.* 2011;16:775–785. PubMed PMID: 21515799.
62. Lundholt BK, Scudder KM, Pagliaro L. A simple technique for reducing edge effect in cell-based assays. *J Biomol Screen.* 2003;8:566–70. PubMed PMID: 14567784.
63. Benjamini, Y; Hochberg, Y. 1995. "Controlling the false discovery rate: a practical and powerful approach to multiple testing". *Journal of the Royal Statistical Society, Series B (Methodological)* 57: 289–300. MR 1325392.
64. Genovese C., Wasserman Y. *Journal of the Royal Statistical Society: Series B. Statistical Methodology.* 2002;64:499–517.
65. Zhang XD, Lacson R, Yang R, et al. The use of SSMD-based false discovery and false nondiscovery rates in genome-scale RNAi screens. *J Biomol Screen.* 2010;15:1123–31. PubMed PMID: 20852024.
66. Dragiev P, Nadon R, Makarenkov V. Two effective methods for correcting experimental high-throughput screening data. *Bioinformatics.* 2012;28:1775–1782. PubMed PMID: 22563067.
67. Kummel AH, Gubler P. Integration of multiple readouts into the z' factor for assay quality assessment. *J Biomol Screen.* 2010;15:95–101. Gehin, et al. PubMed PMID: 19940084.
68. Collins, MA. 2009. Generating “omic knowledge”: the role of informatics in high content screening. *Combi Chem & high throughput screening.* 12:917-925.
69. Cornelissen F, Cik M, Gustin E. Phaedra, a protocol-driven system for analysis and validation of high-content imaging and flow cytometry. *J. Biomol Screen.* 2012;17:496–508. PubMed PMID: 22233649.



# Advanced Assay Development Guidelines for Image-Based High Content Screening and Analysis

Mark-Anthony Bray, Ph.D.<sup>1</sup> and Anne Carpenter, Ph.D.;<sup>1</sup> Imaging Platform, Broad Institute of MIT and Harvard

Created: July 8, 2017.

## Abstract

Automated microscopes are now widespread in biological research. They enable the unprecedented collection of images at a rate which outpaces researchers' ability to visually inspect them. Whether interrogating hundreds of thousands of individual fixed samples or fewer samples collected over time, automated image analysis has become necessary to identify interesting samples and extract quantitative information by microscopy. This chapter builds on the material presented in the introductory HCS section.

## 1. Experimental design for HCS

### 1.1. Controls

Whenever possible, positive and negative controls should be included in an assay. Using controls is required to calculate a performance envelope for measuring the assay quality and phenotype feature space (see "Assay Quality and Acceptance Criteria for HCS" section below).

However, positive controls may not be readily available. In these situations, an assay measuring a real biological process may still show a phenotype of interest under some conditions that can be observed and measured even if positive controls that induce high levels of cells with the phenotype do not exist. Once a condition is identified and demonstrates such a measurable change, then it can serve as a positive control going forward.

For profiling assays, in which a large variety of cellular features are measured to identify similarities among samples, and hence designed to have multiple readouts, several different positive controls for each desired class of outcomes may be necessary. However, these may not be known in advance. Long running assays will typically accumulate positive controls over time and may even change the perceived limits or dynamic range of the assay.

---

<sup>1</sup> Imaging Platform, Broad Institute, of MIT and Harvard; Email: mbray@broadinstitute.org; Email: anne@broadinstitute.org.

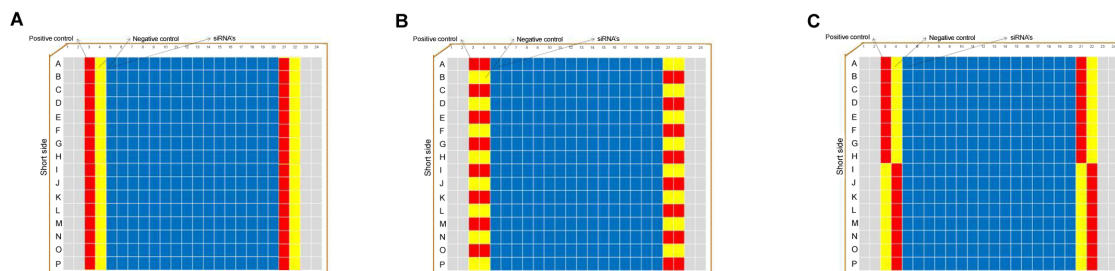


**Figure 1:** Location of sixteen positive controls (red) and sixteen negative controls (yellow) on a 384-well plate. In layout (A), both sets of controls are located on the plate edges in a regular pattern, and are susceptible to edge-based bias. In contrast, layouts (B) and (C) attempt to systematically decrease the edge bias by alternating the spatial position of the controls so that they appear in equal quantity on each of the rows and available columns. Adapted from (1).

Ideally, a positive control is of the same type as the reagents to be screened (e.g. a small molecule control for a small molecule screen, and an RNAi-based control for an RNAi screen). However, any reagent that induces the phenotypic change of interest can serve as a positive control if necessary, even if artificial. For example, expression of a constitutively active form of a tagged protein or knockdown of a target by RNAi can simulate the effects of a sought-after small molecule in a screen. Although differences in modality may complicate direct quantitative analysis of such controls, such 'artificial' controls are often helpful during assay development and optimization, and provide a sense of the dynamic range to be expected in the screen.

In selecting controls, there is a temptation to select reagents with very strong effects as positive controls. This is often the result of undue emphasis on minimum criteria for acceptance for screening, such as a  $Z'$ -factor cutoff. Good judgment should instead prevail, and positive controls should be selected based on the intensity of the hits hoped to find. For example, it is not helpful to select a very strong positive control that yields a high-quality  $Z'$ -factor if it is not comparable to the strength of the expected hits sought in an actual screen. Instead, inclusion of moderate to mild positive controls, or decreasing doses of a strong positive control, is better in gaining a sense of the sensitivity of the assay to realistic hits.

The authors have observed several successful screens with sub-par  $Z'$ -factors or absent a positive control that nonetheless yielded high-value, reproducible, biologically relevant hits. As such, common sense should prevail by factoring in the complexity and value of hits in the screen and the degree of tolerance for false positives that can be filtered out in confirmation screens.

For plates of reagents from vendors, typically only the first and the last columns of a multi-well plate are available for controls, with the treated samples contained in the middle wells.



Unfortunately, this practice renders the assay susceptible to the well-known problem of plate-based edge effects, which lead to over- or under-estimation of cellular responses when normalizing by the control wells.

One strategy to minimize edge effects is to spatially alternate the positive and negative controls in the available wells, such that they appear in equal numbers on each of the available rows and on each of the available columns (1)(2). (Figure 1)

If the screener is creating a custom plate for an HCS run, ideally the control wells should be randomly placed across the plate in order to avoid spatial bias. However, this approach is rarely practical in large screens as it must be performed manually. Therefore, the chance of introducing a spatial bias effect by using a non-random control placement is an accepted practice due to the difficulty in creating truly random plate arrangements.

For screens run in multiple batches where the controls need to be prepared such as lentiviral shRNA screens which necessitate the creation of viral vectors, variation in viral preparation may be confounded with assay variation. One helpful strategy in this situation is to make a plate containing controls in one batch, freeze them and then thaw and use them a few at a time as the screen progresses. This method can help identify assay drift or batch specific problems.

For analytical approaches to correcting inter- and intra-plate bias, see the section "Normalization of HCS data" below.

## 1.2. Replicates

Like all HTS assays, the cost of replicates should be weighed against the cost of cherry-picking hits and performing a confirmation screen. HCS assays with complex phenotypes are often more difficult to score so more replicates are often needed. Experiments are normally performed in duplicate or higher replicate numbers in order to decrease both false positive and false negative rates. Performing replicate treatments offers the following advantages (2):

1. Taking the mean or median of the replicate measurements yields lower variability than with single measurements only.
2. Replicate measurements provide direct estimates of variability and are useful for evaluating the probability of detecting true hits. When combined with control measurements, a statistically significant change can be determined by comparing (a) the ability to distinguish treated wells from the controls, and (b) the ability to distinguish replicates of the same treatment.
3. Replicates reduce the number of false negatives without increasing the number of false positives.

Despite the multitude of good reasons for high replicate numbers, almost all large screens are performed in duplicate. Increasing the replicate number from 2 to 3 is a 50% increase in reagent cost which in the case of an HCS screen involving the tens or hundreds of thousands of samples can determine whether the screen is performed at all. HCS screens

are normally performed by first screening all the samples, usually at a single concentration in duplicate, and then retesting all the hits in confirmation assays. The confirmation assays serve to filter out the false positives and are performed on a much smaller scale where it is easier to increase the replicate number and perform dose response studies if needed. In an HCS screen, preference is given to reducing false negatives because if a hit is missed during the first round of screening, it is irretrievable unless the screen is performed.

The number of treatment replicates needed is empirical and largely dictated by the subtlety of the observed cellular behavior: If a given treatment produces a strong biological response, fewer replicates will be required by virtue of a high signal-to-noise ratio. In certain cases, up to 7 replicates may be needed (3) but 2 - 4 is more typical.

Placement of replicate wells is subject to the same considerations in placement of control wells (see "Controls" above). Although randomization of the sample placement from one replicate to another is ideal, this is rarely done and for practical reasons, plates follow the same layout for all replicates. Where possible, both inter- and intra-plate replicate wells should be used for the purposes of ensuring robust normalization (see "Normalization of HCS data" below).

## 2. Assay Quality AND Acceptance Criteria for HCS

**Z'-factor** (not to be confused with z-score): While there are a number of different measurements of assay performance, the most widely used measurement to assess an assay is the so-called Z'-factor.

- *Definition:* This criteria for primary screens has gained wide acceptance in the HTS community and is defined as (4):

$1 - \frac{3(\sigma_p + \sigma_n)}{|\mu_p - \mu_n|}$  where  $\mu_p$  and  $\sigma_p$  are the mean and standard deviation values of the positive control (or alternately, the treated samples) and  $\mu_n$  and  $\sigma_n$  are those of the negative control.

- *Range and interpretation:* The Z'-factor has the range of  $-\infty$  to 1, and is traditionally interpreted as follows: (Table 1).

It should be noted that the "ideal" case of  $Z' = 1$  implies that the dynamic range  $\rightarrow \infty$  or  $\sigma_p = \sigma_n = 0$  (no variation). Neither of these scenarios represent realistic assays.

For moderate assays, the screener should consider the utility of mining hits that fall into the  $Z' = 0 - 0.5$  range. Given the screening cost of eliminating a false positive (which is hopefully low) as compared to that of eliminating a false negative (potentially very costly, as mentioned above), a decision will need to be made whether to follow up on such hits or instead cherry-pick and repeat treatments, or re-screen entire plates.

- *Advantages:* While  $Z' > 0.5$  has become a de facto cutoff for most HTS assays,  $0 < Z' \leq 0.5$  is often acceptable for complex HCS phenotype assays, because those hits may

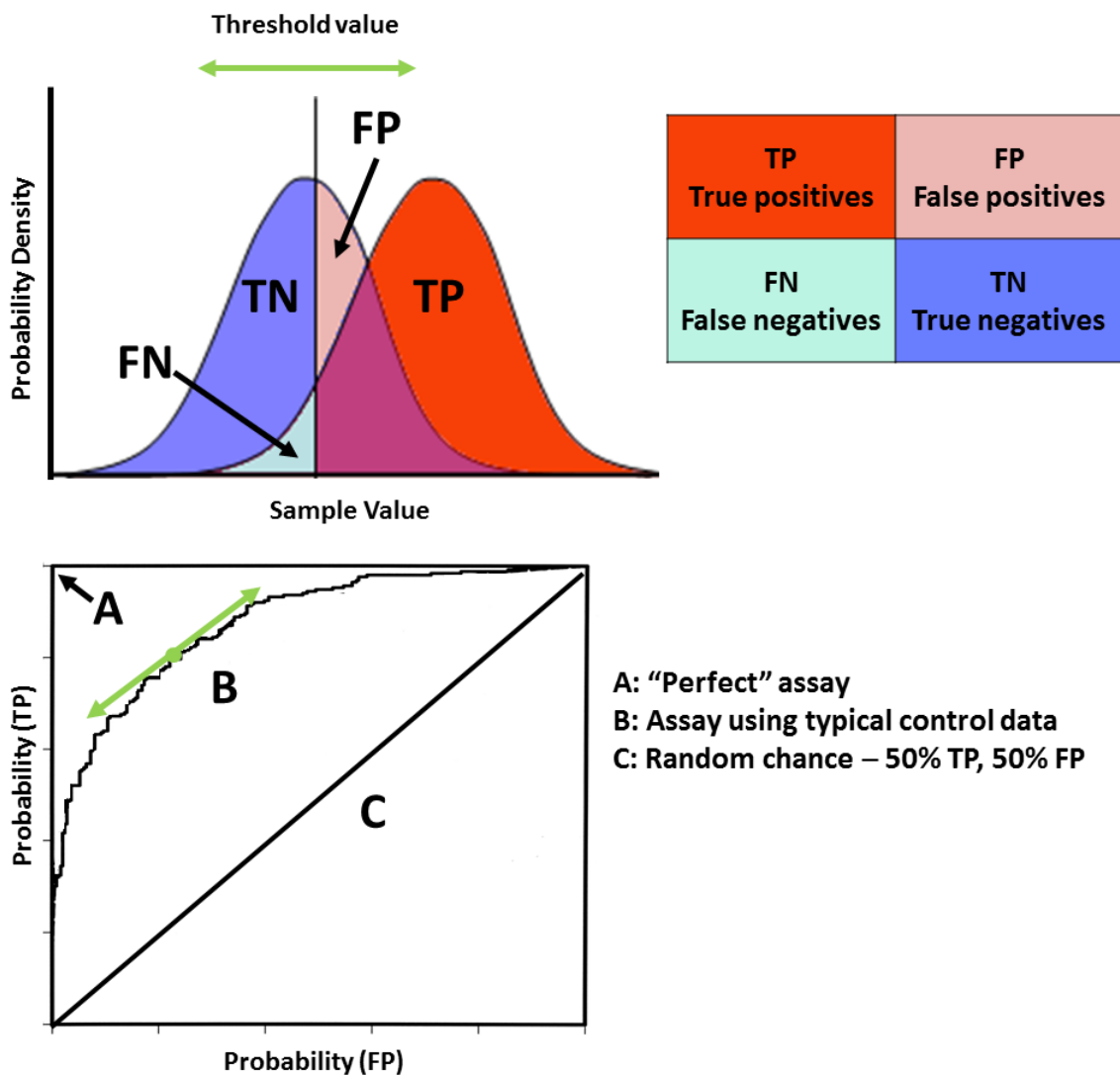


**Figure 2:** Details of a receiver characteristic curve. "Top:" Probability distributions of a hypothetical pair of control data. As a threshold value is varied, the proportions of actual and predicted positives and negatives drawn from the two distributions will also vary. "Bottom:" Three hypothetical ROC curves based on the table below. Adapted from (10).

be more subtle but still valuable. In comparison to other assay robustness metrics (5), advantages of the  $Z'$ -factor include:

- Ease of calculation.
- Accounts for the variability in the compared groups while properly ignoring the absolute background signal.
- Often found in both commercial and open-source software packages.
- *Disadvantages:*

- Does not scale linearly with signal strength. That is, an increased target reagent or a very strong positive control may achieve a higher Z'-factor that is disproportionate to the phenotype strength. The above ranges may not realistically represent more moderate screening positives which may still be biologically meaningful, e.g., RNAi screens where the signal-to-background ratio is lower than that of small-molecule screens (6).
- The use of sample means and standard deviation. Statistically, this condition assumes that the negative and positive control values follow a normal (i.e., Gaussian) distribution. The presence of outliers or asymmetry in the distributions can violate this constraint. Such is often the case for cell-based assays but is rarely verified, and can yield a misleading Z'-factor. Conversely, attempting to correct for this by transforming the response values to yield a normal distribution (e.g., log scaling) may yield an artificially high Z'-factor (7).
- The sample mean and sample standard deviation are often not robust estimators of the distribution mean and standard deviation. In the presence of outliers, these statistics can easily lead to an inaccurate measure of control distribution separation.

**One-tailed Z' factor:** This measure is a variant of the Z'-factor formulation which is more robust against skewed population distributions. In such cases, long tails opposite to the mid-range point lead to a high standard deviation for either population, which results in a low Z' factor even though the population means and samples between the means may be well-separated (unpublished work).

- *Definition:* This statistic has the same formulation as the Z'-factor, with the difference that only those samples that lie between the positive/negative control population medians are used to calculate the standard deviations.
- *Range and interpretation:* Same as that for the Z'-factor.
- *Advantages*
  - Attempts to overcome the Gaussian limitation of the original Z'-factor formulation.
  - Informative for populations with moderate or high amounts of skewness.
- *Disadvantages*
  - Still subject to the scaling issues described above for the original Z'-factor formulation.
  - Not available as part of most analysis software packages.

**V-factor:** The V-factor is a generalization of the Z'-factor to a dose-response curve (8).

*Definition:* Calculated as either:

$1 - 6 \frac{\sigma_{fit}}{|\sigma_p - \sigma_n|}$  where  $\sigma_{fit} = \sqrt{\frac{1}{N} \sum_{i=1}^N (f_{exp} - f_{mod})^2}$ , i.e, the root-mean-square deviation of a logistic model to the response data, and  $\sigma_p$  and  $\sigma_n$  are defined as above; or

$1 - 6 \frac{\text{mean}(\sigma)}{|\sigma_p - \sigma_n|}$  if no model is used, i.e., the average of several replicates where  $\sigma$  are the standard deviations of the data.

- *Range and interpretation:* Same as that for the Z'-factor.
- *Advantages*
  - Decreased susceptibility to saturation artifacts, which reduce the variability of the controls.
  - Taking the entire response curve into account makes the V-factor robust against dispensing errors (which typically occur towards the middle of the dose curve, rather than the extremes as for the positive/negative controls).
  - The V-factor formula has the same value as the Z'-factor if only two doses are considered.
- *Disadvantages:*
  - Requires dose response data, which requires many more samples than statistics relying solely on positive and negative controls.
  - Not available as part of most analysis software packages (CellProfiler is an exception).

**Strictly standardized mean difference (SSMD, denoted as  $\beta$ ):** This measure was developed to address limitations in the Z' factor in experiments with control of moderate strength.

- *Definition:* The SSMD measures the strength of the difference between two controls, using the formulation is (9)(10):

$$\beta = \frac{\mu_n - \mu_p}{\sqrt{\sigma_n^2 + \sigma_p^2}}$$

where  $\mu_n$ ,  $\sigma_n^2$ ,  $\mu_p$  and  $\sigma_p^2$  are defined as above for the Z' factor.

- *Range and interpretation:* Acceptable screening values for SSMD depend on the strength of the positive controls used, as described in the following table (11) (these threshold values assume that the positive control response is larger than that of the negative control; if the converse is true, the threshold values are negative and the inequality signs are reversed): (Table 2).

Zhang *et al* (10) make the following recommendations to choosing the appropriate criterion:

- In chemical compound assays (which typically have positive controls with strong/extremely strong effects), use criterion (4) or (3).
- For RNAi assays in which cell viability is the measured response, use criterion (4) for the empty control wells (i.e, wells with no cells added).
- If the difference is not normally distributed or highly skewed, use criterion (4).
- If only one positive control is present in the experiment, use criterion (3).
- For two positive controls, use criterion (3) for the stronger control and criterion (2) for the weaker control.
- *Advantages* (6)
  - Ease of calculation.
  - Accounts for the variability in the compared groups.
  - Accommodates the effect size of the controls, through the use of different thresholds.

- Lack of dependence on sample size.
- Linked to a rigorous probability interpretation.
- *Disadvantages* (6)
  - Not available as part of most analysis software packages (CellProfiler is an exception).
  - Not intuitive for many biologists.
  - The thresholds are based on a subjective classification of control strength.

### **Area under the receiver operating characteristic curve (AUC) (12):**

- *Definition:* The receiver characteristic curve (ROC) is a graph showing the proportion of true and false positives given a range of possible thresholds between the positive and negative control distributions (see figure). This pictorial information can be summarized as a single value by taking the area under the ROC curve (also known as the AUC) (Figure 2).
- *Range and interpretation:* The AUC can assume a value between 0 and 1. An assay which generates both true and false positives at random would result in a diagonal line between (0, 0) and (1, 1) on the ROC. For such a case, the AUC would equal 0.5. Therefore, a usable assay must therefore have an  $AUC > 0.5$  (and ideally much higher) although no cutoff criteria has been agreed upon by the community (Table 3).

Given that most screens will require a false positive rate of less than 1%, the right side of the ROC is typically less relevant than the left-most region. An alternate metric is to calculate the AUC from only the left-most region (12).

- *Advantages* (6)
  - Allows for the viewing the dynamic range of the data given positive and negative controls.
  - Does not assume that control distributions are normal (i.e, Gaussian)
  - Multiple thresholds for defining positives and the resulting trade-offs between true positive and true negative detection can be evaluated simultaneously.
- *Disadvantages* (6)
  - Requires a large sample size for calculation. Ideally, many replicates of positive and negative controls are needed.
  - Some information is lost when the AUC is used exclusively rather than visual inspection of the complete ROC. For example, two classifiers under consideration may have the same AUC but one may do better than the other at different parts of the ROC graph (that is, their curves intersect at some point). In this case, the relative accuracy no longer becomes a measure of the global performance, and restricting the AUC calculation to only a portion of the ROC graph is recommended.
  - Not available as part of most analysis software packages (though GraphPad's [Prism](#) is a commonly-used exception).

**Table 1:** Interpretation of  $Z'$  values

| Value             | Interpretation   |
|-------------------|--|
| $Z' = 1$          | An ideal assay   |
| $1 > Z' \geq 0.5$ | Excellent: Good separation between the populations       |
| $0.5 > Z' \geq 0$ | Marginal: Moderate to no separation of the distributions |
| $Z' = 0$          | Nominal: Good only for a yes/no response                 |
| $Z' < 0$          | Unacceptable: Screening is essentially impossible        |

**Table 2:** Interpretation of SSMD values (positive control response > negative control response)

| Quality Type | 1 Moderate Control   | 2 Strong Control   | 3 Very Strong Control | 4 Extremely Strong Control |
|--------------|----------------------|--------------------|-----------------------|----------------------------|
| Excellent    | $\beta \geq 2$       | $\beta \geq 3$     | $\beta \geq 5$        | $\beta \geq 7$             |
| Good         | $2 > \beta \geq 1$   | $3 > \beta \geq 2$ | $5 > \beta \geq 3$    | $7 > \beta \geq 5$         |
| Inferior     | $1 > \beta \geq 0.5$ | $2 > \beta \geq 1$ | $3 > \beta \geq 2$    | $5 > \beta \geq 3$         |
| Poor         | $\beta < 0.5$        | $\beta < 1$        | $\beta < 2$           | $\beta < 3$                |

**Table 3:** Interpretation of AUC values

| Value     | Interpretation                                      |
|-----------|---|
| AUC = 1   | A "perfect" assay.                                  |
| AUC = 0.5 | Poor: Performance is only as good as random chance. |
| AUC < 0.5 | Worse than random chance.                           |

### 3. Quality Control for HCS

Unlike most HTS assays, HCS data can be visually and sometimes automatically checked to identify and remove artifacts. In HCS assays, several fluorescent probes are often used simultaneously to stain cells, each labeling distinct cellular components in each sample. For screens in which the goal is to identify a small number of hits for a particular, known phenotype of interest, the candidate hits can often be screened by eye to eliminate false-positive artifacts. However, large screens and profiling experiments probing a broad spectrum of subtle morphological responses require more automated methods to detect and remove artifacts and systematic aberrations.

In general, the best approach to avoid imaging artifacts is to adjust the image acquisition settings to optimize the image quality (see the section "Capturing a Good Image" in the introductory [HCS chapter](#) of the AGM for more details). However, despite the screener's best efforts at acquisition and sample preparation, anomalies will still appear and end up polluting otherwise high-quality microscopy data.

Common artifacts that can confound image analysis algorithms are out-of-focus images, debris, image overexposure, and fluorophore saturation, among others. Because these anomalies affect a wide variety of intensity, morphological, and textural measurements in different ways, a single quality control (QC) metric that captures all types of artifacts, without also triggering on the unusual appearance of hits of interest, is not realistic. Instead, it is recommended to use either multiple metrics targeting the various artifacts that arise, or a supervised machine-learning approach.

### 3.1. Using targeted features for QC

#### 3.1.1. Cell count as a quality control measure

Depending on the experimental context, a simple measure of quality is the calculated cell count. This metric can help identify problems with the following situations:

- **Per-image object segmentation:** If the screener has an idea of the typical number of cells in a given image, deviations from this range at the per-image level can be indicative of improper object segmentation. An unusually low apparent number may mean that neighboring cells are getting merged together or are absent due to cell death or incorrect cell plating, whereas a high apparent count may mean that cellular objects are being split apart incorrectly or an artifact such as compound precipitation is present.
- **Per-well heterogeneities:** Uneven distribution of cells have effects on cellular adhesion and morphology, and in multiwell plates, low cell counts may characterize the wells of the edge of the plate. Computation and display of per-well cell counts in a plate layout heatmap format can reveal the presence of such systemic artifacts, which can be corrected at the sample preparation stage (14).

#### 3.1.2. Features for detecting out-of-focus images

Despite the use of autofocusing routines on automated microscopes, out-of-focus images are a common and confounding artifact in HCS. The rate of occurrence can depend on the cell type being examined and how adherent the cells are to the bottom of the well. Two measures are particularly useful in out-of-focus image detection (15):

- **Power log-log slope (PLLS):** This measure evaluates the slope of the power spectral density of the pixel intensities on a log-log scale; the power spectrum density shows the strength of the spatial frequency variations as a function of frequency. It is always negative, and decreases in value as blur increases and high-frequency image components are lost. Typical in-focus values are in the range of  $-1.5 \sim -2$ ; very negative values indicate a steep slope which means that the image is composed mostly of low spatial frequencies. It is recommended to plot the PLLS for a given channel as a histogram and examine outliers that are substantially less than  $-2$ .
  - **Advantages:** Because the PLLS of natural images is relatively invariant, this metric is useful as an unbiased estimator of focus.



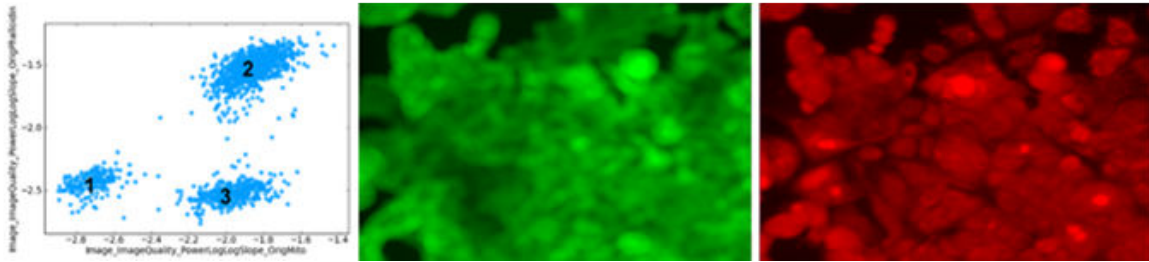


**Figure 3:** Illustration of PLLS performance for in-focus/out-of-focus MCF7 images. *Left panel:* Scatter plot of PLLS from the mitochondrial channel (x-axis) vs the phalloidin channel (y-axis) on a whole-image basis. If both channels were simultaneously blurred, we would expect that the measurements would cluster along a line. In this case, though, there are three clusters are apparent: clusters 1 and 2 represent images in which both channels are blurred/in-focus, and cluster 3 where one channel is in focus but the other is not. An example image from cluster 3 is shown, both the blurry mitochondrial (center panel) and in-focus phalloidin channels (right panel).

- **Disadvantages:** The presence of bright artifacts (e.g, fluorescent debris) in an otherwise in-focus image can produce artificially low PLLS values (Figure 3).
- **Textural correlation:** This measure evaluates the dependency of each pixel on the grayscale value of its neighbors, for a given spatial scale. Given the proper spatial scale, this measure shows the separation between blurry/in-focus images: as the correlation of an image increases, the blurriness of the image also increases. Of particular importance is the choice of spatial scale: a smaller spatial scale will pick up the blurring of smaller image features first, increasing the sensitivity. In general, it should be no larger than the diameter for a typical object (e.g, nucleus, speckle) in the channel of interest.
  - **Advantages:** Performance is generally insensitive to the amount of cell coverage.
  - **Disadvantages:** Dependence upon proper *a priori* selection of spatial scale. If the scale is too small, this metric starts reflecting the smaller in-focus image features rather than the amount of blur; too large a value, and it reflects the spatial proximity of similar cellular features.

The situation is more complicated if only a portion of the image is out-of-focus rather than the entire image (e.g., a section of a confluent cell cultures lifting off and "rolling up", causing a local change in the depth of field). In this case, the difference between such images and in-focus images will not be as distinct, but a more moderate shift in the metric values may still aid in establishing a reasonable cutoff.

### 3.1.3. Features for detecting images containing saturated fluorescent artifacts

Saturation artifacts are another common aberration encountered in HCS. Unusually bright regions in an image can be caused by debris contamination, aggregation of fluorescent dye, and/or inappropriately high exposure time or detector gain settings. Such regions can produce inaccurate intensity measurements and may impair cell identification even when such a region is small or not terribly bright.

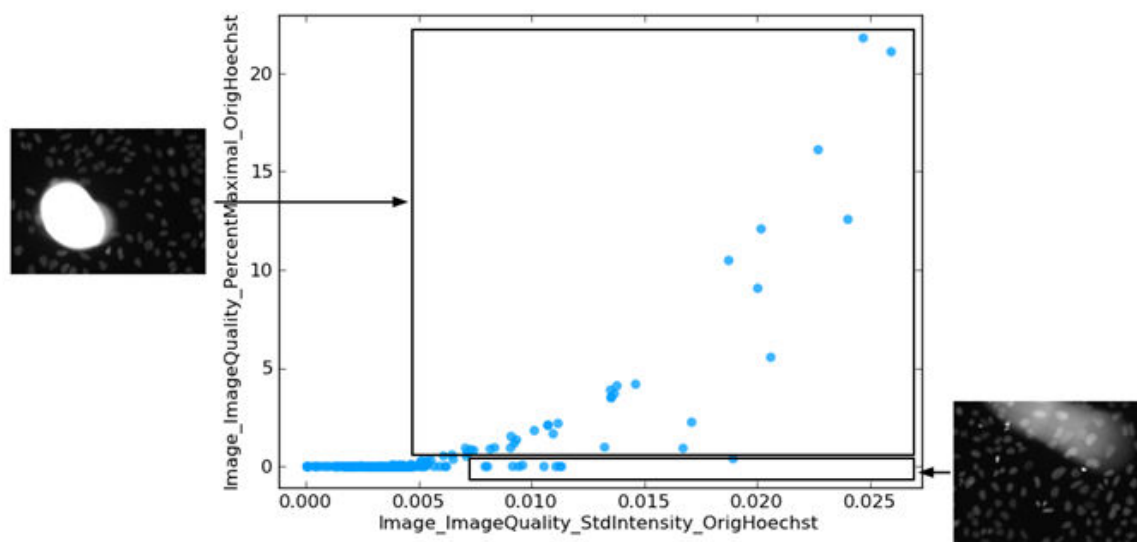


**Figure 4:** Illustration of performance of the percentage of pixels at maximum intensity and the standard deviation of the pixel intensities. The inset to the left shows a example image from the box at top where the percentage measure is high. The inset to right shows an example image from the box at bottom where the image standard deviation is high but the percentage measure is low.

The following metrics can be measured and examined to detect saturation artifacts:

- A useful measure is the percentage of the image that is occupied by saturated pixels. (Here, we define *saturation* as the maximum value in the image as opposed to the maximum bit-depth allowed by the image format.) In normal cases, only a small percentage of the image is at this value. Images with a high percentage value typically indicate either bright artifacts or saturated objects (e.g., non-artifactual dead cells). Further examination is required to determine which is the case, and whether the image is salvageable.
- The standard deviation of the pixel intensity is also useful for detection of images where a bright artifact is present but is not bright enough to cause saturation (Figure 4).

### 3.2. Using machine learning for QC

Machine learning provides a more intuitive way to train a computer to differentiate unusable from acceptable images on the basis of a sample set of each (the training set) and is particularly useful for detection of unforeseen aberrations. PhenoRipper is an open-source unsupervised machine-learning tool that can detect major classes of similar images and can be useful for artifact detection (16). The advantage of taking the machine learning approach is that it does not require a priori knowledge of the important features which identify the artifact(s). Disadvantages include the time required to create the training set and the expertise to run the analysis (17)

For more on machine learning applications, see the section "Machine learning for HCS" below.

## 4. Normalization of HCS data

In the process of performing an HCS screen, invariably small differences between samples, including replicates, appear despite the screener's best efforts at standardization of the experimental protocol. These include both systematic (i.e., stemming from test conditions and procedure) and random errors (i.e., stemming from noise). Sources of systematic error include (18):

1. Errors caused by reagent aging, or changes to compound concentrations due to reagent evaporation or cell decay.
2. Anomalies in liquid handling, malfunction of pipettes, robotic failures and reader effects
3. Variation in incubation time and temperature differences, temporal drift while measuring multiple wells and/or multiple plates and reader effects, and lighting or air flow present over the course of the entire screen

The combination of these effects may generate repeatable local artifacts (e.g., border, row or column effects) and global drifts recognizable as consistent trends in the per-plate measurement means/medians which result in row and/or column measurements that systematically over- or underestimate expected results (19).

In addition, the cellular population context (e.g. cell density) has a profound influence of cell behavior and may account significantly to cell-to-cell variability in response to treatment (20); correcting for these effects involve sophisticated methods of modeling the cellular population response (21).

The overall impact of these variations depends upon the subtlety of the cellular response in question. For example, even if a positioned plate layout is used (rather than a random layout), a strong biological response may be sufficient to overcome any plate effects that may occur by virtue of a high signal-to-noise ratio.

If this is not the case, normalization is necessary to remove these systematic variations and allow the detection of variation originating from experimental treatments. The following results are ideal:

1. The feature ranges observed across different wells with the same treatment should be similar.
2. The feature distributions of the controls (whether positive or negative) should be similar.

Examples of software packages that include a variety of plate normalization techniques include GeneData Screener (<http://www.genedata.com>) and Bioconductor (22).

## 4.1. Inter-plate normalization

For screening purposes, ideally the control wells should be present on all plates. Negative controls should be present at minimum, but preferably both positive and negative, and subject to the criteria described in the "Controls" section above, with the expectation that the cellular response in the control wells is consistently similar between all samples. However, this is rarely the case; it is not uncommon for the means and standard deviations of the collected measurements to vary from plate to plate. Hence, *inter-plate normalization* is needed to reduce variability between samples across plates.

The choice of normalization method will depend on the particular assay. Methods of inter-plate normalization include the following (6)(2):

- **Fraction or percent of controls:** The most straightforward approach is division of each sample value by the mean of the (negative or positive) control measurement of interest. This approach requires a large number of controls for sufficient estimation of the mean (see "Replicates" above), and is appropriate in instances where the data is tightly distributed and close to normal. Because information about the sample variation is not included, this measure is sensitive to outliers in the controls. A more robust version of this calculation is to substitute the median for the mean (although the sample variation is still not taken into account).
- **Normalized percent inhibition:** When a reliable positive control is available, this approach is calculated as  $x'_i = \frac{H - x_i}{L - x_i} \times 100\%$  where  $x_i$  is the measured value,  $x'_i$  is the evaluated percentage,  $H$  is the mean of the high controls,  $L$  is the mean of low controls. However, see the caveats with the use of positive controls in "Controls" section above.
- **Fraction or percent of samples:** When a high proportion of wells are expected to produce little to no response (e.g., many RNAi studies), the mean of all samples on a plate can be used for the percent of controls formula in lieu of a negative control. A more robust version of this calculation is to substitute the median for the mean, subject to the caveats above.
  - This approach is recommended if the assay lacks good negative controls that work effectively across all plates, and can provide more accurate measures due to the larger number of samples as compared to controls while reducing the need for large numbers of controls (6).
  - A variation on this approach that is unique to HCS is normalization of nuclei intensity measures by the DNA content using the mode of the DNA intensities, in cases where the large majority of the cells are in interphase in the cell cycle.
  - However, the assumption that the reagents have no biological effect should be confirmed for the particular assay. For example, it is not recommended where most of the wells have been chosen precisely because the response is differentially expressed or the overall response level between samples is changed. The following screens would violate this assumption:

1. Confirmation screens in which phenotype-positive reagents are evaluated on the same assay plate.
  2. Primary screens targeting structurally or functionally related genes.
- **Z-score (or standard score) and robust z-score:** The z-score transforms the measurement population distribution on each plate to a common distribution with zero mean and unit variance. The formula is  $x'_i = \frac{x_i - \mu}{\sigma}$  where  $x_i$  is the measured value,  $x'_i$  is the normalized output value and  $\mu$  and  $\sigma$  are the mean and standard deviations, respectively. An advantage of this approach is the incorporation of the sample variation into the calculation. However, the method assumes a normal Gaussian distribution to the underlying data (which is often not the case in HCS) and is sensitive to outliers or otherwise non-symmetric distributions. For an approach which is more robust against outliers, the robust z-score uses the median for the mean and the median absolute deviation (MAD) for the standard deviation.
  - **Robust linear scaling:** In this method, distributions are normalized by mapping the 1st percentile to 0 and the 99th percentile to 1 (21). This approach does not make assumptions about similarity of the distribution shape. However, this approach does not guarantee that the distributions of the controls will be identical between plates.

## 4.2. Intra-plate normalization

On a given plate, systematic errors generate repeatable local artifacts and smooth global drifts. These artifacts often become more noticeable upon visualization of the measurements and it is helpful to display well values graphically in their spatial layout, such as through the use of positional boxplots, heat maps of assay measurements on a plate layout and trellis map overviews of heat maps across multiple plates (23) (Figure 5).

In general, it is highly recommended to prospectively avoid such artifacts through sample preparation optimization. For example, plate edge effects can be substantially mitigated by simply allowing newly cultured plates to incubate at room temperature for a period of time (14). Another approach is to simply avoid the edge effect by leaving the edge wells filled with liquid but unused for samples; special plates exist for this purpose (e.g., Aurora plates from Nexus Biosystems). However, in experiments that require a large number of samples to be processed, leaving the edge wells empty may not be practical in terms of cost.

### 4.2.1. Correction of systematic spatial effects

The following analytical approaches may be used if there is an observed positional effect:

1. **Global parametric fitting:** This approach fits a smooth function to the data based on the physical plate layout. The corresponding per-cell measurements at each position are then divided by the smoothed function. Care must be taken in selecting the function parameters. If the function is too smooth, it is then unable to accurately model the spatial variation due to systemic error; if the function is too rigid, it will over-fit the measurements and will not generalize to new data. Using splines to create the parametric surface is common.

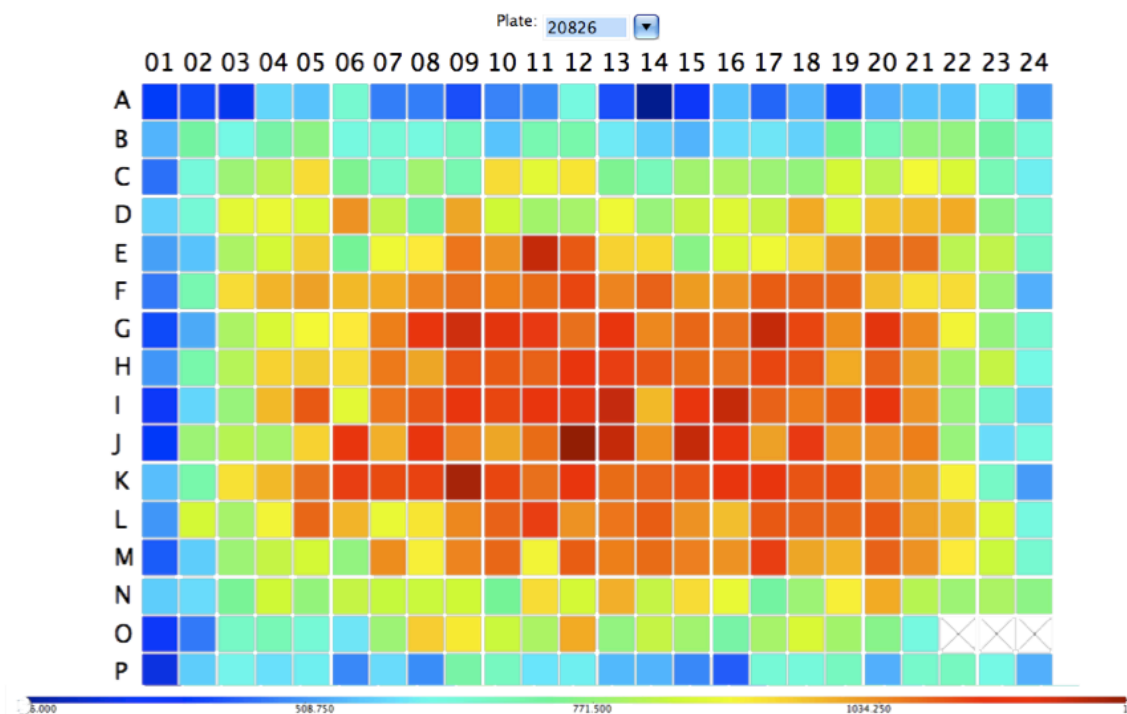


**Figure 5:** Heat map of values from a hypothetical 384-well plate containing edge effects.

2. **Local filtering:** Similar to the global parametric fitting approach, this method takes the physical plate layout into account. Assuming that the aberration is highly spatially localized, the measurements for each well are "denoised" using measures from adjacent wells, often the median calculated from a square neighborhood centered on the well to be normalized.
3. **B-Score:** This method locally corrects for systematic positional effects by iterative application of the Tukey median polish algorithm (19)(24). This approach is robust to outliers. However, it assumes that most samples in a plate have no biological effect (essentially using the entire plate as a negative control) and can produce artifacts if this assumption is violated.
4. **Model-based:** In either of the above cases, consideration must be given to whether all the samples on a plate can be used or just a subset. In a primary screen where the majority of the reagents can be assumed to have negligible or minor effect, the full set of samples can be used. In a confirmation screen, the spatial variation may be caused by samples that exhibit a moderate to large effect; hence, the representative samples should be drawn from the control wells. In this case, correction may be achieved using a diffusion model based on the control wells even though the location of the controls is often spatially constrained (25).

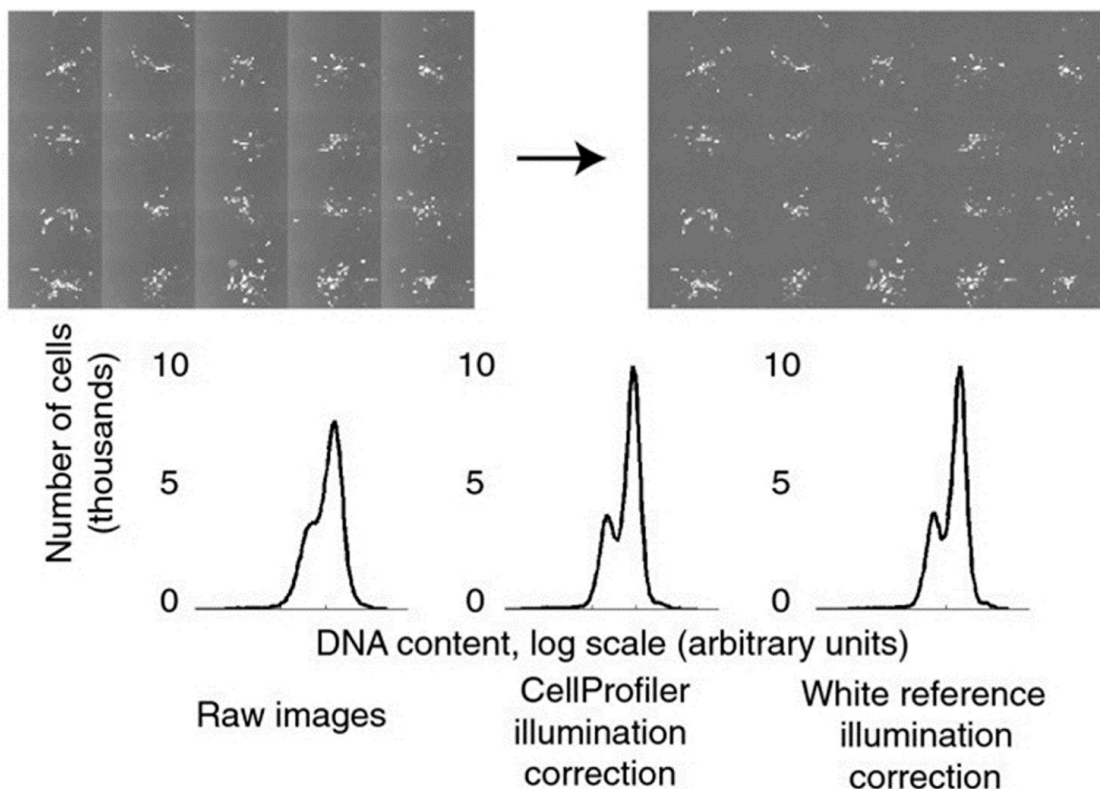


**Figure 6:** *Top left:* Example of uneven illumination from the left to the right within each field of view in a tiled grid of 5 x 4 images from a cell microarray. *Top right:* Correction of anomalies by CellProfiler. *Bottom:* Impact of anomalies and correction on *Drosophila* Kc167 DNA content data. Adapted from (27), copyright Carpenter et al.

#### 4.2.2. Illumination correction

The quantification of cellular fluorescence intensities and accurate segmentation of images is often hampered by variations in the illumination produced by the microscope optics and light sources. It is not uncommon for illumination to vary 1.5- to 2-fold across a single image when using standard microscope hardware.

Image acquisition software may mitigate these artifacts through the use of a reference image of a uniformly fluorescent sample (e.g. free fluorescent dye), which is then divided or subtracted from each collected image. This approach is described in "Image Optimization and Background Correction" section in the introductory [HCS chapter](#) and has the advantage of convenience and utility in cases where the illumination might change over time, e.g., light source aging. Disadvantages of this approach include:

- The underlying assumption is that the screener properly creates the appropriate referencing images and that conditions do not change between the acquisition of the reference images and the collection of the experimental images.

- Some software only allows one white reference image to be used to correct all wavelengths, which ignores differences in their respective optical paths and spectral characteristics.
- The fact that a uniformly fluorescent control is in a different chemical environment than a real sample is not taken into account.
- Typical methods do not account for different exposure times between the standard image and each collected image, although more sophisticated software allows for using a linear fit based on a series of images using a variety of exposure times for each wavelength.

A retrospective (i.e., post image acquisition) approach is an alternative (26). It bases the correction on all (or a sufficiently large subset of) the images from a plate for a given wavelength. This approach assumes that the actual cellular intensity distribution is distorted by a multiplicative non-uniform illumination function (additional sources of bias may also be considered if needed). This approach is applied to each wavelength condition because the spectral characteristics of the filters differ in addition to non-uniformities introduced by the excitation lamp. Furthermore, it should be applied to each plate for a given image acquisition run unless it can be shown that observed patterns are consistent across plates. The methodology is as follows:

1. For all images of a given wavelength, smooth the image by applying a median filter. Because we do not want the small-scale cellular features to obscure the underlying large-scale illumination heterogeneity, the size of the filter should be large enough that any cells in the image are heavily blurred.
2. Estimate the illumination function by calculating the per-pixel average of all the smoothed images.
3. Rescale the illumination function so that the range is  $(1, \infty)$  by dividing by the minimum pixel value, or more robustly, by the 2<sup>nd</sup> percentile pixel value (to avoid division-by-zero problems)
4. Obtain the corrected image by dividing the original image by the illumination correction function (Figure 6).

## 5. Measurement of image features

The quantitative extraction and measurement of features is performed by biological image analysis tools (e.g., CellProfiler (27), Fiji (28) and commercial software sold with HCS instruments). In addition to features that are straightforwardly related to the intended biological question, the extraction of additional features lends itself to serendipitous discoveries if mined correctly. A couple of examples illustrate this point:

- A phenotypic screen of 15 diverse morphologies in *Drosophila* cells revealed that cells with actin blebs and actin located in the periphery also tended to contain a 4N DNA content, a cell cycle relationship that would most likely not have been uncovered outside of an HCS context (29).



- Another study used a diffuse GFP reporter to look for clathrin-coated pit (plasma membrane) and intracellular vesicle formation. The researchers also took the opportunity measure GFP signal representing translocation to the nucleus. Unexpectedly, such an effect was uncovered which was compound-specific effect and not previously described in literature (30).

Measured image features fall into the following types (31) (some of which are described under "Feature Extraction" in the introductory [HCS chapter](#)):

- **Counts:** The number of objects or sub-cellular objects per compartment (e.g., foci per cell in a DNA damage experiment). The number of objects per image may also be useful as a quality control statistic.
- **Size and shape:** Size is a descriptor of the pixel area occupied by a specific labelled compartment and includes such measures as area, perimeter and major axis length. Shape measures describe specific spatial features. Some examples include the aspect ratio (ratio of the height vs width of the smallest enclosing rectangle) as a measure of elongation, or compactness (ratio of the squared perimeter and the area). Zernike features (coefficients of a Zernike polynomial fit to a binary image of an object) are also useful as descriptors of shape.
- **Intensity:** The amount of a particular marker at a pixel position, assuming that the total intensity is proportional to the amount of substance labeled. The idea is that the presence or absence of the marker reflects a specific cellular state. For example, the total intensity of a DNA label in the nucleus is related to DNA content, which is useful for cell-cycle phase identification. Intensity measurements include the minimum, maximum, various aggregate statistics (sum, mean, median) as well as correlation coefficients of intensity between channels with different markers (useful for co-localization). If the target marker changes position, e.g. translocation from the nucleus from the cytoplasm, then the correlation coefficient of the stain between the two sub-compartments can provide a larger signal dynamic range than only measuring intensity in either the sub-compartment independently.
- **Texture:** A description of the spatial regularity or smoothness/coarseness of an object, which is useful for characterizing the finer patterns of localization. Textural features can be statistical (statistical properties of the grey levels of the points comprising a surface), structural (arrangements of regular patterns), or spectral (periodicity in the frequency domain).
- **Location:** The position of an object with respect to some other feature. Typically, the (x,y) location of an object within the image is not itself biologically relevant. However, relative positional features (e.g., absolute distance of foci from the border of an enclosing organelle) may be indicative of some physiological change.
- **Clustering:** A description of the spatial relationship of an object with respect to other objects. Examples of measures include the percentage of the perimeter touching a neighboring object and the number of neighbors per object.

It should be noted that while some of the suggested features are often difficult to use as direct readouts and are not biologically intuitive to interpret (e.g., texture and some shape

features), they are often beneficial for machine learning approaches (see the section "Machine learning for HCS" below for more details). While spreadsheets are commonly used for storing cellular measurements, in order to contain the vast amount of per-cell information, across millions of cells, a database is a more feasible option for data storage and interrogation.

## 6. Machine learning for HCS

Generically, *machine learning* is defined as the use of algorithms capable of building a model from existing data as input and generalizing the model to make predictions about unknown data as output (32). The measurement of a large number of features lends itself to the use of machine-learning approaches for automated scoring of samples, especially in cases where visual inspection or hand-annotation of images is time- and cost-prohibitive. In the context of HCS, machine-learning algorithms make predictions about images (or regions of images) based on prior training. We describe below two domains in HCS where machine-learning has proven useful: identifying regions of interest in images and scoring phenotypes (a brief discussion of machine-learning for quality control application is above).

### 6.1. Machine learning for image segmentation

Typically, the first step to an HCS workflow is the identification of the image foreground from the background, i.e, finding which pixels belong to each object of interest. For fluorescent images, often one of a number of thresholding algorithms is suitable for this purpose (33).

However, in cases where the pixel intensity of the foreground is not markedly different from that of the background (e.g, brightfield images), machine-learning approaches can be useful in classifying pixels as foreground and background based on other features, such as local intensity variation or texture. Because it is not trivial to choose *a priori* features that identify the foreground, a common approach is to extract a large number of image features, hand-select example foreground and background regions and then use machine learning to find combinations of features that identify the foreground class (or classes) of pixels from the background.

One open-source pixel classification tool is Ilastik (34). It classifies each pixel in an image by calculating sets of features that are linear combinations of the intensities of neighborhood pixels in order to identify textures and edges in the neighborhood of the pixel (35). The software then calculates a membership probability for each class based on these features using supervised machine learning based on hand-annotated pixels.

### 6.2. Machine learning for scoring phenotypes

Machine-learning can in theory be used to identify samples of interest based on features calculated from entire images. However, the actual application of this approach is rare in HCS, so we focus more on machine-learning based on per-cell features.

### 6.2.1. Feature extraction and normalization

Using one or two features for scoring phenotypes is a common approach, especially when the biological relevance of the features of interest are well-defined (17). However, hand-selecting the features necessary to distinguish phenotypes of interest versus negative controls is often intractable, especially if the phenotype is subtle, or simple linear combinations are insufficient. A machine learning approach lends itself well to this task, provided a sufficient variety of features are provided as "raw material." For more details on the types of features that can be extracted see the section "Measurement of image features" above. For complex phenotypes, the features that will contribute to the discriminating power of the classifiers will probably not be known in advance. Thus, in general, it is advisable to extract as many features as is practical and to use a machine-learning algorithm capable of choosing among them.

In many HCS experiments, the phenotype is dramatic enough that plate-to-plate variation and batch effects are the only confounding effects of concern and they can be removed adequately using the techniques mentioned in the prior section.

However, for more subtle phenotypes, the screener will need to model and remove the confounding effects more precisely in order to avoid obscuring the distinctions between phenotypes of interest.

For further details related to normalization, see the "Normalization" section above.

### 6.2.2. Supervised machine-learning for identification of particular phenotype sub-populations

For rare phenotypes that are nonetheless recognizable by eye, a researcher can generate a classifier to recognize cells with the phenotype of interest. Software packages that perform this task are Definiens Cellenger (36) and CellProfiler Analyst (29). Here we describe the workflow for CellProfiler Analyst, which is open-source (available at <http://www.cellprofiler.org>).

#### 6.2.2.1. Creating a classifier

In CellProfiler Analyst, an interactive training session with iterative feedback is used to create a classifier for supervised machine learning as follows:

1. The software presents cells to the researcher for sorting, either selected randomly from the assay or taken from a specific plate with positive or negative controls. The screener manually sorts these into phenotypic "bins" to create a *training set*. Preferably, the screener will sort clear examples of the phenotype(s) in question; cells with an uncertain phenotype can be ignored, while keeping in mind that all cells will eventually be scored by the computer. Here, we refer to cells showing a phenotype of interest as "positives" (Figure 7).

Additional bins can be added, but as few bins as necessary should be used for the

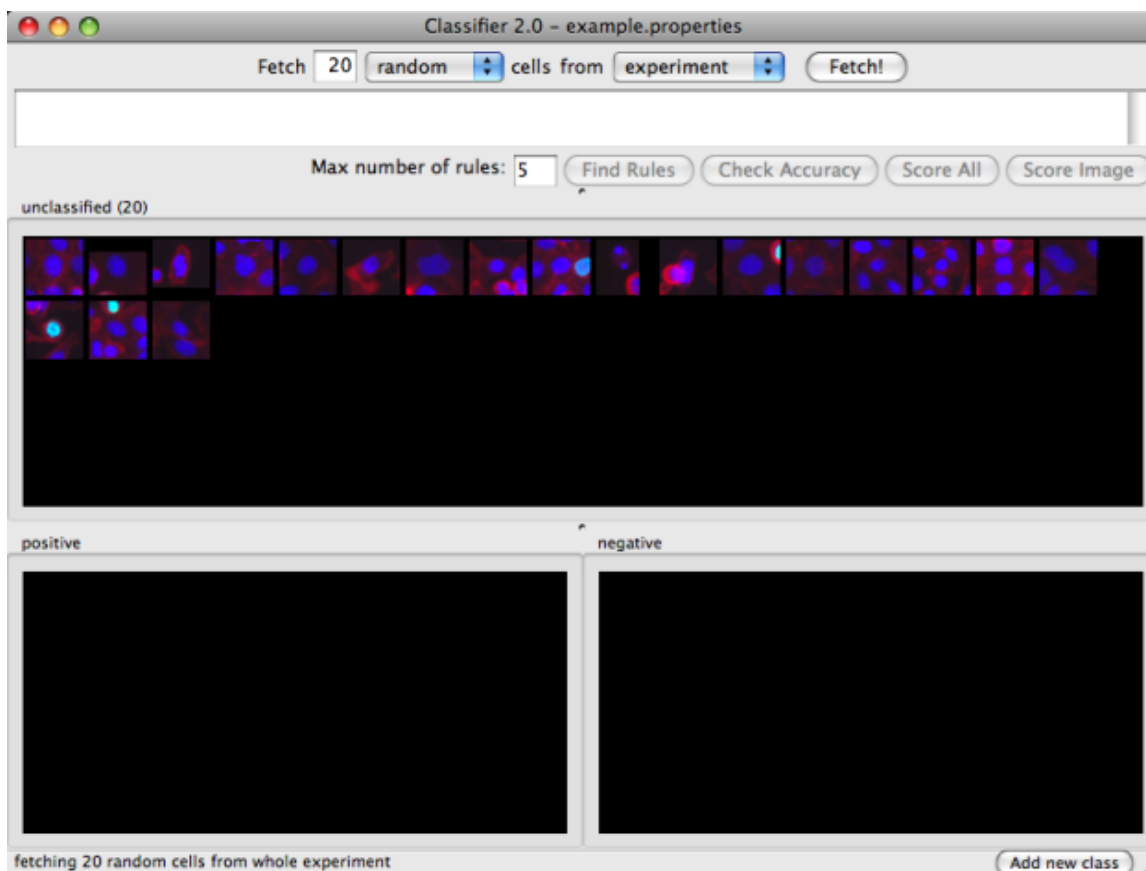


**Figure 7:** Twenty unclassified cells are presented to the screener for initial sorting using the CellProfiler Analyst phenotype classification tool.

relevant downstream analysis as adding too many bins can decrease the overall accuracy.

If uncertain about the classification of a particular object, it can be ignored or removed from the list of objects under consideration. However, keep in mind that the final scoring will ultimately assign **all** objects to a class.

A note of caution: Sampling of a phenotype from only the control samples can lead to "overfitting," a scenario in which the machine-learning algorithm preferentially learns features which are irrelevant to the phenotype itself (e.g., spatial plate effects), leading to a classifier which does not generalize well and has poor predictive performance. It is thus preferred to select individual cells from a variety of images in the experiment.

2. After enough initial examples are acquired for the training set (typically, a few dozen or so), the screener then requests the computer to generate a tentative classifier based on the sorted cells. The screener sets the number of rules for distinguishing the cells in each of the classification bins. Here, we define a *rule* as a

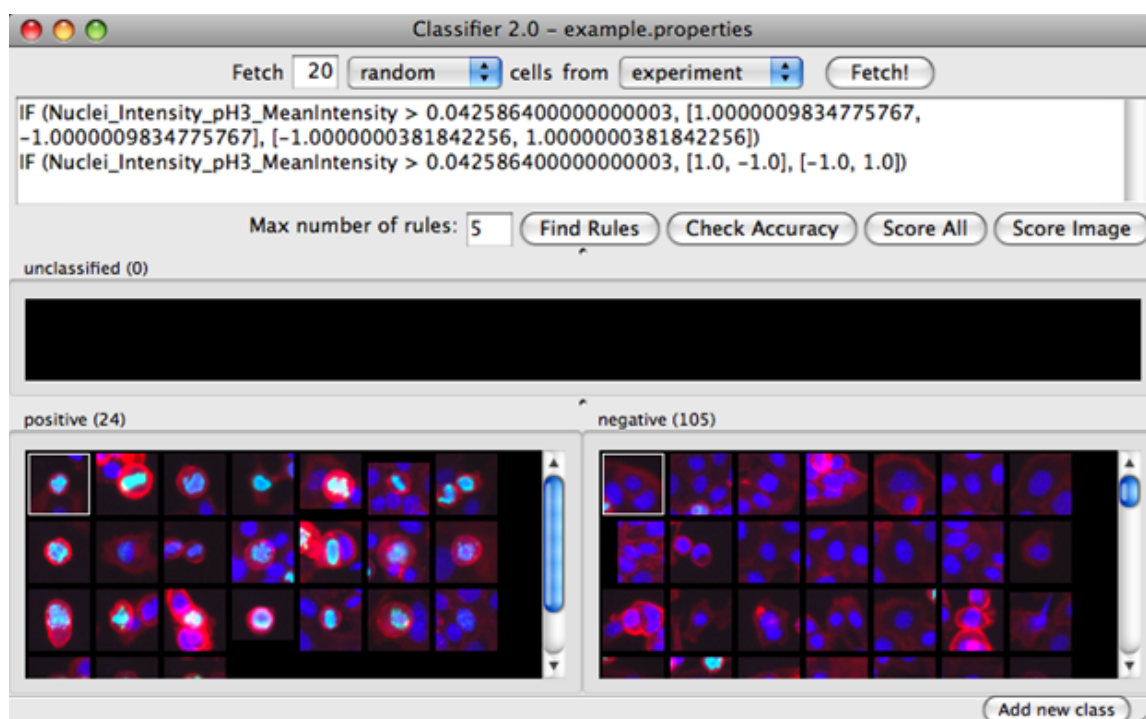


**Figure 8:** The set of rules after initial sorting using the CellProfiler Analyst classifier tool. In this example, only 2 rules were found out of the specified maximum of 5, both pertaining to the mean pH3 intensity of the nuclei channel, indicating that this feature was sufficient to achieve perfect classification on the training set.

feature and cutoff representing a decision about the cell. It is recommended to use a smaller number of rules (e.g., five) at the early stages of defining a training set in order to accumulate cells spanning the full range of the phenotype and avoid training for a too-narrow definition of the phenotype (Figure 8).

3. At this point, the goal is to refine the rules by adding more cells to the training set. The screener then requests cells that the classifier deems as belonging to a particular phenotype.
4. The screener refines the training set, correcting errors by moving misclassified cells to the correct bin and re-training the classifier by generating a new set of rules (Figure 9).
5. By repeating the two steps above, the classifier becomes more accurate. If needed, the number of rules should be increased to improve accuracy (see below). At this point, the screener should save the training set for future refinement, to re-generate scores and for experimental records. It is advisable to do so before proceeding to scoring the entire experiment because scoring may take a long time for large screens.
6. When the accuracy of the classifier is sufficient, the screener can then scores all cells in the experiment so that the number of positive cells in each sample can be calculated (Figure 10).

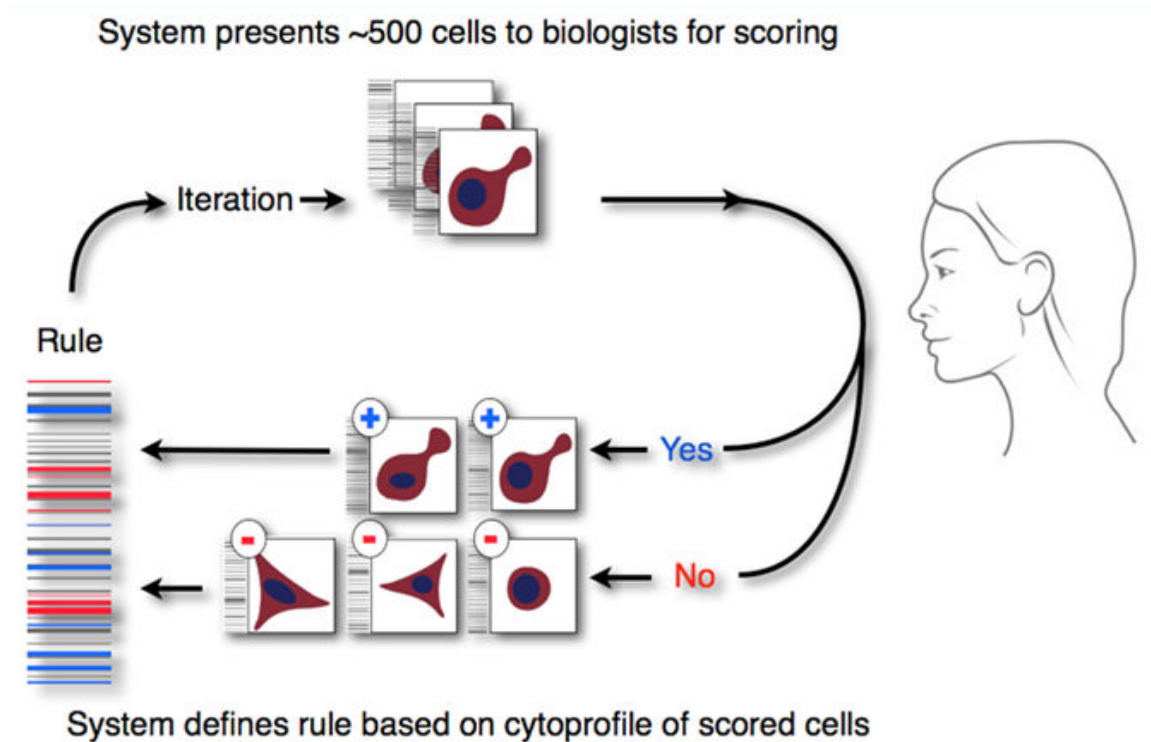


**Figure 9:** Illustration of the iterative machine learning workflow. Adapted from (29), copyright The National Academy of Sciences of the USA.

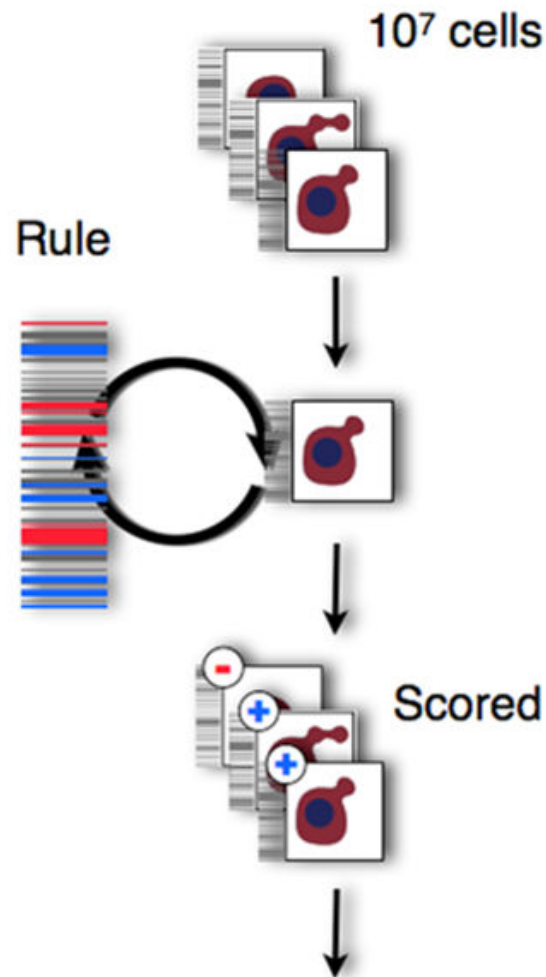
### 6.2.2.2. Obtaining rules during the training phase and assessing classifier accuracy

When the first pass at sorting sample cells is finished, the maximum number of rules allowed needs to be specified prior to generating the initial set of rules.

During the initial training step, it is best to use a small number of rules (typically 5 to 10) in order to avoid defining the phenotype too narrowly. Doing so will help insure identification of the minimal set of features covering the wide range of object characteristics represented in the training set.

As training proceeds, if the number of misclassifications does not improve, the number of rules may be increased to allow the machine-learning algorithm to capture more subtle distinctions between phenotypes. However, using more rules does not always result in greater accuracy. In particular, increasing the number of rules above 100 is unlikely to improve classification accuracy and is computationally expensive to calculate.

Based on prior experience with 14 phenotypes in human cells, an upper limit of 50 rules is recommended for complex object classes (that is, to the human eye, one that involves the assessment of many features of the objects simultaneously) (29).



**Scored cells are sorted by well:  
identify samples with a high proportion of positive cells**

**Figure 10:** Illustration of the final cell scoring workflow. Adapted from (29), copyright The National Academy of Sciences of the USA.

The most accurate way to gauge the performance of a classifier is to fetch a large number of objects of a given phenotype from the whole experiment. The fraction of the retrieved objects correctly matching the requested phenotype indicates the classifier's general performance. For example, if a screener fetches 100 positive objects but find upon inspection that 5 of the retrieved objects are not positives, then the classifier is estimated to have a positive predictive value of 95% on individual cells. Note that the classifiers' ability to detect positives and negatives must be interpreted in the context of the actual prevalence of individual phenotypes, which may be difficult to assess a priori. For studies

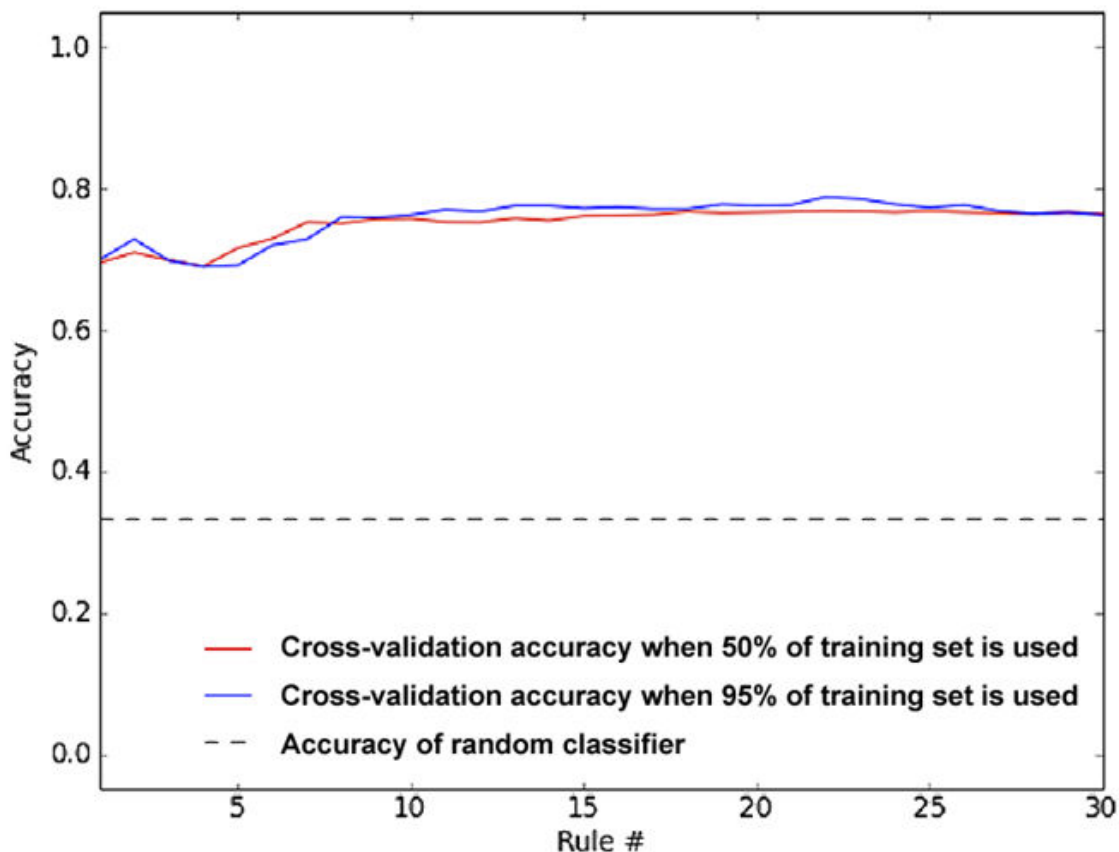


**Figure 11:** Plot displaying the cross-validation accuracy of a 3-class classifier with 30 rules. Note that the accuracy does not increase for more than 10 rules.

or screens where the data is gathered over time, re-training the classifiers on the larger data set can increase their robustness.

*Cross-validation* is a standard method for estimating classifier accuracy, with important caveats discussed below. One version of this approach is to use a sub-sample of the training set for training a classifier and then use the remainder of the training set for testing. The optimal number of rules may be assessed by plotting the cross-validation accuracy for the training set as an increasing number of rules are used, where values closer to 1 indicate better performance. Two features of the plot are useful for guiding further classification:

1. If the accuracy increases (that is, slopes upward) at larger numbers of rules, adding more rules is likely to help improve the classifier (if the line slopes downward, this may indicate more training examples are needed).
2. If the accuracy is displayed for two sub-sampling percentages (say, 50% and 95% of the examples are used for training), and the two curves are essentially the same, adding more cells to the training set is unlikely to improve performance.



A note of caution: The accuracy in these plots should not be interpreted as the actual accuracy for the overall experiment. These plots tend to be pessimistic, as the training set usually includes a disproportionate number of difficult-to-classify examples (Figure 11).

The relationship between accuracy on individual cells versus accuracy for scoring wells for follow-up is complicated, because false positives and false negatives are often not evenly distributed across wells in an experiment. In practice, improving accuracy on individual cells leads to better accuracy on wells, and in general, the actual goal is per-well accuracy more than per-cell accuracy.

## 7. Whole-organism HCS

For those experiments in which the molecular mechanisms in question cannot yet be reduced to biochemical or cell-based assays, screeners can search for chemical or genetic regulators of biological processes in whole model organisms rather than isolated cells or proteins. The advantages of performing HCS in an intact, physiological system include the increase in likelihood that the findings from such experiments accurately translate into the context of the human body (e.g., in terms of toxicity and bioavailability), simplification of the path to clinical trials, and reduction of the failure of potential therapeutics at later stages of testing.

While a number of small animals are amenable to whole-organism HCS (e.g., zebrafish embryos, *Drosophila* fruit fly larvae, etc), this section of the chapter will focus on novel HCS techniques developed for the *Caenorhabditis elegans* roundworm.

### 7.1. *C. elegans* HCS

The nematode *C. elegans* is an increasingly popular choice for enabling HCS in whole organisms due to the following advantages:

- Manually-analyzed RNAi and chemical screens are well-proven in this organism, with dozens completed (37).
- Many existing assays can be adapted to HCS; instrumentation exists to handle and culture *C. elegans* in HTS-compatible multi-well plates.
- Its organ systems have high physiologic similarity and genetic conservation with humans.
- *C. elegans* is particularly suited to assays involving visual phenotypes: physiologic abnormalities and fluorescent markers are easily observed because the worm is mostly transparent.
- The worms follow a stereotypic development pattern that yields identically-appearing adults, such that deviations from wild-type are more readily apparent.

Microscopy imaging and flow cytometry are the primary HCS methods for *C. elegans*, as plate readers do not offer per-worm or morphological readouts and often cannot measure bulk fluorescence from worm samples due to their spatial heterogeneity within the well.

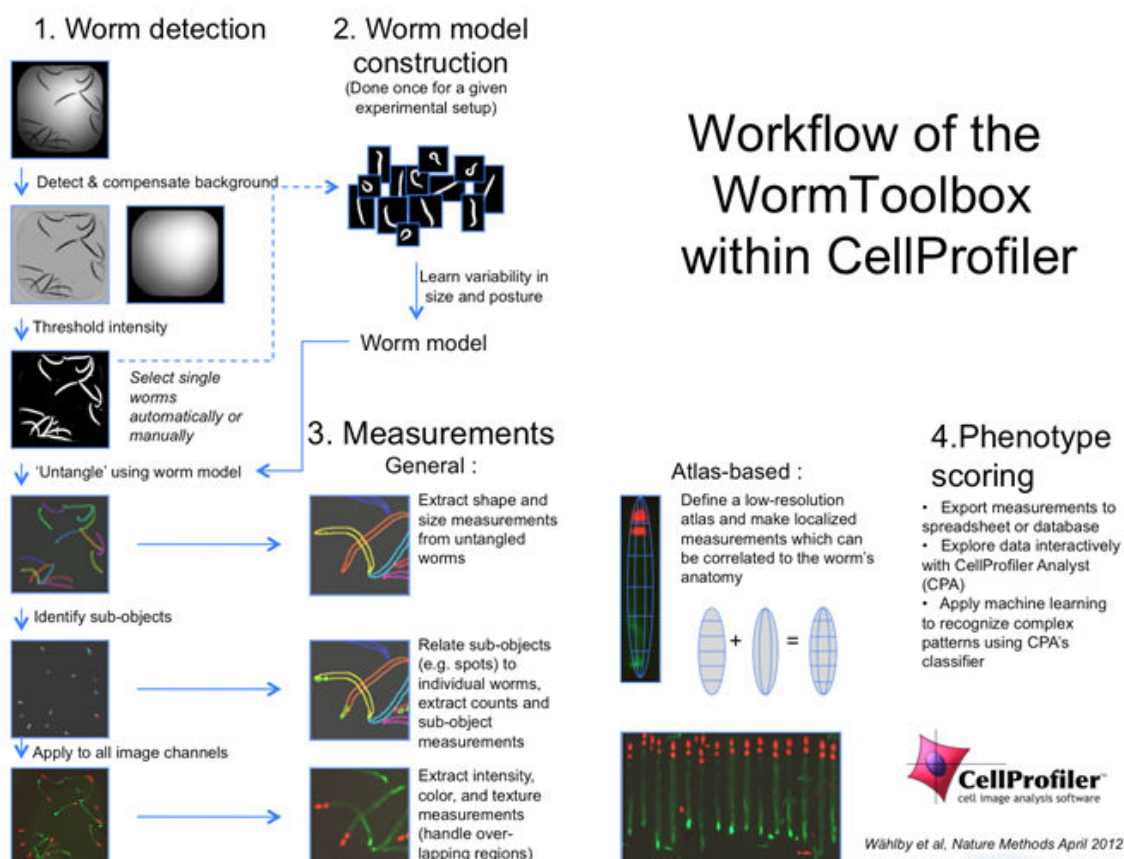


**Figure 12:** Workflow of the WormToolbox in CellProfiler. Adapted from (42), contributed by Carolina Wählby.

- Flow cytometers:** Systems such as the COPAS Biosort (Union Biometrica) can be used for the automatic sorting of various "large" objects, including *C. elegans*, using the object size and intensity of fluorescent markers. Such a system is capable of differentiating some phenotypes using fluorescent intensity changes as the readout (e.g., isolating of mutants with reduced RFP-to-GFP intensity ratios as compared to wild-type worms (38) or signature extraction based on GFP intensity profiles created along the length of the worm (39)). One limitation of this approach is low spatial resolution. Another disadvantage is that retrieval of worms from the multi-well plates typically used in screening becomes a rate-limiting step, reducing the throughput.
- Automated microscopy:** Defining worm phenotypes in HCS has also been enabled through the use of image data. Standard 6- or 12-well assays can be miniaturized to 96- or 384 well plates by dispensing a precise number of worms within a specified size/age range into the desired number of multiwell plates (using a COPAS sorter, for example). The worms are typically transferred from agar to liquid media to minimize imaging artifacts. A paralytic drug may be added to slow worm

movement, minimizing misalignment between subsequently imaged channels. Alternately, microfluidics may also be used to stabilize worm position (40).

Below is an HCS image analysis workflow tailored for worms dispensed into multi-well plates (41), using brightfield images of each well, along with the corresponding images from additional fluorescence wavelengths:

1. **Well identification:** In order to restrict worm detection to the region of interest, delineate the well boundary within the brightfield image; the well interior is typically brighter than the well exterior, lending itself to simple thresholding. In order to avoid artifacts at the well edge, use morphological erosion to contract the well border by a few pixels.
2. **Illumination correction and masking of pixel intensities:** Often the brightfield image will exhibit illumination heterogeneities which must be corrected prior to worm detection (see the "Illumination\_correction" section above). Calculate an illumination correction function (ICF) from the brightfield image and then correct the image by dividing by the ICF. It is recommended to mask the image using the eroded well image and use the result for creating the ICF, otherwise the ICF will be distorted by the sharp features at the well edge. At this point, the illumination-corrected image is then masked with the eroded well image in order to restrict worm identification to the well area.
3. **Worm foreground identification:** Identify the worms as the image foreground using image thresholding on the brightfield image. Because the brightfield images are usually high-contrast, an automatic thresholding method such as Otsu is typically effective here. It is helpful to impose size criteria in order to remove objects that are likely to be spurious, e.g, debris, embryos, and other artifacts.
4. **Make population-averaged measurements if desired:** At this point, quantification of the additional fluorescent markers within the worm regions can be performed. For example, if a viability stain (e.g., SYTOX Orange) was used as part of a live/dead assay, image segmentation (i.e. partitioning the foreground pixels into individual worms) is not necessary, and the workflow would continue by identifying the SYTOX-positive pixels from the fluorescent image using automatic thresholding, measuring the total pixel area occupied by the worm foreground and the SYTOX foreground, and calculating the ratio of the SYTOX foreground total area and the worm foreground area to yield the final per-well readout of worm death.
5. **Make per-worm measurements if desired:** For some assays, it is preferable to identify individual animals rather than a whole-well readout (e.g., pathogen screens). While non-touching worms can usually be delineated in brightfield images based on the differences in intensities between foreground and background, image intensity alone is not sufficient for touching and overlapping worms. For these assays, algorithms are required that separate touching and overlapping worms. Moreover, edges and intensity variations within the worms often mislead conventional segmentation algorithms. Here, we describe a recent algorithm that employs a probabilistic shape model using intrinsic geometrical

properties of the worms (such as length, width profile, and limited variability in posture) as part of an automated segmentation method (distributed as a toolbox in CellProfiler) (42) (Figure 12)

- a. **Identify worms as described in the above workflow:** in this case, however, only the brightfield images are acquired from each well
- b. **Construct a worm "model":** Once the worm foreground is obtained, construct a model of the variations in worm morphology by creating a training set of non-touching representative worms. This is done by saving binary images of a number of non-touching worms and using the "Training" mode of the UntangleWorms module in the CellProfiler worm toolbox.
- c. **Apply the worm model to worm clusters:** Once the model is created, apply the model on the images using the "Untangle" mode of the UntangleWorms module. The result of this operation will be identify the individual worms from the worm clusters as well as exclude artifacts such as debris, embryos, etc.
- d. **Quantify fluorescent markers:** Measure the various features available for each worm, such as morphology, intensity, texture, etc. The delineated worms can also be mapped to a common atlas (using StraightenWorms) so that spatial distribution of staining patterns may be quantified (Figure 12).

## 8. Acknowledgements

This material is based upon work supported by the National Institutes of Health (R01 GM089652 to AEC, U54 HG005032 to Stuart Schreiber, and RL1 HG004671 to Todd Golub, administratively linked to RL1 CA133834, RL1 GM084437, and UL1 RR024924), the National Science Foundation (DB-1119830 to MAB), and Eli Lilly & Company.

## 9. References

1. Kozak K, Agrawal A, Machuy N, Csucs G. Data mining techniques in high content screening: A survey. (2009). *J Comput Sci Syst Biol.* 2009;2:219–239.
2. Malo N, Hanley JA, Cerquozzi S, Pelletier J, Nadon R. Statistical practice in high-throughput screening data analysis. *Nat Biotechnol.* 2006;24(2):167–75. PubMed PMID: 16465162.
3. Genovesio A, Kwon YJ, Windisch MP, Kim NY, Choi SY, Kim HC, Jung S, Mammano F, Perrin V, Boese AS, Casartelli N, Schwartz O, Nehrbass U, Emans N. Automated genome-wide visual profiling of cellular proteins involved in HIV infection. *J Biomol Screen.* 2011;16(9):945–58. PubMed PMID: 21841144.
4. Zhang JH, Chung TDY, Oldenburg KR. A simple statistical parameter for use in evaluation and validation of high throughput screening assays. *J Biomol Screen.* 1999;4(2):67–73. PubMed PMID: 10838414.
5. Iversen PW, Eastwood BJ, Sittampalam GS, Cox KL. A comparison of assay performance measures in screening assays: signal window, Z'factor, and assay variability ratio. *J Biomol Screen.* 2006;11(3):247–52. PubMed PMID: 16490779.

6. Birmingham A, Selfors LM, Forster T, Wrobel D, Kennedy CJ, Shanks E, Santoyo-Lopez J, Dunican DJ, Long A, Kelleher D, Smith Q, Beijersbergen RL, Ghazal P, Shamu CE. Statistical methods for analysis of high-throughput RNA interference screens. *Nat Methods*. 2009;6(8):569–75. PubMed PMID: 19644458.
7. Sui Y, Wu Z. Alternative statistical parameter for high-throughput screening assay quality assessment. *J Biomol Screen*. 2007;12(2):229–34. PubMed PMID: 17218666.
8. Ravkin I, Temov V, Nelson AD, Zarowitz MA, Hoopes M, Verhovsky Y, Ascue G, Goldbard S, Beske O, Bhagwat B, Marciniak H. Multiplexed high-throughput image cytometry using encoded carriers. *Proc SPIE*. 2004;2004(5322):52–63.
9. Zhang XHD. A pair of new statistical parameters for quality control in RNA interference high-throughput screening assays. *Genomics*. 2007;89(4):552–61. PubMed PMID: 17276655.
10. Zhang XHD (2011). *Optimal High-Throughput Screening: Practical Experimental Design and Data Analysis for Genome-scale RNAi Research*. Cambridge University Press, 2011 ISBN 978-0-521-73444-8.
11. "Strictly standardized mean difference." *Wikipedia, The Free Encyclopedia*. *Wikimedia Foundation*, Available at: [http://en.wikipedia.org/wiki/Strictly\\_standardized\\_mean\\_difference](http://en.wikipedia.org/wiki/Strictly_standardized_mean_difference)
12. Fawcett T. An introduction to ROC analysis. *Pattern Recognit Lett*. 2006;27(8):861–874.
13. "Receiver operating characteristic", *Wikipedia, The Free Encyclopedia*. *Wikimedia Foundation*, Available at: [http://en.wikipedia.org/wiki/Receiver\\_operating\\_characteristic](http://en.wikipedia.org/wiki/Receiver_operating_characteristic)
14. Lundholt BK, Scudder KM, Pagliaro L. A simple technique for reducing edge effect in cell-based assays. *J Biomol Screen*. 2003;8(5):566–70. PubMed PMID: 14567784.
15. Bray MA, Fraser AN, Hasaka TP, Carpenter AE. Workflow and metrics for image quality control in large-scale high-content screens. *J Biomol Screen*. 2012;17(2):266–74. PubMed PMID: 21956170.
16. Rajaram S, Pavie B, Wu LF, Altschuler SJ. PhenoRipper: software for rapidly profiling microscopy images. *Nat Methods*. 2012;9(7):635–637. PubMed PMID: 22743764.
17. Logan DL, Carpenter AE. Screening cellular feature measurements for image-based assay development. *J Biomol Screen*. 2010;15(7):840–846. PubMed PMID: 20516293.
18. Dragiev P, Nadon R, Makarenkov V. Systematic error detection in experimental high-throughput screening. *BMC Bioinformatics*. 2011;12:25. PubMed PMID: 21247425.
19. Brideau C, Gunter B, Pikounis B, Liaw A. Improved statistical methods for hit selection in high-throughput screening. *J Biomol Screen*. 2003;8(6):634–47. PubMed PMID: 14711389.
20. Snijder B, Pelkmans L. Origins of regulated cell-to-cell variability. *Nat Rev Mol Cell Biol*. 2011;12(2):119–25. PubMed PMID: 21224886.
21. Perlman ZE, Slack MD, Feng Y, Mitchison TJ, Wu LF, Altschuler SJ. Multidimensional drug profiling by automated microscopy. *Science*. 2004;306(5699):1194–8. PubMed PMID: 15539606.
22. Gentleman RC, Carey VJ, Bates DM, Bolstad B, Dettling M, Dudoit S, Ellis B, Gautier L, Ge Y, Gentry J, Hornik K, Hothorn T, Huber W, Iacus S, Irizarry R, Leisch F, Li C, Maechler M, Rossini AJ, Sawitzki G, Smith C, Smyth G, Tierney L, Yang JY, Zhang J.

- Bioconductor: open software development for computational biology and bioinformatics. *Genome Biol.* 2004;5(10):R80. PubMed PMID: 15461798.
23. Gunter B, Brideau C, Pikounis B, Liaw A. Statistical and graphical methods for quality control determination of high-throughput screening data. *J Biomol Screen.* 2003;8(6):624–33. PubMed PMID: 14711388.
  24. Makarenkov V, Zentilli P, Kevorkov D, Gagarin A, Malo N, Nadon R. An efficient method for the detection and elimination of systematic error in high-throughput screening. *Bioinformatics.* 2007;23(13):1648–57. PubMed PMID: 17463024.
  25. Carralot JP, Ogier A, Boese A, Genovesio A, Brodin P, Sommer P, Dorval T. A novel specific edge effect correction method for RNA interference screenings. *Bioinformatics.* 2012;28(2):261–8. PubMed PMID: 22121160.
  26. Jones TR, Carpenter AE, Sabatini DM, Golland P (2006) Methods for high-content, high-throughput image-based cell screening. *Proceedings of the Workshop on Microscopic Image Analysis with Applications in Biology (MIAAB)*. Metaxas DN, Whitaker RT, Rittcher J, Sebastian T (Eds). Copenhagen, Denmark, October 5, pp 65-72.
  27. Carpenter AE, Jones TR, Lamprecht MR, Clarke C, Kang IH, Friman O, Guertin DA, Chang JH, Lindquist RA, Moffat J, Golland P, Sabatini DM. CellProfiler: image analysis software for identifying and quantifying cell phenotypes. *Genome Biol.* 2006; 2006;7(10):R100. PubMed PMID: 17076895.
  28. Schindelin J, Arganda-Carreras I, Frise E, Kaynig V, Longair M, Pietzsch T, Preibisch S, Rueden C, Saalfeld S, Schmid B, Tinevez JY, White DJ, Hartenstein V, Eliceiri K, Tomancak P, Cardona A. Fiji: an open-source platform for biological-image analysis. *Nat Methods.* 2012;9(7):676–82. PubMed PMID: 22743772.
  29. Jones TR, Carpenter AE, Lamprecht MR, Moffat J, Silver SJ, Grenier JK, Castoreno AB, Eggert US, Root DE, Golland P, Sabatini DM. Scoring diverse cellular morphologies in image-based screens with iterative feedback and machine learning. *Proceedings of the National Academy of Sciences USA.* 2009;106(6):1826–31. PubMed PMID: 19188593.
  30. Garippa RJ, Hoffman AF, Gradl G, Kirsch A. High Throughput Confocal Microscopy for Beta Arrestin Green Fl. uorescent Protein Translocation: G Protein-Coupled Receptor Assays Using the Evotec (Perkin-Elmer) Opera. *Methods in Enzymology: Measuring Biological Responses with Automated Microscopy*, Vol. 414. Ed. By James Inglese, Elsevier Academic Press, San Diego, CA. 2006. PubMed PMID: 17110189.
  31. Ljosa V, Carpenter AE. Introduction to the quantitative analysis of two-dimensional fluorescence microscopy images for cell-based screening. *PLoS Comput Biol.* 2009;5(12):e1000603. PubMed PMID: 20041172.
  32. Tarca AL, Carey VJ, Chen XW, Romero R, Drăghici S. Machine learning and its applications to biology. *PLoS Comput Biol.* 2007;3(6):e116. PubMed PMID: 17604446.
  33. Sahoo PK, Soltani S, Wong AK, Chen YC. A survey of thresholding techniques. *Comput Vision Graph Image Process.* 1988;41:233–260.
  34. ilastik: Interactive Learning and Segmentation Toolkit. Available at: <http://www.ilastik.org/>

35. Hamprecht FA (2010) Ilastik: Interactive learning and segmentation tool kit. 2011 IEEE International Symposium on Biomedical Imaging. URL Available at: <http://hci.iwr.uni-heidelberg.de/download3/ilastik.php>.
36. Baatz M, Arini N, Schäpe A, Linszen B. Object-oriented image analysis for high content screening: detailed quantification of cells and sub cellular structures with the Cellenger software. *Cytometry A*. 2006;69(7):652–8. PubMed PMID: 16680706.
37. O'Rourke EJ, Conery AL, Moy TI. Whole-animal high-throughput screens: the *C. elegans* model. *Methods Mol Biol*. 2009;486:57–75. PubMed PMID: 19347616.
38. Doitsidou M, Flames N, Lee AC, Boyanov A, Hobert O. Automated screening for mutants affecting dopaminergic-neuron specification in *C. elegans*. *Nat Methods*. 2008;5(10):869–72. PubMed PMID: 18758453.
39. Dupuy D, Bertin N, Hidalgo CA, Venkatesan K, Tu D, Lee D, Rosenberg J, Svrzikapa N, Blanc A, Carnec A, Carvunis AR, Pulak R, Shingles J, Reece-Hoyes J, Hunt-Newbury R, Viveiros R, Mohler WA, Tasan M, Roth FP, Le Peuch C, Hope IA, Johnsen R, Moerman DG, Barabási AL, Baillie D, Vidal M. Genome-scale analysis of in vivo spatiotemporal promoter activity in *Caenorhabditis elegans*. *Nat Biotechnol*. 2007;25(6):663–8. PubMed PMID: 17486083.
40. Chung K, Crane MM, Lu H. Automated on-chip rapid microscopy, phenotyping and sorting of *C. elegans*. *Nat Methods*. 2008;5(7):637–43. PubMed PMID: 18568029.
41. Moy TI, Conery AL, Larkins-Ford J, Wu G, Mazitschek R, Casadei G, Lewis K, Carpenter AE, Ausubel FM. High-throughput screen for novel antimicrobials using a whole animal infection model. *ACS Chemical Biology*. 2009;4(7):527–33. PubMed PMID: 19572548.
42. Wählby C, Kamensky L, Liu ZH, Riklin-Raviv T, Conery AL, O'Rourke EJ, Sokolnicki KL, Visvikis O, Ljosa V, Irazoqui JE, Golland P, Ruvkun G, Ausubel FM, Carpenter AE. An image analysis toolbox for high-throughput *C. elegans* assays. *Nat Methods*. 2012;9(7):714–6. PubMed PMID: 22522656.





# Nuclear Factor Kappa B (NF- $\kappa$ B) Translocation Assay Development and Validation for High Content Screening

O. Joseph Trask, Jr, BS<sup>1</sup>

Created: October 1, 2012.

## Abstract

In this assay study design, activation through stimulation or inhibition of the Nuclear Factor  $\kappa$ B (NF- $\kappa$ B) pathway demonstrates translocation of NF- $\kappa$ B protein from the cytoplasm to nucleus as measured using automated fluorescent microscopy computer-assisted image analysis technology better known as high content screening (HCS), High Content Analysis (HCS), High Content Imaging (HCI), or Image Cytometry (IC). This approach offers a better understanding of novel drug targets by examining the sub-cellular spatial distribution of the target proteins and the effects of target perturbation on cellular processes. Cell imaging provides multi-probe detection and is advantageous over other methods in quantifying spatial measurements such as protein translocation or redistribution, receptor internalization, cell morphology, cell motility, cell cycle, cell signaling, and others. The limitation of traditional microscopy and image analysis has been a log jam of sample throughput, day-to-day variability, poor standardization and of the need for specialized personnel to operate and oversee instrumentation. Automated fluorescent microscopy systems offer one solution for studying cell function in a “high content screening” (HCS) mode that allows the capability of measuring multiple cellular characteristics in a non-biased fashion. This chapter details the assay development, optimization, and validation for running a compound screening campaign and includes descriptions of the cell model, stimuli to activate NF- $\kappa$ B pathway, time course kinetics, effects of serum on assay window, validation of proinflammatory cytokines, reference control inhibitor compound optimization, and examples of nomenclatures used by many manufactures of HCS instruments or software algorithms.

## Introduction and background

There is still much that remains unknown within the biology of NF- $\kappa$ B despite the fact that in the year 2011 NF- $\kappa$ B celebrated its 25 year anniversary (1). NF- $\kappa$ B, also referred to as the Rel family of proteins, was first described in 1986 as a protein which binds to specific decameric DNA sequences (ggg ACT TTC C) in mature B-cells nuclear fraction

---

<sup>1</sup> The Hamner Institutes for Health Sciences; Email: jtrask@thehamner.org.

✉ Corresponding author.

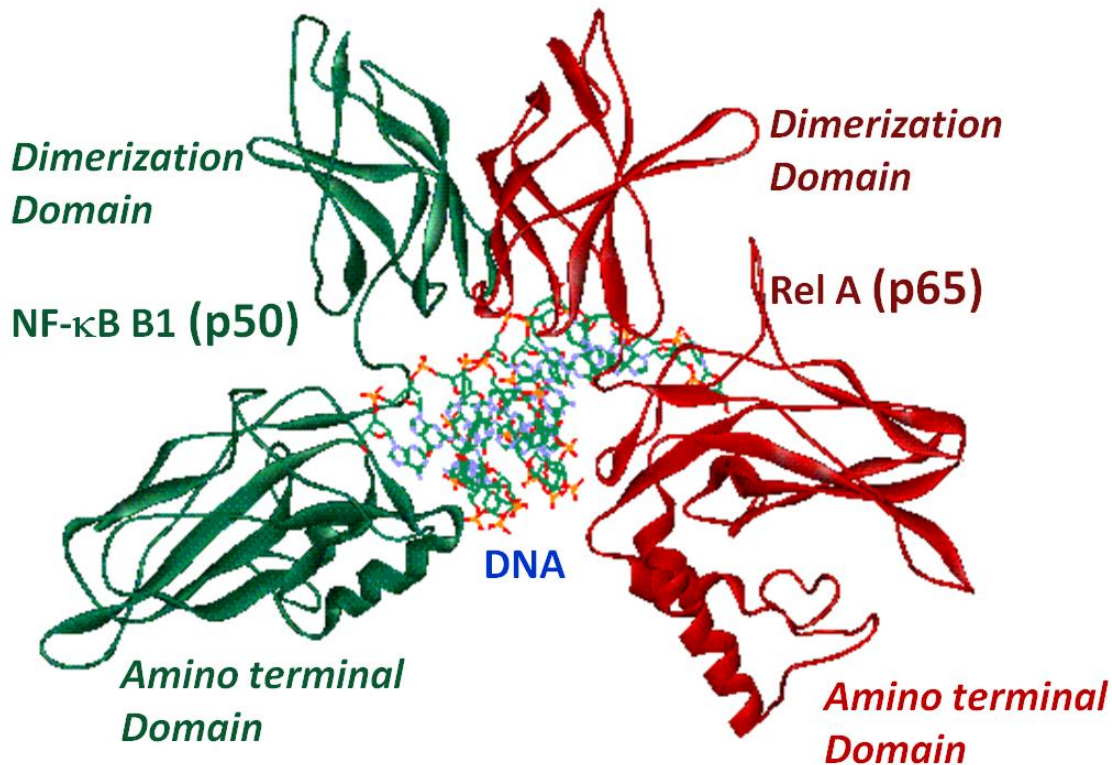


**Figure 1: Structure of the NF- $\kappa$ B/DNA complex.** There are two subunits of NF- $\kappa$ B, p50 (green) and p65 (red). The representation of the ribbon structure is viewed down the DNA helix axis with hydrophobic core. Adapted from Chen F, et al (33).

and the immunoglobulin kappa light chain enhancer of plasma cells (2). The subunits of NF- $\kappa$ B or Rel family proteins are part of a structurally related family; currently five different proteins have been identified: p50, p52, p65, Rel-B and c-Rel. The structure of NF- $\kappa$ B resembles a “butterfly” in appearance with DNA binding in a pocket between two domains (Figure 1) (3). All identifiable Rel proteins contain a conserved N-terminal region, called the Rel Homology Domain (RHD). The RHD contains the DNA-binding and dimerization domains and the nuclear localization signal of the Rel proteins. p50 (also called NF- $\kappa$ B B1) and p65 (RelA) were the first NF- $\kappa$ B proteins to be identified. In 1988, I $\kappa$ B was described as a specific inhibitor of the NF- $\kappa$ B ability to translocate and turn on transcription factors (4). Seven known I $\kappa$ B’s have been identified: I $\kappa$ B- $\alpha$ , I $\kappa$ B- $\beta$ , I $\kappa$ B- $\gamma$ , I $\kappa$ B- $\epsilon$ , Bcl-3, p100 and p105. All known I $\kappa$ B’s contain ankyrin repeats (30-33aa) that mediate non-covalent interaction between I $\kappa$ K and NF- $\kappa$ B. NF- $\kappa$ B p50 subunit crystal structure was first described by two groups (5, 6). NF- $\kappa$ B has similarities with NF-AT family of proteins with both having interaction with members of FOS and Jun family of proteins (7). Activation of NF- $\kappa$ B signaling is triggered in a series of steps through either the classical canonical pathway, the alternative non-canonical pathway, or the atypical I $\kappa$ K independent pathway (8-11) (Figure 2). NF- $\kappa$ B was initially discovered in B-cells, although B-cells do not express NF- $\kappa$ B until stimulated by LPS or cytokines (12). NF- $\kappa$ B is

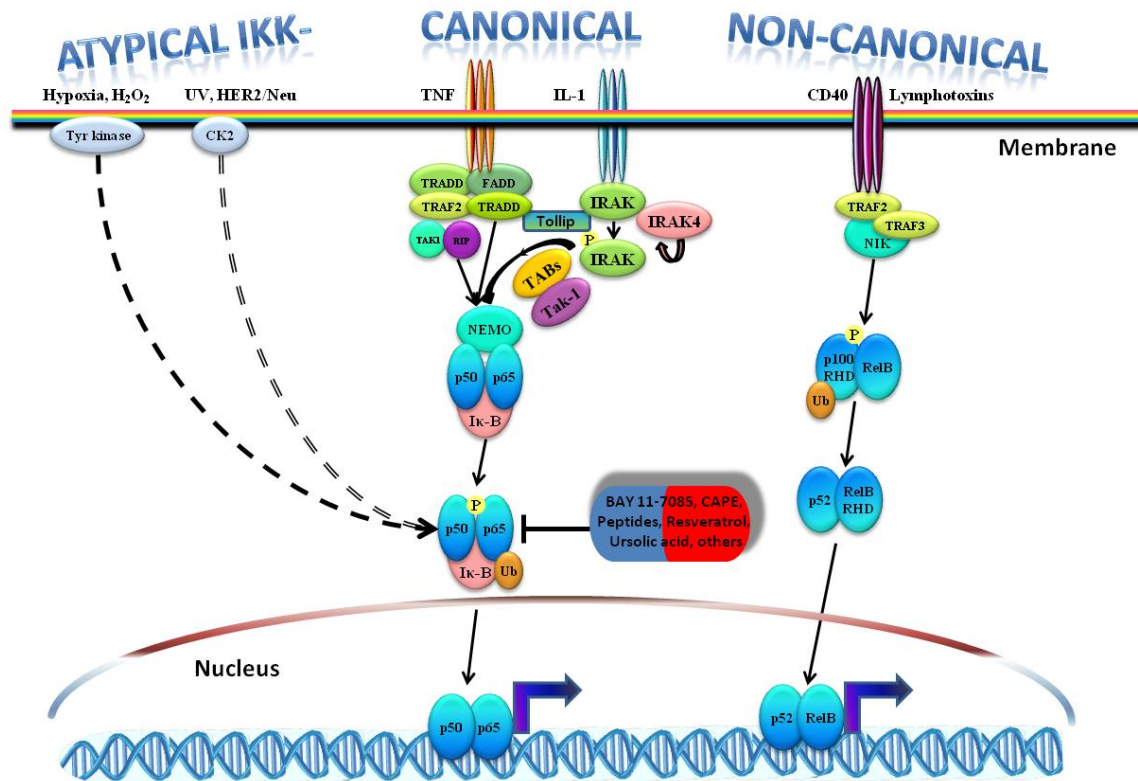


**Figure 2: Activation of NF- $\kappa$ B Signaling Pathway.** There are currently three recognizable pathways to activate NF- $\kappa$ B, the canonical, the non-canonical, and the atypical I $\kappa$ K independent pathways. NF- $\kappa$ B is naturally inhibited by I $\kappa$ B. Upstream activating signal (e.g., binding of TNF- $\alpha$ , IL-1 $\alpha$ , LPS, CD40, Lymphotoxin, UV, HER2/Neu, H<sub>2</sub>O<sub>2</sub>, or other unknown ligands to its receptor) causes phosphorylation of I $\kappa$ B by I $\kappa$ K (I $\kappa$ B kinase). This triggers the degradation of I $\kappa$ B through the ubiquitin system (Ub), where the target molecule is masked by a chain of ubiquitins for degradation by the 26S proteasome. The free unbound NF- $\kappa$ B can then translocates to the nucleus and activates transcription (22). NF- $\kappa$ B translocation is reduced by inhibitor compounds such as BAY 11-7085, other I $\kappa$ B kinase inhibitor compounds, and other means.

generally thought to be constitutively active and located in the cytoplasm in most cell types, until induced by a stimulus to migrate to the nucleus. Exceptions are corneal keratinocytes and vascular smooth muscle cells, which have been shown to have nuclear NF- $\kappa$ B in the absence of activation (13). Following activation, translocation, and transcription of NF- $\kappa$ B in the nucleus, re-accumulation of I $\kappa$ B $\alpha$  in the cytoplasm is thought to occur within 60 minutes (14, 15). Furthermore, if I $\kappa$ B $\alpha$  is re-synthesized it may enter the nucleus and then interacts with NF- $\kappa$ B complexes and inhibit DNA binding (16). Dimerization of NF- $\kappa$ B subunits results in the association of NF- $\kappa$ B proteins with DNA. The C-terminal region of the Rel homology domain is where dimerization takes place. The nuclear localization sequence (NLS) that regulates transport of activated NF- $\kappa$ B complexes into the nucleus is located near the end of the C-terminal end of the Rel homology domain. With the exception of Rel B, all Rel protein family members contain a phosphorylation site for PKA approximately 25aa to the N-terminal of the NLS (17).

Translocation of NF- $\kappa$ B is a critical step in the coupling of extracellular stimuli to the transcriptional activation of specific target genes. NF- $\kappa$ B is activated by pro-inflammatory cytokines (IL-1 $\alpha$ , IL-1 $\beta$ , TNF- $\alpha$ ); bacterial toxins (LPS, exotoxin B); viral products (HIV-1, HTLV-1, HBV, EBV, Herpes Simplex); and cell death stimuli (O<sub>2</sub>-free radicals, UV light,  $\gamma$ -radiation) (17, 18). I $\kappa$ B proteins are rapidly phosphorylated following induction by triggering cytokine receptors. I $\kappa$ K- $\alpha$  and I $\kappa$ K- $\beta$  are both responsible for modification of I $\kappa$ B complex. NF- $\kappa$ B in response to activation of these cytokines is associated with triggering cellular defense genes (17). Upon cell stimulation, the nuclear localization signal on NF- $\kappa$ B becomes exposed and the protein translocates to the nucleus, where it turns on transcription factors and induces specific gene expression.

The NF- $\kappa$ B activation has direct screening applications for drug discovery for many pharmaceutical companies and in medicine for several therapeutic indications, most notably, inflammatory tissue injury, where NF- $\kappa$ B controls the gene expression of a variety of pro-inflammatory mediators (11, 19, 20). In addition, NF- $\kappa$ B regulates a number of genes that are involved in mediating tumorigenesis, metastasis, proliferation (21, 22) and apoptosis (23-26). Vascular cell adhesion molecule-1 (Vcam-1) found on endothelial cells following exposure to cytokines or LPS is involved in regulation of NF- $\kappa$ B (2, 21), however, it requires an IRF-1 site that is located 3' to the TATA box (27). Other genes that regulate NF- $\kappa$ B and are involved in the immune response and inflammation include peptide transporter (TAP-1), proteasome subunit LMP2 (28), MHC class II variant chain genes (29), and other unknown genes. Inducible nitric oxide synthase (iNOS) is regulated by NF- $\kappa$ B activation, which results in an increase in nitric oxide production (30) and the inducible cyclooxygenase (COX-2), which generates prostanoids (31). Transcriptional regulation of p53, c-myc, and ras gene can be controlled by NF- $\kappa$ B activation (32).

## Principle of the Assay

NF- $\kappa$ B is typically present and resides in the cytoplasm of most cells as a complex with members of I $\kappa$ B inhibitor family of proteins. Both the size of this complex and I $\kappa$ B masking of the nuclear localization sequence of NF- $\kappa$ B prevents NF- $\kappa$ B entry through the nuclear membrane. Once I $\kappa$ B is phosphorylated and degrades, the nuclear localization sequences become assessable and NF- $\kappa$ B is free to translocate to the nucleus (Figure 3). Microscopy images reveal strong evidence of the redistribution of NF- $\kappa$ B from the cytoplasm to the nucleus following cytokine stimulation (Figure 4).

## Assay Development Considerations

### Image Analysis Algorithm to Detect NF- $\kappa$ B Translocation

The basic principle to detect NF- $\kappa$ B translocation is dependent on identifying the nucleus of a cell using one of many nucleic acid probe reporters, typically Hoechst, DAPI, or DRAQ5.

Once the nucleus is identified using image analysis process it is masked, and then a secondary mask overlay is created to either encompass the entire cell boundaries or a

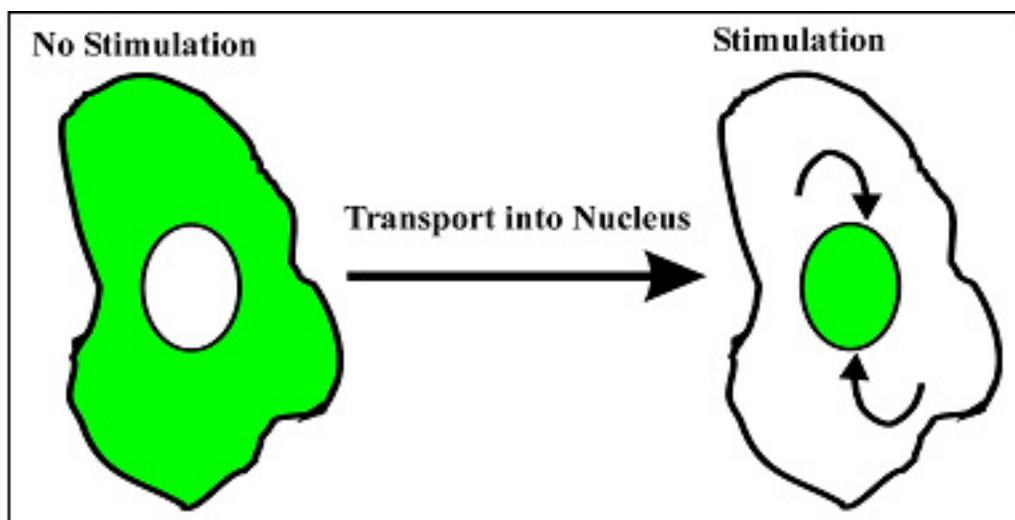


**Figure 3: Diagrammatic view of the principle of NF- $\kappa$ B activation.** NF- $\kappa$ B (green), normally resides in the cytoplasm, once activated by stimuli (IL-1 $\alpha$ , TNF- $\alpha$ , etc) it translocates to the nucleus.

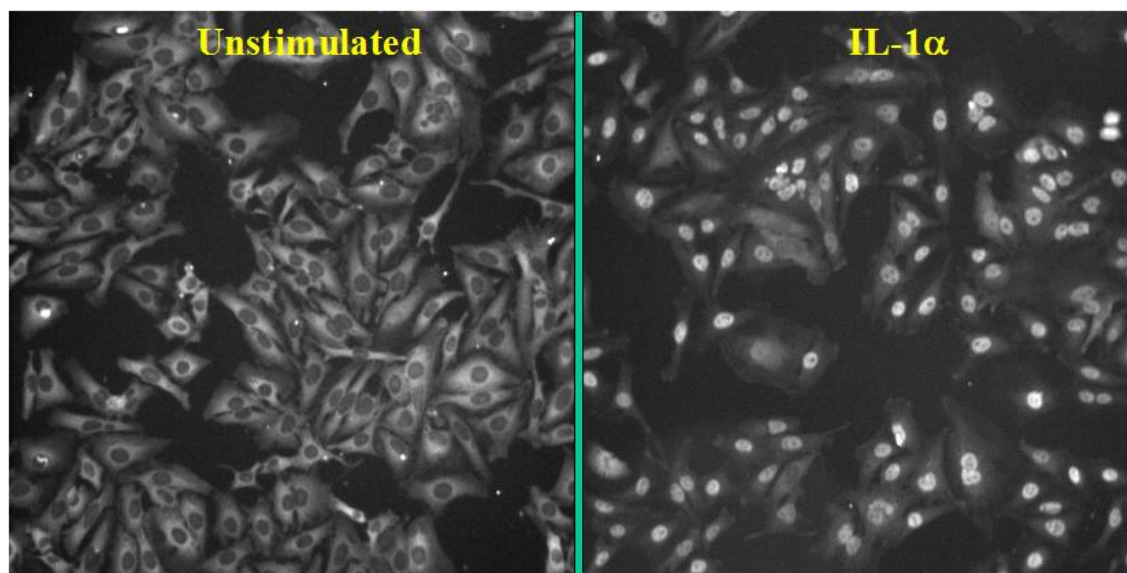


**Figure 4:** HeLa cells unstimulated or stimulated with 25 ng/ml IL-1 $\alpha$  for ~40 minutes. Cells were then fixed and labeled with NF- $\kappa$ B-p65 polyclonal antibody and secondary AlexaFluor488 with counterstain of Hoechst 33342. (Left). Unstimulated cells showing a shaded cytoplasm containing NF- $\kappa$ B-p65 with a dark nucleus “donut hole” counter stain. (Right). Following activation of NF- $\kappa$ B, the nucleus appears bright as represented in white and the cytoplasm is no longer shaded indicating the protein translocated from the cytoplasm to the nucleus.

subset area of the cytoplasmic area. Within this secondary masked area (nucleus and/or cytoplasm) labeled NF- $\kappa$ B can then be quantified. Most available algorithms report two critical features; (A) NF- $\kappa$ B intensity in the nucleus and (B) NF- $\kappa$ B intensity in the

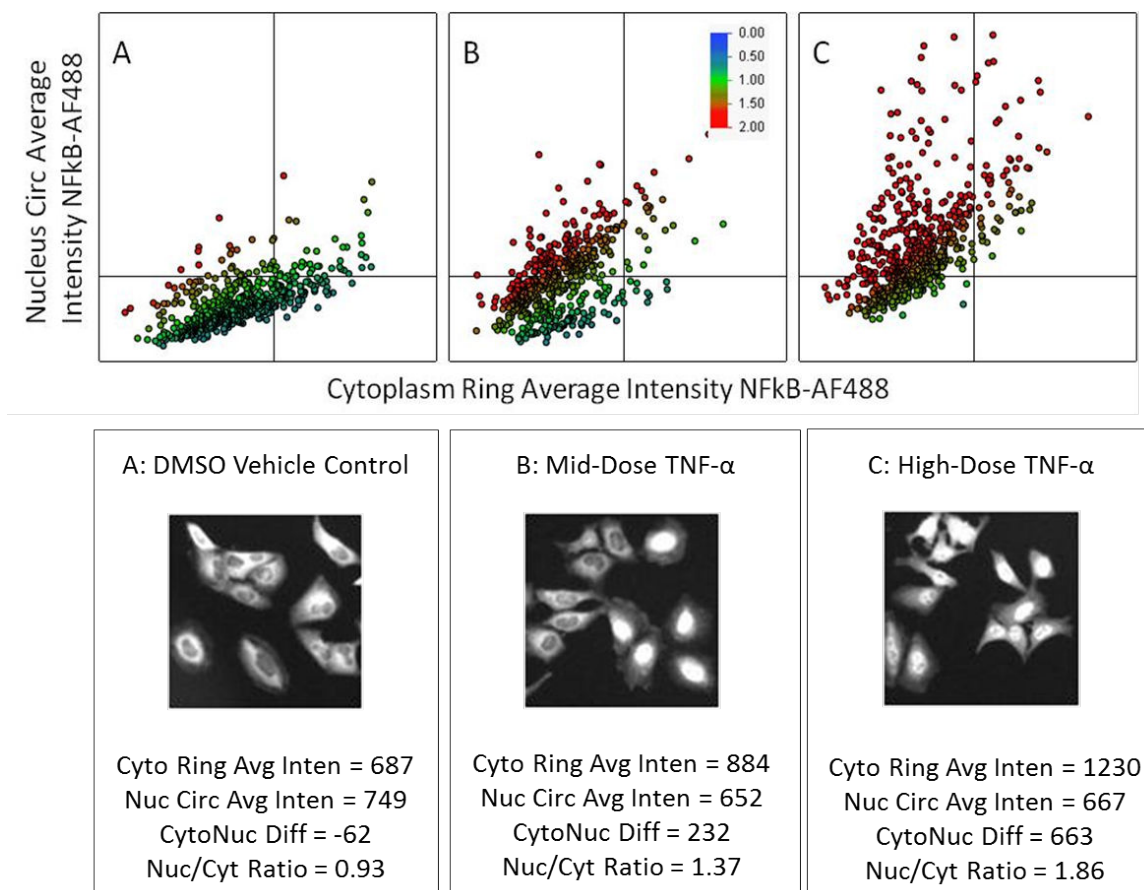


**Figure 5:** Multiparametric plot (Top) and corresponding images (Bottom) of NF- $\kappa$ B-AF488 average cytoplasm ring and nucleus circ intensities at the single cell level in HeLa cells following TNF- $\alpha$  dosing for 35 minutes. Each “dot” or “bubble” represents a single cell with a total of approximately 550 cells per graph; xy axis crossbar set at grayscale intensity value of 900. The color difference from blue to red is dependent on ratiometric calculation of NF- $\kappa$ B-AF488 Nucleus Circ Average Intensity divided by the Cytoplasm Ring Average Intensity (Nuc/Cyt Ratio); scale is display in graph B for all. (A) Vehicle control (B) Mid dose of TNF- $\alpha$  (C) High dose of TNF- $\alpha$ . Note the cell objects shift from cytoplasm ring average intensity (x-axis) to the nuclear circ average intensity (y-axis) and increase in Nuc/Cyt Ratio (red bubbles) with increasing TNF- $\alpha$  concentration.

cytoplasm. Once determined, a translocation value is calculated by measuring the average intensity of “difference” of the NF- $\kappa$ B protein between the identified cytoplasmic region and nuclear region (Cyto-Nuc Difference). Additionally, a “ratio” of the average intensity of the nuclear region to average intensity of the cytoplasmic region can be calculated to represent this translocation value; Nuc/Cyt Ratio. Both the “difference” and “ratio” features reflect a biological phenotype of NF- $\kappa$ B translocation. The data feature output from images is commonly reported as a well summary value but the calculation begins at the single cell level as shown in Figure 5. An example of well level data nomenclature describing these key features from different imaging platforms is showcased in Table 1. Representative images and algorithm overlays of HeLa cells in a dose response with IL-1 $\alpha$

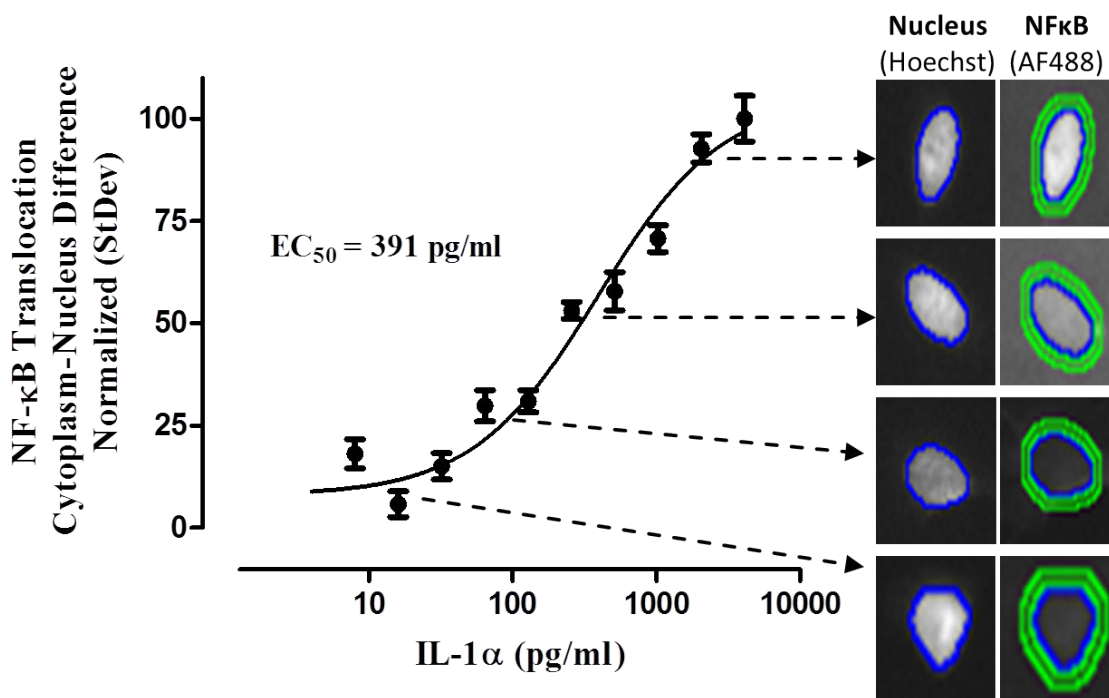


**Figure 6: Nuclear Factor  $\kappa$ B Translocation in HeLa cells following 30 minute incubation with IL-1 $\alpha$ .**

Cells labeled with Hoechst 33342 are masked with a blue ring outline to identify the nuclear area. Dilution of this mask to identify cytoplasm area is masked and highlighted with two green rings to identify fluorescence of NF- $\kappa$ B-p65 antibody labeling. Note, the first green ring (inner) is dilated away from the outer nuclear boundary; it is then copied and expanded to represent the outer ring. The area between these two rings represents the cytoplasm area measured. The algorithm can output either the difference between the average intensities in the green and blue mask area or output a ratio of between the blue and green mask areas. Although difficult to see in these images NF- $\kappa$ B is expressed in the cytoplasm at low doses of IL-1 $\alpha$ .

are shown in Figure 6. Differences at the plate level (96 wells) in cells treated with stimuli (Max) or with DMSO or inhibitor compound (Min) are used to calculate Z-factor values (34) using CytoNuc Difference and Nuc/Cyt Ratio, highlighted in Table 2.

Additional, there are other valuable HCS output features that are useful including identifiable objects (cells), variability of intensity across area within the nucleus or cytoplasm, morphological measurements including the size, shape, length, aspects of individual cells or objects within a cell. For compound screening, the use of nucleus or cytoplasm area intensity may also be helpful to identify nuisance fluorescent compounds that display the same or similar spectral properties as the probes used in the assay design and development. However, keep in mind that these compounds could also be classified as “false positive” activate compounds from the screen. In this case, careful follow ups needs to be employed by measuring basal autofluorescence levels in cells without fluorescent reporters and with compound(s) in question.

**Table 1: Algorithm nomenclature output comparison of HCS feature data to measure NF-κB autofluorescence only.**

| Feature   | BD AttoVision      | Cell Profiler | Definiens Developer | GE HealthCare      | MDC MetaXpress              | Perkin Elmer                                  | Thermo Scientific |
|---|--------------------|---------------|---------------------|--------------------|-----------------------------|---|-------------------|
| Intensity inside the cytoplasm area   | Cyt (Variable)     | Variable      | Variable            | Cell Intensity     | Outer Area                  | Intensity cytoplasm Alexa nnn mean (Variable) | RingAvgInten      |
| Intensity inside the nucleus area   | Nuc (Variable)     | Variable      | Variable            | Nuc Intensity      | Inner Area (AF488)          | Intensity nucleus Alexa nnn mean (Variable)   | CircAvgInten      |
| Difference, between intensity in cytoplasm area minus the intensity in nucleus area | Nuc-Cyt (Variable) | Variable      | Variable            | N/A                | N/A                         | Variable                                      | CytoNuc Diff      |
| Ratio, intensity in nucleus area divided by the intensity in the cytoplasm area     | Nuc/Cyt (Variable) | Variable      | Variable            | Nuc/Cell Intensity | Inner/Outer Intensity Ratio | Variable                                      | NucCyt Ratio      |

**Table 2: NF-κB-p65-AF488 HCS feature data output comparison of Nuc/Cyt Ratio and CytoNuc Difference measurements in HeLa cells. The minimum (min) signal is the baseline constitutive expression of NF-κB and the maximum (max) is NF-κB response following ~35 minute incubation with either 25ng/ml IL-1α or 25ng/ml TNF-α; data includes the percent coefficient of variation (% CV) from 96-wells. The Z factor is calculated as described in literature (34)**

| IL-1α              | Ratio: Nuc/Cyt | Difference: Cyto-Nuc Diff | TNF-α              | Ratio: Nuc/Cyt | Difference: Cyto-Nuc Diff |
|--------------------|----------------|---------------------------|--------------------|----------------|---------------------------|
| Signal (Min / Max) | 1.0<br>1.84    | -75.2<br>523              | Signal (Min / Max) | 0.957<br>1.86  | -38.3<br>495              |
| % CV (Min / Max)   | 4%<br>8.1%     | 3.5%<br>4.5%              | % CV (Min / Max)   | 2.4%<br>6.7%   | 3.7%<br>5.4%              |
| Z factor           | 0.64           | 0.76                      | Z factor           | 0.73           | 0.73                      |



## Assay Detection and Limitation

The assay described below will quantify the redistribution of NF- $\kappa$ B from the cytoplasm to the nucleus upon activation using antibodies to NF- $\kappa$ B p65 subunit in intact cells following fixation. Stimulating cells with proinflammatory cytokines such as IL-1 $\alpha$  and TNF- $\alpha$  activates the canonical NF- $\kappa$ B pathway and therefore the noncanonical pathway (CD40, LT), or the atypical I $\kappa$ B independent pathway (UV, Hypoxia) will likely be non-responsive in this assay format. In addition, this assay can indirectly measure I $\kappa$ B degradation since phosphorylation of I $\kappa$ B is required before degradation of I $\kappa$ B $\alpha$  and subsequent translocation of NF- $\kappa$ B subunit to the nucleus. This assay does not directly measure phosphorylation of NF- $\kappa$ B protein.

This assay can be multiplexed with other biofluorescent probes. For example, other kinase related bioprobes to measure MAPK kinase pathways such as phospho-JNK-1/2 or viability indicators may provide important information about the biology or selectivity of the compound. The critical consideration for developing this assay is the dose and time using more than one stimulus to triggering multiple signaling pathways.

## Assay Development

### Cell Model

HeLa cells are endothelial cells from the American Tissue Culture Corporation (ATCC), catalogue number CCL-2, original isolated from the cervix of a 31yo black female with adenocarcinoma, were selected as the cell line as choice for this assay for several reasons. (A) HeLa cells are well documented in the literature to illustrate NF- $\kappa$ B redistribution; (B) HeLa cells are relatively flat once seeded in plates and therefore image well using widefield 2-D bright-field and fluorescent microscopy; (C) there are commercial available validated kits and antibodies to detect redistribution of NF- $\kappa$ B.

**Note:** Other cells such as Swiss 3T3, BHK, HepG2-C3A, Rat hepatocytes, LLCPK, HMVEC, CHO-K1, HT1080, HCT-116, U 2-OS, and others are also known to express NF- $\kappa$ B but before adopting one of these cell lines or other unlisted cell models, it is recommended to validate assay performance with a known cell line such as HeLa.

### Cell culturing and harvesting

Maintenance of the HeLa cell line or cell of choice should be carried out following recommendations from the ATCC or the source of the cell line. Typically splitting cells 2-3 times per week is required for optimal growth and performance in the assay. Do not allow cells to become over confluent in tissue culture flasks. If this occurs, it will be necessary to thaw a new vial of cells before proceeding with assay development, validation, or screening. Grow cells in complete media, and then adjust serum concentration prior to cell seeding as necessary (see [Effects of Serum](#) for additional information). Upon harvest of cells with trypsin or other cell detachment methodology it is recommended to filter the cells through a cell strainer (40-70 microns) to remove large

clumps before cell counting and seeding. If aggregates are not removed this will negatively impact cell object identification and segmentation with image analysis algorithms.

## Cell Seeding Number Determination

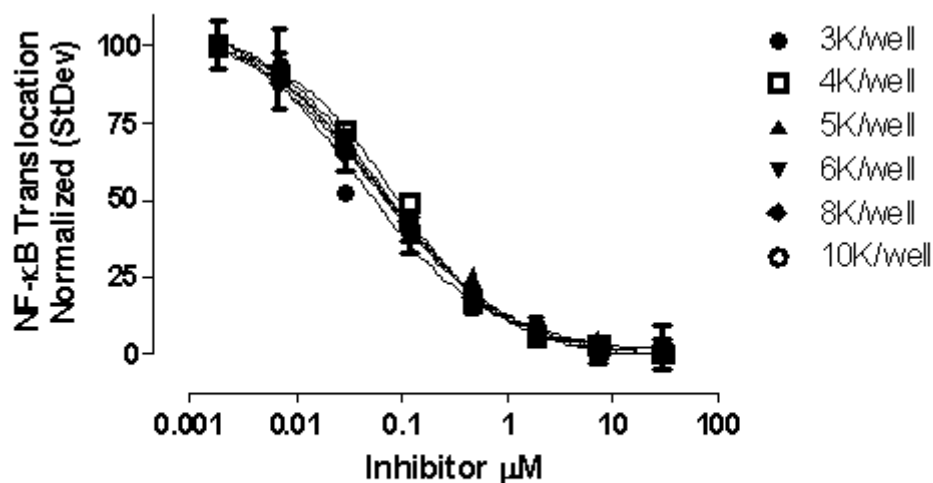
Determine the optimal cell seeding density as described in the assay development HCS chapter by seeding cells at approximately 5,000 cells/well for a 96-well plate as the median starting point; then dilute or increase the cell density by approximately 40-50%. (*Note: In 384-well plates, approximately 2,500 cells/well is recommended*). Incubate cells overnight, and then label as described in subsequent sections with reporter probes. There is some variability but no significant difference in cell number (3,000 to 10,000 cells/well) in 96-well plate format from the NF- $\kappa$ B inhibitor compound IC<sub>50</sub> curves (Figure 7). However, since identification and segmentation of individual cells in the well is optimal for accurate image analysis measurement of NF- $\kappa$ B, 5,000 cells/well was chosen. An NF- $\kappa$ B reference compound inhibitor, IK202, was used to determine cell number. The number of cells per well was optimized based on reviewing images to observe cell-to-cell contact. Higher concentrations of cells per well resulted in rejection of more cells due to piling of cells, massive cell contact clumps, and poor image analysis segmentation. However, the number of fields required to collect 500 cells, the assay defined threshold, was decreased (Figure 8). The optimal cell seeding density for HeLa cells is 5,000 cells/well for 96-well plate. *{data not shown}*.

## Cell Passage Limitations

It is critical to gauge the number of cell passages in the assay before a noticeable decline is observed. Cells with many passages may not survive, become contaminated, or fail to respond in the assay over time. If possible, continue passaging cells at the onset of development with a fresh thaw of cells and maintain a weekly stock over time; then measure NF- $\kappa$ B response in comparison with lower passage cells. HeLa cells with different cell splitting passage numbers up to 40 from ATCC and the same lot were tested to compare sensitivity to TNF- $\alpha$  cytokine to activate translocation of NF- $\kappa$ B and to determine if the response was altered. Even though the R<sup>2</sup> of the curve fitting was similar; there was a significant shift in the NF- $\kappa$ B translocation EC<sub>50</sub> response to cytokines in cells with high passage number. A significant loss in responsiveness of NF- $\kappa$ B translocation was observed with an increase in calculated EC<sub>50</sub> values directly correlated with increasing passage number (Figure 9). Based on these findings it is recommended to use cells with as low passage number as possible and as a general rule never exceed passage of 20.

## Activators of the NF- $\kappa$ B Signaling Pathway

Activating NF- $\kappa$ B pathway using cellular cytokines as described in the introduction is critical to establish an assay window. Although several stimuli have been identified in activating NF- $\kappa$ B pathway, three cytokines, IL-1 $\alpha$ , IL-1 $\beta$ , and TNF- $\alpha$  gave the most robust and best EC<sub>50</sub> values of all stimuli tested (Figure 10). IL-1 $\alpha$ , IL-1 $\beta$  family members and



|      | 3K/well | 4K/well | 5K/well | 6K/well | 8K/well | 10K/well |
|------|---------|---------|---------|---------|---------|----------|
| EC50 | 0.03777 | 0.09116 | 0.06331 | 0.06138 | 0.06414 | 0.05735  |

**Figure 7:** Cell Number Determination. HeLa cells seeded overnight, treated with reference compound inhibitor for 15 minutes and subsequent 25ng/ml TNF- $\alpha$  for ~35 minutes, and then fixed and stained for NF- $\kappa$ B-p65-AF488. Plates were analyzed on HCS imager to determine NF- $\kappa$ B translocation using CytoNuc Difference; data was normalized to control and plotted in GrapPad Prism using non-linear regression 3-parameter fit.

TNF- $\alpha$  cytokines activate NF- $\kappa$ B through different up-stream mechanisms. Platelet-derived growth factor (PDGF) also activates the translocation events of the NF- $\kappa$ B pathway to a lesser extent and is described to work through Ras and PI3 kinase signaling. (33). Lymphotoxin (LT)  $\alpha$ 1/ $\beta$ 2, LT  $\alpha$ 2/ $\beta$ 1, and IFN- $\gamma$  showed little or no activation of NF- $\kappa$ B (the latter stimuli data is not shown). Additionally, anisomycin and phorbol-12-myristate-13-acetate (PMA) were also tested but did not show NF- $\kappa$ B-p65 activation as robustly as IL-1 $\alpha$ , IL-1 $\beta$ , or TNF- $\alpha$  stimulus. This knowledge is important if considering multiplexing NF- $\kappa$ B with other signaling pathways. In this assay design, development, and validation, HeLa cells will be stimulated with both IL-1 $\alpha$  and TNF- $\alpha$  following compound treatment, however, for compound profiling and screening, either stimuli alone will work and choice of cytokine is depended on the upstream or downstream target and biology.

## Plate Type

The NF- $\kappa$ B assay is considered a very robust HCS assay using HeLa cells and likely can be adapted to many different SLAS standard plate types including 384-well or even 1536-well formats, however it is recommended to first perform the proof of concept in a validated format such as the 96-well, as discussed within, then move to another well plate format. In this assay sterile 96-well tissue cultured treated Perkin Elmer (Packard) View plates were chosen with no extracellular matrix proteins or PDL substrate coating.

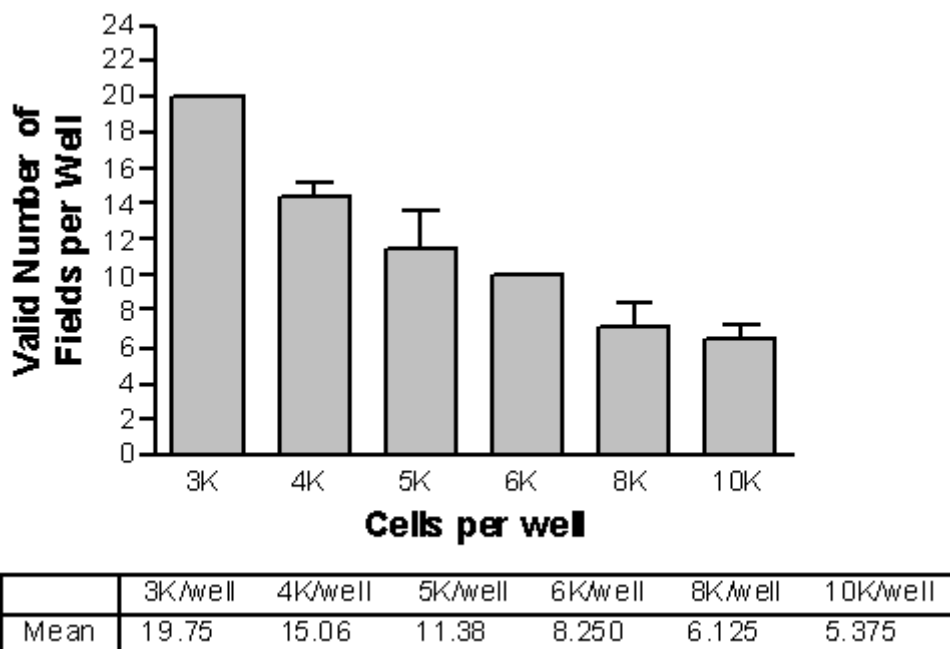
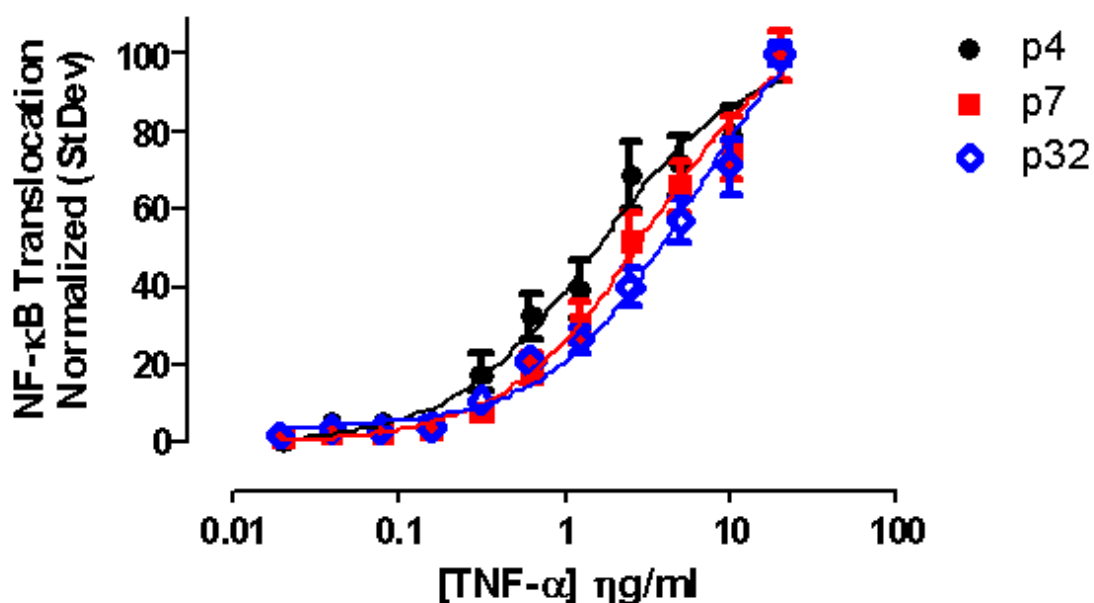


**Figure 8:** Field numbers required to collect 500 objects (cells) using a 10X/0.3NA objective, no magnifier and a 1392x1024 camera pixel array sensor.

## Reagent & Probes

There are a few validated assay kits and antibodies in market that can be used for this assay, or alternatively development of an in-house or “homebrew” assay protocol kit can be developed. In the next section, details of developing and comparing with a commercially available kit are described. The primary advantage of using a commercial kit is it is “ready to use” with “cookbook” instructions included. If just measuring a few plates, then this is a preferable option. The benefit of developing an in-house “homebrew” kit is to know what antibodies, buffers, and reagents are being used in the assay as this may not be disclosed by commercial sources of kits. In addition, the cost for running many plates is reduced once an in-house kit is developed. This chapter should reduce development time and costs. An example comparing a commercial kit with an in-house kit using alternative antibody sources and the process to cross validate their relative performance is described in next section.

**Note:** Before beginning the assay development process determine if a fixed endpoint assay is appropriate for the biological question. Alternatives to the classic antibody recognition and binding approach is the use of a fusion protein of NF- $\kappa$ B with a fluorescent protein reporter such as GFP, mCherry, or HaloTag® (Promega, Madison, WI) are other options to consider for measuring protein function.



|      | p4    | p7    | p32   |
|------|-------|-------|-------|
| EC50 | 1.556 | 3.228 | 5.881 |

**Figure 9:** Cell Passage Number Comparison. Different cell splitting passages of HeLa cells seeded at 5,000 cells/well overnight and treated with dose response of TNF- $\alpha$  for ~35 minutes, then fixed and stained to measure NF- $\kappa$ B translocation. Plates were analyzed on HCS imager to determine NF- $\kappa$ B translocation using CytoNuc Difference calculation; data was normalized to control and plotted in GraphPad Prism using non-linear regression 3-parameter fit.

## Commercial Kit Validation & Development of In-house “Home-Brew” Kit

The initial assay development was performed using commercial available validated kits for NF- $\kappa$ B. Additional, several different commercial available antibodies were screened for signal-to-noise ratio performance that targeted the p65 subunit of NF- $\kappa$ B (Appendix-1). Although other antibodies worked well in the evaluation, based on performance and comparable EC<sub>50</sub> calculated values, the rabbit polyclonal IgG NF- $\kappa$ B-p65 antibody from Santa Cruz (SC-372) was used for assay development and validation procedures (see Figure 11).

Since the commercial kit contains other unknown and perhaps proprietary reagents, i.e., antibody, buffers, and reagents including PBS; PBS containing 0.5% Triton X-100; PBS containing 0.01% Tween-20 for testing and comparison with “in-house” buffers and commercial kit; it is always important to verify the signal-to-noise ratio window and insure that assay variability is not sacrificed.

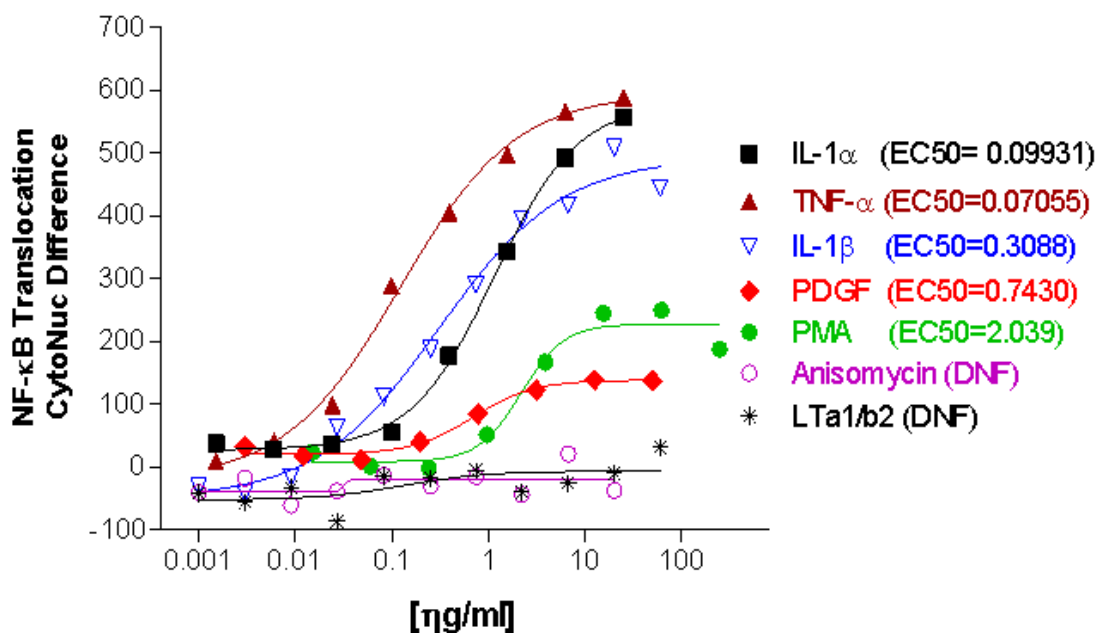


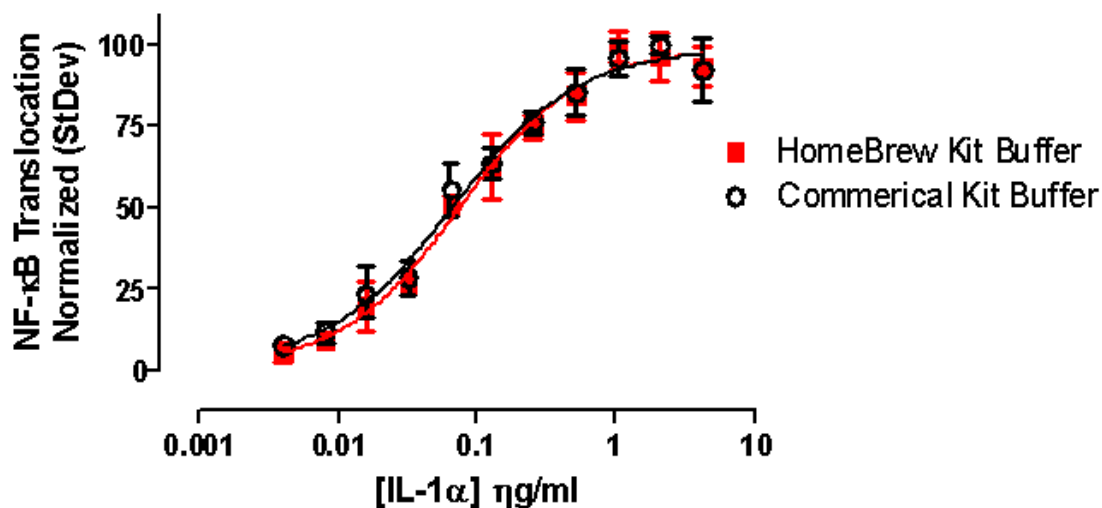
**Figure 10: Activation of NF- $\kappa$ B-p65 with Different Stimuli.** HeLa cells seeded at 5,000 cells/well overnight and treated with stimuli for 30 minutes, then fixed and labeled with NF- $\kappa$ B-p65-AF488 and Hoechst33342 to measure NF- $\kappa$ B translocation. Plates were analyzed on HCS imager to determine NF- $\kappa$ B translocation using CytoNuc Difference calculation; data expressed as raw unit values (y-axis) from algorithm using non-linear regression 3-parameter fit was done in GraphPad Prism; standard deviation error bars (n=3) was removed for visualization.

Comparisons of different lots of NF- $\kappa$ B antibody from Santa Cruz were done at three different concentrations of primary antibody following stimulation with IL-1 $\alpha$ . There were no significant differences observed (Figure 12). Lot-to-lot variability was evaluated several times with new antibody lot shipments and no significant differences in the calculated EC<sub>50</sub> values were observed.

### Fixation comparison of two different forms of formaldehyde solution

Formaldehyde, 37% stock solution (Sigma) and Ultra-pure Formaldehyde, methanol-free 10% stock solution (Polysciences) were compared. HeLa cells were treated with IL-1 $\alpha$  for about 30 minutes, followed by 1:10 dilution of fixation buffer in PBS for 10 minutes. An approximately 3-fold shift in the EC<sub>50</sub> values was observed (Figure 13). For this assay, 3.7% formaldehyde from Sigma containing methanol was used. It is possible higher concentrations of Ultrapure formaldehyde may be used but this needs confirmation by testing.

**Note:** At the time of testing 16-20% paraformaldehyde solution was not readily available from commercial sources and should be considered as alternative source.



|      | HomeBrew Kit Buffer | Commercial Kit Buffer |
|------|---------------------|-----------------------|
| EC50 | 0.07322             | 0.06533               |

**Figure 11: Comparison of Commercial and HomeBrew Buffers.** HeLa cells seeded at 5,000 cells/well overnight and treated with dose response of IL-1 $\alpha$  for ~35 minutes, then fixed and stained to measure NF- $\kappa$ B translocation using SC-372 antibody. Plates were analyzed on HCS imager to determine NF- $\kappa$ B translocation using CytoNuc Difference calculation; data was normalized to control and plotted in GraphPad Prism using non-linear regression 3-parameter fit.

Please refer to institutional safety guidelines before working with formaldehyde; suggestions are in Safety Consideration Guidelines Precautions. Formaldehyde is specifically regulated by OSHA, so be sure you are in compliance with the OSHA standard ([http://www.osha.gov/pls/oshaweb/owadisp.show\\_document?p\\_id=10075&p\\_table=STANDARDS](http://www.osha.gov/pls/oshaweb/owadisp.show_document?p_id=10075&p_table=STANDARDS)).

## Stability and Lot Variability of Cytokines

Variability of cytokines lots were measured to determine variability of the assay if new reagents were introduced to the assay during the screening campaign or used in subsequent screens. Please note, it is highly recommended to order all reagents before the start of the experiment and/or screen. From this experiment and several other experiments, both IL-1 $\alpha$  (data not shown) and TNF- $\alpha$  EC<sub>50</sub> responses and calculated EC<sub>50</sub> values indicated very high reproducibility (Figure 14). In addition, the activity and stability of cytokine performance was measured after one or more freeze-thaw cycles (Figure 15).

## Stability of NF- $\kappa$ B detection in cells following fixation

The NF- $\kappa$ B protein in HeLa cells is stable for several days at 4°C prior to staining with NF- $\kappa$ B antibody following fixation with 3.7% formaldehyde for 10 minutes, washed and stored

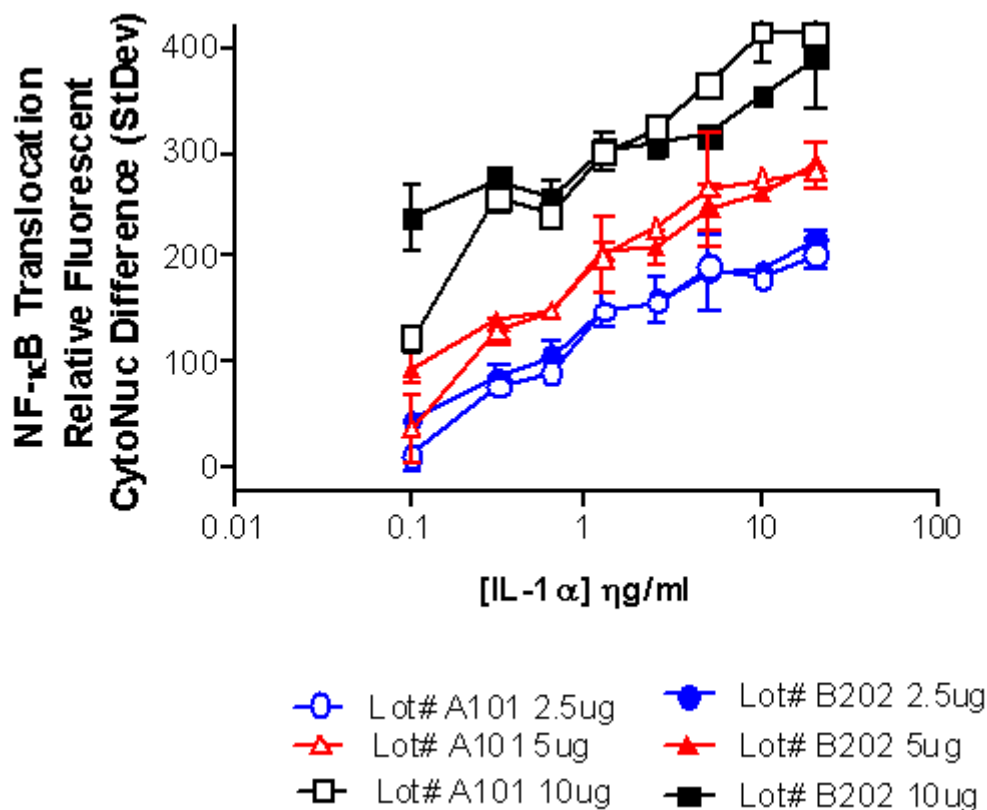


**Figure 12: Lot-to-Lot Variability Comparison of Santa Cruz SC-372 NF-κB-p65 Antibody.** HeLa cells seeded at 5,000 cells/well overnight and treated with dose response of IL-1α for ~35 minutes, then fixed and stained to measure NF-κB translocation using two different lots of SC-372 antibody and at different concentration dilutions. Plates were analyzed on HCS imager to determine NF-κB translocation using CytoNuc Difference calculation; data was not normalized and plotted with “raw” numbers in GraphPad Prism.

in PBS. This provides flexibility in screening operations if a “Stop Point” is required in the workflow. It is recommended that cells stained with NF-κB antibody be imaged as soon as possible, and not to exceed 14-days (Figure 16). For logistics in screening operations including robotics, liquid handling, and cell plate handling to reduce fluctuations in pH and temperature, 35 minutes was chosen.

### Time Course of Cytokine Stimulation

Determine the optimal time window for NF-κB translocation by performing a time dependent stimulation with known stimuli. HeLa cells seeded at 5,000 cells/well in a 96-well plate overnight were then treated with 50 ng/ml of IL-1α to establish a time course for activation and redistribution of NF-κB. Following incubation with cytokine, cells were fixed at different times and then labeled with NF-κB antibody using an indirect staining method with secondary fluorescent antibody. Images of cells expressing fluorescent



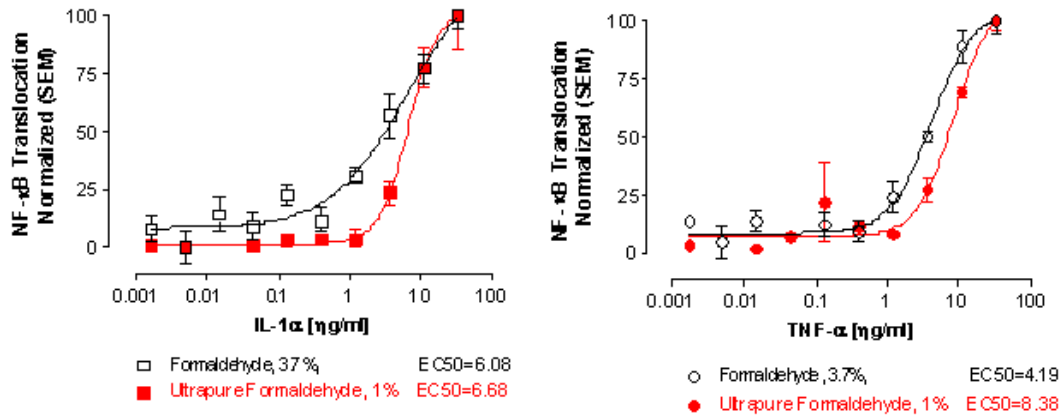


**Figure 13: Comparison of Formaldehyde Fixatives.** HeLa cells seeded at 5,000 cells/well overnight and treated with either dose response of IL-1α (left) or TNF-α (right) for ~35 minutes, then fixed with either 3.7% formaldehyde or 1% Ultrapure Formaldehyde and stained to measure NF-κB translocation. Plates were analyzed on HCS imager to determine NF-κB translocation using CytoNuc Difference calculation; data was normalized to control and plotted in GraphPad Prism using non-linear regression 3-parameter fit.

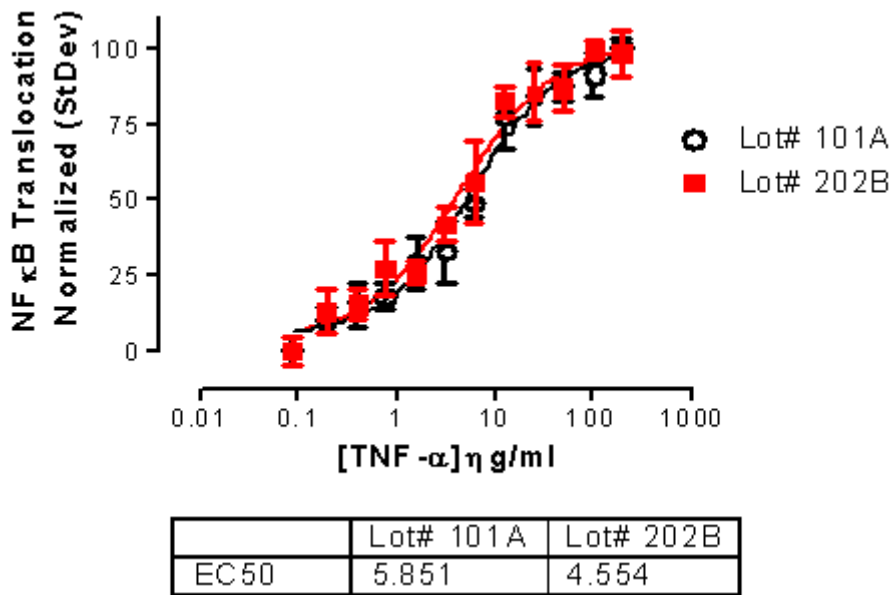


**Figure 14: Lot variability of tumor necrosis factor alpha.** HeLa cells seeded at 5,000 cells/well overnight and treated with dose response of TNF-α for ~35 minutes, then fixed and stained to measure NF-κB translocation. Plates were analyzed on HCS imager to determine NF-κB translocation using CytoNuc Difference calculation; data was normalized to control and plotted in GraphPad Prism using non-linear regression 3-parameter fit.

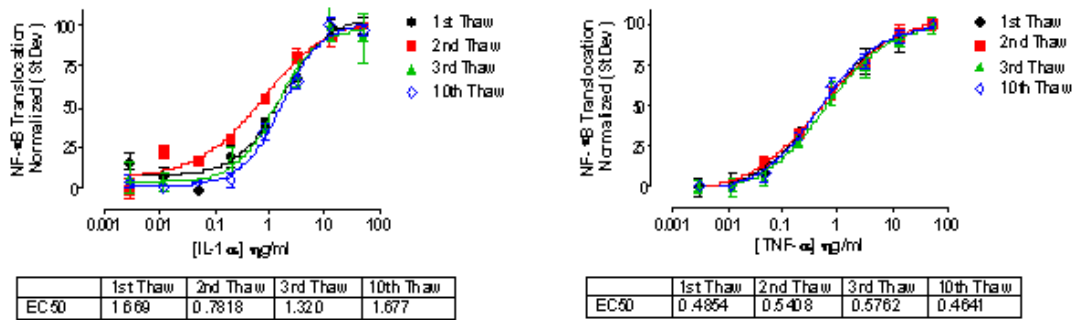


**Figure 15: Stability of cytokines following multiple freeze-thaw cycles.** Following the reconstitution of the cytokine per manufacture suggestion, cytokine reagents were store at  $-80^{\circ}\text{C}$ , and then allowed to thaw at room temperature before use. Samples were then re-frozen at  $-80^{\circ}\text{C}$  multiple times. Translocation of NF- $\kappa$ B was performed on HeLa cells following treatment with IL-1 $\alpha$  (left) or TNF- $\alpha$  (right) as previously described and data was normalized to control and plotted in GraphPad Prism using non-linear regression 3-parameter fit.

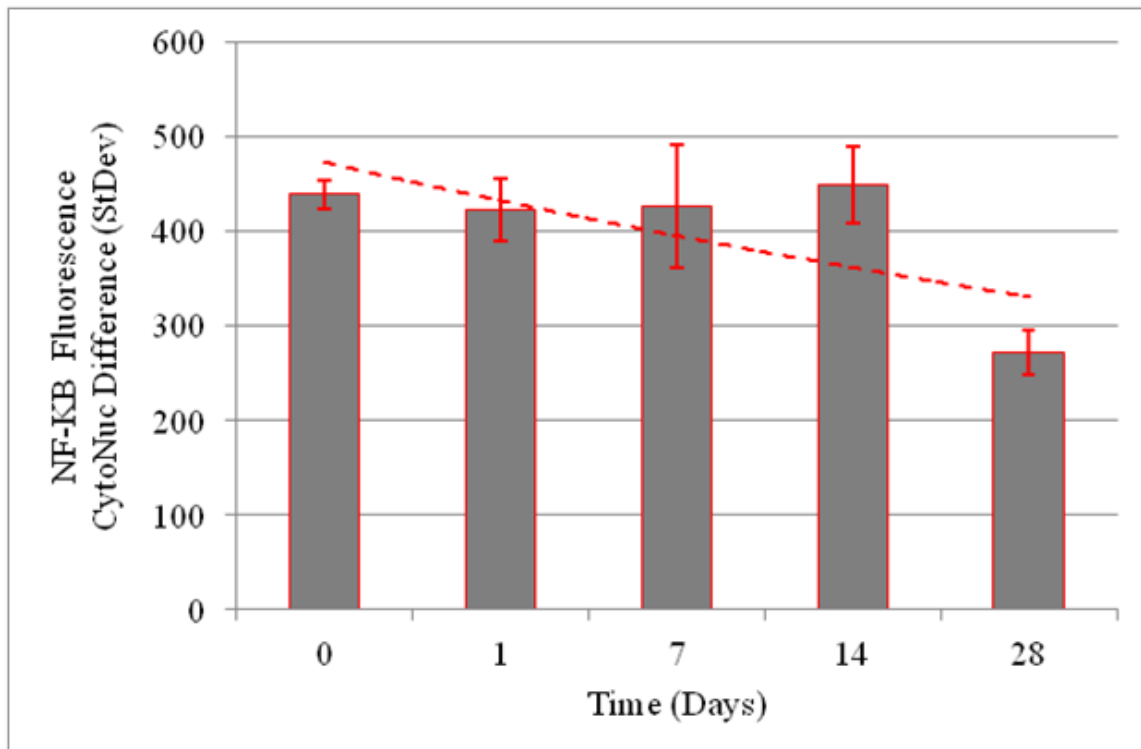


**Figure 16: Stability of NF- $\kappa$ B-p65-AF488 complex post staining and fixation.** Using several plates, HeLa cells seeded at 5,000 cells/well overnight and treated with 25 $\eta$ g/ml of TNF- $\alpha$  for  $\sim$ 35 minutes, then fixed and stained to measure NF- $\kappa$ B translocation at the maximum signal. At different time points (days), plates were analyzed on HCS imager to determine NF- $\kappa$ B translocation fluorescent intensity measurements using CytoNuc Difference calculation; raw data was used and plotted for comparison.

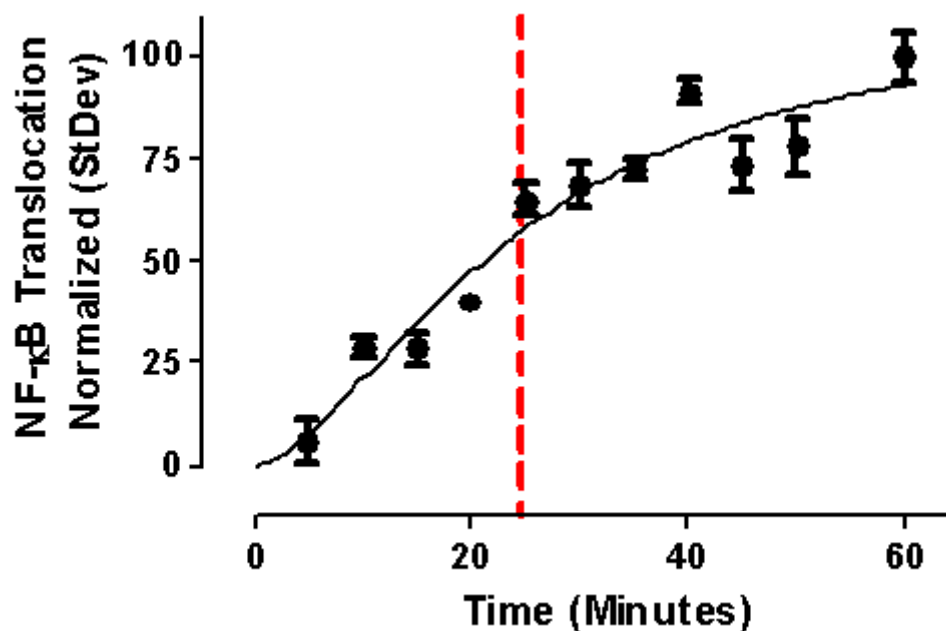


**Figure 17: NF- $\kappa$ B Translocation time course kinetics.** HeLa cells seeded at 5,000 cells/well overnight and treated with 25ng/ml of IL-1 $\alpha$  over time, at 5 or 10 time minute intervals, cells were fixed and then stained to measure NF- $\kappa$ B translocation. Plates were analyzed on HCS imager to determine NF- $\kappa$ B translocation using CytoNuc Difference calculation; data was normalized and plotted in GraphPad Prism using non-linear regression one-site binding to calculate the  $\frac{1}{2}$  time response, 24 minutes.

antibody are captured using HCS imager and analyzed for NF- $\kappa$ B expression. Time  $\frac{1}{2}$  = 24 minutes (Figure 17). Based on these results 30-60 minutes proved to be an excellent window to capture NF- $\kappa$ B translocation.

## Effects of Serum

HeLa cells treated with cytokines IL-1 $\alpha$  and TNF- $\alpha$  were tested with different concentrations of fetal bovine serum (FBS) to determine if serum affects the assay performance and window. While the assay window did not diminish with concentration of serum, the sensitivity of cytokine stimulation as calculated by EC<sub>50</sub> values of NF- $\kappa$ B translocation was significantly different; IL-1 $\alpha$  sensitivity with 0.5% FBS increased ~3-fold as compared to 10%FBS, while TNF- $\alpha$  sensitivity increased by ~ 2.5-fold using 0.5%FBS as compared to 10%FBS (see Figure 18). Based on this data and subsequent data 0.5% FBS concentration was chosen for validation experiments.

## DMSO Tolerance

HeLa cells seeded at 5,000 cells/well in 100 $\mu$ L media containing 0.5%FBS were allowed to attach overnight. Cells were then incubated with DMSO concentrations up to 10% for 30 minutes (2X the dosing time for compound treatment) followed by 30-minute incubation

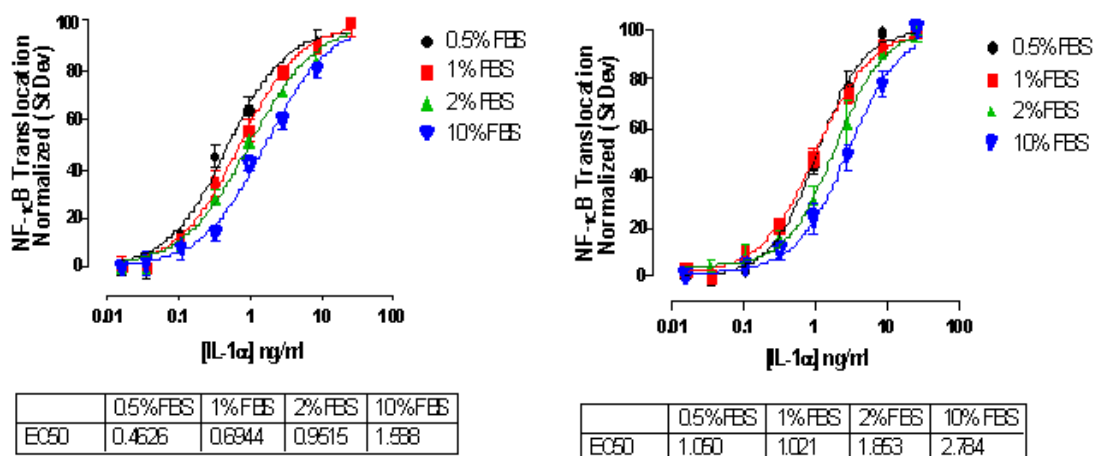


**Figure 18: NF- $\kappa$ B translocation effects from serum concentrations.** HeLa cells seeded at 5,000 cells/well overnight in 10% Fetal Bovine Serum (FBS), were then removed from complete serum by washing with serum-free media and replaced with 0.5%, 1%, 2%, or 10% FBS and treated with dose response of either IL-1 $\alpha$  (left) or TNF- $\alpha$  (right) for ~35 minutes. Cells were then fixed and stained to measure NF- $\kappa$ B translocation. Plates were analyzed on HCS imager to determine NF- $\kappa$ B translocation using CytoNuc Difference calculation; data was normalized and plotted in GraphPad Prism using non-linear regression 3-parameter fit.

of cytokine. The increase and subsequent decrease in signal at DMSO concentrations greater than 1% on the graph is a result in change in cell morphology and cytotoxicity respectively (Figure 19). At 5% DMSO, the cell's cytoplasm area shrunk as a result of increase in nuclear size, thus the image analysis algorithm measurement is reflective in the data showing an increase in CytoNuc translocation (see figure 19). At 10% DMSO, the cells are fragmented, dissociated, or detached from the plate and therefore not possible to quantify cytoplasm or nuclear fluorescent expression.

## Reference Compounds

### Dosing Time of compounds on Cells

It is highly recommended to pre-determine the duration of exposure dose of an inhibitor compound prior to stimulation with secondary stimuli such as cytokines or growth factors. Please keep in mind and consider the following:

- Is it possible to co-add the inhibitor compound and stimuli simultaneously?
- How does this affect the S:N window or assay variability?
- Is a pre-incubation required to maximize window and assay variability?
- Is there an advantage for the workflow in screening operations?

For this assay a 15 minute pre-incubation of inhibitor compound was chosen to make certain the compound exposure to the cells was saturated prior to stimulating with cytokines. Comparative data suggests simultaneous co-addition of both the inhibitor

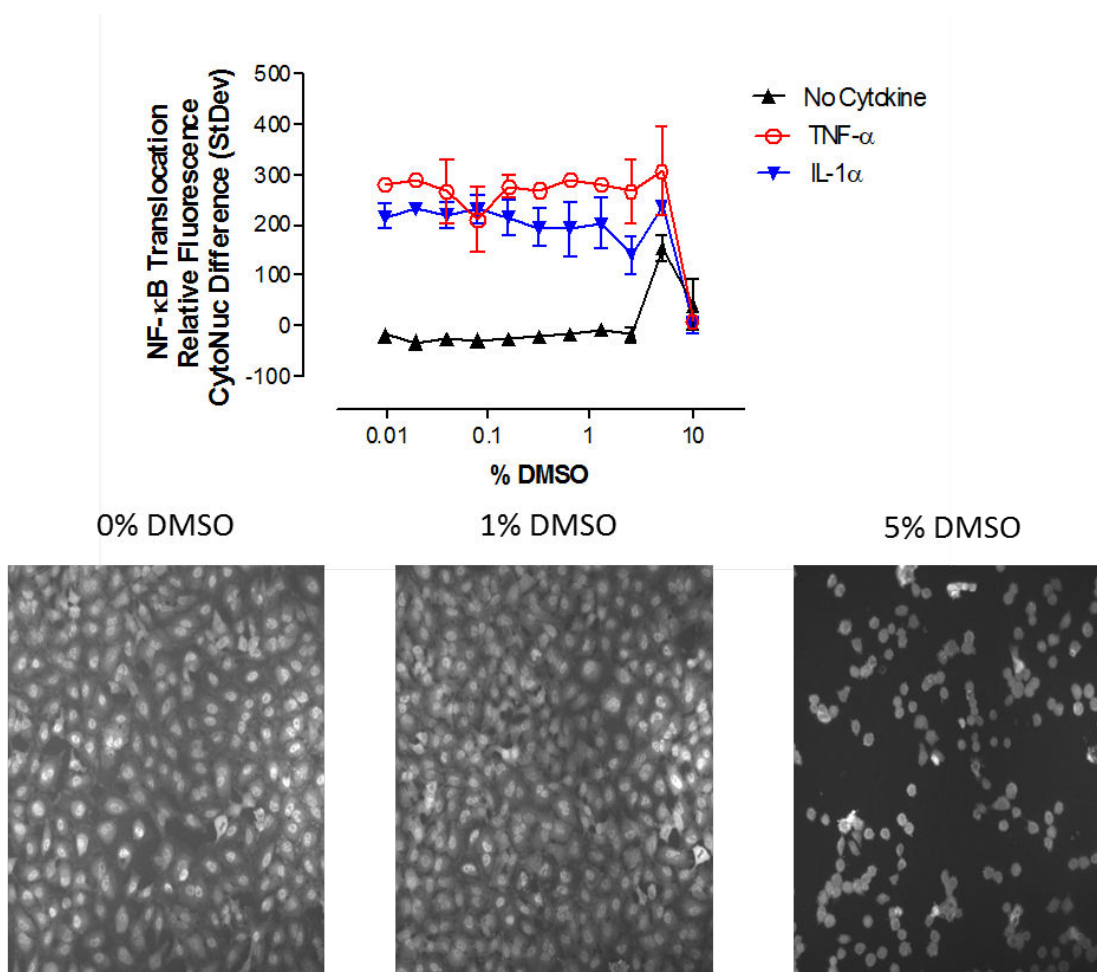


**Figure 19:** DMSO tolerance. HeLa cells seeded at 5,000 cells/well overnight and treated DMSO for 15 minutes followed by stimulation with either media only containing 0.5% FBS, 25ng/ml IL-1 $\alpha$ , or 25ng/ml TNF- $\alpha$  for ~35 minutes. Cells were then fixed and stained to measure NF- $\kappa$ B translocation. Plates were analyzed on HCS imager to determine NF- $\kappa$ B translocation using CytoNuc Difference calculation; raw data was used and plotted for comparison (top) and images captured using 10X/0.3NA objective (bottom) show differences in concentration.

compound and stimuli does not affect the performance of the assay window (data not shown). But keep in mind these are reference compounds and unknown chemicals in a compound library may not readily penetrate cells before NF- $\kappa$ B is activated.

### Inhibitors of NF- $\kappa$ B Pathway

There are several known inhibitors of NF- $\kappa$ B pathway that have been published such as Bayer's compound, BAY 11-7085, which was initially selected as the control inhibitor reference compound for assay development and validation because it was commercially available and showed IC<sub>50</sub> activity of about 10  $\mu$ M (Figure 20). Additionally there were two compounds identified in-house named IK101 and IK202 with improved potency. These compounds were chosen as reference compounds in the assay validation, although

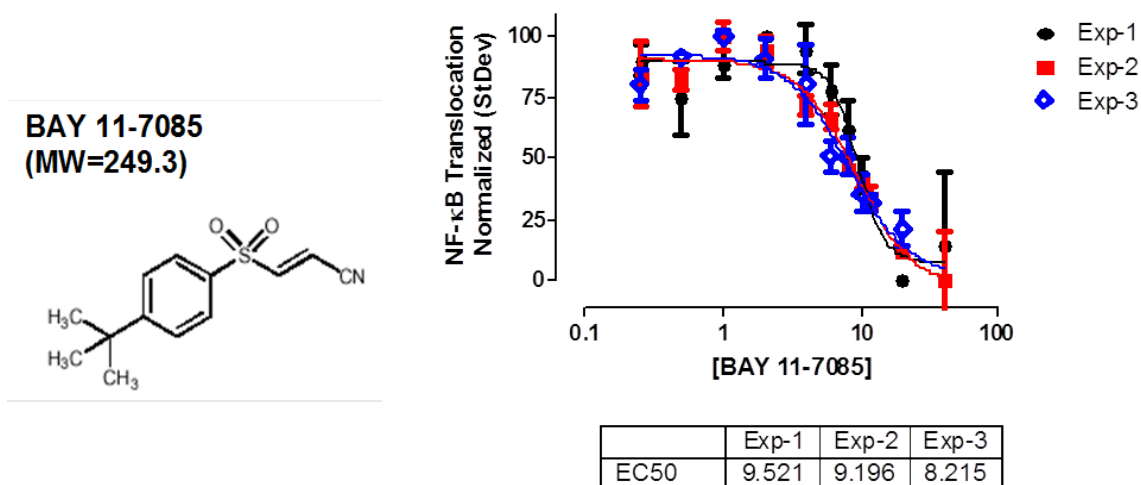


**Figure 20: BAY 11-7085 structure and NF- $\kappa$ B translocation inhibition experimental variability.** From 3 experiments, HeLa cells seeded at 5,000 cells/well overnight and treated in dose response with reference compound inhibitor, BAY11-7085 for 15 minutes followed by stimulation with 25ng/ml TNF- $\alpha$  for ~35 minutes. Cells were then fixed and stained to measure NF- $\kappa$ B translocation. Plates were analyzed on HCS imager to determine NF- $\kappa$ B translocation using CytoNuc Difference calculation; data was normalized and plotted in GraphPad Prism using non-linear regression 3-parameter fit.

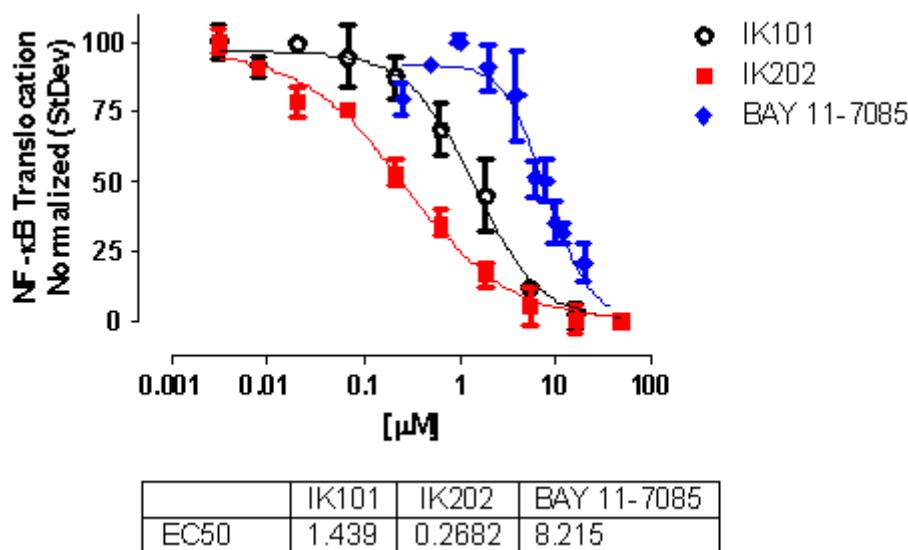


**Figure 21: Comparison of NF- $\kappa$ B translocation inhibition using reference compound inhibitor compounds BAY 11-7085, IK101 and IK202.** HeLa cells seeded at 5,000 cells/well overnight and treated in dose response with reference compound inhibitors, BAY11-7085, IK101, or IK202 for 15 minutes followed by stimulation with 25ng/ml TNF- $\alpha$  for ~35 minutes. Cells were then fixed and stained to measure NF- $\kappa$ B translocation. Plates were analyzed on HCS imager to determine NF- $\kappa$ B translocation using CytoNuc Difference calculation; data was normalized to control and plotted in GraphPad Prism using non-linear regression 3-parameter fit.

BAY 11-7085 and BAY 11-7082 compounds both could serve as reference compounds. The IK101 and IK202 compounds, with  $IC_{50}$  values of less than 2  $\mu$ M and 0.3  $\mu$ M, respectively, were used for demonstration and performance for assay validation purposes (Figure 21). Inhibitor compounds were pre-incubated with cells for 15 minutes followed by cytokine addition for about 30 minutes.

## Reference Compound Stability of Freeze-Thaw Cycles

HeLa cells treated with reference compounds (IK101 or IK202) that underwent multiple freeze-thaw cycles over a course of several weeks were tested for stability and/or loss of activity. Compounds were dissolved in 100% DMSO and aliquoted in cryovials and stored at  $-80^{\circ}\text{C}$  for later use. After up to 10 freeze-thaw cycles there is no significant evidence of loss of compound activity (Figure 22).

## Performance and Validation Pre-Screen

Following the optimization in the prior steps it is critical to validate the process procedure for screening operations before testing unknown chemicals. In Figure 23 and Figure 24, the reproducibility of cytokine stimuli is determined over a course of three independent assays and at least 3 different days to mimic the time it may take to screen an entire library. This requires independent harvesting of cells from flasks, cell seeding, and so on over 3 or more days. In Figure 25, the reference compound inhibitor IK202 was tested for reproducibility over 3 independent experiments, again to mimic screening operations. The results were acceptable for proceeding with Z-factor determination.

To determine the robustness and variability of single dose addition across the entire plate using liquid handling and robotics, at least 2 full plates with minimum and maximum responses are required to calculate a Z-factor. Z-factor is calculated using the formula  $1 - [3 \times (\text{standard deviation of positive control} + \text{standard deviation of negative control}) / (\text{mean of positive control} - \text{mean of negative control})]$  (33). The values from the Z-factor are indicative of the variability of the data, values of less than 0 is considered too much overlap in the positive and negative signal; 0 – 0.5 is considered a marginal assay and 0.5 – 1 is considered an excellent assay.

For the NF- $\kappa$ B assay, the maximum response (Max or positive) is cytokine addition and the minimum (Min or negative) response is the reference compound inhibitor, i.e., IK202 + cytokine. Additionally a Mid response can be added to verify ~50% reduction in the assay window. As mentioned earlier and throughout this chapter measuring translocation of NF- $\kappa$ B with HCS can use one or more HCS data features, namely intensities of the Cytoplasm-Nucleus Difference (CytoNuc Diff) or the Nucleus to Cytoplasm Ratio (Nuc/Cyt Ratio). In Figure 26 (IL-1 $\alpha$ ) and Figure 27 (TNF- $\alpha$ ), both the CytoNuc Diff and Nuc/Cyt Ratio is reported. Interestingly, the TNF- $\alpha$  stimuli showed equivalent Z-factor values, however, the IL-1 $\alpha$  stimuli Z-factor was significantly different; the CytoNuc Diff was 0.76 and the Nuc/Cyt Ratio was 0.64. Both are considered excellent screenable assays.

Reagents for assay are listed in Table 3.

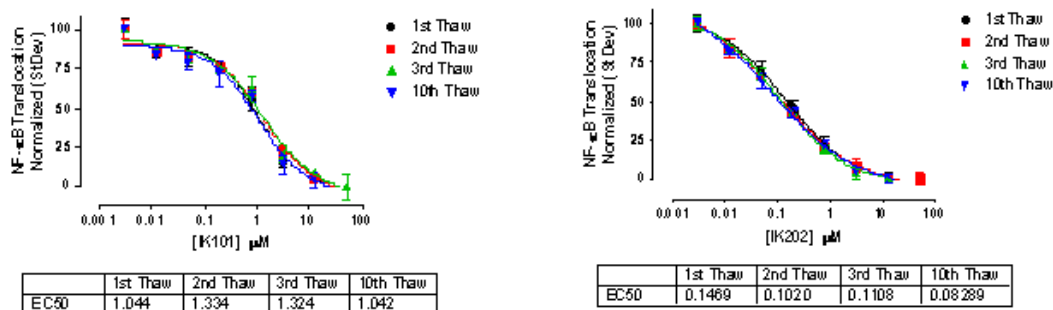


**Figure 22: Freeze-thaw cycle stability of reference compound inhibitors IK101 and IK202.** Reference inhibitor compounds were made at 10mM in DMSO and stored at  $-80^{\circ}\text{C}$ , and then allowed to thaw at room temperature before use. Compound vial samples were then re-frozen at  $-80^{\circ}\text{C}$  multiple times following thaw. HeLa cells seeded at 5,000 cells/well overnight and treated in dose response with reference compound inhibitors IK101 (left) or IK202 (right) for 15 minutes followed by stimulation with 25ng/ml TNF- $\alpha$  for ~35 minutes. Cells were then fixed and stained to measure NF- $\kappa$ B translocation. Plates were analyzed on HCS imager to determine NF- $\kappa$ B translocation using CytoNuc Difference calculation; data was normalized to control and plotted in GraphPad Prism using non-linear regression 3-parameter fit.



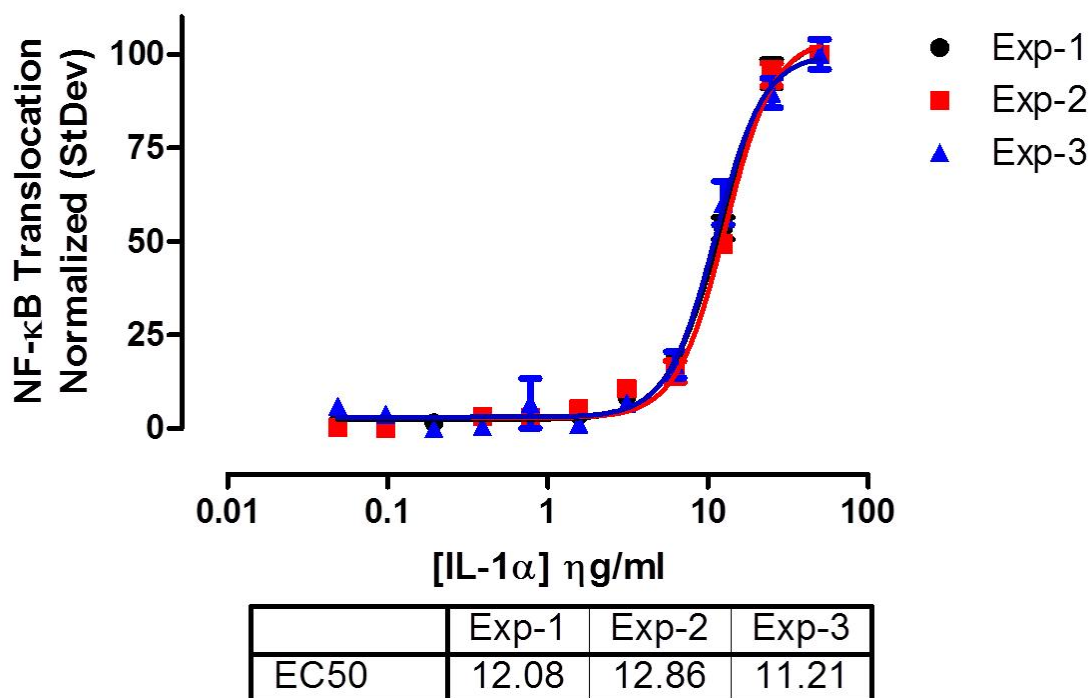


**Figure 23: IL-1 $\alpha$  dose response experimental variability.** HeLa cells seeded at 5,000 cells/well overnight and treated with IL-1 $\alpha$  in dose response for ~35 minutes were fixed and then stained to measure NF- $\kappa$ B translocation. Plates were analyzed on HCS imager to determine NF- $\kappa$ B translocation using CytoNuc Difference calculation; data was normalized and plotted in GraphPad Prism using non-linear regression 3-parameter fit.

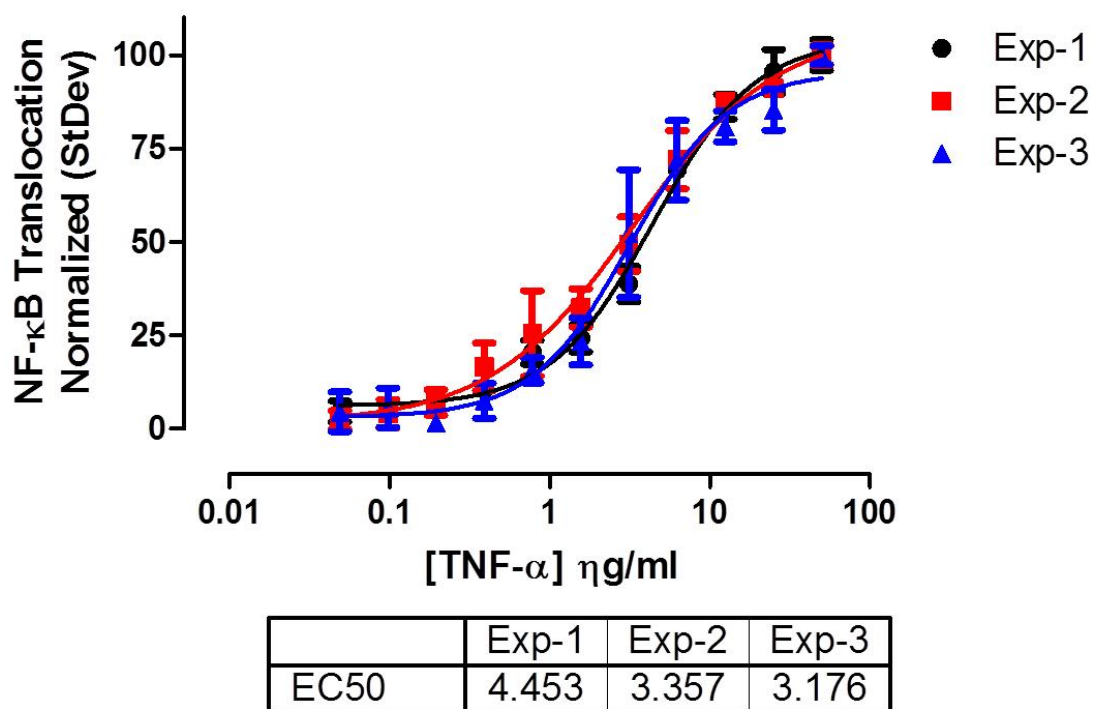
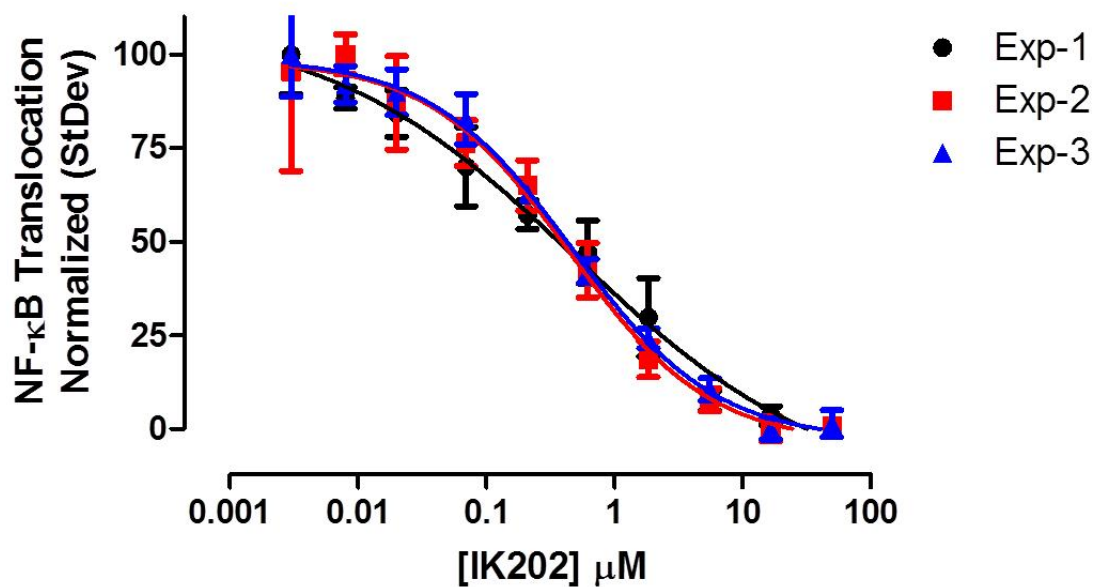


**Figure 24: TNF- $\alpha$  dose response experimental variability.** HeLa cells seeded at 5,000 cells/well overnight and treated with TNF- $\alpha$  in dose response for ~35 minutes were fixed and then stained to measure NF- $\kappa$ B translocation. Plates were analyzed on HCS imager to determine NF- $\kappa$ B translocation using CytoNuc Difference calculation; data was normalized and plotted in GraphPad Prism using non-linear regression 3-parameter fit.



|      | Exp-1  | Exp-2  | Exp-3  |
|------|--------|--------|--------|
| EC50 | 0.4985 | 0.4474 | 0.4717 |

**Figure 25: Reference compound inhibitor IK202 dose response 3 day experimental variability.** HeLa cells seeded at 5,000 cells/well overnight and treated in dose response with reference compound inhibitors IK202 for 15 minutes followed by stimulation with 25ng/ml TNF- $\alpha$  for ~35 minutes. Cells were then fixed and stained to measure NF- $\kappa$ B translocation. Plates were analyzed on HCS imager to determine NF- $\kappa$ B translocation using CytoNuc Difference calculation; data was normalized to control and plotted in GraphPad Prism using non-linear regression 3-parameter fit.

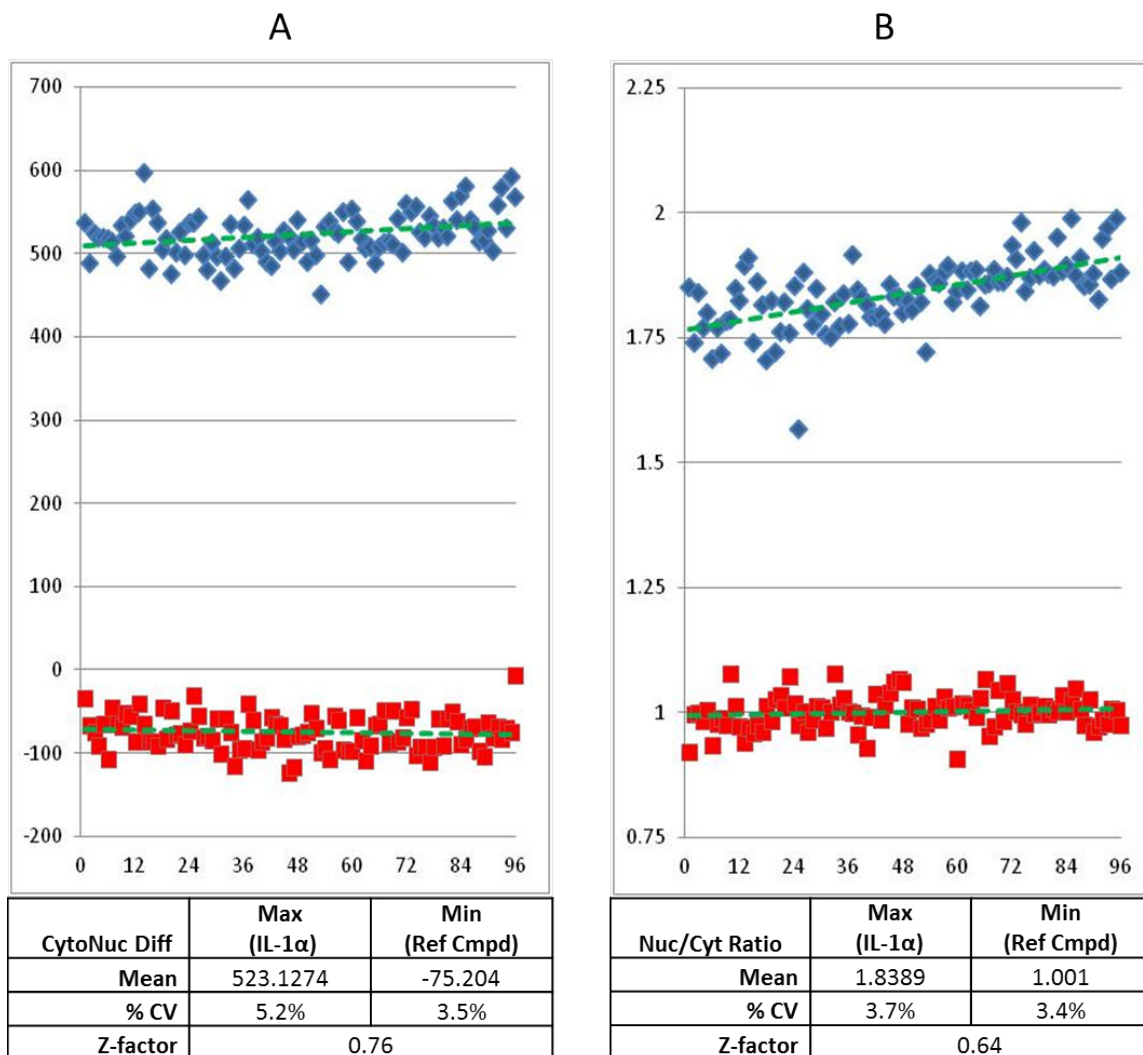


**Figure 26: NF-κB translocation IL-1α stimuli Z-factor calculation & graph display.** HeLa cells seeded at 5,000 cells/well overnight into 3 different 96-well plates were treated with 0.5% DMSO for maximum response (Red), media for unstimulated (green), and reference compound inhibitors IK202, 50μM for minimum response (blue) for 15 minutes followed by stimulation with 25ng/ml IL-1α for ~35 minutes. Cells were then fixed and labeled to measure NF-κB translocation. Plates were analyzed on HCS imager to determine NF-κB translocation using CytoNuc Difference (Panel A) or Nuc/Cyt Ratio (Panel B) calculation. Raw data values from HCS instrument were used to calculate the mean response (left axis) and standard deviation (right axis). Z-factor was calculate using the formula  $1 - [3 * (\text{standard deviation of positive control} + \text{standard deviation of negative control}) / (\text{mean of positive control} - \text{mean of negative control})]$  (33).

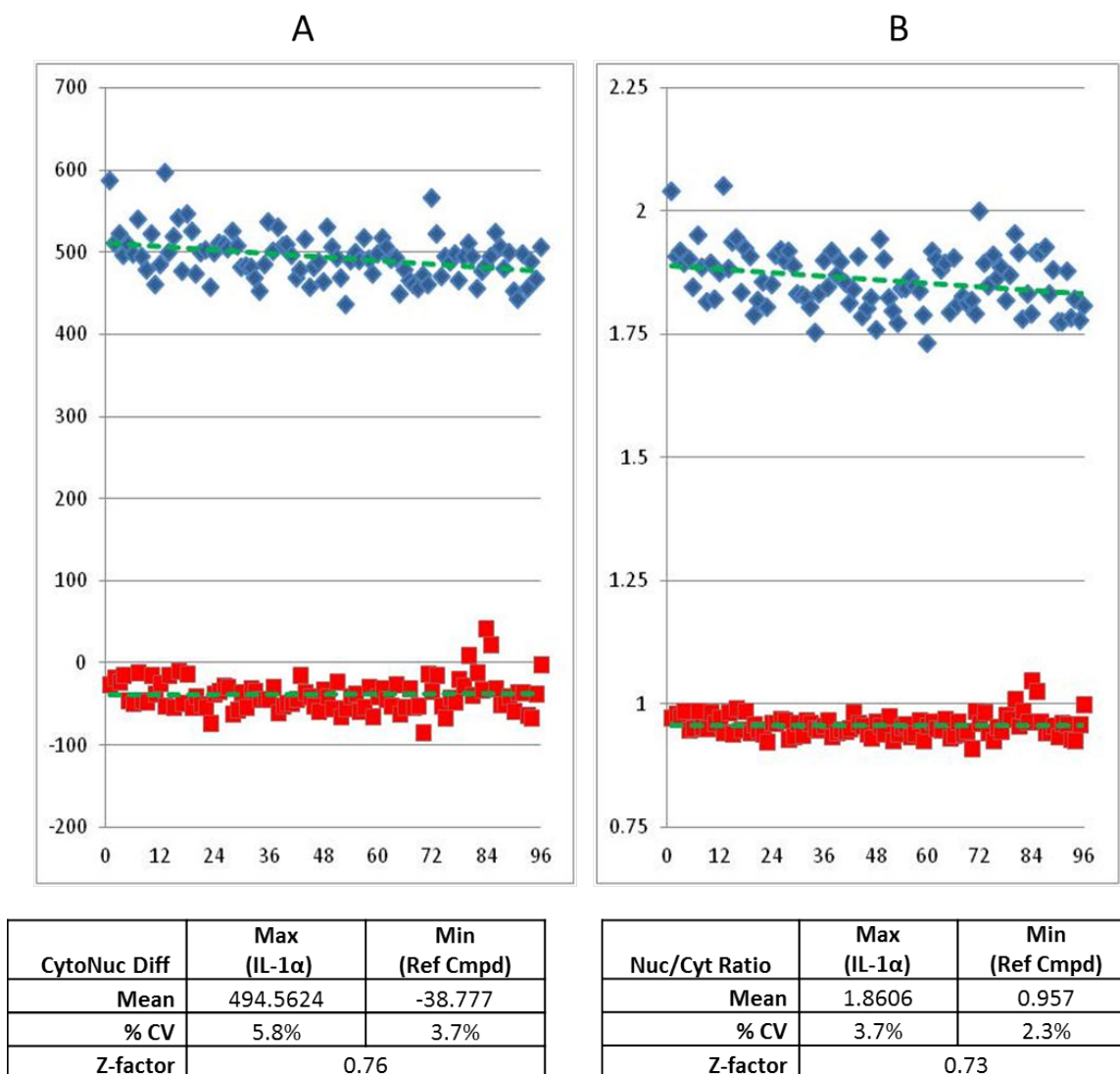


**Figure 27: NF- $\kappa$ B translocation TNF- $\alpha$  stimuli Z-factor calculation & graph display.** HeLa cells seeded at 5,000 cells/well overnight into 3 different 96-well plates were treated with 0.5% DMSO for maximum response (Red), media for unstimulated (green), and reference compound inhibitors IK202, 50 $\mu$ M for minimum response (blue) for 15 minutes followed by stimulation with 25ng/ml TNF- $\alpha$  for ~35 minutes. Cells were then fixed and labeled to measure NF- $\kappa$ B translocation. Plates were analyzed on HCS imager to determine NF- $\kappa$ B translocation using CytoNuc Difference (Panel A) or Nuc/Cyt Ratio (Panel B) calculation. Raw data values from HCS instrument were used to calculate the mean response (left axis) and standard deviation (right axis). Z-factor was calculated as previously described.

**Table 3: List of materials and reagents**

| Reagents   | Vendor           | Cat #     |
|--|------------------|-----------|
| Alexa 488 goat anti-rabbit IgG (H+L, 2 mg/ml)          | Invitrogen       | A-11008   |
| Albumin from Bovine Serum (BSA)                        | Sigma            | A-2153    |
| Dimethylsulfoxide (DMSO), 78.13 g/mole                 | Thermo           | 20684     |
| DPBS (PBS), Mg <sup>2+</sup> and Ca <sup>2+</sup> free | Lonza            | 17-512Q   |
| Fetal Bovine Serum, Defined                            | Thermo           | Sh30070   |
| Formaldehyde, 37%                                      | Sigma            | F-1268    |
| <i>*Formaldehyde, Ultrapure, MeOH free, 10%</i>        | Polysciences     | 04018     |
| <i>*Paraformaldehyde, Ultrapure, MeOH free, 16%</i>    | Polysciences     | 18814-20  |
| HeLa cells   | ATCC             | CCL-2     |
| Hoehst 33342   | Invitrogen       | H-21492   |
| L-Glutamine, 200 mM                                    | Lonza            | 17-605E   |
| Minimum Essential Medium Eagle (EMEM)                  | Lonza            | 12-662F   |
| NF-κB p65 (C-20) Rabbit Polyclonal IgG, 200 μg/ml      | Santa Cruz       | SC-372    |
| Penicillin/Streptomycin, 10000 Units                   | Lonza            | 17-602E   |
| Polyoxyethylensorbitan monolaurate (Tween-20) 10%      | Roche            | 1332465   |
| Recombinant Interleukin -1α (rh IL-1α)                 | R&D Systems      | 200-LA    |
| Recombinant Tumor Necrosis Factor-α (rh TNF-α)         | R&D Systems      | 210-TA    |
| t-Octylphenoxypoly-ethoxyethanol (Triton X-100), 10%   | Roche            | 1332481   |
| Trypsin-EDTA, 1X (0.05%)                               | Invitrogen/Gibco | 25300-054 |
| Water, Reverse Osmosis (RO-H <sub>2</sub> O)           | House            |           |
| <b>Reference Compound(s)</b>                           |                  |           |
| BAY 11-7082  | Enzo             | BML-EI278 |
| BAY 11-7085  | Enzo             | BML-EI279 |
| <b>Consumables</b>                                     |                  |           |
| 12-Place Dilution Reservoir                            | USA Scientific   | 1301-1212 |
| 150 cm <sup>2</sup> Cell Culture Flask (T-150)         | Corning          | 430825    |
| 96-well Packard View Plates                            | Perkin Elmer     | 6005182   |
| 96-well V-bottom Plates                                | Nunc             | 245128    |
| Backing Tape, Black                                    | Perkin Elmer     | 6005189   |
| Cell Strainer, 70 μM                                   | BD Falcon        | 352350    |

\* Alternative fixative solution; recommend a final solution of 4% paraformaldehyde but test in assay model to verify performance.

Table 3 continues on next page...

Table 3 continued from previous page.

| Reagents                    | Vendor           | Cat #        |
|-----------------------------|------------------|--------------|
| Plate Seals                 | Excel Scientific | 100-SEAL-PLT |
| Reagent Reservoir, 50 ml    | Corning (Costar) | 4870         |
| Storage Mats, 96-well plate | Corning (Costar) | 3092         |

\* Alternative fixative solution; recommend a final solution of 4% paraformaldehyde but test in assay model to verify performance.

## Preparation of Stock Reagents:

1. Reference compound (IK202), 10 mM: Make a 10mM stock solution by dissolving 10mg IK202 compound (MW=202.3) into 4.95 ml DMSO. Store at  $-80^{\circ}\text{C}$ .
2. Hoechst 33342, 2 mg/ml: Make a 2 mg/ml stock solution by dissolving in 100% DMSO. Protect from light. Store aliquots at  $-80^{\circ}\text{C}$  ~indefinitely.
3. IL-1 $\alpha$ , 10  $\mu\text{g/ml}$ : Make a 10  $\mu\text{g/ml}$  stock solution by dissolving in PBS containing 0.1% BSA. Store aliquots at  $-80^{\circ}\text{C}$  for up to 6 months.
4. TNF- $\alpha$ , 10  $\mu\text{g/ml}$ : Make a 10  $\mu\text{g/ml}$  stock solution by dissolving in PBS containing 0.1% BSA. Store aliquots at  $-80^{\circ}\text{C}$  for up to 6 months.

## Working Solutions per 96-well Plate (Prepared daily)

1. Inhibitor compound: Dilute in EMEM media without serum at 5X final concentration (50  $\mu\text{M}$  final at 250  $\mu\text{M}$ ). For IK202 compound, dilute 25  $\mu\text{l}$  of 10mM stock into 1ml of EMEM media. Note final DMSO concentration should not exceed 1%.
2. IL-1 $\alpha$ : Make working solution at 6X (150 $\eta\text{g/ml}$ ) the final assay concentration, which is 25 $\eta\text{g/ml}$ . Dilute 15  $\mu\text{l}$  of 10  $\mu\text{g/ml}$  cytokine into every 1ml of EMEM media needed to complete the assay. For one 96-well plate dilute 45  $\mu\text{l}$  of 10  $\mu\text{g/ml}$  cytokine stock in 3ml of EMEM. Note, for EC<sub>50</sub>, start at 40 $\eta\text{g/ml}$  final and dilute 1:3 in PBS or medium. For time course or kinetics study, use 25  $\eta\text{g/ml}$ .
3. TNF- $\alpha$ : Make working solution at 6X (150 $\eta\text{g/ml}$ ) the final assay concentration, which is 25 $\eta\text{g/ml}$ . Dilute 15  $\mu\text{l}$  of 10  $\mu\text{g/ml}$  cytokine into every 1ml of EMEM media needed to complete the assay. For one 96-well plate dilute 45  $\mu\text{l}$  of 10  $\mu\text{g/ml}$  cytokine stock in 3ml of EMEM. Note, for EC<sub>50</sub>, start at 40  $\eta\text{g/ml}$  final and dilute 1:3 in PBS or medium. For time course or kinetics study, use 25  $\eta\text{g/ml}$ .
4. Formaldehyde: Dilute 37% formaldehyde 1:10 with PBS. Warm to  $37^{\circ}\text{C}$  before use, this must be prepared fresh with each assay run.
5. 0.1% Triton X-100: Dilute 250  $\mu\text{l}$  of 10% Triton X-100 in 24.75 ml of PBS. Prepare fresh daily.
6. 0.01% Tween-20: Dilute 50  $\mu\text{l}$  of 10% Tween-20 in 50ml of PBS. Prepare fresh daily.
7. Primary Rabbit anti-NF- $\kappa$ B-p65 polyclonal antibody: Make 5  $\mu\text{g/ml}$  1<sup>o</sup> antibody solution by diluting antibody 1:40 in PBS (137.5  $\mu\text{l}$  of antibody into 5.5ml of PBS). Prepare fresh daily.

- Goat anti-Rabbit Alexa-488 Secondary Antibody / Hoechst Stain: Make a 10 µg/ml 2<sup>o</sup> antibody solution by diluting antibody 1:400 in PBS (27.5 µl of 2<sup>o</sup> antibody into 5.5ml of PBS). Add 5.5 µl of 2 mg/ml Hoechst 33342 stock solution for a 2 µg/ml solution (1:1000 dilution). Prepare fresh daily and protect from light.

## Plate Layout

Plate controls used as experimental references can be placed in any wells throughout the plate as long as the “data analysis calculator” is programmed to interrupt the plate layout conditions and concentrations of compound. For simplicity and a guideline use the example plate layout illustrated in Box 1 with controls on the outside columns and all test compounds in the center of the plate. Edge effects for the assay are minimal because of the short incubation period.

### Box 1: Example of a Plate Layout.

|   | 1    | 2 | 3 | 4 | 5 | 6 | 7 | 8 | 9 | 10 | 11 | 12   |
|---|------|---|---|---|---|---|---|---|---|----|----|------|
| A | DMSO |   |   |   |   |   |   |   |   |    |    | DMSO |
| B | DMSO |   |   |   |   |   |   |   |   |    |    | DMSO |
| C | MIN  |   |   |   |   |   |   |   |   |    |    | MAX  |
| D | MIN  |   |   |   |   |   |   |   |   |    |    | MAX  |
| E | MIN  |   |   |   |   |   |   |   |   |    |    | MAX  |
| F | MIN  |   |   |   |   |   |   |   |   |    |    | MAX  |
| G | DMSO |   |   |   |   |   |   |   |   |    |    | DMSO |
| H | DMSO |   |   |   |   |   |   |   |   |    |    | DMSO |

## Protocol for finding Inhibitors (Antagonist) in the NF-κB Pathway

Note: All washes and buffers are at 100µl unless indicated otherwise. Assays can be performed with automated hand-held pipettes for less than 10-plates. For more than 10-plates it is recommended to use automated plate washers and liquid handling devices.

### Day-1

- Seed approximately 5,000 cells/well in 100 µl volume of EMEM media containing 0.5% FBS, 2 mM L-Glutamine in 96-well plate (recommend using automated cell dispensing device for uniformity)
- Allow cells to attach overnight in complete medium at 37°C, 5% CO<sub>2</sub>, 95% relative humidity.



**Day-2**

3. Transfer 25  $\mu$ l 37°C pre-warmed compound from v-bottom compound plates to cell plate using automated liquid handling device.
4. Incubate for 15 minutes at 37°C, 5% CO<sub>2</sub>, 95% relative humidity.
5. Transfer 25  $\mu$ l 37°C pre-warmed cytokine (IL-1 $\alpha$  or TNF- $\alpha$ ) from v-bottom compound plates to cell plate using automated liquid handling device.
6. Incubate for 35 minutes at 37°C, 5% CO<sub>2</sub>, 95% relative humidity.
7. Remove all media using hand-held aspirator or with automated liquid handling device.

*Note: option to add high concentration of fixative directly to the cells or remove media and add final concentration of fixative buffer.*

8. Immediately fix cells by adding 100  $\mu$ l of “pre-warmed” 3.7% formaldehyde solution in a vented hood or with an automated liquid handling device.
9. Incubate at room temperature for 10 minutes with plate lid.

10. Remove formaldehyde and replace with 100  $\mu$ l of PBS using an automated liquid handling device. Please read safety precautions before working with formaldehyde.

*Note: At this step, you can stop the experiment and store plate at 4°C for several days by filling wells with salt solution and sealing to prevent evaporation.*

11. Add 100  $\mu$ l of 0.1% Triton X-100/PBS working solution and incubate 5 minutes at room temperature (RT). Use automated liquid handling device as needed.
12. Wash plate 2X with 100  $\mu$ l PBS at RT, leaving PBS on cells.
13. Use 96-head aspirator to remove buffer or use an automated liquid handling device. DO NOT ALLOW WELLS TO DRY.
14. Immediately add 50  $\mu$ l of 1<sup>o</sup> antibody using hand-held pipettor or automated liquid handling device. Incubate for 60 min at RT.
15. Remove antibody and discard. Wash plate 1X with 100  $\mu$ l of 0.01% Tween 20/PBS.
16. Incubate for 15 minutes at RT.
17. Wash 2X with 100  $\mu$ l PBS at RT, leaving PBS on cells.
18. Use 96-head aspirator or automated liquid handling device to remove buffer. DO NOT ALLOW WELLS TO DRY.
19. Immediately add 50  $\mu$ l of 2<sup>o</sup> antibody containing Hoechst dye per well.
20. Incubate 1-hour in the dark at RT. Protect from light by using black tape plate lids or foil.

21. Wash with 100  $\mu$ l of 0.01% Tween20/PBS. Incubate for 10 minutes at RT.
22. Wash plate with 100  $\mu$ l PBS at RT
23. Add 200  $\mu$ l PBS and seal plates.
24. Analyze plates on High Content Imaging device. If required, plates can be store at 4°C in dark for future analysis. Do not freeze plates.

## Protocol for Activators (Agonist) of NF $\kappa$ B Pathway

*Note: All washes and buffers are at 100  $\mu$ l unless indicated otherwise. Assays can be performed with automated hand-held pipettes such as Matrix for less than 10-plates. For more than 10-plates, automated plate washers, Multidrop, or MultiMek should be used.*

### Day-1

1. Plate approximately 5,000 cells/well in 100  $\mu$ l volume of EMEM media containing 0.5% FBS, 2mM L-Glutamine in 96-well plate (Multidrop)
2. Allow cells to attach overnight in complete medium at 37°C, 5% CO<sub>2</sub>, 95% relative humidity.

### Day-2

1. Transfer 25  $\mu$ l of 37°C pre-warmed unknown agonist or known agonist such as cytokines (IL-1 $\alpha$  or TNF- $\alpha$ ) from v-bottom compound plates to cell plate using automated liquid handling device.
2. Incubate for 35 minutes at 37°C, 5% CO<sub>2</sub>, 95% relative humidity.
3. Remove all media using hand-held aspirator or with automated liquid handling device.

*Note: option to add high concentration of fixative directly to the cells or remove media and add final concentration of fixative buffer.*

4. Immediately fix cells by adding 100  $\mu$ l of “pre-warmed” 3.7% formaldehyde solution in vented hood or with an automated liquid handling device.
5. Incubate at room temperature for 10 minutes with plate lid.
6. Remove formaldehyde and replace with 100  $\mu$ l of PBS using an automated liquid handling device. Please read safety precautions before working with formaldehyde.

*Note: At this step, you can stop the experiment and store plate at 4°C for several days by filling wells with salt solution and sealing to prevent evaporation.*

7. Add 100  $\mu$ l of 0.1% Triton X-100/PBS working solution and incubate 5 minutes at room temperature (RT). Use automated liquid handling device as needed.
8. Wash plate 2X with 100  $\mu$ l PBS at RT, leaving PBS on cells.

9. Use 96-head aspirator to remove buffer or use an automated liquid handling device. DO NOT ALLOW WELLS TO DRY.
10. Immediately add 50  $\mu$ l of 1<sup>o</sup> antibody using hand-held pipettor or automated liquid handling device. Incubate for 60 minutes at RT.
11. Remove antibody and discard. Wash plate 1X with 100  $\mu$ l of 0.01% Tween20/PBS.
12. Incubate for 15 minutes at RT.
13. Wash 2X with 100  $\mu$ l PBS at RT, leaving PBS on cells.
14. Use 96-head aspirator or automated liquid handling device to remove buffer. DO NOT ALLOW WELLS TO DRY.
15. Immediately add 50  $\mu$ l of 2<sup>o</sup> antibody containing Hoechst dye per well.
16. Incubate for 1-hour in the dark at RT. Protect from light by using black tape plate lids or foil.
17. Wash with 100  $\mu$ l of 0.01% Tween20/PBS. Incubate for 10 minutes at RT.
18. Wash plate with 100  $\mu$ l PBS at RT
19. Add 200  $\mu$ l PBS and seal plates.
20. Analyze plates on High Content Imaging device. If required plates can be store at 4<sup>o</sup>C in dark for future analysis. Do not freeze plates.

Note: Cells will respond to cytokines in the presence of serum and NF- $\kappa$ B will translocate to nucleus. For step-3, be sure to adjust either the volume of medium or the amount of cytokine.

## Logistics Analysis of Protocol

1. Projected # plates/day: state number of plates that can be processed per day
2. Suggested equipment: automated cell dispensing devices, automated liquid handling devices, 96-well aspirator, HCS imager
3. Timing issues, stop points: After fixation step
4. Stability and process studies: Compound and cytokine freeze-thaw stability acceptable
5. Dealing with multiple lots of reagents: None
6. Reagent and supplies availability: None
7. Flow Chart: None
8. Safety considerations: Example, formaldehyde use, see appendix-6
9. Data Collection Issues: state electronic location of data storage
10. Estimated throughput: state number of plates that can be processed per day
11. Batching Plates/Stop Points:

12. 3.7% formaldehyde fixation – STOP POINT - plates can be stored for several days at 4°C in PBS.
13. Permeabilization with 0.1% Triton X-100 – BATCHING – handle as many plates that can be processed under 15-minute incubation period.
14. Wash steps – BATCHING – do not allow wells to dry and do not introduce air bubbles during wash and aspiration steps. Handle one plate at a time unless automation devices are used.
15. Post staining, after plate is sealed – STOP POINT – store plates at 4°C in the dark and read on HCS Imager within 14-days.

## Cell Based Screen

1. Cell Handling for HeLa cells
  - a. Cell Bank – *location of cells in the cell bank*
  - b. Continuous Passage – Yes, maximum passage is not known.
  - c. Transfection – No
  - d. Proposed Schedule – continuous passage
  - e. Cell Culturing Guidelines:
    - i. Subculturing: Remove medium, and rinse with PBS. Remove the solution and rinse cell monolayer with Trypsin-EDTA solution. Remove and allow flask to sit at room temperature for 3-5 minutes or until the cells round up. Lightly tap flask to detach cells. Add fresh culture medium containing at least 0.5%FBS, aspirate and dispense into new culture flasks.
    - ii. Split Ratio: A subcultivation ratio from 1:2 to 1:10 is recommended
    - iii. Fluid Renewal: 2 to 3 times per week
2. Propagation: Suggested medium: Minimum essential medium Eagle with 2 mM L-glutamine, fetal bovine serum, 10%; 1% (100Units/ml) Penicillin/Streptomycin.  
Temperature: 37°C , 5%CO<sub>2</sub>
3. Freeze Medium: culture medium 90%; DMSO, 10%

## Compound Libraries

It is recommended to use a library of compounds to test the sensitivity and robustness of the assay for both negative and positive responses. There is a unique NF-κB inhibitor set of 14 -compounds available from Calbiochem (Cat#481487 InhibitorSelect™ NF-κB Signaling Pathway Inhibitor Panel). There are now 4 versions of this library with the latter ones containing IκK inhibitors. Additionally there are other larger compound library collections commercially available for purchase including LOPAC. For this assay the Calbiochem kinase Library, otherwise known as the Millipore EMD 539744 InhibitorSelect™ 96-Well Protein Kinase Inhibitor Library-I was the only commercial library available. Interestingly, this 80 chemical compound library contains no NF-κB or IκK inhibitor compounds and this is reflected in the results. For single point determination at 50 μM, two compounds showed an increase in NF-κB CytoNuc difference as a result of changes in the morphological characteristics of the cell in assay

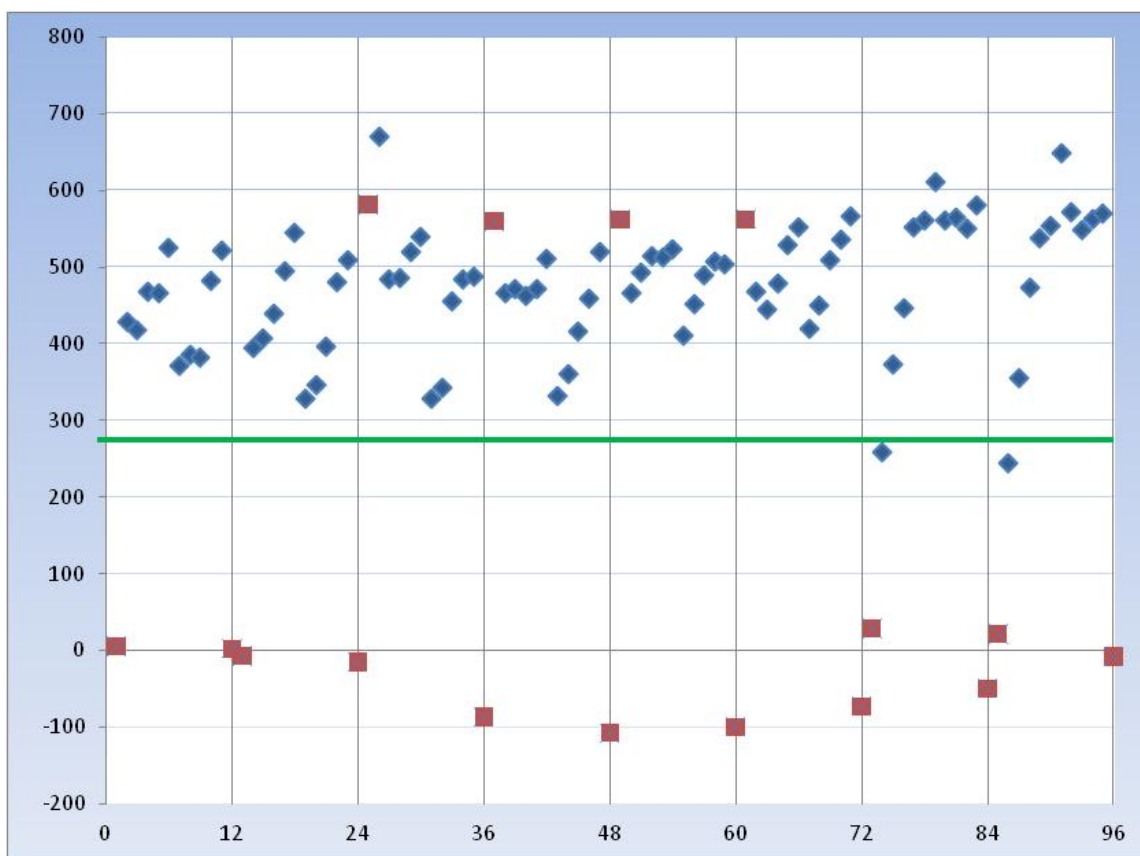


**Figure 28: Results from Calbiochem kinase library (EMD 539744 InhibitorSelect™) screen.** HeLa cells seeded at 5,000 cells/well overnight and dosed with a single dose of 50 $\mu$ M compound for 15 minutes followed by stimulation with 25 $\eta$ g/ml TNF- $\alpha$  for ~35 minutes. Cells were then fixed and labeled to measure NF- $\kappa$ B translocation. Plates were analyzed on HCS imager to determine NF- $\kappa$ B translocation using CytoNuc Difference calculation. Raw data values from HCS instrument were used to calculate the mean response. Controls represented as “red squares” and compound tested shown in “blue triangles”. Green line represents ~50% activity; points below this line are considered “hits”. No inhibitors were confirmed; one compound showed an increase in NF- $\kappa$ B Nuc-Cyt difference that was a result in changes in the morphological characteristics of the cell in assay both with IL-1 $\alpha$  and TNF- $\alpha$  stimulation. Images not shown.

both with IL-1 $\alpha$  and TNF- $\alpha$  stimulation (Figures 28 and 29). No activates were confirmed with IL-1 $\alpha$  or TNF- $\alpha$  stimulation IC<sub>50</sub> curves follow-ups from 50 $\mu$ M, 3-fold in duplicates.

## Other Considerations

### Detection of Cytotoxicity and Fluorescent Compounds in NF- $\kappa$ B Translocation Assay

One of the powers of HCS is providing the capability to measure morphological and intensities of bioprobe markers at the single cell level. The combination of these capabilities allows the ability to measure cell populations and subpopulations captured in

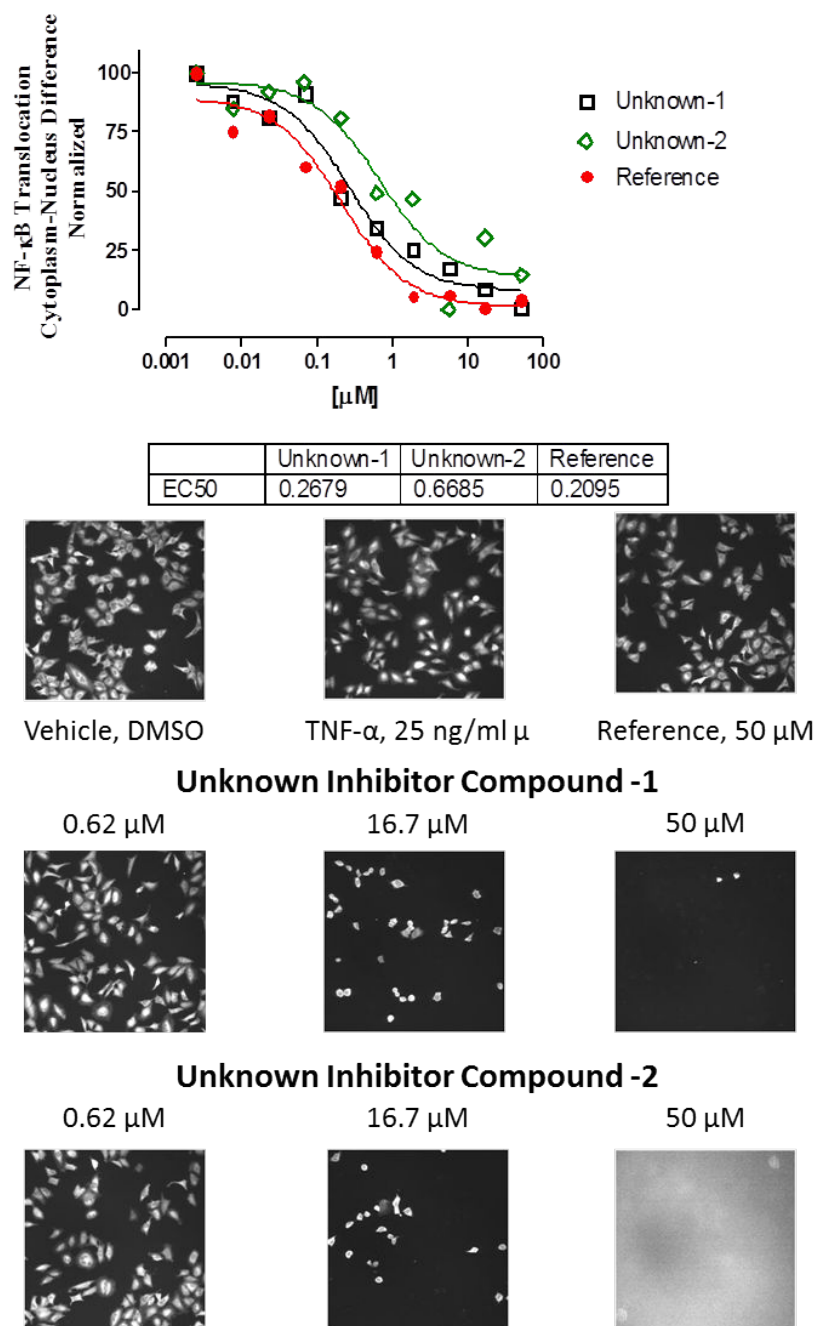


**Figure 29: Reference compound and unknown inhibitor dose response with corresponding images.** Top panel is a comparison of reference compound inhibitor and two unknown inhibitors identified as actives in screen. HeLa cells seeded at 5,000 cells/well overnight and treated in dose response with reference compound inhibitors IK202 or two unknown inhibitor compounds for 15 minutes followed by stimulation with 25ng/ml TNF- $\alpha$  for ~35 minutes. Cells were then fixed and stained to measure NF- $\kappa$ B translocation. Plates were analyzed on HCS imager to determine NF- $\kappa$ B translocation using CytoNuc Difference calculation; data was normalized to control and plotted in GraphPad Prism using non-linear regression 3-parameter fit. Bottom panel of images: (A) vehicle (DMSO) control; (B) TNF- $\alpha$ , 25ng/ml control; (C) IK202, 50 $\mu$ M reference compound inhibitor; (D) Unknown inhibitor compound-1, 0.62 $\mu$ M; (E) Unknown inhibitor compound-1, 16.7 $\mu$ M; (F) Unknown inhibitor compound-1, 50 $\mu$ M; (G) Unknown inhibitor compound-2, 0.62 $\mu$ M; (H) Unknown inhibitor compound-2, 16.7 $\mu$ M; (I) Unknown inhibitor compound-2, 50 $\mu$ M.

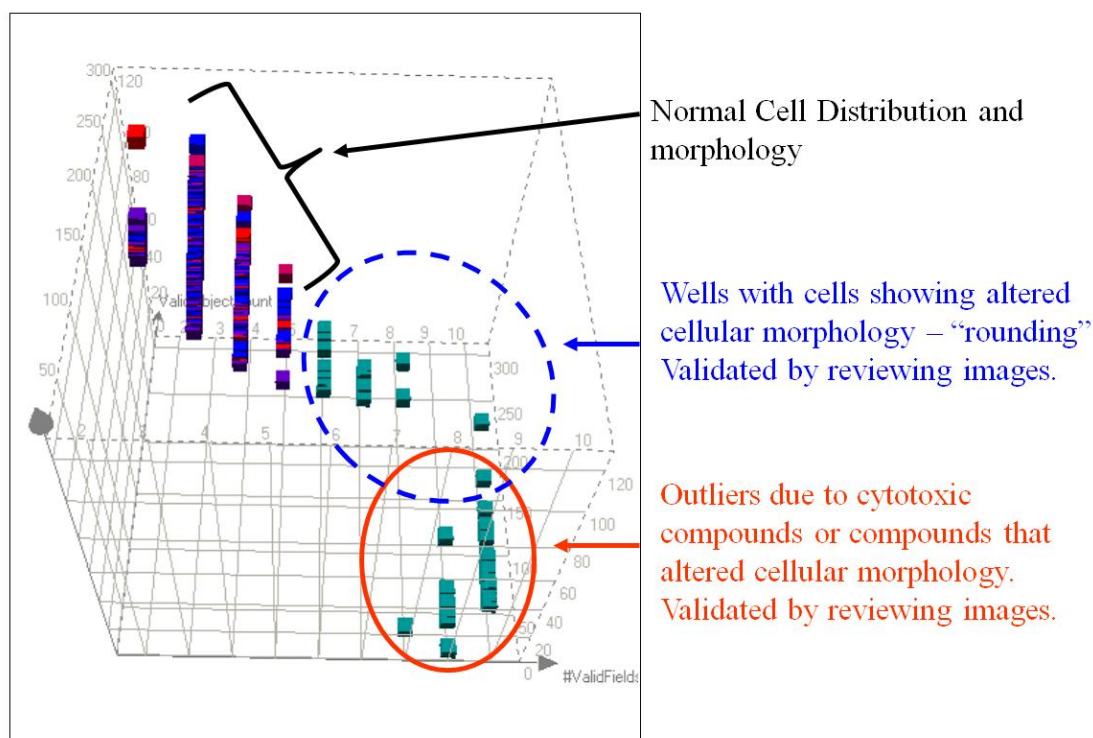


**Figure 30: SpotFire 3-D graph visualization:** well level plate HCS features showing separation between normal cell distribution, altered morphology, or cell loss and/or cytotoxic effects. X axis = number of valid fields; Y axis = valid object count; Z axis = average cell density/field

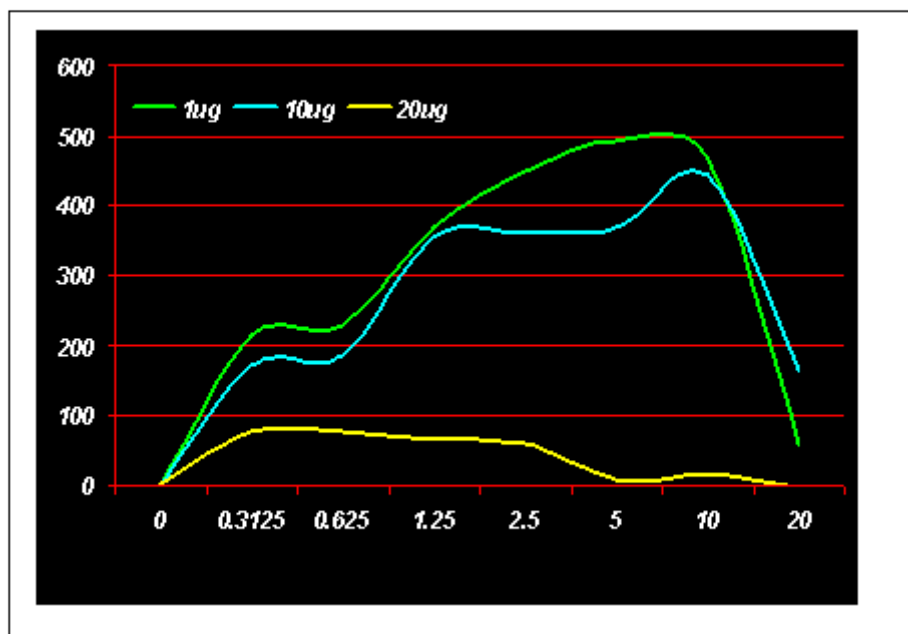
the image. If a compound dosing concentration is the direct or indirect cause of cytotoxicity it is often measurable with good precision by using population statistics of the number of cell objects detected in the well in comparison to a vehicle control well. Optional, cytotoxic and viable dyes can be used in combination with the biomarker indicator as a reporter. HeLa cells seeded overnight, then pre-incubated with 10-point compound dose response starting at 50 $\mu$ M,  $\frac{1}{2}$  log for 15 minutes and subsequently treated with TNF- $\alpha$  for 35 minutes, were stained with NF $\kappa$ B antibody as previously described. The inhibition of NF- $\kappa$ B in the presence of the known reference compound recorded an IC<sub>50</sub> of 0.2095  $\mu$ M using 3-parametric fit in GraphPad Prism, whereas the unknown inhibitor compounds recorded an IC<sub>50</sub> of 0.2679  $\mu$ M and 0.6685  $\mu$ M. The differences in these values is somewhat subtle in the curve fitting; however, the key difference is observed in the loss of cells with increasing concentration of the compound above the recorded IC<sub>50</sub> value. It is important to always review and record the number of cellular objects, fields, or other HCI feature parameters that provide information about an alteration in the cell seeding density in the well in addition to other key HCS feature values including reviewing the images to validate the results (Figure 30).

To determine if an unknown compound(s) is fluorescent in the visible spectra when screening a chemical compound library using HCS assays can be achieved by using intensity measurements in the nucleus or cytoplasm regions of interests (ROI). These compounds can create a false positive and are not commonly identified until follow ups are underway in protein redistribution assay such as NF $\kappa$ B where fluorescence can occupy both the cytoplasm and nuclear ROI. If a suspect compound is thought to be fluorescent in the HCS assay, this can verify using a high content imager by measuring the baseline autofluorescence of cells using vehicle control, then measure any increase in fluorescence following compound treatment. Evidence of compound fluorescence in the cells is typically observable using fluorescent microscopy images not shown.

## Screening Commercially Available NF- $\kappa$ B Antibodies (Appendix 1)

NF- $\kappa$ B Antibody Staining (Santa Cruz, SC-372)

Secondary labeling concentration; 1, 10, 20 $\mu$ g/ml.

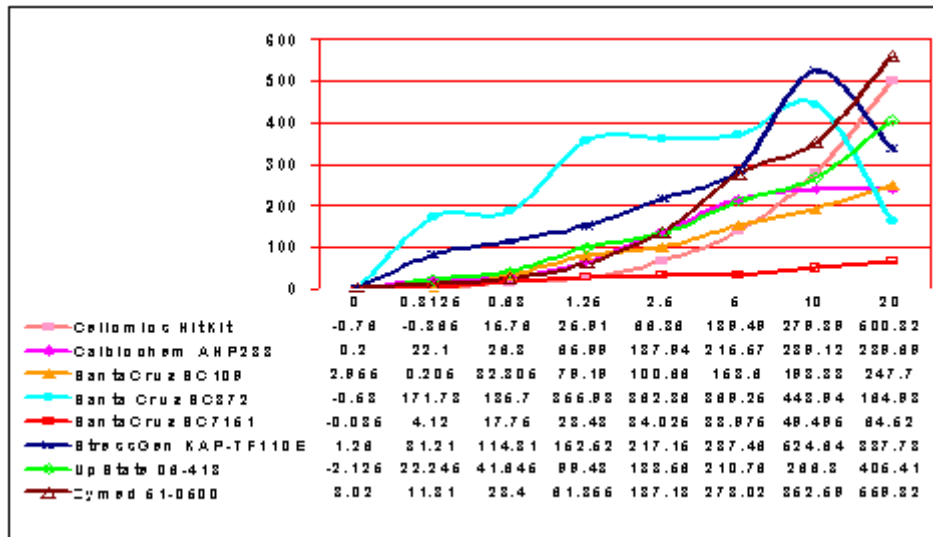


### Graph of commercially available antibodies evaluated

X-axis represents 1<sup>o</sup>Ab concentration with 10 $\mu$ g/ml 2<sup>o</sup>Ab;

Y-axis represents average fluorescent intensity of NF- $\kappa$ B difference between the cytoplasm and nucleus subtracted from the 2<sup>o</sup>Ab control. Values listed below x-axis are the raw data (CytoNuc Diff).





## Safety Considerations: Guidelines & Precautions (Appendix 2)

Please follow institutional laboratory safety considerations and special precautions with regard to formaldehyde and paraformaldehyde use. Training is commonly required for all personnel using formaldehyde and paraformaldehyde

### Formaldehyde and Paraformaldehyde Use Guidelines in the Laboratory:

1. All stock solutions greater than 4% must be maintained in a fume hood.
2. Working solution of less than 4% and less than 37°C can be used in the following areas:
  - Fume hood
  - Biosafety cabinet
  - Automation liquid handling robots with standard setup with <4% formaldehyde solution in appropriate reservoir positions. Following addition of formaldehyde, plate lids must cover open plates to minimize formaldehyde exposure during a 10-15 minute incubation period. Transfer of formaldehyde to and from the liquid handling robot reservoir requires a safety container that is larger than the stock reservoir container to collect any spill. It is recommended that the volume of working solution of formaldehyde does not exceed 100ml at any given time. If additional formaldehyde solution volume is required than add as needed.
3. Transport of formaldehyde working solution between laboratories and pre-warming to 37°C requires standard lid cover to prevent potential exposure.
4. Formaldehyde waste should be less than 0.1% before it is discarded; be sure to verify per institution or government ordinance.
5. Formaldehyde mixture with DMSO requires normal DMSO disposal procedures.

6. Stock solutions of 37% formaldehyde contains methanol and disposal of this stock solution should be treated as flammable if appropriate.
7. Report any excessive spill of formaldehyde to your safety department

## Acknowledgements

This work began at Sphinx Laboratories, Division of Eli Lilly in 2001, knowledge and effort gained at Eli Lilly as well as several years at Abbott Laboratories, Duke University Medical Center, and the Hamner Institutes for Health Sciences made it possible to put this manuscript together.

## References

1. Celebrating 25 years of NF- $\kappa$ B. *Nat Immunol.* 2011;12:681. PubMed PMID: 21772274.
2. Sen R, Baltimore D. Inducibility of kappa immunoglobulin enhancer-binding protein NF-kappa B by a posttranslational mechanism. *Cell.* 1986;47:921–928. PubMed PMID: 3096580.
3. Chen FE, Huang DB, Chen YQ and Ghosh G. 1998. Crystal structure of p50/p65 heterodimer of transcription factor NF-B bound to DNA *Nature*, 391:410- 413.
4. Baeuerle P, Baltimore D. I kappa B: a specific inhibitor of the NF- $\kappa$ B transcription factor. *Science.* 1988;242:540–46. PubMed PMID: 3140380.
5. Ghosh G, Van Duyne G, Ghosh S, Sigler P. Structure of NF- $\kappa$ Bp50 homodimer bound to a  $\kappa$ B site. *Nature.* 1995;373:303–10. PubMed PMID: 7530332.
6. Muller C, Rey F, Sodeoka M, Verdine G, Harrison S. Structure of the NF- $\kappa$ B p50 homodimer bound to DNA. *Nature.* 1995;373:311–17. PubMed PMID: 7830764.
7. Nolan G. NF-AT-AP-1 and Rel-bZIP: hybrid vigor and binding under the influence. *Cell.* 1994;77:795–98. PubMed PMID: 8004669.
8. M. Karin. 1999. The beginning of the end: IkappaB kinase (IkK) and NF-kappaB activation. *J. Biol. Chem.* 274: 27339–27342
9. Gilmore T. D. Introduction to NFkB: players, pathways, perspectives. *Oncogene.* 2006;25:6680–6684. PubMed PMID: 17072321.
10. Schreiber S., Nikolaus S., Hampe J. Activation of nuclear factor kappa B inflammatory bowel disease. *Gut.* 1998;42:477–484. PubMed PMID: 9616307.
11. Tergaonkar V. NFkB Pathway: A good signaling paradigm and therapeutic target. *Int J. Biochem. Cell Biol.* 2006;38:1647–1653. PubMed PMID: 16766221.
12. Grilli M, Jason JS, Lenardo M. NF-kB and rel-participants in a multiform transcriptional regulatory system. *Int. Rev. Cytol.* 1993;43:1–62. PubMed PMID: 8449662.
13. Lawrence R, Chang LJ, Siebenlist U, Bressler P, Sonenshein G. Vascular smooth muscle cells express a constitutive NF- $\kappa$ B-like activity. *J. Biol. Chem.* 1994;269:28,913–18. PubMed PMID: 7961853.
14. Baeuerle P, Henkel T. Function and activation of NF- $\kappa$ B in the immune system. *Annu. Rev. Immunol.* 1994;12:141–79. PubMed PMID: 8011280.

15. Siebenlist U, Franzoso G, Brown K. Structure, regulation and function of NF- $\kappa$ B. *Annu. Rev. Cell Biol.* 1994;10:405–55. PubMed PMID: 7888182.
16. Arenzana-Seisdedos F, Thompson J, Ro-driguez M, Bachelier F, Thomas D, Hay R. Inducible nuclear expression of newly synthesized I $\kappa$ B $\alpha$  negatively regulates DNA-binding and transcriptional activation of NF- $\kappa$ B. *Mol. Cell. Biol.* 1995;15:2689–96. PubMed PMID: 7739549.
17. A.S. Baldwin, Jr., 1996. The NF-kappa B and I kappa B proteins: new discoveries and insights. *Annu. Rev. Immunol.* 14:649–683.
18. Ding GJ, Fischer PA., Boltz RC., Schmidt JA., Colaianne JJ., Gough A., Rubin RA., Miller DK. Characterization and Quantitation of NF- $\kappa$ B Nuclear Translocation Induced by Interleukin-1 $\alpha$  and Tumor Necrosis Factor- $\alpha$ . *J Biol Chem.* 1998;273:28897–28905. PubMed PMID: 9786892.
19. Ghosh S., May M.J., Kopp E.B. NF- $\kappa$ B and Rel proteins: evolutionarily conserved mediators of immune responses. *Annu. Rev. Immunol.* 1998;16:225–260. PubMed PMID: 9597130.
20. Heiss E, Herhaus C, Klimo K, et. al. 2001. Nuclear factor kappa B is a molecular target for sulforaphane-mediated anti-inflammatory mechanisms. *J. Biol. Chem.* 276: 32008–32015.
21. Bharti AC, Aggarwal BB. Nuclear factor-kappa B and cancer: its role in prevention and therapy. *Biochemical Pharmacology.* 2002;64:883–888. PubMed PMID: 12213582.
22. Baldwin AS, 2001. Control of oncogenesis and cancer therapy resistance by the transcription factor NF-kappaB. *J. Clin. Invest.* 107:241–246
23. Chen F, Castranova V, and Shi X, 2001. New insights into the role of nuclear factor-kappaB in cell growth regulation. *Am. J. Pathol.* 159: 387–397.
24. Beg AA and Baltimore D. 1996. An essential role for NF-kappaB in preventing TNF-alpha-induced cell death. *Science* 274:782–784.
25. Wang CY, Mayo MW and Baldwin AS Jr, 1996. TNF- and cancer therapy-induced apoptosis: potentiation by inhibition of NF-kappaB. *Science* 274: 784–787.
26. Van Antwerp DJ, Martin SJ, Kafri T, et. al. 1996. Suppression of TNF-alpha-induced apoptosis by NF-kappaB. *Science* 274: 787–789.
27. Ahmad M, Marui N, Alexander R, Medford R. Cell type-specific transactivation of the VCAM-1 promoter through an NF- $\kappa$ B enhancer motif. *J. Biol. Chem.* 1995;270:8976–83. PubMed PMID: 7536741.
28. Wright K, White L, Kelly A, Beck S, Trowsdale J, Ting J. Coordinate regulation of the human TAP1 and LMP2 genes from a shared bidirectional promoter. *J. Exp. Med.* 1995;81:1459–71. PubMed PMID: 7699330.
29. Brown A, Linhoff M, Stein B, Wright K, Baldwin A, Basta P, Ting J. Function of NF- $\kappa$ B/Rel binding sites in the MHC class II invariant chain promoter is dependent on cell-specific binding of different NF- $\kappa$ B/Rel subunits. *Mol. Cell. Biol.* 1994;14:2926–35. PubMed PMID: 8164652.
30. Zie QW, Kashiwabara Y, Nathan C. Role of transcription factor NF- $\kappa$ B/Rel in induction of nitric oxide synthase. *J. Biol. Chem.* 1994;269:4705–8. PubMed PMID: 7508926.

31. Pahl H.L. Activators and target genes of Rel/NF- $\kappa$ B transcription factors. *Oncogene*. 1999;18:6853–6866. PubMed PMID: 10602461.
32. Wu H, Lozano G. 1994. NF- $\kappa$ B activation of p53: a potential mechanism for suppressing cell growth in response to stress. *J. Biol. Chem.* 269:20,067–74
33. Romashkova JA, Makarov SS. NF- $\kappa$ B is a target of AKT in anti-apoptotic PDGF signaling. *Nature*. 1999;401:86–90. PubMed PMID: 10485711.
34. Zhang JH, Chung TDY, Oldenburg KR. A simple statistical parameter for use in evaluation and validation of high throughput screening assays. *J. Biomol Screen.* 1999;4:67–73. PubMed PMID: 10838414.

# High Content Screening with Primary Neurons

Hassan Al-Ali,<sup>1</sup> Murray Blackmore,<sup>2</sup> John L Bixby,<sup>1</sup> and Vance P. Lemmon<sup>✉1</sup>

Created: October 15, 2013; Updated: October 1, 2014.

## Abstract

Advances in microscopy, instrumentation, and image analysis software, combined with improved protocols for acquiring and maintaining primary neuronal cultures, have made high content analysis (HCA) with primary neurons a routine procedure in many labs. Additional improvements in robotics and automation allow the high-throughput application of HCA in high-content screening (HCS). Given its multiplexed nature, HCS provides an unprecedented amount of multiparametric kinetic and morphogenic information from cells. It holds promise for better understanding of molecular signaling networks, and for easing the bottleneck in the drug discovery process, particularly relating to neurological disorders. Here we describe protocols for preparing different neuronal types and discuss advantages, challenges, pitfalls, and detailed workflows for utilizing them in HCS with various perturbagens.

## 1. Introduction

High-content screening (HCS) has emerged as a new approach for drug target validation and lead optimization before costly animal testing (1,2), as well as a valuable tool for understanding complex molecular processes in a cellular context (3). Despite years of progress, in understanding the etiology and genetics of numerous disorders afflicting the nervous system, the number of disease modifying therapeutics remains modest. HCS offers a number of advantages over conventional high-throughput screening (HTS) approaches when studying neurons, which will be discussed below.

### 1.1. What is HCS?

HCS is a screening method based on multiparametric analyses of large scale image data extracted from multiple targets in thousands or millions of cells in multiwell plates (1,2,4). Thus, although high-content analysis (HCA) refers to the extraction of multiparametric information from image data, HCS is the automated medium-to-high-throughput application of HCA in screening campaigns. The concept of HCA dates back to the late 1990s, when the Cellomics<sup>TM</sup> initiative conceptualized it as a strategy for cataloging multiple molecular processes inside intact cells (5). The initiative was bolstered by the development of fluorescent-protein biosensors that allowed time-dependent examination

---

<sup>1</sup> Miami Project to Cure Paralysis, University of Miami Miller School of Medicine. <sup>2</sup> Department of Biomedical Sciences, Marquette University.

✉ Corresponding author.

of processes ranging from membrane activity and cell signal transduction to energy metabolism and cell physiology (2). By utilizing the correct combination of probes, and by spatially (and sometimes temporally) resolving readouts of individual cells, HCA can provide quantitative measurements of nuclear size/shape, DNA content, organelle shape and function, protein modification and intracellular localization, cell movement, and cell shape. HCS can thus produce an enormous amount of morphometric and kinetic outputs.

## 1.2. Why HCS?

The majority of drug discovery campaigns have utilized HTS methods as originally introduced by the pharmaceutical industry (6). Most HTS assays screen for *in vitro* interactions with a single target, typically using a spectrophotometric or fluorescent readout (7,8). This approach has been extremely successful in identifying probes and drug-like molecules with a wide range of selectivities towards intended targets. However, the rate at which new drugs have been reaching the clinic has decreased (9,10). One possible explanation is the difficulty of capturing the complexity of interactions that occur within cells or whole tissues using target-based screening. Although target-based HTS offers a streamlined pipeline for sifting through millions of compounds and conditions, the added burden of performing screens in more complex systems with expanded assay readouts may well be worth the effort (1). However, cell-based screening is usually agnostic to molecular mechanisms of action, hence subsequent determination of drug targets and lead compound optimization can be quite difficult. Fortunately, advancements in chemical proteomics and comprehensive activity panels are quickly improving the outlook for target identification.

The informational gain from investigating signaling networks using unbiased genetic screens in cellular systems, by way of HCS, has also been highlighted (3). Most of our knowledge of signal transduction pathways has come from forward genetic screens in model organisms. These methods have been extremely successful in delineating many of the canonical pathways and their major transducers, they do not sufficiently address the spatial and temporal complexities of signal transduction within cells. For example, different neuronal cell types exhibit significantly distinct RNA expression profiles (11) that likely underlie distinct physiologies. Cell-based genetic screens using various genetic perturbagens, gain- or loss-of-function analyses, will be vital for elucidating the intricate signaling circuitry within specific neuronal types. This may prove essential for identifying appropriate drug targets for the notoriously cell-specific neurological diseases.

The technology for high content analysis (HCA) is becoming more affordable and readily available to both industry and academia, encouraging such endeavors as HCS in primary neurons (12). Technical obstacles have, until recently, hindered screening with primary neuronal systems, including the difficulty of obtaining, culturing, and transfecting primary neurons (13,14). However, new culturing and transfection methodologies now offer a more practical platform for HCA, and by extension HCS, in these cells.

## 2. Preliminary Assay considerations

Therapeutic agent discovery in the nervous system has thus far trailed behind other areas, implying the need for more relevant screening models (15,16). Choosing a cell type for HCS may be the most important element of the experimental design, while also being the most challenging. Many of the conditions and reagents of the experiment are tailored to the chosen cell type, upon which large investments of time, effort, and money are ultimately made. Thus, a well-reasoned choice of the most relevant cellular model is critical. Additional consideration must be given to the usually narrow range of conditions in which the assay yields the largest separation between positive and negative controls. Choosing the most relevant substrate, treatment conditions, incubation time, and immunostaining protocols can all pose additional challenges that must be overcome before an HCA assay is considered to be appropriate for screening. Detailed protocols appear at the end of this chapter.

### 2.1. Neuronal Type

Several options are currently available for HCS, each with its own advantages and drawbacks (17). Primary cells are far more physiologically relevant than immortalized cell lines (18), and neurons differentiated *in vivo* best recapitulate actual neuronal subpopulations (12). Primary neurons have gene and protein expression profiles that better resemble those of differentiated cells *in vivo*, and are thus more appropriate for drug target validation (12). Numerous considerations factor into the choice of age and type of primary neurons to be used.

#### 2.1.1. Embryonic versus adult neurons

Historically, primary neurons isolated from embryonic brain have been more frequently utilized than neurons isolated from postnatal or mature brain. This is due to the relative ease of isolating embryonic neurons, in addition to increased viability, improved regenerative ability, and reduced glial growth in embryonic cultures compared to their adult derived counterparts (19–23). Terminally differentiated CNS neurons are post-mitotic in culture, although neuronal cultures may contain precursors that divide in permissive culture conditions (24). Reduced glial numbers in embryonic brains combined with culture conditions that retard glial growth and proliferation (25) allow for the preparation of relatively homogenous low density neuronal cultures, which can be useful in simplifying immunostaining, HCA readout, and culture consistency. However, the improved regenerative and survival capacity of embryonic neurons combined with the lack of additional cell types that would more reliably recapitulate the biological environment can, for example, lead to false hits (or false negatives) in a screen for neuroprotective agents relevant to the adult CNS. Thus, one should be aware of the balance between choosing the most relevant cellular model and maintaining assay screening suitability. It may prove most efficient to perform HCS with a more convenient cellular model, and to use a secondary filtering assay, such as a slice culture that better

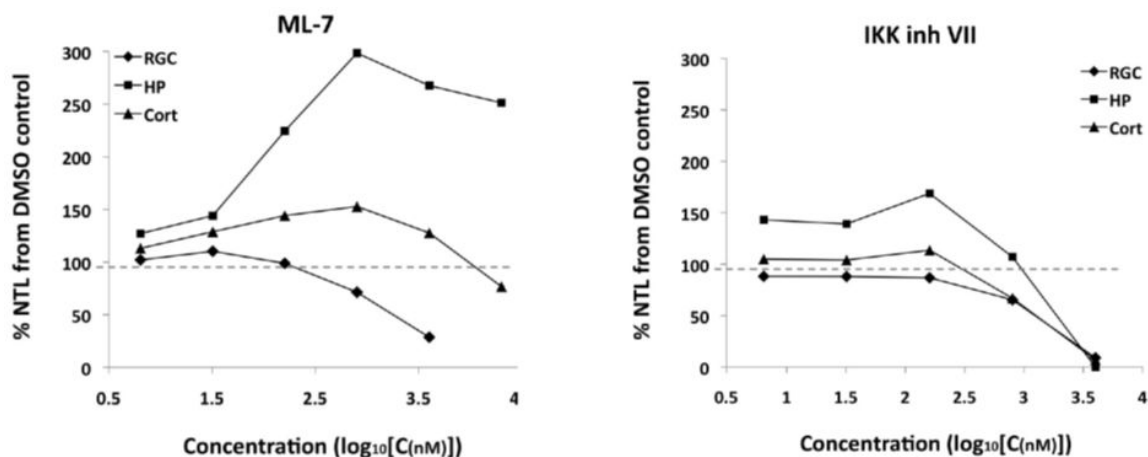


**Figure 1:** Neurite total length (NTL) in various neuronal cell types treated for 2DIV with protein kinase inhibitors ML-7 and IKK inh VII, relative to DMSO treated controls. HP: E18 hippocampal neurons, CGN: postnatal (P8) cerebral granules neurons, Cort: postnatal (P5) Cortical neurons, RGC: postnatal (P8) retinal ganglion neurons (*unpublished data*).

recapitulates the cellular and molecular environment of the CNS, to reduce numbers of false positives prior to animal testing (26,27).

### 2.1.2. Choosing the source of primary neurons

Many types of primary neurons of mouse, rat, or human origin have been successfully used in cell-based screening, and in particular HCS. Regardless of species, neuronal cells of the same type and anatomical origin tend to behave similarly in culture. Cortical neurons have been used in large scale overexpression screens for neurite growth promoting genes (28). Hippocampal neurons have also been used in overexpression (29) and chemical (26) screens for agents that promote neurite growth. Cerebellar granule neurons (CGNs) have been used in overexpression studies, knockdown screening with siRNA (30), and neurotoxicity testing (31). Dorsal root ganglion (DRG) neurons have been used in chemical screens for compounds that mitigate neuronal injury in hyperglycemic conditions (32) as well as knockdown studies of axonal degeneration (33). Retinal ganglion cells (RGCs) have been used to screen, by overexpression, developmentally regulated genes (34). Given the differences in gene expression profiles, as well as morphological dissimilarities among different neuronal types, variability in their respective responses to certain perturbagens is expected (Figure 1). This highlights the importance not only of choosing primary neurons over cells lines, but also specifically selecting the neuronal cell type that best recapitulates the target cell population.

## 2.2. Choosing a substrate

In most cases, it is preferable to perform HCS with purified neurons attached directly to a culture substrate rather than on or around non-neuronal cells. Non-neuronal cells can rapidly outgrow neuronal counterparts in culture, or confound phenotypic analysis due to



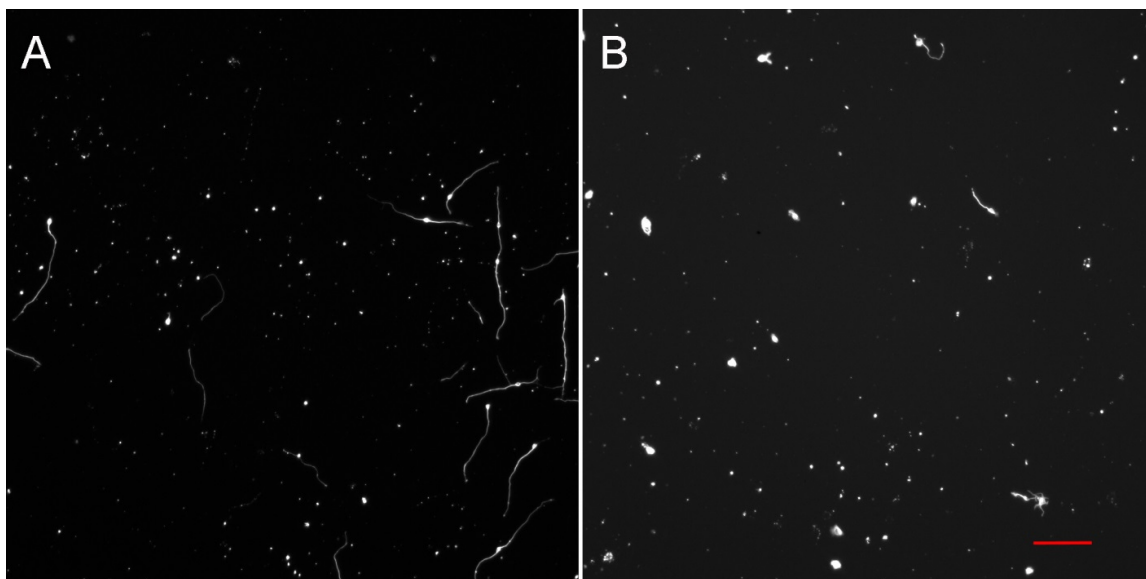


**Figure 2:** Postnatal (P8) CGN cells grown on (A) PDL/Laminin and (B) PDL/Laminin/CSPG. Scale bar 100  $\mu\text{m}$  (*unpublished data (29,71,74)*).

neuronal attachment and subsequent migration of non-neuronal cells. Additionally, studying cultures that contain mixed cell types requires the consideration of indirect effects mediated by non-neuronal cells, which can complicate mechanistic interpretations. Therefore, protocols have been developed for either purifying neuronal cells prior to culturing or optimizing conditions for neuronal growth at the expense of other proliferating cell types, such as glia. The elimination of a non-neuronal cell scaffold, however, creates the requirement for an alternative substrate to allow cell adhesion and neurite growth. Polylysine treated surfaces promote cell adhesion and viability of primary neurons (35). Polylysine also promotes reproducible neurite growth in low-density cultures. Both poly-D-lysine (PDL) and poly-L-lysine (PLL) have been used with success, and early studies showed that while the D isomer minimizes aggregation of neurons better than the L isomer, the two elicit little difference otherwise (35). More recently, polyethylenimine was reported to allow adhesion and growth of primary neurons while completely immobilizing the cells after adhesion (36). Polylysine can also constitute a basal adhesive substrate upon which proteins can be loaded. For example, laminin allows growth and spreading of cultured neurons (37) and promotes extension of longer neurites (38) than those grown on polylysine alone. This can be desirable when searching for agents that inhibit axon growth, as it can increase the dynamic range of the assay readout. Inversely, neurite growth inhibitory components, such as chondroitin sulfate proteoglycans (CSPG) and/or myelin derived proteins (39–45) can be applied to inhibit neurite growth and increase biological relevance of the assay when searching for agents that can promote neurite growth on inhibitory substrates (Figure 2). Naturally, any modifications to the substrate will add complexity to the assay and data interpretation.

## 3. Assay Development

### 3.1. Cell culture media

Synthetic media require serum supplementation to maintain survival of cultured primary neurons. In certain cases, supplementation with growth or trophic factors may be necessary. Low density cultures can be sustained directly by an astrocyte feeder layer (46), or indirectly using glial condition media (47,48). Serum supplements, however, introduce significant experimental variability as a result of differences in donor age, sex, nutrition, and physiological state (49). Similar variability can result from conditioned media. To circumvent this problem, defined media supplements were developed to replace serum (49–51). The widely used supplement, B27, was developed and optimized in conjunction with a DMEM derived formulation, Neurobasal, and the B27/Neurobasal combination has been shown to support growth of various neuronal types (25). The B27 supplement was later reformulated into SN21 to further minimize lot variability and enhance the quality of cultures (52). Other reformulations, such as the NeuroCult™ SM1 supplement, are optimized to give reproducibly high numbers of functional neurons and reduced glial cell contamination.

Despite attempts to fully define the culture media, lot and vendor variability can introduce significant noise into the experiment. It is thus preferable to test different lots of reagents and then obtain enough of well-qualified reagents for an entire screening campaign. Of course it is essential that appropriate positive and negative controls be run to ensure reproducibility.

### 3.2. Cell density and plating method

Desired plating density depends on the application and readout of the assay. High density cultures are required for HCS protocols utilizing neural networks or cellular monolayers, and may be more amenable for screens of neurotoxic or neuroprotective agents (53). Low density cultures, on the other hand, are required for HCS protocols focused on cellular (particularly neuritic) morphology. Unfortunately, however, neurons grow relatively poorly at low density, and small variations in local densities can cause significant differences in neurite morphology (Figure 3). Thus, a sufficient number of cells must be evaluated to accommodate the large variability and non-normal distribution of morphological properties within low density cultures. Usually, 96-well plates offer sufficient area for a low density culture screen with enough neurons per condition/well, although the duration of the experiment depends on the rate at which the neurons extend and overlap processes (overlapped processes render automated cell feature extraction [segmentation] difficult or impossible). For assays that allow or require higher cell densities, 384 well plates may be used. If cells become overlapped sooner than the effect of treatment can be observed, lowering the cell density may be required. This can be achieved by seeding fewer cells or switching to larger area wells. However, because low cell number can dramatically increase noise in the data, it may be more prudent to switch to a larger well size rather than decrease cell number. This is especially true for screens

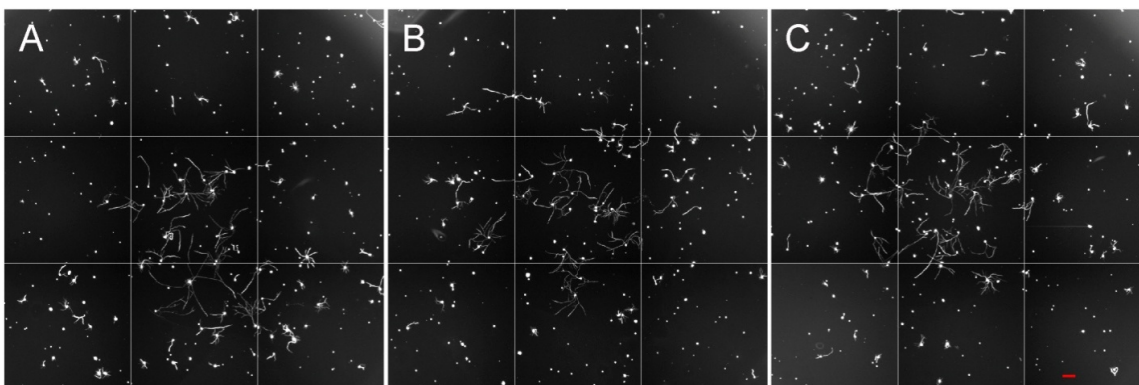


**Figure 3:** A, B,& C, 9 field image montages of RGC cells grown inside wells of 96-well plates, showing differences in neurite length correlated with cell location and cell density (*unpublished data*).

involving transfection, which is often inefficient (transfection rates of 10-50%), and also decreases neuronal viability.

Edge effects are widely recognized in screening departments and can lead to high well-to-well variability and deterioration of overall assay performance (54). Numerous factors can contribute to edge effects, including thermal gradients and differential evaporation rates. An easy work around is to load peripheral wells with water or buffer and avoid using them in the assay.

When seeding cultures of any density, it is best to keep the neurons as uniformly dispersed as possible within the wells. This minimizes perturbations due to variations in local conditions and maximizes the number of cells that can be included in the analysis. When loading cells pre-diluted in media, it helps to do so at low speed to avoid creating too much turbulence which can lead to patterning of cells as they sediment to the bottom. If, on the other hand, cells are being spread in a relatively small volume over a larger volume of media pre-equilibrated within the well, it helps to gently lift and release the entire volume once or twice to insure proper dispersion.

### 3.3. Endpoint assays and fixation

It has been suggested that the full potential of HCS will be realized with time-lapse imaging of live cells (12). Temporal analysis of cellular behaviors can lead to improved understanding of the phenomena underlying observations made in a phenotypic screen and allow for better differentiation between primary and secondary consequences of treatment (55). However, the magnitude and technical requirement for such an undertaking might be inconvenient for medium to high throughput screens, or perhaps unnecessary for endpoint assays. Additionally, longer-term time-lapse studies, especially those using fluorescence, can result in damage or cell death (though current imaging with sensitive cameras and low light levels can mitigate this problem). Live imaging can also limit the types of features that can be easily measured, such as phospho-epitopes on signaling proteins (which require antibody staining), making an endpoint assay more

information-rich. This raises the question of when to terminate the experiment and how to fix the cultures for imaging. Ideally, incubation times should be calibrated to give maximum separation between positive and negative controls (see Section 3.8). This information is normally acquired empirically. The fixation method will depend on the subsequent steps for analyzing the cultures. Typically, cells are fixed in 4% paraformaldehyde in phosphate buffer. Sucrose can be added to the fixative to enhance preservation of membrane structure and processes during cross-linking. Sucrose also increases the density of the fixing solution, which causes it to drop to the bottom of the wells and ensure rapid fixation. In certain cases, paraformaldehyde can mask antigenic epitopes from recognition by specific antibodies. In those cases, other fixatives, such as cold methanol, can be used.

### 3.4. Washing

Post-fixation, cultures require multiple rounds of washing, to remove fixative and other reagents. It is important to adopt a washing procedure that is gentle enough to avoid washing away cells and preserve their delicate processes while also being rapid and efficient. A plate washer can be used if the proper settings can be deployed to avoid harsh suction or excessive flushing. It is prudent to avoid complete drying of cells during washing. If a plate washer is used, it is best to leave a few millimeters of wash buffer over the cells at times during the wash cycle. If plates are being washed manually, it is best to use a multichannel suction adapter with pins shorter than the full depth of the well. It helps to take out and dispense fluid gently and at low speed, preferably along the wall of the well rather than directly over the cells.

### 3.5. Permeabilization and blocking

Labeling with primary antibodies prior to permeabilization ensures that only surface proteins are identified. However, the fixation step itself can cause permeabilization, even if no detergent is present (56). Therefore, it is important to perform staining for the protein of interest along with an exclusively intracellular protein to identify instances of compromised plasma membrane integrity. For staining intracellular proteins, a permeabilization step is normally required, usually with Triton X-100 (0.2-0.3%, 5-10 mins). Milder detergents, such as digitonin and leucoperm, may be useful when Triton X-100 compromises antigenicity. Saponin (0.02%) can be used to permeabilize cell membranes while keeping intracellular organelle membranes intact. Preparation and storage of solutions of Digitonin and Saponin is not always straightforward so it is helpful to consult the literature (57). In all cases, non-specific binding sites should be blocked to decrease background staining. This can be achieved with a 10% bovine serum albumin solution, fish gelatin, or goat serum. As an example, goat serum may help with background caused by nonspecific binding of secondary antibodies raised in goat. By adding detergent to the block, the permeabilization and blocking steps can be combined to minimize wash steps. In this case, a lower percentage of Triton X-100 (0.03%) can be used to slow down the permeabilization process, allowing sufficient time for blocking (up to one day).

### 3.6. Staining and visualization

Quantitative HCA measurements of neuronal morphology are commonly carried out using immunohistochemistry with fluorescent dyes. Hoechst and DAPI dyes are routinely used to stain DNA and identify nuclei. Immunostaining of cytoskeletal markers, such as tubulin, is commonly used for visualizing cell morphology. Tubulin  $\beta$ III-specific monoclonal antibodies that preferentially label neurons can be used for preparations that contain a substantial number of non-neuronal cells. Tubulin antibodies will also allow for the detection of neurites; however, other antibodies need to be used to distinguish dendrites from axons. Antibodies to dendrite-selective markers, such as MAP-2, or axon-specific markers, such as Tau1, can be used for that purpose. For quantification of synapse formation, co-localization of presynaptic markers, such as synapsin, with postsynaptic puncta can be measured (58,59). It is generally convenient to also stain for tubulin because automated HCA software will typically require a complete cell body mask in order to correctly assign structures to their corresponding cell body. Co-staining of other markers can be done simultaneously, provided antibody compatibility is ensured. Primary antibodies for different antigens, such as MAP2 or  $\beta$ III tubulin, must be raised in different species (for example mouse and rabbit) if they are to be used simultaneously in the assay. Secondary antibodies should preferably be from the same species (for example goat or donkey). It is important to pre-absorb secondary antibodies with potentially cross-reacting primary antibodies. Thus, a goat-anti-mouse secondary antibody should be preabsorbed on a rabbit IgG column to eliminate cross reactivity. Pre-absorbed antibodies are readily available from commercial sources. It is crucial to ensure that the optical filter sets used for imaging have appropriate excitation/emission filters so as to capture relevant signals from a given combination of fluorophores, while minimizing “bleed-through” from one channel to another. An alternative method to secondary immunostaining is to use primary antibodies that are directly conjugated to fluorescent tags. These are readily available from various suppliers. Conjugation kits are also available for labeling primary antibodies with a variety of fluorophores, infrared dyes, and quantum dots.

Plasma membrane specific dyes can be used for delineating cell bodies and neurites. CellMask™ Deep Red has been used with success in a neurite growth assay, where it was applied in the fixative solution along with a nuclear stain, dramatically decreasing the time and reagents required for the staining process (60). However, while these stains do survive fixation, they do not survive permeabilization, and so their use must be reserved for assays where external morphology and/or extracellular staining are the only endpoints.

### 3.6. Data analysis

In addition to HCS parameters that can be extracted from virtually all cell types, which include cellular/nuclear/organelle size and brightness, HCS with neurons can produce readout parameters related to neuron-specific morphologies, such as axon and dendrite count, branching, and length. All vendors of major HCS imaging systems provide image analysis software solutions for neuronal HCS (e.g., Figure 4).

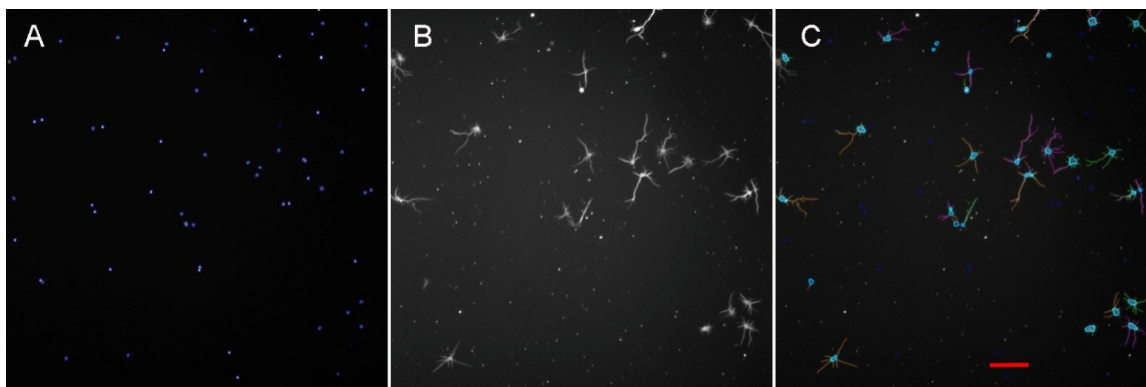


**Figure 4:** HCA of neurons in culture. Neurons in 96 well plates immunostained for nuclei (Hoechst – Panel A) and  $\beta$ III-tubulin (cell bodies and neurites – Panel B). The images were automatically traced using the Neuronal Profiling BioApplication (Cellomics) to yield dozens of morphological measurements for each neuron in the well (Panel C). Scale bar 100  $\mu$ m (*unpublished data*).

Additionally, there are other commercial (61) and open source (62–64) feature extraction solutions. Given the sheer amount of data produced from HCS image analysis, it is helpful to develop batch processing scripts to facilitate data analysis and quality control.

### 3.7. Assay suitability and quality control

The suitability of a screening assay is a measure of its ability to reproducibly distinguish positive from negative controls. Due to inter-prep variability and differences in the behaviors of dissociated primary neurons in culture, it is essential to run the proper controls in every screening experiment to evaluate the consistency of responses to treatment. Because of variability in absolute readout values, means, coefficients of variation, and signal to noise ratios, it is difficult to compare assay performance across multiple assay formats or even within repetitions of the same assay. To resolve this issue, a dimensionless statistical parameter,  $Z'$ -factor, was defined to assess the “screening window” of a bioassay (65). A  $Z'$ -factor value of  $\geq 0.5$  reflects a large separation band between the populations of positive and negative control readouts, and thus indicates good screening suitability (Figure 5).

The  $Z'$ -factor is, however, based on a single selected readout. HCS offers the option of collecting a large number of readouts per screen. Incorporating additional parameters in the definition of assay hits can distinguish between actives with distinct mechanisms of action. For that purpose, a multiparametric  $Z'$ -factor was proposed (66). This multiparametric value is calculated by scaling  $Z'$  values from multiple readouts, and thus requires post hoc calculation of a weight for each considered readout. A potentially more objective metric for distinguishing actives in a screen is the multidimensional perturbation value (mp-value) (67). The strength of this approach lies in evaluating exactly how similar or dissimilar treatments are from each other or from controls, and thus no *a priori* definition of hits is required. However, this can make the definition of hits

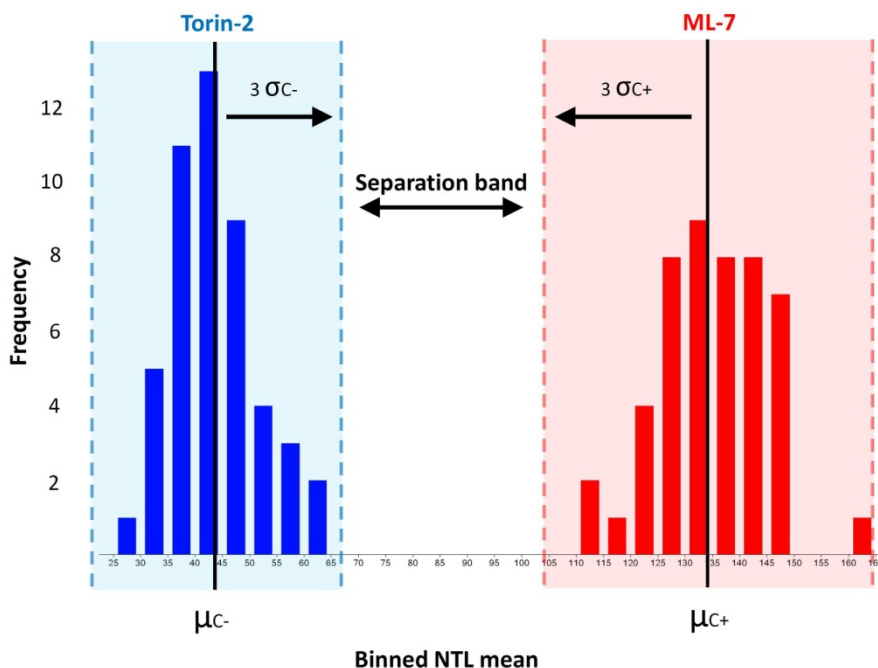


**Figure 5:** Bar plot representing binned values of neurite total length (NTL) averages from wells (96-well plates) containing cultured hippocampal neurons treated with ML-7 (neurite growth promoter) or Torin-2 (neurite growth inhibitor). Each block shows the mean of the population with three standard deviations above and below. This pair of controls yields a  $Z'$ -factor  $>0.7$ , as evidenced by the complete separation of the two populations (*unpublished data*).

less clear-cut. In most cases, HCS focuses on one select parameter, and the suitability of the assay is evaluated using a one dimensional  $Z'$ -factor.

## 4. Additional Considerations

### 4.1. Controls

Due to the complex morphology of neurons compared to most other cells types, these cells manifest a relatively large range of measurable phenotypes. Consequently, a number of factors can influence the phenotypes of cultured primary neurons, including preparation, reagents, and culture conditions. This introduces a significant amount of variability (noise) in the data that can mask effects from treatment. It is possible to minimize circumstantial variability and improve detection of treatment effects by including normalization controls within individual plates (29). A sufficient number of controls is important for reliable normalization (68). Negative controls in compound screens usually receive the equivalent amounts of solvent (e.g. DMSO)—it is important to determine beforehand whether the solvent at relevant concentrations has any discernible effects on the assay readout. Choosing controls for RNA/DNA screens is less straightforward. “Control” plasmids or oligonucleotides may unevenly influence phenotypic parameters. It may be necessary to screen a large number of different

constructs to determine population behavior and select controls that yield population mean values.

## 4.2. Cell viability assessment

Accurate quantification of cell death is a critical component of HCS with primary neurons. Cell viability is the most important readout in neurotoxicity screens, but is important when analyzing data for any screen. As mentioned previously, certain phenotypes have non-normal distribution in low-density neuronal cultures, and a minimum number of viable (or valid) cells is required to obtain reliable and reproducible results. Thus, it is important for quality control purposes that individual data points on cellular phenotypes are obtained from healthy neurons in suitable numbers. Therefore an assessment of cell viability is required. Several methods exist that assess viability by interrogating different aspects of the cell - nuclear morphology, caspase activation, membrane integrity, and mitochondrial function. Each of these indicators answers the question of viability in a different way. For example, examining caspase activation using antibodies against activated caspase 3 or 9 is a measure of apoptotic death. Dying cells tend to have smaller nuclei that stain more brightly with DNA stains (due to DNA compacting and fragmentation), hence the nuclear morphology and staining intensity can be used as an indicator of cells death (Figure 6 unpublished data), provided the proper controls are considered (29).

This, however, may not work equally well for all neuronal types. In the case of live cell imaging, cell viability can be assessed by examining membrane integrity. Membrane impermeable fluorescent dyes can be used to identify dead cells by positive or negative selection. For example, a DNA-binding fluorescent impermeable dye like SYTOX® will fluoresce inside dead or dying cells with breached cellular and nuclear membranes. Inversely, a cell permeable dye like Calcein AM will enter live cells where it will be cleaved into a fluorescent membrane-impermeable derivative, thus fluorescing inside live cells. Another widely used marker for cell viability is mitochondrial function as indicated by the presence of a mitochondrial membrane potential, which can be examined using commercially available dyes such as MitoTracker® or Tetramethylrhodamine, Ethyl Ester, Perchlorate (TMRE).

## Considerations for small molecule screening

### 4.3.1. Concentration of small molecules

Choosing a single concentration for a cell-based small-molecule screen is complicated by a multitude of factors including, but not limited to, differences in solubility, membrane permeability, binding affinity, selectivity, and toxicity. A single concentration screen accepts the caveat of exaggerated false negatives. Ideally, a concentration of a compound that is close to  $IC_{50}$  or  $K_D$  of the target should be tested. However, even slight chemical modifications can dramatically alter the binding affinity within a group of chemically related compounds, making it unrealistic to find a single concentration that elicits effects in all actives. Of course, in cell-based screenings, most molecular targets are unknown.



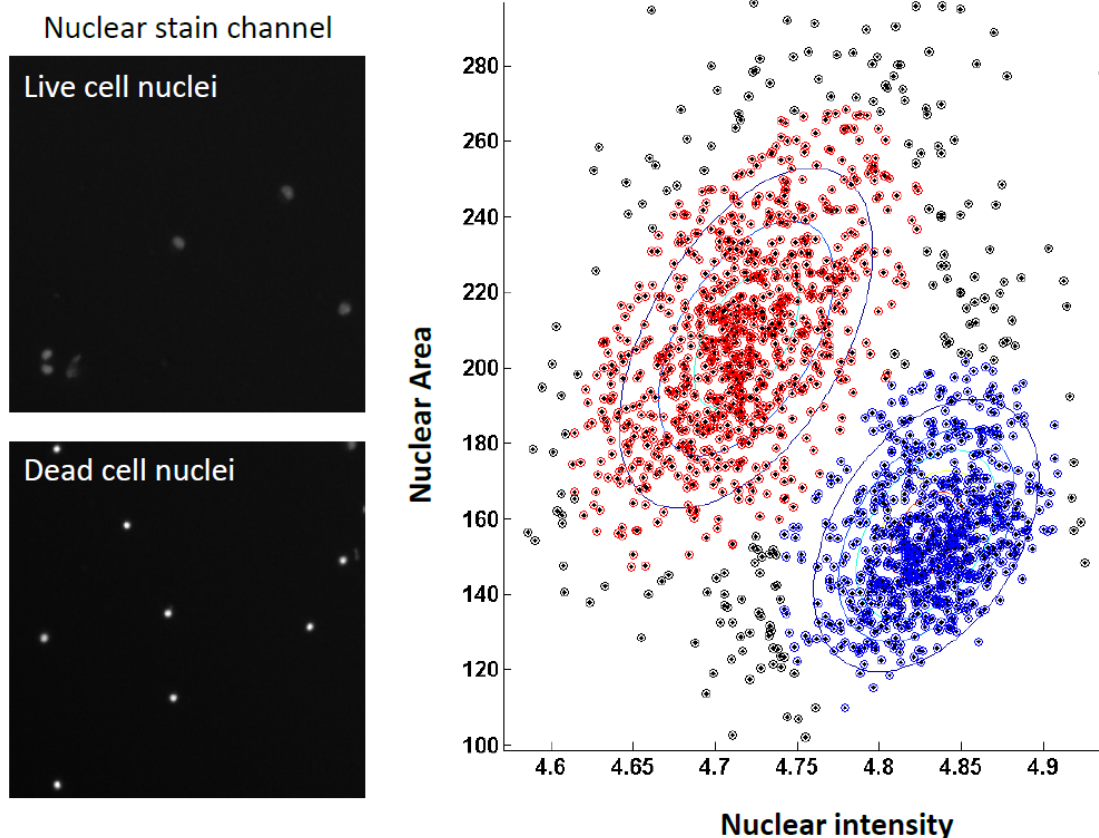


**Figure 6:** Small and bright nuclei are the result of heterochromatin condensation, while big dim nuclei correspond to cells that are alive. This distinction can be used to measure cell survival in nuclei-stained cultures. A Gaussian fit searches for two clusters within the population as live [large nucleus, low intensity] or dead [small nucleus, high intensity] (*unpublished data and 29*).

Therefore, it is highly desirable to obtain a dose response in HCS of primary neurons, typically in the low nanomolar to micromolar range.

#### 4.3.2. Time and duration of treatment

Two important considerations for cell-based screening of small molecules include time of administration of the compounds and duration of incubation. Depending on the experimental model, the exact time for adding the compounds may be of biological relevance or purely technical relevance. Low density cultures are often allowed a recovery period before perturbation (typically a few hours to a day). Assays that examine effects on networks of neuronal processes, for example, will require the necessary time for such networks to form following plating. Thus, pre-treatment time should be considered in the overall time of the assay and cultures must be verified to remain viable and healthy over the course of the entire experiment. It is most helpful if the duration of incubation is calibrated to maximize the dynamic range of the readout. To achieve this, the  $Z'$ -factor

can be calculated for control positives (promoters) and negatives (inhibitors) at multiple time points, and the window with the largest  $Z'$ -factor can be adopted for the screen.

### 4.3.3. DMSO tolerance

DMSO is by far the most commonly used solvent for small-molecule and drug-like compound libraries. DMSO can induce toxicity in neurons at concentrations greater than 0.5% v/v. At high enough concentrations, DMSO can also affect neuronal morphology and function (Figure 7). It is thus advisable to keep final DMSO concentrations as low as possible, preferably below 0.5% v/v. It is also useful to keep DMSO concentrations constant in serial dilutions of stock compounds in media, to eliminate DMSO concentration effects as a confounding variable.

## 4.4. Considerations for genetic screening

### 4.4.1. Overexpression vs knockdown

Overexpression screens with primary neurons have identified developmentally regulated transcription factors (34), kinases, and phosphatases (29) involved in axon regeneration. Knockdown screens have also been used to identify regeneration associated kinases (30) as well as kinases involved in neurodegeneration (53). The choice between overexpression and knockdown depends on the exact question that the assay is attempting to answer; each method brings its own advantages and drawbacks. Overexpression can produce false negatives due to issues arising from auto-regulation, inappropriate posttranslational modification, novel activities at high expression levels, and lack of activation by stoichiometrically insufficient trans-activators. Knockdown with RNAi can suffer from severe off-target effects (69), and may be less efficient in neurons compared to other cell types (70). Ultimately, a validation with one approach of hits identified using the other approach will increase the likelihood of biological relevance.

### 4.4.2. Transfection

Transfecting primary neurons can be challenging for multiple reasons, including difficulties in obtaining sufficient quantities of purified neurons and problems encountered in automated liquid handling. Traditional lipid-based methods yield low transfection rates in neurons and induce cell death. Electroporation can yield more efficient transfection for HCS, and is likely preferable (29,71). RNAi is reported to be less efficient in neurons than in other cell types (70), and longer turnover rates of proteins can lead to false negatives. Magnetic transfection may enhance siRNA introduction into neurons (53). Viral transduction, which overcomes many of these problems, has been successfully used in HCS with primary neurons (33).

### 4.4.3. Identification of transfected or transduced cells

A common issue with overexpression of cDNA libraries is the lack of a tag or a co-expressed marker. Thus, for transfection or transduction efficiencies below 100%, a marker is required for identifying modified cells. New libraries are more commonly being

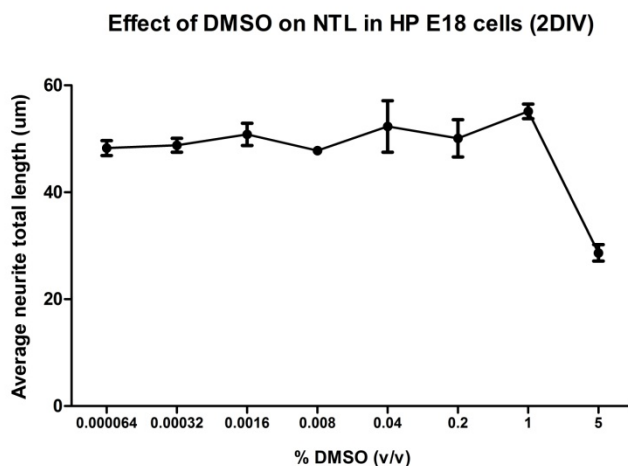


**Figure 7:** Effect of DMSO concentration on neurite length in E18 hippocampal neurons. Each point represents an average of 6 data points  $\pm$  SEM. These data suggest that it would be best to keep the final DMSO concentration below 1% to avoid complicating any analysis related to neurite length (*unpublished data*).

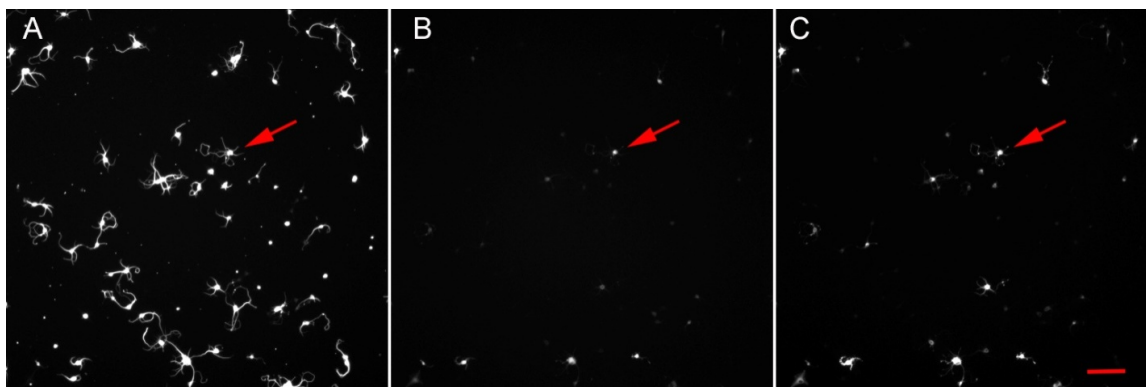


**Figure 8:** Postnatal (P5) cortical neurons (1) simultaneously transfected with GFP (1) and mCherry (1). Arrows indicate a cell exhibiting fluorescence in both green (1) and red (1) channels, indicating double transfection. The high co-transfection rate suggests that a fluorescent marker can be used as a marker for transfected cells in this experiment. Scale bar 100 um (*unpublished data*)

made with tags, such as Myc or FLAG. If tagged constructs are used, a follow-up validation experiment with the untagged proteins may be required to eliminate possible false positives, though false negatives would persist (as discussed before).

Alternatively, a coexpressed fluorescent protein can be introduced via an Internal Ribosomal Entry Site (IRES) (72). Another strategy is to use plasmids expressing the self-cleaving 2A peptide (73), though such plasmids may exhibit variability in expression of the second (reporter) gene. Finally, a co-transfection strategy can be used in which the gene of interest is administered at a 4-6X molar ratio relative to a reporter plasmid. This

generally results in 80-90% of fluorescently marked cells also expressing the gene of interest (29) (Figure 8).

## 5. Protocols for HCS with Primary Neurons

### 5.1. Small molecule screening with hippocampal neurons - Overview

This bioassay utilizes primary hippocampal neurons isolated from embryonic (E18) rat brain and is optimized for identifying small molecules that can promote neurite growth in those neurons. The cells are cultured on a semi-permissive substrate, poly-D-lysine, which produces moderate neurite growth and allows for a large dynamic range in neurite length readout (growth promoters can reach 300-400% of control neurite growth). The assay typically produces a very good Z' factor and has low false discovery rate. In its current format, it is suited for low throughput screening (with a practical average of 100-200 compounds per experiment), though the high Z'-factor makes it suitable for higher throughput screening.

#### 5.1.1. Reagents

1. NbActiv4 Cell-culture media (BrainBits cat. no. Nb4-500)
2. NeuroCult™ SM1 Supplement (Stemcell cat. no. 05711)
3. Hibernate E (Brainbits-HE-Ca-500mL)
4. 2.5% (wt/vol) trypsin; aliquot for single use (0.5 ml) and store at  $-20\text{ }^{\circ}\text{C}$
5. DNase 30 mg/mL in ddH<sub>2</sub>O (Sigma-Aldrich cat. no. D-5025)
6. Polylysine solution,  $0.5\text{ mg mL}^{-1}$  in HBSS (prepared from poly-L-lysine, molecular weight 30,000–70,000 kDa; Sigma-Aldrich, cat. no. P2636)
7. HBSS (LifeTechnologies cat. no. 14175-103)
8. 4% PFA 4% Sucrose in PBS
9. PBS
10. DMSO
11. Blocking and permeabilization buffer (0.2% fish gelatin, 0.03% Triton X-100, in PBS + 0.02% azide)
12. Mouse anti-tubulin  $\beta$ III antibody
13. Hoechst solution (10 mg/mL)
14. Alexa Fluor® 488 Goat Anti-Mouse IgG (H+L) (Lifetechnologies cat. no. A-11029)

#### 5.1.2. Equipment

1. Laminar flow hood, able to accommodate a dissecting microscope
2. Tissue culture incubator at  $35.5\text{ }^{\circ}\text{C}$  with humidified 5% CO<sub>2</sub> atmosphere
3. Water bath at  $37\text{ }^{\circ}\text{C}$
4. Dissecting microscope
5. Dissecting tools (sterilized): fine-tipped forceps, microdissecting scissors
6. Hemacytometer or automated cell counter
7. Sterile plasticware: 5-, 10- and 25 mL serological pipettes, tissue culture dishes and bacteriological dishes, 15 mL and 50 mL conical centrifuge tubes

8. Sterile glass Pasteur pipettes
9. 96-well plates
10. Filter-plugged pipette tips (1200, 200, and 20  $\mu\text{L}$ )

### 5.1.3. Pre-coating culture plates

1. On the day before the experiment, load PDL solution in 96-well plates to coat (50  $\mu\text{L}/\text{well}$ )
2. Wash plates next morning with HBSS or PBS (150  $\mu\text{L} \times 4$  washes) then leave in buffer until plating

Comment: For larger well size, the volume of PDL coating solution should be increased roughly proportional to the well area.

### 5.1.4. Preparing the Cells

1. Euthanize timed pregnant rat carrying E18 embryos using an IACUC approved method
2. In a laminar flow hood, remove the embryos and place in a petri dish containing Hibernate E
3. Dissect pup brains and collect hippocampi in 15 ml conical tube containing Hibernate E with SM1 (2% v/v)
4. Prepare dissociation media by combining 4.5 ml of Hibernate E (without SM1) with 0.5 mL of Trypsin and 100  $\mu\text{L}$  of DNase solution
5. Carefully decant hippocampi then add dissociation solution. Incubate at 37  $^{\circ}\text{C}$  for 15-20 min, occasionally swirling the tube
6. Using cotton plugged Pasteur pipettes (flame polished), remove dissociation media then add 5 mL of Hibernate E containing SM1. Swirl the tube to thoroughly wash the tissue. Allow the tissue to settle to the bottom of the tube then carefully remove the rinse solution. Repeat this step 5 times to dilute out trypsin and DNase and remove debris from lysed cells
7. Remove final rinse media from the tube then add 1 pipette-full of rinse media
8. Using the narrow-bore flame-polished Pasteur pipette (pre-wetted with rinse media), triturate until all cells are dissociated and no chunks of tissue remain. It's best to perform less than ten triturations as it adversely affects cell viability
9. Bring volume up to 8-12 mL using Hibernate E containing SM1, then mix well and determine cell concentration

Comment: Plating cells immediately after trituration will prevent clumping and improve overall quality of the culture.

### 5.1.5. Plating

1. Dilute cells in culture media to a final concentration of 10,000 cells/ml
2. Aspirate HBSS from PDL coated plates
3. Load 150  $\mu\text{L}$  of cell solution in the middle 48 wells (See Figure 9)

| A01 | A02 | A03         | A04         | A05         | A06         | A07         | A08         | A09         | A10         | A11 | A12 |
|-----|-----|-------------|-------------|-------------|-------------|-------------|-------------|-------------|-------------|-----|-----|
| B01 | B02 | 150 $\mu$ L | 150 $\mu$ L | 150 $\mu$ L | 150 $\mu$ L | 150 $\mu$ L | 150 $\mu$ L | 150 $\mu$ L | 150 $\mu$ L | B11 | B12 |
| C01 | C02 | 150 $\mu$ L | 150 $\mu$ L | 150 $\mu$ L | 150 $\mu$ L | 150 $\mu$ L | 150 $\mu$ L | 150 $\mu$ L | 150 $\mu$ L | C11 | C12 |
| D01 | D02 | 150 $\mu$ L | 150 $\mu$ L | 150 $\mu$ L | 150 $\mu$ L | 150 $\mu$ L | 150 $\mu$ L | 150 $\mu$ L | 150 $\mu$ L | D11 | D12 |
| E01 | E02 | 150 $\mu$ L | 150 $\mu$ L | 150 $\mu$ L | 150 $\mu$ L | 150 $\mu$ L | 150 $\mu$ L | 150 $\mu$ L | 150 $\mu$ L | E11 | E12 |
| F01 | F02 | 150 $\mu$ L | 150 $\mu$ L | 150 $\mu$ L | 150 $\mu$ L | 150 $\mu$ L | 150 $\mu$ L | 150 $\mu$ L | 150 $\mu$ L | F11 | F12 |
| G01 | G02 | 150 $\mu$ L | 150 $\mu$ L | 150 $\mu$ L | 150 $\mu$ L | 150 $\mu$ L | 150 $\mu$ L | 150 $\mu$ L | 150 $\mu$ L | G11 | G12 |
| H01 | H02 | H03         | H04         | H05         | H06         | H07         | H08         | H09         | H10         | H11 | H12 |

**Figure 9:** Plating schematic

4. Allow cells to adhere for 2 hours in tissue culture incubator prior to treatment

Comment: Use a multichannel manual pipette and load cells gently. Alternatively, use the slowest speed setting on an automated pipette. This helps avoid patterning in the plated cells and promote even spreading.

### 5.1.6. Preparing Compound Dilution Plates

1. Place culture media in a 96-well plate (new – uncoated) as shown in Figure 10 (solution A = culture media, solution B = culture media + 0.8% DMSO)
2. Add 1  $\mu$ L of compound stock solution to each of the top wells containing 124  $\mu$ L. This will produce a final DMSO concentration of 0.8% and final compound concentration of 80  $\mu$ M (starting with a 10 mM stock solution in DMSO). Control wells receive 1  $\mu$ L of DMSO
3. Using a multichannel manual p200 pipette, mix the solutions in the top row then move 25  $\mu$ L to the below row. This creates a 1:5 dilution of compound while DMSO is held constant at 0.8%. Repeat serial dilutions until the last row. This format allows for screening 3 compounds per plate at 6 concentrations with duplicate wells per condition.
4. Place compound dilution plates in tissue culture incubator for 1-2 hours to equilibrate

For calculating the  $Z'$ -factor of the assay, include an additional plate (or more) with the corresponding treatment format as shown in the schematic in Figure 11 ( $C_+$  is a compound that produces the desired bioassay readout – in this case neurite growth promotion, and  $C_-$  is a compound that produces the opposite effect – or neurite growth inhibition. Both compounds must be prepared at 4X the corresponding concentration where their maximal effects are observed. See Figure 11)

### 5.1.7. Treatment

1. Using a multichannel manual p200 pipette, aspirate 50  $\mu$ L from the final dilution (row G) and slowly add to corresponding row of recipient cell plate (4X dilution, 50  $\mu$ L of compound solution into 150  $\mu$ L of cell culture). Repeat going up the rows

| A01 | A02 | Compound 1 |         | Compound 2 |         | Compound 3 |         | DMSO    |         | A11 | A12 |
|-----|-----|------------|---------|------------|---------|------------|---------|---------|---------|-----|-----|
| B01 | B02 | 124 (A)    | 124 (A) | 124 (A)    | 124 (A) | 124 (A)    | 124 (A) | 124 (A) | 124 (A) | B11 | B12 |
| C01 | C02 | 100 (B)    | 100 (B) | 100 (B)    | 100 (B) | 100 (B)    | 100 (B) | 100 (B) | 100 (B) | C11 | C12 |
| D01 | D02 | 100 (B)    | 100 (B) | 100 (B)    | 100 (B) | 100 (B)    | 100 (B) | 100 (B) | 100 (B) | D11 | D12 |
| E01 | E02 | 100 (B)    | 100 (B) | 100 (B)    | 100 (B) | 100 (B)    | 100 (B) | 100 (B) | 100 (B) | E11 | E12 |
| F01 | F02 | 100 (B)    | 100 (B) | 100 (B)    | 100 (B) | 100 (B)    | 100 (B) | 100 (B) | 100 (B) | F11 | F12 |
| G01 | G02 | 100 (B)    | 100 (B) | 100 (B)    | 100 (B) | 100 (B)    | 100 (B) | 100 (B) | 100 (B) | G11 | G12 |
| H01 | H02 | H03        | H04     | H05        | H06     | H07        | H08     | H09     | H10     | H11 | H12 |

**Figure 10:** Schematic of compound dilution plate

| A01 | A02 | A03               | A04               | A05               | A06               | A07               | A08               | A09               | A10               | A11 | A12 |
|-----|-----|-------------------|-------------------|-------------------|-------------------|-------------------|-------------------|-------------------|-------------------|-----|-----|
| B01 | B02 | 4X C <sub>H</sub> | 4X C <sub>H</sub> | 4X C <sub>H</sub> | 4X C <sub>H</sub> | 4X C <sub>L</sub> | 4X C              | 4X C              | 4X C <sub>L</sub> | B11 | B12 |
| C01 | C02 | 4X C <sub>H</sub> | 4X C <sub>H</sub> | 4X C <sub>H</sub> | 4X C <sub>H</sub> | 4X C <sub>L</sub> | 4X C <sub>L</sub> | 4X C <sub>L</sub> | 4X C <sub>L</sub> | C11 | C12 |
| D01 | D02 | 4X C <sub>H</sub> | 4X C <sub>H</sub> | 4X C <sub>H</sub> | 4X C <sub>H</sub> | 4X C <sub>L</sub> | 4X C <sub>L</sub> | 4X C <sub>L</sub> | 4X C <sub>L</sub> | D11 | D12 |
| E01 | E02 | 4X C <sub>H</sub> | 4X C <sub>H</sub> | 4X C <sub>H</sub> | 4X C <sub>H</sub> | 4X C <sub>L</sub> | 4X C <sub>L</sub> | 4X C <sub>L</sub> | 4X C <sub>L</sub> | E11 | E12 |
| F01 | F02 | 4X C <sub>H</sub> | 4X C <sub>H</sub> | 4X C <sub>H</sub> | 4X C <sub>H</sub> | 4X C <sub>L</sub> | 4X C <sub>L</sub> | 4X C <sub>L</sub> | 4X C <sub>L</sub> | F11 | F12 |
| G01 | G02 | 4X C <sub>H</sub> | 4X C <sub>H</sub> | 4X C <sub>H</sub> | 4X C <sub>H</sub> | 4X C <sub>L</sub> | 4X C <sub>L</sub> | 4X C <sub>L</sub> | 4X C <sub>L</sub> | G11 | G12 |
| H01 | H02 | H03               | H04               | H05               | H06               | H07               | H08               | H09               | H10               | H11 | H12 |

**Figure 11:** Schematic for additional assay plate containing corresponding treatment

(increasing concentration). Final compound concentration in screen: 0.0064, 0.032, 0.16, 0.8, 4, and 20  $\mu\text{M}$  (in 0.2% DMSO)

2. Be sure to avoid creating too much turbulence in the wells to avoid detaching recently adhered cells.
3. Return plates to incubator and culture for 48 hours

Comment: Do this for 5 or less plates at a time to avoid leaving the cells too long out of the incubator, which could lead to changes in the pH of culture media and affect cell viability.

### 5.1.8. Fixing the cultures

1. Remove media from plates and immediately replace with 100  $\mu\text{L}$  of warm (37  $^{\circ}\text{C}$ ) PFA/sucrose solution. Gently inverting plates will remove media without damaging delicate neurites
2. Fix for 15-20 min
3. Rinse with PBS (200  $\mu\text{L}$  /well  $\times$  3)

Comment: Exercise sufficient care when handling PFA and perform all steps inside a fume hood with sufficient protection. Be sure to properly dispose of waste PFA solution

### 5.1.9. Staining and imaging

1. Remove PBS and add 100  $\mu\text{L}$  of blocking/permeabilization buffer (PBS, 0.2% fish gelatin, 0.03% Triton X-100, 0.02% azide) and incubate overnight at 4  $^{\circ}\text{C}$  (can be

stored over the weekend). If faster permeabilization and blocking are required, cells can be permeabilized in a higher Triton X-100 concentration (0.3% in PBS) for 1 hour and then blocked for 1 hour.

2. Add 100  $\mu\text{L}$  of primary antibody solution (mouse anti-Beta III tubulin in blocking buffer) and incubate overnight at 4  $^{\circ}\text{C}$ .
3. Rinse wells with PBS (200  $\mu\text{L} \times 3$ )
4. Remove PBS and add 100  $\mu\text{L}$  of secondary antibody solution (Goat anti-mouse Alexa 488, 10  $\mu\text{g}/\text{mL}$  Hoechst, 0.2% fish gelatin, 0.02% azide, in PBS). Shake gently on a rotating shaker for 2 hours.
5. Rinse wells with PBS (200  $\mu\text{L} \times 5$ )
6. Image plates using a Celloomics ArrayScan VTI in 2 different channels for nuclear staining (Hoechst) and cell body/neurite staining ( $\beta\text{III-tubulin}$ ). Typically, nine fields per well are imaged with a 5X objective and automatically traced by the Neuronal Profiling Bioapplication. To get reliably reproducible results, at least 200-300 cells should be measured per condition.

### 5.1.10. Data analysis

1. Export plate data in Excel sheet format.
2. Filter out artifacts, cells that died upon plating, debris, and so on. This can usually be achieved by applying filters on phenotypic parameters. A set that works well for this assay includes the following cut off (NeuriteTotalLength > 10  $\mu\text{m}$ , NeuriteMaxLengthWithoutBranching < 500  $\mu\text{m}$ , MinCellBodyArea > 100  $\mu\text{m}^2$ , MaxCellBodyArea < 3000  $\mu\text{m}^2$ , MaxNeuriteBranching < 50). Additional parameters can be derived empirically and added as required. This leaves only the valid neurons in each well.
3. For each drug condition, normalize the data to the controls in the corresponding row. For example, to calculate the effect of Compound 1 on neurite total length (NTL) at 20  $\mu\text{M}$ , use the following formula

$$\text{Compound1 \%NTL (20 uM)} = \frac{\text{AVG}(B3_{\text{NTL}} + B4_{\text{NTL}})}{\text{AVG}(B9_{\text{NTL}} + B10_{\text{NTL}})} \times 100$$

Where B3NTL and B4NTL are the averages of neurite total length in wells B3 and B4, and B9NTL and B10NTL are the averages of neurite total length in wells B9 and B10.

4. Calculate the Z-score for each attribute using the following formula

$$\text{Compound1 Z-score NTL (20 uM)} = \frac{\text{AVG}(B3_{\text{NTL}} + B4_{\text{NTL}}) - \text{AVG}(B9_{\text{NTL}} + B10_{\text{NTL}})}{\sigma_{\text{controls}}}$$

Where  $\sigma_{\text{controls}}$  is the standard deviation in all DMSO wells within the plate (columns 9[B→G] and 10[B→G])



5. Calculate the Z'-factor for the assay using the positive and negative control (CH/CL) plate(s) according to the following formula

$$Z'\text{-factor} = 1 - \frac{(3\sigma_{C_H} + 3\sigma_{C_L})}{|\mu_{C_H} - \mu_{C_L}|}$$

Where  $\mu_{C_H}$  and  $\mu_{C_L}$  are the means for the positive and negative (neurite growth promoter and neurite growth inhibitor) control wells respectively, and  $\sigma_{C_H}$  and  $\sigma_{C_L}$  are the respective standard deviations.

Comment: Hits can be identified as compounds that fulfill the following criteria: %NTL > 130% & NTL Z-score > 1.5 & % valid neurons > 60% & valid neurons Z-score > -4. Hits must be confirmed in two independent screens. These criteria usually yield an average false discovery rate of ~ 10%.

Comment: Considering the rather large size of datasets generated from this kind of experiment, it is advisable to automate the data analysis process, provided that sufficient attention is given to quality control and validation of all data points.

## 5.2. Plasmid DNA screening with cortical neurons – Overview

This bioassay uses mixed cortical cells from early postnatal rat pups, aged P1 to P7, and is optimized for delivery of plasmid DNA via electroporation. The use of postnatal neurons, as opposed to embryonic, is beneficial when screening for genes or compounds that may be relevant to age-related reductions in neurite outgrowth. Such cultures, however, are subject to challenges associated with isolating and maintaining postnatal neurons. As animals age postnatally between P1 and P7 neurons become increasingly difficult to dissociate, and the mechanical force needed to remove neurons from the surrounding matrix increases, which leads to increased mortality during cell preparation. Sequential digestion with papain followed by trypsin, continual agitation during enzyme treatments, and brief triturations are critical to balance the relative difficulty in dissociating cells with the need for large numbers of viable cells to support screening efforts. It is also important that cells be provided with appropriate survival factors in the growth media. This protocol utilizes a relatively complex growth media, which is then conditioned by exposure to glial cultures. Glial conditioning increases cell viability and neurite outgrowth. This procedure will yield approximately 5 million cells from three rat pups, with transfection efficiencies of approximately 40%.

### 5.2.1. Preparing 1mg/mL poly d-lysine (PDL) stock solution

#### Reagents:

1. PDL: Poly-D Lysine (Hydrobromide) Mol. Wt. 30,000-70,000  
PDL 100 mg Powder (Sigma P7886).
2. 10X HBSS: Hank's Balanced Salt Solution: KCl 53.7 mM, KH<sub>2</sub>PO<sub>4</sub> 4.4 mM, NaCl 1.3 M, NaHCO<sub>3</sub> 41.66 mM, Na<sub>2</sub>HPO<sub>4</sub> 3.38 mM, Hepes 99.87 mM.

3. This recipe makes 10x, should be pH 7.2, to 1Liter
  - a. 4 g KCl (MW: 74.5)  
0.6 g KH<sub>2</sub>PO<sub>4</sub> (MW: 136)  
76.5 g NaCl (MW: 58.4)  
3.5.g NaHCO<sub>3</sub> (MW: 84)  
35.8 g Na<sub>2</sub>HPO<sub>4</sub> (MW: 142)  
23.8 g HEPES (MW: 238.3)
  - b. After adjusting pH, sterilize by filtration
  - c. Dilute to 1x with water before use

**Tools:**

1. Sterile hood (Bio-safety cabinet)
2. 0.22 µm Filter (Nalgene 595-4520)
3. Multichannel pipette trough
4. 96-Well Falcon Plate (Falcon 353072)
5. 15 mL Falcon tubes (Falcon 352097)
6. 100 mL Bottle
7. 10 mL and 50 mL Pipette (Falcon 357551 and 357550)

**Protocol:**

1. All preparation should be done in the HOOD
2. Spray inside of the Hood with ethanol to kill Bacteria before use
3. If PDL ships as 100 mg powder, make it into a 10x solution (stock PDL) as follows.
4. Using a 50 mL pipette, transfer 100 ml 1x HBSS into the PDL container.
5. Mix with the pipette in order to dissolve powder.
6. Filter the stock PDL solution through a 0.22 µm filter into the 100 mL bottle attached to the vacuum.
7. Using a 10 mL pipette, make 10 mL aliquots of the PDL solution in 15 mL tubes.
8. Label the tubes with the date/ Name/ PDL concentration (1 mg/mL)/ Cat No. / Lot No.
9. Store @ -20°C for further use.

**5.2.2. Pre-coating plates with PDL (100 µg/mL) for further laminin coating**

**Purpose:** Coat plates with PDL to augment cell adhesion, final concentration of 100 µg/mL.

**Reagents and Tools:**

1. Multichannel pipette trough
2. Multichannel pipette (1200 µL)
3. 1x HBSS (Gibco 14175)
4. Box of 1200 µL Tips

5. 96-Well Falcon Plate (Falcon 353072)
6. 5 mL and 50 mL Pipette (Falcon 357543 and 357550)
7. 100 mL Bottle

### **Protocol:**

#### **20 x 96 Well Plates: 90 mL 1x HBSS, 10 mL PDL Stock Solution**

1. Thaw one aliquot of 10 mL PDL Stock solution on the 37 °C water bath
2. Using a 50 mL pipette, transfer 90 mL of 1x HBSS into a 100 mL Bottle
3. Add the 10 mL PDL stock solution and mix
4. Transfer the total volume to a trough
5. Using multi-channel fill 100 µL/well in the inner 48 wells of the 96-well plates
6. Store the plates inside a plastic box in the cold room over night or until use

#### **10 x 24 Well Plates: 90 mL 1x HBSS, 10 mL PDL Stock Solution**

Follow exactly the same procedure but filling 400 µL/well.

### **5.2.2. Coating plates with laminin (10 µg/mL) after PDL pre-coating**

#### **Reagents and Tools:**

1. Falcon PDL-coated plates
2. 1x HBSS (Gibco 14175)
3. Mouse Laminin I, 1 mg/mL, 100 µL aliquot (Cultrex 3500-010-01)
4. Multichannel pipette (1200 µL)
5. Multichannel pipette trough
6. Pasteur glass pipette
7. 15 mL Falcon tubes

### **Protocol:**

#### **1 x 96 well Plates: 3 mL 1x HBSS, 30 µL Laminin**

1. Thaw laminin aliquot on ice
2. Using Pasteur glass pipette with vacuum remove the PDL from wells or invert the plate gently.
3. Wash 5 times with sterile distilled water. Leave the last wash while you do step 4.
4. In a 15 mL tube add 30 µL of laminin solution per 3 mL of HBSS per plate and transfer to a multichannel trough.
5. Remove the water from the wells and add 60 µL of laminin solution in the inner 48 wells of the 96-well plates.
6. Incubate plates overnight @ 37 °C, 5%CO<sub>2</sub> in the incubator.

#### **1 x 24 well Plate: 7.5 mL 1x HBSS, 75 µL Laminin**

Follow exactly the same procedure but adding 75  $\mu$ L of laminin solution per 7.5 mL of HBSS per plate and filling the wells with 300  $\mu$ L of Laminin solution final concentration 10  $\mu$ g/mL.

### 5.2.3. Preparing the transfection reagents: intraneuronal buffer (INB) stock solutions and INB solution

#### Reagents:

1. Potassium Chloride, Powder (KCL) FW: 74.55 (J.T.Baker-3052-01)
2. HEPES Sodium Salt FW: 260.29 (Omnipur-5380)
3. Calcium Chloride ( $\text{CaCl}_2$ ) FW: 147.02 (Fisherbiotech-BP510-500)
4. Ethylene glycol-bis(2-aminoethyl-ether)-N,N,N',N'-tetraacetic acid (EGTA) FW: 380.35 (sigma-E4378-25g)
5. Magnesium chloride hexahydrate ( $\text{MgCl}_2$ ) FW: 203.31 (sigma-M2670-500g)

#### Protocol:

1. Prepare the following solutions:
  1. 1 M KCL
  2. 1 M HEPES
  3. 0.5 M EGTA (Needs to be dissolved @ pH8 with 10 M NaOH Solution)
  4. M  $\text{CaCl}_2$
  5. M  $\text{MgCl}_2$
2. Check the pH for the solutions

#### INB Preparation

1. Add in a 50 ml Falcon tube:
  - H<sub>2</sub>O: 42 mL
  - 1 M KCL: 6.75 mL
  - 1 M HEPES: 0.5 mL
  - 0.5 M EGTA: 0.5 mL
  - M  $\text{CaCl}_2$ : 0.1 mL
  - M  $\text{MgCl}_2$ : 0.1 mL
2. Check the pH of the INB; it should be about 7-8.
3. In the white hood, filter the INB through a 0.22  $\mu$ m filter and leave 10 mL (labeled as filtered INB) in a Falcon tube for the transfection itself and pour the rest in a multichannel through to wash the transfection plate (BTX plate).

### 5.2.4. Preparing culture media: enhanced neuronal buffer (END) supplement recipe

1. 50 ml 100x Sato Stock:
  - Add the following to 50ml Neurobasal medium:

- 0.5 g transferrin [Sigma #T1147]
  - 0.5 g BSA [Sigma #A4161]
  - 12.5  $\mu$ L progesterone [Sigma #P8783] (from stock: 2.5 mg/100  $\mu$ L EtOH)
  - 80 mg putrescine [Sigma #P7505]
  - 500  $\mu$ L sodium selenite [Sigma #S5261] (from stock: 4 mg/100  $\mu$ L 0.1N NaOH + 10 mL NB)
2. 50 mL 100X T3 [Sigma #T6397-100 mg]:
    - Dissolve 3.2 mg triido-thyronine [Sigma #T6397] in 400  $\mu$ L 0.1 N NaOH
    - Add 30  $\mu$ L to 60 mL DPBS [Invitrogen #14287072]
    - Filter 0.22  $\mu$ m filter, DISCARDING the first 8 mL
    - Aliquot and store at -20 °C
  3. 10 ml 1000X NAC [Sigma #A8199-10G]:
    - Dissolve 50 mg N-acetyl cysteine in 10 mL NB (will be yellowish in color)
    - Make aliquots and store at -20 °C

To prepare an aliquot to add to 100 mL Neurobasal (calcium free) [Invitrogen 12348017] add:

- 1 mL 100X Pen/Strep [Invitrogen #15140122]
- 1 mL Sato stock
- 1 mL 100X T3
- 1 mL 100X L-glutamine [Invitrogen #25030149]
- 100  $\mu$ L 1000X NAC
- 2 mL 50X B27 [Invitrogen #17504044] (This was replaced by Neurocult supplement SM1 from Stemcell Technologies, item #:05711)

Mix:

- 50 mL of Pen/Strep
- 50 mL of Sato (1)
- 50 mL of T3 (2)
- 50 mL of L-Glutamine
- 5 mL of NAC (3)
- 100 mL of SM1 supplement

Make aliquots of 6.1 mL and freeze at -20 °C.

### 5.2.5. Glial cell culture

#### Culture Media

1. 430 mL MEM with Earle's Salts (Gibco 11095-080)
2. 15 mL Glucose 20% in 1X PBS
3. Dissolve and filter through a 0.22  $\mu$ m filter to sterilize
4. 5 mL Anti-Anti (Antibiotic/Antimycotic) (Gibco 15240)
5. 50 mL Horse Serum (Gibco 26050-070)

## Dissociation Media

1. 18 mL HibernateE (-CaCl) (Brainbits-HE-Ca-500 mL)
2. 2 mL Trypsin (2.5%, Gibco 15090)

## Prepare for Culture

1. Prepare 500 mL Culture Media (see above)
2. Prepare 20 mL Dissociation Media
3. Thaw two 50  $\mu$ L aliquots of DNase (30 mg/mL, Sigma-D5025) on ice
4. Prepare Culture Dishes
  - a. Place 4 mL Culture Media in Falcon 3002 dishes
  - b. Place 25 mL Culture Media in T75 Flask (Thermoscientific-156499)
5. Thaw at least 6 mL of horse serum
6. Set up in hood
  - a. 2 forceps
  - b. 1 spatula (to transfer slices)
  - c. 1 scalpel
  - d. 1 razor blade
  - e. 1 Petri Dish
  - f. 20 mL Hibernate E on ice
  - g. Pasteur pipette with bulb

## Protocol

1. Remove at least 4 P1 or P2 rat brains and place in ice-cold Hibernate E (-CaCl)
2. Under dissecting scope, remove meninges and make 2 transverse slices of brain using scalpel.
3. Using forceps as tiny clippers, remove cortex from brain slices.
4. Once all the cortex pieces are collected, transfer to lid of Petri dish. Mince with razor blade.
5. Using Pasteur pipette, transfer minced cortex to dissociation media (get rid of bubbles).
6. Add 1 aliquot of DNase to trypsin solution
7. Incubate in trypsin for 15 minutes with constant shaking.
8. Prepare a 50 mL tube with 3 mL of Horse serum in the bottom.
9. Place tube containing cortical cells and trypsin solution in hood and let the pieces settle to the bottom (takes a few minutes).
10. Remove supernatant and place in tube with horse serum (to stop trypsin reaction)
11. Add another 10 mL of dissociation media to the tube with the cortex pieces. Add 1 aliquot of DNase.
12. Incubate another 15 minutes, 37 °C, with constant shaking.
13. Add 3 ml of horse serum to second dissociation. Triturate 10 times with 10 mL pipette attached to electric pipette aid.

14. Filter the original supernatant and the new triturated cells supernatant through a 70  $\mu\text{m}$  filter, and into a fresh 50 mL tube.
15. Pellet cells at 180G for five minutes.
16. Remove supernatant and resuspend in 10 mL of culture media.
17. Plate 1 mL of resuspended cells per T75 flask or more if desired.

#### Comments:

1. Cell viability will be quite low the next day and large amounts of cellular debris will be visible. This is not a cause for concern. After consistent media changes over the next few weeks, the surviving cells will proliferate and make a nice monolayer in about 2-3 weeks.
2. To help prevent the overgrowth of microglial cells, when changing the media, strike the flask sharply to dislodge microglia, which tend to be loosely adherent, prior to replacing the media.

### 5.2.6. Passage of glial cultures

**Comment:** 1 confluent Glial flask can be split into 5 new flasks.

#### Culture Media

1. 430 mL MEM with Earle's Salts (Gibco 11095-080)
2. 15 mL Glucose 20% in 1X PBS pH-7.4 (Gibco-70011)
3. Dissolve and filter to sterilize
4. 5 mL Anti-Anti (Antibiotic/Antimycotic) (Gibco 15240)
5. 50 mL Horse Serum (Gibco 26050-070)

#### Protocol

1. Prepare Glial media and add 25 mL per flask (Thwermoscientific-256499).
2. Incubate at 37 °C until plate the cells.
3. Take the Glial flask to split and remove the media.
4. Add 10 mL of 1X HBSS (Gibco-14175) to wash the Glial culture. Move gently to the sides.
5. Remove the HBSS and add 5 mL of trypsin 0.05%(Invitrogen-25300062-500 mL).
6. Gently move the flask to spread the trypsin.
7. Incubate for 5 min, 37 °C.
8. Add 5 mL of Glial media to stop the trypsin (volume of trypsin=volume of media).Move the flask to spread the media evenly.
9. Transfer the suspended Glial culture to a 50 mL tube.
10. Centrifuge at 1000rcf for 5 min. Remove supernatant.
11. Resuspend using 1 ml of Glial media first and then add more media (1 mL of media per each new flask).
12. Put 1 mL of cells into each pre-warmed T75 flask. Gently move flask to spread cells evenly.

### 5.2.7. 24-well transfection of cortical neurons

#### Reagents

1. Hibernate E (Brainbits-HE-Ca-500 mL)
2. 24-well Falcon plates coated with PDL + laminin
3. Papain (Worthington, #3126)
4. ENB Media 50% Glia Conditioned
5. Intraneuronal Buffer solution(INB)
6. 50X SM1 Neuronal Supplement (Stemcell-05711)
7. DNase solution (Sigma-D-5025)
8. Trypsin 2.5% (Gibco-15090)

#### Tools

- Sharp forceps
- Spatula (for transferring brain slices)
- Razor blade
- Scalpel
- BTX Transfection plate (BTX-45-0450)

#### Protocol

- The day before the experiment: Prepare ENB media (see protocol)
- On the day of the experiment prepare INB transfection buffer (see protocol)

#### Fill culture plates with media

1. Filter the ENB Media.
2. Optional: add forskolin to the ENB Media (1  $\mu$ l of 5 mM stock per ml). Mix thoroughly.  
Note: forskolin can be used to increase transcription from CMV promoters and in this way enhance expression from plasmids. Researchers should weigh this technical advantage against the potentially confounding effects of elevated cAMP signaling.
3. Add 400  $\mu$ L per well of the media to the 24-well plate. Be sure to avoid air bubbles at the bottom of the wells. If you get air bubbles, tap the plate to make the bubbles go up.
4. Put the plate on the incubator until use.

#### Prepare Hibernate E solutions

1. In a 50 mL Falcon tube place 20 mL of room temperature Hibernate E (for rinsing papain)
2. In another 50 mL Falcon Tube place 50 mL of Hibernate E + SM1 (add 1 mL 50X SM1)



### Prepare 15 mL tube for Papain incubation

1. Put 10 mL of hibernate E in tube, put at room temp.
2. Add enough Papain to have 20 U/mL. usually 160-210  $\mu\text{L}$ .  
 $200\text{U}/(\text{U}/\text{mg} \times \text{mg}/\text{mL}) = \text{mL} \rightarrow \times 10^{-3} = \mu\text{L}$  Papain
3. Place tube in water bath.
4. Transfer brain to a Petri dish containing ice-cold hibernate E (-CaCl)

### Prepare Transfection plate

1. Before using the INB buffer (Intraneuronal Buffer), filter it using a 10 mL syringe and 0.22  $\mu\text{m}$  filter.
2. Rinse BTX plate with 150  $\mu\text{L}$ /well of INB, 5 times.
3. Leave in the hood to dry. Put under the UV light for 15 min if you are reusing the transfection plate.

### Set up Hood for Dissection

1. Tools (forceps, scalpel, razor blade, transfer spatula)
2. Pipette with bulb
3. Ethanol
4. 60 mm Petri dish
5. Start thawing DNase and Trypsin aliquots on ice.

### Harvest Brains and dissecting cortex out

1. Let the pups sleep on ice for 10 min
2. Cut head off P1 rat with large scissors
3. Using small scissors make incision along midline of scalp. Clear the skin away.
4. Make cuts through skull, starting at the base of the skull and working around the later edges. This creates a large flap that can be peeled off.
5. Scoop whole brain into a 10 cm dish containing 10-12 mL ice-cold Hibernate E.
6. Remove meninges from brain (Back to Front)
7. Use scalpel to prepare a thick transverse section of middle 2/3 of brain.
8. Remove cortex from section (see Figure 12)
9. Repeat process for another brain, placing pieces of cortex from both brains together.
10. Get the dissociation media ready
11. Remove Papain solution from water bath and place in hood with cap open.
12. Add 50  $\mu\text{L}$  of DNase solution to papain.
13. Place a suction bulb on a glass pipette.
14. Using a flat spatula, transfer pieces of cortex to the lid of a Petri dish.
15. Using razor blade, mince the pieces of cortex.
16. Use pipette to transfer pieces of cortex into papain. This will take several repetitions. Be careful to avoid bubbles. Use the pipette to remove any bubbles.

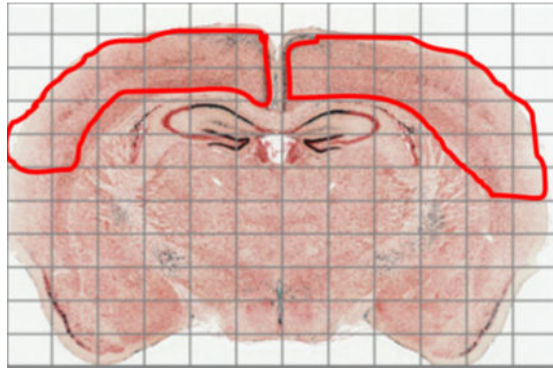


**Figure 12:** Diagram of rat cortex (outlined in red) in rat brain section.

17. Place conical tube with Papain + DNase solution and cortex in 37° C incubator on a shaker. Incubate for 30 minutes.

### **During incubation, prepare the following:**

1. Clean up hood and organize pipettes and tip boxes
2. Be sure that Trituration Media (Hibernate E + SM1) is waiting at room temperature.
3. Lightly fires polish a glass pipette and attach it to suction bulb.
4. Attach a glass pipette to the vacuum.
5. Label 3 15 mL conical tubes as follows:
6. “Cell collection”
7. “Cell count”
8. “Transfection”
9. Set out 5 mL of buffer INB at room temperature.

### **Rinse Papain, triturate, add Trypsin**

1. Spin cortex at 10G for 1 minute.
2. Remove supernatant; replace with 5 mL Hibernate E + SM1.
3. Spin cortex at 10G for 1 minute.
4. Remove supernatant, replace with 1.5 mL Hibernate E + SM1
5. Add 5  $\mu$ L DNase.
6. Triturate 3 times.
7. Spin cortex at 10G for 1 minute.
8. Remove supernatant; replace with 10 mL Hibernate E (NO SM1).
9. Spin cortex at 10G for 1 minute.

10. Remove supernatant; replace with 9 mL Hibernate E (NO SM1).
11. Add 1 mL trypsin + 50  $\mu$ L DNase.
12. Incubate 30 minutes, 37 °C, shaking.
13. During incubation start loading the plasmids in the transfection plate. First, the INB, then each plasmid. When each column is loaded, cover it with tape to avoid confusion and evaporation.

### **Rinse, Triturate**

The purpose of this trituration paradigm is to minimize the number of times a dissociated cell passes through the pipet tip. Tissue aggregates are triturated briefly, resulting in dissociation of cells from their surface. These cells are then removed to a separate container before further trituration of the aggregates. This approach is critical to maintain viability.

1. Spin cortex at 10G for 1 minute.
2. Remove supernatant; replace with 5 mL Hibernate E + B27.
3. Spin cortex at 10G for 1 minute.
4. Remove supernatant, replace with 1.5 mL Hibernate E + B27
5. Add 5  $\mu$ L DNase.
6. Triturate 3 times.
7. Let cortex settle for 2 minutes (set timer).
8. Remove the supernatant and place in “collection tube”.
9. Repeat steps 4-8 about five or six times, until about 10-12 mL of cell suspension is collected.

### **Determine Cell Concentration**

1. Gently invert “Cell Collection” tube until the cells are evenly distributed (some probably settled to a pellet on the bottom during triturations).
2. Transfer 1ml of media to “Cell Count” tube.
3. Spin “Cell Count” tube at 80G, 3 minutes, room temperature.
4. Remove supernatant, and re-suspend pellet in 1 mL of Hibernate E + SM1.
5. Combine 90  $\mu$ L of cells with 10  $\mu$ L of trypan blue. Use hemacytometer to count number of HEALTHY cells.

### **Transfection and plating of cells**

1. Calculate the volume needed for 1 million cells (We use 500,000 cells per column)
2. Vol. needed= amount of cell we want/ Cell count
3. Transfer that volume from “Cell Collection” tube to “Transfection” tube.
4. Spin down cells, 80G, 5 minutes, room temperature.
5. Resuspend cells in 500  $\mu$ L INB (250  $\mu$ L per column of BTX plate). INB IS TOXIC TO CELLS. FROM THIS POINT ON, WORK AS FAST AS YOU CAN WITHOUT MAKING MISTAKES.

6. Place 25  $\mu$ l of INB + cells in each well for transfection. Mix just one time, gently.
7. Cover transfection plate with tape. Use razor blade to make sure tape is not blocking the contact points.
8. Transfect cells with electroporator (350V, 300us, 1x)
9. Remove tape from transfection plate.
10. Add 100 ml of Hibernate E + SM1 to each well. Gently mix 2x.
11. Using multichannel pipette, transfer 25  $\mu$ l to wells in culture plate.
12. Let grow for two days, 37°C, and proceed with the Immunohistochemistry.

### 5.2.8. Fixative: paraformaldehyde 4%, sucrose 4%

Comment: Paraformaldehyde (PFA) fixative is very dangerous and much care should be taken while following this procedure! PFA in powdered form is very dangerous. Wear a mask and measure in a chemical fume hood! Do not allow yourself or anyone in the lab to be exposed to the powder or fumes coming from the hot water.

#### Materials

Set everything in the fume hood before starting:

1. Scale, spatula and weight plate.
2. PFA (Sigma P6148-500g)
3. Sucrose (FLUKA Biochemika\_84097-1kg)
4. PBS 10x
5. 1 N NaOH
6. Glacial Acetic Acid
7. Distilled H<sub>2</sub>O

For 250 mL:

- 10 g PFA
- 10 g Sucrose
- 200 mL H<sub>2</sub>O
- 25 mL 10X PBS

#### Procedure:

**For a 250 mL solution: 10 g of PFA and 10 g of Sucrose**

1. Heat water (200 mL) to 60°C (don't allow it to go above 65 °C) and stir continuously
2. Weigh the PFA. Clean the scale of any remaining PFA.
3. Add the PFA and the sucrose to the water. Let stir for a few minutes.
4. Add 1 pellet of NaOH (or a few hundred  $\mu$ l of NaOH 1N). Add only one at a time and wait a few minutes to see if more is necessary (until the solution turns clear).
5. Add 25 mL of 10X PBS.
6. Adjust pH near to 7.4 with pH strips using Glacial Acetic Acid.
7. Take to final volume with distilled water.

8. Filter and aliquot (12 mL/tube).

Note that the immunohistochemistry protocol calls for two distinct solutions: a BLOCKING BUFFER, which is used in the initial blocking step, and then an ANTIBODY BUFFER in which antibodies are applied.

### **Antibody Buffer**

1. 200 mL ddH<sub>2</sub>O
2. 1.75g NaCl (Sigma-Aldrich-S9625- 10 kg)
3. 1.2g Trizma Base (Sigma-T1503- 1 kg)
4. 2g BSA (Sigma-A9418- 100g )
5. 3.5g lysine (Sigma L2513- 25 g)
6. 0.02% Na Azide (2 mL of stock solution, which is 2 g in 100 mL H<sub>2</sub>O)

Adjust to pH 7.4 and filter sterilize

### **Blocking Buffer:**

To Antibody Buffer Add

1. 20% Normal Goat Serum (Gibco-16210): 2 mL/10 mL Antibody solution
2. 0.2% TritonX: 200  $\mu$ L from 10% Triton solution (prepared from 1 mL Triton X-100 (Omnipure-9410) in 9 mL 1XPBS).

Blocking is done for 30 minutes @ room Temperature

Antibody incubations are done in Antibody Buffer only (no serum or triton)

## **5.2.9. Immunohistochemistry for cortical neurons on 24-well falcon plates**

### **Reagents & Instruments**

1. Multichannel pipette P 1200.
2. Triton X 10% (1 mL Triton X-100 (Omnipure-9410) in 9 mL 1XPBS)
3. Goat Serum (Gibco-16210)
4. Blocking Buffer
5. 4% PFA/4% Sucrose solution
6. Hoechst (Sigma-2495-100 mg)

### **Procedure**

1. In the fume hood: Remove the media from the plates (use a tray for easy handling).
2. Add 400  $\mu$ L per well of PFA4%/Sucrose4% and incubate for 30 min.
3. Discard the PFA and wash with 400  $\mu$ L/well of PBS 1X at least 5 times. Wait a few seconds between washes.

4. Prepare the blocking solution: 10 mL of Blocking Buffer (enough for 1 plate) 20% of Goat Serum: 2 mL/ 2% of Triton X: 200  $\mu$ L Triton 10%.
5. Remove the last wash and add 400  $\mu$ L/well of the Blocking Buffer.
6. Incubate for 30 min.
7. Prepare the Primary antibody in Antibody Buffer (for example Rb anti- $\beta$ -tubulin III, 1:500) (Sigma-T2200-200  $\mu$ L)
8. Discard the Blocking Buffer and add 400  $\mu$ L/well of the primary antibody in Antibody Buffer. Incubate overnight at 4 °C.
9. Wash at least 5 times with PBS 1X, 400ul/well.
10. Prepare the Secondary Antibody in Antibody Buffer. Ex: Alexa Fluor GaRb 647 1:500 (invitrogen-A21244) and Hoechst 1:1000.
11. Add 400  $\mu$ L/well of the secondary antibodies and incubate for 1-2 hr in the dark.
12. Rinse the plate with PBS 1X at least 5 times.

## Acknowledgments

The authors would like to thank the contributions of the many members of our laboratory over the past ten years in developing these methods. Special thanks to W. Buchser, O. Gutiérrez Arenas, J. Lerch, D. Motti, J. Pardinás, T. Slepak, R. Smith, and L. Usher. This work was supported by National Institutes of Health grants HD057632 (to V.P.L.), and NS059866 (to J.L.B.), NS080145 and DOD grant W81XWH-05-1-0061 (to V.P.L. and J.L.B.), the Buoniconti Fund and the Walter G. Ross Distinguished Chair in Developmental Neuroscience (to V.P.L.).

## References

1. Giuliano K. A. High-Content Screening: A New Approach to Easing Key Bottlenecks in the Drug Discovery Process. *J. Biomol. Screen.* 1997;2:249–259.
2. Giuliano K. A., Taylor D. L. Fluorescent-protein biosensors: new tools for drug discovery. *Trends Biotechnol.* 1998;16:135–40. PubMed PMID: 9523461.
3. Friedman A., Perrimon N. Genetic screening for signal transduction in the era of network biology. *Cell.* 2007;128:225–31. PubMed PMID: 17254958.
4. Krausz E. High-content siRNA screening. *Mol. Biosyst.* 2007;3:232–40. PubMed PMID: 17372651.
5. Giuliano K. A., Johnston P. A., Gough A., Taylor D. L. Systems cell biology based on high-content screening. *Methods Enzymol.* 2006;414:601–19. PubMed PMID: 17110213.
6. Hertzberg R. P., Pope A. J. High-throughput screening: new technology for the 21st century. *Curr. Opin. Chem. Biol.* 2000;4:445–51. PubMed PMID: 10959774.
7. Macarrón R., Hertzberg R. P. Design and implementation of high throughput screening assays. *Mol. Biotechnol.* 2011;47:270–85. PubMed PMID: 20865348.
8. Macarrón R., Hertzberg R. P. Design and implementation of high-throughput screening assays. *Methods Mol. Biol.* 2009;565:1–32. PubMed PMID: 19551355.
9. Zhang J. H., Chung T. D., Oldenburg K. R. Confirmation of primary active substances from high throughput screening of chemical and biological populations: a statistical

- approach and practical considerations. *J. Comb. Chem.* 2:258–65. PubMed PMID: 10827934.
10. Houston J. B., Galetin A. Methods for predicting in vivo pharmacokinetics using data from in vitro assays. *Curr. Drug Metab.* 2008;9:940–51. PubMed PMID: 18991591.
  11. Lerch J. K., Kuo F., Motti D., Morris R., Bixby J. L., Lemmon V. P. Isoform diversity and regulation in peripheral and central neurons revealed through RNA-Seq. *PLoS One.* 2012;7:e30417. PubMed PMID: 22272348.
  12. Daub A., Sharma P., Finkbeiner S. High-content screening of primary neurons: ready for prime time. *Curr. Opin. Neurobiol.* 2009;19:537–43. PubMed PMID: 19889533.
  13. Zeitelhofer M., Vessey J. P., Xie Y., Tübing F., Thomas S., Kiebler M., Dahm R. High-efficiency transfection of mammalian neurons via nucleofection. *Nat. Protoc.* 2007;2:1692–704. PubMed PMID: 17641634.
  14. Halterman M. W., Giuliano R., Dejesus C., Schor N. F. In-tube transfection improves the efficiency of gene transfer in primary neuronal cultures. *J. Neurosci. Methods.* 2009;177:348–54. PubMed PMID: 19014969.
  15. Kola I., Landis J. Can the pharmaceutical industry reduce attrition rates? *Nat. Rev. Drug Discov.* 2004;3:711–5. PubMed PMID: 15286737.
  16. Adams C. P., Brantner V. V. Estimating the cost of new drug development: is it really 802 million dollars? *Health Aff. (Millwood).* 25:420–8. PubMed PMID: 16522582.
  17. Eglen R. M., Gilchrist A., Reisine T. An overview of drug screening using primary and embryonic stem cells. *Comb. Chem. High Throughput Screen.* 2008;11:566–72. PubMed PMID: 18694393.
  18. Nolan G. P. What's wrong with drug screening today. *Nat. Chem. Biol.* 2007;3:187–91. PubMed PMID: 17372598.
  19. Banker G. A., Cowan W. M. Rat hippocampal neurons in dispersed cell culture. *Brain Res.* 1977;126:397–42. PubMed PMID: 861729.
  20. Bartlett W. P., Banker G. A. An electron microscopic study of the development of axons and dendrites by hippocampal neurons in culture. I. Cells which develop without intercellular contacts. *J. Neurosci.* 1984;4:1944–53. PubMed PMID: 6470762.
  21. Brewer G. J. Thrombin causes cell spreading and redistribution of beta-amyloid immunoreactivity in cultured hippocampal neurons. *J. Neurochem.* 1996;67:119–30. PubMed PMID: 8666982.
  22. Brewer G. J. Isolation and culture of adult rat hippocampal neurons. *J. Neurosci. Methods.* 1997;71:143–55. PubMed PMID: 9128149.
  23. Brewer G. J., Price P. J. Viable cultured neurons in ambient carbon dioxide and hibernation storage for a month. *Neuroreport.* 1996;7:1509–12. PubMed PMID: 8856709.
  24. Brewer G. J. Regeneration and proliferation of embryonic and adult rat hippocampal neurons in culture. *Exp. Neurol.* 1999;159:237–47. PubMed PMID: 10486191.
  25. Brewer G. J., Torricelli J. R., Evege E. K., Price P. J. Optimized survival of hippocampal neurons in B27-supplemented Neurobasal, a new serum-free medium combination. *J. Neurosci. Res.* 1993;35:567–76. PubMed PMID: 8377226.
  26. Al Ali H., Schuerer S. C., Lemmon V. P., Bixby J. L. Chemical Interrogation of the neuronal kinome using a primary cell-based screening assay. *ACS Chem. Biol.* 2013.;130312133627001. PubMed PMID: 23480631.

27. Blackmore M. G., Wang Z., Lerch J. K., Motti D., Zhang Y. P., Shields C. B., Lee J. K., Goldberg J. L., Lemmon V. P., Bixby J. L. Krüppel-like Factor 7 engineered for transcriptional activation promotes axon regeneration in the adult corticospinal tract. *Proc. Natl. Acad. Sci. U. S. A.* 2012;109:7517–22. PubMed PMID: 22529377.
28. Blackmore M. G., Moore D. L., Smith R. P., Goldberg J. L., Bixby J. L., Lemmon V. P. High content screening of cortical neurons identifies novel regulators of axon growth. *Mol. Cell. Neurosci.* 2010;44:43–54. PubMed PMID: 20159039.
29. Buchser W. J., Slepak T. I., Gutierrez-Arenas O., Bixby J. L., Lemmon V. P. Kinase/ phosphatase overexpression reveals pathways regulating hippocampal neuron morphology. *Mol. Syst. Biol.* 2010;6:391. PubMed PMID: 20664637.
30. Loh S. H. Y., Francescut L., Lingor P., Bähr M., Nicotera P. Identification of new kinase clusters required for neurite outgrowth and retraction by a loss-of-function RNA interference screen. *Cell Death Differ.* 2008;15:283–98. PubMed PMID: 18007665.
31. Götte M., Hofmann G., Michou-Gallani A.-I., Glickman J. F., Wishart W., Gabriel D. An imaging assay to analyze primary neurons for cellular neurotoxicity. *J. Neurosci. Methods.* 2010;192:7–16. PubMed PMID: 20620166.
32. Vincent A. M., Feldman E. L. Can drug screening lead to candidate therapies for testing in diabetic neuropathy? *Antioxid. Redox Signal.* 2008;10:387–93. PubMed PMID: 17961065.
33. Gerdtts J., Sasaki Y., Vohra B., Marasa J., Milbrandt J. Image-based screening identifies novel roles for IKK and GSK3 in axonal degeneration. *J. Biol. Chem.* 2011;286:28011–8. PubMed PMID: 21685387.
34. Moore D. L., Blackmore M. G., Hu Y., Kaestner K. H., Bixby J. L., Lemmon V. P., Goldberg J. L. KLF family members regulate intrinsic axon regeneration ability. *Science.* 2009;326:298–301. PubMed PMID: 19815778.
35. Brewer G. J., Cotman C. W. Survival and growth of hippocampal neurons in defined medium at low density: advantages of a sandwich culture technique or low oxygen. *Brain Res.* 1989;494:65–74. PubMed PMID: 2765923.
36. Soussou W. V., Yoon G. J., Brinton R. D., Berger T. W. Neuronal network morphology and electrophysiology of hippocampal neurons cultured on surface-treated multielectrode arrays. *IEEE Trans. Biomed. Eng.* 2007;54:1309–20. PubMed PMID: 17605362.
37. Liesi P. Do neurons in the vertebrate CNS migrate on laminin? *EMBO J.* 1985;4:1163–70. PubMed PMID: 4006911.
38. Manthorpe M., Engvall E., Ruoslahti E., Longo F. M., Davis G. E., Varon S. Laminin promotes neuritic regeneration from cultured peripheral and central neurons. *J. Cell Biol.* 1983;97:1882–90. PubMed PMID: 6643580.
39. Gopalakrishnan S. M., Teusch N., Imhof C., Bakker M. H. M., Schurdak M., Burns D. J., Warrior U. Role of Rho kinase pathway in chondroitin sulfate proteoglycan-mediated inhibition of neurite outgrowth in PC12 cells. *J. Neurosci. Res.* 2008;86:2214–26. PubMed PMID: 18438921.
40. Shen Y., Tenney A. P., Busch S. A., Horn K. P., Cuascat F. X., Liu K., He Z., Silver J., Flanagan J. G. PTPsigma is a receptor for chondroitin sulfate proteoglycan, an inhibitor of neural regeneration. *Science.* 2009;326:592–6. PubMed PMID: 19833921.



41. Shields L. B. E., Zhang Y. P., Burke D. A., Gray R., Shields C. B. Benefit of chondroitinase ABC on sensory axon regeneration in a laceration model of spinal cord injury in the rat. *Surg. Neurol.* 2008;69:568–77discussion 577. PubMed PMID: 18486695.
42. Sivasankaran R., Pei J., Wang K. C., Zhang Y. P., Shields C. B., Xu X.-M., He Z. PKC mediates inhibitory effects of myelin and chondroitin sulfate proteoglycans on axonal regeneration. *Nat. Neurosci.* 2004;7:261–8. PubMed PMID: 14770187.
43. Lee J. K., Geoffroy C. G., Chan A. F., Tolentino K. E., Crawford M. J., Leal M. A., Kang B., Zheng B. Assessing spinal axon regeneration and sprouting in Nogo-, MAG-, and OMgp-deficient mice. *Neuron.* 2010;66:663–70. PubMed PMID: 20547125.
44. Lee J. K., Zheng B. Role of myelin-associated inhibitors in axonal repair after spinal cord injury. *Exp. Neurol.* 2011. PubMed PMID: 21596039.
45. Hsieh S. H., Ferraro G. B., Fournier A. E. Myelin-associated inhibitors regulate cofilin phosphorylation and neuronal inhibition through LIM kinase and Slingshot phosphatase. *J Neurosci.* 2006;26:1006–1015. PubMed PMID: 16421320.
46. Kaech S., Banker G. Culturing hippocampal neurons. *Nat. Protoc.* 2006;1:2406–15. PubMed PMID: 17406484.
47. Engele J., Schubert D., Bohn M. C. Conditioned media derived from glial cell lines promote survival and differentiation of dopaminergic neurons in vitro: role of mesencephalic glia. *J. Neurosci. Res.* 1991;30:359–71. PubMed PMID: 1686785.
48. Meberg P. J., Miller M. W. Culturing hippocampal and cortical neurons. *Methods Cell Biol.* 2003;71:111–27. PubMed PMID: 12884689.
49. Bottenstein J. E., Sato G. H. Growth of a rat neuroblastoma cell line in serum-free supplemented medium. *Proc. Natl. Acad. Sci. U. S. A.* 1979;76:514–7. PubMed PMID: 284369.
50. Romijn H. J., van Huizen F., Wolters P. S. Towards an improved serum-free, chemically defined medium for long-term culturing of cerebral cortex tissue. *Neurosci. Biobehav. Rev.* 1984;8:301–34. PubMed PMID: 6504415.
51. Romijn H. J. Development and advantages of serum-free, chemically defined nutrient media for culturing of nerve tissue. *Biol. Cell.* 1988;63:263–8. PubMed PMID: 3066424.
52. Chen Y., Stevens B., Chang J., Milbrandt J., Barres B. A., Hell J. W. NS21: re-defined and modified supplement B27 for neuronal cultures. *J. Neurosci. Methods.* 2008;171:239–47. PubMed PMID: 18471889.
53. Welsbie D. S., Yang Z., Ge Y., Mitchell K. L., Zhou X., Martin S. E., Berlinicke C. A., Hackler L., Fuller J., Fu J., Cao L.-H., Han B., Auld D., Xue T., Hirai S.-I., Germain L., Simard-Bisson C., Blouin R., Nguyen J. V, Davis C.-H. O., Enke R. A., Boye S. L., Merbs S. L., Marsh-Armstrong N., Hauswirth W. W., Diantonio A., Nickells R. W., Inglese J., Hanes J., Yau K.-W., Quigley H. A., Zack D. J. Functional genomic screening identifies dual leucine zipper kinase as a key mediator of retinal ganglion cell death. *Proc. Natl. Acad. Sci. U. S. A.* 2013;110:4045–50. PubMed PMID: 23431148.

54. Lundholt B. K., Scudder K. M., Pagliaro L. A simple technique for reducing edge effect in cell-based assays. *J. Biomol. Screen.* 2003;8:566–70. PubMed PMID: 14567784.
55. Neumann B., Held M., Liebel U., Erfle H., Rogers P., Pepperkok R., Ellenberg J. High-throughput RNAi screening by time-lapse imaging of live human cells. *Nat. Methods.* 2006;3:385–90. PubMed PMID: 16628209.
56. Glynn M. W., McAllister A. K. Immunocytochemistry and quantification of protein colocalization in cultured neurons. *Nat. Protoc.* 2006;1:1287–96. PubMed PMID: 17406413.
57. Bridges C. D. A method for preparing stable digitonin solutions for visual pigment extraction. *Vision Res.* 1977;17:301–2. PubMed PMID: 867852.
58. Bixby J. L., Reichardt L. F. The expression and localization of synaptic vesicle antigens at neuromuscular junctions in vitro. *J. Neurosci.* 1985;5:3070–80. PubMed PMID: 3932606.
59. Harrill J. A., Robinette B. L., Mundy W. R. Use of high content image analysis to detect chemical-induced changes in synaptogenesis in vitro. *Toxicol. In Vitro.* 2011;25:368–87. PubMed PMID: 20969947.
60. Yeyeodu S. T., Witherspoon S. M., Gilyazova N., Ibeanu G. C. A rapid, inexpensive high throughput screen method for neurite outgrowth. *Curr. Chem. Genomics.* 2010;4:74–83. PubMed PMID: 21347208.
61. Giordano, G., and Costa, L. G. (2012) Morphological assessment of neurite outgrowth in hippocampal neuron-astrocyte co-cultures. *Curr. Protoc. Toxicol. Chapter 11*, Unit 11.16.
62. Wang D., Lagerstrom R., Sun C., Bishof L., Valotton P., Götte M. HCA-vision: Automated neurite outgrowth analysis. *J. Biomol. Screen.* 2010;15:1165–70. PubMed PMID: 20855562.
63. Fanti Z., Martinez-Perez M. E., De-Miguel F. F. NeuronGrowth, a software for automatic quantification of neurite and filopodial dynamics from time-lapse sequences of digital images. *Dev. Neurobiol.* 2011;71:870–81. PubMed PMID: 21913334.
64. Dehmelt L., Poplawski G., Hwang E., Halpain S. NeuriteQuant: an open source toolkit for high content screens of neuronal morphogenesis. *BMC Neurosci.* 2011;12:100. PubMed PMID: 21989414.
65. Zhang J. J.-H., Chung T., Oldenburg K. A Simple Statistical Parameter for Use in Evaluation and Validation of High Throughput Screening Assays. *J. Biomol. Screen.* 1999;4:67–73. PubMed PMID: 10838414.
66. Kümmel A., Gubler H., Gehin P., Beibel M., Gabriel D., Parker C. N. Integration of multiple readouts into the z' factor for assay quality assessment. *J. Biomol. Screen. Off. J. Soc. Biomol. Screen.* 2010;15:95–101. PubMed PMID: 19940084.
67. Hutz J. E., Nelson T., Wu H., McAllister G., Moutsatsos I., Jaeger S. A., Bandyopadhyay S., Nigsch F., Cornett B., Jenkins J. L., Selinger D. W. The multidimensional perturbation value: a single metric to measure similarity and activity of treatments in high-throughput multidimensional screens. *J. Biomol. Screen.* 2013;18:367–77. PubMed PMID: 23204073.

68. Zhang X. D., Heyse J. F. Determination of sample size in genome-scale RNAi screens. *Bioinformatics*. 2009;25:841–4. PubMed PMID: 19223447.
69. Collinet C., Stöter M., Bradshaw C. R., Samusik N., Rink J. C., Kenski D., Habermann B., Buchholz F., Henschel R., Mueller M. S., Nagel W. E., Fava E., Kalaidzidis Y., Zerial M. Systems survey of endocytosis by multiparametric image analysis. *Nature*. 2010;464:243–9. PubMed PMID: 20190736.
70. Sasaguri H., Mitani T., Anzai M., Kubodera T., Saito Y., Yamada H., Mizusawa H., Yokota T. Silencing efficiency differs among tissues and endogenous microRNA pathway is preserved in short hairpin RNA transgenic mice. *FEBS Lett*. 2009;583:213–8. PubMed PMID: 19084527.
71. Buchser W., Pardinas J., Shi Y., Bixby J., Lemmon V. 96-Well electroporation method for transfection of mammalian central neurons. *Biotechniques*. 2006;41:619–624. PubMed PMID: 17140120.
72. Howe D. G., McCarthy K. D. A dicistronic retroviral vector and culture model for analysis of neuron-Schwann cell interactions. *J. Neurosci. Methods*. 1998;83:133–42. PubMed PMID: 9765126.
73. Kim J. H., Lee S.-R., Li L.-H., Park H.-J., Park J.-H., Lee K. Y., Kim M.-K., Shin B. A., Choi S.-Y. High cleavage efficiency of a 2A peptide derived from porcine teschovirus-1 in human cell lines, zebrafish and mice. *PLoS One*. 2011;6:e18556. PubMed PMID: 21602908.
74. Hutson T. H., Buchser W. J., Bixby J. L., Lemmon V. P., Moon L. D. F. Optimization of a 96-Well Electroporation Assay for Postnatal Rat CNS Neurons Suitable for Cost-Effective Medium-Throughput Screening of Genes that Promote Neurite Outgrowth. *Front. Mol. Neurosci*. 2011;4:55. PubMed PMID: 22207835.



# Phospho-ERK Assays

Kim E. Garbison,<sup>1</sup> Beverly A. Heinz, Mary E. Lajiness, Jeffrey R. Weidner,<sup>\*</sup> and G. Sitta Sittampalam<sup>†</sup>

Created: May 1, 2012; Revised: June 25, 2015.

## Abstract

Extracellular signal-related kinase (ERK1/2 or p42/44) is a kinase in the mitogen-activated protein kinase (MAPK) family and phosphorylation of ERK (p-ERK) can be used as a common end point measurement for the activation of many classes of G protein coupled receptors (GPCR). This chapter addresses the use of PerkinElmer's AlphaScreen<sup>®</sup> SureFire<sup>™</sup> assay to measure ERK phosphorylation. This chapter is intended to assist in the development and optimization of p-ERK assays by providing sample protocols, factors to consider during assay optimization and data analysis details for the agonist and antagonist modes.

## Introduction

Extracellular signal-related kinase (ERK1/2 or p42/44) is a serine/threonine kinase that acts as an essential component of the Mitogen-Activated Protein Kinase (MAPK) signal transduction pathway. There are two MAPKs which play an important role in the MAPK/ERK cascade, MAPK1/ERK2 and MAPK3/ERK1. Many biological functions are mediated by this pathway through the regulation of transcription, translation, and cytoskeletal rearrangements, including cell growth, adhesion, survival and differentiation. The MAPK/ERK cascade also plays a role in the initiation and regulation of meiosis, mitosis, and postmitotic functions in differentiated cells by phosphorylating a number of transcription factors. About 160 substrates have been identified for ERKs and many of these substrates are localized in the nucleus to participate in the regulation of transcription. However, there are other substrates located in the cytosol or in other cellular organelles that are responsible for processes. The MAPK/ERK cascade is also involved in the regulation of lysosome processing and endosome cycling through the perinuclear recycling compartment (PNRC); as well as in the fragmentation of the Golgi apparatus during mitosis.

Activation of ERK1/2 is commonly used to measure the functional outcomes for G protein coupled receptors (GPCRs). The  $\alpha$ -subunit of G proteins can be categorized into different subclasses,  $G_{\alpha i/o}$ ,  $G_{\alpha q}$ , and  $G_{\alpha s}$ , that trigger different signaling cascades. For GPCR targets, one utility of measuring p-ERK is its relevance across multiple receptor

---

<sup>1</sup> Eli Lilly & Company, Indianapolis, IN.

\* Editor

† Editor

### GPCR signaling pathways via ERK 1/2

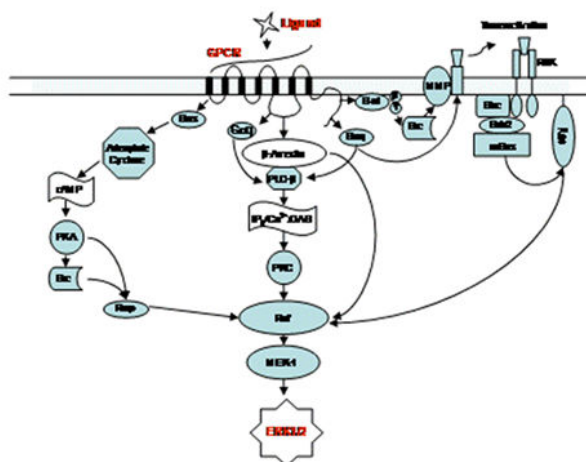


**Figure 1:** ERK1/2 can be activated by GPCRs which couple to different G protein subclasses and transduce the signal by different pathways. Functional separation of these signals is achieved by spatially distinct pools of ERK1/2 within the cell (1).

classes ( $G_{\alpha q}$ ,  $G_{\alpha i/o}$ , and some  $G_{\alpha s}$ ).  $G_{\alpha s}$ -coupled receptors increase cAMP and  $G_{\alpha i}$  receptors decrease cAMP levels through the stimulation or inhibition of the adenylyl cyclase pathway.  $G_{\alpha q}$ -coupled receptors are known to work through the activation of the Phospholipase-C (PLC) pathway, causing increases in intracellular calcium. The advantage of measuring phosphorylated ERK (p-ERK) is that it is a common endpoint, despite initialization from different  $\alpha$ -subunits and therefore different cascades. Now due to newer technology, there are options for developing cell-based screening assays with high throughput capability (Figure 1).

Measuring p-ERK can provide an alternative read-out for receptors. Detection of p-ERK can also potentially provide some advantages that supplement calcium and cAMP assay results when assessing GPCR drug candidates.

**Note:** *The content of the Assay Guidance Manual will be updated quarterly with contributions and new chapters to ensure the manual stays relevant to the current technologies and best practices used in the rapidly changing field of drug discovery and development. The chapter is currently in the process of being updated to reflect the current state of the field with respect to p-ERK assays and technologies. Therefore, it is possible that the most up-to-date information may not yet be included, but will be added in forthcoming chapter updates.*

## Overview of Technology

There are multiple methods currently used to measure p-ERK:

- AlphaScreen<sup>®</sup> SureFire<sup>™</sup> ERK Assay – High throughput capability using bead proximity-based AlphaScreen technology.
- ELISA - Enzyme linked immunosorbent assays require wash steps and long incubations (often overnight). However, measurement with an Acumen reader can provide images of cells if this is desirable.
- Meso-Scale Discovery Assays – Electrochemiluminescence-based method providing medium to high throughput screening.
- LICOR - Infrared fluorescence-based method providing medium to high throughput screening.
- Western Blot Analysis – This method can be labor intensive and offers limited throughput.

## AlphaScreen SureFire ERK Assay

### General Background

Detection of activated ERK is enabled by immuno-sandwich capture of endogenous phosphorylated ERK in cell lysates. Antibody-coated AlphaScreen beads generate a highly amplified signal when in close proximity, due to binding of p-ERK (Figure 2; <http://www.PerkinElmer.com>, <http://www.TGR-Biosciences.com>).

### Characteristics of the AlphaScreen SureFire ERK Assay

Measurement of p-ERK can be done in many ways, but the kit combining PerkinElmer's AlphaScreen technology and TGR BioSciences' SureFire cellular ERK assay is a popular method of measurement. Published work indicates that ERK1/2 activation is pharmacologically similar to previously established responses in other assay formats (1). Here are some characteristics of this assay format:

- Can be used with primary or cultured cells (adherent or non-adherent)
- Cloned or endogenous receptors (transient or stable transfection)
- Non-radioactive
- Detects agonists, antagonists, or orphans
- Homogeneous assay
- No wash steps
- One day assay
- Automatable for high throughput (384- or 1536-wells)
- Highly sensitive and low background
- Can detect broad affinities
- Specialized reader is required

### Sample Protocol

See the PerkinElmer protocol for AlphaScreen SureFire p-ERK assay kits or the TGR Biosciences SureFire Cellular ERK assay protocol for more detailed information.

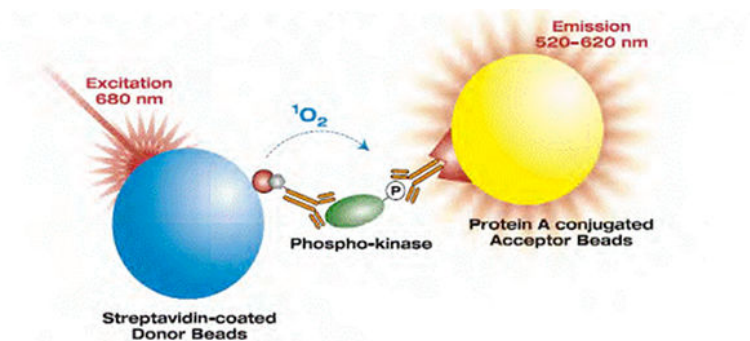


**Figure 2:** AlphaScreen SureFire ERK Assay Principle.

Additional information is also available for one versus two plate protocols and non-adherent cells.

Suggested Assay plate: PerkinElmer, Proxiplate-384 well plate (half volume), #6006280

## Schematic Outline of the SureFire Cellular ERK Assay

1. Plate cells into 96- or 384-well proxiplate for 24 hours at 37°C
2. Starve cells with low serum or serum-free medium. This optional step helps to keep the basal phosphorylation levels low (times vary based on the cell type).
3. Add inhibitors (time may vary)
4. Add agonist for 5 to 15 minutes
5. Lyse cells for 10 minutes at room temperature
6. Transfer 6 µl lysate to assay plate
7. Add 10 µl reaction mix containing beads for 2 hours at room temperature
8. Read plate

## Assay Formats

### Agonist Mode:

- a. Cells are stimulated with agonist and optimal time and temperature for stimulation are determined.
- b. Max response is maximum p-ERK produced by full agonist stimulation (Figure 3).
- c. Min response is p-ERK produced in the presence of stimulation buffer without agonist.
- d. Relative EC<sub>50</sub> is obtained from the concentration response curve.
- e. Detection of GPCR-induced ERK1/2 activation in transfected cell lines (Figure 4).

### Antagonist Mode:

- a. Cells are pretreated with diluted test antagonist at 37°C for 1-2 hours.
- b. Agonist is added at the EC<sub>80</sub> concentration and incubated at room temperature for 15 minutes.



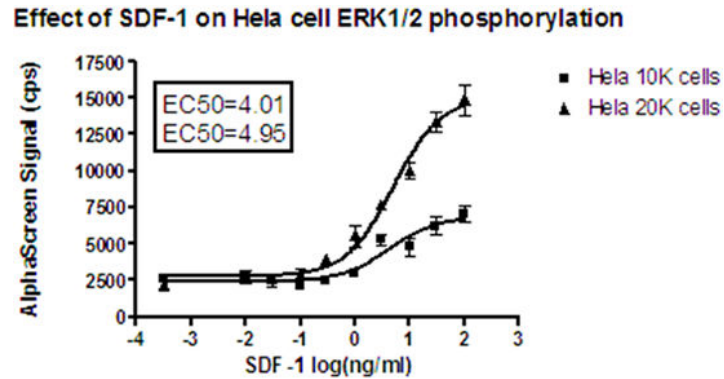


**Figure 3:** Agonist concentration response curves. ERK1/2 activation with cells expressing endogenous GPCRs.

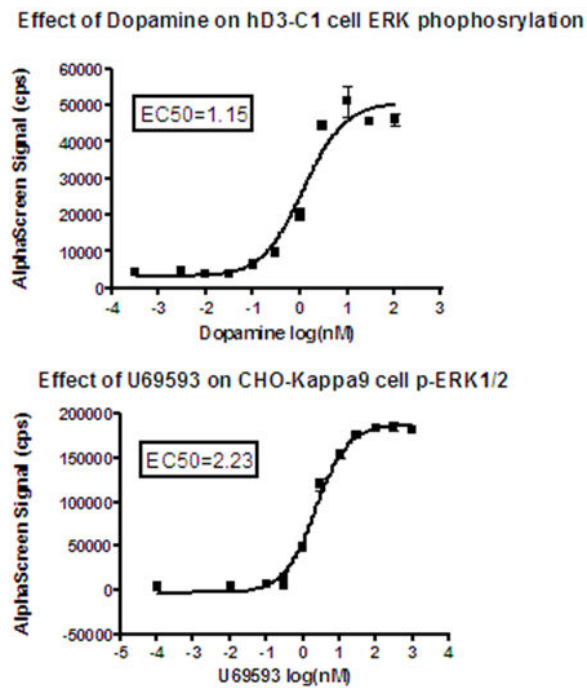


**Figure 4:** Detection of GPCR-induced ERK1/2 activation in transfected cell lines. A) Effect of dopamine on hD3-C1 cell ERK phosphorylation. B) Effect of U69593 on CHO-Kappa9 cell p-ERK1/2.

- c. Inhibition of the agonist response is quantified.
- d. Max response is maximum p-ERK produced by full agonist stimulation.
- e. Min response is p-ERK produced in the presence of stimulation buffer without agonist.
- f. Relative IC<sub>50</sub> is determined from the concentration response curve (Figure 5).

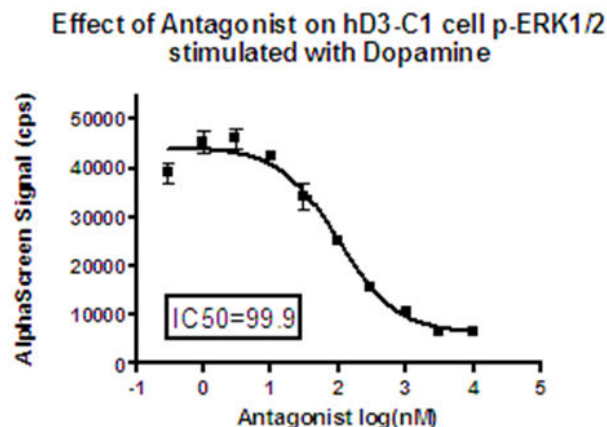


Figure 5: Antagonist concentration response curve.

## Assay Optimization

The following conditions should be optimized for the best assay performance:

- Cell titration to minimize the baseline ERK1/2 phosphorylation level and to maximize the signal window.
- Serum starvation parameters (if required). This may be necessary to reduce background.
- DMSO tolerance study.
- Time course for compound incubation.
- Time course for agonist stimulation.
- Optimization of instrument set-up.

## Helpful Hints for Performing SureFire AlphaScreen ERK Assays

- Cells are grown to confluence in microplate wells prior to assaying for ERK1/2. This is important because contact inhibition significantly lowers the level of background ERK1/2 phosphorylation, synchronizes the responsiveness of the cells, and maximizes the signal window.
- Cells should be harvested from flasks for seeding into microplates at approximately 70-90% confluence. Cells should be detached from the flasks using conditions as mild as possible and allowed to adhere to plates for at least 24 hours prior to the assay.
- Monitor the cell passage number; determine empirically whether the cells will lose responsiveness at passages beyond a maximum limit.
- Assay incubation temperature should be at least 22°C.
- To eliminate “edge effects”, increase the reaction volumes from 11  $\mu$ l (4  $\mu$ l cell lysate and 7  $\mu$ l reaction mix) to 16  $\mu$ l (6  $\mu$ l cell lysate and 10  $\mu$ l reaction mix).
- Avoid bubbles in the assay wells.

- g. Because AlphaScreen beads are light sensitive, add beads and incubate assay plates in low light conditions.
- h. Read the plates using the Envision Alpha Turbo module to avoid an “edge effect” in data consistency.

## Websites

[www.TGR-Biosciences.com](http://www.TGR-Biosciences.com)

[www.PerkinElmer.com](http://www.PerkinElmer.com)

## References

### Literature Cited

1. Osmond RIW, Sheehan A, Borowicz R, Barnett E, Harvey G, Turner C, Brown A, Crouch MF, Dyer AR. GPCR Screening via ERK 1/2: A Novel Platform for Screening G protein-Coupled Receptors. *J. Biomol. Screen.* 2005;10(7):730–737. PubMed PMID: 16129779.

### Additional References

Luttrell DK, Luttrell LM. Signaling in time and space: G protein-coupled receptors and mitogen-activated protein kinases. *Assay Drug Dev Tech.* 2003;1:327–338. PubMed PMID: 15090198.

Luttrell LM. G protein-coupled receptor signaling in neuroendocrine systems. ‘Location, location, location’: activation and targeting of MAP kinases by G protein-coupled receptors. *J. Molec. Endocrinology.* 2003;30:117–126.

Schulte G, Fredholm BB. Signalling from adenosine receptors to mitogen-activated protein kinases. *Cellular Signalling.* 2003;15:813–827. PubMed PMID: 12834807.



# IP-3/IP-1 Assays

Kim E. Garbison,<sup>1</sup> Beverly A. Heinz, and Mary E. Lajiness

Created: May 1, 2012.

## Abstract

Activation of G-protein coupled receptors (GPCR) that couple to  $G_{\alpha\theta}$  and  $G_{\beta\gamma}$  and subsequent activation of phospholipase C  $\beta$  (PLC- $\beta$ ) can be detected through the measurement of D-myo-inositol 1,4,5-triphosphate (IP3) in cells. This chapter describes technologies that can be used to develop robust assays for screening compounds, more specifically the use of Homogeneous Time-Resolved Fluorescence Assay (HTRF) for IP3 measurement. A sample preparation protocol, parameters for assay optimization and examples of data analysis are provided.

## Introduction

**Note: The content of the Assay Guidance Manual will be updated quarterly with contributions and new chapters to ensure the manual stays relevant to the current technologies and best practices used in the rapidly changing field of drug discovery and development. The chapter is currently in the process of being updated to reflect the current state of the field. Therefore, it is possible that the most up-to-date information may not yet be included, but will be added in forthcoming chapter updates.**

Agonist stimulation of G protein coupled receptors that are coupled to  $G_{\alpha q}$  (or to  $G_{\beta\gamma}$  subunits) leads to activation of phospholipase C  $\beta$  (PLC- $\beta$ ) followed by production of D-myo-inositol 1,4,5-triphosphate (IP3). IP3 initiates the release of  $Ca^{2+}$  from intracellular stores before it is rapidly degraded to IP2 then IP1 (Figure 1). Activation of this pathway is usually measured by detection of intracellular calcium using fluorescent calcium indicator dyes and fluorescence plate readers (FLIPR). Although calcium assays are robust and easily amenable to HTS, there are some important limitations: calcium flux is very rapid and transient, and does not allow detection of constitutive activity (or inverse agonism); interference by fluorescent and nuisance compounds is a problem; and sensitivity is often insufficient to allow the use of primary cells. Alternatively, it is possible to measure IP3 production directly or indirectly as a read-out of PLC- $\beta$  activation.

## Overview of Technology

Traditional assays for total inositol phosphate accumulation used radioactivity and were complicated and not amenable to HTS. In addition, IP3 production is very rapid and transient before it is metabolized to IP2 and IP1. There are a few alternative technologies

---

<sup>1</sup> Eli Lilly & Company, Indianapolis, IN.

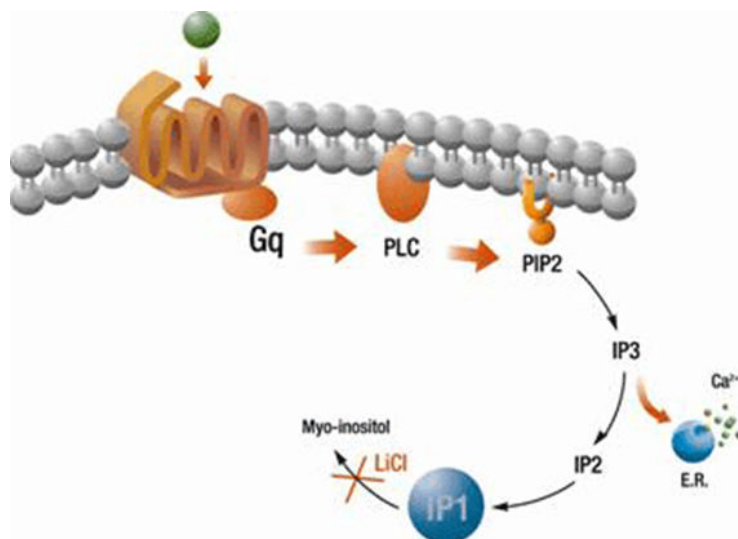


**Figure 1:** Activation of  $G_{\alpha q}$  Pathway ( Reprinted from Cisbio with permission).

available for measurement of IP-3 including AlphaScreen (Perkin Elmer) and HitHunter™ Fluorescence Polarization (DiscoverRx). Recently a homogeneous time resolved fluorescence assay for IP1 (IP-One HTRF®), has been developed by Cisbio (see below). This assay format takes advantage of the fact that lithium chloride (LiCl) inhibits the degradation of IP1, the final step in the inositol phosphate cascade, allowing it to accumulate in the cell, where it can be measured as a substitute for IP3. Data from Cisbio show that the assay can be used with endogenously or heterologously expressed receptors in either adherent or suspension cells, to quantitate the activity of agonists, antagonists, and inverse agonists. Agonist  $EC_{50}$ 's and antagonist  $IC_{50}$ 's using the IP-One HTRF® assay correlate very well with those from calcium assays and traditional IP3 detection assays.

## IP-One HTRF® Technology (Cisbio)

### General Background

The IP-One HTRF® assay kit allows direct quantification of myo-Inositol 1 phosphate (IP1) in cultured cells. The assay is a competitive immunoassay. IP1 produced by cells (in the presence of LiCl) after receptor activation competes with an IP1 analog coupled to a d2 fluorophore (acceptor) for binding to an anti-IP1 monoclonal antibody labeled with Eu Cryptate (donor). The resulting signal is inversely proportional to the concentration of IP1 in the sample. A standard curve is constructed to convert raw data to IP1 concentration (Figure 2).

See the following link for more information: <http://www.htrf.com/products/gpcr/ipone/>

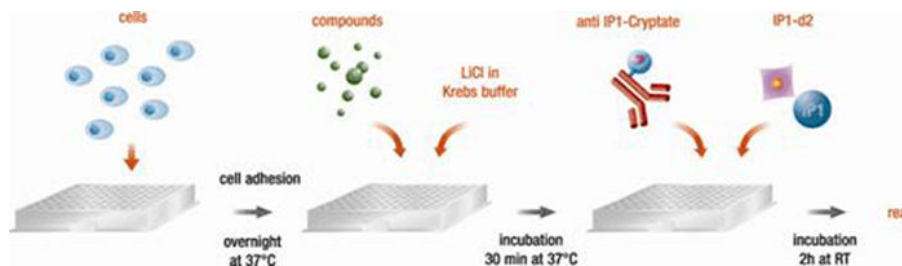


**Figure 2:** IP1 HTRF Assay Protocol (Reprinted from Cisbio with permission).

## Sample Preparation Protocol

Assay may be conducted in 96-well, 384-well or 1536-well formats. Only white plates should be used for IP-One HTRF. Suggested plate types:

- 96 half-well plate Costar cat # 3688 (white, opaque flat bottom, TC-treated). Total working volume = 100  $\mu$ l.
  - 96-well Costar cat # 3917 (white, opaque flat bottom, TC-treated). Total working volume = 200  $\mu$ l.
  - See the following link for additional plate recommendations: <http://www.htrf.com/technology/assaytips/microplate/>
1. Adherent cells may be seeded into tissue culture treated, white microplates 24 hours before assay. Just before the assay, media is removed from adherent cells and replaced with Stimulation Buffer (included in the kit). Note: buffers containing phosphate can not be used.
  2. Alternatively, cells may be prepared in suspension using the Stimulation Buffer provided in the kit, and plated immediately before the assay.
  3. Serial dilutions of the IP1 standard included in the kit are made using Stimulation Buffer, and pipetted into the assay plate for the standard curve.
  4. Cells are pre-treated with antagonist compounds prepared in Stimulation Buffer for 15-30 minutes at 37°C, 5% CO<sub>2</sub>.
  5. Agonist prepared in Stimulation Buffer is added and plates are incubated at 37°C, 5% CO<sub>2</sub> for required stimulation time (to be optimized).
  6. Diluted IP1 d2 conjugate is added to wells.
  7. Diluted anti-IP1 Eu Cryptate is added to wells.
  8. Plates are incubated for 1 hour at room temperature.
  9. Plates are read on an HTRF<sup>®</sup> compatible reader (eg: Envision, Tecan GENios, BMG Rubystar). See the following link for other readers: [http://www.htrf.com/technology/htrfmeasurement/compatible\\_readers/](http://www.htrf.com/technology/htrfmeasurement/compatible_readers/)
  10. Excitation is at 320 nm. CisBio recommends using a ratiometric measurement for HTRF<sup>®</sup> emissions at both 620 nm and 665 nm. Emissions at 620 nm are used as an internal reference and emissions at 665 nm reflect the biological response. The

ratio of 665/620 allows normalization for well-to-well variability and interference due to assay components.

Signal Stability: plates may be read repeatedly for determination of kinetics, and signal is stable for at least 24 hours at RT.

## Results and Data Analysis

The ratio of absorbance 665/ absorbance 620 nm emissions is calculated. A standard curve is plotted of Ratio 665/620 vs IP-1 concentration using non-linear least squares fit (sigmoidal dose response variable slope, 4PL). Unknowns are read from the standard curve as nM concentration of IP1. Ratio 665/620 of unknowns should fall on the linear portion of the standard curve. Increased accumulation of IP-1 will result in a decrease in signal (Figure 3).

## Assay Formats

### Agonist Mode:

Cells are stimulated with agonist for optimum time and increase in IP1 produced by receptor activation is quantified. Max response is maximum IP1 produced by full agonist stimulation. Min response is IP1 produced in the presence of stimulation buffer and the absence of agonist. Relative EC<sub>50</sub> and Relative Efficacy (% maximum activity of a test compound relative to the reference agonist) may be obtained from concentration response curve (Figure 4).

### Antagonist Mode:

Cells are treated with test antagonist compound for approximately 15 minutes. Agonist is then added at approximately EC<sub>80</sub> concentration and incubated for optimum time. Inhibition of the agonist response is quantified. Max response is IP1 produced by EC<sub>80</sub> concentration of agonist in the absence of compound. Min response is IP1 produced in the presence of stimulation buffer and the absence of agonist or test compound. Relative IC<sub>50</sub> may be obtained from concentration response curve and used to calculate antagonist K<sub>b</sub> (Figure 5).

### Inverse Agonist Mode:

Cells expressing a constitutively active receptor are treated with test compound for optimum time (in the absence of agonist). Inhibition of the basal response (IP1 produced in the presence of stimulation buffer alone) by test compound is quantified. Max response is basal level of IP1 produced in cells expressing the constitutively active receptor during the incubation time. Min response is basal level of IP1 produced in cells without the receptor. Relative EC<sub>50</sub> Inverse and Relative Efficacy Inverse (% maximum response of reference inverse agonist) may be obtained from concentration response curve (Figure 6).



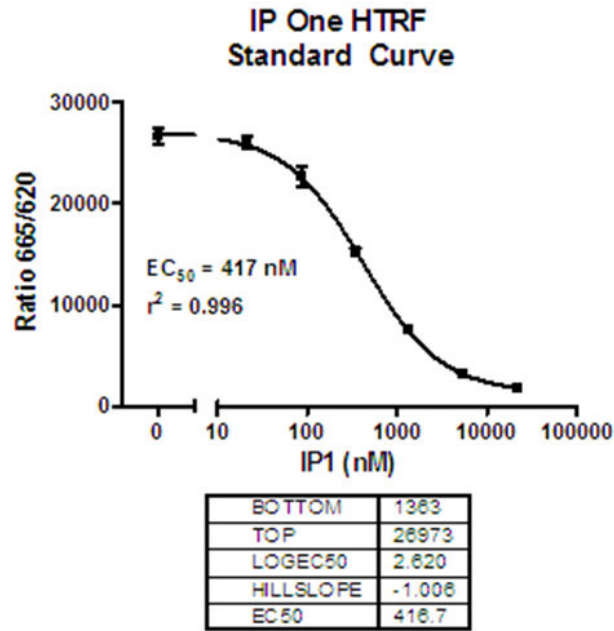


Figure 3: 1 Standard Curve.

## IP-One HTRF® HEK293 GPCR X

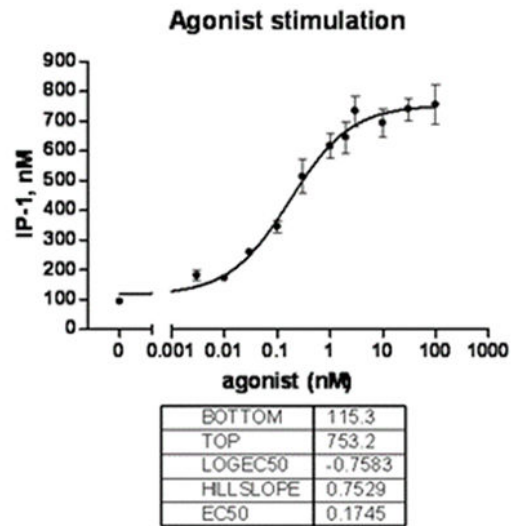
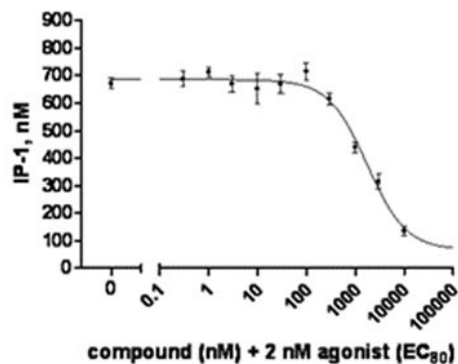


Figure 4: Agonist concentration response curve

## IP-One HTRF® HEK293 GPCR X

Inhibition of agonist stimulated IP-1 accumulation

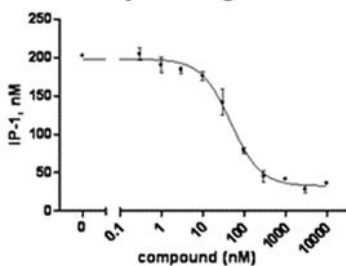


|           |        |
|-----------|--------|
| BOTTOM    | 66.03  |
| TOP       | 885.5  |
| LOGEC50   | 3.245  |
| HILLSLOPE | -1.097 |
| EC50      | 1760   |
| KI        | 141.6  |

Figure 5: Antagonist concentration response curve

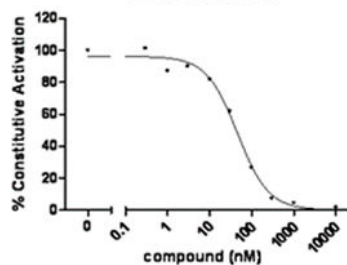
## IP-One HTRF® HEK293 GPCR Y

Inhibition of constitutive IP-1 accumulation by inverse agonist



|           |        |
|-----------|--------|
| BOTTOM    | 32.67  |
| TOP       | 198.2  |
| LOGEC50   | 1.678  |
| HILLSLOPE | -1.212 |
| EC50      | 47.68  |

Normalized data



|           |        |
|-----------|--------|
| BOTTOM    | 0.2155 |
| TOP       | 96.22  |
| LOGEC50   | 1.659  |
| HILLSLOPE | -1.179 |
| EC50      | 45.62  |

Figure 6: Inverse agonist concentration-response curve

## Assay Optimization

The following parameters should be optimized to ensure that the level of IP-1 produced in the wells falls within the linear range of the standard curve, signal window is maximized and variability is acceptable:

- cell number
- preincubation of cells with stimulation buffer

- agonist stimulation time
- incubation time after addition of conjugates

See the following link for Cisbio recommendations for assay optimization: <http://www.htrf.com/files/resources/ip-one%20nature.pdf>

## Web Sites

<http://www.htrf.com/resources/>

## References

- Eglen RM. Functional G protein-coupled receptor assays for primary and secondary screening. *Combinatorial Chemistry & High Throughput Screening*. 2005;8(4):311–318. PubMed PMID: 16101007.
- Inglese J., Johnson R.L., Simeonov A., Xia M., Zheng W., Austin C.P., Auld D.S. High-throughput screening assays for the identification of chemical probes. *Nature Chemical Biology*. 2007;3(8):466–479. PubMed PMID: 17637779.
- McLoughlin D.J., Bertelli F., Williams C. The A, B, Cs of G-protein-coupled receptor pharmacology in assay development for HTS. *Expert Opinion on Drug Discovery*. 2007;2(5):603–619. PubMed PMID: 23488953.
- Trinquet E., et al. D-myo-Inositol 1-phosphate as a surrogate of d-myo-inositol 1,4,5-trisphosphate to monitor G protein-coupled receptor activation. *Analytical Biochemistry*. 2006;358(1):126–135. PubMed PMID: 16965760.



# Cardiomyocyte Impedance Assays

Sarah D. Lamore, PhD,<sup>✉1</sup> Clay W Scott, PhD,<sup>2</sup> and Matthew F. Peters, PhD<sup>3</sup>

Created: February 25, 2015.

## Abstract

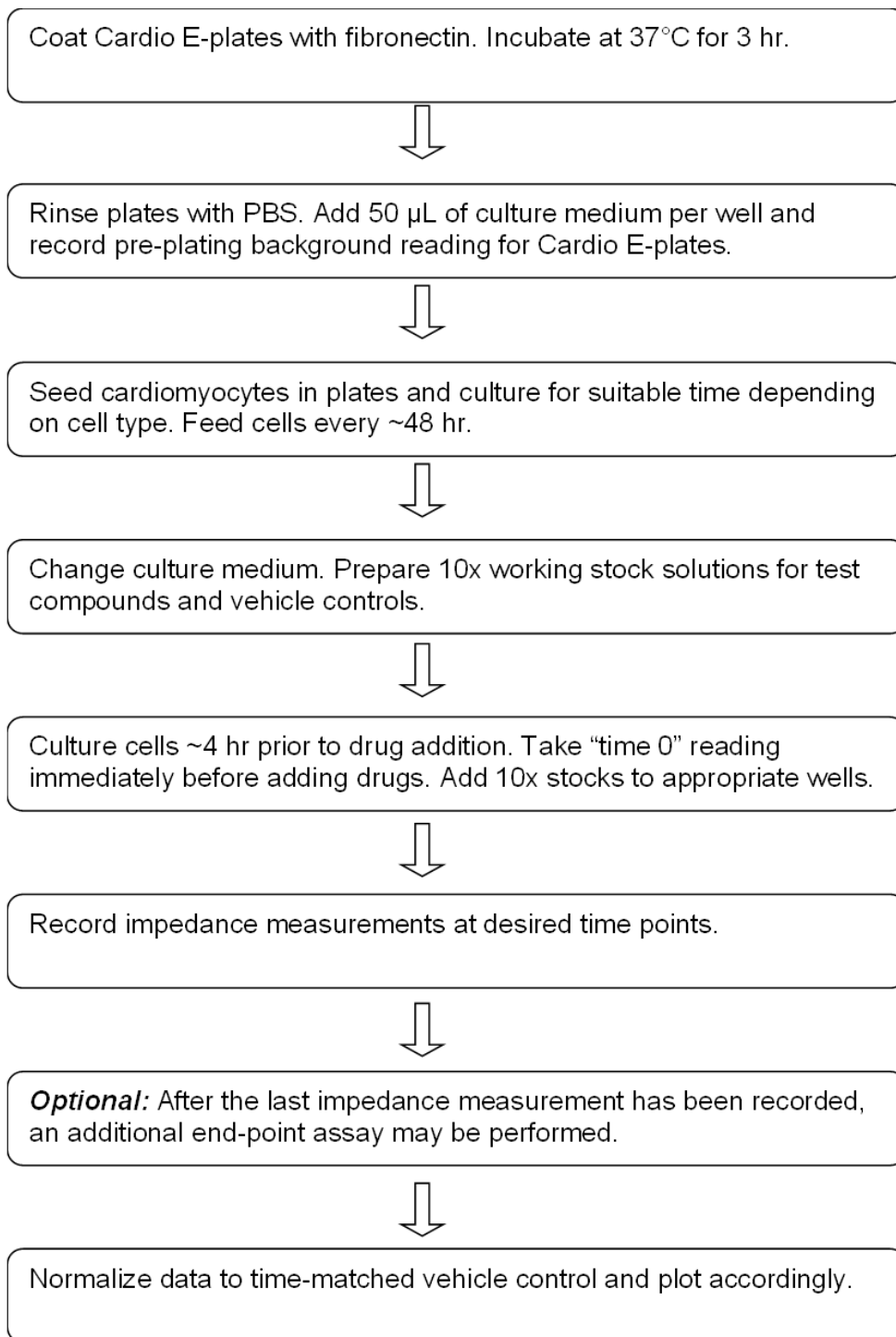
Cellular impedance assays have been broadly utilized as a label-free approach for toxicity and drug discovery screening. The xCELLigence RTCA Cardio instrument sets itself apart from other impedance technologies by its rapid data acquisition rate (12.9 msec). This speed is fast enough to detect the contractile activity of beating cardiomyocytes, offering a relatively high throughput and robust strategy to noninvasively monitor the effects of test compounds on cardiomyocyte function. This chapter introduces the fundamentals and applications of cardiomyocyte impedance assays. A protocol detailing cardiomyocyte culture, data acquisition, and data analysis using the xCELLigence RTCA Cardio system is provided and considerations for assay design and data interpretation are discussed.

---

<sup>1</sup> Drug Safety and Metabolism, AstraZeneca Pharmaceuticals, Waltham, MA; Email: sarah.lamore@astrazeneca.com. <sup>2</sup> Drug Safety and Metabolism, AstraZeneca Pharmaceuticals, Waltham, MA; Email: clay.scott@astrazeneca.com. <sup>3</sup> Drug Safety and Metabolism, AstraZeneca Pharmaceuticals, Waltham, MA; Email: matt.peters@astrazeneca.com.

<sup>✉</sup> Corresponding author.

## Flowchart



## Introduction

Cellular impedance assays have proved to be a robust and versatile label-free approach to study whole cellular behavior. The technology utilizes electrodes that are incorporated into the bottom of each well of tissue culture plates. Weak alternating current (AC) is applied between the electrodes with tissue culture medium as the electrolyte. Impedance is calculated using the AC version of Ohm's law where impedance ( $Z$ ) is the ratio of voltage ( $v$ ) / current ( $I$ ). Cells are seeded into the wells and attach to the bottom of the well. The cell layer covers the electrodes, thus impeding current flow between the electrodes to varying degrees, depending on cell number, morphology, adhesion, and cell-cell contacts. Cell morphology and adhesion changes are therefore quantified without exogenous detection labels or dyes, allowing noninvasive, continuous, and label-free monitoring of cellular events.

After cells adhere to the bottom of an impedance plate, current flows between the electrodes through a combination of extracellular and transcellular paths. The frequency of the electrical current influences the preferred path; lower frequency currents tend to take extracellular (paracellular) paths while higher frequency currents have a propensity to pass capacitively through cell membranes (transcellular) (1, 2). Because these paths are preferentially sensitive to different cellular functions and/or events, controlling current frequencies has allowed researchers to tailor cellular impedance platforms to suit diverse screening applications. Different instruments have been used to quantitatively measure a wide variety of cellular events, including cell viability and growth, migration, cell-cell and cell-matrix contact, and GPCR and kinase signaling (reviewed in 3).

Application of impedance to cardiomyocytes has recently been introduced by the xCELLigence RTCA Cardio instrument (ACEA Biosciences, San Diego, CA) that produces a single frequency ( $10^4$  Hz) to enable accelerated data acquisition (12.9 msec) (4, 5). The number of data points collected per second ( $\sim 78$ ) easily allows for quantitative monitoring of impedance changes associated with the physical movement of spontaneous, synchronously beating cardiomyocytes. This relatively high throughput, label-free approach to detect cardiomyocyte beating has several advantages: 1) it allows for continuous, real-time monitoring without the need of exogenous detection reagents, 2) it produces robust, quantitative data, and 3) it offers versatile data analysis.

## Concept and Overview of xCELLigence RTCA Cardio System

The xCELLigence Real-Time Cell Analysis (RTCA) Cardio instrument exploits impedance changes across the cardiac monolayer to evaluate both cardiomyocyte health status and contraction-induced morphology changes. Cardiomyocytes are cultured on 96-well Cardio E-Plates, which contain interdigitated gold microelectrodes incorporated into the bottom of each well. Spontaneously beating cardiomyocytes from several sources, including freshly isolated rat neonatal cardiomyocytes as well as human stem cell-derived cardiomyocytes have been used successfully with the RTCA Cardio system.

## RTCA Cardio Control Unit

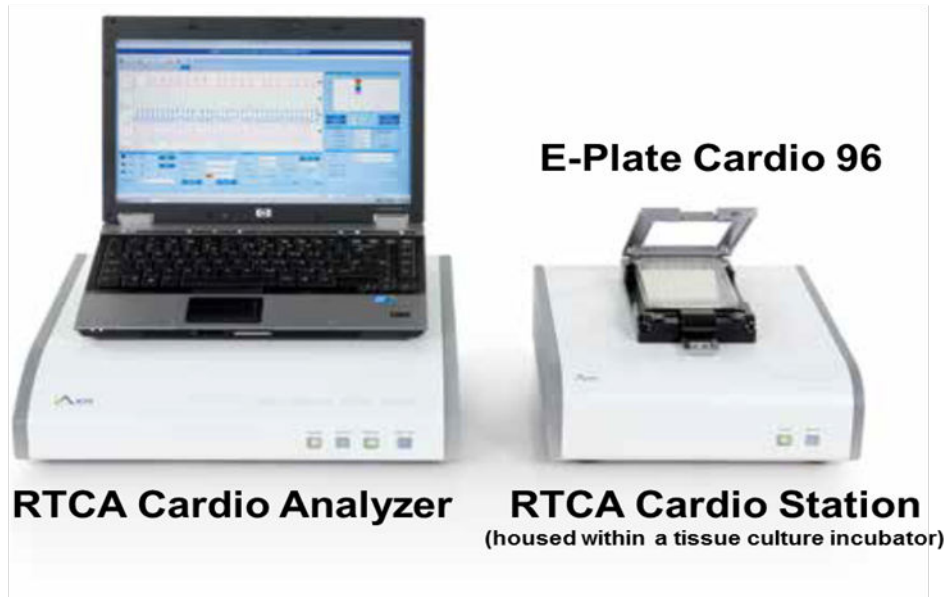


**Figure 1:** xCELLigence RTCA Cardio instrument (ACEA Biosciences). The RTCA Analyzer and Control Unit (left) connect to the RTCA Cardio Station (right), which is housed within a standard tissue culture incubator.

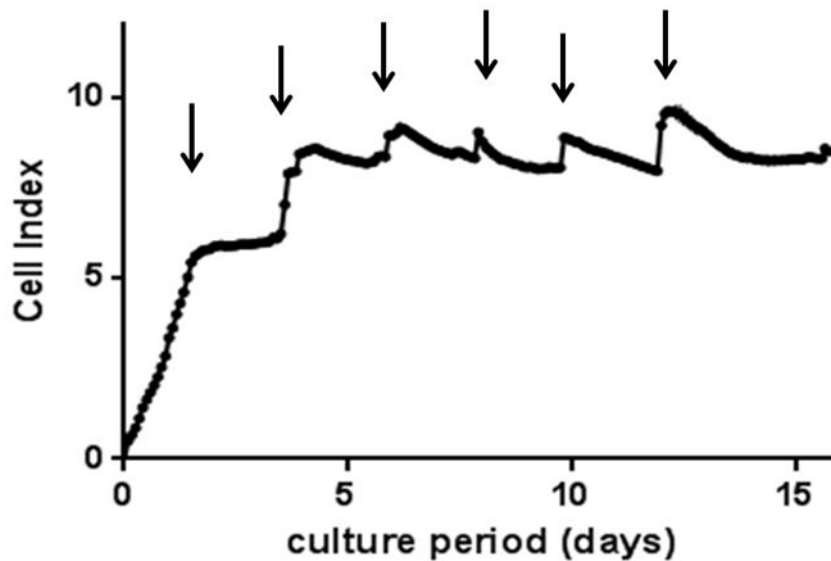


**Figure 2:** Changes in cell index over the course of cardiomyocyte culture. iPSC (30,000 plateable iCell® cardiomyocytes per well) were seeded on an E-plate 96 and overall impedance, displayed as cell index, was monitored for 16 days (mean  $\pm$  SD of 3 wells). Medium changes indicated by black arrows.



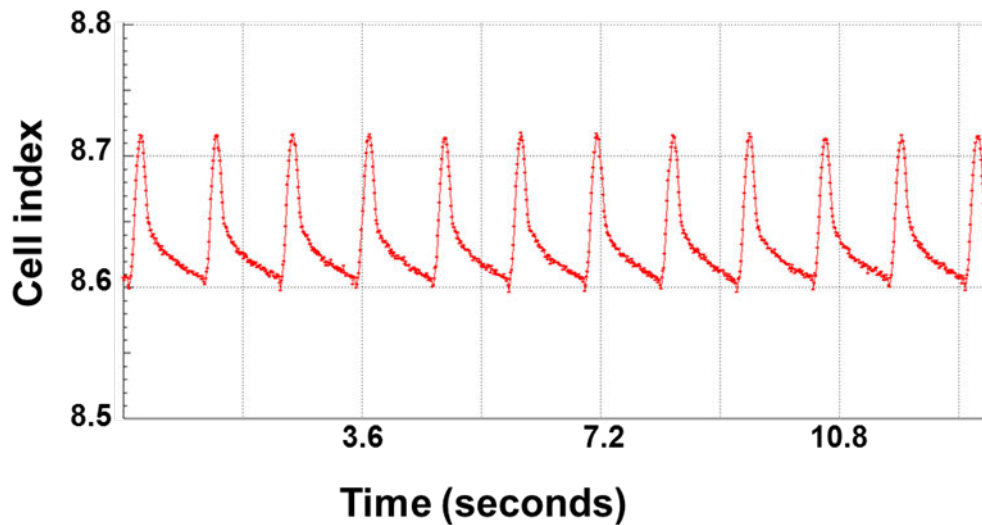


**Figure 3:** Change in cell index of beating cardiomyocytes. Note the relatively small fluctuation in cell index (8.6-8.7) compared to the overall cell index of  $\sim 8.6$ , equaling an  $\sim 0.09\%$  change in impedance.

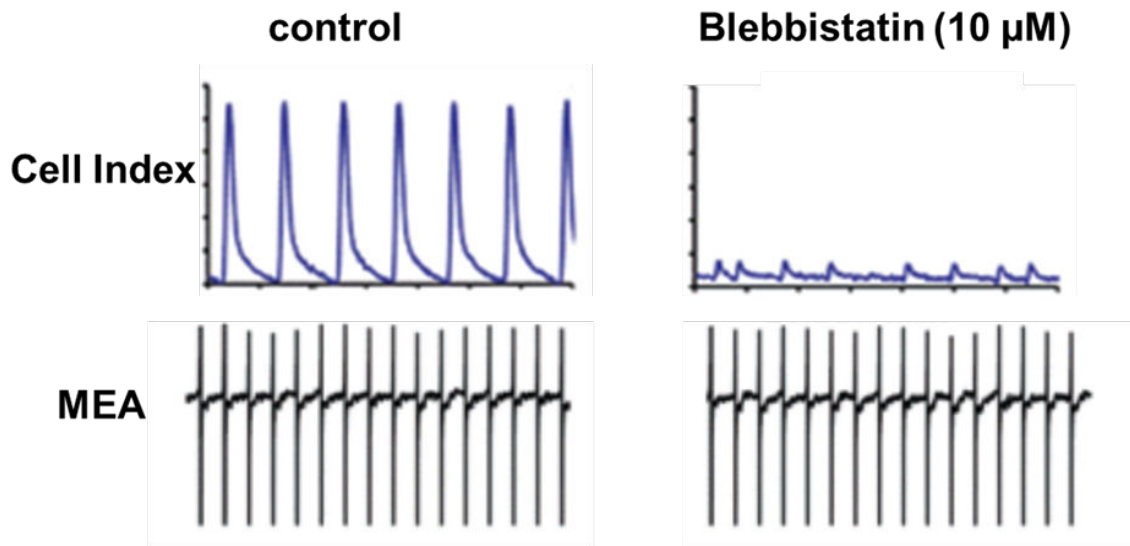


**Figure 4:** Effect of blebbistatin, a myosin II inhibitor, on mouse embryonic stem cell-derived cardiomyocyte impedance and MEA profiles (Adapted from 5). Blebbistatin treatment ( $10 \mu\text{M}$ ) results in inhibition of impedance signals but does not have an effect on field potential recordings measured by MEA.

The system is composed of the RTCA Cardio Station, the RTCA Control Unit, and the RTCA Analyzer (Figure 1). To monitor impedance, the Cardio E-plate is placed in the RTCA Cardio Station, which is housed within a standard tissue culture incubator. The analyzer connects to the station through a ribbon cable that passes through the sealed door of the incubator. The control unit operates the software and acquires and displays the

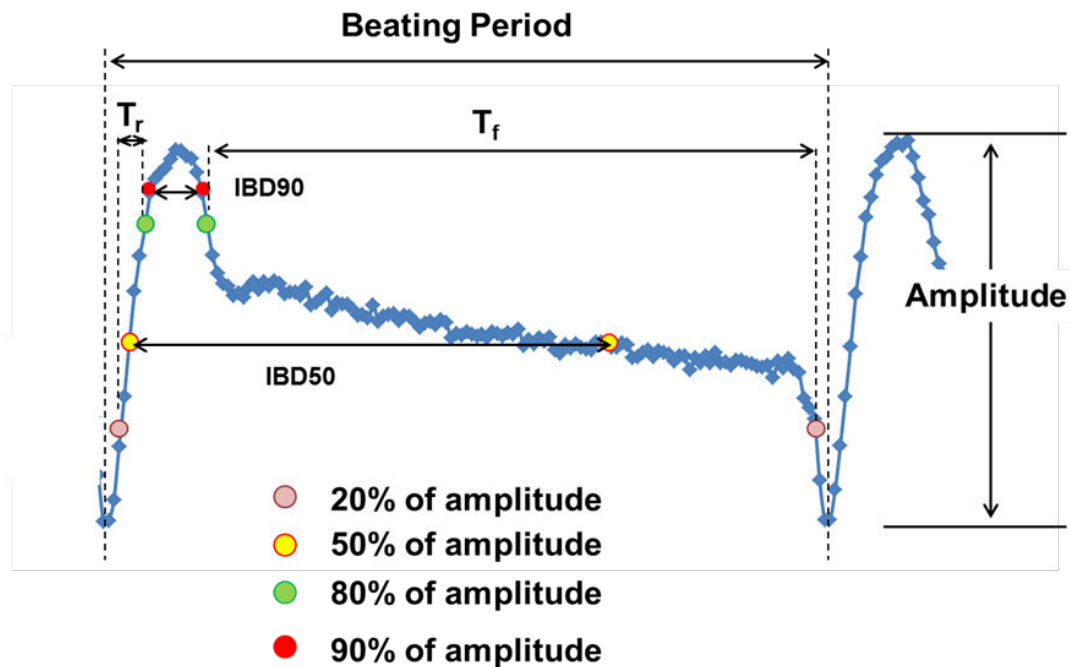


**Figure 5:** Definition of beat parameters. RTCA Cardio Software identifies and quantifies several beat parameters including amplitude, beating period,  $T_f$ ,  $T_r$ , IBD<sub>50</sub>, and IBD<sub>90</sub>.

data in real time, while the analyzer sends and receives the electronic signals between the control unit and the station. Impedance is measured and Cell Index (CI) is calculated by subtracting base line impedance from impedance at any given time and dividing by a constant value (6). Because cell index is a relative measure of impedance, it is exquisitely sensitive to changes in cell number, attachment, and morphology. Change in any of these factors produces a measurable change in CI values and thus allows for determination of cell status over assay time (Figure 2).

The contractile activity of beating cardiomyocytes results in small transient changes in impedance that are a fraction (generally 0.1%) of the overall impedance (Figure 3). The hallmark feature of the xCELLigence RTCA Cardio System is the fast data acquisition rate (12.9 msec), allowing the detection of minute morphological changes of a spontaneously beating cardiomyocyte monolayer, thereby enabling a readout that is downstream of both mechanical and electrical elements of contraction. A demonstration that impedance measures the physical movement of contraction rather than the electrophysiological properties of cardiomyocyte beating can be seen with blebbistatin, a small molecule myosin II inhibitor, which causes a reduced impedance beating pattern in the absence of altering the action potential as detected by multi-electrode array (MEA) (Figure 4). The current version of the analysis package of the RTCA Cardio Instrument Software is capable of quantifying several beat parameters including beat rate (BR), beat amplitude (amp), beat duration (IBD<sub>50</sub>, IBD<sub>90</sub>), rising time ( $T_r$ ), falling time ( $T_f$ ), beating pattern similarity (BS), and beating rhythm irregularity (BRI) (Table 1 and Figure 5). Therefore, in

addition to monitoring changes in overall cellular status (morphology/attachment/viability), changes in beating characteristics can also be assessed.

A few publications have cross-validated the Cardio System with other detection methods using positive control compounds with well-established molecular mechanisms of action. For example, Guo et al (7) tested 28 compounds covering different known cardioactive mechanisms (inhibitors of various cardiac ion channels, GPCR agonists, etc) and showed comparable detection with both impedance and electrical field potential using microelectrode arrays (MEA). In a follow-up study, this group demonstrated concordance between impedance and patch clamp electrophysiological data using compounds with established clinical arrhythmic liability (8). Scott et al (9) demonstrated similar assay performance metrics between the impedance assay and a field stimulation IonOptix (optical-based) measure of cardiomyocyte contractility, using 30 inotropes and 19 non-inotropes. These compounds were recently tested for effects on  $Ca^{2+}$  transients using the FLIPR Tetra instrument, and gave results comparable to that seen with IonOptix and impedance (10). Thus, impedance data overlaps favorably with that derived from other detection methods, and in some cases can detect compounds that are not detected in methods that quantify “upstream” endpoints such as the action potential and calcium flux (e.g. blebbistatin, Figure 4). Finally, high-content imaging has been used to detect structural cardiotoxins (i.e. causing morphological damage and toxicity as opposed to affecting the mechanical properties of the cardiomyocyte) (11). Such compounds have not yet been systematically tested in the Cardio System. It will be interesting to determine the overlap between these two methods for detecting structural cardiotoxicity.

**Table 1:** Definition of beat parameters. RTCA Cardio Software identifies and quantifies several beat parameters.

| Parameter                   | Abbreviation                          | Definition   |
|-----------------------------|---------------------------------------|--|
| Beat rate                   | BR                                    | Number of beats per minute   |
| Beat amplitude              | amp                                   | Cell Index difference between one negative peak to the following positive peak                                     |
| Beat duration               | IBD <sub>50</sub> , IBD <sub>90</sub> | Duration between two adjacent points sitting at 50% or 90%, respectively, of maximal amplitude                     |
| Rising time                 | T <sub>r</sub>                        | Time the signal rises from 20% peak height to 80% peak height  |
| Falling time                | T <sub>f</sub>                        | Time the signal falls from 80% peak height to 20% peak height  |
| Beating period              |                                       | Time between each positive or negative peak  |
| Beating rhythm irregularity | BRI                                   | The CV (SD/avg) of all of the beating periods in one sweep   |
| Beating pattern similarity  | BS                                    | A comparison of the beating compared to a selected base time (score 1 for exactly the same -1 to exactly opposite) |

## Sample Protocol

This protocol provides basic instructions for cardiomyocyte culture, compound treatments, data acquisition, and analysis using the RTCA Cardio system. As an example, a description of how to culture commercially available induced pluripotent stem cell-derived cardiomyocytes (iPSC-CM) from CDI International (Madison, WI) for use with the RTCA Cardio system is offered. These cells can be maintained for extended durations ( $\geq 3$  weeks), thereby enabling measurement of acute and sub-acute drug-induced effects.

### Cell Plating and Culture

1. Dilute fibronectin (Sigma cat# F1141) to 10  $\mu\text{g}/\text{mL}$  with sterile DPBS.
2. Coat wells of E-plate Cardio 96 (ACEA cat# 06417051001) with 50  $\mu\text{L}$  of 10  $\mu\text{g}/\text{mL}$  fibronectin. Incubate plates at 37°C for 3 hr. Alternatively plates can be incubated at 4°C overnight.
3. Aspirate fibronectin solution and rinse wells once with 200  $\mu\text{L}$  DPBS.
4. Add 50  $\mu\text{L}$  of iCell® plating medium (CDI cat# CMM-100-110) to each well.
5. Record pre-plating background impedance measurement for each plate.
6. Thaw iCell® cardiomyocytes (CDI International) for 4 min in a 37°C water bath. Transfer cells to a 50 mL conical tube and slowly add room-temperature plating medium drop-wise to a final volume of 5 mL plating medium/vial of cells. (Note: iCell® cardiomyocyte viability is highly dependent on the thawing process. Be sure to follow instructions provided by the manufacturer.)
7. Count cells and, taking into account the plating efficiency for the specific lot number of cells, dilute the cell suspension in plating medium to a final concentration of  $6 \times 10^5$  plateable cells/mL.
8. Seed 30,000 plateable cells per well by pipeting 50  $\mu\text{L}$  of the cell suspension/well. (Note: Significant edge effects can occur with the beating pattern. Therefore it is suggested that the outer wells are filled with buffer and not used for experimentation. This results in 60 wells of each plate being used per experiment.)
9. Allow cells to settle undisturbed for 30 min at room temperature to ensure even distribution of cardiomyocytes.
10. Culture cells undisturbed for 2 days at 37°C / 7%  $\text{CO}_2$ .
11. Aspirate medium and add 100  $\mu\text{L}$  maintenance medium (CDI cat# CMM-100-120) per well. (Note: Take caution when replacing the maintenance medium. When aspirating spent medium, do not touch the bottom of the well as this might result in the removal of cells and cause an altered beating rhythm. Gently and slowly add fresh maintenance medium to the side of each well to reduce disturbance to the monolayer.)
12. Culture cells for an additional 10-12 days, carefully replacing maintenance medium every other day.

## Compound Addition and Data Acquisition

1. Cells will have a consistent, stable, and synchronous beating pattern after approximately 10-14 days in culture; this window is the optimum time for compound addition and data acquisition.
2. On the day of compound addition, replace maintenance medium with 90  $\mu$ L fresh medium ~4 hr before taking time zero reading and return cells to incubator.
  - a. Temperature decreases reduce myocyte beating, and therefore several steps should be taken to reduce the time that cell cultures are out of the incubator (< 2 min). Maintenance medium should always be warmed to 37°C, for both cell culture and for preparing 10x stocks of test compounds. If possible, liquid handling steps should be automated.
3. Prepare 1000x stocks of test compounds in appropriate vehicle. Dilute stocks and vehicle controls 1:100 in maintenance medium for a 10x working stock in a 96-well cell culture plate. (Note: Vehicle should not exceed 0.1% final concentration and vehicle controls should always be included in the assay.)
4. Take time zero reading for each plate immediately before compound addition.
5. Add 10  $\mu$ L of working stock to appropriate wells.
6. Collect data at desired time points (3 sweeps at 30-60 sec per time sweep). iCell® cardiomyocytes have a relatively long-term stable beating pattern and therefore cardiomyocyte beating function can be monitored for  $\geq$  72 hr.
7. If desired, an additional end-point assay can be performed AFTER the last reading is taken (e.g., cell viability can be assessed using commercial kits such as CellTiter-Glo® Luminescent Cell Viability Assay, Promega cat# G7570).

## Data Analysis and Results

1. The total impedance and each of the beating parameters are recorded for every sweep performed by the RTCA software.
2. Under the “plot” tab, the beating pattern can be visualized by selecting the desired wells (right side of screen) and time (under “axis scale”). The RTCA software will identify the negative and positive peaks for each of the beats. The peaks can be visualized by checking the box next to “peaks” under “axis scale”. A “+” indicates a positive peak and a “-“ indicates a negative peak identified by the software. In most cases, the default settings correctly identify the positive and negative peaks. However, in some cases, the settings may need to be adjusted by tuning the waveform peak shape, threshold, and noise filter in order to correctly identify the peaks of the beating pattern.
  - a. After verifying correct peak identification, export the desired beat parameters into excel for data manipulation (Figure 6).
    - i. Select the desired beat parameters (left hand box).
    - ii. Select the desired time points (upper right hand box).
    - iii. Export parameters into excel in list and/or plate format (lower right box).

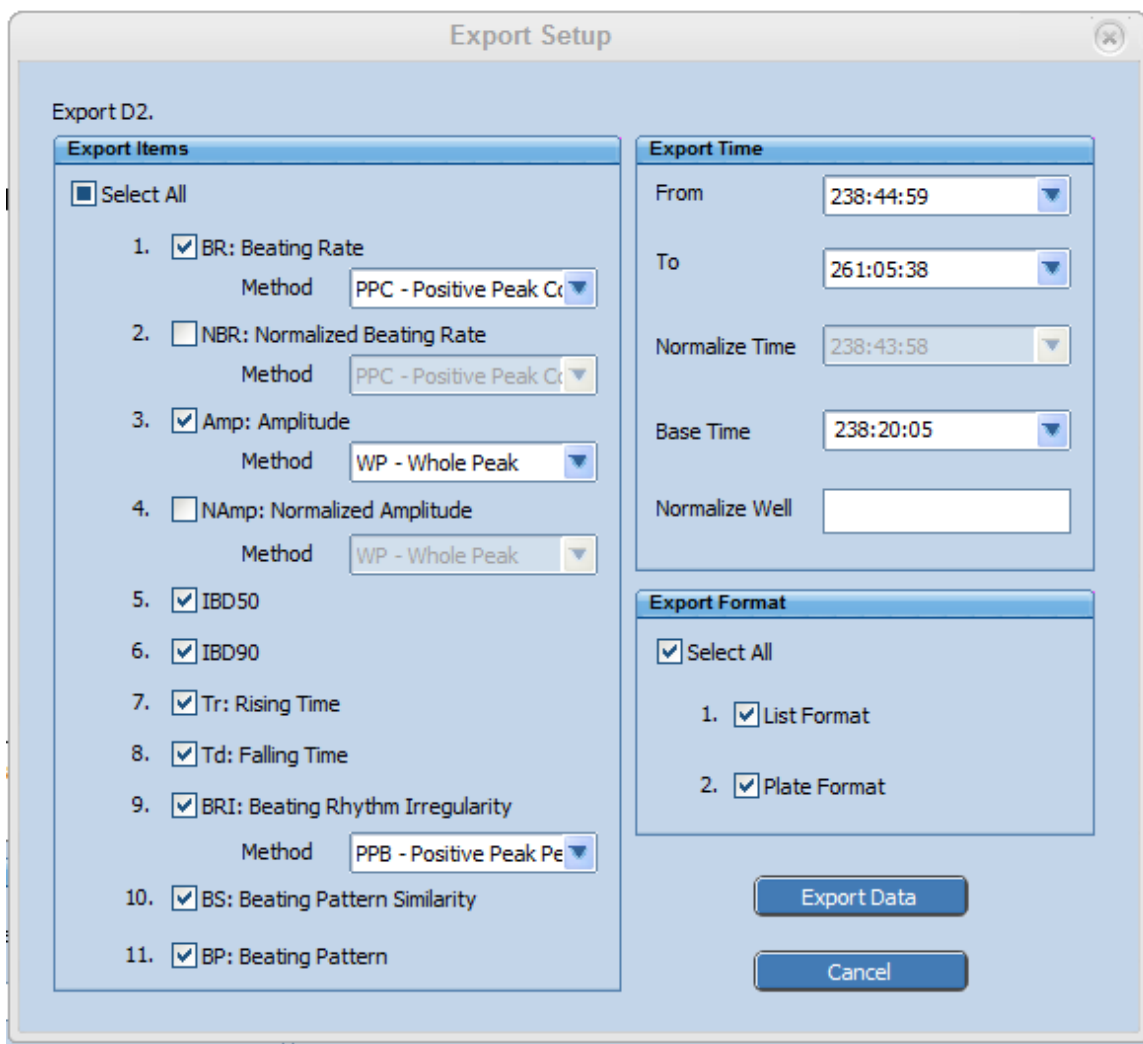


**Figure 6:** Screen shot of beat parameter export setup page. Beat parameters can be selected (left hand box) for the desired time points (upper right hand box). Parameters can be exported into excel in list and/or plate format (lower right box).

- b. Export CI values into excel and calculate changes over the treatment period (Figure 7). CI changes provide valuable information on cell health, attachment, and morphology status.
      - i. Select the desired wells (upper right of screen).
      - ii. Select the desired time points (under “axis scale”).
      - iii. Right click on the cell index graph (upper left of screen).
      - iv. Click on “copy data in list format” or “copy data in matrix format”.
3. Total impedance and beating characteristics will vary slightly between wells, and therefore treating each well as an independent unit will improve the data precision. To compare the effect of tested compounds, data should be transformed first to percent of time zero reading for each well and subsequently to percent of time-

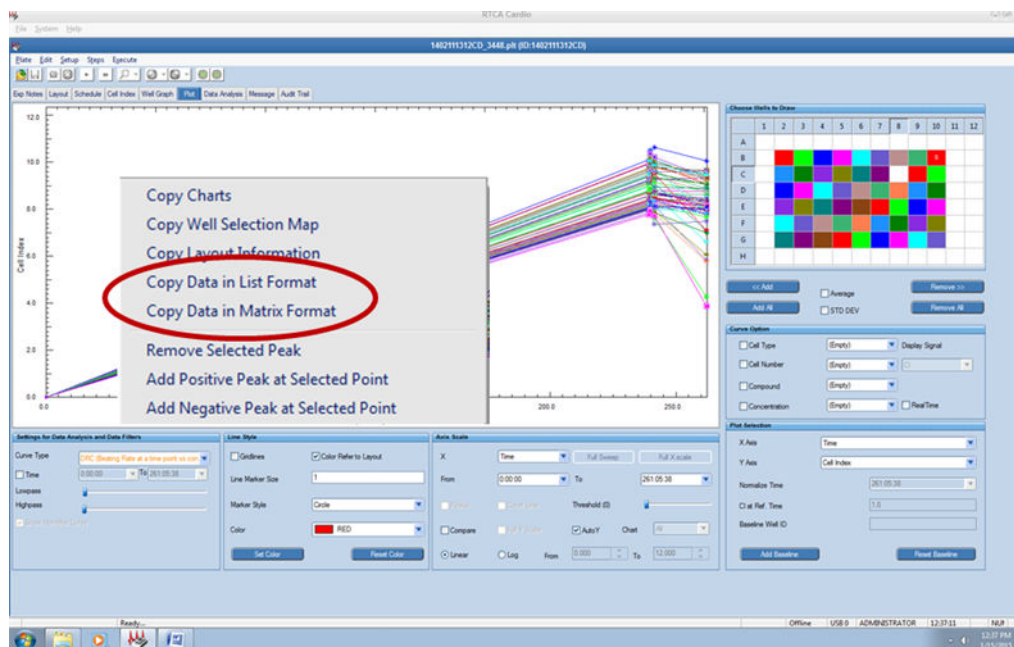


**Figure 7:** Screen shot of cell index export page. Cell index can be exported (left hand graph) for the desired time points (selected under “axis scale”). Parameters can be exported into excel in list and/or plate format.

matched vehicle control. Concentration-response curves can then be generated and  $EC_{50}$  /  $IC_{50}$  values can be calculated (Figure 8).

4. An emphasis on caution interpreting overall CI changes: several factors contribute to the impedance readout and a decrease in cell index is not always indicative of cell death. As an example, treatment of cardiomyocytes with blebbistatin causes a decrease in CI after a 20 hr exposure period. However, an end-point assay performed using CellTiter-Glo<sup>®</sup> Luminescent Cell viability Assay shows that cellular ATP levels remain comparable to that of control (Figure 9), indicating that while cells have detached from the surface of the well, they are still viable. This example illustrates the importance of a secondary assay to measure viability in conjunction with cell index information to judge cytotoxic effects.

## Assay Optimization

- Cell number per well
- Time of cardiomyocyte culture prior to drug addition
- Time points for impedance measurements to encompass acute versus subacute effects
- Number of sweeps and sweep time for robust data
- Tolerability of cardiomyocytes to appropriate compound vehicles

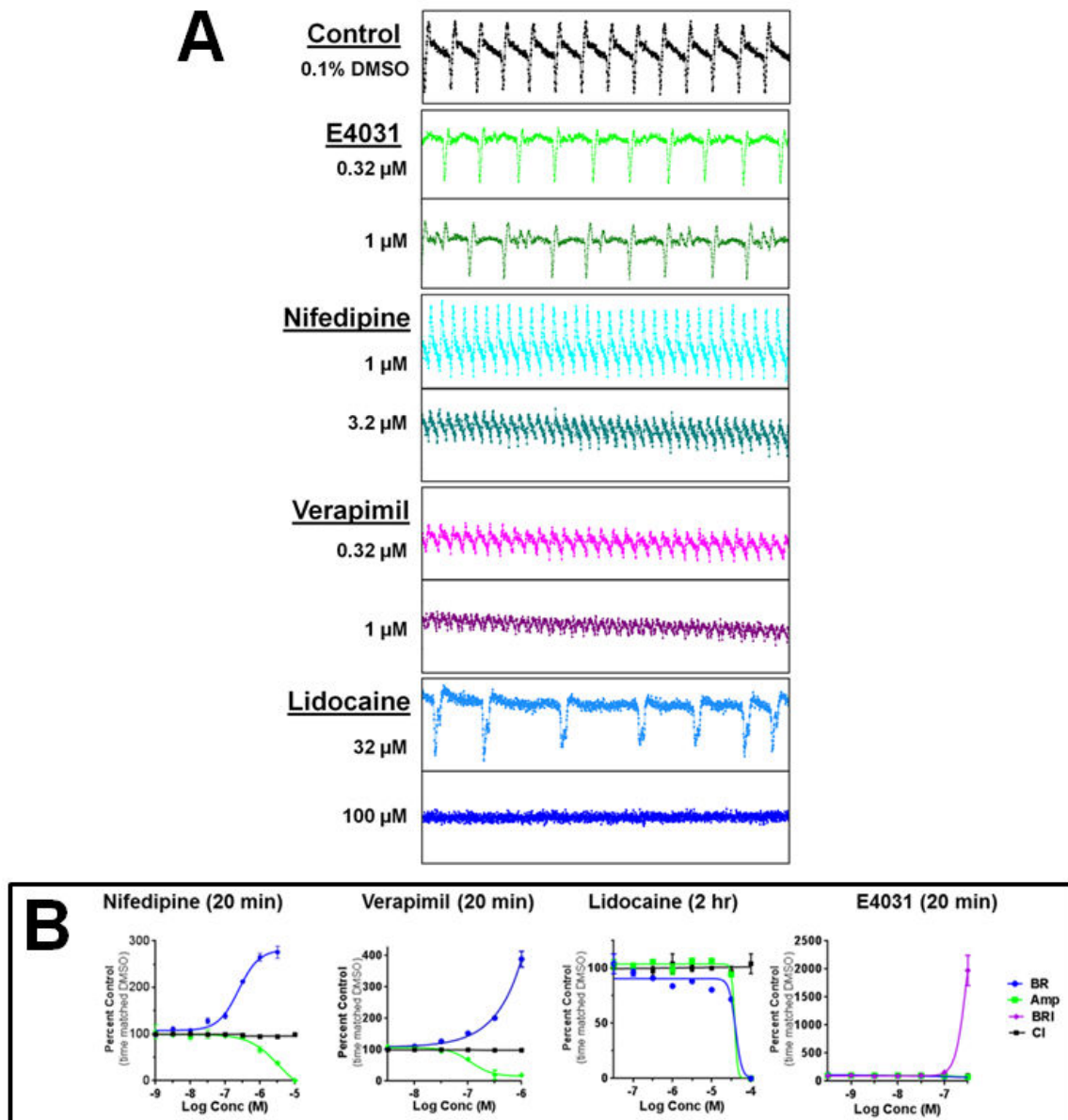


**Figure 8:** Examples of compound-induced changes in CM impedance profiles. Effects of a hERG-I<sub>kr</sub> blocker (E4031, 20 min), sodium channel blocker (lidocaine, 2 hr), and L-type calcium channel blockers (nifedipine and verapamil, both 20 min). Shown as (A) raw traces and (B) concentration response curves (mean  $\pm$  SD) for beat rate, beat amplitude, and BRI (E4031 only). Concentration-response curves were derived for each parameter by first calculating percent of time zero for each well and then percent of time-matched vehicle control.



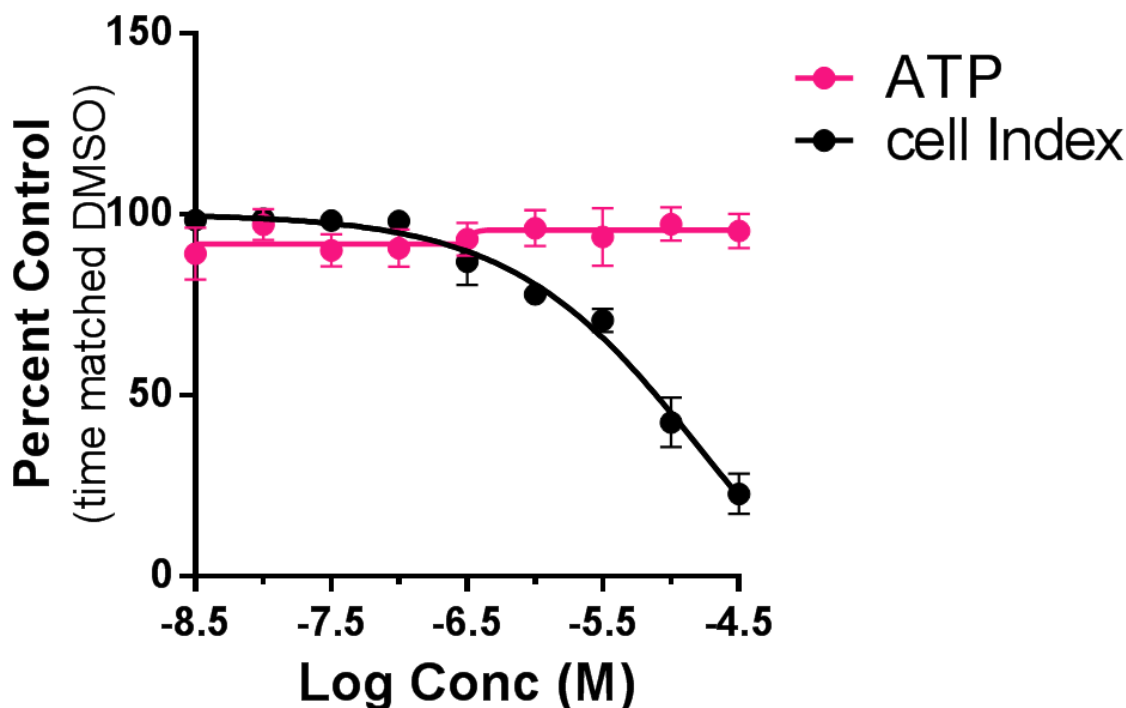


**Figure 9:** Effect of blebbistatin (20 hr) on CI and cellular ATP levels. Concentration-response of blebbistatin (20 hr) on cellular ATP levels and cell index (mean  $\pm$  SD). Concentration-response curves were derived for each parameter by first calculating percent of time zero for each well and then percent of time-matched vehicle control.

## References

### Literature Cited

1. Ciambone, et al. Cellular dielectric spectroscopy: a powerful new approach to label-free cellular analysis. *J Biomol Screen.* 2004;9(6):467–480. PubMed PMID: 15452333.
2. Ramasamy, et al. Drug and bioactive molecule screening based on a bioelectrical impedance cell culture platform. *Int J Nanomedicine.* 2014;(9):5789–5809. PubMed PMID: 25525360.
3. Peters, et al. Evaluation of cellular impedance measures of cardiomyocyte cultures for drug screening applications. *Assay Drug Dev Technol.* 2012;10(6):525–532. PubMed PMID: 22574652.
4. Xi, et al. Functional cardiotoxicity profiling and screening using the xCELLigence RTCA Cardio System. *J Lab Autom.* 2011;16(6):415–421. PubMed PMID: 22093298.
5. Abassi, et al. Dynamic monitoring of beating periodicity of stem cell-derived cardiomyocytes as a predictive tool for preclinical safety assessment. *Br J Pharmacol.* 2012;165(5):1424–1441. PubMed PMID: 21838757.

6. Peters, et al. Human Stem Cell-Derived Cardiomyocytes in Cellular Impedance Assays: Bringing Cardiotoxicity Screening to the Front Line. *Cardiovasc Toxicol.* 2015;15(2):127–39. PubMed PMID: 25134468.
7. Guo, et al. Refining the human iPSC-cardiomyocyte arrhythmic risk assessment model. *Toxicol Sci.* 2013;136(2):581–594. PubMed PMID: 24052561.
8. Guo, et al. Estimating the risk of drug-induced proarrhythmia using human induced pluripotent stem cell-derived cardiomyocytes. *Toxicol Sci.* 2011;123(1):281–289. PubMed PMID: 21693436.
9. Scott, et al. An Impedance-Based Cellular Assay Using Human iPSC-Derived Cardiomyocytes to Quantify Modulators of Cardiac Contractility. *Toxicol Sci.* 2014;142(2):331–338. PubMed PMID: 25237062.
10. Pointon, et al. Assessment of Cardiomyocyte Contraction in Human-Induced Pluripotent Stem Cell-Derived Cardiomyocytes. *Toxicol Sci.* 2015;144(2):227–237. PubMed PMID: 25538221.
11. Pointon, et al. Phenotypic Profiling of Structural Cardiotoxins In Vitro Reveals Dependency on Multiple Mechanisms of Toxicity. *Toxicol Sci.* 2013;132(2):317–326. PubMed PMID: 23315586.

## Additional References

- Lamore, et al. Cellular impedance assays for predictive preclinical drug screening of kinase inhibitor cardiovascular toxicity. *Toxicol Sci.* 2013;135(2):402–413. PubMed PMID: 23897988.
- Himmel (2013) Drug-induced functional cardiotoxicity screening in stem cell-derived human and mouse cardiomyocytes: effects of reference compounds. *J Pharmacol Toxicol Methods* 68 (1), 97-111.
- Jonsson, et al. Impedance-based detection of beating rhythm and proarrhythmic effects of compounds on stem cell-derived cardiomyocytes. *Assay Drug Dev Technol.* 2011;9(6): 589–599. PubMed PMID: 22085047.

# Screening for Target Engagement using the Cellular Thermal Shift Assay - CETSA

Hanna Axelsson, MSc,<sup>1</sup> Helena Almqvist, MSc,<sup>1</sup> Brinton Seashore-Ludlow, PhD,<sup>1</sup> and Thomas Lundbäck, PhD<sup>✉1</sup>

Created: July 1, 2016.

## Abstract

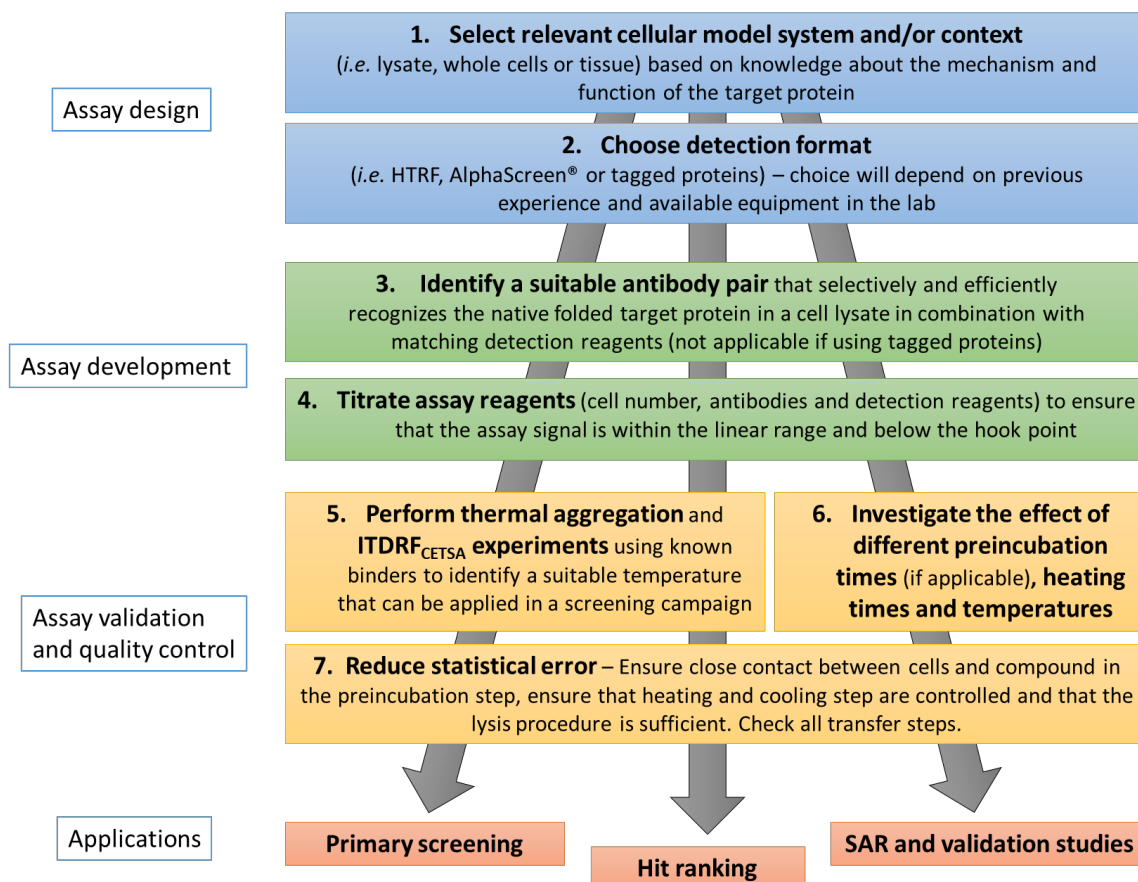
The direct measurement of drug-protein interactions in living cells is a major challenge in drug discovery research. Using the cellular thermal shift assay or CETSA such measurements can be achieved, in principle, in any cell samples and in microtiter-plate format. This chapter starts with an overview of CETSA and then continues to provide thorough guidance in the development, optimization and application of a microplate-based protocol using AlphaScreen® as the detection format. Significant parts of the experimental descriptions are applicable also to other detection modalities. Each step in the assay development and validation process is exemplified by real case data from the development and validation of a fully screen-compatible live-cell assay for thymidylate synthase (TS; encoded by TYMS). When possible, the descriptions are kept general such that it allows for translation to other target proteins and efforts are made to point out crucial steps and considerations in the experimental design. At the end of the chapter there is a section devoted to insights from our screen adaptation experiences, troubleshooting and a discussion on tentative applications of microplate-based CETSA.

---

<sup>1</sup> Karolinska Institutet; Email: hanna.axelsson@ki.se; Email: helena.almqvist@ki.se; Email: brinton.seashore-ludlow@ki.se; Email: thomas.lundback@ki.se.

<sup>✉</sup> Corresponding author.

## Flow Chart



## Introduction

Confirmation of direct binding to the intended target proteins in living systems, *i.e.* target engagement, is critical in the pharmacological validation of new chemical probes and drug candidates (1,2). Several exciting methodologies to achieve this are currently emerging, many of which are based on measurements of proximal biomarkers or the use of labelled molecules (tracers) or proteins to follow the binding process in microplate format (3–5). Here, we focus on the complementary use of thermal shift assays in live cells. These assays rely solely on ligand-induced thermodynamic stabilization of proteins, thus eliminating the requirements for tracer generation and protein engineering. As such this methodology provides a particularly attractive alternative for screening in primary cells, tissues, animal models and patient-derived material (6–8). Together with other developments, this technology opens up the possibility to track drug target engagement throughout the discovery process, in principle from primary screening to the treated patient. This information will help to ensure resources are invested on the best candidate compounds in target-based drug discovery programs.

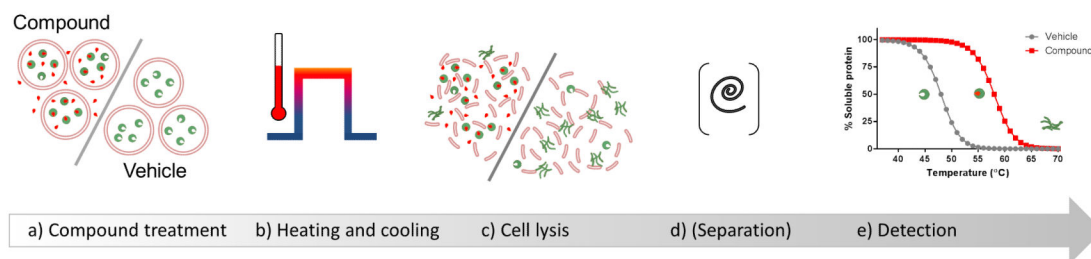


**Figure 1: Illustration of the general assay procedure.** The cells are incubated with compounds or controls followed by a transient heating step, cell lysis, an optional step in which the irreversible aggregates are separated from the soluble proteins and finally detection illustrated by the graph showing remaining levels of soluble target protein.

## CETSA Background

As with traditional melting temperature ( $T_m$ ) shift assays (9–14), CETSA relies on protein stabilization as a result of ligand binding. Simply explained, when unbound proteins are exposed to a heat gradient, they begin to unfold or “melt” at a certain temperature. The mid-point of these transitions, *i.e.* where the concentrations of native and denatured proteins are the same, is generally referred to as the apparent melting temperature. Ligand-bound proteins, however, are stabilized by their interacting partner and will therefore melt at a higher temperature when exposed to the same heat gradient, resulting in a so called  $T_m$  shift. This term is however reserved for equilibrium processes, whereas CETSA is based on quantification of remaining levels of stabilized protein following irreversible aggregation of thermally unfolded proteins (see Figure 1 for a schematic outline). Thus to reflect the non-equilibrium nature of these experiments, the ligand-induced stabilization is more appropriately referred to as thermal aggregation temperature ( $T_{agg}$ ) shifts.

In practice a typical CETSA experiment involves the following steps:

1. Drug treatment of the cellular system of choice (lysate, whole cells or tissue samples).
2. Transient heating of the cells to thermally denature and precipitate proteins that are not stabilized by ligand.
3. Controlled cooling and lysis of the cells.
4. Removal of precipitated proteins (if necessary).
5. Detection of remaining soluble protein in the supernatant/soluble fraction.

Based on the nature of the studied target protein and the cellular system chosen, experimental aspects of these steps will vary. Examples of possible variations include the

choice of protein source (cell lysate, intact cells, biopsies or tissue homogenates), the length and means of sample treatment with ligand before heating, the heating time and temperature range applied and the procedure used for cell lysis (if applicable). The need for sample workup, such as the separation of the remaining stabilized protein from the denatured and precipitated material, as well as the ways to do so, is directly linked to the choice of detection method. This, in turn, depends on the demands for sample throughput, as well as prior knowledge and instrumentation available in the laboratory.

## Experimental Formats

In general CETSA experiments assess drug target engagement in two different modes. The first setup serves the purpose of comparing the apparent  $T_{agg}$  curves for a target protein in the presence and absence of ligand when subjected to a temperature gradient. The aim is to assess the potential ligand-induced thermal stabilization (Figure 2a). The second alternative is to generate a so called isothermal dose-response fingerprint (ITDRF<sub>CETSA</sub>). Here, the stabilization of the protein is studied as a function of increasing ligand concentration while applying a heat challenge at a single temperature (Figure 2b). It is common practice to first establish the  $T_{agg}$  curve for the unliganded protein, such that the isothermal challenge can be applied at a suitable temperature around or above the  $T_{agg}$ . Both formats allow for the ranking of compound affinities to a single protein target, but for structure activity relationship (SAR) studies ITDRF<sub>CETSA</sub> experiments are often more suitable.

## Assay Design

Before performing a CETSA experiment on a new target protein, some important considerations and choices must first be made to ensure that the ligand treatment and transient heating steps reflect the biology of interest in the best possible way. Naturally this means selecting an appropriate cellular model system in which the target protein is expressed, but considerations should also be made with regards to culture conditions and cellular status if these factors are suspected or known to affect the protein levels, regulation or ability to bind ligands. In addition, depending on affinity reagent availability, throughput demands and equipment in the lab, a suitable detection technology that is amenable to microplate-based measurements must be decided upon. A general overview to these considerations is summarized in Figure 3 and the following sections intend to discuss the various aspects of assay design in more detail.

## Model Systems

The CETSA method has been validated for a range of different cellular model systems of various complexity and relevance to clinical situations (6,15). An important prerequisite of the CETSA experiments is that they are performed under conditions where protein unfolding results in irreversible precipitation, such that ligand-induced stabilization can be assessed through remaining levels of soluble protein. Hence experiments can be performed in cell lysates if the endogenous protein is difficult to express and purify in a

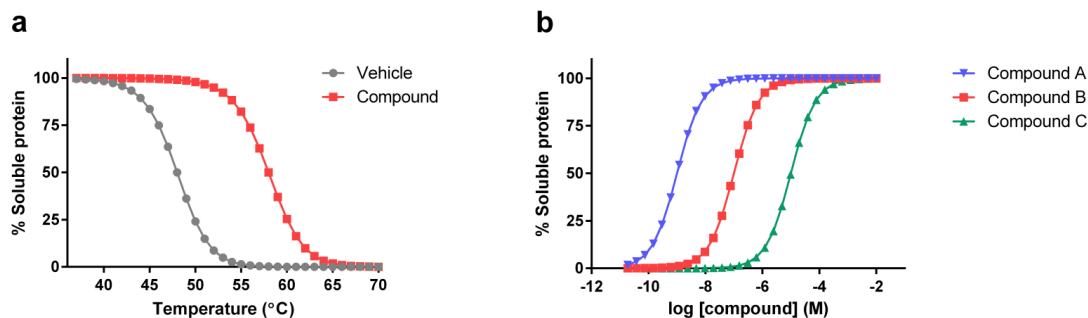


**Figure 2:** Anticipated results from CETSA experiments performed in two different ways. a) Example  $T_{agg}$  curve for a target protein in the presence (red squares) and absence (grey circles) of ligand when subjected to a heat gradient. b) Example ITDRF<sub>CETSA</sub> curves for three compounds with different apparent potencies.

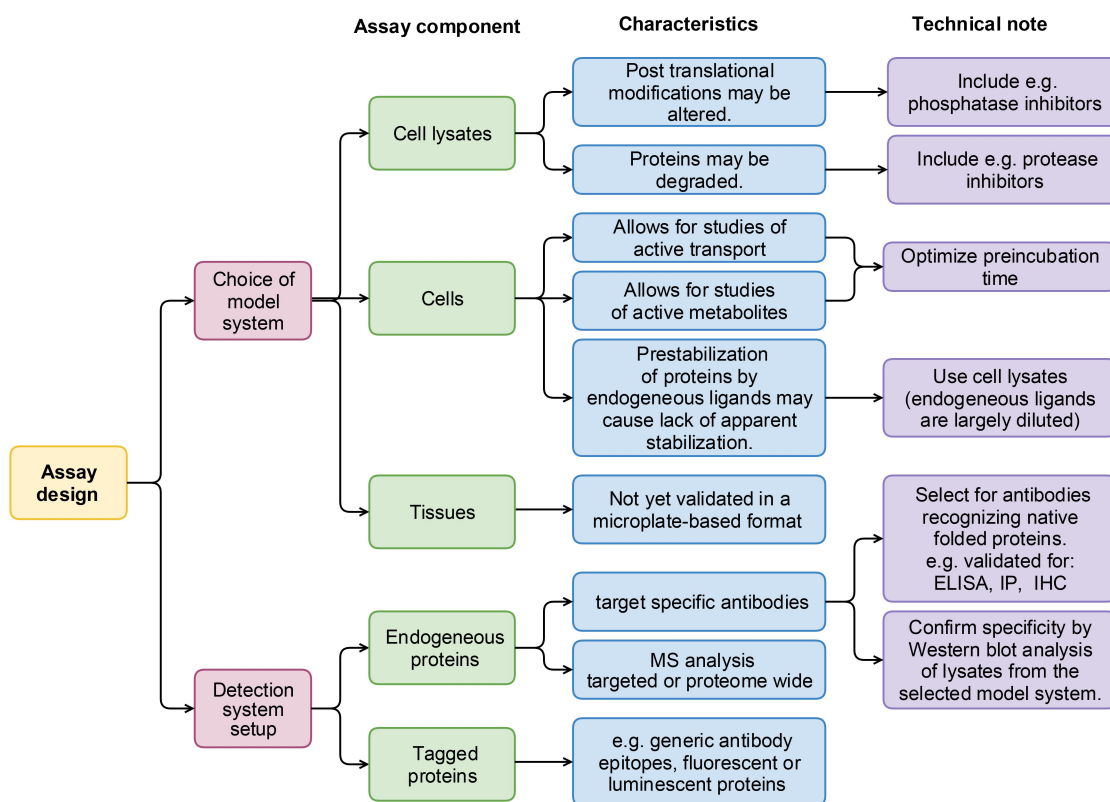


**Figure 3:** Illustration of general considerations and technical notes related to assay design. Figure created using Gliffy software.

relevant form for more traditional target-based screening or if it is desirable to avoid the barriers of serum binding and cell permeability associated with live cell assays. These

aspects can, on the other hand, be addressed by the use of relevant cellular model systems as exemplified by drug efficacy, drug transport, drug activation, off-target effects and drug resistance studies in the original CETSA publication, which also included an example of monitoring drug distribution in animals (6).

It is likely that the level of complexity of the model system will increase with the maturity of a drug discovery program and potentially start with cell lysates or cells that overexpress a tagged protein to facilitate detection. This will likely be more prevalent for novel target proteins as these generally come with a less mature repertoire of affinity reagents to support detection of endogenous protein levels. As the project matures and enters late preclinical and clinical phases there will be a need to confirm response in primary cells, which is feasible if there are affinity tools available for achieving the protein quantification. Recent developments in the mass spectrometry (MS) field (16) may also come to support such efforts in case suitable affinity reagents are missing.

## Detection Formats

As already mentioned, the basis of CETSA is that the vast majority of proteins denature and precipitate at elevated temperatures, whereas ligand-bound proteins are stabilized and thus remain folded in solution. In the original publication the stabilized protein in the soluble fraction of the samples was detected using western blotting (WB) (6). WB-based detection has since been adopted in the majority of reported applications of CETSA in the literature (15), with the aim to study the effect of only one or a few compounds on individual target proteins. In general, WB-based CETSA experiments are relatively simple to establish because they only require one affinity reagent, namely a specific antibody directed towards the protein target of interest, and utilize equipment already available in most biochemistry labs. A detailed protocol for this procedure was recently published (7).

Many CETSA applications will, however, require a more systematic, parallel processing of samples. This includes, for example, hit qualification activities where thousands of hits from high-throughput screening campaigns are ranked based on their concentration-dependent responses in downstream follow-up assays. In such cases it is necessary to move CETSA to a microplate-based (or equivalent) format so that all addition and treatment steps can be performed using automated liquid handling and the transient heating and cooling can be achieved using plate-compatible equipment. Naturally such microplate formatting of the assay involves miniaturization and a minimization of the number of assay steps to improve on assay throughput. This reduction of steps also serves to diminish well-to-well variability and consequently improve on assay quality.

Detection of the amount of remaining soluble protein can be achieved using a broad range of available protein quantification assays. These include, but are not limited to enzyme-linked immunosorbent assay (ELISA) and variations thereof, proximity ligation assays and dot blots. Although these methods are compatible with a microtiter-plate format, the throughput is limited due to the requirement of wash steps and/or separation steps before detection. An optimal detection method should instead be homogenous and allow for the quantification of remaining soluble protein against a background of the same protein in



denatured and aggregated forms, such that the separation step can be eliminated. The detection must also be achieved against a cell lysate background to avoid the sample workup and wash steps. Well-proven homogeneous detection methods in which antibodies or other affinity reagents recognize the folded protein structure in a cell lysate are, for example, AlphaScreen® (Amplified Luminescent Proximity Homogeneous Assay Screen) or time-resolved fluorescence resonance energy transfer (TR-FRET)-based assays. Applications are also emerging where the detection is greatly facilitated by using engineered proteins in which a signaling entity is incorporated (*e.g.* the Society for Laboratory Automation and Screening (SLAS) 5<sup>th</sup> Annual International Conference & Exhibition) (17,18).

Although not generally applicable to high-throughput microplate formats, even though this may be changing (16), it is worthwhile noting that detection can also be achieved using MS. This was recently adopted in an extension of the CETSA methodology in a technique referred to as thermal proteome profiling (TPP) or thermal-stability profiling, which allows for the simultaneous measurement of the entire melting proteome (19–21). Consequently this method allows for studies of the apparent selectivity of individual compounds or for unbiased target identification activities for compounds with unknown mechanisms of action in cell lysates and live cells. However, great care must be taken to ensure that these studies are undertaken with an understanding of the thermodynamic prerequisites for the magnitude of thermal shifts as these vary broadly among proteins and ligands (22). As a consequence,  $T_{\text{agg}}$  shift signatures must be considered highly apparent unless they are extended to include multiple ligand concentrations and temperatures such that the difference in shift sizes for different binding events can be accounted for (23).

## Assay Development

The following section provides a detailed description of the various assay development and optimization steps to establish a homogeneous CETSA assay in live cells. Each step is illustrated by experimental data for human thymidylate synthase (TS) and specific consideration is given to point out potential challenges in the assay development and to provide guidelines for resolving such complications. A major aim in establishing this assay was to enable the detection of endogenous protein levels, with the intent to demonstrate potential utility for primary cells, thus requiring the use of a homogeneous immunoassay for detection. Although the following descriptions and illustrations will largely reflect this choice of assay readout, attempts will be made to separate specific issues from more general considerations that are also applicable to other readouts. In the case of tagged proteins with a signaling entity, the reader is directed to the Assay Validation section.

## Antibody Screening

AlphaScreen® is a proximity assay based on two bead types referred to as donor and acceptor beads, both of which possess a relatively large surface area for conjugation of

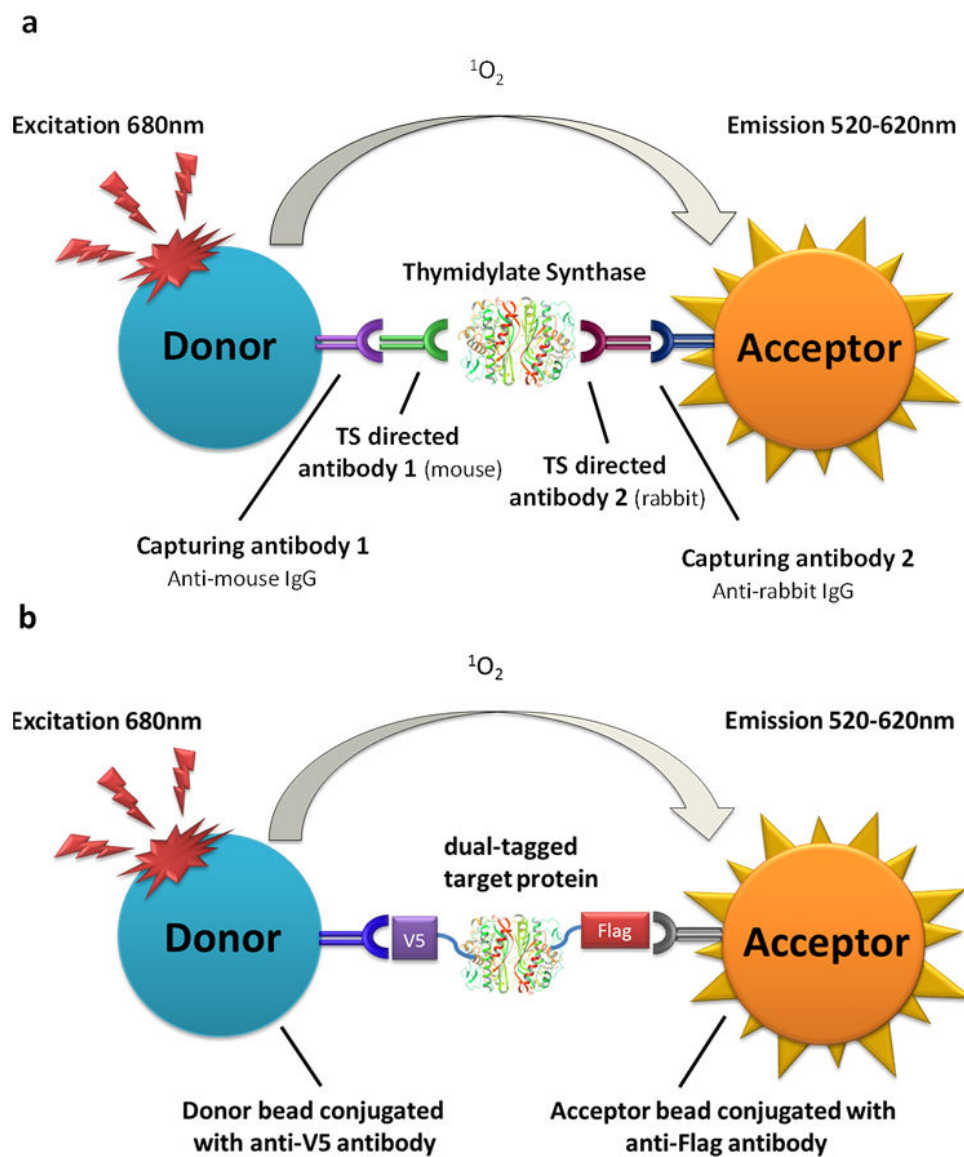


**Figure 4: Illustration of two AlphaScreen® setups for detection of endogenous and tagged proteins, respectively.** Both setups are based on the formation of a multicomponent complex consisting of the donor and acceptor beads functionalized with different affinity reagents that recognize the target protein of interest. a) Setup for detection of endogenous protein, in this case exemplified by TS, consisting of donor and acceptor beads functionalized with capturing antibodies (anti-mouse IgG and anti-rabbit IgG) recognizing anti-target antibodies (from mouse and rabbit) raised against different epitopes of the target protein. b) Example of a tentative setup for the detection of tagged proteins with dual epitopes, allowing the use of generic beads conjugated with antibodies towards these epitopes. Other options include for example GFP, luciferase and beta-galactosidase tagged proteins to circumvent the need for an immunoassay.

biomolecules (24). Excitation of the donor beads results in the generation and release of singlet oxygen, which travels in solution and results in excitation and light emission from the acceptor beads when they are close in space, *e.g.* only when a complex is formed that

involves both bead types. The system allows for the formation of complexes consisting of these beads functionalized with affinity reagents that recognize the target molecule of interest. An advantage of the AlphaScreen® technology, compared to *e.g.* TR-FRET assays, is the significantly longer distance tolerated for the proximity signal (24). This supports the use of multicomponent complexes in which the target-directed affinity reagents are recognized by capture antibodies or other affinity reagents on generic conjugated beads (25), prompting us to adopt this detection modality in the screening for suitable antigen-directed antibodies (7,8).

A starting point and prerequisite for the development of any homogenous, antibody-based assay is to identify a suitable antibody pair with sufficient affinity and selectivity for the target protein. Each pair consists of two antibodies that simultaneously recognize the native soluble target protein in a complex background of denatured and aggregated proteins. If the antibodies also recognize the denatured and aggregated protein it will be necessary to separate soluble from denatured protein prior to detection, *e.g.* by centrifugation or filtration. Depending on the number and quality of antibodies available, the strategies for selection of a good pair will vary. If there are numerous available antibodies it is recommended to test as many combinations as possible. A general guideline is to acquire and test antibodies that are validated to recognize the target protein in a fully folded form *i.e.* antibodies validated for ELISA, immunoprecipitation (IP) or immunohistochemistry (IHC). It is also good to include antibodies raised against different epitopes of the target protein (C-terminal, N-terminal and internal regions).

It should be pointed out that a key limiting factor in the selection of antibodies is the possible appearance of ligand-induced suppression of antibody recognition and thereby quenching of the anticipated signal (7,8). This is likely due to a conformational change of the target protein upon ligand binding. Failure to carefully validate the affinity reagent pair comes with an obvious risk for false negatives or unnecessarily large reagent investments if this is discovered late in the process. Known binders, ideally from a broad range of different structural classes, are therefore included in the very first experiments and throughout assay validation.

Herein the establishment of a microplate-based CETSA will be exemplified based on donor and acceptor beads functionalized with capturing antibodies directed towards mouse-derived and rabbit-derived IgG respectively (Figure 4a). Once a suitable antibody pair has been identified it is an option to conjugate the antibodies directly to the AlphaScreen® beads. This serves to improve the assay signal, as it shortens the distance between the beads, but most importantly it removes the need to carefully titrate multiple assay components. Alternatively the user has the option to move to alternative screening compatible assay formats such as TR-FRET assays. If the project aim does not require the use of primary non-engineered cells, assay development can be further simplified by the use of proteins with different reporter functionalities (Figure 4b).

### Experimental Setup:

In this experiment all combinations of the selected antibodies are tested at a single concentration. The initial antibody screen is preferably done using recombinant protein; however, it can also be performed in a cell lysate if follow-up experiments ensure that the correct protein is selected for. A good starting point is to use antibody and protein concentrations at or slightly below the binding capacity of the AlphaScreen® beads. It is also worthwhile mentioning that screening scenarios in which the protein exists in multiple forms with regards to post-translational modifications may exist. If so this fact must be carefully considered in the antibody selection process. As a rule of thumb it is useful to always compare the observed data with those obtained using WB-based detection (or possibly mass spectrometry) as the size resolution helps to identify the presence of multiple forms.

As already mentioned, ligand binding can result in suppression of the anticipated signal; thus it is strongly recommended to include known binders in the very first experiments (if available), preferably from different structural classes (7,8). These controls are then included throughout the assay development and validation process to ensure that the selected antibody combinations produce a robust signal to background without any impact of the compound on the protein quantification.

It is important to also include a negative control lacking the target protein. If recombinant protein is not available, the negative control can consist of a lysate that has been heated well above the aggregating temperature of the target protein. Although this procedure also removes a significant portion of other proteins it can serve as a first estimate of the background signal. As described below, we also recommend that seeding experiments are used to validate the specificity of the signal, *i.e.* addition of recombinant protein to a non-modified cell lysate to see that the signal scales linearly with added protein concentration.

### Assay Protocol:

All additions are made directly to an AlphaScreen® compatible detection plate.

- a. Add recombinant protein (or cell lysate) and preincubate with known binders or only buffer (or heated lysate) at room temperature. Depending on the sensitivity of the target protein it may be necessary to add specific supplements to the buffers such as protease or phosphatase inhibitors to avoid degradation or alterations of post-translational modifications.
- b. Prepare solutions of all different antibody combinations and add to the samples and incubate for a minimum of 30 minutes at room temperature.
- c. Add acceptor and donor beads, seal the plate, centrifuge briefly and incubate for 2 hours or overnight at room temperature under subdued light before reading the plate in an AlphaScreen® compatible plate reader.

The results of such an example antibody selection screen based on four mouse-derived and three rabbit-derived antibodies are shown below in Figure 5. Note that depending on the affinity reagents and bead types it can be possible to add a mixture of these reagents at

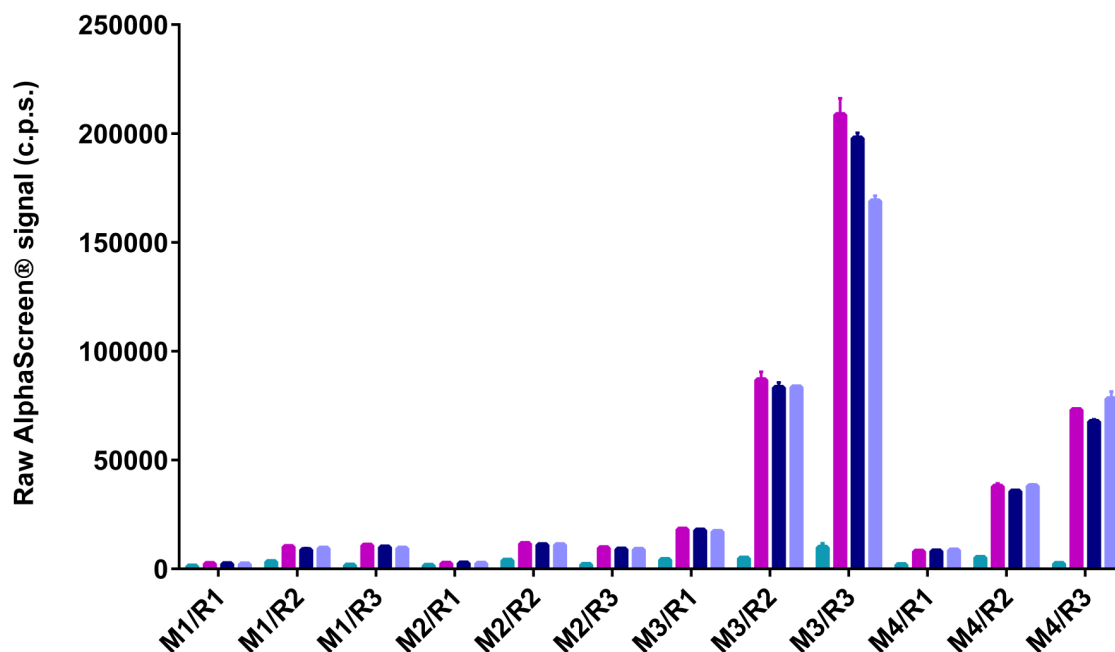


**Figure 5:** Illustration of the results from a screen of antibody pairs for recognition of recombinant TS. All combinations of four mouse-derived (M1-M4) and three rabbit-derived antibodies (R1-R3) were evaluated. Colors denote buffer only (teal), the presence of 2 nM of TS (magenta) or the addition of two known binders: 100 μM deoxyuridine monophosphate (dUMP) (dark blue) and 100 μM dUMP and 10 μM raltitrexed (lavender) to the 2 nM TS condition. Known inhibitors were included to investigate the risk of compound induced loss of target recognition. In this case, four antibody pairs (M3/R2, M3/R3, M4/R2 and M4/R3) were selected for further testing. Data are provided as the average and range from experiments done in duplicate at one independent test occasion. Adopted with permission from Macmillan Publishers Ltd: Nat. Commun. 7 (2016), copyright (2016) <http://www.nature.com/ncomms/2016/160324/ncomms11040/abs/ncomms11040.html>

the same time. In some cases better results are achieved when the acceptor and donor beads are added separately with an incubation time in between the additions (see generic AlphaScreen® guidelines if necessary).

### Kinetics of the Antibody Recognition:

A factor that may be significantly altered when moving from an assay system using recombinant protein to a more complex system, such as a cell lysate, is the time required to establish equilibrium for all interactions involved in the detection system. The kinetics of antibody recognition of the target protein in a cell lysate may be impacted if the antibodies also bind to other proteins. A relatively fast establishment of the equilibrium and a signal that remains stable over time is desirable as this provides maximal flexibility in the assay procedure and allows accommodation of both smaller and larger screen batches. The experiment is also essential to establish that the target protein is stable and

that the aggregates formed during the heat challenge do not resolubilize in the buffers and conditions applied for detection.

### Experimental Setup:

This experiment serves to investigate the kinetics of antibody recognition by comparing the influence of different incubation times (for example 2h, 6h and overnight). Included in the incubations is the pair of antibodies and AlphaScreen® beads together with a cell lysate containing the target protein at endogenous levels. Because it is not recommended to read an AlphaScreen® sample multiple times (due to light induced signal deterioration) it is necessary to prepare one set of samples for each incubation time and antibody pair. A negative control consisting of a heated lysate to represent the background signal is also included for all conditions.

### Assay Protocol:

All additions are made directly to an AlphaScreen® compatible detection plate.

- a. Add lysate samples.
- b. Add solutions of the selected antibody combinations.
- c. Add acceptor and donor beads, seal the plate, centrifuge briefly and incubate for 2 hours, 6 hours or overnight at room temperature under subdued light before reading the plate in an AlphaScreen® compatible plate reader.

The results of such an example examination of antibody recognition kinetics are shown for four different antibody pairs recognizing human TS in Figure 6.

### Titration of Assay Reagents

Given the nature of many immunoassays, *i.e.* the use of a multi-component complex involving several saturable components (binding capacity of antibodies and beads) to generate the assay signal, it is essential to carefully titrate both antibody and target protein concentrations. Titrations could also involve the AlphaScreen® beads, but in general we have stayed with the recommended concentrations. The aim of the experiment is to ensure that the assay is applied below the hook point and that an increase in target protein scales linearly with the assay signal (26). Titrations are still necessary, but much simplified, in assays using fewer components such as TR-FRET with the labels placed directly on the antibodies or the use of tagged proteins carrying a signaling entity.

### Experimental Setup:

This experiment serves to perform a crosswise titration of both target-directed antibodies using cell lysate from unheated cells. The purpose is to identify the optimal concentration of each antibody and the experiment should include an appropriate control, such as lysates from cells heated sufficiently above the protein  $T_{agg}$ . Once optimal conditions have been established, a titration of the target protein must be performed by making a serial dilution of the lysate using the optimized antibody concentrations for detection. Depending on the outcome of these two experiments it may be necessary to make another

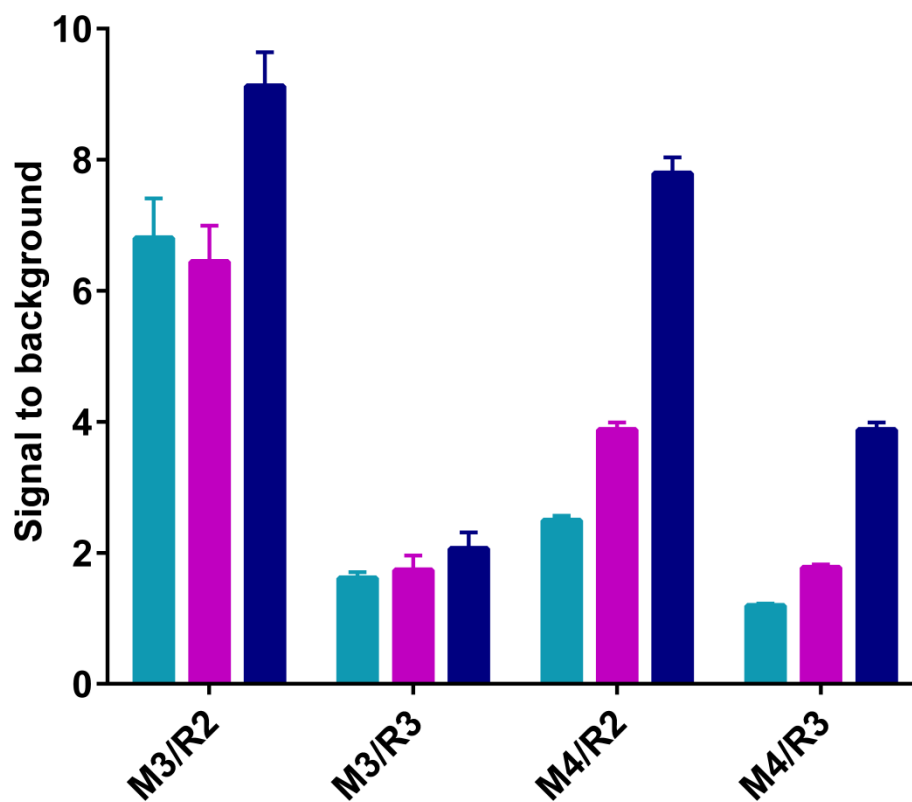


**Figure 6:** Illustration of the kinetics of antibody recognition of TS in K562 cell lysates. The signal to background of the different antibody pairs is given as a function of time after addition of antibodies and beads: 2h (teal), 6h (magenta) and 18h (dark blue). The combination of M3 and R2 was selected for further assay development based on a relatively fast and stable signal development and a high signal to background. Data are provided as the average and standard error of mean (SEM) from experiments done in triplicate at one test occasion. Adopted with permission from Macmillan Publishers Ltd: Nat. Commun. 7 (2016), copyright (2016) <http://www.nature.com/ncomms/2016/160324/ncomms11040/abs/ncomms11040.html>

iteration of the antibody titration, *e.g.* if the result from the lysate titration indicates that the first experiment was performed at target protein concentration at or above the hook point. Another option is to do a cross-titration of both antibodies against several dilutions of the lysate in order to accomplish both titrations at once.

### Assay Protocol for the Initial Antibody Titration:

All additions are made directly to an AlphaScreen® compatible detection plate.

- Add the lysate samples.
- Prepare a crosswise titration of the two antibodies and add these to the lysate samples.
- Add acceptor and donor beads, seal the plate, centrifuge briefly and incubate for 2 hours or overnight at room temperature (depending on outcome of the above

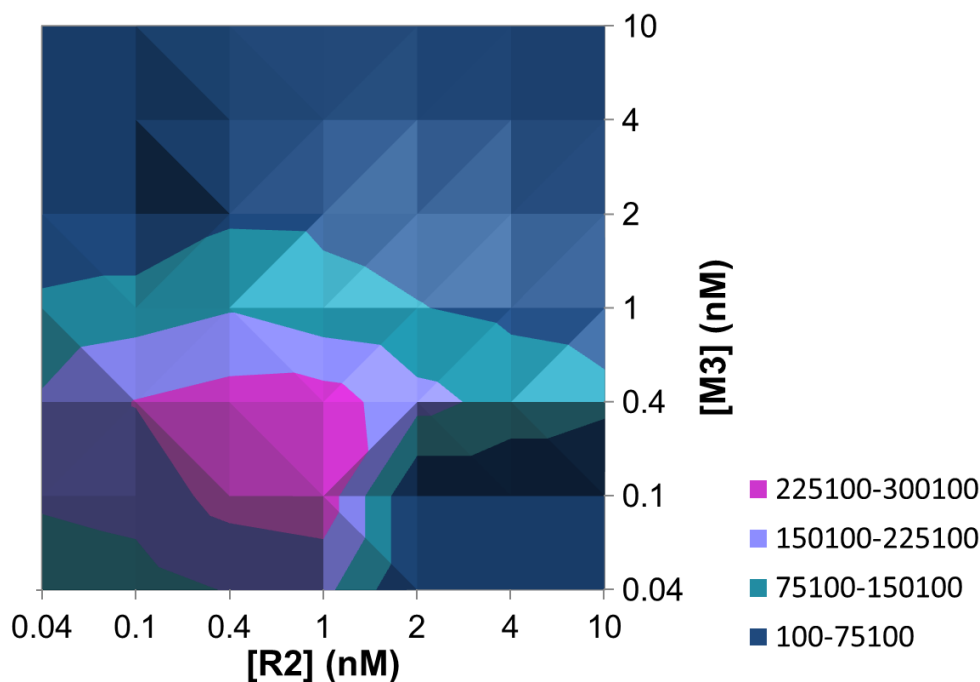


**Figure 7:** Illustration of the results from a crosswise titration of an antibody pair for the recognition of TS in a K562 cell lysate. Data are shown as a 3D contour graph where the concentrations of the antibodies directed towards TS are varied on the x-axis (R2) and y-axis (M3). The color scale is based on raw AlphaScreen® signal (c.p.s.). Based on these results 0.4 nM M3 and 1.0 nM R2 was selected for the final assay. Note the hook effect occurring at elevated concentrations of either antibody. Data are provided as the average from experiments done with  $n=2-4$  for each condition obtained at one test occasion. Adopted with permission from Macmillan Publishers Ltd: Nat. Commun. 7 (2016), copyright (2016) <http://www.nature.com/ncomms/2016/160324/ncomms11040/abs/ncomms11040.html>

described experiments) under subdued light before reading the plate in an AlphaScreen® compatible plate reader.

The result of such a crosswise titration is shown in Figure 7 for the selected antibody pair recognizing human TS.

### Assay Protocol for the Target Protein/Cell Number Titration:

All additions are made directly to an AlphaScreen® compatible detection plate.

- a. Prepare a dilution series of the cell lysate and transfer samples into the detection plate.
- b. Add antibodies at optimized concentrations to the lysate samples.
- c. Add acceptor and donor beads, seal the plate, centrifuge briefly and incubate for 2 hours or overnight at room temperature under subdued light before reading the plate in an AlphaScreen® compatible plate reader.

Example of the result of such a cell lysate titration is shown in Figure 8 for human TS.



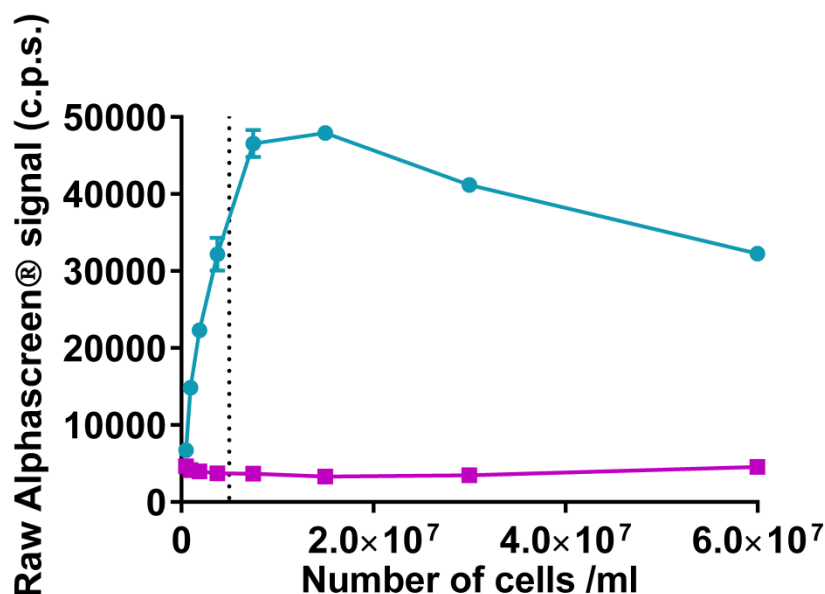


**Figure 8: Illustration of a K562 cell lysate titration for recognition of TS.** Cell lysate from unheated K562 cells are represented by teal circles and heated cells by magenta squares respectively. Based on these results it was decided to use 5 million cells per ml (dotted line) in the final assay to ensure that the assay is performed within the linear range of detection. Data are shown as the average and SEM from triplicate samples obtained at one test occasion. Adopted with permission from Macmillan Publishers Ltd: Nat. Commun. 7 (2016), copyright (2016) <http://www.nature.com/ncomms/2016/160324/ncomms11040/abs/ncomms11040.html>

## Addressing the Specificity of the Antibodies

Even if the selected antibodies may show excellent specificity one by one in a WB-based detection setup, it is necessary that this holds true also in a dual recognition homogenous assay format.

### Experimental Setup for Examining Antibody Specificity:

Such validation can be achieved by seeding a dilution series of recombinant protein in a cell lysate from both unheated and heated cells, as well as in cell medium. It is advised to use a fairly low lysate concentration for this experiment in order to ensure that the experiment is performed below the hook point of the detection system. A proportional increase in signal suggests that the signal is specific for the target protein and that recognition can be achieved in the context of a diluted cell lysate. Additional experiments that can be performed include competition experiments with antigen peptides for each of the antibodies and these can be performed at higher cell lysate concentration to further demonstrate sufficient selectivity.

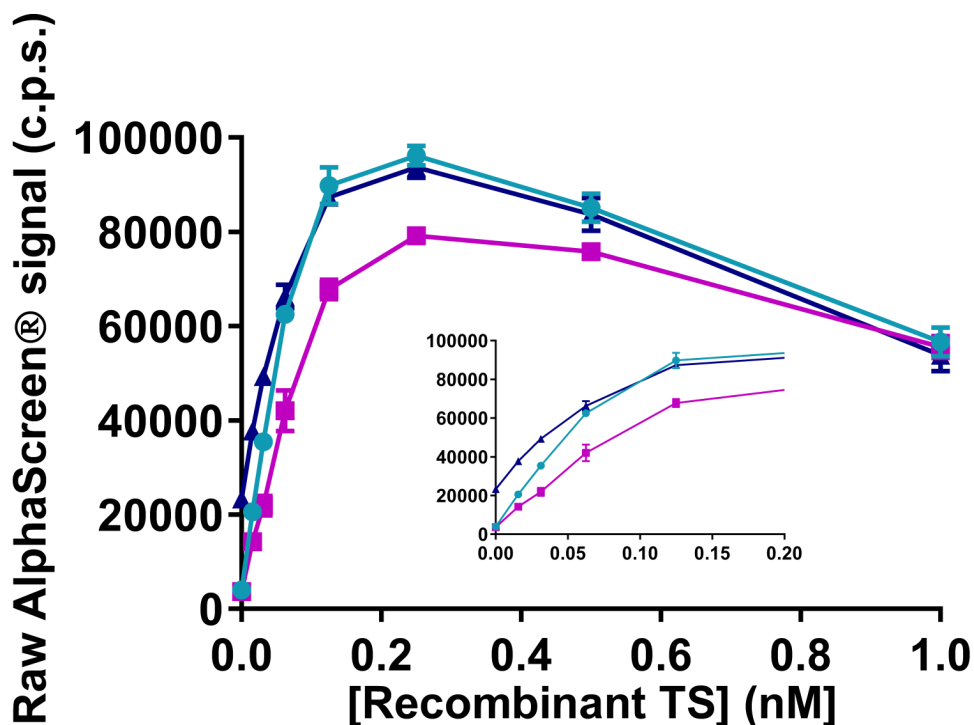


**Figure 9: Illustration of the results from a seeding experiment addressing antibody specificity.** Data are shown as a function of added recombinant human TS seeded in unheated cell lysates (blue triangle), lysate from heated cells (magenta square), or to cell medium without any cells (teal circle). The insert illustrates the same data, but restricted to the 0-0.2 nM concentration range. To ensure that at least the initial part of the titration is performed below the hook point it is necessary to use a rather diluted cell lysate for this experiment. In this case the cell lysate background corresponded to 1 million K562 cells per ml. A signal increase in line with the increasing concentration of seeded recombinant TS is observed in both unheated and heated lysates, although the background levels in the absence of TS are different which reflects the TS levels in K562 cells. In the absence of the cell lysate background the signal increase is somewhat steeper. Based on these data we conclude that the antibodies selectively recognize TS also in the cell lysates. Data are shown from one test occasion as the average and SEM from triplicate samples. Adopted with permission from Macmillan Publishers Ltd: Nat. Commun. 7 (2016), copyright (2016) <http://www.nature.com/ncomms/2016/160324/ncomms11040/abs/ncomms11040.html>

### Assay Protocol for Examining Antibody Specificity:

All additions are made directly to an AlphaScreen® compatible detection plate.

- Add lysate and medium samples.
- Prepare and add a dilution series of recombinant protein (including the appropriate post-translational modifications if this is the purpose of the assay).
- Add antibodies at optimized concentrations to the samples.

- d. Add acceptor and donor beads, seal the plate, centrifuge briefly and incubate for 2 hours or overnight at room temperature under subdued light before reading the plate in an AlphaScreen® compatible plate reader.

Results from an example of a seeding experiment based on recombinant human TS are illustrated in Figure 9.

## Assay Validation

The following sections intend to give an overview of suggested procedures for the validation and optimization of a microplate-based CETSA assay. The different steps are illustrated by experimental data from the development of a live cell assay for TS including the final screening protocol. As for earlier sections the aim is to highlight generic considerations that are applicable also to other readouts.

### $T_{agg}$ Curves and $ITDRF_{CETSA}$ Experiments

As already mentioned CETSA experiments are principally designed in two different ways.  $T_{agg}$  curve experiments are carried out to assess any apparent ligand induced stabilization of the target protein, whereas  $ITDRF_{CETSA}$  experiments are used to study the apparent stabilization as a function of increasing ligand concentration. A pharmacological validation of the homogenous assay may be achieved by quantitatively comparing  $T_{agg}$  and  $ITDRF_{CETSA}$  data with those obtained using an alternative, validated readout. This confirmation could for example be achieved using the original WB approach. Such assay validation is optimally performed for a broad range of known binders. If ligands of different structural classes or compounds that bind to different binding sites are available, it is highly recommended to include examples of all of these.

#### Experimental Setup $T_{agg}$ Curves:

For CETSA, as with other thermal shift assays, it is recommended to use saturating compound concentrations in order to achieve sufficiently sized apparent shifts in aggregating temperature (22). Hence it is often necessary to perform the  $T_{agg}$  experiments at higher compound concentrations than with other assays (see below for more quantitative qualifications of these recommendations). A suggested starting point is 5-20 times above the cellular  $EC_{50}$  value provided that solubility and toxicity is not a problem. If the cellular  $EC_{50}$  is not known one should consider also potential cell permeability and serum binding properties of the compounds when estimations are done based on biochemical  $IC_{50}$  values. The experiment must include temperatures both above and below the expected aggregating temperature to cover the complete aggregation curve.

#### Assay Protocol $T_{agg}$ Curves:

Compound treatment is performed in a PCR plate and the detection is done in an AlphaScreen® compatible detection plate.

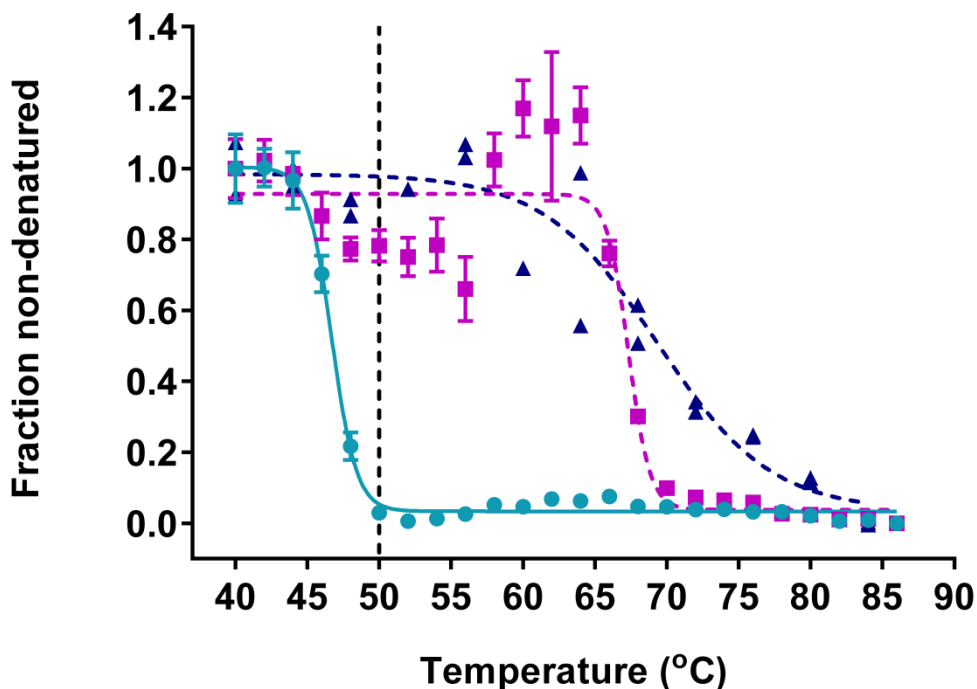


**Figure 10: Illustration of  $T_{agg}$  curves for TS in K562 cells.** Data are shown for unliganded TS in the presence of DMSO (green circle), floxuridine (blue triangle) and raltitrexed (magenta square). The vertical dotted line at 50°C represents the temperature selected for the isothermal experiment. Note that high  $T_{agg}$  values should not be considered as reliable measures of potency and permeability as these temperatures may influence cell membrane integrity (6). Data are provided as the average and SEM from two independent experiments performed in duplicate for raltitrexed and as individual data points from one experiment in duplicate for floxuridine. Adopted with permission from Macmillan Publishers Ltd: Nat. Commun. 7 (2016), copyright (2016) <http://www.nature.com/ncomms/2016/160324/ncomms11040/abs/ncomms11040.html>

- Prepare two cell aliquots. Treat one with compound and the other with the corresponding concentration of DMSO and preincubate both samples at 37°C (see the section “Variation of the preincubation time probes cellular uptake and metabolism” for more details).
- Transfer aliquots of samples from each treatment to a PCR plate.
- Subject the PCR plate to a transient heat gradient (see the section “Variations to the transient heating step” for details regarding the heating time) in a PCR machine with separate heat zones (PCR machines with a plate gradient option could alternatively be used). Make sure to always include a controlled cooling step back to room temperature as the aggregation that occurs downstream of target protein denaturation may occur also during this step. Failure to carefully control both the heating and cooling between all wells of the microtiter plate may result in plate edge effects.

- d. Add lysis buffer to the PCR plate and mix thoroughly to ensure complete lysis of the cells.
- e. Transfer aliquots of the samples to the detection plate and add antibodies.
- f. Add acceptor and donor beads, seal the plate, centrifuge briefly and incubate for 2 hours or overnight at room temperature under subdued light before reading the plate in an AlphaScreen® compatible plate reader.

An example of  $T_{agg}$  data and ligand-induced stabilization are illustrated for TS in Figure 10.

### Experimental Setup ITDRF<sub>CETSA</sub>:

The choice of temperature for the transient heat challenge in ITDRF<sub>CETSA</sub> experiments is selected based on the results observed in the preceding  $T_{agg}$  experiments. A general rule of thumb is to select a temperature near or above the apparent  $T_{agg}$  such that a sufficiently large assay window is obtained. The best assay windows are obtained if a temperature is chosen such that the target protein levels of the unliganded  $T_{agg}$  curve is close to baseline, although the user should be aware that much elevated temperatures is associated with a loss of response to the ligand (see below for further details).

### Assay Protocol ITDRF<sub>CETSA</sub>:

Compound treatment is performed in a PCR plate and the detection is done in an AlphaScreen® compatible detection plate.

- a. Serially dilute compounds and transfer the dilution series to a PCR plate.
- b. Add cells to the plate and preincubate at 37°C (see the section “Variation of the preincubation time probes cellular uptake and metabolism” for more details).
- c. Subject the PCR plate to a transient heat challenge (see the section “Variations to the transient heating step” for details) in a PCR machine. Include a controlled cooling step to room temperature.
- d. Add lysis buffer to the PCR plate and mix thoroughly to ensure complete lysis of the cells.
- e. Transfer aliquots of the samples to the detection plate and add antibodies.
- f. Add acceptor and donor beads, seal the plate, centrifuge briefly and incubate for 2 hours or overnight at room temperature under subdued light before reading the plate in an AlphaScreen® compatible plate reader.

Example data from an ITDRF<sub>CETSA</sub> experiment for TS are illustrated in Figure 11.

### Variation of the Preincubation Time Probes Cellular Uptake and Metabolism

One factor that may influence the apparent stabilization of the target protein in a live cell-based system is the length of the preincubation time with compound. When working with live cells it is important to allow enough time for the compounds to cross the cellular membrane and where it applies allow for the subsequent intracellular metabolic activation

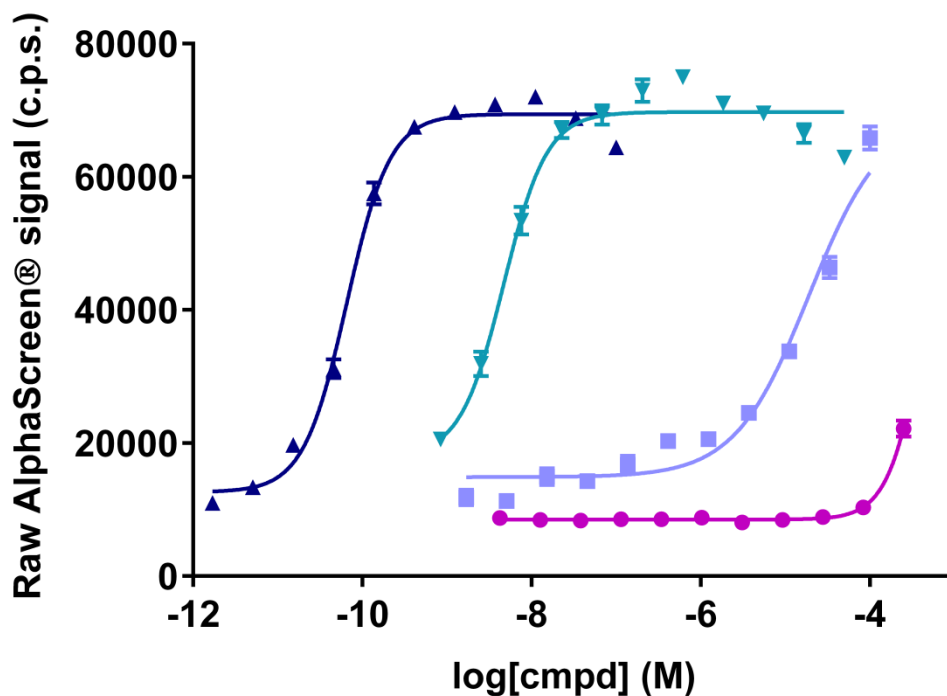


**Figure 11: Results of ITDRFCETSA experiments in K562 cells with known and a novel TS ligands.** ITDRFCETSA data illustrating the apparent stabilization of TS after 2 hour preincubation with floxuridine (blue upwards triangle), 5-fluorouridine (FUR) (teal downwards triangle), and 5-FU (lavender square) and for the novel TS ligand CBK115334 (magenta circle). Data are provided as the average and SEM from one independent experiment done in quadruplicate. Adopted with permission from Macmillan Publishers Ltd: Nat. Commun. 7 (2016), copyright (2016) <http://www.nature.com/ncomms/2016/160324/ncomms11040/abs/ncomms11040.html>

of the compounds. In general 30–60 minutes is enough, but in the cases where metabolic activation is required prior to target engagement, longer preincubation times may be necessary (8). One should be aware that longer preincubation times may alter protein levels and post-translational modifications, thus impacting measured protein levels for reasons other than ligand-induced target protein stabilization.

### Experimental Setup Preincubation Time with Compounds:

The appropriate choice of preincubation time varies with target protein and perhaps more importantly the nature of the ligands. In cases where there is reason to believe that cellular uptake is slow or that intracellular activation is required prior to target protein binding it is useful to conduct preliminary experiments in which the preincubation time is varied. This can be done by applying the same ligand concentration series to multiple plates, on which preincubation times prior to the transient heating step are varied.

*Assay Protocol Preincubation Time with Compounds:*

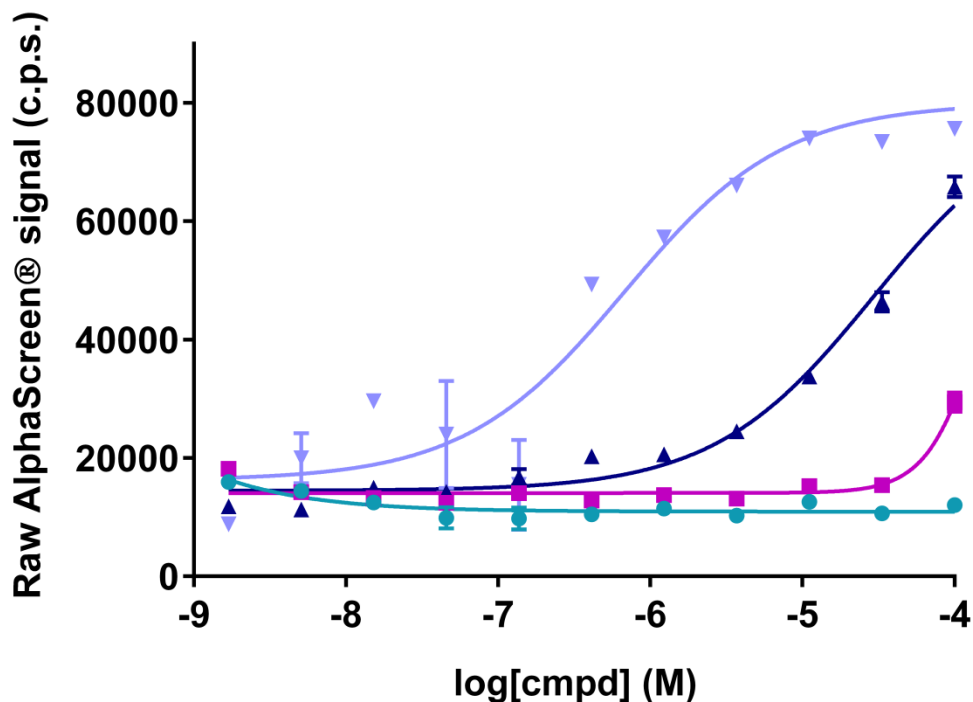


**Figure 12:** Illustration of a preincubation time experiment with 5-fluorouracil (5-FU) using K562 cells. ITDRF<sub>CETSA</sub> data obtained after various lengths of preincubation time, as shown here for 10 min (teal circle), 30 min (magenta square), 2h (blue upwards triangle) and 6h (lavender blue downwards triangle). 5-FU is an example of a compound requiring metabolic activation prior to target engagement. Data are provided as the average and SEM from experiments done in quadruplicate at a single test occasion. Adopted with permission from Macmillan Publishers Ltd: Nat. Commun. 7 (2016), copyright (2016) <http://www.nature.com/ncomms/2016/160324/ncomms11040/abs/ncomms11040.html>

Compound treatment is performed in a PCR plate for variable times at 37°C. Detection is done in an AlphaScreen® compatible detection plate.

- Serially dilute compounds and transfer the dilution series to multiple PCR plates.
- Add cells to the plate and preincubate at 37°C for several different time periods, e.g. for 30 min, 1h, and several hours.
- Subject the PCR plates to a transient heat challenge in a PCR machine. Include a controlled cooling step to room temperature.
- Add lysis buffer to the PCR plates and mix thoroughly to ensure complete lysis of the cells.
- Transfer aliquots of the samples to the detection plate and add antibodies.
- Add acceptor and donor beads, seal the plates, centrifuge briefly and incubate for 2 hours or overnight at room temperature under subdued light before reading the plate in an AlphaScreen® compatible plate reader.

Data from this type of experiment is illustrated in Figure 12 for TS. As the known drugs targeting TS require intracellular enzymatic activation it serves as a clear example of the

importance of the preincubation time. In most cases such a dramatic change in apparent potency over time will not occur, but it illustrates the potential to use this technology for measuring kinetics of ligand uptake and metabolism.

## Variations to the Transient Heating Step

As already mentioned, CETSA technology is based on measurements of remaining levels of soluble protein following a transient heat challenge, which serves to thermally denature and irreversibly precipitate proteins that are not stabilized by ligand. The majority of studies reported in the literature have adopted the procedure described in the original study (15), which involved a three minute transient heating step with the temperature range adjusted to fit the thermal stability of the protein of interest. Importantly, it has been shown that transient heating up to 60-65°C for this time period does not have an acute impact on cell membrane integrity (6,7). It is, however, important to emphasize that the non-equilibrium nature of this procedure results in apparent measures of target protein stability and that both  $T_{agg}$  and  $ITDRF_{CETSA}$  values are expected to change with both the temperature and the duration of the heat challenge (7,23). Consequently users must be aware that the choice of temperature and duration of the heat challenge can also affect the relative ranking of compounds and that this will be especially pronounced when studying ligands with long off-rates or ligands from different structural classes where the binding thermodynamics can vary greatly.

The careful generation of CETSA data in which the transient heating step is varied in a systematic way for several model systems will allow a better understanding of what models to apply for more quantitative interpretations. From the extensive literature on equilibrium systems, it is known that temperatures well above the  $T_{agg}$  of the unliganded protein and excessive heating times should be avoided as they drive the continuous unfolding and aggregation process (14). However, the possibility to use temperatures around or even below the apparent  $T_{agg}$  will be strongly dependent on the assay statistics obtained as the signal to background of the assay is dependent on the unfolding of a sufficiently large portion of the protein. There is an option to reproduce what is done in isothermal denaturation assays, *i.e.* to apply a temperature challenge well below the  $T_{agg}$  for prolonged periods of time, but this comes with an increased risk of heat stress responses, at least in live cells. Practically, however, a further reduction of assay volumes to facilitate rapid and homogeneous sample heating, as well as alternative means to achieve this more efficiently are potential future developments of the technology.

## Screening Protocol for a 384-well based CETSA Assay

For screening purposes, the same conditions as in the  $ITDRF_{CETSA}$  experiments are applied, although in most cases only one compound concentration will be tested. An example of a screening protocol applied in the case for human TS is outlined below, while a schematic illustration of the assay procedure is available in Figure 13.



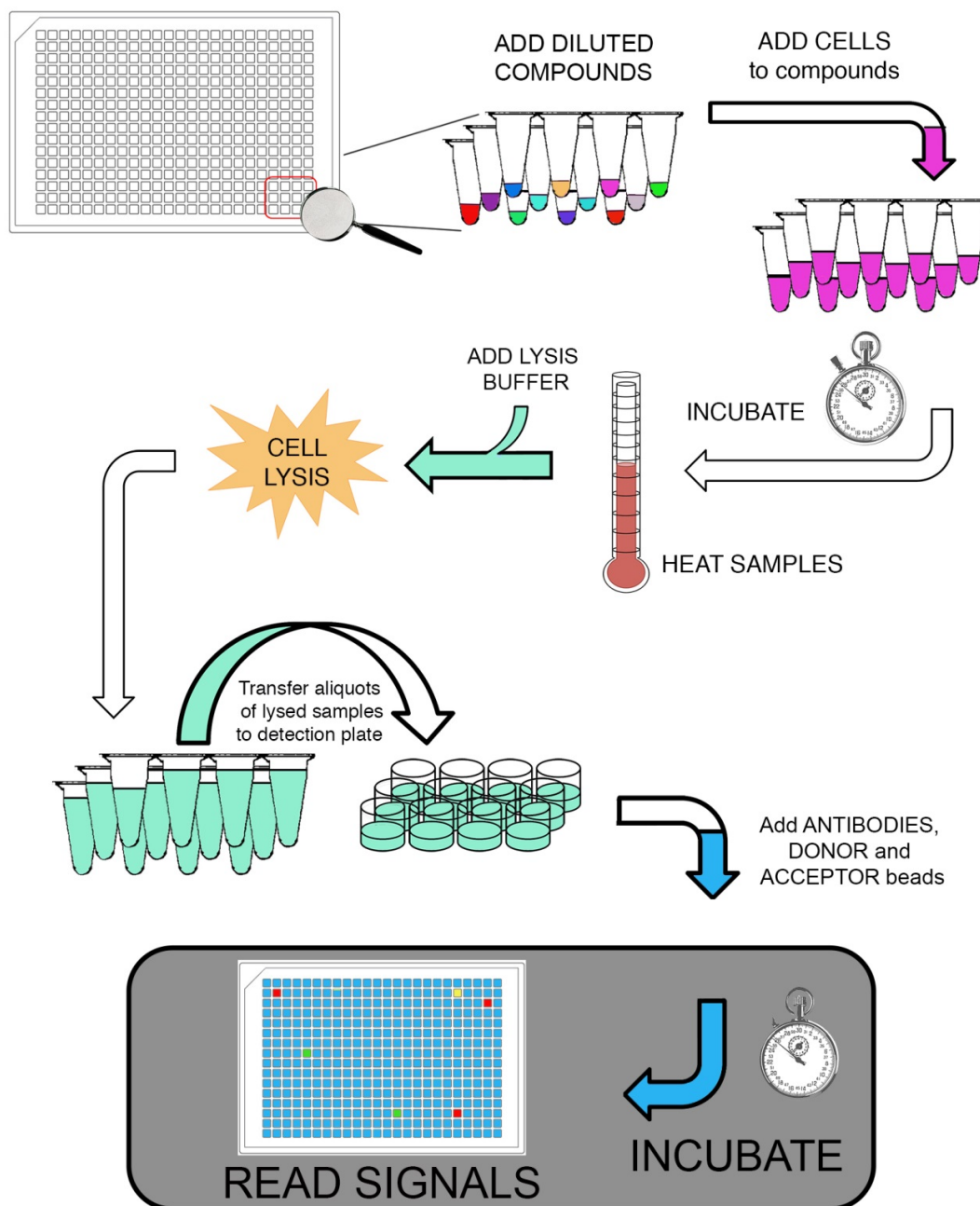


**Figure 13:** Schematic outline of the assay procedure and screening logistics as applied in the screening campaign on human TS using CETSA. Compounds and controls were predisposed to 384-well plates (Echo 550) and subsequently diluted with cell medium (Multidrop™ Combi). Next, the diluted compounds were transferred to 384-well PCR plates (Bravo liquid handling instrument). Cells were then added using a multipipette followed by preincubation for 2h in a cell incubator at 37°C. After the incubation the plates were transiently heated to 50°C for three minutes followed by a controlled cooling to 20°C (Roche LightCycler®480). The plates were then centrifuged briefly, lysed by addition of lysis buffer (Flexdrop IV). To ensure sufficient lysis the samples were thoroughly mixed using a 384-well tip head (Bravo). A small aliquot of the lysates were then transferred to detection plates followed by the addition of a solution of the detection reagents (Multidrop™ Combi) under subdued light. The plates were incubated overnight at room temperature before detection (Envision plate reader). Reprinted by permission from Macmillan Publishers Ltd: Nat. Commun. 7 (2016), copyright (2016) <http://www.nature.com/ncomms/2016/160324/ncomms11040/abs/ncomms11040.html>

### Assay Protocol Screen Format:

- a. Transfer of 5  $\mu$ l diluted compound solutions into individual wells of a 384-well PCR plate using a Bravo liquid handling instrument.
- b. Addition of 5  $\mu$ l K562 cell suspension to all wells.
- c. Preincubation of samples for 2h at 37°C.
- d. Heating to 50°C for 3 min in a PCR machine, followed by controlled cooling down to 20°C.
- e. Lysis by addition of 10  $\mu$ l lysis buffer using a Flexdrop IV.
- f. Thorough mixing to achieve complete cell lysis followed by transfer of 3  $\mu$ l of the diluted samples to a 384-well Proxiplate using a Bravo liquid handling instrument.
- g. Addition of a mix of antibodies, acceptor and donor beads under subdued light to the 384-well Proxiplate using a Multidrop™, centrifuge briefly and incubate for 2 hours or overnight at room temperature under subdued light before reading the plate in an EnVision plate reader.

In this protocol the majority of intracellular TS will denature and irreversibly aggregate unless stabilized by ligand. Inclusion of controls at relevant positions of the plate allows for standard normalization of the data to compare the potential stabilizing effects of the tested compounds with those of the positive controls. Further details on data analysis are available in the original study (8).

### Materials and Reagents

The following materials and reagents were used in the development and optimization of a microplate based live cell CETSA assay for TS using AlphaScreen® as the detection format. The assay was developed and validated as outlined above and successfully applied in a screening campaign for known and novel inhibitors (8).

- Human myelogenous leukemia cell line K562 (ATCC No. CCL-243)
- Echo 550 liquid handler (Labcyte)
- Bravo liquid handling platform (Agilent)
- PCR machine (ProFlex™, Applied Biosystems)
- Real-time PCR machine (LightCycler®480 system, Roche)
- EnVision microplate reader with AlphaScreen modality (PerkinElmer)
- Multidrop™ Combi reagent dispenser (Thermo Scientific)
- PlateLoc thermal microplate sealer (Agilent)
- Labcyte 384 LDV plates (LP-0200)
- 384-well polypropylene plates (784201, Greiner)
- 384-well hardshell PCR plate (HSR480, BIORAD)
- Peelable Aluminium seal (24210-001 Agilent)
- Breathable plate seal (3345, Corning)
- AlphaScreen® SureFire® Lysis Buffer (TGRLB100ML, PerkinElmer)
- AlphaLISA buffer (AL000F, PerkinElmer)
- ProxiPlate (#6008280, PerkinElmer)

- AlphaScreen® anti-mouse donor beads (#AS104D, PerkinElmer)
- AlphaScreen® anti-rabbit acceptor beads (#AL104C, PerkinElmer)
- Mouse monoclonal anti-TS IgG sc-376161 (Santa Cruz)
- Rabbit polyclonal anti-TS IgG (15047-1-AP, Proteintech)

## Reduction of Assay Variability and Troubleshooting

When transferring an assay into a high-throughput format for screening purposes it is of great importance to reduce assay variability in order to obtain reliable statistics and accurate results. The screen formatting procedure usually also involves an attempt to reduce the number of assay steps to simplify the logistics, which generally results in reduced well-to-well variability and consequently improved assay quality. This section serves to outline some of the most critical aspects in the experimental procedure as we understand them today. Examples of unexpected technical challenges that have been encountered and solutions thereof are also discussed. A brief schematic overview of the different steps, including a practical guidance on how to reduce variability, is available in Figure 14. It is important to remember that the technology is young and is expected to develop and mature with each investigated model system and target protein.

### Compound Treatment:

In order to obtain accurate results it is crucial that the cells in each well of the PCR plate are exposed to the intended compound concentration. A somewhat unexpected challenge when moving the assay to a plate-based format was a random lack of contact between compounds predisposed by means of acoustic nanodispensing and cells added with a bulk dispenser such as a MultiDrop™. This problem was caused by the formation of air bubbles trapped in the bottom of the wells in the PCR plate preventing contact between compound and cells. If instead larger volumes (µl) of diluted compounds are transferred to the PCR plates prior to addition of cells, this issue can easily be circumvented. Alternatively the user can consider the inclusion of a brief centrifugation step.

### Transient Heating, Cooling and Lysis:

For this part of the procedure it is of great importance to identify a PCR plate that will not be distorted after the transient heating and the subsequent cooling to room temperature. This is essential to obtain an even transfer of the heated and lysed samples to the detection plate. In cases where no transfer step is necessary, *i.e.* the detection is done directly in the PCR plate, it will be important for the safe stacking and detection of the plates in a microplate reader.

One challenge in the microplate-formatting of the CETSA assay has been to obtain consistent and reliable cell lysis with little variability between wells. An uneven cell lysis will greatly impact assay quality and it is recommended to keep this step under careful control. The use of lysis buffer with thorough sample mixing will greatly improve the throughput compared to the repeated freeze/thawing procedure applied in the original protocol (6). A possible concern using lysis buffers is that the presence of detergents may

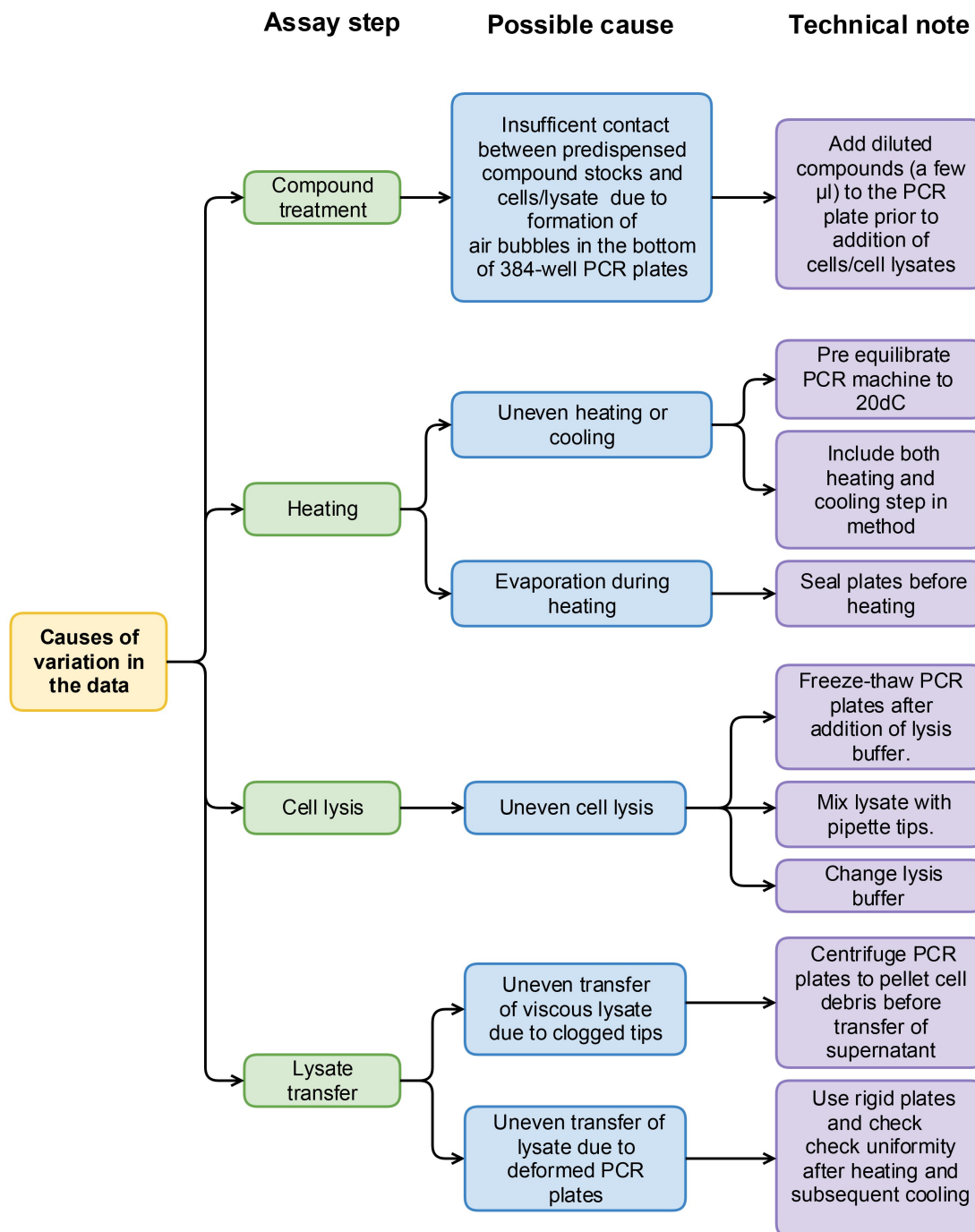


**Figure 14.** Outline of some critical aspects that influence assay variability in the plate-based CETSA procedure. Figure created using Gliffy software.

resolubilize irreversible aggregates of denatured proteins, and thereby negatively affect the quantification of remaining soluble protein after the heating step. In the assay

development process it is therefore advisable to examine this carefully for each individual case. This can for example be done by comparing the results from  $T_{agg}$  and ITDRF<sub>CETSA</sub> experiments with those obtained using the original WB protocol (6). Worth noting is that a recent study reports no signs of resolubilization for a broad range of proteins upon treatment of the irreversible aggregates with a variety of different detergents, with the exception being high concentrations of SDS that thus should be avoided (20). If insufficient lysis is observed with the lysis buffers an inclusion of a freezing and subsequent thawing step may improve the results.

### Separation of Soluble and Denatured Proteins:

Separation of the irreversible aggregates of unfolded proteins from the soluble pool of proteins by means of centrifugation and the subsequent transfer of the supernatant (or a filtration step) is not an ideal setup for a microplate-based screening assay. Such steps will have a negative impact on both throughput and assay variability and should if possible be avoided. However, if the aggregated proteins are resolubilized, or if the antibodies cannot discriminate between native and denatured protein, a separation step is necessary.

### Detection

One of the biggest challenges in the homogeneous assay setup with immunoassay detection is the observation that ligand binding can cause significant quenching of the signal due to loss of antibody recognition (7,8). This is not related to the CETSA approach per se but is instead associated with the detection step, as it was also found to be the case in the absence of heating. Since this has been observed for all proteins tested so far, the identification of a suitable antibody pair requires careful testing for this effect or screening for conditions to overcome this phenomenon (7,8,23). It is therefore recommended to include known binders of the target protein throughout the assay development process in order to identify and avoid such problems. Cellular systems that are not dependent on recognizing epitopes of native proteins are less likely to be affected in this way, provided the signaling tags are situated in such a way that their accessibility is not affected by ligand binding.

### Tentative Applications

The original Science publication from 2013 now has over 100 citations in the scientific literature (as of June 1, 2016). The majority of these are based on studies of target engagement for a few molecules using the WB-based approach, while there are relatively few examples of more systematic studies for libraries or series of compounds in microplate format. Besides its potential utility for looking at patient responses or even for patient stratification we foresee its application in at least three stages in the preclinical drug discovery process.

First, given the abundance of available methodologies for target-based high-throughput screening, it is perhaps most likely that CETSA will be applied as a generic tool for prioritization and cleaning of hit lists in primary cells of relevance for the intended

clinical indication.  $T_m$  shift assays are generally accepted as robust methods for the purpose of removing misbehaving compounds as they positively select for stabilizing compounds. Furthermore, CETSA in live cells allows for an early assessment of other aspects of the identified hits such as serum protein binding and cell permeability, while still being focused on the intended target protein rather than a proximal biomarker or a phenotypic response that could potentially be influenced by nearby pan-targets or completely different mechanisms.

Additionally, in the case of unknown functions for e.g. an orphan target protein or difficulties in expressing and purifying a particular target protein in a relevant form to support screening, CETSA could provide a viable means for identifying chemical starting points in a screening campaign. Most importantly though CETSA offers, similar to other target engagement assays that can be applied in live cells, a possibility to examine the structure-activity relationships for target engagement and thus allows for comparison with those relationships observed in various functional and phenotypic readouts. Such studies offer a great complement to other target validation tools and should be considered as a prerequisite for the validation of chemical probes.

## References

1. Bunnage ME, Chekler ELP, Jones LH. Target validation using chemical probes. *Nat Chem Biol.* 2013;9(4):195–9. PubMed PMID: 23508172.
2. Cook D, Brown D, Alexander R, March R, Morgan P, Satterthwaite G, et al. Lessons learned from the fate of AstraZeneca's drug pipeline: a five-dimensional framework. *Nat Rev Drug Discov.* 2014;13(6):419–31. PubMed PMID: 24833294.
3. Robers MB, Dart ML, Woodroffe CC, Zimprich CA, Kirkland TA, Machleidt T, et al. Target engagement and drug residence time can be observed in living cells with BRET. *Nat Commun.* 2015;6 [10.1038/ncomms10091](https://doi.org/10.1038/ncomms10091). DOI. PubMed PMID: 26631872.
4. Schulze J, Moosmayer D, Weiske J, Fernandez-Montalvan A, Herbst C, Jung M, et al. Cell-based protein stabilization assays for the detection of interactions between small-molecule inhibitors and BRD4. *J Biomol Screen.* 2015;20(2):180–9. PubMed PMID: 25266565.
5. Kaniskan HU, Szewczyk MM, Yu Z, Eram MS, Yang X, Schmidt K, et al. A potent, selective and cell-active allosteric inhibitor of protein arginine methyltransferase 3 (PRMT3). *Angew Chemie - Int Ed.* 2015;54(17):5166–70. PubMed PMID: 25728001.
6. Martinez Molina D, Jafari R, Ignatushchenko M, Seki T, Larsson EA, Dan C, et al. Monitoring drug target engagement in cells and tissues using the cellular thermal shift assay. *Science.* 2013;341(6141):84–7. PubMed PMID: 23828940.
7. Jafari R, Almqvist H, Axelsson H, Ignatushchenko M, Lundbäck T, Nordlund P, et al. The cellular thermal shift assay for evaluating drug target interactions in cells. *Nat Protoc.* 2014;9(9):2100–22. PubMed PMID: 25101824.
8. Almqvist H, Axelsson H, Jafari R, Dan C, Mateus A, Haraldsson M, et al. CETSA screening identifies known and novel thymidylate synthase inhibitors and slow

- intracellular activation of 5-fluorouracil. *Nat Commun.* 2016;7 [10.1038/ncomms11040](https://doi.org/10.1038/ncomms11040). DOI. PubMed PMID: 27010513.
9. Pantoliano MW, Petrella EC, Kwasnoski JD, Lobanov VS, Myslik J, Graf E, et al. High-density miniaturized thermal shift assays as a general strategy for drug discovery. *J Biomol Screen.* 2001;6(6):429–40. PubMed PMID: 11788061.
  10. Lo MC, Aulabaugh A, Jin G, Cowling R, Bard J, Malamas M, et al. Evaluation of fluorescence-based thermal shift assays for hit identification in drug discovery. *Anal Biochem.* 2004;332(1):153–9. PubMed PMID: 15301960.
  11. Senisterra GA, Markin E, Yamazaki K, Hui R, Vedadi M, Awrey DE. Screening for ligands using a generic and high-throughput light-scattering-based assay. *J Biomol Screen.* 2006;11(8):940–8. PubMed PMID: 17092916.
  12. Epps DE, Sarver RW, Rogers JM, Herberg JT, Tomich PK. The ligand affinity of proteins measured by isothermal denaturation kinetics. *Anal Biochem.* 2001;292(1):40–50. PubMed PMID: 11319816.
  13. Sarver RW, Rogers JM, Epps DE. Determination of ligand-MurB interactions by isothermal denaturation: application as a secondary assay to complement high throughput screening. *J Biomol Screen.* 2002;7(1):21–8. PubMed PMID: 11897052.
  14. Senisterra GA, Soo Hong B, Park H-W, Vedadi M. Application of high-throughput isothermal denaturation to assess protein stability and screen for ligands. *J Biomol Screen.* 2008;13(5):337–42. PubMed PMID: 18448703.
  15. Molina DM, Nordlund P. The Cellular Thermal Shift Assay: A Novel Biophysical Assay for In Situ Drug Target Engagement and Mechanistic Biomarker Studies. *Annu Rev Pharmacol Toxicol.* 2015;56(30):1–21. PubMed PMID: 26514198.
  16. Sinclair I, Stearns R, Pringle S, Wingfield J, Datwani S, Hall E, et al. Novel Acoustic Loading of a Mass Spectrometer: Toward Next-Generation High-Throughput MS Screening. *J Lab Autom.* 2016;21(1):19–26. PubMed PMID: 26721821.
  17. McNolty D, Bonnette L, Ho T, Qi H, Annan R, Holgate M. Revving up CETSA: Evaluating Drug Target Engagement in Living Cells via Cellular Thermal Shift Assay. 2016; Poster at the SLAS 5th Annual International Confer.
  18. Menichelli E, Lun A, Ciceri P, Treiber D. HitHunter Pulse: A Novel Biochemical and Cellular Target Engagement Assay Platform for Drug Discovery. 2016; Poster at the SLAS 5th Annual International Confer.
  19. Savitski MM, Reinhard FBM, Franken H, Werner T, Savitski MF, Eberhard D, et al. Tracking cancer drugs in living cells by thermal profiling of the proteome. *Science.* 2014;346(6205) [10.1126/science.1255784](https://doi.org/10.1126/science.1255784). DOI. PubMed PMID: 25278616.
  20. Reinhard FBM, Eberhard D, Werner T, Franken H, Childs D, Doce C, et al. Thermal proteome profiling monitors ligand interactions with cellular membrane proteins. *Nat Methods.* 2015;12(12):1129–31. [Internet]. PubMed PMID: 26524241.
  21. Franken H, Mathieson T, Childs D, Sweetman GMA, Werner T, Tögel I, et al. Thermal proteome profiling for unbiased identification of direct and indirect drug targets using multiplexed quantitative mass spectrometry. *Nat Protoc.* 2015;10(10):1567–93. doi: [10.1038/nprot.2015.101](https://doi.org/10.1038/nprot.2015.101). Available from: <http://dx.doi.org>. PubMed PMID: 26379230.
  22. Cimperman P, Baranauskiene L, Jachimoviciute S, Jachno J, Torresan J, Michailoviene V, et al. A quantitative model of thermal stabilization and

- destabilization of proteins by ligands. *Biophys J.* 2008;95(7):3222–31. PubMed PMID: 18599640.
23. Seashore Ludlow B, Axelsson H, Almqvist H, Jenmalm Jensen A, Lundbäck T. Quantitative Interpretation of Target Engagement and Specificity from Cellular Thermal Shift Assays; Manuscript in preparation.
  24. Eglen RM, Reisine T, Roby P, Rouleau N, Illy C, Bossé R, et al. The use of AlphaScreen technology in HTS: current status. *Curr Chem Genomics.* 2008 Jan;1:2–10. PubMed PMID: 20161822.
  25. Bembenek ME, Burkhardt A, Ma J, Li Z, Loke HK, Wu D, et al. Determination of complementary antibody pairs using protein A capture with the AlphaScreen assay format. *Anal Biochem.* 2011;408(2):321–7. PubMed PMID: 20868646.
  26. Illy C, St.Pierre JA, Bouchard N, Wenham D. Development of High-Throughput Screening Assays for Kinase Drug Targets Using AlphaScreen<sup>TM</sup> Technology. In: Minor LK, editor. *Handbook of Assay Development in Drug Discovery.* Boca Raton, FL, USA: CRC Press; 2006. p. 53–70.



# Measurement of cAMP for $G_{\alpha_s}$ - and $G_{\alpha_i}$ Protein-Coupled Receptors (GPCRs)

Tao Wang,<sup>1</sup> Zhuyin Li,<sup>1</sup> Mary Ellen Cvijic,<sup>1</sup> Litao Zhang,<sup>1</sup> and Chi Shing Sum<sup>1</sup>

Created: November 20, 2017.

## Introduction

Cyclic adenosine monophosphate (cAMP) is an important intracellular second messenger in GPCR signal transduction. Agonist activation of GPCRs that couple to the  $G_{\alpha_s}$  protein leads to an increased production of intracellular cAMP levels, whereas activation of GPCRs that couple to the  $G_{\alpha_i}$  protein leads to reduced production of intracellular cAMP levels. Both of these intracellular cAMP changes are mediated through the modulation of adenylate cyclase activity. cAMP regulates the activity of cAMP-dependent protein kinase A (PKA), which plays an important role in a variety of downstream cellular processes.

A number of reagent kits are available on the market that can be used to measure intracellular cAMP levels. These include the HTRF cAMP kit from Cisbio, the LANCE cAMP kit from PerkinElmer, the HitHunter cAMP kit from DiscoverX and the cAMP Direct Immunoassay Kit from Abcam and BioVision. These assays are all based on the use of antibodies that specifically recognize both intracellular cAMP and an exogenous labeled cAMP conjugate that acts as a competitor, followed by detection of the labeled cAMP conjugate by a variety of detection technologies, including fluorescence resonance energy transfer (FRET) or enzymatic reactions. In addition, the antibody-independent GloSensor cAMP assay from Promega employs semi-split luciferase, which reassembles when bound to cAMP. The advantages and disadvantages of the various cAMP assay technologies are given in Table 1. This chapter focuses on the Cisbio HTRF cAMP kit to illustrate the methodology and considerations for development of assays that measure intracellular cAMP. The assay development principles discussed here can be easily applied to similar cAMP measurement kits or various other detection methodologies.

**Table 1.** Comparison of popular cAMP assay technologies

| Technology | Vendor | Principle  | Advantages   | Disadvantages  |
|------------|--------|--|--|--|
| HTRF       | Cisbio | <ul style="list-style-type: none"> <li>A time-resolved assay technology based on fluorescence</li> </ul> | <ul style="list-style-type: none"> <li>Homogeneous assay</li> <li>Ratiometric readout</li> </ul> | <ul style="list-style-type: none"> <li>Generally lower signal-to-background compared to</li> </ul> |

*Table 1. continues on next page...*

Table 1. continued from previous page.

| Technology    | Vendor      | Principle   | Advantages   | Disadvantages   |
|---------------|-------------|---|--|---|
|               |             | <p>resonance energy transfer between a long-lifetime Europium cryptate fluorescent donor (<math>\text{Eu}^{3+}</math>) and a fluorescent acceptor (XL665 or d2).</p> <ul style="list-style-type: none"> <li>• Recognition of a fluorescent acceptor labeled cAMP by a fluorescent donor labeled anti-cAMP leads to energy transfer signal.</li> <li>• Competition from endogenous cAMP for the antibody results in reduced energy transfer signal.</li> <li>• Loss-of-signal measurement: the level of cellular cAMP is inversely related to the signal.</li> </ul> | <ul style="list-style-type: none"> <li>• Anti-cAMP antibodies available with different affinities toward cAMP for desired assay sensitivities</li> <li>• Does not require any recombinant protein expression for detection</li> <li>• Permits absolute quantification of cellular cAMP level by means of a standard curve</li> </ul> | <p>other technologies</p>   |
| LANCE TR-FRET | PerkinElmer | <ul style="list-style-type: none"> <li>• A time-resolved assay technology based on fluorescent resonance energy transfer between a long-lifetime Europium chelate fluorescent donor</li> </ul>  | <ul style="list-style-type: none"> <li>• Homogeneous assay</li> <li>• Ratiometric readout</li> <li>• Does not require any recombinant protein expression for detection</li> </ul>  | <ul style="list-style-type: none"> <li>• Generally lower signal-to-background compared to other technologies</li> </ul> |

Table 1. continues on next page...

Table 1. continued from previous page.

| Technology | Vendor    | Principle   | Advantages  | Disadvantages   |
|------------|-----------|---|---|---|
|            |           | <p>(Eu<sup>3+</sup>) and a fluorescent acceptor (<i>ULight</i>).</p> <ul style="list-style-type: none"> <li>• Recognition of a fluorescent donor labeled cAMP by a fluorescent acceptor labeled anti-cAMP leads to energy transfer signal.</li> <li>• Competition from endogenous cAMP for the antibody results in reduced energy transfer signal.</li> <li>• Loss-of-signal measurement: the level of cellular cAMP is inversely related to the signal.</li> </ul> | <ul style="list-style-type: none"> <li>• Permits absolute quantification of cellular cAMP level by means of a standard curve</li> </ul>   |   |
| HitHunter  | DiscoverX | <ul style="list-style-type: none"> <li>• An enzyme fragment complementation (EFC) technology-based assay that uses two fragments of <i>E. coli</i> β-galactosidase (β-gal): a large protein fragment (enzyme acceptor, EA) and a small peptide fragment (enzyme donor, ED). Separately, these fragments</li> </ul>  | <ul style="list-style-type: none"> <li>• Homogeneous assay</li> <li>• High signal-to-background</li> <li>• Does not require any recombinant protein expression for detection</li> <li>• Permits absolute quantification of cellular cAMP levels by means of a standard curve</li> </ul> | <ul style="list-style-type: none"> <li>• Compounds that block the recombination or inhibit the activity of β-gal could lead to false positives/negatives</li> </ul> |

Table 1. continues on next page...

Table 1. continued from previous page.

| Technology | Vendor  | Principle  | Advantages   | Disadvantages   |
|------------|---------|--|--|---|
|            |         | <p>are inactive, but in solution they rapidly recombine to form active <math>\beta</math>-gal enzyme, which can hydrolyze substrate to produce a luminescent signal.</p> <ul style="list-style-type: none"> <li>cAMP from cell lysates and ED-labeled cAMP (ED-cAMP) compete for anti-cAMP antibody binding. Unbound ED-cAMP is free to complement EA to form active enzyme, which subsequently produces a luminescent signal. The amount of signal produced is proportional to the amount of cAMP in the cell lysate.</li> <li>Gain-of-signal assay: increased cAMP level leads to increased signal.</li> </ul> |  |   |
| Glosensor  | Promega | <ul style="list-style-type: none"> <li>A luciferase biosensor-based assay that uses genetically</li> </ul>   | <ul style="list-style-type: none"> <li>Homogeneous assay</li> <li>Real-time live-cell kinetic</li> </ul> | <ul style="list-style-type: none"> <li>Requires expression of cAMP-dependent</li> </ul> |

Table 1. continues on next page...

Table 1. continued from previous page.

| Technology                  | Vendor            | Principle   | Advantages   | Disadvantages   |
|-----------------------------|-------------------|---|--|---|
|                             |                   | <p>encoded biosensor with cAMP binding domain fused to a luciferase.</p> <ul style="list-style-type: none"> <li>• Binding of cAMP to the cAMP binding domain changes the conformation of the biosensor, leading to the activation of luciferase. The intensity of the luciferase signal is proportional to the amount of cAMP in the cells.</li> <li>• Gain-of-signal assay: increased cAMP level leads to increased signal.</li> </ul> | <p>measurement possible</p> <ul style="list-style-type: none"> <li>• Two different biosensors with different sensitivities to cAMP are available</li> <li>• Sensitivity may be high enough that activity of G<sub>αi</sub> receptor can be assessed without the need to first stimulate cAMP production</li> </ul> | <p>luciferase in cells</p> <ul style="list-style-type: none"> <li>• No cAMP calibration curves with an external standard</li> </ul> |
| cAMP Direct Immunoassay Kit | Abcam / Biovision | <ul style="list-style-type: none"> <li>• A competitive immunoassay by immobilizing anti-cAMP antibody in assay wells.</li> <li>• cAMP-HRP conjugate directly competes with cAMP from samples for binding to the cAMP antibody on the plate.</li> <li>• The signal intensity is</li> </ul>   | <ul style="list-style-type: none"> <li>• Washing step removes potential interferences from compounds or cell culture medium</li> <li>• Does not require any recombinant protein expression for detection</li> <li>• Permits absolute quantification</li> </ul>   | <ul style="list-style-type: none"> <li>• Non-homogeneous assay</li> </ul>   |

Table 1. continues on next page...

Table 1. continued from previous page.

| Technology | Vendor | Principle   | Advantages  | Disadvantages |
|------------|--------|---|---|---------------|
|            |        | inversely proportional to the concentration of cAMP in samples. | of cellular cAMP level by means of a standard curve |               |

## Flowchart of Assay Development Guidelines

### 1. Select cell lines or primary cells

- Recombinant cells generally produce greater signal change due to receptor expression .
- Endogenously expressed receptor from cell lines or primary cells can be used for more physiological relevance.

### 2. Select cAMP assay reagents of desired sensitivity

- cAMP antibody is available as femto2, dynamic2 or HiRange kit for different sensitivity.
- The choice is dependent on the cells and the density of assay format (i.e, 96-, 384-, or 1536-well).

### 3. Optimize cell density and forskolin concentration (G<sub>i</sub>-coupled receptor)

- Cell density and forskolin concentrations should be titrated simultaneously to maximize potential assay window while keeping the measured signals within the linear range of the cAMP calibration curve.

### 4. Determine agonist dose-response relationships and potency values

- The measured signals are converted to cAMP levels, which are then used to determine the EC<sub>50</sub> or EC<sub>80</sub> values.

### 5. Determine antagonist dose-response relationships and EC<sub>50</sub> values by stimulating with EC<sub>50-80</sub> agonist concentration

- The measured signals are converted to cAMP levels, which are then used to determine the EC<sub>50</sub> or EC<sub>80</sub> values.

### 6. Assess assay performance statistics, including Z', signal-to-background ratio, reproducibility of potency data

- Ensure Z' > 0.5 and reproducibility over multiple runs are within acceptable limits.

## Overview of the Assay Technology

The Cisbio cAMP assay uses homogeneous time-resolved fluorescence technology (HTRF) to measure cAMP in a non-separation, high throughput format. These kits are based on a competitive immunoassay using Eu<sup>3+</sup> cryptate-labeled anti-cAMP antibody and d2-labeled cAMP (Figure 1). Detailed guidance on various immunoassay methods are described in the chapter “Immunoassay Methods” within this NIH Assay Guidance Manual (1). In the HTRF cAMP assay, binding of these two molecules will bring the long-lived fluorescent donor Eu<sup>3+</sup> cryptate and short-lived fluorescent acceptor d2 into close proximity, which facilitates fluorescence resonance energy transfer to occur between the donor and the acceptor. The long fluorescent lifetime of Eu<sup>3+</sup> cryptate allows the introduction of a time delay of approximately 50 to 150 microseconds between the system excitation and fluorescence emission measurement. Together with the large Stokes shift of

<sup>1</sup> Bristol-Myers Squibb Company, NJ.

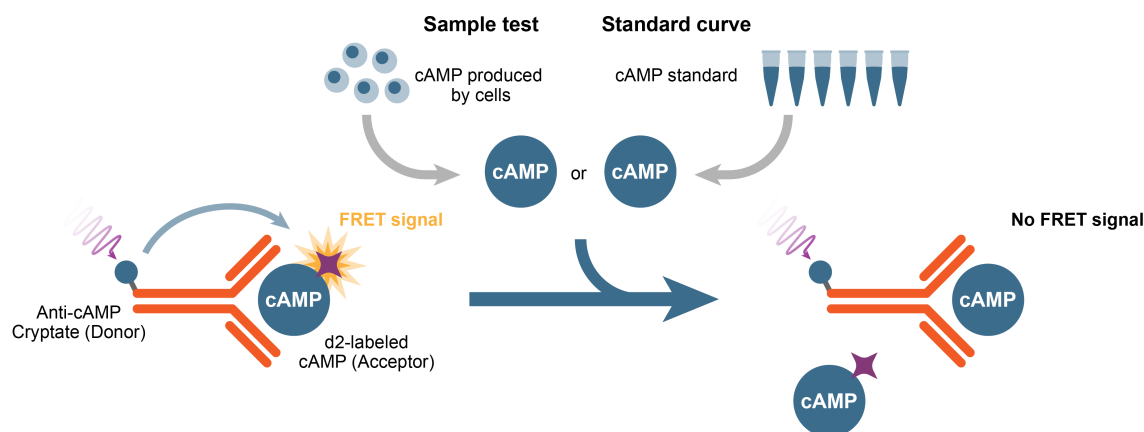


**Figure 1. Principles of the HTRF cAMP Assay.** Anti-cAMP cryptate and d2-labeled cAMP are the two main components of the detection reagents. cAMP produced intracellularly is detected following cell lysis via competition between the intracellular cAMP and d2-labeled cAMP for the anti-cAMP antibody. An increase in intracellular cAMP leads to disruption of FRET signal, whereas a decrease in intracellular cAMP results in higher FRET signal (2).

the donor fluorophore (337 nm excitation to 620 nm emission), the Eu<sup>3+</sup> cryptate-based time-resolved fluorescent technology eliminates non-specific short-lived emissions (e.g. fluorescence from compounds or plastic plates) (2). Furthermore, the use of a ratiometric readout between donor emission at 620 nm and acceptor emission at 665 nm is advantageous, particularly for reducing well-to-well variations or plate edge effects that are often seen in homogeneous assay formats. Cisbio has several cAMP kits that differ in the affinity of the antibody for cAMP and are suitable for detection of intracellular cAMP levels over several relative concentration ranges.

The use of positive and negative controls is important to define the dynamic range of the assay within each plate and for proper quality control from plate to plate and run to run. The inclusion of one or more reference compounds for concentration-response analysis is valuable for assessing the incidence of assay drift. More details can be found in the AGM chapters HTS Assay Validation (3) and Assay Operations for SAR Support (4).

## Importance of cAMP Standard Curve

To establish the relationship between the actual cellular response and the assay readout, a cAMP standard curve should be included with each run as an assay control. The level of cAMP is measured indirectly through competition with a labeled cAMP competitor for binding to the cAMP antibody. The more cAMP produced, the lower the measured signal, and vice versa. The actual cAMP level is determined by using a standard curve in which the signals are measured using various known concentrations of cAMP. The cAMP standard curve is usually represented in a semi-log plot of  $Em_{665}/Em_{615} \times 10^4$  versus cAMP concentration (Figure 2A). The measured signal ratio displays an inverse sigmoidal

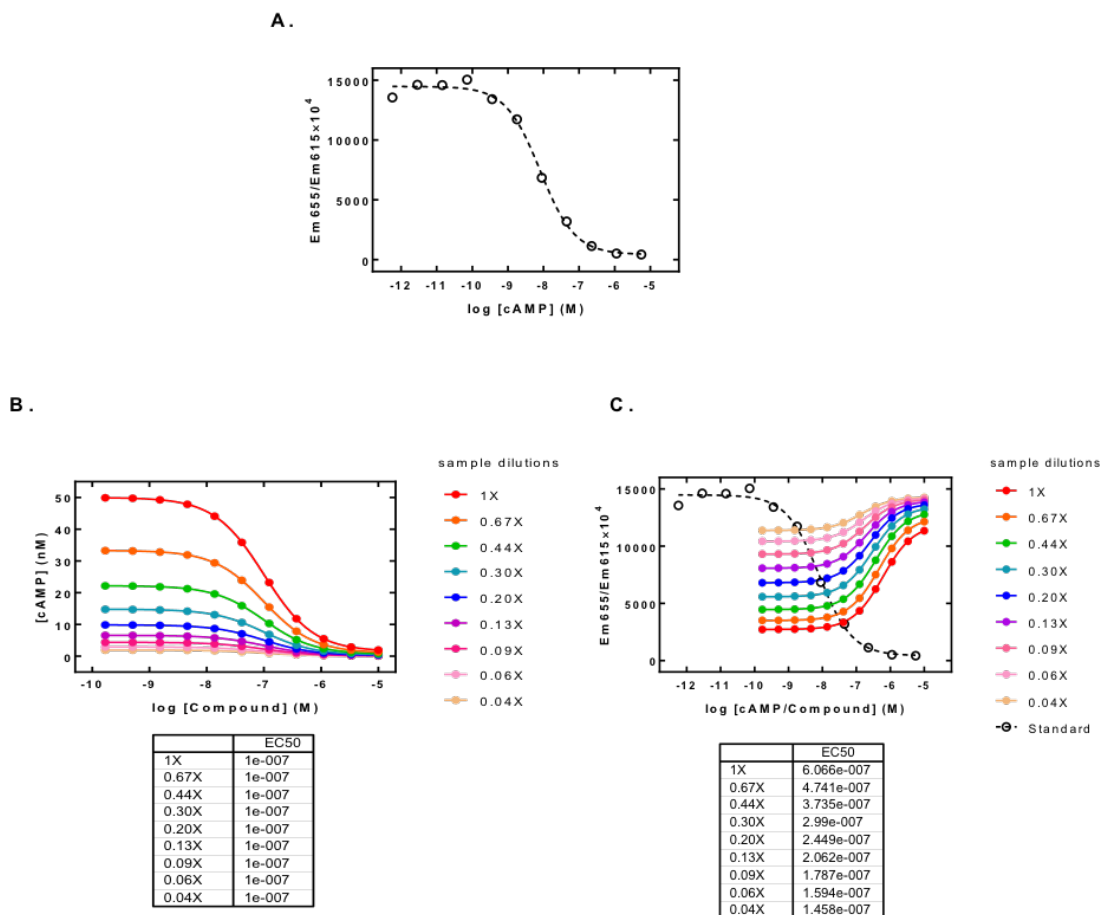


**Figure 2.** Illustration of the importance of estimating potency values using concentration-response curves expressed in cAMP levels instead of HTRF signal. Panel A. A typical cAMP standard curve. Panel B. Agonist concentration-response curves expressed in cAMP levels and the estimated EC<sub>50</sub> values. Panel C. Corresponding concentration-response curves expressed in HTRF signal and the estimated EC<sub>50</sub> values.

relationship with the log concentration of cAMP. The cAMP level from an assay reaction is determined via interpolation from the standard curve (1).

During assay development, it is important that the assay conditions (e.g. cell density, forskolin concentration, and agonist stimulation) are optimized so that the measured signals fall within the linear range of the standard curve. Due to the sigmoidal relationship between the signal and the cAMP level, signals at the top region of the cAMP standard curve can be too sensitive to changes in cAMP level, whereas signals at the bottom region can be too insensitive to the changes.

Figure 2 illustrates the importance of converting the measured signals to cAMP levels to accurately determine the potency values from concentration-response curves. Figure 2A shows a typical cAMP standard curve. Figure 2B is a series of concentration response



curves simulated to closely resemble actual data from the response characteristics of an agonist that mediates inhibition of forskolin-stimulated cAMP production in a G<sub>αi</sub>-coupled receptor. Increasing the concentration of the agonist causes a reduction in intracellular cAMP levels. Each of the nine curves shown in the panel represents different dilutions from the original lysate from 1X to 0.04X dilutions. Since the curves are simply generated by dilution of the same lysates, the agonist EC<sub>50</sub> values are the same for all the curves (i.e., 100 nM). For illustration purposes, if these agonist curves are converted back to HTRF signal in accordance with the standard curve, another series of curves is generated as shown in Figure 2C. The estimated EC<sub>50</sub> values from Figure 2C erroneously increase over a 4-fold range but none of these values accurately reflect the actual EC<sub>50</sub> value. This phenomenon is a result of the semi-logarithmic relationship between the measured signal and cAMP level. Similar discussion on the importance of using a cAMP standard curve to convert measured signal ratios to levels of cAMP and how basing the activity measurement on HTRF ratio may skew the potency and efficacy estimation are also described in the literature (5,7). Furthermore, the use of a calibration curve and the selection of an appropriate model is thoroughly discussed in the AGM chapter Immunoassay Methods (1).

## Assay Development and Optimization Guidelines

As indicated in the above flowchart, assay development should start from selecting the appropriate endogenously expressing cells or transfecting cells to overexpress the target receptor. If cell lines stably expressing the receptors are generated, multiple clones can be selected initially either by FACS to assess the surface protein expression or by qPCR for gene expression. The level of receptor expressed on the cell surface impacts both the potency and efficacy of agonists. Figure 3 illustrates how the estimated potency values increase for a set of agonists as the expression level of target receptor increases. Furthermore, a partial agonist may behave as a full agonist due to a high level of receptor expression, which leads to high receptor reserve. During the early lead discovery phase, it may be advantageous to utilize cell lines of high receptor expression to enhance the sensitivity of detecting hit compounds. Nevertheless, it would be important to assess multiple cell clones expressing receptors at various levels if correlation with other assay readouts is desirable in the lead optimization phase.

Once a cellular model is selected or generated, for a G<sub>αs</sub>-coupled receptor, assay development may begin by determining the concentration-response relationship of a known agonist at various cell densities. Figure 4 shows an example of such agonist and cell density titration curves. As shown in the figure, it is important to note that when there are too many cells, the signal-to-background may be adversely affected. The agonist concentration-response curves are examined to identify concentrations in which the response falls within the linear detection range of the cAMP standard curve. A cell density that produces the best dynamic range and expected EC<sub>50</sub> value of the agonist is selected.

For a G<sub>αi</sub>-coupled receptor, its activation needs to be assessed under a detectable cAMP level. This can be achieved using forskolin or a known agonist of a G<sub>αs</sub>-coupled receptor

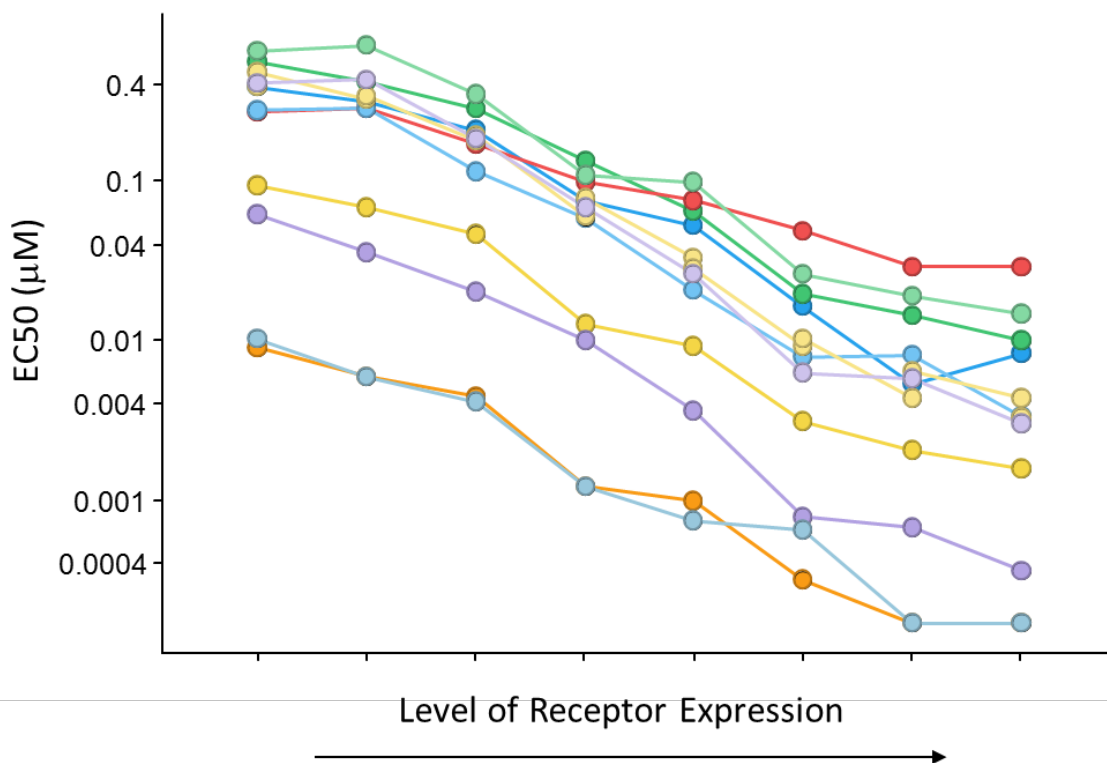


**Figure 3.** Dependence of agonist potency ( $EC_{50}$  values) on the level of receptor expression. Shown are individual compound potency values that were measured in cells lines expressing a given level of receptor. Different compounds are shown in symbols and lines of different colors.

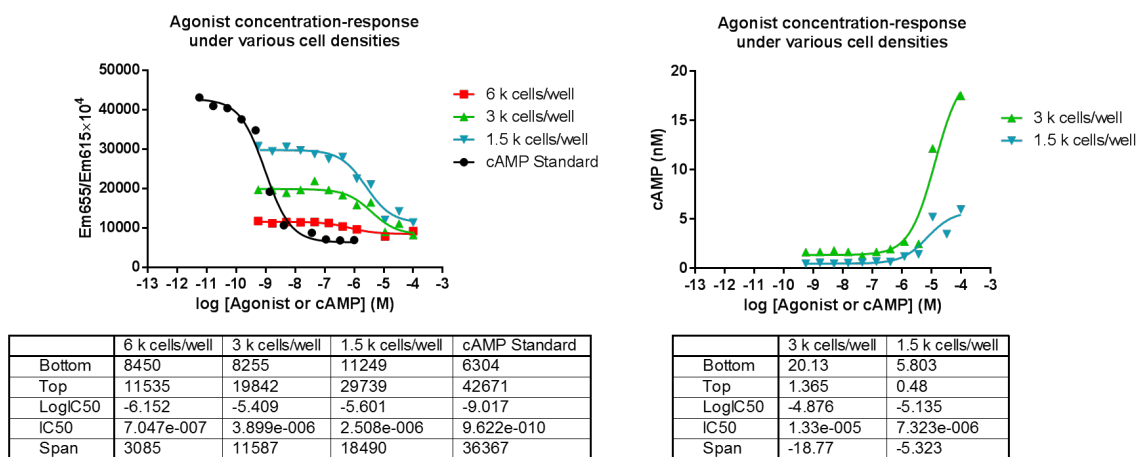


**Figure 4.** Examples of (A) agonist-concentration response curves at various cell densities for a  $G_{\alpha s}$ -coupled receptor and (B) agonist-concentration response curves expressed in cAMP level. In this example, when the cell density is too high as with 6 k/cells, the signals produced exceeded the optimal range of cAMP level (panel A) and therefore the curve cannot be converted to cAMP value (panel B).

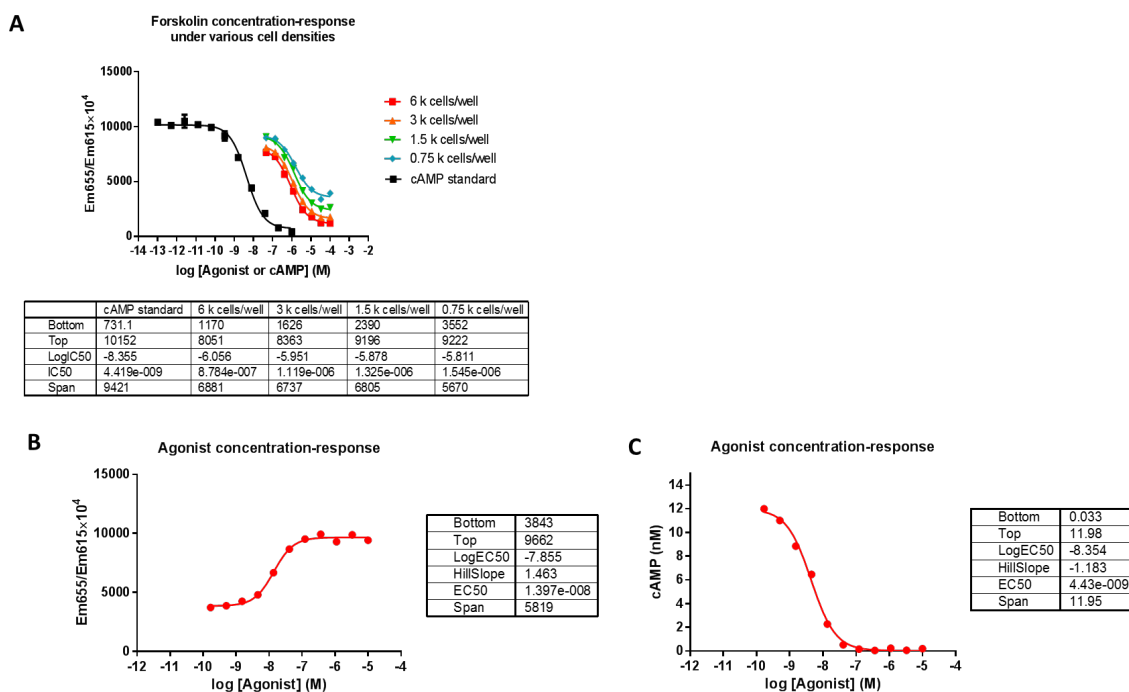


**Figure 5.** Examples of (A) forskolin concentration response-curves at various cell densities for a G<sub>α<sub>i</sub></sub>-coupled receptor, (B) an agonist concentration-response assayed at 3 μM forskolin and 1,500 cells/well as selected from Panel A, and (C) the agonist concentration-response from Panel B expressed in cAMP level.

to stimulate cAMP production, as shown in Figure 5. Similarly, a combination of appropriate forskolin concentration and cell density that can stimulate cAMP production to a level that is within the linear detection range and generate optimal assay dynamic range would be selected. Subsequently, the agonist response can be assessed at the chosen conditions to ensure its potency agrees with anticipated values.

For either G<sub>α<sub>s</sub></sub>- or G<sub>α<sub>i</sub></sub>-coupled receptors, following the determination of agonist response, the potency of antagonist can be assayed at a selected agonist concentration between EC<sub>50</sub> to EC<sub>80</sub>. A summary of assay optimization and troubleshooting guidelines is given in Table 2.

**Table 2.** Key assay optimization parameters and troubleshooting guidelines

| Problem  | Possible reason              | Solution   |
|--|------------------------------|--|
| <i>G<sub>α<sub>s</sub></sub> agonist assay</i>   |                              |  |
| Basal cAMP falls out of the lowest measurable limit in the linear part of the cAMP standard curve (i.e., cAMP level too low) | Insufficient number of cells | Increase the number of cells in the assay reaction |

Table 2. continues on next page...

Table 2. continued from previous page.

| Problem   | Possible reason  | Solution   |
|---|--|--|
| Basal cAMP exceeds the highest measurable limit in the linear part of the cAMP standard curve (i.e., cAMP level too high) | Too many cells   | Decrease the number of cells in the assay reaction   |
| Agonist-stimulated cAMP level undetectable (i.e., cAMP level too low)   | cAMP rapidly degraded by endogenous phosphodiesterase  | Include phosphodiesterase inhibitors such as IBMX  |
|   | Cells not expressing sufficient quantities of receptor | Select for higher expressing clones as determined by qPCR or by FACS                             |
|   | Compounds not efficacious                              | Test other compounds known to be efficacious in modulating cAMP production                       |
|   | Insufficient compound binding to the receptor          | Allow for longer incubation of the assay reactions   |
| Agonist-stimulated cAMP level exceeds the linear part of the cAMP standard curve (i.e., cAMP level too high)              | Phosphodiesterase inhibition too strong                | Test the presence and absence of phosphodiesterase inhibitor                                     |
|   | cAMP detection antibody too sensitive                  | Select for an anti-cAMP antibody with lower affinity for cAMP                                    |
|   | Too many cells   | Decrease the number of cells in the assay reaction   |
| <i>Gai agonist assay</i>  |  |  |
| Basal cAMP falls out of the lowest detection limit in the cAMP standard curve (i.e., cAMP level too low)                  | Insufficient number of cells                           | Increase the number of cells in the assay reaction   |
| Forskolin-stimulated cAMP not achieving high enough level (i.e., cAMP level too low)                                      | Not enough cells                                       | Increase the number of cells in the assay reaction   |
|   | cAMP rapidly degraded by endogenous                    | Include phosphodiesterase inhibitors such as IBMX  |
|   | Forskolin concentration too low                        | Increase the concentration of forskolin as determined in forskolin concentration-response curves |
| Forskolin stimulated cAMP exceeded the linear part of the cAMP standard curve (i.e., cAMP level too high)                 | Too many cells   | Decrease the number of cells in the assay reaction   |
|   | Forskolin concentration too high                       | Reduce the concentration of forskolin as determined in forskolin concentration-response curves   |
| Agonist-stimulated change in cAMP level undetectable  | Cells not expressing sufficient quantities of receptor | Select for higher expressing clones as determined by qPCR or by FACS                             |

Table 2. continues on next page...

Table 2. continued from previous page.

| Problem   | Possible reason   | Solution   |
|---|---|--|
|   | Compounds not efficacious                                 | Test other compounds known to be efficacious in modulating cAMP production |
|   | Insufficient compounds binding to the receptor            | Allow for longer incubation of the assay reactions                         |
| <i>G<sub>αs</sub> antagonist assay</i>  |   |  |
| Antagonist compounds do not antagonize the agonist-stimulated response or not giving expected potency | Insufficient antagonist compounds binding to the receptor | Allow for longer pre-incubation of the antagonist compounds                |
|   | Compounds not efficacious                                 | Test other compounds known to be efficacious in modulating cAMP production |
|   | Agonist stimulation too strong                            | Reduce agonist concentration used for stimulation                          |
| <i>G<sub>αi</sub> antagonist assay</i>  |   |  |
| Antagonist compounds do not antagonize the agonist-stimulated response or not giving expected potency | Insufficient antagonist compounds binding to the receptor | Allow for longer pre-incubation of the antagonist compounds                |
|   | Compounds not efficacious                                 | Test other compounds known to be efficacious in modulating cAMP production |
|   | Agonist stimulation too strong                            | Reduce agonist concentration used for stimulation                          |
|   | Accumulated cAMP not degraded                             | Test presence or absence of phosphodiesterase inhibitor                    |

## cAMP Assays for Receptors Coupled to G<sub>αs</sub> Protein

The following guidelines were developed for assays using suspension cells for high throughput mode; however, the assay can be adapted easily for adherent cells. Volumes are given for a 384-well assay (20 μL assay reaction) and can be adjusted proportionally to other plate densities.

### G<sub>αs</sub>-Coupled Agonist Format

The activation of adenylylate cyclase by G<sub>αs</sub>, in the presence of an agonist, the generation of intracellular cAMP and its measurement by HTRF technology is shown in Figure 6.

### Sample Protocol for G<sub>αs</sub>-Coupled Agonist Assays

Step 1: Grow cells in tissue culture flasks for 1-3 days in the corresponding cell culture medium.

- Select a cell line containing the target GPCR of interest.

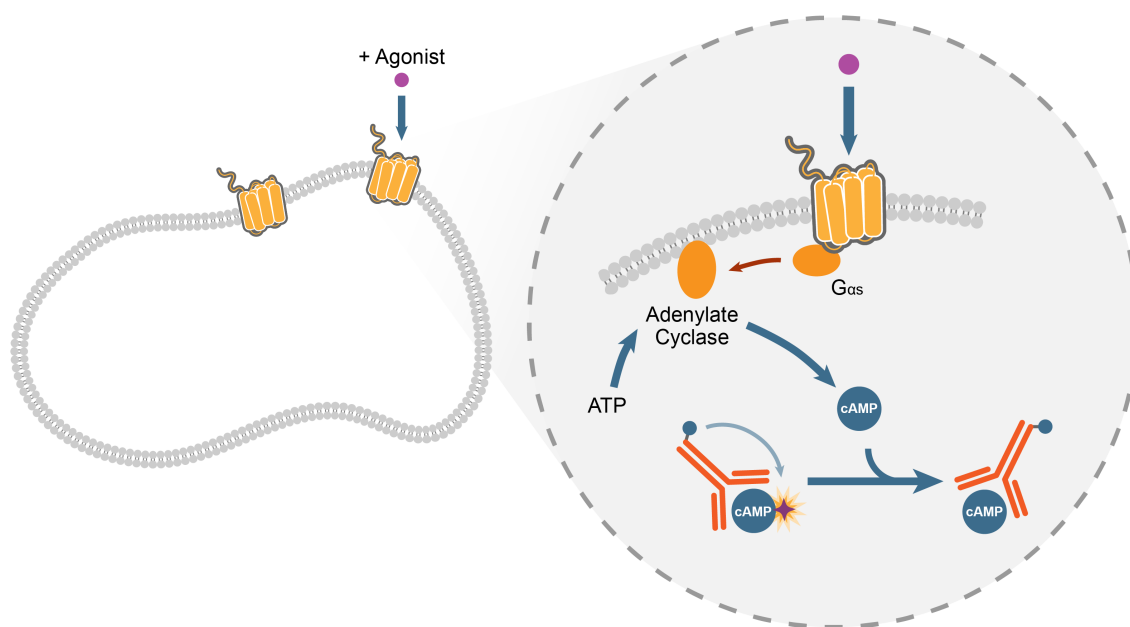


**Figure 6. cAMP Measurement for Agonists of a G $\alpha_s$ -Coupled Receptor.** Activation of the receptor by an agonist causes an exchange of GDP for GTP in the G protein complex that subsequently dissociates into a G $\beta\gamma$  dimer and a G $\alpha_s$  monomer. The activated G $\alpha_s$  subunit binds to adenylate cyclase resulting in the generation of intracellular cAMP, which is measured using the specific Eu $^{3+}$ -labeled anti-cAMP antibody and d2-labeled cAMP in a competitive HTRF assay.

- A negative control cell line as a counter screen may either be the parental cell line devoid of the target or a cell line expressing an unrelated GPCR that couples to the same G protein.
- Make sure the cells are healthy and active in the log phase of growth and are maintained in the same way in all experiments, as the state of the cells may affect the receptor response.
- Limit cell passage in concordance with assay performance statistics. Ideally, to avoid variation in cellular response due to changes in the state of the cells or receptor expression, expand the cell culture to the quantities required for the entire screening campaign in one large batch of a single passage and prepare cryopreserved cells as one batch. Various manufacturers of cell culture reagents offer different cryopreservation reagents and methods. During screening, recover the cells and use them as needed.

Step 2: Dissociate the cells from the flask and centrifuge at 1000 rpm for 5 minutes.

- Use of Trypsin or other enzymatic/non-enzymatic cell dissociation agents should be tested prior to screening.
- Some receptor proteins may tolerate trypsinization, but other enzymatic reagents such as TrypLE (Thermo) or non-enzymatic reagents such as CellStripper (Corning) may be used if needed.

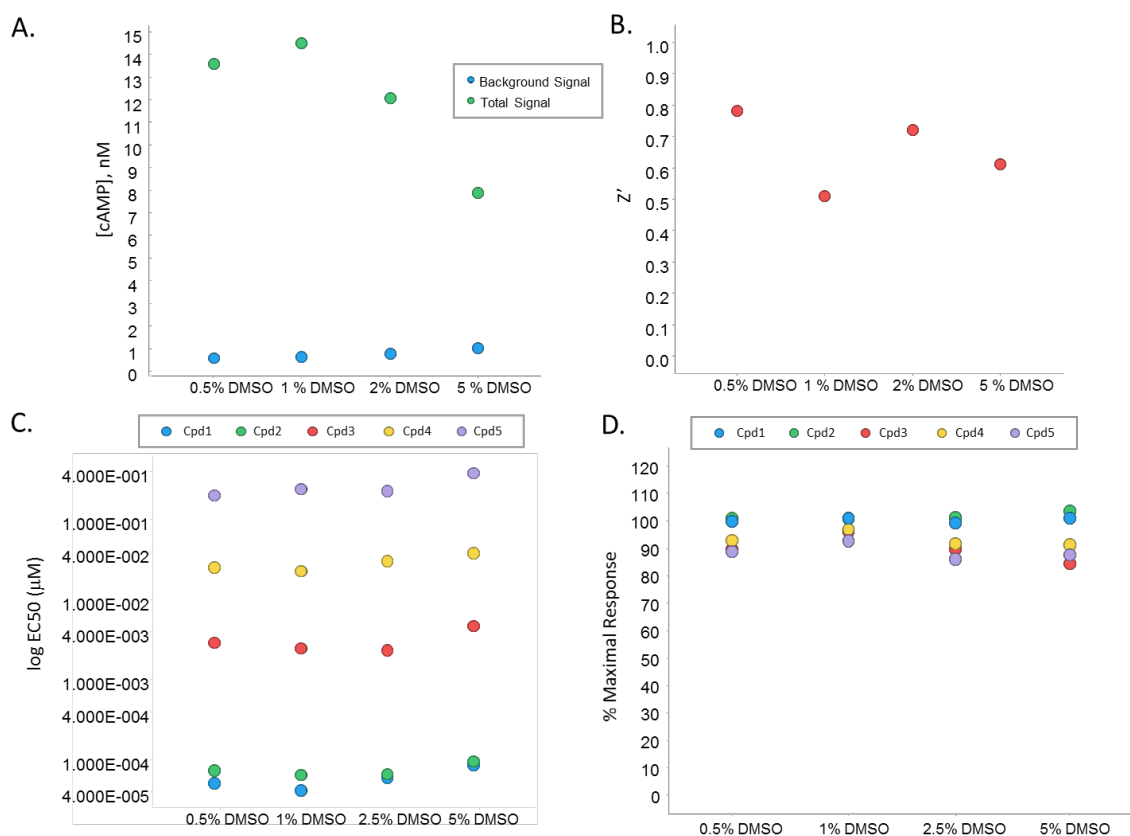


**Figure 7.** An example of a DMSO tolerance test carried out by conducting the cAMP assay in the presence of different concentrations of DMSO. Various parameters are assessed to identify the acceptable range of DMSO without adversely affecting the performance of the assay and the pharmacological measurements. The parameters are: (A) levels of cAMP in the presence of an agonist (total signal) and absence of the agonist (background signal), (B)  $Z'$  as described in (6), (C) agonist  $EC_{50}$  values, and (D) % maximal agonist response. In panels C and D, symbols of different colors denote different agonists.

**Step 3:** Aspirate the medium and re-suspend the cells in assay buffer. Count and dilute the cells to the proper densities in assay buffer.

- In most cases, HBSS or Dulbecco's PBS (DPBS) buffers can be used: 1X HBSS/20mM HEPES with or without 0.1% BSA (fat acid-free) or DPBS with  $Ca^{2+}/Mg^{2+}$  with or without 0.1% BSA.
- Cell densities should be determined during assay development in cell titration experiments such that the measured signal falls within the linear range of the cAMP standard curve while yielding the best assay window determined with a reference agonist.
- Using too many cells, and hence the presence of too many receptors, may reduce the effective free concentrations of ligands and cause the assay to bottom-out and therefore limit the ability to differentiate potent compounds. Too many cells may also saturate the cAMP assay reagents.

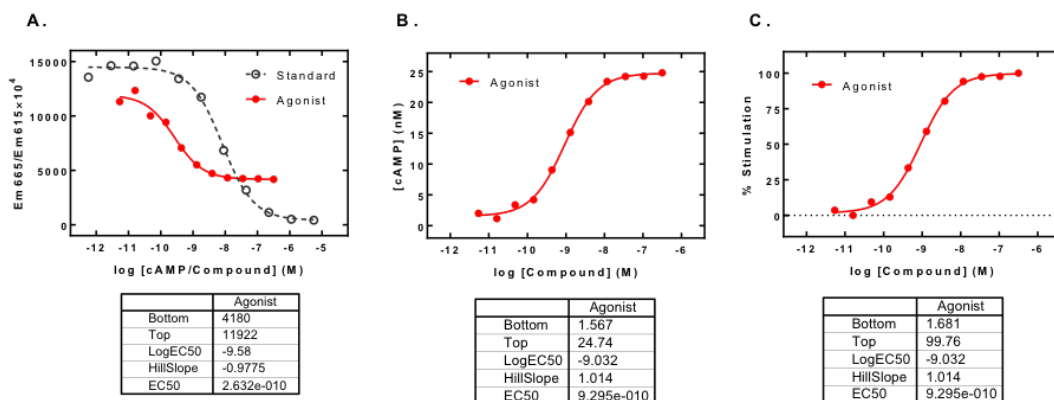


**Figure 8.** An example of an agonist concentration-response curve in  $G_{\alpha s}$ -coupled receptors. Panel A. The agonist response is plotted as the HTRF ratio ( $Em665/Em615 \times 10^4$ ) along with the cAMP standard curve. Note that the agonist produces signals that are within the linear portion of the standard curve. Panel B. The agonist response is plotted as the cAMP level to determine the  $EC_{50}$  values. Panel C. The same agonist response is plotted as % stimulation. Data are analyzed using a four-parameter logistic regression.

Step 4: Add 3-isobutyl-1-methylxanthine (IBMX) or other phosphodiesterase inhibitor to the cell suspension. IBMX is a competitive nonselective *phosphodiesterase inhibitor* which inhibits the degradation intracellular cAMP. It is generally used at a final concentration of 0.1 mM in the assay, but the impact of phosphodiesterase inhibitor on compound potency and the required concentration should be determined according to the assays and cell lines being used. Dispense 10  $\mu$ L of cells to assay plates pre-dotted with compounds. (*Note that depending on the extent of activity of phosphodiesterase in the cells, the use of inhibitor is optional.*)

- IBMX can be made at high concentration (0.5 M) and aliquoted and stored at  $-20^{\circ}\text{C}$  to avoid multiple freeze-thaw cycles.
- Different assay plates may be tested. Please refer to Cisbio website for microplate recommendations (<http://www.cisbio.com/usa/drug-discovery/htrf-microplate-recommendations>).
- The cell suspension is best prepared only when it is ready for dispensing to avoid deterioration of cellular response. In a large screening campaign, longevity of the cell suspension should be determined from the concentration-response curves.
- Compounds dissolved in DMSO can be pre-dotted into assay plates in sub-microliter volume using an acoustic dispenser, such as Labcyte Echo or EDC Biosystems ATS, or pre-diluted in an assay buffer prior to addition. Tolerance of the cellular response to DMSO should be investigated during assay development. Most cells can tolerate up to 1% DMSO in the assay. An example of a DMSO tolerance test is shown in Figure 7.
- Cells and other reagents can be dispensed by various peristaltic pump-based liquid handlers, such as Thermo Combi-drop or the BioTek Washer Dispenser, or any of the widely available tip-based liquid handlers.



Step 5: Cover the assay plate and incubate for 30 minutes at room temperature (RT).

- The duration of assay incubation depends on the kinetic properties of the compounds. Potency values can be underestimated if the incubation is insufficient to achieve steady state conditions.

Step 6: Prepare the cAMP standard curve according to the manufacturer's instructions.

Step 7: Dispense 5 μL/well of diluted d2-labeled cAMP conjugate followed by 5 μL/well of cryptate-labeled anti-cAMP antibody to the cell plate and standard curve plate. Both MultiDrop and Tempest liquid handling instruments are compatible for HTRF reagents.

- d2-labeled cAMP conjugate and cryptate-labeled anti-cAMP antibody are reconstituted per manufacturer's instructions.
- Working solutions are prepared by diluting the concentrated stock 20-fold using lysis buffer provided in the kit.

Step 8: The plates are incubated for 1 hour at RT and read using instruments such as a PerkinElmer Envision with a protocol that is set and optimized for HTRF detection.

- Fluorescence intensity is measured at emission of 665 nm and 615 nm (Em665 and Em615), with excitation at 350 nm.
- Plates can be read repeatedly to ensure that the antibody binding reaches steady state.

Step 9: Convert the results from the reader into cAMP levels using the cAMP standard curve.

- Readings are generally expressed as  $Em665/Em615 \times 10^4$ , but may vary depending on the exact detection instrument being used.

Step 10: Data analysis. See Figure 8.

## G<sub>αs</sub>-Coupled Antagonist Format

In this format, an antagonist displaces an agonist for a G<sub>αs</sub> coupled receptor and the resulting inhibition of adenylate cyclase is measured using the HTRF assays, as shown in Figure 9.

## Sample Protocol for G<sub>αs</sub>-Coupled Antagonist Assays

The procedure for determination of antagonist activity of a G<sub>αs</sub>-coupled receptor using cAMP measurement is essentially the same as the procedure described above for detection of agonist activity. In the antagonist format, an agonist is added at concentrations that trigger 50-80% of the maximum response (EC<sub>50-80</sub>) of the agonist. The rationale and precautions for each step can be referred to in the above agonist assay protocol, except for those specific to antagonist assays. All compounds of interest should also be tested in the agonist mode to ensure the absence of agonist activities.

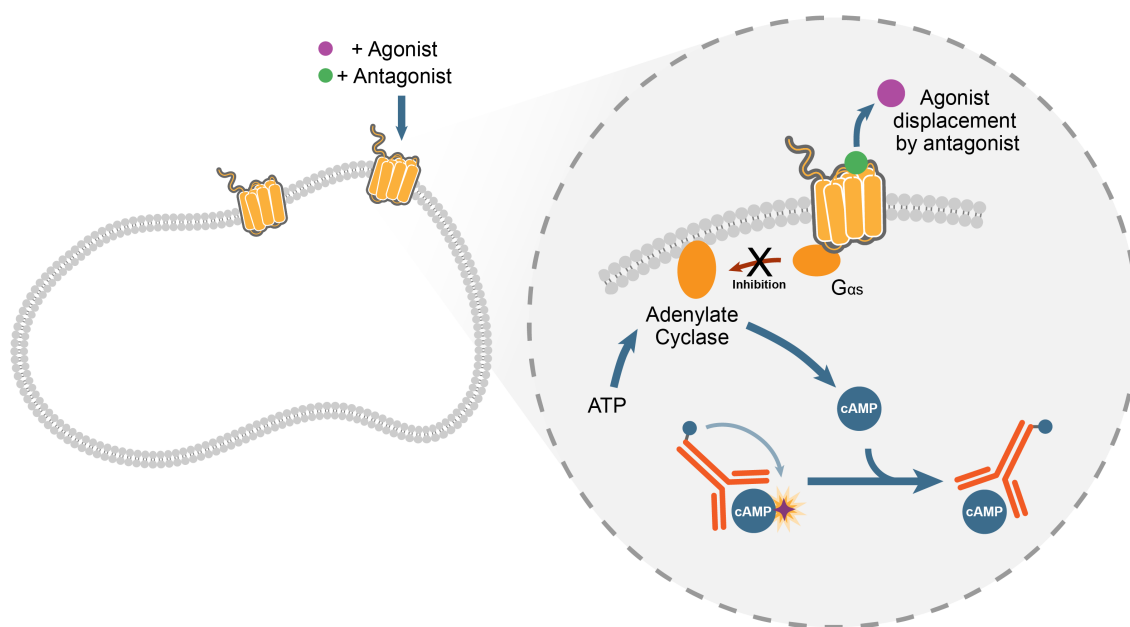


**Figure 9. cAMP Measurement for Antagonists of a G $\alpha_s$ -Coupled Receptor.** An antagonist prevents the activation of the receptor by an agonist which prevents G protein complex dissociation. The adenylate cyclase is not activated and the generation of intracellular cAMP does not occur.

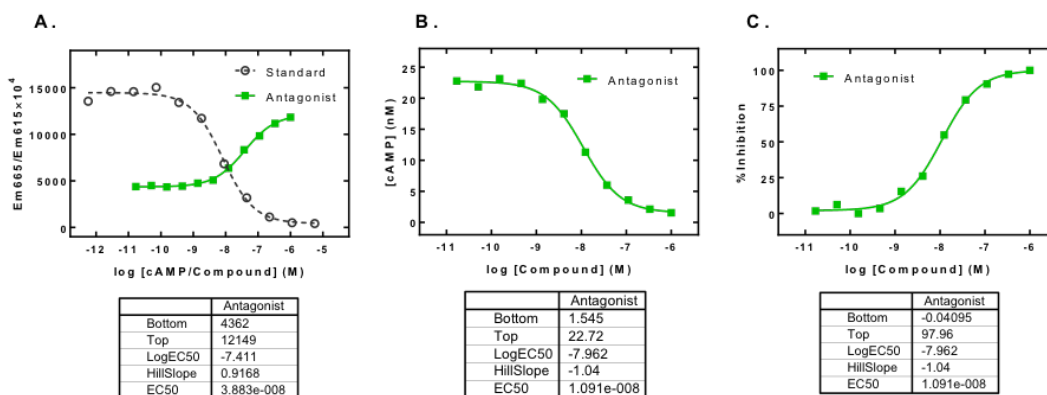


**Figure 10.** An example of antagonist concentration-response curves in G $\alpha_s$ -coupled receptors. Panel A. The antagonist response is plotted as the HTRF ratio ( $Em665/Em615 \times 10^4$ ) along with the cAMP standard curve. Note that the antagonist produces signals that are within the linear portion of the standard curve. Panel B. The antagonist response is plotted as the cAMP level to determine the IC<sub>50</sub> values, respectively. Panel C. The same antagonist response is plotted as % Inhibition. Data are analyzed using four-parameter logistic regression.

Step 1: Grow cells in flask for 1-3 days in the corresponding cell culture medium.

Step 2: Dissociate the cells from the flask and centrifuge at 1000 rpm for 5 minutes.

Step 3: Aspirate the medium and re-suspend the cells in assay buffer. Count and dilute the cells to the desired concentration in assay buffer.

- The working concentration of the cell suspension is twice as much as in agonist mode due to the volume difference. For example, if  $1 \times 10^6$  cell/ml is used in the agonist assay, then  $2 \times 10^6$  cells/ml is prepared for the antagonist assay.

Step 4: Add IBMX, which is generally used at a final concentration of 0.1 mM in the assay, but the impact of phosphodiesterase inhibitor on compound potency and the required concentration should be determined according to the assays and cell lines being used. Dispense 5  $\mu$ L of cells into assay plates that have been pre-dotted with test compound in DMSO or pre-diluted in an assay buffer. (*Note that depending on the extent of activity of phosphodiesterase in the cells, the use of inhibitor is optional.*)

Step 5: Cover the plate and incubate for 15-30 minutes at room temperature (RT).

- Depending on the kinetic properties of test compounds relative to the agonist used for stimulation, this step can be adjusted from no incubation to an extended incubation time as needed.

Step 6: Add 5  $\mu$ L of the agonist solution diluted in assay buffer. Incubate the plates at RT for 30 minutes.

- The final concentration of the agonist chosen should result in 50 to 80% of the maximum response of the agonist, as determined during development of the agonist assay.
- The working concentration is prepared at 2X the desired final concentration.
- At the chosen EC<sub>50-80</sub> concentration of agonist, the measured agonist response should not exceed the linear range of the cAMP standard curve.

Step 7: Prepare the standard curve according to the manufacturer's instructions.

Step 8: Dispense 5  $\mu$ L of diluted d2-labeled cAMP conjugate followed by 5  $\mu$ L of cryptate-labeled anti-cAMP antibody into the cell plate and the standard curve plate.

Step 9: Incubate the plates for 1 hour at RT and measure the signal with a PerkinElmer Envision reader (or equivalent) using a protocol that is optimized for HTRF measurements.

Step 10: Convert the results from the reader into cAMP levels using the cAMP standard curve.

- Readings are generally expressed as  $Em_{665}/Em_{615} \times 10^4$ .

Step 11: Data analysis. See Figure 10.

## cAMP Assays for Receptors Coupled to $G_{\alpha i}$ Protein

The following guidelines are developed for assays carried out using suspension cells for high-throughput mode, although the assay can be adapted easily for adherent cells. Volumes are given for a 384-well assay (20  $\mu$ L assay reactions) and can be adjusted proportionally to other plate density formats.

### $G_{\alpha i}$ -Coupled Agonist Format

In assaying a  $G_{\alpha i}$ -coupled receptor, forskolin is typically used to increase the level of cAMP so that the lowering of the cAMP level due to receptor negative regulation of adenylate cyclase can be observed (Figure 11). Alternatively, the cells can be stimulated to produce cAMP by an agonist to a  $G_{\alpha s}$ -coupled receptor that is also present in the cells.

### Sample Protocol for $G_{\alpha i}$ -Coupled Agonist Assays

Step 1: Grow cells in tissue culture flasks for 1-3 days in the corresponding cell culture medium.

- Select a cell line containing the target GPCR of interest.
- A negative control cell line as a counter screen may either be the parental cell line devoid of the target or a cell line expressing an unrelated GPCR that couples to the same G protein.
- Make sure the cells are healthy and active in the log phase of growth and are maintained in the same way in all experiments, as the state of the cells may affect the receptor response.
- Control cell passage number based on assay performance. Ideally, to avoid variation in cellular response due to changes in the state of the cells or receptor expression, expand the cell culture to the quantities required for the entire screening campaign in one large batch of a single passage and prepare cryopreserved cells as one batch. Various manufacturers of cell culture reagents offer different cryopreservation reagents and methods. During screening, recover the cells and use them as needed.

Step 2: Dissociate the cells from the flask and centrifuge at 1000 rpm for 5 minutes.

- Use of Trypsin or other enzymatic/non-enzymatic cell dissociation agents should be tested prior to screening.
- Some receptor proteins may tolerate trypsinization, but other enzymatic reagents such as TrypLE (Thermo) or non-enzymatic reagents such as CellStripper (Corning) may be used if needed.

Step 3: Aspirate the cell culture medium and re-suspend the cells in assay buffer. Count and dilute the cells to the proper densities in assay buffer.

- In most cases, HBSS or Dulbecco's PBS (DPBS) buffers can be used: 1X HBSS/20mM HEPES with or without 0.1% BSA (fat acid-free) or DPBS with  $Ca^{2+}/Mg^{2+}$  with or without 0.1% BSA.

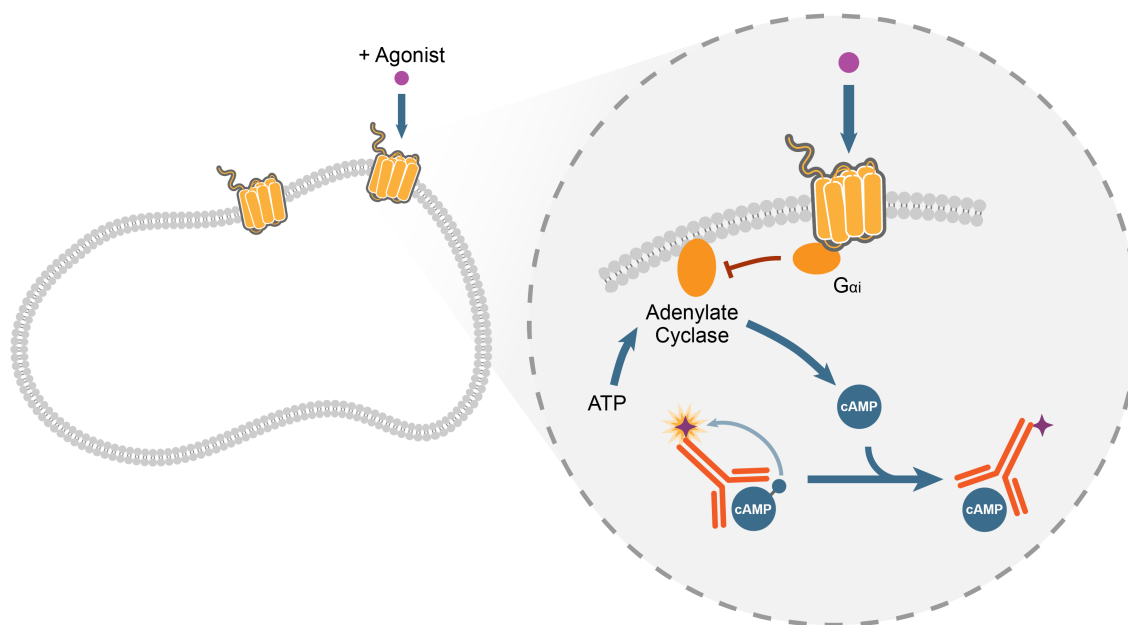


**Figure 11. cAMP Measurement for Agonists of a G<sub>αi</sub>-Coupled Receptor.** Treatment of cells with forskolin results in an increase in cellular cAMP levels. The addition of an agonist decouples the G protein complex that subsequently dissociates into a G<sub>βγ</sub> dimer and a G<sub>αi</sub> monomer. The activated G<sub>αi</sub> subunit binds to adenylate cyclase resulting in the negative regulation of intracellular cAMP (no intracellular cAMP is generated).

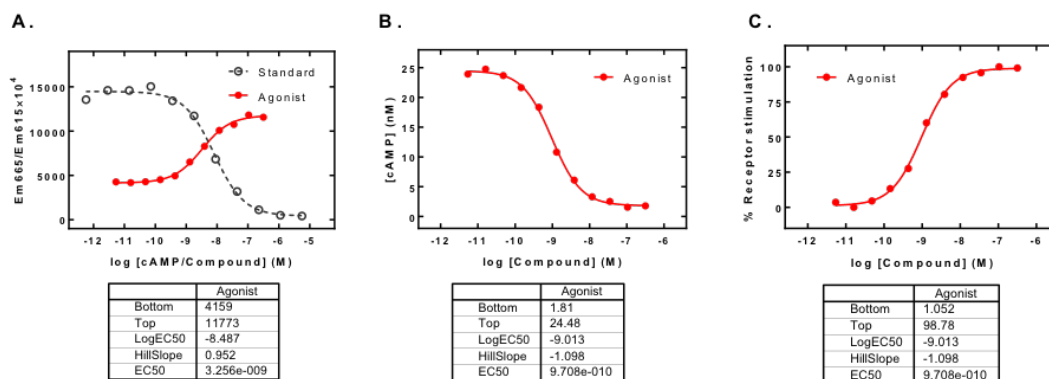


**Figure 12.** An example of agonist concentration-response curves in G<sub>αi</sub>-coupled receptors. Panel A. The agonist response is plotted as the HTRF ratio ( $Em665/Em615 \times 10^4$ ) along with the cAMP standard curve. Note that the agonist produces signals that are within the linear portion of the standard curve. Panel B. The agonist response is plotted as the cAMP level to determine the IC<sub>50</sub> values, respectively. Panel C. The same agonist response is plotted as % Inhibition. Data are analyzed using a four-parameter logistic regression.

- Cell densities should be determined during assay development in cell titration experiments such that the measured signal falls within the linear range of the cAMP standard curve while yielding the best assay window.
- Using too many cells, and hence the presence of too many receptors, may reduce the effective free concentrations of ligands and cause the assay to bottom-out and therefore limit the ability to differentiate potent compounds. Too many cells may also saturate the cAMP assay reagents.

Step 4: Prepare a solution containing the desired amount of forskolin (to stimulate cAMP production so that the inhibitory effect of agonist on the cAMP level can be detected.) Add IBMX, generally at a final concentration of 0.1 mM, or other phosphodiesterase inhibitor and dispense 5  $\mu$ L of the mixture into assay plates pre-dotted with compounds, followed by dispensing 5  $\mu$ L of cell suspension. *(Depending on the extent of activity of phosphodiesterase in the cells, the use of an inhibitor is optional. The impact of a phosphodiesterase inhibitor on compound potency and the required concentration should be determined according to the assays and cell lines being used.)*

- Forskolin can be prepared as a 10 mM stock in DMSO in a glass vial and kept at RT.
- The concentration of forskolin to be used in the assay should be optimized to ensure that the measured signal falls within the linear range of the cAMP standard curve while yielding the best assay window. Cell density and forskolin concentration can be optimized simultaneously by a three-way titration that includes cells and forskolin at different concentrations in the absence and presence of a reference agonist.
- IBMX can be made at high concentration (0.5 M), aliquoted and stored at  $-20^{\circ}\text{C}$  to avoid multiple freeze-thaw cycles.
- Different assay plates may be tested. Please refer to the Cisbio website for microplate recommendations (<http://www.cisbio.com/usa/drug-discovery/htrf-microplate-recommendations>).
- The cell suspension is best prepared only when it is ready for dispensing to avoid deterioration of cellular response. In a large screening campaign, longevity of the cell suspension should be determined from the concentration-response curves.
- Compounds dissolved in DMSO can be pre-dotted into assay plates in sub-microliter volume using an acoustic dispenser, such as Labcyte Echo or EDC Biosystem ATS, or pre-diluted in an assay buffer prior to addition. Tolerance of the cellular response to DMSO should be investigated during assay development. We found that most cells can tolerate up to 1% DMSO in the assay.

Step 5: Cover the assay plate and incubate for 30 minutes at room temperature (RT).

- The duration of assay incubation depends on the kinetic properties of the compounds. Potency values can be underestimated if the incubation is insufficient to achieve equilibrium.

Step 6: Prepare the cAMP standard curve according to the manufacturer's instructions.

Step 7: Dispense 5 μL/well of diluted d2-labeled cAMP conjugate followed by 5 μL/well of cryptate-labeled anti-cAMP antibody to the cell plate and cAMP standard curve plate.

- d2-labeled cAMP conjugate and cryptate-labeled anti-cAMP antibody are reconstituted per manufacturer's instructions.
- Working solutions are prepared by diluting the concentrated stock 20-fold using lysis buffer provided in the kit.

Step 8: The plates are incubated for about 1 hour at RT and read using an instrument such as the PerkinElmer Envision with a protocol that is set and optimized for HTRF detection.

- Fluorescence intensity is measured at Em665 and Em615, with excitation at 350 nm.
- Plates can be read repeatedly to ensure that the antibody binding reaches steady state.

Step 9: Convert the results from the reader into cAMP levels using the cAMP standard curve.

- Readings are generally expressed as  $Em665/Em615 \times 10^4$ .

Step 10: Data analysis. See Figure 12.

## G<sub>αi</sub>-Coupled Antagonist Format

In this format, an antagonist displaces an agonist for a G<sub>αi</sub> coupled receptor and the resulting inhibition of adenylate cyclase is measured using the HTRF assays, as shown in Figure 13.

## Sample Protocol for G<sub>αi</sub>-Coupled Antagonist Assays

The procedure for determination of antagonist activity of a G<sub>αi</sub>-coupled receptor using cAMP measurement is essentially the same as the procedure described above for detection of agonist activity. In the antagonist format, an agonist is added at concentrations that trigger 50-80% of the maximum response (EC<sub>50-80</sub>) of the agonist. The rationale and precautions for each step can be referred to in the above agonist assay protocol, except for those specific to antagonist assays. All compounds of interest should also be tested in the agonist mode to ensure the absence of agonist activities.

Step 1: Grow cells in flask for 1-3 days in the corresponding cell culture medium.

Step 2: Dissociate the cells from the flask and centrifuge at 1000 rpm for 5 minutes.

Step 3: Aspirate the medium and re-suspend the cells in assay buffer. Count and dilute the cells to the desired concentration in assay buffer. Dispense 5 μL of cells into assay plates that have been pre-dotted with compounds in DMSO or pre-diluted in an assay buffer. Incubate the plate at RT for 15-30 minutes.

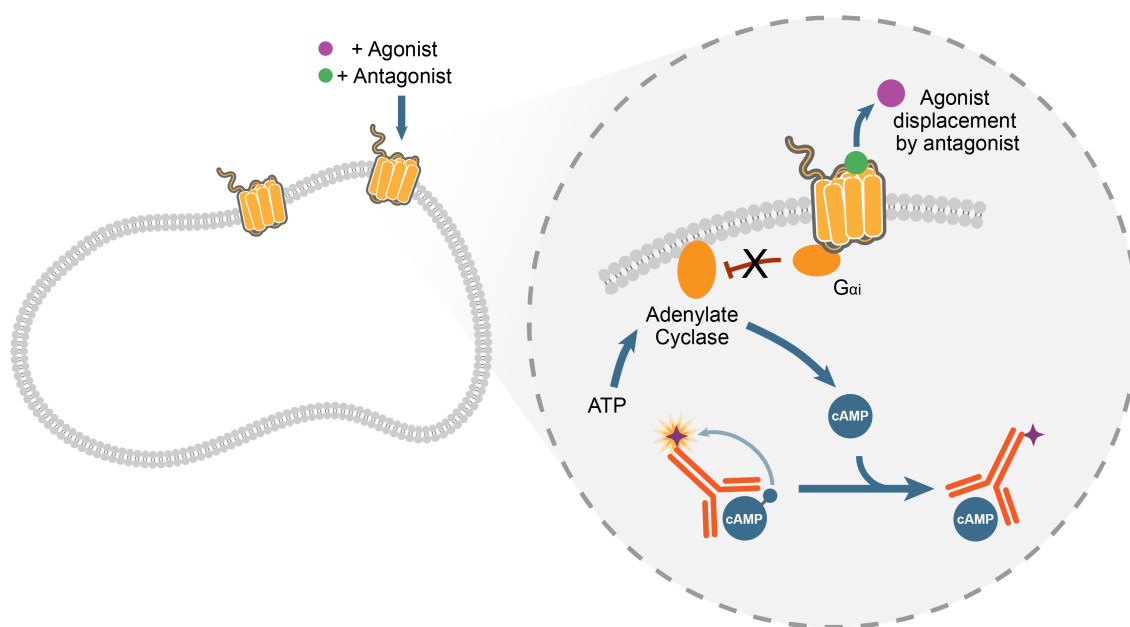


**Figure 13. cAMP Measurement for Antagonists of a G<sub>αi</sub>-Coupled Receptor.** Treatment of cells with forskolin results in an increase in cellular cAMP levels. The addition of an agonist decouples the G protein complex that subsequently dissociates into a G<sub>βγ</sub> dimer and a G<sub>αi</sub> monomer. The activated G<sub>αi</sub> subunit binds to adenylate cyclase resulting in the negative regulation of intracellular cAMP (no intracellular cAMP is generated). The presence an antagonist causes the release of the cAMP inhibition through competition between the antagonist and the agonist. Consequently, the level of cAMP level increases.

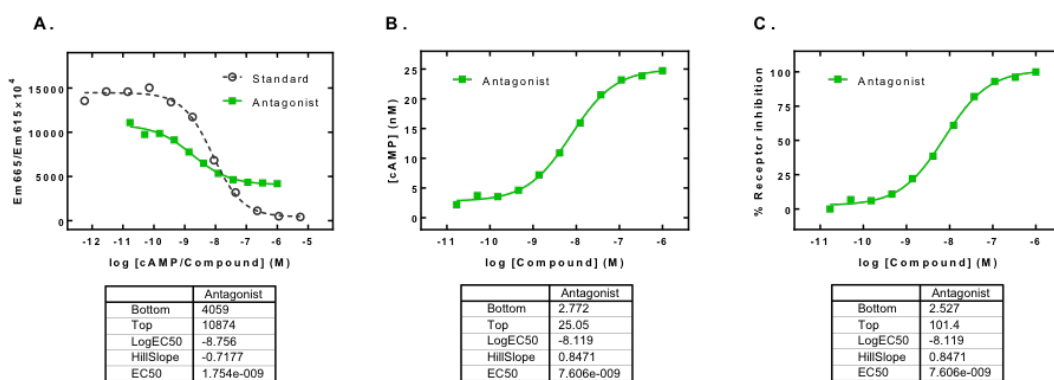


**Figure 14.** Examples of agonist and antagonist concentration-response curves in G<sub>αi</sub>-coupled receptors. Panel A. The agonist and antagonist responses are plotted as the HTRF ratio (Em665/Em615×10<sup>4</sup>) along with the cAMP standard curve. Note that both types of response produce signals that are within the linear portion of the standard curve. Panel B. The agonist and antagonist responses are plotted as the cAMP level to determine the EC<sub>50</sub> and IC<sub>50</sub> values, respectively. Data are analyzed using four-parameter logistic regression.



- Depending on the kinetic properties of the test compounds relative to the agonist used for stimulation, this step can be adjusted from no incubation to an extended incubation time as needed.

Step 4: Prepare a solution containing the desired concentration of forskolin, IBMX (generally at a final concentration of 0.1 mM) and agonist, and dispense 5 μL of the mixture into the assay plates pre-dotted with compounds. (*Depending on the extent of activity of phosphodiesterase in the cells, the use of inhibitor is optional. The impact of phosphodiesterase inhibitor on compound potency and the required concentration should be determined according to the assays and cell lines being used.*)

- The final concentration of the agonist chosen should result in 50 to 80% of the maximum response of the agonist, as determined during development of the agonist assay.
- The working concentration of forskolin, IBMX and agonist solution mixture is prepared at 2X the desired final assay concentration.
- At the chosen EC<sub>50-80</sub> concentration of agonist, the measured agonist response should not exceed the linear range of the cAMP standard curve.

Step 5: Cover the plate and incubate for 30 minutes at room temperature (RT).

Step 6: Prepare the standard curve according to the manufacturer's instructions.

Step 7: Dispense 5 μL diluted d2-labeled cAMP conjugate followed by 5 μL of cryptate-labeled anti-cAMP antibody into the cell plate and the standard curve plate.

Step 8: Incubate the plates for 1 hour at RT and measure the signal with a PerkinElmer Envision using a protocol that is optimized for HTRF detection.

Step 9: Convert the results from the reader into cAMP levels using the cAMP standard curve.

- Readings are generally expressed as  $Em_{665}/Em_{615} \times 10^4$ .

Step 10: Data analysis. See Figure 14.

## Acknowledgements

The authors would like to thank Nathan Cheadle, Jie Pan and Melissa Yarde for the review of this guidance.

## References

1. Cox KL, Devanarayan V, Kriauciunas A, Manetta J, Montrose C, Sittampalam S. Immunoassay Methods. In: Sittampalam GS, Coussens NP, Brimacombe K, Grossman A, Arkin M, Auld D, et al., editors. Assay Guidance Manual. Bethesda (MD)2004.
2. Available from: [https://en.wikipedia.org/wiki/Stokes\\_shift](https://en.wikipedia.org/wiki/Stokes_shift).

3. Iversen PW, Beck B, Chen YF, Dere W, Devanarayan V, Eastwood BJ, et al. HTS Assay Validation. In: Sittampalam GS, Coussens NP, Brimacombe K, Grossman A, Arkin M, Auld D, et al., editors. Assay Guidance Manual. Bethesda (MD)2004.
4. Beck B, Chen YF, Dere W, Devanarayan V, Eastwood BJ, Farmen MW, et al. Assay Operations for SAR Support. In: Sittampalam GS, Coussens NP, Brimacombe K, Grossman A, Arkin M, Auld D, et al., editors. Assay Guidance Manual. Bethesda (MD)2004.
5. Hill SJ, Williams C, May LT. Insights into GPCR pharmacology from the measurement of changes in intracellular cyclic AMP; advantages and pitfalls of differing methodologies. *British journal of pharmacology*. 2010;161(6):1266–75. PubMed PMID: 21049583.
6. Zhang JH, Chung TD, Oldenburg KR. A Simple Statistical Parameter for Use in Evaluation and Validation of High Throughput Screening Assays. *J Biomol Screen*. 1999;4(2):67–73. PubMed PMID: 10838414.
7. Burford NT, Watson J, Alt A. Standard Curves Are Necessary to Determine Pharmacological Properties for Ligands in Functional Assays Using Competition Binding Technologies. *Assay and Drug Development Technologies*. 2017;15(7):320–329. PubMed PMID: 29120673.

# Measurement of $\beta$ -Arrestin Recruitment for GPCR Targets

Tao Wang,<sup>1</sup> Zhuyin Li,<sup>1</sup> Mary Ellen Cvijic,<sup>1</sup> Carol Krause,<sup>1</sup> Litao Zhang,<sup>1</sup> and Chi Shing Sum<sup>1</sup>

Created: November 20, 2017.

## Introduction

$\beta$ -Arrestins are ubiquitously expressed in all cell types, and function in the desensitization of G-protein coupled receptors (GPCRs), the control of GPCR intracellular trafficking, and the activation of GPCRs to multiple signaling pathways (1-4). Therefore,  $\beta$ -arrestin-mediated signaling constitutes an important part of GPCR signaling in addition to G protein-mediated signaling. As many GPCRs are found to recruit  $\beta$ -arrestin, the  $\beta$ -arrestin recruitment assay has found important use in drug discovery, especially in the discovery of ligands for orphan GPCRs and in situations where the second messenger signaling is unknown (5,6). Furthermore, the discovery of biased GPCR ligands and the findings that distinct G-proteins versus  $\beta$ -arrestin signaling preferences may offer therapeutic advantages over conventional ligands imply that a screening campaign should be designed to focus on the most disease relevant pathways (7-10). In this aspect, the  $\beta$ -arrestin recruitment assay has added an important piece to the repertoire of assay tools in drug discovery.

There are four major *in vitro* assay technologies available on the market that are capable of measuring ligand-induced  $\beta$ -arrestin recruitment: PathHunter  $\beta$ -arrestin Assay (DiscoverX) (11), Tango GPCR Assay (Thermo Fisher Scientific) (12), LinkLight GPCR/ $\beta$ -arrestin Signaling Pathway Assay (BioInvenu) (13), and Transflour Assay (Molecular Devices) (14). The PathHunter  $\beta$ -arrestin Assay, Tango GPCR Assay System and LinkLight GPCR/ $\beta$ -arrestin Signaling Pathway Assays are homogenous, high throughput assays while the Transflour Assay is a fluorescence image-based assay. All four assays involve the expression of the  $\beta$ -arrestin as a fusion protein with another protein or fragment, while the PathHunter, Tango and LinkLight assays require fusion of the GPCR to another peptide or protein moiety as well. Table 1 compares the principles of these technologies as well as their advantages and limitations.

This guideline uses PathHunter  $\beta$ -arrestin from DiscoverX to illustrate the concepts for performing GPCR  $\beta$ -arrestin recruitment assay. The principle behind this guideline can be applied to all the  $\beta$ -arrestin assay technologies.

---

<sup>1</sup> Bristol-Myers Squibb Company, NJ.

**Table 1.** Comparison of various  $\beta$ -arrestin assay technologies as well as their advantages and limitations.

| Technologies                                | Vendor                   | Principles  | Advantages   | Limitations  |
|---|--------------------------|---|--|--|
| PathHunter $\beta$ -arrestin Assay          | DiscoverX                | A $\beta$ -galactosidase enzyme fragment complementation technology-based assay. $\beta$ -Arrestin recruitment brings about reconstitution of an active $\beta$ -galactosidase, which is split into a PK fragment fused to the GPCR and an enzyme acceptor protein fused to the $\beta$ -arrestin. The active enzyme catalyzes a chemiluminescence reaction from an exogenous substrate to generate a chemiluminescence readout.  | <ul style="list-style-type: none"> <li>• Signal is specific to the GPCR of interest tagged to the PK fragment off-target signal is minimized.</li> <li>• High signal-to-background from chemiluminescence readout.</li> </ul>                      | <ul style="list-style-type: none"> <li>• Requires construction of fusion proteins for both the GPCR and <math>\beta</math>-arrestin proprietary detection reagents.</li> </ul>   |
| Tango GPCR Assay                            | Thermo Fisher Scientific | A reporter gene assay that is based on the use of a non-native transcription factor linked to the GPCR via a protease cleavage site. $\beta$ -Arrestin recruitment causes the irreversible cleavage and release of the transcription factor mediated by a protease-tagged $\beta$ -arrestin. The freed transcription factor promotes the expression of a $\beta$ -lactamase reporter, which in turns catalyzes the turnover of an exogenous substrate to generate a fluorescent signal. | <ul style="list-style-type: none"> <li>• Signal is specific to the GPCR of interest tagged to the transcription factor and off-target signal is minimized.</li> <li>• Two color ratiometric FRET readout can reduce experimental noise.</li> </ul> | <ul style="list-style-type: none"> <li>• Requires the construction of fusion proteins for both the GPCR and <math>\beta</math>-arrestin, and a cell line harboring the reporter gene.</li> <li>• Longer assay duration due to the need for expression of the reporter gene.</li> </ul> |
| LinkLight GPCR/ $\beta$ -arrestin Signaling | BioInvenu                | $\beta$ -Arrestin is fused to a permutated luciferase. Recruitment causes the irreversible cleavage of the luciferase mediated by a non-native  | <ul style="list-style-type: none"> <li>• Signal is specific to the GPCR of interest tagged to the transcription factor</li> </ul>  | <ul style="list-style-type: none"> <li>• Requires construction of fusion proteins for</li> </ul>   |

*Table 1. continues on next page...*

Table 1. continued from previous page.

| Technologies     | Vendor            | Principles  | Advantages   | Limitations  |
|------------------|-------------------|---|--|--|
|                  |                   | protease fused to the GPCR. Subsequent refolding of the luciferase into an active enzyme can be detected by an exogenous substrate to generate a chemiluminescence readout. | <p>and off-target signal is minimized.</p> <ul style="list-style-type: none"> <li>Compatible with any existing luciferase substrates.</li> </ul>   | both the GPCR and $\beta$ -arrestin.   |
| Transfluor Assay | Molecular Devices | Recruitment of a GFP-tagged $\beta$ -arrestin and the concomitant intracellular translocation is visualized and quantified by bioimaging method.                            | <ul style="list-style-type: none"> <li>Amenable to studies of the intracellular spatial-temporal relationship of GPCR activation and <math>\beta</math>-arrestin recruitment.</li> </ul> | <ul style="list-style-type: none"> <li>Requires the use of GFP fusion protein of <math>\beta</math>-arrestin.</li> </ul> |

## Flowchart of Assay Development Guidelines

1. Select a GPCR target cell line and a control cell line expression another GPCR, preferably with similar total and background.

- The control cell line allows for detection of off-target activity.

2. Determine agonist dose-response relationships and potency values while optimizing cell density and determining the time course and desired temperature of  $\beta$ -arrestin recruitment

- The three parameters (cell density, temporal profile and temperature) for  $\beta$ -arrestin recruitment can be optimized simultaneously.
- The measured chemiluminescent signals are used to determine the  $EC_{50}$  or  $EC_{80}$  values.
- Since the assay is an end-point assay, multiple reactions need to be set up for all combinations.

3. Determine antagonist dose-response relationships and  $IC_{50}$  values by stimulating with  $EC_{50-80}$  agonist concentration

- The measured chemiluminescent signals are used to determine the  $IC_{50}$  value.

4. Assess assay performance statistics, including  $Z'$ , signal-to-background ratio, reproducibility of potency data

- Ensure  $Z' > 0.5$  and that reproducibility over multiple runs are within acceptable limits

## Overview of the $\beta$ -Arrestin Recruitment Assay

The PathHunter GPCR  $\beta$ -arrestin assay is based on proprietary Enzyme Fragment Complementation technology from DiscoverX. PathHunter  $\beta$ -arrestin GPCR cells are engineered to co-express the ProLink (PK) tagged GPCR and the Enzyme Acceptor (EA) tagged  $\beta$ -arrestin. Activation of the GPCR-PK induces  $\beta$ -arrestin-EA recruitment, facilitating complementation of the two  $\beta$ -galactosidase enzyme fragments (EA and PK). The resulting functional enzyme hydrolyzes the Galacton Star substrate to generate a chemiluminescent signal (Figure 1).

PathHunter  $\beta$ -arrestin GPCR cells can be purchased from DiscoverX (<https://www.discoverx.com>) directly as stable expressing cell lines, or generated using

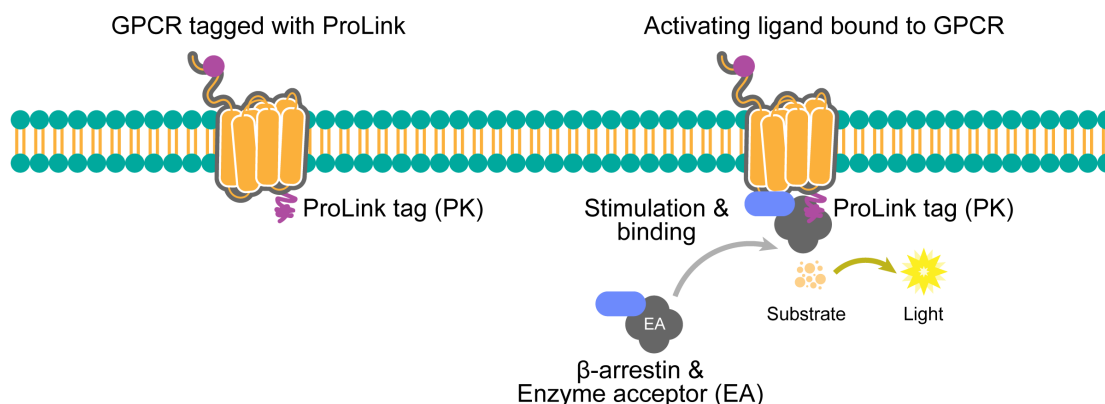


**Figure 1.** The GPCR  $\beta$ -arrestin recruitment assay principle.

PathHunter parental cells engineered to express  $\beta$ -arrestin1 or  $\beta$ -arrestin2-EA fusion protein. Also, retroviral particles are available to generate the parental cells in various cellular backgrounds. Various types of ProLink vectors can be chosen to create the GPCR construct carrying the ProLink (PK) tagged GPCR. Specific detection reagents can be purchased from DiscoverX.

The use of positive and negative controls is important to define the dynamic range of the assays in each plate and monitor the overall assay quality. Inclusion of one or multiple reference compounds for concentration-response analysis is valuable for assessing the incidence of assay drift and robustness. More details can be found in the AGM chapters HTS Assay Validation (15) and Assay Operations for SAR Support (16). As in other assays, performing a counter-screen assay with an unrelated GPCR in the same technology readout is crucial to ensure on-target interaction. The signal may be subject to interference from compounds that inhibit the  $\beta$ -galactosidase enzymatic activity, or those that inhibit the GPCR  $\beta$ -arrestin complex formation.

## Guidelines and Sample Protocol for Agonist Assays

Step 1: Grow cells in tissue culture flasks for 1-3 days in the corresponding cell culture medium.

- Select a DiscoverX PathHunter cell line expressing the tagged GPCR target of interest.
- A negative control cell line as a counter screen may be either the DiscoverX  $\beta$ -arrestin parental cell line devoid of the target or a DiscoverX  $\beta$ -arrestin cell line expressing an unrelated GPCR.
- Make sure the cells are healthy and active in the log phase of growth and are maintained the same way in all experiments, since the growth state of the cells may affect the receptor response.

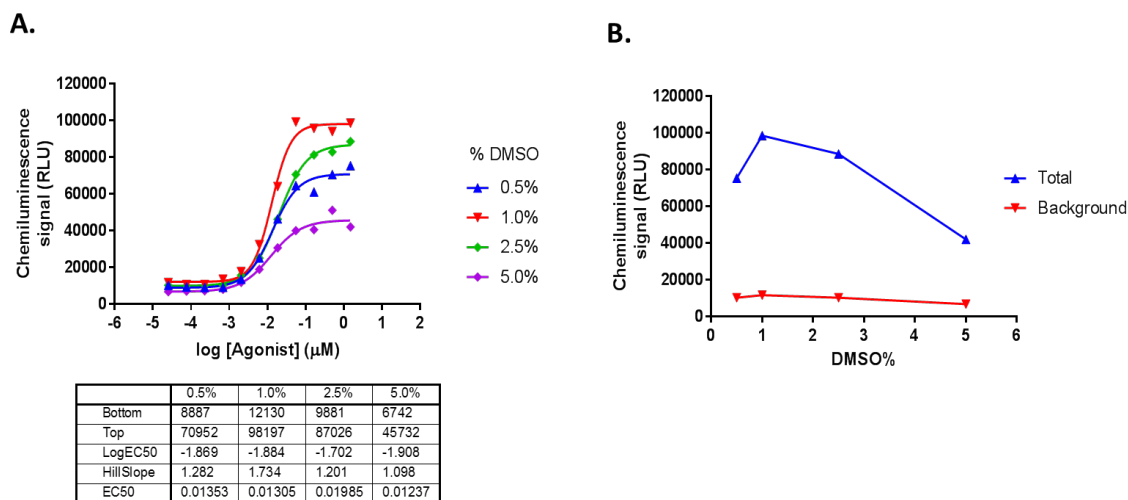


**Figure 2.** DMSO tolerance test. (A) The effect of DMSO on agonist-stimulated response is shown in relationship to the agonist concentration-dependent responses. In this example, DMSO concentrations at 5% or higher reduce the maximal responses by over 50% without affecting the EC<sub>50</sub> values. (B) The effect of DMSO is examined in terms of the effect on total and background signals. The total signal is seen to decline dramatically beyond 2.5% DMSO. Similar analysis can be performed to determine DMSO effects on Z'.

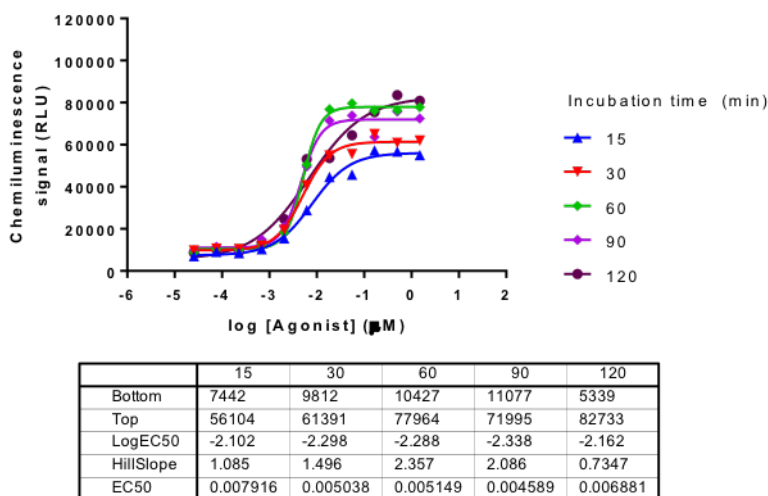


**Figure 3.** Determination of compound incubation time in an agonist assay. A known agonist is used to assess the time it takes to achieve steady-state cellular response by incubating the agonist for increasing periods of time. In this example, the maximal response elicited by the agonist is slightly higher upon longer incubation; however, the potency remains largely the same. If available, agonists with different potencies may be used to assess the kinetic behavior of various compounds in order to determine the best timing that yields the expected potency.

- Cell passage number should be tightly controlled based on assay performance statistics. Ideally, to avoid variation in cellular response due to changes in the state

of the cells or level of receptor expression, expand the cell culture to the quantities required for the entire screening campaign in one large batch of a single passage, “assay-ready” cryopreserved cells in appropriate aliquot sizes (17). DiscoverX has a suggested cryopreservation method and cryopreservation reagent for its cell lines outlined in the instruction manual. Other cryopreservation methods and reagents are available from various manufacturers of cell culture reagents. These can be tested as well for suitability to identify a method that provides high viability and receptor functionality. Frozen cell aliquots can be stored for some time and recovered as needed during a screen.

Step 2: Dissociate the cells from the flask and centrifuge at 1000 rpm for 5 minutes to pellet the cells.

- Use of Trypsin or other enzymatic/non-enzymatic cell dissociation agents should be tested prior to screening. Some receptor proteins may tolerate trypsinization, but other enzymatic reagents such as TrypLE (Thermo Fisher) or non-enzymatic reagents such as Cellstripper (Corning) may be used if the system under study does not tolerate treatment with proteases.

Step 3: Aspirate the cell culture medium and re-suspend the cells in cell plating medium. Count and dilute the cells to the proper densities in cell plating medium.

- Cells should be dissociated well enough so that no cell clumps are observed during cell counting. For troublesome cell lines, optimize the dissociation condition and filter the cells through an appropriate strainer (e.g. BD Cell Strainer).
- In most cases, basal medium supplemented with 0.5 to 10% FBS can be used. Sensitivity of the cells and compound activity to serum should be tested.
- Cell densities should be determined during assay development in cell titration experiments. Generally, a range of 5,000–20,000 cells/well will be suitable for 384-well assay.

Step 4: Dispense cells in plating medium into 384-well microplate and incubate the cells overnight at 37°C at 95% O<sub>2</sub>/5% CO<sub>2</sub>.

- Cells and other reagents can be dispensed by various peristaltic pump-based liquid handlers, such as Thermo Combi-drop or the BioTek Washer Dispenser, or any of those widely available tip-based liquid handlers.
- Tissue culture-treated or poly-D-lysine plates may be used depending on the cell type.
- The PathHunter  $\beta$ -arrestin assay may be run as a suspension assay. In that case, the cells diluted in assay buffer can be seeded directly into assay plates and used immediately for assays.

Step 5: Remove plating medium and replace with serum-free or low serum assay medium if needed.



- At this step, cells can be serum-starved for 4-16 hours depending on application. Serum starvation helps minimize basal signaling, which is especially important if agonists for the GPCR target are present in the serum.

Step 6: Dispense test compounds into the plates.

- Compounds dissolved in DMSO can be pre-dotted into assay plates in sub-microliter volume using an acoustic dispenser such as the Labcyte Echo, or pre-diluted in an assay buffer prior to addition.
- Tolerance of the cellular response to DMSO should be tested. Maintaining DMSO concentration under 1% is preferred. An example of DMSO tolerance test is shown in Figure 2.

Step 7: Incubate the cell plates at 37°C for 90 minutes (or other optimized condition).

- GPCR- $\beta$ -arrestin interaction is known to exhibit two distinguishable characteristics, known as Class A and Class B interactions. Class A interaction refers to the formation of transient GPCR- $\beta$ -arrestin complexes which dissociate during receptor trafficking. Class B interaction is more sustained, and the complex co-localizes to subcellular compartments during receptor translocation (18).
- Incubation time of the assay should be optimized for each GPCR. For some GPCRs, the assay can also be performed at room temperature.
- With the PathHunter  $\beta$ -arrestin assay, the PK tag on the engineered GPCR may have some degree of intrinsic affinity for the EA fragment. This may influence the GPCR- $\beta$ -arrestin interaction. A time-course experiment may be performed to assess how this may affect Class A and Class B profiles.

See figure 3 for determination of compound incubation time.

Step 8: Prepare a solution of PathHunter Detection Reagent (1 part Galacton Star, 5 parts Emerald II Solution and 19 parts PathHunter Cell Assay Buffer according to manufacturer's instruction).

- If cells are incubated with compounds at 20  $\mu$ l of volume, then 10  $\mu$ l of detection reagent is needed for each well.
- The detection reagent can be added directly to the compound-treated cells using any of the peristaltic pump-based liquid handlers (e.g., Combi-drop from Thermo Fisher or BioTek Washer Dispenser).
- If compound interference is suspected, a wash step using DPBS with  $\text{Ca}^{2+}/\text{Mg}^{2+}$  can be carried out prior to the addition of detection reagent.

Step 9: Incubate for 60 minutes at room temperature and measure chemiluminescent signal using plate readers such as the PerkinElmer EnVision. The output signal is relative light units (RLU). The absolute RLU scale may vary depending on the detector.

The final cell density, temperature and the selection of optimal time point is based on the Z' and the expected potency (15).

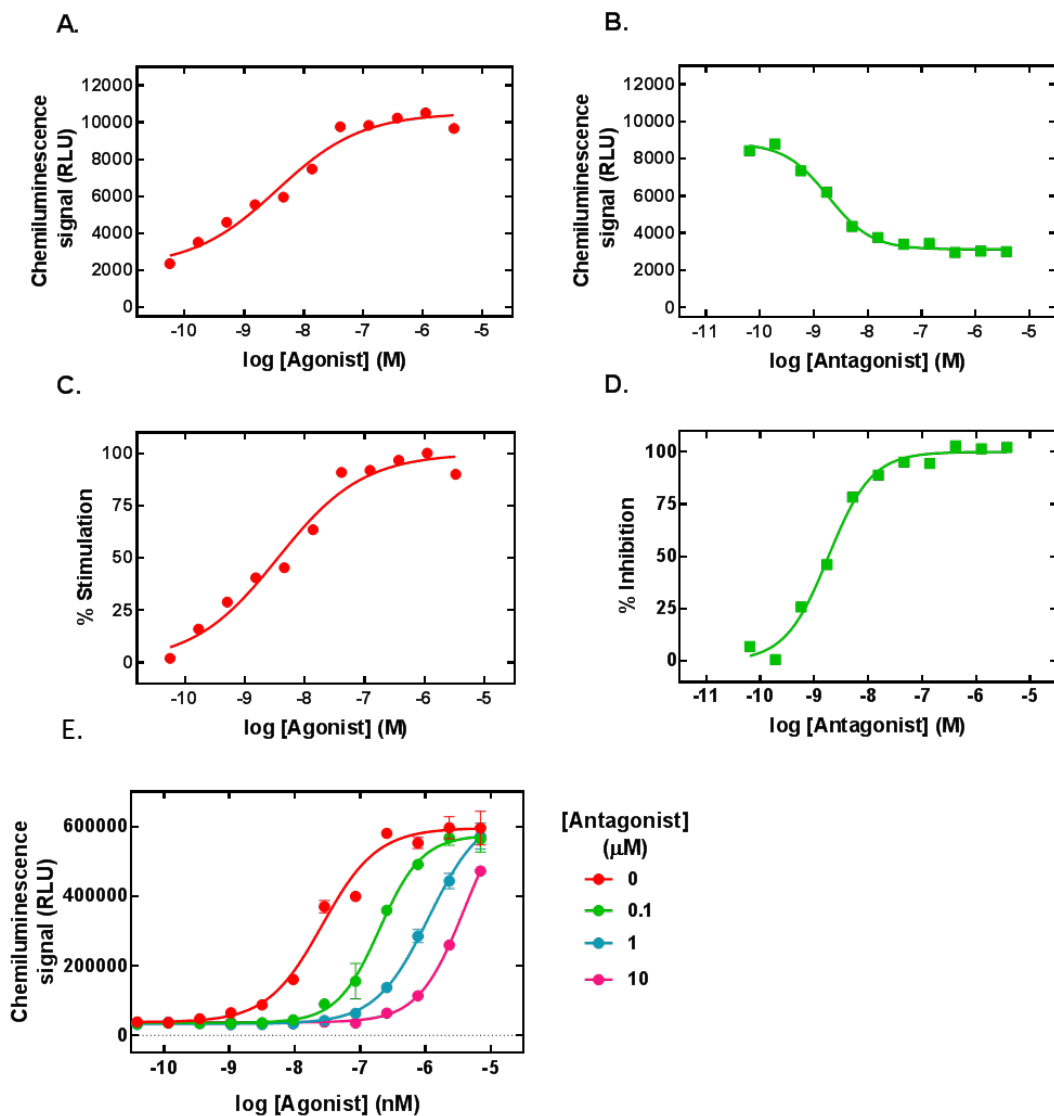


**Figure 4.** Examples of agonist and antagonist concentration-response curves in GPCR-β-arrestin recruitment assays in agonist mode (A, C), antagonist mode (B, D) and Schild dose-shift assay (E). Raw data from chemiluminescence readout are illustrated in Panels A and B, with the normalized data given in Panels C and D. % Stimulation =  $[(\text{RLU signal} - \text{Min RLU}) / (\text{Max RLU} - \text{Min RLU})] \times 100$ . % Inhibition =  $[1 - (\text{RLU signal} - \text{Min RLU}) / (\text{Max RLU} - \text{Min RLU})] \times 100$ . Panel E. Schild dose-shift assay can be performed to assess the surmountability of antagonism and to determine the affinity of the antagonist (19), as implemented in the GraphPad Prism software. Data are analyzed using four-parameter logistic regression.

## Guidelines and Sample Protocol for Antagonist Assays

Prior to setting up an antagonist-characterization assay, the agonist to be used for stimulating the cells during the antagonist mode should be tested to determine the potency. The  $\text{EC}_{50-80}$  of the agonist (determined from a concentration response curve)

can be selected for use in the antagonist assay. The assay procedure is similar to the agonist mode with an additional step for agonist stimulation ( $EC_{50-80}$  value) after incubation of cells with test compounds. All test compounds should also be assessed in the agonist mode to examine any agonist activities.

Step 1: Grow cells in tissue culture flasks for 1-3 days in the corresponding cell culture medium.

- Select a DiscoverX PathHunter cell line expressing the tagged GPCR target of interest.
- A negative control cell line as a counter screen may be either the DiscoverX  $\beta$ -arrestin parental cell line devoid of the target or a DiscoverX  $\beta$ -arrestin cell line expressing an unrelated GPCR.
- Make sure the cells are healthy and active in the log phase of growth and are maintained in the same way in all experiments, as the growth state of the cells may affect the receptor response.
- Cell passage number should be tightly controlled based on assay performance statistics. Ideally, to avoid variation in cellular response due to changes in the state of the cells or level of receptor expression, expand the cell culture to the quantities required for the entire screening campaign in one large batch of a single passage, “assay-ready” cryopreserved cells in appropriate aliquot sizes (17). DiscoverX has a suggested cryopreservation method and cryopreservation reagent for its cell line that is available in the instruction manual. Other cryopreservation methods and reagents are available from various manufacturers of cell culture reagents. These can be tested as well for suitability to identify a method that provides high viability and receptor functionality. Frozen cell aliquots can be stored for some time and recovered as needed during a screen.

Step 2: Dissociate the cells from the flask and centrifuge at 1000 rpm for 5 minutes to pellet the cells.

- Use of Trypsin or other enzymatic/non-enzymatic cell dissociation agents should be tested prior to screening.
- Some receptor proteins may tolerate trypsinization, but other enzymatic reagents such as TrypLE (Thermo Fisher) or non-enzymatic reagent such as Cellstripper (Corning) may be used if needed.

Step 3: Aspirate the cell culture medium and re-suspend the cells in cell plating medium. Count and dilute the cells to the proper densities in cell plating medium.

- Cells should be dissociated well enough so that no cell clumps are observed during cell counting. For troublesome cell lines, optimize the dissociation and filter the cells through an appropriate strainer (e.g. BD Falcon Cell Strainer).
- In most cases, basal medium supplemented with 0.5 to 10% FBS can be used. Sensitivity of the cells and compound activity to serum should be tested.

- Cell densities should be determined during assay development in cell titration experiments. Generally, a range of 5,000–20,000 cells/well will be suitable for 384-well assay.

Step 4: Dispense cells in plating medium into 384-well microplate and incubate the cells overnight at 37°C at 95% O<sub>2</sub>/5% CO<sub>2</sub>.

- Tissue culture-treated or poly-D-lysine plates may be used depending on the cell type.
- The PathHunter  $\beta$ -arrestin assay may be run as a suspension assay. In that case, the cells diluted in assay buffer can be seeded directly into assay plates and used immediately for assays.

Step 5: Remove plating medium and replace with serum-free or low serum assay medium if needed.

- At this step, cells can be serum-starved for 4-16 hours depending on application. Serum starvation helps minimize basal signaling, which is especially important if agonists for the GPCR target are present in the serum.

Step 6: Dispense test compounds into the plates.

- Tolerance of the cellular response to DMSO should be tested. Maintaining DMSO concentration under 1% is preferred.

Step 7: Incubate the cell plates at 37°C for 15-30 minutes (or other optimized condition), then dispense the proper amount of the *EC*<sub>50-80</sub> concentration of agonist.

Step 8: Incubate the cell plate at 37°C (or other optimized condition) for the desired length of time according to the time-course experiment.

- GPCR- $\beta$ -arrestin interaction is known to exhibit two distinguishable characteristics. Class A interaction is transient, and the GPCR-  $\beta$ -arrestin complex may dissociate during receptor trafficking. Class B interaction is more sustained, and the complex co-localizes during receptor translocation (18).
- Appropriate incubation time of the assay can be optimized for each GPCR. For some GPCRs, the assay can also be performed at room temperature.
- With the PathHunter  $\beta$ -arrestin assay, the PK tag on the engineered GPCR may have some degree of intrinsic affinity for the EA fragment. This may influence the GPCR- $\beta$ -arrestin interaction. Tests may be performed to assess how this may affect the Class A and Class B profiles.

Step 9: Prepare a solution of PathHunter Detection Reagent (1 part Galacton Star, 5 parts Emerald II Solution and 19 parts PathHunter Cell Assay Buffer according to manufacturer's specification).

- The detection reagent can be added directly to the compound-treated cells using any of the peristaltic pump-based liquid handlers (e.g., Combidrop from Thermo Fisher or BioTek Washer Dispenser).

- If compound interference is suspected, a wash step using DPBS with  $\text{Ca}^{2+}/\text{Mg}^{2+}$  can be carried out prior to addition of detection reagent.

Step 10: Incubate for 60 minutes at RT and measure chemiluminescent signal using plate readers such as EnVision.

The final cell density, temperature and the selection of optimal time point is based on the Z' and the expected potency (15).

See figure 4 for examples of agonist and antagonist concentration-response curves in GPCR- $\beta$ -arrestin recruitment assays.

An overall guideline of the assay workflow is shown in the following table.

| Assay Step  | Typical Range                        | Instrumentation   |
|---|--------------------------------------|---|
| Grow cells  |                                      | CO <sub>2</sub> incubator   |
| Harvest cells   |                                      | Centrifuge  |
| Plate cells   | 5,000 – 20,000 cells per well (384w) | Combi-drop (Thermo Fisher), BioTek Washer Dispenser, or tip-based liquid handler            |
| Dispense compounds  | 0.1 nM – 10 $\mu$ M                  | Echo, ATS Gen5, or tip-based liquid handler   |
| Incubate cells  | Room temperature or 37°C             | CO <sub>2</sub> incubator   |
| Dispense agonist (for antagonist assay)                     | EC <sub>50</sub> – EC <sub>80</sub>  | Combi-drop (Thermo Fisher), BioTek Washer Dispenser, or tip-based liquid handler            |
| Wash cells with PBS (if compound interference is suspected) |                                      | BioTek Washer, BlueWasher (BlueCatBio), or manually inverted the plate to remove the liquid |
| Stop reaction by addition of lysis and detection reagents   |                                      | Combi-drop (Thermo Fisher), BioTek Washer Dispenser, or tip-based liquid handler            |
| Incubate detection reagents                                 | Room temperature                     |   |
| Measure chemiluminescence                                   |                                      | Envision, or other luminometer  |

## Troubleshooting

Key assay optimization parameters and troubleshooting guidelines are available in Table 2.

**Table 2.** Key assay optimization parameters and troubleshooting guidelines

| Problem   | Possible reason  | Solution  |
|---|--|---|
| Background signal higher than expected          | Presence of endogenous agonist(s) in serum   | Perform serum starvation for different periods of time.   |
|   | Constitutive receptor signaling  | Examine multiple clones of different receptor expression levels.  |
| Agonist-stimulated response low or undetectable | Receptor intrinsically not recruiting $\beta$ -arrestin or the subtype of $\beta$ -arrestin being used | Assess $\beta$ -arrestin recruitment with various subtypes by other methods such as co-immunoprecipitation if feasible.   |
|   | Cells not expressing sufficient quantities of receptor or $\beta$ -arrestin                            | Examine multiple clones of different receptor and $\beta$ -arrestin expression levels.  |
|   | Compound is not efficacious  | Test other compounds known to be efficacious in triggering $\beta$ -arrestin recruitment.   |
|   | Insufficient compound binding to receptors   | Perform time-course and temperature experiments for optimal activity.   |
| Agonist/antagonist potency not as expected      | Insufficient compound binding to receptors   | Perform time-course and temperature experiments for optimal activity.   |
|   | Dynamics of receptor- $\beta$ -arrestin recruitment may be transient                                   | Perform time-course and temperature experiments for optimal $\beta$ -arrestin recruitment.  |
|   | Intrinsic signaling bias   | Confirm signaling bias with an orthologous $\beta$ -arrestin recruitment assay.   |
|   | Influence of $\beta$ -galactosidase activity in detection step   | Perform orthologous $\beta$ -arrestin recruitment assay or counter screen assay with another cell line expressing a GPCR known to recruit $\beta$ -arrestin; incorporate a wash step to remove compounds from cells prior to detection. |

## Acknowledgements

The authors would like to thank Nathan Cheadle, Jie Pan and Melissa Yarde for the review of this guidance.

## References

1. Gurevich EV, Gurevich VV. Arrestins: ubiquitous regulators of cellular signaling pathways. *Genome Biol.* 2006;7(9):236. doi: [10.1186/gb-2006-7-9-236](https://doi.org/10.1186/gb-2006-7-9-236). PubMed PMID: 17020596.

2. Lefkowitz RJ, Shenoy SK. Transduction of receptor signals by beta-arrestins. *Science*. 2005;308(5721):512–7. doi: [10.1126/science.1109237](https://doi.org/10.1126/science.1109237). PubMed PMID: 15845844.
3. Moore CA, Milano SK, Benovic JL. Regulation of receptor trafficking by GRKs and arrestins. *Annu Rev Physiol*. 2007;69:451–82. doi: [10.1146/annurev.physiol.69.022405.154712](https://doi.org/10.1146/annurev.physiol.69.022405.154712). PubMed PMID: 17037978.
4. Tian X, Kang DS, Benovic JL. beta-arrestins and G protein-coupled receptor trafficking. *Handb Exp Pharmacol*. 2014;219:173–86. doi: [10.1007/978-3-642-41199-1\\_9](https://doi.org/10.1007/978-3-642-41199-1_9). PubMed PMID: 24292830.
5. Kroeze WK, Sassano MF, Huang XP, Lansu K, McCorvy JD, Giguere PM, et al. PRESTO-Tango as an open-source resource for interrogation of the druggable human GPCRome. *Nat Struct Mol Biol*. 2015;22(5):362–9. doi: [10.1038/nsmb.3014](https://doi.org/10.1038/nsmb.3014). PubMed PMID: 25895059.
6. Southern C, Cook JM, Neetoo-Isseljee Z, Taylor DL, Kettleborough CA, Merritt A, et al. Screening beta-arrestin recruitment for the identification of natural ligands for orphan G-protein-coupled receptors. *J Biomol Screen*. 2013;18(5):599–609. doi: [10.1177/1087057113475480](https://doi.org/10.1177/1087057113475480). PubMed PMID: 23396314.
7. Rominger DH, Cowan CL, Gowen-MacDonald W, Violin JD. Biased ligands: pathway validation for novel GPCR therapeutics. *Curr Opin Pharmacol*. 2014;16:108–15. doi: [10.1016/j.coph.2014.04.002](https://doi.org/10.1016/j.coph.2014.04.002). PubMed PMID: 24834870.
8. Violin JD, Crombie AL, Soergel DG, Lark MW. Biased ligands at G-protein-coupled receptors: promise and progress. *Trends in pharmacological sciences*. 2014;35(7):308–16. doi: [10.1016/j.tips.2014.04.007](https://doi.org/10.1016/j.tips.2014.04.007). PubMed PMID: 24878326.
9. Kenakin T, Christopoulos A. Signalling bias in new drug discovery: detection, quantification and therapeutic impact. *Nat Rev Drug Discov*. 2013;12(3):205–16. doi: [10.1038/nrd3954](https://doi.org/10.1038/nrd3954). PubMed PMID: 23411724.
10. Luttrell LM, Maudsley S, Bohn LM. Fulfilling the Promise of "Biased" G Protein-Coupled Receptor Agonism. *Molecular pharmacology*. 2015;88(3):579–88. doi: [10.1124/mol.115.099630](https://doi.org/10.1124/mol.115.099630). PubMed PMID: 26134495.
11. Zhao X, Jones A, Olson KR, Peng K, Wehrman T, Park A, et al. A homogeneous enzyme fragment complementation-based beta-arrestin translocation assay for high-throughput screening of G-protein-coupled receptors. *J Biomol Screen*. 2008;13(8):737–47. doi: [10.1177/1087057108321531](https://doi.org/10.1177/1087057108321531). PubMed PMID: 18660457.
12. Barnea G, Strapps W, Herrada G, Berman Y, Ong J, Kloss B, et al. The genetic design of signaling cascades to record receptor activation. *Proc Natl Acad Sci U S A*. 2008;105(1):64–9. doi: [10.1073/pnas.0710487105](https://doi.org/10.1073/pnas.0710487105). PubMed PMID: 18165312.
13. Eishingdrelo H, Cai J, Weissensee P, Sharma P, Tocci MJ, Wright PS. A cell-based protein-protein interaction method using a permuted luciferase reporter. *Curr Chem Genomics*. 2011;5:122–8. doi: [10.2174/1875397301105010122](https://doi.org/10.2174/1875397301105010122). PubMed PMID: 22207892.
14. Oakley RH, Hudson CC, Cruickshank RD, Meyers DM, Payne RE Jr, Rhem SM, et al. The cellular distribution of fluorescently labeled arrestins provides a robust, sensitive, and universal assay for screening G protein-coupled receptors. *Assay Drug Dev Technol*. 2002;1(1 Pt 1):21–30. doi: [10.1089/154065802761001275](https://doi.org/10.1089/154065802761001275). PubMed PMID: 15090153.

15. Iversen PW, Beck B, Chen YF, Dere W, Devanarayan V, Eastwood BJ, et al. HTS Assay Validation. In: Sittampalam GS, Coussens NP, Brimacombe K, Grossman A, Arkin M, Auld D, et al., editors. Assay Guidance Manual. Bethesda (MD)2004.
16. Beck B, Chen YF, Dere W, Devanarayan V, Eastwood BJ, Farmen MW, et al. Assay Operations for SAR Support. In: Sittampalam GS, Coussens NP, Brimacombe K, Grossman A, Arkin M, Auld D, et al., editors. Assay Guidance Manual. Bethesda (MD)2004.
17. Zaman GJ, de Roos JA, Blomenrohr M, van Koppen CJ, Oosterom J. Cryopreserved cells facilitate cell-based drug discovery. *Drug Discov Today*. 2007;12(13-14):521–6. doi: [10.1016/j.drudis.2007.05.008](https://doi.org/10.1016/j.drudis.2007.05.008). PubMed PMID: 17631245.
18. Pierce KL, Lefkowitz RJ. Classical and new roles of beta-arrestins in the regulation of G-protein-coupled receptors. *Nat Rev Neurosci*. 2001;2(10):727–33. doi: [10.1038/35094577](https://doi.org/10.1038/35094577). PubMed PMID: 11584310.
19. Colquhoun D. Why the Schild method is better than Schild realised. *Trends in pharmacological sciences*. 2007;28(12):608–14. doi: [10.1016/j.tips.2007.09.011](https://doi.org/10.1016/j.tips.2007.09.011). PubMed PMID: 18023486.



# Genome Editing Using Engineered Nucleases and Their Use in Genomic Screening

Joana R. Costa, Ph.D.,<sup>1</sup> Bruce E. Bejcek, Ph.D.,<sup>2</sup> James E. McGee, Ph.D.,<sup>3</sup> Adam I. Fogel, Ph.D.,<sup>4</sup> Kyle R. Brimacombe, M.S.,<sup>5</sup> and Robin Ketteler, Ph.D.<sup>✉1</sup>

Created: November 20, 2017.

## Abstract

Understanding gene function is critical for developing therapeutic strategies to target disease. Common approaches to understanding gene function in a systematic and unbiased way include loss-of-function and gain-of-function genomic screening. Some of these rely on artificially increasing the copy number of gene transcripts using cDNA expression libraries. Others interrogate endogenous protein expression through genetic loss-of-function approaches such as siRNA screening. Over the past two decades, targeted approaches that reduce the endogenous expression level of genes or proteins have been developed that facilitate a much better understanding of genes in the context of the living cell. Technologies have been developed that enable precise modification of the genome rather than reduction at the transcript level. These include zinc finger nucleases, TALENs and the CRISPR/Cas9 technology. The use of these systems in large-scale high-throughput screening is an emerging field and we herein highlight recommendations for such applications.

## Introduction

The ability to modify the expression of single genes and proteins has become one of the most important tools in molecular and cellular biology. Several methodologies have been developed to allow for specific gene manipulation in tissue culture cells, which have become colloquially known as “genome-editing”. These rely on nucleases that are engineered to cut specific genomic target sequences, including *Zinc Finger Nucleases* (ZFN), *Transcription Activator-like Effector Nucleases* (TALEN) and *Clustered Regularly Interspaced Short Palindromic Repeats* (CRISPR) nucleases (1). Homing meganucleases have also been used for these purposes but because they have not achieved widespread use they will not be discussed further.

---

<sup>1</sup> MRC Laboratory for Molecular Cell Biology, University College London; Email: j.costa@ucl.ac.uk; Email: r.ketteler@ucl.ac.uk. <sup>2</sup> Western Michigan University; Email: Bruce.bejcek@wmich.edu. <sup>3</sup> Eli Lilly; Email: McGee\_james\_e@lilly.com. <sup>4</sup> Biogen Inc.; Email: adam.fogel@biogen.com. <sup>5</sup> NIH/NCATS; Email: kyle.brimacombe@nih.gov.

✉ Corresponding author.

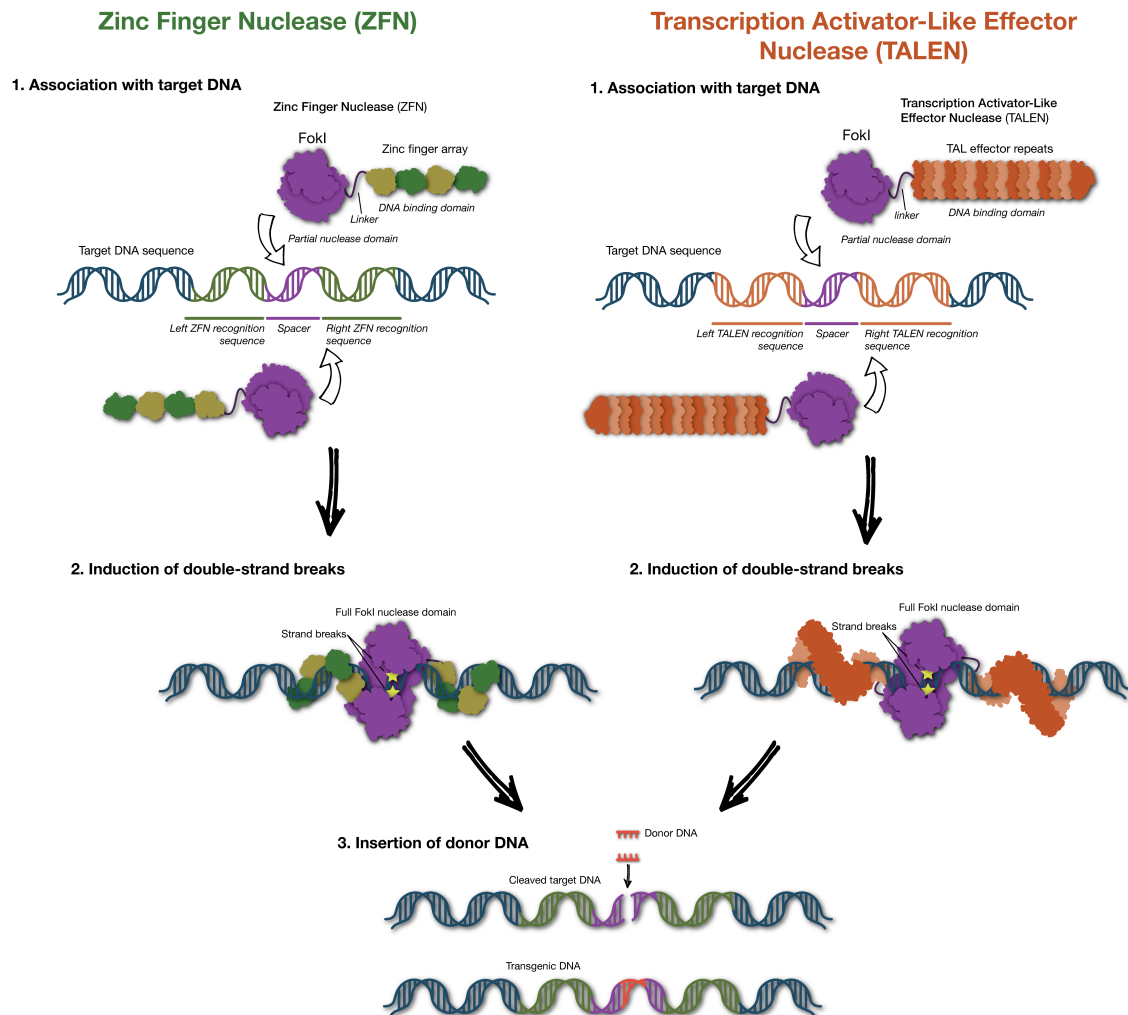


**Figure 1:** Overview of genome editing by zinc finger nucleases (ZFNs) and Transcription Activator-Like Effector Nucleases (TALENs). Zinc finger nucleases are composed of the Fok I endonuclease and an array of zinc finger binding domains that recognize the target DNA sequence. The action of two ZFNs on both strands of the DNA will result in a double strand break. A donor DNA provided in trans can then be integrated at the site of the break, resulting in a transgenic DNA sequence. In the absence of a donor template, the double strand break will be repaired by the host machinery, often resulting in insertions/deletions (indels) that disrupt the open reading frame. For TALENs, the zinc finger array is replaced by TAL effector repeats that guide targeting to the DNA.

The ZFNs, TALENs, and CRISPR/Cas9 (CRISPR associated) enzymes create double stranded breaks in the target DNA sequence which the cell will then repair using one of two pathways (Figure 1, Figure 2). The first of these processes is non-homologous end joining (NHEJ), which occurs without the use of a repair template. NHEJ results in a deletion or insertion (indel), the resulting sequence of which is essentially random and impossible to control. Practically, this pathway is useful in generating loss-of-function (knockout) of the gene of interest. The second pathway is homology-directed repair

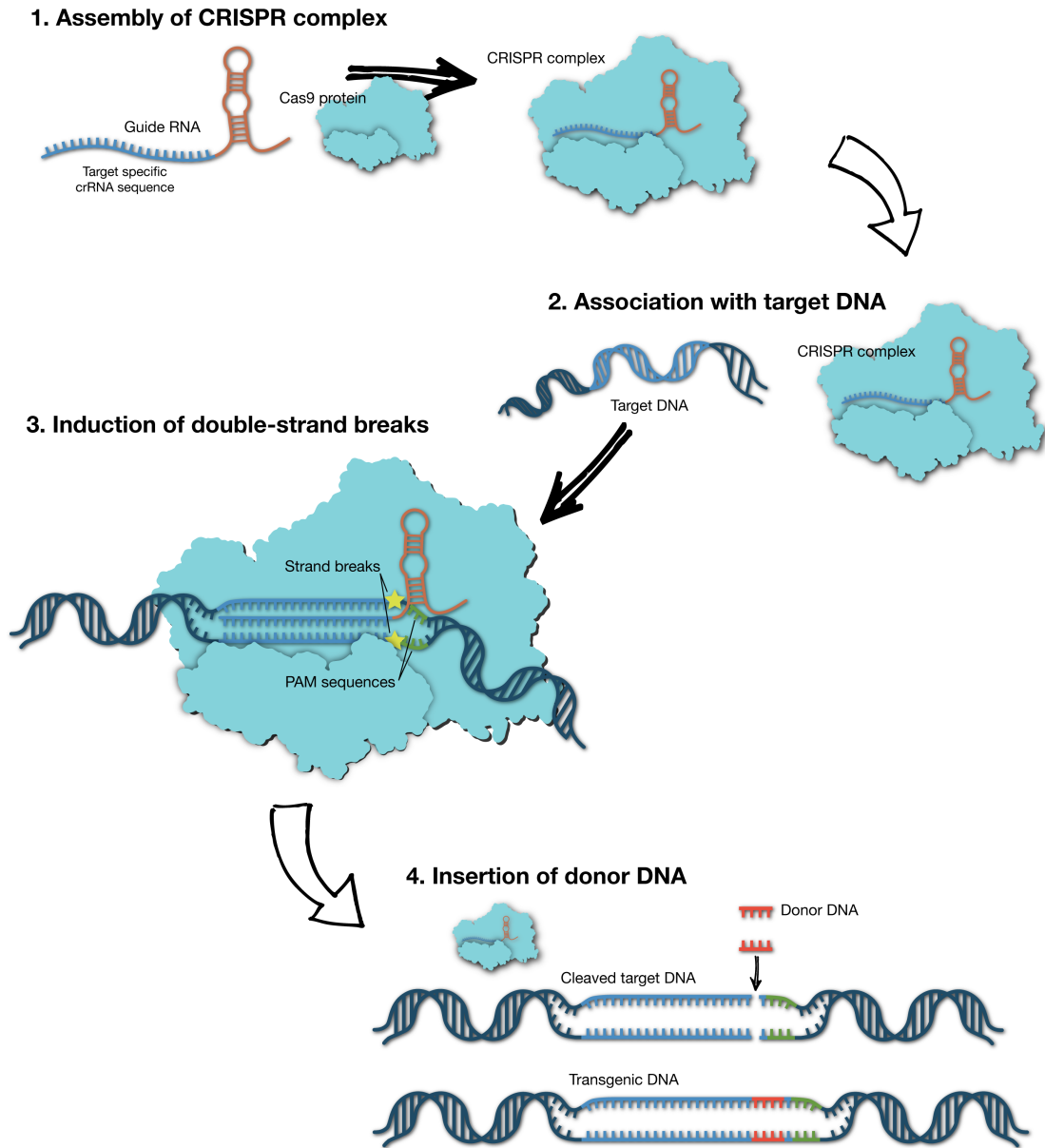


**Figure 2:** Mechanism of CRISPR/Cas9 genome editing. CRISPR/Cas9 genome editing requires a single guide (sg) RNA that directs the Cas9 endonuclease to a specific region of the genomic DNA, resulting in a double strand break. By providing a donor DNA in trans, a transgenic DNA can be created, whereas in the absence of a donor DNA, the double strand break will be repaired by the host cell, resulting in an insertion or deletion, thus potentially disrupting the open reading frame of a gene.

(HDR), which utilizes a repair template that contains homology to the sequences proximal to the DNA break (the endogenous template in cells is the sister chromatid). This pathway allows for precise control of the resulting insertion, but requires additional DNA sequences to be transfected, and is often less efficient than the NHEJ pathway.

In addition to these methods, *recombinant Adeno-Associated Viral vectors* (rAAVs) have been used to modify specific genomic DNA targets as well (2) (reviewed in (3) and (4)). The rAAV methodology for genomic modification does not rely on the activity of an exogenously derived nuclease but relies on the replacement of sequences carried on a rAAV for the endogenous cellular homologue. rAAV methods will not be discussed further in this chapter.

All of these methods can be used in a wide variety of cell types to modify specific DNA sequences. In this chapter, we discuss the general application of different genome editing techniques for cell line generation and the specific use of CRISPR as a scalable platform for genetic screening.

## A. Zinc Finger Nucleases (ZFNs)

Typically, genome editing platforms require two key features: an endonuclease that can cut a target location in the genome; and a sequence-specific adaptor that targets the endonuclease to a specified region on the DNA.

Zinc finger nucleases are chimeric proteins comprised of a DNA binding domain composed of zinc fingers (based on zinc finger transcription factors) and an endonuclease (5) (Figure 1, reviewed in (6)). Zinc fingers are ~30 amino acids that can bind to a limited combination of ~3 nucleotides. By using a combination of different zinc fingers, a unique DNA sequence within the genome can be targeted. Similarly, it was discovered that the *Fok I* type IIS restriction endonuclease had distinct and separable DNA binding and DNA cleavage domains, and the cleavage domain only has activity when there is dimerization (7). Making a chimera of the zinc finger binding domain with the *Fok I* digestion domain resulted in an artificial nuclease with a specificity that can theoretically be tailored to any sequence. When used in whole live cells it has become a powerful tool for the creation of cells that have single, insertion/deletion (indel) mutations in a region of interest in the genome.

The concept of use for zinc finger nucleases is relatively straightforward. Two chimeras are produced. Each chimera recognizes a specific and unique DNA sequence where the two sequences are relatively close to each other. When these chimeras are bound to the DNA they cut the DNA to create a fragment that is released, resulting in the activation of the cellular repair machinery in the form of NHEJ. NHEJ results in indels of various sizes and thus can disrupt open reading frames and result in a nonfunctional protein or a lack of an exon. Alternatively, a fragment of DNA can be also supplied to the cell, resulting in replacement of the sequence between the two cut sites by homologous recombination. The replacement fragment can be a normal or mutant form of the gene that is to be replaced.

There are some drawbacks with this technique:

Cost and time to engineer. ZFNs were the original platform used for genome editing and date back to the 1980s (8). Their use has always been hampered by the need to computationally predict and then iteratively engineer and test for sequence specificity. In

comparison with the modular nature of TALE repeat binding, or the direct Watson-Crick affinity pairing of the CRISPR/Cas system, this makes the ZFNs much slower to develop and much costlier to pursue for a given target. This is the major reason why this technique has fallen out of favor in recent years.

Targeting specificity. Although the sequence that is targeted for digestion may be unique within the genome and the ZFN may have a high affinity for this sequence, off-target binding and cleavage of other DNA sequences can occur and result in undesired genome modification at other sites. For this interaction to result in digestion of DNA that will be repaired by NHEJ both halves of the ZFN must recognize sequences around the target site. Although this probability is small there are known zinc fingers that have off-site digestion patterns that will result in disruption of more than one site. Such off-target activities can be determined by sequencing the entire genome, but this is time consuming and costly. The best way to determine whether off-target activities might be influencing the biology of interest is to create more than one ZFN to digest the DNA at different sites (and presumably different off-target sites). When assessing knockout function, it is also imperative that the phenotype is rescued with a reintroduction of a functional gene in order to demonstrate the phenotype achieved is due to disruption of the gene of interest.

## B. TALENs

TALE-Nucleases (TALENs) are based on the transcription activator-like effector (TALE) proteins from *Xanthomonas* bacterial species (reviewed in (9,10)) that have a DNA binding domain and an effector domain (Figure 1). The DNA binding domain consists of several subdomains of slightly variable length (~34 amino acids) but have a nearly identical amino acid sequence. There is a region at the 12<sup>th</sup> to 13<sup>th</sup> amino acids that is highly variable (the repeat variable dinucleotide, RVD) and known to mediate nucleotide specificity (see Table 1). The combination of these ~34 amino acid regions and the RVD dictate which DNA sequence is bound. Therefore, the engineering of a sequence specific binding domain is more easily accomplished than with ZFNs as this is a more modular approach. It requires only varying the RVD nucleotides and not the rest of the repeat backbone to achieve specificity with reasonable avidity. As with ZFNs, this DNA recognition domain can then be fused with a variety of proteins including the *Fok I* catalytic domain.

Like ZFNs, TALENs can be used to make a site-specific cut in genomic DNA, which results in either indel mutations or allows for replacement specific pieces of DNA if a suitable HDR template is delivered. Since the TALE domains allow for a more highly predictable, modular creation of binding domains, they gained immediate popularity when compared with ZFNs because they obviated the need for expensive and time-consuming engineering. Cloning TALEN constructs could be done in 1-2 weeks and the highly modular nature of the binding domains made binding fidelity much more likely. They have been used in cells from a variety of species both in tissue culture as well as *in vivo*. The advantages of TALENs over ZFNs are increased predictability of binding of the TALE domain to the desired target sequence and cost.

Like ZFNs, TALEN construction requires verification *in vitro* to demonstrate an adequate level of cleavage efficiency before they can be employed in experiments. Due to the modular nature of the TALE repeats, the probability of rationally designing a TALEN that will be specific for a particular sequence appears to be greater than that for ZFNs, however it is not possible to rule out off-target cleavage in a given cell line without extensive testing.

**Table 1.** Nucleotide binding by amino acids of the RVD.

| Amino acids in the repeat variable dinucleotide (RVD) at aa 12 and 13 | Nucleotide(s) recognized |
|---|--------------------------|
| HG  | T, A, C                  |
| NG  | T                        |
| N*  | C, T                     |
| HD  | C                        |
| NN  | G, A                     |
| NS  | A, C, G, T               |
| NI  | A                        |

## C. CRISPR

The identification of clustered regularly interspaced short palindromic repeats (CRISPR) along with the CRISPR associated (Cas) protein is the most recent development and is even more rapid and modular than the TALEN platform. The CRISPR/Cas9 technology is a three-component system consisting of an endonuclease (Cas9), a sequence-specific targeting element (the crRNA), and another RNA that links Cas9 with the crRNA, the tracrRNA (Figure 3) (11). Both crRNA and tracrRNA can be combined in a single molecule termed single guide (sg) RNA (12,13). Since an RNA molecule acts as the guide in this system, and the technology for cloning DNA oligonucleotides has been well developed, this system results in a methodology that is simpler and more rapid to develop than TALENs and ZFNs. CRISPR/Cas9 is now widely used in multiple organisms, both *in vitro* and *in vivo*.

The mechanism of action for the CRISPR/Cas system relies on the expression of at least two components: an effector enzyme and a guide RNA (Figure 2). The effector enzyme most commonly used to date is Cas9 from the type II CRISPR/Cas system from *Streptococcus pyogenes*. Although there are three different types of CRISPR/Cas systems currently known, the type II enzymes are preferable as they are single polypeptides. To be used in this system the CAS9 protein must be expressed and translocated to the nucleus. Several laboratories have created codon-optimized versions with nuclear translocation signal sequences (NLS).

The crRNA recognizes and pairs with a sequence of 20 nucleotides in length within the targeted genome (Figure 3). Targeting relies on sequences at the 3' end of the desired site for digestion. These sequences, known as protospacer adjacent motifs (PAMs), are critical

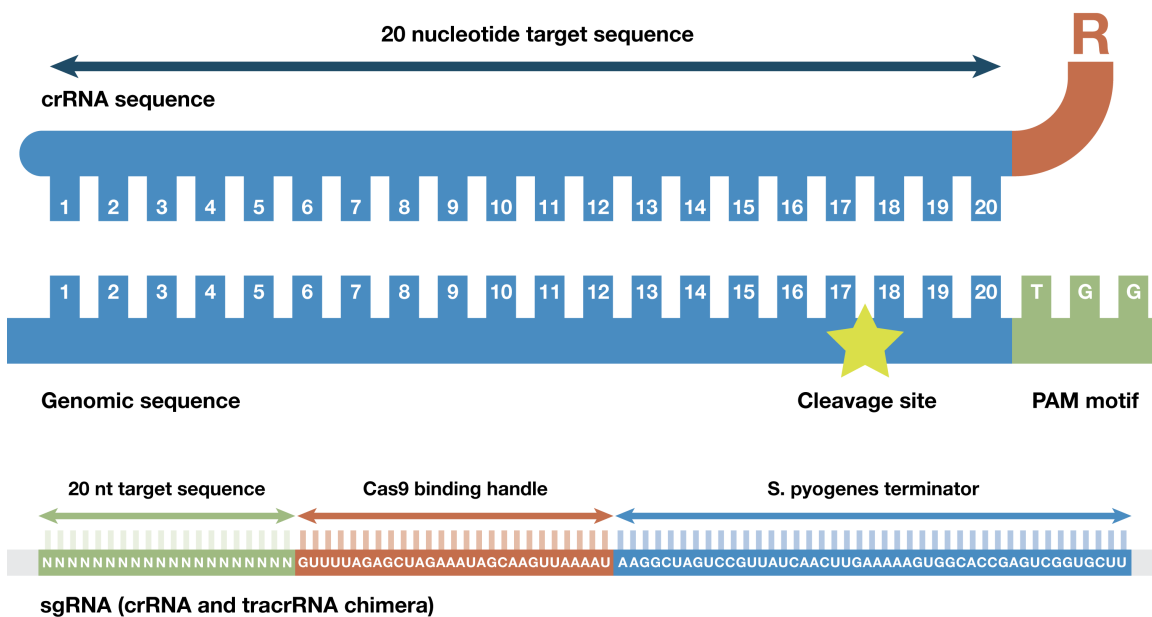


**Figure 3:** Anatomy of a single guide (sg) RNA. The sgRNA is composed of a crRNA sequence that is fused to the tracrRNA. The crRNA contains a 20 nt sequence that is identical to the genomic target DNA sequence. A pre-requisite for binding of the sgRNA to the target site is the presence of a PAM motif following the 20 nt recognition sequence. “R” denotes the remaining part of the sgRNA, consisting of a Cas9 binding handle and the *S. pyogenes* terminator sequence. Cleavage occurs at the -3 position upstream of the PAM motif.

and unique to the CAS9 proteins isolated from different species. Alternative endonucleases such as the type V Cpf1 exist that utilize different PAM motifs for targeting (14), thus expanding the repertoire of potential target sites (see Table 2). While the requirement for a PAM motif in the genome is a major restriction in this technique, it is estimated that every gene harbors multiple sites, allowing disruption of virtually any gene.

One advantage of the CRISPR/Cas9 technology is its great versatility. In effect, the sgRNA directs the endonuclease to a specific site in the genome. By attaching functional domains to Cas9, it is possible to target any functionality to a specific genomic location, including promoter sites and introns. For instance, using a translational fusion of catalytically inactive Cas9 to transcriptional activators, such as multimers of the VP16 peptide, and targeting a promoter region, it is possible to activate gene expression (15). Similarly, systems for gene repression, histone modification and epigenetic alterations have been created (16,17,18). In addition, the system can be used to specifically paint genomic sequences or tag sequence regions with a fluorescent protein or protein tag (19,20). It is also possible to generate an inducible CRISPR/Cas9 system either using classical repressor

systems or small molecule inhibitors of Cas9 (21). The inventiveness of researchers to create novel applications of this technology seems to be infinite.

**Table 2:** Endonucleases with different PAM specificity.

| Name             | Organism   | PAM            | Type | Ref       |
|------------------|--|----------------|------|-----------|
| SpCas9           | <i>Streptococcus pyogenes</i>                    | 5'-NGG-3'      | II   | (11)      |
| SpCas9 VQR       | <i>Streptococcus pyogenes</i>                    | 5'-NGAN-3'     | II   | (105,106) |
| SpCas9 EQR       | <i>Streptococcus pyogenes</i>                    | 5'-NGNG-3'     | II   | (105,106) |
| SpCas9 VRER      | <i>Streptococcus pyogenes</i>                    | 5'-NGCG-3'     | II   | (105,106) |
| SaCas9           | <i>Staphylococcus aureus</i>                     | 5'-NNGRRT-3'   | II   | (105,107) |
| NmCas9           | <i>Neisseria meningitides</i>                    | 5'-NNNNGATT-3' | II   | (108)     |
| St1Cas9          | <i>Streptococcus thermophiles</i>                | 5'-NNAGAAW-3'  | II   | (109)     |
| St3Cas9          | <i>Streptococcus thermophiles</i>                | 5'-NNGGNG-3'   | II   | (109)     |
| BlCas9           | <i>Brevibacillus laterosporus</i>                | 5'-NNNCND-3'   | II   | (110)     |
| AsCpf1<br>LbCpf1 | <i>Acidaminococcus</i><br><i>Lachnospiraceae</i> | 5'-TTTC-3'     | V    | (14)      |
| C2c1             | <i>A. acidoterrestris</i>                        | 5'-TTC-3'      | V    | (111)     |

## Comparison of the Various Genome Editing Technologies

While commercial availability and technical aspects of design, assembly, and delivery are significant criteria when choosing a nuclease, performance is of equal importance. Factors that govern performance are influenced by the model system of choice (cell line, model species, etc.), the efficiency of nucleic acid delivery, and the presence of polymorphisms in the target region. Indeed, there are examples for each of the major genome editing technologies where very high frequency of modification is observed. Targeting efficiencies of 1%-50% have been reported for TALENs and ZFNs (22,23,24) and efficiencies of up to 70% have been reported for CRISPRs (13,25,26).

Despite the growing amount of data using these systems, there are very few examples of side-by-side comparisons, making it difficult to evaluate which system will work most effectively for an unvalidated target gene or sequence. Recently, the efficiency of TALENs was directly compared to that of CRISPR/Cas9. Site-specific editing of an EGFP transgene in mammalian cells showed that CRISPR/Cas9 is more efficient and precise than TALENs in the absence of a homology-repair DNA template. Contrarily, when supplied with a repair template, TALENs performed more efficiently (27).

Another study has focused on the signature of TALENs and ZFNs (insertions vs deletions). TALENs introduced mostly deletions whereas ZFNs introduced both insertions and deletions (28). However, a more systematic comparison of these techniques is required to draw any conclusions.



Very recently, a direct comparison of CRISPR, CRISPR-interference (CRISPRi) and shRNA on gene modulation was established by using a lethality screen (essential genes). Targeting of 46 essential and 47 nonessential genes showed that CRISPR performed better than the shRNA and CRISPRi methodologies as it allowed a better distinction of the two groups of genes. In this experiment, shRNA-mediated knockdown resulted in more noise (29).

A key aspect of genome editing technologies is their potential use in high-throughput screening applications for understanding gene function and drug target identification. While in principle all mentioned genome editing techniques are suitable for production of gene targeting libraries, there are some practicalities that make the use of the CRISPR/Cas9 the primary choice for such applications. In the next section, we will discuss the advantages of CRISPR/Cas9 in this context and its use in screening.

## Screening

Cell-based high-throughput screening in the pharmaceutical industry serves two main purposes: a) the identification of genes underlying phenotypes that correlate with disease (identification of drug targets); and b) the identification of chemical or biological agents that bind to or modulate the activity of such drug targets in cell-based assays (phenotypic screening). Of particular interest in recent years has been high-content screening, due to the ease of use, the potential for multiplexing several readouts, and the high amount of information that can be recorded from relatively simple experiments (30). Nonetheless, enzymatic reporter assays and general viability assays are also very powerful tools even in the age of HCS (31).

Traditionally, modulation of gene expression using genomic libraries has been achieved with siRNA/shRNA libraries (see book-part://[cbrnai]). Although successful in many applications, the use of these libraries presents some challenges. Notably, off-target activities of siRNAs or shRNAs and incomplete knockdown represent major sources of false positives and false negatives, respectively. Nonetheless, the technology has been widely used and been successful for the identification of gene function in multiple organisms. Further, siRNA-based approaches (but also CRISPR/Cas9 activation and repression screens; see below) are preferable when identifying the gene function of essential genes, since in this case complete knockout will obscure any functional readout by disruption of cellular function. The two key reasons why genome editing technologies may overtake the widespread use of siRNA technology in the near future are: 1) *the possibility to create a “clean” knockout of a gene, where residual activity is not present and can be neglected; and 2) the reduced confusion created by off-target activities.*

The use of genome editing technologies in high-throughput approaches has not yet reached the same ease of automation and throughput as other technologies, but protocols are being developed by industry and academic laboratories that will address the current limitations (32).

There is general consensus that the applicability of both TALENs and ZFNs methodologies in screening approaches is more reduced than that of CRISPR. To date, there has been very little use of TALENs, ZFNs and AAV-related techniques for functional genomic screening. This is due to the design complexity and time-consuming generation of TALENs and ZFNs, relative to CRISPR. Nevertheless, an innovative cloning system has recently allowed the generation of a TALEN library comprising TALEN plasmids for 18,740 protein-coding genes (33,34). In a pilot study targeting 126 of those genes, the efficiency was around 90%. Moreover, TALEN-mediated knockout of genes involved in the NF- $\kappa$ B pathway performed better than siRNA knockdown (35). However, no large-scale screens or using TALENs have been published to date. Therefore, we will focus below mainly on the use of CRISPR/Cas9 in screening applications.

The main advantage of the CRISPR/Cas9 technology for screening approaches is that the DNA-targeting molecule is a short RNA. Single guide RNA and crRNA libraries can be produced easily and cost-effectively, thus putting this technology at the forefront of functional genomic screening.

When using genomic libraries to modulate genome sequences such as those mentioned above, two types of screening approaches can be designed: 1. Pooled screening, and 2. Arrayed screening (32). Both have very different requirements in terms of library design, assay design, screen optimization, quality control, hit selection and post-screen validation that is summarized in Table 3 and discussed below.

**Table 3:** Advantages and disadvantages of pooled vs arrayed screening.

|               | Pooled screening   | Arrayed screening  |
|---------------|--|--|
| Advantages    | <ul style="list-style-type: none"> <li>• simple setup</li> <li>• requires no automation and specialized equipment</li> <li>• requires less experimental manipulation</li> <li>• suitable for cell viability/proliferation assays identification of drug resistance genes</li> <li>• comprehensive profiling of genome-wide library</li> <li>• cost-effective</li> </ul>  | <ul style="list-style-type: none"> <li>• easy genotype-phenotype correlation</li> <li>• suitable for high-content screening assays</li> <li>• multi-parametric readouts possible</li> <li>• suitable for primary cells and neurons</li> <li>• custom-made libraries are available</li> </ul>   |
| Disadvantages | <ul style="list-style-type: none"> <li>• requires high cell number</li> <li>• not suitable for primary cells and neurons</li> <li>• not suitable for high-content screening</li> <li>• biosafety considerations for virus libraries</li> <li>• requires a selection step</li> <li>• analysis depends on the availability of next-generation sequencing (NGS)</li> <li>• rare gene transcripts may be more difficult to identify</li> <li>• limited number of readouts</li> </ul> | <ul style="list-style-type: none"> <li>• requires specialized equipment (lab automation)</li> <li>• costly and time-consuming</li> <li>• quality control difficult (internal controls and statistical adjustments may be needed)</li> <li>• genome editing efficiency and transfection efficiency may be low</li> <li>• plate and well variability high</li> </ul> |

## Pooled Library Screening

CRISPR/Cas9 screens can be performed in two different formats (arrayed vs. pooled libraries). Most CRISPR-based screens performed to date utilize pooled libraries. In short, a pooled library is a single preparation of many different sgRNA plasmids. The use of pooled libraries requires a positive or negative selection step, and thus has limited use for high-content screening approaches. However, there is great potential for pooled library screening as the setup is relatively simple and does not require extensive automation and high-throughput screening capabilities. Usual readouts include cell viability and/or proliferation measurements, and the identification of drug resistance genes (36). Several studies reported in the literature comprise investigations in several fields, such as for the identification of cancer tumour suppressor genes (37), viral infection (38), cell cycle regulation and DNA replication. CRISPR/Cas9 screens have been successfully performed not only in mammalian cells but also in *Drosophila* cells (39) and Zebrafish (40). Recently, a resource summarizing all high-throughput CRISPR/Cas9 screens has been published and is frequently updated (41).

In general, pooled lentiviral screening with CRISPR/sgRNA libraries uses several of the same principles as pooled shRNA screening. This is likely the main reason why pooled

screening approaches have been developed very quickly, with essentially all the technology for library production, screening workflow and hit identification already established in key laboratories. Many of these principles can be found in book-part:// [cbrnai] and will not be discussed in detail here. However, there are key differences in terms of library design, assay optimization, hit identification and validation that will be outlined below.

## Library Design

Pooled Libraries consist of a pool of sgRNAs in a lentiviral vector backbone that is used to transfect or transduce in bulk the cell line of interest. Several tools exist for identification of guide RNA target sequences in the genome. The two key features in producing a high-quality library is a) identification of unique target sites in the genome as to limit potential off-target activities; and b) to predict highest efficiency for genome editing. The identification of unique target sites is usually done by a search for PAM motifs combined with a BLAST algorithm (<https://blast.ncbi.nlm.nih.gov/Blast.cgi>) to remove similar regions. Deleterious consequences of off-target activity can be mitigated by strategies described above, and improvements to Cas9-based platforms have been occurring at a rapid pace in the last couple of years resulting in increased fidelity (42,43,44).

The rules for predicting the highest efficiency genome editing sequence targets are not well understood and are lagging behind our understanding of how to select good siRNA molecules. Nonetheless, recent progress has made it clear that there are key determinants that improve design of sgRNA sequence. A recent study has investigated the cleavage activity of sgRNAs on single nucleotide mismatched targets (45). The study found a 4 nucleotide sequence located at +4 to -7 upstream of the PAM motif that can help in the design of gene specific sgRNAs. Another study found nucleotides both at PAM distal and proximal sites to be important for on-target activity (46). Another feature that has been recognized to interfere with genome editing efficiency is PAM density, reasoning that sites harboring multiple PAMs are less amenable to editing (47). Further determinants for improved design have been made (48), suggesting that G is preferred at the -1 and -2 positions proximal to the PAM sequence, a preference for C at the -3 position, a preference for A in positions from -5 to -12 and for G in positions from -14 to -17. However, this prediction is based on a limited set of data and the overall design rules for efficient guide RNAs need to be further investigated.

Several online CRISPR design tools now exist, and these enable the prediction of off-target sites, along with the probability of those events based on the individual sgRNA designs. Some of these are summarized in recent reviews (49,50). A list of online tools and websites for sgRNA design can be found in the appendix.

A very interesting experimental approach to generate sgRNA libraries from any gene without the need for bioinformatics prediction of target sequences has recently been described as an alternative (51). This method relies on the use of a semi-random primer containing a PAM complementary sequence and standard molecular biology tools to

generate a sgRNA library. This method is particularly useful for generating sgRNA libraries for species where limited sequence information is available.

Several companies have developed their own sgRNA design tools, which make it easy to design and order the reagents with a very simple two-click system. Often, the problem is that too many sequences are identified and selection becomes a matter of being spoiled for choice. Given that most sgRNA sequences work reasonably well, it might be best to opt for location in the gene sequence rather than predicted efficiency. For instance, sequences close to the 5'-end of a gene might be favorable, but one should keep in mind that alternative start sites might result in expression of a downstream gene fragment. Also, ribosomal frameshifting (52) and “illegitimate translation” (53) can result in expression of a gene from out-of-frame alleles. An alternative is to target within a functional or catalytic domain. Often, even an in-frame insertion can result in disruption of protein function, as we have observed for the ATG4B protease (Robin Ketteler, unpublished observation).

Currently available libraries are listed in the appendix.

## Assay Optimization

A pooled CRISPR screen typically requires three components: the sgRNA library, Cas9 endonuclease, a cell model of interest and a sequence analyzer for hit identification.

Cells: When choosing the right cell line, the first choice should always be that the most relevant cell type is used to address the specific biological question. However, one might want to consider the ploidy of cells. For instance, in diploid cells, one would need to edit two alleles in order to get a complete loss of function phenotype. In polyploid cells, this might be more complicated. To date there is no evidence that the number of alleles has an effect on genome editing efficiency, although it has been suggested that the efficiency may be lower with increasing number of alleles (54). Another consideration is that 1 in 3 modifications can result in an in-frame indel, thus potentially not leading to a loss of gene function. Identified phenotypes can therefore be a consequence of mosaicism in gene function in a certain cell. Furthermore, interfering with the endogenous DNA repair mechanism may interfere with genome editing efficiencies. All of these caveats will require addressing when validating individual hits from pooled library screening.

Delivery of library: Often, the pooled library is supplied as a glycerol stock where each plasmid needs to be amplified before use. This is a critical step, as during amplification one has to ensure that the representation of each sgRNA is maintained. In a next step, the plasmids will be delivered to producer cells that produce the lentivirus particles for transduction of the target cells. This step is critical and assessment of virus titer is necessary. During transduction of target cells, the key requirement is that each cell receives only one virus on average. This can be best achieved by transducing cells with a mixture of lentiviral particles at a low multiplicity of infection that allows a single integration per cell. On the other hand, one has to ensure that each plasmid is represented in the infected cell population. Therefore, an excess of cells is usually used, at least 100-fold higher than the number of plasmids. This also means that a large portion of cells will

not be transduced. Another consideration in pooled lentiviral screening that affects the number of cells required for hit identification is that each transcript is represented at high enough numbers so that even rare transcripts can be identified. For this reason, the number of cells in the beginning of the screen should be sufficiently high to enable such representation. Typically, 100-200 million cells are transduced and screened.

Delivery of Cas9 endonuclease: The CAS9 endonuclease can be delivered in conjunction with the sgRNA (using the same vector) or provided in trans, either in the form of a stable Cas9 expressing cell line or through transient delivery of the Cas9 gene or protein into cells. Some studies have suggested that the transient delivery of Cas9 protein can be advantageous to reduce off-target effects when compared to a stable Cas9 expressing cell line. However, for practical reasons and to reduce variability between batches, a stable Cas9 cell line is often used.

Selection: In the next step, a positive or negative selection will be applied to allow the identification of sgRNA-mediated editing events that lead to a desired phenotype. In a positive selection screen, a positive selective pressure will eliminate all cells that do not survive the selection (e.g. treatment with puromycin). The few cells that survive can then be sequenced and the underlying sgRNA identified. Positive selection screens are typically very robust, if the selection pressure is very strong. Obviously, the right amount of selective pressure has to be optimized in a first experiment on a control population. In a negative selection screen, most cells will survive. Therefore, one has to perform next-generation sequencing on the starting population, apply selection, and perform another round of next-generation sequencing on the surviving cells. By comparing the results from the initial population with the selected population, one can identify the list of gRNAs that are underrepresented during negative selection. For both, positive and negative selection screens, access to next-generation sequencing platforms is essential. An alternative to positive or negative selection is the use of a fluorescent marker protein and cell sorting.

Pooled library screening is not feasible for cell types that have limited proliferative potential or a limited passage number such as neurons or primary cells. Also, pooled screening is limited for identification of morphological phenotypes, such as those typically observed in high-content screening assays.

## Hit Identification

Pooled screens require a selection step in order to enrich for cells displaying the desired phenotype. Ultimately, this will result in the differential representation of transcripts in the selected cell population that can be identified by next-generation sequencing. The identity of each sgRNA in the final population can be determined by one of two approaches: the sgRNA sequence can be determined by designing primers for PCR amplification that recognize the vector backbone and are flanking the sgRNA, thus effectively directly sequencing the sgRNA. An alternative is to use sgRNA-specific barcodes in the lentiviral vector backbone that are sequenced and then infer the corresponding sgRNA sequence. The advantage of a barcode approach is that probe

sequences can be designed so that optimal hybridization settings can be obtained for each plasmid, resulting in equal PCR amplification and representation of transcripts.

Identification of sequences can be done by microarrays (55) or deep sequencing. Recently, a multiplexed barcoded library approach has been developed that allows hit identification in a high-throughput manner (56). In order to capture underrepresented sgRNAs, it is important to reach a high level of transcript representation, and – as mentioned above – to start with a sufficiently high cell number. There are a few things worth noting:

Sequencing Depth: A key consideration is sequencing depth. It has been estimated that more than  $1 \times 10^7$  reads are required for a complex library. While normalization is usually not required, it is important to assess the representation of each sgRNA in the initial library before selection. Therefore, a cumulative distribution normalized to the total number of reads may help in this. This can also be important for quality control, as deviations from this curve may indicate a loss of diversity in the starting population.

Representation/Reads: After determination of the representation of each sgRNA, it is important to apply statistical measures to determine the significance of the results. Several user-friendly programs have been designed to aid in statistical analysis, including RIGER (57), RSA (58), HitSelect (59) and MaGeCK (60).

Recently, an R package for data analysis and documentation of pooled CRISPR library screens has been developed (caR pools (61)).

## Validation

Post-screen validation of hits from pooled and arrayed library screening use common principles and will be discussed below.

## Arrayed Library Screening

The use of arrayed libraries is still in its early days and only recently have they become available. Arrayed libraries present a broader applicability, allowing direct analysis of image-based phenotypes as well as biochemical readouts based on intensity (colorimetric/fluorescence/luminescence). In this sense, the use of arrayed libraries is more direct. In some cases a selection step for the cells that incurred a genetic modification may be required, whereas for robust biochemical readouts (such as luminescence), this step might be unnecessary. The same is true when the targeting efficiency is very high.

## Library Design

Guide RNA design follows very similar rules for arrayed libraries as for pooled libraries. Tools for identifying target sequences are described above and listed in the appendix. Here, we will only focus on particular requirements for arrayed libraries.

An arrayed library usually consists of guide or crRNAs targeting a single gene within each well in a multi-well microplate format. In some cases, there is more than one sgRNA/crRNA per well, but the key point is that each well contains agents that target the same

single gene. The main advantage is that the gene-function correlation can be much more easily established than by selection of over- or underrepresented sequences in a mixed pool.

Unlike pooled libraries, arrayed libraries can occur in many different formats.

Lentiviral arrayed libraries are available, and these often contain the same vectors and sequences as the corresponding pooled libraries. The use of lentiviral libraries provide an efficient delivery to almost any cell type, but may require a selection step and culture of the cells for extended time (>7 days) before analysis.

Synthetic crRNA libraries: Synthetic libraries of small RNA molecules have been successfully delivered to cells at high efficiency and with similar protocols developed for siRNA oligonucleotides. In this case, high transfection efficiency is essential as there is no ability to select cells. Experiments are on a shorter time frame (within a few days). When using crRNAs, the tracrRNA has to be provided in trans alongside the Cas9 endonuclease.

In vitro transcribed sgRNA libraries: Another format that is being offered, although usually at lower scale due to the cost in manufacturing, is an *in vitro* transcribed sgRNA library. These are being offered as custom libraries and it is unlikely that they will be provided as an off-the-shelf solution for large libraries.

It is worth noting that chemically synthesized crRNAs have been suggested to be more versatile due to the possibility of having incorporated chemical modifications that increase gene editing efficiency (see review (62)). It can be expected that further improvements in this area may result in alternative library design in the future.

The key advantages of arrayed libraries are that the gene-function correlation is much easier to establish, the handling can be automated using standard liquid handlers, and an arrayed format is easily adaptable to high-content screening technologies. Also, it is possible to deliver the Cas9-sgRNA as a ribonucleoprotein complex, which has been suggested to reduce off-target activities (63). A key disadvantage is the cost of arrayed libraries, plus uncertainties associated with the genome editing efficiency, which may be below the detection limit of conventional high-content screening assays (see Table 3).

The libraries currently available are designed to target the whole genome, individual classes of genes (e.g. tumour suppressors, hormone receptors) and specific pathways (e.g. angiogenesis, apoptosis, cell cycle). Additionally, custom-made libraries that match the need of the research community are also available. Resources for pooled and arrayed libraries are listed in the appendix.

## Assay Optimization

An optimal assay is one that delivers the maximum number of reproducible positive hits and a minimum of false negatives. In arrayed CRISPR library screening, very similar measures can be applied as in siRNA or small molecule library based approaches. Thus, the optimization of an assay starts with evaluation of a positive (i.e. exerting the



maximum known phenotypic effect) and a negative (i.e. neutral) control. A good signal-to-noise window is necessary and statistical measures for effect size such as a  $Z'$ -factor can be used to evaluate the reagents (64). One complication in CRISPR based approaches is that penetrance of a phenotype is typically much lower than for siRNA or small molecule screening approaches. For instance, if genome editing efficiency is below 20%, it becomes hard to identify a phenotype in image-based approaches (unless the phenotype is an off-on switch of a fluorescently labeled reporter gene). Assays with a low background noise and a high signal-to-noise window obviously perform better than assays that record morphological changes in organelle structure or number.

The main issue is to ensure that the observed phenotype is indeed linked to the desired mutation or edited locus.

The parameters that will affect this are:

- transfection efficiency (the phenotype should only be observed in cells that have been transfected)
- genome editing efficiency (the phenotype should only be observed in cells that have been successfully edited)
- off-target activity (the phenotype should only be observed in cells that have been edited at the correct location)

Accordingly, controls should be deployed to test each of these steps.

- For transfection/transduction efficiency, one could include a control such as a plasmid encoding for a fluorescent protein that can be easily quantified. Alternatively, a reagent that results in cell death can be used, such as sgRNAs targeting the *Plk1* gene, which is often used as readout for the setup of RNAi screens. As a negative control, one could use a scrambled sgRNA or a sgRNA targeting an exogenous gene such as firefly luciferase or GFP.
- Assessing genome editing efficiency during a screen is often difficult. Ideally, a positive control could be used here, targeting a gene that is known to exert a strong phenotypic effect. Genes often used are *HPRT1*, *TK* or *DHFR*, which can be used as selection markers.
- Off-target activity is most often assessed post-screening, when secondary assays are used to validate hits. However, off-target effects can be potentially reduced by selecting the right library in the beginning, as discussed above.

Depending on the method of delivery, the optimal conditions of transfection/transduction should be determined beforehand. For lentiviral particles, the multiplicity of infection (MOI) that gives the best transduction and genome editing efficiency must be empirically determined. Unlike pooled screens where it is crucial to have one integrant per cell, in arrayed screening it is less important to restrict the number of integrations per cell as all viral particles within one well will target the same gene. Therefore much higher MOIs are typically used. We recommend the use of an MOI of 2-5 for the sgRNA particles.

Assessing genome editing efficiency is usually done for identified hits post-screening. There are possibilities for investigating genome editing in a high-throughput manner, though, and if costs for such methods decrease in the coming years, it is in principle feasible to do this important quality control step while screening. The technologies for assessment of genome editing efficiency will be discussed below in the “validation” section.

## Hit Identification

Hits in arrayed CRISPR library screening can be identified by the commonly used Z score measures that incorporate sample size and deviations from normal distribution to identify genes that enhance or reduce a phenotype. When edge effects might interfere with the assay, a B score can be applied post-screening to normalize for these effects. Often, a simple signal to background calculation is sufficient to identify the strongest phenotypes.

## Validation

For high-throughput screening using genome editing technologies, it is very important to attribute the phenotypic effect to a successfully edited genome modification. There are multiple methods available, from a very simple setup requiring only a PCR instrument to very complex technologies that rely on next-generation sequencing (Table 4).

Accordingly, the cost, but most importantly the potential of each technique is very different and requires careful assessment before choosing the appropriate method.

**Table 4:** Overview of validation methods.

| Method                                      | Cost     | Resolution | High-throughput potential | Equipment              | Comments  |
|---|----------|------------|---------------------------|------------------------|---|
| Sanger sequencing                           | low      | high       | yes                       | Sequencer              | needs sub-cloning, time-consuming; can use deconvolution software |
| Mismatch Cleavage Detection Assay           | low      | low        | no                        | Standard lab equipment | not sensitive, not quantitative                                   |
| Poly-acrylamid gel electrophoresis          | low      | low        | no                        | Standard lab equipment | simple, cheap method, but non-quantitative                        |
| Indel Detection by Amplicon Analysis (IDAA) | moderate | moderate   | yes                       | PCR machine            | simple method with good resolution                                |
| High Resolution Melt analysis (HRM)         | low      | high       | yes                       | RT-PCR machine         | simple, cheap method with high resolution                         |

*Table 4 continues on next page...*

Table 4 continued from previous page.

| Method                     | Cost | Resolution | High-throughput potential | Equipment                   | Comments  |
|----------------------------|------|------------|---------------------------|-----------------------------|---|
| Competitive PCR            | low  | moderate   | yes                       | PCR machine                 | simple and cheap method, but non-quantitative   |
| Digital Droplet PCR        | high | high       | yes                       | Digital Droplet PCR machine | simple method with high resolution, amenable to 96-well format                            |
| Next generation sequencing | high | high       | yes                       | Next generation sequencer   | most comprehensive analysis of genome editing; has potential to detect off-target effects |

### PCR based assays

**Mismatch Cleavage Detection Assay:** Technologies with relatively low throughput include mismatch cleavage assay detection (65) such as the Surveyor assay (Invitrogen) and GeneArt Genomic Cleavage Detection Kit (ThermoFisher) that utilize the properties of an error-prone polymerase for amplification of fragments that harbor mismatch mutations.

**PCR-PAGE:** An alternative is the use of poly-acrylamide gel electrophoresis, where PCR fragments are generated from the genomic region, subjected to denaturation and re-annealing, and analysis of differential patterns of migration by homo- or heteroduplexes (66).

**High Resolution Melting Curve Analysis:** An alternative with higher throughput is high resolution melting (HRM) curve analysis (67). HRM makes use of different melting curve patterns for two individual PCR products and is efficient to detect indels with a resolution close to 1 nucleotide.

**Indel Detection by Amplicon Analysis (IDAA):** Another PCR-based method termed Indel Detection by Amplicon Analysis (IDAA) relies on tri-primer labeling of a PCR product and detection by gel electrophoresis (68).

**Competitive PCR:** A simple and cheap semiquantitative method to identify mutated cells based on competition-based PCR has been developed, where a mixture of three primers with one primer overlapping the Cas9 cleavage site can be used (69).

**Digital Droplet PCR:** Recently, Digital Droplet PCR has been used to detect genome editing events in a high-throughput manner (70). This method is based on partitioning of PCR reactions on single targets into droplets and using a fluorescence-based readout for each individual droplet PCR to visualize changes in the DNA sequence. Quantification of edited and wild-type alleles can be done in the same sample. More recent versions of this

approach have enabled the simultaneous detection of NHEJ and HDR events in a single reaction mixture (71).

### Sequencing based assays

**Sanger Sequencing:** Traditionally, genome editing has been assessed for single genes by sub-cloning the affected locus followed by Sanger sequencing. However, this method is time-consuming and not amenable to large-scale interrogation of genome editing events.

**Next-Generation Sequencing:** One caveat of the PCR based assays is that they only detect that a mutation has occurred but they do not detect the specific sequence alterations exerted by genome editing. Next-generation sequencing technologies can overcome this limitation. For instance, a variant of next generation sequencing, CRISPR Genome Analyzer (CRISPR-GA), can be used to map the specific alterations detected (72). CRISPR-GA provides information on size and location of indels, as well as the efficiency of NHEJ and HDR events. This is a huge advantage in terms of validation, as one could use this to determine if the phenotype corresponds to an edited site. An alternative is BATCH-GE (73), which provides batch analysis features, thus reducing the time required for analysis.

### Additional validation steps

After a cell is identified as carrying the appropriate mutation additional steps are necessary for validation that the phenotype is directly the result of the known mutation and not due to some other effect. This can be done using secondary phenotypic assays which can include one or more of the following:

1. Rescue of the phenotype by expression of an exogenous normal copy of the mutated gene. This can be achieved by transfection or transduction of a plasmid or retrovirus particle, respectively. One caveat is that overexpression may result in a higher copy number, thus not representing the original endogenous levels.
2. Reversion of the genome modification back to wild-type by genome editing. In this approach it is important to include controls to demonstrate that the mutated cell line has been rescued and that the initial unmutated cell line has not been “reisolated” due to contamination. This can be easily accomplished by including insertion of silent mutations into the reversion step.

## Conclusion

In summary, genome editing technologies have greatly advanced over the last decade and provided new insights into the function of genes and proteins. Recently, these technologies have been applied to high-throughput screening applications, with the CRISPR/Cas9 system at the forefront of this development. It can be expected that further improvements to this technology will be made in this fast-moving field and some of the challenges such as delivery and efficiency will be overcome in the not too distant future.

### Acknowledgements

This work was supported by the Medical Research Council, grant number MC\_U12266B.

## Appendix

### Commercial availability of ZFNs, TALENs, CRISPR/Cas9

ZFNs, TALENs and rAAVs may be custom synthesized or created. They may be ordered either by user design or by having the company design and synthesize and clone the relevant protein. There is a consortium for the development of ZFNs.

As of 2017, the following companies are known to provide ZFN synthesis services and/or reagents to create ZFNs:

- Sigma-Aldrich ([www.sigma-aldrich.com](http://www.sigma-aldrich.com))
- Available through Addgene ([www.addgene.com](http://www.addgene.com))
  - Oligomerized Pool Engineering
  - Context dependent assembly
  - Modular assembly (Barbas kit, Joung kit, Wolfe system)

As of 2017, the following companies offer Tal synthesis services and or reagents to create TALENs:

- Collectis Bioresearch (<http://www.collectis.com/>)
- Life Technologies ([www.lifetechnologies.com](http://www.lifetechnologies.com))
- Available through Addgene ([www.addgene.com](http://www.addgene.com))
  - FLASH assembly
  - Modular assembly (Voytas kit, Joung kit, Zhang kit)

As of 2017, the following companies offer CRISPR/Cas9 development services:

- Agilent
- Dharmacon/GE
- Genecopeia
- Horizon Genomics
- IDT
- MolDiag Solutions
- Sigma/Merck
- Synthego
- ThermoFisher

### Online Resources for Guide and crRNA Design

When choosing the best design algorithm for sgRNA, there are multiple choices (see below). All have in common a basic search algorithm for a PAM motif sequence and some blast search against potential off-target effects, i.e. similar sequences. The most useful websites are the ones that provide clear information and visualization of results, for

example when displaying the location of the cut site, providing a suggestion of potential sequencing primers and scores about similar sequences that are easy to understand.

| Design tools   | Considerations   | Reference |
|--|--|-----------|
| sgRNA Scorer 2.0                                     | Identify putative guide sequences and assign a predicted activity. Considers off-target effects. Uses CasFinder algorithm.                               | (74)      |
| CRISPR-DO (CRISPR Design and Optimization)           | Predicts sgRNA efficiency and off-target scoring; applied to several genomes   | (75)      |
| Drosophila RNAi Screening Center (DRSC) Find CRISPRs | Very good graphical visualization in JBrowse. Considers off-target effects.  | (76)      |
| ge-CRISPR  | Evaluates potential off-target sequences; very user-friendly tool  | (77)      |
| CT-Finder  | Graphical visualization on JBrowse. Considers off-target effects. Applied to several genomes   | (78)      |
| CHOPCHOP   | Considers off-target effects. Very informative table. Cas9 nuclease, Cas9 nickase, Cpf1 and TALEN  | (79)      |
| Breaking-Cas   | Interactive design   | (80)      |
| Cas-Database   | Graphical visualization in JBrowse. Both Cas9 and Cpf1   | (81)      |
| CLD (CRISPR Library Designer)                        | Design of CRISPR/Cas9 libraries. Also suitable for targeting non coding regions.   | (82)      |
| WU-CRISPR  | Human or mouse genomes. No graphical visualization.  | (83)      |
| CRISPR-GA (Genome Analyzer)                          |  | (72)      |
| CRISPRscan   | Predictions are available as tracks that can be uploaded in the UCSC genome browser. Applies to several species  | (84)      |
| CRISPR-ERA   | Editing, repression and activation; Cas9 nuclease and Cas9 nickase. Predictions are available as tracks that can be uploaded in the UCSC genome browser. | (85)      |
| Protospacer Workbench                                |  | (86)      |
| WGE   Sanger Institute                               | Along with Gibson assembly PCR oligo designer. Geniverse browser   | (87)      |
| E-CRISP  |  | (88)      |
| Phyto-CRISP-Ex                                       | Protist genomes, 2 sequential filters are applied.   | (89)      |
| CRISPR-P   | Applicable to Plants   | (90)      |

*Table continues on next page...*

Table continued from previous page.

| Design tools   | Considerations  | Reference |
|--|---|-----------|
| Off-Spotter  | Interactive way of selecting the seed sequence                  | (91)      |
| CRISPR Direct  |   | (92)      |
| CRISPRseek   | Bioconductor package  | (93)      |
| sgRNAs9  | Software package  | (94)      |
| GPP Web portal<br>sgRNA designer for CRISPRa and CRISPRi | Gene activation and gene repression. No graphical visualization | (95)      |

## Available Libraries for Screening

As of this date (2017), the following libraries for screening using CRISPR/Cas9 are available:

|            |  |
|------------|--|
| Commercial | Sanger Whole Genome & Sigma CRISPR arrayed libraries<br>Thermo Fisher (LentiArray CRISPR Libraries, TrueGuide CRISPR Libraries)<br>Dharmacon (synthetic guide RNA and lentiviral guide RNA)<br>Genecopeia<br>GenScript<br>Horizon<br>Adgene<br>Agilent   |
| Academic   | <u>Pooled lentiviral libraries:</u><br>Mouse genome-wide lentiviral CRISPR-gRNA library (96)<br>Human and mouse genome-wide lentiviral CRISPR/-gRNA library (GECKO) (97,98)<br>Human genome-wide lentiviral CRISPR/gRNA library (99)<br>Drosophila genome-wide CRISPR library (39)<br>Human genome-wide lentiviral library (Toronto KnockOut TKO) (100)<br>Human and mouse CRISPRi and CRISPRa libraries (101)<br>Human lncRNA targeting library (102)<br><u>Arrayed libraries:</u><br>Human genome-wide, sequence-verified, arrayed lentiviral CRISPR library (103)<br>Human and mouse lentiviral arrayed library (104) |

## References

1. Gaj T, Gersbach CA, Barbas CF 3rd. ZFN, TALEN, and CRISPR/Cas-based methods for genome engineering. *Trends in biotechnology*. 2013;31:397–405. PubMed PMID: 23664777.
2. Hirata R, Chamberlain J, Dong R, Russell DW. Targeted transgene insertion into human chromosomes by adeno-associated virus vectors. *Nature biotechnology*. 2002;20:735–738. PubMed PMID: 12089561.
3. Daya S, Berns KI. Gene therapy using adeno-associated virus vectors. *Clinical microbiology reviews*. 2008;21:583–593. PubMed PMID: 18854481.
4. Russell DW. AAV vectors, insertional mutagenesis, and cancer. *Molecular therapy : the journal of the American Society of Gene Therapy* **15**, 1740-1743 (2007).

5. Kim YG, Cha J, Chandrasegaran S. Hybrid restriction enzymes: zinc finger fusions to Fok I cleavage domain. *Proceedings of the National Academy of Sciences of the United States of America*. 1996;93:1156–1160. PubMed PMID: 8577732.
6. Durai S, Mani M, Kandavelou K, Wu J, Porteus MH, Chandrasegaran S. Zinc finger nucleases: custom-designed molecular scissors for genome engineering of plant and mammalian cells. *Nucleic acids research*. 2005;33:5978–5990. PubMed PMID: 16251401.
7. Li L, Wu LP, Chandrasegaran S. Functional domains in Fok I restriction endonuclease. *Proceedings of the National Academy of Sciences of the United States of America*. 1992;89:4275–4279. PubMed PMID: 1584761.
8. Miller J, McLachlan AD, Klug A. Repetitive zinc-binding domains in the protein transcription factor IIIA from *Xenopus* oocytes. *The EMBO journal*. 1985;4:1609–1614. PubMed PMID: 4040853.
9. Mussolino C, Cathomen T. TALE nucleases: tailored genome engineering made easy. *Current opinion in biotechnology*. 2012;23:644–650. PubMed PMID: 22342754.
10. Joung JK, Sander JD. TALENs: a widely applicable technology for targeted genome editing. *Nature reviews Molecular cell biology*. 2013;14:49–55. PubMed PMID: 23169466.
11. Jinek M, East A, Cheng A, Lin S, Ma E, Doudna J. RNA-programmed genome editing in human cells. *eLife*. 2013;2:e00471. PubMed PMID: 23386978.
12. Cong L, et al. Multiplex genome engineering using CRISPR/Cas systems. *Science*. 2013;339:819–823. PubMed PMID: 23287718.
13. Mali P, et al. RNA-guided human genome engineering via Cas9. *Science*. 2013;339:823–826. PubMed PMID: 23287722.
14. Zetsche B, et al. Cpf1 is a single RNA-guided endonuclease of a class 2 CRISPR-Cas system. *Cell*. 2015;163:759–771. PubMed PMID: 26422227.
15. Gilbert LA, et al. CRISPR-mediated modular RNA-guided regulation of transcription in eukaryotes. *Cell*. 2013;154:442–451. PubMed PMID: 23849981.
16. Qi LS, et al. Repurposing CRISPR as an RNA-guided platform for sequence-specific control of gene expression. *Cell*. 2013;152:1173–1183. PubMed PMID: 23452860.
17. Larson MH, Gilbert LA, Wang X, Lim WA, Weissman JS, Qi LS. CRISPR interference (CRISPRi) for sequence-specific control of gene expression. *Nature protocols*. 2013;8:2180–2196. PubMed PMID: 24136345.
18. Hilton IB, Gersbach CA. Enabling functional genomics with genome engineering. *Genome research*. 2015;25:1442–1455. PubMed PMID: 26430154.
19. Chen B, et al. Dynamic imaging of genomic loci in living human cells by an optimized CRISPR/Cas system. *Cell*. 2013;155:1479–1491. PubMed PMID: 24360272.
20. Ma H, Naseri A, Reyes-Gutierrez P, Wolfe SA, Zhang S, Pederson T. Multicolor CRISPR labeling of chromosomal loci in human cells. *Proceedings of the National Academy of Sciences of the United States of America*. 2015;112:3002–3007. PubMed PMID: 25713381.
21. Rauch BJ, et al. Inhibition of CRISPR-Cas9 with Bacteriophage Proteins. *Cell* **168**, 150-158 e110 (2017).



22. Miller JC, et al. A TALE nuclease architecture for efficient genome editing. *Nature biotechnology*. 2011;29:143–148. PubMed PMID: 21179091.
23. Mussolino C, Morbitzer R, Lutge F, Dannemann N, Lahaye T, Cathomen T. A novel TALE nuclease scaffold enables high genome editing activity in combination with low toxicity. *Nucleic acids research*. 2011;39:9283–9293. PubMed PMID: 21813459.
24. Maeder ML, et al. Rapid "open-source" engineering of customized zinc-finger nucleases for highly efficient gene modification. *Molecular cell*. 2008;31:294–301. PubMed PMID: 18657511.
25. Hwang WY, et al. Heritable and precise zebrafish genome editing using a CRISPR-Cas system. *PloS one*. 2013;8:e68708. PubMed PMID: 23874735.
26. Feng Z, et al. Efficient genome editing in plants using a CRISPR/Cas system. *Cell research*. 2013;23:1229–1232. PubMed PMID: 23958582.
27. He Z, Proudfoot C, Whitelaw CB, Lillico SG. Comparison of CRISPR/Cas9 and TALENs on editing an integrated EGFP gene in the genome of HEK293FT cells. *SpringerPlus*. 2016;5:814. PubMed PMID: 27390654.
28. Kim Y, Kweon J, Kim JS. TALENs and ZFNs are associated with different mutation signatures. *Nature methods*. 2013;10:185. PubMed PMID: 23396284.
29. Evers B, Jastrzebski K, Heijmans JP, Grenrum W, Beijersbergen RL, Bernards R. CRISPR knockout screening outperforms shRNA and CRISPRi in identifying essential genes. *Nature biotechnology*. 2016;34:631–633. PubMed PMID: 27111720.
30. Ketteler R, Kriston-Vizi J. High-Content Screening in Cell Biology. *Waltham, MA: Academic Press* 4, 234-244 (2016).
31. Ketteler R. The Feynman trajectories: determining the path of a protein using fixed-endpoint assays. *Journal of biomolecular screening*. 2010;15:321–326. PubMed PMID: 20130209.
32. Agrotis A, Ketteler R. A new age in functional genomics using CRISPR/Cas9 in arrayed library screening. *Frontiers in genetics*. 2015;6:300. PubMed PMID: 26442115.
33. Reyon D, Tsai SQ, Khayter C, Foden JA, Sander JD, Joung JK. FLASH assembly of TALENs for high-throughput genome editing. *Nature biotechnology*. 2012;30:460–465. PubMed PMID: 22484455.
34. Reyon D, et al. Engineering customized TALE nucleases (TALENs) and TALE transcription factors by fast ligation-based automatable solid-phase high-throughput (FLASH) assembly. *Current protocols in molecular biology / edited by Frederick M Ausubel [et al]* **Chapter 12**, Unit 12 16 (2013).
35. Kim Y, et al. A library of TAL effector nucleases spanning the human genome. *Nature biotechnology*. 2013;31:251–258. PubMed PMID: 23417094.
36. Kurata M, et al. Using genome-wide CRISPR library screening with library resistant DCK to find new sources of Ara-C drug resistance in AML. *Scientific reports*. 2016;6:36199. PubMed PMID: 27808171.
37. Katigbak A, Cencic R, Robert F, Senecha P, Scuoppo C, Pelletier J. A. CRISPR/Cas9 Functional Screen Identifies Rare Tumor Suppressors. *Scientific reports*. 2016;6:38968. PubMed PMID: 27982060.
38. Park RJ, et al. A genome-wide CRISPR screen identifies a restricted set of HIV host dependency factors. *Nature genetics*. 2017;49:193–203. PubMed PMID: 27992415.

39. Bassett AR, Kong L, Liu JL. A Genome-Wide CRISPR Library for High-Throughput Genetic Screening in *Drosophila* Cells. *Journal of genetics and genomics = Yi chuan xue bao* **42**, 301-309 (2015).
40. Shah AN, Davey CF, Whitebirch AC, Miller AC, Moens CB. Rapid reverse genetic screening using CRISPR in zebrafish. *Nature methods*. 2015;12:535–540. PubMed PMID: 25867848.
41. Rauscher B, Heigwer F, Breinig M, Winter J, Boutros M. GenomeCRISPR - a database for high-throughput CRISPR/Cas9 screens. *Nucleic acids research*. 2017;45:D679–D686. PubMed PMID: 27789686.
42. Cho SW, et al. Analysis of off-target effects of CRISPR/Cas-derived RNA-guided endonucleases and nickases. *Genome research*. 2014;24:132–141. PubMed PMID: 24253446.
43. Fu Y, Sander JD, Reyon D, Cascio VM, Joung JK. Improving CRISPR-Cas nuclease specificity using truncated guide RNAs. *Nature biotechnology*. 2014;32:279–284. PubMed PMID: 24463574.
44. Ran FA, et al. Double nicking by RNA-guided CRISPR Cas9 for enhanced genome editing specificity. *Cell*. 2013;154:1380–1389. PubMed PMID: 23992846.
45. Zheng T, et al. Profiling single-guide RNA specificity reveals a mismatch sensitive core sequence. *Scientific reports*. 2017;7:40638. PubMed PMID: 28098181.
46. Liu X, Homma A, Sayadi J, Yang S, Ohashi J, Takumi T. Sequence features associated with the cleavage efficiency of CRISPR/Cas9 system. *Scientific reports*. 2016;6:19675. PubMed PMID: 26813419.
47. Malina A, Cameron CJ, Robert F, Blanchette M, Dostie J, Pelletier J. PAM multiplicity marks genomic target sites as inhibitory to CRISPR-Cas9 editing. *Nature communications*. 2015;6:10124. PubMed PMID: 26644285.
48. Xu H, et al. Sequence determinants of improved CRISPR sgRNA design. *Genome research*. 2015;25:1147–1157. PubMed PMID: 26063738.
49. Chuai GH, Wang QL, Liu Q. In Silico Meets In Vivo: Towards Computational CRISPR-Based sgRNA Design. *Trends in biotechnology*. 2017;35:12–21. PubMed PMID: 27418421.
50. Mohr SE, Hu Y, Ewen-Campen B, Housden BE, Viswanatha R, Perrimon N. CRISPR guide RNA design for research applications. *The FEBS journal*. 2016;283:3232–3238. PubMed PMID: 27276584.
51. Arakawa H. A method to convert mRNA into a gRNA library for CRISPR/Cas9 editing of any organism. *Science advances*. 2016;2:e1600699. PubMed PMID: 27574704.
52. Ketteler R. On programmed ribosomal frameshifting: the alternative proteomes. *Frontiers in genetics*. 2012;3:242. PubMed PMID: 23181069.
53. Makino S, Fukumura R, Gondo Y. Illegitimate translation causes unexpected gene expression from on-target out-of-frame alleles created by CRISPR-Cas9. *Scientific reports*. 2016;6:39608. PubMed PMID: 28000783.
54. Miles LA, Garippa RJ, Poirier JT. Design, execution, and analysis of pooled in vitro CRISPR/Cas9 screens. *The FEBS journal*. 2016;283:3170–3180. PubMed PMID: 27250066.

55. Brummelkamp TR, et al. An shRNA barcode screen provides insight into cancer cell vulnerability to MDM2 inhibitors. *Nature chemical biology*. 2006;2:202–206. PubMed PMID: 16474381.
56. Wong AS, et al. Multiplexed barcoded CRISPR-Cas9 screening enabled by CombiGEM. *Proceedings of the National Academy of Sciences of the United States of America*. 2016;113:2544–2549. PubMed PMID: 26864203.
57. Luo B, et al. Highly parallel identification of essential genes in cancer cells. *Proceedings of the National Academy of Sciences of the United States of America*. 2008;105:20380–20385. PubMed PMID: 19091943.
58. Konig R, et al. A probability-based approach for the analysis of large-scale RNAi screens. *Nature methods*. 2007;4:847–849. PubMed PMID: 17828270.
59. Diaz AA, Qin H, Ramalho-Santos M, Song JS. HiTSelect: a comprehensive tool for high-complexity-pooled screen analysis. *Nucleic acids research*. 2015;43:e16. PubMed PMID: 25428347.
60. Li W, et al. MAGeCK enables robust identification of essential genes from genome-scale CRISPR/Cas9 knockout screens. *Genome biology*. 2014;15:554. PubMed PMID: 25476604.
61. Winter J, et al. caRpoools: an R package for exploratory data analysis and documentation of pooled CRISPR/Cas9 screens. *Bioinformatics*. 2016;32:632–634. PubMed PMID: 26508755.
62. Kelley ML, Strezoska Z, He K, Vermeulen A, Smith A. Versatility of chemically synthesized guide RNAs for CRISPR-Cas9 genome editing. *Journal of biotechnology*. 2016;233:74–83. PubMed PMID: 27374403.
63. Liang X, et al. Rapid and highly efficient mammalian cell engineering via Cas9 protein transfection. *Journal of biotechnology*. 2015. PubMed PMID: 26003884.
64. Zhang JH, Chung TD, Oldenburg KR. A Simple Statistical Parameter for Use in Evaluation and Validation of High Throughput Screening Assays. *Journal of biomolecular screening*. 1999;4:67–73. PubMed PMID: 10838414.
65. Langhans MT, Palladino MJ. Cleavage of mispaired heteroduplex DNA substrates by numerous restriction enzymes. *Current issues in molecular biology*. 2009;11:1–12. PubMed PMID: 18541926.
66. Zhu X, et al. An efficient genotyping method for genome-modified animals and human cells generated with CRISPR/Cas9 system. *Scientific reports*. 2014;4:6420. PubMed PMID: 25236476.
67. Thomas DK, et al. Comparative variation within the genome of *Campylobacter jejuni* NCTC 11168 in human and murine hosts. *PloS one*. 2014;9:e88229. PubMed PMID: 24516617.
68. Yang Z, et al. Fast and sensitive detection of indels induced by precise gene targeting. *Nucleic acids research*. 2015;43:e59. PubMed PMID: 25753669.
69. Harayama T, Riezman H. Detection of genome-edited mutant clones by a simple competition-based PCR method. *PloS one*. 2017;12:e0179165. PubMed PMID: 28586390.
70. Nelson CE, et al. In vivo genome editing improves muscle function in a mouse model of Duchenne muscular dystrophy. *Science*. 2016;351:403–407. PubMed PMID: 26721684.

71. Miyaoka Y, et al. Systematic quantification of HDR and NHEJ reveals effects of locus, nuclease, and cell type on genome-editing. *Scientific reports*. 2016;6:23549. PubMed PMID: 27030102.
72. Guell M, Yang L, Church GM. Genome editing assessment using CRISPR Genome Analyzer (CRISPR-GA). *Bioinformatics*. 2014;30:2968–2970. PubMed PMID: 24990609.
73. Boel A, et al. BATCH-GE: Batch analysis of Next-Generation Sequencing data for genome editing assessment. *Scientific reports*. 2016;6:30330. PubMed PMID: 27461955.
74. Chari R, Mali P, Moosburner M, Church GM. Unraveling CRISPR-Cas9 genome engineering parameters via a library-on-library approach. *Nature methods*. 2015. PubMed PMID: 26167643.
75. Ma J, et al. CRISPR-DO for genome-wide CRISPR design and optimization. *Bioinformatics*. 2016;32:3336–3338. PubMed PMID: 27402906.
76. Housden BE, Lin S, Perrimon N. Cas9-based genome editing in *Drosophila*. *Methods in enzymology*. 2014;546:415–439. PubMed PMID: 25398351.
77. Kaur K, Gupta AK, Rajput A, Kumar M. ge-CRISPR - An integrated pipeline for the prediction and analysis of sgRNAs genome editing efficiency for CRISPR/Cas system. *Scientific reports*. 2016;6:30870. PubMed PMID: 27581337.
78. Zhu H, Misel L, Graham M, Robinson ML, Liang C. CT-Finder: A Web Service for CRISPR Optimal Target Prediction and Visualization. *Scientific reports*. 2016;6:25516. PubMed PMID: 27210050.
79. Labun K, Montague TG, Gagnon JA, Thyme SB, Valen E. CHOPCHOP v2: a web tool for the next generation of CRISPR genome engineering. *Nucleic acids research*. 2016;44:W272-276. PubMed PMID: 27185894.
80. Oliveros JC, et al. Breaking-Cas-interactive design of guide RNAs for CRISPR-Cas experiments for ENSEMBL genomes. *Nucleic acids research*. 2016;44:W267-271. PubMed PMID: 27166368.
81. Park J, Kim JS, Bae S. Cas-Database: web-based genome-wide guide RNA library design for gene knockout screens using CRISPR-Cas9. *Bioinformatics*. 2016;32:2017–2023. PubMed PMID: 27153724.
82. Heigwer F, et al. CRISPR library designer (CLD): software for multispecies design of single guide RNA libraries. *Genome biology*. 2016;17:55. PubMed PMID: 27013184.
83. Wong N, Liu W, Wang X. WU-CRISPR: characteristics of functional guide RNAs for the CRISPR/Cas9 system. *Genome biology*. 2015;16:218. PubMed PMID: 26521937.
84. Moreno-Mateos MA, et al. CRISPRscan: designing highly efficient sgRNAs for CRISPR-Cas9 targeting in vivo. *Nature methods*. 2015;12:982–988. PubMed PMID: 26322839.
85. Liu H, Wei Z, Dominguez A, Li Y, Wang X, Qi LS. CRISPR-ERA: a comprehensive design tool for CRISPR-mediated gene editing, repression and activation. *Bioinformatics*. 2015;31:3676–3678. PubMed PMID: 26209430.
86. MacPherson CR, Scherf A. Flexible guide-RNA design for CRISPR applications using Protospacer Workbench. *Nature biotechnology*. 2015;33:805–806. PubMed PMID: 26121414.

87. Hodgkins A, et al. WGE: A CRISPR database for genome engineering. *Bioinformatics*. 2015. PubMed PMID: 25979474.
88. Heigwer F, Kerr G, Boutros M. E-CRISP: fast CRISPR target site identification. *Nature methods*. 2014;11:122–123. PubMed PMID: 24481216.
89. Rastogi A, Murik O, Bowler C, Tirichine L. PhytoCRISP-Ex: a web-based and stand-alone application to find specific target sequences for CRISPR/CAS editing. *BMC bioinformatics*. 2016;17:261. PubMed PMID: 27363443.
90. Lei Y, Lu L, Liu HY, Li S, Xing F, Chen LL. CRISPR-P: a web tool for synthetic single-guide RNA design of CRISPR-system in plants. *Molecular plant*. 2014;7:1494–1496. PubMed PMID: 24719468.
91. Pliatsika V, Rigoutsos I. "Off-Spotter": very fast and exhaustive enumeration of genomic lookalikes for designing CRISPR/Cas guide RNAs. *Biology direct*. 2015;10:4. PubMed PMID: 25630343.
92. Naito Y, Hino K, Bono H, Ui-Tei K. CRISPRdirect: software for designing CRISPR/Cas guide RNA with reduced off-target sites. *Bioinformatics*. 2015;31:1120–1123. PubMed PMID: 25414360.
93. Zhu LJ, Holmes BR, Aronin N, Brodsky MH. CRISPRseek: a bioconductor package to identify target-specific guide RNAs for CRISPR-Cas9 genome-editing systems. *PloS one*. 2014;9:e108424. PubMed PMID: 25247697.
94. Xie S, Shen B, Zhang C, Huang X, Zhang Y. sgRNAs9: a software package for designing CRISPR sgRNA and evaluating potential off-target cleavage sites. *PloS one*. 2014;9:e100448. PubMed PMID: 24956386.
95. Doench JG, et al. Rational design of highly active sgRNAs for CRISPR-Cas9-mediated gene inactivation. *Nature biotechnology*. 2014;32:1262–1267. PubMed PMID: 25184501.
96. Koike-Yusa H, Li Y, Tan EP, Velasco-Herrera Mdel C, Yusa K. Genome-wide recessive genetic screening in mammalian cells with a lentiviral CRISPR-guide RNA library. *Nature biotechnology*. 2014;32:267–273. PubMed PMID: 24535568.
97. Shalem O, et al. Genome-scale CRISPR-Cas9 knockout screening in human cells. *Science*. 2014;343:84–87. PubMed PMID: 24336571.
98. Sanjana NE, Shalem O, Zhang F. Improved vectors and genome-wide libraries for CRISPR screening. *Nature methods*. 2014;11:783–784. PubMed PMID: 25075903.
99. Wang T, Wei JJ, Sabatini DM, Lander ES. Genetic screens in human cells using the CRISPR-Cas9 system. *Science*. 2014;343:80–84. PubMed PMID: 24336569.
100. Hart T, et al. High-Resolution CRISPR Screens Reveal Fitness Genes and Genotype-Specific Cancer Liabilities. *Cell*. 2015;163:1515–1526. PubMed PMID: 26627737.
101. Horlbeck MA, et al. Compact and highly active next-generation libraries for CRISPR-mediated gene repression and activation. *eLife*. 2016;5 PubMed PMID: 27661255.
102. Liu SJ, et al. CRISPRi-based genome-scale identification of functional long noncoding RNA loci in human cells. *Science*. 2017;355 PubMed PMID: 27980086.
103. Erard N, Knott SRV, Hannon GJ. A CRISPR Resource for Individual, Combinatorial, or Multiplexed Gene Knockout. *Molecular cell* **67**, 348-354 e343 (2017).
104. Metzakopian E, et al. Enhancing the genome editing toolbox: genome wide CRISPR arrayed libraries. *Scientific reports*. 2017;7:2244. PubMed PMID: 28533524.

105. Kleinstiver BP, et al. Engineered CRISPR-Cas9 nucleases with altered PAM specificities. *Nature*. 2015. PubMed PMID: 26098369.
106. Anders C, Bargsten K, Jinek M. Structural Plasticity of PAM Recognition by Engineered Variants of the RNA-Guided Endonuclease Cas9. *Molecular cell*. 2016;61:895–902. PubMed PMID: 26990992.
107. Ran FA, et al. In vivo genome editing using *Staphylococcus aureus* Cas9. *Nature*. 2015;520:186–191. PubMed PMID: 25830891.
108. Hou Z, et al. Efficient genome engineering in human pluripotent stem cells using Cas9 from *Neisseria meningitidis*. *Proceedings of the National Academy of Sciences of the United States of America*. 2013;110:15644–15649. PubMed PMID: 23940360.
109. Muller M, *et al.* *Streptococcus thermophilus* CRISPR-Cas9 Systems Enable Specific Editing of the Human Genome. *Molecular therapy : the journal of the American Society of Gene Therapy* **24**, 636-644 (2016).
110. Karvelis T, et al. Rapid characterization of CRISPR-Cas9 protospacer adjacent motif sequence elements. *Genome biology*. 2015;16:253. PubMed PMID: 26585795.
111. Yang H, Gao P, Rajashankar KR, Patel DJ. PAM-Dependent Target DNA Recognition and Cleavage by C2c1 CRISPR-Cas Endonuclease. *Cell* **167**, 1814-1828 e1812 (2016).

## Suggested Reading

Iizumi et al, Simple one-week method to construct gene-targeting vectors: application to production of human knockout cell lines, *Biotechniques* 41:311-316 2006

Jantz and Berg, Probing the DNA-binding affinity and specificity of designed zinc finger proteins *Biophys J* 98:852-860, 2010

Klug, Towards therapeutic applications of engineered zinc finger proteins *FEBS Letters* 579:892-894 2005

Perez-Pinera et al, Advances in targeted genome editing, *Curr Opin Chem Biol* 16:268-277, 2012

## Suggested Websites

[www.addgene.com](http://www.addgene.com)

[www.agilent.com](http://www.agilent.com)

[www.cellectis.com](http://www.cellectis.com)

[www.genecopoeia.com](http://www.genecopoeia.com)

[www.horizondiscovery.com](http://www.horizondiscovery.com)

[www.idtdna.com](http://www.idtdna.com)

[www.lifetechnologies.com](http://www.lifetechnologies.com)

[www.moldiag.in](http://www.moldiag.in)

[www.sigma-aldrich.com](http://www.sigma-aldrich.com)

[www.synthego.com](http://www.synthego.com)





# Inhibition of Protein-Protein Interactions: Cell-Based Assays

Mark Wade, Ph.D.,<sup>1</sup> Jacqui Méndez, M.S.,<sup>2</sup> Nathan P. Coussens, Ph.D.,<sup>3</sup> Michelle R. Arkin, Ph.D.,<sup>4</sup> and Marcie A. Glicksman, Ph.D.<sup>5</sup>

Created: November 20, 2017.

## Abstract

There is a strong interest in discovering compounds that inhibit protein-protein interactions. High-throughput screening (HTS) approaches include formats using purified proteins (see AGM chapter Inhibition of Protein-Protein Interactions: Non-Cellular Assay Formats) (1) and those using whole cells. This chapter describes two types of cell-based HTS assays, energy transfer (Förster resonance energy transfer and bioluminescence resonance energy transfer) and protein complementation (fluorescence or enzymatic, e.g. luciferase).

## Introduction

Protein-protein interactions (PPI) are a diverse and challenging group of targets for small-molecule discovery efforts (2). PPI interfaces come in a wide variety of sizes (from 4 amino acids to thousands of Å<sup>2</sup>) and vary greatly in their binding affinities, dynamics, and complexity (from two proteins to tens of proteins in a complex). In order to capture the complexity of the PPI environment and maintain the integrity of the PPI complex, several groups have developed assays to monitor protein complexes in cells.

Cellular PPI assays offer different advantages and disadvantages when compared to biochemical approaches using purified proteins *in vitro*. Biochemical formats offer the advantage that the targets are studied in isolation, and hits from such screens are likely to interact directly with one of the proteins (see AGM chapter Inhibition of Protein-Protein Interactions: Non-Cellular Assay Formats) (1). However, the cellular context is lost in a protein-based assay. In cells, proteins are in their native environment, including discrete subcellular locations and formation of multi-protein complexes. This complexity provides additional mechanisms of interaction for a small molecule, and ensures that active compounds are cell permeable and able to reach the PPI target.

---

<sup>1</sup> Center for Genomic Science of IIT@SEMM, Fondazione Istituto Italiano di Tecnologia; Email: Mark.Wade@iit.it. <sup>2</sup> Promega Corp.; Email: Jacqui.mendez@promega.com. <sup>3</sup> National Center for Advancing Translational Sciences, National Institutes of Health; Email: coussensn@mail.nih.gov. <sup>4</sup> University of California, San Francisco; Email: Michelle.arkin@ucsf.edu. <sup>5</sup> Orig3n Inc.; Email: Marcie@orig3n.com.

This chapter describes the development of energy transfer and protein complementation screening assays for identifying small molecules that modulate PPI in cells. General introductions to assay development for HTS, cell culture for HTS, and high content imaging can be found in dedicated chapters in this *Assay Guidance Manual*.

## Background

Energy transfer assays include Förster resonance energy transfer (FRET) and bioluminescence resonance energy transfer (BRET). In a FRET assay, the fluorescence energy from the donor protein is transferred to the acceptor protein, which then emits light; in BRET, luciferase-induced chemiluminescence provides the donor energy that is then transferred to a fluorescent protein or dye. For energy transfer assays, donor and acceptor proteins are fused to each partner of a PPI. Formation of the PPI complex brings the two proteins close enough to undergo energy transfer.

Bimolecular protein complementation assays utilize a reporter protein that has been genetically split into two chains that do not fold into active protein on their own. Each chain is fused to one of the target protein partners; when the protein partners come into contact, the split reporter protein is reconstituted and its fluorescence or enzymatic activity is restored. Protein fragment complementation assays fall into 'indirect' and 'direct' reporter classes. For direct reporters, complementation of the two fragments leads to reconstitution of reporter function – such as fluorescence (for example, GFP) or enzymatic activity (such as luciferase). Indirect reporters trigger additional events that lead to the assay readout, such as transcription via the 2-hybrid assay (3-6). The direct reporter system provides a more proximal measurement of a PPI, and is therefore generally preferred for the discovery of PPI inhibitors.

Table 1 contrasts the energy-transfer and protein-complementation formats. All methods rely on generating fusion proteins with the reporter pairs. The signals that derive from energy transfer and protein complementation require that the two proteins of interest be in molecular contact. These assay formats are distinct from co-localization assays that are used to demonstrate that two proteins are in the same subcellular region.

The selection of a cell-based energy transfer versus protein complementation assay depends on several factors. Due to its relatively low signal and narrow dynamic range, FRET is generally read through an imaging-based assay or flow cytometry; by contrast, enzyme complementation and BRET assays utilize a standard multi-modal plate reader. An important distinction among formats is whether they are reversible. Upon reading out a dynamic process, it is highly advantageous for the reporter signal to also be reversible. FRET, BRET and bimolecular luminescence protein complementation (BiLC) are reversible (7-12), whereas bimolecular fluorescent protein complementation (BiFC),  $\beta$ -galactosidase complementation, and  $\beta$ -lactamase complementation are generally not reversible (6, 13-23).

**Table 1:** Cell-based PPI assays described in this chapter

| Format   | Notable features   |
|--|--|
| <b>Förster Resonance Energy Transfer (FRET)</b>  | <b>Read out:</b> high content imaging or flow cytometry<br><b>Benefits:</b> reversibility, suited to live-cell assay<br><b>Limitations:</b> low signal/dynamic range, photobleaching, need to correct spectral overlap   |
| <b>Bioluminescence resonance energy transfer (BRET, NanoBRET)</b>  | <b>Read out:</b> plate reader with luminescence detection<br><b>Benefits:</b> reversibility, high signal/low background, suited to live-cell assay, cell-permeable chemiluminescent substrates and fluorescent tags available<br><b>Limitations:</b> Older configurations of BRET have too much spectral overlap resulting in narrow dynamic range                   |
| <b>Bimolecular fluorescent protein complementation (BiFC)</b>  | Generally not reversible   |
| <b>Bimolecular luminescence protein complementation (BiLC)</b>   | <b>Read out:</b> plate reader with luminescence detection<br><b>Benefits:</b> reversibility, high signal/low background, suited to live-cell assay, cell-permeable chemiluminescent substrates available<br><b>Limitations:</b> signals vary depending on fusion constructs and selection of luciferase species/substrate; compounds can inhibit luciferase directly |
| <b>Other enzyme protein complementation (<math>\beta</math>-galactosidase, <math>\beta</math>-lactamase)</b> | <b>Read out:</b> plate reader with fluorescence detection<br><b>Benefits:</b> high signal/low background, suited to live-cell assay, cell-permeable substrates available<br><b>Limitations:</b> generally not reversible   |

## General Considerations for Developing Cell-Based PPI Assays

**Yeast versus mammalian cells:** Methods to measure PPI in mammalian cell-based assays are robust and in most cases provide sufficient throughput to serve as primary screening formats. We therefore recommend using cells of the same species as the target PPI. *Saccharomyces cerevisiae* (yeast) has been extensively used to discover protein-protein interactions and has also been used to discover the mechanisms of action and off-target effects of bioactive compounds (24). Several of the assays described below can be used in yeast cells. However, there are some drawbacks to yeast expression of mammalian proteins. First, yeast lacks some proteins that might be required to form multi-protein complexes and might not produce the posttranslational modifications required for some mammalian PPIs. Second, accumulation of some test compounds in yeast is prevented by the expression of multidrug transporters, though yeast strains with increased drug sensitivity are available (25).

**Cell type considerations:** Any transfectable cell line can be used, but there is an increasing trend towards using cell lines and primary cells that best recapitulate the native biology. For instance, primary astrocytes have been stably transfected and used in a high-throughput screen to detect neuronal cells (26). An important factor for run-to-run reproducibility is to maintain a consistent passage number for cells. We highly

recommend that a screen-sized batch of cells are grown and frozen in single-use aliquots prior to initiating the screen.

**Transient versus stable transfection:** If at all possible, stable transfection is highly preferable to transient transfection. First, stable transfection increases run-to-run reproducibility, which is critical for high-throughput screening (HTS). Second, expression levels can be selected based on resistance markers or FACS-based selection. Higher expression levels are often obtained through transient transfection, which can increase signal strength but might decrease physiological relevance.

**Orientation of the protein fusions:** In protein-complementation (BiFC and BiLC) assays, steric hindrance can sometimes prevent reconstitution/proper folding of the split protein. For example, GFP N- and C-terminal regions might not be oriented correctly upon protein-protein interaction, and thus fluorescence will not be observed. FRET and BRET efficiencies depend on distance and angle (see **Equations 2 and 3** in the next section), so orientation can also affect energy-transfer efficiency. Therefore, fusions to the PPI partners should be tested in all orientations and combinations to determine the optimal pair. In some cases, the biology of the PPI under study will limit the configuration options. For example, fusion of polypeptides to the C-terminus of the *really interesting new gene* (RING) domain can inhibit biological function. Additionally, placing a linker (such as a serine/glycine sequence) between the proteins of interest and each half of the split protein is recommended to reduce steric hindrance. Including an epitope tag in this linker region can also be useful for quantifying the relative amount of each fusion partner present in the cell.

**Full-length versus fragments of the proteins of interest:** There are biological and practical considerations to consider. The use of full-length proteins is recommended when possible, because additional domains remote from the primary site of interaction can sometimes contribute to binding. However, steric effects or alterations in the stability, expression level, or localization of the proteins are sometimes prohibitive. In this case, fragments rather than full-length proteins might be required for interrogating some PPIs.

**Making the system inducible:** Consistent expression of the PPI is preferable if the protein pair is constitutively expressed in the native case. On the other hand, there are potential advantages for regulated expression of the fusion proteins. First, if the system is under a doxycycline-regulated promoter (Dox-on), graded expression of the protein can be achieved by titrating in the amount of inducer. This aids assay development, as the minimal amount of fusion protein required to generate sufficient signal can be determined. Second, an inducible system allows cells to be pre-incubated with compounds before expression of the interacting partners. This might increase the number of compounds identified in the primary screen if the PPI is essentially irreversible.

**To lyse or not to lyse:** Sometimes the term 'cell-based' PPI assay is used when the cells are lysed before the complex is measured. *An important issue with this assay format is that protein-protein and protein-small molecule interactions will re-equilibrate during lysis and dilution.* These assays might therefore be more precisely defined as 'lysate-based' PPI

assays. There are situations in which a lysate-based assay is beneficial. For instance, when the PPI is difficult to express in a native form, one could express the interacting protein partners in the cell and prepare lysates before performing the screen. In this way, one can also perform large-scale preparations from cells grown in bulk and generate assay-ready lysate that can be stored. It is also noteworthy that compounds that are not cell-permeable can still be identified through a lysate-based assay. However, if the goal is to screen for PPI inhibitors in whole cells, a non-lytic format should be used.

**Demonstrate that the PPI under study drives the complementation and not vice-versa:**

For fragment complementation assays, it is important to demonstrate that the affinity of the PPI of interest is not significantly altered by the addition of the protein fragments. Control constructs containing point mutation(s) that destroy the PPI can be used for this purpose. If available, a known small molecule inhibitor should be used as a positive control. As with any type of screen, the controls for specificity and selectivity of ‘hits’ identified in protein fragment complementation screens are critical.

**Statistical Considerations:** The  $Z'$ -factor should be used to evaluate the quality or performance of the optimized assay prior to implementing HTS (27). The  $Z'$ -factor takes into account the measurement variability for the high-signal ( $c^+$ ) and low-signal controls ( $c^-$ ) in addition to the overall dynamic range of the assay signal as shown below where  $\sigma_{c^+}$  and  $\sigma_{c^-}$  are the standard deviation and mean values for the high-signal and low-signal controls, respectively (**Equation 1**):

$$Z' \text{ factor} = 1 - \frac{(3\sigma_{c^+} + 3\sigma_{c^-})}{|\mu_{c^+} - \mu_{c^-}|}$$

An assay with a  $Z'$ -factor value between 0.5–1 is considered to be robust with low assay variability and suitable for HTS. Variability within the plate, between plates, and between days needs to be established. Hits should be defined by a threshold of three standard deviations from the baseline and the percent coefficient of variation (in the absence of a positive control) should be less than 10%. For additional information on assay validation see the AGM Chapter HTS Assay Validation.

**Assay artifacts and interferences:** Prior to selecting an assay for optimization, it is important to carefully consider all potential sources of artifacts and interferences. In comparing multiple assay approaches for high-throughput screening, the primary assay should be selected to minimize susceptibility to interferences, provided that the assay is robust, feasible and of suitable quality for screening. Counter screens can be developed to identify compounds that interfere with the detection method or have intractable mechanisms of action. Additionally, orthogonal assays can be optimized that are susceptible to different types of artifacts compared with the primary assay, and also increase the evidence for on-target activities of hit compounds (see AGM chapters Interferences with Luciferase Reporter Enzymes and Interference with Fluorescence and Absorbance) (28, 29). Depending on the design and readout, assays have different susceptibilities to artifacts and interferences. The methodologies described in this chapter rely on the measurement of fluorescence and luminescence (luciferase) light as a readout.

Test compounds in chemical libraries can interfere with the detection measurement due to autofluorescence properties, scattering of light, or by absorbing light at the excitation or emission wavelengths (inner filter effect) (28, 29). Fluorescence spectroscopic profiling studies of large compound libraries indicated that interference is most prominent in the UV and blue range, whereas it is substantially reduced for red-shifted readouts (30, 31). Therefore one can reduce library compound interferences by simply selecting the most red-shifted detection reagents that are available and applicable. Luciferase assays are susceptible to interference by colored compounds that can quench luminescence as well as enzymatic inhibitors (see AGM chapters Interferences with Luciferase Reporter Enzymes and Interference with Fluorescence and Absorbance) (28-30, 32). It is critical to ensure that the signals being measured are in the linear range of the detection instrumentation and that the appropriate hardware (such as filters and mirrors) are in place. While some interference mechanisms are assay or readout dependent, other mechanisms such as chemical reactivity (see AGM chapter Assay Interference by Chemical Reactivity) (33) and aggregation (see AGM chapter Assay Interference by Aggregation) (34) can affect a wide range of methodologies and should be tested for by appropriate assays during the hit triage process.

## Förster Resonance Energy Transfer (FRET)

### Introduction

Förster Resonance Energy Transfer (FRET) occurs when energy from an excited fluorophore (donor) is absorbed by another molecule (acceptor). FRET is a powerful method for measuring distances between two fluorophores and is used in unimolecular systems (e.g., the donor and acceptor on the same protein) and biomolecular systems (e.g., the donor and acceptor on two interacting proteins; **Figure 1**).

The underlying principles of FRET were introduced over fifty years ago (reviewed in (35)). Cell-based FRET was first used in flow cytometry (11), but it is also an established format for high content assays and plate-reader formats.

For a FRET assay, the donor and acceptor molecules must be in close proximity to one another (typically 10-100 Å). In addition, there must be overlap between the fluorescence emission spectrum of the donor and the excitation spectrum (usually the same as the absorption spectrum) of the acceptor (**Figure 2**). The extent of overlap is referred to as the spectral overlap integral ( $J$ ). Förster demonstrated that the efficiency ( $E$ ) of the energy transfer depends on the inverse sixth-distance between donor and acceptor (36) (**Equation 2**):

$$E = \frac{R_0^6}{(R_0^6 + r^6)}$$

Where  $R_0$  is the Förster distance at which half the energy is transferred to the acceptor and  $r$  is the distance between donor and acceptor. Förster distance ( $R_0$ ) is dependent on a number of factors, including the fluorescence quantum yield of the donor in the absence

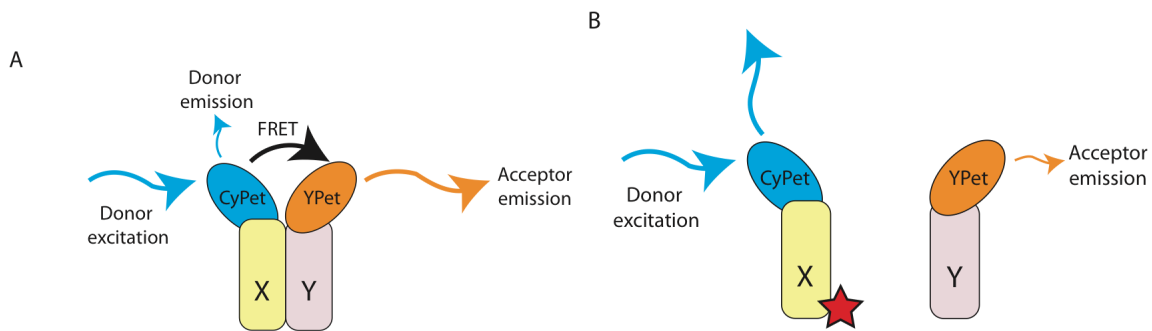


**Figure 1.** Schematic representation of FRET between two proteins (X and Y) fused to donor- and acceptor fluorescent proteins (CyPet and YPet, respectively). When excited, CyPet emits light, unless that energy is transferred to the YPet acceptor molecule. The YPet then emits light at its characteristic wavelength. If the PPI is inhibited (e.g., by a small molecule, red star) the CyPet donor and YPet acceptor are no longer in proximity, and FRET is reduced.

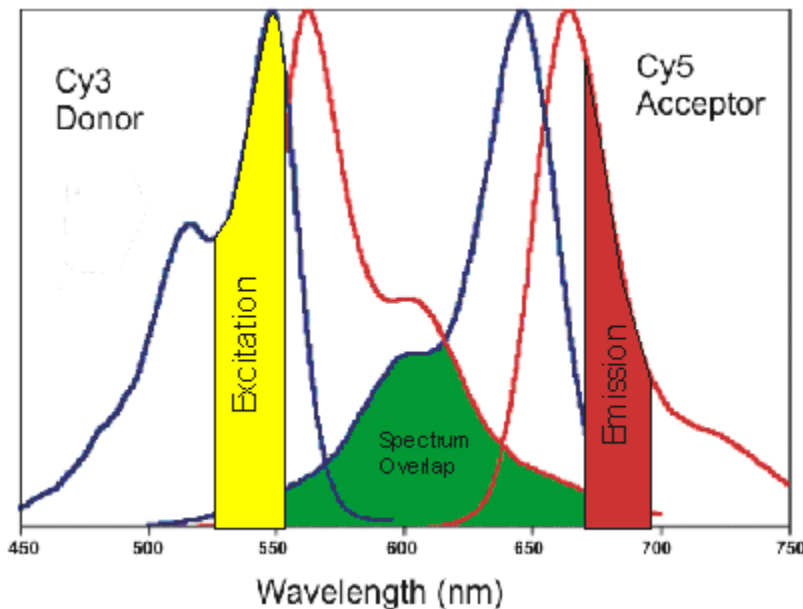


**Figure 2.** Spectral overlap and FRET. The donor (Cy3) is excited at a maximal wavelength of 550 nm, and emits with light at 650 nm. The acceptor (Cy5) absorbs light at 570 nm and emits at 670 nm. Energy transfer occurs due to the spectral overlap between the emission of the donor and excitation spectrum of the acceptor (shown in green). Crosstalk occurs when donor emission overlaps with acceptor emission, such that the donor emission is counted as FRET; similarly, the acceptor can be directly excited during donor excitation if their absorbance spectra overlap (as they do here).

of acceptor ( $\epsilon_d$ ), the refractive index of the solution ( $\eta$ ), the dipole angular orientation of each molecule ( $k^2$ ), and the spectral overlap integral of the donor and acceptor ( $J$ ) (Equation 3):

$$R_o = 9.78 \times 10^3 \times (\eta^{-4} \times f_d \times k^2 \times J)^{\frac{1}{6}} \times \text{\AA}$$

The  $R_o$  distance is between 30-50 Å for the FRET pairs in Table 2. While this range could be important for large complexes, FRET pairs are generally chosen based on spectral characteristics rather than  $R_o$ . Energy transfer leads to a reduction in donor fluorescence and an increase in acceptor fluorescence, and is usually reported as the ratio donor emission/acceptor emission. Cell-based FRET generally uses fluorescent proteins, which have broad excitation and emission peaks and small Stokes shift (the distance between the emission and excitation wavelengths). It is therefore important to carefully select the donor and acceptor fluorescent proteins to maximize the distance between fluorescence wavelengths of donor and acceptor, and use narrow bandpass filters to avoid counting the overlap between the donor and acceptor (called cross-talk). Crosstalk should be measured and corrected (see below).

**Table 2.** Common Donor/Acceptor pairs for intracellular FRET

| Donor (ex/em)         | Acceptor (ex/em)   | Reference |
|-----------------------|--------------------|-----------|
| Sirius (355/424)      | mseCFP (434/474)   | (62)      |
| mTagBFP (402/457)     | sfGFP (485/510)    | (63)      |
| CFP (433/475)         | eYFP (514/527)     |           |
| CFP (433/475)         | Venus (515/528)    |           |
| mTurquoise2 (434/474) | Venus (515/528)    | (64)      |
| CFP (433/475)         | mCitrine (516/529) |           |
| mTFP1 (462/492)       | mCitrine (516/529) | (65)      |
| eCFP (439/476)        | YPet (517/530)     | (66)      |
| CyPet (435/477)       | YPet (517/530)     |           |
| Venus (515/528)       | mKOκ (551/563)     | (67)      |
| mAmetrine (406/526)   | tdTomato (554/581) | (65)      |
| Sapphire (399/511)    | DsRed (558/583)    | (62)      |
| CFP (433/475)         | mRFP (584/607)     | (68)      |
| CFP (433/475)         | mCherry (587/610)  | (64)      |
| eYFP (514/527)        | mCherry (587/610)  | (64)      |
| Venus (515/528)       | mCherry (587/610)  |           |
| mOrange (548/562)     | mCherry (587/610)  | (66)      |
| mKOκ (551/563)        | mLumin (587/621)   | (67)      |

## Assay Development

**Instrumentation:** For imaging, there are a number of instruments well suited for high-throughput imaging assays (e.g. Molecular Devices' Image Express, GE Healthcare InCell



Analyzer, PerkinElmer Operetta). Many commercial plate readers can be used to detect the signal from FRET, and are appropriate for lysate-based assays. These include TECAN's Safire (now TECAN M1000), BMG's PherastarFS, BioTek's Synergy2 and -4, PerkinElmer's Envision.

Plates: Black solid or clear bottom plates are compatible with FRET. For imaging assays, there are plates optimized for microscopy with flat bottom, uniform, and thin plastic wells to minimize distortion (e.g., from Aurora Biotechnologies, Costar, and Greiner).

Cell types: FRET has been performed in many cell types including U2OS, HEK293, HeLa, COS-7, CHO, HCT-116. Selecting the most relevant cell type generally leads to identification of more relevant hits.

Buffers: For cell-based HTS in intact cells, phenol red-free medium should be used. The medium should be buffered against changes in pH by the addition of HEPES, for example.

Choice of FRET pair: Select the appropriate fluorescent protein pair to use in FRET (see Table 2). Ideal pairs have maximal overlap of donor emission and acceptor excitation, but minimal direct excitation of the acceptor at the excitation maximum of the donor. Historically, CFP/YFP has been the choice for FRET. However, with the continual expansion of the fluorescent protein palette, a large number of additional pairs are now available. Commonly used pairs include modified GFP/Venus (37, 38) and CyPet/YPet (12). Many of the newer pairs contain red-shifted acceptors, as this provides the opportunity for multiplexing with green-shifted acceptors in order to study more than one interaction simultaneously. Red-shifted variants are also advantageous as they can reduce the noise generated by cellular autofluorescence, which is generally in the green range. However, caution should be taken when choosing earlier versions of red-shifted proteins (such as DsRed or mRFP), as they generally have lower quantum yields than green fluorescent proteins.

For measuring PPI on the cell membrane, one can use donor and acceptor labeled antibodies raised against the proteins of interest. This method has been successfully used to detect changes in the interaction between the ERBB1/ERBB2 heterodimer, for example. (39)

Assay Conditions: The ratio of the donor and acceptor is critical for accurate FRET. This can be tricky for bimolecular FRET, where two fusion proteins are expressed at different levels or have different stabilities. This might lead to an excess of emission donors that do participate in the PPI, which will in turn mask the true FRET signal. An excess of acceptor can also complicate interpretation of the FRET signal, particularly if the acceptor is susceptible to direct excitation. In addition to expression level, other factors such as pH and temperature (in the case of live cell FRET) can interfere with the assay readout because they alter the rate of acceptor or donor maturation, and thus affect their concentrations.

## Data Analysis

The type of analysis performed is linked to the precise FRET methodology used in the screen. In the simplest version, the ratio between acceptor and donor emission following donor excitation is calculated before and after compound addition. In order to overcome the issue of spectral cross-talk (in which the acceptor is excited directly by the donor excitation wavelength, or in which donor emission is present in the acceptor channel), filter cubes with bandpasses very specific for each FRET pair should be used. Ideally, several additional control cell lines should also be used in order to obtain a more accurate measurement of FRET efficiency. These include untransfected cells, and cells that express either the donor or the acceptor FRET partner. Measuring the fluorescence emission in these cells following excitation at donor and acceptor wavelengths provides information that can be used to calibrate the system. FRET is a powerful method but it does require careful analysis of images including measurement of bleed-through from each signal and normalization if the expression levels are different.

Alternatively, where ratio is not 1:1, the acceptor photobleaching (donor dequenching) FRET method might be considered, as the FRET efficiency calculated using this approach is independent of the ratio (see (39) for an example of FRET calculated using this method). In terms of HTS, however, this technique is relatively low throughput, as it generally requires laser scanning microscopy and high magnification, and bleaching times can be in the order of minutes for some photostable proteins.

Fluorescence lifetime microscopy (FLIM) is a third alternative to the measurement of FRET. This technique is independent of the ratio between donor and acceptor, as it only measures changes in donor fluorescence lifetime following illumination. Specifically, participation of the donor in FRET reactions with the acceptor alters the donor fluorescence lifetime, which can then be used to estimate changes in FRET efficiency in the presence and absence of compounds. However, conventional FLIM is unsuitable for HTS as its measurement is time-consuming and requires sophisticated instrumentation. Recently, FLIM microplate readers compatible with SBS standard labware have been introduced on the market (for example, see <http://www.fluorescenceinnovations.com/cells.html>). Furthermore, the throughput of FLIM has been improved, to give 96 well plate reads of tens of minutes, rather than hours (40). Because spectral bleed-through is not an issue with this technique, additional control cell lines expressing individual FRET proteins are not required. However, quantification of FLIM does require a series of calculations following image segmentation (for examples see (40) and (41)).

## Assay Validation Steps

1. Test which orientation of the donor and acceptor fluorescent protein fusions produces the most robust FRET signal (depending on the protein of interest, validation of correct subcellular localization or biochemical activity might also be prudent). Also determine whether full-length proteins or only the interaction domains should be used for the FRET constructs. Inclusion of an epitope tag in the

linker between the donor and acceptor fluorescent proteins and the proteins of interest can help determine relative ratio. If one member of the pair is more highly expressed, this protein should be selected as the acceptor because it reduces the potential of free donors contributing to spectral cross talk.

2. In the absence of small molecule positive controls, create point mutants or deletion constructs that disrupt the interaction under investigation.
3. Generate cells in which neither, or only one of the FRET pair is expressed in order to establish the degree of spectral cross-talk and bleed-through from each fluorophore.
4. Select specific filters based on the FRET pair chosen (i.e., it is not sufficient to use a general 'YFP' filter for all of the new yellow acceptor fluorescent protein variants). Use of dual band excitation/emission filters to allow simultaneous read of donor and acceptor emission can reduce variability during plate reads.
5. Optimize the illumination conditions for FRET: low illumination might result in poor signal to noise, whereas strong illumination can lead to photobleaching, both of which will complicate ratiometric analysis.
6. For automated image acquisition, minimize the exposure time for auto-focusing in order to avoid photobleaching effects.

## Statistical Considerations for FRET

Enough cells should be prepared in bulk to run the full screen to avoid passage-number variation. Batch-to-batch (day-to-day) variations can also be significant with FRET. Inclusion of the same control on all plates within and between batches is recommended. The same statistics that have been described for other HTS methods apply to FRET-based assays, See the AGM chapter (see the AGM Chapter HTS Assay Validation) (42). See the overall statistical considerations section at the beginning of this chapter.

## Sample Validation Data

**Example 1.** Development of FRET Assay into Quantitative and High-throughput Screening Technology Platforms for Protein-Protein Interactions by Song and colleagues (12). This manuscript describes development of a FRET-based assay for measuring the signaling cascade of SUMOylation using the FRET pair CyPet and YPet. Assay development and a pilot high-throughput screen in 384-well plates is described. Compounds are incubated with the stably transfected HEK293 cells for two hours, before reading the signal in a Molecular Devices FlexStation reader.

**Example 2.** Förster resonance energy transfer (FRET)-based subcellular visualization of pathogen-induced host receptor signaling by Buntru and colleagues (43). This study measures a protein-protein interaction in intact live cells using flow cytometry measurements. The authors further validated their assay with confocal microscopy and acceptor photobleaching to localize the sites of bacteria-host cell contact. This assay could be adopted for high-throughput screening.

## Troubleshooting Guide

**No or low FRET:** The absence of energy transfer might be related to the actual FRET donor and acceptor constructs. Steric issues might prevent optimal FRET, while some combinations of fluorescent proteins and interacting proteins might be inherently unstable. Check expression of all orientations of N- and C-terminal fusions of fluorescent proteins for both donor and acceptor during assay development. An excess of free donor can reduce apparent FRET efficiency, and in this case one should titrate the FRET pairs during transfection optimization to favor an excess of acceptor. Suboptimal filter sets can significantly compromise FRET; thus the bandpass of the filters should be tailored to precisely match the absorption/emission spectra for the fluorescent proteins. If FRET is being estimated ratiometrically, care must be taken to avoid photobleaching. Reduce illumination intensity using neutral density filters, and illuminate only donor when scanning plates to identify cells to analyze. In order to maximize FRET efficiency, choose partners with minimal excitation of acceptor at maximal excitation of donor, and maximal overlap of donor emission and acceptor excitation.

**Low signal-to-noise:** Low signal-to-noise can be due to a low FRET signal (see above) or due to fluctuations in the light source. It is critical that the light source is stable for this assay. Another trivial explanation for low signal-to-noise is the mislabeling of donor and acceptor images during analysis.

**Ratio is very high or low:** In microscopy-based FRET, outliers with very high or low FRET ratios can be due to analysis of out-of-focus images or differences in expression in transient transfections or pooled transfectants. In this case, different ROIs or cells must be selected and re-analyzed.

**High FRET with negative controls:** The fluorescent proteins should incorporate mutations to prevent oligomerization (44). If the genetic controls using binding-deficient mutants give a high FRET signal, this might indicate that the fluorescent proteins are oligomerizing and driving a non-specific interaction. Alternatively the expression level of the FRET pair might be too high and in this case re-optimization of expression is required. Also one should examine the signal overlap between donors and acceptors. Another possibility is that the interaction under investigation is more complex than originally thought. The investigator should validate the sequences of plasmid DNAs to confirm the presence of disruptive mutations.

## Bioluminescence Resonance Energy Transfer (BRET)

### Introduction

Bioluminescence Resonance Energy Transfer (BRET) is also a proximity-based assay that measures the energy transfer from a donor to an acceptor, in this instance luciferase is used as the donor, and a fluorescent protein as the acceptor (10). The NanoBRET method employs a NanoLuc fusion protein as the bioluminescent donor and a fluorescently labeled HaloTag fusion protein as the acceptor (**Figure 3**). The optimized blue-shifted

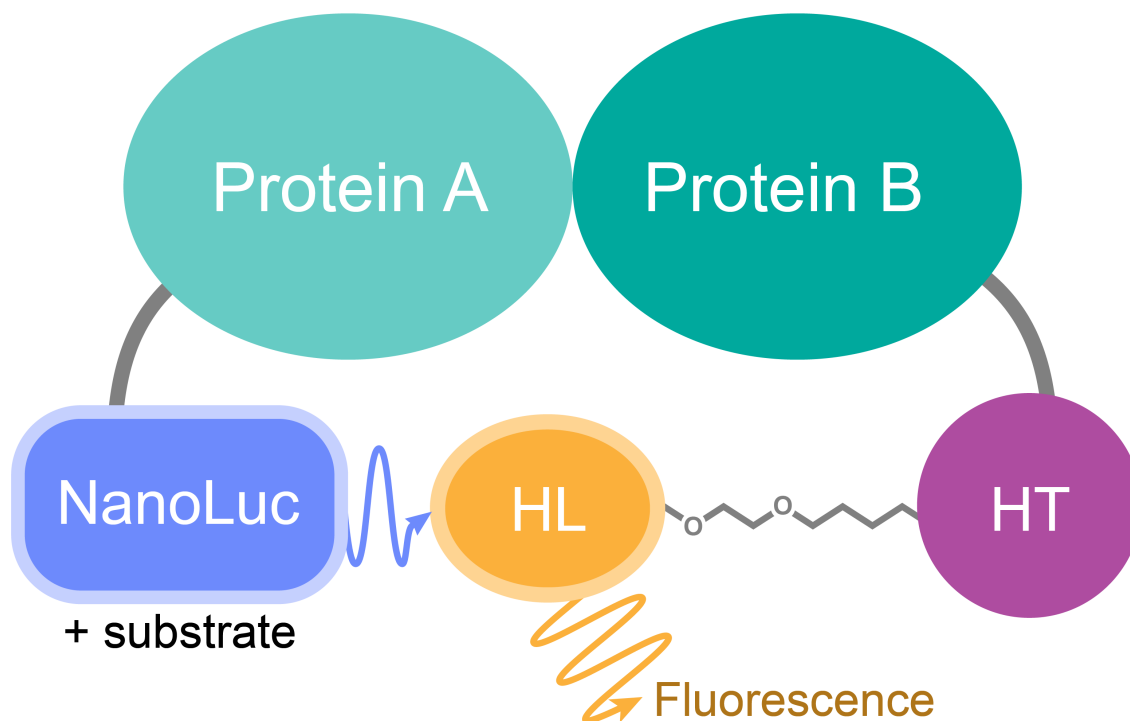


**Figure 3.** Overview of the NanoBRET assay principle. Energy is transferred from a NanoLuc-Protein A fusion (energy donor) to a fluorescently labeled HaloTag-Protein B fusion (energy acceptor) upon interaction of Protein A and Protein B.

NanoLuc donor paired with the red-shifted HaloTag acceptor minimizes spectral overlap, resulting in low bleed-through and improved signal-to-background and dynamic range. The extremely bright and stable NanoLuc® also allows for expression of the donor at or near physiological levels further reducing background and improving sensitivity.

### Assay Development

**Instrumentation:** To measure BRET assays, an instrument capable of sequentially measuring dual-filtered luminescence values equipped with appropriate filters is required. For the NanoBRET configuration the ideal filter setup will include a band pass (BP) filter centered around 460nm to measure the donor signal (Ex. Emission 450nm/BP 80nm) and a long pass (LP) filter starting at around 600–610nm to measure the acceptor signal (Ex. Emission 610nm/LP). Filters outside of these ranges will miss critical measurements and compromise data quality. Commercial plate readers pre-equipped with the proper filter set up include Promega's GloMax Discover and BMG's CLARIOstar. Instruments that can be equipped with optional filters include Thermo's Varioskan (Edmunds Optics filters: donor 450nm CWL, 25mm diameter, 80nm FWHM, Interference Filter and acceptor 1 inch diameter, RG-610 Long Pass Filter) and PerkinElmer's EnVision (Chroma filters: Emission Filter (for EmSlot4) Cat. # AT600LP and Second Emission Filter (for EmSlot1) Cat. #AT460/50m).

For instruments using mirrors, select the luminescence mirror. An integration time of 0.2–1 second is typically sufficient. Ensure that the gain on the photomultiplier tube is optimized to capture the highest donor signal without reaching instrument saturation.

Plates: White tissue culture grade plates are preferred. Black plates can quench luminescence. Formats include 96 and 384 wells. 1,536 well formats might require optimization and a specialized instrument.

Cell types: NanoBRET can be performed in any cell line that can be transfected including HEK293, HeLa, HCT-116, NIH3T3, CHO, and Jurkats. For difficult to transfect cells, optimization might be required. Generation of stable cell lines expressing one or both protein partners is highly preferred, for the reasons described above.

Media: To avoid interference with the acceptor signal, phenol red-free medium should be used. Reduced serum media such as Opti-MEM + 4% FBS is recommended. The use of higher amounts of FBS can increase variability in 384 and 1,536 well formats.

Assay conditions: Find the optimal ratio of donor and acceptor expression levels to minimize unbound donor, which reduces background and maximizes dynamic range (see Assay Validation Steps below). Cells are transfected and grown under typical tissue culture conditions. Because the HT protein is not intrinsically fluorescent, a set of samples without ligand can be plated and used as a background control. The non-lytic assay is completed by the addition of the NanoLuc substrate furimazine and donor and acceptor signal measurements.

Kits and reagents: Kits for generating NanoLuc and HaloTag fusion clones and kits containing HaloTag ligand and NanoLuc substrate reagents are available from Promega.

## Data Analysis

It is critical to use the appropriate filters to capture the specific donor and acceptor signals for NanoBRET, generic filters for other BRET configurations might not be applicable.

The donor emission occurs at 460nm, a band pass (BP) filter that covers close to 460nm with a band pass range of 8–80nm is preferred. A short pass (SP) filter that covers the 460nm area also can be used but it might result in an artificially large value for the donor signal measuring the bleed-through into the acceptor peak. This artificially large value could compress the ratio calculation and reduce the assay window. The acceptor emission occurs at 618nm. To measure the acceptor signal, a long pass filter starting at 600–610nm is preferred.

To calculate the BRET ratio the acceptor signal is divided by the donor signal (**Equation 4**):

$$\frac{618 \text{ nm}_{Em}}{460 \text{ nm}_{Em}} = \text{Raw NanoBRET ratio} = BU$$

To convert raw BRET units (typically decimal values) to milliBRET units (mBU; whole numbers), multiply each raw BRET value by 1,000 (**Equation 5**):

$$\frac{618 \text{ nm}_{Em}}{460 \text{ nm}_{Em}} = BU \times 1000 = mBU$$

To account for any background contribution, the mean ratio from the no ligand control samples is subtracted from the ligand containing samples to yield a corrected ratio (**Equation 6**):

$$\text{Mean } mBU(\text{experimental}) - \text{Mean } mBU(\text{no ligand control}) = \text{Mean corrected } mBU$$

### Assay Validation Steps

1. Determine the donor and acceptor configuration with the optimal distance and geometry for efficient energy transfer between the protein partners. There might be instances when there is prior knowledge of the protein biology that would prevent a certain terminus from being tagged. If no such constraints exist, both proteins of interest can be tagged with either NanoLuc or HaloTag on either the N- or C-terminus resulting in up to 8 possible constructs and 8 possible combinations. Full-length proteins or protein domains might be used. Test the various combinations in the assay to see which one(s) give the most robust ratio(s).
2. Optimize transfection conditions for the top pair configuration(s). This is done by finding the ratio of donor to acceptor DNA that minimizes unbound donor, reducing the background and maximizing dynamic range. Generally, the amount of HaloTag DNA is kept at a higher concentration while the NanoLuc DNA is reduced to 1/10<sup>th</sup> to 1/1,000<sup>th</sup> relative to the amount of HaloTag DNA.
3. If a known modulator of the interaction is available, either an inhibitor or an activator, confirm the proper biological response. In some cases the highest possible ratio pair might not always equate the most robust response to the modulator. It is advisable to test more than one combination to find the most responsive to the expected biology. In addition, some small molecules might have been developed against a particular isolated domain or using *in vitro* assays and might not elicit the same response when using full-length proteins or inside the cell.
4. If no known modulator is available, donor saturations assays (DSA) might be performed to show assay specificity (8). In a DSA, the amount of NanoLuc donor DNA is kept constant while steadily increasing the amount of acceptor DNA. As the acceptor-to-donor (A/D) ratio increases, a specific BRET assay will show ratios that increase in a hyperbolic manner and reach a plateau representing complete saturation of all donors with acceptor molecules. Non-specific interaction, as it can be tested with a negative control protein, will generate much weaker ratios that plot in a linear manner known as bystander BRET (**Figure 4**).

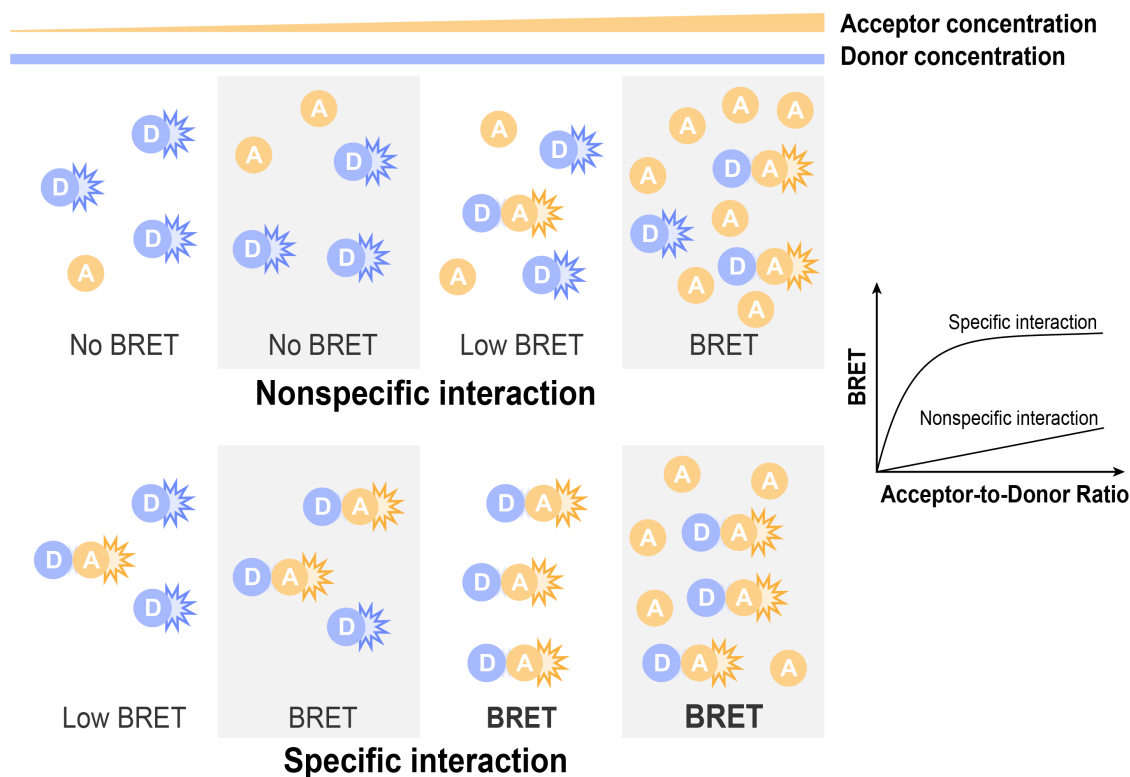


**Figure 4.** Principle of the Donor Saturation Assay (DSA) to validate BRET assay specificity.

## Statistical Considerations for BRET

The ratiometric nature of the BRET assay intrinsically results in low variability. Use the corrected mBU and standard deviation values to calculate the  $Z'$ -factor (see **Equation 1**).

## Sample Validation Data

**Example 1.** NanoBRET—A Novel BRET Platform for the Analysis of Protein–Protein Interactions by Machleidt and colleagues (9). In this example, the authors describe the development of the NanoBRET configuration of BRET and its application to a novel assay developed for analyzing the interactions of bromodomain proteins with chromatin in living cells.

**Example 2.** Generation of a Selective Small Molecule Inhibitor of the CBP/p300 Bromodomain for Leukemia Therapy by Picaud and colleagues (45). The authors report the development and preclinical evaluation of a novel, potent inhibitor targeting CBP/p300 bromodomains that impairs aberrant self-renewal of leukemic cells. This is a good example of a small molecule that when studied in live cells, exhibits differential inhibitory profiles in full-length proteins vs. individual protein domains



## Troubleshooting Guide

### No or low BRET:

- a. Ensure filters are specific for NanoBRET: 460nm (with 8–80nm band pass) for donor signal and 600–610nm long pass for acceptor signal. Make sure the gain on the photomultiplier tube is set to detect donor signal without instrument saturation. Confirm ratio calculation is acceptor divided by donor values (618nm/460nm).
- b. Test all possible donor/acceptor combinations to find best pair.
- c. Ensure protein expression by checking luminescence for NanoLuc constructs. Expression for HaloTag constructs can be checked by fluorescently labeling with a HaloTag ligand such as TMR which can then be run on SDS-PAGE and analyzed using a fluorescence scanner.
- d. Optimize transfection conditions and relative amounts of donor and acceptor DNA. Excess donor will compress assay window.
- e. Some PPI might be dependent on specific biological events or stimuli to activate specific pathways. Ensure proper pathway activators are added. If possible, check proper phenotypical responses by other means.
- f. Confirm cell health by a viability assay (see AGM chapter Cell Viability Assays).
- g. Absolute raw values and ratios will vary among PPI systems. Absolute BRET values depend on the proximity of the protein partners, the affinity of the interaction, the relative occupancy with other interacting proteins and the instrument setup. When possible, check specificity with a known modulator such as an inhibitor or by the Donor Saturation Assay (DSA).

**High variability:** Optimize all parameters of the assay aiming for  $Z'$ -factors between 0.5 and 1. If the assay parameters have been optimized, consider automated dispensing to reduce variability.

**Unable to detect proper expected biology in the presence of small molecule:** Increase the concentration of small molecule, treat overnight or both to see maximum effect. If the compound was developed *in vitro* against the domain or region alone, it might not disrupt the interaction of the full-length proteins. Test region or domain alone versus full-length protein. Always consider the possibility that the compound might affect the luciferase activity without actually disrupting the PPI (see next section).

## Fluorescent Protein Fragment Complementation

### Introduction

Direct reporter complementation assays have split reporter proteins fused to the protein partners of interest; formation of the PPI causes reconstitution of the reporter protein and induction of fluorescence or enzymatic activity (**Figure 5**).

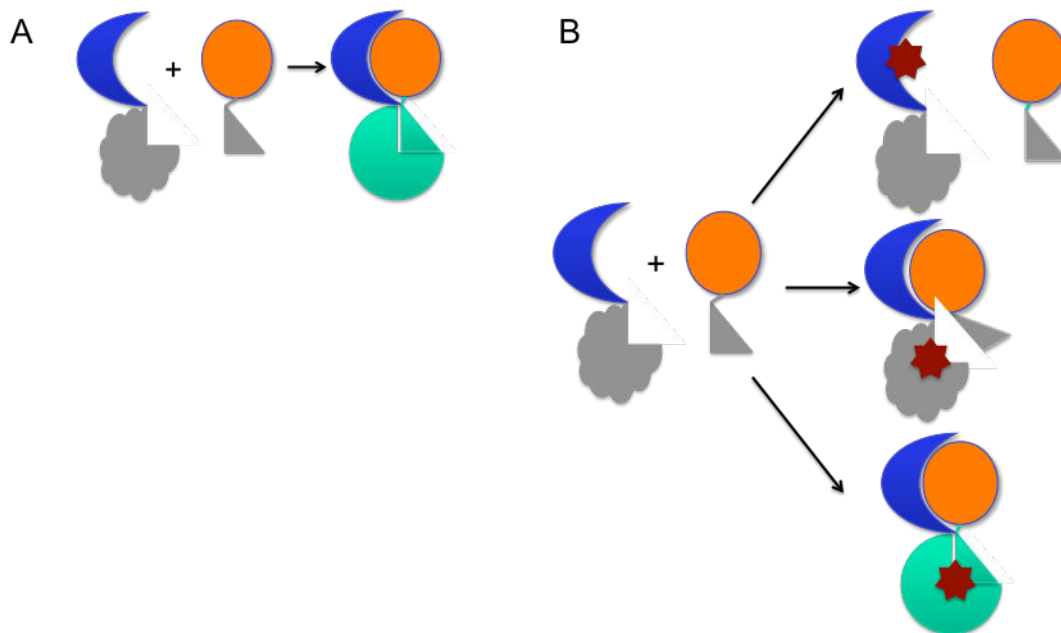


**Figure 5:** Principle of protein fragment complementation. (A) Two interacting proteins (blue) are fused to N- and C-terminal fragments of a reporter protein such as GFP or luciferase (gray). Following interaction, the reporter is reconstituted (green). (B) A small molecule (red star) can affect the reporter signal in several ways. The molecule might bind to and specifically inhibit the PPI under interrogation, a ‘true positive’ (top). Alternatively, false positive compounds could interfere with reconstitution of the reporter protein (middle) or block the catalytic activity of the reporter (bottom). Secondary screens are required to identify such false positive events.

The use of split GFP as a PPI reporter was first described by Regan and colleagues (46). In this method, a GFP variant was separated between residues 157 and 158 into two polypeptides, each of which were fused to interacting leucine zippers. Reconstitution of fluorescence was not observed when the GFP fragments were co-expressed without the leucine zippers, indicating that PPI could be reliably detected using this method. GFP and additional fluorescent proteins were rapidly adopted for the study of PPIs. Hu and Kerppola extended the use of split GFP to measure protein-protein interactions in mammalian cells (16). This so-called ‘*Bimolecular Fluorescence Complementation*’ (BiFC) has been extended to many other fluorescent proteins, greatly expanding the potential combinations that could be applied *in vivo*. BiFC offers some advantages over other fluorescence-based methods for PPI detection. For example, FRET requires careful control of the ratio between interacting partners, and is also less sensitive than BiFC due to the presence of background fluorescence emitted by the acceptor fluorophore (**Section 2**) (47). Many BiFC pairs have been demonstrated (**Table 3**).

Because the primary amino acid sequence of different fluorescent proteins varies at only a few residues, it is possible to ‘multiplex’ BiFC. For example, the C-terminal amino acid sequences of GFP, YFP, and BFP are identical after amino acid 155, whereas their N-terminal sequences differ at several residues. In this way, the interaction of one protein

with 2 potential partners can be interrogated simultaneously. For example, interaction of the bJun transcription factor with its binding partners bFos and bATF2 has been demonstrated (16).

Despite its versatility, BiFC does suffer from some limitations. First, refolding of the fluorescent chromophore fragments is essentially irreversible (48, 49). While this might be advantageous for detecting weak or transient PPIs, the irreversible nature of BiFC in its present form greatly complicates its application as a discovery platform for inhibitors of PPIs. To get around this issue, one can engineer an inducible BiFC reporter (using a doxycycline-responsive promoter, for example); the reporter cell lines can then be incubated with compounds prior to expression of the BiFC constructs, providing a time window in which their activity can be detected.

A second issue with BiFC (and other complementation assays in general) is that the signal intensity, compared to that achieved with the full-length protein, is often orders of magnitude lower. Although the background of BiFC is low, the reduced signal can sometimes reduce the robustness of the HTS assay. Variants of Venus (a YFP derivative) have been reported to significantly improve the signal/background for complementation (13).

Finally, a fluorescence-maturation step follows re-association of the split chromophore. In some cases, this maturation is temperature-dependent; the BiFC signal from some YFP fragments and from mCherry is greatly enhanced if the temperature is lowered to 25-30 °C prior to readout (13, 17). This change in temperature presents an additional logistical consideration and potential source of variability for BiFC-based HTS campaigns.

**Table 3.** Examples of BiFC partners

| Fluorescent Protein | N-terminus    | C-terminus | Comments   | Reference |
|---------------------|---------------|------------|--|-----------|
| GFP                 | 1-157         | 158-238    | Utilized a brighter variant of wtGFP   | (69)      |
| Venus               | 1-154         | 155-238    | A brighter variant of YFP  | (13)      |
| Venus               | 1-210 (V150A) | 210-238    | Additional mutations added to Venus to improve S/N ratio   | (14)      |
| YFP                 | 1-154         | 155-238    | Increasingly replaced by other 'yellow' variants (Citrine and Venus) due to sensitivity to high temperatures | (15)      |
| CFP                 | 1-154         | 155-238    |  | (16)      |
| mCitrine            | 1-172         | 173-238    |  | (70)      |
| mCherry             | 1-159         | 160-237    | Sensitive to high temperatures, requires longer maturation times   | (17)      |
| mLumin              | 1-151         | 152-233    | Brighter mKate variant, less sensitive to high temperature compared to other red variants                    | (71)      |

## Assay Development

**Chromophore selection:** **Table 3** lists common fluorescent proteins used in split constructions. Each reference contains additional variations in terms of the location of the split, and point mutations to improve fluorescence emission or stability in the BiFC application. Splitting chromoproteins can also slightly alter the maximum excitation and emission spectra compared to the full-length proteins, and wavelength scanning to identify the optimal excitation and emission is therefore recommended when using new BiFC pairs.

**Instrumentation:** BiFC can be measured on high content fluorescence microscopes (e.g., Molecular Devices Image Express and Image Express Ultra, GE Healthcare INCell Analysts 2200 or 6000, or the PerkinElmer Operetta or Opera) or flow cytometry (e.g., BD Biosciences, Intellicyte). If the fluorescence intensity is sufficiently high, the assay might be readable on a fluorescent plate reader (e.g., TECAN Safire<sup>2</sup> or M1000, BMG Pherastar, BioTek Synergy series, Molecular Devices M5 or Flexstation, PerkinElmer Envision). Reading fluorescence from the bottom of the well is less sensitive to the effects of fluorescence interference from the medium, but top reading plates with a z-plane optimization function can also be used. If a new BiFC reporter is being evaluated, monochromator-based readers can be useful to determine the peak emission of the reporter during assay development.

**Plates:** Due to the fluorescent readout, black-walled plates are recommended. Clear bottom plates, such as  $\mu$ Clear plates from Greiner, are suitable for imaging or for detecting fluorescence from the bottom of the plate.

**Cell types:** a variety of cells have been used for BiFC assays, including U2OS osteosarcoma, HEK293, COS-1, HeLa and NIH3T3. A primary consideration for high content imaging applications is that the cells should adhere well to the plate. For plate-reader based assays, it might be necessary to perform multiple reads per well (several plate readers allow reading at different spots within a well) to compensate for unequal cell distribution.

**Buffers:** Cells can be grown in the medium recommended by ATCC. However, for maximal signal (especially when using GFP) it is preferable to use phenol red-free and low-glucose medium in live cells, or switch to PBS if fixed cells are used. These solutions can overcome some of the issues associated with autofluorescence coming from medium components. Fixation should be optimized to reduce quenching of fluorescent proteins.

**Assay Conditions:** In general, lower temperatures (between 4 °C and RT) favor fluorescence complementation. However, fluorescence is reconstituted in many BiFC pairs (for example, mCherry) following incubation at higher temperatures (RT to 30 °C). With newer versions such as Venus, the temperature dependence might be less critical. The temperature and time of incubation for each BiFC pair must be determined empirically, and binding-deficient mutants should be included to control for non-specificity of the BiFC reporter. This is particularly important at lower temperatures, where

complementation can occur independently of the proteins to which the fragments are fused. Following completion of the screen, cells might be visualized live, or can be washed in PBS and fixed in 4% paraformaldehyde and stored protected from light until examination. Include additional negative control wells where possible (medium in the absence of cells, for example) to determine the background auto-fluorescence.

## Data Analysis

General considerations: Stably transfected cells are highly preferable due to the improved run-to-run stability and ability to subsequently separate cells with the desired expression profiles. If the BiFC screen is performed by transient transfection, however, it is critical to co-transfect a full-length fluorescent protein that is spectrally distinct from the BiFC pair as an internal control for transfection efficiency. In this way, the BiFC signal can be normalized to the full-length fluorescent protein signal on a per cell basis, and the results plotted as a histogram. Ideally, the control protein is expressed from the same plasmid as the BiFC pair; otherwise, not all cells will receive both the BiFC and the full-length fluorescent protein with the same ratio. During assay development, plates should include cells with genetic controls for non-interacting mutants (e.g. N- and C-terminal fragments of the fluorescent protein fused to point or deletion mutants of one of the interacting pair). These constructs can be used to validate that PPI formation drives BiFC and set background readings for the assay.

Imaging-based assays: a nuclear stain (e.g., Hoechst 33342) is added to live or fixed cells. Plates are imaged at the appropriate resolution (typically 10x) with the appropriate fluorescence filters for the nuclear stain and fluorescent protein. Cells are identified by nuclear stain and by the intensity and localization of the fluorescent protein. Fluorescence can be monitored in several ways, such as intensity/cell, number of cells above an appropriate threshold, or number or intensity of puncta/cell. The most reproducible and robust measure should be used to calculate the signal for high-signal and low-signal controls and to determine  $Z'$ -factor values (see **Equation 1**). Normalization of fluorescence to cell number is important to account for inconsistencies in cell plating or cell-growth and to identify toxic compounds. Dead or dying cells can be excluded by morphological criteria (e.g., cell rounding, nuclear condensation) during image segmentation.

Plate-reader based assays: If a plate reader is used for the BiFC measurement, readings are best performed in cells that have been washed to remove dead and floating cells that can give confounding bright fluorescent signals. Normalization of the BiFC to cell number is important to exclude false positives that are toxic. With a genetically engineered system, this normalization can be achieved using an IRES driving expression of a second fluorescent protein or luciferase. Alternatively, a fluorescent indicator of cellular viability (such as resazurin or CellTiter-Fluor) can be used as an indirect measure of cell number. Care should be taken to ensure the spectral overlap between this marker and the BiFC pair is minimal.

## Assay Validation

Note: many of the assay validation considerations are similar to those described for BRET.

Optimal protein pair configuration: Determine the optimal orientation of the fusion proteins for both partners testing both N- and C-terminal orientations (total of 8 combinations). Linker design is also a critical factor at this stage; Gly-Ser rich sequences of varying lengths, as well as RPACKIPNDLKQKVMNH and AAANSSIDLISVPVDSR have been used successfully. In order to validate expression by western blot, an epitope tag such as HA or FLAG can also form part of the linker.

Assay validation controls: Known small-molecule inhibitors are ideal, but if no such modulator is available, design a negative control construct where one of the interacting proteins is mutated to disrupt binding. Alternatively, donor saturation can be used (see Assay Validation Steps for NanoBRET).

Optimize expression: Optimize transfection conditions by varying the ratio of the donor and acceptor plasmids. Determine the optimal temperature and time following induction to yield maximal fluorescence. Ideally, fast maturing fluorescent proteins should be chosen, although due to the split, the maturation times for the BiFC pairs might differ from the full-length fluorescent proteins. If the assay is to be performed transiently, titrate the BiFC pair in order to give the most stable signal with the lowest expression of protein. Also establish the shortest time at which the signal is stable, to avoid issues associated with overexpression. Perform both microscopy and plate reader based analyses at this step. Note that the level of fluorescence from split fluorescent proteins is far less than the full-length counterparts, so adjust gain accordingly. Maximal emission might be slightly offset compared to the full-length protein, which must be taken into account when selecting filters. Determine whether the subcellular localization (and if possible biochemical activity) of the BiFC pair is consistent with the biology. For a multiwell format and especially if the reading will be high content, optimize cell seeding density. If individual cells need to be segmented, then aim for a final confluence at measurement of around 50-60%.

Determine the timing of compound addition: Because BiFC for most (if not all) fluorescent proteins is irreversible, it is recommended that compounds are added either before or concomitantly with introduction of the BiFC pair. Set high-signal (vehicle only) low-signal (known inhibitor, mutated PPI pair, etc.) controls.

## Statistical Considerations for Fluorescent Protein Fragment Complementation

For an assessment of assay robustness, the  $Z'$ -factor can be used (see **Equation 1**). Ideally the low-signal control should be a known small molecule inhibitor of the PPI under investigation. Otherwise, the non-interacting genetic control can be substituted, although this might give an artificially low BiFC signal compared to actual small molecule inhibitors. For initial hit determination, each sample can be compared to the plate-based

mean BiFC signal, with a cutoff defined as between 1 and  $3 \times \sigma$  from the mean, depending on the assay robustness. Secondary screens should be in place in order to test for selectivity (for instance, a different PPI using the same BiFC fluorescent reporter) and for assay interference (for example, test the putative hits against the original PPI, but using split luciferase instead of BiFC).

## Sample Validation Data

**Example 1.** Drug screening for autophagy inhibitors based on the dissociation of Beclin 1-Bcl2 complex using BiFC technique and mechanism of eugenol on anti-influenza A virus activity by Dai and colleagues (50). The goal of this study was to identify compounds that disrupt the interaction between Beclin and Bcl2, thereby increasing autophagy. BiFC used mCherry (N-terminal mCherry aa1-169-Bcl2 and C-terminal mCherry aa160-262-Beclin1). For 96-well plate assays, A549 cells were transfected with BiFC constructs before compound addition for 8 h. The cell-based assay using a microplate reader gave a  $Z'$ -factor of 0.5. Known autophagy inhibitors (ERK inhibitor, MAPK inhibitor) increased the BiFC signal, whereas activators (anisomycin,  $H_2O_2$ ) reduced the signal.

## Troubleshooting Guide

No or low BiFC signal: Check all orientations of the fusion proteins and linker lengths to find maximal signal and check for expression by western analysis. Ensure that the filter is correct; this can also be optimized by performing a wavelength scan on monochromatic instruments. Determine the optimal temperature for the maturation of the fluorescent BiFC construct (a range is from 4 °C for 1 h through 37 °C). Due to the lower fluorescence intensity of split fluorescent proteins, reads of multiwell plates should be performed in optically clear medium, and might require significant optimization of the photomultiplier tube gain.

BiFC signal not affected by positive controls: The level of the BiFC constructs might be too high. In that case, switch to weaker promoters, shorter incubation times, or use a lower dose of the inducing agent if using an inducible system. Pre-dose cells with compound prior to expression of the BiFC constructs. Also, older fluorescent proteins used for BiFC can be more prone to self-assembly. Use newer variants such as Venus (V150A mutant, split at 1-210 and 210-238) (14).

## Luciferase Enzyme Fragment Complementation

### Introduction

*Bimolecular luciferase complementation (BiLC)* is proving to be a powerful tool in many discovery projects (51). For example, PPIs involved in pathways associated with cancer (52, 53), Alzheimer's disease (54) and plant signaling (55) have all been interrogated with this method. Compared with BiFC, luciferase complementation has three distinct advantages. First, the interaction between the two fragments does not require covalent bond formation, and is therefore completely reversible (49). Second, background

luminescence is extremely low because the overlapping luciferase fragments, have no activity on their own, and can reassemble into an active enzyme when the proteins they are fused to are brought into close proximity by the interacting proteins of interest. In addition, the affinity of the split luciferase fragments for each other is much weaker than that of the interacting proteins of interest to which they are fused. Finally, the enzymatic activity of luciferase combined with a very low background leads to robust assays when evaluated by common screening metrics such as the Z'-factor (27). Several groups have also reported the use of BiLC in xenograft studies in mice (7, 53, 56), opening the possibility of further characterization of lead compounds during preclinical studies. **Table 4** highlights the many flavors of BiLC. Some of these enzymes require ATP (e.g., firefly), while others do not (e.g. Renilla).

As discussed above for fluorescent protein fragment complementation assays, BiLC can also be multiplexed. Multiplexing is possible because the N-terminus within a particular luciferase family determines its spectral characteristics, whereas the C-terminus contributes the enzymatic function (57, 58). Ozawa and colleagues (52) have identified mutations in the C-terminus of click beetle red (CBR) that allow complementation with N-terminal fragments of firefly, CBR and click beetle green (CBG) luciferases. Thus, the interaction of a 'bait' protein (fused to the C-terminus of CBR) with two competing proteins (each of which is fused to a different N-terminal luciferase fragment) can be interrogated. In a second study, complementing CBR and CBG fragments were rationally designed using a 'bait' fused to the C-terminus of CBG and prey fused to either the N-terminus of CBG or CBR (59).

The multiplexed BiLC setup allows the detection of multiple PPIs using one common substrate (D-Luciferin or commercial reagents), but also requires careful selection of imaging medium, luminescence emission filters, and software to perform spectral deconvolution of the data. In terms of HTS, the time taken to image each microwell plate will depend on the total photon output, which in turn will be determined by the expression level of the constructs and the strength of their interaction.

BiLC also has some limitations, such as sensitivity to false positives (inhibitors of luciferase enzymatic activity, for example) and false negatives (such as autofluorescent test compounds). Additionally, as with all protein fragment complementation assays, the choice and orientation of fusion partners might be limited to some extent by steric effects. Controls for normalization of cell number or transfection efficiency are also critical in this assay. Suitable controls include co-transfection or IRES-driven expression of a reporter such as Renilla luciferase or fluorescent protein. Finally, because the chemiluminescent reaction requires molecular oxygen, this assay might be affected in HTS screens performed at low oxygen concentrations or those performed in strictly anaerobic organisms.



## Assay Development

**Instrumentation:** Many commercial multimodal plate readers can be used to detect the signal from BiLC. These include Promega's GloMax, TECAN's Safire<sup>2</sup> (now TECAN M1000), BMG's Pherastar, BioTek's Synergy series, PerkinElmer's Envision.

**Choice of luciferase species:** There are multiple choices for luciferase species. Click beetle luciferases show little color sensitivity to pH and temperature changes as opposed to firefly luciferase, in which the maximal emission color can vary by as much as 40 nm under different reaction conditions (59).

**Plates:** Solid white plates (for example Corning 3570) are recommended. If the assay is performed with live cells and is to be combined with a fluorescence readout, then black walled Greiner  $\mu$ Clear plates can be used.

**Cell types:** BiLC has been performed in many cell types including U2OS, SaOS-2, HEK293, H4 neuroglioma, HeLa, COS-7, CHO.

**Buffers:** For kinetic BiLC studies in intact cells, phenol red-free medium containing 100  $\mu$ M D-luciferin (made from a concentrated stock solution) should be used. The medium should be buffered by the addition of HEPES, for example. For endpoint assays in which the cells are lysed, phenol red-free medium is still recommended.

**Kits:** For large numbers of plates in HTS format, commercially available luciferase detection reagents can be beneficial due to the batch-to-batch consistency. Although these reagents are frequently added at a 1:1 (reagent:medium) ratio, lower ratios still produce robust signals and can be optimized during assay development.

**Titration of reagents:** In a 384-well format, a cell density between 2000 and 15000 per well is recommended, depending on the cell type. This is based on a stable cell line system; if the assay will be performed using transient transfection, the optimal cell density might differ.

**Assay Conditions:** If stable cell lines with constitutive expression are used, it is important to screen several clones and pick those that exhibit a robust signal with the minimum amount of overexpression. An alternative (but more labor-intensive) option is to develop a bidirectional, doxycycline-inducible reporter system, where each pair of the fragment complementation module is expressed following addition of doxycycline to the medium. This can aid in control of the level of expression, permit compounds to be added before protein complexes are formed, and restrict the expression of potentially toxic fragment pairs.

**Timing:** the optimal time for detection of luminescence will vary according to the experimental setup. For example, if a doxycycline inducible system is used, robust signal can be detected 6-10 h following the addition of doxycycline. One advantage of a short incubation time is that secondary compound effects, such as cytotoxicity, are likely to be avoided.

As with conventional luciferase assays, it is important to equilibrate the plates to room temperature for up to 30 min before reading. This improves plate Z'-factors. In comparison with full-length luciferase, the window for detection of the BiLC signal might be significantly shorter when using reagents such as SteadyGlo. Therefore during assay development the time post-lysis at which optimal luciferase activity is detected must be determined. This will dictate the number of plates that can be processed per unit time while maintaining acceptable plate metrics.

## Data Analysis

Using real-time analysis of click beetle green and click beetle red luciferase heteroprotein fragment complementation, the hybrid proteins rapidly and directly reconstitute an enzymatic reporter activity within the cell, offering the potential benefit of real-time analysis and enhanced sensitivity for detecting weakly interacting proteins.

## Assay Validation Steps

To validate the assay, well-characterized binding partners would be useful. For example, the rapamycin-binding domain of human mTOR (residues 2024–2113) and human FK506-binding protein-12 can provide a well-characterized macromolecular interaction platform to validate protein fragment complementation pairs. In the case of Villalobos et al., the N-terminal fragments of all luciferase PCA constructs were each fused to a flexible G-S linker and the C-terminus of the rapamycin-binding domain of human mTOR, while the C-terminal fragments of all constructs were each fused to a flexible G-S linker and the N-terminus of FK506 binding protein-12 (59). Subsequently, HEK293T cells were used for the validation and the protein interactions were analyzed by live cell bioluminescence imaging.

It is important to establish that the half-life of the protein of interest was unaffected by the addition of the fusion protein. To rule out that any change is related to a change in the half-life of the protein, monitor the stability of the protein complex in real time using a HeLa TetOn stable line expressing the two binding partners. Ilagan et al. used the luciferase complementation activity in live  $\Delta E$ -NLuc/CLuc-RBP $\kappa$ -expressing cells that was monitored continuously for 6 h in the presence or absence of the protein translation inhibitor cycloheximide (60). The decay in bioluminescence indicated a Notch intracellular domain half-life of ~180 minutes, consistent with the half-life obtained by pulse-chase experiments in HeLa cells.

Another way to validate PPI assays is to use known inhibitors of the interaction if they are available. This allows the demonstration that the complementarity can be inhibited. Without the availability of a known inhibitor, a peptide can be selected that will block the two complementary fragments.

## Statistical Considerations for Luciferase Enzyme Fragment Complementation

The investigator should calculate the  $Z'$ -factor (see **Equation 1**) to gauge assay quality and suitability for HTS (27). For the low-signal control, omission of the substrate, an inhibitor (small molecule or peptide), or the cell line expressing only one of the complementary fusion proteins can be used.

### Sample Validation Data

**Example 1:** Dual-color click beetle luciferase heteroprotein fragment complementation assays by Villalobos and colleagues (59). This paper describes a set of reversible, multicolored heteroprotein complementation fragments based on the click beetle luciferases that utilize the same substrate as firefly, D-luciferin. Using luciferase fragment complementation a dual-color quantification was performed with two discreet pairs of interacting proteins simultaneously or two distinct proteins interacting with a third shared protein in live cells with real-time analysis. The proteins examined were  $\beta$ -TrCP, an E3-ligase that regulates both  $\beta$ -catenin and  $\text{I}\kappa\text{B}\alpha$ , and GSK3 $\beta$  as the kinase that regulates  $\text{I}\kappa\text{B}\alpha$  processing.

**Example 2:** Real time imaging of notch activation with a luciferase complementation reporter by Ilagan and colleagues (60). This paper measures ligand binding of Notch with a luciferase complementation assay. Notch receptors undergo ectodomain shedding followed by  $\gamma$ -secretase-mediated release of the Notch intracellular domain. The Notch intracellular domain translocates to the nucleus and associates with the DNA-binding protein CBF1/RBPjk/Su(H)/Lag and then subsequently activates gene expression. The activation of specific Notch paralogs was monitored in live cells and in real time using luciferase complementation imaging. In order to validate the system, kinetic analyses of Notch signaling with agonist- and ligand-dependent activation were conducted in live cells.

## Alternative Enzyme Complementation Assays

Two other enzyme complementation formats –  $\beta$ -lactamase and  $\beta$ -galactosidase – are also used for cell-based assays. The luciferase approach offers reversibility and the ability to multiplex PPI readouts, which are clear advantages. Because the assay development and troubleshooting will be analogous to the luciferase complementation described above, an extensive assay description is not included here. Nevertheless, a couple of important points are worth noting for each system.

Beta-galactosidase is a natural example of protein fragment complementation, because two polypeptides ( $\text{lac}\alpha$  and  $\text{Lac}\omega$ ) derived from the LacZ gene assemble to form the active enzyme. Mutagenesis studies led to the identification of weakly complementing  $\Delta\alpha$  and  $\Delta\omega$  polypeptides, whose interaction is driven by the protein partners to which they are fused (6). One advantage of this system is that there are diverse methods for the detection

of  $\beta$ -galactosidase activity, including immunohistochemical, fluorescent and chemiluminescent detection reagents. Thus, PPIs measured using split  $\beta$ -galactosidase can be detected on plate readers, flow cytometers and conventional microscopic systems. Furthermore, a choice of  $\beta$ -galactosidase reagents with different spectral characteristics facilitates multiplexing of this assay with other readouts. As with the BiLC approach, the enzymatic nature of split  $\beta$ -galactosidase assays can also lead to high signal-to-noise ratios, and a robust format for HTS (for examples, see (23)). Measuring PPI by  $\beta$ -galactosidase fragment complementation can also be used as a surrogate measure of other cellular processes, such as GPCR activation (DiscoverX PathHunter), proteolysis, and cytoplasmic-nuclear translocation (61).

Beta-lactamase is also amenable to protein fragment complementation (21). Because  $\beta$ -lactamase is a smaller protein, its usage might be advantageous in situations where  $\beta$ -galactosidase complementation is perturbed by steric hindrance. Beta-lactamase has been used to monitor the interaction between components of the Bcl2 pathway (18), GPCRs and arrestin (22) and proteins involved in Toll-like receptor signaling, and it provides a robust assay for HTS (19, 20).

## Suggested Websites

### Engineering split GFP

<http://www.stanford.edu/group/boxer/gfp.html>

[http://en.wikipedia.org/wiki/Green\\_fluorescent\\_protein](http://en.wikipedia.org/wiki/Green_fluorescent_protein)

### Protein folding from fragments

<http://www.ncbi.nlm.nih.gov/pmc/articles/PMC2211703/?tool=pubmed>

### FRET considerations

<http://www.olympusmicro.com/primer/techniques/fluorescence/fret/fretintro.html>

<https://www.biotek.com/resources/white-papers/fluorescent-proteins-filters-mirrors-and-wavelengths/>

### Luciferase

Harvard luciferase blackboard green and red (firefly) luciferase

<http://2009.igem.org/Team:Harvard/Split>

Spectra for different luciferases

<http://www.targetingsystems.net/drug-discovery.php>

Click Beetle differences

[http://www.promega.com/products/reporter-assays-and-transfection/reporter-vectors-and-cell-lines/chroma\\_luc-vectors/](http://www.promega.com/products/reporter-assays-and-transfection/reporter-vectors-and-cell-lines/chroma_luc-vectors/)

## References

1. Arkin MR, Glicksman MA, Fu H, Havel JJ, Du Y. Inhibition of Protein-Protein Interactions: Non-Cellular Assay Formats. In: Sittampalam GS, Coussens NP, Brimacombe K, Grossman A, Arkin M, Auld D, Austin C, Baell J, Bejcek B, Chung TDY, Dahlin JL, Devanaryan V, Foley TL, Glicksman M, Hall MD, Hass JV, Inglese J, Iversen PW, Kahl SD, Kales SC, Lal-Nag M, Li Z, McGee J, McManus O, Riss T, Trask OJ, Jr., Weidner JR, Xia M, Xu X, editors. *Assay Guidance Manual*. Bethesda (MD)2004.
2. Arkin MR, Tang Y, Wells JA. Small-molecule inhibitors of protein-protein interactions: progressing toward the reality. *Chem Biol*. 2014;21(9):1102–14. doi: [10.1016/j.chembiol.2014.09.001](https://doi.org/10.1016/j.chembiol.2014.09.001). Epub 2014/09/23. PubMed PMID: 25237857.
3. Bruckner A, Polge C, Lentze N, Auerbach D, Schlattner U. Yeast two-hybrid, a powerful tool for systems biology. *Int J Mol Sci*. 2009;10(6):2763–88. doi: [10.3390/ijms10062763](https://doi.org/10.3390/ijms10062763). PubMed PMID: 19582228.
4. Karimova G, Pidoux J, Ullmann A, Ladant D. A bacterial two-hybrid system based on a reconstituted signal transduction pathway. *Proc Natl Acad Sci U S A*. 1998;95(10):5752–6. PubMed PMID: 9576956.
5. Pelletier JN, Campbell-Valois FX, Michnick SW. Oligomerization domain-directed reassembly of active dihydrofolate reductase from rationally designed fragments. *Proc Natl Acad Sci U S A*. 1998;95(21):12141–6. PubMed PMID: 9770453.
6. Rossi F, Charlton CA, Blau HM. Monitoring protein-protein interactions in intact eukaryotic cells by beta-galactosidase complementation. *Proc Natl Acad Sci U S A*. 1997;94(16):8405–10. PubMed PMID: 9237989.
7. Luker GD, Luker KE. Luciferase protein complementation assays for bioluminescence imaging of cells and mice. *Methods Mol Biol*. 2011;680:29–43. doi: [10.1007/978-1-60761-901-7\\_2](https://doi.org/10.1007/978-1-60761-901-7_2). PubMed PMID: 21153371.
8. Bacart J, Corbel C, Jockers R, Bach S, Couturier C. The BRET technology and its application to screening assays. *Biotechnol J*. 2008;3(3):311–24. doi: [10.1002/biot.200700222](https://doi.org/10.1002/biot.200700222). PubMed PMID: 18228541.
9. Machleidt T, Woodroffe CC, Schwinn MK, Mendez J, Robers MB, Zirnmerman K, Otto P, Daniels DL, Kirkland TA, Wood KV. NanoBRET-A Novel BRET Platform for the Analysis of Protein-Protein Interactions. *Acs Chem Biol*. 2015;10(8):1797–804. doi: [10.1021/acscchembio.5b00143](https://doi.org/10.1021/acscchembio.5b00143). PubMed PMID: 26006698.
10. Pflieger KD, Eidne KA. Illuminating insights into protein-protein interactions using bioluminescence resonance energy transfer (BRET). *Nat Methods*. 2006;3(3):165–74. doi: [10.1038/nmeth841](https://doi.org/10.1038/nmeth841). PubMed PMID: 16489332.
11. You X, Nguyen AW, Jabaiah A, Sheff MA, Thorn KS, Daugherty PS. Intracellular protein interaction mapping with FRET hybrids. *Proc Natl Acad Sci U S A*. 2006;103(49):18458–63. doi: [10.1073/pnas.0605422103](https://doi.org/10.1073/pnas.0605422103). PubMed PMID: 17130455.
12. Song Y, Madahar V, Liao J. Development of FRET assay into quantitative and high-throughput screening technology platforms for protein-protein interactions. *Ann Biomed Eng*. 2011;39(4):1224–34. doi: [10.1007/s10439-010-0225-x](https://doi.org/10.1007/s10439-010-0225-x). PubMed PMID: 21174150.

13. Kodama Y, Hu CD. An improved bimolecular fluorescence complementation assay with a high signal-to-noise ratio. *Biotechniques*. 2010;49(5):793–805. doi: [10.2144/000113519](https://doi.org/10.2144/000113519). PubMed PMID: 21091444.
14. Ohashi K, Kiuchi T, Shoji K, Sampei K, Mizuno K. Visualization of cofilin-actin and Ras-Raf interactions by bimolecular fluorescence complementation assays using a new pair of split Venus fragments. *Biotechniques*. 2012;52(1):45–50. doi: [10.2144/000113777](https://doi.org/10.2144/000113777). PubMed PMID: 22229727.
15. Hu CD, Chinenov Y, Kerppola TK. Visualization of interactions among bZIP and Rel family proteins in living cells using bimolecular fluorescence complementation. *Mol Cell*. 2002;9(4):789–98. PubMed PMID: 11983170.
16. Hu CD, Kerppola TK. Simultaneous visualization of multiple protein interactions in living cells using multicolor fluorescence complementation analysis. *Nat Biotechnol*. 2003;21(5):539–45. doi: [10.1038/nbt816](https://doi.org/10.1038/nbt816). PubMed PMID: 12692560.
17. Fan JY, Cui ZQ, Wei HP, Zhang ZP, Zhou YF, Wang YP, Zhang XE. Split mCherry as a new red bimolecular fluorescence complementation system for visualizing protein-protein interactions in living cells. *Biochem Biophys Res Commun*. 2008;367(1):47–53. doi: [10.1016/j.bbrc.2007.12.101](https://doi.org/10.1016/j.bbrc.2007.12.101). PubMed PMID: 18158915.
18. Galarneau A, Primeau M, Trudeau LE, Michnick SW. Beta-lactamase protein fragment complementation assays as in vivo and in vitro sensors of protein protein interactions. *Nat Biotechnol*. 2002;20(6):619–22. doi: [10.1038/nbt0602-619](https://doi.org/10.1038/nbt0602-619). PubMed PMID: 12042868.
19. Lee HK, Brown SJ, Rosen H, Tobias PS. Application of beta-lactamase enzyme complementation to the high-throughput screening of toll-like receptor signaling inhibitors. *Mol Pharmacol*. 2007;72(4):868–75. doi: [10.1124/mol.107.038349](https://doi.org/10.1124/mol.107.038349). PubMed PMID: 17615244.
20. Lee HK, Dunzendorfer S, Tobias PS. Cytoplasmic domain-mediated dimerizations of toll-like receptor 4 observed by beta-lactamase enzyme fragment complementation. *J Biol Chem*. 2004;279(11):10564–74. doi: [10.1074/jbc.M311564200](https://doi.org/10.1074/jbc.M311564200). PubMed PMID: 14699116.
21. Wehrman T, Kleaveland B, Her JH, Balint RF, Blau HM. Protein-protein interactions monitored in mammalian cells via complementation of beta -lactamase enzyme fragments. *Proc Natl Acad Sci U S A*. 2002;99(6):3469–74. doi: [10.1073/pnas.062043699](https://doi.org/10.1073/pnas.062043699). PubMed PMID: 11904411.
22. Zhao CK, Yin Q, Li SY. A high-throughput screening system for G-protein-coupled receptors using beta-lactamase enzyme complementation technology. *Acta Pharmacol Sin*. 2010;31(12):1618–24. doi: [10.1038/aps.2010.154](https://doi.org/10.1038/aps.2010.154). PubMed PMID: 21102483.
23. Graham DL, Bevan N, Lowe PN, Palmer M, Rees S. Application of beta-galactosidase enzyme complementation technology as a high throughput screening format for antagonists of the epidermal growth factor receptor. *J Biomol Screen*. 2001;6(6):401–11. doi: [10.1089/108705701753364896](https://doi.org/10.1089/108705701753364896). PubMed PMID: 11788058.
24. Smith AM, Ammar R, Nislow C, Giaever G. A survey of yeast genomic assays for drug and target discovery. *Pharmacol Ther*. 2010;127(2):156–64. doi: [10.1016/j.pharmthera.2010.04.012](https://doi.org/10.1016/j.pharmthera.2010.04.012). PubMed PMID: 20546776.

25. Rogers B, Decottignies A, Kolaczowski M, Carvajal E, Balzi E, Goffeau A. The pleiotropic drug ABC transporters from *Saccharomyces cerevisiae*. *J Mol Microbiol Biotechnol*. 2001;3(2):207–14. PubMed PMID: 11321575.
26. Colton CK, Kong Q, Lai L, Zhu MX, Seyb KI, Cuny GD, Xian J, Glicksman MA, Lin CL. Identification of translational activators of glial glutamate transporter EAAT2 through cell-based high-throughput screening: an approach to prevent excitotoxicity. *J Biomol Screen*. 2010;15(6):653–62. doi: [10.1177/1087057110370998](https://doi.org/10.1177/1087057110370998). PubMed PMID: 20508255.
27. Zhang JH, Chung TD, Oldenburg KR. A Simple Statistical Parameter for Use in Evaluation and Validation of High Throughput Screening Assays. *J Biomol Screen*. 1999;4(2):67–73. PubMed PMID: 10838414.
28. Auld DS, Inglese J. Interferences with Luciferase Reporter Enzymes. In: Sittampalam GS, Coussens NP, Brimacombe K, Grossman A, Arkin M, Auld D, Austin C, Baell J, Bejcek B, Chung TDY, Dahlin JL, Devanaryan V, Foley TL, Glicksman M, Hall MD, Hass JV, Inglese J, Iversen PW, Kahl SD, Kales SC, Lal-Nag M, Li Z, McGee J, McManus O, Riss T, Trask OJ, Jr., Weidner JR, Xia M, Xu X, editors. *Assay Guidance Manual*. Bethesda (MD)2004.
29. Simeonov A, Davis MI. Interference with Fluorescence and Absorbance. In: Sittampalam GS, Coussens NP, Brimacombe K, Grossman A, Arkin M, Auld D, Austin C, Baell J, Bejcek B, Chung TDY, Dahlin JL, Devanaryan V, Foley TL, Glicksman M, Hall MD, Hass JV, Inglese J, Iversen PW, Kahl SD, Kales SC, Lal-Nag M, Li Z, McGee J, McManus O, Riss T, Trask OJ, Jr., Weidner JR, Xia M, Xu X, editors. *Assay Guidance Manual*. Bethesda (MD)2004.
30. Simeonov A, Jadhav A, Thomas CJ, Wang Y, Huang R, Southall NT, Shinn P, Smith J, Austin CP, Auld DS, Inglese J. Fluorescence spectroscopic profiling of compound libraries. *J Med Chem*. 2008;51(8):2363–71. doi: [10.1021/jm701301m](https://doi.org/10.1021/jm701301m). PubMed PMID: 18363325.
31. Jadhav A, Ferreira RS, Klumpp C, Mott BT, Austin CP, Inglese J, Thomas CJ, Maloney DJ, Shoichet BK, Simeonov A. Quantitative analyses of aggregation, autofluorescence, and reactivity artifacts in a screen for inhibitors of a thiol protease. *J Med Chem*. 2010;53(1):37–51. doi: [10.1021/jm901070c](https://doi.org/10.1021/jm901070c). PubMed PMID: 19908840.
32. Auld DS, Southall NT, Jadhav A, Johnson RL, Diller DJ, Simeonov A, Austin CP, Inglese J. Characterization of chemical libraries for luciferase inhibitory activity. *J Med Chem*. 2008;51(8):2372–86. doi: [10.1021/jm701302v](https://doi.org/10.1021/jm701302v). PubMed PMID: 18363348.
33. Dahlin JL, Baell J, Walters MA. Assay Interference by Chemical Reactivity. In: Sittampalam GS, Coussens NP, Brimacombe K, Grossman A, Arkin M, Auld D, Austin C, Baell J, Bejcek B, Chung TDY, Dahlin JL, Devanaryan V, Foley TL, Glicksman M, Hall MD, Hass JV, Inglese J, Iversen PW, Kahl SD, Kales SC, Lal-Nag M, Li Z, McGee J, McManus O, Riss T, Trask OJ, Jr., Weidner JR, Xia M, Xu X, editors. *Assay Guidance Manual*. Bethesda (MD)2004.
34. Auld DS, Inglese J, Dahlin JL. Assay Interference by Aggregation. In: Sittampalam GS, Coussens NP, Brimacombe K, Grossman A, Arkin M, Auld D, Austin C, Baell J, Bejcek B, Chung TDY, Dahlin JL, Devanaryan V, Foley TL, Glicksman M, Hall MD, Hass JV, Inglese J, Iversen PW, Kahl SD, Kales SC, Lal-Nag M, Li Z, McGee J,

- McManus O, Riss T, Trask OJ, Jr., Weidner JR, Xia M, Xu X, editors. Assay Guidance Manual. Bethesda (MD)2004.
35. Tsien RY. The green fluorescent protein. *Annu Rev Biochem.* 1998;67:509–44. doi: [10.1146/annurev.biochem.67.1.509](https://doi.org/10.1146/annurev.biochem.67.1.509). PubMed PMID: 9759496.
  36. Forster T. \*Zwischenmolekulare Energiewanderung Und Fluoreszenz. *Ann Phys-Berlin.* 1948;2(1-2):55–75.
  37. Zimmermann T, Rietdorf J, Girod A, Georget V, Pepperkok R. Spectral imaging and linear un-mixing enables improved FRET efficiency with a novel GFP2-YFP FRET pair. *FEBS Lett.* 2002;531(2):245–9. PubMed PMID: 12417320.
  38. van der Krogt GN, Ogink J, Ponsioen B, Jalink K. A comparison of donor-acceptor pairs for genetically encoded FRET sensors: application to the Epac cAMP sensor as an example. *PLoS One.* 2008;3(4):e1916. doi: [10.1371/journal.pone.0001916](https://doi.org/10.1371/journal.pone.0001916). PubMed PMID: 18382687.
  39. Roszik J, Toth G, Szollosi J, Vereb G. Validating pharmacological disruption of protein-protein interactions by acceptor photobleaching FRET imaging. *Methods Mol Biol.* 2013;986:165–78. doi: [10.1007/978-1-62703-311-4\\_11](https://doi.org/10.1007/978-1-62703-311-4_11). PubMed PMID: 23436412.
  40. Alibhai D, Kelly DJ, Warren S, Kumar S, Margineau A, Serwa RA, Thion E, Alexandrov Y, Murray EJ, Stuhmeier F, Tate EW, Neil MA, Dunsby C, French PM. Automated fluorescence lifetime imaging plate reader and its application to Förster resonant energy transfer readout of Gag protein aggregation. *J Biophotonics.* 2013;6(5):398–408. doi: [10.1002/jbio.201200185](https://doi.org/10.1002/jbio.201200185). PubMed PMID: 23184449.
  41. Sun Y, Hays NM, Periasamy A, Davidson MW, Day RN. Monitoring protein interactions in living cells with fluorescence lifetime imaging microscopy. *Methods Enzymol.* 2012;504:371–91. doi: [10.1016/B978-0-12-391857-4.00019-7](https://doi.org/10.1016/B978-0-12-391857-4.00019-7). PubMed PMID: 22264545.
  42. Iversen PW, Beck B, Chen YF, Dere W, Devanarayan V, Eastwood BJ, Farmen MW, Iturria SJ, Montrose C, Moore RA, Weidner JR, Sittampalam GS. HTS Assay Validation. In: Sittampalam GS, Coussens NP, Brimacombe K, Grossman A, Arkin M, Auld D, Austin C, Baell J, Bejcek B, Chung TDY, Dahlin JL, Devanaryan V, Foley TL, Glicksman M, Hall MD, Hass JV, Inglese J, Iversen PW, Kahl SD, Kales SC, Lal-Nag M, Li Z, McGee J, McManus O, Riss T, Trask OJ, Jr., Weidner JR, Xia M, Xu X, editors. Assay Guidance Manual. Bethesda (MD)2004.
  43. Buntru A, Zimmermann T, Hauck CR. Fluorescence resonance energy transfer (FRET)-based subcellular visualization of pathogen-induced host receptor signaling. *Bmc Biol.* 2009;7. doi: Art 81 doi: [10.1186/1741-7007-7-81](https://doi.org/10.1186/1741-7007-7-81).
  44. Zacharias DA, Violin JD, Newton AC, Tsien RY. Partitioning of lipid-modified monomeric GFPs into membrane microdomains of live cells. *Science.* 2002;296(5569):913–6. [10.1126/science.1068539](https://doi.org/10.1126/science.1068539). doi: DOI. PubMed PMID: 11988576.
  45. Picaud S, Fedorov O, Thanasopoulou A, Leonards K, Jones K, Meier J, Olzscha H, Monteiro O, Martin S, Philpott M, Tumber A, Filippakopoulos P, Yapp C, Wells C, Che KH, Bannister A, Robson S, Kumar U, Parr N, Lee K, Lugo D, Jeffrey P, Taylor S, Vecellio ML, Bountra C, Brennan PE, O'Mahony A, Velichko S, Muller S, Hay DC, Daniels DL, Urh M, La Thangue NB, Kouzarides T, Prinjha R, Schwaller J, Knapp S.



- Generation of a Selective Small Molecule Inhibitor of the CBP/p300 Bromodomain for Leukemia Therapy. *Cancer Res.* 2015;75(23):5106–19. doi: [10.1158/0008-5472.Can-15-0236](https://doi.org/10.1158/0008-5472.Can-15-0236). PubMed PMID: 26552700.
46. Ghosh I, Hamilton AD, Regan L. Antiparallel leucine zipper-directed protein reassembly: Application to the green fluorescent protein. *Journal of the American Chemical Society.* 2000;122(23):5658–9. doi: [10.1021/ja994421w](https://doi.org/10.1021/ja994421w). doi: DOI.
  47. Kerppola TK. Design and implementation of bimolecular fluorescence complementation (BiFC) assays for the visualization of protein interactions in living cells. *Nat Protoc.* 2006;1(3):1278–86. doi: [10.1038/nprot.2006.201](https://doi.org/10.1038/nprot.2006.201). PubMed PMID: 17406412.
  48. Magliery TJ, Wilson CG, Pan W, Mishler D, Ghosh I, Hamilton AD, Regan L. Detecting protein-protein interactions with a green fluorescent protein fragment reassembly trap: scope and mechanism. *J Am Chem Soc.* 2005;127(1):146–57. doi: [10.1021/ja046699g](https://doi.org/10.1021/ja046699g). PubMed PMID: 15631464.
  49. Stefan E, Aquin S, Berger N, Landry CR, Nyfeler B, Bouvier M, Michnick SW. Quantification of dynamic protein complexes using Renilla luciferase fragment complementation applied to protein kinase A activities in vivo. *Proc Natl Acad Sci U S A.* 2007;104(43):16916–21. doi: [10.1073/pnas.0704257104](https://doi.org/10.1073/pnas.0704257104). PubMed PMID: 17942691.
  50. Dai JP, Zhao XF, Zeng J, Wan QY, Yang JC, Li WZ, Chen XX, Wang GF, Li KS. Drug Screening for Autophagy Inhibitors Based on the Dissociation of Beclin 1-Bcl2 Complex Using BiFC Technique and Mechanism of Eugenol on Anti-Influenza A Virus Activity. *Plos One.* 2013;8(4). doi: ARTN e61026 doi: [10.1371/journal.pone.0061026](https://doi.org/10.1371/journal.pone.0061026).
  51. Verhoeef L, Wade M. Visualization of Protein Interactions in Living Cells Using Bimolecular Luminescence Complementation (BiLC). *Curr Protoc Protein Sci.* 2017;90:30 5 1- 5 14. Epub 2017/11/02. doi: [10.1002/cpps.42](https://doi.org/10.1002/cpps.42).
  52. Hida N, Awais M, Takeuchi M, Ueno N, Tashiro M, Takagi C, Singh T, Hayashi M, Ohmiya Y, Ozawa T. High-sensitivity real-time imaging of dual protein-protein interactions in living subjects using multicolor luciferases. *PLoS One.* 2009;4(6):e5868. doi: [10.1371/journal.pone.0005868](https://doi.org/10.1371/journal.pone.0005868). PubMed PMID: 19536355.
  53. Luker KE, Piwnicka-Worms D. Optimizing luciferase protein fragment complementation for bioluminescent imaging of protein-protein interactions in live cells and animals. *Methods Enzymol.* 2004;385:349–60. doi: [10.1016/S0076-6879\(04\)85019-5](https://doi.org/10.1016/S0076-6879(04)85019-5). PubMed PMID: 15130748.
  54. Hashimoto T, Adams KW, Fan Z, McLean PJ, Hyman BT. Characterization of oligomer formation of amyloid-beta peptide using a split-luciferase complementation assay. *J Biol Chem.* 2011;286(31):27081–91. doi: [10.1074/jbc.M111.257378](https://doi.org/10.1074/jbc.M111.257378). PubMed PMID: 21652708.
  55. Gehl C, Kaufholdt D, Hamisch D, Bikker R, Kudla J, Mendel RR, Hansch R. Quantitative analysis of dynamic protein-protein interactions in planta by a floated-leaf luciferase complementation imaging (FLuCI) assay using binary Gateway vectors. *Plant J.* 2011;67(3):542–53. doi: [10.1111/j.1365-313X.2011.04607.x](https://doi.org/10.1111/j.1365-313X.2011.04607.x). PubMed PMID: 21481030.

56. Paulmurugan R, Umezawa Y, Gambhir SS. Noninvasive imaging of protein-protein interactions in living subjects by using reporter protein complementation and reconstitution strategies. *Proc Natl Acad Sci U S A*. 2002;99(24):15608–13. doi: [10.1073/pnas.242594299](https://doi.org/10.1073/pnas.242594299). PubMed PMID: 12438689.
57. Branchini BR, Southworth TL, Murtiashaw MH, Wilkinson SR, Khattak NF, Rosenberg JC, Zimmer M. Mutagenesis evidence that the partial reactions of firefly bioluminescence are catalyzed by different conformations of the luciferase C-terminal domain. *Biochemistry*. 2005;44(5):1385–93. doi: [10.1021/bi047903f](https://doi.org/10.1021/bi047903f). PubMed PMID: 15683224.
58. Nakatsu T, Ichiyama S, Hiratake J, Saldanha A, Kobashi N, Sakata K, Kato H. Structural basis for the spectral difference in luciferase bioluminescence. *Nature*. 2006;440(7082):372–6. doi: [10.1038/nature04542](https://doi.org/10.1038/nature04542). PubMed PMID: 16541080.
59. Villalobos V, Naik S, Bruinsma M, Dothager RS, Pan MH, Samrakandi M, Moss B, Elhammali A, Piwnica-Worms D. Dual-color click beetle luciferase heteroprotein fragment complementation assays. *Chem Biol*. 2010;17(9):1018–29. doi: [10.1016/j.chembiol.2010.06.018](https://doi.org/10.1016/j.chembiol.2010.06.018). PubMed PMID: 20851351.
60. Ilagan MX, Lim S, Fulbright M, Piwnica-Worms D, Kopan R. Real-time imaging of notch activation with a luciferase complementation-based reporter. *Sci Signal*. 2011;4(181):rs7. doi: [10.1126/scisignal.2001656](https://doi.org/10.1126/scisignal.2001656). PubMed PMID: 21775282.
61. Zhu PJ, Zheng W, Auld DS, Jadhav A, Macarthur R, Olson KR, Peng K, Dotimas H, Austin CP, Inglese J. A miniaturized glucocorticoid receptor translocation assay using enzymatic fragment complementation evaluated with qHTS. *Comb Chem High Throughput Screen*. 2008;11(7):545–59. PubMed PMID: 18694391.
62. Tomosugi W, Matsuda T, Tani T, Nemoto T, Kotera I, Saito K, Horikawa K, Nagai T. An ultramarine fluorescent protein with increased photostability and pH insensitivity. *Nat Methods*. 2009;6(5):351–3. doi: [10.1038/nmeth.1317](https://doi.org/10.1038/nmeth.1317). PubMed PMID: 19349978.
63. Su T, Pan S, Luo Q, Zhang Z. Monitoring of dual bio-molecular events using FRET biosensors based on mTagBFP/sfGFP and mVenus/mKOkappa fluorescent protein pairs. *Biosens Bioelectron*. 2013;46:97–101. doi: [10.1016/j.bios.2013.02.024](https://doi.org/10.1016/j.bios.2013.02.024). PubMed PMID: 23517824.
64. Woehler A. Simultaneous quantitative live cell imaging of multiple FRET-based biosensors. *PLoS One*. 2013;8(4):e61096. doi: [10.1371/journal.pone.0061096](https://doi.org/10.1371/journal.pone.0061096). PubMed PMID: 23613792.
65. Ai HW, Hazelwood KL, Davidson MW, Campbell RE. Fluorescent protein FRET pairs for ratiometric imaging of dual biosensors. *Nat Methods*. 2008;5(5):401–3. doi: [10.1038/nmeth.1207](https://doi.org/10.1038/nmeth.1207). PubMed PMID: 18425137.
66. Ouyang M, Sun J, Chien S, Wang Y. Determination of hierarchical relationship of Src and Rac at subcellular locations with FRET biosensors. *Proc Natl Acad Sci U S A*. 2008;105(38):14353–8. doi: [10.1073/pnas.0807537105](https://doi.org/10.1073/pnas.0807537105). PubMed PMID: 18799748.
67. Su T, Zhang Z, Luo Q. Ratiometric fluorescence imaging of dual bio-molecular events in single living cells using a new FRET pair mVenus/mKOkappa-based biosensor and a single fluorescent protein biosensor. *Biosens Bioelectron*. 2012;31(1):292–8. doi: [10.1016/j.bios.2011.10.034](https://doi.org/10.1016/j.bios.2011.10.034). PubMed PMID: 22088261.

68. Galperin E, Verkhusha VV, Sorkin A. Three-chromophore FRET microscopy to analyze multiprotein interactions in living cells. *Nat Methods*. 2004;1(3):209–17. doi: [10.1038/nmeth720](https://doi.org/10.1038/nmeth720). PubMed PMID: 15782196.
69. Ghosh PS, Hamilton AD. Noncovalent template-assisted mimicry of multiloop protein surfaces: assembling discontinuous and functional domains. *J Am Chem Soc*. 2012;134(32):13208–11. doi: [10.1021/ja305360q](https://doi.org/10.1021/ja305360q). PubMed PMID: 22839643.
70. Shyu YJ, Liu H, Deng X, Hu CD. Identification of new fluorescent protein fragments for bimolecular fluorescence complementation analysis under physiological conditions. *Biotechniques*. 2006;40(1):61–6. PubMed PMID: 16454041.
71. Chu J, Zhang Z, Zheng Y, Yang J, Qin L, Lu J, Huang ZL, Zeng S, Luo Q. A novel far-red bimolecular fluorescence complementation system that allows for efficient visualization of protein interactions under physiological conditions. *Biosens Bioelectron*. 2009;25(1):234–9. doi: [10.1016/j.bios.2009.06.008](https://doi.org/10.1016/j.bios.2009.06.008). PubMed PMID: 19596565.



# *In Vivo* Assay Guidelines

Viswanath Devanaryan, PhD, Joseph V. Haas, MS, and Philip W. Iversen, PhD



# In Vivo Assay Guidelines

Joseph Haas, MS,<sup>✉1,\*</sup> Jason Manro, MS,<sup>1</sup> Harlan Shannon, PhD,<sup>2</sup> Wes Anderson, MS,<sup>1,\*\*</sup> Joe Brozinick, PhD,<sup>1</sup> Arunava Chakravartty, PhD,<sup>3</sup> Mark Chambers, PhD,<sup>1</sup> Jian Du, PhD,<sup>1</sup> Brian Eastwood, PhD,<sup>1</sup> Joe Heuer, PhD,<sup>1</sup> Stephen Iturria, PhD,<sup>4</sup> Philip Iversen, PhD,<sup>1,\*\*\*</sup> Dwayne Johnson, BS,<sup>1</sup> Kirk Johnson, PhD,<sup>1</sup> Michael O'Neill, PhD,<sup>1</sup> Hui-Rong Qian, PhD,<sup>1</sup> Dana Sindelar, PhD,<sup>1</sup> and Kjell Svensson, PhD<sup>1</sup>

Created: May 1, 2012; Updated: October 1, 2012.

## Abstract

This document is intended to provide guidance for the design, development and statistical validation of *in vivo* assays residing in flow schemes of discovery projects. It provides statistical methodology for pre-study, cross-study (lab-to-lab transfers and protocol changes), and in-study (quality control monitoring) validation. Application of the enclosed methods will increase confidence in data from *in vivo* assays in the critical path and enable better decisions about SAR directions and compound prioritization. Screens using both single dose and multiple dose *in vivo* assays are discussed, along with acceptance criteria at different stages of validation.

## Flow Chart

This document is intended to provide guidance for the development and statistical validation of *in vivo* assays residing in flow schemes of discovery projects. It provides statistical methodology for pre-study, cross-study (lab-to-lab transfers and protocol changes), and in-study (quality control monitoring) validation. Application of the enclosed methods will increase confidence in data from *in vivo* assays in the critical path and enable better decisions about SAR directions and compound prioritization.

---

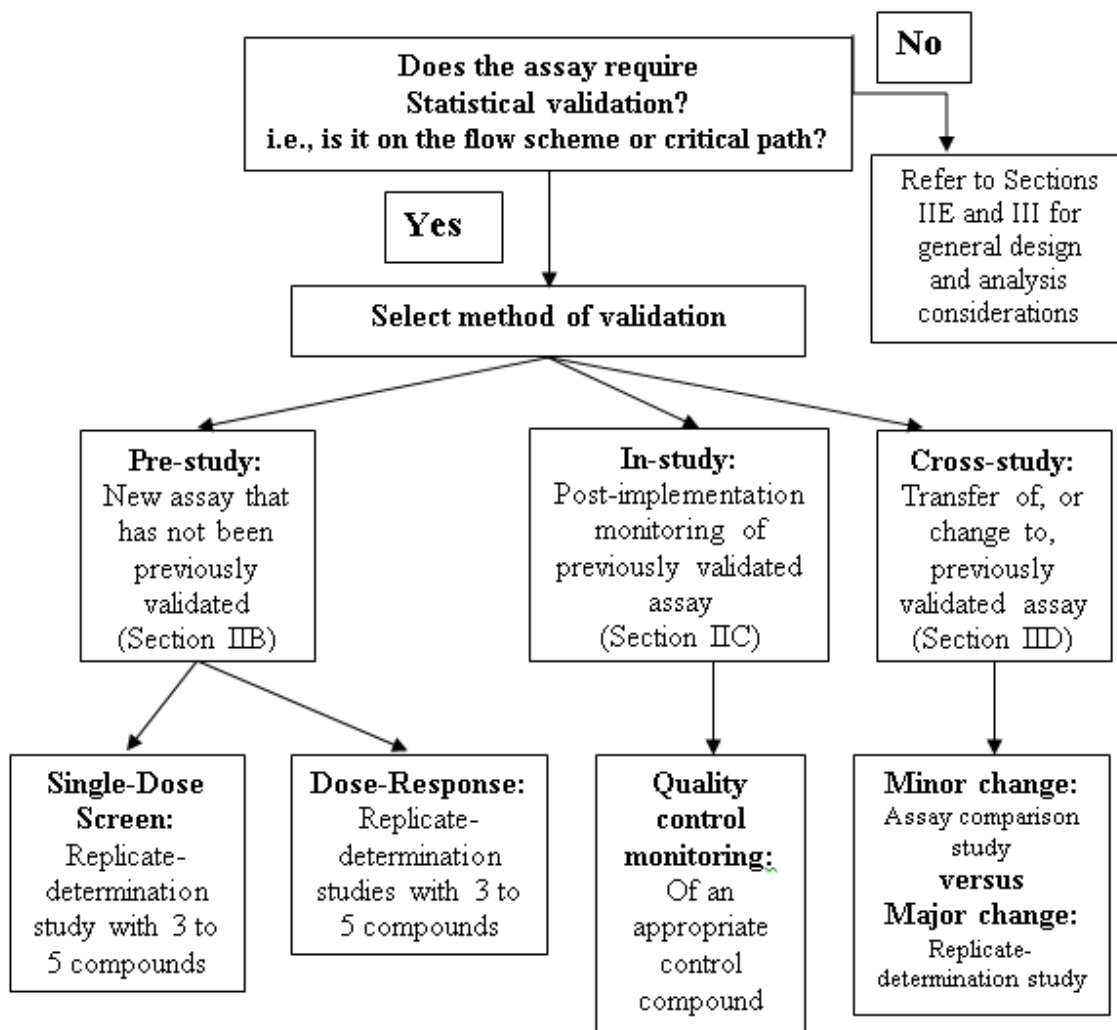
<sup>1</sup> Eli Lilly & Company, Indianapolis, IN. <sup>2</sup> Indiana University Purdue University at Indianapolis, Indianapolis, IN. <sup>3</sup> Abbott Laboratories, Chicago, IL. <sup>4</sup> Monsanto, Ankeny, IA.

<sup>✉</sup> Corresponding author.

\*Principal Author

\*\*Co-Author

\*\*\*Editor



The document is organized into three sections, and includes several examples. The Introduction (Section 1) provides general definitions of biological assays and provides general concepts in assay development and validation. Assay Validation (Section 2) contains the procedures and statistical details for *in vivo* assay validation, while Background Material (Section 3) covers general statistical concepts related to the design and analysis of *in vivo* experiments.

## 1. Introduction

This document is written to provide guidance to investigators who are developing and statistically validating *in vivo* assays for the evaluation of structure-activity relationships and/or compound collections to identify chemical probes that modulate the activity of biological targets. Specifically, this manual provides guidelines for:



- a. Identifying potential assay formats of *in vivo* models compatible with **Single Dose Screens** (SDSs) and **Dose-Response Curves** (DRCs) for evaluating structure-activity relationships (SAR).
- b. Statistical validation of the assay performance parameters (pre-study, in-study, and cross-study validation).
- c. Optimizing assay protocols with respect to sensitivity, dynamic range, and stability.

### 1.1. General definition of biological assays

A biological assay is defined by a set of methods that produce a detectable signal allowing a biological process to be quantified. In general, the quality of an assay is defined by the *robustness and reproducibility* of this signal in the absence of any test compounds or in the presence of inactive compounds. This robustness will depend on the type of signal measured (biochemical, physiological, behavioral, etc.), and the analytical and automation instrumentation employed. The quality of the SDS is then defined by the behavior of this assay system when screened against a collection of compounds. These two general concepts, assay quality and screen quality, are discussed with specific examples in this manual.

### 1.2. General Concepts in Method (Assay) Development and Validation of an *In vivo* Model

The overall objective of any method validation procedure is to demonstrate that the method is *acceptable for its intended purpose*. Usually, the purpose is to determine the biological and or pharmacological activity of new chemical entities (NCE). The acceptability of a measurement procedure or bioassay method begins with its design and construction, which can significantly affect its performance and robustness.

The validation process originates during identification and/or design of a model and method development and continues throughout the assay life cycle (Figure 1). During method development, assay conditions and procedures are selected that minimize the impact of potential sources of invalidity (e.g. so-called false positives or false negatives) on the measurement of analyte or the biological end point (e.g. biochemical, physiological or behavioral changes). There are three fundamental general areas in method development and validation: (a) Pre-study (Identification and Design phase) validation (b) In-study (Development and Production phase) validation, and (c) Cross-validation or method transfer validation. These stages encompass the systematic scientific steps in an assay development and validation cycle.

#### 1.2.1. Pre-study validation:

This validation occurs prior to implementing the assay. At this stage the choice of an assay format is made. Close attention must be paid to factors such as the selection of methods with appropriate specificity and stability. It is important that the assay be designed and the protocol written to facilitate the statistical analysis (i.e. appropriate design and analysis method, and adequate sample size), and that proper randomization techniques be used.

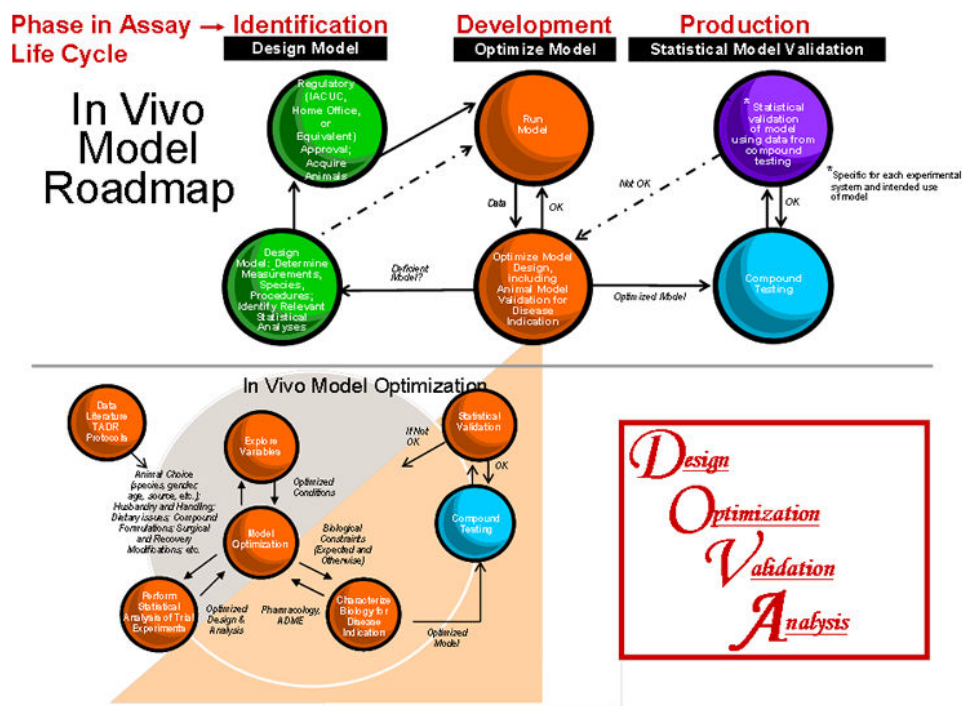


Figure 1: The *In vivo* Model Assay Development Cycle.

This requires the generation and statistical analysis of confirmatory data from planned experiments to document that analytical results satisfy pre-defined acceptance criteria. Within-run statistical measures of assay performance such as the Minimum Significant Difference (MSD) for SDSs and Minimum Significant Ratio (MSR) for DRCs are calculated. If available, the assay sensitivity and pharmacology is evaluated using control compounds.

### 1.2.2. In-study validation:

These procedures are needed to verify that a method remains acceptable *during its routine use*. In order to compare data for compounds tested at different times, the pre-study statistical measures of assay performance (MSD or MSR) are updated to include between-run variability. Each run of the assay should contain appropriate {maximum and minimum} control groups or treatments to serve as quality controls of each run and to check overall performance. (Maximum and/or minimum quality controls differ conceptually from an “active” positive or negative controls; see Control Compounds or Treatment Groups.) This will allow the investigator to check for procedural errors and to evaluate stability of the method over time. Control Charts illustrates procedures which may be used to evaluate assay performance over time (i.e., control chart monitoring).

### 1.2.3. Cross validation:

This portion includes the *assay hand-off* from the individual investigator’s team to another laboratory or a screening center. More broadly, this procedure is used at any stage to

verify that an acceptable level of agreement exists in analytical results before and after procedural changes in a method as well as between results from two or more methods or laboratories. Typically, each laboratory assays a subset of compounds and the agreement in results is compared to predefined criteria that specify the allowable performance of the assay.

#### 1.2.4. Resources:

The validation guidelines described here should be applicable to most *in vivo* models encountered in drug discovery research. However, situations could arise in which their verbatim application would be impractical given resource constraints, intended use of the assay, or other reasons. In these situations, and in general, the following principles should apply:

- Some form of statistical validation should always be performed and is better than no validation.
- The amount of resources, including time, spent on validation should be kept to a reasonably small fraction of the total resources to be used for testing compounds. What is “reasonable” will have to be determined by the key personnel involved with each project.

*These guidelines are intended to be used as “guidelines” and not exact “requirements.”* The specified assay performance measures serve to quantify how well the assay is performing and should be used to guide proper interpretation of the data. Determining whether an assay is “fit for its intended purpose” should be based on a combination of these assay performance measures and sound scientific judgment of the team.

## 2. Assay Validation Procedures

### 2.1. Overview

The statistical validation requirements for an assay vary, depending upon the prior history of the assay. The four main components of the statistical validation are:

1. Adequate study design and data analysis method.
2. Proper randomization of animals.
3. Appropriate statistical power and sample size.
4. Adequate reproducibility across assay runs.

Assays should be designed so that all biologically meaningful effects are statistically significant. In an exploratory study, this “meaningful effect” might correspond to any effect that is pharmacologically relevant. For a project/program team, it might correspond to an effect that meets the critical success factors (CSFs) defined in the compound development flow scheme. Power and sample size analyses are especially relevant for experiments that are designed to address key endpoints in a flow scheme. It is not acceptable to set a CSF equal to the effect size that is statistically significant since that effect size may or may not be biologically relevant. A CSF should be established based

upon its biological relevance to the discovery effort. The assay is designed, optimized and validated so that biologically meaningful effects (e.g., CSFs) are statistically significant. Quantifying the reproducibility of an *in vivo* flow scheme assay will enable a team to discern whether compounds tested in different runs of the assay are exhibiting differential activity. This will result in better decisions about SAR directions and compound prioritization.

If the assay is new, or has never been previously validated relative to the targeted purpose, or mechanism of action, of the assay, then full validation should be performed. If the assay has been previously validated in a different laboratory, and is being transferred to a new laboratory, then a Replicate-Determination study (Pre-Study Validation) and a formal comparison between the new assay and the existing (old) assay (i.e., cross-study validation; Cross Validation) should be performed. If an assay is being transferred, it is considered validated if it has previously been assessed by all the methods in Section 2.2, and is being transferred to a new laboratory without undergoing any substantive changes to the protocol. If the intent is to store the data under the same Assay Method Version (or AMV) in an electronic database as the previous laboratory's AMV, then an assay comparison study (Cross Validation) should be done as part of the Replicate-Determination study. Otherwise only the intra-laboratory part of the Replicate-Determination study (Pre-Study Validation) is recommended.

If the assay is updated from a previous version run in the same facility then the requirements vary, depending upon the *extent of the change*. Major changes require a validation study equivalent to the validation of a new assay. Minor changes require bridging studies that demonstrate the equivalence of the assay before and after the change. See Section 2.4 - Cross Validation for examples of major and minor changes.

An assay methodology which has been previously validated for a different target or mechanism of action should be validated in full when used for a new or different target or mechanism as the variability, in particular, and reproducibility may be quite different for different mechanisms even though the methods may be very similar or identical. This concept is analogous to separately validating receptor binding assays for different receptors.

## 2.2. Pre-Study Validation: Replicate-Determination Study for Single-Dose Screens and Dose-Response Curves

### 2.2.1. Overview and Rationale

It is important to verify that assay results from multiple determinations or assay runs have acceptable reproducibility with no material systematic trends in the key endpoints. In this section, we define how to quantify assay variability and determine assay equivalence. We also explain the rationale for the statistical methods employed in calculating reproducibility of activity and potency. *We strongly recommend consultation with a statistician before designing experiments to estimate variability, and the sources thereof, described below.* In particular, you should discuss with a statistician alternatives for assays

with significant time, resource, or expenditure constraints as well as assays which will be used to test a minimal number of compounds to properly balance validation requirements with these constraints.

Replicate-Determination studies with two runs are used to formally evaluate the *within-run* assay variability (i.e., pre-study validation), or to formally compare a new assay to an existing (old) assay (i.e., cross-study validation). Replicate-Determination studies also allow a preliminary assessment of the *overall* or *between-run* assay variability, but two runs are not enough to adequately assess overall variability. In-study methods (In-Study Validation) are used to formally evaluate the overall variability in the assay in routine use. Note that the Replicate-Determination study is a diagnostic and decision tool used to establish that the assay is ready to go into production by showing that the endpoints of the assay are reproducible over a range of efficacies or potencies. It is not intended as a substitute for in-study monitoring or to provide an estimate of the *overall* MSD or MSR.

It may seem counter-intuitive to call the differences between two independent assay runs “within-run.” However, the terminology results from the way those terms are defined. Experimental variation is categorized into two distinct components: *between-run* and *within-run* sources.

Consider the following examples:

- **Between-run variation:** If there is variation in the concentrations of the components in the vehicle between two runs then the assay results could be affected. However, assuming that the same vehicle is used with all compounds within the run, each compound will be equally affected and so the difference will only show up when comparing the results of two runs: one run will appear higher on average than the other run. This variation is called *between-run* variation.
- **Within-run variation:** If the concentration of one compound in the vehicle varies from the intended concentration (or dose) then all animals receiving that compound will be affected. However, animals receiving other compounds will be unaffected. This type of variation is called *within-run* as the source of variation affects different compounds in the same run differently. Therefore, it is necessary to compare results for one compound on each of two occasions.
- **Some sources of variability affect both *within- and between-run* variation.** For example, environmental conditions in an animal room have the potential to contribute to both types of variability. Suppose within a run of a particular *in vivo* assay, the temperature in the animal room exhibits spatial variation and animal response is sensitive to temperature. Animals will then respond differently depending upon their location in the room, and these differences are *within-run* as not all animals are equally affected. In comparison, suppose that during a particular run of the assay the room temperature on average is higher or lower than in previous runs. In this instance, the animals will respond differently on average during this run relative to other runs, and since all animals are affected this is

*between-run* variation. Thus, a variable such as animal room temperature can be a source of both within- and between-run variation.

The *total variation* is the sum of both sources of variation. When comparing two compounds across runs, one must take into account both the within-run and between-run sources of variation. But when comparing two compounds in the same run, one must only take into account the within-run sources, since, by definition, the between-run sources affect both compounds equally.

In a Replicate-Determination study, the between-run sources of variation cause one determination to be on average higher than another determination. However, it would be very unlikely that the difference between the two determinations would be exactly the same for every compound in the study. These individual compound “differences from the average difference” are caused by the within-run sources of variation. The higher the within-run variability the greater the individual compound variation within assay runs.

The analysis approach used in the Replicate-Determination study is to estimate and factor out between-run variability, and then estimate the magnitude of within-run variability.

**Note:** The between- and within-run sources of variability assessed during assay validation calculations apply to the treatment group means, not to the animal level data. Animal-to-animal variability is obviously present in *in vivo* experiments and this variability affects the reproducibility of the resulting treatment group means, but as shown subsequently, the animal-to-animal variability is not directly used in the calculation of the MSD and MSR. It is used to assess whether a data transformation is needed, and to assess sample size adequacy. See Section 2.5 for additional information about sources of variability in an *in vivo* assay.

### 2.2.2. Procedure (Steps)

All assays should have a reproducibility comparison (Steps 1 – 3). Single-dose screens should be validated separately from dose-response curve determinations, but it may be possible to validate both methods concurrently (consult with a statistician for options; also see Section 2.2.7 for an example). If the assay is to replace an existing assay using the same AMV code then an assay comparison study should also be done (Step 4).

1. Select a minimum of 3 to 5 compounds that have activities covering the effect range of interest and, if applicable, potencies that cover the dose-range to be tested. The compounds should be well spaced over these ranges.
2. All of the compounds should be tested in each of two runs of the assay.
3. Compare the two runs (as per Section 2.2.5 – 2.2.6.2.)
4. If the assay is to replace an existing assay:
  - a. All compounds should be tested in a single run of the former assay as well as in two runs of the new assay. If a single run of the former assay already exists that meets the requirements in Step 1, it can be used for validation as long as the run is reasonably contemporaneous in time with the run of the new assay.

- b. Compare the results of the two assays, or labs, by analyzing the first run of the new assay with the single run of the former assay.

### 2.2.3. Summary of Acceptance Criteria (discussed in detail below)

1. For new assays, in Step 3 conduct reproducibility and equivalence tests for activity (single-dose screens and dose-response assays) and/or potency (dose-response assays) comparing the two runs. The assay should have an MSD < 20% and both Limits of Agreement on Differences (LsAd) between -20% and +20% for % activity. For potency results, recommendations are an MSR < 3 and both Limits of Agreement (LsA) between 0.33 and 3.0.
2. For assay transfer purposes, in Step 3 conduct reproducibility and equivalence tests for activity (single-dose screen and dose-response assays) and/or potency (dose-response assays) comparing the two runs in the new lab. The assay should have an MSD < 20% and both Limits of Agreement between -20% and +20% for % activity, and an MSR < 3 and both Limits of Agreement between 0.33 and 3.0 for potency.
3. For assay transfer purposes, in Step 4b conduct reproducibility and equivalence tests for activity and/or potency comparing the first run of the new lab to the single run of the old lab. The assays should have Limits of Agreement between -20% and +20% for % activity and Limits of Agreement between 0.33 and 3.0 for potency to be declared equivalent.

### 2.2.4. Notes

1. The Replicate-Determination study as laid out in Sections 2.2.2 and 2.2.3, assumes that the entire study is accomplished in just two runs of the assay (i.e. selected compounds are tested in each of two runs). While this design is preferred, it may not be possible for low-throughput assays in which only a small number of compounds can be tested per run. Alternatives are available in which each half of the replicate determination spans multiple runs (i.e., selected compounds are tested in each of a set of assay runs). Teams should discuss possible design alternatives and the appropriate analysis with their statistician. See also Section 2.2.7 for one possible alternative design and analysis.
2. *The acceptance criteria summarized above should be considered guidelines*, and may in fact be too stringent for some assays. Failure to meet the acceptance guidelines does not necessarily mean that the assay is unusable. Teams should consult with their statistician to understand the ramifications of missing the recommended criteria, and how it affects setting the CSF for the project and making decisions about compounds. For example, if the CSF is >80% and the MSD is 30%, then the assay will fail too many efficacious compounds, since even a 90%-active compound will fall below the CSF some of the time when the MSD is 30%. A more appropriate CSF in this situation might be 70 or even 60%. Furthermore, a 30% MSD indicates that a compound would need an activity test result of at least 80% to be considered to have differential activity from a compound with an activity test result of 50%. If the team desires increased power to discriminate among test

compounds, the assay may need to be re-optimized to identify and reduce sources of variability (see Section 2.5 for additional details).

3. If a project is very new, there may not be 3 to 5 unique compounds with activity *in vivo* (where activity means some measurable activity above the minimum threshold of the assay). In that case it is acceptable to test compounds more than once, and/or at different doses, to get an acceptable sample size. For example, if there are only 2 active compounds then test each compound twice at the same two or three doses in each determination. However, when doing so, (a) it is important to biologically evaluate them as though they were different compounds, including independent sample preparation (i.e., weighing and solubilization), and (b) label the compounds and/or doses as “a”, “b” etc. so that it is clear in the Replicate-Determination analysis which results are being compared across runs.
4. Dose-response assays need to be compared for both potency (ED<sub>50</sub>) and efficacy (% maximum response). It is acceptable to use the same compounds for both single-dose and dose-response assays.

An assay may pass the reproducibility assessment (Steps 1-3 in the procedure [Section 2.2.2]), but may fail the assay comparison study (Step 4 in the procedure [Section 2.2.2]). The assay comparison study may fail either because of an absolute Mean Difference (MD) > 5% (or Mean Ratio (MR) different from 1), or a high MSD (or MSR) in the assay comparison study. If it's the former then there is an activity or potency shift between the assays. You should assess the values in the assays to ascertain their validity (e.g., which assay's results compare best to those reported in the literature?). If it fails because the assay comparison study MSD (or MSR) is too large (but the new assay passes the reproducibility study) then the old assay lacks reproducibility. In either case, if the problem is with the old assay, then the team should consider re-running key compounds in the new assay to provide comparable results to compounds subsequently run in the new assay.

### 2.2.5. Activity/Efficacy; Single Dose Screens

#### 2.2.5.1. Analysis: Activity\Efficacy; Single Dose Screens

The points below describe and define the terms used in the acceptance criterion summarized in Section 2.2.3 and discussed in the Diagnostic Tests (Section 2.2.5.2). Individual animal data should be normalized to the positive (maximally effective) and negative (minimally effective) control averages to yield % activity for each animal. The computations that follow should then be made on the % activity averages for each compound, not the individual animal % activities.

1. Compute the difference in activity (first minus second) between the first and second determination for each compound. Let  $\bar{d}$ , and  $s_d$  be the sample mean and standard deviation of the difference in activity.
2. Compute the **Mean-Difference**:  $MD = |\bar{d}|$  This is the average difference in activity between the two determinations.



3. Compute the **Difference Limits**:  $DLs = \bar{d} \pm 2s_d / \sqrt{n}$ , where n is the number of compounds. This is a 95% confidence interval for the Mean-Difference.
4. Compute the **Minimum Significant Difference**:  $MSD = 2s_d$ . This is the smallest activity difference between two compounds that is statistically significant.
5. Compute the **Limits of Agreement**:  $LsAd = \bar{d} \pm 2s_d$ . Most of the compound activity differences should fall within these limits (approximately 95%).
6. For each compound compute the **Difference** (first minus second) of the two activities, and the **Mean** activity (average of first and second).

Items 2-6 can be combined into one plot: the Difference-Mean plot (see example below).

### 2.2.5.2. Example

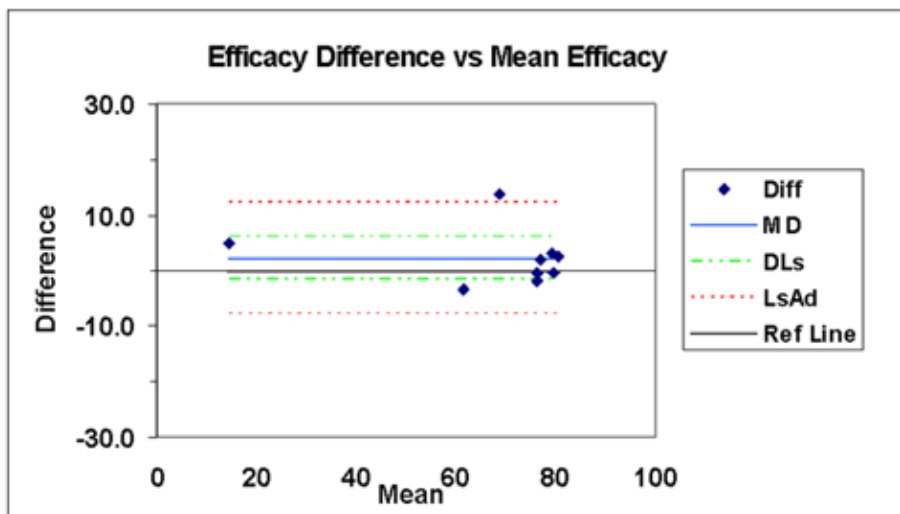
What follows is an example of an *in vivo* assay which measures the inhibition of EnzymeX Desaturase Index in rats, and which was transferred to Lab B from Lab A. Nine compounds were tested in each of two runs in Lab B with n=5 rats per compound. Table 1 displays the % inhibition averages of 5 rats per compound, along with the differences in compound averages. The MD, MSD, and Limits of Agreement are also shown which are computed from the average and standard deviation of the differences. This particular assay easily meets the acceptance criteria summarized in Section 2.2.3.

The compound averages can also be entered directly into the Replicate-Experiment template developed for *in vitro* assays and available on the NIH website. This template will perform the MD, MSD, and LsAd calculations and display them in the Difference-Mean plot.

Figure 2 shows the desired result of pure chance variation in the difference in activities between runs. The blue solid line shows the Mean Difference, i.e. the *average* relationship between the first and second run. The green long-dashed lines show the 95% confidence limits (or Difference Limits) of the Mean Difference. These limits should contain the value 0, as they do in this case. The red short-dashed lines indicate the Limits of Agreement between runs. They indicate the *individual compound* variation between the first and second run. You should see all, or almost all, the points fall within the red dashed lines. The lower line should be above -20, while the upper line should be below +20, which indicates a 20% difference between runs in either direction. The MD should be less than 5%, as it is in this example.

As this assay originated in Lab A, the lab comparison described in Step 4 of Section 2.2.2 was also completed. Eight of the nine compounds tested in the Lab B Replicate-Determination were also tested in Lab A. The eight compound averages of n=5 rats were entered into the template along with the corresponding eight compound averages from the first run in Lab B. Figure 3 shows the results, which meet the acceptance criteria summarized in Part 3 of Section 2.2.3.

**Note:** Although this assay achieved a successful transfer from Lab A to Lab B, demonstrating reproducibility within Lab B, as well as equivalence between labs, the validation has a shortcoming with respect to the selected compounds. *The selected*



#### Equivalence Test Results

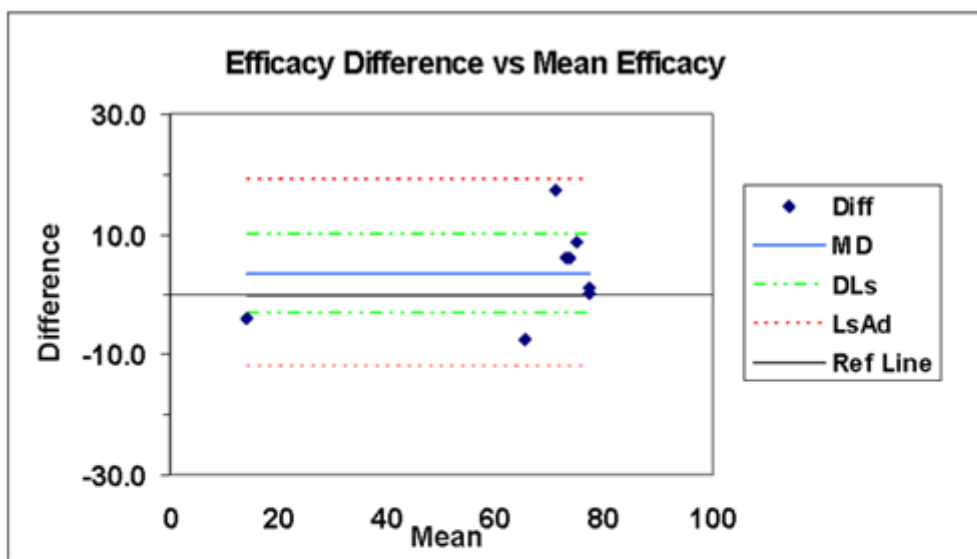
|     |               |
|-----|---------------|
| N   | 9             |
| MD  | 2.20          |
| DLs | -1.67<br>6.07 |

#### Reproducibility Test Results

|                  |                |
|------------------|----------------|
| MSD (Within-Run) | 10.06          |
| LsAd             | -7.87<br>12.26 |

Figure 2: Result of reproducibility and equivalence tests for activity comparing the two runs in the new lab, Lab B. This example shows the desired result of pure chance variation in the difference in activities between runs.

*compounds are not well spaced over the activity range of interest, with most compound activities clustered together and falling well above the CSF of 50%. Since the reproducibility of a compound result from a given assay could depend on the activity level of the compound, it is very important to make an effort to cover the range of potential activity, and in particular to include compounds with activity bracketing the CSF (recognizing that this may be difficult depending on the maturity of a particular project).*



**Equivalence Test Results**

|     |       |
|-----|-------|
| N   | 8     |
| MD  | 3.49  |
| DLs | -3.03 |
|     | 10.01 |

**Reproducibility Test Results**

|                  |        |
|------------------|--------|
| MSD (Within-Run) | 15.60  |
| LsAd             | -12.10 |
|                  | 19.09  |

Figure 3: Result of reproducibility and equivalence tests for activity comparing the first run of the new lab (Lab B) to the single run of the old lab (Lab A). This example shows results that meet the acceptance criteria.

**Table 1: EnzymeX Desaturase Index Assay Replicate-Determination in Lab B.**

| Compound                      | Test1 %Inh | Test2 %Inh   | Difference |
|-------------------------------|------------|--------------|------------|
| A                             | 76.19      | 76.68        | -0.49      |
| B                             | 17.01      | 12.21        | 4.79       |
| C                             | 80.78      | 77.76        | 3.02       |
| D                             | 75.49      | 61.77        | 13.72      |
| E                             | 77.87      | 76.04        | 1.83       |
| F                             | 59.78      | 63.13        | -3.35      |
| G                             | 79.47      | 79.84        | -0.36      |
| H                             | 75.28      | 77.26        | -1.98      |
| I                             | 81.92      | 79.30        | 2.61       |
| <b>MD = AVG of diffs</b>      |            | <b>2.20</b>  |            |
| <b>MSD = 2 x STD of diffs</b> |            | <b>10.06</b> |            |

Table 1: continues on next page...

Table 1: continued from previous page.

|   |       |       |
|---|-------|-------|
| <b>LSAd = MD ± MSD</b><br><b>(2.20 ± 10.06)</b> | -7.87 | 12.26 |
|---|-------|-------|

### 2.2.5.3. Diagnostic Tests and Acceptance Criterion: Activity\Efficacy; Single Dose Screens

1. If the MSD  $\geq 20\%$  then there is poor agreement for **individual** compounds between the two determinations. This problem occurs when the *within-run* variability of the assay is too high. An assay meets the MSD acceptance criterion if the (within-run) MSD  $< 20\%$ .
2. If the Difference Limits do not contain the value 0, then there is a statistically significant **average** difference between the two determinations. Within a lab (Step 3) this is due to high *between-run* assay variability. Between labs (Step 4), this could be due to a systematic difference between labs, or high between-run variability in one or both labs. Note that it is possible with a very “tight” assay (i.e., one with a very low MSD) or with a large set of compounds to have a statistically significant result for this test that is not very material, i.e., the actual MD is small enough to be ignorable. If the result is statistically significant then examine the MD. If it is between -5% and +5% then the average difference between runs is deemed immaterial.
3. The MD and the MSD are combined into a single interval referred to as the **Limits of Agreement**. An assay that either has a high MSD and/or an MD different from 0 will tend to have poor agreement of results between the two determinations. An assay meets the Limits of Agreement acceptance criterion if both the upper and lower limits of agreement are between -20 and +20.

## 2.2.6 Potency; Dose-response curves

### 2.2.6.1. Analysis: Potency; Dose-response curves

The points below describe and define the terms used in the acceptance criterion summarized in Section 2.2.3 and discussed in the Diagnostic Tests (Section 2.2.6.2). See Section 3.5 for guidelines for fitting *in vivo* dose-response curves.

1. Compute the difference in log-potency (first minus second) between the first and second determination for each compound. Let  $\bar{d}$ , and  $s_d$  be the sample mean and standard deviation of the difference in log-potency. Since ratios of ED<sub>50</sub> values (relative potencies) are more meaningful than differences in potency (1 and 3, 10 and 30, 100 and 300 have the same ratio but not the same difference), we take logs in order to analyze ratios as differences.
2. Compute the **Mean-Ratio**:  $MR = 10^{\bar{d}}$ . This is the geometric average fold-difference in potency between two determinations.
3. Compute the **Ratio Limits**:  $RLS = 10^{\bar{d} \pm 2s_d / \sqrt{n}}$ , where  $n$  is the number of compounds. This is the 95% confidence interval for the Mean-Ratio.

4. Compute the **Minimum Significant Ratio**:  $MSR = 10^{2s}$ . This is the smallest potency ratio between two compounds that is statistically significant.
5. Compute the **Limits of Agreement**:  $L_{95A} = 10^{z \pm 2s}$ . Most of the compound potency ratios (approximately 95%) should fall within these limits.
6. For each compound compute the **Ratio** (first divided by second) of the two potencies, and the **Geometric Mean** potency:  $GM = \sqrt{\text{first} \times \text{second}}$ .

Items 2-6 can be combined into one plot: the Ratio-GM plot. The plot is very similar to the Difference-Mean plot described previously in Section 2.2.5 except that both axes are on the log scale instead of the linear scale.

### 2.2.6.2. Diagnostic Tests and Acceptance Criterion: Potency; Dose-response curves

1. If the  $MSR \geq 3$  then there is poor agreement for **individual** compounds between the two runs. This problem occurs when the *within-run* variability of the assay is too high. An assay meets the MSR acceptance criterion if the (within-run)  $MSR < 3$ .
2. If Ratio Limits do not contain the value 1, then there is a statistically significant **average** difference between the two determinations. Within a lab (Step 3) this is due to high *between-run* assay variability. Between labs (Step 4), this could be due to a systematic difference between labs, or high between-run variability in one or both labs. Note that it is possible with a very “tight” assay (i.e., one with a very low MSR), or with a large set of compounds, to have a statistically significant result for this test that is not very material, i.e., the actual MR is small enough to be ignorable. If the result is statistically significant then examine the MR. If it is between 0.67 and 1.5 then the average difference between runs is less than 50% and is deemed immaterial. Note that there is no direct requirement for the MR, but values that are outside 0.67 and 1.5 are unlikely to pass the Limits of Agreement criterion in step 3 below.
3. The MR and the MSR are combined into a single interval referred to as the **Limits of Agreement**. An assay that either has a high MSR and/or an MR different from 1 will tend to have poor agreement of results between the two determinations. An assay meets the Limits of Agreement acceptance criterion if both the upper and lower limits of agreement are between 0.33 and 3.0.

### 2.2.7. Other Approaches for Assessing Reproducibility

#### 2.2.7.1 Retrospective Assessment of Reproducibility

The preferred method for validating an in-vivo assay is by the Replicate-Determination Study described in Sections 2.2.1 – 2.2.6.2. This prospective approach provides an up-front assessment of the capability of an assay to reproducibly identify active compounds prior to placing the assay into production.

It is also possible to validate an assay retrospectively, that is, to collect validation data while screening test compounds. For example, a Single Dose Screen that has been

adequately designed and powered, and that will use proper randomization and analysis techniques could be placed immediately into production. One could then include a “quality control” (see Sections 2.3.1 and 3.1 for a description) in each run of test compounds in order to assess the reproducibility component of assay validation. After six or more runs of the assay, the quality control data could be used to calculate an MSD for the assay.

One obvious risk in using the retrospective approach is that six or more runs of test compound data will be generated before knowing whether or not the reproducibility of the assay is adequate for a team’s needs. This can be an efficient approach provided the resulting MSD is acceptably small; if it is not, the assay may need to be re-optimized to identify and reduce sources of variability (see Section 2.5 for additional details).

*We strongly recommend consultation with a statistician before embarking on this approach to assessing the reproducibility component of assay validation.* Teams should also consult a statistician regarding the calculation and interpretation of the MSD once the data are collected. Note also that this approach produces an “overall” MSD (see Section 2.1 for a description), since in addition to within-run variation, the resulting MSD also encompasses between-run variation from more than six runs.

#### **2.2.7.1.1. Example**

What follows is an example of an *in vivo* assay run in Lab B, which measures the inhibition of EnzymeX Desaturase Index in rats, and which was transferred to Lab B from Lab A and discussed in Section 2.2.5. The assay was retrospectively validated in Lab A by including a quality control in each of seven runs. These data are shown in Figure 4, which displays % inhibition data for individual animals as well as the averages for each run (connected by the blue line in the plot). The overall MSD of 16% is calculated from the standard deviation of the seven % inhibition averages and meets the validation criteria of  $MSD < 20\%$ . The variability chart also indicates a decrease in animal-to-animal variation over time, as well as a slight increase in the activity of the quality control over time.

The % inhibition averages can also be entered into the control chart template (see Section 2.3.2 for additional details), which will calculate the overall MSD and allow monitoring of the averages over time. Output from the template is displayed in Figure 5.

#### **2.2.7.2. Concurrent Validation of SDSs and DRCs**

As mentioned in Section 2.2.2, SDSs should be validated separately from DRCs, but it is possible to validate both methods concurrently. Rather than beginning with the SDS validation via a Replicate-Determination Study (described in Section 2) using several compounds at a single dose, one could proceed directly to the DRC Replicate-Determination Study using a smaller number of compounds tested in dose-response format. The pairs of % activity determinations for the individual doses of each compound can be used to calculate an MSD that is applicable to the assay in single-dose format, while the pairs of ED<sub>50</sub> determinations can be used to calculate an MSR that is applicable to the assay in dose-response format.

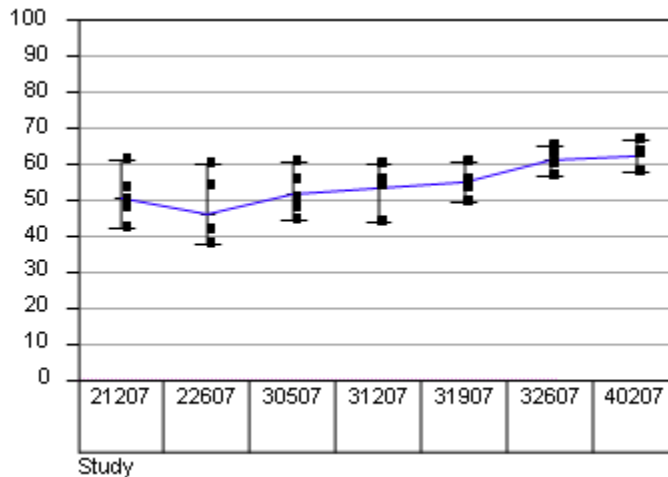


Figure 4: Variability chart of EnzymeX Desaturase Index versus Study.

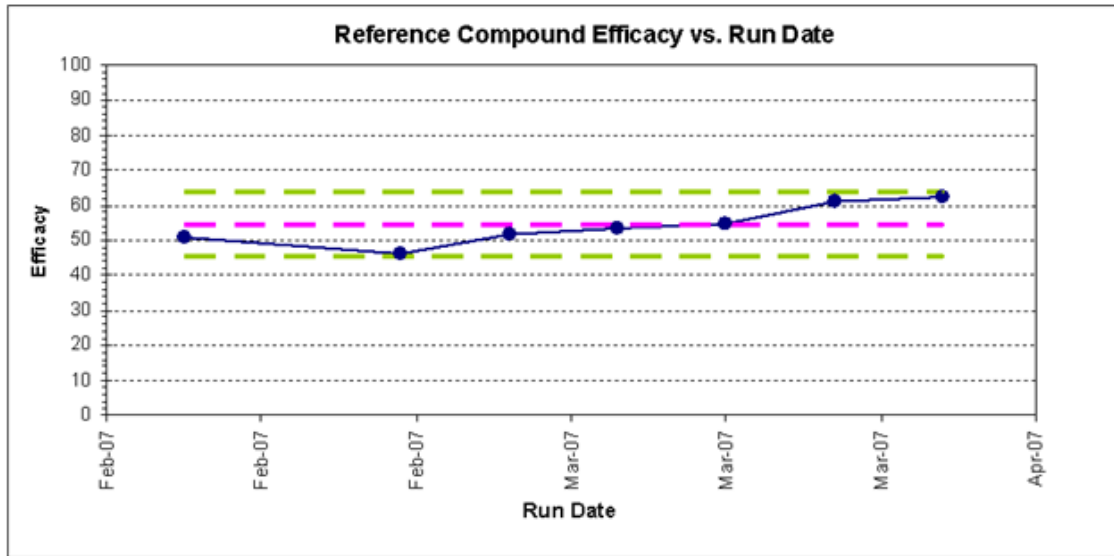
### 2.2.7.2.1. Example

The Capsaicin-Induced Eye Wipe Assay evaluates the ability of compounds to alleviate conjunctival irritation caused by exposure to capsaicin, as measured by inhibition of eye wiping in rats. The assay was developed and validated in Lab A, and upon completion of these activities, the assay was transferred to Lab B. Since the operator in the receiving laboratory was well-trained with respect to running the assay, and since no other major changes to the protocol were made, a bridging study or “Single-Determination Study” was utilized to validate the transfer (see Section 2.4 for additional details).

Three compounds were selected and tested in dose-response format with  $n=6$  rats per each of four doses plus a capsaicin control for a total of 30 animals. The three compounds were tested once in the originating lab and once in the receiving lab. Percent inhibitions of the capsaicin-induced numbers of eye wipes are displayed in the variability chart (Figure 6). One compound was lost for technical reasons in one of the labs, so only two are charted.

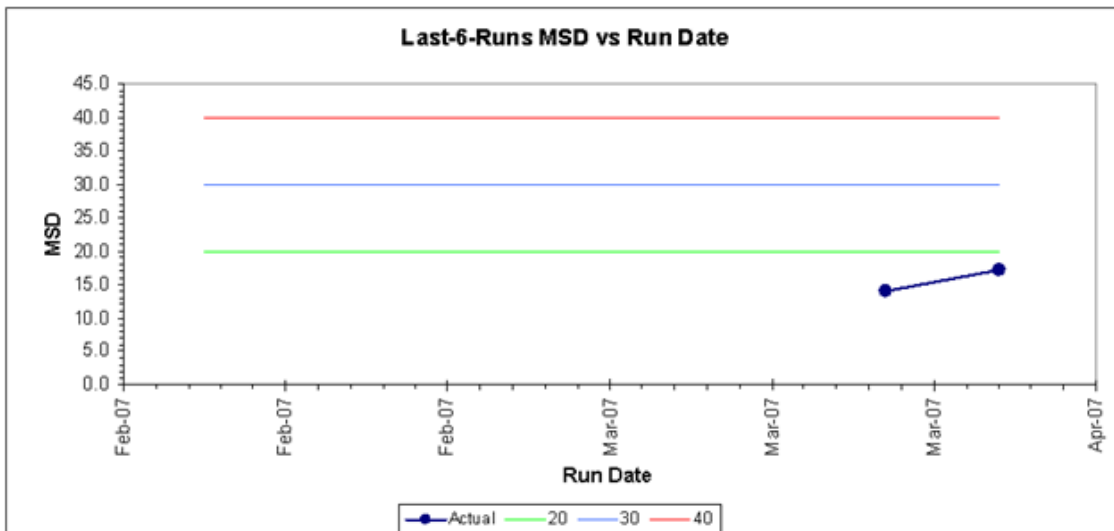
The variability chart indicates similar-dose response relationships for the two compounds between labs. There does however appear to be a consistent shift in the % inhibition for the individual compounds between labs. Also note that there is not complete overlap in the tested doses between labs, but each lab has four doses plus capsaicin available for estimation of the  $ED_{50}$  and 6 pairs of single-dose % inhibitions for calculation of the Mean Difference, Minimum Significant Difference, and Limits of Agreement.

This Single-Determination Study is also an example in which each lab’s set of three determinations spanned multiple runs of the assay (i.e., each compound was tested in a separate run) as described in Section 2.2.4 Note 1. Teams should consult their statistician for appropriate MD, MSD, and LsAd calculations when determinations span multiple runs.



**Control Limits**

|                     |       |
|---------------------|-------|
| Mean (Center Line)  | 54.38 |
| Upper Control Limit | 63.60 |
| Lower Control Limit | 45.16 |



**Mean Summary**

|         |       |
|---------|-------|
| High    | 62.48 |
| Low     | 46.20 |
| Overall | 54.38 |
| Current | 62.48 |

**MSD Summary**

|         |       |
|---------|-------|
| High    | 17.15 |
| Low     | 14.02 |
| Overall | 16.31 |
| Current | 17.15 |

Figure 5: Output from entering percent inhibition averages into the control chart template.



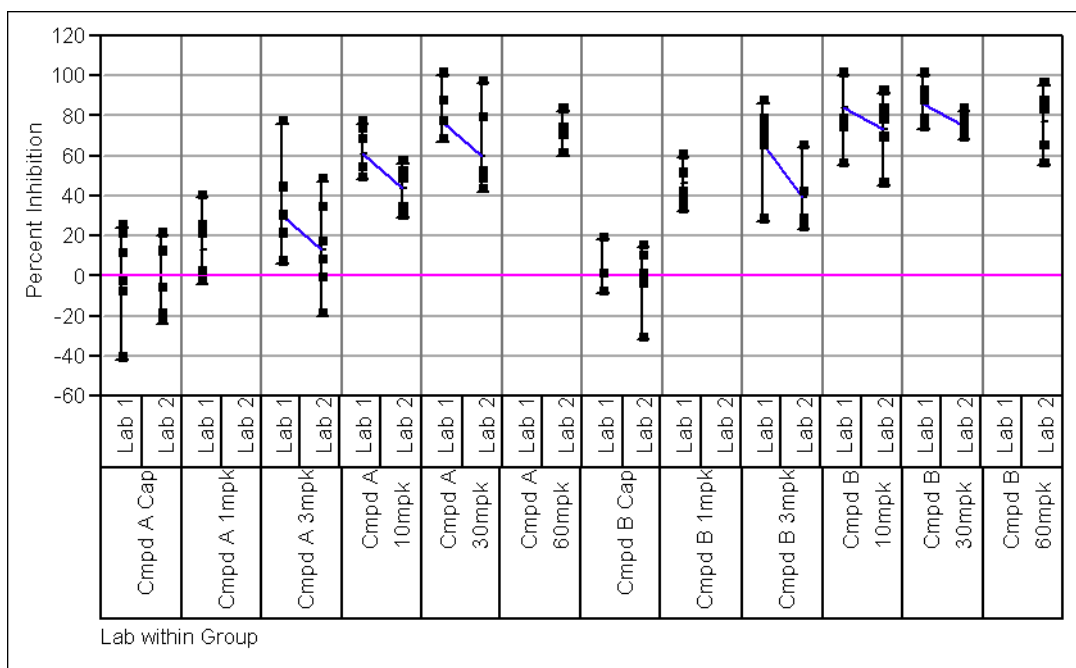


**Figure 6: Variability chart for percent inhibition in a Single-Determination Study.**

For the data in this example, the MD is 17%, the MSD is 11%, and the LsAd are 5.1% and 28%. While the MSD is excellent at 11%, the LsAd do not fall between -20% to +20% due to the 17% average shift in % inhibition between labs. While ED<sub>50</sub>s from just two compounds are not enough to calculate an MSR, the ED<sub>50</sub>s estimated from a four-parameter logistic fit also exhibited a shift in potency between labs, but the magnitude of the shift was less than 3-fold for both compounds.

Even though the LsAd did not meet the within  $\pm 20\%$  criterion, the transfer validation was accepted and the assay was implemented in the receiving laboratory. This decision was based on discussion with scientists regarding possible explanations for the shift, as well as implications for the projects the assay supports. While the LsAd failed the  $\pm 20\%$  criterion, the limits did fall within  $\pm 30\%$ , and the ED<sub>50</sub>s from the two compounds fell within 3-fold, which taken together was considered acceptable for the teams' needs. No MSR could be calculated, but since each compound's dose-response curve consisted of 30 independently tested animals (thereby providing confidence in the resulting ED<sub>50</sub>s), and the ED<sub>50</sub>s agreed to within 3-fold, the transfer was considered to be validated in both single-point and dose-response formats. Close monitoring of a quality control was also recommended for the assay going forward.

Another alternative approach is to include the dose used for the single-dose screen in dose-response determinations, and using the resulting repeats to calculate an MSD.

## 2.3. In-study Validation (Single-Dose Screens)

As mentioned previously in Section 2.2.1, the Replicate-Determination study is used to formally evaluate *within-run* assay variability. The study also provides a preliminary assessment of the *overall* assay variability, but typically does not involve enough assay runs to adequately assess *overall* variability. Overall assay variability consists of both within-run and *between-run* sources of variability, and hence needs to be estimated from several runs of the assay.

Post-implementation monitoring of the measured activity of a control compound that is regularly included in runs of the assay is an effective means for estimating the overall variability in the assay, which can then be used to calculate an overall MSD. The resulting MSD will likely be larger than the Replicate-Determination MSD, since the between-run variability is now included, but it is the appropriate MSD for comparing and prioritizing compounds tested in different runs of the assay.

Continuous monitoring of a regularly tested control compound is also an effective means of tracking assay performance over time, thereby ensuring high quality data for compound prioritization. Control charting the activity of the same compound over time ensures that the activity remains stable without appreciable “assay drift,” and enables identification of suspect runs. Tracking assay performance over time will also ensure that the reproducibility of the assay (i.e., the MSD) remains at an acceptable level.

### 2.3.1. Control Compounds or Treatment Groups

Control compounds in *in vivo* experiments serve three purposes: (i) as comparator for the test compounds, (ii) to normalize responses across assay runs, and (iii) as a quality control marker. A **negative (minimally effect) control** is typically included in all runs of an assay and serves as the comparator for test compounds. A **positive (maximally effective) control** is also often included to establish that the assay is working and to normalize the response over assay runs. While these so-called minimum and maximum controls can be monitored over time to ensure that adequate separation is maintained, they may not be the best choice for monitoring assay performance and reproducibility as described in Section 2.3. Since these controls lie at the extremes of the dynamic range of the assay, they may not accurately represent the level of variability present within the interior of the range (i.e., assay variability may be different for low, medium, and high activity levels). Since interest often lies in prioritizing compounds whose activities fall in the middle to upper end of the dynamic range (but not necessarily at the top of the range), an additional control compound with a normalized (to positive and negative controls) activity of 50 to 70% should also be included to adequately monitor assay performance and reproducibility. This **quality control** should be included in each run of the assay, if possible, but could be included periodically (e.g. every other or every third run) if practical limitations (cost, time, resources etc.) exist for the assay.

### 2.3.2. Control Charts

Monitoring assay performance can be accomplished with a simple scatter plot of the % activity of the quality control versus run date, which should be updated after each run of the assay. Assay drift (trends up or down) can be identified visually, and problems investigated and corrected as they occur. Suspect runs should also be investigated and repeated if warranted.

Full-fledged control charts that calculate and display control limits are preferred, since the limits can assist with identifying trends or steps in the data. Control chart monitoring templates that produce scatter plots, as well as the preferred control charts, for *in vivo* assays are available (check with your statistician). Both templates can be used for *in vivo* data by first normalizing the individual animal data to the positive and negative control averages in each run, and entering the % activity averages for the quality control from each run into the templates.

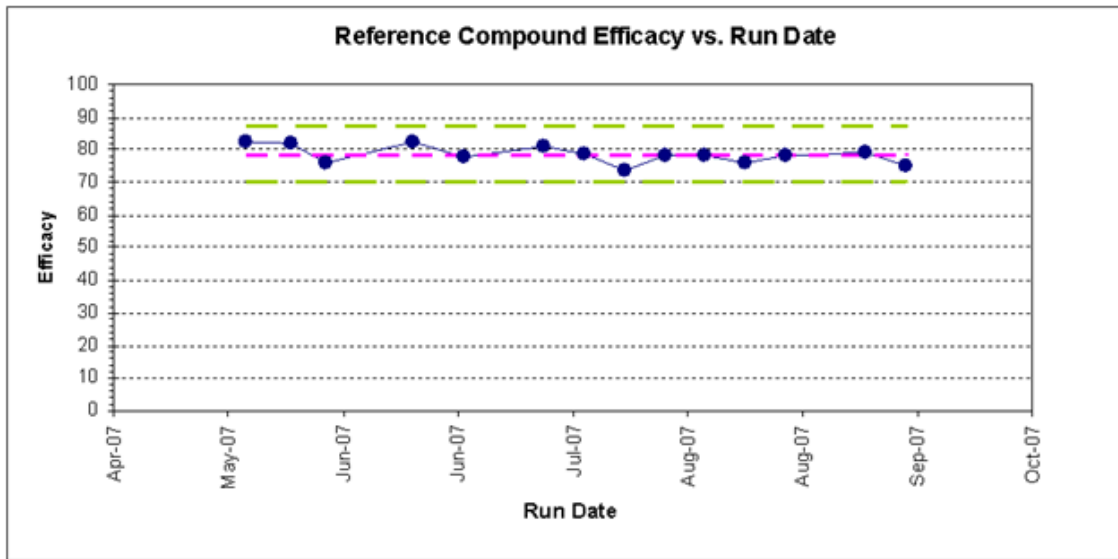
After six runs, both templates will also calculate the overall MSD, which incorporates both within-run and between-run sources of variability (in contrast to the Replicate-Determination MSD, which encompasses only within-run variability). As such, it is expected that inclusion of the within-run variability will inflate the overall MSD as compared to the Replicate-Determination MSD. Teams should consult with their statistician about the interpretation of the overall MSD and how it affects comparing activities of compounds (and subsequent prioritization) tested in different runs of the assay. After each subsequent run, a running MSD (i.e., last-6-runs MSD computed from last six runs) is also computed and displayed graphically to enable monitoring of the reproducibility of the assay over time to ensure that it remains at an acceptable level.

#### 2.3.2.1. Example

What follows is an example of an *in vivo* assay which measures the inhibition of EnzymeX Desaturase Index in DIO rats, and which was discussed previously in Section 2.2.5. A control compound was included in 14 runs of the assay. After normalizing the individual animal EnzymeX DIs to the positive and negative controls within each run, the average % inhibition (n=5 animals per group) of EnzymeX DI for the control compound in each run was entered into the control chart template. The output is shown in Figure 7.

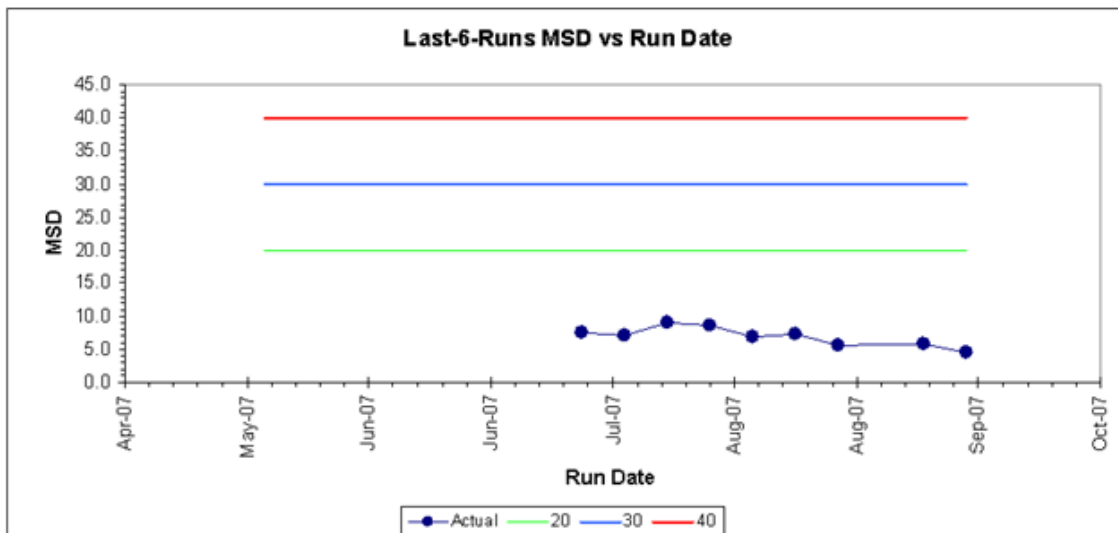
Note the very stable activity of the quality control over the first 14 runs of the assay in the control chart of % activity versus run date. The % activity of the quality control tracks closely to the average of 79% over the 14 runs, with no material drifts or jumps in activity apparent in the chart.

Also note the very stable level of reproducibility in the Last-6-Runs MSD versus run date chart (in fact, the reproducibility looks to be improving slightly over time). The running MSDs are well below 20% (actually fall below 10%), and the overall MSD is excellent at 7.6%, suggesting plenty of power to discriminate among compounds tested in different runs of the assay. However, it is important to note that the overall MSD of 7.64, which incorporates both within-run and between-run variability, is actually smaller than the



**Control Limits**

|                     |       |
|---------------------|-------|
| Mean (Center Line)  | 78.54 |
| Upper Control Limit | 87.24 |
| Lower Control Limit | 69.83 |



**Mean Summary**

|         |       |
|---------|-------|
| High    | 82.46 |
| Low     | 73.77 |
| Overall | 78.54 |
| Current | 75.31 |

**MSD Summary**

|         |      |
|---------|------|
| High    | 9.07 |
| Low     | 4.45 |
| Overall | 7.64 |
| Current | 4.45 |

Figure 7: Output from entering average percent inhibition of EnzymeX DI into the control chart template.

Replicate-Determination MSD of 10.06 (Section 2.2.5), which incorporates only the within-run variability. This could be the result of the operator simply getting better at running the assay (the slight improvement in the running MSDs noted above provides some evidence for this), or it could be due to the fact that the quality control is quite active. While not maximally effective, the % activity of the quality control was certainly outside the recommended range of 50 to 70% activity for a quality control. Since variability (and hence reproducibility) may depend on the activity level of the control (with more active compounds expected to be less variable), the 79% active control may in fact be overestimating the true reproducibility of the assay.

## 2.4. Cross Validation: Bridging Studies for Assay Upgrades/Minor Changes versus Major Changes

Sections 2.2 and 2.3 cover the validation of entirely new assays, or assays that are intended to replace existing assays. The replacement assays are “different” from the original assay, either because of facility changes, personnel differences, or substantively different measurement and recording or automation equipment. Assay upgrades and changes occur as a natural part of the assay life cycle. Requiring a full validation for every conceivable change is impractical and would serve as a barrier to implementing assay improvements. Hence, full validation following every assay change is not recommended. Instead, bridging studies or “mini-validation” studies are recommended to document that the change does not degrade the quality of the data generated by the new assay. In addition, if the assay is to report results in an Assay Method Version (AMV) previously reported into by another assay then it has to be verified that the two labs produce equivalent results.

The level of validation recommended has two tiers, either a Single-Determination Study (Tier I), or a Replicate-Determination Study (Tier II) similar to the full validation package of Section 2.2. Examples of changes within each Tier are given below, along with the recommended validation study for that tier. Note that if the study indicates the change will have an adverse impact on assay quality (i.e., the study indicates there are problems), then the cause should be investigated, corrected, and a full validation should be done. If the results from that study indicate the assays are not equivalent, but the new assay is acceptable, then a new AMV should be established for the assay.

The following guidelines apply principally to changes in biological components of the protocol. If changes are made to the data analysis protocol then these can ordinarily be validated without generating any new data, but rather by comparing the results using the original and new data analysis protocols on a set of existing data. Discuss any changes with a statistician. If changes are made to both the data analysis and biological components of the protocol then the appropriate tier should be selected according to the severity of the biological change as discussed below. The data analysis changes should be validated on the new validation data.

### 2.4.1. Tier I: Single Step and/or Minor Changes to the Assay

Tier I modifications are single changes in an assay such as a change in the person running the assay, an assay condition, instrumentation, or to a *reagent*, that is made either to improve the assay quality or increase the capacity without changing the assay quality. The changes can also be made for reasons unrelated to assay throughput or performance (e.g., change of a supplier for cost savings). Examples of such changes are

- Changes in supplier of animals
- Change in barrier facility used by the supplier
- Changes in recording instruments with similar or comparable electronics. E.g.: blood pressure recording instruments, clinical chemistry equipment, HPLCs, spectrophotometers, behavioral testing equipment such as locomotor activity instruments or operant conditioning chambers. A performance check for signal dynamic range, and signal stability is recommended prior to switching instruments.
- For *ex vivo* analysis of tissues, changes in liquid handling equipment with similar or comparable volume dispensing capabilities. Volume calibration of the new instrument is recommended prior to switching instruments. [Note that plate and pipette tip materials can cause significant changes in derived results ( $IC_{50}$ ,  $EC_{50}$ ). This may be due to changes in the adsorption and wetting properties of the plastic material employed by vendors. Under these conditions a full validation may be required].
- Changes in dilution protocols covering the same concentration range for the concentration–response curves. A bridging study is recommended when dilution protocol changes are required.
- Lot changes of critical reagents such as a new lot of receptor membranes or a new lot of serum antibodies.
- Assay moved to a new laboratory without major changes in instrumentation, using the same reagent lots, same operators (or operators with similar experience and/or training), and assay protocols.
- Assay transfer to an associate or technician within the same laboratory having substantial experience in the assay platform, biology and pharmacology. No other changes are made to the assay.

The purpose of the validation study is to document that the change does not reduce the assay quality.

#### 2.4.2.1. Protocol and Analysis

Conduct the assay comparison portion of the Replicate-Determination Study discussed in Section 2.2, i.e., compare one run of a minimum of 3 to 5 compounds using the existing assay to one run of the assay under the proposed format. If the compound set used in the original validation is available then one need to only run the set again in the new assay protocol, and compare back to Run 1 of the original Replicate-Determination Study. The acceptance criterion is the same as for the assay comparison study: the assay should have

Limits of Agreement between -20% and +20% for % activity, and an MSR < 3 and Limits of Agreement should be between 0.33 and 3.0 for potency.

#### 2.4.2. Tier II: Substantive Changes

Substantive changes requiring full assay validation: when substantive changes are made in the assay procedures, measured signal responses, target pharmacology and control compound activity values may change significantly. Under these circumstances, the assay should be re-validated according to methods described in Section 2.2. The following changes constitute substantive changes, particularly when multiple changes in factors listed below are involved:

- Changes in strain of animals: e.g., SD to Fischer
- Transfer of the assay to a different laboratory location, with distinctly different instrumentation, QB practices or training.
- Changes in detection instruments with significant difference in the optics and electronics. For example, blood pressure monitors, behavioral test equipment, counting equipment, spectrophotometers, and plate readers.
- Changes in assay platform: e.g.: filter binding to LS/MS detection for ex vivo binding assays.
- Changes in assay reagents (including lot changes and supplier) that produce significant changes in assay response, pharmacology and control activity values. For example, changes in enzyme substrates, isozymes, cell-lines, label types, control compounds, calibration standards, (radiolabel vs. fluorescent label), plates, tips and bead types, major changes in buffer composition and pH, co-factors, metal ions, etc.
- Changes in liquid handling equipment with significant differences in volume dispensing capabilities.
- Changes in liquid handling protocol with significant differences in volume dispensing methods.
- Changes in assay conditions such as shaking, incubation time, or temperature that produce significant change in assay response, pharmacology and control activity values.
- Major changes in dilution protocols involving mixed solvents, number of dilution steps and changes in concentration range for the concentration-response curves.
- Change in analyst/operator running the assay, particularly if new to the job and/or has no experience in running the assay in its current format/assay platform.
- Making more than one of the above-mentioned changes to the assay protocol at any one time.

Substantive changes typically require full validation, i.e., a complete Replicate-Determination Study. If the intent is to report the data in the same AMV then an assay comparison study must be conducted as part of the Replicate-Determination study.

## 2.5. How to Deal with High Assay Variability

As mentioned previously, the sources of variation in an assay include the between- and within-run sources of variability. In addition, the animal-to-animal variability as well as variability in measuring the response of the subject also contributes to the overall variability in the assay. In order to optimize an assay and/or when an assay fails to meet the acceptance criteria, it is important to specifically assess each of these sources of variability. The variance, which is the square of the standard deviation, can be used to estimate the magnitude, or relative contribution, of each of these sources of variability. Variance is useful because the sources of variation are additive on the variance scale, but not on the standard deviation scale. When an assay fails to meet the acceptance criteria, it is necessary to determine the source of the high assay variability in order to be able to make changes to reduce the relevant variability. For example, simply increasing the number of animals per group may not necessarily reduce between-run variability.

### 2.5.1. Example: Analyzing Variability in an Ex Vivo Binding Assay

In an *ex vivo* receptor binding assay, subjects (5 rats per dose group) were administered a dose of a test compound orally, sacrificed 1 hour later, the cerebellum removed and stored at  $-70^{\circ}$  until used in the binding assay. For the *ex vivo* receptor binding assay, the tissue was homogenized and incubated for 30 minutes at  $37^{\circ}\text{C}$  in a water bath. The tissue from each animal was aliquoted into 8 tubes, together with radioligand and buffer, and incubated for 2 hours. Four tubes were used to measure total binding and four tubes to measure non-specific binding. Each tube was centrifuged at  $12000 \times g$  for 5 minutes, washed and then placed in a gamma counter and counted. Counts for each tube were converted to DPM and recorded. A plot of the data from each of the vehicle treated animals for each of 3 experiments is presented in Figure 8. The variance in the assay is summarized in Table 2.

The total variance was partitioned statistically into study-to-study, animal-to-animal, and tube-to-tube variability. In this example, the result for each of the four tubes is the difference between the DPM in one of the four tubes used to estimate total binding minus the mean of the four tubes used to estimate nonspecific binding. Thus, each of the four tubes represents a different measurement of one subject and the variability among the four tubes from one animal represents variability in the measurement of binding in that animal. In this example, study-to-study variability accounts for approximately 68% of the total (Table 2, far right column). In order to optimize the assay and reduce the overall variability, reducing the study-to-study variability would have the greatest impact. One way of reducing study-to-study variability is to normalize the data within each study in order to compare results across each study. In this example, the radiolabel was  $^{125}\text{I}$ , and its relatively short half-life is the major source of the study-to-study variability; normalizing the data within each study would reduce study-to-study variability due to isotopic decay. The need to normalize, rather than using raw counts, is well known and accepted for *in vitro* binding studies, but this practice is not common for *in vivo* assays. It is appropriate to compare raw signals across studies only when the study-to-study



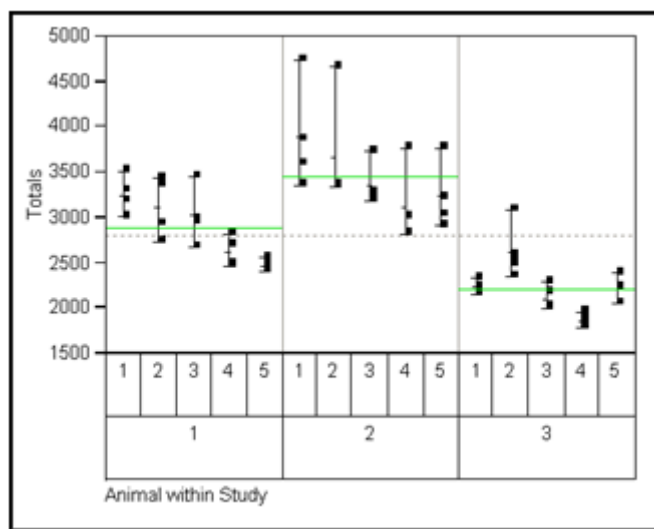


Figure 8: Plot of the vehicle treated animals in an *ex vivo* binding assay. The ordinate (y-axis) is total specific binding in DPM in each of the four tubes used to assess specific binding. Data for 5 animals in each of three studies is represented.

variation is negligible. Note that increasing the sample size would not reduce this source of variability. The second largest source of variability, approximately 18%, is tube-to-tube, that is, the variability in measuring each animal. In order to reduce this source of variability, additional measurements of each animal would be needed. Using 5 tubes to assess specific binding, rather than 4, and only 3 tubes to assess nonspecific binding (which is typically not highly variable) would reduce this source of variability. If only one measurement on an animal is made, the measurement-to-measurement variability still exists, but cannot be calculated. (Another example is that of measuring tumor volume with calipers – measuring only once at a given assessment versus measuring multiple times at a given assessment.) Note that increasing the sample size would not reduce this source of variability. Multiple measurements of the response for one subject are the exception rather than the rule for *in vivo* experiments, and yet variability in the measurement process may be a major source of variance in the study. It is important during assay development and optimization to assess the potential contribution of measurement variability on the total variability in the assay and address this potential source as needed, for example by taking the average (or median) of multiple measures on a given subject. The smallest source of variability in the present example, approximately 13% of the total, was due to animal-to-animal variability. Thus, increasing sample size would have impacted the smallest source of variability. The relative contributions of “animal” and “measurement” variation can be used to determine the optimal number of measurements per animal, as well as number of animals. In conclusion, the relative contribution from different sources of variability needs to be directly assessed during assay development and optimization. This assessment allows one to directly address the most relevant sources of variability in order to optimize and statistically validate an assay.

Table 2: Estimated variance contributed by study-to-study variability, animal-to-animal variability, and tube-to-tube variability in an *ex vivo* binding assay.

| Source of Variation | Estimated Variance | Estimated Std Dev | Pct of Total (%) |
|---------------------|--------------------|-------------------|------------------|
| Study               | 373088             | 610.8             | 68.3             |
| Animal              | 72819              | 269.9             | 13.3             |
| Tube                | 100033             | 316.3             | 18.3             |
| Total               | 545941             |                   | 100              |

### 2.5.2. High Variation in Single Dose Determinations

Table 3 below can be used as a reference to determine the sample size necessary for single dose or dose-response assays with high variability. For a given **coefficient of variation** (CV) of the raw data values based on a sample size of 1 subject, the table shows the number of subjects per dose needed for the CV of a mean to be less than or equal to 10 or 20%.

Increasing sample size to reduce variability will also reduce the capacity (i.e., throughput) of the assay to test compounds. Further optimization of the assay could reduce variability and maintain or increase its capacity. The decision to further optimize or to increase sample size will have to be made for each assay.

Table 3: Sample size necessary to reduce the coefficient of variation (CV) to less than 10 or 20%, given a known CV when the sample size is one.

| CV for Individual Subjects | Number of Subjects so that CV Mean < 10% | Number of Subjects so that CV Mean < 20% |
|----------------------------|--|--|
| <10                        | 1  | 1  |
| 10.1-14.1                  | 2  | 1  |
| 14.2-17.3                  | 3  | 1  |
| 17.4-20.0                  | 4  | 1  |
| 20.1-22.3                  | 5  | 2  |
| 22.4-24.4                  | 6  | 2  |
| 24.5-26.4                  | 7  | 2  |
| 26.5-28.2                  | 8  | 2  |
| 28.3-30                    | 9  | 3  |
| 30.1-31.6                  | 10                                       | 3  |
| 31.7-33.1                  | 11                                       | 3  |
| 33.2-34.6                  | 12                                       | 3  |
| 34.7-36.0                  | 13                                       | 4  |

Table 3: continues on next page...

Table 3: continued from previous page.

|           |    |   |
|-----------|----|---|
| 36.1-37.4 | 14 | 4 |
| 37.5-38.7 | 15 | 4 |
| 38.8-40.0 | 16 | 4 |

### 2.5.3. High Variation in Dose-Response Determinations

If in Section 2.2 the assay fails either test ( $MSR > 3$  or Limits of Agreement outside the interval 0.33-3) then the variability of the assay is too high for typical purposes. The following options should be considered to reduce the assay variability:

1. Optimizing the assay to lower the variability in the raw data values. Check that the dose range is appropriate for the compound results. Increasing the number of doses and/or subjects per dose may improve the results. A minimum of 6 doses at 2X intervals, and analyzing the data using nonlinear curve-fitting techniques, is recommended. In general, it is better to have more doses rather than more subjects per dose. The doses should cover the expected range of the assay, e.g., 0-100%, as much as possible.
2. Consider increasing sample size as discussed below. Note that the impact of increasing sample size may decrease capacity, and so the Replicate-Determination Study, and a detailed analysis of the sources of variation, should be used to assess whether increasing the number of subjects per dose will achieve the objective.
3. Adopt as part of the standard protocol to re-test compounds. For example, each compound may be tested 2 or more times in different runs of the assay. Averaging the results from multiple runs will reduce the assay variability (**NB.** In such cases the individual run results may be stored in the database and then the data mining/query tools are used to average the results).

To investigate the impact of increasing sample size in the dose-response assay you should conduct the Replicate-Determination Study with the maximum number of subjects contemplated (e.g., 5 subjects / dose). The data can be analyzed first using all available subjects. Then one subject per group can be removed at random and the data re-analyzed. This step is repeated until the smallest sample size is found that still meets the acceptance criteria. An example below will illustrate this idea.

An *in vivo* receptor occupancy assay was run using 1 subject per dose and the Replicate-Determination Study did not meet the acceptance criteria. To examine if replication (i.e., increasing the number of subjects per dose) would help, a new Replicate-Determination Study was conducted using 4 subjects per dose. Table 4 shows the results of fitting  $ED_{50}$  curves and re-evaluating the MSR and LsA for 2, 3, or 4 subjects per group:

From Table 4 we can see that it takes all 4 subjects to meet the MSR acceptance criteria, and more than 4 subjects would be needed to meet LsA acceptance criterion. It should be noted that the LsA results are close to being acceptable with 4 subjects per group.

Table 4: Results of fitting ED<sub>50</sub> curves and re-evaluating the MSR and LsA for 2, 3, or 4 subjects per group.

| Subjects | MSR  | LsA         |
|----------|------|-------------|
| 2        | 3.62 | 0.35 – 4.59 |
| 3        | 3.32 | 0.43 – 4.74 |
| 4        | 2.44 | 0.53 – 3.16 |

## 3. Design, Sample Size, Randomization, and Analysis Considerations

### 3.1. Assay (Experimental) Design Considerations

Good experimental design is important in order to answer the research question of interest in a way that is free of bias, can be generalized to the desired or targeted population, and is of sufficient size to properly answer the question. This includes such things as determining the measurements to make, timing, dosing frequency and route, the species to use, etc. It also includes identifying the relevant statistical analyses, determining appropriate sample sizes, and determining a randomization scheme.

Several expectations for good experimental design and analysis include:

- An a priori statement of objectives/hypotheses
- Appropriate experimental design methods
- Sufficient, but not excessive, sample size to ensure statistical significance of biologically relevant effects
- A priori determination of appropriate statistical methods

#### 3.1.1. Objectives and/or Hypotheses

State the objectives and/or the hypotheses you wish to accomplish or test with an assay before beginning an experiment. If a hypothesis is formed after collecting the data, the results may be biased. The objectives should be defined in terms of well defined end-point(s). Examples of objectives include comparison of food consumption between a test compound and control, comparison of survival rates between the treated and untreated groups, comparison of the effect level or the ED<sub>50</sub> between a test compound and control, etc.

#### 3.1.2. Design Strategy

*In vivo* studies should be designed in such a way that all meaningful biological effects are statistically significant. In an exploratory study, this “meaningful effect” might correspond to any effect that is pharmacologically relevant. For a project/program team, this meaningful effect might correspond to an effect that meets the CSFs defined in the flow scheme. Power and sample size analysis is especially relevant for assays that are designed to address key endpoints and make decisions as to whether a compound meets the assay’s

CSF. Biologically meaningful effects are not always well-known in advance, in which case a range of plausible effects could be considered.

To a great extent, experimental design is about identifying and determining a strategy to deal with different kinds of variables. The types of variables encountered in research include:

- Manipulated variable (*independent/explanatory variable*)
- Response variable (*dependent/outcome variable*)
- Extraneous variables (*uncontrolled/random*)

The manipulated variable is a purposeful attempt to introduce variability into the experiment by, for example, administering different doses of a drug. If the manipulated variable were the only source of variability, then research design would be quite simple.

Extraneous variables can encroach upon an experiment and can change the results in ways that we do not want or of which we are unaware. Examples of extraneous variables could include inherent animal variation, time of day, baseline body weights or glucose levels, operator ability or skill, lab noise or activity, etc. **To a great extent, experimental design is about having a strategy to deal with extraneous variables.** To ignore them can all too often lead to biased results and the requirement of larger sample sizes. Fixing (holding them constant) or eliminating them, such as by considering only a subgroup of animals, can reduce bias and sample sizes, but can also reduce the generalizability of the results to only those conditions considered in the experiment. Another approach is to control for them by incorporating them into the experimental design, ideally at the design stage, or at the statistical analysis stage if the former is not possible.

Some additional design considerations include:

- Appropriate random allocation of animals to treatment groups.
- Blinding of observers to drug treatment allocation, whenever possible, especially when subjective evaluations are to be made by observers.
- Proper selection of dose levels.
- Optimal selection of control groups.
- Optimal time points to collect samples.
- Proper statistical methodology.

Different design strategies should be carefully considered to minimize variability and maximize information from the experiment.

The design issues stated above should be addressed in the context of the key endpoints (or summary measures) from the study. Examples of such endpoints may include survival rate, glucose normalization, etc. When there are several endpoints of interest from an assay, certain design questions such as the power of the study should be assessed with respect to the endpoints that are considered to be most important by the scientist and the project team.

### 3.1.3. Endpoints

The key endpoints from the study must be identified first, as all other design choices should be tailored to these outcomes. Typical outcomes include:

- Statistical significance from control using Analysis of Variance (ANOVA).
- ED<sub>50</sub> (either absolute or relative) from a dose-response model such as the 4-parameter logistic model (4PL)

Note that the latter can be determined using a variety of methods, and it is important to define the pharmacologically “effective dose,” as well.

### 3.1.4. Control Groups

Control groups serve three purposes: (i) a comparison to the test groups, (ii) as a quality control marker, and (iii) to normalize the response for comparison across studies. A “negative” control is used in all studies and serves as the comparison group. An active or “positive” control is a compound that has a different response from the negative control, and normally represents the maximal response of a standard treatment. A positive control is used when normalization is necessary to stabilize the response across runs of the assay or to illustrate the range of signal available in a particular run of the assay. If a positive control fails to separate from the negative control then there is an increased chance of a false negative outcome. Since normalized responses may still lack reproducibility across runs, a third control may be employed to monitor the reproducibility of the normalized response across runs of the experiment. This control would be a second positive control, but at an activity level lower than the first positive control. These are used as a quality control marker to establish that each run of the experiment is performing as expected, and hence are often called a “quality control.” The activity of a “quality control” should be at a level of activity desired for the advancement of test compounds (see Section 2.3).

### 3.1.5. Statistical Analysis Plan and Implementation

Before developing and validating an assay to be used on a flow scheme, appropriate statistical methods including data transformations and software for analyzing the data from these experiments should be determined.

There are several statistical methods available to analyze any given experiment/data set, and the choice of these methods and the way a certain class of methods is implemented can significantly impact the conclusions from the experiment. For example, there are certain statistical considerations one should take into account when using the analysis of variance (ANOVA) method, including the distribution of the data, equality of variances, baseline variables, methods for comparing different groups, etc. Also, a two-sample *t*-test might often seem appropriate for several types of experiments, but upon careful examination of the study design, the *t*-test might turn out to be less appropriate than some of the other statistical analysis methods for such experiments.

If the study design is changed at any time during a series of experiments, appropriate analysis methods and implementation strategy should once again be examined in light of these changes.

**The basic types of experimental designs are:**

- Parallel group
- Randomized block
- Repeated measures
- Cross-over design

### **3.1.5.1. Parallel Groups Design**

In a parallel groups design, subjects are randomly assigned to groups and each group receives one level of a treatment, for example, one dose of a drug, so each group is independent of every other group. This basic design assumes that there are no important *extraneous variables* that we can identify which will influence or bias the results.

Features of a parallel groups design:

- Simplest design.
- Subjects are randomly assigned to groups, and groups are typically, but not necessarily, of equal size.
- Each group receives one level of a treatment, e.g., one dose of a drug
- Use when randomization is possible.
- Does not account for extraneous variables that influence or bias the results. The variation caused by extraneous variables is attributed to the overall assay variability.

### **3.1.5.2. Randomized Block Design**

A second basic design type is called a Randomized Block Design. Randomized block designs are used when an extraneous variable can be identified prior to randomization and subjects can be divided into subgroups based on values of the extraneous variable. Like a parallel groups design, each treatment group is an independent group of subjects. However, subjects are not assigned to treatment groups in an entirely random manner. Rather, subjects are first placed into one of several subgroups based on a blocking or matching factor (such as baseline values, time of day, gender, baseline body weight, etc.) and then subjects in each block are randomized to the treatment groups.

It is necessary for each subgroup (or “block”) to contribute equally to each treatment. Each subgroup must contribute an equal number of subjects to each treatment. Thus, there must be at least as many subjects in each subgroup as there are treatments. For example, if there are 4 treatments, there must be at least 4 or ideally a multiple of 4 subjects in each subgroup.

It is important that a separate randomization be performed on each block so that high or low values of each subgroup are not always placed into one treatment. This strategy forces the extraneous variable to be balanced across treatment groups.

One disadvantage of the randomized block design is that it is not always logistically feasible. For example, the investigator may be aware of an extraneous variable, but not be able to measure it before the randomization process, such as the size of a cardiac or cerebral infarct.

Features of a randomized block design:

- An extraneous variable can be identified and measured before starting the experiment.
- Subjects can be divided into subgroups based on values of the extraneous variable.
- Each subgroup (“block”) has as many subjects as there are treatment levels.
- Within each block, treatments are randomly allocated to subjects.
- A separate randomization is performed in each block.
- Forces the extraneous variable to be balanced across treatment groups.
- Not always logistically feasible.

Note: we refer to a factor as a “blocking” factor when it is a continuous measure, for example baseline blood glucose levels, that we can divide into different levels, such as high, medium and low. We refer to a factor as a “stratification” factor when it is not continuous, such as gender and we can stratify the groups on the basis of that parameter.

In a randomized block design, it is necessary for all subjects within a block to be as similar as possible. There are several ways in which blocking can be accomplished:

One of the most common ways to “match” subjects is to rank all of the subjects (e.g., 1 through 20) according to each subject’s value of the blocking factor. Subgroups of subjects are then grouped into individual blocks (e.g., subjects 1 – 4 as block 1, subjects 5 – 8 as block 2, etc.). So, within a block, there are similar values of the blocking factor. This minimizes the variance due to the blocking factor (“extraneous variable”).

### **3.1.5.3. Analysis of Covariance (ANCOVA)**

Sometimes it is not possible to identify or account for an extraneous variable at the beginning of a study or design phase. In these instances, it may be still be possible to remove the effect of an extraneous variable during the analysis. One technique is to employ an Analysis of Covariance or ANCOVA. Note that if the treatment affects both the response and the covariate then ANCOVA must not be used, because any observed effect may be due to actions of the treatment on the covariate rather than on the response variable.

An ANCOVA model is most useful when there is a linear relationship between the response and the covariate within each group, and when these slopes are similar. If there is sufficient sample size, it is relatively straightforward to test for these conditions. If the slopes aren’t different from zero then there is little to no benefit in the ANCOVA model. If the slopes aren’t parallel then the interpretation of the treatment comparisons depends on the level of the covariate.



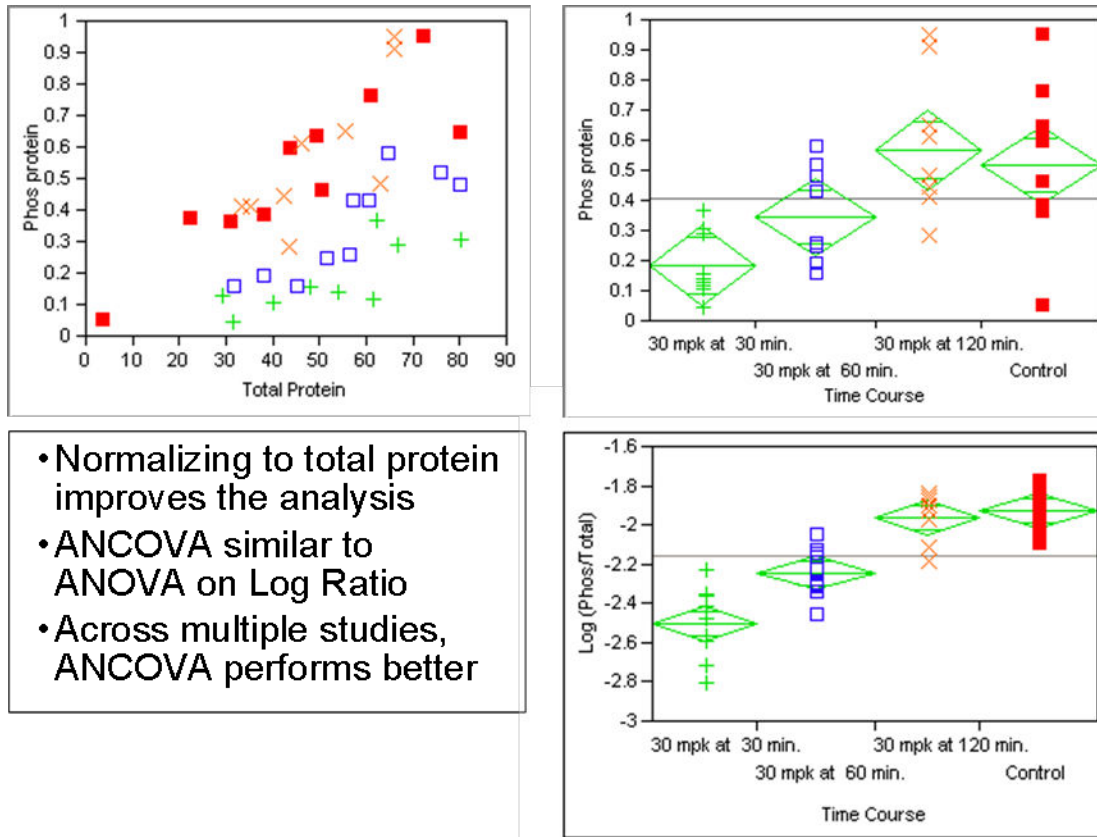


Figure 9: Examples of Analysis of Covariance (ANCOVA).

It is also very important that the values of the covariate overlap among the treatments. If the values for the covariate don't overlap, then you are extrapolating into regions where you have no data and the results could be incorrect. Use of proper randomization techniques will usually prevent this situation.

If the experiment was designed as a randomized block design, it is generally best to analyze it as a randomized block design and avoid using ANCOVA.

You may be able to avoid an ANCOVA model by using the baseline to normalize the response (i.e., change from baseline, ratio, etc.; Figure 9).

### 3.1.5.4. Repeated Measures and Cross-over Designs

Another popular design is to use each subject as a block and test each subject at each of several time points (repeated measures design) or under each treatment condition (cross-over design). With this approach there is only one subject within a block and this minimizes the variance by using each subject as its own control. Repeated measures and crossover designs are just special cases of a randomized block design.

Some examples:

- When a subject receives a dose of drug and is tested at multiple time points.
- When a subject receives all doses of drug. This type of design is also a repeated measures design, but it is a special case of repeated measures and is referred to as a crossover design because each subject is “crossed over” to each treatment or treatment level.
- In a crossover design, different sequences of treatments are identified, and each subject is randomized to one sequence.
- Cross-over designs assume that the effects of each treatment dissipate or don’t interfere with the response of the next treatment (i.e., no carryover). If this is not the case, then the cross-over is not an appropriate design.

Repeated measures designs allow us to separate out the variability due to individual differences (that is, to use each individual as their own control) and therefore better evaluate the effects of the manipulated, or independent variable. This increases the power of the analysis and means that fewer subjects are needed to have adequate statistical power.

### 3.2. Statistical Analysis Considerations

Once the experimental design has been selected, the appropriate statistical analysis then follows:

#### Parallel groups

- One factor with **only two levels**: t-test or ANCOVA
- One factor with more than two levels: one-way ANOVA or ANCOVA
- Two factors: two-way ANOVA or ANCOVA

#### Randomized blocks

- One factor: two-way ANOVA
  - Block as the second factor
- Two factors: three-way ANOVA
  - Block as the third factor
- Crossover & repeated measures: two-way and repeated-measures ANOVA
- Stratified designs: two-way ANOVA

The main analysis issues deal with how well the response data match the probability model assumed by the statistical analysis.

For ANOVA to identify statistically significant treatments or doses, the main issues are to verify the following.

- The residuals of the response or dependant variable are normally distributed with constant variability across groups
- Techniques to handle outliers are appropriate (see below)
- Appropriate multiple comparison techniques are employed for the study objectives

- If concomitant variables such as baseline measures are used, the analysis should appropriately adjust for these variables

For dose-response studies to estimate an ED<sub>50</sub>, the main issues to be examined are the following:

- Whether the variability is constant or varies with the magnitude of the mean response
- Suitability of the dose range for the dose-response model
- Suitability of the dose-response model for the biological effects being examined.

For example, to fit a 4 parameter logistic model successfully, a wide dose-range allowing for well-defined tops and bottoms is required. In practice that is difficult to achieve, and often the top or the bottom is fixed at some pre-specified value. This imposes additional biological assumptions that should be assessed.

### 3.2.1. Outliers

The occurrence of an occasional outlier is not uncommon with *in vivo* experiments, and their presence can sometimes have a large impact on calculated means and, in particular, standard deviations. An observation isolated far above (or below) the bulk of the rest of data can “pull” the calculated mean toward it and result in an overestimate (or underestimate) of the true mean. Since the standard deviation involves a squared term, the impact of an outlier can be even more dramatic, making the standard deviation larger.

In addition to negatively affecting the calculation of summary statistics, outliers can also affect the accuracy of the p-values generated by statistical tests, such as the paired and two-sample t-tests, and the ANOVA. One possible remedy is to perform the statistical test on transformed data (typically the square root or log transform). Transformation is indicated when variability is not constant (e.g., across treatment groups in a one-way ANOVA) and/or when the data are skewed (i.e., longer tail) to the right, but a transformation can also eliminate apparent outliers in some cases (Figure 10).

Another remedial approach is to employ a non-parametric or rank-based statistical test, in which raw data are replaced by their ranks. These are indicated when the data at hand are not adequately modeled by the normal (symmetric, bell-shaped) distribution. Statistical tests based on ranks also down-weight any outliers present in the data. Non-parametric analogs of the paired and two-sample t-tests, and the ANOVA are respectively the Wilcoxon signed rank test, the Mann-Whitney U test, and the Kruskal-Wallis test.

It is acceptable to report the usual summary statistics when presenting data from an *in vivo* experiment for which a transformation or nonparametric test was used for the statistical analysis. However, as mentioned above, outliers can distort the mean and standard deviation, so a better approach is to report summary statistics consistent with the chosen remedial measure (e.g., use the antilog of the mean for log-transformed data; use the median for rank-based tests). Consult a statistician for the appropriate method of reporting summary statistics when outliers are present.

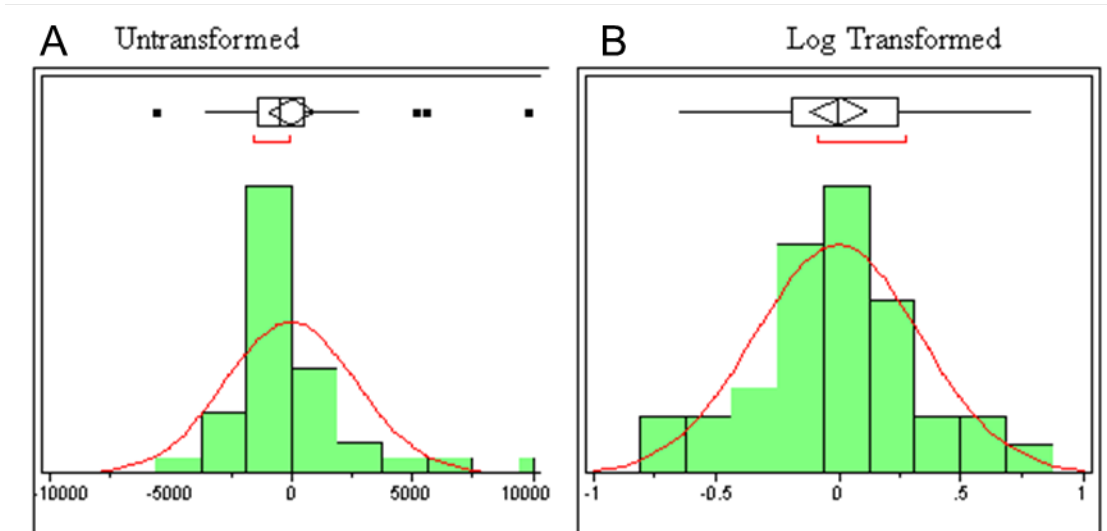


Figure 10: Results of a transformation eliminating outliers. (A) The residuals from a one-way ANOVA fit to the raw AUCs. (B) The residuals from a one-way ANOVA fit to log-transformed AUCs.

Another approach to dealing with outliers is to simply remove them, but this of course requires one to be able to discern which observations are truly erroneous and which simply represent the underlying variability in the assay. The outlier boxplot is a commonly employed and effective tool for identifying outliers. **However, detection of an outlier by this (or other methods) does not automatically mean the observation can be removed.** It simply identifies observations that have the potential to disrupt the statistical analysis and that should be investigated.

If a valid, assignable cause can be identified for an outlying result, or if the result is simply inconsistent with what is being measured and suggests an error was made, the observation can be removed. Otherwise, the analysis should be performed with and without the outlier(s), with both results reported. **If an observation is removed for cause, it should be documented that the data point existed along with the reason for removing it.** Ad hoc rules based on distance in standard deviations units from the mean should not be used.

Outlier box-plots are shown above the histograms in Figure 10. The box is formed by the first and third quartiles and represents the middle 50% of the data. The length of the box (i.e., third quartile minus first quartile) is the inter-quartile range (IQR). The vertical line within the box is the median, and the horizontal lines connected to the box extend to the extremes of the data that fall within 1.5 times the IQR. Any observations falling outside 1.5 times the IQR from the first or third quartiles appear as points on the box-plot and are potential outliers.

A minimum of 10 observations are recommended to generate a box-plot, but in the context of an experiment comparing several compound activities, each individual

compound may be tested in fewer than 10 animals. In that case, the desired statistical model (e.g., a one-way ANOVA) can be fit and the outlier box-plot generated on the residuals from the model fit.

Residuals are automatically calculated in most statistical software, and in some cases are very simple to calculate. For example, the residuals from a one-way ANOVA of compound activities are simply the data “centered” by subtracting the respective compound mean. Consult a statistician for help with generating residuals from statistical models.

Figure 10 is an example of dog plasma exposures for 8 formulations of a single compound (4 dogs per formulation). The residuals from a one-way ANOVA fit to the raw AUCs appear in the box-plot and histogram in Figure 10A. Note that the histogram suggests right skew for the AUCs, and there are potential outliers in the box-plot, particularly on the upper end of the distribution.

Right skew with outliers (along with increasing variability with increasing mean) are telltale signs that a log transform may be needed. The residuals from a one-way ANOVA fit to log-transformed AUCs appear in Figure 10B. Note that the distribution is much more symmetric, and the box-plot does not identify any outliers on the log scale. The bell-shaped normal distribution (superimposed on the histogram) appears to more adequately model the log-transformed AUCs.

In summary:

- Outlier box-plots can be used to identify potential outliers. Other methods, such as number of standard deviations from the mean, are not recommended.
- An outlier can be removed from an analysis if it has an assignable cause or is clearly erroneous, but this should be documented.
- When there are outliers that do not have a known cause and are not clearly erroneous, analyze the data with and with the suspected outliers and report all results.
- Transforming the response variable can sometimes make outliers become non-outliers and satisfy standard analysis assumptions better than non-transformed data.
- Non-parametric analysis methods can be used to minimize the impact of outliers on analysis results without removing them from the analysis.

### 3.3. Randomization

There are a number of randomization techniques that are available. Certain study designs require specific randomization techniques, (e.g. randomized block designs, stratified designs, etc.). Random numbers should be obtained from an acceptable random number generator, (e.g., Excel, JMP, SAS, random number table, randomization web tool, etc.).

It is also very important to appropriately randomize subjects to treatment groups, as this reduces opportunities for bias. Randomization requires extra time and effort, but it can be more costly to not use it. Non-random strategies for assigning animals to treatment

groups, when applied consistently across studies, will tend to introduce flaws, or bias, into the study results. By looking at the performance of a strategy across a series of studies we can then examine how well or poor a particular strategy is working. A truly random selection process is one where each subject is equally likely to be selected for any treatment group. The word “random” has a specific meaning that implies a formal random process such as a random number table or a computer generated random list has been used to make animal selections. **Using a computer-generated random list or method is the preferred method.**

*Intentionally assigning subjects to different groups in order to balance one or more baseline variables is not an acceptable randomization method.* While it might appear that the goals of randomization have been achieved, other unknown biases could be introduced.

- Randomization:
- Prevents implicit/explicit bias in treatment assignment
  - Approximately balances groups with respect to all extraneous variables affecting response
  - Does add to logistical complexity
  - Is the primary technique for assigning animals to groups
- Work with a statistician to
  - Design a workable randomization
  - Incorporate known covariate information

### 3.4. Power

The study should be planned so that the minimum pharmacologically relevant change or the flow scheme CSF has a high probability (usually 80%) of being statistically significant. The probability that a relevant change will be statistically significant is referred to as statistical power.

Note that since the total number of animals available for an assay run may be constrained by practical considerations such as a processing capacity, etc., the power analysis often determines how many dose groups may be examined within a single study.

The statistical power is a function of the following key elements.

- Assay variability (the lower the assay variability the higher the statistical power for a given sample size and effect size)
- Effect size (the larger the effect size the larger the statistical power for a given sample size and level of assay variability)
- Total number of animals in the test group
- Total number of groups and the number of animals per group in the study (in both cases the more animals the higher the statistical power).

Standard convention is to use 80% power to detect the minimum biologically significant effect with a false positive rate of 5% when evaluating or setting sample size. Declaring statistical significance when p-values are less than 0.05, along with appropriate

multiplicity corrections, ensures the false positive rate is 5%. In general, a minimum of three runs of an assay with the format to be used in production should be used to estimate the experimental error. The power calculation should account for multiplicity corrections. The number of animals used should be sufficient so that all relevant drug effects are statistically significant.

When setting CSFs for an *in vivo* study, the CSF should be set above the minimum detectable difference if the CSF is defined on the response scale (e.g. percent inhibition > x % at y dose, body weight change > x grams, etc.). For potency CSFs, the study should be powered to exceed the minimum biologically significant effect. Following this paradigm, it is unlikely that you will have sufficient sample size to declare statistical significance at the minimum biologically significant effect, but you should power the study to be able to detect statistical significance at some dose.

In a dose-response study to estimate an ED<sub>50</sub>, two compounds will have statistically different ED<sub>50</sub>s if the ratio of the ED<sub>50</sub>s (larger::smaller) exceeds the minimum significant ratio (MSR) of the assay (see Section 2.2). Thus, the latter should be small enough to discriminate all pharmacologically relevant differences. The MSR depends upon the number of animals, the number of concentrations used, and the spacing of the doses with respect to the ED<sub>50</sub>. The number of doses should either be large enough to estimate an ED<sub>50</sub> over a reasonably wide range and/or adjusted for each compound based on the efficacy demonstrated in a single dose screen. If a large number of doses are used, the number of animals per dose may be quite small.

### 3.5. Analysis of Dose-Response Curves: Principles and Practice

In considering how to statistically evaluate dose-response curves, it is informative to review some of the historical context of how dose-response curves have been analyzed. When pharmacologists were first determining dose-response curves, in the very early days of pharmacology, they often plotted the data on an arithmetic scale (Figure 11A), that being the simplest and, perhaps, most familiar, to them.

In order to summarize and compare different dose-response curves, scientists attempted to describe these curves mathematically. However, the curves, a type of parabola, require rather complicated equations to describe. Prior to the invention of calculators and computers, it was too laborious and time-consuming to solve these equations. Scientists therefore searched for other ways of plotting and summarizing their data which might be readily described by equations. One way of doing this was to plot the dose-response curve on a semi-logarithmic plot, as shown for the same data in Figure 11B.

The semi-log plot of the data is the familiar sigmoidal (S-shaped) plot of many dose-response curves. This type of plot had the important advantage that **the middle part of the curve was approximately linear** (Figure 12). The portion of the curve from 16% efficacy to 84% efficacy can be described by a linear equation ( $y = mx + b$ ) which can be solved without the aid of calculators or computers. However, data outside of this range (below 16% and above 84%) was off the linear portion of the curve and therefore was

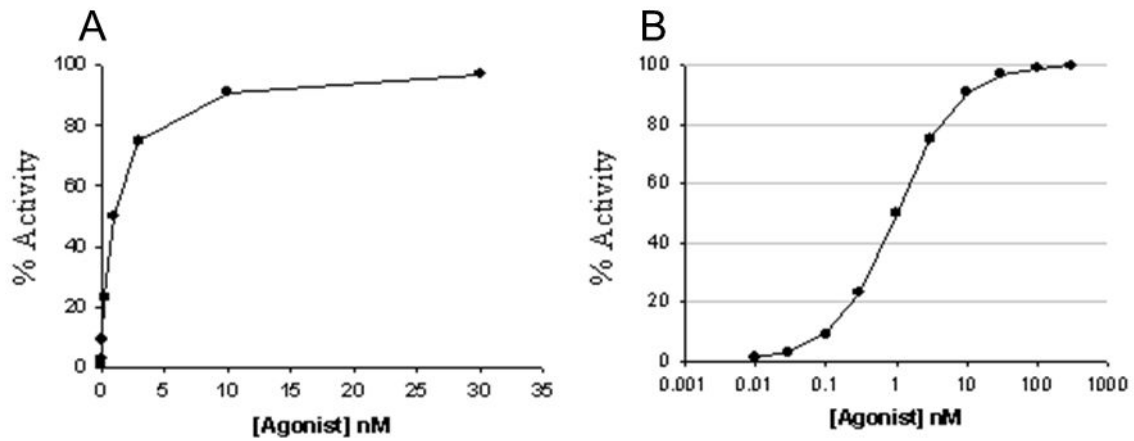


Figure 11: (A) Linear versus (B) semi-logarithmic plots of the same set of theoretical data.

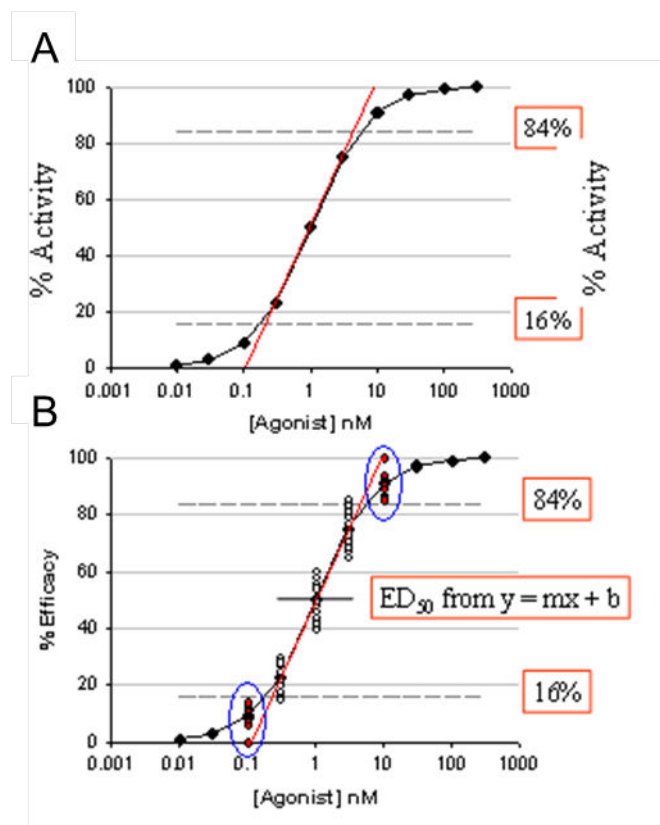


Figure 12: (A) Illustration of the linear portion of a sigmoidal dose-response curve and (B) the influence of data points which lie outside of the 16 – 84% region of the dose-response curve on the calculation of the slope of the line and potentially on the dose producing a 50% effect (ED<sub>50</sub>).

excluded from the analysis since the inclusion of such data would alter the slope of the line.



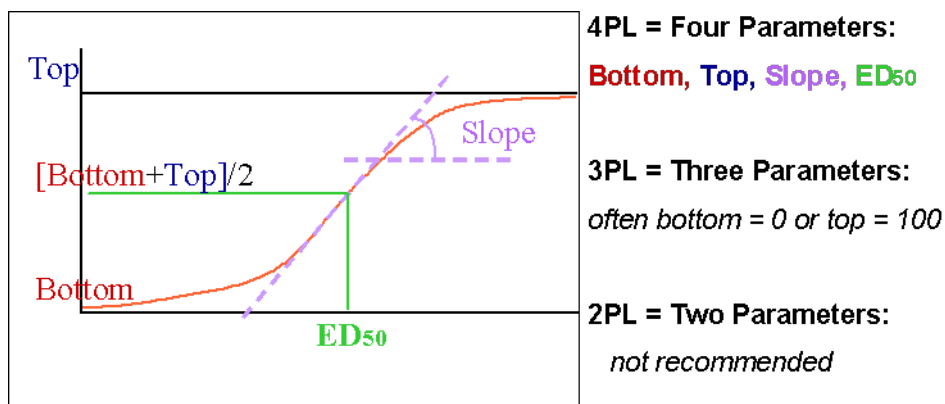


Figure 13: Illustration of the parameters of a 4-parameter logistic model of sigmoidal-shaped curves.

Pharmacologists wanted to have a single number to describe the dose-response plots of their data. For this purpose, the dose which produced a 50% effect ( $ED_{50}$ ) seemed ideal since it was in the middle of the linear portion of the curve and could be calculated from the linear regression. These types of considerations led pharmacologists to design experiments which emphasized the middle, linear portion of the curve. Pharmacologists therefore primarily designed studies to have three groups (the minimum number of points needed to describe a line), and to have large numbers of animals in each group (to have a robust estimate of each mean).

**A problem with this approach was that if the means of any groups fell outside of the 16 to 84% range, they were of little use in solving the linear equation.** Many text books taught that data outside of the 16 – 84% range should be excluded, particularly the results of any groups where the mean was 0% or 100%. However, data at the extremes, or asymptotes, were very important data as they defined the top and bottom of dose-response curves. Moreover, it was difficult to calculate confidence limits on the slope and  $ED_{50}$ . Thus, using only linear regression and the linear portion of the curve had substantial limitations.

Since sigmoidal curves are nonlinear, a non-linear regression algorithm should be used to fit the data. Today, with computers to solve complex equations very rapidly, we can use non-linear curve fitting techniques to model, or mathematically describe sigmoidal-shaped dose-response curves. From the non-linear curve-fit, specific parameters are estimated which describe the dose-response curve. The parameter estimates can then be used to compare dose-response curves for different compounds.

Sigmoidal dose-response curves can be described using four different parameters:

- The top, or maximum effect
- The bottom, or minimum effect
- The  $ED_{50}$ , or mid-point on the curve
- The slope of the curve

Using four parameters to describe a non-linear curve is called a 4 parameter logistic model, as illustrated in Figure 13.

The 4-Parameter Logistic (4PL) Model generates a family of curves using the four parameters of top, bottom, middle and slope. With these parameters, and using nonlinear regression, we can describe most sigmoidal curves. On occasion, there may be a practical or theoretical reason to define what the bottom and/or the top of a curve will be; for example, it may be known from the experimental methods or pharmacological theory that the bottom will be 0% or the top will be 100%. In such cases, only three parameters may be needed to describe the data. In such a case, a 3-parameter logistic model may be used to describe the data. Three parameter models are used most commonly when the dose range is imperfect (too high or too low) with respect to the potency of the compound, and we do not have doses which yield data near the top or bottom.

One also could fix both the top and bottom at constant values (a 2-parameter logistic model). However this approach makes some strong assumptions and one should let the data estimate the top and bottom whenever possible.

### 3.5.1. Analyzing Dose-Response Data

One way of analyzing data from dose-response determinations is to use ANOVA with a Dunnett's test to determine if there is an overall effect of the drug, and which doses produced an effect was statistically different from the control group. However, this analysis doesn't allow one to estimate a dose producing a 50% effect nor estimate the minimal and maximal effects or the slope. The dose producing a 50% effect will typically lie between two of the doses tested, and therefore requires interpolation to estimate. Interpolation requires some type of regression analysis.

In certain situations, for example with a limited number of dose groups, linear regression may be the best approach. However, the linear regression approach has several limitations:

1. Interpolating between two doses does not use all the data and hence can be inefficient. If one uses more than two doses, a straight-line fit may not be appropriate and the result will be a distorted (biased) estimate of the ED<sub>50</sub>.
2. It is not trivial to quantify the precision (i.e. calculate a standard error) of the estimate of the ED<sub>50</sub> from linear regression. Thus, it is not trivial to determine if two ED<sub>50</sub> values are statistically significantly different.
3. There is no ability to identify the minimum and maximum effect, nor the precision of the estimates, with linear regression.

By using a nonlinear regression model, one can get a better fit to **all** of the data, as well as calculate estimates and 95% confidence limits for the ED<sub>50</sub>, slope, maximum effect and minimum effect.

In the process of assay validation, methods for analyzing dose-response data must be selected and the method should remain constant for a validated assay. However, there may be situations where deviations are appropriate. Consult with a statistician for how to most

appropriately deal with specific situations, or datasets, where deviations from pre-determined data analysis approaches may be appropriate.

### 3.5.2. Experimental design requirements for linear vs. nonlinear analysis

For analysis by linear regression or ANOVA followed by a Dunnett's test, 3 or 4 groups of usually 5 to 10 animals per group traditionally has been required to provide precise estimates of the mean and variation for each treatment group and thus, sufficient power to identify all important treatment effects. To estimate potency results, such as ED<sub>50</sub>, the requirements are quite different; having data over the entire range of the dose-response curve is required, and estimates of the mean at each individual dose do not need to be as precise. That is, with nonlinear regression, one is not estimating a given point (or mean), but rather the parameters of the entire curve; modest deviations in a single point are less likely to substantially impact the parameters of the overall curve. On the other hand, not having data points at, for example, the top or bottom, can substantially impact the analysis. Therefore, it is necessary to have a larger number of groups with fewer animals per group. With experimental designs for nonlinear analysis, it may even be possible to reduce the total number of animals needed. Diagnostic checking of the resulting curve fit is essential; the ED<sub>50</sub> and asymptotes must make sense. Further, the confidence limits should be sufficiently precise to meet research objectives. Therefore, it is critically important to carefully consider the selection of doses in an experimental design with nonlinear regression analysis. For example, using 6 dose levels with 4 animals per group would be far more appropriate than using 3 dose levels with 8 animals per group. Also for nonlinear regression analysis, it is best to have doses that are equally-spaced on the log scale. *When an assay is statistically validated, the number of groups and animals per group needed should be verified with a statistician.*

As an illustration, the effects of a drug on decreasing ethanol consumption in a behavioral assay were compared under two different experimental designs. For these experiments, animals were trained to drink an ethanol solution over a period of several weeks. Animals were then randomized to treatment groups which receive either vehicle or a dose of the test drug. The drug produced a dose-related decrease in ethanol consumption (Figure 14). In the more traditional experimental design (Figure 14A), vehicle and 4 doses of drug were administered to groups of 6 animals each, for a total of 30 animals. When the data were analyzed by ANOVA and a Dunnett's test, doses of 3, 10 and 30 were significantly different from vehicle. There were only 2 doses on the linear portion of the dose-response curve (16 – 84%), an insufficient number to properly use linear regression, and therefore an ED<sub>50</sub> and confidence limits could not be calculated with any degree of robustness. If nonlinear regression analysis is applied to the data in the left panel, an ED<sub>50</sub> value of 0.6 mg/kg is obtained (a value which appears to be too low based on visual inspection of the data) and confidence limits can be obtained only for the parameter Top. The bottom could be fixed at zero, which provides a better estimate of the ED<sub>50</sub>, but its lower confidence limit could not be calculated using JMP software. When a nonlinear-compatible design was used (Figure 14B), 6 doses of drug were administered to groups of 3 animals each for a total of 18 animals. A low, inactive dose of drug was used in place of vehicle, allowing for

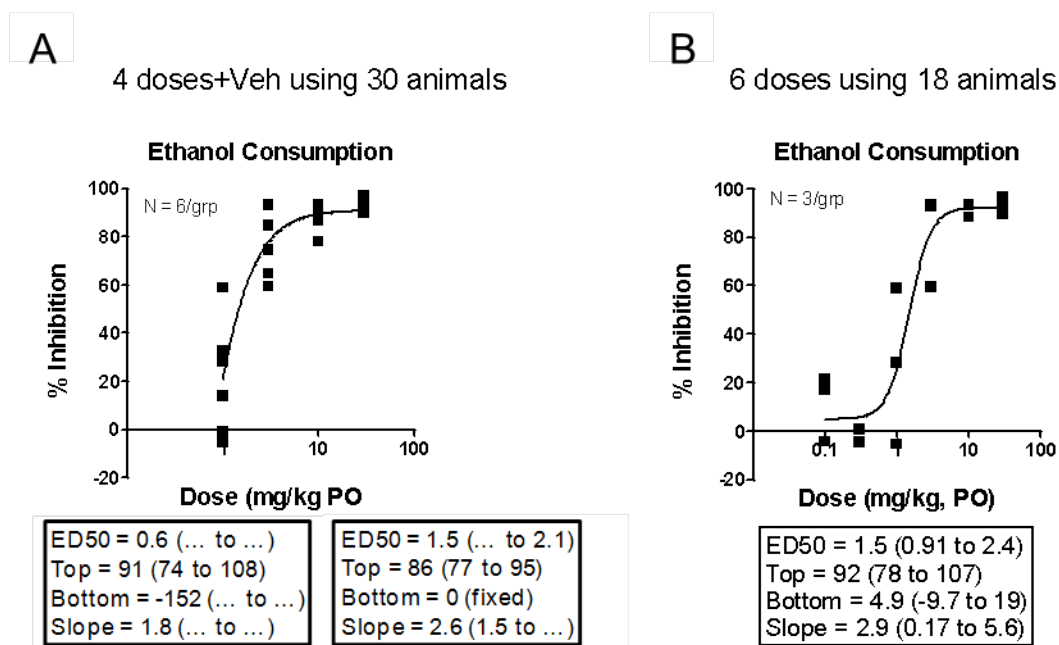


Figure 14: Comparison of (A) results with a more traditional experimental design using vehicle plus 4 doses of drug and 6 animals per dose and (B) results from a nonlinear-compatible design with 6 doses of drug and 3 animals per dose.

a better estimate of Bottom in this experiment. A vehicle group could also have been included. (Note: results from a vehicle treated group can, if appropriate, be incorporated into the nonlinear analysis; however, since there is no “zero” point on a log scale, vehicle is typically assigned a dose-value two to three orders of magnitude below the lowest dose tested; consult with a statistician for ways to incorporate a vehicle group into a nonlinear analysis). From nonlinear regression, an ED<sub>50</sub> value of 1.5 mg/kg is obtained (which appears reasonable based on visual inspection of the data) as well as 95% confidence limits (0.91 to 2.4 mg/kg). In addition, estimates of the Top, Bottom and Slope, along with their respective confidence limits, are obtained. Thus, if the primary goal is to obtain an ED<sub>50</sub> value together with confidence limits, a nonlinear-compatible design yields more results with far greater precision, and may also require fewer animals.

### 3.5.3. Key points in the analysis of dose-response curves

#### Analysis Key Points:

- Regression is needed for interpolation
- 4 parameter logistic model is primary model for dose-response work
- Diagnostic checking is essential
  - Reasonable asymptotes
  - Numerically complete answer
  - Try fixing top or bottom as necessary

Design Key Points:

- Doses need to be spaced across a broad dose range
  - Doses may need to be in 2X steps rather than 3X (i.e., half-log)
- Preferable to use more groups but may need fewer animals per group
  - Nonlinear approaches can provide more information with fewer animals

## 4. Abbreviations

**3PL**, 3-parameter logistic

**4PL**, 4-parameter logistic

**AMV**, Assay method version

**CSF**, Critical success factor

**DLs**, Difference Limits

**DRC**, Dose-response curve

**ED<sub>50</sub>**, Dose which produces 50% effect (Effective Dose 50%)

**Relative ED<sub>50</sub>**: Dose which produces 50% of the maximal response produced by that drug in the test system; considered to be relative measure of affinity

**Absolute ED<sub>50</sub>**: Dose which produces 50% of the maximal response which can be observed in the test system by a positive control; theoretically a drug could produce an effect greater than the maximum that can be measured

**GM**, Geometric Mean

**LsA**, Limits of Agreement

**LsAd**, Limits of Agreement on differences

**MD**, Mean Difference

**MR**, Mean Ratio

**MSD**, Minimum Significant Difference

**MSR**, Minimum Significant Ratio

**RLs**, Ratio Limits

**SAR**, Structure-activity relationship

**SDS**, Single-dose screen

## 5. Suggested Reading

Landis SC, Amara SG, Asadullah K. et al. A call for transparent reporting to optimize the predictive value of preclinical research. *Nature*. 2012;490(7419):187–91. PubMed PMID: 23060188.

# *In Vivo* Receptor Occupancy in Rodents by LC-MS/MS

Cynthia D. Jesudason, Ph.D,<sup>1</sup> Susan DuBois, BS,<sup>1</sup> Megan Johnson, BS,<sup>1</sup> Vanessa N. Barth, Ph.D,<sup>1</sup> and Anne B. Need, Ph.D<sup>1</sup>

Created: March 9, 2017.

## Abstract

Receptor (or enzyme) Occupancy (RO) is a quantitative measure of what percentage of the total number of available target receptors is engaged by or bound to a *particular* ligand. In drug discovery, it is important to determine the relationship of a receptor's occupancy to its final observed pharmacological efficacy and/or toxicological readout. RO is related to but distinct from a ligand's potency and maximal efficacy. Different compounds may achieve different percentages and durations of occupancy. Receptor occupancy/exposure relationships as well as the duration of occupancy have been used to project clinical doses.

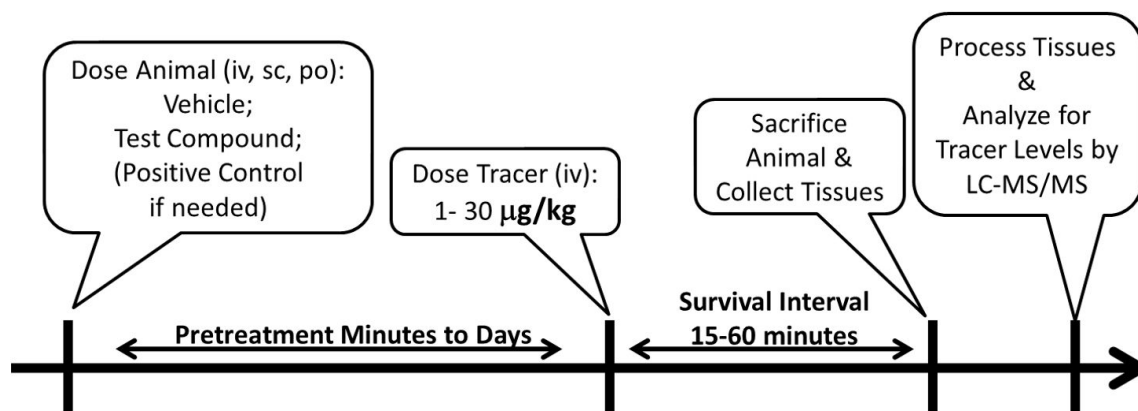
The drug discovery lead optimization flow scheme can be improved by inclusion of a receptor occupancy assay that determines the level of target engagement to allow rational triage and selection of compounds to advance into more labor intensive and longer duration efficacy studies.

In the clinic, RO is measured using radioisotopically labeled tracer ligands whose distributions can be determined by non-invasive imaging methods, most commonly positron emission tomography (PET) and single photon emission computed tomography (SPECT) (1). Recent advances in the sensitivity of LC-MS/MS detectors have enabled determination of RO in preclinical studies without the need for a radiotracer (2, 3). This chapter will cover the details of performing an *in vivo* receptor occupancy assay using an LC-MS/MS methodology. This chapter assumes that a tracer exists for the target for which occupancy measures are being made, and will **not** detail the process of identifying a novel tracer (4, 5). A suitable LC-MS/MS tracer should be selective and have high affinity for the pharmacologic target, be readily tissue-penetrant, have low nonspecific binding, and exhibit suitable kinetics.

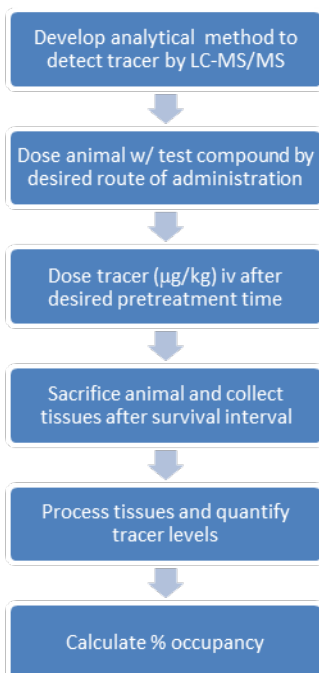
---

<sup>1</sup> Eli Lilly & Company; Email: jesudasoncd@lilly.com; Email: dubois\_susan\_l@lilly.com; Email: watson\_megan\_a@lilly.com; Email: barth\_vanessa\_nicole@lilly.com; Email: need\_anne\_b@lilly.com.

## Experimental Design



## Flowchart



## Materials and Methods

### Animals

Adult rats and mice are group housed in rooms with a 12-hour light/dark cycle. Room temperature is maintained at  $21 \pm 3^\circ\text{C}$ . Food and water are available *ad libitum* until the beginning of the experimental protocol. Animals are allowed 3-5 days of acclimation to the housing environment prior to testing. In the most ideal case, the RO assay will be



performed in the same strain of animals used for the efficacy/toxicology assay. The choice of animal strain will also be influenced by any differences in expression level of the receptor or enzyme between rats and mice (6). Pharmacology differences between rodents and humans due to differences in the target protein sequence can be overcome by utilizing “humanized” animals.

## Test Compounds

Test compounds refer to the compounds for which receptor occupancy is to be assessed. These compounds can be administered through any desired route with any pretreatment time in a suitable vehicle. Animals may be fasted overnight if test compounds are to be administered by oral gavage. We note that the stress induced by oral gavage can be a confounding variable in many studies, so proper training in the procedure should be undertaken. In the most ideal case, the dose, vehicle and route of administration would match those used in other assays in the drug discovery flow scheme to build occupancy, efficacy/toxicology, and exposure relationships (7, 8).

## Tracer

Tracer refers to the compound that is administered at low doses to characterize receptor occupancy at a specific target. The likelihood of finding a tracer is dependent on a number of factors as illustrated in Figure 1.

Compounds with low nonspecific binding will be more likely to exhibit a favorable differential distribution *in vivo* consistent with the biology. This differential distribution is directly related to the density of the target ( $B_{max}$ ) and the affinity of the compound to the target. The physiochemical properties of a good tracer molecule have been described in the literature based on analyses of existing PET ligands (9, 10).

The tracer is administered intravenously in the lateral tail vein in a dose volume of 0.5 mL/kg for rats and 5 mL/kg for mice following the desired pretreatment time of the test compound. It is typically administered in the range of 1-30  $\mu\text{g}/\text{kg}$ . The survival interval between tracer administration and animal sacrifice is typically in the range of 15-60 minutes. The dose of the tracer and the survival interval will differ for each tracer, and will need to be optimized prior to setting up an RO assay to obtain the largest signal to noise window with the shortest survival interval. An example of a tracer optimization study is shown in Figure 2 in which the striatum expresses the target of interest while the cerebellum does not (i.e. null region), and is a measure of nonspecific binding of the tracer.

## Analytical Method Development

The tracer of interest is diluted in 50:50 (acetonitrile:water) with 0.1% formic acid to 1  $\mu\text{g}/\text{kg}$ . This is infused into the mass spectrometer using a 1 mL syringe (Hamilton Cat. No. 4023184) at 10  $\mu\text{L}/\text{min}$  and the precursor and product ions are identified. The compounds are quantified after elution from the HPLC using a triple quad mass spectrometer with

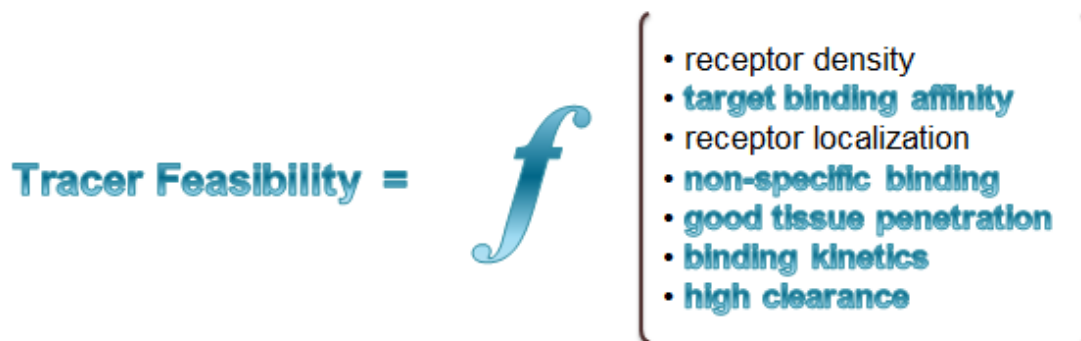


**Figure 1:** Tracer properties

multiple reaction monitoring (MRM methods) and monitoring parent and product ion pairs in positive or negative mode as appropriate for the tracer. A sample LC trace and MS/MS for the tracer PBR28 is shown in Figure 3.

## Live Phase

Mice or rats (n=4) receive either vehicle alone, test compound, or a positive control (PC) if no null region exists. After the desired pretreatment time the animals are administered the tracer. Following the survival interval they are euthanized by cervical dislocation followed by decapitation. Trunk blood is collected in EDTA coated 1.5 mL conical polypropylene centrifuge tubes and stored on wet ice until study completion.

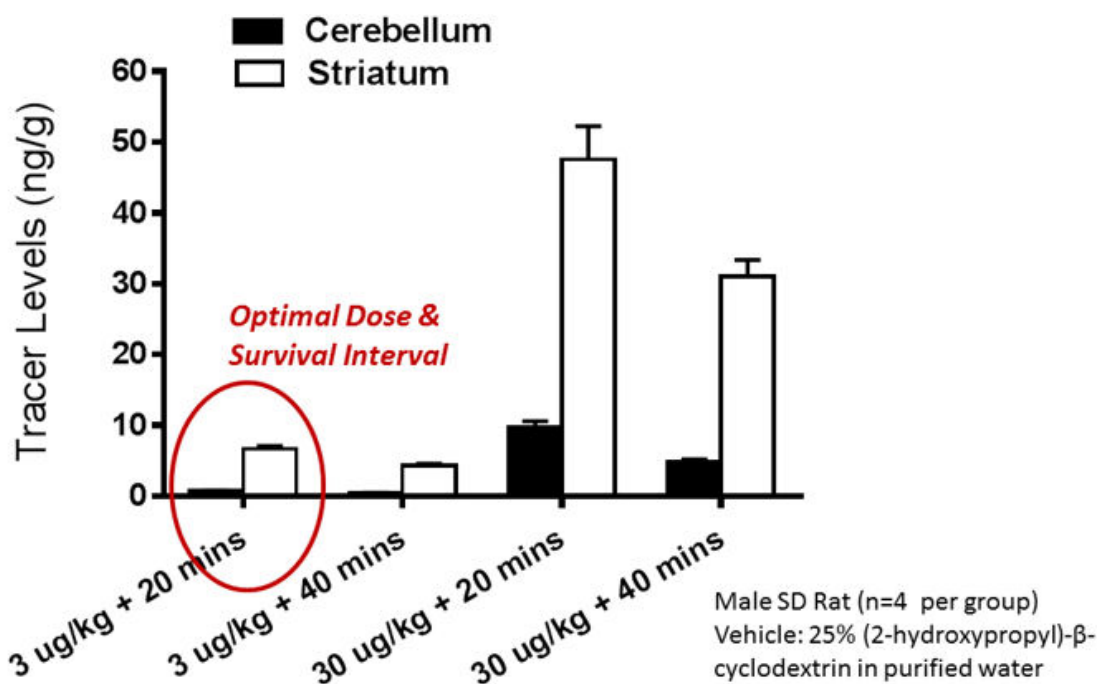
**Central Occupancy:** Brains are removed and rinsed with sterile water. The regions of interest are dissected, placed in 1.5 mL conical polypropylene centrifuge tubes and stored on wet ice until completion of the live phase. Regions of interest should include a brain region with a high expression of the target of interest as well as a null region with little or no receptor density, if available.

**Peripheral Occupancy:** Peripheral tissues are dissected, rinsed with cold saline, placed in 1.5 mL conical polypropylene centrifuge tubes, minced to fine pieces using fine point scissors, weighed, and stored on wet ice until completion of live phase study.

## Tissue Preparation and Analysis

Blood samples are collected at the time of sacrifice via trunk blood collection into 1.5 mL EDTA coated Eppendorf tubes and stored on wet ice until the study completion. Whole blood is centrifuged at  $15,000 \times g$  for 20 minutes to obtain plasma. Finally, 50  $\mu\text{L}$  of plasma are added to Eppendorf tubes containing 200  $\mu\text{L}$  of acetonitrile containing 0.1% (v/v) formic acid and vortexed to mix.

Tissue samples are collected at the time of sacrifice, rinsed with sterile water, stored in a 1.5 mL Eppendorf tube, weighed and stored on wet ice until the study completion. Stainless steel beads (NextAdvance SSB14B) are added to peripheral tissue and the tubes



### Tracer Dose and Survival Interval

| Tracer Dose, Survival Interval | BP | % SUV |
|--------------------------------|----|-------|
| 3 ug/kg, 20 min                | 7  | 224   |
| 3 ug/kg, 40 min                | 10 | 146   |
| 30 ug/kg, 20 min               | 5  | 159   |
| 30 ug/kg, 40 min               | 6  | 104   |

**Binding Potential (BP)** = (Striatal levels/cerebellar levels) – 1

**Standardized Uptake Value (SUV)** = (Striatal tracer levels /injected tracer dose) x 100

**Figure 2:** Example Tracer Optimization Study

are placed in a Bullet Blender for 5 minutes. Acetonitrile containing 0.1% (v/v) formic acid is added to all tissues at a volume of four times the tissue sample weight in milligrams. All tissues are homogenized by using an ultrasonic dismembrator probe (Fisher Scientific Model 100, Pittsburgh, PA). Homogenized tissue and plasma are centrifuged at 15,000  $\times$  g for 20 minutes. An aliquot of supernatant containing the tracer is diluted in water to an acetonitrile content less than that of the mobile phase and 10  $\mu$ L is injected by an autosampler onto an HPLC employing a suitable column, such as ZORBAX Eclipse XDB-C18 column (part no. 971700-902, Agilent Technologies, Wilmington, DE). Separation is achieved using isocratic or gradient conditions and a mobile phase of water/ acetonitrile containing 0.1% (v/v) formic acid. Individual standards for the tracer and plasma are prepared by adding known concentrations of tracer to naïve tissue or plasma

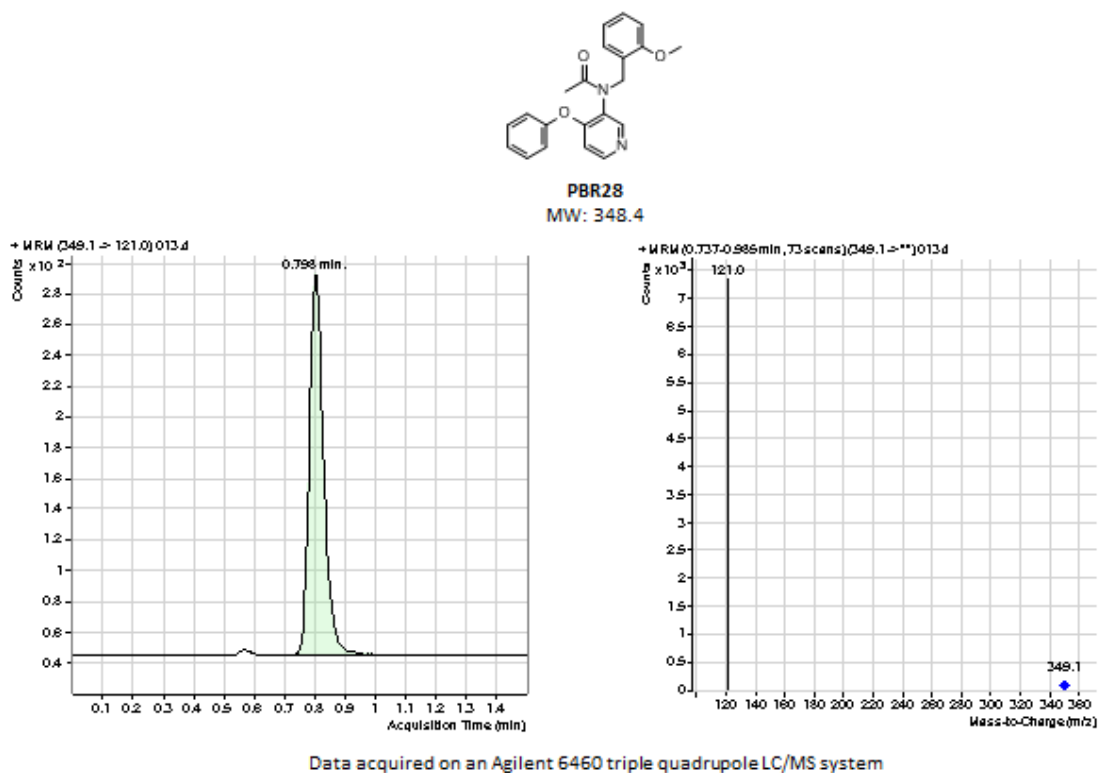


**Figure 3:** Example LC & MS/MS Trace

and processed in the same manner as the samples. This process could potentially be automated to increase throughput but we are not aware of any group that has implemented this. A typical standard calibration curve is shown in Figure 4 (n=2, R<sub>2</sub> >95%)

## Determination of Occupancy

Receptor Occupancies can be calculated by using one of two different methods, the ratio method and the positive control method.

### The Ratio Method

The ratio method is preferred when a null region is available in the same organ because this can correct for the potential variations in exposure of the tracer as a result of a number of variables including changes in blood flow (both increases or decreases), as well as changes in tracer efflux caused by pretreatment of the test compound. It is more difficult to identify nonspecific binding regions within a particular peripheral organ or another peripheral organ that truly represents nonspecific tracer binding. Therefore, with peripheral occupancy studies, 100% occupancy is pharmacologically defined and

| LC-MS/MS Calibration Curve for Tracer in Tissue |                     |         |
|---|---------------------|---------|
| Matrix =  | Brain Tissue (ng/g) |         |
| Levels  | 1st Run             | 2nd Run |
| 0.3   | 0.304               | 0.292   |
| 1   | 1.08                | 0.985   |
| 3   | 3.01                | 2.78    |
| 10  | 10.3                | 10.2    |
| 30  | 31.4                | 29.5    |
| 60  | 58.7                | 57.5    |
| <b>R2 = 0.9978</b>                              |                     |         |

| LC-MS/MS Calibration Curve for Tracer in Tissue |                    |         |
|---|--------------------|---------|
| Matrix =  | Lung Tissue (ng/g) |         |
| Levels  | 1st Run            | 2nd Run |
| 0.3   | 0.290              | 0.305   |
| 1   | 0.962              | 1.09    |
| 3   | 2.93               | 3.04    |
| 10  | 10.3               | 9.96    |
| 30  | 29.5               | 28.9    |
| <b>R2 = 0.9976</b>                              |                    |         |

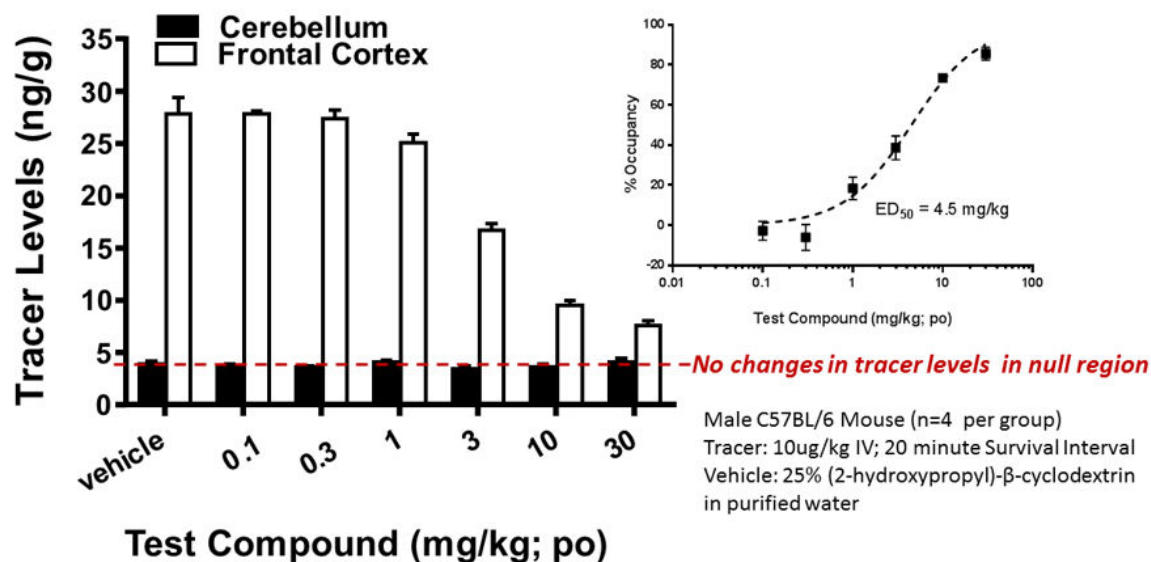
| LC-MS/MS Calibration Curve for Tracer in Plasma |                |         |
|---|----------------|---------|
| Matrix =  | Plasma (ng/mL) |         |
| Levels  | 1st Run        | 2nd Run |
| 0.3   | 0.322          | 0.275   |
| 1   | 0.987          | 1.02    |
| 3   | 3.17           | 3.04    |
| 10  | 10.0           | 9.82    |
| 30  | 29.3           | 29.0    |
| <b>R2 = 0.9970</b>                              |                |         |

**Figure 4:** Example Calibration Curve in Tissues & Plasma

experimentally determined for each tracer within a single tissue using the positive control method described later.

Receptor Occupancies are calculated using the well-described ratio method (7), but substituting the tracer concentrations determined by LC-MS/MS for the radiolabeled tracer levels determined with scintillation spectrometry.

The following equation is employed:



| Test Compound (mg/kg) po   | % Occupancy         | SEM  |
|----------------------------|---------------------|------|
| 0.1                        | -2.83               | 4.74 |
| 0.3                        | -6.10               | 6.43 |
| 1                          | 18.4                | 5.67 |
| 3                          | 38.6                | 5.93 |
| 10                         | 73.6                | 1.51 |
| 30                         | 85.6                | 3.24 |
| <b>Abs ED<sub>50</sub></b> | <b>4.5 mg/kg po</b> |      |

**Figure 5: Receptor Occupancy Dose Response Curve Using the Ratio Method.** Occupancy is summarized by treatment group mean % occupancy  $\pm$  standard error of the mean. All dose occupancy curves were plotted using the software program GraphPad Prism. Absolute ED<sub>50</sub> was estimated from the sigmoidal dose-occupancy curve analysis using the proper constraints.

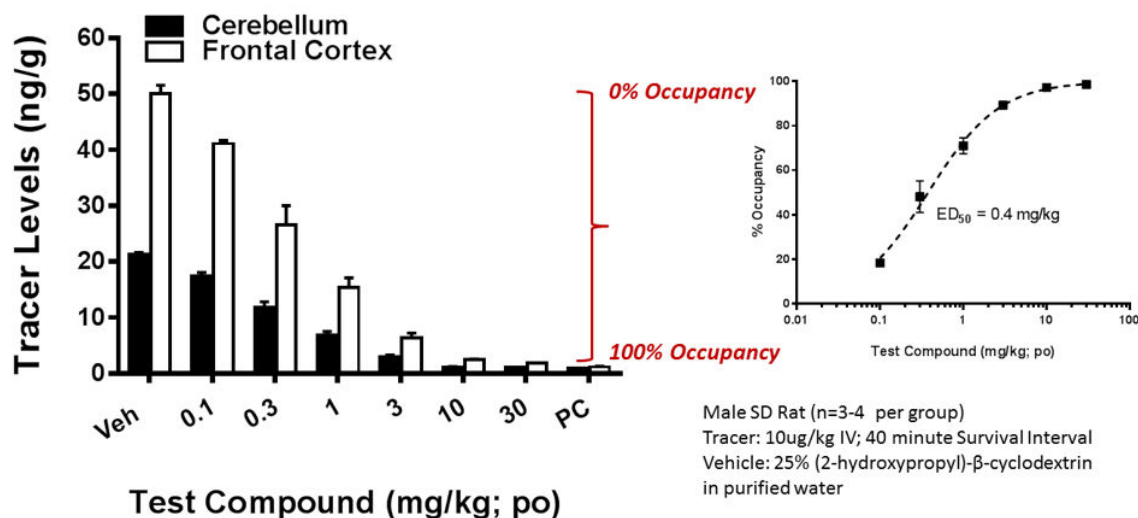
$$\% \text{ Occupancy} = \left( 1 - \left[ \frac{(\text{Ratio}_t - 1)}{(\text{Ratio}_c - 1)} \right] \right) \times 100$$

Each Ratio refers to the ratio of tracer in a brain area rich in target receptor to the tracer detected in a null region with little or no receptor density. Ratio<sub>t</sub> refers to animals treated with test compound, while Ratio<sub>c</sub> refers to the average ratio in vehicle-treated animals.

An example of a receptor occupancy dose response using this methodology is shown in Figure 5 in which the cerebellum is the null region, and the frontal cortex expresses the target.

### The Positive Control Method

This method is utilized when no null region is available for brain occupancy and for all peripheral occupancy assays. Average vehicle tracer levels in the target rich region represent 0% occupancy. Average tracer levels observed in this tissue from the positive



| Test Compound (mg/kg) po | % Occupancy         | SEM |
|--------------------------|---------------------|-----|
| 0.1                      | 18.3                | 1.1 |
| 0.3                      | 48.1                | 7.1 |
| 1                        | 71                  | 3.6 |
| 3                        | 89.3                | 1.7 |
| 10                       | 97.3                | 0.2 |
| 30                       | 98.7                | 0.1 |
| <b>Abs ED50</b>          | <b>0.4 mg/kg po</b> |     |

**Figure 6: Receptor Occupancy Dose Response Curve Using the Positive Control Method.** Occupancy is summarized by treatment group mean % occupancy ± standard error of the mean. All dose occupancy curves were plotted using the software program GraphPad Prism. Absolute ED<sub>50</sub> was estimated from the sigmoidal dose-occupancy curve analysis using the proper constraints.

control group represents 100% occupancy. The intermediate tracer levels from the test compound pretreated group are interpolated linearly between the tracer levels in the vehicle-treated animals (0% occupancy) and in the positive control animals (100% occupancy) in order to determine the percent occupancy. The positive control dose is identified as a dose that is well on the top asymptote of the receptor occupancy curve for this test compound or another previously tested compound known to bind to the target (11).

$$\begin{aligned}
 \text{Intercept} &= \text{Average} \left( \text{all vehicle} \frac{\text{ng (tracer)}}{\text{g (tissue)}} \right) \\
 \text{Slope} &= \frac{\text{Average} \left( \text{all positive control} \frac{\text{ng (tracer)}}{\text{g (tissue)}} \right) - \text{Average} \left( \text{all vehicle} \frac{\text{ng (tracer)}}{\text{g (tissue)}} \right)}{100} \\
 \% \text{ Occupancy} &= \frac{\left( \frac{\text{ng (tracer)}}{\text{g (tissue)}} \right) - \text{intercept}}{\text{slope}}
 \end{aligned}$$

This method is dependent on having access to a suitable positive control compound that demonstrates 100% occupancy at the desired target, and this can often be a challenge for

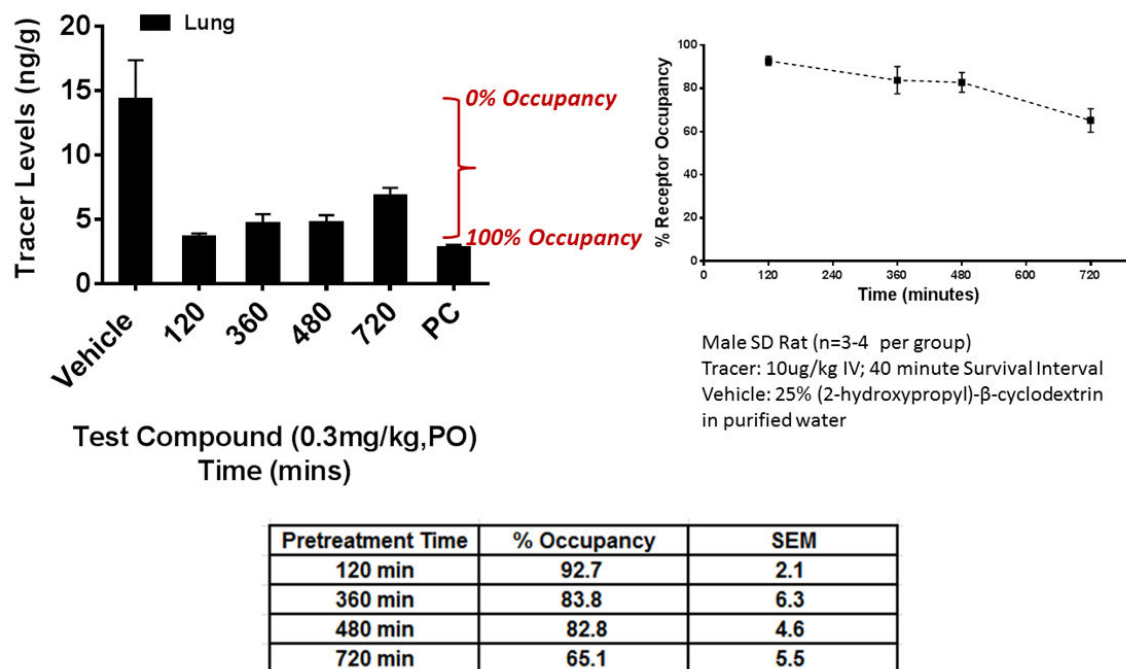


**Figure 7: Time Course Occupancy Using the Positive Control Method.** Occupancy is summarized by treatment group mean % occupancy  $\pm$  standard error of the mean.

new targets where there are no known reference compounds available and limited chemical SAR information.

An example of a receptor occupancy dose response using this methodology is shown in Figure 6 in which both the frontal cortex and the cerebellum express the target and show dose-dependent reduction in measured tracer levels.

The duration of occupancy is also an important feature of clinical candidates, and an example of a time course peripheral occupancy study using the positive control method is shown in Figure 7.

## Graphical Analysis

Prism (GraphPad Software Inc., San Diego, CA) software can be employed for calculations, curve fitting and graphics (Figures 5-7).

## References

- George N., Gean E. G., Nandi A., Frolov B., Zaidi E., Lee H., Brasic J. R., Wong D. F. Advances in CNS Imaging Agents: Focus on PET and SPECT Tracers in Experimental and Clinical Use. *CNS Drugs*. 2015;29(4):313–330. PubMed PMID: 25948171.
- Need A. B., McKinzie J. H., Mitch C. H., Statnick M. A., Phebus L. A. *In vivo* rat brain opioid receptor binding of LY255582 assessed with a novel method using LC/MS/MS



- and the administration of three tracers simultaneously. *Life Sciences*. 2007;81(17-18): 1389–1396. PubMed PMID: 17935738.
3. Chernet E., Martin L. J., Li D., Need A. B., Barth V. N., Rash K. S., Phebus L. A. Use of LC/MS to assess brain tracer distribution in preclinical *in vivo* receptor occupancy studies: Dopamine D2, serotonin 2A and NK-1 receptors as examples. *Life Sciences*. 2005;78(4):340–346. PubMed PMID: 16139310.
  4. Joshi E. M., Need A., Schaus J., Chen Z., Benesh D., Mitch C., Morton S., Raub T. J., Phebus L., Barth V. Efficiency Gains in Tracer Identification for Nuclear Imaging: Can *In vivo* LC-MS/MS Evaluation of Small Molecules Screen for Successful PET Tracers? *ACS Chemical Neuroscience*. 2014;5(12):1154–1163. PubMed PMID: 25247893.
  5. Need A, Kant N, Jesudason C, Barth V. Approaches for the discovery of novel positron emission tomography radiotracers for brain imaging. *Clinical and Translational Imaging*. 2017.:1–10. doi: [10.1007/s40336-017-0221-3](https://doi.org/10.1007/s40336-017-0221-3).
  6. Pope G. R., Roberts E. M., Lolait S. J., O'Carroll A-M. Central and peripheral apelin receptor distribution in the mouse: Species differences with rat. *Peptides*. 2012;33(1): 139–148. PubMed PMID: 22197493.
  7. Wadenberg, M-L. G.; Kapur, S.; Soliman, A.; Jones, C.; Vaccarino, F.; Dopamine D2 receptor occupancy predicts catalepsy and the suppression of conditioned avoidance response behavior in rats. *Psychopharmacology (Berlin)* (2000), 150(4), 422-429. PubMed PMID: 10958084.
  8. Barth V., Need A. B., Tzavara E. T., Giros B., Overshiner C., Gleason S. D., Wade M., Johansson A. M., Perry K., Nomikos G. G., Witkin J. M. In vivo occupancy of dopamine D3 receptors by antagonists produces neurochemical and behavioral effects of potential relevance to attention-deficit-hyperactivity disorder. *Journal of Pharmacology and Experimental Therapeutics*. 2013;344(2):501–510. PubMed PMID: 23197772.
  9. Zhang L., Villalobos A., Beck E., Bocan T., Chappie T., Chen L., Grimwood S., Heck S., Helal C., Hou X., Humphrey J., Hu J., Skaddan M., McCarthy T., Verhoest P., Wager T., Zasadny K. Design and selection parameters to accelerate the discovery of novel central nervous system positron emission tomography (PET) ligands and their application in the development of a novel phosphodiesterase 2A PET ligand. *Journal of Medicinal Chemistry*. 2014;56(11):4568–4579. PubMed PMID: 23651455.
  10. Barth V, Need A. Identifying Novel Radiotracers for PET Imaging of the Brain: Application of LC-MS/MS to Tracer Identification. *ACS Chemical Neuroscience*. 2014;5(12):1148–1153. PubMed PMID: 24828747.
  11. Need A. B., Davis R.J., Alexander-Chacko J. T., Eastwood B., Chernet E., Phebus L. A., Sindelar D. K., Nomikos G. G. The relationship of *in vivo* central CB1 receptor occupancy to changes in cortical monoamine release and feeding elicited by CB1 receptor antagonists in rats. *Psychopharmacology*. 2006;184(1):26–35. PubMed PMID: 16328376.



# Assay Artifacts and Interferences

Michelle Arkin, PhD, Douglas Auld, PhD, Jonathan Baell, PhD, Kyle Brimacombe, MS, Jayme L. Dahlin, MD, PhD, Timothy L. Foley, PhD, James Inglese, PhD, and Stephen C. Kales, PhD



# Assay Interference by Chemical Reactivity

Jayne L. Dahlin, MD, PhD,<sup>1</sup> Jonathan Baell, PhD,<sup>2</sup> and Michael A. Walters, PhD<sup>3</sup>✉

Created: September 18, 2015.

## Abstract

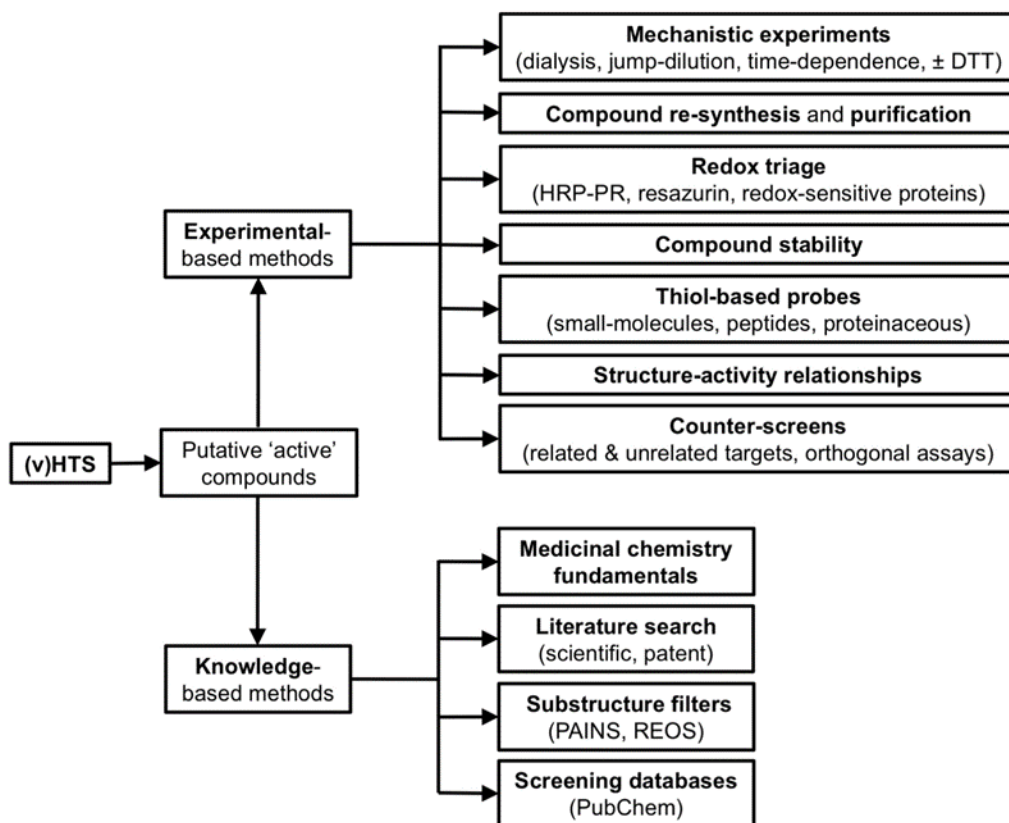
Real and virtual high-throughput screens (HTS) are crucial components of the modern drug discovery process. Assays that determine the biological activity of compounds found by both of these approaches may be subject to interference by a variety of processes, one of which is non-specific chemical reactivity. Within this mode of assay interference, test compounds can chemically react with assay reagent(s) or biological molecule(s), confounding the assay readout by producing apparent biological activity. Failure to identify and triage (remove from consideration) these compounds can result in wasted resources and project dead-ends. This chapter contains practical strategies to mitigate the impact of assay interference by compound chemical reactivity. Two general approaches are described to identify and triage reactive compounds in the context of drug discovery and development: knowledge-based and experimental-based methods. Knowledge-based strategies covered in this chapter include substructure filters, literature and database searches, and the consulting of experienced medicinal chemists. Experimental-based strategies covered in this chapter include mechanistic experiments, thiol-based probes and multiple types of counter-screens. Employing a well-designed and comprehensive screening tree that incorporates these strategies should reduce the likelihood of pursuing reactive assay artifacts and intractable hits from HTS campaigns.

---

<sup>1</sup> Mayo Clinic College of Medicine, Rochester, MN. <sup>2</sup> Monash Institute of Pharmaceutical Sciences, Monash University, Melbourne, Australia. <sup>3</sup> Institute for Therapeutics Discovery and Development, University of Minnesota, Minneapolis, MN.

✉ Corresponding author.

## Flow Chart



## Abbreviations

ALARM NMR, a La assay to detect reactive molecules by nuclear magnetic resonance; BME,  $\beta$ -mercaptoethanol; BSA, bovine serum albumin; CoA, coenzyme A; CPM, *N*-[4-(7-diethylamino-4-methylcoumarin-3-yl)phenyl]maleimide; DMSO, dimethyl sulfoxide; DTT, dithiothreitol; ELSD, evaporative light scattering detection; GSH, glutathione; HMQC, heteronuclear multiple quantum coherence; HPLC, high-performance liquid chromatography; HRP-PR, horseradish peroxidase-phenol red; HTS, high-throughput screen or high-throughput screening; IC<sub>50</sub>, half maximal inhibitory concentration; *m/z*, mass-to-charge ratio; MS, mass spectrometry; NMR, nuclear magnetic resonance; PAINS, pan assay interference compounds; PDA, photo diode array; REOS, Rapid Elimination Of Swill; SAR, structure-activity relationship; SIR, structure-interference relationship; UPLC, ultra-performance liquid chromatography.

## Introduction and Background

### Section Introduction

Some classes of compounds display activity that is associated with non-specific or generalized chemical reactivity rather than target binding. Many useful therapeutics that bind and react with their target are known. However, such reactivity was not rationally sought but generally unearthed after therapeutic relevance was demonstrated. Other, rationally designed, covalent-irreversible and covalent-reversible inhibitors are typically fit-for-purpose. That is, testing is performed with the full knowledge of potential target reactivity, or compound reactivity with the target is purposefully designed into the chemical leads to promote greater affinity (1-4). Additionally, throughout the lead optimization process, the contributions of covalent and non-covalent interactions to target binding are characterized. For example, the FDA approved drugs afatinib (EGFR; conjugate addition of protein cysteine to  $\alpha,\beta$ -unsaturated amide) (5), captopril (ACE; thiol binding of active-site zinc) (6, 7), carfilzomib (proteasome; double nucleophilic addition of N-terminal threonine to epoxyketone) (8), and telaprevir (hepatitis NS3/4A serine protease; serine addition to  $\alpha$ -ketoamide) (9), all function by well-designed, targeted reactivity (target; mechanism of action). While these mechanisms can clearly prove efficacious when well-characterized, they are not necessarily appropriate for upstream discovery: when searching for a new starting point for a given biological target, non-covalent inhibition is desirable since a reactivity-driven screening hit has an extremely low chance of yielding to successful optimization. Undesired compound-target reactions have become recognized as a significant and costly source of assay artifacts (10-13). This section will discuss artifacts that may be caused by undesired and surreptitious compound reactivity\*. Herein we will use the term 'active' to describe compounds that display activity in an assay. The term 'hit' will be reserved for compounds that have activity at a well-defined target.

\*In this chapter, many of the examples and nomenclature will refer to target-based assays, specifically for enzymatic inhibition. This is meant to aid in readability. However, many of the general principles will hold true for non-enzymatic targets, such as transcription factors, protein-protein interactions, surface receptors and ion channels, as well as cell-based and organism-based (*in vivo*) systems.

### Chemical Reactivity Interference in Target-Based Assays

Chemical reactivity interference typically involves chemical modification of reactive protein residues or, less frequently, modification of nucleophilic assay reagents. Typical protein-modifying reactions include (A) oxidation of the cysteine sulfur (see Redox section, *vide infra*), (B) nucleophilic addition to activated unsaturation (referred to as Michael addition), (C) nucleophilic aromatic substitution, and (D) disulfide formation by reaction with thiol-containing compounds (Figure 1). Reaction of protein residues with highly electrophilic functional groups (such as acid halides, epoxides,  $\alpha$ -halo carbonyls, and aldehydes) is also common.

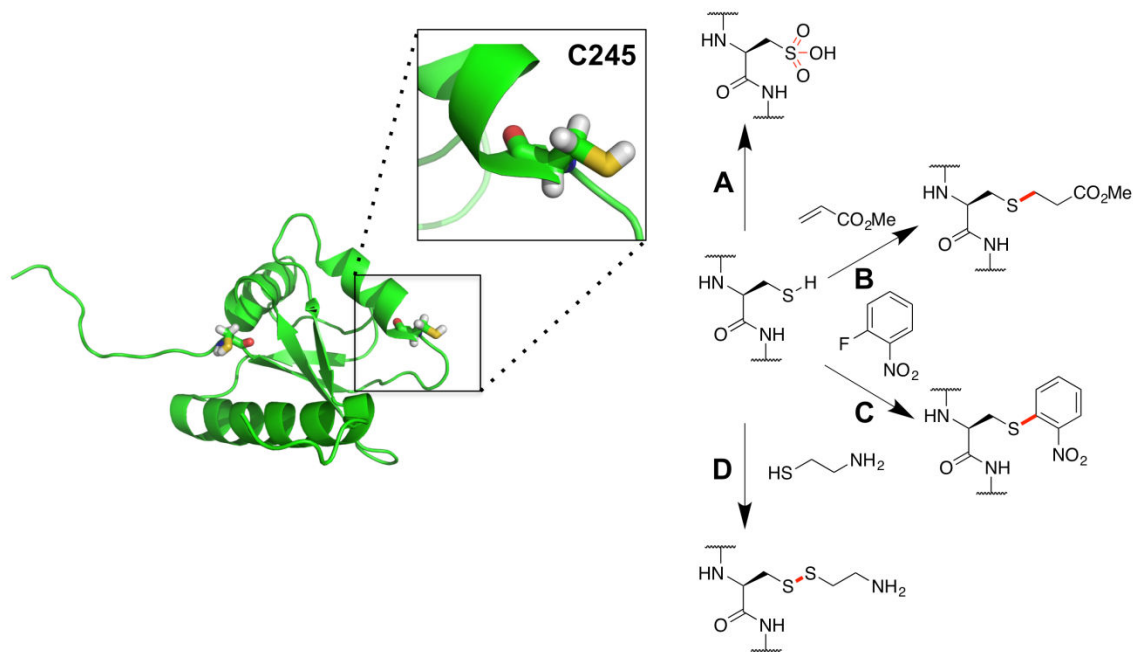


**Figure 1:** Typical reactions that are responsible for reaction-mediated assay interference involving cysteine reacting as a nucleophile with various electrophiles. (A) cysteine oxidation, (B) Michael-addition of the cysteine-thiol to an activated, unsaturated group, (C) nucleophilic-aromatic substitution, and (D) disulfide bond formation. The human La protein PDB ID 1OWX is used here for illustrative purposes (14). The bonds formed in these reactions are indicated in red.

While reactions of cysteine are highlighted in Figure 1, electrophilic reactions have also been observed at amino acid side chains such as Asp, Glu, Lys, Ser, and Tyr (15). In simple peptide models (6-12 mer), reactivity was shown to be Cys >> Lys >> Ser, Tyr with a small selection of electrophilic compounds (16). On the other hand, some probes that can undergo nucleophilic aromatic substitution have been observed to selectively react with Lys over Cys in proteomic experiments (15). Of relevance here is work that suggests that vinyl ketones readily react with protein cysteines, whereas tosylate esters readily react with a variety of residue types, including Asp, Glu, and Tyr (17). Protein microenvironment can greatly influence side-chain reactivity by altering the  $pK_a$  of amino acids (18). Therefore, while simplified models of amino acid reactivity may be helpful, they may not provide true evidence of non-interference of compounds in the context of a target protein.

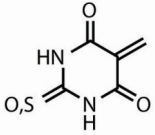
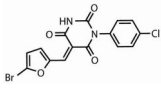
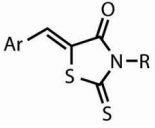
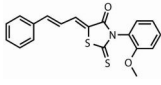
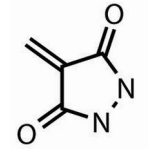
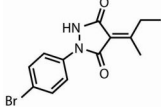
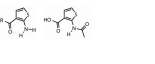
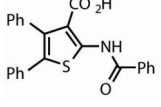
Reactive moieties such as acid halides and aldehydes are easily recognized as covalent modifiers. Typically these can be discarded from screening 'actives' without further consideration. Many of these substructures can also be recognized by filters such as REOS (Rapid Elimination of Swill) (19). It is important to recognize that chemical reactivity is context specific. The reactivity of biological nucleophiles is affected by protein structure, electrophile structure, and reaction (assay) conditions. For example, not all epoxides (or other functional groups) in all molecules will be reactive under all assay conditions. The same holds true for other electrophilic or oxidizing species. For example, gradations of



nitrile reactivity are well-documented (20). However, as a general rule compounds containing known reactive moieties should always be considered guilty (liable to cause false activity) until proven innocent by orthogonal assays.

Recently, several further classes of compounds, beyond those that are easy to spot and discard, have been added to the list of compound classes that can cause apparent bioactivity by reactive mechanisms. These classes of compounds, called PAINS (pan assay interference compounds), contain defined substructures that are more difficult to recognize as being potentially reactive. The most common of these structures are shown in Table 1. These classes have been fully described (21-23). While not every PAINS substructure has a defined mechanism of assay interference, most of the substructures are presumed to be reactive. Certain PAINS classes can also interfere via metal chelation, and aggregation, but these chemical mechanisms of interference will not be discussed in this section.

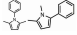
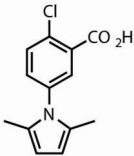
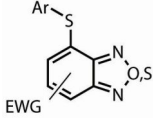
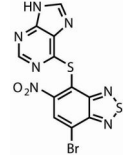
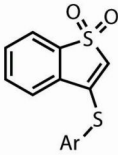
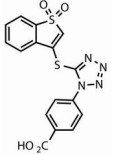
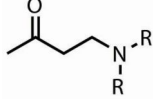
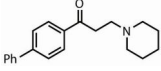
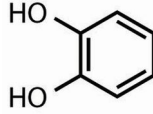
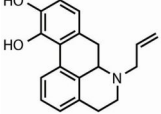
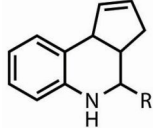
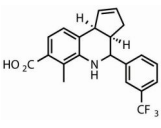
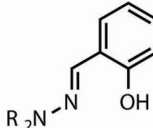
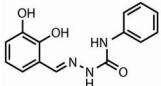
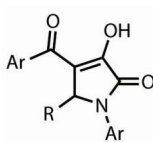
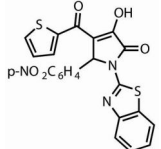
**Table 1:** Examples of non-selective covalent modifiers commonly encountered in HTS triage. Shown are particularly notorious substructures linked to non-selective reactivity (in alphabetical order) and representative examples found in the scientific literature. This list is by no means comprehensive. Also included are noteworthy references describing the chemical basis of non-selective covalent reactivity for each class shown.

| Substructure  | Structure (example)   | Class name                                  | MOA comment <sup>a</sup>            |
|---|---|---|-------------------------------------|
|  |  | Alkyldene barbiturates and thiobarbiturates | Reactive                            |
|  |  | Alkyldene rhodanines                        | Reactive, photo-reactive, chelation |
|  |  | Alkyldene pyrazolidinediones                | Reactive                            |
|  |  | 2-Amino-3-carbonylthiophenes                | Redox-active                        |

<sup>a</sup> Commonly encountered reactive mechanisms of action (MOA) for this series.

Table 1 continues on next page...

Table 1 continued from previous page.

| Substructure  | Structure (example)   | Class name  | MOA comment <sup>a</sup>  |
|---|---|---|---|
|    |    | Aralkyl pyrroles  | Reactive, can form bioactive polymers (24)  |
|    |    | Benzofurazans, Benzothiadiazoles (S-linked aromatic LGs)        | Reactive (nucleophilic aromatic substitution) (25)                                    |
|    |    | Benzo[ <i>b</i> ]thiophene 1,1-dioxides (S-linked aromatic LGs) | Reactive (addition-elimination) (25)  |
|   |   | Beta-amino ketones  | Elimination to form reactive species  |
|  |  | Catechols   | Chelator; redox-active, oxidizes to quinones  |
|  |  | Cyclopentene-fused tetrahydroquinolines                         | Reaction catalyst impurities and/or formation of an electrophilic by-product in vitro |
|  |  | Hydroxyphenylhydrazones   | Chelation   |
|  |  | 3-Hydroxy-pyrrolidin-2-ones                                     | Reactivity, protein disruptors  |

<sup>a</sup> Commonly encountered reactive mechanisms of action (MOA) for this series.

Table 1 continues on next page...

Table 1 continued from previous page.

| Substructure | Structure (example) | Class name                               | MOA comment <sup>a</sup>  |
|--------------|---------------------|--|---|
|              |                     | N-(4-Hydroxynaphthalen-1-yl)sulfonamides | Redox-active; reactive; buffer instability to form reactive quinones (25) |
|              |                     | Isothiazolones                           | Reactive  |
|              |                     | Maleimides                               | Reactive (25)   |
|              |                     | Phenolic Mannich bases (Betti bases)     | Reactive  |
|              |                     | Quinones                                 | Redox-active; reactive  |
|              |                     | Succinimides (S-linked aromatics)        | Buffer instability to form reactive maleimide (25)                        |
|              |                     | 1,2,4-Thiadiazole salts                  | Reactive (reversible, ring-opening disulfide bond formation) (25)         |

<sup>a</sup> Commonly encountered reactive mechanisms of action (MOA) for this series.

## Chemical Reactivity Interference in Cell-Based and Phenotypic Assays

While this chapter focuses on target-based and cell-free assays, a critical point is that cell-based or phenotypic assays are also subject to interference by non-specific chemical reactivity. A prime example is the case of PTC124, a small-molecule that was discovered in a firefly luciferase-based assay targeting nonsense codon suppression (26). Several studies have provided evidence that this compound reacts with ATP to produce an adduct (PTC124-AMP) capable of stabilizing the firefly reporter enzyme, which ultimately

confounds the cell-based assay readout by yielding apparent activation (27, 28). It is important to note that amphiphilic compounds, in particular those that are cationic in nature, can interfere with membranes and hence give artifactual results, not just in cell-based assays but also in membrane-associated target-based assays (29).

If a test compound has non-specific target activity, then it is highly unlikely that any observed effect could be specifically attributed to a well-defined compound-target interaction in a complex biological system such as a cell. Researchers performing cell-based screens should therefore be aware of the potential for off-target effects due to compound reactivity.

## Prevalence in HTS

Most screening libraries contain reactive compounds and this must be considered in HTS triage. Natural products, which can be part of screening libraries, can also be electrophilic and highly reactive (30). Table 2 shows a comparison of the number of compounds found by HTS, REOS (19), and PAINS filters (*vide infra*) in a few general screening libraries (MLSMR: the Molecular Library Small Molecule Repository), Academic A and B (two representative academic screening libraries), and two recent (2014-2015) versions of eMolecules; a collection of commercially-available compounds). It has been suggested that PAINS compounds are often those that are easily prepared by high-throughput synthesis (formerly referred to as combinatorial synthesis) and, thus, would most likely be highly represented in large, unfiltered collections of compounds. The HTS filter used here is the one implemented in Pipeline Pilot, and recognizes reactive compounds, metals, etc. REOS filters were designed to remove compounds likely to cause assay interference but also those that might be anticipated to cause late stage project failures because of toxicity (so-called ‘toxicophores’). PAINS filters were carefully developed based on the actives in a select group of assays performed on a specific compound library. They recognize compounds that would likely interfere with assays. PAINS filters do not recognize the most reactive structural moieties because those functional groups were not included in the library upon which the filters were based. Other useful filtering strategies for removing potential interference compounds from data sets have been published (31, 32). The seminal point here is that the apparent hit rate due to PAINS compounds exceeds the typical 0.5 – 2% hit rates from screening of broad small molecule chemical libraries, so left unfiltered, authentic hits might not be identified from primary screening.

**Table 2:** Almost all libraries contain potential interference compounds. MLSMR: Molecular Library Small Molecule Repository (2014); Academic A and B: representative academic screening libraries; eMolecules: two versions of a curated library of commercially-available compounds (2014-2015); HTS: high-throughput screening filter in Pipeline Pilot (Accelrys); REOS: Rapid Elimination of Swill; PAINS: Pan assay interference compounds. REOS and PAINS filters as implemented in Schrödinger.

| Collection | Compounds (n) | HTS  | REOS   | PAINS  | PAINS (%) |
|------------|---------------|------|--------|--------|-----------|
| MLSMR      | 314,651       | 7160 | 79,695 | 18,654 | 6         |

Table 2 continues on next page...

Table 2 continued from previous page.

| Collection | Compounds (n) | HTS     | REOS           | PAINS   | PAINS (%) |
|------------|---------------|---------|----------------|---------|-----------|
| Academic A | 208,887       | 5082    | 59,041         | 10,098  | 5         |
| Academic B | 234,304       | 3287    | 41,134         | 9831    | 4         |
| eMolecules | 6,580,176     | 200,805 | NC             | 366,939 | 6         |
|            | 5,498,347     |         | 982,150 (~20%) |         |           |

## Section Summary

Compounds that are known to be reactive with proteins are likely to be found as “actives” in any primary HTS screen. The next sections will offer strategies to help triage these compounds so that resources can be directed to what might be better compound classes.

## Knowledge-Based Strategies to Minimize Impact of Interference Compounds

### Section Introduction

All libraries will most likely contain compounds capable of causing assay interference. Therefore, it is essential that a combination of knowledge and assay-based strategies be used to separate the true from false actives. There are several other knowledge-based strategies that will help the project team focus on the best chemical matter.

### Understand Medicinal Chemistry Concepts and Reactive Substructures

Screening collections will inevitably contain reactive molecules, despite their limited potential utility as chemical leads. Many of these compounds represent synthetic intermediates submitted to corporate and commercial screening collections, or were developed for antineoplastic or antimicrobial projects. Many of these reactive functional groups have been characterized (Table 3). These can include acyl chlorides or aldehydes, for example. Medicinal chemists can usually identify these more obvious reactive groups.

Many of these functional groups are relatively straightforward to identify, and many cheminformatics programs have filters to rapidly identify the more conspicuous ‘reactophores’. For example, the cheminformatics platform in Pipeline Pilot has an ‘HTS filter’ that efficiently removes compounds with many of these problematic substructures. The NIH Molecular Libraries Small Molecule Repository has a similar set of functionality filters available. Another free and useful site for compound filtering currently available is FAF-Drugs3 (33). Compounds bearing these reactive groups should generally be avoided. However, not every reactive substructure filter can be all-inclusive, and in practice it is prudent to have trained medicinal chemists examine the results of a filtering process (34).

**Table 3:** Examples of notoriously reactive substructures. X, halogen; R/R'/R'', alkyl.

| Functional group            | Structure | Functional group                     | Structure   |
|-----------------------------|-----------|--------------------------------------|-------------|
| Acyl halides                |           | $\alpha$ -Halocarbonyls              |             |
| Aldehydes                   |           | $\beta$ -Heterosubstituted carbonyls |             |
| Aliphatic esters            |           | Heteroatom-heteroatom single bonds   |             |
| Aliphatic ketones           |           | Imines                               |             |
| Alkyl halides               |           | Michael acceptors                    |             |
| Anhydrides                  |           | Perihalo ketones                     |             |
| Aziridines                  |           | Sulfonate esters                     |             |
| $\alpha,\beta$ -dicarbonyls |           | Sulfonyl halides                     |             |
| Epoxides                    |           | Thioesters                           |             |
|                             |           | Thiols                               | <b>R-SH</b> |

## Computational Methods

Computational strategies have been described to help identify reactive compounds and frequent hitters. One of the most straightforward methods available to academic researchers to flag problematic compounds is the use of substructure filters. In addition to filtering out compounds with the well-characterized reactive functional groups described above, screening actives should be flagged for PAINS substructures. In practice, this can be accomplished by several means. The computational chemistry suites from Tripos and Schrödinger have built-in, user-friendly PAINS filters. PAINS filtering can also be accomplished with open-source software, such as KNIME, or using the FAF-Drugs3 server (33, 35). Compounds that are not flagged as PAINS by substructure filters can still represent problematic compounds. This may be partly explained by the fact that the original PAINS substructures were identified by six HTS campaigns using AlphaScreen, and specific substructures were designed with specific cut-off criteria. Compounds closely resembling PAINS substructures may therefore not be flagged.

The potential for chemical reactivity can also be modeled and predicted using computational methods (36). These models can provide clues about the potential for reactivity, but they are not a substitute for experimental evidence.

## Search Scientific Literature and Databases

In evidence-based medicine, systematic reviews and meta-analyses are routinely conducted to answer clinical questions. This consists of a thorough literature search, and expert synthesis of the available data to formulate a clinical guideline. Similarly, promising compounds should be put in the context of previous studies to formulate recommendations about future studies (34). This includes assessing the ‘natural history’ of a compound and related analogs. There are several resources that can be used for this purpose (Table 4).

A straightforward practice is to first search for potential lead compounds by their structure to examine what data, if any, are available for the parent compound. For example, one can search PubChem to see how a particular compound behaved in any NIH-funded HTS. Often, a compound will have been screened in tens to hundreds of assays with different targets and assay formats. This can provide valuable clues about bioassay promiscuity including potential reactivity (37-39). A useful web application that offers a convenient window into standardized data from PubChem assays is BADAPPLE (bioactivity data associative promiscuity pattern learning engine) (40). BADAPPLE serves as a plug-in for BARD, the standardized BioAssay Research Database of the MLP (NIH Molecular Libraries Project). The algorithm embedded in BADAPPLE accepts query structures and generates a pscore (promiscuity score) based on a statistical analysis of the bioactivity data in BARD associated with scaffolds present in the query molecule (41).

There is also important information that can be gained from examining related chemical analogs in the databases listed in Table 4. We have found it useful to examine structurally similar compounds, and most chemical search engines have options to search by 2-D

similarity. It is important to realize, however, that substructure searching can be more useful than similarity searching when there is specific interest in core SAR. Some relevant questions to ask include:

- Has this compound (or chemical analogs) been screened before? If so, how often has this compound been active? What percentage of assays has this compound been active in and against how many targets?
- Has the compound (or chemical analogs) been published in the scientific literature? If so, what claims were made about the compound? How was the compound tested? Based on how the compound was tested, is there a possibility that the results could be explained by non-specific chemical reactivity?
- Has this compound (or chemical analogs) been included in any scientific patents? If so, ask similar questions as above.
- How has the compound been synthesized? What are some possible bioactive contaminants? Are there alternative synthetic routes?

Compounds and chemical classes that show up repeatedly in unrelated screens and in different assays should raise suspicion about non-specific reactivity and other non-therapeutically interesting mechanisms of bioassay activity. Performing this exercise can prevent wasted follow-up on promiscuous compounds, or thoroughly investigated compounds, including reactive entities. These search activities can be time intensive, and in practice this step is optimal when the number of candidate compounds has been culled to a handful of chemical series.

**Table 4:** Examples of databases for examining compound natural histories.

| Resource  | Remarks  |
|-----------|--|
| SciFinder | Useful for searching patent literature; very comprehensive; subscription service ( <a href="http://www.cas.org/products/scifinder">http://www.cas.org/products/scifinder</a> ) |
| PubChem   | Provides important information about bioassay promiscuity; open-access ( <a href="https://pubchem.ncbi.nlm.nih.gov/">https://pubchem.ncbi.nlm.nih.gov/</a> )                   |
| Reaxys    | Chemical database for searching scientific literature by chemical structure; subscription service ( <a href="https://www.reaxys.com">https://www.reaxys.com</a> )              |
| ChEMBL    | Compounds and activities; open-access ( <a href="https://www.ebi.ac.uk/chembl/">https://www.ebi.ac.uk/chembl/</a> )  |

## Section Summary

The application of fundamental medicinal chemistry principles is key to identifying intractable reactive screening hits. Cheminformatic resources can help researchers efficiently flag screening actives containing well-known reactive functional groups, and other more subversive reactive substructures like PAINS. Freely available resources can allow researchers to check the ‘natural histories’ of the compounds that turn up as actives in their HTS. For both the HTS novice and experienced chemists, consulting experts in HTS triage is strongly advised when analyzing HTS results. As detailed in the next



section, promiscuous or potentially reactive compounds should be followed up with rigorous experiments to prove that they are selectively hitting the target of interest.

## Experimental-Based Strategies to Mitigate the Impact of Reactive Interference Compounds

### Section Introduction

Non-specific reactive compounds have the potential to derail drug discovery and development projects if they are not identified promptly. Fortunately, there are many experimental tools available to researchers to mitigate this potential problem. In this section, experimental strategies to identify and triage reactive screening compounds are described. Each method has advantages and disadvantages, and a pragmatic approach is to employ several of these strategies. The use of these counter-screens is applicable to screening compounds derived from both target-based and phenotypic screens, and both real and virtual screens. While much of the text refers to enzymatic inhibitors, the counter-screens and overall concepts discussed herein are applicable to other types of targets and mechanisms of action.

### Characterization of Assay Sensitivity to Known Reactive Compounds

During the assay development stage, it may be useful to characterize the effect of various reactive entities on the assay performance. As an example, workers at GlaxoSmithKline have developed a screening library of interference compounds that they use to probe the sensitivity of assays to compounds with different modes of assay interference (T Jurewicz *et al.* unpublished results, SLAS 2015 Annual Meeting). This strategy allows them to fine-tune their assays to limit the interference of these compound classes. It also alerts them to potential compounds that will likely show up as spurious actives.

In practice, there are several ways this process can be accomplished. Assays can be challenged with commercially-available thiol-reactive compounds such as maleimides or quinones. Similarly, one can also test an assay readout and performance with established redox-active compounds like  $\beta$ -lapachone and NSC-95397, as well as  $H_2O_2$  itself (42, 43). If an assay readout or target is particularly sensitive to  $H_2O_2$  (and presumably redox-active compounds), then a strategy could be to adjust assay parameters to minimize  $H_2O_2$  production and prioritize a redox-activity counter-screen early in the post-HTS screening tree, for example.

### Use of Scavenging Reagents to Mitigate Impact of and to Identify Thiol-Reactive Compounds

One straightforward approach to mitigating the impact of thiol-reactive compounds in target-based assays is to include scavenging reagents in the assay buffer. For example, assays can include dithiothreitol (DTT), usually in 1-5 mM final concentrations, to accomplish two objectives. First, this agent helps to keep protein cysteines in the reduced

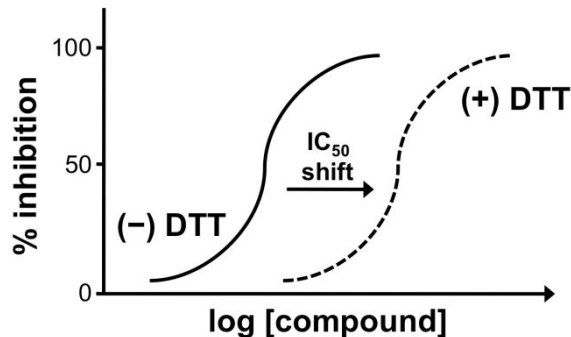


**Figure 2:** Illustrated effect of DTT on  $IC_{50}$  values of reactive compounds in target-based enzymatic assays. Compounds can be tested in the presence and absence of a protein-compatible scavenging agent like DTT. For DTT, this can typically be in the range of 1-5 mM final concentration. Thiol-reactive compounds should in principle show a higher  $IC_{50}$  value in the presence of DTT. In principle, other electrophilic scavengers can be used.

form, which can be required for many protein systems. Second, thiol-reactive compounds can react with the free thiols on DTT. Therefore, DTT can serve as a potential scavenger for thiol-reactive compounds if present in sufficient quantities. Other biological reducing agents may have utility, including  $\beta$ -mercaptoethanol (BME), L-cysteine, *tris*(2-carboxyethyl)phosphine (TCEP; avoids the disulfide exchange possible with DTT) or even non-enzymatic proteins like bovine serum albumin (BSA).

This strategy can be employed from the beginning of the HTS to mitigate the impact of electrophilic compounds. In other words, particularly egregious thiol-reactive compounds would theoretically show reduced activity in the HTS, and would be less likely to be identified among the HTS hits. The ability of DTT to react with some electrophilic compounds can also be exploited in post-HTS assays. One strategy we and others have employed for enzymatic inhibition assays is to measure the  $IC_{50}$  of compounds in both the presence and absence of DTT (Figure 2) (25, 44). Thiol-reactive compounds will often have a significant increase in their  $IC_{50}$  values when sufficient amounts of DTT are added in otherwise identical assay conditions.

### Sample steps | DTT counter-screen

1. Test assay with solvent controls (e.g. DMSO) at several concentrations of DTT (usually 0, 1, 5 mM final concentrations). For each test condition, prepare otherwise identical assay buffer with the appropriate levels of DTT.
2. If assay performance is unaffected by DTT, proceed to step 3. If the assay readout is not compatible with DTT or assay performance suffers, consider testing with other reducing agents (e.g. TCEP, GSH).
3. Test compounds of interest under otherwise identical conditions, ideally in parallel. Include a thiol-reactive positive control to 1) verify the target is sensitive to thiol-reactive compounds, 2) assess overall assay performance, and 3) gauge magnitude of activity differences between different test conditions.

Researchers should consider the following technical points:

- DTT has a limited half-life in aqueous solutions due to oxidation, and stock solutions should ideally be made fresh for each experiment.
- Prior to testing compounds, one should examine the effect of different concentrations of DTT (or comparable reagent) on the assay readout. Certain biological systems or assay readouts may be incompatible with such reagents.
- Significant changes in activity with the addition of DTT should raise concern about thiol-reactive compounds. There is no strict cut-off, but for conventional cell-free enzymatic assays,  $IC_{50}$  changes greater than 3-fold in several independent experiments should raise concerns. With particularly electrophilic compounds, we have seen  $IC_{50}$  changes greater than 10-fold when the  $[DTT] \gg [test\ compound]$ .
- The inclusion of DTT in an assay system does not absolutely prevent the reactivity-based activity or interference of thiol-reactive compounds. Certain compounds may have different reactivity with DTT than with proteinaceous thiols. Another possibility is that the DTT has been oxidized to a form that does not contain free thiols.
- Maleimides such as CPM can be highly useful thiol-reactive positive controls, provided the target of interest is sensitive to thiol-reactive compounds (25).

## Kinetic and Mechanistic Methods to Identify Irreversible-Binding Compounds

Compounds can be tested for evidence of reactivity by kinetic and mechanistic methodologies. The premise is that reactive compounds generally function by irreversible inhibition, and therefore have distinct reaction characteristics compared to well-behaved, reversible inhibitors.

### Assessment of activity time dependence

Reactive compounds typically show time-dependent effects (45-50). Testing can be relatively straightforward. The effect of a compound on a particular target is measured as a function of time. One approach is to vary the amount of time a compound is allowed to incubate with the target before starting an assay ('pre-incubation time'). A time-dependent effect can also be monitored after an assay has been initiated by using continuous reaction monitoring (or sampling assay aliquots), as a reactive compound may show increasing inhibition during the course of an assay as it continues to react with the target. This effect can vary with compound concentration as well. In the case of enzymatic inhibitors, the inhibitory effect of a reactive compound can increase the longer it is allowed to incubate with its reactive target (e.g. an enzyme). One should note, however, that fast-reacting and/or fast-binding compounds may not show time-dependent effects under certain experimental conditions (if, for instance, the incubation times are sufficiently long and the reaction rates are fast). It may not be experimentally feasible to sample short pre-incubation times – this can be due to the time it takes to add reagents, for example. Therefore, a word of caution is that the inability to observe a time-dependent

effect does not necessarily exclude a covalent binding event if the binding and reaction is sufficiently fast.

### Assessment of compound activity reversibility by dialysis methods

Covalent-modifying compounds often irreversibly modulate their target(s). In many cases, the desired profile of a lead compound includes a reversible mechanism of action. For many target-based assays, a test compound can be incubated with the protein(s) of interest, then subjected to dialysis. The target can subsequently be tested for activity after this dialysis to examine for residual bioactivity. The key to interpreting the results is to understand the expected results for both reversible- and irreversible-binding compounds. If a test compound exerts its action by a reversible binding event, the compound should be effectively removed from the system when given sufficient time to equilibrate in a dialysis system (51). Conversely, irreversibly-binding compounds such as reactive screening actives (and also some tight-binding reversible inhibitors) will not be removed by dialysis.

Performing a dialysis experiment is relatively straightforward. The concentration of the test compound should be high enough that it will unequivocally modulate the target at the pre-dialysis concentration. For an enzymatic inhibitor with a Hill slope near 1.0, this may mean incubating the compound at a minimum of 10X its IC<sub>50</sub> value. Testing of the dialyzed target originally treated with the test compound should be compared to a vehicle control (e.g. DMSO-only if the compound is delivered from a DMSO stock solution) subjected to an identical, parallel dialysis procedure (Figure 3). This controls for potential target denaturation or degradation over the course of the dialysis procedure. In principle, compounds that irreversibly modulate their target(s) will retain most of their activity compared to vehicle controls.

### Sample steps | Dialysis counter-screen

1. Prepare stock solutions of compound and protein target.
2. Pre-determine the dose-response of the test compound versus the protein target. Determine the concentration of test compound that reliably results in > 90% target modulation (e.g. enzymatic inhibition). For a compound with a Hill slope of 1.0, this concentration should be greater than 10X IC<sub>50</sub>, which corresponds to 91% inhibition.
3. Incubate compound with protein target for a short duration (e.g. 5-30 min) to ensure equilibration. This incubation can be done with the target at 10X final assay concentrations. This guards against diluting below 1X final assay concentrations during dialysis and prevents against certain proteins that are unstable in dilute solutions. The concentrated solution can still be diluted post-dialysis.
4. Transfer the solution from step 3 to a dialysis vessel with an appropriate molecular weight cut-off.
5. Dialyze compound and target in 1X assay buffer. The length of dialysis and number of buffer changes depends on multiple factors, including the volume of dialysis buffer and the surface area of the dialysis membrane.

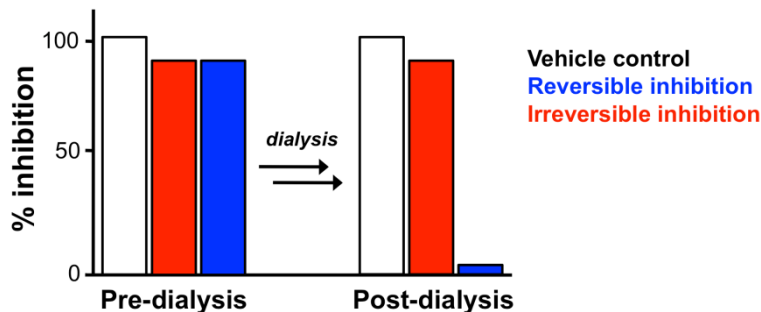


**Figure 3:** Assessment of compound inhibition reversibility by dialysis. Irreversibly-acting compounds (and some slow, tight-binding compounds) can modulate their target(s) even after dialysis. In this experiment, compounds are incubated with target(s) at high compound concentrations, enough that they should achieve near-maximal activity. This solution is then dialyzed. In principle, compounds that are reversibly-bound should pass through the dialysis membrane. After a sufficient period of time, the dialyzed sample is tested for activity and compared to a vehicle control. Reversibly-acting compounds should have activities comparable to the vehicle control, assuming equilibration was reached during dialysis. Shown in the above example is the expected result for an enzymatic assay testing reversible and non-reversible inhibitors.

6. Dilute dialyzed solution with 1X assay buffer to achieve desired concentration of protein target to perform the target assay.
7. Perform target assay.
8. Compare percent modulation to vehicle control and any positive and negative control compounds.

Researchers should consider the following technical points:

- Dialysis can be accomplished quite efficiently with many commercially available cassette systems. Many micro-cassettes allow for smaller volumes of dialysis buffer and fewer amounts of compound and target(s).
- Concentration factors should be accounted for when picking the test compound concentration to achieve a desired final compound concentration capable of near-maximal activity if the mechanism of action is indeed irreversible.
- The activity of the target system can diminish during the dialysis process, especially for certain enzymes sensitive to thermal denaturation or oxidation. Steps to help mitigate this denaturation include using cooler temperatures for dialysis, including carrier proteins in the dialysate, or using concentrated target solutions (see below).
- If dialysis is performed at cooler temperatures (usually done to mitigate target denaturation), remember to use pre-chilled dialysis buffer to avoid transient heating of the sample.
- When dialyzing samples at cooler temperatures (e.g. 4 °C), inspect the sample for signs of compound precipitation. Compounds with poor solubility can sometimes precipitate from solution.
- Consider the use of control compounds, both positive and negative, in this type of experiment. If a target is sensitive to thiol-reactive compounds, then a useful

control is a non-specific thiol-reactive probe like a soluble maleimide. Such a compound should irreversibly modulate the target, even after dialysis.

- Keep in mind that test compounds have the potential to degrade during dialysis. Consider assessing the stability of the compound in buffer to control for compound stability.
- An additional control involves testing compounds prior to initiating dialysis. This can be accomplished by testing aliquots of the compound plus target solutions, along with the corresponding vehicle controls. This control verifies the original activity of the compounds when they are present at high concentrations in the test system.

### Assessment of compound action reversibility by jump-dilution

Another classic experiment to test for irreversible target inhibition involves incubating the test compounds with the target(s) at higher concentrations, diluting the solution, and initiating the assay at the resulting lower concentrations (Figure 4) (51). This is the so-called ‘jump-dilution’ experiment (52-54). In this cell-free experiment, a test compound is typically incubated in a 100X-solution containing the target of interest (e.g. an enzyme), with a test compound concentration of 10-fold its  $IC_{50}$  value in the case of an enzymatic inhibitor with a Hill slope near 1.0. This solution is then rapidly diluted 100-fold into a reaction containing substrate. This dilution creates a 1X-solution of the protein, and dilutes the test compound from 10X the  $IC_{50}$  value to 0.1X the  $IC_{50}$  value. In well-behaved reversible inhibitors having a Hill slope of 1.0, a compound being tested at 10X its  $IC_{50}$  value will show 91% inhibition, while testing at 0.1X its  $IC_{50}$  value will show 9% inhibition. Thus, in general practice, reversible compounds will have a percent inhibition noticeably less than 50%, in contrast to reactive compounds, which will not show a reduction in inhibition because they are still bound to the target even after dilution.

### Sample steps | Jump-dilution counter-screen

1. Determine the dose-response of the test compound versus the protein target. Calculate the  $IC_{50}$  value.
2. Prepare stock solutions of compound and protein target. Be sure to prepare a 1X and 100X solution of the protein target (the highly concentrated target solution is usually prepared with 1X assay buffer unless there are stability issues).
3. Incubate the test compound using 10X  $IC_{50}$  in a solution containing 100X protein target. Mix and incubate to allow for equilibration. Be sure to include a vehicle control
4. Dilute the solution from step 3 100-fold with 1X assay buffer.
5. Add substrate(s) and perform assay using standard procedures.
6. Compare activity of diluted test compound to vehicle control. Positive and negative controls should be included for comparison.

Researchers should consider the following technical points:

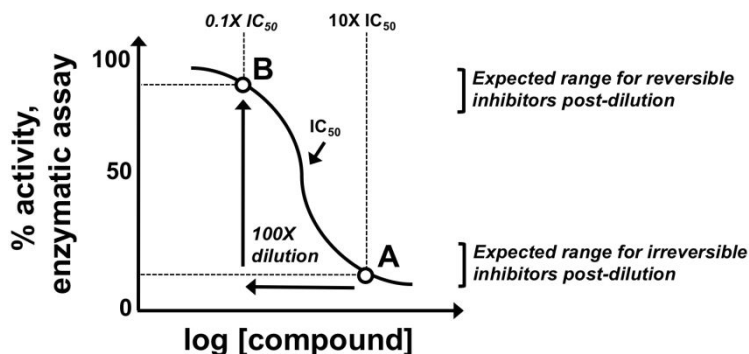


**Figure 4:** Assessment of compound activity reversibility by the jump-dilution method. Shown is an illustration for a compound being evaluated for reversible inhibition in an enzymatic assay, assuming a Hill slope near 1.0. At point (A), the test compound at 10X the  $IC_{50}$  value is initially incubated with the target enzyme at 100X the normal target concentration. After equilibration, this solution is diluted 100-fold with assay buffer. If a compound acts by a completely reversible process, then the expected activity should correspond to a final point (B) after equilibration.

- Prior to performing jump-dilution experiments, it is advisable to have a solid understanding of the compound dose-response. For testing potential enzymatic inhibitors, this means knowing the  $IC_{50}$  value, the Hill slope, and the associated error in both.
- Check for compound precipitation prior to dilution. This is especially true for compounds with poor solubility or weak potencies. A compound with an  $IC_{50}$  of 10  $\mu\text{M}$  will need to be incubated with the target at 100  $\mu\text{M}$  in the aforementioned experiment. A straightforward way to check for compound precipitation is to centrifuge a sample and look for a pellet.
- Ensure the solubility of the proteins/biological target at the 100X concentrations. Look for evidence of protein/target precipitation after brief centrifugation. For example, certain protein complexes or targets sensitive to salt or pH conditions (like histones) may not be entirely soluble at these 100X concentrations.
- Consider the use of control compounds, both positive and negative, in this type of experiment. Targets sensitive to thiol-reactive compounds should retain most of their target modulation even after dilution.
- Testing compounds with Hill slopes that deviate significantly from 1.0 may require adjustments to the suggested dilution steps.
- Note that slow, tight-binding compounds may not show the predicted reversibility, depending on the experimental conditions. If this type of mechanism is suspected, one should carefully scrutinize and investigate the time parameters for each step in the experiment, such as post-dilution incubation time, before the reaction is initiated (55). The time-based effects can be conveniently monitored if a continuous assay readout is available. If this type of inhibition is suspected, we advise consulting an experienced enzymologist.

- Different dilutions or compound concentrations may be used (e.g. 50X, 10X for targets) but one should consider the expected changes in activity (based on the dose-response) and also the experimental errors associated with the assay of choice. For instance, lower magnitude dilutions can potentially make it more difficult to definitively detect reversibility.

## Purification and/or Re-Synthesis of Compounds to Triage Reactive Impurities

As purchased, screening compounds can contain reactive impurities that can lead to assay interference or non-specific activity. These impurities can result from compound degradation, or be the remnants of reactive reagents used in the compound synthesis (56). Screening compounds are typically stored in frozen DMSO, which is a hygroscopic and a mildly reactive solvent. That being the case, prolonged storage of compounds in DMSO or frequent freeze/thaw cycles can cause degradation of screening compounds (57). These degradative transformations can also be catalyzed by trace metal contaminants that may remain from synthetic methods used in the preparation of the compound (58). Metal contaminants such as these can also react with proteins and may not even be detectable by standard measurements of compound purity.

There are several industry-inspired best practices designed to mitigate the risk of reactive impurities (Figure 5). Once a compound is found to be active in HTS, the standards of purity (e.g. LC-MS-PDA-ELDS) and chemical characterization (identity by spectroscopic methods: e.g.  $^1\text{H}$ ,  $^{13}\text{C}$  NMR) become an important consideration (59). These quality control (QC) experiments are required by many funding agencies, including the NIH, which states in several funding announcements that compounds “must be analytically validated in terms of integrity and purity (e.g., use of a re-synthesized powder sample of high purity in the preliminary assays)”. In follow-up assays, the compound of interest should be re-purchased from commercial vendors and subjected to HPLC purification and structural characterization in-house, re-assayed, and its performance compared to the original screening compound. Ideally, the  $\text{IC}_{50}$  values should be nearly identical between the library compound and the re-purchased compound. This step is critical because it allows for QC of the purity and structural identity of the compound of interest. Additionally, the most promising compounds should be re-synthesized in-house, subjected to LC and characterization, and then again re-assayed for comparison to prior samples. If there is a concern about a particular reactive intermediate, compounds can be synthesized by independent routes. Well-behaved compounds should have similar  $\text{IC}_{50}$  values for all batches tested (screening compound, commercial re-purchase, independent re-synthesis). The minimum purity for test compounds entering confirmatory assays should be 95%, as determined by HPLC/MS/PDA/(and, if available, evaporative light scattering detection (ELSD)).



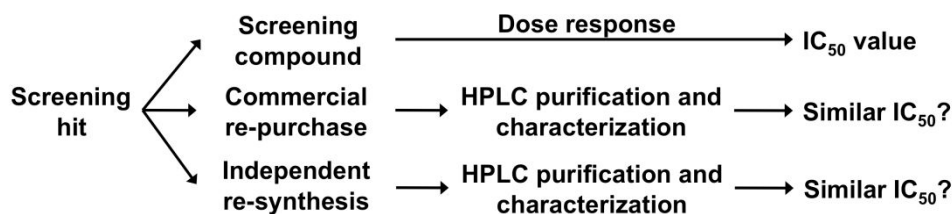


**Figure 5:** Schematic of purification and re-synthesis best practices. Hits derived from screening compound collections should be re-tested with a re-purchased commercial sample that is HPLC purified and characterized for structural identity. Promising compounds should then be re-tested with a sample that has been independently re-synthesized and HPLC purified. All the samples should have reproducible  $IC_{50}$  values.

## Sample steps | Compound purification and re-synthesis

1. Active compounds should be repurchased as solid samples, purified by chromatography, and be subject to rigorous QC standards prior to having their activity confirmed.
2. Purified compounds that have reproducible  $IC_{50}$  values should be prioritized for re-synthesis and retest. Small, focused arrays of analogues made at the same time as the initial active compound can provide SAR that can be used in go/no-go decision making.

Researchers should consider the following technical points:

- QC should consist of LC/MS/PDA (ELSD is also helpful) and NMR ( $^1H$ ,  $^{13}C$ ) assurance of  $\geq 95\%$  purity and identity. PDA = photodiode array
- Low levels of metal impurities (Zn, Pd, Fe, etc.) may cause false positives in some assays. If the assay is sensitive to trace reagent interference, it may be necessary to analyze the purified compounds for metals (detection of trace metals by typical spectroscopic methods is sometimes challenging), to apply resin-based chelators to remove any metals (60, 61), and/or to prepare the compounds by alternative routes that avoid the use of these potential interfering reagents.

## Identification and Triage of Redox-Active Compounds

Several solutions exist to de-risking compounds for redox-activity. A two-fold strategy is recommended whereby 1) the effect of reactive oxygen species (ROS) such as  $H_2O_2$  on the assay system is characterized, and 2) compounds being considered for progression are de-risked for their ability to act as redox-active compounds under the assay conditions.

### Characterization of assay sensitivity to redox activity

This strategy can provide an initial gauge of how likely redox-active compounds are to show up among the assay hits. That is, if a particular assay is found to be sensitive to low micromolar concentrations of  $H_2O_2$ , then any active found should be rigorously evaluated for redox-activity in the post-HTS phase. Different targets may have different

susceptibilities to oxidation. For target-based systems such as *in vitro* enzymatic or protein-protein interaction assays, this can be done by spiking the system with known amounts of H<sub>2</sub>O<sub>2</sub> under assay-like conditions and then measuring the assay readout (25). Similarly, assays can be challenged with known redox-active compounds. For positive control compounds, some suggestions include using  $\beta$ -lapachone and NSC-95397 (42, 43). These approaches can also be performed with cell-based assays, as H<sub>2</sub>O<sub>2</sub> is known to participate in many different cell signaling pathways, and H<sub>2</sub>O<sub>2</sub> and related ROS can be cytotoxins at sufficient exposures (62). It is recommended therefore, that the effect of H<sub>2</sub>O<sub>2</sub> on cell growth and cell signaling markers be measured in cell-based assays where redox-active compounds have the potential to be identified as actives. Even if a particular assay system is not overly susceptible to H<sub>2</sub>O<sub>2</sub> modulation, compounds should still be evaluated for their ability to produce H<sub>2</sub>O<sub>2</sub> because they can contribute to non-specific bioassay activity in other follow-on assays.

### Testing compounds for redox activity

With respect to redox-active compounds, we also recommend that potential lead compounds be de-risked for their ability to act as redox-active compounds, even if this liability is not suspected. This can be done using the simple surrogate assays described below. The advantage of pursuing this strategy is that it can prevent wasted follow-up on intractable compounds early-on in a drug discovery campaign. Additionally, if no redox-activity is identified, it adds a layer of confidence that a candidate compound is displaying activity by a therapeutically relevant mechanism.

One assay to identify H<sub>2</sub>O<sub>2</sub>-producing compounds is a surrogate horseradish peroxidase-phenol red (HRP-PR) assay (43, 63). The experimental procedures outlined in these papers are well-described. The premise of this assay is very straightforward: phenol red produces an absorbance at 610 nm when it is oxidized by HRP in the presence of H<sub>2</sub>O<sub>2</sub>. Therefore, compounds that produce H<sub>2</sub>O<sub>2</sub> *in situ* will lead to a color change (colorless  $\rightarrow$  red) if present in sufficient concentrations. Compounds can be tested for their ability to produce H<sub>2</sub>O<sub>2</sub> in both the presence and absence of the strong reducing agent DTT, as DTT can fuel redox-cycling at low millimolar concentrations, and because some compounds are capable of generating significant amounts of H<sub>2</sub>O<sub>2</sub> even in the absence of DTT (64). We have found the HRP-PR assay very robust, inexpensive, and relatively easy to set-up, as all of the key reagents are commercially available. We have found this robustness extends even to the assay buffer, meaning one can often test for redox-activity with the original HTS-like buffer. Another advantage of this assay is that the assay readout is proportional to the H<sub>2</sub>O<sub>2</sub> concentration.

### Sample steps | HRP-PR redox-activity counter-screen

1. Prepare compounds, reagents and instrumentation.
2. Add vehicle controls (e.g. DMSO) to the appropriate experimental plate wells. These vehicle controls will serve as the negative controls.
3. Add test compounds to the appropriate experimental plate wells.

4. Add  $\text{H}_2\text{O}_2$  to the appropriate experimental plate wells. This will serve as the positive controls. Be careful not to contaminate other wells with  $\text{H}_2\text{O}_2$ .
5. Dispense assay buffer (e.g. the same buffer used in the original HTS) to all experimental plate wells.
6. Dispense assay buffer containing concentrated reducing agent to all experimental wells (except for the wells containing  $\text{H}_2\text{O}_2$  – for these wells, simply add buffer without reducing agent). Note: steps 5 and 6 can be combined in one dispensing step depending on user preferences.
7. Dispense HRP-PR solution to all plate wells.
8. Mix plate contents by plate shaker for 1-2 min.
9. Incubate solutions at room temperature for 20 min.
10. Add NaOH solution to each experimental plate well.
11. Mix plate contents by plate shaker for 1-2 min, then incubate solutions at room temperature for 5 min.
12. Measure  $\text{OD}_{610}$  on plate reader.
13. Analyze data. The  $\text{H}_2\text{O}_2$  wells will serve as the positive controls, while the vehicle controls will serve as the negative controls. Positive control compounds should show a dose-response  $\text{H}_2\text{O}_2$  production.

Researchers should consider the following technical points:

- Additional useful technical details – including recommended dispensing volumes, specific reagents and stock solution compositions – are comprehensively discussed in the original references (43, 63).
- $\text{H}_2\text{O}_2$  can degrade over time. Prepare fresh  $\text{H}_2\text{O}_2$  solutions daily from a stock solution of concentrated  $\text{H}_2\text{O}_2$  stored under the manufacturer's recommended condition.
- Ideally, test compounds should be tested at several concentrations. We typically test between 1-250  $\mu\text{M}$  compound concentrations in triplicate, with several intermediate test points. The number of replicates, dose-response points and test concentrations should be guided by the experimental question and project testing conditions.
- Redox-activity can occur in the presence and/or absence of DTT (or other strong reducing agents). We recommend testing compounds with and without a strong reducing agent like DTT.
- As an interference control, compounds active in this counter-screen should be tested for their ability to interfere with the assay readout in buffer alone, as colored compounds may show a false-positive readout if they absorb light significantly in the 610 nm range.
- In addition to  $\text{H}_2\text{O}_2$  as a positive control, some suggested positive control compounds include using  $\beta$ -lapachone and NSC-95397 (42, 43).
- The threshold for redox-activity inevitably depends on the project. Evidence of a dose-response and  $\text{H}_2\text{O}_2$  production several-fold above baseline values should be flagged for potential triage.

- The addition of catalase to the assay should attenuate the final concentration of  $\text{H}_2\text{O}_2$  and decrease the colorimetric readout. This can serve as an additional confirmatory step.

A second assay for detecting redox-active compounds utilizes a protein-free format to detect redox-cycling compounds. In this assay, compounds are incubated with DTT and the reagent resazurin (65). Redox-active compounds identified by this assay catalyze the reduction of resazurin to resorufin by DTT. The reaction product resorufin can be quantified by measuring fluorescence intensity. Compounds testing positive in this assay are susceptible to producing  $\text{H}_2\text{O}_2$  and superoxide ( $\text{O}_2^-$ ) *in situ*, and are capable of oxidizing protein side chains. The advantages of this assay are that it is protein-free and like the HRP-PR assay, it is straightforward. Disadvantages of this assay are that, unlike the HRP-PR assay, the resorufin product can be formed independently of  $\text{O}_2^-$  or  $\text{H}_2\text{O}_2$ . Therefore, the assay may identify compounds that reduce resazurin but do not necessarily produce reactive oxygen species. Others have suggested that high hit rates and large numbers of false positives may result from this assay (63). Also, compounds cannot be tested in this format in the absence of DTT.

Finally, a lower-throughput option is to test for modification of specific cysteines (as well as other residues like methionine) in redox-sensitive proteins such as certain caspases and cathepsins (64-66). In this type of assay, compounds and redox-sensitive proteins are incubated together, and the protein is analyzed by either LC-MS or LC-MS-MS techniques. The advantage of the latter analytical technique is that it may identify protein residues particularly susceptible to oxidation. These are relatively low-throughput approaches compared to the two aforementioned assays. Using  $\text{H}_2\text{O}_2$  and vehicle controls as positive and negative controls respectively are recommended, as well as known redox-active compounds. Before undertaking these experiments, it is often helpful to consult with researchers with expertise in proteomics to ensure the availability of the necessary instrumentation and to confirm that the assay conditions are compatible with protein mass spectrometry.

## Identification of Unstable Compounds and Reactive Species in Assay Media

Compounds are not always stable in assay media (67). Certain compounds are themselves inert, but can undergo chemical or conformational transformations to form reactive moieties (Figure 6A). For example, we have described a series of succinimides that, when incubated in a basic solution, can undergo elimination to form reactive maleimides. Even reactive compounds can degrade into other reactive compounds, as we have shown with a series of *p*-hydroxyarylsulfonamides that decompose to form reactive quinones (25). Other compounds can oxidize in the presence of air to form reactive products, including certain catechols that can oxidize to form reactive quinones. In principle, many variables can affect the stability of a given compound under typical assay conditions, including:

- Time

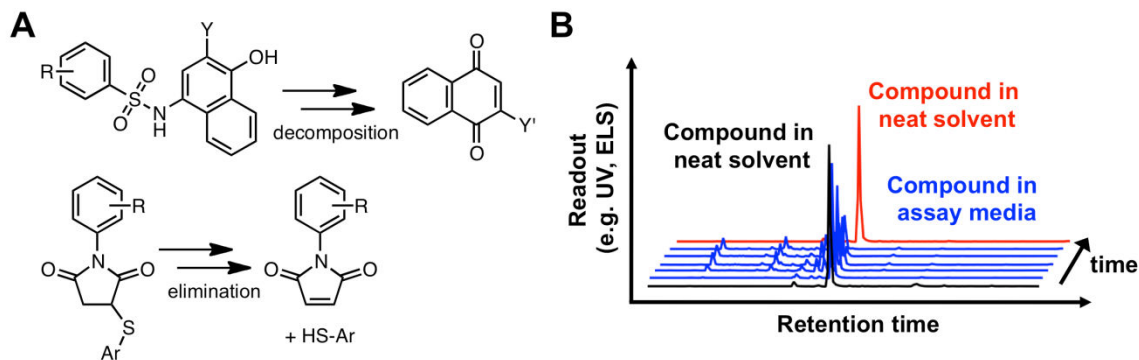


**Figure 6:** Assessment of compound stability in assay buffer. (A) Examples of compound classes showing buffer instability to generate reactive degradation product(s). Y denotes a leaving group such as a halogen or S-linked aromatic group; Ar denotes an aromatic group. (B) Schematic of a sample LC-MS experiment to assess compound stability in assay conditions.

- Temperature
- pH
- Ionic strength
- Gas (atmosphere)
- Concentration (compound and buffer components)
- Stirring
- Presence of certain ions

### Assessing compound stability by chromatography

The stability of test compounds can be monitored in assay buffer over time, using HPLC-based methods (Figure 6B). Compounds are incubated in the assay buffer, and aliquots are analyzed by HPLC or HPLC-MS. Stability can be compared to a control sample in which the compound is incubated in a solvent such as methanol, or another non-reactive solvent. An advantage of HPLC and similar analytical methods include the small amounts of compound needed. We have found benefits to simultaneous reaction monitoring by both evaporative light scattering detection (ELSD) and UV absorption, as reactions monitored by UV can be subject to fluorescent impurities and wavelength-dependent fluorescence properties. Degradation results can also be checked versus a related chemical analogue to draw conclusions about whether the stability is an isolated or series-wide phenomenon.

### Sample steps | HPLC-based assay of compound stability

1. Make stock solution of test compound.
2. Dilute an aliquot of test compound in an inert solvent such as methanol. Run HPLC column to identify parent compound retention time.
3. Titrate concentration of compound and injection volumes to obtain adequate readout intensity without over-saturating detection moiety.
4. Run HPLC column of assay buffer to ensure solvent-instrument compatibility.

5. (Optional) Repeat steps 2-4 as needed to verify consistency of retention time and readout intensity. Optimize instrument settings such as injection volume, buffer gradients, columns, monitoring wavelength (if UV-Vis detection method), ionization settings (if MS detection method), etc.
6. Prepare two master solutions: one containing inert solvent and the other containing 1X assay buffer. Spike each sample with identical amounts of test compound to achieve the desired compound concentrations determined from the previous steps 1-5. Prepare enough solution to allow for multiple injections.
7. Obtain data from test compound in inert solvent.
8. Obtain data from test compound in assay buffer. Resample at multiple time-points.
9. Repeat step 7 at the last time point to control against degradation unrelated to assay buffer.

Researchers should consider the following technical points:

- Care should be taken to omit any buffer components incompatible with liquid chromatography, notably detergents. Many assay buffers now contain detergents like Triton X-100. However, many detergents interfere with proper column function, and should be omitted from the assay buffer.
- For more quantitative measurements, an internal standard can be added to the system to calibrate retention times and analyte concentrations. Samples can be spiked with internal standards for more rigorous quantification. If this strategy is performed, ensure that the internal standard is itself inert and its retention time does not interfere with the analyte.
- Compounds can be analyzed for stability at multiple time points. The minimum time should correspond to the length a test compound is exposed to assay buffer in the parent assay, though as a conservative measure we usually test compound stability for longer time periods.
- An advantage of monitoring HPLC by MS in addition to UV-Vis is the potential to identify the chemical structure of detected degradation products.
- Systems with a calibrated autosampler are ideal, as they allow precise injection volumes.

### **Assessing compound stability by NMR and other methods**

Stability can also be assessed by relatively straightforward NMR experiments. Compounds undergoing chemical or conformational changes as a function of time in assay media may exhibit detectable changes via NMR. However, downsides to this method can be that the high compound concentrations required for NMR detection might not be achievable with lipophilic test compounds, and that deuterated buffer components may be required.

### **Assessment of Compound Reactivity with Known Nucleophiles**

Potential lead compounds should be tested for evidence of reactivity with known biological nucleophiles. Many biologically-relevant nucleophiles are thiols, such as glutathione, coenzyme A, and protein cysteines. There are a variety of thiol-based

nucleophilic probes available to test compounds for chemical reactivity, each with potential advantages and disadvantages (Table 5).

**Table 5:** Examples of nucleophilic probes to detect electrophilic compounds. Shown are the chemical structures of the various nucleophilic probes, select advantages and disadvantages of each test method, and citations to published examples.

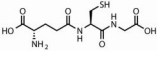
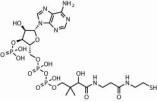
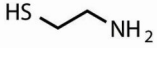
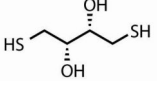
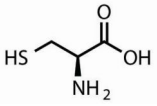
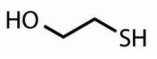
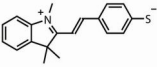
| Probe                     | Structure   | Potential advantages and formats  | Potential disadvantages  | References   |
|---------------------------|---|---|--|--------------|
| Glutathione (GSH)         |    | Inexpensive, HPLC-based, fluorescence-based   | Non-proteinaceous  | (25, 68)     |
| Coenzyme A (CoA)          |    | HPLC-based  | More expensive than GSH, higher MW, non-proteinaceous  | (25, 69)     |
| Cysteamine                |    | Inexpensive, HPLC-based   | Non-proteinaceous  | (70)         |
| Dithiothreitol (DTT)      |    | Inexpensive, HPLC-based   | Short aqueous half-life, non-proteinaceous   | (71)         |
| L-cysteine                |  | Inexpensive, HPLC-based   | Non-proteinaceous  | –            |
| $\beta$ -mercapto-ethanol |  | Inexpensive, HPLC-based   | Odor, Non-proteinaceous  | –            |
| MTSI                      |  | High-throughput capability, fluorescence-based, HPLC-based                            | Oxygen-sensitive, self-dimerization, non-proteinaceous   | (72)         |
| Peptides                  | –   | Protein-like, HPLC-based  | Non-proteinaceous?   | (16)         |
| Proteins                  | –   | Can perform tryptic digest to determine specific adduct sites, LC-based               | Low-throughput, protein requirements, instrumentation requirements, not every peptide/adduct ionizable | (25, 73)     |
| ALARM NMR                 | –   | Protein-based, provides information about conformation changes (non-specific binding) | Expensive (requires non-commercially-available protein), Instrumentation requirements                  | (25, 44, 74) |

Table 5 continues on next page...

Table 5 continued from previous page.

| Probe    | Structure | Potential advantages and formats  | Potential disadvantages   | References |
|----------|-----------|---|---|------------|
| ALARM MS | –         | Protein-based, provides information about adduct structure ( <i>m/z</i> ) | Instrumentation requirements, not every adduct ionizable/stable | (44)       |

## Chromatography-based methods to identify probe-compound adducts

The most straightforward methods to quantifying the reactivity of test compounds with nucleophilic probes involve incubating the test compound with the nucleophilic probe under assay-like conditions, and injecting aliquots into an LC-MS system to look for direct compound-thiol adducts (25, 68, 69). This experimental protocol is highly suited to small-molecule thiol probes including GSH, cysteamine, CoA, and even certain peptides. The disadvantages of these protocols can include the instrumentation required, the potential instability of some adducts to certain chromatographic methods, and the possibility that test compounds may react at different rates with proteinaceous nucleophiles than with the nucleophilic probe employed.

### Sample steps | HPLC adduct counter-screen

1. Prepare stock solutions of compound, thiol probes, and assay buffers.
2. Dilute an aliquot of test compound in an inert solvent. Run HPLC column to identify parent compound retention time.
3. (Optional) Repeat step 2 for thiol probe. Note certain thiol probes may not be detectable by certain detection modalities due to small molecular weight, poor light absorption or poor ionization.
4. Titrate concentration of compounds and thiol probes and injection volumes to obtain adequate readout intensity without over-saturating the detector(s) employed.
5. Run HPLC column of assay buffer to ensure solvent-instrument compatibility.
6. (Optional) Repeat steps 2-5 as needed to verify consistency of retention time and readout intensity. Optimize instrument settings such as injection volume, buffer gradients, columns, monitoring wavelength (if UV-Vis detection method), ionization settings (if MS detection method), etc.
7. Incubate test compound and thiol probe in assay buffer.
8. Run HPLC column of a solution aliquot from step 7.
9. Analyze data for evidence of detectable compound-thiol adducts.

Researchers should consider the following technical points:

- Compounds are usually prepared as 10 mM stock solutions in DMSO. Thiol probes can be prepared as 1 M stock solutions in either water or assay buffer, ideally freshly to mitigate thiol oxidation.



- The ratio of compound to thiol probe can be adjusted, depending on the reactivity of the test compound and the specific experimental question. Usually, this thiol:compound ratio can begin at 1:1 or 2:1. To qualitatively assess whether a test compound can form a detectable adduct, the thiol:compound ratio can be increased.
- Similarly, the length of time and temperature that test compounds and thiols can be allowed to incubate together can vary depending on the specific experimental question. At a minimum, this incubation length and temperature should model the parent assay conditions. Increasing the time and temperature may allow for a greater formation for certain adducts.
- An advantage of monitoring HPLC by MS in addition to UV-Vis is the potential to identify the chemical structure of detected degradation products.
- Systems with a calibrated autosampler are ideal, as they allow precise injection volumes.
- Consider the use of control compounds, both positive and negative.
- Internal standards can be included if more rigorous quantification is desired. If used, such standards should not be reactive or co-elute with the test compound or adduct(s).
- For unstable compounds, consider the possibility of reactive degradation products.
- Note that some adducts may not be stable to certain HPLC conditions, giving misleading results.
- Similarly, certain adducts may be difficult to detect by certain detection modalities. Certain adducts may not be stable to specific MS methods, while certain adducts without a conjugated bond system may be relatively UV-lucent.
- Interpret negative results with healthy skepticism. While a very promising sign in most cases, the failure to detect compound-thiol probe adducts by HPLC or similar methods does not definitively exclude non-specific thiol reactivity.

### Fluorescence-based methods to identify adducts

Thiol reactivity can also be assessed with fluorescence-based methods. For example, compounds that react with the probe MTSI produce a change in fluorescence (72). A similar, fluorescence-based method involves a competition-based assay where the compound competes with GSH for a maleimide-based probe (75). We recently described a similar method using CoA and the thiol-sensitive maleimide probe CPM (25). A disadvantage of these methods is that compounds can interfere with the fluorescent readout by a variety of pathways. Nucleophilic compounds can react with the maleimide-based detection component. Fluorescent or fluorescence-absorbing compounds can also interfere with the assay readout.

#### Sample steps | CoA/GSH-CPM counter-screen

1. Prepare stock solutions of compound, thiol probes, and assay buffers.
2. Add test compounds to experimental plate (96- or 384-well).
3. Add vehicle controls to experimental plate. These wells will be used for controls.

4. Add thiol source to appropriate wells. Mix.
5. Incubate plate from step 4 for > 10 min at 25-37 °C.
6. Add CPM to appropriate wells. Mix.
7. Incubate plate from step 6 for 10 min.
8. Read fluorescence intensity from the experimental plate ( $\lambda_{\text{ex}}$  405 nm,  $\lambda_{\text{em}}$  530 nm).
9. Analyze data. Compare fluorescence intensity of test compound wells with vehicle control wells.
10. Check putative thiol-reactive compounds for fluorescence quenching (25).

Researchers should consider the following technical points:

- Positive and negative controls are necessary. Several positive reaction controls should be included (vehicle controls + assay buffer + thiol source + CPM). Likewise, several negative reaction controls should be included on the same plate (vehicle controls + assay buffer + thiol source; vehicle controls + assay buffer + CPM).
- Positive and negative thiol-reactive control compounds are also recommended.
- A reduction in fluorescence intensity suggests compound-CPM reactivity and/or fluorescence quenching. An increase in fluorescence intensity suggests compound autofluorescence, or the creation of a fluorescent compound-reagent adduct.
- One can confirm fluorescence quenching by determining the absorption and the excitation/emission spectra of putative quenching compounds.
- Compounds are usually prepared as 10 mM stock solutions in DMSO. Thiol probes can be prepared as 1 M stock solutions in either water or assay buffer, ideally freshly to mitigate thiol oxidation. CPM can be prepared as a 1:1 MeOH:H<sub>2</sub>O solution.
- More specifics about stock solutions, concentrations, reagent ratios, dispensing volumes and dispensing steps are described in detail elsewhere (25, 69). Other modified versions of this assay are also described (75, 76).
- The length of time and temperature that test compounds and thiols can be allowed to incubate together can vary depending on the specific experimental question.
- The threshold for thiol-activity inevitably depends on the project. Evidence of a dose-response and significant deviation from vehicle controls (e.g. >20%) baseline values should be flagged for potential triage or follow-up studies.
- Ideally, test compounds should be tested at several concentrations. We typically test between 0.1-100  $\mu\text{M}$  compound concentrations in triplicate, with several intermediate test points. The number of replicates, dose-response points and test concentrations should be guided by the experimental question and project testing conditions.
- This method can be adapted to CoA or GSH as thiol sources. In principle, this method can be adapted for different fluorescence-based maleimide probes besides CPM.

## Other methods

More advanced methods for detecting thiol-reactive screening compounds can involve the use of protein and protein-like (peptide) probes (16). These methods can involve MS or NMR detection methods. MS methods can involve the direct detection of the adduct ion. This can be done with potentially-reactive peptide probes or can involve the native proteins employed in the assay (77). These proteins can be run on a LC system and ionized whole using a LC-MS format. Alternatively, they can be subjected to tryptic-digestion and subjected to LC-MS-MS analysis. The advantages of this latter experiment include information about the specific residue(s) modified. A disadvantage of this approach is that not every peptide is equally prone to ionization, and the amount of time, resources and instrumentation can be prohibitive.

## Assessment of Compound Reactivity with ALARM NMR/MS

The nucleophilicity of cysteine thiols can have significantly different reactivity profiles compared to small-molecule thiols. Therefore, it is possible that certain compounds may not form adducts with GSH, but can react with protein cysteine residues. One solution to identify protein-reactive compounds is ALARM NMR (Figure 7). This technology, developed by Huth and colleagues at Abbott, was adapted after an NMR-based screen to detect small-molecule modulators of the La antigen identified mostly thiol-reactive compounds (44, 74). The La antigen has two cysteine residues, C232 and C245, which are prone to react with electrophilic screening compounds. The formation of covalent adducts between the cysteine residues on the La antigen and test compounds leads to perturbations in several residues, namely L249, L294, and L296. ALARM NMR-positive compounds show characteristic peak shifts and signal attenuation for these particular residues. The inclusion of excess DTT in an otherwise identical reaction is used as a control for non-specific protein perturbations, as electrophilic compounds should react with the excess DTT and spare the protein cysteine residues. ALARM NMR can also detect protein denaturants. This is typically evidenced by complete loss of the characteristic signals for the  $^{13}\text{C}$ -labeled amino acids (44). The protein is enriched with  $^{13}\text{C}$  by including the labeled amino acid precursors during the protein synthesis. In our hands, this assay is medium throughput and robust. Throughput can be increased with the use of an autosampler, a cryoprobe, efficient  $^{13}\text{C}$ -enrichment and optimized pulse sequences. However, unanswered questions about the method include its sensitivity and how to best quantify the results (especially for equivocal findings), answers that may unfold with additional studies.

This method has proven useful in our hands to detect thiol-reactive screening compounds (25). Benefits of this method include its NMR-based readout, which is completely orthogonal to either MS or fluorescent readouts used in other assays. This method also allows for the identification of promiscuous binders and possibly redox-active compounds, as these compounds would perturb the conformation of the La protein in both the presence and absence of DTT. The method is not without its drawbacks, namely

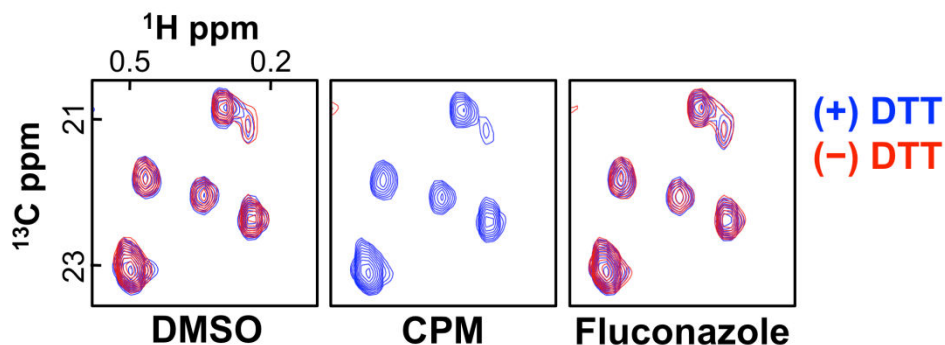


**Figure 7:** Demonstration of ALARM NMR to assess the thiol reactivity of screening compounds. Compounds are incubated with the  $^{13}\text{C}$ -enriched La antigen in either the presence or absence of 20 mM DTT. Shown are the peaks for L249, L294, and L296. Signals were normalized to DMSO controls. Fluconazole is included as a negative thiol-reactive control compound. CPM, a thiol-sensitive maleimide probe, is shown as a positive control compound. Thiol-reactive compounds can cause peak shifts and/or signal attenuation in the absence of DTT, and this effect is significantly attenuated if DTT is included in the reaction mixture.

the instrumentation required, the expense of labeled amino acid precursors and the comparatively higher concentrations of protein and compound required.

ALARM NMR has also been adapted to ALARM MS. The advantages of this approach include the lack of any  $^{13}\text{C}$ -labels as well as spectrometric information about compound-protein adducts, as the  $m/z$  shift resulting from compound-protein adducts can provide clues about the structural nature of the presumed adducts. Potential disadvantages of this approach include the requirement for protein-compatible LC-MS instrumentation and the possibility of compound-protein adduct instability in the LC-MS conditions.

### Structure-Activity Versus Structure-Interference Relationships

The diagnostic importance of SAR in hit compound series has been a point of emphasis in recent literature (78). Closely related analogues of hits (10-25 compounds) prepared by synthetic chemistry should show > 10-fold difference in measured  $\text{IC}_{50}$  values. This exercise can provide confidence along three important lines of evidence that can make or break a compound series: 1) that the activity of the hit is real, 2) that analogues of a hit can be prepared, and 3) that the series has the potential for optimization.

What appear to be structure-activity relationships (SAR) may actually be structure-interference relationships (SIR). Therefore, the term SAR should be employed to describe 'activity' differences between compounds that are known to be non-reactive or have had their target confirmed. Structure-interference relationships can be observed in a compound series, but are typically related to reactivity differences between series members. For example, true SAR in a series for CDK2 inhibitors was confirmed by activity measurements with x-ray crystallography to demonstrate target engagement (79, 80). On the other hand, we have presented several examples of SIR in the context of HTS,

in which structural modifications lead to apparent activity changes, but useful or specific target engagement could not be confirmed (25).

## Orthogonal Assays

Employing orthogonal assays is highly recommended (if not mandatory), in part because reactive compounds can give misleading assay readouts. In some cases, when assays are interrogated by an orthogonal detection method, this apparent activity is lost. A straightforward example is the CPM-based thiol-scavenging assay described previously to indirectly quantify histone acetyltransferase (HAT) activity. In the HAT reaction, an acetyl group from acetyl-CoA is enzymatically transferred to a histone substrate, forming an acetylated histone and free CoA. In this assay format, electrophilic screening compounds can react with free thiols to give a false-positive readout (25, 69). Orthogonal assays that measured the actual acetylated histone products (a Western blot assay and a [<sup>3</sup>H]-acetyl-CoA HAT assay) were critical in identifying thiol-trapping artifacts. Of course, other assay methods may also be susceptible to reactive interference. Therefore, one strategy to mitigate the selection of reactive interference compounds is the use of orthogonal assays.

## Counter-Screens

Non-specific chemical reactivity can also be investigated by performing counter-screens versus related and unrelated targets.

An extremely important, yet usually simple measure to take is to run a counter-screen. This can take place either in parallel during a screening campaign or immediately afterwards once actives are identified. While this will be case-specific for each assay technology, a robust counter-screen typically involves testing the actives in the same type of assay but against a different protein that would not normally be expected to bind the same compound. Actives that hit both assays are likely to be promiscuous or to be interfering with the physics of assay signaling in some way. Care must be taken, however, as any given active can appear to be selective for a biological target over an individual counter-screen, but this is not conclusive proof that the compound will not reveal a reactivity profile when tested against a wider range of targets. Testing in a broad range of assays and proteins is therefore recommended (see below). It is hard to be definitive, but as a compound is optimized towards higher affinity, clear SAR should be revealed for the target of interest concomitant with increased selectivity over any other off-target activity that might have been observed in the screening hit.

Beyond these relatively straightforward counter-screens to detect highly promiscuous substances, compounds should also be shown to be selective against structurally homologous targets (isoforms). These assays should be routinely implemented in-house as they will frequently be used to prioritize hit compounds. Compounds that have been even further refined by optimization should be assayed against targets in the same class (e.g. GPCRs, proteases, kinases, etc.) and, finally, a broad range of targets typically surveyed to provide evidence for lack of off-target toxicity. These assays are typically outsourced to contract research organizations and should be reserved for representative compounds

selected from the best series of compounds. Broad activity in these assays may be indicative of non-selective reactivity.

## Section Summary

Non-specific reactive compounds are a significant risk in early drug discovery and development. In certain cases, irreversible, covalent inhibition is desired. However, in most cases, reactive compounds are not initially sought. In this section, we have highlighted several experimental strategies to identify reactive compounds, including kinetic/mechanistic experiments and tools to specifically identify compound-thiol adducts. This list of experimental approaches is by no means exhaustive. Promising compounds arising from both virtual and real HTS campaigns should be assessed for chemical reactivity. We recommend testing for reactivity even in cases when the compounds of interest are considered benign. This de-risks the compound for later, more resource-intensive experiments.

## Conclusions

Assay readouts are subject to various modes of interference, including chemical reactivity by test compounds. Reactive screening compounds often possess non-specific bioactivity and/or misleading readouts. As such, failure to triage these undesired, non-specific reactive entities can lead to wasted resources and also missed opportunities to pursue more tractable chemical matter with higher chances of downstream project success. Those who tout a compound as a chemical probe or possessing useful biological activity should demonstrate its lack of reactivity interference using a variety of methods (Table 6). Utilizing a two-pronged strategy of knowledge-based and experimental-based methods should enhance the likelihood of identifying reactive nuisance compounds. Within each of these two arms, researchers should aim to perform multiple – and in some cases redundant – experiments to mitigate the risk of pursuing intractable reactive compounds and enhance confidence in biochemically (and therapeutically) useful modes of bioactivity and target engagement.

**Table 6:** Checklist for de-risking reactive compounds.

|  |
|--|
| Cheminformatics  |
| Have the screening hits been filtered for known reactive functional groups?  |
| Have the screening hits been filtered for PAINS?   |
| Have potential lead compounds been reported as active in other assays, patents or scientific papers? How have similar compounds behaved? |
| Reactive compounds   |
| Have potential lead compounds been tested versus at least one nucleophilic probe?  |
| Have potential lead compounds been tested by well-established kinetic experiments for reversibility?                                     |

|  |
|--|
| Redox-active compounds   |
| Has the assay system being tested for susceptibility to H <sub>2</sub> O <sub>2</sub> and redox-active compounds?        |
| Have potential lead compounds been de-risked with respect to redox-activity?   |
| Impurities   |
| Have potential lead compounds been tested by HPLC-purified and characterized commercial samples?                         |
| Have potential lead compounds been tested by HPLC-purified and characterized independently using re-synthesized samples? |

## Suggested Websites

1. SciFinder Scholar (<http://www.cas.org/products/scifinder>). Excellent resource for searching scientific and patent literature by chemical structure. It is highly recommended to search potential lead compounds and structural analogs for literature precedent.
2. PubChem (<http://pubchem.ncbi.nlm.nih.gov/>). An excellent open-access resource containing data from NIH-funded chemical screens. It is highly recommended to search potential lead compounds and structural analogs for their performance in both related and unrelated assays.
3. BADAPPLE (<http://pasilla.health.unm.edu/tomcat/badapple/badapple>). An open-access resource for assessing bioassay promiscuity, which can be used as a supplement to searching PubChem.
4. FAF-Drugs3 (<http://fafdrugs3.mti.univ-paris-diderot.fr/>). An excellent, free site for filtering relatively small sets of compounds.

## Suggested Readings (alphabetical order)

1. Baell, J. B.; Holloway, G. A. *J. Med. Chem.* 2010, 53, 2719.  
Describes in detail the concept of pan-assay interference compounds. Many of these substructures are likely thiol-reactive. A must-read for any researchers engaged in early drug discovery and HTS.
2. Copeland, R. A. *Evaluation of enzyme inhibitors in drug discovery: a guide for medicinal chemists and pharmacologists*; New York: Wiley-Interscience, 2005.  
An excellent text describing kinetic and mechanistic experiments to elucidate the mechanism of action of test compounds. Many of the described experiments and approaches can be adapted to identify reactive compounds.
3. Dahlin, J. L.; Nissink, J. W. M.; Strasser, J. M.; Francis, S.; Zhou, H.; Zhang, Z.; Walters, M. A. *J. Med. Chem.* 2015, 58, 2091.  
Describes in detail multiple experimental strategies to identify thiol-reactive compounds. Illustrative of the havoc that chemical reactivity can have on an HTS campaign if reactive compounds are not identified, and how apparent structure-activity relationships can actually be explained as structure-interference relationships.

4. Huth, J. R.; Mendoza, R.; Olejniczak, E. T.; Johnson, R. W.; Cothron, D. A.; Liu, Y.; Lerner, C. G.; Chen, J.; Hajduk, P. J. *J. Am. Chem. Soc.* 2005, 127, 217.  
Introduces ALARM NMR, a protein-based NMR assay to identify thiol-reactive compounds. Provides data suggesting differential reactivity between glutathione and a protein probe (La antigen).
5. McCallum, M. M.; Nandhikonda, P.; Temmer, J. J.; Eyermann, C.; Simeonov, A.; Jadhav, A.; Yasgar, A.; Maloney, D.; Arnold, L. A. *J. Biomol. Screening* 2013, 18, 705.  
Nicely describes a novel thiol-based fluorescent probe to identify reactive screening compounds adaptable to a high-throughput format.
6. Soares, K. M.; Blackmon, N.; Shun, T. Y.; Shinde, S. N.; Takyi, H. K.; Wipf, P.; Lazo, J. S.; Johnston, P. A. *Assay Drug Dev. Technol.* 2010, 8, 152.  
Describes the prevalence of redox-active compounds in the context of a large-scale HTS, along with detailed protocols describing the HRP-PR assay.
7. Thorne, N.; Auld, D. S.; Inglese, J. *Curr. Opin. Chem. Biol.* 2010, 14, 315.  
Summarizes many of the common sources of compound-dependent assay interference encountered in HTS.
8. Walters, W. P.; Namchuk, M. *Nat. Rev. Drug Disc.* 2003, 2, 259.  
Describes the use of Rapid Elimination Of Swill (REOS) cheminformatics filters.

## References

1. Mah R, Thomas JR, Shafer CM. Drug discovery considerations in the development of covalent inhibitors. *Bioorg Med Chem Lett.* 2014;24(1):33–9. doi: [10.1016/j.bmcl.2013.10.003](https://doi.org/10.1016/j.bmcl.2013.10.003). PubMed PMID: 24314671.
2. Kalgutkar AS, Dalvie DK. Drug discovery for a new generation of covalent drugs. *Expert Opin Drug Discov.* [ doi: [10.1517/17460441.2012.688744](https://doi.org/10.1517/17460441.2012.688744)]. 2012 //;7(7): 561-81.
3. Flanagan ME, Abramite JA, Anderson DP, Aulabaugh A, Dahal UP, Gilbert AM, Li C, Montgomery J, Oppenheimer SR, Ryder T, Schuff BP, Uccello DP, Walker GS, Wu Y, Brown MF, Chen JM, Hayward MM, Noe MC, Obach RS, Philippe L, Shanmugasundaram V, Shapiro MJ, Starr J, Stroh J, Che Y. Chemical and Computational Methods for the Characterization of Covalent Reactive Groups for the Prospective Design of Irreversible Inhibitors. *J Med Chem.* [ doi: [10.1021/jm501412a](https://doi.org/10.1021/jm501412a)]. 2014 //;57(23):10072-9.
4. Singh J, Petter RC, Baillie TA, Whitty A. The resurgence of covalent drugs. *Nat Rev Drug Discovery.* [ doi: [10.1038/nrd3410](https://doi.org/10.1038/nrd3410)]. 2011 //;10(4):307-17.
5. Solca F, Dahl G, Zoephel A, Bader G, Sanderson M, Klein C, Kraemer O, Himmelsbach F, Haaksma E, Adolf GR. Target binding properties and cellular activity of afatinib (BIBW 2992), an irreversible ErbB family blocker. *J Pharmacol Exp Ther.* [ doi: [10.1124/jpet.112.197756](https://doi.org/10.1124/jpet.112.197756)]. 2012 //;343(2):342-50.



6. Klingler F-M, Wichelhaus TA, Frank D, Cuesta-Bernal J, El-Delik J, Mueller HF, Sjuts H, Goettig S, Koenigs A, Pos KM, Pogoryelov D, Proschak E. Approved Drugs Containing Thiols as Inhibitors of Metallo- $\beta$ -lactamases: Strategy To Combat Multidrug-Resistant Bacteria. *J Med Chem*. [ doi: [10.1021/jm501844d](https://doi.org/10.1021/jm501844d)]. 2015 //;58(8):3626-30.
7. Natesh R, Schwager SLU, Evans HR, Sturrock ED, Acharya KR. Structural Details on the Binding of Antihypertensive Drugs Captopril and Enalaprilat to Human Testicular Angiotensin I-Converting Enzyme. *Biochemistry*. [ doi: [10.1021/bi049480n](https://doi.org/10.1021/bi049480n)]. 2004 //;43(27):8718-24.
8. Kim KB, Crews CM. From epoxomicin to carfilzomib: chemistry, biology, and medical outcomes. *Nat Prod Rep*. [ doi: [10.1039/c3np20126k](https://doi.org/10.1039/c3np20126k)]. 2013 //;30(5):600-4.
9. Matthews SJ, Lancaster JW. Telaprevir: A Hepatitis C NS3/4A Protease Inhibitor. *Clinical Therapeutics*. [ doi: [10.1016/j.clinthera.2012.07.011](https://doi.org/10.1016/j.clinthera.2012.07.011)]. 2012 //;34(9):1857-82.
10. Rishton G. Reactive compounds and in vitro false positives in HTS. *Drug Discov Today*. 1997;2:382-4.
11. Jadhav A, Ferreira RS, Klumpp C, Mott BT, Austin CP, Inglese J, Thomas CJ, Maloney DJ, Shoichet BK, Simeonov A. Quantitative analyses of aggregation, autofluorescence, and reactivity artifacts in a screen for inhibitors of a thiol protease. *J Med Chem*. 2010;53(1):37-51. PubMed PMID: 19908840.
12. Thorne N, Auld DS, Inglese J. Apparent activity in high-throughput screening: origins of compound-dependent assay interference. *Curr Opin Chem Biol*. 2010;14(3):315-24. PubMed PMID: 20417149.
13. Sink R, Gobec S, Pecar S. False positives in the early stages of drug discovery. *Curr Med Chem*. 2010;17:4231-55. PubMed PMID: 20939815.
14. Jacks A, Babon J, Kelly G, Manolaridis I, Cary PD, Curry S, Conte MR. Structure of the C-terminal domain of human La protein reveals a novel RNA recognition motif coupled to a helical nuclear retention element. *Structure*. 2003;11:833-43. PubMed PMID: 12842046.
15. Shannon DA, Banerjee R, Webster ER, Bak DW, Wang C, Weerapana E. Investigating the proteome reactivity and selectivity of aryl halides. *J Am Chem Soc*. 2014;136:3330-3. PubMed PMID: 24548313.
16. Wei C, Chupak L, Philip T, Johnson B, Gentles R, Drexler D. Screening and characterization of reactive compounds with in vitro peptide-trapping and liquid chromatography/high-resolution accurate mass spectrometry. *J Biomol Screen*. 2014;19(2):297-307. PubMed PMID: 23796688.
17. Weerapana E, Simon GM, Cravatt BF. Disparate proteome reactivity profiles of carbon electrophiles. *Nat Chem Biol*. [ doi: [10.1038/nchembio.91](https://doi.org/10.1038/nchembio.91)]. 2008 //;4(7):405-7.

18. Baeza J, Smallegan MJ, Denu JM. Site-specific reactivity of nonenzymatic lysine acetylation. *ACS Chem Biol*. 2015;10:122–8. PubMed PMID: 25555129.
19. Walters WP, Namchuk M. A guide to drug discovery: designing screens: how to make your hits a hit. *Nat Rev Drug Discov*. [ doi: [10.1038/nrd1063](https://doi.org/10.1038/nrd1063)]. 2003 //;2(4):259-66.
20. Oballa RM, Truchon J-F, Bayly CI, Chauret N, Day S, Crane S, Berthelette C. A generally applicable method for assessing the electrophilicity and reactivity of diverse nitrile-containing compounds. *Bioorg Med Chem Lett*. 2007;17(4):998–1002. PubMed PMID: 17157022.
21. Baell JB, Ferrins L, Falk H, Nikolakopoulos G. PAINS: relevance to tool compound discovery and fragment-based screening. *Aust J Chem*. 2013;66(12):1483–94.
22. Baell JB. Observations on screening-based research and some concerning trends in the literature. *Future Med Chem*. 2010;2(10):1529–46. PubMed PMID: 21426147.
23. Baell JB, Holloway GA. New Substructure Filters for Removal of Pan Assay Interference Compounds (PAINS) from Screening Libraries and for Their Exclusion in Bioassays. *J Med Chem*. 2010;53(7):2719–40. doi: [10.1021/jm901137j](https://doi.org/10.1021/jm901137j). PubMed PMID: 20131845.
24. Zhu W, Groh M, Haupenthal J, Hartmann RW. A detective story in drug discovery: elucidation of a screening artifact reveals polymeric carboxylic acids as potent inhibitors of RNA polymerase. *Chemistry*. 2013;19:8397–400. PubMed PMID: 23681768.
25. Dahlin JL, Nissink JWM, Strasser JM, Francis S, Zhou H, Zhang Z, Walters MA. PAINS in the assay: chemical mechanisms of assay interference and promiscuous enzymatic inhibition observed during a sulfhydryl-scavenging HTS. *J Med Chem*. 2015;58(5):2091–113. PubMed PMID: 25634295.
26. Welch E, Barton E, Zhuo J, Tomizawa Y, Friesen W, Trifillis P, Paushkin S, Patel M, Trotta C, Hwang S, Wilde R, Karp G, Takasugi J, Chen G, Jones S, Ren H, Moon Y, Corson D, Turpoff A, Campbell J, Conn M, Khan A, Almstead N, Hedrick J, Mollin A, Risher N, Weetall M, Yeh S, Branstrom A, Colacino J, Babiak J, Ju W, Hirawat S, Northcutt V, Miller L, Spatrack P, He F, Kawana M, Feng H, Jacobson A, Peltz S, Sweeney H. PTC124 targets genetic disorders caused by nonsense mutations. *Nature*. 2007;447(7140):87–91. PubMed PMID: 17450125.
27. Auld DS, Lovell S, Thorne N, Lea WA, Maloney DJ, Shen M, Rai G, Battaile KP, Thomas CJ, Simeonov A, Hanzlik RP, Inglese J. Molecular basis for the high-affinity binding and stabilization of firefly luciferase by PTC124. *Proc Natl Acad Sci U S A*. 2010;107(11):4878–83. PubMed PMID: 20194791.
28. Auld DS, Thorne N, Maguire WF, Inglese J. Mechanism of PTC124 activity in cell-based luciferase assays of nonsense codon suppression. *Proc Natl Acad Sci U S A*. 2009;106(9):3585–90. PubMed PMID: 19208811.

29. Baell JB. Screening-Based Translation of Public Research Encounters Painful Problems. *ACS Medicinal Chemistry Letters*. [ doi: [10.1021/acsmchemlett.5b00032](https://doi.org/10.1021/acsmchemlett.5b00032)]. 2015 //;6(3):229-34.
30. Gersch M, Kreuzer J, Sieber SA. Electrophilic natural products and their biological targets. *Nat Prod Rep*. 2012;29(6):659–82. PubMed PMID: 22504336.
31. Bruns RF, Watson IA. Rules for Identifying Potentially Reactive or Promiscuous Compounds. *J Med Chem*. [ doi: [10.1021/jm301008n](https://doi.org/10.1021/jm301008n)]. 2012 //;55(22):9763-72.
32. Pearce BC, Sofia MJ, Good AC, Drexler DM, Stock DA. An Empirical Process for the Design of High-Throughput Screening Deck Filters. *J Chem Inf Model*. [ doi: [10.1021/ci050504m](https://doi.org/10.1021/ci050504m)]. 2006 //;46(3):1060-8.
33. Lagorce D, Sperandio O, Baell J, Miteva M, Villoutreix B. FAF-Drugs3: a web server for compound property calculation and chemical library design. *Nucleic Acids Res*. 2015.piiqkv353. PubMed PMID: 25883137.
34. Dahlin JL, Walters MA. The essential roles of chemistry in high-throughput screening triage. *Future Med Chem*. 2014;6(11):1265–90. PubMed PMID: 25163000.
35. Saubern S, Guha R, Baell JB. KNIME workflow to assess PAINS filters in SMARTS Format. Comparison of RDKit and Indigo cheminformatics libraries. *Mol Inform*. 2011;30(10):847–50.
36. Curpan R, Avram S, Vianello R, Bologna C. Exploring the biological promiscuity of high-throughput screening hits through DFT calculations. *Bioorg Med Chem*. 2014;22:2461–8. PubMed PMID: 24656802.
37. Canny SA, Cruz Y, Southern MR, Griffin PR. PubChem promiscuity: a web resource for gathering compound promiscuity data from PubChem. *Bioinformatics*. 2009;28(1):140–1. PubMed PMID: 22084255.
38. Han L, Wang Y, Bryant SH. A survey of across-target bioactivity results of small molecules in PubChem. *Bioinformatics*. 2009;25(17):2251–5. PubMed PMID: 19549631.
39. Hu Y, Bajorath J. What is the likelihood of an active compound to be promiscuous? Systematic assessment of compound promiscuity on the basis of PubChem confirmatory bioassay data. *AAPS J*. 2013;15(3):808–15. PubMed PMID: 23605807.
40. Bologna C, Ursu O, Oprea T, Yang J. BADAPPLE: Bioactivity data associative promiscuity pattern learning engine. [Accessed: 08-03-2015]; Available from: <http://pasilla.health.unm.edu/tomcat/badapple/badapple>;  
See also: <http://www.slideshare.net/jeremyyang/badapple-bard-talk> ACS National Meeting, Sept. 9, 2013, Indianapolis, IN.
41. Wilkens SJ, Janes J, Su AI. HierS: Hierarchical Scaffold Clustering Using Topological Chemical Graphs. *J Med Chem*. [ doi: [10.1021/jm049032d](https://doi.org/10.1021/jm049032d)]. 2005 //;48(9):3182-93.

42. Fernandez Villamil S, Stoppani AOM, Dubin M. Redox cycling of beta-lapachone and structural analogues in microsomal and cytosol liver preparations. *Meth Enzymol.* 2004;378:67–87. PubMed PMID: 15038958.
43. Soares KM, Blackmon N, Shun TY, Shinde SN, Takyi HK, Wipf P, Lazo JS, Johnston PA. Profiling the NIH Small Molecule Repository for compounds that generate H<sub>2</sub>O<sub>2</sub> by redox cycling in reducing environments. *Assay Drug Dev Technol.* 2010;8(2):152–74. PubMed PMID: 20070233.
44. Huth JR, Mendoza R, Olejniczak ET, Johnson RW, Cothron DA, Liu Y, Lerner CG, Chen J, Hajduk PJ. ALARM NMR: a rapid and robust experimental method to detect reactive false positives in biochemical screens. *J Am Chem Soc.* 2005;127(1):217–24. PubMed PMID: 15631471.
45. Ang K, Ratnam J, Gut J, Legac J, Hansell E, Mackey Z, Skrzypczynska K, Debnath A, Engel J, Rosenthal P, McKerrow J, Arkin M, Renslo A. Mining a cathepsin inhibitor library for new antiparasitic drug leads. *PLoS Negl Trop Dis.* 2011;5(5):e1023. PubMed PMID: 21572521.
46. Zhou W, Hur W, McDermott U, Dutt A, Xian W, Picarro SB, Zhang J, Sharma SV, Brugge J, Meyerson M, Settleman J, Gray NS. A structure-guided approach to creating covalent FGFR inhibitors. *Chem Biol.* 2010;17(3):285–95. PubMed PMID: 20338520.
47. Singh J, Petter RC, Baillie TA, Whitty A. The resurgence of covalent drugs. *Nat Rev Drug Discov.* 2011;10:307–17. PubMed PMID: 21455239.
48. Arnold LA, Estebanez-Perpina E, Togashi M, Jouravel N, Shelat A, McReynolds AC, Mar E, Nguyen P, Baxter JD, Fletterick RJ, Webb P, Guy RK. Discovery of small molecule inhibitors of the interaction of the thyroid hormone receptor with transcriptional coregulators. *J Biol Chem.* 2005;280(52):43048–55. PubMed PMID: 16263725.
49. Kwiatkowski N, Zhang T, Rahl P, Abraham B, Reddy J, Ficarro S, Dastur A, Amzallag A, Ramaswamy S, Tesar B, Jenkins C, Hannett N, McMillin D, Sanda T, Sim T, Kim N, Look T, Mitsiades C, Weng A, Brown J, Benes C, Marto J, Young R, Gray N. Targeting transcription regulation in cancer with a covalent CDK7 inhibitor. *Nature.* 2014;511:616–20. PubMed PMID: 25043025.
50. Han H, Yang Y, Olesen S, Becker A, Betzi S, Schönbrunn E. The fungal product terreic acid is a covalent inhibitor of the bacterial cell wall biosynthetic enzyme UDP-N-acetylglucosamine 1-carboxyvinyltransferase (MurA). *Biochemistry.* 2010;49(19):4276–82. PubMed PMID: 20392080.
51. Copeland RA. Evaluation of enzyme inhibitors in drug discovery: a guide for medicinal chemists and pharmacologists. 1st ed. New York: Wiley-Interscience; 2005.

52. Ghebremariam YT, Erlanson DA, Cooke JP. A novel and potent inhibitor of dimethylarginine dimethylaminohydrolase: a modulator of cardiovascular nitric oxide. *J Pharmacol Exp Ther.* 2014;348:69–76. PubMed PMID: 24135074.
53. Foley TL, Rai G, Yasgar A, Daniel T, Baker HL, Attene-Ramos M, Kosa NM, Leister W, Burkart MD, Jadhav A, Simeonov A, Maloney DJ. 4-(3-Chloro-5-(trifluoromethyl)pyridin-2-yl)-N-(4-methoxypyridin-2-yl)piperazine-1-carbothioamide (ML267), a potent inhibitor of bacterial phosphopantetheinyl transferase that attenuates secondary metabolism and thwarts bacterial growth. *J Med Chem.* 2014;57:1063–78. PubMed PMID: 24450337.
54. Ehmann D, Jahic H, Ross P, Gu R, Hu J, Kern G, Walkup G, Fisher S. Avibactam is a covalent, reversible, non- $\beta$ -lactam  $\beta$ -lactamase inhibitor. *Proc Natl Acad Sci U S A.* 2012;109:11663–8. PubMed PMID: 22753474.
55. Copeland RA, Basavapathruni A, Moyer M, Scott MP. Impact of enzyme concentration and residence time on apparent activity recovery in jump dilution analysis. *Anal Biochem.* 2011;416:206–10. PubMed PMID: 21669181.
56. Tarzia G, Antonietti F, Duranti A, Tontini A, Mor M, Rivara S, Traldi P, Astarita G, King A, Clapper JR, Piomelli D. Identification of a bioactive impurity in a commercial sample of 6-methyl-2-p-tolylaminobenzo[d][1,3]oxazin-4-one (URB754). *Ann Chim.* 2007;97(9):887–94. PubMed PMID: 17970304.
57. Engeloch C, Schopfer U, Muckenschnabel I, Goff FL, Mees H, Boesch K, Popov M. Stability of screening compounds in wet DMSO. *J Biomol Screen.* 2008;13(10):999–1006. PubMed PMID: 19029012.
58. Dotterer SK, Forbes RA, Hammill CL. Impact of metal-induced degradation on the determination of pharmaceutical compound purity and a strategy for mitigation. *J Pharm Biomed Anal.* 2011;54(5):987–94. PubMed PMID: 21163601.
59. Simeonov A, Yasgar A, Klumpp C, Zheng W, Shafqat N, Oppermann U, Austin CP, Inglese J. Evaluation of micro-parallel liquid chromatography as a method for HTS-coupled actives verification. *Assay Drug Dev Technol.* 2007;5(6):815–24. PubMed PMID: 18078381.
60. Barbaras D, Brozio J, Johannsen I, Allmendinger T. Removal of Heavy Metals from Organic Reaction Mixtures: Preparation and Application of Functionalized Resins. *Org Process Res Dev.* [ doi: [10.1021/op900102a](https://doi.org/10.1021/op900102a)]. 2009 //;13(6):1068-79.
61. Dorow RL, Herrinton PM, Hohler RA, Maloney MT, Mauragis MA, McGhee WE, Moeslein JA, Strohbach JW, Veley MF. Development of an efficient synthesis of the pyrrolquinolone PHA-529311. *Org Process Res Dev.* [ doi: [10.1021/op050251y](https://doi.org/10.1021/op050251y)]. 2006 //;10(3):493-9.
62. Paulsen CE, Carroll KS. Orchestrating redox signaling networks through regulatory cysteine switches. *ACS Chem Biol.* 2010;5(1):47–62. PubMed PMID: 19957967.

63. Johnston PA, Soares KM, Shinde SN, Foster CA, Shun TY, Takyi HK, Wipf P, Lazo JS. Development of a 384-well colorimetric assay to quantify hydrogen peroxide generated by the redox cycling of compounds in the presence of reducing agents. *Assay Drug Dev Technol.* 2008;6(4):505–18. PubMed PMID: 18699726.
64. Mirkovic B, Sosič I, Gobec S, Kos J. Redox-based inactivation of cysteine cathepsins by compounds containing the 4-aminophenol moiety. *PLOS ONE.* 2011;6(11):e27197. PubMed PMID: 22073285.
65. Lor LA, Schneck J, McNulty DE, Diaz E, Brandt M, Thrall SH, Schwartz B. A simple assay for detection of small-molecule redox activity. *J Biomol Screen.* 2007;12(6):881–90. PubMed PMID: 17579124.
66. Poljak A, Grantb R, Austinc CJD, Jamiec JF, Willowsc RD, Takikawad O, Littlejohn TK, Truscotte RJW, Walkere MJ, Sachdevf P, Smythea GA. Inhibition of indoleamine 2,3 dioxygenase activity by H<sub>2</sub>O<sub>2</sub>. *Arch Biochem Biophys.* 2006;450:9–19. PubMed PMID: 16624246.
67. Di L, Kerns EH. Stability challenges in drug discovery. *Chem Biodivers.* 2009;6(11):1875–86. PubMed PMID: 19937822.
68. Nagy P, Lechte TP, Das AB, Winterbourn CC. Conjugation of glutathione to oxidized tyrosine residues in peptides and proteins. *J Biol Chem.* 2012;287(31):26068–76. PubMed PMID: 22648418.
69. Dahlin JL, Sinville R, Solberg J, Zhou H, Francis S, Strasser J, John K, Hook DJ, Walters MA, Zhang Z. A cell-free fluorometric high-throughput screen for inhibitors of Rtt109-catalyzed histone acetylation. *PLOS ONE.* 2013;8(11):e78877. PubMed PMID: 24260132.
70. Olson ME, Li M, Harris RS, Harkia DA. Small-molecule APOBEC3G DNA cytosine deaminase inhibitors based on a 4-amino-1,2,4-triazole-3-thiol scaffold. *ChemMedChem.* 2013;8(1):112–7. PubMed PMID: 23180603.
71. Bowers EM, Yan G, Mukherjee C, Orry A, Wang L, Holbert MA, Crump NT, Hazzalin CA, Liszczak G, Yuan H, Larocca C, Saldanha SA, Abagyan R, Sun Y, Meyers DJ, Marmorstein R, Mahadevan LC, Alani RM, Cole PA. Virtual ligand Screening of the p300/CBP histone acetyltransferase: identification of a selective small molecule inhibitor. *Chem Biol.* 2010;17(5):471–82. PubMed PMID: 20534345.
72. McCallum MM, Nandhikonda P, Temmer JJ, Eyermann C, Simeonov A, Jadhav A, Yasgar A, Maloney D, Arnold LA. High-throughput identification of promiscuous inhibitors from screening libraries with the use of a thiol-containing fluorescent probe. *J Biomol Screen.* 2013;18(6):705–13. PubMed PMID: 23446699.
73. Mattras H, Aliau S, Demey E, Poncet J, Borgna J-L. Mass spectrometry identification of covalent attachment sites of two related estrogenic ligands on human estrogen

- receptor alpha. *J Steroid Biochem Mol Biol.* 2006;98:236–47. PubMed PMID: 16513342.
74. Huth JR, Song D, Mendoza RR, Black-Schaefer CL, Mack JC, Dorwin SA, Lador US, Severin JM, Walter KA, Bartley DM, Hajduk PJ. Toxicological evaluation of thiol-reactive compounds identified using a la assay to detect reactive molecules by nuclear magnetic resonance. *Chem Res Toxicol.* 2007;20(12):1752–9. PubMed PMID: 18001056.
75. Epps DE, Taylor BM. A competitive fluorescence assay to measure the reactivity of compounds. *Anal Biochem.* 2001;295(1):101–6. PubMed PMID: 11476550.
76. Chung CC, Ohwaki K, Schneeweis JE, Stec E, Varnerin JP, Goudreau PN, Chang A, Cassaday J, Yang L, Yamakawa T, Kornienko O, Hodder P, Inglese J, Ferrer M, Strulovici B, Kusunoki J, Tota MR, Takagi T. A fluorescence-based thiol quantification assay for ultra-high-throughput screening for inhibitors of coenzyme A production. *Assay Drug Dev Technol.* 2008;6(3):361–74. PubMed PMID: 18452391.
77. Bista M, Smithson D, Pecak A, Salinas G, Pustelny K, Min J, Pirog A, Finch K, Zdzalik M, Waddell B, Wladyka B, Kedracka-Krok S, Dyer MA, Dubin G, Guy RK. On the mechanism of action of SJ-172550 in inhibiting the interaction of MDM4 and p53. *PLoS One.* [ doi: [10.1371/journal.pone.0037518](https://doi.org/10.1371/journal.pone.0037518)]. 2012 //;7(6):e37518.
78. Baell J. Screening-based translation of public research encounters painful problems. *ACS Med Chem Lett.* 2015;6(3):229–34. PubMed PMID: 25941544.
79. Schonbrunn E, Betzi S, Alam R, Martin M, Becker A, Han H, Francis R, Chakrasali R, Jakkaraj S, Kazi A, Sebti S, Cubitt C, Gebhard A, Hazlehurst L, Tash J, Georg G. Development of highly potent and selective diaminothiazole inhibitors of cyclin-dependent kinases. *J Med Chem.* 2013;56(10):3768–82. PubMed PMID: 23600925.
80. Dahlin J, Inglese J, Walters M. Mitigating risk in academic preclinical drug discovery. *Nat Rev Drug Discov.* 2015;14(4):279–94. PubMed PMID: 25829283.





# Interference with Fluorescence and Absorbance

Anton Simeonov<sup>1</sup> and Mindy I. Davis<sup>✉2</sup>

Created: December 7, 2015; Updated: July 1, 2018.

## Abstract

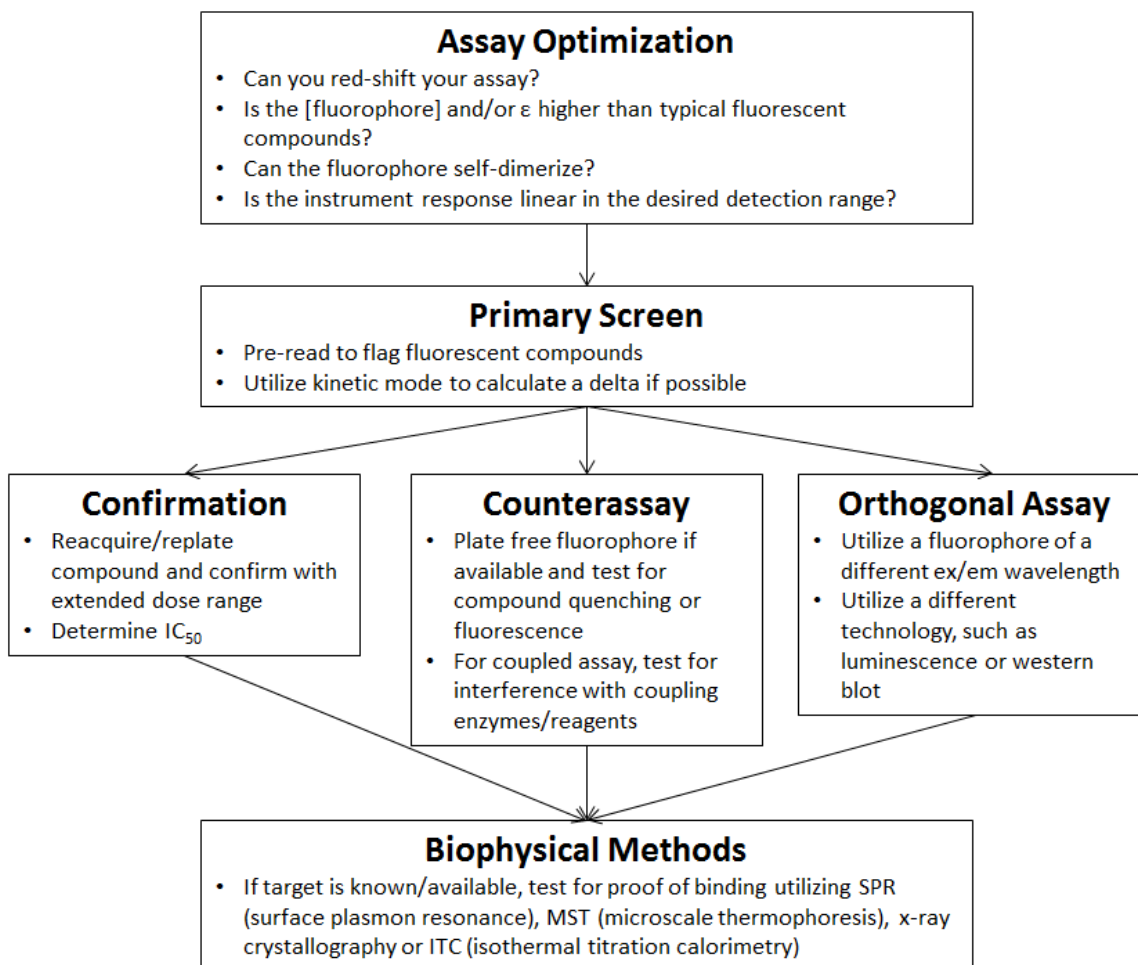
Assays, both high-throughput and lower throughput, are an integral part of the drug discovery process and are used for identifying and validating potential drug candidates. Many biochemical and cell-based assays utilize fluorescence and to a lesser extent absorbance readouts so it is important to consider the impact on the assay quality of a given detection method. There are many fluorophores available that span a wide energy spectrum, and it is important to select the appropriate fluorophore and assay conditions for a given assay to minimize assay interference. Additionally, many of the small molecules found in libraries used for screening are themselves fluorescent, leading to potential false positives through interference. Similarly, for absorbance assays, colored compounds can interfere with the detection method depending on the concentration and extinction coefficient. Assays can be designed to minimize the interference from the library itself, and counterassays can be utilized to identify potential compounds that interfere with the detection method. Orthogonal assays using a different detection method can also be employed to further validate HTS hits. It is important to weed out assay artifacts as early as possible in the drug discovery process to avoid spending time and resources pursuing compounds that are not actually impacting the desired biology but rather are false positives.

---

<sup>1</sup> National Center for Advancing Translational Sciences, National Institutes of Health, Rockville, Maryland, USA. <sup>2</sup> National Center for Advancing Translational Sciences, National Institutes of Health, Rockville, Maryland, USA.

<sup>✉</sup> Corresponding author.

## Flow Chart



## Fluorescence Interferences

### Typical Fluorophores used in High-throughput Screening

Fluorescence is the process by which a molecule absorbs a photon of light exciting an electron to a higher energy state. This electron often relaxes down to the lowest vibrational level of the excited state and then a photon of a longer wavelength (lower energy) is emitted. This shift in energy of the emitted photon relative to excited photon is called a Stokes Shift. Exceptions to this decrease in energy of the emission relative to the excitation can be found in the case of multiphoton excitation, which is beyond the scope of this chapter (1). Fluorescence has been a workhorse for many years in the design of assays for HTS. Examples include fluorescent enzyme substrates or products, coupled assays, fluorescence polarization assays, tracer assays and FRET ratio assays, where in many of these systems detection can be performed in either endpoint or kinetic mode. There is a veritable rainbow of fluorophores described that can be used in assay design (Figure 1).

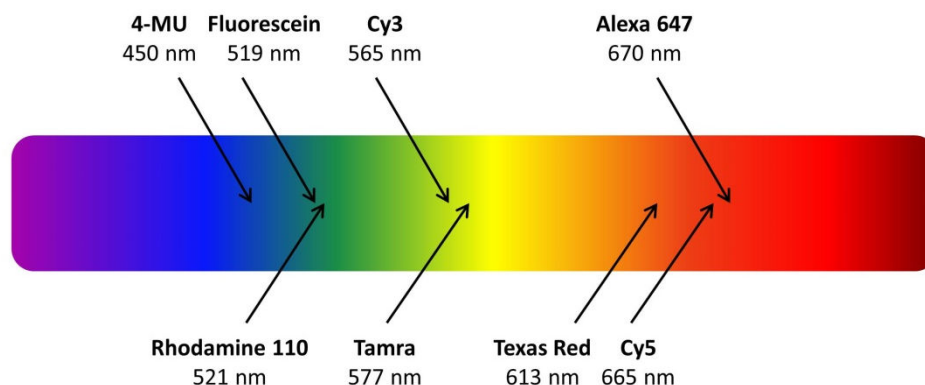


**Figure 1:** Fluorophores are available that span the UV and visible spectrum. Representative commonly used fluorophores are shown with their emission wavelengths indicated.

Table 1 shows eight representative fluorophores commonly used in assays and their excitation (ex) and emission (em) wavelengths. It should be noted that the fluorophores are often not excited at the peak of the excitation spectrum but rather to higher energy to avoid overlap with the emission peak and likewise the emission peak is often detected off of the maximum at lower energy to avoid any bleedover from the excitation peak. There are many spectral viewers and tables of fluorophores available online that can be consulted to select the appropriate wavelength for excitation and emission for a given fluorophore (ex: <http://searchlight.semrock.com/> and <http://www.lifetechnologies.com/us/en/home/life-science/cell-analysis/labeling-chemistry/fluorescence-spectraviewer.html> and <http://aatbio.com/p3400.html>). Additional details on particular fluorophore families can be found in two reviews (2, 3). In addition to using fluorescent molecules in biochemical assays, small molecule fluorophores, such as DAPI/Hoechst dyes, and fluorescent proteins such as GFP (green fluorescent protein), are frequently used in cell-based assay formats. For a given assay design, it is important to recognize the possible sources of false positives due to fluorescence interference as well as false negatives to minimize the cost in time and money for following up on assay artifacts or the cost for missing potential hits, respectively.

It is important to note that fluorophores can have highly conjugated planar systems that can cause issues in assay designs. For example, rhodamine 110 (ex= 497 nm, em= 520 nm), which is planar and has a low net charge, can form dimers, which are detected by the appearance of a higher energy peak (4). Some of the Alexa dyes have higher charge, which can limit the formation of these dimers. Dimer formation results in a decreased assay performance due to self-quenching of the fluorescence, spurious changes in fluorescence polarization as a function of probe concentration, and solubility issues. When a new peptide labeled with rhodamine is ordered, the spectrum can be measured +/- 20% acetonitrile, a condition which dissolves the dimers and should lead to a spectral shift if dimers are present (4). This effect of dimerization is also potentially problematic with

some of the Bodipy dyes, such as Texas Red. Dye pairs with two rhodamines can also be used to develop assay systems for studying protein-peptide interactions, in which an increase in fluorescence upon disruption of the dimer is monitored (4).

**Table 1:** Commonly Utilized Fluorescent Molecules and their Excitation and Emission Wavelengths.

| Fluorophore                               | Excitation (nm) | Emission (nm) |
|---|-----------------|---------------|
| 4-MU <sup>a</sup>                         | 356             | 448           |
| Rhodamine 110 <sup>b</sup>                | 497             | 521           |
| Fluorescein, FITC, Alexa 488 <sup>b</sup> | 492             | 519           |
| Tamra <sup>c</sup>                        | 552             | 577           |
| Cy3 <sup>b</sup>                          | 554             | 565           |
| Texas Red <sup>c</sup>                    | 594             | 613           |
| Alexa 647 <sup>b</sup>                    | 650             | 670           |
| Cy5 <sup>b</sup>                          | 648             | 665           |

Note: the superscript letters after the name of the fluorophore indicate the source of the excitation and emission wavelength information. a = AAT Bioquest, b = Semrock and c = Invitrogen.

## Fluorescence Properties of Small Molecules

The features found in fluorophores, such as conjugated aromatic systems, can also be present in purchased and synthesized compound libraries. Just as luciferase reporter assays could have a hit list overpopulated by luciferase inhibitors, fluorescence assays can have a hit list overpopulated with compounds fluorescent in the region interrogated by the assay (Figure 2) (5, 6). These compounds will likely lead to dose-dependent interference and can thereby mimic a true active in the assay. The majority of assays used in HTS use plate readers with broad band filters. These broad band filters increase the likelihood that a fluorescent compound will interfere with the assay but have the benefit of allowing the same filter set to be used for fluorophores with nearby but not identical excitation and emission.

There are two main mechanisms by which a compound can directly interfere with a fluorescent assay: quenching and autofluorescence. A compound can absorb light itself and through a Beer's Law effect ( $A = \epsilon cl$ ) attenuate the intensity of, i.e., quench, the excitation or emission light from the assay (where  $A$  = absorbance,  $\epsilon$  = extinction coefficient,  $C$  = concentration and  $l$  = pathlength). The unwanted interception of the light entering the assay system or leaving the assay system will affect the readout and could lead to false positives or negatives depending on the particular assay design. This effect is called the inner filter effect and is an intrinsic property of a molecule. The efficiency of quenching is proportional to the extinction coefficient of the molecule and its concentration in the assay.

The second main mechanism is autofluorescence as some compounds found in libraries are themselves fluorescent. If the compound fluorescence overlaps with the region of

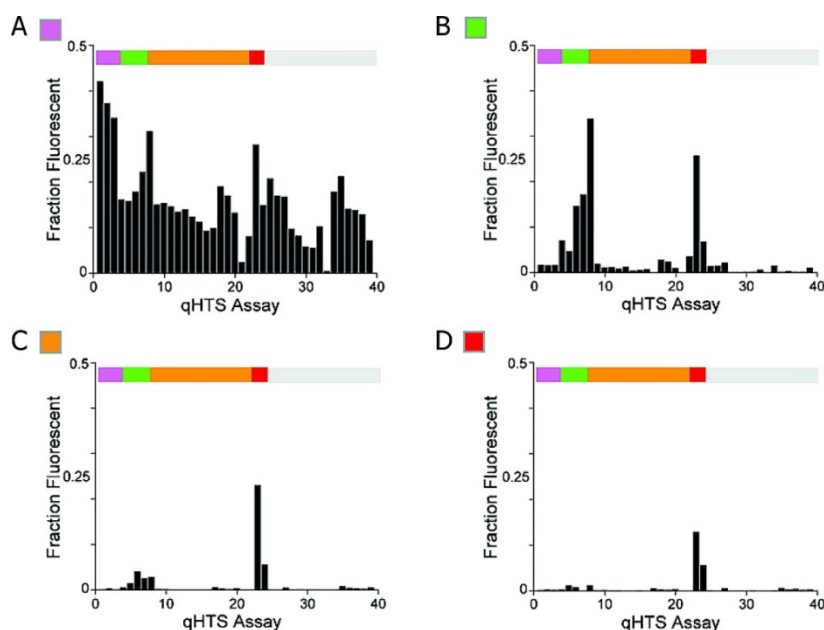


**Figure 2:** Enrichment of fluorescent compounds among the actives in wavelength-relevant regions. A fluorescence profile across 39 qHTS assays is shown, where the fraction of fluorescent compounds out of all actives identified in each screen is plotted for the library members fluorescent in 4-MU (A), fluorescein (B), rhodamine (C), and Texas Red (D) spectral regions. Assays are ordered by the spectral region being measured, ranging from blue (assay 1) to red (assay 24), and assays considered to be wavelength-neutral (assays 25–39, gray overhead bar) Reprinted with permission from (6). Copyright 2008 American Chemical Society.

detection in the assay, the compound can cause interference. The extent of interference will depend on the concentration of the fluorescent molecule in the assay and the concentration of the test compound and their relative fluorescence intensities in the assay conditions. An important consideration is quantum yield  $\phi = (\# \text{ of photons emitted})/(\# \text{ of photons absorbed})$ . Additionally, a compound that is very fluorescent can cause blow out of the signal in adjacent wells, sometimes referred to as a halo effect. Accordingly, fluorescence assays are usually run in black plates, which absorb some of the scattered fluorescence and limit scattering to adjacent wells. For a very weak fluorescent assay, like some HTRF (Homogeneous Time Resolved Fluorescence, Cisbio, <http://www.cisbio.com/usa/drug-discovery/htrf-technology>) assays, white assay plates can be used, such as was used for studying the glucokinase (GCK) and glucokinase regulatory protein (GKRP) interaction (7).

It is important to note that just because a compound is fluorescent or a quencher does not mean that it cannot also have important relevant biological activity. It just means that having an orthogonal method to confirm the activity that would not be subject to fluorescence interference is increasingly important. Examples of successful drugs that are fluorescent include the anthracycline antibiotics doxorubicin, daunorubicin and idarubicin (8).

A detailed fluorescence analysis spanning a 4-log range was conducted on a large chemical library and Table 2 shows the percent of the library that was fluorescent in the different spectral regions at concentrations of test compounds relevant for typical HTS campaigns (6). About 5% of the library was more fluorescent than 10 nM of the UV-active fluorophore 4-methylumbelliferone (i.e., 7-hydroxy-4-methylcoumarin), but by red-shifting the spectral window this rate of interference dramatically dropped (6). In a separate larger library screen, a similar % of the library (5.6%) was found to be auto-fluorescent in the blue spectral region (9). For three assays that utilized readouts in the blue-fluorescent spectral region, blue-fluorescent compounds, which make up just 5% of the tested compounds in the library made up nearly 50% of the identified actives, but when assays employing red-shifted readouts were utilized, the % representation of the blue-fluorescent compounds more closely mirrored their library composition (Figure 2) (6).

**Table 2:** Number and Percentage of Compounds (out of 71 391 Tested) Displaying Fluorescence Equivalents Equal to or Exceeding 100 and 10 nM Standards. Reprinted with permission from (6). Copyright 2008 American Chemical Society.

| Fluorophore standard | >10 nM | % of library | >100 nM | % of library |
|----------------------|--------|--------------|---------|--------------|
| 4-MU                 | 3498   | 4.90         | 1306    | 1.83         |
| AlexaFluor 350       | 3643   | 5.10         | 138     | 1.92         |
| AlexaFluor 488       | 23     | 0.03         | 7       | 0.01         |
| fluorescein          | 119    | 0.17         | 31      | 0.04         |
| resorufin            | 7      | 0.01         | 3       | 0.004        |
| rhodamine            | 7      | 0.01         | 3       | 0.004        |
| Texas Red            | 8      | 0.01         | 1       | 0.001        |
| AlexaFluor 647       | 0      | 0            | 0       | 0            |

## Assay Design Strategies for Common Fluorescence-based HTS Assays to Minimize the Frequency of and Detect Fluorescence Interference

Fluorescent assays are widely used in HTS and direct fluorescence, coupled assays, fluorescence polarization, TR-FRET and DSF will be discussed. A common type of assay includes the consumption or generation of a fluorescent molecule. An example would be IDH1 (isocitrate dehydrogenase 1, an enzyme in the citric acid (TCA) cycle), which utilizes NADP and generates the fluorescent product NADPH, an example of an endogenous fluorophore (10). If the substrates or products of the enzyme reaction of interest are not endogenously fluorescent, a pro-fluorescent substrate can be used that only becomes fluorescent upon enzyme activity. For example, Ubiquitin-rhodamine is frequently used to assess the activity of deubiquitinases, which cleave off the Rhodamine fluorophore leading to an increase in fluorescence (11). These types of assays can be run in either endpoint or kinetic mode, which will be described in more detail below. Using a standard curve, the amount of fluorophore present at the end of the reaction can be calculated and used to design a counterassay that can detect both autofluorescence and

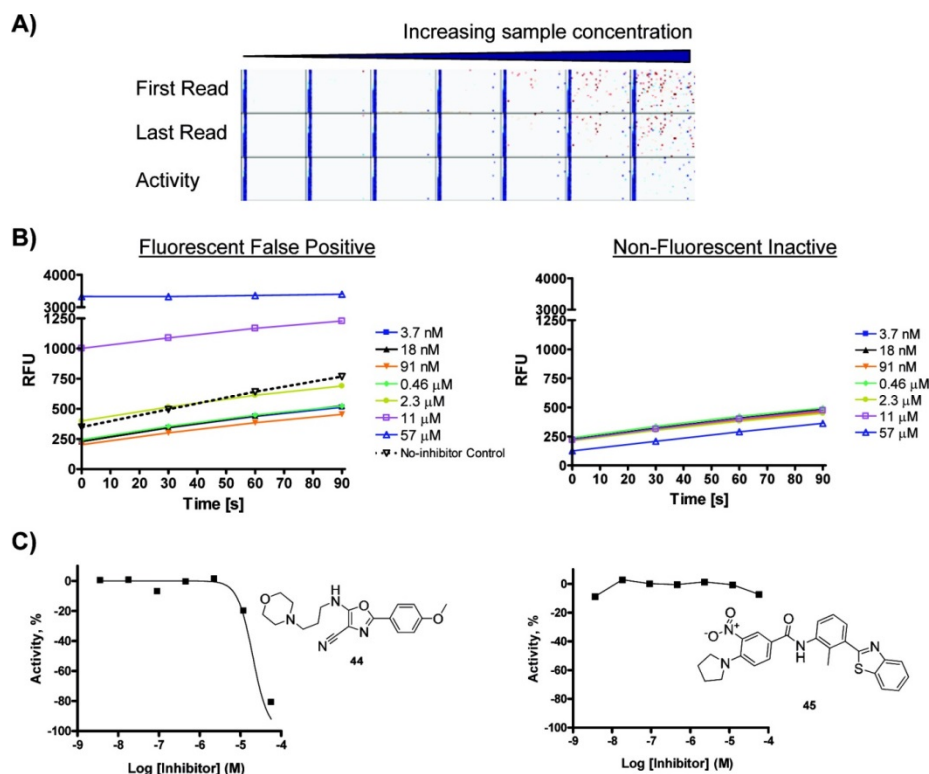


**Figure 3:** Fluorescence interference analysis. (A) Plate heatmaps associated with one seven-concentration compound series in 1536-well format. Shown are the first and last fluorescent reads and the activity calculated from the 60 s initial rates. Subtracting out the higher-than-average but steady fluorescence of some compounds (large number of red dots on heatmaps associated with first and last reads) leads to the significant reduction of interference (small number of blue dots in the activity heatmap). However, for compound 44, which is highly fluorescent (left plots in B and C), the drift in inherent fluorescence within the reaction time course (panel B, left plot) can lead to the erroneous calculation of concentration–response effect (C, left plot). A nonfluorescent inactive compound 45 (right plots in B and C) displays nearly overlapping reaction time courses (B, right plot) and as a consequence the corresponding concentration–response trend is relatively flat, resulting in the correct assignment of inactive phenotype (C, right plot) Reprinted with permission from (9). Copyright 2010 American Chemical Society.

quenchers. The amount of fluorescent substrate and/or products is plated in assay buffer and the effect of compound on the observed fluorescence is measured.

In a typical multistep enzyme reaction, compound is added to enzyme and then after incubation, the reaction is started by the addition of one or more substrates. Prior to initiation of the reaction, a pre-read could be done to assess the intrinsic fluorescence of the added compound. If the assay is run in qHTS format (12) then an  $EC_{50}$  of the fluorescence can be obtained and compared to the  $IC_{50}$  of the reaction. When using a CCD plate reader, such as the Viewlux (PerkinElmer), this pre-read can be very fast and would not impact the overall speed of a large HTS campaign.

Because compound libraries tend to have greater interference in the blue-green spectral region, designing an assay with a red-shifted readout (beyond 500 nm) can dramatically

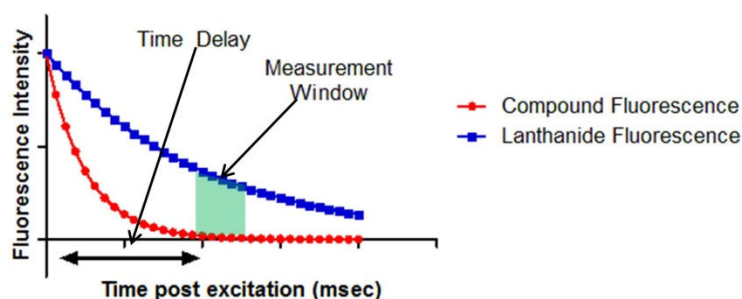


**Figure 4:** TR-FRET principle. By having a time delay between excitation and detection of emission (indicated by double-headed arrow), a measurement window (green trapezoid) can often be obtained in which the compound fluorescence (red) has decayed nearly to baseline and the longer-lived lanthanide (blue) has decayed significantly less.

limit the interference from a library and be a viable option as long as the detector used has effective and sensitive filters for the region of interest (6). This type of strategy has been used successfully for dehydrogenases that produce or use NADPH (ex= 340, em= 435 nm) or NADH, which in turn are substrates for diaphorase, an enzyme that converts resazurin to the fluorescent product resorufin (ex= 530, em= 590 nm) (10). This type of coupled assay can be run in kinetic mode if the product of the enzyme reaction is NADPH or NADH or in endpoint mode if the substrate is NADH or NADPH. The benefits of kinetic mode, when applicable, are described below. As mentioned above, care should be taken not to redshift to a fluorophore that will form dimers under the conditions of your assay (for example, rhodamine).

In some direct fluorescence assay designs, the concentration of the fluorophore is very high in the assay, which will decrease the likelihood of significant interference from the compound library. An example of utilization of a high concentration of fluorophore is an assay for glucocerebrosidase, a target for the treatment of Gaucher disease, in which the  $K_m$  of the pro-fluorescent substrate was very high so its concentration used in the assay was high and the effect of compound fluorescence was negligible (13). This is an example of assay strength where even at low % conversion (5%), the amount of fluorophore generated is high (30  $\mu\text{M}$ ) so there was no observed interference from the compound library even though this assay was in the near UV region. This drop off in interference as the concentration of fluorophore increases is recapitulated in the results shown in Table 2. Additionally, in this case the authors developed two assays that used fluorophores from different spectral regions and interleaved the assays, which can further screen out compounds that interfere with a unique part of the spectral region.

Importantly, rather than using endpoint mode, kinetic mode can be used in which a change in fluorescence readout over time is measured. In most cases, the fluorescence of the test compound will not change in the assay over time so it will be subtracted out. Important exceptions to this would be fluorophores that photobleach in which case the



fluorescence would decrease overtime due to exposure to the excitation light and, likewise, compounds that are exceedingly fluorescent can lead to imperfect subtraction. Kinetic mode is a very powerful method to eliminate many assay artifacts including subtle differences in initial dispense volumes (see Figure 3). For the cysteine protease cruzain, the use of kinetic mode decreased the number of compounds detected as hits due solely to detection interference (9). Additionally, a delta readout can increase the signal-to-background of an assay. For an assay for TGR (thioredoxin glutathionereductase) found in *Schistosoma mansoni* parasites, the signal to background was only 2.1 in endpoint mode but by utilizing kinetic mode a robust assay with a  $Z' = 0.76$  was developed (14). For very fast reactions, the practical implementation of kinetic mode can be challenging due to the finite speed of dispensing reagent, transferring a plate to the reader and reading the plate. By utilizing a plate with a CCD detector, such as the Viewlux, all wells can be detected simultaneously and reactions as short as 5 minutes are feasible by leaving the plate in the detector and collecting readouts in continuous mode every 20-30 seconds. For slower reactions, the readouts can be done in discontinuous mode where after the first read the plate is removed and incubated outside of the plate reader and then reloaded and read at a later time or times. The logistics of these different types of kinetic mode have been described (15).

Another common assay format is fluorescence polarization or FP (16). In this assay design the concentration of the fluorophore tracer can be very high which can affect the apparent  $IC_{50}$  of the test compound but this can be corrected for with the Kenakin equation as described in (17). Conversely if the concentration of the tracer is very low, such as in a Transcreeper assay (BellBrook Labs) that may have tracer in the single digit nM concentration, the assay can be overly sensitive to autofluorescence interferences (even if red-shifted) because the concentrations tested of the library are significantly higher and even the tail of a compound's fluorescence spectrum can overwhelm the tracer signal. For this type of assay, which can be quite prone to interference when the concentration of tracer is quite low, as would be the case for studying a tight-binding pair, in addition to assessing the FP signal, the intensity could be observed and compounds in which the intensity is far greater than the basal would suggest the ability of that compound to interfere with the assay. Just as was done for glucocerebrosidase where two different fluorophores were used in a direct fluorescence assay, this technique was also used in an FP assay for peptidyl prolyl isomerase 1 (Pin1). This FP assay used a peptide tracer labelled with FITC ( $ex = 480$ ,  $em = 540$  nm) or with TAMRA ( $ex = 525$ ,  $em = 598$  nm) as described in Pubchem AID 504891 and 624312. Note that these excitation and emission wavelengths are off of the peak maxima for each fluorophore to avoid bleed-over as described above and also to accommodate available filter sets on the Viewlux plate reader. A compound that was a hit in both assays would be less likely to be the result of fluorescence interference. These two assays could be run either sequentially or in an interleaved fashion (18).

Assay designs in which the fluorophore of interest in the assay has a longer half-life, such as the long half-life of lanthanides, can allow the use of a delay during which the fluorescence of the test compound would dissipate as usual fluorescent half-lives are very

fast and then the emission of the fluorophore in the assay can be measured after the compound autofluorescence has dissipated (Figure 4). A representative delay would be 50-100  $\mu$ s. One type of assay that takes advantage of the longer life of lanthanides is the TR-FRET assay (time-resolved fluorescence resonance energy transfer). An example assay design would be for a protein-protein interaction where each protein is tagged with a unique tag such as GST and a 6x-His tag. Antibodies that are directed at these tags can be labeled with a unique fluorophore. One antibody will have what is called a donor fluorophore on it, this fluorophore will be excited by the instrument excitation energy and will transfer non-radiative energy to the acceptor fluorophore (which is not excited at the same wavelength as the donor) on the other antibody if and only if the two fluorophores are in close proximity, i.e., the proteins that they are targeting are close to each other (7). By monitoring not just the acceptor/donor intensity ratio but also the total intensity, compounds that are autofluorescent or quenchers can be flagged. If dose-dependent effects are seen in both the donor and acceptor channels and not just the acceptor channel, it is probable that the compound is interfering with the detection. There is a helpful paper on reducing compound interference in TR-FRET assays (19). There are two frequently used commercial vendors for TR-FRET assays that have a continually expanding array of assay kits available, as well as toolbox components to develop your own assay (HTRF, Cisbio, <http://www.cisbio.com/usa/drug-discovery/htrf-technology>; Lance, PerkinElmer, <http://www.perkinelmer.com/Resources/TechnicalResources/ApplicationSupportKnowledgebase/LANCE/lance.xhtml> ). The HTRF assay for glucokinase (GCK) and glucokinase regulatory protein (GKRP) interaction is an example that was designed using toolbox reagents targeting the distinct tags on the two proteins (7).

Differential Scanning Fluorimetry (DSF) is another fluorescence-based technique that assesses whether a test compound stabilizes the protein leading to an increase in the melting temperature of the protein, thereby indicating direct binding of the compound to the protein. DSF employs a dye that is sensitive to the hydrophobicity of the environment, with fluorescence increasing with hydrophobicity when the protein melts and such hydrophobic regions are gradually exposed to the solvent, as reviewed in (20). DSF can be miniaturized to 1536 using an instrument such as the Roche Lightcycler enabling this technique to become HTS amenable. Weak binders often need to be screened at high concentrations that may interfere with the detection in much the same way as described above for the other assay types.

It is important to note that for fluorescence-based assays, particularly in the blue/green spectral region, the presence of dust which is often fluorescent in this region can interfere with assay design. Limiting dust and blowing off any observed dust from plates being used for the assay is important. Additionally, running an assay in qHTS mode makes identification of outliers straightforward.

## Absorbance Interferences

For HTS campaigns, fluorescence techniques are far more popular than absorbance based methods. This is due in part to the very short pathlength found in miniaturized assays and the effect of pathlength on the strength of the signal (Beer's law;  $A=\epsilon Cl$ ), causing miniaturized absorbance-based assays to irretrievably lose signal window. For example, in 1536 at a typical assay volume of 5  $\mu\text{L}$  the pathlength of light is  $\sim 0.2\text{--}0.25$  cm, while in a 384-well plate with a typical assay volume of 40  $\mu\text{L}$ , the pathlength is approximately 0.5 cm. In order for the signal to be robust, either the  $\epsilon$  or the concentration, or both, need to be high. Just as fluorescent compounds can interfere with fluorescence assays, colored compounds can interfere with absorbance based assays by the inner filter effect described above. If the  $\epsilon$  is known for the compound of interest the effect on absorbance can be calculated from  $A=\epsilon Cl$  (Beer's Law).

An example of a successful miniaturized absorbance assay is DTNB (Ellman's reagent = 5,5'-Dithiobis(2-nitrobenzoic acid)) that uses mM concentrations of chromophore and since most compounds are assayed in the  $\mu\text{M}$  range, the assay chromophore dominates the readout and little interference will be observed (21). While there are instances where absorbance assays have been successfully employed, oftentimes it is beneficial to seek out fluorescence alternatives as seen in the following example. TGR (thioredoxin glutathionereductase) found in *Schistosoma mansoni* parasites and PRX2 (peroxiredoxin 2) enzymes are important components of the redox cascade in the parasite. A HTS assay was developed to screen for inhibitors of TGR/PRX2 (14). The initial assay design was developed to monitor the decrease in absorbance of NADPH at 340 nm but the authors found that switching to a fluorescent readout lead to an increase in signal strength and minimized quenching and inner-filter effects from the compounds in the library because many of the small molecules and buffer components absorbed in the 340 nm spectral region (14).

## Acknowledgements

The authors would like to acknowledge Steve Titus for his assistance with Table 1 and Figure 1. This work was supported by the NCATS Intramural Research Program and the Molecular Libraries Common Fund Program of the National Institutes of Health. The content of this publication does not necessarily reflect the views of policies of the Department of Health and Human Services, nor does mention of trade names, commercial products, or organizations imply endorsement by the U.S. Government.

## References

1. Denk W, Svoboda K. Photon upmanship: why multiphoton imaging is more than a gimmick. *Neuron*. 1997;18(3):351–7. Epub 1997/03/01. PubMed PMID: 9115730.
2. Lavis LD, Raines RT. Bright ideas for chemical biology. *ACS Chem Biol*. 2008;3(3):142–55. doi: [10.1021/cb700248m](https://doi.org/10.1021/cb700248m). Epub 2008/03/22. doiPubMed Central PMCID: PMC2802578. PubMed PMID: 18355003.

- Lavis LD, Raines RT. Bright building blocks for chemical biology. *ACS chemical biology*. 2014;9(4):855–66. doi: [10.1021/cb500078u](https://doi.org/10.1021/cb500078u). Epub 2014/03/04. doiPubMed Central PMCID: PMC4006396. PubMed PMID: 24579725.
- Geoghegan KF, Rosner PJ, Hoth LR. Dye-pair reporter systems for protein-peptide molecular interactions. *Bioconj Chem*. 2000;11(1):71–7. Epub 2000/01/19. PubMed PMID: 10639088.
- Auld DS, Southall NT, Jadhav A, Johnson RL, Diller DJ, Simeonov A, et al. Characterization of chemical libraries for luciferase inhibitory activity. *J Med Chem*. 2008;51(8):2372–86. doi: [10.1021/jm701302v](https://doi.org/10.1021/jm701302v). Epub 2008/03/28. PubMed PMID: 18363348.
- Simeonov A, Jadhav J, Thomas CJ, Wang Y, Huang R, Southall NT, Shinn P, Smith J, Austin CP, Auld DS, Inglese J. Fluorescence Spectroscopic Profiling of Compound Libraries. *J. Med. Chem*. 2008;51:2363–2371. PubMed PMID: 18363325.
- Rees MG, Davis MI, Shen M, Titus S, Raimondo A, Barrett A, et al. A panel of diverse assays to interrogate the interaction between glucokinase and glucokinase regulatory protein, two vital proteins in human disease. *PloS one*. 2014;9(2):e89335. doi: [10.1371/journal.pone.0089335](https://doi.org/10.1371/journal.pone.0089335). Epub 2014/03/04. doiPubMed Central PMCID: PMC3929664. PubMed PMID: 24586696.
- Perez-Ruiz T, Martinez-Lozano C, Sanz A, Bravo E. Simultaneous determination of doxorubicin, daunorubicin, and idarubicin by capillary electrophoresis with laser-induced fluorescence detection. *Electrophoresis*. 2001;22(1):134–8. doi: [10.1002/1522-2683\(200101\)22:1<134::AID-ELPS134>3.0.CO;2-X](https://doi.org/10.1002/1522-2683(200101)22:1<134::AID-ELPS134>3.0.CO;2-X). Epub 2001/02/24. PubMed PMID: 11197162.
- Jadhav A, Ferreira RS, Klumpp C, Mott BT, Austin CP, Inglese J, et al. Quantitative analyses of aggregation, autofluorescence, and reactivity artifacts in a screen for inhibitors of a thiol protease. *J Med Chem*. 2010;53(1):37–51. doi: [10.1021/jm901070c](https://doi.org/10.1021/jm901070c). Epub 2009/11/17. doiPubMed Central PMCID: PMC2992957. PubMed PMID: 19908840.
- Davis MI, Gross S, Shen M, Straley KS, Pragani R, Lea WA, et al. Biochemical, cellular, and biophysical characterization of a potent inhibitor of mutant isocitrate dehydrogenase IDH1. *J Biol Chem*. 2014;289(20):13717–25. doi: [10.1074/jbc.M113.511030](https://doi.org/10.1074/jbc.M113.511030). Epub 2014/03/29. doiPubMed Central PMCID: PMC4022846. PubMed PMID: 24668804.
- Hassiepen U, Eidhoff U, Meder G, Bulber J-F, Hein A, Bodendorf U, et al. A sensitive fluorescence intensity assay for deubiquitinating proteases using ubiquitin-rhodamine110-glycine as substrate. *Analytical biochemistry*. 2007;371(2):201–7. doi: [10.1016/j.ab.2007.07.034](https://doi.org/10.1016/j.ab.2007.07.034). doi: <http://dx.doi.org>. PubMed PMID: 17869210.
- Inglese J, Auld DS, Jadhav A, Johnson RL, Simeonov A, Yasgar A, et al. Quantitative high-throughput screening: a titration-based approach that efficiently identifies biological activities in large chemical libraries. *Proc Natl Acad Sci U S A*. 2006;103(31):11473–8. doi: [10.1073/pnas.0604348103](https://doi.org/10.1073/pnas.0604348103). Epub 2006/07/26. doiPubMed Central PMCID: PMC1518803. PubMed PMID: 16864780.
- Urban DJ, Zheng W, Goker-Alpan O, Jadhav A, Lamarca ME, Inglese J, et al. Optimization and validation of two miniaturized glucocerebrosidase enzyme assays for high throughput screening. *Comb Chem High Throughput Screen*. 2008;11(10):

- 817–24. Epub 2008/12/17PubMed Central PMCID: PMC2668958. PubMed PMID: 19075603.
14. Simeonov A, Jadhav A, Sayed AA, Wang Y, Nelson ME, Thomas CJ, et al. Quantitative high-throughput screen identifies inhibitors of the *Schistosoma mansoni* redox cascade. *PLoS Negl Trop Dis*. 2008;2(1):e127. doi: [10.1371/journal.pntd.0000127](https://doi.org/10.1371/journal.pntd.0000127). Epub 2008/02/01. doiPubMed Central PMCID: PMC2217675. PubMed PMID: 18235848.
  15. Michael S, Auld D, Klumpp C, Jadhav A, Zheng W, Thorne N, et al. A robotic platform for quantitative high-throughput screening. *Assay and drug development technologies*. 2008;6(5):637–57. doi: [10.1089/adt.2008.150](https://doi.org/10.1089/adt.2008.150). Epub 2008/11/28. doiPubMed Central PMCID: PMC2651822. PubMed PMID: 19035846.
  16. Auld DS FM, Kahl SD, et al. . Receptor Binding Assays for HTS and Drug Discovery. 2012 May 1 [Updated 2012 Oct 1]. 2004-. In: *Assay Guidance Manual* [Internet] Bethesda (MD): Eli Lilly & Company and the National Center for Advancing Translational Sciences [Internet].
  17. Lea WA, Simeonov A. Fluorescence polarization assays in small molecule screening. *Expert Opin Drug Discov*. 2011;6(1):17–32. doi: [10.1517/17460441.2011.537322](https://doi.org/10.1517/17460441.2011.537322). Epub 2012/02/14. doiPubMed Central PMCID: PMC3277431. PubMed PMID: 22328899.
  18. Simeonov A, Yasgar A, Jadhav A, Lokesh GL, Klumpp C, Michael S, et al. Dual-fluorophore quantitative high-throughput screen for inhibitors of BRCT-phosphoprotein interaction. *Analytical biochemistry*. 2008;375(1):60–70. doi: [10.1016/j.ab.2007.11.039](https://doi.org/10.1016/j.ab.2007.11.039). Epub 2007/12/27. doiPubMed Central PMCID: PMC3389998. PubMed PMID: 18158907.
  19. Imbert PE, Unterreiner V, Siebert D, Gubler H, Parker C, Gabriel D. Recommendations for the reduction of compound artifacts in time-resolved fluorescence resonance energy transfer assays. *Assay and drug development technologies*. 2007;5(3):363–72. doi: [10.1089/adt.2007.073](https://doi.org/10.1089/adt.2007.073). Epub 2007/07/20. PubMed PMID: 17638536.
  20. Lea WA, Simeonov A. Differential scanning fluorometry signatures as indicators of enzyme inhibitor mode of action: case study of glutathione S-transferase. *PloS one*. 2012;7(4):e36219. doi: [10.1371/journal.pone.0036219](https://doi.org/10.1371/journal.pone.0036219). Epub 2012/05/05. doiPubMed Central PMCID: PMC3340335. PubMed PMID: 22558390.
  21. Lea WA, Jadhav A, Rai G, Sayed AA, Cass CL, Inglese J, et al. A 1,536-Well-Based Kinetic HTS Assay for Inhibitors of *Schistosoma mansoni* Thioredoxin Glutathione Reductase. *Assay and drug development technologies*. 2008;6(4):551–5. doi: [10.1089/adt.2008.149](https://doi.org/10.1089/adt.2008.149). PubMed PMID: PMC2669305.



# Interferences with Luciferase Reporter Enzymes

Douglas S. Auld<sup>1</sup> and James Inglese<sup>2</sup>

Created: July 1, 2016; Updated: July 1, 2018.

## Abstract

Here we describe the molecular basis underlying interference by inhibitors of reporter enzymes for biochemical and cell-based assays. This understanding is used to create strategies to mitigate the confounding effects reporter enzyme inhibitor interference has on interpreting high throughput screening results, and to aid in evaluating chemical probes derived from reporter gene assays. As well, example compounds that act as potent inhibitors of luciferases are described which can serve as useful tools when developing luciferase-based assays.

## Introduction

This chapter records knowledge learned from studying inhibitors of luciferase enzymes commonly used as reporters in assays. First, an overview of how different types of assays – primary, secondary, counterscreens, and orthogonal, apply to the identification of assay interferences is described. Next, the prevalence of luciferase inhibitors in typical compound screening libraries is shown along with the mechanism by which compounds interfere with luciferases. Inhibitor profiles for ATP-dependent luciferases, such as firefly luciferase, as well as non-ATP-dependent enzymes, such as *Renilla* luciferase, are shown. Finally, methods and strategies that can rapidly identify luciferase inhibitors are defined.

## Assay Artifact Definition

We define artifactual activity as an activity that arises due to a tested substance interfering with the assay signal in a manner that is not related to actual interactions with the biological target/pathway under study or any relationship that is of biological significance to the study. A classic example of such compound-mediated interferences include light scattering or ‘concentration quenching’ the latter of which occurs when a light absorbing compound or impurity, acting through a Beer’s law effect, attenuates the excitation or emission light detected as described in equation 1, where the attenuation of bioluminescence light ( $RLU_0$ ) by a compound with absorbance  $A$  will decrease the emitted light output to  $RLU$  according to equation 1 (1).

$$RLU = RLU_0 \times 10^{-\frac{1}{2}A} \quad (\text{eq. 1})$$

---

<sup>1</sup> Novartis Institutes for BioMedical Research. <sup>2</sup> National Center for Advancing Translational Sciences (NCATS), National Institutes for Health (NIH).

Additional phenomenon resulting in artifactual activity include aggregation of a compound, redox behavior of a compound (2) inhibition of an enzymatic reporter, and complex forms of fluorescence interference by a compound observed in cell-based imaging assay formats (3). We do not include unwanted activity such as cytotoxicity or general transcriptional/translational effects as these have genuine biological mechanisms underlying the activity.

## Role of Primary, Secondary, Orthogonal and Counterscreen Assays in the Identification of Assay Artifacts

Following the primary high throughput screen (HTS), where typically hundreds of thousands to millions of samples are rapidly screened, several types of additional assays are performed with different aims. To avoid confirmation error, the researcher's first goal is to provide evidence for on-target activity through follow-up assay approaches (Figure 1). With this in mind, assays where a negative result is the desired outcome, particularly when this is due to a loss of signal, should be considered carefully before drawing conclusions about the underlying biological mechanism of the observed activity. For example, a typical counterscreen assay employed at the level of early assessment aims to test for direct interference with the detection reagent or cellular system; therefore a negative result in the counterscreen is the desired outcome. In this way, counterscreens only serve to deselect compounds (e.g., a screen for compound fluorescence serving to remove compounds from consideration in a fluorescent assay system) and fail to answer if interesting biological activity is also present. For instance, there is nothing wrong with developing a fluorescent compound provided that there are assays available to accurately measure the activity. Therefore, negative results in counterscreen assays are not as useful as an assay that reinforces *evidence for target activity*.

The most powerful assay for confirming activity of interest is an 'orthogonal' assay which provides *evidence for target activity*. These assays aim to replicate the exact biology as the primary assay but differ in that a single component is changed, such as the method of detection, which should be independent of the targeted biology. In an orthogonal assay a positive result is the anticipated outcome confirming that compound activity does not depend on the detection technology and is likely related to the target/pathway of interest (see flow chart in (4) and 'Orthogonal Cross-Validation Selection Strategy' Table 1 in (5) as examples). On the other hand, a negative result is a strong indication that the primary screen activity was dependent on the detection method, assay format or technique. Positive results in orthogonal assays do not imply that the desired mechanism of activity has been achieved. This requires additional work, for example by the determination of binding affinity and stoichiometry using biophysical techniques for target-based assays (6).

At the early stages of discovery, potentially the least reliable assays to ascertain genuine activity from the primary screen are the so-called secondary assays. There are several reasons for this. By their nature, secondary assays are often low-throughput (e.g. Western analysis, co-culture models, and experiments requiring manual manipulation) and as such



### Counterscreen approach



### Orthogonal approach



### Coincident approach



**Figure 1: General strategies to identify assay interference compounds.** For luciferase assays, counterscreens using the same reporter enzyme but under the control of an alternative promoter or a time course (e.g., for FLuc with D-luciferin for detection) are often used to identify compounds that interfere with luciferase detection, but these approaches only serve to deselect compounds that interfere with the detection. The biological activity of these compounds remains inconclusive unless an orthogonal reporter system is implemented where the same promoter (or biosensor for a pathway) is used in the same cell background but with a different reporter enzyme; ideally two luciferases with inhibitors that are defined by different SARs. In the orthogonal approach, compounds are selected if activity is found in both the primary and orthogonal assays. The coincident approach measures two orthogonal reporter enzymes under the control of a single response element in the same cells using a co-expression strategy, such as the incorporation of ribosome skipping sequences. The coincident approach represents an optimal orthogonal reporter system that can define whether any biological activity of interest is present in one experiment.

require the premature, relatively uninformed selection of HTS actives from an often relatively large pool of candidates. Secondary assays can be less robust, subjected to observation bias, under powered, and are often far less understood in terms of interferences than typical HTS assays. Although, the aim in a secondary assay is to build proof for target activity, positive results often being the goal, negative results may eventually be dismissed if these assays are thought to be of lower quality or have reduced sensitivity. Therefore, before compounds are chosen for secondary assays, we suggest that there be strong positive evidence for target activity obtained in one or more orthogonal assay systems. Finally, throughout the confirmation process the researcher should avoid the “eureka” view and irrational exuberance that often follows the initial identification of potent ‘hits’. Such an attitude can lead one to develop an erroneous narrative from which strong opinions are formed that can persist even when data is subsequently obtained demonstrating the initial findings to be false. Identification of artifacts at the earliest stage possible is crucial to prevent anchoring of misguided opinions.

**Table 1:** Properties of luciferases found as components in HTS assays.

| Enzyme    | Species                                   | MW (kDa) | Em (nm)          | ATP | Substrate               | Stability                   | HTS   |
|-----------|---|----------|------------------|-----|-------------------------|-----------------------------|-------|
| FLuc      | <i>Photinus pyralis</i>                   | 62       | 550-570          | Yes | D-luciferin             | 4.0 hr (cell)               | B & C |
| Ultra-Glo | <i>Photuris pennsylvanica</i> (mutant)    | 61       | 550-570          | Yes | D-luciferin             | >24hrs at 60°C <sup>a</sup> | B     |
| CBLuc     | <i>Pyrophorus plagiophthalmus</i>         | 60       | 537 or 613       | Yes | D-luciferin             | 7.0 hr (cell)               | C     |
| RLuc      | <i>Renilla reniformas</i>                 | 36       | 480              | No  | Coelenterazine          | 4.5 hr (cell)               | B & C |
| RLuc8     | <i>Renilla reniformas</i> (mutant)        | 36       | 480 <sup>5</sup> | No  | Coelenterazine          | 4.5 hr (cell)               | C     |
| GRLuc     | <i>Renilla reniformas</i> (mutant)        | 36       | 530              | No  | Coelenterazine          | 48 hr (cell)                | C     |
| RFLuc     | <i>Luciola cruciata</i> (mutant)          | 62       | 620              | Yes | D-luciferin             | 3.0 hr                      | C     |
| NanoLuc   | <i>Oplophorus gracilirostris</i> (mutant) | 19       | 450              | No  | Furimazine <sup>6</sup> | 6hr (cell) †                | C     |
| GLuc      | <i>Gaussia princeps</i> (mutant).         | 20       | 485              | No  | Coelenterazine          | 60 hr (cell media)          | C     |
| CLuc      | <i>Cypridina noctiluca</i>                | 62       | 465              | No  | Vargulin                | 53 hr (cell media)          | C     |
| TLuc      | <i>Metridia pacifica</i> (mutant)         | 15.7     | 480              | No  | Coelenterazine          | 1 hr (cell) †               | C     |

GRLuc, GLuc-Dura, and RFLuc are mutant forms of the native RLuc enzyme and TLuc (Turbo luciferase) are all commercialized by Thermo Fisher Scientific. GLuc is also available from New England Biolabs. NanoLuc and click beetle luciferases (CBLuc; both green and red emitting variants are available) developed by Promega Corp. The emission of RLuc8 can be blue-shifted to 395 nm using DeepBlueC (coelenterazine-400a). HTS refers to the type of HTS assay where the luciferase is commonly used, B – biochemical, C – cell-based. † Destabilized versions are available with half-lives of <30min in cells.

## Interferences with Reporter Enzymes

### Luciferases as Reporters

One of the most common reporter enzymes employed for constructing HTS assays are luciferases, which generate a bioluminescent signal through oxidation of a luciferin substrate. The two most common luciferases, which have been widely applied in HTS, are firefly luciferase (FLuc; EC 1.13.12.7) from the firefly *Photinus pyralis* and *Renilla* luciferase (RLuc) from the sea pansy *Renilla reniformis*. However, many new luciferases are now available which differ in substrate requirements, stability, emission spectrum and

brightness (Table 1). Luciferases are attractive as assay reporters due to the high signal to background inherent to bioluminescence, largely due to a very low background signal as no excitation light is required to generate a signal (7).

## Prevalence and Structure Activity Relationships of Luciferase Inhibitors

Studies of FLuc inhibitors among large compound libraries show that approximately 5% of the compounds inhibit FLuc at a screening concentration of 11  $\mu$ M (10). In a titration-based screen of the PubChem library against FLuc, 360,864 IC<sub>50</sub> values were determined from a FLuc enzymatic assay (using K<sub>M</sub> levels of D-luciferin and ATP). More than 10K compounds showed potent concentration-response curves and 168 compounds had potencies <100nM with many achieving single-digit nanomolar potency (4). This data is available in PubChem AID: 588342. Screening of the Novartis compound file at 10  $\mu$ M showed a similar hit rate of 4% (at >30% inhibition; (8)). This hit rate is significant as HTS assays using FLuc as a reporter are found to have hit lists which are enriched with FLuc inhibitors. Such enrichments within hit lists can be as high as 98% (9-11).

Common chemotypes which act as inhibitors of FLuc have been published (4, 9, 11-13). The PubChem data (AID: 588342) can also be used as a resource. Here, we provide a summary of the major chemotypes found as inhibitors of FLuc. In general, potent FLuc inhibitors tend to be low molecular weight compounds (published data from PubChem shows a MW<sub>avg</sub> = 325.8  $\pm$  63.3 Da, maximum = 898.8 Da, minimum 122.17 Da; (4)) that have linear, planar structures, while compounds with larger branched configurations show weaker activity. One of the primary classes of inhibitors mimics the D-luciferin (D-LH<sub>2</sub>) structure (2-(6-oxo-1,3-benzothiazol-2-ylidene)-1,3-thiazolidine-4-carboxylic acid; Figure 2) and contain either a benzothiazole, benzoxazole, or benzimidazole core structure (Figure 2; (4, 9)). X-ray co-crystal structures support that simple benzothiazoles bind to the D-luciferin pocket of FLuc (4). Compounds which do not bear resemblance to the D-LH<sub>2</sub> substrate, such as CID:3238892 containing a quinoline core, are also found as enzyme inhibitors. Other inhibitor classes that do not appear to be structurally similar to either D-luciferin or ATP substrates include diaryl structures, such as resveratrol (12) and those containing a 3,5 diaryl-oxadiazole core (4, 9, 14). Compounds containing a *m*-carboxylate group, such as CID:1129835 (PTC124, Translarna<sup>™</sup>; Ataluren), have been shown to be potent inhibitors of the enzyme where the carboxylate group is appropriately positioned in the FLuc active site to form a highly potent adenylate adduct ((14, 15); and see below). Aryl carboxylates with different linkers that have been determined to undergo adenylate formation are shown in Figure 2 (and see (4)). Additionally, certain compounds which bind to the luciferase pocket are large enough and have the appropriate geometry to gain access to at least part of the adenylate pocket (Auld, Inglese *et al.*, unpublished results).

Studies have shown overlap of FLuc inhibitors with some drugs often tested in now popular 'repurposing' studies (see as an example (5), SI Figures 3-5) and important drug target classes. For example, certain FLuc inhibitors are also found as protein kinase inhibitors (PKIs). From a library of 367 PKIs, 10 compounds were found as active against

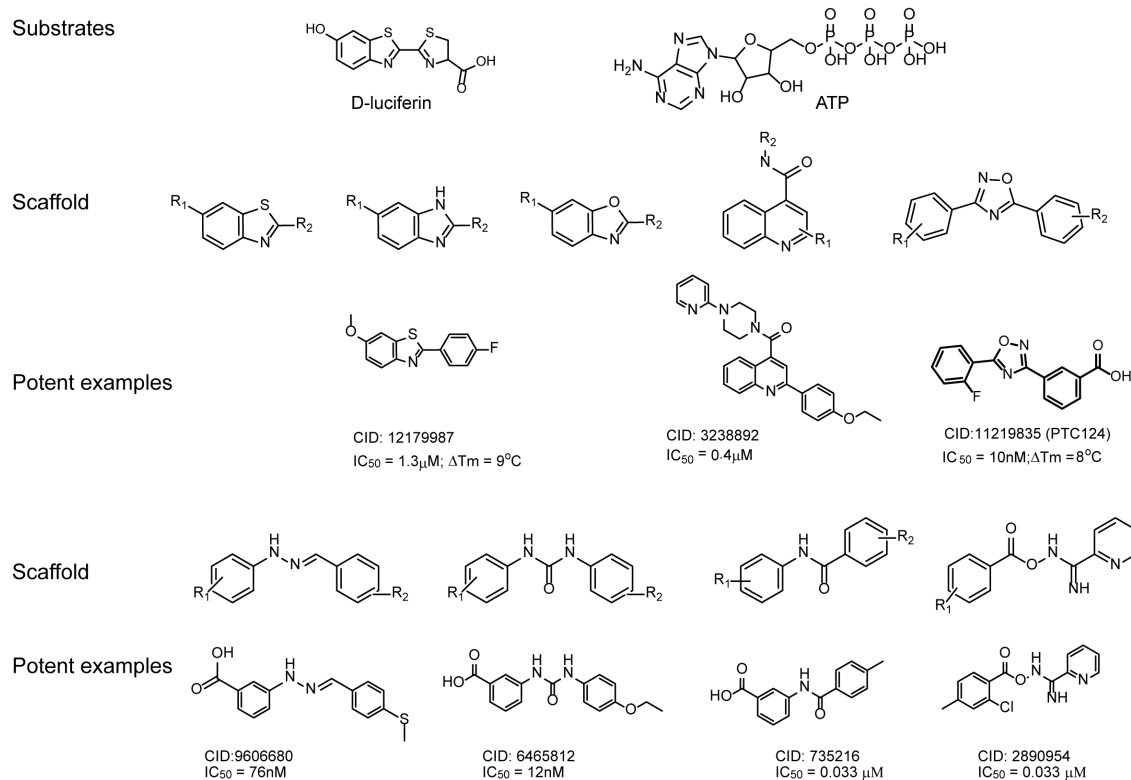


**Figure 2:** Example scaffolds and compounds that are inhibitors of FLuc. Pubchem CIDs are given as well as published potency values and thermal stabilization values when available.

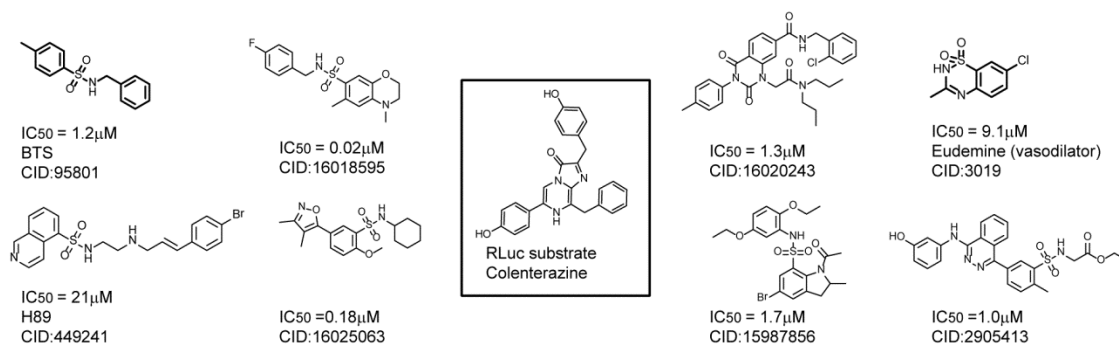


**Figure 3:** Example compounds that are inhibitors of RLuc. Pubchem CIDs are given as well as published potency values (1-4). The substrate for RLuc is shown boxed in the center.

FLuc with IC<sub>50</sub> < 1 μM. FLuc inhibitors were found among tyrosine kinase inhibitors, such as VEGFR-2/TIE-2, as well as GSKβ inhibitors (16). This emphasizes the need for orthogonal assays to determine relevant on-target activity from FLuc inhibitory activity.

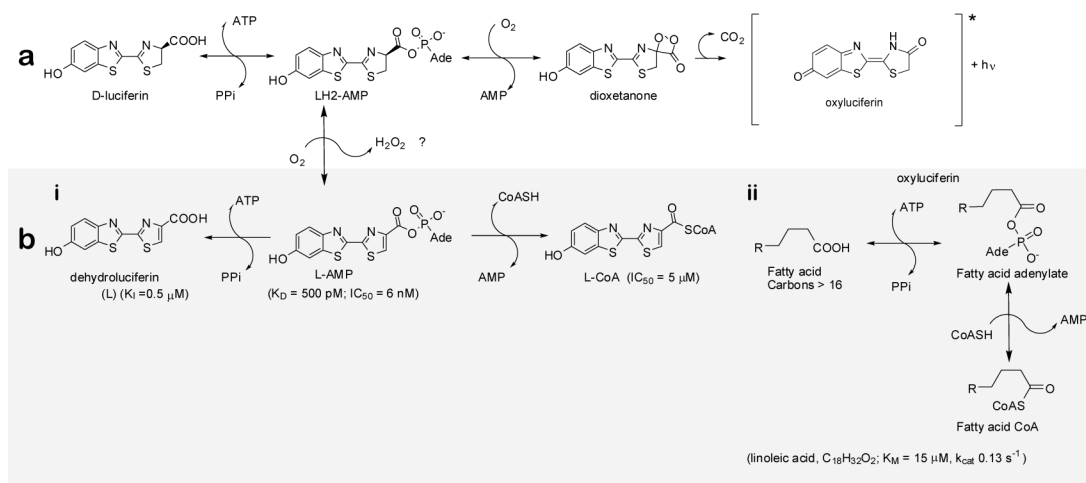


**Figure 5: Reactions catalyzed by FLuc.** (a) The light reaction catalyzed by FLuc. The substrates D-luciferin (D-LH<sub>2</sub>) and ATP are used by FLuc to form a luciferyl-adenylate intermediate (LH<sub>2</sub>-AMP). This intermediate then undergoes nucleophilic attack by molecular oxygen, and upon subsequent displacement of AMP, an unstable dioxetanone is formed, which spontaneously breaks down to form oxyluciferin, and CO<sub>2</sub> with the emission of a photon (6). (b) Dark reactions catalyzed by FLuc are shown in the gray shaded area. (i) One of these involves a side-reaction in which oxidation of LH<sub>2</sub>-AMP occurs to form the potent inhibitor L-AMP, which can undergo pyrophosphorolysis or thiolysis to yield less potent inhibitors, L or L-CoA, respectively (7). (ii) FLuc has also been reported to use certain fatty acids as substrates yielding fatty acyl-CoA metabolites. Kinetic constants for the synthesis of lineoleic acid-CoA are taken from Oba *et al.* (9). Figure adapted with permission from Thorne *et al.*, (10).

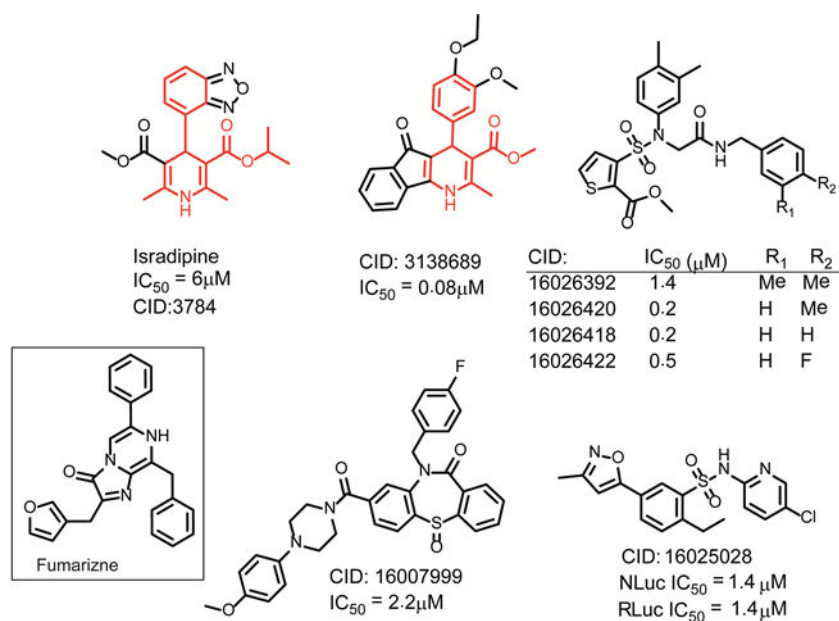


**Figure 4: Example NanoLuc inhibitors.** Common chemotypes acting as inhibitors of NanoLuc include those with a phenyl-1,4-dihydropyridine core as is found in the drug Isradipine. The aryl sulfonamide scaffold found in RLuc inhibitors is also found among NanoLuc inhibitors.

Inhibitors for the commonly used luciferase RLuc have also been published (Figure 3). A prominent class of inhibitors includes those with an aryl sulfonamide core, some of which can achieve potencies of  $<0.1\mu\text{M}$  (8, 17). The well-utilized PKA inhibitor, H89, has this substructure and is an RLuc inhibitor which can confound the interpretation of this compound's activity in cell-based assays using RLuc as a reporter (18). However, in the same library of 367 PKI compounds where FLuc inhibitors were identified, none were potent inhibitors of RLuc, a finding perhaps related to the ATP-independent enzymatic mechanism of RLuc.

A newer luciferase isolated from the deep sea shrimp *Oplophorus gracilirostris* and optimized for stability and brightness by Promega scientists has also been described (Table 1) (19). The optimized luciferase is called NanoLuc™ due to the small molecular weight (19kDa) and superior brightness, partly afforded by the enzyme acting on a colenterazine analog, fumarizine (Figure 4). NanoLuc inhibitors have been described (see Figure 4 for examples) and there is some overlap among RLuc inhibitors (approximately 20%, Figure 4) which is not surprising given the similar substrates used by these enzymes. In contrast, overlap of NanoLuc inhibitors with FLuc inhibitors was found to be approximately ~6% (8, 20).

## Mechanistic Understanding of Firefly Luciferase Inhibitors

The majority of compounds which have been investigated showing luciferase interference act as enzyme inhibitors and many are competitive with the luciferin substrate (4, 8, 9). Ring system analysis of chemotypes that interfere with fluorescent detection shows a different set of scaffolds compared to what is observed in FLuc inhibitors, supporting that FLuc inhibitors are not general light attenuating or light scattering compounds (4, 9). FLuc bioluminescence covers a range of the visible spectrum from 500-600nm and therefore compounds (typically richly colored, blue, black, or red dyes) could quench the luminescent light of FLuc but only at high ( $>10\mu\text{M}$ ) concentrations; attenuation being dependent on the extinction coefficient of the compound at the detection wavelength (9). In contrast, RLuc signal, with an emission maximum near 480nm, can be attenuated by yellow/brown colored compounds that are much more prevalent in typical low molecular weight screening libraries, but again this only becomes significant at high compound concentrations (3, 21).

Firefly luciferase has a complex enzymatic mechanism involving both light producing oxidation of D-LH<sub>2</sub> as well as a few non-luminescent side-reactions (Figure 5). The light producing reaction requires ATP, which FLuc converts to a luciferyl-adenylate intermediate with the release of pyrophosphate (Figure 5a). This intermediate breaks down in the presence of molecular oxygen to form a short-lived dioxetanone intermediate which decays to oxyluciferin with the emission of a photon (Figure 5a). However, it has been known for nearly 50 years that FLuc also forms a dehydroluciferyl-adenylate product which acts as a potent inhibitor of the enzyme (L-AMP; Figure 5b, i) (22). The L-AMP inhibitor can be removed from the enzyme through the binding of CoASH which converts this to a lower affinity L-CoA product. The L-AMP product is an example of a multi-

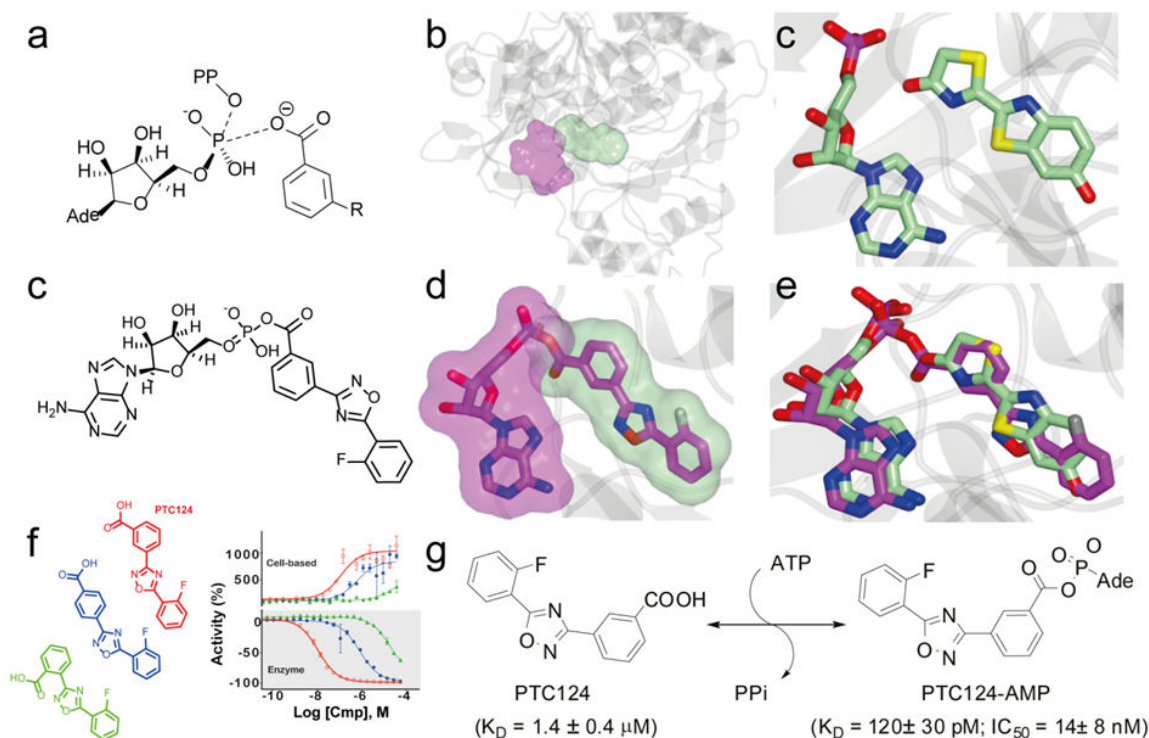


**Figure 6: Mechanism and binding of PTC124 MAI.** (a) The *m*-carboxylate of PTC124 is positioned to attack the  $\alpha$ -phosphate of ATP releasing PTC124-AMP and PPi. (b) The volume of the AMP (purple) and D-LH<sub>2</sub> (green) active site pockets are shown. (c) Relative orientation of AMP and D-LH<sub>2</sub> in the FLuc active site. (c) Structure of PTC124-AMP MAI. (d) X-ray co-crystals showing the bound conformation of PTC124-AMP in the FLuc active site (PDB: 3IES). (e.) Overlay of the FLuc substrates with the MAI. (f) Structures of regioisomers of PTC124 are shown at left and experimental results for the three regioisomers shown at right, for a FLuc RGA (top) and the enzyme assay at  $K_M$  levels of substrate (bottom). Data are from Auld *et al.* (5). (g) MAI formation results in a potent inhibitor, as expected from the product of AMP and PTC124 binding affinities.

substrate adduct inhibitor (MAI) which occurs in some enzymes in rare cases (23). The ability of FLuc to catalyze adenylate formation with certain long chain fatty acids, such as linoleic acid, has also been shown (Figure 5b, ii). These “dark reactions” play a role in the mechanisms of inhibition for certain compounds. A prominent example of a compound that undergoes adenylation by FLuc to form a potent MAI is the compound PTC124 (Translarna™; Ataluren), a compound containing a 3,5 diaryl-oxadiazole that was originally identified in an FLuc-based reporter gene assay (RGA) (24). Mechanistic studies using a variety of analogs, including regioisomers of the aryl carboxylate and X-ray co-crystal structures, have demonstrated that the *m*-carboxylate of PTC124 is in the precise location once bound to the FLuc active site to attack the  $\alpha$ -phosphate of ATP through a  $S_N2$  displacement reaction, forming a phosphoanhydride yielding PTC124-AMP and PPi (Figure 6). The PTC124-AMP ligand binds with high affinity to the FLuc enzyme ( $K_D = 120\text{pM}$ ). Both PTC124 itself and the MAI thermally stabilize the enzyme, but the MAI stabilizes FLuc by more than 10°C (15). X-ray co-crystal structures reveal

that PTC124-AMP binds across the D-LH<sub>2</sub> and ATP sites in FLuc, filling the luciferin pocket and a subspace of the ATP pocket reserved for the adenosine base (Figure 6d). Enzyme stabilization and potency correlate with the apparent activity derived in the FLuc-RGA but not an orthogonal RLuc-RGA and PTC124 is not an inhibitor of RLuc (14, 15). Near-attack conformation modeling and experimental results support that the *m*-carboxylate is optimal for MAI formation with *ortho* and *para* regioisomers showing to be far less optimal for MAI formation, leading to less activity in both the enzyme assay and the FLuc RGA (Figure 6f). The reporter-biased activity of PTC124 has been subsequently confirmed in a study that employed a wide variety of different reporters, demonstrating that PTC124 fails to show activity using alternative RGA systems (25). The basis for this confounding activity lies in the ability of this compound to initially act as a substrate of FLuc, participating in one of the dark reactions, leading to the formation of a potent MAI reminiscent of the naturally occurring L-AMP (Figure 6g). High intracellular ATP concentrations favor MAI formation leading to potent stabilization of FLuc in cells. Ligand-based stabilization leads to a rise in FLuc enzyme levels in compound-treated cells, resulting in an increase in signal relative to untreated cells after cells are lysed and detection reagents are added. Addition of detection reagents, such as BrightGlo, containing high concentrations of substrates, including CoASH, relieves the potent inhibition through formation of PTC124-CoA product, analogous to the L-AMP mechanism. Generally, it has been found that many FLuc inhibitors show increased signals in FLuc-based RGAs when certain detection reagents are used, due to ligand-based stabilization of the enzyme in cells (10). The effect of ligand-based stabilization on FLuc RGAs is described in more detail in the section below.

For coelenterazine non-ATP dependent enzymes, such as RLuc, the mechanisms of inhibition are likely simpler and many appear to be competitive with the coelenterazine substrate. However, to date there is no structural data on RLuc inhibitor complexes analogous to the X-ray co-crystal structures that have been determined for FLuc, so our current understanding on the binding mode of RLuc inhibitors is not well defined.

## Role of Ligand-based Stabilization of Reporter Enzymes in RGA Responses

Protein conformational transitions exist in thermodynamic equilibrium and ligands may bind to a particular conformation, leading to stabilization of that protein state. Ligand-based stabilization of alternative protein conformations forms the basis for allosteric regulation of enzymes (26) and this fundamental property also forms the foundation of many biophysical techniques aimed at confirming ligand binding, including differential scanning calorimetry (27, 28), chemical denaturation experiments (29), as well as methods for identifying the target of compounds (30, 31). In some cases ligand-binding events lead to significant stabilization of the protein structure, although some may decrease stability. However, studies of luciferase inhibitors have shown that many of these act to increase the thermal stability of the enzyme (Figure 7). For the studies of luciferase inhibitors, thermal stabilization is concordant with the potency against the enzyme with potent luciferase inhibitors leading to large  $\Delta T_M$  values ( $\sim 10^\circ\text{C}$ ). The half-life of the free



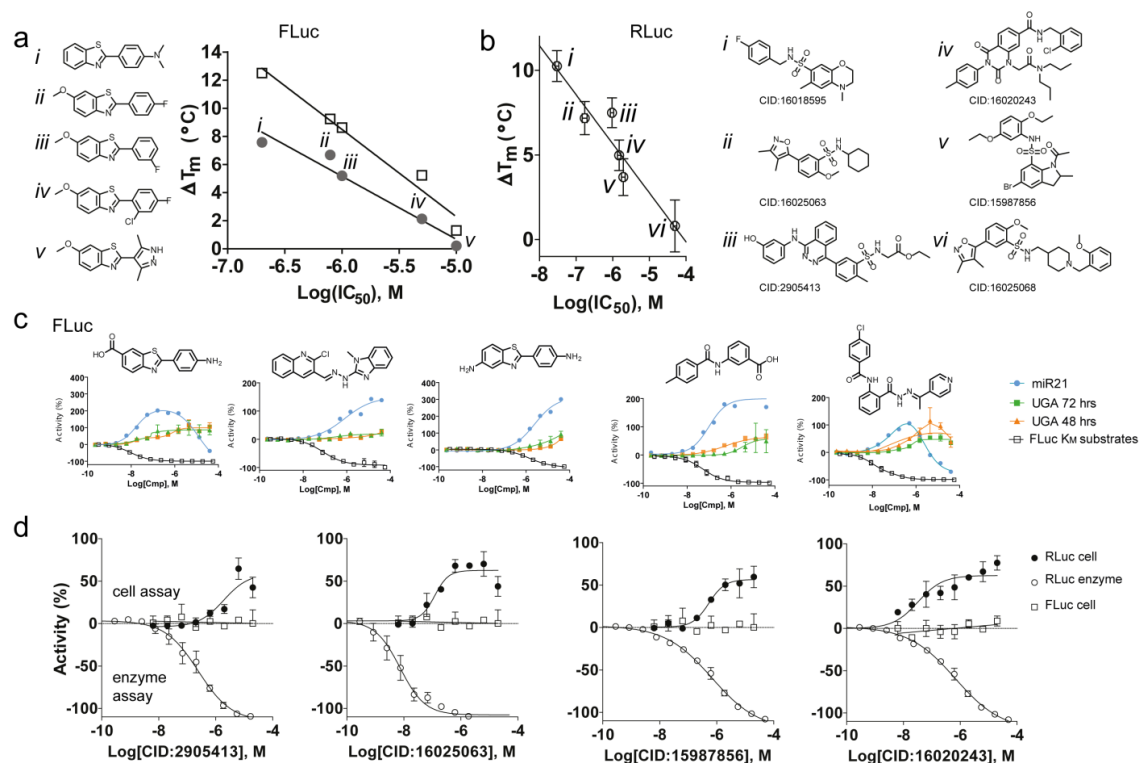


**Figure 7: Thermostabilization of luciferases by inhibitors and effect on cell-based assays. (a).**

Representative simple benzothiazoles and example thermal shift data. The  $\Delta T_M$  values obtained at 100  $\mu\text{M}$  compound in the presence (open squares) or absence (solid circles) of 2 mM ATP are plotted against the potency of each benzothiazole (b) Structures and thermal melt data for RLuc inhibitors. DSF was used to measure the  $T_M$  values of representative RLuc inhibitors differing in potency against the enzyme. Correlation of  $\Delta T_M$  values (taken as the difference between the  $T_M$  at 25  $\mu\text{M}$  compound and apoenzyme) and the measured  $IC_{50}$ 's for the Renilla inhibitors (structures shown in panel B). Compound *vi* showed an estimated  $IC_{50} > 50 \mu\text{M}$  in the enzyme assay. Data shown is from  $n = 3$ , error bars are the SD. (c) CRCs for select FLuc inhibitors comparing their activity in the cell-based assays and biochemical assay. FLuc inhibitors with different MOIs commonly exhibit inhibition of FLuc in the biochemical assay with  $K_M$  concentrations of substrates and produce activation or bell-shaped curves in cell-based assays. The data are the average of replicate determinations ( $n = 3$  or 4, enzyme assay;  $n = 2$  or 3 for cell-based assay), where error bars represent the SD. (d) Behavior of RLuc inhibitors in a FLuc/RLuc-based RGA. Graphs show data from both reporters in the RGA which was provided expression of both FLuc and RLuc in cells from bis-ctronic promoter (data at or above origin; solid circles RLuc activity; open squares FLuc activity, used as an indicator of cell viability in the assay) and the purified RLuc enzyme assay (curves, below origin). Data from RLuc-based RGA ( $n = 2$ ) or enzyme assay ( $n = 4$ ), error bars are SD. All compounds were inactive on FLuc up to 57  $\mu\text{M}$  (FLuc inhibition values taken from PubChem, AID 588342). Figure was adapted with permission from references (4,10).

enzyme in cells for common luciferases such as FLuc and RLuc is  $\sim 4$  hr (see Table 1), therefore inhibitors which stabilize the luciferase can show significant increases in luciferase levels in cells relative to untreated wells within the typical incubation time of most RGAs employed in HTS (12-48 hr). This can lead to the counterintuitive finding where luciferase inhibitors lead to increases in luminescent signal in cell-based assays as

many luciferase inhibitors are competitive with the luciferin substrate and detection reagents contain high concentrations of substrates (4, 9-11). Destabilized luciferases using proteasome targeting sequences, such as PEST, can show greater increases in signal, while more stable enzymes (e.g. NanoLuc) can show a muted activation response due to inhibitors or appear as inhibited in cell-based assays (8). Oftentimes the potency of the activation activity in the cell-based assay will mirror the potency of inhibitory activity in the luciferase enzyme assay (Figure 7).

## Strategies to Mitigate Luciferase Inhibitor Interference

For biochemical assays that employ FLuc to detect ATP levels or use pro-luciferin substrates (e.g. CYP assays and caspases assays; Promega Corp.) one can check for direct interference with the formulated detection mix. For this purpose the enzyme assay can be run to completion or excess product can be added to the assay (in the absence of the enzyme) and detection reagents added to measure if any compounds inhibit the detection reaction (32). For ATP-dependent enzymes, such as protein kinases, orthogonal approaches can be employed through the use of orthogonal readouts, such as TR-FRET or FP, enabled using antibodies toward ADP (33). As well, the use of KinaseGlo and ADPGlo can provide orthogonal assays as the signals for kinase activity proceed in opposite directions, which can be used to test for interferences (34). Promega reagents use an optimized firefly luciferase variant derived from *Photuris pennsylvanica* (UltraGlo, Table 1) and this thermostable variant appears to be less susceptible to inhibitors relative to WT *Photinus pyralis* luciferase (35).

For cell-based assays one can identify luciferase inhibitors using several counterscreen approaches (4). In the case of FLuc, one can detect the activity using D-LH<sub>2</sub> alone (100 $\mu$ M is added to the wells) and the assay can then be read kinetically in live cells (36). In this assay format, FLuc inhibitors will often show inhibition at very early time points. Alternatively, hits can be assayed against the FLuc enzyme using the biochemical enzyme assay that has been described for which all the reagents are commercially available (4, 15). Enzyme assays for RLuc, NanoLuc, and TLuc are also easily constructed for use as counterscreens. For example, Inglese *et al.* used NanoLuc secreted into cell media as a source for a NanoLuc enzyme due to commercial unavailability of purified NanoLuc (37). Comparison to historical datasets using the same reporter can also be used, but one must be cautious when interpreting these results particularly when examining assays that measure an increase in FLuc signal, as the level of activation depends on the basal level of luciferase that is expressed, which is often different between RGA cell lines (4).

Ideally, one should aim to employ an orthogonal reporter to rapidly identify luciferase inhibitors and determine if any activity of interest is present. This approach is superior to the counterscreen approaches mentioned above as these counterscreens can only deselect interfering compounds without being able to determine if these also have interesting activity (Figure 1). Proven orthogonal pairs include FLuc and NanoLuc or FLuc and RLuc (20), FLuc and beta-lactamase (5) and secNLuc and GLuc (37). As mentioned above, FLuc inhibitors overlap little (~6%) with NanoLuc inhibitors while the overlap with FLuc and

RLuc is slightly greater (~10%; (8)). Additional bright luminescent reporter enzymes with a different inhibitor structure activity relationship (SAR) than FLuc include GLuc and TLuc (Table 1). A cell-based orthogonal reporter system has recently been described and is made possible for FLuc/RLuc and FLuc/NLuc as both of these have detection reagents which can be formulated to detect both luciferases from the same well (17, 20). In the optimized reporter system, two orthogonal reporters can be co-expressed in the same cell by incorporating a ribosomal skipping sequence between the two orthogonal reporter pairs which allows for rapid determination of reporter-biased responses using the available dual detection reagents (17). In this so-called coincident reporter system, one seeks to find compounds that are active in both reporter signals; compounds showing activity in only reporter signal are likely reporter inhibitors.

## References

1. Fersht A. Enzyme Structure and Mechanism. 2nd Edition. . W.H. Freeman and Company.; 1984. p. 176.
2. Dahlin JL, Baell J, Walters MA. Assay Interference by Chemical Reactivity: NCBI; 2015 [Sep. 18 2015]. Available from: <http://www.ncbi.nlm.nih.gov/books/NBK53196/>.
3. Simeonov A, Davis MI. Interference with Fluorescence and Absorbance: NCBI; 2015 [December 7, 2015]. Available from: <http://www.ncbi.nlm.nih.gov/books/NBK53196/>.
4. Thorne N, Shen M, Lea WA, Simeonov A, Lovell S, Auld DS, Inglese J. Firefly luciferase in chemical biology: a compendium of inhibitors, mechanistic evaluation of chemotypes, and suggested use as a reporter. *Chem Biol.* 2012;19(8):1060–72. doi: [10.1016/j.chembiol.2012.07.015](https://doi.org/10.1016/j.chembiol.2012.07.015). Epub 2012/08/28. doiPMCID: 3449281. PubMed PMID: 22921073.
5. Jang SW, Lopez-Anido C, MacArthur R, Svaren J, Inglese J. Identification of drug modulators targeting gene-dosage disease CMT1A. *ACS Chem Biol.* 2012;7(7):1205–13. doi: [10.1021/cb300048d](https://doi.org/10.1021/cb300048d). doiPMCID: 3401360. PubMed PMID: 22530759.
6. Klumpp M. Non-stoichiometric inhibition in integrated lead finding - a literature review. *Expert opinion on drug discovery.* 2016;11(2):149–62. doi: [10.1517/17460441.2016.1128892](https://doi.org/10.1517/17460441.2016.1128892). PubMed PMID: 26653534.
7. Fan F, Wood KV. Bioluminescent assays for high-throughput screening. *Assay and drug development technologies.* 2007;5(1):127–36. doi: [10.1089/adt.2006.053](https://doi.org/10.1089/adt.2006.053). PubMed PMID: 17355205.
8. Ho PI, Yue K, Pandey P, Breault L, Harbinski F, McBride AJ, Webb B, Narahari J, Karassina N, Wood KV, Hill A, Auld DS. Reporter Enzyme Inhibitor Study To Aid Assembly of Orthogonal Reporter Gene Assays. *ACS Chem Biol.* 2013;8(5):1009-17. doi: [Doi 10.1021/Cb3007264](https://doi.org/10.1021/Cb3007264). PubMed PMID: WOS:000319720700020.
9. Auld DS, Southall NT, Jadhav A, Johnson RL, Diller DJ, Simeonov A, Austin CP, Inglese J. Characterization of chemical libraries for luciferase inhibitory activity. *J Med Chem.* 2008;51(8):2372–86. doi: [10.1021/jm701302v](https://doi.org/10.1021/jm701302v). Epub 2008/03/28. PubMed PMID: 18363348.

10. Auld DS, Thorne N, Nguyen DT, Inglese J. A specific mechanism for nonspecific activation in reporter-gene assays. *ACS Chem Biol.* 2008;3(8):463–70. doi: [10.1021/cb8000793](https://doi.org/10.1021/cb8000793). Epub 2008/07/02. doiPMCID: 2729322. PubMed PMID: 18590332.
11. Thorne N, Auld DS, Inglese J. Apparent activity in high-throughput screening: origins of compound-dependent assay interference. *Curr Opin Chem Biol.* 2010;14(3):315–24. doi: [10.1016/j.cbpa.2010.03.020](https://doi.org/10.1016/j.cbpa.2010.03.020). Epub 2010/04/27. doiPMCID: 2878863. PubMed PMID: 20417149.
12. Bakhtiarova A, Taslimi P, Elliman SJ, Kosinski PA, Hubbard B, Kavana M, Kemp DM. Resveratrol inhibits firefly luciferase. *Biochemical and biophysical research communications.* 2006;351(2):481–4. doi: [10.1016/j.bbrc.2006.10.057](https://doi.org/10.1016/j.bbrc.2006.10.057). PubMed PMID: 17064666.
13. Thompson JF, Hayes LS, Lloyd DB. Modulation of firefly luciferase stability and impact on studies of gene regulation. *Gene.* 1991;103(2):171–7. PubMed PMID: 1889744.
14. Auld DS, Thorne N, Maguire WF, Inglese J. Mechanism of PTC124 activity in cell-based luciferase assays of nonsense codon suppression. *Proc Natl Acad Sci U S A.* 2009;106(9):3585–90. doi: [10.1073/pnas.0813345106](https://doi.org/10.1073/pnas.0813345106). Epub 2009/02/12. doiPMCID: 2638738. PubMed PMID: 19208811.
15. Auld DS, Lovell S, Thorne N, Lea WA, Maloney DJ, Shen M, Rai G, Battaile KP, Thomas CJ, Simeonov A, Hanzlik RP, Inglese J. Molecular basis for the high-affinity binding and stabilization of firefly luciferase by PTC124. *Proc Natl Acad Sci U S A.* 2010;107(11):4878–83. doi: [10.1073/pnas.0909141107](https://doi.org/10.1073/pnas.0909141107). Epub 2010/03/03. doiPMCID: 2841876. PubMed PMID: 20194791.
16. Dranchak P, MacArthur R, Guha R, Zuercher WJ, Drewry DH, Auld DS, Inglese J. Profile of the GSK published protein kinase inhibitor set across ATP-dependent and-independent luciferases: implications for reporter-gene assays. *PloS one.* 2013;8(3):e57888. doi: [10.1371/journal.pone.0057888](https://doi.org/10.1371/journal.pone.0057888). doiPMCID: 3591448. PubMed PMID: 23505445.
17. Cheng KC, Inglese J. A coincidence reporter-gene system for high-throughput screening. *Nature methods.* 2012;9(10):937. doi: [10.1038/nmeth.2170](https://doi.org/10.1038/nmeth.2170). PubMed PMID: 23018994.
18. Herbst KJ, Allen MD, Zhang J. The cAMP-dependent protein kinase inhibitor H-89 attenuates the bioluminescence signal produced by Renilla Luciferase. *PloS one.* 2009;4(5):e5642. doi: [10.1371/journal.pone.0005642](https://doi.org/10.1371/journal.pone.0005642). doiPMCID: 2680982. PubMed PMID: 19461967.
19. Hall MP, Unch J, Binkowski BF, Valley MP, Butler BL, Wood MG, Otto P, Zimmerman K, Vidugiris G, Machleidt T, Robers MB, Benink HA, Eggers CT, Slater MR, Meisenheimer PL, Klaubert DH, Fan F, Encell LP, Wood KV. Engineered luciferase reporter from a deep sea shrimp utilizing a novel imidazopyrazinone substrate. *ACS Chem Biol.* 2012;7(11):1848–57. doi: [10.1021/cb3002478](https://doi.org/10.1021/cb3002478). doiPMCID: 3501149. PubMed PMID: 22894855.
20. Hasson SA, Fogel AI, Wang C, MacArthur R, Guha R, Heman-Ackah S, Martin S, Youle RJ, Inglese J. Chemogenomic Profiling of Endogenous PARK2 Expression Using a Genome-Edited Coincidence Reporter. *ACS Chem Biol.* 2015. doi: [10.1021/cb5010417](https://doi.org/10.1021/cb5010417). PubMed PMID: 25689131.

21. Simeonov A, Jadhav A, Thomas CJ, Wang Y, Huang R, Southall NT, Shinn P, Smith J, Austin CP, Auld DS, Inglese J. Fluorescence spectroscopic profiling of compound libraries. *J Med Chem.* 2008;51(8):2363–71. doi: [10.1021/jm701301m](https://doi.org/10.1021/jm701301m). PubMed PMID: 18363325.
22. McElroy WD, DeLuca M, Travis J. Molecular uniformity in biological catalyses. The enzymes concerned with firefly luciferin, amino acid, and fatty acid utilization are compared. *Science.* 1967;157(3785):150–60. PubMed PMID: 5339507.
23. Inglese J, Benkovic SJ. Multisubstrate Adduct Inhibitors of Glycinamide Ribonucleotide Transformylase - Synthetic and Enzyme-Assembled. *Tetrahedron.* 1991;47(14-15):2351-64. doi: [Doi 10.1016/S0040-4020\(01\)81773-7](https://doi.org/10.1016/S0040-4020(01)81773-7). PubMed PMID: WOS:A1991FB16500002.
24. Welch EM, Barton ER, Zhuo J, Tomizawa Y, Friesen WJ, Trifillis P, Paushkin S, Patel M, Trotta CR, Hwang S, Wilde RG, Karp G, Takasugi J, Chen G, Jones S, Ren H, Moon YC, Corson D, Turpoff AA, Campbell JA, Conn MM, Khan A, Almstead NG, Hedrick J, Mollin A, Risher N, Weetall M, Yeh S, Branstrom AA, Colacino JM, Babiak J, Ju WD, Hirawat S, Northcutt VJ, Miller LL, Spatrack P, He F, Kawana M, Feng H, Jacobson A, Peltz SW, Sweeney HL. PTC124 targets genetic disorders caused by nonsense mutations. *Nature.* 2007;447(7140):87–91. doi: [10.1038/nature05756](https://doi.org/10.1038/nature05756). PubMed PMID: 17450125.
25. McElroy SP, Nomura T, Torrie LS, Warbrick E, Gartner U, Wood G, McLean WH. A lack of premature termination codon read-through efficacy of PTC124 (Ataluren) in a diverse array of reporter assays. *PLoS biology.* 2013;11(6):e1001593. doi: [10.1371/journal.pbio.1001593](https://doi.org/10.1371/journal.pbio.1001593). doiPMCID: 3692445. PubMed PMID: 23824517.
26. Monod J, Wyman J, Changeux JP. On the Nature of Allosteric Transitions: A Plausible Model. *Journal of molecular biology.* 1965;12:88–118. Epub 1965/05/01. PubMed PMID: 14343300.
27. Ericsson UB, Hallberg BM, Detitta GT, Dekker N, Nordlund P. ThermoFluor-based high-throughput stability optimization of proteins for structural studies. *Anal Biochem.* 2006;357(2):289–98. PubMed PMID: 16962548.
28. Matulis D, Kranz JK, Salemme FR, Todd MJ. Thermodynamic stability of carbonic anhydrase: measurements of binding affinity and stoichiometry using ThermoFluor. *Biochemistry.* 2005;44(13):5258–66. PubMed PMID: 15794662.
29. Mahendrarajah K, Dalby PA, Wilkinson B, Jackson SE, Main ER. A high-throughput fluorescence chemical denaturation assay as a general screen for protein-ligand binding. *Anal Biochem.* 2011;411(1):155–7. doi: [10.1016/j.ab.2010.12.001](https://doi.org/10.1016/j.ab.2010.12.001). PubMed PMID: 21138727.
30. Martinez Molina D, Jafari R, Ignatushchenko M, Seki T, Larsson EA, Dan C, Sreekumar L, Cao Y, Nordlund P. Monitoring drug target engagement in cells and tissues using the cellular thermal shift assay. *Science.* 2013;341(6141):84–7. doi: [10.1126/science.1233606](https://doi.org/10.1126/science.1233606). Epub 2013/07/06. PubMed PMID: 23828940.
31. Nishiya Y, Shibata K, Saito S, Yano K, Oneyama C, Nakano H, Sharma SV. Drug-target identification from total cellular lysate by drug-induced conformational changes. *Anal Biochem.* 2009;385(2):314-20. Epub 2008/12/24. doi: [S0003-2697\(08\)00799-9 \[pii\]](https://doi.org/10.1016/j.ab.2008.12.001)

32. Auld DS, Acker MG. Considerations for the design and reporting of enzyme assays in high-throughput screening applications. *Perspectives in Science*. 2014;1:56–73.
33. Staeben M, Kleman-Leyer KM, Kopp AL, Westermeyer TA, Lowery RG. Development and validation of a transreener assay for detection of AMP- and GMP-producing enzymes. *Assay and drug development technologies*. 2010;8(3):344–55. doi: [10.1089/adt.2009.0254](https://doi.org/10.1089/adt.2009.0254). doiPMCID: 2894640. PubMed PMID: 20158441.
34. Tanega C, Shen M, Mott BT, Thomas CJ, MacArthur R, Inglese J, Auld DS. Comparison of bioluminescent kinase assays using substrate depletion and product formation. *Assay and drug development technologies*. 2009;7(6):606–14. doi: [10.1089/adt.2009.0230](https://doi.org/10.1089/adt.2009.0230). doiPMCID: 3096547. PubMed PMID: 20059377.
35. Auld DS, Zhang YQ, Southall NT, Rai G, Landsman M, MacLure J, Langevin D, Thomas CJ, Austin CP, Inglese J. A basis for reduced chemical library inhibition of firefly luciferase obtained from directed evolution. *J Med Chem*. 2009;52(5):1450–8. doi: [10.1021/jm8014525](https://doi.org/10.1021/jm8014525). doiPMCID: 3430137. PubMed PMID: 19215089.
36. Didiot MC, Serafini S, Pfeifer MJ, King FJ, Parker CN. Multiplexed reporter gene assays: monitoring the cell viability and the compound kinetics on luciferase activity. *Journal of biomolecular screening*. 2011;16(7):786–93. doi: [10.1177/1087057111407768](https://doi.org/10.1177/1087057111407768). PubMed PMID: 21693766.
37. Inglese J, Dranchak P, Moran JJ, Jang SW, Srinivasan R, Santiago Y, Zhang L, Guha R, Martinez N, MacArthur R, Cost GJ, Svaren J. Genome editing-enabled HTS assays expand drug target pathways for Charcot-Marie-tooth disease. *ACS Chem Biol*. 2014;9(11):2594–602. doi: [10.1021/cb5005492](https://doi.org/10.1021/cb5005492). doiPMCID: 4245164. PubMed PMID: 25188731.

# Assay Interference by Aggregation

Douglas S. Auld, Ph.D.,<sup>1</sup> James Inglese, Ph.D.,<sup>2,3</sup> and Jayme L. Dahlin, M.D., Ph.D.<sup>4</sup>

Created: July 26, 2017.

## Abstract

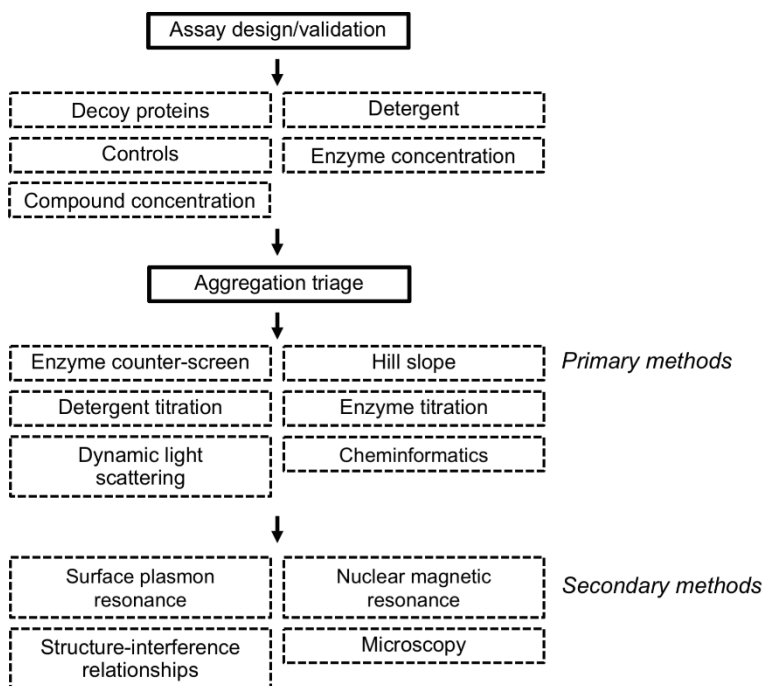
Aggregation is a common mechanism of compound-mediated assay interference encountered in high-throughput screening (HTS) and follow-up experiments. Compounds that form aggregates *in situ* can nonspecifically perturb biomolecules in biochemical and cell-based assays. Nonspecific bioactivity from aggregation can waste significant resources when unaccounted for in assay design and readout interpretation. This chapter describes two general principles: (a) experimental considerations to mitigate the impact of aggregation in bioassays, and (b) counter-screens and other strategies to identify aggregation among bioactive test compounds. This content should be useful for those performing bioassays utilizing small-molecules, including HTS and follow-up assays, chemical biology, and molecular pharmacology.

---

<sup>1</sup> Novartis Institutes for Biomedical Research, Cambridge, MA, USA. <sup>2</sup> National Center for Advancing Translational Sciences, National Institutes of Health, Rockville, MD, USA. <sup>3</sup> National Human Genome Research Institute, Bethesda, MD, USA. <sup>4</sup> Department of Pathology, Brigham and Women's Hospital, Boston, MA, USA; Email: jdahlin@bwh.harvard.edu.

✉ Corresponding author.

## Flowchart



## Abbreviations

|                  |   |
|------------------|---|
| BSA              | bovine serum albumin                          |
| CAC              | critical aggregation concentration            |
| CRC              | concentration response curve                  |
| CMC              | critical micelle concentration                |
| DLS              | dynamic light scattering                      |
| HAT              | histone acetyltransferase                     |
| HTS              | high-throughput screening                     |
| IC <sub>50</sub> | half-maximal inhibitory concentration         |
| K <sub>d</sub>   | dissociation constant                         |
| MLSMR            | Molecular Libraries Small Molecule Repository |
| NMR              | nuclear magnetic resonance                    |
| qHTS             | quantitative HTS                              |
| SIR              | structure-interference relationships          |
| SPR              | surface plasmon resonance                     |
| TEM              | transmission electron microscopy.             |



## Introduction and Background

### Introduction

Drug and chemical probe discovery often utilizes real and virtual high-throughput screening (HTS) to identify chemical matter for subsequent optimization. HTS readouts from biochemical and cell-based systems are subject to a variety of compound-mediated assay interferences, including aggregation (1). The apparent bioactivity derived from aggregation is often difficult to optimize, and if not recognized early in the discovery process, it can result in significant wasted resources and questionable conclusions derived from these experiments. This section provides an overview of the prevalence and mechanistic details of aggregation in HTS.

### Mechanism of Assay Interference by Aggregation

Understanding the mechanisms of aggregation is important because it can inform data interpretation and counter-screen design. Aggregation occurs when susceptible test compounds form aggregates in solution (colloids) (**Figure 1**). For these compounds, aggregation occurs at a critical aggregation concentration (CAC), which is typically in the low-to-mid micromolar compound concentration range. Unlike simple compound precipitation, aggregates can dissolve when diluted below the CAC (2). These solid colloids are composed of up to  $10^8$  small-molecules and are several hundred nanometers in mean diameter (n.b. some polydispersity), present in mid-femtomolar concentrations when formed, and are therefore not typically observed by visual inspection like compound precipitation (2,3). For enzyme systems (the most well-characterized system for aggregators), bioactivity results from a *reversible* association between enzyme and aggregate surface (4,5). It is currently thought that this binding represents protein *adsorption*, rather than *absorption*, with activity modulation occurring by partial protein unfolding (6). This nonspecific binding typically results in enzymatic inhibition. Furthermore, the affinity of aggregate-protein binding is quite strong, with  $K_D$  values in the picomolar range. By contrast, aggregates do not appear to have high affinities for other biomolecules such as DNA or peptides (3). However, aggregates may still interfere with protein-DNA/RNA binding assays through sequestration of the protein component. Individual aggregates can bind up to 10,000 individual enzymes (2). Interestingly, proteins bound to aggregates can retain their activity upon dissociation (“catch and release”) (5).

Notably, certain compounds may form “non-classical”, *smaller* aggregates capable of modulating protein structure and function. For example, the small-molecule JNJ525 showed apparent low micromolar activity in a TNF $\alpha$ -TNFR1/2 TR-FRET protein-protein interaction assay (7). Like conventional aggregators, this compound showed detergent-sensitive activity and steep Hill slopes in the primary biochemical assay. Detailed mechanistic studies including x-ray crystallography revealed JNJ525 binds TNF $\alpha$  as an ordered 5-member aggregate, disrupting the TNF $\alpha$ -TNF $\alpha$  protein-protein interaction and preventing TNF $\alpha$ -TNFR1/2 association.

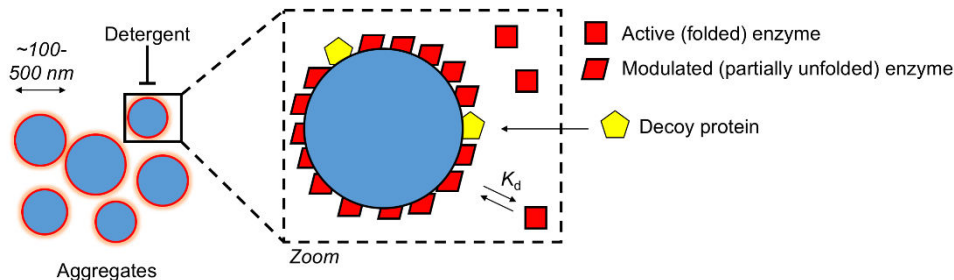


**Figure 1. Current model of aggregation.** Above the CAC, compounds form solid aggregates, typically 100-500 nm in mean diameter. Enzyme then adsorbs to the aggregate surface with high affinities (e.g.,  $K_d$  = picomolar to nanomolar ranges). Adsorbed proteins are partially unfolded, which can modulate activity. Free, unperturbed protein occurs when the aggregates become saturated. When present in sufficient concentrations, detergents can disrupt aggregates. Decoy proteins such as BSA can compete with enzyme for adsorption to aggregate surfaces

Importantly, aggregation can be dependent on multiple experimental factors, including the structure of the test compound, the assay conditions, and the susceptibility of a given target system to aggregates. For example, it is well known that the CAC for aggregators is compound-specific (e.g., some compounds may aggregate at 5  $\mu\text{M}$ , whereas others may only aggregate at 50  $\mu\text{M}$  compound concentrations). In a series of surface plasmon resonance (SPR) experiments, aggregates showed compound-dependent behavior versus the same target (8). In other words, not all aggregates behave the same way versus the same target. Furthermore, studies of the same aggregators versus different targets demonstrate proteins have different susceptibilities to aggregation (9,10).

Such varying responses to different aggregates may reflect differences in specific compound-aggregate affinities. For instance, a given aggregate may have protein-dependent affinities, as recent reports with dye-stabilized compound aggregates demonstrated up to 90-fold differences in apparent affinities between four unrelated proteins (3). These varying responses may also be explained by the nature of specific protein dynamic perturbations induced by a given aggregate. Depending on the tertiary structure of a given protein, aggregate adsorption may significantly perturb protein structural dynamics and function, while in other cases it may cause no appreciable changes.

## Prevalence of Aggregation in HTS

Aggregation is a significant source of nonspecific bioactivity, particularly in HTS. In a seminal study screening a 70,563-member Molecular Libraries Small Molecule Repository (MLSMR) library for AmpC  $\beta$ -lactamase inhibition, 1204/1274 (95%) of the *primary actives* were identified as aggregators (10). Overall, 1.7% of the entire library was flagged as a likely aggregator in this HTS due to detergent-sensitive bioactivity. In another MLSMR HTS for cruzain inhibition, 1.9% of the 197,861-compound library and approximately 90% of the primary actives showed detergent-sensitive inhibition, behavior consistent with aggregation (11). Based on these studies, one could estimate that

compounds capable of forming aggregates constitute less than 5% of HTS libraries. These studies also demonstrate that if an assay is not properly designed, the vast majority of primary actives can result from aggregation. The main consequences of enriching active compounds with aggregation is that significant resources are spent chasing aggregates in place of potentially more tractable chemical matter.

## Section Summary

Aggregation represents a significant source of nonspecific bioactivity and compound-mediated assay interference in HTS and related experiments. Aggregation occurs at compound- and assay-specific critical compound concentrations, and promotes nonspecific activity through partial protein unfolding. Understanding the mechanism of aggregation allows for (a) strategies to mitigate the incidence of aggregation interference, and (b) the design of counter-screens to identify bioactivity due to aggregates.

## Strategies to Mitigate Incidence of Aggregation in Biochemical Assays

### Introduction

This section describes several experimental strategies and technical considerations to reduce the incidence of aggregation in biochemical assays (n.b., strategies for cell-based assays are less characterized). Strategies discussed include the use of detergents and decoy proteins to prevent aggregate formation, the choice of enzyme and compound concentrations to mitigate the effects of aggregates on assay readouts, and control compounds to characterize the effects of aggregation on assay readouts.

### Detergents

Perhaps the single-most effective strategy to prevent aggregation is to include detergents in assay buffers (4,9,12,13). These reagents act by disrupting colloid structure and can raise the CAC. With most aggregators, activity is dramatically attenuated by the inclusion of detergents (**Figure 2**). In many instances, the addition of detergent can also reverse nonspecific protein modulation by aggregation (4). Another benefit of including detergents is the prevention of nonspecific protein adsorption to container walls, thus preventing time-dependent losses in enzyme activity and decreasing the amount of required enzyme.

There are several choices of detergents to prevent colloid formation, with most being nonionic (**Table 1**). The most popular and well-characterized detergent with respect to aggregation is Triton X-100, which is often used at 0.01% (v/v) final concentrations. A common misconception is that using these “default” detergent conditions will completely eliminate assay interference and nonspecific bioactivity from aggregation. While this concentration is a helpful starting point, it does *not* absolutely prevent colloid formation for every compound. Detergents vary greatly in properties (**Table 1**) and detergents such

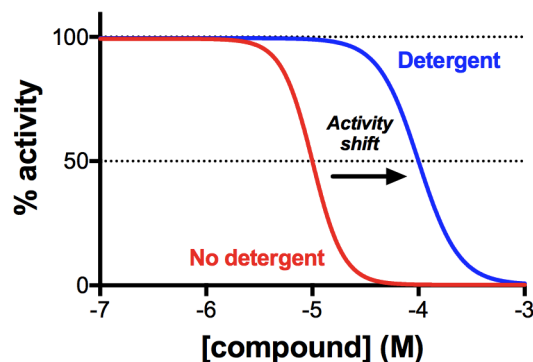


**Figure 2. Detergent-dependent activity of aggregators.** Shown is a simulation of a prototypical aggregator assayed without (red line;  $IC_{50} = 10 \mu M$ ) and with detergent (blue line;  $IC_{50} = 100 \mu M$ ). Sufficient amounts of detergent will typically attenuate bioactivity due to aggregation, as illustrated by the activity shift.

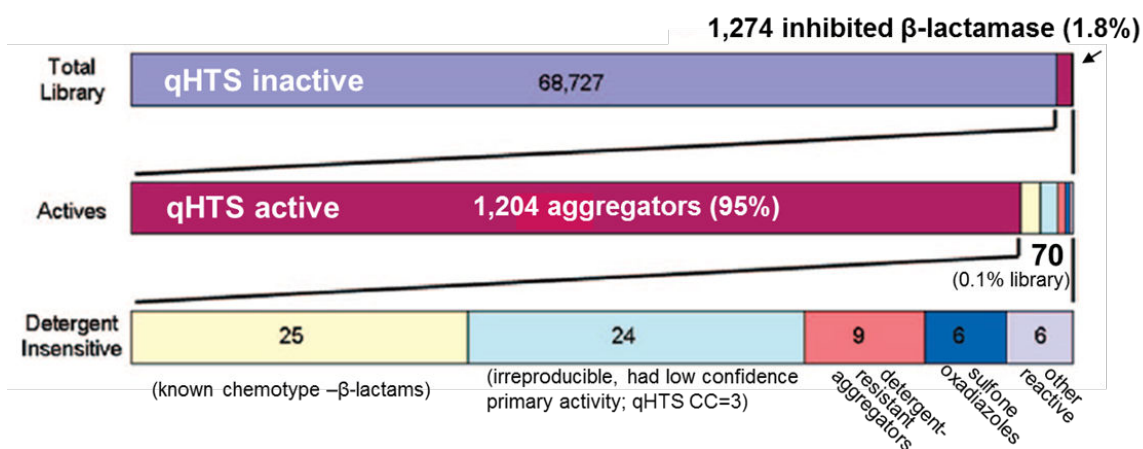


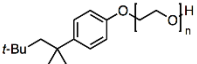
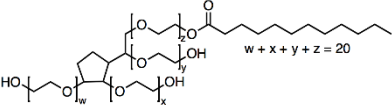
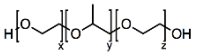
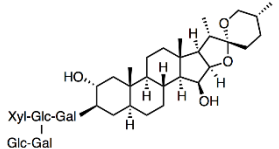
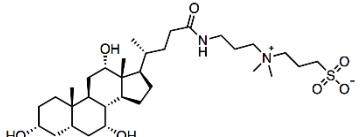
**Figure 3. Mechanistic analysis of actives from a  $\beta$ -lactamase biochemical HTS dominated by aggregators.** Using quantitative HTS (qHTS), ~70 K compounds were assayed for  $\beta$ -lactamase inhibition. The active compounds (1.8%) were analyzed for detergent-sensitive inhibition, which accounted for 95% of the primary qHTS actives. The remaining 5% of detergent-insensitive compounds (70 compounds) included  $\beta$ -lactam-based inhibitors, irreproducible samples, nonspecific reactive substances, and detergent-resistant aggregators. Detergent-resistant aggregators comprise only 0.7% of the aggregators identified. (adapted with permission from K Babaoglu *et al.* *J Med Chem*, 2008) (15)

as Triton X-100 can form very large micelles at concentrations at or above the critical micelle concentration (CMC) which are difficult to remove from proteins. Therefore, detergent concentrations that are well above the CMC should be avoided and one should verify that the complete assay system (e.g., target, reagents, readout, instrumentation) is compatible with the proposed detergent under the conditions to be tested.

A representative example of detergent effects on the distribution of HTS actives can be seen in a comprehensive study exploring the mechanistic basis of the actives from a  $\beta$ -

lactamase HTS (15). Detergent sensitivity was used to establish the preponderance of actives that were a result of aggregation, with remaining mechanisms consisting of nonspecific reactive compounds, PAINS-like compounds, and *bona fide* AmpC  $\beta$ -lactamase inhibitors, the latter comprising < 2% of the HTS actives (**Figure 3**) (1,15,16).

**Table 1.** Example detergents used in biochemical assays. CMC, the critical micelle concentration, or the concentration at which the detergent begins to form micelles. Aggregation number, the number of detergent molecules in a micelle.

| Detergent      | Chemical structure  | Ionic / nonionic | CMC <sup>a</sup>                         | Detergent aggregation number | Technical notes  |
|----------------|---|------------------|--|------------------------------|--|
| Triton X-100   |    | Nonionic         | 0.2-0.9 mM (20-25 °C)<br>0.01% = 0.16 mM | 100-155                      | Often used at 0.01% (v/v) or higher; can produce H <sub>2</sub> O <sub>2</sub> in aqueous solutions (14) (recommend preparing fresh buffers for experiments) |
| TWEEN-20       |  | Nonionic         | 0.06 mM (20-25 °C)<br>0.001% = 0.8 mM    |                              |  |
| Pleuronic F-68 |  | Nonionic         | 0.04 mM (20-25 °C)<br>0.01% = 0.1 mM     |                              |  |
| Saponin        | Variable  | Nonionic         |  |                              |  |
| Digitonin      |  | Nonionic         | < 0.5 mM (20-25 °C)                      | 60                           |  |
| CHAPS          |  | Ionic            | 6 mM<br>0.01% = 1.6 mM                   | 10                           |  |

<sup>a</sup> Data obtained from manufacturer (Sigma-Aldrich)

## Decoy Proteins

Another tactic to mitigate the effects of aggregation is the addition of decoy proteins. The current model for this phenomena involves pre-saturation of aggregates by relatively high concentrations of decoy protein, leaving the biomolecule of interest (e.g., target enzyme) unperturbed by the aggregates.

The prototypic example is the carrier protein bovine serum albumin (BSA). High concentrations of BSA can prevent nonspecific enzymatic modulation by several known aggregators when BSA is present in the assay before the addition of aggregators (17). Importantly, high concentrations of BSA do not routinely reverse enzyme modulation (17).

Several important technical points should be noted:

- A suggested starting concentration for BSA is 0.1 mg/mL.
- Because they do not reverse bioactivity from aggregation, BSA or other proteins should be present in the assay system *before* the addition of test compound.
- Carrier proteins have the potential to sequester monomeric test compounds, lowering the free test compound concentration. This effect may be pronounced at high protein:compound ratios.
- Verify high concentrations of aggregate decoy proteins such as BSA do not interfere with the assay readout or disrupt assay performance. For example, free thiols on untreated decoy proteins may react with assay reagents or electrophilic test compounds.

## Enzyme Concentration

For enzymatic biochemical assays, another proposed tactic to mitigate the effects of nonstoichiometric bioactive compounds (such as aggregators) is to simply increase the concentration of target enzyme (18). This approach is based on a proposed stoichiometric model of enzyme inhibition for aggregators (**Equation 1**) (19):

$$\frac{[I]}{K_d} = \frac{\text{inh \%}}{100 - \text{inh \%}} + \frac{\left[\frac{(\text{inh \%})}{100}\right][E]}{K_d} \quad \text{Equation 1}$$

In this model, enzyme inhibition will appear stoichiometric in cases when enzyme concentration significantly exceeds the  $K_d$  value of the inhibitor. This is not an unreasonable assumption for aggregators (recall that many aggregators appear to have  $K_d$  values in the low picomolar range). In other words, the  $IC_{50}$  value of an aggregator will increase linearly with increases in enzyme concentration. In this model, non-aggregating compounds are not expected to have such dramatic shifts in  $IC_{50}$  values unless they have low  $K_d$  values, which is unlikely when screening non-optimized chemical matter versus a novel target.

This technique is not without its drawbacks. Aside from consuming more enzyme per test compound, a potential downside to this tactic is that by increasing the amount of enzyme,

reactions will proceed faster (18). A practical consequence is that it may be more difficult to sample reactions at low substrate turnover/product formation.

## Compound Concentration

Another approach to prevent the formation of aggregates is to decrease the concentration of test compound. The logic of this approach is to lower compound concentrations below the CAC, so that observed bioactivity would more likely be due to other mechanisms of target engagement. This approach will only prevent colloid formation if the compound test concentrations are below the CAC for the specific experimental condition tested, and may not be effective for compounds with relatively lower CACs. Another drawback to this approach is the increased probability of missing less potent but potentially useful compounds which may only be identified at higher compound concentrations. This dilemma can be addressed by using qHTS should a range of compound concentrations be necessary to limit the false-negative occurrence or comprehensively profile the chemical library (20).

## Controls/Reference Compounds

During assay development and optimization, it may also be advantageous to assess the effect of known aggregators on assay readout (**Table 2**) (21).

This tactic can help guide the optimization of experimental conditions to reduce the incidence of aggregation. For example, if aggregator controls show significant bioactivity, one may wish to modify the concentration(s) of detergent, aggregator decoy proteins, test compounds, and/or enzyme.

A second potential benefit of this approach is that it permits the actual characterization of aggregation on the assay readout. In conventional cell-free enzymatic assays, this effect may be as simple as enzyme inhibition marked by steep concentration-response curves (CRCs). This approach may be especially useful in more complex assays such as multi-step biochemical assays and cell-based assays, where the potential effect(s) of aggregation may not be intuitive. For example, some aggregators exhibit “bell-shaped” CRCs in cell viability assays, a phenomenon which reflects the concentration of bioactive, monomeric compound (**Figure 4**) (22). Taking the time to robustly characterize the effect of aggregation on assay readout may enhance bioactive compound triage. That is, when test compounds produce a similar readout to known aggregators, one may wish to triage such compounds or flag them for subsequent counter-screens (see section “STRATEGIES TO IDENTIFY AGGREGATION”).

A third potential benefit of using aggregator controls is that it may help estimate the incidence of aggregation among bioactive compounds. If a variety of known aggregators are inactive, one might anticipate aggregators would not be particularly enriched among the primary active compounds. On the other hand, if most aggregator controls are active, one might anticipate a formidable proportion of the primary active compounds may owe their bioactivity to aggregation. This estimate may inform the design of the post-HTS

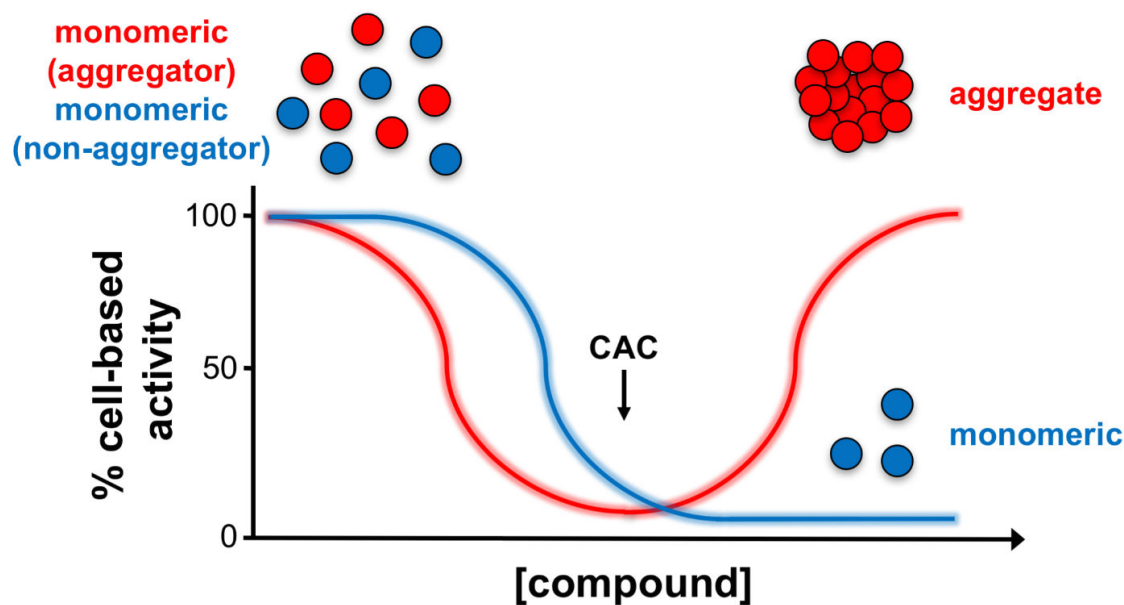


**Figure 4. Cellular CRCs for aggregators.** Some aggregators can exhibit bell-shaped (“U-shaped”) CRC in cell-based assays. At low compound concentrations (below the CAC), monomeric compound is free to interact with the cellular components. Bioactive monomeric compounds will typically exhibit a standard dose-response. However, for aggregators at higher compound concentrations (at or above the CAC), the majority of compound forms an aggregate in the culture media (colloid), effectively sequestering bioactive compound and introducing aggregate-cell interactions.

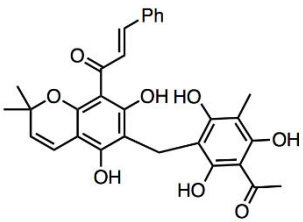
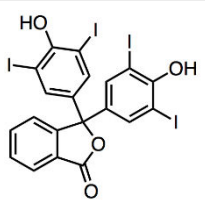
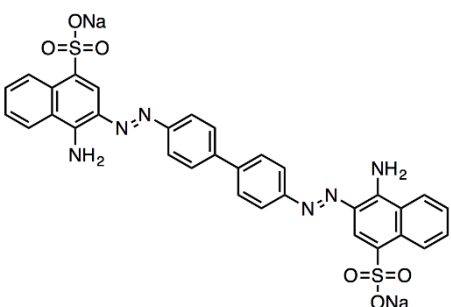
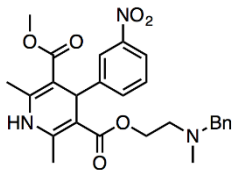
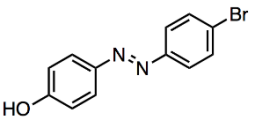
screening tree (23). In the latter scenario, one may wish to perform a series of aggregation counter-screens earlier in the triage process, in order to rapidly discard nonspecific aggregators.

Aggregation can be dependent on the assay conditions, meaning even known aggregators will not form micelles in every assay. Therefore, if using this approach, it is advised to include several different controls to get a more comprehensive assessment of aggregation in a particular assay.

**Table 2.** Suggested commercially available aggregation control compounds. Most of these compounds should form aggregates in the low micromolar range (e.g., 1-50  $\mu\text{M}$ ), though exact CACs will depend on experimental conditions including buffer composition. Additional examples can also be found in several



seminal manuscripts (4,9,10,15,24). Additional examples of potential aggregation controls can be found online at [PubChem](#) (see Table 3 for relevant PubChem AIDs) and [Aggregator Advisor](#).

| Compound    | Chemical structure  | Commercially availability | References |
|-------------|---|---------------------------|------------|
| Rottlerin   |    | Yes                       | (9)        |
| TIPT        |    | Yes                       | (9)        |
| Congo red   |   | Yes                       | (9)        |
| Nicardipine |  | Yes                       | (4)        |
| 4BPAP       |  | Yes                       | (17)       |

## Section Summary

Thoughtful assay design can potentially reduce the impact of nonspecific aggregation. Suggested strategies include the addition of detergents and decoy proteins, and careful consideration of enzyme and test compound concentrations. Assays can also be challenged with previously characterized aggregators to gauge the potential effect(s) of aggregation on assay readouts.

## Strategies to Identify Aggregation

### Introduction

Even with the aforementioned strategies in place, it is still possible to encounter aggregation. Alternatively, one may wish to investigate aggregation in previously identified bioactive compounds. This section describes several counter-screens and experimental strategies to identify aggregation among bioactive compounds. Primary methods to identify aggregators are discussed, including enzymatic counter-screens, CRC analyses, assay component titrations, and dynamic light scattering (DLS). Secondary methods to identify aggregation such as such as SPR, structure-interference relationships (SIR), nuclear magnetic resonance (NMR), and microscopy are also discussed.

### $\beta$ -Lactamase Counter-Screen

The most popular and well-characterized counter-screen for aggregation is an AmpC  $\beta$ -lactamase enzymatic assay (25). The reasons for utilizing this particular enzyme are partly historic, as much of the published characterization of aggregation stems from an HTS targeting AmpC (9). In this assay, compounds are tested for inhibition of the *Escherichia coli* AmpC  $\beta$ -lactamase in the presence and absence of detergent (**Figure 5**). Most compounds should not show activity versus this target, regardless of detergent status, and non-aggregating, well-behaved inhibitors will show detergent-independent enzymatic inhibition. By contrast, aggregators will in many cases show detergent-dependent activity at low micromolar compound concentrations.

It is highly recommended to perform some variation of the AmpC assay as an aggregation counter-screen. This assay has several favorable characteristics: (a) it is highly robust; (b) it requires no specialized instrumentation aside from a standard absorbance plate reader; (c) the enzyme is relatively easy to produce and is also commercially available; and (d) there is an abundance of previously characterized control compounds.

### Sample Steps | AmpC Counter-Screen

1. Prepare compound solutions. For testing compounds at 10  $\mu$ M final concentrations, we prepare 500  $\mu$ M working solutions for compatibility with the following assay protocol.
2. Prepare nitrocefin reagent stock solution. We prepare this solution as 5 mM nitrocefin in neat DMSO. Protect this solution from light. Stock solution is typically stable to multiple freeze-thaw cycles.
3. Prepare assay buffers. First prepare 10X stock solution without detergent. Then prepare two 1X buffer solutions (one without detergent, one with detergent).
4. Prepare enzyme stock solution. Prepare as 30X solution in assay buffer plus 0.0006% Triton X-100 (v/v). The minor amount of detergent prevents nonspecific enzyme adsorption to container walls.

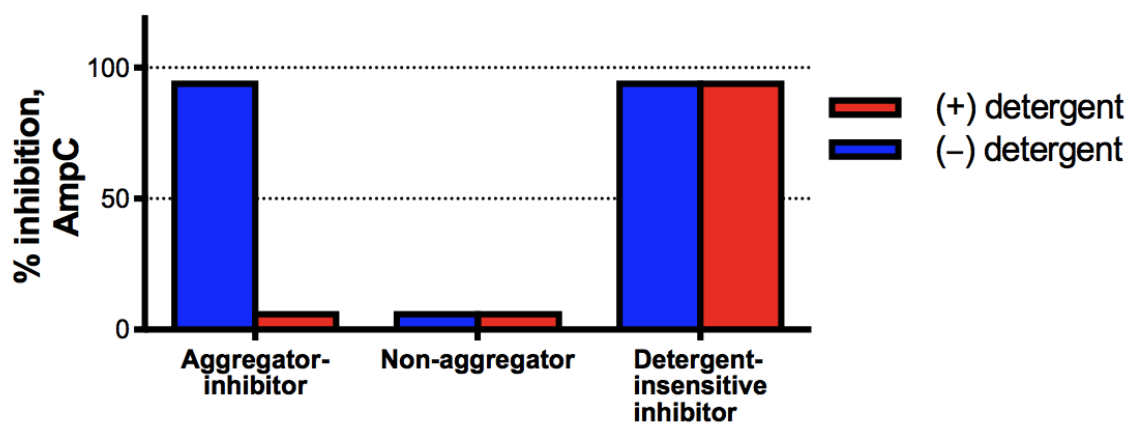


**Figure 5. Representation of AmpC counter-screen for aggregation.** Compounds are tested for inhibition of the AmpC B-lactamase in the absence (blue) and presence (red) of 0.01% Triton X-100 (v/v). Putative aggregators are most often identified by a significant attenuation of activity upon the inclusion of detergent (while not shown, some aggregators can activate AmpC activity). Non-aggregators typically show minimal activity in both the presence and absence of detergent. Detergent-insensitive inhibitors, which can include well-behaved compounds, show similar activity in the presence and absence of detergent.

5. Add 142  $\mu\text{L}$  buffer to plate wells with multichannel pipette. We typically use 96-well plates (e.g., Corning Half-Area UV-transparent plates).
6. Add 5  $\mu\text{L}$  of 30X enzyme solution to plate wells with multichannel pipette.
7. Add 3  $\mu\text{L}$  of compound stock solution to plate wells with pipette. To do this step with a multichannel pipette requires “pre-plating” compound stocks in a separate microplate.
8. Mix by gently pipetting up and down three times. Ensure adequate mixing, as the neat DMSO has a tendency to pool at the bottom of plate wells if not sufficiently mixed.
9. Incubate solution from [Step 8](#) for 5 min at room temperature.
10. Add 3  $\mu\text{L}$  of nitrocefin reagent solution to solution from [Step 9](#).
11. Mix by gently pipetting up and down three times. Ensure adequate mixing, as the neat DMSO has a tendency to pool at the bottom of plate wells if not sufficiently mixed.
12. Monitor reaction at 482 nm for 5 min using plate reader. Begin monitoring reaction as quickly as possible to best capture  $V_{\text{max}}$ .
13. Repeat [Steps 5 through 12](#), substituting detergent-free buffer with detergent-containing buffer.
14. Analyze enzymatic activity using  $V_{\text{max}}$ .
15. Normalize percent activity to vehicle control (e.g., DMSO-only).
16. Compare activities between the detergent-free and detergent-containing reactions. Compounds are flagged as punitive aggregators if there is a significant attenuation\* of bioactivity with the inclusion of detergent.

- \* *Based on historical data in our lab, this is defined as > 20% reduction in activity. Other criteria can include > 3 SD from the negative control (untreated) wells.*

Researchers should consider the following technical points:

- The above protocol is an adaption of a previously published protocol (25).
- For general applicability, this protocol is based on multichannel pipettes rather than liquid-handling instruments.
- Compounds are typically tested at 10  $\mu$ M final compound concentrations. However, it may be necessary to test at alternate concentrations, specifically if the CAC in the relevant assay system is potentially higher than 10  $\mu$ M.
- Always include positive and negative control compounds. For suggested positive aggregation controls, refer to “Controls/reference compounds” section. We have historically used compounds such as lidocaine as negative aggregation control compounds.
- Recombinant *E. coli* AmpC can be prepared in-house, or purchased from a commercial source.
- Note different species of AmpC may have different susceptibilities to aggregation.
- Purification tags may also alter the behavior of a protein with respect to aggregation.
- Different reaction buffers can likely be used for this counter-screen. For example, one may wish to test in the exact buffer as the original HTS. Always verify enzyme activity in any new buffer system.
- Large bubbles can be removed by brief centrifugation or manually by gentle blowing. Excessive bubbling often results from vigorous/turbulent dispensing and mixing, as well as excess detergent (10). To reduce bubbling, mixing should occur below the liquid level of the reaction well (25).
- Prepare detergent solutions fresh for each experiment, as Triton X-100 can produce  $H_2O_2$  in aqueous solution (14).
- Pure detergents can take several minutes to an hour to completely dissolve when transferred to aqueous solutions. Verify detergent is completely dissolved before proceeding with experiments.
- Pure detergents can be highly viscous and difficult to pipette. Prepare 10% solution (v/v) in  $H_2O$  for easier, more precise dispensing.
- Depending on the enzyme source, purity, and method of protein quantification, a necessary experiment is to titrate the concentration of enzyme.
- Keep enzyme solutions on ice when not in use during the course of an experiment.

## Detergent Titration Counter-Screen

As compound aggregates can have varying sensitivities to detergents and also different CACs, another tactic to identify aggregates is to perform a series of detergent titrations in the original assay system. Non-aggregating compounds will have minimal changes in

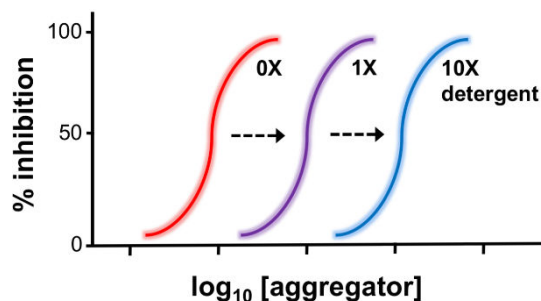


**Figure 6. Representation of a detergent titration experiment to identify aggregation.** For aggregators, the  $IC_{50}$  values can increase with increasing amounts of detergent. Shown is a hypothetical inhibitory aggregator (n.b. steep Hill slope).

bioactivity with increasing concentrations of detergent. By contrast, aggregates may demonstrate decreased potencies with increased concentrations of detergent (**Figure 6**).

### Sample steps | Detergent Titration Counter-Screen

1. Prepare two or more buffer solutions: one containing no detergent, the other(s) containing varying levels of detergent (e.g., 1X, 5X, 10X)
2. Prepare parallel reaction solutions using the detergent and detergent-free buffers.
3. Test compound in the detergent-free buffers.
4. Test compound in the detergent-containing buffers.
5. Compare activity in the presence and absence of detergent.

Researchers should consider the following technical points:

- Verify the target protein(s), test compound(s), assay reagent(s), and assay readout tolerate the specific detergent being used in this counter-screen.
- Because it can prevent protein adsorption to container walls, detergent-containing reactions may have more active enzyme, and consequently, may have greater overall bioactivity than otherwise identical detergent-free reactions.
- Aggregation is suspected when bioactivity is significantly attenuated by the inclusion of detergent. The exact magnitude of this effect will depend on the specific target and assay system. A rule of thumb is rightward shifts in  $IC_{50} > 3X$  should be considered likely aggregate-dependent effects and further analysis with higher detergent concentrations may be warranted if the compound is not immediately eliminated from further follow-up consideration. Depending on assay precision,  $IC_{50}$  values can fluctuate, and a useful tool for assessing the significance of changes in  $IC_{50}$  values is the minimum significant ratio (MSR). For detailed discussion, the reader is referred to Minimum Significant Ratio – A Statistic to Assess Assay Variability.

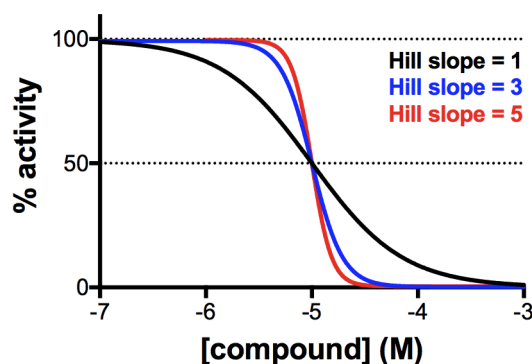


**Figure 7. Hill slope analysis to identify aggregation.** Shown is a simulation of compounds with identical 10  $\mu\text{M}$   $\text{IC}_{50}$  values. Aggregators characteristically have steep CRCs. A well-behaved compound (black line) typically has a Hill slope equal to 1.0, whereas many aggregators have higher Hill slopes (blue, red lines).

## Hill-Slope Analysis

A salient feature of aggregation are steep CRCs (**Figure 7**) (4,10,19,27). This reflects the CAC, the high affinity of the protein-aggregate complex, and the protein-compound stoichiometry. Based on the Hill Equation (**Equation 2**), the “steepness” of a given CRC is quantified by Hill coefficient (“Hill slope”).

$$\varnothing = \frac{[L]^n}{K_d + [L]^n} \quad \text{Equation 2}$$

(where  $\varnothing$  represents fraction of receptor bound to ligand,  $[L]$  represents free (unbound) ligand concentration,  $K_d$  represents apparent dissociation constant,  $n$  represents Hill coefficient)

For example, a well-behaved inhibitor with non-cooperative binding will have a Hill slope of 1.0, with approximately 90% of the bioactivity spanning across two orders of magnitude. In general, many aggregators will have Hill slopes greater than 1.5, some even being greater than 5.0. As a word of caution, a subset of aggregators can also have Hill slopes close to 1.0.

Calculating Hill slopes for CRC data is performed by regression analyses. Many labs will use commercial software packages such as GraphPad Prism. Many default curve-fitting algorithms will assume a fixed slope (Hill slope equal to 1.0), so it is critical to select a “variable slope” curve-fit. For example, a sigmoidal CRC is often fit to a four-parameter variable slope equation (**Equation 3**) (28, 29).

$$Y = \frac{Low + (High - Low)}{1 + 10^{(\log EC_{50} - X)(Hil\ slope)}} \quad \text{Equation 3}$$

(where  $Y$  represents assay activity, Low and High represent the low and high bounds)

Depending on the shape and completeness of the CRC, additional constraints may need to be specified for an accurate curve-fit. For additional details on calculating the Hill slope, refer to Assay Operations for SAR Support.

There are some caveats to using Hill slope analysis for aggregation. First, aggregators with Hill slopes close to 1.0 have been described (10). Second, covalent modifiers can also have steep Hill slopes (10). Third, as mentioned previously, any situation where  $[E] \gg K_d$  of the inhibitor will result in a steep Hill slope.

## Enzyme Concentration Titration

Another relatively straightforward approach to identify nonspecific inhibition by aggregators is to perform a series of enzyme titration experiments (19,25). Based on the aforementioned stoichiometric model of aggregation inhibition, the  $IC_{50}$  value of an aggregator is expected to increase linearly with increases in enzyme concentration (for single-point experiments, percent inhibition should decrease when the concentration of enzyme is increased).

## Sample Steps | Enzyme Titration Counter-Screen

1. Test compound at standard enzyme concentration (i.e., 1X) under standard conditions. Also perform vehicle control in parallel.
2. Determine activity of test compound from Step 1 relative to vehicle control.
3. Test same compound from Step 1, except at 5X enzyme concentration under otherwise standard conditions. Also perform vehicle control in parallel with this same enzyme concentration.
4. Determine activity of test compound from Step 3 relative to vehicle control.
5. Repeat Steps 3 and 4 with increasing concentrations of enzyme (e.g., 10X, 20X)
6. Plot  $IC_{50}$  versus enzyme concentration. A linear relationship is suggestive of stoichiometric inhibition, consistent with aggregation.

Researchers should consider the following technical points:

- If available, include a non-aggregator positive control compound. The activity of such a compound should not proportionally increase with additional enzyme (unless enzyme concentration significantly exceeds the  $K_d$  value of the inhibitor).
- Verify the effect of increased enzyme on reaction progress. With increased enzyme, reactions will proceed quicker and not approximate steady-state conditions due to increased product formation. Also verify assay readout is within the dynamic range of the detection system.

## Centrifugation Counter-Screen

Aggregators will often show a pronounced decrease in bioactivity when reaction solutions are centrifuged (4). This process effectively pellets the aggregates, leaving only monomeric compound (and non-sequestered protein if present) in the supernatant (**Figure 8**).

Notably, this counter-screen does not identify potential aggregators based on differential

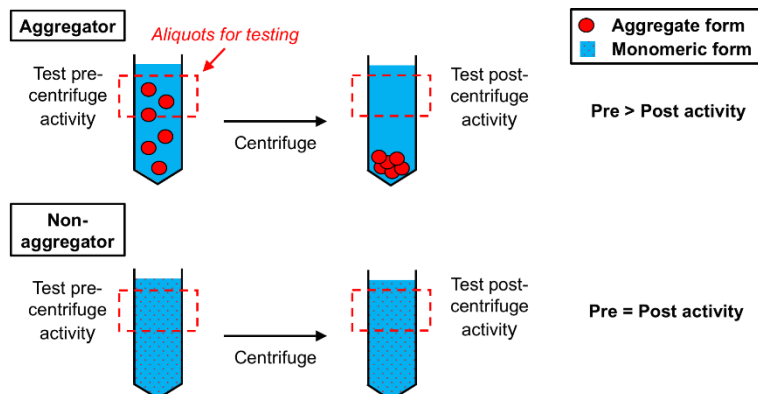


**Figure 8. Centrifuge-based experiment to identify aggregation.** Aggregates (top panel) can usually be removed by brief centrifugation of samples. For aggregators, post-centrifugation supernatant aliquots should show reduced bioactivity compared to pre-centrifugation samples. By contrast, non-aggregators (bottom panel) should have similar activity pre- and post-centrifugation.

bioactivity in the presence and absence of detergents. For this reason, *this particular counter-screen may be especially useful in assay systems intolerant to detergents or decoy proteins.*

## Sample Steps | Centrifugation Counter-Screen

1. Incubate test compound in assay buffer for 5 min.
2. Remove supernatant aliquot from Step 1 for testing.
3. Centrifuge mixture from Step 1 at approximately 15,000 g for 30 min at 4 °C. Potential aggregates should form a sediment.
4. Remove supernatant aliquot from Step 3 for testing.
5. Test and compare bioactivity of aliquots from Steps 2 and 4 by adding remaining assay reagents (e.g., target enzyme(s), substrate(s), co-factor(s), etc.).

Researchers should consider the following technical points:

- Include a vehicle-only control (e.g., DMSO-only) to control for changes in enzyme activity during the centrifugation process.
- Also include a known non-aggregating positive control compound (if known).
- Both types of controls should be tested for bioactivity using pre- and post-centrifuged aliquots.
- For poorly soluble compounds, also consider simple precipitation of compound rather than colloid formation.
- As a control for the centrifugation process, store the pre-centrifugation aliquots in conditions similar to the centrifugation (e.g., 4 °C).



## Pre-incubation Counter-Screen

A simple mechanistic counter-screen for suspected aggregators is to modify the compound-protein pre-incubation time. Aggregators will often show more potent activity when allowed to pre-incubate with the target protein (4,9). In an AmpC assay, the magnitude of this effect varied from several-fold to greater than 50-fold changes in IC<sub>50</sub> values (9).

Notably, this counter-screen does not identify potential aggregators based on differential bioactivity in the presence and absence of detergents. For this reason, *this particular counter-screen may be useful in assay systems intolerant to detergents or decoy proteins, or to follow-up on those compound activities that may fall into the aggregator detergent-insensitive class* (see **Figure 4**).

The counter-screen premise is relative simple. For a conventional enzymatic assay, compounds are tested in two different reaction systems: (1) compounds and proteins are pre-incubated together for 5 min, then the reaction is initiated by addition of non-proteinaceous substrate, and (2) compounds and non-proteinaceous substrate are incubated together, then the reaction is initiated by addition of protein. In the first reaction, when aggregates and protein are allowed to incubate together for even 5 min, most of the protein will adsorb to the aggregates (in the absence of other strategies to mitigate aggregation such as detergents and/or decoy protein). In the second reaction, no such adsorption occurs between the non-proteinaceous assay components and aggregates when incubated together. When this second reaction is initiated by the addition of protein, there is a higher initial concentration of unbound (and unmodulated) protein.

This tactic is generally best when performed as a counter-screen, rather than in the HTS phase where one may consider reducing pre-incubation times to reduce assay interference from potential aggregation. Reducing pre-incubation times is difficult in many HTS settings due to instrumentation and scale. Furthermore, pre-incubation is often purposefully designed to allow for equilibration purposes.

1. Incubate test compound and protein for 5 min. Also perform vehicle control.
2. Initiate reaction by adding non-proteinaceous substrate to mixture from Step 1.
3. Determine activity from reaction from Step 2 relative to vehicle control.
4. In a separate reaction, incubate test compound with non-proteinaceous assay components for 5 min. Also perform vehicle control.
5. Initiate reaction by adding proteins (e.g., target enzyme) to mixture from Step 4.
6. Determine activity from reaction from Step 5 relative to vehicle control.
7. Compare activities from Steps 3 and 6.

Researchers should consider the following technical points:

- Include a known non-aggregating positive control compound (if known).
- The suggested length of pre-incubation is 5 min, though it is possible this interval may need to be extended for slower-forming aggregate-protein complexes.

- Recall the differential activity of aggregators will depend on the formation of aggregates during the pre-incubation phase. If sufficient amounts of detergent to dissolve aggregates are already present in the assay, minimal differential activity may be observed.
- For compounds showing increased bioactivity with protein pre-incubation, one should also consider the possibility of irreversible, time-dependent target modulation. Refer to Assay Interference by Chemical Reactivity for additional details on the identification of reactivity.

## Dynamic Light Scattering

Dynamic light scattering (DLS) is a biophysical technique used to determine particle sizes in solution. Compounds are dissolved in solution, and if aggregation occurs, the size of aggregates can be quantified by measuring temporal fluctuations in light scattering and generating an autocorrelation function (**Figure 9**). There are several examples of DLS used in the identification and characterization of aggregates (2,4,6,24,30). Modern instruments utilize either cuvettes or microplates, the latter being amenable to higher-throughput counter-screens. This technique provides direct, physical evidence of aggregate formation, though it does not provide functional information about any detected aggregates. Another advantage is that the assay is not dependent on the particular target (protein-free), and in theory it can be adapted to model assay specific buffer conditions. Depending on available instrumentation and desired throughput, DLS can be a highly useful primary counter-screen for aggregation.

## Structure-Interference Relationships

Structure-activity relationships (SAR) can often be explained by assay interference, so-called structure-interference relationships (SIR). Analysis for SIR in the context of HTS can help identify potential aggregators by analyzing specific bioactive chemotypes in-depth. This approach can be especially helpful for equivocal analyses, where it is unclear whether a bioactive chemotype is a function of aggregation or useful target engagement. If the apparent SAR appears to correlate with aggregation, then it can facilitate triage of related analogs and also inform the design of related chemotypes to prevent the formation of colloids. As with conventional SAR analyses, this approach is most helpful with multiple compounds. Bioactivity analysis should focus not just on the active compounds and close analogs, but also on structurally-related inactive compounds. If a chemotype is particularly important for a project, this analysis can be aided by SAR-by-commerce, in which closely related analogs (active and inactive) can be purchased and tested for activity in the original assay and aggregation counter-screens.

This approach was particularly helpful in the post-HTS triage of a 3-hydroxy-pyrrolidin-2-one core active against the fungal histone acetyltransferase (HAT) Rtt109 (**Figure 10**). In this case, clues that an apparent SAR actually reflected an aggregation-dependent SIR included: (a) little change in activity with minor aromatic substituent changes, (b) correlation of bioactivity with increased lipophilicity and molecular weight,

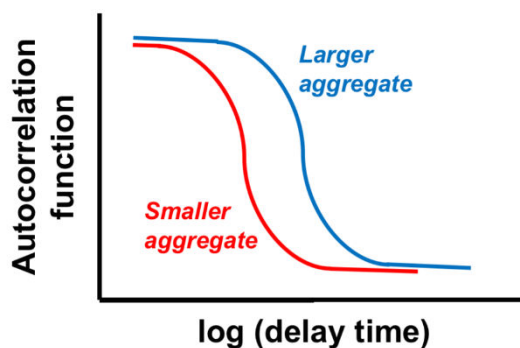


**Figure 9. Dynamic light scattering for the characterization of aggregates.** Due to their sizes, aggregates will scatter light. The size of aggregates can be characterized by DLS by plotting the autocorrelation function as a function of delay time. Larger aggregates will maintain a higher correlation for longer delay times relative to smaller aggregates (compare blue and red curves).

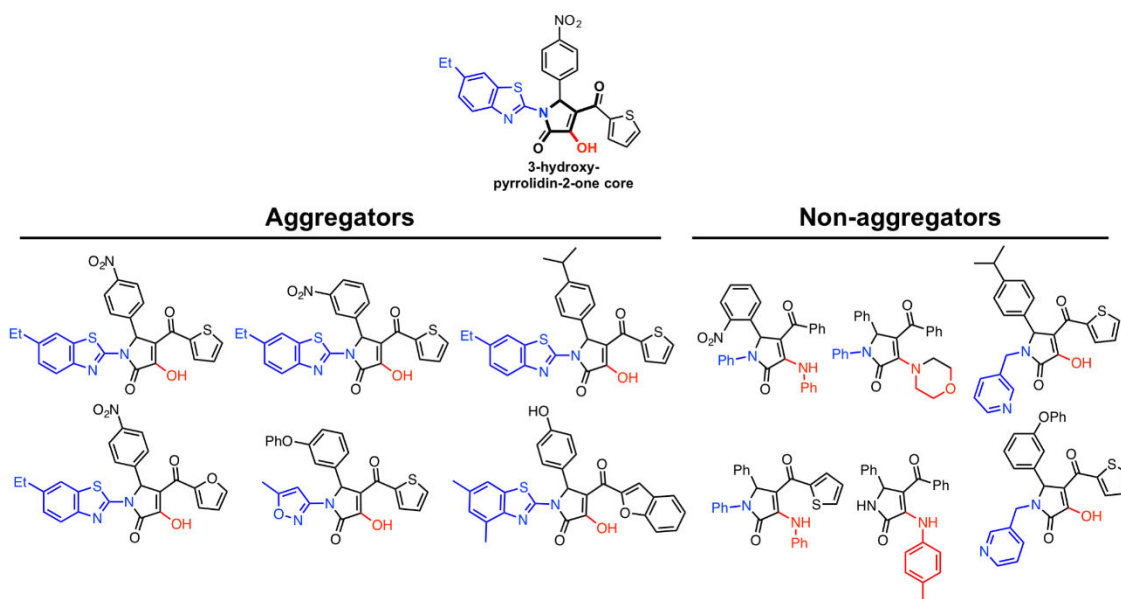


**Figure 10. Structure-interference relationships of aggregators.** Analysis of analogs can help identify bioactivity due to aggregation. In this example from an HTS for inhibitors of yeast Rtt10930, most compounds with the 3-hydroxy-pyrrolidin-2-one core are active at low micromolar compound concentrations versus Rtt109, and are also flagged as aggregators by the AmpC aggregation counter-screen. Compounds without the C3-hydroxy group were inactive versus Rtt109 and inactive in the AmpC counter-screen (C3 substituents highlighted in red). Compounds with alkyl substituents at the N1-position were also inactive versus Rtt109 and inactive in the AmpC counter-screen (N1 substituents highlighted in blue).

and (c) a precipitous drop in activity with the removal of the C3-hydroxy group. Of course, these findings could also be explained by true bioactivity, which should also be considered in any such analysis. In this example the correct identification of aggregation as the primary source of bioactivity ultimately depended on correlation with other

experimental data (AmpC counter-screen, steep Hill slopes, detergent titration, mechanism of action studies) (31). By determining the specific components contributing to aggregation, there was high confidence in discontinuing work on this chemotype.

## Computational Approaches

Cheminformatics can also be utilized to help identify potential aggregators, especially in the context of the large datasets inherent to HTS. Since the factors contributing to aggregation are multifactorial, most current cheminformatics tools for aggregation triage are based on chemical similarity to known aggregators.

A helpful, open-resource for flagging potential aggregators is [Aggregator Advisor](#) (32). In this method, compound structures in the form of SMILES can be submitted to a database of known aggregators. Compounds with a high-degree of similarity to known aggregators are flagged. This page also contains an extensive list of aggregators (“Rogues’ Gallery”).

Datasets from several HTS campaigns in the presence and absence of detergents are also publically available *via* [PubChem](#), which can facilitate additional data analyses and method development (**Table 3**).

**Table 3.** PubChem HTS data relevant to aggregation.

| PubChem Assay  | PubChem Assay ID |
|--|------------------|
| qHTS Inhibitors of AmpC Beta-Lactamase (assay without detergent)                     | 485341           |
| qHTS Inhibitors of AmpC Beta-Lactamase (assay with detergent)                        | 485294           |
| qHTS Assay for Promiscuous and Specific Inhibitors of Cruzain (without detergent)    | 1476             |
| qHTS Assay for Promiscuous and Specific Inhibitors of Cruzain (with detergent)       | 1478             |
| Promiscuous and Specific Inhibitors of AmpC Beta-Lactamase (assay without detergent) | 585              |
| Promiscuous and Specific Inhibitors of AmpC Beta-Lactamase (assay with detergent)    | 584              |

## Nuclear Magnetic Resonance

Two different nuclear magnetic resonance (NMR) techniques have been described to identify aggregates, one protein-free (“ligand-based”) and the other utilizing a protein probe (“protein-based”).

In one counter-screen, standard proton NMR can be used to identify aggregates without the need for target protein (33). Compared to monomeric (non-aggregating) forms, aggregates can exhibit characteristic chemical shift patterns due to the additional intermolecular effects from compounds in close proximity. These chemical shift perturbations revert to the monomeric chemical shift patterns upon dilution, with the addition of detergent, or after centrifugation (**Figure 11**). These chemical shift patterns include chemical shift change(s), additional peak(s), and change(s) in peak shape. The advantages of this technique include its lack of required protein, its use of relatively

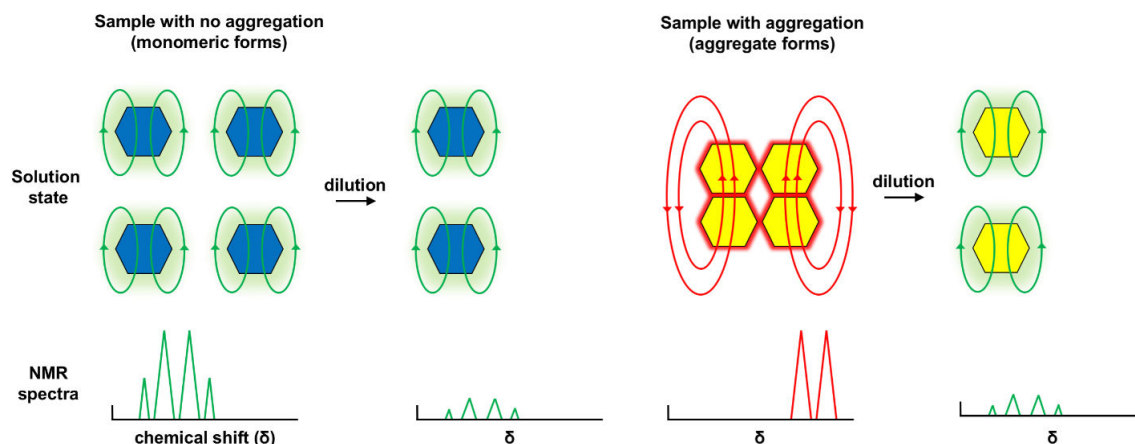


**Figure 11. NMR-based detection of aggregation.** (Left) Non-aggregating compounds (blue) exist in monomeric form, producing characteristic chemical shifts (depicted as green lines). Dilution of the sample does not produce chemical shifts, just dilution of signal intensity. (Right) Aggregating compounds (yellow) will exist as aggregates, producing a set of chemical shifts specific for the aggregate form (red lines). Dilution of the sample below the CAC disrupts the aggregate to form monomeric compound, which have a different chemical shift pattern (green lines).

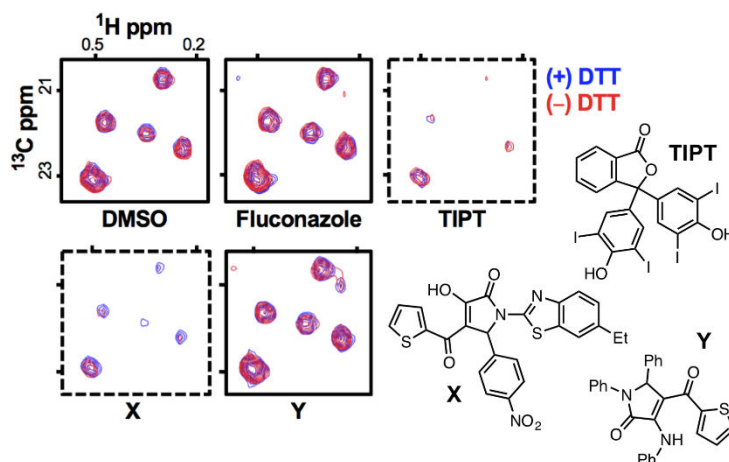


**Figure 12. ALARM NMR readout sensitive to aggregation.** Known aggregators TIPT and compound X perturb the La antigen conformation independent of DTT (9,31). Compound Y, a structural analog of X, is used as an aggregation negative control compound. Fluconazole included as additional non-reactive, non-aggregation control compound. Dashed border, ALARM NMR-positive.

standard instrumentation (i.e., proton NMR), and a biophysical readout. The main disadvantage of this assay is its comparatively lower throughput. Like DLS and microscopy, it can detect aggregation but does not inform the functional consequence of these aggregates on bioactivity. For details on performing this counter-screen, see the original manuscript for an excellent experimental walkthrough (33).

Another technique, a La assay to detect reactive molecules by nuclear magnetic resonance (ALARM NMR), is sensitive to nonspecific protein perturbation by known aggregators (31). This assay is an industry-developed [ $^1\text{H}$ - $^{13}\text{C}$ ]-HMQC counter-screen originally developed to identify nonspecific thiol-reactive screening compounds by their ability to induce DTT-dependent conformational shifts in the La antigen (34,35). As they exert their bioactivity through non-covalent interactions, aggregators can perturb the La antigen conformation independent of DTT (**Figure 12**). An advantage of using ALARM NMR is its ability to identify nonspecific thiol-reactivity *and* aggregation. However, potential drawbacks of this method are the specialized instrumentation required, its medium throughput (approximately 50 samples per day), and the relatively high concentrations of compound required for testing (i.e., mid-micromolar). As the La antigen may not be sensitive to every aggregator (JL Dahlin, unpublished observations) and the experimental conditions may not approximate the relevant original screening conditions, we recommend following up critical results with additional counter-screens.

## Surface Plasmon Resonance

Another biophysical technique for detecting aggregation utilizes surface plasmon resonance (SPR) biosensors. Aggregates can produce characteristic readouts in SPR experiments, most notably superstoichiometric binding (**Figure 13**) (8). An interesting finding from this original study is that the nature of any given aggregate-protein interactions can vary depending on the particular compound *or* the target protein identity. This technique can capture multiple modes of aggregation-target interactions, including stoichiometry and the kinetics of aggregate association and dissociation. Like many of the other aforementioned aggregation counter-screens, aggregation in this SPR setup is generally attenuated by the addition of detergent. The advantages of this technique include its general applicability to any target amenable to SPR, and its biophysical readout, which provides information about the kinetics of direct aggregate-protein interactions. The main disadvantages of this technique are its instrumentation requirements (i.e., non-standard in many academic labs), need for protein immobilization (“on chip”), and overall throughput. For details on performing this counter-screen, we refer to the original manuscript for several example aggregation readouts (8).

## Microscopy

While not a routine tool due to the specific instrumentation required and the relatively low throughput, aggregates can also be directly visualized through specialized microscopy. The most common microscopy method for observing aggregates is transmission electron microscopy (TEM) (4,9,36,37). A general procedure involves preparing the compound aggregate in assay buffer, then transferring to a carbon-coated grid, followed by negative staining with uranyl acetate or ammonium molybdate. Aggregates can also be indirectly visualized with fluorescent microscopy when incubated with fluorescent proteins, which can adsorb to the surface of aggregates (4). The direct observation of adducts should be correlated with additional bioactivity and mechanistic data.

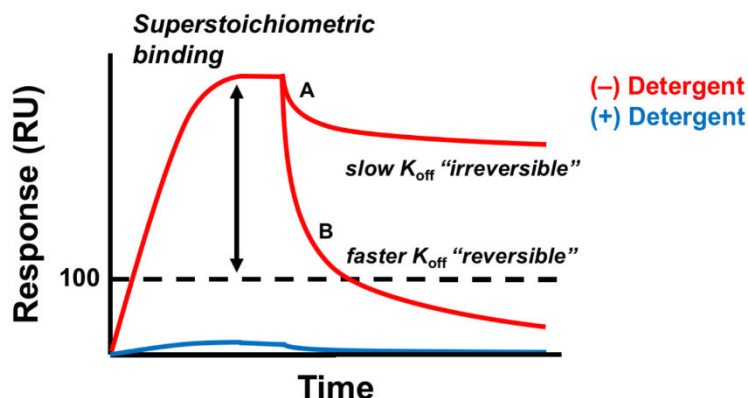


**Figure 13. SPR characterization of aggregators.** Shown is a simulation of a prototypical aggregator in a standard SPR experiment. In this example, response is normalized to a well-behaved inhibitor that binds the protein in a 1:1 ratio (RU = 100). Aggregators can produce superstoichiometric binding (characterized by large responses) and can display detergent-dependent protein binding (compare red and blue lines). Aggregates can display either slow dissociation mimicking irreversible binding (curve A) or faster dissociation (curve B).

## Section Summary

Bioactivity due to nonspecific aggregation can be identified through several strategies. Initial tests to evaluate for aggregation typically include enzymatic counter-screens, CRC analyses, DLS, and simple mechanistic experiments. More advanced and/or resource-intensive methods include SPR, NMR, and microscopy. In addition to triaging nonspecific compounds, these strategies can also be useful for de-risking compounds as they proceed along the discovery and development pipeline.

## Frequently Asked Questions

This section seeks to answer some common questions about aggregation in the context of drug and chemical probe discovery, including some common misconceptions (adapted from [advisor.bkslab.org](http://advisor.bkslab.org)).

### 1 Can aggregation affect cell-based assay readouts?

Yes. There are several examples of aggregators modulating cell-based readouts. Interference and nonspecific bioactivity can result from direct interaction with membrane-bound receptors (38), a reduction in bioactive monomeric compound (37), or interactions with other extracellular factors (36). Aggregators have also been associated with cytotoxicity and changes in cellular histone acetylation (JL Dahlin *et al.*, forthcoming results). It is unclear if aggregates can form intracellularly. Studies with Evans blue suggest aggregates do not transverse individual cell membranes intact (e.g., by endocytosis) (22). Some known aggregators exhibit U-shaped curves due to aggregation at high compound concentrations which effectively prevents cell penetration (22). Other studies with Evans

blue suggest certain aggregates may cross certain tissue structures such as tumor blood vessels via increased permeability (37). Compounds can potentially form aggregates *in vivo*, based on simulated intestinal fluid studies (39). Therefore, it is highly advised to consider the use of aggregator controls in cell-based assays, especially when testing compounds at micromolar concentrations. It is currently unclear which strategies, including the use of detergents and decoy proteins, can most effectively mitigate aggregation in cell-based experiments, especially without perturbing cell function.

## **2. Several FDA-approved drugs are aggregators. How can this observation be reconciled with the recommendation to triage aggregators?**

Several drugs can form aggregates in enzymatic assays at micromolar concentrations (24). However, many of these drugs have been extensively optimized for potency and selectivity, and are typically used at nanomolar compound concentrations, well below their CACs.

## **3. Can one predict aggregation based on chemical structure (e.g., *in silico*)?**

Several methods have been described to flag potential aggregators based on structure and other properties (24,30,32,40,41). As with any model, there is always the potential for false-positive and false-negative predictions. While helpful for economically analyzing large numbers of compounds, these tools should not be used as sole substitutes for well-designed experimental counter-screens for aggregation.

## **4. Do aggregators always inhibit enzyme activity?**

No. While the most common effect of partial protein unfolding by aggregation in enzymatic assays is inhibitory, it is possible to actually enhance target activity (10). For example, we have observed several reproducible cases of reported HAT inhibitors actually increasing AmpC activity (JL Dahlin *et al.*, forthcoming results). The mechanistic basis of this phenomenon is unclear, but it may be influenced by reaction volume and/or compound solubility.

## **5. Can a compound aggregate in all assay conditions?**

No. Aggregation (i.e., CAC) depends on multiple factors, including assay buffer components, ionic strength, pH, and detergent (42). Other experimental factors such as pre-incubation time, temperature, mixing procedures, and organic solvents (e.g., DMSO) may also alter aggregation behavior. These factors, combined with the actual compound concentration, determine whether a compound aggregates or not.

## **6. Do aggregators always show a complete concentration-response?**

Not necessarily. Aggregator CRCs can plateau before achieving a complete dose-response due to compound precipitation (19).

## **7. What other HTS phenomenon can be attributed to aggregators?**



Gain-of-signal outputs have been observed, possibly the result of an aggregation phenomenon. In one case, an HTS TR-FRET assay identified a very large number of primary actives (a compound-dependent positive FRET signal). Given it was unlikely that a productive protein-protein interaction would be facilitated by these compounds, the possibility exists this effect was caused under a situation where aggregates created a surface upon which donor and acceptor labeled proteins adhered and resulted in a non-mechanism relevant proximity, thereby producing the positive FRET signal (J Inglese, personal observation ca. 2003).

Additionally, there is also the possibility for aggregates to interfere with antibody-based assays by sequestering immunoglobulin reagents.

## Conclusions

Aggregation represents a significant source of compound-mediated assay interference and nonspecific bioactivity in biological assays which utilize small molecules. The incidence of aggregation by test compounds can usually be mitigated by careful assay design, such as the use of detergents and the optimization of enzyme and test compound concentrations. Aggregators can be identified by several strategies (**Table 4**), including enzymatic counter-screens, DLS, and various titration experiments. Cheminformatics and advanced strategies such as microscopy, NMR, and SPR can also identify aggregators.

Several recommendations are made to prevent wasted follow-up on aggregators in the context of HTS, chemical biology, and related fields.

1. Proactively design assays to mitigate the effect and the prevalence of aggregation.
2. Empirically test bioactive compounds for aggregation by at least one method (i.e., test regardless of whether aggregation is suspected or not).
3. Compounds with a high index of suspicion for aggregation should be evaluated by multiple methods.
4. Testing for aggregation should attempt to approximate the relevant biological assay conditions.

Following these strategies should triage intractable chemical matter and de-risk more promising bioactive compounds.

**Table 4.** Summary of aggregation counter-screens.

| Assay                   | Pros   | Cons  | Notes   |
|-------------------------|--|---|---|
| AmpC $\beta$ -Lactamase | -Well-characterized<br>-Robust<br>-Medium-to-high throughput<br>-Requires relatively standard instrumentation (i.e., plate reader) | -AmpC assay conditions might not be compatible with target assay conditions<br>-Not all aggregators modulate AmpC | -AmpC commercially available<br>-Provides additional information about target specificity<br>-Assay subject to other forms of compound- |

*Table 4. continues on next page...*

Table 4. continued from previous page.

| Assay               | Pros  | Cons   | Notes  |
|---------------------|---|--|--|
|                     |   |  | mediated interference<br>-Indirect evidence of aggregation   |
| Detergent titration | -Utilizes original assay target and assay technique<br>-Assays target modulation by aggregates                                    | Detergents might not be compatible with target assay conditions  | -Assay subject to other forms of compound-mediated interference<br>-Indirect evidence of aggregation |
| Hill slope          | Can analyze existing CRC data   | Aggregators do not always exhibit steep Hill slopes  | Indirect evidence of aggregation   |
| Enzyme titration    | -Utilizes original assay target and assay technique<br>-Assays target modulation  | May require significantly adjusting assay time points and other variables  | -Assay subject to other forms of compound-mediated interference<br>-Indirect evidence of aggregation |
| Centrifugation      | -Utilizes original assay target and assay technique<br>-Assays target modulation  | High-force centrifugation generally lower throughput   | Assay subject to other forms of compound-mediated interference                                       |
| Cheminformatics     | -Requires only chemical structure as input<br>-High-throughput  | -Training sets based on specific assay conditions, targets; applicability to other experimental variables unknown<br>-Susceptible to false-positive and false-negative results | Experimental confirmation strongly recommended   |
| DLS                 | -Biophysical evidence of aggregates<br>-Medium throughput<br>-Direct observation of aggregates                                    | -Requires non-standard instrumentation<br>-Does not assay target modulation  |  |
| NMR                 | -Biophysical evidence of aggregates<br>-Does not require protein (ligand-based)   | -Lower throughput<br>-Does not assay target modulation<br>-Requires non-standard instrumentation   | Indirect evidence of aggregation   |
| ALARM NMR           | -Biophysical evidence of aggregates<br>-Provides additional information about target specificity and nonspecific thiol reactivity | -Lower throughput<br>-Requires relatively high protein and compound concentrations<br>-Protein may not be universally susceptible to aggregates                                | Indirect evidence of aggregates  |

Table 4. continues on next page...

Table 4. continued from previous page.

| Assay      | Pros   | Cons   | Notes                           |
|------------|--|--|---------------------------------|
|            |  | -Requires non-standard instrumentation   |                                 |
| SPR        | -Biophysical evidence of aggregates<br>-Can be adapted to target or surrogate proteins | -Lower throughput<br>-Requires non-standard instrumentation<br>-Does not assay target activity | Indirect evidence of aggregates |
| Microscopy | -Lower throughput<br>-Direct observation of aggregates                                 | -Requires non-standard instrumentation<br>-Does not assay target activity                      |                                 |

## Suggested Web Resources

1. Aggregator Advisor ([advisor.bkslab.org](http://advisor.bkslab.org)).

An excellent web-based cheminformatics resource for identifying potential aggregators. The input is test compounds in SMILES format, and the output is a similarity score relative to known aggregators.

2. PubChem ([pubchem.ncbi.nlm.nih.gov](http://pubchem.ncbi.nlm.nih.gov)).

A free resource for several HTS campaigns for aggregation.

## Suggested Readings (alphabetical order)

1. Babaoglu, K.; Simeonov, A.; Irwin, J. J.; Nelson, M. E.; Feng, B.; Thomas, C. J.; Cancian, L.; Costi, M.P.; Maltby, D. A.; Jadhav, A.; Inglese, J.; Austin, C. P.; Shoichet, B. K. *J Med Chem*, **2008**, *51*, 2505.

A detailed follow-up mechanistic analysis of aggregators from a biochemical HTS campaign (accompanies Suggested Reading #3).

2. Feng, B. Y.; Shoichet, B. K. *Nat Protoc*, **2006**, *1*, 550.

An easy to follow step-by-step guide describing the AmpC  $\beta$ -lactamase counter-screen for aggregation.

3. Feng, B. Y.; Simeonov, A.; Jadhav, A.; Babaoglu, K.; Inglese, J.; Shoichet, B. K.; Austin, C. P. *J Med Chem*, **2007**, *50*, 2385.

A representative example of the prevalence of aggregation in a biochemical HTS campaign, demonstrating ~95% of primary actives were detergent-sensitive aggregators (accompanies Suggested Reading #1).

4. McGovern, S. L.; Helfand, B. T; Feng, B.; Shoichet, B. K. *J Med Chem*, **2003**, *46*, 4265.

An excellent discussion of the biochemical mechanisms of aggregation.

## Acknowledgements

JLD acknowledges Dr. Michael A. Walters for helpful discussions and research support.

## REFERENCES

1. Thorne N., Auld D. S., Inglese J. Apparent activity in high-throughput screening: origins of compound-dependent assay interference. *Curr. Opin. Chem. Biol.* 2010;14:315–324. PubMed PMID: 20417149.
2. Coan K. E. D., Shoichet B. K. Stoichiometry and physical chemistry of promiscuous aggregate-based inhibitors. *J. Am. Chem. Soc.* 2008;130:9606–9612. PubMed PMID: 18588298.
3. Duan D., Torosyan H., Elnatan D., McLaughlin C. K., Logie J., Shoichet M. S., Agard D. A., Shoichet B. K. Internal structure and preferential protein binding of colloidal aggregates. *ACS Chem. Biol.* 2017;12:282–290. PubMed PMID: 27983786.
4. McGovern S., Helfand B., Feng B., Shoichet B. K. A specific mechanism of nonspecific inhibition. *J. Med. Chem.* 2003;46:4265–4272. PubMed PMID: 13678405.
5. McLaughlin C., Duan D., Ganesh A., Torosyan H., Shoichet B., Shoichet M. Stable colloidal drug aggregates catch and release active enzymes. *ACS Chem. Biol.* 2016;11:992–1000. PubMed PMID: 26741163.
6. Coan K. E. D., Maltby D. A., Burlingame A. L., Shoichet B. K. Promiscuous aggregate-based inhibitors promote enzyme unfolding. *J. Med. Chem.* 2009;52:2067–2075. PubMed PMID: 19281222.
7. Blevitt J., Hack M., Herman K., Jackson P., Krawczuk P., Lebsack A., Liu A., Mirzadegan T., Nelen M., Patrick A., Steinbacher S., Milla M., Lumb K. Structural basis of small-molecule aggregate induced inhibition of a protein-protein interaction. *J. Med. Chem.* 2017;60:3511–3517. PubMed PMID: 28300404.
8. Giannetti A. M., Koch B. D., Browner M. F. Surface plasmon resonance based assay for the detection and characterization of promiscuous inhibitors. *J. Med. Chem.* 2008;51:574–580. PubMed PMID: 18181566.
9. McGovern S. L., Caselli E., Grigorieff N., Shoichet B. K. A common mechanism underlying promiscuous inhibitors from virtual and high-throughput screening. *J. Med. Chem.* 2002;45:1712–1722. PubMed PMID: 11931626.
10. Feng B. Y., Simeonov A., Jadhav A., Babaoglu K., Inglese J., Shoichet B. K., Austin C. P. A high-throughput screen for aggregation-based inhibition in a large compound library. *J. Med. Chem.* 2007;50:2385–2390. PubMed PMID: 17447748.
11. Jadhav A., Ferreira R. S., Klumpp C., Mott B. T., Austin C. P., Inglese J., Thomas C. J., Maloney D. J., Shoichet B. K., Simeonov A. Quantitative analyses of aggregation, autofluorescence, and reactivity artifacts in a screen for inhibitors of a thiol protease. *J. Med. Chem.* 2010;53:37–51. PubMed PMID: 19908840.

12. Ryan A. J., Gray N. M., Lowe P. N., Chung C.-W. Effect of detergent on “promiscuous” inhibitors. *J. Med. Chem.* 2003;46:3448–3451. PubMed PMID: 12877581.
13. Duan D., Doak A., Nedyalkova L., Shoichet B. Colloidal aggregation and the in vitro activity of traditional Chinese medicines. *ACS Chem. Biol.* 2015;10:978–988. PubMed PMID: 25606714.
14. Miki T., Orii Y. The reaction of horseradish peroxidase with hydroperoxides derived from Triton X-100. *Anal. Biochem.* 1985;146:28–34. PubMed PMID: 3993940.
15. Babaoglu K., Simeonov A., Irwin J., Nelson M., Feng B., Thomas C., Cancian L., Costi M., Maltby D., Jadhav A., Inglese J., Austin C., Shoichet B. Comprehensive mechanistic analysis of hits from high-throughput and docking screens against beta-lactamase. *J. Med. Chem.* 2008;51:2502–2511. PubMed PMID: 18333608.
16. Dahlin, J. L.; Baell, J. B.; Walters, M. A. Assay interference by chemical reactivity. In *Assay Guidance Manual*, Sittampalam, G.; Coussens, N., Eds. Eli Lilly and the National Center for Advancing Translational Science: Bethesda, 2015.
17. Coan K. E. D., Shoichet B. K. Stability and equilibria of promiscuous aggregates in high protein milieus. *Mol. Biosyst.* 2007;3:208–213. PubMed PMID: 17308667.
18. Habig M., Blechschmidt A., Dressler S., Hess B., Patel V., Billich A., Ostermeier C., Beer D., Klumpp M. Efficient elimination of nonstoichiometric enzyme inhibitors from HTS hit lists. *J. Biomol. Screen.* 2009;14:679–689. PubMed PMID: 19470716.
19. Shoichet B. K. Interpreting steep dose-response curves in early inhibitor discovery. *J. Med. Chem.* 2006;49:7274–7277. PubMed PMID: 17149857.
20. Inglese J., Auld D., Jadhav A., Johnson R., Simeonov A., Yasgar A., Zheng W., Austin C. Quantitative high-throughput screening: a titration-based approach that efficiently identifies biological activities in large chemical libraries. *Proc. Nat. Acad. Sci. U.S.A.* 2006;103:11473–11478. PubMed PMID: 16864780.
21. Redhead M., Satchell R., Morkunaite V., Swift D., Petrauskas V., Golding E., Onions S., Matulis D., Unitt J. A combinatorial biophysical approach; FTSA and SPR for identifying small molecule ligands and PAINS. *Anal. Biochem.* 2015;479:63–73. PubMed PMID: 25837771.
22. Owen S., Doak A., Ganesh A., Nedyalkova L., McLaughlin C., Shoichet B., Shoichet M. Colloidal drug formulations can explain “bell-shaped” concentration-response curves. *ACS Chem. Biol.* 2014;9:777–784. PubMed PMID: 24397822.
23. Dahlin J., Walters M. The essential roles of chemistry in high-throughput screening triage. *Future Med. Chem.* 2014;6:1265–1290. PubMed PMID: 25163000.
24. Seidler J., McGovern S. L., Doman T. N., Shoichet B. K. Identification and prediction of promiscuous aggregating inhibitors among known drugs. *J. Med. Chem.* 2003;46:4477–4486. PubMed PMID: 14521410.
25. Feng B. Y., Shoichet B. K. A detergent-based assay for the detection of promiscuous inhibitors. *Nat. Protoc.* 2006;1:550–553. PubMed PMID: 17191086.
26. Nelson K., Dahlin J., Bisson J., Graham J., Pauli G., Walters M. The essential medicinal chemistry of curcumin. *J. Med. Chem.* 2016;60:1620–1637. PubMed PMID: 28074653.
27. Shoichet B. K. Screening in a spirit haunted world. *Drug Discov. Today.* 2006;11:607–615. PubMed PMID: 16793529.

28. Gubler H., Schopfer U., Jacoby E. Theoretical and experimental relationships between percent inhibition and IC50 data observed in high-throughput screening. *J. Biomol. Screen.* 2013;18:1–13. PubMed PMID: 22853931.
29. Prinz H. Simplification traps. *J. Chem. Biol.* 2012;5:1–4. PubMed PMID: 23226811.
30. Feng B., Shelat A., Doman T., Guy R., Shoichet B. High-throughput assays for promiscuous inhibitors. *Nat. Chem. Biol.* 2005;1:146–148. PubMed PMID: 16408018.
31. Dahlin J. L., Nissink J. W. M., Francis S., Strasser J., John K., Zhang Z., Walters M. A. Post-HTS case report and structural alert: promiscuous 4-aryl-1,5-disubstituted-3-hydroxy-2H-pyrrol-2-one actives verified by ALARM NMR. *Bioorg. Med. Chem. Lett.* 2015;25:4740–4752. PubMed PMID: 26318992.
32. Irwin J., Duan D., Torosyan H., Doak A., Ziebart K., Sterling T., Tumanian G., Shoichet B. An aggregation advisor for ligand discovery. *J. Med. Chem.* 2015;58:7076–7087. PubMed PMID: 26295373.
33. Laplante S. R., Carson R., Gillard J., Aubry N., Coulombe R., Bordeleau S., Bonneau P., Little M., O'Meara J., Beaulieu P. L. Compound aggregation in drug discovery: implementing a practical NMR assay for medicinal chemists. *J. Med. Chem.* 2013;56:5142–5150. PubMed PMID: 23730910.
34. Huth J. R., Mendoza R., Olejniczak E. T., Johnson R. W., Cothron D. A., Liu Y., Lerner C. G., Chen J., Hajduk P. J. ALARM NMR: a rapid and robust experimental method to detect reactive false positives in biochemical screens. *J. Am. Chem. Soc.* 2005;127:217–224. PubMed PMID: 15631471.
35. Huth J. R., Song D., Mendoza R. R., Black-Schaefer C. L., Mack J. C., Dorwin S. A., Lador U. S., Severin J. M., Walter K. A., Bartley D. M., Hajduk P. J. Toxicological evaluation of thiol-reactive compounds identified using a la assay to detect reactive molecules by nuclear magnetic resonance. *Chem. Res. Toxicol.* 2007;20:1752–1759. PubMed PMID: 18001056.
36. Feng B., Toyama B., Wille H., Colby D., Collins S., May B., Prusiner S., Weissman J., Shoichet B. Small-molecule aggregates inhibit amyloid polymerization. *Nat. Chem. Biol.* 2008;4:197–199. PubMed PMID: 18223646.
37. Owen S. C., Doak A. K., Wassam P., Shoichet M. S., Shoichet B. K. Colloidal aggregation affects the efficacy of anticancer drugs in cell culture. *ACS Chem. Biol.* 2012;7:911–919. PubMed PMID: 22625864.
38. Sassano M., Doak A., Roth B., Shoichet B. Colloidal aggregation causes inhibition of G protein-coupled receptors. *J. Med. Chem.* 2013;56:2406–2414. PubMed PMID: 23437772.
39. Doak A., Wille H., Prusiner S., Shoichet B. Colloid formation by drugs in simulated intestinal fluid. *J. Med. Chem.* 2010;53:4259–4265. PubMed PMID: 20426472.
40. Hsieh J., Wang X., Teotico D., Golbraikh A., Tropsha A. Differentiation of AmpC beta-lactamase binders vs. decoys using classification kNN QSAR modeling and application of the QSAR classifier to virtual screening. *J. Comput. Aided Mol. Des.* 2008;22:593–609. PubMed PMID: 18338225.
41. Rao H., Li Z., Li X., Ma X., Ung C., Li H., Liu X., Chen Y. Identification of small molecule aggregators from large compound libraries by support vector machines. *J. Comput. Chem.* 2010;31:752–763. PubMed PMID: 19569201.

42. Pohjala L., Tammela P. Aggregating behavior of phenolic compounds - a source of false bioassay results? *Molecules*. 2012;17:10774–10790. PubMed PMID: 22960870.





# Assay Validation, Operations and Quality Control

Viswanath Devanaryan, PhD, Timothy L. Foley, PhD, Madhu Lal-Nag, PhD,  
Jeffrey R. Weidner, PhD, and Mary Jo Wildey, PhD



# Development and Applications of the Bioassay Ontology (BAO) to Describe and Categorize High-Throughput Assays

Uma D. Vempati<sup>1</sup> and Stephan C. Schürer<sup>2</sup>

Created: May 1, 2012; Updated: October 1, 2012.

## Abstract

Ontologies are important tools to organize information and formalize knowledge in a subject domain. In this chapter, the authors introduce Bioassay Ontology (BAO), the first ontology to describe and categorize chemical biology and drug screening assays and their results. BAO has been applied to standardize, organize and annotate assays and screening results to enable analysis and information extraction across multiple and diverse data sets, with the goal to infer new knowledge about the molecular mechanism of action of small molecules in the assay model systems. The authors provide an overview of BAO and present several applications, including the annotation of a large number of HTS assays and an assay annotation tool (BioAssayAnnotationTemplate). BAO has also been used in a software tool (BAOsearch) to enable query and exploration of assay experiments and results via a simple user interface. BAO is an evolving ontology with a growing number of applications and user community.

## Introduction

High-throughput screening (HTS) of small molecules is one of the most important strategies to identify novel entry points projects for drug discovery projects (1). For several decades, HTS and ultra-high throughput screening (uHTS) have primarily been in the realm of the pharmaceutical industry, where huge amounts of data have been generated using these technologies. In 2003, NIH made HTS accessible to public sector research via the Molecular Libraries Program (MLP), the aim of which is to advance translational research (2). MLP projects leverage innovative assay technologies to develop compounds, termed chemical probes, which are effective at modulating specific biological processes or disease states via novel targets. The program has established publicly funded screening centers, along with a common screening library (the Molecular Libraries Small Molecule Repository, or MLSMR) and a data repository, PubChem (3). One of the visions of the MLP is to generate a complete data matrix screening the same compound library

---

<sup>1</sup> Center for Computational Science, University of Miami Miller School of Medicine. University of Miami, Florida. <sup>2</sup> Department of Molecular and Cellular Pharmacology, University of Miami Miller School of Medicine. University of Miami, Florida.



**Figure 1.** Chapter overview: Development and applications of the Bioassay Ontology (BAO) to describe and categorize high-throughput assays.

across a large and diverse biological space, thereby producing the most comprehensive public chemical biology data resource.

The ability to identify suitable leads for novel probes or drug development candidates requires carefully designed screening campaigns. Such campaigns are typically a series of assays performed to select a suitable class of compounds that show the desired biological effect, and to establish that the observed effect is based on a perturbation of the biological system by the small molecule (and not, for example, due to interference with the assay system). It is particularly desirable to establish the molecular mechanism of action (MOA) of a lead compound. A screening campaign typically includes primary screens (screening a large number of compounds very fast), confirmatory screens (replicates), concentration response screens, and various types of secondary assays, such as orthogonal or counter assays. If suitable compound series are identified, SAR (structure activity relationship) studies are performed, and a project can then move forward onto lead optimization. In the context of the MLP, it should be noted that the NIH Chemical Genomics Center (NCGC) developed an innovative screening protocol combining primary and concentration response screening, called quantitative HTS (qHTS) (4). Using the qHTS approach, an entire compound library is screened at several concentrations, enabling the identification of SAR directly from the primary screening results; thus, the discovery process is accelerated, while also producing a more information rich data matrix. For assays run at the MLP and deposited to PubChem, the results and conclusions from a screening campaign are in most cases deposited as a separate “assay” called the “summary

assay”. However, in PubChem, it is not easy to retrieve all assays from a campaign together with their particular purpose (primary, confirmatory, secondary) and various other important characteristics, because relationships between assays to describe campaigns and other critical metadata are not captured in a way that would allow systematic querying.

Similarly to the HTS datasets produced in the pharmaceutical industry, the public sector screening data are considered a valuable resource, which has received wide-spread attention. However, their diversity and quantity also present enormous challenges to organizing, standardizing, and integrating the data to maximize their scientific, and ultimately, their public health impact. In response to calls for HTS standards (5), we have taken the initiative in defining a knowledge model and terminology to describe bioassays, such as those produced by the MLP and deposited into PubChem. A recent report describing Minimum Information About a Bioactive Entity (MIABE) (6) further emphasizes the need for controlled terminologies and standardized approaches to describe chemical biology assays and their outcomes. We are working towards establishing a community standard to formally describe probe and drug discovery assays and screening results. Our approach is similar to the one taken in other fields such as microarray experimentation, where minimum information specifications (Minimum Information About a Microarray Experiment or MIAME 2.0), multiple data models (MicroArray Gene Expression Object Model or MAGE-OM) and the MGED (Microarray and Gene Expression Data) ontology (7) have been developed and incorporated into Web Services such as the Gene Expression Omnibus (8) to facilitate data exchange. Having such standards in place and implemented in an appropriate informatics infrastructure (9) will facilitate a) the re-use of assay results beyond an individual project (screening campaign) for the purpose of identifying compounds based on established or hypothesized molecular MOA; and, b) the evaluation of screening results in the context of all available information, for example to remove promiscuous compounds, or to perform global analyses of chemical versus biological space. Comprehensive and standardized assay annotations will also facilitate the design of screening campaigns and aid in the development and implementation of new assays. Here, we focus on the Bioassay Ontology (BAO, <http://bioassayontology.org/>) to formally describe and categorize biological screening assays and their results.

Ontologies have been used in biology to organize information within a domain, and to a lesser extent, to annotate experimental data. The most successful and highly-used biomedical ontology is the Gene Ontology (GO) (10), which consists of terms to describe gene product biological processes, cellular localization and molecular function. Several hundred ontologies are hosted by the Open Biological and Biomedical Ontologies (OBO) Foundry (102, counted on 4/15/2011) (11) as well as the National Center for Biomedical Ontologies (NCBO, 263 ontologies counted on 4/15/2011) (12), centered on domains ranging from African traditional medicine to Zebrafish anatomy. However, no public ontology to describe assays in the drug and probe discovery domain exists. Moreover, there is no ontology to describe the screening outcomes. The most obvious reason for this is that HTS datasets have not been publically accessible until recently, with the

establishment of PubChem. We created the BioAssay Ontology (BAO) for the purpose of standardizing, organizing and semantically describing these biological assays and screening results. The BAO is under active development, and we refer the reader to our website (<http://bioassayontology.org/>) and the BAO Wiki (<http://bioassayontology.org/wiki>), which contain the most current information related to this project.

In this article, we briefly discuss the main concepts required to describe important details of bioassay experiments and screening results. Then, we report the development of the ontology (BAO) and provide an overview/outline of the BAO with examples of how some of the concepts are implemented in the BAO; we also discuss related resources incorporated into the BAO. Subsequently, we describe applications of the BAO. Most importantly, the annotation of assays including the annotation process, statistics of the distribution of assays in PubChem based on the main BAO concepts, and an example of a screening campaign using the BAO are described. We also show how BAO annotations can be leveraged to analyze data across many assays to derive novel insights that are not readily obtained from any individual screening campaign. The BAO supports inferences within the functionality of Web Ontology Language (OWL) 2.0, raising the possibility of formally reasoning across the data, with several possible applications. To simplify assay annotations and to enable a large community to annotate assays, we generate a prototypical annotation template. Finally, we briefly describe BAOsearch, a Semantic Web software application to explore screening assays and results in the context of BAO. Figure 1 shows a high level overview of the contents of this chapter

## The BAO to organize screening assays, results and campaigns

### Organizing bioassays into interpretable categories

One of the goals of the BAO was to organize assays by several main concepts describing their most important characteristics, and enabling the meaningful categorization of assays, for example, by biology or technology. Such a classification of assays enables the identification of related or similar assays, either for the purpose of data analysis or assay development. These main categories were determined based on competency questions such as:

- i. What is known about the biological target of the assay?
- ii. Was the assay performed on a purified protein or in a cellular system (assay format)?
- iii. What are the characteristics of the perturbing agent (e.g. small molecule)?
- iv. How was the perturbation converted into a detectable signal?
- v. What was the physicochemical method on which the detection is based?

To answer such questions across a large and diverse assay space, we organized the BAO into the main hierarchies describing assay format, design, target, and detection technology (described in Overview of BAO). For example, cell-based assays can be divided into the following broad categories, based on the assay design: reporter-gene,

viability, cell morphology, redistribution (protein/second messenger/metal/dye redistribution), membrane potential, binding, second messenger (cAMP, calcium), and enzymatic assays. To illustrate this further, assays utilizing luciferase technology can be classified into subcategories, such as luciferase reporter gene, viability, adenosine triphosphate (ATP)-coupled, luciferin-coupled, and luciferase enzyme activity assays. All of the main BAO concepts can also be further specified. For example, to describe a permanent cell line, it will be relevant to describe growth mode (adherent or in suspension), cell line culturing components (including the culture medium and assay medium), cell line modifications (such as transfection or viral transduction), and transfection attributes (DNA construct and transfection agent) used to modify a cell-line. Having such information about cell lines used in assays would make it possible to delineate the role of the different attributes to the outcome of an assay, and thus, would facilitate assay design and optimization.

### Describing screening outcomes/results

Another important question to analyze assay results is: How were the results reported/quantified? Although the BAO covers many assay types, including endpoint and kinetic assays and the corresponding outcomes, we specifically focused on describing the most important HTS types, such as single concentration response type and concentration response assays. Typical endpoints of assays include  $IC_{50}$ ,  $EC_{50}$ , and percent inhibition, percent activation, respectively (described in the Overview of BAO section). Further specifications about assays endpoints, for example the curve fit method or normalization, are also described.

### Describing screening campaigns

To describe screening campaigns, we need concepts to describe the assay stage (primary, confirmatory, secondary), the measurement throughput quality (single concentration, concentration response, single measurement, and multiple replicates), a campaign name, and relationships to define how one assay is related to another in a screening campaign, including typical confirmatory and counterassays. These annotations are needed to define business rules to aggregate assay results across an entire screening campaign. Moreover, in combination with the assay categories above, the overarching goal is to enable the meaningful aggregation of assay outcomes across many campaigns to identify compounds with known or likely molecular mechanism of action (MMOA).

## Ontology development and overview of the BAO

### Ontology Development

During the last 10 years, tremendous progress has been made in developing Semantic Web (13) technologies with the goals being the formalization of knowledge, linking information across different domains, and integrating complex, diverse, and large data sets. Semantic Web technologies can solve many data integration problems, because they

formally define semantics and support descriptive formal knowledge representations (14). Ontologies, like controlled vocabularies and thesauri, describe what things mean by linking terms to a human-readable definition. As such, ontologies are used for sharing knowledge in a common language, as well as to organize that knowledge. Beyond controlled vocabularies and thesauri linking terms to human-readable definitions and Uniform Resource Identifiers (URIs), ontologies can be used to formalize knowledge in explicit (logical) axioms defining classes, their properties and relationships. Thus, ontologies enable a computational system to reason formally on the content, with the potential to discover new knowledge by inference or to identify possible sources of errors.

The BAO was constructed using Protégé version 4.1 (15) in the OWL 2.0 (16), which supports description logic (DL). A number of available plugins were used throughout the development process, including OWLViz2 (17) and OntoGraf (18) for visualization, and DL reasoning engines HermiT (19) and Pellet (20). Our ontology development follows established ontology engineering methodologies using a combination of top-down (domain expert-driven) and bottom-up (data-driven) approaches (21). The BAO is instantiated in a well-specified syntax and designed to share a common space of identifiers. The ontology has a formally specified and clearly delineated content. All terms in the ontology have textual definitions. The BAO is developed using version control and the derived products; for example, an annotation tool or BAO annotated content (described in Application of the BAO) are developed to correspond to a specific BAO release. In the development of the BAO, we also make use of existing ontologies and database (described in Integration of BAO with Existing Ontologies and Databases). The BAO (v1.4b1158) has SROIQ(D) (22) expressivity and consists of 1035 classes, 47 object properties (relations), 9 data properties, and 27 individuals (not including individuals from annotated assays or endpoints).

## Overview of BAO

In the following, we use ‘single quotes’ to denote BAO classes and *italic* font to denote the relationships in the BAO. The main class hierarchies in the BAO include ‘format’, ‘design’, ‘meta target’, ‘detection technology’ and ‘endpoint’, which were described in a recent publication (23). ‘Format’ and ‘perturbagen’ have direct relationships to ‘bioassay’; ‘meta target’, ‘detection technology’, ‘design’, and ‘endpoint’ are linked to ‘bioassay’ via ‘measure group’. ‘Measure group’ is a concept created to group experimental outcomes into sets, and thus enables the modeling of multiplexed and multi-parametric assays. Each BAO class hierarchy includes multiple levels of sub-classes and is also linked to a corresponding specification class hierarchy (Figure 2). Specification classes contain additional details and attributes about a specific BAO assay component class. In addition, the BAO includes general assay specifications such as footprint (plate density), assay conditions (including pH, incubation time), readout content, quality measurement (including z-factor, z’-factor, signal to noise, coefficient of variation), measurement throughput quality, and assay stage to describe campaigns, among others.



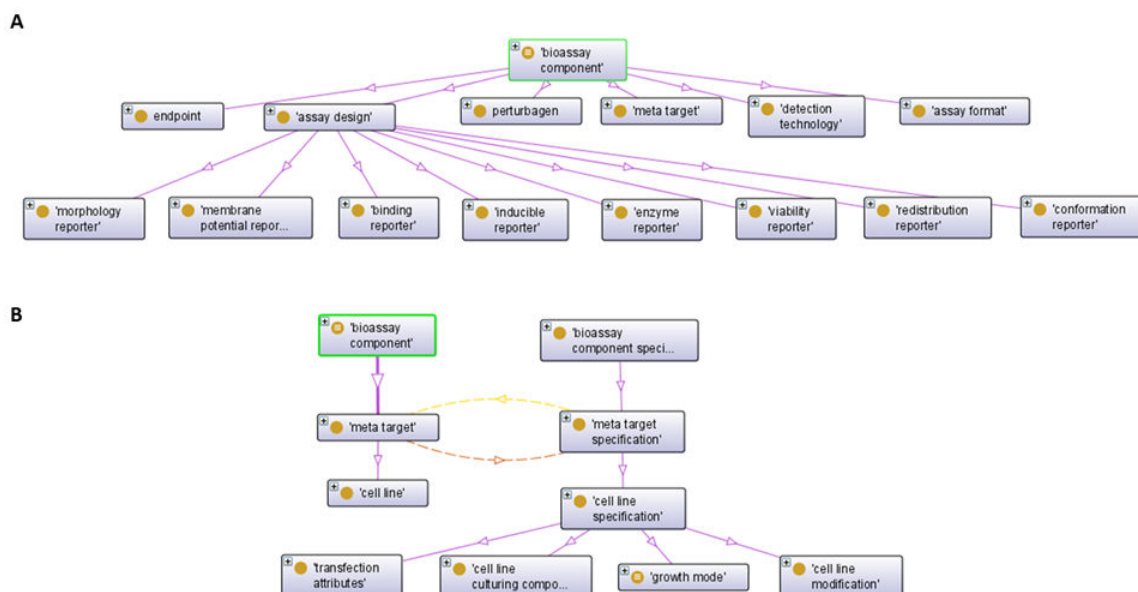


**Figure 2.** (A) Illustration of the major BAO class hierarchies, including the top level classes of ‘assay design.’ (B) The ‘cell line’ concept and its corresponding specification class hierarchy.

As the BAO is under active development, we want to refer readers to the BAO website (<http://bioassayontology.org/>) for the most current classes and their exact definitions. Here, we briefly define the main class hierarchies. ‘Assay format’ is a conceptualization of assays based on the biological and/or chemical features of the experimental system, and includes several broad categories: ‘biochemical format’, ‘cell-based format’, ‘cell-free format’, ‘tissue-based format’, ‘organism-based format’, and ‘physicochemical format’. ‘Assay design’ describes the assay methodology and implementation of the way in which the perturbation of the biological system is translated into a detectable signal. Specifically, the ‘assay design’ is organized into various types of reporters, including ‘binding reporter’, ‘conformation reporter’, ‘enzyme reporter’, ‘inducible reporter’, ‘membrane potential reporter’, ‘morphology reporter’, ‘redistribution reporter’, and ‘viability reporter’ (Figure 2A). Each of these have several subclasses and attributes (specifications); for example, luciferase reporter gene assays (‘luciferase induction’) that were analyzed below are a subclass of reporter gene assays, and several assay kits are available to quantitate that, as described in the corresponding specifications. The BAO describes the physicochemical method of signal detection used in bioassays as ‘detection technology’. It includes ‘spectrophotometry’, ‘fluorescence’, ‘luminescence’, ‘radiometry’, ‘label free’, and ‘microscopy’. Assay ‘meta target’ describes what is known about the biological system and/or its components interrogated in the assay (and influenced by the perturbagen). ‘Meta target’ can be directly described as a ‘molecular target’ (e.g. a purified protein or a protein complex), or indirectly by a ‘biological process’ or event (e.g. ‘regulation of transcription’). In the case of cell-based assays, the BAO defines important attributes of a ‘permanent cell line’ in an assay (Figure 2B). The BAO cell line specifications include: ‘growth mode’, which describes whether it grows ‘adherent’ or in ‘suspension’; a ‘cell line

culturing component' that includes the 'culture medium' and 'assay medium'; a 'cell line modification' that describes the type of modification that the cell line underwent, e.g. 'transfection', 'viral transduction', etc.; and 'transfection attributes', namely the 'DNA construct' and the 'transfection agent' used to modify a cell-line.

An assay 'endpoint' describes a quantitative or qualitative result of the bioassay. The main classes that we identified are concentration- and response-type endpoints. Simple examples include 'IC<sub>50</sub>', 'EC<sub>50</sub>', and 'percent inhibition', 'percent activation', respectively. In the BAO, the concept 'endpoint' is described using DL by classifying them (among others) into 'response' and 'perturbagen concentration' endpoints, and formalizing how these are related. Endpoints are linked to what type of change they quantify, such as 'inhibition' or 'activation', and the BAO also formalizes relationships between different types of endpoints; for example, the fact that an IC<sub>50</sub> corresponds to the perturbagen concentration at which 50 percent response (and specifically inhibition) is observed. This allows the querying of screening results by a mechanism of action, such as inhibition or activation, or a query based on type of results (IC<sub>50</sub>, EC<sub>50</sub> vs. percent inhibition, activation) and the retrieval of semantically equivalent results (described in Inference and Reasoning Using the BAO) (23).

In addition to annotating individual assays, the BAO is also suited to defined screening campaigns. As mentioned above, the BAO includes classes to define a campaign name (purpose), an 'assay stage' ('primary', 'confirmatory', 'secondary') and a 'measurement throughput quality' including 'single concentration single measurement' (which we also define as HTS), 'single concentration multiple replicates', 'concentration response single measurement' (defined as qHTS), and 'concentration response multiple replicates'. Relationships to define how one assay relates to another in a screening campaign include '*is confirmatory assay of*', '*has confirmatory assay*', '*is counter assay of*', '*has counter assay*', '*uses orthogonal technology to*', and '*uses same technology as*', etc. Relationship characteristics are also defined; for example, the inverse relationships are '*is confirmatory assay of*' and '*has confirmatory assay*'. Based on these classes and relationships, it is possible to define business rules to aggregate results within one screening campaign, and potentially across many campaigns, to prioritize compounds of a known or hypothesized MMOA. Table 1 shows examples of sets of assays comprising screening campaigns (partial view) and their (informal) BAO annotations and relationships.

**Table 1.** Partial (informal) view of BAO annotations and relationships to describe assays related to the screening campaigns, "Identification of inhibitors of Kruppel-like factor 5" and "Novel allosteric modulators of the M5 muscarinic receptor."

|                         |   |                    |                 |
|-------------------------|---|--------------------|-----------------|
| <b>Screen. campaign</b> | "Identification of inhibitors of Kruppel-like factor 5" |                    |                 |
| <b>AID</b>              | 1700  | 1973               | 1825            |
| <b>Assay Stage</b>      | Primary Assay   | Confirmatory Assay | Secondary Assay |

Table 1. continues on next page...

Table 1. continued from previous page.

|   |   |   |   |
|---|---|---|---|
| <b>Relationship</b>                         | has confirmatory assay 1973,<br>has counter assay 1825      | has primary assay 1700                        | has primary assay 1700                        |
| <b>Assay Measurement Throughput Quality</b> | Single concentration<br>single measurement                  | Concentration response<br>multiple replicates | Single concentration<br>single measurement    |
| <b>Endpoint</b>                             | % Inhibition  | IC <sub>50</sub>                              | % Inhibition                                  |
| <b>Assay Format</b>                         | Cell-based format   | Cell-based format                             | Cell-based format                             |
| <b>Assay Design</b>                         | Luciferase induction  | Luciferase induction                          | Viability reporter, ATP<br>content            |
| <b>Meta Target</b>                          | Regulation of<br>transcription                              | Regulation of<br>transcription                | Cell death                                    |
| <b>Detection Technology</b>                 | Luminescence  | Luminescence                                  | Luminescence                                  |
| <b>Measured Entity</b>                      | Luciferase  | Luciferase                                    | ATP   |
| <b>Screen. campaign</b>                     | "Novel allosteric modulators of the M5 muscarinic receptor" |   |   |
| <b>AID</b>                                  | 2665  | 2194  | 2206  |
| <b>Assay Stage</b>                          | Primary   | Confirmatory                                  | Secondary                                     |
| <b>Relationship</b>                         | has confirmatory assay 2194,<br>has counter assay 2206      | has primary assay 2665                        | has primary assay 2665                        |
| <b>Assay Measurement Throughput Quality</b> | Single concentration<br>single measurement                  | Concentration response<br>multiple replicates | Concentration response<br>multiple replicates |
| <b>Endpoint</b>                             | Maximal activation  | EC <sub>50</sub>                              | EC <sub>50</sub>                              |
| <b>Assay Format</b>                         | Cell-based format   | Biochemical format                            | Cell-based format                             |
| <b>Assay Design</b>                         | Calcium redistribution                                      | Radioligand binding                           | Calcium redistribution                        |
| <b>Meta Target</b>                          | Muscarinic acetylcholine<br>receptor M5                     | Muscarinic acetylcholine<br>receptor M5       | Muscarinic acetylcholine<br>receptor M1       |
| <b>Detection Technology</b>                 | Fluorescence intensity                                      | Scintillation counting,<br>filter assay       | Fluorescence intensity                        |
| <b>Measured Entity</b>                      | Calcium   | (3H)-NMS                                      | Calcium                                       |

## Integration of BAO with existing ontologies and databases

We analyzed existing biomedical ontologies with respect to their coverage of concepts required to describe HTS assays performed for probe and drug discovery projects. Although no resource existed to describe the experiments and data types, including biochemical and cell-based assays of various technologies and assay designs using small molecules, a number of existing ontologies and bioinformatics databases contain information that are needed to define parts of concepts related to HTS. We leverage these existing resources in the BAO. For example, GO (10) 'biological process' and Cell Line Ontology (CLO) (24) 'cell line' classes, along with additional parameters, are used in the

BAO ‘meta target’ and ‘meta target specifications’. CLO is currently being extended as a collaborative effort to cover cell lines relevant for biological screening (25). Organism names associated with targets were imported from NCBITaxon (26). Protein target names and IDs were referenced from UniProt (27). From Unit Ontology (UO) (28), ‘concentration unit’, ‘time unit’, and ‘length unit’ terms were imported into the BAO. The Ontology for Biomedical Investigation (OBI) also includes relevant information, although it describes different types of experiments (29). We are also currently working on importing the disease terminology from the human disease (DOID) ontology, which would facilitate linking targets studied in a bioassay directly to a disease (30).

We have used standard practices that allow modular reuse of external ontologies. Towards this, we have used two methods: OntoFox (31) and the module and axiom extraction facilities built into the OWL3 API (32). We have added the additional general concept inclusion axioms (GCIs) to the BAO to bridge the host concepts and the imported axioms, and we checked the safety and the satisfiability of the knowledge base using the Hermit reasoned in Protégé.

## Application of the BAO

### Expert annotation of PubChem assays using the BAO

#### Annotation Process

Using the BAO, a large number of assays were annotated by domain experts (Ph.D. biologists with expertise in HTS). To aid in manual annotation, assays were first clustered based on textual descriptions. We achieved this by initially generating a text fingerprint from all words used in title, description, protocol, and source using the Pipeline Pilot 8.0 (Accelrys, San Diego, CA) text analytics component collection. The assay “documents” were then clustered based on the fingerprints using the Tanimoto similarity metric. This method grouped together similar assays very effectively; for example, assays from the same screening campaign, by center, or assays with the same procedure or assay design, such as NCGC toxicity assays, were grouped together. Following cluster preprocessing, assays were manually annotated by assay format, design, detection technology, and other BAO categories, which included over 100 distinct concepts. The assay annotations from each assay were cross-checked, and then loaded into a Resource Description Framework (RDF) triple store. Screening outcomes (endpoints) were loaded into a relational database.

#### Statistics of PubChem Assay Categories

Using BAO annotations, assays can be readily categorized. We performed statistics on the 1,008 PubChem assays that we manually curated so far (Figure 3). For categorizations based on ‘assay stage’ there were: 286 primary assays, 425 confirmatory assays, 242 secondary assays, and 55 summary assays. In terms of ‘assay format’, the majority of assays were of ‘cell-based format’ [548] or ‘biochemical format’ [372]. There are also a few assays having ‘organism-based format’ [13], ‘cell-free format’ [12], and ‘tissue-based format’ [8]. The ‘assay design’ was curated as ‘binding reporter’ [241], ‘enzyme reporter’

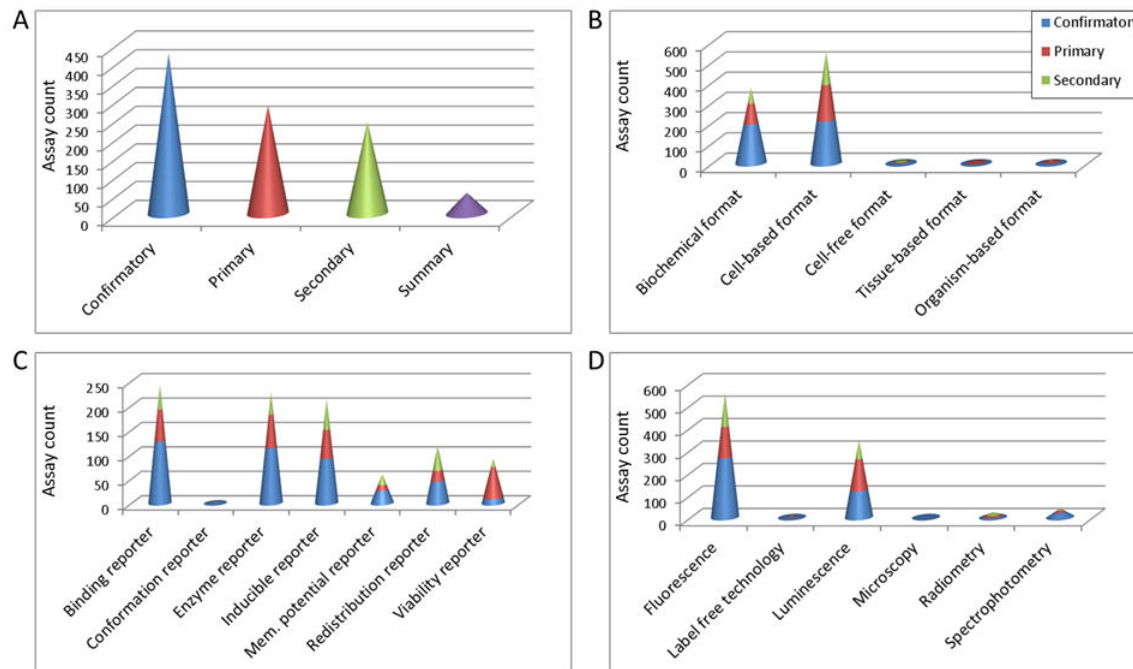


**Figure 3.** PubChem Assay counts based on BAO annotations of assays by 'assay stage' (A) 'assay format' (B), 'assay design' (C), and 'detection technology' (D) of 1,008 assays.

[227], 'inducible reporter' [212], 'redistribution reporter' [117], 'viability reporter' [91] and a few 'membrane potential reporter' [59] and 'conformation reporter' [5] types. Assays were annotated with the following 'detection technologies': 'fluorescence' [553], 'luminescence' [342], 'spectrophotometry' [39], 'radiometry' [11], 'label free technology' [6], and 'microscopy' [1]. A high level 'bioassay type,' based on compound properties and processes that are interrogated in the assay, was assigned to PubChem assays as follows: 'functional' [722], 'binding' [193], and 'ADMET' [33]. The types of assay classifications given above are relevant to interpret screening results; for example, biochemical assays provide direct evidence of the mechanism of action (e.g. inhibition of an enzyme), while activity in cell-based assays implies that a compound is cell permeable.

### Annotating Screening Campaigns Using the BAO

In addition to the above annotations, the BAO can be used to group assays into screening campaigns and to organize them by assay stage, measurement throughput quality, and various assay relationships, among other categories. Table 1 provides a partial (informal) view of the BAO annotations and relations of a screening campaign to identify inhibitors of Kruppel-like factor 5 performed at the Scripps Research Molecular Screening Center (33).

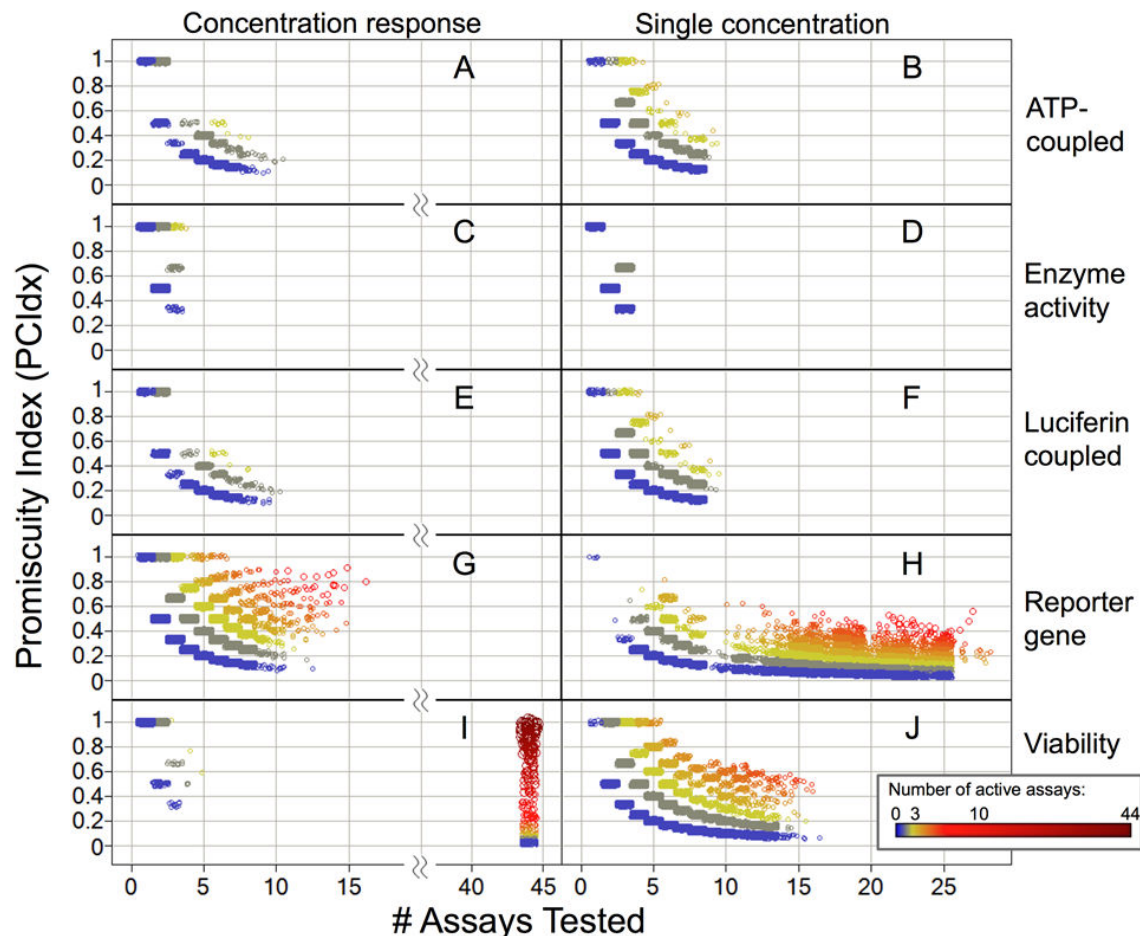


**Figure 4.** Compound promiscuity by luciferase assay technologies. For each compound, the Promiscuity Index versus number of tested assays is depicted. (A, B) Adenosine triphosphate (ATP)-coupled enzyme activity (e.g., kinase activity, not viability). (C, D) Luciferase enzyme activity. (E, F) Luciferin-coupled enzyme activity (e.g., P450). (G, H) Luciferase reporter gene assays. (I, J) Cell viability assays (ATP coupled). (A, C, E, G, I) Concentration-response assays. (B, D, F, H, J) Single-concentration assays. Color and size indicate the number of assays (of the particular luciferase assay type) in which a compound was active. In total, 87,615 data points with at least one active assay are shown: (A) 3,457, (B) 5,619, (C) 2,313, (D) 3,646, (E) 3,457, (F) 5,619, (G) 14,200, (H) 36,685, (I) 1,413, (J) 11,206. Figure reprinted from reference (34) with permission from Sage publications.

## Cross Assay Data Analyses Using the BAO

In the following example, we leveraged BAO annotations of PubChem assays to elaborate on compounds that are promiscuously active in assays that employ a luciferase-based design, which is one of the most widely used assay technologies. We were also interested in suggesting possible mechanisms underlying their promiscuous activity (34). Luciferase-assays were classified into five subcategories:

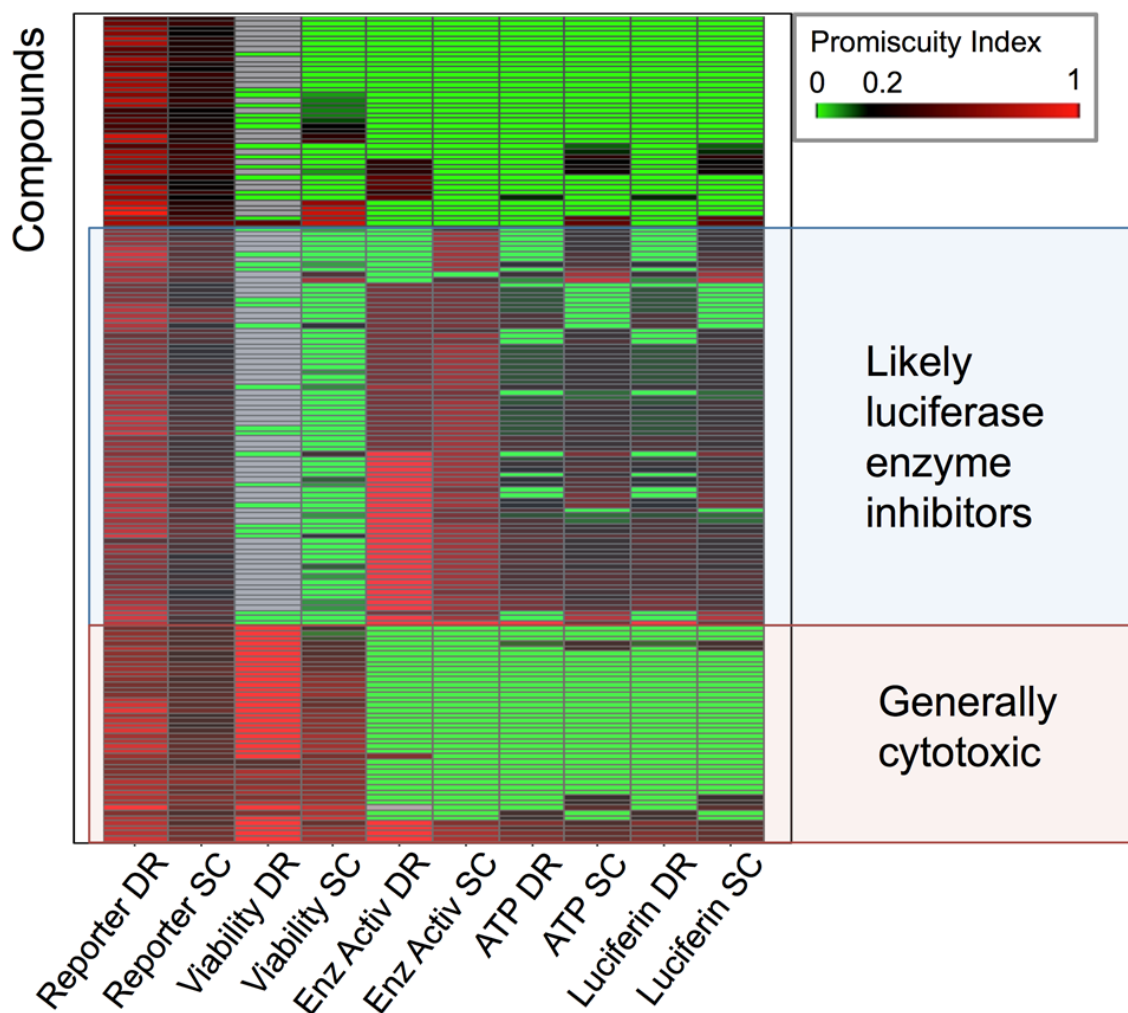


**Figure 5.** Heat map of the 161 most promiscuous compounds in luciferase reporter gene assays, which are active in at least 5 concentration-response and 5 single concentration (luciferase reporter) assays. DR and SC denote “dose response” and “single concentration,” respectively. Shown are the promiscuity indices of all compounds in the different luciferase assay categories for both concentration-response and single concentration assays, respectively, clustered by their PCI<sub>dx</sub> profiles. Two groups of promiscuous reporter gene compounds were apparent, suggesting the mechanism for reporter gene assay promiscuity; this mechanism is one in which compounds were also active in viability assays (red shade) and the other where compounds were also active in luciferase enzyme assays (blue shade). Figure reprinted from reference (34) with permission from Sage publications.

1. Reporter gene assays: use the luciferase gene downstream of a promoter of interest. The amount of luciferase expressed is quantified by the intensity of light (luminescence) produced in the presence of substrates, ATP and luciferin.
2. Viability assays: estimate the proportion of living cells in an assay by measurement of ATP content in a luciferase-catalyzed reaction
3. Adenosine triphosphate (ATP)-coupled assays: measure the residual amount of ATP (e.g, after a kinase reaction) by a coupled luciferase reaction.

4. Luciferin-coupled assays: measure the amount of luciferin generated after detoxification by cytochrome P450 enzyme activity
5. Luciferase enzyme activity assays: quantify the luciferase enzyme activity by the amount of light produced in a biochemical reaction.

Figure 4 illustrates the promiscuity of compounds in these five types of assays tested at either a single concentration or concentration-response. The promiscuity index (PCIdx) was simply defined as the ratio of the number of assays in which a compound was found active, and the number of assays in which it was tested.

Centered on this analysis, compounds can be classified based on their likely mechanism of promiscuity, and this mechanism can be related to their chemical structure. For example, we looked specifically at compounds most frequently active in luciferase reporter gene assays and analyzed their promiscuity in the other types of assays using luciferase (Figure 5). Two clusters emerged, one in which compounds were also active in the majority of viability assays and which are therefore likely toxic, and another where compounds are active in luciferase enzyme inhibition assays and whose activity is therefore likely related to interference with the luciferase enzyme. Several chemotypes were identified, which were consistent with the respective proposed mechanisms (34).

In other examples, as the BAO allows the annotation of important reagents used in an assay, it may thus be applied to identify and analyze the influence of subtle differences in the assay conditions, e.g., the presence of ‘detergent’, ‘reducing agent’, etc. In PubChem AIDs 584, 585, 1002 and 1003, compounds were screened to identify AmpC beta-lactamase inhibitors, both in the presence and absence of 0.01% Triton X-100. These assays were performed at the NCGC, where they used the aggregation profiling approach to identify sensitivity of aggregate formation of compounds to detergent (35, 36). In another campaign, the investigators screened for inhibitors of caspase-1 (AIDs 888, 929) and used reagents with different redox potential to eliminate false positives that could result from compound-generated reactive oxygen species (37, 38). In annotating PubChem assays using the BAO, we capture these types of reagents, facilitating later identification and analysis of the effects of those reagents on screening outcomes.

## Inference and reasoning using the BAO

In addition to identifying assays and subsequently analyzing their results based on BAO class annotations (as described above), the BAO also provides the potential to infer annotations and to identify assays and screening results that are semantically equivalent to a query of interest, but involve query terms not explicitly matched, and therefore could not be easily identified by a classical (relational) search. These types of functionalities are made possible by the open-world reasoning/inference capabilities of the system. For example, the BAO formally (using DL) defines an ‘IC<sub>50</sub>’ endpoint as the ‘perturbagen concentration’ that results in ‘50 percent inhibition’. As described above, both ‘IC<sub>50</sub>’ and ‘percent inhibition’ are specified as quantifying ‘inhibition’ (mode of action). These formal descriptions, among others, enable the retrieval of both IC<sub>50</sub> or percent inhibition results in queries for active compounds, as specified by response and screening concentration



cutoffs (23). BAO inverse relations linking perturbagens, endpoints, and measure groups further enable the identification (by inference) of assays that are active in a certain number of assays. Several SPARQL (Simple Protocol and RDF Query Language) query examples are available from our website (<http://www.bioassayontology.org/>).

In other possible applications, reasoning can be leveraged to identify potential annotation errors, because BAO axioms do not allow all possible combinations of annotations. In a simple example, 'cell-based format' may be associated with specific subclasses of 'assay design' such as 'inducible reporter', 'viability reporter', or 'redistribution reporter', while biochemical assays may be associated with 'enzyme activity'. Because the various subclasses of 'assay design', as well as cell-based and biochemical assays are disjointed, errors could readily be identified via reasoning.

## Assay Annotation Tool to facilitate adaptation of the BAO

To enable biologists to report sufficiently annotated and standardized screening data using the BAO, we developed a proto-typical Excel-based annotation tool called the BioAssay Annotation Template (BAT) (39, 40). To create the BAT, we first generated a BAO-derived dictionary file in which the major BAO class hierarchies are flattened out. The resulting BAO-derived dictionary file includes all the leaf nodes of the BAO with a label/name that reflect the original BAO hierarchy. The IDs of these terms correspond to the original BAO leaf nodes (Figure 6). This flattened version of the BAO was then used in RightField (40), an open-source tool for adding ontology terms to Excel spreadsheets, to generate an annotation template by mapping BAO terms to corresponding Excel cells and exposing them as drop down menus. The Excel-based BAT includes the metadata field names to be annotated with the corresponding BAO terms. It is organized by the main BAO categories. For many of the annotation fields, the template specifies a range of allowed terms from the BAO, which are presented as a drop-down list/menu. To illustrate the use of BAT to annotate data, we illustrate the annotation of a PubChem assay (partial view, Table 2).

As the BAO is version controlled, any BAT corresponds to a specific BAO release. Because the BAO leaf node IDs correspond to the dictionary terms, annotations made based on a previous version of the BAT can (in most cases) be mapped to an updated version. This is critical, because the terminology will likely be optimized over time and new terms may be added corresponding to new assay designs, technologies, etc. We envision the BAO to be established as a standard to describe probe and drug discovery assays, and we will maintain the BAO in the public domain. BAO-derived products, such as dictionary files and an annotation tool (conceptually similar to BAT) will thus enable the community to annotate assays using the same centrally and publically maintained terminology, identified by BAO IDs, since the derived products correspond to a specific recent release of the BAO.

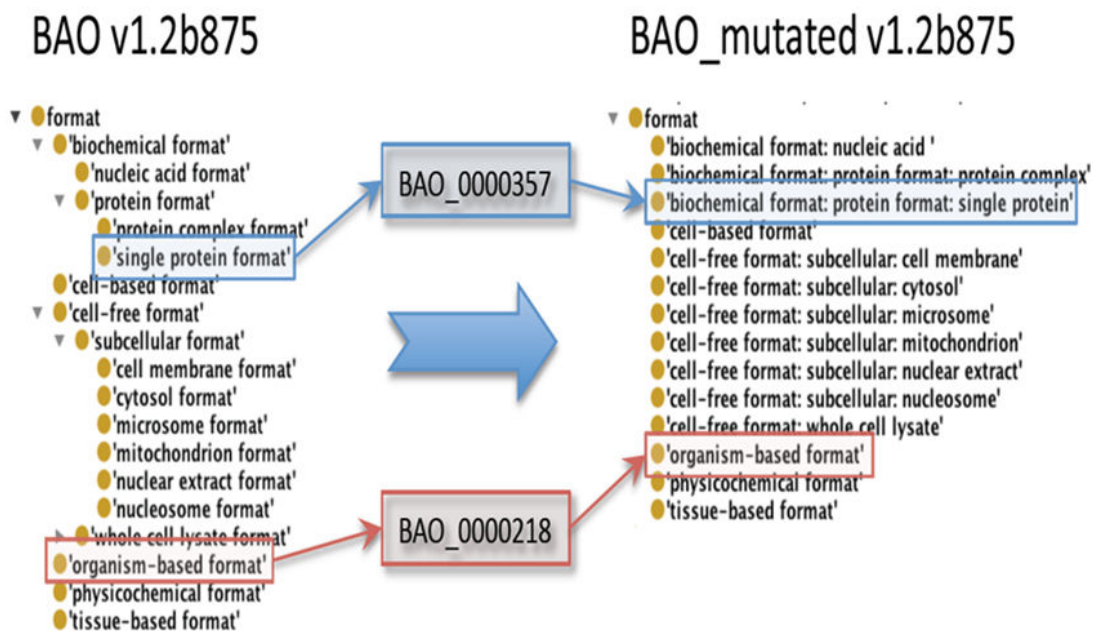


**Figure 6.** Flattening of the BAO class hierarchy generates a BAO-derived dictionary file, which contains only the most specific leaf nodes for the main BAO categories. The BAO leaf node IDs were maintained in this process. The labels/names in the flat dictionary file reflect the original class BAO hierarchy.

**Table 2.** Partial view of annotation of a PubChem assay (AID1700) using BAT

| BAO Concept   | BAO Annotation Terms  |
|---|---|
| id specification: bioassay id: <b>pubchem aid</b>   | 1700  |
| bioassay specification: <b>screening campaign name</b>  | Identification of inhibitors of Krüppel-like factor 5   |
| bioassay specification: <b>assay title</b>  | Primary cell-based high throughput screening assay to identify inhibitors of Krüppel-like factor 5 (KLF5) |
| bioassay specification: <b>assay stage</b>  | primary   |
| bioassay specification: <b>bioassay type</b>  | functional  |
| bioassay specification: <b>assay measurement throughput quality</b>                           | single concentration single measurement   |
| bioassay specification: <b>assay measurement type</b>   | endpoint assay  |
| bioassay specification: <b>content readout type</b>   | single readout  |
| bioassay specification: <b>assay readout method</b>   | regular screening   |
| bioassay specification: pubchem specification: <b>assay source</b>                            | The Scripps Research Institute Molecular Screening Center   |
| <b>assay format</b>   | cell-based format   |
| assay format detail: <b>assay phase characteristic</b>  | heterogeneous assay   |
| meta target: <b>biological process target</b>   | regulation of transcription   |
| meta target: <b>permanent cell line</b>   | IEC-6   |
| meta target detail: cell line specification: <b>cell modification</b>                         | stable transfection   |
| meta target detail: cell line specification: transfection specification: <b>dna construct</b> | luciferase gene with Kruppel-like factor 5-promoter   |
| <b>assay design</b>   | luciferase induction  |
| assay design detail: <b>measured entity</b>   | luciferase  |
| assay design detail: <b>signal direction</b>  | signal decrease   |
| assay design detail: assay kit information: <b>name</b>                                       | SteadyLite-HTS reagent  |
| assay design detail: assay kit information: <b>manufacturer</b>                               | Perkin Elmer  |
| <b>perturbagen</b>  | small molecule  |
| perturbagen detail: <b>compound library</b>   | MLSMR   |
| <b>detection technology</b>   | luminescence  |
| detection technology detail: <b>detection instrumentation</b>                                 | ViewLux CCD imager  |
| detection technology detail: <b>detection instrumentation manufacturer</b>                    | Perkin Elmer  |
| <b>endpoint</b>   | percent inhibition  |
| endpoint detail: <b>pubchem tid</b>   | 1   |
| endpoint detail: response endpoint: <b>response unit</b>                                      | percent   |
| endpoint detail: <b>screening concentration</b>   | 5   |
| endpoint detail: screening concentration: <b>concentration unit</b>                           | micromolar  |
| endpoint detail: curve fit specification: <b>number concentration values</b>                  | 1   |
| endpoint detail: curve fit specification: <b>number replicates</b>                            | 1   |
| endpoint detail: <b>endpoint mode of action</b>   | inhibition  |

## BAOSearch software application

We have developed a prototype Semantic Web software application, BAOSearch (41). BAOSearch is a web-based application for querying, browsing and downloading small molecule bioactivity data by using concepts defined in the BAO. BAOSearch is available at <http://baosearch.ccs.miami.edu/>. BAOSearch is a multi-tier, web-based, AJAX-enabled application written primarily in Java and built following a RESTful Web Services paradigm (Representational State Transfer (REST)), which is a software architecture for multi-platform on-demand content delivery (42, 43); all data are stored in MySQL. SPARQL Database (SDB (44)) is used for the triple-store to store asserted and inferred assay annotations encoded in OWL. Numerical data associated with screening results and chemical structure information are stored in the associated relational schema and accessed using Hibernate (45) in order to enable fast searching of these types of data. The free-text search functionality is enabled using the Lucene text search library (46, 47). This is done using a modified version of the VIVO indexer (48, 49), which pulls new annotations from the triple-store, adds associated information from the BAO based on the subsumption hierarchies, and then processes this information using the Lucene

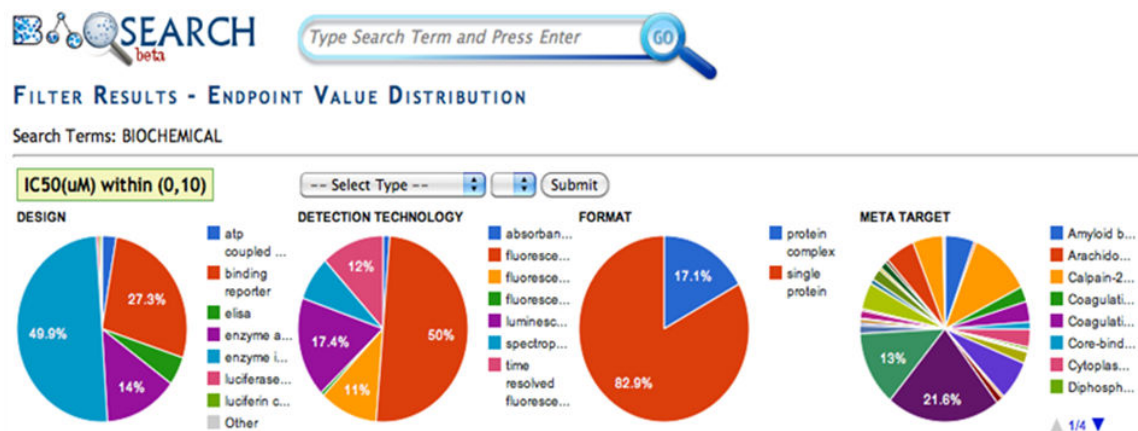


**Figure 7.** BAOsearch facilitates querying, browsing and downloading of small molecule chemistry and bioactivity data by using concepts defined in the BAO.

library to build the free-text search indexes. This is illustrated in Figure 7, where a query was run (by concept search) for identifying biochemical assays having IC<sub>50</sub> endpoints of less than 10 micromolar concentration. The endpoints that satisfy the set search criteria were categorized based on the major BAO concepts, namely, 'assay design', 'detection technology', 'assay format' and 'meta target', as displayed in the results page.

## Summary and conclusion

Large amounts of data are generated by HTS in private and public organizations. Nevertheless, large scale screening capabilities have so far not translated to increased numbers of approved drugs (50). One likely reason is that available data is used inefficiently. It remains a challenge to effectively translate increasing amounts of data into actionable knowledge; at the very least, this is the case for the current public domain data. To address this challenge, we have developed the BioAssay Ontology (BAO) to describe biological assays and their outcomes by concepts that are relevant to interpret, analyze and integrate screening data. The BAO addresses: 1) development of standardized terminology and uniform standards to report HTS and lower throughput probe and drug discovery assays and results; and 2) a semantic description of bioassays and their results to formalize domain knowledge and to facilitate semantic integration with diverse other resources (10, 25, 26, 28). We have used the BAO to annotate PubChem assays, provide statistics, and show that BAO concepts are useful to categorize and analyze screening results (34). Beyond individual assay and results, the BAO also describes screening campaigns. The BAO supports inferences within the functionality of OWL 2.0, raising the possibility to formally reason across the data with potential to discover novel insights or detect possible errors sources and inconsistencies by inference. We are developing the BAO into a community standard to describe assays and their results, with the goal of enabling the integration of diverse datasets and facilitating the interpretation and global comparison and analysis of assay experiments and screening outcomes. The BAO also

includes information to enable linking external content, such as pathway databases. The overarching goal of the BAO is to better organize the available assay space in the context of bioinformatics and chemical biology resources, and in doing so, to enable inference or prediction of MMOA of small molecules based on the corpus of available screening data. The BAO will thus enable the biological research community to better utilize increasingly large and diverse chemical biology screening datasets to develop and test scientific hypotheses. We also see potential for the BAO to facilitate cross-disciplinary collaborations, for example, among screening biologists, chemical biologists, engineers, medicinal chemists, and cheminformaticians, because the BAO provides formal definitions (including relationships) of concepts that relate to several disciplines.

The BAO is openly available and under active development. For the most current release and a wide variety of information related to the BAO project, we refer to our website (<http://www.bioassayontology.org/>) and Wiki (<http://www.bioassayontology.org/wiki>). We continue to annotate assays develop software tools related to the BAO. Our BAOsearch Semantic Web application makes it very easy to query, search, explore, and download BAO-annotated assays, standardized screening results, and chemical structures. It is available at <http://baosearch.ccs.miami.edu/>.

## Acknowledgements

The work presented here was supported by NIH grant RC2 HG005668. We acknowledge resources from the Center for Computational Science at the University of Miami.

## References

1. Posner BA. High-throughput screening-driven lead discovery: meeting the challenges of finding new therapeutics. *Current opinion in drug discovery & development*. 2005;8:487–94. PubMed PMID: 16022185.
2. Austin CP, Brady LS, Insel TR, Collins FS. NIH Molecular Libraries Initiative. *Science*. 2004;306:1138–1139. PubMed PMID: 15542455.
3. Wang Y, Xiao J, Suzek TO, Zhang J, Wang J, Bryant SH. PubChem: a public information system for analyzing bioactivities of small molecules. *Nucleic Acids Res*. 2009;37:W623-33. PubMed PMID: 19498078.
4. Inglese J, Auld DS, Jadhav A, Johnson RL, Simeonov A, Yasgar A, Zheng W, Austin CP. Quantitative high-throughput screening: a titration-based approach that efficiently identifies biological activities in large chemical libraries. *Proc Natl Acad Sci U S A*. 2006;103:11473–11478. PubMed PMID: 16864780.
5. Inglese J, Shamu CE, Guy RK. Reporting data from high-throughput screening of small-molecule libraries. *Nat Chem Biol*. 2007;3:438–441. PubMed PMID: 17637769.
6. Orchard S, Al-Lazikani B, Bryant S, Clark D, Calder E, Dix I, Engkvist O, Forster M, Gaulton A, Gilson M, Glen R, Grigorov M, Hammond-Kosack K, Harland L, Hopkins A, Larminie C, Lynch N, Mann RK, Murray-Rust P, Lo Piparo E, Southan C, Steinbeck C, Wishart D, Hermjakob H, Overington J, Thornton J. Minimum

- information about a bioactive entity (MIABE). *Nature reviews. Drug discovery*. 2011;10:661–9. PubMed PMID: 21878981.
7. Whetzel PL, Parkinson H, Causton HC, Fan L, Fostel J, Fragoso G, Game L, Heiskanen M, Morrison N, Rocca-Serra P, Sansone S-A, Taylor C, White J, Stoeckert CJ. The MGED Ontology: a resource for semantics-based description of microarray experiments. *Bioinformatics (Oxford, England)*. 2006;22:866–73. PubMed PMID: 16428806.
  8. Edgar R, Domrachev M, Lash AE. Gene Expression Omnibus: NCBI gene expression and hybridization array data repository. *Nucleic acids research*. 2002;30:207–10. PubMed PMID: 11752295.
  9. Schürer S, Tsinoremas N: Screening Informatics. In *A Practical Guide to Assay Development and High-Throughput Screening in Drug Discovery*. edited by Chen T CRC Press Taylor and Francis; 2009:233-263.
  10. Ashburner M, Ball CA, Blake JA, Botstein D, Butler H, Cherry JM, Davis AP, Dolinski K, Dwight SS, Eppig JT, Harris MA, Hill DP, Issel-Tarver L, Kasarskis A, Lewis S, Matese JC, Richardson JE, Ringwald M, Rubin GM, Sherlock G. Gene ontology: tool for the unification of biology. The Gene Ontology Consortium. *Nat Genet*. 2000;25:25–29. PubMed PMID: 10802651.
  11. Smith B, Ashburner M, Rosse C, Bard J, Bug W, Ceusters W, Goldberg LJ, Eilbeck K, Ireland A, Mungall CJ, Leontis N, Rocca-Serra P, Ruttenberg A, Sansone SA, Scheuermann RH, Shah N, Whetzel PL, Lewis S. The OBO Foundry: coordinated evolution of ontologies to support biomedical data integration. *Nat Biotechnol*. 2007;25:1251–1255. PubMed PMID: 17989687.
  12. Whetzel PL, Noy NF, Shah NH, Alexander PR, Nyulas C, Tudorache T, Musen MA. BioPortal: enhanced functionality via new Web services from the National Center for Biomedical Ontology to access and use ontologies in software applications. *Nucleic acids research*. 2011;39 Suppl 2:W541-5. PubMed PMID: 21672956.
  13. Berners-Lee T, Hendler J, Lassila O. The Semantic Web. *Scientific American*. 2001.;5. PubMed PMID: 11323639.
  14. Baker CJO, Cheung K-H: *Semantic Web: Revolutionizing Knowledge Discovery in the Life Sciences*. 1st edition. Springer; 2007.
  15. Noy NF, Crubezy M, Ferguson RW, Knublauch H, Tu SW, Vendetti J, Musen MA. Protege-2000: an open-source ontology-development and knowledge-acquisition environment. *AMIA Annu Symp Proc*. 2003.:953. PubMed PMID: 14728458.
  16. OWL 2 Web Ontology Language ( Available at: <http://www.w3.org/TR/owl2-overview/>).
  17. OWLViz. (<http://code.google.com/p/code-owl-plugins/wiki/OWLViz>).
  18. Ontograf. ( Available at: <http://protegewiki.stanford.edu/wiki/OntoGraf>).
  19. Shearer R, Motik B, Horrocks I: Hermit: a highly-efficient OWL reasoner. In *5th International Workshop on OWL: Experiences and Directions (OWLED 2008)*. Karlsruhe, Germany: Universität Karlsruhe; 2008:10.
  20. Sirin E, Parsia B: Pellet system description. In *Proceedings of the International Workshop on Description Logics (06)*. edited by Parsia Sattler, U., Toman, D. B Lake District, UK: CEUR; 2006, 189.

21. Guarino N, Oberle D, Staab S: What Is an Ontology? Handbook on Ontologies 2009:1-17.
22. Horrocks I, Kutz O, Sattler U: The even more irresistible SROIQ. In Knowledge Representation (KR). edited by Doherty P, Mylopoulos J Lake District of the UK: AAAI; 2006:57-67.
23. Visser U, Abeyruwan S, Vempati U, Smith RP, Lemmon V, Schurer SC. BioAssay Ontology (BAO): A Semantic Description of Bioassays and High-Throughput Screening Results. BMC bioinformatics. 2011;12:257. PubMed PMID: 21702939.
24. Sarntivijai S, Ade AS, Athey BD, States DJ. A bioinformatics analysis of the cell line nomenclature. Bioinformatics. 2008;24:2760–2766. PubMed PMID: 18849319.
25. Sarntivijai S, Xiang Z, Meehan T, Diehl A, Vempati U, Schurer S, Pang C, Malone J, Parkinson H, Athey B, He Y. S: Cell Line Ontology: Redesigning Cell Line Knowledgebase to Aid Integrative Translational Informatics. In Proceedings of the International Conference on Biomedical Ontology (ICBO). 2011:in press.
26. Organismal Classification NCBI ( Available at: <http://bioportal.bioontology.org/ontologies/1132>).
27. UniProt, Available at: <http://www.uniprot.org/> ( Available at: <http://www.uniprot.org/>).
28. Units of Measurement (UO). ( Available at: <http://bioportal.bioontology.org/visualize/45500/>).
29. Brinkman RR, Courtot M, Derom D, Fostel JM, He Y, Lord P, Malone J, Parkinson H, Peters B, Rocca-Serra P, Ruttenberg A, Sansone SA, Soldatova LN, Stoeckert CJ Jr, Turner JA, Zheng J. Modeling biomedical experimental processes with OBI. J Biomed Semantics. 2010;1 Suppl 1:S7. PubMed PMID: 20626927.
30. Du P, Feng G, Flatow J, Song J, Holko M, Kibbe WA, Lin SM. From disease ontology to disease-ontology lite: statistical methods to adapt a general-purpose ontology for the test of gene-ontology associations. Bioinformatics. 2009;25:i63–8. PubMed PMID: 19478018.
31. Xiang Z, Courtot M, Brinkman RR, Ruttenberg A, He Y. OntoFox: web-based support for ontology reuse. BMC Res Notes. 2010;3:175. PubMed PMID: 20569493.
32. Grau BC, Kazakov Y, Sattler U HI: Modular Reuse of Ontologies: Theory and Practice. Journal of Artificial Intelligence Research. 2008;31:273–318.
33. Bialkowska A, Crisp M, Bannister T, He Y, Chowdhury S, Schurer S, Chase P, Spicer T, Madoux F, Tian C, Hodder P, Zaharevitz D, Yang VW: Identification of Small-Molecule Inhibitors of the Colorectal Cancer Oncogene Kruppel-Like Factor 5 Expression by Ultrahigh-Throughput Screening. Molecular cancer therapeutics 2011:1535-7163.MCT-11-0550-.
34. Schürer SC, Vempati U, Smith R, Southern M, Lemmon V. BioAssay Ontology Annotations Facilitate Cross-Analysis of Diverse High-Throughput Screening Data Sets. Journal of Biomolecular Screening. 2011;16:415–426. PubMed PMID: 21471461.
35. Feng BY, Shoichet BK. A detergent-based assay for the detection of promiscuous inhibitors. Nature protocols. 2006;1:550–3. PubMed PMID: 17191086.
36. Coan KED, Maltby DA, Burlingame AL, Shoichet BK. Promiscuous aggregate-based inhibitors promote enzyme unfolding. Journal of medicinal chemistry. 2009;52:2067–75. PubMed PMID: 19281222.

37. Smith GK, Barrett DG, Blackburn K, Cory M, Dallas WS, Davis R, Hassler D, McConnell R, Moyer M, Weaver K. Expression, preparation, and high-throughput screening of caspase-8: discovery of redox-based and steroid diacid inhibition. *Archives of biochemistry and biophysics*. 2002;399:195–205. PubMed PMID: 11888206.
38. Baell JB, Holloway GA. New substructure filters for removal of Pan Assay Interference Compounds (PAINS) from screening libraries and for their exclusion in bioassays. *Journal of Medicinal Chemistry*. 2010;53:2719–2740. PubMed PMID: 20131845.
39. Vempati U, Przydzial M, Abeyruwan S, Schürer S: BAO Annotation Template. 2011.
40. RightField. ( Available at: <http://www.sysmo-db.org/rightfield>).
41. Abeyruwan S, Chung C, Datar N, Gayanilo F, Koleti A, Lemmon V, Mader C, Ogihara M, Puram D, Sakurai K, Smith R, Vempati U, Venkatapuram S, Visser U, Schürer S: BAOsearch: A Semantic Web Application for Biological Screening and Drug Discovery Research. In *Semantic Web Challenge, 9th International Semantic Web Conference (ISWC)*. Shanghai, China: 2010.
42. Abeyruwan S, Chung C, Datar N, Gayanilo F, Koleti A, Lemmon V, Mader C, Ogihara M, Puram D, Dakurai K, Smith R, Vempati U, Venkatapuram S, Visser U, Schurer S: PrOntoLearn: Using Lexico-Semantic Ontology Generation using Probabilistic Methods. In *Workshop on Uncertainty Reasoning for the Semantic Web at the 9th International Semantic Web Conference, ISWC 2010*. edited by Bobillo F, Carvalho R, Costa PCGD, D'Amato C, Fanizzi N, Laskey KB, Laskey KJ, Lukasiewicz T, Martin T, Nickles M, Pool M Shanghai, China: 2010:25-36.
43. Richardson L, Ruby S: RESTful web services. O'Reilly Media, Inc. 2007.
44. Open Jena SDB ( Available at: <http://openjena.org/SDB>).
45. Hibernate Relational Persistence for Java and .NET ( Available at: <http://www.hibernate.org>).
46. Ding Y, Yi K, Xiang R: Design of Paper Duplicate Detection System Based on Lucene. *Wearable Computing Systems, Asia-Pacific Conference on 2010*, 0:36-39.
47. The Apache Lucene Project. ( Available at: <http://lucene.apache.org>).
48. Krafft DB and C, Nicholas A. and Caruso, Brian and Corson-Rikert, Jon and Devare, Medha and Lowe, Brian J. and VIVO Collaboration: VIVO: Enabling National Networking of Scientists. In *Proceedings of the WebSci10: Extending the Frontiers of Society On-Line*. Raleigh, NC: 2010.
49. VIVO. ( Available at: <http://vivoweb.org/>).
50. Mayr LM, Bojanic D. Novel trends in high-throughput screening. *Curr Opin Pharmacol*. 2009;9:580–588. PubMed PMID: 19775937.

## Glossary of BAO terms (partial list)

As the definition of terms will evolve, be optimized over time, and BAO terms will evolve over time, we are maintaining a glossary of BAO terms on our BAO Wiki: [http://bioassayontology.org/wiki/index.php/BAO\\_Glossary](http://bioassayontology.org/wiki/index.php/BAO_Glossary). Here, we provide a current partial list of the most important BAO terms.



**Absorbance wavelength** — In absorbance measurements, it is the wavelength at which light is absorbed by a biological entity or a dye.

**Assay biosafety level** — The level of biocontainment required to isolate hazardous biological agents in an enclosed facility; it ranges from the lowest biosafety level of 1 to the highest at level 4.

**Assay design** — The underlying method (technology) and assay strategy used to determine the action of the perturbation in the assay system.

**Assay footprint** — This describes the physical format, such as plate density, in which an assay is performed; this is generally a microplate format, but it can also be an array format.

**Assay format** — Assay Format is a conceptualization of assays based on the biological and/or chemical features of the experimental system.

**Assay kit information** — Manufacturer Information about the name of the company that created the kit/component used in the assay.

**Assay kit informationName** — The title of the kit/biologicals used in the assay.

**Assay measurement throughput quality** — Describes the quality of the measurements performed on each sample, such as single concentration, single repetition, concentration-response, multiple repetitions, etc.

**Assay measurement type** — This describes whether a change in an assay is measured once at one fixed end-point or over a period of time at several time points.

**Assay medium** — The cell culture broth used while performing an assay on cells; it is optimized for each assay type. Some interfering additives such as serum, growth factors, buffers, amino acids, antibiotics, etc. might be eliminated in this medium.

**Assay phase characteristic** — Refers to whether all assay components are in solution or in solid phase, which determines their ability to scatter light.

**Assay readout method** — This describes the difference in the number of detection parameters used in HTS versus HCS assays.

**Assay serum** — The serum used in assay medium while performing an assay on cells; it is optimized for each assay type.

**Assay source** — The screening center at which the assay was performed. Most of the assays deposited in PubChem were performed at one of the MLPCN screening centers.

**Assay stage** — It describes the purpose of the assay in an assay campaign. Assay stage also relates to the order of assays in a screening campaign. For example, the primary assay, which is performed first, identifies some hits. The primary hits are then confirmed in a confirmatory assay. Subsequent secondary assays are run to eliminate compounds that are

not of interest or to confirm hits using an alternate design/technology, or to further characterize compounds.

**Assay temperature** — The temperature at which the assay was performed.

**Assay title** — The name of a bioassay, which is associated with each assay ID (AID).

**Background control** — It is the reading obtained from wells to which the sample or one of the reagents was not added. This is subtracted from all of the experimental readings prior to further analysis.

**Bioassay type** — Categorization of bioassays based on the property or process that the assay is interrogating, e.g. ADMET, functional, etc.

**Biological process target** — A biological process is a process of a living organism. It is a recognized chemical reaction or molecular function with a defined beginning and an end.

**b-score** — It is calculated by first computing a two-way median to account for row and column effects of the plate; then, this is divided by their median absolute deviation to standardize for plate-to-plate variability.

**Buffer** — A mixture of a weak acid and its conjugate base or a weak base and its conjugate acid.

**Cell modification** — The type of alterations performed on the cell line, which include plasmid transfection, viral transduction, cell fusion, etc.

**Coefficient of variation** — Measure of the signal dispersion  $CV=100 \times [\text{StdDev}(\text{sample}) / \text{Avg}(\text{sample})]$

**Cofactor** — A nonprotein component of enzymes required for the enzyme's activity, e.g., coenzyme A (CoA).

**Compound library manufacturer** — The name of the company that synthesized a compound library.

**Compound library** — The name of a perturbation collection from one source, which can be either commercial or academic, e.g., MLSMR, LOPAC, etc.

**Concentration unit** — This describes the most common unit used in calculating volumetric stoichiometry molarity. Units include molar, millimolar, micromolar, nanomolar.

**Content readout type** — It is the throughput and information content generated in an assay. Categorizes multiplexed (i.e. multiple targets measured simultaneously), multiparametric assays, high content (image-based) and regular (plate reader) assays.

**Coupled substrate incubation** — It is the interval of time between the addition of a coupled enzyme substrate and the reaction stopping procedure in a coupled enzyme assay.

**Coupled substrate** — It is an enzyme substrate whose concentration is regulated by the activity of a different enzyme.

**Culture medium** — The liquid broth used to grow cells, which is optimized for each cell type and includes additives such as growth factors, buffers, amino acids, antibiotics, etc.

**Culture serum** — Cultured cells require serum or growth factors for growth by cell division. Each cell type is grown in a medium supplemented with a variable concentration of serum, which is optimized for its growth.

**Curve fit model** — A mathematical model/equation to which the data is fitted (using the curve fit method/algorithm). The Hill equation is commonly used to estimate the number of ligand molecules that are required to bind to a receptor to produce a functional effect.

**Curve fit specification** — input dataIt identifies whether the data has been normalized (by Z and Z' factors, signal to background, signal to noise, and coefficient of variance), or if it was an immediate readout obtained from a HTS assay.

**Curve fit specification** — number concentration valuesIt is the number of concentrations at which the perturbation is screened to obtain the curve fit endpoint.

**Curve fit specification** — number replicatesIt is the number of replicate measurements (repetitions) per concentration value used in the curve fit procedure.

**Detection instrumentation manufacturer** — The name of the company that created the detection instrumentation.

**Detection instrumentation** — Lists the type of equipment used for measurement/readout from an assay, e.g. FLIPR, ViewLux plate reader, PHERAstar, etc.

**Detection technology** — The physical method (technology) used to measure/readout the effect caused by the perturbation in the assay environment.

**Detergent** — A surfactant used in biological assays to lyse the cells and tissues by solubilizing the membrane lipids, and to unfold the proteins by disrupting the bonds.

**Disposition** — This describes the status of a tissue, and whether it is from a normal or a diseased tissue.

**DMSO** — It stands for dimethyl sulfoxide, which is a common organic solvent used to solubilize the chemical compounds prior to their addition to an assay; it is often used as a control.

**DNA construct** — A brief description of the recombinant DNA created by the insertion of a gene or siRNA encoding DNA of interest into a vector. It includes information on the type of vector, the type of promoter, the selectable markers, etc.

**Dye** — Molecules used as optical probes, which have fluorescence/colorimetric properties.

**EC number** — A unique identifier of an enzyme based on the chemical reaction that it catalyzes. It is created by the Enzyme Commission.

**Emission wavelength** — For fluorescence measurements, it is the wavelength at which an excited fluorophore emits fluorescence.

**Endpoint mode of action** — This refers to the effect of the perturbagen on the target of an assay, and whether it brings about inhibition, activation, cytotoxicity, etc.

**Endpoint** — An abstract concept representing a measurement or parameter quantifying or qualifying a perturbation.

**Entrez gene accession number** — A unique identifier of a gene, e.g., GeneBank ID.

**Enzyme activity measurement** — The different methods by which an enzyme function can be measured, such as product formation or substrate depletion.

**Enzyme reaction** — The interval of time during the enzyme activity measurement in a kinetic assay.

**Excitation wavelength** — For fluorescence measurements, it is the wavelength at which a fluorophore is excited.

**Growth mode** — Refers to the manner in which cells grow in culture, either in suspension (without being attached to a surface) or adherent (cells requiring a surface, such as tissue culture plate).

**High control** — The high control contains the substrate titration without inhibitor to reflect the maximum activity at each substrate concentration.

**Inducer** — An inducer is a molecular entity that is required to initiate a biological process, e.g., interferon-gamma is an inducer of the transcription factor STAT-1.

**Inhibitor reagent** — A known blocker of a target used to lower the activity of that target prior to screening for selective activator compounds of that target.

**Interaction** — The molecule or entity to which the protein binds in a binding reaction, e.g. protein, DNA, RNA, etc.

**Low control** — The low control contains the substrate titration without enzyme or substrate and without inhibitor. The low controls should reflect the signal expected for no enzyme activity at each substrate concentration.

**Measure group** — It is an abstract concept to group and link multiple (different) sets of experimental results to one bioassay. Measure groups thus facilitate the description of multiparametric (or multiplexed) assays that measure more than one effect of the perturbagen on the system that is screened. They would also facilitate the definition of profiling assays, e.g. assays that test compounds against multiple (protein) targets.

**Measured entity** — A molecular entity, which is the output of a biological reaction or process that is quantitated either directly (by the presence of a tag or probe) or indirectly in a coupled reaction.

**Metal salt** — An ionic compound (principally consisting of Na, K, Li, Ca, and Mg as cation) that is used as an additive in an assay.

**Mode of perturbagen introduction** — The reagent used to introduce siRNA into the cell, e.g. lipofectamine, Fugene, etc.

**Molecular target** — It is either a protein or a nucleic acid of interest, which is modulated by a perturbagen in an assay.

**Monoclonal antibody** — Highly specific antibodies produced by the clones of a single hybrid cell, which is generated by the fusion of a B cell with a tumor cell. They recognize a unique epitope of an antigen.

**NCBI taxonomy ID** — The unique identification number pertaining to the classification of an organism. It is obtained by referring to the NCBI taxonomy database.

**Negative control** — The control is used to determine the base-line to compare the effect of the test perturbagen. Often the negative control is the solvent (e.g. DMSO) in which the perturbagen was dissolved.

**Normalized percent inhibition** — Data normalization obtained by dividing the difference of mean of the positive controls and sample measurement by the difference of the mean of the positive controls and mean of the negative control.

**Occluder** — A compound that impedes interaction of promiscuous perturbagens with co-expressed proteins; it is used to limit non-specific interactions of the perturbagen.

**Organism name** — Entity from which protein / cell line was derived.

**Percent control** — A measure of the compound activity calculated by dividing the raw measurement obtained with the compound by the mean of the measurements with the controls multiplied by 100.

**Permanent cell line** — Immortalized cell, which has undergone transformation and can be passed indefinitely in culture.

**Perturbagen delivery** — This describes whether the perturbagens are tested individually or as mixtures/pools.

**Perturbagen incubation** — The interval of time between the addition of a perturbagen and the measurement of change, as observed by a detection/readout in a bioassay.

**Perturbagen library type** — A collection of perturbagens, e.g., compounds, siRNA, miRNA, etc., which are sold by different vendors, or generated in academic institutions.

**Perturbagen origin** — The source of perturbagen, whether it is purified from a natural source or it is a synthetic compound, etc.

**Perturbagen** — The agents used to alter the activity of the target of interest in a bioassay.

**pH** — Assay pH approximates the negative logarithm (base 10) of the molar concentration of dissolved hydronium ions in a solution.

**PMIDA PMID** — (PubMed Identifier or PubMed Unique Identifier) is a unique number assigned to each PubMed citation.

**Polyclonal antibody** — Antibodies produced by immunizing a mammal such as a mouse, rabbit or goat with an antigen. They are a mixture of antibodies produced from different B cells raised against any of the different epitopes of that antigen.

**Positive control** — It is a chemical compound or reagent used in each plate of an assay to normalize the response of the test perturbagens (by plate).

**Potentiator** — A known activator of a target/pathway, used prior to screening the compounds for selective inhibitor indications (e.g., forskolin is a potentiator for Gi/o pathway of G-proteins).

**Pressure** — It is the force per unit area applied in a direction perpendicular to the surface of an object in an assay.

**Primary cell line** — Cells that are cultured from a subject (tissue or tumor) and which are not immortalized. They can undergo only a limited number of cell divisions prior to reaching senescence.

**Protein form** — It describes whether changes were introduced into a protein sequence and the type of changes, e.g., fusion, mutation, deletion, post-translational modifications.

**Protein preparation method** — The method by which a protein is purified from its source.

**Protein purity** — The steps involved in isolating a protein from either its natural or recombinantly expressed sources.

**PubChem AID** — It is the unique identification number of a bioassay.

**PubChem assay comment** — This is the PubChem assay statement that can be assigned by depositors to a bioassay.

**PubChem assay depositor** — The organization or individual that added the assay to PubChem.

**PubChem assay description** — This contains the background information and rationale for performing a bioassay, and is found on the PubChem website associated with each assay ID (AID). It also includes the assay design and some information on the related bioassays.

**PubChem assay protocol** — This includes the methodology used to perform a particular bioassay and is found on the PubChem website associated with each assay ID (AID). It includes the assay components and the order in which they were added, the incubation times, detection method and the kit used, etc.

**PubChem assay provider** — The investigator who provided the assay to be run at the screening center.

**PubChem summary comment** — The statement deposited by the assay provider, which summarizes the screening campaign with respect to the identification of lead compounds and chemical probes.

**PubChem TID** — It is an endpoint ID of a bioassay deposited at PubChem.

**Redox reagent** — Redox reagents either accept or donate electrons to facilitate the oxidation-reduction reactions, e.g. dithiothreitol (reducing agent), hydrogen peroxide (oxidizing agent).

**Response unit** — Units of endpoints/results, which are obtained from testing perturbagen at a single concentration, e.g., percent, count, ratio. Response endpoints quantify the magnitude of the perturbation.

**Screening campaign name** — A title used to describe a set of assays that are performed to achieve a screening campaign goal, e.g., to identify leads for a drug development program.

**Screening concentration** — It is the concentration of the perturbagen used in an assay to elicit the biological effect or perturbation.

**Signal direction** — It is the trend of measured readout signal, whether it increases or decreases in perturbagen treated wells, as compared to the untreated or carrier-treated wells in an assay.

**Signal to noise** — Measure of signal strength:  $S/N = \frac{\text{Avg}(\text{pos control}) - \text{Avg}(\text{neg control})}{[\text{StdDev}(\text{pos control}) + \text{StdDev}(\text{neg control})]}$

**Signal window** — Difference of signal between positive and negative controls; assay dynamic range  $SW = \frac{\text{Avg}(\text{pos control}) - \text{Avg}(\text{neg control}) - 3 \times [\text{StdDev}(\text{pos control}) + \text{StdDev}(\text{neg control})]}{\text{StdDev}(\text{pos control})}$

**Substrate incubation** — The interval of time between the addition of an enzyme substrate and the measurement of change, as observed by a detection/ readout in a bioassay.

**Substrate** — The substance on which the enzyme acts to generate a product.

**Tracer** — A radioisotope used as a tag in a biological assay, e.g. 3-H thymidine used as a tracer to detect DNA-replication.

**Transfection agent** — The agent used to introduce the nucleic acid of interest into cells, e.g., lipofectamine, Fugene, etc.

**UniProt ID** — It is a unique identifier of a protein sequence.

**z factor** — It describes the assay dynamic range considering range and data variation:  
 $Z = 1 - \{3x[\text{StdDev}(\text{sample}) + \text{StdDev}(\text{neg control})] / [\text{Avg}(\text{sample}) - \text{Avg}(\text{neg control})]\}$ . It is not to be confused with z-score.

**z-prime factor** — It describes the assay dynamic range considering range and data variation  
 $Z' = 1 - \{3x[\text{StdDev}(\text{pos control}) + \text{StdDev}(\text{neg control})] / [\text{Avg}(\text{pos control}) - \text{Avg}(\text{neg control})]\}$

**Z-score** — Random and systematic error can induce either underestimation (false negatives) or overestimation (false positives) of measured signals. Z-score indicates how many standard deviations an observation is above or below the mean. For calculating this value, the average of the plate values is subtracted from individual raw values, and the difference divided by the standard deviation estimated from all measurements of the plate.



# Data Standardization for Results Management

Robert M. Campbell,<sup>1</sup> Julia Dymshitz,<sup>2</sup> Brian J. Eastwood,<sup>3</sup> Renee Emkey,<sup>4</sup> David P. Greenen,<sup>5</sup> Julia M. Heerding,<sup>6</sup> Dwayne Johnson,<sup>7,\*</sup> Thomas H. Large,<sup>8</sup> Thomas Littlejohn,<sup>9</sup> Chahrzad Montrose,<sup>10</sup> Suzanne E. Nutter,<sup>11</sup> Barry D. Sawyer,<sup>12</sup> Sandra K. Sigmund,<sup>13</sup> Martin Smith,<sup>14</sup> Jeffrey R. Weidner,<sup>15,†</sup> and Richard W. Zink<sup>16</sup>

Created: May 1, 2012; Updated: October 20, 2017.

## Abstract

Raw data collected in screening assays should be appropriately analyzed to derive activity expressed as potency or efficacy values of tested compounds (IC<sub>50</sub> or EC<sub>50</sub> values). In this chapter the authors discuss standardized approaches to processing radioligand binding, enzyme and functional assays used in HTS and lead optimization. Detailed account is given in processing normalizing raw data and curve fitting. A glossary is also included defining the terms used for consistency in processing raw data in a standardized manner.

## Introduction

### Definitions of Result Levels

**Raw data:** Individual measurements as produced by the instruments used in the experiment.

**Normalized well level:** Individual data values that have been transformed to provide a consistent, biologically relevant context. This is often done using vehicle and maximally efficacious compound controls. (Inhibition, Stimulation, etc; in most cases Inhibition and Stimulation are expressed as a % of the dynamic range of the assay)

**Aggregate:** median (preferred) or mean normalized well level data when replicates exist in a single run (Inhibition, Stimulation, etc.). This level provides for a consistent determination of n as it applies to *in vitro* results.

---

<sup>1</sup> Eli Lilly & Company, Indianapolis, IN. <sup>2</sup> Eli Lilly & Company, Earlwood Manor, UK. <sup>3</sup> Eli Lilly & Company, Earlwood Manor, UK. <sup>4</sup> Amgen Inc., Boston, MA. <sup>5</sup> Eli Lilly & Company, Indianapolis, IN. <sup>6</sup> Eli Lilly & Company, Indianapolis, IN. <sup>7</sup> Eli Lilly & Company, Indianapolis, IN. <sup>8</sup> Sunovion Pharmaceuticals Inc., Boston, MA. <sup>9</sup> Eli Lilly & Company, Indianapolis, IN. <sup>10</sup> Eli Lilly & Company, Indianapolis, IN. <sup>11</sup> Eli Lilly & Company, Indianapolis, IN. <sup>12</sup> Eli Lilly & Company, Indianapolis, IN. <sup>13</sup> Eli Lilly & Company, Indianapolis, IN. <sup>14</sup> Eli Lilly & Company, Indianapolis, IN. <sup>15</sup> AbbVie, Chicago, IL. <sup>16</sup> Eli Lilly & Company, Indianapolis, IN.

\* editor

† editor

**Derived data:** Results calculated from groups normalized or aggregate well level data based upon the fit of this data to a mathematical model. ( $IC_x$ , Relative  $IC_x$ ,  $EC_x$ ,  $K_i$ ,  $K_b$ , etc.)

**Summarized data:** Statistical summarization of results across multiple runs. (geometric mean  $IC_x$ , Relative  $IC_x$ ,  $K_i$ ,  $K_b$  or average Inhibition, Stimulation, etc.)

## Absolute $IC_{50}$ , Relative $IC_{50}$ or Relative $EC_{50}$

For assays described in this chapter, absolute  $IC_{50}$  (abs  $IC_{50}$ ), relative  $IC_{50}$  (rel  $IC_{50}$ ) and relative  $EC_{50}$  (rel  $EC_{50}$ ) are predominantly used to derive a value that can be used to compare results within and across runs in the same assay, as well as between different assays. Abs  $IC_{50}$  and rel  $IC_{50}$  are used when different assumptions are applied; the selection of either is at the discretion of the scientist but should be applied consistently and not changed for a defined assay.

For consistency, rel  $IC_{50}$  is used for inhibition assays while rel  $EC_{50}$  is used for stimulation assays, even though there is no fundamental difference between them. Because of their relative simplistic composition, biochemical *in vitro* assays can be easily labeled as either “Stim” or “Inh”, while every biochemical whole cell assay can be either as “Stim” or “Inh” depending on multiple factors. Therefore, the guideline for defining whole cell biochemical assays is to use the label that better reflects the perceived pharmacology, regardless of the direction (increasing or decreasing with test substance concentration) of the raw signal. How an assay is defined can also drive which result type label to use. For instance, if an assay categorized by cell cycle modulation is attempting to inhibit the cell cycle, the rel  $IC_{50}$  should be used.

## Guidelines for Curve Fitting

- Three or four parameter logistic curve fits are acceptable.
- Under appropriate conditions, the top may be fixed to 100 (maximum or compound control level) and the bottom may be fixed to 0 (minimum or vehicle control level).
- It is recommended that the Hill Coefficient not be preset to any fixed number, unless supported by a statistician.
- Cubic spline curve fits *are not recommended*, unless supported by a statistician.
- The Fitting Error of the  $IC_{50}/EC_{50}$  should not exceed 100%, unless supported by a statistician. (*It should be noted that this “standard error” is a measure of “goodness of fit” of the data to the curve fitting equation and not the “standard error” of aggregate data values*).

## Normalizing Data using a Positive Control Curve

In some cases (such as where there is a non-linear standard curve for the analyte), it is preferable to use a reference curve to define the dynamic range of the assay. In those cases, the fitted top of the reference curve is substituted for the max while the fitted bottom of

the reference curve is substituted for the min in normalization calculations. This may be particularly useful in agonist assays where the use of a reference agonist curve is strongly recommended. It is still preferable to define the dynamic range on each plate so that individual plate drift is assessed and single plates can pass/fail. Additionally, the upper and lower asymptote of the reference curve should be established by the data in order to use them for dynamic range determination.

## Application of a Standard Curve

Use of a standard curve is required wherever possible when the raw data is not a linear function of the biological response. For example, optical densities, fluorescence units and luminescence units often cannot be directly used for calculations of activity as they are often non-linear functions of the concentration of the relevant biological product. A standard curve is used to convert the raw data to concentration of biological substance. The calculated concentrations are then used to calculate the *Normalized Result*, as discussed in most thoroughly in the [Immunoassay chapter](#). The standard curve data should be generated with an appropriate number of points and concentration range, fit by an appropriate concentration-response model so that bias and precision are within acceptable limits. All raw data within the scope of the assay can be converted to the biological response.

## Data Types and Associated Rules for Radioligand Binding Assays: Inhibition Mode

### Normalized Results

For radioligand binding methods, the use of Inhibition is recommended to quantify the ability of individual concentrations of a substance to inhibit the total specific binding of radioligand. The use of % bound *for normalization is discouraged*, but it's recommended that biologists calculate and track changes to % bound as a measure of assay performance.

Calculation:

$$\text{Inhibition (\%)} = 100 - \left[ \frac{(\text{Measured Binding} - \text{Min})}{(\text{Max} - \text{Min})} \right] \times 100$$

Max = maximum binding

Min = non-specific binding

### Derived Results: Absolute IC<sub>50</sub> and Relative IC<sub>50</sub>

Absolute IC<sub>50</sub> = the molar concentration of a substance that reduces the specific binding of a radioligand to 50% of the maximum specific binding.

Relative IC<sub>50</sub> = the molar concentration of a substance that reduces the specific binding of a radioligand to 50% of the range of the binding curve (Top – Bottom) for that particular substance.

Notes:

- For incomplete curves, the response data should span above 50% for an IC<sub>50</sub> to be used for the determination of a K<sub>i</sub>.
- The Top and Bottom parameters should be within +/- 20% of the Top and Bottom dynamic range control values.

### Derived Results: K<sub>i</sub>

The equilibrium dissociation constant of a test compound (K<sub>i</sub>) should be calculated using the standard Cheng-Prusoff equation:

$$K_i = \frac{IC_{50}}{1 + \frac{[R]}{K_d}}$$

[R] = concentration of radioligand used in the assay

K<sub>d</sub> = the equilibrium dissociation constant of the radioligand in the assay

Notes:

- K<sub>i</sub> carries the same prefix as the IC<sub>50</sub> from which it is derived.
- For competitive binding mechanisms, a K<sub>i</sub> is recommended to be reported for radioligand binding assays, from IC<sub>50</sub> values generated using 3 or 4-parameter curve fitting methods.
- For uncompetitive or complex (ill-defined) binding mechanisms, an IC<sub>50</sub> is preferred, because one of the main assumptions for the use of the Cheng-Prusoff equation is based on a competitive, bimolecular interaction.

## Data Types and Associated Rules for Enzymatic Assays: Inhibition Mode

### Normalized Results

Inhibition with a Unit of Measurement (UOM) of % based on complete enzyme inhibition (dynamic range of the assay)

Calculation:

$$\text{Inhibition (\%)} = 100 - \left[ \frac{(\text{Activity of Enzyme with Test Cmpd \& Substrate} - \text{Min})}{(\text{Max} - \text{Min})} \right] \times 100$$

Max = observed enzyme activity measured in the presence of enzyme, substrate(s) and cofactors utilized in the method.

Min = observed enzyme activity measured in the presence of substrate(s) and cofactors utilized in the method, and (a) in the absence of enzyme, or (b) in the presence of a fully inhibited enzyme.

### Derived Results: Absolute IC<sub>50</sub>, Relative IC<sub>50</sub>

Relative IC<sub>50</sub> = the molar concentration at which 50% of maximal inhibition for that substance is observed.

Absolute IC<sub>50</sub> = the molar concentration of a substance that reduces the enzymatic activity to 50% of the total enzymatic activity.

## Data Types and Associated Rules for *In Vitro* Functional Assays

### Antagonists

#### Normalized Results

Inhibition with a UOM of % should be calculated for responses to individual concentrations of test substances.

Calculation:

$$\text{Inhibition (\%)} = 100 - \left[ \frac{(\text{Response in presence of Test Cmpd \& Ref Agonist} - \text{Min})}{(\text{Max} - \text{Min})} \right] \times 100$$

Max = response in presence of some concentration of a reference agonist challenge dose.

Min = (a) response in the presence of diluents and in the absence of test substance and agonist; or (b) response in the presence of maximally effective antagonist and challenge dose of agonist.

#### Derived Result: Rel IC<sub>50</sub>

Relative IC<sub>50</sub> = the molar concentration of a substance (antagonist) that reduces the efficacy of the reference agonist or the constitutive activity of the biological target by 50% of the antagonist curve (Top-Bottom) for that particular test substance.

### Derived Result: $K_b$

Calculation of  $K_b$  by Schild analysis isn't standard practice due to throughput and cost disadvantages. Consequently, the Cheng-Prusoff equation is typically used to reduce the data and subsequently assigned the label of  $K_b$ .

Calculation: Use standard Cheng-Prusoff equation for functional assays.

$$K_b = \frac{IC_{50}}{1 + \frac{[A]}{EC_{50}}}$$

[A] = the concentration of the reference agonist that is being inhibited

$EC_{50}$  = the Relative  $EC_{50}$  of the reference agonist determined in the same run of the assay.

If the slope of the curve for the reference agonist deviates significantly from 1, the use of the modified Cheng-Prusoff equation is recommended.

### Other Derived Results:

#### Schild $K_b$

Schild  $K_b$  is measure of affinity for a competitive antagonist that is calculated using the ratios of equi-active concentrations of a full agonist (most typically  $EC_{50}$  concentrations are used) in the absence and presence of one or more concentrations of the antagonist. Schild  $K_b$  offers a true evaluation of a test compound's ability to mechanistically perform as an antagonist. This process exposes toxic effects and compound precipitation as false positive activity, and therefore, should be used when time and cost are not limitations.

#### $E_{min}$

The maximum activity of an antagonist test substance relative to a reference agonist. This is obtained by first generating a fitted top from a %Inhibition curve and then converting that to the corresponding %Stimulation of the reference agonist curve. The  $E_{min}$  value for antagonist mode should equal the relative efficacy for agonist mode for competitive inhibitors. In order to make use of  $E_{min}$ , the selected agonist concentration (i.e.  $EC_{80}$ ) should produce an activity above the expected  $E_{min}$  value (Figure 1).

### Notes:

- $K_b$  carries the same prefix as the  $IC_{50}$  from which it is derived.
- The use of Abs  $IC_{50}$  is discouraged.
- Because partial antagonists exist, a full response curve with defined Top & Bottom can be achieved even if the %Inh doesn't exceed 50%.
- A concentration response curve for the reference agonist should be determined in each experimental run if a  $K_b$  is to be determined. The frequency within the run

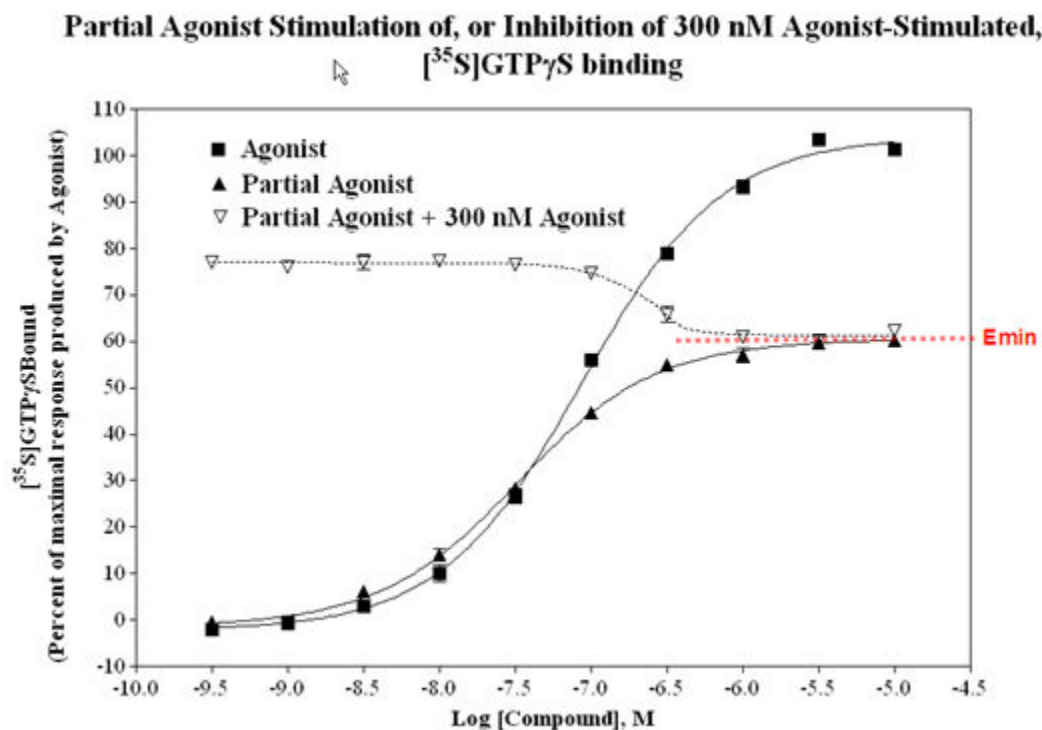


**Figure 1:** Partial agonist stimulation or inhibition of 300 nM agonist-stimulated [35S]GTP $\gamma$ S binding

depends on assay variability. A statistician should be consulted concerning this frequency during the assay validation process.

## Agonists

### Normalized Data

Stimulation with a UOM of % should be calculated for responses to individual concentrations of test substances.

Calculation:

$$\text{Stim (\%)} = \left[ \frac{(\text{Response in presence of Test Cmpd} - \text{Min})}{(\text{Max} - \text{Min})} \right] \times 100$$

Min = the fitted Bottom of a 4 parameter logistic curve fitting equation applied to data generated from the positive control (reference agonist).

Max = (a) the maximum activity of a positive control agonist determined by the fitted Top of a 4 parameter logistic curve fitting equation applied to a concentration response curve from the positive control; or (b) the maximum activity of a positive control in Max wells, which should represent the empirically-derived saturating concentration of the positive control.

## Derived Results: Relative EC<sub>50</sub> and Relative Efficacy

Relative EC<sub>50</sub> = the molar concentration of a substance that produces 50% of that test substance's maximum stimulation.

Relative Efficacy = the maximum activity of a test substance relative a reference agonist. The UOM for Relative efficacy is %.

Calculation:

$$\text{Rel Eff (\%)} = \left[ \frac{\text{Fitted Top of Test Cmpd}}{\text{Fitted Top of Reference Agonist}} \right] \times 100$$

## Other Derived Results:

### Fold Activity and Fold Activity Max

The fold activity (or fold activity max) result is useful when comparing *test compounds evaluated across multiple functional assays* because varying levels of efficacy can be observed amongst the different or same reference agonists.

The intended use of this calculation is to provide additional information to reduce or define differences between assays, so that differences between compound activities can be further quantified. For example, a compound run in an assay normalized to a *reference agonist with low efficacy* would appear to be more efficacious when compared to another compound run in a separate assay normalized to a *reference agonist with high efficacy*. Comparing folds activities, which looks at the magnitude of compound-induced activity relative to baseline, enables a scientist to make a conclusion that is not influenced by differences in reference agonist responsiveness. Also, the fold activity result of a control compound can be useful to quality control chart, tracking changes in assay responsiveness over time.

Calculation:

$$\text{Fold Act \& Fold Act Max} = \frac{\text{Raw data response in presence of Test Cmpd}}{\text{Min}}$$

Min = Raw basal activity of constitutive receptor.

### Relative AUC

Relative AUC (Area Under the Curve) is defined as the ratio of the area under the fitted concentration-response curve for the test compound to the area under the fitted concentration-response curve for the reference compound. Specifically, areas are calculated as the area under the curve that lies above the horizontal line  $y = 0\%$ . The area calculation corresponds to the shaded region in the figure below, where the contribution to the area as one move along the concentration axis is proportional to the log of the concentration distance covered, **not** the linear concentration distance covered. One



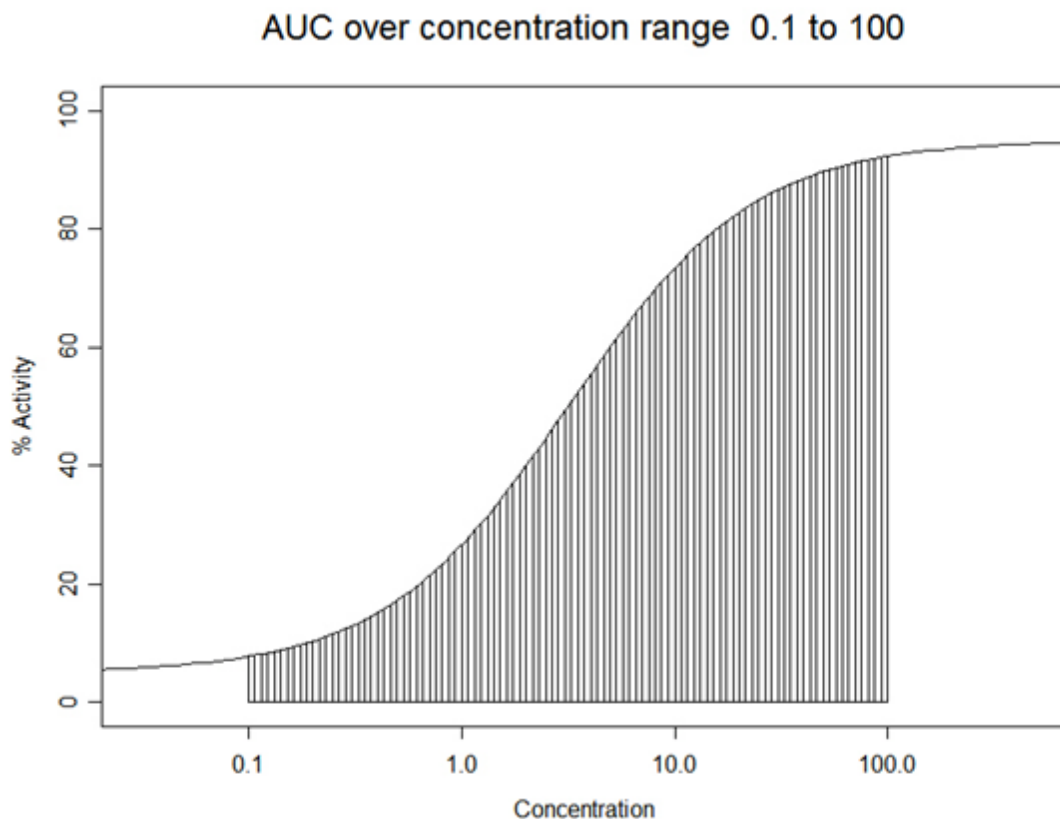


**Figure 2:** The “area of activity” that is used in the calculation as Rel AUC.

should calculate the area using an exact formula when it is available, as is the case for the 4PL and 3PL models. Otherwise, one may use an approximation method, such as the trapezoid rule. In either case, for the calculated value of relative AUC to be meaningful, the areas for both the test and reference compounds should be computed in the same concentration range. Likewise, the comparison between two relative AUCs is only meaningful when each is computed in the same concentration range. If the same concentration range was not used for assaying the test and reference compounds, the equations for the fitted curves may be used for extrapolation in order to compute the components of the relative AUC over the same concentration range.

Rel AUC is useful with functional assays in which compounds are measured with varying efficacies (agonists and partial agonists) and potencies. Because Rel AUC measures the area of activity, *both efficacy and potency data are essentially combined, generating a value that provides an overall assessment of activity and selectivity between tested compounds.* However, Rel AUC should not be a substitute but rather a supplement to individual efficacy and potency data during the analysis process. Figure 2 illustrates the “area of activity” that is used in the calculation as Rel AUC.

Calculation:

$$\text{Rel AUC} = \left[ \frac{\text{AUC of Test compound}}{\text{AUC of Reference compound}} \right]$$

### Notes:

- A four-parameter curve fit should be used for the Ref Agonist.
- The maximum and minimum asymptotes should be defined by the data for the Ref Agonist
- Calculation of Rel Eff assumes that both the test compound and positive control each have a defined Top asymptote.

## Orphan Receptors – Stimulation Mode

Assays exist for which there are no identified positive control or reference agonist compounds. An example of this situation is an assay that utilizes an “orphan” target as a bio-entity. An “orphan” target is a bio-entity that has a primary sequence suggesting it is a member of one of the super families of biological targets; however, *no ligand for this “receptor” has been identified*. Generally, it is the aim of the research effort to identify ligands for this “orphan” so that a protocol for a validated assay can be developed. Until at least enough data is gathered to identify a ligand for these types of bio-entities, assays utilizing them will be considered “validated” at only the hit to lead level. During this period, responses to individual concentrations of test substances can be normalized by one of the following formulae, which either make use of a known nonspecific activator or simply use basal activity of the constitutive receptor.

### Orphan Receptors Normalized to Nonspecific Activator

Stimulation with a UOM of % should be calculated for responses to individual concentrations of test substances.

$$\text{Stim (\%)} = \left[ \frac{(\text{Response in presence of Test Cmpd} - \text{Min})}{(\text{Max} - \text{Min})} \right] \times 100$$

Max = fully activated by nonspecific activator.

Min= constitutive basal activity of the receptor (no activation)

### Orphan Receptors Normalized to Constitutive Receptor

Responses to individual concentrations of test substances that increase the measured activity of the orphan target are normalized to the basal level of activity of the target measured in the absence of the test substance. These responses can be expressed as either a percent of the basal activity or as a fold of the basal activity using one of the following

Calculation:

$$\text{Fold Act \& Fold Act Max} = \frac{\text{Raw data response in presence of Test Cmpd}}{\text{Min}}$$

Min = Raw basal activity of the constitutively active receptor

### Notes:

- Results from this equation can generate percents much greater than 100.
- Expression of Fold Act or Fold Act Max should only be determined until either a nonspecific activator or ligand is identified; and should only be used to rank order compounds tested in the same assay.
- The calculated Fold Act or Fold Act Max value is expected to be greater than 1 for an agonist. If the calculated value is less than 1, the test compound could be an inverse agonist.

### Potentiators

Potential assays measure the ability of an *test substance to augment the response produced by a relatively low concentration of an active substance in some biological system*. Currently, these assays are run in *one of two modes*. The following paragraphs address the most frequently used mode.

The first mode involves the addition of one or more concentrations of a test substance in the presence of a fixed concentration of the known active substance called the “Reference Agonist”. In this mode, potentiation is the response produced by the combination of substances minus the response produced by the specific concentration of Reference Agonist alone. *But, how does one normalize this response?*

It is recognized that potentiation assays might be executed when no known potentiator exists. However, no potentiation assay should be run without the existence of a known Reference Agonist. Therefore, the response to the specific concentration of the Reference Agonist plus the test substance (potentiation) should be normalized to the fitted Top of a concentration response curve of the Reference Agonist, determined at least once in every run of the assay. The frequency of the determination of the concentration response curve of the Reference Agonist for the purpose of normalizing other responses in any potentiation assay would be depend upon other factors such as plate variability and run-to-run reproducibility.

### Normalized Data

Stimulation with a UOM of % should be calculated for responses to the Reference Agonist.

Potentiation with a UOM of % should be calculated for responses to individual concentrations of test substances.

Calculation:

$$\text{Pot (\%)} = \left[ \frac{(\text{Response in presence of Test Cmpd \& Challenge Dose} - \text{Min})}{(\text{Max} - \text{Min})} \right] \times 100$$

Min = Response in the presence of challenge dose EC<sub>10</sub> of reference agonist

Max = Response in the presence of full agonist dose

### Notes:

- This provides for a Potentiation equal to 0% when the response to the combination of test substance and Reference Agonist is equal to the response to the Reference Agonist alone (e.g. a test substance that is not a potentiator).

### Derived Data

Relative EC<sub>50</sub> = the molar concentration of a substance that produces 50% of that test substance's maximum stimulation.

Relative Potentiator Efficacy: There is little if any discussion in the scientific literature addressing a standard term or calculation of efficacy of a potentiator. It is suggested that this result type be termed Relative Potentiator Efficacy (or Rel Pot Eff) to distinguish it from the Relative Efficacy of an agonist. It is equal to the fitted Top of the potentiation curve minus the normalized response to the specific concentration of Reference Agonist alone divided by 100 minus the normalized response to the specific concentration of Reference Agonist alone. Figure 3 illustrates the above decisions.

### Inverse Agonists

According to multiple models of drug-receptor interaction, receptors have been demonstrated to exist in equilibrium between two states. These two states are R\*, the active form of the receptor, and R, the inactive form.

*Agonists exhibit higher affinity for the active form of the receptor.* When an agonist binds to a receptor, it stabilizes the active form of the receptor, shifts the equilibrium toward the active state and produces a response in the biological system under investigation. Substances that produce this effect possess positive intrinsic activity.

*Antagonists exhibit equal affinity for both forms of the receptor.* When an antagonist binds to a receptor, it stabilizes the initial equilibrium between the active and inactive forms of the receptor. Therefore, no observable change in the activity of the biological system occurs. Substances of this type possess zero intrinsic activity.

*Inverse agonists exhibit higher affinity for the inactive state of the receptor.* When an inverse agonist binds to a receptor, it stabilizes the inactive form of the receptor, shifts the equilibrium toward that state and produces an opposite response in the biological system. These substances possess negative intrinsic activity.

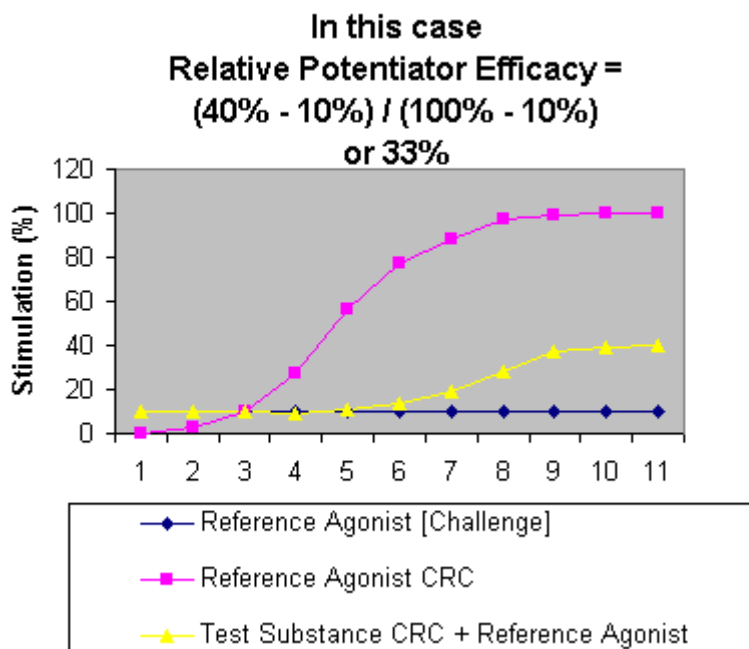


**Figure 3:** Relative Potentiator Efficacy example plot.

Receptors have been demonstrated to exist in a constitutively active state both *in vitro* and *in vivo*. *In vitro*, the constitutive activity observed in assays utilizing transfected cell lines is generally attributed to the over expression of the receptor at levels hundreds to thousands of times higher than occur *in vivo*. Under these conditions, the total number of receptors in the active state is sufficiently high to produce a measurable response even when no exogenous substance has been added to the system. *The addition of an inverse agonist to the system produces a decrease in the measured response.* The magnitude of the decrease is related to the amount of negative intrinsic efficacy of the inverse agonist.

The possibility for confusion exists when one desires to quantify results for potential drug candidates that are inverse agonists. Some of the questions that arise are:

1. Because the measured response is a decreased activity produced by an inverse agonist, is the normalized result type Inhibition or Stimulation?
2. What is the algorithm for normalized results?
3. What is the algorithm for fitting concentration response curves?
4. Is the result type describing potency of a test substance a Relative EC<sub>50</sub> or a Relative IC<sub>50</sub> or another measure?
5. How is the result type describing potency of a potentiator differentiated from the potency result type for an agonist?
6. Is Relative Efficacy a negative number?

There are no absolute answers to these questions provided by the current literature; however, there is a consistent theme.

1. The most frequently used normalized result type is Inhibition with a unit of measure of % activity.
2. The dynamic range for inverse agonists is the difference between activity in the absence of, or fully inhibited, biological target and the constitutive activity. *Use of the “absence” method is preferable in early development of inverse agonist assays because it eliminates the dependency on a pre-existent known inverse agonist to compare responses of test substances to.* However, as with other functional assays, as soon as an appropriate inverse agonist has been found, it should be utilized as a positive control in the assay for the purpose of calculating relative efficacies.

## Assays Normalizing Data to an Inverse Agonist Control

### Normalized Data

Inhibition with a UOM of % should be calculated for responses to individual concentrations of test substances.

Calculation:

$$\text{Inh (\%)} = \left[ \frac{(\text{Response in presence of Test Cmpd} - \text{Min})}{(\text{Max} - \text{Min})} \right] \times 100$$

Min = Response activity in presence of constitutively active receptor alone

Max = Response activity in presence of positive control and receptor

### Derived Data

Relative EC<sub>50</sub> Inverse = the molar concentration of a substance that produces 50% of the range of inverse agonist curve (Top – Bottom) for that particular test substance.

Rel Efficacy Inverse = 100 x (Fitted Top of the test substance expressed as %/Fitted Top of the Positive Control Reference Inverse Agonist expressed as %)

Calculation:

$$\text{Rel Eff Inv (\%)} = \left[ \frac{\text{Fitted Top of Test Cmpd}}{\text{Fitted Top of Reference Inverse Agonist}} \right] \times 100$$

### Notes:

- Because inverse agonist response curve profiles look similar to profiles generated by toxic compounds, it's advised that a confirmation assay be used to provide more evidence that a given test compound is an inverse agonist.
- Hill Coefficient and Rel Efficacy Inverse values are positive.
- The calculated Fold Act or Fold Act Max value is expected to be greater than 1 for an agonist. If the calculated value is less than 1, the test compound could be an inverse agonist.

## Assays Normalizing Data to No Receptor Control (Orphan Receptor)

### Normalized Data

Inhibition with a UOM of % should be calculated for responses to individual concentrations of test substances.

Calculation:

$$\text{Inh (\%)} = \left[ \frac{(\text{Response in presence of Test Cmpd \& Receptor} - \text{Min})}{(\text{Max} - \text{Min})} \right] \times 100$$

Min = Response activity in the presence of the constitutively active receptor alone

Max = Response activity in the absence of the receptor

### Derived Data

Relative EC<sub>50</sub> Inverse = the molar concentration of a substance that produces 50% of the range of inverse agonist curve (Top – Bottom) for that particular test substance.

### Notes:

- Because inverse agonist response curve profiles look similar to profiles generated by toxic compounds, it's advised that a confirmation assay be used to provide more evidence that a given test compound is an inverse agonist.
- Hill Coefficient and Rel Efficacy Inv values are positive.
- The calculated Fold Act or Fold Act Max value is expected to be greater than 1 for an agonist. If the calculated value is less than 1, the test compound could be an inverse agonist.

## Assays Normalizing Data to Reference Agonist:

### Normalized Data

Stimulation with a UOM of % should be calculated for responses to individual concentrations of test substances.

Calculation:

$$\text{Stim (\%)} = \left[ \frac{(\text{Response in presence of Test Cmpd} - \text{Min})}{(\text{Max} - \text{Min})} \right] \times 100$$

Min = the fitted Bottom of a 4 parameter logistic curve fitting equation applied to data generated from the Reference Agonist

Max = the maximum activity of a Reference Agonist determined by the fitted Top of a 4 parameter logistic curve fitting equation applied to a concentration response curve from the positive control.

**Notes:**

- % Stimulation values will be negative for inverse agonist test compounds.

**Derived Data**

Relative EC<sub>50</sub> Inverse = the molar concentration of a substance that produces 50% of that test substance's inverse agonism.

Relative Efficacy = the maximum activity of a test substance relative to a Reference Agonist. The UOM for Relative efficacy is %.

Calculation:

$$\text{Rel Eff Inv (\%)} = \left[ \frac{\text{Fitted Bottom of Test Cmpd}}{\text{Fitted Top of Reference Agonist}} \right] \times 100$$

**Notes:**

- Rel Efficacy and Hill Coeff values for inverse agonists will be negative.
- Calculation of Rel Eff assumes the test compound has a defined Bottom asymptote and Reference Agonist have a defined Top asymptote.
- Because inverse agonist response curve profiles look similar to profiles generated by toxic compounds, it's advised that a confirmation assay be used to provide more evidence that a given test compound is an inverse agonist.
- The calculated Fold Act or Fold Act Max value is expected to be greater than 1 for an agonist. If the calculated value is less than 1, the test compound could be an inverse agonist.

**Reference**

1. Neubig RR, Spedding M, Kenakin T, Christopoulos A. International Union of Pharmacology Committee on Receptor Nomenclature and Drug Classification. XXXVIII. Update on terms and symbols in quantitative pharmacology. *Pharmacol Rev.* 2003;55(4):597-606. doi: [10.1124/pr.55.4.4](https://doi.org/10.1124/pr.55.4.4). PubMed PMID: WOS: 000186910700007.

**Glossary****Abs IC<sub>50</sub>**

Absolute IC<sub>50</sub>; the molar concentration of a substance that inhibits 50% of the dynamic range of the assay. In contrast to Rel IC<sub>50</sub>, Abs IC<sub>50</sub> is not the inflection point of the curve. It's determined to be the concentration at which 50% inhibition is realized.



**Bottom**

The lower asymptote of a logarithmically derived curve. The Bottom value can be determined with real values or predicted using the logarithm applied to the result data set.

**CRC**

Concentration-response curve mode. The mode to describe an assay performed with multiple concentrations of a given test substance, which might then render a logarithmically-derived graph curve.

**E<sub>min</sub>**

The maximum activity of an antagonist test substance relative to a reference agonist. This is obtained by first generating a fitted top from a %Inhibition curve and then converting that to the corresponding %Stimulation of the reference agonist curve. The E-min value for antagonist mode should equal the relative efficacy for agonist mode for competitive inhibitors.

**Fold Activity**

The ratio of biological activity in the presence of an exogenous substance to that in its absence. It is the test compound's observed response (raw data value) divided by the median of the same plate's Min wells. This result type is used exclusively with single point assays. If the value is greater than 1, the test compound is likely an agonist. If the calculated value is less than 1, the test compound could be an inverse agonist.

**Fold Activity Max**

The maximum observed Fold Activity in a concentration response curve whether it was excluded or not. It is the test compound's observed response (raw data value) divided by the median of the same plate's Min wells. If the value is greater than 1, the test compound is likely an agonist. If the calculated value is less than 1, the test compound could be an inverse agonist.

**Fold Activity Max (FA)**

The maximum observed Fold Activity in a concentration response curve whether it was excluded or not. The (FA) indicates that this result type is summarized. Because activity can be detected at different test substance concentrations, the summarized value must be viewed with this knowledge.

**Hill Coeff**

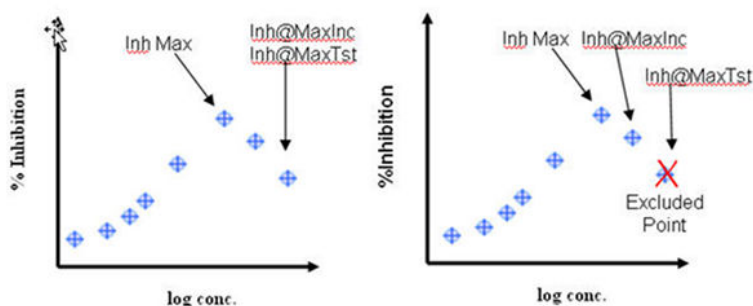
Derived slope a three or four parameter logistic curve fit. Should not be fixed to any given value without consultation with a statistician. It should not be a negative value except for inverse agonist assays.

**Inh**

Activity determined for a single point inhibition assay. Unit of Measure is always %.

### Inh @ Max Inc

Inhibition observed at the highest included (i.e. not excluded) concentration of a substance tested in a concentration response mode method version regardless of whether it was included in the parametric fit to produce derived results. (See Illustration below)



### Inh @ Max Tst

Inhibition observed at the maximum concentration of a substance tested in a concentration response mode method version regardless of whether it was included in the parametric fit to produce derived results. (See Illustration below)

### Inh Max

Maximum inhibition produced by any concentration that was included for the application of a curve fit algorithm (See Illustration below).

### Inh Max (FA)

Maximum inhibition produced by any concentration that was included for the application of a curve fit algorithm. This result type differs from Inh Max by allowing summarization to occur; the FA is defined as 'for averaging'. Because this result type could yield an average value from multiple test substance concentrations, the value should be used with this knowledge and therefore with caution.

### $K_i$

Result from the Cheng-Prusoff equation or from a slightly modified derivation. This label is used primarily with binding assays (see standard texts for formula) and represents the affinity of a compound for a receptor. Documentation of the formula and any changes to the Cheng-Prusoff should be noted in the assay protocol.

### $K_b$

Result from the Cheng-Prusoff equation or from a slightly modified derivation. This label is used primarily with functional antagonist assays (see standard texts for formula) and represents the affinity of a compound for a receptor. This label doesn't represent results mechanistically determined via the Schild analysis; rather the label Schild  $K_b$  is used in those calculations.

**Pot**

Potential result type for single point mode. Many potentiation assays involve the addition of one or more concentrations of a test substance in the presence of a fixed concentration of the known active substance called the Reference Agonist. In this mode, potentiation is the response produced by the combination of substances minus the response produced by the specific concentration of Reference Agonist alone.

**Pot @ Max Inc**

Potentiation observed at the highest included concentration of a substance from an analysis of a concentration response curve.

**Pot @ Max Tst**

Potentiation observed at the maximum concentration of a single substance tested in a concentration response mode method version regardless of whether it was included in the parametric fit to produce derived results.

**Pot Max**

The maximum potentiation observed for a substance in a single run of a potentiation concentration response mode method regardless of whether it was included in the parametric fit to produce derived results.

**Rel AUC**

Defined as the ratio of the area under the fitted concentration-response curve for the test compound to the area under the fitted concentration-response curve for the reference compound.

**Rel EC<sub>50</sub>**

Relative EC<sub>50</sub>; the molar concentration of a substance that stimulates 50% of the curve (Top – Bottom) for that particular substance. It can also be described as the concentration at which the inflection point is determined, whether it's from a three- or four-parameter logistic fit.

**Rel EC<sub>50</sub> Inv**

The Relative EC<sub>50</sub> of an inverse agonist.

**Rel Eff**

The maximum activity of a test substance relative to a standard positive control agonist. The result is expressed as percent from the following formula: 100 x Fitted Top of the test substance divided by the Fitted Top of an Agonist control. The agonist control should have a four parameter curve fit with defined lower and upper asymptotes but can have the Bottom fixed to zero in certain cases. The test compounds should have a four parameter curve fit but can have a three parameter fit with the bottom fixed to zero if the data warrants it.

**Rel Eff Inv**

The maximum activity of a test substance relative to a standard positive control inverse agonist. The result is expressed as percent from the following formula:  $100 \times \text{Fitted Top of the test substance} / \text{Fitted Top of the Inverse Agonist control}$ . The inverse agonist control should have a four parameter curve fit with defined lower and upper asymptotes but can have the Bottom fixed to zero in certain cases. The test compounds should have a four parameter curve fit but can have a three parameter fit with the bottom fixed to zero if the data warrants it.

**Rel IC<sub>50</sub>**

Relative IC<sub>50</sub>; the molar concentration of a substance that inhibits 50% of the curve (Top – Bottom) for that particular substance. It can also be described as the concentration at which the inflection point is determined, whether it's from a three- or four-parameter logistic fit.

**Rel Pot Eff**

The fitted top of the potentiation curve minus the normalized response to the specific concentration of Reference Agonist alone divided by 100 minus the normalized response to the specific concentration of Reference Agonist alone.

**Stim**

Activity determined for a single point stimulation assay. Unit of Measure is always %.

**Stim @ Max Inc**

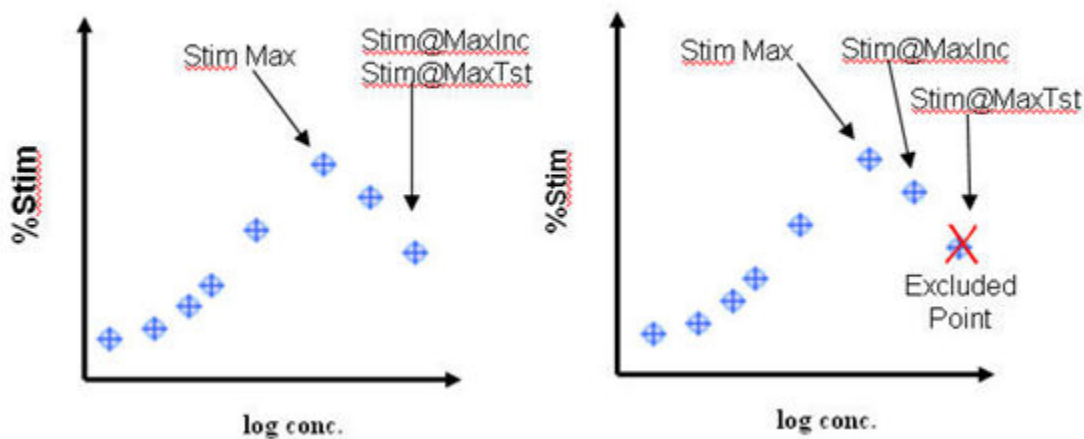
Stimulation observed at the highest included (i.e. not excluded) concentration of a substance tested in a concentration response mode method version regardless of whether it was included in the parametric fit to produce derived results. (See illustration below)

**Stim @ Max Tst**

Stimulation observed at the maximum concentration of a substance tested in a concentration response mode method version regardless of whether it was included in the parametric fit to produce derived results. (See illustration below)

**Stim Max**

Maximum stimulation produced by any concentration that was included for the application of a curve fit algorithm (See illustration below)



### Stim Max (FA)

Maximum stimulation produced by any concentration that was included for the application of a curve fit algorithm. This result type differs from Stim Max by allowing summarization to occur; the FA is defined as 'for averaging'. Because this result type could yield an average value from multiple test substance concentrations, the value should be used with this knowledge and therefore with caution.

### Schild $K_b$

A measure of affinity for a competitive antagonist that is calculated using the ratios of equi-active concentrations of a full agonist (most typically  $EC_{50}$  concentrations are used) in the absence and presence of one or more concentrations of the antagonist. See pp. 335-339, Pharmacologic Analysis of Drug-Receptor Interaction, 3rd Ed. by Terry Kenakin.

### SP

Single point mode. Assay performed with once concentration of test substance. Common result types used include Inh and Stim. Result values should always include the concentration of the test substance used to determine the activity.

### Stephenson's $K_p$

A measure of affinity for a partial agonist that is calculated through the comparison of equi-active concentrations of a full agonist in the absence and presence of a single concentration of the partial agonist. See pp. 284-286, Pharmacologic Analysis of Drug-Receptor Interaction, 3rd Ed. by Terry Kenakin.

### Top

The upper asymptote of a logarithmically derived curve. The Top value can be determined with real values or predicted using the logarithm applied to the result data set.



# HTS Assay Validation

Philip W. Iversen, PhD,<sup>✉1,\*</sup> Benoit Beck, PhD,<sup>2</sup> Yun-Fei Chen, PhD,<sup>1</sup> Walthere Dere, MS,<sup>3</sup> Viswanath Devanarayan, PhD,<sup>4</sup> Brian J Eastwood, PhD,<sup>1</sup> Mark W. Farnen, PhD,<sup>1</sup> Stephen J. Iturria, PhD,<sup>5</sup> Chahrzad Montrose, PhD,<sup>1</sup> Roger A. Moore, MS,<sup>6</sup> Jeffrey R. Weidner, PhD,<sup>8,†</sup> and G. Sitta Sittampalam, PhD<sup>7,‡</sup>

Created: May 1, 2012; Updated: October 1, 2012.

## Abstract

Assays employed in HTS and lead optimization projects in drug discovery should be rigorously validated both for biological and pharmacological relevance, as well as for robustness of assay performance. This chapter addresses the essential statistical concepts and tools needed in assay performance validation developed in the pharmaceutical industry, specifically for higher throughput assays run exclusively in 96-, 384- and 1536-well formats using highly automated liquid handling and signal detection systems. In this context, it is assumed that the biological and pharmacological validation of the assay system has already been established, and the high throughput performance characteristics requires validation. This is an essential chapter for these who design and implement HTS and lead optimization assays to support SAR projects in pre-clinical drug discovery.

## 1. Overview

The statistical validation requirements for an assay vary, depending upon the prior history of the assay. Stability and Process studies (Section 2) should be done for all assays, prior to the commencement of the formal validation studies. If the assay is new, or has never been previously validated, then full validation is required. This consists of a 3-day Plate Uniformity study (Section 3) and a Replicate-Experiment study (Section 4). If the assay has been previously validated in a different laboratory, and is being transferred to a new laboratory, then a 2-day Plate Uniformity study (Section 3) and a Replicate-Experiment study (Section 3) are required. An assay is considered validated if it has previously been assessed by all the methods in this section, and is being transferred to a new laboratory without undergoing any substantive changes to the protocol. If the intent is to store and use data and results from the previous laboratory, then an assay comparison study

---

<sup>1</sup> Eli Lilly & Company, Indianapolis, IN 46285. <sup>2</sup> Axiosis, Inc., Brussels, Belgium. <sup>3</sup> GSK Biologicals, Brussels, Belgium. <sup>4</sup> Charles River Laboratories, <sup>5</sup> Monsanto, Ankeny, IA. <sup>6</sup> Retired. <sup>7</sup> National Institutes of Health. <sup>8</sup> QualSci Consulting, LLC.

<sup>✉</sup> Corresponding author.

\* Editor

† Editor

‡ Editor

(Section 4) should be done as part of the Replicate-Experiment study. Otherwise only the intra-laboratory part of the Replicate-Experiment study (Section 4) is recommended.

If the assay is updated from a previous version run in the same facility then the requirements vary, depending upon the extent of the change in methodology, equipment, operator and reagents. Major changes require a validation study equivalent to a laboratory transfer. Minor changes require bridging studies that demonstrate the equivalence of the assay before and after the change. See Section 5 for examples of major and minor changes.

These techniques are intended to be applied to  $\geq 96$ -well primary and functional assays. Discussion with a statistician is necessary for alternatives for assays that require significant time, resource or expenditure to scientifically balance validation requirements with these constraints.

## 2. Stability and Process Studies

### 2.1. Reagent Stability and Storage Requirements

It is important to determine the stability of reagents under storage and assay conditions.

- Use the manufacturer's specifications if the reagent is a commercial product.
- Identify conditions under which aliquots of the reagent can be stored without loss of activity.
- If the proposed assay will require that the reagent be frozen and thawed repeatedly, test its stability after similar numbers of freeze-thaw cycles.
- If possible, determine the storage-stability of all commercial and in-house reagents.
- If reagents are combined and aliquoted together, examine the storage-stability of the mixtures.

### 2.2. Reaction Stability Over Projected Assay Time

Conduct time-course experiments to determine the range of acceptable times for each incubation step in the assay. This information will greatly aid in addressing logistic and timing issues.

#### 2.2.1. Reagent Stability During Daily Operations; Use Of Daily Leftover Reagents

The stability studies will require running assays under standard conditions, but with one of the reagents held for various times before addition to the reaction. The results will be useful in generating a convenient protocol and understand the tolerance of the assay to potential delays encountered during screening.

If possible, reagents should be stored in aliquots suitable for daily needs. However, appropriate stability information pertinent to storing leftover reagents (particularly expensive ones) for future assays should be obtained.



New lots of critical reagents should be validated using the bridging studies with previous reagent lots.

## 2.3. DMSO Compatibility

Test compounds are delivered at fixed concentrations in 100% DMSO, thus solvent-compatibility of assay reagents should be determined. The validated assays should be run in the absence of test compounds and in the presence of DMSO concentrations spanning the expected final concentration. Typically, DMSO concentrations from 0 to 10% are tested. Note that the DMSO compatibility of the assay should be completed early, since remaining validation experiments such as the variability studies, should be performed with the concentration of DMSO that will be used in screening. For cell based assays, it is recommended that the final % DMSO be kept under 1%, unless demonstrated by other experiments that higher concentrations can be tolerated.

## 3. Plate Uniformity and Signal Variability Assessment

### 3.1. Overview

All assays should have a plate uniformity assessment. For new assays the plate uniformity study should be run over 3 days to assess uniformity and separation of signals, using DMSO concentration to be used in screening. For the transfer of validated assays to other laboratories, the plate uniformity study can be performed over 2 days to establish that the assay transfer is complete and reproducible (see Section 1 for the definition of an assay transfer). Uniformity assays should be performed at the maximum and minimum signal or response levels to ensure that the signal window is adequate to detect active compounds during the screen.

The variability tests are conducted on three types of signals.

- *“Max” signal*: This measures the maximum signal as determined by the assay design. In in-vitro assays that measure receptor-ligand binding or enzyme activity measurement with substrate conversion to products, maximum signal represents a readout signal in the absence of test compounds. For cell-based agonist assays this parameter would be the maximal cellular response of an agonist; for potentiator assays “Max” signal is measured with an EC<sub>10</sub> concentration of a standard agonist plus maximal concentration of a standard potentiator. The observed response is as per validated assay protocol, and may exceed 10% in some cases. For inhibition assays the “Max” signal would be the signal response obtained with an EC<sub>80</sub> concentration of a standard agonist. Again the observed response is as per protocol, and may not be 80%. For inverse agonist assays “Max” signal would be the untreated constitutively active response of the cells in the presence of DMSO alone.
- *“Min” signal*: This measures the background signal as determined by the assay design. In in-vitro assays that measure receptor-ligand binding or enzyme activity measurement with substrate conversion to products, minimum signal represents a readout signal in the absence of test compounds, labeled ligand or the

enzyme substrate. For cell-based agonist assays this is the basal signal. For potentiator assays this is an EC<sub>10</sub> concentration of agonist. For inhibitor assays, including receptor-binding assays, this is an EC<sub>80</sub> concentration of the standard agonist plus a maximally inhibiting concentration of a standard antagonist (preferred) or unstimulated reaction.

- “Mid” signal: This parameter estimates the signal variability at some point between the maximum and minimum signals. Typically, for agonist assays the mid-point is reached by adding an EC<sub>50</sub> concentration of a full agonist/activator compound; for potentiator assays it is an EC<sub>10</sub> concentration of agonist plus EC<sub>50</sub> concentration of a potentiator; and for inhibitor assays it is an EC<sub>80</sub> concentration of an agonist plus an IC<sub>50</sub> concentration of a standard inhibitor to each well. In receptor-ligand binding or enzyme activity measurement based assays, this parameter represents the mid-point signal measured using EC<sub>50</sub> concentration of a control compound.

*N.B If calibration of the analytical signals is required for compound activity measurements, the Max, Min and Mid signals correspond to calibration curve responses, and not the raw plate reader counts. It is a requirement that the raw signals lie within the range of the calibration curve. Not more than 1-2% of the wells should be outside the calibration range (i.e. above the fitted top or below the fitted bottom of the calibration curve).*

Two different plate formats exist for the plate uniformity studies: an **Interleaved-Signal** format where all signals are on all plates, but varied systematically so that on all plates, on a given day, each signal is measured in each plate. This approach can also be used in concentration-response curve (CRC) plate formats where a reference compound is tested at multiple concentrations with production control wells (Max and Min). Uniform signal plates for “Max” and “Min” are also included where each signal is run uniformly across entire plates. The Interleaved-Signal format can be used in all instances and requires fewer plates. The CRC format is usually easier to run, since it closely conforms to the production process for the assay, including automated pipeting. It is also useful for detecting non-uniform signals, but usually takes more plates in total and the data analysis is more complex. The uniform-signal plates should be interpreted with caution if signals vary across plates on a given day. See Section 3.3.5 for examples and more information.

## 3.2. Interleaved-Signal Format

### 3.2.1. Procedure

The following plate layout is recommended for which the Excel analysis templates have been developed. These layouts have a combination of wells producing “Max”, “Min”, and “Mid” signals on a plate with proper statistical design. Use the same plate formats on all days of the test. Do not change the concentration producing the mid point signal over the course of the test. See Section 3.2.4 for a further discussion about midpoint accuracy. The trials should use *independently* prepared reagents, and preferably be run on *separate* days. Data Analysis Templates are available (from the online eBook) for [96-](#) and [384-well plates](#).

**Plate 1**

| Row | C1 | C2 | C3 | C4 | C5 | C6 | C7 | C8 | C9 | C10 | C11 | C12 |
|-----|----|----|----|----|----|----|----|----|----|-----|-----|-----|
| 1   | H  | M  | L  | H  | M  | L  | H  | M  | L  | H   | M   | L   |
| 2   | H  | M  | L  | H  | M  | L  | H  | M  | L  | H   | M   | L   |
| 3   | H  | M  | L  | H  | M  | L  | H  | M  | L  | H   | M   | L   |
| 4   | H  | M  | L  | H  | M  | L  | H  | M  | L  | H   | M   | L   |
| 5   | H  | M  | L  | H  | M  | L  | H  | M  | L  | H   | M   | L   |
| 6   | H  | M  | L  | H  | M  | L  | H  | M  | L  | H   | M   | L   |
| 7   | H  | M  | L  | H  | M  | L  | H  | M  | L  | H   | M   | L   |
| 8   | H  | M  | L  | H  | M  | L  | H  | M  | L  | H   | M   | L   |

H=Max, M=Mid, L=Min

**Plate 2**

| Row | C1 | C2 | C3 | C4 | C5 | C6 | C7 | C8 | C9 | C10 | C11 | C12 |
|-----|----|----|----|----|----|----|----|----|----|-----|-----|-----|
| 1   | L  | H  | M  | L  | H  | M  | L  | H  | M  | L   | H   | M   |
| 2   | L  | H  | M  | L  | H  | M  | L  | H  | M  | L   | H   | M   |
| 3   | L  | H  | M  | L  | H  | M  | L  | H  | M  | L   | H   | M   |
| 4   | L  | H  | M  | L  | H  | M  | L  | H  | M  | L   | H   | M   |
| 5   | L  | H  | M  | L  | H  | M  | L  | H  | M  | L   | H   | M   |
| 6   | L  | H  | M  | L  | H  | M  | L  | H  | M  | L   | H   | M   |
| 7   | L  | H  | M  | L  | H  | M  | L  | H  | M  | L   | H   | M   |
| 8   | L  | H  | M  | L  | H  | M  | L  | H  | M  | L   | H   | M   |

H=Max, M=Mid, L=Min

**Plate 3**

| Row | C1 | C2 | C3 | C4 | C5 | C6 | C7 | C8 | C9 | C10 | C11 | C12 |
|-----|----|----|----|----|----|----|----|----|----|-----|-----|-----|
| 1   | M  | L  | H  | M  | L  | H  | M  | L  | H  | M   | L   | H   |
| 2   | M  | L  | H  | M  | L  | H  | M  | L  | H  | M   | L   | H   |
| 3   | M  | L  | H  | M  | L  | H  | M  | L  | H  | M   | L   | H   |
| 4   | M  | L  | H  | M  | L  | H  | M  | L  | H  | M   | L   | H   |
| 5   | M  | L  | H  | M  | L  | H  | M  | L  | H  | M   | L   | H   |
| 6   | M  | L  | H  | M  | L  | H  | M  | L  | H  | M   | L   | H   |
| 7   | M  | L  | H  | M  | L  | H  | M  | L  | H  | M   | L   | H   |
| 8   | M  | L  | H  | M  | L  | H  | M  | L  | H  | M   | L   | H   |

H=Max, M=Mid, L=Min

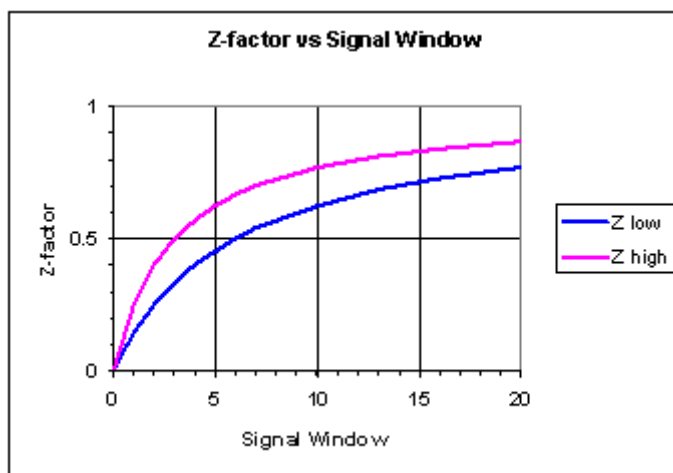


Figure 1: Z-Factor interval versus Signal Window.

### 3.2.2. Summary Signal Calculations and Plate Acceptance Criteria

Calculations and acceptance criteria are described below. The overall requirement is that the raw signals are sufficiently tight and that there is significant separation between the “Max” and “Min” signals to conduct screening.

1. Outliers should be flagged with an asterisk in the plate input section. The outliers should be “obvious”, and the rate of outliers should be less than 2 percent (i.e. on average less than 2 wells on a 96-well plate, 8 wells on a 384-well plate).
2. Compute the mean (AVG), SD, and CV (of the mean) for each signal (Max, Min and Mid) on each plate. Note that the CV is calculated taking into account the number of wells per test compound per concentration to be used in the production assay. For example, if in the production assay duplicate wells will be run for each concentration of each test substance, then  $CV = (SD/\sqrt{2})/AVG$ . More generally, if there will be  $n$  wells per test compound per concentration, then  $CV = (SD/\sqrt{n})/AVG$ . The acceptance criteria are that the CV’s of each signal be less than or equal to 20%. Note that the Min-signal often fails to meet this criterion, especially for those assays whose Min-signal mean is very low. An alternate acceptance criterion for the Min-signal is  $SD_{min} \leq$  both  $SD_{mid}$  and  $SD_{max}$ . All plates should pass all signal criteria (ie all Max, and Mid- signals should have CV’s less than 20% and all “Min” signals should either pass the CV criteria or the SD criteria).

For each of the “Mid”-signal wells, compute a percent activity for agonist or stimulation assay relative to the means of the (Max and Min- signals on that plate, i.e.,

$$\% \text{Activity} = \frac{\text{well}_{mid} - \text{AVG}_{min}}{\text{AVG}_{max} - \text{AVG}_{min}} \times 100$$

For inhibition assays compute percent inhibition for each mid-signal well, where  
 $\%Inhibition = 100 - \%Activity$ .

3. Compute the mean and SD for the “Mid”-signal percent activity values on each plate. The acceptance criterion is  $SD_{mid} \leq 20$  on all plates.
4. Compute a Signal Window (SW) or Z' factor (Z') for each plate, as described below. The acceptance criterion  $SW \geq 2$  or  $Z' \geq 0.4$  on all plates (either all SW's  $\geq 2$  or all Z'  $\geq 0.4$ ).

The formula for the signal window is

$$SW = \frac{\left( AVG_{max} - 3SD_{max} / \sqrt{n} \right) - \left( AVG_{min} + 3SD_{min} / \sqrt{n} \right)}{SD_{max} / \sqrt{n}}$$

where  $n$  is the number of replicates of the test substance that will be used in the production assay. Instead of the SW the Z' factor can be used to evaluate the signal separation, where the only difference is the denominator ( $AVG_{max} - AVG_{min}$ ) is used instead of  $SD_{max}$ . The complete formula is

$$Z' = \frac{\left( AVG_{max} - 3SD_{max} / \sqrt{n} \right) - \left( AVG_{min} + 3SD_{min} / \sqrt{n} \right)}{AVG_{max} - AVG_{min}}$$

If one assumes that the SD of the “Max”, signal is at least as large as the SD of the “Min” signal, then the Z' factor will be within a specific range for a given signal window, as illustrated in Figure 1. Note that Z' values greater than 1 are possible only if  $AVG_{max} < AVG_{min}$ , and so the templates also check that all Z' values are less than 1.

The recommended acceptance criterion is Z' factor  $\geq 0.4$ , which is comparable to a  $SW \geq 2$ . Either measure could be used.

### 3.2.3. Spatial Uniformity Assessment

A scatter plot (see examples below) can reveal patterns of drift, edge effects and other systematic sources of variability. The response is plotted against well number, where the wells are ordered either by row first, then by column, or by column first, then by row. The overall requirement is that plates do not exhibit material edge or drift effects. In general drift or edge effects  $< 20\%$  are considered insignificant. Effects seen only on a single or few plates, and not a predominant pattern, are also considered insignificant. Some guidelines for detecting and dealing with these problems follow.

#### 3.2.3.1. No drift or edge effects

Figure 2 (A, B) shows two plots (of the same data) show an example where there are no edge effects or drift.

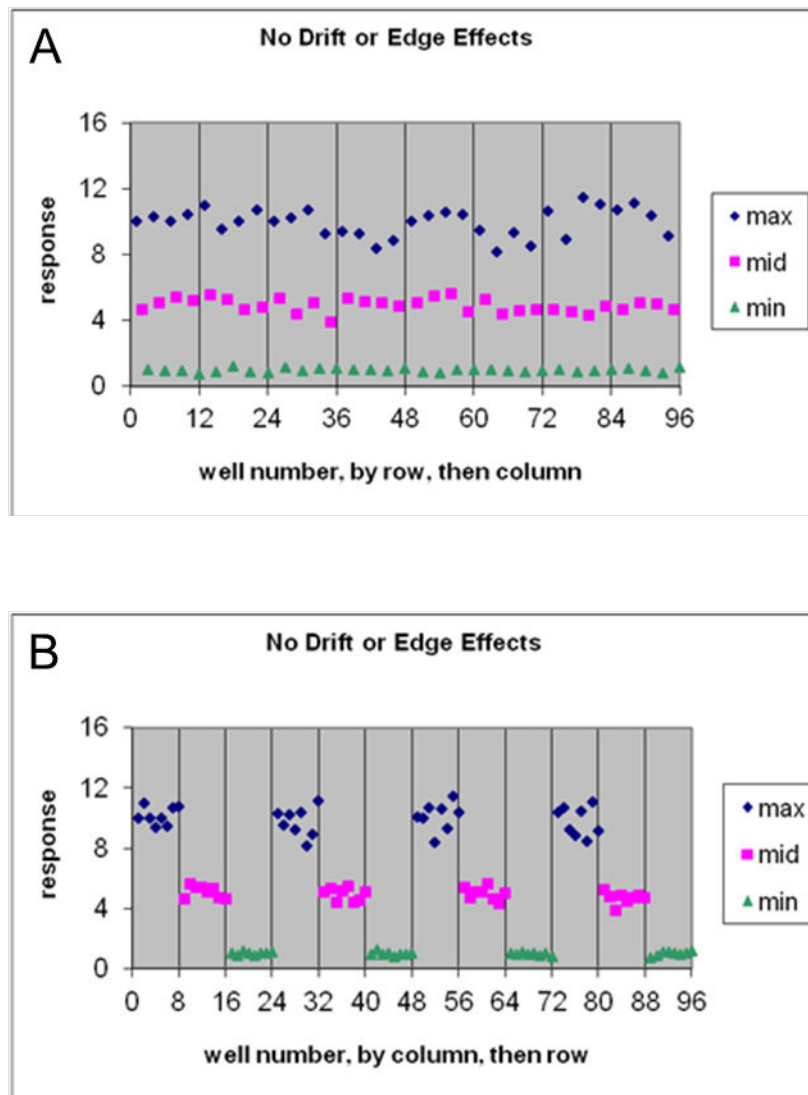


**Figure 2 A and B:** Example with no drift or edge effects. The data in both plots come from the same set.

### 3.2.3.2. Drift

Use the Max and Mid signals to assess for drift. Look for significant trends in the signal from left-to-right and top-to-bottom. If you observe drift that exceeds 20% then you have material drift effects. In Figure 3 (A, B) the mean of column 1 is 10.6, while the mean of column 10 is 13.8, and the overall mean is 12.2. The drift is 26%  $[(13.8-10.6)/12.2]$ , and therefore the cause of this drift should be investigated.

### 3.2.3.3. Edge Effects

Edge effects can contribute to variability, and spotting them can be a helpful troubleshooting technique. Edge effects are sometimes due to increased evaporation from outer wells that are incubated for long periods of time. Edge effects can also be caused

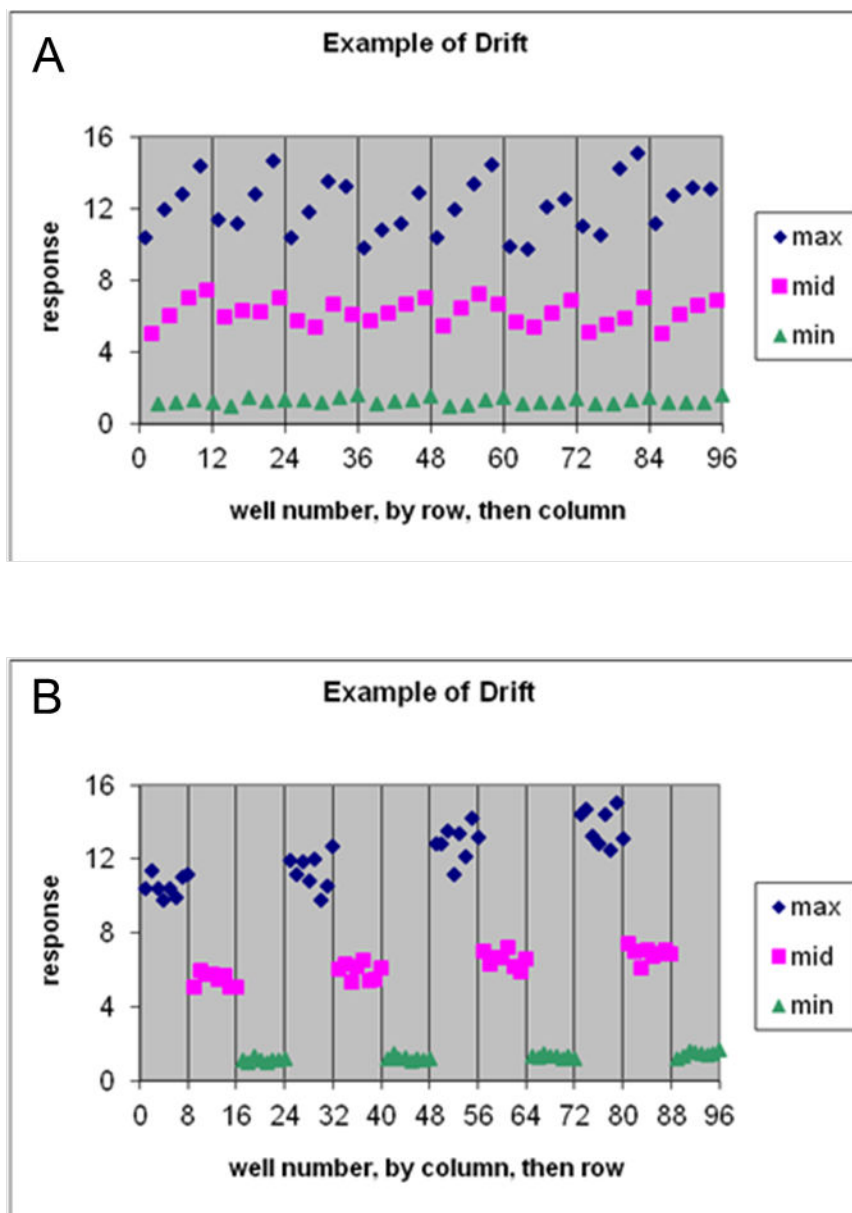


**Figure 3 A and B:** Example of material drift effects. The data in both plots come from the same set.

either by a short incubation time or by plate stacking – these conditions allow the edge wells to reach the desired incubation temperature faster than the inner wells. Edge effects are demonstrated in Figure 4.

### 3.2.4. Inter-Plate and Inter-Day Tests

The normalized Mid signal should not show any significant shift across plates or days. “Significant shift” depends to a certain extent on the typical slopes encountered in dose response curves. Thus plate-to-plate or day-to-day variation in the mid point percent activity needs to be assessed in light of the steepness of the dose-response curves of the

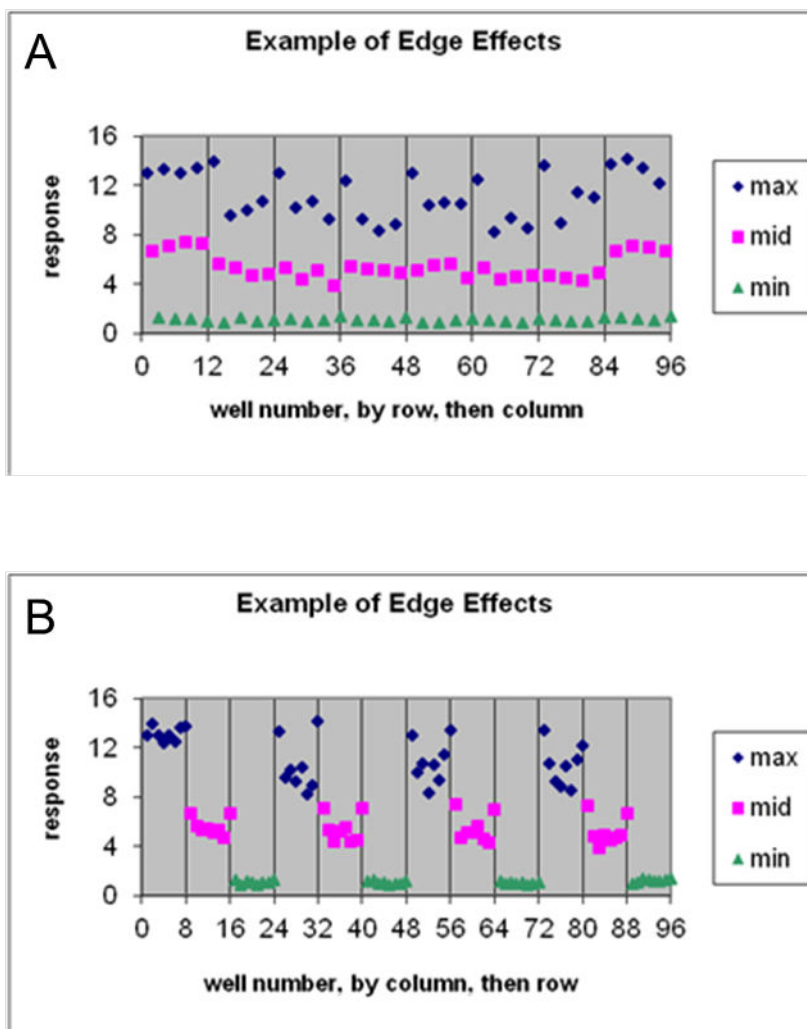


**Figure 4 A and B:** Example of edge effects. The data in both plots come from the same set. N.B., Because of the vertical axis scale, problems in the Min and even Mid signals may not be visible. Adjusting the scale to highlight the edge effect may be necessary to properly examine these signals.

assay. For receptor binding assays, and other assays with a slope parameter of 1, a 15% difference can correspond to a two-fold change in potency. The template will translate the mean normalized Mid signal to potency shifts across plates and days. There should not be a potency shift  $>2$  between any two plates within a day, or  $>2$  between any two average day Mid point % activities. For functional assays whose slopes may not equal 1 you can enter a “typical” slope into the template. This should be derived from the slope of a dose-response curve for the substance used to generate the Mid point signal.

For these calculations to have utility the Mid-point % Inhibition/Activity should be “near” the midpoint. Values within the range of 30-70% are ideal. Studies with mean values outside this range should be discussed with a statistician, especially before any studies are



repeated solely for this reason. Also note that the conditions used to obtain the midpoint should not be changed over the course of the plate uniformity study.

### 3.2.5. Summary of Acceptance Criteria

1. **Intra-plate Tests:** Each plate should have a  
 $CV_{\max}$  and  $CV_{\text{mid}} \leq 20\%$ ,  
 $CV_{\min} \leq 20\%$  or  $SD_{\min} \leq \min(SD_{\text{mid}}, SD_{\max})$ ,  
Normalized  $SD_{\text{mid}} \leq 20$ ,  
 $SW \geq 2$  or  $Z' \geq 0.4$ .
2. **No material (or insignificant) edge, drift or other spatial effects.** Note that the templates do not check this criterion.
3. **Inter-plate and Inter-Day Tests:** The normalized average Mid-signal should not translate into a fold shift  
> 2 within days,  
> 2 across any two days.

### 3.2.6. 384-well Plate Uniformity Studies

384-well plates contain 16 rows by 24 columns, and one 384-well plate contains the equivalent of four 96-well plates. Two different formats of interleaved plate uniformity templates have been developed. The first layout expands the 96-well plate format into four squares (Figure 5).

The second is useful for assays using certain automation equipment such as Tecan and Beckman (Figure 6). For these instruments column 1 of the 96-well plate corresponds to columns 1 and 2 of the 384-well plate, and is laid out in 8 pairs of columns.

The analysis and acceptance criteria are exactly the same as for 96-well format Plate Uniformity Studies. See Section 3.2.5 for a summary of the acceptance criterion.

## 3.3. Concentration-Response Curve (CRC) plus Uniform-Signal Plate Layouts

CRC plus Uniform-Signal plate layouts are an alternative format to conduct the plate uniformity studies. Their main advantage is easier execution since it is more amenable to automated pipetting per the production process for the assay. In the uniform-signal plates, all wells on each plate are exactly the same, and together with heat maps provide for a straightforward assessment of spatial properties. Optionally, the opposite production controls (Max and Min) can be included on the uniform-signal plates to assess within-plate Z factors. The CRC plates have a single reference compound serially diluted across every row or every column, along with Max and Min-control wells, per the planned production layout.

| Plate 1 |    |    |    |    |    |    |    |    |    |     |     |     |     |     |     |     |     |     |     |     |     |     |     |     |
|---------|----|----|----|----|----|----|----|----|----|-----|-----|-----|-----|-----|-----|-----|-----|-----|-----|-----|-----|-----|-----|-----|
| Row     | C1 | C2 | C3 | C4 | C5 | C6 | C7 | C8 | C9 | C10 | C11 | C12 | C13 | C14 | C15 | C16 | C17 | C18 | C19 | C20 | C21 | C22 | C23 | C24 |
| 1       | H  | M  | L  | H  | M  | L  | H  | M  | L  | H   | M   | L   | H   | M   | L   | H   | M   | L   | H   | M   | L   | H   | M   | L   |
| 2       | H  | M  | L  | H  | M  | L  | H  | M  | L  | H   | M   | L   | H   | M   | L   | H   | M   | L   | H   | M   | L   | H   | M   | L   |
| 3       | H  | M  | L  | H  | M  | L  | H  | M  | L  | H   | M   | L   | H   | M   | L   | H   | M   | L   | H   | M   | L   | H   | M   | L   |
| 4       | H  | M  | L  | H  | M  | L  | H  | M  | L  | H   | M   | L   | H   | M   | L   | H   | M   | L   | H   | M   | L   | H   | M   | L   |
| 5       | H  | M  | L  | H  | M  | L  | H  | M  | L  | H   | M   | L   | H   | M   | L   | H   | M   | L   | H   | M   | L   | H   | M   | L   |
| 6       | H  | M  | L  | H  | M  | L  | H  | M  | L  | H   | M   | L   | H   | M   | L   | H   | M   | L   | H   | M   | L   | H   | M   | L   |
| 7       | H  | M  | L  | H  | M  | L  | H  | M  | L  | H   | M   | L   | H   | M   | L   | H   | M   | L   | H   | M   | L   | H   | M   | L   |
| 8       | H  | M  | L  | H  | M  | L  | H  | M  | L  | H   | M   | L   | H   | M   | L   | H   | M   | L   | H   | M   | L   | H   | M   | L   |
| 9       | H  | M  | L  | H  | M  | L  | H  | M  | L  | H   | M   | L   | H   | M   | L   | H   | M   | L   | H   | M   | L   | H   | M   | L   |
| 10      | H  | M  | L  | H  | M  | L  | H  | M  | L  | H   | M   | L   | H   | M   | L   | H   | M   | L   | H   | M   | L   | H   | M   | L   |
| 11      | H  | M  | L  | H  | M  | L  | H  | M  | L  | H   | M   | L   | H   | M   | L   | H   | M   | L   | H   | M   | L   | H   | M   | L   |
| 12      | H  | M  | L  | H  | M  | L  | H  | M  | L  | H   | M   | L   | H   | M   | L   | H   | M   | L   | H   | M   | L   | H   | M   | L   |
| 13      | H  | M  | L  | H  | M  | L  | H  | M  | L  | H   | M   | L   | H   | M   | L   | H   | M   | L   | H   | M   | L   | H   | M   | L   |
| 14      | H  | M  | L  | H  | M  | L  | H  | M  | L  | H   | M   | L   | H   | M   | L   | H   | M   | L   | H   | M   | L   | H   | M   | L   |
| 15      | H  | M  | L  | H  | M  | L  | H  | M  | L  | H   | M   | L   | H   | M   | L   | H   | M   | L   | H   | M   | L   | H   | M   | L   |
| 16      | H  | M  | L  | H  | M  | L  | H  | M  | L  | H   | M   | L   | H   | M   | L   | H   | M   | L   | H   | M   | L   | H   | M   | L   |

| Plate 2 |    |    |    |    |    |    |    |    |    |     |     |     |     |     |     |     |     |     |     |     |     |     |     |     |
|---------|----|----|----|----|----|----|----|----|----|-----|-----|-----|-----|-----|-----|-----|-----|-----|-----|-----|-----|-----|-----|-----|
| Row     | C1 | C2 | C3 | C4 | C5 | C6 | C7 | C8 | C9 | C10 | C11 | C12 | C13 | C14 | C15 | C16 | C17 | C18 | C19 | C20 | C21 | C22 | C23 | C24 |
| 1       | L  | H  | M  | L  | H  | M  | L  | H  | M  | L   | H   | M   | L   | H   | M   | L   | H   | M   | L   | H   | M   | L   | H   | M   |
| 2       | L  | H  | M  | L  | H  | M  | L  | H  | M  | L   | H   | M   | L   | H   | M   | L   | H   | M   | L   | H   | M   | L   | H   | M   |
| 3       | L  | H  | M  | L  | H  | M  | L  | H  | M  | L   | H   | M   | L   | H   | M   | L   | H   | M   | L   | H   | M   | L   | H   | M   |
| 4       | L  | H  | M  | L  | H  | M  | L  | H  | M  | L   | H   | M   | L   | H   | M   | L   | H   | M   | L   | H   | M   | L   | H   | M   |
| 5       | L  | H  | M  | L  | H  | M  | L  | H  | M  | L   | H   | M   | L   | H   | M   | L   | H   | M   | L   | H   | M   | L   | H   | M   |
| 6       | L  | H  | M  | L  | H  | M  | L  | H  | M  | L   | H   | M   | L   | H   | M   | L   | H   | M   | L   | H   | M   | L   | H   | M   |
| 7       | L  | H  | M  | L  | H  | M  | L  | H  | M  | L   | H   | M   | L   | H   | M   | L   | H   | M   | L   | H   | M   | L   | H   | M   |
| 8       | L  | H  | M  | L  | H  | M  | L  | H  | M  | L   | H   | M   | L   | H   | M   | L   | H   | M   | L   | H   | M   | L   | H   | M   |
| 9       | L  | H  | M  | L  | H  | M  | L  | H  | M  | L   | H   | M   | L   | H   | M   | L   | H   | M   | L   | H   | M   | L   | H   | M   |
| 10      | L  | H  | M  | L  | H  | M  | L  | H  | M  | L   | H   | M   | L   | H   | M   | L   | H   | M   | L   | H   | M   | L   | H   | M   |
| 11      | L  | H  | M  | L  | H  | M  | L  | H  | M  | L   | H   | M   | L   | H   | M   | L   | H   | M   | L   | H   | M   | L   | H   | M   |
| 12      | L  | H  | M  | L  | H  | M  | L  | H  | M  | L   | H   | M   | L   | H   | M   | L   | H   | M   | L   | H   | M   | L   | H   | M   |
| 13      | L  | H  | M  | L  | H  | M  | L  | H  | M  | L   | H   | M   | L   | H   | M   | L   | H   | M   | L   | H   | M   | L   | H   | M   |
| 14      | L  | H  | M  | L  | H  | M  | L  | H  | M  | L   | H   | M   | L   | H   | M   | L   | H   | M   | L   | H   | M   | L   | H   | M   |
| 15      | L  | H  | M  | L  | H  | M  | L  | H  | M  | L   | H   | M   | L   | H   | M   | L   | H   | M   | L   | H   | M   | L   | H   | M   |
| 16      | L  | H  | M  | L  | H  | M  | L  | H  | M  | L   | H   | M   | L   | H   | M   | L   | H   | M   | L   | H   | M   | L   | H   | M   |

| Plate 3 |    |    |    |    |    |    |    |    |    |     |     |     |     |     |     |     |     |     |     |     |     |     |     |     |
|---------|----|----|----|----|----|----|----|----|----|-----|-----|-----|-----|-----|-----|-----|-----|-----|-----|-----|-----|-----|-----|-----|
| Row     | C1 | C2 | C3 | C4 | C5 | C6 | C7 | C8 | C9 | C10 | C11 | C12 | C13 | C14 | C15 | C16 | C17 | C18 | C19 | C20 | C21 | C22 | C23 | C24 |
| 1       | M  | L  | H  | M  | L  | H  | M  | L  | H  | M   | L   | H   | M   | L   | H   | M   | L   | H   | M   | L   | H   | M   | L   | H   |
| 2       | M  | L  | H  | M  | L  | H  | M  | L  | H  | M   | L   | H   | M   | L   | H   | M   | L   | H   | M   | L   | H   | M   | L   | H   |
| 3       | M  | L  | H  | M  | L  | H  | M  | L  | H  | M   | L   | H   | M   | L   | H   | M   | L   | H   | M   | L   | H   | M   | L   | H   |
| 4       | M  | L  | H  | M  | L  | H  | M  | L  | H  | M   | L   | H   | M   | L   | H   | M   | L   | H   | M   | L   | H   | M   | L   | H   |
| 5       | M  | L  | H  | M  | L  | H  | M  | L  | H  | M   | L   | H   | M   | L   | H   | M   | L   | H   | M   | L   | H   | M   | L   | H   |
| 6       | M  | L  | H  | M  | L  | H  | M  | L  | H  | M   | L   | H   | M   | L   | H   | M   | L   | H   | M   | L   | H   | M   | L   | H   |
| 7       | M  | L  | H  | M  | L  | H  | M  | L  | H  | M   | L   | H   | M   | L   | H   | M   | L   | H   | M   | L   | H   | M   | L   | H   |
| 8       | M  | L  | H  | M  | L  | H  | M  | L  | H  | M   | L   | H   | M   | L   | H   | M   | L   | H   | M   | L   | H   | M   | L   | H   |
| 9       | M  | L  | H  | M  | L  | H  | M  | L  | H  | M   | L   | H   | M   | L   | H   | M   | L   | H   | M   | L   | H   | M   | L   | H   |
| 10      | M  | L  | H  | M  | L  | H  | M  | L  | H  | M   | L   | H   | M   | L   | H   | M   | L   | H   | M   | L   | H   | M   | L   | H   |
| 11      | M  | L  | H  | M  | L  | H  | M  | L  | H  | M   | L   | H   | M   | L   | H   | M   | L   | H   | M   | L   | H   | M   | L   | H   |
| 12      | M  | L  | H  | M  | L  | H  | M  | L  | H  | M   | L   | H   | M   | L   | H   | M   | L   | H   | M   | L   | H   | M   | L   | H   |
| 13      | M  | L  | H  | M  | L  | H  | M  | L  | H  | M   | L   | H   | M   | L   | H   | M   | L   | H   | M   | L   | H   | M   | L   | H   |
| 14      | M  | L  | H  | M  | L  | H  | M  | L  | H  | M   | L   | H   | M   | L   | H   | M   | L   | H   | M   | L   | H   | M   | L   | H   |
| 15      | M  | L  | H  | M  | L  | H  | M  | L  | H  | M   | L   | H   | M   | L   | H   | M   | L   | H   | M   | L   | H   | M   | L   | H   |
| 16      | M  | L  | H  | M  | L  | H  | M  | L  | H  | M   | L   | H   | M   | L   | H   | M   | L   | H   | M   | L   | H   | M   | L   | H   |

Figure 5: Standard Interleaved 384-well Format Plate Layouts.

### 3.3.1. Procedure

Max and Min signals are prepared as defined in Section 3.1. Two plates are run for each signal. Two CRC plates are also run, for a total of six plates per day. The number of days required is the same as the Interleaved-Signal layout: three days for new assays, two days for transfers of previously validated assays.

| Plate 1 |    |    |    |    |    |    |    |    |    |     |     |     |     |     |     |     |     |     |     |     |     |     |     |     |
|---------|----|----|----|----|----|----|----|----|----|-----|-----|-----|-----|-----|-----|-----|-----|-----|-----|-----|-----|-----|-----|-----|
| Row     | C1 | C2 | C3 | C4 | C5 | C6 | C7 | C8 | C9 | C10 | C11 | C12 | C13 | C14 | C15 | C16 | C17 | C18 | C19 | C20 | C21 | C22 | C23 | C24 |
| 1       | H  | H  | M  | M  | L  | L  | H  | H  | M  | M   | L   | L   | H   | H   | M   | M   | L   | L   | H   | H   | M   | M   | L   | L   |
| 2       | H  | H  | M  | M  | L  | L  | H  | H  | M  | M   | L   | L   | H   | H   | M   | M   | L   | L   | H   | H   | M   | M   | L   | L   |
| 3       | H  | H  | M  | M  | L  | L  | H  | H  | M  | M   | L   | L   | H   | H   | M   | M   | L   | L   | H   | H   | M   | M   | L   | L   |
| 4       | H  | H  | M  | M  | L  | L  | H  | H  | M  | M   | L   | L   | H   | H   | M   | M   | L   | L   | H   | H   | M   | M   | L   | L   |
| 5       | H  | H  | M  | M  | L  | L  | H  | H  | M  | M   | L   | L   | H   | H   | M   | M   | L   | L   | H   | H   | M   | M   | L   | L   |
| 6       | H  | H  | M  | M  | L  | L  | H  | H  | M  | M   | L   | L   | H   | H   | M   | M   | L   | L   | H   | H   | M   | M   | L   | L   |
| 7       | H  | H  | M  | M  | L  | L  | H  | H  | M  | M   | L   | L   | H   | H   | M   | M   | L   | L   | H   | H   | M   | M   | L   | L   |
| 8       | H  | H  | M  | M  | L  | L  | H  | H  | M  | M   | L   | L   | H   | H   | M   | M   | L   | L   | H   | H   | M   | M   | L   | L   |
| 9       | H  | H  | M  | M  | L  | L  | H  | H  | M  | M   | L   | L   | H   | H   | M   | M   | L   | L   | H   | H   | M   | M   | L   | L   |
| 10      | H  | H  | M  | M  | L  | L  | H  | H  | M  | M   | L   | L   | H   | H   | M   | M   | L   | L   | H   | H   | M   | M   | L   | L   |
| 11      | H  | H  | M  | M  | L  | L  | H  | H  | M  | M   | L   | L   | H   | H   | M   | M   | L   | L   | H   | H   | M   | M   | L   | L   |
| 12      | H  | H  | M  | M  | L  | L  | H  | H  | M  | M   | L   | L   | H   | H   | M   | M   | L   | L   | H   | H   | M   | M   | L   | L   |
| 13      | H  | H  | M  | M  | L  | L  | H  | H  | M  | M   | L   | L   | H   | H   | M   | M   | L   | L   | H   | H   | M   | M   | L   | L   |
| 14      | H  | H  | M  | M  | L  | L  | H  | H  | M  | M   | L   | L   | H   | H   | M   | M   | L   | L   | H   | H   | M   | M   | L   | L   |
| 15      | H  | H  | M  | M  | L  | L  | H  | H  | M  | M   | L   | L   | H   | H   | M   | M   | L   | L   | H   | H   | M   | M   | L   | L   |
| 16      | H  | H  | M  | M  | L  | L  | H  | H  | M  | M   | L   | L   | H   | H   | M   | M   | L   | L   | H   | H   | M   | M   | L   | L   |

| Plate 2 |    |    |    |    |    |    |    |    |    |     |     |     |     |     |     |     |     |     |     |     |     |     |     |     |
|---------|----|----|----|----|----|----|----|----|----|-----|-----|-----|-----|-----|-----|-----|-----|-----|-----|-----|-----|-----|-----|-----|
| Row     | C1 | C2 | C3 | C4 | C5 | C6 | C7 | C8 | C9 | C10 | C11 | C12 | C13 | C14 | C15 | C16 | C17 | C18 | C19 | C20 | C21 | C22 | C23 | C24 |
| 1       | L  | L  | H  | H  | M  | M  | L  | L  | H  | H   | M   | M   | L   | L   | H   | H   | M   | M   | L   | L   | H   | H   | M   | M   |
| 2       | L  | L  | H  | H  | M  | M  | L  | L  | H  | H   | M   | M   | L   | L   | H   | H   | M   | M   | L   | L   | H   | H   | M   | M   |
| 3       | L  | L  | H  | H  | M  | M  | L  | L  | H  | H   | M   | M   | L   | L   | H   | H   | M   | M   | L   | L   | H   | H   | M   | M   |
| 4       | L  | L  | H  | H  | M  | M  | L  | L  | H  | H   | M   | M   | L   | L   | H   | H   | M   | M   | L   | L   | H   | H   | M   | M   |
| 5       | L  | L  | H  | H  | M  | M  | L  | L  | H  | H   | M   | M   | L   | L   | H   | H   | M   | M   | L   | L   | H   | H   | M   | M   |
| 6       | L  | L  | H  | H  | M  | M  | L  | L  | H  | H   | M   | M   | L   | L   | H   | H   | M   | M   | L   | L   | H   | H   | M   | M   |
| 7       | L  | L  | H  | H  | M  | M  | L  | L  | H  | H   | M   | M   | L   | L   | H   | H   | M   | M   | L   | L   | H   | H   | M   | M   |
| 8       | L  | L  | H  | H  | M  | M  | L  | L  | H  | H   | M   | M   | L   | L   | H   | H   | M   | M   | L   | L   | H   | H   | M   | M   |
| 9       | L  | L  | H  | H  | M  | M  | L  | L  | H  | H   | M   | M   | L   | L   | H   | H   | M   | M   | L   | L   | H   | H   | M   | M   |
| 10      | L  | L  | H  | H  | M  | M  | L  | L  | H  | H   | M   | M   | L   | L   | H   | H   | M   | M   | L   | L   | H   | H   | M   | M   |
| 11      | L  | L  | H  | H  | M  | M  | L  | L  | H  | H   | M   | M   | L   | L   | H   | H   | M   | M   | L   | L   | H   | H   | M   | M   |
| 12      | L  | L  | H  | H  | M  | M  | L  | L  | H  | H   | M   | M   | L   | L   | H   | H   | M   | M   | L   | L   | H   | H   | M   | M   |
| 13      | L  | L  | H  | H  | M  | M  | L  | L  | H  | H   | M   | M   | L   | L   | H   | H   | M   | M   | L   | L   | H   | H   | M   | M   |
| 14      | L  | L  | H  | H  | M  | M  | L  | L  | H  | H   | M   | M   | L   | L   | H   | H   | M   | M   | L   | L   | H   | H   | M   | M   |
| 15      | L  | L  | H  | H  | M  | M  | L  | L  | H  | H   | M   | M   | L   | L   | H   | H   | M   | M   | L   | L   | H   | H   | M   | M   |
| 16      | L  | L  | H  | H  | M  | M  | L  | L  | H  | H   | M   | M   | L   | L   | H   | H   | M   | M   | L   | L   | H   | H   | M   | M   |

| Plate 3 |    |    |    |    |    |    |    |    |    |     |     |     |     |     |     |     |     |     |     |     |     |     |     |     |
|---------|----|----|----|----|----|----|----|----|----|-----|-----|-----|-----|-----|-----|-----|-----|-----|-----|-----|-----|-----|-----|-----|
| Row     | C1 | C2 | C3 | C4 | C5 | C6 | C7 | C8 | C9 | C10 | C11 | C12 | C13 | C14 | C15 | C16 | C17 | C18 | C19 | C20 | C21 | C22 | C23 | C24 |
| 1       | M  | M  | L  | L  | H  | H  | M  | M  | L  | L   | H   | H   | M   | M   | L   | L   | H   | H   | M   | M   | L   | L   | H   | H   |
| 2       | M  | M  | L  | L  | H  | H  | M  | M  | L  | L   | H   | H   | M   | M   | L   | L   | H   | H   | M   | M   | L   | L   | H   | H   |
| 3       | M  | M  | L  | L  | H  | H  | M  | M  | L  | L   | H   | H   | M   | M   | L   | L   | H   | H   | M   | M   | L   | L   | H   | H   |
| 4       | M  | M  | L  | L  | H  | H  | M  | M  | L  | L   | H   | H   | M   | M   | L   | L   | H   | H   | M   | M   | L   | L   | H   | H   |
| 5       | M  | M  | L  | L  | H  | H  | M  | M  | L  | L   | H   | H   | M   | M   | L   | L   | H   | H   | M   | M   | L   | L   | H   | H   |
| 6       | M  | M  | L  | L  | H  | H  | M  | M  | L  | L   | H   | H   | M   | M   | L   | L   | H   | H   | M   | M   | L   | L   | H   | H   |
| 7       | M  | M  | L  | L  | H  | H  | M  | M  | L  | L   | H   | H   | M   | M   | L   | L   | H   | H   | M   | M   | L   | L   | H   | H   |
| 8       | M  | M  | L  | L  | H  | H  | M  | M  | L  | L   | H   | H   | M   | M   | L   | L   | H   | H   | M   | M   | L   | L   | H   | H   |
| 9       | M  | M  | L  | L  | H  | H  | M  | M  | L  | L   | H   | H   | M   | M   | L   | L   | H   | H   | M   | M   | L   | L   | H   | H   |
| 10      | M  | M  | L  | L  | H  | H  | M  | M  | L  | L   | H   | H   | M   | M   | L   | L   | H   | H   | M   | M   | L   | L   | H   | H   |
| 11      | M  | M  | L  | L  | H  | H  | M  | M  | L  | L   | H   | H   | M   | M   | L   | L   | H   | H   | M   | M   | L   | L   | H   | H   |
| 12      | M  | M  | L  | L  | H  | H  | M  | M  | L  | L   | H   | H   | M   | M   | L   | L   | H   | H   | M   | M   | L   | L   | H   | H   |
| 13      | M  | M  | L  | L  | H  | H  | M  | M  | L  | L   | H   | H   | M   | M   | L   | L   | H   | H   | M   | M   | L   | L   | H   | H   |
| 14      | M  | M  | L  | L  | H  | H  | M  | M  | L  | L   | H   | H   | M   | M   | L   | L   | H   | H   | M   | M   | L   | L   | H   | H   |
| 15      | M  | M  | L  | L  | H  | H  | M  | M  | L  | L   | H   | H   | M   | M   | L   | L   | H   | H   | M   | M   | L   | L   | H   | H   |
| 16      | M  | M  | L  | L  | H  | H  | M  | M  | L  | L   | H   | H   | M   | M   | L   | L   | H   | H   | M   | M   | L   | L   | H   | H   |

Figure 6: HHMMLL 384-well Plate Uniformity Plate Layouts

### 3.3.2. Summary Calculations and Plate Acceptance Criterion

The calculations will be performed by the Excel template provided. Details of the calculations are as follows:

1. Compute the mean (AVG), standard deviation (SD) and Coefficient of Variation (CV) for the Max and Min plates (as per the Interleaved-Signal format the CV's should reflect the number of wells per test-condition envisioned in the production assay). Also compute these quantities using the Max and Min control wells on the CRC plates. Requirements are the same as for Interleaved-Signal format: The CV of each plate should be less than 20%. Alternatively, the Min plates should have  $SD \leq \text{smaller of } SD_{\text{mid}} \text{ and } SD_{\text{max}}$ .
2. For the CRC plates, determine which concentration has mean activity across all plates that is closest to 50%. Designate this concentration as the "Mid" signal. Then compute the percent activity for agonist or stimulation assays, and percent

inhibition for antagonist or inhibition assays (including binding assays). In this format the calculation is

$$\% \text{Activity} = \frac{\text{well}_{\text{mid}} - \text{AVG}_{\text{min}}}{\text{AVG}_{\text{max}} - \text{AVG}_{\text{min}}} \times 100$$

3. where  $\text{AVG}_{\text{min}}$  is the average of the on-plate Min control wells, and  $\text{AVG}_{\text{max}}$  is the average of the on-plate Max control wells. Percent Inhibition = 100 - %Activity.
4. Compute the SD of the normalized signals on each Mid signal. The acceptance criterion is  $\text{SD}_{\% \text{mid}} \leq 20$ .
5. Compute the Z' factor and/or the SW for each plate where Max and Min controls are present, and for the Max and Min uniform plates, if the opposite production control wells were included. Z' factor and SW can also be calculated within a day across plates, pooling all of the Max and Min wells, but this is only useful if the raw signal levels are consistent between plates. The formulas are the same as in Section 3.2.2. The acceptance criterion is either all  $Z' \geq 0.4$  or all  $\text{SW} \geq 2$ .

### 3.3.3. Spatial Uniformity Assessment

Heat maps or similar types of plots can be generated for the raw plate data. The criterion for acceptance is the same as for the interleaved format: No drift or edge effects that exceed 20% of the mean. Also as in the Interleaved-Signal format, the presence of these effects should be apparent as the predominant effect, and not seen just in single isolated plate for the assay to be failed by this criterion.

Using the Max and Min uniform plates, Figure 7 illustrates a spatially uniform result, an edge effect, and a drift effect. Uniform Mid signal plates were used in this example instead of CRC plates. Day 1 shows an acceptably uniform result. Day 2 shows an assay with a significant edge effect (25% from the mean edge value to the mean of the interior), and Day 3 shows an assay with significant drift (25% change in mean value from left to right as compared to the average in the middle). If patterns are similar or worse than those depicted in Day 2 or Day 3 then the assay **does not pass** the spatially uniform requirement.

### 3.3.4. Inter-Plate and Inter-Day Tests

The Inter-plate and inter-day tests are the same as in Section 3.2.4, except the definitions of % Activity and % Inhibition defined above (Section 3.3.1) are used in the tests. In addition,  $\text{EC}/\text{IC}_{50}$ s can be calculated from the CRC data, and fold shifts in mean  $\text{EC}/\text{IC}_{50}$  between plates and days can be examined directly to assess variability. In addition, a preliminary Minimum Significant Ratio (MSR) can be calculated from the CRC plates, as follows. An  $\text{EC}/\text{IC}_{50}$  can be calculated for each row on each plate. For higher density plates (384-wells and above), there could be more than one CRC curve fit per row. Compute the standard deviation (S) of all the  $\text{Log IC}_{50}$ s across plates and days (Alternatively, a variance components analysis could be used to separate within-plate,

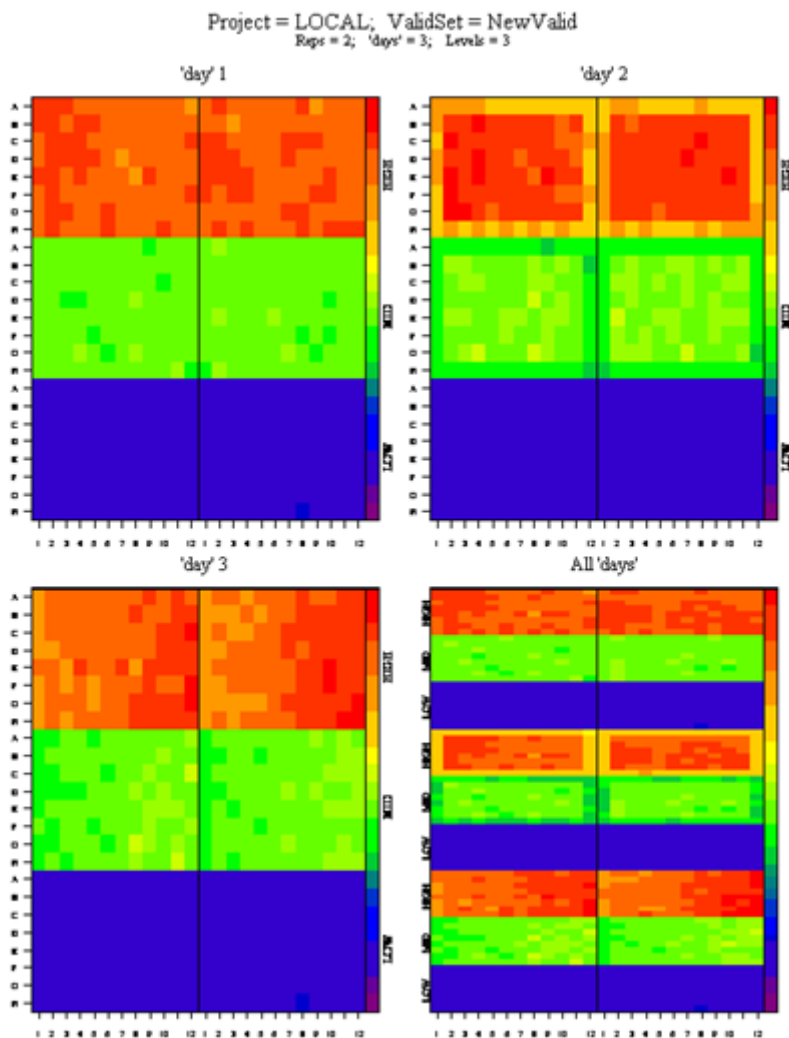


**Figure 7:** Illustrates a spatially uniform result (Day 1), an edge effect (Day 2), and a drift effect (Day 3). Mid signal plates were used in place of CRC plates.

within-day and between-day variability). The MSR is  $10^{(2 \cdot \sqrt{2}) \cdot S}$ , and this value is the smallest ratio between two  $IC_{50}$ s that is statistically significant. A common criterion is for the MSR to be less than 3. This MSR should be considered a preliminary and optimistic estimate of the assay MSR, because it is based on a single compound and because the  $IC_{50}$ s derived from different rows on the same plate, or even different plates on the same day, will most often not reflect all of the sources of variability in the assay.

### 3.3.5. Impact of Plate Variation on Validation Results

Uniform-Signal plates in the CRC format make the assumption that plate variation within each run day is negligible. If this assumption is not correct, then some of the diagnostic

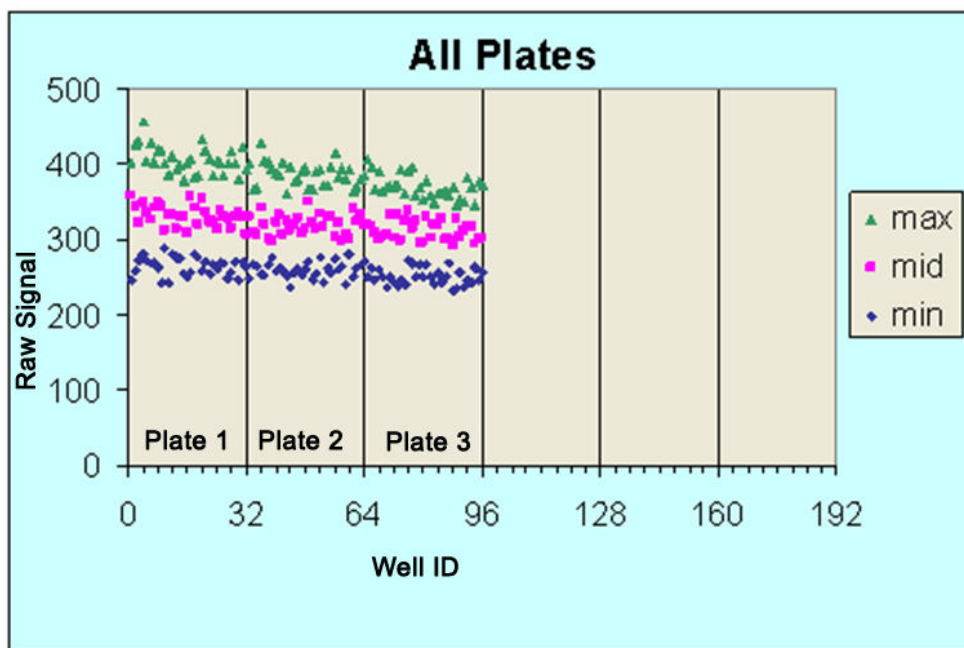


**Figure 8:** Raw data values for 3 plates of an Interleaved-Signal Plate Uniformity Study. Plates 1-3 show the actual plate values obtained on one day of the test.

tests described here will be misleading. In that case, one should either include opposite production control wells (Max and Min) on the uniform-signal plates, or use the Interleaved-Signal format instead. In particular,  $Z'$  factors and/or Signal Windows computed across plates or across days may be incorrect in either direction, and the Inter-plate and Inter-Day tests could unnecessarily fail acceptable assays.

The following example illustrates the problem. The raw signals of one day of an Interleaved-Signal format Plate Uniformity Study are shown in Figure 8. The Max and Mid raw signals vary across the 3 plates (Figure 8, Plates 1-3), but note that the % Activity is very stable across the 3 plates (Figure 9, Plates 1-3). The maximum fold shift across plates is 1.2.

The Midpoint Percent Activity plot (Figure 9) shows what happens when on-plate Max and Min controls are not used. The three left-hand panels show the plates, normalized to their own controls while, to mimic the Uniform-Signal protocol with its off-plate controls, the three right-hand panels of Figure 9 show each plate's mid signal normalized to the plate 3 controls:

**Plate 4** shows the plate 1 mid signal data normalized to the plate 3 Max and Min signals,

**Plate 5** shows the plate 2 mid signal data normalized to the plate 3 Max and Min signals and

**Plate 6** is the same as plate 3.

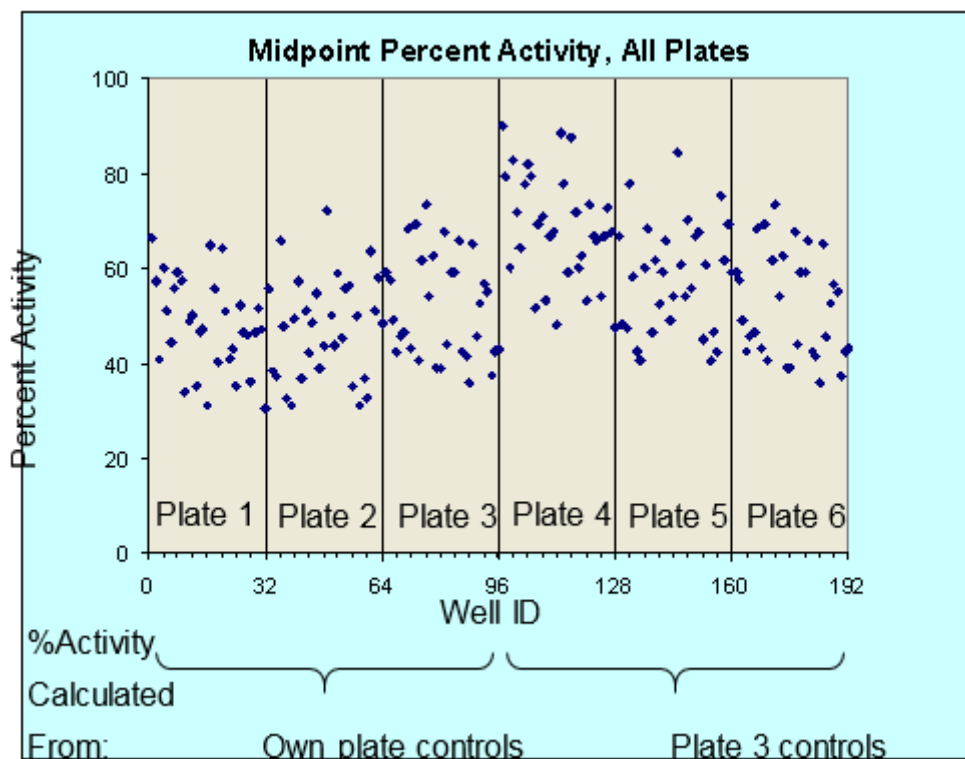


**Figure 9:** Normalized midpoint values for 3 plates of an Interleaved-Signal Plate Uniformity Study. Plates 1-3 show the actual plate midpoints normalized to the on-plate controls. Plates 4-6 show the same midpoints all normalized to the Plate 3 Min and Max controls. Notice the shift in activity for plates 4 vs. 1 and 5 vs. 2.

In the presence of variation in the uniform-signal plates, off-plate controls do not effectively normalize the assay. As Figure 9 shows, plate-to-plate variation in the raw signals can induce the appearance of significant mid-point variation when in fact there is little variation in signals properly normalized to on-plate controls. In this example using off-plate controls, Plates 1-3 have a max fold shift of 2.0 which does not pass the inter-plate acceptance criterion.

**Table 1:** Reference for the number of replicates necessary for assays with high variability.

| CV using 1 well | Number of wells so that CV < 20% | Number of wells so that CV < 20% |
|-----------------|----------------------------------|----------------------------------|
| <10             | 1                                | 1                                |
| 10.1-14.1       | 2                                | 1                                |
| 14.2-17.3       | 3                                | 1                                |
| 17.4-20.0       | 4                                | 1                                |
| 20.1-22.3       | 5                                | 2                                |

Table 1 continues on next page...

Table 1 continued from previous page.

| CV using 1 well | Number of wells so that CV < 20% | Number of wells so that CV < 20% |
|-----------------|----------------------------------|----------------------------------|
| 22.4-24.4       | 6                                | 2                                |
| 24.5-26.4       | 7                                | 2                                |
| 26.5-28.2       | 8                                | 2                                |
| 28.3-30.0       | 9                                | 3                                |
| 30.1-31.6       | 10                               | 3                                |
| 31.7-33.1       | 11                               | 3                                |
| 33.2-34.6       | 12                               | 3                                |
| 34.7-36.0       | 13                               | 4                                |
| 36.1-37.4       | 14                               | 4                                |
| 37.5-38.7       | 15                               | 4                                |
| 38.8-40.0       | 16                               | 4                                |

**Table 3: MSR and LsA evaluation of Replicate-Experiment study using both replicates, and then re-calculated using just the first replicate.**

| Replicates Used | Assay 1 |           | Assay 2 |           |
|-----------------|---------|-----------|---------|-----------|
|                 | MSR     | LsA       | MSR     | LsA       |
| Rep 1 Only      | 2.27    | 0.44-2.27 | 3.30    | 0.28-3.08 |
| Both Reps       | 1.71    | 0.57-1.67 | 2.15    | 0.44-2.03 |

**Table 2: MSR and LsA evaluation of Replicate-Experiment study using the first 2 replicates, first 3 replicates, and all 4 replicates.**

| Reps | MSR  | LsA       |
|------|------|-----------|
| 2    | 3.62 | 0.35-4.59 |
| 3    | 3.32 | 0.43-4.74 |
| 4    | 2.44 | 0.53-3.16 |

## 4. Replicate-Experiment Study

### 4.1. Overview

It is important to verify that the assay results are reproducible, i.e. that the variability of key end points of the assay are acceptably low. In addition, if the assay is to report results previously reported by another assay, then it is necessary to verify that the two labs produce equivalent results. In this section, we define how to quantify assay variability and determine assay equivalence. It is important to read the entire section below to understand the rationale for the statistical methods employed in calculating



reproducibility of potency and efficacy. We strongly recommend consultation with a statistician before designing experiments to estimate variability described below.

#### 4.1.1. Rationale

Replicate-Experiment studies are used to formally evaluate the *within-run* assay variability and formally compare the new assay to the existing (old) assay. They also allow a preliminary assessment of the *overall* or *between-run* assay variability, but two runs are not enough to adequately assess overall variability. Post-production methods (Section 3) are used to formally evaluate the overall variability in the assay. Note that the Replicate-Experiment study is a diagnostic and decision tool used to establish that the assay is ready to go into production by showing that the endpoints of the assay are reproducible *over a range of potencies*. It is not intended as a substitute for post-production monitoring or to provide an estimate of the *overall* Minimum Significant Ratio (MSR).

It may seem counter-intuitive to call the differences between two independent assay runs as “within-run” variability. However, the terminology results from how assay runs are defined. Experimental variation is categorized into two distinct components: *between-run* and *within-run* sources. Consider the following examples:

- If there is variation in the concentrations of buffer components between 2 runs, then the assay results could be affected. However, assuming that the same buffer is used with all compounds within one run, each compound will be equally affected and so the difference will only show up when comparing one run to another run, i.e. in two runs, one run will appear higher on average than the other run. This variation is called *between-run* variation.
- If the concentration of a compound in the stock plate varies from the target concentration then all wells where that compound is used will be affected. However, wells used to test other compounds will be unaffected. This type of variation is called *within-run* as the source of variation affects different compounds in the same run differently.
- Some sources of variability affect both within- and between-run variation. For example, in a FLIPR assay cells are plated and then incubated for 24-72 hours to achieve a target cell density taking into account the doubling time of the cells. For example, if the doubling time equals the incubation time, and the target density is 30,000 cells/well, then 15,000 cells/well are plated. But even if exactly 15,000 cells are placed in each well there won't be exactly 30,000 cells in each well after 24 hours. Some will be lower and some will be higher than the target. These differences are *within-run* as not all wells are equally affected. But also suppose in a particular run only 13,000 cells are initially plated. Then the wells will on average have fewer than 30,000 cells after 24 hours, and since all cells are affected this is *between-run* variation. Thus cell density has both within- and between-run sources of variation.

The total variation is the sum of both sources of variation. When comparing two compounds across runs, one must take into account both the *within-run* and *between-run* sources of variation. But when comparing two compounds in the same run, one must only

take into account the within-run sources, since, by definition, the between-run sources affect both compounds equally.

In a Replicate-Experiment study the between-run sources of variation cause one run to be on average higher than the other run. However, it would be very unlikely that the difference between the two runs were exactly the same for every compound in the study. These individual compound “differences from the average difference” are caused by the within-run sources of variation. The higher the within-run variability the greater the individual compound variation in the assay runs.

*The analysis approach used in the Replicate-Experiment study is to estimate and factor out between-run variability, and then estimate the magnitude of within-run variability.*

## 4.2. Procedure

All assays should have a reproducibility comparison (Steps 1-3). If the assay is to replace an existing assay and combine the data, then an assay comparison study should also be done (Steps 4 and 5).

1. Select 20-30 compounds that have potencies covering the concentration range being tested and, if applicable, efficacy measures that cover the range of interest. The compounds should be well spaced over these ranges.
2. All compounds should be run in each of two runs of the assay.
3. Compare the two runs as per Section 4.3-4.6.
4. Assay comparison: Same compound set should be run in a single run of the previous assay.
5. Compare the results of the two assays by analyzing the first run of the new assay with the single run of the previous assay.

## 4.3. Analysis (Potency)

For the reproducibility comparison, paste potency values from the two runs into the Run-1 and Run-2 data columns. All tests are analyzed and computed by the spreadsheet, which also provides additional plots and diagnostics to assist in judging the results.

For the assay comparison study, paste the potency values for the first run of the new assay into the Run-1 column and the potency values for the (single) run of the previous assay into the Run- column. Potency values should be calculated according to the methods of Section 3. A template for the [Replicate-Experiment data analysis](#) is available for download from the online eBook.

The points below describe and define the terms used in the template and the acceptance criterion discussed in the Diagnostic Tests section below.

1. Compute the difference in log-potency (= first – second) between the first and second run for each compound. Let  $\bar{d}$ , and  $s_d$  be the sample mean and standard deviation of the difference in log-potency. Since ratios of EC<sub>50</sub> values (relative potencies) are more meaningful than differences in potency, we take logs in order

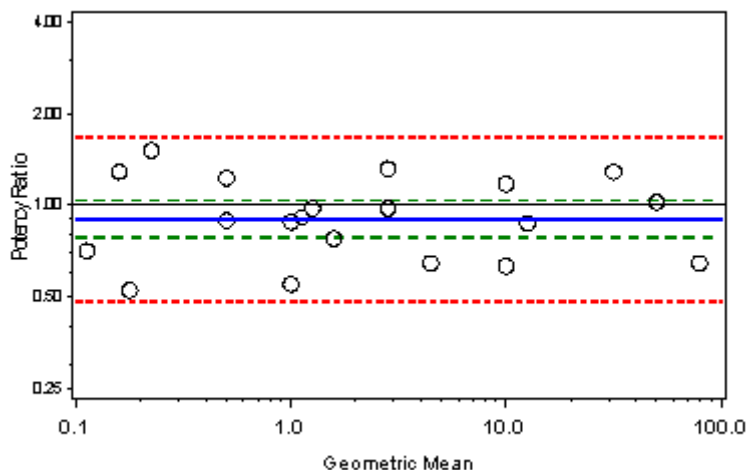


**Figure 10:** Potency Ratio versus GM Potency. This is a typical example for an acceptable assay: The MR=0.90, RLs=(0.78-1.03) [contains the value 1.0], MSR=1.86 [under 3.0], LsA=(0.48-1.67) [between 0.33 and 3.0]. The blue-solid, green long-dashed and red short-dashed lines represent the MR, RLs and LsA values respectively

to analyze ratios as differences. (Note: hypothetical potency values of 1 and 3, 10 and 30, 100 and 300 have the same ratio but not the same difference),

2. Compute the **Mean-Ratio**:  $MR = 10^{\bar{d}}$ . This is the geometric average fold difference in potency between two runs.
3. Compute the **Ratio Limits**:  $RLS = 10^{\bar{d} \pm 2s/\sqrt{n}}$ , where  $n$  is the number of compounds. This is the 95% confidence interval for the Mean-Ratio.
4. Compute the **Minimum Significant Ratio**:  $MSR = 10^{2s}$ . This is the smallest potency ratio between two compounds that is statistically significant.
5. Compute the **Limits of Agreement**:  $LsA = 10^{\bar{d} \pm 2s}$ . Most of the compound potency ratios (approximately 95%) should fall within these limits.
6. For each compound compute the **Ratio** (=first/second) of the two potencies, and the **Geometric Mean** potency:  $GM = \sqrt{\text{first} \times \text{second}}$ .

Items 2-6 can be combined into one plot: the Ratio-GM plot. An example is in Figure 10. The points represent the compounds; the blue-solid, green long-dashed and red short-dashed lines represent the MR, RLs and LsA values respectively.

Figure 10 shows the desired result of pure chance variation in the difference in activities between runs. The blue solid line shows the geometric mean potency ratio, i.e. the *average* relationship between the first and second run. The green long-dashed lines show the 95% confidence limits of the mean ratio. These limits should contain the value 1.0, as they do in this case. The red short-dashed lines indicate the limits of agreement between runs. They indicate the *individual compound* variation between the first and second run. All or almost all, the points should fall within the red dashed lines. The lower line should be

above 0.33, while the upper line should be below 3.0, which indicates a 3-fold difference between runs in either direction. The MSR should be less than 3.0, as it is in this example.

#### 4.4. Diagnostic Tests and Acceptance Criterion (Potency)

1. If the  $MSR \geq 3$  then there is poor **individual** agreement between the two runs. This problem occurs when the *within-run* variability of the assay is too high (Figure 11A). An assay meets the MSR acceptance criterion if the (within-run) **MSR** < 3.
2. If Ratio limits do not contain the value 1, then there is a statistically significant **average** difference between the two runs. Within a lab (Step 3) this is due to high *between-run* assay variability. Between labs (Step 4), this could be due to a systematic difference between labs, or high between-run variability in one or both labs. See Figure 11B for an illustration. Note that it is possible with a very “tight” assay (i.e. one with a very low MSR) or with a large set of compounds to have a statistically significant result for this test that is not very material, i.e., the actual MR is small enough to be ignorable. If the result is statistically significant then examine the MR. If it is between 0.67 and 1.5 then the average difference between runs is less than 50% and is deemed immaterial. However, in Figure 2(b) the  $MR=2.01$ , indicating a 101% difference between runs, which is too high to be considered “equivalent”. Note that there is no direct requirement for the MR, but values that are this extreme are unlikely to pass the Limits of Agreement criterion in step 3 below.
3. The MR and the MSR are combined into a single interval referred to as the **Limits of Agreement**. An assay that either has a high MSR and/or an MR different from 1 will tend to have poor agreement of results between the two runs. An assay meets the Limits of Agreement acceptance criterion if both the upper and lower limits of agreement are between 0.33 and 3.0. Note that assays depicted in both Figure 11 A and B do not have Limits of Agreement inside the acceptance region and thus do not meet the acceptance criterion.

#### 4.5. Analysis (Efficacy)

The points below describe and define the terms used in the template and the acceptance criterion discussed in the Diagnostic Tests section. Note that the methods described here are intended for functional full/partial assays and non-competitive antagonist assays. Some potentiator assays, as well as assays normalized by fold stimulation may best be analyzed with the techniques described in the potency section rather than the methods described here. Consult a statistician for the best method of analysis.

1. Compute the difference in efficacy (= first – second) between the first and second run for each compound. Let  $\bar{d}$ , and  $s_d$  be the sample mean and standard deviation of the difference in efficacy.
2. Compute the **Mean-Difference**:  $MD = |\bar{d}|$ . This is the average difference in efficacy between the two runs.

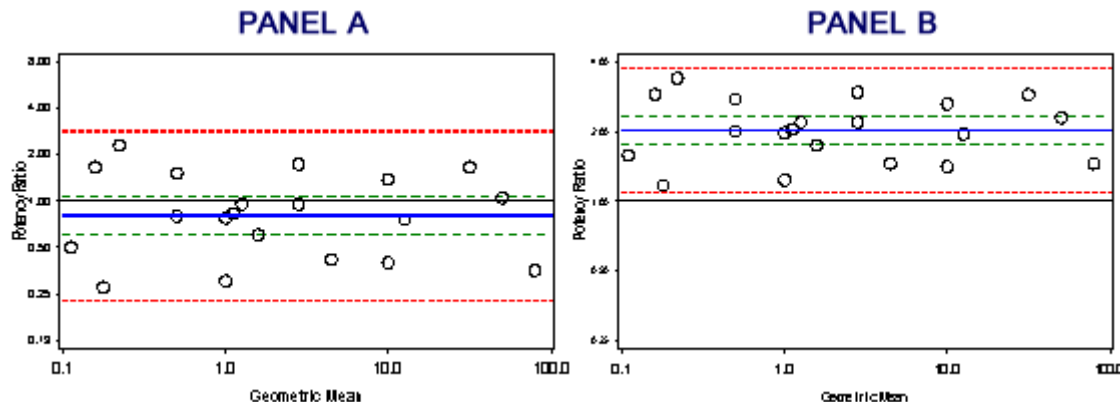


**Figure 11:** Potency Ratio vs. GM Potency. (A) Shows a case where the within-run variability is too large (MR= 0.8, RLs= (0.61-1.07), MSR= 3.54, and LsA= (0.23-2.84), and (B) shows a case where the LsA are outside the acceptable range because the Mean Ratio is too large, i.e., there is a tendency for the activity values in run 1 to be larger than in run 2 (MR= 2.01, RL= (1.75-2.32), MSR= 1.86, and LsA= (1.08-3.75). In both cases the reason(s) for these conditions should be investigated.

3. Compute the **Difference Limits**:  $DLs = \bar{d} \pm 2s_d / \sqrt{n}$ , where  $n$  is the number of compounds. This is a 95% confidence interval for the Mean-Difference.
4. Compute the **Minimum Significant Difference**:  $MSD = 2s_d$ . This is the smallest efficacy difference between two compounds that is statistically significant.
5. Compute the **Limits of Agreement**:  $LsAd = \bar{d} \pm 2s_d$ . Most of the compound efficacy differences should fall within these limits (approximately 95%).
6. For each compound compute the **Difference** (= first-second) of the two efficacies, and the **Mean** efficacy (average of first and second).

Items 2-6 can be combined onto one plot: the Difference-Mean plot (not shown). The plot is very similar to the Ratio-GM plot except that both axes are on the linear scale instead of the log scale.

#### 4.6. Diagnostic Tests (Efficacy)

Generally the same two problems discussed under potency need to be judged for efficacy as well. However, a general acceptance criterion for efficacy has not been established as there is not a consensus on efficacy standards and for most projects potency is the primary property of interest. As guidelines, the MD should be less than 5 (i.e., less than 5% average difference between runs) and the MSD should be less than 20 (e.g., 20% activity). More importantly, the MD and MSD should be used to judge the appropriateness of any efficacy CSF's a project may have. For example, if the CSF for efficacy is >80%, and the MSD is 30%, then the assay will fail too many efficacious compounds - a 90%-active compound would fall below the CSF 25% of the time. A more appropriate CSF in this situation would be 70 or even 60%.

## 4.7. Summary of Acceptance Criteria

1. In Step 3, conduct reproducibility and equivalence tests for potency comparing the two runs in the new lab. The assay should pass both tests ( $MSR < 3$  and both Limits of Agreement should be between 0.33 and 3.0).
2. In Step 5, conduct reproducibility and equivalence tests for potency comparing the first run of the new lab to the single run of the old lab. The assays should pass both tests to be declared equivalent (Limits of Agreement between 0.33 and 3.0).
3. For full/partial agonist assays and non-competitive antagonist assays, repeat points 1 and 2 for efficacy. Use the informal guidelines discussed above, and project efficacy CSFs to judge acceptability of results.

## 4.8. Notes

1. If a project is very new, there may not be 20-30 unique active compounds (where active means some measurable activity above the minimum threshold of the assay). In that case it is acceptable to run compounds more than once to get an acceptable sample size. For example, if there are only 10 active compounds then run each compound twice. However, when doing so, (a) it is important to biologically evaluate them as though they were different compounds, including the preparation of separate serial dilutions, and (b) label the compounds “a”, “b” etc. so that it is clear in the test-retest analyses which results are being compared across runs.
2. Functional assays need to be compared for both potency ( $EC_{50}$ ) and efficacy (%maximum response). This may well require a few more compounds in those cases.
3. In binding assays, it is best to compare  $K_i$ 's, and in functional antagonist assays it is best to compare  $K_b$ 's.
4. An assay may pass the reproducibility assessment (Steps 1-3 in the procedure [Section 4.2.]), but may fail the assay comparison study (Steps 4-5 in the procedure [Section 4.2]). The assay comparison study may fail either because of a MR different from 1 or a high “MSR” in the assay comparison study. If it's the former then there is a potency shift between the assays. You should assess the values in the assays to ascertain their validity (e.g. which assay's results compare best to those reported in the literature?). If it fails because the Lab Comparison study is too large (but the new assay passes the reproducibility study) then the old assay lacks reproducibility. In either case, if the problem is with the old assay, then the team should consider re-running key compounds in the new assay to provide comparable results to compounds subsequently run in the new assay.

## 5. How to Deal with High Assay Variability

### 5.1. High Variation in Single Concentration Determinations

Table 1 can be used as a reference to determine the number of replicates necessary for assays with high variability. For a given CV of the raw data values based on 1 well, it shows the number of replicates needed for the CV of a mean to be less than or equal to 10 or 20%. This table does not indicate how the  $IC_{50}/K_i/K_b$  variability will be affected (See Section 5.2 for high variation in  $IC_{50}/K_i/K_b$  responses).

Adding replicates to reduce variability will also reduce the capacity (i.e., throughput) of the assay to test compounds. Further optimization of the assay could reduce variability and maintain or increase its capacity. The decision to further optimize or add replicates will have to be made for each assay.

### 5.2. Excess Variation in Concentration-Response Outcomes ( $EC_{50}$ , $IC_{50}$ , $K_i$ , or $K_b$ )

If in Section 4 the assay fails either test ( $MSR > 3$  or Limits of Agreement outside the interval 1/3-3) then the variability of the assay is too high. The following options should be considered to reduce the assay variability:

1. Optimizing the assay to lower variability in the signal (see Section 6) of the raw data values. Check that the concentration range is appropriate for the compound results. Adding more concentrations and/or replicates may improve the results. A minimum of 8 concentrations at half-log intervals is recommended. In general, it is better to have more concentrations (up to 12) rather than more replicates.
2. Consider adding replicates as discussed below. Note that the impact of adding replication may be minimal, and so the Replicate Experiment Study should be used to assess whether increasing the number of replicates will achieve the objective.
3. Adopt as part of the standard protocol to re-run results. For example, each compound may be tested once per run on 2 or more runs. Then averaging the results will reduce the assay variability (**Note:** In such cases the individual run results are stored in the database, and the data mining/query tools are used to average the results).

To investigate the impact of adding replicate wells in the concentration-response assay conduct the Replicate-Experiment study with the maximum number of wells contemplated (typically 3-4 wells / concentration). To examine the impact of replication compute the MSR versus number-of-replicates curve. To construct this curve, make all data calculations using only the first replicate of each concentration to evaluate the MSR and Limits of Agreement for 1 well per concentration. Then repeat all calculations using the first two replicates per concentration, and so on until you are using all replicates. If the assay does not meet the acceptance criterion when all replicates are used then replication will not sufficiently impact the assay to warrant the replication. If it does meet the

criterion using all replicates, ascertain how many replicates are needed by noting the smallest number of replicates that are required to meet the Replicate-Experiment acceptance criterion. Two examples below will help illustrate the steps.

**Example 1:** A binding assay was run using 1 well per concentration and the Replicate-Experiment study did not meet the acceptance criterion. To examine if replication would help, a new Replicate-Experiment study was conducted using 4 wells per concentration. Using only the first replicate from each concentration, the results were normalized, curves fit, and  $K_i$ 's were calculated for each concentration-response curve. The MSR and LsA were evaluated. The entire calculation steps were repeated using the first 2 replicates, first 3 replicates and all 4 replicates, with the results listed in Table 2.

From Table 2, it is evident that i all 4 replicates are needed to meet the MSR acceptance criterion, and no amount of replication (up to 4 replicates) will meet LsA acceptance criterion.

**Example 2:** In a second study, a pair of uptake inhibition assays (the project had two targets, each measured by one assay) the Plate Uniformity Study indicated two replicates would be required to meet the Plate Uniformity Signal acceptance criteria in Assay 2. However, plate uniformity criteria concerning replication do not readily translate to dose-response requirements, and so the requirements were investigated in both assays. The Replicate-Experiment Study was conducted using two replicates. The calculations were performed using both replicates, and then re-calculated using just the first replicate. The MSR and LsA are summarized in Table 3.

Using two replicates both assays meet all acceptance criterion. Using only a single replicate, Assay 1 still meets all criteria, while Assay 2 does not. Note that in this instance both assays benefited from increased replication. However, Assay 1 is a very tight assay and hence this benefit is not really needed. So in this example, the replication requirements were the same for both single dose screening and concentration -response studies, but in general this will not be the case.

## 6. Bridging Studies for Assay Upgrades and Minor Changes

### 6.1. Overview

Sections 3 and 4 cover the validation of entirely new assays, or assays that are intended to replace existing assays. The replacement assays are “different” from the original assay, either because of facility changes, personnel differences, or substantively different reagents, detection and automation equipment. Assay upgrades and changes occur as a natural part of the assay life cycle. Requiring a full validation for every conceivable change is impractical and would serve as a barrier to implementing assay improvements. Hence full validation following every assay change is not recommended. Instead bridging studies or “mini-validation” studies are recommended to document that the change does not degrade the quality of the data generated by the new assay.



The level of validation recommended has 3 tiers: A small plate uniformity study ([Tier I](#)), to an assay comparison portion of the Replicate-Experiment study ([Tier II](#)), to a full validation package of Sections 3 and 4 ([Tier III](#)). Examples of changes within each Tier are given below, along with the recommended validation study for that Tier. Note that if the study indicates the change will have an adverse impact on assay quality (i.e. the study indicates there are problems), then the cause should be investigated and a full (Tier III) validation should be done. If the results from that study indicate the assays are not equivalent, but the new assay has to be implemented, then the results should not be combined into one set.

The following applies principally to changes in biological components of the protocol. If changes are made to the data analysis protocol then these can ordinarily be validated without generating any new data, by comparing the results using the original and new data analysis protocols on a set of existing data. Discuss any changes with a statistician. If changes are made to both the data analysis and biological components of the protocol, then the appropriate Tier should be selected according to the severity of the biological change as discussed below. The data analysis changes should be validated on the new validation data and any additional validation work may be needed as judged by the statistician.

## 6.2. Tier I: Single Step Changes to the Assay

Tier I modifications are single changes in an assay such as a change to a reagent, instrumentation, or assay condition that is made either to improve the assay quality or increase the capacity without changing the assay quality. Changes can also be made for reasons unrelated to assay throughput or performance (e.g. change of a supplier for cost savings). Examples of such changes are

- Changes in detection instruments with similar or comparable optics and electronics. E.g.: plate readers, counting equipment, spectrophotometers. A performance check for signal dynamic range, and signal stability is recommended prior to switching instruments.
- Changes in liquid handling equipment with similar or comparable volume dispensing capabilities. Volume calibration of the new instrument is recommended prior to switching instruments. [Note that plate and pipette tip materials can cause significant changes in derived results (IC<sub>50</sub>, EC<sub>50</sub>). This may be due to changes in the adsorption and wetting properties of the plastic material employed by vendors. Under these conditions a full validation may be required].

The purpose of the validation study is to document the change and not reduce the assay quality (see Figure 12).

### 6.2.1. Protocol

Conduct a 4-plate Plate Uniformity Study using the layouts in the “2 Plates per Day” tab of the Plate Uniformity Template (the layouts are the same as Plates 1 and 2 of Section

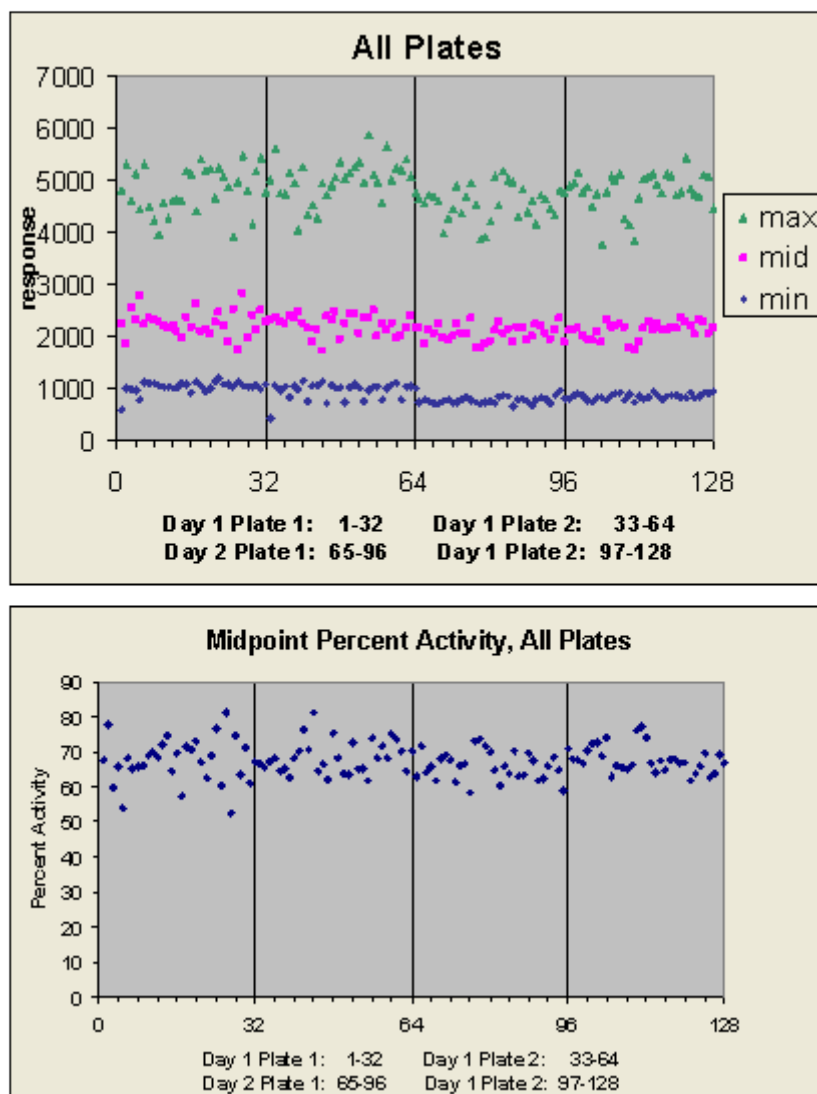


**Figure 12:** Tier I validation study comparing manual pipetting (plates 1 and 2) versus multidrop pipetting (plates 3 and 4) in GTP $\gamma$ S assay.

3.2). Plates 1 and 2 should be done using the existing protocol, and Plates 3 and 4 done using the new protocol on the same day using the same reagents and materials (except for the intentional change). Use the 2-Day / 2-Plates per Day template to conduct the analysis.

### 6.2.2. Analysis

The main analysis is a visual inspection of the “all plates” plots to ensure that the signals have not changed in either magnitude and/or variability. The mean and SD calculations for each plate can help, but visual inspection is usually sufficient.

### 6.2.3. Example

An assay was changed by replacing a manual pipetting step with a multidrop instrument. A 4-plate Plate Uniformity study was run as per the protocol, with the manual pipetting done in plates 1 and 2, and the multidrop in plates 3 and 4. The results show that the mean percent activity is the same and the multidrop's variability superior (i.e. lower) to the manual pipetting (Figure 12).

## 6.3. Tier II: Minor Assay Changes

Tier II changes are more substantive than Tier I changes, and have greater potential to directly impact EC<sub>50</sub>/IC<sub>50</sub> results. Examples of such changes are

- Changes in dilution protocols covering the same concentration range for the concentration–response curves. A bridging study is recommended when dilution protocol changes are required.
- Lot changes of critical reagents such as a new lot of receptor membranes or a new lot of serum antibodies.
- Assay moved to a new laboratory without major changes in instrumentation, using the same reagent lots, same operators and assay protocols.
- Assay transfer to an associate or technician within the same laboratory having substantial experience in the assay platform, biology and pharmacology. No other changes are made to the assay.

### 6.3.1. Protocol and Analysis

Conduct the assay comparison portion of the Replicate Experiment Study discussed in Section 4, i.e. compare one run of 20-30 compounds of the assay using the existing assay to one run of the assay under the proposed format and compare the results. If the compound set used in the original validation is available then run the same set again in the new assay protocol, and compare back to Run-1 of the original Replicate-Experiment Study. The acceptance criterion is the same as for the assay comparison study: Both Limits of Agreement should be between 1/3 and 3.0.

## 6.4. Tier III: Substantive Changes

Substantive changes requiring full assay validation: When substantive changes are made in the assay procedures, measured signal responses, target pharmacology and control compound activity values may change significantly. Under these circumstances, the assay should be re-validated according to methods described in Sections 3 and 4. The following changes constitute substantive changes, particularly when multiple changes in factors listed below are involved:

- Changes in assay platform: e.g.: Filter binding to Fluorescence polarization for kinase assays.
- Changes in assay reagents (including lot changes and supplier) that produce significant changes in assay response, pharmacology and control activity values. For

example, changes in enzyme substrates, isozymes, cell-lines, label types, control compounds, calibration standards, (radiolabel vs. fluorescent label), plates, tips and bead types, major changes in buffer composition and pH, co-factors, metal ions, etc.

- Transfer of the assay to a different laboratory location, with distinctly different instrumentation, QB practices or training.
- Changes in detection instruments with significant difference in the optics and electronics. For example, plate readers, counting equipment, spectrophotometers.
- Changes in liquid handling equipment with significant differences in volume dispensing capabilities.
- Changes in liquid handling protocol with significant differences in volume dispensing methods.
- Changes in assay conditions such as shaking, incubation time, or temperature that produce significant change in assay response, pharmacology and control activity values.
- Major changes in dilution protocols involving mixed solvents, number of dilution steps and changes in concentration range for the concentration-response curves.
- Change in analyst/operator running the assay, particularly if new to the job and/or has no experience in running the assay in its current format/assay platform.
- Making more than one of the above-mentioned changes to the assay protocol at any one time.

Substantive changes require full validation, i.e. a three day Plate Uniformity Study and Replicate Experiment Study. If the intent is to report the data together with the previous assay data then an assay comparison study should be conducted as part of the Replicate Experiment study.

## 7. References

Sittampalam GS, Iversen PW, Boadt JA, Kahl SD, Bright S, Zock JM, Janzen WP, Lister MD. Design of Signal Windows in High Throughput Screening Assays for Drug Discovery. *J Biomol Screen.* 1997;2:159–169.

Zhang J-H, Chung TDY, Oldenburg KR. A simple statistical parameter for use in evaluation and validation of high throughput screening assays. *J Biomol Screen.* 1999;4:67–73. PubMed PMID: 10838414.

Taylor PB, Stewart FP, Dunnington DJ, Quinn ST, Schulz CK, Vaidya KS, Kurali E, Tonia RL, Xiong WC, Sherrill TP, Snider JS, Terpstra ND, Hertzberg RP. Automated Assay Optimization with Integrated Statistics and Smart Robotics. *J. Biomol Screen.* 2000;5:213–225. PubMed PMID: 10992042.

Iversen PW, Eastwood BJ, Sittenpalam GS. A Comparison of Assay Performance Measures in Screening Assays: Signal Window,  $Z'$ -Factor and Assay Variability Ratio. *J of Biomol Screen.* 2006;11:247–252. PubMed PMID: 16490779.

Bland JM, Altman DG. Statistical methods for assessing agreement between two methods of clinical measurement. *Lancet.* 1986;I:307–310. PubMed PMID: 2868172.

Eastwood BJ, Farmen MW, Iversen PW, Craft TJ, Smallwood JK, Garbison KE, Delapp N, Smith GF. The Minimum Significant Ratio: A Statistical Parameter to Characterize the Reproducibility of Potency Estimates from Concentration-Response Assays and Estimation by Replicate-Experiment Studies. *J Biomol Screen*. 2006;11:253–261. PubMed PMID: 16490778.

Eastwood, BJ, Chesterfield, AK, Wolff MC, and Felder CC: Methods for the Design and Analysis of Replicate-Experiment Studies to Establish Assay Reproducibility and the Equivalence of Two Potency Assays, in Gad, S (ed): *Drug Discovery Handbook*, John Wiley and Sons, New York, 2005, 667-688



# Assay Operations for SAR Support

Benoit Beck,<sup>1</sup> Yun-Fei Chen, Walthere Dere, Viswanath Devanarayan, Brian J. Eastwood, Mark W. Farnen, Stephen J. Iturria, Phillip W. Iversen,<sup>2</sup> Steven D. Kahl, Roger A. Moore, Barry D. Sawyer, and Jeffrey Weidner\*

Created: May 1, 2012; Updated: November 20, 2017.

## Abstract

Most biological assays measure potency of compounds as an activity coefficient, frequently known as molar concentration of inhibitor at 50% response (IC<sub>50</sub>) or an agonist concentration at 50% biological activity (EC<sub>50</sub>). Since biological response responses are non-linear and generally sigmoidal in shape, appropriate curve fitting is important. In addition, the variability in measured IC<sub>50</sub>/EC<sub>50</sub> should be monitored to ensure reliable and robust data analysis of the assay curves to support expensive SAR operations in drug discovery. This chapter addresses in detail significant concepts in curve-fitting techniques and statistical concepts and tools required SAR support.

## A. Determination of EC<sub>50</sub>/IC<sub>50</sub>

### Models and Curve Fitting Guidelines

For competitive binding assays and functional antagonist assays the most common summary measure of the dose-response curve is the IC<sub>50</sub>, the concentration of substance that provides 50% inhibition. For agonist/stimulator assays the most common summary measure is the EC<sub>50</sub>, the concentration giving 50% of that compound's maximal response. Substantial variation in the methodology used to derive these values exists, and this variation has been shown to substantially impact overall assay variability. This section discusses important issues to consider and provides some guidelines on how to proceed. They are based on the [Data Standardization for Results Management](#) chapter of this book. Consult that document for the specifics for each assay type. Consult a statistician to see if these guidelines are appropriate for your assay, and if other outcomes such as AUC or a threshold dose should be used.

Before fitting a concentration -response curve to obtain the EC<sub>50</sub>/IC<sub>50</sub>, each well should be converted to either percent activity or percent inhibition with respect to positive and negative controls (note: for simplicity all text below is stated for determining IC<sub>50</sub>'s; determining EC<sub>50</sub>'s is identical). Percent activity of all replicate wells from a given run, (including multiple plates per run) for a given concentration, should be averaged either by taking the mean, or preferably, taking the median. *Outliers less influence the median values*

---

<sup>1</sup> Eli Lilly & Company, Indianapolis, IN. <sup>2</sup> Eli Lilly & Company, Indianapolis, IN.

\* Editor

when there are 3 or more replicates. Thus only one averaged point per concentration per run is used to fit the dose-response equation to the data. This is because replicate wells on either the same or different plates are often correlated with each other and, thus, do not provide true replication of the experiment.

The four parameter logistic model (4PL), also called the *Hill-Slope model*, is the most common equation fit to in vitro concentration-response data. One form of the equation is

$$y = bot + \frac{(top - bot)}{1 + (x/IC_{50})^{slope}}$$

where,  $y$  is the percent activity and  $x$  is the corresponding concentration. The fitted  $IC_{50}$  parameter is the **relative**  $IC_{50}$ , and is defined as the concentration giving a response half way between the fitted top and bottom of the curve. Some software, such as ActivityBase, also provides the **absolute**  $IC_{50}$ , which is defined as the concentration giving exactly a 50% response. The relative  $IC_{50}$  is recommended for most assays (see notes below and [Glossary](#) for definitions). You should also report the **fitting error**, which is usually called the standard error by most software packages (we use the term fitting error to differentiate it from the standard error of the mean [SEM] derived from multiple determinations of a compound).

The 4PL model is the best model for concentration -response data, but there are cases where it should not be used. In some cases, due to the potency of the compound falling outside the concentration range, the data may not fully describe the bottom or top asymptote of the curve. In those cases, respectively, the bottom (3PLFB) or top (3PLFT) can be fixed to improve the curve fit. If you observe a substantial reduction in the % Fitting Error, and a better concentration-response plot of the fitted curve with respect to the actual data then you should switch to either the 3PLFB or 3PLFT model as appropriate.

## Examples

All examples below are from receptor binding data fitting % Activity versus concentration (expressed by ActivityBase as log-concentration in the plots). For this type of assay, the top, bottom and slope parameters should in theory be 100, 0 and -1, respectively.

Figure 1 is a concentration-response best fit by the 4PL model. Both asymptotes are defined by the data, and the fitting error is approximately the same with all 3 models. Note that even though the fitting error is smallest with the top fixed (8.63% versus 9.51%), the reduction is not small enough to warrant the fixed top model, nor is there any material change in the  $IC_{50}$ . The fixed bottom model is clearly inappropriate as the data clearly defines a bottom  $>0$ .

The fitting error is expressed here as a percentage of the fitted parameter value. For example, if the  $IC_{50}$  is 0.061 and its fitting error is 0.0058, then the % Fit Error is 9.51%.



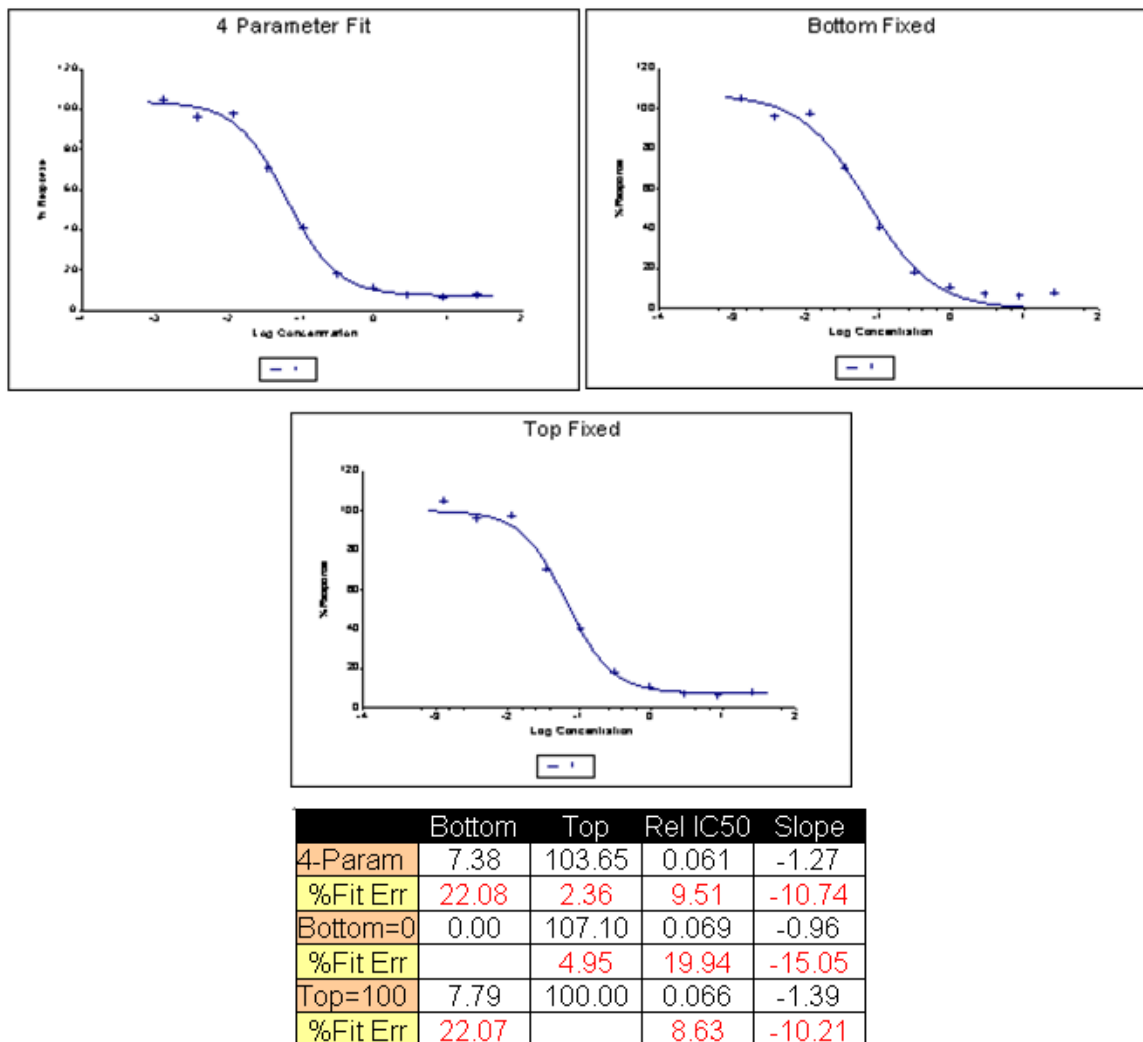


**Figure 1:** Curve fit results for a dose-response best fit by a 4PL model.

Figure 2 is best fit by the fixed top (3PLFT) model. The data does not define a top asymptote, and the fitted top (128.32) and slope (-0.58) from the 4PL model are inappropriate for this (binding) data. By fixing the top at 100% the fitting error is reduced from 57.54 to 21.55%, and the IC<sub>50</sub> increases by more than two-fold. Thus the 3PLFT model should be selected over the 4PL.

Figure 3 is best fit by a fixed bottom (3PLFB) model. Note that the data does not define the bottom asymptote, and the fitted bottom (41.54) and fitted slope (-1.83) from the 4PL are inappropriate for binding data. The fixed bottom model reduces the fitting error from 80.19% to 20.85%, while the IC<sub>50</sub> increases by more than two-fold. The fitted IC<sub>50</sub> (20.88 nM) is inside the dose-range (0.001-25 nM), and so it is appropriate to report this value. Note in this case Activity Base was unable to fit a fixed top model.

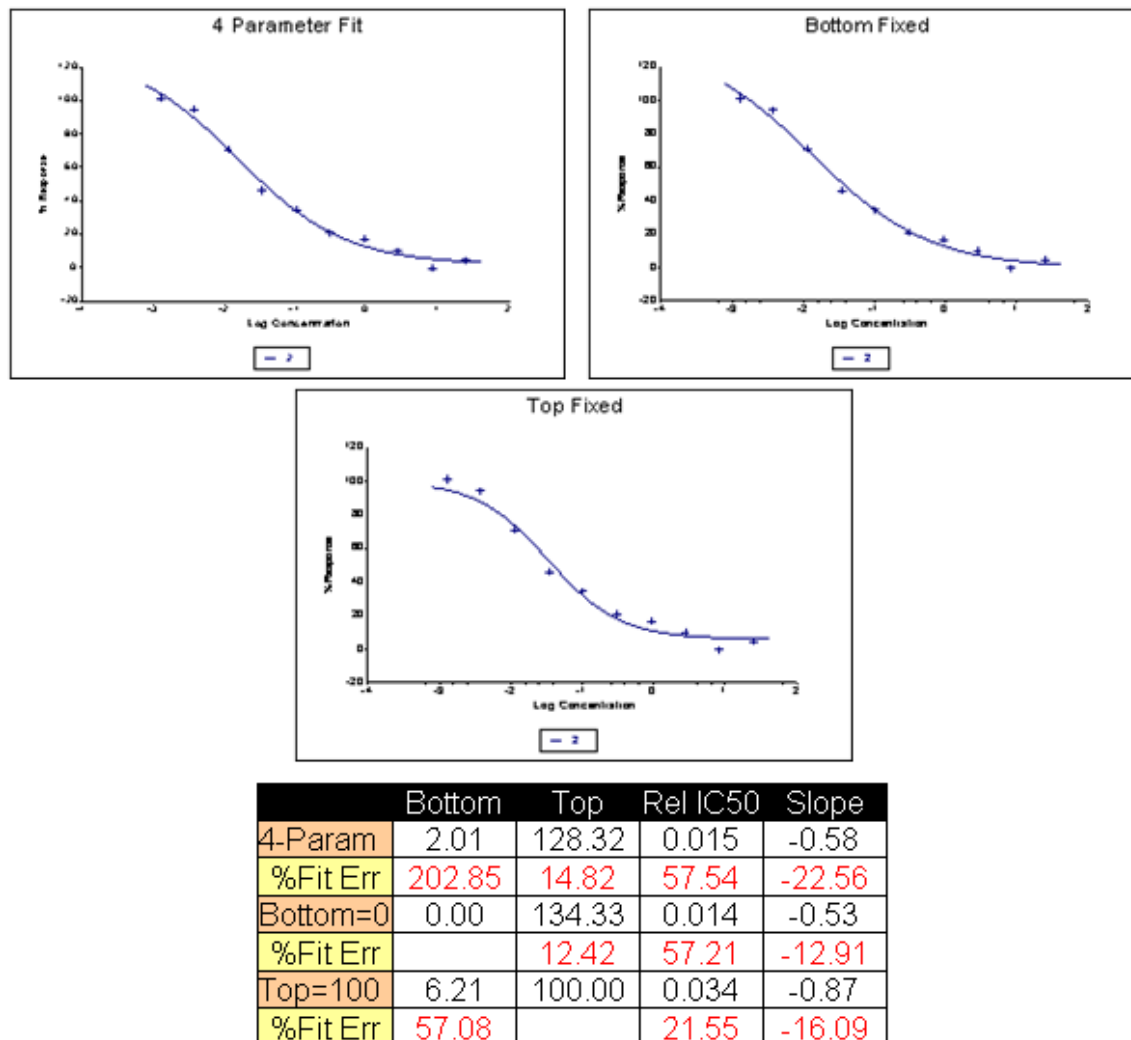


**Figure 2:** Curve fit results for a dose-response best fit a by a 3PLFT model.

Figure 4 illustrates the definition and *effect of outliers* (Figure 4 A). Outliers are single, vertically isolated points that are clearly inappropriate. The point is “obviously” erroneous. The effect of the outlier in this case is to bias the estimate of the bottom upwards, pulling it away from the other points of the data. In general, outliers can bias either the top, bottom or slope parameter depending upon where they occur in the concentration - response curve. It is appropriate to remove the outlier (Figure 4 B) and refit the points. Fixing top or bottom did not materially improve the curve fit (not shown).

Figure 5 illustrates the effect of *high assay variation*. No single point stands out as “obviously erroneous”, and therefore it would be inappropriate to remove any points from the curve fit. Fixing top or bottom does not materially improve the curve fit, and so the 4PL model should be used. Note that the estimates themselves are not implausible, but the fitting error is 33.83%, which is caused by the relatively high assay variation.

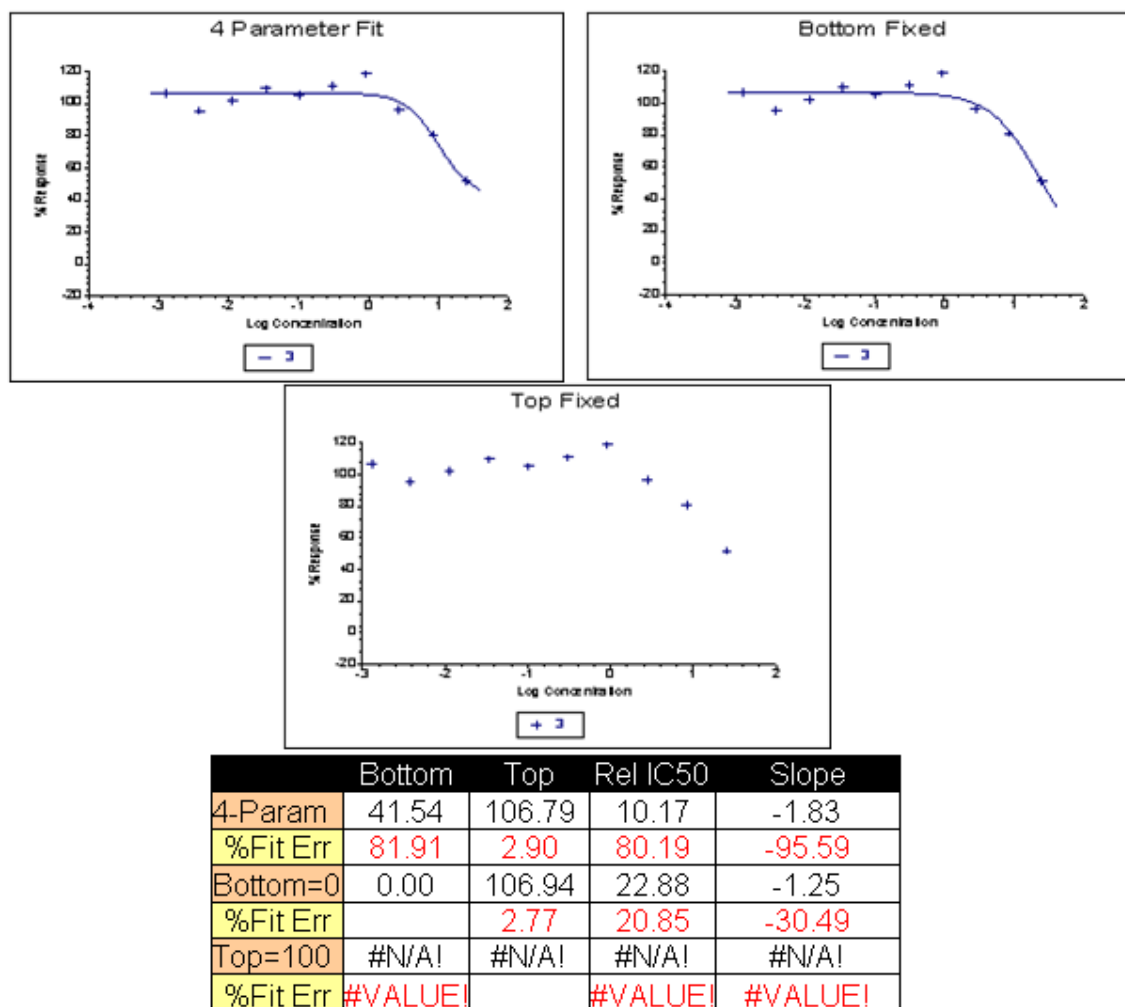
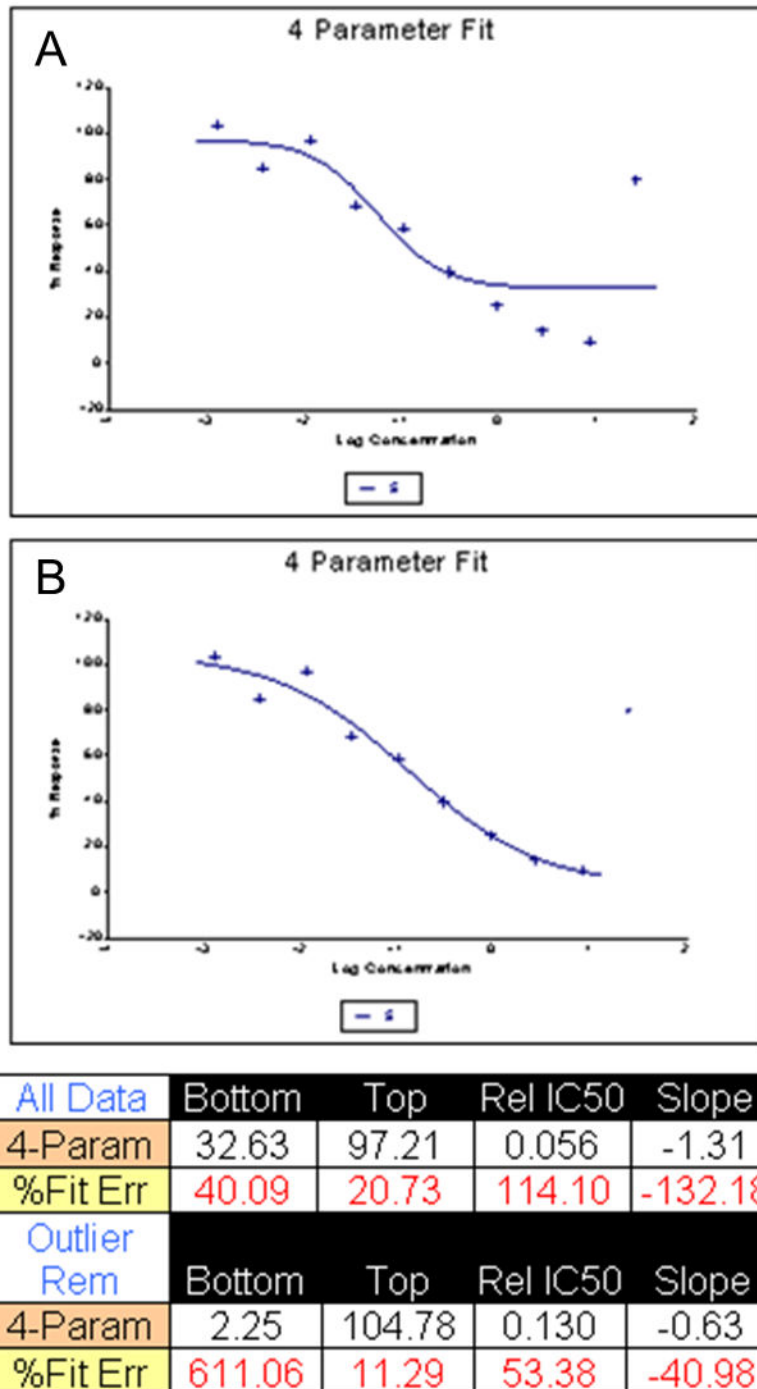


Figure 3: Curve fit results for a dose-response best fit by a 3PLFB model.

Notes:

1. This equation can be fit to the data using Activity Base, Bravo Curve fit, JMP, Graphpad Prism or Sigma Plot. Note that the form of the equation varies from one software package to the next. Some, such as Graphpad Prism, fit Log-IC<sub>50</sub> instead of IC<sub>50</sub>, and the equation looks quite different, but the results are the same as that shown above.
2. The terms **absolute** and **relative** IC<sub>50</sub> are not universal. Both are usually just called the “IC<sub>50</sub>”, and it’s left unstated which value is actually used.
3. If your software toll reports Log-IC<sub>50</sub> then convert both the estimate and the % fitting error (%FE) according to the formulas  
 $IC_{50} = 10^{\text{Log-IC}_{50}}$  and  $\%FE(IC_{50}) = FE(\text{Log-IC}_{50}) \times \ln(10) \times 100$
4. There should be at least one point on both sides of the reported IC<sub>50</sub>, i.e. the reported IC<sub>50</sub> should lie inside the concentration -range used in the assay. The



**Figure 4:** Curve fit results for a dose-response containing an outlier. (A) The effect of the outlier in this case is to bias the estimate of the bottom, pulling it away from the other points of the data. (B) Results once the outlier is removed and the curve refit to the points.

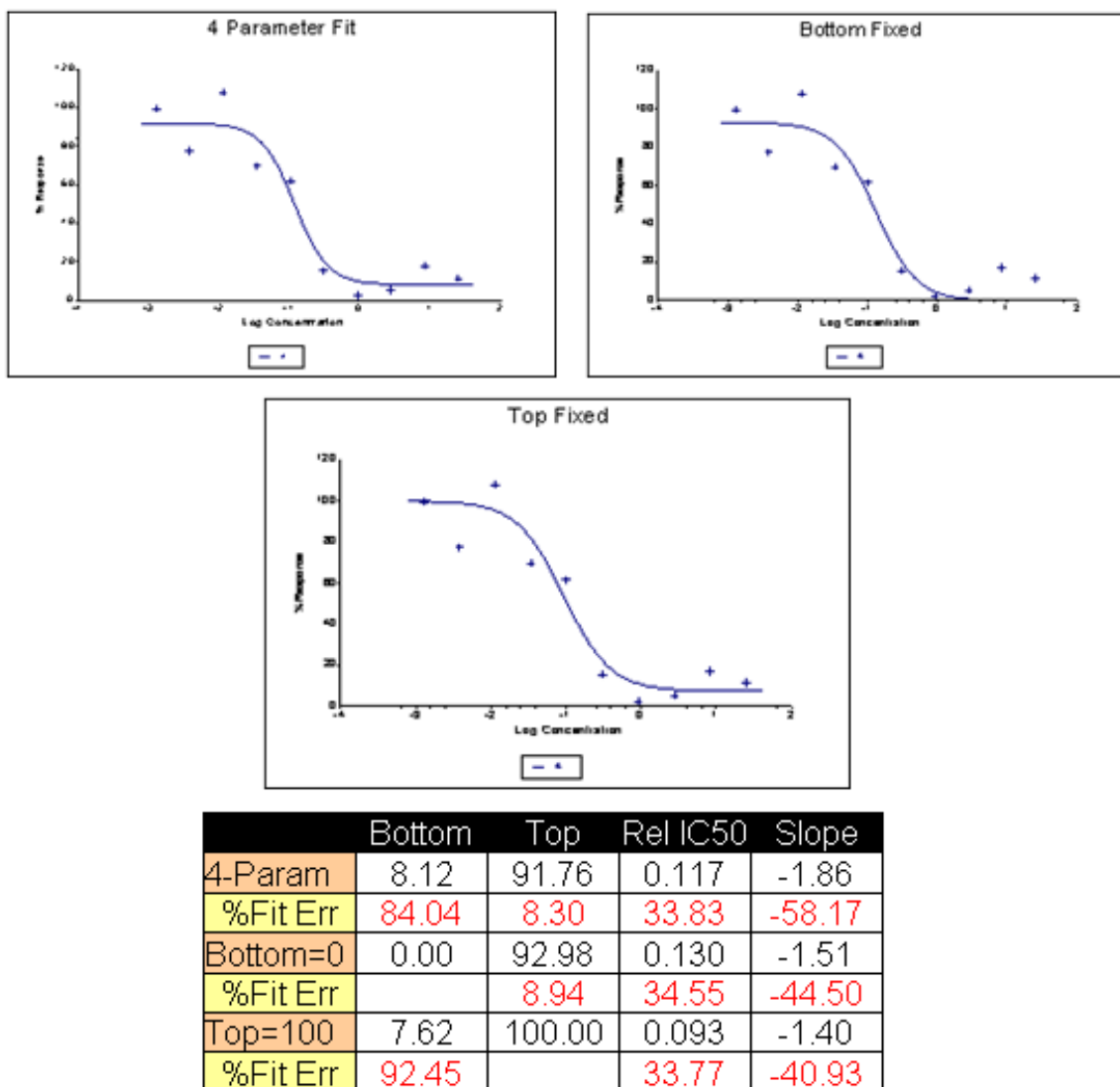


Figure 5: Curve fit results for a dose-response with high assay variability, but no outliers.

intent of this rule is to make the IC<sub>50</sub> estimate an interpolation of generated data and not an extrapolation of generated data. Cases not satisfying this rule should not have an IC<sub>50</sub> reported or reported with a comment that indicates the value is extrapolated. If a value is reported, it should be “<X<sub>min</sub>” or “>X<sub>max</sub>”, as appropriate, where X<sub>min</sub> is the lowest concentration and X<sub>max</sub> is the largest concentration included in the analysis.

- It is a good idea to remove obvious outliers and then refit the curve without the outliers. Note that if it isn't obvious, it isn't an outlier. See examples 4 and 5 above to distinguish high variability from outliers.
- For competition assays, such as radioligand binding assays and competitive inhibition assays, the fitted slope should be within 2 (slope) fitting errors of the

value 1, and slope estimates outside this range indicate assay problems that need to be investigated.

## B. Production Monitoring

Production assays can be monitored in two basic ways: running control (reference) compounds and retrospective studies of compounds that have repeat evaluations that accumulate as part of the normal SAR process. Of the two methods, running control compounds allows problems to be identified prospectively and corrected, whereas retrospective studies are limited to verification of past activity. However, retrospective studies can be useful supplements, especially when conducted prior to important milestones where demonstration of “*valid biological assays*” is a requirement. Below are comments on the setup/selection of controls and the analysis of retrospective studies, and the use of bridging studies to verify that changes to assay protocols have no effect on the assay results.

### Control Compounds

Key assays in a project and assays where problems are suspected should have *two control compounds, a primary and a secondary* (this is referred to as **Close Monitoring**). All other assays should have at least a primary control (**Regular Monitoring**). Both compounds need to be run once per run, unless plate variability is suspected. In that case the primary control compound needs to be run once per plate. The purpose of the primary control is to ensure that there isn't any “assay drift”, i.e. that the same compound has a stable  $K_i/K_b/EC_{50}$  over time, and that the assay reproducibility (MSR, is stable over time. (MSR: Minimum Significant Ratio; see [HTS Assay Validation](#)).

The purpose of the secondary control is to examine the stability of results over a concentration -range. If problems do develop, then it is important to examine whether the entire concentration -range is *equally affected* (a small problem) or whether the concentration -range is *differentially affected* (a big problem). Also, two controls permit direct calculation of both the within-run and overall MSR's, and a check that the MSR is consistent over a range of potencies.

The activity of the primary control should be at or near the most potent compound available, and ideally should be the Lead compound. There should also be sufficient stock of a single lot of the compound so that it can be run on a continuous basis for some period of time. Since the control compound is supposed to be representative of the test compounds, it should receive the same sample handling as all the test compounds, and not be specifically prepared and added to the assay outside of normal test compound procedures.

For the secondary control,  $IC_{50}$  should be *>100 fold less* potent than the primary control. Otherwise it has the same requirements as the primary control. As the SAR develops the potency traditionally improves. So when the “best” compounds are more than 100-fold more potent than the primary control then select a new primary control. If the assay has a

secondary control then the old primary control becomes the new secondary control, and the existing secondary control is dropped. If there is no secondary control, then it is suggested to run both primary controls over the first 6 runs of the new primary control.

A *scatter plot* for control compound for the values of  $\log\text{-}K_i/K_b/EC_{50}$  versus run date should be updated after every run and checked for problems. For assays with two control compounds the difference in  $\log\text{-}K_i/K_b/EC_{50}$  versus run date should be plotted, and for agonist and non-competitive antagonist assays the efficacy versus run date should also be plotted. Outliers and trends in the values of  $\log\text{-}K_i/K_b/EC_{50}$ , either up or down (assay drift) should be checked visually, and problems investigated and corrected as they occur. Runs with significant numbers of outliers should be repeated.

After 6 runs compute the overall MSR of the assay based on the control compounds according to formula:  $MSR = 10^{2s^2}$

where  $s$  is the standard deviation of the  $\log\text{-}K_i/K_b/EC_{50}$  values. This MSR is the total or *overall* MSR (whereas the one computed in a test-retest study encompasses only the within-run variability), and should be less than or equal to 7.5. This standard comes from practical experience obtained thus far with assays in the company, and not theoretical statistical considerations. Note that this is a minimum standard that all assays should meet, and in practice chemistry requirements may indicate a smaller MSR (as low as 2-3) is required for some or all assays. The Project/Program Team should discuss this issue with a statistician to set appropriate MSR's for their assays.

After each run, a *running MSR plot* should be maintained (i.e. computed from the last 6 runs) and checked to ensure the continued good reproducibility of the assay. The [attached template](#) (available from the online eBook) can be used to generate this with MSR values calculated from the last 6 runs.

## Examples

Figure 6 illustrates results for an assay *with a single control*. Figure 6A shows the potency versus run date scatter plot, Figure 6B shows the moving MSR chart. The MSR points are based on the last 6 runs of the assay, i.e. the first point is computed using runs 1-6, the second point uses runs 2-7, etc. The Mean Summary section indicates the highest/lowest/last  $IC_{50}$ 's in the period were 22.63, 4.42 and 11.25  $\mu\text{M}$  respectively (chart units are in nM). The overall average was 10.17  $\mu\text{M}$ . The potency has no apparent temporal trends, and no unusual observations. Figure 6B shows the trends in MSR over time, which appears to increase until mid Feb-2002, and then decrease. However, the magnitude of the increase trends is quite small and well within the variation of an estimate based on a sample of size 6. The highest/lowest/latest MSR's are 6.8, 2.7 and 2.7 respectively. The overall MSR is 4.4, which is not the average of the 6-run MSR's but instead is a single estimate derived using the entire sample (18 data points in this case). This is a stable assay with moderate assay variation ( $3 < MSR < 5$ ).

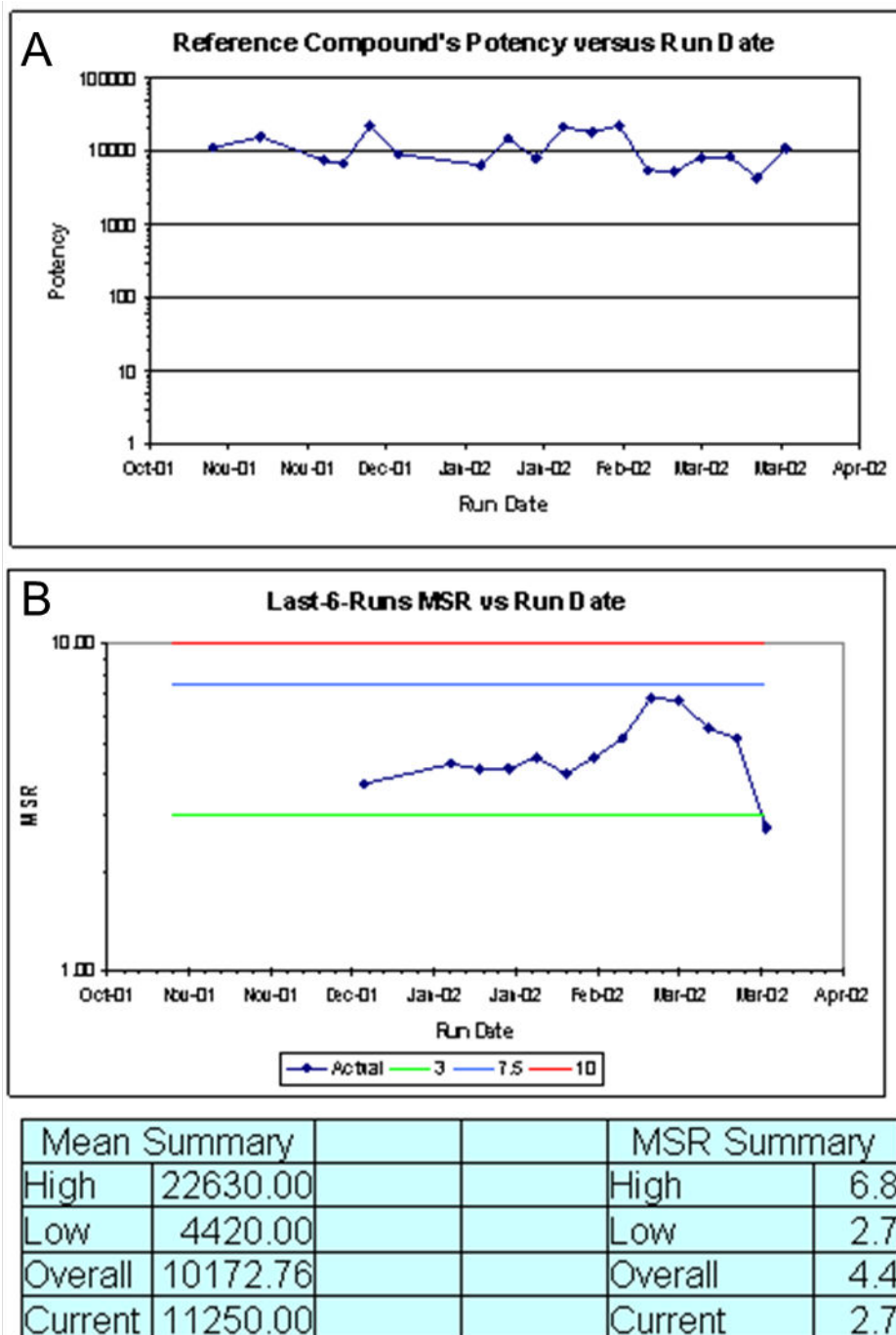
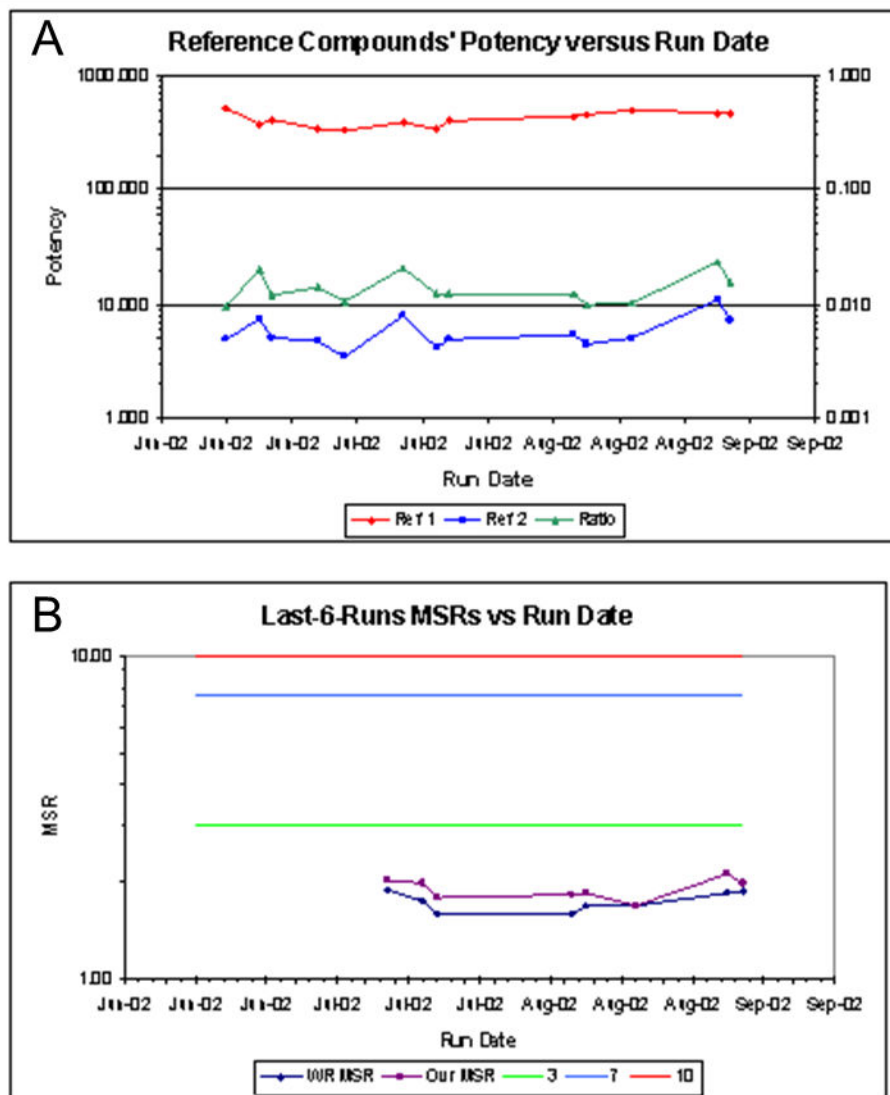


**Figure 6:** Potency, MSR chart, and summary statistics for an assay with one control.

Figure 7 illustrates an assay *with two controls*. In Figure 7A, the red and blue lines represent the two compounds, and are positioned using the left axis. The green line is the potency ratio between the two compounds and is positioned using the right axis. Figure 7B shows the moving MSR values both within run and overall. The Overall-Overall MSR





|         | Mean Summary |       |       |         | MSR Summary |         |
|---------|--------------|-------|-------|---------|-------------|---------|
|         | Ref 1        | Ref 2 | Ratio |         | WR          | Overall |
| High    | 505.26       | 10.84 | 0.02  | High    | 1.9         | 2.1     |
| Low     | 324.19       | 3.42  | 0.01  | Low     | 1.6         | 1.7     |
| Overall | 409.51       | 5.53  | 0.01  | Overall | 1.8         | 2.0     |
| Current | 462.99       | 7.21  | 0.02  | Current | 1.9         | 2.0     |

Figure 7: Potency, MSR chart, and summary statistics for an assay with two controls.

is the value to be reported. The within-run MSR's are only for comparison backwards to the test-retest study results, and for times when compounds are compared within the same run of an assay. As with Figure 6, there are no apparent temporal problems, i.e. this

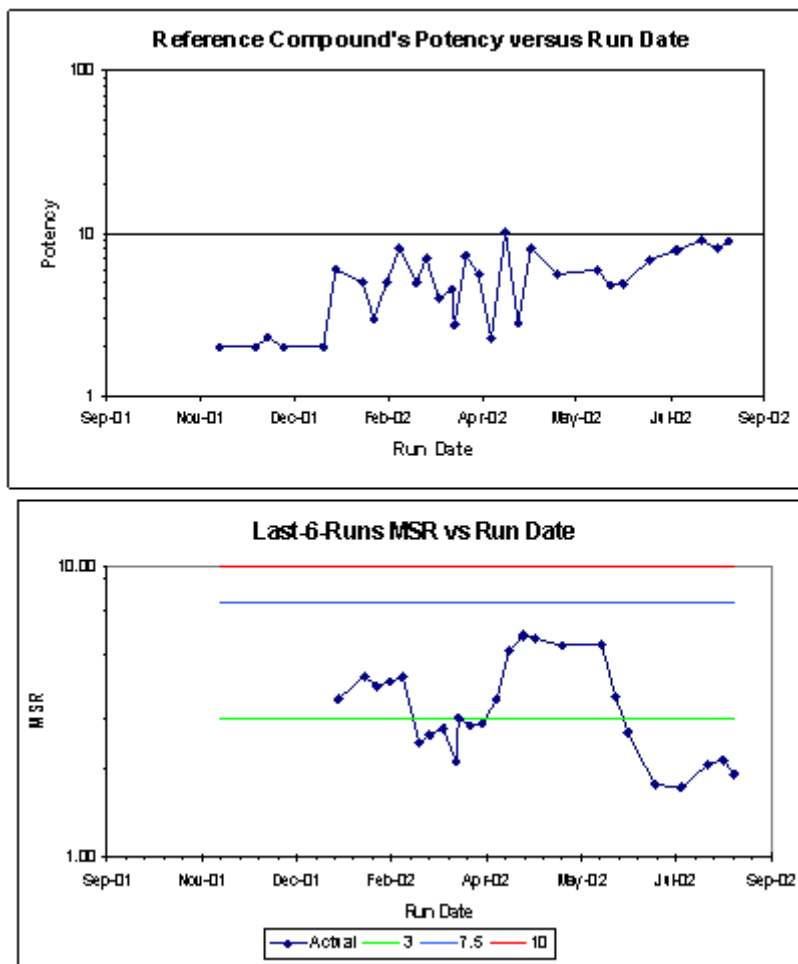


**Figure 8:** Potency and MSR chart illustrating assay drift.

is a stable assay with an overall MSR of 2.0. This assay is less variable than the assay in Figure 6.

Figures 8 and 9 illustrate problems with a *shift in compound potency*. Figure 8 illustrates a steady degradation in potency over time, whereas Figure 9 illustrates a more sudden shift in potency at a particular point in time. In Figure 8 the assay variability appears to be shrinking, while in Figure 9 it appears to be stationary. Repetitive freeze-thaw cycles of a compound may cause a slow degradation in potency whereas a change in lot of a key assay ingredient may result in a sudden potency shift.

In both cases it is important to identify the cause and correct it as soon as possible.

Figure 10 illustrates an *assay with stable potency, but in June the assay variability increased*. The moving MSR was stable around 3, but after June increased to over 10, and remained there. This also is most likely caused by a change in the assay process around that time. Again it is important to identify and correct the cause as soon as possible. Note however

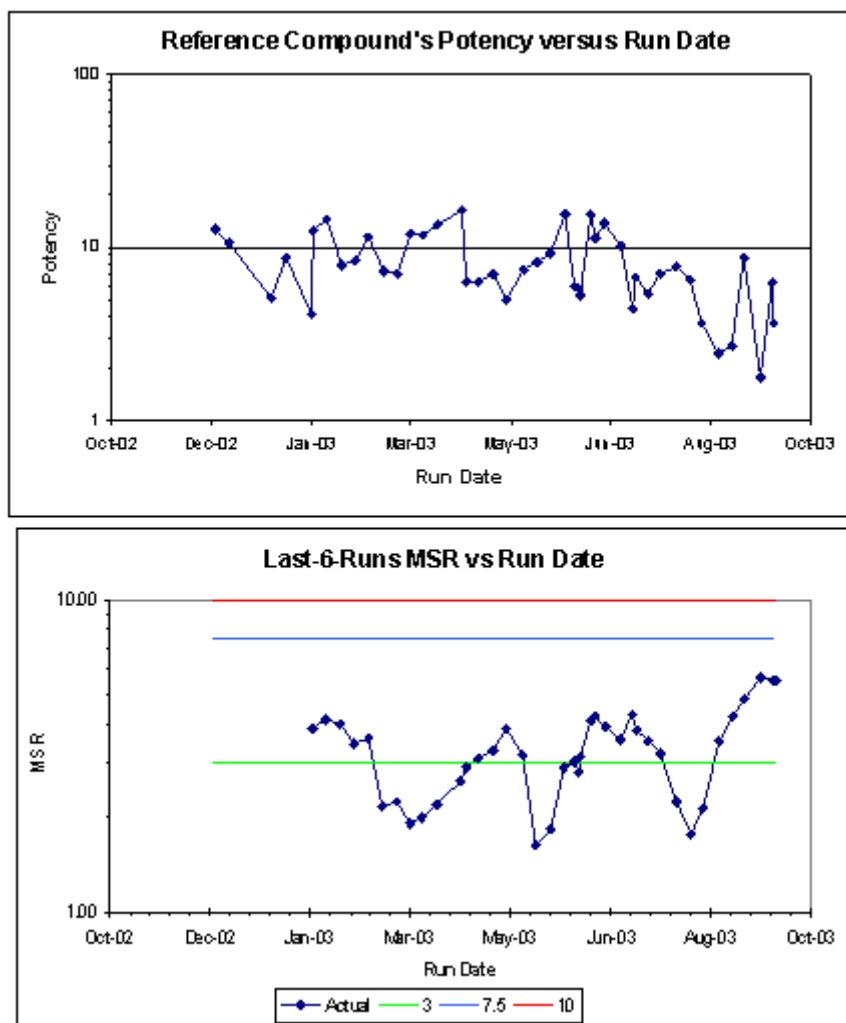


**Figure 9:** Potency and MSR chart illustrating sudden change in potency.

that a single outlier will cause the MSR chart to increase for the next 6 runs, and so it usually takes more time to correctly distinguish a change in assay variability from a single outlier result.

## Retrospective Studies

During the course of project/program development numerous compounds are repeatedly evaluated and stored in archival databases. This data can be mined to examine the reproducibility of assay results. This work should always be done by a statistician as the repeated compounds are not a random selection of all compounds, and may be biased with respect to time of evaluation, potency, structure and “assayability” (the latter term is meant to reflect conditions such as solubility, quenching, stickiness to plastic and other practical problems). In spite of these potential problems retrospective studies can be a

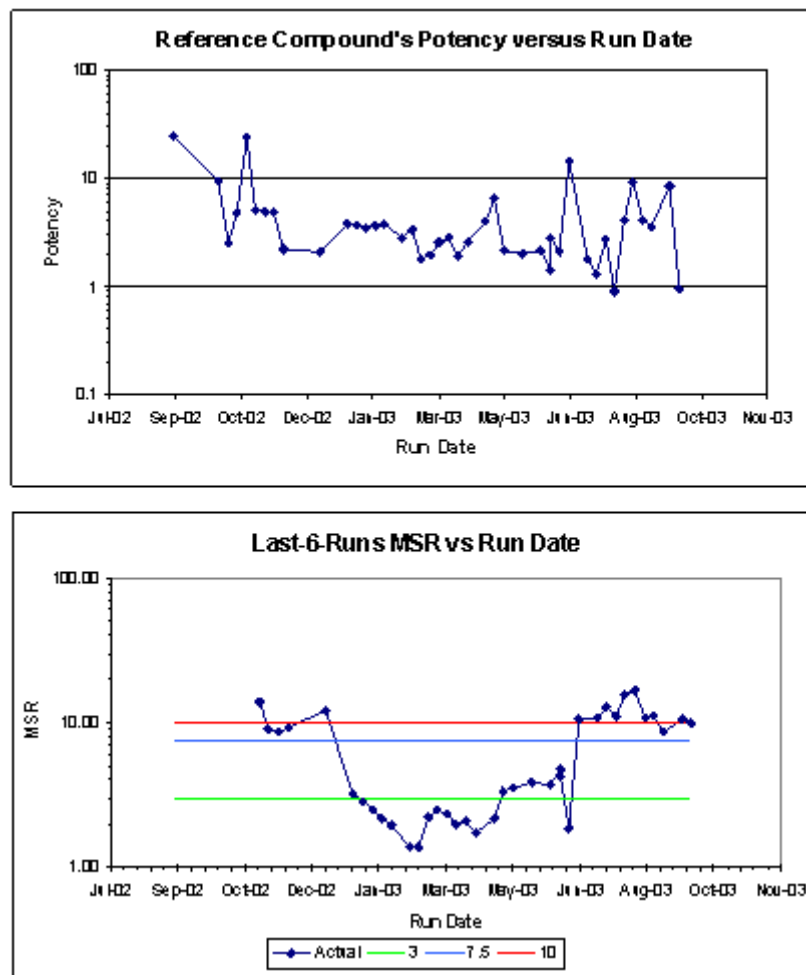


**Figure 10:** Potency and MSR chart for change in assay variability.

very useful exercise, particularly in establishing the acceptability of older assays that have never been formally evaluated for reproducibility. In addition, the MSR can be examined over various subsets such as potency range, structure and run date to check that the control compound MSR's are representative of the test compounds with respect to potency range, structure and run date.

## Bridging Studies

If a key aspect of an assay changes, such as an equipment change or lot of a reagent, then a test-retest study should be conducted to verify equivalence of the two protocols. A judgment should be made on a case-by-case basis of whether the full protocol outlined in the [HTS Assay Validation](#) chapter needs to be made, or only a single run under old and new conditions (i.e. one might do just Step 4 of the procedure, or one might do both Steps 3 and 4 depending upon the severity of the protocol change). Also in cases of specific modifications such as replacing equipment for a particular step in the assay an experiment

can be designed to validate that the replacement is equivalent to the original in the conduct of that step of the assay.

### Dimethylsulfoxide: biological compatibility and compound storage.

Dimethylsulfoxide (DMSO) is a universal solvent for all compounds tested in high, medium and low throughput screens (HTS, MTS and LTS). Compounds are initially dissolved in 100% DMSO and further diluted in 100% DMSO screening and IC<sub>50</sub> or K<sub>i</sub> determinations. So many assays may require an additional dilution step in water or assay buffer to reduce the DMSO concentration to a level that is acceptable for the assay, depending upon the specific capabilities of the equipment being used. It is extremely important that the DMSO compatibility of biological reagents such as enzymes, receptors, protein/peptide reagents and cells be established to ensure that the screening assays are not adversely affected. In general, the final DMSO concentrations in cell-based assays are <0.2% and are <1% in biochemical assays. It is highly recommended that the tolerable DMSO concentration be determined individually for each validated assay.

DMSO is also used as a cryoprotectant in the freezing of cell cultures at ATCC. The product is cell culture grade and has been tested to ensure cell viability. Each lot is also tested for the absence of bacteria, fungi, and endotoxin.

When solubilized compounds are stored in DMSO, it is important to understand the stability of these compounds under various storage conditions and freeze-thaw cycles. A detailed study of these effects was published recently (1). It is believed that the degradation of DMSO solubilized compounds is mainly due to moisture absorbed from the air. This can happen during frequent freeze-thaw cycles of compounds stored frozen in DMSO, or frequent exposure to air during repeated access for biological testing (cherry-picking).

#### Recommended storage conditions for DMSO solubilized compounds:

- Polypropylene plates.
- Storage temperature: 10 degree C or room temperature.
- Inert gas atmosphere: argon flush.
- Minimal exposure to moist environments

## References

1. Cheng. X., Hochlowski J, Tan H, Hepp, D, beckner C, Kantor S, Schmitt R, Studies on Repository Compound Stability in DMSO Under Various Conditions. J Biomol Screening. 2003;8(3):292–304.
2. Kozikowski BA, Burt TM, Tirey DA, Williams LE, Kuzmak, BR, Stanton, DT, Morand, KL, and Nelson, SL The Effect of Room-Temperature Storage on the Stability of Compounds in DMSO. J Biomol Screen. 2003;8:205–209. PubMed PMID: 12844442.



# Minimum Significant Ratio – A Statistic to Assess Assay Variability

Joseph V. Haas, MS,<sup>1</sup> Brian J. Eastwood, PhD,<sup>2</sup> Philip W. Iversen, PhD,<sup>3</sup> Viswanath Devanarayan, PhD,<sup>4</sup> and Jeffrey R. Weidner, PhD<sup>5</sup>

Created: November 1, 2013; Updated: November 20, 2017.

## Abstract

The MSR is a statistical parameter that characterizes the reproducibility of potency estimates from *in vitro* concentration-response assays. Biological activity expressed as potency of compounds is an important parameter in screening and drug discovery. Standard potency estimates are expressed as IC<sub>50</sub>, EC<sub>50</sub> or simply as AC<sub>50</sub> values derived from concentration-response (CRC) assays designed to measure activation, inhibition or modulation of targets and pathways of pharmacological significance. Concepts of Minimum Significant Ratio (MSR) discussed below address how the reproducibility of potency values is derived quantitatively using standard or control compounds of known activity and test compounds that have been tested in multiple runs. MSR values inform the scientists the extent of reliability of assays designed to support new compound selection through Structure-Activity Relationships (SAR) of chemical libraries.

## 1. Introduction

The chapter on HTS Assay Validation (Section 4) provides a detailed discussion of the Minimum Significant Ratio (MSR) in the context of the Replicate-Experiment study. The MSR is a statistical parameter that characterizes the reproducibility of potency estimates from *in vitro* concentration-response (CRC) assays and can be estimated from the Replicate-Experiment study (1). The chapter on Assay Operations for SAR Support also discusses the MSR (Section B) in two contexts: running control (reference) compounds and retrospective studies of compounds that have repeat evaluations that accumulate as part of the normal SAR process. This chapter provides additional detail on the calculation and interpretation of the MSR and further demonstrates the value of this parameter to characterize the reliability of an *in vitro* assay.

---

<sup>1</sup> Eli Lilly and Company; Email: haas\_joseph\_v@lilly.com. <sup>2</sup> Eli Lilly and Company; Email: eastwood\_brian\_j@lilly.com. <sup>3</sup> Eli Lilly and Company; Email: iversen\_philip\_w@lilly.com. <sup>4</sup> Charles River Laboratories; Email: Viswanath.Devanarayan@crl.com. <sup>5</sup> AbbVie; Email: jeffrey.weidner@abbvie.com.

## 2. Common Types of MSR

### 2.1. Overview

Potency measurements from concentration-response assays are usually log-normally distributed and as such,  $\log_{10}AC_{50}$  (log concentration at half maximal activity) is preferred for statistical analysis and modeling, including estimation of the MSR. *The MSR is defined as the smallest ratio between the potencies of two compounds that is statistically significant* and is calculated as  $MSR = 10^{2\sqrt{2}s}$ , where  $s$  is an estimate of the standard deviation of a log potency for one compound. The variability estimate  $s$  can be estimated in different ways depending on available data and associated analysis method (e.g., within-run, between-run, and other sources of variability). The common ways to estimate assay variability are detailed below.

### 2.2. Replicate Experiment MSR

As detailed in the chapter on HTS Assay Variability (Section 4), the Replicate-Experiment MSR is a diagnostic and decision tool used to establish that an assay is ready to go into production. It is estimated from two independent runs of 20-30 compounds and is calculated as  $MSR = 10^{2S_d}$ , where  $s_d$  is the standard deviation of the paired differences in log potency across the two runs. A template for the Replicate-Experiment data analysis is [available for download](#) from the online eBook.

Two runs are not considered adequate to estimate between-run variability so the Replicate-Experiment MSR focuses only on within-run variability. Use of the standard deviation of the paired differences factors out the between-run variability. The chapter also specifies the Limits of Agreement (LsA) as an assessment of between-run reproducibility, but is necessarily a preliminary assessment as it is based on only two runs.

Variability due to reagents is limited and sample management variability is not typically represented in the Replicate-Experiment, so the resulting MSR is considered to be the most optimistic estimate of the reproducibility of an assay. The Replicate-Experiment MSR should be  $< 3$  to move an assay into production.

### 2.3. Control Compound MSR

As discussed in the chapter on Assay Operations for SAR Support (Section B), concentration-response assays should include a control compound in every run for process monitoring over time. This enables prospective identification and correction of problems (e.g., drifts or shifts in the  $AC_{50}$ ) as well as estimation of assay reproducibility via the MSR and determination of whether the MSR is stable over time. A minimum of six runs is considered adequate to estimate between-run variability, and the Control Compound MSR can be calculated from six or more runs as  $MSR = 10^{2\sqrt{2}s}$ , where  $s$  is the standard deviation of the  $\log_{10}AC_{50}$  values across runs, assuming one  $AC_{50}$  result per run. The [attached template](#) (available from the online eBook) can be used to generate this with MSR values calculated from the last 6 runs.



While the Control Compound MSR captures between-run variability, compounds chosen for QC monitoring are typically the most potent compound available to a project team and are generally well-behaved. Additionally, common sources of sample variation may not be represented. As such, while the Control Compound MSR is more representative of the reproducibility of an assay due to inclusion of between-run variability, it is still somewhat optimistic because it is based on a single well-behaved compound. Given the  $< 3$  criteria for the Replicate-Experiment MSR, it is not unusual to observe a Control Compound MSR as high as 4, depending on the level of between-run variability.

If a control compound is independently repeated in each run (e.g., on each plate), within-run variability can also be estimated and incorporated into the calculation of the MSR in addition to between-run variability. The MSR is calculated as  $10^{2\sqrt{2}s}$ , but  $s$  is the square root of the sum of the run date and residual variance components from the fit of a random effects model (2).

## 2.4. Database MSR

Retrospective studies are also discussed in the chapter on Assay Operations for SAR Support (Section B). These studies make use of potency results for compounds with repeat evaluations in multiple runs, including the control compound, to estimate the reproducibility of an assay. It is likely that numerous repeat evaluations will accumulate during the course of a project with results stored in databases for ready access to the data for estimation of the MSR.

The Database MSR captures both within-run and between-run variability from multiple compounds, and is considered the most representative estimate of assay reproducibility (subject to the caveats below). A minimum of six runs is desired. The MSR is calculated as  $MSR = 10^{2\sqrt{2}s}$ , where  $s$  is the square root of the sum of the run date and residual variance components from the fit of a mixed effects model with compound as a fixed effect and run date as a random effect (2).

It is important to note that the database MSR reflects variability from all parts of the compound testing process including, but not limited to:

- Compound synthesis
- Compound handling
- Assay preparation
- Assay operation
- Data analysis

As such, Database MSRs can be in the 4-5 range even when an assay had a Replicate-Experiment MSR  $< 3$ . When this occurs, it does not necessarily imply there is a problem with the assay itself. There are many potential sources of variability being captured by a single number – differences in structural classes, properties of individual compounds (solubility, quenching, stickiness to plastic, etc.), temporal effects, etc. Diagnostic work is often needed, and the Database MSR can be calculated and compared over various

subsets, such as potency range, structural class, time periods, etc. Database MSR's can also be calculated with and without the control compound to determine how well the control compound represents the test compounds. Plots of residuals from a one-way analysis of variance (ANOVA) with compound as the fixed effect (2) are also effective tools for identifying possible causes of an elevated Database MSR. For example, plotting residuals versus run date can be useful for identifying temporal effects.

## 2.5. Robust Database MSR

### 2.5.1. Overview

As mentioned in Section 2.4, various compound specific problems (solubility, quenching, stickiness to plastic, etc.) can contribute to assay variability and/or produce extreme values. Extreme values can also arise due to errors in the compound testing process (compound handling, assay preparation, assay operation, etc.). A high occurrence of such outliers is not typically expected, but some number will undoubtedly arise over the course of a project where large numbers of compounds are tested. Although the mixed model described in Section 2.4 is the preferred method for calculating a Database MSR, even a small number of outliers can inflate the variability estimates and artificially inflate the MSR.

### 2.5.2. Diagnostic Plots and Exclusion of Data

One approach to dealing with outliers and high variability for individual compounds is to identify them with diagnostic plots and exclude them from the calculation of the MSR. Figure 1 is a plot of residuals versus run date for compounds with repeat evaluations in multiple runs of an assay. The residuals are from a one-way analysis of variance (ANOVA) of the  $\log_{10}AC_{50}$ s with compound as the fixed effect (2). Five compounds are identified in Figure 1 as having large residuals. Figure 1 also identifies some unusual runs where all the residuals lie above or below the 0 reference line. Normally you should expect a random scatter about this line. The Database MSR = 10.0 with all data included compared to 5.8 without the five compounds identified in the residual plot. See Section 2.5.5 for additional diagnostic plots for this assay.

### 2.5.3. Robust Estimates of Variability

Another approach to dealing with outliers and high variability for individual compounds is to use variability estimates that are less sensitive to the presence of extreme values. At the simplest level, estimating assay variability amounts to calculating the standard deviation of log potencies from compound repeats. Let  $X_j$  represent repeat  $AC_{50}$ s for a control compound

$$SD = \sqrt{\frac{\sum (x_i - \text{mean}(x_i))^2}{n-1}} \quad MSR = 10^{(2\sqrt{2SD})}$$

Even a small number of extreme values can artificially increase or decrease the mean, and to an even greater extent artificially increase the SD due to squared term. The median

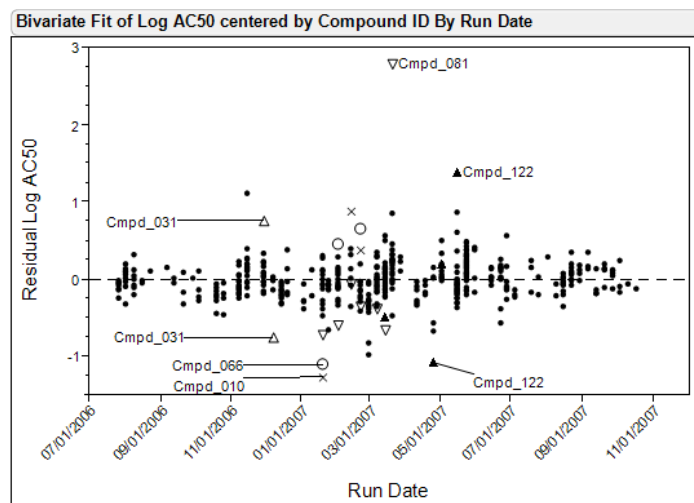


**Figure 1:** Compound  $\text{Log}_{10}\text{AC}_{50}$  Residuals vs. Run Date

absolute difference is a robust estimator of variability that is less sensitive to extreme values (3).

$$\text{MAD} = \text{median}(|x_i - \text{median}(x_i)|) \quad \text{MSR} = 10^{(2\sqrt{2}(\text{MAD}/0.6745))}$$

The MAD makes use of the median rather than the mean, which is less sensitive to outliers, and uses the absolute value instead of the square. These differences make the MAD more robust to outliers compared to the standard deviation. The 0.6745 scale factor is needed for the MAD to be consistent estimator of the standard deviation under the normal distribution.

The median and the MAD can also be used to calculate a Robust Database MSR as an alternative to the Database MSR calculated via the mixed model in Section 2.4. The resulting MSR is robust to the presence of a small number of outliers and provides a more accurate representation of the reproducibility of an assay. For the example assay in Section 2.5.2, the Robust Database MSR = 5.9, which is very similar to the Database MSR of 5.8 calculated without the five compounds with large residuals.

#### 2.5.4. Calculation of the Robust Database MSR

There are many robust methods that could potentially be used to calculate a Robust Database MSR. One obvious approach is M-estimation (3) applied to the mixed model fit described in Section 2.4. M-estimation involves using iteratively reweighted least squares (IRLS) with a weighting function (e.g., Tukey's bi-square) applied to the mixed model residuals at each iteration. The weighted residuals of iterations are used as weights in the next iteration until the process converges. This has the effect of down-weighting potencies with large residuals and results in variability estimates (and hence MSRs) that are not artificially inflated by outliers.

M-estimation in the context of a mixed model is computationally intensive and can have convergence issues due to the presence of both fixed and random effects in the model. To avoid these issues, especially in an industrial setting where there are assays with large numbers of repeat evaluations and/or where there are large numbers of assays, a method of moments approach using medians and MADs is recommended for the Robust Database MSR.

The small sample properties of the resulting Robust Database MSR dictate a minimum of 100 observations for adequate performance. The 100 or more observations can be repeat evaluations of a single control compound across  $\geq 100$  runs or a combination of within- and between-run repeats of the compound across at least six runs to generate a Robust Control Compound MSR. The Robust Database MSR is calculated by adding test compounds with repeat evaluations in at least two runs, including within-run repeats where available.

For a CRC assay with 100 or more observations from compounds with two or more  $AC_{50}$ s across at least six or more runs, the Robust Database MSR is calculated as below.

Steps 1-11 are performed on each compound, step 12 is the summary across compounds, and step 13 is the Robust Database MSR calculation.

1. Compute within-run  $Median_{(W-R)_i}$  as median of  $\log AC_{50i}$  for each run  $i$ . If a run has no within-run repeats,  $Median_{(W-R)_i}$  is the single  $\log AC_{50}$  for that run.
2. Compute  $Median_{All}$  as the median of all  $\log AC_{50}$ s for a given compound
3. Compute between-run  $MAD^2_{B-R}$  as  $(\text{median}(|Median_{(W-R)_i} - Median_{All}|)) / 0.5725)^2$
4. Compute within-run  $MAD^2_{(W-R)_i}$  for each run as  $(\text{median}(|\log AC_{50i} - Median_{(W-R)_i}|) / 0.5725)^2$
5. Compute  $N_{(W-R)_i}$  as # of within-run repeats for each run
6. Compute within-run  $MAD^2_{W-R}$  as  $\sum_i((N_{(W-R)_i} - 1) \times MAD^2_{(W-R)_i}) / \sum_i(N_{(W-R)_i} - 1)$
7. Compute  $N^2_{(W-R)_i}$  as # of within-run repeats squared for each run
8. Compute  $N_{Run}$  as # of runs for a given compound
9. For each compound, compute  $N_0$  as  $(\sum_i(N_{(W-R)_i} - 1) - \sum_i N^2_{(W-R)_i} / \sum_i(N_{(W-R)_i} - 1)) / (N_{Run} - 1)$
10. For compounds without within-run repeats, compute  $RobustVar_{Cmpd}$  as  $N_0 \times MAD^2_{B-R}$
11. Otherwise, compute  $RobustVar_{Cmpd}$  as  $MAD^2_{W-R} + ((N_0 \times MAD^2_{B-R}) - MAD^2_{W-R}) / N_0$
12. Compute RobustVar across all compounds as the median of the pair-wise averages (i.e., Walsh Averages) of  $RobustVar_{Cmpd}$  as described in (4)
13. Compute the Robust Database MSR as  $10^{2\sqrt{2s}}$ , where  $s$  is the square root of RobustVar

The calculation of the Robust Database MSR is somewhat complicated. An alternative when Steps 1-13 is prohibitive is a one-way ANOVA with compound as the fixed effect

(2). The same MSR formula (Step 13) is used, but  $s$  is the root mean square error from the one-way ANOVA. The diagnostic plots discussed in Section 2.5.2 would also be needed to identify and exclude outliers from the calculation of the MSR.

### 2.5.5. Automated Calculation of the Robust Database MSR

Due to lack of convergence issues and fast computational time, the Robust Database MSR described in Section 2.5.4 is amenable to automation. The Robust Database MSR can be calculated for all assays publishing to a database and regularly re-calculated (e.g., weekly or even nightly) as assays publish new potency results to the database. This provides consumers of *in vitro* potency data an up-to-date estimate of the reliability of an assay.

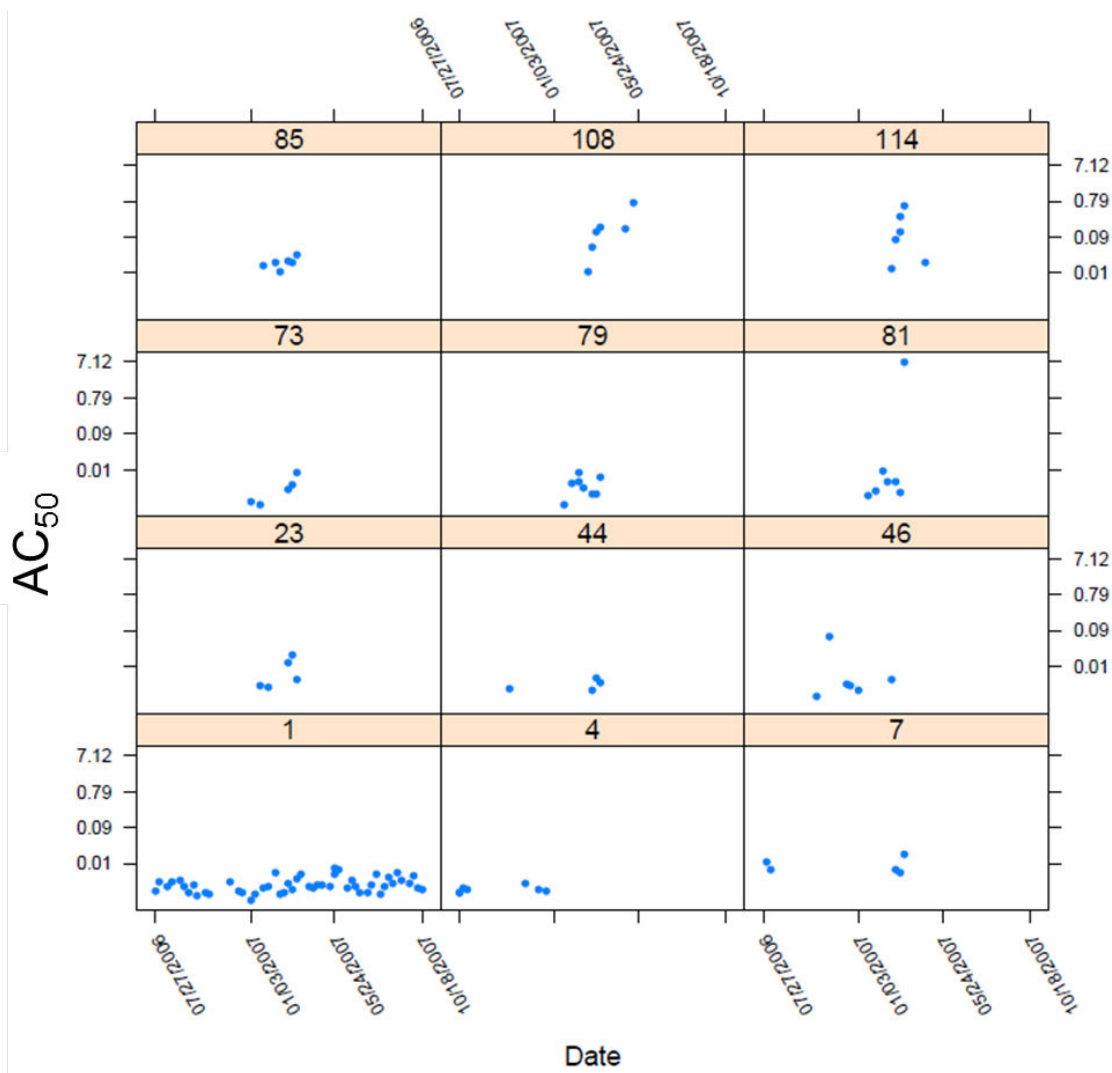
What follows are figures and tables from an implementation of the automated Database MSR for the sample assay discussed in Section 2.5.2. The Robust Database MSR is calculated as described in Section 2.5.4, and the Non-Robust Database MSR is calculated by method of moments. Method of moments was chosen over the preferred mixed model approach for the Non-Robust Database MSR for computational speed and consistency with the robust method of moments approach. For balanced datasets, the method of moments approach is equivalent to the mixed model and is a reasonable approximation to the mixed model for the unbalanced datasets that typically arise over the course of a project.

Figure 2 displays  $AC_{50}$ s for the twelve compounds with the most repeat evaluations for an assay, including the control compound in the lower left panel. This is intended as a quick visual assessment of reproducibility of potency for the compounds with the most repeat evaluations.

Figure 3 is a plot of compound  $\log_{10}AC_{50}$ s in order of decreasing potency for all compounds with repeat evaluations. The compounds identified as having extreme residuals in Section 2.5.2 are also marked in the plot. The entire collection of repeat evaluations for this assay consists of 510 evaluations of 182 compounds in 55 runs. The non-robust MSR = 10.6 and the robust MSR = 5.9. Note that the robust MSR is considerably smaller than the non-robust MSR, as the former is less sensitive to the extreme values seen in Figure 3.

Figure 4 is a plot of compound  $\log_{10}AC_{50}$ s in order of decreasing potency for the last twelve months of repeat evaluations, which consists of 457 evaluations of 165 compounds in 44 runs. The non-robust MSR = 11.6 and the robust MSR = 6.01 with the robust MSR considerably smaller due to being less sensitive to the extreme values.

Several diagnostic plots can also be included in the Automated Database MSR output. Figure 5 is a plot of the Non-Robust (red line) and Robust (black line) Database MSRs in twelve-month periods (only one in this particular example) that is useful for assessing the stability of the MSR over time. Numbers of observations are captured as tick marks on the x-axis. Figures 6 & 7 plot the residuals from a one-way ANOVA with compound as the fixed effect versus compound and run date respectively. The plot of residuals versus compound shows that the variability in  $\log_{10}AC_{50}$  can be different for different



**Figure 2:** Twelve Compounds with the Most Repeat Evaluations

compounds. The plot of residuals versus run date can identify unusual runs as noted in Section 2.5.2.

### 3. Other Considerations

#### 3.1. Precision of Replicate $AC_{50}$ s for Individual Compounds

The MSR estimates the overall reproducibility of  $AC_{50}$ s for an assay, but not the precision of specific compound  $AC_{50}$  estimates. When repeat evaluations are available for a compound, it is appropriate to report the results for the compound as the geometric mean of the replicate  $AC_{50}$ s ( $10^{\text{MeanLog}}$ , where MeanLog is the arithmetic mean of the  $\log_{10}AC_{50}$ s) and 95% confidence interval for the mean ( $10^{\text{LCL}}$  to  $10^{\text{UCL}}$ , where LCL and UCL are lower and upper confidence limits of the 95% CI for the arithmetic mean of



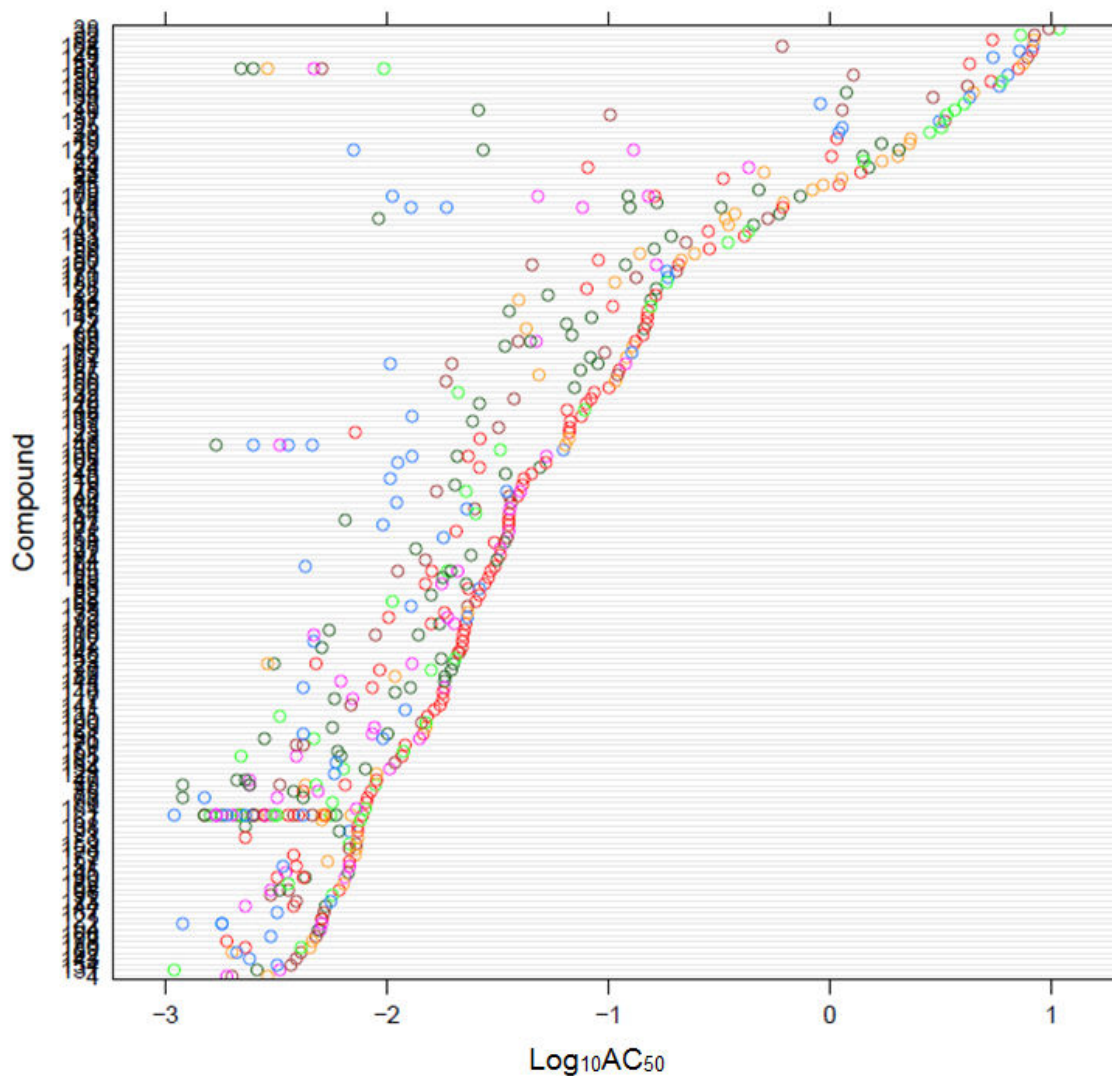


**Figure 4:** Compound Log<sub>10</sub>AC<sub>50</sub>s in Order of Decreasing Potency for Last Twelve Months of Repeat Evaluations

### 3.2. Value of Additional Replication

As mentioned previously, an adequate number of repeat evaluations can be expected to accrue over the course of a typical project. Even so, the vast majority of compounds are typically only tested once in an assay as shown in the histogram of compound replicates in Figure 8, which is based on actual experience in a large pharmaceutical company. As such, project teams may also elect to repeatedly evaluate a small set of compounds at regular intervals to increase confidence in the Database MSR estimate and provide additional process monitoring over time beyond what is provided by including a control compound in every run.



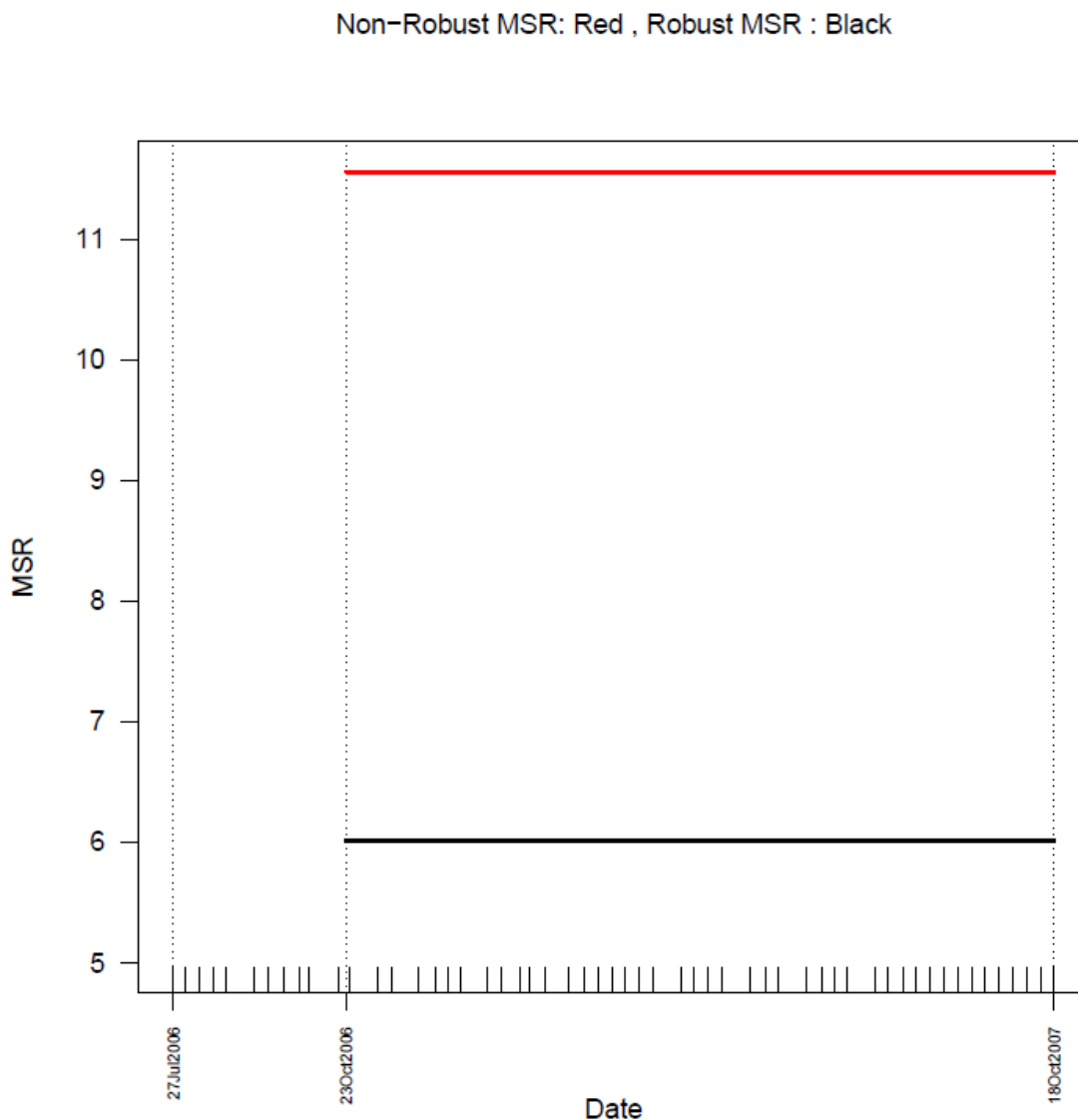


**Figure 5:** Non-Robust and Robust Database MSR in Twelve Month Time Periods

A project team may also elect to institute repeat testing of all important compounds (e.g., repeat all compounds in the lead optimization phase  $n=3$  times) when the Database MSR is large (i.e., approaching or exceeding 5). In this paradigm, geometric mean potencies are compared between compounds which has the effect of reducing the MSR, since the MSR for the comparison of means is  $MSR = 10^{2\sqrt{2}(s/\sqrt{n})}$ , where  $n$  is the number of times each compound has been tested (assumed to be the same across compounds). The preferred approach to dealing with a highly variable assay is to thoroughly investigate potential sources of variability and eliminate them, but depending on assay costs, replication can be an effective way to manage variability.

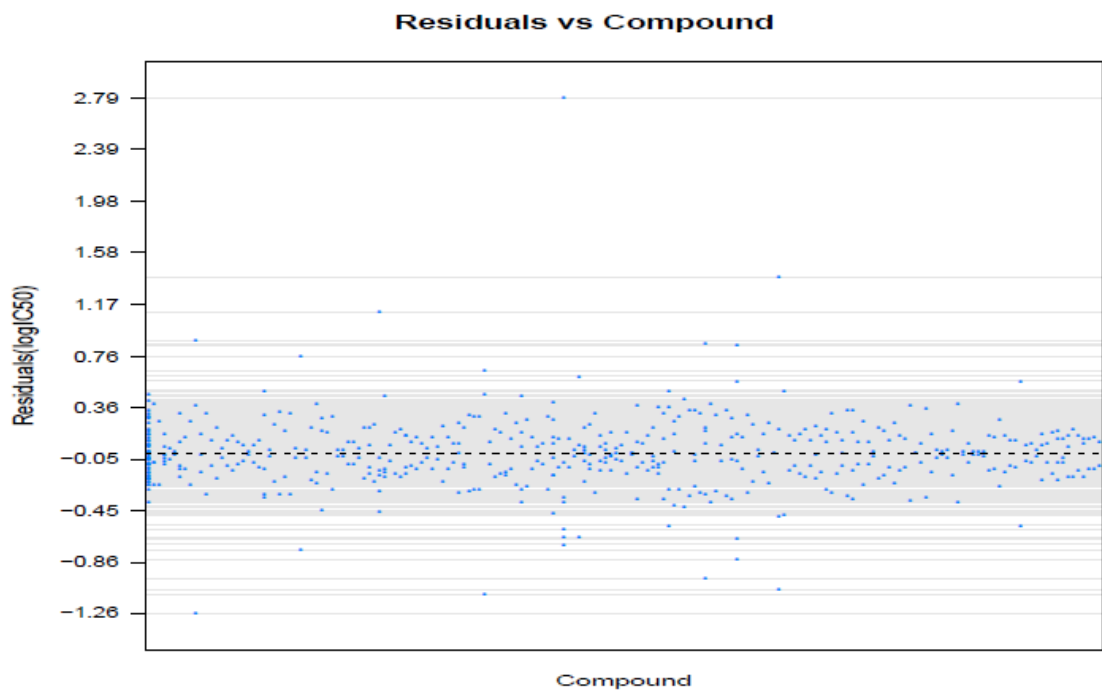


Figure 6: One-Way ANOVA Residuals vs. Compound for All Available Data

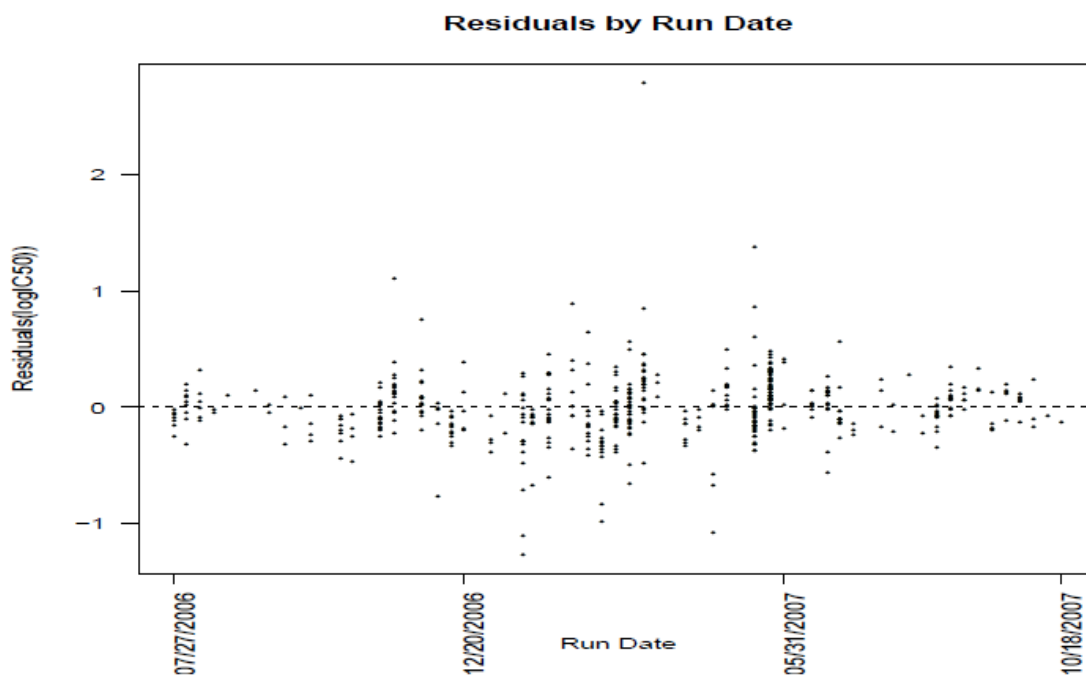


Figure 7: One-Way ANOVA Residuals vs. Run Date for All Available Data

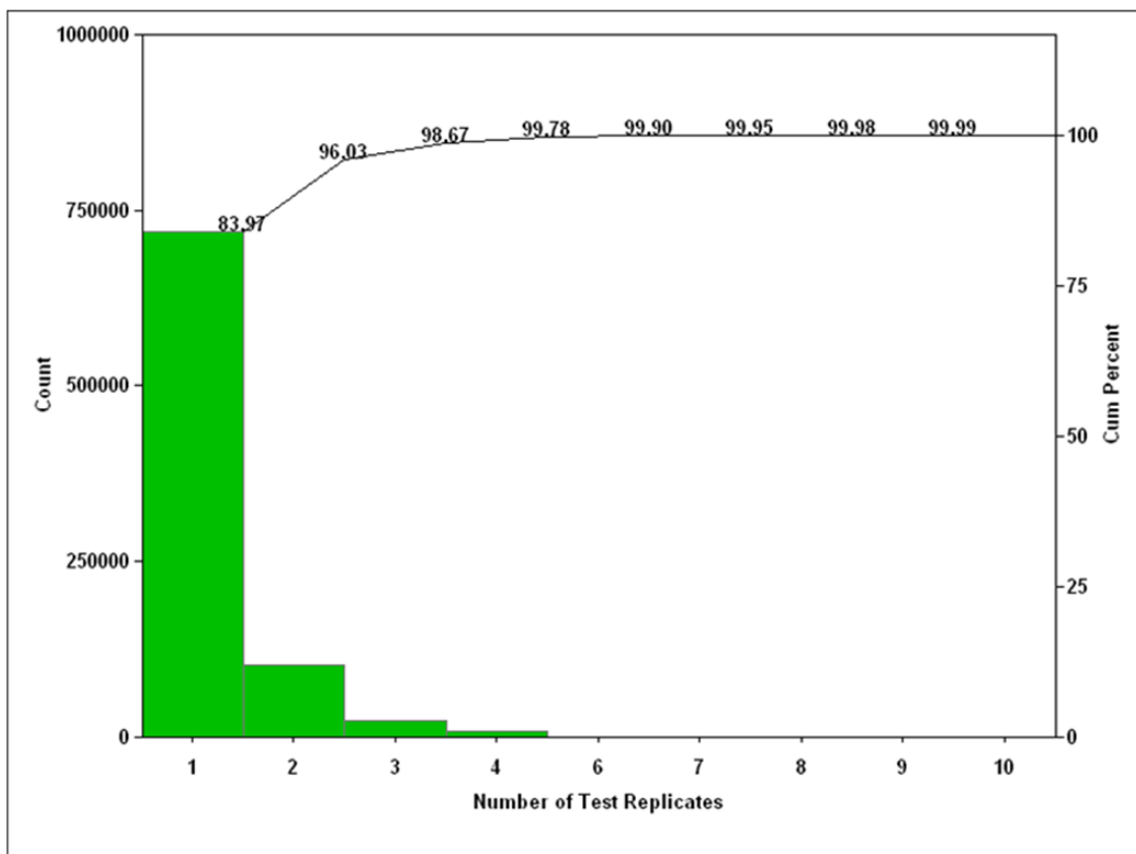


Figure 8: Data from Lots Created in 2008 and Run in CRC Assays in 2008-09

### 3.3. Effect of Compound Lot on Database MSR

Although a single lot represents most compounds in a typical project, important compounds will likely require the synthesis of multiple lots. Multiple lots are presumed to be thoroughly characterized by chemists to ensure equivalence between lots, so multiple lots should not be expected to have substantively different potencies.

Figure 9 compare MSRs – with and without accounting for sample lot – of 15 assays. The results indicate no substantive differences in calculated MSRs. Note also that the MSR sample size can increase or decrease based on distribution of lots for multiple lot compounds.

While multiple lots are not typically expected to be substantively different, the potential for large impact is always there, so it should at least be considered for assays with large MSR.

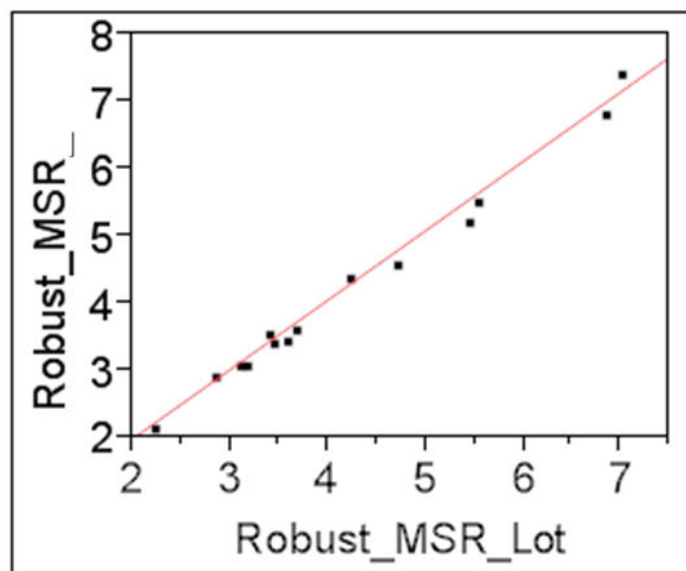


**Figure 9:** Robust MSR (Compound) vs. Robust MSR (Compound & Lot) for 15 Sample Assays with Line of Agreement

## 4. Conclusion

The MSR is a statistical parameter that characterizes the reproducibility of potency estimates from *in vitro* concentration-response assays. It is also a valuable tool for assessing the reliability of an *in vitro* assay throughout its life cycle. The Replicate-Experiment MSR is a diagnostic and decision tool that establishes an assay's readiness to go into production. Once an assay is in production, the Control Compound MSR enables prospective identification and correction of problems (e.g., drifts or shifts in potency), as well as assessment of the stability of the MSR over time. The Database MSR is considered the most representative estimate of assay reproducibility and is calculated from compounds with repeat evaluations that accumulate during the course of a project. The Database MSR can be calculated automatically for assays publishing to a database giving consumers of *in vitro* potency data up-to-date estimates of assay reliability. Outliers can arise over the course of a project for a variety of reasons and even a small number can artificially inflate the Database MSR. Diagnostic plots are needed to identify and exclude these values or a Robust Database MSR can be calculated that is less sensitive to the presence of a few extreme values.

## 5. References

1. Eastwood BJ, Farmen MW, Iversen PW, Craft TJ, Smallwood JK, Garbison KE, Delapp N, Smith GF. The Minimum Significant Ratio: A Statistical Parameter to Characterize the Reproducibility of Potency Estimates from Concentration-Response Assays and

- Estimation by Replicate-Experiment Studies. *J Biomol Screen*. 2006;11:253–261. PubMed PMID: 16490778.
2. Montgomery DC. *Design and Analysis of Experiments*. John Wiley and Sons, New York, 2012.
  3. Staudte RG and Sheather SJ. *Robust estimation and testing*. John Wiley and Sons, New York, 1990.
  4. Hollander M and Wolfe DA: *Nonparametric Statistical Methods*. John Wiley and Sons, New York, 1999.
  5. Bland JM, Altman DG. Statistical methods for assessing agreement between two methods of clinical measurement. *Lancet*. 1986;I:307–310. PubMed PMID: 2868172.
  6. Eastwood, BJ, Chesterfield, AK, Wolff MC, and Felder CC: *Methods for the Design and Analysis of Replicate-Experiment Studies to Establish Assay Reproducibility and the Equivalence of Two Potency Assays*, in Gad, S (ed): *Drug Discovery Handbook*, John Wiley and Sons, New York, 2005, 667-688.



# Assay Technologies

Michelle Arkin, PhD, Douglas Auld, PhD, Kyle Brimacombe, MS, Thomas D.Y. Chung, PhD, Nathan P. Coussens, PhD, Marcie Glicksman, PhD, Zhuyin Li, PhD, James McGee, PhD, Owen McManus, PhD, and G. Sitta Sittampalam, PhD





# HPLC-MS/MS for Hit Generation

Stefan Jon Thibodeaux, M.S.,<sup>1,\*</sup> David A Yurek, M.S.,<sup>2,†</sup> and James E McGee, Ph.D.<sup>3,‡</sup>

Updated: July 8, 2017.

## Abstract

Mass Spectrometry based screening has allowed researcher's to employ native substrates for screening, screen previously intractable targets, and eliminate the need to use coupled reactions. Recently, many instrumentation advances have been made to increase throughput, thus allowing routine access to this technology. This chapter details the different instrumental set-ups which will enable mass spectrometry based screening, and issues and solutions likely to be encountered during assay development.

## Introduction

The use of LC-MS/MS as an assay platform for hit generation has enabled the development of assay methodologies that were previously difficult or impossible using conventional means of detection (2-4). These instruments are able to identify and quantify low levels of analytes in complex matrices (5). Their ability to detect unmodified natural substrates and products is also an advantage as modified substrates may impact the quality of hits (6, 7). Additionally, the near universality of detection gives LC-MS/MS a wide range of applications. Historically, LC-MS/MS detection techniques were too slow for screening applications. However, with the clever use of valves and pumps, several researchers are beginning to exploit LC-MS/MS and have implemented this strategy for routine screening (8-10). Liquid chromatography techniques encompass no chromatography (flow injection), to isocratic, and to gradient methods using short columns, and to staggered injections on multiple columns. Early versions of LC-MS/MS screening utilized Gilson's 8-probe liquid handler and staggered injection systems (8, 9). A few years ago, a company employing a unique autosampler, (RapidFire™, Agilent) was spun out of Pfizer with LC-MS/MS screening as their mainstay (10). In the past few years, other manufacturers have offered autosamplers capable of the high sampling rates required for this technique. This manual will focus on four systems which are proven to deliver the through-put necessary for hit generation for a 100,000-200,000 compound screen in a few weeks. Also, the technical details ranging from assay buffer components to data processing will be discussed.

---

<sup>1</sup> Eli Lilly and Company; Email: thibodeaux\_stefan@lilly.com. <sup>2</sup> Eli Lilly and Company; Email: yurek\_david\_a@lilly.com. <sup>3</sup> Eli Lilly and Company; Email: Mcgee\_james\_e@lilly.com.

\* Author

† Author

‡ Editor

## Assay Components

Ideally, only buffers and detergents which are compatible with the mass spectrometer should be used in the bio-chemical assay mixture. However, enzyme systems commonly require the presence of non-volatile buffers, proteins, and/or detergents for optimal activity. The levels to which non-volatile components can be tolerated in the bio-chemical system is directly related to the chromatographic system employed (Table 1). For example, the flow injection mode is most sensitive to ion suppression and requires the most sample clean-up or only mass spectrometry friendly components. Whereas chromatographic separation methods can tolerate less stringent sample clean up and less mass spectrometry friendly components can be employed.

The buffers of choice for the biochemical assay are ammonium acetate and ammonium bicarbonate as these buffers are compatible with the mass spectrometer due to their volatility. If these buffers are not compatible with the enzyme assay, then conventional buffers can be used. However, for flow injection significant sample cleanup would need to occur. Detergents represent the most troublesome assay components as these are normally retained on reverse phase resins. Typically, replacing or avoiding SDS and polymeric detergents such as TWEEN, Triton, and NP50 is the best course of action. Polymeric surfactants are mixtures of several molecules of varying polarities and masses, which interfere by eluting in a broad time window and flooding the system with a large number of ions that will greatly suppress the desired signals or cause “cross talk”(11). If these cannot be replaced with the more mass spec friendly detergents, then these should be used at the lowest effective concentration. When detergents must be used, single molecule forms are best e.g. CHAPS, octyl  $\beta$ -D-glucopyranoside or dodecyl  $\beta$ -D-glucopyranoside. Then, only one component needs to be separated from the analytes to enable detection.

**Table 1:** Volatile HPLC Modifiers used in LC-MS/MS

| Volatile Modifiers       | Abbreviation | Concentration Used | pKa | pH range | Comments  |
|--------------------------|--------------|--------------------|-----|----------|---|
| <b>Acids</b>             |              |                    |     |          |   |
| Trifluoro-Acetic Acid    | TFA          | 0.02-0.1%          | 0.3 | 1-2      | Forms ion-pairs in gas phase, suppresses positive ionization, gives strong negative ion |
| Formic Acid              | FA           | 0.1-1%             | 3.8 | 2-3      |   |
| Acetic Acid              | HOAc         | 0.1-1%             | 4.8 | 3.8-5.8  |   |
| Propionic Acid           |              | 1-5%               |     | 2.5-4.5  | Used as post-LC additive to break ion-pairing   |
| Heptafluoro-Butyric Acid | HFBA         | 0.10%              |     | 1.5-3.5  | Forms ion-pairs in gas phase, suppresses  |

*Table 1 continues on next page...*

Table 1 continued from previous page.

| Volatile Modifiers            | Abbreviation       | Concentration Used | pKa       | pH range  | Comments                                       |
|-------------------------------|--------------------|--------------------|-----------|-----------|--|
|                               |                    |                    |           |           | positive ionization, gives strong negative ion |
| Bicarbonate                   | HCO <sub>3</sub>   | 10-50 mM           | 6.3, 10.3 | 6.8-11.3  | Prepare fresh daily                            |
| <b>Bases</b>                  |                    |                    |           |           |  |
| Ammonia                       | NH <sub>3</sub>    | 10 mM              | 9.2       | 8.2-10.3  | Prepare fresh daily                            |
| Triethylamine                 | TEA                | 10 mM              | 10.7      | 9.7-11.7  | Prepare fresh daily                            |
| Piperidine                    |                    | 1-10 mM            | 10.0      | 9-11      |  |
| 1-Methyl-Piperidine           |                    | 1-10 mM            | 10.2      | 9.3-11.3  |  |
| Morpholine                    |                    | 1-10 mM            | 8.4       | 7.4-9.4   |  |
| 4-Methyl-Morpholine           |                    | 1-10 mM            | 8.4       | 7.4-9.4   |  |
| Pyrrolidine                   |                    | 1-10 mM            | 11.3      | 10.3-12.3 |  |
| <b>Common Buffers</b>         |                    |                    |           |           |  |
| Ammonium Acetate              | AmOAc              | 10-200 mM          |           | 7.0       |  |
| Ammonium Formate              | AmF                | 10-200 mM          |           | 6.3       |  |
| Ammonium Bicarbonate          | AmHCO <sub>3</sub> | 10-100 mM          |           | 8-10      | Prepare fresh daily                            |
| Triethyl-Ammonium Bicarbonate | TEAB               | 10-100 mM          |           | 8-10      | Prepare fresh daily                            |

## Mass Spectrometers

The choice of mass spectrometer will have significant impact on the ability to perform MS based screening. A triple quadrupole is the preferred instrument because it delivers the best combination of sensitivity, selectivity, scan speed, and dynamic range. A triple quadrupole instrument is usually run in multiple reaction monitoring (MRM) mode. MRM works by selecting the ion of interest in the first quadrupole, fragmenting the ion of interest in the second quadrupole, and finally selecting one of the fragments in the third quadrupole for detection by the detector. Typically, one unique product ion is selected for each parent, but more than one product ion can be selected as a confirmatory ion. Also, quadrupole-time-of-flight or orbit trap instruments are being used for screening. Quadrupole-time-of-flight or orbit trap instruments provide the ability to obtain accurate mass measurements of the ions of interest. Due to this capability a narrow mass range window can be used to obtain specificity rather than fragmenting the molecule as in a triple quadrupole instrument. This can be a significant advantage when dealing with small molecules which have poor fragmentation efficiency or do not fragment to produce a dominant ion (12). The mass range, resolution, and speed of the quadrupole-time-of-flight or orbit trap enable the use of small proteins as substrates that may generate multiple enzymatic products. It is not necessary to have standards for the products as the entire mass range is captured in the TOF scan, enabling all the products to be measured

simultaneously. For example, a small protein which undergoes multiple phosphorylations could be analyzed directly to determine if inhibitors give different phosphorylation patterns. The drawbacks to the use of Q-ToF instruments for screening are the large data files produced and the limited data processing software available. However, instrument companies are actively working to remove these barriers.

The short LC columns or flow-injection used in mass spectrometry based screening places additional demands and restraints on the mass spectrometry system. The reduced chromatography used in these rapid assays typically does not separate substrate and the product, therefore; the use of unique MRM transitions or exact masses for identification and quantitation are needed. Generally, no problems are seen if the compounds are not isobaric as unique molecular ions are observed. Occasionally, cross-talk between analytes may occur if the collision cell of the MS is not sufficiently cleared between analyte transitions (seen only in older instruments), or if an analyte converts to the other analyte in the source. If analytes have the same molecular ion and the fragment selected for analyte A also appears as a fragment for analyte B, then a pure sample of A will produce a peak in B and vice versa. If A and B are separated in time, this is not a problem. However, analytes are normally not separated in these rapid assays and unique fragments are then required. This may necessitate the use of lower sensitivity fragments to assure uniqueness. Typically, sensitivity is not an issue for these screening assays. As an illustration, a major fragment at 271 is seen in the analysis of several prostaglandins that would be optimal for sensitivity; if the analyte did not co-elute with other components also producing this fragment. Selection of other less abundant fragments allows unique identification of specific prostaglandin analytes. The isomeric prostaglandins PGE2 and PGD2 may be identified by their fragmentation pattern (13). Also the 5-, 12-, and 15-HETEs are good examples of isobaric molecules which can be identified and quantitated by their fragmentation patterns even though signal intensity is lost compared to the most abundant fragment (14).

To deal with the inherently variable process of generating and measuring ions in a mass spectrometer, internal standards are used. The best internal standards are isotopically labeled analogues with a mass shift of +4 or greater. If an isotopically labeled product is not available, then a structural analog should be used. The internal standard should be added as soon as possible, (normally when the reaction is quenched) and its concentration should be half way between the maximum and minimum concentration of the product. The internal standard normalizes the analyte response to a known amount of material that has undergone identical sample handling. Therefore, once the internal standard is added, the ratio of analyte to internal standard is fixed regardless of decomposition, sample handling differences, and variances inherent in the mass spectrometry process. If the substrate and product for a reaction are close in structure and the calibration curves are parallel then the substrate can be used as in a ratio with the product. If the substrate is completely different than the product or the product and substrate calibration curves are not parallel, then an internal standard should be used.

The high flow rates used to obtain the through-put necessary to enable an MTS campaign place increase desolvation demand on the mass spectrometer. The source temperature is usually set to the highest allowed value and the source gas flow rates are set very close to the maximum allowed. Also, the high volume of samples injected on the mass spectrometer is greater than the typical sample work load. These special circumstances necessitate a more frequent cleaning schedule compared to that typically recommended by the instrument vendor. When running 100 or more 384-well plates a week, the instrument should be cleaned every two weeks or earlier depending upon the signal degradation. This can be monitored by plotting the response of the control wells over time. When the area counts decrease twenty-five percent or more then cleaning should occur.

For typical bioanalytical assays, linearity of triple quadrupole instrument response to analyte concentration may be established over >4 orders of magnitude. For screening assays, only 2-3 orders of magnitude are needed as activity of the reaction is measured from 0-100% inhibition. It is important to monitor the analytes in the linear range of the instrument response because calculation of percent inhibition assumes a linear function. Also, the signal to noise ratio for the product should be sufficient to measure 99% inhibition of the enzyme. The response of the non-inhibited wells should therefore be at least 100-fold signal to noise.

The mass spectrometer can ionize molecules using four basic modes of ionization electrospray positive, electrospray negative, atmospheric pressure chemical ionization positive and atmospheric pressure chemical ionization negative. While any ionization mode may be used, typically, electrospray ionization is used; as most compounds will have a fixed or inducible charge or be able to form adducts with an appropriate modifier. The topic of electrospray ionization is beyond the scope of this article. Here are a number of reviews and books on this topic (15-18)

## Sample Preparation

Normally, some clean-up of screening samples is required prior to chromatography (Figure 1). At the very least, a stop reagent that halts the reaction and engenders stability to the final mixture is required, as the samples may sit in the autosampler or freezer for an extended time. The stop reagent may consist of a low or high pH buffer, organic solvent, quenching reagent, derivatizing reagent, etc; similar to normal screening methods. Again, volatile reagents should be used to avoid contamination of the MS system. The internal standard(s) is normally added in the stop reagent (see MS parameters section).

The most common stop reagents are acetonitrile or methanol with or without modifier, and water with formic or trifluoroacetic acid. Acetonitrile (ACN) or methanol ratios of 1:1 to 1:4 sample to solvent are generally used. The high levels of ACN or methanol will cause the proteins in the sample to precipitate, and require the plates to be centrifuged or filtered prior to analysis. If the biochemical system cannot be stopped with ACN or methanol due to chromatographic issues, then water with formic or trifluoroacetic acid at 1-10% (v/v) should be tried. This type of sample preparation leaves the salts and buffers in

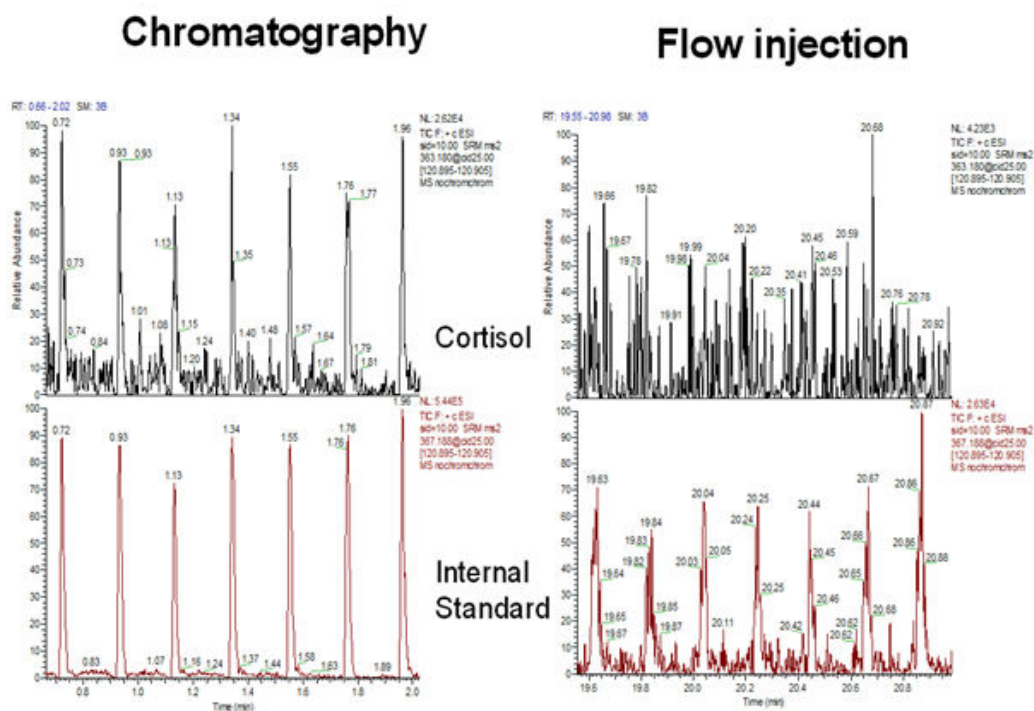


**Figure 1:** Comparison between ballistic chromatography and flow injection for 10 ng/mL of cortisol. Intensity of internal standard for flow injection was  $2.6 \times 10^4$  compared to  $5.4 \times 10^5$  for the ballistic chromatography setup.

the sample. Therefore, the system must include a divert valve or “dump valve” between the column and the MS to remove the salts to waste and preserve the cleanliness of the MS. Alternatively, the analytes may be captured from the assay mix by liquid/liquid or solid phase extraction, followed by drying and reconstitution or dilution with water. Analysis of the subsequent samples often does not require a “dump valve” system as these methods result in cleaner samples with salts, proteins, and detergents typically removed. Liquid/liquid extraction methods may be automated using robotics, but require easily achieved modifications to the normal robotics and use of solvent resistant plates. Venting of the robot to remove organic solvent(s) vapors is necessary for safety (Figure 2; see instrument set-up section). Also, organic solvents used in liquid/liquid extraction are not tolerated by the plates normally used for the assays Table 2. Of the common polymers used, only polypropylene is resistant to some of these solvents (see manufacturer’s specifications). However, Teflon-like plates are available in 96 and 384 formats. These Teflon-like plates are typically used for combinatorial chemistry applications, and are more expensive than the plates normally employed in screening. However, in many cases, they may be washed

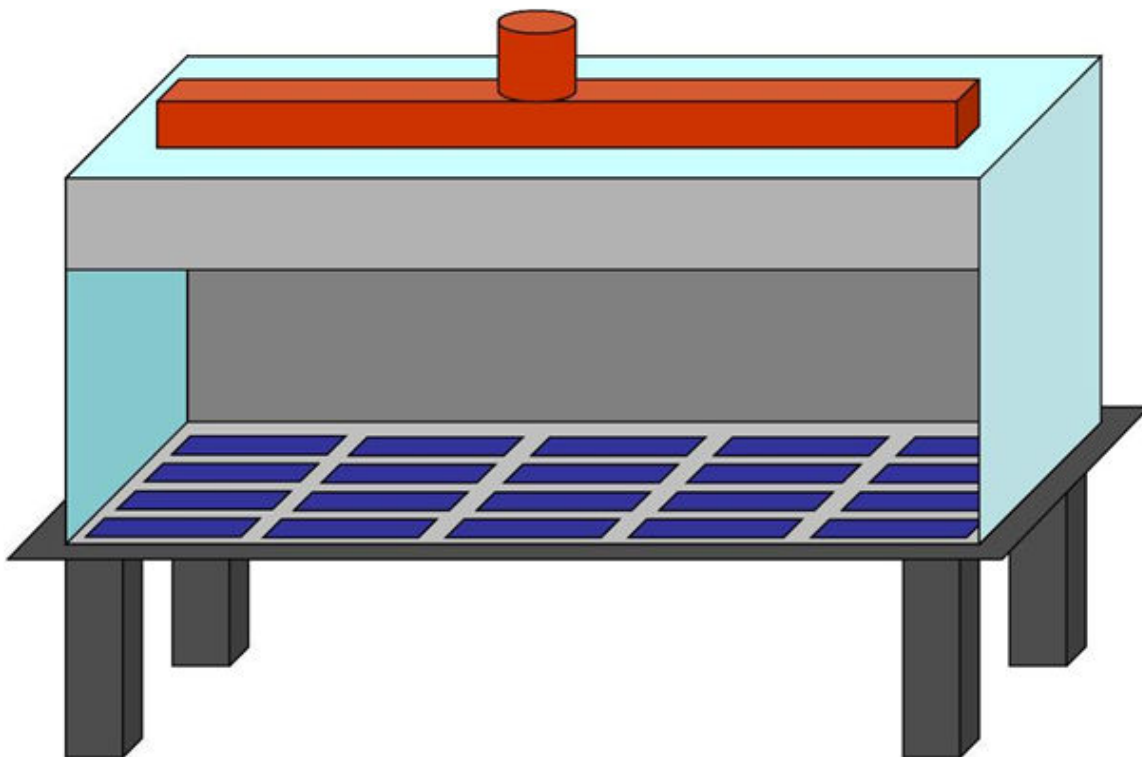


**Figure 2:** Schematic for Modified BioMek FX for Organic Solvents

and re-used. Also, reagent reservoirs containing solvents on the robot deck must also be made of solvent-resistant materials (e.g. metal, glass, Teflon). As pipette tips are constructed from polypropylene, they tend to be resistant to solvents, especially as they are only in contact with the solvent for a short time. However, compatibility should be checked prior to use. Although 96 and 384-well plate based SPE phases are available, these tend to be cost prohibitive when considering the number of samples to be processed in a typical screen.

Derivatization of the analytes can make them amenable to extraction or detection. This is beneficial when the analytes are difficult to chromatograph due to sticking to surfaces, broadening of peaks, or poor retention. However, this does add further complexity to the screen and may affect the assay statistics if the reactions are not optimized or complete. If derivatization is required for sensitivity or to overcome some other property, both substrate and product should react to the same level of completion or a stable-labeled internal standard will be necessary.

**Table 2:** Extraction Solvents

| Extraction Solvent | Solvent Strength | Polarity | BP  | Dielectric Constant | % of Solvent in Water | % of Water in Solvent |
|--------------------|------------------|----------|-----|---------------------|-----------------------|-----------------------|
| Heptane            | 0.01             | 0        | 98  | 1.92                | 0.0003                | 0.01                  |
| Toluene            | 0.29             | 2.4      | 110 | 2.4                 | 0.67                  | 0.046                 |
| MTBE               | 0.47             | 2.5      | 55  | 4                   | 4.8                   | 1.5                   |
| Diethyl ether      | 0.38             | 2.8      | 35  | 4.3                 | 6.89                  | 1.3                   |
| Methylene Chloride | 0.42             | 3.1      | 40  | 9.08                | 1.6                   | 0.17                  |
| Chloroform         | 0.4              | 4.1      | 61  | 4.81                | 0.815                 | 0.072                 |
| Ethyl Acetate      | 0.58             | 4.4      | 77  | 6.02                | 8.7                   | 9.8                   |
| Butanol            | 0.7              | 3.9      | 117 | 17.8                | 7.8                   | 20.1                  |

## Chromatography

In the most common situation, chromatography is required to avoid ion suppression from the sample matrix (Figure 2). The goal is to keep the analysis time as short as possible while providing acceptable separation of the analytes from the suppressing contaminants. A chart of sample analysis cycle time and daily throughput is shown in Table 3. In the realm of analysis times <20 seconds/sample, assay screens of 50-100K samples become feasible. However, even an increase of a few seconds/sample will raise the total screen time significantly. This restricts the use of chromatography to ballistic or snap gradients – essentially “on-line SPE” with little or no separation of the analytes from each other, requiring unique MRM transition channels for each analyte or unique parent masses for accurate mass instruments. In these methods, the sample is loaded with a retaining mobile phase while unretained components are diverted to waste (via a dump valve), followed by a very rapid mobile phase switch to elute the analytes to the MS.

The two most used types of chromatography for medium through-put screening are reverse-phase and HILIC. Reverse-phase chromatography uses a hydrophobic stationary phase, usually a C18 alkyl chain bonded to a silica particle. The C18 alkyl chain can be replaced by a C4, C8, phenyl, or cyano, but the same methodology applies. The initial mobile phase is water with or without some amount of organic, plus a modifier. Typical modifiers and their concentrations are located in the table (Table 1). The elution solvent is then acetonitrile or methanol with the same or possibly different modifiers. The analytes are retained on the alkyl phase due to its hydrophobic nature and then elute with the higher percentage of organic solvent. This type of chromatography is excellent for the majority of analytes which will be screened by mass spectrometry. Reverse phase chromatography is also versatile due to the ability to change modifiers which adjust the retention of the analytes. Two of the most significant advances with this type of chromatography are the increase in pH range and the ability to use 100 percent aqueous solvent systems. The bonded phase is typically only stable to pH 7; however, with the introduction of hybrid particles, pH stability up to twelve is possible. This allows for the



use of high pH mobile phases to retain molecules that are not well behaved at lower pH. Also, increase in pH can dramatically improve peak shape and can sometimes dramatically effect sensitivity in the mass spectrometer. Using 100% aqueous phases may cause phase collapse for older resins, resulting in non-reproducible retention times. However, resins are currently manufactured which are compatible with 100% aqueous phases. For a more in-depth discussion of reverse-phase chromatography, please refer to the following references (19-26).

HILIC (Hydrophilic Interaction Chromatography) is very good for retention of polar analytes. This type of partition chromatography can use the same solvents as reverse-phase chromatography but in the reverse order. The compounds are loaded in high organic (typically 95% acetonitrile) and eluted by increasing the water content. The samples are also typically in a high percentage of organic solvent, which couples well with stopping the reaction with acetonitrile and then direct analysis of the samples. The stationary phases for HILIC are quite different from reverse-phase chromatography. Typically HILIC stationary phases are bare silica, diol, amino, amide or specialty stationary phases which have dual functional groups. Unlike reverse-phase columns where exchanging one manufacturer's C18 column for another may provide minimum changes in peak shape or retention, changing from one HILIC packing material to another may produce significant changes in retention, peak shape, and carry-over. For this reason, typically 5 or 6 different HILIC stationary phases are tested using the same mobile phase composition. For a more in depth discussions on HILIC chromatography please refer to these reviews (23, 25, 27, 28).

**Table 3.** Sample Analysis Rates

| Cycle Time (sec) | Samples/Minute | Samples/Hour | 384-well Plates /Hour | Samples/Day | 384-well Plates /Day | Days for 50K Screen* |
|------------------|----------------|--------------|-----------------------|-------------|----------------------|----------------------|
| 3                | 20             | 1200         | 3.13                  | 28800       | 75                   | 2.1                  |
| 5                | 12             | 720          | 1.88                  | 17280       | 45                   | 3.5                  |
| 8                | 7.5            | 450          | 1.17                  | 10800       | 28.13                | 5.6                  |
| 10               | 6              | 360          | 0.94                  | 8640        | 22.5                 | 7.0                  |
| 12               | 5              | 300          | 0.78                  | 7200        | 18.75                | 8.4                  |
| 15               | 4              | 240          | 0.63                  | 5760        | 15                   | 10.5                 |
| 20               | 3              | 180          | 0.47                  | 4320        | 11.25                | 14.0                 |
| 25               | 2.4            | 144          | 0.38                  | 3456        | 9                    | 17.4                 |
| 30               | 2              | 120          | 0.31                  | 2880        | 7.5                  | 20.9                 |
| 60               | 1              | 60           | 0.16                  | 1440        | 3.75                 | 41.9                 |

\* 320 samples and 64 controls/plate, continuous operation

## Instrument Set Up

In this section, several arrangements of instruments are described. Although other arrangements are possible, these have proven robust in our hands.

### Modified Gilson 8-probe

For extracted or generally clean samples, an isocratic system, developed employing a Gilson 8-probe that uses a mobile phase and column allowing for slight separation of the void volume and analytes (8). The setup is pictured in Figures 3 and 4. The Gilson 8-probe was modified by addition of a 10-port column-switching valve that is used to route pump flow to each of the eight sample injection valves in sequence, each sample injection valve linked directly to the corresponding positions on the switching valve. The two remaining positions on the switching valve (9 & 10) are used to by-pass the Gilson, routing flow directly to the column. During operation, the eight samples are loaded to the corresponding sample injection valve loops (load position) with the switching valve in the by-pass position (#10). Then, all sample valves are switched to the inject position. Because there is no flow through the sample valves, the samples are locked in the loops. Each sample valve is then selected in turn by rotating the switching valve through positions #1-8 using a time program of contact closures from the Agilent HPLC pump. Position #9 is passed over to wait at #10 for the next eight samples. As each sample injection valve is selected, the isocratic flow (2 ml/min) sweeps the sample from its loop to the column, where it is separated, and on to the MS, where it is detected. Each sample valve is selected for 6 seconds. The analytes are partially retained on the column, separating slightly from the void volume. The pressure spike observed on switching the 10-port valve causes a blip in the data trace from the MS and timing of its occurrence is adjusted away from the appearance of the peaks to enable facile integration.

During the rotation of the switching valve, the Gilson's 8-probes and injection ports are washed using a modified washing system. The needles are washed at the wash station, both inside and out, using the syringe working solvent in the normal manner. The injection ports are washed using a modified washing system incorporating a HPLC pump, a two-position switching valve, and an 8-way splitter. Flow of wash solution from the pump (16 ml/min) proceeds through the two-position switching valve that directs flow to the pump solvent reservoir or the injection ports, thus recycling solvent when not in use. When the injection ports are selected, flow proceeds through the 8-way splitter creating a flow of 2 ml/min to the exit/waste ports of the sample valves and up through the needle entrance of the ports, back-flushing the ports. The overflow from the ports is collected in the drainage moat surrounding the ports and exits via a drain tube to a waste bottle that is under constant negative pressure using an exhaust trunk. This method reduces carryover to essentially zero and also clears any plugging of the injection ports.

For high-throughput operation, the Agilent HPLC pump, degasser, and column compartment, and the AB Sciex API-4000 are controlled by the Sciex Analyst software. To facilitate the rapid analysis, data was acquired into a single data file for each iteration of

## Modified Gilson 8-probe Autosampler – Injection

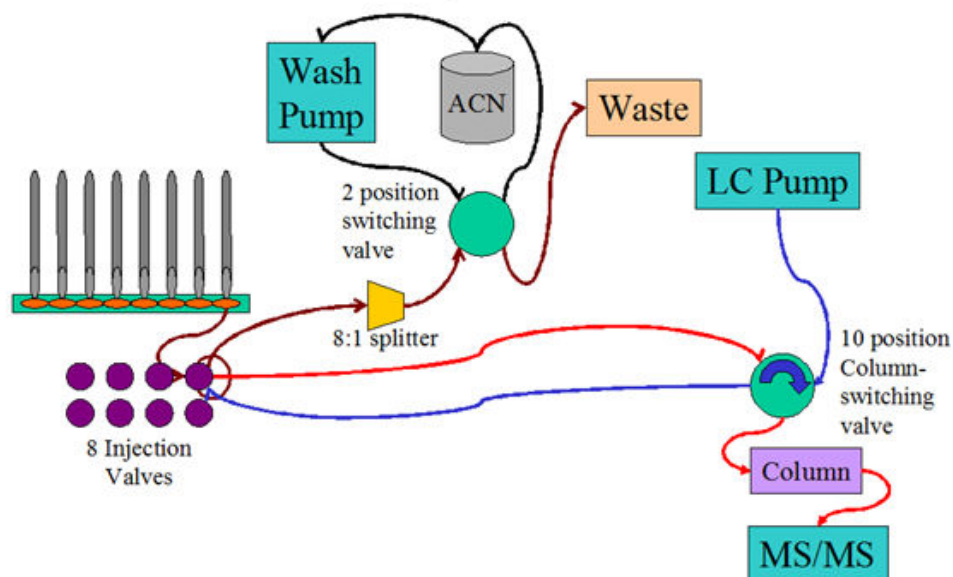


**Figure 3:** Schematic of Modified Gilson 8-probe Autosampler in the injection position. All peek lines have been replaced metal.

the Gilson 8-probe, yielding 8 samples per file (Figure 5). The movement of the column switching valve used to select the individual sample injection valves on the Gilson 8-probe was controlled by the inject start contact closure from the 8-probe and a time program of contact closures from the Agilent HPLC pump. The washing pump was set up to run continuously, with its switching valve controlled via the AB Sciex software. The Gilson 8-probe was run in stand-alone mode using Trilution software, but with a Ready-Out contact closure signal required from the LC-MS/MS. The 8-probe also sent an inject start contact closure to the MS to start the acquisition. Thus, if the autosampler failed, the MS would not start. Also, if the LC-MS/MS failed, the autosampler would not proceed. This dual “handshake” saves samples in the event of equipment failure. To prevent failures due to leaks in the plumbing that are missed by the leak detection resistors on the Agilent equipment, the low pressure setting on the pump is set to 34 bar. Also, as PEEK tubing will fail after prolonged exposure to ACN, all lines up to the column were plumbed with stainless steel. Data handling utilized a method written in the vendor software with analytes 1-8 representing samples 1-8 of each iteration of the 8-probe. After integration, the results were transferred to Excel and transposed with a template to 384-well format.

## Modified Gilson 8-probe Autosampler – Wash

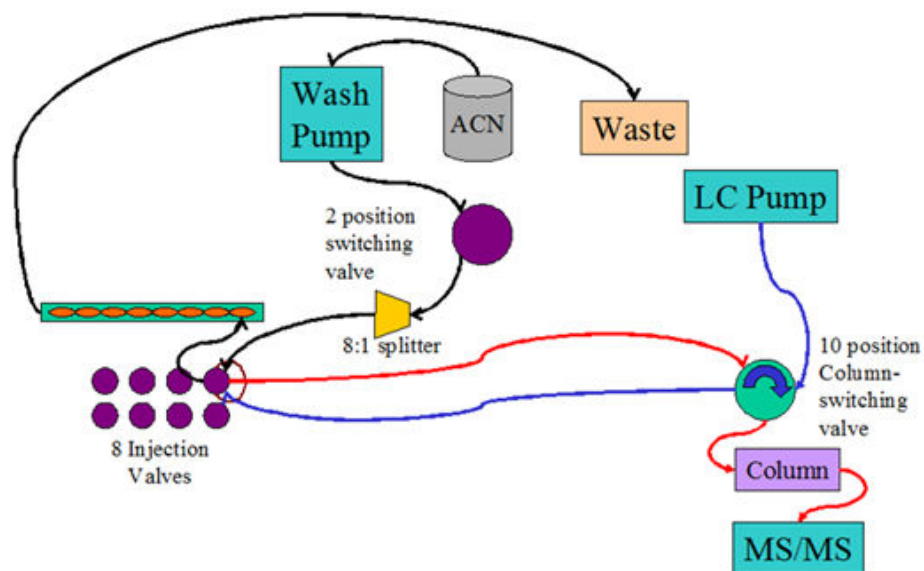


**Figure 4:** Schematic of Modified Gilson 8-probe Autosampler in Wash position. All peek tubing has been replaced with steel.

### Off-the-shelf MTS system

For analyses requiring a ballistic gradient, the Shimadzu Prominence system offers a practical alternative. A typical set up utilizes a 10-port two position valve to select pumps and route flow to either waste or the MS. During equilibration and sample injection, flow proceeds from the loading LC pump to the autosampler, to the 10-port valve, through the column, and exiting to waste. Flow from the eluting LC pump proceeds through the same 10-port valve to the MS. After the sample is injected, the analytes are retained on the column while unretained materials are sent to waste. The valve switch moves the column from the loading pump flow to the eluting pump stream and sweeps the analytes into the MS. After the analytes have eluted, the valve is switched again and the column re-equilibrated with the loading pump flow.

Figure 6 illustrates the layout of the pumps, autosampler, 10 port valve and mass spectrometer. This arrangement provides for instantaneous delivery of the elution and re-equilibration solvents to the column through the 10 port valve. Also, solvent B is continuously pumped to the MS, either bypassing the column or through the column.

Figure 7a depicts the wiring diagram which starts both the pumps and the mass spectrometer simultaneously. With each injection, the autosampler sends a start signal to

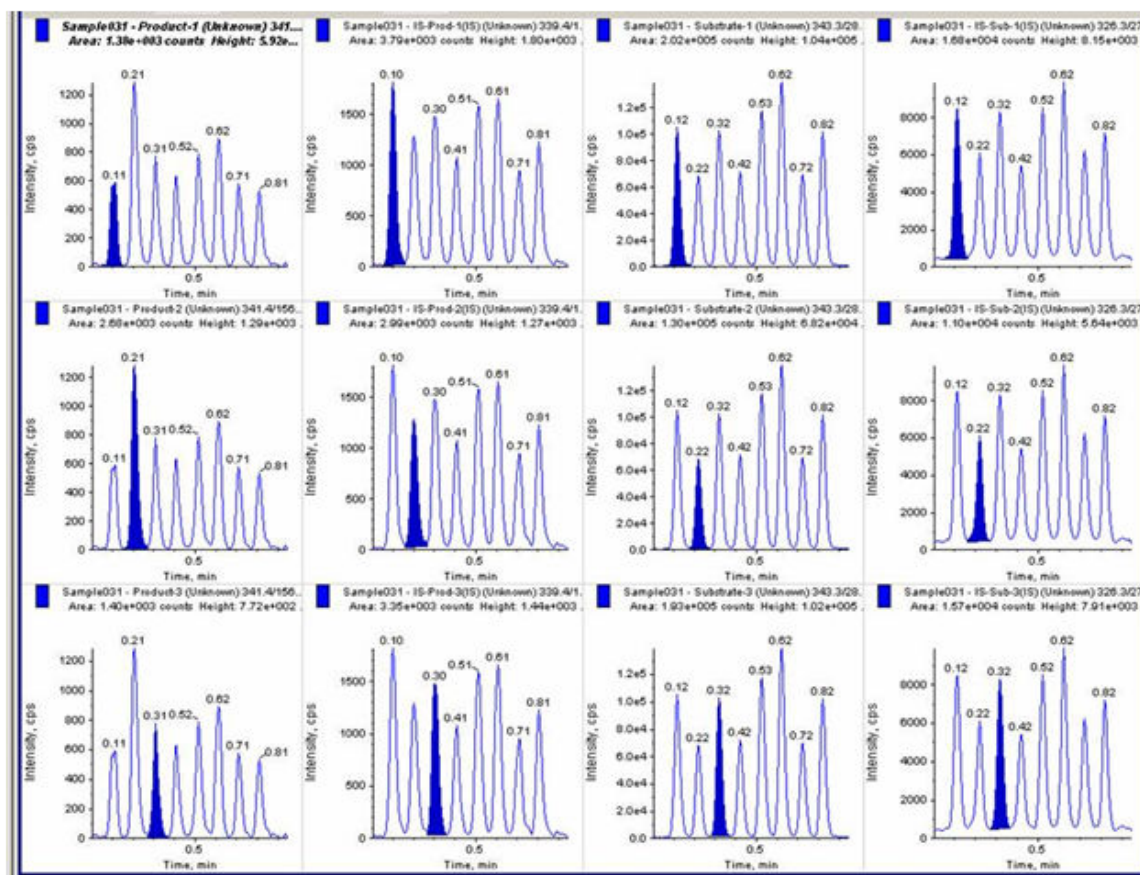


**Figure 5:** Example of data obtained with Gilson 8-probe. Gilson 8-probe was connected to AB SCIEX 4000 and the data was processed using Analyst®.

the pumps to begin the pump's time programs and to the mass spectrometer. However, the mass spectrometer ignores any further start signals from the autosampler until the time programmed into the mass spectrometer method has elapsed. The time program for pump A controls the switching valve and the pump's shut off time. The time program for pump B controls its shut off time. The flow rates for pump A and B are  $2.5 \text{ mL min}^{-1}$  until 2.9 minutes, with a drop to  $0 \text{ mL min}^{-1}$  at 3 min. With this set-up the pumps will stop flowing if they do not receive a start signal before 3.0 minutes. Therefore, after the 12th plate has run or if an error occurs, the pumps will shut off, allowing for unattended operation of the system.

Figure 7b depicts the wiring diagram enabling a pump error to stop the autosampler while running in local mode. After the wiring is connected, the External Signal Functions (EXT-S) parameter in each pump is set to 2. Without this configuration, the autosampler would continue to inject samples even though the pumps are not working. There is no need the change the wiring connections and the EXT-S settings when switching between MTS mode and normal bio-analytical mode.

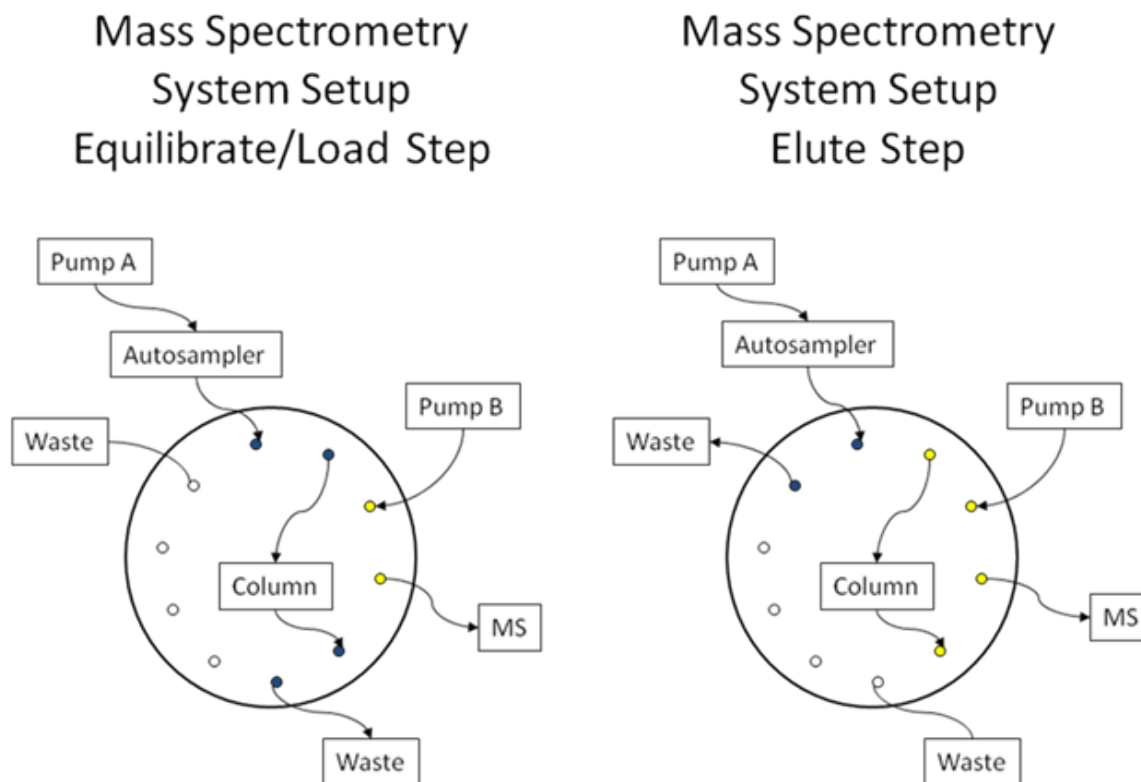


**Figure 6:** Schematic of MS-MTS system using the 20 AC Shimadzu auto-sampler, 20 AD Shimadzu pumps, 10 port valve, and a mass spectrometer.

## Commercially-built System for MTS

A commercially available instrument was built to perform rapid ballistic gradients with a computerized interface to facilitate automated mass spectrometry based screening. Therefore, this instrument has significant advantages in ease of use, speed, and robustness over the previous two platforms. The instrument consists of three isocratic pumps and one peristaltic pump, four valves, a vacuum system for sample loading, column holder, refractive index detector, and a plate changer. Another vital component is the software to integrate the data which is further discussed in the data handling section. Unlike most sample inlet systems, this commercially built instrument uses vacuum to remove sample from the sample plate. The sample is pulled through the tubing, through the injector loop, and to an optical window. A refractive index change is detected when the sample liquid appears, which then triggers the injection valve to switch and load the column with the sample. If the sample is not loaded by the time specified in the method, the valve will still inject and that well will be missed. If a specified number of missed injections occur, the system will shut down. The three isocratic pumps work in concert with the valves to provide low carryover and rapid sample clean up. Pump 1 is used to load the compound onto the column, wash the sample, and re-equilibrate the system. Pump 2 is used to wash the sample flow path. The solvents from pump 2 do not interact with the sample. This

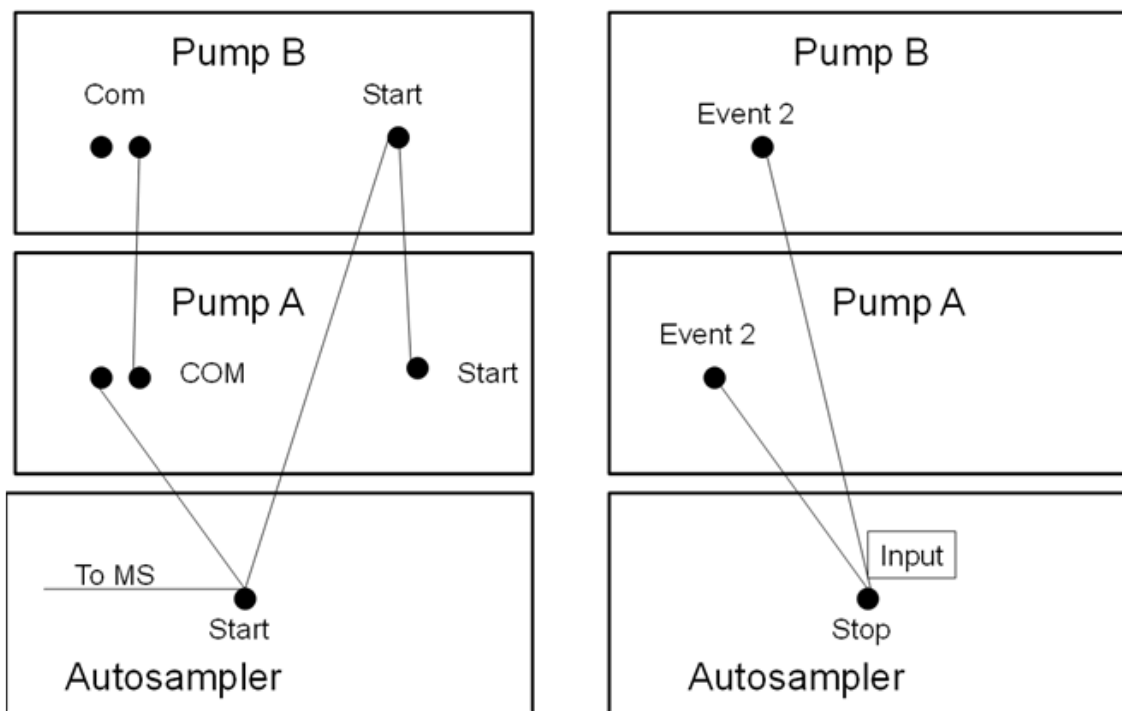


**Figure 7:** Schematic of wiring. A) Wiring setup for starting the pumps and auto-sampler simultaneously. B) Wiring setup for sending a stop signal to the auto-sampler if the pumps' pressure fall below minimum pressure setting, or detects a leak.

allows for the possibility of using a very aggressive wash in pump 2 if needed to reduce carryover; however, this solvent is usually the same as the elution solvent. Pump 3 elutes the sample from the column, with flow either to the mass spectrometer or through the column to the mass spectrometer. When the system switched from load to elute, pump 2 is then flushing the system while pump 3 is eluting the sample. The column compartment on this instrument can hold up to 6 columns. When performing method development these can range from cyano to C18 phase. In production mode these are the same stationary phase. If during a run the backpressure is above the limit specified and there is another column of the same packing material available, then the instrument will automatically change to the new column and resume the analysis. The standard packing materials supplied in their catalog are cyano, C4, C8, C18, silica, HILIC and Hypercarb columns. Custom packed columns can be obtained; however, by modifying the plumbing the system can be made to accept a multitude of columns. This is especially useful when trying to decide on the best column or if a high pH compatible stationary phase either for reverse-phase or HILIC is necessary. The one drawback to modifying the plumbing is the loss of the automated column switching capability. But the ability to use more column types is a worthwhile trade off. This system is best illustrated by the Agilent Rapidfire™ (2, 4, 29-31).

## Staggered Injection System

The staggered injection system is the only true HPLC system of the four discussed. These systems are typically composed of four HPLC pumps, two or four auto-samplers, four columns, a column switcher, and advanced software to integrate and control these components (32-34). The injections are staggered in time so that the compounds are eluting at different times into the mass spectrometer. These systems allow true gradient elution instead of only a ballistic gradient. Therefore, this type of system may be able to successfully overcome more complex matrixes than the systems previously described. The price paid for this increased chromatographic resolving power is speed. The fastest this system can inject is about one sample per minute; therefore, the best through-put this system can achieve is 4-5 samples per minute. The biggest shortcoming to this system is all the parts that have to keep running to achieve this through-put. Recent versions of software controlling this system will compensate for loss of one channel by redistributing the samples across the other three channels. This system (like the Shimadzu system previously discussed) can be used to perform other functions besides MTS screening making it a versatile option for any lab thinking about screening on infrequent basis. This system is best illustrated by the Aria System from Thermofisher.

## Data Handling

In years past, processing MTS data was a challenge using vendor software; however, this is now not the case. The most complete solution is provided using the Rapidfire<sup>®</sup> because that system has its own data integration software capable of integrating data from Thermo Fischer Scientific, AB Sciex and Agilent mass spectrometers. Using the Agilent platform integration software it is quite easy to process data from samples contained in 10 to 20 plates collected in a single file. After straight-forward data integration, the software can display the data in either plate format or column format. The software will do an excellent job processing data in screening mode; however, if calibration curves are needed, then the software has limitations depending upon the MS instrument used. If the Rapidfire<sup>®</sup> is connected to an Agilent mass spectrometer, then making in-plate calibration curves will be straight-forward as the system is fully integrated into the Agilent Mass Hunter software. If the Rapidfire<sup>®</sup> is connected to a Thermo Fischer Scientific or AB Sciex mass spectrometer, obtaining a calibration curve requires data to be imported into a program like Excel or JMP for further processing or will require using the mass spectrometry vendor's software to process the data.

All three brands major brands of mass spectrometers (Agilent, ThermoFisher Scientific and AB Sciex) may be used to obtain data from the Gilson 8-probe or the Shimadzu autosampler options described. Using the Gilson allows the normal vendor quantitation software to be used for data integration of the eight peaks per data file, with further processing in Excel or similar programs. The Shimadzu set up requires use of vendor specific software to process the data as the entire plate data is contained in a single file. For the Agilent, this will be done using their Mass Hunter software. For the ThermoFisher Scientific instrument, data processing is performed using GMSU/QuickCalcCalculation, a



separate software package from their standard package. For AB Sciex, data processing is performed using their Multiquant™ software package, also purchased separately. As opposed to the Rapidfire® integration software, these vendor solutions work better if each 384/96 well plate is contained in a single file. These software packages also work better if an internal standard (or the substrate which can act as the internal standard) is used as an injection marker for processing the data. After the data is processed and exported to a spread sheet, percent conversion or area ratio can be calculated. Mass spectrometry data running in MTS mode is inherently more variable when only the product of the reaction is considered; however, because the product of the reaction is made from the substrate, a percent conversion calculation may be used to normalize the data. This should only be done if the instrument response slopes for the substrate and product standard curves are parallel. If the lines are not parallel an internal standard must be used. The calculation for percent conversion is:

$$\% \text{ Conversion} = \text{Product}/(\text{Product} + \text{Substrate})$$

If the biochemical system allows for percent conversion to be used, this will result in the least amount of assay variance as it negates the variance caused by the robotics systems used to add substrate to the assay plates. Addition of internal standard will only account for the variance occurring after its addition at the stoppage of the reaction.

## Other Notes

Some time is generally required for the screening lab personnel to become accepting of this new technique and its ability to pinpoint problem areas in assay methods and practice. In this process, robust experiments with adequate controls are needed that allow the data to speak for itself without equivocation. MRM transitions may be included that monitor each component of the reaction, allowing any errors or trends to be seen and facilitating rapid assay development. This will quickly highlight the new LC-MS/MS techniques as rapid assay development tools.

Collaborative efforts initiated with analytical departments containing the equipment and assay personnel are recommended as the purchase of the LC-MS/MS equipment requires significant capital expenditure, and its operation requires the incorporation of trained, experienced staff with the screening lab personnel.

## Example Initiation of a New Screen

The following is a typical example of what occurs when developing a new MTS assay:

1. Order product or products of the reaction and obtain substrate or substrates.
2. Infuse the substrate/s and product/s into the triple quadrupole instrument to obtain the MRM transitions. Ascertain from infusion if molecule will ionize in positive mode only or negative mode only or both. Usually three MRM channels are obtained per analyte and tested.

3. From the structure or from literature discern if reverse-phase or HILIC chromatography will retain and elute the compounds.
4. Using a traditional HPLC system run a quick gradient from 100 percent water to 95 percent organic in reverse-phase mode or 95 percent organic to 10 percent organic in HILIC mode. Determine if peak is eluted from column with good peak shape and low carry-over. Determine minimum amount of organic tolerated for reverse-phase ie. 95/5, 90/10, 80/20 water/organic.
5. Inject the substrate at 1  $\mu$ M concentration to determine if cross talk into the product channel occurs. If there is less than 0.5% cross talk then proceed to next step. If significant cross talk is observed determine the reason.
  - a. Substrate is not pure and contains some product. This analysis needs chromatographic resolution between the product and substrate.
  - b. The MRM channel chosen is not specific enough. Re-infuse the analytes and obtain more MRM channels to test.
6. Run a calibration curve in the assumed range of the reaction. We usually prepare our calibration curves by serial dilutions either 1:2 or 1:3 dilutions in water for reverse-phase and 1:3 water/ACN for HILIC. This will generate an ideal state/sensitivity.
7. Determine if the reaction can be stopped with organic and at what ratio or does the reaction have to be stopped with water which will usually contain 10% formic acid in a 1:1 ratio.
8. Rerun calibration curve in buffer system stopping with conditions developed in step 7.
9. Now decrease the chromatographic run time by doing a step gradient i.e. hold for 6 seconds to wash and then elute at 90/10 organic/water for reverse-phase and 10/90 for HILIC.
10. Rerun calibration curve with substrate and product to determine new limit of quantitation, linearity, and parallelism of substrate and product.
11. If Substrate and product response are parallel, use percent conversion for screen. If slopes are not parallel, then obtain an analog IS or stable labeled IS.
12. Analytical assay is now ready to test biochemical samples.
13. Run minimum and maximum experiments with calibration curves to determine if the product concentration is in the previously established linear range.
14. Run standard biochemical assay development experiments.

## References

1. Slavicek J.M., Hayes-Plazolles N. The Lymantria dispar nucleopolyhedrovirus contains the capsid-associated p24 protein gene. *Virus Genes*. 2003;26(1):15–8. PubMed PMID: 12680688.
2. Highkin M.K., et al. High-throughput screening assay for sphingosine kinase inhibitors in whole blood using RapidFire(R) mass spectrometry. *J Biomol Screen*. 2011;16(2):272–7. PubMed PMID: 21297110.
3. Lunn C.A. Label-free screening assays: a strategy for finding better drug candidates. *Future Med Chem*. 2010;2(11):1703–16. PubMed PMID: 21428840.

4. Jonas M., LaMarr W.A., Ozbal C. Mass spectrometry in high-throughput screening: a case study on acetyl-coenzyme a carboxylase using RapidFire--mass spectrometry (RF-MS). *Comb Chem High Throughput Screen.* 2009;12(8):752–9. PubMed PMID: 19531010.
5. Hopfgartner G.r., Bourgoigne E. Quantitative high-throughput analysis of drugs in biological matrices by mass spectrometry. *Mass Spectrometry Reviews.* 2003;22(3): 195–214. PubMed PMID: 12838545.
6. Beher D., et al. Resveratrol is Not a Direct Activator of SIRT1 Enzyme Activity. *Chemical Biology & Drug Design.* 2009;74(6):619–624. PubMed PMID: 19843076.
7. Pacholec M., et al. SRT1720, SRT2183, SRT1460, and Resveratrol Are Not Direct Activators of SIRT1. *Journal of Biological Chemistry.* 2010;285(11):8340–8351. PubMed PMID: 20061378.
8. Morand K.L., et al. Techniques for increasing the throughput of flow injection mass spectrometry. *Anal Chem.* 2001;73(2):247–52. PubMed PMID: 11199973.
9. Xu R., et al. Application of parallel liquid chromatography/mass spectrometry for high throughput microsomal stability screening of compound libraries. *J Am Soc Mass Spectrom.* 2002;13(2):155–65. PubMed PMID: 11841071.
10. Quercia A.K., et al. High-throughput screening by mass spectrometry: comparison with the scintillation proximity assay with a focused-file screen of AKT1/PKB alpha. *J Biomol Screen.* 2007;12(4):473–80. PubMed PMID: 17478485.
11. Annesley T.M. Ion suppression in mass spectrometry. *Clin Chem.* 2003;49(7):1041–4. PubMed PMID: 12816898.
12. Zhang N.R., et al. Quantitation of small molecules using high-resolution accurate mass spectrometers - a different approach for analysis of biological samples. *Rapid Commun Mass Spectrom.* 2009;23(7):1085–94. PubMed PMID: 19263405.
13. Masoodi M., Nicolaou A. Lipidomic analysis of twenty-seven prostanoids and isoprostanes by liquid chromatography/electrospray tandem mass spectrometry. *Rapid Communications in Mass Spectrometry.* 2006;20(20):3023–3029. PubMed PMID: 16986207.
14. Masoodi M., et al. Simultaneous lipidomic analysis of three families of bioactive lipid mediators leukotrienes, resolvins, protectins and related hydroxy-fatty acids by liquid chromatography/electrospray ionisation tandem mass spectrometry. *Rapid Communications in Mass Spectrometry.* 2008;22(2):75–83. PubMed PMID: 18059001.
15. Banerjee S., Mazumdar S. Electrospray ionization mass spectrometry: a technique to access the information beyond the molecular weight of the analyte. *Int J Anal Chem.* 2012;2012:282574. PubMed PMID: 22611397.
16. Liuni P., Wilson D.J. Understanding and optimizing electrospray ionization techniques for proteomic analysis. *Expert Rev Proteomics.* 2011;8(2):197–209. PubMed PMID: 21501013.
17. Cole, R.B. and Editor, *Electrospray And MALDI Mass Spectrometry: Fundamentals, Instrumentation, Practicalities, And Biological Applications, Second Edition.* 2010: John Wiley & Sons, Inc. 847 pp.
18. Cooper, B.T., *Applied Electrospray Mass Spectrometry. Practical Spectroscopy Series. Volume 32. Edited by Birendra N. Pramanik (Schering-Plough Research Institute,*

- Kenilworth, NJ), A. K. Ganguly (Stevens Institute of Technology, Hoboken, NJ), and Michael L. Gross (Washington University, Saint Louis). Marcel Dekker: New York and Basel. 2002. viii + 434 pp. \$185.00. ISBN 0-8247-0618-8. J. Am. Chem. Soc., 2002. 124(Copyright (C) 2012 American Chemical Society (ACS). All Rights Reserved.): p. 13638-13639.
19. West C., Elfakir C., Lafosse M. Porous graphitic carbon: a versatile stationary phase for liquid chromatography. *J Chromatogr A*. 2010;1217(19):3201–16. PubMed PMID: 19811787.
  20. Gerber F., et al. Practical aspects of fast reversed-phase high-performance liquid chromatography using 3 microm particle packed columns and monolithic columns in pharmaceutical development and production working under current good manufacturing practice. *J Chromatogr A*. 2004;1036(2):127–33. PubMed PMID: 15146913.
  21. Roses M., Subirats X., Bosch E. Retention models for ionizable compounds in reversed-phase liquid chromatography: effect of variation of mobile phase composition and temperature. *J Chromatogr A*. 2009;1216(10):1756–75. PubMed PMID: 19167714.
  22. Novakova L., Vlckova H. A review of current trends and advances in modern bio-analytical methods: chromatography and sample preparation. *Anal Chim Acta*. 2009;656(1-2):8–35. PubMed PMID: 19932811.
  23. Lloyd R. Snyder, J.J.K., John W. Dolan, ed. *Introduction to Modern Liquid Chromatography* 3rd ed. 2010, John Wiley & Sons, Inc.
  24. Lough, W.J., I.W. Wainer, and Editors, *High Performance Liquid Chromatography: Fundamental Principles and Practice*. 1996: Blackie. 276 pp.
  25. Snyder, L.R., et al., *Introduction to Modern Liquid Chromatography, Third Edition*. 2010: John Wiley & Sons, Inc. 912 pp.
  26. Rohrs, H.W., *LC/MS: A practical user's guide*, by Marvin C. McMaster, Wiley-Interscience Hoboken, NJ, 07030, USA. J. Am. Soc. Mass Spectrom., 2006. 17(Copyright (C) 2012 American Chemical Society (ACS). All Rights Reserved.): p. 1193.
  27. Buszewski B., Noga S. Hydrophilic interaction liquid chromatography (HILIC)—a powerful separation technique. *Analytical and Bioanalytical Chemistry*. 2011;402(1): 231–247. PubMed PMID: 21879300.
  28. Hsieh Y. Hydrophilic interaction liquid chromatography-tandem mass spectrometry for drug development. *Curr Drug Discov Technol*. 2010;7(3):223–31. PubMed PMID: 20843291.
  29. Hutchinson S.E., et al. Enabling lead discovery for histone lysine demethylases by high-throughput RapidFire mass spectrometry. *J Biomol Screen*. 2012;17(1):39–48. PubMed PMID: 21859681.
  30. Wu X., et al. In vitro ADME profiling using high-throughput rapidfire mass spectrometry: cytochrome p450 inhibition and metabolic stability assays. *J Biomol Screen*. 2012;17(6):761–72. PubMed PMID: 22460176.
  31. Leveridge M.V., et al. Lead discovery for microsomal prostaglandin E synthase using a combination of high-throughput fluorescent-based assays and RapidFire mass spectrometry. *J Biomol Screen*. 2012;17(5):641–50. PubMed PMID: 22337655.

32. Briem S., Pettersson B., Skoglund E. Description and validation of a four-channel staggered LC-MS/MS system for high-throughput in vitro screens. *Anal Chem.* 2005;77(6):1905–10. PubMed PMID: 15762603.
33. Roddy T.P., et al. Mass spectrometric techniques for label-free high-throughput screening in drug discovery. *Anal Chem.* 2007;79(21):8207–13. PubMed PMID: 17902631.
34. Li, S., et al., *Full utilization of a mass spectrometer using on-demand sharing with multiple LC units.* *J. Mass Spectrom.*, 2012. **47**(Copyright (C) 2012 American Chemical Society (ACS). All Rights Reserved.): p. 1074-1082.



# Impedance-Based Technologies

Kim E. Garbison,<sup>1</sup> Beverly A. Heinz,<sup>2</sup> Mary E. Lajiness, Jeffrey R. Weidner,<sup>3,\*</sup> and G. Sitta Sittampalam<sup>4,†</sup>

Created: May 1, 2012.

## Abstract

Activation of endogenous receptors (GPCR, tyrosine kinase and nuclear receptors) results in changes in the cytoskeleton and related morphological changes in cells. Changes in electrical impedance associated with these morphological changes in the presence of agonists and antagonists of these receptors can be used to evaluate hits from HTS assays. In this chapter, the basics of impedance assays and the use of two instruments available for these applications are discussed. Examples of GPCR activation and a sample protocol are also provided for the benefit of beginners and experienced investigators.

## Introduction

***Note: The content of the Assay Guidance Manual will be updated quarterly with contributions and new chapters to ensure the manual stays relevant to the current technologies and best practices used in the rapidly changing field of drug discovery and development. This chapter is currently in the process of being updated to reflect the current state of the field with respect to impedance-based technologies. Therefore, it is possible that the most up-to-date information may not yet be included, but will be added in forthcoming chapter updates.***

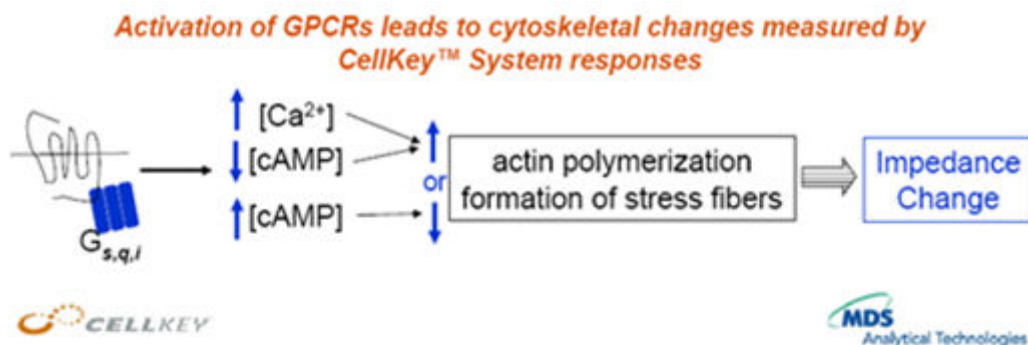
Impedance-based assay systems for cell-based assays measure changes in electrical impedance relative to a voltage applied to a cell monolayer. They allow measurement of activation of all receptor types including G-protein coupled receptors, tyrosine kinase receptors, and some nuclear receptors. Upon activation of cell surface receptors, signal transduction pathways are initiated causing cellular morphological changes. Production of intracellular effectors results in changes in the cellular cytoskeleton which are reflected as changes in the flow of current across, and between the cells in the monolayer. This change in the flow of current around and through cells is represented in a single well by an overall change in the impedance within that well (Figure 1). Impedance-based assay technologies are universal and require no labels or special reagents. They may be used with either transfected or endogenous receptors and for primary cells.

---

<sup>1</sup> Eli Lilly & Company, Indianapolis, IN. <sup>2</sup> Eli Lilly & Company, Indianapolis, IN. <sup>3</sup> AbbVie, Chicago, IL; Email: jeffrey.weidner@abbvie.com. <sup>4</sup> National Institutes of Health, Rockville, MD; Email: gurusingham.sittampalam@nih.gov.

\* Editor

† Editor



**CellKey™ System**  
(MDS Analytical Technologies)



**RT-CES®**  
(Acea Biosciences)

**Figure 1:** Two example impedance-based assay platforms are the RT-CES® from Acea Biosciences and the CellKey™ System from MDS Analytical Technologies.

## Overview of ACEA Biosciences RT-CES®

Cells are seeded into the ACEA RT-C ES® 96-well plate which contains electrodes in the bottom of each well. After monitoring cell impedance through an equilibration period, the plate is removed from the instrument and compound additions are made, either manually or with external liquid handling instrumentation. The plate is returned to the incubator and the connection with the instrument is re-established. Monitoring of impedance continues. Responses are reported as “Cell Index”, a parameter derived from impedance measurements.

### Features:

- System is set up in an incubator, so cells may be continuously monitored over long periods (eg. for growth curves and proliferation assays).



- With optional RT-CIM<sup>®</sup> module, cell invasion and migration assays may be performed

## Overview of CellKey™ System

The CellKey™ System is based on a label-free technology called Cellular Dielectric Spectroscopy (CDS), which is capable of measuring complex impedance changes in cell monolayers. Impedance ( $Z$ ) is related to the ratio of voltage to current ( $Z=V/I$ ) as described by Ohm's law. Cells are seeded onto a CellKey™ microplate that contains electrodes at the bottom of each well. The CellKey™ instrument applies voltage across the electrodes producing electrical currents that flow around and between cells (extracellular current,  $i_{ec}$ ) and through cells (transcellular current, etc) (Figure 2A).

The CellKey™ System measures changes in impedance that occur in each well upon stimulation of cell surface receptors. Contributors to the impedance as measured in each well are changes in cell adherence to substrate, changes in cell shape and volume, and changes in cell-cell interactions. These dynamic cellular changes affect the flow of extracellular and transcellular current and hence the magnitude and characteristics of the impedance measured. In practice, the extracellular current is what contributes most of the signal.

Changes in impedance are captured in real time and are quantified. In addition, the unique response profiles produced after receptor activation are indicative of the G-protein coupling type (Figure 2B). Applications of this technology include receptor panning, signal pathway identification and deconvolution, hit identification, enhanced selectivity screening, and pharmacological profiling for potency and efficacy.

### Features:

- Built in liquid handling allows continuous monitoring of responses from the moment of compound addition.
- May be integrated with lab automation.
- Both adherent and suspension cells may be used as well as primary cells.
- Assays may be run at either 37°C or room temperature.
- Response profiles have been correlated to G-protein coupling status.
- Small sample 96-well plates are available with 1/20 the well surface area as the standard 96-well plate, allowing a 75% or greater reduction in cells required as well as savings on test compounds.
- Easy to use software for data analysis

## Sample Protocol for CellKey™ (MDS Analytical Technologies)

Also see CellKey™ Assay Development Guide provided by MDS Analytical Technologies and the CellKey™ Operator's Manual.

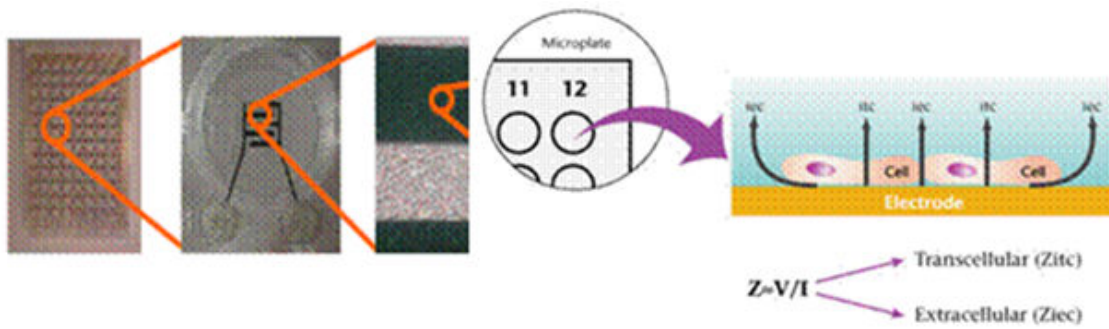


**Figure 2A:** CellKey™ Standard 96W microplate (left), and individual assay well with close-up view of interdigitated electrodes (center left), and live cells plated on and between the electrode fingers (center right) and diagram highlighting flow of extracellular (iec) and transcellular (itc) current (right).

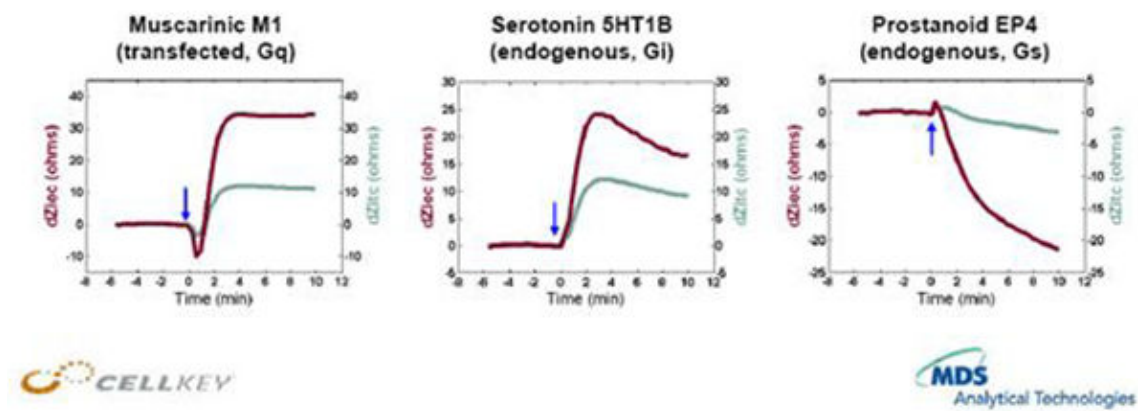


**Figure 2B:** Typical CellKey™ Response Profiles for  $G_q$ ,  $G_i$  and  $G_s$  coupled GPCR

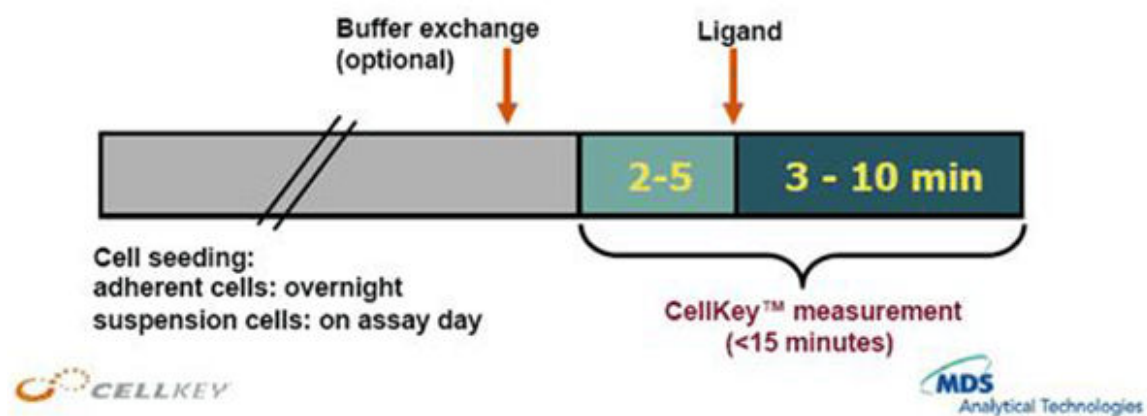


**Figure 3:** CellKey™ System Assay

1. Assay Buffer: Hank's Balanced Salt Solution (HBSS) with  $\text{Ca}^{2+}$  and  $\text{Mg}^{2+}$ , 20 mM HEPES, 0.1% BSA. If BSA is included, it should be fatty acid-free (Sigma #A0281 or #A6003) to avoid activation of endogenous fatty acid receptors on cells. (Other buffers such as Tyrodes, PBS, or culture media may also be used.)
2. Harvest, count, and resuspend cells to yield the appropriate density determined during assay optimization. Cells should be just confluent at the time of assay. Seed cell plate with 150  $\mu\text{l}$ /well.
  - Adherent cells are usually plated the day before the assay in culture medium and incubated at 37°C, 5%  $\text{CO}_2$  overnight. The CellKey™ 96-well microplates may be treated with surface coatings such as collagen or poly-d-lysine to improve adherence if desired.
  - Suspension cells are harvested, washed three times in assay buffer, counted and resuspended to the appropriate concentration in assay buffer. 135  $\mu\text{l}$  of cell suspension is dispensed into each well. Cells are allowed to settle for a minimum of 30 minutes at room temperature before assay.
3. Prepare 10X agonist and antagonist compounds in assay buffer in 96-well plates.
4. Load cell plate, pipet tips, compound plate, and reservoir with assay buffer into the CellKey™ System.
5. Default protocols are available for fluid exchange and stimulation/data acquisition, depending on whether cells are adherent or suspension, or if agonist or antagonist responses are to be measured. These protocols may be edited or used as written. These protocols control the fluidic parameters (tip height, volumes, speed, etc) as well as assay temperature.
6. Stimulation and data acquisition may be performed at either 37°C or room temperature.
7. Fluid exchange is performed on adherent cells plated in culture media. It may be done using the CellKey™ System or off-line with other liquid handling instrumentation. It consists of aspiration of culture media, washing the wells 3 times with assay buffer, and leaving 135  $\mu\text{l}$  of assay buffer in the wells. There is no need to perform fluid exchange on suspension cells.
8. Generally, cells are equilibrated for 20 minutes after fluid exchange. If antagonists are to be added, they are pipetted by the CellKey™ System immediately after fluid exchange so pre-incubation can proceed during the equilibration period. 15  $\mu\text{l}$  of 10X antagonist is added to 135  $\mu\text{l}$  well volume (Figure 3).
9. The agonist stimulation protocol is initiated after equilibration. Generally 15  $\mu\text{l}$  of 10X agonist is added to 135  $\mu\text{l}$  in the plate. If an antagonist has been added previously, well volume = 150  $\mu\text{l}$ , and 16.5  $\mu\text{l}$  of 10X agonist is added.
10. For data collection, default settings in the CellKey™ System software are provided for most adherent cells (for example HEK293 and CHO). Details are found in the Operator's Manual. Response time is usually 5-15 minutes following a 2 minute baseline data collection. Quantifying responses is typically done by calculation of the maximum change from baseline.
11. In addition to quantifying the response, qualitative MOA information may be obtained by examination of kinetic response profiles.

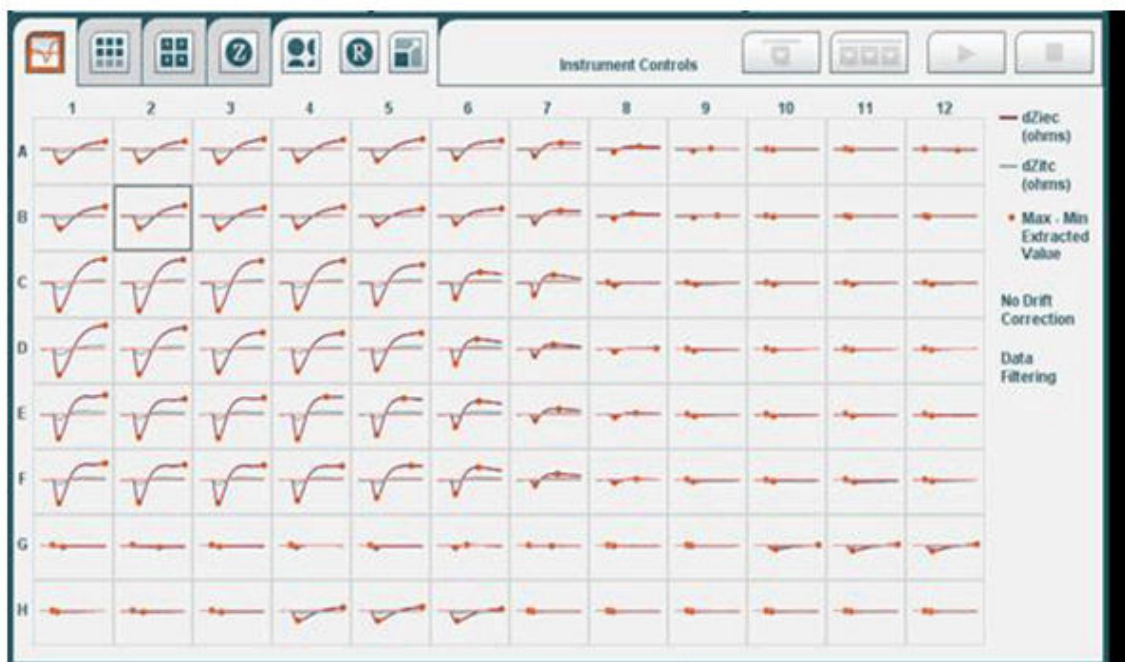


Figure 4A: Kinetic profiles from 96-well plate

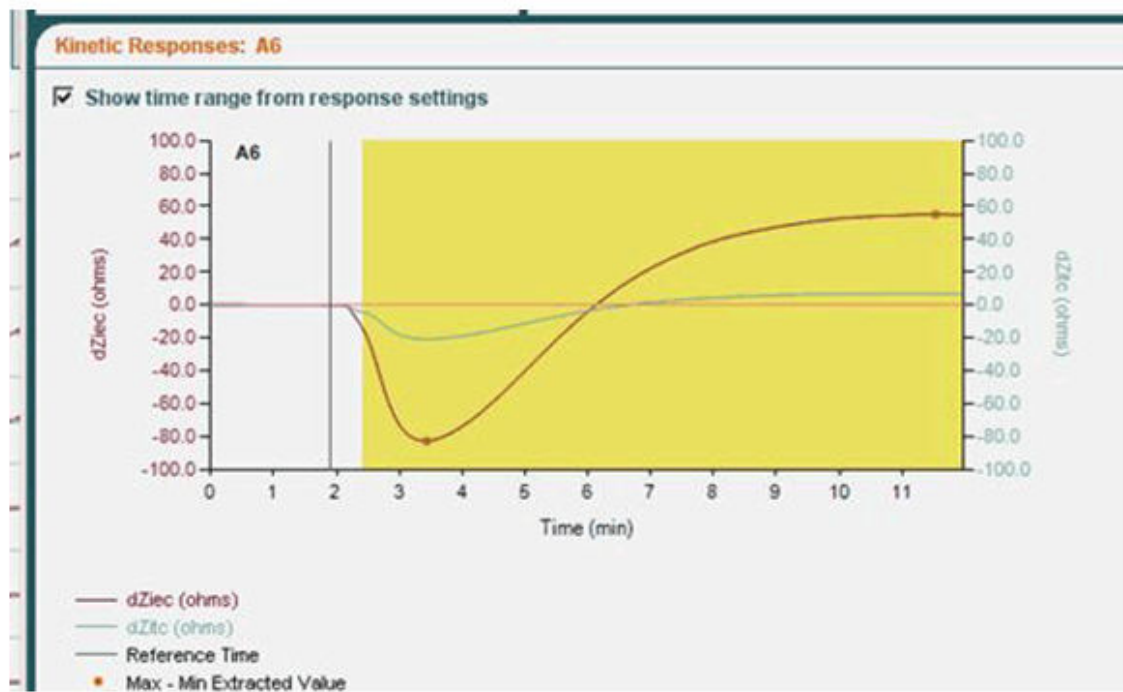


Figure 4B. Kinetic Profile from individual well

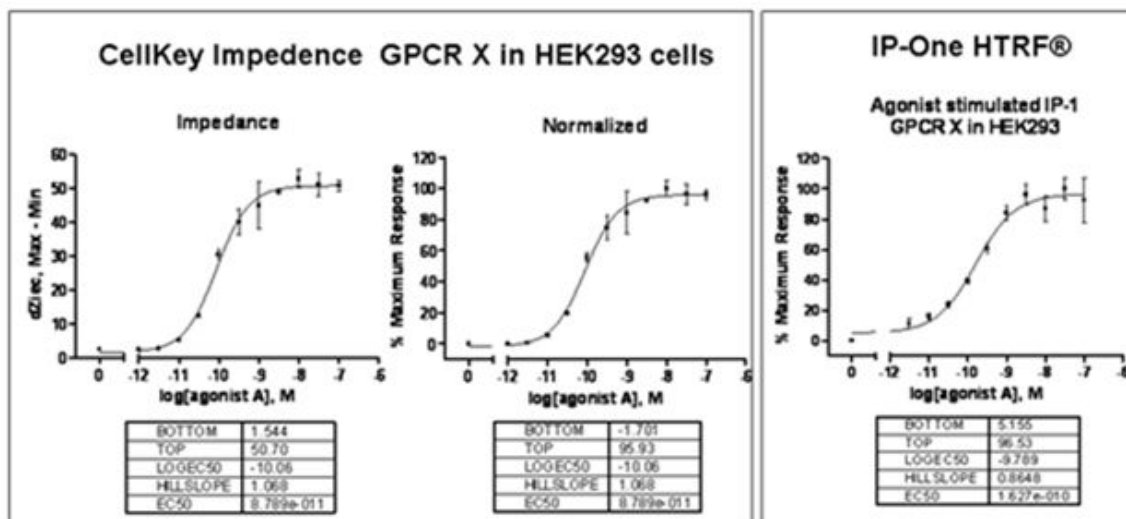


Figure 5. Example: Agonist concentration response curve EC50 for agonist stimulated increase in impedance for a Gq coupled GPCR correlates with the EC50 for IP-1 accumulation using IP-One HTRF®.

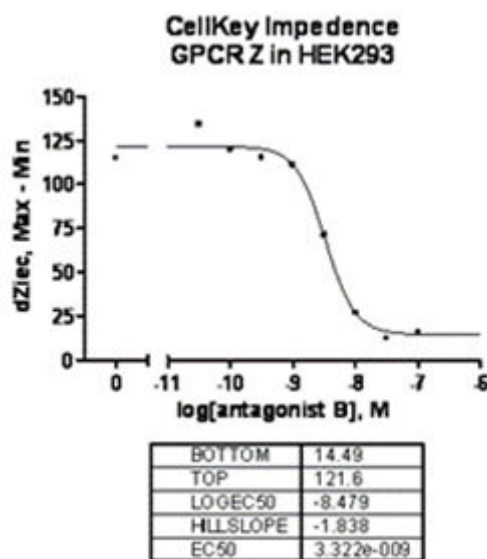


Figure 6. Example: Antagonist concentration response curve

## CellKey™ System Results and Data Analysis

1. Kinetic responses for a selected individual well or all wells are displayed on the screen. dZiec (extracellular current) responses are quantified by the instrument software (Figure 4A and 4B) by either, subtraction of the minimum impedance reading from the maximum impedance reading, the maximum impedance reading

from baseline, or the impedance reading at a specified point in time during the stimulation period. Data is exported to Excel and saved.

2. Maximal – minimal dZiec responses can be plotted vs compound concentrations to generate concentration response curves and calculate EC<sub>50</sub> / IC<sub>50</sub> (Figures 5 and 6). (Please refer to [Data Standards for Results Management](#).)

## Helpful Hints for Performing CellKey™ Assays

- Allowing cell plates to rest for at least 15 minutes before placing in the incubator for overnight incubation allows cells to settle evenly to the bottom of the well and improves variability.
- Evaporation control: Media evaporation during overnight incubation can lead to “edge effects” due to effects on cell growth. Use of MicroClime™ Environmental Lids (Labcyte Inc. #LLS-0300) or BREATHseal™ (Greiner Bio-One #676051) is recommended on cell plates to reduce evaporation.
- Changes in buffer components such as DMSO, BSA and cations, can lead to responses in cells reflected by changes in impedance. Buffer constituents should be consistent between the cells in the microplate and compounds added. If the final DMSO concentration will be higher than 0.1%, it is necessary to include the same concentration of DMSO in the equilibration buffer.
- In order to avoid changes in compound concentration due to evaporation before or during incubation in the instrument, a pre-scored plate seal such as the EZ Pierce Plate Sealing films (Sigma) should be used on the compound plates.
- Make sure compound plate is warmed to at least room temperature before running the assay to avoid temperature differences between cell plate and compounds.
- For characterization of receptor-mediated response profiles, best results are obtained at 28°C rather than 37°C. This may be due to slower kinetics at the lower temperature.
- CellKey™ Small Sample 96-well plates are available that have the footprint of a 96-well plate but the well area of a 1536-well plate. This allows a reduction of at least 75% in cells required, and also reduces volume of compound needed. CellKey™ System Technical Note 1 details special considerations when using these plates.
- CellKey™ System microplates may be coated with collagen (Sigma C9791) or poly-d-lysine (Sigma P6407) or any other coating material of interest. If using poly-d-lysine, be sure to rinse plates before plating cells as it is toxic to the cells when free in solution. Use the following procedure for coating plates:
  1. Pipet 50 µl/well of 50 mg/ml poly-d-lysine (in sterile water).
  2. Incubate plate at room temperature for 1 hour.
  3. Aspirate contents and pipet in 100 µl sterile water to wash wells.

Aspirate water out and immediately plate cells. (Do not allow to dry as crystals may form causing the electrode on the bottom of the wells to lift.)

## Additional References

- Atienza JM, et al. Dynamic and label-free cell-based assays using the real-time cell electronic sensing system. *Assay and Drug Development Technologies*. 2006;4(5):597–607. PubMed PMID: 17115930.
- Cooper MA. Non-optical screening platforms: the wave in label-free screening? *Drug Discovery Today*. 2006;11(23-24):1068–1074. PubMed PMID: 17129825.
- McGuinness R. Impedance-based cellular assay technologies: recent advances, future promise. *Current Opinion in Pharmacology*. 2007;7:535–540. PubMed PMID: 17900985.
- Peters MF, et al. Evaluation of Cellular Dielectric Spectroscopy, a whole-cell, label-free technology for drug discovery on Gi-coupled GPCRs. *Journal of Biomolecular Screening*. 2007;12(3):312–319. PubMed PMID: 17307886.
- Yu, et al. Real-time monitoring of morphological changes in living cells by electronic cell sensor arrays: an approach to study G protein-coupled receptors. *Analytical Chemistry*. 2006;78(1):35–43. PubMed PMID: 16383308.
- Leung G, et al. Cellular Dielectric Spectroscopy: A Label-Free Technology for Drug Discovery. *JALA*. 2005;10:258–269.
- CellKey™ System Assay Development Guide, MDS Analytical Technologies. 1021420 Rev B.

## Acknowledgements

Contributing author to this chapter: John Proctor, Ph.D. - Application Scientist MDS Analytical Technologies





# Instrumentation

Marcie Glicksman, PhD, James McGee, PhD, and G. Sitta Sittampalam, PhD



# Basics of Assay Equipment and Instrumentation for High Throughput Screening

Eric Jones,<sup>1</sup> Sam Michael,<sup>2</sup> and G. Sitta Sittampalam<sup>3</sup>

Created: May 1, 2012; Updated: April 2, 2016.

## Abstract

This chapter contains a synopsis of general and specialized instrumentation used in screening and lead optimization laboratories. The instrument type is described along with the general principles of operation to familiarize readers considering equipping drug discovery laboratories, principally directed to new investigators. The descriptions are introductory and detailed information on installation and applications should be obtained from instrument vendors and experienced drug discovery scientists and engineers.

## Introduction

Instruments employed in quantitative biology laboratories can be broadly categorized into microplates, microplate readers, microplate handling equipment, liquid handling equipment and other miscellaneous instruments such as safety equipment, centrifuges, incubators, electronic balances, microscopes, pH meters, spectrophotometers and other bench-top equipment routinely used in high throughput screening (HTS) assay development laboratories. It is absolutely important to familiarize yourself with the equipment and its proper use.

## Common Equipment in HTS Labs

1. **Microplates**
2. **Microplate Readers**
3. **Liquid Handling Equipment**
4. **Microplate Handling Systems**
5. **Misc. Benchtop Equipment**
6. **Hoods, Incubators & Freezers**

## Microplates

The microplate is the standard format of miniaturization and automation for bioassays (Biochemical and cell-based assays) associated with drug discovery. Within each

---

<sup>1</sup> National Center for Advancing Translational Sciences, National Institutes of Health. <sup>2</sup> National Center for Advancing Translational Sciences, National Institutes of Health. <sup>3</sup> National Center for Advancing Translational Sciences, National Institutes of Health.

microplate is a 2D array of wells with a limited volume for the experimentation to take place. The most common well densities for screening come in 96, 384 and 1536 wells per plate. Numerous manufacturers make microplates in a wide range of materials specific to equipment and customer needs. The footprint of the microplate and well locations has been standardized by ANSI (American National Standards Institute) and SLAS (Society for Laboratory Automation and Screening).

In HTS laboratories, microplates are generally categorized into “Compound Plates” and “Assay Plates”. Compound plates are for storage of the molecular library to be screened against and durable such the same plate can be used for extended periods and across several screens. Assay plates are where the experimentation takes place, selected based on the assay conditions and only used for the extent of an individual screen.

## Available Plate Configurations

- 24-well (Figure 1)
- 96-well & 96-well half-area (Figure 2)
- 384-well (Figure 3)
- 1536-well (Figure 4)

Most commonly used microplates in HTS applications have 96-wells (12 columns × 8 rows) with 250-300 volume  $\mu\text{L}$  capacity. Recent introductions include 96-well half area, 384- and 1536-well plates using the same outside plate dimensions (or foot print). The 96-well half area and 384-well plates use less reagents (75-100  $\mu\text{L}$  capacity), and a major advantage is the reduced reagent consumption. However, these plates require special care during reagent delivery. The 1536-well plates are used less commonly, and require special liquid delivery equipment.

## Plate Color

Microplates are typically offered in opaque white, opaque black or translucent. Compound plates are typically translucent such that compound volumes and color can be seen. Opaque plates are used to enhance detection technologies. Generally white assay plates are for luminance assays and black assay plates are for fluorescence assays. The bottom material of an opaque plate may be clear to support bottom reads and colorimetric (absorbance) assays.

## Microplate Materials

Microplates are available in numerous materials that have different characteristics and, as such, may be more appropriate for specific applications. The list below provides some examples of microplate materials, their characteristics, and applications for the different plate materials.

- Polystyrene (PS)
  - Typical material for assay plates
  - Low production cost



**Figure 1:** 24 Well Microplate, Source PerkinElmer <http://www.perkinelmer.com>



**Figure 2:** 96 Well Microplate, Source PerkinElmer <http://www.perkinelmer.com>

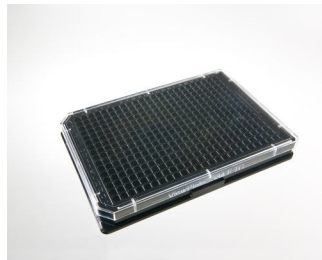


**Figure 3:** 384-Well Microplate, Source PerkinElmer <http://www.perkinelmer.com>



**Figure 4:** 1536-Well Microplate, Source PerkinElmer <http://www.perkinelmer.com>

- Rigid and brittle
- Some natural binding properties to biomolecules
- Cyclic Olefin Copolymer (COC)

- Material for assay and compound plates
- Works well for acoustic dispensing
- Less susceptible to breakage during handling
- DMSO resistant
- Polypropylene (PP)
  - Typical material for compound plates
  - DMSO resistant
  - Thermal Stability
  - More durable than PS

## Well Bottom Shape

The shapes of the wells in microplates vary with the application. Flat bottoms are standard and also required for some detection technologies that use transmission of light through the bottom material. Round bottoms can aid in cell washing and V-bottoms reduce dead volumes when transferring volumes between plates.

## Plate Bottom Material

The bottom material of a plate is often specific to the detection technology. Many assays require reading the plate from underneath therefore the plate bottom material must be optically clear. The thickness and quality of clarity varies with the materials used, often a plastic or glass. Microscopy biased detection systems with higher objectives would require more optical clarity than most microplate readers and therefore consideration in comparing materials to costs should be made.

## Surface Treatments

To aid in assay performance many surface treatment options are available. Polystyrene inherently binds biomolecules with large hydrophobic regions through passive interactions without treatment. Surface treatment options can enhance or minimize this effect. Tissue culture treated surfaces are also common to aid in cell attachment. These either affect the binding of biomolecules to microplate surfaces or improve the attachment of cell lines.

## Microplate Sealing

For the purpose of maintaining specific microplate well conditions there are several options for controlling environmental exposure and contamination including plate lids and plate seals.

## Plate Lids

Plate lids rest on the top of a microplate and allow ease of access for biologists and are supported by many automated systems. The material may be machined metal or plastic with a gasket to seal along the perimeter of the plate. Automated systems may use a

vacuum holding system, specific features built into the lid shape or an empty plate nest to store the lid while the microplate wells are accessed for compound and reagent additions. Assay plate lids may also have a system such as an array of holes for gas exchange.

## Plate Seals

The plate seal is an adhesive film that is pressed onto the top of the microplate. The material for the seal and the adhesive can be selected for the application and chemical compatibility required.

## Automated Plate Sealing Systems

Automated plate sealing systems can be fed by hand or by robot (Figure 5). Most sealers use a thermal process where the microplate is pressed against a hot plate with the sealing material between. The seal adhesive, and to some extent the top of the microplate, melt making a seal. The seal can be permanent or removed by hand. Besides thermal sealing, there are automated plate sealing systems using press on adhesives. Press-on seals do not have the potential damaging effects of a thermal system such as plate deformation or having a significant heat source in close proximity to the microplate well contents. In addition to sealing plates, there is also instrumentation with the ability to robotically remove seals.

## Microplate Readers

The microplate reader is designed to detect and quantify biological, chemical or physical events found within the well of a microplate. There is currently a wide range of detection technologies to suit specific assay requirements many of which can be combined into single multi-purpose instrumentation.

## Single & Multi-Mode Readers

Single and multi-mode microplate readers are used for fluorescence, luminescence, absorbance and other light based detection technologies (Figure 6). These detection technologies share many of the same components differing in the light paths through the sample. Single mode microplate readers can be small and economical tailored to a specific technology. A bit larger and costlier than single mode readers, a multi-mode reader can be very advantageous for a lab combining multiple technologies and detection modes into a single more versatile unit. In many cases the use of a detection reagent is required to quantify a specific event.

## Common Detection Technologies

- Fluorescence Intensity (FI) - A light source of a specific wavelength illuminates fluorescent molecules within a sample causing the simultaneous light emission from the sample (Figure 7). If the emission light is of a different wavelength it can be filtered from the excitation source light and can then be measured using a light detector such as a photomultiplier tube (PMT). Some variations of the technology.



**Figure 5:** PlateLoc™ Thermal Microplate Sealer, Source Agilent Technologies <http://www.chem.agilent.com>



**Figure 6:** Synergy HT Multi-Mode Microplate Reader, Source Biotek <http://www.biotek.com>

- Time-Resolved Fluorescence (TRF) - Uses specific fluorescent molecules called lanthanides that have long light emission times following the removal of an excitation source. The excitation light source is pulsed and the light detector measures the sample after other fluorescent molecule emissions have diminished resulting in lower backgrounds than FI however there is less assay compatibility and higher reagent costs.
- Fluorescence Polarization - Polarization refers to the orientation waves, in this case waves of light. Similar to FI with the addition of polarizing light filters for the excitation light source and sample emission. Fluorescence polarization measures the mobility of fluorescent molecules. Fluorescent molecules attached to larger objects will rotate relatively slowly and will emit more polarized light when excited by a polarized light source. Smaller molecules will rotate more rapidly and the light emission will become depolarized. Useful in measuring molecular binding.



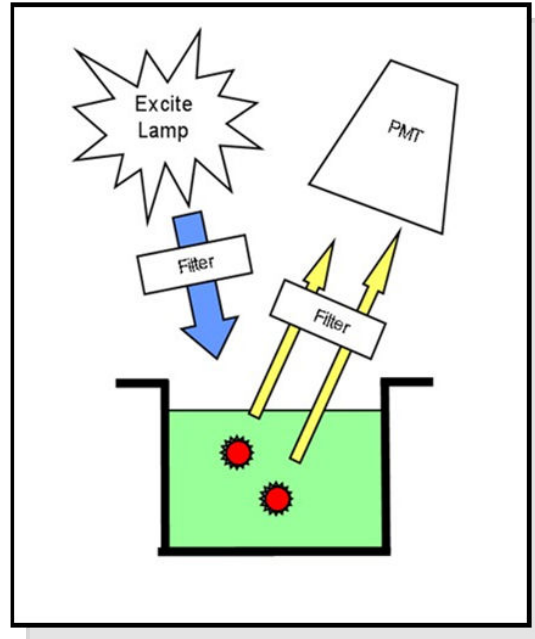


**Figure 7:** Simplified Fluorescence Detection

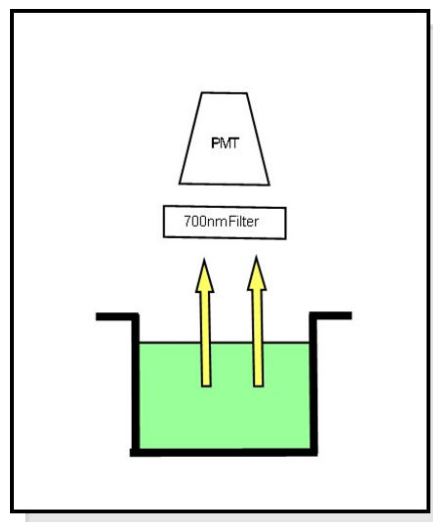


**Figure 8:** Simplified Luminescence Detection

- Luminescence - Measurement of light emission caused by a chemical or biochemical reaction (Figure 8). Luminescence does not require an excitation light source. Used in many luciferase-based assays such as gene expression, cytotoxicity and ATP detection.
- Absorbance - Measuring the amount of light absorbed as it passes through the well. A light source of a selected wavelength illuminates the sample while the detector

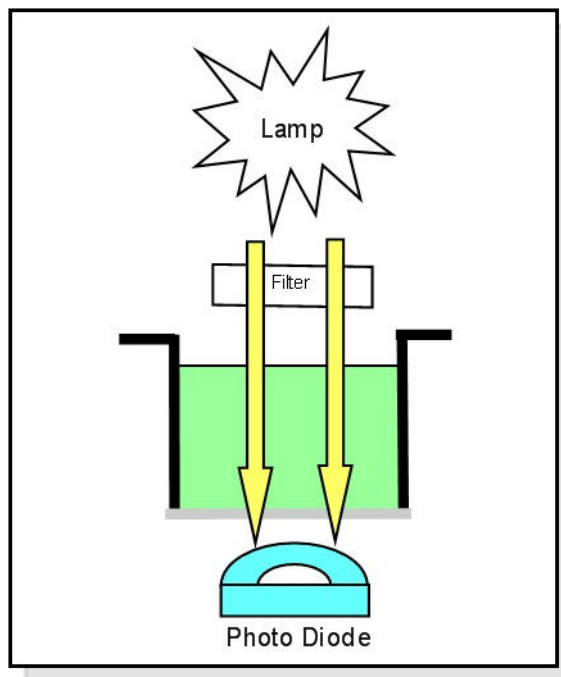


**Figure 9:** Simplified Absorbance Detection

measures the amount of light from the opposing side of the well (Figure 9). The amount of light absorbed can be related to the biology of interest.

- AlphaScreen - Assay technology developed using bead-based chemistry to study bimolecular interactions through homogeneous proximity. Binding of molecules of interest captured on anode and cathode beads leads to an energy transfer from one bead to the other producing a signal when subjected to a specific excitation. Requires the use of a 680nm laser excitation not available on all microplate readers.

## Filters and Monochromators

Filters and monochromators are two competing wavelength selection technologies integral to microplate reader design. Both have their advantages.

- Monochromator - A diffraction grating separates white light into a spectrum such that a slotted material can be positioned isolating the specific wavelength of light. Used for both excitation and emission filtering.
  - Convenient and flexible, does not require an inventory of compatible filters
  - Can perform a spectral scan to characterize unknown fluorophores or spectral shifts
  - Reduction of signal/sensitivity due to the significant loss of light in diffraction gratings
- Filter Based - Optical filters with specific wavelengths and bandwidths are incorporated into the excitation and detection light paths.
  - Less expensive components compared with monochromators

- Minimal signal loss and effective separation of excitation and emission wavelengths
- Several filters are typically maintained within the equipment and/or accessed for changing by the equipment operator.
- Cannot perform spectral scan
- An initial inventory of commonly used filters is required with the likelihood of purchasing more filters over time to accommodate changing needs

Many microplate readers are modular with numerous upgrade paths.

### Common Options to Consider

- Top Read, Bottom Read or Both - Single mode microplate readers often have the detector light path set to read from only the top or bottom of the plate depending on the detection technology while multimode readers are often adapted to read plates from either the top or bottom of the microplate.
  - Bottom reads require a clear bottom microplate such that light can pass through often used for absorbance assays and fluorescence intensity often performs better for cells adherent to the bottom of the plate.
  - Top reads perform best with solid bottom plates and work well for detection of molecules that are suspended in solution.
- Temperature Control & Incubation
- Gas Purging
- Reagent Injection- Some assays kits signals decay rapidly and require near simultaneous detection that can only be achieved by delivering reagents within the microplate reader.

Major manufacturers of microplate readers include:

- PerkinElmer
- Tecan
- Thermo Scientific
- BMG Labtech
- Molecular Devices
- Biotek

### Ultra High Throughput Screening Microplate Reader

The ViewLux™ uHTS Microplate Imager is a commonly used device in high throughput screening with some unique features of note (Figure 10). The ViewLux™ operates on similar light based detection technologies as other microplate readers however, while most readers provide excitation light and detection on a well to well basis, the ViewLux™ excites the entire microplate at once and using a highly sensitive CCD camera to capture an image of the emission signal. The image is rapidly processed to correct for any parallax error and to provide a numerical representation for each individual well. Though many microplate readers are more sensitive and considerably less



**Figure 10:** ViewLux™, Source PerkinElmer <http://www.perkinelmer.com>

costly the time to process an entire microplate on the ViewLux can be reduced from minutes to seconds. Due to its size and cost, the ViewLux™ is typically reserved for assay development and automated screening of a high volume of compounds (manufactured by PerkinElmer).

## High Content Imagers

High Content Screening (HCS) an extension of HTS utilizing much of the same processes and equipment for screening except that the microplate read portion of the assay is performed using an automated microscope or high content imager. Much more than a standard microscope, a high content imager incorporates an automated platform for plate handling and image processing software to quantify the data collected under specified parameters. Using one or more fluorescent dyes different excitation light sources can be applied and images saved of the emission. A separate image showing each fluorescent emission is taken in rapid succession and then overlaid onto each other resulting in a high resolution image of the results. High content imagers are able to collect data other microplate readers cannot such as cell morphology or spatially localized proteins.

Excitation light is provided using a lamp, lasers or light emitting diodes (LED). LEDs are currently the optimal choice due to their long life span and stable output. Emission light is collected from the bottom of the plate through microscope objectives that can be changed to different magnifications and the image is captured using a digital camera. Some high content imagers can be equipped with a confocal microscope system. Considerably more

complex and expensive, a confocal system can provide further depth resolution and improved contrast by rejecting light from out of focus sources. A confocal system is particularly useful in imaging small or 3D cellular systems/structures and samples with strong background fluorescence.

Manufactures include:

- GE
- Thermo Scientific
- PerkinElmer
- Molecular Devices
- Yokogawa

## Laser Scanning Cytometers

Laser scanning cytometers in comparison to other microplate readers can be classified as medium content imaging. Excitation is by laser across the surface of a microplate, as a molecule excites and fluoresces it is detected by photo multiplier tube. The technology is effective at detecting cells, colonies and model organisms but not subcellular features or processes. Has large depth of focus allowing differentiation between low and high concentration of signals.

Manufactures include:

- TTP Labtech
- Molecular Devices
- Hamamatsu

## Label Free Detection

Label free detection refers to the quantification of biological, chemical or physical events without the use of detection reagents. Detection reagents can be of considerable cost and though they are not used for label free detection the money saved is more than offset by the need of specialized plates. There are currently two methods of label-free detection on the market, monitoring the change in impedance and detecting shifts of the refractive index from the bottom of the plate.

Impedance-based label-free readers use microplates with integrated electrodes molded to bottom of the wells. A voltage is applied to each well and electrical currents flow around, between and through cells. The measurement of impedance or resistances to electrical flow is recorded during the duration of the event to be monitored. The microplate and electrical connections are often routed through and access port of an incubator to maintain environmental conditions while monitoring over long periods. Changes in cell adherence, shape, volume and interactions ultimately affect the recorded impedance logged in real time.

Using a specialized microplate changes near the bottom surface of the well are detected by monitoring the reflected wavelength. A refractive waveguide biosensor grating is

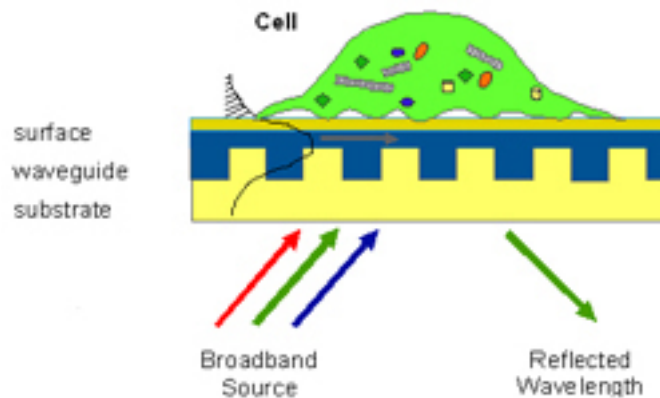


**Figure 11:** Epic Label Free Detection System, Source Corning [http://www.corning.com/lifesciences/epic/en/products/epic\\_system.aspx](http://www.corning.com/lifesciences/epic/en/products/epic_system.aspx)

imbedded into the bottom surface of the microplate. As a broadband light source illuminates the bottom of the well a reflected wavelength is detected indicating the refractive index near the well bottom. After a cell binding event or intracellular protein movement a shift in the refractive index occurs and is then detected by the change in the reflected wavelength (Figure 11).

Manufactures include:

- Corning
- PerkinElmer
- Molecular Devices
- SRU Biosystems

## Spectrophotometry

The electromagnetic spectrum stretches from radio waves to gamma rays (Figure 12).

### Spectrometric Techniques

- Absorption
- Emission
- Scattering
- Ultraviolet and Visible Absorption Spectroscopy
- Dual-beam uv-vis spectrophotometer
- Fluorescence Spectroscopy

## Electromagnetic Spectrum

Spectroscopy is the use of the absorption, emission, or scattering of electromagnetic radiation by atoms or molecules (or atomic or molecular ions) to qualitatively or quantitatively study the atoms or molecules, or to study physical processes. The

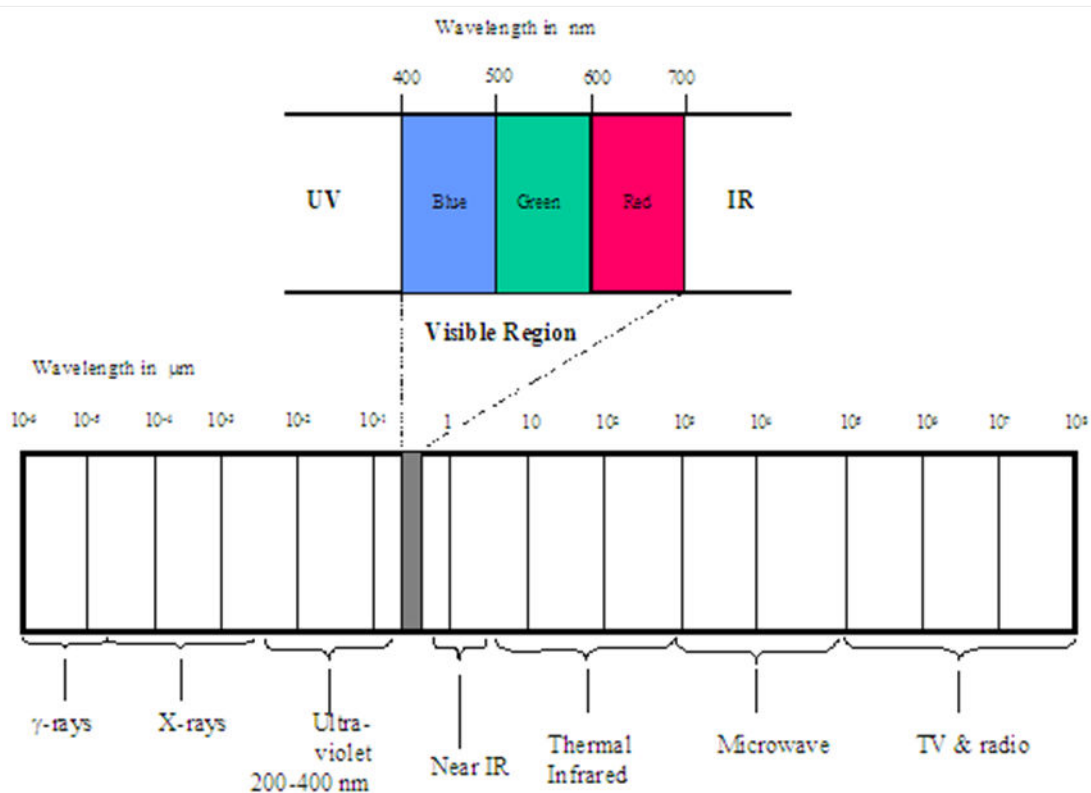
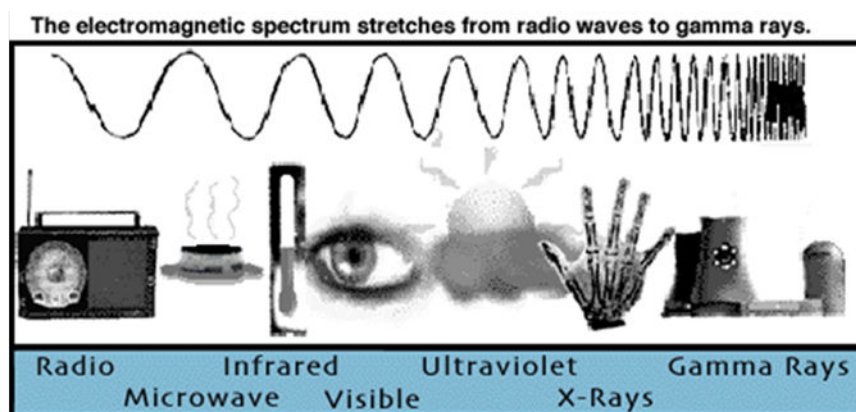
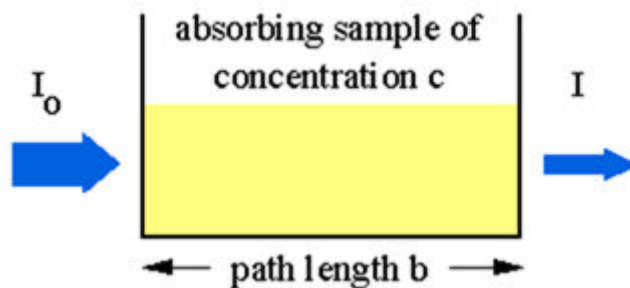


Figure 12: Schematic depictions of the electromagnetic spectrum.

interaction of radiation with matter can cause redirection of the radiation and/or transitions between the energy levels of the atoms or molecules. A transition from a lower level to a higher level with transfer of energy from the radiation field to the atom or molecule is called **absorption**. A transition from a higher level to a lower level is called **emission** if energy is transferred to the radiation field or non-radiative decay if no radiation is emitted. Redirection of light due to its interaction with matter is called



**Figure 13:** Schematic of Beer-Lambert law

**scattering**, and may or may not occur with transfer of energy, i.e., the scattered radiation has a slightly different or the same wavelength.

## Absorption

When atoms or molecules absorb light, the incoming energy excites a quantized structure to a higher energy level. The type of excitation depends on the wavelength of the light. Electrons are promoted to higher orbitals by ultraviolet or visible light, vibrations are excited by infrared light, and microwaves excite rotations. An absorption spectrum is the absorption of light as a function of wavelength. The spectrum of an atom or molecule depends on its energy level structure, and absorption spectra are useful for identification of compounds. Measuring the concentration of an absorbing species in a sample is accomplished by applying the *Beer-Lambert Law*.

The Beer-Lambert law (or Beer's law) is the linear relationship between absorbance and concentration of an absorbing species. The general *Beer-Lambert law* is usually written as:

$$A = a(\lambda) \cdot b \cdot c$$

where  $A$  is the measured absorbance,  $a(\lambda)$  is a wavelength-dependent absorptivity coefficient,  $b$  is the path length, and  $c$  is the analyte concentration. When working in concentration units of molarity, the *Beer-Lambert law* is written as:

$$A = \epsilon \cdot b \cdot c$$

where  $\epsilon$  is the wavelength-dependent molar absorptivity coefficient with units of  $M^{-1} \text{ cm}^{-1}$ . Experimental measurements are usually made in terms of transmittance ( $T$ ), which is defined as  $T = I / I_0$ , where  $I$  is the light intensity after it passes through the sample and  $I_0$  is the initial light intensity (Figure 13). The relation between  $A$  and  $T$  is:

$$A = -\log T = -\log(I/I_0).$$

The linearity of the Beer-Lambert law is limited by chemical and instrumental factors. Causes of nonlinearity include:



- Deviations in absorptivity coefficients at high concentrations ( $>0.01$  M) due to electrostatic interactions between molecules in close proximity.
- Scattering of light due to particulates in the sample.
- Fluorescence or phosphorescence of the sample.
- Changes in refractive index at high analyte concentration.
- Shifts in chemical equilibria as a function of concentration.
- Non-monochromatic radiation. (Deviations can be minimized by using a relatively flat part of the absorption spectrum such as the maximum of an absorption band).
- Stray light leaking into the sample compartment.

## Emission

Atoms or molecules that are excited to high energy levels can decay to lower levels by emitting radiation (emission or luminescence). For atoms excited by a high-temperature energy source this light emission is commonly called atomic or optical emission (see atomic-emission spectroscopy), and for atoms excited with light it is called atomic fluorescence (see atomic-fluorescence spectroscopy). For molecules it is called molecular fluorescence if the transition is between states of the same spin and phosphorescence if the transition occurs between states of different spin. The emission intensity of an emitting substance is linearly proportional to analyte concentration at low concentrations, and is useful for quantifying emitting species (Figure 14).

## Scattering

When electromagnetic radiation passes through matter, most of the radiation continues in its original direction but a small fraction is scattered in other directions. Light scattered at the same wavelength as the incoming light is called Rayleigh scattering. Light that is scattered in transparent solids due to vibrations (phonons) is called Brillouin scattering. Brillouin scattering is typically shifted by  $0.1$  to  $1\text{ cm}^{-1}$  from the incident light. Light that is scattered due to vibrations in molecules or optical phonons in solids is called Raman scattering. Raman scattered light is shifted by as much as  $4000\text{ cm}^{-1}$  from the incident light.

## Ultraviolet and Visible Absorption Spectroscopy

UV-vis spectroscopy is the measurement of the wavelength and intensity of absorption of near-ultraviolet and visible light by a sample. Ultraviolet and visible light are energetic enough to promote outer electrons to higher energy levels. UV-vis spectroscopy is usually applied to molecules and inorganic ions or complexes in solution. The UV-vis spectra have broad features that are of limited use for sample identification but are very useful for quantitative measurements. Measuring the absorbance at some wavelength and applying the Beer-Lambert Law can determine the concentration of an analyte in solution. The light source is usually a hydrogen or deuterium lamp for UV measurements and a tungsten lamp for visible measurements. The wavelengths of these continuous light sources are selected with a wavelength separator such as a prism or grating

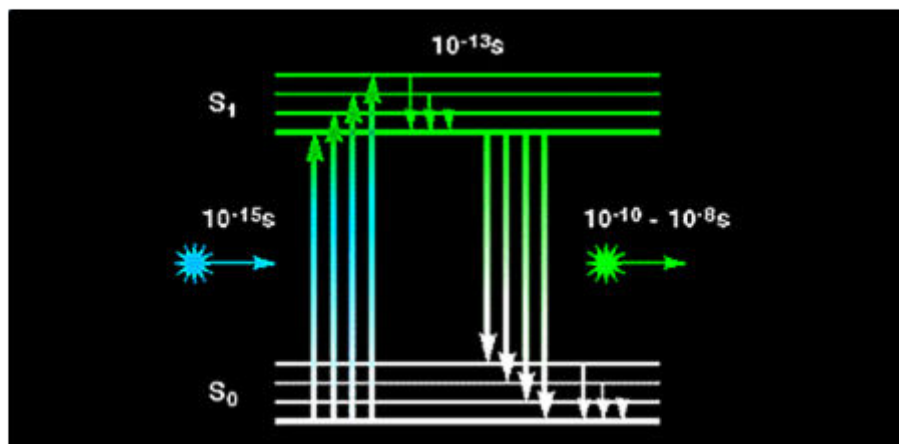


Figure 14: Jablonski Diagram

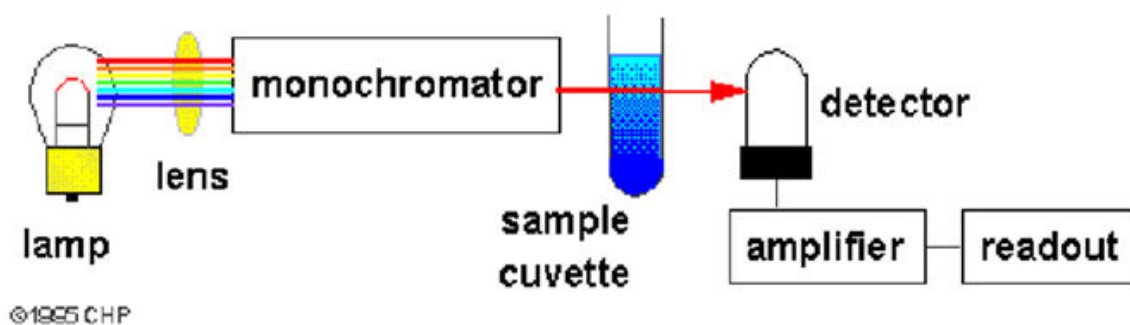
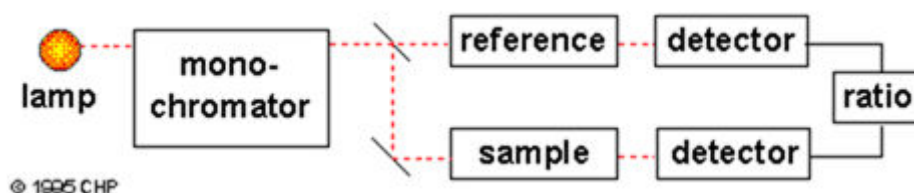


Figure 15: Schematic of a single beam UV-vis spectrophotometer

monochromator. Spectra are obtained by scanning the wavelength separator and quantitative measurements can be made from a spectrum or at a single wavelength (Figure 15).

### Dual-beam UV-VIS spectrophotometer

In single-beam UV-vis absorption spectroscopy, obtaining a spectrum requires manually measuring the transmittance (see the Beer-Lambert Law) of the sample and solvent at each wavelength. The double-beam design greatly simplifies this process by measuring the transmittance of the sample and solvent simultaneously (Figure 16). The detection electronics can then manipulate the measurements to give the absorbance. Table 1 provides specifications for a typical spectrophotometer.



**Figure 16:** Schematic of a dual-beam UV-VIS spectrophotometer.

**Table 1:** Specifications of a typical spectrophotometer:

|                            |   |
|----------------------------|---|
| Wavelength range:          | 200~800 nm                                      |
| Spectral Band width:       | 2 nm  |
| Wavelength Accuracy:       | 1 nm  |
| Stray Light:               | Less than 0.002%(300 nm, 630 nm)                |
| Photometric Range:         | Absorbance-1~3 Abs                              |
| Transmittance:             | 0~200%T   |
| Photometric Accuracy:      | 0.5%T   |
| Photometric Repeatability: | 0.3%T   |
| Light Source:              | Tungsten Lamp, Deuterium Lamp                   |
| Monochromator:             | Diffraction grating single monochromator system |
| Cell:                      | Max. 4 turrets                                  |
| Dimension:                 | 500mm(L) x 380 mm(W) x 230 mm(H)                |
| Power Requirements:        | 110/220V, 3A, 50/60 Amps.                       |

## Fluorescence Spectroscopy

Light emission from atoms or molecules can be used to quantify the amount of the emitting substance in a sample. The relationship between fluorescence intensity and analyte concentration is:

$$F = k \cdot QE \cdot P_0 \cdot (1 - 10^{-\epsilon \cdot b \cdot c})$$

where F is the measured fluorescence intensity, k is a geometric instrumental factor, QE is the quantum efficiency (photons emitted/photons absorbed),  $P_0$  is the radiant power of the excitation source,  $\epsilon$  is the wavelength-dependent molar absorptivity coefficient, b is the path length, and c is the analyte concentration (, b, and c are the same as used in the Beer-Lambert law). Expanding the above equation in a series and dropping higher terms gives:

$$F = k \cdot QE \cdot P_0 \cdot (2.303 \cdot \epsilon \cdot b \cdot c)$$

This relationship is valid at low concentrations ( $<10^{-5}$  M) and shows that fluorescence intensity is linearly proportional to analyte concentration. Determining unknown concentrations from the amount of fluorescence emitted from a sample requires

calibration of a fluorimeter with a standard (to determine  $k$  and  $QE$ ) or by using a working curve.

Many of the limitations of the Beer-Lambert law also affect quantitative fluorimetry. Fluorescence measurements are also susceptible to inner-filter effects. These effects include excessive absorption of the excitation radiation (pre-filter effect) and self-absorption of atomic resonance fluorescence (post-filter effect).

## pH Meters

The pH meter measures the pH of a solution using an ion-selective electrode (ISE) that responds to the  $H^+$  concentration of the solution. The pH electrode produces a voltage that is proportional to the concentration of the  $H^+$  concentration, and making measurements with a pH meter is therefore a form of potentiometry. The pH electrode is attached to control electronics that convert the voltage to a pH reading and display it on a meter. A pH meter consists of a  $H^+$ -selective membrane (ISE), an internal reference electrode, an external reference electrode, and a meter with control electronics and display (Figure 17). Commercial pH electrodes usually combine all electrodes into one unit that are then attached to the pH meter.

An ion-selective electrode (ISE) produces a potential that is proportional to the concentration of an analyte. Making measurements with an ISE is therefore a form of potentiometry. The most common ISE is the pH electrode, which contains a thin glass membrane that responds to the  $H^+$  concentration in a solution. The potential difference across an ion-sensitive membrane is

$$E = K - (2.303RT/nF)\log(a)$$

where  $K$  is a constant to account for all other potentials,  $R$  is the gas constant,  $T$  is temperature,  $n$  is the number of electrons transferred,  $F$  is Faraday's constant, and  $a$  is the activity of the analyte ion. A plot of measured potential versus  $\log(a)$  will therefore give a straight line. ISEs are susceptible to several interferences. Samples and standards are therefore diluted 1:1 with total ionic strength adjuster and buffer (TISAB). The TISAB consists of 1 M NaCl to adjust the ionic strength, acetic acid/acetate buffer to control pH, and a metal complexing agent. ISEs consist of the ion-selective membrane, an internal reference electrode, an external reference electrode, and a voltmeter. A typical meter is shown in the document on the pH meter. Commercial ISEs often combine the two electrodes into one unit that are then attached to a pH meter.

**NOTE:** All pH meters should be calibrated daily, and preferably, before each use. It is important to know that the ISE potential can drift due to drying of the LaF3 membrane and the evaporation of internal reference solutions.

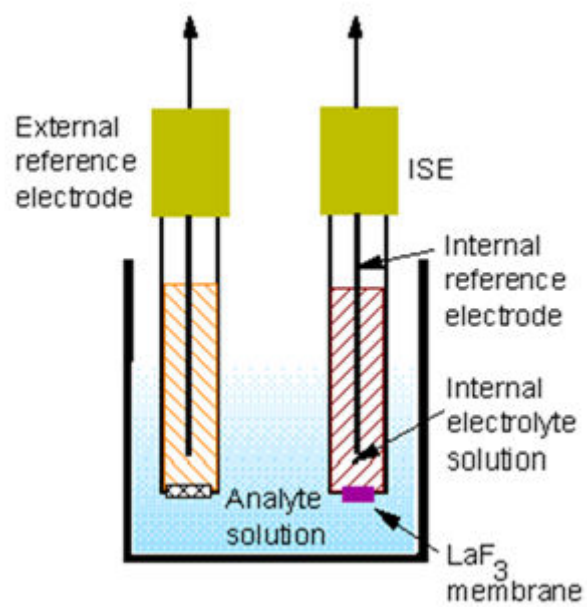


**Figure 17:** Schematic of an ISE measurement.



**Figure 18:** Representative image of a balance.

## Electronic Balances

Analytical balances are accurate and precise instruments to measure weights (Figure 18). They require a draft-free location on a solid bench that is free of vibrations. Modern balances have built-in calibration weights to maintain accuracy. Older balances should be calibrated periodically with a standard weight. A few weighing tips follow:

- Do not bump or place objects on the bench after zeroing the balance.
- Weigh powders on weighing paper or in weighing dishes. Handle objects with tongs, gloves, or weighing paper to prevent fingerprints.
- Let hot objects cool before weighing.
- Weigh hygroscopic materials rapidly since they will absorb water during weighing.
- When making repetitive weighings always use the same procedure.
- Ensure that the balances are calibrated routinely.
- It is absolutely important to keep the balance pans and the area around precision balances clean. Clean up after each use for safety and convenience of others.
- In dry cold weather, weighing fine powders can be a problem due to static charges that develop on particles. Devices are now available for neutralizing electric charges of the material while it is still in the container. Use of these devices is highly recommended for accurate weighings.

## Microscopes

- Microscopes
- Microscope Parts
- Objectives
- Condensers
- Iris Diaphragm
- Eyepiece
- 2.5 Field Limiting Aperture

A microscope is not designed to magnify small objects. For example, you can find in any hobby or toy store a \$49.95 instrument capable of magnifying objects to 1200 times. And that includes a zoom lens and light source. Most student and research microscopes magnify no more than 1000 times with costs starting at around \$1500.00, with research microscopes going into the tens of thousands of dollars. Is the academic community being taken for a ride? No. The \$49.95 microscope only gives you an image that is a soft blur at 1000x magnification, whereas the research microscope's image is crystal sharp. This is called resolution, the ability to see fine details. Once you can resolve fine details then you can magnify them. Every optical system has a finite resolution; if you magnify objects beyond the resolution the result will be empty magnification. **So, the actual purpose of a microscope is to see small things clearly.**

A desirable attribute of a microscope is depth of field, which is the range of depth that a specimen is in acceptable focus. A microscope that has a thin depth of field will have to be

continuously focused up and down to view a thick specimen. A third feature that a microscope has is its mechanism for contrast formation. Contrast is the ratio between the dark and the light. Typically, most microscopes use absorption contrast; that is, the specimen is subjected to stains in order to be seen. This is called bright field microscopy. There are other types of microscope that use more exotic means to generate contrast, such as phase contrast, dark field, and differential interference contrast. The fourth desirable feature is a strong illumination source. The higher a microscope magnifies the more light will be required. Also, there will be more optical trade off leeway when more light is present. The illumination source should also be at a wavelength (color) that will facilitate the interaction with the specimen. All microscopes fall into either of two categories based on how the specimen is illuminated. In the typical compound microscope the light passes through the specimen and is collected by the image forming optics. This is called diascopic illumination. Dissecting (stereo) microscopes generally use episcopic illumination for use with opaque specimen. The light is reflected onto the specimen and then into the objective lens. The four attributes of an optical system may have trade-offs with each other. For example, resolution and brightness is antagonistic towards contrast and depth of field. One cannot have maximum resolution and maximum contrast simultaneously. Theoretically speaking, if you had an infinite resolving system there would be no contrast to discern the image. It is up to the microscopist to decide which attribute is needed to view a particular specimen. All of which are controlled by the iris diaphragm.

## Microscope Parts

### Objectives

The objective lens is the lens that is closest to the object or specimen (Figure 19). It is essentially the information-gathering lens of an optical system. Therefore, it is regarded as the most important lens of the microscope. There are many different types of objective lenses. The most common and inexpensive is the achromat. This lens is usually found on student microscopes. It is corrected for spherical aberration for only green light.

Chromatic aberration is corrected in only two colors. The apochromat objective is far superior and generally very expensive. Chromatic aberration is corrected for all three colors and it is spherically corrected for two colors. These objectives quite often will require a special compensating eyepiece. Semiapochromat objectives have correction in between the apochromat and achromat. Flat field or plano objectives compensate for curvature of field and are excellent for histology work. The flat field objectives can be optically constructed to be also an achromat, semiapochromat or apochromat. In the latter case the lens would be called a plano apochromat which is generally regarded as the finest lens available. The price of a single plano apochromat will run into the many thousands of dollars. Figure 20 provides a comparison of the resolution using different types of objectives.

Each objective has information critical for the maximum resolution possible written on the side of the barrel. Generally the magnification is printed in the largest text with the manufacturer type designation. The second value is the numerical aperture. Beneath that,



**Figure 19:** Image of objective lens

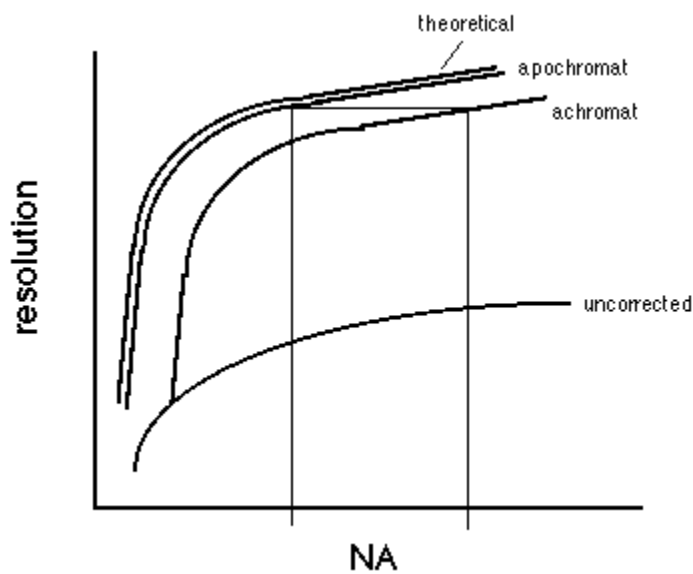


**Figure 20:** Comparison of the resolution using different types of objectives.

in a smaller font the tube length and the cover glass thickness is given. Any special information will also be added such as if it is an oil lens, infinity etc. The tube length usually 160 refers to the distance between the objective and the eyepiece in millimeters. It must be maintained if the aberrations are to be corrected. You can recognize a superior microscope if when adjusting the interpupillary distance you can see the eyepiece extend which happens to maintain the proper tube length. The cover slip thickness usually around 0.17mm is also critical. This corresponds to a cover glass of No. 1.5. The more sophisticated objectives even have a cover glass compensation control that you dial in the thickness of the cover glass.

## Condensers

The sub-stage condenser of a microscope is designed to focus the light onto the specimen. In addition it must also fill the numerical aperture of the objective (Figure 21). Like objective lenses there are several different types. The most common being the Abbe



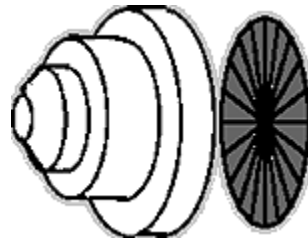


**Figure 21:** Example of a substage microscope condenser.

condenser. This type is not corrected for optical aberrations. The achromatic condenser is corrected for both spherical and chromatic aberrations. Both types of condenser have their numerical aperture printed on the side. This needs to be of equal or greater value than that of the objective N.A., otherwise, the full resolution of the objective will not be utilized. Most substage condensers can use immersion oil like that of the objectives to achieve their full N. A. This is not recommended unless you are doing very demanding photomicroscopy work.

### Iris Diaphragm

The iris diaphragm is the most important single control on the microscope (Figure 22). There is a misconception that it is used to regulate the amount of light. The light intensity control is the sole means to adjust the brightness. The iris diaphragm is the resolution versus contrast control. It does this by varying the size of the numerical aperture of the objective lens. Usually, lenses such as those found on cameras have the iris diaphragm built in the objective lens. In a microscope objective the iris diaphragm would have to be very small, which would be difficult to manufacture. So the optical engineers put the iris diaphragm at the optical equivalent of being in the objective lens, in the condenser assembly. This is one of the reasons why the condenser lens has to be set at the correct distance to the objective. In addition the iris diaphragm controls the depth of field.

### Eyepiece

The eyepiece is basically a projection lens system (Figure 23). There are three types generally used in light microscopy. The most common is the Huygenian type. This eyepiece is used with low and medium magnification and is designed to project the image into a human eye. Some of these eyepieces will have a long eyepoint, the spot where your eye should be, so you can focus with your glasses on. If you suffer from astigmatism you should wear your glasses while using the microscope. If you are near or far sighted then you can adjust the eyepiece for your personal correction using the diopter corrector and leave your glasses off. The second type of eyepiece is the compensating eyepiece and is generally used with apochromate or flat field objectives. These provide superior image quality. The third type is the photo eyepiece. These are designed to project a corrected image onto film plane in a camera. These are generally considered the finest of eyepieces. All eyepieces will have a relative magnification written on the side of the barrel. They

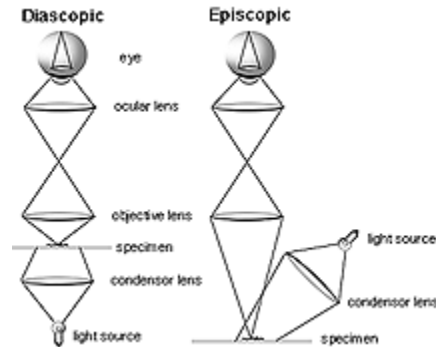


**Figure 22:** Schematic of iris diaphragm control.

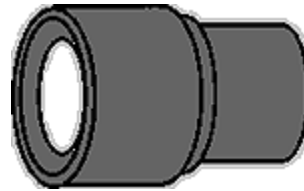


**Figure 23:** Example of a microscope eyepiece.

range in magnification from 2.5X to 15X with the lower magnifications used with the photo eyepiece.

### Field Limiting Aperture

The field-limiting aperture is used to determine the correct position and center of the condenser lens. It is used in conjunction with the condenser centering knobs to place the illumination in the center. It also helps in reducing the amount of optical flare.

## Liquid Handling Devices

The high throughput screening lab has several liquid handling applications and device technologies are chosen to best suit the specific task.

### Hand-held Pipette

The pipette transfers precise volumes of liquids through movement of a piston and the displacement of air (Figure 24). Pipettes have specified volume ranges and the user selects the increment. The usable range of volume is 100nl to 1ml. Pipette tips are disposable and available in numerous shapes, sizes and treatments. Accurate manual pipetting is a lab skill acquired with practice. Common variations of pipettes are as follows.

- Single-channel
- Multi-channel – Typically 8 or 12 simultaneous channels
- Electronic



**Figure 24:** Example pipettes

- Repeaters – Allows for multiple dispenses following a single aspiration

## Automated Pipetting Devices

Automated pipetting platforms are scalable to the application and level of automation desired (Figure 25). Microplates are positioned in specific locations on the instrument deck or into a plate stacker. The number of available positions can range from 2 - >16 positions and further plate capacity can be added when using stackers. The head, consisting of the liquid handling apparatus, may be outfitted with a single tip, single column of tips or 96/384 2D array of tips for accommodating whole plate transfers referred to as plate stamping. Tips used may be disposable or reusable with washing applications.

Creating methods on these devices can be very involved and uses elements of programming logic such as variable parameters, database access and conditional looping. Once a method is optimized it is then very reproducible. These devices are often used as the main integrating platform for compact systems with options to include plate transferring capabilities and auxiliary equipment.

Major manufacturers of automated pipetting systems include:

- Beckman Coulter
- Hamilton
- Perkin Elmer
- Cybio
- Agilent
- Tecan

## Solenoid Valve Based Dispensers

Using a pressurized bottle of fluid, a fast acting valve and robotic positioning, these systems can deliver precise volumes (>0.1  $\mu\text{l}$ ) into the microplate well at very high rates of speed. Assuming a constant air pressure in the bottle, the volume to be dispensed is controlled by adjusting valve timing.



**Figure 25:** 96 Channel Automated Pipette, Source Tecan <http://www.tecan.com>

Most systems offer the ability to dispense multiple fluids simultaneously using separate valves and fluid paths. Dispensing is controlled by a spreadsheet correlating the specific valve and volume to the microplate well. Common fluids for this equipment include cell media, buffers and detection reagents. Dispensing of viscous fluids or cells prone to clumping can be problematic and interfere with valve operation. Dispensing DMSO is possible though may cause rapid valve degeneration.

Most components of the equipment fluid path are reused and therefore cleaning operations are a must. In most cases a combination of 70% ethanol, cleaning detergents and high purity water are sufficient.

These systems are used heavily in high throughput screening due to their dispense accuracy and speed of operation. Dispensing a nominal volume across an entire microplate can take 1 to 3 minutes.

Manufacturers of Solenoid Valve Based Dispensers:

- Beckman Coulter
- Thermo Fisher Scientific

## Peristaltic Pump Based Dispensers

Peristaltic pumps are found in numerous applications in the laboratory and medical fields (Figure 25). Peristaltic pumps move fluids using positive displacement by pinching flexible tubing with rotating sets of rollers. The pumping liquid is maintained within the tubing and no external contact is made between pump components and fluid. This lack of contact allows for a large range of chemical capabilities based solely on the tubing material. Tubing is intended to be removed or replaced. Direction and speed are easily varied.

For microplate dispensing the peristaltic pump has some specific features. The fluid path is part of a cassette assembly consisting of tubing, tips, tension adjustment screws and plastic housing. The cassettes are consumable with lifespans varied by manufacturer and operating volume ranges. The equipment has a plate positioning system, motor controlled rotating rollers and the user interface.

The main disadvantage of the peristaltic pump microplate dispenser is the cost of consumable cassettes. Each cassette costs \$500-\$1000 and is considered accurate for dispensing a few hundred plates. The lifespan may be increased by proper cleaning, storage and recalibration techniques. The advantage is that cassettes are accurate out of the box.

Manufacturers of Peristaltic Pump Based Dispensers:

- Thermo Fisher Scientific
- Biotek

## Pintools

The pintool is used for fixed low volume liquid transfers between microplates. For HTS this equipment is used for the transfer of compounds from the library into the assay plate. The pins are stainless steel with precision machined features to set the volume of liquid transfer (Figure 26). As the pin enters the source, pin surfaces make liquid contact. When the pin is withdrawn, small amounts of liquid adhere to the surfaces until the pin is submerged again and surface tension of the adherent liquid can be broken. Following any liquid transfer, pintool pins must be washed and dried prior to their next use. Washing steps typically include solvent baths, blotting and air drying.

The pintool head is the fixture to hold the pins the proper positions (Figure 27). The head is made to match the diameter of the pins used and plate density, typically 96, 384 or 1536 pins to be used with 96-, 384-, or 1536-well plates, respectively. Though fixtures can be made for hand held operations, higher density plates require higher levels of precision for accurate transfers thus necessitating the need for robotic control. Most liquid handling robotic systems can be adapted to use pintools, while dedicated systems are also available.

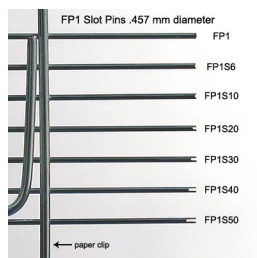


**Figure 26:** Example Slotted Pin Selection, Source V&P Scientific <http://www.vp-scientific.com>



**Figure 27:** Example Pintool Head, Source V&P Scientific <http://www.vp-scientific.com>

The pintool is advantageous for HTS due to its high speed and direct correlation of compound plate well position to assay plate well position. The principal provider of pintool pins and fixtures is V&P Scientific.

## Acoustic Dispensers

Acoustic dispensers use focused bursts of sound energy to propel 1-10 nanoliter (nL) sized droplets between source and destination microplates without direct liquid contact (Figure 28). Droplet dispenses are very rapid and the final volume transfer is achieved using increments of droplet size. Contamination is minimized since there is no contact carryover between operations. Contrasting the pintool, the acoustic dispensers is exceedingly flexible using a user-created dispense map that specifically defines source well, destination well and volume for each transfer.

The acoustic dispenser brings flexibility into the screening workflow. In addition to 1-1 plate stamping complex liquid handling operations can easily be achieved at low volumes

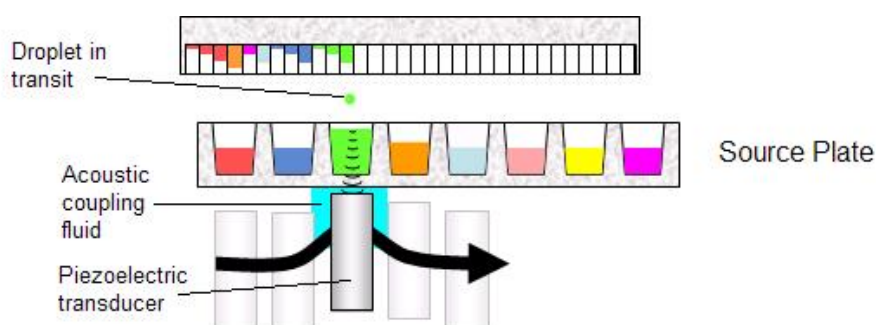


**Figure 28:** Simplified Acoustic Dispense, Source [http://en.wikipedia.org/wiki/File:Acoustic\\_transfer1.jpg](http://en.wikipedia.org/wiki/File:Acoustic_transfer1.jpg)

such as dispensing into dry wells, serial dilutions, matrix/poly-pharmaceutical screening and cherry picking. Dispensing compound into dry plates then storing for later use is known as making “Assay Ready” plates. An “Assay Ready” plate can be created in advance of a screen as resources are available and on a separate system. If screening multiple compound concentrations, the number of concentrations multiplies the number of compound plates needed. Using an acoustic dispenser, different concentrations can be achieved from a single stock greatly reducing the number of compound plates needed. Follow up assays often require the creation compound plates with compounds of specific interest at different concentrations. The creation of a single follow up plate can take a considerable amount of resources. Using the acoustic dispenser screening of only the specific follow up compounds is possible without the need of new plates and potentially done on the fly.

The advantages of acoustic dispensing have some contrasting limitations. The cost for equipment varies with model and options but is typically >\$300k per unit. The speed of operation is significantly slower when compared to the pintool requiring multiple units to maintain throughput. A 384-well transfer can take about 4min while 1536 wells can take > 10min. The compound plate must have 384 or 1536 wells and be acoustically compatible, meaning that the well shape and material must effectively transfer sound energy. Many

microplate venders are now offering microplates for this specific purpose. The droplet destination can be any labware that fits into an SLAS/SBS microplate footprint though it must be inverted for operation. For 384 and 1536 plates, liquid tension maintains fluids in the well during inversion though other labware may have to be initially dry.

Manufacturers of Acoustic Dispensers:

- Labcyte
- EDC Biosystems

The quality of assay data depends critically on the ability of individual scientists to use the liquid delivery devices appropriately. It is highly recommended that you make yourself familiar with all pipetting equipment in your lab. Also note that these liquid dispensers will have to be calibrated on a regular basis. For automated liquid handlers, special procedures recommended by the manufacturers are employed. These procedures usually involve serial dilutions of dyes from stock solutions and the determination of the accuracy and precision of the dilutions.

## Suggested Websites and Resources

1. Analytical Instrumentation Review. ( Available at: <http://www.uam.es/docencia/quimcursos/Scimedia/chem-ed/analytic/ac-meths.htm>).
2. Corning Microplate Selection Guide. ( Available at: [http://catalog2.corning.com/lifesciences/media/pdf/productselectionguide\\_microplates11\\_02\\_cls\\_mp\\_014.pdf](http://catalog2.corning.com/lifesciences/media/pdf/productselectionguide_microplates11_02_cls_mp_014.pdf))
3. Corning Life Sciences | Corning® Epic® Technology | Corning Epic System ( Available at: [http://www.corning.com/lifesciences/epic/en/products/epic\\_system.aspx](http://www.corning.com/lifesciences/epic/en/products/epic_system.aspx))
4. Agilent PlateLoc Thermal Microplate Sealer Consumables Selection Guide. ( Available at: [http://www.chem.agilent.com/Library/selectionguide/Public/5990-3659en\\_lo%20CMS.pdf](http://www.chem.agilent.com/Library/selectionguide/Public/5990-3659en_lo%20CMS.pdf))
5. Everything You Need To Know About Pin Tools But Were Afraid To Ask. ( Available at: [http://www.vp-scientific.com/pin\\_tools.htm](http://www.vp-scientific.com/pin_tools.htm))

## Suggested Readings (alphabetical order)

1. Buchser W, Collins M, Garyantes T, Guha R, Haney S, Lemmon V, Li Z, Trask OJ., Assay Development Guidelines for Image-Based High Content Screening, High Content Analysis and High Content Imaging. In: Sittampalam GS, Coussens NP, Nelson H, Arkin M, Auld D, Austin C, Bejcek B, Glicksman M, Inglese J, Iversen PW, Li Z, McGee J, McManus O, Minor L, Napper A, Peltier JM, Riss T, Trask OJ Jr., Weidner J, editors. Assay Guidance Manual [Internet]. Bethesda (MD): Eli Lilly & Company and the National Center for Advancing Translational Sciences; 2004-. 2012 Oct 1 [updated 2014 Sep22].
2. Eglen RM, Reisine T, Roby P, Rouleau N, Illy C, Bossé R, et al. The use of AlphaScreen technology in HTS: current status. *Current chemical genomics*. 2008;1(1) PubMed PMID: 20161822.



3. Garbison KE, Heinz BA, Lajiness ME, Weidner JR, Sittampalam GS., Impedance-Based Technologies. In: Sittampalam GS, Coussens NP, Nelson H, Arkin M, Auld D, Austin C, Bejcek B, Glicksman M, Inglese J, Iversen PW, Li Z, McGee J, McManus O, Minor L, Napper A, Peltier JM, Riss T, Trask OJ Jr., Weidner J, editors. Assay Guidance Manual [Internet]. Bethesda (MD): Eli Lilly & Company and the National Center for Advancing Translational Sciences; 2004-. 2012 May 1.
4. Millar DP. Time-resolved fluorescence spectroscopy. *Curr Opin Struct Biol.* 1996;6(5): 637–42. PubMed PMID: 8913686.
5. Phillips D. Luminescence lifetimes in biological systems. *Analyst.* 1994;119(4):543–50. PubMed PMID: 8024118.



# Calculations and Instrumentation used for Radioligand Binding Assays

Steven D. Kahl, G. Sitta Sittampalam,<sup>\*</sup> and Jeffrey Weidner<sup>†</sup>

Created: May 1, 2012; Updated: October 1, 2012.

## Abstract

Radioligand binding assays are a “work horse” in biological laboratories and have been adapted for HTS and lead optimization support in drug discovery. The instrumentation is highly specialized to measure radioactivity of the labels on binding ligands and requires specialized calculation procedures. In this chapter, the author thoroughly and systematically describes the instrumentation and calculation principles used in data analysis. Sample calculations are shown along with definitions of terms and important steps in setting up the instrumentation. This is a very useful chapter for beginners, as well as a refresher for experienced investigators.

## Introduction

The purpose of this chapter is to 1) describe common calculations used in radioligand binding assays and 2) outline steps for setting up and using microplate scintillation counters (Microbeta Trilux and TopCount).

When performing calculations such as those described on the following pages, it is advised to use unit dimension equations. This ensures that values have the appropriate units for the designated purpose. Unit dimension equations are used through this chapter.

## Radioactive Calculations

### Determination of Counting Efficiency

Microplate scintillation counters, used for reading Scintillation Proximity Assay (SPA) and filtration assays, detect flashes of light (photons) that occur when a released radioactive particle interacts with and excites a fluor molecule. Not all of the radioactive particles emitted will be detected as photons by the counting instrument. The output from the scintillation counter is the number of photons detected per unit time, typically expressed in counts per minute (CPM). The ratio between CPM detected by the instrument and actual disintegrations per minute (DPM) of the isotope is termed **efficiency**. The efficiency of counting depends on the geometry of the detector, scintillation properties of the fluor and the energy of the particular isotope. Determination of DPM is important for making conversions to calculate molar

---

<sup>\*</sup> Editor

<sup>†</sup> Editor

concentrations of radioligands, and it is also important if a comparison between different instruments is required. For data that will be normalized (e.g. % Inhibition), CPM can be used as a direct readout from the instrument.

The efficiency for each isotope counting condition should be independently determined for an instrument. Steps to determine average instrument efficiency are shown in the example below for an SPA assay using a [<sup>3</sup>H]-labeled radioligand and YSi SPA beads:

### Example Determination of Efficiency

[<sup>3</sup>H]-labeled SPA Beads can be prepared by incubating [<sup>3</sup>H]-labeled biotin with YSi streptavidin beads and washing them (using centrifugation) to remove any unbound radioactivity. Alternatively, a reaction associated with an assay (e.g. WGA beads, membranes, radioligand) can be used.

1. Remove a 300 µl aliquot of [<sup>3</sup>H]-SPA beads to a 1.5 ml polypropylene tube.
2. Centrifuge the tube for 5 seconds in a microfuge to pellet the [<sup>3</sup>H]-SPA beads.
3. Remove the supernatant. Dispose of it properly, treating it as potential radioactive waste.
4. Add 300 µl of PBS and mix beads. Repeat centrifugation and remove supernatant.
5. Resuspend in a final volume of 300 µl PBS.
6. For a Microbeta, pipette 25 µl of beads into three different wells of a microplate. Add 175 µl of PBS. Allow the beads to settle overnight.
7. Count the microplate and determine the average CPM for the three replicates (example: 52,800 CPM).
8. Add 25 µl of beads to three different scintillation vials containing scintillation cocktail. Count the vials on a liquid scintillation counter, which is capable of returning results in DPM, and determine the average for the three replicates (example: 140,582 DPM).
9. Determine efficiency using the following equation:

$$\text{Efficiency} = \frac{\text{CPM}}{\text{DPM}} = \frac{52,800}{140,582} = 0.38$$

For [<sup>125</sup>I], a gamma counter with a known efficiency can be used for the determination of the total DPM.

Some typical instrument efficiencies for common isotope configurations on a Trilux Microbeta are shown in Table 1.

These are approximate efficiencies for comparison. Actual efficiencies for your instrument should be determined independently. In addition, some counting conditions require special “window settings” that can impact the apparent efficiency. Alterations or repairs to an instrument (e.g. adjustment of photomultiplier tubes (PMT's)) may also require determination of an updated efficiency value.

**Table 1: Typical instrument efficiencies for common isotope configurations on a Trilux Microbeta. These are approximate efficiencies for comparison and actual efficiencies for your instrument should be determined independently.**

| Isotope          | Scintillation Mode | Efficiency |
|------------------|--------------------|------------|
| $^3\text{H}$     | Filtration         | 0.32       |
| $^3\text{H}$     | SPA (PVT)          | 0.23       |
| $^3\text{H}$     | SPA (YSi)          | 0.34       |
| $^{125}\text{I}$ | Filtration         | 0.45       |
| $^{125}\text{I}$ | SPA (PVT)          | 0.38       |
| $^{125}\text{I}$ | SPA (YSi)          | 0.56       |

## Conversion from CPM to DPM

DPM are calculated from the equation shown below, where efficiency is expressed as a decimal percent. Determination of instrument efficiency (Eff) is described above.

$$\text{DPM} = \frac{\text{CPM}}{\text{Efficiency}}$$

### Example:

1000 CPM detected in an assay using Polyvinyltoluene (PVT) SPA beads and  $^3\text{H}$ .

The instrument efficiency was determined to be 22%.

|     |   |                |
|-----|---|----------------|
| DPM | = | CPM/Efficiency |
|     | = | 1000/0.22      |
|     | = | 4545           |

## Specific Activity (SA)

The amount of radioactivity per unit mole for a radioligand is referred to as the **specific activity** (often abbreviated as SA) and is typically given in units of Ci/mmol by the manufacturer. Since raw data from assays using radioactivity are in CPM or DPM, conversion of the specific activity from Ci/mmol to CPM/fmol or DPM/fmol is usually more convenient for further data analysis.

Conversion Factors:  $1 \text{ Ci} = 2.22 \times 10^{12} \text{ DPM}$

$10^{12} \text{ fmol} = 1 \text{ mmol}$

### Equation to convert Ci/mmol to DPM/fmol:

$$\text{DPM/fmol} = [\text{Specific activity (Ci/mmol)}] \times [2.22 \times 10^{12} \text{ DPM/Ci}] \times [\text{mmol}/10^{12} \text{ fmol}] = \text{SA} \times 2.22$$

**Example:** SA = 2000 Ci/mmol

$$\text{DPM/fmol} = \text{SA} \times 2.22 = 2000 \times 2.22 = \underline{4440 \text{ DPM/fmol}}$$

**Equation to Convert Ci/mmol to CPM/fmol:**

$$\begin{aligned} \text{CPM/fmol} &= [\text{SA (Ci/mmol)}] \times [2.22 \times 10^{12} \text{ DPM/Ci}] \times [\text{mmol}/10^{12} \text{ fmol}] \times \text{Efficiency} \\ (\text{CPM/DPM}) &= \text{SA} \times 2.22 \times \text{Eff} \end{aligned}$$

**Example:** Instrument efficiency = 40%, SA = 2000 Ci/mmol

$$\text{CPM/fmol} = \text{SA} \times 2.22 \times \text{Eff} = 2000 \times 2.22 \times 0.4 = \underline{1776 \text{ CPM/fmol}}$$

## Nominal Concentration of a Radioligand

The theoretical or nominal concentration of a radioligand stock solution can be calculated from the stated radioactive concentration (RAC, in  $\mu\text{Ci/ml}$ ) and the specific activity (SA, in Ci/mmol) using the equation shown below:

$$[\text{Radioligand}] = \text{RAC}/\text{SA}$$

**Example:** Radioactive concentration (RAC): 50  $\mu\text{Ci/ml}$

Specific Activity (SA): 2000 Ci/mmol

Conversion factor: 1 Ci =  $10^6$   $\mu\text{Ci}$

$$[\text{Radioligand}] = \text{RAC}/\text{SA} = (50 \mu\text{Ci/ml} \div 2000 \text{ Ci/mmol}) \times 1 \text{ Ci}/10^6 \mu\text{Ci} = 2.5 \times 10^{-8} \text{ mmol/ml}$$

$$= 2.5 \times 10^{-8} \text{ M}$$

$$= \underline{25 \text{ nM}}$$

This is the nominal concentration of the stock on the reference date. To estimate the concentration on any other day, see the **Radioactive Decay** section to determine the fraction remaining and the resulting concentration. See also the **Dilution of Stock** section to prepare a dilution of a stock radioligand.

## Actual Concentration of a Radioligand

When performing radioligand binding assays, a rough estimate for the concentration of radioligand used in the assay can be computed using the information supplied with the material. This is called the theoretical or nominal concentration (shown above). In order to calculate the **actual** concentration of the radioligand used in an assay more accurately, one should count an aliquot of the stock mix and obtain the CPM or DPM for that aliquot, then use the equation below.

**Equation to convert CPM to pM:**

$$\text{pM} = \frac{\text{CPM}/\text{SA (CPM/fmol)}}{\text{Volume (ml)}} \times \frac{0.001 \text{ pmol/fmol}}{0.001 \text{ liter/ml}} = \frac{\text{CPM}/\text{SA}}{\text{Vol}}$$

**Example:** Counted a 50  $\mu\text{l}$  aliquot of a stock mix, which yielded 50,000 CPM; SA = 1776 CPM/fmol (see above for calculation).

$$\text{pM} = \frac{50,000 \text{ CPM}/1776 \text{ CPM/fmol}}{0.05 \text{ ml}} = \underline{\underline{563 \text{ pM}}}$$

If values are in DPM, one should use specific activity (SA) expressed in DPM/fmol. Use appropriate unit conversions to determine the concentration in nM,  $\mu\text{M}$ , etc.

It is best practice to use the **actual** concentration of radioligand determined for each assay in calculations such as  $K_i$ , rather than the theoretical or nominal concentration.

## Radioactive Decay

Radioactive decay is a random event and follows an exponential decay trend. You can calculate the fraction remaining in a radioactive sample if you know the date (reference date) when the specific activity or radioactive concentration was known using the following equation:

$$\text{Fraction Remaining} = e^{(-0.693/t_{1/2}) \cdot \text{time}}$$

where  $t_{1/2}$  is the half-life of the isotope (time it takes for half the isotope to decay), and time is the number of days before or after the known reference date. The term  $(-0.693/t_{1/2})$  is also referred to as the decay rate constant,  $K_{\text{decay}}$ .

**Example:** [ $^{125}\text{I}$ ] radioligand with a known specific activity on 10/1/07.

Half-life for [ $^{125}\text{I}$ ] = 60 days.

Fraction remaining on 10/20/07 (20 days):

$$\text{Fraction Remaining} = e^{(-0.693/60) \cdot 20} = 0.794 \text{ or } 79.4\% \text{ remaining}$$

The fraction remaining following radioactive decay can also be determined from tables. Note that for the activity on a day prior to the stated reference date, the fraction remaining will be greater than 1.

An assumption typically made is that radioactive decay results in unlabeled decay product(s), which no longer bind to the target or receptor of interest. This implies that the specific activity remains constant over time and that the concentration of ligand changes with time. This assumption may not be valid with all radioligands used.

## Half-Life

Table 2 shows half-lives (time for half of the isotope to decay) for common isotopes, along with typical values for specific activity of a single-labeled molecule. One should always consult the manufacturer's information for the exact specific activity of a radioligand.

Note that half lives (even for the same isotope) can vary from one manufacturer to another. In addition, if software is used for tracking of decay of isotope inventories, one must make sure that the half life value used is consistent throughout.

**Table 2: Half-lives for common isotopes and typical values for specific activity of a single-labeled molecule. One should always consult the manufacturer's information for the exact specific activity of a radioligand.**

| Isotope          | Half-life   | Specific Activity |
|------------------|-------------|-------------------|
| <sup>3</sup> H   | 12.43 years | 85.0 Ci/mmol      |
| <sup>125</sup> I | 60 days     | 2000 Ci/mmol      |
| <sup>32</sup> P  | 14.3 days   | 9128 Ci/mmol      |
| <sup>35</sup> S  | 87.4 days   | 1493 Ci/mmol      |
| <sup>14</sup> C  | 5730 years  | 0.064 Ci/mmol     |

## Dilution of Stock

To calculate the amount of a radioligand stock solution required to prepare a specific volume of a dilution, the parameters listed below will be needed. The values listed for each parameter are for use in the example calculations.

Radioactive Concentration (RAC): 50  $\mu$ Ci/ml

Specific Activity (SA): 2000 Ci/mmol

Half-life for isotope: 60 days (I-125)

Reference date: 10/1/07

Date of preparation: 10/20/07

Volume of final diluted mix: 50 ml

Desired concentration of final diluted mix: 0.1 nM

- 1 Determine nominal stock concentration – described above in **Stock Concentration** section:

$$[\text{Radioligand}] = \text{RAC}/\text{SA} = (50 \mu\text{Ci}/\text{ml} \div 2000 \text{ Ci}/\text{mmol}) \times 1 \text{ Ci}/10^6 \mu\text{Ci} = 2.5 \times 10^{-8} \text{ mmol}/\text{ml}$$

$$= 2.5 \times 10^{-8} \text{ M}$$



= 25 nM

2) Determine stock concentration on day of use – described in **Radioactive Decay** section above:

Date of use – Reference Date = 20 days

Fraction Remaining =  $e^{(-0.693/60) \cdot 20} = 0.794$  or 79.4% remaining

Therefore, stock concentration on day of use =  $0.794 \times 25 \text{ nM} = \underline{19.85 \text{ nM}}$

3) Determine amount of stock required:

$C_1V_1 = C_2V_2$  solving for  $V_1$ , yields  $V_1 = C_2V_2/C_1 = (50 \text{ ml} \times 0.1 \text{ nM})/19.85 \text{ nM} = \underline{0.252 \text{ ml}}$

This is the theoretical or nominal concentration. To determine actual concentration, count an aliquot of the diluted mix and calculate as shown in the **Actual Concentration of Radioligand** section above.

## Instrumentation

### Microbeta Trilux

#### General Concepts

A Microbeta Trilux comes with either 6 or 12 detectors. Each detector is comprised of two photomultiplier tubes (PMT's), one on top of the sample and one on the bottom. The PMT's operate using conventional coincidence circuitry, as shown in Figure 1.

Each detector counts only a portion of a 96-well microplate (16 wells per detector on the 6-detector Microbeta model, ~9 wells on the 12-detector model). The area of the plate counted by each detector of a 6- or 12-detector model is shown in Figure 2.

Although the use of multiple detectors can increase throughput, since the performance of PMT's are not identical, a calibration procedure (Normalization) is required. An identical sample is counted by all of the detectors, and a relative efficiency (fractional value) is determined. If an activity (DPM) for the sample is known, this can be inputted into the software, and the detectors are normalized to this activity. This will result in the efficiency factors being lower than if the detectors are normalized against each other. As an example, the typical efficiency relative to activity for [3H] with SPA beads is 0.20 – 0.30. When the detectors are normalized against each other, the relative efficiencies should be 0.9 – 1.0.

#### Modes of Normalization

There are two ways to normalize the Trilux with a single sample in well G11 (for 96 well plate):

1. Relative to the detector with the highest reading (CCPM = CPM)

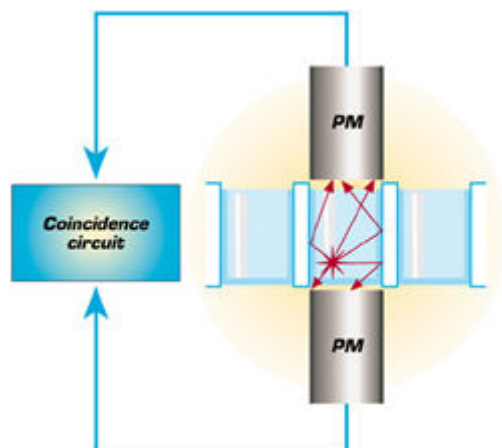
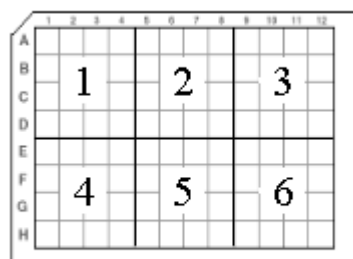
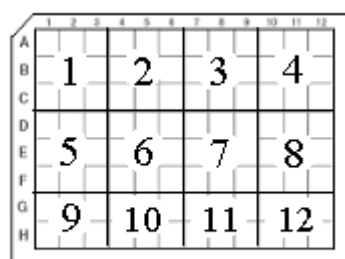


**Figure 1:** Diagram of a Microbeta Detector. Each detector includes two photomultiplier tubes that operate in coincidence counting mode. In this mode, background photons not related to the sample are eliminated because they do not possess the energy required for both PMT's to distinguish it in a discrete amount of time. The lower PMT can be disabled to count opaque-bottomed microplates. (Diagram from Perkin Elmer Life and Analytical Sciences Document 1450-1017-07).



**6-Detector Model**



**12-Detector Model**

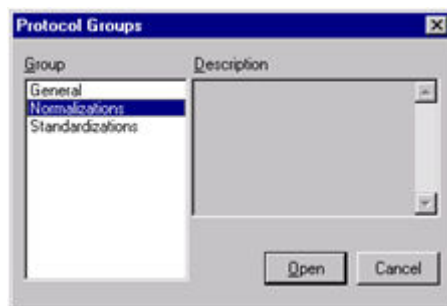
**Figure 2:** The area of the plate counted by each detector of a 6- or 12-detector model of a Microbeta Detector.

2. Relative to the activity inputted in well G11 (CCPM = DPM)

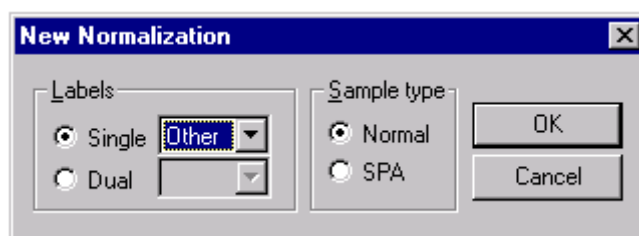
The basic principle for each of these modes is shown at the end of this section. The sample to be used for normalization must be in well G11. Both normalization protocols are set up the same way, with one additional step for mode 2, when results in DPM are desired. There are other features for Standardization (e.g. using quench curves) or Easy DPM, Paralux, etc. that are not discussed in this document.

### Setup of a Normalization Protocol

1. Click on the Protocols button at the top of the Microbeta software toolbar.
2. Select **Normalizations** followed by the **Open** button.



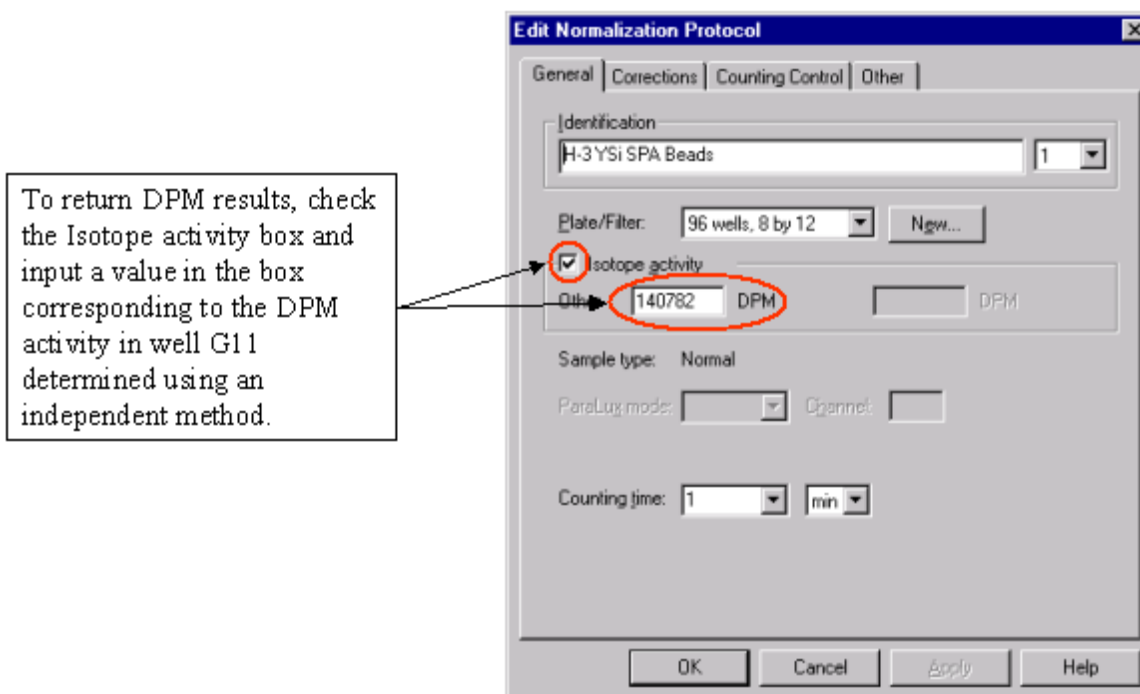
3. Click on the **New** button to create a new normalization protocol.
4. Select the appropriate label from the pull-down menu in the pop-up dialog box and click **OK**. Do not check SPA unless you want to use Paralux counting mode (consult instrument manual).



In many cases, particularly with YSi SPA beads, you should select **Other** and use the manual energy spectrum window settings shown in the table below in Step 6. The default settings were designed for PVT SPA beads.

5. Under the **General** tab, type in a name for the protocol and select a number for the protocol from the pull-down list (only unused, available protocol numbers are listed).

**If it is desired to express results in DPM:** Check the **Isotope activity** box and input a number for the activity (in DPM) that is in well G11. This activity should be determined by counting an identical aliquot in a liquid scintillation counter (for 3H) or a gamma counter (for 125I) that has a known efficiency ( $DPM = CPM/Efficiency$ ). In this example, replicate aliquots of YSi SPA beads were counted in a liquid scintillation counter with an average of 140,782 DPM. An identical aliquot was placed in well G11 of a microplate for normalization. The value 140,782 is entered into the area on the General tab, as shown below.

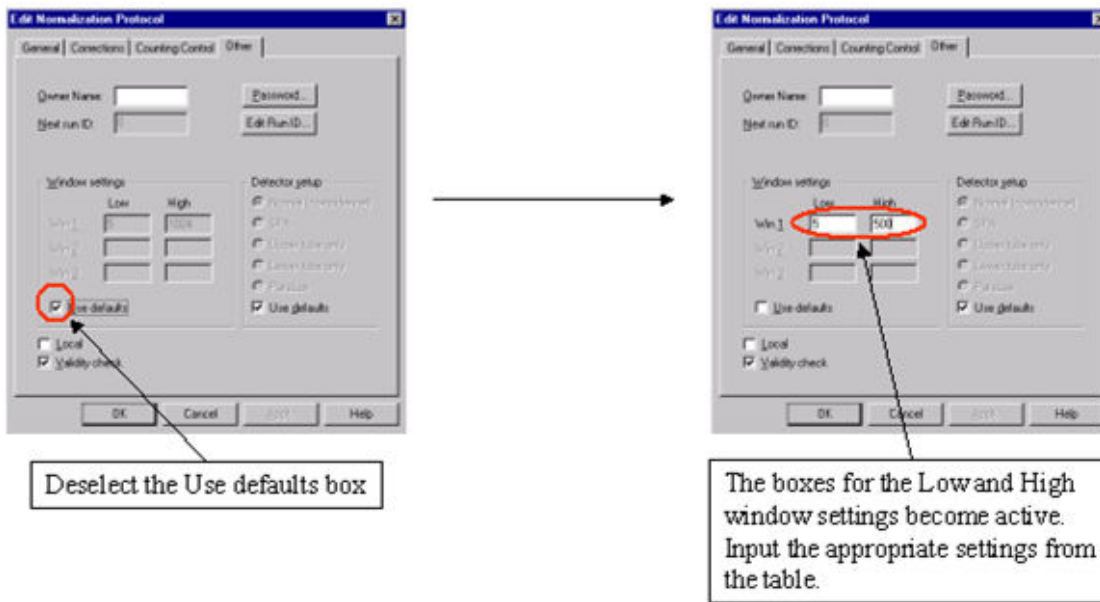


6. If **Other** was selected as the label, the energy spectrum window settings may need to be manually defined. By default it will appear under the Other tab as a window from 5 to 1024, an open energy spectrum window.

Uncheck the box next to **Use defaults**. The window settings for Low and High can now be changed.

Table 3 indicates the suggested settings for several isotopes and types of SPA beads and Cytostar-T plates. The screen capture below shows the **Other** tab, after new window settings have been inputted for tritium YSi SPA beads and the Microbeta (Table from [www.perkinelmer.com](http://www.perkinelmer.com)).

Under the *Other* tab:



7. Click OK to save the normalization protocol.

**Table 3:** suggested settings for several isotopes and types of SPA beads and Cytostar-T plates

| ISOTOPE                               | SPA PVT   |           | SPA Yttrium silicate |           | Cytostar-T microplates |           |
|---------------------------------------|-----------|-----------|----------------------|-----------|------------------------|-----------|
|                                       | MicroBeta | TopCount  | MicroBeta            | TopCount  | MicroBeta              | TopCount  |
| Tritium                               | 5 - 360   | 1.5 - 35  | 5 - 500              | 0 - 50    | 5 - 250                | 1.5 - 45  |
| Iodine-125                            | 5 - 530   | 1.5 - 100 | 5 - 650              | 0 - 100   | 5 - 350                | 1.5 - 50  |
| Phosphorus-33                         | 5 - 650   | 2.9 - 256 | 5 - 750              | 2.9 - 256 | 5 - 700                | 1.5 - 100 |
| Sulphur-35                            | 5 - 600   | 2.9 - 256 | 5 - 700              | 2.9 - 256 | 5 - 500                | 1.5 - 60  |
| Carbon-14                             | 5-650     | 2.9 - 256 | 5 - 750              | 2.9 - 256 | 5 - 500                | 1.5 - 60  |
| Calcium-45                            |           |           |                      |           | 5 - 550                | 1.5 - 60  |
| Rubidium-86<br>[energy range<br>HIGH] |           |           |                      |           |                        | 2.9 - 256 |

### 12 Detector Trilux Microbeta Normalization Process

Normalization Protocol

**Relative Detector Efficiency**

All 12 detectors read well G11 and report CPM values. The efficiency of each detector, relative to all of the detectors is determined as follows:

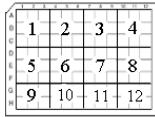
$$\text{Rel Efficiency} = \text{CPM} / \text{Highest CPM value detected}$$

| Detector # | CPM in G11 | Rel Eff |
|------------|------------|---------|
| 1          | 9,875      | 0.9875  |
| 2          | 9,908      | 0.9908  |
| 3          | 9,789      | 0.9789  |
| 4          | 10,000     | 1.0000  |
| 5          | 9,700      | 0.9700  |
| 6          | 9,650      | 0.9650  |
| 7          | 9,991      | 0.9991  |
| 8          | 9,809      | 0.9809  |
| 9          | 9,900      | 0.9900  |
| 10         | 9,799      | 0.9799  |
| 11         | 9,867      | 0.9867  |
| 12         | 9,809      | 0.9809  |

Normalization Protocol is run only once - Detector efficiencies are stored with Normalization Protocol information.

General Protocol

Normalization Protocol linked to General Counting Protocol.



Microplate counted with 12 different detectors, each detector counting either 9 or 6 wells depending on location.

Raw CPM values for each well are corrected using the corresponding Relative Efficiency values determined in the Normalization Protocol (CCPM).

General Protocol

| CPM | 1    | 2    | 3    | 4    | 5    | 6    | 7    | 8    | 9    | 10   | 11   | 12  |
|-----|------|------|------|------|------|------|------|------|------|------|------|-----|
| A   | 1971 | 2182 | 2115 | 2182 | 2183 | 1941 | 1982 | 2020 | 2050 | 1880 | 1980 | 189 |
| B   | 1977 | 1938 | 2015 | 2201 | 2032 | 1930 | 2124 | 1938 | 1244 | 2451 | 1825 | 189 |
| C   | 2286 | 2139 | 2131 | 1981 | 1938 | 1813 | 2058 | 1815 | 2257 | 2332 | 1795 | 182 |
| D   | 2147 | 2020 | 1938 | 1911 | 1937 | 2033 | 2138 | 1938 | 1782 | 2188 | 1919 | 180 |
| E   | 2288 | 2215 | 2216 | 2285 | 2218 | 2011 | 1927 | 2032 | 2138 | 2387 | 2140 | 209 |
| F   | 2288 | 2215 | 2216 | 2285 | 2218 | 2011 | 1927 | 2032 | 2138 | 2387 | 2140 | 209 |
| G   | 2192 | 2032 | 2038 | 2273 | 2015 | 2011 | 2084 | 1919 | 2019 | 2275 | 1934 | 182 |
| H   | 2288 | 2215 | 2216 | 2285 | 2218 | 2011 | 1927 | 2032 | 2138 | 2387 | 2140 | 209 |

| CCPM | 1    | 2    | 3    | 4    | 5    | 6    | 7    | 8    | 9    | 10   | 11   | 12  |
|------|------|------|------|------|------|------|------|------|------|------|------|-----|
| A    | 1980 | 2180 | 2140 | 2200 | 2170 | 1980 | 1990 | 2030 | 2100 | 1880 | 1980 | 189 |
| B    | 2000 | 2020 | 2030 | 2300 | 2110 | 2000 | 2200 | 1950 | 1250 | 2450 | 1825 | 189 |
| C    | 2290 | 2150 | 2140 | 1970 | 1940 | 1820 | 2060 | 1820 | 2260 | 2340 | 1795 | 182 |
| D    | 2150 | 2030 | 1940 | 1920 | 1940 | 2030 | 2140 | 1940 | 1790 | 2190 | 1910 | 180 |
| E    | 2290 | 2210 | 2210 | 2280 | 2210 | 2010 | 1930 | 2030 | 2140 | 2390 | 2140 | 209 |
| F    | 2290 | 2210 | 2210 | 2280 | 2210 | 2010 | 1930 | 2030 | 2140 | 2390 | 2140 | 209 |
| G    | 2190 | 2030 | 2030 | 2270 | 2010 | 2010 | 2080 | 1910 | 2010 | 2270 | 1930 | 182 |
| H    | 2290 | 2210 | 2210 | 2280 | 2210 | 2010 | 1930 | 2030 | 2140 | 2390 | 2140 | 209 |

### 12 Detector Trilux Microbeta Normalization Process

Normalization Protocol

**Detector Efficiency: Relative to DPM**

All 12 detectors read well G11 and report CPM values. The efficiency of each detector, relative to an inputted DPM activity is determined as follows:

$$\text{Efficiency} = \text{CPM} / \text{DPM of inputted sample}$$

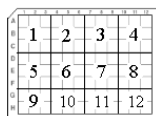
Example DPM inputted: 10,000 DPM (from liq. scint.)

| Detector # | CPM in G11 | Rel Eff |
|------------|------------|---------|
| 1          | 3,200      | 0.3200  |
| 2          | 3,189      | 0.3189  |
| 3          | 3,345      | 0.3345  |
| 4          | 3,098      | 0.3098  |
| 5          | 3,234      | 0.3234  |
| 6          | 3,290      | 0.3290  |
| 7          | 3,129      | 0.3129  |
| 8          | 3,400      | 0.3400  |
| 9          | 3,209      | 0.3209  |
| 10         | 3,334      | 0.3334  |
| 11         | 3,205      | 0.3205  |
| 12         | 3,199      | 0.3199  |

Normalization Protocol is run only once - Detector efficiencies are stored with Normalization Protocol information.

General Protocol

Normalization Protocol linked to General Counting Protocol.



Microplate counted with 12 different detectors, each detector counting either 9 or 6 wells depending on location.

Raw CPM values for each well are corrected using the corresponding Detector Efficiency values determined in the Normalization Protocol (CCPM).

General Protocol

| CPM | 1    | 2    | 3    | 4    | 5    | 6    | 7    | 8    | 9    | 10   | 11   | 12  |
|-----|------|------|------|------|------|------|------|------|------|------|------|-----|
| A   | 1971 | 2182 | 2115 | 2182 | 2183 | 1941 | 1982 | 2020 | 2050 | 1880 | 1980 | 189 |
| B   | 1977 | 1938 | 2015 | 2201 | 2032 | 1930 | 2124 | 1938 | 1244 | 2451 | 1825 | 189 |
| C   | 2286 | 2139 | 2131 | 1981 | 1938 | 1813 | 2058 | 1815 | 2257 | 2332 | 1795 | 182 |
| D   | 2147 | 2020 | 1938 | 1911 | 1937 | 2033 | 2138 | 1938 | 1782 | 2188 | 1919 | 180 |
| E   | 2288 | 2215 | 2216 | 2285 | 2218 | 2011 | 1927 | 2032 | 2138 | 2387 | 2140 | 209 |
| F   | 2288 | 2215 | 2216 | 2285 | 2218 | 2011 | 1927 | 2032 | 2138 | 2387 | 2140 | 209 |
| G   | 2192 | 2032 | 2038 | 2273 | 2015 | 2011 | 2084 | 1919 | 2019 | 2275 | 1934 | 182 |
| H   | 2288 | 2215 | 2216 | 2285 | 2218 | 2011 | 1927 | 2032 | 2138 | 2387 | 2140 | 209 |

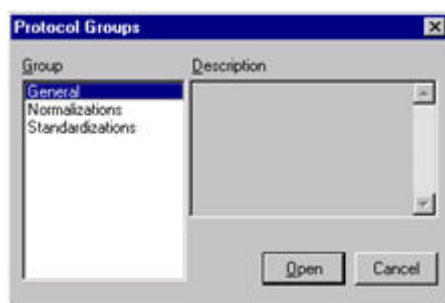
| CCPM | 1    | 2    | 3    | 4    | 5    | 6    | 7    | 8    | 9    | 10   | 11   | 12   |
|------|------|------|------|------|------|------|------|------|------|------|------|------|
| A    | 1984 | 1980 | 1980 | 1981 | 1981 | 1981 | 1981 | 1981 | 1981 | 1981 | 1981 | 1981 |
| B    | 1973 | 1924 | 1921 | 1933 | 1980 | 1920 | 1920 | 1920 | 1920 | 1920 | 1920 | 1981 |
| C    | 1983 | 1933 | 1931 | 1981 | 1981 | 1981 | 1981 | 1981 | 1981 | 1981 | 1981 | 1981 |
| D    | 1981 | 1982 | 1979 | 1983 | 1983 | 1981 | 1981 | 1981 | 1981 | 1981 | 1981 | 1981 |
| E    | 1983 | 1933 | 1931 | 1981 | 1981 | 1981 | 1981 | 1981 | 1981 | 1981 | 1981 | 1981 |
| F    | 1983 | 1933 | 1931 | 1981 | 1981 | 1981 | 1981 | 1981 | 1981 | 1981 | 1981 | 1981 |
| G    | 1983 | 1933 | 1931 | 1981 | 1981 | 1981 | 1981 | 1981 | 1981 | 1981 | 1981 | 1981 |
| H    | 1983 | 1933 | 1931 | 1981 | 1981 | 1981 | 1981 | 1981 | 1981 | 1981 | 1981 | 1981 |

Figure 3: Linking of a Normalization protocol to a General counting protocol for a 12-detector Trilux using either a relative detector efficiency set up or an efficiency relative to a known activity.

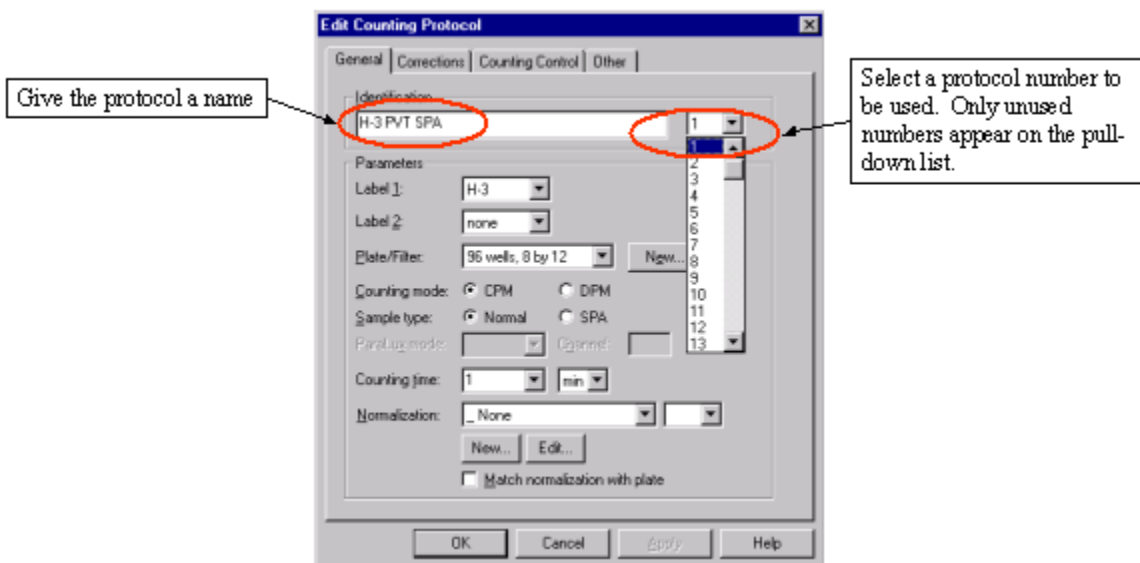
## Setup of a General Counting Protocol

A Normalization protocol is linked to a General Counting protocol, in order to define the counting parameters (i.e. isotope, window settings, etc.) and the detector efficiencies (relative to the highest detector reading or relative to DPM activity) needed to correct raw counting data.

1. Click on the Protocols button at the top of the Microbeta software toolbar.
2. Select **General** followed by the **Open** button.

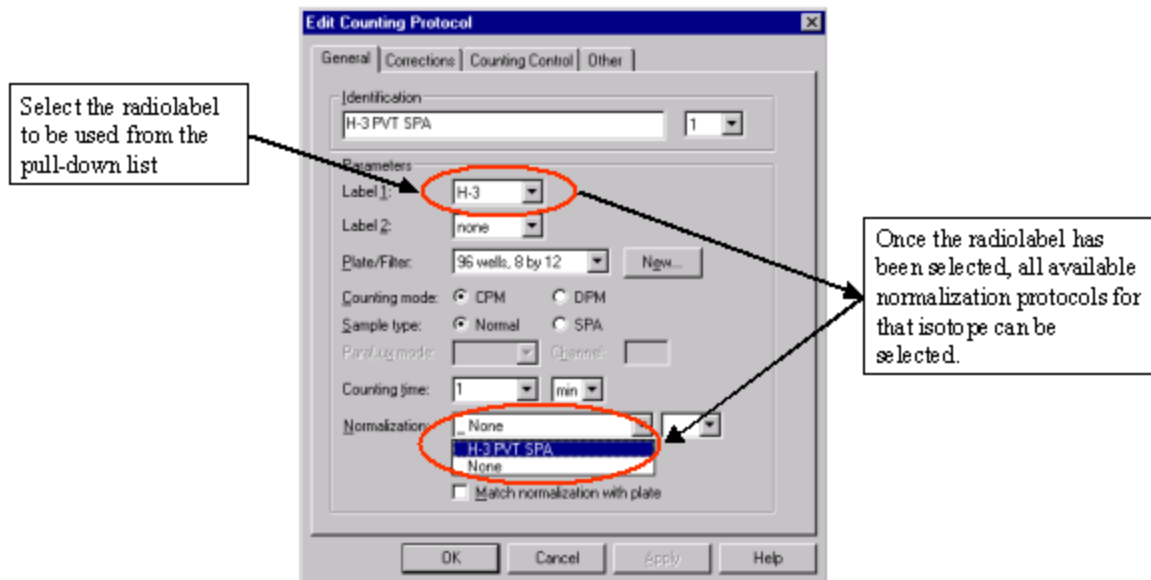


3. Click on the **New** button to create a new General counting protocol.
4. In the Edit Counting Protocol window, type in a name for the protocol in the **Identification** space. Select a protocol number from the pull-down list to the right of the **Identification** name. Only unused protocol numbers will appear in this pull-down list.



5. Select the isotope from the pull-down list. Once the isotope is selected, Normalization protocols that have been created using that isotope will appear in the Normalization pull-down area. Select the appropriate Normalization protocol to link to the General counting protocol. Note that an underscore (\_) before the name of a Normalization protocol

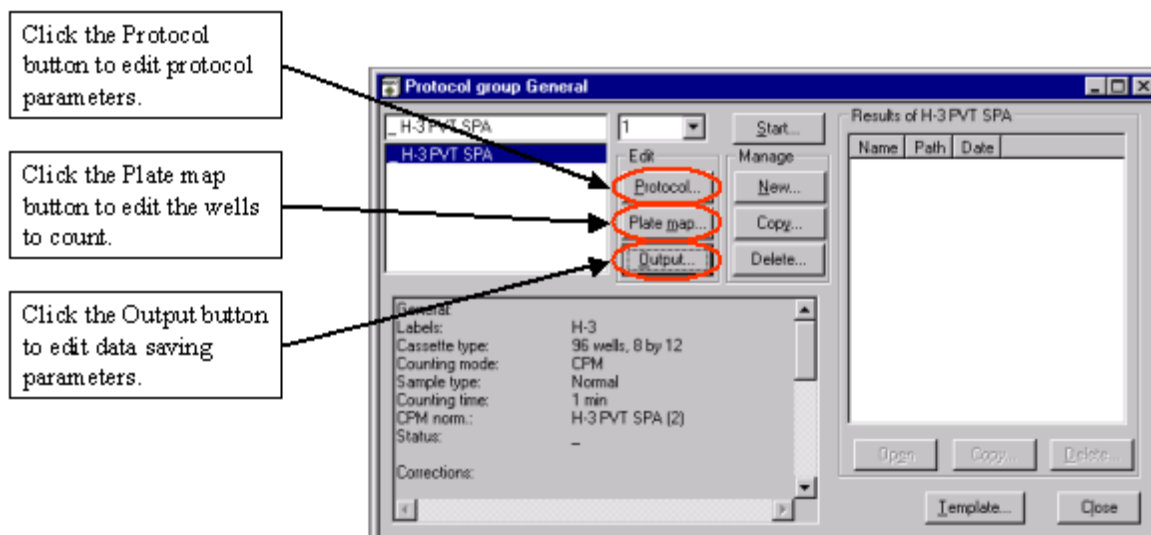
indicates that the Normalization plate has not been counted yet. Once the Normalization data has been stored, an (n) will appear before the name of the Normalization protocol.



6. Change the Counting time if desired (default is 1 min). The other tabs in the Edit Counting Protocol window (*Corrections*, *Counting Control*, *Other*) usually do not need to be modified unless special counting circumstances are being used.

7. Click OK to save the General counting protocol. Click Yes on the dialog box that pops up.

8. From the *Protocol group General* window, the General counting protocols can be edited.



9. The Protocol button allows editing of the protocol parameters (i.e. counting time).



10. The Plate map button allows selection of microplate wells to count (default set to entire plate).

11. The Output button allows selection of file and printing options. There are a couple of changes that should be made in the output as outlined below:

If the instrument is connected to a network and does not have a dedicated printer attached to the PC controller, it may be desirable to deselect the printing option. Quality printouts of the data directly from the instrument to a network laser printer are difficult. Deselect Generate print output in the **Print** tab.

Under the **File 1** tab, it is advisable to change the path where data files are electronically stored. By default, they are stored in the Results subdirectory where the Microbeta software is stored. This can be dangerous, as the Normalization parameters are also stored in that subdirectory. Accidental deletion or moving of Normalization protocol results files will render the Normalization protocols useless. To prevent this, direct General counting output to a different subdirectory.

Under the **File 1** Items tab, if you do not want the electronic data file to have the data expressed as 96 numbers in a column (for a 96-well plate), deselect the Column section box. The data file will have results in plate format only (8 x 12 array for 96-well microplates).

The suggested outline shown above is for general counting conditions. One should consult instrument owners or the manufacturer for advanced counting options such as cross-talk correction, background correction or manual setting of count windows.

Figure 3 demonstrates the linking of a Normalization protocol to a General counting protocol for a 12-detector Trilux using either a relative detector efficiency set up or an efficiency relative to a known activity. Similar linking occurs for a 6 detector instrument.

## TopCount

### General Concepts

The TopCount is different than the Microbeta because it uses a single photomultiplier tube (PMT) counting from the top of the microplate instead of one PMT on top and one on bottom. Consequently, the TopCount determines background from true photon events using a time-resolved discrimination method of scintillation counting. This means that appropriate scintillators (known as slow scintillators) must be used for proper signal detection (Figure 4). The TopCount is available in 6- and 12-detector models.

Normalization of the TopCount is similar to the Microbeta, except that **Well A10** is used by the detectors as the common read well. In addition, the TopCount NXT software does not have a provision to enter in an activity (in DPM) for the normalization amount on the

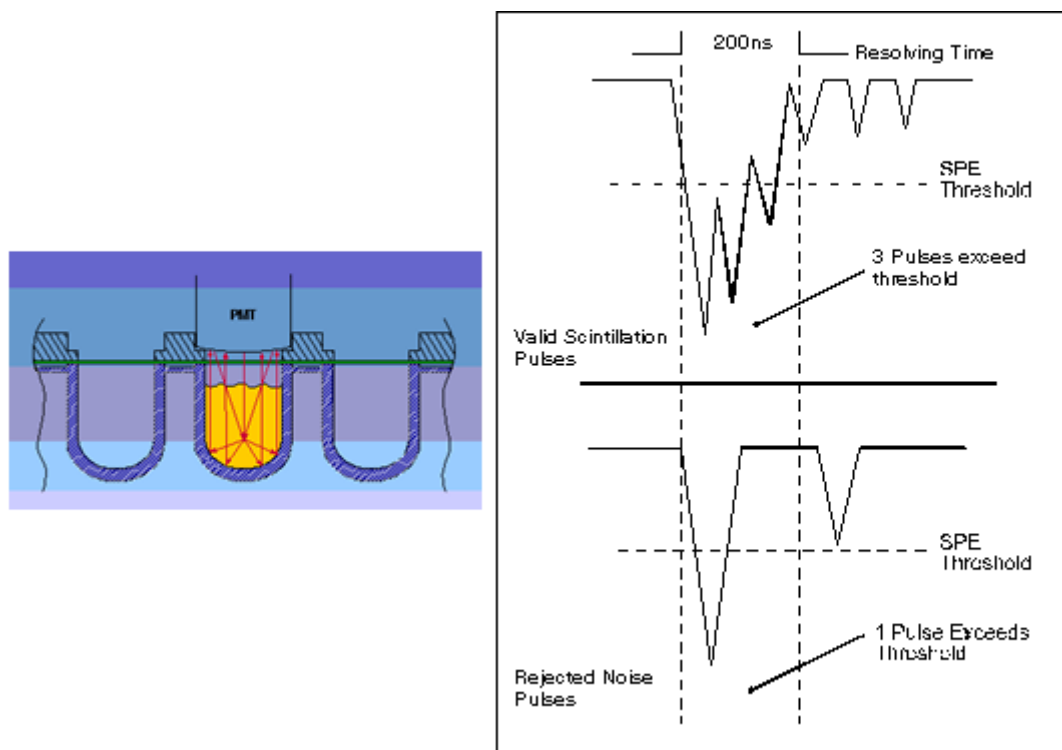


**Figure 4:** Diagram of TopCount Pulse Discrimination. Appropriate slow scintillators must be used to allow the photon energy to dissipate in a time resolved manner (multiple pulses detected during resolving time). Single pulses detected by the PMT during the resolving time would be eliminated as background noise. The TopCount uses a single PMT positioned on top. Diagrams from Perkin Elmer Life and Analytical Sciences (Document TCA-003).

plate. Therefore, results are always reported in corrected CPM, with the detectors normalized relative to each other. Efficiency of the TopCount must be determined manually, and the correction factor must be applied to determine DPM activity. Further information about normalization procedures and applications for the TopCount can be obtained from the manufacturer.

A stepwise procedure for setting up a counting protocol on a TopCount NXT is shown below.

### Setup of Counting Assay

1. Click on the Assay Wizard icon located in the tool bar at the top of the software window (hold the mouse over a button to obtain a description of each icon).
2. Select Create a New Assay.
3. Define the assay name and number; select CPM as the Assay Type; select the desired plate type if requested.
4. Accept the default selection of Unknowns, unless you need to add Totals and Blanks for additional calculations.

5. Select Counting Options including delays and repeats, and select the Radionuclide from the drop-down list. Table 4 lists preset window settings on the TopCount NXT.
6. Define printed and ASCII file outputs, as well as post-processing user application programs.
  7. Select Instrument Correction Factors.
  8. Establish Instrument Correction Factors.
  9. Define Sample Map and finish Setup.
  10. The first time the Assay Protocol is selected, a normalization plate with a sample of activity in well A10 will be expected. Future runs will count plates using the stored normalization parameters.

**Table 4: Preset window settings on the TopCount NXT.**

| Name                       | Scintillator | Energy |             | Efficiency |            | Channels  |           |
|----------------------------|--------------|--------|-------------|------------|------------|-----------|-----------|
|                            |              | Range  | Mode        | Region A   | Region B   |           |           |
| Polyvinyltoluene (PVT) SPA |              |        |             |            |            |           |           |
| 3H-PVT-SPA                 |              |        | Liq/Plastic | Low        | Normal     | 1.5-35.0  | 1.5-256.0 |
| 125I-PVT-SPA               |              |        | Liq/Plastic | Low        | Normal     | 1.5-100.0 | 1.5-256.0 |
| 33P-PVT-SPA                |              |        | Liq/Plastic | Low        | Normal     | 2.9-256.0 | 2.9-256.0 |
| 35S-PVT-SPA                |              |        | Liq/Plastic | Low        | Normal     | 2.9-256.0 | 2.9-256.0 |
| Yttrium Silicate (YS) SPA  |              |        |             |            |            |           |           |
| 3H-YS-SPA                  |              |        | Glass       | Low        | High Sens. | 0.0-50.0  | 0.0-256.0 |
| 125I-YS-SPA                |              |        | Glass       | Low        | High Sens. | 0.0-100.0 | 0.0-256.0 |

## Uniformity Plate

To test instrument detector variation, a uniformity plate with the same level of radioactivity in all wells is generated. The counting results are analyzed for each detector, as well as across the plate by columns and rows, to determine if any detectors require adjustment. Periodic counting of a uniformity plate (called a Performance Check) can identify detector drift or other instrument problems. This procedure can be performed regardless of the instrument type or the number of detectors.

Since many assays are performed in a concentration response mode, a gradient signal across the plate is an expected result. An example of how a Performance Check using a uniformity plate can assist in reducing instrument variability is shown in Figure 5.

To generate a 96-well microplate for [ $^{125}\text{I}$ ] SPA beads, labeled beads are prepared using WGA beads, [ $^{125}\text{I}$ ]-ligand and receptor membranes. A brief procedure is described below:

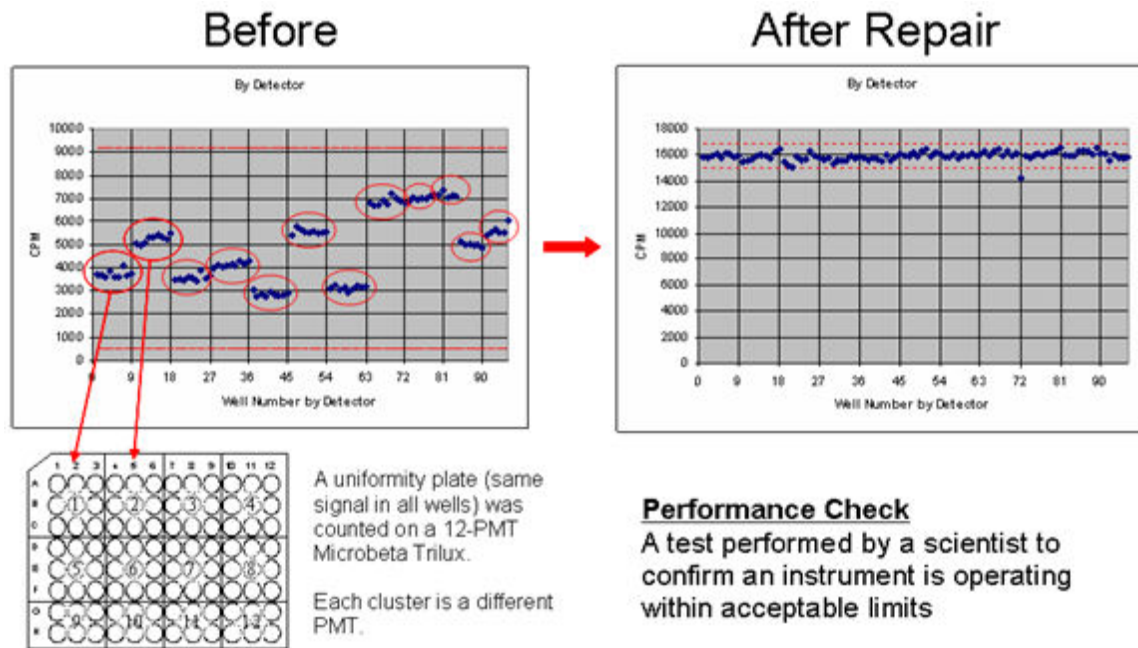


**Figure 5:** Example a performance check, which reduces instrument variability.

Add receptor membranes, [ $^{125}\text{I}$ ]-ligand and WGA SPA beads in an appropriate buffer in a single tube. After a incubation time (consistent with the biological system), add 200  $\mu\text{l}$  of diluted bead mixture per well using a 12-channel pipette. Change tips for each row. Allow beads to settle overnight (stable counting conditions) or centrifuge if the receptor/ligand interaction is not stable. Count radioactivity in Microbeta (use clear bottom plate) or TopCount (use opaque bottom plate)

Results for a typical read using a clear bottom plate and a 12-detector Microbeta Trilux are shown in Figure 6. The relative efficiency between all 12 detectors is >95%.

## Color Quench Correction

If colored compounds are to be tested and are present during the counting step (as in a non-separation technique such as SPA) color quenching may be present. This occurs when the photons emitted by the fluor are absorbed by the colored compound resulting in attenuation of signal. The emission spectra (~420 nm max) of SPA beads detectable in the Trilux and TopCount and the absorption spectra for common colors are shown in Figure 7.

For the Trilux and TopCount, compounds that are red, yellow or orange (absorption max ~400 nm) have the biggest impact on signal attenuation (with PVT or YSi SPA beads) if they are present while reading the plates.

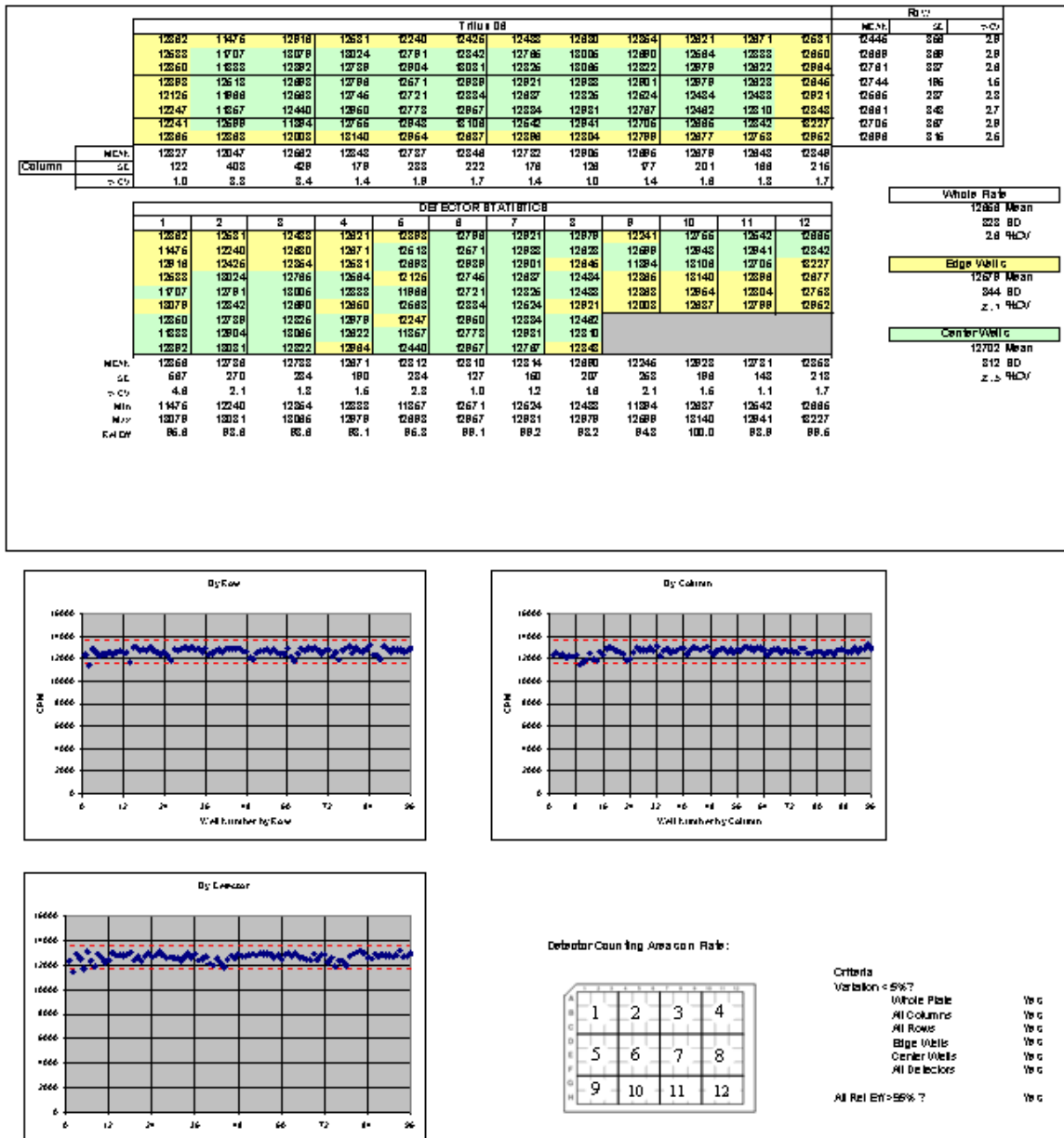
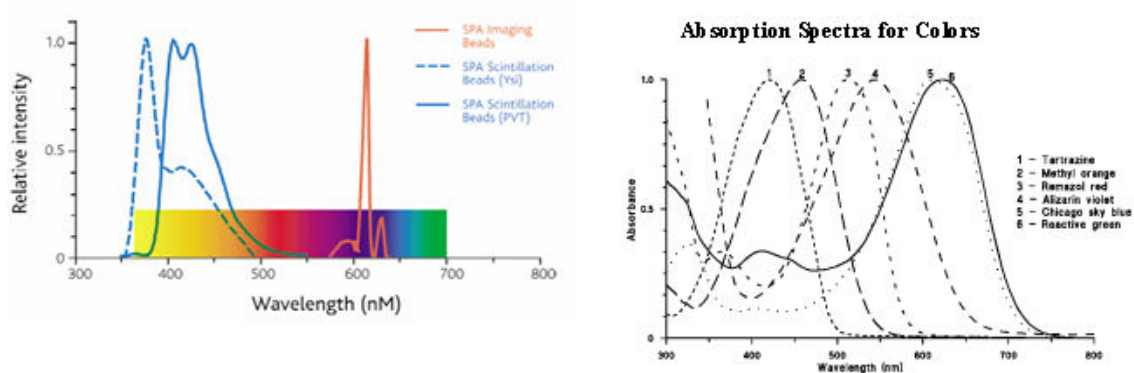


Figure 6: Results for a typical read using a clear bottom plate and a 12-detector Microbeta Trilux.

Correction of color quenching can be performed within the software of the Trilux or TopCount using a prepared quench curve. Typically, this is performed with a yellow dye, such as tartrazine.



**Figure 7:** The emission spectra (~420 nm max) of SPA beads detectable in the Trilux and TopCount and the absorption spectra for common colors. Diagrams from PE LAS.

## Abbreviations

**CPM** = Counts per minute

**DPM** = Disintegrations per minute

**SA** = Specific activity, example: Ci/mmol

**RAC** = Radioactive concentration, example:  $\mu\text{Ci/ml}$  or  $\text{mCi/ml}$

**Eff** = Efficiency, defined as  $\text{CPM/DPM}$

**PMT** = Photomultiplier tube, detects photons of light emitted by a source (e.g. fluor)

**SPA** = Scintillation Proximity Assay

**YSi** = Yttrium silicate, a rare earth metal based SPA bead

**PVT** = Polyvinyltoluene, a plastic-based SPA bead

**PE LAS** = Perkin Elmer Life and Analytical Sciences

# Pharmacokinetics and Drug Metabolism

Editor: Xin Xu, PhD





# *In Vitro* and *In Vivo* Assessment of ADME and PK Properties During Lead Selection and Lead Optimization – Guidelines, Benchmarks and Rules of Thumb

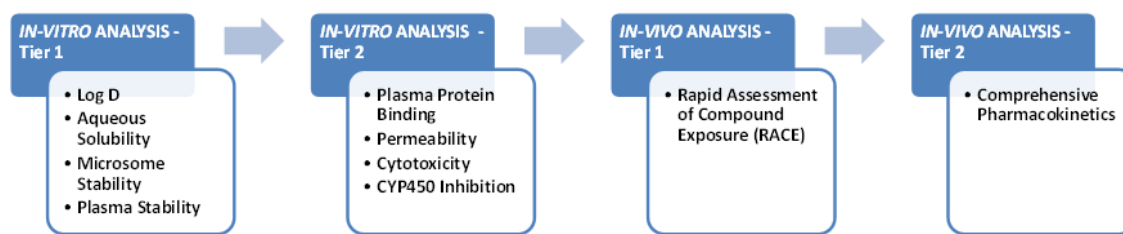
Thomas D.Y. Chung,<sup>1</sup> David B. Terry,<sup>2</sup> and Layton H. Smith<sup>3</sup>

Created: September 9, 2015.

## Abstract

Assessment of the pharmacological properties of small molecule chemical compounds is critical to the initial selection or identification of a chemical lead, and during the further lead optimization to elucidate the Structure-Activity Relationships (SAR) and Structure Property Relationships (SPR), and ultimately to select the compound(s) that will enter Investigational New Drug (IND)-enabling studies. While extensive discussion of how Absorption, Distribution, Metabolism, and Excretion (ADME) of compounds affects their ultimate pharmacokinetics (PK) is beyond the scope of this chapter, herein, we provide guidelines for ADME and PK assessments, benchmarks and practical “rules of thumb” for selecting compounds with sufficient PK to be viable efficacious drugs.

## Flow Chart of a Two-tier Approach for *In Vitro* and *In Vivo* Analysis



## Background

As well-reviewed in the Assay Guidance Manual (AGM) chapter on Early Drug Discovery and Development Guidelines, there is an evolving paradigm for drug discovery and early

<sup>1</sup> Conrad Prebys Center for Chemical Genomics, Sanford Burnham Prebys Medical Discovery Institute, La Jolla, CA. <sup>2</sup> Conrad Prebys Center for Chemical Genomics, Sanford Burnham Prebys Medical Discovery Institute at Lake Nona, Orlando, FL. <sup>3</sup> Conrad Prebys Center for Chemical Genomics, Sanford Burnham Prebys Medical Discovery Institute at Lake Nona, Orlando, FL.

development with the academic and non-profit enterprises focused on delivering innovative, novel, new chemical entities (NCE) through collaboration, partnering and licensing optimized leads for final clinical development to pharmaceutical companies. That chapter outlined the overall process, critical steps and key decision points at each step. Each of these steps and associated technologies, protocols, techniques, and case examples are covered elsewhere in the AGM. Ultimately, an exemplary compound(s) emerges from systematic elucidation of the Structure Activity Relationship (SAR) through examining the potency, specificity and selectivity of analogs around a chemical scaffold. This comprises identification of a chemical lead, where the most potent, specific and selective compound(s) are chosen.

Assessments of the pharmacological properties of Absorption, Distribution, Metabolism, and Excretion (ADME) of a candidate chemical lead(s) are critical to their initial selection, and establishes benchmarks against which compounds synthesized during lead optimization can be evaluated. Further improvements in ADME properties during lead optimization are sought, while preserving the potency and selectivity of the chemical lead(s), though sometimes more efficacious compounds have lower *in vitro* potencies, but better ADME properties.

These activities often reside in an exploratory pharmacology group that provides *in vitro* and *in vivo* pharmacologic and physicochemical property analysis of biologically active small molecules in support of small molecule probe/drug discovery projects. Early pharmacological assessment has been adopted within the pharmaceutical industry as a critical feature of a robust drug/probe discovery process. This is because the development and optimization of useful molecules is a multi-parameter process. Simply designing new analogs and developing a SAR for increased potency against the biological target is inadequate for the development of small molecule probes or drugs suitable for cellular, tissue, or whole animal disease model(s). The assessment and optimization of Structure-Pharmacologic/Property-Relationships (SPR) is a further critical step for efficacy evaluation. In addition to assessing compound characteristics such as solubility, protein binding, and serum stability, the data allows the chemistry team to prioritize different structural classes and rank order them not only based on potency but also in relation to potential downstream absorption or metabolism liabilities. An excellent additional overview of pharmacokinetics (PK) can be found on the online version of the Merck Manual (<http://www.merckmanuals.com/professional/clinical-pharmacology/pharmacokinetics/overview-of-pharmacokinetics>)

Prior to actual dosing in animals, a number of relatively rapid and cost effective *in vitro* assays can serve as surrogates and indicators of the ADME fate of compounds *in vivo*. Improvements in ADME properties of compounds translate to their improved PK properties. Simply stated, if a compound is rapidly absorbed, well distributed, minimally metabolically degraded and not rapidly eliminated, while not being toxic, then it more likely will rapidly achieve peak levels in the blood, maintain the desired levels (n-fold above the IC<sub>50</sub>) for a longer duration, before falling to low trough levels, and ultimately being cleared by the body.

In the sections below, we describe the basic component and provide high level protocols for a two-tiered approach for these key *in vitro* ADME assays (see Flow Chart). We provide an example of an ADME table, and benchmarks for a series of probe compounds developed through the NIH Molecular Libraries Program (MLP) by our group when we were part of the Molecular Libraries Probe Production Centers Network (MLPCN). We then summarize a two-tiered approach to doing pharmacokinetic studies (see Flow Chart). First an abbreviated “rapid” assessment for compound exposure (R.A.C.E.) developed by us (LHS), then the more typical “comprehensive” pharmacokinetic analysis used during late lead optimization toward candidate selection for final preclinical IND.

Ultimately, the *in vivo* efficacy of an optimized lead will be better served by having good pharmacological properties, so that the compound administered at a given dose actually achieves the required concentration, for sufficient duration in the target tissue to achieve the desired biological effect, while minimizing any undesired off target effects. Improvement in these ADME properties is sought prior to actual dosing in animals to assess PK, and certainly for larger compound efficacy studies, since animals are expensive and the ethics of sacrificing animals in poorly designed studies uninformed by pharmacological guidance are indefensible.

## *In Vitro* Analysis - Low Compound Requirements and Relative Moderate Capacity

### Lipophilicity

Pharmacologic question addressed: “*Will my parent compound be stored in lipid compartments or how well will my parent compound bind to a target protein?*”

Lipophilicity is an important physicochemical property of a potential drug. It plays a role in solubility, absorption, membrane penetration, plasma protein binding, distribution, CNS penetration and partitioning into other tissues or organs such as the liver and has an impact on the routes of clearance. It is important in ligand recognition, not only to the target protein but also CYP450 interactions, HERG binding, and PXR mediated enzyme induction.

Lipophilicity is typically measured as the neutral (non-ionized) compound distribution between non-aqueous (octanol) and aqueous (water) phase and the result is expressed as a 10-base logarithm of the concentration ratios between these phases (partition coefficient), log P.

Another common measure for lipophilicity is the distribution coefficient, log D, which takes into account the compound’s ionized and non-ionized forms, and therefore the measurement is done at different pH values. Typically the most interesting is pH 7.4, since the majority of known drugs contain ionizable groups and are likely to be charged at physiological pH.

### Assay Design:

- Test articles are assayed in triplicate
- One concentration of test article (typically 10  $\mu\text{M}$ )
- n-Octanol is the partition solvent
- Ratio of buffer: Octanol is 1:1 (other ratios available)
- Positive control: Testosterone (high log  $D_{7.4}$  value)
- Negative control: Tolbutamide (low log  $D_{7.4}$  value)

**Analysis:** LC/MS/MS measurement of parent compound

**Report:** Log  $D_{7.4}$  value

**Quantity of test article required:** 1.0 - 2.0 mg

#### Summary of Assay:

Lipophilicity of compounds is assessed using the golden standard “shake-flask” method. The compound is dissolved in a solution with equal amounts of octanol and water, shaken for 3 hours, and then measured for the amount of compound in each phase. Log D values are calculated by the log ( $[\text{compound}]_{\text{octanol}} / [\text{compound}]_{\text{buffer}}$ ).

## Solubility

Pharmacologic question addressed: “*What is the bioavailability of my compound?*”

Aqueous solubility, another common physicochemical parameter for drug discovery compounds, is an important analysis as it reflects the bioavailability of the compound. The ability of a compound to dissolve in a solvent to give a homogenous system is one of the important parameters to achieve a desired concentration of drug in systemic circulation for the desired (anticipated) pharmacological response. Formulation and routes of administration, especially oral dosing, are challenging for poorly soluble drugs, as it limits the absorption of compound from the gastrointestinal tract. Also, poor solubility will affect other AMDE/DMPK analyses, if some fraction of the compound precipitates and is unavailable (e.g. in assays for metabolite stability and various CYP identification/inhibition/induction assays). Also, since the majority of known drugs contain ionizable groups, the aqueous solubility is assessed over a range of pH values.

#### Assay Design:

- Test articles are assayed in duplicate
- One concentration of test article (typically 1  $\mu\text{M}$ )
- Phosphate buffered solution (other buffers available)
- Three point pH range (5.0, 6.2, 7.4)
- Positive control: Diclofenac (high solubility)
- Negative control: Dipyridamole (low solubility)
- Background control: DMSO only

**Analysis:** UV spectrophotometry measurement of parent compound

**Report:** Amount of compound dissolved ( $\mu\text{M}$ )

**Quantity of test article required:** 1.0 - 2.0 mg

**Summary of Assay:**

The compound is dissolved in buffer solutions at the indicated pH values. The compound is allowed to reach thermodynamic equilibrium by incubating for 18 hours. Compound UV absorption is compared to fully saturated solution in 1-propanol.

## Hepatic Microsome Stability

Pharmacologic question addressed: *“How long will my parent compound remain circulating in plasma within the body?”*

The assay uses subcellular fractions of liver, microsomes, to investigate the metabolic fate of compounds. Liver microsomes consist mainly of endoplasmatic reticulum and contain many drug-metabolizing enzymes, including cytochrome P450s (CYPs), flavin monooxygenases, carboxylesterases, and epoxide hydrolase (1). Liver microsomes are available commercially (example, Xenotech, LifeTechnologies and DB Biosciences) as frozen preparations that are usually prepared in bulk with pooled livers from sacrificed mice, rat or human cadavers. As a result, hepatic microsomal metabolic activity can vary significantly from batch to batch. Therefore, in critical studies, it is recommended that planning to obtain the same lot of microsomes be considered in the experimental plans. If lots of microsomes do run out, a few bridging comparisons to establish comparable values for microsomal stability of reference compounds, should be done.

**Assay Design:**

- Test articles are assayed in triplicate
- Human liver microsomes (or other species as needed) (0.5 mg/mL)
- One concentration of test article (typically 10  $\mu$ M)\*
- Two time points  $t = 0$  and  $t = 60$  min\*
- Positive control: Substrates with known activity
- Negative control: NADPH deficient

**Analysis:** LC/MS/MS measurement of parent compound at specific time points

**Report:** % metabolism of the test article (single time point); also, intrinsic clearance and half-life (multiple time points)\*

**Quantity of test article required:** 1.0 - 2.0 mg

**Summary of Assay:**

Metabolic stability of compounds are assessed at a single concentration (typically 10  $\mu$ M) at  $t = 0$  and at  $t = 60$  min. Stability of compounds are tested in human (other species available) liver microsomes. Compounds are tested in triplicate with or without NADP wells as a negative control for P450 metabolism. Each assay will include a substrate with known activity (such as the CYP3A4 substrate testosterone) as a positive control (2).

\*Note: the number of concentrations/time points in the assay can be expanded for drug development SAR efforts.

## Plasma Stability

Pharmacologic question addressed: “*Is my compound degraded in plasma?*”

In addition to hepatic metabolism, compounds are also subjected to degradation/modification by enzymes in plasma, particularly hydrolysis and esterases. Thus, the stability of test compounds in plasma is an important parameter, which not only affects *in vivo* results, but also the bioanalytical assay strategy and design. Investigation of plasma stability should be performed early in the discovery process in order to assess potential degradation and/or protein binding issues.

### Assay Design:

- Test articles are assayed in triplicate
- Two concentrations (10  $\mu\text{M}$  and 100  $\mu\text{M}$  or if known  $C_{\text{max}}$  and 10x  $C_{\text{max}}$ )
- Two time points  $t = 0$  and  $t = 180$  min
- Positive control: Procaine (50  $\mu\text{M}$ )
- Negative control: Procainamide (50  $\mu\text{M}$ )

**Analysis:** LC/MS/MS detection of the remaining test article

**Report:** % parent compound remaining

**Quantity of test article required:** 1.0 - 2.0 mg

### Summary of Assay:

A solution of test compound in plasma is prepared and incubated for a predetermined time period. Aliquots are removed at pre-defined time points and analyzed by LC/MS/MS. The peak area for the parent compound is compared to the time zero sample in order to assess the amount of compound still available.

## Plasma Protein Binding

Pharmacologic question addressed: “*What percent of the compound plasma protein is bound, to which component (sub-fraction), and what is the free fraction available to cover the target?*”

The binding of test compounds to plasma proteins is an important factor affecting drug efficacy, metabolism and pharmacokinetic properties. In many cases, drug efficacy is determined by the concentration of free drug (unbound), rather than the total concentration in plasma. If the drug is highly bound to plasma proteins, the amount of drug available to reach the target is reduced. Subsequently, the efficacy of that compound may be significantly reduced. Therefore, information on the free drug fraction is essential for drug development and may be helpful in correlating with *in vivo* efficacy.

Rapid equilibrium dialysis (RED) is an accurate and reliable method for determining the degree to which a compound binds to plasma proteins. Plasma spiked with test compound is added to the center chamber of a commercial plate based RED device. Blank, isotonic sodium phosphate buffer is added to the peripheral chamber of the RED device and the plate is incubated at 37°C for 4 hours. Equilibrium of free compound is achieved by the diffusion of the unbound compound across the dialysis membrane. Several manufacturers provide RED devices (Thermo Scientific). Aliquots of the buffer and the plasma are taken at pre-determined time points and the concentration of free and bound test compound is determined by LC/MS/MS analysis.

**Assay Design:**

- Test articles are assayed in duplicate
- Test articles are mixed with human plasma (other species available)
- One concentration of test article (10 µM, different concentrations available)
- One time point ( $t = 4$  hours at 37°C)
- Positive control: Propranolol (high binding) and Metoprolol (low binding)
- Negative control: No plasma (PBS only)

**Analysis:** LC/MS/MS detection of the test compound in plasma and in buffer

**Report:** % compound bound

**Quantity of test article required:** 1.0 - 2.0 mg

**Summary of Assay:**

Human or specific species of interest plasma in the sample chamber are spiked with test compounds at 100x dilution of stock solution (typically 10 mM in DMSO). The chamber is sealed, and the compound is dialyzed against PBS, pH 7.4 at 37°C for 4 hours. Aliquots from each chamber (plasma and PBS) are collected and the concentrations of compound in each sample are determined by LC/MS/MS. Adjustments are made for non-specific binding.

## Screening Cytotoxicity / Hepatotoxicity Test

Pharmacologic question addressed: “*Is my compound too toxic to be therapeutic?*”

Cytotoxicity is a well-established and easily accessible endpoint to gather early information about the general / acute toxic potential of a test article. The *in vitro* cytotoxicity test with primary hepatocytes is used to identify the cytotoxic potential of a test substance. The relative cell viability upon incubation with test article compared to the solvent control is determined (single point).

The ATP-lite 1step Cytotoxicity Assay (PerkinElmer) is a single reagent addition, homogeneous, luminescence ATP detection assay that measures the number of live cells in culture wells.

**Assay Design:**

- Primary hepatocytes (other cells available)
- 12-dose concentration response curve (CRC) of the test article (100x IC<sub>50</sub> or 50 µM maximum concentration)
- Two replicates of CRC
- One incubation time 24 hours
- Positive control: Compounds with known toxicity
- Negative control: Compound with known non-toxicity
- Background control: Vehicle only

**Analysis:** Luminescence is measured from 550 - 620 nm.

**Report:** IC<sub>50</sub>

**Quantity of test article required:** 1.0 - 2.0 mg

#### **Summary of Assay:**

Hepatocyte cells are incubated for 24 hours with known toxic and non-toxic compounds at a range of different concentrations. At the end of the incubation period the cells are loaded with the ATP-lite™ 1step ATP monitoring reagent and scanned using an automated plate reader with luminescence detection (Tecan Infinite M200 reader) to determine the number of active cells.

#### **CYP450 Inhibition Profiling**

This assay extends the findings of the microsomal stability assay. Pharmacologic question addressed: “*Does my compound inhibit a key oxidative metabolic enzyme that would lead to subsequent drug-drug interactions?*”

Cytochrome P450s (CYPs) are a superfamily of heme-containing enzymes that mediate the inactivation and metabolism of many drugs as well as endogenous substances. Compounds that inhibit P450s may cause the toxic accumulation of other substrates. CYP inhibition profiling examines the effects of a test compound on the metabolism of other known enzyme substrates of the five primary drug human metabolizing CYP: 1A2, 2B6, 2C9, 2D6, 3A4. The levels of the CYP isoform marker substrate and metabolites are measured in the presence and absence of a test compound by LC/MS/MS.

#### **Assay Design:**

- Five CYP isoenzymes: 1A2, 2B6, 2C9, 2D6, 3A4
- Test articles are run in triplicate
- One concentration of human liver microsomes (0.5 mg/mL)
- One concentration of test item (10 µM)
- One time point 0.5 hours
- Positive control: CYP marker reaction (Table 1)
- Negative control: NADPH deficient reaction control

**Analysis:** LC/MS/MS detection (appearance of metabolite)



**Report:** Data are expressed as % inhibition of selected metabolites formation for each CYP450 enzyme (1A2, 2B6, 2C9, 2D6, 3A4).

(See FDA guideline for CYP substrates:

<http://www.fda.gov/Drugs/DevelopmentApprovalProcess/DevelopmentResources/DrugInteractionsLabeling/ucm093664.htm>)

**Quantity of test article required:** 1.0 - 2.0 mg

### Summary of Assay:

In an assay similar to the metabolic stability assay, liver microsomes are used to determine the CYP450 inhibition profile of test compounds by measuring the % metabolism of a known substrate. Microsomes (and NADPH regenerating system) are dispensed into a 96-well plate containing a substrate and test compound (10  $\mu$ M), and the reaction is allowed to proceed for 0.5 hours at 37°C with shaking. The reaction is quenched by the addition of MeOH, centrifuged and the amount of product is measured by LC/MS/MS. Each plate will contain a known inhibitor of each CYP450 profiled as positive control and NADP-/- negative controls.

**Table 1:** Inhibition profiling for the five primary drug human metabolizing cytochrome P450s.

| CYP Enzyme | Substrate        | Metabolite                     | Known Inhibitor |
|------------|------------------|--------------------------------|-----------------|
| 1A2        | Phenacetin       | Acetaminophen                  | Furafylline     |
| 2B6        | Bupropion        | Hydroxybupropion               | Ticlopidine     |
| 2C9        | Diclofenac       | 4-hydroxydiclofenac            | Tienilic Acid   |
| 2D6        | Dextromethorphan | Dextrorphan                    | Paroxetine      |
| 3A4        | Testosterone     | 6 $\beta$ -hydroxytestosterone | Azamulin        |

## Permeability

Pharmacologic question addressed: “How well is my drug absorbed in the gastrointestinal tract?”

Evaluating compound permeability through a cell monolayer is a good indication of intestinal permeability and oral bioavailability. The Parallel Artificial Membrane Permeability Assay (PAMPA) provides a high throughput, non-cell based method for predicting passive, transcellular intestinal absorption, the process by which the majority of small molecule drugs enter circulation. In the PAMPA method, an artificial membrane immobilized on a filter is placed between a donor and acceptor compartment. The compound is introduced in the donor compartment. Following the permeation period, the amount of compound in the donor and acceptor compartments are quantified using scanning UV spectrophotometry.

The gastrointestinal tract (GT) has a pH range from pH 1 – 8. The pH of the blood is constant at pH 7.4; therefore it is possible for a pH gradient to exist between the GT and

the plasma that can affect the transport of ionizable molecules. In an effort to mimic this pH gradient *in vitro*, alternative assays with pH 7.4 for the acceptor compartment and pH values 5.0, 6.2, and 7.4 in the donor compartment are used.

PAMPA is a well-established and predictive assay that models the absorption of drugs in the gut. However, PAMPA is an artificial system that may provide inaccurate and potentially misleading results. Despite these limitations, PAMPA can be a useful tool to prioritize lead compounds in early stages of development. The colon carcinoma (Caco-2) cell permeability assay is the industry standard for *in vitro* prediction of intestinal absorption of drugs, but it too has limitations. Caco-2 cells require extensive culturing (>20 days), and often fail to form the cohesive monolayer necessary for uniform transport of compounds across the cell layer. The assay requires a significant amount of compound to perform the assay (typically ~20 mg). Together, the limitations of time and compound consumption decrease the value of the results obtained by Caco-2 at the early stages of drug discovery. One variant of PAMPA is the Blood Brain Barrier (BBB) PAMPA in where the artificial monolayer contains brain specific membrane components, such as sphingolipids.

**Assay Design:**

- Test articles are run in triplicate
- One concentration (25  $\mu$ M)
- One time point (18 hours)
- One pH (7.4) or three point pH range (5.0, 6.2, 7.4) for acceptor compartment
- Single polar membrane lipid (phosphatidylcholine in dodecane)
- Multiscreen PVDF membrane (0.45  $\mu$ m)
- Positive control: Verapamil (high permeability)
- Negative control: Theophylline (low permeability)

**Analysis:** The concentration of the compound remaining in the donor well, diffused through the membrane and into the acceptor well, and reference compounds are measured by UV spectrophotometry

**Report:** Bin the results as high, medium, or low predicted absorption and report direct permeability units ( $10^{-6}$  cm/s)

**Quantity of test article required:** 5.0 - 7.0 mg

**Summary of Assay:**

A lipid bilayer is established on a membrane filter and a test compound solution is added to the top of the membrane-lipid interface. The ability of compounds to passively diffuse through the lipid treated membrane is an indication of the overall compound permeability. This approach is helpful in compound profiling and supporting the relative rank ordering of compounds.

## Example of *In Vitro* ADME Profiling Assays

Table 2 below shows an example tabulation of the ADME properties assessed and evaluated as a requirement for nomination of a chemical probe in the Molecular Libraries Program (MLP) for probes ML301, ML314 and a few key related analogs, as described in the NCBI MLP probe report: <http://www.ncbi.nlm.nih.gov/books/NBK184496/> that describes a novel small molecule agonist for the Neurotensin 1 Receptor (NTR1).

ADME profile of ML301 (Probe 1) and related compounds: ML301, its intriguing naphthyl analog (MLS-0446079), and the prior art, pyrazole, were evaluated in a detailed *in vitro* ADME screen as shown in Table 2. Despite its structural similarity (imidazole vs. pyrazole) to the prior art compound, ML301 exhibited substantial advantages in this testing, especially with regard to plasma and microsomal stability. These three compounds all exhibited good solubility due to the presence of the carboxylic acid moiety.

The PAMPA assay is used as an *in vitro* model of passive, transcellular permeability. The compounds exhibited good overall permeability, inversely related to the pH of the donor compartment. Because these NTR1 agonists are envisioned as predecessors of psychoactive drugs, a preliminary assessment of their potential to cross the BBB was performed. When incubated with an artificial membrane that models the BBB, much lower permeability was observed. These observations are also consistent with the carboxylic acid function in the compounds, and may present an opportunity for future enhancements.

Plasma protein binding is a measure of a drug's efficiency of binding proteins within blood plasma. The less bound a drug is, the more efficiently it can traverse cell membranes or diffuse. Drugs that are highly bound to plasma proteins are confined to the vascular space, thereby having a relatively low volume of distribution. In contrast, drugs that remain largely unbound in plasma are generally available for distribution to other organs and tissues. The imidazole scaffold compounds (ML301 and its MLS-0446079) exhibited substantial protein binding, but significantly lower than that of the prior art, pyrazole.

The stability of small molecules and peptides in plasma may strongly influence *in vivo* efficacy. Drug candidates are susceptible to enzymatic processes, such as those mediated by proteases or esterases in plasma. They may also undergo intramolecular rearrangement or bind irreversibly (covalently) to proteins. ML301 showed excellent stability in plasma, significantly better than that of either analog.

The microsomal stability assay is commonly used to rank compounds according to their metabolic stability, which influences how long the candidate may remain intact while circulating in plasma. ML301 showed excellent stability in human and modest stability in mouse liver homogenates, which was much better than that observed for the prior art analog, MLS-0437103. None of the compounds showed toxicity (>50  $\mu\text{M}$ ) toward human hepatocytes.

ADME profile of ML314 (Probe 2): As described above for ML301, *in vitro* ADME screening was also conducted for ML314. Consistent with its aqueous solubility data, ML314 exhibited high permeability in the PAMPA assay with increasing pH of the donor compartment. When incubated with an artificial membrane that models the BBB, ML314 was found to be highly permeable. ML314 was highly bound to plasma protein and exhibited very high plasma stability. ML314 was metabolized rapidly when incubated *in vitro* with human and mouse liver microsomes. This result is not completely surprising because of the presence of several unsubstituted aryl and alkyl positions and Ar-OMe ethers, which are prone to oxidation, hydrolysis, conjugation and other metabolic reactions. ML314 showed a >15-fold window for toxicity (LC<sub>50</sub> = 30 μM) towards human hepatocytes. Improving the metabolic stability and toxicity profile of ML314 represents a challenge as well as an avenue for further optimization studies in the future.

**Table 2:** Summary of *in vitro* ADME/T properties of NTR1 agonists ML301 (& analogs) and ML314.

| ADME/T Assay Panel Component  |                    | MLS-0437103<br>( <i>prior art pyrazole</i> ) | MLS-0446079<br>( <i>ML301-naphthyl analog</i> ) | ML301<br>(Probe 1)                   | ML314<br>(Probe 2)<br><i>β-arrestin biased</i> |
|---|--------------------|--|---|--------------------------------------|--|
| <b>Aqueous Solubility</b> in pION's buffer (μg/mL) [ <i>μM</i> ] <sup>a</sup><br>pH 5.0/6.2/7.4                       |                    | 52.9 / >155 / >155<br>[113 / >296 / >296]    | 102.6 / >145 / >145<br>[247 / >297 / >297]      | >52 / >52 / >52<br>[>99 / >99 / >99] | >125 / 9.0 / 0.52<br>[>297 / 21.4 / 1.2]       |
| <b>Aqueous Solubility</b> in 1x PBS, pH 7.4 (μg/mL) [ <i>μM</i> ] <sup>a</sup>  |                    | ND   | ND  | ND                                   | 0.45 [1.1]                                     |
| <b>PAMPA Permeability, P<sub>e</sub></b><br>(x10 <sup>-6</sup> cm/s)<br>Donor pH: 5.0 / 6.2 / 7.4<br>Acceptor pH: 7.4 |                    | 1267 / 725 / 70                              | 953 / 145 / 12                                  | 363 / 17 / 6                         | 1163 / 2145 / 2093                             |
| <b>BBB-PAMPA Permeability, P<sub>e</sub></b><br>(x10 <sup>-6</sup> cm/s)<br>Donor pH: 7.4 Acceptor pH: 7.4            |                    | 4.8  | 1.1   | 1.2                                  | 399  |
| <b>Plasma Protein Binding</b> (% Bound)   | Human 1 μM / 10 μM | 99.60 / 99.71                                | 97.93 / 97.96                                   | 98.69 / 98.70                        | 99.45 / 99.22                                  |
|   | Mouse 1 μM / 10 μM | 96.63 / 97.10                                | 96.43 / 95.41                                   | 92.15 / 91.36                        | 99.67 / 98.84                                  |
| <b>Plasma Stability</b> (% Remaining at 3 hrs) Human/Mouse  |                    | 88.94 / 70.74                                | 76.00 / 75.97                                   | 100 / 100                            | 100 / 99.55                                    |
| <b>Hepatic Microsome Stability</b><br>(% Remaining at 1hr) Human/Mouse  |                    | 75.50 / 45.67                                | 100 / 75.70                                     | 100 / 59.48                          | 1.36 / 0.16                                    |

<sup>a</sup> Solubility also expressed in molar units (μM) as indicated in *italicized [bracketed values]*, in addition to more traditional μg/mL units. ND = Not Determined

Table 2 continues on next page...

Table 2 continued from previous page.

| ADME/T Assay Panel Component  | MLS-0437103<br>( <i>prior art pyrazole</i> ) | MLS-0446079<br>( <i>ML301-naphthyl analog</i> ) | ML301<br>(Probe 1) | ML314<br>(Probe 2)<br><i>β-arrestin biased</i> |
|---|--|---|--------------------|--|
| <b>Toxicity</b> Towards Fa2N-4 Immortalized Human Hepatocytes LC <sub>50</sub> (μM) | >50  | >50   | >50                | 29.6   |

<sup>a</sup> Solubility also expressed in molar units (μM) as indicated in *italicized [bracketed values]*, in addition to more traditional μg/mL units. ND = Not Determined

## In Vivo Analysis - High Compound Requirements and Low Capacity

### Rapid Assessment of Compound Exposure (R.A.C.E.)

This experiment is a rapid and efficient compressed *in vivo* PK screening method to determine the pharmacokinetic attributes of novel chemical probes (3). A small cohort of animals (4 mice or 2 rats/experiment), is administered compound orally (*p.o.*) or by intraperitoneal injection (*i.p.*) at a single dose (5 - 50 mg/kg). Blood samples are collected at 20 and 120 minutes. The plasma samples are analyzed with a mini-standard curve (Figure 1). This experiment provides a snapshot of compound exposure sufficient to estimate total compound exposure as the area under the curve (AUC<sub>(20-120 min)</sub>), providing a rank order of estimated AUC values to prioritize compounds for further investigation.

Another utilization for R.A.C.E. is to evaluate varying formulation excipients for improving solubility and absorption. Generally, formulation excipients approved by the FDA are available for this assay. Please refer to reference (4) for FDA approved excipients and amounts.

#### Assay Design:

- Test articles are formulated for *p.o.* or *i.p.* dosing
- One dose of test article (5 - 50 mg/kg)
- Two time points (*t* = 20 min and 120 min)

**Analysis:** LC/MS/MS detection of the test compound(s) in plasma samples

**Report:** Estimated AUC<sub>(20-120 min)</sub> and a rank order of compound exposure

**Quantity of test article required:** 5.0 - 50.0 mg

### Comprehensive Pharmacokinetic Analysis

Compounds that show promising PK profiles or that are further developed, can be subjected to a comprehensive pharmacokinetic analysis and metabolite identification

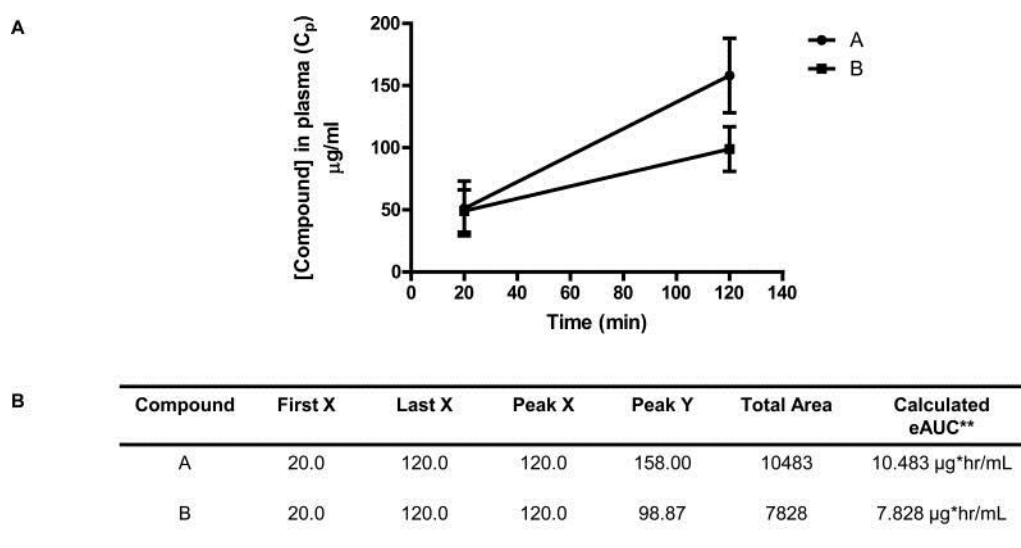


**Figure 1:** Example of data from a previously performed RACE study. The purpose of this study was to select which compound from a series exhibited the highest estimated exposure. (A) Representative exposure data from two compounds in a series obtained by sequential RACE studies (n=3 mice/time point; vehicle mice showed no compound in the plasma, data not shown). (B) Results from the GraphPad Prism5 AUC analysis. \*\*eAUC (estimated exposure (AUC<sub>20-120 min</sub>)) using a “trapezoidal” estimation of AUC (Copyright © 2012 John Wiley & Sons, Inc., republished with permission from (3)).

study. An example set of graphs representing typical time course drug plasma concentrations following oral dosing can be found in Wikipedia <http://en.wikipedia.org/wiki/Pharmacokinetics> and are reproduced to illustrate the key related parameters: time to reach ( $t_{max}$ ) maximal concentration ( $C_{max}$ ) of compound, time to reduce concentration by half of the initial value ( $t_{1/2}$ ), dosing interval ( $\tau$ ), and area-under-curve (AUC) or total compound exposure (Figure 2).

A minimum of six 300 gram rats are required, per compound tested, for appropriate sampling. For each drug, the compound will be formulated in suitable vehicle to typically 1.0 mg/mL (final concentration) and administered to 3 rats at 1 mg/kg *i.v.* into a femoral vein catheter. The same substance is administered to an additional 3 rats at 2 mg/kg by oral gavage (*direct dosing of compound into the stomach through a feeding tube*). Blood is drawn (0.25 mL) via the femoral artery catheter at 5, 15, and 30 minutes and at 1, 2, 4, 6, 8 and 24 hours post dose for a total maximum volume of 2.25 mL. Plasma samples are analyzed by LC/MS/MS. A comprehensive PK analysis requires 6-12 animals and blood collections at 8 time points.

#### Assay Design:

- Single test article is formulated for both *p.o.* and *i.v.* dosing
- *I.v.* and *p.o.* doses of test article (e.g., 1.0 mg/kg and 2.0 mg/kg)
- Nine time points (5, 15, and 30 min and at 1, 2, 4, 6, 8 and 24 hours).

**Analysis:** LC/MS/MS detection of the test compound(s) in individual plasma samples

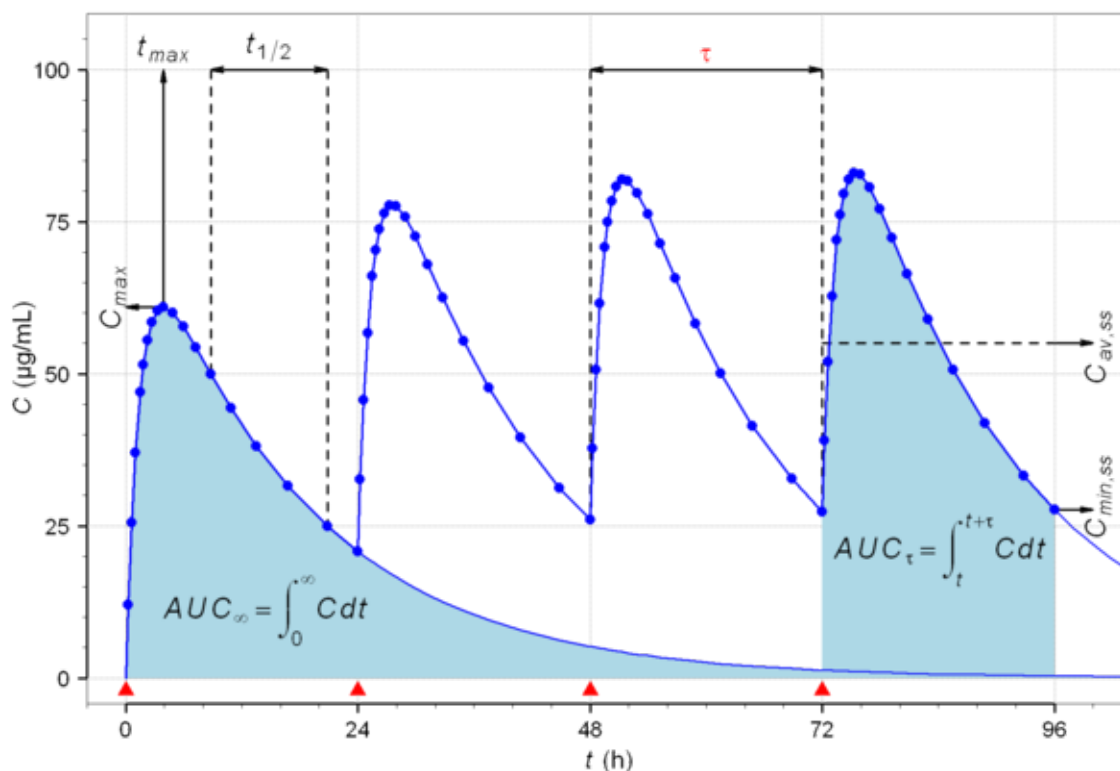


**Figure 2:** Time course of drug plasma concentrations over 96 hours following oral administrations every 24 hours ( $\tau$ ). Absorption half-life is 1 hour and elimination half-life is 12 hours. Note that in steady state and in linear pharmacokinetics  $AUC_{\tau} = AUC_{\infty}$ . Steady state is reached after about  $5 \times 12 = 60$  hours (courtesy of Helmut Schütz).

**Report:** Time course of plasma drug concentration versus time, PK parameters (for example, AUC,  $t_{1/2}$ , oral bioavailability) and metabolite identification

**Quantity of test article required:** 10 - 100 mg

## Suggested Equipment and Resources

**Automated workstation:** A flexible versatile high-throughput/high-capacity workstation system for automated liquid handling is a useful work horse of the pharmacology lab. The system should be capable of processing compound solutions for analysis and executing the various *in vitro* profiling assays. A variable spanning 8 channel pipette arm, a 96-well multichannel pipetting head, and plate gripper arm are useful for reformatting samples between vials, tubes, and 96-well plates. Specialized devices include vacuum filtration and magnetic separation modules, as well as integrated devices for heating, cooling, and shaking samples.

**Multimodal Plate Reader:** A multi-mode plate reader capable of UV/Vis, top/bottom fluorescence, and flash/glow luminescence read modes accessible to the plate gripper arm of a workstation is useful for unattended reading for a batch of samples.

**Liquid Chromatography/Mass Spectrometric/Mass Spectrometry (LC/MS/MS):** This technology is the workhorse of all ADME/T and PK analyses of samples from both the *in vitro* and *in vivo* assay. After extraction of biomatrix from small molecules, the small molecule sample and any related compounds (metabolized, hydrolyzed, or broken down compounds) are first separated through high-performance liquid chromatography (HPLC). The effluent from the HPLC are monitored in real-time for ultraviolet absorbance at 254 and 280 nm, and absorbing samples are diverted into an on-line electrospray unit to introduce samples into the mass spectrometer, followed by sequential quadrupole selection and detection of mass/charge ( $m/z$ ) distributions of samples that are characteristic of parent and derived molecules. For example, we use a Shimadzu UPLC coupled with an automated AB Sciex API 4000 MS/MS system with QTRAP detection. This is a high performance hybrid triple quadrupole/linear ion trap system with excellent dynamic range and sensitivity. However, this is a very mature sector of the MS market and several vendors with comparable instruments exist.

**Microplate Scintillation and Luminescence Counter:** For studies with radiolabeled compounds, scintillation devices are still required. Currently a few manufacturers still make multi-wall, microtiter plate based scintillation counters (e.g. PerkinElmer TopCount NXT™), these devices can also plate luminescence readers.

## References

### Literature Cited

1. Yan Z, Caldwell GW. Metabolism profiling, and cytochrome P450 inhibition & induction in drug discovery. *Curr Top Med Chem*. 2001 Nov;1(5):403–25. [Review]. PubMed PMID: 11899105.
2. White RE. High-throughput screening in drug metabolism and pharmacokinetic support of drug discovery. *Annu Rev Pharmacol Toxicol*. 2000;40:133–57. [Review]. PubMed PMID: 10836130.
3. McAnally D, Vicchiarelli M, Siddiquee K, Smith LH. In Vivo Rapid Assessment of Compound Exposure (RACE) for Profiling the Pharmacokinetics of Novel Chemical Probes. *Curr Protoc Chem Biol*. 2012 Dec 1;4(4):299–309. PubMed PMID: 23788556.
4. Strickley RG. Solubilizing excipients in oral and injectable formulations. *Pharm Res*. 2004 Feb;21(2):201–30. [Review]. PubMed PMID: 15032302.

### Additional References

5. Guengerich FP. Characterization of human microsomal cytochrome P-450 enzymes. *Annu Rev Pharmacol Toxicol*. 1989;29:241–64. [Review]. PubMed PMID: 2658771.
6. Li AP. Screening for human ADME/Tox drug properties in drug discovery. *Drug Discov Today*. 2001 Apr 1;6(7):357–66. PubMed PMID: 11267922.



7. Banker MJ, Clark TH, Williams JA. Development and validation of a 96-well equilibrium dialysis apparatus for measuring plasma protein binding. *J Pharm Sci.* 2003 May;92(5):967–74. [Comparative Study]. PubMed PMID: 12712416.
8. Liu H, Sabus C, Carter GT, Du C, Avdeef A, Tischler M. In vitro permeability of poorly aqueous soluble compounds using different solubilizers in the PAMPA assay with liquid chromatography/mass spectrometry detection. *Pharm Res.* 2003 Nov; 20(11):1820–6. [Comparative Study]. PubMed PMID: 14661927.
9. Bermejo M, Avdeef A, Ruiz A, Nalda R, Ruell JA, Tsinman O, Gonzalez I, Fernandez C, Sanchez G, Garrigues TM, Merino V. PAMPA--a drug absorption in vitro model 7. Comparing rat in situ, Caco-2, and PAMPA permeability of fluoroquinolones. *Eur J Pharm Sci.* [Comparative Study Research Support, Non-U.S. Gov't]. 2004 Mar;21(4): 429-41.
10. Di L, Kerns EH, Gao N, Li SQ, Huang Y, Bourassa JL, Huryn DM. Experimental design on single-time-point high-throughput microsomal stability assay. *J Pharm Sci.* 2004 Jun;93(6):1537–44. [Comparative Study]. PubMed PMID: 15124211.
11. Kansy M, Avdeef A, Fischer H. Advances in screening for membrane permeability: high-resolution PAMPA for medicinal chemists. *Drug Discov Today Technol.* 2004 Dec;1(4):349–55. PubMed PMID: 24981614.
12. Avdeef A, Artursson P, Neuhoff S, Lazorova L, Grasjo J, Tavelin S. Caco-2 permeability of weakly basic drugs predicted with the double-sink PAMPA pKa(flux) method. *Eur J Pharm Sci.* [Research Support, Non-U.S. Gov't]. 2005 Mar;24(4): 333-49.
13. Di L, Kerns EH, Hong Y, Chen H. Development and application of high throughput plasma stability assay for drug discovery. *Int J Pharm.* 2005 Jun 13;297(1-2):110–9. PubMed PMID: 15876500.
14. Avdeef A, Tsinman O. PAMPA--a drug absorption in vitro model 13. Chemical selectivity due to membrane hydrogen bonding: in combo comparisons of HDM-, DOPC-, and DS-PAMPA models. *Eur J Pharm Sci.* 2006 May;28(1-2):43–50. PubMed PMID: 16476536.
15. Bendels S, Tsinman O, Wagner B, Lipp D, Parrilla I, Kansy M, Avdeef A. PAMPA - excipient classification gradient map. *Pharm Res.* 2006 Nov;23(11):2525–35. PubMed PMID: 17053953.
16. Avdeef A, Bendels S, Di L, Faller B, Kansy M, Sugano K, Yamauchi Y. PAMPA--critical factors for better predictions of absorption. *J Pharm Sci.* 2007 Nov;96(11): 2893–909. PubMed PMID: 17803196.
17. Kerns EH, Di L, Carter GT. In vitro solubility assays in drug discovery. *Curr Drug Metab.* 2008 Nov;9(9):879–85. [Review]. PubMed PMID: 18991584.
18. Sinko B, Garrigues TM, Balogh GT, Nagy ZK, Tsinman O, Avdeef A, Takacs-Novak K. Skin-PAMPA: a new method for fast prediction of skin penetration. *Eur J Pharm Sci.* [Research Support, Non-U.S. Gov't]. 2012 Apr 11;45(5):698-707.



# Glossary



# Glossary of Quantitative Biology Terms

Viswanath Devanarayan,<sup>1</sup> Barry D. Sawyer, Chahrzad Montrose, Dwayne Johnson, David P. Greenen, Sitta Sittampalam,<sup>2</sup> Terry Riss,<sup>3</sup> and Lisa Minor<sup>4</sup>

Created: April 15, 2012; Updated: September 22, 2014.

## Abstract

In this chapter, the authors have provided standardized definitions of cell culture and quantitative biology terms generally employed in assays for HTS and lead optimization. The quantitative biology terms include definitions both biological and statistical concepts used assay design, development and validation. These definitions are intended to facilitate streamlined communications across multiple disciplines of scientists involved in drug discovery and development research.

## Cell Culture Terms

**Acclimatization** — Adaption of a culture to different environments such as temperature, humidity or CO<sub>2</sub>.

**Anaerobic Growth** — Growth of an organism in the absence of ambient O<sub>2</sub>.

**Anchorage Dependent (Attached) Cells** — Cells that require a substrate to survive in culture.

**Apoptosis** — A process in cells leading to programmed cell death.

**Batch Culture** — Cells or microbes cultured in a bioreactor that contains all nutrients needed until all is harvested as a unit.

**Bioreactor** — Environmentally controlled vessel for creation of biological products.

**Carry** — To maintain a cell line by subculturing in tissue culture medium containing nutrients that will maintain the phenotype and genotype.

**Cell Clone** — Cell line derived from a single cell and therefore all cells are identical

**Cell Culture** — Establishment and maintenance of cells derived from dispersed tissue taken from original tissues, primary culture, or from a cell line or cell strain.

**Cell Line** — Immortalized cell that has undergone transformation and can be passed indefinitely in culture.

---

<sup>1</sup> Eli Lilly & Company, IN. <sup>2</sup> National Center for Advancing Translational Sciences (NIH), MD. <sup>3</sup> Promega Corp. WI. <sup>4</sup> In Vitro Strategies, LLC, NY.

**Cell Passage** — The splitting (dilution) and subsequent redistribution of a monolayer or cell suspension into culture vessels containing fresh media, also known as subculture.

**Cell Strain** — Cells which can be passed repeatedly but only for a limited number of passages.

**Cell Transformation** — Permanent alteration in cell genotype that results in phenotypic change from the original cell. It may result in a primary cell becoming immortalized.

**Chemically Defined** — Solution such as culture medium in which the ingredients are completely known.

**Cloning Efficiency** — Percent of cells that can become a clone when plated at single cell densities.

**Confluency** — Based on the amount of space between the cells on the growth surface. A culture is confluent if no plate can be seen between cells. Degrees of confluency is based on percent of culture dish that is covered. Thus 100% to lower percent exists. The confluency of the culture may influence cell division and gene expression.

**Cytopathic** — Causing cell pathology.

**Cytotoxic** — Causing cell death.

**Density-Dependent Growth Inhibition** — Reduced proliferation of cells upon reaching a threshold density, i.e. reaching confluence.

**Differentiation** — Property of cells to exhibit tissue-specific properties in culture.

**Endotoxin** — a material that is part of the cell wall of some bacteria. It can be released upon bacterial death and cause cell sepsis. Medias and media components are routinely tested for its presence.

**Generation Time** — Time it takes for a cell to complete a cycle of division from same stage to same stage.

**Growth Curve** — A plot of cell number vs. time. Should demonstrate exponential log phase growth up to stationary phase.

**Hatch** — To bring cells out of the freezer; to start a culture from a freezer stock.

**Heat Inactivation** — heating serum at 56C for 30 minutes to inactivate complement proteins that can affect cell growth of some cell lines.

**Mycoplasma** — Prokaryotic organism. Smallest form of bacteria with no cell walls. It can cause infections in plants and animals. It can infect cultured cells without obvious change in cellular morphology but can result in alterations in cellular behaviors. Its presence is routinely monitored.

**Monolayer** — A layer of cells one cell thick, grown in a culture.

**Primary Cells** — Cells resulting from the seeding of dissociated tissues, i.e. HUVEC cells. Primary cultures will eventually die or lose their original phenotype and genotype with passaging.

**Pass** — See cell passage or subculture

**Selective Medium** — culture medium containing a factor to limit the growth of particular organisms. It could be used in transfection (contain antibiotic) to eliminate cells that are not transfected and do not receive the antibiotic resistance factor from transfection.

**Serum Free Medium (SFM)** — culture growth solution that does not contain serum but may contain other components as supplements.

**Split** — To subculture/passage cells; see cell passage.

**Stable Cell Line** — Cell line that stably expresses a transfected product. Typical systems that exist include resistance to antibiotics such as neomycin phosphotransferase, conferring resistance to G418, etc. The culturing of the cells can be done as a mixed population or by single cell culture to obtain cell clones from one single integration event.

**Sterile Techniques** — methods to ensure lack of contamination with microorganisms.

**Suspension Culture** — Cells which do not require attachment to a substrate to proliferate, i.e. anchorage independent. Cell cultures derived from blood are typically grown in suspension. Cells can grow as single cells or as clumps. To subculture, the cultures that grow as single cell suspension can simply be diluted. However, cultures containing clumps must have the clumps disassociated prior to subculturing.

**Surfactant** — A substance used to minimize the shear stress of water or medium. It can be used in media designed for suspension culture. A common one is Pluronic.

**Transient Transfection** — The introduction of foreign DNA into a cell to allow the expression of DNA and protein. The DNA does not incorporate into the genome therefore, with cell division, the effect is lost (diluted out) making the event transient (transient transfection). Cells capable of being transfected are referred to as “competent”. Protocols are available for opening transient “holes” in the cell membranes allowing introduction of plasmids or siRNA.

**Thaw** — Same as hatch.

## Quantitative Biology Terms

### Absolute EC50

The molar concentration of a substance that increases the measured activity in an agonist assay to 50% of the range of activity expressed relative to maximum and minimum controls.

### Absolute IC50

The molar concentration of an inhibitor required to block a given response by 50%, half way between the maximum and minimum controls if the response is expressed relative to the maximum and minimum controls.

### Accuracy

A measure of the closeness of agreement of a measured test result obtained by the analytical method to its theoretical true (or accepted reference) value. This is relevant only for calibration-curve based applications where a purified or relative reference standard material is available to quantify the analyte levels in test samples.

### Accuracy Profile

A plot of the mean percent recovery (or percent relative error) and its confidence interval versus the concentration of the spiked standards (validation or QC samples). It is used to judge the quality of a calibration-curve based assay in terms of total error (bias plus variance).

### Assays/Methods

- **Assay-Biochemical:** Biological measurements performed with purified or crude biochemical reagents.
- **Assay-Cell-based:** Biological measurements performed in which at least one of the reagents consists of a population of live cells.
- **Assay Design:** see Multivariate (Factorial Experiments), aka, Experimental Design.
- **Assay-In vitro:** From the Latin meaning 'in glass'. Any assay (biochemical or cell-based) conducted in a synthetic container (e.g. microtiter plate, microfluidic cell).
- **Assay-In vivo:** From the Latin meaning 'in life'. Typically used for assays conducted in living animals (e.g. mice, rats, etc.) with the exception of microorganisms (e.g. yeast, bacteria or *C. elegans*).
- **Assay Platform:** Technology used to measure response or output. (e.g. Fluorescence polarization or Radiometric counting).
- **Assay-Phenotypic:** An assay where the measured signal corresponds to a complex response such as cell survival, proliferation, localization of a protein, nuclear translocation etc. The molecular target is not assumed.
- **Assay-Primary:** The first assay performed in a testing scheme to identify biologically active chemical entities in a screening mode.
- **Assay-Secondary:** Assays that follow the primary assays to confirm the biological activity of chemical entities identified in the primary assays. This can also include selectivity and specificity assays.
- **Assay-Selectivity/Specificity:** Assays employed to elucidate the specificity of biologically active chemical entities towards a set of closely related disease targets.
- **Assay Validation:** see Validation
- **Assay-Separation:** Prior to detection a physical separation of at least one component from the assay is performed. (Standard ELISA, filtration, HPLC etc.)



- **Assay-non-separation:** Any assay where a physical separation is not required prior to detection.
- **Assay-Target based:** An assay where the measured response can be linked to a known set of biological reagents such as a purified enzyme, domain or a reporter gene.

### **Biological Target**

A macromolecule or a set of macromolecules in a biochemical pathway that is responsible for the disease pathology.

### **Bottom**

The lower asymptote of a logarithmically derived curve. The Bottom value can be determined with real values or predicted using the logarithm applied to the result data set.

### **Calibration Curve**

Also called “standard curve”, a calibration curve is a regression of the assay response on the known concentrations in “standard” samples. It is a model that fits data from standards and is used for calculating (calibrating) values of unknown test samples. For example, measurement of protein/biomarker expression levels of various compounds from in-vitro and in-vivo samples.

### **Central Composite Designs**

A type of multi-factor experiment that is used to optimize the most important factors in an assay (usually 3 to 5 factors).

### **Classification & Regression Tree Models**

A set of statistical methods in which observations are classified into groups based on a set of predictor variables and their relationship with a response variable. These models can be used for multivariate correlation analysis.

### **Cluster Analysis**

A set of statistical methods in which objects (e.g., compounds) are divided into groups such that objects within a group are similar across a set of 2 or more variables.

### **Concordance Correlation Coefficient**

A measure of agreement between two variables, i.e., how closely the paired values match. That is, it measures the degree of closeness of the data to the agreement line ( $Y=X$  line). Since the Pearson's correlation measures the degree of departure of the data from the best straight line, which can be considerably different from the agreement line, the concordance correlation coefficient is more stringent than the Pearson's correlation.

### **Control Compound**

A compound that is routinely run in the same manner as the test compounds in every run of the assay. This term does not refer to the plate controls used to define the maximum

and minimum responses, and they may or may not be a “literature standard” or “reference” compound.

### **CRC**

Concentration-response curve mode. The mode to describe an assay performed with multiple concentrations of a given test substance, which might then render a logarithmically-derived graph curve.

### **Dynamic Range**

It is the interval between the upper and lower concentration of the analyte in the sample for which the assay has been demonstrated to have acceptable level of accuracy, precision, linearity, etc.

### **EC50**

The effective concentration of an agonist, which produces 50% of the maximum possible response for that agonist.

### **Emin**

The maximum activity of an antagonist test substance relative to a reference agonist. This is obtained by first generating a fitted top from a %Inhibition curve and then converting that to the corresponding %Stimulation of the reference agonist curve. The E-min value for antagonist mode should equal the relative efficacy for agonist mode for competitive inhibitors.

### **Factor**

An assay variable that can be changed by the user. Examples include the amount of a reagent, incubation time, buffer type, etc.

### **False Positive**

A hit where the signal modulation is not related to the targeted activity. The sources of false positives include, random or systematic errors in liquid handling, spectrophotometric or fluorescence interference of the assay signal by chemical compounds, reagent instability etc. It is important to note that false positives can be reproducible when they are not related to random errors (as in the case of compound interference).

### **Fold Activity**

The ratio of biological activity in the presence of an exogenous substance to that in its absence. It is the test compound's observed response (raw data value) divided by the median of the same plate's Min wells. This result type is used exclusively with single point assays. If the value is greater than 1, the test compound is likely an agonist. If the calculated value is less than 1, the test compound could be an inverse agonist.

### Fold Activity Max

The maximum observed Fold Activity among the concentrations included in a concentration response curve. It is the test compound's observed response (raw data value) divided by the median of the same plate's Min wells. If the value is greater than 1, the test compound is likely an agonist. If the calculated value is less than 1, the test compound could be an inverse agonist.

### Four Parameter Logistic Model

A non-linear regression model commonly used for fitting dose-response and concentration-response data. The four parameters are Minimum (response at zero dose), Maximum (response at infinite dose), Relative EC50 (or IC50, ED50, etc.) and Slope. The 4PL model can be written in several mathematically equivalent versions. Two popular versions are given below.

$$Y = bottom + \frac{top - bottom}{1 + \left(\frac{x}{EC50}\right)^{slope}}$$

$$Y = bottom + \frac{top - bottom}{1 + 10^{(\log(x) - \log(EC50)) \cdot slope}}$$

### Fractional Factorial Experiments

A type of multi-factor experiment in which only a subset of factor level combinations is tested. These experiments are very efficient for screening a large number of factors prior to optimizing the most important factors.

### Generalized Additive Models

Statistical models in which more general (e.g., nonlinear) relationships between variables can be examined. These models can be used for multivariate correlation analysis.

### High Throughput Screening (HTS)

Greater than 100,000 compounds screened per screen.

### Homogeneous Assay

All assay components exist in solution phase at the time of detection (e.g. none of the components are in beads or cells). Technically no component scatters light.

### Heterogeneous Assay

One or more assay components are present in solid phase at time detection. (e.g.: SPA, cells or IMAP).

### Hill Coefficient

Derived slope a three or four parameter logistic curve fit. Should not be fixed to any given value without consultation with a statistician. It should not be a negative value except for inverse agonist assays.

## Inhibition

Reduction of a predefined stimulus. Unit of Measure is always % when normalized to the dynamic range of the assay.

### Inhibition at Max Included Concentration

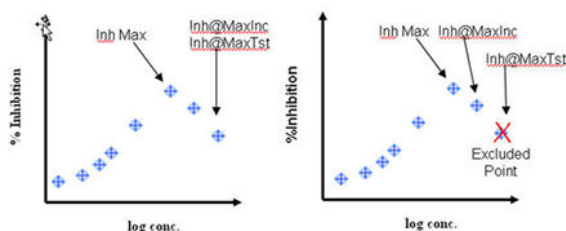
Inhibition observed at the highest included (i.e. not excluded) concentration of a substance tested in a concentration response mode method version regardless of whether it was included in the parametric fit to produce derived results. (see Illustration below)

### Inhibition at Max Tested Concentration

Inhibition observed at the maximum concentration of a substance tested in a concentration response mode method version regardless of whether it was included in the parametric fit to produce derived results. (see Illustration below)

### Inhibition Max

Maximum inhibition produced by any concentration that was included for the application of a curve fit algorithm (see Illustration below)



## Inverse Agonist

When an inverse agonist binds to a receptor, it stabilizes the inactive form of the receptor, shifts the equilibrium toward that state and produces a response opposite to that produced by an agonist in the biological system under investigation. These substances possess negative intrinsic activity.

## Least Squares (Pearson's) Correlation Coefficient

A measure of linear correlation between two variables.

## LsA (Limits of Agreement)

These are statistical limits that define the region that contains 95% of all potency ratios.

## Mean Ratio (MR)

The average ratio of potencies between the two runs.

## Multivariate (Factorial) Experiments (Experimental Design)

A system of experimentation for optimizing assays in which multiple factors are varied simultaneously in such a way that the effect of each factor can still be determined. In

addition, one can also measure interactions between factors and use this information to more efficiently optimize an assay.

### **Multiple Linear Regression**

A statistical method where the response variable is a linear function of several predictor variables. This can be used for multivariate correlation analysis.

### **Multivariate Correlation Analysis**

A statistical analysis method where correlative relationships between 3 or more variables are examined.

### **Nonlinear Regression**

Statistical methodology for fitting models that is nonlinear in their parameters, for example, the four-parameter logistic model.

### **One Factor at a Time Experiments**

A series of experiments in which one factor is changed at a time. Once the “best” condition for one factor is found, it is fixed at that setting for subsequent experiments. This approach to assay optimization will not find the optimum conditions if at least one factor interacts with another, i.e., the best level of one factor depends on the levels of another factor.

### **Overall MSD (Minimum Significant Difference)**

The minimum difference in efficacies of two compounds evaluated in different runs that is statistically significant, i.e. that should be considered a real change in efficacy. The Overall MSD is defined for a single run of each compound.

### **Overall MSR (Minimum Significant Ratio)**

The minimum ratio in potencies of two compounds evaluated in different runs that is statistically significant, i.e. that should be considered real change in potency. The Overall MSR is defined for a single run of each compound.

### **Optimization**

The process of developing an assay (prior to validation) wherein the variables affecting the assay are elucidated (e.g., Antibody concentration, incubation time, wash cycles, etc.). This process is ideally carried out using a multi-variate factorial approach where the interdependence between multiple variables/parameters can be taken into account.

### **Orphan Receptor**

A biological target that has a primary sequence suggesting it is a member of one of the super families of biological targets; however, no ligand for this “receptor” has been identified. Generally, it is the aim of the research effort to identify ligands for this “orphan” so that a protocol for a validated assay can be created.

### **Percent Recovery**

The calibrated value of a standard or validation sample divided by its expected value (known concentration), expressed as a percentage.

### **Plate Format**

Microtiter plate well density (e.g., 96-, 384- or 1536-well) and plate composition (e.g., clear bottom black or clear bottom polystyrene, etc.)

### **Potentialiation**

Many assays involve the addition of one or more concentrations of a test substance in the presence of a fixed concentration of the known active substance called the Reference Agonist. In this mode, if an increased stimulus is observed the test compound is deemed a potentiator. Potentialiation is the response produced by the combination of substances minus the response produced by the specific concentration of Reference Agonist alone.

### **Precision**

A quantitative measure (usually expressed as standard deviation, coefficient of variation, MSR) of the random variation between a series of measurements from multiple sampling of the same homogenous sample under the prescribed conditions.

### **Precision Profile**

A plot of the variability of calibrated values (expressed as a CV) versus concentration of standard. It is used to judge the quality of a calibration curve in terms of the variability in the calibrated values. It also determines the working range of a calibration curve.

### **Production MSD (Minimum Significant Difference)**

The minimum difference in efficacies of two compounds evaluated in different runs that is statistically significant, taking into account the number of runs routinely applied to all compounds in the assay. For example, if all compounds are routinely tested twice on separate days then the average of both runs will have greater precision than each individual run, and the Production MSD reflects this increased precision.

### **Production MSR (Minimum Significant Ratio)**

The minimum ratio in potencies of two compounds evaluated in different runs that is statistically significant, taking into account the number of runs routinely applied to all compounds in the assay. For example, if all compounds are routinely tested twice on separate days then the average of both runs will have greater precision than each individual run, and the Production MSR reflects this increased precision.

### **Quantitative Biology**

A set of skills that is essential for the design, optimization and validation of reproducible and robust assays/methods to establish the pharmacological profiles of biologically active chemical entities. The practice of quantitative biology requires the understanding of how cellular, biochemical and pharmacological principles can be integrated with analytical and

automation technologies, employing appropriate statistical data analysis and information technology tools.

### **Relative AUC**

Defined as the ratio of the area under the fitted concentration-response curve for the test compound to the area under the fitted concentration-response curve for the reference compound.

### **Relative EC50**

Relative EC50; the molar concentration of a substance that stimulates 50% of the curve (Top – Bottom) for that particular substance. It can also be described as the concentration at which the inflection point is determined, whether it's from a three- or four-parameter logistic fit.

### **Relative EC50 Inv**

The Relative EC50 of an inverse agonist.

### **Relative Efficacy**

The maximum activity of a test substance relative to a standard positive control agonist. The result is expressed as percent from the following formula:  $100 \times \text{Fitted Top of the test substance} / \text{Fitted Top of an Agonist control}$ . The agonist control should have a four parameter curve fit with defined lower and upper asymptotes but can have the Bottom fixed to zero in certain cases. The test compounds should have a four parameter curve fit but can have a three parameter fit with the bottom fixed to zero if the data warrants it.

### **Relative Efficacy Inv**

The maximum activity of a test substance relative to a standard positive control inverse agonist. The result is expressed as percent from the following formula:  $100 \times \text{Fitted Top of the test substance} / \text{Fitted Top of the Inverse Agonist control}$ . The inverse agonist control should have a four parameter curve fit with defined lower and upper asymptotes but can have the Bottom fixed to zero in certain cases. The test compounds should have a four parameter curve fit but can have a three parameter fit with the bottom fixed to zero if the data warrants it.

### **Relative IC50**

Relative IC50; the molar concentration of a substance that inhibits 50% of the curve (Top – Bottom) for that particular substance. It can also be described as the concentration at which the inflection point is determined, whether it's from a three- or four-parameter logistic fit.

**Relative Potentiator Efficacy**

The fitted top of the potentiation curve minus the normalized response to the specific concentration of Reference Agonist alone divided by 100 minus the normalized response to the specific concentration of Reference Agonist alone.

**Response Surface Analysis**

A statistical analysis method that is used for central composite designs. A quadratic polynomial model is fit to the data in order to find the optimum conditions for an assay.

**Repeatability**

Repeatability is the precision of repeated measurements within the same analytical run under the same operating conditions over a short interval of time. It is also termed intra-assay or intra-batch precision.

**Reproducibility (Run to Run)**

A general term to describe the precision of results generated from multiple runs of a compound (or any homogenous test sample) in an assay. An assay may lack reproducibility because of either high within-run or across-run variability, or because of systematic trend (drift) over time in the response. An assay that is reproducible across runs is one that has variation within acceptable limits and has no material systematic trends.

**Reproducibility (Lab to Lab)**

Reproducibility across labs expresses the precision between laboratories. It is useful for assessing the “transferability” of an assay and/or the validity of comparing results from samples that are run in two or more laboratories.

**Robustness/Ruggedness of the Assay**

Robustness is a measure of the capacity of the assay to remain unaffected by small, but deliberate changes in method parameters and provides an indication of its reliability during normal run conditions.

**Schild Kb**

A measure of affinity for a competitive antagonist that is calculated using the ratios of equi-active concentrations of a full agonist (most typically EC50 concentrations are used) in the absence and presence of one or more concentrations of the antagonist. See pp. 335-339, Pharmacologic Analysis of Drug-Receptor Intercation, 3rd Ed. by Terry Kenakin.

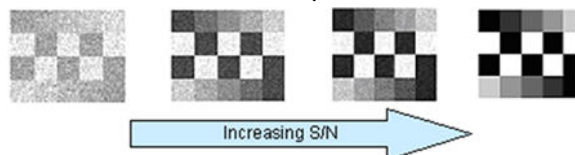
**Signal-to-background (S:B or S/B)**

The ratio between the mean max signal and the mean minimum or background signal. This definition has been useful for describing the dynamic range of the assay.



### Signal to Noise Ratio (S:N or S/N)

Defined as the mean signal (eg. Max or Min signal) divided by the standard deviation of this signal. This definition has been useful for describing the “signal strength” of an assay. The figure below illustrates how a two signals (black= background or Min and white=max) may appear as the “noise” in the system varies.



### Signal Window

A measure of separation between max. and min. controls in an assay that accounts for the amount of variability in the assay. The formula is:

$$SW = \frac{mean_{max} - mean_{min} - 3(SD_{max} + SD_{min})}{SD_{max}}$$

### Simple Linear Regression

A statistical method for fitting a straight line to paired (X, Y) data.

### Spearman's Correlation Coefficient

A nonparametric measure of correlation between two variables. It is applied to ranked values of the data and is therefore robust to outliers in the data.

### Specificity

The ability of the assay to determine unequivocally the analyte in the presence of components that may be expected to be present in the sample.

### Spike

Addition of a known quantity of a specific reference material or positive control to a sample matrix for recovery studies.

### Stephenson's Kp

A measure of affinity for a partial agonist that is calculated through the comparison of equi-active concentrations of a full agonist in the absence and presence of a single concentration of the partial agonist. See pp. 284-286, Pharmacologic Analysis of Drug-Receptor Interaction, 3rd Ed. by Terry Kenakin.

### Stimulation

Increase of a measured output. Unit of Measure is always % when normalized to the dynamic range of the assay (Min and Max control wells). Note that this calculation can generate percents much higher than 100.

### Stimulation at Max Included

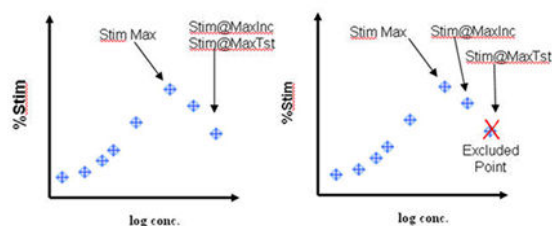
Stimulation observed at the highest included (i.e. not excluded) concentration of a substance tested in a concentration response mode method version regardless of whether it was included in the parametric fit to produce derived results. (See illustration below)

### Stimulation at Max Tested

Stimulation observed at the maximum concentration of a substance tested in a concentration response mode method version regardless of whether it was included in the parametric fit to produce derived results. (See illustration below)

### Stimulation Max

Maximum stimulation produced by any concentration that was included for the application of a curve fit algorithm (See illustration below)



### Target Platform

A set of biochemically and biologically related targets implicated in disease pathologies. Examples include G-protein coupled receptors (GPCRs), nuclear hormone receptors (NHRs), Kinases, Proteases, Transporters, Ion channels and Chemokines.

### Testing Flow Scheme

Stages of testing NCEs as it progresses from active to hit to lead to a clinical candidate. Tests include in-vitro assays, animal model tests, ADME assays biopharmaceutical and toxicological tests.

### Test-retest experiment

An experiment in which a set of (usually) 20-30 compounds is tested in two independent runs of an assay. Its purpose is to estimate the MSR (for dose-response assays) or the MSD (for single-point assays or an efficacy measure in dose-response assays). This experiment will provide a reliable estimate of only the within-run MSR.

### Top

The upper asymptote of a logarithmically derived curve. The Top value can be determined with real values or predicted using the logarithm applied to the result data set. The Unit of Measure is always %.

### Ultra High Throughput Screening (uHTS)

Greater than 500,000 compounds screened per screen.

## Validation

Validation includes all the laboratory investigations that demonstrate that the performance characteristics of an assay are suitable and reliable for its intended analytical use. It describes in mathematical and quantifiable terms the performance characteristics of an assay.

### Validation/QC Samples

Samples of standard material that are prepared independently of the standards used for a calibration curve. They are not used to fit the calibration curve, but they are calibrated against it to determine percent recovery.

### Within-Run MSD (Minimum Significant Difference)

The minimum difference in efficacies of two compounds evaluated in the same run that is statistically significant, i.e. that should be considered a real change in efficacy.

### Within-Run MSR (Minimum Significant Ratio)

The minimum ratio in potencies of two compounds evaluated in the same run that is statistically significant, i.e. that should be considered real change in potency.

### Z'-Factor

Another measure of separation between maximum and minimum controls in an assay that accounts for the amount of variability in the assay. The formula is:

$$Z'\text{-Factor} = 1 - \frac{(3\sigma_+ + 3\sigma_-)}{|\mu_+ - \mu_-|}$$

## Genetics Terms

**Allelic drop-out** — Failure to detect an allele in a sample or failure to amplify an allele during PCR.

**Allelic ladder** — Comprised of DNA fragments that represent common alleles at a locus.

**Allele** — A different form of a gene at a particular locus. The characteristics of a single copy of a specific gene or of a single copy of a specific location on a chromosome. For example, one copy of a specific STR region might have 10 repeats, while the other copy might have 11 repeats. These would represent two alleles of that STR region.

**Heterozygous** — Having two different alleles at the same locus.

**Homozygous** — Having two of the same alleles at the same locus.

**Off Ladder (OL) Alleles** — Alleles that size outside allele categories represented in the ladder.

**Phenotype** — The detectable outward manifestations of a specific genotype; the physical characteristics of a living object.

**Polymerase Chain Reaction (PCR)** — A technique for enzymatically replicating DNA without using a living organism.

**Polymorphism** — Variations in DNA sequences in a population that are detected in human DNA identification testing.

**Short Tandem Repeats (STR)** — Multiple copies of a short identical DNA sequence arranged in direct succession in particular regions of chromosomes.